F1103

ACADÉMIE DE LA RÉPUBLIQUE SOCIALISTE DE ROUMANIE

REFERÁLVA
R

REVUE ROUMAINE DE CHIMIE

TOME 26
N° 1
Janvier 1981

EDITURA ACADEMIEI REPUBLICII SOCIALISTE ROMÂNIA

Rev. Roumaine Chim.

RRCHAX, **26**, *1*, p. 1–158 (1981), Bucarest

ACADÉMIE DE LA RÉPUBLIQUE SOCIALISTE DE ROUMANIE

COMITÉ DE RÉDACTION

Rédacteur en chef:

I. G. MURGULESCU, membre de l'Académie de la République Socialiste de Roumanie

Rédacteurs en chef adjoints:

A. T. BALABAN et V. EM. SAHINI, membres correspondants de l'Académie de la République Socialiste de Roumanie

Collège de rédaction:

EM. BRATU, ELENA CEAUȘESCU, ECATERINA CIORĂNESCU-NENITZESCU, CR. SIMIONESCU, membres de l'Académie de la République Socialiste de Roumanie; P. SPACU, membre correspondant de l'Académie de la République Socialiste de Roumanie; MARGARETA AVRAM, M. BANCIU, I. HAIDUC, D. I. MARCHIDAN, I. MOLDOVAN, G. NIAC et D. SĂNDULESCU

La Revue Roumaine de Chimie paraît 10 fois par an. Toute commande de l'étranger pour les travaux parus aux Editions de l'Académie de la République Socialiste de Roumanie sera adressée à ILEXIM, Departamentul Export-Import Carte (Livres)/Departamentul Export-Import Presă (Revues), P.O.B. 136—137, télex 11226, 3, str. 13 Decembrie, 79517 Bucarest, Roumanie

Les manuscrits, les livres et les revues proposés en échange, ainsi que toute correspondance seront envoyés à la rédaction :

REVUE ROUMAINE DE CHIMIE

125, Calea Victoriei, 79717 Bucarest, Roumanie, téléphone 50 76 80

EDITURA ACADEMIEI REPUBLICII SOCIALISTE ROMÂNIA
125, Calea Victoriei, 79717 Bucarest, Roumanie, téléphone 50 76 80

REVUE ROUMAINE DE CHIMIE

Tome 26, N° 1 Janvier, 1981

V. E. SAHINI and LILIANA TELEA, CNDO/2 calculations of anisidine isomers . . . 3–7

D. FERRO, V. PIACENTE and M. PELINO, Measurements of the vapour pressure of β-bromonaphthalene . . . 9–15

MIHAELA HILLEBRAND, I. BACIU and G. MAXIM, ESR and electronic study of the 1,4-benzo-*p*-dioxin [2,3-b] thioxanthone anion-radical . . . 17–20

G. CHITHAMBARATHANU PILLAI, J. RAJARAM and J. C. KURIACOSE, The oxidation of butan-2-one by vanadium (V) in aqueous perchlorate media. Kinetics and mechanism . . . 21–27

DELIA ISAC, M. MRACEC, N. PROŞTEANU and Z. SIMON, The kinetics of thermal and photochemical decomposition of aromatic diazonium salts . . . 29–35 R

I. M. SIDAHMED, S. M. SALEM and F. M. ABDEL HALIM, Alkaline hydrolysis of formamide in water-organic solvent mixtures . . . 37–42

D. GEANĂ, Chemical equilibrium in multicomponent reaction systems . . . 43–53 R

N. PETRESCU and LUCIA GANOVICI, Self-diffusion of tellurium in liquid Tl_2Te alloy . . . 55–64 C

SILVIA PLOŞTINARU and P. SPACU, Mixed ligand compounds of lanthanides with neutral ligands containing donor oxygen atoms. III. Chlorosalicylates of lanthanides with 2,2′-dipyridyl-1,1′-dioxide . . . 65–70

VICTORIA COLDEA, M. COLDEA and I. HAIDUC, Proton magnetic resonance spectra of some di- and triorganotion mono- and dithiocarboxylates . . . 71–79

M. S. K. YOUSSEF and KH. M. HASSAN, Synthesis of some new thienylazetidin-2-ones and thienylthiazolidin-4-ones . . . 81–86

MARIA BRUMĂ and GABRIELA NEAMŢU, Poly-1,3,4-oxadiazoles. IX. Ordered poly-1,3,4-oxadiazole-amide-imides . . . 87–93

M. ABDALLA, A. ESSAWY, M. A. EL-HASHASH and A. M. EL-GENDY, Action of aromatic hydrocarbons, active methylene compounds and Grignard reagents on α-3-benzylidene-5-[1′(2′-methylnaphthalenyl)]-2(3H) furanone and 4-benzylidene-1-*p*-tolyl-2-[1′(2′-methylnaphthalenyl)]-2-pyrroline-5-one . . . 95–99

M. A. EL-HASHASH, M. E. SHABAN and M. M. HABASHY, Some reactions of 3,4-methylenedioxybenzylidene-*p*-isopropylacetophenone . . . 101–108

EM. GEORGESCU, I. DRUTA and MAGDA PETROVANU, Dipolar derivatives in the quinazoline series. I. Synthesis of pyrrolo[1,2,-c] quinazolines (in French) 109–116

M. A. MATEESCU, H. C. SCHELL, M. DIMONIE, T. BENŢIA, C. DIMITRIU and O. MAIOR, Cationic beaded PVA ion exchangers. I. Reticulation, derivatisation and some physical-chemical properties (in German) . . . 117–124

DOINA GAVRILĂ, Experimental studies bearing upon the behaviour of polyvinyl chloride in heavy fields of nuclear radiations . . . 125–130

M. DIMA, S. OPREA and E. DUMITRIU, Reactivity of acrylic monomers. III. Copolymerization of N,N-dimethylaminoethyl-methacrylate with N,N-diethylacrylamide . . .

ANDREI FL. DĂNEŢ, Study of extraction and complexing of palladium (II) 131–139 with 1-(*p*-nitrophenyl), 3-(*p*′-azobenzene)-triazene and 1-(*p*-nitronaphthyl), 3-(*p*′-azobenzene)-triazene . . . 141–149

A. M. QURESHI and A. N. PATEL, A new acid-base indicator . . . 151–153

BOOK REWIEVS . . . 155–157

|Rev. Roumaine Chim.| 33 **26**, *1*, 1–158, (1981) Bucarest

Revue Roumaine de Chimie, **26**, *1*, 3–7 (1981)

CNDO/2 CALCULATIONS OF ANISIDINE ISOMERS

V. E. SAHINI and LILIANA TELEA
Center of Physical Chemistry Bucharest, Splaiul Independenţei 202, Bucharest, Romania

Received April 16, 1980

CNDO/2 Molecular Orbital Method is used to study the conformations and charge distributions of anisidine isomers. Theoretical charge distributions correlate with pK_a values and NMR chemical shifts. Calculated dipole moments prove the presence of a weak intramolecular hydrogen bond in *ortho*-anisidine, and equal amount of both *cisoid* and *transoid* form in the *meta* isomer and a single conformation for the *para* anisidine, in agreement with experimental data.

INTRODUCTION

The interaction between the substituents and the benzene ring plays a very important part in determining the structure and stabilities of aromatic derivatives.

Our previous studies[1,2] concerning the structure and some physicochemical properties of anisidines have mainly taken into account the π interactions between the substituents and the aromatic system and very little the effects of σ electrons, which also may influence the energy of interaction and the molecular conformation.

These considerations led us to the idea of performing a semiempirical calculation that takes account of all valence electrons in order to investigate two aspects :

a) Calculation of charge distribution and the dipole moment and
b) Determination of the most stable conformation of isomers.

Molecular Orbital calculation in CNDO/2 approximation [3] has been carried out. The charge distributions have been compared with literature data concerning chemical shifts $\delta^{13}C$ of aromatic carbons [4] and δNH_2 of amino proton. [5,6]

The dipole moment calculated values have been compared with the corresponding experimental data. [1,7,8]

METHOD OF CALCULATION

The closed shell version of Pople and Beveridge CNINDO program [9] has been modified and adapted for 47 basis orbitals on the Felix C–256.

The input geometrical parameters, including bond lengths and valence angles are given in table 1.

The coordinate system has been chosen so that the aromatic cycle was in the $x-y$ plane, hence the $2p_z$ orbital has been considered as π orbital. A tetrahedral structure for the N atom has been considered,[10] but, in order to optimize the amino group interaction with the π system, a zero degree dihedral angle with respect to the benzene plane has been assumed.[11] An sp^2 hybridization for the methoxy oxygen has been considered.[12] The methoxy group rotation described by the angle θ between the ring plane and the $C_{(Ar)}-O-C_{(CH_3)}$ plane results from the balance of two opposing effects [12]: an effect which tends to place the OCH_3 group coplanar with the ring in order to obtain the maximum overlap of the oxygen $2p_z$ orbital with the aromatic π system, and a counteracting effect, the steric repulsion of the *ortho* substituent which tends to diminish the coplanarity of the methyl group with the ring.

TABLE 1

Geometrical parameters for CNDO/2 calculations of anisidine isomers

Bond	Length, Å	Bond angles	Degrees
$C-N$	1.420	$H-N-C$	109.47
$N-H$	1.040	$H-N-H$	109.47
$C=C$	1.397		
$C_{Ar}-H$	1.084	$H-C-H_{(CH_3)}$	109.47
$C_{Ar}-O$	1.360		
$O-C_{(CH_3)}$	1.360	other angles	120.00
$C_{(CH_3)}-H$	1.090		

RESULTS AND DISCUSSIONS

The dipole moment values and the energy calculated for various conformations (corresponding to different θ values) of the anisidines are given in table 2.

The results indicate a maximum stability for a dihedral θ angle between 90−130° in the case of the *ortho* isomer. The best agreement of the calculated dipole moment with the experimental values is obtained for $\theta = 110°$. Obviously, the conformation corresponding to $\theta = 0°$ has a maximum repulsion, the CH_3 group coplanar with the ring raises the potential energy of the molecule.

The twisting of the methyl hydrogen about the O−C bond diminishes the repulsion of this group with the aminic proton, but the dipole moment values are little improved (Table 3).

For the *meta* isomer the conformations obtained for $\theta = 0°$ and $\theta = 180°$ have the same stability. From the comparison of the corresponding dipole moments with the experimental value an equal amount of both conformers results.

In the case of *para* isomer a greater stability is obtained for a $\theta = 90°$, but the calculated dipole moments are in better agreement with the observed values for the identical conformations corresponding to $\theta = 0°$ and 180°.

We suppose that an improvement of the calculated dipole moment values for *para*-anisidine can be obtained if a modification of the amino group conformation is adopted taking into account the noncoplanarity with the aromatic ring.[13]

TABLE 2

Energies and dipole moments for various conformations of anisidines

Isomer	θ degrees	E (eV)	$\mu^{theor.}$ (D)	μ^{exp} and references (D)
ortho-anisidine	0	−85.954	2.017	1.42[1] ; 1.51[7]
	60	−86.669	1.884	
	90	−86.670	1.615	
	110	−86.667	1.364	
	120	−86.668	1.225	
	130	−86.669	1.081	
	160	−86.664	0.693	
	180	−86.661	0.576	
meta-anisidine	0	−86.664	2.433	1.84[1] ; 1.86[8]
	60	−86.668	2.230	
	90	−86.669	1.998	
	180	−86.664	1.189	
para-anisidine	0	−86.659	2.048	1.72[1] ; 1.82[7]
	30	−86.664	2.056	
	90	−86.665	2.161	
	180	−86.659	2.047	

If the HNH valence angle is modified, using the values obtained from IR spectra[14] corresponding to an intermediate sp^3-sp^2 hybridization, the isomer stability increases but a better agreement of the dipole moment values is obtained for a tetrahedral angle. The values of charge distributions on the ring carbons calculated for the most stable conformation are in good agreement with the corresponding $^{13}C-NMR$ chemical shifts (Table 4).

TABLE 3

Influence of φ angle on the dipole moment and stability of *ortho*-anisidine conformers

θ (degrees)	φ (degrees)	μ (D)	E^{tot} (eV)
0	0	2.017	−85.954
	60	1.996	−86.642
	90	1.977	−86.623
90	0	1.615	−86.670
	30	1.604	−86.667
	60	1.589	−86.668

A π-charge transfer from the nitrogen toward the cycle and a simultaneous growth of σ charge on the aminic nitrogen is found (Tables 4 and 5). The inductive effect of methoxy group transferred through the σ framework is opposed by a dominant π donation of the oxygen lone pair, and

TABLE 4

Correlation of CNDO/2 charge distribution in the benzene ring with $^{13}C-NMR$ chemical shifts

Isomer	Atom	C_1	C_2	C_3	C_4	C_5	C_6
ortho-anisidine	ρ^{π}	0.9716	1.0338	1.0198	1.0365	0.9983	1.0643
	$\rho_{2p}^{\pi+\sigma}$	2.9122	2.8842	3.0136	3.0093	2.9833	3.0353
	ρ_{2p+2s}^{total}	3.9036	3.8737	4.0281	4.0121	3.9910	4.0419
	$\delta^{13}C^4$ (ppm)	138.6	147.6	111.7	117.7	122.1	115.2
meta-anisidine	ρ^{π}	0.9079	1.1372	0.9219	1.1088	0.9469	1.1149
	$\rho_{2p}^{\pi+\sigma}$	2.8494	3.1063	2.7940	3.0804	2.9593	3.0760
	ρ_{2p+2s}^{total}	3.8387	4.1157	3.7894	4.0863	3.9701	4.0793
	$\delta^{13}C^4$ (ppm)	151.0	101.0	161.5	102.9	130.08	108.2
para-anisidine	ρ^{π}	0.9634	1.0553	1.0335	1.0044	1.0297	1.0568
	$\rho_{2p}^{\pi+\sigma}$	2.8942	3.0280	3.0225	2.8560	3.0164	3.0293
	$\rho_{2\pi+2s}^{total}$	3.8798	4.0354	4.0383	3.8456	4.0270	4.0362
	$\rho^{13}C^4$ (ppm)	143.2	116.5	115.8	152.0	115.8	116.5

an inhibition of delocalization of the nitrogen lone pair on the aromatic ring results. The competition between the inductive and conjugative effects of the methoxy group dissapears in the *meta* isomer where only the inductive effect operates. In this case the effective nitrogen π charge has the lowest value. As the charge on the nitrogen diminishes, a simultaneous increase of the charge distributions on the NH bonds takes place that leads to the unshielding of H atoms and their protonisation.

TABLE 5

Variation of the nitrogen charge distribution with the basicity and amino proton chemical shift

Isomer	ρ_N^{π}	ρ_N^{2p}	$\delta NH_2^{5,6}$	pK_a^5
para-anisidine	1.9182	4.0496	4.50	5.34
ortho-anisidine	1.9159	4.0478	4.60	4.53
meta-anisidine	1.9089	4.0466	4.92	4.23

Indeed as it has been expected, the charge density variation on the amino nitrogen correlates with the pK_a values and the amino proton chemical shifts.[5,6]

CONCLUSIONS

The CNDO/2 calculations provide a good description of the charge distribution in the three isomeric anisidines, in agreement with their basicity and chemical shifts. The calculated dipole moment values are in relatively good agreement with the experimental ones.

The conformational energies and dipole moment values obtained by CNDO/2 method prove the presence of a weak intramolecular hydrogen bond in *ortho* anisidine (an intermediate conformation between the free — *cisoid* and completly chelated — *transoid* form is favoured), an equal amount of both conformers in the *meta* isomer case and a single conformation for the *para* anisidine.

REFERENCES

[1] V. E. Şahini and L. Telea, *Rev. Roumaine Chim.*, **21**, 321 (1976).
[2] V. E. Şahini and L. Telea, *Rev. Roumaine Chim.*, **21**, 645 (1976).
[3] J. A. Pople, D. P. Santry and G. A. Segal, *J. Chem. Phys.*, **43** S, 129, 136 (1965).
[4] C. Nagata, O. Hamada and S. Tanaka, *Nippon Kagaku Kaishi*, **7**, 1029 (1976).
[5] B. M. Lynch, *Tettrahedron Letters*, **1969**, 1357.
[6] E. V. Titov, *J. Molec. Structure*, **19**, 301 (1973).
[7] A. L. McClellan, "Tables of Experimental Dipole Moments", W. H. Freeman, San Francisco, 1963.
[8] S. K. Jatkar, V. K. Phansalkar, and C. A. Chinchwadkar, *Indian J. Chem.*, **7**, 93 (1969).
[9] J. A. Pople, and D. L. Beveridge "Aproximate Molecular Orbital Theory", McGraw Hill, New York, 1970.
[10] D. G. Lister and J. K. Tyler, *Chem. Comm.*, **1966**, 152.
[11] G. Adler and R. L. Lichter, *J. Org. Chem.*, **39**, 3457 (1974).
[12] W. J. Hehre, L. Radom and J. A. Pople, *J. Amer. Chem. Soc.*, **94**, 1496 (1972).
[13] G. L. Butt and R. D. Topsom, *Spectrochim. Acta*, **34A**, 975 (1978).
[14] V. E. Sahini and L. Telea, *Rev. Roumaine Chim.*, **23**, 483 (1978).

contributions of delocalization of the nitrogen lone pair on the aromatic ring results. The competition between the inductive and [illegible] effects of the [illegible] group [illegible] in the [illegible] where only the inductive effect operates. In this case the [illegible] charge has

TABLE [illegible]

[illegible] of the nitrogen charge [illegible] with the [illegible] and amino proton chemical shift

the lowest value. As the charge on the nitrogen diminishes, a [illegible] increase of the charge [illegible] on the NH bonds [illegible] leads to the [illegible] of [illegible] and their [illegible].

Indeed as it has been expected, the charge [illegible] on the amino nitrogen correlates with the pK_a values and the amino proton chemical shifts.[14]

DISCUSSION

The CNDO/2 calculations provide a good description of the charge distribution in the three isomeric [illegible], in agreement with basicity and chemical shifts. The calculated dipole moment values are in relatively good agreement with the experimental values.

The conformational energies and dipole moments values obtained by CNDO/2 method prove the presence of a weak intramolecular hydrogen bond in ortho-[illegible] (an intermediate conformation between the free [illegible] and completely chelated [illegible] form is favoured); an equal amount of both conformers in the meta isomer and only a single conformation for the para [illegible].

REFERENCES

[illegible]

Revue Roumaine de Chimie, 26, 7, 9–15 (1981)

MEASUREMENTS OF THE VAPOUR PRESSURE OF ß-BROMONAPHTHALENE *

D. FERRO, V. PIACENTE and M. PELINO
Instituto di Chimica Fisica, Università degli Studi, Roma

Received August 8, 1979

Employing different techniques, the vapour pressure of β-bromonaphthalene was determined in the temperature range 275–378 K.
The following pressure-temperature equations :

solid → gas $\lg P(\mathrm{kPa}) = (8.77 \pm 0.50) - (3360 \pm 200)/T$

liquid → gas $\lg P(\mathrm{kPa}) = (5.68 \pm 0.50) - (2320 \pm 250)/T$

are determined. Thermodynamic functions as free energy function and entropy for gaseous and liquid phases were derived.

A number of investigations on the physico-chemical properties of β-bromonaphthalene are reported in literature.[1,2] D.T.A. and X-ray diffraction analyses of the solid compound show that some phase transitions occur. However, as concerns the vaporization behaviour, apparently no vapour pressure determination has been carried out as yet. As a part of a program for the study of vaporization thermodynamics of selected pure organic substances,[3,4] the vapour pressure of β-bromonaphthalene was determined by using different techniques.

The results are reported in this paper.

EXPERIMENTAL AND RESULTS

The β-bromonaphthalene employed (99% pure) was supplied by Fluka AG Buch SG. The vapour pressure of this compound was measured by using the torsion, effusion, the Knudsen-effusion and the transpiration techniques.

A. TORSION-EFFUSION METHOD

Details of the technique and the experimental apparatus have been reported previously.[4] The values of the vapour pressure in equilibrium with bromonaphthalene were derived from the torsion angles α of the effusion cell by using the well known relation :

$$P = 2K\alpha/(a_1 l_1 f_1 + a_2 l_2 f_2)$$

where K is the torsion constant of the suspension tungsten wire, a_1 and a_2 are the areas of the two effusion holes of the cell, l_1 and l_2 their respective distances from the rotation axis, and f_1 and f_2 the corresponding geometrical correction factors.

---

* This work has been supported by Consiglio Nazionale delle Ricerche, Roma.

Three cells, similar to that schematized in figure 1 but with different geometrical constants (Table 1), were employed in this study. Cell temperatures were determined with a calibrated chromel-alumel thermocouple inserted in a second blank cell placed below the torsion effusion cell. In order to test the apparatus, prior to the β-bromonaphthalene vaporization experiments, the vapour pressures of iodine, naphtalene and

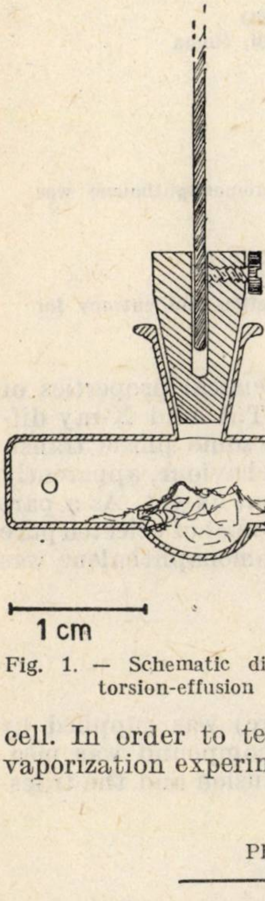

Fig. 1. — Schematic diagram of the torsion-effusion cell.

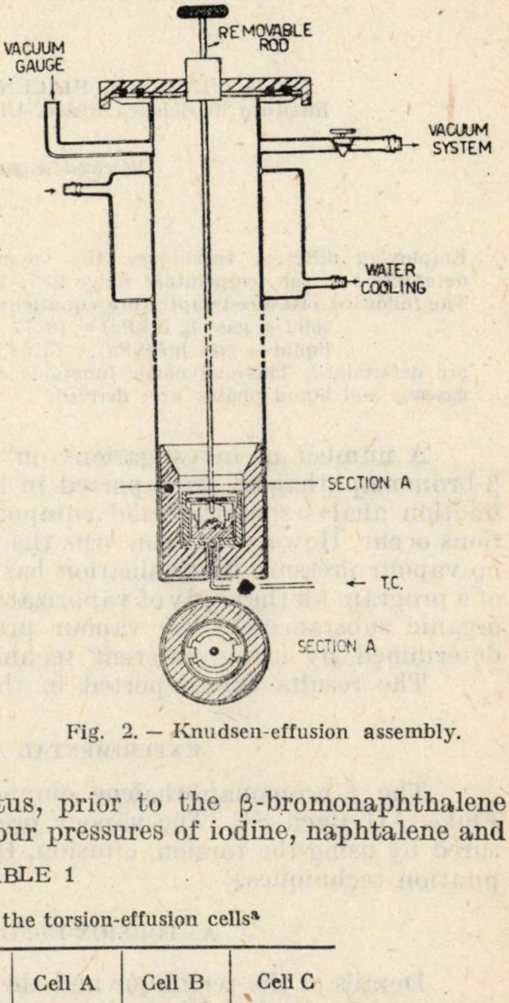

Fig. 2. — Knudsen-effusion assembly.

TABLE 1

Physical constant of the torsion-effusion cells[a]

		Cell A	Cell B	Cell C
Orifice area of the cells[b] (10^{-3} ± ±0.05 cm^2)	(1)	31.40	1.13	6.36
	(2)	31.40	1.13	5.03
Force correction factors [5]	(1)	0.880	0.306	0.430
	(2)	0.875	0.306	0.398
Moment arm (cm)±0.01	(1)	0.66	1.10	0.97
	(2)	0.69	1.01	1.05

[a] The torsion constant K of tungsten wire (length (34.8±0.2) cm, diameter 30 μm) is equal to 0.346±0.003 dyne cm rad^{-1}.

[b] Measured by photographic enlargement.

sulfur were measured. The agreement between the sublimation enthalpy values for these substances derived by the vapour data and those reported in literature [6,7] was excellent and this has been considered a proof that thermodynamic equilibrium conditions were obtained within the cell and that temperature measurements were reliable. The vaporization of the bromonaphthalene was studied in five runs over the temperature range 275—359 K.

The results are listed in table 2 and fitted as plot of lg *P vs* 1/*T* in figure 2. Because of the high vapour pressure of the compound at the

TABLE 2

Vapour pressure of β-bromonaphthalene measured by torsion-effusion method

Run	*T* (K)	*P* (kPa)	Run	*T* (K)	*P* (kPa)
B.01	275	4.13 10^{-4}	B.02	309	8.85 10^{-3}
	282	8.26 ,,		312	1.18 10^{-2}
	288	1.65 10^{-3}		315	1.33 ,,
	293	2.06 ,,		317	1.48 ,,
	295	2.48 ,,		318	1.62 ,,
	297	3.30 ,,		319	1.77 ,,
	304	3.71 ,,		320	1.92 ,,
	312	1.03 10^{-2}		324	2.95 ,,
	315	1.20 ,,		327	3.40 ,,
	317	1.24 ,,		329	3.54 ,,
	318	1.32 ,,		330	3.69 ,,
	324	2.19 ,,			
	325	2.85 ,,	B.03	305	3.40 10^{-3}
	326	3.35 ,,		308	4.53 ,,
	328	4.58 ,,		313	7.92 ,,
	328	3.88 ,,		317	1.02 10^{-2}
	329	4.09 ,,		318	1.13 ,,
	330	4.47 ,,		320	1.58 ,,
	331	4.67 ,,		327	3.05 ,,
	332	5.00 ,,		329	3.51 ,,
	333	5.37 ,,		340	7.73 ,,
	334	5.58 ,,		342	8.28 ,,
				344	9.75 ,,
				347	1.09 10^{-1}
				348	1.17 ,,
				349	1.18 ,,
				350	1.20 ,,
				354	1.37 ,,
				355	1.41 ,,
B.04	309	5.66 10^{-3}	B.05	310	7.03 10^{-3}
	315	9.06 ,,		312	8.20 ,,
	320	1.58 10^{-2}		313	9.37 ,,
	328	3.51 ,,		317	1.05 10^{-2}
	332	5.32 ,,		318	1.17 ,,
	339	7.00 ,,		320	1.28 ,,
	340	7.92 ,,		321	1.52 ,,
	341	8.65 ,,		322	1.75 ,,
	347	1.18 10^{-1}		324	1.87 ,,
	352	1.45 ,,		325	2.11 ,,
	356	1.61 ,,		327	2.34 ,,
	357	1.67 ,,		329	2.58 ,,
	358	1.69 ,,		331	2.70 ,,
	359	1.38 ,,			

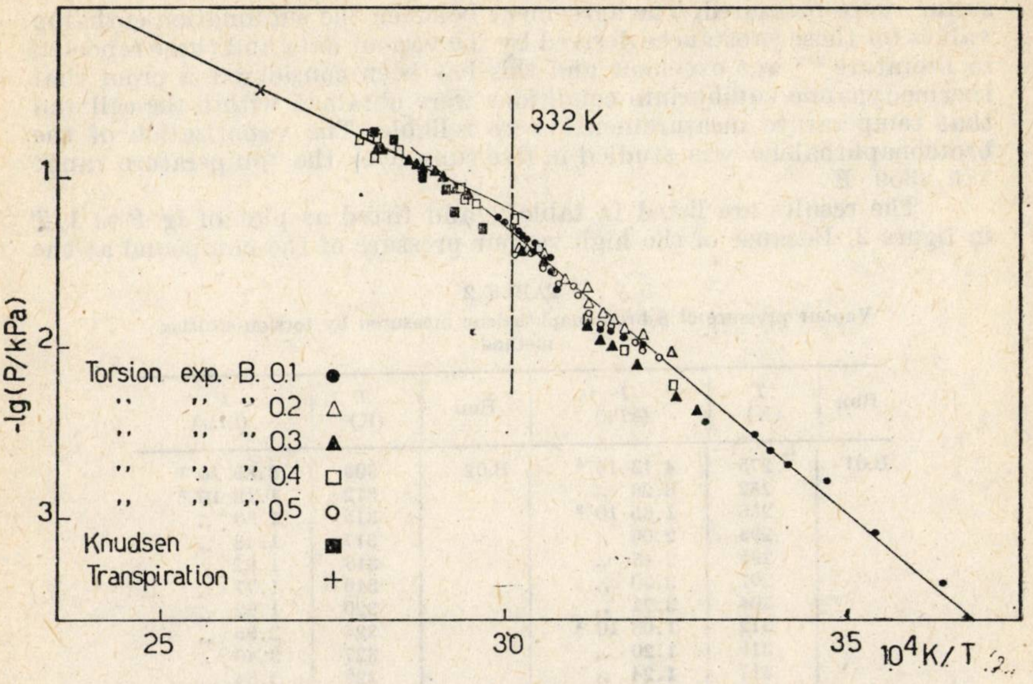

Fig. 3. — Experimental values of vapour pressure of the β-bromonaphthalene

room temperature, the zero torsion angle was measured at the end of each run when the sample was completely vaporized. Considering that in the covered temperature range the β-bromonaphthalene melts, two pressure-temperature equations, corresponding to the vaporization from the solid and liquid compound by the least-square treatment of the data, were derived :

$$\text{solid}: \quad \lg P\,(\text{kPa}) = (8.77 \pm 0.16) - (3363 \pm 51)/T \qquad (1)$$

$$\text{liquid}: \quad \lg P\,(\text{kPa}) = (5.11 \pm 0.28) - (2111 \pm 98)/T \qquad (2)$$

where the associated errors on the slopes and intercepts are standard deviations.

B. KNUDSEN-EFFUSION TECHNIQUE

Some vapour pressure values over liquid β-bromonaphthalene were determined by the Knudsen-effusion method.[8]

The experimental apparatus is reported in figure 3. The heating of the cell was obtained utilizing an oil-bath and the temperatures were measured by a calibrated Cupper-Constantan thermocouple inserted into the effusion cell. At any fixed temperature, the vapour pressure value was derived from the mass-loss of the sample through the relation :

$$P(\text{kPa}) = 2.29\, K_c m (T/M)^{1/2}/A\Delta t$$

where m is the mass of the vapour effused from the cell in the time Δt through the effusion hole of area A, M is the molar mass of the gas, T the cell temperature and K_c the Clausing's factor.[9] In each run the vaporization time was evaluated by opening and closing the effusion hole of the cell. The amount of vapour effused was determined by weighing the cell before and after each experiment.

Also in this case, calibration runs using pure iodine and sulfur were performed. The measured vapour pressure compares fairly well with those reported in literature.[6]

TABLE 3

Vapour pressure of the β-bromonaphthalene (1) measured by Knudsen effusion method

Run	T (K)	Substance evaporated (mg)	t (s)	P (kPa)
1	338±3	627	90	$4.36\ 10^{-2}$
2	342±2	616	60	$6.46\ 10^{-2}$
3	344±2	847	60	$8.91\ 10^{-2}$
4	348±2	1 025	60	$1.10\ 10^{-1}$
5	353±3	2 440	98	$1.62\ 10^{-1}$
6	356±2	1 277	60	$1.38\ 10^{-1}$

In table 3 and figure 2 the obtained data are reported, assuming that β-bromonaphthalene is the only gaseous species in thermodynamic equilibrium with the liquid phase by analogy with α-bromonaphthalene.[3]

C. TRANSPIRATION METHOD

A set of vapour pressure values at 378 K was determined by the transpiration method. The method and the apparatus were described in a previous work.[10] The pressure P_i is derived from the weight of the vapour condensed in a water cooled collector (m_i) in the time Δt by the equation :

$$P_i = m_i^0/(m_i^0 + P^0 \Delta t \Phi M_i / RT^0)$$

where Φ is the flow-rate of the carrier gas measured by a flowmeter placed at the inlet of a furnace, P^0 and T^0 the pressure and the temperature of the carrier gas in the flowmeter, R is the gas constant and M_i the molecular weight of the vapour. The optimal range of the carrier gas flow rate, argon in our case, that ensures the saturation of the carrier gas, was determined experimentally. The vapour pressures were measured varying the carrier gas and the condensation time. The amount of condensed vapour was determined by a gain of mass of the collector after each experiment.

Because of the high vapour pressure of the compound at room temperature, at the end of each measurement the collector, as soon as drawn out of the furnace, was sealed with two tephlon caps. The weight of the condensate was opportunely corrected to take into account the sublimation of the sample from the collector at the temperature of the cooling water during the experiment time. In table 4 the vapour pressure values

TABLE 4

Vapour pressure of β-bromonaphthalene measured by transpiration method

T (K)	Vapour condensed (mg)	Time (min)	Φ (ml/min)	P (kPa)
379±1	48.1	10	171±8	3.24 10^{-1}
378±1	77.1	17	173±8	3.02 „
378±1	87.6	17	209±6	2.82 „
376±1	59.2	12	164±10	3.47 „
377±1	65.1	14	169±5	3.16 „
			Average (3.1±0.2) 10^{-1}	

measured at 378 ± 1 K are summarized; from these data the value $P = (3.1 \pm 0.2)\ 10^{-1}$ kPa was derived.

CONCLUSION

On the gound of the results obtained by the torsion-effusion method, the vapour pressure of the solid bromonaphthalene follows the equation :

$$\lg P\ (kPa) = (8.77 \pm 0.50) - (3360 \pm 200)/T \qquad (3)$$

where the associated errors were estimated taking into account the incertainties in the temperature measurements and in the calibrated factors. From the slope of this equation, the second-law sublimation enthalpy at the average temperature of 357 K derived from the slope is $\Delta H^\circ_{298} = 44 \pm 5$ kJ mol^{-1}. The sublimation enthalpy at 298 K was also calculated by the third-law procedure. The necessary free energy functions, $(G^\circ_T - H^\circ_{298})/T$, of gaseous β-bromonaphthalene were calculated in the usual way by the mechanical-statistical formulae adopting, for the molecule, a planar configuration and bond lenghts and angles equal to those proposed by Chanh et al.[2] for the solid phase. The necessary vibrational frequencies were determined experimentally by the infrared matrix isolation technique with a procedure similar to that described elsewhere.[11] It is interesting to note that our data agree with those obtained by Sharma et al.[12] studying the solid sample mulled with organic solvent.

In table 6 are reported the third-law vaporization enthalpies at each experimental temperature. The average value $\Delta H^\circ_{298} = 53 \pm 1$ kJmol^{-1} agrees enough with that determined by the second law, $\Delta H^\circ_{298} = 46 \pm 5$, reduced at 298 K by using the heat contants reported in table 5. The value $\Delta H^\circ_{298} = 49 \pm 6$ kJ/mol for the vaporization of liquid β-bromonaphthalene is proposed. This value used in conjunction with the sublimation enthalpy reported above gives, for the fusion enthalpy of β-bromonaphthalene, the value $\Delta H^0_{fus} = 15 \pm 9$ kJ mol^{-1}. By using the equations (3) and (4) the melting point 336 K is derived, which agrees with the value 332 K reported in literature.[2] These agreements could be taken as further proof that the absolute vapour pressure values and the temperature measurements are reliable.

TABLE 5

Thermodynamic functions of the β-bromonaphthalene

T (K)	Liquid		Gas	
	$H^0_T - H^0_{298}$ (kJ mol^{-1})	$-(G^0_T - H^0_{298})/T$ (J mol^{-1} K^{-1})	$H^0_T - H^0_{298}$ (kJ mol^{-1})	$-(G^0_T - H^0_{298})/T$ (J mol^{-1}K^{-1})
300	0.3	283	0.3	378
320	3.9	283	3.4	378
340	7.7	284	6.7	379
360	11.7	285	10.1	380
380	15.9	287	13.8	382
400	20.4	289	17.6	384

REFERENCES

[1] See for example : B. W. Cox, M. A. Keenan, R. D. Topson and G. J. Wright, *Spectrochimica Acta*, **21**, 1663 (1965).

[2] N. B. Chanh, Y. Haget, F. Leroy and F. Hannoteaux, *Acta Cryst.* **B.29**, 1469 (1973).

[3] M. Urbani, R. Gigli and V. Piacente, *J. Chem. Eng. Data* (1979).

[4] R. D. Freeman, Momentum Sensor in "The Characterization of High Temperature Vapours" J. L. Margrave Editor, Wiley, New York 1967 ; V. Piacente and G. De Maria, *Ric. Sci.*, **39**, 549 (1969).

[5] R. D. Freeman and A. W. Searcy, *J. Chem. Phys.*, **22**, 762 (1954).

[6] R. Hultgren, R. L. Or and K. K. Kelley, "Supplement to Selected Values of Thermodynamic Properties of Metals and Alloys" Dep. of Mineral Technology, Univ. of California, Berkley, California, 1967.

[7] O. Shuzo "Computer Aided Data Book of Vapour Pressures", Data Book Publishing Company Tokio, Japan 1967.

[8] M. Knudsen, *ANN. Phys.*, **28**, 75 (1909).

[9] S. Dushman, "Scientific Foundation of Vacuum Technique", Wiley, New York, 1958, pp 90–111.

[10] V. Piacente and G. Balducci, *Rev. Roumaine Chim.*, **18**, 2083 (1973).

[11] L. Bencivenni, S. Nunziante Cesaro, S. Maltese and M. Spoliti, *High Temp. Sci.* (1979).

[12] O. P. Sharma and R. D. Singh, *Ind. J. of pure Appl. Phys.*, **11**, 618 (1973).

Revue Roumaine de Chimie, 26, 7, 17–20 (1981)

ESR AND ELECTRONIC STUDY OF THE 1,4-BENZO-*p*-DIOXIN [2,3-b] THIOXANTHONE ANION-RADICAL

MIHAELA HILLEBRAND, I. BACIU and G. MAXIM
Department of Physical Chemistry, the Polytechnic,
Bd. Republicii 13, Bucharest, Romania

Received December 19, 1979

The ESR and optical spectra of the anion-radical obtained by electrochemical reduction from 1,4-benzo-*p*-dioxin [2,3-b] thioxanthone are reported and discussed. The experimental hyperfine splittings and the McLachlan spin densities underline the predominant effect of the thioxanthone moiety on the spin distribution.

The influence brought about by the presence of an acceptor group (nitro, benzoyl, acetyl) on the oxido-reduction properties of a donor molecule was previously investigated for some substituted anthracene heteroanalogs. It was thus observed that for dibenzo-*p*-dioxin,[1] phenoxatellurine,[2] and even for phenothiazine,[3] the strongest donor in the series, the presence of nitro groups ensured sufficient reducibility to the molecules so that stable anion-radicals, with well resolved ESR spectra, might be obtained besides the expected cation-radicals. When four nitro groups were substituted on phenothiazine, an inverse effect was also noted, that is the loss of the donor capacity of the molecule, reflected by the failure of cation-radical formation. From the other electron-acceptor groups studied, benzoyl was found strong enough to lead to anion-radicals from dibenzo-*p*-dioxin and phenoxathiin,[4] while the attempts to prepare anion-radicals starting from the acetyl derivatives of the same heterocycles failed.[5]

In all the anion-radicals obtained from the anthracene heteroanalogs, the spin distribution was determined by the substituent, while in the cation-radicals it was similar to that of the unsubstituted radicals.

In the following, we have continued the same study and have been interested in the behaviour on oxidation and reduction of 1,4-benzo-*p*-dioxin [2,3-b] thioxanthone (I) which is derived from dibenzo-*p*-dioxin but contains a fragment which is easily reducible, thioxanthone (II).

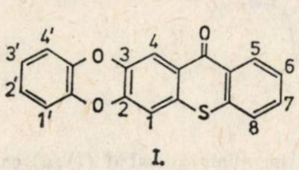

I.

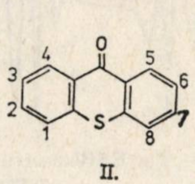

II.

EXPERIMENTAL AND MO CALCULATIONS

1,4-Benzo-p-dioxin [2,3-b] thioxanthone was synthetized by the condensation method described previously.[6] The anion-radical was generated electrochemically by an *in situ* technique both for ESR and optical investigations. The cells were equipped with platinum electrodes and as supporting electrolyte we used tetrabutylammonium perchlorate. The experiments were performed in dimethylsulfoxide (DMSO) and dimethylformamide (DMF). The ESR spectrum was recorded on a JES-3B spectrometer, operating in the X band frequency. The hyperfine splittings (hfs) and the g factor were measured against peroxylaminedisulfonate ($a_N - 1.3$ mT ; $g - 2.0055$). The optical spectrum was recorded on a SPECORD UV-VIS spectrophotometer.

To obtain the cation-radical, the standard method consisting in the dissolution in sulfuric acid was tried, but without results.

The McLachlan spin densities were calculated using the resonance and coulombian parameters given in table 1.

TABLE 1

Semiempirical parameters used in McLachlan spin density calculations

X	O	S	O(C=O)
h_x	2.00	1.2	1.3
k_{CX}	0.71	0.57	1.6

RESULTS AND DISCUSSION

The ESR spectrum of the anion-radical of (I), consisting of four distinct groups is presented in figure 1 and is interpreted with the hfs from table 2. Table 2 contains also the hfs reported for the anion-radical

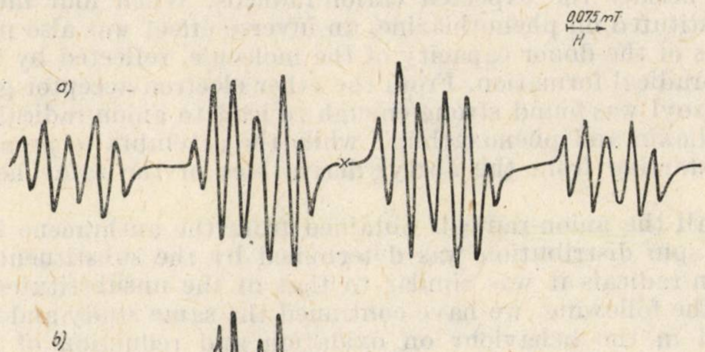

Fig. 1. — The ESR spectrum of the anion-radical of (I) ; a) experimental spectrum ; b) simulated spectrum.

II by Urberg and Kaiser.[7] Inspection of both sets of hfs reveals that two couplin ; constants are missing in the spectrum of I comparatively to II (those belonging to protons 2 and 3 in II), but the others do not differ in a significant manner and consequently the same assignment can be made. Urberg and Kaiser assigned the largest values in the range of 0.35 mT to the *para* positions relative to the carbonyl group, in agreement with the calculated spin densities and the assignment made for the benzophenone anion-radical. Considering the same assignment, for I we observe that the hyperfine splittings belonging to the *ortho* positions relative to the carbonyl group, namely 4 and 5, are no more equivalent, and both are somewhat larger than in II. Another difference to be noted consists in a slight inequivalence of the protons 1 and 8.

TABLE 2

Experimental and calculated hyperfine splittings (mT) for the anion-radicals I and II, and the *g* factor values ; $Q_{\mathrm{H}}^{\mathrm{CH}} = /2.7/$ mT

Radical	Position	1	2	3	4	5	6	7	8	1′, 2′, 3′, 4′	*g*
I	Exp.	0.043	—	—	0.352	0.384	0.091	0.390	0.037	<0.020	2.0036
	Calc.	0.043	—	—	0.343	0.373	0.121	0.408	0.022	0.000	
II	Exp.[7]	0.034	0.375	0.095	0.338	0.338	0.095	0.375	0.034	—	2.0035
	Calc.	0.024	0.380	0.115	0.353	0.353	0.115	0.380	0.024		

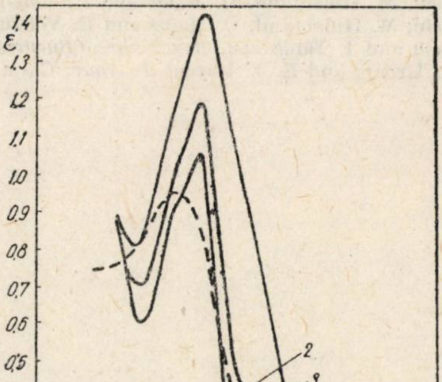

Fig. 2. — The electronic spectrum recorded during the electrochemical reduction of (I) in DMSO : 1) initial solution of (I) in DMSO ; 2, 3) the spectrum during the electrochemical reduction ; 4) the spectrum after the interruption of the electrolysis and decomposition of the anion-radical.

The similitude between the two ions and the lack of coupling constants to be assigned to the dibenzo-*p*-dioxin cycle point out the reduced influence of this fragment, the resulted anion-radical I conserving the electronic spin distribution of the thioxanthone radical.

The calculated spin densities for both ions agree very well with the experimental data. It must be remarked that the spin densities on the dibenzo-*p*-dioxin moiety are close to zero, confirming the experimental observation about the predominant character of the thioxanthone fragment and the delocalization of the odd electron mainly on it.

The electronic spectrum recorded during the electrochemical reduction of I in DMSO is presented in figure 2. We ascribe the absorption in the range of 420—425 nm (22—24 kK) to the anion-radical I, since it appears in time during the electrolysis and disappears when the solution is aerated. The final absorption near 400 nm is probably due to a by-product.

The spectral features of the anion-radical I, together with the failure of the cation-radical formation, lead to the conclusion that in 1,4-benzo-*p*-dioxin [2,3-b] thioxanthone, the donor effect of the dibenzo-*p*-dioxin fragment is surpassed by the acceptor part, which determines the character of the whole molecule.

REFERENCES

[1] I. Baciu, M. Hillebrand, V. Sahini and E. Volanschi, *Rev. Roumaine Chim.*, **21,** 485 (1976).
[2] A. Gioabă, V. Sahini and E. Volanschi, *J. Chem. Soc. Perkin II*, **1977,** 529.
[3] M. Hillebrand and M. Răileanu, *Rev. Roumaine Chim.*, **19,** 1227 (1974).
[4] I. Baciu, M. Hillebrand, O. Maior and E. Volanschi, to be published.
[5] I. Baciu, M. Hillebrand, O. Maior and E. Volanschi, to be published.
[6] I. Baciu and I. Tănăsescu, *Rev. Chim. (Bucureşti)*, **1971,** 645.
[7] M. M. Urberg and E. T. Kaiser, *J. Amer. Chem. Soc.*, **89,** 5179 (1967).

Revue Roumaine de Chimie, 26 1, 21—27 (1981)

THE OXIDATION OF BUTAN-2-ONE BY VANADIUM (V) IN AQUEOUS PERCHLORATE MEDIA. KINETICS AND MECHANISM

G. CHITHAMBARATHANU PILLAI, J. RAJARAM and J. C. KURIACOSE
Department of Chemistry, Indian Institute of Technology, Madras 600036, India

Received July 12, 1979

The oxidation of butan-2-one by vanadium (V) in aqueous perchlorate media is completely acid catalysed and the orders in ketone and vanadium (V) are one in each, while that in acid is nearly one. The addition of salts like NaCl, $NaClO_4$, $NaHSO_4$ and Na_2SO_4 increase the rate to different extents. The solvent isotope effect, $k_{D_2O}/k_{H_2O}=3.6$, suggests the involvement of the enolic form of ketone in a reaction that takes place through free radical intermediates.

INTRODUCTION

Vanadium (V) has been investigated as an oxidising agent for many organic and inorganic substrates.[1-5] The oxidation of butan-2-one by alkaline hexacyanoferrate (III) ion,[6] chloramine-T[7] and Cr(VI)[8] has been reported. The results of a detailed study of the oxidation of butan-2-one by vanadium (V) in dilute perchloric acid medium are presented here.

EXPERIMENTAL

Reagents :

Vanadium (V) solutions were prepared by dissolving ammonium metavanadate (AR, Hungary) with aqueous $HClO_4$ (reagent grade). Butan -2-one was purified by distillation and its purity checked by GLC. Solutions of butan-2-one were prepared just before use. $NaClO_4$ (AR, Riedel) was used for adjustment of ionic strength.

Procedure :

Vanadium (V) was determined by adding a known amount of ferrous ammonium sulphate solution in 5N H_2SO_4 and titrating the excess with $K_2Cr_2O_7$ using N-phenylanthranilic acid as indicator.

The rate of the reaction was followed by quenching an aliquot of the reaction mixture in a measured excess of ferrous ammonium sulphate and back titrating the unreacted Fe^{2+} against standard dichromate using N-phenylanthranilic acid as indicator. All the kinetic experiments have been carried out in a thermostat constant to ±0.2, at two different temperatures, 40° and 50°C.

RESULTS AND DISCUSSIONS

The stoichiometry of the reaction is found to be 2 gm ions of vanadium (V) to one mole of the ketone. Formic acid is found to be one of the products by the chromotropic acid test.[9] Vanadium (IV) is the reduction product as shown by the absorption around 700 nm at the end of the reaction.

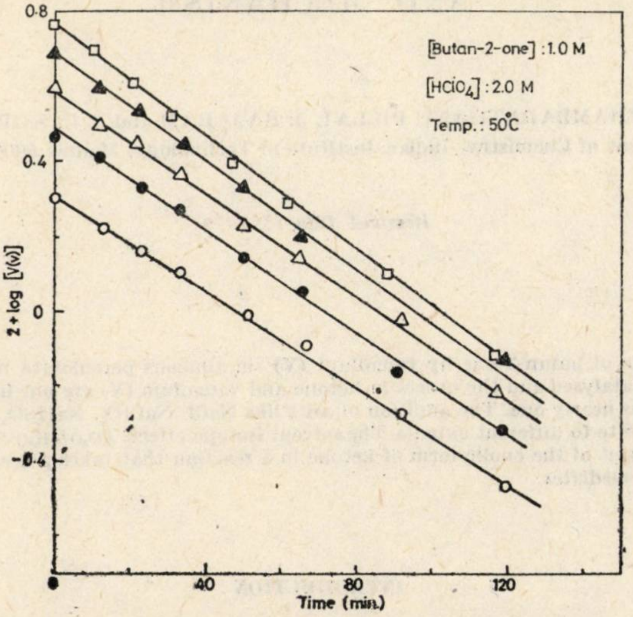

Fig. 1. — First order plots for different initial concentrations of vanadium (V).

All the kinetic experiments were carried out under pseudo first order conditions with [butan-2-one] $\gg$ [Vanadium (V)]. Figure 1 shows the first order plots of log vanadium (V) *vs* time for different initial concentrations of V (V). Figure 2 shows the first order plots for different ketone concentrations (0.75 M — 2.5 M) at a constant concentration of Vanadium (V) and acid and at constant ionic strength. Figure 3 shows the plots of k_{obs} as a function of [butan-2-one] indicating that the order in ketone is one.

The slope of the plot of log k_{obs} *vs.* log [$HClO_4$] is 0.9 (Figure 4). To determine whether the fractional value has any significance, a plot of $1/k_{obs}$ *vs* $1/HClO_4$ was made and found to be linear with a positive slope and intercept (Figure 5). This suggests that the acid is involved in complex formation.

The rate of the reaction is increased by an increase in the proportion of acetic acid in the solvent. A plot of log k_{obs} *vs.* $1/D$ is linear (Figure 6), which permits the calculation of r, the radius of the transition state complex.[10] It is found to be 1.5×10^{-8}cm. Salts like $NaClO_4$, $NaHSO_4$, NaCl

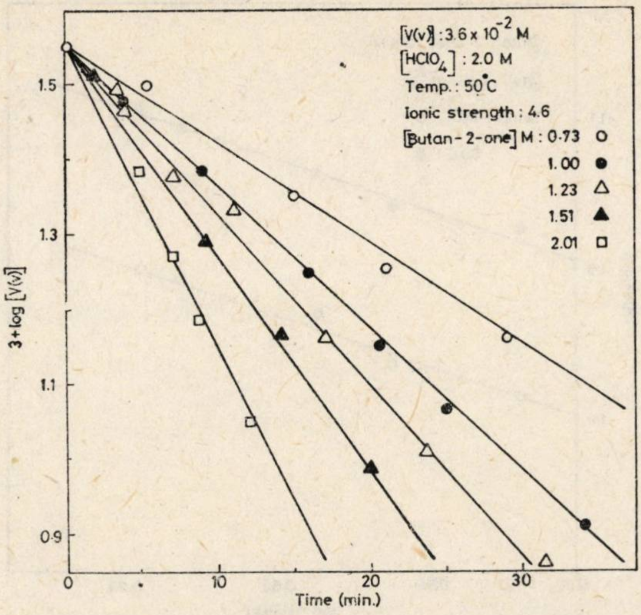

Fig. 2. — First order plots for different concentrations of butan -2-one.

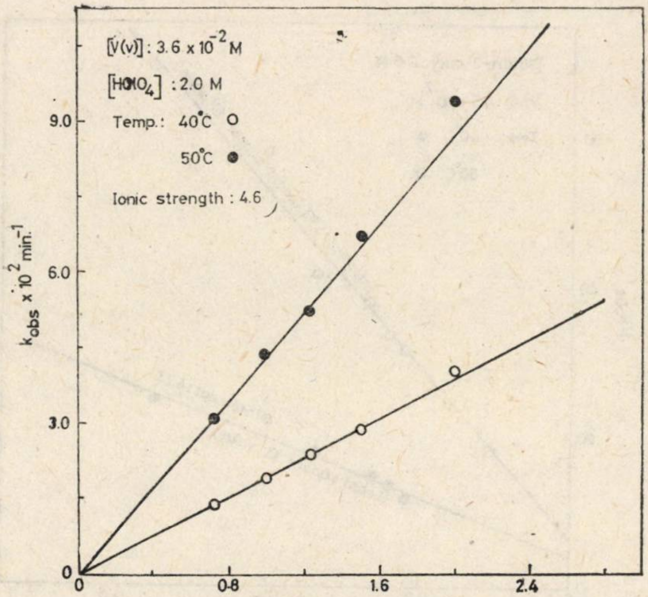

Fig. 3. — Plots of observed rate constant *vs.* concentration of butan-2-one.

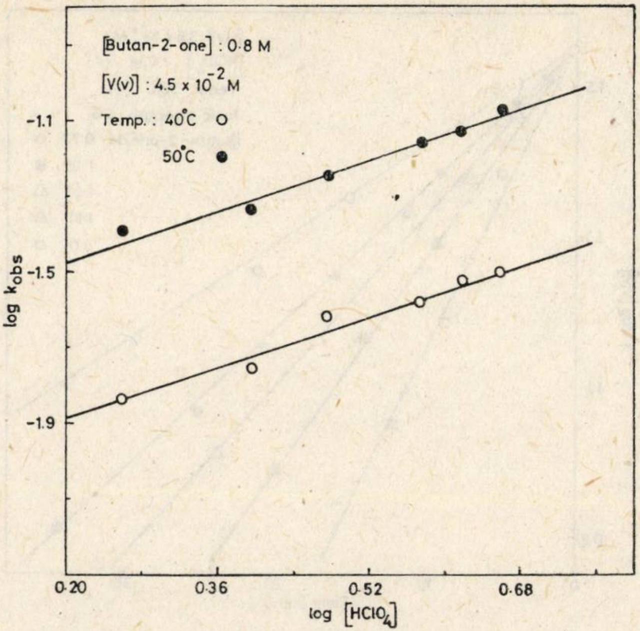

Fig. 4. — Plots of log k_{obs} *vs* log [perchloric acid].

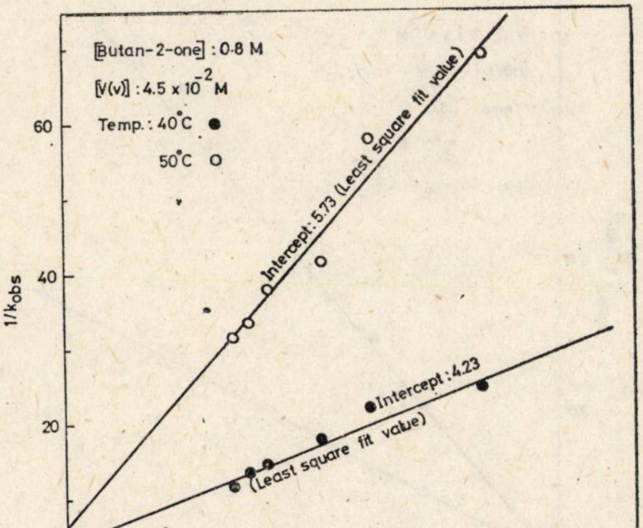

Fig. 5. — Plots of $1/k_{obs}$ *vs*.1/[perchloric acid].

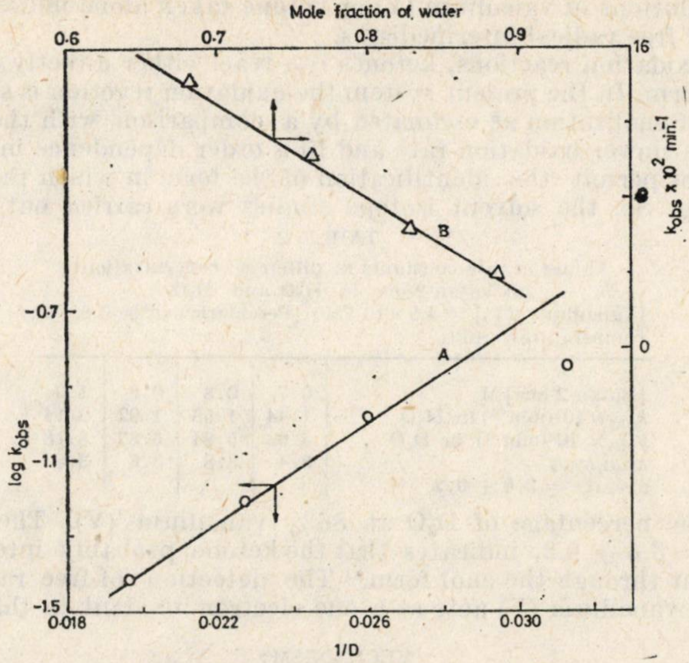

Fig. 6. — Plots of log k_{obs} *vs.*1/D and k_{obs} *vs.* mole fraction of water.

and Na_2SO_4 increase the rate, but to different extents, as seen in table 1, $NaHSO_4$ having the maximum effect. The difference in the rate due to the addition of these salts suggests the formation of different active vanadium (V) species. In pure perchloric acid medium, $V(OH)_3^{2+}$ is considered to be the active species.[3]

TABLE 1

Values of rate constants at different concentrations of salts
[Butan-2-one] = 1 M ; [Perchloric acid] = 2M ;
[Vanadium (V)] = 4.2 × 10^{-2}M ; Temperature : = 50°C

[Salt]M	$k_{obs.} \times 10^2$ (min^{-1}) when salt is			
	$NaHSO_4$	$NaClO_4$	NaCl	Na_2SO_4
0	1.96	1.96	1.96	1.96
0.5	2.70	2.20	2.17	2.35
1.0	3.91	2.55	3.25	3.00
1.5	5.20	3.27	4.71	—
2.0	6.77	4.49	6.27	—
2.5	7.80	4.68	7.10	—

Induced polymerization of methyl methacrylate or acrylonitrile during the reaction and the absence of polymerization of these monomers in solutions of vanadium (V) or ketone taken alone indicate the formation of free radical intermediates.

In oxidation reactions, ketones can react either directly or through the enol form. In the present system the oxidation reaction is slower than the rate of enolization as estimated by a comparison with the bromination.[8] This slower oxidation rate and first order dependence in vanadium (V) do not permit the identification of the form in which the ketone is interacting. So, the solvent isotope studies were carried out (Table 2), keeping the percentage of D_2O at 86% vanadium (V). The value of $k_{D_2O}/k_{H_2O} = 3.6 \pm 0.2$, indicates that the ketone probably interacts with the oxidant through the enol form.[11] The detection of free radicals suggests that vanadium (V) acts as a one electron oxidant in this system.[3]

TABLE 2

Values of rate constants at different concentrations of butan-2-one in H_2O and D_2O
[Vanadium (V)] = 4.5×10^{-2}M ; [Perchloric acid] = 0.83 M ;
Temperature = 40°C

[Butan-2-one] M	0.7	0.8	0.9	1.0
$k_{obs} \times 10^3 (min^{-1})$ in H_2O	1.44	1.56	1.92	2.14
$k_{obs} \times 10^3 (min^{-1})$ in D_2O	4.93	5.94	6.87	8.18
k_{D_2O}/k_{H_2O}	3.4	3.8	3.6	3.8
average = 3.6 ± 0.2				

MECHANISM:

The kinetic results observed indicate that the rate expression will be of the form,

$$\text{Rate} = \frac{-d[V(V)]_T}{dt} = \frac{k\,[\text{butan-2-one}]\,[H^+][V(V)]_T}{1 + \text{const.} \times [H^+]}$$

A mechanism involving the formation of an active vanadium (V) species in an equilibrium step and its interaction with the enolic form of the ketone in a slow step to give a free radical which gives the product, is proposed.

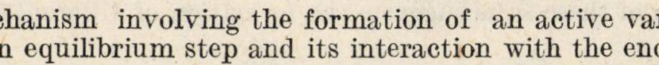

$$CH_3-\underset{\underset{O}{\|}}{C}-CH_2-CH_3 \rightleftharpoons CH_3-\underset{\underset{OH}{|}}{C}=CH-CH_3 \qquad (1)$$

$$VO_2^+ + H_3O^+ \overset{K_1}{\rightleftharpoons} V(OH)_3^{2+} \qquad (2)$$

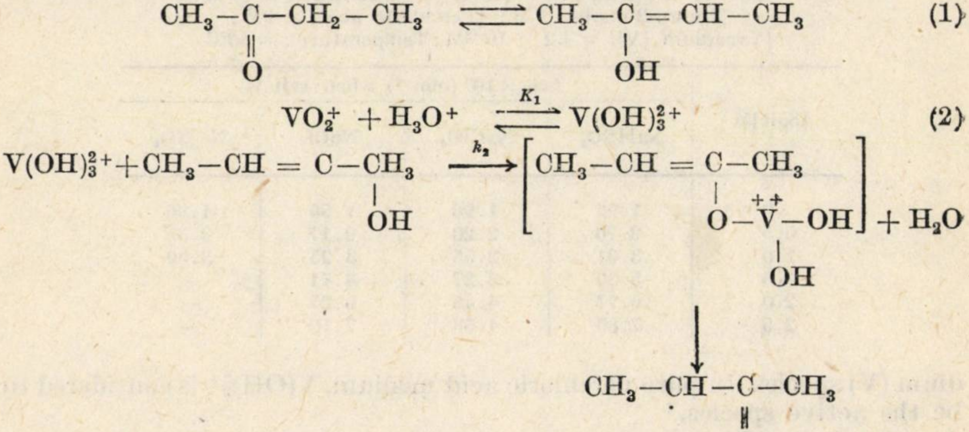

$$V(OH)_3^{2+} + CH_3-CH=\underset{\underset{OH}{|}}{C}-CH_3 \xrightarrow{k_2} \left[CH_3-CH=\underset{\underset{O-\overset{++}{V}(-OH)(-OH)}{|}}{C}-CH_3\right] + H_2O \longrightarrow CH_3-CH-\underset{\underset{O}{\|}}{C}-CH_3 + V(OH)_2^{2+} \qquad (3)$$

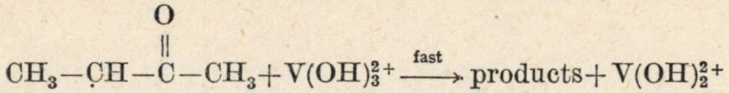

$$CH_3-\underset{\cdot}{C}H-\overset{\overset{O}{\|}}{C}-CH_3+V(OH)_3^{2+}\xrightarrow{\text{fast}}\text{products}+V(OH)_2^{2+} \quad (4)$$

The above mechanism gives the rate law,

$$\text{Rate} = \frac{-\mathrm{d}[V(V)]_T}{\mathrm{d}t} = \frac{k_2K_1[\text{butan-2-one}][H^+][V(V)]_T}{1 + K_1[H^+]}$$

where $[V(V)]_T$ is the total concentration of vanadium (V).

$$k_{obs} = k_2K_1[\text{butane-2-one}][H^+]/(1 + K_1[H^+]) \quad \text{(ii)}$$

At constant [butan-2-one] = 'm'M,

$$1/k_{obs} = 1/mk_2K_1[H^+] + 1/mk_2 \quad \text{(iii)}$$

From the slope and intercept of the plot of $1/k_{obs}$ *vs.* $1/[H^+]$, the values of k_2 and K_1 can be calculated. At constant acid concentration a plot of k_{obs} *vs.* [butan-2-one] gives a straight line with a positive slope passing through the origin. Equation (ii) has a slope equal to $k_2K_1[H^+]/$ $/(1 + K_1[H^+]) = X$. From the values of k_2 and K_1, calculated using the plot of $1/k_{obs}$ *vs.*$1/[H^+]$, the value of 'X' can be computed and compared with the values of 'X' obtained from the plot according to equation (ii).

Values of 'X' computed through the plots of $1/k_{obs}$ *vs.* $1/[H^+]$ (eqn. iii) and k_{obs} *vs.* [butan-2-one] (eqn.ii) are given below.

Temperature	Eqn. (ii)	Eqn. (iii)
40°	1.96×10^{-2}	1.94×10^{-2}
50°	4.44×10^{-2}	5.27×10^{-2}

The good agreement in values supports the proposed mechanism. Since the values of k_2 and K_1 are known at two temperatures, $\Delta H^{\neq}$ for complex formation and the energy of activation for the rate determining step are calculated and are found to be 17.2 kcal/mole and 6.8 kcal/mole respectively.

REFERENCES

[1] W. A. Waters, *Rev. Chim. (Bucureşti)*, **7**, 1371 (1962).

[2] R. N. Mehrotra, *J. Chem. Soc. (B)*, **1968**, 1563.

[3] W. A. Waters, and J. S. Littler, "Oxidation in Organic Chemistry", Part A, edited by K. B. Wiberg, Academic Press, New York, 1965, p. 204.

[4] J. S. Littler and W. A. Waters, *J. Chem. Soc.*, **1959**, 4046.

[5] J. R. Jones and W. A. Waters, *J. Chem. Soc.*, **1962**, 2068.

[6] V. N. Singh, H. S. Singh and B. B. L. Saxena, *J. Amer. Chem. Soc.*, **91**, 2643 (1969).

[7] S. P. Mushran, R. Sanehi and M. C. Agarwal, *Z. Naturforsch*, **27b**, 1161 (1972).

[8] S. K. Tandon, K. K. Banerjee and G. V. Bakore, *Indian J. Chem.*, **1971**, 677.

[9] F. Feigl, "Spot Tests in Organic Chemistry", Elsevier Publishing, Amsterdam, 1960, p. 349.

[10] E. S. Amis, *Analyt. Chem.*, **27**, 1672 (1955).

[11] S. Saccubai and M. Santappa, *Indian J. Chem.*, **8**, 533 (1970).

[illegible] + [illegible] $\rightleftharpoons$ products [illegible] (i)

The above mechanism gives the rate law

$$\text{Rate} = [illegible]$$

where [illegible] is the total concentration of [illegible]

$$k_{obs} = [illegible] \qquad (ii)$$

At constant [illegible]

$$[illegible] \qquad (iii)$$

From the slope and intercept of the plot of [illegible] values of [illegible] and [illegible] can be calculated at constant [illegible] concentration, a plot of [illegible] gives a straight line with a positive slope passing through the origin. Equation (ii) has a slope equal to [illegible] = X. From the values of [illegible] and [illegible] calculated using the plot of [illegible] the value of X can be computed and compared with the values of X obtained from the [illegible] according to equation (ii).

Values of X computed through the plot of [illegible] (iii) and [illegible] are given below.

Temperature	Eqn. (ii)	Eqn. (iii)
40°	1.50 × 10[illegible]	1.44 × 10[illegible]
30°	[illegible] × 10[illegible]	[illegible] × 10[illegible]

The good agreement in values supports the proposed mechanism. From the values of [illegible] and [illegible] at two temperatures, ΔH° for complex formation and the energy of activation for the rate determining step are calculated and are found to be [illegible] kcal mole and [illegible] kcal/mole respectively.

REFERENCES

[1] W. A. Waters, [illegible] (1958).
[2] [illegible] J. Chem. Soc. [illegible]
[3] W. A. Waters and [illegible] [illegible] Academic Press, New York, 1965, p. [illegible]
[4] [illegible] and W. A. Waters, J. Chem. Soc. [illegible]
[5] [illegible] and W. A. Waters, J. Chem. Soc. [illegible]
[6] [illegible] and [illegible] J. Amer. Chem. Soc. [illegible]
[7] [illegible]
[8] [illegible] Indian J. Chem. [illegible]
[9] [illegible]
[10] [illegible]
[11] [illegible] Indian J. Chem. [illegible]

Revue Roumaine de Chimie, **26**, *1*, 29–35 (1981)

THE KINETICS OF THERMAL AND PHOTOCHEMICAL DECOMPOSITION OF AROMATIC DIAZONIUM SALTS

DELIA ISAC, M. MRACEC, N. PROŞTEANU and Z. SIMON
Chemical Research Laboratory "Solventul" Timişoara, ICECHIM CCMP, spl. N. Titulescu, nr. 31, Timişoara, 1900, Romania

Received November 27, 1979

The kinetics of thermal decompositions in solution of diazonium salts of sulphanilic acid and sulphanilamide and also the photodecomposition of diazonium salt of *p*-dimethylaminoaniline were followed spectrophotometrically. The following activation energies (*E*) and preexponent (*A*) were obtained for thermal decompositions of benzenediazonium salts : for the sulphanilic acid derivative $E= 127.19$ kJ/mol, $A=6.0\ 10^{15}s^{-1}$, for the sulphanilamide derivative $E = 124.2$ kJ/mol, $A = 4.0\ 10^{15}s^{-1}$; the *p*-dimethylaminoaniline derivative presents a higher thermal stability, but undergoes photochemical decomposition in visible light.

The thermal and photochemical decompositions of the aromatic diazonium salts formally take place according to the same radical or ionic mechanism, depending on the medium and the reacting substances.[1,2]

A homolitic process has been reported for basic medium, in buffer alcoholic solutions, or in organic solvents as mixtures (benzene-tetramethylsulphone, or nitrobenzene-tetramethylsulphone) when the decomposition of the diazonium salts leads to the formation of an arylether.[3,4] This mechanism is proved by the magnetochemical investigation which indicates the presence of the free radical, during the decomposition.[2,5]

In acidic medium water solutions, the thermal or photochemical decompositions follow a heterolytic mechanism with the formation of the phenol. [1,3,6-8] The first rate determining step is the heterolytic monomolecular dissociation of the C—N bond with the formation of N_2 and of the phenylcarbonium ion.

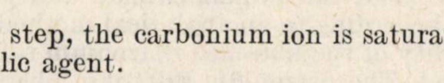

In the second rapid step, the carbonium ion is saturated owing to the attack of a nucleophilic agent.

$$C_6H_5^+ + H_2O \rightarrow C_6H_5 - OH_2^+ \rightarrow C_6H_5 - OH + H^+$$

The coupling reaction between the diazonium cation and the phenol obtained from its decomposition can be neglected.[9]

When adding salt (NaCl solution), the distribution of reaction products depends upon the competition between Cl^- and H_2O for the carbonium ion.[3,10]

The kinetics of the thermal and photochemical decompositions of diazonium salts in water solutions, neutral or slightly alkaline, are of the first order. [11-14]

$$v = -\frac{d[Ar\overset{+}{N}_2]}{dt} = k_1[Ar\overset{+}{N}_2]$$

In D_2O the thermal decomposition reaction rate of the diazonium salts is the same as in H_2O.[13] There was established that the decomposition rate of the diazonium salts in different solvents increases in the order :[10] water < ethanol < ether-ethanol. The decomposition reaction rate is practically independent of the concentration and nature of the acids present in solution.[15]

The *p*-substituted benzenediazonium salts follow the same photodecomposition process as the benzenediazonium salts.[16] The thermal stability of the *p*-amino and N substituted *p*-aminophenyldiazonium salts at room temperature is relativety high and the photochemical effects can be easily distinguished.[14]

There is a surprising effect of substituents upon reaction rates.[15,17] The substituents with — M and — I effect in *meta* or *para* positions decrease the reaction rates. Electron donor substituents in *meta* position increase the reaction rates, but the same substituents in *para* position strongly decrease the reaction rates. It is supposed that this stabilization is due to a resonance effect that increases the C—N bond order.[14,18] The effect of electronegative substituents on the photochemical stability of the diazo compounds is inverse as compared to their effect upon thermal stability.[8]

The purpose of this paper is to contribute to the knowledge of the thermal and photochemical stability of some diazonium salts.

The variations of concentration with time at different temperatures for the thermal and photochemical decompositions were followed spectrophotometrically in UV and visibly on spectrophotometer SPECORD UV—VIS (Karl Zeiss Jena).

RESULTS AND DISCUSSION

The sulphanilic acid, the sulphanilamide and *p*-dimethylaminoaniline were diazotized according to an analytical method.[19] The thermal and photochemical stability of the obtained diazonium salts was verified by a spectrometric method. The diazonium salts of sulphanilic acid and sulphanilamide are photochemically stable up to 353 K, but thermally instable ; that is why the kinetics of their decomposition could be followed in the UV domain. The diazonium salt of *p*-dimethylaminoaniline is thermally stable, but very sensitive photochemically, which allows the qualitative study of its photodecomposition in the UV and visible domain.

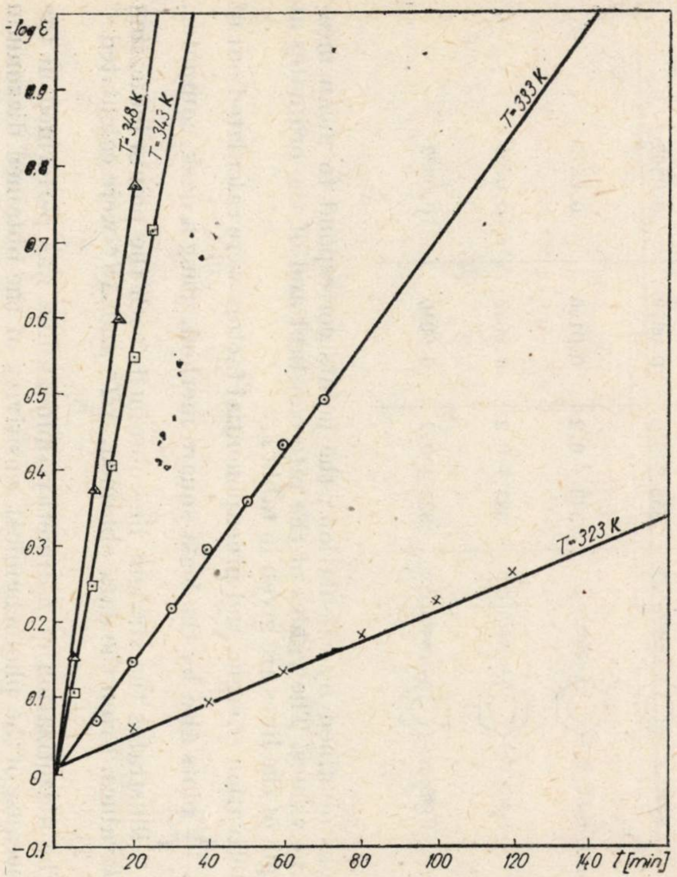

Fig. 1. — — log ε *versus* time (min.) for the thermal decomposition of the diazonium salt of sulphanilic acid at different temperatures (× : $T = 323 \pm 0.2$ K, ⊙ : $T = 333 \pm 0.2$K, ⊡ : $T = 343 \pm 0.2$ K, △ : $T = 348 \pm 0.2$ K).

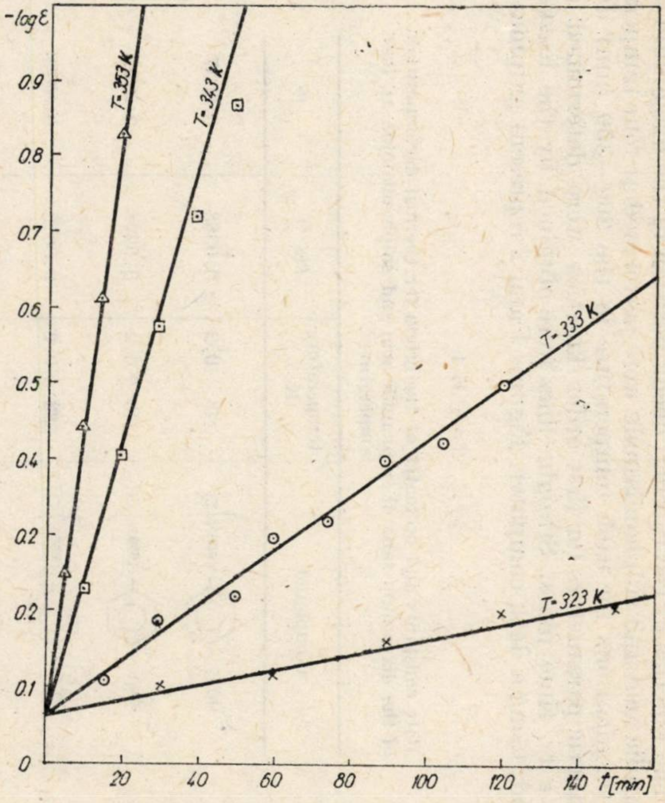

Fig. 2. — — log ε *versus* time (min.) for the thermal decomposition of the diazonium salt of sulphanilamide at different temperatures (× : $T = 323 \pm 0.2$ K, ⊙ : $T = 333 \pm 0.2$ K, ⊡ : $T = 343 \pm 0.2$ K, △ : $T = 353 \pm 0.2$ K).

The kinetics of the thermal decomposition of the diazonium salts of sulphanilic acid and sulphanilamide were performed at four temperatures, six determinations for each temperature in the 200—350 (nm) domain. The kinetic parameters for first order kinetics were determined out of —log ε *vs*. time plots. Straight lines were obtained by the least-square method, using a desk computer. Figures 1 and 2 represent graphically the equations obtained by calculation; the points correspond to mean measurement values. The values of the rate constant and of the ordinates at the origin of the lines are given in table 1.

TABLE 1

Rate constants and ordinates at the origin for thermal decomposition of the diazonium salts of sulphanilic acid and sulphanilamide at four temperatures.

Compound	temperature K	$k(s^{-1})$	a
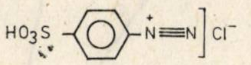	348 ± 0.2	0.0388	−0.0037
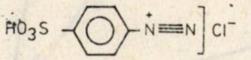	343 ± 0.2	0.0296	−0.0207
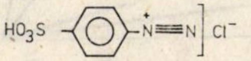	333 ± 0.2	0.0070	0.0074
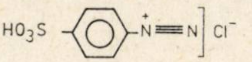	323 ± 0.2	0.0020	0.0159
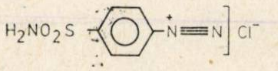	353 ± 0.2	0.0379	0.0567
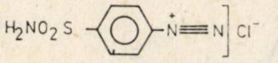	343 ± 0.2	0.0156	0.0873
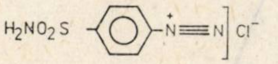	333 ± 0.2	0.0035	0.0706
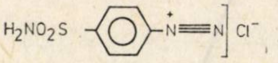	323 ± 0.2	0.0010	0.0632

Activation energies and preexponential factors were calculated out of $\ln k$ *vs*. $\frac{1}{T}$ plots also by the least-square method, using a desk computer. Figure 3 illustrates the straight line obtained, with the points indicating the $\ln k$ values. From the data obtained, $\Delta H^{\neq}$ and $\Delta S^{\neq}$ were calculated [20] (Table 2).

The diazotization of *p*-dimethylaminoaniline was performed in the dark, because of the photochemical sensitivity of the obtained diazonium salt. The diazonium salt of the *p*-dimethylaminoaniline is stable in the dark (several hours at 353 K); the visible absorption curves do not change. Diffuse neon light (of the laboratory) produces a sensible decrease of visible absorption even after 10 minutes. Absorption curves (diffuse neon light) were registered every ten minutes. The obtained spectra are shown in figures 4 and 5. Recordings in UV demonstrate also that the diazonium

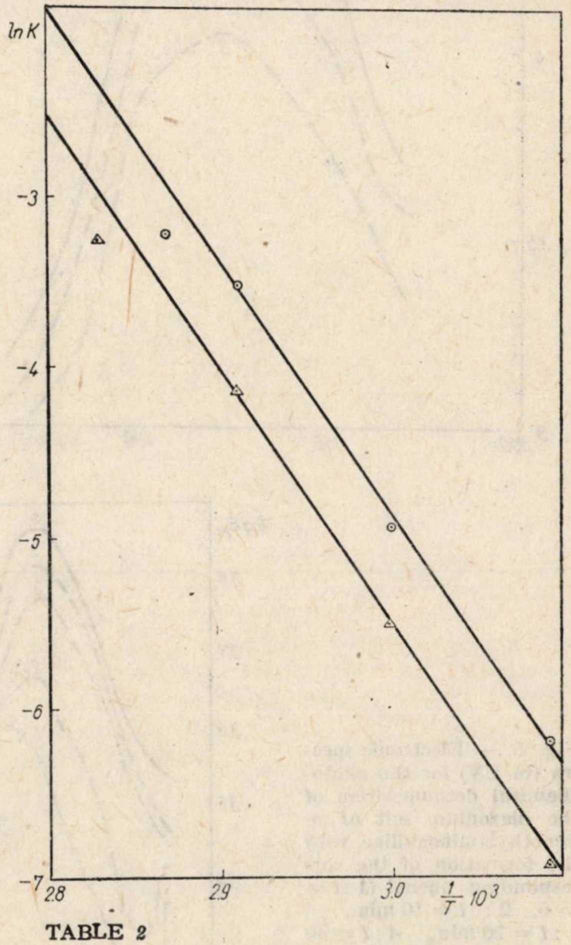

Fig. 3. — ln *k* versus $\frac{1}{T}\cdot 10^3$ for the thermal decomposition of the diazonium salts of sulphanilic acid and sulphanilamide (△ = the diazonium salt of sulphanilic acid, ⊙ = the diazonium salt of sulphanilamide).

TABLE 2

Activation energies, preexponential factors, activation enthalpies and entropies for thermal decomposition of the diazonium salts of sulphanilic acid and sulphanilamide

Compound	E_a kJ/mol	$A(s^{-1})$	$\Delta H^{\neq}$ kJ/mol	$\Delta S^{\neq}$ J/mol·grad
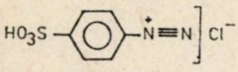	127.194	6.10^{15}	124.683	48.116
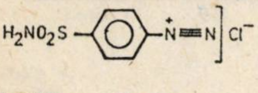	124.265	4.10^{15}	121.336	44.350

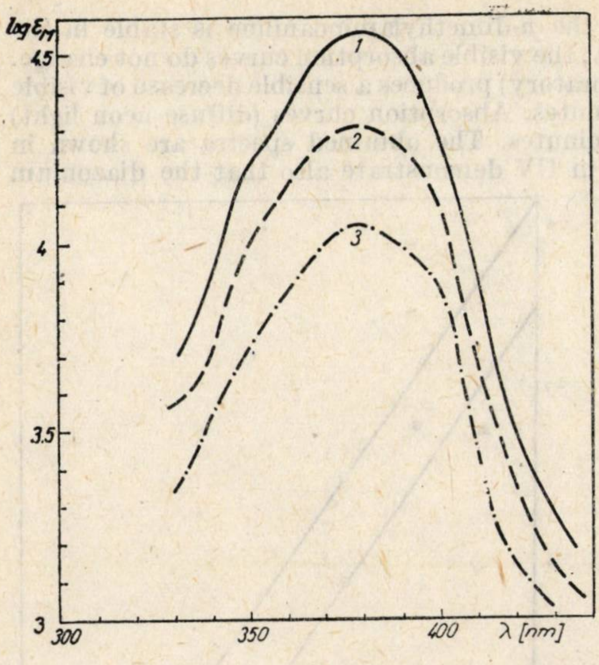

Fig. 4. — Electronic spectra (visible) for the photochemical decomposition of the diazonium salt of *p*-dimethylaminoaniline (1 : $t = 0$, 2: $t=10$ min., 3: $t=20$ min.)

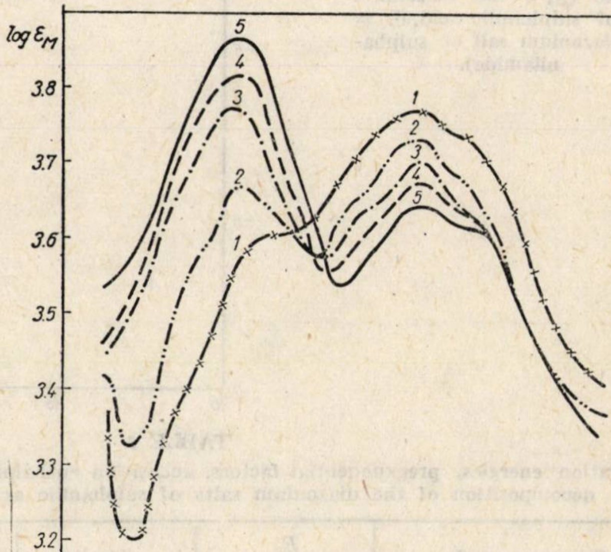

Fig. 5. — Electronic spectra (in UV) for the photochemical decomposition of the diazonium salt of *p*-dimethylaminoaniline, with the formation of the corresponding phenol (1 : $t = 0$, 2 : $t = 10$ min., 3 : $t = 20$ min., 4 : $t = 30$ min., 5 : $t = 40$ min).

salt of *p*-dimethylaminoaniline is instable and decomposes under the action of visible light. The determinations performed every ten minutes of figure 5 illustrate the photodecomposition of the diazonium salt and the formation of the corresponding phenol.

The diazonium salts of the sulphanilic acid and sulphanilamide with electron attractive substituents in *para* positions are photochemically stable, but thermally instable.

The thermal stability at the room temperature of the diazonium salt of *p*-dimethylaminoaniline is due to the presence of the electron donor substituent in *para* position and allows the qualitative observation of the photochemical effects.

REFERENCES

[1] H. Baril Jr., *J. Chem. Phys.*, **22**, 1275 (1954).
[2] E. A. Boudreaux and E. Boulet, *J. Amer. Chem. Soc.*, **80**, 1588 (1958).
[3] W. E. Lee, J. G. Calvert and E. W. Malmberg, *J. Amer. Chem. Soc.*, **83**, 1928 (1961).
[4] R. A. Abramovitch and F. F. Gadallah, *J. Chem. Soc. B*, **1968**, 497.
[5] P. J. Zandstra and E. M. Evleth, *J. Amer. Chem. Soc.*, **86**, 2664 (1964).
[6] J. Jonge, R. Dijkstra and G. L. Wiggerink, *Rec. Trav. chim.*, **71**, 846 (1952).
[7] M. Breitenbach, K. H. Heckner and D. Jäkel, *Z. phys. Chem. (Leipzig)*, **244**, 377 (1970).
[8] M. M. A. Seyewetz and D. Mounier, *Bull. Soc. chim. France*, **43**, 827 (1928).
[9] B. Demian, Thesis, Timişoara, 1972.
[10] E. S. Lewis, R. E. Halliday and L. D. Hartung, *J. Amer. Chem. Soc.*, **91**, 430 (1969).
[11] H. Zollinger "Azo and Diazo Chemistry", Interscience, New York, 1961, p. 139.
[12] D. Schulte-Frohlinde, H. Blume and H. Güsten, *J. Phys. Chem.*, **66**, 2489 (1962).
[13] M. L. Crossley, R. H. Kienle and C. H. Benbrook, *J. Amer. Chem. Soc.*, **62**, 1400 (1940).
[14] R. Barraclough, F. Jones, D. Patterson and A. Tetlow, *J. Soc. Dyers Colour*, **88**, 22 (1972).
[15] D. F. De Tar and S. Kwong, *J. Amer. Chem. Soc.*, **78**, 3921 (1956).
[16] M. Sukigara and S. Kikuchi, *Bull. Chem. Soc. Japan*, **40**, 461 (1967).
[17] D. F. De Tar and A. R. Ballentine, *J. Amer. Chem. Soc.*, **78**, 3916 (1956).
[18] C. K. Ingold, "Structure and Mechanism in Organic Chemistry", G. Bell, London, 1953, p. 800.
[19] G. Ciuhandu and M. Mracec, *Z. analyt. Chem.*, **238**, 104 (1968).
[20] J. M. Lehn, *Fortschr, Chem. Forsch.*, **15**, 311 (1970).

Revue Roumaine de Chimie, 26 7, 37–42 (1981)

ALKALINE HYDROLYSIS OF FORMAMIDE IN WATER-ORGANIC SOLVENT MIXTURES

I. M. SIDAHMED, S. M. SALEM and F. M. ABDEL HALIM
Chemistry Department, Faculty of Science, Moharram Bey, Alexandria, Egypt

Received August 8, 1979

The alkaline hydrolysis of formamide was carried out in aqueous-methanol, ethanol, *n*-propanol, isopropanol, *tert*-butanol or ethylene glycol solutions at 25°C. The bimolecular rate constants were found to decrease steadily with the progressive addition of the normal alcohols (methanol, ethanol and *n*-propanol) to the aqueous formamide solution, while curves with minima were observed on adding branched alcohols or glycol to the reaction medium. Moreover, the minimum shifted towards the water rich side for ethylene glycol, and *tert*-butanol, rather than for isopropanol-water mixtures. The results are discussed in the light of the "Back-strain" effect and solvation phenomena, and a mechanism for the alkaline hydrolysis of formamide is proposed.

INTRODUCTION

The effect of media on the rate constants of the reactions involving the hydrolysis of amides in aqueous organic solvents is attributed to many different factors.[1,2]

Although the dielectric constant of the medium, in some cases, has been successfully used for interpretation of the kinetic data, however, the plausible theories of solvent effects [3] could not be applied in many cases as found in the present work, since the macroscopic dielectric constant gives no indication of the solvent effects on the rate.

EXPERIMENTAL

Materials : Formamide (B.D.H.) was used after purification.[4] Organic solvents used (Merck grade) were further purified.[4] Carbonate free sodium hydroxide solution was prepared and standardized against standard hydrochloric acid solution.

Preparation of solutions : The appropriate amount of the organic solvent was introduced into a measuring flask containing the weighed amount of formamide, affording a 0.05 M solution on completion to the mark. After attainment of thermal equilibrium, the volume of sodium hydroxide solution, corresponding to 0.05 M, was added to the flask containing the formamide solution ; the mixture was then completed to the mark and placed throughout the experiment in a thermostat at 25°C ± 0.02°.

Rate determination : The ion exchange resin procedure [5] was used to follow the rate of the hydrolysis reaction. At suitable time intervals, 5 ml samples of the reaction mixture were withdrawn and allowed to flow through the ion exchanger containing the cationic Amberlite

resin, IR—120 (H). The liberated formic acid solution was titrated against standard sodium hydroxide solution to the phenolphthalein end point. Complete hydrolysis was assumed to be attained when the experimental and the calculated infinity values became almost identical.

RESULTS AND DISCUSSION

The hydrolysis reaction was found to follow the second order rate equation

$$k_2 = \frac{x}{a(a - x)t} \tag{1}$$

A typical example of the plots for the reaction at 25°C in methanol-water mixtures is shown in figure 1. Table 1 contains the interpolated values for k_2, which originally have been obtained from such plots.

The theories of the solvent effects [3] failed in the interpretation of the present data as shown in the example given in figure 2.

From the rate profiles shown in figure 3, we may predict that the change in the base activity, which is accompanying the progressive addition of the organic solvent component, has a predominating effect on the rate of the reaction relative to any other effective factor.

TABLE 1

Interpolated values of the rate constants for the alkaline hydrolysis of formamide in aqueous-organic solvent at 25°C

	$10^4\, k_2$ (in $\mathrm{l.mole^{-1}.s^{-1}}$)					
Solvent (wt. %)	methanol	ethanol	*n*-propanol	*iso*-propanol	*t*-butanol	ethylene glycol
0	22.86	22.86	22.86	22.86	22.86	22.86
5	21.69	21.61	21.51	20.14	21.50	21.34
10	20.46	20.34	20.20	17.70	20.07	19.79
15	19.32	19.20	19.03	15.93	18.71	18.31
20	18.19	18.01	17.85	14.52	17.39	16.80
25	17.02	16.78	16.80	13.65	16.07	17.20
30	15.88	15.52	15.90	13.18	16.52	18.24
35	14.77	14.40	15.10	12.95	17.60	19.29
40	13.59	13.12	14.29	12.92	18.65	20.37
45	12.47	11.94	13.65	13.05	19.74	21.44
50	11.27	10.70	13.12	13.33	20.83	22.55
55	10.09	9.58	12.62	13.82	21.90	23.61
60	8.94	8.37	12.08	14.43	—	—
65	7.75	7.16	11.59	15.15	—	—
70	6.59	5.95	11.12	16.02	—	—
75	5.45	4.78	10.74	17.07	—	—
80	4.31	3.73	10.34	18.40	—	—
85	3.24	2.69	9.95	20.20	—	—
90	2.15	1.72	9.58	22.19	—	—

It has been reported that when sodium hydroxide is dissolved in ethanol (or methanol) the solutions would mainly contain ethoxide (or methoxide) rather than hydroxide ions,[6-8] and many puzzling facts have been explained in the light of this assumption. [9,10]

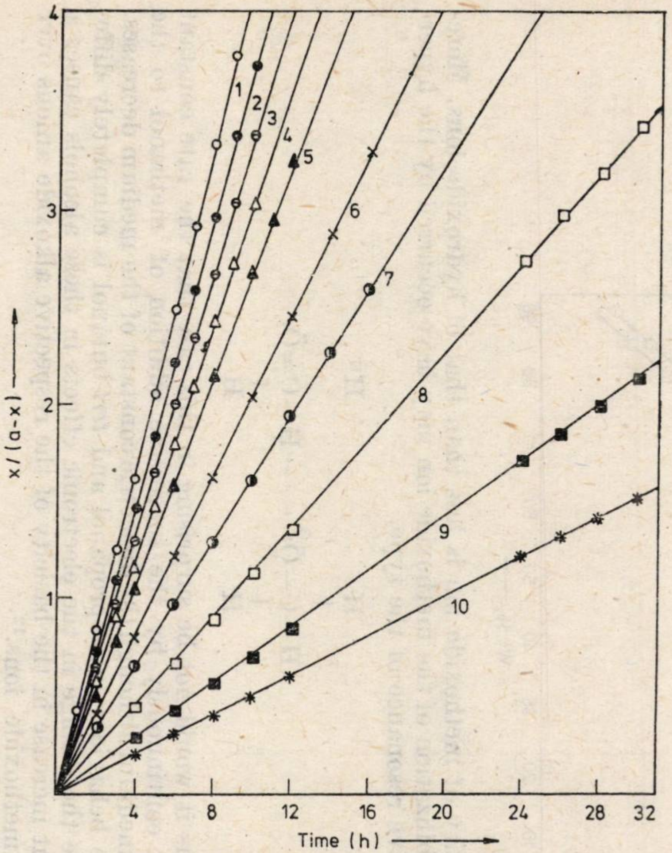

Fig. 1. — Second order plots for the alkaline hydrolysis of formamide at 25°C in methanol-water mixtures (the figures indicate the percent of methanol) : *1.* 0.00 ; *2.* 9.79 ; *3.* 19.74 ; *4.* 26.67 ; *5.* 35.84 ; *6.* 49.15 ; *7.* 59.52 ; *8.* 71.27 ; *9.* 82.00 ; *10.* 86.53.

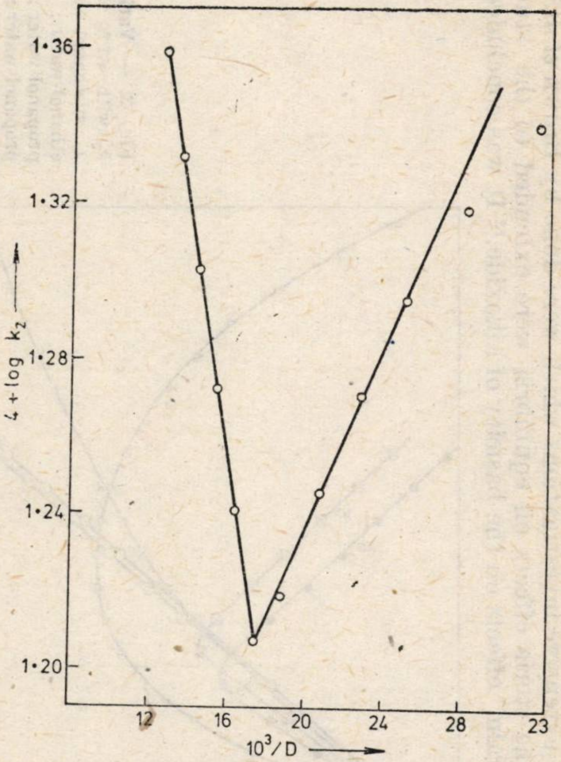

Fig. 2. — Variation of log k_2 with $1/D$ for the hydrolysis in *tert*-butanol-water mixtures.

The extensive investigations which were done by Brown *et al.*[11] concerning the steric effects on equilibria were extended to the study of "Back strain" effects on the basicity of alkoxide.[12] It was concluded that the basicity of methoxide ion is less than that of hydroxide ions. Moreover, stabilization of the methoxide ion may have occurred by the hyperconjugative resonance of the type.

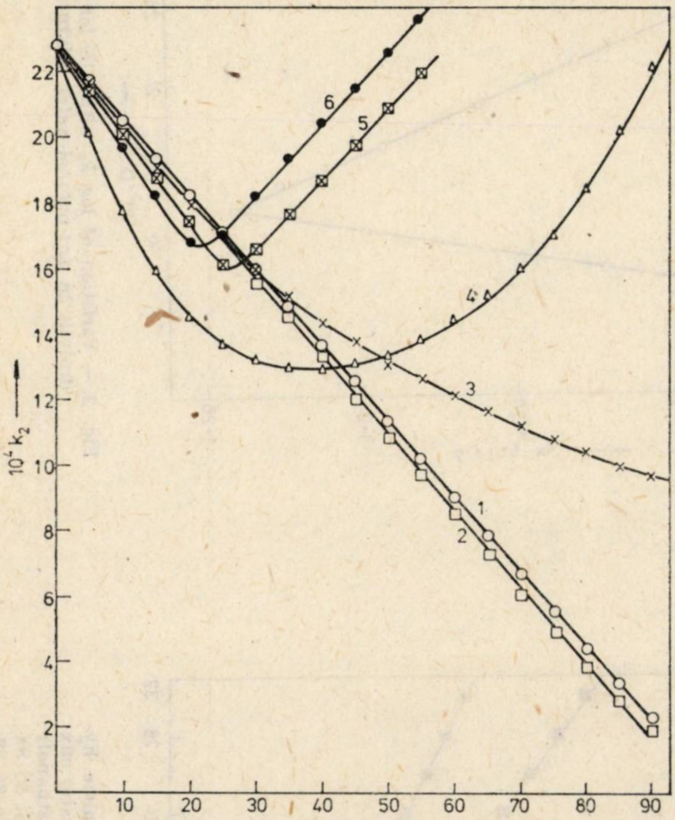

Fig. 3. — Variation of k_2 with wt % alcohol: *1.* methanol-water; *2* ethanol-water; *3.* *n*-propanol-water; *4.* *iso*-propanol-water; *5.* *tert*-butanol-water; *6.* ethylene glycol-water.

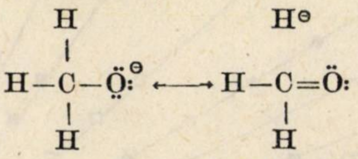

$$\mathrm{H{-}\overset{\displaystyle H}{\underset{\displaystyle H}{C}}{-}\ddot{O}{:}^{\ominus}} \longleftrightarrow \mathrm{H{-}\overset{\displaystyle H^{\ominus}}{\underset{\displaystyle H}{C}}{=}\ddot{O}{:}}$$

Thus it would not be surprising in this case that the rate constant decreases continuously by the successive addition of methanol to the reaction medium although the dielectric constant of the medium decreases.

The behaviour in isopropanol and *tert*-butanol is completely different since the change in the electronic effects in these alcohols causes a significant increase in the basicity of the respective alkoxide anions over that of methoxide ions.[12]

Since the rate of the reaction is dependent on the stoichiometric concentration of the base anion, it is expected that the rate will decrease due to the decrease in the stoichiometric concentration of the hydroxide ion by the addition of the organic solvent component, according to the equation :

$$\bar{O}H + ROH \rightleftharpoons R\bar{O} + H_2O \qquad (2)$$

where the effective base in the water rich side will be the hydroxide and not the alkoxide ions. As the concentration of the alcohol increases, the concentration of the alkoxide ion predominates and becomes the effective base in the medium. The activity of the alkoxide ions formed at higher water concentration is expected to diminish, due to solvation effects, even more than their activity in media of lower water concentration. Accordingly, it is expected that the rate of the reaction increases due to the increase in the reactivity of the alkoxide ions at the range of low dielectric constant.

In methanol-water mixtures the rate of hydrolysis reaction is influenced by both decrease of dielectric constant and decrease in basicity. It is proposed that the latter factor will be predominating in the case of methanol-water mixtures which leads to a continual decrease in rate.

In the case of isopropanol and *tert*-butanol the above two effects act parallelly and favour the increase in reaction rate in low dielectric constant mixtures.

The anion of ethylene glycol may be stabilized by intramolecular hydrogen bonding of an unreacted hydroxyl group and the alkoxide oxygen atom[13]; the activity of such anion may be enhanced at the lower dielectric constant region, since the charge is somewhat dispersed through this hydrogen bonding.

It is well known that the solvation energies of ions increase as their charge to size ratios increases and this may render high activity for *tert*-butoxide over that of isopropoxide and, consequently, the minimum shifts towards the higher dielectric constant region.

The trend of increasing basicity through the series of alcohols begins its appearance when the reaction is carried out in *n*-propyl alcohol, and we can say for the present work that the order of increasing basicity is as follows :

$$\mathrm{Me\bar{O}} \simeq \mathrm{Et\bar{O}} < n\text{-}\mathrm{pr\bar{O}} < iso\text{-}\mathrm{pr\bar{O}} < tert\text{-}\mathrm{Bu\bar{O}} < \text{ethylene glycoxide.}$$

The order of magnitude of nucleophilicities of any two reagents may be reversed as the substrate is changed.[13] Similarly, in the present investigation, the rate constant is not expected to be always the same under the same conditions, but it is basically dependent on the nature of the substrate.

Proposed mechanism : The change in the relative concentration of the hydroxide and alkoxide ions due to the change in the solvent composition is accomodated by the equilibrium represented by equation (2). Accordingly, the overall reaction rate may be represented by equation (3),

$$\text{Rate} = K_2[\text{Amide}]\,[\text{Base}] \qquad (3)$$

where $[\mathrm{Base}] = [\bar{\mathrm{O}}\mathrm{H}] + [\mathrm{R}\bar{\mathrm{O}}]$
Accordingly, equation (3) becomes,

$$\mathrm{Rate} = [\mathrm{Amide}]\ \{k'[\bar{\mathrm{O}}\mathrm{H}] + k''[\mathrm{R}\bar{\mathrm{O}}]\} \qquad (4)$$

by substitution for $[\bar{\mathrm{O}}\mathrm{H}]$ in equation (4) from the equilibrium (2) and rearrangement, we obtain :

$$\mathrm{Rate} = [\mathrm{Amide}]\,[\mathrm{R}\bar{\mathrm{O}}]\left\{\frac{k'[\mathrm{H_2O}]}{K[\mathrm{ROH}]} + k''\right\} \qquad (5)$$

therefore,

$$k_{\mathrm{obs}} = \frac{k'[\mathrm{H_2O}]}{K[\mathrm{ROH}]} + k'' \qquad (6)$$

Where k' and k'' are the specific rate constants for the reaction catalysed by $\bar{\mathrm{O}}\mathrm{H}$ and $\mathrm{R}\bar{\mathrm{O}}$ ions respectively and K is the equilibrium constant represented by equation (2).

In the case of methanol, the increase in alcohol content will cause a decrease in k'' and hence k_{obs}. will also decrease, while in the cases of isopropanol, *tert*-butanol and ethylene glycol, k'' is still small at the region of high dielectric constant due to the specific solvation of the anion by the highly polar solvent, water. At the low dielectric constant region, the increase in k'' may overcome the decrease in the first term of the right hand side of equation (6), which results in an increase in the value of k_{obs}. at low dielectric constant region.

REFERENCES

[1] A. Streitwieser, Jr., "Solvolytic Displacement Reactions", McGraw-Hill, New York, 1962.

[2] J. F. Bunnett, *Ann. Rev. Phys. Chem.*, **14**, 271, (1963).

[3] E. S. Amis, "Solvent Effects on Reaction Rates and Mechanisms", Academic Press, New York, 1966.

[4] A. I. Vogel, "A Text-Book of Practical Organic Chemistry", 3*rd* Ed., 1971 ; p. 166, 169, 170, 171, 285, 886.

[5] M. M. Elsemongy, M. S. Abu Elamayem and M. Moussa, *Z. phys. Chem. (Frankfurt)*, **95**, 215 (1975).

[6] E. F. Caldin and G. Long, *J. Chem. Soc.*, **1954**, 3737.

[7] R. F. Caldin and J. C. Trickett, *Trans. Faraday Soc.*, **49**, 772 (1953).

[8] J. W. Baker and A. J. Neale, *Nature*, **172**, 588 (1953).

[9] J. F. Bunnett and R. E. Zahler, *Chem. Rev.*, **49**, 339, 340, 348 (1951).

[10] Landolt-Börnstein, "Tabellen", Springer, Berlin, 5*th* Ed., 1931, p. 1110 ; Erg. II b, 1923, p. 1068.

[11] H. C. Brown and R. B. Johannesen, *J. Amer. Chem. Soc.*, **75**, 1953, 16 ; G. S. Hammond, "Steric Effects in Organic Chemistry", Newman, Wiley, Inc. , 1956, p. 454—460.

[12] J. Hine and M. Hine, *J. Amer. Chem. Soc.*, **74**, 5266 (1952).

[13] E. S. Gould, "Mechanism and Structure in Organic Chemistry", Holt, Rinehart and Winston, Inc. New York, 1959.

Revue Roumaine de Chimie, 26, 7, 43–53 (1981)

CHEMICAL EQUILIBRIUM IN MULTICOMPONENT REACTION SYSTEMS

D. GEANĂ
Dept. of Physical Chemistry, The Polytechnical Institute,
Bucharest, str. Polizu 1, Romania

Received January 30, 1980

A formulation of the problem of chemical equilibrium based on the atomic matrix of reaction system is suggested. A transformation is presented of the equation system thus obtained, permitting the rigorous introduction of De Donder variable vector to multicomponent reaction systems. In order to solve the chemical equilibrium, an algorithm is presented together with its application to the reaction system of generator gas.

NOTATION

$\boldsymbol{A}$ — stoichiometric matrix
$\boldsymbol{B}$ — vector of initial abundance of chemical elements
b_i — initial abundance of chemical element i
C — number of chemical components
$\boldsymbol{E}$ — vector of reaction extents
F — function obtained by eq. (38)
f_i — function defined by eq. (37)
G — free enthalpy of system
$\boldsymbol{I}$ — matrix unity
$\boldsymbol{K}$ — vector of equilibrium constants
K_k — equilibrium constant of reaction k
M — number of chemical elements
$\boldsymbol{N}$ — moles number vector
n_j — moles number of component j
P — total pressure
R — number of reactions
T — temperature
$\boldsymbol{W}$ — atomic matrix
$\boldsymbol{Y}$ — matrix in eq. (32)
Greek symbols
α_{ij} — number of atoms of element i in component j
ν_{kj} — stoichiometric coefficient of component j in reaction k
ξ_k — De Donder variable (extent of reaction k)

Superscripts

(n) — expressed by means of mole number
(P) — expressed by means of partial pressure
$^{\circ}$ — initial value
T — transposition for matrices

INTRODUCTION

The problem of the chemical equilibrium within a multicomponent reaction system can be mathematically formulated in two ways[1] :

a) minimization of a criterion function for thermodynamic equilibrium of the system (*e.g.* free enthalpy) with corresponding physical restrictions : balance equations of mass and non-negativity of mole number. It is the "optimization approach".

b) nonlinear equation system based on mass action law with the same mentioned physical constraints, which is the "nonlinear equations approach".

Both formulations will naturally lead to identical solutions of the problem. This results from the fact that formulation (b) is derived from (a) through the method of Lagrangian multipliers.[1]

Virtually, depending on the particular reaction system one or another of the formulations can have advantages over the other one with regard to the numerical calculation, convergence etc.

Due to this reason in literature there have been proposed quite a lot of solving methods for the chemical equilibrium according to both mathematical formulations.[1] One of them acquired a particular popularity as it is the case of Rand method proposed by White, Johnson and Danzig [2] or nonlinear equation method known as Brinkley method.[1] More recently, the problem of simultaneous chemical and phase equilibrium was also considered.[3, 4]

The non-uniqueness of the solution of chemical equilibrium in nonideal systems with condensed phases was recently discussed.[5-7] We hereinafter will consider the chemical equilibriun as having a unique solution that is the criterion function of equilibrium (i.e.G) has a single extremum (minimum) and the stability conditions are also met.

In a recent work, Park [8] suggested new calculation methods to solve the problem of chemical equilibrium formulated as alternative (b). These methods (called prime and dual ones), starting with concepts specific to the electrical networks, transform the initial system of equations by means of suitable changes of variable. The resulting advantages consist in convergence rate and stability of numerical method.

Following Park's ideas,[8] the present paper suggests a formulation of the problem of chemical equilibrium, in alternative (b), based on the atomic matrix of reaction system. A transformation is described of the equation system thus obtained, permitting the rigorous introduction of De Donder variable (reaction extent) [9] to multicomponent systems. In order to solve the chemical equilibrium, a calculation algorithm is presented together with its application to the reaction system of generator gas (or coal gaseification).

ATOMIC MATRIX AND STOICHIOMETRIC MATRIX OF A MULTICOMPONENT REACTION SYSTEM

The atomic matrix ($\boldsymbol{W}$) of a multicomponent reaction system has the dimensions $M \times C$ and contains as elements, α_{ij}, scalars equal to the number of atoms of chemical element i in compound j.

The special properties of this matrix and the significance of its rank are dealt with in a number of works.[10–13]
We shall consider hereinafter that atomic matrix is of rank M. This matrix, which can be easily constructed for a system knowing its components, permits to obtain a stoichiometric matrix based on the equation :

$$\boldsymbol{A}\boldsymbol{W}^{T} = 0 \tag{1}$$

$\boldsymbol{A}$ is a stoichiometric matrix of the reaction system with dimensions $R \times C$ (R — number of reactions, C — number of chemical components). Its elements are stoichiometric coefficients, ν_{kj}, of component j in reaction k. This matrix has also a number of special properties. [8,12]

Matrix $\boldsymbol{A}$ can be partitioned into two matrices :

$$\boldsymbol{A} = \boldsymbol{A}_1 | \boldsymbol{A}_2 \tag{2}$$

having the dimensions $\boldsymbol{A}_1(R \times R)$ and $\boldsymbol{A}_2(R \times (C-R))$.
Likewise, matrix $\boldsymbol{W}$ can be partitioned

$$\boldsymbol{W} = \boldsymbol{W}_1 | \boldsymbol{W}_2 \tag{3}$$

the undermatrices having the dimensions $M \times (C-M)$ and $M \times M$ respectively.

Since [10–13] there are the identities $C-M = R$ or $M = C-R$, equation (1) can be written :

$$\boldsymbol{A}_1\boldsymbol{W}_1^T + \boldsymbol{A}_2\boldsymbol{W}_2^T = 0 \tag{4}$$

or

$$\boldsymbol{A}_2\boldsymbol{W}_2^T = -\boldsymbol{A}_1\boldsymbol{W}_1^T \tag{5}$$

After multiplication on the right by $(\boldsymbol{W}_2^T)^{-1}$ it yields :

$$\boldsymbol{A}_2 = -\boldsymbol{A}_1\boldsymbol{W}_1^T(\boldsymbol{W}_2^T)^{-1} \tag{6}$$

In the easiest of cases one can assume $\boldsymbol{A}_1 = \boldsymbol{I}$ where $\boldsymbol{I}$ is matrix unity of dimensions $R \times R$. Thus the equation (6) becomes :

$$\boldsymbol{A}_2 = -\boldsymbol{W}_1^T(\boldsymbol{W}_2^T)^{-1} \tag{7}$$

permitting the calculation of $\boldsymbol{A}_2$ matrix. A stoichiometric matrix is thus obtained

$$\boldsymbol{A} = \boldsymbol{I} | \boldsymbol{A}_2 \tag{8}$$

for the considered system.

FORMULATION OF EQUILIBRIUM PROBLEM

For a multicomponent reaction system one can obtain, based on atomic matrix $\boldsymbol{W}$, a stoichiometric matrix $\boldsymbol{A}$ corresponding to a set of linear independent reactions R.

Equilibrium can be formulated for R reactions on the basis of the equilibrium constants $K_k^{(n)}$ forming a column-vector $\mathbf{K}^{(n)}$ of dimension R.

$$K_k^{(n)} = \prod_{j=1}^{C} n_j^{\nu_{kj}} \qquad (k = 1,2 \dots R) \tag{9}$$

where $K_k^{(n)}$ is the equilibrium constant of reaction k expressed by means of moles number n_j of each component of the system.

Using the two modes of matrix equations, the sigma mode (notation in [ ]) and the pi mode (notation in { }) as suggested by Park[8], equation (9) can be written as follows:

$$\{\boldsymbol{K}^{(n)} = \boldsymbol{A}\boldsymbol{N}\} \tag{10}$$

where $\boldsymbol{N}$ is column vector of the number of moles n_j $(j = 1,2..C)$.

The system of nonlinear equations (10) is completed by M balance equations of the number of moles symbolically written using the sigma mode of Park[8]:

$$[\boldsymbol{W}\boldsymbol{N} = \boldsymbol{B}] \tag{11}$$

where $\boldsymbol{B}$ is column vector of b_i elements standing for the initial (given) abundance of chemical element i in the system.

Knowing the numbers of moles initially introduced in the system, n_j° $(j = 1,2\,..C)$ and forming the corresponding column vector $\boldsymbol{N}^{\circ}$, $\boldsymbol{B}$ vector can be calculated by the equation:

$$[\boldsymbol{B} = \boldsymbol{W}\boldsymbol{N}^{\circ}] \tag{12}$$

In this form the problem of equilibrium consists in solving the equation system (10—11) (C equations with C unknowns) for positive mole numbers.

The system was solved in this form by Anthony and Himmelblau[14] and we shall revert to it in the example below. The various methods suggested by literature[1] (forming the "nonlinear equations" approach group) differentiate one another by the way they transform the problem formulated in equations (10—11) and numerical method practically used.

We further describe a new transformation of the problem (10—11). For this, one can use partitions (2) and (3) of matrices $\boldsymbol{A}$ and $\boldsymbol{W}$ and also the partitions of the vectors:

$$\boldsymbol{N}^T = \boldsymbol{N}_1 \,|\, \boldsymbol{N}_2\,;\ (\boldsymbol{N}^{\circ})^T = \boldsymbol{N}_1^{\circ} \,|\, \boldsymbol{N}_2^{\circ} \tag{13}$$

where $\boldsymbol{N}_1$ and $\boldsymbol{N}_1^{\circ}$ have the dimension R while $\boldsymbol{N}_2$ and $\boldsymbol{N}_2^{\circ}$ the dimension $C - R = M$.

Equation (10) can be written:

$$\{\mathbf{K}^{(n)} = \boldsymbol{A}_1\boldsymbol{N}_1 + \boldsymbol{A}_2\boldsymbol{N}_2\} \tag{14}$$

Whereas equation (11) is written:

$$[\boldsymbol{W}_1\boldsymbol{N}_1 + \boldsymbol{W}_2\boldsymbol{N}_2 = \boldsymbol{W}_1\boldsymbol{N}_1^\circ + \boldsymbol{W}_2\boldsymbol{N}_2^\circ] \tag{15}$$

It results from equation (15);

$$[\boldsymbol{N}_2 = \boldsymbol{W}_2^{-1}\boldsymbol{W}_1\boldsymbol{N}_1^\circ + \boldsymbol{N}_2^\circ - \boldsymbol{W}_2^{-1}\boldsymbol{W}_1\boldsymbol{N}_1] \tag{16}$$

Substituting $\boldsymbol{N}_2$ from (16) in (14) it results:

$$\{\mathbf{K}^{(n)} = \boldsymbol{A}_1\boldsymbol{N}_1 + \boldsymbol{A}_2(\boldsymbol{N}_2^\circ - \boldsymbol{W}_2^{-1}\boldsymbol{W}_1(\boldsymbol{N}_1 - \boldsymbol{N}_1^\circ))\} \tag{17}$$

Using the matrix equation:

$$\boldsymbol{W}_2^{-1}\boldsymbol{W}_1 = -\boldsymbol{A}_2^T(\boldsymbol{A}_1^T)^{-1} \tag{18}$$

easily resulting from (1), equation (17) can be written:

$$\{\mathbf{K}^{(n)} = \boldsymbol{A}_1\boldsymbol{N}_1 + \boldsymbol{A}_2(\boldsymbol{N}_2^\circ + \boldsymbol{A}_2^T(\boldsymbol{A}_1^T)^{-1}(\boldsymbol{N}_1 - \boldsymbol{N}_1^\circ))\} \tag{19}$$

At this stage, vector $\boldsymbol{E}$ can be introduced according to the equation:

$$[\boldsymbol{E} = (\boldsymbol{A}_1^T)^{-1}(\boldsymbol{N}_1 - \boldsymbol{N}_1^\circ)] \tag{20}$$

or transforming

$$[\boldsymbol{N}_1 = \boldsymbol{N}_1^\circ + \boldsymbol{A}_1^T\boldsymbol{E} \tag{21}$$

It may be noticed that $\boldsymbol{E}$ represents column vector having as elements the extents of reaction $\xi_k(k = 1,2\ldots R)$ introduced by De Donder.[9]

Substituting (20) and (21) in (19) it yields:

$$\{\mathbf{K}^{(n)} = \boldsymbol{A}_1(\boldsymbol{N}_1^\circ + \boldsymbol{A}_1^T\boldsymbol{E}) + \boldsymbol{A}_2(\boldsymbol{N}_2^\circ + \boldsymbol{A}_2^T\boldsymbol{E})\} \tag{22}$$

Since $\boldsymbol{A}_1 = \boldsymbol{I}$ and $\mathbf{A}_2$ is given by equation (7) it results:

$$\{\mathbf{K}^{(n)} = (\boldsymbol{N}_1^\circ + \boldsymbol{E}) - \boldsymbol{W}_1^T(\boldsymbol{W}_2^T)^{-1}(\boldsymbol{N}_2^\circ - \boldsymbol{W}_2^{-1}\boldsymbol{W}_1\boldsymbol{E})\} \tag{23}$$

This matrix equation represents the formulation of chemical equilibrium problem based on atomic matrix.

Equation (22) can be written in the final form as:

$$\{\mathbf{K}^{(n)} = \boldsymbol{A}(\boldsymbol{N}^\circ + \boldsymbol{A}^T\boldsymbol{E})\} \tag{24}$$

where from it results :

$$[N = N^\circ + A^T E] \tag{25}$$

Equations (21, 25) permit a rigorous mathematically introduction of De Donder variable vector to multicomponent reaction systems.

Matrix equation (24) corresponds to the system of R nonlinear equations :

$$K_k^{(n)} = \prod_{j=1}^{C} \left(n_j^\circ + \sum_{k=1}^{R} \nu_{jk}\xi_k \right)^{\nu_{kj}} \tag{26}$$

Equation (26) represents the transformation of equilibrium problem (10—11). It is worth mentioning now that the value of the equilibrium constant $K_k^{(n)}$ cannot be obtained directly from thermo-chemical data. It can for instance be obtained from the well known relation

$$K_k^{(n)} = K_k^{(P)} \left(P^{-1} \sum_{j=1}^{C} n_j \right)^{\sum_{j=1}^{C} \nu_{kj}}, \qquad (k = 1,2,..R) \tag{27}$$

in the case of an ideal system in gaseous phase. P is the total pressure in the system while $K_k^{(P)}$ the equilibrium constant of reaction k expressed in partial pressures (possibly to be calculated from standard free enthalpy of reaction). Equation (26) becomes :

$$K_k^{(P)} = \left(P \left(\sum_{j=1}^{C} n_j \right)^{-1} \right)^{\sum_{j=1}^{C} \nu_{kj}} \prod_{j=1}^{C} \left(n_j^\circ + \sum_{k=1}^{R} \nu_{jk}\xi_k \right)^{\nu_{kj}} \tag{28}$$

In this form the nonlinear equation system (28) can be directly solved by a usual numerical method. To avoid difficulties connected to convergence one can apply first a Gauss transformation of stoichiometry as suggested by Park.[8] His prime method is a special case of equation (28).

It has to be noticed that the final form (28) reached is well-known to physical chemist, being generally used for calculation of equilibrium in systems with one chemical reaction. [9,11,15] Equations like (28) were also used for systems with two simultaneous reactions by intuitional generalization of the one reaction case.[15,16] Such methods were not considered in the review book by van Zeggeren and Storey.[1]

It is also worth mentioning that equations (22) and (25) (by which the vector of De Donder variable is rigurously introduced) are used, [9–13,15] being introduced as mass balance equations by generalization of one reaction case.

ALGORITHM FOR SOLVING THE EQUILIBRIUM PROBLEM

Considering the formulations of the chemical equilibrium problem dealt with in the previous chapter, one can give a calculation algorithm of a numerical solution. A reaction system being given by components C, temperature T, total pressure P and vector N° one can calculate composition at equilibrium as follows :

a) the atomic matrix of the system, $\boldsymbol{W}$, is constructed

b) a stoichiometric matrix of the system is obtained with equations (7–8)

c) equilibrium constants $K_k^{(P)}$ corresponding to chemical reactions set obtained under (b) are calculated by usual methods. A matrix method based on standard free enthalpies of formation was recently proposed.[17]

d) the nonlinear equation system (28) is solved by a suitable numerical method. The vector of De Donder variable, $\boldsymbol{E}$, is obtained at equilibrium.

e) the composition at equilibrium is calculated (vector $\boldsymbol{N}$) by equation (25).

EXAMPLE OF APPLICATION OF ALGORITHM

For ilustration of the above method one has chosen the reaction system of generator gas (coal gaseification). This system was also calculated by Anthony and Himmelblau [14] and Scully.[18] This permits the comparison of results.

Atomic matrix of the system having the components CO_2, H_2O, CH_4, CO, H_2, C is :

$$\boldsymbol{W} = \begin{array}{c} \\ \\ \\ \\ \end{array}\begin{array}{ccc|ccc|c} CO_2 & H_2O & CH_4 & CO & H_2 & C & \\ \hline 1 & 0 & 1 & 1 & 0 & 1 & C \\ 2 & 1 & 0 & 1 & 0 & 0 & O \\ 0 & 2 & 4 & 0 & 2 & 0 & H \\ \hline \multicolumn{3}{c}{\boldsymbol{W}_1} & \multicolumn{3}{c}{\boldsymbol{W}_2} & \end{array} \qquad (29)$$

From equation (7) it results :

$$\boldsymbol{A}_2 = \begin{vmatrix} -2 & 0 & 1 \\ -1 & -1 & 1 \\ 0 & -2 & -1 \end{vmatrix} \qquad (30)$$

Stoichiometric matrix corresponding to (8) is :

$$\boldsymbol{A} = \begin{array}{cccccc} CO_2 & H_2O & CH_4 & CO & H_2 & C \\ \hline 1 & 0 & 0 & -2 & 0 & 1 \\ 0 & 1 & 0 & -1 & -1 & 1 \\ 0 & 0 & 1 & 0 & -2 & -1 \end{array} \qquad (31)$$

Matrix $\boldsymbol{A}$ is arbitrary at any nonsingular transformation, for instance by matrix $\boldsymbol{Y}$ of dimensions 3×3 (generally $R \times R$) with condition that $\det \boldsymbol{Y} \neq 0$.

Naturally the problem can be solved with the obtained matrix $\boldsymbol{A}$. In order to use the initial data from [14] the stoichimetric matrix $\boldsymbol{A}$ is transformed by matrix:

$$\boldsymbol{Y} = \begin{vmatrix} -1 & 0 & 0 \\ 0 & -1 & 0 \\ 0 & 0 & 1 \end{vmatrix} \tag{32}$$

A new stoichiometric matrix (noted $\boldsymbol{A}$ too) is thus obtained in the form:

$$\boldsymbol{A} = \begin{array}{c} \begin{array}{cccccc} CO_2 & H_2O & CH_4 & CO & H_2 & C \end{array} \\ \begin{vmatrix} -1 & 0 & 0 & 2 & 0 & -1 \\ 0 & -1 & 0 & 1 & 1 & -1 \\ 0 & 0 & 1 & 0 & -2 & -1 \end{vmatrix} \end{array} \tag{33}$$

This matrix corresponds to the set of chemical reactions used in the calculation of equilibrium in [14] At temperature $T = 700°C$ and total pressure $P = 1$ atm the vector of equilibrium constants is :[14]

$$\boldsymbol{K}^{(P)} = \begin{Vmatrix} 1.07266 \\ 1.66179 \\ 0.031769 \end{Vmatrix} \tag{34}$$

Vectors $\boldsymbol{N}^\circ$ and $\boldsymbol{N}$ are:

$$\boldsymbol{N}^\circ = \begin{Vmatrix} 0.17335 \\ 0.17451 \\ 0. \\ 0. \\ 0. \end{Vmatrix} ; \quad \boldsymbol{N} = \begin{Vmatrix} 0.17335 - \xi_1 \\ 0.17451 - \xi_2 \\ \xi_3 \\ 2\xi_1 + \xi_2 \\ \xi_2 - 2\xi_3 \end{Vmatrix} \tag{35}$$

The values of vector $\boldsymbol{N}^\circ$ elements are those used in.[14] The presence of $n^{\circ}_{N_2} = 0.65214$ moles nitrogen (inert) is also considered in the system. Carbon constitutes the solid phase and it is considered present in sufficient amount in the system so that reactions reach the equilibrium. The sum of moles number in gaseous phase is:

$$\sum_{j=1}^{C} n_j = 1 + \xi_1 + \xi_2 - \xi_3 \tag{36}$$

There are all the elements to obtain the nonlinear equations system (28). Since the equilibrium is heterogeneous, the system is reduced to 5 components (in gaseous phase) therefore the matrix $\boldsymbol{A}$ contains only the first 5 columns (size 3×5). The system of resulting equations can be formally written:

$$f_i(\xi_1, \xi_2, \xi_3) = 0 \qquad (i = 1, 2, 3) \tag{37}$$

The numerical method used for solving the system (37) is minimization of function:

$$\min F = \sum_{i=1}^{3} f_i^2(\xi_1, \xi_2, \xi_3) \tag{38}$$

The problem (38) is an optimization problem. It is subject to restrictions:

$$\begin{aligned} 0 &< \xi_1 < 0.17335 \\ 0 &< \xi_2 < 0.17451 \\ 0 &< \xi_3 < 0.5\,\xi_2 \end{aligned} \tag{39}$$

A series of known methods [19, 20] are disponible in order to solve the optimization problem with restrictions (38, 39). Hooke–Jeeves method was chosen for its simplicity. This method (called "direct search") was also used in [14] to solve this problem in formulation (10, 11) that is in 6 variables. Although Hooke-Jeeves method is generally used to solve optimization problems without restrictions it can be easily modified to introduce constraints such as (39).

Using such a modification, problem (38, 39) was solved on the computer using a FORTRAN program.

The results of calculations using two initial points at which iterations started are given in table 1. The values of function F are also given for the initial and equilibrium values of vector $\boldsymbol{E}$.

TABEL 1

Chemical equilibrium in reaction system of generator gas.
$P = 1$ atm. $T = 700$°C

	I	II
$\boldsymbol{E}$ (initial)	0.05 0.05 0.02	0.15 0.15 0.02
F (initial)	$0.4664587 \cdot 10^{5}$	$0.3686981 \cdot 10^{2}$
$\boldsymbol{E}$ (equil.)	0.09065 0.15047 0.00057	0.09063 0.15049 0.00057
F (equil.)	$0.4177226 \cdot 10^{-6}$	$0.8405592 \cdot 10^{-6}$
No. iterations	30	28
$\boldsymbol{N}$ (equil)	0.08270 0.02404 0.00057 0.33177 0.14933	0.08272 0.02402 0.00057 0.33175 0.14935

The convergence test was $\Delta\xi_i \leqslant 10^{-5}$. One can notice that first vector $\boldsymbol{E}$ is closer to the solution of the problem having the final value of the function lower. The values of $\boldsymbol{N}$ vector elements were obtained by equation (35) and agree excellently with those reported in.[14] There are no data in [14] to compare the convergence rate. Therefore the problem in formulation (10,11) was solved by Hooke-Jeeves method, that is similarly to .[14]

The results show that convergence rate is much lower; after 300 iterations one obtains values close to those given above, but the function value is still $\sim 10^{-4}$.

At least for two reasons, the reduction of the number of variables and the increase of convergence rate, the formulation suggested by the present paper to solve the chemical equilibrium in multicomponent systems shows advantages over other formulations. Of course, it is necessary to test the method in the case of more complex problems but the advantage of a minimum number of variables will be maintained for any situation. The method can be extended to consider real behaviour of the systems as in the literature.[21-23]

APPENDIX

It may be of interest the fact that, from formulation (10—11) of equilibrium and using partitionings (2,3) and (13) one can obtain the equation system constituting the Brinkley method for solving the problem of chemical equilibrium.

Thus from

$$\{\boldsymbol{K}^{(n)} = \boldsymbol{A}_1\boldsymbol{N}_1 + \boldsymbol{A}_2\boldsymbol{N}_2\} \qquad (A_1)$$

and

$$[\boldsymbol{W}_1\boldsymbol{N}_1 + \boldsymbol{W}_2\boldsymbol{N}_2 = \boldsymbol{B}] \qquad (A_2)$$

one obtains

$$\{\boldsymbol{N}_1 = \boldsymbol{A}_1^{-1}\boldsymbol{K}^{(n)} - \boldsymbol{A}_1^{-1}\boldsymbol{A}_2\boldsymbol{N}_2\} \qquad (A_3)$$

and

$$[\boldsymbol{N}_2 = \boldsymbol{W}_2^{-1}\boldsymbol{B} - \boldsymbol{W}_2^{-1}\boldsymbol{W}_1\boldsymbol{N}_1] \qquad (A_4)$$

Considering the equation

$$[\boldsymbol{W}_2^{-1}\boldsymbol{W}_1 = -\boldsymbol{A}_2^T(\boldsymbol{A}_1^T)^{-1}] \qquad (A_5)$$

one obtains

$$[\boldsymbol{N}_2 = \boldsymbol{W}_2^{-1}\boldsymbol{B} + \boldsymbol{A}_2^T(\boldsymbol{A}_1^T)^{-1}\,\boldsymbol{N}_1] \qquad (A_6)$$

The system of equations (A_3) and (A_6) can be solved using Brinkley algorithm. Matrix equations have a simpler form if we consider $\boldsymbol{A}_1 = \boldsymbol{I}$. Thus:

$$\{\boldsymbol{N}_1 = \boldsymbol{K}^{(n)} - \boldsymbol{A}_2\boldsymbol{N}_2\} \qquad (A_7)$$

$$[\boldsymbol{N}_2 = \boldsymbol{W}_2^{-1}\boldsymbol{B} + \boldsymbol{A}_2^T\boldsymbol{N}_1] \qquad (A_8)$$

N_2 corresponds to the "system components" while N_1 to "derived species" of Brinkley.[1]

Formulation of Park's duale method [8] can also be obtained based on equations (A_1) and (A_2).

REFERENCES

[1] F. van Zeggeren and S. H. Storey, "The Computation of Chemical Equilibria", University Press, Cambridge, 1970.

[2] W. B. White, S. M. Johnson and G. B. Danzig, *J. Chem. Phys.*, **28**, 751 (1958).

[3] F. P. Boynton, *J. Chem. Phys.*, **32**, 1880 (1960).

[4] R. V. Sanderson and H. H. Y. Chien, *Ind. Eng. Chem. Proc. Des. Dev.*, **12**, 81 (1973).

[5] H. S. Caram, and L. E. Scriven, *Chem. Eng. Sci.*, **31**, 163 (1976).

[6] H. G. Othmer, *Chem. Eng. Sci.*, **31**, 993 (1976).

[7] R. A. Heidemann, *Chem. Eng. Sci.*, **33**, 1517 (1978).

[8] D. J. M. Park, *J. Chem. Phys.*, **65**, 3085 (1976).

[9] I. Prigogine and R. Defay, "Chemische Thermodynamik", VEB Deutscher Verlag, Leipzig 1962.

[10] R. Aris, "Introduction to the Analysis of Chemical Reactors", Prentice-Hall, New-Jersey, 1966.

[11] K. Denbigh, "Principles of Chemical Equilibrium", University Press, Cambridge, 1955.

[12] N. F. Stepanov, M. E. Erl'kina and G. G. Filippov, "Methods of Linear Algebra in Physical Chemistry", Izd. Mosk. Univ., Moskow, 1976 (russ.).

[13] E. J. Henley and E. M. Rosen, "Material and Energy Balances Computations", Wiley, New-York, 1969.

[14] R. G. Anthony and D. M. Himmelblau, *J. Phys. Chem.*, **67**, 1080 (1963).

[15] J. G. Kirkwood and I. Oppenheim, "Chemical Thermodynamics", McGraw-Hill, New-York, 1961.

[16] B. F. Dodge, "Chemical Engineering Thermodynamics", McGraw-Hill, New-York, 1944.

[17] D. Geană, *Rev. Chim. (Bucureşti)*, **28**, 1058 (1977).

[18] D. B. Scully, *Chem. Eng. Sci.*, **17**, 977 (1962) ; **18**, 725 (1963).

[19] G. S. Beveridge and R. S. Schechter, "Optimization — Theory and Practice", McGraw-Hill, New-York, 1970.

[20] D. Geană and D. Popescu, *Rev. Chim. (Bucureşti)*, **29**, 433 (1978).

[21] S. Peter and H. Wenzel, *Chemie-Ing.-Techn.*, **45**, 572 (1973).

[22] D. Geană and F. E. Daneş, *Bul. Inst. Politeh. (Bucureşti)*, **40**, 31 (1978).

[23] F. E. Daneş and D. Geană, *Rev. Chim. (Bucureşti)*, **30**, 244 (1979).

Revue Roumaine de Chimie, **26**, *1*, 55–64 (1981)

SELF-DIFFUSION OF TELLURIUM IN LIQUID Tl_2Te ALLOY

N. PETRESCU * and LUCIA GANOVICI **

*Department of Metallurgy, The Polytechnic Institute of Bucharest, Spl. Independenţei 212, Romania

** Centre of Physical Chemistry, Spl. Independenţei 202, Bucharest, Romania

Received April 24, 1980

The paper presents the results of the determinations of the self-diffusion coefficients of tellurium in the liquid alloy of stoichiometric composition Tl_2Te. The experimental determinations have been made by the capillary-reservoir method, using radioactively labelled tellurium in the composition of the alloy in the reservoir. The experimental results, interpreted in terms of the thermally activated processes, have emphasized two distinct temperature ranges with different Arrhenius equations : the pre-freezing range (450—500°) having an abrupt rise of the diffusivity and the range of higher temperatures (over 500°) having a slower rise of diffusivity *versus* temperature. A successful attempt has been made to interpret the diffusion process in the melt in terms of the rigid spheres theory. Using diffusion model proposed by Protopapas and considering the Tl_2Te association in the melt as the structural entity for diffusion, a very good agreement has been obtained between the experimental and theoretical values in the pre-freezing range. This points the fact that the Tl_2Te groups are stable in the melt only close to the freezing point and they dissociate at higher temperatures.

Diffusion coefficients determinations in molten alloys are not numerous, and much still remains to be done in this field of research. Our knowledge on metallic melts results especially from the determinations of other properties which can be used to evaluate if an alloy system shows a monotonous variation of its properties in agreement with the simple laws of the mixtures, or, on the contrary, it shows singular variations at certain compositions pointing to peculiar processes or transformations in the melt. Difficult problems face the theory of liquid state in order to explain these processes, but on the other hand such processes offer a precious material for deriving information about the structure of the melts.[1]

The liquid Tl_2Te alloy chosen for our diffusion studies has a special position in the Tl— Te system showing pronounced singularities in its properties. The molten Tl — Te alloy shows a strong decrease of the electric conductivity[2,3] in the vicinity of the Tl_2Te compound, so that the very composition of the compound is marked by a sharp peak of the resistivity (Fig. 1).

The thermoelectric power[4,5] also shows strong variations in the vicinity of the stoichiometric composition Tl_2Te, the Seebeck coefficient passing through zero at this composition after having shown a maximum and

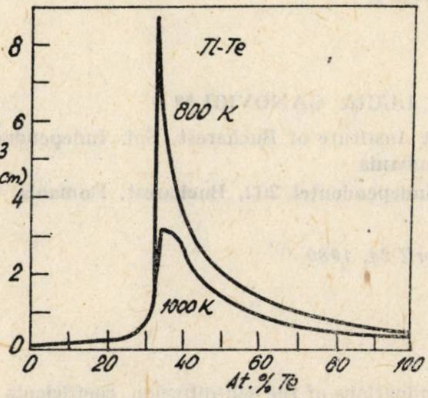

Fig. 1. — Resistivity isotherms in liquid Tl—Te alloys.

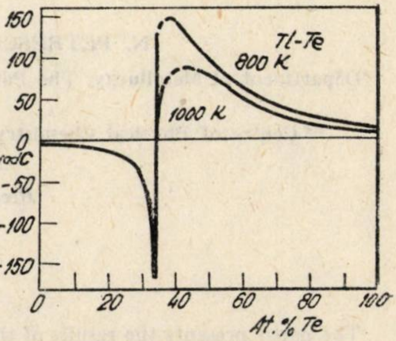

Fig. 2. — Thermoelectric power isotherms in liquid Tl—Te alloys.

a minimum at the adjacent compositions (Fig. 2). This behaviour is similar to that of a solid semiconductor compound for which minute deviations from the stoichiometry are equivalent to an impurification with donor or acceptor elements.

In figures 1 and 2 a pronounced symmetry is manifest in the two domains adjacent to the $p-n$ transition. On the Tl rich side, where the Seebeck coefficient (S) is negative, S and ρ change rapidly with composition but are almost temperature independent. The behaviour in this region has been assigned to a dispersion of Tl^{3+} ions in the matrix formed by Tl_2Te molecules. On the Te rich side S and ρ change slowly with composition but decrease rapidly as the temperature rises. This behaviour has been interpreted in terms of the electronic structure of the melts, as a result of the generation of holes on account of acceptor electronic levels created by the chemical reactions in the melt.

The study of the thermodynamics of the Tl—Te system points to a strong decrease of the mixing entropy [6] and a pronounced minimum of the mixing heat [7] in the melt at the composition of Tl_2Te compound. The measurements of the Hall coefficient and of magnetic properties [8] also show strong anomalies at the composition of Tl_2Te compound.

Singular behaviour of the excess molar volume and of the viscosity in Tl — Te melts in the vicinity of the stoichiometric composition Tl_2Te has been established in the experiments of Nakamura and Shimoji,[4,9] who have studied the density and the viscosity in Tl—Te melts of different compositions and temperatures (Figs 3 and 4).

These facts show that the molten Tl_2Te compound has clear cut peculiar properties of great theoretical interest and this urged us to study the diffusive mass transport properties at this very composition.

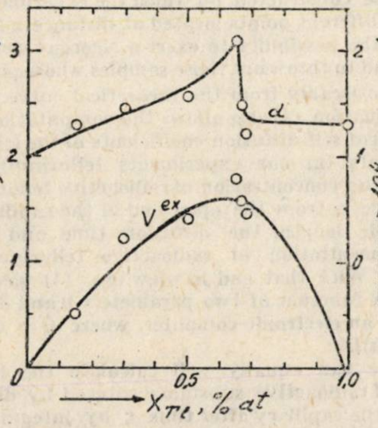

Fig. 3. — Excess molar volume V^{ex} and thermal dilatation coefficients α at 500°C in the Tl—Te system in liquid state.

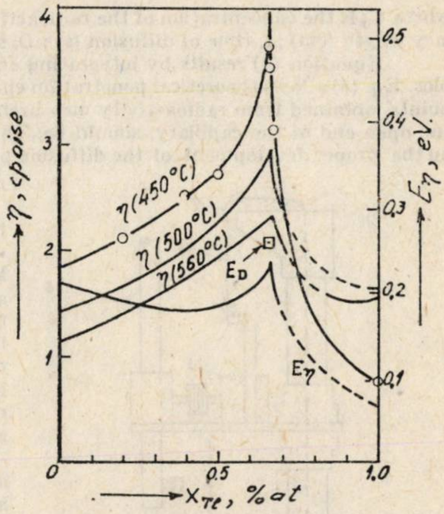

Fig. 4. — Viscosity isotherms and activation energy for viscous flow, E_η, in Tl—Te system in liquid state.

EXPERIMENTAL

For determining the self-diffusion coefficients of tellurium in liquid Tl—Te alloys, we used the capillary — reservoir method. Both capillary and reservoir were filled with alloy of the same composition, but part of the tellurium used for preparing the alloy in the reservoir was radioactively labelled. The capillary was sunken in the melt in the reservoir and diffusion took place at the open end of the capillary through the contact surface with the bath. The labelling with radioactive tellurium allowed the diffusion process to be studied quantitatively. The distribution of the radioactive tellurium entered into the capillary, varies in time according to a function resulting by integrating Fick's second law :

$$\frac{\partial C}{\partial t} = D \frac{\partial^2 C}{\partial x^2} \tag{1}$$

To carry out the integration, the proper initial and limit conditions in the experimental diffusion couple are needed. For capillaries of length l open at one end and filled with non-radioactive alloy, the initial conditions are :

$$t = 0; \quad C = 0; \quad 0 < x < l \tag{2}$$

and limit conditions are :

$$\begin{aligned} C = C_0; \quad x = 0; \quad t > 0 \\ \frac{\partial C}{\partial x} = 0; \quad x = l; \quad t > 0 \end{aligned} \tag{3}$$

For these conditions, the concentration distribution of the radioactive tellurium in the capillary, after a diffusion time t, is given by the relation :

$$\frac{C(x,t)}{C_0} = 1 - \frac{4}{\pi} \sum_{n=0}^{\infty} \frac{1}{(2n+1)} \sin \frac{(2n+1)\pi}{2} \frac{x}{l} \exp\left[-\frac{(2n+1)^2\pi^2}{4} \frac{Dt}{l^2}\right] \tag{4}$$

where C_0 is the concentration of the radioactive tellurium in the reservoir at time $t = 0$; l, capillary length (cm) ; t, time of diffusion (s) ; D, self-diffusion coefficient (cm²/s) of labelled element.

Equation (4) results by integrating eq. (1) through the method of separating the variables. Eq. (4) allows theoretical penetration curves to be constructed, on which the experimental points, obtained from radioactivity measurements in different points located at distance x from the open end of the capillary, should lie. This offers the possibility to exert a rigorous control on the proper development of the diffusion process, and to throw out those samples whose points deviate noticeably from the theoretical curve.

Equation (4) also allows the computation of the values of self-diffusion coefficients of the labelled elements (in our experiments tellurium), by knowing the concentration of radioactive tellurium at distance x from the open end of the capillary, the sample length, the diffusion time and the initial concentration of radioactive tellurium in the bath. With that end in view, eq. (4) was tabulated in function of two parameters θ and δ, by means of an electronic computer, where $\theta = Dt/l^2$ and $\delta = x/l$.

One can equally well calculate the total amount of radioactive substance entered by diffusion into the capillary after time t, by integrating eq. (4) on the whole length of the capillary ; one obtains the average concentration $\bar{C}$ in the capillary :

$$\frac{\bar{C}}{C_0} = 1 - \frac{8}{\pi^2} \sum_{n=0}^{\infty} \frac{1}{(2n+1)^2} \exp\left[-\frac{(2n+1)^2\pi^2}{4} \frac{Dt}{l^2}\right] \tag{5}$$

Equation (5) tabulated in function of the parameter $\theta = Dt/l^2$ allows the calculation of the diffusion coefficient from a single radioactivity measurement, namely that of the whole capillary after diffusion.

The diffusion process has been carried out in an apparatus made in our laboratory, which was specially designed to take into account the specific conditions of the metallic melts.

The diffusion apparatus outlined in figure 5 comprises a diffusion chamber made of quartz, a furnace 1 containing inside the reservoir of liquid metal 2, and a passing zone separated from the diffusion chamber by a quartz tap 3, which, when turned off, allows the diffusion samples to be changed without need to solidify the liquid metal in the reservoir.

A mechanical device 4, operated by means of the electrical motor 5, serves to move down or lift the diffusion samples for introducing them into or taking them out from the reservoir of liquid metal. The mechanical device 4 comprises a screwed rod 6 attached at its lower end to a stainless steel rod 7 which slides through the air tight passing 8 in the metallic body 9. This metallic body 9 ends with a polished vent which closes the quartz passing zone 11.

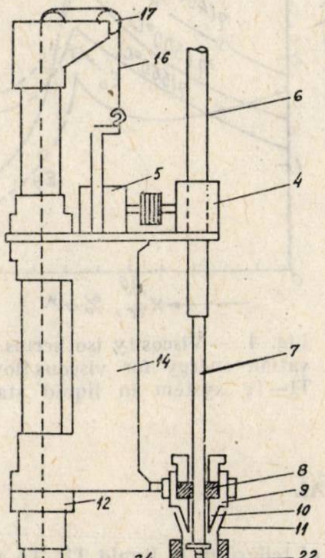

Fig. 5. — Diffusion apparatus.

To close or open the diffusion chamber one lets down or lifts the metallic taper fastened to ring 12 which slides on holder 13. This device is drived by means of an electrical motor and a mechanical system fitted up on a metallic platform fastened on plate 14 (not shown in figure 5). The weight of the whole moving device is conterbalanced by weights 15 hanging to a flexiblle metallic cable 16 which passes through a pulley system 17.

The heating system comprises a kanthal ribbon wound in a helicoidal groove cut in the very quartz wall of the diffusion chamber around the reservoir, so that a hot zone without thermal gradient can be established on a length of about 30 cm. The outer quartz tube 18 serves as a thermal insulator.

The temperature has been measured by means of a Pt — PtRh thermocouple put in quartz sheath 19, which serves at the same time as a holder for the crucible containing the liquid metal bath. To ensure a constant temperature during the diffusion run, within ±1°C, a potentiometric device was used.

The capillaries 20 holding the diffusion samples were made of graphite and they were fastened to a hanging system 21 connected with a stainless steel rod 7 by means of the link part 22. Clamp 23 serves to center the system.

Before a diffusion run, the apparatus is connected alternatively to the vacuum pump and to a pure argon supply by means of a taps system 24.

The diffusion sample was contained within a capillary hole of 0.8—1 mm diameter and 20—25 mm length drilled in a spectral pure graphite rod. Sintered alumina tubes sealed at one end have been sometimes used to contain the diffusion samples. The capillaries, either of graphite or of sintered alumina, were filled with the liquid Tl_2Te alloy by vacuum pumping them and introducing the liquid alloy under argon pressure.

The diffusion sample holding device is shown in figure 6.

The capillary containing the diffusion sample 1 is screwed into a small graphite disc 2 fastened to the holding graphite rod 3, linked in its turn to a quartz rod 4 by means of a stainless steel coupling 5. A similar coupling 6 serves to link the whole system to the stainless steel rod which lets down or lifts the diffusion samples in order to introduce them into or to take them out from the liquid bath in the reservoir.

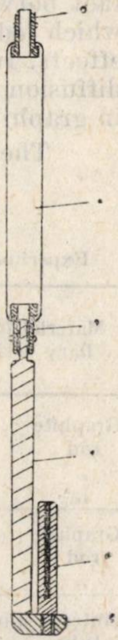

Fig. 6— Diffusion samples holding device.

The alloy of stoichiometric composition corresponding to Tl_2Te compound has been prepared in sealed quartz ampoules at a temperature of 600°. Tellurium and thallium of high purity (99.999%) have been used to prepare the alloy. For the alloy in the reservoir, part of the stoichiometrically necessary tellurium was radioactive.

After the diffusion run, the radioactivity of the capillary sample was measured integrally by means of a scintillation counter. The time of counting was chosen long enough to ensure a relative standard deviation less than 1%.

For reference, the radioactivity of the bath in the reservoir was measured on a capillary of the same length and diameter filled with the alloy of the bath, using the same filling technique as for diffusion sample.

RESULTS AND DISCUSSION

The self-diffusion coefficients of tellurium in liquid Tl_2Te alloy and their variation with temperature have been studied in the present work in the temperature range 450—600°C. The upper limit of the studied temperature range was set by rapid increase with temperature of the vapour tension of liquid tellurium.

Measurements were made at six different temperatures, using two samples for each diffusion run; several diffusion runs have been made at the same temperature. From the total number of the diffusion samples which participated at the diffusion runs, only about 50% have been taken into consideration. The remaining 50% of the samples were rejected because they didn't agree with the conditions imposed at the integration of eqs (4) and (5). These disagreements were due to interruption of the contact between bath and capillary either because of hydrodynamic effects which led to pulling out of the top of the capillary or to surface tension effects. In order to remove this latter cause of perturbations, a series of diffusion runs has been carried out with diffusion samples contained not in graphite capillaries but in sintered alumina ones.

The experimental results of the diffusion runs are given in table 1.

TABLE 1

Experimental results on the self-diffusion coefficients of tellurium in liquid Tl_2Te alloy

Material for capillary recipient	Diffusion temperature (°C)	Diffusion time (s)	Capillary length (cm)	$D.10^5$ (cm²/s)	$(\bar{D} \pm \sigma_D) \cdot 10^5$ (cm²/s)
Graphite rod	450	5,415	1.690	2.05	2.27±0.13
,,	450	5,415	1.903	2.49	
,,	450	5,400	1.863	2.26	
Graphite rod	475	4,500	1.946	2.85	3.04±0.19
,,	475	4,500	2.032	3.23	
Sintered alumina tube	500	4,500	2.163	3.74	4.31±0.34
,,	500	4,500	2.093	5.13	
,,	500	4,500	2.124	3.69	
,,	500	4,500	2.144	4.66	
Graphite rod	525	4,500	2.092	5.07	4.96±0.11
,,	525	4,500	2.120	4.85	
Graphite rod	575	3,600	1.886	6.02	6.11±0.09
,,	575	3,600	1.923	6.21	
Sintered alumina tube	600	3,600	1.855	7.86	6.74±0.98
,,	600	3,600	1.653	5.62	

The variation of the self-diffusion coefficients of tellurium *versus* reciprocal of the absolute temperature is given in figure 7 in semilogarithmic scale.

It is obvious from our experimental data that the decrease of the diffusion coefficients of tellurium is very abrupt in the pre-freezing region of the Tl_2Te alloy, namely in a temperature range of about 60°C above the solidification point (~440°C) of the Tl_2Te compound. On this account, we have decided to interpret the experimental results in terms of the activated process law (Arrhenius equation) distinctly for the pre-freezing range and for the upper temperature range. Thus, we have established the following Arrhenius equation for the temperature variation of the self-diffusion coefficient of tellurium in liquid Tl_2Te alloy in the pre-freezing range (440—500° C):

$$D = 411.10^{-3} \exp\,(-14100/RT) \tag{6}$$

For the upper temperature range (above 500°C), the corresponding equation is:

$$D = (12.14 \pm 1.90).10^{-3} \exp\left(-\frac{6001 \pm 158}{RT}\right) \tag{7}$$

The main feature put in evidence by these two equations is a larger value of the activation energy for diffusion in the pre-freezing range.

The large activation energy and the rapid decrease of the diffusion coefficient in the pre-freezing range, suggest that considerable structural changes take place in the melt. This supposition is supported too by the results of Nakamura and Shimoji [9] on the density and viscosity of the molten Tl — Te alloys. These determinations show that both the excess molar volume and viscosity isotherms have pronounced peaks in the vicinity of the stoichiometric composition Tl_2Te (Figures 3 and 4).

In figure 4 it is obvious that the viscosity peaks at the stoichiometric composition are higher and higher as the temperature approaches the solidification point. In order to emphasize this feature we have plotted in figure 4 not only the viscosity isotherms given by Nakamura and Schimoji at 500 and 560°C, but also the isotherm at 450°C close to the solidification point of Tl_2Te compound. For obtaining the 450 isotherm we have used the viscosity data of the above quoted authors for different compositions in the liquid Tl—Te system.

The low values of the diffusion coefficients in the proximity of the solidification point, obtained in our experimental determinations agree with the viscosity maxima in the same temperature range.

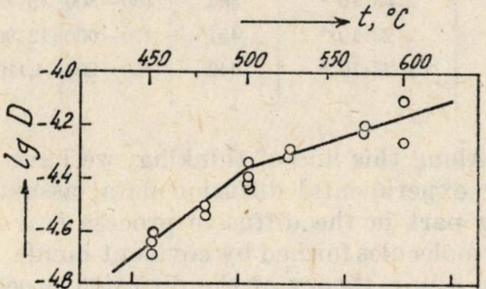

Fig. 7. — Temperature variation of the self-diffusion coefficients of tellurium in liquid Tl_2Te alloy.

In the upper temperature range, the value of the activation energy for diffusion derived from our experimental data ($E_D = 6\,001$ cal/mol.g), compares well with the activation energy for viscous flow ($E_\eta = 5\,200$ cal/mol.g) that we have calculated from the viscosity data.

The peculiar variation of the diffusion coefficient in the pre-freezing range can be assigned to a weakening of the ionic character of the Tl—Te bonds and the appearance of covalent bonds which result in the stable molecular groups of composition Tl_2Te.

The slower temperature variation of the diffusion coefficient at higher temperatures ($> 500°C$) can be assigned to a dissociation of the molecular Tl_2Te groups.

In some previous paper [10, 11] we have determined the self-diffusion coefficients in pure liquids Te and Tl. Using these values at 450°C and comparing them with the self-diffusion coefficient of tellurium in Tl_2Te alloy at the same temperature, we can see that the diffusivity in the liquid compound close to its solidification point is lower than in the pure component elements.

The data in table 2 also show that the activation energy for diffusion in the Tl_2Te alloy is much larger than the activation energy for diffusion in pure components. This fact is in good agreement with the assumption of the weakening of the ionic character of the Tl—Te bonds in the vicinity of the stoichiometric composition of the stable Tl_2Te compound and the appearance of stronger bonds of covalent type between the component elements of the compound.

TABLE 2

Comparison of self-diffusion data in pure liquid components (Tl and Te) and in liquid Tl_2Te alloy

Diffusion system	Self-diffusion coefficient at 450°C (cm²/s)	Melting point °C	Arrhenius eq. for diffusion $D = D_0 \exp(-Q/RT)$ derived from experimental data			Source
			Temperature range °C	D_0 (cm²/s)	Q (cal/mol.g)	
Tl	$2.55 \cdot 10^{-5}$	304	350—800	$(3.17 \pm 0.27) \cdot 10^{-4}$	$3,620 \pm 130$	**10**
Te	$2.73 \cdot 10^{-5}$	451	470—600	$(12.90 \pm 0.31) \cdot 10^{-4}$	$5,550 \pm 297$	**11**
Te in Tl_2Te	$2.27 \cdot 10^{-5}$	442	450—500	$4,110 \cdot 10^{-4}$	14,000	**Present paper**

Along this line of thinking, we have undertaken the interpretation of our experimental diffusion data, assuming that the structural entity taking part in the diffusive process is a molecular group, namely the Tl_2Te molecules formed by covalent bonds. With this aim in view we have chosen a new theory of the diffusion process, based on the concept of a rigid spheres model for fluids. This theory, first proposed by Ascarelli and Paskin [12] and developped by Protopapas and coworkers [13], considers the fluid composed of rigid spheres in which the atomic transport is described by the Enskog theory,[14] with the necessary corrections derived from molecular dynamics computations carried out by using the Dymond and Alder [15] approximations and the state equation of Carnahan — Starling [16].

The expression for the temperature variation of the diffusion coefficient in the melt proposed by Protopapas [13] is :

$$D = \frac{(\pi RT/M)^{1/2}\, \sigma(T)C(\eta)\,(1-\eta)^3}{8\eta(2-\eta)} \tag{8}$$

where M is the molecular weight of the diffusing particle, $C(\eta)$ is a correction factor depending on the packing density η calculated and tabulated by Alder [17] and $\sigma(T)$ is the rigid spheres diameter for which a computation relation is available. [13]

Protopapas and coworkers have checked their model for the self-diffusion in ten pure liquid metals and they have found a good agreement between the values of the self-diffusion coefficient calculated from eq. (8) and the experimental values.

In the present paper we have undertaken to check this theory for a liquid alloy and we applied eq. (8) for computation of the self-diffusion coefficients of tellurium in molten Tl_2Te compound. To do this we have assumed that the structural entity taking part in the diffusive process is a molecular group containing two thallium atoms and one tellurium atom having a molecular mass $M = 536.41$. As the atomic diameters of the two atomic species are very close ($\sigma_{Tl} = 3.18$ Å and $\sigma_{Te} = 3.20$ Å) we have considered a compact packing of the three atoms, so that the diameter of the molecular group Tl_2 Te at the solidification temperature is twice the diameter of any of the component atoms. For higher temperatures we have considered a temperature variation of the diameter of this structural entity according to the following equation established by Protopapas [13] :

$$\sigma = \sigma_{T_m}[1 - B(T/T_m)^{1/2}] : (1 - B) \tag{9}$$

where B is a constant having a value $B = 0.112$ for liquid metals.

Using eqs (8) and (9) we have calculated the theoretical values of the self-diffusion coefficients of tellurium in liquid Tl_2Te alloy plotted *versus* temperature in figure 8. On the same plot we have put our experimental values.

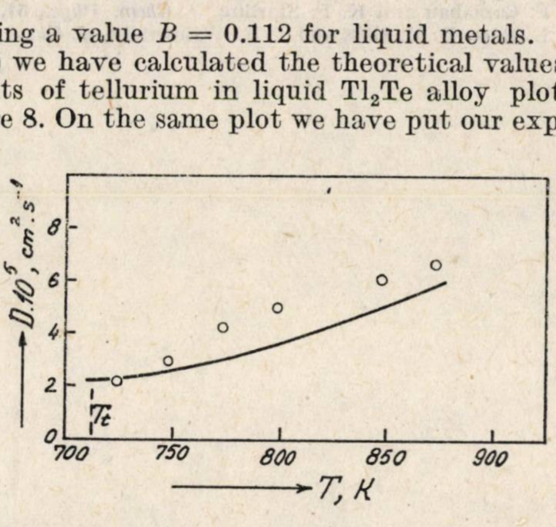

Fig. 8. — Comparison of experimental values of the self-diffusion coefficients of tellurium in molten Tl_2Te compound (o) with theoretical values calculated from a rigid sphere model (solid line).

Figure 8 shows that the model we have supposed for the structure of the liquid Tl_2Te compound in the pre-freezing range, in the framework of the theory of Protopapas is in very good agreement with the experimental data. So, at 450°C there is a perfect agreement between the theoretical and experimental values, at 475°C the results are still very close but at 500°C a divergence between the theoretical and the experimental values becomes obvious.

The trends manifested in figure 8 are a strong support for our assumption concerning the structure of the liquid Tl_2Te compound : in the prefreezing range the molten compound is composed of molecular entities of Tl_2Te, which progressively decompose as the temperature rises so that above 500°C the diffusion particles are no more molecular groups but individual atoms.

REFERENCES

[1] N. H. Nachtrieb, "Atomic Transport Properties in Liquid Metals", Academic Press New-York, 1976.
[2] M. Cutler and C. E. Mallon, *J. Appl. Phys.*, **36**, 201 (1965).
[3] J. E. Enderby and C. J. Simons, *Phyl. Mag.*, **20**, 125 (1969).
[4] Y. Nakamura and M. Shimoji, *Trans. Faraday Soc.*, **65**, 1509 (1969).
[5] M. Cutler and C. E. Mallon, *Phys. Rev.*, **144**, 642 (1966).
[6] Y. Nakamura and M. Shimoji, *Trans. Faraday Soc.*, **67**, 1270 (1971).
[7] T. Maekawa, T. Yokokawa and K. Niwa, *J. Chem. Thermodyn.*, **3**, 143 (1971).
[8] D. Brown, D. S. Moore and E. F. W. Seymour, *Phil. Mag.*, **23**, 1249 (1971).
[9] Y. Nakamura, and M. Shimoji, "The Properties of Liquid Metals", Proc. Second Int. Conf. Tokyo, 3—8 Sept. 1972, Taylor and Francis LTD, London, 1973.
[10] N. Petrescu and L. Ganovici, *Rev. Roumaine Chim.*, **21**, 1293 (1976).
[11] E. Nicoloiu, L. Ganovici and I. Ganovici, *Rev. Roumaine Chim.* **15**, 1713 (1970).
[12] P. Ascarelli and A. Paskin, *Phys. Rev.*, **165**, 222 (1968).
[13] D. Protopapas, F. C. Anderson and N. A. D. Parlee, *J. Chem. Phys*, **59**, 15 (1973).
[14] S. Chapman and T. G. Cowling, "The Mathematical Theory of Non-Uniform Gases", Cambridge, 1970.
[15] J. H. Dymond and B. J. Alder, *J. Chem. Phys.*, **45**, 2061 (1966).
[16] M. F. Carnahan and K. F. Starling, *J. Chem. Phys.*, **51**, 635 (1969).
[17] B. J. Alder, D. M. Gass and T. E. Wainwright, *J. Chem. Phys.*, **53**, 3813 (1970).

Revue Roumaine de Chimie, 26, 7, 65–70 (1981)

MIXED LIGAND COMPOUNDS OF LANTHANIDES WITH NEUTRAL LIGANDS CONTAINING DONOR OXYGEN ATOMS. III[1,2]

CHLOROSALICYLATES OF LANTHANIDES WITH 2,2′-DIPYRIDYL-1,1′-DIOXIDE

SILVIA PLOŞTINARU and P. SPACU
ICECHIM-Center of Physical Chemistry, Splaiul Independenţei 202, Bucharest, Romania

Received February 7, 1980

The methods of synthesis and properties of some lanthanide compounds of the $Ln(dipyO_2)(ClSal)_3 \cdot H_2O$ form, where dipy O_2 = 2,2′-dipyridyl-1,1′-dioxide and ClSal = 5-chlorosalicylic acid are presented. The obtained compounds were characterized according to their chemical composition and thermogravimetrical behaviour. The coordination type of the ligands was established by the study of their IR spectra. The electronic spectra give information on the hypersensitivity effect and allow us to calculate the nephelauxetic ratio and covalency degree of the Pr(III) and Nd (III) compounds.

In some previous papers,[3,4] we studied a series of complexes of lanthanides hydroxycarboxylates formed with neutral bidentate ligands as aromatic amines, containing nitrogen as donor atom. These ligands are known as being strong σ donors. This fact is confirmed by the high values of the complex formation constants as well as by their ability to form stable complexes with the majority of the chemical elements.[5,6] The σ bonding of these ligands with the rare earth elements is however, weaker than that with the *d* transition metals.[7]

Due to the affinity of the rare earth ions to the oxygen, in the last years, complexes of lanthanides with oxides of the aromatic amines have been studied.

The aim of the present paper is to investigate the coordination ability of the neutral bidentate ligand 2,2′-dipyridyl-1,1′-dioxide with the rare earth ions. This ligand has two donor oxygen atoms which may coordinate to the central metal ion, to form a ring of seven atoms. Recent works[8,9] describe the donor properties of this ligand against some transition and nontransition metal ions, oxycations and lanthanides.

There are few studies devoted to the description of the donor properties of this ligand in the complexes formed with the lanthanide hydroxycarboxylates.

EXPERIMENTAL

Reagents used. Ln_2O_3 99.9% purity (Mathey and Johnson); 5-chlorosalicylic (Fluka A G); and 2,2′-dipyridyl—1,1′-dioxide. Ln_2O_3 were transformed in nitrates and the neutral ligand, 2,2′-dipyridyl — 1,1′-dioxide, was prepared by oxidation of the dipyridyl.[10] The product was purified by crystallization, by adding an appreciable amount of acetone to the warm aqueous solution. A white powder, dried under vacuum in desiccator, on *di*—P_2O_5, was obtained. The purity was checked by means of melting point and elemental analysis. *Synthesis of complexes.* The complexes were isolated from aqueous solutions containing the soluble salt of lanthanide treated in excess with a solution of 2,2′-dipyridyl-1,1′-dioxide. The soluble cationic complexes $[LndipyO_2]^{3+}$ such obtained was treated with the amonium salt of the chlorosalicylic acid (pH = = 7—7.5). A precipitate, which was quantitatively separated was immediately obtained. After repeteadly washing with hot water, the precipitate was filtered, washed with water and small portions of alcohol and then dried on *di*—P_2O_5 in a desiccator under vacuum. Irrespective of the added amount of ligand and the nature of the rare earth ion, the following compounds were always obtained:

$Ln(dipyO_2)\,(ClSal)_3.H_2O$ where: Ln = La, Pr, Nd, Sm, Eu, Tb, Dy, Er.

$dipyO_2$ = 2,2′-dipyridyl-1,1′-dioxide.

ClSal = 5-chlorosalicylic acid

The formula was established using the data of the chemical analysis (Table 1).

TABLE 1

Analytical data

Formula of the compounds	Ln%		C%		H%		N%	
	calcd.	found	calcd.	found	calcd.	found	calcd.	found
La $(dipyO_2)\,(ClSal)_3\cdot H_2O$	16.05	16.38	43.29	43.68	2.56	2.94	3.26	3.38
Pr $(dipyO_2)\,(ClSal)_3\cdot H_2O$	16.36	16.58	43.19	42.85	2.55	2.97	3.25	3.36
Nd $(dipyO_2)\,(ClSal)_3\cdot H_2O$	16.68	16.72	43.03	43.04	2.54	2.85	3.24	3.33
Sm $(dipyO_2)\,(ClSal)_3\cdot H_2O$	17.26	17.48	42.72	42.88	2.52	2.56	3.21	3.55
Eu $(dipyO_2)\,(ClSal)_3\cdot H_2O$	17.42	17.68	42.64	42.91	2.52	2.91	3.21	3.55
Tb $(dipyO_2)\,(ClSal)_3\cdot H_2O$	17.96	17.86	42.31	42.04	2.50	2.75	3.18	3.37
Dy $(dipyO_2)\,(ClSal)_3\cdot H_2O$	18.29	18.54	42.14	41.91	2.49	2.86	3.17	3.41
Er $(dipyO_2)\,(ClSal)_3\cdot H_2O$	18.88	19.05	41.89	42.07	2.47	2.82	3.15	3.40

Equipment. The elemental analysis (C,H,N) was made by microcombustion. The metal was determined gravimetrically, as oxide.

The thermodifferential measurements were performed with a OD—102 derivatograph (system F. Paulik, J. Paulik and L. Erdey). Al_2O_3 was used as reference. The heating within the interval 20—1000°C is made with the rate of 10°/minut.

The IR spectra were recorded between 700—3600 cm^{-1} by means of a UR-10 Zeiss-Jena spectrophotometer, using KBr pellets.

The electronic spectra were recorded by means of a VSU-2 Zeiss-Jena spectrophotometer on ethanol and methanol solutions of 10^{-4}—10^{-5} mol/l for the domain 210—340 nm and benzene, acetone, chlorophorm and DMF solutions of 10^{-2}mol/l concentration for the domain 360—950 nm.

The reflectance spectra were recorded by means of a VSU-1 spectrophotometer, using MgO as standard.

RESULTS AND DISCUSSION

The IR spectra may give information concerning the complex formation and the coordination of the ligands. To this purpose, the IR spectra of the mixed ligand complexes, of the free ligands, hydroxycarboxylic acid and 2,2′-dipyridyl-1,1′-dioxide, as well as of the simple salt $Nd(ClSal)_3$ were recorded in the domain 700—3600 cm^{-1} (Table 2). Due to the complexity of the spectra, we shall present only those bands of which assignment is reliable and which are useful to emphasize the coordination of the ligands

TABLE 2

IR spectral data
(cm^{-1})

ClSal acid	$Nd(ClSal)_3$	$dipyO_2$	Ln $(dipyO_2)$ $(ClSal)_3.H_2O$			Assignment
			Nd	Dy	Er	
3400	3400		3400	3400	3400	$\nu(OH)$
	3050	3040	3090	3080	3080	
1670	—		—	—	—	$\nu(C=O)$
		1500	1620	1620	1620	$\nu(C-H)$
	1550		1580	1580	1580	$\nu_{as}(COO^-)$
1470	1465	1475	1470	1470	1475	
1440	1435	1425	1430	1430	1428	$\nu(C=C)$, $\nu(C=N)$
	1365		1370	1370	1370	$\nu_s(COO)^-$
1290	1290					
		1262	1248	1245	1245	
		1255	1220	1220	1218	$\nu(N-O)$
830	830					
		852	834	835	835	$\delta(N-O)$
		841	818	818	818	
		775	775	780	780	$\gamma(C-H)$
		730	730	730	730	

The coordination of the chlorosalycilic acid to the rare earth ion may be put in evidence studying the position of the characteristic band of the carbonyl group. The monobasic aliphatic acids show intense bands between 1705—1720 cm^{-1}, ascribed to the carbonyl group. For the chlorosalicylic acid, which may form strong intramolecular hydrogen bonds the characteristic frequency of the carbonyl group is shifted towards lower wave numbers (1670 cm^{-1}). As a consequence of complex formation, the band of the carbonyl group from the carboxylic group disappears, being substituted by the two bands of the COO^- group. This group has an asymmetric stretching vibration (1550—1610 cm^{-1}) and a symmetric one (1300—1400 cm^{-1}). For the coordinated chlorosalicylic ion, they appear at 1580 cm^{-1} (ν_{as}) and 1370 cm^{-1} (ν_s), respectively. It should be mentioned that for the simple salt of Nd-chlorosalicylate, ν_{as} occurs at 1550 cm^{-1}. Higher wave numbers for the mixed ligand complexes may be interpreted as being due to the higher covalency of the chemical bonds, as compared with those of the simple salts.

The neutral ligand (dipy O_2) presents many vibrations active in IR. Some of them are perturbed by coordination. The other ones, occurring at higher wave numbers than 1400 cm^{-1}, due to $C = C$ vibrations, are overlapped with those of coordinated chlorosalicylic ion. For this reason we have analyzed only the frequencies of $\nu(N-O)$ and $\delta(N-O)$ which are more sensitive to the metal-ligand bond formation (Table 3). The assignment is mainly based on the spectrum of free $dipyO_2$, compared with the spectra of other molecules such as Py, PyN-O, diphenyl, etc.[11] The ligand 2,2'-dipyridyl-1,1'-dioxide is actually a molecule of substituted diphenyl, having a nonplanar structure. This is proved by its IR spectrum on solid state, where two intense bandsd ue to ν(N—O) are present. If the molecule were symmetric (planar) only a band of ν(N—O) should be observed.

TABLE 3

IR spectral data

Formula of the compound	ν(N—O) cm^{-1}	Δν(N—O) cm^{-1}	δ(N—O) cm^{-1}	Δδ(N—O) cm^{-1}
dipyO$_2$	1262 1255	—	852 841	— —
Pr(dipyO$_2$) (ClSal)$_3$ ·H$_2$O	1248 1220	−14 −35	834 818	−18 −23
Er (dipyO$_2$) (ClSal)$_3$ ·H$_2$O	1245 1218	−17 −37	835 820	−17 −21

As may be seen, in table 3, there are some changes of the bands, corresponding to ν(N—O) and δ(N—O) frequencies, due to the metal-ligand bond formation in the mixed ligand complexes. The bands corresponding to the stretching vibration ν(N—O) (1255 cm^{-1} and 1262 cm^{-1} in the free ligand) occur as shifted towards lower wave numbers in the complexes (Table 3). The shift is 14—37 cm^{-1}. These changes are, probably, due to the weakness of the π_{N-O} chemical bond, caused by the coordination of the oxygen to the central metal ion. It should be mentioned that the observed shifts are lower than in the similar complexes of the *d* transition metal ions. This fact shows that the lanthanide oxygen bonds are weaker than those of the *d* metal ions.

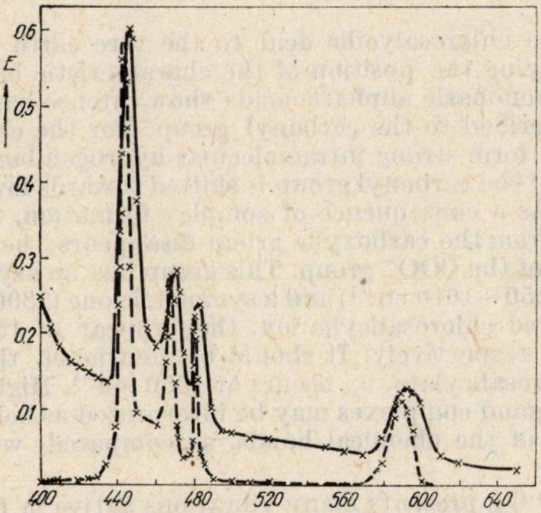

Fig. 1.—Absorption spectra of : —×—×— Pr(dipyO$_2$) (ClSal)$_3$ · H$_2$O ; — — x — — x Pr (NO$_3$)$_3$ H$_2$O.

The other two bands, occurring at 841 cm^{-1}, and 853 cm^{-1}, in the free ligand are attributed to the bending vibration $\delta N-O$. In the complexes studied they occur practically with the same intensities, their shift being of about 20 cm^{-1}.

Information regarding the hypersensitivity and the nephelauxetic effect has been obtained from electronic spectra. These spectra have been recorded between 400–900 nm for solutions using different solvents as well as for the solid compounds. The absorption bands are very sharp and are due to intra-shell $f-f$ transitions of the f^n electronic configuration.

Interesting results were obtained for Pr(f^2) and Nd(f^3) complexes. Obvious changes in maxima and intensity are observed with some absorption bands, due to the coordination. The spectrum of aqua ion Ln $(NO_3)_3 \cdot {}_xH_2O$ has been taken as reference. Figure 1 shows the spectra of the mixed ligand complex of Pr (III) and of the corresponding aqua ion.

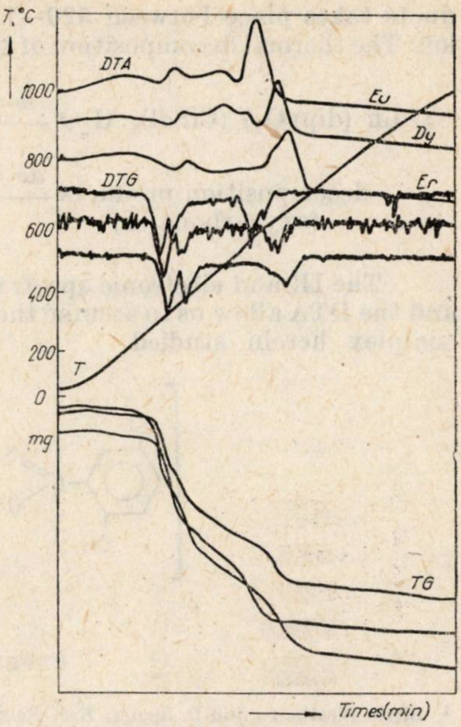

Fig. 2. — Thermal curves for Ln $(dipyO_2(ClSal)_3 \cdot H_2O$.

The nephelauxetic parameter 1 — β and the covalency degree of the metal-ligand bond have been calculated for the Pr (III) and Nd(III) complexes. Their values are close to those for other mixed ligand complexes elsewhere studied.[1,2] It has been observed that the shifts of the absorption bands depend on the filling with electrons of the f-shell. As the f-shell is filled up with electrons, the f orbitals are less involved in chemical bonding. For this reason band shifts are no more observed.

As results from chemical analysis, the mixed ligand complexes here reported crystallize with one water molecule. This fact is proved by the differential thermal analysis. As may be seen (Figure 2) on the TG curve, the dehydration of the complexes takes place at about 100°C. The existence of the anhydrous complex is evidenced by the slope of TG curve, between 100–280°C. This fact is in agreement with the chemical analysis performed for complexes dehydrated at 105–110°C. The decomposition of the anhydrous complexes begins over 280°C. The process is endothermal at 300°C, 310°C and 320°C, depending on the nature of the central metal ion.

The neutral ligand is removed, together with the partial decomposition of the organic ligand. The exothermal oxidation of the decomposition products takes place between 520—710° and depends on the central metal ion. The thermal decomposition of the complexes may be thus represented :

$$\mathrm{Ln\ (dipyO_2)\ (ClSal)_3.H_2O} \xrightarrow{80-100^\circ} \mathrm{Ln\,(dipyO_2)\ (ClSal)_3} \xrightarrow{280-500^\circ}$$

$$\underset{\text{(oxycarbonates)}}{\text{decomposition products}} \xrightarrow{520-700^\circ} \mathrm{Ln_2O + CO_2} \xrightarrow{>700^\circ} \mathrm{Ln_2\,O_3}$$

The IR and electronic spectral data, as well as the chemical analysis and the DTA allow us to assume the chemical formula for the mixed ligand complex herein studied.

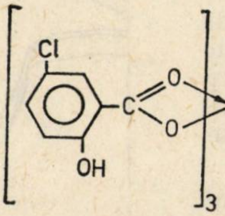

REFERENCES

[1] Silvia Ploştinaru and P. Spacu, *Rev. Roumaine Chim.*, **18**, 2051 (1973).
[2] S. Ploştinaru and P. Spacu, *Rev. Roumaine Chim.*, **19**, 567 (1974).
[3] P. Spacu and S. Ploştinaru, *Rev. Roumaine Chim.*, **17**, 697 (1972).
[4] P. Spacu and S. Ploştinaru, *Rev. Roumaine Chim.*, **18**, 971 (1973).
[5] E. König, *Coord. Chem. Rev.*, **3**, 471 (1968).
[6] G. S. Malik, S. P. Singh and J. P. Tandon, *Monatsh.*, **108**, 163 (1977).
[7] J. H. Forsberg, *Coord. Chem. Rev.*, **11**, 373 (1973).
[8] P. C. Simpson, D. Vicinguera and J. V. Quagliano, *Inorg. Chem.*, **2**, 286 (1963).
[9] S. K. Madan and W. E. Bull, *J. Inorg. Nuclear Chem.*, **26**, 2211 (1964).
[10] P. C. Simpson, D. Vicinguera and j. v. Quagliano, *Inorg. Chem.* **2**, 282 (1963).
[11] J. E. Katon and E. R. Lippincott, *Spectrochim. Acta*, 15, 627 (1959).

Revue Roumaine de Chimie, 26, *1*, 71—79 (1981)

PROTON MAGNETIC RESONANCE SPECTRA OF SOME DI- AND TRIORGANOTIN MONO- AND DITHIOCARBOXYLATES

VICTORIA COLDEA * M. COLDEA ** and I. HAIDUC ***
* Institute of Hygiene, Cluj-Napoca, Romania
** Physics Department, University of Cluj-Napoca, R-3400 Cluj-Napoca, Romania
*** Department of Chemistry, University of Cluj-Napoca, Romania

Received April 2, 1980

Chemical shifts and *J*(H—H) and *J*(Sn—H) coupling constants in 13 organotin mono- and dithiocarboxylates, i.e. Me_2SnX_2 ($X = C_6H_5CS_2$, $C_6H_5C(O)S$, $Br C_6H_4CS_2$, $C_6H_5CH_2CS_2$), Ph_3SnX ($X = C_6H_5CS_2$, $C_6H_5C(O)S$, p-$BrC_6H_4CS_2$, $C_6H_5CH_2CS_2$), Cy_3SnX ($X = C_6H_5C(O)S$, $C_6H_5CH_2CS_2$) $\cdot Bu_2SnX_2$($X = C_6H_5CS_2$, $C_6H_5C(O)S$, $C_6H_5CH_2CS_2$) were determined. The long-range coupling constants *J* (Sn—H) are analysed in terms of the Fermi contact interaction. The percentage *s* character of the tin orbital in the Sn—C bond, for the Me_2SnX_2 compounds is derived as 0.36.

1. INTRODUCTION

The study of proton chemical shifts and of the spin-spin coupling constants *J*(H—H) and *J* (M—M), where M is a metal with non-zero nuclear spin, in organometallic compounds, provides information concerning both their structure and the degree of *s* character of the M orbitals directed towards the carbon atom.

The changes in the percentage *s* character of the M—C bond orbitals for different compounds of the same element should also be reflected in the long-range coupling constant *J*(M—H), because the electronic structure of the molecular fragment separating the nuclei M and H, depends on the electronic distributions around atom M.

The good agreement between experimental and theoretical values for long-range coupling constants for group IV A elements and the proton, in the Me_4M methyl compounds, seems to indicate that the Fermi contact interaction is the most important part of the spin coupling Hamiltonian. This is also true for some other organometallic compounds (difuryl- and diethylmercury [1]). In addition, a proportionality was found between long-range metal-proton coupling constants and the corresponding proton-proton coupling constants. [2] The review of Barbieri et al.[3] gives detailed account of those organometallic compounds for which this affirmation is true.

The aim of this paper was to study the proton chemical shifts and the coupling constants $J(H-H)$ and $J(M-H)$ in the four series of organotin compounds, which involve different molecular fragments, in order to gain some information concerning their structure and bonding.

2. EXPERIMENTAL

A number of 13 organotin mono- and dithiocarboxylates have been synthesized. Details about their preparation, analysis and other spectral data are given elsewhere.[4]

The proton magnetic resonance (^1H-NMR) spectra were recorded in CCl_4 solution with hexamethyldisiloxane as internal standard, with a TESLA BS487 B spectrometer operating at 80 MHz.

3. RESULTS AND DISCUSSION

The ^1H-NMR spectra of all 13 investigated compounds confirmed the expected structure. Only for compound $C_6H_5CS_2SnPh_3$ some summary ^1H-HMR data are reported in the literature.[5] Although the ^1H-NMR spectrum is relatively complicated, consisting of three bands (Fig. 2), it was shown that all 20 aromatic protons give a single signal at $\delta = 7.33$ ppm.[5]

The results of ^1H-NMR studies for all compounds are given in tables 1–4. The grouping was made according to the nature of organic substituent at tin.

In table 1 are given the ^1H-NMR characteristics for dimethyltin compounds Me_2SnX_2, where $X = C_6H_5CS_2$, $C_6H_5C(O)S$, p-$BrC_6H_4CS_2$ and $C_6H_5CH_2CS_2$.

TABLE 1

Chemical shifts (ppm) and long-range coupling constants (Hz) for dimethyltin derivatives

Compound	δ_0	δ_m	δ_p	$\delta_0-\delta_m$	$\delta(CH_2)$	$\delta(CH_3)$	$J(^{117}Sn-C-H)$	$J(^{119}Sn-C-H)$
$(C_6H_5CS_2)_2SnMe_2$	8.20	7.23	7.45	0.97	—	1.37	76	80
$[C_6H_5C(O)S]_2SnMe_2$	7.92	7.26	7.42	0.66	—	1.05	72.6	76.4
$(BrC_6H_4CS_2)_2SnMe_2$	8.05	7.37	—	0.68	—	1.31	75.2	79
$(C_6H_5CH_2CS_2)_2SnMe_2$	7.1	7.1	7.1	0	4.10	1.05	77.8	81.2

The ^1H-NMR spectra for these compounds consist of three bands, (Fig. 1) corresponding to *ortho-*, *meta-* and *para-*protons from phenyl groups in the dithiocarboxylate ligand and to those from methyl groups bonded to tin.

The bands corresponding to aromatic protons present a first-order splitting with a coupling constant $J(H-H) \simeq 8Hz$.

Inductive effects in the substituted benzene produce a change in the electron distribution between the different positions (*ortho*, *meta* and *para*) and consequently the protons are not identical, as in the case of compounds $(C_6H_5CS_2)_2SnMe_2$ and $[C_6H_5C(O)S]_2SnMe_2$. Nevertheless, one can observe only a single proton signal for compound $(C_6H_5\,CH_2CS_2)_2\,SnMe_2$.

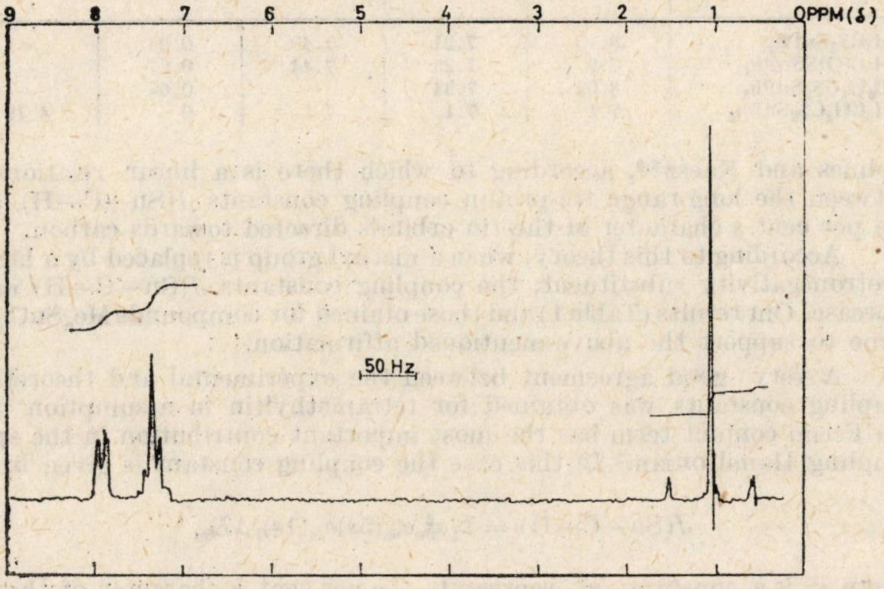

Fig. 1. – ^1H-NMR spectrum of $[C_6H_5C(O)S]_2SnMe_2$.

This is a case in which the inductive effect is absent or it is compensated by a conjugation effect.[6] The difference between the chemical shifts of the *ortho-*, *meta-* and *para*-protons is affected by the group bonded to the aromatic ring. As expected, the chemical shift of *ortho*-protons is the most affected by the substituted groups, compared to the chemical shift of the protons from unsubstituted benzene ($\delta = 7.27$ ppm).

The signal of methyl-protons is flanked by satellites with proper intensities showing that they arise from long-range $^{117/119}$ $Sn-C-H$ coupling in the $Sn-CH_3$ groups. The good resolution of the spectra allowed us to determine the indirect coupling constants for both isotopes (Fig. 1).

For each compound, the ratio of coupling constants $J(^{117}Sn-C-H)/J\,(^{119}Sn-C-H)$ is very close to the ratio of the magnetic moments of the two isotopes, *i.e.* $-0.9949/-1.0409 = 0.95581$.[7]

In these compounds the coupling constants $J\,(^{119}Sn-C-H)$ are ca 25 Hz larger than those found in tetramethyltin, where $J(^{119}\,Sn-C-H) = 54.3$ Hz, but are close to those obtained in the compound Me_2SnCl_2.[7] The increase of the coupling constant value in our compounds as well as in methyltin chlorides Me_nSnCl_{4-n} $(n = 1,2,3)$[7] compared to that found in tetramethyltin was expected. Our results and those obtained by Vladimiroff and Malinowski for Me_nSnCl_{4-n} compounds[7] confirm the theory advanced by

TABLE

Chemical shifts (ppm) and long-range coupling constants

Compound	δ_a	δ_b	δ_c	$\delta_a-\delta_b$	$\delta(CH_2)$
$C_6H_5CS_2SnPh_3$	8.15	7.21	7.43	0.94	—
$C_6H_5C(O)SSnPh_3$	7.9	7.23	7.44	0.67	—
$BrC_6H_4CS_2SnPh_3$	8.02	7.34	—	0.68	—
$C_7H_5CH_2CS_2SnPh_3$	7.1	7.1	7.1	0	4.15

Holmes and Kaesz[8,9], according to which there is a linear relationship between the long-range tin-proton coupling constants $J(\mathrm{Sn-C-H})$ and the per cent *s* character of the tin orbitals directed towards carbon.

According to this theory, when a methyl group is replaced by a higher electronegativity substituent, the coupling constants $J(\mathrm{Sn-C-H})$ must increase. Our results (Table 1) and those otained for compounds Me_nSnCl_{4-n}[7]. come to support the above-mentioned affirmation.

A very good agreement between the experimental and theoretical coupling constants was obtained for tetramethyltin in assumption that the Fermi contact term has the most important contribution in the spin-coupling Hamiltonian.[2] In this case the coupling constant is given by :

$$J(\mathrm{Sn-C-H}) = k_1 \alpha^2_{\mathrm{Sn}} a_{\mathrm{Sn}}(5s) a_{\mathrm{H}}(1s)/\Delta E_{\mathrm{Sn}} \tag{1}$$

where k_1 is a constant, α^2_{Sn} represents the per cent *s* character of the Sn orbitals in the Sn—C bonds, $a_{\mathrm{Sn}}(5s)$ and $a_{\mathrm{H}}(1s)$ are the hyperfine coupling constants for Sn and H, and ΔE_{Sn} is the mean singlet-triplet excitation energy. The above equation may be applied also for H—C—H bond with $\alpha^2_{\mathrm{H}} = 1$, i.e.

$$J(\mathrm{H-C-H}) = k_2 [a_{\mathrm{H}}(1s)]^2/\Delta E_{\mathrm{H}} \tag{2}$$

When the Sn—C—H bond angle is equal to that of the H—C—H bond, the constants k_1 and k_2 have the same value. In the case of compounds Me_4M (M = metal IV A) and of our compounds, the angle of Sn—C—H can be assumed as tetrahedral.

The ratio of equation (1) and (2) gives the following relation between the two coupling constants :

$$J(\mathrm{Sn-C-H}) = \alpha^2_{\mathrm{Sn}} (\Delta E_{\mathrm{H}}/\Delta E_{\mathrm{Sn}}) \; [a_{\mathrm{Sn}}(5s)/a_{\mathrm{H}}(1s)] J(\mathrm{H-C-H}) \tag{3}$$

Taking into account that in methane $J(\mathrm{H-C-H}) = 12.5$ Hz[10] and for our compounds the mean value of the coupling constant $J(^{119}\mathrm{Sn-C-H})$ is 79 Hz and taking $\Delta E_{\mathrm{H}} = 8.75$ eV and $\Delta E_{\mathrm{Sn}} = 6.7$ eV, the values used by Smith[11] and the hyperfine coupling constants $a_{\mathrm{Sn}}(5s) = 0.62\ \mathrm{cm}^{-1}$ and $a_{\mathrm{H}}(1s) = 0.047\ \mathrm{cm}^{-1}$, the values calculated by Goudsmith[12], one obtains for the per cent *s* character in the Sn—C bond, the value $\alpha^2_{\mathrm{Sn}} \cong 0.36$. This value is larger than the value $\alpha^2_{\mathrm{Sn}} = 0.25$ used by Smith in the calcu-

2

(Hz) for triphenyltin derivatives

δ_d	δ_e	δ_f	$\delta_d-\delta_e$	J(Sn−C−H_d)	J(Sn−C−H_e)
7.52	7.17	7.14	0.35	58.4	26.8
7.52	7.18	7.15	0.34	53.2	23.2
7.51	7.24	7.15	0.27	55.8	24.2
7.4	7.15	7.15	0.25	59.8	27.8

lations.[2] Consequently, the replacing of the two methyl groups with X leads to an increase of the per cent *s* character in the Sn—C bond and adequately its decrease in the Sn—S bond. This change of the α^2_{Sn} parameter is due to the hybridization change in the Sn—C bond.

The ^{1}H—NMR spectral data for triphenyltin compounds Ph_3SnX, where X is the same as above, are listed in table 2.

The spectra exhibit three major bands and are relatively complicated, while the phenyl groups bonded directly to tin atom give a spectrum of A_2B_2C type, which is superposed on the signal of *meta-* and *para*-protons from X (Fig. 2).

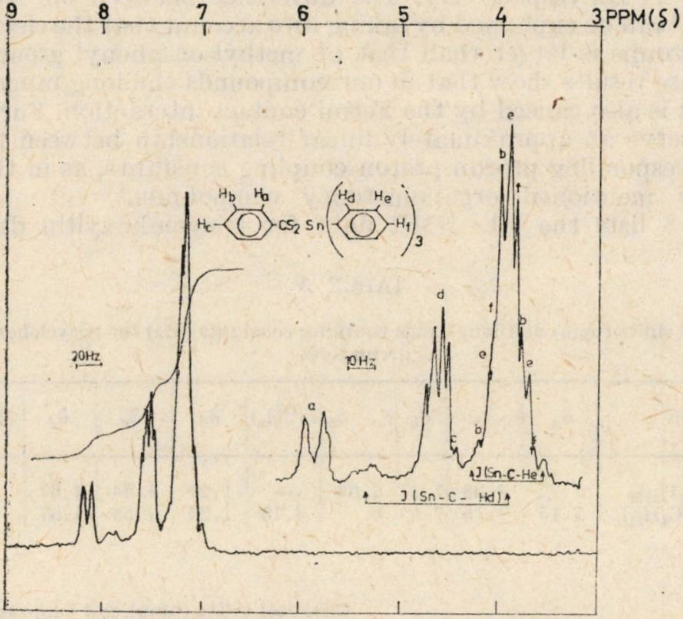

Fig. 2. ^{1}H—NMR spectrum of $C_6H_5CS_2SnPh$.

The spectra point out the interaction of the $^{117/119}$Sn spins with that of the protons from aromatic rings bonded directly to tin and on the other hand, the interaction of *ortho*-protons from these aromatic rings with those from *meta* and *para* positions.

The data obtained for compounds listed in table 1 were used for the assignment of the various peaks.

The chemical shifts determined for protons of the phenyl group from X given in table 1 remain practically the same, even if the methyl groups at tin are replaced by phenyl groups, because there are at least five bonds separating them.

The band at higher magnetic field represents a superposition of the *meta*- and *para*-proton signals from the four aromatic rings.

The signals from the *ortho*- and *meta*-protons of phenyl groups bonded directly to tin are flanked by satellites caused by the long range coupling between tin and protons from these positions. The middle band, which consists of four peaks, is due to the *ortho*-protons of phenyl groups. The splitting of this band in a quartet produced by the interaction of these protons with both *meta*- and *para*-protons, resulting for the corresponding coupling constants the values $J_{ortho} \simeq 7.2$ Hz and $J_{para} \simeq 3$ Hz.

The assignment of the various peaks is visualised in figure 2 where the same letters were used for the resonance peaks and the corresponding protons in the chemical formula.

The long-range coupling constants between Sn and the *ortho*- and *meta*-protons are smaller than those obtained by Kula et al.[13] in the compounds $Ph_nSn(CH_3)_{4-n}(n = 1,2,3)$, i.e. $J(Sn-C-H_0) = 49$ Hz and $J(Sn-C-H_p) = 17$ Hz respectively. The difference between our values and those cited,[13] can be explained by taking into account that the electronegativity of X groups is larger than that of methyl or phenyl groups. Consequently, these results show that in our compounds the long-range tin-proton coupling is also caused by the Fermi contact interaction. Furthermore, one can observe an approximately linear relationship between tin-proton and the corresponding proton-proton coupling constants, as in the case of the already mentioned organomercury compounds.[1]

Table 3 lists the ^1H-NMR data for tricyclohexyltin derivatives.

TABLE 3

Chemical shifts (ppm) and long-range coupling constants (Hz) for tricyclohexyltin derivatives

Compound	δ_a	δ_b	δ_c	$\delta_a-\delta_b$	$\delta(CH_2)$	δ_d	δ_e	δ_f	$J(Sn-C-H_d)$
$C_6H_5C(O)SSn(C_6H_{11})_3$	7.92	7.28	7.37	0.64	—	1.27	1.54	1.67	96
$C_6H_5CH_2CS_2Sn(C_6H_{11})_3$	7.15	7.15	7.15	0	4.16	1.24	1.55	1.67	91.4

TABLE

Chemical shifts (ppm) and long-range coupling

Compound	δ_a	δ_b	δ_c	$\delta_a-\delta_b$	$\delta(CH_2)$	α $\delta(CH_2)$	β $\delta(CH_2)$
$(C_6H_5CS_2)SnBu_2$	8.2	7.22	7.45	0.98	—	0.79	1.21
$C_6H_5C(O)S_5SnBu_3$	7.95	7.27	7.41	0.68	—	0.8	1.22
$(C_6H_5CH_2CS_2)_2SnBu_3$	7.14	7.14	7.14	0	4.12	0.66	1.05

The spectra of these compounds consist of three bands : the two bands at low magnetic field are given by the aromatic protons from **X**.

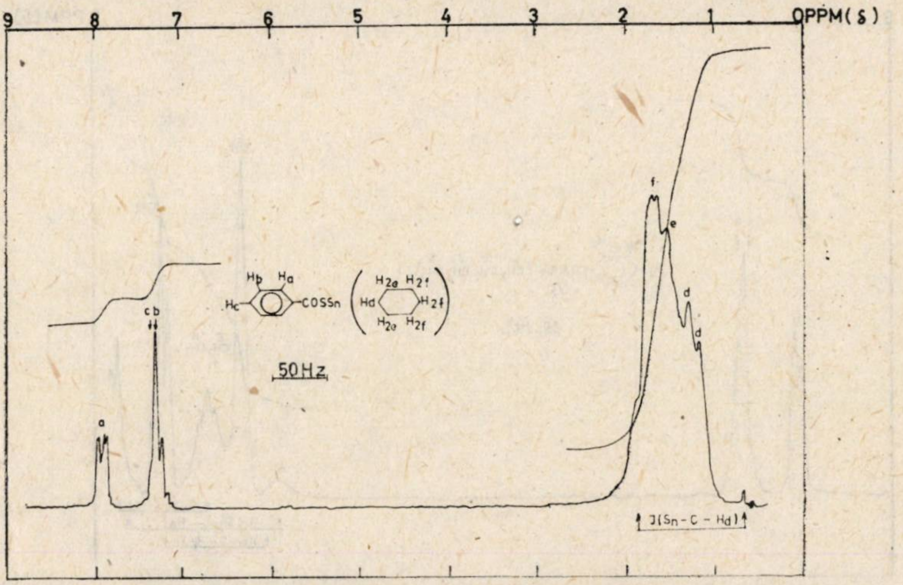

Fig. 3. — ^1H-NMR spectrum of $C_6H_5C(O)SSn(C_6H_{11})_3$.

The high field band (at ca $\delta = 1.5$ ppm) is a very broad resonance line and results from the cyclohexyl protons. In fact this band is a superposition of many signals with close chemical shifts and which were not resolved. Nevertheless, this band presents three marked peaks which can be assigned to the central signals of the cyclohexyl protons from the three different positions. The assignment of various peaks can be followed in figure 3 and was done taking into account the number of protons in each position and that the tin is electropositive. Therefore, the higher field signal is due to the geminal proton from d position. The long-range proton coupling with tin and the values of coupling constants are given in table 3.

Finally, in table 4 the ^1H-NMR spectral data for the dibutyltin derivatives are given. The spectra of this series of compounds consist of many bands (Fig. 4) and their identification may be followed according to the notations on the figure.

4

constants (Hz) for dibutyltin derivatives

$\delta(\overset{\gamma}{CH_2})$	$\delta(CH_3)$	$J(Sn-C-H_\alpha)$	$J(Sn-C-H_\beta)$	$J(Sn-C-H_\gamma)$
1.36	1.8	79	148	84
1.39	1.67	80	136	87
1.2	1.63	60	140	78

The first two low field bands are attributed to aromatic protons from X and the high field bands are given by different groups from butyl.

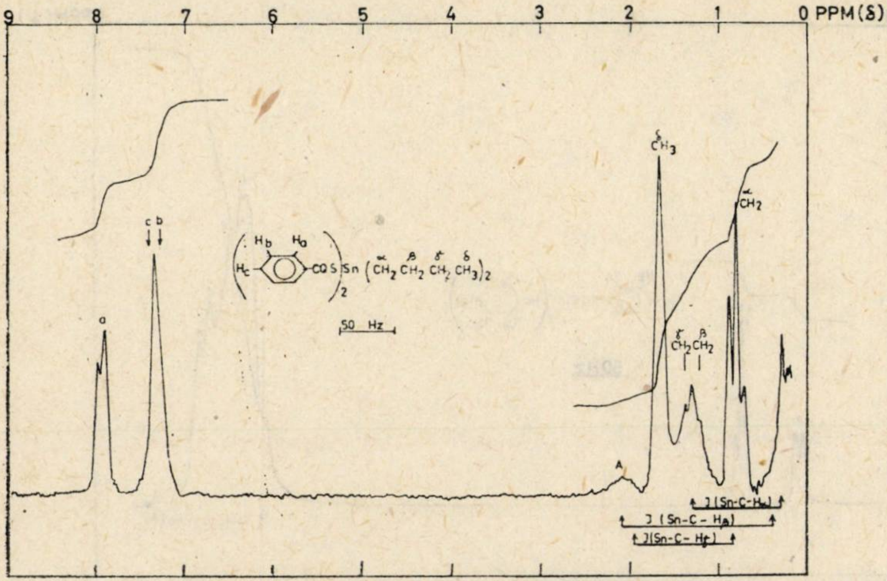

Fig 4. — ^1H—NMR spectrum of $[C_6H_5C(O)S]_2SnBu_2$.

Tin, being electropositive, will shield much more the protons of CH_2 group from α position and this shielding will decrease from α to δ position. The band corresponding to CH_2 group from α position and which presents the first-order splitting has a stronger low field peak than usual. This suggests that there is here a contribution from other signal. This band is flanked by satellites caused by the tin-proton long-range interaction. In figure 4 the size of this interaction is given through the coupling constant $J(Sn-C-H\alpha)$. The rigorous analysis of the spectra pointed out also the existence of long-range Sn—H coupling with protons from β and γ positions. The broad signal A from the left of the butyl group bands may be attributed to a number of similar coupling constants. Figure 4 shows the size of these interactions and the corresponding coupling constants are given in table 4.

The values of these coupling constants, for all three positions (α, β and γ) are larger than the corresponding values from compounds R_4Sn with R = Me, Et, nPr, Me_3CCH_2 [3] and this is also due to the electronegative groups X, as shown earlier, thus confirming again the major role of the Fermi contact term in the long-range coupling.

4. CONCLUSIONS

The examination of ^1H—NMR data listed in tables 1—4 shows that the aromatic protons of the thiocarboxylate ligand are not influenced by the alkyl and aryl groups bonded to tin, because these groups are separated from aromatic protons through at least five bonds.

In the dithiophenylacetic derivatives, the signal from methylene protons of the $C_6H_5CH_2CS_2$ group appears always at $\delta \simeq 7.1$ ppm, showing that these protons are not influenced by the groups bonded directly to tin. One may conclude that the methylene protons signal is determined both by the inductive and ring current effects.

In all compounds investigated long-range strong tin-proton interactions of Fermi contact type are observed, the orbital and dipolar contributions in the coupling Hamiltonian being negligible.

The replacement of two methyl groups in the compound Me_4Sn with two X groups leads to an increase of the *s* character of the Sn—C bond orbital from 0.25 to 0.36 per cent.

REFERENCES

[1] L. Lunazzi, M. Tieco, C. A. Boicelli and F. Taddei, *J. Mol. Spectroscopy*, **35**, 190 (1970).
[2] G. W. Smith, *J. Chem. Phys.*, **42**, 435 (1965).
[3] C. Barbieri , R. Benassi and F. Taddei, *Gazz. chim. Ital.*, **105**, 807 (1975).
[4] V. Coldea and I. Haiduc, *Synth. React. Inorg. Metal-Org. Chem.*, **10**, 417 (1980).
[5] S. Kato, T. Kato, T. Yamauchi, Y. Shibahoshi, E. Kakuda, M. Mizuta and Y. Yshii, *J. Organometall. Chem*, **76**, 215 (1974).
[6] R. H. Bible, "Interpretation of NMR Spectra", Plenum Press, New York, 1965.
[7] T. Vladimiroff and E. R. Malinowski, *J. Chem. Phys.*, **42**, 440 (1965).
[8] J. R. Holmes and H. D. Kaesz, *J. Amer. Chem. Soc.*, **83**, 3903 (1961).
[9] G. P. van der Kelen, *Nature*, **193**, 1069 (1962).
[10] M. Karphus, *J. Chem. Phys.*, **30**, 11 (1959).
[11] G. W. Smith, *J. Chem. Phys.*, **40**, 2037 (1964).
[12] S. Goudsmith, *Phys. Rev.*, **43**, 636 (1933).
[13] M. R. Kula, E. Auberger and K. K. Mayer, *Chem. Ber.*, **98**, 634 (1965).

Revue Roumaine de Chimie, 26, 7, 81—83 (1981)

SYNTHESIS OF SOME NEW THIENYLAZETIDIN-2-ONES AND THIENYLTHIAZOLIDIN-4-ONES

M. S. K. YOUSSEF[a] and KH.M. HASSAN
Chemistry Department, Faculty of Science, Assiut University, Assiut, Egypt

Received July 21, 1979

A series of thienylidene anils (1a, b—6 a, b) have been prepared by interaction of thiophene-2-carboxaldehyde (or its 5-bromo-derivative) with heterocyclic amines. Cyclocondensation reaction of chloroacetyl chloride or mercaptoacetic acid with thienylidene anils (1a, b—6a, b) gives thienylazetidin-2-ones (7a, b—12 a, b) and thienylthiazolidin-4-ones (13 a, b—18 a, b) respectively.

Currently, there is much interest in the chemotherapeutic efficiency of sulphur bearing compounds for their technological uses in drug synthesis.[1] In view of the fact that several sulphur derivatives possess useful antiinflammatory, antileprotic, bactericidal, insecticidal and antituberculous properties,[2-4] it is of interest to incorporate such molecules into a well known antimicrobial nucleus (e.g. azetidinone and/or thiazolidinone[5,6]) in order to evaluate the resulting compounds for their pharmacological activity.

Since the introduction of penicillins and cephalosporines which contain a β-lactam moiety, a continual problem has been the emergence of drug-resistant strains of bacteria, which has led to an interest in the synthesis of functionally substituted β-lactams. In many cases the resistance arises from the production of β-lactamases, enzymes which degrade these antibiotics.[7] Synthesis of new functionally substituted β-lactams having a modified microbiological spectrum, is important to keep pace with the appearance of these resistant bacterial strains.

RESULTS AND DISCUSSION

We wish to report a simple and efficient synthesis of the hitherto unreported thienylazetidinones and thienylthiazolidinones which are potential precursors of various functionally substituted β-lactams and thiazolidinones.

---

[a] Author to whom all correspondence should be addressed.

Thus, thiophene-2-carboxaldehyde or its 5-bromo-derivative have been condensed with some heterocyclic amines in absolute ethanol in the presence of piperidine as a catalyst giving a good yield of 2-thienylidene (or 5-bromo-2-thienylidene)-2-amino-thiazole **(1 a, b)**;-2-amino-1,3,4-thiadiazole **(2 a, b)**;-2-amino-benzothiazole **(3a, b** analogously **4 a, b)**, -2-aminopyridine **(5a)** and -2-amino-5-chlorobenzoxazole **(6a, b)** respectively.

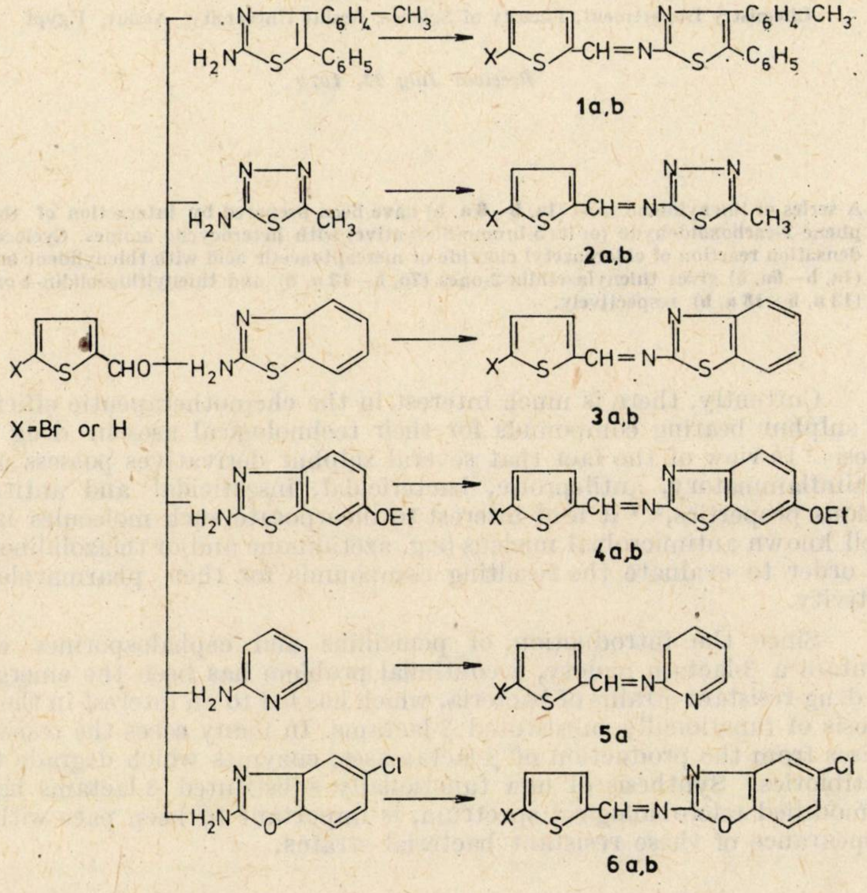

The structures of these compounds **1a, b** — **6a, b** were supported by their elemental analyses (cf. Table 1) and IR spectra which showed an absorption band at 1660 cm^{-1} (due to the $C = N$ group).[8]

A widely used method of β-lactam (azetidinone) synthesis consists in the reaction of an acid chloride with an imine in the presence of a base.[9] The cyclocondensation reactions of chloroacetyl chloride with thienylidene anils (**1 a, b**—**6 a, b**) were carried out in dry dioxane in the presence of triethylamine as an acid binding agent giving the corresponding 1-(2′-thiazolyl)-4-(2″-thienyl)-(**7 a, b**), 1-(2-thiadiazolyl)-4-(2″-thienyl)-(**8 a, b**), 1-(2′-benzothiazolyl)-4-(2″-thienyl)-(**9 a, b** and **10 a, b**), 1-(2′-pyridyl)-4-(2″-thienyl)-(**11a**) and 1-(2′-benzoxazolyl)-4-(2″-thienyl)-(**12 a, b**)-3-chloroazetidin-2-ones respectively, in poor yield.

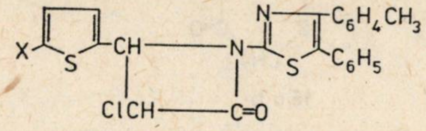
X
S
CH
N
C6H4CH3
C6H5
ClCH
C=O

7a,b

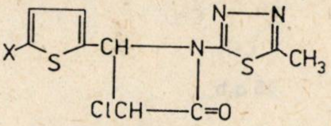
X
S
CH
N—N
CH3
ClCH
C=O

8a,b

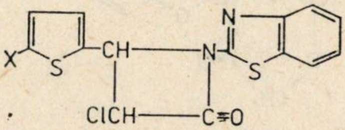
X
S
CH
N
ClCH
C=O

9a,b

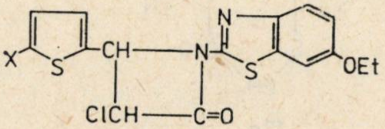
X
S
CH
N
OEt
ClCH
C=O

10a,b

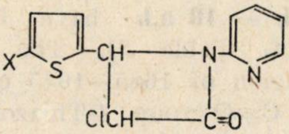
X
S
CH
N
ClCH
C=O

11a,b

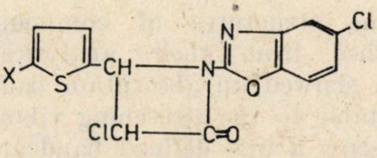
Cl
X
S
CH
N
O
ClCH
C=O

12a,b

The structures of compounds **7 a, b–12 a, b** have been demonstrated by a combination of elemental (cf. Table 2) and IR spectral analyses. The IR spectra reveal an absorption band around 1760–1720 cm^{-1} assignable to ν(C=O) of monocyclic β-lactams.[8]

Surrey and others[10] intensively investigated the cyclocondensation reaction of mercaptoacetic acid with substituted anils. They found in most cases that the product has the cyclic structure of a thiazolidinone.

In our investigation the cyclocondensation of mercaptoacetic acid with thienylidene anils (**1 a, b–6 a, b**) proceeded in dry benzene within 10–12 hrs. with a reflux system using a dean-stark trap giving a moderate yield of the corresponding 3-(2′-thiazolyl)-2-(2″-thienyl)-(**13 a, b**), 3-(2′-thiadiazolyl)-2-(2″-thienyl)-(**14 a, b**), 3-(2′-benzothiazolyl)-2-(2″-thienyl)-(**15 a, b** and **16 a, b**), 3-(2′-pyridyl)-2-(2″-thienyl)-(**17a**) and 3-(2′-benzoxazolyl)-2-(2″-thienyl)-(**18a, b**)-thiazolidin-4-ones respectively.

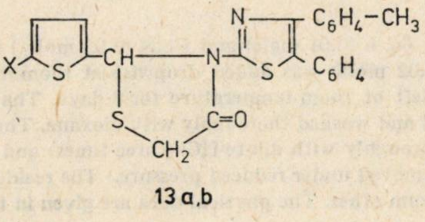
X
S
CH
N
C6H4–CH3
C6H4
S
C=O
CH2

13a,b

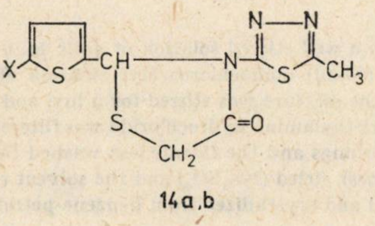
X
S
CH
N—N
CH3
S
C=O
CH2

14a,b

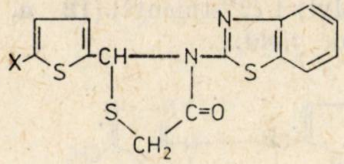

15 a,b

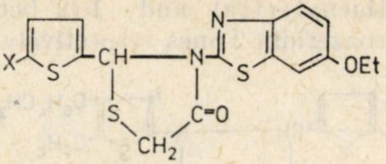

16 a,b

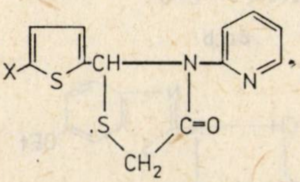

17a

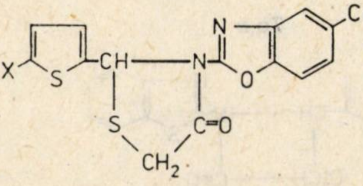

18 a

The structures of compounds **13 a, b — 18 a,b** have been established from their analytical data (cf. Table 3). The IR spectra showed an absorption band in the region of 1685—1645 cm^{-1} attributable to the stretching vibration of the C=O group. 4-Thiazolidinones show a well defined band at 1690 cm^{-1} due to the C=O group.[8]

EXPERIMENTAL

Completion of the reaction and purity of the compounds prepared were checked by TLC. Melting points are uncorrected. The IR (KBr) spectra were recorded on a Unicam SP 200G spectrophotometer.

THIENYLIDENE ANILS (**1a, b—6a, b**)

Equimolecular amounts of thiophene-2-carboxaldehyde (or its 5-bromo derivative) and heterocyclic amines were refluxed in dry ethanol in the presence of piperidine for 3 hrs. The reaction mixture was concentrated and cooled. The solid mass was filtered, washed with ether and crystallized from ethanol. The results are listed in table 1.

SUBSTITUTED 4-THIENYLAZETIDIN-2-ONES (**7a, b—12 a, b**)

To a well stirred solution of anils **1a, b—6a, b** (0.01 mole) and Et_3N (0.02 mole) in dry dioxane (50 ml) monochloroacetyl chloride (0.02 mole) was added dropwise at room temperature ; the mixture was stirred for 5 hrs. and left at room temperature for 3 days. The precipitated triethylamine hydrochloride was filtered and washed thoroughly with dioxane. The combined washings and the filtrate was washed thoroughly with dilute HCl (three times) and water three times), dried (Na_2SO_4) and the solvent removed under reduced pressure. The residue was (collected and crystallized from benzene-petroleum ether. The physical data are given in table 2

TABLE 1

Thienylidene anils **1 a, b—6 a, b**

Compound No.	m.p. °C	Yield %	Molecular formula	Analysis (Calcd./ Found) %			
				C	H	N	Br
1a	183—184	80	$C_{21}H_{15}N_2S_2Br$	57.40	3.41	6.37	18.22
				57.33	3.55	6.41	18.20
2a	217—218	77	$C_8H_6N_3S_2Br$	33.33	2.08	14.58	27.77
				33.30	2.09	14.60	27.80
3a	160—161	75	$C_{12}H_7N_2S_2Br$	44.58	2.16	8.66	24.76
				44.60	2.15	8.64	24.70
4a	148—149	83	$C_{14}H_{11}N_2OS_2Br$	45.77	2.99	6.62	21.79
				45.78	3.00	6.52	21.78
5a	93— 94	73	$C_{10}H_7N_2SBr$	44.94	2.62	10.48	29.96
				44.97	2.70	10.47	29.99
6a	181—182	70	$C_{12}H_6N_2OSBrCl$*	42.16	1.75	8.19	23.42
				42.17	1.85	8.20	23.50
1b	140—141	78	$C_{12}H_{16}N_2S_2$	57.14	6.34	11.11	—
				57.15	6.40	11.12	—
2b	224—225	85	$C_8H_7N_3S_2$	45.93	3.34	20.09	—
				45.94	3.35	20.10	—
3b	82— 83	72	$C_{12}H_8N_2S_2$	59.01	3.27	11.47	—
				59.04	3.30	11.50	—
4b	116—117	74	$C_{14}H_{12}N_2OS_2$	58.33	4.16	9.72	—
				58.32	4.18	9.90	—
5b	170—171	76	$C_{12}H_7N_2OSCl$**	54.85	2.66	10.66	—
				54.96	2.70	10.56	—

* Analysis for Cl : Calcd. 10.39 ; Found 10.49%.
** Analysis for Cl : Calcd. 13.52 ; Found 13.50%.

TABLE 2

Substituted thienylazetidin-2-ones **7a ,b—12 a, b**

Compound No.	m.p. °C	Yield %	Molecular formula	Analysis (Calcd./Found) %				
				C	H	N	Br	Cl
7a	155—156	7	$C_{23}H_{16}N_2OS_2BrCl$	53.54	3.10	5.43	15.51	6.88
				53.55	3.11	5.44	15.61	6.89
8a	182—183	10	$C_{10}H_7N_3OS_2BrCl$	32.92	1.92	11.52	21.94	9.73
				32.94	1.94	11.53	21.95	9.82
9a	149—150	9	$C_{14}H_8N_2OS_2BrCl$	42.05	2.00	7.00	20.03	8.88
				42.07	2.04	7.03	20.04	8.90
10a	171—172	12	$C_{16}H_{12}N_2O_2S_2BrCl$	43.29	2.70	6.31	18.03	8.00
				43.30	2.80	6.41	18.04	8.03
11a	161—162	5	$C_{12}H_8N_2OSBrCl$	41.92	2.32	8.15	23.35	10.33
				41.99	2.35	8.17	23.27	10.34
12a	190—191	6	$C_{14}H_7N_2O_2SBrCl_2$	40.19	1.67	6.69	19.13	16.95
				40.17	1.66	6.68	19.11	16.99
7b	125—126	8	$C_{14}H_{17}N_2OS_2Cl$	51.14	5.17	8.52	—	10.80
				51.24	5.20	8.54	—	10.93
8b	180—181	10	$C_{10}H_8N_3OS_2Cl$	42.03	2.80	14.71	—	12.43
				42.07	2.86	14.73	—	12.44
9b	162—163	13	$C_{14}H_9N_2OS_2Cl$	52.41	2.80	8.73	—	11.70
				52.42	2.90	8.74	—	11.90
10b	148—149	15	$C_{16}H_{13}N_2O_2S_2Cl$	52.67	3.56	7.68	—	9.73
				52.77	3.60	7.80	—	9.76
12b	130—131	10	$C_{14}H_8N_2O_2SCl_2$	49.55	2.35	8.25	—	20.94
				49.56	2.43	8.30	—	20.99

SUBSTITUTED 2-THIENYLTHIAZOLIDIN-4-ONES (13a, b—18a, b)

A mixture of anils **1 a, b—6a, b** (0.02 mole) and mercaptoacetic acid (0.02 mole) in dry benzene (100 ml) was refluxed using a water separator until the theoretical amount of water had been collected. After most of the benzene had been removed the residue was dissolved in ether and seeded. In some cases the thiazolidinone separated out directly from benzene solution. The results are summarized in table 3.

TABLE 3

Substituted thienylthiazolidin-4-ones **13a, b—18 a, b**

Compound No.	m.p. °C	Yield %	Molecular formula	Analysis (Calc./Found) %			
				C	H	N	Br
13a	86— 87	30	$C_{23}H_{17}N_2OS_2Br$	53.80	3.31	5.45	15.59
				53.90	3.33	5.46	15.60
14a	186—187	40	$C_{10}H_8N_3OS_3Br$	34.88	2.31	12.13	23.12
				34.69	2.40	12.22	23.22
15a	75— 76	34	$C_{14}H_9N_2OS_3Br$	42.31	2.26	7.05	20.15
				42.30	2.30	7.09	20.35
16a	118—119	40	$C_{16}H_{13}N_2O_2S_3Br$	43.53	2.94	6.34	18.14
				43.55	2.99	6.40	18.19
17a	130—131	35	$C_{12}H_9N_2OS_2Br$	42.22	2.63	8.21	23.46
				42.23	2.73	8.21	23.55
18a	174—175	33	$C_{14}H_8N_2O_2S_2BrCl$*	40.43	1.92	6.73	19.25
				40.49	1.93	6.73	19.24
13b	112—113	29	$C_{14}H_{18}N_2OS_3$	51.53	5.52	8.58	—
				51.61	5.55	8.61	—
14b	198—199	45	$C_{10}H_9N_2OS_3$	31.33	2.34	10.96	—
				31.44	2.40	10.99	—
15b	136—137	42	$C_{14}H_{10}N_2OS_3$	52.83	3.14	8.80	—
				52.94	3.15	8.90	—
16b	142—143	38	$C_{16}H_{14}N_2O_2S_3$	53.03	3.86	7.73	—
				53.02	3.93	7.83	—
18b	180—182	44	$C_{14}H_9N_2O_2S_2Cl$**	49.92	2.67	8.32	—
				49.90	2.70	8.42	—

* Analysis for Cl : Calcd. 8.54; Found 8.52%.

** Analysis for Cl : Calcd. 10.54; Found 10.61%.

REFERENCES

[1] A. Burger, "Medicinal Chemistry", Interscience Publishers, New York a division of Wiley and Sons, 2nd ed., 1960.

[2] Martindale, "The Extra Pharmocopoeia", Edited by Norman W. Blacow, XXIV, 1972, p. 1770.

[3] E. D. Bergmann and D. Lavie, *J. Amer. Chem. Soc.*, **74**, 4948 (1952).

[4] U. P. Pasa, J. Sci. Club Antituberculous Action of Streptomycin, Thiosemicarbazones Sulphones : *Chem. Abstr.*, **48**, 1033 (1954).

[5] H. T. Clarke, J. R. Johnson and R. Robinson, "The Chemistry of Penicillin", Princeton University Press, 1949.

[6] A. R. Surrey, *J. Amer Chem. Soc.*, **71**, 3354 (1949).

[7] E. I. Edwards, R. Epton and G. Marr, *J. Organometallic Chem.*, **107**, 351 (1976).

[8] L. J. Bellamy, "The Infrared Spectra of Complex Molecules", Methuen and Co. Ltd., London, 2nd ed., 1958.

[9] A. K. Bose, Y. H. Chiang and M. S. Manhas, *Tetrahedron Letters*, **1971**, 4091.

[10] A. R. Surrey, *J. Amer. Chem. Soc.*, **69**, 2911 (1947).

Revue Roumaine de Chimie, 26, 1, 87–93 (1981)

POLY-1,3,4-OXADIAZOLES. IX[1]
ORDERED POLY-1,3,4-OXADIAZOLE-AMIDE-IMIDES

MARIA BRUMĂ and GABRIELA NEAMŢU
"Petru Poni" Institute of Macromolecular Chemistry, Aleea Gr. Ghica Vodă, 41 A
Iaşi, Romania

Received December 4, 1979

Ordered poly-1,3,4-oxadiazole-amide-imides have been synthesized by polycondensation reaction of 2,5-bis(*p*-aminophenyl)-1,3,4-oxadiazole with diacid chlorides of certain aromatic acids containing a preformed imide ring. The polycondensation was carried out using equimolecular quantities of the two monomers, at low temperature, in polar aprotic solvents and inert atmosphere.

The obtained polymers have been characterized by inherent viscosity, IR absorption and thermal stability values. The maximum inherent viscosity of a 0.5% solution is 2.2 dl/g. Thermogravimetric analysis shows that the polymers decompose in air over 440°C. From 10% polymer solutions, flexible and transparent films have been cast with good mechanical and dielectric properties.

INTRODUCTION

Among heterocyclic polymers having high thermal stability, poly-1,3,4-oxadiazoles are of particular interest owing to the superior thermal stability of the 1,3,4-oxadiazole unit in oxidative atmosphere.[2] Preston and Black[3,4] have established the following order of the thermal stability of certain polymers having similar structures, which contain various heterocycles :

in inert atmosphere : imide > benzimidazole > thiazole > 1,3,4-oxadiazole > 4-phenyl-1,2,4-triazole ;

in air : 1,3,4-oxadiazole > imide > 4-phenyl-1,2,4-triazole > benzimidazole > thiazole.

Synthesis of certain macromolecular structures which contain both oxadiazole and imide units has led to materials which had a very good thermal stability in oxidative atmosphere as well as excellent mechanical properties given by the imide units.[5]

Poly-1,3,4-oxadiazole-imides produced by the two-steps method from aromatic diamines containing preformed oxadiazole ring and aromatic dianhydrides have a moderate stability to hydrolysis as the conversion of the intermediate polyamic acid can only be achieved up to 75–80%.[6] Another method which was used to produce polyoxadiazole-imides from ditetrazoles and diacid chlorides, resulted in insoluble low molecular weight polymers which showed great processing difficulties.[7]

We have synthesized ordered poly-1,3,4-oxadiazole-amide-imides from monomers which contained both oxadiazole and imide units preformed, introducing amide groups between aromatic and heteroaromatic rings to provide an increased solubility of the final polymer.

RESULTS AND DISCUSSION

The technique used was the low-temperature polycondensation of 2,5-bis (*p*-aminophenyl)-1,3,4-oxadiazole (I)

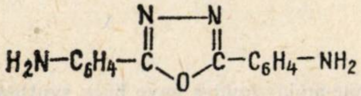

I

with two types of diacid chlorides containing preformed imide units. The type IIa was obtained from trimellitic anhydride and *p*- or *m*-aminobenzoic acid, treating the intermediate dicarboxylic acid with thionyl chloride :

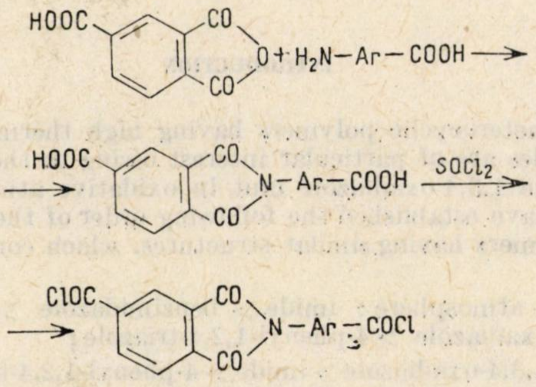

IIa

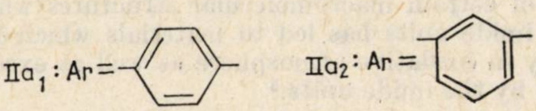

The type IIb was obtained from trimellitic anhydride and aromatic diamines, such as 4-4′-diamino-diphenyl-methane, 4,4′-diamino-diphenylether and 4,4′-diamino-diphenyl-sulphone, also treating the intermediate dicarboxylic acid with thionyl chloride :

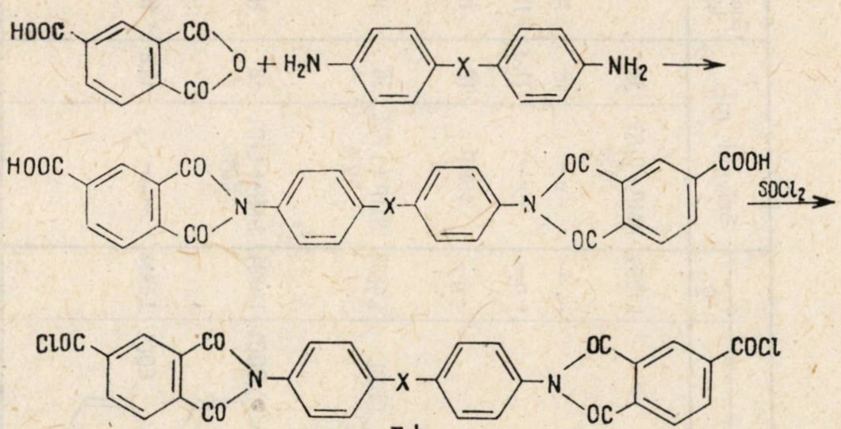
HOOC
CO
O
CO
H₂N
X
NH₂
HOOC
CO
N
X
N
OC
COOH
SOCl₂
ClOC
CO
N
X
N
OC
COCl

II b

II b_1: X = O   II b_2: X = CH_2 II b_3: X = SO_2

The polycondensation of monomer I with diacid chlorides of type IIa led to partially ordered poly-1,3,4-oxadiazoleamide-imides IIIa, while the polycondensation of monomer I with diacid chlorides of type IIb led to ordered poly-1,3,4-oxadiazoleamide-imides IIIb :

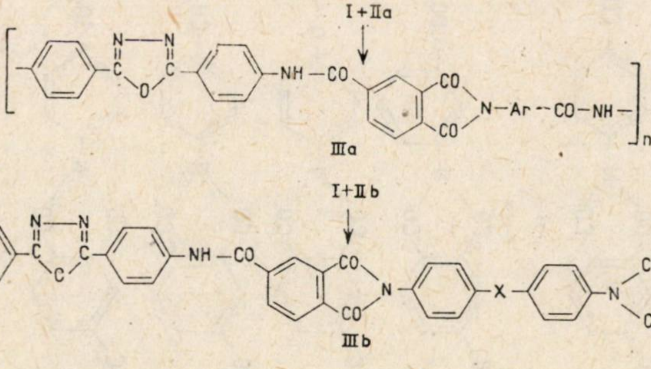
I + IIa
N—N
C
C
O
NH—CO
CO
N—Ar—CO—NH—
CO
n

IIIa

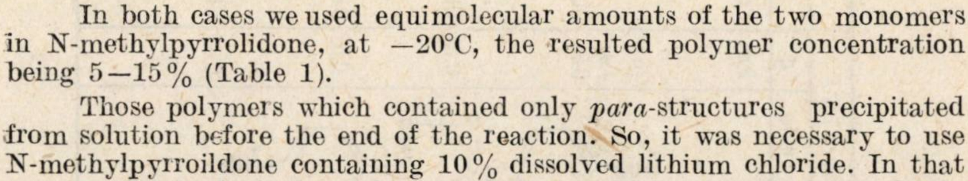
I+II b
N—N
C
C
C
NH—CO
CO
N
X
N
CO
CO—NH—
CO
CO
n

IIIb

In both cases we used equimolecular amounts of the two monomers in N-methylpyrrolidone, at −20°C, the resulted polymer concentration being 5−15% (Table 1).

Those polymers which contained only *para*-structures precipitated from solution before the end of the reaction. So, it was necessary to use N-methylpyrroildone containing 10% dissolved lithium chloride. In that case we obtained viscous polymer solutions, which were precipitated into water. The inherent viscosities are 0.9−2.2 in NMP + 10% lithium chloride at a concentration of 0.5 g polymer/100 ml solvent at 20°C (Table 2).

TABLE 1

Preparation of the polymers III

Poly-mer.	Amine		Diacid chloride		Solvent, ml.		Conc. %	Temp. °C
	Formula	g.	Formula	g.				
IIIa_1	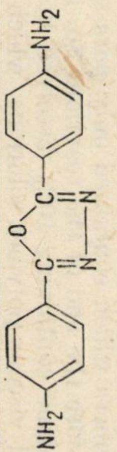	0.84	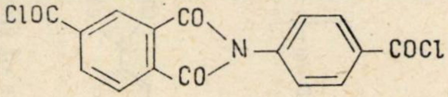	1.1604	NMP+ LiCl 10%	38	5	−20
		−„−	−„−	−„−	−„−	18	10	−20
		−„−	−„−	−„−	−„−	11.3	15	
IIIa_2		0.84	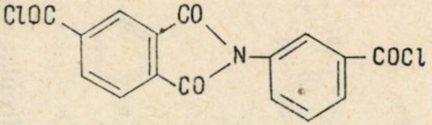	−„−	NMP	18	10	−20
IIIb_1		0.63	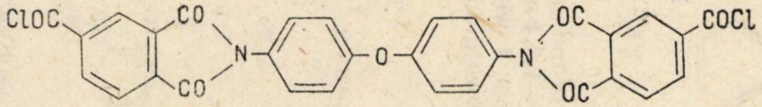	1.4633	NMP+ LiCl 10%	18	10	−20
IIIb_2		0.63	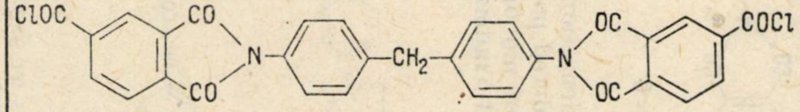	1.4884	NMP+ LiCl 10%	18	10	− 20
IIIb_3		0.63	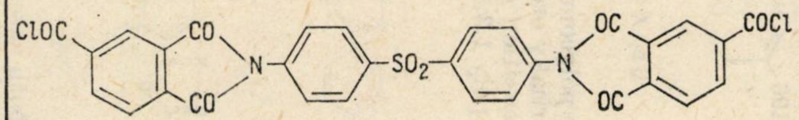	1.5834	−„−	19.8	10	−20

TABLE 2

Properties of polymers

Polymer	Aspect	η inh.[1] dl/g	Solubility in NMP	T.G.A. weight loss, %[3]		Elemental analysis N %[4]	
				at 400°C	at 500°C	calc.	found
$IIIa_1$	gel	—	—	—	—	—	—
$IIIa_2$	fibrous	1.5	+	1.8	17.3	15.31	15.02
$IIIb_1$	powder	2.2	+[2]	1.0	12.5	12.25	12.15
$IIIb_2$	—,,—	0.9	—,,—	2.0	19	12.38	12.22
$IIIb_3$	—,,—	1.7	—,,—	1.5	14.0	12.06	11.96

[1] Measured at a concentration of 0.5 g/100 ml in NMP + LiCl 10%, at 20°C

[2] Soluble in NMP + LiCl 10%

[3] Determined in air on "Derivatograph" Paulik-Paulik, at a heating rate of 9.8°/min.

[2] Determined by Dumas method.

Infrared spectra showed absorption bands at 730, 1720 and 1780 cm^{-1} assigned to the imide ring[8] and 1190 cm^{-1} and 960 cm^{-1} assigned to the oxadiazol ring.[9]

Thermogravimetric analysis of the synthesized polymers, performed in air, at a heating rate of 9.8°/minut, showed no weight loss up to 360°C; at 400°C they only lose 1—2%, at 440—460°C a rapid decomposition takes place and at 500°C the weight loss is 12—19% (Table 2). The best thermal stability is that of the polymer $IIIb_1$, which has on ordered structure built from oxadiazole, benzene and imide rings bound by amide and ether groups. The lowest thermal stability is that of the polymer $IIIb_2$ which contains methylene groups instead of ether groups. If we compare the polymers synthesized in the present paper with similar polymers having no imide cycles, that is polyoxadiazoleamides which we synthesized in a previous paper,[10] we can see that polyoxadiazole-amide-imides have a higher thermal stability. Polyoxadiazole-amides begin to decompose at about 360°C, while polyoxadiazole-amide-imides decompose over 440°C (Fig. 1).

The polymers sythesized in the present paper showed good mechanical and insulating properties, as it can be seen from the values of the dielectric loss tangent which is $2.33-4.02 \times 10^{-3}$ (Table 3). They were compared with the polyimide obtained from pyromellitic dianhydride and *p-p'*-oxydianiline (film H).

TABLE 3

Mechanical and insulating properties of polyoxadiazole-amide-imide $IIIa_2$*

Properties	Polymer $IIIa_2$	Film H
Tensile strength (Kgf/cm^2)	11.6	12.16
Dielectric loss	0.0023	0.003
Dielectric constant	3.00	3.5
Volume resistivity (Ω.cm)	5.3×10^{15}	0.9×10^{17}

* All data were obtained on films of 30 μ.

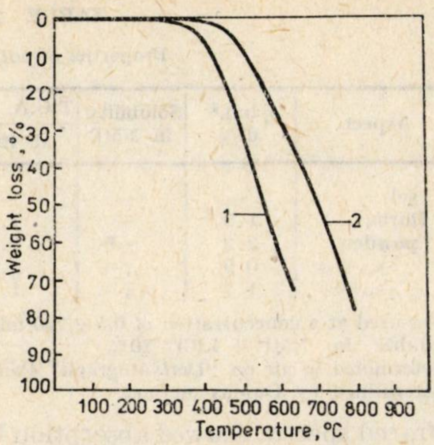

Fig. 1. — Thermogravimetric analysis of structurally related polymers.

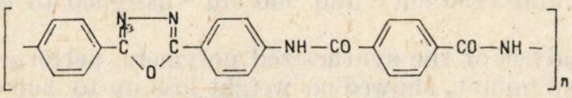

1. Polyoxadiazole-amide

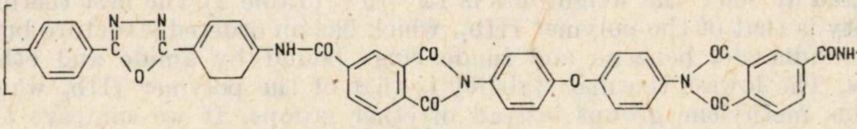

2. Polyoxadiazole-amide-imide

EXPERIMENTAL

PREPARATION OF MONOMERS

2,5-Bis-(*p*-aminophenyl)-1,3,4-oxadiazole (I) was prepared according to a known procedure,[11] from *p*-aminobenzoic acid and hydrazine hydrate in polyphosphoric acid, at 125—130°C. The reaction mixture was poured into cold water and the diamine was precipitated with 20% sodium hydroxide solution. It was purified by recrystallization from ethanol; m.p.259°C.

*4-Carboxy-N(*p*-carboxyphenyl) phthalimide and 4-carboxy-N* (m-*carboxyphenyl) phthalimide* were prepared by the condensation of equimolecular amounts of *p*- or *m*-aminobenzoic acid with trimellitic anhydride in dimethylformamide at reflux temperature, for 2 h. The precipitate was filtered and washed with acetone. It was purified by dissolving in DMF containing 5% dissolved lithium chloride and precipitated with acetone. Then it was washed with acetone and dried in a vacuum oven at 150°C. Melting point of 4-carboxy-N (*p*-carboxyphenyl) phthalimide > 350°C. Melting point of 4-carboxy-N (*m*-carboxyphenyl) phthalimide > 350°C.[12]

*4-Chloroformyl—N(*p*-chloroformylphenyl) phthalimide* (IIa_1) *and 4-chloroformyl-N*(m-*chloroformylphenyl)phthalimide* (IIa_2) were prepared by refluxing dicarboxy-compounds with excess thionyl chloride on a water bath. Few drops of dimethylformamide were added to the reaction mixture and the heating was continued for 3 h. Excess of thionyl chloride was removed by distillation and the residue was recrystallized from n-hexane. M.p. of $IIa_1 = 174-175$°C; m.p. of $IIa_2 = 194-195$°C.

Oxy-bis-N(4-phenylene)-4′(chloroformyl)phthalimide(IIb_1) was prepared from 4,4′-diaminodiphenylether (1 mol) and trimellitic anhydride (2 mol) in N-methylpyrrolidone at reflux temperature, 40 minutes.[13] The resultant water was distilled off. The precipitate was filtered and purified by recrystallization from dimethylacetamide, washed with acetone and dried in vacuum oven at 150°. The diacid was then refluxed for 3 h with excess thionyl chloride and a few drops of dimethylformamide. The yellow product was filtered, washed with n-hexan and dried in vacuum at 100°C. M.p. 238—239°C.

Methylene-bis-N(4-phenylene)-4'(chloroformyl) phthalimide (IIb_2) was prepared by the reaction of 4,4'-diaminodiphenyl-methane (1 mol) and trimellitic anhydride (2 mol) in N-methylpyrrolidone under the same conditions as used for the oxy-derivative.[14] On heating with excess thionyl chloride a yellow diacid chloride was obtained. M.p. 264—265°C.

Sulfuryl-bis-N(4-phenylene)-4'(chloroformyl) phthalimide (IIb_3) was prepared by the reaction of 4,4'-diaminodiphenyl-sulphone (1 mol) and trimellitic anhydride (2 mol) in N-methylpyrrolidone under the same conditions as used for the oxy-derivative. On heating with excess thionyl chloride, a white crystalline diacid chloride was obtained. M.p. 307—308°C.[15]

N-methylpyrrolidone was dried over sodium hydroxide pellets and distilled over phosphorous pentoxide under reduced pressure and was stored over molecular sieves.

PREPARATION OF POLYMERS

Polycondensation was run under anhydrous conditions, in a nitrogen atmosphere, equimolecular amounts of diamine and diacid chloride being used. A three necked flask fitted with stirrer and drying tube was flushed with nitrogen and charged with diamine and N-methylpyrrolidone to obtain a 5—15% final solution of polymer. The flask was cooled below —15°C and the diacid chloride (as a finely divided powder) was added all at once with stirring. The flask content was kept below —10°C for 30 minutes then slowly raised to room temperature within other 30 minutes, and kept at room temperature for 2—3 h. The clear yellow viscous solution was then neutralized with pyridine. When diacid chlorides of formula IIb were used, the polymer precipitated out of solution and it became necessary to add 10% lithium chloride and to heat on a steambath in order to redissolve the polymer.

Films were prepared by casting 10% NMP solutions on a glass plate and evaporating the solvent at 100°C 30 min. and 150°C for 1 h.

The following example illustrates the general procedure : 0.84 g 2,5-bis (*p*-aminophenyl)-1,3,4-oxadiazole (I) were placed in a three necked flask and dissolved in 18 ml N-methylpyrrolidone. The solution was cooled to —20°C and 1.1604 g 4-chloroformyl-N (m-chloroformylphenyl) phthalimide (IIa_2) was added with stirring. The flask content was kept below — 10°C for 30 minutes, then slowly raised to room temperature within another 30 minutes and kept at room temperature for 2 h. 0.5 g pyridine were added to the clear polymer solution for neutralization. The inherent viscosity measured for a 0.5% concentration in NMP at 20°C is 1.5 dl/g.

A flexible, transparent film was obtained by casting the 10% polymer solution on a glass plate and evaporating the solvent at 100°C for 30 minutes and 150°C for 1 h.

The dielectric tangent loss is 2.3×10^{-3}. It was measured on polymer films at room temperature, frequency 800 Hz, using a differential bridge with transformer, of the type TT (303).

REFERENCES

[1] M. Brumă and L. Stoicescu-Crivetz, *Rev. Roumaine Chim.*, **16**, 1591 (1971).

[2] A. H. Frazer and T. A. Reed, *J. Polymer Sci.*, *C*, **19**, 89 (1967).

[3] J. Preston and W. B. Black, *J. Polymer Sci.*, B, **3**, 845 (1965).

[4] J. Preston and W. B. Black, *J. Polymer Sci.*, *A—1*, **5**, 2429 (1967).

[5] C. E. Sroog, A. L. Endrey, S. V. Abramo, C. E. Beer, W. M. Edwards and K. L. Olivier, *J. Polymer Sci.*, *A*, **3**, 1373 (1965).

[6] J. H. Hodkin, *J. Appl. Polym. Sci.*, **20**, 2309 (1967).

[7] M. Brumă, L. Stoicescu-Crivetz and I. Zugrăvescu, *Rev. Roumaine Chim.*, **16**, 935 (1971).

[8] N. A. Adrova, M. I. Bessonov, L. A. Laius and A. P. Rudakov, "Poliimidynovyi klass termostoikih polymerov", Akad. Nauk S.S.S.R., 1968, p. 90.

[9] C. I. Abshire and C. S. Marvel, *Makromol. Chem.*, **44**, 388 (1961).

[10] L. Stoicescu-Crivetz, M. Brumă and I. Zugrăvescu, *Rev. Roumaine Chim.*, **13**, 1069 (1968).

[11] A. Siegrist, Swiss. Pat. 383.985 ; *Chem. Abstr.* **62**, 14867 (1965).

[12] M. Strul, Neamţu G., El. Măntăluţă and I. Zugrăvescu, *Rev. Roumaine Chim.*, **16**, 941 (1971).

[13] B. A. Jubanov. S. A. Mashkevitch and S. R. Rafikov, *Vysokomol. Soedineniya*, A, **14**, 22 (1972).

[14] Brit. pat. 1, 155, 230 (1969) ; *Chem. Abstr.*, **71**, 40319 (1969).

[15] W. Wrasidlo and J. M. Augl, *J. Polymer Sci.*, *A—1*, **7**, 321 (1969).

Revue Roumaine de Chimie, 26, 1, 95–99 (1981)

ACTION OF AROMATIC HYDROCARBONS, ACTIVE METHYLENE COMPOUNDS AND GRIGNARD REAGENTS ON α-3-BENZYLIDENE-5-[1′(2′-METHYLNAPHTHALENYL)]-2(3H) FURANONE AND 4-BENZYLIDENE-1-p-TOLYL-2-[1′(2′-METHYLNAPHTHALENYL)]-2-PYRROLINE-5-ONE

M. ABDALLA, A. ESSAWY, M. A. EL-HASHASH * and A.M.EL-GENDY
Faculty of Science, Zagazig University, Egypt

* Faculty of Science, Ain Shams University, Egypt

Received August 26, 1979

α-3-Benzylidene-5-[1′(2′-methylnaphthalenyl)]-2 (3H) furanone (**1**) reacts with dichloromethane or benzene in the presence of anhydrous $AlCl_3$ to give 4-[1′(2′-methylnaphthalenyl)]-2-naphthoic acid (**3**). Compound **1** reacts with toluene, *o*-chlorotoluene and *o*-xylene to give 2-benzylidene 1-aryl-4-[1′(2′-methylnaphthalenyl)]-1,4-butandiones (**4**). The action of Grignard reagents on furanone **1** affords the addition products **5**. Michael reaction of **1** with diethyl malonate and benzyl methyl ketone gives the Michael adducts **6**. Pyrrolone **2** also reacts with acetylacetone, benzyl methyl ketone and diethyl malonate to give the corresponding Michael adducts **7**.

Earlier,[1-3] we described the synthesis and some reactions of 3-arylidene-5-substituted-2 (3H) furanone and 4-benzylidene-1-aryl-2-substituted pyrroline-5-one. Now, we extend our investigation to 3-benzylidene-5-[1′(2′-methyl naphthalenyl)] —2 (3H). furanone (**1**) and 4-benzylidene -1-p-tolyl-2-[1′(2′-methyl naphthalenyl)]-2-pyrroline-5-one **(2)**.

In the present paper we have examined the reactivity of the furanone and pyrrolone systems (by introducing 2′-methyl naphthalenyl group instead of substituted phenyl group) towards aromatic hydrocarbons, Grignard reagents and active methylene compounds. It is known that the highly conjugated carbon chain in arylidene furanones is a reactive site for the Friedel — Crafts reaction.[1,2 4,5] Thus, 3-benzylidene-5-[1′(2′-methyl naphthalenyl)] -2 (3H) furanone (**1**) reacts with $AlCl_3$ in the presence of benzene or dichloromethane to give 4-[1′(2′-methyl naphthalenyl)] -2-naphthoic acid (**3**). Alkylation of the aromatic compounds such as toluene, *o*-chlorotoluene and *o*-xylene by **1** in the presence of anhydrous $AlCl_3$ gave 1-aryl-2-benzylidene-4-[1′ (2′-methyl naphthalenyl]) buta-1,4-diones, **4 a—c.** 3-Benzylidene-5-[1′(2′-methyl naphthalenyl)] -2(3H)-furanone **1** also reacted with Grignard reagents,[2,6] namely phenyl magnesium bromide and methyl magnesium iodide, affording 3-diphenyl methyl-5- [1′(2′-methyl naphthalenyl)] 2-(3H) furanone (**5a**) and 3-phenyl ethyl-5-[1′(2′-methyl naphthalenyl)] -2(3H) furanone (**5b**) respectively by 1,4 addition to α, β unsaturated carbonyl moiety of **1**. The reaction of **1** with compounds containing active methylene group was also investigated. Thus, **1** reacted with diethyl malonate and / or benzyl methyl ketone in the presence of sodium ethoxide in boiling ethanol to give 1,2 dipolar adducts α-3-(β-acetyl — α, β-diphenyl ethyl)-5-[1′(2′-methyl naphthalenyl)] -2(3H) furanone (**6a**) and α-3-(β, β-diethyl-α-phenyl ethyl)-5-[1′ (2′-methyl naphthalenyl)]-2 (3H) furanone (**6b**). The active methylene compounds, namely acetyl acetone, benzyl methyl ketone and diethyl malonate reacted with **2** under Michael reaction conditions in the presence of sodium ethoxide / ethanol and yielded the Michael adducts[3] 4-(β, β-diacetyl-α-phenyl ethyl) -1-*p*-tolyl-2-[1′(2′-methyl naphthalenyl)] -2-pyrroline-5-one (**7a**), 4-(β-acetyl-α, β-diphenyl ethyl)-1-*p*-tolyl -2-[1′(2′-methyl naphthalenyl)] -2-pyrroline-5-one (**7b**) and 4-(β, β-diethyl-α-phenyl ethyl) -1-*p*-tolyl-2-[1′(2′-methyl naphthalenyl)]-2-pyrroline-5-one (**7c**).

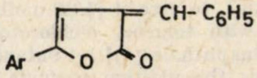

1

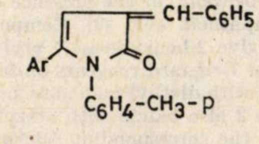

2

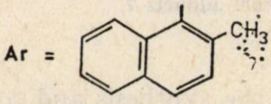

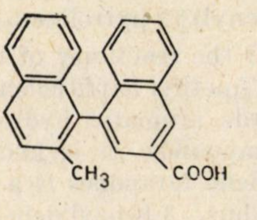

3

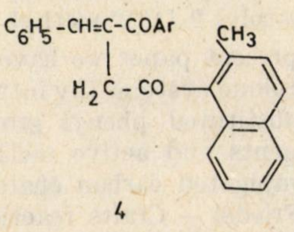

4

a, Ar = $C_6H_4-CH_3-p$

b, Ar = $C_6H_3-Cl, CH_3)-2,3$

c, Ar = $C_6H_3(CH_3)_2-2,3$

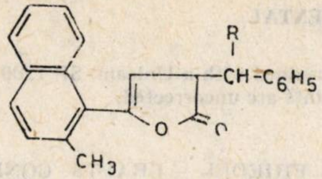

5

a, R = C_6H_5
b, R = CH_3

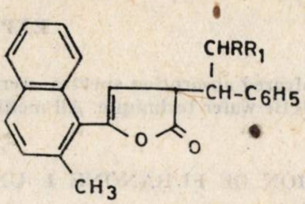

6

	R	R_1
a,	$COCH_3$	C_6H_5
b	$COOC_2H_5$	$COOC_2H_5$

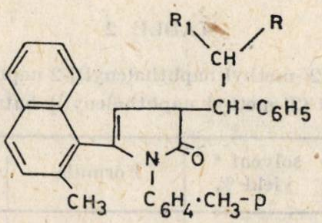

7

	R	R_1
a,	CH_3CO	CH_3CO
b,	CH_3CO	C_6H_5
c,	$COOC_2H_5$	$COOC_2H_5$

The IR spectra of the compounds **3**—**7** are presented in table 1.

TABLE 1

IR spectra of compounds **3**—**7**

Compd.	IR absorption (cm^{-1})								
	ν(CO) (aryl acid)	ν(CO) (aryl ketone)	ν(CO) (α, β-unsaturated ketone)	ν(CO) (saturated open chain ketone)	ν(CO) (ester)	ν(C=C)	ν(CH) (out of plane deformation)	ν(CO) (unsaturated γ lactone)	ν(CO) (unfused γ-lactone)
3	1695								
4a		1675	1690				815		
4b		1670	1685				810		
4c		1670	1680				815		
5a						1615		1795	
5b						1620		1790	
6a				1720				1785	
6b					1742			1790	
7a				1725					1710
7b				1715					1700
7c					1742				1705

EXPERIMENTAL

The infrared absorption spectra were determined with a Unicam SP 1200 spectrophotometer using KBr wafer technique. All melting points are uncorrected.

REACTION OF FURANONE 1 UNDER FRIEDEL – CRAFTS CONDITIONS

To a mixture of dichloromethane or an aromatic solvent and anhydrous $AlCl_3$ (10 g, 0.06 mole) a solution of **1** in dichloromethane or in an aromatic hydrocarbon was added gradually. After stirring for 15 hrs the reaction mixture was decomposed with dil. HCl and the solvent removed by steam distillation. The solid products were crystallized from suitable solvents (Table 2).

TABLE 2

Physical data of 4-[1′(2′-methyl naphthalenyl)]-2-naphthoic acid (**3**) and 1-aryl-2-benzylidene-4-[1′(2′-methyl naphthalenyl)] butan-1,4-diones **4 a–c**

Compound	m.p°C	solvent * yield %	Formula	Analysis (%) Found	Analysis (%) Required
3	175	B	$C_{22}H_{16}O_2$	C 84.60	84.62
		70		H 5.01	5.13
4a	160	B	$C_{29}H_{24}O_2$	C 86.2	86.14
		60		H 5.89	5.94
4b	180	T	$C_{29}H_{23}ClO_2$	C 79.29	79.36
		65		H 5.32	5.25
				Cl 8.3	8.10
4c	195	M	$C_{30}H_{26}O_2$	C 86.06	86.12
		70		H 6.25	6.22

* B = benzene ; T = toluene ; M = methanol

REACTION OF 1 WITH GRIGNARD REAGENTS

To Mg metal (0.7 g) in anhyd. ether (30 ml) an aryl / or alkyl halide (0.03 mole) in dry ether (15 ml) was added dropwise. The reaction mixture was refluxed and **1** (0.01 mole) in dry ether (50 ml) added in portions during 2 hrs. The mixture was further refluxed for 3 hrs, left overnight and decomposed with dil. HCl. The ethereal layer was washed with water, dried over anhydrous sodium sulphate and evaporated by air blowing to give a solid which was crystallized from a suitable solvent. The results obtained are given in table 3.

TABLE 3

Characterization of products **5a** and **5b**

Compound	m.pC°	solvent* yield %	Formula	Analysis (%) Found	Analysis (%) Required
5a	250	T	$C_{28}H_{22}O_2$	C 86.21	86.15
		60		H 5.63	5.64
5b	235	E	$C_{23}H_{20}O_2$	C 84.23	84.15
		55		H 6.0	6.1

* T = toluene ; E = ethanol.

REACTION OF FURANONE **1** WITH DIETHYL MALONATE OR BENZYL METHYL KETONE UNDER MICHAEL CONDITIONS FORMATION OF **6a** AND **6b**

Benzyl methyl ketone (0.01 mole) or diethyl malonate (0.01 mole) was added to an alcoholic solution of sodium ethoxide which has been prepared from sodium (0.3 g ; 0.013 g atom) and 140 ml of absolute ethyl alcohol, then **1** (0.01 mole) was added and the resulting solution was heated under reflux for 7 hrs. The reaction mixture was diluted with water and extracted with ether. The aqueous layer was acidified with ice-cold dilute hydrochloric acid. The solid that separated was filtered, dried and crystallized from the proper solvent to give **6a** and **6b** ; (yield 60%). Results are given in table 4.

TABLE 4

Characterisation of Michael adducts **6a** and **6b**

Compound	mp°C	Solvent* yield %	Formula	Analysis (%)	
				Found	Required
6a	145	E	$C_{31}H_{26}O_3$	C 83.3	83.41
		60		H 5.67	5.83
6b	245	A	$C_{29}H_{28}O_6$	C 73.82	73.73
		65		H 5.91	5.93

* E = ethanol ; A = acetic acid.

REACTION OF ACETYLACETONE, BENZYL METHYL KETONE AND DIETHYL MALONATE WITH (**2**)

A mixture of **2** (0.1 mole) in ethanol (80 ml) and acetylacetone, benzyl methyl ketone or diethyl malonate (0.1 mole) was heated under reflux with sodium methoxide (0.1 mole) for 7 hrs. The reaction mixture was diluted with water and extracted with ether. The aqueous layer was acidified with ice-cold dilute hydrochloric acid. The solid which separated was filtered, dried and crystallized from the proper solvent to give (**7a-c**), yield 70% The results are given in table 5.

TABLE 5

Physical data of Michael adducts **7 a—c**

Compound	m.p°C	Solvent* yield %	Formula	Analysis (%)	
				Found	Required
7a	195	B	$C_{34}H_{31}NO_3$	C 81.43	81.44
		75		H 6.18	6.19
				N 2.78	2.79
7b	168	B	$C_{28}H_{33}NO_2$	C 85.12	85.2
		70		H 6.32	6.2
				N 2.7	2.6
7c	180	M	$C_{36}H_{35}NO_5$	C 77.2	77.01
		65		H 6.24	6.23
				N 2.42	2.5

* B = benzene ; M = methanol.

REFERENCES

1. A. Sammour, M. Abdalla and A. Essawy, *Pakistan J. Sci. Res.*, **26**, 200 (1974) (under pubication).
2. M. Abdalla and A. Essawy, *Indian J. Chem.*, **15**, 523 (1977)
3. A. Essawy and A. A. Hamed, *Indian J. Chem.*, **15**, 694 (1977)
4. Y. Shyam Sunder Rao, *Chem. Rev.*, **64**, 353 (1964).
5. R. Filler and H. A. Leipod, *J. Org. Chem.*, **27**, 4440 (1962).
6. R. Filler, E. J. Piasek and L. H. Mark, *J. Org. Chem.*, **26**, 2659 (1961).

Revue Roumaine de Chimie, 26, 7, 101–108 (1981)

SOME REACTIONS OF 3,4-METHYLENEDIOXYBENZYLIDENE-*p*-ISOPROPYLACETOPHENONE

M. A. EL-HASHASH, M. E. SHABAN and M. M. HABASHY
Faculty of Science, Ain Shams University, Abbasia, Cairo, Egypt

Received September 19, 1979

3,4-Methylenedioxybenzylidene-*p*-isopropylacetophenone (**1**) reacts with hydrogen peroxide to give the oxirane derivative **2**. The cleavage of the strained oxirane ring with sodium hydroxide afforded the corresponding 1,2-diketone, **3**, and glycolic acid derivative **4**. The reaction of **1** with methylene compounds (under Michael conditions), aromatic hydrocarbons (under Friedel-Crafts conditions), hydrazines, hydroxylamine, benzylamine and bromine has been described. Also, the reaction of the dibromide **12** with hydroxylamine, phenylhydrazine and toluene in presence of anhydrous aluminium chloride has been investigated.

In general, hydrogen peroxide reacts with α, β-unsaturated ketones producing the corresponding epoxyketones.[1,2] In this study, this reaction was applied to the 3,4-methylenedioxybenzylidene-*p*-isopropylacetophenone (**1**). Thus, treatment of the alcoholic solution of **1** with hydrogen peroxide in alkaline medium yielded the epoxide **2**.

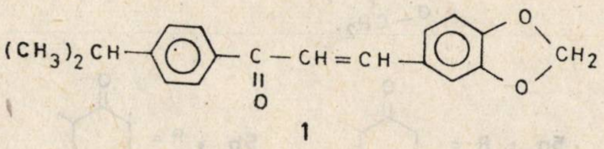

1

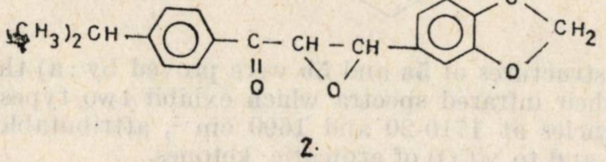

2

The proposed structure of **2** was supported by : a) its analytical data, b) the infrared spectrum which showed strong absorption bands at 1685 cm^{-1} (ν(CO)) and at 1250 cm^{-1} (epoxide linkage), and c) treatment of **2** with sodium hydroxide solution,[3] which gave a mixture of two products ; the 1-(*p*-isopropylphenyl)-3-(3′,4′-methylenedioxyphenyl) propane-1,2-dione **(3)** and *p*-isopropylphenyl-3,4-methylenedioxyphenylmethylglycolic acid (**4**),

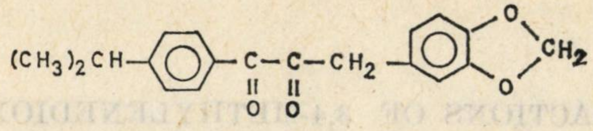

3

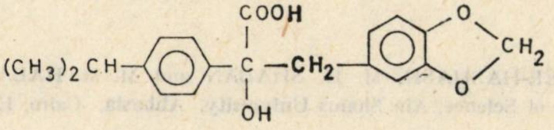

4

The structure of the 1,2-diketone **3** was proved by : a) analytical data and b) the infrared spectrum which showed strong absorption bands in the carbonyl region at 1710 and 1690 cm^{-1} characteristic of 1,2-diketones. Also, the structure of the glycolic acid derivative **4** was confirmed by its analytical data and the infrared spectrum which showed strong bands characteristic of ν(CO) (1700 cm^{-1}), ν(OH) of carboxylic group (3010 cm^{-1}) and ν(OH) band (3450 cm^{-1}).

The Michael condensation of compound **1** in presence of sodium methoxide with cyclohexanone or cyclopentanone gave the 2-[β-(*p*-isopropylbenzoyl)-α-(3,4-methylenedioxyphenyl)-]-cyclohexanone (**5a**) and -cyclopentanone (**5b**), respectively.[4-6]

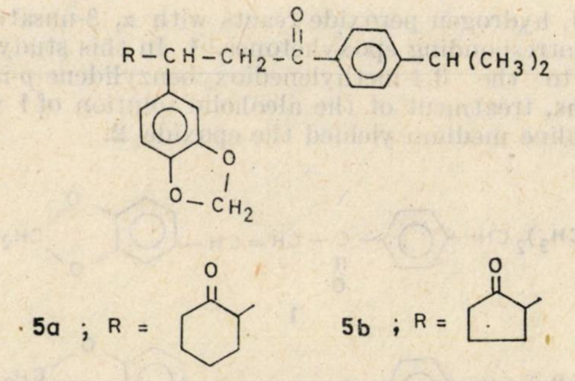

The assigned structures of **5a** and **5b** were proved by : a) their analytical data and b) their infrared spectra which exhibit two types of carbonyl groups frequencies at 1710-20 and 1690 cm^{-1}, attributable to ν(CO) of cyclic ketones and to ν(CO) of aromatic ketones.

Recently,[7,8] it has been reported that chalcones reacted with malononitrile, giving rise to pyridine derivatives. In the present work, 3,4-methylenedioxybenzylidene-*p*-isopropylacetophenone (**1**) was condensed with malononitrile in the presence of ammonium acetate in a 1 : 1 molar ratio to give 2-amino-6-(*p*-isopropylphenyl)-4-(3′, 4′-methylenedioxyphenyl)-nicotinonitrile (**6**) through Michael reaction (with the elimination of one mole each of water and hydrogen), beside the colourless 2-amino-3-cyano-

6-(*p*-isopropylphenyl)-4-(3′, 4′-methylenedioxyphenyl) hexahydropyridine (**7**).

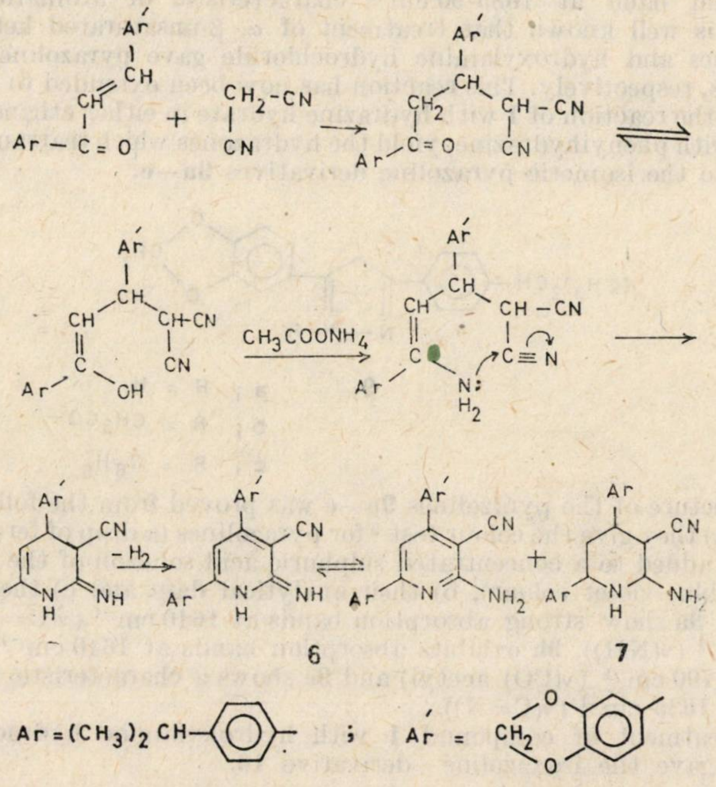

The structure of **6** is evidenced by its analytical and spectral data. Thus, its infrared spectrum shows bands at 2222 cm^{-1} (conjugated ν(C≡N)), 3470 cm^{-1} (ν(NH)), and δ(NH_2) (1630 cm^{-1}).

The reaction of aromatic hydrocarbons with α, β-unsaturated ketones under Friedel-Crafts conditions has been reported.[1] Thus, the reaction of compound **1** with benzene or *p*-xylene in presence of anhydrous aluminium chloride, gave 1-(phenyl- or *p*-xylyl)-1-(3′, 4′-methylenedioxyphenyl)-2-isopropylbenzoylethane (**8a**) and (**8b**).

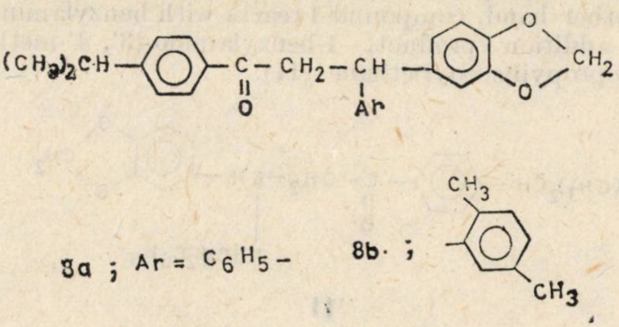

The structures of **8a** and **8b** were substantiated from the following evidence : a) their analytical data and b) their infrared spectra which show a strong absorption band at 1685-90 cm^{-1} characteristic of aromatic ketones.

It is well known that treatment of α, β-unsaturated ketones with hydrazines and hydroxylamine hydrochloride gave pyrazolines and isoxazolines, respectively. This reaction has now been extended to compound **1**. Thus, the reaction of **1** with hydrazine hydrate in either ethanol or acetic acid or with phenylhydrazine, yield the hydrazones which rearranged immediately to the isomeric pyrazoline derivatives **9a—c**.

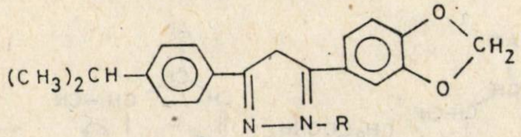

9 a ; R = H
b ; R = CH_3CO-
c ; R = C_6H_5

The structure of the pyrazolines **9a—c** was proved from the following evidence : a) they give the colour test [9] for pyrazolines (a drop of ferric chloride solution added to a concentrated sulphuric acid solution of the compound gives a blue-violet colour), b) their analytical data and c) their infrared spectra : **9a** show strong absorption bands at 1640 cm^{-1} (ν(C=N)) and at 3340 cm^{-1} (ν(NH)), **9b** exhibits absorption bands at 1640 cm^{-1} (ν(C=N)) and at 1700 cm^{-1} (ν(CO) acetyl) and **9c** shows a characteristic absorption band at 1635 cm^{-1} (ν(C=N)).

Treatment of compound **1** with hydroxylamine hydrochloride in ethanol gave the isoxazoline derivative **10**.

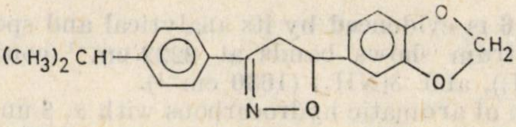

10

The structure of **10** was proved by its analytical data and its infrared spectrum which reveal the presence of C=N group.

On the other hand, compound **1** reacts with benzylamine in ethanol to give the addition product, 1-benzylamino-(3′, 4′-methylenedioxyphenyl)-2-(*p*-isopropylbenzoyl)ethane (**11**).

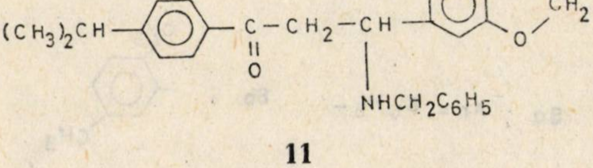

11

The structure of **11** is evidenced by analytical as well as spectral data. Thus, its infrared spectrum shows absorption bands at 1690 cm^{-1} and 3340 cm^{-1} attributable to $\nu(CO)$ and $\nu(NH)$.

Treatment of **1** with bromine in carbon tetrachloride yields the corresponding dibromide **12**.

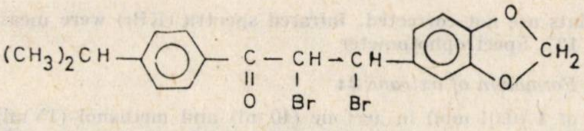

12

The proposed structure of **12** was proved by its analytical data and its infrared spectrum which shows a band at 1690 cm^{-1} ($\nu(CO)$ ketone).

The chalcone dibromide **12** was converted into the pyrazole derivative **13** by the reaction with phenylhydrazine in boiling acetic acid.[10-12] As a point of interest, the dibromide **12** was condensed with hydroxylamine hydrochloride in boiling acetic acid when the isoxazole derivative **14** was obtained.

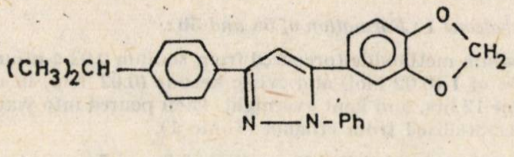

13

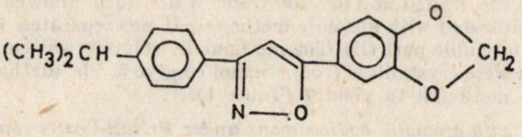

14

The structures of **13** and **14** were established from : a) their analytical data and b) their infrared spectra which exhibit a band attributable to C=N group at 1625–1630 cm^{-1}.

The reaction of the dibromide **12** with benzene or toluene in presence of anhydrous aluminium chloride, gave **15a** and **b**, respectively.

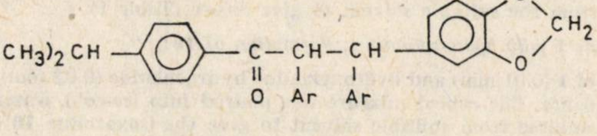

15

a ; $Ar = C_6H_5-$

b ; $Ar = p-CH_3-C_6H_4-$

The structures of **15a** and **b** were confirmed by their analytical data and their infrared spectra which reveal the presence of aromatic CO group of ketones.

EXPERIMENTAL

Melting points are not corrected. Infrared spectra (KBr) were measured on a Perkin-Elmer Infracord 137 Spectrophotometer.

Epoxidation of **1** ; *Formation of oxirane* **2**:

A solution of **1** (0.01 mol) in acetone (40 ml) and methanol (15 ml) was treated with 8% aqueous sodium hydroxide (12 ml), followed by hydrogen peroxide (30% ; 5 ml). The solution was shaken and brought to boiling point during one hour, then left overnight at room temperature. A white crystalline product was separated and recrystallised from light petrol (80—100°) (Table 1).

Action of sodium hydroxide on the oxirane **2** ; *Formation of diketone* **3** *and glycolic acid* **4**:

The crystalline oxirane **2** (2g) was refluxed with ethanol (5 ml) and 10% aqueous sodium hydroxide (2 ml) for 3 hrs. The ethanol was evaporated and water (20 ml) was added to the residue. The alkaline solution was extracted with ether. The alkaline layer was acidified to give the glycolic acid **4**. The ethereal extract was evaporated to yield the diketone **3**. The products were crystallised from the suitable solvent (Table 1).

Michael reaction with chalcone **1** ; *Formation of* **5a** *and* **5b**:

A solution of sodium methoxide (prepared from sodium 0.02 g-atoms in 15 ml methanol) was added to a solution of **1** (0.02 mol) and cyclic ketone (0.02 mol) in methanol (50 ml). The mixture was refluxed for 12 hrs, and kept overnight, then poured into water. The solid products were filtered off and crystallised from ethanol (Table 1).

Reaction of chalcone **1** *with malononitrile; Formation of* **6** *and* **7**:

A mixture of malononitrile (1.32 g, 0.02 mol), chalcone **1** (0.01 mol) and ammonium acetate (2.31 g, 0.03 mol) was heated at 140—150°C for 8 hrs, then allowed to cool. The orange residue product was triturated with absolute methanol. It was separated in two parts, a methanolic part (A) and an insoluble part (B). The methanolic solution was concentrated to yield colourless crystals which were crystallised from ethanol to give **6**. The methanol insoluble part (B) was crystallised from methanol to yield **7** (Table 1).

Reaction of chalcone **1** *with aromatic hydrocarbons under Friedel-Crafts conditions; Formation of* **8a** *and* **8b** :

To a cooled stirred mixture of anhydrous aluminium chloride (0.03 mol) in 30 ml of dry benzene or *p*-xylene at 10°C, a solution of **1** (0.01 mol) in 20 ml of aromatic hydrocarbon was added. Stirring was continued for an additional 3 hrs at room temperature and 3 hrs at 100°C. The complex was decomposed with 250 ml of dilute (1 : 15) hydrochloric acid. The mixture was extracted with ether and the solvent evaporated under reduced pressure. The product was crystallised from suitable solvent to give **8a** and **b** (Table 1).

Reaction of chalcone **1** *with hydrazines; Formation of* **9a—c**:

A solution of **1** in ethanol (30 ml) was treated with hydrazine hydrate or phenylhydrazine (0.03 mol). The mixture was refluxed for 6 hrs. The yellow products obtained after cooling were crystallised from the suitable solvent to give **9a—c** (Table 1).

Reaction of chalcone **1** *with hydroxylamine* ; *Formation of* **10**:

A mixture of **1** (0.01 mol) and hydroxylamine hydrochloride (0.02 mol) in ethanol (30 ml) was refluxed for 6 hrs. The cooled mixture was poured into ice-cold water and the product obtained was crystallised from suitable solvent to give the isoxazoline **10** (Table 1).

Reaction of chalcone **1** *with benzylamine; Formation of* **11**:

A solution of **1** (0.01 mol) in ethanol and benzylamine (0.02 mol) was refluxed for 6 hrs. The cooled solution was poured into ice-cold dilute hydrochloric acid. The pale yellow solid was crystallised from the suitable solvent to give **11** (Table 1).

TABLE 1

Characterisation of compounds 2—15

Compound	m.p.	Solvent * Yield %	Formula	Analysis % (Found/Calcd.) C	H	N
2	113—15	L.P. (79%)	$C_{19}H_{18}O_4$	73.54 73.96	5.80 5.65	
3	122—3	M (71%)	$C_{19}H_{18}O_4$	73.54 74.10	5.80 6.01	
4	168—70	E (64%)	$C_{19}H_{20}O_5$	69.51 69.95	6.09 6.12	
5a	148—50	E (59%)	$C_{25}H_{28}O_4$	76.53 77.04	7.14 6.83	
5b	139—41	E (61%)	$C_{24}H_{26}O_4$	76.19 76.72	6.87 6.98	
6	128—9	E (75%)	$C_{21}H_{20}N_2O_2$	75.90 76.12	6.02 6.38	8.43 8.84
7	116—18	M (79%)	$C_{22}H_{24}N_3O_2$	72.92 73.34	6.62 6.39	11.60 11.70
8a	233—5	B (69%)	$C_{25}H_{24}O_3$	80.64 81.10	6.45 6.39	
8b	260—2	E (72%)	$C_{27}H_{28}O_3$	81.00 81.55	7.00 7.32	
9a	115—17	E (79%)	$C_{19}H_{20}N_2O_2$	74.02 74.38	6.49 6.10	9.09 8.75
9b	122—3	A (77%)	$C_{21}H_{22}N_2O_3$	72.00 72.48	6.28 5.94	8.00 8.22
9c	155—7	E (76%)	$C_{25}H_{24}N_2O_2$	78.12 78.58	6.25 6.08	7.29 7.64
10	174—6	E (69%)	$C_{19}H_{19}NO_3$	73.78 74.28	6.14 6.57	4.53 4.85
11	103—5	E (73%)	$C_{26}H_{27}NO_3$	77.80 78.32	6.73 6.31	3.49 3.71
12	143—5	B (76%)	$C_{19}H_{18}Br_2O_3$	50.22 50.01	3.96 3.94	*Br* 35.24 35.35
13	215—7	E (69%)	$C_{25}H_{22}NO_2$	81.52 81.80	5.97 5.82	*N* 3.80 3.77
14	192—3	E (70%)	$C_{19}H_{17}NO$	82.90 82.72	6.18 6.03	5.09 5.20
15a	220—2	B (65%)	$C_{31}H_{28}O_3$	83.03 83.39	6.25 6.00	
15b	229—31	B—L.P. (68%)	$C_{33}H_{32}O_3$	83.19 83.42	6.72 6.50	

*** L.p. = Light petrol (80—100°) ; M = Methanol ; E = Ethanol ; B = Benzene and A= Acetic acid.**

Action of bromine on **1**; *Formation of the chalcone dibromide* **12** :

A stirred solution of **1** (0.01 mol) in carbon tetrachloride (30 ml), was treated with bromine (0.01 mol) in carbon tetrachloride (20 ml). The mixture was left overnight and the solvent was evaporated under reduced pressure to give a reddish solid which was crystallised from light petrol (100—120°) to yield the dibromide **12** (Table 1).

Reaction of chalcone dibromide **12** *with phenylhydrazine; Formation of the pyrazole* **13** :

A solution of **12** (0.01 mol) in ethanol (30 ml) and phenylhydrazine (0.01 mol) was refluxed for 8 hrs. The cooled mixture was poured into ice-cold dilute hydrochloric acid and the product was crystallised from suitable solvent to give the pyrazole **13** (Table 1).

Reaction of chalcone dibromide **12** *with hydroxylamine hydrochloride; Formation of isoxazole* **14** :

A solution of **12** (0.01 mol) in ethanol (30 ml) and hydroxylamine hydrochloride (0.01 mol) was refluxed for 8 hrs. The cooled mixture was poured into ice-cold water. The product was crystallised from suitable solvent to give the isoxazole **14** (Table 1).

Reaction of chalcone dibromide **12** *with aromatic hydrocarbons; Formation of* **15a** *and* **15b** :

A solution of **12** (0.01 mol) in a dry aromatic hydrocarbon (50 ml), namely (benzene or toluene) was added gradually to a cold suspension of anhydrous aluminium chloride (0.04 mol) in a large excess of the same hydrocarbon (100 ml). The temperature of the mixture was not allowed to rise above 60°. The suspension was stirred at 60° for 5 hrs, then poured into ice-cold hydrochloric acid mixture. The organic layer was separated and steam distilled. The reaction product was extracted with ether. Evaporation was accompained under reduced pressure. The product was crystallised from suitable solvent to give **15a** and **b** (Table 1).

REFERENCES

[1] A. Sammour and M. El-Kasaby, *U.A.R., J. Chem.*, **13**, 151 (1970).
[2] H. H. Wasserman and E. N. Aubry, *J. Amer. Chem. Soc.*, **77**, 590 (1955).
[3] M. A. El-Hashash and M. El-Kady, *Rev. Roumaine Chim.*, **23**, 1581 (1978).
[4] D. W. Hill, *J. Chem. Soc.*, **1935**, 11115.
[5] W. Dilthey, O. Trosken, K. Plum and W. Schommer, *J. prak. Chem.*, **141**, 231 (1934).
[6] L. A. Carpiné, *J. Org. Chem.*, **30**, 736 (1965).
[7] A. Sammour, Y. Akhnoukh and H. Jahine, *U.A.R., J. Chem.*, **13**, 421 (1970).
[8] A. Sammour and M. A. El-Hashash, *Egypt J. Chem.*, **16**, 381 (1973).
[9] V. Knorr, *Liebigs Ann. Chem.*, **238**, 200 (1887).
[10] N. Coker and M. Fields, *J. Org. Chem.*, **27**, 2226 (1962).
[11] K. H. Johnston and R. G. Shotter, *J. Chem. Soc., C*, **1968**, 1774.
[12] A. Sammour, M.I.B. Selim and G. H. El-Sayed, *U.A.R., J. Chem.*, **14**, 235 (1971).

Revue Roumaine de Chimie, 26, 7, 109—116 (1981)

DÉRIVÉS DIPOLAIRES EN SÉRIE QUINAZOLINIQUES. I

SYNTHÈSE DE PYRROLO [1, 2—c] QUINAZOLINES

EMILIAN GEORGESCU, IOAN DRUTA et MAGDA PETROVANU

Institut Polytechnique « Gh. Asachi », Laboratoire de Chimie organique, Jassy, 11, str. 23 August, Roumanie

Reçu le 13 Décembre 1979

On a obtenu, pour la première fois, des dérivés pyrolo [1,2-c] quinazoliniques de type VI (a, b) et VII (a, b, c, d) par des réactions de cycloadditions [3 + 2] dipolaires des quinazolinium-ylures (IV B) obtenus « in situ » sur l'acétylènedicarboxylate de méthyle et le propiolate d'éthyle.

★

The first synthesis of the pyrolo [1,2-c] quinazoline derivatives of the type VI (a, b) and VII (a, b, c, d) is described through a [3 + 2] dipolar cycloaddition between quinazolinium ylides IV B generated *in situ* and dimethyl acetylenedicarboxylate or ethyl propiolate.

Dans le cadre des recherches plus amples dans le domaine des diazinium-ylures [1] nous avons commençé à étudier les possibilités d'obtention et la réactivité des quinazolinium-ylures.

A notre connaissance il n'existe jusqu'à ce moment aucun indice concernant les quinazolinium-ylures.

Le but du présent travail est de préciser les possibilités de synthèse et la réactivité des quinazolinium-ylures de type IV vis-à-vis des alcynes activés par un ou deux substituents électro-attracteurs et d'étudier le mécanisme et la stéréochimie des diverses réactions.

Dans la première étape de nos recherches nous avons essayé d'obtenir les quinazolinium-ylures IV par la méthode du sel. [2] En faisant réagir la quinazoline (I) avec des dérivés α-halogénocarbonyliques tels que les bromures de phénacyle (II a, R = H), *p*-nitrophénacyle (II b, R = NO_2), *p*-bromophénacyle (II c, R = Br) *p*-méthoxyphénacyle (II d, R = OCH_3) nous avons obtenu les bromures de cycloimmonium correspondants (III a, R=H ; III b, R = NO_2 ; III c, R = Br ; III d, R = OCH_3).

A l'exception du bromure de N-phénacyle-3-quinazolinium (III a) nous n'avons pas réussi à obtenir les sels (III) à l'état pur à cause du phénomène d'hydration covalente très caractéristique pour les dérivés quinazolinique.[3a, b, c, d]

Nous avons quand même essayé d'obtenir les ylures (IV) correspondants en traitant les sels impurs par des bases mais nous n'avons pas réussi à les isoler.

L'échec des réactions d'obtention des ylures (IV) nous a conduit à l'idée de faire réagir simultanément la quinazoline, le dérivé α-halogénocarbonylique et un agent dipolarophyle en milieu basique dans le but d'obtenir directement les adduits cycliques, par suite des réactions d'additions [3 + 2] dipolaires des quinazolinium-ylures (IV) intermédiaires non isolables, sur les dipolarophyles. En effet, nous avons réussi à obtenir par cette voie des produits pyrrolo [1,2-c] quinazoliniques ayant la structure générale suivante.

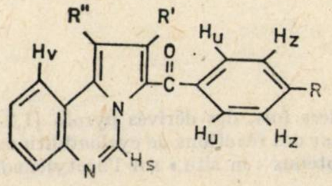

Nous avons choisi premièrement comme agent dipolarophyle un alcyne symétriques, l'acétylènedicarboxylate de méthyle. En portant à reflux un mélange de quinazoline, bromure de phénacyle para substitué (II a, b) et acétylène dicarboxylate de méthyle en solution époxydique, nous avons obtenu les pyrrolo [1,2-c]- quinazolines (VI a, R = H ; VI b, R = NO_2) ; on a utilisé comme solvants le propène oxyde ou l'épichlorhydrine qui sont des bases suffisamment fortes pour extraire l'acide bromhydrique des sels de quinazolinium (III a, b) mais pas assez puissantes pour réagir avec le dérivé α-halogéno-carbonylique.

La structure des adduits cycliques VI (a, b) a été déterminée par voie chimique et spectrale.

Ainsi dans les spectres I.R. des produits VI (a, b) les deux groupements CO estériques présentent des absorptions très différentes. Les bandes d'absorptions aux nombres d'ondes plus grands 1740 cm^{-1} (VI a) et 1733 cm^{-1} (VI b) sont fournies par les groupements estériques en position 2. Le phénomène est dû à l'influence stérique exerçée par les deux groupements voisins (cétonique et estérique) ; ceux-ci provoquent tant la distorsion des groupements estériques en position 2, que la déviation à partir de la coplanarité, ce qui a comme conséquence une annulation partielle de la conjugaison $\pi-\pi$ entre le groupement C=0 et le noyau pyrrolique. Ce fait conduit à l'augmentation de l'ordre de la liaison C=0, donc au déplacement des bandes d'absorption vers des nombres d'ondes plus grands.

D'autre part, les absorptions à des nombres d'ondes particulièrement bas dues aux groupements estériques en position 1, 1712 cm^{-1} (VI a) et 1728 cm^{-1} (VI b) ne peuvent être expliquées que si l'on admet une participation importante des structures limites B et C.

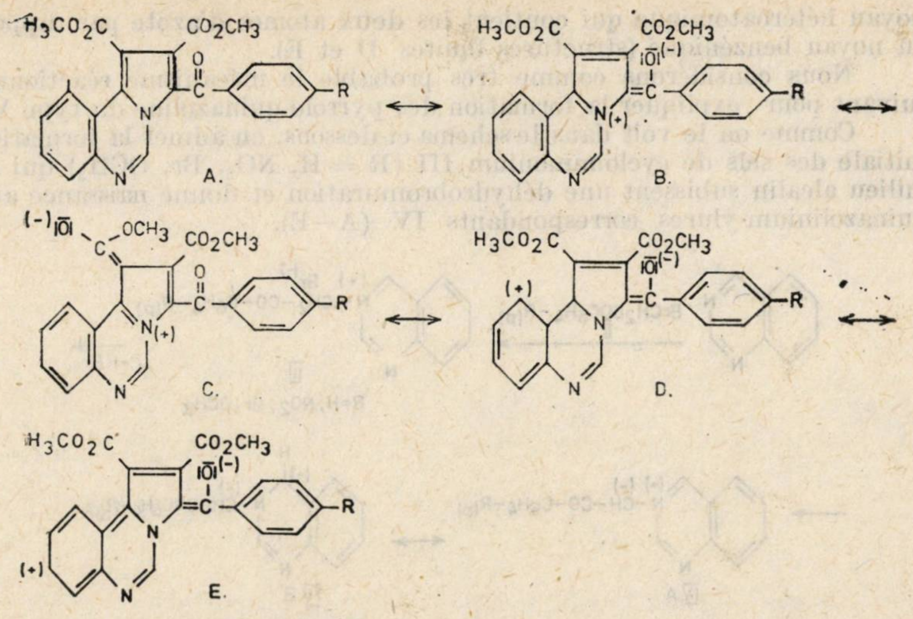

D'ailleurs une analyse plus minutieuse des structures limites met en évidence la vinilogie entre la structure A et les amides diaryliques (B)[4] respectivement les esters carbamiques (C),[5] les deux classes connues pour la valeur réduite des nombres d'ondes des absorptions des groupements CO par suite d'une forte conjugaison p—π. En plus, la participation des structures limites du type B explique la très petite différence $\Delta\nu = \nu_{CO}$ (VI b) — ν_{CO} (VI a) = 2 cm^{-1} par le fait que les effets — I et —E des groupements nitriques se propagent en grande partie sur tout le système aromatique, la liaison C = 0 cétonique étant moins affectée.

Par la position et la forme des signaux les spectres ^1H—RMN confirment les structures proposées. Ainsi l'existence des deux singulets fournis par le proton H_s ainsi que celle des signaux des protons aromatiques et dans des rapports d'intensité correspondants confirme la formation des produits VI a, VI b.

Un plus grand intérêt présentent les multiplets à $\delta = 0,88-9,09$ ppm (VI a) et $\delta = 9,23-9,43$ ppm (VI b) attribués aux protons H_v. Les déplacement chimiques importants de ces protons par rapport aux autres protons aromatiques peuvent être causés tant par les effets de champ dus à leur position « péri », que par les effets d'anisotropie dus aux groupements CO estériques en positions 1.

La participation considérable des structures limites du type B et C pour le produit VI b est prouvée par la valeur accrûe des différences $\Delta\delta H_s = \delta H_s(\text{VI b}) - \delta H_s(\text{VI a}) = 1,15$ ppm, tandis que la différence $\Delta\delta H_v = \delta H_v$ (VI b) $- \delta H_v$(VI a) $= 0,34$ ppm indique la participation de structures limites du type D et E.

En plus, la différence $\Delta\delta H_s - \Delta\delta H_v = 1,15-0,34$ ppm $= 0,81$ ppm met en évidence la localisation préférentielle de la charge positive sur le noyau hétéroatomique qui contient les deux atomes d'azote par rapport au noyau benzénique (structures limites D et E).

Nous considérons comme très probable le mécanisme réactionnel suivant pour expliquer la formation des pyrrolo-quinazoline du type VI.

Comme on le voit dans le schema ci-dessous, on admet la formation initiale des sels de cycloimmonium III (R = H, NO_2, Br, OCH_3) qui en milieu alcalin subissent une déhydrobromuration et donne naissance aux quinazolinium-ylures correspondants IV (A—E).

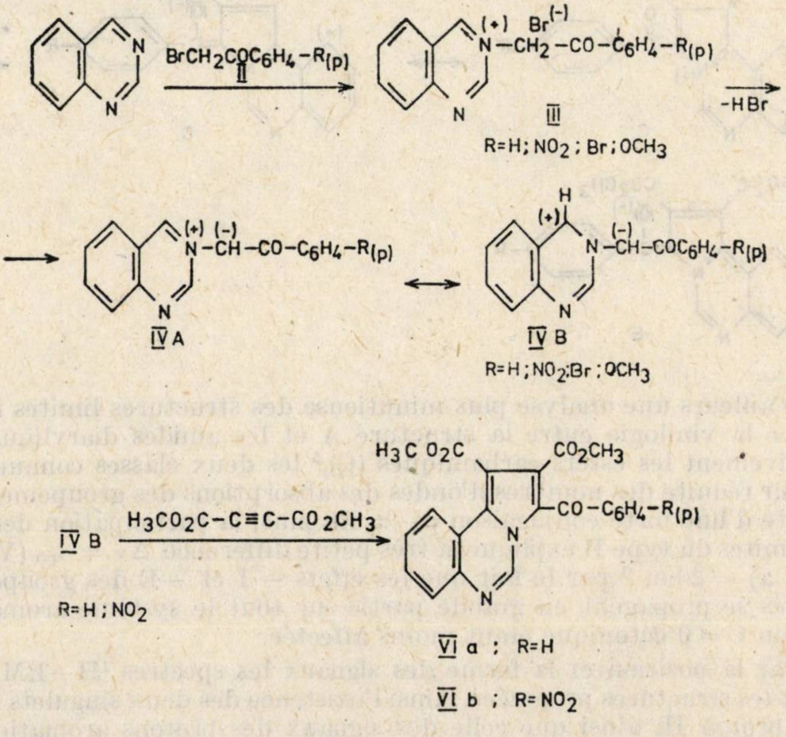

N
N
$BrCH_2COC_6H_4-R_{(p)}$
II
(+)
$Br^{(-)}$
$N-CH_2-CO-C_6H_4-R_{(p)}$
III
R=H; NO_2; Br; OCH_3
-HBr
(+) (-)
$N-CH-CO-C_6H_4-R_{(p)}$
IV A
H
(+)
(-)
$N-CH-COC_6H_4-R_{(p)}$
IV B
R=H; NO_2; Br; OCH_3
IV B
$H_3CO_2C-C\equiv C-CO_2CH_3$
R=H; NO_2
H_3CO_2C
CO_2CH_3
$CO-C_6H_4-R_{(p)}$
VI a ; R=H
VI b ; R=NO_2

Comme tous les cycloimmonium-ylures, les quinazolinium-ylures admettent à côté d'une structure « octet » (IV A), une structure « sextet » de dipole 1,3 (IV B). Grace à cette structure (IV B) ces ylures réagissent avec les agents dipolarophyles présents dans le mélange réactionnel (dans notre cas l'acétylène dicarboxylate de méthyle) et fournissent les adduits cycliques VI (a, b).

Tenant compte des données de la littérature concernant la quaternisation préférentielle de l'atome N^3 du noyau quinazolinique[3b,6] ainsi que de la structure des adduits cycliques obtenus nous avons admis que dans notre cas aussi la quaternisation touche à l'atome d'azote N^3, plus basique que l'atome d'azote N^1.

Poursuivant nos recherches, nous avons utilisé comme agent dipolarophyle un alcyne dissymétrique, le propiolate d'éthyle.

Dans ce cas il faut tenir compte de la régiosélectivité de la réaction d'addition de l'ylure à l'alcyne dissymétrique.

Comme on le sait, lorsque l'agent dipolarophyle est dissymétrique, l'addition peut conduire à deux adduits cycliques, par suite des deux sens d'addition possibles.

Dans notre cas l'addition pouvait conduire à deux adduits cycliques isomères.

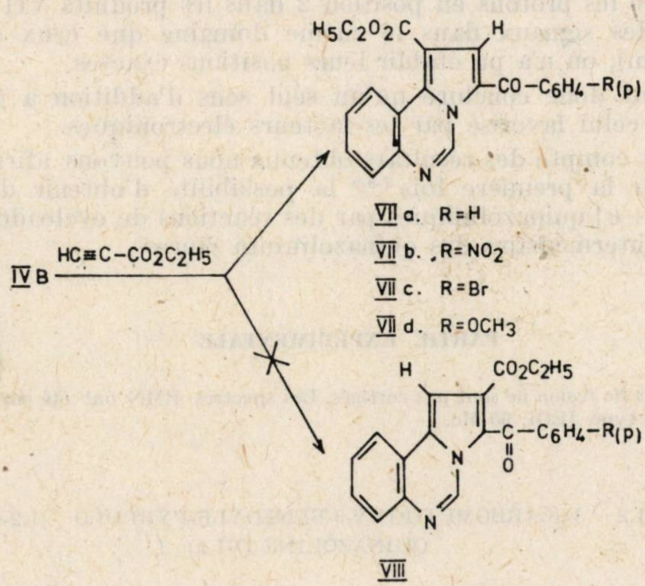

VII a. R=H

VII b. R=NO2

VII c. R=Br

VII d. R=OCH3

VIII

Dans les produits du type VII (a—d) le carbanion ylurique et lié à l'atome de carbone positivé du dipolarophyle, c'est à dire l'addition a eu lieu dans le sens favorisé par les facteurs électroniques.

Par contre, une structure du type VIII prendrait naissance par suite d'une addition inverse à la première.

Les données analytiques et spectrales plaident en faveur des structures VII (a, b, c, d).

Ainsi les spectres IR et ^1H—RMN des produits VII (a, b, c, d) ressemblent beaucoup à ceux des produits VI (a, b, c, d).

Les valeurs extrêmement réduites des nombres d'ondes d'absorptions des groupements C=O estériques et spécialement de ceux cétoniques dans les produits VII a (1710 cm^{-1} et 1630 cm^{-1}) et VII d (1715 cm^{-1} et 1635 cm^{-1}) indiquent une participation plus importante des structures limites des types B et C en comparaison avec les produits VI (a, b).

Evidemment, l'absence d'un groupement carbéthoxylique en position 2 élimine les effets d'encombrements stériques permettant une meilleure coplanarité et une conjugaison $\pi-\pi$ plus accentuée des liaisons C=O avec les noyaux aromatiques dans le cas des produits du type (VII) en comparaison avec les produits (VI). En plus, dans les produits VI (a et b), le groupement estérique en position 2 détermine l'augmentation de l'ordre des liaisons C=O qui se trouvent dans les positions 1 et 3 en déplaçant leurs absorptions vers des nombres d'ondes plus grands.

Dans les spectres ^1H-RMN on a pu mettre en évidence les signaux des protons H_v et H_s sur la base des considérations concernant les produits VI (a et b) mentionnés plus haut. En général, les positions des signaux fournis par les protons des produits VII (a, b, c, d) ne diffèrent par trop de ceux fournis par les mêmes protons dans les produits VI (a et b).

Puisque les protons en position 2 dans les produits VII (a, b, c, d) présentent des signaux dans le même domaine que ceux aromatiques (7,4—8,7 ppm), on n'a pu établir leurs positions exactes.

On peut donc conclure qu'un seul sens d'addition a été observé, précisément celui favorisé par les facteurs électroniques.

Tenant compte des résultats obtenus nous pouvons afirmer d'avoir montré, pour la première fois [7,8,9] la possibilité d'obtenir des systèmes pyrrolo [1,2—c] quinazoliniques par des réactions de cycloadditions dipolaires par l'intermédiaire des quinazolinium ylures.

PARTIE EXPÉRIMENTALE

Les points de fusion ne sont pas corrigés. Les spectres RMN ont été enregistrés sur un spectromètre de type JEOL 60 Mc.

1,2 — DICARBOMÉTHOXY-3-BENZOYLE-PYRROLO [1,2-c] QUINAZOLINE (VI a)

On suspend 3,29 g (10 mmol) bromure de N-phénacyle-3-quinazolinium III ; R=H ; p.f. 145—50° dans 50 ml de propène oxyde et on ajoute 1,22 ml (10 mmol) d'acétylènedicarboxylate de méthyle. On agite 24 h à température ambiante. On évapore une partie du solvant et on filtre les cristaux jaunes séparés ; p.f. 217—21° (produit non identifié) ; on chasse le solvant sous vide et on recristallise le résidu dans du propanol.

Après une nouvelle recristallisation dans un mélange chloroforme-éther éthylique on obtient 1,34 g cristaux aciculaires blancs à p.f. 160—161°. Rd. 34,5 %. Analyse pour $C_{22}H_{16}N_2O_5$ (388) calculé : C% 68,04 ; H% 4,12 ; N% 7,21 ; trouvé : C% 68,31 ; H% 4,37 ; N% 7,45. Spectre IR (KBr cm^{-1}) ; 1740, 1712 (CO estérique) ; 1650 (C=O cétonique) ; 1180, 1202, 1228 (C—O—C). Spectre ^1H-RMN ($CDCl_3$, TMS, δ pp m) singulet 3,28 (3H ; CH_3) ; singulet 3,93 (3H ;CH_3) ; multiplet 7,41—7,9 (8H ; aromatiques) ; multiplet 8,88—9,09 (1H ; CH_v) ; singulet 9,68 (1H ; H_v).

1,2-DICARBOMÉTHOXY-3-(4'-NITRO-BENZOYLE)-PYRROLO [1,2-c] QUINAZOLINE (VI b)

On dissout 1,3 g (10 mmol) quinazoline et 2,44 g (10 mmol) de bromure de *p*-nitrophénacyle dans 50 ml de propène oxyde ; on ajoute 1,22 ml (10 mmol) acétylènedicarboxylate de méthyle et on agite pendant 24 h à la température ambiante.

On chasse une partie du solvant et on abandonne la solution au réfrigérateur pendant la nuit. On filtre le précipité obtenu, on le lave sur le filtre à l'éther et on le recristallise dans un mélange $CHCl_3$ — éther éthylique. On obtient 1,13 g de cristaux aciculaires jaunes pales à p.f. 243—44°. Rd. 26 %. Analyse pour : $C_{22}H_{15}N_3O_7$ (433) calculé : C% 60,96 ; H% 3,46 ; N% 9,70 ; trouve : C% 61,10 ; H% 3,68 ; N% 9,88. Spectre IR (KBr cm^{-1}) : 1733, 1718 (CO estérique) ; 1652 (CO cétonique) ; 1535 (NO_2 assym.) ; 1355 (NO_2 sym.) ; 1179, 1203, 1232 (C—O—C). Spectre RMN (TFA, TMS, δ ppm) : singulet 3,61 (3H ; CH_3) ; singulet 4,21 (3H ; CH_3) ; multiplet 8,08—8,66 (7H ; aromatiques) ; multiplet 9,23—9,43 (1H, H_v) ; singulet 11,01 (1H ; H_s).

1-CARBETHOXY-3-BENZOYLE-PYRROLO [1,2-c] QUINAZOLINE (VII a)

On dissout 1,3 g (10 mmol) de quinazoline et 1,99 g (10 mmol) de bromure de phénacyle dans 50 ml de propène oxyde et on ajoute 1,1 ml (10 mmol) de propiolate d'éthyle. On agite pendant 24 h à température ambiante, on évapore une partie du solvant et on ajoute du méthyle-cyclohexane. Le précipité est filtré et recristallisé dans un mélange alcoole éthylique-chloroforme. On obtient 1,2 g cristaux aciculaires à p.f. 151—53°Rd. 1,45 g (42,15%). Analyse pour $C_{21}H_{16}N_2O_3$ (344) ; calculé : C% 73,25 ; H% 4,65 ; N% 8,13 ; trouvé : C%73,61 ; H% 4,90 ; N% 8,34 ; Spectre IR (KBr cm^{-1}) : 1711 (CO estérique) ; 1632 (CO cétonique) ; 1188 (C—O—C). Spectre RMN ($CDCl_3$, δppm) : triplet (3H ; CH_3) ; 1,40 ; $J = 7Hz$; quadriplet (2H ; CH_2) 4,41 ; $J = 7$ Hz ; multiplet (9H aromatiques) 7,43—805 ; multiplet (1H ; H_v) 9,60—9,81 ; singulet (1H ; H_3) 10,30.

1-CARBÉTHOXY-3-(4'-NITROBENZOYLE)-PYRROLO [1,2-c] QUINAZOLINE (VII b)

On traite un mélange de 1,3 g (10 mmol) quinazoline et 2,44 g (10 mmol) bromure de 4-nitrophénacyle dans 50 ml de propène oxyde par 1,1 ml (10 mmol) propiolate d'éthyle et on agite pendant 24 h à température ambiante. On chase une partie du solvant et on filtre le précipité obtenu. Après recristallisation dans du chloroforme on obtient 1,65 g de cristaux aciculaires jaunes à op.f. 236—237°. Rd. 42,4%. Analyse pour : $C_{21}H_{14}N_3O_5$ (389) : calculé : C% 64,78 ; H% 3,85 ; N% 10,78 ; trouvé : C% 64,48 ; H% 4,10 ; N% 10,85. Spectre IR (KBr cm^{-1}) : 1715 (CO estérique) ; 1636 (CO cétonique) ; 1526 (NO_2 assym.) ; 1355 (NO_2 sym.) ; 1198 (C—O—C). Spectre RMN (TFA, TMS, δppm) : triplet (3H ; CH_3) 1,60 ; $J = 7$ Hz ; quadriplet (2H ; CH_2) 4,74 ; $J = 7$ Hz ; multiplet (8H aromatiques, 8,13—8,75 ; multiplet (1H ; H_v) 9,85—10,11 ; singulet (1H ; H_8) 11,55.

1-CARBÉTHOXY-3-(4'-BROMOBENZOYLE)-PYRROLO [1,2-c] QUINAZOLINE (VII c)

On dissout 1,3 g (10 mmol) de quinazoline et 2,78 g (10 mmol) de bromure de 4-bromophénacyle dans 50 ml propène oxyde, on ajoute 1,1 ml (10 mmol) de propiolate d'éthyle et on agite 24 h à température ambiante. On évapore la moitié du solvent, on ajoute de l'éther éthylique et on filtre le précipité obtenu. Après recristallisation dans un mélange chloroforme-éther éthylique on obtient 1,3 g de cristaux aciculaires jaunes à p.f. 193—[illegible]° ; Rd. 1,75 g (40,66%). Analyse pour : $C_{21}H_{14}BrN_2O_3$ (423) : calculé : C% 59,57 ; H%3,54 ; N% 6,61 ; trouvé : C% 59,84 ; H% 3,81 ; N% 6,84. Spectre IR (KBr cm^{-1}) : 1715 (CO estérique) ; 1634 (CO cétonique) ; 1195 (C—O—C). Spectre RMN ($CDCl_2$, TMS, δppm) : triplet (3H ; CH_3) 1,43, $J = 7$ Hz ; quadriplet (2H ; CH_2) 4,43 (1H ; H_v) $J = 7$ Hz ; 9,66—9,86 ; singulet (1H ; H_8) 10,34.

1-CARBÉTHOXY-3-(4'-MÉTHOXY-BENZOYLE)-PYRROLO [1,2-c] QUINAZOLINE (VII d)

On traite un mélange de 1,3 g (10 mmol) quinazoline et 2,3 g (10 mmol) de bromure de 4-méthoxyphénacyle dans 50 ml propène oxyde par 1,1 ml (10 mmol) de propiolate d'éthyle et on agite 24 h à température ambiante. On évapore une partie du solvant et on ajoute de l'éther éthylique. Le précipité obtenu est filtré et lavé à l'éther éthylique. Après recristallisation dans un mélange chloroformeéther éthylique on obtient des cristaux aciculaires blancs à p.f. 177—8°. Rd. 1,51 g (40,3 %). Analyse pour : $C_{22}H_8N_2O_4$ (374) ; calculé : C% 70,58 ; H% 4,81 ; N% 7,48 ; rouvé : C% 70,32 ; H% 4,97 ; N% 5,72. (Spectre IR (KBr, cm^{-1}) : 1728 (CO estérique) ; 1630 CO cétonique) ; 1169, 1178, 1206 (C—O—C). Spectre RMN $CDCl_3$, TMS, δppm): triplet (3H; CH_3)

3,91, $J = 7$Hz ; singulet (3H ; CH_3) 3,91 ; quadriplet (2H ; CH_2) 4,43, $J = 7$Hz ; doublet (2H ; Hz) 7,05, $J = 9$ Hz ; multiplet 7,58–8,08 (6H aromatiques parmi lesquels à 7,9 doublet 2H, (H_u) $J = 9$Hz, multiplet (1H ; H_v) 9,61–9,81 ; singulet (1H ; H_8) 10,25.

BIBLIOGRAPHIE

[1] I. Zugrăvescu et M. Petrovanu, « N-Ylid Chemistry », McGraw-Hill, London, 1976.

[2] F. Kröhnke, *Ber. dtsch. chem. Ges.*, **68,** 1177 (1935).

[3] a. A. Albert, W. L. F. Armarego et E. Sprinner, *J. Chem. Soc.*, **1961,** 2689 ; b. *Ibid.* 5267 ; c. W. L. F. Armarego, *J. Chem. Soc.*, **1962,** 561 ; d. J. N. Bunting et D. D. Perrin, *J. Chem. Soc.*, **1967**, 950.

[4] M. St. C. Flett, *Spectrochim. Acta.*, **18,** 1537 (1962).

[5] R. Mecke et A. Lütringhaus, *Chem. Ber.*, **90,** 975 (1957).

[6] J. W. Bunting et W. G. Meathrel, *Canad. J. Chem.*, **48,** 2449 (1970).

[7] E. Ajello, *Atti Acad. Sci. Lett. Arti Palermo*, **30,** 237 (1969–70) *Chem. Abstr.*, **77,** 152, 110 (1972).

[8] S. Beveridge et J. L. Huppatz, *Austral J. Chem*, **23,** 781 (1970).

[9] J. W. Lown et K. Matsumoto, *Canad. J. Chem.*, **49,** 3119 (1971).

Revue Roumaine de Chimie, 26, 1, 117–124 (1981)

SAURE PERLFÖRMIGE IONENAUSTAUSCHER DES VERNETZTEN POLYVINYLALKOHOLS. I

VERNETZUNG, EINFÜHRUNG VON IONENAUSTAUSCHGRUPPEN UND EINIGE PHYSIKALISCH-CHEMISCHE EIGENSCHAFTEN

M. A. MATEESCU, H. D. SCHELL, M. DIMONIE *, T. BENŢIA, C. DIMITRIU und O. MAIOR*

Institut für biologische Wissenschaften zu Bukarest, Abteilung für Enzymologie, Splaiul Independenţei 296, 77748 Bukarest 17, Rumänien

* Polytechnisches Institut zu Bukarest, Lehrstuhl für Chemie und organische Technologie, Rumänien

Eingegangen am 22. März 1980

Wird perlförmiger Polyvinylalkohol in basischem Milieu mit Epichlorhydrin vernetzt, so werden unlösliche Polyvinylalkohol-Gele erhalten, deren Vernetzungsgrad von der angewandten Menge des Vernetzungsagenten abhängt. Bei höheren Vernetzungsgraden erhält man im Falle des PVA — zum Unterschied von andern Plyhydroxyverbindungen — Produkte mit loseren Strukturen und einem grösseren Wasseraufnahme vermögen, als es bei Gelen mit geringerem Vernetzungsgrad der Fall ist. Diese erlauben nämlich die Bildung von Wasserstoffbrücken zwischen den kettenförmigen PVA-Molekülen, was ein dichteres Netzwerk mit einem geringeren Wasseraufnahmevermögen bedingt. Durch Einführen von sauren Ionenaustauschgruppen in das Molekül des vernetzten PVA wurden Ionenaustauscher, wie CM-, SE- und P-PVA erhalten, deren Austauschkapazitäten von der Anzahl der in das Molekül eingeführten Ionenaustauschgruppen bestimmt ist. Durch die Vernetzung und das Einführen der Ionenaustauschgruppen wird die perlförmige und poröse Struktur der PVA-Gele nicht verändert.

By the epichlorohydrine treatment of beaded, porous PVA in alkaline medium, insoluble crosslinked PVA-gels are obtained, with a different degree of reticulation, as a function of the amount of the crosslinking agent used. At the higher degree of reticulation, the swelling properties are more pronounced than in the case of the smaller reticulation degree. This peculiar behaviour of PVA-gels relative to other polyhydroxilated stationary phases is due to some interchain hydrogen bonds which are more frequent in the gels with a small reticulation degree. By introduction of ion exchange groups, ion-exchangers of CM-, SE- and P-PVA types, with different capacities, are obtained. By reticulation and derivatisation, the beaded and porous structure is preserved.

Neben andern wirksamen Methoden, die zur Isolierung und Reinigung von organischen hochmolekularen Verbindungen, wie Peptide, Proteine, Enzyme, Hormone, Nukleinsäuren, Nukleotide und Polysaccharide, angewendet werden, nimmt die Ionenaustauschchromatographie zur Zeit einen wichtigen Platz ein. Die Ionenaustauschchromatographie ist Dank ihrer vielseitigen Möglichkeiten sowohl für analytische, als auch für prä-

---

Verwendete Abkürzungen : PVA = Polyvinylalkohol ; CM = Carboxymethyl ; SE = Sulfoäthyl ; SP = Sulfopropyl ; *P* = Phosphat.

parative Zwecke von besonderem Interesse und ergänzt oft in nützlicher Weise andere chromatographische Verfahren.

Zur Darstellung von sauren und basischen Ionenaustauschern wurden ausser Styrol-Divinylbenzol-Kopolymere [1] besonders zahlreiche Polyhydroxyverbindungen, wie Dextran, [2] Cellulose, [3] Agarose [4] und Amylose [5,6] verwendet. Die meisten der erzielten Verbindungen, wie z.B. CM- und SP-Sephadex, [2] CM- und P-Cellulose, [7] CM-, SE- und P-Agarose,[8,9] CM-Sepharose CL,[10] CM-Amylose [5,6] sind patentiert worden und werden auch von verschiedenen Firmen geliefert.

In der Fachliteratur sind auch Ionenaustauscher auf PVA-Basis schon beschrieben worde,[11-13] deren Darstellungsverfahren sich aber von den weiter unten beschriebenen unterscheiden.

In der vorliegenden Arbeit berichten wir über die Vernetzung von perlförmigem von Dimonie und Mitarb.[14] dargestellten PVA, die Einführung von Ionenaustauschgruppen in das vernetzte PVA-Molekül sowie über einige physikalisch-chemische Eigenschaften der erzielten Verbindungen. Der perlförmige und poröse Zustand der Gelpartikel ermöglicht die Erzielung von optimalen Durchflussgeschwindigkeiten in den Chromatographiesäulen, was sich günstig auf die Auftrennungsfähigkeit auswirkt.

Weiter unten sind die während der Synthese der in dieser Arbeit beschriebenen Ionenaustauscher ablaufenden chemischen Reaktionen schematisch dargestellt *.

MATERIAL UND METHODIK

Der in unserer Arbeit verwendete PVA wurde in Form poröser Perlen im Chemischen Kombinat „Victoria" nach einem von Dimonie und Mitarb.[14] beschriebenen Verfahren dargestellt.

Vernetzung des perlförmigen PVA. Es wurden 100 g PVA in 150 ml eisgekühlte 5 N Natriumhydroxidlösung eingetragen und nach 30 min unter Rühren im Eisbad mit 20 g Epichlorhydrin behandelt. Nach weiteren 30 min und gelegentlichem Umrühren wurde das Reaktionsgemisch dann auf dem Wasserbad zunächst 30 min auf 40—45°C und dann abschliessend noch 60 min auf 60—75°C erwärmt. Der erzielte vernetzte PVA (PVA-X-20) wurde

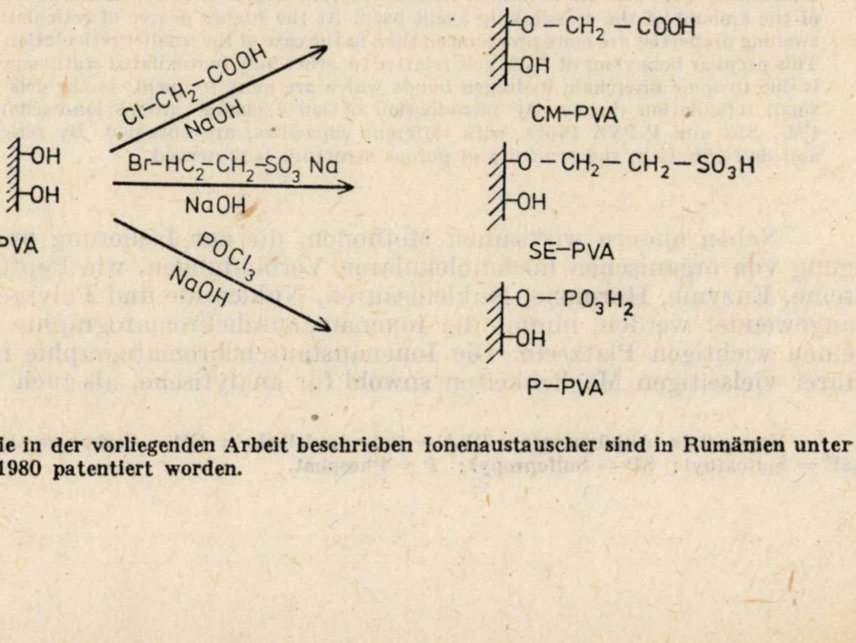

* Die in der vorliegenden Arbeit beschrieben Ionenaustauscher sind in Rumänien unter nr. 74486/1980 patentiert worden.

sodann auf dem Büchner-Trichter an der Wasserstrahlpumpe bis zur völligen Entfernung des Natriumhydroxids gewaschen*.

In der gleichen Weise wurden noch drei weitere PVA-Verbindungen mit unterschiedlichem Vernetzungsgrad, und zwar PVA-X-5, PVA-X-10 und PVA-X-30 hergestellt, wobei an Stelle der 20 g Epichlorhydrin diesmal 5, 10, respektive 30 g zur Anwendung gelangten.

Für die darauffolgenden Synthesen der verschiedenen Ionenaustauscher verwendeten wir den PVA-X-20 mit einer Körnergrösse von 0,1—0,4 mm.

Bei der Synthese der PVA-Ionenaustauscher berücksichtigten wir die von Schell und Gheție [8,9] im Falle der analogen Agarose-Ionenaustauscher gemachten Angaben, wobei einige Reaktionsbedingungen aber auch etwas abgeändert wurden.

Darstellung des vernetzten CM—PVA. 100 ml in destilliertem Wasser abgesetztes perlförmiges Gel von vernetztem PVA wurden an der Wasserstrahlpumpe abgenutscht, darauf in einem Berzelius-Becher mit 100 ml eisgekühlter 10 N NaOH-Lösung behandelt und nach 30 min Aufbewahrung im Eisbad unter Rühren mit 20 g in 10—15 ml destilliertem Wasser gelöster Monochloressigsäure versetzt. Danach wurde das Reaktionsgemisch auf dem Wasserbad 100—200 min auf 65—70°C erhitzt und abschliessend das Reaktionsprodukt bis zur völligen Entfernung des NaOH (neutrale Reaktion des Waschwassers) gewaschen. Zwecks Aktivierung wurde das Reaktionsprodukt für einige Minuten mit Eisessig behandelt und dann mit viel Wasser neutral gewaschen.

Durch Anwendung von 40 g Monochloressigsäure wurde ein Produkt mit einer höheren Austauschkapazität erhalten.

Darstellung des vernetzten P—PVA. In 100 ml eisgekühlte 10 N NaOH-Lösung wurden 100 ml in destilliertem Wasser abgesetztes perlförmiges Gel des vernetzten PVA eingetragen und unter gelegentlichem Rühren 25—30 min stehen gelassen. Darauf wurde unter Rühren tropfenweise (Tropftrichter) 90 ml einer aus 30 ml $POCl_3$ und 60 ml Äthyläther bestehenden Mischung hinzugegeben, wobei die Tropfgeschwindigkeit so gehalten wurde, dass die Temperatur des Reaktionsgemisches 30—35°C nicht überschritt (Reaktionsdauer etwa 60—90 min). Das Reaktionsprodukt wurde nach Beendigung der Reaktion in kaltem Wasser aufgeschwemmt und dann auf dem Büchner-Trichter an der Wasserstrahlpumpe bis zur Erzielung neutraler Waschwasser gewaschen.

Ein Produkt mit höherer Austauschkapazität wurde erzielt, indem 100 ml perlförmiges PVA-X-20-Gel in 150 ml 10 N NaOH-Lösung eingetragen und wie weiter oben mit einer aus 45 ml $POCl_3$ und 90 ml Äthyläther bestehenden Mischung behandelt wurden.

Darstellung des vernetzten SE-PVA. 100 ml in destilliertem Wasser abgesetztes perlförmiges Gel von vernetztem PVA wurden an der Wasserstrahlpumpe abgenutscht und in 100 ml eisgekühlte 10 N NaOH-Lösung eingetragen. Nach 30 min und gelegentlichem Umrühren wurden sodann 15 g Natriumbromäthylsulfonat in 30 ml Wasser unter Rühren hinzugefügt und darauf 3 Stunden in Stichstoffatmosphäre auf dem Wasserbad bei 60°C erhitzt. Abschliessend wurde das Reaktionsprodukt ausgiebig mit destillieetem Wasser gewaschen, dann zwecks Aktivierung in 150—200 ml 0,5 N H_2SO_4 für einige Minuten eingetragen und abschliessend mit destilliertem Wasser bis zur neutralen Reaktion des Waschwassers gewaschen.

Ein Produkt mit höherer Austauschkapazität wurde erhalten, indem wie weiter oben verfahren, doch 130 ml 10 N NaOH-Lösung und 20 g Natriumbromäthylsulfonat zur Anwendung gelangten.

Die *Austauschkapazitäten* der erzielten Ionenaustauscher wurden durch potentiometrische Titration mit 0,1 N NaOH-Lösung ermittelt, wobei 5 ml Gel verwendet wurden und die Austauschkapazitäten pro ml Gel ausgedrückt sind.

Das *Wasseraufnahmevermögen* (water regain) wurde wie üblich bestimmt, [15] indem eine genau abgewogene Menge der trockenen PVA-Verbindung zum Quellen in destilliertes Wasser eingetragen, dann an der Wasserstrahlpumpe abgenutscht und schliesslich erneut abgewogen wurde. Die Ergebnisse sind in g H_2O/g Trockensubstanz ausgedrückt.

Der in Prozenten ausgedrückte *Feuchtigkeitsgehalt* (g H_2O/g Trockengewicht) wurde bestimmt, indem eine bestimmte Menge der betreffenden PVA-Verbindung gleich nach Erzielung der Gewichtskonstantz bei 105 °C und nach 24 Stunden Aufbewahrung in offenem Gefäss bei Zimmertemperatur genau abgewogen wurde.[16]

Das *Quellvolumen* oder *Quellvermögen* wurde bestimmt, indem eine bekannte Menge der zu untersuchenden PVA-Verbindung in einem Messzylinder in destilliertem Wasser zum Quellen belassen und dann nach beendetem Quellen das erzielte Gelvolumen abgelesen wurde.[17] Die erzielten Ergebnisse sind in ml Gel/g Trockensubstanz ausgedrückt.

---

* Der Buchstabe X weist darauf hin, dass der PVA vernetzt ist, während die darauffolgende Zahl die Menge des zur Vernetzung von 100 g PVA verwendeten Epichlorhydrins (in g) angibt.

Die *Trocknung* der PVA-Gele wurde so, wie es von Schell undGheţie[18,19] für Agarosederivate beschrieben worden ist, durch schrittweise Entwässerung mittels Aceton vorgenommen.

Die *IR-Spektralanalyse* wurde vorgenommen, nachdem die vernetzten PVA-Verbindungen erst 1 Stunde auf 105°C zwecks völliger Entfernung des adsorbierten Wassers erhitzt worden waren, so dass die charakteristischen Banden der assoziierten OH-Gruppen nur von den interkatenaren Wasserstoffbrücken herrühren konnten. Die Bestimmungen wurden mit Hilfe eines IR-Spektralphotometers (Specord IR 75, C. Zeiss, Jena) ausgeführt, wobei Proben zu 2,75 mg vernetztem PVA, die zusammen mit 400 mg KBr zu Pillen verarbeitet worden waren, zur Anwendung gelangten.

Die rasterelektronenmikroskopischen Untersuchungen fanden an mit Chrom einheitlich metallisierten Proben statt, deren Metallschicht eine Dicke von 1000 Å[20] aufwies.

ERGEBNISSE UND DISKUSSIONEN

Durch Vernetzung des perlförmigen PVA mit Epichlorhydrin werden unlösliche Gele mit dichterem oder loserem Netzwerk — je nach der Menge des angewandten Vernetzungsagenten — erhalten. Die Eigenschaften dieser Gele sind in Table 1 widergegeben.

TABELLE 1

Physikalisch-chemische Eingenschaften einiger PVA-Gele mit unterschiedlichem Vernetzungsgrad

Gel-Tpy	Quellvermögen (Quellvolumen) ml Gel/g Trockensubstanz	Wasseraufnahmevermögen (water regain) g H_2O/g Trockensubstanz	Feuchtigkeitsgehalt g H_2O/100 g Trockensubstanz
PVA-X-5	3,33	1,39	5,31
PVA-X-10	3,90	1,86	5,48
PVA-X-20	4,45	2,28	5,66
PVA-X-30	3,90	1,98	3,98

Die so erzielten Gele des vernetzten PVA unterscheiden sich in ihrem Verhalten von anderen in der Chromatographie als stationäre Phasen verwendeten vernetzten Polyhydroxyverbindungen, wie es z. B. die Verbindungen des Dextrans (Sephadex)[21], der Agarose [22] oder der Amylose [23] darstellen, und zwar bezüglich der Abhängigkeit gewisser physikalisch-chemischer Eigenschaften vom Vernetzungsgrad derselben. So verleiht — im Falle der letztgenannten Gele — ein geringer Vernetzungsgrad diesen ausgeprägte hydrophile Eigenschaften. Das lose Netzwerk dieser Gele bedingt ein hohes Quellvermögen (grosses Quellvolumen), eine erhöhte Wasseraufnahmefähigkeit und einen gesteigerten Feuchtigkeitsgehalt, während mit fortschreitendem Vernetzungsgrad eine stetige Verminderung dieser hydrophilen Eigenschaften zu beobachten ist (das Quellvermögen sinkt, es vermindern sich auch die Wasseraufnahmefähigkeit und der Feuchtigkeitsgehalt). Dieses Verhalten ist dadurch zu erklären, dass die erwähnten Polyhydroxylverbindungen sich durch ihre Hydroxylgruppen mit den im Milieu befindlichen Wassermoleküle assoziieren (und diese so auch in das Innere des Raumgitters gelangen), wobei ein bedeutendes Quellen der Gelpartikel hervorgerufen wird. Ein fortgeschrittenerer Vernetzungsgrad vermindert aber die Quellfreudigkeit im wässrigen Milieu, da die Makromoleküle durch die steigende Anzahl von Querverbindungen (Vernetzung) immer enger zusammengehalten werden.

Im Falle der PVA-Gele konnten wir überraschenderweise gerade ein umgekehrtes Verhalten beobachten, und zwar, dass bei geringeren Vernetzungsgraden auch die aquophilen Eigenschaften, wie z. B. das Quellvermögen, weniger stark ausgeprägt waren (Abb. 1). Bei PVA-Gelen mit fortgeschritteneren Vernetzungsgraden aber konnten wir — bis zu einem gewissen Grad der Vernetzung — eine Intensivierung der hydrophilen Eigenschaften (grösseres Quellvolumen, grösseres Wasserafnahmevermögen, grösseren Feuchtigkeitsgehalt) beobachten, wonach die PVA-Gele dann, bei noch höheren Vernetzungsgraden ein normales Verhalten — also eine Verringerung der hydrophilen Eigenschaften — aufweisen. Eine mögliche Erklärung dieser Verhaltensweise der Gele des vernetzten PVA ist weiter unten schematisch dargelegt (Schema I). Das unterschiedliche Verhalten der vernetzten PVA-Verbindugen, gegenüber anderen vernetzten Polyhydroxylverbindungen, kann durch die besondere Verteilung der Hydroxylgruppen, die sich in einer regelmässigen Aufeinanderfolge derselben im kettenförmigen PVA-Molekül äussert, erklärt werden, was die Möglichkeit zur Ausbildung einer grossen Zahl von Wasserstoffbrücken zwischen den Hydroxylgruppen benachbarter PVA-Moleküle schafft. Je weiter die queren Glyzerinätherbrücken voneinander entfernt sind (PVA-X-5), um so grösser ist die Zahl der Wasserstoffbrücken, die sich zwischen den PVA-Kettenmolekülen ausbilden können und eine kompaktere Struktur des dreidimensionalen Netzwerks bewirken. Wenn die Glyzerinätherbrücken (deren Länge etwa 8,34 Å beträgt) etwas dichter beieinander stehen (PVA-X-10, PVA-X-20), so können sich zwischen den PVA-Kettenmolekülen keine Wasserstoffbrücken ausbilden, da diese für ihr Zustandekommen eine Entfernung von 1,0—1,7 Å zwischen den dabei einbegriffenen H- und O-Atomen und eine Entfernung von höchstens 5,5 Å zwischen den betreffenden PVA-Molekülen benötigen, was als Folge eine loser Struktur bedingt. In diesem Fall ist das räumliche Netzwerk also etwas lockerer und es können mit den Wassermolekülen des Milieus Verbindungsbrücken geschlagen werden (Hydratierung der Hydroxylgruppen). Um unsere Hypothese zu überprüfen, nahmen wir die IR-Spektren der PVA-Gele mit dem geringsten Vernetzungsgrad und der kontraktiertesten Struktur (PVA-X-5) und auch derjenigen mit einem fortgeschritteneren Vernetzungsgrad und einer loseren Struktur (PVA-X-20) auf. Aus den am IR-Spektrophotometer erhaltenen Aufzeichnungen konnte festgestellt werden, dass der Frequenzbereich der für die an der Wasserstoffbrückenbildung beteiligten Hydroxylgruppen charakteristischen Bande im Falle des PVA-X-5 bedeutend breiter ist (2980—3650 cm^{-1}), verglichen mit dem an PVA-X-20 erzielten (3090—3610 cm^{-1}), was beim PVA-X-5-Gel aut die Anwesenheit einer grösseren Zahl von an Wasserstoffbrücken beteiligten Hydroxylgruppen schliessen lässt. Andererseits beobachtet man im Falle des PVA-X-20-Gels eine ausgeprägtere Bande bei = 3450 cm^{-1}, die für die Hydroxylgruppen charakteristisch ist, was bei diesem Gel auf eine grössere Zahl von freien OH-Gruppen, als im Falle des PVA-X-5-Gels hinweist.

Aus den beim Rasterelektronenmikroskop erzielten Bildern geht hervor, dass die PVA-Partikel ihre poröse Perlenform auch nach der Vernetzung und Einführung von Ionenaustauschgruppen beibehalten (Abb. 2). An den am Rasterelektronenmikroskop erzielten Abbildungen konnte für die Poren der Gelperlen ein Durchmesser von 0,5—3,8 μ festgestellt werden.

Tabelle 2 enthält einige Eigenschaften der sauren Ionenaustauscher, die vom PVA-X-20-Gel ausgehend erzielt wurden.

TABELLE 2

Einige physikalisch-chemische Eigenschaften der sauren Ionenaustauscher, die vom vernetzten PVA erzielt wurden.
(Die Buchstaben *a* und *b* beziehen sich auf die erste bzw. zweite Variante der im Kap. „Material und Methodik" angegebenen Versuchsbedingungen)

Gel-Typ	Variante der Synthese	Austauschkapazität		Quellvermögen (Quellvolumen) ml Gel/g Trockensubstanz	Wasseraufnahmevermögen (water regain) g H_2O/g Trockensubstanz
		mval/ml Gel	mval/g Trockensubstanz		
PVA-X-20		0	0	4,45	2,28
CM-PVA-X-20	a	0,060	0,290	4,49	2,29
	b	0,087	0,478	4,83	2,85
SE-PVA-X-20	a	0,017	0,080	4,70	2,70
	b	0,026	0,145	5,55	2,85
P-PVA-X-20	a	0,027	0,123	4,55	3,23
	b	0,044	0,248	9,75	4,50

Aus den in Tabelle 2 zusammengefassten Versuchsergebnissen geht klar hervor, dass durch Einführung der sauren Ionenaustauschgruppen eine Steigerung der hydrophilen Eigenschaften der Gele eintritt. Diese vom vernetzten PVA erzielten Ionenaustauscher bilden weisse, glänzende, poröse Gelperlen mit vorzüglichen mechanischen Eigenschaften.

In einer künftigen Mitteilung werden wir über andere Eigenschaften dieser Ionenaustauscher, wie ihr Verhalten gegenüber osmotischen Schocks, Porösität der Gelperlen u.a.m. berichten.

Die Verfasser danken Herrn Dr. S. Moldoveanu für die Ausführung der IR-Spektralanalysen und die wertvollen Ratschläge sowie Frau Elena Iaport für die technische Unterstützung.

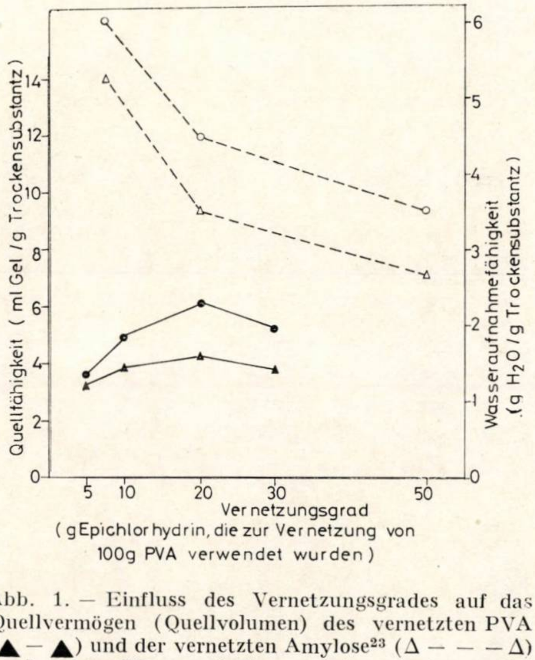

Abb. 1. — Einfluss des Vernetzungsgrades auf das Quellvermögen (Quellvolumen) des vernetzten PVA (▲ — ▲) und der vernetzten Amylose[23] (Δ — — — Δ) sowie auf das Wasseraufnahmevermögen (water regain) des vernetzten PVA (● — ●) und der vernetzten Amylose (0— — — 0)

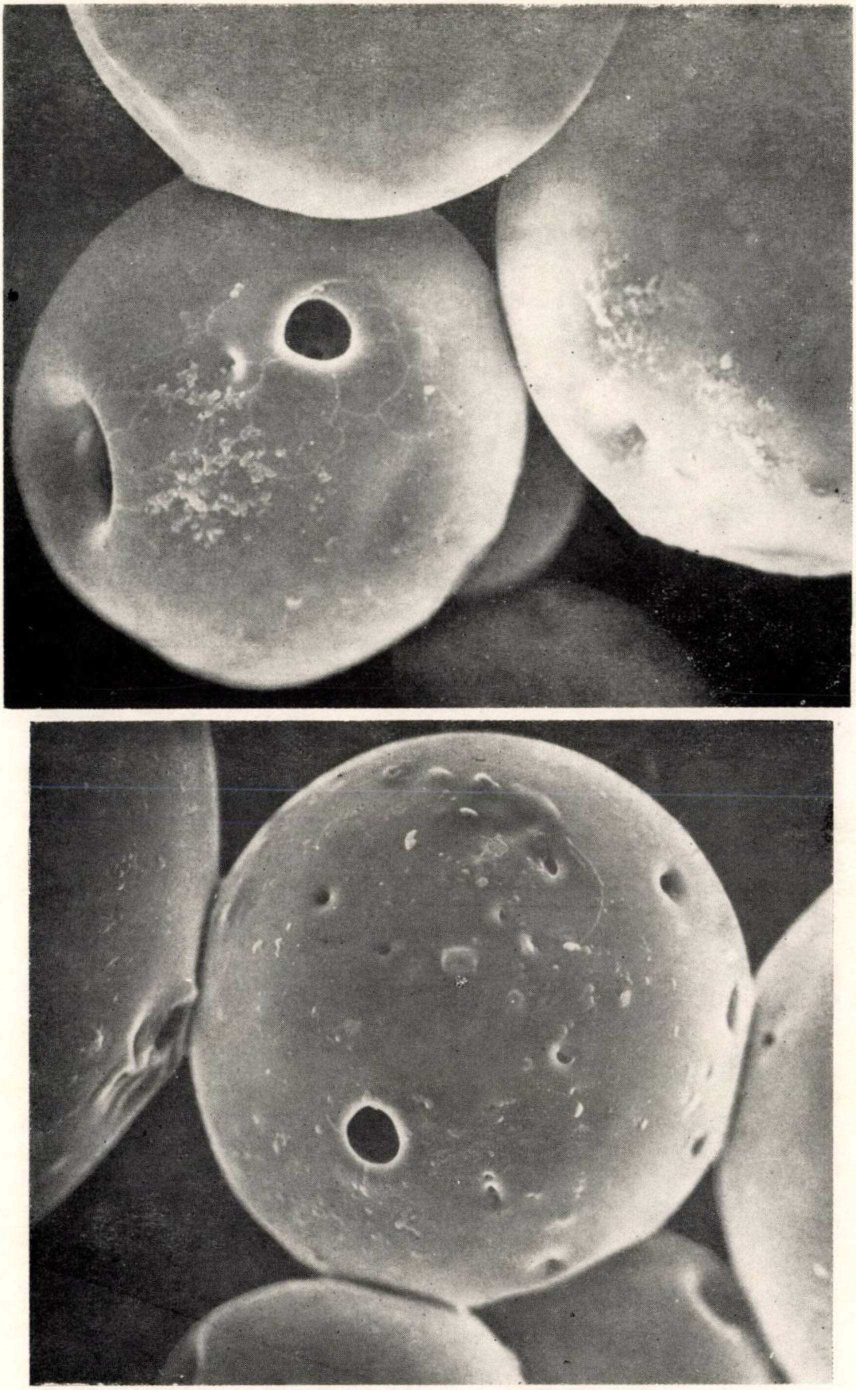

Abb. 2. – Mit dem Rasterelektronenmikroskop erzielte Abbildungen einiger PVA-Partikel.

a) Rasterelektronenmikroskopisches Bild des PVA-X-20 (direkte Vergrösserung 200 mal, Endvergrösserung 450 mal)

b) Rasterelektronenmekroskopisches Bild des CM-PVA-X-20 (direkte Vergrösserung 200 mal, Endvergrösserung 450 mal).

SCHEMA 1

Schematische Darstellung der hypothetischen Struktur von PVA-Gelen mit unterschiedlichem Vernetzungsgrad

Gel-Typ	Hypothetische Struktur eines Molekülfragmentes von vernetztem PVA-Gel (Schematische Darstellung)	Quellvolumen (ml Gel/g Trockensubstanz)	Bemerkungen
PVA-X-5	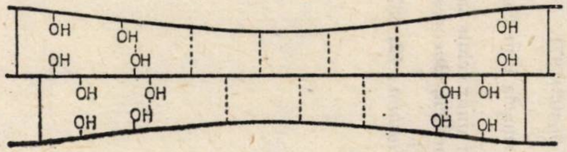	3,33	Geringer Vernetzungsgrad ; kontraktierte Gelstruktur wegen der grossen Anzahl von Wasserstoffbrücken, die sich zwischen den kettenförmigen PVA-Molekülen ausbilden können.
PV-X-10	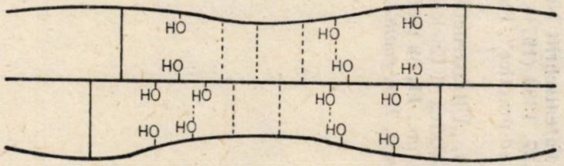	3,90	Weniger kontraktierte Gelstruktur ; die etwas dichter liegenden Glyzerinäterbrücken verhindern die Ausbildung einer grösseren Zahl von Wasserstoffbrücken
PVA-X-20	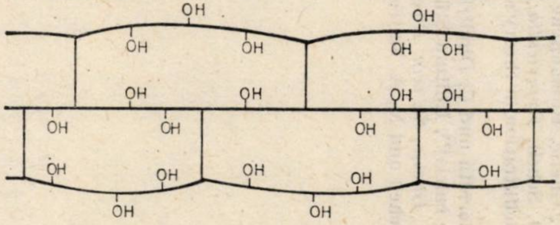	4,45	Fortgeschrittener Vernetzungsgrad ; äusserst lose Raumstruktur ; die zahlreichen Glyzerinäthergruppen verhindern die Ausbildung von Wasserstoffbrücken zwischen den einzelnen PVA-Molekülen.
PVA-X-30	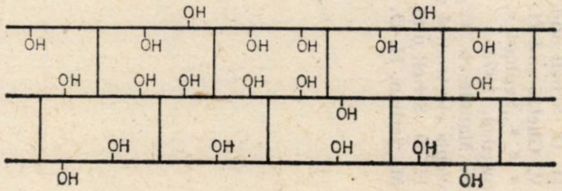	3,90	Noch mehr fortgeschrittener Vernetzungsgrad ; wegen der grossen Anzahl von quervernetzenden Glyzerinätherbrücken kontraktierte Raumstruktur.

— = PVA-Ketten ; | = Glyzerinätherbrücken ; ¦ = Wasserstoffbrücken zwischen OH-Gruppen, die verschiedenen PV ren

A

LITERATUR

[1] C. Sabău, „Schimbul ionic — teoria și aplicațiile sale în chimia analitică", Editura Academiei R.S. România, București, 1967.

[2] * * * "Sephadex Ion Exchangers", Pharmacia Fine Chemicals, Uppsala, Sweden, 1973.

[3] * * * "Serva Cellulose Ionenaustauscher", Serva Entwicklungslabor, Heidelberg, 1962.

[4] H. D. Schell, T. Bentia und M. A. Mateescu, Rumänische Patentschrift Nr. 65382/1977.

[5] H. D. Schell, M. Șerban, M. A. Mateescu und T. Bentia, *Rev. Roumaine Chim.*, **23**, 1143 (1978).

[6] H. D. Schell, M. Șerban und M. A. Mateescu, Rumänische Patentschrift Nr. 62322/1977.

[7] * * * "Ionenaustauscher auf Zellulosebasis", Reanal, Budapest Ungarn.

[8] H. D. Schell, und V. Ghetie, Rumänische Patentschrift Nr. 52785/1971.

[9] V. Ghetie und H. D. Schell, Rumänische Patentschrift Nr. 52786/1971.

[10] * * * „DEAE-Sepharose CL—6B, CM-Sepharose CL—6B for ion exchange chromatography", Pharmacia Fine Chemicals, Uppsala, Sweden, 1976.

[11] P. G. M. Flodin, P. J. A. O. Johansson und S. A. I. Carlsson, U.S.A. Patentschrift Nr. 3275576/1966.

[12] P. G. M. Flodin, U.S.A. Patentschrift Nr. 3208994/1965.

[13] * * * Aktiebolaget Pharmacia Uppsala (Schweden), B.R.D. Patentschrift Nr. 1443359/1968.

[14] M. Dimonie, M. Georgescu, C. Oprescu, J. Rogoz, D. Emil, M. Corobea und M. Tomescu, Rumänische Patentschrift Nr. 58177/1971.

[15] P. Flodin, „Dextran Gels and their Applications in Gel Filtration", Meijels Bokindustri, Uppsala, Sweden, 1962.

[16] M. E. Carsten, „Ion Exchange Celluloses Bibliography", California Corporation Research, Los Angeles, 1962.

[17] M. Ryban, Z. Brada und I. M. Hais, „Säulenchromatographie an Cellulose-Ionenaustauscher", VEB Gustav Fischer Verlag, Jena, 1966, p. 100.

[18] H. D. Schell und V. Ghetie, Rumänische Patentschrift Nr. 56403/1971.

[19] V. Ghetie und H. D. Schell, *Experientia*, **27**, 1384 (1971).

[20] * * * „Sephadex, Gelfiltration in theory and practice", Pharmacia Fine chemicals, Uppsala, Sweden, 1973.

[21] N. Manolescu, V. Ciocnitu und C. Dimitriu, „Ultrastructura unor celule sanguine în microscopia electronică de baleiaj", Editura Științifică și Enciclopedică, București, 1979.

[22] H. D. Schell und V. Ghetie, *St. cerc. Biochim.*, **11**, 69 (1968).

[23] M. Șerban, H. D. Schell und M. A. Mateescu, *Rev. roum. Biochim.*, **12**, 187 (1975).

Revue Roumaine de Chimie, **26**, *7*, 125–130 (1981)

EXPERIMENTAL STUDIES BEARING UPON THE BEHAVIOUR OF POLYVINYL CHLORIDE IN HEAVY FIELDS OF NUCLEAR RADIATIONS

DOINA GAVRILĂ
Department of Physics, The Polytechnic Institute of Bucharest, Splaiul Independenţei, 313, Romania

Received September 14, 1979

The variation of the breaking elongation and the resistance to traction are studied ; the influence of γ radiation on the electric properties (surface and volume resistivity, dielectric rigidity, permittivity and loss angle tangent) is determined and several correlations are established between these quantities and the polymer structure as determined by infrared spectroscopy.

The first works concerned with polyvinyl chloride belong to Burr and Garrison, who studied the change of mechanical characteristics to irradiation in the reactor. Further on, Byrne et al.[1] studied the mechanical features of nonplastified polyvinyl chloride when irradiated with γ-rays obtained from a ^{60}Co source ; at room temperature and at an over—200 Mrad dose, a slight increase of the resistance to tearing was observed.

Chapiro,[2] Pinner[3], and Miller[4] showed that in the presence of some extra polyfunctional monomers, the reticulation processes predominate over the destructive ones.

If irradiation is carried out in vacuum, the specimens irradiated at over — 20 Mrad doses do not get torn, not even at a 250°C temperature.

Popovic[5] gave some polyvinyl chloride — with plastifier specimens a total γ-ray dose of 150 Mrad and observed that following irradiation both the resistance and elongation to tearing decreased.

The main reaction which develops in irradiated polyvinyl chloride is dehydrochlorination ; the reticulation phenomenon is due just to some reactions of this kind, the reticulated product appearing intensely colored.[6,7]

EXPERIMENTAL

Upon experimenting with polyvinyl chloride, granules for 1 KV isolation (PVC type I) obtained from a K-wert 70 suspension of polyvinyl chloride with plastifier were used.

The characteristic features of type M—2 polyvinyl chloride specially used for cable coverings (PVC type M) were also studied. The plates required for measurements (maximal thickness 1.5 mm) were obtained by high-temperature pressing. Test specimens specific to mechanical and electrical trials were subsequently obtained by punching.

The materials were irradiated by pure γ radiations supplied by a ^{60}Co source (output dose $1.2 \, . \, 10^6$ rad/h) or by an electron beam and by breaking radiations supplied by the 3 MeV linear electron-accelerator.

With the object of evidencing the chemical changes elicited by radiations infrared examinations were resorted to, namely the kalium bromide tablet method.

EXPERIMENTAL RESULTS AND DISCUSSIONS

Figure 1 graphically presents how breaking elongation depends upon the integral absorbed dose in both polymer types.

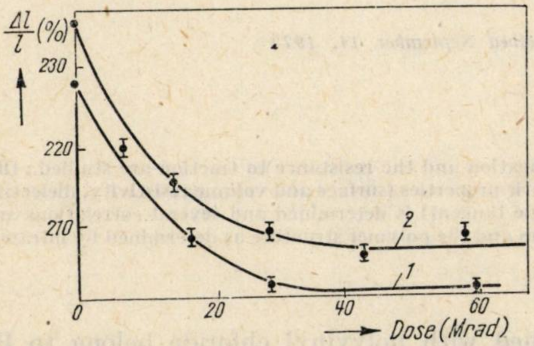

Fig. 1.—Dependence of breaking elongation upon dose. **1.** PVC type I irradiated at the electron accelerator by an output dose of $7.2.10^8$ Rad/h. 2. PVC type M with γ rays (output dose $1.2.10^6$ Rad/h).

Table 1 shows the dependence of limiting tensile strenght upon dose.

TABLE 1

Mean values of limiting tensile strength at different irradiation dose

Dose (Mrad)	0	15	30	45	60	75	100	120
PVC type I	258.7	283.8	250.6	248.3	240.3	242.5	242.8	251.3
PVC type M	218.0	210.6	200.8	198.4	209.4	—	—	—

From the two graphs in figure 1 it may be seen that the shape similar in both curves obtained : up to a ~ 40 Mrad dose, breaking elongation records more marked decreases as compared to doses which exceed this value.

Resistance to tearing generally lessens in both polymers according to the increase of dose (Table 1).

The observations above allowed us to conclude that the degradation phenomena are predominating due to irradiation in the air, this events developing concurrently with slight reticulation processes.

Assumption was made that the reticulation process is due to intermolecular dehydrochlorination ; this reaction may also lead to formation of polyene structures, the existence of alyl and polyenyl radicals being confirmed by Salovey et al.[7]

This mechanism was also corroborated by the infrared spectra obtained, which showed a slight increase of the absorption maxima corresponding to the double vinyl linkings (910 cm^{-1}) and to the 945 cm^{-1} stripe attributed to the allyl radicals.

The degradation process is mainly a consequence of the fact the specimens were irradiated in the air; oxygen interferes leading to breakage of the principal catenary as proved by the appearance of CO (1.730 cm^{-1}) and OH (3.450 cm^{-1}) groups. One should also mention that in type I PVC color changes occur which go intensifying as the irradiation dose increases, and are assigned to the appearance of polyene groups, a fact also pointed out by other authors.[8]

The electrical characteristics of irradiated polyvinyl chloride have been less studied so far than the mechanical features. That is why they are granted special attention in the present work.

The variation of irreversible changes of the electrical characteristics of polyvinyl chloride types I and M was followed up according to both the whole irradiation dose and the output dose. The results related to the dependence of volume and respectively surface resistivities upon the irradiation dose are given in figure 2.

The analysis of these results shows that both parameters decrease as the dose increases, a fact which points out that in both polymers conductivity grows accordingly.

It may be observed that the decrease of surface resistivity is more marked as against the fall of volume resistivity. This phenomen is undoubtedly accounted for by the more intense degree of degradation phenomena elicited at the polymer surface by the action of the external factors which influence this parameter: moisture, atmospheric oxygen, impurities, etc.

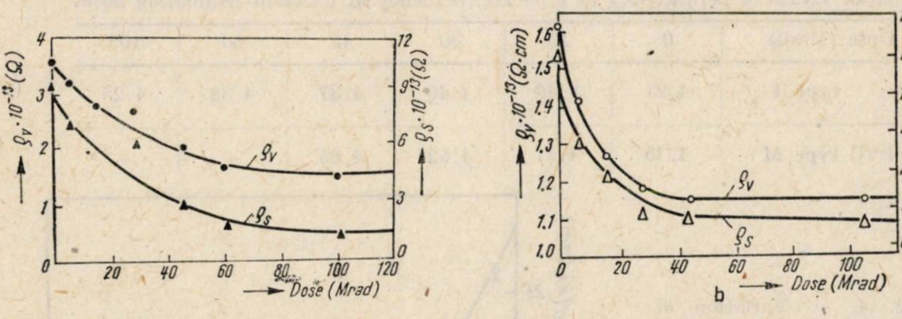

Fig. 2. — Dependence of volume and respectively surface resistivity upon absorbed dose; a. PVC type I; b. PVC type M.

It is already known that the increase of polymer material conductivity through irradiation is owed to the destructive radiation-induced processes which lead to an increase of electron — ion and free radicals. The appearance of allyl-, dienyl- and polyvinyl radicals, in the case of polyvinyl chloride, as evidenced by infrared spectroscopy, has a clearcut significance for the increase in concentration of π mobile electrons, and obviously contributes to the growth of conductivity of the material studied.

The loss angle tangent at the industrial 50 Hz frequency varies according to dose, as seen in figure 3.

One may notice that the curve shape is similar in both cases, which means an increase in losses at low irradiation doses; further on, an ankle occurs on the curve, as well as a stabilizing tendency at large doses. The increase of losses is explained in this case, too, by the appearance of polar CO and OH groups, while the stabilization tendency is attributed to the limited diffusion rate of oxygen within the specimens. The variation of the polarization state of irradiated polyvinyl chloride should represent a cause of permittivity variation following irradiation.

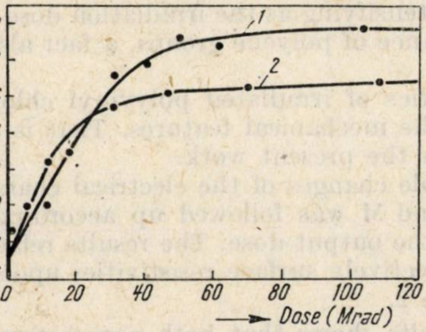

Fig. 3. — Dependence of tg δ at 50 Hz frequency upon dose.
1. PVC type I; 2. PVC type M.

With the aim of checking this hypothesis, permittivity values at 50 Hz frequency were calculated at different doses, and then summarized in table 2.

TABLE 2

Mean values of permittivity at a 50 Hz frequency at different irradiation doses

Dose (Mrad)	0	15	30	45	60	105
type I	4.21	4.40	4.49	4.37	4.33	4.25
PVC type M	4.45	4.57	4.52	4.65	—	—

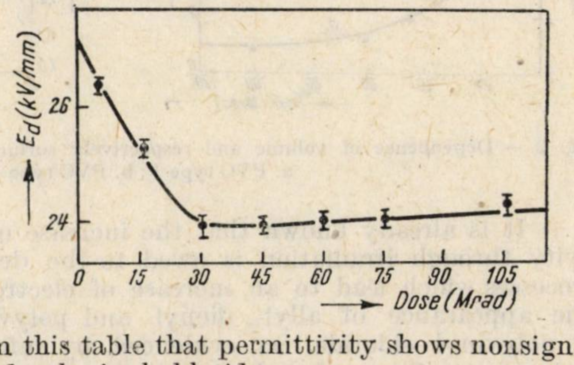

Fig. 4. — Variation of dielectric rigidity of irradiated PVC type I according to irradiation dose.

It may be inferred from this table that permittivity shows nonsignificant variations in irradiated polyvinyl chloride.

Another parameter which is influenced by the emergence of ions, electrons and free radicals is dielectric rigidity (Fig. 4).

At the beginning, a slight decrease of rigidity followed by a bend and further on by a slight increase may be seen on the curve.

As a matter of fact, the increase of carrier concentration leads to a fall in the electric penetration pressure due to both the phenomenon of thermic piercing and intrinsic piercing. As mentioned before, one of the aims of this work was to study the way the irreversible changes of the electrical characteristics of irradiated polymers depend on the output dose used. To this end, type I PVC irradiations were carried out by means of electron accelerator in the air, at a total dose of 30 Mrad.

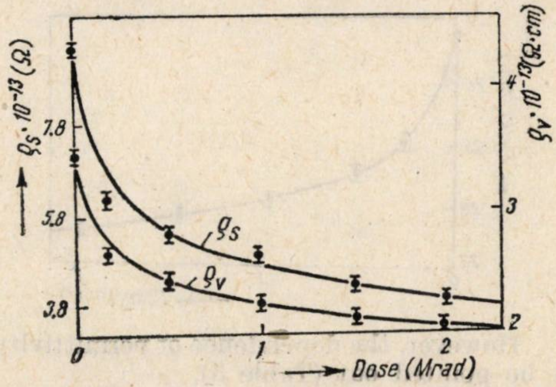

Fig. 5. — Variation of ρ_s and ρ_v in type I PVC according to output dose. Total absorbed dose 30 Mrad.

The variation of volume and surface resistivities in terms of output dose is graphically illustrated in figure 5.

By analyzing these curves it may be seen that both parameters decrease as the output dose gets larger, a fact which points out the correspondent increase of conductivity; a somewhat more marked decrease may be observed with surface resistivity and may be accounted for by some causes analogous to those previously quoted.

The increase of conductivity in irradiated dielectric materials is concordant with the formulas below.[8, 9]

In that circumstance, the increase of conductivity of the irradiated material may be explained just by a correspondent increase of free-pair concentration.

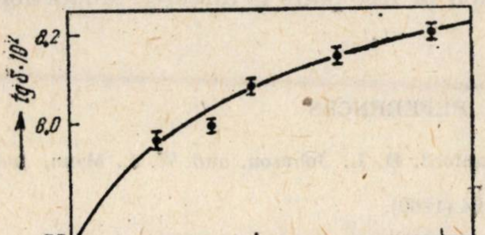

Fig. 6. — Variation of tg δ ($f = 50$ Hz) in terms of output dose in PVC type I. Total absorbed dose = 30 Mrad.

The effects described are much more outstanding when referring to the reversible changes of conductivity, but they also occur, though to a lesser extent, with the irreversible changes of this parameter (see graphs already presented).

Another parameter which varied in terms of output dose is the loss angle tangent at a 50 Hz frequency (Fig. 6).

The increase of losses shows once more the polarizing capacity of the material raised. Confirmation of this fact may be also obtained by analyzing the infrared spectra : for an output dose of 2 Mrad/s the concentration of OH groups increased almost twice as against an output dose of only 1 Mrad/s, at a total dose of 30 Mrad.

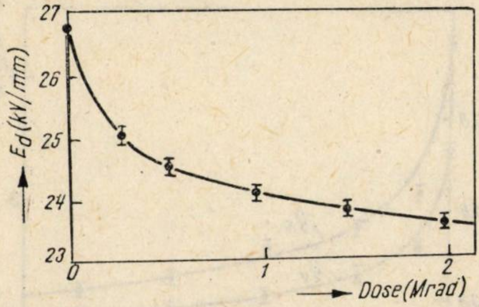

Fig. 7. — Variation of dielectric rigidity of PVC type I according to output dose. Total dose 30 Mrad.

However, the dependence of permittivity upon the output dose could not be pointed out (Table 3).

TABLE 3

Mean values of PVC type I permittivity ($f = 50$ Hz) at various output doses. Integral absorbed dose = 30 Mrad

Output dose (Mrad/s)	0	0.5	0.8	1	1.5	2
	4.22	4.27	4.19	4.15	4.31	4.21

The last parameter whose variation in terms of output dose was studied is dielectric rigidity (Fig. 7).

One may observe the decrease of dielectric rigidity in irradiated polyvinyl chloride type I as the output dose increases, a fact which proves once again that the concentration of free-pairs is directly proportional to the output dose.

REFERENCES

[1] J. Byrne, I. W. Costikyan, V. B. Kanford, D. L. Johnson, and W. L. Mann, *Ind. Eng. Chem. (Analyt. Ed.)*, **45**, 2549 (1953).
[2] A. Chapiro, *J. Chem. Phys.*, **47**, 747, 764 (1960).
[3] A. Pinner, *Nature*, **183**, 1108 (1959).
[4] A. A. Miller, *J. Phys. Chem.*, **63**, 1755 (1959).
[5] B. Popovic, *S.P.E.E.J.*, **26**, 10, 89 (1971).
[6] R. Solovey, J. P. Luongo, *J. Polymer Sci. A—1*, **8**, 209 (1970).
[7] G. J. Atihinson, *J. Appl. Polymer Sci.*, **7**, 1471 (1963).
[8] E. L. Frankevici, *Khim. Vysochih Energhii*, **1**, 567 (1967).
[9] B. S. Iacovlev and E. L. Frankevici, *J. Chem. Phys*, **40**, 1327 (1966).

Revue Roumaine de Chimie, 26, 7, 131–139 (1981)

REACTIVITY OF ACRYLIC MONOMERS. III[1] COPOLYMERIZATION OF N,N-DIMETHYLAMINOETHYL METHACRYLATE WITH N,N-DIETHYLACRYLAMIDE

M. DIMA, S. OPREA and E. DUMITRIU

Department of Chemical Organic Technology, Faculty of Chemical Technology,
Bahlui Stînga 71, Jassy 6600, Romania

Received November 29, 1979

The copolymerization of N,N-dimethylaminoethyl methacrylate (M_1) with N,N-diethylacrylamide (M_2) was investigated. The reactivity ratios, $r_1 = 0.484$ and $r_2 = 0.565$ were determined by various methods. The values of reactivity ratios show an important tendency to alternate of the two monomers. The tendency to alternate was explained on the basis of differences in polarities between the double bonds.

One can notice a high interest in general for copolymers and especially for those of the dimethylaminoethyl methacrylate both in the scientific researches and in practice. The interest shown is determined by the numerous applications of copolymers of this acrylic monomer : coatings,[2–7] thickening agents,[8] additives for oils, [9–13] lacquers, [14–15] photo and electroconductive materials, [11–18] flocculants, etc. Because the applications of the copolymers of dimethylaminoethyl methacrylate present a special interest, the theoretical studies as regards the behaviour of this monomer in the copolymerization process will be of real utility.

The present paper has as aim the study of copolymerization process of N, N-dimethylaminoethyl methacrylate with N, N-diethylacrylamide — monomer which presents a similar field of applications.

EXPERIMENTAL

MATERIALS

N,N-Diethylacrylamide was prepared and purified as previously described.[1]

N,N-Dimethylaminoethyl methacrylate (Merck) was distilled under vacuum and nitrogen to remove the inhibitor. The middle fraction was collected, b.p. 64°/5 mm Hg, $n^{20} = 1.4376$.

2,2′-Azobis (isobutyronitrile), (AIBN), was used after three recrystallizations from ethanol. A stock solution of 0.2% AIBN in dioxane was prepared and stored at room temperature. The used dioxane was refluxed on natrium wire after which it was distilled.

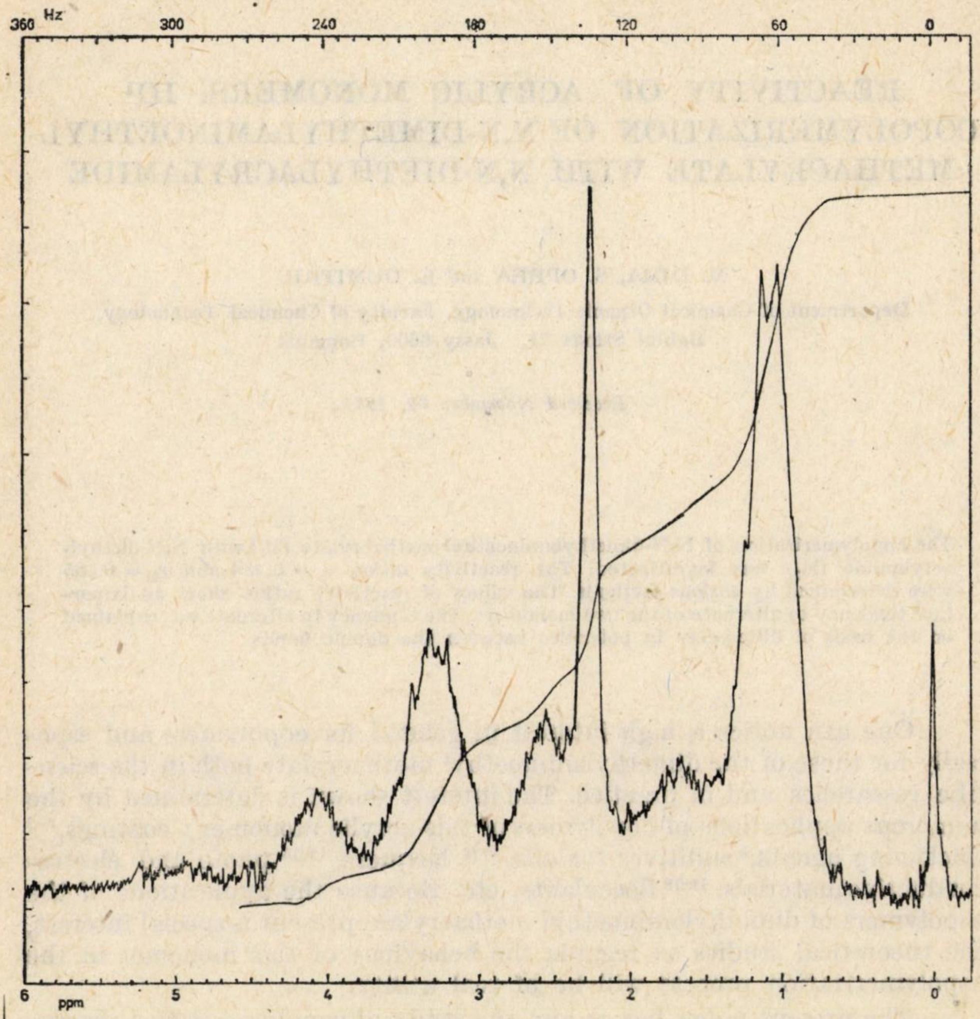

Fig. 1.—NMR spectra for the dimethylaminoethyl methacrylate-diethylacrylamide copolymer (29.4% mole dimethylaminoethyl methacrylate).

COPOLYMERIZATION

The copolymerization of dimethylaminoethyl methacrylate with diethylacrylamide was carried out in dioxane solution in a similar manner as previously described.[1] The copolymers obtained at low conversions were purified by reprecipitation from the dioxane-light petroleum system (solvent and nonsolvent), then they were dried at 50°C under vacuum.

The copolymer compositions were determined by NMR analysis on a JEOL C-60 HL spectrometer. In figures 1 and 2 the spectra of the two copolymers are shown. The reaction conditions and the results are presented in table 1.

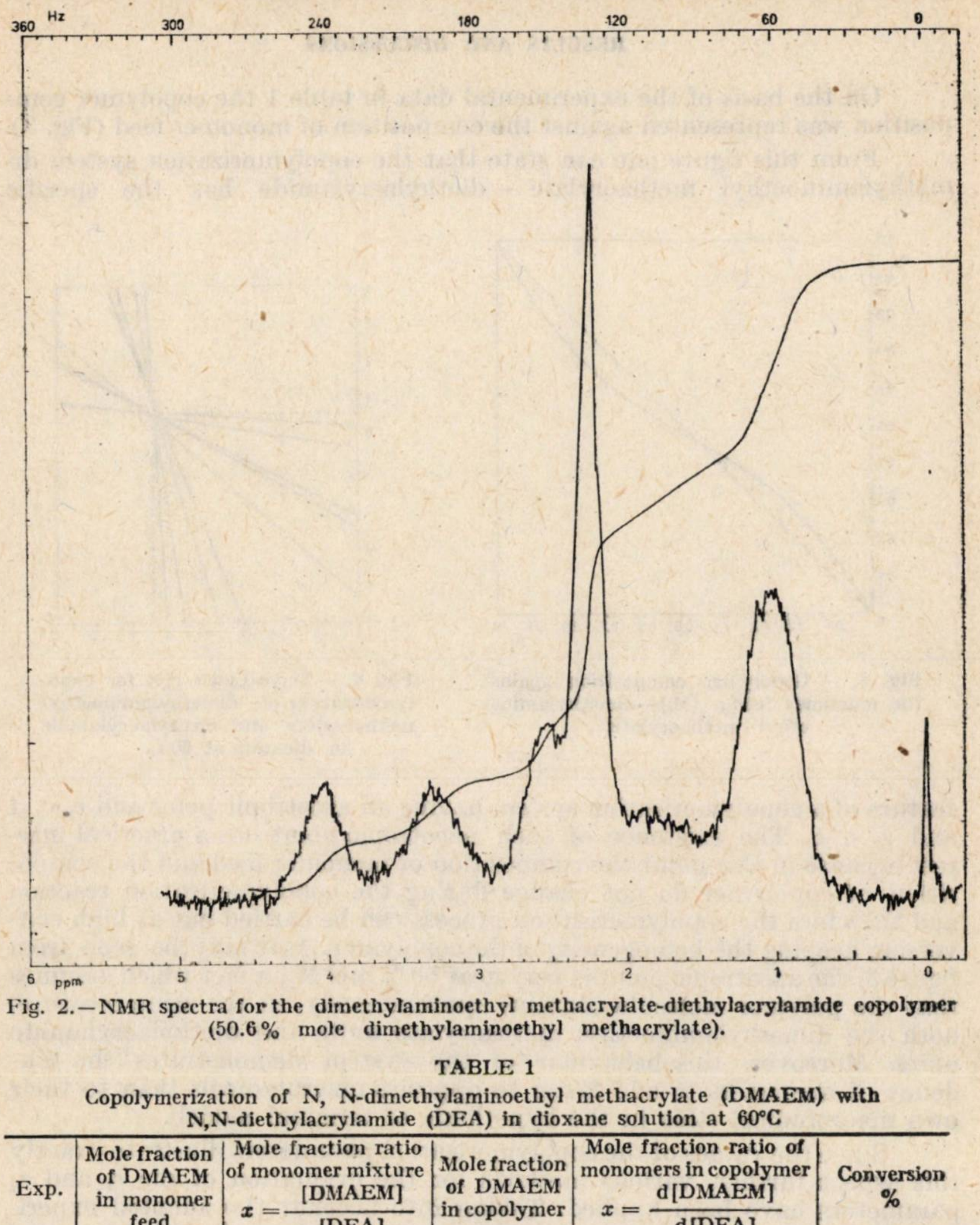

Fig. 2.—NMR spectra for the dimethylaminoethyl methacrylate-diethylacrylamide copolymer (50.6 % mole dimethylaminoethyl methacrylate).

TABLE 1

Copolymerization of N, N-dimethylaminoethyl methacrylate (DMAEM) with N,N-diethylacrylamide (DEA) in dioxane solution at 60°C

Exp.	Mole fraction of DMAEM in monomer feed	Mole fraction ratio of monomer mixture $x = \frac{[DMAEM]}{[DEA]}$	Mole fraction of DMAEM in copolymer	Mole fraction ratio of monomers in copolymer $x = \frac{d[DMAEM]}{d[DEA]}$	Conversion %
1	0.1	0.111	0.138	0.160	8.41
2	0.2	0.250	0.294	0.416	8.17
3	0.3	0.429	0.361	0.565	6.67
4	0.4	0.667	0.414	0.706	7.16
5	0.5	1.000	0.506	1.024	9.15
6	0.6	1.500	0.543	1.188	7.59
7	0.7	2.333	0.619	1.625	8.23
8	0.8	4.000	0.723	2.610	7.38
9	0.9	9.000	0.838	5.173	6.30

RESULTS AND DISCUSSIONS

On the basis of the experimental data in table 1 the copolymer composition was represented against the composition of monomer feed (Fig. 3).

From this figure one can state that the copolymerization system dimethylaminoethyl methacrylate — diethylacrylamide has the specific feature of a copolymerization system having an azeotropic point and $r_1 < 1$ and $r_2 < 1$. The existence of such azeotropic point has a practical interest because in this point the composition of monomer feed and the composition of copolymer do not change during the copolymerization reaction and therefore the copolymerization process can be carried out at high conversion keeping the homogeneity of the copolymer. As it may be seen from figure 3, the azeotropic point is very near 50 % mol M_1, a fact which assumes that the polymer molecule contains approximately, in the same measure, both the dimethylaminoethyl methacrylate units and diethylacrylamide units. Moreover, this behaviour of the system demonstrates the tendency of monomers to add faster to opposite macroradicals than to their own macroradical (this in the hypothesis of terminal model).

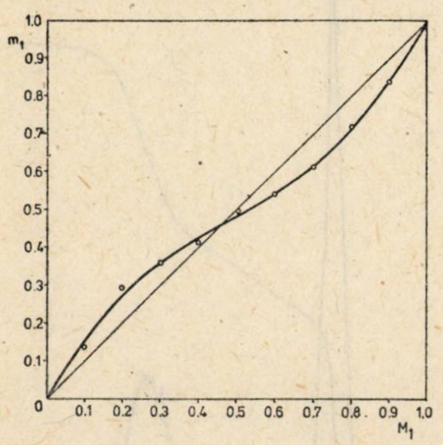

Fig. 3. — Copolymer composition against the monomer feed; (M_1)—dimethylaminoethyl methacrylate.

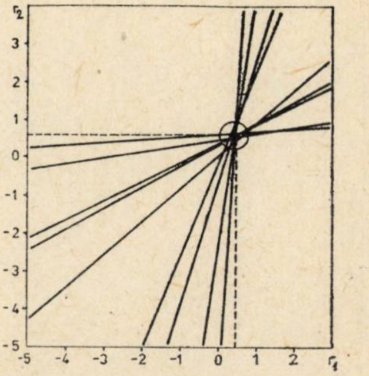

Fig. 4. — Mayo-Lewis plot for copolymerization of dimethylaminoethyl methacrylate and diethylacrylamide in dioxane at 60°C.

Since the values of the copolymerization parameters illustrate exactly this aspect further, various methods for the evaluation of the r_1 and r_2 parameters have been applied. Taking into account the adopted experimental technique, the methods used for the copolymerization parameter evaluation are based on the differential equation of composition.

$$\frac{d[M_1]}{d[M_2]} = \frac{[M_1]}{[M_2]} \cdot \frac{r_1[M_1] + [M_2]}{[M_1] + r_2[M_2]}$$

The first method applied, the interception method,[19] leads to the following graphical representation (Fig. 4).

From the interception of the experimental lines the r_1 and r_2 values have been established (Table 2). Because the estimation of the r_1, r_2 values is made with some inaccuracy by this method, in order to confirm the values obtained, the Fineman-Ross method[20] can be applied (Figure 5).

As it may be observed from figure 5, the Fineman-Ross method was applied in both ways while the lines were drawn using the least square method.

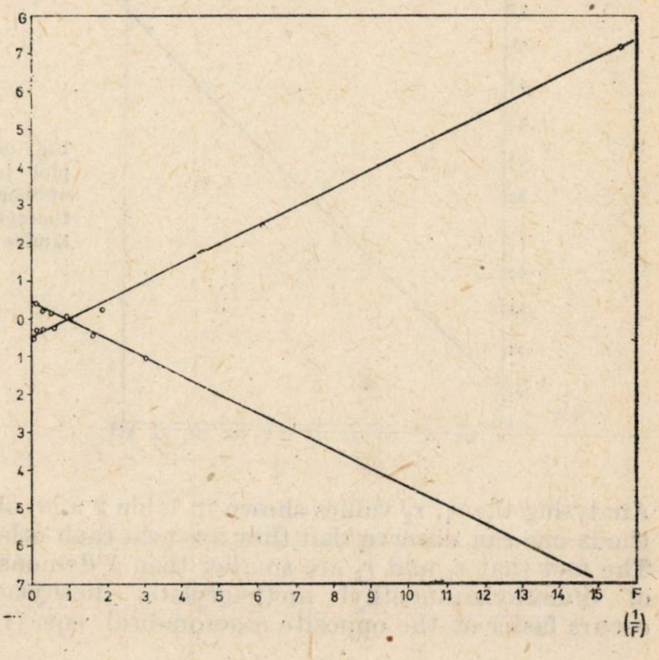

Fig. 5. — Fineman-Ross plot for copolymerization of dimethyl-amino-ethyl methacrylate and diethylacrylamide in dioxane at 60°C.

The values of copolymerization parameters are shown in table 2, too. One can observe that the two methods give similar values for the reactivity ratios. As it is known, another disadvantage of the Fineman-Ross method (if one except the wellknown disadvantages of the differential methods) is due to the unequal weight of the experimental data. The data obtained under extreme experimental conditions have the greatest influence on the

TABLE 2

Copolymerization parameters of N,N-dimethylaminoethylmethacrylate-diethylacrylamide system

Monomer	Reactivity ratio	Mayo-Lewis method	Fineman-Ross method	Kelen-Tüdös method	Q	e
Dimethyl-amino-ethyl methacrylate	r_1	0.49	0.497	0.484	1.346 [23]	0.751
Diethyl-acrylamide	r_2	0.55	0.574	0.565	0.19 [22]	−0. 64

slope of the line, therefore the Kelen-Tüdös method[21] was applied; this method provides a much uniform distribution of the experimental data. The experimental line was obtained by the least square method and from its parameters (slope and interception), r_1 and r_2 were calculated (Table 2).

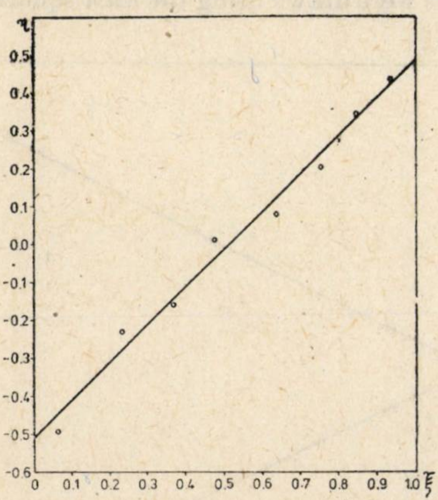

Fig. 6. — Kelen-Tüdös plot for copolymerization of dimethylaminoethyl methacrylate and diethylacrylamide in dioxane at 60°C.

Analysing the r_1, r_2 values shown in table 2 and obtained by various methods one can observe that they are near each other and very near to 0.5. The fact that r_1 and r_2 are smaller than 1 demonstrates that the addition of dimethylaminoethyl methacrylate, diethylacrylamide respectively, occurs faster at the opposite macroradical, eqs. (1) and (2):

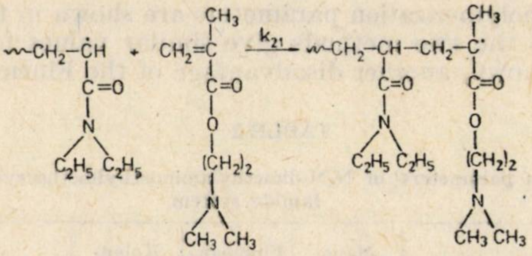

(1)

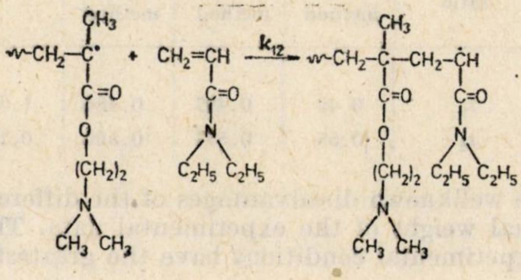

(2)

more than the addition at its macroradical, eqs. (3) and (4).

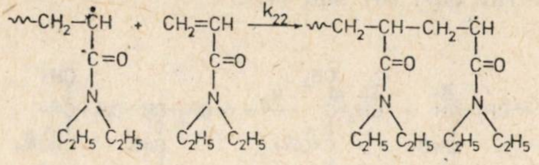

(3)

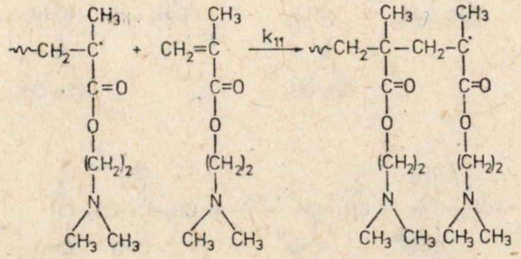

(4)

Also, as in the propagation step, the growing macroradical ended in any of these two monomers prefers the opposite monomer, one can suppose a polarization of the monomers. Such a polarization is possible because the substituents of the two monomers, by their nature, cause the electrons of the double bond to take part in the electronic system of the substituents. As it was shown in a previous paper,[22] the diethylacrylamide molecule is such polarised that the vinyl group is presented as the negative part of a dipole, while the substituent due to its electron-donating nature represents the positive part.

In a similar manner one can suggest a positive polarization of the double bond of dimethylaminoethyl methacrylate, scheme (5):

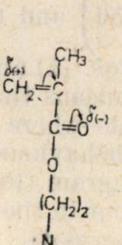

(5)

This supposition regarding the electronic influences of the substituents can be confirmed by the *e* values from the Price-Alfrey scheme (see Table 2). As a consequence of the above mentioned statements, we can attribute to the dimethylaminoethyl methacrylate-diethylacrylamide copolymerization system a behaviour with a strong tendency to alternate the monomer units in the copolymer chains ; thus, the propagation step of the chain may be illustrated by the eqs. (6) and (7) :

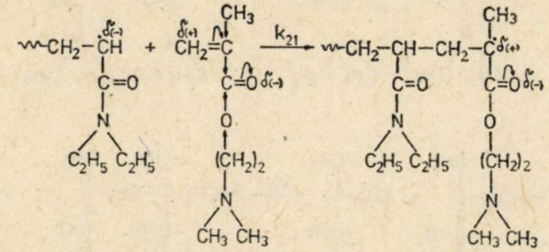

(6)

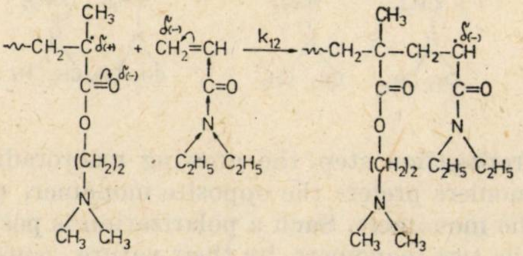

(7)

Such a tendency to alternate has been observed also in the case of the copolymerization of diethylacrylamide with methyl acrylate [22] both by the copolymerization data and by the NMR analysis of the sequence distribution. But, if we referred strictly to the values of the copolymerization parameters it would be shown that in our case r_1 $\left(r_1 = \frac{k_{11}}{k_{12}} = 0.48\right)$ is smaller than r_2 $\left(r_2' = \frac{k_{22}}{k_{21}} = 0.56\right)$ and therefore between the two preferred additions described by eqs. (1) and (2), the addition described by eq. (2) is much preferred. This means that one will find a number of sections in the copolymer molecule where two or more diethylacrylamide units succeed each other. This behaviour in the sequences distribution is reflected in the composition diagram (Fig. 3), by the fact that the inflexion point is near 50 % mol M_1 but in the range of lower concentrations of the dimethylaminoethyl methacrylate.

Another interesting observation results if one compares the reactivity ratios obtained for the system dimethylaminoethyl methacrylate-diethylacrylamide (by Fineman-Ross method $r_{\mathrm{ester}} = 0.497$ and $r_{\mathrm{amide}} = 0.574$) with those obtained for the system methyl acrylate-diethylacrylamide [22] ($r_{\mathrm{ester}} = 0.52$ and $r_{\mathrm{amide}} = 0.40$). One may easily state that the r_{ester} values are roughly identical while the r_{amide} values differ for the two systems, being greater for the dimethylaminoethyl methacrylate-diethylacrylamide system. If the penultimate units have no influence and the ended diethylacrylamide macroradical shows the same reactivity in both systems, it means that the magnitude differences between the two values of r_{amide} are due to the different reactivities of the acrylic esters. Evidently, in the first analysis, the methyl acrylate is more reactive than the dimethylaminoethyl methacrylate, the later having a bulky ester group and a substituent in the α position.

REFERENCES

[1] Part. II: Sp. Oprea, E. Dumitriu and M. Dima, *Rev. Roumaine Chim.*, **25**, 605 (1980).

[2] J. M. Craven, U.S. Part. 3, 689, 470, 16 Oct. 1973; *Chem. Abstr.*, **80**, 97417 (1960).

[3] Mitsubishi Rayon Co., Jap. Pat. 74 10, 526, 11 Mar. 1974; *Chem. Abstr.*, **81**, 122964 (1974).

[4] Nippon Oils and Fatts Co., Ltd., Jap. Pat. 74 10, 815, 13 Mar. 1974; *Chem. Abstr.*, **81**, 123097 (1974).

[5] Soken Chemical Engineering Co., Ltd., Jap. Pat. 75 134, 030, 23 Oct. 1975; *Chem. Abstr.*, **84**, 75866 (1976).

[6] Konsai Paint Co., Ltd., Jap. Pat. 74 08, 578, 25 Jan. 1974; *Chem. Abstr.*, **81**, 65355 (1974).

[7] Toa Gosei Chemical Industry Co., Ltd., Jap. Pat. 72 45, 176, 14 Nov. 1972; *Chem. Abstr.*, **80**, 28611 (1974).

[8] Styrene Co-Polymers Ltd., Brit. Pat. 1, 057, 723, 8 Feb. 1967; *Chem. Abstr.*, **66**, 116656 (1967).

[9] A. Morduchowitz, I. D. Rubin, Ger. Pat. 2, 422, 609, 4 Dec. 1975; *Chem. Abstr.* ,**84**, 124326 (1976).

[10] A. Morduchowitz and I. D. Rubin, U.S. Pat. 3, 816, 315, 11 Jun. 1974; *Chem. Abstr.*, **81**, 93866 (1974).

[11] W. P. Dunworth, U. S. Pat. 3, 336. 124, 15 Aug. 1967; *Chem. Abstr.*, **67**, 83698 (1967).

[12] G. J. Briggs, E. J. Buckler and Y. K. Wei, Ger. Pat. 2, 528, 142, 15 Jan. 1976; *Chem. Abstr.*, **84**, 136975 (1976).

[13] E. M. Stanley and G. B. Tupper, S. Afr. Pat. 70 07, 570, 29 Jun. 1971; *Chem. Abstr.*, **76**, 143177 (1971).

[14] W. M. Finn and F.L.Mc Carthy, U.S. Pat. 3, 541, 037, 17 Nov. 1968; *Chem. Abstr.*, **74**, 32780 (1971).

[15] Toa Gosei Chemical Industry Co., Ltd., Jap. Pat. 71 11, 429, 23 Nov. 1971; *Chem. Abstr.*, **76**, 7384 (1972).

[16] S. Tomari, H. Yamagami, Y. Sakamoto and K. Tsuchiya, Jap. Pat. 73 102, 633, 24 Dec. 1973; *Chem. Abstr.*, **81**, 31850 (1974).

[17] A. E. Gilchrist, U.S. Pat., 3, 922, 212, 25 Nov. 1975; *Chem. Abstr.*, **84**, 75862 (1976).

[18] A. M. Usmani, U.S. Pat. 3, 776, 724, 4 Dec. 1973; *Chem. Abstr.*, **81**,, 56635 (1974).

[19] F. R. Mayo and F. M. Lewis, *J. Amer. Chem. Soc.*, **66**, 1594 (1944).

[20] M. Fineman and S. D. Ross, *J. Polymer Sci.*, **5**, 259 (1950).

[21] T. Kelen and F. Tüdös, *J. Macromol. Sci.-Chem.*, **A9**, 1 (1975).

[22] E. Dumitriu, Sp. Oprea, S. Maxim, A. Nathanson and M. Dima, *Kolloid Z. —Z. Polymere*, **257**, 1203 (1979).

[23] A. P. Francis, D. H. Solomon and T. H. Spurling, *J. Macromol. Sci.-Chem.*, A8, 469 (1974)

Revue Roumaine de Chimie, 26, 1, 141–149 (1981)

STUDY OF EXTRACTION AND COMPLEXING OF PALLADIUM(II) WITH 1-(*p*-NITROPHENYL), 3-(*p'*-AZOBENZENE)-TRIAZENE AND 1-(*p*-NITRONAPHTHYL), 3-(*p'*-AZOBENZENE)-TRIAZENE

ANDREI FLORIN DĂNEŢ

Department of Analytical Chemistry, Faculty of Chemical Technology, The Polytechnical Institute, Splaiul Independenţei, 202, Bucharest, Romania

Received January 22, 1980

Palladium(II) forms with urotropine and the two reagents (noted as HR), $Pd(C_6H_{12}N_4)R_2$-type complexes. The repartition constant of 1-(*p*-nitrophenyl), 3-(*p'*-azobenzene)-triazene in the chloroform-water system (with a 3% urotropine content) is $2.06.10^3$, and that of its complex with palladium and urotropine is $1.22.10^4$; the extraction constant of palladium is 0.203 and the formation constant, β_2, of the complex in aqueous phase is $10^{24.25}$. The value of the extraction constant of palladium (II) with 1-(*p*-nitronaphthyl), 3-(*p'*-azobenzene)-triazene in chloroform is 1.097 and the conditional formation constant of the palladium complex with this reagent is $3.29.10^{10}$ in 50% alcohol and 3% urotropine. The IR spectra of the reagents and palladium complexes were carried out and the corresponding absorption bands were attributed to the vibration of the Pd–N bond. The derivatograms of the 1-(*p*-nitrophenyl), 3-(*p'*-azobenzene)-triazene and the formed complex were obtained.

The data on complexing palladium(II) ion, as well as other metallic ions, with triazenic derivatives are rather scarce in literature. Palladium complexes with 1,3-diphenyltriazene [1,2] were prepared and characterized and the structure of one of the complexes was determined by means of X-ray diffraction.[3] The triazenic derivatives also form stable complexes with mercury(II),[1,4,5] silver(I),[1,2] copper(I, II) [2,3,5] and nickel(II).[3,6]

This paper represents a study on the complexing equilibria in aqueous phase in the presence of urotropine and the extraction in chloroform of palladium(II) with 1-(*p*-nitrophenyl), 3-(*p'*-azobenzene)-triazene (Cadion A) and 1-(*p*-nitronaphthyl), 3-(*p'*-azobenzene)-triazene (Cadion 2B).

A study was also made on the palladium complexes obtained in the solid state.

The Cadions A and 2B were previously employed in the selective spectrophotometric determination of palladium.[7,8]

EXPERIMENTAL

REAGENTS AND APPARATUS

Palladium perchlorate solution of 200 μg Pd (II)/ml titre in 0.5 N perchloric acid, prepared by solving the corresponding amounts of metallic palladium in a very small quantity of concentrated perchloric acid and then the removing of nitric acid by heating.
10% urotropine-water solution.
Cadion A, Austranal and Cadion 2B, B.D.H., from which the solutions in alcohol and chloroform were prepared.

All the substances were p.a. grade reagents.
The absorption spectra were drawn on a DB model Beckman spectrophotometer and the absorbance measurements were performed with a VSU-2G, Carl Zeiss-Jena apparatus. For the pH measurements, the Radelkis OP-205 pH-meter was employed. The derivatograms were obtained on Paulik, Paulik, Erdey system derivatograph, type 2895.

PROCEDURE

The determination of palladium(II) extraction efficiency as a function of the pH of the aqueous phase and repartition constants of the reagents and palladium complexes. In 100 ml separation funnels, previously dried, 0.1 ml palladium perchlorate solution and 3 ml 10% urotropine solution were introduced and then the volume was brought up to 9 ml. The pH was adjusted for different values with either perchloric acid solution or sodium hydroxyde, the volume being then completed to 10 ml with distilled water. 10 ml reagent solution in chloroform were added and the samples were mechanically stirred for two hours. The distilled water and urotropine solution were formely equilibrated with chloroform, while the reagent solution in chloroform was equilibrated with a 3% urotropine aqueous solution. The palladium extraction efficiency was determined by measuring the absorbances of chloroformic extracts at the wavelength corresponding to the maximum absorbance for the formed complexes.

The repartition constants for the reagents and palladium complexes were calculated on the grounds of solubility of these compounds in the two phases. In doing so, the saturated solutions of the compounds were obtained by mechanical stirring for two hours of the solution with the solid compound added in excess. For determining the solubility in the aqueous phase of the palladium complexes, 10^{-4}M $Pd(ClO_4)_2$ was added in order to regress the complex dissociation. The solutions were then filtered, diluted when necessary, and the absorbance was determined at maximum absorption wavelength. As the molar absorbance of a compound may be different for the two phases, the absorbance measurements were performed only in the organic phase, the saturated solution of the compound in the aqueous phase being extracted with a corresponding volume of organic phase. Having known the molar absorbance of the compounds, their solubilities in the two phases could be determined and the repartition constant calculated from the solubility ratio. The working temperature was 25 ± 0.5°C. Only the repartition constants for Cadion A and its complex with palladium and urotropine were determined by this method, as the Cadion 2B and its complex have too low a solubility in the aqueous phase to be spectrophotometrically measured.

Preparation of the solid state compounds. 0.25 g palladium chloride dissolved in a small quantity of 1N HCl was added to a solution containing 30 g urotropine in 200 ml water. The solution together with the precipitate were brought to boiling (when a fraction of precipitate got dissolved) and added over a hot solution containing 1 g Cadion A, or alternatively 1.16 g Cadion 2B, in 300 ml methylic alcohol. The solution was maintained warm and was stirred for another 0.5 hour. A brick-red precipitate was obtained with Cadion A and a brown one with Cadion 2B; either was then filtered through a G—3 crucible. The complexes are hardly soluble in water, little soluble in alcohol and soluble in benzene, acetone and chloroform. The complexes were washed with distilled water and after drying, with benzene. For the complex with Cadion A, Pd = 11.28% and N = 24.12% and for the one with Cadion 2B, Pd = 10.30% and N = = 21.27%. The most probable formula for these compounds is Pd $(C_6H_{12}N_4)R_2$ (the reagent was noted HR), for the two compounds corresponding, respectively, $Pd_t = 11.36\%$, $N_t = 23.92\%$ and $Pd_t = 10.26\%$, $N_t = 21.59\%$.

RESULTS AND DISCUSSIONS

The spectra of the solutions in chloroform of the Cadion A (1), Cadion 2B (2) and complexes formed with palladium(II) (3,4) in urotropine medium are presented in figure 1.

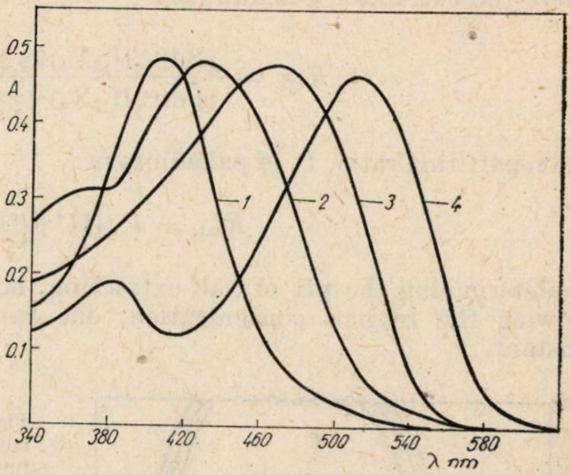

Fig. 1. — The spectra of some solutions in chloroform: $1.5.10^{-5}$M Cadion A and 2B (*1*, *2*) and $0.75.10^{-5}$M complexes formed with palladium and urotropine (*3*, *4*).

The Cadion A has an absorption maximum at 405 nm and its palladium complex at 473 nm. The spectra of the reagents and complexes in benzene and acetone are much alike those in chloroform. The benzene has a hypsochromic effect on the absorption maximum, while the acetone a bathochromic one. The above statement holds for the absorption maxima of both reagent and complex. The combination ratio Pd(II)/reagent in the formed complexes is 1/2 and it was determined by Job[9] method and spectrophotometric titration method. The extraction was made from a 3% urotropine medium. In the absence of urotropine, the extraction efficiency of palladium with the studied reagents decreases drastically. Palladium perchlorate is used, as the palladium(II) ion does not form complexes with the perchlorate ion, that is, the occurrence of any competitive equilibria is avoided.

Under these conditions the palladium is bound within $Pd(C_6H_{12}N_4)^{2+}$ ion, where n is usually 1 and 2 and less probably 3 and 4. For the complexes obtained in the solid state, $n = 1$. The palladium(II) ion forms stable hydroxocomplexes, with the total formation constants $K_1 = 5.01.10^{12}$ and $K_2 = 1.41.10^{26}$.[10] We consider that by co-ordinating the urotropine to the palladium ion (urotropine in great excess), the stability constants of the formed hydroxocomplexes decrease 5—6 orders of magnitude on the analogy of the hydroxocomplexes due to $Ptpy^{2+}$ [11] and $Pt(NH_3)^{2+}$.[12], the palladium(II) ion being similar to the platinum(II). We have concluded that in a reaction medium with a pH value lower than 4, the palladium is practically wholly found as a cation. We consider that the palladium extraction with the studied reagents takes place according to the equilibrium (the compound in the organic phase is noted with 0, while Cadion A and Cadion 2B with HR) :

$$Pd(C_6H_{12}N_4)^{2+} + 2(HR)_0 \rightleftharpoons (Pd\ (C_6H_{12}N_4)\ R_2)_0 + 2H^+ \quad (1)$$

where the extraction constant is :

$$K_{ext.} = \frac{[Pd(C_6H_{12}N_4)R_2]_0[H^+]^2}{[Pd(C_6H_{12}N_4)^{2+}]\ [HR]_0^2} \quad (2)$$

The repartition ratio, *P*, of palladium is :

$$K_{ext.} = P\ ([H^+]^2/[HR]_0^2) \quad (3)$$

By determining the pH of half-extraction, noted as $pH_{1/2}$ ($P = 1$), and knowing the reagent concentration, one can calculate the extraction constant.

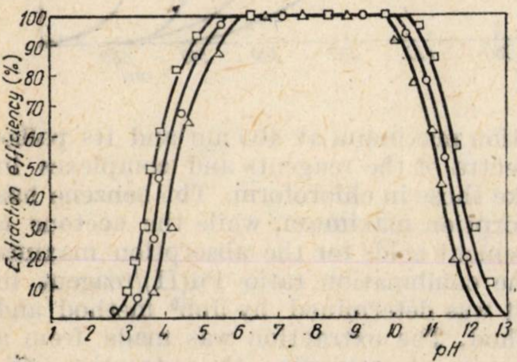

Fig. 2. — The variation of the palladium extraction efficiency as a function of the pH in the aqueous phase, at chloroform extraction of the complex formed with Cadion A and urotropine. The initial concentration in palladium(II) is 1.88.10^{-5}M. The concentrations of the Cadion A solution :

□ – 4.8.10^{-4}M

△ – 1.2.10^{-4}M

○ – 2.4.10^{-4}M

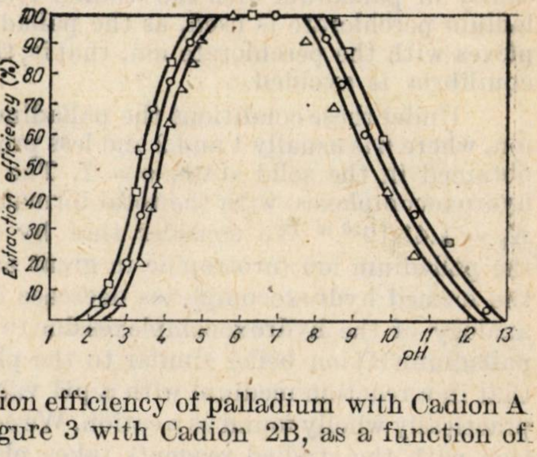

Fig. 3. — The variation of the palladium extraction efficiency as a function of the pH in the aqueous phase, at chloroform extraction of the complex formed with Cadion 2B and urotropine. The initial concentration in palladium(II) is 1.88.10^{-5}M. The concentration of the Cadion 2B solution :

□ – 4.8.10^{-4}M

△ – 1.2.10^{-4}M

○ – 2.4.10^{-4} M

The variation of the extraction efficiency of palladium with Cadion A is presented in figure 2 and in figure 3 with Cadion 2B, as a function of the pH in the aqueous phase.

The values of reagent concentrations together with those of $pH_{1/2}$ and K_{ext} for palladium extraction with Cadion A and Cadion 2B are listed in tables 1 and 2, respectively.

TABLE 1

The reagent concentrations, pH 1/2's and K's for the extraction in chloroform of the palladium complex with urotropine and Cadion A

Reagent concentration	pH 1/2	$K_{ext.}$
$4.8.10^{-4}$M	3.70	0.172
$2.4.10^{-4}$M	3.95	0.218
$1.2.10^{-4}$M	4.25	0.219

Mean value $K_{ext.} = 0.203$

For the most cases, the repartition constant of a compound between two immiscible phases is practically equal to the solubility ratio of the compound in the two phases ; this finding is in good agreement with many experimental data.[13] In table 3, the solubilities and repartition constants of Cadion A and its complex with palladium and urotropine in the chloroform-water system are presented.

TABLE 2

The reagent concentrations, $pH_1/_2$'s and $K_{ext.}$'s for the extraction in chloroform of the palladium complex with urotropine and Cadion 2B

Reagent concentration	$pH_1/_2$	$K_{ext.}$
$4.8.10^{-4}$M	3.30	1.09
$2.4.10^{-4}$M	3.60	1.10
$1.2.10^{-4}$M	3.90	1.10

Mean value $K_{ext.} = 1.096$

TABLE 3

The solubilities and repartition constants of Cadion A and its complex with palladium and urotropine in the $CHCl_3-H_2O$ system

Compound	S. in aq. phase	S. in org. phase	Repartition constant
Cadion A	$8.36.10^{-3}$M	$4.06.10^{-6}$M	$2.06.10^{3}$
The Pd complex	$2.59.10^{-2}$M	$2.13.10^{-6}$M	$1.22.10^{4}$

The formation constant of the -NH- group in the Cadion A molecule was determined spectrophotometrically from the pH influence on the reagent dissociation in a solution of 3% urotropine in chloroform — saturated water, and has a value $K_{HR} = 11.2$.

We assume that the palladium complex formation with the urotropine and studied reagents occurs according to the equilibrium :

$$Pd(C_6H_{12}N_4)^{2+} + 2R^- \rightleftharpoons Pd(C_6H_{12}N_4)R_2 \qquad (4)$$

with a stability constant :

$$\beta_2 = \frac{[Pd(C_6H_{12}N_4)R_2]}{[Pd(C_6H_{12}N_4)^{2+}][R^-]^2} \qquad (5)$$

If P_{MR_2} and P_{HR} are the repartition constants of the complex and reagent respectively, and K_{HR} is the formation constant of the -NH- group from the reagent molecule, one gets the following xpression for $K_{ext.}$:

$$K_{ext.} = \frac{\beta_2 P_{MR_2}}{P_{HR}^2 K_{HR}^2} \qquad (6)$$

Knowing $K_{ext.}$, P_{MR_2} and P_{HR}, as previously determined, one can calculate β_2, which is $10^{24.25}$ for the complex formed by palladium with Cadion A and urotropine.

The conditional formation constant, β_2', of the palladium complex with Cadion 2B and urotropine was calculated by both Sakelaridis's [14] and Klausen's [15] methods. In both cases the determinations were made at a pH value of 7, in a 1–1 alcohol-water and 3% urotropine medium. We assume that, under these conditions, practically the whole amount of palladium is found as hydroxocomplex and the whole amount of reagent as HR. The complex formation equilibrium is thus :

$$Pd(C_6H_{12}N_4)(OH)_2 + 2\,HR \rightleftharpoons Pd\,(C_6H_{12}N_4)R_2 + 2H_2O \qquad (7)$$

with a conditional formation constant :

$$\beta_2' = \frac{[Pd(C_6H_{12}N_4)R_2]}{[Pd(C_6H_{12}N_4)(OH)_2]\,[HR]^2} \qquad (8)$$

The experimental data allowing for the calculation of the Sakelaridis's method are presented in figure 4.

The β_2' mean value for three experimental runs is $3.10.10^{10}$.

The Klausen's method for determining the stability constants is based on the variation of the complex dissociation extent as a function of its dilution. Therefore, the absorbance is measured for some solutions containing the central group and the ligand at the same stoichiometric ratio as in complex, as a function of their dilution. The experimental data are compared with the theoretical ones obtained by means of an electronic computer. We present in table 4 the experimental data obtained for a C value (the sum of reagent and palladium(II) concentrations) of 3.10^{-5} M, and in table 5 the β_2' C^2 values graphically determined from plotting $f(C/q, C)$-lg $\beta_2'C^2$, where q has values ranging between 2 and 10 and $f(C/q,$ $C)$ is the ratio of optical absorptions of some solutions of concentrations C/q and C, measured in cells of thicknesses ql and l cm. The plot was drawn using the theoretical data from Klausen's work.[15] The β_2' value calculated by Klausen's method, as an average for two values of the C concentration, 3.10^{-5} and 5.10^{-5} M, is $\beta_2' = 3.49.10^{10}$.

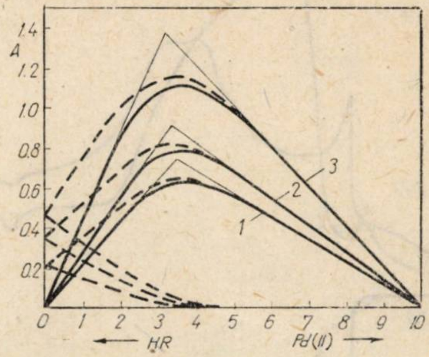

Fig. 4. — The Job curves obtained for isomolar solutions of Cadion 2B and palladium (II) in 1/1 ethanol-water, 3% urotropine medium. The sum of concentrations, Pd(II) + Cadion 2B, is $4.69.10^{-5}$M(*1*), $6.26.10^{-5}$M (*2*) and 9.40 10^{-5}M (*3*).

TABLE 4

The absorbance of some solutions with Pd(II)/Cadion 2B molar ratio 1/2 and the C value 3.10^{-5}M

Sum of concentration	Cell thickness	Absorbance		
		Complex	Reagent	Difference
$2C = 6.0.10^{-5}$M	$l/2 = 0.5$ cm	0.375	0.093	0.282
$C = 3.0.10^{-5}$M	$l = 1$ cm	0.330	0.093	0.237
$C/2 = 1.5.10^{-5}$M	$2l = 2$ cm	0.261	0.092	0.175
$C/3 = 1.0.10^{-5}$M	$3l = 3$ cm	0.233	0.094	0.139

TABLE 5

The absorbance rations and lg (β_2' c^2) values for the palladium complex with urotropine and Cadion 2B for $C = 3.10^{-5}$M

Absorbance ratio	lg($\beta_2'C^2$)	lg ($\beta_2'C^2$) values corrected by 0.60
$f(C/2, C) = 0,740$	1.45	1.45
$f(C/3, C) = 0,590$	1.50	1.50
$f(C, 2C) = 0,840$	2.10	1.50
$f(C/2, 2C) = 0,620$	2.10	1.50

$\beta_2' = 3.41.10^{10}$

The IR spectra of the reagents and complexes with palladium and urotropine were carried out within the 2400—300 cm^{-1} range, in a KI pellet. The spectra of complexes are much more complicated than those of the reagents. The supplementary absorption bands were attributed to the co-ordinated urotropine and to the Pd—N bond vibrations. The absorption bands at 475 cm^{-1} (s), 555 cm^{-1} (s) and 575 cm^{-1} (s), in the case of the complex formed by Cadion 2B, and those at 475 cm^{-1} (s), 525 cm^{-1}(s) and 505 cm^{-1} (f.s.), in the case of the complex formed by Cadion A, may be attributed to the Pd—N bond vibrations. The literature data[16,17] show that, although very variable as intensity, the Pd—N bonds absorb radiations in the 480—575 cm^{-1} range.

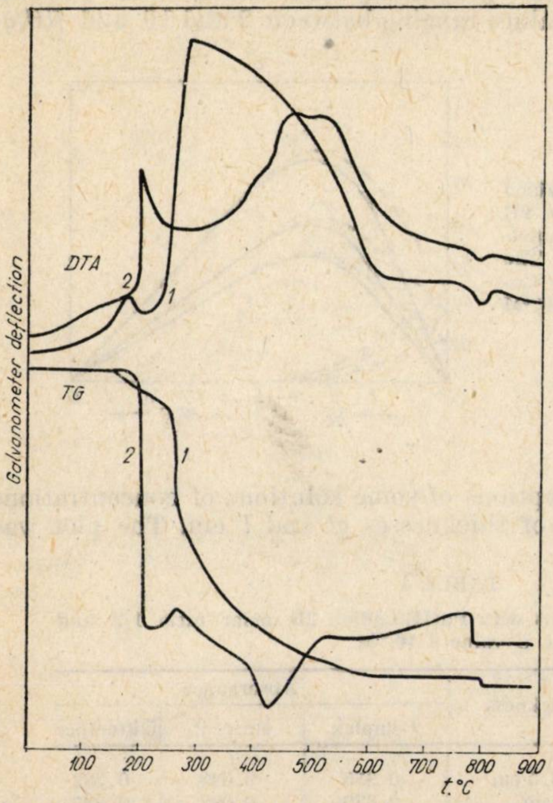

Fig. 5. — The DTA and TG curves for Cadion A(*1*) and its complex with palladium and urotropine (*2*).

The TG and DTA curves for Cadion A and its complex with palladium and urotropine are presented in figure 5. The palladium complex is stable up to 200°C.

CONCLUSIONS

The palladium (II) forms with urotropine and 1-(*p*-nitrophenyl), 3-(p^1-azobenzene)-triazene (Cadion A) and 1-(*p*-nitronaphthyl), 3-(p'-azobenzene)-triazene (Cadion 2B) stable complexes of the general formula Pd $(C_6H_{12}N_4)R_2$, hardly soluble in water and extractable in chloroform. The extraction constant of palladium with Cadion 2B (1.096) is higher than that corresponding to the Cadion A extraction (0.203); the above finding was explained in terms of solubility of Cadion 2B and its complex with palladium and urotropine: the solubility is lower in the aqueous phase and higher in the organic one. The formation constant of the palladium complex with Cadion A and urotropine was determined from the extraction equilibria of both reagent and complex and has a value of $10^{24,25}$, indicating the formation of a very stable complex. The complex formed by palladium (II) with Cadion 2B in 1/1 water-alcohol and 3% urotropine medium has a conditional formation constant of $3.29 . 10^{10}$ (mean value by two methods).

Some of the absorption bands in the IR spectra of the complexes were attributed to the Pd—N bond vibrations.

The formed complexes have a well-known composition, are easily filtrable and stable up to 200°C and they can be used in the gravimetric determination of palladium.

We consider that the most probable formula for the two complexes is the one in which Cadion, A or 2B, works as a unidentate ligand which is bound to the palladium by substituting the hydrogen atom in the triazenic group, leaving behind free co-ordination sites to be occupied by the urotropine.

REFERENCES

[1] C. M. Harris, F. B. Hoskins and R. H. Martin, *J. Chem. Soc.*, **1959**, 3728.

[2] F. P. Dwyer, *J. Amer. Chem. Soc.*, **63**, 78 (1941).

[3] M. Corbett, B. F. Hoskins, N. J. Mc Leod and B. P. O'Day, *Austral. J. Chem.*, **28**, 2377 (1975).

[4] A. P. Terentev, T. V. Ershova and E. G. Ruhadze, *Zhur. obshchei Khim.*, **36**, 1046 (1966).

[5] T. V. Ershova, E. G. Ruhadze and A. P. Terentev, *Zhur. obshchei Khim.*, **39**, 303 (1969).

[6] F. P. Dwyer and D. P. Mellor, *J. Amer. Chem. Soc.*, **63**, 81 (1941).

[7] Gr. Popa and A. F. Dăneţ, "Proceedings of the 3rd Conference on Analytical Chemistry",3rd Vol. Braşov, 1971, p. 209.

[8] Gr. Popa, and A. F. Dăneţ, *Chim. Analit.*, **1**, 86 (1971).

[9] P. Job, *Ann. Chim. (Paris)*, **10**, 113 (1928).

[10] R. M. Izatt, D. Eatough and J. J. Christensen, *J. Chem. Soc. (A)*, **1967**, 1301.

[11] J. R. Perumareddi and A. W. Adamson, *J. Phys. Chem.*, **72**, 414 (1968).

[12] A. A. Grinberg, Kh. I. Gildenyershel and F. P. Panteleeva, *Zhur. neorg. Khim.*, **67**, 2605 (1963).

[13] Yu. A. Zolotov, "Extraction of Chelate Compounds" Ann Arbor-Humphrey Science Publishers, 1970, p. 70.

[14] C. Luca and O. Enea, "Determinarea constantelor analitice. Metode electrometrice şi optice", Editura didactică şi pedagogică, Bucureşti, 1971, p. 71.

[15] K. S. Klausen, *Analyt. Chim. Acta*, **44**, 377 (1969).

[16] G. W. Watt and D. S. Klett, *Spectrochim. Acta*, **20**, 1053 (1964).

[17] D. B. Powell and N. Sheppard, *Spectrochim. Acta*, **17**, 68 (1961).

reaction medium has a conditional formation constant of $3.29 \cdot 10^{8}$ (mean value by two methods).

Some of the absorption bands in the IR spectrum of the complexes were attributed to the C—N bond vibrations.

The isolated complexes have a well-known composition, are easily filterable and stable up to 200°C and they can be used in the gravimetric determination of palladium.

We consider that the most probable formula for the two complexes is the one in which cation, A or AH, works as a monodentate ligand which is bound to the palladium by substituting the hydrogen atom of the [illegible] zene group, leaving behind free coordination sites to be occupied by the [illegible].

REFERENCES

1 [illegible], J. Chem. Soc., 1969, 1225.
2 [illegible], J. Amer. Chem. Soc., 63, 78 (1941).
3 [illegible], Austral. J. Chem., 22, 537 (1969).
4 [illegible], Zhur. Neorg. Khim., 18, 1046 (1973).
5 [illegible], Zhur. Anal. Khim., 16, 563 (1961).
6 [illegible] and [illegible], J. Amer. Chem. Soc., 63, 81 (1941).
7 [illegible], "Proceedings of the 3rd Conference on Analytical Chemistry", 2nd Vol., Prague, 1971, p. 208.
8 [illegible], Chim. Analyt., 1, 60 (1972).
9 [illegible], Anal. Chem. (Japan), 10, 112 (1958).
10 [illegible] and [illegible], J. Chem. Soc. (A), 1967, 150.
11 [illegible] and [illegible], J. Phys. Chem., 72, 414 (1968).
12 [illegible], Zhur. Neorg. Khim., 14, [illegible] (1969).
13 [illegible], "[illegible] of Organic Compounds", [illegible] Science Publish., [illegible] 1971, [illegible].
14 [illegible] and C. Luca, "Determinarea constantelor de stabilitate [illegible] Metode electrometrice şi optice", Editura didactică şi pedagogică, Bucureşti, 1971, p. 61.
15 [illegible], Analyt. Chim. Acta, 44, 177 (1969).
16 [illegible] and D. S. [illegible], Spectrochim. Acta, 20, [illegible] (1964).
17 [illegible] and N. Sheppard, Spectrochim. Acta, 17, [illegible] (1961).

Revue Roumaine de Chimie, 26, *1*, 151–153 (1981)

A NEW ACID-BASE INDICATOR

A. M. QURESHI * and A. N. PATEL **

* Department of Chemistry, Bayero University, Kano, Nigeria
** Department of Chemistry, University of Nigeria, Nsukka, Nigeria

Received August 4, 1979

The acid dissociation constant of zolon red, a pyrazolone, dye, has been determined. The dye can be used as an acid-base indicator in the titration of strong acids with strong and weak bases.

INTRODUCTION

Zolon red, an organic dye, was reported in the literature to form coloured precipitate with few metal ions.[1] The nature of zolon red has recently been investigated.[2] It is the enol form of the condensation product of glutaconic aldehyde with two molecules of 1-phenyl-3-methylpyrazol-5-one (Fig. 1). It is a weak acid with a single dissociable hydrogen ion. This work describes the determination of acid dissociation constant of zolon red and its possible use as an acid-base indicator.

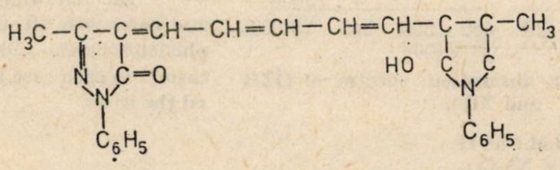

Fig. 1. — Structure of zolon red.

EXPERIMENTAL

Zolon red was prepared by the method of Gehauf and Goldenson.[1] Optical densities were measured on a Unicam SP 600 Spectrophotometer and pH measurements were made on a D-812 Weilheim direct reading pH-meter.

Solution A : 8.80 mg zolon red was dissolved in 100 ml absolute ethanol.

Solution B : The dissociated form of zolon red was prepared by diluting 10 ml solution A and 25 ml 0.04 M sodium acetate to 100 ml with water.

Solution C : The undissociated form of zolon red was prepared by diluting 10 ml solution A and 10 ml 0.1 M HCl to 100 ml with water.

Absorption spectra of dissociated (solution B) and undissociated (solution C) forms of zolon red were recorded over the range 345–540 nm. Molar extinction coefficients of solutions

B and C were plotted against wavelength (Fig. 2). The wavelengths for maximum absorption of dissociated and undissociated forms of zolon red are 480 nm and 420 nm respectively. The molar extinction coefficients of the two forms of zolon red at 420 nm and 480 nm are given below.

λ	ε_{ZR^-}	ε_{HZR}
420 nm	0652.2	2446.0
480 nm	4426.0	1691.0

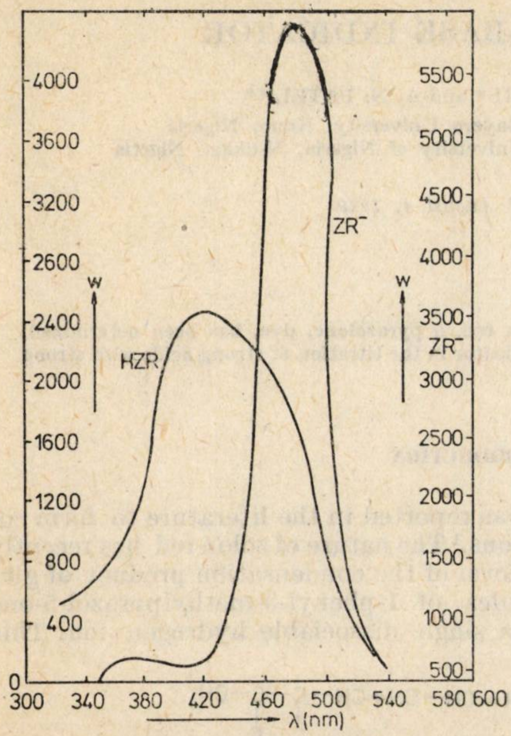

Fig. 2. — Electronic absorption spectra of HZR and ZR⁻.

Solutions of 0.04M—$NaCH_3COO$; 0.02M—CH_3COOH; 0.01 M—HCl and 10^{-3} M—HCl were used to prepare zolon red solutions of different pH and their optical densities were recorded. The concentration of dissociated and undissociated forms of zolon red present in these solutions were calculated using molar extinction coefficients of ZR^- and HZR at 420 nm and 480 nm. The results are shown in table 1.

Standard sodium carbonate solutions were prepared by dissolving 2.544 g and 1.3515 g of Analar anhydrous sodium carbonate in 250 ml water each. Sodium hydroxide solutions were standardized with potassium hydrogenphthalate. HCl, H_2SO_4 and HNO_3 were standardized with sodium hydroxide solution.

The following solutions of acids and bases were titrated using zolon red, phenolphthalein and methyl orange indicators. In each case the burrette contained the bases.

0.098 M and 0.0503 M NaOH
0.096 M and 0.051 M Na_2CO_3
0.103 M and 0.054 M HCl
0.114 M and 0.055 M H_2SO_4
0.108 M and 0.046 M HNO_3

TABLE 1

pK values of zolon red

Solution No	Observed pH	Optical density at 420 nm	Optical density at 480 nm	$[ZR^-]$ $M\times10^{-6}$	$[HZR]$ $M\times10^{-6}$	pK_a
1	5.30	0.155	0.950	212.0	6.8	3.80
2	4.80	0.130	0.660	143.7	14.8	3.81
3	4.55	0.190	0.832	176.5	30.6	3.79
4	3.10	0.332	0.359	33.1	126.9	3.70

DISCUSSION

The orange coloured saturated ethanolic solution (10^{-3}M) of zolon red, which will be referred as HZR in subsequent discussion, changes to yellow on addition of aqueous acids and to red by aqueous alkalies. The electronic absorption spectra of dissociated (ZR^-) and undissociated (HZR) forms are shown in figure 2. It has a pK_a value 3.78 ± 0.04.

The behaviour of HZR as an indicator can possibly be explained by the following dissociation equilibrium

$$HZR \rightleftharpoons H^+ + ZR^-$$

The undissociated compound, HZR, is yellow while the anion ZR^-, is red. The equilibrium position would move to the left if the hydrogen ion concentration is high and undissociated zolon red predominates ; the solution appears yellow. The addition of a base reduces the hydrogen ion concentration and the solution becomes red because the equilibrium position shifts to the right. The transition interval lies between pH 3.5 and 6.0. The colour changes from yellow to orange at pH 3.5 and the first red colour appears at pH 6.0.

HZR has been found quite suitable for the titration of strong acids with strong and weak bases. It gives permanent red colour at the end-point. Consistent results were obtained when the accuracy of titration was checked using phenolphthalein and methyl orange indicators. However, inconsistent results were obtained with weak acids. Zolon red indicator does not need screening with a blue dye and in this way it has an advantage over methyl orange. Zolon red, thus, deserves a place in the list of acid-base indicators.

REFERENCES

[1] B. Gehauf and J. Goldenson, *Analyt. Chem.*, **27**, 420 (1955).
[2] A. M. Qureshi and A. N. Patel, *Z. Naturforsch.*, **33b**, 450 (1978).

Revue Roumaine de Chimie, 26, 1, 155—157 (1981)

COMPTES RENDUS

Recent Developments in the Chemistry of Natural Carbon Compounds, Volume IX, R. Bognar, V. Bruckner and Cs. Szantay — editors, Akadémiai Kiadó, Budapest, 1979, 420 pages.

The first part of this book, "Synthetic chemistry of insect pheromones and juvenile hormones" (198 pages) is written by Kenji Mori, one of the well-known contributors of this domain. In spite of the 50 years which have passed from the classical Butenandt synthesis of bombykol (the sex phermone of *Bombix mori*) none of the available monographs on pheromones has been written with a special emphasis on synthetic problems. This review provides "a compilation of synthetic works in insect chemistry" (up to June 1976). The first chapter describes general synthetic methods useful in insect chemistry. A special attention is payed to stereoselective routes to trisubstituted olefins starting from the idea that "a review on juvenile hormone synthesis is almost equivalent to a review on the synthesis of trisubstituted olefins". The second chapter presents the synthesis of about sixty insect pheromones classified after their chemical structure (e. g. pheromones with E — respectively Z — olefinic linkage, pheromones with conjugated —, respectively non-conjugated diene system, terpenoid pheromones etc.). Optically active pheromones are thoroughly reviewed. The third chapter describes the synthesis of insect juvenile hormones (J. H.). After a relatively short enumeration of non-stereoselective syntheses of J. H., the greatest part of the chapter is dedicated to stereoselective syntheses, summarized chronologically (starting with the first famous stereoselective synthesis of Corey) with a specification of the key-reaction used (e.g. Claisen rearrangement, Julia cleavage, Witting reaction, Biellmann coupling, organosulfur reactions etc.). As in the case of pheromones, a special attention is payed to syntheses of optically active J. H.

The entire text of this part is limited only to general and conclusive problems but this test is completed in a beautiful manner by many reaction schemes containing practically all the useful data for a first information. Interesting contributions from the author's laboratory (e.g. Mori syntheses of J. H. I and J. H. II etc.) are included. A rich reference list (about 380 references) and a short index are added.

The second part of the book, "Composition of bulgarian rose flower concrete ; the structure and biogenesis of its components") (80 pages ; 141 references) is written by B. Stoianova-Ivanova. The paper describes the results of the author's group concerning the composition of the wax and "absolute" from concrete of the bulgarian rose (the concrete was obtained by extraction and not by hydrodistillation as before). The author presents in detail all the important components of the wax : hydrocarbons, fatty acids, alcohols, ketones, diols and cyclic compounds. The quantitative changes in the compounds of the wax during the developments of buds into the flowers are also mentioned. The main components of the absolute, as results from the recent author's works, are presented underlining the importance of modern physical methods (chromatography, IR, MS etc.) in this domain. An interesting chapter concerning the problems of biogenesis of the long chain components of natural waxes is also included. An original scheme for biosynthesis of even-membered paraffins and odd-membered fatty acids (components identified only recently in plant waxes) is proposed.

The third part of the book, "Chalcone epoxides in flavonoid chemistry", (113 pages ; 346 references) by Gy. Litkey, summarizes the results obtained in the chemistry of chalcone epoxides (including the problems of Agar-Flynn-Oyamada oxidation) during the years 1963—1973. The connexions between the chalcone epoxides and flavonoids are presented under several headings : oxidation of chalcones, conversions of 2′-OR- chalcone epoxides, rearrangement reactions, structure studies. The importance of other epoxides (flavene, aurone and flavindogenide) in flavonoid chemistry is also stressed. The last part of the paper is devoted to Agar-Flynn-Oyamada reaction (oxidation of 2-hydroxychalcone or flavanone derivatives with alkaline hydrogen peroxyde to 3-hydroxyflavanones or 3-hydroxyflavones ; reaction supposed to occur through chalcone epoxides). Numerous details (e.g. structure and mechanism studies using NMR and UV — spectroscopy) are thoroughly analysed.

M. Banciu

L. LÁNG, Editor, *Absorption Spectra in the Infrared Region*, Akadémiai Kiadó, Budapest, Volume 4, 1978, 319 pages, and Volume 5, 1980, 319 pages.

The well known compilation of infrared spectra started by Professor Láng in 1975 has now reached its 4th and 5th volumes.

These continue publishing the absorption IR spectra of newly isolated or synthesized organic and biochemical compounds, specifying the conditions in which the spectra were obtained, and other data of interest. All the spectra were run (or re-run) on the UR-10 and UR-20 Zeiss-Jena spectrophotometers in various Hungarian laboratories, in the range 4000—400 cm^{-1}, most of them as KBr pellets. As a beneficial corollary of this, their appearance is uniform, thereby facilitating comparison with spectra of unknown species.

Unfortunately, visual comparison of spectra becomes more and more difficult and tedious today, when their number has become so large and when computers are so easily available. Like in other spectra compilations built up on the same principles as this one, the retrieval of spectra for reasons of comparing them with the spectrum of an unknown substance is difficult. This comparison would have been greatly facilitated if assignment of at least some of the absorption bands, *e.g.* those corresponding to group vibrations, would have been given. By default, a good alphabetical index, cumulated over all the previous volumes of the collection and set up on the basis of the structural name of each compound, would have been very helpful. Both these facilities are lacking.

The books are nevertheless useful, mainly for offering the researcher the yet unreported IR absorption spectra of a large variety of organic and biochemical compounds.

Alex. Butucelea

RICHARD L. LIBOFF, Introduction to the theory of kinetic equations, Robert E. Krieger Publishing Company, Huntington, New York 1979, 397 pages.

Kinetic theory deals with non-stationary effects in large systems of particles. Hence almost in every place where something really happens in a many-body system (i.e. a process is going on) kinetic effects are usually involved. Non-kinetic effects are responsible only for the incipient stages of the process. There is not any risk to overestimate the interest in kinetic theories. This fact and the great complexity of the problem, explain the great amount of research in this field.

However, introductory books in this field are rather scarce. As known, in the Landau's courses such a book was intended to be the ninth volume — but it has never been written. The present introduction by Professor Richard L. Liboff from Cornell University, is such a book — and an excellent one.

The book is self-consistent, so that references to background knowledge in order to understand it are not necessary. It begins with a review of classical mechanics, which is the starting point in any classical kinetics theory. The Lagrangian and Hamiltonian formalisms, Poisson brackets and canonical transformations, action — angle variables, Hamilton-Jacobi Theory, and Poincaré invariants, all are reviewed in Chapter 1. Well selected problems and exercises accompany them, and one can safely estimate that the text would be well accessible to a self-studying student. This assertion holds for any chapter in this book, so that it will not be repeated.

The classical mechanics is the starting point, but the development of mechanics into a kinetic theory can be made on several ways. Thus, in chaper 2 a rigorous approach starting from the Louville equation (the method of Prigogine, and the method of the BBGKY chain) is considered. Another approach is to make a Markov assumption from the beginning. On this line, the Chapman-Kolmogorov equation is presented.

In a process an initial stage, a kinetic stage, and a hydrodynamical one can be distinguished. The characteristic of the kinetic stage is that all the properties are functionals of the one-particle distribution (the hydrodynamical stage is only a remarkably simple case of the former one). In this stage, the time evolution of the one particle distribution is determined by a kinetic equation. Obviously, the main object of a kinetic theory is the derivation of the kinetic equation. The essential features explained above (which are by no meansobvious) are treated in Chapter 3. The treatment is based on the Bogoliubov analysis of the BBGKY equations, and also on the cluster expansion technique. Very general kinetic equations can be obtained in this way, but tractable, though approximate equations, are also very useful. As a straightforward example, the streaming equation and the Vlassov equation are given here.

Kinetic equations can also be derived in a more direct approach beginning with the analysis of the collision concept. This is done in Chapter 4. The equations of Boltzmann, Krook-Bhatnager-Gross, and Fokker-Planck are derived with great care for details. The author has carefully examined the properties of the corresponding collision operators, and also the corresponding H-theorems, i.e. the irreversible behaviour. All these equations are derived in several ways, and the corresponding domain of applicability is always properly analysed. The chapter is closed with two applications to plasma kinetic theory, namely the Landau, and the Balescu-Lennard kinetic equations.

The approach to equilibrium, and the methods of solving kinetic equations are dealt with in Chapter 5. They are illustrated with the Boltzmann equation, but this gives standard methods which are not limited to this particular case. The chapter starts with the definition of the local variables in terms of the one particle distribution. Phenomenologically, these variables obey the hydrodynamical equations, which include the definition of the transport coefficients. The purpose is to obtain statistical expressions for the transport coefficients. This is done by the Chapman-Enskog method, and also by the Grad's technique (the method of moments), which are given in detail. The last part of this chapter is concerned with the approach to equilibrium, and there is a discussion on the particular features of the irreversible behaviour. The nature of irreversibility is a challenging subject even today, and the last section of the book is devoted to this subject.

There is a large number of problems and exercises accompanying the main text. Besides, each chapter of the book is completed with very valuable references (there are about 500 references in all). The references are selected for a student interested in further study and are very handily systematized according to the subject. Still, all these remain enumerable details, while this book deserves to be described as a whole. In fact it is a very original book, and, as such, it carries a kind of "soul" of its own. The mark of the book is the passion for deep physical analysis embeded in a clear mathematical treatment. The book has originated from a course attended by aero, mechanical, and electrical engineering students, and also by physics and space science students. These students need precise methods in the theory of kinetic equations, and also a deep physical grasp on the subject. The book does satisfy these requirements, and is outstandingly written by an outstanding professor and scientist.

Gh. Vasu

NOTE POUR LES AUTEURS

La Revue Roumaine de Chimie publie des articles en anglais, français, russe, allemand ou espagnol. Les auteurs sont priés d'envoyer des articles et des comptes rendus inédits.

Les manuscrits seront dactylographiés à deux intervalles. La bibliographie, les tableaux et la légende des figures seront placés après le texte.

Si l'article fait partie d'une série numérotée, le titre de la partie précédente sera indiqué dans une note au bas de la première page.

Chaque article sera précédé d'un résumé comprenant quinze lignes au maximum.

Les références bibliographiques dans le texte seront faites par des exposants sans parenthèses et paraîtront à la fin de l'ouvrage.

Les publications périodiques mentionnées dans la bibliographie seront présentées suivant les prescriptions internationales ; le nom de l'auteur précédé de l'initiale du prénom, le titre du périodique abrégé conformément à « Chemical Abstracts » et souligné par une ligne, le numéro du tome indiqué par des chiffres arabes et souligné par deux lignes, suivi de la première page de l'article : à la fin, l'année de la parution sera placée entre parenthèses. Le numéro de la revue ne sera pas indiqué, si les pages du volume sont numérotées consécutivement.

Les textes des livres ou traités inclueront : les noms des auteurs, les initiales du prénom, le titre du livre entre guillemets et sans être sougliné, le numéro du tome précédé par l'abréviation « vol. » (ou « Bd. »), le numéro de l'édition, les éditions (the publisher), la localité de la parution du livre, l'année de la parution et la page de la référence précédée(s) par l'abréviation « p » (ou « S »).

Les brevets seront indiqués comme suit : l'auteur ou la firme, le pays et le numéro du brevet, la date et la revue (Chem. Abstr.) Par ex. : M. Jones (to Union Carbide Co.), Brit. Pat. 601 238, 2 Sept. 1959, *Chem. Abstr.*, **54**, 12808 (1960).

Les diagrammes seront tracés à l'encre de Chine sur papier calque. Les tableaux et les figures (en nombre strictement nécessaire) seront numérotés par des chiffres arabes. Les courbes dans les figures seront numérotées par des chiffres arabes et leur explication sera donnée dans la légende des figures. Prière de ne pas inscrire les mêmes données dans les tableaux et les figures. Chaque tableau aura un titre. On indiquera dans le texte la place approximative des tableaux et des figures. Les formules chimiques seront incluses dans le texte : en outre, elle seront transcrites sur papier calque, à l'encre de Chine.

Les auteurs sont priés d'indiquer les caractères italiques (en soulignant les lettres au crayon), ainsi que tout autre caractère spécial : les préfixes *ortho*, *meta*, *para*, *cis*, *trans*, etc. seront soulignés pour indiquer leurs caractères italiques, et ne seront jamais écrits avec des majuscules.

Aucune correction à la main ne sera admise sur le manuscrit. Les corrections seront frappées à la machine. Les lettres grecques ou autres symboles spéciaux seront insérés à la main à l'encre clairement.

Le manuscrit sera signé par l'auteur.

Le colonne-titre aura 50 lettres au maximum.

L'entière responsabilité du contenu des articles appartient aux auteurs.

PRINTED IN ROMANIA

ORSZÁGOS MŰSZAKI KÖNYVTÁR ÉS DOKUMENTÁCIÓS KÖ
180

TRAVAUX PARUS AUX ÉDITIONS DE L'ACADÉMIE DE LA RÉPUBLIQUE SOCIALISTE DE ROUMANIE

ELENA CEAUŞESCU, **Polimerizarea stereospecifică a izoprenului** (La polymérization stéréospécifique de l'isoprène), 1979, 306 p.

CR. SIMIONESCU, VALERIA GORDUZA, **Polimeri biocombatibili şi biologic activi** (Polymèrs biocompatibles et biologiquement actifs), 1980, 479 p.

MIHAIL FLORESCU, **Metode ştiinţifice în dezvoltarea industriei chimice moderne** (Méthodes scientifiques dans le développement de l'industrie chimique moderne), 1979, 256 p.

CONST. GH. MACAROVICI, **Analiza chimică cantitativă anorganică** (L'Analyse chimique quantitative inorganique), 1979, 457 p.

Ş. MOLDOVEANU, A. SAVIN, **Aplicaţii în chimie ale metodelor semiempirice de orbitali moleculari** (Applications en chimie des méthodes semi-empiriques d'orbitaux moléculaires), 1980, 286 p.

A. T. BALABAN, I. GĂLĂŢEANU, G. GEORGESCU, LIGIA SIMIONESCU, **Compuşi marcaţi şi radiofarmaceutici cu aplicaţii în medicina nucleară** (Composés marqués et radiopharmaceutiques à application en médecine nucléaire), 1979, 495 p.

I. E. TEODORESCU et MARIA FITI, **Iradierea tehnologică** (L'Irradiation technologique), 1979, 216 p.

I. G. MURGULESCU, E. SEGAL, **Introducere în chimia fizică vol. II. 1. Teoria molecular-cinetică a materiei** (Introduction à la chimie physique. IIe vol. 1. La Théorie moléculaire-cinétique de la matière) 1979, 1033 p.

I. G. MURGULESCU, V. EM. SAHINI, **Introducere în chimia fizică, vol. I. 2. Structura şi proprietăţile moleculelor** (Introduction à la chimie physique. Ier vol. 2. La structure et les propriétés des molécules), 1978, 604 p.

S. STERNBERG, FL. DANEŞ, **Termodinamica chimică aplicată** (La thermodynamique chimique appliquée), 1978, 400 p.

D. PURDELA (sous la direction), **Nomenclatura chimiei anorganice** (La nomenclature de la chimie inorganique), 1977, 153 p.

C. DRĂGULESCU, E. PETROVICI, **Chimia structurală modernă. Chimia coordinanţei 8** (La chimie structurale moderne. La Chimie de la coordinence 8), 1977, 947 p.

I. ZUGRAVESCU, MAGDA PETROVANU, **N-ylid chemistry**, coédition avec McGraw-Hill International Book Company, U.S.A., 1977, 396 p.

I. G. MURGULESCU, **Introducere în chimia fizică, vol. I.1. Atomi, molecule, legătură chimică** (Introduction à la chimie physique, Ier vol. 1. Atomes. Molécules. Liaison chimique), 1976, 560 p. 2 pl.

P. BALTĂ, E. BALTĂ, **Introduction to the physical chemistry of the vitreous state**, coédition avec Abacus Press, 1976, 287 p.

I. GĂLĂŢEANU, **Radiochimia aplicată. Metode şi probleme** (La radiochimie appliquée. Méthodes et problèmes), 1976, 307 p.

CONST. V. UGLEA, **Cromatografia pe gel permeabil. Noi domenii de aplicare** (La chromatographie sur gel perméable. Nouveaux domaines d'application), 1976, 122 p.

CONST. GH. MACAROVICI, D. MACAROVICI, **Chimia oxizilor dubli şi utilizările lor** (La chimie des oxydes doubles et leur utilisation), 1975, 195 p.

ELENA CEAUŞESCU, **Research work on synthesis and characterization of macromolecular compounds. Contributions**, 1974, 251 p.

CR. SIMIONESCU, VIORICA RUSAN, V. POPA, **Chimia algelor marine** (La chimie des algues marines), 1974, 212 p., 1 pl.

1981 MAI 1 1

I.P.I. 2634

43426

Lei 25. —
$ 55 (price per year)

F 1103

ACADÉMIE DE LA RÉPUBLIQUE SOCIALISTE DE ROUMANIE

REFERÁLVA

R

REVUE ROUMAINE DE CHIMIE

TOME 26
N° 2
Février 1981

EDITURA ACADEMIEI REPUBLICII SOCIALISTE ROMÂNIA

Rev. Roumaine Chim.

RRCHAX, 26, 2, p. 159–330 (1981), Bucarest

ACADÉMIE DE LA RÉPUBLIQUE SOCIALISTE DE ROUMANIE

COMITÉ DE RÉDACTION

Rédacteur en chef :

I. G. MURGULESCU, membre de l'Acadèmie de la République Socialiste de Roumanie

Rédacteurs en chef adjoints :

A. T. BALABAN et V. EM. SAHINI, membres correspondants de l'Académie de la République Socialiste de Roumanie

Collège de rédaction :

EM. BRATU, ELENA CEAUŞESCU, ECATERINA CIORĂNESCU-NENITZESCU, CR. SIMIONESCU, membres de l'Académie de la République Socialiste de Roumanie ; P. SPACU, membre correspondant de l'Acadèmie de la République Socialiste de Roumanie ; MARGARETA AVRAM, M. BANCIU, I. HAIDUC, D. I. MARCHIDAN, I. MOLDOVAN, G. NIAC et D. SĂNDULESCU

La Revue Roumaine de Chimie paraît 10 fois par an. Toute commande de l'étranger pour les travaux parus aux Editions de l'Académie de la République Socialiste de Roumanie sera adressée à ILEXIM, Departamentul Export-Import Carte (Livres)/Departamentul Export-Import Presă (Revues), P.O.B. 136—137, télex 11226, 3, str. 13 Decembrie, 79517 Bucarest 12, Roumanie

Les manuscrits, les livres et les revues proposés en échange ainsi que toute correspondance seront envoyés à la rèdaction :

REVUE ROUMAINE DE CHIMIE

125, Calea Victoriei, 79717 Bucarest, Roumanie, téléphone 50 76 80

EDITURA ACADEMIEI REPUBLICII SOCIALISTE ROMÂNIA
125, Calea Victoriei 79717, Bucarest, Roumanie, téléphone 50 76 80

KÖNYVTÁR ÉS ... KÖZPONT

REVUE ROUMAINE DE CHIMIE

Tome 26, N° 2 Février, 1981

RODICA VÎLCU and A. CIOCHINĂ, Steady state hot wire thermal conductivity set-up for fluids . . . . 161—174

CR. CONŢESCU and M.I. VASS, FEM study of silver layers adsorbed on tungsten. II. Surface structure and surface migration . . . . 175—183 Bc

V. T. POPA and E. SEGAL, Adsorption on heterogeneous surfaces : on the ''Condensation approximation'' . . . . 185—195

DOMNINA POPESCU, V. GOŞA, R. H. SCHUSTER, N. I. IONESCU and D. OANCEA, The explosive combustion of the vinylacetylene—air mixtures initiated by a hot nickel—chromium wire . . . . 197—202 R

F. DOMKA, J. MICIUKIEWICZ and W. ZMIERCZAK, Catalytic properties of Fe_2O_3—Nd_2O_3 system (in French) . . . . 203—210

F. DOMKA and M. ŁANIECKI, The effect of synthesis conditions on the activity of iron-chromium oxide catalysts for water gas shift reaction (in French) . . . . 211—215

I. V. NICOLESCU and I. SĂNDULESCU, Relations between the methods of preparation, properties and activity of Bi—Mo—Fe—O catalyst in oxidative dehydrogenation of n-butenes in butadiene . . . . 217—228

B. LENARCIK and E. BEZAK, A study for optimum conditions of extraction of transition metal complexes with pyridine derivatives. Extraction of the Co(II), Ni(II) and Zn(II) complexes of 3,5-dimethylpyridine . . . 229—235

J. ZSAKÓ and T. LÁSZLÓ, Complex compounds of some diosphenolic type carotenoids. Astacene complexes. Spectrophotometric study of the system Fe(III)—astacene. . . . . 237—243

A. ESSAWY, M. EL-GARBY YOUNES, M.M. BADRAN and A.Z.M. HEIKAL, Synthesis and reactions of 3-cinnamoyl-4-phenyl-6-[1′(2′-methoxynaphthalenyl]-2-pyridone and of 2-methyl-(b)-2′-[α(β-methoxynaphthalenyl)--4′-phenyl-3′, 4′-dihydropyridyl]-azachromone . . . . 245—252

GUY RICART, CHARLES GLACET and DANIEL COUTURIER, Synthesis and stereochemistry of 2-dialkylamino-3-(2-tetrahydropyranyl)-tetrahydropyrans (in French) . . . . 253—268

V. VÂNTU, NORA RĂDULESCU, MARIANA IONESCU and C. SÂRBU, Leaving group effect in the reaction of 5-substituted-2-pentanones with sodium methoxide . . . . 269—273

Revue Roumanie Chim. **26**, *2*, 159—330 (1981) Bucarest

R

M. CHATZOPOULOS and J.P. MONTHEARD, Radicalic cyclizations of unsaturated aldehydes (in French) . . . . 275—282

M.M. HABASHY, A. ESSAWY and M.M.M. HAMAD, Epoxidation of 2,6-diarylidenecyclohexanones and some reactions of the corresponding epoxides . . 283—290

CLEOPATRA VASILIU-OPREA and M. POPA, Mechano-chemical reactions of poly (vinyl chloride). 9. Characterization of the obtained products by mixing PVC-S with aromatic diamines (in German) . . . . 291—303

DAN S. VASILESCU, Alternating tendency in copolymerization. V. Equimolecular copolymers and dimers of 1,1-diphenylethylene . . . . 305—313

ALEXANDER J. CORPACIUS, Quantitative analysis of chromatographic observations . . . . 315—325

BOOK REVIEWS . . . . 327—330

Revue Roumaine de Chimie, 26, 2, 161–174 (1981)

STEADY STATE HOT WIRE THERMAL CONDUCTIVITY SET-UP FOR FLUIDS

RODICA VÎLCU * and A. CIOCHINĂ **

* Polytechnical Institute, Department of Physical Chemistry, Bd. Republicii 13, Bucharest, Romania
** ICECHIM, Centre of Physical Chemistry, Spl. Independenţei 202, Bucharest, Romania

Received May 16, 1980

Some theoretical principles as well as mounting of a set-up including a potential lead cell for the absolute measurement of the thermal conductivity of fluids by the steady state hot wire method are presented. The experiments were carried out on nitrogen, oxygen, carbon dioxide, propane, n-butane and acetylene. The precision is about 0.3% and the accuracy better than 2%, as estimated from both computation of errors and comparison with the available data in literature.

1. INTRODUCTION

The thermal conductivity of fluids is a thermophysical property important for both technology and knowledge of fundamental phenomenon governing the heat exchange processes. As the estimation methods for single fluids and mixtures are suitable only in some particular cases, the accurate measurement of this property has become necessary. Despite the simplicity of the steady state hot wire method, a proper construction of the cell and set-up have to fulfil a lot of conditions. The mathematical model for the cell offers the solutions for computation of the heat losses at the wire ends and through the potential leads, as well as for the geometric cell constant corrections. Supposing these known, the accuracy and precision of the results are influenced by two main factors : a phenomenological one, natural convection and thermal radiation, and an instrumental one, related to the accuracy of the temperature and geometric dimension measurement.

2. PRINCIPLE OF THE METHOD

A metal wire is stretched along the inside axis of a hollow cylinder (cell tube). The wire performs the dual function of heater and resistance thermometer.

For steady state temperature conditions at the hot wire surface and inner surface of the cell tube, the thermal conductivity, λ, of the fluid located in-between the two concentric cylinders is calculated with the relation [1] :

$$\lambda = [\ln (d_2/d_1)Q] / [2\pi L(T_1 - T)] \tag{1}$$

where d_1 and d_2 are the wire diameter and the inner diameter of the cell tube, respectively ; L is the length of the wire between the potential leads ($d_1 \ll d_2 \ll L$) ; Q is the electric power dissipated by conduction through the fluid layer ; T_1 and T are the hot wire temperature and cell tube inner wall temperature, respectively. The thermal conductivity of the fluid is determined at the experimental presure, P, and average temperature $\overline{T} = (T_1 + T)/2 = T + (\theta/2)$, where $\theta = T_1 - T$.

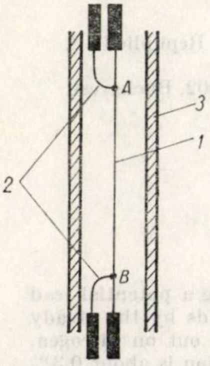

Fig. 1. — Diagram of a hot wire potential lead cell : 1 — axial wire ; 2 — potential leads ; 3 — cell tube.

3. EXPERIMENTAL ASSEMBLY

The experimental assembly consists of : measurement cell, thermostat unit, vacuum unit and electric circuit.

3.1. Measurement cell

The cell tube was made of glass (Pyrex or Jena) ; the axial wire and potential leads were made of platinum. The experimental cell was presented in figure 2.

The diameter of the wire, $d_1 = 2r_1 = 0.050 \pm 0.0005$ mm, was measured under microscope. The length between the potential leads, $L = 2l = 180.3 \pm 0.02$ mm, was measured by means of a cathetometer. The potential lead diameter was $d_3 = 2r_3 = 0.031 \pm 0.0005$ mm and the length of each lead $l_3 \simeq 30 \pm 0.1$ mm. The inner diameter, $d_2 = 2r_2 = 3.59 \pm 0.01$ mm, and the outer diameter, $d_e = 2r_e = 5.08 \pm 0.01$ mm of the cell tube were measured with a micrometer. The eccentricity of the centering system at the cell ends, $\varepsilon \leqslant 0.1 \pm 0.03$ mm, was measured by means of magnifying glasses. All linear measurements on the cell are conducted at ambient temperature T_a. The geometric cell constant, A_a, at the temperature T_a, is $A_a = [\ln (d_2/d_1)] / (2\pi L) = 3.7727$ m^{-1}. The corrected cell constant for the eccentricity is calculated as :

$$A' = [\ln (x + \sqrt{x^2 - 1})] / (2\pi L) \tag{2}$$

$$x = \frac{1}{2}\left[\frac{d_1}{d_2} + \frac{4(r_2 - \varepsilon)}{d_1}\left(1 - \frac{r_2 - \varepsilon}{d_2}\right)\right] \tag{3}$$

Using the percentage eccentricity, $E = 100\ \varepsilon/r_2$, the relation (3) becomes :

$$x = \frac{1}{2}\left[\frac{d_1}{d_2} + \frac{d_2}{d_1}(1 - 10^{-4} E^2)\right] \tag{4}$$

With $E = 5.6\%$, one gets $A' = 3.7699$ m^{-1}, that is a correction of -0.074%.

3.2. Thermostating unit

The measurement cell was immersed into a thermostating vessel (Fig. 3), connected to a (U — 10 — type) thermostat.

After reaching the thermal equilibrium, the long-run temperature fluctuation within the cell was less than 0.01 K and vertical temperature gradient was smaller than 0.1 K/0.25 m.

3.3. Vacuum unit

In order to evacuate and fill up the cell with gases or vapours, a classical vacuum unit for pressures down to about 10^{-5} torr was made. The gas mixtures were prepared volumetrically or according to the partial pressure law. The organic liquid vapours were obtained by injecting a known amount of liquid into the cell (in vacuo).

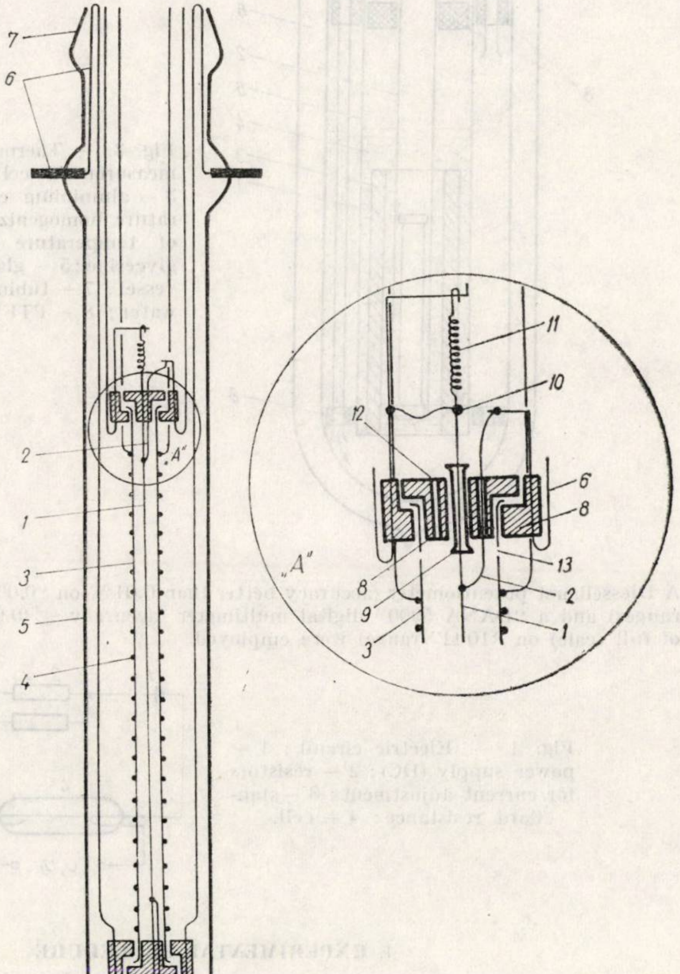

Fig. 2. — Measurement cell : 1 — axial wire ; 2 — potential lead ; 3 — cell tube ; 4 — platinum thermoresistance ; 5 — external glass tube ; 6 — thick platinum leads ; 7 — conical ground joint (or spherical joint with "0" ring) ; 8 — PTFE parts ; 9 — glass capillary ; 10 — insulating glass bead ; 11 — tungsten coil ; 12, 13 — channels and respectively orifices as cell inlets for fluid.

3.4. Electric circuit

The electric circuit has to allow for the following measurements : calibrating as thermoresistance, $R(T)$, of the platinum wire (determination of the temperature coefficient, α, of the electrical resistance) ; measurement of the electric resistances, R and R_1, of the wire at the temperature T of the initial thermal equilibrium, respectively at the temperature T_1

of the hot wire after having reached the steady state ; measurement of the total electric power Q_t fed into the wire, at steady state. The electric circuit is presented in figure 4 and the measurements are run potentiometrically.

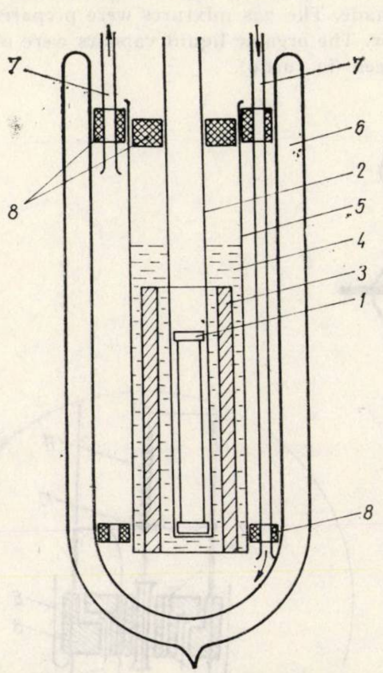

Fig. 3. — Thermostating unit : 1 — measurement cell ; 2 — glass tube ; 3 — aluminium cylinder for temperature homogenization and damping of temperature fluctuations ; 4 — glycerine ; 5 — glass tube ; 6 — Dewar vessel ; 7 — tubing for thermostated water ; 8 — PTFE centering pieces.

A Diesselhorst potentiometer (accuracy better than 0.01% on "0.001 V", "0.01 V" and "1 V" ranges) and a "DANA 5900" digital multimeter (accuracy ± (0.003% of reading + 0.005% of full scale) on "10 Ω" range) were employed.

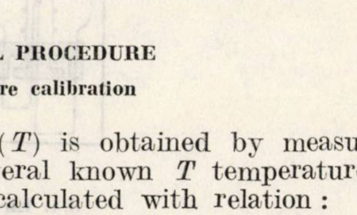

Fig. 4. — Electric circuit : 1 — power supply (DC) ; 2 — resistors for current adjustment ; 3 — standard resistance ; 4 — cell.

4. EXPERIMENTAL PROCEDURE

4.1. Platinum wire calibration

The experimental equation $R(T)$ is obtained by measuring the wire electrical resistance, R, at several known T temperatures. [2] The resistance R at temperature T is calculated with relation :

$$R = R_{sd}\, U/U_{sd} \qquad (5)$$

where U, U_{sd} are the voltages measured between the potential leads and respectively between the R_{sd} standard resistance terminals, when

I_0 is the measuring current through the circuit. The T temperature is measured with a thermometer with a precision $\delta T = 0.02$ K. The heating effect due to the measuring current is calculated as:

$$\theta_0 = [RI_0^2 \ln (d_2/d_1)] / (2\pi L\lambda) \tag{6}$$

For $R = 10\ \Omega$, $I_0 \leqslant 10^{-3}$ A, $L = 0.18$ m, $\lambda \geqslant 0.1$ W/(mK), one gets $\theta_0 < 3.8 \times 10^{-4}$ K.

Within the 293—353 K temperature range, due to the limited accuracy in the measurement of both electrical resistance and temperature, the obtained $R(t)$ experimental equation is:

$$R = R_0(1 + \alpha_0 t) \tag{7}$$

where R, R_0 are the electrical resistances at the temperatures t(°C) and 0°C, respectively, or:

$$R = R_a[1 + \alpha_{t_a}(t - t_a)] \tag{8}$$

R_a being the electrical resistance at temperature t_a.

$$\alpha_{t_a} = \alpha_0/(1 + \alpha_0 t_a) \tag{9}$$

For this cell, $R_0 = 10.103\ \Omega$ and $\alpha_0 = 3.925 \times 10^{-3}\ (°\mathrm{C})^{-1}$ were obtained.

4.2. Heating current

In order to perceive a temperature difference of 10^{-n} K, from the hot wire temperature T_1, the heating current variations have to be:

$$\Delta I_1 < (10^{-n}\pi L\lambda) / [R_1 I_1 \ln (d_2/d_1)] \tag{10}$$

$$\Delta I_1 / I_1 < 10^{-n} / (2\theta) \tag{11}$$

4.3. Measurement of T_1, Q_t an $\alpha\,\theta$ parameters

The resistance R_1 of an L length hot wire, fed with an I_1 heating current, is calculated with relation:

$$R_1 = R_{sd}\, U_1 / U_{sd,1} \tag{12}$$

where U_1 and $U_{sd,1}$ are the voltages measured between the potential leads and respectively between the standard resistance terminals. The T_1 temperature is calculated from the $R(T)$ equation.

The total electrical power, Q_t, generated in the wire is:

$$Q_t = U_1 U_{sd,1} / R_{sd} \tag{13}$$

For *pure conduction*, T_1 is proportional to Q_t and therefore R_1 is a linear function of I_1^2; the pairs of experimental values (R_1 and Q_t) lay on a straight line (Fig. 5).

This finding enables us to determine, by linear extrapolation, the resistance R and temperature T of the wire at $Q_t = 0$ $(I_1 = 0)$, corresponding to the cell inner wall temperature, at thermal equilibrium. One obtains :

$$\theta = (R_1 - R)/(R\alpha_T) \quad (14)$$

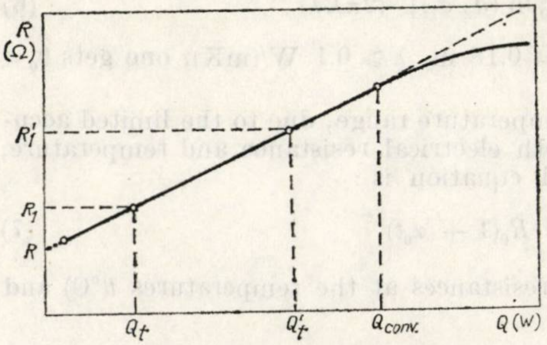

Fig. 5. — Measurement principle of the wire temperature raise and establishing of the pure conduction range.

When steady state measurable T_1 and T_e (cell outer wall temperature) values are employed, one gets :

$$\lambda = \ln (d_2/d_1)\left[2\pi L\left(\frac{T_1 - T_e}{Q_t}\right) - \frac{1}{\lambda_2}\ln (d_e/d_2)\right]^{-1} \quad (15)$$

where λ_2 is the thermal conductivity of the cell tube material.

To eliminate T_e = constant, two values T_1 and T'_1 are chosen for Q_t and Q'_t, within the pure conduction range (linear domain, Fig. 5).

$$\lambda = \ln (d_2/d_1)\left[2\pi L\left(\frac{T'_1 - T_1}{Q'_t - Q_t}\right) - \frac{1}{\lambda_2}\ln (d_e/d_2)\right]^{-1} \quad (16)$$

At 293 K, λ_2(Pyrex) = 1.06 W/(mK).[1,3] Since the $[\ln (d_e/d_2)/\lambda_2]$ term is anyway smaller than 5% of the $[2\pi L(T_1 - T_e)/Q_t]$ value, an error of 10% for λ_2 leads to an error smaller than 0.5% for λ.

4.4. Experimental tests for temperature jump and natural convection

In gases and vapours, at low pressures, the molecular mean free path becomes equal to or longer than the thickness of the gas layer in the cell. The resultant effect is a temperature jump[1] : the real temperature difference, $\theta = T_1^0 - T^0$, across the gas layer is smaller than the measured difference, $\theta_{ac} = T_1 - T$. This temperature jump, related to the accomodation phenomenon of the gas molecules at the solid-gas interfaces, is proportional to the temperature gradient and inversely proportional to the absolute pressure, P, of the gas in the cell :

$$\theta_{ac} = \theta + C_{ac}(1/P) \quad (17)$$

The plot $\theta_{ac}(1/P)$ is a straight line having a positive slope, C_{ac}, and an intercept θ. This is the experimental test for phenomenon identification and it permits establishing the working pressure at which this perturbatory effect vanishes. The test becomes uncertain for polar fluid vapours for which a $\lambda(P)$ dependence due to a molecular association in the vapour phase has been pointed out.[4]

The conductive heat flow, Q, is independent of both θ and fluid layer thickness, $\dot{r} = r_2 - r_1$, while the convective heat flow, Q_{conv}, is proportional to θ^2 and $\dot{r}^3$. The deviation from the linear behavior $Q_t(\theta)$ is an experimental evidence of the onset of convection. The experimental test for convection absence consists in measuring λ at different θ values, respectively at different Q_t values (or in cells with different d_2 for the same Q_t and T values). The $\lambda(Q_t)$ or $\lambda(d_2)$ dependence indicates the convection occurrence; by progressively reducing the heat flow and thus the temperature gradient (or d_2), a point will be found at which λ remains constant. It is a doubtful procedure to derive λ values from measurments affected by convection, by extrapolating the results to $\theta = 0$. For gases, the absence of convection can be checked by getting constant λ values for experiments at different pressures (viscosities), because λ is pressure independent as stated in the kinetic theory.[5] The pressure is not reduced down to values low enough to occur a temperature jump due to the accomodation phenomenon. The temperature jump effect lessens with the pressure increase, while the convection is minimized by decreasing the gas pressure in the cell. In order to eliminate the two effects, both experimental tests and a correct design of the cell are obligatory.[6-8] It has been established theoretically as well as experimentally that the natural convection is negligible if $\mathrm{Ra} = \mathrm{Gr} \times \mathrm{Pr} < 1\,000$, where Ra, Gr, and Pr are the adimensional Rayleigh, Grashof and Prandtl numbers.[1] The maximum admitted temperature gradient, $Q_{\mathrm{conv}} = (T_1 - T)_{\mathrm{conv}}$, is calculated with the relation:

$$(T_1 - T)_{\mathrm{conv}} < (1\,000\eta\lambda)/(g\beta\dot{r}^3\rho^2 c_p) = (1\,000\nu\lambda)/(g\beta\dot{r}^3\rho c_p) \qquad (18)$$

where ν, ρ, c_p, η, β are kinematic viscosity, density heat capacity at constant pressure, dynamic viscosity and volumetric expansion coefficient of the fluid at temperature $\bar{T}$ respectively; $g = 9.81$ m/s^2 is gravity constant; $\dot{r} = r_2 - r_1$ is fluid layer thickness. For gases, at T and P far away from the respective critical values, $\beta = 1/\bar{T}$. For liquids:

$$\beta = [1/(T_1 - T)]\,[(\rho_T/\rho_{T_1}) - 1]$$

In table 1, the θ_{conv} values as calculated with relation (18) are listed for several fluids, together with physical properties as given in literature.[9]

Table 1 shows the very great difference between the θ_{conv} values for gases and liquids. For most liquids, $\theta_{\mathrm{conv}} < 1$ K.

TABLE 1 A

Calculated θ_{conv} values for some gases

Gas (P = 1 bar)	T (K)	ρ (kg/m³)	c_p (J/(kg.K))	$10^2\lambda$ (W/(mK))	$10^5\eta$ (N s/m²)	$10^3\beta$ (l/K)	θ_{conv} (K)
argon	290	1.66	521.3	1.722	2.21	3.45	1413
	370	1.30	520.8	2.103	2.71	2.70	4190
nitrogen	290	1.16	1039 7	2.524	1.74	3.45	1660
	370	0.90	1041.7	3.065	2.10	2.70	5080
oxygen	290	1.33	917.8	2.592	2.02	3.45	1700
	370	1.03	933.4	3.204	2.44	2.70	5500
hydrogen	290	0.0837	14280.7	17.67	0.88	3.45	>10000
	370	0.0658	14433.4	21.06	1.03	2.70	>10000
carbon dioxide	290	1.835	842.7	1.585	1.45	3.45	436
	370	1.434	913.5	2.206	1.81	2.70	1440
methan	290	0.668	2208.8	3.29	1.08	3.45	1930
	370	0.522	2439	4.40	1.32	2.70	5950
chloroform	290	4.087	607	0.07	1.00	3.45	36.84
benzene	290	4.0	1090	1.01	0.74	3.45	22.64

TABLE 1 B

Calculated θ_{conv} values for some liquids

Liquid (P = 1 bar)	T (K)	ρ (kg/m³)	c_p (J/(kg.K))	λ (W/(mK))	$10^4\eta$ (N s/m²)	$10^3\beta$ (l/K)	θ_{conv} (K)
n-pentane	290	629.1	2301	0.121	2.46	1.56	0.39
	300	619.3	2357.6	0.118	2.26	1.62	0.33
n-octane	290	704.6	2191.7	0.134	5.69	1.14	1.13
	370	637.7	2469	0.111	2.62	1.37	0.39
ciclohexane	290	781.4	1839	0.125	9.72	1.21	1.65
benzene	290	891.3	1712.5	0.1465	6.75	1.13	1.18
	350	827.1	1902.4	0.1313	3.31	1.38	0.45
carbon tetrachloride	290	1599.8	853	0.1055	10.2	1.20	0.76
	350	1482.4	908.7	0.094	4.86	1.34	0.31
ethylene glycol	290	1113	2382	0.250	213.2	0.64	51.93
	370	1056	2742	0.263	24.03	0.67	5.68
glycerine	300	1246.5	2384	0.2880	86.40	0.40	30.90
	370	1210.4	2771.3	0.2972	1.54	0.66	0.31
water	290	998.9	4181.3	0.5918	10.02	0.15	17.43
	370	960.3	4213.3	0.6797	2.89	0.72	1.29

4.5. Geometric cell constant

The geometric constant, A, at temperature $\overline{T}$ is [1,3]:

$$A = [1 + (\delta A'/A')]A' \qquad (19)$$

where:

$$\frac{\delta A'}{A'} = \frac{\overline{T} - T_a}{\ln (d_2 / d_1)} \{\beta_2 - \beta_1 [1 + \ln (d_2/d_1)]\} \qquad (20)$$

and β_1, β_2 are thermal expansion coefficients of the wire (platinum) and cell tube, respectively. With $\beta_1 = 9 \times 10^{-6}$ K^{-1}, β_2 (Pyrex) $= 3.2 \times \times 10^{-6}$ K^{-1} (or β (Jena) $= 5 \times 10^{-6}$ K^{-1}), mean values [1,3] over the 273–373 K range, and $(\overline{T} - Ta) \leqslant 100$ K, one gets $A = 3.7660$ m^{-1}, that is a correction of $-0.104\,\%$.

4.6. Heat loss determination

Assuming that both limiting surfaces are "grey", the radiative heat flow, Q_{rad}, emitted by radiation from the wire towards the inner wall of the cell, across the fluid layer, is estimated with the relation [1]:

$$Q_{\text{rad}} = 4\sigma\varepsilon_1\pi\, d_1 L \overline{T}^3 (T_1 - T) \qquad (21)$$

where $\sigma = 5.67 \times 10^{-8}$ W/(m^{2}K^4) is Stephan-Boltzmann constant and ε_1 is the emissivity of the wire.

$$Q_{\text{rad}}/Q = 4\sigma\varepsilon_1 \overline{T}^3 r_1 \ln (d_2/d_1)/\lambda \qquad (22)$$

The emissivity for polished surface pure platinum in air or reducing atmosphere is estimated over the $400 \leqslant T \leqslant 1\,500$ K range with the relation [1]:

$$\varepsilon_1 = 1.05 \times 10^{-4}\, T + 8 \times 10^{-3}$$

For $\overline{T} \leqslant 370$ K, $\varepsilon_1 \simeq 0.05$ and $\lambda \geqslant 0.01$ W/(mK), it results $Q_{\text{rad}}/Q \leqslant 0.6\,\%$. The heat loss, $Q_{A,\,B}$, through the wire ends and potential leads can be calculated [3] with a precision better than $0.5\,\%$. The $Q_{A,\,B}$ value increases along with λ, being still low ($Q_{A,\,B}/Q < 0.3\,\%$) even for $\lambda = 0.7$ W/(mK).

The total heat flow, Q_t, generated in the wire is generally made up of the following components:

$$Q_t = Q + (Q_{\text{rad}} + Q_{\text{conv}} + Q_{A,B}) \qquad (23)$$

If the experimental test shows an absence of convection, the conductive heat flow is:

$$Q = Q_t - (Q_{\text{rad}} + Q_{A,\,B})$$

In vacuo, $Q = 0$ because $\lambda = 0$. As Q_{rad} and $Q_{A,\,B}$ are pressure independent:

$$Q_t^v = Q_{\text{rad}} + Q_{A,B} \qquad (24)$$

where Q_t^v is the total electrical power measured in vacuo.

$$Q = Q_t - Q_t^v \qquad (25)$$

This is the experimental procedure for overall heat loss determination.

5. EXPERIMENTAL DATA

Since for most liquids $\theta_{conv} < 1$ K and error analysis (Appendix) proved that the θ measurement error was very high, the thermal conductivity measurements were carried out for the following single gases: nitrogen, oxygen, carbon dioxide, propane, n-butane and acetylene. The gases were dried up by passing over the anhidrone columns. Their purity, cromatographically checked, was better than 99%. The measured thermal conductivity, λ_e, values are given in table 2.

TABLE 2

Experimental λ_e thermal conductivity values

nitrogen	$\bar{T}$(K)	306.0	313.4	321.0	330.0	334.9	338.6	345.2	354.7	
	$10^3\ \lambda_e$(W/(mK))	26.7	27.0	27.6	28.2	28.3	28.5	29.3	29.8	
oxygen	$\bar{T}$ (K)	310.1	317.5	325.8	332.4	338.3	342.3	351.2	354.8	360.8
	$10^3\lambda_e$(W/(mK))	27.8	28.6	29.3	29.5	30.1	30.4	30.9	31.3	31.8
carbon dioxide	$\bar{T}$ (K)	307.1	313.2	316.4	325.8	330.6	336.5	344.1	350.7	358.2
	$10^3\ \lambda_e$(W/(mK))	17.3	17.6	18.1	18.7	19.2	19.7	20.2	20.8	21.4
propane	$\bar{T}$ (K)	305.1	315.1	323.0	333.1	337.5	347.0	353.7		
	$10^3\ \lambda_e$(W/(mK))	19.4	20.5	21.5	22.6	23.3	24.0	24.5		
n-butane	$\bar{T}$ (K)	312.5	321.1	324.8	330.0	335.0	341.5	349.9	356.1	
	$10^3\ \lambda_e$(W/(mK))	17.0	17.6	18.2	18.5	19.0	19.9	20.8	21.5	
acetylene	$\bar{T}$ (K)	309.3	316.0	324.0	330.0	334.0	345.0	347.2	354.8	
	$10^3\ \lambda_e$(W/(mK))	23.1	23.5	25.0	25.5	26.0	27.0	27.5	28.1	

In table 3, the literature data [10] on thermal conductivity, λ_t, are listed together with our values $\lambda_e(c)$ as calculated from the experimental $\lambda_e(\bar{T})$ equation.

TABLE 3

λ_t and $\lambda_e(c)$ thermal conductivity values

	$\bar{T}$(K) λ(W/(mK))	300	310	320	330	340	350
nitrogen	$10^3\ \lambda_t(2\%)$	25.98	26.71	27.41	28.08	28.74	29.39
	$10^3\ \lambda_e(c)$	26.21	26.85	27.50	28.14	28.79	29.44
oxygen	$10^3\ \lambda_t(1\%)$	26.74	27.53	28.31	29.07	29.82	30.56
	$10^3\ \lambda_e(c)$	27.19	27.94	28.69	29.44	30.19	30.94
carbon dioxide	$10^3\ \lambda_t(2\%)$	16.62	17.40	18.17	18.95	19.73	20.50
	$10^3\ \lambda_e(c)$	16.67	17.48	18.30	19.11	19.92	20.73
propane	$10^3\ \lambda_t(3\%)$	18.3	19.3	20.4	21.5	22.6	23.7
	$10^3\ \lambda_e(c)$	19.0	20.0	21.1	22.2	23.3	24.3
n-butane	$10^3\ \lambda_t(2\%)$	15.99	16.94	17.93	18.95	19.97	21.01
	$10^3\ \lambda_e(c)$	15.49	16.55	17.60	18.66	19.71	20.76
acetylene	$10^3\ \lambda_t(5\%)$	21.3	22.4	23.5	24.6	25.8	26.9
	$10^3\ \lambda_e(c)$	22.0	23.1	24.3	25.4	26.5	27.7

Our data are in good agreement with those in literature within the estimated accuracy ($\leqslant 2\%$). Continuing these determinations and those already published in a previous paper, [11] we will give to print the data concerning the organic vapours and binary gas mixtures.

APPENDIX

ERROR ANALYSIS

A.1. Random errors

If $y = y(x_1, \ldots, x_n)$ and $\delta x_1 \ldots, \delta x_n$ are the probable errors associated with $x_1, \ldots, x_n$ respectively, then the most probable random error of y is :

$$\delta^2 y = \left(\frac{\partial y}{\partial x_1}\right)^2_{x_2, \ldots, x_n} \delta^2 x_1 + \ldots + \left(\frac{\partial y}{\partial x_n}\right)^2_{x_1, \ldots, x_{n-1}} \delta^2 x_n$$

This equation will be applied to each of the measurements made in the experimental work. Here is an example for $R_0 = 10\ \Omega$, $L = 0.18$ m and $\alpha_0 = 3.9 \times 10^{-3}$ (°C)$^{-1}$.

a) $$\delta R_{sd} = 8 \times 10^{-4}\ \Omega\,;\ \delta R_{sd}/R_{sd} = 8 \times 10^{-5}$$

b) $$R = R_{sd} \mathrm{U}/\mathrm{U}_{sd}$$

$$\delta^2 R = \frac{\mathrm{U}^2}{\mathrm{U}_{sd}^2}\,\delta^2 R_{sd} + \frac{R_{sd}^2}{\mathrm{U}_{sd}^2}\,\delta^2 \mathrm{U} + \frac{\mathrm{U}^2 R_{sd}^2}{\mathrm{U}_{sd}^4}\,\delta^2 \mathrm{U}_{sd}$$

$$\frac{\delta^2 R}{R^2} = \frac{\delta^2 \mathrm{U}}{\mathrm{U}^2} + \frac{\delta^2 \mathrm{U}_{sd}}{\mathrm{U}_{sd}^2} + \frac{\delta^2 R_{sd}}{R_{sd}^2}$$

$$\delta^2 R/R^2 \leqslant (10^{-4})^2 + (10^{-4})^2 + (8 \times 10^{-4})^2/10^2$$

$$\delta^2 R/R^2 \leqslant 2.64 \times 10^{-8}$$

$$\delta R/R \leqslant 1.62 \times 10^{-4}$$

The values of $\delta^2 R$ error are given in Table A.1.

TABLE A.1

Values of $\delta^2 R$ error

t (°C)	0	10	20	30	40	50	60	70	80	90	100
$10^3 \alpha$(°C)$^{-1}$	3.90	3.75	3.62	3.49	3.37	3.26	3.16	3.06	2.97	2.89	2.81
R (Ω)	10.00	10.39	10.78	11.17	11.56	11.95	12.34	12.73	13.12	13.51	13.90
$10^6\ \delta^2 R(\Omega)^2$	2.64	2.85	3.07	3.29	3.53	3.77	4.02	4.28	4.54	4.82	5.10

c) $$\alpha_t = (R' - R)/[R(\Delta t)]\,;\quad \Delta t = t' - t$$

$$\delta^2\alpha_t = \frac{1}{R^2(\Delta t)^2}\,\delta^2 R' + \frac{R'^2}{R^4(\Delta t)^2}\,\delta^2 R + \frac{\alpha_t^2}{(\Delta t)^2}\,(\delta^2 t' + \delta^2 t)$$

$$\frac{\delta^2\alpha_t}{\alpha_t^2} = \left(1 + \frac{1}{\alpha_t\,\Delta t}\right)^2 \left(\frac{\delta^2 R'}{R'^2} + \frac{\delta^2 R}{R^2}\right) + \frac{\delta^2 t' + \delta^2 t}{(\Delta t)^2}$$

For $t = 20°\mathrm{C}$ and $\delta t = \delta t' = 0.02°\mathrm{C}$, the values of $\delta\alpha_t/\alpha_t$ relative error are presented in Table A.2.

d) $$\Delta t = (R' - R)/(R\alpha_t)\,;\quad \Delta t = t' - t$$

$$\delta^2(\Delta t) = \frac{1}{R^2\alpha_t^2}\,\delta^2 R' + \frac{R'^2}{R^4\alpha_t^2}\,\delta^2 R + \frac{(\Delta t)^2}{\alpha_t^2}\,\delta^2\alpha_t$$

$$\frac{\delta^2(\Delta t)}{(\Delta t)^2} = \left(1 + \frac{1}{\alpha_t\Delta t}\right)^2 \left(\frac{\delta^2 R'}{R'^2} + \frac{\delta^2 R}{R^2}\right) + \frac{\delta^2\alpha_t}{\alpha_t^2}$$

The values of $\delta(\Delta t)/\Delta t$ relative error calculated for $t = 20°\mathrm{C}$ and $\delta^2\alpha_t/\alpha_t^2 = 1.46 \times 10^{-6}$ are given in Table A.2.

TABLE A.2

Values of $\delta\alpha_t/\alpha_t$ and $\delta(\Delta t)/\Delta t$ relative errors

t' (°C)	30	40	50	60	70	80	90	100
$10^{11}\ \delta^2\alpha_t$ (°C)$^{-2}$	67.1	17.8	8.38	4.98	3.37	2.46	1.91	1.54
$10^{6}\ \delta^2\alpha_t/\alpha_t^2$	51.2	13.6	6.39	3.80	2.57	1.88	1.46	1.17
$10^{3}\ \delta\alpha_t/\alpha_t$	7.16	3.69	2.53	1.95	1.60	1.37	1.21	1.08
$10^{3}\ \delta^2(\Delta t)$ (°C)^2	4.47	5.22	6.26	7.61	9.26	11.2	13.5	16.0
$10^{6}\ \delta^2(\Delta t)/(\Delta t)^2$	44.7	13.0	6.96	4.76	3.70	3.11	2.75	2.50
$10^{3}\ \delta(\Delta t)/(\Delta t)$	6.68	3.61	2.64	2.18	1.92	1.76	1.66	1.58

e) $$R_1 = R_{sd}\mathrm{U}_1/\mathrm{U}_{sd,1}$$

$$\delta^2 R_1 = \frac{\mathrm{U}_1^2}{\mathrm{U}_{sd,1}^2}\,\delta^2 R_{sd} + \frac{R_{sd}^2}{\mathrm{U}_{sd,1}^2}\,\delta^2\mathrm{U}_1 + \frac{\mathrm{U}_1^2 R_{sd}^2}{\mathrm{U}_{sd,1}^4}\,\delta^2\mathrm{U}_{sd,1}$$

$$\frac{\delta^2 R_1}{R_1^2} = \frac{\delta^2\mathrm{U}_1}{\mathrm{U}_1^2} + \frac{\delta^2\mathrm{U}_{sd,1}}{\mathrm{U}_{sd,1}^2} + \frac{\delta^2 R_{sd}}{R_{sd}^2}$$

$$\delta^2 R_1/R_1^2 \leqslant 2.64 \times 10^{-8}$$

$$\delta R_1/R_1 \leqslant 1.62 \times 10^{-4}$$

f)
$$\theta = (R_1 - R)/(R\alpha_t)$$

$$\delta^2\theta = \frac{1}{R^2\alpha_t^2}\,\delta^2 R_1 + \frac{R_1^2}{R^4\alpha_t^2}\,\delta^2 R + \frac{\theta^2}{\alpha_t^2}\,\delta^2\alpha_t$$

$$\frac{\delta^2\theta}{\theta^2} = \left(1+\frac{1}{\theta\alpha_t}\right)^2\left(\frac{\delta^2 R_1}{R_1^2}+\frac{\delta^2 R}{R^2}\right)+\frac{\delta^2\alpha_t}{\alpha_t^2}$$

The values of $\delta\theta/\theta$ relative error calculated with $\delta^2\alpha_t/\alpha_t^2 = 1.46 \times 10^{-6}$ are presented in Table A.3.

TABLE A.3

Values of $\delta\theta/\theta$ relative error

t (°C)	θ(°C)	$\delta\theta/\theta$ (%)	t(°C)	θ(°C)	$\delta\theta/\theta$ (%)
20	0.5	12.7	70	0.5	15.0
	1	6.37		1	7.53
	2	3.20		2	3.78
	3	2.14		3	2.53
	4	1.61		4	1.90
	5	1.30		5	1.53
30	0.5	13.2	80	0.5	15.5
	1	6.61		1	7.76
	2	3.32		2	3.89
	3	2.22		3	2.60
	4	1.67		4	1.96
	5	1.35		5	1.57
40	0.5	13.7	90	0.5	15.9
	1	6.84		1	7.97
	2	3.43		2	4.00
	3	2.30		3	2.68
	4	1.73		4	2.01
	5	1.39		5	1.62
50	0.5	14.1	100	0.5	16.4
	1	7.07		1	8.20
	2	3.55		2	4.11
	3	2.38		3	2.75
	4	1.79		4	2.07
	5	1.44		5	1.66
60	0.5	14.6			
	1	7.30			
	2	3.66			
	3	2.45			
	4	1.84			
	5	1.48			

g)
$$Q_t = \mathrm{U}_1\mathrm{U}_{\mathrm{sd},1}/R_{\mathrm{sd}}$$

$$\delta^2 Q_t = \frac{\mathrm{U}_1^2}{R_{\mathrm{sd}}^2}\,\delta^2\mathrm{U}_{\mathrm{sd},1} + \frac{\mathrm{U}_{\mathrm{sd},1}^2}{R_{\mathrm{sd}}^2}\,\delta^2\mathrm{U}_1 + \frac{\mathrm{U}_1^2\mathrm{U}_{\mathrm{sd},1}^2}{R_{\mathrm{sd}}^4}\,\delta^2 R_{\mathrm{sd}}$$

$$\frac{\delta^2 Q_t}{Q_t^2} = \frac{\delta^2\mathrm{U}_1}{\mathrm{U}_1^2} + \frac{\delta^2\mathrm{U}_{\mathrm{sd},1}}{\mathrm{U}_{\mathrm{sd},1}^2} + \frac{\delta^2 R_{\mathrm{sd}}}{R_{\mathrm{sd}}^2}$$

$$\delta^2 Q_t/Q_t^2 \leqslant 2.64 \times 10^{-8}$$

$$\delta Q_t/Q_t \leqslant 1.62 \times 10^{-4}$$

A.2. Systematic errors

h)
$$A = \ln(d_2/d_1)/(2\pi L)$$

$$\frac{\delta^2 A}{A^2} = \frac{1}{[\ln(d_2/d_1)]^2}\left[\left(\frac{\delta d_2}{d_2}\right)^2 + \left(\frac{\delta d_1}{d_1}\right)^2\right] + \frac{\delta^2 L}{L^2} = \frac{1}{(4.28)^2}\left[\left(\frac{10^{-2}}{3.6}\right)^2 + \left(\frac{5\times 10^{-4}}{0.05}\right)^2\right] + \left(\frac{0.02}{180}\right)^2$$

$$\delta^2 A/A^2 = 5.9 \times 10^{-6}$$

$$\delta A/A = 2.4 \times 10^{-3}$$

i) Cell eccentricity correction : $<0.1\%$

j) Correction for the temperature drop across the glass wall of the cell : $<0.5\%$

k) Correction for the heat loss through the wire ends and potential leads : $<0.2\%$

l) Correction due to the heat loss by thermal radiation : $<0.2\%$

Finally, the overall error in λ determination is :

$$\frac{\delta^2\lambda}{\lambda^2} = \frac{\delta^2 A}{A^2} + \frac{\delta^2 Q}{Q^2} + \frac{\delta^2\theta}{\theta^2}$$

For gases ($\theta \geqslant 5$ K) one obtains :

$$\delta^2\lambda/\lambda^2 \leqslant 5.9 \times 10^{-6} + 2.64 \,.\, 10^{-8} + 10^{-4}$$

$$\delta^2\lambda/\lambda^2 \leqslant 1.06 \times 10^{-4}\,;\ \delta\lambda/\lambda \leqslant 1.03 \times 10^{-2}$$

The error in thermal conductivity measurement is determined by the error in θ measuring. For liquids, where $\theta < 1$ K, the error in thermal conductivity measurement is 8–20%

REFERENCES

[1] "Thermal Conductivity", ed. R.P. Tye, vol. II, Acad. Press, London, 1969.

[2] D.I. Marchidan and M. Ciopec, "Temperatura, scări, metode și mijloace de măsurare", Ed. Științifică și enciclopedică, București, 1977.

[3] N.V. Tsederberg, "Thermal Conductivity of Gases and Liquids", Edward Arnold Ltd., London, 1965.

[4] L.A. Bennett and R.G. Vines, *J. Chem. Phys.*, **23**, 1587 (1955).

[5] J. Hirschfelder, C. Curtiss and B. Bird, "Molecular Theory of Gases and Liquids", Wiley, New York, 1954.

[6] J. A. A. Snel, Thesis, Amsterdam, 1973.

[7] R. Vîlcu and A. Ciochină, *Studii și Cercetări de Chimie, Acad. R.S.R.*, **21**, 571 (1973).

[8] R. Vîlcu and A. Ciochină, *Studii și Cercetări de Chimie, Acad. R.S.R.*, **21**, 643 (1973).

[9] N. B. Vargaftik, "Spravocinik po teplofiziceskim svoistvam gazov i zhidkostei", Nauka, Moscova, 1972.

[10] Y. S. Touloukian, P. E. Liley and S. C. Saxena, "Thermophysical Properties of Matter", vol. 3, TPRC Data Series, Plenum Press, New York, 1970.

[11] R. Vîlcu and A. Ciochină, *Rev. Roumaine Chim.*, **17**, 1679 (1972).

Revue Roumaine de Chimie, 26, 2, 175–183 (1981)

FEM STUDY OF SILVER LAYERS ADSORBED ON TUNGSTEN. II.[1]

SURFACE STRUCTURE AND SURFACE MIGRATION

CR. CONȚESCU and M. I. VASS
Institute for Chemical Research, Center of Physical Chemistry, Spl. Independenței 202,
77208 Bucharest, Romania

Received May 20, 1980

The values of diffusion coefficient (D), activation energy (E_{diff}), activation entropy and jump frequency in surface diffusion of silver atoms within the first monolayer adsorbed on clean tungsten surface were measured for three characteristic surface directions. It is found that E_{diff} depends on the moving direction relative to tungsten planes, whereas the preexponential factors D_0 have anomalously low values. The former is caused by steric constraints of the motion and is related to local surface atomic structures, while the latter shows that motion of adsorbed atoms is correlated because of interatomic interactions.

1. INTRODUCTION

The methods of Field Emission Microscopy (FEM) and Field Ion Microscopy (FIM) offer the unique possibility of surveying the dynamics of adsorbed atoms in relation to atomic arrangement of solid surfaces. Indeed, in their motion over the substrate surface, adsorbed atoms map the contour of surface potential fields acting on them along the moving direction. As a general rule, surface diffusion on close packed single crystal planes needs small activation energy but the rougher the surface on the atomic scale, the higher the corresponding diffusion barrier. On several crystal planes there are preferential directions of atomic migration. A good example is the W (211) plane, where surface atoms migrate easily along the parallel atomic rows [111] oriented but never on the perpendicular [$0\bar{1}1$] direction.[2]

We previously studied surface diffusion of silver layers adsorbed on tungsten.[1] Two different diffusion mechanisms were observed for deposits with thickness in the range of 3 to 4 atomic layers, depending on the initial deposit configuration and temperature range. Migration was always highly anisotropic in respect of tungsten substrate and showed the occurrence of limiting surface barriers, passing through some high index planes with pronounced surface atomic roughness. In the present work the results on surface migration of silver atoms within the first adsorbed monolayer are given. [3] The experimental work was done using the same FEM apparatus and procedure described elsewhere. [1]

2. RESULTS AND DISCUSSIONS

The change of emission patterns during migration of a submonolayer silver film adsorbed on tungsten single crystal is shown in figure 1. By dosing the clean tungsten surface (Fig. 1, a) with silver at room temperature, a deposit is formed only on the emitter regions facing directly the vapor source, namely on the (111) plane (Fig. 1, b). By heating this layer between 400 and 500 K, silver atoms move rapidly over the (110) plane and concentrate on (111) and its vicinals and also around the (100) planes (Fig. 1, c-e). Since adsorbed silver increases the surface work function, [1,3] migration of silver atoms towards (100) can be followed by the graduate darkening of the invaded areas (Fig. 1). Finally silver is uniformly spread over the surface region limited by $(21\bar{1})$, (110), (211), (100) planes (Fig. 1, f, g), excepting a small area around (301). At this stage, the mean coverage degree determined from the work function value (4.56 eV) and the known intensity of vapor flux is $\bar{\theta} = 0.75$.

Assuming that surface migration takes place by independent jumps of adsorbed atoms, the well-known relationships

$$\overline{(\Delta\bar{x})^2} = CDt \tag{1}$$

$$D = D_0 \exp\left(-E_{\mathrm{diff}}/kT\right) \tag{2}$$

$$D_0 = \frac{\nu a^2}{2\alpha} \tag{3}$$

$$\nu = \frac{kT}{h} \exp\left(\Delta S_{\mathrm{diff}}/k\right) \tag{4}$$

might be used to calculate the diffusion coefficient D, activation energy E_{diff} and activation entropy ΔS_{diff}. In the above equations $\Delta\bar{x}$ is the mean distance traversed by the boundary in time t, ν is the frequency of elementary jumps, a is the mean jump length, $C \approx 1$ and $\alpha = 2$ for two-dimensional diffusion.

Although very familiar, the above expressions make necessary some cautionary remarks in connection with their using on surface diffusion. They have been deduced in the usual approach of the absolute rate theory and assuming that migration takes place by individual atomic jumps, *i.e.* by neglecting the possibility of correlated motion. In most work on bulk diffusion, this point is not very important, since the diffusing impurity atoms or crystal defects are usually in quite low concentration. Since diffusion species on the surfaces may be much more concentrated, lateral interactions may be serious and the event of correlated

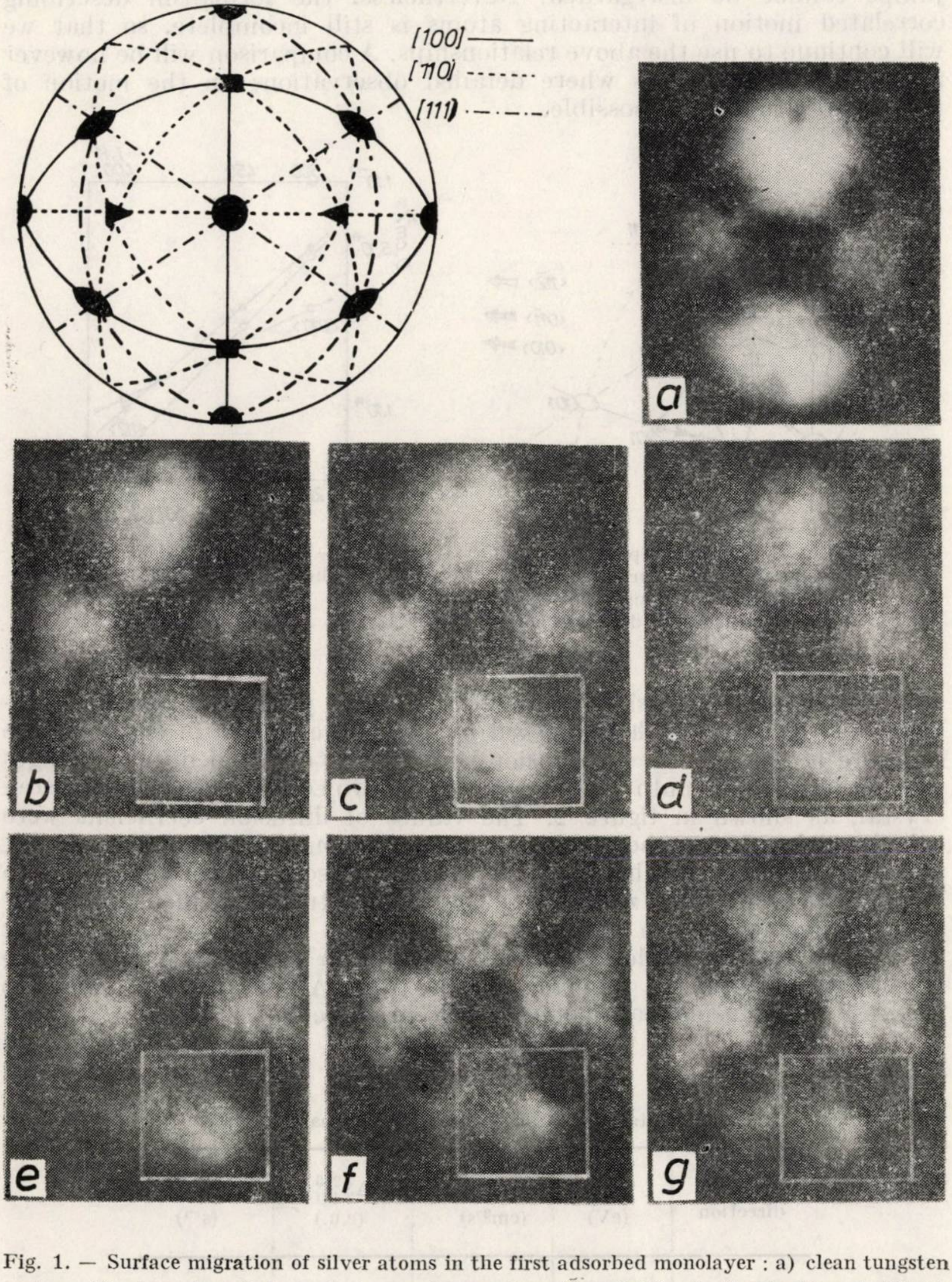

Fig. 1. — Surface migration of silver atoms in the first adsorbed monolayer : a) clean tungsten surface ; b) silver deposit formed at room temperature ($\bar{\theta} = 0.75$) ; c) after heating at 400 K, 1 minute ; d) at 400 K, 4 minutes ; e) at 450 K, 4 minutes ; f) at 500 K, 1 minute ; g) at 500 K, 2 minutes. On the top left are shown the stereographic projection and main zone lines of a b.c.c. crystal.

jumps cannot be disregarded. Nevertheless, the formalism describing correlated motion of interacting atoms is still incomplete, so that we will continue to use the above relationships. A comparison will be however made with other works where detailed observations on the motion of individual atoms are possible.

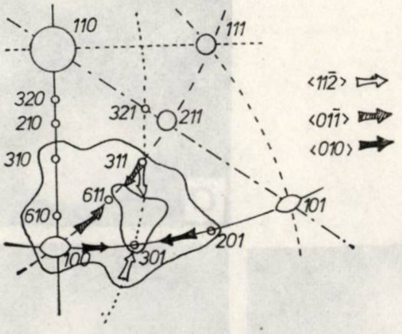

Fig. 2. -- Crystallographic map of the square figure marked on emission patterns showing the initial and final positions of diffusion boundary.

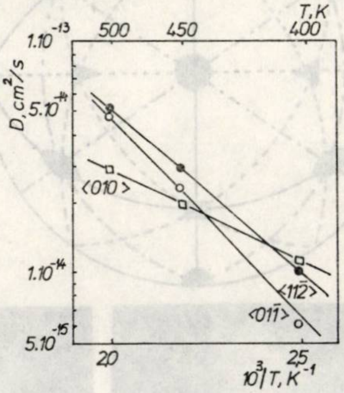

Fig. 3. — Temperature dependence of the diffusion coefficients.

To evaluate diffusion parameters, a small portion of emission patterns was chosen, which is marked by the white square in the sequence of figure 1. The contour of diffusion boundary at different diffusion stages was then mapped onto the stereographic projection of b.c.c. tungsten crystal, as shown in figure 2. The values of diffusion coefficient were calculated by timing the motion of diffusion boundary at 400 K, 450 K and 500 K on three characteristic surface directions, corresponding to $[11\bar{2}]$, $[010]$ and $[01\bar{1}]$ zone lines. The temperature dependence of diffusion coefficients, shown in figure 3, allowed us to determine E_{diff} and D_0 for the three considered directions. A jump length of 3 Å, close to the lattice constant of tungsten crystal (3.17 Å) was used to calculate the rest of diffusion parameters given in table 1.

TABLE 1

Experimental values of surface diffusion parameters

Surface direction	E_{diff} (eV)	D_0 (cm²/s)	$\Delta S_{\text{diff}}^{273}$ (e.u.)	ν (s⁻¹)
[010]	0.19	$2.49.10^{-12}$	−38.9	$1.11.10^{4}$
$[11\bar{2}]$	0.27	$2.41.10^{-11}$	−35.1	$1.07.10^{5}$
$[01\bar{1}]$	0.36	$2.35.10^{-10}$	−30.6	$1.04.10^{6}$

It is found that surface migration of adsorbed silver atoms is strongly dependent on the moving direction relative to substrate. Activation energy, although smaller than the mean value reported by Jones[4] for the same system (0.55 eV) is characteristic for a true surface migration process. Jump frequency is also well compared with Jones' values ($6.10^5 - 5.10^8\ s^{-1}$).

It is interesting that activation entropy has negative values. According to the kinetic model of diffusion based on absolute rate theory, ΔS_{diff} is always positive for perfect elastic crystals.[5] Negative values of ΔS_{diff} were however experimentally observed in migration of copper[6] and gold[7] films on tungsten, associated with surface potential barriers passing through (301) planes. These evidences of apparent negative diffusion entropy are indications for a migration process where the moving atoms are trapped in nonequivalent surface sites. Taking for example $\Delta S = -40$ cal/mole.K and $T = 400$ K, it can be simply shown that $\Delta G \leqslant 0$ implies $\Delta H \leqslant -1.6$ kcal/mole $= -0.07$ eV. This could be a good estimation for the variation of adsorption energy between different crystal planes.

One can further observe from table 1 that values of D_0 between $10^{-10} - 10^{-12}$ cm²/s are very small compared with values characteristic for surface diffusion of individual atoms (usually in the range of $10^{-3} - 10^{-5}$ cm²/s). They rather approach the order of magnitude of D_0 for diffusion processes taking place through correlated jumps of small atomic groups (dimers, trimers).[8,9] On the other hand, activation energy, which is much less than the mean adsorption energy (2.38 eV),[3] is rather characteristic for diffusion of small atomic groups than of individual atoms. The above-mentioned things allow us to conclude that the surface migration of silver atoms in the first chemisorbed layer is a cooperative phenomenon, taking place by correlated jumps of neighbor adsorbed atoms, at least in the proximity of (100) planes. This is in agreement with recent works of Ehrlich,[8,9] who found that pairs or triplets of adsorbed atoms can diffuse as a unit and their motion is characterized by low values of both D_0 and E_{diff}.

The unexpected importance of mutual interactions for correlated motion of neighbor adsorbed atoms is perhaps one of the most important results of recent studies on surface diffusion.[8-11] They throw a new light upon the complexity of surface diffusion and reveal the role of still ignored factors, needing theoretical explanations. For the system studied here we may assume that the reasons of correlated motion of adsorbed silver atoms are dipole – dipole interactions within the first adsorbed monolayer. These interactions should be more important at $\overline{\theta} = 0.75$, which is the coverage corresponding to the maximum increase of the mean work function.[1]

3. THE ROLE OF STRUCTURAL FACTORS

Experimental data given in table 1 show that activation energy has different values for various moving directions on tungsten surface. This is clearly the effect of local arrangement of substrate atoms and it could be related either to the microstructure of a given plane or to macrostructure of the entire emitter surface. It can be well assumed, as Gomer did, [12] that a relatively small number of surface sites may exist for silver atoms to be adsorbed on tungsten surface. Various substrate planes differ mainly in the number, but not in the type of trap sites. Since atomic jumps in diffusion occur between pairs of equivalent trap sites, we will find on each plane a limited number of surface paths for elementary atomic jumps, associated to given crystallographic directions. For each direction, the initial and final positions of a jumping atom are stable adsorption positions. They are however separated by some intermediate surface sites where the moving atoms are held in the state of activated complex. According to this atomistic picture, the activation energy for a given surface direction may be correlated to the number and kind of intermediate activated positions, i.e. it depends on the steric constraints of the motion.

Marble models are suited to represent the surface microstructure of metals on an atomistic scale. The equilibrium position of the adsorbate may be obtained using the hypothesis of pairwise interactions, which works well in adsorption of metals on metals, provided charge transfer is small and covalent bonding is likely. [13] It is found that stable adsorption sites are those where adatoms contact the maximum number of substrate atoms. Since the difference of atomic radii is not very large for Ag/W system, these positions should be in a fairly good correspondence with "lattice" sites (L) of substrate atoms in the next adjacent plane. Taking the example of (110), (111) and (211) planes of b.c.c. W, let us examine on structural models on a clean surface (Fig. 4) what kind of intermediate activated positions a moving atom meets when jumping between two equivalent "lattice" sites.

There are four kinds of surface sites on W (110) plane : a centered one on top of a tungsten atom (C), the "bridge" position (B), the "saddle" one (S) and the normal "lattice" position (L). The sequences of intermediate positions traversed in an elementary jump between two neighbor "lattice" sites are L→C→L in [010] direction and L→S→C→S→→L in $[01\bar{1}]$ direction. The jump lengths are also different : $a_{[010]} = 3.17$ Å and $a_{[01\bar{1}]} = 4.47$ Å. The state of activated complex should then be identified with C positions for surface migration in [010] direction but it is more complicated and consists of a combination of (S — C — S) positions along $[01\bar{1}]$. The corresponding activation barrier should be smaller for [010] than for $[01\bar{1}]$ and this is precisely what we observed (0.19 eV compared with 0.36 eV).

Surface sites on W (111) are of three kinds : centered on top of a tungsten atom in the outermost layer (C), "fault" positions (F) onto a second layer atom and true "lattice" sites (L) onto a third layer atom. The energetic difference between F and L positions is not very large, [14] so that atomic jumps parallel to $[11\bar{2}]$ direction may occur between L→F positions with an activation energy of 0.27 eV. It corresponds to "turning " of a silver atom around the saddle existing between a couple of tungsten atoms of the outermost layer, parallel to [011] direction. In contrast with this, elementary jumps along $[01\bar{1}]$ take place by "clim-

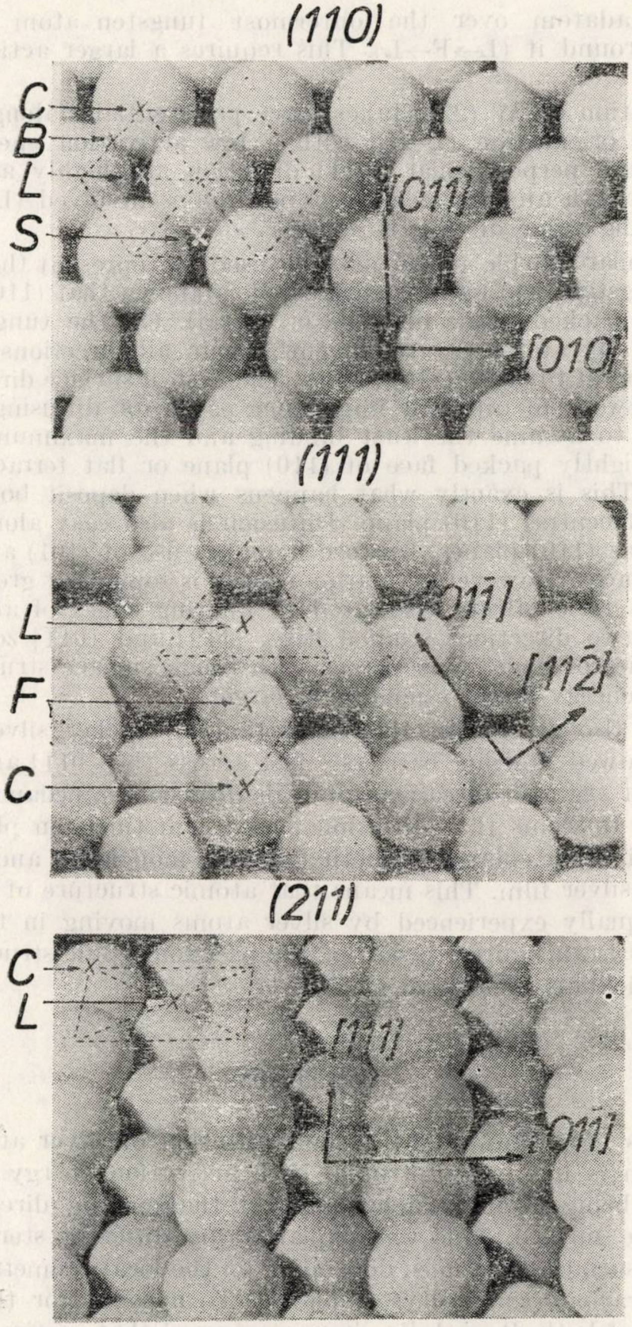
(110)
C
B
L
S
[01$\bar{1}$]
[010]
(111)
L
[01$\bar{1}$]
[11$\bar{2}$]
F
C
(211)
C
L
[1$\bar{1}$1]
[01$\bar{1}$]

Fig. 4. — Marble models of surface atomic structure on (110), (111) and (211) tungsten planes showing the geometry of some surface sites available for adsorbed atoms.

bing" an adatom over the outermost tungsten atom (L→C→L) or by going around it (L→F→L). This requires a larger activation energy (0.36 eV).

Migration on W (211) takes place preferentially along atomic rows with [111] orientation (L→L) with a low activation energy. [2] Atomic jumps in the perpendicular [01$\bar{1}$] direction are highly activated, since a sequence with an intermediate C position is involved (L→C→L). The corresponding value of E_{diff} is 0.36 eV.

A similar marble model may be used to represent the macrostructure of tungsten field emitter surface. It is known that (110) plane is the most close packed plane of a b.c.c. crystal. On the tungsten tip it is sorrounded by atomically rough surfaces in all directions except [111] zones, linking it to other (110) planes. The rest of surface directions constitutes a network of different impedance paths for diffusing atoms. It is reasonably to assume the least binding and the maximum mobility on the most tightly packed face of (110) plane or flat terraces with (110) structure. This is exactly what happens when deposit boundary meets the edge of central (110) plane. Diffusion is also easy along [010] zone line, towards (110) planes, because it makes use of (101) and (10$\bar{1}$) close packed terraces. However activation energy is somewhat greater (0.19 eV) because of steric effects associated to limiting edges of above terraces. The other two directions studied here, [11$\bar{2}$] and [01$\bar{1}$] zone lines, traverse a series of high index planes with rough surface structure and the activation energy is correspondingly larger.

It is also significant that migration of thicker silver layers ($\bar{\theta} = 4-5$) showed limiting barriers [1] just across the [01$\bar{1}$] and [11$\bar{2}$] zone lines, which are also directions of high diffusion impedance in the first monolayer. It seems that diffusion over rough tungsten planes requires a large activation energy for both the first monolayer and next atomic layers of a silver film. This means that atomic structure of tungsten substrate is equally experienced by silver atoms moving in the outermost layers. This is an indirect proof for the pseudomorphic structure of silver films at thickness of several monolayers. [1,3]

4. CONCLUSIONS

It has been shown that surface diffusion of silver atoms adsorbed on tungsten is highly anisotropic, both activation energy and diffusion coefficient being strongly dependent on the moving direction relative to substrate surface. This was explained by different steric constraints on various surface directions, depending on the local geometry of tungsten atoms on various single crystal planes. To account for the anomalous low values of both D_0 and E_{diff} it was assumed that motion of neighbor adsorbed atoms is correlated. This may be a consequence of dipole — dipole interactions in silver layers when the surface coverage corresponds to the maximum work function increase.

REFERENCES

[1] Part I: M.I. Vass and Cr. Conţescu, *Rev. Roumaine Chim.*, **20**, 1253 (1975).

[2] G. Ehrlich and F. G. Hudda, *J. Chem. Phys.*, **44**, 1039 (1966).

[3] Cr. Conţescu, Thesis, National Institute for Chemistry, Bucharest, (1979).

[4] J. P. Jones, *Surface Sci.*, **32**, 29 (1972).

[5] J. W. Christian, "The Theory of Transformation in Metals and Alloys", Pergamon Press, Oxford, 1967.

[6] J. P. Jones, *Proc. Roy. Soc.*, **A 284**, 469 (1965).

[7] J. P. Jones, in "Surface Phenomena of Metals", Monograph No. 28, Soc. Chem. Ind., 1967.

[8] W. R. Graham and G. Ehrlich, *Phys. Rev. Letters*, **31**, 1047 (1973).

[9] W. R. Graham and G. Ehrlich, *Thin Solid Films*, **25**, 85 (1975).

[10] G. E. Rhead, *Surface Sci.*, **47**, 205 (1975).

[11] T. T. Tsong, P. Cowan and G. Kellog, *Thin Solid Films*, **25**, 97 (1975).

[12] R. Gomer, "Field Emission and Field Ionization", Harvard Univ. Press, Cambridge, Massachusetts, 1961.

[13] E. Bauer, *J. Physique (Colloque C 4)*, **38**, C4 – 146 (1977).

[14] G. Ehrlich, *Surface Sci.*, **63**, 422 (1977).

Revue Roumaine de Chimie, **26**, *2* 185–195 (1981)

ADSORPTION ON HETEROGENEOUS SURFACES: ON THE "CONDENSATION APPROXIMATION"

V.T. POPA and E. SEGAL

Polytechnical Institute of Bucharest, Department of Physical Chemistry and Electrochemical Technology, Bucharest, Bd. Republicii 13, Romania

Received May 13, 1980

The method of the condensation approximation is presented following essentially Roginski's approach. Some new mathematical and physical features of the problem are revealed. A new general procedure of getting the expression of the inferior limit of integration, characteristic of this method, is proposed. This new expression is shown to be physically consistent and mathematically more suitable than the "classical" one, in the case of Langmuir local behaviour.

I. INTRODUCTION

The framework of the present paper is the so-called "homotattic patch" model,[1,2] describing adsorption on heterogeneous surfaces. In the following, we shall restrict ourselves to localized monolayer adsorption – independent systems – on heterogeneous surfaces.[3] Under these circumstances, the fundamental relation we shall make use of, is:

$$\vartheta(p) = \int_{\Delta\epsilon} \theta(p, \epsilon)\, \chi(\epsilon)\, \mathrm{d}\epsilon \tag{1}$$

where

– $\vartheta(p)$ is the overall adsorption (coverage) on the heterogeneous surface, also called "total" isotherm, being the analytical expression of the experimental data;

– $\Delta\epsilon$ is the range of possible values of the adsorption energy, ϵ; with a proper definition of the function $\chi(\epsilon)$, $\Delta\epsilon$ is usually taken equal to $[0, \infty)$;

– $\chi(\epsilon)$ is the "energetic" distribution of the adsorption sites, *i.e.* $\chi(\epsilon)\mathrm{d}\epsilon$ is the fraction of the total number of adsorption sites with adsorption energies in the range $[\epsilon, \epsilon + \mathrm{d}\epsilon]$; in probabilistic terms $\chi(\epsilon)$ has the meaning of a probability density;

– $\theta(p, \epsilon)$, called "local" isotherm, is the expression of a *postulated* adsorption mechanism, assumed *the same* for the whole adsorption energy, $\Delta\epsilon$, and pressure, Δp, experimental ranges. Considering heterogeneity from a strictly energetic point of view, the expression of $\theta(p, \epsilon)$

has to be one of some (kinetically or statistically derived) isotherms on a (energetically) homogeneous surface. For localized monolayer adsorption the following boundary conditions are fulfilled:

$$\begin{cases} \theta(p,\ 0) = 0 \\ \theta(p,\infty) = 1 \end{cases} \tag{2}$$

$$\begin{cases} \theta(0,\ \epsilon) = 0 \\ \theta(\infty, \epsilon) = 1; \end{cases} \tag{3}$$

the adsorption (coverage) monotoneously increases with both adsorption energy and pressure. Moreover, $\theta(p, \epsilon)$ has another important property:

$$\int_0^{\infty} [1 - \theta(p, \epsilon)]\, d\epsilon = \varepsilon_1(p) \tag{4}$$

where $\varepsilon_1(p)$ has the dimensions of an energy and, taking into account (3) it fulfils the following boundary conditions:

$$\begin{cases} \varepsilon_1(0) = \infty \\ \varepsilon_1(\infty) = 0 \end{cases}, \quad 0 \leqslant \epsilon < \infty. \tag{5}$$

$\vartheta(p)$ is subject to the boundary conditions:

$$\begin{cases} \vartheta(0) = 0 \\ \vartheta(\infty) = 1 \end{cases}. \tag{6}$$

Introducing the second conditions of (6) and (3) in (1) we get the normalization requirement for the distribution function:

$$\int_{\Delta\epsilon} \chi(\epsilon)\, d\epsilon = 1 \tag{7}$$

Mathematically, equation (1) represents a Fredholm integral equation of the first kind, when $\Delta\epsilon = [0, \infty)$, the solution of which caused (and still causes) a large amount of theoretical work. Two excellent review papers are an older one of Honig [4] and a more recent one of Cerofolini. [5]

The exact solution of equation (1) is a rather difficult problem. There are many attempts, out of which the Sips [6] and Cerofolini [5] methods have been largely used and commented upon in subsequent papers. Unfortunately, none of the rigorous methods is free of inconveniencies. For example, the Sips one, based on the formalism of the Stieltjes transform, imposes severe restrictions on the acceptable analytical form of $\vartheta(p)$, thus being of restricted use in the interpretation of the experimental data. The method proposed by Cerofolini [5] and developed later [7,8], consists of Fourier series expansion of the functions ϑ, θ and $\varkappa$ and does not need an analytical expression of the experimental data, $\vartheta(p)$, but involves a large amount of computations. The method was criticized [9] and improved [10] by Smutek, whose conclusion is unfavourable: even the improved formalism involves tedios iterations and the resulting distribution function may still be irrelevant for the experimental data. Smutek recommends an alternative method [11] based on the Γ-distributions.

In most cases, "exact" (or, more precisely, rigorous) methods of evaluating the function $\chi(\epsilon)$, although involving a great deal of (numeric) calculations, lead more or less to some approximation of the experiment. The reason of this fact must be looked for either in the mathematical restrictions imposed on the experimental data, $\vartheta(p)$, (in the case of analytical methods), or in the intrinsic difficulties of the computing formalism (in the case of numerical methods).

Consequently, it was quite natural to derive some (essentially) approximate but mathematically convenient methods. It is an act of justice rendering to quote under this circumstance the name of Roginski[12,13] who seems to have been forgotten in the last ten years published papers. Roginski gave the first systematic approach to the problem of approximate solving of the equation (1). Twenty years later, Harris [14] used the term "condensation approximation" (C.A.) for a (formally but not essentialy) different treatment of the problem. In addition to some applications of the C.A., Harris presented a procedure of evaluating the errors involved in using this method.

In the following, apart from the general presentation of the method, we shall outline some features of the problem which, as far as we know, have not been dealt with, till now. We shall adopt and (we hope) improve Roginski's approach which seems more appropriate to the physical picture of the method than the unanimously followed (in subsequent papers) approach of Harris.

II. THE CONDENSATION APPROXIMATION

Equation (1) is considerably simplified by replacing the kernel (local isotherm) $\theta(p, \epsilon)$ with a step-function :

$$\theta_a(p, \epsilon) = \begin{cases} 0 \; \epsilon < \varepsilon_a(p) \\ 1 \; \epsilon \geqslant \varepsilon_a(p) \end{cases} \tag{8}$$

For $\epsilon_m \leqslant \epsilon \leqslant \epsilon_M$, a much simpler equation results, containing under the integral sign only an *approximate* distribution function, $\chi_a(\epsilon)$

$$\vartheta(p) = \int_{\varepsilon_a(p)}^{\epsilon_M} \chi_a(\epsilon)\, d\epsilon \tag{9}$$

which, assuming the existence of the inverse function, $p = p_a(\epsilon)$, can be readily obtained :

$$\chi_a(\epsilon) = \frac{\partial \vartheta[p_a(\epsilon)]}{\partial \epsilon} \tag{10}$$

The main mathematical problem of this method consists in the choice of the function $\varepsilon_a(p)$ so that the approximate function, $\chi_a(\epsilon)$, to be as close as possible to the "true" one, $\chi(\epsilon)$. Several mathematical procedures (and physical arguments) for obtaining $\varepsilon_a(p)$ were reported,[5,12–14] all of them giving the same final result (at least in the case of Langmuir local behaviour). The general way is to impose certain conditions to the local isotherm and to explicitate a relation between $\epsilon = \varepsilon_a$ and p. Such a condition [13] is :

$$\frac{\partial^2 \theta(p, \epsilon)}{\partial \epsilon^2} = 0 \tag{11}$$

which gives $\varepsilon_a(p)$ as the inflexion abscissa of the function $\theta(p = \text{ct.}, \epsilon)$, which will be denoted $\varepsilon_0(p)$. We must outline that the sigmoid form of the function $\theta(p = \text{ct.}, \epsilon)$, with a sharp leap around the inflexion point, led Roginski (in the case of the Langmuir local isotherm) to the idea of replacing it with a step-function and expressing $\varepsilon(p)$ by means of (11). This idea may be generalized. *Monotonously increasing* functions $\theta(p, \epsilon)$ having such a behaviour are suited for the approximation, owing to a simple physical picture : they describe a local behaviour which suggests neglecting the adsorption on patches weakly covered (with $\epsilon < \varepsilon_a(p)$) and its overestimation on patches strongly covered (with $\epsilon > \varepsilon_a(p)$) [13]. We shall prove (convincingly, we hope) in the next section that the choice expressed by $\varepsilon_0(p)$ is inconvenient and leads to serious error. In fact, Harris himself came to the same conclusion [14].

We offer the following alternative, based on the convergence property (4); for $\Delta\epsilon = [\epsilon_m, \epsilon_M]$ the "condensation" adsorption energy, denoted $\varepsilon_1(p)$ is given by

$$\varepsilon_1(p) = \epsilon_m + \int_{\epsilon_m}^{\epsilon_M} [1 - \theta(p, \epsilon)]\,d\epsilon \tag{4'}$$

Replacing in (4′) $\epsilon_m = 0$; $\epsilon_M = \infty$, we obtain Eq. (4).

Some geometrical interpretation of $\varepsilon_1(p)$ will be given in the next section. Meanwhile, it is easy to write down the boundary conditions analogous to (5) :

$$\begin{cases} \varepsilon_1(0) = \epsilon_M, \\ \varepsilon_1(\infty) = \epsilon_m \end{cases} \quad \epsilon_m \leqslant \epsilon \leqslant \epsilon_M \tag{5'}$$

We can assign the following physical meaning to Eqs. (5) and (5′) : assuming that adsorption proceeds with increasing pressure on patches with decreasing adsorption energy, $\varepsilon_1(p)$ exhibits the correct boundary behaviour, *i.e.* near zero pressure the occupancy of the most active (maximum adsorption energy) patches and at infinite pressure that of the less active (minimum adsorption energy) patches takes place. As it will be seen, it is not the case with the expression of $\varepsilon_0(p)$: for $p \to \infty$, $\varepsilon_0(p) \to -\infty$, thus allowing for unrealistical values of the adsorption energy. To overcome this problem, Harris [14] had to impose some conditions on the function $\vartheta(p)$ which describes the experimental data, thus coming to the same sort of inconvenience as in the case of the Sips nonapproximate method.

III. THE C.A. IN THE CASE OF LANGMUIR LOCAL BEHAVIOUR

The Langmuir isotherm [15] is (historically) the first choice of describing the local adsorption mechanism on heterogeneous surfaces, its utilization being suggested for the first time by Langmuir himself. [16] It was and still is the most used expression for $\theta(p, \epsilon)$ and will be also adopted here. Its explicit form is given by

$$\theta(p, \epsilon) = \left[1 + \frac{p_L}{p} e^{-\epsilon/RT}\right]^{-1} \quad (12)$$

where p_L is a characteristic constant (having pressure dimensions), generally assumed independent of ϵ. Figure 1 clearly illustrates the above mentioned features of the function $\theta(p = \text{const.}, \epsilon)$. The arrows indicate the shifting of the curve with increasing or decreasing p. By means of Eqs (11) and (12) or some other conditions imposed on $\theta(p, \epsilon)$,[5] the same expression, $\varepsilon_0(p)$, was obtained and made use of, till now:

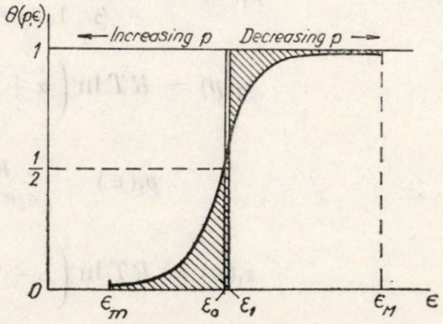

Fig. 1. — Plot of the function $\theta(p = \text{const.}, \epsilon)$ versus ϵ.

$$\varepsilon_0(p) = RT \ln \frac{p_L}{p} \quad (13)$$

allowing for unrealistic negative values of the adsorption energy for $p > p_L$. This major shortcoming leads, in spite of a convenient mathematical manipulation, to serious error in evaluating the distribution function. The inverse function to be used in Eq. (10) is

$$p_0(\epsilon) = p_L e^{-\epsilon/RT} \quad (14)$$

and the corresponding approximate distribution function will be denoted $\chi_0(\epsilon)$.

The alternative procedure proposed in the preceeding section is geometrically equivalent to the equality of the shaded areas in figure 1. For some finite range of ϵ variation

$$RT \ln \alpha = \epsilon_m \leqslant \epsilon \leqslant \epsilon_M = RT \ln \beta, \quad \beta > \alpha \geqslant 1 \quad (15)$$

equations (12) and (4′) yield

$$\varepsilon_1(p) = RT \ln\left(\alpha \frac{p + p_L/\alpha}{p + p_L/\beta}\right), \quad (16)$$

with the inverse dependence:

$$p_1(\epsilon) = \frac{p_L}{\beta} \, \frac{\beta - e^{\epsilon/RT}}{\alpha - e^{\epsilon/RT}} \quad (17)$$

From (16) and (17) we get the following expressions corresponding to particular values of α and β in (15):

$$\varepsilon_1(p) = RT \ln \frac{p + p_L}{p + p_L/\beta}, \quad 0 \leqslant \in \leqslant RT \ln \beta; \tag{16'}$$

$$p_1(\in) = -\frac{p_L}{\beta} \frac{\beta - e^{\in/RT}}{1 - e^{\in/RT}}, \quad 0 \leqslant \in \leqslant RT \ln \beta; \tag{17'}$$

$$\varepsilon_1(p) = RT \ln \left(\alpha + \frac{p_L}{p} \right), \quad RT \ln \alpha \leqslant \in < \infty \tag{16''}$$

$$p_1(\in) = \frac{p_L}{e^{\in/RT} - \alpha}, \quad RT \ln \alpha \leqslant \in < \infty \tag{17''}$$

$$\varepsilon_1(p) = RT \ln \left(1 + \frac{p_L}{p} \right), \quad 0 \leqslant \in < \infty \tag{16'''}$$

$$p_1(\in) = \frac{p_L}{e^{\in/RT} - 1}, \quad 0 \leqslant \in < \infty \tag{17'''}$$

Eqs. (16‴) and (17‴) also result from (4) and (12).

The estimated value of p_L [17] is of the order 10^6 torr, much higher than the usual adsorption experimental values. It might seem that the uprisen objection on $\varepsilon_0(p)$ is useless due to the fact that adsorption isotherms are commonly determined within a pressure range far enough from p_L (we may recall, however, the well-known catalytical synthesis of ammonia where adsorption phenomena take place at pressures of the order 10^6 torr); moreover, the higher the pressure the less the local probability of monolayer adsorption, *i.e.* the less the local behaviour can be described by the Langmuir isotherm. Thus one might conclude that ε_0 is good enough in *common experimental conditions*, within which the whole model holds.

We reject this conclusion by the following argument. It is a general request of any physical model to have mathematical (and physical) consistency; as neither the general equation of the actual adsorption model (1) nor the Langmuir one (12) imply the upper limiting of the pressure range, the same should happen to $\varepsilon_a(p)$. It is the case with $\varepsilon_1(p)$, whereas with $\varepsilon_0(p)$ it is not. On consistency grounds, we may expect to get better results using $\varepsilon_1(p)$, particularly for pressure near p_L where $\varepsilon_0(p)$ completely fails. The evidence should (and will) be first of all of mathematical nature, as we are dealing with a method of calculation of some distribution function.

In figure 2 the functions $\varepsilon_0(p)/RT$ and $\varepsilon_1(p)/RT$ (Eq. (16‴)) are represented against p/p_L. Their values practically coincide for $p \simeq 0.1\, p_L$, so that within the pressure range $(0,\, 0.1\, p_L)$ both $\varepsilon_0(p)$ and $\varepsilon_1(p)$ lead to the same (numerical) result. The corresponding distribution functions, $\chi_0(\in)$ and $\chi_1(\in)$, although different in their analytical form, will exhibit close (practically identical) numerical values till $\epsilon \simeq 3\ RT$. The expression $\varepsilon_1(p)$ will be far more advantageous when considering an experimentally more realistic *limited range* for the adsorption energy; indeed, Eqs (16–16″) show the dependence of $\varepsilon_1(p)$ on the (finite) limits of integration whereas $\varepsilon_0(p)$ conserves its form. In this case, the differences between the two functions may extend over a larger pressure range, as figure 3 clearly illustrates. At the intersection point, $(1/\sqrt{\alpha\beta}, \ln\sqrt{\alpha\beta})$, $\varepsilon_0 = \varepsilon_1$. The two functions are close to one another within a relatively small pressure range (near $p = p_L/\sqrt{\alpha\beta}$) outside of which they are quite different. Accordingly, the two distribution functions will have close values within a relatively small range of the adsorption energy (near $\epsilon = RT \ln\sqrt{\alpha\beta}$).

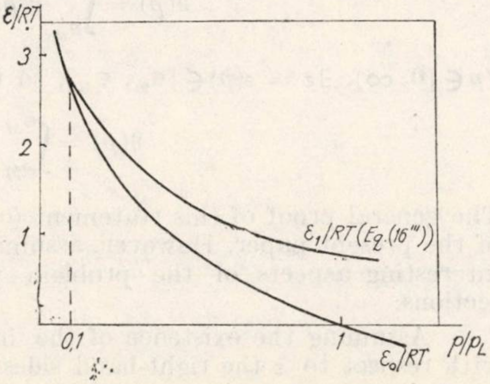

Fig. 2. – Plot of the functions $\varepsilon_0(p)/RT$ and $\varepsilon_1(p)/RT$ (given by Eq (16‴)) versus p/p_L

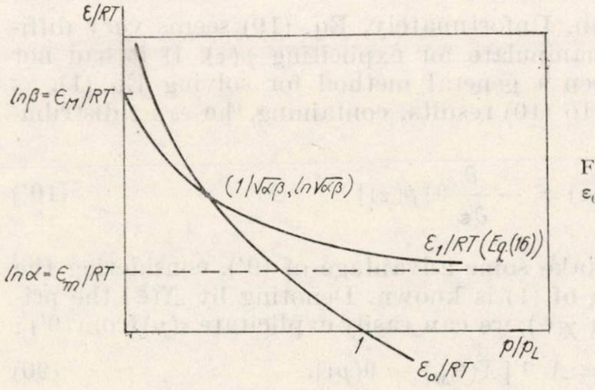

Fig. 3. – Plot of the functions $\varepsilon_0(p)/RT$ and $\varepsilon_1(p)/RT$ (given by Eq. (16)) versus p/p_L)

IV. THE "EXACT APPROXIMATION"

This paradoxical formulation is supported by the idea of transforming the condensation approximation into a nonapproximate (exact) method, by means of some purely mathematical speculation. Indeed, the monotony and boundary properties (Eqs (2), (3) and (6)) of the local and overall isotherms together with the normalization condition for the distribution function suggest the following statement: considering the integral equation (1)

$$\vartheta(p) = \int_{\in_m}^{\in_M} \theta(p, \in)\, \chi(\in)\, d\in, \tag{1}$$

$\forall p \in [0, \infty)$, $\exists \varepsilon = \varepsilon(p) \in [\in_m, \in_M]$, so that

$$\vartheta(p) = \int_{\varepsilon(p)}^{\in_M} \chi(\in)\, d\in \tag{9'}$$

The general proof of this statement (or its contrary) is beyond the scope of the present paper. However, assuming its validity, we can reveal some interesting aspects of the problem we dealt with in the preceeding sections.

Assuming the existence of the inverse function $p(\varepsilon)$ and deriving with respect to ε the right-hand sides of (1) and (9′) we get

$$\chi(\varepsilon) = \int_{\in_m}^{\in_M} \left\{ -\frac{\partial}{\partial \varepsilon} \theta\,[p(\varepsilon), \in] \right\} \chi(\in)\, d\in \tag{18}$$

so getting the condition

$$-\frac{\partial}{\partial \varepsilon}\, \theta\,[p(\varepsilon), \in] = \delta(\in - \varepsilon) \tag{19}$$

where δ is the Dirac function. Unfortunately, Eq. (19) seems very difficult (if not impossible) to manipulate for expliciting $p(\varepsilon)$. If it had not been so, this could have been a general method for solving Eq. (1), as from (9′) a similar equation to (10) results, containing the *exact* distribution function, $\chi(\in)$:

$$\chi(\varepsilon) = -\frac{\partial}{\partial \varepsilon} \vartheta\,[p(\varepsilon)] \tag{10'}$$

However, we can still take some advantage of (9′), considering the case when the exact solution of (1) is known. Denoting by $X(\in)$ the primitive of the known function $\chi(\in)$, we can easily explicitate $\varepsilon(p)$ from (9′):

$$\varepsilon(p) = X^{-1}\,[X(\in_M) - \vartheta(p)], \tag{20}$$

where X^{-1} is the inverse function of X; the inversability of this function conditions the existence of $\varepsilon(p)$ in an explicit form. Similarly, the existence of the function $p(\varepsilon)$

$$p(\varepsilon) = \vartheta^{-1}\,[X(\in_M) - X(\varepsilon)] \tag{21}$$

is conditioned by the inversability of ϑ.

Eqs (20) and (21) are useful for testing some particular approximate method. This can be done calculating the approximate distribution, $\chi_a(\in)$, by means of Eq. (10) for some special isotherms, $\vartheta(p)$, the corresponding distributions of which, $\chi(\epsilon)$, were exactly determined (*e.g.* by the Stieltjes transform method) and comparing the two functions. Another way is to compare the chosen approximate function $\varepsilon_a(p)$ (or $p_a(\epsilon)$) with the exact one, given by (20) or (21). We may point out an interesting fact: whereas $\varepsilon_a(p)$ results from some condition imposed only on the local isotherm, $\theta(p, \epsilon)$, *i.e.* it depends only on the form of this function, $\varepsilon(p)$ explicitly depends on the form of both $\vartheta(p)$ and $\chi(\epsilon)$ (and only implicitly on $\theta(p, \epsilon)$, through which ϑ and χ are connected in the integral equation (1)). It appears that a better choice of $\varepsilon_a(p)$ should be obtained taking into account the form of $\vartheta(p)$ (beside that of $\theta(p, \epsilon)$) *for each particular case.* Anyhow, this problem exceeds the framework of this paper in which we are dealing with the "classical" condensation approximation only.

To conclude this section, an example will be given which convincingly illustrates the superiority of $\varepsilon_1(p)$ on $\varepsilon_0(p)$. Consider the so-called semilogarithmic isotherm investigated by Temkin [18] and experimentally by Romanushkina, Kiperman and Temkin: [19]

$$\vartheta(p) = \frac{1}{\ln\frac{\beta}{\alpha}} \ln \frac{\beta p + p_L}{\alpha p + p_L} \tag{22}$$

whose exact distribution function is the constant one:

$$\chi(\epsilon) = \begin{cases} (RT\ln\beta/\alpha)^{-1} & \epsilon \in [RT\ln\alpha,\ RT\ln\beta] \\ 0 & \epsilon \notin [RT\ln\alpha,\ RT\ln\beta] \end{cases}, \quad \beta > \alpha \geqslant 1. \tag{23}$$

Introducing (22) and (13) into (10) the corresponding χ_0 approximate function results:

$$\chi_0(\epsilon) = \begin{cases} \dfrac{\beta - \alpha}{RT\ln\dfrac{\beta}{\alpha}} \dfrac{e^{\epsilon/RT}}{(e^{\epsilon/RT} + \beta)(e^{\epsilon/RT} + \alpha)} & RT\ln\alpha \leqslant \epsilon \leqslant RT\ln\beta \\ 0 & \text{elsewhere} \end{cases}; \tag{24}$$

It is easy to check that χ_0 is unnormalized. The error involved was estimated by Harris [14] as an application of his general procedure of evaluating the errors occurring in the C.A. method. It is not necessary to calculate the corresponding χ_1 function as, making use of Eqs (20), (22) and (23), we get for the "exact" function $\varepsilon(p)$ precisely the expression derived for $\varepsilon_1(p)$ (Eq. 16)), *i.e.* in this particular case:

$$\varepsilon(p) = \varepsilon_1(p) = RT\ln\alpha\frac{p + p_L/\alpha}{p + p_L/\beta}. \tag{16^{IV}}$$

The distribution function χ_1 is obviously identical with the exact distribution, given by (23).

An additional proof to this somehow surprising result will be presented, making use of some simple mathematical manipulations. In fact, from (1) and (9′) we get

$$\int_{\epsilon_m}^{\epsilon_M} \theta(p, \epsilon)\,\chi(\epsilon)\,d\epsilon = \int_{\varepsilon(p)}^{\epsilon_M} \chi(\epsilon)\,d\epsilon$$

and further,

$$\int_{\epsilon_m}^{\epsilon_M} [1 - \theta(p, \epsilon)]\,\chi(\epsilon)\,d\epsilon = \int_{\epsilon_m}^{\varepsilon(p)} \chi(\epsilon)\,d\epsilon$$

wherefrom, taking into account that $\chi(\epsilon) = \text{const.}$, we get the general definition of $\varepsilon_1(p)$ given in Section II, irrespective of the particular form of $\theta(p, \epsilon)$:

$$\varepsilon(p) \equiv \varepsilon_1(p) = \epsilon_m + \int_{\epsilon_m}^{\epsilon_M} [1 - \theta(p, \epsilon)]\,d\epsilon \qquad (4')$$

Physically, the constant distribution corresponds to what Temkin called "uniform nonhomogeneous" surfaces. [18] In terms of C.A., the error involved considering $\theta(p, \epsilon) = 0$ within the range $[\epsilon_m, \varepsilon_a)$ and $\theta(p, \epsilon) = 1$ within the range $[\varepsilon_a, \epsilon_M]$ is compensated in this case by the correct choice of $\varepsilon_a \equiv \varepsilon_1$, given by (4′); in fact, the magnitude of the excluded integration range equals $\int_{\epsilon_m}^{\epsilon_M} [1 - \theta(p, \epsilon)]\,d\epsilon$, which represents *the total uncovered surface* (the total number of free adsorption sites).

Obviously, for any other distribution, $\varepsilon_1(p)$ becomes an approximate expression, but anyway it is a better approximation than $\varepsilon_0(p)$, as we shall show in a subsequent paper.

V. CONCLUSIONS

The approach to the approximate working out of integral equation (1) presented here is an extension of Roginski's one and appears to be physically more consistent than the usual C.A. approach.

The new procedure of determining the "key" function, $\varepsilon_a(p)$, leads in the case of uniform inhomogeneity to exact results, irrespective of the specific form of the local behaviour. The resulting expression, $\varepsilon_1(p)$, is physically consistent within the framework of the considered model: localized monolayer adsorption without lateral interactions. The superiority of the function $\varepsilon_1(p)$ on the classical one, $\varepsilon_0(p)$, is clearly demonstrated, on general physical and mathematical grounds and in the particular case of Langmuir local behaviour.

BIBLIOGRAPHY

[1] C. Sanford and S. Ross, *J. Phys. Chem.*, **58**, 288 (1954).
[2] S. Ross and J.P. Olivier, "On Physical Adsorption", Interscience, New York, 1964.
[3] A. Clark, "The Theory of Adsorption and Catalysis", Academic Press, New York, 1970.
[4] J. M. Honig, *Ann. N. Y. Acad. Sci.*, **58**, 741 (1954).
[5] G. F. Cerofolini, *Thin Solid Films*, **23** 129 (1974).
[6] R. Sips, *J. Chem. Phys.*, **16**, 490 (1948) ; **18**, 1 024 (1950).
[7] W. Rudzinski, M. Jaronic, S. Sokolowski and G. F. Cerofolini, *Czech. J. Phys.*, **B 25,** 891 (1975).
[8] S. Sokolowski, M. Jaroniec and G. F. Cerofolini, *Surface Sci.*, **47**, 429 (1975).
[9] M. Smutek, *Czech. J. Phys.*, **B 25**, 902 (1975).
[10] M. Smutek, *Czech. J. Phys.*, **B 26**, 1179 (1976).
[11] M. Smutek, *Czech. J. Phys.*, **B 26**, 699 (1976).
[12] S. Z. Roginski, *Doklady Akad. Nauk S.S.S.R.*, **45**, 61 (1944) ; **45** 194 (1944).
[13] S. Z. Roginski, "Adsorbzia i kataliz na neodnorodnyh poverhnostiah", Izdatelstvo Akad. Nauk S.S.S.R, Moskva — Leningrad, 1948.
[14] L. B. Harris, *Surface Sci.*, **10**, 128 (1968) ; **13**, 377 (1969), **15**, 182 (1969).
[15] I. Langmuir, *J. Amer. Chem. Soc.*, **40**, 1361 (1918).
[16] I. Langmuir, *J. Amer. Chem. Soc.*, **54**, 2798 (1932).
[17] J. P. Hobson, *Canad. J. Phys.*, **43** 1934 (1965).
[18] M. Temkin, *Zhur. fiz. Khim.*, **15**, 296 (1941).
[19] A. E. Romanushkina, S. L. Kiperman and M. Temkin, *Zhur. fiz. Khim.*, **27**, 1181 (1953).

Revue Roumaine de Chimie, 26, 2, 197–202 (1981)

THE EXPLOSIVE COMBUSTION OF THE VINYLACETYLENE–AIR MIXTURES INITIATED BY A HOT NICKEL–CHROMIUM WIRE

DOMNINA POPESCU*, V. GOŞA *, R. H. SCHUSTER *, N. I. IONESCU *
and D. OANCEA **

* Center of Physical Chemistry, Bucharest, Spl. Independenţei 202, Romania
** Department of Physical Chemistry and Electrochemical Technology of the Polytechnic Institute, Bucharest, Bd. Republicii 13, Romania

Received August 4, 1979

The study of the explosive combustion of vinylacetylene–air mixtures, initiated by a heated nickel–chromium wire, indicates the existence of three combustion ranges. Each of them can be characterized by differences in the parameters of the explosive reaction.

In a previous paper [1] we pointed out several problems concerning the explosion limits of the vinylacetylene–air system. In the present paper, we extended our study on the same system initiated by a heated Ni–Cr filament, emphasizing the existence of different combustion ranges depending on the composition of the explosive mixtures.

EXPERIMENTAL

The measurements were carried out with the equipment and following the procedure described elsewhere. [1] The fuel was a mixture of the following composition : 93% vinylacetylene, 6% vinyl chloride and 1% argon. Throughout the paper, this mixture was considered as vinylacetylene (VAc). The initiation source was a heated Ni–Cr filament ($r = 143\ \Omega\cdot m^{-1}$; $\Phi = 0.1$ mm ; $l = 200$ mm). As during the combustion the wire surface underwent changes which altered the heat transfer from the source to the system, the filament was replaced after a certain number of experiments.

RESULTS AND DISCUSSIONS

Since the explosive combustion was accompanied by a light emission, this emission was the criterion that an explosion occurred.

The experiments were carried out within the concentration range 0–53% VAc in air (v/v) at subatmospheric pressures. The range 0–15% VAc was particularly investigated owing to the interest in antiexplosive protection.

The plot of the lowest initial pressure for which the explosion could be detected (minimum explosion pressure) against VAc concentration is given in figure 1. In order to emphasize the existence of three distinct regions (I, II, III) on the pressure/concentration curve, only the data up to 200 mmHg were plotted in this figure. The plot shows that at lower VAc concentrations (under 2.5%) the minimum explosion pressure increases steeply when VAc concentration decreases, establishing the lower explosion limit at 1.5–1.7% VAc for 760 mmHg initial pressure. This figure is in good agreement with the literatura values: 2.2[2]; 1.8[3,5]; 1.6–1.8[4]; 1.7–1.9[6]% VAc, although the experimental conditions were quite different, indicating that the lower explosion limit does not seem to depend significantly upon the initiation source.

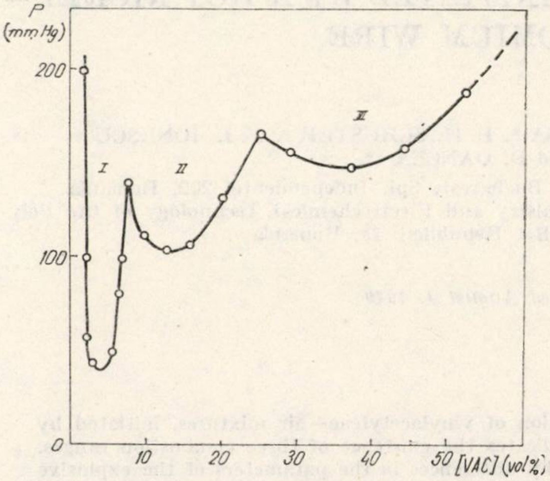

Fig. 1. — The dependence of the minimum explosion pressure on the vinylacetylene concentration for the VAc—air system.

The plot in figure 1 indicates the existence of three minima having different shapes. They are situated at increasing pressures and VAc concentrations. The first minimum of 40 mmHg is situated at 3.5% VAc, the second of 100 mmHg at ~12% VAc and the third of 150 mmHg at ~33–38% VAc. It can be observed that while the first minimum is quite sharp, the last is comparatively broader. The upper explosion limit obtained in this study is higher than the literature data: 9.2[2]; 53–53.2[3]; 40–43[4]; 40[5] and 42%[6], showing a marked dependence upon the experimental conditions.

The existence of three ranges on the plot of minimum explosion pressure against VAc concentration can be associated with changes in the explosive combustion mechanism, supported also by characteristic changes in flame colour and propagation. Within the first range, the flame is blue up to 6% VAc and turns gradually to green between 6 and 8% VAc. The second range is characterized by a white-yellowish flame, producing slight traces of carbon black when VAc concentration exceeds 15%. Within the third range, the flame is yellow and yields noticeable quantities of carbon black.

The flame propagation is also dependent upon VAc concentration: while within the first and second ranges the flame propagates both upwards and downwards, only an upward propagation was observed within the third range.

The final pressure in the explosion cell after combustion and thermal equilibration was lower, approximately equal or larger as compared to the initial pressure, for the blue, green and yellow flames, respectively.

Since the experiments were performed using a cell which opened when the inside pressure exceeded the atmospheric pressure, it was possible to delimit a range of initial pressures within which the maximum pressure reached during explosion was able to open the cell. From the measured heating time and the known voltage across the filament of known initial resistance [1], the critical energy needed to initiate the explosion could be calculated. The critical energy, uncorrected for the resistance change during the heating period, increases when the initial pressure is lowered. Plots of critical energy against the initial pressure are given in figure 2, for several mixtures of different compositions. It is evident that the critical energy is strongly dependent on the mixture composition. Within the first explosive range (I.Fig. 1), the critical energy reaches a minimum around 6–8% VAc, a value up to twice larger than the stoichiometric concentration. As the critical energy is strongly dependent on the source nature as well as on the different experimental details, the data obtained by different authors are quite scattered and an absolute value is meaningful only under some particular circumstances [7]. Using a slow dissipating source, not only the critical energy but also the source power seems to be important, because the source temperature is higher when the power increases. When VAc concentration is larger than 8% (range II, Fig. 1), an explosive combustion occurs if the source power is large enough, but only a slow combustion on the filament occurs if the source power is low. In this latter case, if the explosion can't occur, when the power supply is disconnected, the filament remains still incandescent 3 to 15 seconds. The data reported in this paper for the minimum explosion pressures were obtain-

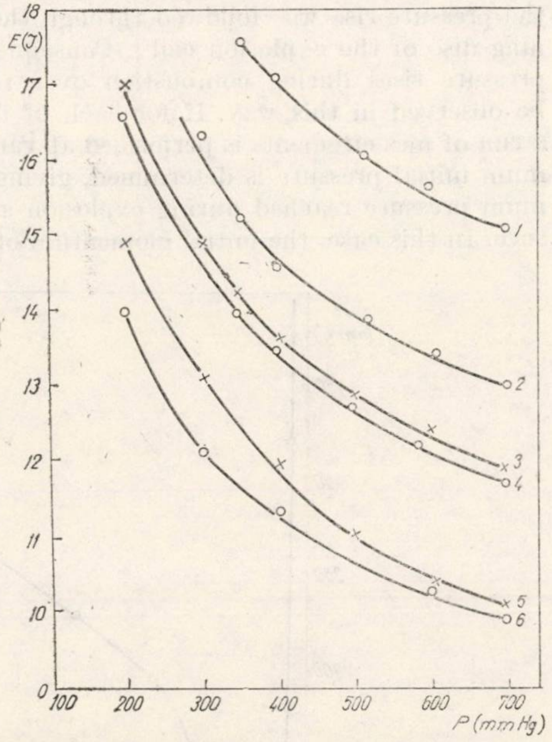

Fig. 2. — The dependence of the critical energy on the initial pressure for the vinylacetylene—air system, at various VAc concentrations : 1—1.8% ; 2—2.5% ; 3—2.9% ; 4—3.7% ; 5—4.5% ; 6—5.0% vol.

ed using large source powers, to avoid the slow combustion on the filament.

The explosive combustion could also be characterized by the maximum pressure reached during the explosion. Because the simple equipment used in this work was not provided with a pressure transducer, the pressure rise was followed through the initial momentum of the opening disc of the explosion cell [1]. Consequently, only the range where the pressure rises during combustion over the atmospheric pressure could be observed in this way. If for each of the different VAc–air mixtures, a run of measurements is performed at variable initial pressures, a minimum initial pressure is determined, giving the limit for which the maximum pressure reached during explosion still equalizes the external pressure. In this case, the initial momentum of the opening disc is zero. When plotted against the mixture composition, these limit initial pressures give a curve shown in figure 3 designated in this paper as "zero initial momentum curve".

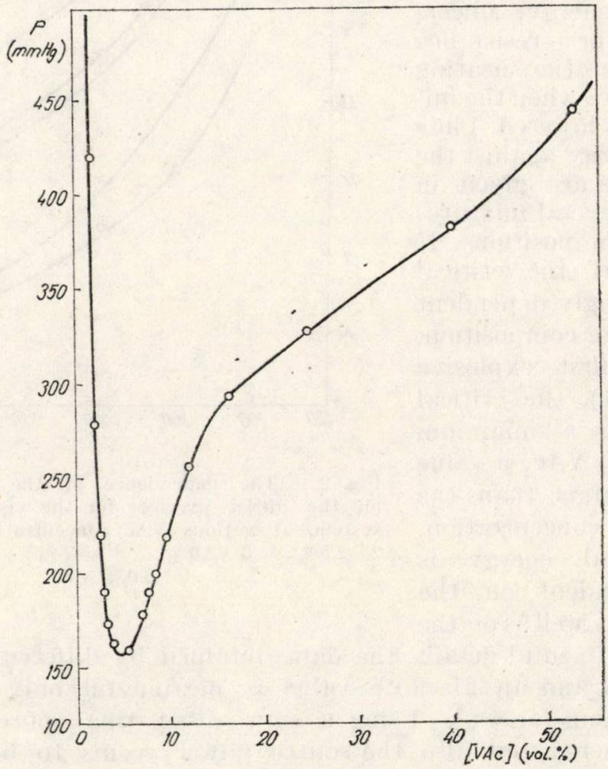

Fig. 3. — Zero initial momentum curve for the vinylacetylene–air system.

The curve exhibits a marked lobe between the lower explosion limit and ~16 % VAc, with a minimum at 5 % VAc. It must be specified that this range exhibits the largest pressure rise (measured from the initial to atmospheric pressure) with a maximum at 5 % VAc, and corresponds to those mixtures which burn without carbon black formation. When VAc concentration exceeds 15 % and the mixture burns with carbon black formation, the pressure rise during explosion is lower and the limit pressure has a steady but slower increase.

For a given composition, the plot of the initial momentum of the opening disc against the initial pressure gives a straight line, as illustrated in figure 4 for several mixtures.

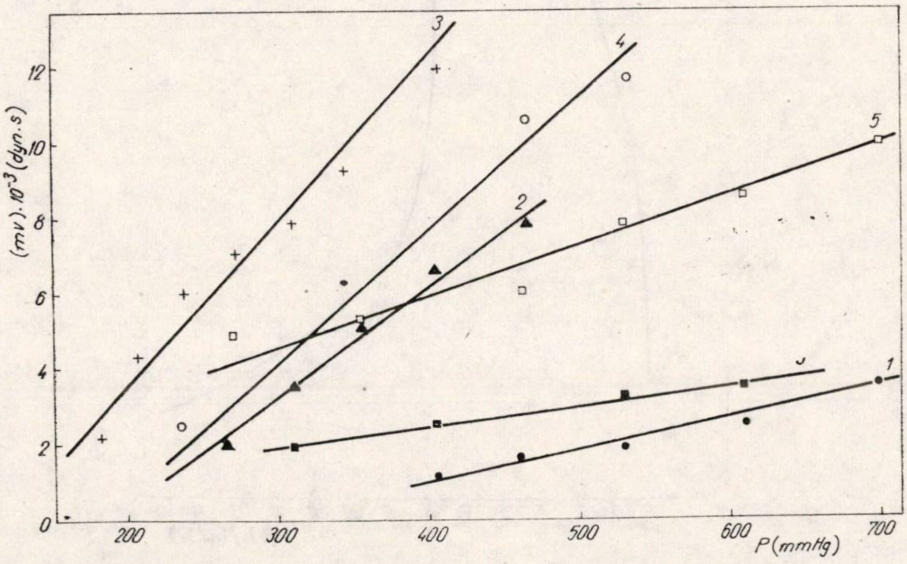

Fig. 4. — The dependence of the initial momentum of the opening disc on the initial pressure for the vinylacetylene—air system, at several mixture concentrations : 2.0(.—.—.— (curve 1) ; 2.5(▲—▲—▲) (curve 2) ; 5.0(+—+—+) (curve 3) ; 7.6(○—○—○) (curve 4) ; 8.4(□—□—□) (curve 5) ; 14.5(■—■—■) vol. %VAc (curve 6).

The slopes of these lines are very sensitive to the mixture composition and can be used to characterize the explosive combustion. A plot of these slopes [d(mv)/dp] against VAc concentration is shown in figure 5. The slope reaches a maximum around 6 % VAc, emphasizing that the mixtures of about 5 % VAc exhibit a maximum instability. Within 8 % and 15 % VAc, the slope decreases slowly, reaching a relatively constant value over 15 % VAc.

Our experiments concerning the behaviour of explosive VAc—air mixtures at subatmospheric pressures revealed the existence of three distinct combustion ranges characterized by obvious differences in several simple, but illustrative parameters of an explosive gas reaction.

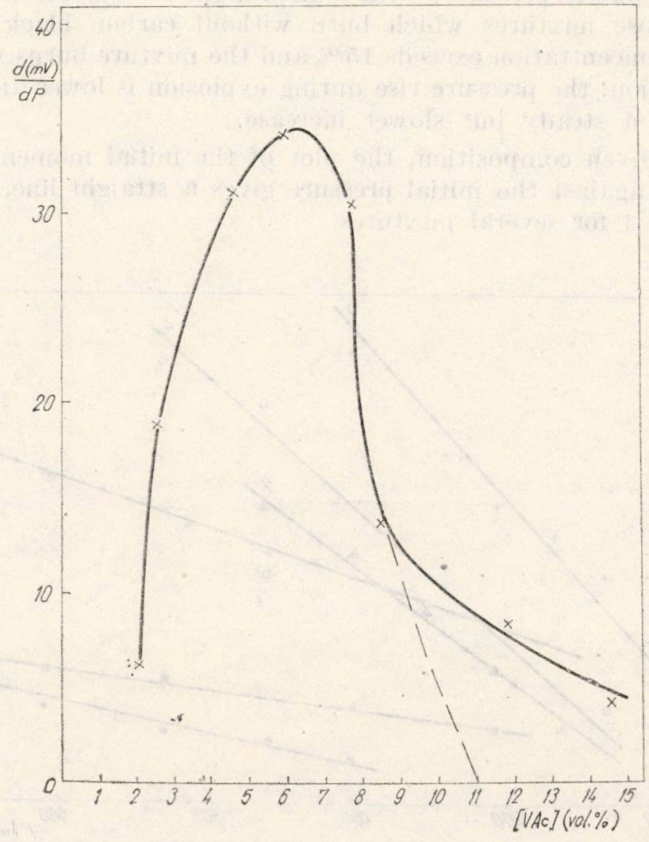

Fig. 5. — Diagram of the slope of initial momentum — pressure lines against vinylacetylene concentration for the VAc—air system.

REFERENCES

[1] R. H. Schuster, N. I. Ionescu, D. Popescu and D. Oancea, *Rev. Roumaine Chim.*, **24**, 531 (1979).

[2] T. Ikegami, *Rev. Phys. Chem. Japan*, **32**, 13 (1963).

[3] R. Mushii and F. Moshcovici, *Zhur. Vses. Khim. Obshchestv.*, **12**, 318 (1967).

[4] R. Mushii and M. Glikin, *Vestn. Tekhn. i Ekon. Inform. Naucinyh Issled.*, **1963**, 28.

[5] T. Kitagawa, C. Kitagawa and T. Nishimura, *Kogyo Kagaku Zasshi*, **67**, 1570 (1974).

[6] R. Mushii, *Zhur. priklad. Khim.*, **41**, 19 (1968).

[7] B. Lewis and G. von Elbe, "Combustion, Flames and Explosion of Gases", Academic Press, New York, 1961, chapter V.

Revue Roumaine de Chimie, **26**, *2*, 203–210 (1981)

LES PROPRIÉTÉS CATALYTIQUES DU SYSTÈME DE Fe_2O_3—Nd_2O_3

F. DOMKA, J. MICIUKIEWICZ et W. ZMIERCZAK
Laboratoire de Cinétique et de Catalyse, Institut de Chimie UAM, 60–780 Poznań, Pologne

Reçu le 9 septembre 1979

On a constaté que l'activité catalytique de l'oxyde de fer dépend de son procédé de préparation et n'est pas en relation avec les changements de la surface spécifique provoqués par le promoteur Nd_2O_3 introduit.

It has been found that the catalytic activity of ferricoxide depends on its preparation procedure, whereas there is no correlation between changes in surface area caused by the Nd_2O_3 promoter introduced.

Parmi plusieurs facteurs physiques et chimiques qui conditionnent l'activité catalytique ce sont les propriétés de la surface du solide qui jouent le rôle prédominant.

Ceci concerne en particulier les oxydes de fer qui ont la capacité de catalyser la conversion de l'oxyde de carbone par la vapeur d'eau. [1-4] D'après les travaux d'Adwood, d'Arnold [2] et d'Uchida et ses collaborateurs, [5] on sait que l'activité des catalyseurs ferrochromiques dépend de la façon dont on a procédé pour préparer les oxydes de fer qui se trouvent dans ces catalyseurs en quantité de 93% environ.

Le promoteur Cr_2O_3 n'influence pas cette activité et ne joue qu'un rôle secondaire. [1]

Il est intéressant de rappeler à cette occasion que la grande majorité de promoteurs, étudiés et cités dans la littérature (plus de 40), n'influence pas l'activité catalytique de l'oxyde de fer dans la réaction de conversion de CO par la vapeur d'eau mais joue le rôle d'un élément stabilisant la surface spécifique en la rendant résistante au frittage. [2,3] Ce point de vue est représenté par Yoshimura, [6] Domka et ses collaborateurs. [2,3] D'autres auteurs comme Rienäcker et Heint, [7] Mars [8] ou Boreskov [9] accordent au promoteur Cr_2O_3 le rôle d'un modificateur de la texture poreuse et de la surface spécifique des catalyseurs. De cette façon on a trouvé la corrélation entre l'activité et la surface accessible. [8]

En continuant nos études précédentes nous avons déterminé l'influence des conditions de l'élaboration de l'oxyde de fer et aussi du promoteur, oxyde de Nd^{22} sur les changements de la surface spécifique, de l'activité catalytique et de la résistance thermique des catalyseurs au fer pour la conversion de CO par la vapeur d'eau dans le domaine des températures élevées.

PARTIE EXPÉRIMENTALE

On a étudié trois séries de catalyseurs obtenus à partir de $Fe(OH)_3$ (série A), à partir de γ-FeOOH (série B) et à partir de δ-FeOOH (série C) qui contenaient jusqu'à 5% en poids de Nd_2O_3 (teneur Nd%). Pour obtenir ces catalyseurs on a profité des méthodes décrites par Krause, [10–12] et le néodyme a été introduit par la voie de coprécipitation par l'ammoniaque à la température ambiante. Les catalyseurs préparés ont été soumis, avant la réduction, à une activation thermique, pendant 3 heures, aux températures entre 300°C et 800°C dans un courant d'air. La composition chimique des oxydes de fer et de néodyme a été ensuite vérifiée par la méthode gravimétrique et par titrimétrie.

Les essais d'A.T.D. ont été faits à l'air dans un creuset de Pt. On a utilisé l'appareillage MOM, type OD-102. Comme substance neutre de point de vue thermique on a utilisé α-Al_2O_3. [13]

Les photos au microscope éléctronique ont été faites sur le microscope de skaning Cambridge Instr., type Stereoscan 150.

La surface spécifique a été déterminée par la méthode de la dessorption thermique d'argon (par chromatographie). [14]

Le test de conversion de l'oxyde de carbone par la vapeur d'eau a été réalisé par une méthode dynamique dans l'appareillage représenté sur la fig. 1.

L'oxyde de carbone 1 provenait d'une bouteille (FLUKA) et la vapeur d'eau a été produite dans un saturateur. [15–17] Le mélange réactionnel dont le rapport H_2O/CO est égal à 2,5 a été dirigé sur 500 mg de catalyseur [18] dilué par les brins de quartz, [19] placé dans un réacteur en quartz. [11] Avant la réaction, le catalyseur a été soumis pendant 60 min. à une réduction par le mélange réactionnel. La température de conversion a été fixée à 350°±0,5°C. Les produits de la réaction ont été analysés toutes les 20 min. par la méthode chromatographique. L'activité a été exprimée par le taux de conversion (en %). Le débit du gaz réactionnel a été fixé à 1 500 ml/h.

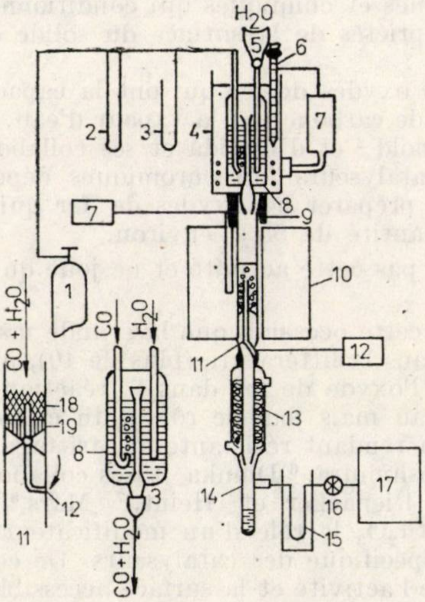

Fig. 1. — L'appareillage utilisé dans l'étude du processus de conversion du CO par la vapeur d'eau (1—bouteille avec CO, 2—débitmètre, 3—manomètre, 4,10—thermostat du saturateur et du réacteur, 5—récipient de H_2O, 6—thermomètre à contact, 7—régulateur électronique de temperature, 8—saturateur, 9—écran thermique, 11—« poche » du thermocouple, 12—mesureur du thermocouple, 13—réfroidisseur, 14—récepteur de H_2O, 15—traiteur au froid, 16—soupape du dosage, 17—chromatographe, 18—catalyseur, 19—ouate de quartz).

RÉSULTATS EXPÉRIMENTAUX

D'après les données de l'analyse thermique différentielle nous avons étudié les modifications qui accompagnent la formation des catalyseurs Fe_2O_3—Nd_2O_3. Le promoteur de néodyme, introduit dans une proportion de 5% en poids, produit un certain déplacement des maximums sur les courbes d'A.T.D., caractéristiques des préparations ferriques, [13,15] vers les températures plus élevées. Ceci en relation avec le déplacement de la température de formation de la phase $\alpha-Fe_2O_3$ qu'on observe aussi sur les autres exemples [3] et qui prouve qu'il arrive ici une augmentation d'amorphisme et de stabilité de surface des oxydes actives par les promoteurs de néodyme. On n'a pas enrégistré de formation de phases qui proviendraient d'une combinaison entre Fe_2O_3 et Nd_2O_3. Les pics exothermiques de cristallisation de la phase $\alpha-Fe_2O_3$ [13] ont été observés dans le domaine de températures entre 400°C et 600°C (max. a 512°C) pour les préparations de la série A ; entre 455°C et 540°C (max. 500°C) pour les préparations de la série B ; entre 260°C et 320°C pour celles de la série C. Ces écarts entre les températures de formation de Fe_2O_3 proviennent de la vitesse et du degré de réduction des catalyseurs avant la réaction.

D'après les données du tableau I il apparaît que le type du composé ferrique de départ ainsi que la température de calcination influencent la valeur de la surface spécifique et aussi l'activité catalytique. Ceci est en rapport étroit avec la composition des différentes phases du système Fe_2O_3/H_2O [13] qui conduit à la formation de la phase active Fe_3O_4.

La nature des phases des catalyseurs réduits ainsi que les conditions optimales de la réduction seront présentées dans un travail ultérieur.

Dans le tableau sont comparées les propriétés catalytiques des composés ferriques étudiés, groupés en trois séries. Il faut noter également les modifications de la surface spécifique des préparations contenant Nd_2O_3 jusqu'à 5% en poids. Les propriétés catalytiques de ces masses de contact ne sont pas en relation avec les valeurs de leur surface spécifique. La structure active se forme pendant la 1ère étape de synthèse et d'activation thermique, comme nous l'avons signalé dans les travaux antérieurs. [16,17]

D'après les résultats expérimentaux répresentés sur les figures 2, 3 et 4 il apparaît que le promoteur Nd_2O_3 ne favorise pas un accroissement de la surface spécifique des oxydes de fer en particulier dans le cas de la série C. En plus, la présence du promoteur rend les oxydes de fer plus résistants à la cuisson dans les limites de température jusqu'à 800°C (Fig. 8—11). Les préparations les moins sensibles à cet effet sont celles de la série B provenant de γ-FeOOH. Au-dessus de la température d'activation de 500°C (excepté les préparations de la série C), on observe une importante diminution de la surface spécifique. Ceci est en rapport avec la formation de la phase cristalline $\gamma-Fe_2O_3$ de faible aire superficielle à cette température, non influencée par la présence de Nd_2O_3.

Il est intéressant de constater que la résistance thermique à la cuisson jusqu'à une température de 800°C des préparations formées à partir de δ-FeOOH et $Nd/OH/_3$ est assez grande. Nous avons observé et décrit un phénomène semblable dans le cas du système iso-ortho-$Fe/OH/_3$-$Cr/OH/_3$ [18] dont les particules ressemblent aux produits de la cuisson de δ-FeOOH. [15]

La valeur de la surface spécifique n'est pas en relation avec les propriétés catalytiques de toutes ces préparations dans la réaction de conversion de CO par la vapeur d'eau. A la température d'activation de

TABLEAU 1

Résultats expérimentaux de la surface spécifique et du taux de conversion de CO par la vapeur d'eau des trois séries de catalyseurs ferriques dotés par l'hydroxyde de néodyme et activés aux différentes températures

Temp. de la réaction = 350°C $H_2O/CO = 2,5$

Température d'activation	Série A ortho-$Fe(OH)_3 + Nd(OH)_3$				Série B γ-$FeOOH + Nd(OH)_3$				Série C δ-$FeOOH + Nd(OH)_3$			
S [m²/g]	Teneur en Nd [%] dans le catalyseur $Fe_2O_3 - Nd_2O_3$											
α [%]	—	1,0	3,0	5,0	—	1,0	3,0	5,0	—	1,0	3,0	5,0
300	98,00	158,84	135,46	220,46	112,30	113,12	147,69	140,83	123,28	159,40	177,77	214,52
	30,56	30,26	22,22	23,68	24,35	37,87	13,33	17,89	29,33	22,61	11,57	5,31
400	52,40	89,62	83,86	152,37	80,85	66,23	88,70	83,29	62,71	122,10	145,93	170,69
	30,01	40,78	25,00	19,74	28,66	39,21	31,33	23,07	36,33	34,61	13,79	8,64
500	33,11	41,31	28,81	57,22	32,12	35,78	62,10	55,92	26,67	71,45	112,70	124,86
	21,33	31,16	27,63	9,70	27,01	27,27	24,55	28,26	20,15	27,50	7,17	6,25
600	20,52	15,91	20,91	19,40	20,11	21,68	30,93	33,94	17,83	45,40	69,73	90,02
	10,14	23,07	31,50	8,49	18,76	36,36	32,68	28,04	15,61	27,25	6,52	10,20
800	6,41	14,81	15,42	18,41	8,61	18,51	21,42	24,37	8,20	20,18	40,61	50,42
	3,64	21,52	25,99	6,01	7,97	16,34	13,56	13,99	5,24	20,12	5,01	8,10

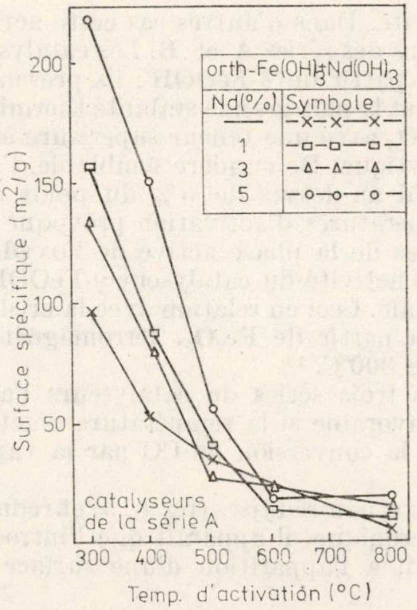

Fig. 2. — Influence de la température d'activation sur la surface spécifique des préparations obtenues à partir d'ortho $Fe(OH)_3 + Nd(OH)_3$ (série A).

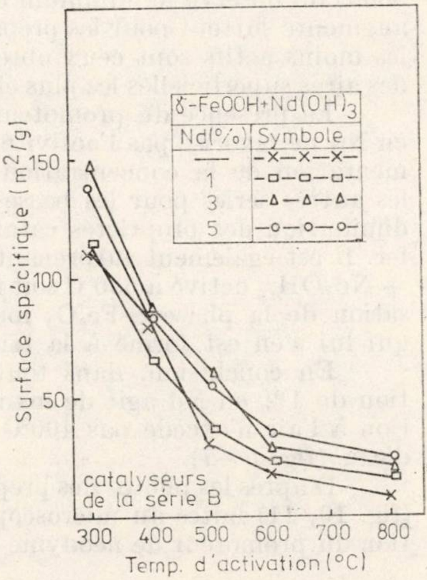

Fig. 3. — Influence de la température d'activation sur la surface spécifique des préparations obtenues à partir de γ-$FeOOH + Nd(OH)_3$ (série B).

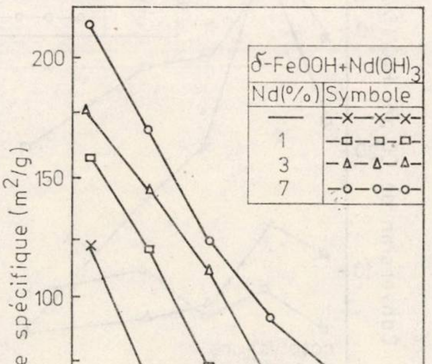

Fig. 4. — Influence de la température d'activation sur la surface spécifique des préparations obtenues à partir de δ-$FeOOH + Nd(OH)_3$ (série C).

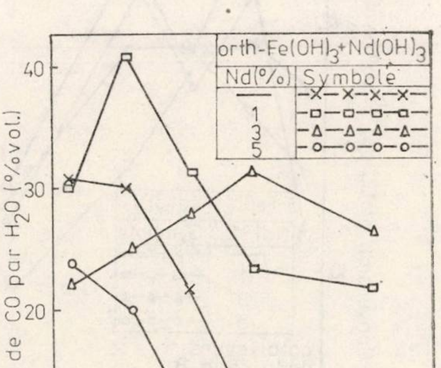

Fig. 5. — Influence de la température d'activation des préparations de la série A sur le degré de conversion de CO par la vapeur d'eau.

500°C on observe le minimum d'activité. Dans d'autres cas cette activité augmente surtout pour les préparations des séries A et B. Les catalyseurs les moins actifs sont ceux obtenus à partir de δ-FeOOH ; ils présentent des aires superficielles les plus élevées et la plus grande stabilité thermique.

La présence du promoteur Nd_2O_3 avec une teneur supérieure à 1% en Nd ne favorise pas l'activité catalytique. De manière semblable, l'augmentation de la concentration en Nd au-dessus de 5% du poids dans les autres séries pour les basses températures d'activation provoque une diminution des propriétés catalytiques de la phase active de l'oxyde de fer. Il est également surprenant que l'activité du catalyseur γ-FeOOH + + Nd/OH/$_3$ activé à 500°C soit minimale. Ceci en relation avec la cristallisation de la phase α-Fe_2O_3 formée à partir de Fe_2O_3, ferromagnétique qui lui s'en est formé à la temp. de 300°C. [13]

En conclusion, dans toutes les trois séries de catalyseurs l'addition de 1% en Nd agit de manière favorable si la température d'activation à l'air n'excède pas 400°C pour la conversion de CO par la vapeur d'eau (fig. 5 –7).

D'après les photos des préparations non-réduites (fig. 8, 9) et réduites (fig. 10, 11) faites au microscope élécronique, il apparaît que l'introduction du promoteur de néodyme conduit à l'apparition d'une surface rugueuse caracterisée par une fragmentation accrue (fig. 9, 11) en comparaison avec une surface agglomérée des préparations α-Fe_2O_3 non-activées.

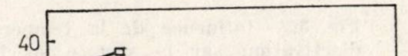

Fig. 6. – Influence de la température d'activation des préparations de la série B sur le degré de conversion de CO par la vapeur d'eau.

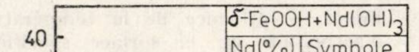

Fig. 7. – Influence de la température d'activation des préparations de la série C sur le degré de conversion de CO par la vapeur d'eau.

A cette étape d'étude nous n'avons pas pu observer l'influence de deux variétés cristallographiques de Nd_2O_3 connues (cubique et hexagonale) sur les propriétés catalytiques de Fe_2O_3. Le passage de la phase cubique à l'hexagonale de Nd_2O_3 se fait à la température de 750°C.[19]

A la lumière de la présente étude il est possible d'affirmer que l'utilisation du promoteur Cr_2O_3 dans Fe_2O_3 pour les catalyseurs de la conversion de CO par la vapeur d'eau est beaucoup plus avantageuse puisque les mailles cristallines de α-Cr_2O_3 et de α-Fe_2O_3 (oxydes isomorphiques) se ressemblent.[20, 21] Dans les conditions de la réaction, la phase méta-

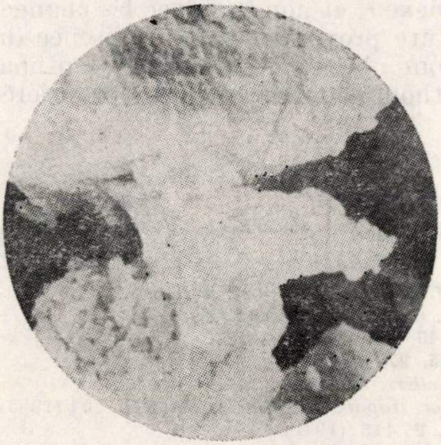

Fig. 8. — La photo faite au microscope électronique de α-Fe_2O_3 obtenu à partir d'ortho $Fe(OH)_3$ à la température 800°C (agr. 10000x).

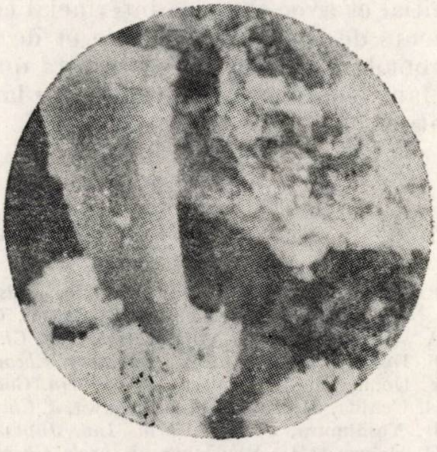

Fig. 9. — La photo faite au microscope électronique de $Fe_2O_3 . Nd_2O_3$ (5 %Nd) — série ortho (A).

La préparation a été activée à 800°C (agr. 10000x).

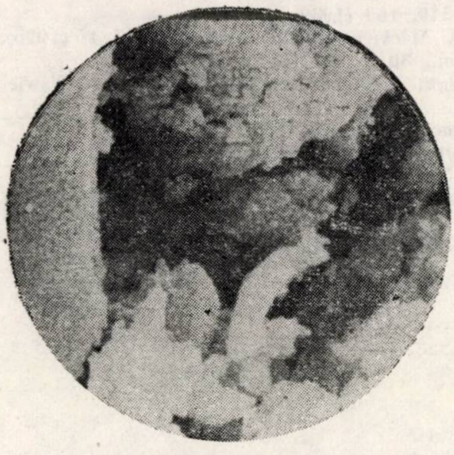

Fig. 10. — La photo faite au microscope électronique de α-Fe_2O_3 réduit, obtenu à partir d'ortho $Fe(OH)_3$ à la température 400°C (agr. 20000x).

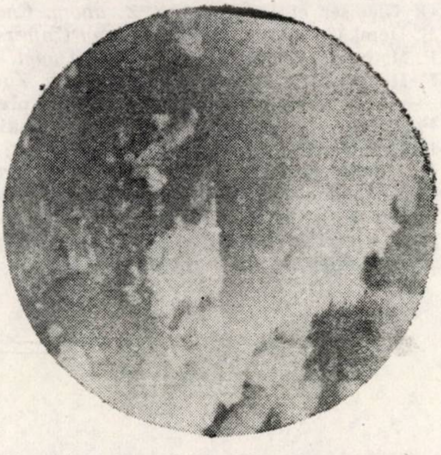

Fig. 11. — La photo faite au microscope électronique de $Fe_2O_3 . Nd_2O_3$ 5 % Nd réduit— série A (ortho). La préparation a été activée à 400°C (agr. 10000 x).

stable γ-Ce_2O_3 ne peut exister qu'en relation avec la phase α-Fe_2O_3. Dans le cas du néodyme qui forme un réseau cubique stable, une telle relation n'est pas observée.

D'après l'étude faite on voit que l'activité des catalyseurs à base d'oxydes de fer est plutôt en relation avec la structure de l'oxyde de Fe initial et avec l'espace interfacial complexe [22] et non pas avec les changements de l'aire superficielle et de texture provoqués par la présence du promoteur Nd_2O_3. Il en résulte que pour obtenir un catalyseur optimal il faut chercher la relation entre la méthode d'obtention et les propriétés catalytiques de ce catalyseur.

BIBLIOGRAPHIE

[1] P. S. Pulatonow et Z. P. Jovonovic, *Glasnik Chem. Druszt.*, **35**, 279 (1970).
K. Laudien et H. Witzmann, *Chem. Techn.*, **18**, 485 (1966).

[2] A. Atwood et M. R. Arnold, *Ind. Eng. Chem.*, **45**, 424 (1953).

[3] F. Domka et M. Łaniecki, *Z. anorg. Chem.*, **435**, 273 (1977).

[4] F. Domka et M. Łaniecki, *Reac. Kin. Catal. Letters*, **3**, 261 (1975).

[5] H. Uchida, M. Kurita et K. Ogawa, *J. Chem. Soc. Japan, Ind. Chem. Sect.*, **56**, 754 (1953).

[6] R. Yoshimura, *J. Soc. Chem. Ind. Japan*, **34**, 27 113 (1931).

[7] H. Heinze et G. Rienäcker, *J. prak. Chem.*, **6**, 315 (1958).

[8] P. Mars, M. J. Goroels et P. Zwietering, «Actes II-éme Congrès International de Catalyse», vol. 2, **2429** (1961).

[9] T. M. Jurjewa, G. K. Boreskow et W. S. Gruwer, *Kinetika i Kataliz.*, **10**, 294 (1969).
M. I. Markina, G. K. Boreskow, F. P. Iwanowskij et B. G. Ljudkowskaja, *Kinetika i Kataliz*, **2**, 867 (1961).

[10] A. Krause et A. Lewandowski, *Z. anorg. Chem.*, **206**, 328 (1932).

[11] A. Krause, Pat. PRL 34 471, 1951.

[12] O. Glemser et E. Gwinner, *Z. anorg. Chem.*, **240**, 163 (1939).

[13] F. Domka, *Cahiers scientifiques de l'Université A. Mickiewicz, Chemia, Poznań*, **17**, 15 (1975).

[14] F. M. Nelson et F. T. Eggertsen, *Analyt. Chem.*, **30**, 1 387 (1958).

[15] F. Domka, M. Łaniecki, L. Domka, W. Zmierczak, J. Miciukiewicz, I. Wolska et I. Wświeczorek, *Chem. Techn.* (sous presse).

[16] F. Domka, M. Łaniecki et Z. Ruszkowski, *Reac. Kinet. Letters*, **2**, 171 (1975).

[17] F. Domka et M. Łaniecki, *Matériaux du 1e Symp. PAN*, (1976) p. 207.

[18] F. Domka et M. Łaniecki, *Surface Technol.*, **5**, 303 (1977).

[19] L. A. Sazanow et H. G. Łogwinienko, *Kinetika i Kataliz*, **3**, 161 (1962).

[10] F. Domka et Z. Ruszkowski, *Matériaux de la conférence du PTCh, ZB 411* (1976).

[11] D. E. Cox, W. I. Takei et G. Shirane, *J. Phys. Chem. Solids*, **24**, 405 (1963).

[12] J. Miciukiewicz, *Dissertation* (1979).

Revue Roumaine de Chimie, 26, 2, 211–215 (1981)

INFLUENCE DES CONDITIONS DE SYNTHÈSE SUR L'ACTIVITÉ DES CATALYSEURS FERRO-CHROMIQUES DANS LA CONVERSION DE CO PAR LA VAPEUR D'EAU

F. DOMKA et M. ŁANIECKI

Laboratoire de Cinétique et de Catalyse, Institut de Chimie UAM à Poznań, Pologne

Reçu le Septembre 9, 1979

On a étudié la relation entre les conditions de la synthèse, le traitement thermique des oxydes de fer et l'activité catalytique des catalyseurs ferrochromiques obtenus à partir des modifications polymorphiques différentes de l'oxyde de fer hydraté. On a constaté, que pour obtenir une activité optimale des catalyseurs il faut utiliser 2,4 ou 8 % de Cr_2O_3 suivant le composé de fer initial.

The relation has been studied between synthesis and thermal treatment conditions of iron oxides and the activity of iron-chromium oxide catalysts prepared from different polymorphic modifications of iron oxide hydrates.
It has been found that a maximal catalytic activity is achieved in the case of the catalysts containing 2,4 or 8% of Cr_2O_3 used as a catalyst stabilizer.

Dans plusieurs cas, la structure active des catalyseurs se forme, à partir du matériel initial déjà dans le premier stade de la synthèse. [1–3]

Ceci concerne aussi les catalyseurs ferrochromiques qui jusqu'à maintenant ont été utilisés dans la conversion de CO par la vapeur d'eau aux températures élevées. [4–7]

Il résulte de plusieurs études que ces catalyseurs ne jouent que le rôle secondaire, [5, 8–12] et que l'élément actif c'est l'oxyde de fer modifié.[5,11] C'est pour cela que notre attention s'est portée sur la relation entre les conditions de la synthèse, le traitement thermique des oxydes de fer et l'activité des catalyseurs ferrochromiques obtenus à partir des hydroxydes ou des oxyhydroxydes de fer biographiquement différents.

PARTIE EXPÉRIMENTALE

Trois séries de catalyseurs ont été obtenues à partir d'ortho-$Fe(OH)_3$, d'iso-ortho-$Fe(OH)_3$ [13] et de γ-FeOOH. [14] .

Les préparations de la série ortho-$Fe(OH)_3$ (O-) ont été obtenues par coprécipitation d'une solution d'ammoniaque (25 %), d'un mélange d'hydroxydes et des solutions de nitrates de fer ($Fe(NO_3)_3$ $9H_2O$ — pur pour analyse) et de chrome ($Cr(NO_3)_3 . 9H_2O$ — pur pour analyse) dosés dans des rapports correspondants.

Les préparations de la série iso-ortho-$Fe(OH)_3$ (I-) ont été obtenues en deux étapes. D'abord on a précipité iso-orthohydroxyde de fer par une méthode décrite par Krause. [13] Le précipité a été séché à la température ambiante ensuite on l'a fait passer au tamis (le diamètre de la maille = 0,12 mm). Le précipité a été placé dans une solution de nitrate de chrome (0,03 N — pur pour analyse). Le précipité de $CrOH_3$ qui s'était formé à la surface de l'hydroxyde de fer a été obtenu à l'aide d'une solution de NH_3OH (0,1 N)[5] à la température 70°C en le mélangeant tout le temps jusqu'à l'obtention du pH = 8. La préparation ainsi obtenue a été séchée à l'air, ensuite on l'a soumise à un traitement thermique.

Les préparations de la série γ-FeOOH (G-) ont été obtenues de la façon suivante : pendant la première étape on a préparé γ-FeOOH[14] par une forte oxydation à l'air d'une suspension de $FeOH_2$. Les autres opérations ont été faites comme dans la série I. De cette façon on a obtenu les trois séries de catalyseurs ferrochromiques (jusqu'à 10% en poids de Cr_2O_3), ainsi que les oxydes de fer (préparations étalon), qui ont été activés pendant trois heures dans un flux d'air qui passait avec une vitesse de 20 l/h.

L'activité catalytique dans la réaction de conversion de CO par la vapeur d'eau a été étudiée dans un réacteur intégral d'après le schéma déjà décrit dans un travail antérieur.[3] L'oxyde de carbone a été pris d'une buteille Fluka.

Le temps de la réaction est 4 heures, la temperature 350°C le débit de CO = 1500 cm^3/h, le rapport H_2O : CO est de 2,5. Les produits de la réaction ont été analysés par la méthode chromatographique dans une colonne de 3 m remplie de carbone actif (20—35 mesh.).

La surface spécifique des catalyseurs avant et après la réaction a été mesurée par la méthode de dessorption thermique d'argone.[15]

RÉSULTATS EXPÉRIMENTAUX

Dans le tableau sont présentés les résultats suivants : l'activité catalytique et la surface spécifique des catalyseurs activés aux températures comprises entre 400°C et 800°C obtenus à partir de trois composés différents. On a pris en considération l'influence de Cr_2O_3 sur la grandeur de la surface spécifique et sur les propriétés catalytiques. La relation entre l'activité catalytique, la quantité de Cr_2O_3 et la température d'activation est présenté sur les fig. 1, 2 et 3. En général on voit bien les différences dans les propriétés catalytiques des préparations qui diffèrent d'après les modifications du matériel initial et d'après la teneur en Cr_2O_3.

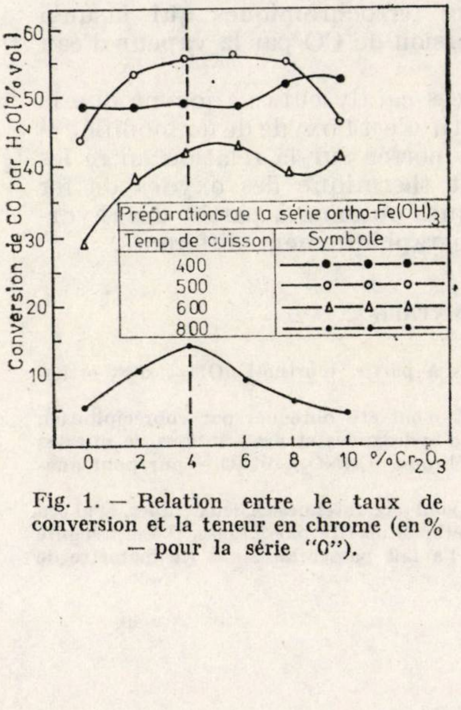

Fig. 1. — Relation entre le taux de conversion et la teneur en chrome (en % — pour la série "0").

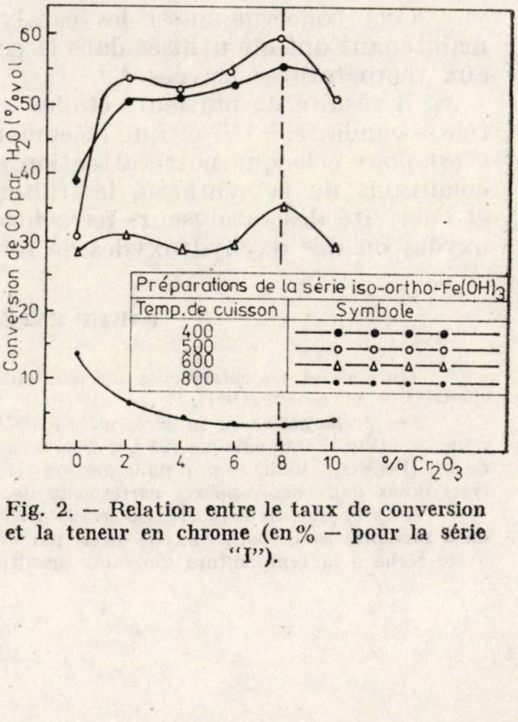

Fig. 2. — Relation entre le taux de conversion et la teneur en chrome (en % — pour la série "I").

Par contre aux résultats des études de Mars et ses collaborateurs [9] on n'a pas observé une relation entre la surface spécifique et l'activité catalytique. L'oxyde de chrome introduit dans toutes les trois préparations ferriques initiales favorise une augmentation assez regulière de la surface spécifique en fonction de l'augmentation de concentration. Avec l'augmentation de la température d'activation des catalyseurs on observe un abaissement systématique de la surface spécifique ; pour les préparations qui contiennent Cr_2O_3 activées à 800°C cette surface est comprise entre 0,75 et 3,4 m^2/g (G-10), pour celles qui n'en contiennent pas la surface est comprise entre 0,3 et 1,8 m^2/g. Pour les préparations activées à 400°C la surface des oxydes de fer est comprise entre 48 (0) et 74 m^2/g (G-O), tandis que pour les catalyseurs entre 60 (0 —2) et 127 m^2/g (I-10). À la température 800°C nous avons à faire à un processus extensif d'activation des surfaces dans des oxydes pures et dans des mélanges d'oxydes. L'activité spécifique n'augmente qu'après l'introduction de Cr_2O_3 dans le γ-FeOOH et pratiquement ne dépend pas de la quantité d'oxyde de chrome (tableau). Cette activité varie beaucoup aux températures élevées d'activation et pour les préparations qui ne contiennent pas de chrome. Ceci s'explique par le rôle stabilisateur de Cr_2O_3 vis-à-vis de la surface de Fe_2O_3 lequel a été décrit par Yoshimura, [16] Mars, [9] Domka et Łaniecki. [5] L'oxyde de chrome agit en tant que stabilisateur thermique et ne permet pas la formation de l'alliage fritté à la température plus basse que 500°C. [5]

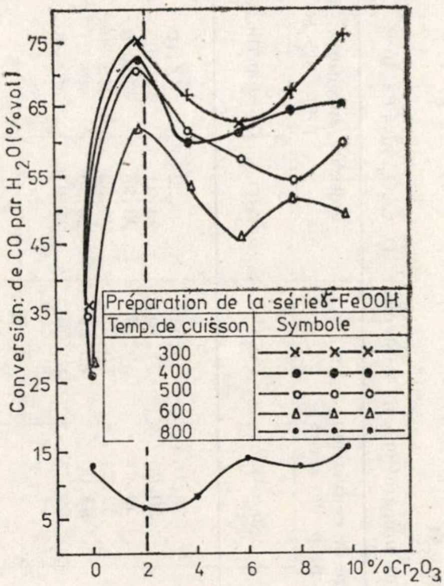

Fig. 3. — Relation entre le taux de conversion et la teneur en chrome (en % — pour la série "G").

Le manque de relation entre la grandeur de la surface spécifique et l'activité catalytique est lié à la fonction protectrice de Cr_2O_3 qui se dépose sur la surface d'agglomérats de la phase active de Fe_3O_4 et à la diminution partielle de micropores. [5,11] Dans le cas des catalyseurs de la série « ortho » la quantité de 6% de Cr_2O_3 permet la formation d'une couche de protection et favorise l'activité optimale. Pour la série iso-ortho-$FeOH_3$ il faut 8% de Cr_2O_3 pour obtenir l'activité optimale, et pour la série γ-FeOOH seulement 2% de Cr_2O_3. Ces différentes quantités de Cr_2O_3 sont nécessaires pour que la couche de protection se forme pour une certaine préparation ferrique. [5,11]

Ce fait peut être utilisé dans la synthèse des catalyseurs dont la teneur en Cr_2O_3, qui coûte cher, est basse. D'après les figures 1, 2 et 3 qui montrent la relation entre l'activité et la teneur en Cr_2O_3, en pour-cent, pour les trois séries de préparations, il apparaît que la température de calcination optimale est de 500°C.

TABLEAU

Superficie effective et activité catalytique 350°C des préparations du système Fe_2O_3/Cr_2O_3 jusqu'à 10 %

% en Cr_2O_3 et la temp. de cuisson [°C]	Superficie effective [m^2/g] prép. des séries /prép. après la réduction/			Degré de conversion [%] prép. des séries			Activité spécifique [$cm^3/h.m^2$] prép. des séries		
	ortho	iso-ortho	γ-FeOOH	ortho	iso-ortho	γ-FeOOH	ortho	iso-ortho	γ-FeOOH
0—400	48,31	62,92	74,41	48,66	38,16	25,94	30,22	18,19	10,46
2—400	60,06	93,60	74,62	49,03	50,20	71,10	24,31	16,09	28,58
4—400	61,41	109,39	86,08	48,66	50,91	59,26	23,95	13,96	20,65
6—400	58,91	121,47	105,59	48,15	52,24	60,91	24,52	12,90	17,31
8—400	60,28	123,96	91,32	51,73	55,00	63,61	25,75	13,31	20,89
10—400	58,17	127,04	77,44	52,48	53,28	64,50	27,07	12,58	24,99
0—500	18,24/ 9,63	35,65/10,52	43,96/14,74	44,12	30,49	27,41	72,57	25,66	18,71
2—500	27,80/21,14	56,28/40,33	44,25/39,16	53,32	53,30	70,80	57,54	28,41	48,00
4—500	28,24/24,22	57,69/42,81	50,31/37,62	55,47	53,96	60,43	58,93	27,02	36,03
6—500	29,87/24,29	56,70/44,68	50,18/40,94	55,62	54,61	56,71	55,87	28,89	33,90
8—500	32,66/25,31	58,08/46,35	49,12/44,59	54,54	59,28	53,59	50,10	30,62	32,73
10—500	32,81/27,68	56,19/50,83	47,28/40,39	46,61	50,11	58,92	42,62	26,75	37,38
0—600	8,25	14,50	25,32	29,16	28,09	27,74	106,04	58,12	30,24
2—600	10,77	18,85	27,52	38,25	30,93	61,22	106,55	49,22	72,54
4—600	12,16	20,88	30,79	40,31	29,09	52,84	99,45	41,79	51,48
6—600	12,73	21,63	29,45	42,69	29,09	45,06	100,60	40,35	45,90
8—600	14,30	21,45	27,71	38,30	35,18	50,68	80,35	49,20	54,87
10—600	15,66	18,74	27,05	40,97	29,09	48,22	78,49	46,57	53,48
0—800	0,32	1,83	1,53	5,48	13,47	13,00	513,75	220,82	254,90
2—800	0,75	2,08	2,45	10,49	6,28	6,18	419,60	90,58	75,67
4—800	0,65	3,48	1,92	13,79	4,07	8,03	636,46	35,09	125,47
6—800	0,76	2,48	2,40	8,35	3,83	13,27	329,61	46,33	165,88
8—800	1,07	2,82	3,11	6,00	2,92	11,61	168,22	31,06	111,99
10—800	1,22	3,05	3,41	4,10	4,05	14,71	100,82	39,84	129,41

En conclusion, la plus grande activité d'un catalyseur ferrochromique, ainsi que la quantité optimale de Cr_2O_3 introduite, dépendent de la manière dont on procède à la synthèse de l'oxyde de fer. Nous avons décrit ce problème plus précisément dans les travaux antérieurs. [5,11]

BIBLIOGRAPHIE

[1] F. Domka et M. Łaniecki, *Wyd. Nauk. UAM*, **17**, 12 (1975).
[2] J. Hoogschagen et P. Zwietering, *J. Chem. Phys.*, **21**, 2 224 (1953).
[3] F. Domka, M. Łaniecki et Z. Ruszkowski, *React. Kinet. Catal. Letters*, **3**, 261 (1975).
[4] L. Piesche et H. Witzmann, *Chem. Techn.*, **18**, 478, 482, 485 (1966).
[5] F. Domka et M. Łaniecki, *Z. anorg. Chem.*, **435**, 273 (1977).
[6] D. Allen, *Fert. Sci. Technol. Ser.*, **2**, 3 (1974).
[7] J. Rajagopala Rao et B. R. Sant, *Chem. Age India*, **24**, 695 (1973).
[8] F. Domka et Z. Ruszkowski, Pat. PRL nr 191060 (1976).
[9] P. Mars, M. J. Gorgeles et P. Zwietering, "Actes du Deuxième Congrès Int. de Catalyse", vol. **2**, (1961), p. 2 429.
[10] K. Atwood et R. Arnold, *Ind. Eng. Chem.*, **45**, 424 (1953).
[11] F. Domka et M. Łaniecki, *Surf. Technol.*, **7**, 217 (1978).
[12] M. Uchida, M. Kurita et K. Ogawa, *J. Chem. Soc. Japan Ind. Chem. Sect.*, **56**, 754 (1953).
[13] A. Krause et J. Garbaczówna, *Z. anorg. Chem*, **211**, 296 (1933).
[14] A. Krause, Patent PRL nr. 34471.
[15] F. M. Nelsen et F. T. Eggertsen, *Analyt. Chem.*, **30**, 1387 (1958).
[16] R. Yoishimura, *Chem. News*, **143**, 267 (1931).

Revue Roumaine de Chimie, 26, 2, 217–228 (1981)

RELATIONS BETWEEN THE METHODS OF PREPARATION, PROPERTIES AND ACTIVITY OF Bi–Mo–Fe–O CATALYST IN OXIDATIVE DEHYDROGENATION OF n-BUTENES IN BUTADIENE

I. V. NICOLESCU and I. SĂNDULESCU
National Institute of Chemistry, Department of Technology and Catalysis, Bucharest, Romania,
Splaiul Independenţei 202

Received April 4, 1979

The present work deals with a mechano-topochemical reaction for catalyst synthesis. The new method has been used for the preparation of Bi–Mo–O and Bi–Mo–Fe–O catalysts.

Physical-structural properties of catalysts as well as their activity in oxidative dehydrogenation of n-butenes are reported. The presence of Fe_2O_3 in ternary catalysts Bi–Mo–Fe–O highly increases the catalytic activity. We have suggested that the activity of these catalysts is related to an active catalytic complex formed from the Erman phase, iron-molybdate and double hexamolybdate of iron and bismuth. Correlations between the kinetics of the reaction and some textural characteristics of catalysts are also discussed.

I. INTRODUCTION

Conversion in catalytic dehydrogenation of n-butenes to butadiene, is related to the thermodynamic equilibrium conditions of the endothermic reaction :

$$\Delta H = +28 \text{ kcal/mol} \quad C_4H_8 \rightleftharpoons C_4H_6 + H_2$$

Owing to these conditions, even at 560–600°C, the yield is limited to 17–20% and selectivity at 75–80% per run.

Recently, the industrial catalytic process of oxidative dehydrogenation of n-butenes has been performed introducing a hydrogen acceptor, halogen or oxygen. [1-5] Under these conditions the reaction equilibrium has been strongly displaced, so that practically the conversion might be not related to equilibrium conditions.

$$\Delta H_{700} = -31 \text{ kcal/mol} \quad C_4H_8 + 1/2\ O_2 \rightarrow C_4H_6 + H_2O$$

So, the butadiene yield increases to about 65–70% and selectivity to 90–95%, per run, at 400–460°C. Since the reaction is highly exothermic, a great deal of conventional fuel is saved.

There is a great diversity of literature concerning the catalytic systems and preparation methods. That makes very difficult to find correlations between the nature and the structure of the active components, the genesis, the activity, as well as the selectivity of the catalyst in the above reaction.[6-9]

To establish such correlations we have studied the following binary and ternary catalytic systems: $Bi_2O_3-MoO_3$; $Bi_2O_3-Fe_2O_3$; $MoO_3-Fe_2O_3$; $Bi_2O_3-MoO_3-Fe_2O_3$. The influence of the nature of the active components, the ratio among the components, the preparation methods, the textural and structural properties, as well as the activity and selectivity of these catalysts have been investigated.

II. EXPERIMENTAL RESULTS AND DISCUSSIONS

The purity of n-butenes used was 97.8%, with 61.4% butene-1 and 36.4% butene-2.

Hydrogen acceptor was atmospheric oxygen and the diluent the steam. The reaction was carried out in a dynamic microreactor using 5g of 2.0—2.5 mm pellets catalyst. Pellet size was picked out to avoid diffusional effects.

The products were analysed by gas-chromatography; yield (R), selectivity (S), and conversion (C) were calculated with the following relations:

$$R_{\text{butadiene}} = \frac{\text{mols butadiene}}{\text{mols butenes fed}}$$

$$C_{\text{butenes}} = \frac{\text{mols butene converted}}{\text{mols butenes fed}}$$

$$S_{\text{butadiene}} = \frac{\text{mols butadiene}}{\text{mols butenes converted}}$$

II.1. PREPARATION OF THE CATALYSTS

There were three methods used for preparation of catalysts:

a. Mixing equivalent quantities of oxidic components, in order to obtain the desired atomic ratio, followed by thermic treatment;

b. Mixing equivalent quantities of some metallic compounds (bismuth nitrate, iron nitrate, molybdic acid) followed by thermic treatment;

c. The new "mechano-topochemical" method.

The last one consists in the mechanical mixing of component salts (in solid phase, as crystal-hydrates) with an alkaline component (ammonium carbonate or bicarbonate) also in solid phase. The solid-solid interface reaction took place in a dense fluid medium made up of crystal water according to a topochemical reaction mechanism.[10]

The activities of some catalysts, Bi : Mo : Fe = 0.5 : 1.0 : 1.2 (atomic ratio) prepared by the above methods are presented in table 1.

The test was carried out under the following conditions : temperature 400—480°C, volumetric flow rate of n-butenes 600 h^{-1}; molar ratio n-butene : air : steam = 1.0 : 3.5 : 7.5

TABLE 1

The influence of preparation method on activity of ternary system Bi/Mo/Fe = 0.5/1.0/1.2

Preparation method	Reaction temperature °C	Conversion n-butenes % wt	Butadiene yield % wt	Butadiene selectivity % wt
Method described under *a*	400	46.5	41.1	88.4
	440	49.4	42.6	86.2
	480	54.8	43.1	78.6
Method described under *b*	400	52.2	46.8	89.6
	440	56.2	49.8	88.4
	480	59.3	46.1	77.8
Method described under *c*	400	60.3	57.2	94.8
	440	67.2	62.0	92.3
	480	68.1	60.8	89.0

In the further experiments, we used only the catalysts prepared by the mechano-topochemical method due to their obvious higher performances.

II.2. ACTIVITY AND SELECTIVITY OF CATALYSTS

The activity and selectivity of the binary and ternary catalysts were determined under the following conditions : temperature 400—520°C ; volumetric flow rate 600 h^{-1} for n-butenes ; molar ratio n-butene : air : steam = 1.0 : 3.5 : 7.5.

The C, R and S values of reactions with no catalyst, or with individual oxidic consituents of the catalysts have been compared with the same parameters of catalytic process.

II.2.1. Thermal oxidative dehydrogenation of n-butenes

The thermal oxidative process was carried out, both with and without steam, under the previous conditions. Results are shown in figure 1.

Oxygen (air) introduction results in lower yields of butadiene, namely 0.65 at 400°C and 3.15% at 520°C with the selectivity below 40%. The selectivity decreases noticeably with the increase of the temperature.

The steam considerably decreases conversion as well as yield of butadiene and fairly increases selectivity.

Therefore the oxygen will act as an acceptor for hydrogen from hydrocarbon only under specific activation on the catalyst.

II.2.2. Oxidative dehydrogenation of n-butenes on Bi_2O_3, MoO_3, and Fe_2O_3

The presence of the oxidic constituents of the active catalysts increases the conversion. Nevertheless, the activity and the selectivity are still insignificant over the temperature range investigated. The results are shown in figure 2.

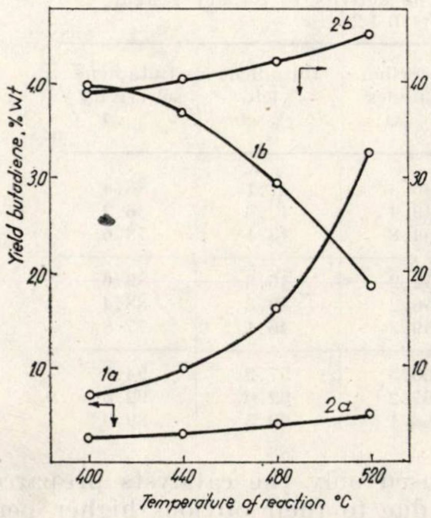

Fig. 1. — Thermal oxidative dehydrogenation of n-butenes. *1-a, b* — in the absence of steam; *2-a, b* — in the presence of steam.

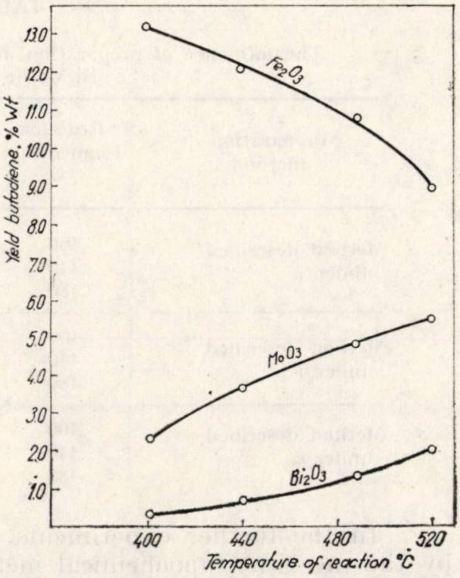

Fig. 2. — Yield of the butadiene in oxidative dehydrogenation of the butenes on metallic oxides. $V_v = 600\ h^{-1}$/n-butenes; n-butenes : air : steam ratio = 1.0 : 3.5 : 7.5.

The butadiene yields range in the order: $Fe_2O_3 > MoO_3 > Bi_2O_3$ and selectivity in the order: $MoO_3 > Fe_2O_3 > Bi_2O_3$.

In oxidic ternary systems, Fe_2O_3 will improve to a greater extent the activity and MoO_3, the selectivity.

II.2.3. Binary catalytic systems

Figure 3 represents the activity of catalytic systems of type $Bi_2O_3 - MoO_3$, versus atomic ratio Bi/Mo ranging between 0.5/1.0 and 2.0/1.0.

As far as the yield is concerned, the atomic ratio between the components strongly affects the activity of catalysts. The most active is the Bi/Mo = 1.0/1.0 system for which the yield in butadiene is 52% at temperature 520°C. The minimum activity is exhibited by the Bi/Mo = = 0.6/1.0 atomic ratio system, for which the yield in butadiene is 12%.

The selectivity and activity of these catalytic systems are varying irregularly with atomic ratio but stay within a range of values close to 90%, for most of the ratios.

The study of the catalytic activity of the other binary systems of the type $Bi_2O_3-Fe_2O_3$ and $MoO_3-Fe_2O_3$ showed that they are inactive or have small activity in oxidative dehydrogenation of n-butenes.

II.2.4. Ternary catalytic systems

In the binary catalytic system $Bi_2O_3-MoO_3$, we have studied the influence of a third component, namely Fe_2O_3 on catalytic activity. The best results were obtained in the case of the ternary catalytic systems $Bi_2O_3-MoO_3-Fe_2O_3$, having the atomic ratio Bi/Mo = 0.5/1.0, with the lowest concentration of Bi_2O_3.

The study of the catalytic activity of the ternary systems as a function of the concentration of the Fe_2O_3 — figure 4 — has shown that a slight decrease of the yield in butadiene at the low concentrations of Fe_2O_3 takes place. The continuous increase of the amount of Fe_2O_3 leads to a ternary catalytic system with the significant activity in the oxidative dehydrogenation process. Thus, at the atomic ratio Bi/Mo/Fe = = 0.5/1.0/1.2, the yield increases up to a maximum value of 62% at 440°C. We have previously mentioned that the binary system Bi/Mo = = 0.5/1.0 presents a yield of only 40% in butadiene.

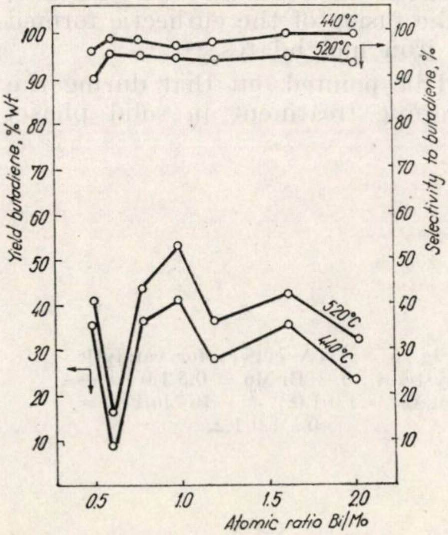

Fig. 3. — The activity and selectivity of binary catalysts, $Bi_2O_3.MoO_3$ as a function of atomic ratio Bi/Mo. $V_v = 600$ h^{-1}/n-butenes ; n-butenes : air : steam ratio = = 1.0 : 3.5 : 7.5.

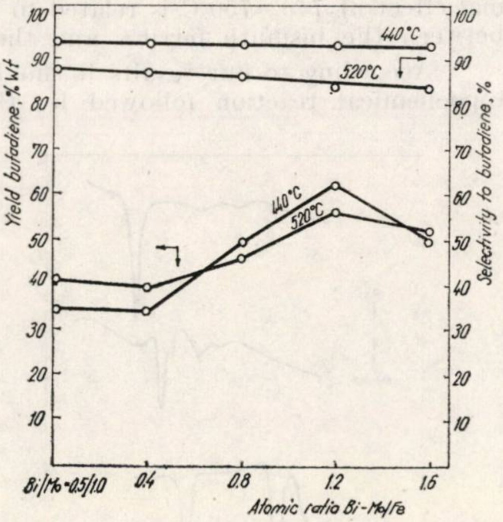

Fig. 4. — The activity and selectivity of ternary catalysts Bi—Mo—Fe as a function of atomic ratio Bi : Mo = 0.5 : 1.0/Fe. V_v = = 600 h^{-1}/n-butenes ; n-butenes : air : steam ratio = 1.0 : 3.5 : 7.5.

Further increase in the amount of Fe_2O_3 results in a decrease of the activity of the ternary system, but selectivity still has values over 90%, at temperatures under 500°C.

II.3. PHYSICAL-STRUCTURAL PROPERTIES OF CATALYSTS

II.3.1. Thermodifferential analysis

DTA curves for binary and ternary systems have been carried out. Figure 5 shows the DTA curves for the $Bi_2O_3-MoO_3$ systems with the atomic ratio Bi/Mo = 0.5/1.0 and 1.0/1.0, and the ternary systems $Bi_2O_3-MoO_3-Fe_2O_3$ with the atomic ratio Bi/Mo/Fe = 0.5/1.0/1.2.

The binary system Bi/Mo = 0.5/1.0 exhibits a small exothermal effect at 420°C probably due to the reaction between the free Bi_2O_3 and MoO_3 with formation of bismuth molybdate. An euthectic which melts at 620°C, producing a marked endothermal effect, is formed between the bismuth molybdate and the excess of molybden oxide.

The DTA curve of the catalytic system Bi/Mo = 1.0/1.0 exhibits an endothermal effect at 580°C. It may be assumed that this is the temperature where the phase transformation of the Bi/Mo = 1.0/1.0 compound into the Bi/Mo = 2/3 and respectively the Bi/Mo = 2/1 compounds occurs. At 660°C the exothermal effect closely followed by a strong endothermal effect at 690°C may be attributed to the fusion of the euthectic produced out from the high temperature compounds of Bi/Mo = = 1.0/1.0 dissociation.[11]

In ternary system, the endothermal effects at 580–590°C are due to the polymorphic transformation of the iron molybdates. The endothermal effect at 740–750°C is related to the fusion of the euthectic formed between the bismuth ferrites and the iron molybdates.[12]

According to our results it should be pointed out that during the topochemical reaction followed by thermic treatment in solid phase, iron and bismuth complex molybdates as well as bismuth ferrites are formed.

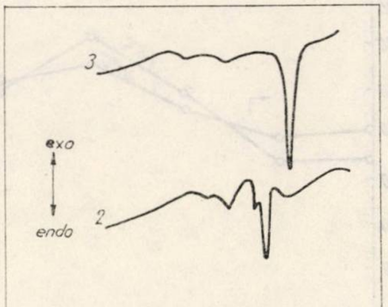

Fig. 5. — DTA curves for catalytic systems. *1* — Bi/Mo = 0.5/1.0 ; *2* — Bi/Mo = 1.0/1.0 ; *3* — Bi/Mo/Fe = 0.5/1.0/1.2.

The phases produced out, with the above-mentioned structure and the catalytic performance in the oxidative dehydrogenation are in good agreement.

II.3.2. Texture of catalysts

The main textural characteristics of some binary and ternary catalysts are shown in table 2.

The real density of the binary catalysts increases with the amount of Bi_2O_3 while the apparent density is unaffected.

The total volume of the pores ranges between 0.13545 cm^3/g for binary system Bi/Mo = 0.5/1.0, and 0.1604 cm^3/g for ternary system.

TABLE 2

Textural characteristics of binary and ternary catalysts

Catalytic system	Real density g/cm^3	Apparent density g/cm^3	Surface area m^2/g	Total volume of pores cm^3/g	Macropores volum cm^3/g	R_M Å
Bi/Mo = 1.5/1.0	5.81	3.58	2.4	0.13545	0.12155	3, 400
Bi/Mo = 0.8/1.0	6.32	3.32	2.86	0.1429	0.1377	1,000
Bi/Mo = 1.0/1.0	6.53	3.38	3.34	0.1517	0.1377	1,000 and 8,500
Bi/Mo = 1.2/1.0	6.92	3.34	1.92	0.1845	0.1380	1,600
Bi/Mo = 1.6/1.0	7.83	3.68	1.15	0.1441	0.079	2,500
Bi/Mo/Fe =0.5/1.0/1.2	5.4	2.9	3.4	0.1604	0.1474	400 and 25,000

Figure 6 shows the pores distribution by radius for the binary systems Bi/Mo = 0.5/1.0 and 1.0/1.0, and for the ternary system Bi/Mo/Fe = = 0.5/1.0/1.2.

The increase of the amount of Bi_2O_3 in the binary catalysts shifts the medium pores to lower values, and the surface area under the maximum becomes broader; there is also noticed an apparent bimodal distribution of the pores. Fe_2O_3 addition changes the distribution of the medium pores and of the macropores. The ternary catalyst Bi/Mo/Fe = 0.5/1.0/1.2 exhibits a heterogenous porous structure with medium pores and macropores having radia of 400 and respectively 25,000 Å.

There is also evident that, with the addition of Fe_2O_3 some differences in the structural properties of binary and ternary catalysts appear.

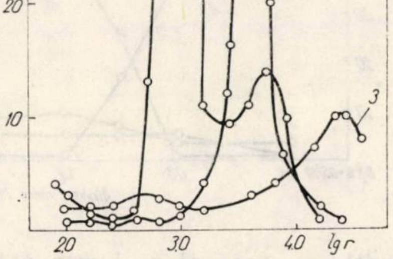

Fig. 6. — Pores distribution by the radius. 1 — Bi/Mo = 1.0/1.0; 2 — Bi/Mo = = 0.5/1.0; 3 — Bi/Mo/Fe = 0.5/1.0/1.2.

II.3.3. Determination of active catalytic phases

The X-ray study of the oxides, of the binary and ternary catalytic systems allows to draw some conclusions regarding the structure of catalysts.

It was established that the ternary catalytic systems display the following phases : [13]

a. A compound which appears gradually in the system with increase of the amount of Fe_2O_3. This compound is the same as the so-called X compound, found by Batist et al. [14] This compound was also identified in catalysts after the catalytic reaction (figure 7, curve 1);

b. $Bi_2O_3.3MoO_3$ which appears in the samples with a lower amount of Fe_2O_3 (figure 7, curve 2);

c. $Fe_2O_3.(3-4)MoO_3$, which appears in each sample in small quantities (figure 7, curve 3);

d. α-Fe_2O_3 which appears in catalysts with higher Fe_2O_3 content (figure 7, curve 4).

Figure 7 shows the phase mixture composition, as a function of the atomic ratio Mo/Fe in the catalysts.

In ternary catalysts with lower Fe_2O_3 contents, the Bi/Mo = 2/3 compound is prevailing. The increase in the Fe_2O_3 content results in the decrease of the intensity line of this compound, with the subsequent appearance and increase of the characteristic line of X compound (curve 2). The maximum of the latter compound is found in the Bi/Mo/Fe = 0.5/1.0/1.2 system, which also displays the best catalytic activity.

From phase distribution in ternary catalysts, it may be concluded that the X compound is an iron and bismuth double hexamolybdate $Bi_2Fe_2(MoO_4)_6$.

Our results lead to the assertion that the ternary catalyst activity in the oxidative dehydrogenation is due to an active catalytic complex made up of the Erman phase (Bi/Mo = 1/1), iron molybdate ($Fe_2O_3.4MoO_3$) and iron and bismuth double hexamolybdate $Bi_2Fe_2(MoO_4)_6$, and not to any of these phases taken separately. Each phase exhibits with no exception, lower catalytic activity than the above-mentioned equilibrium-compound.

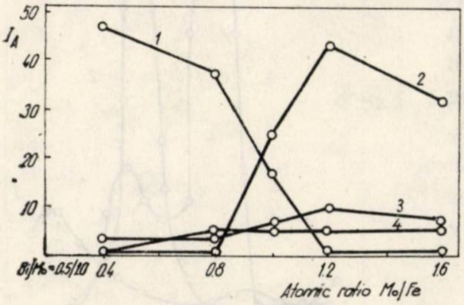

Fig. 7. — Variation of the relative concentrations of various phases in Bi-Mo-Fe catalytic system, as a function of the atomic ratio Mo/Fe (atomic ratio Bi/Mo = = 0.5/1.0). *1* — Bi_2O_3. $3MoO_3$; *2* — X-Compound ; *3* — Fe_2O_3. $(3-4MoO_3)$; *4* — αFe_2O_3.

We have calculated the distribution of molybden oxide among the three specified phases which formed the catalytic complex :

17.5% in the Erman phase

49.1% in the bismuth and iron double molybdate
33.4% in the iron molybdate

After the reaction, X-ray patterns of the nonstoichiometric molybden oxides of type $MoO_{2.88}$ or Mo_9O_{26} have been identified in the ternary catalysts. The existence of these oxides indicates that the oxidative dehydrogenation has been performed at the expense of the n-butenes oxidation with the oxygen from the catalyst lattice, the latter being restored with oxygen from the reaction medium.[15]

In the intermediary stage a Mo-O bond splits and it is then restored through the adsorption of oxygen from the reaction medium by a hole in the lattice, as follows:

$$C_4H_8 + O^{2-} + \square_d \rightleftharpoons C_4H_7^- + OH^-$$

$$2OH^- \rightarrow H_2O + \square_d + O^{2-}$$

$$C_4H_7^- + O^{2-} \rightarrow C_4H_6 + \square_r + OH^- + 2e^-$$

$$\square_r + 1/2O_2 + 2e^- \rightarrow O^{2-}$$

It is likely that this oxygen acceptor-donor mechanism occurs on the $Bi_2Fe_2(MoO_4)_6$ phase, which contains most of the Mo-O bonds.

II.4. CORRELATIONS BETWEEN TEXTURAL PARAMETERS AND THE ABSOLUTE RATE OF THE CATALYTIC OXIDATIVE DEHYDROGENATION REACTION OF THE n-BUTENES

As already mentioned we intended to set out some correlations between activity, expressed as local reaction rate and the textural parameters of the catalysts, such as macroporosity, the macropore volume, the pore radius, retention time of the reactant inside the macropore.[16]

In this order, we have studied comparatively the catalytic system Bi/Mo = 0.5/1.0 and Bi/Mo = 1.0/1.0 and Bi/Mo/Fe = 0.5/1.0/1.2.

It is known that in general reaction rate formula, the retention time $d\tau$ of the reactant flow rate V_0 (cm^3/s) within the reactor volume dV_r (reactor cross section infinitely small) is given by the expression:

$$d\tau = \frac{dV_r}{V_0}$$

By the substitution of the term which stands for the reactor volume, dV_r, with the volume of macropores V_M, granting that the reactant flows through them, one obtains the next expressions:

$$d\tau = \frac{dV_r}{F_{A_0}} = \frac{V_M}{F_{A_0}} = \tau_M$$

$$S_M = \frac{2V_M}{r_M}$$

$$-r_A = F_{A_0} \cdot X_A$$

$$F'_M = -r_A \tau_A \qquad F'_M = \frac{-r_A}{F_{A_0}} V_M$$

where : F_A — feeding flow rate (mol/g.sec)
X_A — moles butenes transformed per second and gram of catalyst
τ_M — retention time of the reactants in the macropores
S_M — internal surface area of macropores
r_M — mean radius of macropores
F_M — moles butenes transformed as a function of retention time inside the macropores
r_A — total reaction rate (moles/g.sec)

Figure 8 shows the variation of the apparent reaction rate with the feeding rate for the catalysts Bi/Mo=0.5/1.0 and Bi/Mo/Fe = 0.5/1.0/1.2 taking into account the global flow rate of the reactants.

We notice a linear dependence between the reaction rate and the reactant flow rate up to a certain value. The linear range corresponds to our experiment conditions. Apparent reaction order calculated from slope has fractionary values closed to zero, which shows that the mechanism is more complex when some of reaction mixtures of 1-butene and 2-butene are used.

Figure 9 shows the flow rate of the reaction products plotted against the retention time of the reactants inside the macropores, for the same catalysts. In both cases, a linear dependence is noticed up to retention time ranging from 1.0 to 1.5 s.

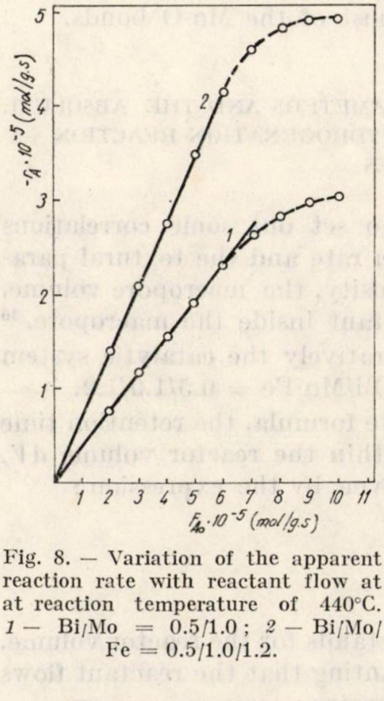

Fig. 8. — Variation of the apparent reaction rate with reactant flow at at reaction temperature of 440°C. *1* — Bi/Mo = 0.5/1.0 ; *2* — Bi/Mo/Fe = 0.5/1.0/1.2.

Figure 10 shows the simultaneous variation of the reaction rate and of the butadiene yield with the retention time of the reactant inside the macropores for three catalysts : Bi/Mo = 0.5/1.0, Bi/Mo = 1.0/1.0 and Bi/Mo/Fe = 0.5/1.0/1.2.

A correlation between the reaction rate and the yield as function of the considered parameter may be noticed.

These experimental data suggest certain dependences between the kinetic parameters of the reaction and some textural characteristics of the catalysts which could be meaningful when criteria for selecting the catalysts are involved.

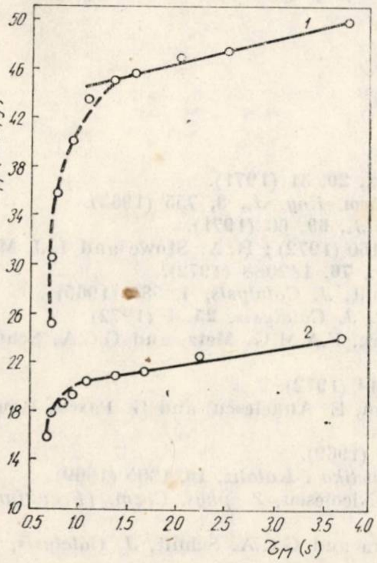

Fig. 9. — Variation in the flow of the reaction products with the stationary time of reactants inside the macropores. Reaction temperature 440°C. *1* — Bi/Mo = 0.5/1.0 ; *2* — Bi/Mo/Fe = 0.5/1.0/1.2.

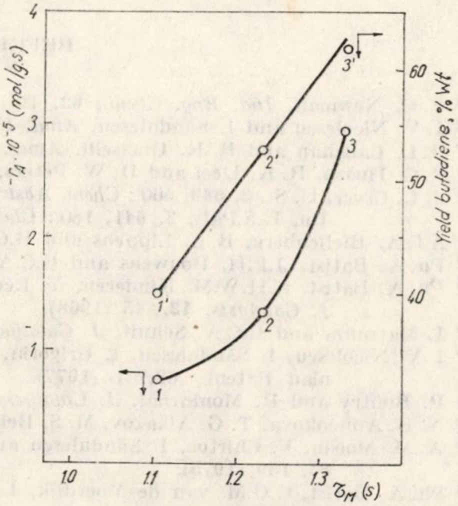

Fig. 10. — Dependence of the reaction rate and of the butadiene yield with the stationary time of reactants inside the macropores. Reaction temperature 440°C. *1,1'* — Bi/Mo = 0.5/1.0 ; *2,2'* — Bi/Mo = 1.0/1.0 ; *3,3'* — Bi/Mo/Fe = 0.5/1.0/1.2.

CONCLUSIONS

1. A new mechano-topochemical method of catalysts synthesis has been tested. This method enhaces reproducibility of the preparation and highly improves the activity and selectivity against the same catalysts prepared by classical methods.

The interface reaction of the solid hydrated particles provides a better interaction among the components of the reaction mixture, thus favouring the formation of the active catalytic phases.

2. Addition of Fe_2O_3 to the binary catalytic systems Bi—Mo—O substantially increases their activity.

3. In the case of the catalyst Bi/Mo/Fe = 0.5/1.0/1.2, the oxidative dehydrogenation is ensured by an active catalytic complex formed out of $Bi_2O_3 . 2MoO_3$ (Erman phase), iron molybdate $Fe_2O_3 . 4MoO_3$ and iron and bismuth double hexamolybdate $Bi_2O_3 . Fe_2O_3 . 6MoO_3$.

4. The research carried out has shown the existence of some interdependences between the kinetic parameters of the reaction and some textural characteristics of the catalysts (the area included in the macropores, the retention time of the reactant inside the macropores) which could be emphasized as criteria for selecting a particular catalyst.

REFERENCES

[1] F. C. Newman, *Ind. Eng. Chem.*, **62**, 41 (1970).

[2] I. V. Nicolescu and I. Săndulescu, *Anal. Univ. Buc.*, **20**, 31 (1971).

[3] J. L. Callahan and R. K. Grasselli, *Amer. Inst. Chem. Eng. J.*, **9**, 755 (1963).

[4] P. C. Husen, R. K. Deel and D. W. Peters, *Oil Gas J.*, **69**, 60 (1971).

[5] J. L. Croce, U. S., 3, 649, 560 ; *Chem. Abstr.*, **77**, 21160 (1972) ; R. A. Stowe and I. J. Martin, U.S.Pat., 3, 641, 180 ; *Chem. Abstr.*, **76**, 142088 (1972).

[6] A.C.A. Bleijenberg, B. C. Lippens and G.C.A. Schuit, *J. Catalysis*, **4**, 581 (1965).

[7] Ph. A. Batist, J.F.H. Bouwens and G.C.A. Schuit, *J. Catalysis*, **25**, 1 (1972).

[8] Ph. A. Batist, A.H.W.M. Kinderen, Y. Leeuwenburg, F.A.M.G. Metz, and G.C.A. Schuit, *J. Catalysis*, **12**, 45 (1968).

[9] I. Matsuura and G.C.A. Schuit, *J. Catalysis*, **25**, 314 (1972).

[10] I .V. Nicolescu, I. Săndulescu, I. Grigoriu, T. Crişan, E. Angelescu, and G. Pascu, Romanian Patent, 62,701 (1977).

[11] P. Boutry and R. Montarnal, *J. Catalysis*, **13**, 75 (1969).

[12] Y. B. Annenkova, T. G. Alkazov, M. S. Belenki, *Kinetika i Kataliz*, **10**, 1305 (1969).

[13] A. M. Moisin, V. Chirtoc, I. Săndulescu and I. V. Nicolescu, *Z. phys. Chem. (Frankfurt)*, **95**, 159 (1975).

[14] Ph. A. Batist, C.G.M. van de Moesdijk, I. Matsuura and G.C.A. Schuit, *J. Catalysis*, **20**, 40 (1968).

[15] W.H.M. Sachtler and N. de Boer, "Proceeding 3rd International Congress Catalysis", vol. 1, Amsterdam, 1965, p. 252.

[16] I. V. Nicolescu, E. Angelescu, I. Grigoriu, T. Crişan and C. Grigoriu, *Chim. Ind., Génie Chimique*, **104**, 1731 (1971).

Revue Roumaine de Chimie, **26**, *2*, 229–235 (1981)

A STUDY FOR OPTIMUM CONDITIONS OF EXTRACTION OF TRANSITION METAL COMPLEXES WITH PYRIDINE DERIVATIVES. EXTRACTION OF THE Co(II), Ni(II) AND Zn(II) COMPLEXES OF 3,5-DIMETHYLPYRIDINE

B. LENARCIK and E. BEZAK

Institute of Chemistry, Pedagogical College, 25–020 Kielce, Poland

Received July 12, 1979

The extraction of the Co(II), Ni(II) and Zn(II) complexes of 3,5-dimethylpyridine with several solvents has been studied.

The extraction percent, E, characterizing the extraction, has been shown to correlate well with the formation degrees, α_n, of some complexes. Based on the dependence $E = f(\alpha_n)$, a procedure has been developed for the determination of the composition of extractable species. Over a certain concentration range, the Ni(II) complexes of 3,5-dimethylpyridine occurred as square planar species in the organic phase.

INTRODUCTION

Extraction methods have found a variety of applications both in scientific and technical investigations.[1,2] For instance, they can be employed for extraction of rare-earth metals from aqueous solutions in the form of their complexes.[3,4] Extraction has also been used for studies of the composition and stability of complexes in aqueous solution.[5] The probability of transfer of a complex from aqueous phase to organic one has been found to increase as water molecules in the co-ordination sphere of a metal become substituted for those of organic ligands. This is especially valid for large molecules of organic compounds which are hydrophobic in nature. According to a commonly accepted model,[6] the extraction of a metallic complex should increase upon change of the octahedral structure to tetrahedral or square planar ones.

The objective of this work was to explore the possibility of extraction of the Co(II), Ni(II) and Zn(II) complexes of 3,5-dimethylpyridine 3,5-lutidine. Previously,[7] the compound was shown to form relative by stable complexes with metals. With zinc, an equilibrium between tetrahedral and octahedral species was observed. The ligand itself is fairly hydrophobic, being sparingly soluble in water.

Another reason which prompted us to undertake this study was a report[8] of other authors who found that in organic solvents pyridines formed readily octahedral or tetrahedral complexes with cations of the first row of transition metals.

EXPERIMENTAL

Reagents

3,5-Dimethylpyridine (Fluka AG) was purified by fractional distillation, a fraction boiling at 171—172°C being collected. The purity of the distillate was checked chromatographically. Nitric acid (anal. grade reagent manufactured by Nitrogen Works, Tarnów) was properly diluted and standardized against Na_2CO_3 or $Na_2B_4O_7 . 10H_2O$. Solutions of metal nitrates were prepared from doubly crystallized salts (anal. grade reagents, Nitrogen Works, Chorzów). The concentrations of the metals were determined by titration with a di-Na EDTA solution and gravimetrically. The concentration of the KNO_3 solution was determined gravimetrically in form or sulphate.

As extractions, the following solvents were used : acetylacetone, ethyl acetylacetate, cyclohexanol, benzene, tributyl phosphate /TBT/, amyl alcohol, isoamyl alcohol and solutions of 3,5-dimethylpyridine in *iso*-amyl alcohol. The solvents were purified by distillation.

Apparatus

The pH measurements were made by using a digital pH meter PHM-64 (Radiometer, Copenhagen) and a GK230iC combined electrode.

Absorption spectra were taken on a UV-VIS Specord spectrophotometer (C. Zeiss, Jena). Quartz cuvettes with the path lengths of 1 and 2 cm were used. The magnetic susceptibility measurements were made by employing the Gouy's method.

Procedure

All measurements were carried out at 25°C and 1.00 ionic strength (KNO_3). To prevent hydrolysis of the complexes in the aqueous phase, the concentration of 3,5-dimethylpyridine nitrate was held constant (0.50 M) in all solutions.

In order to prepare solutions for extraction, the so-called basic and acidic ones were placed in 50 cm^3 volumetric flasks. The former contained a weighed quantity of the ligand and known volumes of the standardized HNO_3. KNO_3 and a metal nitrate solutions. The acidic solutions were different from the basic ones in the absence of the ligand only. By mixing together proper volumes of the acidic and basic solutions, 10 cm^3 samples were obtained ; they had the same levels of metal and bonded 3,5-dimethylpyridine acid and differred in the level of the free base only.

Extraction experiments were run with 9 cm^3 of the solution and equal volume of an organic solvent. Tightly closed test tubes were shaken for 15—20 min to speed up attaining the equilibrium. As soon as the extraction was completed, the pH of the aqueous phase and the metal level in it were measured. When calculating the metal concentration, changes in the volume of aqueous phase, which had taken place during extraction, were accounted for.

Calculations

The extraction percent, E, was calculated from the equation

$$E = \frac{C_M^0 - C_M}{C_M}$$

where C_M^0 and C_M are the metal concentrations in the aqueous phase prior to and after extraction, respectively.

The knowledge of the pH of the aqueous phase allowed to calculate the free ligand concentration, [L], after reaching equilibrium, from the equation

$$[L] = \frac{K_a \, C_k}{[H_3O^+]}$$

where K_k is the ionization constant of the conjugate acid of 3,5-dimethylpyridine and C_k is the nitric acid concentration. The K_a value of 1.03×10^{-6} has been accepted for calculations.[7] Further, for each system studied, the formation degrees of individual complexes, α_n, were calculated for arbitrary ligand concentrations from the equation

$$\alpha_n = \frac{\beta_n [L]^n}{\sum\limits_{n=0}^{n=N} \beta_n [L]^n}$$

The values of the overall stability constants, β_n, have been taken from [7].

RESULTS AND DISCUSSION

With the solvents tested, the highest E values were obtained using a solution of 3,5-dimethylpyridine in *iso*-amyl alcohol, *iso*-amyl alcohol alone or cyclohexanol. For the systems considered, cyclohexanol turned out to be an inferior extractant to *iso*-amyl alcohol due to a poorer electrondonating power of the former. Accordingly, extraction experiments were performed with *iso*-amyl alcohol or with the 3,5-dimethylpyridine solutions in the alcohol.

Addition of the base to the alcohol resulted in an increase in the partition coefficient value, since the level of the base increased in both phases. At the same time the complexation degree of the metal in the aqueous phase increased. The results of extraction, in terms of a dependence between E and the free ligand concentration are shown in figures 1—3. In these figures, also the distribution of the central ion concen-

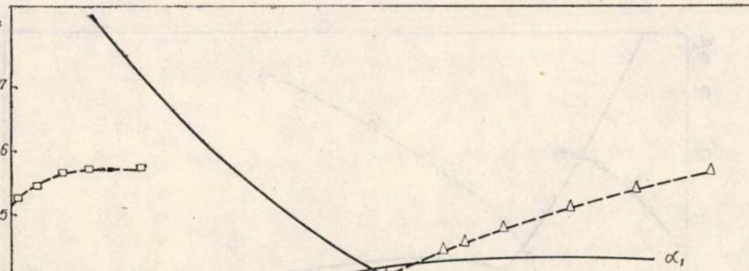

Fig. 1. — Extraction percent of the Co(II) — 3,5-dimethylpyridine complexes between water and cyclohexanol (□), *iso*-amyl alcohol (○) and solutions of 3,5-dimethylpyridine in *iso*-amyl alcohol (△) *vs.* free ligand concentration in the aqueous phase along with degrees of formation of individual complexes.

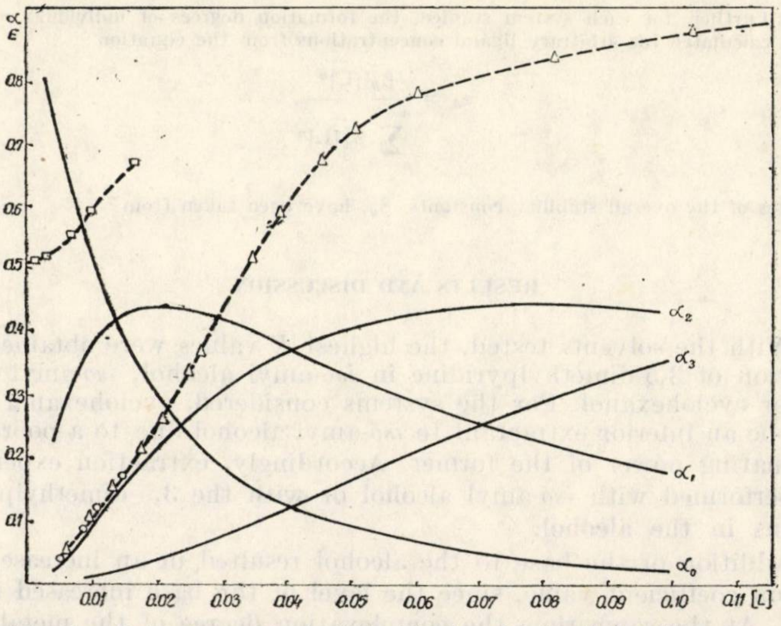

Fig. 2. — Extraction percent of the Ni(II) — 3,5-dimethylpyridine complexes between water and cyclohexanol (□), *iso*-amyl alcohol (○) and solutions of 3,5-dimethylpyridine in *iso*-amly alcohol (△) *vs.* free ligand concentration in the aqueous phase along with degrees of formation of individual complexes.

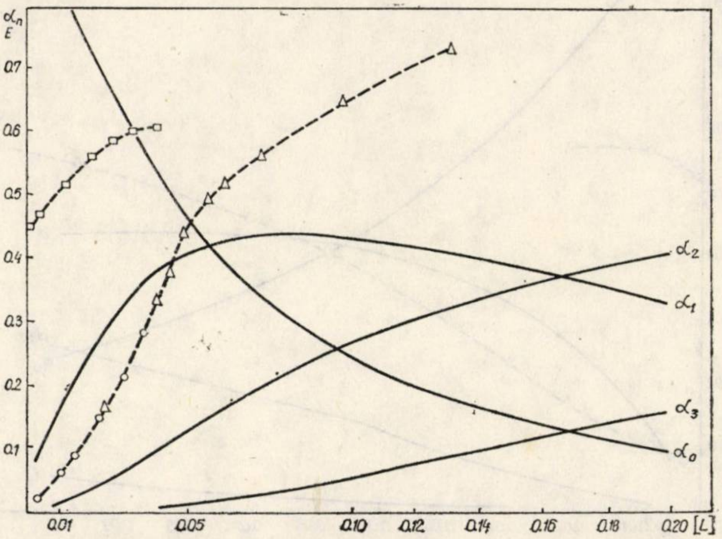

Fig. 3. — Extraction percent of the Zn (II) — 3,5-dimethylpyridine complexes between water and cyclohexanol (□), *iso*-amyl alcohol (○) and solutions of 3,5-dimethylpyridine in *iso*-amyl alcohol (△) *vs.* free ligand concentration in the aqueous phase along with degrees of formation of individual complexes.

tration, C_M, among the formation degrees of individual complexes is shown as a function of the free ligand concentration in aqueous phase. In our opinion, both the shape and position of the $E = f([L])$ curves resemble closely the course of the functions $\alpha_n = f([L])$. In all systems involving *iso*-amyl alcohol, the shape of the extraction curves resembles that of the curve for α_2, thus indicating that a complex containing two 3,5-dimethylpyridine molecules passes to the organic phase. This similarity is particularly evident for the Co(II) and Ni(II) compounds. The extraction curve in the cyclohexanol system is situated at higher E values, thus indicating that the alcohol molecules solvate metallic ions very strongly.

To examine in detail the relationship between E and α_n, we paid attention to that between E and α_2 for all three systems (cf. Fig. 4). In these systems, the partition coefficient, E, turned out to be directly proportional to α_2 over a certain range. However, for Ni(II), the $E = f(\alpha_2)$ graph deviated towards higher E values, thus indicating that along with ML_2, species richer in the pyridine ligand are being extracted. A reverse situation was noted with the Co(II)—3,5-dimethylpyridine and Zn(II) —3,5-dimethylpyridine systems. This can be explained in terms of passing several complexes to the organic phase. The extraction of the Ni(II) complexes with *iso*-amyl alcohol was accompanied by change in colour, from blue to red. To elucidate the cause for this change, we took absorption spectra of the complexes in both phases, prior and after the extraction (cf. Fig. 5). Analogous experiments were made with the Co(II) complexes which revealed one strong band at 19,800 cm^{-1} assigned to the $^4T_{1g} \rightarrow {}^4T_{2g}$ pink-coloured transition, characteristic for octahedral complexes of the metal.[9] The spectra of the aqueous and organic layers were similar to each other. This suggests that the extraction of the Co(II) complexes was not accompanied by a change in configuration of the co-ordination sphere of the metal.

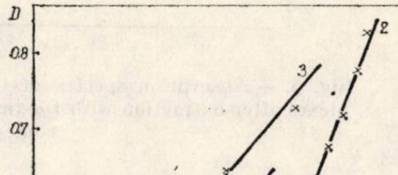

Fig. 4. — Dependence extraction percent of degrees of formation of individual complexes : 1. — Ni (II), $E = f(\alpha_2)$; 2. — Co(II), $E = f(\alpha_2)$; 3. — Zn (II), $E = f(\alpha_2)$.

In the Ni(II) —*iso*-amyl alcohol system, complexes in the aqueous and organic phases are likely to differ in the structure of the co-ordination sphere. In the aqueous phase, two bands characteristic for octahedral Ni(II) complexes were observed.[10] The first band 24,800 cm^{-1} corresponds to the $^3A_{2g} \rightarrow {}^3T_{1g}(P)$ transition and the other (14,500 cm^{-1}) to the $^3A_{2g} \leftarrow {}^3T_{1g}(F)$ one. The red-coloured organic phase displayed one absorption band at 19,200 cm^{-1}.

After Gray [11] the band can be assigned to tetra-co-ordinate planar Ni(II) complexes. This assumption was further supported by results

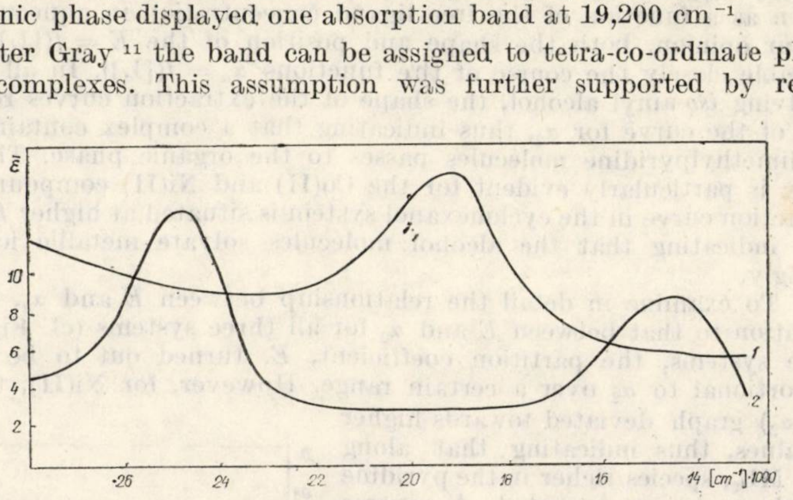

Fig. 5. — Absorption spectra of the Ni(II) — 3,5-dimethylpyridine complexes after extraction with *iso*-amyl alcohol. 1 — organic phase, 2 — aqueous phase.

of magneto-chemical measurements. The negative values of the magnetic susceptibility of the Ni(II) complex in the organic phase (-0.785×10^{-6} c.g.s.u.) indicates a diamagnetic substance. It has long been known that the diamagnetism of the Ni(II) complexes is due to square planar species only. [11, 12] Consequently, the equilibrium reached during extraction of the Ni(II) complexes is accompanied by a configurational equilibrium, since in the aqueous phase six-coordinate species occur whilst in the organic phase square planar ones. Another picture was observed during extraction of Ni(II) with 3,5-dimethylpyridine solutions in *iso*-amyl alcohol. Absorption spectra of the aqueous and organic phases did not show any change in the co-ordination sphere of the metal after extraction. In this case the equilibrium octahedron ⇌ planar square was strongly shifted towards the formation of octahedral species at a large concentration of the amine in solution.

The foregoing facts allow to establish the most probable compoition of complexes passing from the aqueous phase to the organic one. Some difficulty was encountered in the determination of the manner of combining nitrate ions in the extracted complexes and simultaneous determination of the number of molecules of *iso*-amyl alcohol combined in the co-ordination sphere. The extraction experiments were carried out at a considerable ionic strength (1.0) maintained by means of nitrate. The anion exhibits moderate complex-forming properties. On this basis the ions have been assumed to be combined in the co-ordination sphere. The probable composition of the extractable complexes is given in table 1.

TABLE 1

Probable composition of complexes passing to the organic phase

Metal	Extractant	Composition of extractable complex *
Co(II)	*iso*-amyl alcohol	$[Co(lu)S_3(NO_3)_2]$
	iso-amyl alcohol + + 3,5-lutidine	$[Co(lu)_2S_2(NO_3)_2]$
Ni(II)	*iso*-amyl alcohol	$[Ni(lu)_2(NO_3)_2]$
	iso-amyl alcohol + + 3,5-lutidine	$[Ni(lu)_3S(NO_3)_2]$
Zn(II)	*iso*-amyl alcohol	$[Zn(lu)S_3(NO_3)_2]$
	iso-amyl alcohol + + 3,5-lutidine	$[Zn(lu)_2S_2(NO_3)_2]$

* lu = 3,5-lutidine ; S = molecule of extractant or water

CONCLUSIONS

1. Extraction curves, $E = f([L])$, show a correlation with the graphs of the formation degrees of some complexes, $\alpha_n = f([L])$.

2. The composition of complexes passing to the organic phase can be found from the dependence $E = f(\alpha_n)$.

3. The transfer of a complex from the aqueous phase to an organic one may be accompanied by a change in the structure of the co-ordination sphere.

REFERENCES

[1] I. Stary, "Proceedings of the International Conference Held at Gothenburg, Sweden", North-Holland Publishing Company, Amsterdam, 1967, p. 7.

[2] B., Jezowska-Trzebiatowska, S. Kopacz and T. Mikulski, "Pierwiastki rzadkie (Rare Elements)", PWN, Warszawa-Wrlocław, 1967.

[3] J. Minczewski, J. Chwastowska and R. Dybczynski, "Analiza śladowa. Metody rozdzielania i zagęszczania (Trace Analysis. Methods of Separation and Concentration)", WNT, Warszawa, 1973.

[4] S. Kopacz, "Ekstrakcja związków nieorganicznych tlenowymi ekstrahentami w układach siarczanowych (Extraction of Inorganic Compounds with Oxygen-Containing Extractants in Sulphate Media)" Politechnika Wrocławska, Wrocław, 1977.

[5] F. J. C. Rossotti and H. Rossotti, "The Determination of Stability Constants and Other Equilibrium Constants in Solution", Academic Press, New York, 1961.

[6] W. Libuś, "Structure of Complex Compounds", Pergamon Press and WNT, Warszawa, 1964, p. 537.

[7] B. Lenarcik and M. Rzepka, *Roczniki Chem.*, in press.

[8] C. J. Ballahausen and C. K. Jorgensen, *Acta Chem. Scand.*, **9**, 397 1955.

[9] B. Jeżowska-Trzebiatowska, "Structure of Complex Compounds", Pergamon Press, WNT, Warszawa, p. 254.

[10] F. Cotton, "Advanced Inorganic Chemistry", Mir, Moscow, 1969.

[11] H. B. Gray and C. J. Balhausen, *J. Amer. Chem. Soc.*, **85**, 260 (1963).

[12] R. S. Nyholm, *Chem. Revs.*, **53**, 262 (1953).

Revue Roumaine de Chimie, 26, 2, 237–243 (1981)

COMPLEX COMPOUNDS OF SOME DIOSPHENOLIC TYPE CAROTENOIDS

ASTACENE COMPLEXES. SPECTROPHOTOMETRIC STUDY OF THE SYSTEM Fe (III) — ASTACENE

J. ZSAKÓ[a] and T. LÁSZLÓ[b]

[a]Faculty of Chemical Technology, "Babeş-Bolyai" University, str. Arany János 11, 3400 — Cluj-Napoca, Romania

[b]Department of Chemistry and Biochemistry, Institute of Agronomy "Petru Groza", str. Mănăştur 3, 3400 — Cluj-Napoca, Romania

Received March 10, 1980

By testing the colour reactions of astacene with some metal salts in alcoholic solutions, the complex formation with Al, Cr(III), Cu(II), Fe(III) and Hg(II) salts has been observed ; the diosphenolic tautomer form of the astacene is presumed to give these complexes. A spectrophotometric study of the system Fe(III) nitrate — astacene showed the formation of a rather stable complex with a metal to ligand ratio equal to 1 : 1. A new method has been tested, consisting in direct titrations performed in the spectrophotometric cell, by using a special device.

INTRODUCTION

The cyclic α-diketones able to give keto-enol tautomery, as well as organic compounds containing phenyl groups with at least two neighbouring OH groups, form complex compounds with some metal ions.

E. Bayer and co-workers [1] have shown the flowers of *Centaurea cyanea* to contain a chelate compound of Fe(III) and Al with the anhydro base of cyanin. Similar chelates are formed by the other anthocyanines, respectively anthocyanidines, flavonols, flavosemiquinones and flavoquinones. [2]

The diosphenol (bucocamphor), which is an α-diketone, showing keto-enol tautomery, gives a dark green colour with $FeCl_3$. [3]

Since some carotenoids contain a tautomeric diosphenol group, they can be presumed to give chelate type complexes. Such carotenoids are e.g. the following : astacene (3, 4, 3′, 4′-tetraketo-β-carotene), 2,3-dehydro-adonirubin (3,4,4′-triketo-β-carotene), 2,3-dehydro-adonixanthin or β-doradecin (3,4-diketo-3′-hydroxy-β-carotene), euglenanone or dehydro-hydroxy-echinenone (3,4-diketo-β-carotene),[4–10] 3,4′-dihydroxy-dehydro-echinenone (3,4′-dihydroxy-4-keto-2,3 dehydro-β-carotene), [11,12] dehydroflexixanthin, [13] α-doradecin (3,4-diketo-3′-hydroxy-α-carotene), [14] roserythrin. [15,16]

It is worth mentioning, that the 3-hydroxy-4-keto-carotenoids, like the 3-hydroxy-echinenone, give dark blue colour with KOH in ethanol, in the absence of air. Presumably, the potassium salt of the endiol form is obtained. [17-19] One can presume these compounds to be able to form also chelate type complexes.

A great number of other type complexes of the carotenoids have been reported, too. Such complexes are formed with $TiCl_4$ by the following carotenoids: β-carotene, zeaxanthin, physalien, [20] cryptoxanthin palmitate, [21] canthaxanthin, rhodoxanthin, β-apo-8′-carotenal [22] and some 5,8-epoxy-carotenoids. [23] Complex compounds are formed also by other epoxy-carotenoids as violaxanthin, luteochrom, cryptoflavin with Hg(II) chloride, [24,25] the inchain epoxides of canthaxanthin and of astacene with Hg(II), Fe(III) and Al chlorides, [26-29] violaxanthin and neoxanthin with $AlCl_3$, [30] peridinin with europium complexes [31] etc. The formation of π-complexes with iron-carbonyl has been reported in the case of β-carotene, lycopene [32] and of related compounds, like β-ionone and vitamin A. [33]

In the present paper the behaviour of the astacene ($C_{40}H_{50}O_4$) has been studied, with respect to its possibility to form complex compounds. The diosphenolic and α-diketo tautomeric forms of the all-trans-astacene are the following:

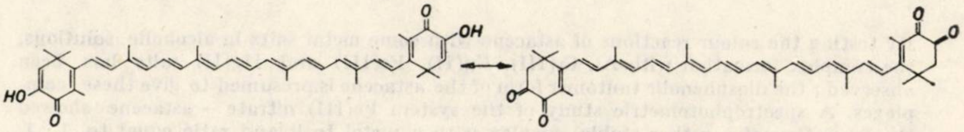

TESTING OF COMPLEX FORMATION

To an ethanolic solution of astacene, having a light orange colour, ethanolic solutions of different salts have been added drop by drop. The effects observed are presented in table 1. By using methanol as solvent, the results are the same.

The change of colour indicates the formation of complex compounds. Since similar tests performed with other carotenoids (β-carotene, zeaxanthin, canthaxanthin) showed a quite different behaviour of these compounds, one can presume the diosphenolic or the α-diketo groups to be responsible for the complex formation.

In the presence of diluted HCl or acetic acid the colour reactions given in table 1 do not occur and by adding these acids to the coloured solutions containing the complexes, their colour turns into light yellow, indicating the decomposition of the complexes. Since acids shift the tautomeric equilibrium towards the α-diketo form, the above effect shows the enolic (diosphenolic) form to participate in the complex formation as a bidentate ligand. This conclusion is in agreement with literature data. [13, 34]

The coloured solutions of astacene complexes of Al, Cu(II), Fe(III) and Hg(II) are rather stable. They can be diluted with water or acetone, without any significant colour change. By adding some drops of diluted

TABLE 1

Testing of complex formation in astacene solutions in ethanol

Salt	Colour	Other effects
$AlCl_3$	red-violet	—
$Al_2(SO_4)_3$	—	opalescence
$Cr_2(SO_4)_3$	dark orange	opalescence
$CuCl_2$	red-violet	—
$CuSO_4$	brown-violet	—
$FeSO_4$	—	opalescence
$FeCl_3$	red-brown	—
$Fe(NO_3)_3$	red-brown	—
$Fe_2(SO_4)_3$	red-violet	—
$HgCl_2$	red-violet	—

ammonia solution, a precipitate is formed, having a darker colour than the initial solutions.

The presence of KOH hinders the complex formation and the coloured complex solutions turn into yellow by adding several drops of 1 N KOH or NaOH solution. This means that the complex formation occurs only in a definite pH range.

From the red-brown alcoholic solution of Fe(III)nitrate and astacene, after a standing of 24 hours, red-brown crystals are formed. The m.p. of this product is 355°C.

SPECTROPHOTOMETRIC STUDY OF THE SYSTEM ASTACENE – $Fe(NO_3)_3$

In order to determine the most suitable wavelength to the investigation of the complex formation, the UV and visible spectra of $Fe(NO_3)_3$, of astacene and of their mixture have been recorded. Results are given in figure 1. As seen from this figure, the astacene (L) has an absorption maximum at about 478–480 nm in ethanol. The absorption of the Fe(III) salt (M) is very low and above $\lambda = 500$ nm it is quite insignificant. The astacene – Fe(III) salt mixture, corresponding to the metal to ligand ratio 1 : 1, shows an increased absorption at $\lambda > 540$ nm (as compared to the astacene) and a decreased one below this wavelength value. This indicates the formation of a complex compound. For the further study the wavelength $\lambda = 600$ nm has been chosen (indicated by an arrow in Fig. 1), since the absorption of the complex is relatively high at this λ, but the absorption of L and of M are very low.

By using Job's method,[35] an isomolar series with a total concentration $c_M + c_L = 4 \times 10^{-5}$ mole/l has been prepared in ethanol (c_M and c_L stand for the analytical concentrations of $Fe(NO_3)_3 . 9H_2O$ and of astacene, respectively). The absorptions of the samples are presented in figure 2 (curve 1). Since both components show a slight absorption at this wavelength, a corrected absorption has been calculated (curve 2), by substracting from curve 1 the sum of the absorption of M and of L, corresponding to the concentrations c_M and c_L, respectively (curve 3). As seen, curve 2 presents a clear maximum at the molar ratio $r = c_L/(c_M + c_L)$ equal to 0.5, *i.e.* the ligand to metal ratio is 1 : 1 in the complex formed.

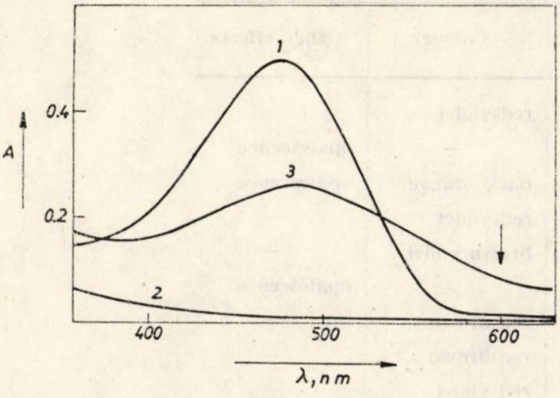

Fig. 1. — UV and visible spectra in ethanolic solutions in 1 cm cell: 1 — astacene, 4×10^{-5} mole/l; 2 — $Fe(NO_3)_3 . 9H_2O$, 4×10^{-5} mole/l; 3 — astacene, 4×10^{-5} mole/l + $Fe(NO_3)_3 . 9H_2O$, 4×10^{-5} mole/l.

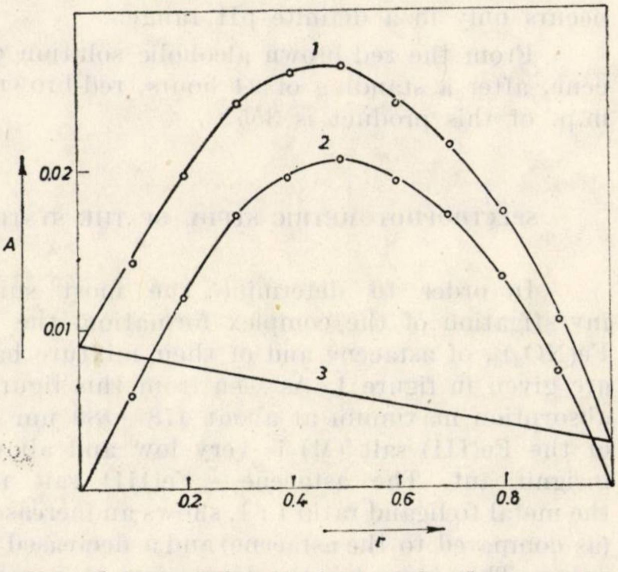

Fig. 2. — Curve Job in ethanol. $\lambda = 600$ nm. $c_M + c_L = 4 \times 10^{-5}$ mole/l, 20°C. 1 cm cell: 1 — absorption measured; 2 — absorption corrected; 3 — hypothetic absorption in the absence of complex formation.

The same study has been repeated in methanol solutions by using the method of isomolar titrations, described in the experimental part. The corrected absorption values, as function of the ratio r, are presented in figure 3. The maximum at $r = 0.5$ indicates the formation of the same complex 1:1.

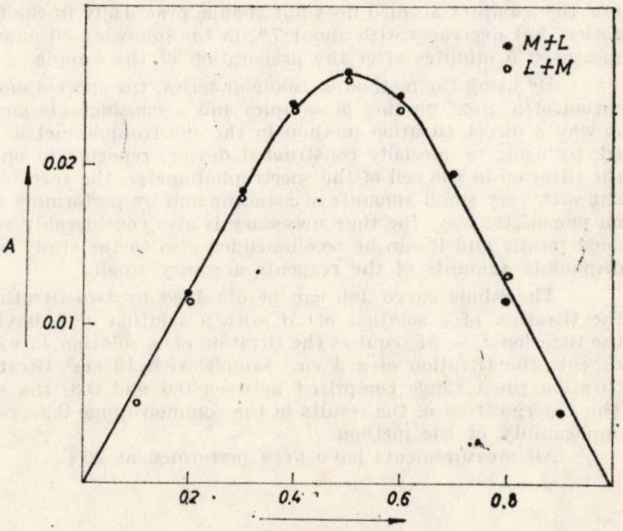

Fig. 3. — Curve Job in methanol, obtained by means of isomolar titration in the cell, with 4×10^{-5} mole/l solutions. $\lambda = 600$ nm. 20°C. 1 cm cell. Titration of Fe $(NO_3)_3 \cdot 9H_2O$ with astacene (M + L) and of astacene with $Fe(NO_3)_3 \cdot 9H_2O$ (L + M).

Since the stability of the complex depends on the pH of the system, it can be determined only in buffer solutions. The apparent stability constant, derived from our absorption data, obtained in non-buffered systems is of $\log \beta \approx 5.9$.

EXPERIMENTAL PART

Preparation of astacene. The astacene has been extracted from the petals of *Adonis aestivalis*, as described in the literature.[36] M.p. 208—210°C. It does not give any "*cis*-peak" in the spectral range between 320 and 360 nm, which means that it is the all-*trans* isomer, respectively it does not contain mono-*cis* isomers.[37, 38]

Astacene solutions have been prepared by using methanol or ethanol of p.a. purity and freshly distilled before utilization. Since the solubility of the astacene is very low in alcohols, the preparation of solutions of known concentrations presents some difficulties. Solutions have been obtained by using a special device for directed dissolution, described in an earlier paper.[39]

The concentration of the astacene has been determined colorimetrically on the basis of the specific absorption coefficient $A^{1\%}_{1\,\mathrm{cm}}$.[40] The $A^{1\%}_{1\,\mathrm{cm}}$ value of the astacene is known only for pyridinic solutions at $\lambda = 498$ nm and it is equal to 1690.[41]

The $A^{1\%}_{1\,\mathrm{cm}}$ value in ethanol and in methanol has been determined in the following way: the absorption $A^{x}_{1\mathrm{cm}}$ of the ethanolic or methanolic solution has been measured at $\lambda = 498$ nm. 10 cm³ samples of the solutions have been evaporated at room temperature *in vacuo*. The residue has been solved in 10 cm³ pyridine and the concentration (x) has been determined colorimetrically, by using the literature $A^{1\%}_{1\,\mathrm{cm}}$ value.[41]

The specific absorption coefficient values obtained as the mean of 6 experimental data in ethanol, and of 8 data in methanol at $\lambda = 498$ nm, are the following:

$$\text{in ethanol } A^{1\%}_{1\,\mathrm{cm}} = 1750 \pm 68$$

$$\text{in methanol } A^{1\%}_{1\,\mathrm{cm}} = 1730 \pm 62$$

Testing of complex formation. To samples of 3—4 ml solutions of astacene in ethanol (respectively in methanol), 1 N solutions of the salts indicated in table 1, solved in the same solvent, have been added drop by drop.

Spectrophotometric measurements have been performed by means of a VSU-1 type universal spectrophotometer Zeiss in 1 cm cells. Since the absorption of the samples containing the complex studied does not change practically in the first 10 minutes after their preparation, but decreases with about 7% in the following 30 minutes, absorption values have been measured 5 minutes after the preparation of the sample.

By using the method of isomolar series, the spectrophotometric study implies the preparation of a great number of samples and a considerable amount of astacene is needed. This is why a direct titration method in the spectrophotometric cell has been proposed and tested, by using a specially constructed device, reported in our earlier paper.[42] By performing the titration in the cell of the spectrophotometer, the spectrophotometric study can be carried out with very small amounts of astacene and by performing the homogenization of the sample on pneumatic way, the time necessary is also considerably shortened. This method gave very good results and it can be recommended also to the study of other systems, especially if the disponible amounts of the reagents are very small.

The whole curve Job can be obtained by two titrations. The titration $M + L$ means the titration of a solution of M with a solution of L having the same concentration and the titration $L + M$ requires the titration of a solution L, with a solution of M. In our experiments the titration of a 4 cm^3 sample with 16 cm^3 titrating solution covered in the first titration the r range comprised between 0.0 and 0.8, the second one between 0.2 and 1.0. The superposition of the results in the common range $0.2 \leqslant r \leqslant 0.8$ (Fig. 3), showed the perfect applicability of the method.

All measurements have been performed at 20°C.

REFERENCES

[1] E. Bayer, H. Egeter, A. Funk, K. Nether and K. Wegmann, *Angew. Chem.*, **78**, 834 (1966).
[2] F. Müller, P. Hemmerich and A. Ehrenberg, *European J. Biochem.*, **5**, 158 (1968).
[3] C. D. Nenițescu, "Chimie organică", Ed. Didactică și Pedagogică, București, vol. II, p. 87.
[4] A. Seybold and T. W. Goodwin, *Nature*, **184**, 1714 (1959).
[5] K. Egger, *Phytochem.*, **4**, 609 (1965).
[6] H. Kleinig and K. Egger, *Phytochem.*, **6**, 611 (1967).
[7] K. Egger and H. Kleinig, *Phytochem.*, **6**, 905 (1967).
[8] N. J. Krinsky and T. H. Goldsmith, *Arch. Biochim. Biophys.*, **91**, 271 (1960).
[9] O. Isler, "Carotenoids". Birkhäuser Verlag, Basel-Stuttgart, 1971, p. 806.
[10] C. Bodea, E. Nicoară, Gh. Illyés and M. Șerban, *Stud. și Cercetări Biochim.*, **8**, 271 (1965).
[11] I. Baldas, Q. N. Porter, A. P. Leftwick, R. Holzel, B. C. L. Weedon and I. Szabolcs, *Chem. Comm.*, **1969**, 415.
[12] H. Kleinig and F. C. Czygan, *Z. Naturforsch.*, **24 B**, 927 (1969).
[13] A. I. Aasen and S. Liaaen-Jensen, *Acta Chem. Scand.*, **20**, 1970 (1966).
[14] T. Katayama, H. Yokoyama and C. O. Chichester, *Internat. J. Biochem.*, **1**, 438 (1970).
[15] S. Liaaen-Jensen, *Pure and Applied Chem.*, **35**, 81 (1973).
[16] G. W. Francis, S. Herzberg, R. R. Upadyay and S. Liaaen-Jensen, *Acta. Chem. Scand.*, **26**, 1097 (1972).
[17] C. Bodea, "Tratat de biochimie vegetală", Part I. "Fitochimie", Ed. Acad. R.P.R., București, 1964, vol., I., p. 561.
[18] G. Neamțu, V. Tămaș and C. Bodea, *Rev. Roumaine Biochim.*, **3**, 305 (1966).
[19] R. Kuhn and N. A. Sørensen, *Ber. dtsch. chem. Ges.*, **71**, 1879 (1938).
[20] V. Tămaș and C. Bodea, *Rev. Roumaine Chim.*, **12**, 1517 (1967).
[21] V. Tămaș and C. Bodea, *Rev. Roumaine Chim.*, **14**, 405 (1969).
[22] V. Tămaș and C. Bodea, *Rev. Roumaine Chim.*, **14**, 141 (1969).
[23] V. Tămaș and C. Bodea, *Rev. Roumaine Chim.*, **15**, 655 (1970).
[24] H. Yamamoto, C. O. Chichester and T. O. M. Nakayama, *Analyt. Chem.*, **33**, 1792 (1961).
[25] C. Subbarayan, F. G. Jungalwala and H. R. Cama, *Analist. Biochem.*, **12**, 275 (1965).
[26] D. Oșianu, E. Nicoară and C. Bodea, *Rev. Roumaine Chim.*, **16**, 765 (1971).
[27] D. Oșianu, E. Nicoară and C. Bodea, "Third Internat. Symposium on Carotenoids other than Vitamin A", 1972, Cluj, Romania, Abstracts of Communications, p. 30.

[28] D. Oșianu, E. Nicoară and C. Bodea, *Rev. Roumaine Chim.*, **19**, 1203 (1974).

[29] D. Oșianu, E. Nicoară and C. Bodea, *Rev. Roumaine Chim.*, **25**, 261 (1980).

[30] C. Costes and B. Monties, "Third Internat. Symposium on Carotenoids other than Vitamin A", 1972, Cluj, Romania, Abstracts of Communications, p. 28.

[31] H. Kjøsen and S. Liaaen-Jensen, "Third Internat. Symposium on Carotenoids other than Vitamin A", 1972, Cluj, Romania, Abstracts of Communications, p. 5.

[32] M. Ichikawa, M. Tsutsui and F. Volwinkel, *Z. Naturforsch.*, **22 B**, 376 (1967).

[33] M. Cais and N. Maoz, *J. Organomet. Chem.*, **5**, 370 (1966).

[34] N. Arpin, "Les caroténoides des discomycetes". Univ. Lyon, Doctor Thesis, 1968, p. 53.

[35] P. Job, *Ann. Chim.*, **9**, 113 (1928).

[36] G. Neamțu, V. Tămaș and C. Bodea, *Rev. Roumaine Biochim.*, **3**, 305 (1966).

[37] T. W. Goodwin, "Chemistry and Biochemistry of Plant Pigments", Academic Press, London, 1965, p. 116.

[38] Ch. Gansser and L. Zechmeister, *Helv. Chim. Acta*, **182**, 1757 (1957).

[39] T. László, *Rev. Chim. (București)*, **29**, 781 (1978).

[40] T. W. Goodwin, "Chemistry and Biochemistry of Plant Pigments", Academic Press, London, 1965, p. 529.

[41] H. M. Rauen, "Biochemisches Taschenbuch", Springer Verlag, Berlin, 1964, vol. I, p. 367.

[42] T. László, *Rev. Chimie Analitică (București)*, **1**, 203 (1971).

Revue Roumaine de Chimie, 26, 2, 245–252 (1981)

SYNTHESIS AND REACTIONS OF 3-CINNAMOYL-4-PHENYL-6-[1′(2′-METHOXYNAPHTHALENYL]-2-PYRIDONE AND OF 2-METHYL-(b)-2′-[α(β-METHOXY-NAPHTHALENYL)-4′-PHENYL-3′,4′-DIHYDROPYRIDYL]-AZACHROMONE

A. ESSAWY, M. EL-GARBY YOUNES, M. M. BADRAN * and A. Z. M. HEIKAL
Chemistry Department, Faculty of Science, Zagazig University, Egypt
* Faculty of pharmacy, Cairo University, Egypt

Received September 19, 1979

Reactions of 3-cinnamoyl-4-phenyl-6-[1′(2′-methoxy naphthalenyl)]-2-pyridone (**3**), with hydrazine hydrate, phenylhydrazine, hydroxylamine hydrochloride, urea and thiourea and reactions of 2-methyl azachromone **4b** with aromatic aldehydes, hydrazine, phenylhydrazine, maleic anhydride and diethylmaleate are described.

Earlier we described [1] the synthesis and some reactions of 6-substituted-3-cinnamoyl-4-phenyl-2-pyridone and related compounds. Now, we extend our investigation to 3-cinnamoyl-4-phenyl-6-[1′(2′-methoxy naphthalenyl)]-2-pyridone (**3**). Thus, 3-cinnamoyl pyridone derivatives (**3a-e**) were synthesized by the Claisen-Schmidt condensation [1-3] of an appropriate aldehyde with 3-acetyl-2(1H) pyridone (**1**). Compound **1** was also fused with ethyl methyl ketone, ninhydrine or diacetyl at 200°C in the presence of anhydrous $ZnCl_2$ and gave compounds **5**, **6** and **7** respectively, (for IR and UV spectra see Table 1). The condensation of 3-cinnamoyl-2-pyridones **3** with hydrazine hydrate or phenyl hydrazine was carried out in 1 : 1 molar ratio with elimination of two molecules of water producing pyrazolines **8a-c**, (IR spectra, Table 1). The products gave the colour test for pyrazolines. [1] Condensation of the 3-cinnamoyl pyridone **3a** with hydroxylamine hydrochloride in boiling ethanol in the presence of sodium hydroxide yielded the isoxazoline derivative **9**.

The 3-cinnamoyl pyridone **3a** reacted easily with urea or thiourea in the presence of a few drops of sulphuric acid and ethanol to form 3-pyrimidones **10a** and **10b** respectively (IR spectra, see Table 1). 2-Methyl azachromone (**4b**) was synthesized by the Claisen condensation [4] of 3-acetyl-4-phenyl-6-[1′ (2′-methoxy naphthalenyl)] -2-oxo-1,2,3-tetrahydro pyridine (**2**) with ethyl acetate, in the presence of sodium hydride, followed by cyclization of the intermediate diketone (**4a**) using ethanolic hydrogen chloride. This route paralles the general synthesis of chromones from O-hydroxy acetophenones. [5] Condensation of **4b** with benzaldehyde or anisaldehyde in the presence of sodium ethoxide gave **11a** and **11b** respec-

TABLE 1

IR and UV spectra

Compound	IR spectra (KBr, cm^{-1})											UV spectra	
	ν(CO) pyridone	ν(CO) α,β-unsat.	ν(C=C)	ν(C=N)	ν(OH)	ν(NH)	ν(C=S)	ν(N–C=S)	ν(CO) exocyclic	ν(CO) azachromone	ν(CO) ester	$CHCl_3$ λ max^3 (nm)	ϵ_{max}
3a	1700	1680	1640										
3b	1705	1685	1620										
3d	1710	1680	1630									242	81575
												344	9300
4a	1740		1605		3450	3350			1670				
4b			1615							1680			
5	1710	1655	1600									244.3	8183
												343	1995
6	1720	1650	1610										
7	1713	1640	1615									243	62650
8a	1710			1615	3350	3300							
8b	1705			1620	3500	3400							
9	1715			1615	3500	3450							
10a	1710			1630	3500	3350							
10b	1720			1625	3300	3250	1290	1475					
11a			1605	1630						1710			
12a	1710			1625	3540	3450							
13				1610						1770			
15				1610						1700	1730		

tively, (IR spectra, see Table 1). The diene system in **11a** reacted with maleic anhydride yielding the corresponding Diels – Alder adduct **13**. Hydrolysis of adduct **13** gave the corresponding dibasic acid **14**, which can be also prepared by reaction of **11a** with maleic acid. The structure of the dibasic acid **14** was further proved by esterification yielding the corresponding diester **15** which was also obtained by Diels – Alder reaction of **11a** with diethylmaleate (IR spectra, see Table 1). [6]

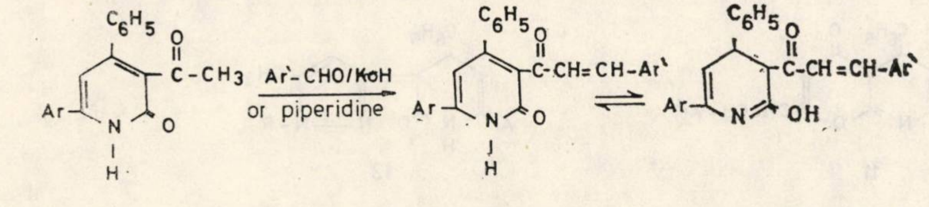

1 3a 3b

Ar`

a C_6H_5
b $C_6H_4-OCH_3$ (p-)
c $C_6H_3-O_2CH_2-3,4$
d $C_6H_4-NO_2$ (m-)
e C_6H_4-Cl (p-)

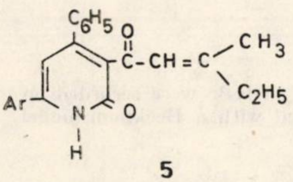

5

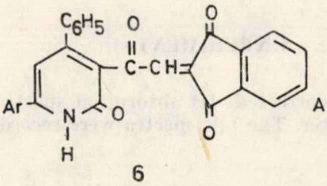

6

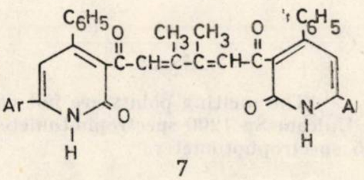

7

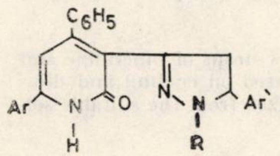

8

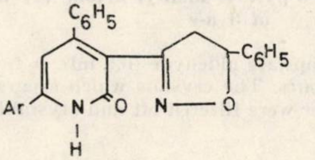

9

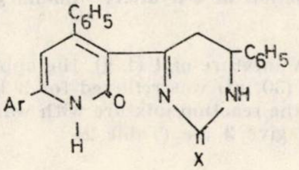

10

a X = O

b X = S

	Ar`	R
a	C_6H_5	H
b	C_6H_5	C_6H_5
c	C_6H_4-Cl (p-)	H

Ar =

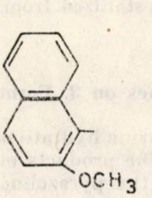

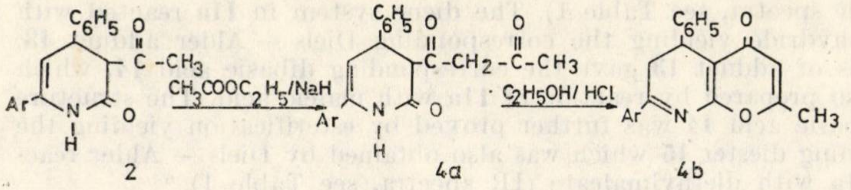

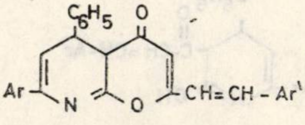

11

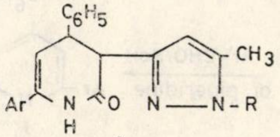

12

a $Ar' = C_6H_5$

b $Ar' = C_6H_4-OCH_3$ (*p*-)

a $R = H$

b $R = C_6H_5$

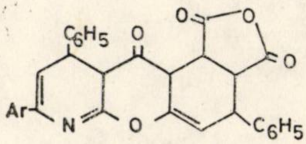

13

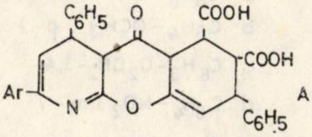

14

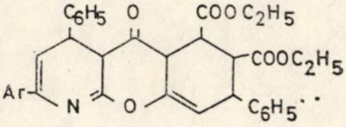

15

EXPERIMENTAL

The melting points are not corrected. IR absorption spectra in KBr were recorded on a Unicam Sp 1200 spectrophotometer. The UV spectra were recorded with a Beckman model 25 spectrophotometer.

Condensation of 2-hydroxy -4,6-diaryl-3-pyridyl methyl ketone (1) with aldehydes. Formation of 3 a-e

A mixture of **1** (1 g), the appropriate aldehyde (0.5 ml), a few drops of piperidine and ethanol (30 ml) was refluxed for 3 hours. The crystals which separated on cooling and dilution of the reaction mixture with water were filtered off and crystallized from the suitable solvent to give **3 a-e** (Table 2).

Condensation of 2-hydroxy -4,6- diaryl -3-pyridyl methyl ketone 1 with ketones and diketones. Formation of 5, 6 and 7

A mixture of **1** (0.01 mole), the ketone or diketone (0.015 mole) and anhydrous zinc chloride (0.5 g) was heated on an oil bath at 200—230°C for 6 hours. After cooling, the reaction mixture was washed with water and crystallized from the proper solvent to give **5**, **6** or **7**. The results are listed in table 3.

Action of hydrazines on 3. Formation of 8a-e

A solution of **3** (0.01 mole), hydrazine hydrate or phenyl hydrazine (0.01 mole) in ethanol (30 ml), was refluxed for 4 hours. The products obtained after concentration and colling were crystallized from ethanol to give the pyrazoline derivatives **8a-e** (table 4).

TABLE 2

Characterization of compounds **3 a-e**

Compound	m.p(°C)	Solvent * yield (%)	Formula	Analysis %) Found	Calc.
3a	165	B/P 60	$C_{31}H_{23}NO_3$	C 81.3 H 5.1 N 3.0	81.4 5.0 3.0
3b	167	B/P 70	$C_{32}H_{25}NO_4$	C 78.9 H 5.0 N 2.8	78.85 5.1 2.87
3c	190	E 70	$C_{33}H_{25}NO_4$	C 79.4 H 5.0 N 2.7	79.3 5.0 2.8
3d	170	E 70	$C_{31}H_{22}N_2O_5$	C 74.0 H 4.3 N 5.4	74.1 4.3 5.5
3e	60	P 70	$C_{31}H_{21}NO_3Cl$	C 75.7 H 4.5 N 2.9	75.8 4.3 2.8

* B/P = benzene/light petrol (60−80°C) ; E = ethanol ; P = light petrol(60−80°C).

TABLE 3

Characterization of compounds **5**, **6** and **7**

Compound	m.p (°C)	Solvent* yield (%)	Formula	Analysis (%) Found	Calc.
5	165	B/P 60	$C_{28}H_{25}NO_3$	C 79.3 H 6.0 N 3.3	79.4 5.9 3.3
6	230	E 70	$C_{33}H_{21}NO_5$	C 77.6 H 4.1 N 2.6	77.4 4.1 2.7
7	175	B/P 70	$C_{52}H_{40}N_2O_6$	C 79.2 H 5.1 N 3.5	79.19 5.08 3.5

* B/P = benzene/light petrol (60−80°C) ; E = ethanol.

TABLE 4

Characterization of compounds **8a-c**

Compound	m.p (°C)	Solvent* yield (%)	Formula	Analysis (%) Found	Calc.
8a	235	E 70	$C_{31}H_{24}N_3O_2$	C 79.1 H 5.2 N 8.8	79.1 5.1 8.9
8b	210	E 70	$C_{37}H_{28}N_3O_2$	C 81.2 H 5.0 N 7.8	81.3 5.1 7.69
8c	130	B/P 75	$C_{31}H_{24}N_3O_2Cl$	C 72.6 H 4.7 N 8.1	72.7 4.7 8.2

* B/P = benzene/light petrol (60/80°C) ; E = ethanol.

Action of hydroxylamine hydrochloride on 3a. Formation of 9

A mixture of **3a** (0.01 mole), hydroxylamine hydrochloride (0. 012 mole) and pyridine (20 ml) was heated under reflux for 4 hours. The cooled reaction mixture was poured into 10% cold acetic acid and the product obtained was crystallized from the proper solvent to give the oxazole derivative **9** (Table 5).

TABLE 5

Characterization of compounds **4**, **9** and **10**

Compound	m.p (°C)	Solvent* yield (%)	Formula	Analysis (%)	
				Found	Calc.
9	175	B/P 70	$C_{31}H_{23}N_2O_3$	C 78.8	78.9
				H 4.9	4.88
				N 6.0	5.9
10a	225	B 70	$C_{32}H_{25}N_3O_3$	C 76.8	76.9
				H 5.1	5.0
				N 8.2	8.4
10b	80	E 60	$C_{32}H_{25}N_3O_2S$	C 74.6	74.5
				H 4.8	4.8
				N 7.9	8.1
4a	130	B 80	$C_{26}H_{24}NO_4$	C 72.2	75.3
				H 5.8	5.79
				N 3.4	3.38
4b	80	M 80	$C_{26}H_{22}NO_3$	C 78.6	78.7
				H 5.6	5.5
				N 3.4	3.5

* B = benzene ; B/P = benzene/light petrol (40—60°C) ; M = methanol ; E = ethanol

Condensation of 3a with urea or thiourea. Formation of 10a and 10b

A cold solution of **3a** (0.01 mole) and urea or thiourea (0.01 mole) in absolute ethanol (40 ml) was treated with concentrated sulphuric acid (2 ml). The mixture was set aside at room temperature for 24 hours. The reaction mixture was neutralized with sodium carbonate solution. The solid product separated was crystallized from the proper solvent to give **10a** and **10b** respectively (Table 5).

Condensation of 2 with ethyl acetate. Formation of 4a

A mixture of **2** (1 g), ethyl acetate (3 ml), dry dioxane (20 ml), and 50% suspension of sodium hydride in oil (1.2 g) was refluxed for 30 minutes, cooled, poured into water (50 ml) and 2 N hydrochloric acid (5 ml) and stirred. The product was crystallized from the suitable solvent to give **4a** (Table 5).

Conversion of 4a to 4b

One gram of **4a** was heated under reflux for one hour with 10% ethanolic hydrogen chloride (10 ml). The mixture was cooled and neutralized with aqueous sodium bicarbonate. The solid obtained was crystallized from the proper solvent to give **4b** as pale yellow crystals (Table 5).

Condensation of 2-methyl azachromone derivative 4b with aromatic aldehydes. Formation of 11a and 11b

Compound **4b** (0.006 mole) was dissolved in absolute ethanol and treated at room temperature with an alcoholic C_2H_5ONa solution (0.006 mole). The appropriate aldehyde (0.006 mole) was then added and the mixture was kept 24 hours at room temperature. The condensation product was filtered off and crystallized from the proper solvent to give **11a** and **11b**. (Table 6).

TABLE 6

Characterization of compounds 11—15

Compound	m.p (°C)	Solvent* yield (%)	Formula	Analysis (%) Found		Calc.
11a	155	B	$C_{33}H_{25}NO_3$	C	82.0	81.9
		80		H	5.1	5.1
				N	2.7	2.8
11b	150	B/P	$C_{34}H_{27}NO_4$	C	79.4	79.5
		70		H	5.1	5.2
				N	2.7	2.7
12a	88	P	$C_{26}H_{23}N_3O_2$	C	76.3	76.2
		70		H	5.5	5.6
				N	10.0	10.2
12b	128	B/P	$C_{32}H_{27}N_3O_2$	C	78.9	79.1
		88		H	5.5	5.5
				N	8.5	8.6
13	230	B	$C_{37}H_{26}NO_6$	C	76.6	76.5
		60		H	4.3	4.4
				N	2.5	2.4
14	315	E	$C_{37}H_{29}NO^7$	C	74.2	74.1
		60		H	4.7	4.8
				N	2.4	2.3
15	180	B/P	$C_{41}H_{37}NO_7$	C	75.0	75.1
		60		H	5.5	5.6
				N	2.0	2.1

* B = benzene ; B/P = benzene/light petrol (60—80°C) ; P = light petrol (100—120°C) ; E = ethanol.

Action of hydrazine hydrate and phenyl hydrazine on 4b. Formation of 12a and 12b

A mixture of **4b** (0.01 mole), hydrazine hydrate or phenyl hydrazine (0.02 mole) in acetic acid (30 ml), was refluxed for 3 hours. The products obtained after cooling were crystallized from the proper solvent to give (**12a** and **12b**) respectively (Table 6).

Reaction of 11a with maleic anhydride. Formation of 13

A mixture of **11a** (0.004 mole), maleic anhydride (0.004 mole) and dry xylene (30 ml) was refluxed for 15 hours. The crystals which separated on cooling the reaction mixture were filtered off and crystallized from the suitable solvent to give **13** (Table 6).

Hydrolysis of 13. Formation of 14

A solution of the anhydride **13** (2 g), sodium hydroxide (2 g) was refluxed for 2 hours. The reaction mixture was acidified with ice-cold dilute hydrochloric acid. The solid product separated was crystallized from the proper solvent to give the dibasic acid **14** (Table 6).

Preparation of an authentic sample of 14

A mixture of **11a** (2 g), maleic acid (5 g) and dry xylene (30 ml) was refluxed for 10 hours. After concentration and cooling, the solid product was identified to be **14** by m.p. and mixed m.p. determination. Yield 65%.

Esterification of 14. Formation of 15

A solution of the dibasic acid **14** (2 g) in ethanol (50 ml) was treated with gaseous hydrogen chloride for 2 hours. The product obtained after concentration and cooling was crystallized from the suitable solvent to give **15** (Table 6).

Preparation of authentic sample of 15

A mixture of **11a** (2 g), diethyl maleate (5 ml) and dry xylene (50 ml) was refluxed for 10 hours. The solid obtained after concentration and cooling was crystallized from C_6H_6/light petrol (60–80°C) to give a compound identified to be **15** by m.p. and mixed m.p. determination, yield 60%.

REFERENCES

[1] A. Essawy, M. Abdalla and A. Deeb, *Pakistan J. Sci. Indust. Res.* (in press).

[2] N. S. Vulfson and G. M. Sukhotina, *Khim. Geterotsikl. Soedin.*, **4**, 682 (1967) ; *Chem. Abstr.*, **68**, 39 432 (1968).

[3] M. Cussac and A. Boucherle, *Chim. Ther.*, **2**, 101 (1967).

[4] M. Abdalla, A. Essawy and A. Deeb, *Indian. J. Chem.*, **16** B, 332, (1978).

[5] G. Wittig, Fr. Bangert and H. E. Richter, *Liebigs, Ann., Chem.*, **446**, 155 (1925).

[6] A. Sammour, *J. Org. Chem.*, **25**, 1458 (1960).

Revue Roumaine de Chimie, **26**, *2*, 253–268 (1981)

SYNTHÈSE ET STÉRÉOCHIMIE DES DIALKYLAMINO-2 (TÉTRAHYDROPYRANNYL-2)-3 TÉTRAHYDROPYRANNES

GUY RICART, CHARLES GLACET et DANIEL COUTURIER
Laboratoire de Chimie Organique I, U.E.R. de Chimie, Université des Sciences et Techniques de Lille I, B.P. 36, 59650 Villeneuve d'Ascq (France)

Reçu le 20 Septembre 1979

Les dialkylamino-2 (tétrahydropyrannyl-2)-3 tétrahydropyrannes **8** sont obtenus dans leur configuration *trans* indépendamment de la méthode de préparation : ils se composent d'un mélange de diastéréoisomères R*R* et R*S* en proportions variables. Un mécanisme permettant l'interprétation des résultats expérimentaux est proposé. L'étude par spectrométrie RMN ^{1}H et l'analyse dipolmétrique permettent l'attribution des configurations et des conformations de ces composés.

2-Dialkylamino-3-(2-tetrahydropyranyl)-tetrahydropyrans **8** are obtained in *trans* configuration independently of the synthesis way, but diastereoisomers R*R*, R*S* proportions are variable. A mechanism is suggested for the interpretation of experimental results. Configurations and conformations of these compounds are established by dipolmetric analysis and ^{1}H NMR study.

Récemment nous avons fait état du comportement particulier en RMN ^{1}H des dialkylamino-2 tétrahydropyrannes aussitôt après dissolution dans l'acide acétique. Nous observons en effet une coalescence des signaux des protons H_{-3}, H_{-4}, H_{-5} et surtout H_{-6} axial et équatorial tandis que le proton H_{-2} n'est jamais dédoublé et garde sensiblement la même largeur à mi-hauteur.[1] Il ne peut s'agir du ralentissement de l'inversion de cycle, se faisant d'ailleurs à température plus basse. La barrière d'énergie évaluée ici est nettement supérieure à celle de l'inversion du cycle tétrahydropyrannique.[2]

Nous avons suggéré l'existence d'une interconversion rapide oxonium cyclique ⇄ immonium linéaire pour expliquer ce phénomène de coalescence.[1]

L'étude détaillée des réactions chimiques présentées dans ce mémoire confirme cette hypothèse ; les dialkylamino-2 tétrahydropyrannes **1** réagissent lentement avec l'acide acétique pour donner les dialkylamino-2 (tétrahydropyrannyl-2)-3 tétrahydropyrannes **8** ; ces produits se forment aussi si l'acide acétique est remplacé par l'eau ou par aminolyse de l'hydroxy-2 **10** ou diméthylamino-2 **8a** (tétrahydropyrannyl-2)-3 tétrahydropyranne.

RÉSULTATS

A) Action des acides acétique et formique sur les dialkylamino-2-tétrahydropyrannes

Au cours du temps et à température ambiante, les bases **1** évoluent dans le mileu acétique pour donner le composé **8** : on obtient essentiellement l'isomère *trans* (le terme *trans* indique les positions relatives du groupement amino et du substituant en **3** par rapport au cycle tétrahydropyrannique) qui est constitué par un mélange de diastéréoisomères R*R* et R*S* (configuration relative au niveau $C_{(3)}-C_{(8)}$). La cinétique de la réaction est fonction de la nature des N-substituants : c'est avec les dérivés N-diéthylés que la transformation est la plus rapide. L'addition au milieu d'acétate d'amine (ex. acétate de pipéridine pour la transformation de **1c**) se traduit par un enrichissement en dérivé **8** R*R* et la présence de dihydropyranne ou d'un autre solvant ralentit la réaction sans modifier les proportions des diastéréoisomères.

L'introduction d'un méthyle en position 3 ou 4 de l'hétérocycle oxygéné empêche toute évolution en produit de type **8** ; par augmentation de la température, on forme les acétoxy-2 tétrahydropyrannes isomères.

Avec l'acide formique, les amines N-tétrahydropyrannylées **1** sont transformées en dialkylamino-5 pentanols-1 **11** ; si l'on substitue le cycle tétrahydropyranne, il y a un ralentissement très net de la réaction et formation en petite quantité de dialkylformamide identifié (tableau 2). L'acide formique totalement deutérié conduit à partir du réactif **1a** au diméthylamino-5 deutério-5 pentanol-1 **11d** avec substitution isotopique au niveau de l'oxygène (H : D ~ 1,8) et du carbone 4(H : D ~ 2,1).

B) Action de l'eau sur les amines tétrahydropyrannylées 1

L'eau en excès transforme aussi les bases tertiaires **1** en donnant les composés **8**, deutériés en partie sur les sommets 3 (~80 %) et 9 (~45 %) si l'on utilise l'oxyde de deutérium ; dans ces conditions, le diméthylamino-2 tétrahydropyranne **1'a** récupéré a subi l'échange isotopique au niveau du carbone 3 (D : H ~ 1,2).

C) Synthèse au départ de l'hydroxy-2 tétrahydropyranne 10

L'action d'une amine secondaire sur le composé **10** (mélange de diastéréoisomères) permet aussi l'accès aux produits **8** *trans* RR, RS. Si l'amine secondaire est en défaut, nous observons un enrichissement en hémiacétal vraisemblablement *cis* RS. Une aziridine en net excès provoque un clivage de la liaison $C_{(2)}$ —O [3] pour former l'aminohydrine : la transformation est réversible.

D) Synthèse par échange d'amine

Le chauffage prolongé de l'amine **8a** avec une amine secondaire telle que la pipéridine permet l'obtention du produit **8c** de configuration *trans* : les proportions relatives en diastéréoisomères RR, RS sont celles du produit de départ.

ÉTUDE CONFIGURATIONNELLE ET CONFORMATIONNELLE

La configuration au niveau C_{-2}, C_{-3} est déterminée à partir de la constante du couplage $J_{H-2, H-3} = 9$ Hz, valeur en parfait accord avec une disposition axiale des hydrogènes en position 2 et 3 sur le cycle tétrahydropyrannique. [4]

L'attribution de la configuration relative au niveau C_{-3}, C_{-8} est basée sur une étude comparative en RMN du proton H_{-2} : le glissement chimique et le ΔEu sont nettement différents ; la chromatographie en phase gaz permet la séparation des diastéréoisomères R*R* et R*S*. La conformation privilégiée est établie par analyse dipolmétrique en tenant compte des résultats obtenus pour les α-dialkylaminotétrahydropyrannes simples.

A) Calcul théorique des moments dipolaires des différentes conformations des dialkylamino-2 tétrahydropyrannes

L'analyse par RMN^{1}H [5] des N-(tétrahydropyrannyl-2) dialkylamines a montré que l'orientation équatoriale du substituant NR_2 était privilégiée : pour l'α-diméthylaminotétrahydropyranne **1a**, la valeur du glissement chimique et la distance de 11 Hz en milieu acétique [1] entre les composantes extrêmes du signal du proton anomère sont très proches de celles du méthyl-4 α-diméthylaminotétrahydropyranne. Les résultats dipolmétriques montrent que le rotamère à « paire libre » antiparallèle à la liaison $C_{(2)}-O$ est favorisé.

Les moments dipolaires des différentes conformations des dialkylamino-2 tétrahydropyrannes ont été calculés en prenant pour base les valeurs expérimentales respectives de 1,55D, [6] 0,86D [7,8] et 0,73D [8] pour le tétrahydropyranne, la triméthylamine et la t-butylpipéridine. Il est admis que l'angle $OC_{(2)}N$ est de $\theta = 110°$. [9]

Ainsi le moment résultant est le vecteur somme de deux composantes :

1) Celle due au groupe amino de grandeur 0,86D (comme pour la triméthylamine dans le benzène) agissant selon un angle φ, voisin de 110°C par rapport à la liaison $C_{(2)}-N$, [10] dans le plan bissecteur de CNC.

2) Celle du groupe étheroxyde de valeur 1,55D (comme pour le tétrahydropyranne dans le benzène) dirigée selon la bissectrice de l'angle des liaisons $C_{(2)}-O-C_{(6)}$.

Les relations nécessaires au calcul sont établies par addition vectorielle des moments dipolaires projetés suivant trois axes Ox, Oy, Oz ; le système xyz se définit selon : Oz est confondu avec la liaison $C_{(2)}N$ et Ox orienté selon la projection de la bissectrice de l'angle $C_{(2)}-O-C_{(6)}$ sur le plan perpendiculaire à la droite $C_{(2)}N$ (ex. fig. 1). Ces expressions sont fonction de l'angle de rotation α du vecteur dipolaire μ_{tma} autour de la liaison $C_{(2)}N$ et s'écrivent respectivement pour les moments résultants de la substitution d'un groupement dialkylamino équatorial et axial :

$$\mu_{eq} = \left(\mu_{thp}^2 + \mu_{tma}^2 + 2\,\mu_{thp} \cdot \mu_{tma} \left(\sin\frac{\theta}{2} \cdot \sin\varphi \cos\alpha - \cos\frac{\theta}{2} \cdot \cos\varphi \right) \right)^{1/2}$$

$$\mu_{ax} = \left(\mu_{thp}^2 + \mu_{tma}^2 + 2\mu_{thp} \cdot \mu_{tma} \left(\sin\frac{\theta}{2} \cdot \sin\varphi \cos\alpha + \cos\frac{\theta}{2} \cdot \cos\varphi \right) \right)^{1/2}$$

Dans l'hypothèse peu probable de la libre rotation du substituant autour de la liaison C_2—N, les moments moyens résultants deviennent :

$$(\mu_{eq})_m = \left(\mu_{thp}^2 + \mu_{tma}^2 - 2\mu_{thp}\mu_{tma} \cos\frac{\theta}{2} \cos\varphi \right)^{1/2}$$

$$(\mu_{ax})_m = \left(\mu_{thp}^2 + \mu_{tma}^2 + 2\mu_{thp}\mu_{tma} \cos\frac{\theta}{2} \cos\varphi \right)^{1/2}$$

Si l'approche dipolmétrique (tableau 1) ne permet pas d'apprécier l'équilibre conformationnel axial-équatorial (en raison de l'identité des deux moments dipolaires théoriques), elle autorise, en tenant compte des données RMN énoncées précédemment, à choisir le rotamère E comme le plus peuplé (fig. 1) ; l'examen des modèles moléculaires confirme que pour une substitution équatoriale, le rotamère E est considérablement favorisé en raison d'interactions électrostatiques moindres (pas de répulsions synaxiales entre les orbitales des atomes d'azote et d'oxygène) et stériques moins défavorables. L'hypothèse de la libre rotation peut-être rejetée au vu des résultats expérimentaux.

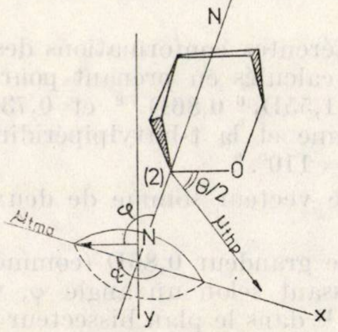

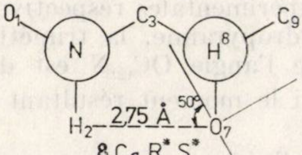

1 équatorial
(définition du système xyz)

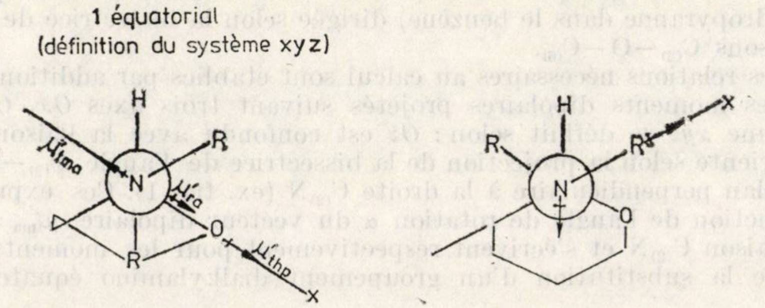

1a eq. (α = 180°) 1a ax. (α = 120°)

Figure 1. — Géométrie des dérivés tétrahydropyrannylés

TABLEAU 1

Moment dipolaire calculé et expérimental pour l'amine **1**.

	équatorial				axial			
rotamères α (degrés)	60	180	300	libre	0	120	240	libre
μ(D) calc.	2,16	1,27(*)	2,16	1,91	2,16	1,26	1,26	1,62

(*) = 1,28 en prenant le moment de la t-butylpipéridine.

R	CH_3	n-C_3H_2	$(CH_2)_4$	$(CH_2)_5$
μtr.	1,20	1,20	1,19	1,18
	1,16(*)			

(*) selon la méthode d'Onsager ; $\varepsilon 20 = 3{,}32$.

B) Etude conformationnelle des (tétrahydropyrannyl-2)-3 diméthylamino-2-tétrahydropyrannes *trans* R*R* et R*S*

Pour les N-(tétrahydropyrannyl-2)-dialkylamines, le moment dipolaire μ_{ra} de grandeur 1,20D est dans le plan $O-C_2-N$ et l'angle $OC_2\vec{\mu}_{ra}$ peut être évalué à 88,5° ; si l'origine du vecteur $\vec{\mu}_{ra}$ est portée en C_3, sa direction est contenue dans le plan $H_{3e}-C_3-C_4$ parallèle au plan $O-C_2-N$ et l'angle $H_{3e}C_3\vec{\mu}_{ra} = \varphi_1$ vaut 91°5.

Dans ces conditions, le moment résultant de la substitution d'un groupement diméthylamino-2 tétrahydropyrannyl-3 équatorial est obtenu par addition vectorielle des moments du diméthylamino-2 tétrahydropyranne $\vec{\mu}_{ra}$ et du tétrahydropyranne $\vec{\mu}_{thp}$ en fonction de l'angle de rotation α_1 (angle dièdre $O_7-C_8-C_3-\vec{\mu}_{ra}$) autour de la liaison C_3-C_8, par la relation :

$$\mu = \left(\mu_{thp}^2 + \mu_{ra}^2 + 2\mu_{thp}\,\mu_{ra}\left(\sin\frac{\theta}{2}\cdot\sin\varphi_1\cdot\cos\alpha_1 - \cos\frac{\theta}{2}\cdot\cos\varphi 1\right)\right)^{1/2}$$

Le système d'axe est celui de la figure 1, mais transféré sur le carbone 3 de la molécule **8** : C_2, N, μ_{tma}, φ, α deviennent respectivement C_8, C_3, μ_{ra}) φ_1, α_1. Le tableau de la figure 2 indique les valeurs calculées, à partir de cette expression, des moments dipolaires correspondant aux différents rotamères :

1 — Si Y est l'oxygène et X le méthylène, la méthode dipolmétrique permet de retenir les conformations C_a et C_c ; l'examen des modèles moléculaires montre que le rotamère C_a est énergiquement favorisé car si dans C_a existent les interactions de type γ-gauche (interaction H_{9a}/H_{4a} et H_{9e}/H_{2a}), par contre pour C_c nous avons les interactions $\ddot{O}_{7a}/H_{2a}$ et $\ddot{O}_{7e}/H_{4a}$ auxquelles s'ajoute une interaction répulsive non liante $\ddot{N}/H_{9a}$ sévère.

2 — Si X est l'oxygène et Y le méthylène, la dipolmétrie autorise les conformations C_a et C_b ; cependant l'interaction non liante $\ddot{N}/H_{9e}$ fortement répulsive, défavorise le conformère C_b au profit du conformère C_a.

La RMN du proton H_{2a} du diastéréoisomère RS indique que le signal subit un effet blindant dû vraisemblablement, dans la conformation C_a, à la proximité de l'atome d'oxygène en position 7 ; pour le rotamère C_b, ce même proton devrait résonner pour une fréquence voisine de celle de la molécule RR dans sa géométrie *a*, et avoir un glissement chimique proche de celui des diméthylamino-2 tétrahydropyrannes,[1] en tenant compte de l'éloignement de cet oxygène 7 et de l'effet quasi nul d'un groupement cyclohexyle sur le proton axial adjacent.[11] A partir des figures spatiales d'anisotropie magnétique schématisant les surfaces limites proposées pour un oxygène d'éther[12] il est possible d'interpréter le déplacement vers les champs forts du signal du proton H_2 de l'isomère RS ; dans sa conformation C_a, cet hydrogène doit vraisemblablement se situer dans la zone positive (ou diamagnétique) qui est l'intérieur d'un cône dirigé suivant l'axe perpendiculaire au plan bissecteur des deux liaisons de l'oxygène 7 : l'angle que fait cet axe avec la direction O_7-H_2 et la distance O_7-H_2 sont respectivement de l'ordre de 50° et 2,75 Å (figure 1).

Nous avons complété cette analyse par une étude RMN avec le tri(dipivalométhanate) d'europium. Si nous admettons que les « LSR » (Lanthanides Shift Reagents) sont des acides durs, les interactions seront meilleures avec les bases dures qu'avec les bases molles.[13] Pour les α-dialkylaminotétrahydropyrannes, l'ordre de basicité proposé est $NR_2 > -O-$[5] ; ceci est en accord avec l'ordre d'affinité décroissante proposé par la littérature.[14] Donc pour le composé **8** aux basses concentrations en « LSR », la fonction basique la plus forte (N) sera dominante. En général de grands changements dans la conformation du substrat ne doivent pas être attendus à cause de la faible coordination de l'ion lanthanide avec la molécule substrat ; cependant dans les états stériques privilégiés le site de coordination n'est pas facilement accessible par LnIII et si des modifications de conformations doivent intervenir, ce sera pour favoriser la liaison LSR — substrat : ainsi les modèles $C_b(X=CH_2,\ Y=O)$ et $C_c(X=O,\ Y=CH_2)$ peuvent former un complexe chélaté (bidentate) qui doit provoquer une augmentation remarquable (fonction de la participation du « LIS » (Lanthanide Induced shift)[15] nettement supérieure pour C_bRR étant donné qu'il n'existe pas les interactions répulsives H_{9a}/H_{2a} et H_{9e}/H_{4a} comme dans C_cRS : il doit donc y avoir une participation nettement supérieure de C_bL à l'équilibre que de C_cL (schéma 2) d'où un LIS plus important, ce que nous vérifions (Tableau 3).

$$\begin{tikzcd}
\text{RR}\quad X=CH_2\quad Y=O & C_aL \arrow[r, shift left] \arrow[r, leftarrow, shift right] \arrow[d, shift left, leftarrow] \arrow[d, shift right] & C_bL\ \text{(chélaté)} \arrow[r, leftarrow, shift left] \arrow[r, shift right] \arrow[d, shift left, leftarrow] \arrow[d, shift right] & C_cL \arrow[d, shift left, leftarrow] \arrow[d, shift right] \\
 & C_a+L \arrow[r, shift left] \arrow[r, leftarrow, shift right] \arrow[d, shift left, leftarrow] \arrow[d, shift right] & C_b+L \arrow[r, shift left] \arrow[r, leftarrow, shift right] \arrow[d, shift left, leftarrow] \arrow[d, shift right] & C_c+L \arrow[d, shift left, leftarrow] \arrow[d, shift right] \\
\text{RS}\quad X=O\quad Y=CH_2 & C_aL \arrow[r, shift left] \arrow[r, leftarrow, shift right] & C_bL \arrow[r, shift left] \arrow[r, leftarrow, shift right] & C_cL\ \text{(chélaté)}
\end{tikzcd}$$

Schéma 2

En résumé, nous pouvons dire que pour les dialkylamino-2 tétrahydropyrannes complexes **8** la constante de couplage $J_{H2,\ H3}$ confirme une orientation *trans*-équatoriale des groupements NR_2 et tétrahydropyrannyle. Des moments dipolaires identiques, l'examen des modèles moléculaires, des « LIS » et des « δ » nettement différents permettent de préciser la géométrie privilégiée des produits de la réaction soient **8** R*R* Ca et 8 R*S* Ca *trans* (fig. 2).

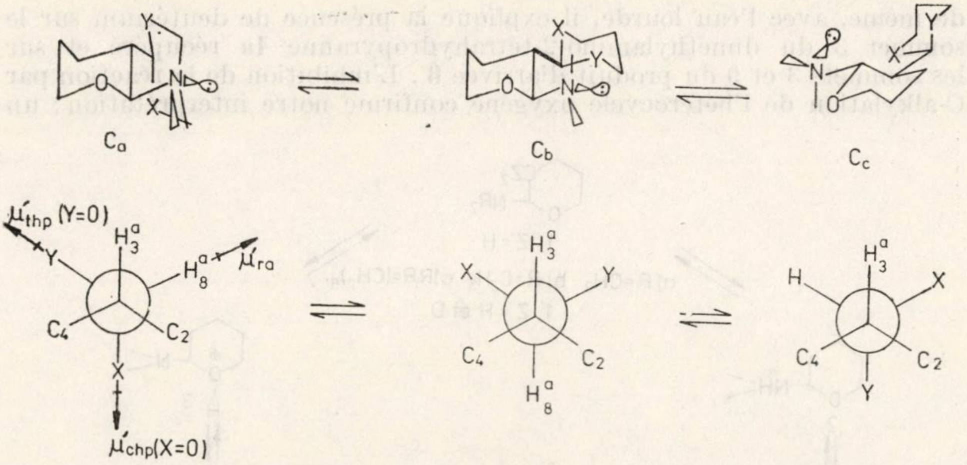

	R^*R^* si X=CH_2 et Y=0			R^*S^* si X=0 et Y=CH_2		
rotamère	C_b	C_a	C_c	C_c	C_b	C_a
α_1	0	120	240	0	120	240
μ_{calc}	2,63	1,54	1,54	2,63	1,54	1,54

Figure 2. — Equilibre conformationnel des diméthylamino-2 (tétrahydropyrannyl-2)-3 tétrahydropyrannes *trans* **8a**

DISCUSSION

Deux mécanismes peuvent être invoqués pour expliquer la formation du produit **8** :

— l'ammonium **2** conduit à l'ion tétrahydropyrannylium *4* qui donne naissance et se condense avec le dihydropyranne **5** ; l'intermédiaire **7** fixe l'amine et fournit le produit attendu **8** (schéma 1).

— l'oxonium cyclique **3**, beaucoup plus réactif par nature que l'ammonium **2** engendre le N-(ω-hydroxypentylidène) dialkylammonium **6** qui évolue par addition du groupement hydroxylé sur la fonction immonium, soit en rendant l'oxonium **3**, soit entre deux molécules de **6** pour donner, avec départ de dialkylamine, le produit **8**, via l'intermédiaire **9** : des condensations de ce type ont déjà été postulées. [16]

Or l'expérience nous enseigne que l'addition de dihydropyranne au milieu réactionnel n'a pas l'effet attendu (le dihydropyranne n'intervient pas en tant que réactif) mais que l'acide formique, connu pour réduire les immoniums en amines [17] transforme la base **1** en aminoalcool **11** via **6**. Nous savons aussi que les (tétrahydropyrannyl-2) alkylamines secondaires non substituées sur le cycle oxygéné présentent la tautomérie cycle-chaîne (Tableau 2). Sur ces indications il est permis de rejeter la première interprétation pour ne retenir que la seconde. L'intermédiaire immonium **6** rend aussi compte de l'enrichissement isotopique du carbone 4 du diméthyl-amino-5-pentanol-1 **11d** avec un acide formique deutérié ;

de même, avec l'eau lourde, il explique la présence de deutérium sur le sommet 3 du diméthylamino-2-tétrahydropyranne **1a** récupéré et sur les sommets 3 et 9 du produit d'arrivée **8′**. L'inhibition de la réaction par C-alkylation de l'hétérocycle oxygéné confirme notre interprétation ; un facteur d'origine stérique peut être invoqué, à savoir que l'introduction d'un substituant sur la chaîne **6** gêne la libre rotation des liaisons simples entraînant une diminution du degré de liberté du système favorable à la cyclisation[18] ; nous avons placé le groupement méthyle en position 4, afin de lever toute ambiguité à propos de l'encombrement qu'il pourrait provoquer en position 3 ; d'autres expériences rendent compte de l'influence d'un substituant sur la stabilité accrue de la liaison C_α—O (tableau 2) et démontrent la généralité de l'effet. Pour l'hydroxy-2 tétrahydropyranne **10**, l'intermédiaire **9** est celui qui explique le mieux le passage *trans* RS → *cis* RS via l'aminal avec départ d'amine : on suppose, ce qui est vraisemblable, que la configuration au niveau $C_{(3)}$—$C_{(8)}$ est gardée quand la fonction hydroxyle est remplacée par l'amine ; l'hémiacétal **10** en solution dans le benzène en présence d'eau lourde, soumis aux conditions de l'expérience, ne s'isomérise pas (ou du moins pas de façon significative même en présence d'amine tertiaire) : ceci écarte toute participation directe de l'eau libérée par cette réaction.

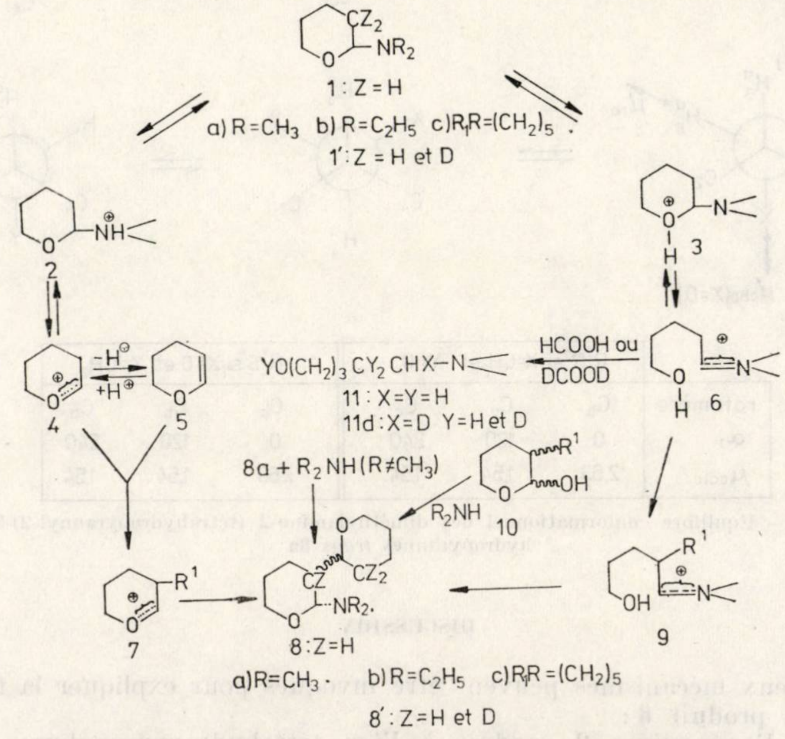
CZ2
NR2
O
1 : Z = H
a) R=CH3 b) R=C2H5 c) R1R=(CH2)5 .
1′ : Z = H et D
NH
2
N
3
H
6
HCOOH ou
DCOOD
YO(CH2)3 CY2 CHX–N
11 : X=Y=H
11d : X=D Y=H et D
H⊕
+H⊕
4
5
8a + R2NH (R≠CH3)
R1
OH
10
R2NH
CZ
CZ2
NR2.
7
8 : Z=H
9
a)R=CH3 . b)R=C2H5 c)RR=(CH2)5
8′ : Z=H et D

Schéma 1. — Interprétation de la formation des composés **8**.

TABLEAU 2

Etude du comportement de 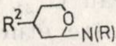 dans différents milieux

Réactifs	T°	Substituants		Taux de coupure (%)	
				$C_\alpha-O$	$C_\alpha-N$
HCOOH	70−80°	$R^2=H$	R = alkyle	100	
		$R^2=CH_3$	$R=CH_3$ $R=(CH_2)_5$	90 96	10 4
CH_3COOH	20°	$R^2=H$ $R^2=CH_3$	R = alkyle $R=CH_3$	100 0	0(33 à 60°)
Ac_2O[19]	65°	$R^2=H$ ou $R^2=H$ $R^2=CH_3$	CH_3 $R=CH_3$ R = alkyle $R=-(CH_2)_5$	100	100 41 (a)
acide picrique ($EtOH/H_2O$)	20°	$R^2=H$ $R^2=CH_3$	R = alkyle $R=CH_3$	100 (b) 0 (c)	
Hydrogène/Ni Raney	20°	$R^2=H$ $R^2=CH_3$	$R=CH_3$	100 (d) 100 (d)	
		$R^2=H$ $R^2=CH_3$	$N(R)_2=NHR$	8 (e) 0	

a) Formation des acétoxy-2 tétrahydropyrannes diastéréoisomères. b) picrate de $(R)_2NH$. c) Picrate stable. d) Obtention de $HO(CH_2)_2CHR^2(CH_2)_2N(R)_2$ avec $v_{R^2=H} \sim 3v_{R^2=CH_3}$. e) $(THP)-2NHR \leftrightarrows HO(CH_2)_4CH=NR$.

La stéréosélectivité au niveau C_{-2}, C_{-3} de la réaction s'explique en admettant avec Nguyen Trong Anh[20] que pour l'induction asymétrique 1, 2, il suffit de considérer les modèles de Felkin. Lors de l'addition nucléophile intramoléculaire de l'hydroxyle sur le groupe immonium du substrat **9**, la faible énergie relative (d'autant plus que R^1 est un gros substituant) de l'état de transition viendra de l'antipériplanéité des liaisons $HO \rightarrow C_{(1)}$ et $C_{(2)}-R^1$. L'apparition d'une interaction importante type « contrainte A (1,3) »[21] défavorise fortement les conformations telle que *I* (figure 3) susceptible de conduire au diastéréoisomère **8** *cis*. L'application du concept d'antipériplanéité associé à l'idée de « contrainte A(1,3) » permet donc de ne retenir que l'état de transition *II* qui donne le produit **8** dans sa géométrie *trans*. Par contre avec les modèles issus de l'ion mésomère **4**, on devrait aboutir selon le même critère au composé **8** de configuration *cis* majoritaire ce qui est contraire au résultat expérimental.

Pour conclure, nous pouvons rappeler qu'il existe quatre méthodes de synthèse des composés **8** ; elles peuvent être décrites comme diastéréosélectives si l'on n'envisage que la configuration relative au niveau des carbones 2 et 3. L'isomère *trans* obtenu est un mélange d'isomères R*R* et R*S* (configuration au niveau C_{-3}, C_{-8}). Les configurations et l'équilibre conformationnel ont pu être étudiés par RMN^{1}H et dipolmétrie. La structure des produits des différentes réactions découle d'un même

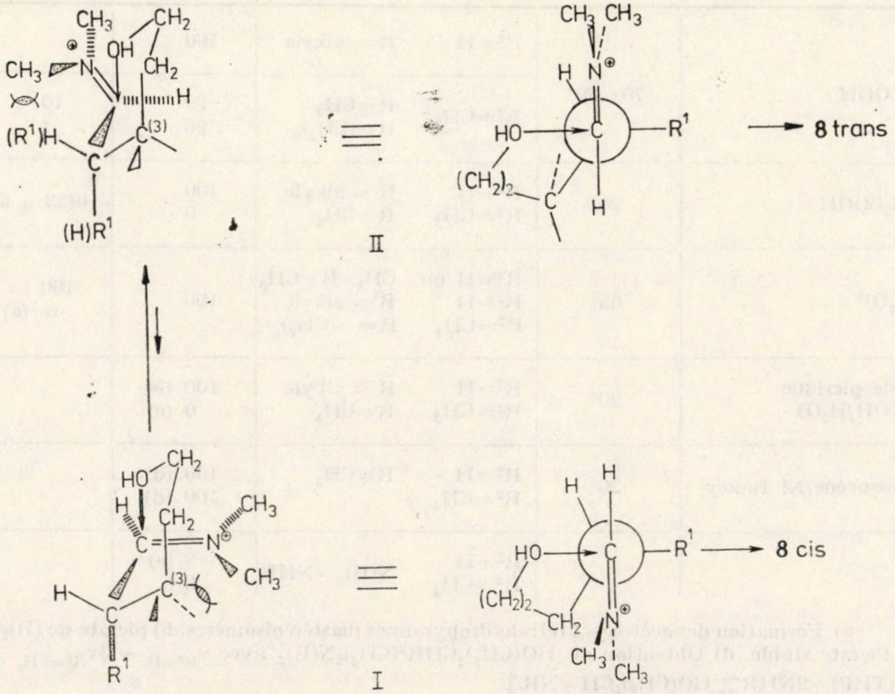

Figure 3. — Interprétation de la stéréochimie des produits **8** formés.

intermédiaire : l'immonium **6**. Nous vérifions ainsi que cet intermédiaire réagit de façon intermoléculaire (eau, acides acétique et formique) et intramoléculaire par un retour au composé **1** (l'eau deutériée forme les isotopomères **1'**) avec cependant deux possibilités de refermeture ce qui se traduit par la coalescence en RMN^{1}H des protons H–3, H–4, H–5, H–6 sans modification apparente du signal $H-2^1$ (schéma 3).

PARTIE EXPÉRIMENTALE

Le chromatographe en phase vapeur utilisé est un appareil Girdel de la série 3000. Les spectres infrarouges ont été enregistrés sur un spectrophotomètre Beckman modèle 4210. Les spectres de RMN ^{1}H ont été réalisés avec un appareil Varian A-60 ; les déplacements chimiques vers les champs faibles sont donnés en ppm à partir du TMS en référence interne ; les constantes de couplage sont données en hertz ; les abréviations suivantes sont utilisées : s : singulet ; d : doublet ; t : triplet q : quadruplet. Les spectres de masse ont été obtenus au moyen d'un spectromètre Hitachi RMU 6E avec une énergie d'ionisation de 70 et 10eV (dosage

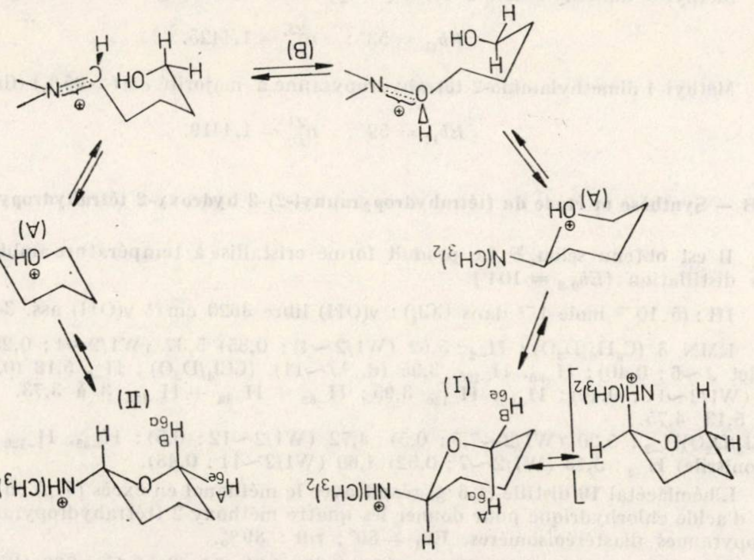

Schéma 3. — Interprétation de l'échange entre les deux sites pour les produits **1** en solution dans l'acide acétique.

isotopique) et d'un Ribermag R10-10. Les points de fusion sont déterminés avec un appareil Mettler. Les dosages d'azote par l'acide perchlorique en milieu acétique ont été faits pour tous les produits aminés.

A — Préparation des α-aminotétrahydropyrannes C_{-3} et C_{-4} méthylés

Les produits **1**[22] sont couramment utilisés au laboratoire. La synthèse des dérivés C_{-3} et C_{-4} méthylés est faite à partir des dihydropyrannes correspondants par l'intermédiaire des hydroxy-2 tétrahydropyrannes.

a) *Obtention des dihydropyrannes :*

L'éthoxy-2 méthyl-3 ou -4 tétrahydropyranne, contenant en poids 0,5 % d'acide paratoluènesulfonique, est chauffé à 140°C avec agitation ; on distille un mélange d'éthanol et de méthyl-3 ou -4 Δ^2-dihydropyranne. La réaction doit être menée rapidement pour éviter une trop grande résinification de l'étheroxyde vinylique, mais tout en minimisant l'entraînement d'éthoxy-2 tétrahydropyranne. Le distillat est dilué avec l'éther et porté à doux reflux ; l'alcool est consommé par le sodium.

Méthyl-3 et méthyl-4 Δ^2-dihydropyranne : $Eb_{760} = 114°$[23] et 103°.[19]

b) *Obtention des hémiacétals :*

Le dihydropyranne (0,15 mole) en solution dans 100 ml d'acide chlorhydrique 0,1 N est agité fortement pour bien émulsionner. La réaction est conduite à 20°C ; la dissolution progressive permet de suivre son avancement qui peut être précisé par CPV. Après 1h30 de contact, on neutralise par la soude 3N, sature en carbonate et extrait au chloroforme (rendement : 75 %).

Méthyl-3 (*cis* : 35 % *trans* : 65 %) et méthyl-4 (*cis* : 47 % *trans* : 53 %) hydroxy-2 tétrahydropyrannes : $Eb_{0,4} = 40°$ et $Eb_{0,7} = 56°$.[24]

c) *Passage aux α-aminotétrahydropyrannes :*

A 0,2 mole d'hémiacétal refroidi à 0°C, on ajoute 0,4 mole d'amine en solution benzénique ; la réaction est menée en présence de tamis moléculaire 3Å ; on laisse pendant 18 h à 40°C. Les rendements sont de l'ordre de 80 %.

Méthyl-3 diméthylamino-2 tétrahydropyranne *trans* (fig. 3 $R^1 = CH_3$)

$$Eb_{11} = 53° ; \quad n_D^{23} = 1,4425.$$

Méthyl-4 diméthylamino-2 tétrahydropyranne à majorité *cis* (> 95 %) (fig. 3 Me en $C_{(3)}$)

$$Eb_{12} = 59° ; \quad n_D^{23} = 1,4419.$$

B — Synthèse et étude du (tétrahydropyrannyl-2)-3 hydroxy-2 tétrahydropyranne 10 :

Il est obtenu selon.[25] Le produit formé cristallise à température ambiante 24 heures après distillation ($Eb_{0,2} = 104°$).

IR : (5.10^{-3} mole 1^{-1} dans CCl_4) : ν(OH) libre 3620 cm^{-1} ν(OH) ass. 3470 cm^{-1}.

RMN δ (C_6H_6/D_2O) : H_{-2} : 5,62 (W1/2∼4) ; 0,35) 5,37 (W1/2∼4 ; 0,25) 4,96 (aspect doublet $J \sim 6$; 0,40) ; H_{-6e}, H_{-12e}, 3,95 (d, $^2J \sim 11$). (CCl_4/D_2O) : H_{-2} 5,18 (0,35) 5,05 (0,25) 4,65 (W1/2∼11 ; 0,40) ; H_{-6e}, H_{-12e} 3,95 ; $H_{-6a} + H_{-8a} + H_{-12a}$ 3 à 3,73. (hexane) H_{-2} : 5,32 5,13 4,75.
($CDCl_3/D_2O$)H_{-2} : 5,20 (W1/2∼7,5 ; 0,5) 4,72 (W1/2∼12 ; 0,5) ; H_{-6e}, H_{-12e} : 4(d, $^2J \sim 11$). (acétonitrile) H_{-2} : 5,13 (W1/2∼7 ; 0,52) 4,60 (W1/2∼11 ; 0,48).

L'hémiacétal **10** distillé (1,6 g) réagit avec le méthanol en excès (5 g) en présence d'une trace d'acide chlorhydrique pour donner les quatre méthoxy-2 (tétrahydropyrannyl-2)-3 tétrahydropyrannes diastéréoisomères. $Eb_1 = 80°$; rdt : 89 %.

RMN H_{-2} (C_6H_6) : 5,17 (W1/2∼4,5 ; 0,38) 4,91 ($^3J \sim 3$; 0,15) 4,68 (W1/2∼4,5 ; 0,26) 4,51 ($^3J \sim 5,5$; 0,21). (CCl_4) : 4,70 4,53 4,48 4,24. ($CDCl_3$) : 4,84 4,68 4,62 4,38.

Etude de la réaction entre l'hémiacétal **10** recristallisé dans l'éther (1.10^{-5} mole dont 7.10^{-5} mole d'isomère *cis* RS) et la pipéridine (les résultats sont exprimés en mole × 10^{-3} :

10 *cis* RS	pipéridine	amines **8c** formées	
		RR	RS
0,07	0	0	0
0,12	0,5	0,41	0,09
0	1,15	0,66	0,34

C — Synthèse des dialkylamino-2 (tétrahydropyrannyl-2)-3 tétrahydropyrannes 8

1) L'amine tétrahydropyrannylée **1** en solution dans l'acide acétique est laissée à température ambiante pendant plusieurs heures (tableau 4) ; on dilue avec l'éther ; le milieu, refroidi à −5°C, est neutralisé par la soude aqueuse.

Influence de la présence d'un solvant : l'amine **1a** ($16,8.10^{-3}$ mole) avec l'acide acétique (50.10^{-3} mole) donne après 95h. de réaction à 20°C, $4,7.10^{-3}$ mole de **8a** ; en présence de 1,5 cm^3 de dihydropyranne, de tétrahydropyranne ou de chloroforme, cette valeur devient respectivement 3,02, 3,36 et 2,94 pour un même temps de contact.

2) Avec l'eau, le mélange initial, homogène dans le cas **1a** (hétérogène dans le cas de **1b**) est abandonné (agité) pendant plusieurs jours ; le produit lourd décante ; on extrait avec l'éther, récupère l'amine légère **1** non transformée et distille le produit lourd **8**.

a) *Diméthylamino-2 (tétrahydropyrannyl-2)-3 tétrahydropyrannes* **8a** :

RMN ^1H de l'amine **1a** : les protons en position 3,4 et 5 donne un massif large et mal résolu situé vers 1,70 ppm qui se dédouble par refroidissement (∼1,62 et ∼1,87 ppm). L'enthalpie libre d'activation s'obtient en employant l'expression $\Delta G^*_{T_c} = 4,57\ T_c\ [9,97 + \log T_c / ((\nu_A - \nu_B)^2 + 6J^2_{AB})^{1/2}]$ [26] ; les paramètres utilisés sont T_c : température de coalescence ∼287°K, $(\nu_A - \nu_B) = \nu_{H-6e} - \nu_{H-6a} \sim 31$ Hz, $J_{AB} \sim 11$Hz, d'où $\Delta G^* \sim 14,2$ kcal.mole^{-1}. Pour les figures de coalescence avec les conditions détaillées (solvant, concentration) on se reportera à [1].

$$Eb_{0,1} = 69° ; \; n_D^{20} = 1,4793 ; \; d_4^{20} = 1,010 ; \; \varepsilon^{20} = 3,61 ; \; \mu = 1,48.$$

TABLEAU 3

Synthèses des amines **8**

Réactifs (moles 10^{-2})		$T°$ (°C)	Temps (h.)	Produits **8** formés *trans*			
				pourcent. relatifs en		Rdt (%)	Résines (g.)
				RR	RS		
(4,8)	AcOH (14)	20	168	30	70	65	0,10
(1,2)	$(Me)_2NH/C_6H_6$ 6N (10 cm^3)	47	22	57	43	95(a)	
(28,6)	H_2O (145)	20	70j	54	46	72(b)	
(7,2)	D_2O (32,5)	20	90j	57	43	52(c)	
(7)	AcOH (18)	20	68	41	59	51	1,5
	H_2O	20		68	32		
(2,75)	pipéridine (3,7)	105	12	54	46	92	
(6,6)	AcOH (20)	20	93	25	75	68	0,3
(7,2)	AcOH (27,7) pipéridine (6,6)	20	93	50	50	3	

a) partir de l'hémiacétal **10** distillé. b) **1a** récupéré : 27%. c) **1a** récupéré : 37%.

Analyse $C_{12}H_{23}NO_2$: N% calc. 6,57 ; N% tr. 6,60.

CPV : Carbowax 20M : KOH (15 : 5) L : 0,5 m $T°$ colonne 160° ; ordre d'élution : R*R* puis R*S*

RMN (CCl_4) δ : H_{-2} 3,57 (d, $^3J \sim 9$) et 3,85 (d, $^3J \sim 9$) ; $NC\underline{H}_3$ 2,30 et 2,29

Masse : m/e 58 (100%) $\overbrace{CH_2 \overset{\cdots}{-} N(CH_3)_2}^{\oplus}$; (pic moléculaire) : 213

m/e 58 (100%) ; 213, 214, 215, 216 (pics moléculaires) pour le produit **8a** formé avec D_2O ; spectre de masse de l'amine **1a** récupérée après réaction avec D_2O : m/e 58 (100%) ; 129, 130, 131 (pics moléculaires des isotopomères).

Etude du glissement induit par un lanthanide : L'addition de complexe de lanthanide tel que le tri (dipivalométhanate) d'europium à la solution d'amine **8a** dans le chloroforme deutérié, induit des variations des glissements chimiques vers les champs faibles dont l'amplitude croit avec le rapport molaire $Eu(DPM)_3$/Soluté **8a**. Les valeurs des déplacements $\Delta Eu = \delta_{Eu(DPM)_3} - \delta_0$ sont extrapolées pour des rapports molaires égaux à 1. Pour le calcul de la distance entre les atomes O_7 et H_2 du diastéréoisomère RS dans sa conformation C_a, nous avons pris comme longueur des liaisons C—C, C—O, C—H, les valeurs respectives de 1,54, 1,43, 1,1 Å. Nous avons admis que le cycle tétrahydropyranne adopte la forme chaise parfaite.

TABLEAU 4

Déplacements chimiques $\delta \times 10^6$) par rapport au tétraméthylsilane pour les diméthylamino-2 tétrahydropyrannes *trans* RR et RS **8a**.

	RR				RS	
	H^2	$NC\underline{H}_3$	$H_e^{6,12}$	$H_a^{6,8,12}$	H^2	$NC\underline{H}_3$
CCl_4	3,85 (3,84)	2,29	3,90 ($^2J =$ = 11,5)	3–3,70	3,57 (3,55)	2,30
$CDCl_3$	3,97	2,33	3,97	3,07–3,73	3,67	2,33
C_6H_6	4,17 d, $^3J = 9$ (4,17 W1/2 = 3,5)	2,42	3,95	3–3,74	3,70 d, $^3J = 9$ (3,70 W1/2 = 3,5)	2,38
$\Delta E_u(10^{-6})$	13,8	8,1			6,1	2,9

Les valeurs entre parenthèses sont celles du produit deutérié en position 3.

TABLEAU 5

RMN ^{13}C des composés **8** : déplacements chimiques ($\delta \times 10^6$) proposés (a)

Carbones n° / Isomères	2	3(b)	8(c)	9(b)	6	12	4	5	10	11	$N\underline{C}H_3$
R*R*	94,68	43,36	76,30	29,30	66,74	68,37	23,14	26,72	24,47	26,72	39,514
R*R*	94,68	43,02	77,09	26,00	67,05	68,65	24,10	26,72	24,10	26,92	39,446

a) Les spectres rmn ont été enregistrés sans solvant sur un appareil Brüker WP80 fonctionnant a 20,15 mégahertz avec le tétraméthylsilane comme standard interne ; les δ ^{13}C du produit **1a** sont donnés par [36].

b) fortement réduits pour le composé **8′a**.

c) **8′a** R*R* : 76,20 ; R*S* : 76,98.

b) *Diéthylamino-2 (tétrahydropyrannyl-2)-3 tétrahydropyranne* **8b** :

RMN ^1H de l'amine **1b** δ (CCl_4) H_{-2} 3,95 ; H_{-6e} 3,98 ; H_{-6a} 3,31 ; $NC\underline{H}_2$ 2,73 ; $C\underline{H}_3$ 1. (AcOH avec AcOH : **1b** = 1,20) H_{-2} 4,23 (t, $\Sigma J{\sim}11$) ; H_{-6} 3,70 ; $NC\underline{H}_2$ 2,90 ; CH_3 1,08. (AcOH avec AcOH : **1b** = 2,20) H_{-2} 4,77 ; H_{-6} 3,75 ; $NC\underline{H}_2$ 3,15 ; $C\underline{H}_3$ 1,17.

$Eb_{0,2} = 89°$; $n_D^{20} = 1,4801$.
Analyse $C_{14}H_{27}NO_2$: N% calc. 5,80 ; N% tr. 5,69.

RMN (CCl_4) δ : H_{-2} 3,72 (d, $^3J{\sim}9$) et 3,98 (d, $^3J{\sim}9$) ; $H^{\alpha}_{eq.}$ 3,88. (C_6H_6)H_{-2} 3,83 et 4,26 ; $H^{\alpha}_{eq.}$ 3,91. ($CDCl_3$) H_{-2} 3,80 et 4,07. $H^{\alpha}_{eq.}$ 3,94.

Masse : *m/e* 86 (100 %) $\overbrace{CH_2{=}N}^{\oplus}(C_2H_5)_2$; 241 (pic moléculaire).

c) *Pipéridino-2 (tétrahydropyrannyl-2)-3 tétrahydropyrannes* **8c** :

$Eb_{0,1}$ 105° ; $F = 58,5 - 59°$ (R R = 25 % R S = 75 %)
$F = 45,5 - 46°$ (R R = 50 % R S = 50 %)

RMN (CCl_4) δ H_{-2} 3,56 (d, $^3J{\sim}9$) et 3,89 (d, $^3J{\sim}9$) ; $H^{\alpha}_{eq.}$ 3,92 ($^2J{\sim}11,5$). (C_6H_6) H_{-2} 3,68 et 4,06. ($CDCl_3$) H_{-2} 3,66 et 3,92 ; $H^{\alpha}_{e2.}$ 3,97.

Masse : *m/e* 98 (100 %) $\overbrace{CH_2{=}N}^{\oplus}(CH_2)_5$.

Etude dipolmétrique

1) Appareillage : Les mesures des constantes diélectriques ont été effectuées avec un dipolmètre WTW type DMO1 dans une cellule DFL1 et DFL2.

2) Solvant : Les constantes physiques du benzène anhydre utilisé sont $n_D^{20} = 1{,}5008$; $d_4^{20} = 0{,}879$; $\varepsilon_1 = 2{,}2825$.

3) Détermination des moments dipolaires : Le procédé de calcul pour la détermination du moment dipolaire dans les solutions étendues est celui proposé par Hesdest rand. [27] Plus récemment Guggenheim, [28] Smith, [29] Lippert [30] et Hurwic [31] ont apporté leurs témoignages en faveur de cette méthode.

$$\mu^2 = \frac{27\,kT}{4\pi N}\,\frac{1}{\rho^1(\varepsilon_1 + 2)^2}\,(a_\varepsilon - a_n)M_2$$

Dans cette expression, k est la constante de Boltzmann, T la température absolue, $\rho 1$ la masse volumique du solvant, ε_1 la permittivité du solvant, a_ε et a_n les pentes des droites représentées respectivement par les équations $\varepsilon_{12} - \varepsilon_1 = a_\varepsilon W_2$ et $(n_{D_{1,2}})^2 - n_{D_1}^2 = a_n W_2$ (W_2 fraction massique du soluté) et M_2 masse molaire de la substance dissoute considérée.

Nous nous sommes aussi servis de la théorie d'Onsager [32] utilisée par Böttcher [33] pour calculer le moment dipolaire à partir du liquide pur à l'aide d'une équation de la forme :

$$\mu^2 = (9kT/4\pi N)\ M/\rho(\varepsilon - n^2)\,(2\varepsilon + n^2)/\varepsilon(n^2 + 2)^2$$

et en prenant pour l'indice de réfraction n, la valeur n_D déterminée pour la raie D de la lumière monochromatique du sodium (petitesse de la polarisation atomique). Les valeurs de μ (Onsager) sont assez proches de celles obtenues en solution diluée par la méthode Guggenheim et Smith quoique légèrement inférieures ; on retrouve le même phénomène pour les triméthyl [34] et triéthyl [35] amines.

D — Réaction des amines tétrahydropyrannylées 1 avec l'acide formique.

a) *Diméthylamino-5 pentanol 1*

Un mélange en quantité équimoléculaire d'amine **1a** et d'acide formique est abandonné à la température de la salle jusqu'à la cessation du dégagement de gaz carbonique ; on porte ensuite à 70°C pendant 9 heures. Après addition de carbonate de potassium, on purifie l'aminoalcool par distillation (Rdt : 80 %).

$Eb_{2,5} = 78°$, [22]

Masse : m/e : 58 (100 %, $\overbrace{\mathrm{CH_2} \stackrel{\text{—}}{\cdots} \mathrm{N}}^{\oplus}(\mathrm{CH_3})_2$) ; 131 (pic moléculaire).

m/e : 59 (100 %, $\overbrace{\mathrm{CHD} \stackrel{\text{—}}{\cdots} \mathrm{N}}^{\oplus}(\mathrm{CH_3})_2$) ; 132, 133, 134, 135 (pics moléculaires) pour l'aminoalcool obtenu avec l'acide formique deutérié.

RMN δ 5,22 $\mathrm{C\underline{H}}$ (s) ; 3,50 $\mathrm{C\underline{H}_2O}$; 2,27 $\mathrm{NC\underline{H}_2}$; 2,18 $\mathrm{NC\underline{H}_3}$; 1,42 $\mathrm{\underline{CH}_2}$.

b) Diéthylamino-5 pentanol-1.

Rdt 77 % ; $Eb_1 = 87°$; $n_D^{20} = 1{,}4545$.

RMN ($\mathrm{CCl_4}$) δ 5,10 $\mathrm{O\underline{H}}$; 3,5C $\mathrm{C\underline{H}O_2}$; 2,5 $\mathrm{C\underline{H}_2N}$; 1,40 $\mathrm{C\underline{H}_2}$; 0,97 $\mathrm{C\underline{H}_3}$.

E — Etude de la réaction de l'acide acétique avec le méthyl-4 diméthylamino-2 tétrahydropyranne

Le mélange (rapport molaire acide/base = 9 : 1) est laissé pendant 7 h à 6 °C ; on reprend à l'éther et neutralise avec la soude aqueuse. Nous obtenons les méthyl-4 acétoxy-2 tétrahydropyrannes isomères (*trans/cis*∼2,8) avec un rendement de 33 % ; on récupère 28 % d'α-aminotétrahydropyranne non transformé. Nous n'avons pas mis en évidence les diméthylamino-2 (tétrahydropyrannyl-2)-3 tétrahydropyrannes C-méthylés qui résulteraient d'un clivage de la liaison $C_\alpha - O$.

Méthyl-4 acétoxy 2 tétrahydropyrannes :

Les constantes physiques sont en accord avec celles énoncées par [19].
IR : 1 750 cm^{-1} ester).
RMN ($CDCl_3$) δ : H_2 *cis* 5,60 ; H_2 *trans* 6,12.

BIBLIOGRAPHIE

[1] G. Ricart, C. Glacet et D. Couturier, *Compt. rend. C.*, **284**, 319 (1977).
[2] R. K. Harris et R. A. Spragg, *J. Chem. Soc. (B)*, **1968**, 684.
[3] G. Ricart, D. Couturier et C. Glacet, *Compt. rend., C*, **280** 953 (1975).
[4] R. U. Lemieux et S. Levine, *Canad. J. Chem.*, **42**, 1 473 (1964).
[5] J. Tesse, C. Glacet et D. Couturier, *Compt. rend. C*, **280**, 1 525 (1975).
[6] R. A. Y. Jones, A. R. Katritzky et D. L. Trepanier, *J. Chem. Soc. (B)*, **1971**, 1 300.
[7] A. L. Mc Clellan, «Tables of Experimental Dipole Moments » Freeman, San Francisco, 1963.
[8] R. J. Bishop, D. Dineen, R. A. Y. Jones, A. R. Katritzky, L. E. Sutton et R. J. Wyatt, *J. Chem. Soc. (B)*, **1967**, 493.
[9] M. Gelin, Y. Bahurel et G. Descotes, *Bull. Soc. chim. France*, **1970**, 3 723.
[10] C. P. Smyth, «Dielectric Behavior and Structure », Mc Graw-Hill Book Compagny, Inc. New-York, 1955.
[11] H. Booth, N. C. Franklin et G. C. Gidley, *Tetrahedron*, **21**, 1 077 (1965).
[12] a) L. M. Jackman et S. Sternhell, « Applications of Nuclear Magnetic Resonance Spectroscopy in Organic Chemistry », 2nd edition, Pergamon Press, London, 1969, p. 81.
b) M. L. Martin et G. J. Martin, « Manuel de Résonance Magnétique Nucléaire », Azoulay éditeur, Paris, 1971, p. 43.
[13] T. C. Morrill, R. J. Opitz et R. Mozzer, *Tetrahedron Letters*, **1973**, 3 715.
[14] J. K. M. Sanders et D. H. Williams, *J. Amer. Chem. Soc.*, **93**, 641 (1971).
[15] G. E. Wright et T. Y. Tang Wei, *Tetrahedron*, **29**, 3 775 (1973).
[16] a) N. J. Leonard et W. J. Musliner, *J. Org. Chem.*, **31**, 639 (1966).
b) G. Bianchetti, P. Dalla Crose et D. Pocur, *Tetrahedron Letters*, **1965**, 2 039.
c) A. A. Yasnikov et K. I. Matkovskii, *Ukrain. Khim. Zhur.*, **28**, 210 (1962) ; *Chem. Abstr.*, **58**, 3 306, (1963).
d) N. V. Volkova et A. A. Yasnikvov, *Doklady. Akad. Nauk S.S.S.R*, **149**, 94 (1963) ; *Chem. Abstr.* **59**, 5 011 (1963).
e) L. A. Paquette et H. Stucki, *J. Org. Chem.*, **31**, 1 232 (1966).
f) F. J. Bond et W. E. Musa, *Chem. Ind.*, **1966**, 1 380.
[17] « Enamines Synthesis, Structure and Reactions », edited by A. Gilbert Cook, Marcel Dekker New York 1969, 162, 189—191, 288.
[18] R. Escale et J. Verducci, *Bull. Soc. chim. France*, **1974**, 1 203.
[19] G. Ricart, C. Glacet et D. Couturier, *J. Heterocyclic Chem.*, **14**, 497 (1977).
[20] J. Huet, Y. Maroni-Barnaud, Nguyen Trong Anh et J. Seyden-Penne, *Tetrahedron Letters*, **1976**, 159, et références citées.
[21] a) F. Johnson et S. K. Malhotra, *J. Amer. Chem. Soc.*, **87**, 5 492 (1965).
b) G. Ricart et D. Couturier, *Bull. Soc. chim. France*, **1976**, 569.
[22] a) A. Gaumeton et C. Glacet, *Bull. Soc. chim. France*, **1959**, 1 501.
b) C. Glacet et A. Gaumeton, *Bull. Soc. chim. France*, **1955**, 224.
[23] G. Descotes, B. Giroud-Abel et J. C. Martin, *Bull. Soc. chim. France*, **1967**, 2 475.
[24] Y. R. Nave, P. Oschner, F. Thomas, *Bull. Soc. chim. France*, **1963**, 1 608.
[25] J. Cologne et P. Corbet, *Bull. Soc. chim., France*, **1960**, 283.
[26] M. L. Martin et G. J. Martin, « Manuel de Résonance Magnétique Nucléaire », Azoulay Editeur, Paris, 1971, p. 159.
[27] G. Hedestrand, *Z. phys., Chem.*, B **2**, 428 (1929).
[28] E. A. Guggenheim, *Trans. Faraday Soc.*, **45**, 714 (1949).
[29] J. W. Smith, *Trans. Faraday Soc.*, **46**, 394 (1950).
[30] F. Mollet et E. Lippert, *Z. Elektrochem*, **58**, 553 (1954).
[31] J. Hurwic, *L'Actualité Chimique*, **6**, 5 (1975).
[32] L. Onsager, *J. Amer. Chem. Soc.*, **58**, 1 486 (1936).
[33] C. J. F. Böttcher, *Physica*, **6**, 59, (1939) ; C. J. F. Böttcher, « Theory of Electric Polarization », Elsevier Publ. Co., Amsterdam, 1952.
[34] R. J. W. Lefevre et P. Russell, *Trans. Faraday, Soc.*, **43**, 374 (1947).
[35] G. A. Barlay, R. J. W. Lefevre et B. M. Smythe, *Trans. Faraday Soc.*, **46**, 812 (1950).
[36] A. J. de Hoog, *Org. Magn. Resonance*, **6**, 233 (1974).

Revue Roumaine de Chimie, 26, 2, 269–273 (1981)

LEAVING GROUP EFFECT IN THE REACTION OF 5-SUBSTITUTED-2-PENTANONES WITH SODIUM METHOXIDE

V. VÂNTU *, NORA RĂDULESCU, MARIANA IONESCU and C. SÂRBU
Chemical and Pharmaceutical Research Institute, Şos. Vitan nr. 112, Bucharest, Romania
* Gas and Petroleum Institute, Ploieşti, Romania

Received May 13, 1980

The leaving group effect in the γ-elimination from 5-substituted-2-pentanones was investigated studying the reaction kinetics of 5-chloro-, 5-bromo-, 5-iodo- and 5-0-tosyl-2-pentanone with sodium methoxide. The second order rate constants and the activation parameters were established and assumptions were made concerning the reaction mechanisms.

Our previous work [1] has studied the solvent and the medium basicity effect on the reaction of 5-chloro-2-pentanone with sodium methoxide. Assumptions were made concerning the assignment of the studied reaction between the generally accepted E_1cb and E_2 eliminations mechanisms.

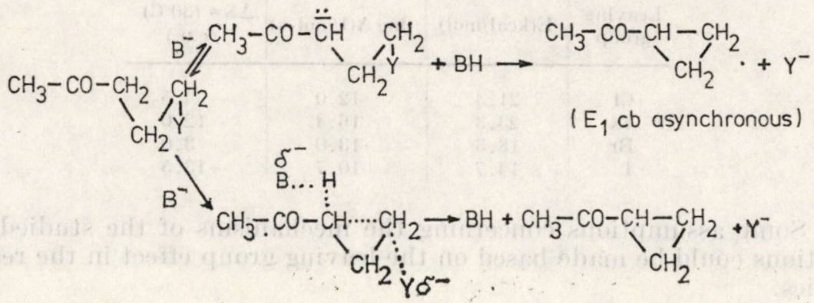

The observed solvent and medium basicity effect pointed out that a transition state having a carbanionic character as in an E_1cb mechanism could be involved in the formation of methyl-cyclopropyl ketone from 5-chloro-2-pentanone with sodium methoxide.

The present work extended our researches on the various 5-substituted-2-pentanones. In order to establish the leaving group effect on the

γ-elimination kinetics the behaviour of 4 various substrates (5-chloro-, 5-bromo-, 5-iodo- and 5-0-tosyl-2-pentanone) was studied in the reaction with sodium methoxide.

Using vapour phase and thin layer chromatography it was stated that for all studied substrates the only reaction product was methylcyclopropyl ketone *via* γ-elimination. This observation simplified the kinetic experiments. The analyses were carried out by the argentimetric titration (for halogen ion) or by acidimetric titration of alkalinity (for tosyl ion). The results of kinetic experiments are summarized in table 1 and the activation parameters in table 2.

TABLE 1

Second order rate constants $k_2.10^3$ l/mols in the reactions of 5-substituted-2-pentanones with sodium methoxide in 9 : 1 benzen : methanol at various temperatures

[substrate] = 0.05 mol/l [MeONa] = 0.1 mol/l

t°C eaving group	0	5	10	20	30	40
Cl	—	—	0.4	1.6	5.5	15.8
O−Ts	—	—	20.0	23.0	300.0	
Br	17.0	32.0	63.0	192.0	—	—
I	76.0	124.0	190.0	500.0	—	—

TABLE 2

Activation parameters in the reaction of 5-substituted-2-pentanones with sodium methoxide in benzene : methanol 9 : 1

Leaving group	E(kcal/mol)	log A(l/mol.s)	ΔS≠ (30°C) (e.u.)
Cl	21.3	12.0	− 4.5
O−Ts	23.3	16.4	12.0
Br	18.3	13.0	3.0
I	14.7	10.7	−13.5

Some assumptions concerning the mechanisms of the studied γ-eliminations could be made based on the leaving group effect in the reaction kinetics.

In an E_1cb carbanionic mechanism, the breaking of C−Y bond in the transition state is negligible, and the reaction rate is mainly determined by the ease of the proton release, therefore, the expected order of the reaction rate is Cl > Br > I, in agreement with the increasing of the inductive effect of the leaving group.

In an E_2 synchronous mechanism having a significant C−Y bond breaking in the transition state, a different reaction rate order, namely Cl < Br < I, was expected in agreement with the decreasing of C−Y bond energies.

For some β-elimination, having an E_1cb carbanionic mechanism, references [2] were recently found in the literature concerning the increase of the reaction rate with the inductive effect of the leaving group, measured by σ_I Taft's parameter.

Figure 1 illustrates the correlation $\log k = f(\sigma_I)$ in β-elimination from β-substituted ethylsulphones (E_1cb mechanism) [2] and the same correlation for β-elimination from β-substituted phenyl-ethanes (E_2 mechanism).[3] The correlation established on the basis of the results presented in table 1, for γ-elimination from 5-substituted-2-pentanone with sodium methoxide is shown in the same figure.

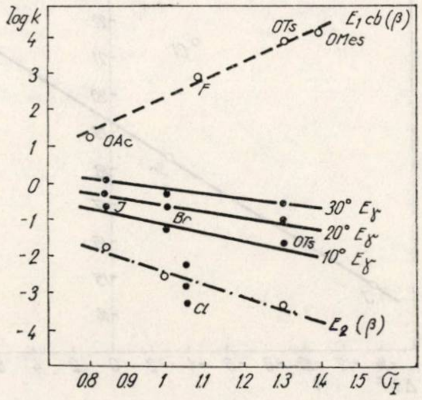

Fig. 1. — Plot of $\log k = f(\sigma_I)$ for β-elimination via E_1cb mechanism (...), via E_2 mechanism (—) and for elimination from 5-substituted-2-pentanones with sodium methoxide (-·-·-·)

The observed dependence in γ-elimination from 5-substituted-2-pentanones having I, Br and O-tosyl as leaving group (slope $= -2.4$) is close to those previously established for the β-synchronous E_2 elimination (slope $= -3.5$) and very far from that of β-carbanionic E_1cb elimination (slope$=4.9$). Therefore it is possible to assume for the γ-elimination from 5-iodo-, 5-bromo- and 5-0-tosyl-2-pentanone with sodium methoyide, a transition state close to an E_2 mechanism. 5-Chloro-2-pentanone is out of the correlation line, in agreement with our previous assumptions, [1] its reaction with sodium methoxide going probably through a transition state close to an E_1cb mechanism.

The plot $\Delta S^{\neq} = f(\Delta H)^{\neq}$ in figure 2, based on the results from table 2, checks up an isokinetic relation proving similar mechanism for the γ-eliminations from 5-iodo-, 5-bromo- and 5-0-tosyl-2-pentanone. 5-Chloro-2-pentanone is here out of the correlation line too.

The observed leaving group effect on the reaction rate and the checking up of an isokinetic relation allow the assumption of an E_2 synchronous like mechanism in the reaction of 5-iodo-, 5-bromo- and 5-0-tosyl-2-pentanone and an E_1cb carbanionic like mechanism in the reaction of 5-chloro-2-pentanone with sodium methoxide in agreement with our previous work.[1]

CONCLUSIONS

The reactions of 5-chloro-, 5-bromo-, 5-iodo- and 5-0-tosyl-2-pentanone with sodium methoxide were studied in solution 9 : 1, benzene-methanol at temperatures ranging from 0° to 40°C ; the only reaction observed was the formation of methyl cyclopropylketone *via* γ-elimination. No leaving group effect on the reaction products was noticed.

Kinetic experiments emphasized a remarkable leaving group effect on the rate of γ-elimination. The correlation established between rate constants and Taft's σ_I parameters besides checking up an isokinetic relation, pointed out that an E_2 synchronous like mechanism could be involved in the γ-elimination from 5-bromo-, 5-iodo- and 5-0-tosyl-2-pentanone with sodium methoxide. In good agreement with our previous work,[1] an E_1cb carbanionic like mechanism was presumed for the γ-elimination from 5-chloro-2-pentanone.

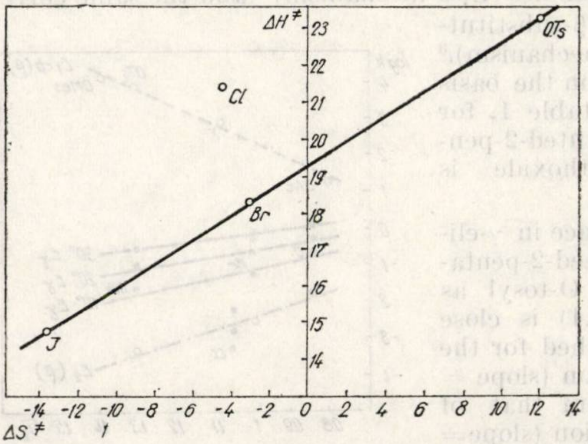

Fig. 2. — Plot of $\Delta S^{\neq} = f(\Delta H^{\neq})$ for the γ-elimination from 5-substituted-2-pentanones with sodium methoxide in 9 : 1 benzene : methanol.

EXPERIMENTAL

5-Halo-2-pentanones [1,4] were prepared from α-acetyl-γ-butirolactone and aqueous soln. of halohydric acids (molar ratio 1 : 3) in benzene, under stirring and heating at temperatures ranging from 40—60°C. The vacuum distillation of benzene extracts, previously dried on anhydrous sodium sulfate, yielded 80—90% of 5-chloro-2-pentanone, b.p. 80—82°/30 mm, 5-bromo-2-pentanone b.p. 94—95°/20 mm and 5-iodo-2-pentanone b.p. 123°/50 mm.

Methyl cyclopropyl ketone was prepared from 5-chloro-2-pentanone and sodium hydroxide in aqueous solution [5] : b.p. 110—112°C, n_D^{25} 1,4226.

5-0-Tosyl-2-pentanone [6] was prepared starting from 5-hydroxy-2-pentanone and *p*-toluenesulfonyl chloride using pyridine as the reaction medium : n_D^{20} 1,5030 (literature n_D^{20} 1,5036).

The solvents : anhydrous methanol reagent grade ("Reactivul") was distilled over magnesium ; commercial benzene was dried on sodium and distilled.

Kinetic experiments. Measured amounts of 5-substituted-2-pentanones and sodium methoxide at given concentrations were placed in two concentric isolated spaces of the same glass ampoule. The ampoules were stoppered, thermostated at the desired temperature for 2 minutes and the reagents mixed up by upsetting the ampoules. At the established times, the ampoule was opened and the reaction was quenched by addition of a 1 : 1 mixture of methanol : acetic acid (for 5-halo-2-pentanones reactions) and icy distilled water (for 5-0-tosyl-2-pentanone reaction). The halogen ion content was titrated with 0.01 N silver nitrate solution in the presence of eosine as indicator and the tosyl anion was appreciated by titration of the remanent alkalinity with 0.01 N hydrochloric acid using phenolphthaleine as indicator. The errors of these determinations were about ± 8%.

REFERENCES

[1] N. Rădulescu and C. Sârbu, *Rev. Roumaine Chim.*, **23**, 197 (1978).

[2] D. R. Marshall, P. T. Thomas and C. J. M. Stirling, *J. Chem. Soc. Perkin II.*, **1977**, 1 898.

[3] J. F. Bunnet, *Angew. Chem.*, **74**, 731 (1962).

[4] N. Rădulescu, M. Iulian, I. P. Ambruș and V. Tamaş, Romanian Pat. 77626, 12 febr. 1974.

[5] C. W. Cannon, R. C. Ellis and I. R. Leal, "Organic Synthesis Collective", Vol. IV, Wiley, New York, 1963, p. 597.

I. I. Grandberg and I. Zuianova, *Khim. Geterotsikl. Soedin.*, **1968**, 845.

Revue Roumaine de Chimie, **26**, *2*, 275–282 (1981)

CYCLISATIONS RADICALAIRES D'ALDÉHYDES ÉTHYLÉNIQUES*

M. CHATZOPOULOS et J. P. MONTHEARD

Laboratoire de Chimie Organique — U.E.R. de Sciences 23, rue du Docteur Paul Michelon — 42023 Saint-Etienne Cédex

Reçu le 5 Octobre 1979

Sept aldéhydes éthyléniques ont été cyclisés en présence de peroxyde de di-terbutyle ou de peroxyde de benzoyle. Dans le cas où il y a compétition entre la formation de cyclopentanone et de cyclohexanone, on observe seulement l'addition du radical carbonyle avec création d'un cycle hexacarboné. Les réactions de bicyclisations avec des aldéhydes biéthyléniques restent minoritaires ou inexistantes.

Seven ethylenic aldehydes have been cyclised in the presence of diterbutyl peroxide or benzoyl peroxide. In the cases when there is a choice between formation of a cyclopentanone or a cyclohexanone, only the addition of carbonyl radical was observed together with the creation of hexacarbon cycle. The bicyclisation reaction with biethylenic aldehydes are few or inexistent.

INTRODUCTION

Il existe de très nombreuses réactions de cyclisations radicalaires qui peuvent appartenir à trois principales catégories :

1. La substitution radicalaire aromatique.[1]
2. La duplication de radicaux.[2]
3. L'addition de radicaux libres sur les doubles ou triples liaisons.[3]

Dans cette dernière catégorie, de très nombreuses fonctions organiques se prêtent à la cyclisation radicalaire : cyano-esters, esters, diesters nitriles, cétones, alcools, chlorures d'acides, diènes.[4] Peu d'études ont été consacrées aux aldéhydes éthyléniques [5, 6] qui sont relativement difficiles à obtenir par synthèse : le but de ce travail a donc été d'étendre cette étude à un maximum d'exemples afin de déterminer les facteurs influençant la réaction (nature de la liaison insaturée, taille du cycle, bicyclisation) et pour cela quelques aldéhydes, dérivés de produits naturels et commerciaux, ont été préparés. De plus, en comparaison avec les aldéhydes précédents, un essai de cyclisation avec un ester et une cétone éthylénique ont été tentés.

---

* Une partie de ce travail a fait l'objet d'une note préliminaire.
M. CHATZOPOULOS et J. P. MONTHEARD. *Compt. rend.*, **280**, 28 (1975).

(Les formules des composés I à VII sont représentées dans le tableau I).

a) Norpinène-2 diméthyl-6,6 butyraldéhyde-2 (I).

Cet aldéhyde est obtenu par chauffage, à l'autoclave, du mélange acroléine plus β-pinène. [7] La même réaction entre l'acroléine d'une part et, d'autre part, le méthylène-cyclohexane ou le méthylène-6 norbornène-2 ne donne lieu qu'à la formation d'éther cyclique au lieu d'aldéhyde éthylénique.

b) Le diméthyl-3,7 vinyl-3 octène-6 al (II) est préparé par pyrolyse de l'éther résultant de la condensation de l'éther-oxyde de vinyle et d'éthyle sur le géraniol. [8]

c) L'aldéhyde III (R = H) est préparé à partir du farnésal, par hydrogénation de la double liaison située en α de la fonction carbonyle. [9] L'aldéhyde III (R = CH_3) résulte de la méthylation en β du farnésal par l'intermédiaire d'un complexe cuivreux.

d) L'aldéhyde IV (R=CH_3) est préparé par oxydation chromique de l'éthyl-linalol en éthyl-citral suivie de l'hydrogénation signalée pour III (R = H). Cette même méthode de réduction est utilisée pour la préparation de l'aldéhyde IV (R = H) à partir du nonadiénal-2,6, produit commercial.

e) La préparation de V s'effectue par alcoylation avec le bromure d'allyle de l'aldéhyde α-campholénique. [10; 11]

f) Le diméthyl-2,6 heptène-5 al (VI) est un produit commercial.

g) La diméthyl-4,8 nonène-7 one-2 (VII) est obtenue par addition du magnésien de l'iodure de méthyle sur le citronellal suivie d'oxydation chromique.

h) Le diméthyl-5,9 décadiène-4,8 al (VIII) résulte de la condensation de l'oxyde de vinyle et d'éthyle sur le linalol. [12]

i) Le norpinène-2 diméthyl-6,6 butanoate de méthyle-2 (IX) est préparé par chauffage de l'acrylate de méthyle dans les mêmes conditions opératoires que pour I.

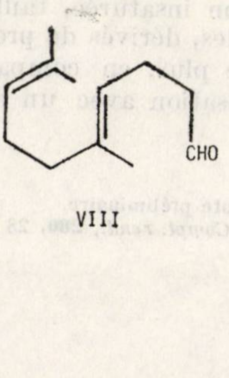

VIII

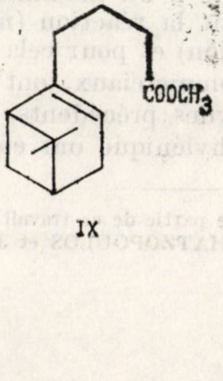

IX

RÉSULTATS (Tableau I)

La cyclisation des aldéhydes éthyléniques s'effectue par addition du radical carbonyle obtenu par arrachement de l'hydrogène aldéhydique en présence de peroxyde organique, le méchanisme est analogue à celui de l'addition des aldéhydes sur les alcènes :

$$R-CHO + R'' \rightarrow R-C\dot{O} + R'H$$

$$R-CO^{\cdot} + CH_2 = CH - \rightarrow R-CO-CH_2-\dot{C}H -$$

Les aldéhydes étudiés sont $\gamma-\delta$, $\delta-\varepsilon$, ou $\varepsilon-\eta$ éthyléniques ; les conditions expérimentales retenues sont les suivantes :

1°) Chauffage de l'aldéhyde à 135°C avec du peroxyde de di-tert-butyle sans solvant.

2°) Chauffage à l'autoclave avec le cyclohexane utilisé comme solvant et le peroxyde de di-tert-butyle.

3°) Emploi du peroxyde de benzoyle en solution dans le cyclohexane à 75°.

En fonction des rendements, le mélange réactionnel est soit soumis à une oxydation pour éliminer l'aldéhyde résiduel, puis chromatographié ; soit directement purifié par chromatographie en phase vapeur préparative.

a) Norpinène-2 diméthyl-6,6 butyraldéhyde-2 (I).

L'addition du radical carbonyle sur la double liaison devrait conduire à une cétone tricyclique ; les données spectrales de la cétone obtenue après purification ne sont compatibles qu'avec l'isopropyl-8 bicyclo (4.4.0) decène-5 one-1 (A) : absence de protons éthyléniques en RMN, absorption UV à 247 nm et 303 nm, $\varepsilon = 11\,400$ et 120. Ce composé résulte de l'ouverture du radical I' par rupture du pont cyclobutane en radical isomère I''.

Sauf dans le cas des thiols ou dérivés, [13] toutes les additions radicalaires sur le β-pinène donnent lieu à un phénomène analogue (fig. 1) :

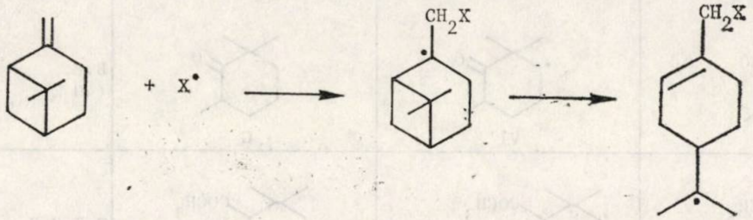

b) La cyclisation du diméthyl-3,7 vinyl-3 octène-6 al (II) s'effectue en deux étapes, tout d'abord formation du radical II' évoluant vers les « vinylmenthones » isomères (B) (liaisons vinyliques décelées par IR et RMN), puis addition du radical isopropyl sur la liaison insaturée conduisant, par bicyclisation, à la tétraméthyl-1,2,3,3 bicyclo [2.2.2] octanone-5 (C) ; la cétone C représente environ 70 % du mélange total de cyclisation.

TABLEAU 1

CYCLISATIONS RADICALAIRES DE QUELQUES DÉRIVÉS CARBONYLES

CARBONYLES	RADICAUX	CETONES	PEROXYDES * ET RENDEMENT
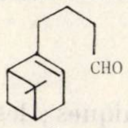 I	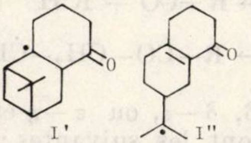 I' I''	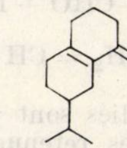	D.T.B.P. (40 %)
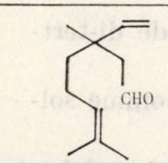 II	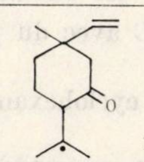 II'	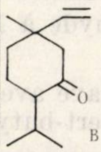 B 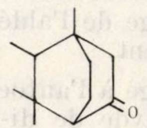 C	D.T.B.P. (40 %) **
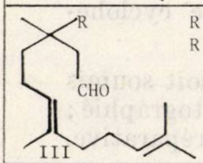 III R = H R = CH_3	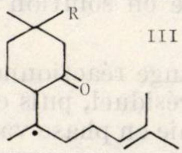 III'	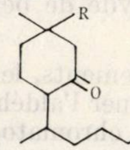 D	D.T.B.P. (R = CH_3) (40 %) B.P (R = H) (20 %)
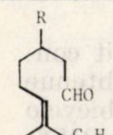 IV R = H R = CH_3	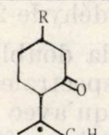 IV'	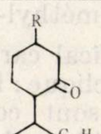 E	B.P. (R = H) (20 %) B.P (R = CH_3) (20 %) D.T.B.P. (R = CH_3) (80 %)
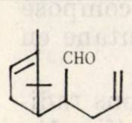 V	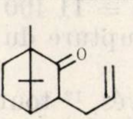 V'	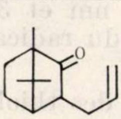 F	B.P (20 %) D.T.B.P (0 %) **
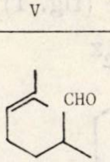 VI	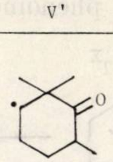 VI'	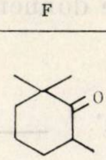 G	B.P. (40 %)
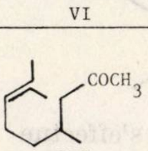 VII	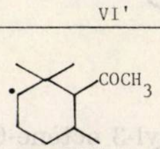 VII'	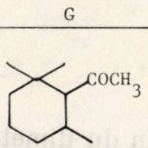 H	D.T.B.P. (30 %)

* D.T.B.P. : Peroxyde de Diterbutyle ; B.P. = Peroxyde de Benzoyle.

** La stéréochimie du méthyle-2 dans C et du groupe allyle dans V n'a pas été déterminée.

c) Quel que soit l'agent radicalaire employé, les aldéhydes III ($R = H$, $R = CH_3$) sont transformés en cétones de monocyclisation D ($R = H$, $R = CH_3$) caractérisées au moyen des données spectrales ; on n'observe pas de bicyclisation à partir du radical III'.

d) Le diméthyl-3,7 nonène-6 al IV ($R = CH_3$) et le nonène-6 al IV ($R = H$) forment, avec des rendements variables suivant le peroxyde utilisé, les cétones E ($R = CH_3$, $R = H$) ; la n-propyl cyclohexanone E ($R = H$) est identifiée par comparaison avec un échantillon authentique.

e) On ne constate, avec l'aldéhyde V, que l'existence de l'α-allyl camphre F par réaction avec le peroxyde de benzoyle. Il n'y a ni formation de cétone bicyclique, ni formation de cyclopentanone par addition sur la liaison allyle (fig. 2).

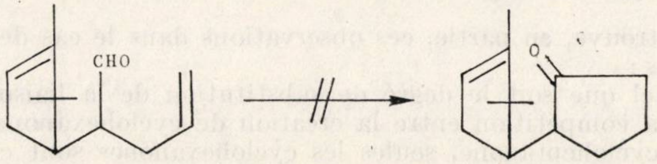

f) Le diméthyl-2,6 heptène-5 al est cyclisé en présence de peroxyde de benzoyle (solvant cyclohexane) en triméthyl-2,2,6 cyclohexanone.

g) La cétone VII, chauffée à 135°C en présence de peroxyde de di-tert-butyle, à l'autoclave avec le cyclohexane comme solvant, conduit au triméthyl-2,2,6 acétyl-1 cyclohexane.

L'aldéhyde VIII et l'ester IX, quel que soit le mode opératoire, restent inchangés.

DISCUSSION

Les quelques essais effectués sur des modèles éthyléniques différents permettent, néanmoins, de faire différentes remarques quant à l'influence de la substitution de la double liaison et de l'agent radicalaire ; il n'est, cependant, pas inutile de rappeler les principaux résultats obtenus par JULIA et collaborateurs sur les α-cyano-esters.[14, 15, 16]

a) La cyclisation en C_5 d'un cyano-ester sur une liaison vinylique non substituée n'est pas possible alors qu'elle est effectuée sur la liaison substituée (fig. 3).

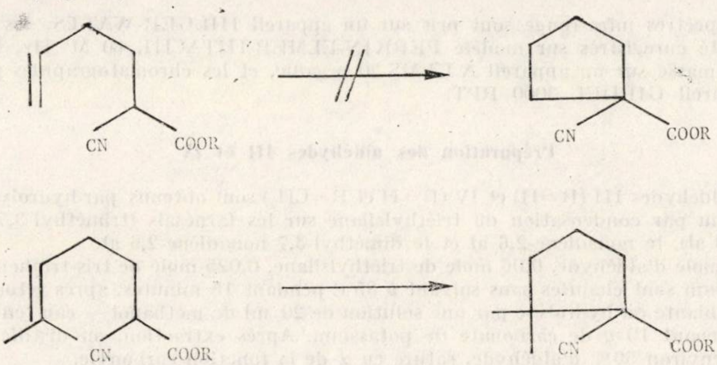

b) Lorsqu'il y a compétition entre la création d'un cycle en C_5 et d'un cycle en C_6, c'est ce dernier qui est formé par suite de l'éventuelle rééquilibration du cycle en C_5 (cas du cyano-6 oate de méthyle [15]).

c) Enfin, la cyclisation sur les doubles liaisons en $\varepsilon - \eta$ dépend du degré de substitution, cependant, il n'y a pas formation de composé bicyclique [16] (fig. 4).

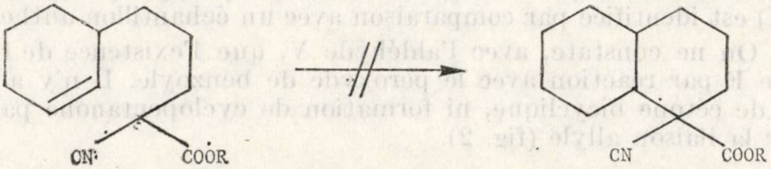

On retrouve, en partie, ces observations dans le cas des aldéhydes éthyléniques :

a) Quel que soit le degré de substitution de la liaison insaturée lorsqu'il y a compétition entre la création de cyclohexanone, cyclopentanone ou cycloheptanone, seules les cyclohexanones sont caractérisées (aldéhydes I, II, III, V, cétone IX).

Dans le cas de l'ester IX où, par arrachement d'un radical $H^{\bullet}$ en α du groupe carboxylate, seul un cyclopentane peut être formé, on observe, en dépit des conditions expérimentales (chauffage à 140°C en présence de D.T.B.P.), l'absence de cyclisation.

b) Au contraire, le degré de substitution semblerait favoriser la cyclisation en cyclopentanones ; il n'y a pas addition de carbonyles sur les liaisons vinylique et allylique dans les aldéhydes II et V, mais dans ces conditions, la non transformation de l'aldéhyde VIII reste inexpliquée.

c) Enfin, il n'a pas été possible d'expliquer l'absence de cyclisation de l'aldéhyde V en présence de peroxyde de diterbutyle, cyclisation qui réussit, avec un faible rendement, en présence de peroxyde de benzoyle. Avec le D.T.B.P., on retrouve l'aldéhyde inchangé sans déceler, par exemple, des fractions dues à la décarbonylation.

PARTIE EXPÉRIMENTALE

Les spectres infra-rouge sont pris sur un appareil HILGER-WATTS, les spectres de RMN ont été enregistrés sur modèle PERKIN-ELMER-HITACHI, 60 M Hz, R 24 A, les spectres de masse sur un appareil A EI MS 20 organic, et les chromatographies préparatives sur un appareil GIRDEL 3000 RPT.

Préparation des aldéhydes III et IV

Les aldéhydes III (R=H) et IV (R=H et R=CH_3) sont obtenus par hydrolyse de l'éther d'énol obtenu par condensation du triéthylsilane sur les farnésals (triméthyl-3,7,11 dodécatriène-2,6,10 al), le nonadiène-2,6 al et le diméthyl-3,7 nonadiène-2,6 al.

0,05 mole d'aldéhyde, 0,06 mole de triéthylsilane, 0,025 mole de tris-triphényl-phosphochloro rhodium sont chauffés sans solvant à 85°C pendant 15 minutes, après retour à la température ambiante ou hydrolyse par une solution de 20 ml de méthanol + eau (en proportions égales) contenant 10 g de carbonate de potassium. Après extraction, on distille le mélange et on isole environ 50 % d'aldéhyde, saturé en α de la fonction carbonyle.

Les données spectrales des aldéhydes III et IV sont les suivantes :

— *III :* Triméthyl-3,7,11 dodécadiène-6, 10 al ou dihydro-farnésal ; IR (liquide cm^{-1}) : 2 750 (CHO), 1 735 (C=O) ; RMN (δppm : CHO 9,6 (t), H éthyléniques 5,3 (m).

— *IV* (R=CH_3) : IR (liquide cm^{-1}) : 2 750 (C$\underline{H}$O), 1 735 (C=O) ; RMN δppm) : CHO 9,6 (t), H éthylénique 5,3 (m).

Préparation de l'aldéhyde V

Ce composé est préparé à partir de l'aldéhyde α-campholénique.[10, 11]
IR (liquide cm^{-1}) : 2 750 (CHO) ; 1 735 (CO), 1650 et 920 ($-CH=CH_2$) ;
RMN (δppm) ; : H aldéhydique 9,5 (d) ; H éthylénique 4,9 (t), H allyliques 5,1 et 6,6 (d et m).

Mode opératoire des cyclisations

1 — Les aldéhydes I, II et III (R=CH_3) sont cyclisés par chauffage à 135° à l'autoclave de 0,045 mole d'aldéhyde avec 0,015 mole de peroxyde de di-tert-butyle dans 50 ml de cyclohexane ou par chauffage de 0,025 mole d'aldéhyde à 135°C avec 0,015 mole de peroxyde ajouté à intervalles réguliers.

Dans chacun des trois exemples, on récupère environ 70 % du mélange réactionnel par distillation, ce qui permet la séparation des fractions lourdes (télomérisation). Ce mélange (composé à 60 % de cétones de cyclisation) est ocydé par l'oxyde d'argent pour éliminer l'aldéhyde résiduel et purifié par chromatographie en phase vapeur préparative.

Cétone **A** : *isopropyl-8 bicyclo[4.4.0] décène-5 one-1*

IR (liquide, cm^{-1}) : 1 670 (C=O), 1 650 (C=C)
UV$_{max}$ = 247 nm (ε = 11 400), 303 nm (ε = 120)
RMN (δppm) CH_3 0,9 (d), absence de proton éthylénique
Masse : M^+ = 192 ; fragments : 149, 135, 93, 55, 41.

Cétone **B** : *méthyl-1 vinyl-1 isopropyl-4 cyclohexanone-3*

IR (liquide, cm^{-1}) : 1 710 (C=O), 1 645 (C=C)
RMN (δppm) = $-CH=CH_2$ 4,86 (m) ; CH_3 et $(CH_3)_2$ vers 1
Masse : M^+ = 180 ; fragments : 138, 95, 70, 55, 41.

Cétone **C** : *tétramethyl-1,2,3,3 bicyclo [2.2.2]octanone-5*

IR (liquide, cm^{-1}) : 1 740 (C=O)
RMN (δppm) = CH_3 0,85 (J = 6 c/s) ; $(CH_3)_2$ 0,9 — 0,95 ; CH_3 1,05 (s)
Masse : M^+ = 180 ; fragments : 115, 123, 109, 95, 82, 69.

Cétone **D** (*R=CH_3*) *: diméthyl-1,1 (méthyl-6 heptène-5 yl-2)-4 cyclohexanone 3*

Infrarouge (liquide, cm^{-1}) : 1 710 (C=O)
RMN (δppm) : $(CH_3)_2$ 0,9 ; CH_3-CH 1,05 (d) ; $(CH_3)_2 = C-(CH_3)$ 1,65 (d) (j = 6 c/s).

2 — Les aldéhydes III (R=H) IV et V ont été cyclisés en présence de peroxyde de benzoyle : 0,015 mole d'aldéhyde sont dissous dans 30 ml de cyclohexane chauffés avec 0,01 mole de peroxyde de benzoyle ajouté par petites portions ; après neutralisation par une solution de carbonate de sodium et évaporation, les cétones sont isolées par chromatographie préparative.

Cétode **D** (*R=H*) *: méthyl 1 (méthyl 6 heptène-5 yl-2)-4 cyclohexanone-3*

Infrarouge (liquide, cm^{-1}) : 1 720 (C=O)
RMN (δppm) : CH_3, $(CH_3)_2-CH$ 1,6—2 (d) ; H éthylénique 5,1 (t)
Masse : M^+ = 222 ; fragments à 152, 139, 123, 112, 109, 95, 82.

Cétone **E** (*R=H*) *: n-propyl-2 cyclohexanone*

Le produit isolé est identifié par comparaison avec un échantillon authentique.

Cétone **E** (*R*=*CH*$_3$) : *méthyl-1 (butyl-2) 4 cyclohexanone-3*

Infrarouge (liquide, cm^{-1} : 1 720 (C=O)
RMN (δppm) : CH$_3$ 0,8–1 (m)
Masse : M$^+$ 16 ; fragments à 149, 129, 112, 105, 97, 82, 55.

Cétone **F** : *triméthyl-1,7,7 allyl-3 norbornanone-2*

Infrarouge (liquide, cm^{-1}) : 3 150, 1 650, 920 (CH=CH$_2$), 1 750 (C=O)
RMN (δppm) : H vinylique 5,1 (d) et 5,6 (m)
Masse : M$^+$ 192 ; fragments à 149, 123, 108, 95, 83, 77, 69, 55, 41.

Cétone **G** : *triméthyl-2,2,6 cyclohexanone*

Infrarouge (liquide, cm^{-1}) : 1 715 (C=O)
RMN (δppm : CH$_3$ 1–1,5 s)
Masse : M$^+$ 140 ; fragments à 105, 83, 71, 69, 55, 43.

Cétone **H** : *triméthyl 2,6,6 acétyl-1 cyclohexane*
Infrarouge (liquide, cm^{-1}) : 1 715 (C=O)
RMN (δppm) : CH$_3$CO 2,1 (5) ; CH : massif vers 1.

BIBLIOGRAPHIE

[1] « Free Radicals Rearrangements », Tome II p. 433, J. W. Witt, « Free Radicals », J. K. Kochi Editeur, Wiley-Interscience, New York, 1973.
[2] A. I. Scott, *Quat. Rev.*, **19**, 1 (1965).
[3] *Réf* 1, p. 418.
[4] Z. Cekovic, *Tetrahedron Letters*, **1972**, 752.
[5] a) R. Dulou, Y. Chretien Bessiere et H. Desalbres, *Compt. rend.*, **258**, 603 (1964).
b) Jp. Montheard, *Compt. rend.*, **260**, 575 (1965).
[6] a) M. Julia et P. Dostert, *Compt. rend.*, **259**, 2 872 (1964).
b) Jc. Chottard et M. Julia, *Bull. Soc. chim. France*, **1968**, 3 700.
[7] C. Kruk, Jc. V. Velzen et Th. de Boer, *Rec. Trav. chim.*, **1969**, 139.
[8] S. Julia, M. Julia, H. Linares et J. C. Blondel, *Bull. Soc. chim. France*, **1962**, 1947.
[9] J. Ojima, M. Nihonnyanagi, T. Kogure, M. Kimugai, S. Horiuchi, K. Nakatzugawa et Y. Nagai, *J. Organo metall. Chem.*, **94**, 449 (1975).
[10] G. Stork et S. R. Dowd. *J. Amer. Chem. Soc.*, **85**, 2 178 (1963).
[11] Jp. Bras, *Thèse de 3e Cycle*, Paris, 1970.
[12] R. Marbet et G. Saucy, *Helv. Chem. Acta.*, **1967**, 2 095.
[13] Jp. Claisse et D. I. Davies, *J. Chem. Soc. (C)*, **1970**, 258.
[14] M. Julia et F. le Goffic, *Bull. Soc. chim. France*, **1964**, 1 129.
[15] M. Julia et M. Maumy, *Bull. Soc. chim. France*, **1966**, 434.
[16] M. Julia, Jm. Surzur et L. Katz, *Bull. Soc. chim. France*, **1964**, 1 109

Revue Roumaine de Chimie, 26, 2, 283–290 (1981)

EPOXIDATION OF 2,6-DIARYLIDENECYCLOHEXANONES AND SOME REACTIONS OF THE CORRESPONDING EPOXIDES

M. M. HABASHY*, A. ESSAWY ** and M. M. M. HAMAD **

* Faculty of Science, Ain Shams University, Cairo, Egypt
** Faculty of Science, Zagazig University, Zagazig, Egypt

Received October 5, 1979

2,6-Diarylidenecyclohexanones react with hydrogen peroxide in alkaline medium to give the corresponding mono- and diepoxy derivatives. The reactions of these epoxides with amines, phenylhydrazine, hydroxylamine hydrochloride, Grignard reagents and aromatic hydrocarbons are described.

Recently, [1] it has been reported that some α, β-unsaturated ketones can give the mono- and diepoxides, upon treating with hydrogen peroxide in alkaline medium. Treatment of 2,6-dibenzylidenecyclohexanone (**1a**) with hydrogen peroxide in alkaline medium, —followed in the present work — gave the corresponding mono- and diepoxy compounds **2** and **3a**. On the other hand, upon treating 2,6-di-*p*-chlorobenzylidenecyclohexanone (**1b**) with hydrogen peroxide under similar conditions, in an attempt to isolate the two corresponding epoxy compounds, only the diepoxide **3b** was isolated.

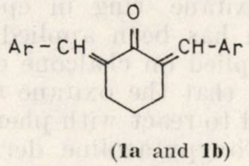

(1a and 1b)

a ; Ar = C_6H_5
b ; Ar = p–ClC_6H_4

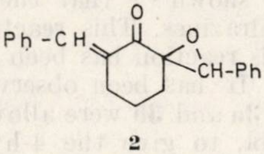

2

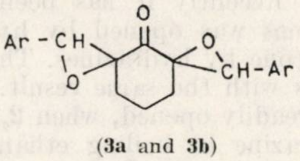

(3a and 3b)

a ; Ar = C_6H_5
b ; Ar = p–ClC_6H_4

The assigned structures of these epoxides **2**, **3a** and **3b** were proved by the following : *i*) Analytical data. *ii*) The infrared spectrum of the monoepoxide **2** showed absorption bands at 1680 cm^{-1} and at 1600 cm^{-1}, characteristic for ν(CO) of conjugated six-membered cyclic ketones and for ν(C=C) respectively, beside a band at 1 250 cm^{-1} attributable to the oxirane linkage. The infrared spectra of the diepoxides **3a** and **3b**, exhibit ν(CO) of saturated six-membered cyclic ketones (1 715 cm^{-1}) and the oxirane linkage (1 255 cm^{-1}). *iii*) The mass spectra of compounds **2** and

3a: The fragmentation patterns of **2** and **3b** show that the molecular ion (M^+) of **2** is 290, corresponding to molecular formula $C_{20}H_{18}O_2$, whereas the molecular ion (M^+) of **3a** is 306, corresponding to molecular formula $C_{20}H_{18}O_3$ The mass spectra exhibit peaks of high intensities, the most characteristic fragments being: $PhCH{=}\overset{+}{O}H$ ($m/e = 107$), $Ph{-}\overset{+}{C}HO$ ($m/e = 106$), $Ph{-}C{\equiv}\overset{+}{O}$ ($m/e = 105$), $Ph{-}\overset{+}{C}H_2$ ($m/e = 91$) and $\overset{+}{Ph}$ ($m/e = 77$). This fragmentation pattern supports the structure of the epoxy compounds, since these fragments reveal the presence of the oxirane linkage.

It was previously reported [2,3] that epoxides are cleaved under the influence of amines. In this investigation, the mono epoxide **2** reacts with benzylamine or *p*-toluidine in boiling ethanol to give the hitherto unknown products **4a** and **4b**. Whereas, treatment of the diepoxides **3a** and **3b** with benzylamine or *p*-toluidine in boiling ethanol gave compounds **5a-c**.

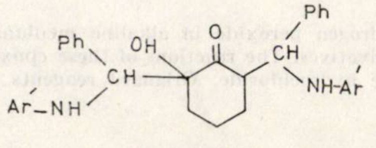

(4a and 4b)

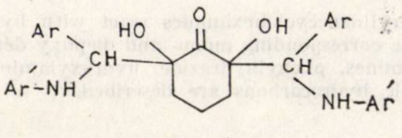

(5a–c)

	Ar′	Ar	Ar′
a	$C_6H_5{-}CH_2$	C_6H_5	$C_6H_5{-}CH_2$
b	$p{-}CH_3{-}C_6H_4$	$p{-}ClC_6H_4$	$C_6H_5{-}CH_2$
c		$p{-}ClC_6H_4$	$p{-}CH_3{-}C_6H_4$

The proposed structure of the products **4a** and **4b** and **5a-c** was substantiated from their analytical data and their infrared spectra which show strong absorption bands in the region 1 720–1 730 cm^{-1} (ν(CO) of saturated six-membered cyclic ketones) and near 3 420–3 450 cm^{-1} (ν(NH) of secondary amines and ν(OH)).

Recently it has been shown [4-6] that the oxirane ring in epoxy ketones was opened by hydrazines. This reaction has been applied on chalcone by hydrazines. This reaction has been applied on chalcone epoxides with the same result. It has been observed that the oxirane ring got readily opened, when **2**, **3a** and **3b** were allowed to react with phenylhydrazine in boiling ethanol, to give the 4-hydroxypyrazoline derivatives **6**, **7a** and **7b** respectively.

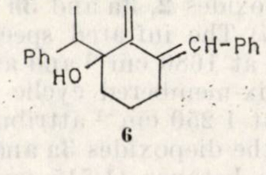

6

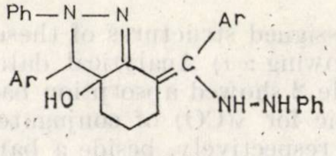

(7a and 7b)

Ar
a ; C_6H_5
b ; $p{-}ClC_6H_4$

The assigned structure of the products **6**, **7a** and **7b** was confirmed by the following observations: *i*) analytical data, *ii*) they give the colour test for pyrazolines [7] and *iii*) the infrared spectrum of compound **6** shows bands at 1 540 cm $^{-1}$ and 3 420 cm $^{-1}$ characteristic of $\nu(C{=}N)$ (conjugated cyclic) and $\nu(OH)$ respectively. The infrared spectra of **7a** and **7b** reveal the presence of bands at 1 600 cm $^{-1}$ ($\nu(C{=}N)$ conjugated cyclic) and at 3 440 cm $^{-1}$ ($\nu(NH)$ and $\nu(OH)$). On the other hand, treatment of the epoxy compounds **2**, **3a** and **3b** with hydroxylamine hydrochloride in boiling pyridine yielded the isoxazole derivatives **8**, **9a** and **9b** respectively.

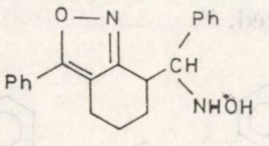

8

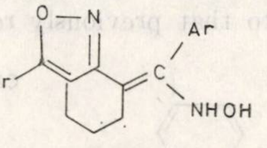

(9a and 9b)

Ar
a ; C_6H_5
b ; $p{-}ClC_6H_4$

The proposed structures of **8**, **9a** and **9b** were proved by their analytical data and their infrared spectra, which exhibit bands at 1 520–1 560 cm $^{-1}$ ($\nu(C{=}N)$ conjugated cyclic) and 3 420–3 440 cm $^{-1}$ ($\nu(NH)$ and $\nu(OH)$).

The reaction of chalcone epoxides with Grignard reagents has been previously reported. [8] In the present study, it has been observed that the mono epoxide **2** reacts with one mole of methylmagnesium iodide or phenylmagnesium bromide to give 2-benzylidene-6-hydroxy-6-methylphenyl- (or diphenyl)carbinylcyclohexanones (**10a**) and (**10b**) respectively, as the main products. Similarly, treatment of the diepoxides **3a** and **3b** with phenylmagnesium bromide or benzylmagnesium chloride, gave 2,6-bis(diarylcarbinyl)-2,6-dihydroxycyclohexanones **11a-c**. The nucleophilic reagent in these reactions, attacks the β-carbon of the epoxy ketone due to the polarization of the C=O group, followed by inductive effect through the oxirane ring and creation of a positive charge on the β-carbon atom.

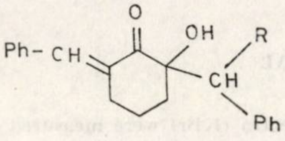

(10a and 10b)

R
a ; CH_3
b ; C_6H_5

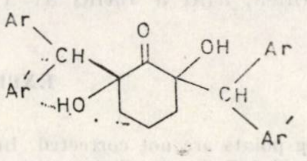

(11a-c)

	Ar	Ar′
a ;	C_6H_5	C_6H_5
b ;	$p{-}ClC_6H_4$	C_6H_5
c ;	$p{-}ClC_6H_4$	$C_6H_5{-}CH_2$

The structures of **10a** and **10b** were established from their analytical data and their infrared spectra, which show a band in the region 1 705–1 695 cm $^{-1}$ ($\nu(CO)$ of conjugated six-membered cyclic ketones), a broad band near 3 400—3 450 cm^{-1} (ν(OH)) and a band at 1 610 cm^{-1} (ν(C=C)). The structure of **11(a-c)** was confirmed by their analytical data and their infrared spectra, which exhibit a band near 1 720—1 725 cm^{-1} (ν(CO) of saturated six-membered cyclic ketones) and a broad band at 3 430 cm^{-1} (ν(OH)).

Alkylation of aromatic hydrocarbons with chalcone epoxides under Friedel-Crafts conditions has been reported.[9, 10] In the present work, treatment of the mono epoxide **2** with benzene in the presence of anhydrous aluminium chloride, gave the fluorene derivative **12**, as the main product. This reaction undoubtedly proceeds by cycloalkylation, which is analogous to that previously reported.[11]

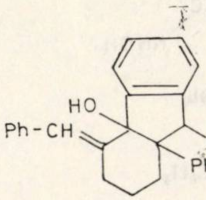

12

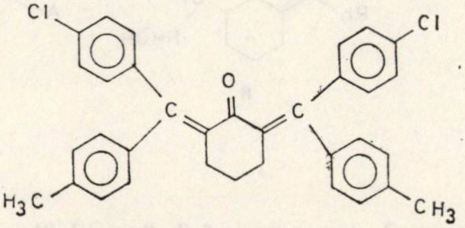

13

The assigned structure of **12** was evidenced by analytical, and infrared spectral data. Thus its infrared spectrum shows a broad band at 3 425 cm^{-1} (ν(OH)) and a weak absorption band near 1 610—1 620 cm^{-1} (ν(C=C)). However, alkylation of toluene with the diepoxide **3b** under Friedel-Crafts conditions, gave compound **13**.

The formation of **13** is probably due to fission of the oxirane ring with subsequent elimination of water. Cyclization failed probably owing to the presence of the two deactivating *p*-chlorophenyl groups in the diepoxide **3b**. The proposed structure of **13** was confirmed by its analytical data and its infrared spectrum which exhibits a sharp band near 1 680—1 690 cm^{-1} attributable to ν(CO) of conjugated six-membered cyclic ketones, and a band at 1 600 cm^{-1} (ν(C=C)).

EXPERIMENTAL

Melting points are not corrected. Infrared spectra (KBr) were measured on a Perkin-Elmer Infracord 137 Spectrophotometer.

Epoxidation of 2,6-diarylidenecyclohexanones 1a and 1b; Formation of 2, 3a and 3b

A solution of 2,6-diarylidenecyclohexanones (**1a** or **1b**) (4 g) in acetone/methanol mixture (40 ml/15 ml) was treated with sodium hydroxide solution (6 ml; 8%) followed by hydrogen peroxide (5 ml; 30%). The reaction mixture was shaken vigorously and brought to the boiling point occasionally during one hour, left overnight at room temperature, then diluted with water. The solid separated was filtered off and recrystallised from the suitable solvent (cf. Table 1).

TABLE 1

2,6 Diarylidenecyclohexanone oxides **2**, **3a** and **3b**

Compound	m.p. (°C)	Solvent* yield %	Formula	Analysis % {Found Calcd.	
				C	H
2	146–7	L.p. 50	$C_{20}H_{18}O_2$	82.49 82.76	6.41 6.21
3a	225–6	B 50	$C_{20}H_{18}O_3$	78.09 78.43	5.63 5.88
3b	205–6	B/L.p. 70	$C_{20}H_{16}Cl_2O_3$	64.23 64.00	4.55 4.27

* L.p. = Light-petrol (60–80°C); B = Benzene and B/L.p. = Benzene/Light-petrol (60–80°C).

Reaction of epoxides 2, 3a and 3b with amines; Formation of 4a and 4b and 5a-c

A solution of **2**, **3a** or **3b** (0.01 mole) and benzylamine or *p*-toluidine (0.02 mole) in ethanol was refluxed for three hours. The solid products separated after concentration and cooling were recrystallised from ethanol to give **4a** and **4b** and **5a-c**. (cf. Table 2).

TABLE 2

Carbinols **4a** and **4b** and **5a-c**

Compound	m.p. (°C)	Yield %	Formula	Analysis % {Found Calcd.		
				C	H	N
4a	230–1	60	$C_{34}H_{36}N_2O_2$	80.72 80.95	6.96 7.14	5.23 5.56
4b	235–6	50	$C_{34}H_{36}N_2O_2$	81.03 80.95	6.95 7.14	5.42 5.56
5a	224–5	55	$C_{34}H_{36}N_2O_3$	78.23 78.46	6.74 6.92	5.42 5.38
5b	175–6	50	$C_{34}H_{34}Cl_2N_2O_3$	69.35 69.27	5.82 5.77	4.39 4.75
5c	156–7	55	$C_{34}H_{34}Cl_2N_2O_3$	69.51 69.27	5.63 5.77	4.57 4.75

Reaction of epoxides 2, 3a and 3b with phenylhydrazine; Formation of 4-hydroxypyrazoline derivatives 6, 7a and 7b

A solution of **2**, **3a** or **3b** (0.01 mole) in ethanol (50 ml) was treated with phenylhydrazine (0.02 mole) and boiled for six hours. The products obtained after concentration and cooling were recrystallised from ethanol to give 4-hydroxypyrazoline derivatives **6**, **7a** and **7b** (cf. Table 3).

TABLE 3

4-Hydroxypyrazoline derivatives **6**, **7a** and **7b**

Compound	m.p. (°C)	Yield %	Formula	Analysis % {Found Calcd. C	H	N
6	130–1	72	$C_{26}H_{24}N_2O$	82.41 82.11	6.19 6.32	7.42 7.37
7a	175–6	75	$C_{32}H_{30}N_4O$	78.97 79.01	6.31 6.17	11.39 11.52
7b	229–30	70	$C_{32}H_{28}Cl_2N_4O$	69.31 69.19	4.98 5.05	10.23 10.09

Reaction of epoxides 2, 3a and 3b with hydroxylamine hydrochloride; Formation of isoxazole derivatives 8, 9a and 9b

A mixture of **2**, **3a** or **3b** (0.01 mole), water (1 ml), pyridine (30 ml) and hydroxylamine hydrochloride (0.02 mole) was refluxed for five hours. The cooled mixture was poured into ice-cold dilute hydrochloric acid and the product obtained was recrystallised from benzene to give the isoxazole derivatives **8**, **9a** and **9b** (cf. Table 4).

TABLE 4

The isoxazole derivatives **8**, **9a** and **9b**

Cmpound	m.p. (°C)	Yield %	Formula	Analysis % {Found Calcd. C	H	N
8	192–3	70	$C_{20}H_{20}N_2O_3$	74.89 75.00	6.36 6.25	8.92 8.75
9a	182–3	75	$C_{20}H_{18}N_2O_2$	75.66 75.47	5.39 5.66	8.59 8.81
9b	234–5	70	$C_{20}H_{16}Cl_2N_2O_2$	62.30 62.02	4.34 4.13	7.38 7.24

Action of Grignard reagents on the epoxides 2, 3a and 3b; Formation of 10a and 10b and 11a-c

A solution of **2**, **3a** or **3b** (0.01 mole) in dry benzene (200 ml) was added to an ethereal solution of the appropriate alkyl (or aryl)-magnesium halide (0.03 mole) during one hour. The reaction mixture was refluxed for six hours, during which time ether was allowed to evaporate, left overnight, hydrolysed with ice-cold saturated ammonium chloride and extracted with ether. The ethereal layer was dried (anhydrous sodium sulphate) and evaporated to give an oil which was triturated with light petrol (40–60°C). The crude solid obtained was recrystallised from the suitable solvent to give the products **10a** and **10b** and **11a-c** (cf. Table 5).

TABLE 5

Carbinols **10a, b** and **11a-c**

Compound	m.p. (°C)	Solvent* yield %	Formula	Analysis % {Found Calcd.	
				C	H
10a	118–9	B/L.p. 60	$C_{21}H_{22}O_2$	82.69 82.35	7.09 7.19
10b	125–6	B/L.p. 55	$C_{26}H_{24}O_2$	84.53 84.78	6.71 6.52
11a	85–6	M 70	$C_{32}H_{30}O_3$	83.33 83.12	6.19 6.49
11b	250–1	M 65	$C_{32}H_{28}Cl_2O_3$	72.51 72.32	5.45 5.27
11c	230–2	/L.p. 70	$C_{34}H_{32}Cl_2O_3$	72.71 72.99	6.09 5.72

* B/L.p. = Benzene/Light-petrol (60–80°C) and M = Methanol.

Reaction of epoxides 2 and 3b with aromatic hydrocarbons; Formation of 12 and 13

A solution of epoxide **2** or **3b** (0.01 mole) in dry aromatic hydrocarbon (benzene or toluene) (100 ml) was added gradually to a cold suspension of anhydrous aluminium chloride (0.04 mole) in a large excess of dry aromatic hydrocarbon (200 ml) and the temperature of the mixture was kept below 30°C. The suspension was stirred at room temperature for eight hours, poured into ice-cold hydrochloric acid solution. The aromatic layer was separated, dried and distilled. The oily residue was triturated with light-petrol (40–60°C) and the crude solid so obtained was recrystallised from the appropriate solvent to give **12** and **13** respectively (cf. Table 6).

TABLE 6

Compounds **12** and **13**

Compound	m.p. (°C)	Solvent* yield %	Formula	Analysis % {Found Calcd.	
				C	H
12	260–1	M 60	$C_{32}H_{28}O$	89.85 89.72	6.69 6.54
13	185–6	E 50	$C_{34}H_{28}Cl_2O$	78.17 78.01	5.21 5.35

* M = Methanol and E = Ethanol.

REFERENCES

[1] C. Pierre and J. L. Pierre, *Bull. Soc. chim. France,* **12,** 2 889 (1974); *Chem. Abstr.,* **84,** 58444 (1976).

[2] N. H. Cromwell, F. H. Schun Acher and J. L. Adeffang, *J. Amer. Chem. Soc.,* **83,** 974 (1961).

[3] I. G. Tischenko and P. M. Malashko, *Jrvest. Akad. Nauk S.S.S.R. Otdel. khim. Nauk*, **6**, 103 (1969) ; *Chem. Abstr.*, **72**, 110717 (1970).

[4] F. Piozzi and C. Fugant, *Ann. Chim. (Ital.)* **56**, 1 248 (1966) ; *Chem. Abstr.*, **67**, 73473(1967).

[5] N. H. Cromwell and J. L. Martin, *J. Org. Chem.*, **33**, 1890 (1968).

[6] G. Kobayaschi, S. Furukawa and Y. Matsuda, *Yalagokuzasshi*, **86**, 115 (1966), *Chem. Abstr.*, **67**, 108594 (1967).

[7] V. Knorr, *Liebigs Ann. Chem.*, **238**, 200 (1887).

[8] E. P. Kohler, N. K. Richtmyer and W. F. Hester, *J. Amer. Chem. Soc.*, **53**, 205 (1931).

[9] J. Colonge and L. Pichat, *Bull. Soc. chim. France*, **16**, 421 (1949).

[10] S. H. Mukherji, O. P. Vig and H. J. Muhauhuray, *J. Indian Chem. Soc.*, **34**, 9 (1957).

[11] A. Sammour, M. Selim and A. A. Hamed, *Egypt. J. Chem.*, **16**, 103 (1973).

Revue Roumaine de Chimie, 26, 2, 291–303 (1981)

MECHANO-CHEMISCHE REAKTIONEN DES POLYVINYLCHLORIDS. 9. CHARAKTERISIERUNG DER ERHALTENEN PRODUKTE DURCH WALZEN VON PVC-S MIT AROMATISCHEN DIAMINEN

CLEOPATRA VASILIU-OPREA und M. POPA

Lehrstuhl für organische und makromolekulare Chemie, Polytechnisches Institut Iassy, Calea 23 August nr. 22 A, Rumänien

Eingegangen am 21. Juli 1979

Vorliegende Arbeit umfasst die physikalisch — chemischen Eigenschaften der durch walzen von Polyvinylchlorid in Anwesenheit aromatischer Diaminen(Benzidin, *m*-Phenylendiamine, *p*-Phenylendiamine) erhaltenen Erzeugnisse. Aufgrund der chemischen und spektralen Charakterisierung wird ein Reaktionsmechanismus des PVC mit den aromatischen Diaminen vorgeschlagen. Es werden ebenfalls einige Feststellungen betreffend die Struktur des modifizierten Polymeren gemacht, und mit den Eigenschaften des Erzeugnisses korreliert.

The paper presents the physico-mechanical properties of the products obtained by mixing the poly(vinyl chloride) with the addition of aromatic diamines (benzidine, *m*-phenylendiamine, *p*-phenylendiamine). On the basis of chemical and spectral data, reaction mechanism of PVC with aromatic diamines was proposed and some specifications are made relating the structure of the modified polymer, which correlates with the whole complex of properties of the obtained products.

Zeits der Verarbeitungsprozesse sind die Polymere starken mechanischen Beanspruchungen ausgesetzt, welche zur Aktivierung einiger chemischen Reaktionen führen können, die anderenfalls schwer einzuleiten sind.

Durch Walzen der PVC mit aromatischen Diaminen, erhält man ein modifiziertes Polymer, dessen mechanische Eigenschaften (Zugfestigkeit), höher als die des Ausgangspolymers sind. [1]

Die Effizienz der Reaktion zwischen dem makromolekularen Produkt und der Diamine, bewertet durch das Anwachsen der Zugfestigkeit, ist von einer Reihe von Faktoren beeinflusst : Diaminenkonzentration, Stabilisatorkonzentration, die mechanischen Bearbeitungsparameter usw., wobei deren systematische Studien in [1] und [2] gezeigt werden.

Die vorliegende Arbeit zeigt die physikalischen und chemischen Eigenschaften des PVC modifiziert durch aromatische Diamine, wobei abschliessend die Struktur des neuen Polymers vorgeschlagen wird sowie der Reaktionsmechanismus, der das starke Anwachsen der physikalischen und mechanischen Kennziffern bezüglich des Ausgangsmaterials erklärt.

Zwecks des Studiums dieser Eigenschaften, wurden die unter verschiedenen Bedingungen erhaltenen Syntheseprodukte, durch die in [1] beschriebene Technik gereinigt, wonach sie den chemischen und spektralen Analysen unterworfen wurden.

1. MOLEKULARGEWICHT

Eine wichtige Eigenschaft der Polymers, bestimmend für deren Eigenschaften ist das Molekulargewicht, welches viskosimetrisch bestimmt wurde. In Abb. 1 —4 wird dessen Änderung in Abhängigkeit der mechanischen Bearbeitungsparameter dargestellt.

So zeigt Abb. 1 die Veränderung des Molekulargewichtes in Abhängigkeit von der Diaminmenge des Ausgangsgemisches. Der Kurvenverlauf ist in allen Fällen der gleiche : zuerst, im Bereich der kleinen Konzentrationen, erhält man einen abfallenden Verlauf, worauf sich ein anwachsender Zweig anschliesst, gleichzeitig mit dem Anwachsen der Diaminmenge. Die drei Kurven (Abb. 1 — Kurve 1, 2 ; Abb. 2) unterscheiden sich folgendermassen : im Falle von *p*-Phenylendiamine wächst das Molekulargewicht bis zu sehr hohen Werten an welche über dreimal den Wert des Molekulargewichtes des Ausgagnspolymers übertreffen, wobei die Proben mit *m*-Phenylendiamine und Benzidyn eine Stabilisationstendenz des Molekulargewichtes erkennen lassen, wenn im Reaktionsgemisch grosse Anteile von Diamine vorhanden sind.

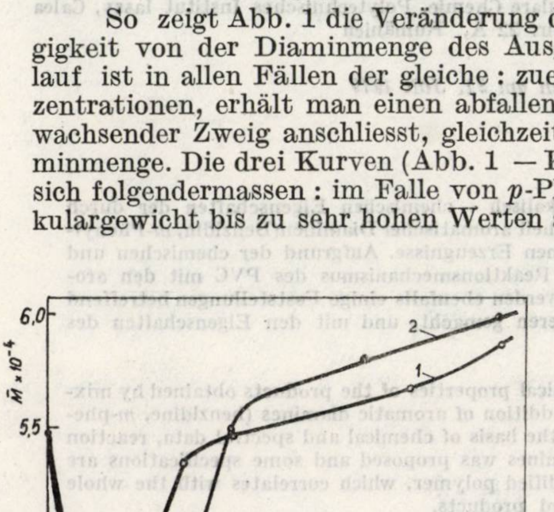

Abb. 1. — Veränderung des Molekulargewichtes in Abhängigkeit von der Diaminenkonzentration. 1) PVC + Benzidyn ; 2) PVC + *m*-Phenylendiamine.

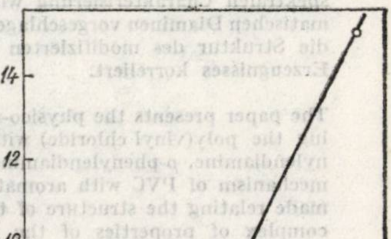

Abb. 2. — Veränderung des Molekulargewichtes in Abhängigkeit von der *p*-Phenylendiaminekonzentration.

Abb. 3 u. 4 zeigen die Veränderung des Molekulargewichtes mit der Reaktionsdauer. Das Verhalten jedes Produktes ist hier verschieden. So, im Falle von *p*-Phenylendiamine kann man ein stetiges Anwachsen weit über den Wert des Ausgangspolymers feststellen. Das nachträgliche Anwachsen des Molekulargewichtes durch Verlängern der Behandlungsdauer ist nicht mehr möglich, da die Proben an der Walze verbrennen.

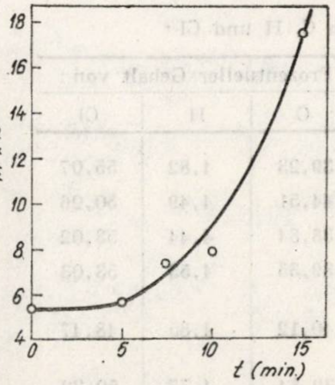

Abb. 3. — Veränderung des Molekulargewichtes in Abhängigkeit von der Behandlungsdauer für PVC-Produkte mit *p*-Phenylendiamine.

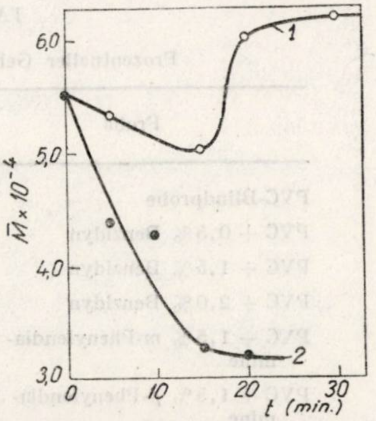

Abb. 4. — Veränderung des Molekulargewichtes in Abhängigkeit von der Behandlungsdauer: 1) PVC + Benzidyn; 2) PVC + *m*-Phenylendiamine.

Die Produkte mit Benzidyn zeigen anfänglich ein Verkleinern des Molekulargewichtes (in den ersten 10 Behandlungsminuten), wonach das Molekulargewicht für längere Behandlungsdauer anwächst und das des Ausgangspolymers übertrifft.

Letztens, im Falle von *p*-Phenylendiamine kann man ein stetiges Verkleinern des Molekulargewichtes festellen, wobei dieses einem Grenzwert gleichzeitig mit dem Anwachsen der Behandlungsdauer zustrebt.

Auf Grund dieses Reaktionsverhaltens kann man auf zwei gleichzeitige Reaktionen im Reaktionssystem schliessen, u.z. eine Abbaureaktion und eine Vernetzung. In einem solchen Fall ist es augenfällig, das bei Verwendung von *p*-Phenylendiamine die Hauptreaktion das Anwachsen des Molekulargewichtes ist, der Reaktionsfreudigkeit beider funktionellen Gruppen der Diamine wegen, wogegen im Falle von *m*-Phenylendiamine die sterischen Verhinderungen der Reaktionskapazität vermindern, vor allem bezüglich der Vernetzung. Die Kurve 2 aus Abb. 4 zeigt eine stetige Verkleinerung des Molekulargewichtes und definiert so einen typischen Abbauprozess.

2. ELEMENTÄRE ANALYSE

Es wurden eine Reihe von Proben, bezüglich deren prozentuellen Gehalt von C, H und Cl, die in verschiedenen Bedingungen synthetisiert worden sind, ausgewählt. Obwohl die erhaltenen Polymere Stickstoff enthalten, was qualitativ durch die Diazotierung der Aminogruppe und Verbindung mit verschiedenen Farbstoffen hervorgehoben wurde, ist in der Tafel 1 diese Charakteristik nicht angegeben, da deren Werte zu klein sind (unter 1%), also im Bereich der experimentellen Fehler. Von diesem Gesichtspunkt aus betrachtet, stimmen die erhaltenen Resultate mit den theoretischen Werten überein, welche zeigen, dass bei der maximalen Diaminmenge mit welcher gearbeitet wurde, es möglich ist im Reaktionsprodukt 0,76% Stickstoff (im Falle von Benzidyn), u. bzw. 1,34% im Falle von *m*-und-*p*-Phenylendiamine vorzufinden.

TAFEL 1

Prozentueller Gehalt von C, H und Cl *

Probe	Prozentueller Gehalt von :		
	C	H	Cl
PVC-Blindprobe	39,23	4,82	55,07
PVC + 0,5% Benzidyn	44,51	4,49	50,26
PVC + 1,5% Benzidyn	38,84	4,44	53,02
PVC + 2,0% Benzidyn	39,35	4,53	53,03
PVC + 1,5% *m*-Phenylendiamine	40,12	4,85	48,47
PVC + 1,5% *p*-Phenylendiamine	39,84	4,77	50,32

*** Die untersuchten Proben erhielt man durch 5 — minutiges Walzen bei einer Temperatur von 170°C.**

Man kann erstens feststellen, dass der prozentuelle Anteil von Chlor in allen Proben kleiner ist als der der PVC-Blindprobe, was zeigt dass diese Produkte tiefen Strukturveränderungen ausgesetzt sind, der chemischen Bindung der aromatischen Komponente mit der Struktureinheit wegen. Auch die Dehydrochlorurierungsrektion ist nicht ausgeschlossen, welche ebenfalls die kleinen Werte des prozentuellen Anteils an Chlor bei den Produkten im Beisein der Diamine erklären könnte.

3. DIE CHEMISCH GEBUNDENE DIAMINEQUANTITÄT

Die Struktur-und-Eigenschaftsveränderungen der Reaktionsprodukten zwischen PVC und aromatischen Diamine, sind durch die chemisch gebundenen Diamine des Polymers bestimmt. Man bestimmte darum die Diaminmenge, wobei die erhaltenen Resultate in Abb. 5 wiedergegeben sind. Man kann augenfällig ein Anwachsen der chemisch gebundenen Diamine feststellen vergleichsweise mit der aus dem Ausgangsgemisch, wobei Benzidyn die grösste Reaktionsfreudigkeit zeigt (Kurve 1) und fast komplett in der Reaktion verbraucht wird. Viel weniger reagiert *p*-Phenylendiamine (Kurve 3), obwohl der Effekt seiner Bindung am Polymer sehr stark das Molekulargewicht beeinflusst.

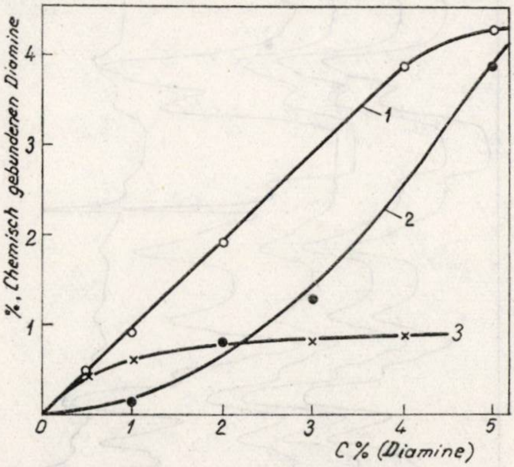

Abb. 5. — Veränderung der chemisch gebundenen Diaminemenge in Abhängigkeit von der Diaminemenge aus dem Ausgangsreaktiongemisch: 1) Benzidyn; 2) *m*-Phenylendiamine; 3) *p*-Phenylendiamine.

4. IR-SPEKTROSKOPIE

Informationen bezüglich der Struktur der erhaltenen Produkte, sowie auch bezüglich der Reaktionsmechanismen, boten die IR-Spektren.

In Abb. 6 sind vergleichsweise die Spektren von zwei Reaktionsprodukten wiedergegeben, erhalten im Beisein maximaler Diaminmen-

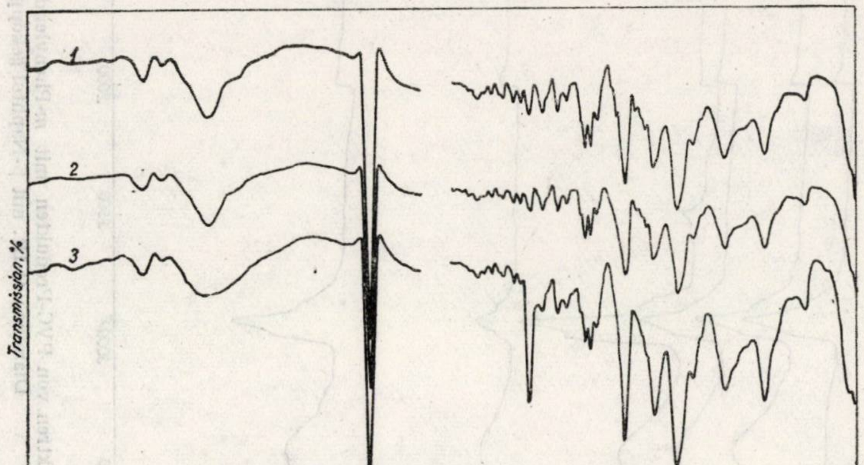

Abb. 6. — IR-Spektren von PVC-Produkten und aromatischer Diamine: 1) PVC + + 4 % *p*-Phenylendiamine; 2) PVC + 5 % Benzidyn; 3) PVC-Blindprobe.

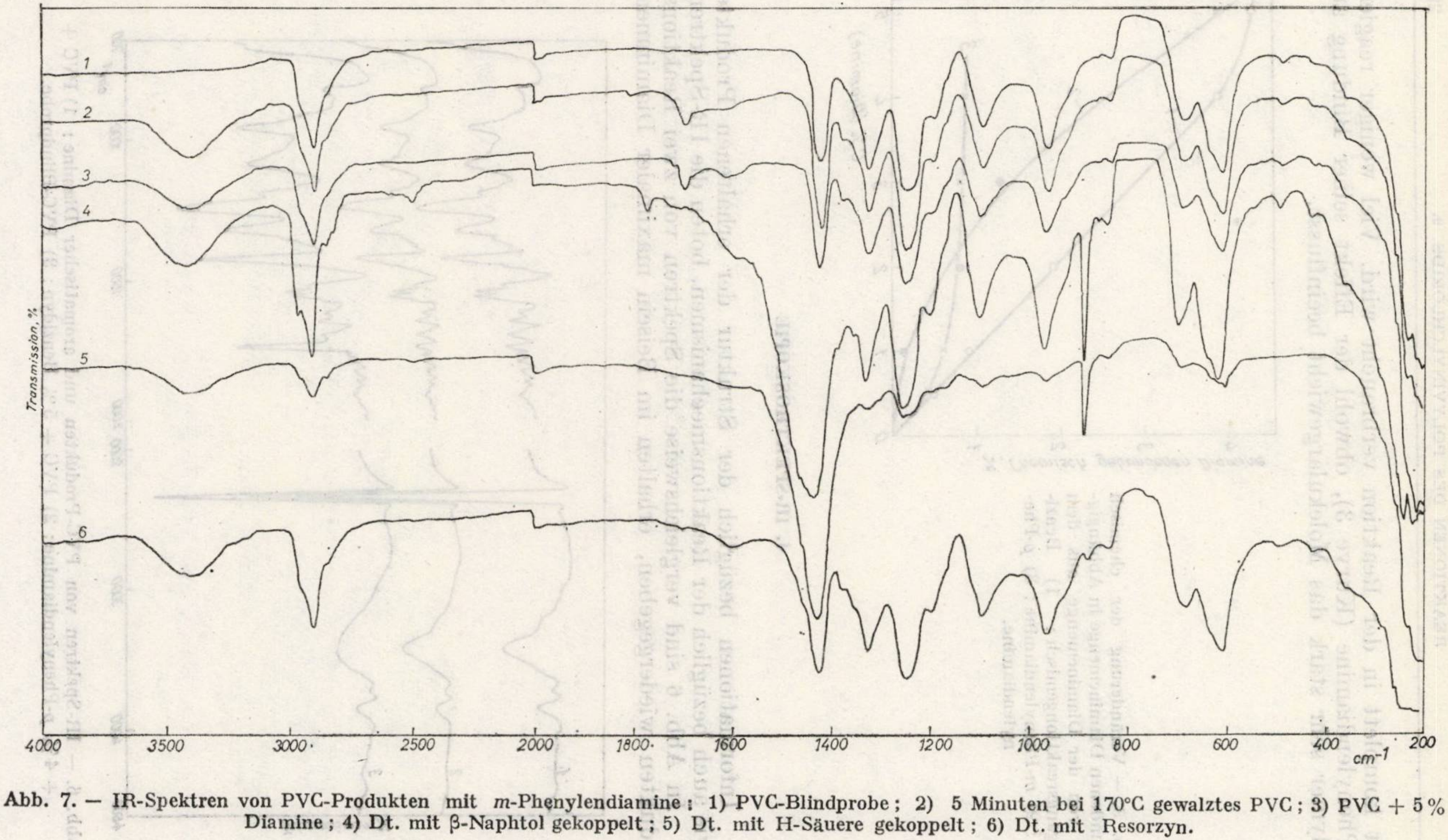

Abb. 7. — IR-Spektren von PVC-Produkten mit *m*-Phenylendiamine; 1) PVC-Blindprobe; 2) 5 Minuten bei 170°C gewalztes PVC; 3) PVC + 5% Diamine; 4) Dt. mit β-Naphtol gekoppelt; 5) Dt. mit H-Säuere gekoppelt; 6) Dt. mit Resorzyn.

gen (5%) und die der Blindprobe (bearbeitet in Abwesenheit von Diamine). Wenn zwischen den Spektren der Produkte mit *p*-Phenylendiamine und Benzidyn (Kurve 1 u. 2) keine Abweichungen auftreten, vergleichweise mit der Blindprobe tritt eine essentielle Abweichung auf u.z. das Wegbleiben des Absorbtionsmaxima bei 1 700 cm^{-1}, was das Verschwinden oder das Verkleinern der Anzahl der Doppelbindungen an der Hauptkette des Polymers zeigt.

In Abb. 7 sind vergleichsweise die Spektren des durch Walzen von PVC mit 5% *m*-Phenylendiamine erhaltenen Produktes und der erhaltenen Produkte durch deren Färben, nach einer vorhergehenden Diazotierung mit H-Säure-Resorzyn-β-Naphtol, wiedergegeben. Man kann dabei das Vergrössern des Peaks bei 1 450 cm^{-1} und das Auftreten eines Peaks bei 860 cm^{-1} bei den Kurven 4, 5 u. 6 feststellen, was die Anwesenheit des Benzolkernes aussagt, auch der Kupplung der Farbstoffe mit aromatischer Struktur wegen.

5. THERMOSTABILITÄT

Es ist bekannt dass die Anwesenheit aromatischer Kerne an der Kette eines Polymers diesem seine Thermostabilität verbessert. Darum untersuchte man die Reaktionsprodukte von dem Gesichtspunkt ihrer Stabilität bei hohen Temperaturen. Man nahm so die Derivatogramme der Reaktionsprodukte mit 1% Diamine, die durch 5-minutiges Walzen bei 170°C erhalten wurden auf, aus welchen die Werte der thermischen Abbauaktivierungsenergien (Tafel 2) berechnet wurden und danach die Kurven bezüglich der Gewichtsabnahme in Abhängigkeit der Zersetzungstemperatur aufgetragen wurde (Abb. 8).

TAFEL 2

Aktievierungsenergie des thermischen Abbaus für Produkte mit 1% Diamine, Walzzeit 5 Minuten bei 170°C.

Probe	Aktievierungsenergie (Kcal/mol)
PVC – Blindprobe	45,6
PVC – + Benzidyn	42,8
PVC + *m*-Phenylendiamine	45,6
PVC + *p*-Phenylendiamine	46,0

Die Kurven aus Abb. 8 zeigen im Allgemeinen den gleichen Verlauf, was die ungefähr gleiche thermische Stabilität der untersuchten Proben beweisst. Das Gleiche geht den Daten der Tafel 2 hervor, wo man sehr naheliegende Werte der thermischen Abbauenergien für alle untersuchten Proben wiederfindet. Bis zu einer Temperatur von 200° C verhält sich die Blindprobe und die mit *m*-Phenylendiamine modifizierte am besten, wobei bei höheren Temperaturen das bessere Verhalten der Produkte mit Benzidyn auffällt.

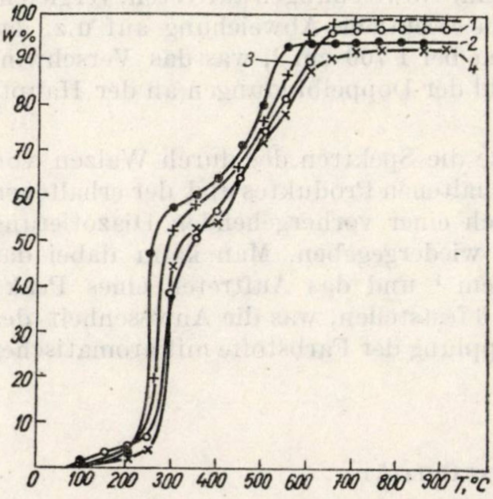

Abb. 8. — Gewichtsverlustveränderung in Abhängigkeit von der Temperatur : 1) PVC+Benzidyn ; 2) PVC + *p*-phenylendiamine ; 3) PVC+ *m*-Phenylendiamine ; 4) PVC Blindprobe.

6. THERMOMECHANISCHE KURVEN

Das Anwachsen der mechanischen Eigenschaften kann von zwei Faktoren bedingt sein :

1) das Anwachsen des Molekulargewichtes, dessen Variation schon in den Abb, 1 –4 besprochen wurde ;

2) das Anwachsen der Kohäsionsenergie auf Grund der physischen Zwischenwirkungen zwischen den Makromolekülen in Anwesenheit der Diamine.

Informationen bezüglich des zweiten Einflussfaktors kann man durch das Aufnehmen der thermomechanischen Kurven erhalten. Die Resultate bezüglich des thermomechanischen Verhaltens sind in Abb. 9 –11 wiedergegeben, wobei die Veränderung der Verformung in Abhängigkeit von der Temperatur für eine konstante Kraft von 50 p registriert wurde.

Auf Grund dieser Registrierungen konnte man die Verglasungstemperaturen berechnen, deren Veränderung in Abhängigkeit von der Diaminmenge aus dem Reaktionsgemisch in Abb. 12 wiedergegeben ist.

Die Veränderung der Verglasungstemperatur (T_g) in Abhängigkeit von der Konzentration ist im Falle von Benzidyn und *p*-Phenylendiamine nicht besonders gross, zeigt aber eine Verkleinerung an. Bei den Produkten mit *m*-Phenylendiamine ist dieser Effekt ausgeprägter. Somit erhält man für eine 5 % *m*-Phenylendiaminemenge im Ausgangsgemisch einen Wert der Verglasungstemperatur von 83°C. Diese Variationsart

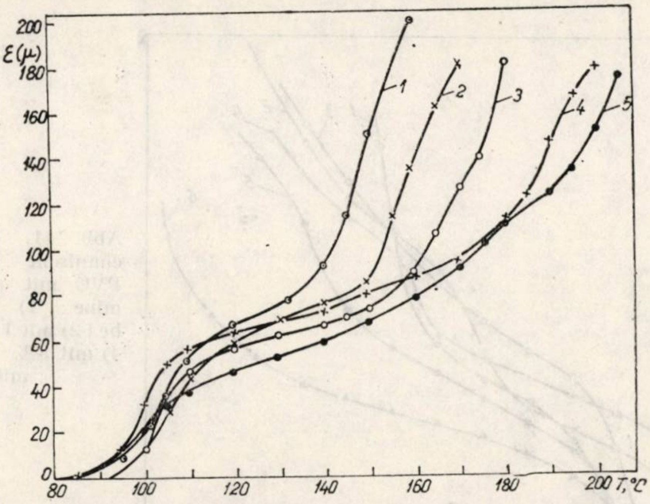

Abb. 9. — Thermomechanische Kurven von PVC mit *p*-Phenylendiamine ; 1) PVC- Blindprobe ; 2) mit 0,5 % ; 3) mit 1 % ; 4) mit 2,5 % ; 5) mit 4 % ; 6) mit 5 %.

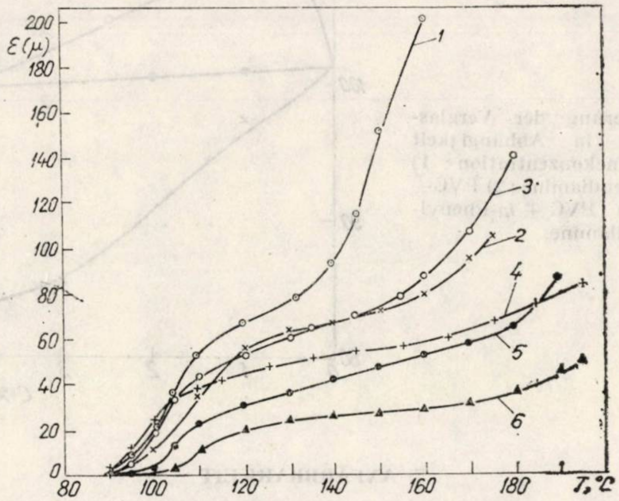

Abb. 10. — Thermomechanische Kurven von PVC mit Benzidyn ; 1) PVC-Blindprobe ; 2) mit 1 % ; 3) mit 2 % ; 4) mit 3 % ; 5) mit 4 % ; 6) mit 5 %.

von T_g zeigt eine Weichmachung an, welche von der chemisch ungebundenen Diamine im Polymer hervorgerufen wird, was auch andere Autoren zeigten. [3,4]

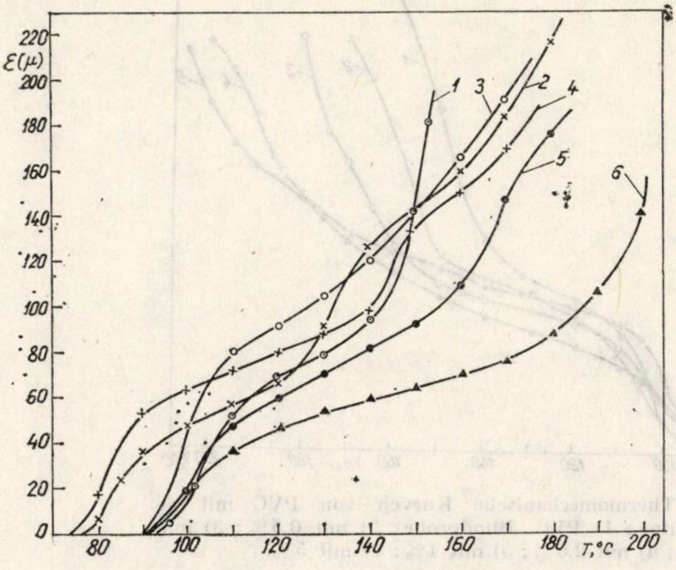

Abb. 11. — Thermomechanische Kurven von PVC mit *m*-Phenylendiamine : 1) PVC-Blindprobe ; 2) mit 1% ; 3) mit 2% ; 4) mit 3% ; 5) mit 4% ; 6) mit 5%.

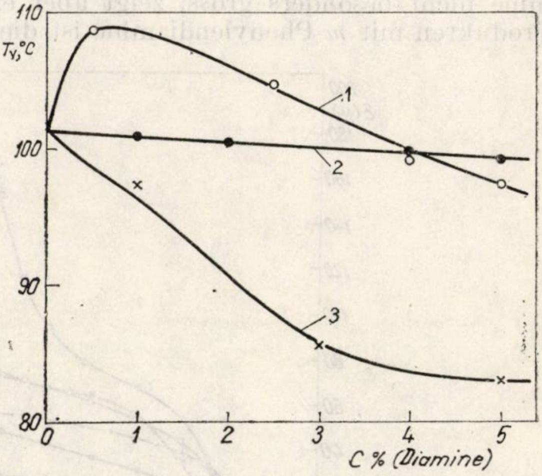

Abb. 12. — Änderung der Verglassungstemperatur in Abhängigkeit von der Diaminekonzentration : 1) PVC+ *p*-Phenylendiamine ; 2) PVC+ +Benzidyn ; 3) PVC + *m*-Phenylendiamine.

7. ANFÄRBBARKEIT

Sowie in dieser Arbeit gezeigt wurde, ist der Stickstoffgehalt in den Reaktionsprodukten gering und fällt in den Bereich der experimentellen Fehler. Um indirekt die Anwesenheit dieses Elementes in den erhaltenen Produkten zu zeigen, bestimmte man qualitativ die freien Aminogruppen aus dem Polymer, durch Diazotierung und Kupplung mit verschiedenen Farbstoffen, sowie mit H-Säure, Resorcyn und β-Naphtol. Man konnte so die Mehrzahl der synthetisierten Produkte intensiv anfärben. Man konnte feststellen, dass für die gleichen Walzzeiten sich die Färbung gleichzeitig mit der Konzentration von Diamine verstärkt, was eine grössere Anzahl von freien Aminogruppen zeigt. Man erhält das gleiche Resultat beim Anwachsen der Walzzeit, wenn die Diaminmenge konstant bleibt.

Man muss unterstreichen, dass die Produkte mit *m*-Phenylendiamine die beste Anfärbbarkeit besitzen, was auch hier eine Anwesenheit einer grossen Anzahl von freien Aminogruppen zeigt.

DISKUSSION

Aller erhaltenen Resultate, bezüglich des mit Diamine reaktioniertem Polymers, nach Absondern der Zusätze und aufmerksamer Reinigung zeigen, dass durch die Walzbearbeitung eine chemische Reaktion zwischen dem Polymer und den verwendeten aromatischen Diamine auftritt. Das bearbeitete Ausgagspolymer PVC unterliegt tiefen strukturellen Veränderungen, was zu dem Verbessern einiger Gebrauchseigenschaften, speziell zum Zugfestigkeitszuwachs führt.

Zeits der Walzbearbeitung spielen sich zwei chemische Reaktionen ab u.z. eine Abbaureaktion und eine Vernetzung.

Die Abbaurektion verfolgt ein hololytisches Zerreissen der makromolekularen Ketten:

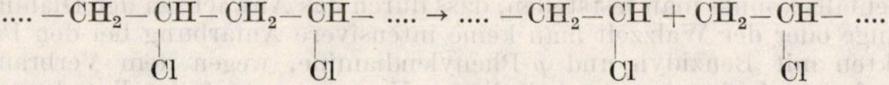

$$\ldots -CH_2-\underset{Cl}{\underset{|}{CH}}-CH_2-\underset{Cl}{\underset{|}{CH}}-\ldots \rightarrow \ldots -CH_2-\underset{Cl}{\underset{|}{\dot{C}H}}+\dot{C}H_2-\underset{Cl}{\underset{|}{CH}}-\ldots \qquad (1)$$

Die Stabilisierung der erhaltenen Makroradikale wird durch Disproportionierung oder Kettenübergang an Diamine erziehlt:

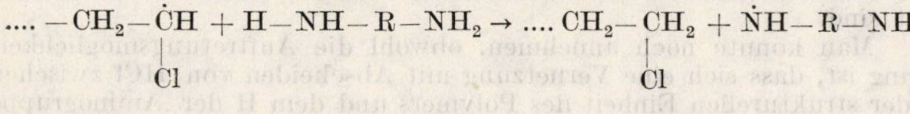

$$\ldots -CH_2-\underset{Cl}{\underset{|}{\dot{C}H}}+H-NH-R-NH_2 \rightarrow \ldots CH_2-\underset{Cl}{\underset{|}{CH_2}}+\dot{N}H-R-NH_2, \qquad (2)$$

wonach eine Wiederverbindung auftritt:

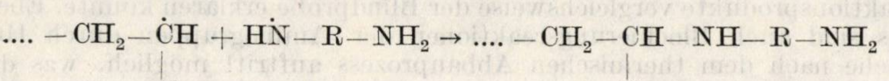

$$\ldots -CH_2-\underset{Cl}{\underset{|}{\dot{C}H}}+H\dot{N}-R-NH_2 \rightarrow \ldots -CH_2-\underset{Cl}{\underset{|}{CH}}-NH-R-NH_2 \qquad (3)$$

Eine solche Reaktion erklärt den Verbrauch der Diamine aus dem Reaktionsmedium, sowie auch die Anwesenheit der freien Aminogruppen, die durch Diazotierung und Kupplung bewiesen wurden. Gleichzeitig erklärt sie die Verkleinerung des Molekulargewichtes des Polymers bei kleinen Behandlungsdauern bzw. kleinen Konzentrationen der Diamine.

Bei grossen Behandlungsdauern kann das Anwachsen des Molekulargewichtes dem bifunktionellen Radikalakzeptoreffekt der Diamine zugewiesen sein, was zur Bindung von Kettenfragmenten und zum Auftreten von Strukturen des Typs

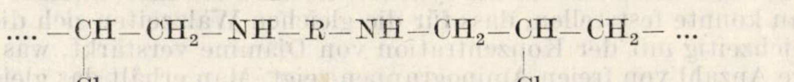

$$\ldots.-\underset{\mathrm{Cl}}{\underset{|}{\mathrm{CH}}}-\mathrm{CH_2-NH-R-NH-CH_2}-\underset{\mathrm{Cl}}{\underset{|}{\mathrm{CH}}}-\mathrm{CH_2}-\ldots \qquad (4)$$

führt.

Die immer schwierigere Lösung der Reaktionsprodukte, gleichzeitig mit dem Anstieg der Walzzeit, sowie auch mit dem Anstieg der Diaminmenge (bis zu 5 % *p*-Phenylendiamine, das Produkt ist praktisch unlöslich) führt zur Annahme von Vernetzungen, die nach unserer Meinung möglich sind, vor allem durch die Addition der Diamine an die Doppelbindungen der Polymerkette :

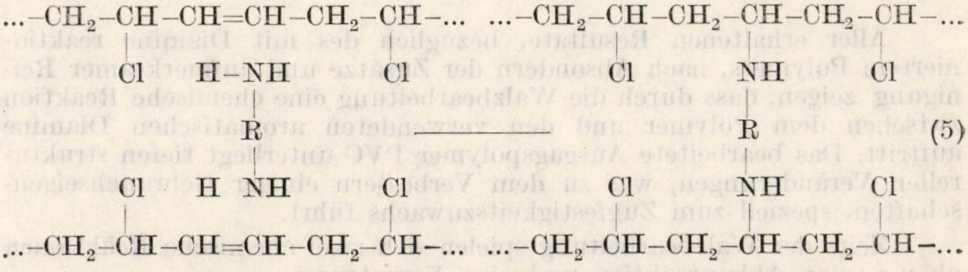

$$\begin{array}{ccccccccccccccc}
\ldots-\mathrm{CH_2}- & \mathrm{CH} & - & \mathrm{CH} & = & \mathrm{CH} & -\mathrm{CH_2}- & \mathrm{CH} & -\ldots\quad\ldots-\mathrm{CH_2}- & \mathrm{CH} & -\mathrm{CH_2}- & \mathrm{CH} & -\mathrm{CH_2}- & \mathrm{CH} & -\ldots \\
 & | & & & & | & & | & & | & & | & & | & \\
 & \mathrm{Cl} & & \mathrm{H} & - & \mathrm{NH} & & \mathrm{Cl} & & \mathrm{Cl} & & \mathrm{NH} & & \mathrm{Cl} & \\
 & & & & & | & & & & & & | & & & \\
 & & & & & \mathrm{R} & & & & & & \mathrm{R} & & & \\
 & & & & & | & & & & & & | & & & \\
 & \mathrm{Cl} & & \mathrm{H} & & \mathrm{NH} & & \mathrm{Cl} & & \mathrm{Cl} & & \mathrm{NH} & & \mathrm{Cl} & \\
 & | & & & & | & & | & & | & & | & & | & \\
\ldots-\mathrm{CH_2}- & \mathrm{CH} & - & \mathrm{CH} & = & \mathrm{CH} & -\mathrm{CH_2}- & \mathrm{CH} & -\ldots\quad\ldots-\mathrm{CH_2}- & \mathrm{CH} & -\mathrm{CH_2}- & \mathrm{CH} & -\mathrm{CH_2}- & \mathrm{CH} & -\ldots
\end{array} \qquad (5)$$

Der Additionsmechanismus an die Doppelbindung kann auch durch das Verschwinden aus den IR-Absorbtionsspektren des Bandes bei 1 700 $\mathrm{cm^{-1}}$, welches den Doppelbindungen angehört, begründet sein. Ebenfalls konnte man feststellen, dass durch das Anwachsen der Diaminemange oder der Walzzeit man keine intensivere Anfärbung bei den Produkten mit Benzidyn und *p*-Phenylendiamine, wegen dem Verbrauch der freien Aminogruppen bei diesen Vernetzungen feststellen konnte. Bei *m*-Phenylendiamine sind diese Reaktionen viel schwieriger erhaltbar, weil die Aminogruppen, die asymetrisch am Benzolkern angeschlossen sind und verschiedene Reaktionsfreudigkeit aufweisen, sterisch verhindert sind.

Man könnte noch annehmen, obwohl die Auftretungsmöglichkeit gering ist, dass sich eine Vernetzung mit Abscheiden von HCl zwischen Cl der strukturellen Einheit des Polymers und dem H der Aminogruppe abspielt, welche Reaktion eventuell den kleinen Gehalt an Chlor der Reaktionsprodukte vergleichsweise der Blindprobe erklären könnte. Ebenfalls sind auch Blockierungsreaktionen der Aminogruppen durch HCl, welche nach dem thermischen Abbauprozess auftritt möglich, was den kleinen Anteil der chemisch gebundenen Diamine im Falle von *p*-Phenylendiamine erklären könnte.

Die vorgeschlagenen Reaktionsabläufe sind durch chemische und spektrale Analysen unterstützt und ermöglichen die Veränderung der Zugfestigkeit aufzuklären. Im Allgemeinen sind die Quellen des Zugfestigkeitszuwachses, die in einer anderen Arbeit besprochen wurden, folgende : Anwachsen des Molekulargewichtes des Polymers, die Vernetzungsreaktionen und die Bildung der Wasserstoffbrücken zwischen den makromolekularen Ketten und dem Überschuss von Diamine.

SCHLUSSFOLGERUNGEN

1. Die Walzbearbeitung von PVC-S im Beisein von aromatischen Diamine, in Abhängigkeit von den Reaktionsbedingungen, führt zu bedeutenden Veränderungen des Molekulargewichtes.

2. Die chemische (Elementaranalyse, die Stickstoffbestimmung nach Kjeldahl, die Diazotierungsreaktionen und die Anfärbbarkeit) und physikalische Analyse (IR-Spektroskopie, Photokolorimetrie) zeigen die chemische Bindung der aromatischen Diamine an die PVC-S-Abbaufragmente.

3. Die thermomechanischen Kurven beweisen, dass der Diamineüberschuss als Weichmacher wirkt.

4. Die hauptsächlichen Zwischenwirkungen (physische und chemische) die sich zeits des Walzens von PVC-S in Anwesenheit von Diamine abspielen und die das bedeutende Anwachsen der Zugfestigkeit erklären, laut einer vorhergehenden Arbeit sind : das Anwachsen des Molekulargewichtes, die Vernetzungsreaktionen und die Bildung von Wasserstoffverbindungen zwischen den Polymerketten und dem Diamineüberschuss.

LITERATURHINWEISE

[1] Cl. Vasiliu Oprea und M. Popa, *Kolloid Zeitschrift und Zeitschrift für Polymeren*, unter Druck.
[2] Cl. Vasiliu Oprea, S. Petrovan, und M. Popa, *Mehanika kompozitnîh materialov*, **6**, 977 (1979).
[3] N. S. Prokhorova, R. G. Timergaleev, V. I. Popov, V. A. Voskresenskii, *Tr. Mezhvuz. 3-ei Konf. Primen. Stroit. Plastmass*, 1970.
[4] V. A. Voskresenskii, N. S. Prokhorova, *Izv. Vyssh. Ucheb., Zaved. Khim. Khim. Tekhnol.*, **14**, 435 (1971).

Revue Roumaine de Chimie, 26, *2*, 305—313 (1981)

ALTERNATING TENDENCY IN COPOLYMERIZATION. V.[1]

EQUIMOLECULAR COPOLYMERS AND DIMERS OF 1,1-DIPHENYLETHYLENE

DAN SORIN VASILESCU

Laboratory of Macromolecular Chemistry, Polytechnical Institute, Calea Victoriei 149, Bucharest
Romania

Received February 5, 1980

As 1,1-diphenylethylene (DPE) represents a monomer unable to homopolymerize, it becomes a useful tool to demonstrate certain reaction mechanisms. In the presence of the complex acrylonitrile—BF_3, DPE participates at two processes, namely alternating copolymerization and cationic dimerization. The noticed kinetic features enabled us to substantiate a mechanism, in agreement with our previous proposals.

1. INTRODUCTION

In our previous papers [1, 2] we have reported that in systems acrylonitrile-$ZnCl_2$-electron donor monomer (such as styrene or vinyl ether) a charge-transfer complex (CTC) is formed. This CTC is present at low concentration and may initiate (according to the reactivity of the electron donor monomer) either the cationic polymerization of vinyl ether or the alternating copolymerization.

In order to substantiate this proposal, we have chosen 1,1-diphenylethylene as the electron donor monomer, since this monomer is well known for its inability to homopolymerize either in a radical or ionic way. The radical affinity of DPE may be considered from the point of view of the steric hindrance in the addition reaction of radical to olefin and also in the terms of the resonance stabilization of the radical; it seems that the former effect may be less important than the latter. [3] Nevertheless, 1,1-diphenylethylene (DPE) can copolymerize with various vinyl monomers, [4] but in the resulting copolymer two successive DPE units do not occur; Ito and Yamashita [5] investigated the triad distribution in the copolymer DPE(M_1)—methyl acrylate(M_2) and found only 222, 221 and 121 triads. Further, DPE cannot homopolymerize by an ionic mechanism. Dimers of DPE may be obtained in the presence of several typical cationic catalysts such as $SnCl_4 . H_2O$ or $SbCl_5 . HCl$. [6] The anion of DPE is also a very stable one and does not produce poly-DPE, but may initiate the anionic polymerization of other monomers [7] or even produce equimolecular copolymers. [8]

Boron trifluoride is a powerful Lewis acid. It has been little used as a complexing agent in alternating copolymerization, despite of the impressive number of papers published on this subject. Ikegami and Hirai [9] have prepared the methyl methacrylate—BF_3 complex and have tried to copolymerize it with styrene at low temperatures, by irradiation with a high pressure mercury lamp; although the temperature was — 75°C, they obtained the 1 : 1 copolymer with a yield of 1%, in admixture with a large amount of polystyrene. Uschold [10] has reported some copolymerization tests between acrylonitrile(AN)—BF_3 and 1-hexene, but the composition of the resulting copolymers seems to be quite obscure. Logothetis and McKenna [11] have reported that copolymerization of acrylate esters—BF_3 complexes with α-olefins such as ethylene, propylene and 1-hexene leads to equimolecular copolymers; when an excess of olefin was used, no cationic polymerization was noticed, but similar attempts made with BF_3—acrylate ester complexes and styrene (or isobutylene) have led only to polystyrene (polyisobutylene).

Some early classical works [12] in the field of cationic polymerization have shown that BF_3 needs a cocatalyst (water, HCl etc.) to initiate the cationic polymerization of styrene.

2. EXPERIMENTAL

2.1. Materials

DPE was prepared according to the method described by Allen [13] from phenyl-magnesium bromide and ethyl acetate; the diphenylmethyl-carbinol intermediately obtained was subsequently dehydrated to DPE. The monomer was purified by double distillation in vacuum (123°/5 mm.Hg) and dried over calcium hydride; the pure, dry DPE was stored in sealed off ampoules.

Acrylonitrile, styrene and solvents were purified according to the usual methods and dried over calcium hydride; after the final fractionation, the pure AN, S or solvents were stored over calcium hydride in vacuum.

Boron trifluoride (purity 98.5%) was used without purification.

Azobisisobutyronitrile was recrystallized from methanol and from chloroform.

2.2. The complex An—BF_3 [14]

A suitable amount of dry AN was cooled down in a three-necked flask equipped with mechanical stirrer, vertical condenser and dropping funnel; a constant argon purge was maintained continously. BF_3 was then slowly added until the complex began to crystallize; during this operation, the temperature was not allowed to rise above 10°C. Subsequently, AN was poured again into the mixture to redissolve the complex; the crude AN—BF_3 mixture was stored in sealed tubes. Further purification was carried out on the vacuum line as follows. The excess of AN was removed by distillation and the remaining 1 : 1 complex was sublimed in the previously weighed ampoule *1* (Fig. 1); consequently, the quantity of AN—BF_3 was measured by double weighing. A known amount of pure AN was distilled into precalibrated ampoule *2* (Fig. 1). The known amounts of complex and free monomer may be mixed after breaking the break seal *3*; the solution obtained was stored in the ampoule *2*, after sealing off the constriction *4*.

The resulting solutions of desired concentration had to be manipulated in the absence of moist air; this led us to adopt the filling system illustrated in figure 2. The ampoule *2* (Figure 1) containing the solution of AN—BF_3 complex in excess of AN was connected to the system presented in figure 2. The apparatus illustrated in figure 2 was flamed out under vacuum to ensure the absence of volatiles and subsequently filled with dry argon. After breaking the break seal *4*, a suitable amount of solution was poured from the ampoule *2* to the measuring tube *3*. The volumes of solution in each bulb *5* were appreciated as differences in volume in the measuring tube *3*. Acid-base titration was used in order to obtain an exact value for the concentration of BF_3 ; bulbs containing a precise volume of solution were broken in excess of NaOH solution and the excess of NaOH estimated by backtitration.[15]

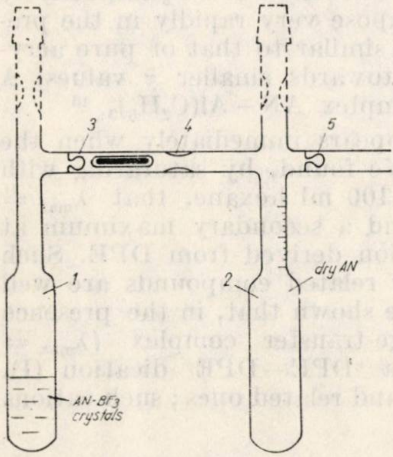

Fig. 1. — Apparatus used for the preparation of the solution of AN/BF_3 complex in excess of acrylonitrile.

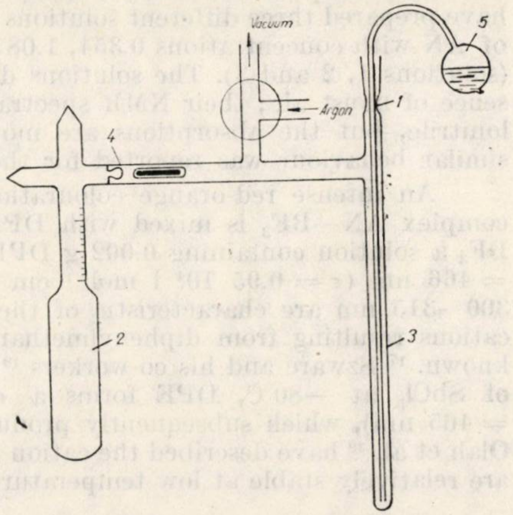

Fig. 2. — System used for introducing the AN/BF_3 complex solution into bulbs ; an argon "cushion" through the narrow neck (1) prevents any contact of the solution with moist air.

2.3. Polymerization and dimerization processes

In these experiments, the ampoules illustrated in figure 3 were used. The type *3a* was suitable for relatively short polymerization times ; a complete sealed off type of reaction vessels has been chosen for longer polymerization times (*3b*). Bulbs containing the $AN-BF_3$ complex and DPE respectively, together with the necessary amount of AIBN were introduced in the reaction vessels. The reaction vessels were evacuated and sealed off ; the bulbs were broken by shaking and the resulted solution homogenized. After an appropriate reaction time, the vessel was opened, the reaction mass diluted with a solvent, filtered off glass debris and poured into a large amount of nonsolvent. The polymers (or crystallized oligomers) were filtrated, dried, weighed. Before analysis, the polymers were reprecipitated in order to remove any incorporated inorganic materials.

2.4. Composition and structure of products

The composition of copolymers was established by elemental analysis ; confirmation of their structure was obtained from their IR (usually KBr pellets) and NMR (60 MHz, external TMS) spectra.

The UV spectra were recorded on very dilute solutions by means of a Unicam SP 8000 ultraviolet spectrophotometer.

Vapour-phase osmometry was used to estimate the molecular weight of oligomers (Hewlett-Packard 302-B vapour phase osmometer).

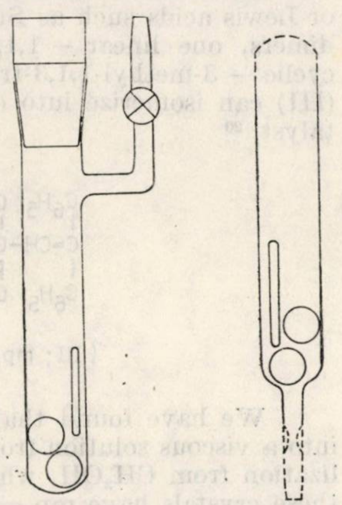

Fig. 3. — Reaction vessels used in the study of the system $AN-BF_3-DPE$.

3. RESULTS AND DISCUSSION

The complex AN$-BF_3$ is a crystalline solid, soluble in AN.[14] We have prepared three different solutions of the AN$-BF_3$ complex in excess of AN with concentrations 0.354, 1.08 and 1.25 mol/l of BF_3 respectively (solutions 1, 2 and 3). The solutions decompose very rapidly in the presence of moist air; their NMR spectra are similar to that of pure acrylonitrile, but the absorptions are moved towards smaller τ values. A similar behaviour was reported for the complex AN$-Al(C_2H_5)_3$.[16]

An intense red-orange colouration appears immediately when the complex AN$-BF_3$ is mixed with DPE. We found, by saturating with BF_3 a solution containing 0.002 g DPE in 100 ml hexane, that $\lambda_{max} = 466$ nm ($\varepsilon = 0.95\ 10^4$ l mol^{-1} cm^{-1}) and a secondary maximum at 300–315 nm are characteristic of the cation derived from DPE. Such cations resulting from diphenylmethane or related compounds are well known.[17] Szwarc and his co-workers[18] have shown that, in the presence of $SbCl_5$ at $-80°C$, DPE forms a charge-transfer complex ($\lambda_{max} = 465$ nm), which subsequently produces a $^{+}DPE-DPE^{+}$ dication (I). Olah et al.[19] have described the cation (II) and related ones; such cations are relatively stable at low temperatures.

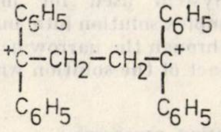

$^{+}C(C_6H_5)_2-CH_2-CH_2-C(C_6H_5)_2^{+}$

(I; $\lambda_{max.}$ =435 and 310 nm)

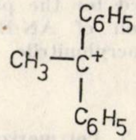

$CH_3-C^{+}(C_6H_5)_2$

(II; $\lambda_{max.}$ =425 and 315 nm)

In solutions containing DPE, its dimers are formed in the presence of Lewis acids such as $SnCl_4$, $BeCl_2$ or $AsCl_3$ at room temperature; two dimers, one linear — 1,1,3,3,-tetraphenyl-1-butene (III) and the other cyclic — 3-methyl-1,1,3-triphenylhydrinden (IV) were found.[20] The dimer (III) can isomerize into (IV) by heating in the presence of an acid catalyst.[20]

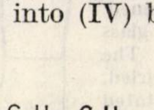

$(C_6H_5)_2C=CH-C(C_6H_5)_2-CH_3$

(III; mp =113°)

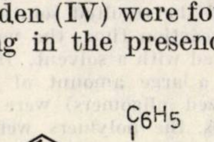

(IV; mp =143°)

We have found that in the presence of BF_3, DPE is transformed into a viscous solution from which, after dissolving in $CHCl_3$ and crystallization from CH_3OH, white crystals may be obtained in high yield; as these crystals have mp = 115°C and MW = 363, we think they consist likely of dimer (III). The same behaviour is found if instead of BF_3, the complex AN$-BF_3$ has been used (see table 1).

TABLE 1

Dimerization of DPE at 25°C; time 27 h

Initial molar fraction			Conversion *) (%)
BF_3	AN	DPE	
0.040	0.491	0.469	30.4
0.062	0.774	0.164	15.2

The production of the initial DPE cation could be the result either of the direct attack of BF_3 on DPE, or of the formation of a charge transfer complex between $AN-BF_3$ and DPE; the latter implies the production of the radical-cation (VIII).

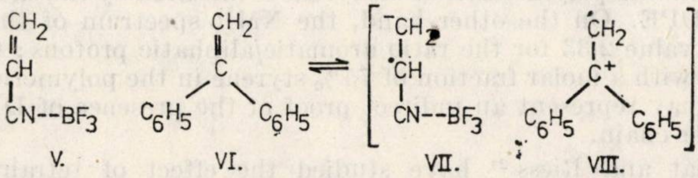

V. VI. VII. VIII.

The role of traces of water in the system, acting as cocatalysts, cannot be excluded; since styrene is very sensitive towards traces of water in cationic polymerization, experiments involving this monomer were also carried out (see table 2).

TABLE 2

Initial tests, involving the $AN-BF_3$ complex and styrene

	Monomers (nmol)			THF (nmol)	Time (min)	Temp. (°C)	Conversion (%)	[η] (dl/g)	Obs.
	AN	S	DPE						
1.	64.0	16.6	–	–	15	25	100	0.24	a, f
2.	60.2	14.8	–	–	5	70	92.3	0.19	a, f
3.	16.9	26.6	27.8	–	60	25	77.5	0.47	a, c, f
4.	13.8	30.1	19.3	–	60	25	106	0.47	a, d, f
5.	34.7	46.1	–	20.7	300	70	17.6	0.34	b, e, g

Observations:

a) Conversion referred to the initial styrene

b) Conversion referred to the initial ([S] + [AN])

c) All the bulbs were simultaneously broken

d) The bulbs containing $AN-BF_3$ and DPE, respectively were broken firstly; after 5 minutes, the bulb containing styrene was broken as well.

e) Styrene was previously mixed with THF

f) $AN/BF_3 = 46.7$

g) $AN/BF_3 = 12.2$

If the bulb containing AN$-$BF$_3$ mixture and the bulb with styrene were broken together, the only product of reaction should be polystyrene (experiments 1 and 2, table 2); the infrared spectra for the polymers obtained are identical with that of polystyrene. The presence of DPE does not hamper the cationic polymerization of styrene. If all the bulbs are simultaneously broken (experiment 3, table 2), the product of reaction is also polystyrene; the elemental analysis has indicated the absence of nitrogen.

In experiment 4 (table 2) the bulbs containing the mixture AN$-$BF$_3$ and DPE respectively were first broken; as usual, the red-orange cation (Likely VIII), characteristic of DPE ? has been formed. After five minutes, the bulb containing styrene was also broken; the colouration of the system disappeared instantaneously and the viscosity of the mixture increased with time. This fact, as well as the observed final conversion (106% with respect to the initial amount of styrene) seem to indicate that the cationic polymerization of styrene is initiated by the cation derived from DPE. On the other hand, the NMR spectrum of the product exhibits a value 2.33 for the ratio aromatic/aliphatic protons; this result may agree with a molar fraction of 75% styrene in the polymeric product. This fact may represent an indirect proof of the presence of DPE in the polystyrene chain.

Cerciat and Riess [21] have studied the effect of tetrahydrofuran (THF) in the copolymerization of AN$-$ZnCl$_2$ or MMA$-$ZnCl$_2$ complexes with styrene; small concentrations of THF of the same order as [ZnCl$_2$] have produced increases in the rate of copolymerization, which remains alternating in essence and hinders the development of cationic polymerization. In our subsequent experiment (5, table 2), the bulb containing styrene was first broken in THF; after homogenization, the bulb containing AN$-$BF$_3$ was broken as well and the ampoule kept at 70°C. The resulting polymer is soluble in toluene and chloroform and insoluble in methanol. The infrared spectrum of this polymer shows an intense peak at 2240 cm^{-1}, characteristic of nitrile group. A ratio aromatic/aliphatic protons $= 0.73$ was obtained by integration of the NMR spectrum; this value corresponds to 44% mole styrene units. These facts may be interpreted in the sense that styrene participates in a charge transfer complex, which is formed in small concentration; this complex has initiated the copolymerization, as no initiator has been used. THF, present in far larger amount than BF$_3$, seems not to hamper the formation of the charge transfer complex, but prevents the propagation of cationic species.

In our previous papers [1, 2] we have proposed the following general mechanism. A charge transfer complex could be formed starting from an acrylic monomer complexed with a Lewis acid and an electron-donor type monomer; the concentration of such a charge transfer complex would be very small, but however it can initiate a polymerization reaction. The type of this process (alternating copolymerization or cationic polymerization) depends on the nature of the donor monomer.

Taking into account that BF$_3$ is a stronger Lewis acid than, let us say, AlCl$_3$ or ZnCl$_2$, it is to be expected that the complex VII$-$VIII may be present in a significant concentration. Knowing also the inability of DPE to form homopolymers, we found it interesting to study the system AN$-$BF$_3$$-$DPE in attempt to verify our previous conclusion.

The previous experiments[4] regarding the radical copolymerization of DPE with AN were carried out at 80 °C, with a rather high concentration of AIBN. We have repeated the experiments involving the AN$-$DPE pair, this time at 70°C and $([AN] + [DPE])/[AIBN] = 10^3$; these new conditions represent a compromise between the appropriate conditions for the decomposition of AIBN and the low reactivity of the copolymerization system. The results are presented in figure 4; all copolymers obtained in the above described manner have practically equimolecular compositions.

We had expected that in the presence of the complex AN$-$BF$_3$ the overall copolymerization rate would have increased and that a more pronounced alternation would take place. The experiments performed did not agree with these initial suppositions.

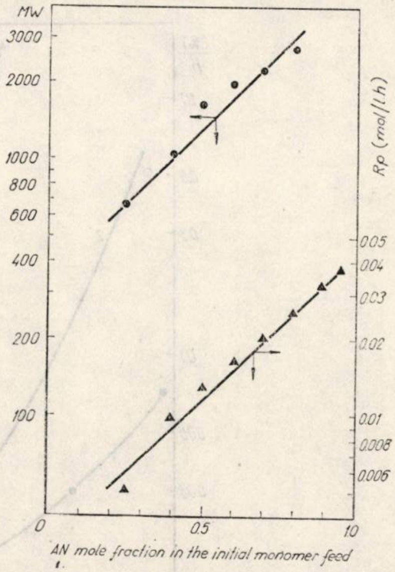

Fig. 4. — The dependence of molecular weight and copolymerization rate on the monomer feed composition for the free radical copolymerization of AN with DPE at 70°C.

Two reactions can take place in the system AN$-$BF$_3$$-$DPE; one is the copolymerization of the pair AN$-$DPE and the other is the dimerization of DPE. The reaction rate (%/h) against monomer feed composition is illustrated in figure 5. For the right branch (copolymerization) the conversion was determined by dividing the copolymer weight by the initial monomer amount, while for the left one (dimerization) the ratio was calculated only with respect to the initial DPE. The presence of BF$_3$ in the AN$-$DPE system causes a decrease of the copolymerization velocity. It may be seen from figure 5 that as the BF$_3$/AN ratio increases, the copolymerization rate decreases; this observation is in conflict with numerous reported experimental facts. Yabumoto et al.,[22] for instance, have shown that in the copolymerization of acrylonitrile with styrene, the copolymerization rate increases twelve times when a ratio ZnCl$_2$/AN $= 0.1$ is used in comparison to the copolymerization in the absence of the salt. The rate of copolymerization diminishes proportionally to the decrease of AN mole fraction in the initial monomer feed, for the same BF$_3$/AN ratio. On the other hand, this decrease is not monotonous; from a certain composition of the monomer feed, a new process, namely the dimerization of DPE, appears. As results from figure 5, the rate of dimerization increases with the content of DPE in the monomer feed; we have eventually obtained a straight line by using a semilogarithmic graph. Of course, the higher the initial BF_3/AN ratio, the faster the dimerization reaction.

The dimer has mp = 146°C and MW = 367; we therefore believe that the product can be identified as the dimer (IV). This substance is also characterized by a UV absorption at $\lambda_{max} = 235$ nm ($\varepsilon = 3.8\ 10^4$ $l.mol^{-1}.cm^{-1}$), value which is close to that found for DPE ($\lambda_{max} = 249$ nm and $= 2.81\ 10^4\ l.mol^{-1}\ cm^{-1}$).

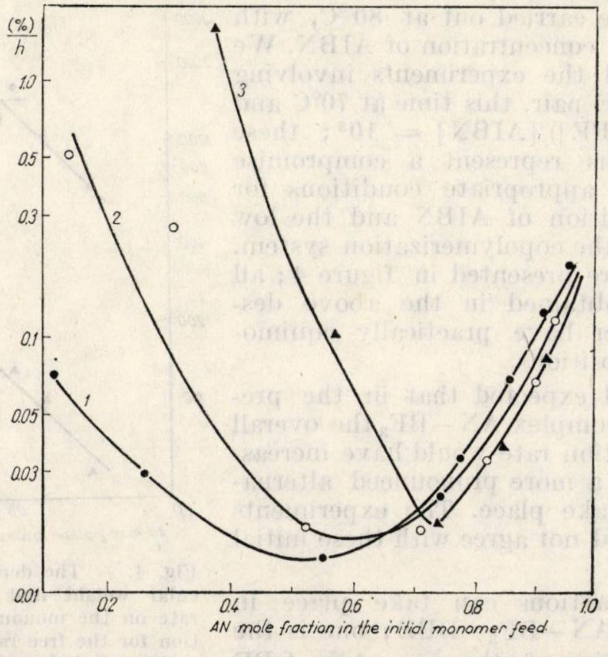

Fig. 5. — Copolymerization of DPE and AN (right branch of curves) and dimerization of DPE (left branch) in the system AN—DPE—BF_3 at 70°C ([AN] + [DPE])/[AIBN] = $= 10^3$; 1) AN/BF_3 = 46.7; 2) AN/BE_3 = 14.3; 3) AN/BF_3 = = 12.2.

We think that these experimental facts can be explained in the following manner. The equilibrium (V + VI ⇌ VII + VIII) is quickly established in the reaction mixture. Unlike other previously described systems, the radical-cation (VIII) is relatively stable; during the copolymerization process, (VIII) may react with a growing radical, or with a primary radical, to give the more stable structure (IX).

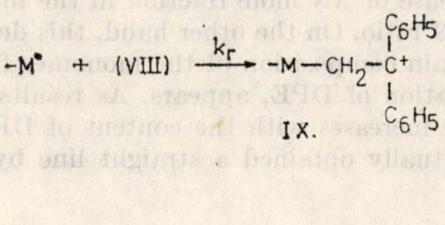

$$\sim M^{\bullet} + (VIII) \xrightarrow{k_r} \sim M-CH_2-\overset{C_6H_5}{\underset{C_6H_5}{C^+}}$$

IX.

This interpretation is in agreement with the fact that as the ratio BF_3/AN increases, the copolymerization rate decreases. If k_r has a high value, the concentration of (VIII) may be small; as a part of the propagating radicals are trapped, the copolymerization rate is slowed down. This explanation is also in agreement with our previous model.[1, 2]

REFERENCES

[1] Part IV : D. S. Vasilescu, *Rev. Roumaine Chim.*, **25**, 000 (1980).

[2] Part III : D. S. Vasilescu, *Rev. Roumaine Chim.*, **25**, 000 (1980).

[3] T. Fueno, T. Tsuruta and J. Furukawa, *J. Polymer Sci.*, **40**, 487 (1959).

[4] Part II. D. S. Vasilescu, *Rev. Roumaine Chim.*, **19**, 1637 (1974).

[5] K. Ito and Y. Yamashita, *J. Polymer Sci.*, *A-1*, **4**, 631 (1966).

[6] A. G. Evans, E. A. James and E. D. Oven, *J. Chem. Soc.*, **1961**, 3532.

[7] S. Penczek, J. Jagur-Grodzinski and M. Szwarc, *J. Amer. Chem. Soc.*, **90** 2174 (1968).

[8] H. Yuki, K. Kasai, S. Murahashi and J. Hotta, *J. Polymer Sci.*, B, **2**, 1121 (1964).

[9] T. Ikegami and H. Hirai, *J. Polymer Sci.*, *A-1*, **8**, 463, (1970).

[10] R. E. Uschold, *Macromolecules*, **4**, 552 (1971).

[11] A. L. Logothetis and J. M. McKenna, *J. Polymer Sci.*, *B*, **12**, 131 (1974).

[12] H. F. Mark, N. G. Gaylord and N. M. Bikales, "Encyclopedia of Polymer Science and Technology", vol. 13, Wiley, New York 1970, p 187.

[13] C. H. F. Allen and S. Converse, "Organic Syntheses", Coll 1, Wiley, New York, 1956, p. 226.

[14] M. Dimonie, D. S. Vasilescu and C. Oprescu (to Petrochemical Combinate — Pitești), Romanian Patent 67230, 9th June 1971.

[15] R. C. Weast (editor), "Handbook of Chemistry and Physics", 51st Edition, The Chemical Rubber Co., Cleveland, 1971, p. B—74.

[16] Y. Koma, S. Kondo and K. Iimura, *J. Polymer Sci.*, *B*, **12**, 133 (1974).

[17] G. Branch and H. Walba, *J. Amer. Chem. Soc.*, **76**, 1564 (1954).

[18] B. E. Fleischfresser, W. J. Cheng, J. M. Pearson and M. Szwarc, *J. Amer. Chem. Soc.*, **90**, 2172(1968).

[19] G. A. Olah, *J. Amer. Chem. Soc.*, **87**, 2 997 (1965).

[20] H. F. Mark, N. G. Gaylord and N. M. Bikales, "Encyclopedia of Polymer Science and Technology", vol. 5, Wiley, New York, 1969, p 121.

[21] B. Cerciat and G. Riess, *J. Polymer Sci.*, *B*, **10**, 879 (1972).

[22] S. Yabumoto, K. Ishii and K. Arita, *J. Polymer Sci.*, *A-1*, **7**, 1 577, (1969) ; **8**, 295 (1970).

Revue Roumaine de Chimie, 26, 2, 315–325 (1981)

QUANTITATIVE ANALYSIS OF CHROMATOGRAPHIC OBSERVATIONS

ALEXANDER J. CORPACIUS
Department of Biochemistry and Biophysics, University of Hawaii, Honolulu, Hawaii

Received May 5, 1979

THEORY OF THE METHOD

Introduction

The chromatographic techniques developed by the Linus Pauling Institute of Science and Medicine are designed for the analysis of urine, breath, blood and saliva. [1–15] These techniques lead necessarily to a very large amount of data due to the many compounds detected in each sample multiplied by the large number of samples involved in the diagnostic process. Obviously, the data are affected by errors coming from multiple sources. In an effort to simplify the overall error picture and to increase the accuracy of data, this paper suggests the elimination of the instrumental errors. If the computed errors are small enough to be negligible, the method would show that the chromatographic system provides highly accurate measurements and, therefore, no error adjustment is necessary. If, on the contrary, the computed errors are large enough to cast doubt on the medical diagnosis, [10] the following adjustment method should be considered.

URINE ANALYSIS

Two New Ideas

The first idea, which I call *the postulate of chromatography*, states that the quantitative value of a sample (S) is the sum of its chromatographic data (ΣCD) and its residual sample (RS), or

$$\Sigma CD + RS - S = 0 \tag{1}$$

The second idea states that chromatographic data enjoy two properties : (a) they are independent data, and (b) they satisfy *the postulate of chromatography*. Both ideas are a part of this theory.

A detailed expression of (1) defines the fundamental conditional equations (2):

$$
\begin{array}{lr}
[(a_1 + v_1^a) + (a_2 + v_2^a) + \ldots (a_n + v_n^a)] + (U_1 + v_1^u) - (S_1 + v_1^s) + \Delta = 0 & \\
[(b_1 + v_1^b) + (b_2 + v_2^b) + \ldots (b_n + v_n^b)] + (U_2 + v_2^u) - (S_2 + v_2^s) + \Delta = 0 & \\
\cdot\ \cdot\ \cdot\ \cdot\ \cdot\ \cdot\ \cdot\ \cdot\ \cdot\ \cdot\ \cdot\ \cdot\ \cdot\ \cdot\ \cdot\ \cdot\ \cdot\ \cdot\ \cdot\ \cdot\ \cdot\ \cdot\ \cdot\ \cdot & (2) \\
[(r_1 + v_1^r) + (r_2 + v_2^r) + \ldots (r_n + v_n^r)] + (U_r + v_r^u) - (S_r + v_r^s) + \Delta = 0 &
\end{array}
$$

where

$a_1, a_2 \ldots . a_n$
$b_1, b_2 \ldots . b_n$ are quantitative values of the chromatographic observations.
$\cdot\ \cdot\ \cdot\ \cdot\ \cdot\ \cdot$
$r_1, r_2 \ldots . r_n$
$U_1, U_2 \ldots . U_r$ are quantitative values of the residual urine.
$S_1, S_2 \ldots . S_r$ are quantitative values of the urine samples.
$v_1^a, v_2^a \ldots . v_n^a$
$v_1^b, v_2^b \ldots . v_n^b$ are unknown random errors attached to the chromatographic observations.
$\cdot\ \cdot\ \cdot\ \cdot\ \cdot\ \cdot$
$v_1^r, v_2^r \ldots . v_n^r$
$v_1^u, v_2^u \ldots . v_r^u$ are unknown random errors attached to the residual urine sample.
$v_1^s, v_2^s \ldots . v_r^s$ are unknown random errors attached to the urine sample.
Δ is an unknown systematic error of the chromatographic apparatus.
n is the number of volatile compounds in urine.
r is the number of urine samples.

Later, in this paper, the systematic error Δ will be numerically determined, as a proper unknown of the chromatographic apparatus. For the time being, it is convenient to eliminate Δ by combining the equations (2) in groups of two equations and subtracting them one from the other. The new type of conditional equations (which are – at least partially – independent of systematic influences of the apparatus) are presented below:

$$
\begin{array}{lr}
(v_1^a - v_1^b) + (v_2^a - v_2^b) + \ldots . (v_n^a - v_n^b) + (v_1^u - v_2^u) - (v_1^s - v_2^s) + w_1 = 0 & \\
(v_1^b - v_1^c) + (v_2^b - v_2^c) + \ldots . (v_n^b - v_n^c) + (v_2^u - v_3^u) - (v_2^s - v_3^s) + w_2 = 0 & \\
\cdot\ \cdot\ \cdot\ \cdot\ \cdot\ \cdot\ \cdot\ \cdot\ \cdot\ \cdot\ \cdot\ \cdot\ \cdot\ \cdot\ \cdot\ \cdot\ \cdot\ \cdot\ \cdot\ \cdot\ \cdot\ \cdot\ \cdot\ \cdot & (3) \\
(v_1^t - v_1^r) + (v_2^t - v_2^r) + \ldots . (v_n^t - v_n^r) + (v_t^u - v_r^u) - (v_t^s - v_r^s) + w_{r-1} = 0 &
\end{array}
$$

The free terms $w_1, w_2 \ldots . w_{r-1}$ are given by:

$$
\begin{array}{lr}
w_1 = (a_1 - b_1) + (a_2 - b_2) + \ldots . (a_n - b_n) + (U_1 - U_2) - (S_1 - S_2) & \\
w_2 = (b_1 - c_1) + (b_2 - c_2) + \ldots . (b_n - c_n) + (U_2 - U_3) - (S_2 - S_3) & \\
\cdot\ \cdot\ \cdot\ \cdot\ \cdot\ \cdot\ \cdot\ \cdot\ \cdot\ \cdot\ \cdot\ \cdot\ \cdot\ \cdot\ \cdot\ \cdot\ \cdot\ \cdot\ \cdot\ \cdot\ \cdot\ \cdot\ \cdot\ \cdot & (4) \\
w_{r-1} = (t_1 - r_1) + (t_2 - r_2) + \ldots . (t_n - r_n) + (U_{r-1} - U_r) - (S_{r-1} - S_r) &
\end{array}
$$

The structure and accuracy of the conditional equations (2) and (3) are important for the practicability of the mathematics to follow and for the validity of the final results of this analysis.

Since the number $r(n + 2)$ of the random errors v is always greater than the number r of samples, the system (3) is undetermined. In order to eliminate the indetermination and to compute the most probable values of v, the following function A is considered.

$$
\begin{aligned}
A = \Sigma v^2 & - 2K_1 \;[(v_1^a - v_1^b) + (v_2^a - v_2^b) + \ldots . (v_n^a - v_n^b) + (v_1^u - v_2^u) - \\
& \qquad - (v_1^s - v_2^s) + w_1] \\
& - 2K_2 \;[(v_1^b - v_1^c) + (v_2^b - v_2^c) + \ldots . (v_n^b - v_n^c) + (v_2^u - v_3^u) - \\
& \qquad - (v_2^s - v_3^s) + w_2] \\
& - 2K_3 \;[(v_1^c - v_1^d) + (v_2^c - v_2^d) + \ldots . (v_n^c - v_n^d) + (v_3^u - v_4^u) - \\
& \qquad - (v_3^s - v_4^s) + w_3] \\
& \cdot \; \cdot \; \cdot \; \cdot \; \cdot \; \cdot \; \cdot \; \cdot \; \cdot \; \cdot \; \cdot \; \cdot \; \cdot \; \cdot \; \cdot \; \cdot \; \cdot \; \cdot \; \cdot \; \cdot \; \cdot \\
& - 2K_{r-1}[(v_1^t - v_1^r) + (v_2^t - v_2^r) + \ldots . (v_n^t - v_n^r) + (v_t^u - v_r^u) - \\
& \qquad - (v_t^s - v_r^s) + w_{r-1}]
\end{aligned}
\tag{5}
$$

where

$K_1, K_2, \ldots . K_{r-1}$ are the Lagrange multipliers, or correlation factors, and Σv^2 is referred to as the sum of the squares of all corrections v. The same corrections v are written with subscripts and superscripts in the brackets of function (5).

The minimum condition applied to the function (5) gives the following explicit structures (6) of all random errors v in function of correlation factors K.

$$
\begin{array}{ll}
v_1^a = +K_1 & v_1^b = -K_1 + K_2 \\
v_2^a = +K_1 & v_2^b = -K_1 + K_2 \\
\cdot \; \cdot \; \cdot \; \cdot \; \cdot \; \cdot & \cdot \; \cdot \; \cdot \; \cdot \; \cdot \; \cdot \; \cdot \; \cdot \\
v_n^a = +K_1 & v_n^b = -K_1 + K_2 \\
v_1^u = +K_1 & v_2^u = -K_1 + K_2 \\
\underline{v_1^s = -K_1} & \underline{v_2^s = +K_1 - K_2} \\
\cdot \; \cdot \; \cdot \; \cdot \; \cdot \; \cdot & \cdot \; \cdot \; \cdot \; \cdot \; \cdot \; \cdot \; \cdot \; \cdot \\
\cdot \; \cdot \; \cdot \; \cdot \; \cdot \; \cdot & \cdot \; \cdot \; \cdot \; \cdot \; \cdot \; \cdot \; \cdot \; \cdot \\
v_1^t = -K_{r-2} + K_{r-1} & v_1^r = -K_{r-1} \\
v_2^t = -K_{r-2} + K_{r-1} & v_2^r = -K_{r-1} \\
\cdot \; \cdot \; \cdot \; \cdot \; \cdot \; \cdot \; \cdot \; \cdot \; \cdot \; \cdot & \cdot \; \cdot \; \cdot \; \cdot \; \cdot \; \cdot \\
v_n^t = -K_{r-2} + K_{r-1} & v_n^r = -K_{r-1} \\
v_{r-1}^u = -K_{r-2} + K_{r-1} & v_r^u = -K_{r-1} \\
\underline{v_{r-1}^s = +K_{r-2} - K_{r-1}} & \underline{v_r^s = +K_{r-1}}
\end{array}
\tag{6}
$$

The "v" expressions of (6) are introduced in the conditional equations (3) and a new general structure of normal equations of correlation factors is obtained.

The solution of the normal equations is given in (7) by the new developments of the correlation factors $K_1, K_2 \dots . K_{r-1}$ which are expressed in function of the free terms $w_1, w_2 \dots . w_{r-1}$ of the normal equations.

$$\begin{aligned} K_1 = & -\frac{1}{r(n+2)}[(r-1)w_1 + (r-2)w_2 + (r-3)w_3 + (r-4)w_4 + \\ & + (r-5)w_5 \dots . + 5w_{r-5} + 4w_{r-4} + 3w_{r-3} + 2w_{r-2} + w_{r-1}] \end{aligned}$$

$$\begin{aligned} K_2 = & -\frac{1}{r(n+2)}[(r-2)w_1 + 2(r-2)w_2 + 2(r-3)w_3 + 2(r-4)w_4 + \\ & + 2(r-5)w_5 \dots . + 10w_{r-5} + 8w_{r-4} + 6w_{r-3} + 4w_{r-2} + 2w_{r-1}] \end{aligned}$$

$$\begin{aligned} K_3 = & -\frac{1}{r(n+2)}[(r-3)w_1 + 2(r-3)w_2 + 3(r-3)w_3 + 3(r-4)w_4 + \\ & + 3(r-5)w_5 \dots . + 15w_{r-5} + 12w_{r-4} + 9w_{r-3} + 6w_{r-2} + 3w_{r-1}] \end{aligned}$$

$$\begin{aligned} K_4 = & -\frac{1}{r(n+2)}[(r-4)w_1 + 2(r-4)w_2 + 3(r-4)w_3 + 4(r-4)w_4 + \\ & + 4(r-5)w_5 \dots . + 20w_{r-5} + 16w_{r-4} + 12w_{r-3} + 8w_{r-2} + 4w_{r-1}] \end{aligned}$$

$$\begin{aligned} K_5 = & -\frac{1}{r(n+2)}[(r-5)w_1 + 2(r-5)w_2 + 3(r-5)w_3 + 4(r-5)w_4 + \\ & 5(r-5)w_5 \dots . + 25w_{r-5} + 20w_{r-4} + 15w_{r-3} + 10w_{r-2} + 5w_{r-1}] \end{aligned}$$

. . . . (7)

. . . .

$$\begin{aligned} K_{r-5} = & -\frac{1}{r(n+2)}[5w_1 + 10w_2 + 15w_3 + 20w_4 + 25w_5 \dots . + \\ & + 5(r-5)w_{r-5} + 4(r-5)w_{r-4} + 3(r-5)w_{r-3} + 2(r-5)w_{r-2} + (r-5)w_{r-1}] \end{aligned}$$

$$\begin{aligned} K_{r-4} = & -\frac{1}{r(n+2)}[4w_1 + 8w_2 + 12w_3 + 16w_4 + 20w_5 \dots . + \\ & + 4(r-5)w_{r-5} + 4(r-4)w_{r-4} + 3(r-4)w_{r-3} + 2(r-4)w_{r-2} + (r-4)w_{r-1}] \end{aligned}$$

$$\begin{aligned} K_{r-3} = & -\frac{1}{r(n+2)}[3w_1 + 6w_2 + 9w_3 + 12w_4 + 15w_5 \dots . + \\ & + 3(r-5)w_{r-5} + 3(r-4)w_{r-4} + 3(r-3)w_{r-3} + 2(r-3)w_{r-2} + (r-3)w_{r-1}] \end{aligned}$$

$$\begin{aligned} K_{r-2} = & -\frac{1}{r(n+2)}[2w_1 + 4w_2 + 6w_3 + 8w_4 + 10w_5 \dots . + \\ & + 2(r-5)w_{r-5} + 2(r-4)w_{r-4} + 2(r-3)w_{r-3} + 2(r-2)w_{r-2} + (r-2)w_{r-1}] \end{aligned}$$

$$\begin{aligned} K_{r-1} = & -\frac{1}{r(n+2)}[w_1 + 2w_2 + 3w_3 + 4w_4 + 5w_5 \dots . + \\ & + (r-5)w_{r-5} + (r-4)w_{r-4} + (r-3)w_{r-3} + (r-2)w_{r-2} + (r-1)w_{r-1}] \end{aligned}$$

The correlation factors (7) are then introduced in (6) for the computation of the random instrumental errors (6) for the computation of the random instrumental errors v.

Finally, without further explanation,

$$\begin{array}{l} A_1 = a_1 + v_1^a ; \quad A_2 = a_2 + v_2^a ; \; \ldots . \; A_n = a_n + v_n^a \\ B_1 = b_1 + v_1^b ; \quad B_2 = b_2 + v_2^b ; \; \ldots . \; B_n = b_n + v_n^b \\ \cdots\cdots\cdots\cdots\cdots\cdots\cdots\cdots\cdots \\ R_1 = r_1 + v_1^r ; \quad R_2 = r_2 + v_r^r ; \; \ldots . \; R_n = r_n + v_n^r \end{array} \tag{8}$$

where A_i, B_i, ... R_i $(i = 1, 2, \ldots . n)$ are the adjusted values of the chromatographic data and the problem is solved; the instrumental errors v are computed and eliminated from data.

DISCUSSION

This mathematical analysis produces two new and interesting peculiarities of the chromatographic data. (However, such peculiarities are known in the Theory of Errors.) According to (6), the errors v of each individual sample are equal; that is:

$$\begin{array}{l} v_1^a = v_2^a = v_3^a \ldots . = v_n^a \text{ are the equal errors of sample } a. \\ v_1^b = v_2^b = v_3^b \ldots . = v_n^b \text{ are the equal errors of sample } b. \\ \cdots\cdots\cdots\cdots\cdots\cdots\cdots\cdots\cdots \\ v_1^r = v_2^r = v_3^r \ldots . = v_n^r \text{ are the equal errors of sample } r. \end{array} \tag{9}$$

Moreover, (6) shows that the total sum of the errors v of the entire group of samples is zero; that is:

$$\sum_{i=1}^{n} v_i^a + \sum_{i=1}^{n} v_i^b + \cdots \sum_{i=1}^{n} v_i^r = 0 \tag{10}$$

Consequently, according to (9), the errors v of each individual sample have a systematic behavior, and according to (10), the errors v of the entire group of samples have a Gauss' or a normal random distribution.

The maximum relative probable error of a single sample found earlier (by Robinson and Pauling, [2] p. 43, and , [10] p. 963, and by Robinson et al., [4] p. 23) is in agreement with (9).

The heart of this study is the totally new idea expressed in (1) which characterizes any chromatographic process. This idea should be accepted universally as a *postulate of chromatography* which leads to the fundamental equations (2). The succeeding mathematics are a rigorous and a tested validity of the classical development of equation (2). Also the generality and yet the practicability of all equations in this paper are due to (2).

The accuracy of the system is improved by the adjustment in a block of all chromatographic data. In this way the bias errors have a better chance to cancel each other, while the overall random errors are numerically determined and eliminated from data. Moreoever, the adjustment in a block would make possible the development of a rigorous study of the error propagation throughout the chromatographic system without resorting to assumptions and/or hypothesis. Classical tools of the Theory of Probability are used throughout. The values (6) are the most probable corrections to all rough chromatographic observations for obtaining the final, improved results (8). The overall mathematical analysis is general and practical; it accepts, for handling, any amount of data and any number of samples.

It should be pointed out that an increasing amount of samples leads to an increasing number of normal equations, hence to increasing difficulty in solving those equations.

The first concern regarding this difficulty was expressed by C. F. Gauss (1777—1855) who did something about it. He discovered the classical Gauss Algorithmus, which is the standard method of solving by hand a large number of normal equations. About 60 normal equations is the largest aggregate ever handled by Gauss Algorithmus.

The high speed computer of our time can handle 2 000—3 000 normal equations.

This study shows that the normal equations do not require any handling. Their general solution is already available in (7), for any number of normal equations. The computations indicated by (7) are algebraic sums of double and triple products only. The simplicity of these computations should indicate that a relatively small computer can handle the computational work load of many thousand normal equations. The developments (7) show a new canonic structure which obviates the laborious and difficult computations of inverting the matrix of a large number of normal equations. A medium size electronic computer should be able to accept the simple algebra of (7) for handing the chromatographic observations of a very large population.

A thorough checking of the mathematics involved in this study is necessary and can be easily performed with the help of (2) and (8). Notice that the only unknown in (2) is the proper systematic error Δ which is still undetermined. The checking consists in obtaining the same value for Δ from each equation (2). After introducing (8) in (2) and after each equation in (2) is solved for Δ, the following equalities are obtained:

$$\begin{aligned}
\boldsymbol{\Delta} &= S_1 - \left(U_1 + \sum_{i=1}^{n} A_i \right) \\
&= S_2 - \left(U_2 + \sum_{i=1}^{n} B_i \right) \\
&= S_3 - \left(U_3 + \sum_{i=1}^{n} C_i \right) \qquad (11) \\
&\cdots\cdots\cdots\cdots\cdots\cdots \\
&= S_r - \left(U_r + \sum_{i=1}^{n} R_i \right)
\end{aligned}$$

The calculus of this analysis and its computer programming are correct if the equalities (11) are rigorously satisfied.

According to this theory, the limitation of chromatographic systems is not only their resolution error (Robinson et al. [4]), but also the quantitation error of samples and samples residues. However, the limitation, or the virtue of chromatographic systems can be uniquely illustrated by their standard deviation; and, the following formula of the standard deviation is one of the products of this theory. But more to my point, one of the immediate and most important practical realities of this theory is the possibility of computing the standard deviation SD of chromatographic data with the help of the formula

$$\mathrm{SD} = \pm\sqrt{\frac{\sum v^2}{r-1}} \tag{12}$$

where $\sum v^2$ is referred to the total number of errors v, and r is the number of samples. Based on all I know about data processing and statistical analysis of data, (12) is the first ever, correct and rigorous formula[16] for computing standard deviation of chromatographic systems.

Because of its singularity $\mathrm{SD} = \pm\infty$ when $r = 1$, the standard deviation can be computed for any number of samples $r > 1$. This standard deviation is the most powerful tool mathematics can offer for assessing the reability of chromatographic systems, pattern recognition, and medical diagnosis. In our computerized world, when at least a small computer is available everywhere, the computation of standard deviation should always be considered, for giving more scientific authority and more practical meaning to chromatographic analysis in relation to health and disease of body and mind, to quantitative analysis of amino acid composition, and other chromatographic applications.

Finally, it should be pointed out that the standard deviation of the adjustment in a block *is the same* for all data involved. This, of course, makes the medical diagnosis more reliable.

APPLICATION

The materials used for analysis and calculation were 1) standard amino acid mixture purchased from Beckman-Spinco Instruments Company and 2) pseudomona putida cytochrome P-450 isolated as described by Gunsalus and Wagner. [17] The analysis was performed with a Beckman-Spinco Model 121 automatic amino acide analyzer to determine the amino acid composition of both materials.

Table 1 illustrates the detailed amino acid composition of these materials. Note that the samples (column II and III) are quite different as far as number and sequence of amino acids are concerned. As already pointed out earlier in this study, these and/or other structural differences among samples do not affect the validity, the prosecution and the results of computation.

TABLE 1

Amino acid composition of the samples

No.	Standard amino acid mixture	*Pseudomona Putida* P-450
I	II	III
1	Aspartic Acid	Asparagine and/or Aspartic Acid
2	Threonine	Threonine
3	Serine	Serine
4	Glutamic acid	Glutamine and/or Glutamic Acid
5	Proline	Proline
6	Glycine	Glycine
7	Alanine	Alanine
8	Cystine	Valine
9	Valine	Isoleucine
10	Moethionine	Leucine
11	Isoleucine	Tyrosine
12	Leucine	Phenylalanine
13	Tyrosine	Lysine
14	Phenylalanine	Histidine
15	Lysine	Arginine
16	Ammonia	
17	Histidine	
18	Tryptophan	
19	Arginine	

Table 2 shows nine distinct groups of computation (column I) which represent a wide variety of sample combinations (column II). We built and performed these nine separate groups of computation — totaling 41 samples and 718 data — in order to prove the generality, the versatility, and the practicability of the method. The different time interval of sample analyses is also presented (column III). Both systematic error Δ (column IV) and standard deviation SD (column V) are two of three items computed by this method. The third item is random error "v" which is attached to each of 718 amino acids (column VI) entering the nine groups of computation.

Table 3 and 4 are intended to show that this computation method leads to improved data. From the bulk of 41 samples, we selected two standard samples. The first sample, table 3 (column III) is one of the most accurate amino acid analyses of our entire body of data, while the second sample, table 4 (column III) is less accurate. Moreover, each of the 19 amino acids of this mixture is in amount of 50 nano moles/milliliter except Cystine which is in amount of 25 nano moles/milliliter.

TABLE 2

Groups of computation and results

No. of groups I	No. of samples in each group II	Time of analysis performed III	Computed Δ nanomoles IV	Computed standard deviation SD nanomoles V	No. of amino acids VI
1	7 standard samples	5.22.79—6.6.79	−0.45860	± 4.76464	133
2	9 standard samples	8.6.79—8.22.79	−0.27435	±14.19112	171
3	13 P-450 samples	8.31.79—9.8.79	−0.04198	±12.35367	195
4	20 samples (No. 1 + No. 3)		−0.21092	±10.21169	328
5	29 samples (No. 1 + No. 2 + No. 3)		−0.23257	±11.32766	499
6	3 standard samples	8.29.79—9.10.79	−0.78988	± 3.41584	57
7	9 standard samples	8.24.79—9.14.79	+3.42539	± 3.93202	162
8	12 samples (No. 6 + No. 7)		+2.34309	± 9.04424	219
9	41 samples (No. 1 + No. 2 + No. 3 + No. 6 + No. 7)		+0.56159	±11.73806	718

TABLE 3

A standard mixture and its amino acid rough and computed data

No. I	Amino acid II	Rough data a_i nM III	$a_i - 50$ IV	$(a_i - 50)^2$ V	Computed data A_i nM VI	$A_i - 50$ VII	$(A_i - 50)^2$ VIII
1	Aspartic acid	50.9460	+0.946	0.8949	50.6474	+0.6474	0.4191
2	Threonine	50.4590	+0.459	0.2107	50.1604	+0.1604	0.0257
3	Serine	50.3940	+0.394	0.1552	50.0954	+0.0954	0.0091
4	Glutamic acid	49.8040	−0.196	0.3842	49.5054	−0.4946	0.2446
5	Proline	49.3610	−0.639	0.4083	49.0624	−0.9376	0.8791
6	Glycine	48.4260	−1.574	2.4775	48.1274	−1.8726	3.5254
7	Alanine	46.4120	−3.588	12.8737	46.1134	−3.8866	15.1057
8	Cystine	22.2380	−2.762	7.6286	21.9394	−3.0606	9.3673
9	Valine	50.9900	+0.990	0.9801	50.6914	+0.6914	0.4780
10	Methionine	49.3030	−0.697	0.4858	49.0044	−0.9956	0.9912
11	Isoleucine	50.0330	+0.033	0.0011	49.7344	−0.2656	0.0771
12	Leucine	49.9210	−0.079	0.0062	49.6224	−0.3776	0.1426
13	Tyrosine	49.2590	−0.741	0.5491	48.9604	−1.0396	1.0808
14	Phenylalanine	49.1720	−0.828	0.6856	48.8734	−1.1266	1.2692
15	Lysine	51.4510	+1.451	2.1054	51.1524	+1.1524	1.3280
16	Ammonia	66.6030	+16.603	275.6596	66.3044	+16.3044	265.8335
17	Histidine	49.6470	−0.353	0.1246	49.3484	−0.6516	0.4246
18	Tryptophan	48.5190	−1.481	2.1934	48.2204	−1.7796	3.1670
19	Arginine	47.7360	−2.264	5.1257	47.4374	−2.5626	6.5669
				$\Sigma = 312.9497$			$\Sigma = 310.9349$

We substracted 50 nano moles (25 nano moles for Cystine) from both rough data (column IV) and computed data (column VII). We also built the squares of these differences (column V and VIII) and their sum. Based on $\sum (a_i - 50)^2 > \sum (A_i - 50)^2$ which is valid for both samples we conclude that *computed data is improved data.*

TABLE 4

A standard mixture and its amino acid rough and computed data

No.	Amino acid	Rough data a_i nM	$a_i - 50$	$(a_i - 50)^2$	Computed data A_i nM	$A_i - 50$	$(A_i - 50)^2$
I	II	III	IV	V	VI	VII	VIII
1	Aspartic acid	49.0170	−0.983	0.9663	51.0544	+1.0544	1.1118
2	Threonine	48.7920	−1.208	1.4593	50.8294	+0.8294	0.6879
3	Serine	50.0470	+0.047	0.0022	52.0844	+2.0844	4.3447
4	Glutamic Acid	46.9970	−3.003	9.0180	49.0344	−0.9656	0.9324
5	Proline	41.2980	−8.702	75.7248	43.3354	−6.6646	44.4169
6	Glycine	41.8320	−8.168	66.7162	43.8694	−6.1306	37.5843
7	Alanine	29.7320	−20.268	410.7918	31.7694	−18.2306	332.3548
8	Cystine	18.0190	−6.981	48.7344	20.0564	−4.9436	24.4392
9	Valine	72.6470	+22.647	512.8866	74.6844	+24.6844	609.3196
10	Methionine	47.4350	−2.565	6.5792	49.4724	−0.5276	0.2784
11	Isoleucine	49.7260	−0.274	0.0751	51.7634	+1.7634	3.1096
12	Leucine	49.9580	−0.042	0.0018	51.9954	+1.9954	3.9816
13	Tyrosine	47.9400	−2.060	4.2436	49.9774	−0.0226	0.0005
14	Phenylalanine	47.8260	−2.174	4.7263	49.8634	−0.1366	0.0187
15	Lysine	49.9330	−0.067	0.0045	51.9704	+1.9704	3.8825
16	Ammonia	46.2790	−3.721	13.8458	48.3164	−1.6836	2.8345
17	Histidine	50.2500	+0.250	0.0625	52.2874	+2.2874	5.2322
18	Tryptophan	48.6820	−1.318	1.7371	50.7194	+0.7194	0.5175
19	Arginine	49.8800	−0.120	0.0144	51.9174	+1.9174	3.6764
			$\Sigma =$	1157.5899		$\Sigma =$	1078.7235

This method is particularly suited as a tool for automatic data analysis of biological processes.

Additional work needs to be done regarding some possible computation refinements.

ACKNOWLEDGEMENTS. To Dr. K. T. Yasunobu, Chairman of the Department, I am deeply thankful for his constructive cooperation and help during the prosecution of this work.

To Dr. Ming-Pi Mi, Director, Data Resources of The Cancer Center of Hawaii, University of Hawaii, I am most grateful for the computer programming and for the generous permission to use the computing facilities of the Cancer Center.

To Mr. Bryd M. Ball, IBM Branch Manager, Honolulu, who previously performed the checking of the canonic structure (7), by using an IBM-APL Small Computer.

REFERENCES

[1] L. Pauling, A. B. Robinson, S. S. Oxley, M. Bergson, A. Harris, P. Cary, J. Blethen and I. T. Keaveny, In David Hawkins and Linus Pauling, eds., "Orthomolecular Psychiatry", W. H. Freeman, San Francisco 1973, pp. 18—33.

[2] A. B. Robinson and L. Pauling, In David Hawkins and Linus Pauling, eds., "Orthomolecular Psychiatry", W. H. Freeman, San Francisco, 1973, pp. 35—53.

[3] A. B. Robinson and F. C. Westall, *J. Ortho. Psych.* **3**, 70 (1974).

[4] A. B. Robinson, D. Partridge, M. Turner, R. Taranishi, and L. Pauling, *J. Chromatog.*, **85**, 19 (1973).

[5] K. E. Matsumoto, D. H. Partridge, A. B. Robinson, L. Pauling, R. A. Flath, R. Mon, and T. Teranishi, *J. Chromatog.*, **85**, 31 (1973).

[6] A. Harris, A. B. Robinson and L. Pauling, *J. Int. Res. Comm.*, **24** 1—10, (1973).

[7] A. B. Robinson, I. T. Keaveny, and L. R. Robinson, *J. Int. Res. Comm.*, **1**, 25 (1973).

[8] A. B. Robinson, P. Cary, B. Dore, I. Keaveny, L. Brenneman, M. Turner, and L. Pauling, *J. Int. Res. Comm.*, **1**, 47 (1974).

[9] A. B. Robinson, F. C. Westall, and G. W. Ellison, *Life Science*, **14**, 1747 (1974).

[10] A. B. Robinson and L. Pauling, *Clinc. Chem.*, **20**, 961 (1974).

[11] H. Dirren, A. B. Robinson, and L. Pauling, *Clin. Chem.*, **21**, 1970 (1975).

[12] A. B. Robinson, M. Weiss, W. R. Reynolds and L. R. Robinson, *Proc. Am. Soc. Mass. Spect.* (May 1975).

[13] A. B. Robinson, R. Willoughby, and L. R. Robinson, *Esp. Geront.*, **11**, 113 (1976).

[14] A. B. Robinson, H. Dirren, A. Sheets J. Miquel, and R. Lundgren, *Esp. Geront.*, **11**, 11 (1976).

[15] R. N. Rosenberg, A. B. Robinson, and D. Partridge, *Clin. Biochem*, **8**, 365 (1975).

[16] F. R. Helmert, "Die Ausgleichungsrechnung nach der Methode der Kleinsten Quadrate", Zweite Auslage, Druck und Verlag von B. A. Teubner, Leipzig 1907, S. 578.

[17] I. C. Gunsalus and A. C. Wagner, *Methods in Enzymology*, **52**, 166 (1978).

Revue Roumaine de Chimie, **26**, *2*, 327—330 (1981)

COMPTES RENDUS

H. DASCH (Editor), "Neutron Diffraction", Springer-Verlag Berlin—Heidelberg—New York, 1978, 357 pages (Volume 6 in the series "Topics in Current Physics").

The sixth volume edited by Hans Dachs in the authoritative Springer-Verlag series "Topics in Current Physics" is entitled "Neutron Diffraction", and deals both with theoretical and practical aspects of this important investigation tool, very useful for a more accurate knowledge of the structure of condensed matter. The volume has 9 papers and a subject index.

The first paper (Principles of Neutron Diffraction, written by Hans Dachs, 40 pages, 22 figures and 72 references) presents comparatively the differences and similitudes between X-ray and neutron diffraction. The different types of interactions of neutrons and X-rays with the condensed matter, the general theory of neutron diffraction and the different experimental techniques are presented.

The second paper (Polarized Neutrons, written by J.B. Hayter, 29 pages, 6 figures, and 84 references) describes the production, handling and possible applications of polarized neutrons. The theoretical and experimental grounds of the investigation of magnetic materials by polarized neutrons are presented.

The third paper (Combining X-Ray and Neutron Diffraction : The study of Charge Density Distributions in solids, written by P. Coppens, 41 pages, 10 figures, 129 references) emphasizes the importance of a complementary use of X-ray and neutron diffraction for ascertaining the crystalline and electronic structure of solids. The results obtained by combining the X-ray and neutron diffraction for the evaluation of charge density distribution in solids are examined.

The fourth paper (The Determination of Magnetic Structures, written by Prandl, 37 pages, 7 figures, 67 references) deals with one of the most important applications of neutron diffraction : the determination of magnetic structure, *i.e.* of the distribution of magnetic moments in the magnetically ordered materials. A clear and concise review of the magnetic point groups and magnetic space groups is made, too.

The fifth paper (Disordered structures, written by W. Schmatz, 46 pages, 30 figures and 109 references) reviews the elastic and quasielastic scattering of neutrons in disordered structures. A discussion is made on the theoretical and experimental aspects of this subject.

The sixth paper (Phase Transitions and Critical Phenomena, written by P.A. Lindgard, 46 pages, 10 figures, 88 references) shortly reviews the theories of phase transitions and critical phenomena, then discusses the implications of these phenomena occurring in different classes of materials on the neutron diffraction patterns, showing that the neutron diffraction study has brought a more intimate knowledge on this subject.

The seventh paper (Application of Neutron Diffraction to Biological Problems, written by G. Zaccaï, 27 pages, 14 figures 34 references) presents the fundamentals of biological uses of neutron diffraction discussed on real examples. The important techniques used in these studies, *i.e.* for the investigation of single crystals, oriented systems and suspensions are presented.

The eighth paper (Liquid Structure Investigation by Neutron Scattering, written by P. Chieux, 32 pages, 8 figures, 50 references) emphasizes the important role played by the neutron diffraction in the understanding of liquid structures. The theoretical and experimental problems of the interpretation of neutron diffraction patterns of liquids are presented, and the advantages of the isotopic substitution and the concentration methods are discussed.

The ninth paper (Dynamical Neutron Diffraction and Its Applications, written by H. Rauch and D. Petrascheck, 49 pages, 31 figures, 116 references) clearly describes the theory of Dynamical Neutron Diffraction and the uses of neutron diffraction for nuclear and solid state — physics investigations.

All papers in this book deal both with theoretical and experimental aspects of the discussed matters and the reviews are clearly and concisely updated. Therefore, the book is a very useful tool for neutron diffraction investigators. Besides, it brings much relevant information for those interested in using neutron diffraction for new applications, and even for beginners in this field.

Dorel Crişan

Ş. MOLDOVEANU and A. SAVIN, "Aplicaţii în chimie ale metodelor semiempirice de orbitali moleculari" (Chemical Applications of the Semiempirical MO Methods), Editura Academiei R. S. România, Bucharest, 1980, 285 pages.

"*Semiempirical* is a word", a known chemist has once remarked, "that tends to make pure quantum chemists irascible and pure experimentalists suspicious". A semiempirical method may indeed be criticizable from the point of view of the rigorous theoretician, but the fact is that it works. This is good news — the more so in a field such as quantum chemistry, where the intricacy of the problems and the difficulties involved in solving them computationally are formidable. Out of the large number of molecular systems known today, only a tiny fraction has been amenable to exact quantum treatment ; these are generally molecules with two or at most three or four atoms. For somewhat larger molecules, approximate methods have to be compulsorily used — and the degree of approximation increases quite fast with the number of atoms. The variety of the approximations' nature, as well as the current easy availability of computers have encouraged "semiempirical" quantum chemists to work out a large spectrum of approximate methods, in which pure quantum chemical procedures are so blended with various experimental data as to give plausible values for other data and for as wide a class of molecules as possible. The experimental data referred to above are taken as pivotal criteria for refining and "fixing" the parameters involved in the quantum equations. The method so adjusted may then be confidently used for predicting some properties of other molecules.

Such methods, though resorting to a heterogeneous, unrigorous approach, have produced satisfactory results so far — in some cases even surprisingly good results — for many molecular systems, including very complex systems such as the biological ones. They have been thus very useful in accounting for many unknown properties of these systems, and in predicting their behaviour under different conditions. In any case, the results may well be taken as a basis for further investigation of the system. The clues provides by the MO calculations, even if only approximate and qualitative, may be used in studies of a largely varied nature. Unlike the *ab initio* MO methods, the semiempirical ones can be applied to reasonably large molecules, to systems which sometimes are very close to the real ones.

The number of books devoted tc approximate methods in quantum chemistry is already quite large and increasing. Any new book on this subject has therefore to be endowed with particular and valuable assets in order to be able to make a real impact upon the development of the field.

The book of Drs. Şerban Moldoveanu and Andrei Savin, from the Polytechnic Institute of Bucharest, dealing specifically with the semiempirical molecular orbital methods and their application in chemistry, has not only one, but two such assets — it is the first book of its kind wholly conceived and written by Romanian researchers and, more important, it is a very good book, even if compared to authoritative texts such as that of Pople and Beveridge or that edited by Segal.

The book begins with a short introduction in the theory of the electronic structure of molecules, then the LCAO-SCF method is treated in detail, based on Roothaan's equations. The main approximate methods of solving them for complex molecular systems are dealt with in Chapters 3 and 6. The systematics of these methods revolves around the various degrees of neglect of the differential overlap between the atomic orbitals involved in a given molecule. Under this heading, the NDDO, CNDO, INDO and PPP methods are reviewed, with due regard to the invariance properties of the equations. Another group of approximate methods treated is that of Hückel, both simple and extended. The semiempirical methods with complete overlap are also mentioned. Various procedures used for simplifying the computation of the multicentric integrals are given, and so is the alternative way of parametrizing and estimating directly the Fock matrix elements. As an example of this latter method, we should mention the TOM method, due in part to one of the authors. The comments on the equivalence between the ZDO-type methods and the complete-overlap methods are very instructive. Details on the nature of the approximations used in each case are given. Since the values of the various parameters are also quoted, any of the methods included can be effectively applied by the interested reader.

Other chapters are devoted to the computation of the molecular integrals for various types of AO's, and to the estimation of the mono-, bi- and multicentric terms in the expression of the electronic energy. Chapter 7 is devoted to the calculation of various physical and chemical properties of substances, using semiempirical methods : determination of equilibrium conformations, heats of formation and atomization, heats of reaction, activation energies, ionization potentials and electron affinities, energy of electronic transitions, electric dipole moments, intensities of infrared transitions, polarizabilities, hyperfine splitting constants in ESR spectra, screening and coupling constants in NMR spectra, reactivity indices, etc. The discussion of the results is critical. (A more thorough comparison of the performance of various methods in this respect would have been nevertheless helpful.) It is comforting to see that many results cited are due to Romanian researchers and that the authors themselves must be credited with a substantial contribution to the field. The final part of the book offers an original version of a computer program based on the CNDO/SW method and suitable for molecules enclosing elements from H to I in the periodic table (except transition metals). The program is written in FORTRAN and was run successfully on the Felix C-256 computer (72K core memory). Finally, an alphabetical index is an aid for locating various items, and the references given at the end of each chapter send the reader to further reading if interested.

As stated above, this is, in the opinion of the reviewer (and of his colleagues working in quantum chemistry) a valuable book. It brings together nearly all the semiempirical methods of quantum chemistry available today, providing all the relevant details and parameters. An extensive chapter is devoted to the approximate calculation of various physico-chemical properties of molecular systems. Moreover, the methods enclosed are treated unitarily and coherently, and the mathematical aspects are fully discussed. The reader has thus on his (or her) desk a self-contained monograph, a real guide, comprising all the necessary data for carrying out computations on real chemical systems.

Alex. Butucelea

BRUNO VOLLMERT, "Grundriss der makromolekularen Chemie", E. Vollmert-Verlag, Karlsruhe, 1979, 1 174 p.

A new edition of the book "Grundriss der makromolekularen Chemie" by Prof. B. Vollmert appeared in Karlsruhe. Both the first edition and the English translation published in the Springer Publishing House in 1962 and 1973, respectively, are well known in our country. Extended and brought up to date, the book represents an excellent universitary textbook of macromolecular chemistry and physical chemistry in which all contributes to the achievement of a work that offers a rapid, accessible and valuable information, beginning with the tackling of the problems and ending with the material disposal in small volumes easy to handle.

The book consists of five volumes with 1 174 pages, 328 figures, 56 tables, about 2 000 references and a subject index. In the broaching manner chosen by the author the attention is paid primarily to the general principles, types of the obtaining reactiones and structures common either to the macromolecular compounds or to a larger polymer group, without treating certain polymers (obtaining, properties etc.).

Typical examples are given which help the reader in familiarizing with the macromolecular compounds particularly important for technical and biological purposes. Thus, by discussing the correlation between the viscoelasticity and the structure of thermoplastic materials some problems regarding the working by injection are elucidated while on the polymerization kinetics the optimizing of technical control of polymerization processes is based.

In the first two volumes the obtaining of polymers is treated while the properties and structural aspects are described in the following two. A short chapter discussing the general structural principles of the polymers is placed before the chapters of polymer syntheses thus allowing a better understanding of the latter.

The obtaining reactions of the macromolecular compounds are divided into two groups : radicalic and ionic chain reactions (vol. I) and reactions of the functional groups (vol. II). A particular attention is paid to the chapter devoted to copolymerization reactions and to the methods of studying the copolymer composition in agreement with their increasing importance for the modern macromolecular chemistry. A large space is given in the second volume to the enzymatic syntheses of nucleic acids and proteins. The overwhelming importance of these syntheses for the living cell as well as their correlation with genetic code entirely justifies the author's attention to these syntheses.

The part devoted to the obtaining of macromolecular compounds ends with a discussion on the polymer reactions which are classified into reactions proceeding with degradation and reactions without modification of the chain length.

In the third volume the properties of the free molecule (macromolecule size and shape) are studied. The chemical and physical methods of determining the molecular weight and the molecular weight distribution are described. The ideal and real random coil is described quantitatively by means of the probabilistic calculation.

In the forth volume the properties of the macromolecules in associated states are treated, namely the macromolecular aggregation states : macromolecular solutions, the gel, highly elastic and glass states. The crystalline state, its morphology and the correlation between the structure and properties are also discussed. Finally the biphase macromolecular systems such as polymers resistant to shock, containing a highly elastic phase, reinforcing polymers as well as the incompatibility problem are treated in short.

The last volume includes the references, a list of the formula and symbols used and a subject index. Besides the literature cited within the text, the author also gives a rich list of monographs and review papers grouped in the same manner as the book content.

The new edition also includes in the fifth volume a list of the commercial names of the principal macromolecular compounds, their constitution and applications as well as the supplying firm.

As regards the nomenclature used, the author generally respects the recommendations of the Nomenclature Commission although he does not give up entirely some usual denominations which would have made the text understanding more difficult.

By the information offered as well as by the impulse to understanding through personal thinking efforts the new edition of the book "Grundriss der makromolekularen Chemie" is particularly useful to those studying the macromolecular chemistry as well as to the industry specialists eager to inform themselves in the macromolecular chemistry fields.

Mihai Dărângă

B. E. READ and G. D. DEAN, "The Determination of Dynamic Properties of Polymers and Composites", Adam Hilger Bristol, 1978, 207 p.

Obtaining new materials with improved physical properties represents a major target of materials science and technology, and the case of the mechanical properties of polymeric materials and composites seems to be one of the most significant and intricate in the field.

The text describes relevant details on several tests and methods developed at the National Physical Laboratory for measuring the dynamic mechanical properties of polymeric materials over a wide range of frequencies and temperatures.

The dynamic mechanical properties of polymers are of considerable fundamental and practical significance. As is well known, they can not only provide a valuable insight into various important aspects of polymer structure but can yield a convenient measure of polymer transition temperatures, fatigue and impact resistance. Moreover, the dynamic mechanical properties of materials are also highly important and are used in applications concerned with structure borne sound for damping.

As a rule, particular attention is paid to the range of linear properties (low-strain mechanical behaviour of linear viscoelastic type) when each test method can be readily handled in relation to the attainable accuracy.

In the first chapter a general introduction is given, a particular attention being paid to the presentation of the physical significance of several dynamic viscoelastic quantities.

The individual techniques are then discussed successively in chapters 2 to 7 (forced non-resonance method, torsion pendulum, audiofrequency resonance methods, flexural resonance, torsional and longitudinal resonance, and the ultrasonic immersion method) and for each the test equipment is described and the underlying theory systematically reviewed on the basis of a pertinent criticism.

Moreover, the limitations and approximations in each case are presented, and the external sources of error are individually discussed and correction procedures suggested.

The lack of awareness of the contributing sources of error in many published data as well as the large discrepancies observed between the data obtained by different techniques or laboratories are discussed in chapter 8, when results obtained by the various techniques are correlated for a selected range of materials.

Intended to serve as a basic guide to all those concerned with the use and development of dynamic mechanical test methods, the monograph, written by two well-known authorities in the field and containing a lot of original as well as previously unpublished results, should be of the greatest assistance to materials research workers in universities, research and industrial laboratories.

Horia Paven

NOTE POUR LES AUTEURS

La Revue Roumaine de Chimie publie des articles en anglais, français, russe, allemand ou espagnol. Les auteurs sont priés d'envoyer des articles et des comptes rendus inédits.

Les manuscrits seront dactylographiés à double interligne. La bibliographie, les tableaux et la légende des figures seront placés après le texte.

Si l'article fait partie d'une série numérotée, le titre de la partie précédente sera indiqué dans une note au bas de la première page.

Chaque article sera précédé d'un résumé comprenant quinze lignes au maximum.

Les références bibliographiques dans le texte seront faites par des exposants sans parenthèse et paraîtront à la fin de l'ouvrage.

Les publications périodiques mentionnées dans la bibliographie seront présentées suivant les prescriptions internationales : le nom de l'auteur précédé de l'initiale du prénom, le titre du périodique abrégé conformément à « Chemical Abstracts » et souligné par une ligne, le numéro du tome, indiqué par des chiffres arabes et souligné par deux lignes, suivi de la première page de l'article ; à la fin, l'année de la parution sera placée entre parenthèses. Le numéro de la revue ne sera pas indiqué si les pages du volume sont numérotées consécutivement. Pour les revues dont les tomes ne sont pas numérotés (par ex. Bull. Soc. Chim. France, etc), l'année de la parution soulignée par deux lignes précèdera l'indication de la page.

Les textes des livres inclueront : les noms des auteurs, les initiales du prénom, le titre du livre entre guillements et sans être souligné, le numéro du tome précédé par l'abréviation « vol. » (ou « Bd. »), le numéro de l'édition, les éditions (the publisher), la localité de la parution du livre, l'année de la parution et la page de la référence précédée par l'abréviation « p ». (ou « S. »).

Les brevets seront indiqués comme suit : l'auteur ou la firme, le pays et le numéro du brevet, la date et la revue (Chem. Abstr.). Par ex. : M. Jones (to Union Carbide Co.), Brit. Pat. 601-238, 2 sept. 1959, *Chem. Abstr.*, 54, 12808 (1960).

Si la référence n'a pas été lue en original, on indiquera aussi la revue de références consultée.

Les diagrammes seront tracés à l'encre de Chine sur papier calque. Les tableaux et les figures (en nombre strictement nécessaire) seront numérotés par des chiffres arabes et leur explication sera donnée dans la légende des figures. Prière de ne pas inscrire les mêmes données dans le tableaux et dans les figures. Chaque tableau aura un titre. On indiquera dans le texte la place approximative des tableaux et des figures. Les formules chimiques seront incluses dans le texte ; en outre, elles seront transcrites sur papier calque, à l'encre de Chine.

Les auteurs sont priés d'indiquer les caractères italiques (en soulignant les lettres au crayon), ainsi que tout autre caractère spécial ; les préfixes *ortho*, *meta*, *para*, *cis*, *trans*, etc. seront soulignés pour indiquer leurs caractères italiques et ne seront jamais écrits avec des majuscules.

Aucune correction à la main ne sera admise sur le manuscrit. Les corrections seront frappées à la machine. Les lettres grecques ou d'autres symboles spéciaux seront insérés à la main à l'encre clairement.

Le manuscrit sera signé par l'auteur.

Le colonne-titre aura 50 lettres au maximum.

L'entière responsabilité du contenu des articles appartient aux auteurs. Pour détails voir le n° 1 (1981).

PRINTED IN ROMANIA

TRAVAUX PARUS AUX ÉDITIONS DE L'ACADÉMIE DE LA RÉPUBLIQUE SOCIALISTE DE ROUMANIE

ELENA CEAUŞESCU, **Polimerizarea stereospecifică a izoprenului** (La polymérisation stéréospécifique de l'isoprène), 1979, 307 p.

CR. SIMIONESCU, VALERIA GORDUZA, **Polimeri biocompatibili şi biologic activi** (Polymèrs biocompatibles et biologiquement actifs), 1980, 479 p.

MIHAIL FLORESCU, **Metode ştiinţifice în dezvoltarea industriei chimice moderne** (Méthodes scientifiques dans le développement de l'industrie chimique moderne), 1979, 256 p.

CONST, GH. MACAROVICI, **Analiza chimică cantitativă anorganică** (L'Analyse chimique quantitative inorganique), 1979, 457 p.

Ş. MOLDOVEANU and A. SAVIN, **Aplicaţii în chimie ale metodelor semiempirice de orbitali moleculari** (Application en chimie des méthodes semi-empiriques des orbitaux moléculaires), 1980, 285 p.

A. T. BALABAN, I. GĂLĂŢEANU, G. GEORGESCU, LIGIA SIMIONESCU, **Compuşi marcaţi şi radiofarmaceutici cu aplicaţii în medicina nucleară** (Composés marqués et radiopharmaceutiques à application en médecine nucléaire), 1979, 495 p.

I. G. MURGULESCU, E. SEGAL, **Introducere în chimia fizică**, vol. II. 1, **Teoria molecular-cinetică a materiei** (Introduction à la chimie physique, IIe vol. 1. (La théorie moléculaire-cinétique de la matière), 1979, 1003 p.

I. E. TEODORESCU, MARIA FITI, **Iradierea tehnologică** (L'Irradiation technologique), 1979, 216 p.

S. STERNBERG, FL. DANEŞ, **Termodinamica chimică aplicată** (La thermodynamique chimique appliquée), 1978, 400 p.

I. G. MURGULESCU, V. EM. SAHINI, **Introducere în chimia fizică**. Vol. I.2. **Structura şi proprietăţile moleculelor** (Introduction à la chimie physique. Vol. I, 2. La structure et les propriétés des molécules), 1978, 604 p.

C. DRĂGULESCU, E. PETROVICI, **Chimie structurală modernă. Chimia coordinanţei 8** (La chimie structurale moderne. La chimie de la coordinence 8). 1977, 947 p.

D. PURDELA (sous la direction de), **Nomenclatura chimiei anorganice** (La nomenclature de la chimie inorganique), 1977, 153 p.

I. ZUGRĂVESCU, MAGDA PETROVANU, **N-ylid chemistry**, 1977, 396 p.

D. NEGOIU, ANGELA KRIZA, **Poluanţi anorganici în aer** (Polluants, inorganiques dans l'air), 1977, 220 p.

I. G. MURGULESCU, **Introducere în chimia fizică. Vol. I. Atomi, molecule, legătură chimică** (Introduction à la Chimie Physique, Ier vol. Atomes, molécules, liaison chimique), 1976, 560 p.

E. P. BALTĂ, E. BALTĂ, **Introduction to the physical chemistry of the vitreous state**, coédition avec Abacus Press, 1976, 287 p.

H. I. GĂLĂŢEANU, **Radiochimia aplicată. Metode şi probleme** (La radiochimie appliquée. Méthodes et problèmes), 1976, 307 p.

CONST. V. UGLEA, **Cromatografia pe gel permeabil. Noi domenii de aplicare** (La chromatographie sur gel perméable. Nouveaux domaines d'application), 1978, 123 p.

CONST. GH. MACAROVICI, D. MACAROVICI, **Chimia oxizilor dubli şi utilizările lor** (La chimie des oxydes doubles et leur utilisation), 1975, 195 p.

ELENA CEAUŞESCU, **Research work on synthesis and characterization of macromolecular compounds. Contributions**, 1974, 251 p.

CR. SIMIONESCU, VIORICA RUSAN, V. POPA, **Chimia algelor marine** (La chimie des algues marines), 1974, 212 p., 1 pl.

I. P. INFORMAŢIA c. 2711

43 426

Lei 25

55 $ (pour un abonnement annuel)

F 1103

REFERÁLVA

R

ACADÉMIE DE LA RÉPUBLIQUE SOCIALISTE DE ROUMANIE

REVUE ROUMAINE DE CHIMIE

TOME 26
N° 3
Mars 1981

EDITURA ACADEMIEI REPUBLICII SOCIALISTE ROMÂNIA

Rev. Roumaine Chim.

RRCHAX, 26, 3, p. 331–506 (1981), Bucarest

ACADÉMIE DE LA RÉPUBLIQUE SOCIALISTE DE ROUMANIE

COMITÉ DE RÉDACTION

Rédacteur en chef:

I. G. MURGULESCU, membre de l'Académie de la République Socialiste de Roumanie

Rédacteurs en chef adjoints:

A. T. BALABAN et V. EM. SAHINI, membres correspondants de l'Académie de la République Socialiste de Roumanie

Collège de rédaction:

EM. BRATU, ELENA CEAUŞESCU, ECATERINA CIORĂNESCU-NENITZESCU, CR. SIMIONESCU, membres de l'Académie de la République Socialiste de Roumanie ; P. SPACU, membre correspondant de l'Académie de la République Socialiste de Roumanie ; MARGARETA AVRAM, M. BANCIU, I. HAIDUC, D. I. MARCHIDAN, I. MOLDOVAN, G. NIAC et D. SĂNDULESCU

La Revue Roumaine de Chimie paraît 10 fois par an. Toute commande de l'étranger pour les travaux parus aux Editions de l'Académie de la République Socialiste de Roumanie sera adressée à ILEXIM, Departamentul Export-Import Carte (Livres)/Departamentul Export-Import Presă (Revues), P.O.B. 136–137, télex 11226, 3, str. 13 Decembrie, 79517 Bucarest, Roumanie

Les manuscrits, les livres et les revues proposés en échange, ainsi que toute correspondance seront envoyés à la rédaction :

REVUE ROUMAINE DE CHIMIE

125, Calea Victoriei, 79717 Bucarest, Roumanie, téléphone 50 76 80

EDITURA ACADEMIEI REPUBLICII SOCIALISTE ROMÂNIA

125, Calea Victoriei, 79717 Bucarest, Roumanie, téléphone 50 76 80

ORSZÁGOS

REVUE ROUMAINE DE CHIMIE

Tome 26, N° 3 Mars, 1981

V. DAVID and Ş. MOLDOVEANU, Interaction between two charge distributions situated into a continuum, infinite and isotropic medium . . . . . . 333–340 Bc

DELIA ISAC, M. MRACEC and Z. SIMON, Structure and reactivity in diazotization reaction. Electronic spectra and molecular orbital calculations for aromatic diazonium salts . . . . 341–348 R

D. BONCHEV and O. MEKENYAN, An estimate of the upper limit of the periodic table based on the Eddington number 349–354

CR. CONŢESCU, FEM study of silver layers adsorbed on tungsten. III. Silver layer growth modes 355–361

D. GEANĂ, On the problem of phase equilibrium in chemical reaction systems 363–376

S. SENENT, L. FERRARI and A. ARRANZ, Kinetic study of the reduction of Cr(VI) by hydroxylamine (in Spanish) 377–382

LUCIA ODOCHIAN, ELENA MIHAI, S. FIŞEL and OLGA MITOŞERIU, Thermogravimetrical analysis of some complex compounds of thiobisnaphthol (in French) 383–388

K. SINGH, P. BAHADUR and P. BAHADUR, Effect of added salt on the colloidal behaviour of alkaline earth metal caprylates . . . . 389–396 R

JEAN GIRAUD, SIROUSSE NOURI and BYOUK BLOURI, On the steam cracking of 6-methyleicosane (in French). 397–405

A. T. BALABAN, Chemical graphs. XXXVII. A simple rule for classifying *peri*-condensed benzenoid hydrocarbons as closed-shell or open-shell (polyradicalic) systems using dualist (characteristic) graphs. 407–413

J. V. SINISTERRA, J. LLAVINA, J. MOREY and J. M. MARINAS, Contribution to mechanism determination of esterification of aliphatic carboxylic acids, catalyzed by $ALPO_4$ and related systems (in Spanish) . . . 415–426

M. S. K. YOUSSEF, Synthesis of some new styryl oxazolophenoxazine cyanines 427–434

A. CHICU and R. BACALOGLU, Nucleophilic substitutions to carbonic acid derivatives. XVII. Kinetics and mechanism of the hydrolysis of N, N, N′-trisubstituted carbonic acid chloramide (in German) 435–440

M. M. MOHAMED, M. A. El-HASHASH, M. A. SAYED and O. A. ABO-BAKER, Studies on the cyclisation of the products of Stobbe condensation with 2,4-dimethylacetophenone 441–448

A. A. El-BARBARY, M. ANWAR, A. A. GHATTAS and A. F. HASHEM, Reaction of 5-aryl-2-thiono-1,3,4-oxadiazoles with some amino- and halo-compounds 449–456

Revue Roumaine Chim. **26,** *3*, p. 331–506 (1981), Bucarest

A. C. RĂZUŞ, V. WERTHEIMER, A. M. GLATZ, ZS. ARVAY and F. BADEA, Kinetics of the thermal rearrangement of benzo[b]bicyclo[3.1.0]hex-2-en-4-yl derivatives 457–470

M. S. K. YOUSSEF, Reaction of diazomethane with anils and mixed azines of thiophene aldehyde or isatin 471–475

S. B. TAMBI, R. K. JAIN and R. L. MITAL, Synthesis of some new fluorosubstituted tricyclic heterocyclics 477–480

DAN SORIN VASILESCU, Alternating tendency in copolymerization. VI. Chain transfer for complexed monomers 481–490

M. THARWAT, A. AWAD and F. RASHWAN, Effect of surfactants on kinetics of reduction of V(V) in universal buffer solutions at the dropping mercury electrode 491–501

BOOK REVIEWS 503–505

Revue Roumaine de Chimie, 26, *3*, 333–340 (1981)

INTERACTION BETWEEN TWO CHARGE DISTRIBUTIONS SITUATED INTO A CONTINUUM, INFINITE AND ISOTROPIC MEDIUM

V. DAVID and Ş. MOLDOVEANU
The Polytechnic, Faculty of Chemical Technology, Analyt. Chem. Dept.,
Splaiul Independenţei 202, Bucharest, Romania

Received April 1, 1980

General mathematical formalism for description of perturbational potentials between two charge distributions in the presence of an outside field is presented.

The potential of N identical molecules is a sum of the two, three,..., N-body potentials, thus:

$$U = \frac{1}{2\,!}\sum_i^N \sum_j^N U_{ij} + \frac{1}{3\,!}\sum_i^N \sum_j^N \sum_k^N U_{ijk} + \dots$$

$$i \neq j \neq k \neq \dots$$

For the systems in the gaseous phase, the contributions of pair potentials are preponderent. The condensed systems are characterised by perturbations of pair potentials from other components.[1,2]

In this paper we have studied an analytical method for the determination of these perturbations, considering that the perturbation of the third body from the rest of (N-2) molecules is equivalent with a perturbation of the surrounding medium taken as infinite, continuous and homogeneous.

BACKGROUND

To determinate the interaction energy between two point charge systems, we begin with the V^i potential created by a charge distribution $q_i (i = 1, 2, \dots, n)$ in a point A, situated at $R = (X, Y, Z)$ from the mass center of the 0 system.[3] Let $r_i = (x_i, y_i, z_i)$ be the position vector for the charge q_i to the 0 origin; therefore

$$V^i = \sum_i \frac{q_i}{|\boldsymbol{R} - \boldsymbol{r}_i|} \tag{1}$$

But:

$$|\boldsymbol{R} - \boldsymbol{r}_i| = [(X - x_i)^2 + (Y - y_i)^2 + (Z - z_i)^2]^{1/2} =$$

$$= \left[\sum_{\rho=1}^{3} (X_\rho - x_{\rho,i})^2\right]^{1/2} \tag{2}$$

Where: $X_1 = X,\ X_2 = Y,\ X_3 = Z$

$$x_{1,i} = x_i,\ x_{2,i} = y_i,\ x_{3,i} = z_i$$

If we introduce:

$$M_0^i \equiv q^i = \sum q_i$$

$$M_1^i \equiv p^i = \sum_i \sum_{\rho_1} q_i x_{\rho_1, i}$$

$$M_2^i \equiv Q^i = \sum_i \sum_{\rho_1} \sum_{\rho_2} q_i x_{\rho_1, i}\, x_{\rho_2, i}$$

$$\cdots\cdots\cdots\cdots\cdots\cdots$$

$$M_\mu^i = \sum_i \sum_{\rho_1} \sum_{\rho_2} \cdots \sum_{\rho_\mu} q_i x_{\rho_1, i}\, x_{\rho_2, i} \cdots x_{\rho_\mu, i}$$

we obtain:

$$V^i = \left[M_0^i + \sum_{\rho_1} M_{\rho_1}^i \frac{\partial}{\partial X_{\rho_1}} + \frac{1}{2!} \sum_{\rho_1} \sum_{\rho_2} M_{\rho_1 \rho_2}^i \frac{\partial^2}{\partial X_{\rho_1} \partial X_{\rho_2}} + \ldots\right] \frac{1}{R} \tag{3}$$

If we consider the term in the brackets as an operator $\mathbf{V}_i$ which acts on a function R^{-1}, we can write:

$$V^i = \mathbf{V}_i R^{-1} \tag{4}$$

$\mathbf{V}_i$ may be called the charge operator because it has the dimension of a charge. In fact the $\mathbf{V}_i$ operator is a sum of operators $\mathbf{T}_{\mu, i}$ written in the form:

$$\mathbf{V}_i = \sum_{\mu=0}^{\infty} \mathbf{T}_{\mu, i} \tag{5}$$

where:

$$\mathbf{T}_{0, i} = M_0^i$$

$$\mathbf{T}_{1, i} = \sum_{\rho_1} M_{\rho_1}^i \frac{\partial}{\partial X_{\rho_1}} = \boldsymbol{p}^i \text{ grad}$$

$$\mathbf{T}_{2, i} = \frac{1}{2!} \sum_{\rho_1} \sum_{\rho_2} M_{\rho_1 \rho_2}^i \frac{\partial^2}{\partial X_{\rho_1} \partial X_{\rho_2}}$$

$$\cdots\cdots\cdots\cdots$$

When A is the mass center of another charge distribution, $q_j (j = 1,2,\ldots,m)$, then the interaction energy between the two systems becomes :

$$U_{ij} = \sum_j q_j V^i(|\boldsymbol{R}_{ij} + \boldsymbol{r}_j|) \tag{6}$$

From Taylor's expansion of $V(|\boldsymbol{R}_{ij} + \boldsymbol{r}_j|)$ one obtains :

$$U_{ij} = \left[M_0^j + \sum_{\rho_1} M^j_{\rho_1} \frac{\partial}{\partial X_{\rho_1}} + \frac{1}{2!} \sum_{\rho_1} \sum_{\rho_2} M^j_{\rho_1 \rho_2} \frac{\partial^2}{\partial X_{\rho_1} \partial X_{\rho_2}} + \ldots \right] V^i(R_{ij}) =$$

$$= \mathbf{V}_j \mathbf{V}_i \frac{1}{R_{ij}} \tag{7}$$

where R_{ij} is the distance between the mass center of q_i and q_j distributions.

If the corresponding operations in (7) are effectuated, we obtain the interaction energy between ions, dipoles, high poles, ions with poles etc.

The commutation of the operators could be easily proved

$$\mathbf{V}_i \mathbf{V}_j = \mathbf{V}_j \mathbf{V}_i$$

Now, we can write U_{ij}, with (5), in the form :

$$U_{ij} = \sum_{\mu=0}^{\infty} \mathbf{T}_{\mu,j} \sum_{\nu=0}^{\infty} \mathbf{T}_{\nu,j} R_{ij}^{-1} \tag{8}$$

THEORY

I. Operational writing of the interaction energy between two charge distributions facilitates the writing of the U'_{ij} interaction energy between two charge distributions in the presence of the perturbational potential created by the surrounding continuum medium ; by analogy with quantum mechanics, we shall introduce perturbational operators in (8), namely, for each $\mathbf{V}$ operator a new one is added, as follows :

$$U'_{ij} = (\mathbf{V}_i + \mathbf{A})(\mathbf{V}_j + \mathbf{B}) R_{ij}^{-1} \tag{9}$$

A, B designating the perturbational operators of the i and j distributions, respectively.

Because the operators do not commute we must write (9) in the form :

$$U'_{ij} = \frac{1}{2} [(\mathbf{V}_i + \mathbf{A})(\mathbf{V}_j + \mathbf{B}) + (\mathbf{V}_j + \mathbf{B})(\mathbf{V}_i + \mathbf{A})] R_{ij}^{-1} \tag{10}$$

For identical molecules, $\mathbf{A} = \mathbf{B}$ and :

$$U'_{ii} = (\mathbf{V}_i + \mathbf{A})(\mathbf{V}_i + \mathbf{A}) R_{ii}^{-1} \tag{11}$$

With U'_{ij} as given by (8) one obtains :

$$U'_{ij} = \frac{1}{2} \sum_{\mu,\nu=0}^{\infty} [(\mathbf{T}_{\mu,i} + \mathbf{A}_\mu)(\mathbf{T}_{\nu,j} + \mathbf{B}_\nu) + (\mathbf{T}_{\nu,j} + \mathbf{B}_\nu)(\mathbf{T}_{\mu,i} + \mathbf{A}_\mu)] R_{ij}^{-1} \tag{12}$$

This means that :

$$\mathbf{A} = \sum_{\mu=0}^{\infty} \mathbf{A}_\mu$$

$$\tag{13}$$

$$\mathbf{B} = \sum_{\nu=0}^{\infty} \mathbf{B}_\nu$$

Expression (12) shows that there is a perturbational potential of the ion-ion, ion-dipole, pole-pole, etc. interactions.

The significance of operators **A** and **B** is simple : the expression (8) of the interacting energy in the presence of the perturbational action of an external field is modified. But the only possibility to modify the operators **V** is to change the pole moments specified for the charge distribution so that with the outside perturbations these poles will be modified with α, β respectively, thus :

$$\mathbf{A} = \alpha_0 + \sum_{\rho_1} \alpha_{\rho_1} \frac{\partial}{\partial X_{\rho_1}} + \frac{1}{2!} \sum_{\rho_1} \sum_{\rho_2} \alpha_{\rho_1\rho_2} \frac{\partial^2}{\partial X_{\rho_1} \partial X_{\rho_2}} + \ldots \tag{14}$$

$$\mathbf{A}_\mu = \frac{1}{\mu!} \sum_{\rho_1} \sum_{\rho_2} \cdots \sum_{\rho_\mu} \alpha_{\rho_1\rho_2\ldots\rho_\mu} \frac{\partial^\mu}{\partial X_{\rho_1} \partial X_{\rho_2} \ldots \partial X_{\rho_\mu}} \tag{14'}$$

Let's call $\mathbf{A}_\mu$ the "perturbational operators" and α_μ will be the variation of the μ order pole. For simplicity we shall denote :

$$\partial^\alpha \equiv \frac{\partial^\mu}{\partial X_{\rho_1} \partial X_{\rho_2} \ldots \partial X_{\rho_\mu}}$$

so that :

$$\mathbf{A}_\mu = \frac{1}{\mu!} \sum_{\rho_1,\rho_2\ldots\rho_\mu} \alpha_{\rho_1\rho_2\ldots\rho_\mu} \cdot \partial^\mu \tag{15}$$

II. The energy function of the system formed by the two interacting charge distributions, can be expressed as :

$$E = T + U$$

(T — kinetic energy, U — potential energy). If we choose a measure system such as $T = 0$, it follows that:

$$E = U$$

The energy of the system composed of the continuum medium and the two charge distributions, not considering the interaction with the medium, may be written:

$$E = E_m + U \tag{16}$$

E_m is the energy of the infinite continuum medium, U — energy of the charge distribution system.

Adding the interaction across the medium, this becomes:

$$E = E'_m + E_k + U' \tag{17}$$

where E_k is the interaction energy between medium and the charge systems, U' is the interaction potential energy between the two charge ditributions in the presence of the perturbational field of the medium, written in the form (12); E'_m is the energy of the medium perturbed in the presence of the charge system. As the medium is supposed to be infinite, a good approximation is:

$$E'_m = E_m$$

Wherefrom it results that:

$$U_{ij} = E_k + U'_{ij} \tag{18}$$

E_k is calculated with the Kirkwood model[4,5,6] and it is given by the medium-charges interaction energy. In this model E_k is:

$$E_k = \sum_{\mu=0}^{\infty} G_\mu \tag{19}$$

Where:

$$G_0 = \frac{1}{2} \cdot \frac{1 - \varepsilon}{\varepsilon} \frac{q^2}{a} \tag{20}$$

$$G_1 = \frac{1 - \varepsilon}{1 + 2\varepsilon} \cdot \frac{p^2}{a^3} \tag{21}$$

$$G_2 = \frac{3}{4a^5} \cdot \frac{1 - \varepsilon}{2 + 3\varepsilon} \left[3Q^2 - \left(\sum_i \sum_\rho q_i x^2_{\rho,i}\right)^2\right] \tag{22}$$

. . . .

(a is the cavity radius, ε — dielectric constant of the medium). From 10 and (18) it follows:

$$\mathbf{V}_i\mathbf{V}_j R_{ij}^{-1} = E_k + \frac{1}{2}[(\mathbf{V}_i + \mathbf{A})(\mathbf{V}_j + \mathbf{B}) + (\mathbf{V}_j + \mathbf{B})(\mathbf{V}_i + \mathbf{A})]R_{ij}^{-1} \tag{23}$$

Using the equations (8) and (12) we can write (18) for identical molecules:

$$\sum_{\nu=0}^{\infty}\sum_{\mu=0}^{\infty} \mathbf{T}_\mu\mathbf{T}_\nu R_{ii}^{-1} = E_k + \sum_{\nu=0}^{\infty}\sum_{\mu=0}^{\infty}(\mathbf{T}_\nu + \mathbf{A}_\nu)(\mathbf{T}_\mu + \mathbf{A}_\mu) R_{ii}^{-1} \tag{24}$$

Wherefrom:

$$-E_k = \sum_{\nu=0}^{\infty}\sum_{\mu=0}^{\infty}(\mathbf{T}_\nu\mathbf{A}_\mu + \mathbf{A}_\nu\mathbf{T}_\mu + \mathbf{A}_\nu\mathbf{A}_\mu) R_{ii}^{-1} \tag{25}$$

Using (19) it follows:

$$-\sum_{\mu=0}^{\infty} G_\mu = \sum_{\nu=0}^{\infty}\sum_{\mu=0}^{\infty}(\mathbf{T}_\nu\mathbf{A}_\mu + \mathbf{A}_\nu\mathbf{T}_\mu + \mathbf{A}_\nu\mathbf{A}_\mu) R_{ii}^{-1} \tag{26}$$

Equation (26), called the equation of perturbation, can be written in the form:

$$\begin{gathered}\sum_{\nu=0}^{\infty}(\mathbf{T}_\nu\mathbf{A}_\mu + \mathbf{A}_\nu\mathbf{T}_\mu + \mathbf{A}_\nu\mathbf{A}_\mu + RG_\mu) R^{-1} = 0 \\ \mu = 0, 1, 2, \ldots \\ R_{ii} \equiv R\end{gathered} \tag{27}$$

The physical meaning of eq. (27) is the following: in the interaction process the potentials of each molecule are very important. These potentials consist of potentials of the poles:

$$V^i = V^i(q, p, Q, \ldots)$$

Formally, the medium acts on the interacting molecules by the components of its potential: a dipole potential of the medium acts on the monopole, dipole, quadrupole, etc. potentials of the two interacting charge distributions. Thus, we can write:

$$\sum_{\nu=0}^{\infty} \mathbf{T}_\nu\mathbf{A}_\mu \neq \mathbf{T}_\mu\mathbf{A}_\mu$$

Because the terms in the parentheses for the different values of ν are linearly independent, we obtain the equation :

$$(\mathbf{T}_\nu \mathbf{A}_\mu + \mathbf{A}_\nu \mathbf{T}_\mu + \mathbf{A}_\nu \mathbf{A}_\mu + RG_\mu) R^{-1} = 0 \tag{28}$$

$$\mu = 0, 1, 2, \ldots$$

$$\nu = 0, 1, 2, \ldots$$

III. Using the forms (5) and (15), it follows that

$$\mathbf{T}_\nu \mathbf{A}_\mu = \frac{1}{\nu!\mu!} \sum_{\rho_1, \ldots, \rho_\nu}^{3} \sum_{\rho'_2, \ldots, \rho'_\mu}^{3} \sum_{b=0}^{\nu} C_\nu^{\nu-b} M_{\rho_1\rho_2..\rho_\nu} \partial^{\nu-b} \alpha_{\rho'_1\rho'_2..\rho'_\mu} \cdot \partial^{\mu+b} \tag{29}$$

$$\mathbf{A}_\nu \mathbf{T}_\mu = \frac{1}{\nu!\mu!} \sum_{\rho_2, \ldots, \rho_\nu}^{3} \sum_{\rho'_1, \ldots, \rho'_\mu}^{3} \alpha_{\rho_1\rho_2..\rho_\nu} M_{\rho'_1\rho'_2..\rho'_\mu} \partial^{\nu+\mu} \tag{30}$$

$$\mathbf{A}_\nu \mathbf{A}_\mu = \frac{1}{\nu!\mu!} \sum_{\rho_2, \ldots, \rho_\nu}^{3} \sum_{\rho'_1, \ldots, \rho'_\mu}^{3} \sum_{b=0}^{\nu} C_\nu^{\nu-b} \alpha_{\rho_1\rho_2..\rho_\nu} \partial^{\nu-b} \alpha_{\rho'_1\rho'_2..\rho'_\mu} \cdot \partial^{\mu+b} \tag{31}$$

Thus, equation (28) can be written in the general form :

$$\sum_{\rho_1, \ldots, \rho_\nu}^{3} \sum_{\rho'_2, \ldots, \rho'_\mu}^{3} \left\{ \sum_{b=0}^{\nu} [C_\nu^{\nu-b} (M_{\rho_1\rho_2..\rho_\nu} + \alpha_{\rho_1\rho_2..\rho_\nu}) \partial^{\nu-b} \alpha_{\rho'_1\rho'_2..\rho'_\mu} \cdot \partial^{\mu+b}] + \right.$$

$$\left. + \alpha_{\rho_1\rho_2..\rho_\nu} M_{\rho'_1\rho'_2..\rho'_\mu} \partial^{\nu+\mu} + \nu!\mu! RG_\mu \right\} R^{-1} = 0 \tag{32}$$

$$\nu = 0, 1, 2, \ldots$$

$$\mu = 0, 1, 2, \ldots .$$

We have thus found (expressions (28) and (32)) which connect the quantities involved in the Kirkwood model and the quantities derived from the perturbational formalism herewith developed.

Further results will be reported in a subsequent paper.

ACKNOWLEDGEMENT **The authors are indebted to Dr. C. I. Lepadatu for helpful and valuable discussions.**

REFERENCES

[1] R. L. Scott, in "Physical Chemistry. An advanced Treatise", vol VIII, ed. D. Henderson, Academic Press, New York, 1971, p. 1.

[2] O. Sinanoglu, in "Intermolecular Forces" ed. J. O. Hirschfelder, Interscience Pub. New York, 1967, p. 283.

[3] H. Margenau, N. R. Kestner, "Theory of Intermolecular Forces", Pergamon Press, New York, 1971.

[4] J. G. Kirkwood, *J. Chem. Phys.*, **1**, 351 (1934).

[5] D. L. Beveridge, G. W. Schnuelle, *J. Phys. Chem.*, **79**, 2562 (1975).

[6] L. Onsager, *J. Amer Chem Soc.*, **58**, 1486 (1936).

Revue Roumaine de Chimie, 26, *3*, 341–348 (1981)

STRUCTURE AND REACTIVITY IN DIAZOTIZATION REACTION

ELECTRONIC SPECTRA AND MOLECULAR ORBITAL CALCULATIONS FOR AROMATIC DIAZONIUM SALTS

DELIA ISAC, M. MRACEC and Z. SIMON
"Solventul" Chemical Research Laboratory, Timişoara, ICECHIM-CCMP spl. N. Titulescu nr. 31, Timişoara, 1900, Romania

Received January 25, 1980

Electronic spectra (200 – 800 nm) are recorded for sulphanilic acid, sulphanilamide and *p*-dimethylaminoaniline, the corresponding hydrochlorides, diazonium salts and hydrolysis products. Molecular orbital calculations by the HMO method are performed for 10 of the above molecules. The positions of absorption maxima are correlated with the calculated transition energies, satisfactory results being obtained.

Kinetic studies performed for the synthesis of aromatic diazonium salts

$$Ar - NH_2 + HONO + HX \rightarrow Ar - \overset{+}{N} \equiv N]X^- + 2H_2O$$

show that HNO_2 does not react as such, but is first transformed in an active nitrosyl cation, in the presence of a mineral acid, at intermediate or high acidities.[1-3]

$$HNO_2 + H^+ \rightleftarrows H_2NO_2^+ (H_2O + NO^+)$$

This cation reacts with the aromatic primary amine, through a succession of reactions, the rate determining step being the reaction in which the attack of the cation on the amine is produced:

$$\underset{(I)}{Ar - NH_2} + \overset{+}{N} = O \rightarrow \underset{(II)}{Ar - \overset{+}{N}H_2 - N = O} \longrightarrow$$

$$\xrightarrow{-H^+} \underset{(III)}{Ar - NH - N = O} \rightarrow \underset{(IV)}{Ar - N = N - OH} \rightleftarrows$$

$$\underset{-H^+}{\overset{+H^+}{\rightleftarrows}} \underset{(V)}{Ar - N = N - \overset{+}{O}H_2} \underset{}{\overset{-H_2O}{\rightleftarrows}} \underset{(VI)}{Ar - \overset{+}{N} \equiv N}$$

Nitrosamine (III) is formed as an intermediate and is rapidly transformed in the diazonium cation (VI), through the diazohydroxid (IV). Studies of the solvent effect on the diazotization kinetics imply, in water, as reaction medium, the following nitrozation agents : NO^+, $NO \cdot OH_2^+$, $NO \cdot NO_3$, $NO \cdot NO_2$. [4]

A mechanism in which the ionized amine reacts with nonionized nitrous acid is also indicated :[5]

$$Ar - NH_3^+ + HNO_2 \rightarrow Ar - NH - NO + H_3O^+$$

$$Ar - NH - NO \rightarrow Ar - N = N - OH$$

$$Ar - N = N - OH \rightarrow Ar - N_2^+ + HO^-$$

$$HO^- + H_3O^+ \rightarrow 2\ H_2O$$

Nevertheless, the formation of nitrosamine from the primary aromatic amine and of the nitrosyl cation is the rate determining step in most cases.

In a strong acid medium, e.g. HCl, the kinetics of the diazotization reaction is of the third order : [6,7]

$$v = k_3\,[H^+]\,[HNO_2]\,[Ar\ NH_2]$$

The diazotization reaction depends on the nature[8] and concentration[7] of the mineral acid used. So, the diazotization is more rapid in H_2SO_4 than in HCl and takes place easier, at greater concentrations of the acid.

As the basicity of amine is increased by electron repelling substituents, but decreased by electron withdrawing substituents, the diazotization reaction rate depends both on the nature of the substituent and on its position relative to the amine group. [9]

Our aim is to contribute to the knowledge of the structure-reactivity relationship in the diazotization reaction. Kinetic studies for this reaction were performed for several aromatic amines and the spectrophotometry was used to follow the concentrations of the reacting species.[10] In this paper we describe the electronic spectra (200—800 nm) of the reacting amines and of their reaction products.

Electronic spectra for sulphanilic acid, sulphanilamide, and -dimethylaminoaniline, the corresponding hydrochlorides, diazonium salts and hydrolysis products are recorded in figures 1, 2 and 3.

The spectra were recorded in identical experimental conditions in order to emphasize the formation of diazonium salts and the correct attribution of spectra transitions.

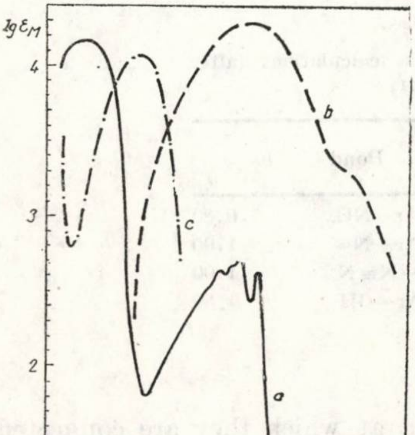

Fig. 1. — Electronic spectra for : a. sulphanilic acid hydrochloride, b. sulphanilic acid diazonium salt, c. hydrolysis product of sulphanilic acid diazonium salt.

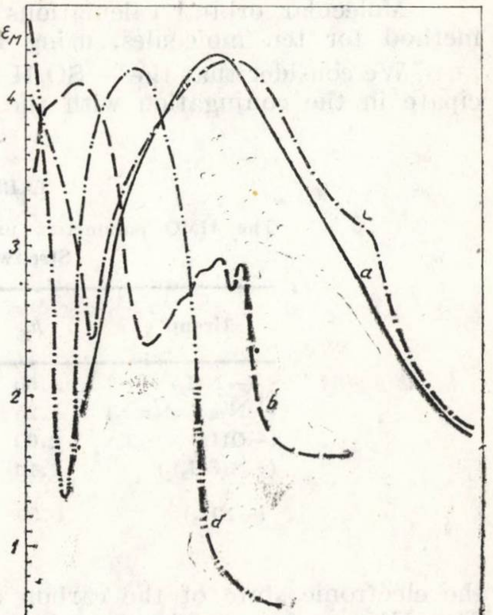

Fig. 2. — Electronic spectra for : a. sulphanilamide in methanol, b. sulphanilamide hydrochloride, c. sulphanilamide diazonium salt, d. hydrolysis product of sulphanilamide diazonium salt.

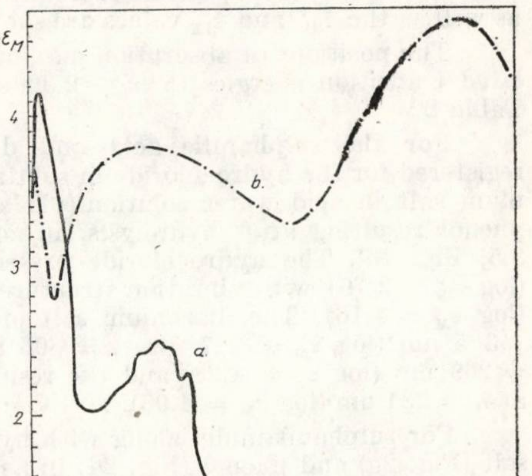

Fig. 3. — Electronic spectra for : a. *p*-dimethylaminoaniline hydrochloride, b. *p*-dimethylaminoaniline diazonium salt.

Molecular orbital calculations were performed through the HMO method for ten molecules, using Streitwieser parameters (Table 1).[11]

We consider that the $-SO_3H$ and $-SO_2NH_2$ groups do not participate in the conjugation with the aromatic cycle and do not disturb the electronic state of the carbon atom at which they are connected. The UV spectra (Table 2) and the spectral data from the literature support these conclusions.[12] The $-SO_3H$ and $-SO_2NH_2$ groups permit symmetrically the ^1L_b transition, increasing the extinction, but do not shift essentially the absorption band as compared to benzene.

TABLE 1

The HMO parameters used in calculations (after Streitwieser[11])

Group	h_X	Bond	k_{Y-X}
$(-NH_2)$	1.50	$Ar-NH_2$	0.80
$(-N\equiv) = (\equiv N)$	1.25	$Ar-N=$	1.00
$(-OH)$	2.00	$-N\equiv N$	1.00
$(-N(CH_3)_2)$	1.10	$Ar-OH$	0.80
$(-\overset{+}{N}H_3)$	0.50		

As 0.5 *n* HCl (pH = 0.5—1) was used, it is expected that the maximal protonated forms (dicationic) should predominate, but in equilibrium, monocationic forms will exist too. In some instances the monocationic forms might have a greater reactivity than the dicationic ones and so they could determine the reaction rate. That is why HMO calculations were performed for all possible protonated forms. The molecular diagrams as well as the ε_{HO} and ε_{LE} values are shown in figures 4, 5 and 6.

The positions of absorption maxima were correlated with the calculated transition energies ($\beta = -2.39$ eV) and the results are shown in Table 2.

For the sulphanilic acid and derivatives the UV spectra were registered for the hydrochloride in solution 0.5 nHCl (Fig. 1a), for diazonium salt in acid water solution (pH approx. 3.5, Fig. 1b) and for the phenol resulting after hydrolysis, in acidic water solution (pH approx. 3.5, Fig. 1c). The hydrochloride presents a maximum at $\lambda = 265$ nm ($\log \varepsilon_M = 2.70$) with vibration structure and a maximum at $\lambda = 214$ nm ($\log \varepsilon_M = 4.16$). The diazonium salt presents a shoulder between 295—305 nm ($\log \varepsilon_M = 3.27$ at $\lambda = 303$ nm) and a maximum at $\lambda = 269$ nm ($\log \varepsilon_M = 4.28$) and the resulting phenol presents a maximum at $\lambda = 231$ nm ($\log \varepsilon_M = 4.06$).

For sulphanilamide, along with hydrochloride (Fig. 2b), diazonium salt (Fig. 2c) and phenol (Fig. 2d) in acid water solution, the spectra in methanol were registered (Fig. 2a) and compared to that one from literature.[13]

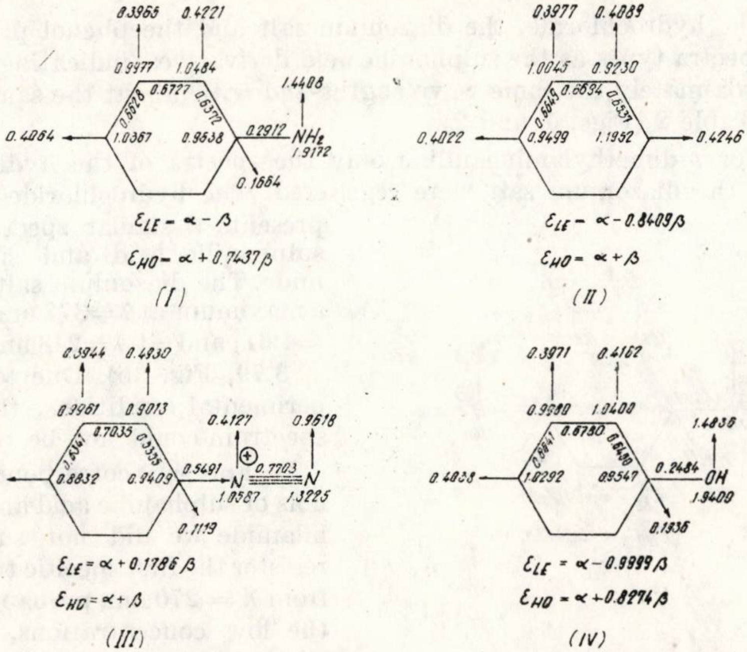
$\mathcal{E}_{LE} = \alpha - \beta$
$\mathcal{E}_{HO} = \alpha + 0.7437\beta$
(I)
$\mathcal{E}_{LE} = \alpha - 0.8409\beta$
$\mathcal{E}_{HO} = \alpha + \beta$
(II)
$\mathcal{E}_{LE} = \alpha + 0.1786\beta$
$\mathcal{E}_{HO} = \alpha + \beta$
(III)
$\mathcal{E}_{LE} = \alpha - 0.9999\beta$
$\mathcal{E}_{HO} = \alpha + 0.8274\beta$
(IV)
NH₂
OH
N
N

Fig. 4. — Molecular diagrams for sulphanilic acid and sulphanilamide (I), corresponding hydrochlorides (II), diazonium salts (III) and their hydrolysis products (IV).

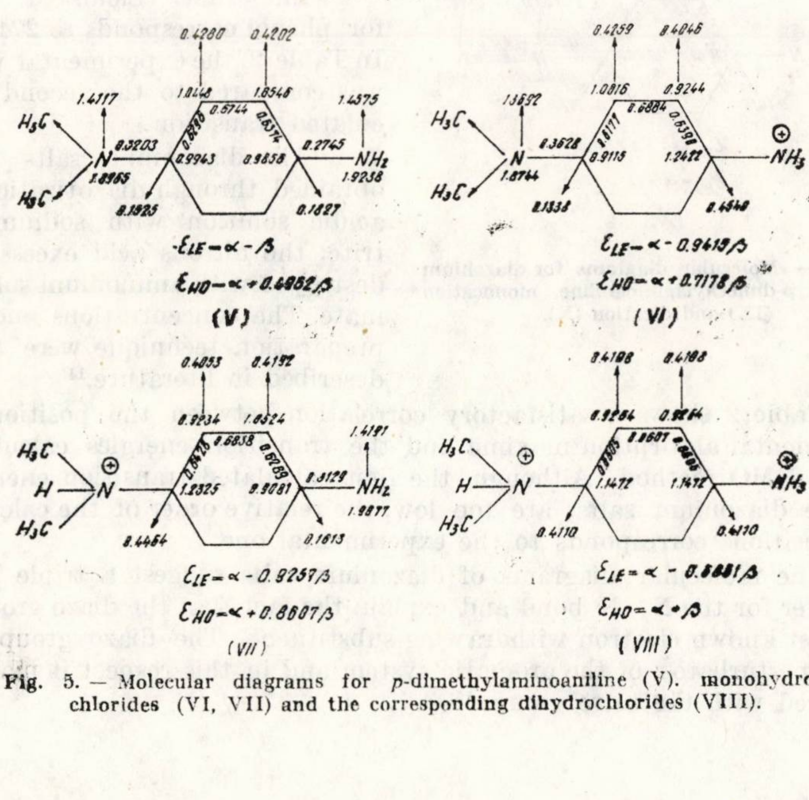
H₃C
H₃C
N
NH₂
$\mathcal{E}_{LE} = \alpha - \beta$
$\mathcal{E}_{HO} = \alpha + 0.6882\beta$
(V)
NH₃
$\mathcal{E}_{LE} = \alpha - 0.9419\beta$
$\mathcal{E}_{HO} = \alpha + 0.7178\beta$
(VI)
H
$\mathcal{E}_{LE} = \alpha - 0.9257\beta$
$\mathcal{E}_{HO} = \alpha + 0.8807\beta$
(VII)
$\mathcal{E}_{LE} = \alpha - 0.8881\beta$
$\mathcal{E}_{HO} = \alpha + \beta$
(VIII)

Fig. 5. — Molecular diagrams for *p*-dimethylaminoaniline (V). monohydrochlorides (VI, VII) and the corresponding dihydrochlorides (VIII).

The hydrochloride, the diazonium salt and the phenol present the same spectra types as the sulphanilic acid derivatives, indicating maxima, at approximately the same wavelengths and with about the same extinctions (Table 2, Figs. 1 and 2).

For *p*-dimethylaminoaniline only the spectra of the hydrochloride and of the diazonium salt were registered. The hydrochloride (Fig. 3a) presents a similar spectrum with sulphanilic acid and sulphanilamide. The diazonium salt presents a maximum at $\lambda=377$ nm ($\log \varepsilon_M = 4.61$) and at $\lambda=248$ nm ($\log \varepsilon_M = 3.79$, Fig. 3b). Due to the experimental conditions, the phenol spectrum could not be registered.

For the corresponding phenols of sulphanilic acid and sulphanilamide we did not succeed to register the first specific transitions from $\lambda = 270$ nm, probably due to the low concentrations, required to register the second, stronger, absorption band.

The first calculated band for phenol corresponds to 274 nm. In Table 2, the experimental value was compared to the second calculated transition.

All diazonium salts were obtained through diazotization in acidic solution with sodium nitrite, the nitrous acid excess was destroyed with ammonium sulphamate. The concentrations and the preparation technique were those described in literature.[14]

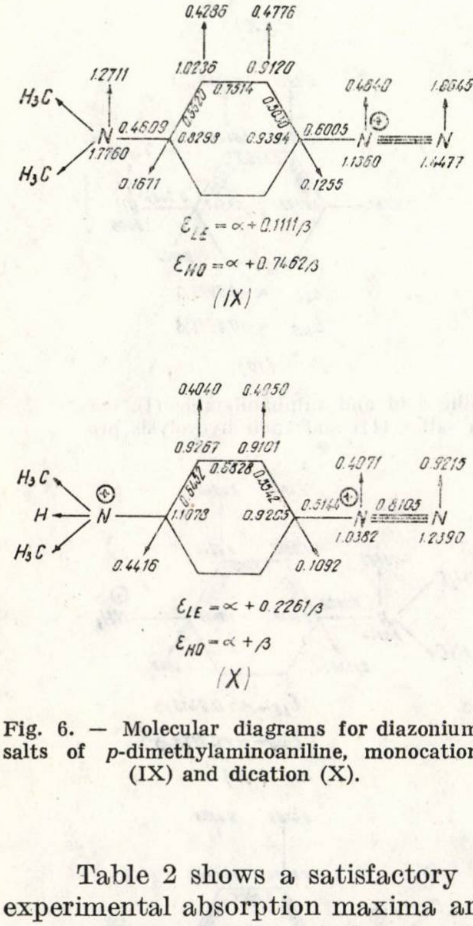
0.4285
0.4776
1.2711
1.0236
0.9120
0.7514
0.5520
0.5030
0.4840
1.6645
H_3C
H_3C
N
0.4609
0.8293
0.9394
0.6005
N
⊕
N
1.7760
1.1360
1.4477
0.1671
0.1255
$\varepsilon_{LE} = \alpha + 0.1111\beta$
$\varepsilon_{HO} = \alpha + 0.7462\beta$
(IX)
0.4040
0.4050
0.9267
0.9101
0.8828
0.5432
0.5042
0.4071
0.9215
H_3C
H
H_3C
⊕
N
1.1078
0.9205
0.5144
⊕
0.8105
N
N
1.0382
1.2390
0.4416
0.1092
$\varepsilon_{LE} = \alpha + 0.2261\beta$
$\varepsilon_{HO} = \alpha + \beta$
(X)

Fig. 6. — Molecular diagrams for diazonium salts of *p*-dimethylaminoaniline, monocation (IX) and dication (X).

Table 2 shows a satisfactory correlation between the positions of experimental absorption maxima and the transition energies calculated by the HMO method. Although, the first calculated transition energies, for the diazonium salts, are too low, the relative order of the calculated transitions corresponds to the experimental one.

The molecular diagrams of diazonium salts suggest a triple bond character for the N—N bond and explain the fact that the diazo group is the most known electron withdrawing substituent. The diazo group is a strong perturbator of the aromatic system and in this respect it may be compared with the nitro group.[15]

TABLE 2

Electronic transitions (nm) and molar extinction coefficients for some aromatic amines, hydrochlorides, the diazonium salts and corresponding hydrolysis products

Compound	Solvent	$\lambda_{exp.}$ (nm)	λ_{calc} (nm)	$\Delta\lambda$* (nm)	log ε_M
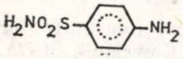	methanol	263	298	35	4.26
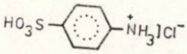	HCL 0.5n	265 214	282 259	17 45	2.70 4.16
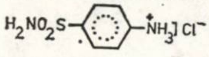	HCL 0.5n	265 219	282 259	17 40	2.91 4.09
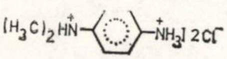	HCL 0.5n	 256 206 	308 (313/291)** 260 (302/279)**	52 (57/35) 54 (96/73)	 2.48 4.16
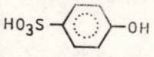	water	231	274	43	4.06
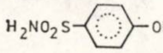	water	237	274	37	4.18
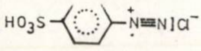	water	303(sh.) 269	633 586	320 317	3.27 4.28
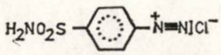	water	313(sh.) 269	633 586	320 317	3.10 4.27
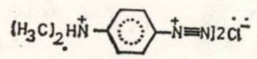	water	 377 248 	672 (818)** 539 (585)**	295 (441) 291 (337)	 4.61 3.79

* $\Delta\lambda = \lambda_{calc.} - \lambda_{exp.}$ (nm)

* * The values in parantheses are calculated for monocations. For *p*-dimethylaminoaniline 313 nm and 302 nm correspond to values calculated in the hypothesis of protonation at the aminic group, while 291 nm and 279 nm in the hypothesis of protonation at the dimethylamino group.

REFERENCES

[1] S. Radu, *St. şi Cerc. chim. Acad. R.S.R.*, **20**, 1287 (1972).

[2] J. Schmid, *Chem.-Ztg.*, **86**, 809 (1962); J. H. RIDD, *Quart. Rev.*, **15** 418 (1961).

[3] R. E. Kirk and D. F. Othmer, "Encyclopedia of Chemical Technology" vol. 5, The Interscience Encyclopedia, New York, 1950, p. 39.

[4] Z. A. Schelly, *J. Phys. Chem.*, **74**, 4062 (1970).

[5] K. Winnacker and E. Weingaertner, "Tehnologie chimică organică", vol. 3, Editura tehnică, Bucureşti, 1959, p. 225.

[6] C. D. Neniţescu, "Chimie Organică", vol. 1, 6-th ed., Editura didactică şi pedagogică, Bucureşti, 1966, p. 577.

[7] A. Aboul-Seoud, *Bull. Soc. chim. belges*, **75**, 249 (1976).

[8] A. Aboul-Seoud and A. Kasem, *Z. Phys. Chem. (Leipzig)*, **235**, 325 (1967).

[9] V. Sterba, Z. Sagner and M. Matrka, *Coll. Czech. Chem. Comm.*, **30**, 3333 (1965).

[10] D. Isac, M. Mracec, N. Prosteanu and Z. Simon, *Rev. Roumaine Chim.* **26**, (1981) in press.

[11] A. Streitwieser Jr., "Molecular Orbital Theory for Organic Chemists", Wiley, New York, 1961, p. 135.

[12] H. H. Jafé and M. Orchin, "Theory and Application of Ultraviolet Spectroscopy", Wiley, New York, 1962, p. 257, p. 484.

[13] J. G. Grasselli and W. M. Ritchey, "Atlas of Spectral Data and Physical Constants for Organic Compounds", vol. 2, 2-nd Edition, C.R.C. Press, Cleveland, 1975, p. 341 (b. 1238).

[14] G. Ciuhandu and M. Mracec, *Z. analyt. Chem.*, **238**, 104 (1968).

[15] E. M. Evleth and R. J. Cox, *J. Phys. Chem.*, **71**, 4082 (1967).

Revue Roumaine de Chimie, 26, 3, 349–354 (1981)

AN ESTIMATE OF THE UPPER LIMIT OF THE PERIODIC TABLE BASED ON THE EDDINGTON NUMBER

D. BONCHEV and O. MEKENYAN
The Department of Physical Chemistry, The Higher School of Chemical Technology, 8010 Burgas, Bulgaria

Received November 8, 1979

Taking the Eddington number 10^{82} as the upper limit of the number of atomic spin-orbital states, $Z_{\max} = 137$ was found. The electron configuration of the element No. 137, as calculated by Fricke, Greiner and Waber in 1971, was proved to coincide best with the above mentioned limiting condition.

INTRODUCTION

The problem of the upper limit of the Periodic Table of chemical elements is one of the most complicated in contemporary theory. According to Mendeleev, if elements heavier than uranium exist, their number should be limited.[1] In 1928 P. Dirac[2] showed that in the electrostatic field of a nuclear point charge, the solution of the basic equation of quantum mechanics became singular at $Z = 137$. Darwin and Gordon[3] have confirmed this result finding $Z_{\max} = 1/\alpha$, where $\alpha \approx \approx 1/137$ is the so-called fine structure constant. The difficulties with the appearance of nonphysical imaginary results for the $1s_{1/2}$ and $2p_{1/2}$ levels for $Z > 137$ were circumvented when an extended nucleus was taken into consideration instead of a point nucleus.[4-8] Nevertheless this difficulty is shifted by this method only near to elements $z = 175$ but does not disappear. It is likely that quantum electrodynamic effects, e.g. vacuum polarization and fluctuation, become so large that the single particle Dirac equation breaks down completely. Theoretical considerations for the quantum electrodynamics of strong fields are given by Rienhardt [2] but practical calculations are still missing. Thus an uncertainty still exists concerning the theoretical estimate of the upper limit of the Periodic Table.

The syntheses of transuranium elements, carried out during the last 30 years, have demonstrated the great instability and short lifetime of superheavy elements. During the sixties, however, the existence of areas of nuclear stability was predicted[10-12] close to the superheavy elements Nos. 114 and 164. The efforts to synthesize these elements have not so far been successful.[13-15]

On the other hand, the problem concerning the possible connection between the parameters of the Universe and those of atoms and elementary particles has risen during the last 40 years.[16–22] One might mention here the conclusions made in these papers concerning the possible variability of the gravitational constant, the fine structure constant, the electron charge and mass, etc. Such studies usually stress the correlation or even the explicit dependence between the parameters of macro- and microcosmos. The physical cause for the existence of these correlations is not discussed, but it is supposed to be elucidated by a future united physical theory.

Related to the above mentioned, an attempt is made in this work to estimate the upper limit of the Periodic Table proceeding from the assumption that the upper limit of physical quantities exists. The largest number having a physical meaning, which is of use in the theory, is the Eddington number, $N_{\max} \approx 10^{82}$, expressing the number of particles in the Universe.[23] We take the number 10^{82} as the upper limit of the number of physically indistinguishable microstates of a given type in the chemical element having the largest possible atomic number, $z_{\max}$. One could suppose that the instability of nuclei increases rapidly when approaching the upper limit of the Periodic Table. Our approach, however, aims solely at indicating the existence of a new connection between some boundary values of the Universe and the atom.

SOME EQUATIONS CONCERNING THE NUMBER OF SPIN-ORBITAL STATES

Let us consider the electron configuration ℓ^N, where ℓ is the angular momentum quantum number, and N — the number of electrons in the ℓth subshell. The coordinate wave function of this electron configuration, in the zero approximation respecting electron interactions, represents a tensor of rank N in the $/2\ell + 1/$ — dimensional space. It is composed as a product of N one-electron functions, called orbitals, which are distinguished by the magnetic quantum number m_i :

$$\psi_{m_1 m_2 \ldots m_N} = \psi_{m_1}(1) \cdot \psi_{m_2}(2) \ldots \psi_{m_N}(N) \tag{1}$$

Taking into account the electron spin, every orbital state will be additionally split into $/2s + 1/^N = 2^N$ substates. Thus, N_0 spin-orbital states are formed :

$$N_0 = [2(2\ell + 1)]^N \tag{2}$$

The greatest number of these states turns out to be forbidden by the Pauli principle. For the number of Pauli allowed spin-orbital states N_a, the formula was derived by the mathematical induction method :

$$N_a = N!\left(C^N_{2\ell+1} \cdot 2^N + \sum_n C^n_{2\ell+1} \cdot C^{N-2n}_{2\ell+1-n} \cdot 2^{N-n-1} \cdot \frac{1}{n} \right) \tag{3}$$

The number of Pauli forbidden spin-orbital states N_p can be defined by subtracting equations (2) and (3). In the formula above, the combination of k-elements taken from m elements without repetition is denoted by C_k^m. Since $C_k^0 = 1$, and $C_k^k = 1$ (including the case $k = 0$), then $C_{2\ell+1-n}^{N-2n}$ will be equal to one when $2\ell + 1 = n$ and $N = 2n$. On the other hand, C_k^m cannot exist by definition at $m > k$, therefore the term containing $C_{2\ell+1}^{N}$ in eqn. (3) will vanish when $N > 2\ell + 1$. In eqn. (3) n is an integer within the range 1 to $2\ell + 1$. It is selected by the condition :

$$n = k, \text{ for } N = 2k \text{ to } 2\ell + 1 + k,$$

where k is each of the integers within the range 1 to $2\ell + 1$. In the electron configuration d^6, for instance, $\ell = 2$, $k = 1, 2, 3$, and $N = 6$ is simultaneously within the ranges $N = 2$ to 6, $N = 4$ to 7, and $N = 6$ to 8. Therefore, $n = 1, 2$, and 3. The case $N = 1$ is not considered here, since then $N_a = N_0$.

A fair number of the Pauli allowed spin-orbital states are indistinguishable, due to the impossibility of discrimination between different electrons. The number of allowed states, also termed microstates, is specified by the Fermi-Dirac statistics :

$$N_M = \frac{X!}{(X - N)!N!} \tag{4}$$

where X is the maximum number of spin-orbitals in the subshell ℓ.

Let the number of the Pauli allowed spino-orbital states (eqn. 3) now be divided by the number of distinguishable states (eqn. 4). In such a way we shall specify the number of the physically indistinguishable spin-orbital states, N_u, by which each of the different microstates in the electron configuration under consideration is realized :

$$N_u = \frac{N_a}{N_M} = \frac{N_0 - N_p}{N_M} \tag{5}$$

Equation (5) holds for the electron configurations of equivalent elctrons only, ℓ^N. In the case of the mixed configuration $\ell_1^{N_1}\ell_2^{N_2}\ldots\ell_k^{N_k}$, in which N_1 electrons are in the subshell ℓ_1, N_2 electrons – in the subshell ℓ_2, etc, the number of physically indistinguishable occurrences of a particular microstate, N_u^{MX}, will be defined by the equation :

$$N_u^{MX} = N_u^{\ell_1} \cdot N_u^{\ell_2} \ldots N_u^{\ell_k} \tag{6}$$

RESULTS AND DISCUSSION

Making use of equations (2) – (5) we have calculated N_u for all possible s^N, p^N, d^N, f^N, and g^N-electron configurations. This quantity was found, in a given, not very large number of electrons ($N \leqslant 5$), to be independent of the type of ℓ-subshell :

$$N_u(\ell_1^N) = N_u(\ell_2^N) = \ldots = N_u(\ell_k^N) = N! \tag{7}$$

The N_u values for some electron configurations are shown in Table 1 together with the total number of spin-orbital states and the number of Pauli forbidden states.

TABLE 1

Number of spin-orbital states for some ℓ^N-electron configurations

Electron config.	N_0	N_p	N_u	Electron config.	N_0	N_p	N_u
p^1	6	0	1	d^8	10^8	$9.75 \cdot 10^7$	56747
p^2	36	6	2	d^9	10^9	$9.93 \cdot 10^8$	$7.26 \cdot 10^5$
p^3	216	96	6	d^{10}	10^{10}	$9.99 \cdot 10^9$	$1.16 \cdot 10^7$
p^4	1 296	936	24	f^7	$1.05 \cdot 10^8$	$8.76 \cdot 10^7$	$5.18 \cdot 10^3$
p^5	7 776	7 060	120	f^8	$1.48 \cdot 10^9$	$1.34 \cdot 10^9$	$4.45 \cdot 10^4$
p^6	46 656	45 696	960	f^9	$2.07 \cdot 10^{10}$	$1.97 \cdot 10^{10}$	$4.69 \cdot 10^5$
d^1	10	0	1	f^{10}	$2.89 \cdot 10^{11}$	$2.83 \cdot 10^{11}$	$6.00 \cdot 10^6$
d^2	10^2	10	2	f^{11}	$4.05 \cdot 10^{12}$	$4.02 \cdot 10^{12}$	$9.09 \cdot 10^7$
d^3	10^3	280	6	f^{12}	$5.67 \cdot 10^{13}$	$5.65 \cdot 10^{13}$	$1.61 \cdot 10^9$
d^4	10^4	4 960	24	f^{13}	$7.94 \cdot 10^{14}$	$7.93 \cdot 10^{14}$	$3.32 \cdot 10^{10}$
d^5	10^5	69 760	120	f^{14}	$1.11 \cdot 10^{16}$	$1.11 \cdot 10^{16}$	$7.97 \cdot 10^{11}$
d^6	10^6	846 400	731.4	g^{17}	$2.19 \cdot 10^{21}$	$2.19 \cdot 10^{21}$	$5.69 \cdot 10^{15}$
d^7	10^7	9 328 000	5 600	g^{18}	$3.93 \cdot 10^{22}$	$3.93 \cdot 10^{22}$	$1.82 \cdot 10^{17}$

Making use of equation (6) and the data in Table 1, the N_u values of the most chemical elements were determined, taking into account all populated ℓ-subshells. The same calculation was made for a certain number of superheavy elements ($Z > 106$). A part of the results obtained are presented in Table 2. The electron configuration of the chemical elements, used in the calculations, were taken from ref.[24]

TABLE 2

Electron configurations and number of indistinguishable spino-orbital states of some heavy and superheavy elements

z	Electron configuration	N_u	z	Electron configuration	N_u
90	$6d^2 7s^2$	$10^{52.42}$	135	$8s^2 8p^2 6f^4 5g^9$	$10^{79.66}$
100	$5f^{12} 7s^2$	$10^{59,33}$	136	$8s^2 8p^2 6f^4 5g^{10}$	$10^{80.72}$
104	$6d^2 7s^2$	$10^{62.33}$	137	$8s^2 8p^2 6f^4 5g^{11}$	$10^{81.85}$
132	$8s^2 8p^2 6f^2 5g^8$	$10^{77.60}$	138	$8s^2 8p^2 6f^4 5g^{12}$	$10^{83.04}$
133	$8s^2 8p^2 6f^3 5g^8$	$10^{78.08}$	139	$8s^2 8p^2 6f^4 5g^{13}$	$10^{84.29}$
134	$8s^2 8p^2 6f^4 5g^8$	$10^{78.68}$	140	$8s^2 8p^2 6f^4 5g^{14}$	$10^{85.59}$

Proceeding from the assumption that an upper limit of physical quantities exists, we have used the Eddington number 10^{82} as a maximum value of the possible physically indistinguishable spin-orbital states, by which a given microstate is brought about :

$$N_u \leqslant 10^{82} \tag{8}$$

It can be seen from Table 2 that the element No. 137 is the closest to this maximum value. Hence, following the assumptions made above, it is with this element that the Periodic Table should end, since the elements having $Z > 137$ would violate condition (8). It is worth while mentioning that our estimation of the upper limit of the Periodic Table coincides with the estimations of Dirac[2], and Darwin and Gordon.[3] An additional justification for this estimation is given by the calculations of N_u performed for the different hypothetical configurations of element No. 137. (Albeit nuclear instability is the physical effect limiting the Periodic Table, one should take into account the consistency existing between the population of electron subshells and nuclear stability.[25-27]

TABLE 3

Hypothetical electron configurations and number of indistinguishable spino-orbital states of element No. 137

No.	Electron configurations	N_u
1	$8s^1 5g^{18}$	$10^{89\cdot33}$
2	$8s^2 5g^{17}$	$10^{88\cdot13}$
3	$8s^2 8p^2 6f^1 5g^{14}$	$10^{84\cdot21}$
4	$8s^2 8p^3 6f^1 5g^{13}$	$10^{83\cdot38}$
5	$8s^2 8p^1 6f^4 5g^{12}$	$10^{82\cdot74}$
6	$8s^2 8p^2 6f^3 5g^{12}$	$10^{82\cdot44}$
7	$8s^2 8p^2 6f^4 5g^{11}$	$10^{81\cdot85}$
8	$8s^2 8p^2 6f^5 5g^{10}$	$10^{81\cdot42}$

As is demonstrated in Table 3, the best coincidence with the number 10^{82} is obtained for the electron configuration $8s^2\,8p^2\,6f^4 5g^{11}$, quoted as the most probable configuration according to the quantum mechanical calculations of Fricke, Greiner, and Waber.[28] It should however be mentioned that it is impossible within our approach to distinguish between this configuration and that in which two electrons populate 7d- instead of 8*p*-subshell (eqn. 7). Relatively more reliable are the results obtained for the number of *g*-electrons in this element.

REFERENCES

[1] D. I. Mendeleev, "Periodicheskii zakon. Osnovnie stat'i", Akad. Nauk USSR, Moscow, 1958.

[2] P. Dirac, *Proc. Roy. Soc.*, **117**, 610 (1928).

[3] B. M. Kedrov and D. N. Trifonov, "O sovremennikh problemakh periodicheskoi sistemi", Atomizdat, Moscow, 1974.

[4] I. Pomeranchuk and Ya. Smorodinsky, *J. Phys. USSR*, **9**, 97, (1945).

[5] D. Liberman, J. Waber, and D. T. Cromer, *Phys. Rev*, **A137** ; 25 (1965).

[6] E. C. Snow, J. Canfield, and J. Waber, *Phys. Rev.*, **A 135**, 969 (1964).

[7] D. Rein, *Z. Physik*, **221**, 423 (1969).

[8] W. Pieper and W. Greiner, *Z. Physik*, **218**, 327 (1969).

[9] P. G. Reinhardt, *Lett. al Nuovo Cimento*, **3**, 313 (1970).

[10] G. T. Siborg, *Ann. Rev. Nucl. Sci.*, **18**, 53 (1968) ; *ibid. J. Chem. Educ.*, **46**, 627 (1969).

[11] S. G. Nielsson, J. R. Nix, A. Sobiczewski, Z. Szymanski, S. Wycech, C. Gustafson, and P. Möller, *Nucl. Phys.*, **A 115**, 545 (1968).

[12] C. F. Tsang and S. G. Nielsson, *Nucl. Phys*, **A 140**, 289 (1970).

[13] G. T. Siborg, "Robert A. Welch Foundation Conference : The Transuranium Elements", Houston, Tex., Nov. 1969.

[14] G. N. Flerov and I. Zvara, Preprint OIYAI D7-6013, Dubna, 1971.

[15] B. Fricke and J. T. Waber, *Actinides Rev.*, **1**, 433 (1971).

[16] P. A. M. Dirac, *Nature*, **139**, 323 (1937) ; *Proc. Roy. Soc.*, **A 165**, 198 (1938).

[17] E. Teller, *Phys. Rev.*, **73**, 801 (1948).

[18] E. R. Harrison, *Nature*, **197**, 1257 (1963).

[19] D. Bonchev, *Jahrb. Hochsch. Chem. Technologie (Burgas)*, **3**, 89 (1966).

[20] G. Gamov, *Phys. Rev. Lett.*, **19**, 759 (1967).

[21] F. G. Dyson, *Phys. Rev. Lett.*, **19**, 1291 (1967).

[22] I. M. Kramarovski and V. Chechev, *Usp. Fiz. Nauk*, **102**, 141 (1970).

[23] A. Eddington, "Space, Time and Gravitation", Cambridge, 1921 ; ibid., "Relativity Theory of Protons and Electrons", Cambridge, 1936.

[24] F. Kotton and J. Wilkinson, "Advanced Inorganic Chemistry", Interscience, New York, 1972.

[25] A. Asunmaa and R. Lepsius, *Naturwiss.*, **38**, 473 (1951).

[26] A. T. Balaban, *Rev. Chim. (București)*, **14**, 158 (1968).

[27] B. Rousseva and D. Bonchev, *Math. Chem. (MATCH)*, **4**, 173. (1978) ; *ibid.*, *Radiochem. Radioanal. Letters*, **40**, 41 (1979).

[28] B. Fricke, W. Greiner, and J. Waber, *Theor. Chim. Acta*, **21**, 235 (1971).

Revue Roumaine de Chimie, **26**, *3*, 355–361 (1981)

FEM STUDY OF SILVER LAYERS ADSORBED ON TUNGSTEN. III[1]

SILVER LAYER GROWTH MODES

CR. CONȚESCU
Institute for Chemical Research,
Center of Physical Chemistry,
Spl. Independenței 202, 77208 Bucharest, Romania

Received May 23, 1980

The change of FEM patterns during condensation of silver on the clean tungsten surface shows that the growth mode and morphology of silver films depend on the substrate temperature. The vertical stack growth mode occurs at low temperature, whereas growth of room temperature deposits is described by the Stranski-Krastanov mode. During heating from 78 to 550 K, the film structure undergoes marked changes, leading to a better atomic ordering and formation of stable structure of equilibrated layers.

1. INTRODUCTION

During condensation of metal vapors onto a solid substrate, the properties of the initial clean surface are gradually lost as the thickness of the deposit increases. Depending on the growth mode, new structures are formed into the growing film, which are not uniquely determined by the nature of the condensing material. The initial stages of growth, when the dimensionality of the film increases from two to three, represent an interesting and serious matter of study because of wide technological applications of thin film devices.

Early studies devoted to the growth mechanism of metallic films were mainly performed on non-crystalline (glass) or pure ionic (alkali halides) substrates. Only in the past few years the increasing interest in technology of epitaxial layers demanded systematic investigations on the growth modes of metallic films onto metallic substrates. They arised the very interesting question of how the lattice adaptation at metal/metal interfaces takes place.

Our previous FEM studies on early stages of growth of silver layers onto the clean surface of tungsten crystal[1-3] illustrated the formation of a coherent interface between two imiscible metals with different crystal structures. The silver lattice is f.c.c., with lattice constant of 4.09 Å, while tungsten has a b.c.c. lattice with lattice parameter of 3.17 Å. In the present work it is shown that, because of strong chemisorptive interactions at the Ag/W interface, tungsten substrate exerts also an important structural influence on very thin deposits, which leads to different growth modes at different temperatures.

2. ADSORPTION, GROWTH AND NUCLEATION OF SILVER ON TUNGSTEN

The experimental arrangement and construction of the Field Emission Microscope (FEM) were described in a previous work.[1] Special attention was paid in outgasing the silver vapor source, so that the pressure of residual gases when operating it was usually less than $5 \cdot 10^{-10}$ torr. The evaporation flux, monitored by means of an electronic circuit, was kept in the range of $5 \cdot 10^{13} - 1 \cdot 10^{14}$ atoms/cm^2·s. The mean thickness ($\bar{\theta}$) of silver layers was calculated assuming that the monolayer coverage ($\bar{\theta} = 1$) corresponds to $1.05 \cdot 10^{15}$ silver atoms/cm^2. Experiments were carried out by evaporating controlled silver doses onto the tungsten emitter held at 78 K or room temperatures. Room temperature deposits were then warmed to 550 K to enable surface diffusion and complete spreading of condensed silver. Thus, the so called equilibrated layers were obtained.

2.1. SUBSTRATE AT 78 K

In figure 1 three representative sequences of emission patterns are shown for silver deposits of approximately same thickness condensed at 78 K (Fig. 1, a—c) and room temperature (Fig. 1, d—f) or spread at 550 K (Fig. 1, g—i). The flux of impinging silver atoms arrived from the left of all emission patterns. Because of hemispherical shape of the emitter sample, the density at substrate surface varies from a maximum in those regions which lie normal to the flux direction to zero in the shadowed areas.

Silver deposits condensed at 78 K have an irregular appearance and are always confined to the surface regions which directly receive the imdinging flux. Because surface diffusion is hindered at this low temperature, each arriving atom is stacked in the position where it impinged on the substrate (or in its close neighborhood). For this reason a dark shadow of (110) terraces appears in figure 1, c on the right of central (110) plane, where silver atoms cannot accede to. The bright collar formed around the lateral $(10\bar{1})$ plane (figure 1, b) shows that condensed atoms agglomerate at step edges of close packed terraces around this plane where the surface density of trapping sites is larger than that on flat compact area of $(10\bar{1})$.

By gentle heating a layer with configuration shown in figure 1, c up to 350 K, the phenomenon of inverse surface migration, described previously as the "back rolling carpet" mechanism,[1] could be observed. It leads to formation of a well-developed, very stable crystallite onto the surface region where the initial thickness of deposits was high. This peculiar behaviour is probably the consequence of a very low cohesion energy of the defective structure formed at 78 K.

2.2. SUBSTRATE AT ROOM TEMPERATURE

First doses condensed at room temperature give rise to layers of more uniform appearance (figure 1, d—f) and almost equal thickness on the whole tungsten surface. A diffuse shadow around the central (110) plane may be observed in figure 1, e, but it does no longer persist by increasing the thickness. At this temperature surface mobility of silver atoms is high enough to enable partial spreading of condensate over surface areas opposite to vapor source.

By further adding silver, layers become non-uniform and nucleation occurs at a certain film thickness, as shown in figure 2. Starting from $\bar{\theta} > 5$, formation of the first silver nuclei is perceptible on those surface areas which are normal to flux direction (Fig. 2, c – e). They arise initially around the lateral $(00\bar{1})$ plane, where the film thickness is obviously larger than on the rest of visible surface. The number and dimensions of silver nuclei increase as the mean thickness increases. At $\bar{\theta} > 7$ bright nuclei develop also in the proximity of $(12\bar{1})$ and $(21\bar{1})$ planes (Fig. 2, f).

From figures 1 and 2 we conclude that silver nuclei grow as isolated islands on the top of an adsorbed multilayer having a critical nucleation thickness. This is not, however, the stable form of silver film, since room temperature nuclei can be destroyed by heating at higher temperatures. Figure 3 shows the results of heating and/or of adding a new silver dose onto a layer spread at subcritical nucleation thickness. The first pattern is of a uniform layer, spread over the entire tungsten surface ($\bar{\theta} = 6.78$). By adding a small silver dose at room temperature the coverage degree becomes $\bar{\theta} = 7.45$ and a bright nucleus arises on $(30\bar{1})$ plane (Fig. 3, b). It is destroyed by heating for 1 minute at 550 K (Fig. 3, c). Much more nuclei appear by further deposition at room temperature (Fig. 3, d), being located on high index planes like $(31\bar{1})$, $(61\bar{1})$, $(31\bar{2})$, $(02\bar{1})$, $(03\bar{1})$, $(20\bar{1})$, $(30\bar{1})$. Thermal dissolution and reappearance of nuclei following a new condensed dose continue at higher thickness, but these processes are somewhat obscured by the increased brightness of thick deposits (Fig. 3, e – i). It is however assumed that islands formed on top of a multilayer film are much less developed when $\bar{\theta} > 10$.

Our observations are in contrast with previous results of Gretz and Pound[4] who reported that silver forms stable three-dimensional nuclei on tungsten even at an adsorbed population of 0.14 monolayers. This led Paunov and Kaishew[5] to advance a model of heterogeneous nucleation according to which nucleation at submonolayer coverage should occur whenever adsorption energy of the first monolayer is smaller than bulk cohesion energy of condensed material. Although this is exactly the case of silver on tungsten,[3] the above predictions disagree with ours and other experimental results.[6-8]

The usefulness of FEM results as a test of nucleation theories was discussed by Jones.[9] Because of the heterogeneity and curvature of their surfaces, field emitter tips are not suitable for a study of nucleation kinetics, but are however well suited to establishing the location of the growth sites for permanent crystallites. As shown by the emission patterns, silver nuclei are always located on high index, rough surface planes. This could be more than a simple manifestation of the intrinsic surface roughness. For example, nuclei could never be observed on (211) or in the middle of (111) planes, which are also regions with some local surface roughness. It seems that nucleation is linked to the existence on the surface of high concentration of kink, edge or corner atoms, acting as very effective traps for adsorbed atoms which arrive by surface diffusion.

2.3. THERMAL EQUILIBRATED LAYERS

Heating the room temperature layers to 550 K leads to uniform spreading of deposits through surface diffusion (Fig. 1, g — i) and also to dissolution of clusters formed on top of thicker layers (Fig. 3). In this way the stable structure of deposits is attained. Emission patterns of thin layers retain much of tungsten symmetry, but a new structure could be detected beyond the critical nucleation thickness.[1]

The work function *vs*. thickness variation of these equilibrated layers was discussed elsewhere.[1,3] We have shown that three different domains may be separated in the structure of a thick equilibrated layer. The first one is a true adsorbed monolayer, giving rise to work function increase on all crystal planes except (110) where surface work function decreases.[10] Then an intermediate layer follows leading to a drastic decrease of the work function on all crystal planes. The last is probably a pseudomorphically adapted transition layer[11] where silver lattice duplicates the b.c.c. lattice of substrate. Some of the properties associated to the transition layer (low work function and cohesion energy) might be successfully explained [1,3] by the existence of an anomalous Ag* (b.c.c.) modification which reduces the lattice misfit between b.c.c. tungsten and f.c.c. silver from 24.7 % to 4.7 %. The pseudomorphic layer has probably different thickness on various crystal planes, depending on the local substrate topography. According to the Frank — van der Merwe model,[12] this layer is stabilized at small thickness through homogeneous elastic strains. It becomes however unstable at larger thickness by spontaneous generation of interface dislocations which gradually diminish the internal strains. By increasing thickness, the normal structure (f.c.c.) and bulk properties of silver appear, including the proper work function value. The change from pseudomorphic to normal silver structure takes probably place beyond the critical thickness where nucleation is firstly observed at room temperature.

3. DISCUSSIONS

Various growth modes are possible during condensation of a film onto a solid substrate, depending on the physico-chemical properties of both the substrate and condensed substance. They may be classified[13,14] as (i) island growth (the Volmer — Weber mode), (ii) layer growth (the Frank — van der Merwe mode), (iii) island growth following layer growth (the Stranski — Krastanov mode) and (iv) vertical stack growth. The first mode occurs whenever the surface energy of the film material (γ_f) is large as compared with that of the substrate (γ_s). The second and third modes are typical of the reverse case, i.e. $\gamma_f < \gamma_s$, and a distinction among them could be made by considering the value of the strain energy (σ) in the film.[13] If $\sigma < \gamma_f$, the film should grow by the Frank — van

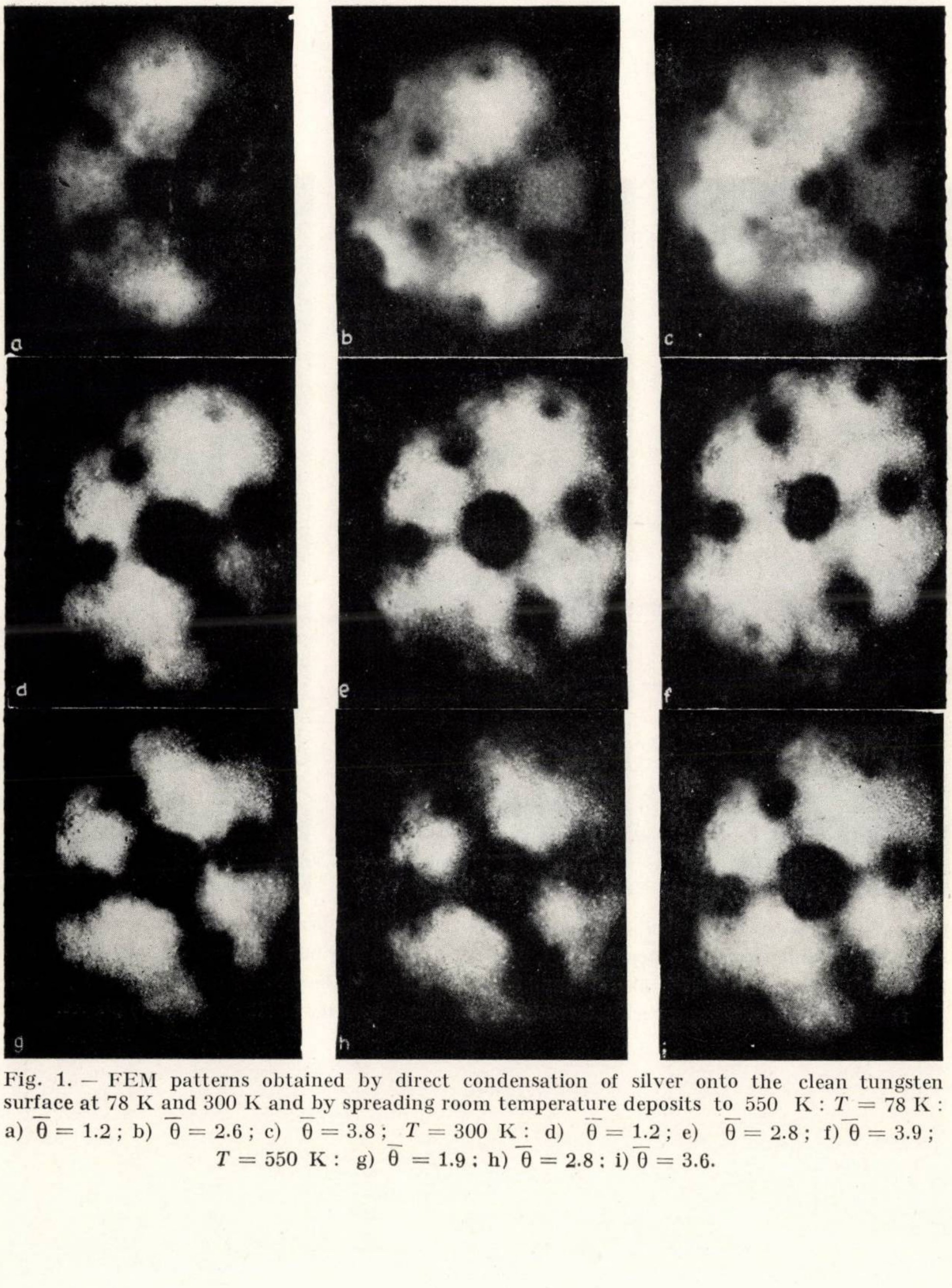

Fig. 1. — FEM patterns obtained by direct condensation of silver onto the clean tungsten surface at 78 K and 300 K and by spreading room temperature deposits to 550 K : $T = 78$ K : a) $\overline{\theta} = 1.2$; b) $\overline{\theta} = 2.6$; c) $\overline{\theta} = 3.8$; $T = 300$ K : d) $\overline{\theta} = 1.2$; e) $\overline{\theta} = 2.8$; f) $\overline{\theta} = 3.9$; $T = 550$ K : g) $\overline{\theta} = 1.9$; h) $\overline{\theta} = 2.8$; i) $\overline{\theta} = 3.6$.

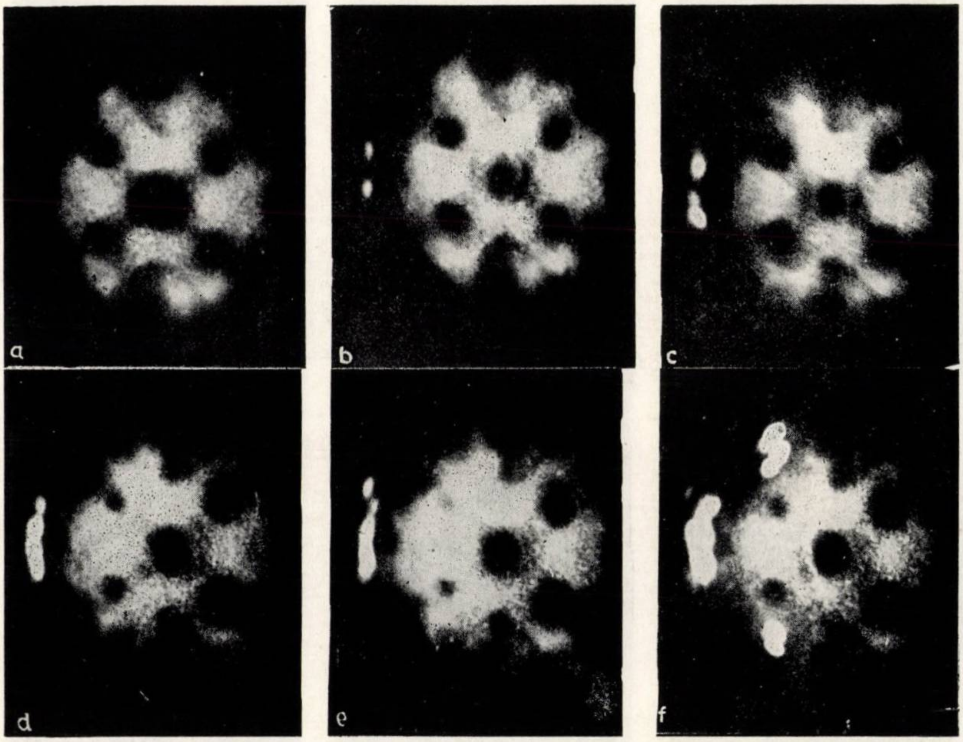

Fig. 2. — Silver nucleation on tungsten surface by room temperature condensation : a) $\bar{\theta} = 2.75$. Nonuniform silver deposit ; b) $\bar{\theta} = 3.70$; c) $\bar{\theta} = 4.60$; d) $\bar{\theta} = 5.25$; e) $\bar{\theta} = 6.15$. Increased thickness on the left half side and nucleation around the directly exposed $(00\bar{1})$ plane ; f) $\bar{\theta} = 7.00$. Nuclei appear as isolated islands in the proximity of $(12\bar{1})$ and $(2\bar{1}\bar{1})$ planes.

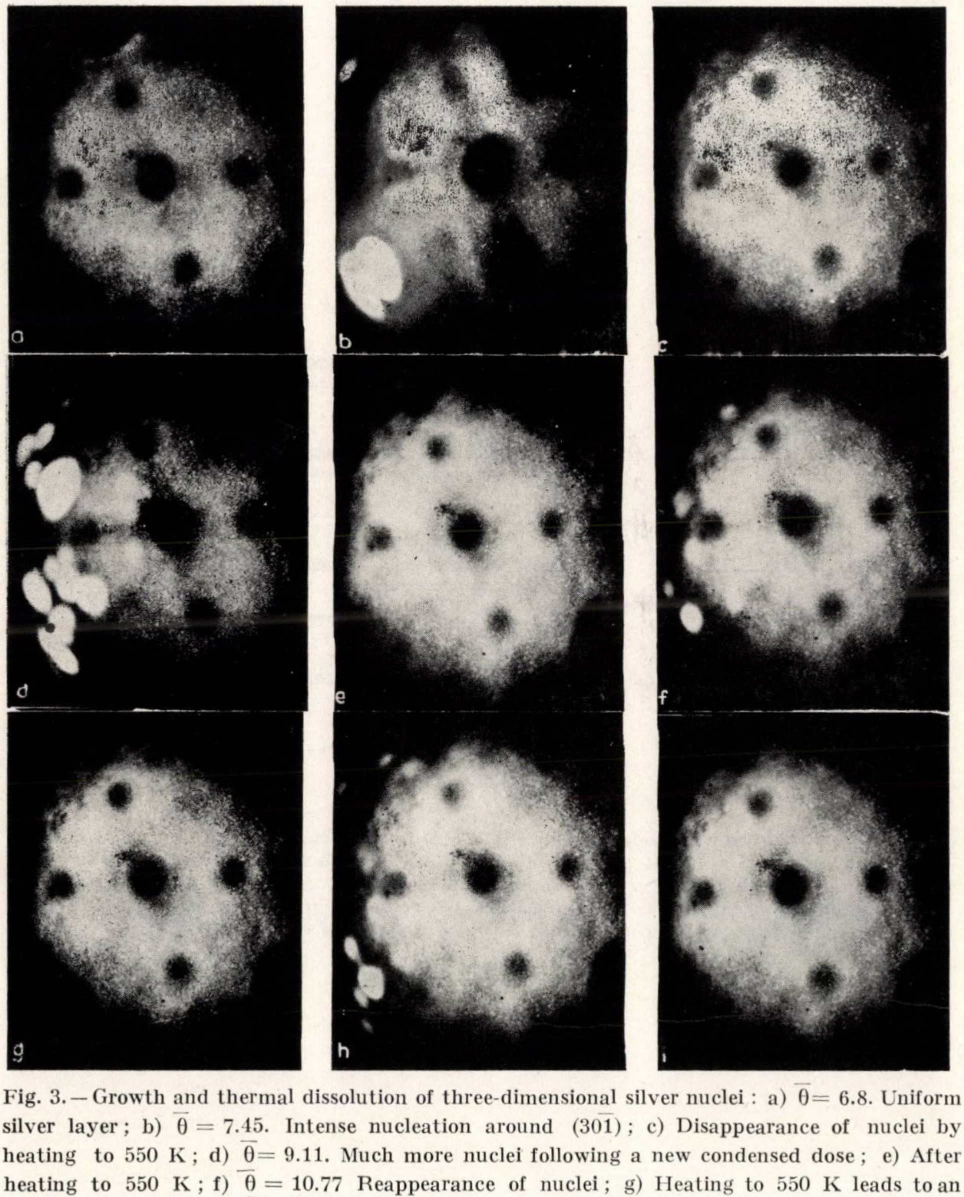

Fig. 3. — Growth and thermal dissolution of three-dimensional silver nuclei : a) $\overline{\theta} = 6.8$. Uniform silver layer ; b) $\overline{\theta} = 7.45$. Intense nucleation around $(30\bar{1})$; c) Disappearance of nuclei by heating to 550 K ; d) $\overline{\theta} = 9.11$. Much more nuclei following a new condensed dose ; e) After heating to 550 K ; f) $\overline{\theta} = 10.77$ Reappearance of nuclei ; g) Heating to 550 K leads to an equilibrated layer ; h) $\overline{\theta} = 11.20$. A new silver dose produces fewer nuclei ; i) Equilibrated layer after heating to 550 K.

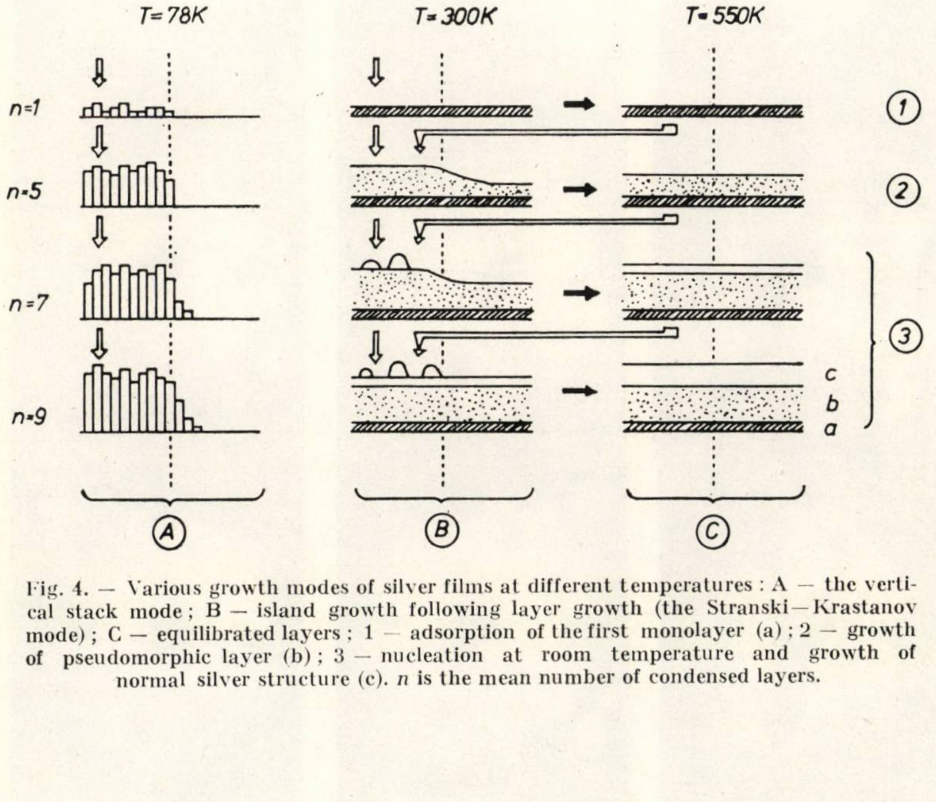

Fig. 4. — Various growth modes of silver films at different temperatures : A — the vertical stack mode ; B — island growth following layer growth (the Stranski—Krastanov mode) ; C — equilibrated layers ; 1 — adsorption of the first monolayer (a) ; 2 — growth of pseudomorphic layer (b) ; 3 — nucleation at room temperature and growth of normal silver structure (c). *n* is the mean number of condensed layers.

der Merwe mechanism. Otherwise (large internal strains) the Stranski–Krastanov mode should occur. The vertical stack growth mode is usually at very low temperatures, where atoms impinging on the substrate surface are held in their arrival positions. Various kinds of growth can occur for the same film/substrate pair at different temperatures.[14] When the film started to grow bidimensionally (modes (ii) and (iii)) the film/substrate interface is always coherent, i.e. the lattice mismatch is entirely eliminated by homogeneous strain in the epitaxial overgrowth. Some atomic alignment may also be achieved at the interface of a film grown initially as isolated islands (mode (i)), but the interface formed in mode (iv) should be considered very irregular.

The above presented results show that various growth modes should be considered for silver films on clean tungsten crystal held at different temperatures. They are sketched in figure 4 together with the most likely structures of silver deposits formed at 78 K, 300 K and 550 K. Open arrows indicate arrival of new silver doses onto the emitter area facing the vapor source (on the left of each draft). Black arrows represent heat induced structural changes.

It is easy to recognize that the sequence of figure 1, a – c indicates the vertical stack growth mode at 78 K. The morphology of deposits is probably columnar and their free surface should be extremely heterogeneous. Even in the limit of a large film thickness the overgrowth maintains probably an essentially two-dimensional character.[14] Previous experiments[1] have shown that silver deposits of type A (Fig. 4) can undergo marked structural changes during a suitable thermal treatment. When the temperature is slowly raised (under conditions enabling the film to achieve an equilibrium configuration) the columns interact with one another and coalesce to form the large crystallite mentioned at the end of surface diffusion ("back rolling carpet" mechanism).[1] The reason is a lower adsorption energy[3] of the first silver monolayer (2.38 eV) compared with cohesion energy of bulk silver (2.96 eV). Since silver is stronger bound to itself than to tungsten substrate, the normal structure of bulk silver can be easily restored starting from the defective structure of type A deposits.

Under conditions of active surface diffusion, the growth mode depends on the relative values of film and substrate surface energy.[13] Because the surface energy of bulk silver ($\gamma_f = 1.1 - 1.3$ J/m^2) is much less than the tungsten surface energy ($\gamma_s = 2.6 - 2.7$ J/m^2) a two-dimensional growth is expected for silver on tungsten. Indeed, at elevated temperatures there is a strong tendency to Frank – van der Merwe growth mode, as already demonstrated by other FEM[8] and LEED – AES[13] studies. For example, at temperatures between 450 and 500 K, the arriving silver atoms spread immediately on the tungsten surface,[7] so that a smooth deposit is formed. Thick silver deposits grown above 700 K are always in defined epitaxial orientations, which for f.c.c./b.c.c. metal pairs depend on the geometry of substrate and the ratio of atomic diameters.[15]

On the basis of above presented FEM patterns we conclude that even at room temperature the early stages of growth which follows chemisorption of the first monolayer are essentially two-dimensional.

The limited surface diffusion at this temperature leads however to nonuniform thickness over the *entire* surface. The silver film, which is strained to coherency with the substrate, has not its normal structure, but an anomalous modification bridging the film/substrate lattice misfit. The appearance of pseudomorphism in very thin silver films (no more than 6 atomic layers) is supported by a quite strong Ag-W bonding. The newly appeared structure, denoted as Ag* (b.c.c.), although very defective and thus unstable, should be considered as intermediate between that of the b.c.c. substrate and f.c.c. bulk condensate. Its formation is shown in the first stages of growth of type B layers in figure 4. As the thickness increases, the film which started to grow coherently under subcritical conditions becomes unstable since accumulated strains exceed surface energy (which should be lower for Ag* (b.c.c.) than for normal f.c.c. silver[1]). The normal lattice structure appears as isolated islands on the top of pseudomorphic layer (and perhaps mixed with it) and is not coherent at room temperature over the underlying film. This is shown by intense nucleation beyond a critical thickness of about 7 monolayers. The processes are shown in the last stages of type B layers.

Thermal equilibrated layers (type C) are the stable form achieved by heating at 550 K. Clearly, some morphological transformations take place during annealing of a room temperature deposit, which result to ordering and a better accomodation of outermost layers. In this way both above mentioned structures become coherent, as shown by the uniform spreading of nuclei on the top of multilayer deposits. It is however unknown how deep this structural change is. Since thermal desorption of thick equilibrated layers gives also the characteristic work function minimum[6,7] we assumed in the model of figure 4 that the thickness of the underlying pseudomorphic layer does not change by heating from room temperature to 550 K.

We conclude therefore that the growth of silver at room temperature, illustrated by emission patterns shown in Figure 1, d – f and figure 2, is an example of Stranski – Krastanov mode. Nevertheless, the growth of an intermediate pseudomorphic layer before three-dimensional nucleation requires an extension of criteria for the occurrence of the Stranski–Krastanov mode, to include layers which cannot be described by the properties of the bulk. Such abnormal structures may form when the first adsorbed monolayer is tightly bound in a structure incompatible with the normal arrangement of the bulk crystal and the ratio of atomic radii of film and substrate is close to unity. Two factors favour the pseudomorphism of ultra-thin metallic films : strong monolayer ordering and low lattice energy of the pseudomorphic form. Under these conditions, several atomic layers will replicate the substrate structure. The larger the bulk cohesion energy of the condensed metal, the stronger the internal strain and the sooner the film can achieve the structure of the bulk. Thus, copper and gold overlayers on tungsten reach the bulk properties at a thickness no larger than 3 or 4 monolayers,[16] whereas silver, whose structure is strongly affected by the substrate, cannot attain the bulk structure in less than 8 or 9 atomic layers.

4. CONCLUSIONS

We have shown that both the growth mode and morphology of silver films condensed on the clean tungsten surface depend strongly on the substrate temperature. By increasing temperature the growth mode changes from the vertical stack mode at 78 K to island growth following layer growth (the Stranski – Krastanov mode) at room temperature. Silver nuclei appear at room temperature on the top of the intermediate pseudormorphic layer with a critical thickness of about 7 monolayers. They are always located on high index planes of tungsten substrate and may be destroyed at higher temperatures. The stable structure resulted by layer growth (the Frank – van der Merwe mode) at elevated temperatures may also be obtained by heating room temperature deposits. Annealing of low temperature deposits leads to structural changes and to a better ordering of the overlayers.

REFERENCES

[1] Part I : M. I. Vass and Cr. Conţescu, *Rev. Roumaine Chim.*, **20**, 1253 (1975).
[2] Part II : Cr. Conţescu and M. I. Vass, *Rev. Roumaine Chim.*, in print.
[3] Cr. Conţescu, Thesis, National Institute for Chemistry, Bucharest, 1979.
[4] R. D. Gretz and G. M. Pound, in "Proceedings Dayton Conference on Condensation and Evaporation", Gordon and Breach, New York, 1963.
[5] M. Paunov and R. Kaishew, *Surface Sci.*, **18**, 268 (1969).
[6] J. P. Jones, *Surface Sci.*, **32**, 29 (1972).
[7] W. Wüstner and D. Menzel, *Thin Solid Films*, **24**, 211 (1974).
[8] A. J. Melmed and R. F. McCarthy, *J. Chem. Phys.*, **42**, 1466 (1965).
[9] J. P. Jones, *Surface Sci.*, **41**, 412 (1974).
[10] M. I. Vass and Cr. Conţescu, in "Heterogeneous Catalysis", Proc. Fourth International Symposium, Varna, 1979, Part. I, p. 33.
[11] H. Mayer, in "Advances in Epitaxy and Endotaxy", vol. I, Ed. G. Schneider, VEB Deutscher Verlag für Grundstoffindustrie, Leipzig, 1971, p. 63.
[12] J. H. van der Merwe, in "Advances in Epitaxy and Endotaxy", vol. I, Ed. G. Schneider, VEB Deutscher Verlag für Grundstoffindustrie, Leipzig, 1971, p. 129.
[13] E. Bauer and H. Poppa, *Thin Solid Films*, **12**, 167 (1972).
[14] G. F. Cerofolini, *Thin Solid Films*, **50**, 69 (1978).
[15] L. A. Bruce and H. Jaeger, *Phil. Mag.*, **A 37**, 337 (1978) ; **A 38**, 223 (1978) ; **A 40**, 97 (1979).
[16] A. Cetronio and J. P. Jones, *Surface Sci.*, **44**, 109 (1974).

Revue Roumaine de Chimie, 26 3, 363–376 (1981)

ON THE PROBLEM OF PHASE EQUILIBRIUM IN CHEMICAL REACTION SYSTEMS

D. GEANĂ
Dept. of Physical Chemistry, Polytechnic Institute,
Spl. Independenţei 313, Bucharest, Romania

Received March 10, 1980

The paper presents two rigorous statements of the problem of phase equilibrium in chemical reaction systems. Both formulations of the problem are equivalent to the dual geometric program. The transformations of "thermodynamic formulations" using geometric programing are presented. Two primal programs associated with the duals are given and some aspects which arise are analysed. The correlation with earlier statements of the problem is discussed. An algorithm for solving a transformed dual geometric program is advanced.

1. INTRODUCTION

In a series of recent papers [1-3] the authors have presented examples of simultaneous chemical and phase equilibria. The problem of phase equilibrium in chemical reaction systems was previously discussed by Boynton.[4] Applications to some practical interesting systems were also given (for example [5,6]). The problem of non-uniqueness in phase and reaction equilibrium computations was analysed too.[1-3,7]

Recently, the problem of chemical equilibrium has theoretically been investigated from a geometric programing point of view.[8-11]

In this paper, the intent is to further extend the treatment based on the geometric programing (GP) to systems with simultaneous chemical and phase equilibrium.

Some new aspects which arise are analysed and the correlation with earlier statements of the problem is discussed. An algorithm for solving a transformed dual geometric program is advanced.

2. THERMODYNAMIC FORMULATION OF PHASE AND REACTION EQUILIBRIUM

We consider a system with N species, F phases and M chemical elements. It is assumed in what follows that each species present in the system is a component of each of the phases. The problem of phase and reaction equilibrium can be formulated thermodynamically, for constant T and P, as a nonlinear program[6]:

$$\min G = \sum_{i,\Phi} n_i^{\Phi} \mu_i^{\Phi} \tag{1}$$

with physical restrictions

$$\sum_{\Phi} n_i^{\Phi} = n_i \quad \begin{matrix} (i = 1, 2 \ldots N) \\ (\Phi = 1, 2 \ldots F) \end{matrix} \tag{2}$$

$$\sum_i a_{ji} n_i = b_j \ (j = 1, 2 \ldots M) \tag{3}$$

$$n_i^{\Phi} \geqslant 0 \tag{4}$$

The restrictions (2,3) can be combined in two different ways:
(a) one substitutes (2) in (3)

$$\sum_{i,\Phi} a_{ji} n_i^{\Phi} = b_j \tag{5}$$

where

$$b_j = \sum_i a_{ij} n_i^0$$

which leads to Boynton's formulation.[4,12] An application to systems with pure condensed phases was presented by the author.[6]
(b) one transforms eq. (3) after[13] to

$$n_i = n_i^0 + \sum_k \nu_{ik} \xi_k \geqslant 0 \quad (k = 1, 2 \ldots \mathscr{R}) \tag{6}$$

by assuming rank $(a_{ji}) = M$, which leads to $\mathscr{R} = N - M$. Now substituting (6) in (2):

$$\sum_{\Phi} n_i^{\Phi} = n_i^0 + \sum_k \nu_{ik} \xi_k \tag{7}$$

Equations (7) are the "balance" conditions given by Prigogine and Defay and used to prove Duhem's theorem.[14] The same equations were used by Heidemann with slight different notations.[3] It is now possible to give two formulations of the phase and reaction equilibrium problem:

a) $\min G(n_i^{\Phi})$ (8)

subject to

$$\sum_{i,\Phi} a_{ji}\, n_i^{\Phi} = b_j \quad (j = 1,\ 2 \ldots M) \tag{9}$$

$$n_i^{\Phi} \geqslant 0 \qquad (i = 1,\ 2 \ldots N) \tag{10}$$

b) $\min G(n_i^{\Phi})$ (11)

subject to

$$\sum_{\Phi} n_i^{\Phi} - \sum_{k} \nu_{ik}\, \xi_k = n_i^0 \quad (i = 1,\ 2 \ldots N) \tag{12}$$

$$n_i^{\Phi} \geqslant 0 \tag{13}$$

The above formulations are equivalent. Because $M < N$ the formulation (a) seems to be simpler, having $M + \Phi N$ restrictions $(9 - 10)$, by comparing with $N + \Phi N$ restrictions of (b).

Algorithms for solving the problem in both formulations were presented in the literature (e.g.[3,4,5]) and will be discussed in relation to the programs transformed.

3. GEOMETRIC PROGRAMING APPROACH

Both formulations (a and b) are equivalent to the dual problem of GP.[8-10] In GP the dual function is $v = \exp(-G/RT)$. The authors specialized in mathematical programing [8-10] have practically used the formulation (a)$(8 - 10)$ by transforming it to a dual geometric program. It must be mentioned that the formulation of some authors [9-11] has a slight mistake, the notions of "component" and "species" being not rightly used. This leads to a number of variables (only N) which is smaller than those herein. The fact has not appeared in applications [9-11] because these were limited to one-phase chemical equilibria. For such systems (generally ideal gaseous systems) the method of GP has revealed some new aspects.[10,11]

In what follows we will transform the formulations (a) and (b), which may be named "chemical thermodynamic formulations", to "GP formulations".

With another distribution of index i, one forms the set I_{NF} :

$$I_{NF} = \left\{\begin{array}{ll} i = 1,2 \ldots N_1, & (\Phi = 1) \\ i = N_1 + 1, \ldots N_2, & (\Phi = 2) \\ \cdot & \\ \cdot & \\ i = N_{F-1} + 1, \ldots N_F & (\Phi = F) \end{array}\right\} \tag{14}$$

or

$$I_{NF} = \{I_1, I_2 \ldots I_F\} \tag{14'}$$

or

$$I_{NF} = \{I_\Phi,\ \Phi = 1 \ldots F\} \tag{14''}$$

where

$$N_F = N \times F$$

3.1. FORMULATION (a)

The problem (8 – 10) can be rewritten :

$$\min G = \sum_{i \in I_{NF}} n_i \mu_i \tag{8'}$$

subject to

$$\sum_{i \in I_{NF}} a_{ji}\, n_i = b_j\ (j = 1, 2, \ldots M) \tag{9'}$$

$$n_i \geqslant 0 \qquad (i \in I_{NF}) \tag{10'}$$

We considered the general model of chemical potential [15] :

$$\mu_i = \mu_i^0(T) + RT \ln C_i + RT \ln \frac{n_i}{n_\Phi} \tag{15}$$

where C_i (in[15] denoted C_i^Φ) is a function dependent on T, P and n_i in the most general case. It is a function characteristic of the phase type (vapour, liquid etc.) and will be determined by the ideal or real model considered (see for example [14,3]). For ideal systems C_i is a function only of T or P.[14] In an ideal vapour (or gas) phase $C_i = P$ and in an ideal liquid phase $C_i = P_i^s$, the vapour pressure. The total mole number in the phase Φ is :

$$n_\Phi = \sum_{i=N_{\Phi-1}}^{N_\Phi} n_i \text{ (with } N_{\Phi-1} = 1 \text{ for } \Phi = 1) \tag{16}$$

Equation (15) can be rearranged to the adimensional form

$$\frac{\mu_i}{RT} = g_i^0 + \ln \frac{n_i}{n_\Phi} \tag{17}$$

where

$$g_i^0 = \frac{\mu_i^0(T)}{RT} + \ln C_i \tag{18}$$

The problem (8′) can be written

$$\min g(n_i) = \frac{G}{RT} = \sum_{i \in I_{NF}} n_i (g_i^0 + \ln(n_i/n_\Phi)) \qquad (19$$

Eq. (19) can be transformed to the dual form of GP:

$$\max v(n_i) = \mathrm{e}^{-g} = \prod_{i=0}^{N_F} \left(\frac{c_i}{n_i} \right)^{n_i} \prod_{\Phi=1}^{F} (n_\Phi)^{n_\Phi} \qquad (20)$$

The problem (20) has dimension $d = N_F - F$ and not $N - F$, as it appears in.[9-11] The notations in (20) are

$$\begin{gathered} n_0 = 1 \;\; c_0 = 1 \\ c_i = \exp[-g_i^0] \quad (i \in I_{NF}) \end{gathered} \qquad (21)$$

The dual problem (20) of GP is subject to restrictions:

$$\begin{gathered} \sum_{i=0}^{N_F} a_{ji}\, n_i = 0 \;\; (j = 1, 2, \ldots M) \\ n_i \geqslant 0 \qquad (n_0 = 1) \end{gathered} \qquad (22)$$

where $a_{00} = 1$ and $a_{j0} = -b_j (j = 1, 2 \ldots M)$. This new matrix a_{ji} is:

$$a_{ji} = \left| \begin{array}{c:c:c:c} 1 & 0 \;\; 0 \;\; 0 \;\; \ldots & 0 \;\; 0 \;\; 0 \;\; \ldots \;\; 0 & \ldots \\ -b_1 & & & \\ -b_2 & a_{jk} & a_{jk} & \\ \cdot & & & \\ \cdot & & & \\ -b_M & & & \cdots \end{array} \right| \qquad (23)$$

$$\underset{(\Phi = 1)}{\left\{ \begin{matrix} j = 1, 2 \ldots M \\ k = 1, 2 \ldots N_1 \end{matrix} \right\}} \quad \underset{(\Phi = 2)}{\left\{ \begin{matrix} j = 1, 2 \ldots M \\ k = N_1 + 1, \ldots N_2 \end{matrix} \right\}}$$

It is possible by the duality theorem,[8,9] to associate with the dual problem (20, 22) a primal program which is:

$$\min \; p_0(z_j) = \prod_{j=1}^{M} z_j^{a_{j0}} \qquad (24)$$

subject to posinomial restrictions

$$p_{\Phi}(z_j) = \sum_{i \in I_{\Phi}} u_i(z_j) = \sum_{i \in I_{\Phi}} c_i z_j^{a_{i1}} z_2^{a_{i2}} \ldots z_M^{a_{iM}} \leqslant 1 \tag{25}$$

$$z_j > 0 \qquad \begin{matrix} (j = 1, 2 \ldots M) \\ (\Phi = 1, 2 \ldots F) \end{matrix}$$

A method for solving the dual problem (in the form (8 — 10)) was given by Boynton,[4] using a "steepest descent" algorithm. This is an extended method of that advanced by White et al[16] for solving one-phase equilibrium problem (see also [12, 17, 6]).

The primal program (24, 25), which is in this paper correctly formulated, seems to present some advantages: small number of variables and restrictions. It rests to be tested with different systems.

3.2. FORMULATION (b)

The problem formulated as (b), eq. (11 — 13), has been recently discussed by Heidemann.[3] Some examples were worked out, especially real systems.

We will present the transformation of this problem in the corresponding dual geometric program.

Using the same set of indices (14) one obtains:

$$\min g(n_i) = \sum_{i \in I_{NF}} n_i \left(g_i^0 + \ln \frac{n_i}{n_{\Phi}} \right) \tag{11'}$$

subject to

$$\sum_{i \in I_{NF}} a_{ji} n_i - \sum_k \nu_{jk} \xi_k = n_j^0 \quad (j = 1, 2 \ldots N) \tag{12'}$$

$$n_i \geqslant 0 \tag{13'}$$

Equation (12′) can be written in the form:

$$\sum_{i \in I_{NF}} a_{ji} n_i = n_j^0 + \sum_k \nu_{jk} \xi_k \quad (k = 1,2 \ldots \mathscr{R}) \tag{26}$$

where matrix a_{ji} is now a block formed of F unity matrix, each of dimension N.

Transforming (11′) to the dual program (20), the formulation arises

$$\max \; v(n_i) \tag{27}$$

subject to new constraints

$$\sum_{i=0}^{N_F} a_{ji} n_i = 0 \, ; \; n_0 = 1 \, ; \; n_i \geqslant 0 \, ; \; (j = 0,1,2 \ldots N) \tag{28}$$

where

$$a_{00} = 1$$

$$a_{j0} = -n_j^0 - \sum_k \nu_{jk}\,\xi_k \quad (k = 1, 2 \ldots \mathcal{R}) \tag{29}$$

Matrix a_{ji} becomes:

$$a_{ji} = \left|\begin{array}{l:llll:llll:l} 1 & 0 & 0 & \ldots & 0 & 0 & 0 & \ldots & 0 & \ldots. \\ -n_1^0 - \sum\limits_k \nu_{1k}\,\xi_k & 1 & 0 & \ldots & 0 & 1 & 0 & \ldots & 0 & \\ -n_2^0 - \sum\limits_k \nu_{2k}\,\xi_k & 0 & 1 & \ldots & 0 & 0 & 1 & \ldots & 0 & \\ \vdots & & & & & & & & & \\ -n_N^0 - \sum\limits_k \nu_{Nk}\,\xi_k & 0 & 0 & \ldots & 1 & 0 & 0 & \ldots & 1 & \ldots. \end{array}\right| \tag{30}$$

$$\underset{(\Phi = 1)}{\begin{Bmatrix} j = 1, 2 \ldots N \\ i = 1, 2 \ldots N_1 \end{Bmatrix}} \quad \underset{(\Phi = 2)}{\begin{Bmatrix} j = 1, 2 \ldots N \\ i = N_1 + 1, \ldots N_2 \end{Bmatrix}} \ldots$$

Now it is also possible to associate with the dual program (27, 28) a corresponding primal:

$$\min p_0(z_j, \xi_k) = \prod_{j=1}^{N} z_j^{a_{j0}} = \prod_{j=1}^{N} z_j^{-(n_j^0 + \sum\limits_k \nu_{jk}\xi_k)} \tag{31}$$

subject to the posinomials:

$$p_\Phi(z_j) = \sum_{i \in I_\Phi} u_i(z_j) = \sum_{i \in I_\Phi} c_i z_1^{a_{i1}} z_2^{a_{i2}} \ldots z_N^{a_{iN}} \leqslant 1 \tag{32}$$

$$z_j > 0 \qquad \begin{array}{l} (j = 1, 2 \ldots N) \\ (\Phi = 1, 2 \ldots F) \end{array}$$

As far as we know such a formulation was not previously given in the literature. This program is only similar to the primal problem (24, 25) but differs in the number of variables and in the matrix a_{ji}. First, this new primal program may appear more complicated (N variables as compared to M), but the matrix a_{ji} (eq. 30) has a remarkable form which make the restrictions (32) linear. These are:

$$\begin{aligned} p_1(z_j) &= c_1 z_1 + c_2 z_2 + \ldots c_{N_1} z_N \leqslant 1 \\ p_2(z_j) &= c_{N_1+1} z_1 + \ldots\ldots c_{N_2} z_N \leqslant 1 \\ &\vdots \\ p_F(z_j) &= c_{N_{F-1}+1} z_1 + \ldots c_{N_F} z_N \leqslant 1 \\ z_j &> 0 \end{aligned} \tag{33}$$

It can be shown that the program (31 — 33) reduces in a particular case, namely $\xi_k = 0$ $(k = 1, 2 \ldots \mathcal{R})$, to the very important problem of phase equilibrium. In this case eq. (26) becomes:

$$\sum_{i \in I_{NF}} a_{ji}\, n_i = n_j^0 \tag{34}$$

This problem was posed in.[15] One obtains a primal program (named "phase equilibrium primal program") similar to the above formulated (31 — 33), which has a simpler objective function and may be useful in applications.

It is interesting to observe that, although the program (31 — 33) is primal in form, it has characteristics of a dual one. So, the program can be reformulated:

$$\max Y = -\ln p_0(z_j,\ \xi_k) \tag{35}$$

subject to (32, 33). This program will be designed as "Y formulation". Using Lagrange's multipliers, $\lambda_\Phi (\Phi = 1, 2 \ldots F)$ and Kuhn-Tucker conditions,[9] one obtains for a stationary point:

$$\frac{\partial Y}{\partial \xi_k} = \sum_j \nu_{jk} \ln z_j = 0 \quad (j = 1, 2 \ldots N)$$

$$\frac{\partial Y}{\partial z_1} = \frac{n_1^0 + \sum_k \nu_{1k}\, \xi_k}{z_1} + \lambda_1 c_1 + \lambda_2 c_{N_1+1} + \ldots \lambda_F c_{N_{F-1}+1} = 0$$

$$\frac{\partial Y}{\partial z_2} = \frac{n_2^0 + \sum_k \nu_{2k}\, \xi_k}{z_2} + \lambda_1 c_2 + \lambda_2 c_{N_1+2} + \ldots \lambda_F c_{N_{F-1}+2} = 0$$

$$\vdots$$

$$\frac{\partial Y}{\partial z_N} = \frac{n_N^0 + \sum_k \nu_{Nk}\, \xi_k}{z_N} + \lambda_1 c_{N_1} + \lambda_2 c_{N_2} + \ldots \lambda_F c_{N_F} = 0 \tag{36}$$

$$\lambda_1(c_1 z_1 + c_2 z_2 + \ldots c_{N_1} z_N - 1) = 0$$

$$\lambda_2(c_{N_1+1} z_1 + c_{N_1+2} z_2 + \ldots c_{N_2} z_N - 1) = 0$$

$$\vdots$$

$$\lambda_F(c_{N_{F-1}+1} z_1 + \ldots c_{N_F} z_N - 1) = 0$$

$$\lambda_\Phi \leqslant 0$$

Equations (36) represent a nonlinear equation system which may be principally solved to find z_j, ξ_k and λ_Φ. It remains also open the question of testing these variants of the "Y formulation" (minimum subject to linear constraints or the nonlinear equation system) on different systems, for deciding on its practical usefulness.

In appendix we come back to give a physical meaning to the "Y formulation" as a nonlinear equation system.

3.3. A TRANSFORMED DUAL PROGRAM

Eq. (26) can be rewritten by expliciting the mole number of components in the phase $\Phi = 1$:

$$n_j = n_j^0 + \sum_k \nu_{jk}\, \xi_k - \sum_j a_{ji}\, n_i \geqslant 0 \qquad (37)$$

$$\left\{ \begin{array}{l} j = 1, 2 \ldots N_1 (= N) \\ i = N_1 + 1, \ldots N_F \end{array} \right\}$$

Transforming (11′) in the dual program (20) and substituting (37), one obtaints after rearrangement :

$$\max\, v(\xi_k, n_i) = K_0 \prod_k K_k^{\xi_k} \prod_i K_i^{-n_i} \prod_j n_j^{-n_j} \prod_i \left(\frac{c_i}{n_i}\right)^{n_i} \prod_\Phi n_\Phi^{n_\Phi} \qquad (38)$$

with the same set of indices as in (37). The significations of notations are :

$$K_0 = \prod_j c_j^{n_j^0} \qquad (39)$$

$$K_k = \prod_j c_j^{\nu_{jk}} \qquad (40)$$

$$K_i = \prod_j c_j^{a_{ji}} \qquad (41)$$

The program (38) subject to restrictions (37) is named [8-9] a "transformed dual problem" in GP. This form leads, after the rearrangement $g = -\ln v$, to expressions well known in chemical thermodynamics. For example, in the case of simple systems, eq. (38) reduces to expressions as those given by Heidemann's equations [3] (29, 37).

The transformed dual program may be solved using a general method from GP. In fact, the problem was solved by Heidemann [3] in the case of butane isomerization, a system with $N = 2$ and $F = 2$. For large systems the problem seems to be very complex, some difficulties being pointed out in.[3]

Another possibility is to meet the conditions of stationarity and obtain:

$$\frac{1}{v(\xi_k, n_i)} \frac{\partial v(\xi_k, n_i)}{\partial \xi_k} = \ln K_k - \sum_j \nu_{jk} \ln n_j + \sum_j \nu_{jk} \ln n_{\Phi=1} = 0 \tag{42}$$

$$\frac{1}{v(\xi_k, n_i)} \frac{\partial v(\xi_k, n_i)}{\partial n_i} = \ln c_i - \ln K_i + a_{ji} \ln n_j - \ln n_i - \\ - a_{ji} \ln n_{\Phi=1} + \ln n_{\Phi(i)} = 0 \tag{43}$$

The sets of indices are those from (37) and the notation $n_{\Phi(i)}$ means the total mole number of the phase which contains the component i.

One arrives in equation (42) to the well-known chemical equilibrium constant relations, for the $\mathscr{R}$ reactions in the system. Equations (43) are also well known, giving the phase equilibrium conditions, i.e. equality of each component chemical potential in all phases. Considering the block form of the matrix a_{ji} (eq. 30), eq. (43) reduces to

$$\ln c_i - \ln K_i + \ln n_j - \ln n_i - \ln n_{\Phi=1} + \ln n_{\Phi(i)} = 0 \tag{44}$$

Applications of eq. (42, 44) to simple systems ($N=2$, $F=2$, $\mathscr{R}=1$) are also found in Heidemann's work.[3] An application to "flash" equilibrium calculations is given by Sanderson and Chien[5] which have solved a nonlinear system of the form (42, 44) by the Marquardt's method.

4. AN ALGORITHM FOR SOLVING THE TRANSFORMED DUAL PROGRAM

We will consider the case of a real system with F phases: a vapor phase (V) and $F-1$ liquid phases. For a component in a liquid phase one can use the "activity" model:

$$C_i^L = f_i^{0L}(T, P_i^s) \cdot \gamma_i(T, P, X_i^L) \tag{45}$$

A component in the vapor phase is described with the "fugacity" model:

$$C_i^V = P \cdot \varphi_i(T, P, X_i^V) \tag{46}$$

The calculation of the functions in the above models can be performed by using thermodynamic equations. For the calculation of $\gamma_i(T, P, X_i^L)$ one chooses a suitable equation, e.g. Wilson's equation or the NRTL equation.[18] The fugacity function $f_i^{0L} = \varphi_i^s P_i^s$ results from the functions $P_i^s(T)$ and $\varphi_i^s(T, P_i^s)$.[18] The function $\varphi_i(T, P, X_i^V)$ can be calculated with a state equation.[18-21]

It is possible to advance an algorithm of computation of phase and reaction equilibrium using the transformed dual program (38, 37, 13′) The steps of the algorithm are:

1. Initial data: $T, P, n_i^0, \mu_i^0(T)$
2. Calculation: $P_i^s(T)$, $\varphi_i^s(T, P_i^s)$, f_i^{0L}

3. Initial approximations : $n_i(i \in I_{NF}/I_1)$, $\xi_k(k = 1, 2, \ldots \mathscr{R})$
4. Calculation : $n_j(j \in I_1)$ with eq. (37)
5. Calculation : $\gamma_i(T, P, X_i^L)$, C_i^L(eq. 45), g_i^0(eq. 18), c_i(eq. 21)
6. Calculation : $\varphi_i(T, P, X_i^V)$, C_i^V(eq. 46), g_i^0(eq. 18), c_i(eq. 21)
7. Solve the dual program (38, 37, 13′) (for example using the projected gradient method of Rosen[9,22]). One obtains new values n_i^{new} $(i \in I_{NF}/I_1)$, $\xi_k^{\text{new}}(k = 1, 2 \ldots \mathscr{R})$
8. Calculation : $n_j^{\text{new}}(j \in I_1)$ with eq. (37)
9. Test stop. If "YES" → End.

If "NOT" → go to 5

The convergence test may be $|n_i^{\text{old}} - n_i^{\text{new}}| \leqslant \varepsilon$.

Application of the above algorithm to real systems in a single phase is presented in another paper.[10] It is possible to follow first a computation by assuming ideal behaviour (without steps 5, 6) and, thereafter, the calculation of the real system. The results obtained with the above method will be presented in a future work.

It must be mentioned that a similar procedure may be developed for solving the "Y formulation" of the primal program (31 − 33).

APPENDIX

We will consider a system with $N = 2$ species ; $F = 2$ phases (say a liquid L and a vapor V) and $\mathscr{R} = 1$ reaction.

The matrix (30) is :

$$a_{ji} = \left|\begin{array}{c:cc:cc} 1 & 0 & 0 & 0 & 0 \\ -n_1^0 - \nu_1\xi & 1 & 0 & 1 & 0 \\ -n_2^0 - \nu_2\xi & 0 & 1 & 0 & 1 \end{array}\right| \begin{array}{l} (j = 0, 1, 2) \\ (i = 0, 1, 2, 3, 4) \end{array} \qquad (\mathrm{A}_1)$$

The problem (31) becomes :

$$\min p_0(z_1, z_2, \xi) = z_1^{-(n_1^0 + \nu_1\xi)} \cdot z_2^{-(n_2^0 + \nu_2\xi)} \qquad (\mathrm{A}_2)$$

subject to

$$p_1(z_1, z_2) = c_1 z_1 + c_2 z_2 \leqslant 1 \qquad (\mathrm{A}_3)$$

$$p_2(z_1, z_2) = c_3 z_1 + c_4 z_2 \leqslant 1$$

and

$$n_i^0 + \nu_i\,\xi \geqslant 0 ; \quad z_1 > 0 ; \quad z_2 > 0$$

The "Y function" (35) is :

$$\max Y = -\ln p_0(z_1, z_2, \xi) = (n_1^0 + \nu_1\xi)\ln z_1 + (n_2^0 + \nu_2\xi)\ln z_2 \qquad (\mathrm{A}_4)$$

The nonlinear equation system (36) becomes :

$$\frac{\partial Y}{\partial \xi} = \nu_1 \ln z_1 + \nu_2 \ln z_2 = 0 \tag{A$_5$}$$

$$\frac{\partial Y}{\partial z_1} = (n_1^0 + \nu_1 \xi)/z_1 + \lambda_1 c_1 + \lambda_2 c_2 = 0 \tag{A$_6$}$$

$$\frac{\partial Y}{\partial z_2} = (n_2^0 + \nu_2 \xi)/z_2 + \lambda_1 c_2 + \lambda_2 c_4 = 0. \tag{A$_7$}$$

$$\lambda_1(c_1 z_1 + c_2 z_2 - 1) = 0 \tag{A$_8$}$$

$$\lambda_2(c_3 z_1 + c_4 z_2 - 1) = 0 \tag{A$_9$}$$

$$\lambda_1 \leqslant 0 ; \quad \lambda_2 \leqslant 0 \tag{A$_{10}$}$$

If both phases coexist at equilibrium, eqs. (A 8 — 10) become :

$$\lambda_1 < 0 ; \quad \lambda_2 < 0 \tag{A$_{11}$}$$

$$c_1 z_1 + c_2 z_2 - 1 = 0 \tag{A 12}$$

$$c_3 z_1 + c_4 z_2 - 1 = 0 \tag{A 13}$$

and the solution of the problem is easily obtained by solving equations (A—12, 13). This arises because the equilibrium is indifferent.[14,3]

Let us now look at a physical meaning of the equations and variables in the nonlinear system (A 5 — 10). It is possible to show by the duality theorem [9] (relations between the primal and dual GP variables) that the monoms in the posinomials (A 3) are equal to the mole fractions of the components in each phase.
Therefore :

$$X_1^L = c_1 z_1 ; \quad X_1^V = c_3 z_1 ; \quad X_2^L = c_2 z_2 \text{ and } X_2^V = c_4 z_2 \tag{A 14}$$

Equations (A 12,13) are in fact the well-known conditions $\sum_i x_i^{\Phi} = 1$.

By substituting (A—12, 13) in eq. (A 6, 7) one obtains the physical significance of λ_1 and λ_2 which are (aside of sign) the total mole number in each phase. Eqs. (A 6, 7) are simply the constraints (7) of the equilibrium problem.

Eq. (A 5) can be rearranged to :

$$z_1^{\nu_1} z_2^{\nu_2} = 1$$

Multiplying (A 11) with $c_1^{\nu_1} c_2^{\nu_2}$ (or $c_3^{\nu_1}\, c_4^{\nu_2}$) and considering (A 12) one obtains :

$$(X_1^L)^{\nu_1} (X_2^L)^{\nu_2} = c_1^{\nu_1}\, c_2^{\nu_2}$$

which, taking into consideration eq. (21), is the well-known equilibrium constant equation.

For ideal systems the solving (A 5 — 10) should be a relatively simple task. For real systems an iterative procedure (as in the algorithm given above) will probably converge to the solution. The direct solving of "Y program" must be considered too.

NOTATIONS

a_{ji} — matrix defined in different equations
b_j — elemental abundance defined in eq. (3, 5)
c_j — function defined in eq. (21)
C_i, C_i^{Φ} — functions defined in eqs. (15), (45), (46)
f_i — fugacity
F — number of phases in the system
g — Gibbs free energy (free enthalpy) of the system defined in eq. (19) (adimensional)
g_i^0 — function defined in eq. (18)
G — Gibbs free energy of the system defined in eq. (1)
I_{NF} — set of indices defined in (14)
K — functions defined in eqs. (39) — (41)
M — number of chemical elements in the system
n_i — mole number of component i
n_i^0 — initial mole number of component i
n_{Φ} — total mole number in phase Φ, eq. (16)
N — number of chemical species in the system
N_F — number of components in all phases ($\equiv N \times F$)
p — posinom
P — pressure
R — gas constant
$\mathscr{R}$ — number of reactions
T — temperature
u_i — monom in a posinomial form
v — dual program function, defined in eq. (20)
X_i — mole fraction
Y — function defined in eq. (35)
z_j — primal program variable

Greek symbols

γ_i — activity coefficient
λ_{Φ} — Lagrange multiplier
μ_i, μ_i^0 — chemical potential and standard chemical potential, respectively
ν_{ji} — stoichiometric matrix (> 0 for products, < 0 for reactants)
ξ_j — extent of reaction j (De Donder variable)
φ_i — fugacity coefficient
Φ — phase index

REFERENCES

[1] H. S. Caram and L. E. Scriven, *Chem. Eng. Sci.*, **31**, 163 (1976).
[2] H. G. Othmer, *Chem. Eng. Sci.*, **31**, 993 (1976).
[3] R. A. Heidemann, *Chem. Eng. Sci*, **33**, 1517 (1978).
[4] F. B. Boynton, *J. Chem. Phys.*, **32**, 1880 (1960).
[5] R. V. Sanderson and H.H. Y. Chien, *Ind. Eng. Chem. Process Dess. Develop.*, **12**, 81 (1973).
[6] D. Geană, *Rev. Chim. (Bucureşti)*, **29**, 1171 (1978).
[7] N. Z. Shapire and L. S. Shapley, *J. Soc. Ind. Appl. Math.*, **13**, 353 (1965).
[8] R. J. Duffin, E. L. Peterson and C. Zener, "Geometric Programming — Theory and Application", Wiley, New York, 1967.
[9] I. Marusciac, "Programare geometrică şi aplicaţii", Ed. Dacia, Cluj-Napoca, 1978.
[10] J. J. Dinkel, and R. Lakshmanan, *Comput. Chem. Eng.*, **1**, 41 (1977).
[11] D. Cartianu, *Rev. Chim. (Bucureşti)*, **30**, 754 (1979).
[12] F. van Zeggern and S. H. Storey, "The Computation of Chemical Equlibrium", Cambridge Univ. Press, 1970.
[13] D. Geană, *Rev. Roumaine Chim.*, **26**, 43 (1981).
[14] I. Prigogine and R. Defay, "Chemische Thermodynamik", VEB Deutscher Verl., Leipzig, 1962.
[15] D. Geană, *Rev. Chim. (Bucureşti)*, **31**, 491 (1980).
[16] W. B. White, S. M. Johnson and G. B. Danzig, *J. Chem. Phys.*, **28**, 751 (1958).
[17] G. Eriksson, Chem. Scr., *4*, 193 (1973); *8*, 100 (1975).
[18] J. M. Prausnitz, C. A. Eckert, R. V. Orye and J.P.O'Connel, "Computer Calculation for Multicomponent Vapor-Liquid Equilibria", Prentice-Hall, New Jersey, 1967.
[19] F. Daneş and D. Geană, *Bulet. Inst. Politehnic (Bucureşti)*, **41** (*4*), 67 (1979).
[20] F. Daneş and D. Geană, *Rev. Roumaine Chim.*, in press.
[21] R. A. Heidemann, Paper presented at the Symposium on the Thermodynamics of Aqueous Systems with Industrial Applications, Calgary, Oct. 1979.
[22] D. Geană, in preparation.

Revue Roumaine de Chimie, 26, *3*, 377–382 (1981)

ESTUDIO CINÉTICO DE LA REDUCCIÓN DEL Cr(VI) POR HIDROXILAMINA

S. SENENT, L. FERRARI y A. ARRANZ
Departamento de Química Física de la Universidad de Valladolid (España)

Recibido, el 27 de Deciembre de 1979

Se ha estudiado espectrofotométricamente la cinética de la reacción entre el Cr(VI) y la hidroxilamina en disoluciones acuosas de ácido perclórico y en exceso de NH_2OH. Los resultados obtenidos se ajustan a una ecuación de velocidad de la forma:

$$-\mathrm{d}[\mathrm{Cr(VI)}]/\mathrm{d}t = \{c_1[\mathrm{HClO_4}] + c_2 + c_3/[\mathrm{HClO_4}]\}[\mathrm{NH_3OH^+}][\mathrm{Cr(VI)}]$$

También se han calculado los parámetros termodinámicos de activación. Se propone un mecanismo de reacción consistente con dicha ecuación.

The kinetics of the reaction between Cr(VI) and hydroxylamine was studied spectrophotometrically in perchloric acid solutions containing excess of NH_2OH. The results agree with the empirical rate law:

$$-\mathrm{d}[\mathrm{Cr(VI)}]/\mathrm{d}t = \{c_1[\mathrm{HClO_4} + c_2 + c_3/[\mathrm{HClO_4}]\}[\mathrm{NH_3OH^+}][\mathrm{Cr(VI)}]$$

The thermodynamic quantities of activation have also been calculated. A mechanism for the reaction, consistent with that law, has been developed.

Muy escasa es la bibliografía existente sobre la oxidación de la hidroxilamina en la que se aborde el estudio cinetoquímico de esas reacciones y se propongan mecanismos de reacción. Se conocen algunos trabajos en los que se han utilizado oxidantes tales como Ce(IV),[1] Mn(III),[2] Co(III)[3] o Ag(II),[4] pero con otros más complejos — por ejemplo Cr(VI) — no se ha pasado de la identificación de los productos finales y determinación de la estequiometría de la reacción,[5,6] que parecen variar de acuerdo con las condiciones iniciales de concentración relativa de los reactivos y acidez del medio. Así, en exceso de hidroxilamina y para disoluciones moderadamente ácidas, la reacción que tiene lugar puede representarse mediante la ecuación:

$$4\,\mathrm{HCrO_4^-} + 6\,\mathrm{NH_3OH^+} + 10\,\mathrm{H^+} \rightarrow 4\,\mathrm{Cr^{3+}} + 3\,\mathrm{N_2O} + 19\,\mathrm{H_2O}$$

Por esta razón, hemos considerado interesante realizar el estudio cinetoquímico del sistema Cr(VI)/hidroxilamina, cuyos resultados y conclusiones constituyen el presente trabajo.

PARTE EXPERIMENTAL

Para seguir la evolución de la reacción en función del tiempo se ha utilizado una técnica espectrofotométrica dinámica, eligiendo como especie química de control el Cr(VI), pues presenta una banda, cuyo máximo aparece a 350 nm, que resulta adecuada en las condiciones de trabajo ya que, aparte de ser intensa, no sufre interferencia alguna con los restantes reactivos ni con los productos de reacción.

Las disoluciones cumplen la ley de Lambert-Beer en los intervalos de concentracion es empleados: $[Cr(VI)] \leqslant 5.10^{-4}$ mol dm^{-3} y $[HClO_4]$ entre 5.10^{-5} y 5.10^{-3} mol dm^{-3}.

Todos los reactivos empleados fueron de pureza ,,para análisis'' : dicromato potásico Merck, hidrocloruro de hidroxilamina FEROSA y ácido perclórico Merck.

Con objeto de mantener constante la fuerza iónica del medio, se agregó en todos los experimentos perclorato sódico Merck.

Dada la rapidez de las reacciones objeto de estudio, resulta recomendable trabajar a temperatura inferior a la ambiente. Por ello se empleó un criostato HAAKE, mod. NK-22, provisto de impulsor centrífugo. El agua lanzada por él bañaba el portacubetas de un espectrofotómetro Perkin-Elmer, mod. 137 U.V., manteniendo la temperatura constante, con un error máximo de ± 0,1°. Las disoluciones de los reactivos; una vez que alcanzaban la temperatura de trabajo en el criostato, se mezclaban e introducían en el espectrofotómetro, en el cual se registraba automáticamente la variación de la absorción en función del tiempo en la longitud de onda elegida, 350 nm.

Las medidas de pH se llevaron a cabo en un pH-metro Radiometer, mod. 26, previamente calibrado con disoluciones reguladoras adecuadas para el intervalo de pH deseado.

RESULTADOS Y DISCUSIÓN

Se ha realizado un estudio sistemático de la influencia de la concentración de los reactivos, acidez del medio y temperatura sobre la velocidad específica de reacción. Los resultados se recogen en las tablas I a III, y pueden resumirse en los siguientes apartados :

1) La pseudoconstante de velocidad, de primer orden, es independiente de la concentración de Cr(VI) en el intervalo de concentraciones estudiado.

2) La relación entre la pseudoconstante de velocidad y la concentración de hidroxilamina puede considerarse directamente proporcional para $[NH_2OH] < 8.10^{-3}$mol dm^{-3}. Para concentraciones superiores se observa cierta desviación de la linealidad, tanto más acusada cuanto mayor es la temperatura.

3) La relación entre los inversos de k_{exp} y los de la concentración de hidroxilamina tambien es lineal, excepto para bajas concentraciones de esta última.

4) La dependencia de la pseudoconstante de velocidad con la acidez es todavía más complicada. En effecto, para $[HClO_4] < 0{,}8 \cdot 10^{-3}$ mol dm^{-3} los datos experimentales se ajustan a una recta de la forma :

$$k_{exp} \cdot [HClO_4] = d\ [HClO_4] + c$$

mientras que cuando $[HClO_4] > 1{,}6 \cdot 10^{-3}$ mol dm^{-3}, la relación lineal aparece al representar k_{exp} frente a $[HClO_4]$, es decir :

$$k_{exp} = b\ [HClO_4] + \ell$$

TABLA 1

Influencia de la concentración de Cr (VI)
Fuerza iónica : 0,38 mol dm^{-3} ; [HClO$_4$] = 5,10 · 10^{-4} mol dm^{-3}

[Cr(VI)]. 10^4 (mol dm^{-3})		1,0	1,5	2,0	2,5	3,0	3,5	4,0	4,5
T/°C	[NH$_2$OH] · 10^3 (mol dm^{-3})	$k_{exp.}$ · 10(min^{-1})							
13	6,0	1,08	1,33	1,10	1,16	1,09	1,29	1,32	—
13	7,0	1,54	1,51	1,52	1,51	1,50	1,49	1,57	—
13	8,0	1,63	1,65	1,63	1,64	1,70	1,58	—	—
23	6,0	2,03	2,02	1,90	1,86	1,91	1,97	2,08	2,26
23	7,0	—	2,95	2,88	2,63	2,64	2,81	—	—

Los coeficientes de correlación oscilan entre 0,9999 y 0,9960

TABLA 2

Influencias de la concentración de hidroxilamina y de la temperatura
Fuerza iónica : 0,38 mol dm^{-3} ; [Cr(VI)] = 4 · 10^{-4} mol dm^{-3} ; [HClO$_4$] = 5 · 10^{-4} mol dm^{-3}

[NH$_2$OH] · 10^3 (mol dm^{-3})	k_{exp} · 10 (min^{-1})					E_a(kJ mol^{-1})	ΔH≠(kJmol^{-1})	ΔS≠(JK^{-1}mol^{-1})
	T °(C) 9,5	12,0	14,5	16,5	20,0			
1,0	0,19	0,21	0,26	0,27	0,32	46	44	−122
3,0	0,46	0,60	0,68	0,76	0,91	42	40	−128
5,0	0,84	1,01	1,38	1,40	1,82	50	48	− 96
7,0	1,17	1,51	2,09	2,12	2,48	49	47	− 96
9,0	1,78	2,09	2,63	3,02	3,79	50	48	− 88

Los coeficientes de correlación oscilan entre 0,9997 y 0,9917 para las constantes de velacidad y entre 0,9992 y 0,9850 E_a, ΔH≠y ΔS≠.

TABLA 3

Influencia de la acidez del medio
Fuerza iónica : 0,38 mol dm^{-3} ; $[Cr(VI)] = 3 \cdot 10^{-4}$ mol dm^{-3}

T (°C)	13	13	13	25	25	25
$[NH_2OH] \cdot 10^4$ (mol dm^{-3})	2	3	5	2^a	3	5
$[HClO_4] \cdot 10^4$(mol dm^{-3})	$k_{exp.} \cdot 10^2(min^{-1})$					
0,5	5,4	7,2	—	—	14,2[b]	33,4[b]
1,0	4,2	6,8	12,9	—	—	30,9
2,0	4,1	6,1	12,1	—	—	—
3,0	4,1	5,8	11,0	—	13,4	24,6
4,0	3,9	5,8	10,6	8,1	15,8	21,1
5,0	4,5	6,2	10,1	—	—	21,0
6,0	5,0	6,4	10,7	—	15,6	24,1[c]
7,0	5,2	6,7	10,8	—	—	25,0[d]
8,0	—	—	—	10,8	17,0	26,8
10,0	6,8	8,9	12,0	11,2	18,9	29,6
11,0	—	—	—	—	20,4	32,5
20,0	12,2	18,5	22,5	17,0	28,4	—
40,0	19,5	28,6	40,1	26,3	45,6	—
50,0	23,2	34,0	48,2	30,6	52,1	—

[a] $[Cr (VI)] = 4.10^{-4}$ mol dm^{-3}.
$[HC10_4] . 10^4$/mol dm^{-3} : [b] 0,9 ; [c] 5,7 ; [d] 6,5.
Los coeficientes de correlación oscilan entre 0,9998 y 0,9939.

Ambas ecuaciones pueden suponerse casos límites de la expresión:

$$k_{exp} [HClO_4] = b[HClO_4]^2 + g[HClO_4] + c$$

en la que el primer y tercer términos llegan a hacerse despreciables en las zonas de baja y alta acidez, respectivamente.

Por consiguiente, la forma más general de la ecuación de velocidad en el intervalo de concentraciones en que la investigación se ha llevado a cabo es:

$$-d[Cr(VI)]/dt = k_{exp}[Cr(VI)] \qquad (1)$$

donde

$$k_{exp} = \{ c_1[HClO_4] + c_2 + c_3/[HClO_4]\}[NH_3OH^+] \qquad (2)$$

Hlasivcová y Novák [6] han identificado los productos finales de esta reacción y su estequiometría para diversas relaciones iniciales $Cr(VI)/NH_2OH$. En condiciones similares a las empleadas en el presente trabajo, comprobaron la presencia de N_2O pero no de N_2 o NO_3^-, y una estequiometría de dos moles de Cr(VI) por tres moles de NH_2OH, por valoración del exceso de hidroxilamina bien polarimétricamente, bien con Ce(IV). Gutch y Waters [7] han detectado por ESR radicales libres de vida corta en reacciones de oxidación de hidroxilamina (tanto en forma de hidrato como de hidrocloruro) con oxidantes monoelectrónicos, a los que atribuyen, en medio ácido, la estructura :

$$\cdot\mathrm{O}-\ddot{\mathrm{N}}\mathrm{H}_2 \leftrightarrow :\bar{\mathrm{O}}-\overset{+}{\underset{\cdot}{\mathrm{N}}}\mathrm{H}_2$$

De acuerdo con estas observaciones y los hechos experimentales anteriormente citados, se propone un mecanismo cuya primera etapa consiste en la formación de un complejo Cr(VI)–hidroxilamina, cuya posible existencia se basa en las mismas pruebas indirectas ya citadas en la discusión del mecanismo de la reacción Cr(VI)–hidracina [8] : linealidad entre los inversos de la pseudoconstante de velocidad y los de la concentración de hidroxilamina y valores negativos encontrados invariablemente para $\Delta S^{\neq}$. Su descomposición lenta da lugar al „intermediato" $NH_2O\cdot$:

$$\mathrm{HCrO_4^-} + \mathrm{NH_3OH^+} \underset{k_{-1}}{\overset{k_1}{\rightleftharpoons}} \mathrm{C} \xrightarrow{k_2} \mathrm{Cr(V)} + \mathrm{NH_2O}.$$

que, con otra molécula $HCrO_4^-$, se oxida a ácido hiponitroso, inestable el cual se descompone en óxido nitroso y agua, aunque no hay que descartar totalmente otras reacciones competitivas de esta última, tal como una posterior oxidación de NHO a HNO_2 que, a su vez, reaccionaría con la hidroxilamina.

En cuanto a la especie $HCrO_4^-$, se supone un comportamiento análogo al indicado en la reacción con la hidracina [8], por lo que no se considera necesario hacer nuevos comentarios sobre las etapas por las que transcurre su reducción.

La aplicación de la aproximación del estado estacionario al mecanismo propuesto, conduce a la ecuación :

$$v = k[\mathrm{HCrO_4^-}][\mathrm{NH_3OH^+}] \qquad (3)$$

donde

$$k = k_1 \cdot k_2/(k_{-1} + k_2) \qquad (4)$$

que es similar a la (1), cuando se mantiene constante la concentración de ácido perclórico.

Para explicar la dependencia de la velocidad de reacción con la acidez, se ha tenido en cuenta los equilibrios :

$$\mathrm{HCrO_4^-} + \mathrm{H_3O^+} \rightleftharpoons \mathrm{H_2CrO_4} + \mathrm{H_2O} \qquad K_1 \simeq 0{,}9\ (25°) \qquad (5)$$

que es el más importante que debe considerarse para las posibles especies crómicas presentes en las condiciones de trabajo, y

$$\mathrm{NH_2OH} + \mathrm{H_3O^+} \rightleftharpoons \mathrm{NH_3OH^+} + \mathrm{H_2O} \qquad K_2 = 6{,}6 \cdot 10^5\ (25°) \qquad (6)$$

Si se supone una serie de reacciones análogas y simultáneas a las del mecanismo propuesto, en las que intervengan las especies H_2CrO_4 y NH_2OH, la ecuación (3) toma la forma:

$$v = k[HCrO_4^-][NH_3OH^+] + k'[H_2CrO_4][NH_3OH^+] +$$

$$+ k''[HCrO_4^-][NH_2OH] + k'''[H_2CrO_4][NH_2OH] \qquad [7]$$

donde k', k'' y k''' son constantes análogas a k [4], que aparecen cuando intervienen las especies H_2CrO_4 y NH_3OH^+, $HCrO_4^-$ y NH_2OH, y H_2CrO_4 y NH_2OH respectivamente. Esta ecuación [7] junto con [5] y [6] conduce a la ecuación [1] y a una expresión de k_{exp} formalmente idéntica a [2], en la que:

$$c_1 = k' \cdot K_1$$

$$c_2 = k + k''' \cdot K_1/K_2$$

$$c_3 = k''/K_2$$

BIBLIOGRAFIA

[1] W. A. Waters y I. R. Wilson, *J. Chem. Soc. (A)*, **1966**, 534.
[2] G. Davies y K. Kustin, *Inorg. Chem.*, **8**, 484 (1968).
[3] B. Srakova, J. Sramek y J. Zyka, *Analyt. Chim. Acta*, **62**, 113 (1972).
[4] D. S. Honig, K. Kustin y J. F. Martin, *Inorg. Chem.*, **11**, 1895 (1972).
[5] P. Kozak y M. Jurecek, *Sb. Ved. Pr. Vys. Sk, Chemicko-technol. Pardubice*, **21**, 43 (1969).
[6] N. Hlasivcová y J. Novák, *Coll. Czechoslov. Chem. Comm.*, **36**, 2027 (1971).
[7] C. J. W. Gutch y W. A. Waters, *J. Chem. Soc. (A)*, **1965**, 751.
[8] S. Senent, L. Ferrari y A. Arranz, *Rev. Roumaine Chim.*, **23**, 179 (1978).

Revue Roumaine de Chimie, **26**, *3*, 383–388 (1981)

CARACTÉRISATION THERMOGRAVIMÉTRIQUE DE CERTAINES COMBINAISONS COMPLEXES DU THIOBISNAPHTOL

LUCIA ODOCHIAN*, ELENA MIHAI*, S. FIŞEL** et OLGA MITOŞERIU ***

* Laboratoire de Chimie Physique;
** Laboratoire de Chimie Analytique et minérale;
Institut Polytechnique de Jassy;
*** Laboratoire de Chimie Physique
Université de Galaţi, Roumanie

Reçu le 29 novembre 1979

On a étudié la décomposition thermique des complexes du thiobisnaphtol avec Cu, Ag, Hg et Pb dans des conditions dynamiques de température à vitesse constante de chauffage de 12,4°/mn en résultant certaines conclusions sur la composition chimique, la thermostabilité et la cinétique de la décomposition thermique. Le rapport de combinaison pour le complexe avec de l'Ag est 1Me : 1 L et pour les complexes avec Cu, Hg et Pb est 1 Me : 2 L. La thermostabilité des produits diminue en partant du thiobisnaphtol vers le complexe avec de l'Hg; le mécanisme de décomposition est complexe et dépend de la nature du métal.

The thermal decomposition of thiobisnaphthol complexes with Cu, Ag, Hg, and Pb was studied under dynamic temperature conditions, at a constant heating rate of 12.4°C/min. Some conclusions were drawn on the chemical composition, thermostability and kinetics of the thermal decomposition. The combination ratios are 1Me : 1 L for the Ag complex and 1 Me : 2 L for the Cu, Hg and Pb complexes. The thermostability decreases from thiobisnaphthol to the Hg complex. The decomposition mechanism is rather complex and depends on the metal nature.

Pour caractériser certains complexes du thiobisnaphtol avec : Cu, Ag, Hg et Pb ayant des applications dans la chimie analytique quantitative,[1] on a effectué, dans le présent ouvrage, la caractérisation thermogravimétrique dans des conditions dynamiques de température, en faisant certaines appréciations concernant la composition chimique, la cinétique de la décomposition thermique et la thermostabilité.

PARTIE EXPÉRIMENTALE

On a utilisé les complexes du thiobisnaphtol avec : Cu, Ag, Hg et Pb.[1]

Comme méthode de travail on a choisi la thermogravimétrie dynamique à vitesse constante d'échauffement en utilisant un dérivatographe MOM — Budapest type Paulik-Paulik-Erdey. Les conditions expérimentales utilisées ont été : vitesse de chauffage de 12,4°/mn, température maximale atteinte 900°, atmosphère ambiante, masse de l'échantillon de 18 mg mélangé à 400 mg Al_2O_3 récemment calciné à 1200°.

RÉSULTATS ET DISCUSSIONS

En analysant les thermogrammes enregistrés on a constaté que la décomposition se produit graduellement.

Le calcul des pertes en poids, ainsi que la quantité et la composition du résidu nous ont permis [2] d'établir la composition des combinaisons étudiées (tabl. 1).

TABLEAU 1

Résultats de l'analyse thermogravimétrique

Formule	W_{total}, mg		Résidue, mg			T_t°	
	calc.	exp.	Nature	Calc.	exp.	Méthodes classiques	DTA
$C_{20}H_{14}O_2S$	18	17,6	—	—	—	220	224
$(C_{20}H_{13}O_2S)_2Cu$	15,9	15,4	CuO noir	2,5	2,1	215	213
$C_{20}H_{13}O_2S$ Ag	13,4	12,2	Ag miroir	5,5	4,6	276	280
$(C_{20}H_{13}O_2S)_2Hg$	18,0	17,8	—	—	—	152	152
$(C_{20}H_{13}O_2S)_2Pb$	9,4	8,8	$PbSO_4$ blanc	9,2	8,6	—	—

Selon les données présentées dans le tableau 1, il résulte que le rapport de combinaison avec le Ag est 1 Me : 1 L, et dans les complexes de Cu, Hg et Pb, 1 Me : 2 L, résultats en concordance avec l'analyse chimique élémentaire (tabl. 2).

TABLEAU 2

Résultats de l'analyse chimique élémentaire

Formule	C %		H %		S %		Me %	
	calc.	exp.	calc.	exp.	calc.	exp.	calc.	exp.
$C_{20}H_{14}O_2S$	68,80	68,20	3,75	3,83	9,18	9,00	—	—
$(C_{20}H_{13}O_2S)_2Cu$	56,49	56,20	3,08	3,12	7,54	7,41	9,10	9,21
$C_{20}H_{13}O_2SAg$	57,51	58,20	3,14	3,20	7,68	8,01	25,36	25,60
$(C_{20}H_{13}O_2S_2)Hg$	57,06	56,80	3,11	3,20	7,62	7,39	—	—
$(C_{20}H_{13}O_2S)_2$ Pb	75,45	75,21	4,40	4,22	10,07	10,01	24,61	24,48

Dans la figure 1 où l'on présente les thermogrammes du thiobisnaphtol, du complexe avec du Pb et avec de l'Hg on a constaté que le mécanisme de décomposition devient plus compliqué dans cette série ; on assiste donc au passage de la décomposition en deux degrés (thiobisnaphtol) à la décomposition en cinq degrés (complexe avec de l'Hg).

TABLEAU 3

Comportement thermique et paramètres cinétiques des processus de décomposition

Formule	I degré			II degré			III degré			IV degré			V degré		
	T_i°	n	E_a kcal/mol	T_i°	n	E_a kcal/mol	T_i°	n	E_a kcal/mol	T_i°	n	E_a kcal/mol	T_i°	n	E_a kcal/mol
$C_{20}H_{14}O_2S$	200	1,7	25,09	478	2,9	46,9	—	—	—	—	—	—	—	—	—
$(C_{20}H_{13}O_2S)_2Cu$	180	2,2	25,30	426	—	92,0	—	—	—	—	—	—	—	—	—
$C_{20}H_{13}O_2S$ Ag	177	2,2	25,30	448	3,75	58,7	—	—	—	—	—	—	—	—	—
$(C_{20}H_{13}O_2S)_2Hg$	102	0,7	19,90	186	—	—	233	1,8	32,77	388	2	51,06	537	7,5	119,6
$(C_{20}H_{13}O_2S)_2Pb$	206	1,0	23,03	502	3,5	131,1	—	—	—	—	—	—	—	—	—

En appliquant la méthode de calcul Freeman-Carroll [3,4] pour les thermogrammes enregistrés on a obtenu les données présentées dans le tableau 3.

On doit remarquer que l'évaluation des paramètres cinétiques par cette méthode n'est pas possible pour tous les degrés de la décomposition. Dans le cas du complexe $(C_{20}H_{12}O_2S)_2Hg$ on ne peut pas appliquer la méthode de calcul avec une précision satisfaisante, parce que la séparation des domaines de décomposition n'est pas toujours nette ou l'intervalle de température est trop mince.

Des données du tableau 3 et des figures 2 et 3 où l'on présente les graphiques de type Freeman-Carroll pour les degrés I et II du thiobisnaphtol et des complexes de Cu, Ag et Pb on constate une modification de l'ordre de réaction qui augmente du premier degré au deuxième et on observe en même temps une modification de l'énergie d'activation avec le déplacement du domaine de température où le processus de décomposition a lieu [5].

Dans la figure 4 on présente le graphique Freeman-Carroll pour la décomposition thermique du complexe $(C_{20}H_{13}O_2S)_2Hg$. On a constaté une augmentation de l'ordre de réaction de 1,8 à 7,5 augmentation correspondant au troisième et au cinquième degré et de l'énergie d'activation que prouve la complexité du mécanisme de décomposition.

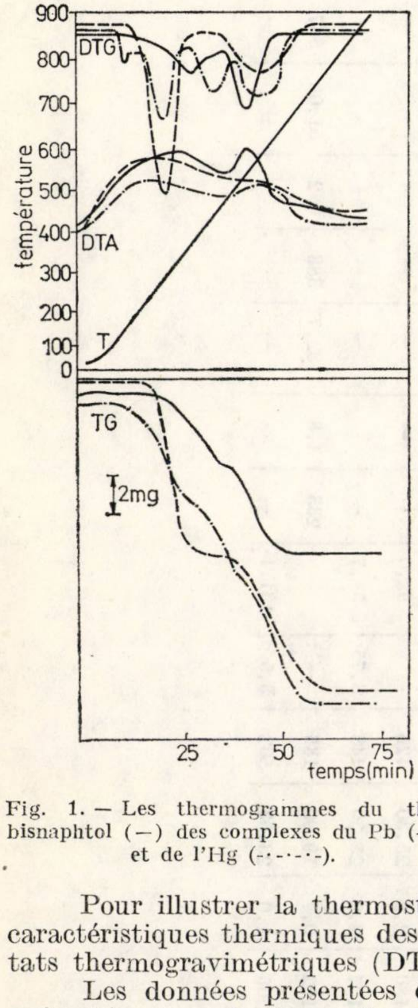

Fig. 1. — Les thermogrammes du thiobisnaphtol (—) des complexes du Pb (----) et de l'Hg (-·-·-·-).

Pour illustrer la thermostabilité, dans le tableau 1 on présente les caractéristiques thermiques des combinaisons étudiées déduites des résultats thermogravimétriques (DTG).

Les données présentées dans le tableau 1 et les courbes DTG [6] présentées dans la figure 5 conduisent à la conclusion que la stabilité thermique diminue dans la série : thiobisnaphtol, complexe du Cu, Ag vers le complexe avec de l'Hg ; le complexe avec du Pb présente une stabilité égale à celle du thiobisnaphtol.

En appliquant le critère cinétique de la thermostabilité on constate : les complexes du thiobisnaphtol avec : Cu, Ag et Pb sont plus stables du point de vue thermique que le complexe avec de l'Hg ; les énergies d'activation du premier degré de décomposition sont plus hautes que l'énergie d'activation du premier degré du complexe avec l'Hg.

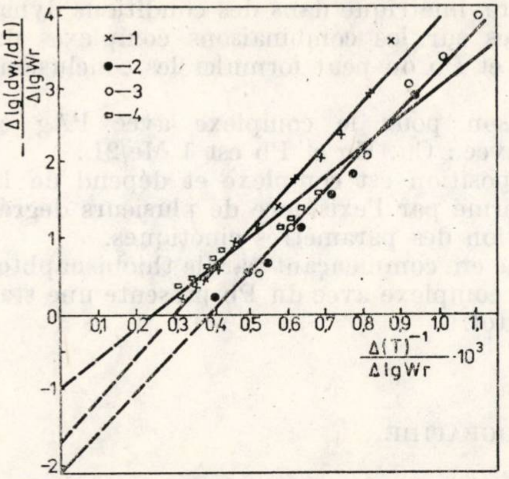

Fig. 2. — Le graphique de type Freeman-Carroll pour le premier degré du thiobisnaphtol et (1) des complexes avec : Cu (2) ; Ag (3) et Pb(4).

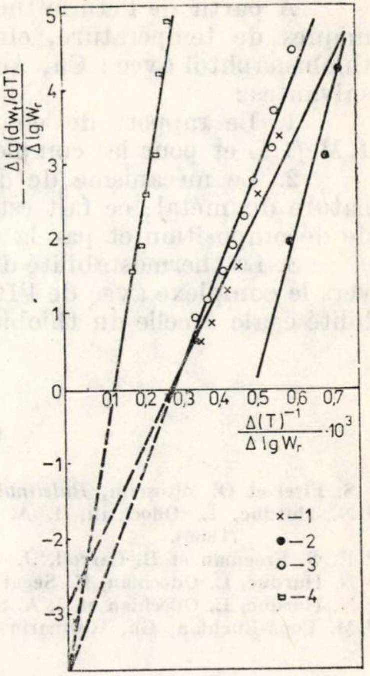

Fig. 3. — Le graphique du type Freeman-Carroll pour le deuxième degré du thiobisnaphtol (1) et des complexes avec : Cu (2) ; Ag(3) et Pb (4).

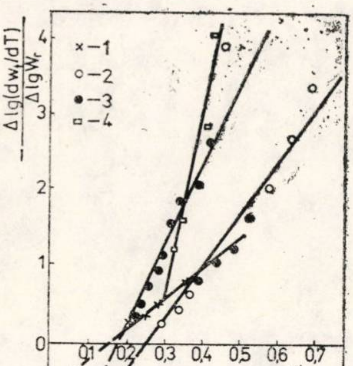

Fig. 4. — Le graphique du type Freeman-Carroll pour le complexe $(C_{20}H_{13}O_2S)_2Hg$ (1) premier degré ; (2) troisième degré et (3) cinquième degré.

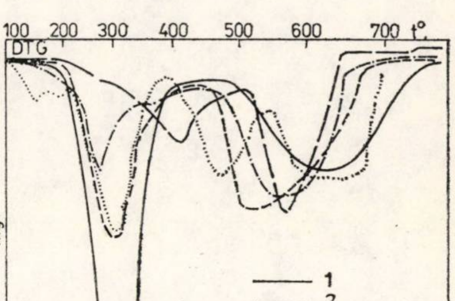

Fig. 5. — Les courbes DTG du thiobisnaphtol : (1) les complexes avec : Cu(2) ; Ag (3) ; Hg (4) et Pb (5).

A partir de l'étude thermogravimétrique dans des conditions dynamiques de température, effectuées sur les combinaisons complexes du thiobisnaphtol avec : Cu, Ag, Hg et Pb on peut formuler les conclusions suivantes :

1. Le rapport de combinaison pour le complexe avec l'Ag et 1 Me/1 L et pour les complexes avec : Cu, Hg et Pb est 1 Me/2L.

2. Le mécanisme de décomposition est complexe et dépend de la nature du métal ; ce fait est confirmé par l'existence de plusieurs degrés de décomposition et par la variation des paramètres cinétiques.

3. La thermostabilité diminue en commençant par le thiobisnaphtol vers le complexe avec de l'Hg ; le complexe avec du Pb présente une stabilité égale à celle du thiobisnaphtol.

BIBLIOGRAPHIE

[1] S. Fişel et O. Mitoşeriu, *Buletinul Universităţii Galaţi*, 1980, **3** (sous presse).

[2] N. Hurduc, L. Odochian, I. A. Schneider et E. Segal, *Rev. Roumaine Chim.*, **11**, 1453 (1966).

[3] E. S. Freeman et B. Carroll, *J. Phys. Chem.*, **62**, 394 (1958).

[4] N. Hurduc, L. Odochian, E. Segal et I. A. Schneider, *Z. phys. Chem.*, **237**, 9 (1968).

[5] N. Hurduc, L. Odochian et I. A. Schneider, *J. Thermal Analysis*, **6**, 17 (1974).

[6] M. Popa-Luchian, Gh. Rozmarin et I. A. Schneider, *J. Thermal Analysis*, **1**, 211 (1969).

Revue Roumaine de Chimie, 26, 3, 389–396 (1981)

EFFECT OF ADDED SALT ON THE COLLOIDAL BEHAVIOUR OF ALKALINE EARTH METAL CAPRYLATES

K. SINGH, P. BAHADUR* and P. BAHADUR**
Department of Chemistry, D.A.V. College, Muzaffarnagar (U.P.), 251001, India

Received May 24, 1978
Revised August 7, 1980

The conductivity measurements have been made to determine the critical micelle concentration (CMC) of alkaline earth metal caprylates in the presence of various salts viz. potassium chloride, nitrate, sulphate, ferricyanide and ferrocyanide. The lowering in CMC of soap solutions by salts was independent of the valency and the concentration of anions. An empirical equation $\log \Lambda_M = A + B \log C$ has been successfully employed to show the intersection of two straight lines corresponding to the CMC of soaps in various salt solutions. The results obtained are in close agreement with those obtained by plotting the deviations against the concentration. The values of constants A and B have been evaluated for two states of soaps in different soap solutions.

INTRODUCTION

Mukerjee and Mysels[1] have reviewed the CMC of surfactants in aqueous solutions. Mysels and Mysels[2] have discussed the problems involved in the determination of CMC of surfactants in the presence of salt solutions and have determined the CMC by plotting the deviations against concentration. Corkill and Goodman[3] have studied the formation of micelles with mixed counter ions and employed the differential conductance curves method for the determination of CMC. Wan and Poon[4] have recorded a shift in CMC at lower concentrations in the presence of salts. Varma and Bahadur[5] have studied the effect of methanol concentration on the micelle formation of aqueous calcium soap solutions. In our previous communication[6] the effect of anion on the colloidal behaviour of alkaline earth metal valerates has been discussed. The present paper deals with the study on micelle formation by alkaline earth metal caprylates in various salt solutions.

EXPERIMENTAL

Materials: **Anala R (BDH) caprylic acid, strontium carbonate, calcium carbonate and magnesium carbonate were used. The acid was purified by distillation under reduced pressure. The electrolyte potassium chloride, nitrate, sulphate, ferricyanide and ferrocyanide were Anala R BDH chemicals.**

*** To whom correspondence should be addressed.**
**** Chemistry Department, Agra College, Agra.**

Preparation of soaps: The calculated amount of metal carbonates was suspended in water and heated to about 80°C. The required amount of acid was added in portions to the suspension under constant stirring till the evolution of carbon dioxide was completely ceased. The products were purified by recrystallization from alcohol and dried in vacuum.

Conductance measurement: The procedure and apparatus used for the conductance measurement of soap solutions were the same as reported in our previous communication [6]. The reproducibility of the experimental data was examined by repeating the measurements several times. The results were reproducible up to 0.1 %.

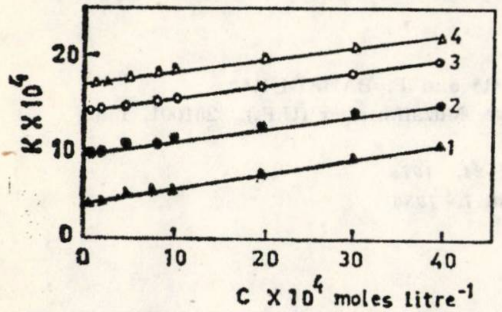

Fig. 1. — Plots of K *vs.* C for calcium caprylate in KNO_3 solution. 1. 0.002N; 2. 0.005N; 3. 0.008N; 4. 0.010N.

RESULTS AND DISCUSSION

The specific conductance K of strontium, calcium and magnesium caprylates has been measured in 0.002, 0.005, 0.008 and 0.010N, potassium chloride, nitrate, sulphate, ferricyanide and ferrocyanide solutions at 40°C. The K values increase with the increasing concentration of soap and electrolyte as well. The plots of K *vs.* C (Fig. 1) were seen almost linear lines which have however represented the intersection of two straight lines at CMC of soaps in aqueous medium.[5,6] A higher degree of precision was, therefore, made to detect micelle formation using the least square method. The specific conductance below the CMC was the best represented by equation (1):

$$K = MC + N \tag{1}$$

where K is the specific conductance and C is the concentration of soap expressed in moles litre^{-1}, M and N are constants recorded in Tables 1 and 2.

TABLE 1

Values of constant M for alkaline earth metal caprylates in electrolytic solutions

Soap	Concentration of electrolyte in g.equiv. litre^{-1}	Constant $M \times 10^4$				
		KCl	KNO_3	K_2SO_4	$K_3Fe(CN)_6$	$K_4Fe(CN)^6$
	0.002	4.68	4.16	3.91	4.42	3.18
Strontium caprylate	0.005	10.19	9.68	—	9.63	8.03
	0.008	15.08	14.60	—	15.07	13.09
	0.010	18.39	17.38	—	18.26	—
	0.002	4.10	3.69	3.93	4.35	4.08
Calcium caprylate	0.005	9.61	9.25	9.42	9.99	8.43
	0.008	15.74	14.13	14.22	15.27	12.78
	0.010	18.56	17.24	17.56	18.74	—
	0.002	4.34	3.98	3.96	4.39	3.17
Magnesium caprylate	0.005	10.14	9.47	9.34	9.99	8.42
	0.008	15.61	14.43	14.09	15.29	13.67
	0.010	16.91	17.60	17.46	18.69	—

TABLE 2

Values of constant N for alkaline earth metal caprylate in electrolytic solutions

Soap	Concentration of electrolyte in g. equiv. litre^{-1}	Constant N				
		KCl	KNO_3	K_2SO_4	$K_3Fe(CN)_6$	$K_4Fe(CN)_6$
Strontium caprylate	0.002	0.160	0.162	0.149	0.148	0.156
	0.005	0.155	0.153	—	0.127	0.121
	0.008	0.166	0.141	—	0.096	0.076
	0.010	0.155	0.132		0.099	—
Calcium caprylate	0.002	0.183	0.183	0.155	0.151	0.060
	0.005	0.172	0.163	0.077	0.101	0.133
	0.008	0.127	0.152	0.093	0.064	0.187
	0.010	0.127	0.139	0.068	0.061	—
Magnesium caprylate	0.002	0.146	0.150	0.136	0.131	0.138
	0.005	0.131	0.136	0.116	0.105	0.083
	0.008	0.119	0.123	0.102	0.076	0.039
	0.010	0.183	0.114	0.093	0.069	—

Each experimental point deviates randomly above the CMC from the line given by this equation with an amount ΔK which is plotted as the ordinate in the figure. The plots of ΔK *vs.* C. (Fig. 2) show the micelle formation at the concentrations 0.007, 0.0015 and 0.004M for strontium, calcium and magnesium caprylate respectively, for all the concentrations of various electrolytes used, supporting the observation made by Corrins and Harkins[7] that the lowering of CMC depends only on the nature and concentration of the ions having charge opposite to that on the micellar aggregate. This shows the effectiveness of salts in lowering the CMC of these soaps which were reported 0.008, 0.002 and 0.005M for strontium[8], calcium[9] and magnesium[10] caprylates in water respectively. The effect of salts on the micelle formation may be attributed to the salting out effect of strong electrolytes. Randall and Failey[11] have reported the relative salting out order of anions and nitrate ions was found to have a lesser salting out property than chloride ions. Since here all the electrolytes show an equal depressant effect on the CMC of soap solutions, it

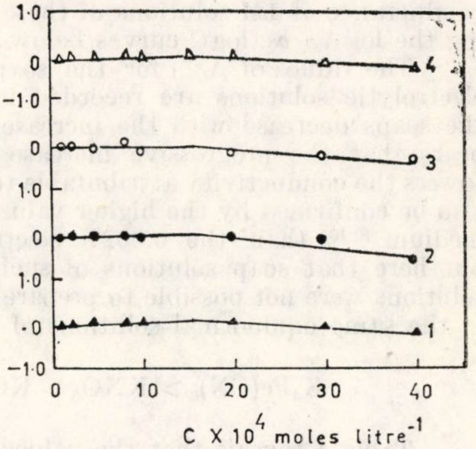

Fig. 2. — Plots of ΔK *vs.* C for calcium caprylate in KNO_3 solution. 1. 0.002N ; 2. 0.005N ; 3. 0.008N ; 4. 0.010N.

is apparent that factors other than salting out action of inorganic salt are involved. The shift of CMC to lower concentration may, therefore, be assumed due to the screening action of the simple electrolyte which lowers the repulsive forces between the polar head groups and as a result of it less electrical work is required in micelle formation.

The molecular conductance, Λ_M of soap solutions in various electrolytic solutions decreases with the increase in concentration and shows the order :

strontium caprylate > calcium caprylate > magnesium caprylate

The plots of Λ_M *vs* $\sqrt{C}$ are concave upwards which may be due to the fact that the factor Λ_M/Λ_O steadily decreases the slope of $\Lambda_M - \sqrt{C}$ plots as the concentration increases and thus shows a concave curve.

An empirical equation (2) has been successfully employed to find out the CMC of the soaps in various electrolytic solutions

$$\log\ \Lambda_M = A + B \log\ C \tag{2}$$

where A and B are constants and C is the concentration of soap expressed in moles litre^{-1}. The plots of log Λ_M *vs.* log$C$ (Fig. 3) are characterized by the intersection of two straight lines corresponding to the CMC of soap solutions. The values of CMC obtained are in close agreement with those obtained from Δk *vs.* C plots. Thus, it may be suggested that equation (2) may also be used as a tool to find out the micelle formation of soaps in electrolytic solutions which have however shown linear curves for these soap solutions in the absence of salts.[8-10] The values of molecular conductance of 1M solutions of these soaps were obtained by extrapolating the logΛ_M *vs.* log$C$ curves below and above the CMC region.

The values of $\Lambda_{C=1}$ for the soaps below the CMC region in different electrolytic solutions are recorded in Table 3. The $\Lambda_{C=1}$ values for all the soaps decrease with the increase in electrolyte concentration. It appears that the progressive increase in the concentration of electrolyte lowers the conductivity attributable to the colloidal electrolyte, which may also be confirmed by the higher values of $\Lambda_{C=1}$ for these soaps in aqueous medium [8-10] than the 0.002N electrolytic solution. It may be pointed out here that soap solutions of such high concentrations in electrolytic solutions were not possible to prepare. The values of $\Lambda_{C=1}$ for all the soaps in the same equinormal solutions of electrolyte exhibit the order :

$$K_4Fe(CN)_6 > KNO_3 > KCl > K_3Fe(CN)_6 > K_2SO_4$$

Table 4 reveals that the values of constant B (i.e. slope of the line in Fig. 3) below the CMC region increase with the increase in electrolyte concentration and are almost constant for equinormal solutions of various electrolytes, which confirms the similar effect of salt on the CMC of soaps.

Table 3 shows that the values of $\Lambda_{C=1}$ calculated from log Λ_M *vs.* log C lines above the CMC region also decrease with increasing electrolyte concentration. It may be due to the increase in micelle size with an increased salt concentration. The micelle size increases with an increased salt

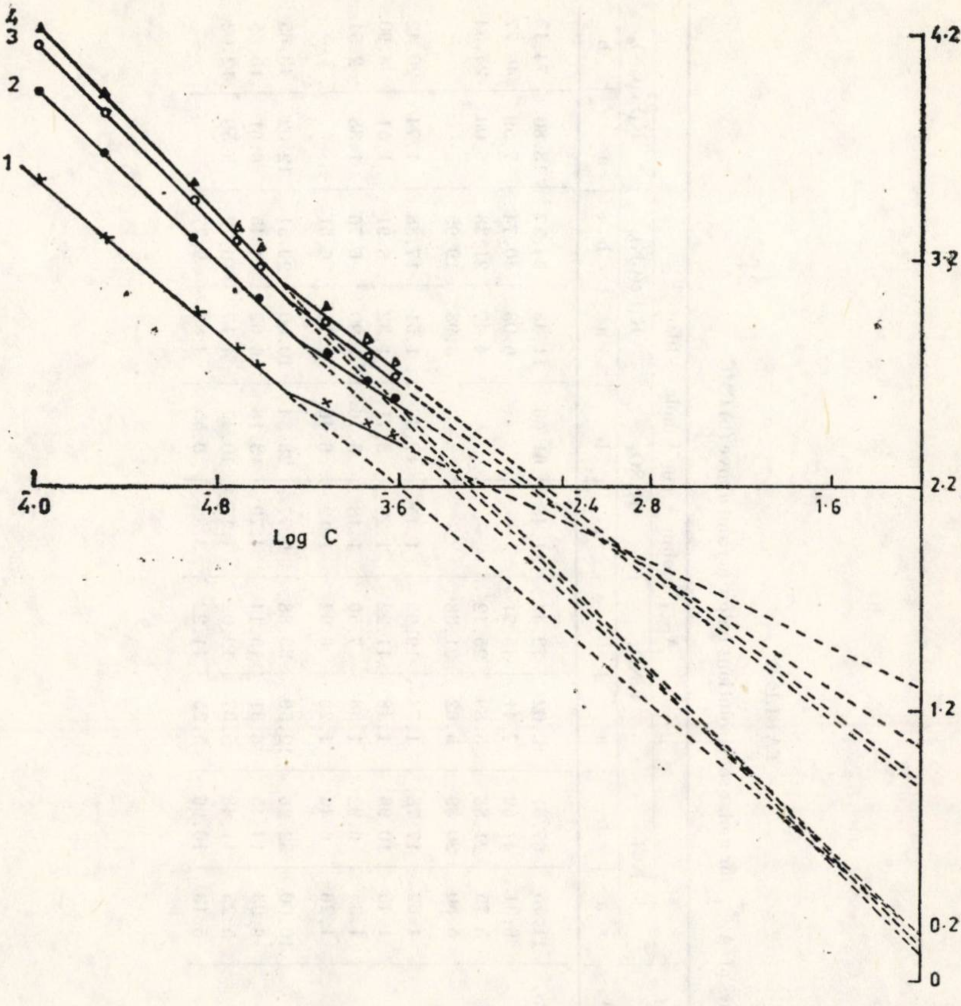

Fig. 3. — Plots of log Λ_M *vs.* log *C* for calcium caprylate in KNO_3 solution. 1. 0.002N; 2. 0.005N; 3. 0.008 N; 4. 0.010N.

concentration due to the reduction in electrical repulsion affecting the balance of forces up on which the size of micelles depends.[12] The values exhibit the order :

$$K_4Fe(CN)_6 > KNO_3 > KCl > K_3Fe(CN)_6 > K_2SO_4$$

The $\Lambda_{C=1}$ values above CMC are higher than the corresponding values below CMC. It may be suggested due to the increase in repulsive forces between the micelles and effective anion which predominates the size effect.

TABLE 3

Values of $\Lambda_{C=1}$ for molar soap solutions below (a) and above (b) CMC

Soap	Concentration of electrolyte in g. equiv. litre $^{-1}$	$\Lambda_{C=1}$ in ohm $^{-1}$ cm $^{-1}$ mole $^{-1}$ litre									
		KCl		KNO_3		K_2SO_4		$K_3Fe(CN)_6$		$K_4Fe(CN)_6$	
		a	b	a	b	a	b	a	b	a	b
Strontium caprylate	0.002	11.75	67.61	12.02	72.44	11.48	61.66	11.48	64.57	13.80	74.13
	0.005	6.31	41.69	7.41	45.71	—	—	6.03	40.74	7.59	46.77
	0.008	5.75	21.88	5.89	25.12	—	—	4.47	21.38	6.03	27.54
	0.010	5.50	20.89	5.62	21.38	—	—	3.98	19.95	—	—
Calcium caprylate	0.002	1.62	17.78	1.74	19.95	1.45	17.38	1.51	17.38	1.74	20.42
	0.005	1.45	10.96	1.48	11.22	1.29	8.71	1.32	8.91	1.51	4.90
	0.008	1.35	6.92	1.38	7.59	1.18	6.76	1.20	6.76	1.38	2.51
	0.010	1.26	6.46	1.29	6.92	1.12	6.46	1.15	6.61	—	—
Magnesium caprylate	0.002	10.00	32.26	12.59	33.88	9.77	28.84	10.00	29.51	12.02	43.65
	0.005	6.03	14.45	6.31	15.14	4.79	13.18	6.62	14.45	6.61	15.85
	0.008	5.25	11.48	5.37	12.02	4.17	10.47	4.17	10.72	5.50	12.02
	0.010	5.13	10.96	5.25	11.22	3.89	9.55	3.89	9.77	—	—

TABLE 4

Values of constant *B* for alkaline earth metal caprylates in electrolytic solutions below (a) and above (b) CMC

Soap	Concentration of electrolyte in g. equiv. litre $^{-1}$	Constant *B*									
		KCl		KNO_3		K_2SO_4		$K_3Fe(CN)_6$		$K_4Fe(CN)_6$	
		a	b	a	b	a	b	a	b	a	b
Strontium caprylate	0.002	0.59	0.24	0.57	0.22	0.57	0.22	0.57	0.22	0.52	0.20
	0.005	0.75	0.39	0.73	0.37	—	—	0.75	0.38	0.70	0.35
	0.008	0.82	0.56	0.82	0.54	—	—	0.83	0.54	0.77	0.48
	0.010	0.83	0.60	0.82	0.58	—	—	0.86	0.59	—	—
Calcium caprylate	0.002	0.82	0.50	0.82	0.48	0.84	0.48	0.84	0.48	0.82	0.43
	0.005	0.95	0.65	0.94	0.64	0.95	0.66	0.95	0.67	0.93	0.74
	0.008	1.00	0.80	1.00	0.77	1.01	0.78	1.02	0.79	1.01	0.90
	0.010	1.03	0.80	1.03	0.80	1.03	0.82	1.04	0.81	—	—
Magnesium caprylate	0.002	0.59	0.38	0.59	0.37	0.58	0.38	0.58	0.39	0.60	0.29
	0.005	0.76	0.58	0.75	0.58	0.77	0.59	0.76	0.58	0.69	0.53
	0.008	0.82	0.68	0.82	0.67	0.84	0.69	0.85	0.68	0.79	0.64
	0.010	0.84	0.70	0.83	0.71	0.87	0.72	0.89	0.73	—	—

Table 4 reveals that the values of B above CMC are constant for an equinormal electrolyte concentration for each soap and increase with the increasing concentration of electrolytes. The higher values of B below CMC than the corresponding values of B above CMC may be due to a slower decrease in molecular conductance.

ACKNOWLEDGEMENTS. The authors are thankful to the college authorities for providing laboratory facilities.

REFERENCES

[1] P. Mukerjee and K. J. Mysels, "Critical Micelle Concentrations of Aqueous Surfactants" NSRDS, Natl. Bureau of Standards, Washington, 1971.

[2] E. K. Mysels and K. J. Mysels, *J. Colloid Sci.*, **20**, 315 (1965).

[3] J. M. Corkill and J. F. Goodman, *Trans. Faraday Soc.* **58**, 206 (1962).

[4] S. C. Wan and K. C. Poon, *J. Pharm. Sci.*, **58**, 1562 (1969).

[5] R. P. Varma and P. Bahadur, *Cellulose Chem. Technol.*, **8**, 27 (1974).

[6] K. Singh, P. Bahadur and P. Bahadur, *Colloid and Polymer Sci.* (in press).

[7] M. L. Corrin and W. D. Harkins, *J. Amer. Chem. Soc.*, **69**, 683 (1947).

[8] R. P. Verma and R. Dayal, *J. Amer. Oil Chemists' Soc.*, **53**, 39 (1976).

[9] R.P. Verma and P. Bahadur, *Cellulose Chem. Technol.*, **9**, 393 (1975).

[10] R. P. Verma and K. Kumar, *Cellulose Chem. Technol.*, **9**, 23 (1975).

[11] M. Randall and C. F. Failey. *Chem. Rev.*, **4**, 271 (1927).

[12] P. H. Elworthy, A. T. Florence and C. B. McFarlane, "Solubilization by Surface Active Agents", Chapman and Hall Ltd., London, 1968.

Revue Roumaine de Chimie, 26, 3, 397–405 (1981)

SUR LE VAPOCRAQUAGE DU MÉTHYL-6-EICOSANE

JEAN GIRAUD, SIROUSSE NOURI et BYOUK BLOURI
Ecole Centrale des Arts et Manufactures
Laboratoire de Génie et Informatique Chimiques
Grande Voie des Vignes-92290-Châtenay Malabry—France

Reçu le 20 novembre 1979

Etude expérimentale du craquage du méthyl-6-eicosane dans un réacteur dynamique construit en acier inoxydable avec des parois passivées par chromaluminisation. L'analyse cinétique montre que l'ordre de la réaction est proche de 1, l'énergie d'activation de la réaction globale est 56,3 kcal et le facteur préexponentiel est égal à $1{,}2.10^{14}$. Ces résultats expérimentaux sont en accord avec la théorie de Rice-Kossiakoff.

Experimental study of cracking of 6-methyl-eicosane in a dynamic stainless steel reactor whose walls had been passivated by a deposit of chromium and aluminium (chromaluminisation). The kinetic analysis shows that the order of reaction is close to 1, the activation energy is of 56.3 kcal. and the pre-exponential factor is $1.2\cdot10^{14}$.

De nombreuses études ont été consacrées au vapocraquage thermique des hydrocarbures, que ceux-ci soient purs ou en mélange ; les conditions expérimentales d'étude étant elles-mêmes très diversifiées.

Le vapocraquage des fuel oils, des gaz oils et même du pétrole brut a été étudié.[1–2]

Cependant la plupart des modèles cinétiques et de simulation reposent en commun sur les théories de Rice et Kossiakoff [3] qui supposent que le craquage thermique se traduit par une chaîne de réactions radicalaires l'état stationnaire étant atteint. Aux faibles taux de conversion et pour des conditions expérimentales douces, ces théories et les résultats expérimentaux sont en accord mais, quel que soit le mécanisme proposé, la plupart des travaux concernent des paraffines normales relativement légères, inférieures ou égales à 16 atomes de carbone.[4] Pour des molécules plus lourdes, nous pourrions citer les travaux de notre propre laboratoire, axés sur l'étude chimique du vapocraquage d'hydrocarbures lourds.[5–6]

Le but de la présente note est de présenter les résultats d'une étude chimique et cinétique du vapocraquage d'un hydrocarbure lourd ramifié : le méthyl-6-eicosane.

PARTIE EXPÉRIMENTALE

Appareillage. Nous avons utilisé un réacteur dynamique composé de trois tubes coaxiaux disposés comme l'indique schématiquement la figure 1. Afin de mieux distinguer les zones de vaporisation et de préchauffage de la zone réactionnelle, l'eau et l'hydrocarbure sont vaporisés et préchauffés dans les zones I et II, respectivement ; la zone III constituant le four proprement dit. Afin d'en améliorer le profil thermique, le four est plongé dans un lit fluidisé de sable (diamètre des particules : 150 μ). La fluidisation est assurée par introduction de 20 ℓ/h d'azote préchauffé à 500°C et traversant une plaque fritée non représentée sur le schéma.

Chaque tube externe mesure 360 mm de long et a pour diamètre 22 et 25 mm. ; chaque tube interne mesure 350 mm de long et a pour diamètre 14 et 16 mm. Les trois parties de l'appareillage sont chauffées par des résistances électriques ($\simeq 20 \Omega$) à pas variable ; les températures sont lues et régulées au moyen de thermocouples Chromel Alumel (1, 2, 3) et les régulateurs.

Le thermocouple 4, mobile, permet de relever le profil thermique du four en fonctionnement. L'isolement thermique est assuré par une couche de Kaolin, la pression des fluides est mesurée au sommet (tubulure 5).

L'hydrocarbure est introduit dans la partie I au moyen d'une seringue et d'un pousse seringue électrique, son débit, constant est de 16 g/h. La température de préchauffage est de 500°C. Une pompe peristaltique est employée pour introduire l'eau dont le débit varie de 20 à 150 g/h ; la température de préchauffage est aussi de 500°C. Les produits de la réaction, évacués par la tubulure 6, sont trempés par un réfrigérant refroidi à l'eau courante puis recueillis dans un piège plongé dans la glace fondante ; les produits gazeux non condensés sont recueillis sur un flacon de Mariotte.

Les effluents sont recueillis lorsque l'appareil est en équilibre, c'est-à-dire un quart d'heure après le début de chaque essai ; auparavant l'appareil est purgé en faisant passer de l'eau durant 1 heure ($\simeq$ 50 g).

Après chaque essai les éventuels dépôts de carbone sont brûlés par un courant d'air chauffé à 600°C.

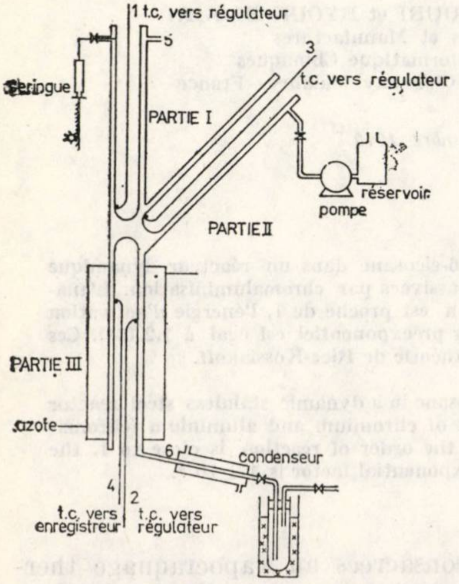

Fig. 1. — Schéma de l'appareillage

Analyse. Les liquides sont analysés en CPV sur un chromatographe GIRDEL équipé d'un détecteur à ionisation de flamme, la surface des pics est déterminée par un intégrateur A.O.I.P. La colonne, en acier inoxydable mesure 3m de long et a un diamètre de 1/8 de pouce, elle est remplie de SE 30 déposé sur chromosorb W/AW 60 — 80 mesh. La température est programmée de 50 à 210°C avec une vitesse linéaire de 10°C/mn.

Les gaz sont analysés sur un chromatographe AérographVarian équipé d'un détecteur à ionisation de flamme en employant deux colonnes en acier inoxydable, chacune ayant 2 m de long et 1/8 de pouce comme diamètre. La première colonne contient du di-octyle sébacate et la seconde du diéthylène glycol + nitrate d'argent.

Le rapport hydrogène/méthane est déterminé en utilisant un chromatographe Hermann Moritz à catharomètre, muni d'une colonne en acier inoxydable de 2m de long et 1/8 de pouce de diamètre remplie de tamis moléculaire 13X.

Synthèse du méthyl-6-eicosane. L'hydrocarbure est préparé en faisant réagir l'heptanone-2 sur le dérivé magnésien du bromo-1-n-tétradécane. L'hydrolyse du complexe intermédiaire conduit à un alcool qui est directement hydrogéné en alcane grâce à un catalyseur de type Adkins, sous une pression d'hydrogène de 100 kg/cm². Sa pureté, déterminée par C.P.V. est 97,5 %.

Effets de parois. Il existe de nombreuses publications soulignant le rôle catalytique des parois sur les réactions de pyrolyse, particulièrement en ce qui concerne les aciers inoxydables.[7 à 9]

Les parois des trois parties du four sont passivées par le procédé de chromaluminisation mis au point par la Société Heurchrome. Ce procédé consiste à déposer, par pulvérisation à chaud, sur la surface à protéger, une couche de 0,01 à 1 mm d'un apport à base de chrome et d'aluminium, ceci confère à l'acier une grande résistance à l'oxydation et à la réduction dans le domaine de température allant jusqu'à 1200°.

Une série préalable d'essais, au cours de laquelle nous avons craqué un mélange de n-paraffines en $C_{24}-C_{25}$ entre 800 et 950°C et en présence d'eau a montré qu'un tube en acier 18/8 ainsi passivé est stable et conduit aux mêmes résultats qu'un tube en quartz, le quartz étant bien connu pour donner de faibles effets catalytiques.[10]

Après 60 heures d'essais (durée moyenne 1h) alternés avec 100 heures de régénérations par passage d'air à 600°C (durée moyenne : 1h30) les résultats sont toujours parfaitement reproductibles contrairement à de nombreux autres aciers spéciaux qui conduisent plus ou moins rapidement à d'importantes quantités de carbone et d'hydrogène.[11]

RÉSULTATS

Les essais ont été effectués entre 550 et 650°C. Le débit d'eau est compris entre 19,8 g/h et 106 g/h, alors que le débit d'hydrocarbure est maintenu constant à 16 g/h. Aux plus forts débits et aux plus hautes températures, le nombre de Reynolds, Re, était égal à 230, ce qui indique que le four fonctionne en régime laminaire. Dans les calculs suivants, nous supposerons que l'écoulement est tampon, dans nos conditions expérimentales cette hypothèse introduit une erreur $\simeq 2\,\%$ sur la répartition des vitesses ainsi que l'a montré.[12]

Cinétique globale du craquage. Une des principales difficultés rencontrées dans la détermination d'énergies d'activation globales à partir d'expériences réalisées en régime dynamique est la détermination du volume réel du réacteur. Dans notre système, malgré la séparation des zones réservées au préchauffage et l'emploi d'un lit fluidisé, le four n'est pas réellement isotherme, aussi avons-nous utilisé le concept de volume équivalent tel qu'il a été défini par.[13]

La température de référence, T_r, est celle qu'indique le régulateur, V étant le volume réel, V_r le volume équivalent, on peut écrire :

$$V_r = \frac{\int_0^V \exp - \dfrac{E}{RT}\,\mathrm{d}V}{\exp - \dfrac{E}{RT_r}}$$

Un programme permet de déterminer V_r à partir des données expérimentales obtenues durant chaque essai en relevant le profil thermique du four. L'énergie d'activation a été fixée a priori à 60 kcal/M, une méthode essais/erreurs programmée permet, par convergence rapide, de déterminer la valeur réelle de l'énergie d'activation.

1) DÉTERMINATION DE L'ORDRE DE LA RÉACTION

Nous avons employé la relation de Kershenbaum et Martin,[14] qui ont montré que pour une température et un profil de pression constants il existe la relation suivante entre la fraction molaire moyenne en hydrocarbure $\overline{X}$, la vitesse initiale de craquage ΔF et de l'ordre de la réaction :

$$\log(-\Delta F) = \mathrm{n} \log(\overline{\mathrm{X}}) + \log k$$

Les essais ont été réalisés pour un faible taux d'avancement. La figure 2 montre le graphe de $\log(-\Delta F)$ en fonction de log X à 2 températures. De ces deux droites nous avons calculé l'ordre n

$$n = 1{,}06 \text{ à } 600°\text{C}$$

$$n = 1{,}16 \text{ à } 650\ °\text{C}$$

2) DÉTERMINATION DE LA CONSTANTE DE VITESSE

Les résultats exposés ci-dessus montrent que l'hypothèse selon laquelle le méthyl-6-eicosane se craque selon une cinétique du premier ordre est fondée. On peut donc écrire :

$$\begin{array}{ccc} A & \xrightarrow{\quad\quad} & B + C \\ (1 - \alpha) & & \alpha + \alpha \end{array}$$

et après détermination expérimentale du taux de conversion α, du volume équivalent et du temps de séjour en résultant t, la tangente à la courbe :

$$\text{Log} \frac{1}{1-\alpha} = f(t)$$

permet de déterminer k. La valeur de l'énergie d'activation est déterminée par le graphe de $\text{Log}\ k = f\,\frac{1}{T}$; puis elle est affinée par la méthode essai/erreur citée ci-dessus.

Nous avons déterminé une valeur globale de l'énergie d'activation :

$$E_a = 56{,}3 \text{ kcal}$$

et une valeur du facteur préexponentiel A :

$$A = 1{,}2\ 10^{+14}$$

Les constantes de vitesse que nous avons déterminées ne sont pas indépendantes de la conversion comme le montre le graphe de $\text{Log} \frac{1}{1-\alpha} = f(t)$ à plusieurs températures (fig. 3).

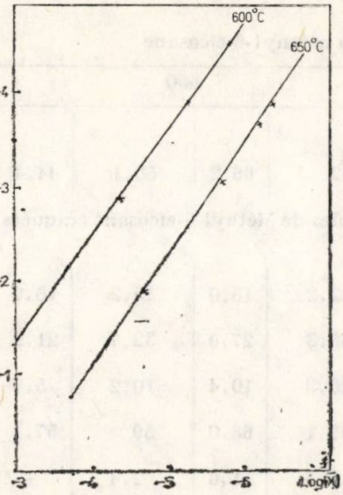

← Fig. 2. — Détermination de l'ordre de la réaction.

Fig. 3. — Détermination de la constante de vitesse *k*.

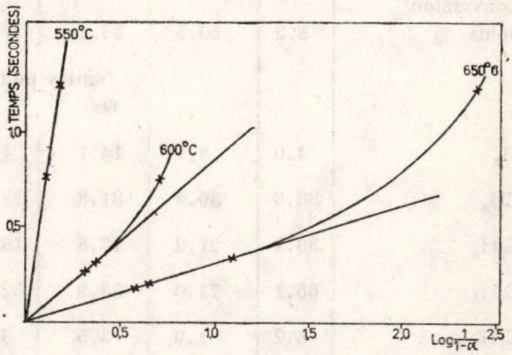

Les vitesses globales moyennes déterminées ainsi sont présentées dans le tableau 1 ci-dessous :

TABLEAU 1

Constantes de vitesse globale du craquage du méthyl-6-eicosane

Température (°C)	k (s^{-1})
550	0,14
600	1,19
650	3,33

Le graphe du logarithme de k en fonction de $1/T$ est indiqué sur la figure 4. Faute de données sur l'énergie d'activation des réactions de craquage de molécules aussi lourdes, il est impossible de comparer la valeur que nous avons déterminée à d'autres. Cependant la corrélation de Voge et Good[15] donne les résultats suivants pour une n paraffine de 21 atomes de carbone :

$$k = 0{,}06 \text{ à } 550°\mathrm{C}\,;\quad k = 0{,}55 \text{ à } 600°\mathrm{C} \text{ et } k = 2{,}8 \text{ à } 650°\mathrm{C}.$$

Ces valeurs, estimées à un facteur 2 ou 3 près, concordent très bien avec les valeurs que nous avons déterminées.

Composition des produits de craquage. Le tableau 2 montre la composition des produits gazeux obtenus dans quelques essais représentatifs. Parce qu'on peut les analyser totalement, les produits gazeux ($\leqslant C_4$) sont distingués des produits liquides qui ne sont analysés que par coupes, selon la longueur de leur chaîne ; exception faite des aromatiques. Comme prévu, l'éthylène est le principal corps formé et constitue de 38 à 44 % en mole des produits gazeux récupérés. La quantité d'éthylène formée croît avec la température, la sélectivité de sa for-

TABLEAU 2

Distribution des produits de craquage du méthyl-6-eicosane

Température °C :	550	600			650			
Conversion poids %	8,2	50,5	33,2	27	92	66,2	50,1	44,4
			moles pour 100 moles de Méthyl-6-eicosane craquées					
			600					
H_2	4,0	8,7	14,1	4,5	22,2	15,0	15,2	16,9
CH_4	38,3	39,8	31,8	23,9	58,3	27,9	32,7	21,2
C_2H_6	36,1	21,2	17,8	16,4	20,3	10,4	10,2	5,7
C_2H_4	63,1	71,0	53,9	52,0	132,1	68,0	59	57,1
C_3H_8	8,2	1,9	3,5	3,2	2,5	1,6	2,4	—
C_3H_6	33,5	32,0	25,5	33,9	66,2	33,0	22,5	20,3
C_4H_{10}	—	—	—	—	—	—	—	—
1-C_4H_8	7,7	4,6	8,5	7,6	21,2	11,1	10,5	6,6
C_4H_6	—	1,7	1,8	—	18,6	4,9	3,9	2,1
			Poids % pour 100 moles de méthyl-6-eicosane craquées					
Liquides en :	18,2	17,4	14,8	14,6	35,0	17,1	17,9	11,9
.C_5-C_9	34,4	25,7	18,48	32,6	33,7	12,7	17,9	22,4
.$C_{10}-C_{15}$	33,3	38,2	38,18	35,5	24,8	44,1	43,7	39,1
.$C_{16}-C_{20}$	13,9	16,3	26,6	16,8	2,5	21,6	17,8	21,2
Aromatiques	t	2,0	0,6	t	3,9	4,2	2,6	5,3

TABLEAU 3

Craquage théorique du méthyl-6-eicosane à 600°C

Moles formées pour 100 Moles craquées

Hydrogène	17
Méthane	41
Ethane	31
Ethylène	102
Propène	44
Butène-1	15

— Liquides de C_5 à C_9 : 66
(13,2 en moyenne, tous isomères confondus)
— Liquides de C_{10} à C_{15} : 40
(6,6 en moyenne, tous isomères confondus)
— Liquides de C_{16} à C_{20} : 26
(5,2 en moyenne, tous isomères confondus).

mation croît lorsque le temps de séjour décroît. Les quantités d'hydrogène et d'hydrocarbures en $C_1 - C_3$ augmentent également avec la conversion, ceci étant dû au fait que les produits de craquage se craquent eux-mêmes lorsque le temps de séjour est grand. Dans ces conditions, le butadiène constitue 7 moles % des produits formés. Nous n'avons jamais identifié le butane, les autres hydrocarbures saturés sont formés en petites quantités : environ 6 moles %.

La figure 5 montre la variation des quantités d'hydrogène, méthane, éthylène, propylène et éthylène recueillis en fonction de la conversion à 600°C. La masse moléculaire moyenne des gaz est de 40,6 elle est indépendante de la conversion et de la température.[4, 16] Les liquides sont composés d'oléfines et d'aromatiques ; les isomères des oléfines sont très nombreux. On remarque que la coupe $C_5 - C_9$ est plus importante que la coupe $C_{10} - C_{15}$ lorsque le taux de conversion est élevé, ce qui peut être dû à un craquage concomitant des produits formés. Les aromatiques sont formés en faible quantité (4 à 5 % en poids au maximum) et uniquement aux températures et temps de séjour importants. Ils sont constitués uniquement de benzène et de toluène.

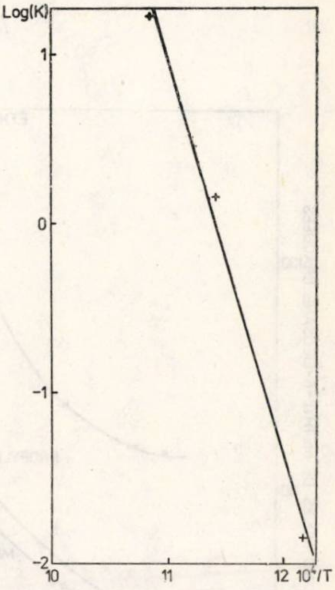

Fig. 4. — Détermination de l'énergie d'activation.

COMPARAISON ENTRE LES RÉSULTATS EXPÉRIMENTAUX ET LA THÉORIE DE RICE

Nous avons appliqué au cas du méthyl-6-eicosane la théorie de Rice et Kossiakoff telle qu'ils l'exposèrent en 1943.[3] D'après cette théorie, il ne se forme pas de paraffine $> C_2$, expérimentalement nous avons trouvé de faibles quantités de propane mais pas de paraffine à chaine plus longue.

La fig. 6 compare les résultats expérimentaux obtenus à 600°C, pour les gaz et pour un taux de conversion de 50 %, aux résultats prévus par la théorie. Celle-ci conduit à des résultats majorés de 35 % environ, sauf pour le méthane où résultats expérimentaux et théorie sont très proches.

Quant aux produits liquides, la théorie prévoit que chaque coupe représente 25 % en poids ; répartis comme e montre le tableau 3. Les résultats expérimentaux s'écartent d'environ 50 % de ces prédictions puisque la coupe en $C_{10} - C_{15}$ représente 38 % en masse et la coupe en $C_{16} - C_{20}$ seulement 16 %. Mais dans l'ensemble, on remarque la bonne concordance entre théorie et résultats expérimentaux.

En conclusion l'étude expérimentale du craquage du méthyl-6-eicosane conduit à la détermination d'un ordre global de réaction égal à 1, et d'une expression de la constante de décomposition

$$k = 10^{+14} \exp - \frac{56.300}{RT}$$

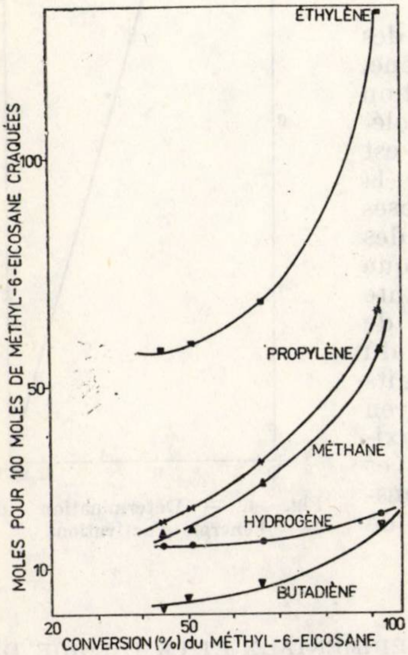

Fig. 5. — Variation des produits de réaction en fonction de la conversion.

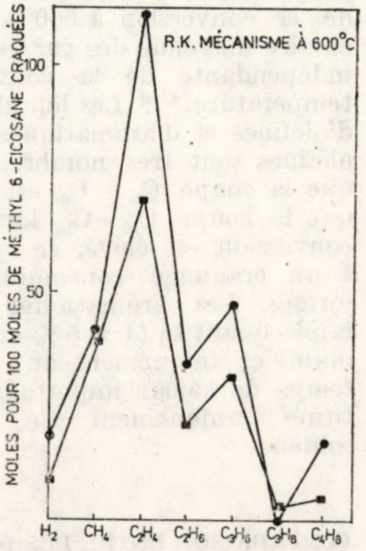

Fig. 6. — Comparaison entre résultats théoriques et expérimentaux du craquage du méthyl-6-eicosane.

qui concorde bien avec les résultats disponibles. Un mécanisme de Rice-Kossiakoff explique la formation des principaux corps obtenus et permet de prévoir quantitativement l'ordre de grandeur de leur formation.

BIBLIOGRAPHIE

[1] E. J. Green, S. B. Zdonik et L. P. Hallee, *Hydrocarbon processing*, **54**, 164 (1975).

[2] L. A. Wilkinson et S. Gomi, *Hydrocarbon processing*, **53**, 109 (1974).

[3] F. O. Rice et A. Kossiakoff, *J. Amer. Chem. Soc.*, **65**, 590 (1943).

[4] B. M. Fabuss et coll., Advances in Petroleum Chemistry and Refining, vol. IX, Interscience, New York, 1964.

[5] B. Blouri, R. Nabavi et P. Rumpf, *Bull. Soc. Chim. France*, 336 (1965).
[6] B. Blouri et J. Giraud, *Information Chimie*, **171**, 229 (1977).
[7] B. L. Crynes et L. F. Albright, *Ind. Eng. Chem. Process. Des. Develop.*, **8**, 25 (1969).
[8] R. F. Marschner, *Ind. Eng. Chem. Process Des. Develop.*, **30**, 554 (1938).
[9] D. L. Trimm, « Coke and Tar Formation During the Pyrolysis of Hydrocarbons », Int. Meeting on steam cracking, 30—31 août 1977, Trondheim, Norvège.
[10] H. Pines et J. T. Arrizo, *J. Amer. Chem. Soc.*, **79**, 4958 (1957).
[11] J. Giraud, B. Blouri et A. R. Partovi, *Information Chimie*, **184**, 111 (1978). 1959.
[12] S. M. Walas, »Reaction Kinetics For Chemical Engineers », McGraw-Hill, New York, 1959.
[13] O. A. Hougen et K. M. Watson, « Chemical Process Principles », vol. III, Wiley, New York, 1947.
[14] L. S. Kershenbaum et J. J. Martin, *AICh. J.*, **13**, 51, 148 (1967).
[15] H. H. Voge et G. M. Good, *J. Amer. Chem. Soc.*, **71**, 593 (1949).
[16] D. Kunzru, Y. T. Shah et E. B. Stuart, *Ind. Eng. Chem. Process. Des. Develop.*, **11**, **4**, 605 (1972).

Revue Roumaine de Chimie, 26, *3*, 407–413 (1981)

CHEMICAL GRAPHS. XXXVII.[1,2]

A SIMPLE RULE FOR CLASSIFYING *PERI*-CONDENSED BENZENOID HYDROCARBONS AS CLOSED-SHELL OR OPEN-SHELL (POLYRADICALIC) SYSTEMS USING DUALIST (CHARACTERISTIC) GRAPHS

ALEXANDRU T. BALABAN
The Polytechnic, Department of Organic Chemistry, Bucharest, Romania

Received August 20, 1980

The number *n* of unpaired spins per molecule of perfusene may be obtained more simply than by the Coulson-Rushbrooke starring procedure of the molecular (constitutional) graph, using the two types of triangles in the corresponding dualist graph : according to Scheme 3A or 3B, these triangles ("black" and "white" ones) point in opposite directions, and *n* is the difference between the numbers of black and white triangles (in absolute values). Examples of perifusene diradicals are given. Thus a very simple rule is available for discriminating normal perifusenes with closed electronic shells ($n = 0$) from perifusene polyradicals with open shells ($n \neq 0$).

1. INTRODUCTION

Previous parts in this series[3,4] have developed the concept of characteristic (or, as we now prefer to say, dualist) graph of a condensed polycyclic benzenoid system (such a system will be called *polyhex* for brevity). A dualist graph is formed by points situated at the centres of benzenoid rings, and by straight lines joining points corresponding to condensed rings. Since the angles between lines (120°, 180° or 240°) are rigid and the lines have constant lengths, the dualist graphs are not to be mistaken for dual graphs as defined in graph theory.[5] By means of dualist graphs, we have proposed a new classification criterion for polyhexes : they are called cata-condensed (for brevity, *catafusenes* will be used instead of cata-condensed benzenoid polycyclic systems) whenever the dualist graph contains no rings (is a "tree" in graph-theoretical language) ;[3,4] when the dualist graph contains only three-membered rings, the polyhex is a *perifusene* (short for peri-condensed benzenoid polycyclic system), and when the dualist graph contains larger rings (possibly in addition to three-membered rings) the polyhex is a *coronafusene* (short for corona-condensed benzenoid polycyclic system).[6]

Dualist graphs of polyhexes, especially of catafusenes, may serve as a basis for their nomenclature and coding[3,4,6] (three-digit coding using digit 0 for denoting annelation with an angle of 180°, and digits

1 or 2 for angles of 120°, or 240°, together with the convention of making the code unique by selecting the lowest possible number resulting from these digits from one end of the catafusene to the other end), for deriving a topological index (L-transform of the three-digit code),[7] for correlating physical,[8] chemical[9] and biochemical[10] properties of polyhexes with their three-digit codes, and for enumerating all possible non-branched[3] or branched catafusenes.[11] The concept of dualist graphs may also be applied to non-benzenoid condensed polycyclic systems for the purpose of coding, nomenclature, enumeration of isomers,[12] and correlation of physical (quantum-chemical) properties.[13] Reviews covering in more detail the concept and applications of dualist graphs are available,[14-16] as well as further uses of such dualist (characteristic) graphs.[17,18]

Perifusenes and coronafusenes are much less amenable to a rigorous mathematical treatment than catafusenes; even the simple problem of enumerating all possible perifusenes has only been explored using computer algorithms.[19-22] Though for a given polyhex recent advances allow the determination of the number of Kekulé structures,[23] in the case of perifusenes the chemical nature of the various possible ring systems is so diversified that, even if the mathematical obstacles for a rational enumeration (for instance by a recursive formula) were surmounted, the chemical aspects still would present difficult problems. Perifusenes may be normal (closed-shell) compounds like pyrene, ovalene or coronene with several Kekulé structures which lead to intermediate bond orders for all C—C bonds; they may be normal (closed-shell) compounds with localized single or double bonds, where all Kekulé structures conserve some single or double bonds like the short double bonds in zethrene (I) or the long single bonds in perylene; they may be open-shell compounds: monoradicals like perinaphthyl (II) or naphthanthryl (III), diradicals* like triangulene (IV),[24] or polyradicals like the triradicals V or VI.

The present paper is devoted to the graph-theoretical treatment of mono- and polyradicals with perifusene structures, in order to provide a means of excluding such systems in an enumeration of chemically "normal" perifusenes, i.e. a graph-theoretical means of partitioning perifusenes into systems with closed and with open electronic shells.

2. CLASSICAL *(COULSON-RUSHBROOKE)* APPROACH

Perifusenes with an odd number of carbon atoms and devoid of side-chains must be $(2k+1)$-radicals where k is a non-negative integer, e.g. monoradicals like perinaphthyl (II) or naphthanthryl (III), or triradicals like V or VI (Scheme 1). Such systems are easy to classify as open-shell systems either by their odd number of carbon atoms, or by the fact that their dualist graphs possess an odd number of independent three-membered rings (like II or VI) or of fused three-membered rings (like III or V).

However, $(2k)$-radicals like the diradical triangulene IV have an even number of carbon atoms and require therefore a special procedure for establishing the fact that they are not "normal" (closed shell), but open-shell compounds. In graph-theoretical terms, a normal Kekulé structure corresponds to a Sachs graph, in particular to a Sachs graph containing only edge-components.[25] In chemical terms, this means that each carbon atom participates in one double bond. An analogous mathematical formulation for constitutional graphs of diradicals (these are the so-called hydrogen-depleted graphs, denoting only the carbon skeleton) is that they admit a decomposition into 1-factors,[26] while the constitutional graphs of $(2k)$-radicals admit no decomposition into 1-factors.

---

* This term is employed as synonym to biradicals.

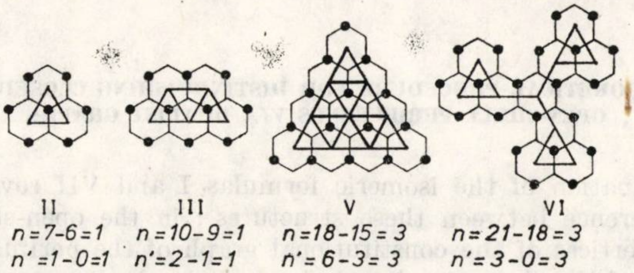

Scheme 1. Polyradicals or monoradicals (n-radicals) with odd $n = 2k + 1$.

The classical approach takes into account that all polyhexes are bipartite (two-colourable) graphs,[5] i.e. alternant hydrocarbons in chemical terms,[27] because they have no odd-membered rings. The Coulson-Rushbrooke starring procedure[28,29] divides all carbon atoms corresponding to the vertices of the constitutional graph into a set of starred and a set of unstarred atoms, so that no atom of one set is adjacent to an atom of the other set. If the numbers of atoms in the two sets are equal, then the compound is normal (closed-shell); if not, the compound is an open-shell n-radical where the number n of odd electrons equals the difference between the cardinals of the two sets.* In Schemes 1 and 2, for convenience, the two sets are distinguished by heavy dots placed at the starred positions, and n is the difference between starred and unstarred vertices of the constitutional graph.

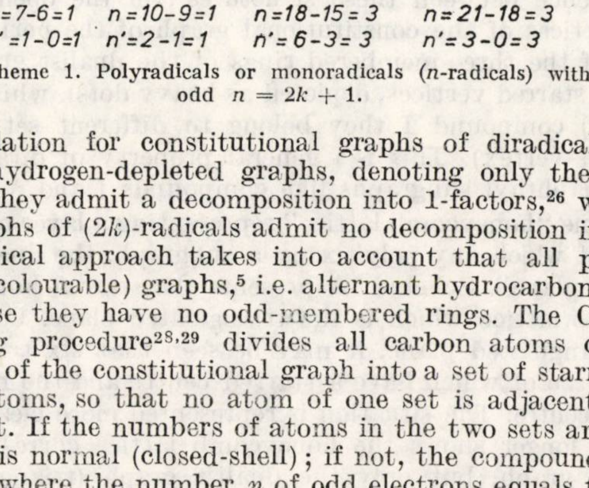

Scheme 2. Normal compounds ($n = 0$) or polyradicals n-radicals) with even $n = 2k$.

For example, zethrene (I) is a normal compound ($n = 0$, Scheme 1) with the two localized double bonds indicated in heavy lines, while the isomeric, topologically different, compound VII, is a diradical like triangulene IV.

---

* The parity of n is relevant, but its sign is not, therefore $|n|$ in absolute values will always be considered in formulas I – VII.

Though this classical approach works, we propose in the present paper an alternative simpler graph-theoretical procedure based on dualist graphs.

3. GRAPH-THEORETICAL PROCEDURE FOR DISTINGUISHING CLOSED-SHELL FROM OPEN-SHELL PERIFUSENES *VIA* DUALIST GRAPHS

Examination of the isomeric formulas I and VII reveals an interesting difference between these structures : in the open-shell diradical VII, both vertices of the constitutional graph of the perifusene lying at the centres of the three-membered rings of the dualist graphs belong to the same set (starred vertices, depicted as heavy dots), while in the closed-shell (normal) compound I they belong to different sets (one starred, one unstarred vertex). This is a general property of diradicals containing two perinaphthyl subgraphs like compounds I and VII.

In a plane "honeycomb lattice" representing a layer of carbon atoms in graphite, of which any polyhex is a subgraph, the dualist graph is a "triangulated plane". Scheme 3A presents the starred honeycomb lattice and its dualist lattice which is the triangulated plane. Considering only the latter triangulated plane, it may be seen that six triangles meet at each point, three of which have a starred centre and the remaining three an unstarred centre. The situation is represented more clearly by Scheme 3B which no longer shows the honeycomb lattice corresponding to the constitutional graph, but only the dualist graph (triangulated plane); in Scheme 3B, the starred- and unstarred-centre triangles are drawn in black and white, respectively. The result is a kind of triangulated chessboard. An essental observation is that for the given orientation of the underlying honeycomb lattice and its dualist triangulated lattice leading to all triangles having horizontally parallel sides, the black triangles always point upwards and that the white ones always point downwards. It is as if there were only two species of triangles (which might be associated with the zoomorphic symbols ♁ and ♂), that we prefer to call *black* and *white triangles* according to Scheme 3B, and which as in Scheme 3A correspond to centre-starred and centre-unstarred triangles, respectively. A similar observation may be traced to Gordon and Davison [3] who had remarked that there exist in a graphite lattice just two types of orientations of bonds around a carbon atom, according to the full lines in Scheme 3C; the corresponding dualist graphs are exactly the two types of triangles (broken lines in Scheme 3C).

If one colours alternatively in black and white the triangles of the dualist graph of any perifusene (or, which is an equivalent procedure, if one superimposes the dualist graph on the bicoloured triangulated plane as in Scheme 3B),* it is easy to obtain n just by calculating the difference n' between the number of black (or centre-starred, or centre-dotted) and white triangles (or centre-unstarred ones). This number n' is always equal to n obtained by the classical Coulson-Rushbrooke starring approach : $n = n'$ as evidenced by the numbers acompanying each of the formulas I — VII, and as it can be demonstrated.

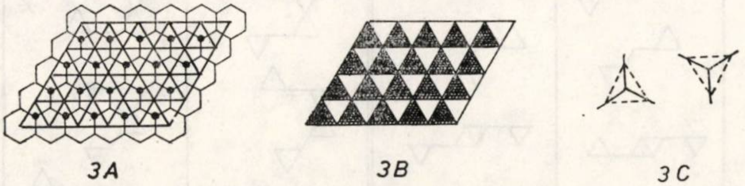

Scheme 3. *A*, the starred honeycomb lattice and its dualist (characteristic) triangulated lattice. *B*, the bicoloured black and white triangulated lattice of dualist graphs. *C*, the two orientations of bonds around carbon atoms in the graphite (honeycomb) lattice indicated by solid lines, and the two types of triangles resulting for the dualist graphs indicated by broken lines.

When the numbers are compared, however, it is seen that the present procedure is much simpler because the dualist graph has a much lower number of triangles than the vertices of the constitutional graph, so that n results as the difference between two relatively large numbers where it is easy to make mistakes, while n' results as the difference between small numbes.

The simplicity of the present graph-theoretical procedure makes it possible to determine $n'=n$ just by visual inspection of the dualist graph, which is not the case with the classical approach.

Therefore, a simple graph-theoretical determination of n for perifusenes based on their dualist graphs is to colour the triangles in black and white according to Scheme 3B and to calculate the absolute value of the difference between the numbers of black and white triangles : for $n = 0$ one obtains normal (closed-shell) compounds, for $n = 1$ one obtains monoradicals, for $n = 2$ one obtains diradicals, etc. As examples, Scheme 4 presents pairwise dualist graphs of normal and diradicalic isomeric perifusenes, where it can be observed by direct visual inspection that the isolated end-triangles (corresponding to perinaphthyl subgraphs) point in the same way in diradicals (i.e. are of the same colour, giving $n = 2$), while in the corresponding normal compounds they point in mutually opposite directions (i.e. are of different colours, cancelling one another and leading to $n = 0$). For comparison with the classical procedure, the reader may write the constitutional graphs corresponding to the dualist graphs exemplified in Scheme 4 ; it may then be seen that finding n is a more cumbersome process by starring the vertices of the constitutional graph, and that it is impossible to decide visually if $n = 0$ or $n = 2$.

---

* This two-colouring of the dualist triangulated *plane* corresponds to the two-colouring of the *vertices* of the bipartite (bicolourable) constitutional graph of the polyhex, but is distinct from it, though it originates in the same cause (graph-theoretical dual relationship).

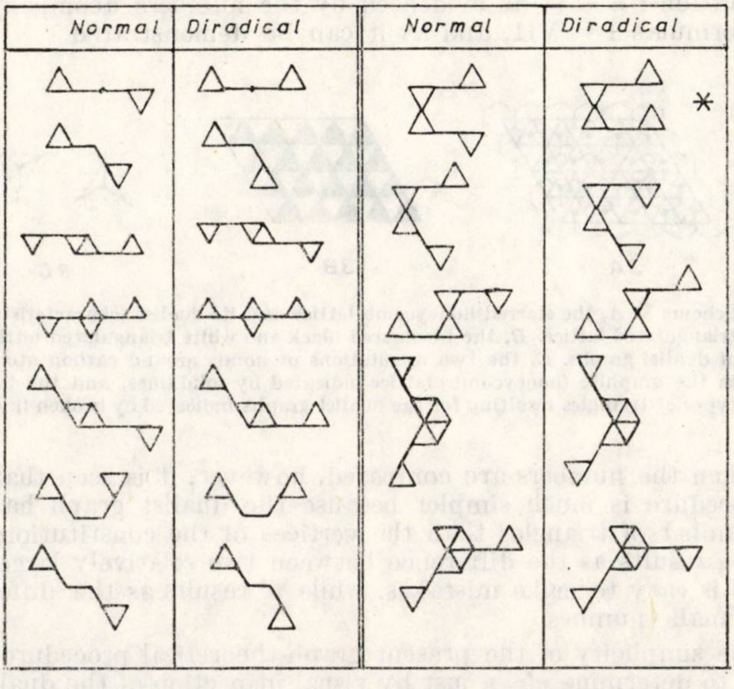

Scheme 4. Dualist graphs of several pairs of isomeric normal (closed-shell) and diradicalic (open-shell) perifusenes. The diradical marked by an asterisk, being a derivative of hexahelicene, cannot be planar owing to steric hindrance.

Note added in proof. Actually the starred atoms should always be the more numerous set, therefore dotted and non-dotted atoms should be interchanged in V. It was pointed out by Dr. R. B. Mallion (personal communication) that there exist alternant diradicals which are not encompassed by the classical or by the present treatments: the diradicals discussed here, or under the name of "non-Kekulé hydrocarbons" by M. J. S. Dewar ("The Molecular Orbital Theory of Organic Chemistry" McGraw-Hill, New York, 1969, p. 232) are not the only possible ones. There exist also diradicals (to be discussed in a future paper) which have equal numbers of starred and unstarred atoms, or of black and white triangles, yet for which one cannot write a Kekulé structure, and the simple HMO method shows that there exist two degenerate half-filled non-bonding molecular orbitals. One such example, included erroneously in Scheme 4, is the middle structure of the right-hand "Normal" column. The correct, normal structure should have both terminal triangles pointing *away* from each other, i. e the left-hand one downwards and the right-hand one upwards and not *towards* each other as in Scheme 4.

REFERENCES

[1] Preceding part, XXXVI : A. T. Balaban and I. Moţoc, *Math. Chem.*, **5**, 197 (1979) ; part XXXVIII is ref. 2. The paper by A. T. Balaban, I. Moţoc and R. Vancea which was announced in ref. 2 as paper XXXVII will appear later as another part of this series.

[2] Part XXXVIII : A. T. Balaban, *Math. Chem.*, **8**, 159 (1980).

[3] A. T. Balaban and F. Harary, *Tetrahedron*, **24**, 2505 (1968).

[4] A. T. Balaban, *Tetrahedron*, **25**, 2949 (1969).

[5] F. Harary, "Graph Theory", Addison-Wesley, Reading, Massachusetts, 1969, pp. 17, 113 R. J. Wilson, "Introduction to Graph Theory", Longman, London, 1972 (reprinted 1978), pp. 17, 72.

[6] D. Bonchev and A. T. Balaban, *Tetrahedron* (in press).

[7] A. T. Balaban, *Rev. Roumaine Chim.*, **22**, 45 (1977).

[8] A. T. Balaban, *Rev. Roumaine Chim.*, **15**, 1243 (1970).

[9] A. T. Balaban et al. (in preparation).

[10] K. Balasubramanian, J. J. Kaufman, W. S. Koski and A. T. Balaban, *J. Computational Chem.*, **1**, 149 (1980).

[11] F. Harary and R. C. Read, *Proc. Edinburgh Math. Soc.*, II, **17**, 1 (1970).

[12] A. T. Balaban, *Rev. Roumaine Chim.*, **15**, 1251 (1970).

[13] A. T. Balaban, *Rev. Roumaine Chim.*, **17**, 1531 (1972).

[14] A. T. Balaban, in "Chemical Applications of Graph Theory" (ed. A. T. Balaban), Academic Press, London, 1976, p. 63.

[15] A. T. Balaban, *Math. Chem.*, **1**, 33 (1975).

[16] D. H. Rouvray and A. T. Balaban, in "Applications of Graph Theory" (eds. R. J. Wilson and L. W. Beineke), Academic Press, London, 1979, p. 177.

[17] A. T. Balaban, *Math. Chem.*, **2**, 51 (1976).

[18] O. E. Polansky and D. H. Rouvray, *Math. Chem.*, **2**, 63, 91 (1976) ; **3**, 97 (1977).

[19] D. Klarner, *Fibonacci Quart.*, **3**, 9 (1965).

[20] R. C. Read, *Can. J. Math.*, **14**, 1 (1962).

[21] W. F. Lunnon, in "Graph Theory and Computing" (ed. R. C. Read), Academic Press, New York, 1972, p. 87.

[22] E. M. Palmer, in "Graph Theory and Applications", Lecture Notes in Mathematics No.303, Springer, New York, 1972, p. 215.

[23] O. E. Polansky and I. Gutman, *Math. Chem.*, **8**, 269 (1980).

[24] E. Clar, "Polycyclic Hydrocarbons", vol. 2, Academic Press (London)—Springer Verlag (Berlin), 1964, pp. 380, 416, 433 for the parent systems of mono- and diradicals ; A. R. Forrester, J. M. Hay and R. H. Thomson, "Organic Chemistry of Stable Free Radicals", Academic Press, London, 1968, p. 77 for perinaphthyl.

[25] A. Graovac, I. Gutman and N. Trinajstić, "Topological Approach to the Chemistry of Conjugated Molecules", Lecture Notes in Chemistry No. 4, Springer, Berlin, 1977, p. 20.

[26] D. M. Cvetković, M. Doob and H. Sachs, "Spectra of Graphs", V.E.B. Deutscher Verlag der Wissenschaften, Berlin, 1980, p. 239.

[27] C. A. Coulson and H. C. Longuet-Higgins, *Proc. Roy. Soc. (London)*, A **191**, 16 (1947).

[28] C. A. Coulson and G. S. Rushbrooke, *Proc. Cambridge Philos. Soc.*, **36**, 193 (1940).

[29] C. A. Coulson, B. O'Leary and R. B. Mallion, "Hückel Theory for Organic Chemists",Academic Press, London, 1978, p. 88.

[30] M. Gordon and W. H. T. Davison, *J. Chem. Phys.*, **20**, 428 (1952).

REFERENCES

[1] Preceding part, XXXV: A. T. Balaban and I. Motoc, Math. Chem. 5, 197 (1979) and XXXVI is ref. 2. The paper by A. T. Balaban, I. Motoc and [illegible], which was announced in ref. 2 as paper XXXVII will appear later as another part of this series.

[2] Part XXXVIII: A. T. Balaban, Math. Chem. 8, 159 (1980).

[3] A. T. Balaban and F. Harary, Tetrahedron, 24, 2505 (1968).

[4] A. T. Balaban, Tetrahedron, 25, 2949 (1969).

[5] F. Harary, "Graph Theory", Addison-Wesley, Reading, Massachusetts, 1969, pp. 17, 143; R. J. Wilson, "Introduction to Graph Theory", Longman, London, 1972 (reprinted 1978), pp. 15, 72.

[6] D. Bonchev and A. T. Balaban, Tetrahedron, in press.

[7] A. T. Balaban, Rev. Roumaine Chim. 22, 45 (1977).

[8] A. T. Balaban, Rev. Roumaine Chim., 15, 1243 (1970).

[9] A. T. Balaban et al. (in preparation).

[10] K. Balasubramanian, J. J. Kaufman, W. S. Koski and A. T. Balaban, J. Computational Chem., 1, 149 (1980).

[11] F. Harary and R. C. Read, Proc. Edinburgh Math. Soc., II, 17, 1 (1970).

[12] A. T. Balaban, Rev. Roumaine Chim., 15, 1251 (1970).

[13] A. T. Balaban, Rev. Roumaine Chim., 17, 1531 (1972).

[14] A. T. Balaban, in "Chemical Applications of Graph Theory" (ed. A. T. Balaban), Academic Press, London, 1976, p. 63.

[15] A. T. Balaban, Math. Chem. 1, 33 (1975).

[16] D. H. Rouvray and A. T. Balaban, in "Applications of Graph Theory" (eds. R. J. Wilson and L. W. Beineke), Academic Press, London, 1979, p. 177.

[17] A. T. Balaban, Math. Chem., 2, 51 (1976).

[18] O. E. Polansky and D. H. Rouvray, Math. Chem. 2, 63, 91 (1976); 3, 97 (1977).

[19] [illegible] Klarner, Fibonacci Quart., 3, 9 (1965).

[20] R. C. Read, Can. J. Math., 14, 1 (1962).

[21] W. F. Lunnon, in "Graph Theory and Computing" (ed. R. C. Read), Academic Press, New York, 1972, p. 87.

[22] F. Harary, in "Graph Theory and Applications", Lecture Notes in Mathematics No. [illegible], Springer, New York, 1972, p. [illegible].

[23] O. E. Polansky and I. Gutman, Math. Chem. 8, 269 (1980).

[24] E. Clar, "Polycyclic Hydrocarbons", vol. 2, Academic Press, London—Springer Verlag, Berlin, 1964, pp. 380, 110, 193 for the current systems of name and the dictionary; [illegible] and [illegible] Thomson, "Organic Chemistry of [illegible] Elements", Academic Press, London, [illegible], p. [illegible].

[25] A. Graovac, I. Gutman and N. Trinajstić, "Topological Approach to the Chemistry of Conjugated Molecules", Lecture Notes in Chemistry No. 4, Springer, Berlin, 1977, p. 22.

[26] D. M. Cvetković, M. Doob and H. Sachs, "Spectra of Graphs", VEB Deutscher Verlag der Wissenschaften, Berlin, 1980, p. [illegible].

[27] C. A. Coulson and H. C. Longuet-Higgins, Proc. Roy. Soc. (London), A 191, 39 (1947).

[28] C. A. Coulson and G. S. Rushbrooke, Proc. Cambridge Phil. Soc., 36, 193 (1940).

[29] C. A. Coulson, B. O'Leary and R. B. Mallion, "Hückel Theory for Organic Chemists", Academic Press, London, 1978.

[30] M. Gordon and W. H. T. Davison, J. Chem. Phys., 20, 428 (1952).

Revue Roumaine de Chimie, 26, *3*, 415–426 (1981)

CONTRIBUCIÓN A LA DETERMINACIÓN DEL MECANISMO DE ESTERIFICACIÓN DE ÁCIDOS ALIFÁTICOS, CATALIZADA POR $AlPO_4$ Y SISTEMAS AFINES

J. V. SINISTERRA, J. LLAVINA, J. MOREY y J. M. MARINAS *
Departamento de Química Orgánica de la Facultad de Ciencias de Palma de Mallorca, España

* Facultad de Ciencias de Córdoba, España.

Recibido : el 17 de Noviembre de 1979

Se ha estudiado el proceso de esterificación con etanol de tres ácidos carboxílicos de cadena normal (acético, propiónico y n-butírico). Se han utilizado como catalizadores sustancias compuestas por $AlPO_4$, Al_2O_3 y SiO_2. Se ha comprobado que la acidez del catalizador (meq/g ó meq/m^2) es el fáctor que más influye sobre la conversión. La expresión cinética que mejor describe el sistema en nuestras condiciones de trabajo, es del tipo $v = \boldsymbol{K}\,P_{AC}P_{AL}$. La energía de activación del proceso es aproximadamente constante, dentro del error experimental en todos los casos ($\approx$ 10 – 12 kcal/mol). Se ha comprobado asimismo que la reacción, utilizando estos catalizadores, presenta una catálisis ácida específica. Se propone un mecanismo tipo $A_{AC}2$ para el proceso, discutiéndose el mismo a la luz de la teoría de los órbitales frontera (F.O.).

The esterification process of ethanol with three carboxylic acids (acetic, propionic and n-butyric) has been studied. The catalysts used in the process are composed of $AlPO_4$, γ-Al_2O_3 and Si_2O_2. It has been shown that the acidity of the catalyst (meq/m^2) is the most influencing property on the yield. The kinetic expression for this process (under our experimental conditions) is of a second order type, $v = \boldsymbol{K}\cdot P_{AC}\cdot P_{AL}$. The apparent activation energy is practically constant in all cases (10–12 kcal/mole). It has been shown that the esterification process exhibits probably specific acid catalysis with these catalysts. An $A_{AC}2$ mechanism is proposed for the reaction, in terms of the Frontier Orbital theory.

INTRODUCCIÓN

La reacción de esterificación es un proceso clásico en Química Orgánica, pudiéndose realizar tanto en fase homogénea (según el método clásico de Fischer y Speir), como en fase heterogénea, con el catalizador en estado sólido y los reactivos en fase gaseosa. En principio, cualquier ácido de Lewis puede ser empleado como catalizador del proceso habiéndose utilizado Al_2O_3 y $SiO_2 - Al_2O_3$,[1-3] zeolitas,[4,5] etc. Dentro de esta línea de investigación cabe encuadrar los trabajos que se vienen realizando sobre la applicación del $AlPO_4$ tipo Kearby, y sistemas afines $Al_2O_3 - AlPO_4$ y $SiO_2 - AlPO_4$ a la reacción de esterificación con fines preparativos[6,7] en los cuales se han puesto de manifiesto la idoneidad de estos catalizadores para el proceso. No obstante dichos trabajos se hallaban faltos del necesario estudio del mecánismo de la reacción orgánica, por lo cual nos propusimos en el presente trabajo intentar determinarlo y analizar la influencia de la variación de la naturaleza del catalizador y de la longitud de la cadena del ácido carboxílico sobre el mismo.

II. PARTE EXPERIMENTAL

II.1. CATALIZADORES

Los catalizadores utilizados fueron denominados :

F — 100 % $AlPO_4$*

F72 — 20 % $AlPO_4$ — 80 % SiO_2*

CF4 — 75 % $AlPO_4$ — 25 % Al_2O_3*

y cuyas síntesis respectivas ya han sido descritas en trabajos precedentes.[8-10] Las propiedades químico-texturales de los mismos aparecen en la tabla 1.

Los catalizadores empleados poseen propiedades muy dispares debido a su diferente constitución. El catalizador F72 es el que presenta una mayor superficie específica, poseyendo por el contrario una menor densidad de centros ácidos. El catalizador F es el que presenta un mayor volumen acumulado de poros.

TABLA 1

Propiedades químico-texturales de los catalizadores utilizados

	F	F72	CF4
S_{esp} (m^2/g)	140,0±10,1	393,0±15,7	135,7±9,4
ΣV_p (ml/g)	0,79±0,06	0,56±0,02	0,37±0,02
*Acidez (meq/g)	0,42±0,02	0,19±0,01	0,37±0,03
Densidad de centros ácidos ($meq/m^2 . 10^3$)	3,00±0,20	0,48±0,03	2,70±0,20

Determina frente a *p*-dimetilaminoazobenceno ($pK_a = + 3,3$), y como base valorante n-$BuNH_2$.

II.2. REACTIVOS UTILIZADOS

Los reactivos utilizados en los ensayos de esterificación han sido etanol y ácido acético de la casa Panreac, de pureza analítica (99,5 %), y ácido propiónico y butírico de la casa MERCK del 99,5 y 98 % respectivamente.

---

* los tanto por ciento indicados son en peso.

II.3. DISPOSITIVO EXPERIMENTAL

El sistema utilizado fue un reactor de flujo continuo cuyas características aparecen ya descritas en la bibliografía.[11] El sistema trabajó como reactor diferencial en condiciones de flujo de pistón durante todos los ensayos cinéticos.

II.4. CONDICIONES EXPERIMENTALES

A fin de minimizar las resistencias a la difusión se trabajó en todos los casos en las siguientes condiciones experimentales:

Tamaño de partícula $\leqslant$ 0,250 mm Ø
Gramos de catalizador empleados:
Acido acético — catalizador F — $w \leqslant 0,4$ g.
Acido acético — catalizador CF4 — $w < 1,0$ g.
Acido acético — catalizador F72 — $w < 2,0$ g.
Acido propiónico — catalizador F72 — — $w < 2,5$ g.
Acido n-butírico — catalizador F72 — $w < 2,5$ g.
Flujo de alimentación $F > 25$ cm³/h.
Flujo de nitrógeno (gas portador) $F_{N_2} > 1$ cm³/s.

RESULTADOS Y DISCUSIÓN

III.1. INFLUENCIA DE LA TEMPERATURA

Como paso previo al estudio cinético, se analizó la variación de la conversión con la temperatura apareciendo los resultados en las Figuras 1 y 2.

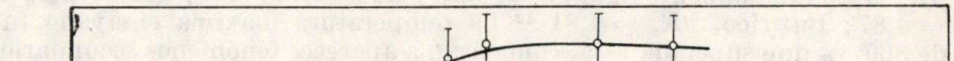

Fig. 1. — Variación de la conversión con la temperatura. Catalizador F72 — $F_{alim} = 30$cm³/h — $F_{N_2} = 6{,}5$cm³/s. ○ Catalítica ; ● Autocatalítica.

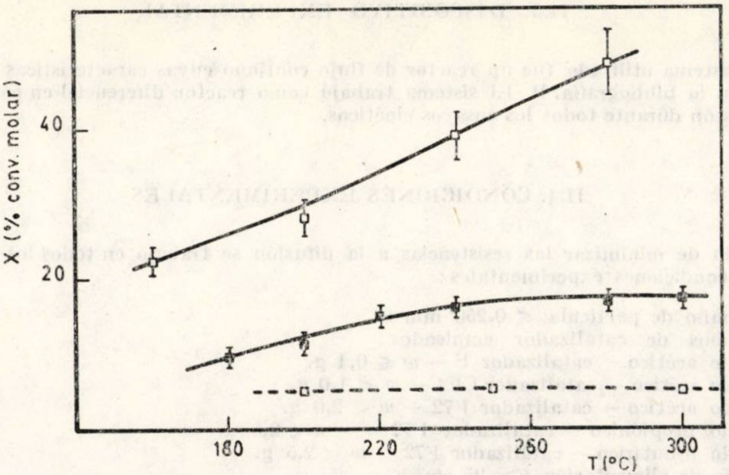

Fig. 2. — Variación de la conversión con la temperatura. Acido acético — $F_{\text{alim}} = 30\ \text{cm}^3/\text{h}$ — $F_{N_2} = 6{,}5\ \text{cm}^3/\text{s}$ □ Catalizador F — $w = 1{,}0$g ; Catalizador CF4 — $w = 0{,}5$g ; ---------- Autocatalítica

En la Figura 1 se representan las curvas obtenidas para los tres ácidos con el catalizador F72, pudiéndose apreciar la gradación de reactividad a temperatura constante, acético > propiónico > butírico, tanto en el caso del proceso catalítico como en el del proceso autocatalítico, lo cual puede correlacionarse con el aumento del impedimento estérico debido a la longitud creciente de la cadena (todos los ácidos poseen un pK_a aproximadamente igual: AcOH, $pK_a = 4{,}75$; Propiónico, $pK_a = 4{,}87$; Butírico, $pK_a = 4{,}81$.[12] La temperatura máxima ensayada fue de 300° ya que superada esta, comienzan a aparecer fenómenos secundarios de pirólisis, eterificación del alcohol, etc. Lo mismo podemos deducir de la Figura 2 donde aparecen las conversiones obtenidaes para el acetato de etilo con los catalizadores F y CF4.

A la luz de estas curvas, pensamos en seleccionar las temperaturas de trabajo para los ensayos cinéticos alrededor de los 200°C a fin de trabajar a bajas conversiones.

III.2. ESTUDIO CINÉTICO

Los ensayos cinéticos se realizaron trabajando en unas condiciones experimentales en las que se minimizaran los fenómenos de resistencia a la difusión (Vease sec. II.4).

El proceso se llevó a cabo variando la relación molar existente entre los tres componentes gaseosos (ácido, etanol, N_2) de forma que la suma $(P_{AC} + P_{AL})$ no fuera constante en ningún caso. En todas las experiencias, las conversiones molares a ester se mantuvieron inferiores a un 15 % a fin de estar seguros de trabajar en la zona de reactor diferencial. Los resultados experimentales obtenidos para los diversos ácidos y catalizadores se muestran en la Tabla 2.

TABLA 2

Resultados experimentales obtenidos en los experimentos cinéticos

Acetato de etilo

$w = 1{,}5$ g. $F_{\text{alim}} = 30$ cm³/h Cat. F72
$T = 200 \pm 5$°C $P_T = 1$ atm $F_{N_2} = 1{,}6$ cm³/s.

P_{N_2}(atm.)	P_{AC}(atm.)	P_{AL}(atm.)	*x (%ácd. conv.)	**v(mol/g.s).10^6
1,000	0	0	0	0
0,382	0,268	0,349	5,68	5,45
0,358	0,278	0,363	6,11	5,86
0,331	0,290	0,378	6,61	6,34
0,317	0,296	0,386	6,98	6,69

Propionato de etilo

$w = 1{,}5$g $F_{\text{alim.}} = 30$ cm³/h Cat. F72 *5*
$T = 220 \pm 5$°C $P = 1$ atm $F_{N_2} = 1{,}6$ cm³/s.

P_{N_2}(atm)	P_{AC}(atm.)	P_{AL}(atm.)	*x (% ácd. conv.)	**v (mol/g.s).10^6
1,000	0	0	0	0
0,396	0,223	0,380	4,3	3,78
0,384	0,227	0,388	4,57	3,94
0,356	0,238	0,406	5,00	4,31
0,341	0,243	0,415	5,23	4,51

Butirato de etilo

$w = 1{,}5$g $F_{\text{alim}} = 30$cm³/h Cat. F72
$T = 240 \pm 5$°C $P_T = 1$atm. $F_{N_2} = 1{,}6$ cm³/s

P_{N_2}(am).	P_{AC}(atm.)	P_{AL}(atm.)	*x(% ácd. conv.)	**v (mol/g.s).10^6
1,000	0	0	0	0
0,426	0,185	0,389	5,36	2,73
0,401	0,193	0,406	5,66	2,97
0,373	0,202	0,425	6,02	3,26
0,358	0,207	0,435	6,22	3,42

Cat. CF4

$w = 0,5$ g $\quad F_{\text{alim}} = 30$ cm^3/h $\quad F_{N_2} = 1,6$ cm^3/s
$T = 200 \pm 5$°C $\quad P_T = 1$ atm.

P_{N_2} (atm.)	P_{AC}(atm.)	P_{AL}(atm.)	* x(% ácd. conv.)	**v (mol/g.s).10^6
1,000	0	0	0	0
0,382	0,268	0,349	4,83	1,39
0,358	0,278	0,363	5,67	1,63
0,331	0,290	0,378	5,91	1,70
0,317	0,296	0,386	6,59	1,90

Cat. F

$w = 0,4$g. $\quad F_{\text{alim}} = 30$cm^3/h $\quad F_{N_2} = 6,75$ cm^3/s
$T = 180 \pm 5$°C $\quad P_T = 1$ atm.

P_{N_2}(atm.)	P_{AC}(atm.)	P_{AL}(atm.)	*x (%ácd. conv.)	**v (mol/g.s).10^5
0,701	0,033	0,266	14,1	4,13
0,699	0,033	0,268	12,4	3,69
0,622	0,041	0,336	14,1	5,93
0,619	0,042	0,339	16,4	6,98
0,617	0,042	0,341	16,0	6,85
0,537	0,051	0,412	16,19	10,00
0,523	0,052	0,424	18,4	11,50
0,464	0,059	0,476	17,5	13,90

Los valores de la velocidad de reacción $v = dx/d(w/F)$ se ajustaron perfectamente a una expresión de segundo orden del tipo [1], dándose a continuación las ecuaciones experimentales obtenidas :

$$v = \boldsymbol{K}\, P_{AC} \cdot P_{AL} \quad [1]$$

— Acético, $T = 200 \pm 5$°C, cat. F72
$v = (7,81 \pm 0,64) \cdot 10^{-5} \cdot P_{AC}P_{AL} - (8,20 \pm 0,90) \cdot 10^{-10}$
$r^2 = 0,999$ [2]
— Propiónico, $T = 220 \pm 5$°C, cat. F 72
$v = (4,45 \pm 0,49) \cdot 10^{-5} \cdot P_{AC}P_{AL} - (1,06 \pm 0,12) \cdot 10^{-9}$
$r^2 = 0,999$ [3]
— Butírico, $T = 240 \pm 5$°C, cat. F72
$v = (3,78 \pm 0,42) \cdot 10^{-5} \cdot P_{AC} \cdot P_{AL} - (2,43 \pm 0,27) \cdot 10^{-10}$
$r^2 = 0,999$ [4]
— Acético, $T = 200 \pm 5$°C, cat. CF4
$v = (1,48 \pm 0,16) \cdot 10^{-4} \cdot P_{AC} \cdot P_{AL} - (6,50 \pm 0,72) \cdot 10^{-9}$
$r^2 = 0,999$ [5]
— Acético, $T = 180 \pm 5$°C, cat. F
$v = (53,2 \pm 5,80) \cdot 10^{-4} \cdot P_{AC} \cdot P_{AL} + (8,56 \pm 0,94) \cdot 10^{-6}$
$r^2 = 0,988$ [6]

En todos los casos, se comprobó que las ordenadas en el origen no eran significativas con un 95 % de certeza, utilizando el test „t" de Student.[13]

Comparando los valores de las pendientes de las rectas [2], [3], [4], puede observarse que la seudoconstante cinética disminuye al aumentar el tamaño del ácido carboxílico, a pesar de haber trabajado a temperaturas crecientes debido a la diferente reactividad de estos. Si se comparan las ecuaciones [2], [5] y [6], puede observarse una gradación en las constantes de velocidad del tipo :

$$K_{\mathrm{F}_{180}} > K_{\mathrm{CF4}_{200}} > K_{\mathrm{F72}_{200°}}$$

Dicho orden está de acuerdo con la densidad de centros ácidos (véase Tabla 1) pero no con la S_{esp} ó ΣV_p. Ello nos indica que la acidez del catalizador es la propiedad químico-textural que más influye en la actividad catalítica de estas sustancias.

III. 3. INFLUENCIA DEL CATALIZADOR

A fin de determinar el tipo de catálisis del proceso se realizaron procesos de esterificación con diferentes gramos de catalizador ; mostrándose en la Figura 3 la variación de la constante cinética K con el número de meq de acidez presentes en cada experimento. Este número se obtiene multiplicando el peso del catalizador por la densidad de centros ácidos (meq/g) de cada catalizador.

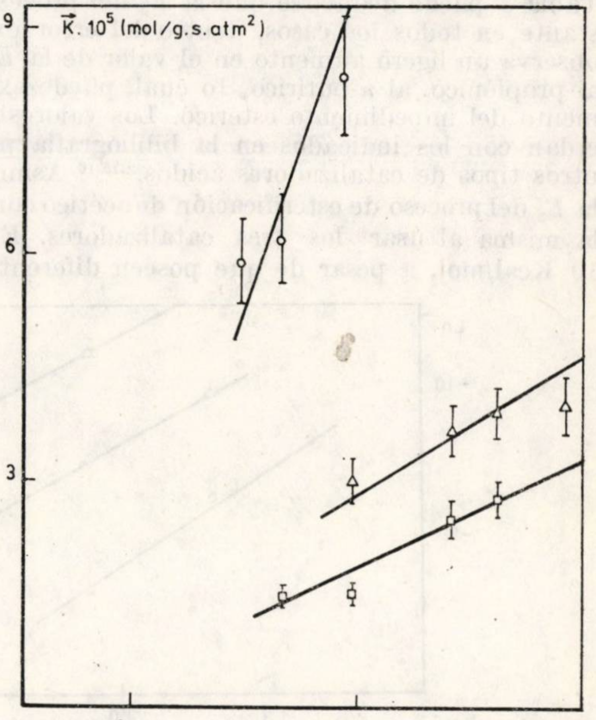

Fig. 3. — Variación de la pseudoconstante cinética con los meq de acidez. Catalizador F72 — — F_{alim} = 30 cm^3/h — F_{N_2} = = 6,5 cm^3/s. ○ Acido acético, T= =200°C ; □ Acido propiónico, T= = 220°C ; △ Acido n-butírico, T = 240°C.

Como puede observarse en dicha figura existe una relación lineal entre ambas magnitudes, por lo que podemos deducir que el proceso sigue posiblemente una catálisis ácida específica esto es que la reacción ocurre mediante una protonación previa de uno de los reactivos el cual reacciona en el paso limitante de la velocidad con la otra molécula de reactivo.[14]

$$\mathrm{A} + \mathrm{H}^+ \rightleftarrows \mathrm{AH}^+ \xrightarrow[\text{lento}]{+\mathrm{B}} \text{Productos}$$

Conclusiones análogas se dedujeron en el caso de la esterificación de acético con etanol utilizando como catalizadores los denominados F y CF4.

III. 4. ENERGÍA DE ACTIVACIÓN

Una vez determinada la ecuación cinética, se procedió a determinar el valor de la E_a del proceso apareciendo la representación de Arrhenius en las Figuras 4 y 5. Los valores de la E_a obtenidos a partir de las mismas aparecen en la Tabla 3. De los resultados indicados en la Tabla 3 puede deducirse que la E_a del proceso es aproximadamente constante en todos los casos, dentro del error experimental. No obstante, se observa un ligero aumento en el valor de la E_a al pasar del ácido acético, al propiónico, al *n*-butírico, lo cual, puede explicarse en función del aumento del impedimento estérico. Los valores observados de la E_a concuerdan con los indicados en la bibliografía para este proceso utilizando otros tipos de catalizadores ácidos.[2,15,16] Asimismo puede observarse que la E_a del proceso de esterificación de acético con etanol es aproximadamente la misma al usar los tres catalizadores. Es decir, aproximadamente 10 Kcal/mol, a pesar de que poseen diferente S_{esp} y acides.

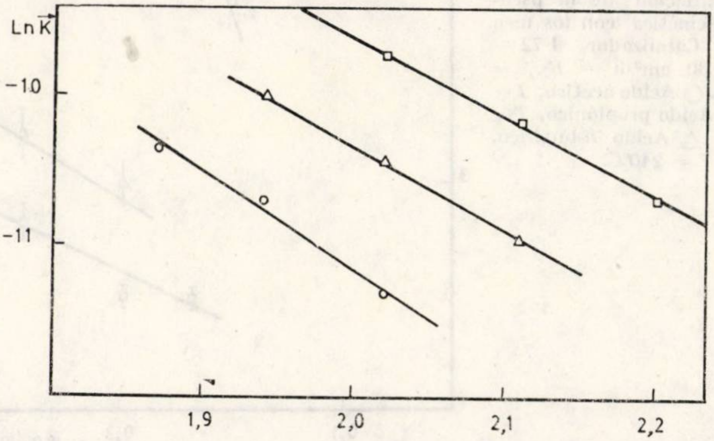

Fig. 4. — Representación de Arrhenius para la esterificación de los diferentes ácidos con el catalizador F72. $F_{\text{alim}} = 30$ cm³/h — — $F_{N_2} = 6{,}5$ cm³/s — Error = 5 %. □ Acido acético ; △ Acido propiónico ; ○ Acido n-butírico.

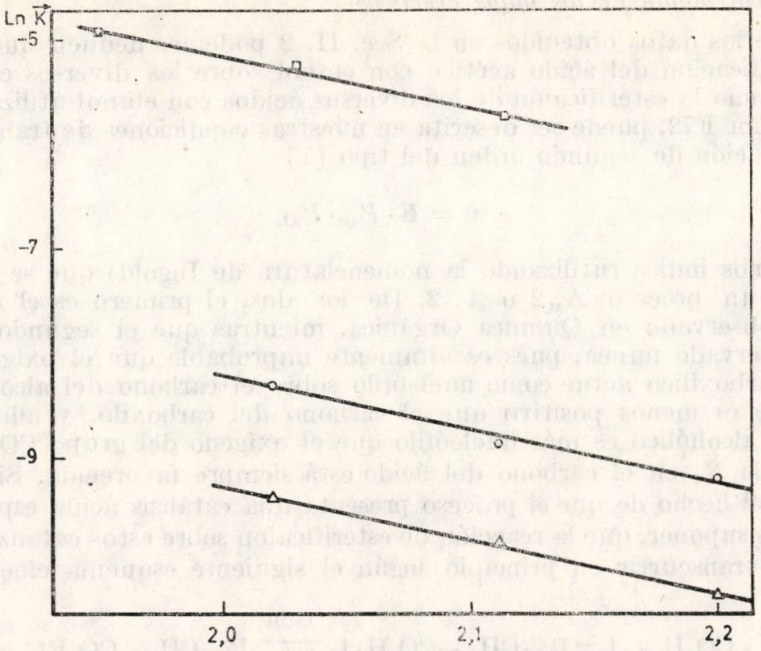

Fig. 5. — Representación de Arrhenius para la esterificación del ácido acético con los diferentes catalizadores. $F_{\mathrm{alim}} = 30$ cm³/h — $F_{N_2} = 6{,}5$ cm³/s — Error = 5 %. □ Catalizador F — $w = 0{,}4$ g; ○ Catalizador CF4 — $w = 0{,}5$ g; △ Catalizador F72 — $w = 1{,}5$ g.

TABLA 3

Valores de la E_a de los procesos esterificación

Acido	Catalizador	S_{esp}(m²/g)	Acidez(meq/g)	E_a(kcal/mol)
Acético	F	140,0±10,1	0,42±0,02	9,79±0,1
Acético	CF4	135,7±9,4	0,37±0,03	9,56±0,1
Acético	F72	393,0±15,7	0,19±0,01	10,34±1,0
Propiónico	F72	393,0±15,7	0,19±0,01	11,19±1,1
n-Butírico	F72	393,0±15,7	0,19±0,01	12,87±1,3

III. 5. MECANISMO DE REACCIÓN

La interpretación mecanística de la reacción orgánica la realizamos en función de los datos cinéticos obtenidos anteriormente y de la aplicación al proceso de la teoría de los orbitales froterizos de Fukui.[17,18]

(a) *Interpretación de los datos cinéticos.*

De los datos obtenidos en la Sec. II. 2 podemos deducir que tanto la esterificación del ácido acético con etanol sobre los diversos catalizadores, como la esterificaión de los diversos ácidos con etanol utilizando el catalizador F72, puede ser descrita en nuestras condiciones de trabajo por una ecuación de segundo orden del tipo [1]

$$v = \boldsymbol{K}\cdot P_{\mathrm{AC}}\cdot P_{\mathrm{AL}} \qquad [1]$$

lo cual nos indica (utilizando la nomenclatura de Ingold) que se trata o bien de un proceso $\mathrm{A_{AC}2}$ o $A_{\mathrm{AL}}2$. De los dos, el primero es el comunmente observado en Química Orgánica, mientras que el segundo no ha sido observado nunca, pues es altamente improbable que el oxígeno del ácido carboxílico actue como nucleófilo sobre el carbono del alcohol, ya que este es menos positivo que el carbono del carboxilo, y ademas el oxígeno alcohólico es más nucleófilo que el oxígeno del grupo CO_2H con lo cual la S_{N} en el carbono del ácido está siempre favorecida. Si a esto unimos el hecho de que el proceso presenta una catálisis ácida específica, podemos suponer, que la reacción de esterificaión sobre estos catalizadores, pudiera transcurrir en principio según el siguiente esquema cinético:

$$\mathrm{R{-}CH_2{-}CO_2H + L \rightleftarrows R{-}CH_2{-}CO_2H\cdot L \xrightleftharpoons[lento]{EtOH} R{-}CH_2{-}CO_2Et + H_2O}$$

$\mathrm{R = H,\ CH_3,\ CH_3{-}CH_2}$
L = Centro activo

La cinética del proceso no nos informa de si la molécula de alcohol está o no adsorbida sobre la superficie del catalizador, aunque presumiblemente podemos suponer que no lo esté debido a que la K depende linealmente del número de equivalentes de ácido presentes (véase Sec. III.3), y de que la K_{ads} del alcohol sobre estos catalizadores (determinada a esta temperatura por otros métodos), es muy pequeña.[19]

(b) *Estudio segun la teoría de F.O.*

El hecho de que las E_a del proceso junto con la expresión cinética y la constante de disociación del ácido, sean análogos para todos los casos estudiados (Mecanismo $A_{\mathrm{AC}}2$), parece indicar que el estado de transición es del mismo tipo para todos los casos.

La interacción entre el ácido carboxílico y el catalizador será una interacción HOMO/LUMO, donde el HOMO sería el orbital X_2 del grupo carboxilo y el LUMO del catalizador presumiblemente sería un orbital σ^*_{OH} del centro ácido P –OH.[20,21]

Dicha interacción habría de ser SUPRA-SUPRA por requerimientos de simetría (Fórmula 1) produciéndose la interacción tipo (I) entre los dos átomos de mayor coeficiente orbitalario, el O_1 del grupo $C = O$ y el H del OH, y habiendo interacciones enlazantes entre los restantes átomos. El término culómbico de la interacción [18,19] tambien dirige el ataque del H^+ del P —OH hacia el mismo

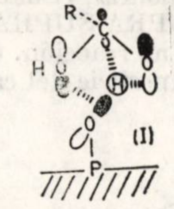

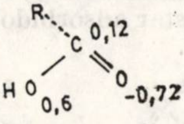

sitio, hacia el oxígeno del C = O que es el que posee mayor carga negativa. Si aceptamos la aproximación de Hückel, por la que al no conjugar R con el grupo CO_2H no afecta a los niveles energéticos de los O.M. del grupo CO_2H, la interacción ácido/catalizador F72 será la misma tanto para el ácido acético como para el propriónico y el n-butírico, y el intermedio (I) podría describir el estado de adsorción activada del ácido sobre el catalizador. Si el estado adsorbido es aproximadamente el mismo, y el alcohol el mismo (EtOH), el estado de transición de la reacción será presumiblemente el mismo, no diferenciándose más que por el distinto grado de impedimento estérico, tal y como observamos en los valores de E_a (véase tabla 3). Una deducción análoga puede hacerse para los diversos

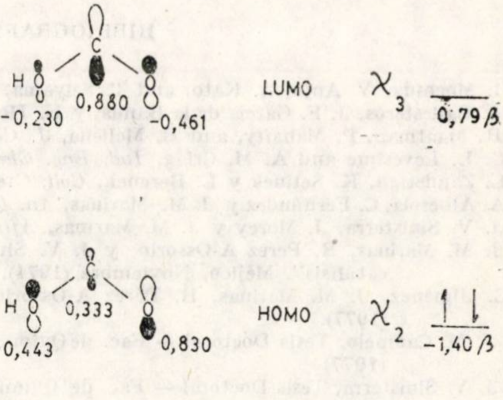

Fig. 6.— Orbitales] moleculares del grupo carboxilico calculados a partir de los datos de la bibliografía (*).

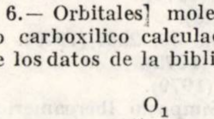

$$R-C_2(=O_1)-O_3-H$$

$H_{11} = \alpha + \beta, H_{22} = \alpha,$

$H_{33} = \alpha + 2\beta, H_{12} = 0{,}8\beta,$

$H_{23} = \beta$

catalizadores en la esterificación del ácido acético con etanol, dicha deducción nos conduciría a decir que muy posiblemente el centro activo de los tres catalizadores sea el mismo, ($E_a \approx$ constante), diferenciándose sólo

---

(*)A. Streitwiesser — "Molecular Orbital Theory ", Wiley and Sons, London (1961).

los catalizadores en el fáctor entrópico ; lo cual coincidiría con otras observaciones existentes de la bibliografía.[13,20,21]

Según todo lo expuesto, el proceso podría visualizarse mediante un mecanismo A_{AC2} con una adsorción SUPRA-SUPRA del ácido carboxílico sobre el centro activo, seguida de una reacción, en la cual el etanol pudiera o no estar adsorbido sobre la superficie del catalizador.

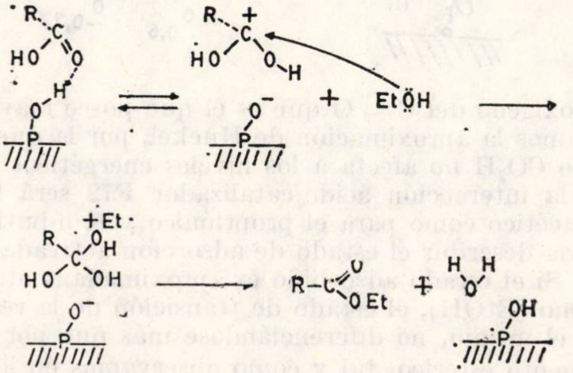

BIBLIOGRAFIA

[1] I. Mochida, Y. Anju, A. Kato, and T. Seiyama, *Bull. Chem. Soc.*, Japan, **44,** 2326 (1971)
[2] A. Ballesteros, J. F. Garcia de la Banda, y E. Hermana, *An. Quim.*, **71,** 179 (1967).
[3] R. Maatman, P. Mahaffy, and R. Mellena, *J. Catalysis*, **35,** 44 (1974).
[4] C. L. Levesque and A. M. Criag, *Ind. Eng. Chem.*, **40,** 96 (1948).
[5] L. Zanderigh, K. Setinek y L. Berenek, *Coll. Czech. Chem. Comm.* **35,** 2367 (1970).
[6] A. Alberola, C. Fernández y J. M. Marinas, *An. Quim.*, **68,** 1399 (1972).
[7] J. V. Sinisterra, J. Morey y J. M. Marinas, *Afinidad*, **36,** 305 (1979).
[8] J. M. Marinas, R. Perez A-Ossorio y J. V. Sinisterra", IV Simposio Iberoamericano de catálisis", Méjico, Noviembre (1974), Comun 3−3.
[9] C. Jiménez, J. M. Marinas, R. Pérez A-Ossorio y J. V. Sinisterra, *An. Quim.*, **73,** 1164 (1977).
[10] J. M. Campelo, Tesis Doctoral — Fac. de Quimicas Univ. Complutense de Madrid, España (1977).
[11] J. V. Sinisterra, Tesis Doctoral — Fac. de Quimicas Univ. Complutense de Madrid, España (1975).
[12] R. C. Weast, "Handbook of Chemistry and Physics", The Chem. Rubber Co. Cleveland, Ohio, 1972.
[13] E. L. Bauer, "Manual de estadistica para químicos", Edt. Alhambra, 1974.
[14] R. W. Alder, R. Baker and J. M. Brown, "Mechanism in Organic Chemistry", Wiley, New York, p. 64.
[15] A. L. Fricke and R. J. Alpeter, *J. Catalysis*, **25,** 33 (1972).
[16] Sharma Nagheswar, *Indian J. Technol.*, **10,** 221 (1972).
[17] K. Fukui, *Accts, Chem. Res.*, **4,** 57 (1971).
[18] K. Fukui, T. Yonezana and H. Saineu, *J. Chem. Phys.*, **29,** 722 (1952).
[19] A. Llobera, J. V. Sinisterra, J. M. Marinas, *Afinidad*, **36,** 299 (1979).
[20] J. B. Peri, *Discuss Faraday Soc.*, **52,** 55 (1971).
[21] J. B. Moffat, *Catal. Rewiews*, **18,** 199 (1978).

Revue Roumaine de Chimie, 26, 3, 427—434 (1981)

SYNTHESIS OF SOME NEW STYRYL OXAZOLOPHENOXAZINE CYANINES

M. S. K. YOUSSEF
Chemistry Department, Faculty of Science, Assiut University,
Assiut, Egypt

Received October 29, 1979

5*H*-Oxazolo (4,5-b) phenoxazine-2-carboxaldehyde (2) reacts with quaternary salt of 2-methyl heterocyclic compounds in the presence of piperidine as a catalyst, giving styryl cyanines 3a-d. Interaction of 2 with non-quaternized heterocyclic compounds afforded the corresponding dimethine bases 4a-d. Also, 5*H*-oxazolo (4,5-b) phenoxazine-2-carboxaldehyde-3-ethiodide (5) interacts with non-quaternized and quaternized salts giving styryl cyanines 6 and 7 respectively. Structural configuration of the synthesized compounds was proved by IR and UV spectral data. The biological activities of the prepared styryl cyanines were screened against some strains of bacteria.

Dimethine or styryl cyanines form an important group of sensitisers, which were prepared in the literature by condensation of quaternary salts of heterocyclic nuclei containing an active methyl group with aromatic aldehydes in the presence of suitable basic or acidic reagents.[1-11] Other heterocyclic aldehydes such as 1,2-diphenyl-indole-3-carboxaldehyde, 4-pyrazolealdehyde, 1-pyrazoline-3-aldehyde and phenothiazine-2-carboxaldehyde were also recommended in the synthesis of cyanine dyes,[12-16] which have been used for production of direct positive photography,[12] as textile dyes[13] and as useful sensitisers for high-energy electrons.[14,15]

Within this respect, 5*H*-oxazolo (4,5-b) phenoxazine-2-carboxaldehyde (**2**) was chosen for the synthesis of new types of cyanine dyes containing two different heterocyclic moieties.

Selective oxidation of 2-methyl-5*H*-oxazolo (4,5-b) phenoxazine (**1**) with selenium dioxide in dioxane/water gave the corresponding 5*H*-oxazolo (4,5-b) phenoxazine-2-carboxaldehyde (**2**), in satisfactory yield.

Interaction of quaternary salts ethiodides of a variety of 2-methyl heterocyclic compounds such as quinaldine, lepidine, α-picoline and 2-methyl benzoxazole with **2** in the presence of dry ethanol and piperidine as a base catalyst gave the corresponding styryl cyanines (**3a-d**) as shown below :

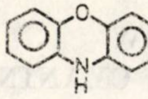

1

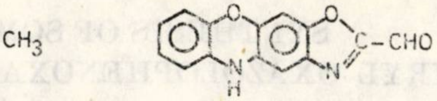

2

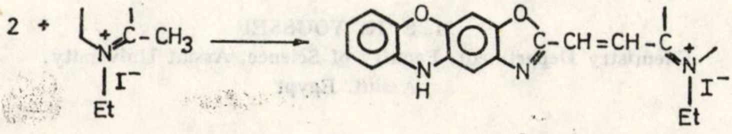

3a - d

3	Heteronucleus
a	quinolino-
b	lepidino-
c	pyridino-
d	benzoxazolo

It is reasonable to assume that the mechanism of this reaction involves a carbanion intermediate,[17] according to the following steps :

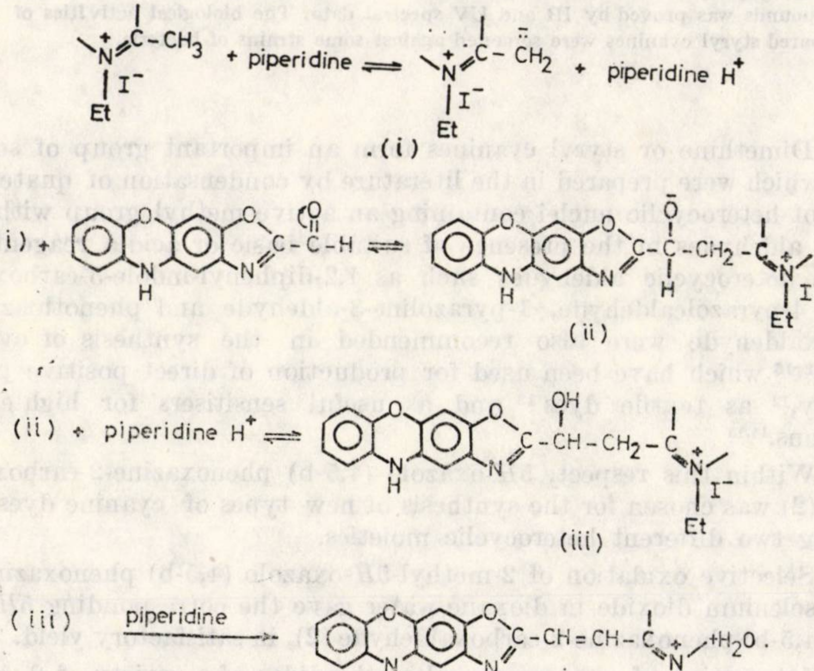
+ piperidine
+ piperidine H⁺
(i)
(i) +
(ii)
(ii) + piperidine H⁺
(iii)
(iii)
piperidine
+H₂O.

3a-d

Piperidine leads to the carbanion (i) formation and polarization of the carbonyl group in the heterocyclic aldehyde. The carbanion (i) adds to the ionized heterocyclic aldehyde forming the aldol anion (ii) which abstracts a proton from the medium (piperidine H+) forming the aldol intermediate (iii). The latter is transformed into the corresponding styryl cyanine **3** on prolonged heating and in the presence of excess piperidine.

The styryl cyanines **3** obtained are highly coloured compounds (from dark brown to reddish-violet), soluble in polar organic solvents. They are readily soluble in concentrated sulphuric acid with liberation of iodine on heating.

The reaction of **2** with non-quaternized heterocyclic compounds under the same conditions for a longer time (15 hrs.) afforded the corresponding styryl bases **4**.

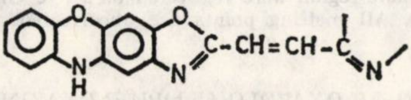

4a – d

a, quinolino– ; b, lepidino–
c, pyridino– ; d, benzoxazolo–

Quaternization of **2** with ethyl iodide in sealed tube under controlled conditions gave the corresponding *5H*-oxazolo (4,5-b) phenoxazine-2-carboxaldehyde-3-ethiodide (**5**). Interaction of **5** with heterocyclic nuclei containing an active methyl group e.*g*. quinaldine, lepidine, α-picoline or 2-methyl benzoxazole, achieved dimethine cyanines **6**.

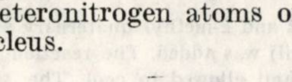

5

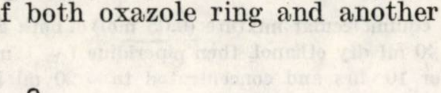

6a – d

The reaction of **5** with quaternary salts of the previous heterocyclic compounds in the presence of absolute ethanol and piperidine as a catalyst gave the corresponding styryl cyanines **7** bearing quaternary salt on heteronitrogen atoms of both oxazole ring and another heterocyclic nucleus.

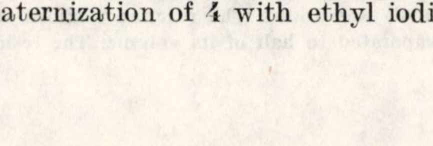

7a – d

Dimethine cyanines of type **7** were prepared by an alternative route, including quaternization of **4** with ethyl iodide in sealed tube at 150 °C for 3 hours.

The photosensitization effect of the prepared oxazolophenoxazine cyanines may be evaluated by considering their absorption spectra in the visible range (cf. Tables 1 –4). It is to be indicated that λ_{max} of these compounds falls usually in the range of 406 –690 nm.

The structure of the above prepared compounds was confirmed by their correct analytical data and infrared spectra which showed absorption bands at 1680 –1539 cm^{-1}, characteristic for oxazole ring structure,[18] at 3340 cm^{-1} (–NH group)[19] of phenoxazine ring and at 1640 –1610 cm^{-1} (–CH = CH–).

EXPERIMENTAL

The infrared spectra were obtained on a Pye Unicam SP 200 G spectrophotometer. Absorption spectra in the visible region were registered on a Pye Unicam SP 8000 ultraviolet recording spectrophotometer. All melting points are uncorrected.

2-METHYL-5*H*-OXAZOLO(4,5-b)PHENOXAZINE (1)

A pure sample of 3-acetylamino-2-acetoxyphenoxazine (20g) was fused at 230°C (*i..e* 5°C above its m.p.) until acetic acid vapours ceased to be evolved (about 5 hrs). The brown melt was extracted with ethanol, the extract was evaporated to half of its volume, cooled and the product precipitated on dilution with water. The solid was collected and crystallized from dilute ethanol to give pale brown needles, m.p. 152°C, yield 11 g. Found : C, 70.36 ; H, 4.36 ; N, 11.58. Calcd. for $C_{14}H_{15}O_2N_2$; C, 70.59 ; H, 4.20 ; N, 11.76 %.

5*H*-OXAZOLO(4,5-b)PHENOXAZINE-2-CARBOXALDEHYDE (2)

2-Methyl-5*H*-oxazolo (4,5-b) phenoxazine (0.01 mol) was dissolved in dioxane (50 ml), a few mls of water were added and the solution was heated with selenium dioxide (0.01 mol) under reflux for 20 hrs whereby selenium was deposited as a red amorphous precipitate which was removed by filtration. The brown filtrate was concentrated to 20 ml from which the aldehyde was separated as brown crystals, m.p. 247 – 50°C, quantitative yield. Found : C, 66.95 ; H, 3.40 ; N, 11.29.C Calcd. for $C_{14}H_8O_3N_2$: C, 66.67 ; H, 3.17 ; N, 11.11 %.

STYRYL CYANINES 3

An equimolecular mixture (0.05 mol) of both **2** and 2-methyl quaternary salts was dissolved in 40 ml dry ethanol, then piperidine (~ 1 ml) was added. The reaction mixture was refluxed for 10 hrs and concentrated to ~ 20 ml and allowed to cool. The solid product separated after acidification with dilute sulphuric acid (0.1 N), was collected, washed with ether and crystallized from dilute ethanol. The results are summarized in table 1.

STYRYL BASES 4

A mixture of *5H*-oxazolo (4,5-b) phenoxazine-2-carboxaldehyde **(2)** (0.03 mol) and the non-quaternized heterocyclic compound (0.03 mol) was dissolved in 30 ml absolute ethanol to which piperidine (0.03 mol) was added. The reaction mixture was allowed to reflux for 15 hrs, filtered hot and evaporated to half of its volume. The residue was cooled, acidified

TABLE 1

Styryl cyanines 3

Compound	mp (C°)	Yield (%)	Molecular formula	λ_{max}* (nm)	$\varepsilon_{max.}$	Analytical data							
						Calculated (%)				Found (%)			
						C	H	N	I	C	H	N	I
3a	290−2	75	$C_{26}H_{20}C_2N_3I$	406,590	9780,18000	58.54	3.75	7.88	23.83	58.62	4.01	7.77	23.50
3b	260	70	$C_{26}H_{20}O_2N_3I$	411,598,670	12135,4400,3065	58.54	3.75	7.88	23.83	58.59	3.83	8.00	23.75
3c	271	55	$C_{22}H_{18}O_2N_3I$	414,592	9450,2970	54.66	3.73	8.69	26.29	55.01	3.89	8.51	26.05
3d	225	61	$C_{24}H_{18}O_3N_3I$	408,590	17800,5500	55.07	3.44	8.03	24.28	55.24	3.22	7.93	24.11

ˣ λ_{max} in 95% ethanol.

TABLE 2

Styryl bases

Compound	mp (°C)	Yield (%)	Molecular formula	λ_{max}* (nm)	$\varepsilon_{max.}$	Analytical data					
						Calculated (%)			Found (%)		
						C	H	N	C	H	N
4a	240	52	$C_{24}H_{15}O_2N_3$	412,592	5765,2305	76.39	3.98	11.14	76.54	4.24	11.17
4b	278	49	$C_{24}H_{15}O_2N_3$	408,592	6690,3015	76.39	3.98	11.14	75.97	4.00	11.03
4c	267	45	$C_{20}H_{13}O_2N_3$	410,515	4045,1720	73.39	3.98	12.84	73.25	4.16	13.10
4d	282	40	$C_{22}H_{13}O_3N_3$	415,563	14700,5775	71.93	3.54	11.44	72.18	3.69	11.38

* λ_{max} in 95% ethanol.

TABLE 3

Styryl cyanines **6**

Compound	mp (°C)	Yiled (%)	Molecular formula	$\lambda_{max.}$* (nm)	$\varepsilon_{max.}$	Analytical data							
						Caculated (%)				Found (%)			
						C	H	N	I	C	H	N	I
6a	320	39	$C_{26}H_{20}O_2B_3I$	600	3640	58.54	3.75	7.88	23 38	58.49	3.81	8.09	23.13
6b	> 330	40	$C_{26}H_{20}O_2N_3I$	588	2585	58.54	3.75	7.88	23.38	58.66	4.00	7.85	23.27
6c	305	34	$C_{22}H_{18}O_3N_3I$	402(sh.), 592	10000,5600	54.66	3.73	8.69	26.29	54.71	3.69	8.80	25.92
6d	210 (dec.)	35	$C_{24}H_{18}O_3N_3I$	412	30680	55.07	3.44	8.03	24.28	55.00	3.19	8.15	25.79

* $\lambda_{max.}$ in 95% ethanol.

TABLE 4

Styryl cyanines **7**

Compound	mp (°C)	Yield (%)	Molecular formula	$\lambda_{max.}$ (nm)	$\varepsilon_{max.}$	Analytical data							
						Calculated (%)				Found (%)			
						C	H	N	I	C	H	N	I
7a	258−9	59	$C_{28}H_{25}O_2N_3I_2$	586,690	24800,9353	53.12	3.63	6.10	36.87	53.36	3.72	6.04	36.66
7b	285	60	$C_{28}H_{25}O_2N_3I_2$	460,600,668	17330,9865,13600	53.12	3.63	6.10	36.87	53.18	3.81	5.95	36.76
7c	185	57	$C_{24}H_{23}O_2N_3I_2$	—	—	45.07	3.60	6.57	39.75	45.23	3.70	6.44	39.88
7d	> 330	55	$C_{26}H_{23}O_3N_3I_2$	440,584	5890,2490	48.00	3.54	6.46	39.08	48.14	3.33	6.29	39.00

* $\lambda_{max.}$ in 95% ethanol.

with a few drops of acetic acid, then diluted with water, whereby the product was precipitated. It was collected and crystallized from an ethanol-water mixture (1 :1) giving the corresponding dimethine bases. The results are listed in table 2.

5*H*-OXAZOLO(4,5-b)PHENOXAZINE-2-CARBOXALDEHYDE-3-ETHIODIDE (5)

In a sealed tube a pure sample of **2** (3 g) was suspended in ethyl iodide (30 ml) and heated in an electric furnance at 130°C for 5 hrs. The tube was cooled, opened and the product was collected and washed with ether. The resulting quaternary salt was pure enough for any further work, however, recrystallization was effected by dissolving the substance in ethanol whereby a brown product was deposited. Yield quantitative, m.p.> 300°C. Found : C, 47.41 ; H, 3.22 ; N, 6.69 ; I, 30,80 ; Calcd. for $C_{16}H_{13}O_3N_2I$: C, 47.06 ; H, 3.19 ; N, 6.86 ; I, 31.13%.

STYRYL CYANINE 6

Equimolecular ratios (0.1 mol) of **5** and the non-quaternized heterocyclic compound were dissolved in absolute ethanol (20 ml) and piperidine (~ 1 ml) was added. The reaction mixture was refluxed for 40 hrs. The usual work-up procedure gave the corresponding styryl cyanines **6** (cf. Table 3).

DIMETHINE CYANINES 7

A mixture of quaternary salt (0.1 mol) and **5** (0.1 mol) was dissolved in 20 ml dry ethanol to which piperidine (0.1 mol) was added. The mixture was heated under reflux for 20 hrs. Following the usual procedure, the corresponding dimethine cyanines were obtained. The results are listed in Table 4.

ANTIMICROBIAL ACTIVITIES

The antimicrobial activities of the prepared styryl cyanines against a variety of microbes were determined. These microorganisms include Gram-positive and Gram-negative bacteria.[20] The bacteria used are : *Bacillus subtilis, Staphylococcus aureus, Pseudomonas aeruginosa, Mycobacterium phlei* and *Escherichia coli.*

The results showed that most of the prepared styryl oxazolophenoxazine cyanines **3**, **6** and **7** proved to range from small to strong activity on the Gram-positive and the Gram-negative bacteria. The activity expressed in percent ranges from 40 – 60%. The most active compounds against the mentioned strains of bacteria are **7a-d**.

REFERENCES

[1] W. H. Mills and J. L. Brieley, *J. Chem. Soc.*, **1922**, 2724.

[2] W. H. Mills and W. J. Pope, *J. Chem. Soc.*, **1922**, 946.

[3] R. M. Anker and A. H. Cook, *J. Chem. Soc.*, **1944**, 489.

[4] A. P. Philips, *J. Org. Chem.*, **12**, 333 (1947).

[5] F. M. Hamer, *J. Chem. Soc.*, **1952**, 3197.

[6] L. Horwitz, *J. Amer. Chem. Soc.*, **77**, 1687 (1955).

[7] A. M. Osman, S.A.M. Metwally and M.S.K. Youssef, *Canad. J. Chem.*, **54**, 37 (1976).

[8] M. R. Mahmoud, Z. H. Khalil and R. M. Issa, *Acta Chim. Acad. Sci. Hung.*, **87**, 121 (1975).

[9] A. M. Osman, Kh. M. Hassan and Z. H. Khalil, *J. Appl. Chem. Biotech.*, **26**, 71 (1976).

[10] A. M. Osman and Z. H. Khalil, *J. Appl. Chem. Biotech.*, **25**, 683 (1975).

[11] A. M. Osman, M.S.K. Youssef and Z. H. Khalil, *J. Appl. Chem. Biotech.*, **26**, 762 (1976).

[12] D. D. Chapman, Ger. Offen, 1,937,251 ; *Chem. Abstr.*, **73**, 89168 (1970).

[13] J. D. Kendall and G. F. Duffin, Ilford British Patent 797,144 ; *Chem. Abstr.*, **53**, 4983 (1959).

[14] A. F. Plue and G., USA Patent 3,013,015 ; *Chem. Abstr.*, **57**, 4801 (1962) ; 3, 073 ; 820 ; *Chem. Abstr.*, **58**, 12711 (1963).

[15] R. Wizinger and CIBA, USA Patent 2,671,783 ; *Chem. Abstr.*, **48**, 12596 (1954).

[16] L. P. Roosens and Gevaert, Photo-Production, British Patent 869,138.

[17] E. S. Gould, "Mechanism and Structure in Organic Chemistry", Holt, Rinehart and Winston, New York, 1950, p. 389.

[18] P. Bassigana, C. Cogrossi and M. Gandino, *Spectrochim. Acta.*, **19**, 1885 (1963).

[19] L. J. Bellamy, "The Infrared Spectra of Complex Molecules", Methuen, London, 2nd Edn, 1958, p. 251.

[20] J. G. Vincent and H. W. Vicent, *Proc. Expl. Biol. Nil.*, **55**, 162 (1944).

Revue Roumaine de Chimie, 26, 3, 435–440 (1981)

NUCLEOPHILE SUBSTITUTIONEN AN KOHLENSÄUREDERIVATEN. XVII[1]

KINETIK UND MECHANISMUS DER HYDROLYSE VON N,N,N'-TRISUBSTITUIERTEN KOHLENSÄURE-CHLORAMIDINEN

A. CHICU und R. BACALOGLU

Technische Hochschule „Traian Vuia", Bocşa Str. 6, 1900 Timişoara, Rumänien

Eingegangen den 27. März 1980

Die Kinetik der Hydrolyse von N,N,N'-substituierten Kohlensäurechloramidinen ist in gutem Einklang mit dem für die Hydrolyse des Kohlensäure-N,N,N'-triphenylchloramidins gefundenen monomolekularen kationischen Reaktionsmechanismus. In den meisten Fällen ist die Ionisierung etwas langsamer als die Folgereaktion des Kations, mit Ausnahme der Fälle in welchen bedeutende sterische Hinderungen oder die katalytische Wirkung der Li-Ionen eingreifen.

N,N,N'-Trisubstituted chloroformamidines hydrolysis kinetics supports the monomolecular mechanism proved for N,N,N'-triphenylchloroformamidine. In the most cases the ionization proceeds slower than the following cation reaction ; the only exception is when important steric hindrance or catalytic effects of Li ions occur.

In der vorangehenden Mitteilung dieser Reihe[1] wurde die Kinetik und der Mechanismus der Hydrolyse von Kohlensäure-N, N, N'-triphenylchloramidinen in wässrigem Dioxan studiert. Es wurde ein Zweistufen-Eliminierungs-Additions-Mechanismus durch kationisches Zwischenprodukt bewiesen :

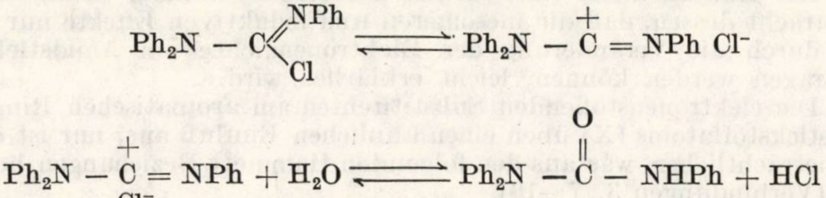

$$Ph_2N-C\genfrac{}{}{0pt}{}{\diagup NPh}{\diagdown Cl} \rightleftharpoons Ph_2N-\overset{+}{C}=NPh\ Cl^-$$

$$Ph_2N-\underset{Cl^-}{\overset{+}{C}}=NPh+H_2O \rightleftharpoons Ph_2N-\overset{\overset{O}{\|}}{C}-NHPh+HCl$$

wobei jeder der zwei Stufen, die vergleichbare Geschwindigkeiten aufweisen, zur langsamen Etappe, in Abhängigkeit von den Reaktionsbedingungen, werden kann.

In der vorliegenden Arbeit wurde die Kinetik und der Mechanismus der Solvolyse einer Reihe von N,N,N'-trisubstituierten Kohlensäurechloramidinen mit verschiedenen Substituenten studiert, zwecks Überprüfung des obenangeführten Mechanismus und zwecks Feststellung der elektronischen und sterischen Einflüsse auf den Reaktionsverlauf.

ERGEBNISSE UND DISKUSSION

In der vorangehenden Arbeit[1] haben wir bewiesen, daß durch die Hydrolyse des Kohlensäure-N,N,N'-triphenylchloramidins in wässrigem Dioxan, sich als einziges Produkt der entsprechende Harnstoff bildet. Auf Grund der Veränderung des Spektrums im UV-Bereich konnte die Reaktionsgeschwindigkeitskonstante pseudo-erster Ordnung bestimmt werden. Im Falle einiger Kohlensäure-N,N,N'-verschieden substituierten Chloramidinen wurde gleichzeitig festgestellt, daß die Hydrolyse in die entsprechenden Harnstoffe durch die Veränderungen der Absorbtionsintensitäten im UV-Bereich verfolgt werden kann.

In Tabelle 1 ist für die verschiedenen studierten Verbindungen, die Wellenlänge eingetragen, bei der die Extinktionsveränderung im Laufe der Reaktion am größten ist und die demnach zur Bestimmung der Geschwindigkeitskonstante für jeden einzelnen Fall verwendet wird. Ebenfalls sind auch die bei 20, 30 und 40°C in wässrigem Dioxan (7 Mol H_2O/kg Lösung), bei Chlorformamidinkonzentrationen zwischen $1 \div 6.10^{-5}$ mol/kg bestimmten Geschwindigkeitskonstanten pesudo-erster Ordnung angegeben. Bestimmt wurden auch die Konstanten pseudo-erster Ordnung für die Reaktion in Gegenwart von $LiClO_4$ ($4{,}2 \cdot 10^{-3}$ mol/kg), in wässrigem Dioxan (3,6 molH_2O/kg), bei derselben Substratkonzentration (Tabelle 1).

Die elektronenstoßenden Substituenten am aromatischen Ring des Amidstickstoffs (Y) begünstigen in allen Fällen die Hydrolyse, was auch durch die entsprechenden Hammett-Beziehungen (Verbindungen 1—6, Tabelle 1) zum Ausdruck kommt:

$$
\begin{array}{lll}
20^\circ & \log k = -2{,}534 - 0{,}87\,\sigma & r = 0{,}959 \\
30^\circ & \log k = -2{,}177 - 0{,}71\,\sigma & r = 0{,}918 \\
40^\circ & \log k = -1{,}916 - 0{,}79\,\sigma & r = 0{,}946 \\
20^\circ\ LiClO_4 & \log k = -1{,}524 - 0{,}90\,\sigma & r = 0{,}990
\end{array}
$$

Der Einfluß dieser Sustituenten ist verhältnismäßig klein, was in Anbetracht dessen, daß die mesomeren und induktiven Effekte nur indirekt durch die Veränderung der Elektronendichte am Amidstickstoff übertragen werden können, leicht erklärlich wird.

Die elektronenstoßenden Substituenten am aromatischen Ring des Iminstickstoffatoms (X) üben einen ähnlichen Einfluß aus, nur ist dieser viel beträchtlicher, was aus den folgenden Hammett-Beziehungen hervorgeht (Verbindungen 3, 7—10).

$$
\begin{array}{lll}
20^\circ & \log k = -2{,}394 - 2{,}50\,\sigma & r = 0{,}991 \\
30^\circ & \log k = -2{,}108 - 2{,}48\,\sigma & r = 0{,}994 \\
40^\circ & \log k = -1{,}815 - 2{,}43\,\sigma & r = 0{,}992 \\
20^\circ\ LiClO_4 & \log k = -1{,}394 - 3{,}26\,\sigma & r = 0{,}992
\end{array}
$$

TABELLE 1

Reaktionsgeschwindigkeitskonstanten pseudo-erster Ordnung der Hydrolyse von Kohlensäure N, N, N'-trisubstituierten Chloramidinen ($1-6\cdot10^{-5}$ Mol/kg) in wässrigem Dioxan in Abwesenheit (7 Mol H_2O/kg) und in Gegenwart von $LiClO_4$(3,6 Mol H_2O/kg, $4,2\cdot10^{-3}$Mol $LiClO_4$/kg)

Nr.	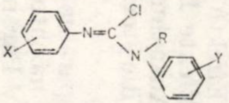 X	R	Y	a) σ X oder Y	b) Σσ* R	b) ΣE_S R	c) $\overline{\forall}$	d) λ nm	k.10³ sec⁻¹ 20°	30°	40°	Aktivierungsparameter ΔS≠ cal/Mol K	ΔH≠ Kcal/Mol	$LiClO_4$ 20° k·10³ sec⁻¹
1	2	3	4	5	6	7	8	9	10	11	12	13	14	15
1	H	CH_3	$4-OCH_3$	−0,27				300	3,72	9,95	17,30	−21,70	13,40	49,30
2	H	CH_3	$4-CH_3$	−0,17				300	4,23	9,59	18,60	−23,37	12,87	51,90
3	H	CH_3	H	0,00	0,60	−2,55	0,98	300	4,34	9,20	16,50	−27,82	11,55	28,30
4	H	CH_3	4−Cl	0,23				305	1,94	3,63	7,17	−30,43	11,27	17,15
5	H	CH_3	3−Cl	0,37				305	1,24	2,41	4,32	−33,06	10,75	12,79
6	H	CH_3	$4-NO_2$	0,78				300	0,58	2,42	3,46	−17,25	15,73	6,48
7	$4-CH_3$	CH_3	H	−0,17				300	9,36	17,30	32,00	−29,69	10,57	148,25
8	$3-CH_3$	CH_3	H	−0,07				300	7,26	12,93	27,68	−26,94	11,54	88,13
9	4−Cl	CH_3	H	0,23				305	0,85	1,91	4,26	−22,59	14,04	7,70
10	3−Cl	CH_3	H	0,37				300	0,54	0,94	1,79	−36,36	10,28	2,55
11	H	C_6H_5	H		1,20	−5,10	1,30	315	0,75	1,63	4,23	−19,30	15,10	5,96
12	H	C_2H_5	H		0,50	−2,48	1,21	300	5,43	13,37	21,80	−25,62	12,07	71,22
13	H	C_2H_5	$C_2H_5^{e)}$		−0,20	−0,14	1,33	275	118,42	165,00	253,00	−39,30	6,29	302,81
14	H	$CH(CH_3)_2$	H		0,41	−2,08		275	26,16	59,68	107,45	−21,95	12,24	85,75
15	H	CH_3	$2,6(CH_3)_2$					290	0,57	0,88	2,28	−30,71	11,94	3,78
16	H	CH_3	$2,6(C_2H_5)_2$					285	0,64	1,03	2,41	−32,26	11,41	3,82
17	$2-CH_3$	CH_3	H					300	0,84	4,65	6,46	− 8,44	18,07	14,53
18	$C_{10}H_7^{f)}$	CH_3	H					325	2,33	5,27	10,16	−24,80	12,80	28,54

a) Hammett-Parameter[2];
b) nichtaddierte Taft-Parameter für die Substituenten vom Amidstickstoff[2];
c) Charton-Parameter für die Amid-NR_2-Gruppen, berechnet laut[3];
d) Die Wellenlänge bei der die Geschwindigkeitskonstanten bestimmt wurden;
e) $-N(C_2H_5)_2-$ Gruppe
f) 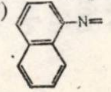 Gruppe

In diesem Fall stellt man fest, daß in Gegenwart von $LiClO_4$ die Substituenteneinflüsse etwas wichtiger sind.

Wird ein Phenylradikal vom Amidstickstoffatom mit einem Äthylradikal ersetzt (Verbindungen 11—13), wächst die Reaktionsgeschwindigkeit stark an. Ein ähnlicher Geschwindigkeitsanstieg, aber von kleinerem Ausmaß, wird bei der Ersetzung des Methylradikals (R) durch Äthyl bzw. iso-Propyl an einem und demselben Amidstickstoffatom festgestellt (Verbindungen 3, 12, 14). Zweifelsohne, rufen diese Substituenten Veränderungen sowohl der elektronischen als auch der sterischen Effekte hervor. Nachdem im ersten Fall durch die Ersetzung des Phenyls durch Äthyl die Elektronendichte am Stickstoff anstieg und die sterische Hinderung abfiel und im Fall der Substitution Methyl-Äthyl-iso-Propyl, sowohl die Elektronendichte am Stickstoff als auch die sterische Hinderung anstieg, können wir den Schluß ziehen, daß die elektronenstoßenden Effekte die Reaktion viel mehr begünstigen als die sterischen Effekte.

Interessant ist, daß für alle diese Verbindungen (3, 11-14) zufriedenstellende Taft-Beziehungen erhalten werden durch die Summierung der sterischen und elektronischen Effekte vom Amidstickstoff:

$$20^\circ \qquad \log k = -1{,}375 - 2{,}28 \sum\sigma^* - 0{,}19 \sum E_S \quad r = 0{,}969$$

$$30^\circ \qquad \log k = -0{,}908 - 2{,}04 \sum\sigma^* - 0{,}11 \sum E_S \quad r = 0{,}942$$

$$40^\circ \qquad \log k = -0{,}900 - 1{,}76 \sum\sigma^* - 0{,}12 \sum E_S \quad r = 0{,}943$$

$$20^\circ\ LiClO_4 \qquad \log k = -0{,}708 - 1{,}39 \sum\sigma^* - 0{,}043 \sum E_S \quad r = 0{,}980$$

Ebenfalls gute Korrelierungen wurden mit den σ^* — Taft und ∀-Charton — Parametern erhalten:

$$20^\circ \qquad \log k = -1{,}992 - 1{,}554 \sum\sigma^* + 0{,}530\ \forall \quad r = 0{,}995$$

$$30^\circ \qquad \log k = -1{,}509 - 1{,}424 \sum\sigma^* + 0{,}320\ \forall \quad r = 0{,}999$$

$$40^\circ \qquad \log k = -1{,}553 - 1{,}255 \sum\sigma^* + 0{,}505\ \forall \quad r = 0{,}996$$

$$20^\circ\ LiClO_4 \qquad \log k = -0{,}932 - 1{,}220 \sum\sigma^* + 0{,}176\ \forall \quad r = 0{,}985$$

Es erscheint nun klar, daß die elektronenstoßenden Effekte einen günstigeren Einfluß auf die Reaktion als die sterischen Effekte haben. Die sterische Hinderung begünstigt alle Reaktionen, mit Ausnahme der Reaktion die in Gegenwart von $LiClO_4$ verläuft und in der die sterischen Einflüsse sehr klein sind.

Ohne in die Polemik über die Bedeutung der σ^*-Taftparameter im Vergleich zu den ∀ — Chartonparametern einzugehen,[4-6] möchten wir hervorheben, daß Korrelierungen ausschließlich mit den ∀-Parametern nicht möglich waren. Dies zeigt, daß die Substituenten meistens durch elektronische Effekte einwirken. Auch wenn man den σ^*-Taftparametern eine bedeutende sterische Rolle zuschreibt, muß man annehmen, daß sie auch ein Ausdruck der elektronischen Effekte sind, was von den ∀ - Parametern auf keinen Fall behauptet werden kann.

Diese Einwendungen sind im Einklang mit dem vorgeschlagenen Mechanismus auf Grund der Lösungsmittel-, der Salz- und der isotopischen Effekte, der katalytischen Wirkung der Metallionen Li^+, Hg^{++}, Ag^+, sowie der Aktivierungsentropien und -enthalpien im Falle der Hydrolyse des N, N, N'-Triphenylchlorformamidins.[1] Es wurde bewiesen, daß dieser Prozeß in zwei Etappen mit vergleichbaren Reaktionsgeschwindigkeiten verläuft und zwar die Ionisierung des Chlorformamidins und die Reaktion zwischen dem Kation und Wasser:

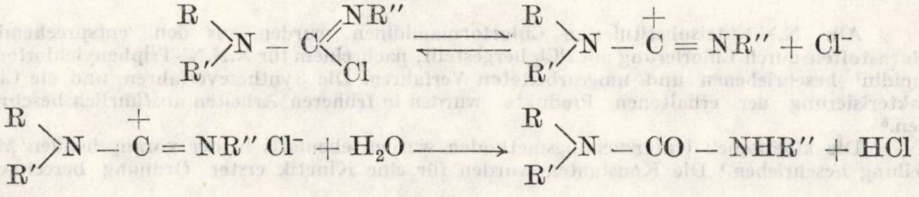

$$\begin{smallmatrix}R\\R'\end{smallmatrix}\!\!>N-C\begin{smallmatrix}\nearrow NR''\\ \searrow Cl\end{smallmatrix} \rightleftharpoons \begin{smallmatrix}R\\R'\end{smallmatrix}\!\!>N-\overset{+}{C}=NR''+Cl^-$$

$$\begin{smallmatrix}R\\R'\end{smallmatrix}\!\!>N-\overset{+}{C}=NR''\,Cl^-+H_2O \longrightarrow \begin{smallmatrix}R\\R'\end{smallmatrix}\!\!>N-CO-NHR''+HCl$$

Bei der Hydrolyse des N,N,N'-Triphenylchlorformamidins[1] in Abwesenheit von Salzen ist die Ionisierung die etwa 3 —4 mal langsamere Etappe und damit entscheidend für die Geschwindigkeit des globalen Prozesses. Auch im Falle verschieden substituierter Verbindungen, spricht die Beschleunigung der Reaktion durch elektronenstoßende Effekte und sterische Hinderung, für diesen Mechanismus.

In Gegenwart von $LiClO_4$ aber, wird die zweite Etappe der Hydrolyse des N,N,N'-Triphenylchlorformamidins [1] etwas langsamer, weil die Li^+-Ionen einen katalytischen Effekt auf beide Prozesse ausüben. Im Falle der substituierten Verbindungen besteht derselbe Effekt, wenigstens für die am Amidstickstoff durch Phenyl-und Äthylradikale substituierten Verbindungen. Die Abnahme der elektronischen Effekte und praktisch die Annulierung der sterischen Effekte in diesem Fall im Vergleich zur Reaktion in Abwesenheit von $LiClO_4$ kann so erklärt werden. Es ist aber nicht ausgeschlossen, daß die elektronenanziehenden Substituenten des aromatischen Rings des Iminstickstoffs den Mechanismus im Sinne einer langsamen Ionisierung verändern. Diese Tatsache wiederspiegelt sich in deren beträchtlichen Effekten auf die Reaktionsgeschwindigkeit. Werden Substituenten am aromatischen Ring in die *orto*-Stellung zu den Stickstoffatomen eingeführt (Verbindungen 15 —18), ist als eine Folge ihrer beträchtlichen sterischen Effekte ein wesentlicher Abfall der Reaktionsgeschwindigkeit zu verzeichnen. Diese Tatsache kann nur dann verstanden werden, wenn wir die in diesen Fällen von der sterischen Hinderung begünstigten Ionisierung als ein rasches Vorgleichgewicht und als langsame Etappe die Reaktion des sterisch gehinderten Kations mit dem Nucleophilen annehmen.

Die verhältnismäßig niedrigen Aktivierungsentropien, zwischen -8 und -40 cal/mol·K sind annehmbar für einen vorwiegend monomolekularen Prozeß. Im Falle des N,N,N'-Triphenylchlorformamidins gliedert sich der Wert von $-19 + -23$ cal/mol·K[1] ebenfalls in diesen Bereich ein.

Wenn in Lösungsmittelgemischen mit einem verhältnismäßig kleinen Gehalt an Wasser gearbeitet wird, erscheinen wenig wichtige Assoziationen zwischen den Lösungsmittelmolekülen. In solchen Systemen setzt die

Ionisierung eine wesentlichere Anordnung der Lösungsmittelmoleküle zum Übergangszustand voraus, also eine kleine Aktivierungsentropie. Hieraus folgt, daß die Solvatierungseffekte eine vorwiegende Rolle in der Aktivierungsentropie spielen.

Da die Aktivierungsenthalpien ziemlich groß sind, sprechen sie ebenfalls für einen monomolekularen Ionisierungsmechanismus.

VERSUCHSTEIL

Alle N,N,N′-trisubstituierten Chlorformamidinen wurden aus den entsprechenden Harnstoffen durch Chlorierung mit PCl_5 hergestellt, nach einem für N,N,N′-Triphenylchlorformamidin[7] beschriebenen und umgearbeiteten Verfahren. Die Syntheseverfahren und die Charakterisierung der erhaltenen Produkte wurden in früheren Arbeiten ausführlich beschrieben.[8]

Die kinetischen Untersuchungsmethoden wurden ebenfalls in der vorangehenden Mitteilung beschrieben.[1] Die Konstanten wurden für eine Kinetik erster Ordnung berechnet.[1]

LITERATURHINWEISE

[1] XVI. Mitt., R. Bacaloglu, A. Chicu und I. Bacaloglu, *J. prakt. Chem.*, unter Druck.

[2] N. B. Chapman und J. Shorter : „Advances in Linear Free Energy Relationships“, Plenum Press, London, 1972, S. 29 und 76.

[3] M. Charton, *J. Org. Chem.*, **42**, 3535 (1977) und die dort zitierte Literatur.

[4] M. Charton, *J. Amer. Chem. Soc.*, **97**, 3691 (1975).

[5] M. Charton, *J. Amer. Chem. Soc.*, **99**, 5687 (1977).

[6] M. Charton, *J. Org. Chem.*, **44**, 903 (1979).

[7] A. Steindorff, *Ber. dtsch. chem. Ges.*, **37**, 964 (1904).

[8] A. Chicu, R. Bacaloglu und C. Csunderlik, *Bul. şt. tehn. I. P. Tmş. Seria Chimie*, unter Druck.

Revue Roumaine de Chimie, 26, *3*, 441—448 (1981)

STUDIES ON THE CYCLISATION OF THE PRODUCTS OF *STOBBE* CONDENSATION WITH 2,4-DIMETHYLACETOPHENONE

M.M. MOHAMED, M. A. El-HASHASH, M. A. SAYED and O. A. ABO-BAKER*
Faculty of Science, Ain Shams University, Abbassia, Cairo, Egypt
* Faculty of Science El-Azhar University.

Received November 29, 1979

2,4-Dimethylacetophenone was condensed with diethyl succinate in the presence of potassium *t*-butoxide and the resulting half-ester was cyclised to naphthalene derivatives **2** or to oxoindenyl acid **8** according to their configuration.

In pursuit of the studies [1,2] concerning the factors (steric and/or polar) that govern the ratio of stereoisomers resulting from the Stobbe condensation, we thought to investigate the effect of some bulky and more polar substituents in the ketonic component (e.g., 2,4-dimethylacetophenone as compared to those used before e.g., 3,4-dimethylacetophenone[3] and *p*-ethylacetophenone[4]), with the aim of deciding what is the prominent factor (steric or polar) which may affect the ratio of stereoisomeric half-esters.

2,4-Dimethylacetophenone condenses with diethyl succinate in the presence of potassium *t*-butoxide to give (E) half-ester [*trans*-(2′, 4′-$(CH_3)_2$ C_6H_3/$COOC_2H_5$)] -3-ethoxycarbonyl-4-methyl-4-(2′, 4′-dimethylphenyl-but-3-enoic acid (**1a**) in a pure crystalline state (73% yield). Besides the crystalline product, an oily half-ester fraction (z-configuration) has been obtained. Previously[3] (E) —configurational product was obtained in a pure crystalline state in 58% yield. Now, we concluded that the polar factor plays a predominat rôle in the acetophenone series.

The position of unsaturation in the products was established by their oxidation to the original ketone. Further evidence for the position of the double bond in **1a** has been obtained from its infrared absorption which shows ν_{max} of two carbonyl groups (at 1727 cm^{-1} and 1718 cm^{-1}) for α,β-unsaturated ester and nonconjugated carboxy group respectively.

CYCLISATION OF THE *trans*-HALF-ESTER (1a)

Assignment of configuration to the crystalline half-ester 1a was made on the basis of its cyclisation with sodium acetate-acetic anhydride to the acetoxynaphthoate 2a. The proposed structure for 2a was supported by

its infrared spectrum which showed strong bands characteristic for two carbonyls (1772 cm^{-1} and 1715 cm^{-1}). Upon hydrolysis it gave the corresponding naphthoic acid **2b**, whose structure was established from its infrared spectrum which showed strong bands characteristic of ν(CO) (1695 cm^{-1}) and of ν(OH) of phenolic hydroxy group (3400 cm^{-1}). The ultraviolet absorption spectrum of **2b** in ethanol indicated λ_{max}^{nm} 247, 304 and 330 –333 infl. (ϵ 37200, 4400 and 2800 respectively) which agreed well with those of analogous naphthalene derivatives.[3] The naphthoic acid derivative **2b** affords the corresponding methoxy naphthoic ester **2c** by methylation and the 4-O-carbethoxymethyl-1,6,8-trimethyl-2-carbethoxymethylnaphthoate (**2d**) by carbethoxymethylation.

The infrared spectrum of **2c** showed the presence of ν(C=O) at 1730 cm^{-1}; in addition, the absorption in the 3μ region disappeared. Compound **2d** showed strong absorption bands for ν_{max} of three carbonyl groups at 1730 cm^{-1}, 1742 cm^{-1} and 1760 cm^{-1} respectively.

Saponification of the methoxy naphthoic ester **2c** and carbethoxymethylnaphthoic ester **2d** gave the corresponding 4-methoxy-1,6,8-trimethyl-2-naphthoic acid (**2e**) and 4-O-carbethoxymethyl-1,6,8-trimethyl-2-naphthoic acid (**2f**) respectively. The latter acids displayed the expected carbonyl absorption at 1700 cm^{-1} for **2e** and at 1695 cm^{-1} and 1725 cm^{-1} for **2f** respectively.

On decarboxylation, the methoxy acid **2e** gave the corresponding 4-methoxy-1,6,8-trimethylnaphthalene (**2g**) in pure crystalline form, whose infrared spectrum does not indicate any absorption either in the 3μ region or in the region specific for the aryl conjugated carboxyl group.

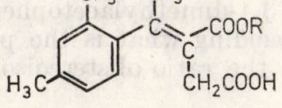

1

a, R = C_2H_5
b, R = H

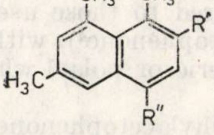

2

	R′	R″
a,	$COOC_2H_5$	$OCOCH_3$
b,	COOH	OH
c,	$COOCH_3$	OCH_3
d,	$COOCH_2COOC_2H_5$	$OCH_2COOC_2H_5$
e,	COOH	OCH_3
f,	COOH	OCH_2COOH
g,	H	OCH_3
h,	$COOCH_2CONHNH_2$	$OCH_2CONHNH_2$

The phenolic acid **2b** could be coupled normally with diazonium salts of aromatic amines to give red dyes **3a-e**.

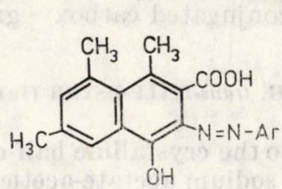

3

	Ar
a,	C_6H_5
b,	o-ClC_6H_4
c,	p-$H_3C\ C_6H_4$
d,	2,4-$(H_3C)_2C_6H_3$
e,	3-Cl-5-CH_3-C_6H_3

Compound **2d** reacted with hydrazine hydrate in boiling ethanol and yielded the expected dihydrazide **2h**, whose structure was elucidated from its infrared spectrum which showed ν_{max} for two carbonyls at 1640 cm^{-1} and 1730 cm^{-1} and other broad band at 3330 cm^{-1} attributable to ν(NH).

In previous works[5-7] it has been reported that anthranilic acid reacts with an excess of benzoyl chloride in pyridine to give 2-phenyl-4H-3,1-benzoxazin-4-one. In the present work, however, we report on the reaction of anthranilic acid with the chloride of 4-methoxy-1,6,8-trimethyl-2-naphthoic acid (**2e**) as a preparative method for 2-substituted 4H-3,1-benzoxazin-4-one for the sake of their pharmacological evaluation. The reaction was performed by treatment of anthranilic acid in pyridine solution with the chloride of acid **2e** in which the 2-(4-methoxy-1,6,8-trimethyl-2-naphthalenyl)-4H-3,1-benzoxazin-4-one (**4**) was obtained.

The infrared spectrum of **4** shows absorption bands at 1742 cm^{-1} and 1645 cm^{-1} attributable to ν(CO) and ν(C=N) respectively.

Compound **4** reacted with hydrazine hydrate in ethanol and gave the N-(4-methoxy-1,6,8-trimethyl-2-naphthyl)-anthranilic acid hydrazide (**5a**), whose structure was established from its infrared spectrum which shows absorption bands at 1660 cm^{-1}, 1640 cm^{-1} and at 3460 cm^{-1}, 3360 cm^{-1}, attributable to ν(CO) and ν(NH) respectively.

On the other hand, compound **4** reacted with hydroxylamine hydrochloride in boiling pyridine and yielded 2-hydroxylaminocarbonyl-4′-methoxy-1′,6′,8′-trimethyl-2′-naphthanilide (**5b**). The infrared spectrum of (**5b**) showed bands attributable to ν(OH), ν(NH) and ν(CO) at 3350 cm^{-1}, 3200 cm^{-1} and 1640 cm^{-1} respectively.

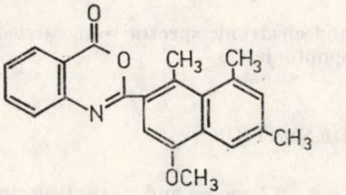

4

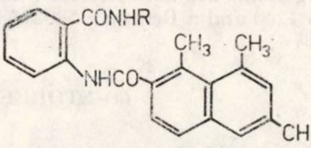

5

R
a, NH_2
b, OH

CYCLISATION OF THE *trans*- DIBASIC ACID 1B

The *trans*-acid **1b** was obtained by hydrolysis both of the crystalline half-ester **1a** and of the oily fraction. The position of unsaturation in the di-acid **1b** was established by its oxidation to the original ketone. Its configuration was proved first by converting it (with acetylchloride) into the corresponding anhydride **6**, which on treatment with aluminium chloride in nitrobenzene gave the naphthoic acid **2b** (about 40% yield). This supports undoubtly the assigned E-configuration of the crystalline dibasic acid **1b**. The infrared spectrum of **1b** shows strong absorptions at 1700 cm^{-1} and 1720 cm^{-1} attributable to ν(CO) of two types of carboxyl groups. The anhydride **6** exhibited the carbonyl coupling bands expected from cyclic five-membered anhydrides, the position of characteristic bands being at 1845 cm^{-1} and 1778 cm^{-1}.

CYCLISATION OF THE *cis*-HALF-ESTER 7

Together with the crystalline di-acid **1b**, an oily acidic fraction was obtained upon hydrolysis of the dimethyl oily half-ester fraction **7**. This acidic fraction was converted (with acetylchloride) into the corresponding oily anhydride which, upon treatment with AlCl$_3$ in acetylene tetrachloride, gave low yield of the oxoindenyl acetic acid **8**. The structure of compound **8** follows from characteristic colour (yellow), solubility in sodium carbonate and from its infrared spectrum which shows strong carbonyl absorption bands at 1715 cm^{-1} and 1690 cm^{-1} which can be correlated with ν(CO) of non-conjugated carboxyl group and α,β-unsaturated ketonic five-membered ring group.

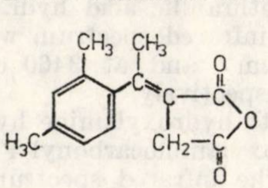

6

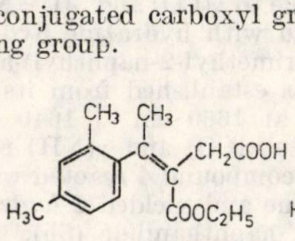

7

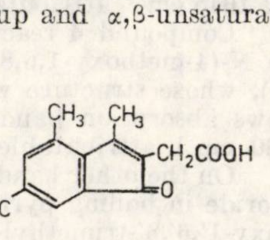

8

EXPERIMENTAL

Melting points are not corrected ; infrared and electronic spectra were carried out using a Unicam Sp 1200 and a Beckman 580216 spectrophotometers.

(a) STOBBE CONDENSATION

A mixture of 2,4-dimethylacetophenone (14.8 g ; 0.1 mole) and diethyl succinate (26.1g ; 0.15 mole) was added during 30 minutes to a boiling stirred solution of potassium *t*-butoxide (4.3 g ; 0.11 mole) in dry *tert*-butanol (25 ml of *t*-butanol per 1 g potassium), boiling and stirring were then continued for 3 hrs. Most of the alcohol was then removed, the cooled residue acidified with dilute hydrochloric acid, and the organic material was taken up in ether and then repeatedly extracted with cold sodium carbonate solution 10 %. The alkaline extract was cooled, acidified with cold dilute hydrochloric acid and the precipitated material extracted with ether. Evaporation of the latter gave an oily half-ester mixture (23 g ; 83 % yield), in which crystalline material started to appear after standing for few days. Crystallisation from light petroleum (b.p. 80—100°C) gave the (E) - configurational half-ester, *trans*-(2′, 4′-$(CH_3)_2C_6H_3$/ /$COOC_2H_5$)-3-ethoxycarbonyl-4-methyl-4-(2′, 4′-dimethylphenyl)-but-3-enoic acid **(1a)** (8.4 g). The results are listed in table 1.

Evaporation of the mother liquor left an oily fraction (14.2 g) whose composition was revealed by later experiments.

Oxidation

To a solution of half-ester (6 g) in 3 % Na_2CO_3 solution (600 ml), 2 % $KMnO_4$ solution (400 ml) was added portionswise while stirring was continued for another hour ; the precipitated manganese dioxide was filtered off, both precipitate and alkaline solutions were thoroughly extracted with ether, then with benzene. Evaporation of the solvent gave the neutral original ketone. Its 2,4-dinitrophenylhydrazone showed no depression upon admixture with authentic derivative prepared from 2,4-dimethylacetophenone.

(b) CYCLISATION OF THE HALF-ESTER

A mixture of the half-ester (5.4 g ; 0.02 mole), freshly fused sodium acetate (2 g ; 0.024 mole) and acetic anhydride (40 ml), was refluxed for 7 hrs. After removal of the excess acetic anhydride under reduced pressure, water was added and the organic material was extracted with ether. The ethereal solution was washed with water, 5% Na_2CO_3 solution, cold 5% NaOH solution and finally with water. Evaporation of the dried ethereal solution gave the neutral cyclised product **2a** (3.5 g ; yield 59.7%) as an oil which failed to solidify.

Saponification of the acetoxy naphthoate 2a

The acetoxy naphthoate **2a** (10 g) was refluxed with 10% aqueous sodium hydroxide solution (*Ca.* 10 ml per 1 g of ester). The solution (which darkened considerably at the end of the reaction) was charcolated, filtered, cooled, and then extracted with ether to remove unsaponified material. The alkaline solution was then acidified with dilute hydrochloric acid and the precipitated material taken up in ether. Evaporation of the dried ethereal solution left 4-hydroxy-1,6,8-trimethyl-2-naphthoic-acid **(2b)** (3.7 g ; 48% yield) in pure crystalline state. The results are listed in table 1.

Methylation and carbethoxymethylation of naphthoic acid 2b

A mixture of naphthoic acid derivative **2b** (1 mole), dimethyl sulphate and/or ethyl chloroacetate (4 mole), anhydrous potassium carbonate (4 mole), and acetone (20 ml per 1 g acid) was refluxed for 20 hrs on a water bath, the solvent was removed and some water added. The organic material was extracted with ether, the ethereal solution was successively washed with water, 10% aqueous sodium hydroxide, and finally with water. Evaporation of the dried ethereal solution gave the methoxy ester **2c** and O-carbethoxymethyl ester **2d** respectively.

2 g of **2b** gave 1.9 g **2c** (85% yield)
2 g of **2b** gave 2.4 g **2d** (71% yield). The results are listed in table 1.

Saponification of the methoxy ester 2c and O-carbethoxymethyl ester 2d

The ester **2c** or **2d** was refluxed with 10% aqueous sodium hydroxide as mentioned for acetoxynaphthoate **2a**.

2 g of **2c** gave 1.6 g of the methoxy acid **2e** (85% yield)
2 g of **2d** gave 1.5 g of the di-acid **2f** (82% yield)
The results are listed in table 1.

Decarboxylation of the methoxy acid 2e. Formation of 2g

The methoxy acid, copper bronze, and quinoline (*Ca.* 1 g and 6 ml, respectively per 1 g of methoxy acid) were refluxed for 3 hrs. The reaction mixture was then poured while hot into dilute hydrochloric acid and the precipitated product extracted with an ether-benzene mixture. The organic extract was washed with dilute hydrochloric acid, sodium carbonate solution, and then with water. Evaporation of the solvent gave 4-methoxy-1,6,8-trimethylnaphthalene (**2g** ; 25% yield) as a semisolid material. The results are listed in table 1.

TABLE 1

Physical data of compounds **1a**, **2(b–h)**, **3(a–e)**, **4**, **5a** and **5b**

Compd.	m.p. (°C) colour	solvent*)	Formula	Analysis %		
					Found	Required
1a	110	P1	$C_{16}H_{20}O_4$	C	69.29	69.24
	colourless			H	7.10	7.30
2b	213	A	$C_{14}H_{14}O_3$	C	73.11	73.02
	colourless			H	6.11	6.13
2c	95	P2	$C_{16}H_{18}O_3$	C	74.68	74.39
	colourless			H	7.00	7.02
2d	76	P2	$C_{22}H_{26}O_7$	C	65.42	65.67
	colourless			H	6.79	6.46
2e	203	X	$C_{15}H_{16}O_3$	C	73.86	73.75
	colourless			H	6.51	6.60
2f	273	X	$C_{16}H_{16}O_5$	C	66.58	66.66
	colourless			H	5.73	5.55
2g	123	P3	$C_{14}H_{16}O$	C	84.10	83.96
	colourless			H	8.22	8.05
2h	240	but.	$C_{18}H_{22}O_5N_4$	C	57.53	57.75
	colourless			H	5.66	5.88
3a	245	E	$C_{20}H_{18}N_2O_3$	C	71.90	71.85
	red			H	5.50	5.38
3b	205	T	$C_{20}H_{17}ClN_2O_3$	C	65.12	64.87
	red			H	4.61	4.76
3c	232	E	$C_{21}H_{20}N_2O_3$	C	72.11	72.41
	red brown			H	5.61	5.74
3d	267	P3	$C_{22}H_{22}N_2O_3$	C	72.61	72.92
	red			H	6.36	6.07
3e	195	E	$C_{21}H_{19}N_2ClO_3$	C	66.02	65.88
	red brown			H	5.10	4.96
4	161	T	$C_{22}H_{19}NO_3$	C	76.82	76.52
				H	5.43	5.50
5a	203	X	$C_{22}H_{23}N_3O_3$	C	70.04	70.02
				H	5.87	6.10
5b	182	X	$C_{22}H_{22}N_2O_4$	C	70.37	69.84
				H	5.46	5.46

***) P1 = light petrol (b.p. 80–100°C) ; P2 = light petrol (b.p. 60–80 °C) ; P3 = light petrol (b.p. 100–120 °C) ; A = glacial acetic acid ; X = xylene ; but. = *n*-butanol ; E = ethanol ; T = toluene.**

Conversion of the di-ester 2d to the di-hydrazide 2h

A solution of **2d** (0.01 mole) and hydrazine hydrate (0.01 mole), in 50 ml ethanol was heated under reflux for 5 hrs; the solid separated on cooling was crystallized from the suitable solvent to give **2h** (61% yield) (cf. Table 1).

Coupling of 2b with diazonium salts of aromatic amines

The phenolic acid **2b** coupled normally with diazonium salts of aromatic amines, namely: aniline, *o*-chloroaniline, *p*-toluidine, 2,4-dimethylaniline and 3-chloro-5-methylaniline and gave the corresponding dyes (**3a-e**) (cf. Table 1).

Action of chloride of the acid 2e on anthranilic acid

To a solution of anthranilic acid (0.01 mole) in 30 ml pyridine the chloride of the acid **2e** (0.02 mole) was added, the mixture was shaken for five minutes and then set aside at room temperature for further one hour. The reaction mixture was poured into cold water and the precipitated solid was filtered off to give the benzoxazinone **4** as pale yellow crystals (yield 61%) (cf. Table 1).

Action of hydrazine hydrate on benzoxazinone 4

A solution of 4 (0.01 mole) and hydrazine hydrate (0.01 mole) in 40 ml ethanol was heated under reflux for 5 hrs. The solid separated on cooling was crystallized from the proper solvent to give the hydrazide **5a** (71% yield) (cf. Table 1).

Action of hydroxylamine hydrochloride on 4

A mixture of **4** (0.01 mole) and hydroxylamine hydrochloride (0.03 mole) in dry pyridine (40 ml) was heated under reflux for 8 hrs. The reaction mixture was poured into cold dilute hydrochloric acid to give the naphthanilide **5b** (66% yield) (cf. Table 1).

(c) SAPONIFICATION OF THE HALF-ESTER 1a. FORMATION OF DI-ACID 1b

The half-ester (8.4 g) was refluxed with 10% aqueous NaOH solution (10 ml per 1g half-ester) for 5 hrs. The alkaline solution was then cooled in ice, acidified with dilute hydrochloric acid, and the precipitated material was taken up in ether. The ethereal solution was washed with water, dried, and then evaporated. The resulting acidic product was obtained as an oil which could be solidified by trituration with light petroleum (b.p. 40—60°C) and gave **1b** (6.1 g; yield 82%). The results are listed in table 2.

Saponification of the oily half-ester fraction

The oily half-ester (14.2 g) was treated as mentioned in (c) and gave an acidic product (10.5 g) whose components were separated on treatment with warm benzene as follows:
(i) a crystalline solid (6.3 g) was identified as 1b by its m.m.p.
(ii) an oily acidic fraction (3.8 g) obtained by evaporation of the mother liquor.

The percentage of the crystalline dibasic acid **1b** in the total acidic product is 60%; this means that the oily half-ester fraction (14.2 g) still contains (*ca.* 8.5 g) of the crystalline (E)-configurational half-ester **1a**.

The relative amounts of products given in (a) should now be modified as follows:

Total half-ester mixture (23 g), (E)-configurational half-ester (8.4 + 8.5 = 16.9 g), the (Z)-configurational half-ester "oily fraction" (6.1g); the (E)-configurational half-ester thus constitutes at least 73% of the product of the Stobbe condensation, involving 2,4-dimethylacetophenone.

TABLE 2

Physical data of compounds **1b**, **6** and **8**

Compd.	m.p.(°C) colour	solvent*	Formula	Analysis %	
				Found	Required
1b	154	B	$C_{14}H_{16}O_4$	C 67.45	67.73
	colourless			H 6.45	6.50
6	123	P	$C_{14}H_{14}O_3$	C 72.93	73.02
	colourless			H 6.30	6.13
8	177	B	$C_{14}H_{14}O_3$	C 73.42	73.02
	yellow			H 6.11	6.13

*) B = benzene ; P = light petrol (b.p. 100 – 120°C)

(d) CONVERSION OF THE DIBASIC ACID 1b TO THE ANHYDRIDE 6

The dibasic acid **1b** (6.3 g) was refluxed with acetylchloride (10 ml, per 1g acid) for 2 hrs. Excess of acetylchloride was then removed by distillation to leave an oily neutral product which could be solidified by trituration with light petroleum (b.p. 40 – 60°C) yielding **6** (5.3 g ; 91 % yield), cf. Table 2 (in the case of the oily dibasic acid, the resulting anhydride could not be solidified).

(e) ACTION OF ALUMINIUM CHLORIDE UPON THE OILY ANHYDRIDE. FORMATION OF 8

To a stirred ice-cold solution of the oily anhydride (1 mole) in dry acetylene tetrachloride (10 ml per 1 g anhydride), powdered anhydrous aluminium chloride (1.1 mole) was added in one portion and stirring was continued for 6 hrs. The reaction mixture was left for two days at room temperature with occasional stirring, then decomposed with ice-cold dilute hydrochloric acid. The acetylene tetrachloride was removed by steam distillation, and the reaction product extracted with ether. The ethereal solution was washed with water, extracted with 5 % sodium carbonate, and the cold alkaline solution was finally acidified. The acidic reaction product was then isolated by extraction with ether.

3.8 g from the oily anhydride gave a viscous acidic product ; repeated extraction with boiling light petroleum (b.p. 100 – 120°C) gave 3,4,6-trimethyl-1-oxo-2-indenylacetic acid (**8**) in yellow crystals (0.3 g ; 8 % yield). The results are listed in table 2.

(f) ACTION OF ALUMINIUM CHLORIDE UPON SOLID ANHYDRIDE

The reaction was carried out using the same procedure described in (e) except that the acetylene tetrachloride was replaced by nitrobenzene. 3 g of compound **6** gave (0.9 g) of the 4-hydroxy-2-naphthoic acid **2b** (30 % yield), which was identified by mmp.

REFERENCES

[1] W. I. Awad, F. G. Baddar, F. A. Fouli, S. M. Omran and M. I.B. Selim, *J. Chem. Soc. (C)*, **1968**, 507.

[2] F. G. Baddar, M. F. El-Newaihy and R. O. Loutfy, *J. Chem. Soc. (C)*, **1970**, 620.

[3] M. F. El-Newaihy and M. A. El-Hashash, *J. Chem. Soc. (C)*, **1971**, 2373.

[4] M. A. El-Hashash and A. A. El-Khamry, *Pakistan J. of Sci. Res.*, **29**, 1 (1977).

[5] D. T. Bain and R. K. Smalley, *J. Chem. Soc. (C)*, **1968**, 1593.

[6] G. Heller and G. Fiesselmann, *Liebigs Ann. Chem.*, **324**, 118 (1902)

[7] R. K. Smalley, H. Suschitzky and E. M. Tanner, *Tetrahedron Letters*, **1966**, 3465.

Revue Roumaine de Chimie, **26**, *3*, 449–456 (1981)

REACTION OF 5-ARYL-2-THIONO-1,3,4-OXADIAZOLES WITH SOME AMINO- AND HALO-COMPOUNDS

A. A. El-BARBARY, M. ANWAR, A. A. GHATTAS and A. F. HASHEM
Chemistry Department, Faculty of Science, Tanta University, Tanta, A. R. Egypt

Received November 8, 1979

5-Aryl-2-thiono-1,3,4-oxadiazoles (I) react with hydrazines, amines and some halo-compounds forming 5-aryl-4-amino-1,2,4-triazole-3-thiones (II) and 2,5-disubstituted-1,3,4-oxadiazoles (III–VIII).

5-Aryl-2-thiono-1,3,4-oxadiazoles (Ia, b) were prepared by the recommended methods.[1-4]

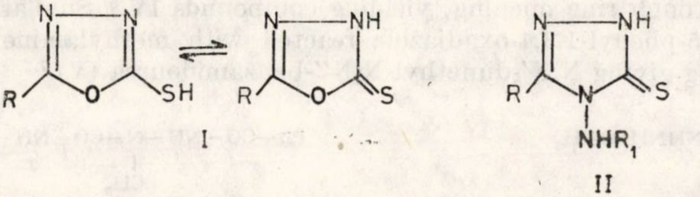

I

II

a, R = $C_6H_4\,CH_3-p$
b, R = C_6H_4OH-*p*

	R	R_1
a,	$C_6H_4CH_3$-*p*	H
b,	$C_6H_4CH_3$-*p*	C_6H_5
c,	$C_6H_4CH_3$-*p*	$C_6H_3(NO_2)_2-2,4$
d,	C_6H_4OH-*p*	H
e,	C_6H_4OH-*p*	C_6H_5

5-Aryl-2-thiono-1,3,4-oxadiazoles (I) react with some hydrazines, namely hydrazine hydrate, phenylhydrazine and 2,4-dinitrophenylhydrazine. The reaction proceeds by cyclization to form 5-aryl-4-amino-1,2,4-triazole-3-thiones (IIa-e) similar to those obtained by Artemov.[5]

The structure of compounds II was established by the following assignments :

(i) Oxidation of IIb with potassium permanganate in acetic acid medium gives the corresponding disulphide III.

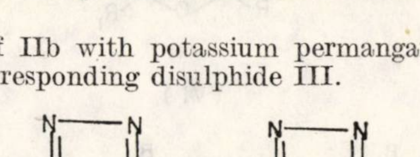

III

(R = $C_6H_4CH_3$-*p*)

(ii) Infrared and ultraviolet spectra.

The infrared spectra of compounds II show the stretching frequencies of ν(NH) at 3370 – 3320 cm^{-1}, and ν(C=S) at 1330-1300 cm^{-1}.

The infrared spectra show also the other functional groups present in each case.

The ultraviolet absorption spectra of these compounds show three main absorption bands in the regions : 215 – 210 nm, 276 – 270 nm and 415 – 410 nm.

(iii) The ^{1}H-N.M.R. spectrum of compound IIb shows the following assignments : a singlet at $\delta = 2.4$ ppm corresponding to 3H(H_3C-aromatic, a multiplet at $\delta = 6.85 - 8.0$ ppm corresponding to 9H aromatic, a singlet at $\delta = 11.8$ ppm corresponding to 1H (N*NH*-Ph) and a singlet at $\delta = 12.45$ ppm corresponding to 1H (triazole *NH*).

The ^{1}H-N.M.R. spectrum of compound IId shows the following assignments : a singlet at $\delta = 3.4$ ppm. corresponding to 3H (H_3C-aromatic, a singlet at $\delta = 5.1$ ppm. corresponding to 1H (N*NH*-aromatic), a multiplet at $\delta = 7.6 - 8.4$ ppm. corresponding to 7H aromatic and a singlet at $\delta = 12.0$ ppm. corresponding to 1H (*NH* triazole).

The reaction of amines with 2-oxo-1,3,4-oxadiazole was found to proceed through ring opening, yielding compounds IV.[6] Similarly, 3-methyl-2-oxo-5-phenyl-1,3,4-oxadiazole reacted with methylamine through ring opening giving N,N′-dimethyl-N,N″-benzamidourea (V).[7]

$R{-}CONHNHCONH_2$

(IV)

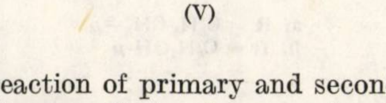

$Ph{-}CO{-}NH{-}\underset{\displaystyle CH_3}{\underset{|}{N}}{-}CO{-}NH{-}CH_3$

(V)

In the present investigation the reaction of primary and secondary amines with 5-aryl-2-thiono-1,3,4-oxadiazoles (I) has been explored. It has been found that amines react with elimination of hydrogen sulphide, forming 2,5-disubstituted-1,3,4-oxadiazoles (VIa-f).

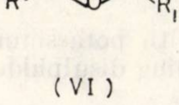

(VI)

	R	R_1		R	R_1
a,	$C_6H_4CH_3$-*p*	NHC_6H_5	d,	C_6H_4OH-*p*	NHC_6H_5
b,	$C_6H_4CH_3$-*p*	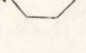	e,	C_6H_4OH-*p*	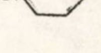
c,	$C_6H_4CH_3$-*p*	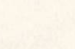	f,	C_6H_4OH-*p*	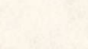

The structure of compounds VI was established by the following:

(i) Infrared and ultraviolet spectra.

The infrared spectra of compounds VI showed the absence of ν(NH) and ν(C=O) absorption bands.

The ultraviolet absorption spectra of compounds VI show the essential absorption band characteristic for 2-substituted-1,3,4-oxadiazoles[8] in the region of 330–320 nm.

(ii) The ^{1}H-N.M.R. spectrum for compound VIa shows the following assignments: a singlet at $\delta = 2.4$ ppm. corresponding to 3H (H_3C-aromatic), a singlet at $\delta = 3.35$ ppm. corresponding to 1H (*HN*-Ph), and a multiplet at $\delta = 7.35 - 8.0$ ppm. corresponding to 9H aromatic.

The ^{1}H-N.M.R. spectrum for compound VIf shows the following assignments: a singlet at $\delta = 1.8$ ppm, corresponding to 6H 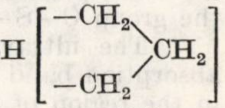 piperidyl, a doublet at $\delta = 3.2$ ppm. corresponding to 4H 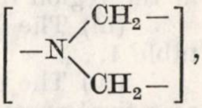, a doublet at $\delta = 7.2-8.0$ ppm. corresponding to 4H aromatic, and a singlet at $\delta = 11.5$ corresponding to 1H (*HO*-aromatic).

Compound Ia reacts with some halo-compounds, namely: methyl iodide, benzylchloride, *p*-toluenesulphonyl chloride, acetylchloride, *o*-bromotoluene and ethylchloroformate, forming 2,5-disubstituted-1,3,4-oxadiazoles (VIIa-f)[9] respectively.

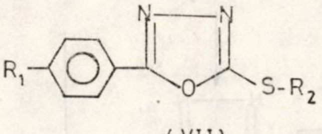

(VII)

	R_1	R_2		R_1	R_2
a,	CH_3	CH_3	f,	CH_3	$COOC_2H_5$
b,	CH_3	$CH_2C_6H_5$	g,	OCH_3	CH_3
c,	CH_3	$SO_2-C_6H_4-CH_3-p$	h,	$OCOCH_3$	$COCH_3$
d,	CH_3	$COCH_3$	i,	CH_3	$CONHNH_2$
e,	CH_3	$C_6H_4-CH_3$-*o*			

Compound Ib reacts with two moles of methyliodide and/or acetylchloride forming compounds VII g, h.

It is worth-mentioning that compounds VIIg,h are obtained even when we use equimolecular amounts of reactants and the reaction was carried out in the cold.

Compound VIIf reacts with hydrazine hydrate yielding the compound VIIi.

The structure of compounds VII was established by the following assignments :

(i) Oxidation of VIIa with potassium permanganate in acetic acid medium gives the corresponding known sulphone VIII.[10]

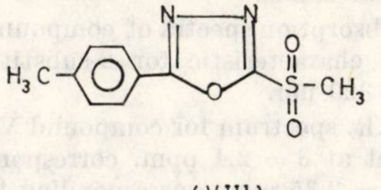

(VIII)

(ii) Infrared and ultraviolet spectra.

Compounds VII show the stretching frequencies attributable to the group C—S—C in the region 720—695 cm^{-1}.

The ultraviolet absorption spectra of compounds VII show the absorption band characteristic for the 2-substituted -1,3,4-oxa-diazoles[8,11] in the region of 335—310 nm.

(iii) The N.M.R. spectral data for compounds VII are listed in table 1.

(iv) The mass spectral data for compounds VIIf can be considered as a final proof for the structure. The ratio of m/e and the relative abundances are given in the following chart :

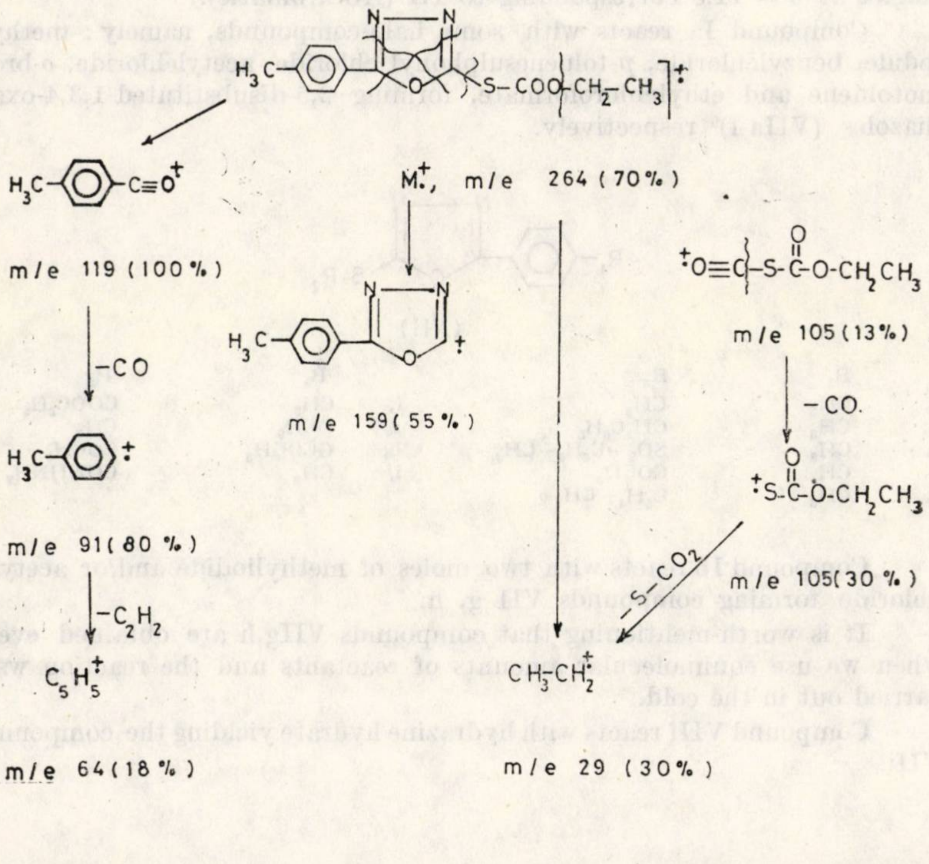
M$^{+\cdot}$, m/e 264 (70%)
m/e 119 (100%)
−CO
m/e 91 (80%)
−C$_2$H$_2$
C$_5$H$_5^+$
m/e 64 (18%)
m/e 159 (55%)
m/e 105 (13%)
−CO
m/e 105 (30%)
−CO$_2$
CH$_3$−CH$_2^+$
m/e 29 (30%)

TABLE 1

The ^{1}H-N.M.R. spectral data for compounds VII*, **

Compound	Phenyl	R_1	R_2
VIIa	7.2−8.0(4H,d.d)	2.45(3H,s)	2.85(3H, s)
VIIc	7.2−8.0(8H,m)	2.48(6H,s)	
VIId	7.2−8.0(4H,d.d)	2.45(3H, s)	2.75(3H, s)
VIIe	7.2−7.9(8H, m)	2.45(6H,s)	
VIIf	7.0−7.8(4H, d.d)	2.45(3H, s)	1.5(3H,t) $\mathrm{CH_2}\mathit{CH_3}$ 4.5(2H,q) $\mathit{CH_2}\mathrm{CH_3}$
VIIg	7.0−7.8(4H,d.d)	3.85(3H, s)	2.6(3H, s)
VIIi	7.25−7.9(4H,d.d)	2.4(3H,s)	5.9(3H, s)$\mathit{NHNH_2}$

* Chemical shifts was determined as δ (ppm)

** s = singlet ; d = doublet ; t = triplet ; q = quartet ; m = multiplet.

EXPERIMENTAL

The IR spectra were recorded with a UNICAM S.P. 1200 spectrophotometer. The KBr pellet technique was used.

The absorption spectra in the U.V region using ethanol as solvent were recorded with a UNICAM S.P. 800 spectrophotometer.

The ^{1}H-N.M.R. spectra were recorded at 60 MHz on a Varian A-60 spectrometer.

Mass spectra were recorded on a V. G. Micromass 7070 F spectrometer operating at 70 eV using direct inlet.

All melting points are uncorrected.

ACTION OF HYDRAZINES ON 5-ARYL-2-THIONO-1,3,4-OXADIAZOLES

5-Aryl 2-thiono-1,3,4-oxadiazoles (I) (0.01 mole) and hydrazines (0.01 mole) in 50 ml dioxane were heated under reflux for 3 hrs. The reaction mixture was concentrated, cooled and filtered. The solid obtained was recrystallized from ethanol to give 5-aryl-4-amino-1,2,4-triazole-3-thiones (IIa-e). Yields 90−95%. The results are given in table 2.

OXIDATION OF IIB WITH POTASSIUM PERMANGANATE

Potassium permanganate solution (0.46 g; 0.003 mole) in the least amount of water was added gradually to a solution of IIb (1 g; 0.003 mole) in acetic acid (50 ml). The reaction mixture was heated on a water-bath for 30 min., concentrated, and cooled. The reaction mixture was poured on ice-cold water, the formed precipitate was filtered off and recrystallized from ethanol to give III in 85 % yield. (See Table 2).

ACTION OF AMINES ON I

5-Aryl-2-thiono-1,3,4-oxadiazoles (I) (0.01 mole) and aniline, piperidine, or morpholine (0.01 mole) in 50 ml absolute ethanol was heated under reflux for 3 hrs. The reaction mixture was concentrated, cooled and filtered. The solid obtained was recrystallized from ethanol to give 2,5-disubstituted-1,3,4-oxadiazoles (IVa-f). Yields 80−85 %. The results are listed in table 3.

TABLE 2

Condensation products of 2-thiono-1,3,4-oxadiazoles with hydrazines

Compound	m.p. (°C)	Formula	Analysis % (Found/Calcd.)			
			C	H	N	S
IIa	198	$C_9H_{10}N_4S$	52.09 52.43	5.12 4.85	26.92 27.18	15.21 15.53
IIb	180	$C_{15}H_{14}N_4S$	63.62 63.83	5.22 4.96	19.74 19.86	11.01 11.35
IIc	191	$C_{15}H_{12}N_6O_4S$	48.00 48.39	3.51 3.23	22.19 22.58	8.81 8.60
IId	265	$C_8H_8N_4OS$	45.86 46.15	4.13 3.85	26.50 26.92	14.96 15.38
IIe	185	$C_{14}H_{12}N_4OS$	59.01 59.15	4.01 4.23	19.53 19.72	11.00 11.27
III	192	$C_{30}H_{26}N_8S_2$	63.62 64.06	5.07 4.63	20.24 19.93	11.01 11.39

TABLE 3

Condensation products of 2-thiono-1,3,4-oxadiazoles with amines

Compound	m.p. (°C)	Formula	Analysis % (Found/Calcd.)		
			C	H	N
VIa	198	$C_{15}H_{13}N_3O$	71.35 71.71	5.00 5.18	16.82 16.73
VIb	203	$C_{13}H_{15}N_3O_2$	63.41 63.67	6.01 6.12	17.00 17.14
VIc	190	$C_{14}H_{17}N_3O$	69.03 69.14	6.84 7.00	17.03 17.28
VId	235	$C_{14}H_{11}N_3O_2$	66.13 66.40	4.62 4.35	12.42 12.65
VIe	245	$C_{12}H_{13}N_3O_2$	57.98 58.30	5.46 5.26	17.01 17.00
VIf	225	$C_{13}H_{15}N_3O_2$	63.92 63.67	5.96 6.12	16.86 17.06

ACTION OF HALOCOMPOUNDS ON Ia

Compound Ia (0.01 mole) and halocompounds (0.01 mole) in 50 ml benzene were heated under reflux for 1 hr. The reaction mixture was concentrated, cooled and the solid obtained was recrystallized from benzene to give VIIa-f. Yields were almost quantitative. The results are given in table 4.

TABLE 4

Condensation products of 2-thiono-1,3,4-oxadiazoles with halocompounds

Compound	m.p. (°C)	Formula	Analysis % (Found/Calcd.)			
			C	H	N	S
VIIa	50	$C_{10}H_{10}N_2OS$	57.92	5.14	13.27	15.31
			58.25	4.85	13.59	15.53
VIIb	203	$C_{16}H_{14}N_2OS$	67.79	5.25	10.06	11.14
			68.09	4.96	9.93	11.35
VIIc	210	$C_{16}H_{14}N_2O_3S_2$	55.23	4.37	8.00	18.27
			55.49	4.05	8.09	18.50
VIId	135	$C_{11}H_{10}N_2O_2S$	56.73	4.35	11.74	13.83
			56.41	4.27	11.97	13.68
VIIe	160	$C_{16}H_{14}N_2OS$	68.02	5.27	10.14	11.00
			68.09	4.96	9.93	11.35
VIIf	200	$C_{12}H_{12}N_2O_3S$	54.35	4.73	10.72	12.01
			54.55	4.55	10.61	12.12
VIIg	130	$C_{10}H_{10}N_2O_2S$	53.79	4.63	12.87	14.09
			54.05	4.50	12.61	14.41
VIIh	115	$C_{12}H_{10}N_2O_4S$	51.72	4.06	10.02	11.39
	(decmp)		51.80	3.60	10.07	11.51
VIIi	160	$C_{10}H_{10}N_4O_2S$	47.89	4.39	22.09	12.67
			48.00	4.00	22.40	12.80

ACTION OF HALOCOMPOUNDS ON Ib

Compound Ib (0.01 mole) and methyliodide and/or acetylchloride (0.02 mole) in 50 ml benzene were heated under reflux for 1 hr. The reaction mixture was concentrated and cooled, the solid obtained was recrystallized from benzene to give VIIg, h in almost quantitative yield. The results are given in table 4.

The same product was obtained when equimolecular amounts of the alkyl halide and Ib were used on cold when and reaction mixture was shaked for 1 hr. The products were identified by m.p. and mixed m.p. with the product obtained as above.

REACTION OF VIIf WITH HYDRAZINE HYDRATE

Compound VIIf (0.01 mole) and hydrazine hydrate (1 ml ; 0.1 mole) in 50 ml ethanol. The reaction mixture was heated under reflux for 1 hr. After concentration and cooling the solid obtained was recrystallized from ethanol to give VIIi. Yield 80%. The data are given in table 4.

OXIDATION OF VIIa WITH POTASSIUM PERMANGANATE

The same method used for the oxidation of IIb was used, affording VIII in 75% yield. The data are given in table 4.

REFERENCES

[1] E. Hoggarth, *J. Chem. Soc.*, **1952**, 4811.

[2] S. Kubota, Y. Kolda, T. Kosaka and O. Kirino, *Chem. Pharm. Bull.*, **18**, 1696 (1970).

[3] R. W. Young, and K. H. Wood, *J. Amer. Chem. Soc.*, **77**, 400 (1955).

[4] G. Ainworth, *J. Amer. Chem. Soc.*, **78**, 4475 (1956).

[5] V. N. Artemov and U. P. Snavaika, *Khim. Geterotsikl. Soedin.* **7**, 905 (1971).

[6] A. Stempel, J. Zelauskas and J. A. Aeschlimann, *J. Org. Chem.* **20**, 412 (1955).

[7] F.M.E. Abdel-Megeid, M.A.F. Elkaschef and A.A.G. Ghattas, *Egypt, J. Chem.*, **20**, 235 (1977).

[8] A. R. Katritzky and A. J. Boulton, "Advances in Heterocyclic Chemistry", vol. 9, Academic Press, New York, 1968, p. 208.

[9] J. H. Boyer, "Heterocyclic Compounds", vol. 7, Elderfield R. C., ed., Wiley, New York, 1961, p. 525.

[10] M. Radha, and V. R. Srinivasan, *Indian J. Chem.*, **7**, 760 (1969).

[11] Yu. N. Sheinker, I. Ya. Postovskii and N. M. Voronian, *Zhur, fiz. Khim.*, **33**, 302 (1959); *Chem. Abstr.*, **54**, 4147 (1960).

Revue Roumaine de Chimie, 26, 3, 457–470 (1981)

KINETICS OF THE THERMAL REARRANGEMENT OF BENZO[b] BICYCLO [3.1.0] HEX-2-EN-4-YL DERIVATIVES

A. C. RĂZUŞ, V. WERTHEIMER, A.M. GLATZ, ZS. ARVAY and F. BADEA
Centre of Organic Chemistry, Spl. Independenţei 202 B, R-78100, Bucharest România

Received August 20, 1980

The epimerisation and the rearrangement reactions of unsubstituted and methyl substituted benzo[b]bicyclo[3.1.0]hex-2-en-4-ols in perchloric acid solutions are studied. The epimerisation of these alcohols proceeds through a cationic intermediate, which can be regarded either as a benzyl cation or as a cyclopropylcarbinyl ion. Both experimental and literature data agreed with a cyclopropane assisted ionization of the title compounds. The rearrangement of the strained bicyclic system affords no driving force in the reaction of the unsubstituted derivative. By contrast, the kinetic data of the epimerisation and rearrangement reactions of the 4-methyl derivative indicate that the migration of the methyl group confers the driving force of the ionization. A 1,3-hydride shift in this case explains better the kinetic behaviour.

The reversible four-electron electrocyclic process, according to Woodward-Hoffmann's rules[1], should proceed either in a conrotatory movement of the termini of the π system, if performed thermally, or disrotatory if the reaction is brought about photochemically. The rule should be observed in both directions of the transformation, either in neutral π systems or in ionic systems, acyclic as well as in cyclic polyenes. An interesting illustration of this rule was discussed by Childs and Winstein.[2-4] In photochemical processes, the well-known benzenium ion, the intermediate of aromatic substitution yields bicyclo[3.1.0]hex-2-en-4-yl cation in a disrotatory electrocyclic process (1). However, the bicyclic ion regenerates benzenium ion on simple heating.

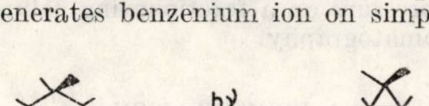

(1)

By contrast, we have found that benzo[b]bicyclo[3.1.0]hex-2-en-4-yl ion generates naphtalenium ion (and thus naphthalene) only in a photochemical reaction,[5] whereas methyl-substituted derivatives give naphthalene both in thermal and in photochemical processes.[6] In a previous paper in this series[7] we have shown that the ring opening in the benzo[b]bicyclo[3.1.0]hexenyl ion actually implies an eight-electron electrocyclic process, requiring lower activation energies. In order to get a better insight into the mechanism of the thermal process suffered by cation **2**, we undertook the kinetic study of the perchloric solvolysis of alcohols **1**.

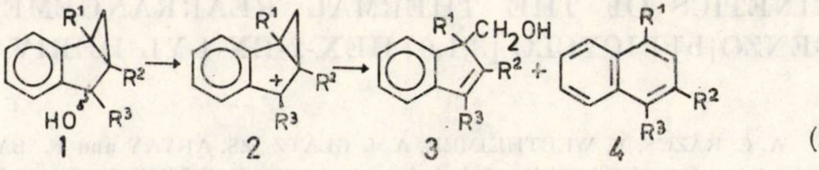

(2)

a. $R^1 = R^2 = R^3 = H$ b. $R^1 = R^2 = H$; $R^3 = CH_3$

c. $R^1 = CH_3$; $R^2 = R^3 = H$ d. $R^1 = R^3 = H$; $R^2 = CH_3$

In the thermal solvolysis, at moderate temperatures (70–90°C), the unsubstituted alcohol **1a** affords only the indenyl bicyclic alcohol **3a**;[5] a similar behaviour is presented by the tertiary bicyclic alchol **1b**. Alcohol **1c** yields the indenyl derivative **3c** as the major reaction product, together with minor amounts of naphthalene **4c**. Unlike other bicyclic secondary alcohols **1**, 1-methylbenzo[b]bicyclo[3.1.0]hex-2-en-4-ol in perchloric acid solutions affords as the single reaction product naphthalene **4d**.[6] Considering the similar behaviour of alcohols **1a** and **1b** under the solvolysis conditions, the tertiary alcohol **1b** was not included in this study.

RESULTS

In the present work, enriched mixtures in the *endo* epimer of alcohols **1** were used. The isolation and identification of the reaction products was reported previously.[5,6]

The rearrangement of alcohols **1** was carried out in 0.3 M perchloric acid solution in dioxane-water (1:1), the concentration of the alcohol being about 0.1 M. The samples after solvolysis were neutralized with 2% sodium hydrogen carbonate solution and extracted several times with ether. The organic layer was dried over magnesium sulfate and the ether removed at normal pressure on a fractionating column. The residue was analysed by gas-chromatography.

1. EPIMERISATION

Alcohol **1a** treated with perchloric acid solution between 44°C and 57°C suffers as the single detectable reaction an *exo-endo* epimerisation.

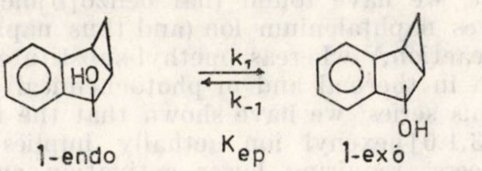

(3)

The equilibrium could be easily followed in this temperature range. At 44°C, the ratio *exo* : *endo* (epimerisation constant, K_{ep}) remains fairly constant after about 20 hours of heating (table 1).

TABLE 1

Epimerisation of benzo[b]bicyclo[3.1.0]hex-2-en-4-ol at 44°C

Time (minutes)	*endo* % moles	*exo* % moles	K_{ep} (=*exo* : *endo*)
0	95	5	
45	90	10	
300	63.55	36.45	
1 320	31.66	67.34	2.12
1 650	31.18	68.28	2.19
1 770	32.60	67.11	2.06

From the mean value of the epimerisation constant (2.12) a free energy difference between the two epimers of 477 cal/mol was calculated. The lower stability of the *endo* isomer is probably due to the repulsion between the hydroxyl group and the *endo* hydrogen atom of the methylene bridge. At higher temperatures, K_{ep} seems to increases from 2.12 at 44°C to 2.82 at 56.7°C. The observed increase is quite unusual, as the rising of temperature should favour the increase of the unstable isomer in the equilibrium mixture.

The sum of the equilibrium rates can be calculated according to the equation (4).

$$k_1 + k_{-1} = \frac{2.303}{t} \lg \frac{A_0 - A_e}{A_t - A_e} \qquad (4)$$

where k_1, k_{-1} = the rate constants in the epimerisation of the *endo* and *exo* isomer, respectively;

A_0 = the initial concentration of the *endo* derivative (the *endo* isomer exceeds the *exo* isomer in the starting material and is less abundant in the equilibrium mixture);

A_t, A_e = the concentration of the *endo* epimer at time t and at equilibrium.

The equilibrium rates were determined at 44°C, 51.2°C and 56.7°C. An example is given in table 2.

From measurements carried out at other temperatures, the activation enthalpy was found to be 25.4 cal/mol and the activation entropy —0.4 e.u.

Above 60°C the rearrangement of **1a** into **3a** prevails, competing the epimerisation reaction. When the temperature is high enough, the ratio *exo*/*endo* remains fairly constant during an experiment (Table 3).

TABLE 2

The epimerisation rate constants of **1a** in perchloric acid solution (dioxane-water 1 : 1) at 44°C

Time (minutes)	*endo* % moles	$10^3(k_1 + k_{-1})$ min^{-1}
0	95	—
75	86.71	1.86
105	83.67	1.87
150	76.88	2.24
225	71.16	2.09
300	63.55	2.29
	31.66	—
		mean value $(2.07 \pm 0.19)10^{-3}$ min^{-1}

TABLE 3

Transformation of *endo*-**1a**, at 95°C, in perchloric acid catalysis

Time (minutes)	*endo* % moles	*exo* % moles	**3a**[a] % moles	K_{ep}
0	95	5	—	
60	29.99	53.80	15.81	1.71
90	29.39	51.75	18.46	1.76
180	22.40	37.48	40.12	1.67
210	18.33	33.90	46.86	1.84
300	10.94	20.16	68.90	1.84
400	6.29	12.24	80.76	1.94
600	2.71	4.67	91.97	1.72
				Mean value (1.79±0.09)

---

[a] Minor amounts of another unidentified product are also formed.

From the value of K_{ep} determined at 90.5°C, a value of 433 cal/mol for ΔG° can be calculated, agreeing well with the value $\Delta G^\circ = 477$ cal/mol calculated at 44°C. We conclude, thus, that the apparent increase of K_{ep} observed at 51.2°C and 56.7°C with respect to K_{ep} determined at 44°C is an artifact of the inset of the rearragement reaction.

Alcohol **1d** is the most reactive derivative of the series. Even at the lowest temperature where determinations were possible, the epimerisation reaction competes with the rearrangement of the bicyclic system. However, at 65.7°C the ratio *exo* : *endo* varies during a run in the limits 1.39 and 3.18 (Table 4). It is clear that at that temperature the epimerisation reaction is not fast enough to attain equilibrium before the ring opening sets in. However, even in that case it was possible to calculate epimerisation rates. Thus, during a run, the reaction mixture was formed of the two epimers and the rection products (mostly 1-methylnaphthalene, see table 4). We may recalculate the proportion of *endo* isomer considering that the reaction mixture is formed only of the two epimers. Then, assuming different values of K_{ep}, we may apply equation (4). In this case the data are best fitted with $K_{ep} = 3.5$ (Table 4).

TABLE 4

Epimerisation of 1-methylbenzo[b]bicyclo[3.1.0]hex-2-en-4-ol (**1d**) in perchloric acid solution at 65.7°C

Time (minutes)	*endo* % moles	(*endo*+*exo*)* % moles	A** % moles	$10^2(k_1 + k_{-1})$*** min^{-1}
0	70	100	70	—
24	33.21	79.41	41.61	3.78
30	28.26	72.16	39.16	3.45
36	28.15	71.83	39.19	2.87
45	23.29	68.49	34.00	3.10
65	18.80	59.52	31.58	2.50
85	12.55	48.38	25.94	3.00
			22.22	—
				Mean value : $(3.11 \pm 0.44)10^{-2}$

---

* Beside the two epimers, the reaction products (mostly naphthalene) are also present in the reaction mixture. ** The *endo* epimer considering only the mixture of the two epimers. *** Calculated from equation (4) with $A_e = 22.22$ %moles.

In the solvolysis of the methyl derivative **1c** an enriched mixture in the *endo* epimer (92%) was used. In contrast to the other derivatives, during a run the *endo* predominates over the *exo* isomer. Thus, at 87.1°, the ratio *exo* : *endo* remains fairly constant through a run, 1 : (10.06 ± 1.27). Even at 97.6°C, the *endo* exceeds the *exo* isomer through most of the reaction (about five half-lives). However, at the end of the reaction (about 98% transformation) the *exo* epimer overtakes the *endo* epimer, the ratio *exo* : *endo* being about 2 :1. We may apply in this case a procedure similar to that used for the methyl derivative **1d** (Table 5).

The data of table 5 clearly show that the epimerisation of **1c** is much slower than the epimerisation of the other derivatives. It seems, thus, that the strikingly different behaviour of **1c** in the acid solvolysis,

TABLE 5

Epimerisation of 5-methylbenzo[b]bicyclo[3.1.0]hex-2-en-4-ol (**1e**) in perchloric acid solution (dioxane-water 1 : 1) at 79.5 °C

Time (minutes)	*endo* % moles	(*endo* + *exo*)* % moles	A** % moles	$10^4(k_1+k_{-1})$*** (min^{-1})
0	92	100	95	—
300	62.73	71.07	88.25	5.18
600	28.54	33.64	84.83	5.38
720	19.66	23.47	83.76	5.29
			34	

* Beside the two epimers, the reaction mixture consists of **3e**, **4e** and minor amounts of unidentified products. ** The *endo* epimer in the mixture of the two epimers. ***Calculated from relation (4) with the assumed value $A = 34\%$ moles.

as compared to that of **1a** and **1d**, is due to lower epimerisation rates as compared to the rearrangement rates. Other data obtained in the course of this work confirm this assumption (see Table 8).

2. REARRANGEMENT

The calculation of the integrated first-order rate constants, independent of the benzo[b]bicyclohexenyl derivative, shows a similar trend : the rates increase with increasing conversion (Tables 6 and 7). This trend may indicate a lower reaction order. Indeed, by plotting conversion *vs.* time a straight line is obtained (Fig. 1) in agreement with zeroth order reaction. The zeroth order reaction is observed only in a narrow temperature range (Fig. 2).

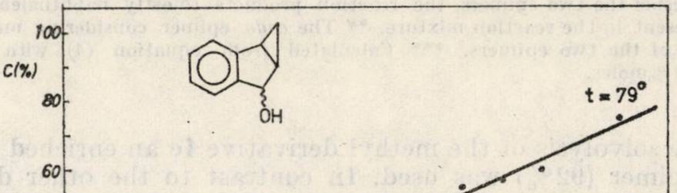

Fig. 1. Conversion *vs.* time of benzo[b]bicyclohexenyl alcohol.

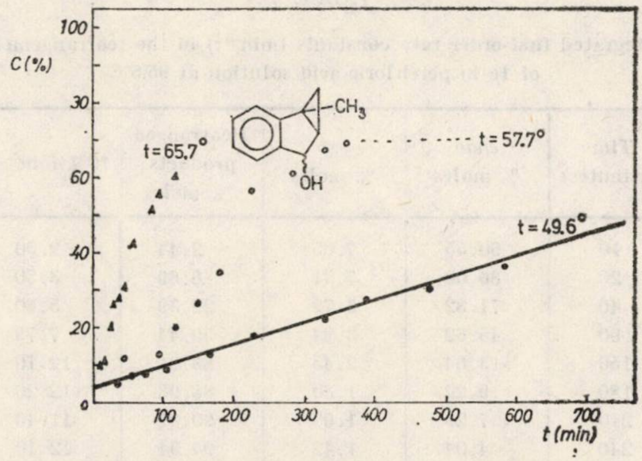

Fig. 2. — The zeroth order reaction is observed only in a narrow temperature range.

TABLE 6

Integrated first order rate constants (min^{-1}) in the rearrangement of **1a**, in perchloric acid solution at 79°C

Time (minutes)	*endo* % moles	*exo* % moles	Rearranged product* % moles	$10^4k(\text{min}^{-1})$
0	95	5		
15	31.35	63.63	1.15	7.83
45	27.57	67.50	2.34	5.27
90	26.42	66.52	3.46	4.12
330	27.00	63.61	15.69	5.18
450	22.91	51.94	21.92	5.50
990	16.81	36.65	43.91	5.84
1470	11.30	26.41	59.08	6.08
1830	6.73	16.56	73.35	7.22
3030	0.64	2.05	90.25	7.68

---

* The indenyl derivative **3a** is the major component of the reaction products. Another unidentified product is also formed in small amounts. The integrated rate constants were calculated considering the overall conversion.

Table 7 shows, nevertheless, that at higher conversions the integrated first-order rate constants become relatively constant. Table 8 summarizes all kinetic data.

TABLE 7

Integrated first-order rate constants (min^{-1}) in the rearrangement of **1c** in perchloric acid solution at 95.5°C

Time (minutes)	*endo* % moles	*exo* % moles	Rearranged products % moles	$10^3k(min^{-1})$
10	90.55	7.05	2.44	2.50
20	86.00	7.31	6.69	3.50
40	71.82	5.79	22.39	5.80
90	45.62	3.94	50.44	7.79
150	13.64	2.45	83.91	12.10
180	9.22	1.80	88.98	12.20
210	7.29	1.90	90.81	11.40
240	4.04	1.42	94.54	12.10
300	0.75	1.73	98.52	11.80

TABLE 8

Kinetic data in the epimerisation and rearrangement of benzo[b]bicyclo[3.1.0] hex-2-en-4-yl derivatives **1** (solvent : dioxane-water 1 : 1 ; catalyst : perchloric acid 0.3M)

Sub-strate	Temp. °C	K_{ep}	Epimerisation		$\Delta S^{\neq}$ e.u.	Rearrangement		$\Delta S^{\neq}$ e.u.
			$k_1 + k_{-1}$ min^{-1}	$\Delta H^{\neq}$ kcal/mol		k^{**} min^{-1}	$\Delta H^{\neq}$ kcal/mol	
1a	44	2.12	$2.07 \cdot 10^{-3}$	25.4	−0.4		33	3−2
	51.2		5.88					
	56.7		10.05					
	69.5					$1.73 \cdot 10^{-4}$		
	79.5		$1.35 \cdot 10^{-1**}$			7.70		
	90.5					30.0		
1c	79.5	2.0	$5.38 \cdot 10^{-4}$			$1.4 \cdot 10^{-3}$	36	17
	87.1		*			3.5		
	95.5		*			$1.2 \cdot 10^{-2}$		
1d	49.6	3.5	$3.7 \cdot 10^{-3}$	27.7	+13	$8.0 \cdot 10^{-4}$	29	7
	57.7		$1.2 \cdot 10^{-2}$			$3.5 \cdot 10^{-3}$		
	65.7		3.1			9.2		
	79.5		$1.37 \cdot 10^{-1**}$					

---

* Not possible to calculate ; the ratio *exo* : *endo* does not change significantly during a run.

** Extrapolated values.

DISCUSSION

1. The epimerisation of alcohols **1** should proceed through the cationic intermediate **5** (Scheme 1).

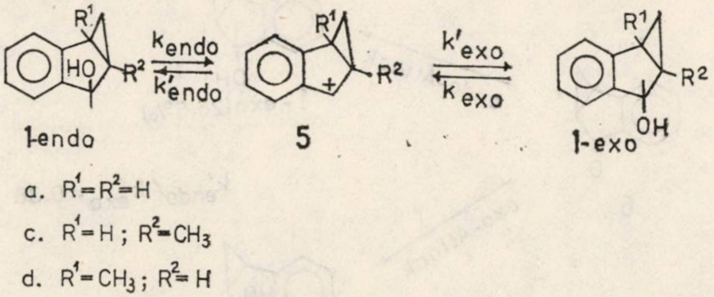

Scheme 1

Intermediate **5** can be regarded either as a benzyl cation or as a cyclopropylcarbinyl ion. We tried to find out from our data whether the neighbouring cyclopropane ring assists the ionization.

It can be easily shown that k_1 and k_{-1} respectively (see equation (4)) are related to the rate constants of scheme 1 through equations (5).

$$k_1 = \frac{k_{endo}}{1 + \dfrac{k'_{endo}}{k'_{exo}}} \tag{5a}$$

$$k_{-1} = \frac{k_{exo}}{1 + \dfrac{k'_{exo}}{k'_{endo}}} \tag{5b}$$

On the other hand, k_1 and k_{-1} are related to the epimerisation equilibrium constant, K_{ep}.

$$K_{ep} = \frac{k_1}{k_{-1}} \tag{6}$$

and thus, k_1 and k_{-1} can be easily calculated from the data of table 8 and equation (6). In order to calculate the ionization rates, k_{endo} and k_{exo}, the ratio of the capture of cation **5**, k'_{endo}/k'_{exo} should be known. As we cannot calculate this ratio from our data, we have used the ratio of epimer formation in the sodium borohydride reduction[6] of ketone **6***. Indeed, the carbonyl group should have at the reaction centre a geometry similar to that of the carbocation **5**.

---

* In the quoted paper[6] the ratio *endo* : *exo* given in the experimental part is actually reversed *(exo* : *endo)*, the *endo* epimer resulting predominantly in the reduction.

Table 9 summarizes the calculated values for the unsubstituted derivative **1a** at 44°C. In order to compare with other values quoted in literature, the data were also extrapolated at 25°C.

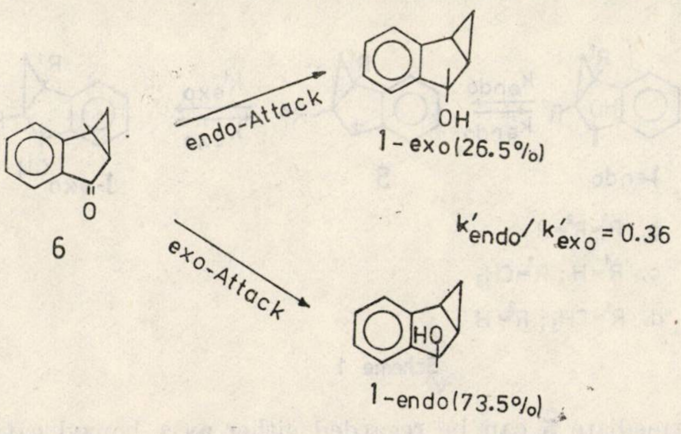

Scheme 2

TABLE 9

Epimerisation rates (k_1 and k_{-1}) and ionization rates (k_{endo} and k_{exo}) for **1a** in 0.3 M perchloric acid in dioxane-water (1 : 1)

Temperature °C	k_1^a s^{-1}	k_{endo}^b s^{-1}	k_{-1}^a s^{-1}	k_{exo}^b s^{-1}
44	$1.64 \cdot 10^{-6}$	$2.23 \cdot 10^{-6}$	$8.20 \cdot 10^{-7}$	$3.09 \cdot 10^{-6}$
25[c]	$1.17 \cdot 10^{-7}$	$1.59 \cdot 10^{-7}$	$5.85 \cdot 10^{-8}$	$2.20 \cdot 10^{-7}$

[a] Calculated from $k_1 + k_{-1}$ and K_{ep}, recorded in table 8.

[b] Calculated from k_1 and k_{-1}, respectively and k'_{exo}/k'_{endo} from scheme 2, using equations(5).

[c] Extrapolated data.

Thus, the two epimers are about as reactive, the *endo* epimer having a slightly lower reactivity than *exo* isomer.

The data of table 9 can be compared with the solvolyses of *p*-nitrobenzoates **7** and **8** in aqueous acetone (80 %), studied by Peters and Brown[8].

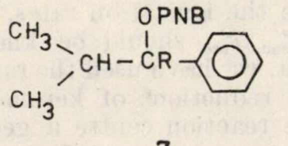

7

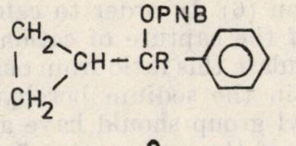

8

R=CH$_3$

$k_7^{25°} = 9.51 \cdot 10^{-9}\ s^{-1}$ $\quad k_8/k_7 = 25300$

The p-nitrobenzoate **7** differs from **1a** by having a tertiary instead of a secondary carbon atom at the reaction centre and having as leaving group the *p*-nitrobenzoate instead of the hydronium group $-\overset{+}{O}H_2$. As far as we know there is no direct comparison in the literature between the leaving-group ability of the two groups. Nevertheless, the data of Bartlett and McCollum[9] suggest that the concentration of the protonated species of alcohol **1a** should be very small, the actual leaving-group ability observed in **1a** should be comparable with that of the *p*-nitrobenzoate. On the other hand, in passing from **7** ($R = CH_3$) to **7** ($R = H$), the tertiary *p*-nitrobenzoate is expected to react a few powers of ten (10^3-10^5) more rapidly than the secondary derivative.[10] Another difference between our runs and those of the solvolyses of **7** and **8** is the more aqueous solvent used in this work. An increase of about 10^2 in the reaction rates should be anticipated on the basis of Y — values for the more diluted solvent.[11] Taking into account all these factors we should expect cyclopropane assistance in the ionization of **1a**, but probably a less efficient one than in the case of the *p*-nitrobenzoate **8**. This conclusion is also supported by the examination of Dreiding models. Indeed, cation **5** cannot adopt a "bisected" geometry, favourable for the cyclopropylcarbinyl cation.[12]

2. REARRANGEMENT

It seems likely that in the solvolysis of **1a** the same intermediate **5a** is involved both in epimerisation and in the rearrangement into the primary alcohol **3a**. Indeed, the impossibility of **5** to adopt the favourable "bisected geometry" of the cyclopropylcarbinyl ion would make energetically more probable the trapping of the ion by water molecules leading to the two epimers (epimerisation reaction), than rearrangement process (7).

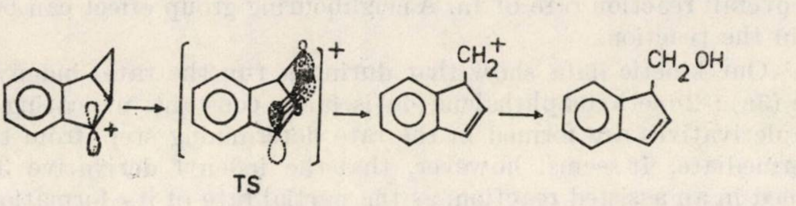

(7)

Table 8 confirms this hypothesis. A high difference in the activation parameters is observed. Although the reaction of **5** is a bimolecular process of low entropy, the activation entropy approaches the value observed for unimolecular reactions. A high energy gap between activation enthalpies of the epimerisation and rearrangement reaction is also noted. We may conclude from these data that the rearrangement of the strained bicyclic system *is not the driving force in ionization*. In other words, the assistance of a neighbouring cyclopropyl ring at a neighbouring ionizing centre does not necessarily lead to cyclopropane ring opening.

Table 8 shows that the epimerisation rates of 1-methylbenzo [b] bicyclo[3.1.0]hex-2-en-4-ol (**1d**) are practically the same as those of the unsubstituted derivative 1a. That means that the 1-methyl substituent does not affect the ionization of **1**. Thus, from the present data there seems to be no reason why the cation **5d** should behave otherwise than cation **5a**. Although **1a** yields only the primary alcohol **3a**, alcohols **3a** and **1d** lead only to 1-methylnaphthalene, we are bound to accept the involvement of cation **5** in both transformations. However, for cation **5d** there must be another pathway which is not available for **5a**.

In the following paper of this series[7] we will show that for the methyl derivatives **1c** and **1d**, the conjugation energies of the benzyl-like cations **5c** and **5d** can justify on otherwise symmetrically forbidden electrocyclic process. If this is true, the kinetics of the reaction of **1c** should be more similar to the kinetics of **1d**, and both derivatives should behave differently from the parent compound **1a**.

Although **1c** yields naphthalene **4c** on heating in acid solution, as does **1d**, the kinetics of its transformation is strikingly opposite to that of derivative **1d**. As table 8 shows, **1c**, in contrast to **1a** and **1d**, suffers a substantially slower epimerisation than the overall transformation reaction. This means that in the formation of the solvolysis products (2-methylnaphthalene and indenyl derivative **3c**) the intermediate is not the same as the one involved in epimerisation.

It is reasonable to admit that cation **5c** is the reaction intermediate in epimerisation. The steric crowding near the reaction centre introduced by the methyl group in position 5 would both lower the protonation equilibrium of alcohol **1c**[9] and hinder the capture of the formed ion. Lower epimerisation rates should be thus expected.

Despite the steric hindrance in epimerisation, table 8 shows a slight increase of the overall rearrangement rate of **1c** as compared to the overall reaction rate of **1a**. A neighbouring group effect can be involved in the reaction.

Our kinetic data show that during a run the ratio indenyl-derivative (**3c**) : 2-methylnaphthalene (**4c**) is fairly constant, indicating that the two derivatives are formed in the rate determining step from the same intermediate. It seems, however, that the indenyl derivative **3c** is not formed in an assisted reaction, as the partial rate of its formation is very close to the rate of **3a** formation. The slight increase in the overall reaction rate can be due to napthalene formation, and this reaction is probably assisted by neighbouring group participation.

Naphthalene formation from any species similar to **1** or **5** should be an electrocyclic process. The single exactly demonstrated ionization process assisted by an electrocyclic ring opening is encountered in the ionization of cyclopropyl derivatives. Woodward and Hoffmann have shown[1] that the ionization concerted with the ring opening to an allyl ion must be stereospecific.

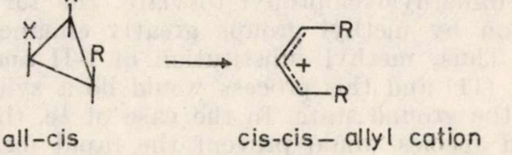
R
X
R
R
+
R
all-cis
cis-cis— allyl cation

(8)

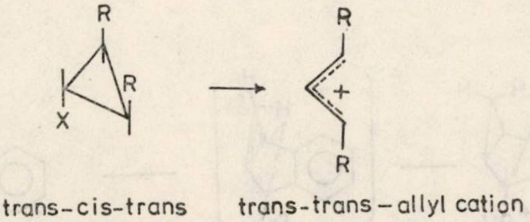
R
R
X
R
+
R
trans-cis-trans
trans-trans—allyl cation

(9)

In bicyclic systems it has been demonstrated[13,14] that only the *all-cis* geometry can afford a ring opening, the *trans-trans* geometry of an allyl cation being highly strained in a cyclic system. Thus, dichlorocarbene addition to alkene **9** yields **11**.[15] It is evident that the addition intermediate **10** has suffered the electrocyclic ring opening (8).

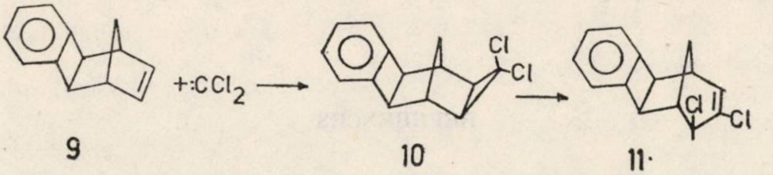
+:CCl₂
Cl
Cl
Cl
Cl
9
10
11

(10)

In cations **5** the *endo*-hydrogen of the methylene bridge can suffer a 1,3 hydride shift in the vacant *p*-orbital. The process should be thermally allowed and concerted with the electrocyclic ring opening of the incipient cyclopropyl cation.

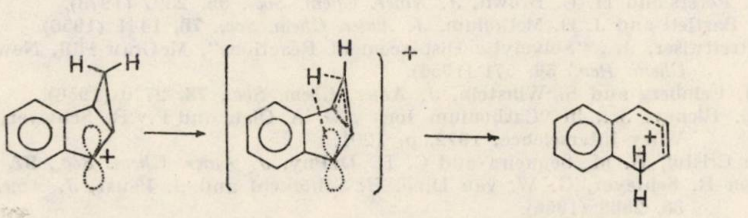

(11)

We may however wonder why cation **5d** can suffer easily this process, as the kinetic data of table 8 show, while cation **5a** prefers to undergo the general ring opening of cyclopropylcarbinyl ions. The answer is probably provided by the data published by Schleyer and coworkers.[14] For *all-cis*-2,3-dimethylcyclopropyl tosylate, the further substitution of the 2,3 position by methyl groups greatly enhances the electrocyclic ring opening. Thus, methyl substitution of 1-H and 5-H in **1a** would favor process (11) and this process would be a symmetry-allowed ring opening from the ground state. In the case of **1c**, the slow formation of the protonated species would prevent the rapid formation of cation **5**. However, hydride ionization of the *endo*-H would assist naphthalenium ion formation.

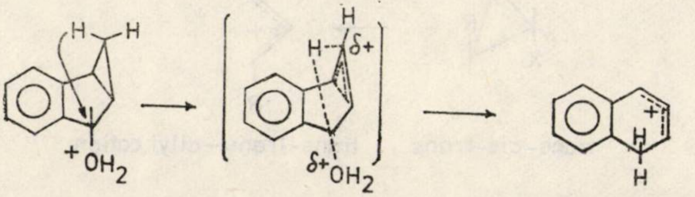

(12)

We believe that the thermal ring opening (1), studied by Childs and Winstein, is another example of a 1,3 shift followed by a concerted ring opening. If that is true, we may conclude, as Woodward and Hoffmann did, that "there is no violation to the conservation of symmetry of the molecular orbitals in a reaction". The apparent violations are in fact other examples (yet not recognized as such) of other symmetry-controlled processes.

REFERENCES

[1] R. B. Woodward and R. Hoffmann, "*The Conservation of Orbital Symmetry*", Verlag Chemie, Weinheim, 1970; *J. Amer. Chem. Soc.*, **87**, 395 (1965).

[2] R. F. Childs, M. Sakai and S. Winstein, *J. Amer. Chem. Soc.*, **90**, 7144 (1968).

[3] R. F. Childs, M. Sakai, B. D. Parrington and S. Winstein, *J. Amer. Chem. Soc.*, **96**, 6403 (1974).

[4] R. F. Childs and S. Winstein, *J. Amer. Chem. Soc.*, **96**, 6409 (1974).

[5] A. C. Răzuş, V. Wertheimer, F. Badea and A. M. Glatz, *Tetrahedron Letters*, **1975**, 1799.

[6] V. Wertheimer, A. M. Glatz and A. C. Răzuş, *Rev. Roumaine Chim.*, **22**, 1505 (1977).

[7] F. Badea, A. M. Glatz and A. C. Răzuş, *Rev. Roumaine Chim.*, **26**, (1981) in print.

[8] E. N. Peters and H. C. Brown, *J. Amer. Chem. Soc.*, **95**, 2397 (1973).

[9] P. D. Bartlett and J. D. McCollum, *J. Amer. Chem. Soc.*, **78**, 1441 (1956).

[10] A. Streitwiser, Jr., "Solvolytic Displacement Reactions", McGraw-Hill, New York, 1962; *Chem. Rev.*, **56**, 571 (1956).

[11] A. H. Feinberg and S. Winstein, *J. Amer. Chem. Soc.*, **78**, 2770 (1956).

[12] H. G. Richey, Jr., in "Carbonium Ions", G. A. Olah and P.v.R. Schleyer, Eds., vol. 3, Wiley-Interscience, 1972, p. 1201.

[13] S. J. Cristol, R. M. Sequeira and C. H. DePuy, *J. Amer. Chem. Soc.*, **87**, 4007 (1965).

[14] P. von R. Schleyer, G. W. van Dine, U. Schölkopf and J. Paust, *J. Amer. Chem. Soc.*, **88**, 2868 (1966).

[15] L. Pârvulescu, Ph. D. Thesis, Bucharest, 1980.

Revue Roumaine de Chimie, 26, *3*, 471–475 (1981)

REACTION OF DIAZOMETHANE WITH ANILS AND MIXED AZINES OF THIOPHENE ALDEHYDE OR ISATIN

M.S.K. YOUSSEF

Chemistry Department, Faculty of Science, Assiut University,
Assiut, Egypt

Received November 19, 1979

Diazomethane reacts with nitro-substituted anils of thiophene aldehyde or isatin and with some asymmetric azines giving rise to 1,2,3,-triazolines. The constitution of the products is discussed.

1,3-Dipolar cycloaddition reactions of diazomethane with Schiff bases were intensively investigated by many contributors.[1-8] The reaction of nitro-substituted anils with diazomethane gave cyclic adducts to which two structures were assigned.[2]

A more extensive study of the addition of diazomethane to anils has been reported by Kadaba.[5] His data confirm the general view that an electron withdrawing group on the amine ring is apparently more effective than a similar group in the benzylidene moiety

From the medicinal point of view, triazoline derivatives are considered to be quite potent as diuretic agents.[9] The present investigation undertakes the synthesis of some new triazolines containing heterocyclic substituents. It was hoped that the new compounds would be of medicinal value.

Thus, thiophene-2-carboxaldehyde or isatin condensed easily with nitroaniline (*o*-, *p*- and *m*-) in absolute ethanol in the presence of piperidine as a catalyst giving good yields of thienylidene nitroanilines (I) and isatylidene nitroanilines (II) respectively, as follows :

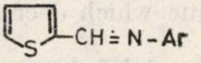

I

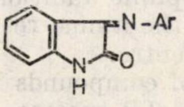

II

a, Ar = $o\text{-}NO_2C_6H_4$
b, Ar = $p\text{-}NO_2C_6H_4$
c, Ar = $m\text{-}NO_2C_6H_4$

On the other hand, thiophene-2-carboxaldehyde hydrazone or isatin-3-hydrazone undergo facile condensation with substituted aromatic aldehydes, ferrocene aldehyde, thiophene aldehyde and its 5-bromo derivative giving in good yields mixed azines, III and IV respectively.

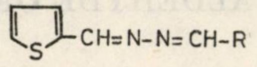

III

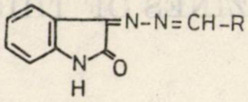

IV

III	R	IV	R
a	o-$NO_2C_6H_4$	a	o-$NO_2C_6H_4$
b	p-$NO_2C_6H_4$	b	p-$NO_2C_6H_4$
c	m-$NO_2C_6H_4$	c	m-$NO_2C_6H_4$
d	p-$(CH_3)_2N\ C_6H_4$	d	C_4H_3S(thienyl)
e	o-HOC_6H_4	e	C_4H_2SBr(5-bromothienyl)
f	C_6H_5-Fe-C_6H_5 (ferrocenyl)		
g	C_4H_3S(thienyl)		
h	C_4H_2SBr(5-bromothienyl)		

The structures of compounds III and IV have been established from the combination of microanalytical and IR data. The IR spectra of the prepared compounds showed absorption bands in the region of 1640–1620 cm^{-1} attributable to $\nu(C{=}N)$ and at 1540–1520 cm^{-1} due to an NO_2-group. The compound III showed an absorption band at 1100–1000 cm^{-1} (unsubstituted cyclopentadienyl ring in ferrocene).[10]

The addition of an ethereal solution of diazomethane on Schiff bases of the type I and II in dioxane proceeded successfully at zero degree for 21 days giving 4-thienyl-3-(o-, p- and m-) nitrophenyl-1,2,3-triazolines (V) and spiro [indolino-3,4′-triazoline]-3′-(o-, p,- and m-) nitrophenyl-2-one (VI) respectively :

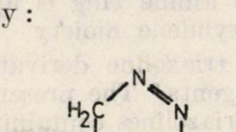

V

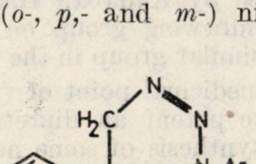

VI

a, Ar = o-$NO_2C_6H_4$
b, Ar = p-$NO_2C_6H_4$
c, Ar = m-$NO_2C_6H_4$

The cyclonucleophilic addition took place easy due to the presence of a-I nitro group in the amine residue which decreases electron density at the unsaturated centre.

The structures of compounds V and VI were proved by the correct elemental analysis and IR spectra. The IR spectra of these compounds showed a characteristic absorption band corresponding to $\nu(N{=}N)$ in the 1590–1580 cm^{-1} region ; a band in the 1260–1240 cm^{-1} range is due to the $-C-N$ group [10] and the absence of the band corresponding to $\nu(C{=}N)$.

In connection with our work on triazolines, it was of interest to synthesize a bis-triazoline system. Attempts to obtain such a molecule by reaction of diazomethane with azines III and IV under the before mentioned conditions were uneffective. Instead, the action of diazomethane on azines III and IV containing an electron withdrawing group (NO_2 group) in the arylidene residue gave 3-thienylidene-amino-4-(*o*-, *p*- and *m*-) nitrophenyl-1,2,3-triazolines (VII) and 3-isatylideneamino-4′-(*o*-, *p*- and *m*-) nitrophenyl-1′, 2′, 3′-triazolines (VIII). However, compounds IIId-h and IVd, e were recovered unreacted from the reaction mixture after a long time of ca 30 days.

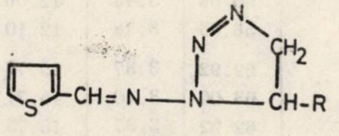

VII

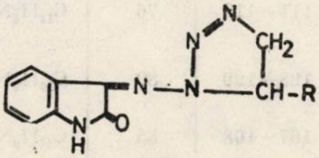

VIII

a, R = o-$NO_2C_6H_4$
b, R = p-$NO_2C_6H_4$
c, R = m-$NO_2C_6H_4$

Elemental analysis as well as IR-spectroscopic analysis of compounds VII and VII are in accordance with the structures suggested. The IR spectra showed beside the foregoing absorption bands, another band at 1620–1615 cm^{-1} attributable to $\nu(C{=}N)$.

EXPERIMENTAL

The infrared absorption spectra were determined with a Unicam SP 200 G spectrophotometer using KBr wafer technique. All melting points are uncorrected.

PREPARATION OF THIENYLIDENE, ISATYLIDENE NITROANILINE (I, II)[a] AND MIXED AZINES (III, IV)[b]

a) Equimolecular amounts of thiophene-2-carboxaldehyde or isatin and the corresponding amine were refluxed in dry ethanol in the presence of piperidine for 10 hrs. The reaction mixture was concentrated and cooled. The precipitate was filtered off and crystallized from ethanol (cf. Table 1).

b) A mixture of equimolecular amounts of thiophene aldehyde hydrazone or isatin 3-hydrazone and the corresponding aldehyde was refluxed in dry ethanol in the presence of piperidine for 5 hrs. The produced mixed azines III and IV were crystallized from ethanol (cf. Table 1).

1,2,3-TRIAZOLINES (V–VIII)

A solution of 1g each of azomethines I–IV in dioxane was treated with excess cold ethereal solution of diazomethane (20 ml). The reaction mixture was kept at 0° for 21 days, during which fresh amounts (10 ml) of ethereal diazomethane solution were added (three times). The solvent was then evaporated and the products were filtered off and crystallized from the proper solvent. The results are listed in table 2.

TABLE 1

Thienylidene, isatylidene nitroaniline and mixed azines (I — IV)

Compd.	m.p. (°C)	Yield (%)	Molecular formula	Analysis (Calcd./Found) %			
				C	H	N	S
Ia	67— 68	70	$C_{11}H_8N_2O_2S$	56.89	3.44	12.06	13.79
				56.87	3.40	12.10	13.81
b	108—109	73	$C_{11}H_8N_2O_2S$	56.89	3.44	12.06	13.79
				56.91	3.43	12.00	13.76
c	111—113	76	$C_{11}H_8N_2O_2S$	56.89	3.44	12.06	13.79
				56.83	3.48	12.10	13.73
IIa	198—199	80	$C_{14}H_9N_3O_3$	62.92	3.37	15.73	—
				63.00	3.40	15.71	—
b	167—168	85	$C_{14}H_9N_3O_3$	62.92	3.37	15.73	—
				62.98	3.35	15.69	—
c	224—225	90	$C_{14}H_9N_3O_3$	62.92	3.37	15.73	—
				62.85	3.36	15.78	—
IIIa	85— 86	65	$C_{12}H_9N_3O_2S$	55.59	3.47	16.21	12.35
				55.61	3.50	16.28	12.41
b	181—182	68	$C_{12}H_9N_3O_2S$	55.59	3.47	16.21	12.35
				55.59	3.44	16.23	13.38
c	155—156	70	$C_{12}H_9N_3O_2S$	55.59	3.47	16.21	12.35
				55.55	3.53	16.20	12.30
d	156—157	62	$C_{14}H_{15}N_3S$	65.36	5.83	16.34	12.45
				65.40	5.90	16.40	12.46
c	133—134	60	$C_{12}H_{10}N_2OS$	62.60	4.34	12.17	13.91
				62.65	4.29	12.13	14.02
f	95— 96	72	$C_{13}H_{14}N_2SFe$	59.62	4.34	8.69	9.93
				59.64	4.44	8.59	10.00
g	158—159	69	$C_{10}H_8N_2S_2$	54.54	3.63	12.72	29.09
				54.45	3.73	12.66	29.11
h	102—103	65	$C_{10}H_7N_2S_2Br$*	40.13	2.34	9.36	21.40
				40.14	2.40	9.41	21.50
IVa	254—255	83	$C_{15}H_{10}N_4O_3$	61.22	3.40	19.07	—
				61.31	3.33	18.92	—
b	280—281	78	$C_{15}H_{10}N_4O_3$	61.22	3.40	19.07	—
				61.25	3.42	19.05	—
c	262—263	76	$C_{15}H_{10}N_4O_3$	61.22	3.40	19.07	—
				61.20	3.40	19.11	—
d	180—182	73	$C_{13}H_9N_3OS$	61.17	3.52	16.47	12.54
				61.11	3.49	16.42	12.50
e	275—276	71	$C_{13}H_8N_3OSBr$**	46.70	2.39	12.57	9.58
				46.80	2.40	12.66	9.60

* Analysis for Br : Calcd. 26.75% ; Found 26.77%.
** Analysis for Br : Calcd. 23.59% ; Found 23.69%.

TABLE 2

1,2,3,-Triazolines (V – VIII)

Compd.	m.p. (°C)	Yield (%)	Molecular formula	Analysis (Calcd./Found) %			
				C	H	N	S
Va	74– 76	38	$C_{12}H_{10}N_4O_2S$	52.55	3.64	20.43	11.67
				52.51	3.50	20.48	11.72
b	143–144	30	$C_{12}H_{10}N_4O_2S$	52.55	3.64	20.43	11.67
				52.49	3.61	20.45	11.69
c	96– 98	33	$C_{12}H_{10}N_4O_2S$	52.55	3.64	20.43	11.67
				52.54	3.60	20.47	11.62
VIa	152–153	35	$C_{15}H_{11}N_5O_3$	58.25	3.55	22.65	—
				58.31	3.45	22.73	—
b	293–294	30	$C_{14}H_{11}N_5O_3$	58.25	3.55	22.65	—
	dec.			58.28	3.62	20.64	—
c	183–184	36	$C_{15}H_{11}N_5O_3$	58.25	3.55	22.65	—
				58.22	3.49	22.69	—
VIIa	201–202	38	$C_{13}H_{11}N_5O_2S$	51.82	3.65	23.25	10.63
				51.92	3.55	23.30	10.68
b	169–170	33	$C_{13}H_{11}N_5O_2S$	51.82	3.65	23.25	10.63
				52.84	3.63	22.26	10.60
c	134–135	35	$C_{13}H_{11}N_5O_2S$	51.82	3.65	23.25	10.63
				51.89	3.65	23.28	10.71
VIIIa	205–206	25	$C_{16}H_{12}N_6O_3$	57.14	3.57	25.00	—
				57.20	3.53	24.92	—
b	239–240	20	$C_{16}H_{12}N_6O_3$	57.14	3.57	25.00	—
				57.16	3.50	25.12	—
c	105–106	20	$C_{16}H_{12}N_6O_3$	57.14	3.57	25.00	—
				57.22	3.57	25.03	—

REFERENCES

[1] H. Meerwein, *Angew. Chem.*, **A60**, 78 (1948).
[2] A. Mustafa, *J. Chem. Soc.*, **1949**, 234.
[3] G. K. Buckley, *J. Chem. Soc.*, **1954**, 1850.
[4] P. K. Kadaba and J. O. Edwards, *J. Org. Chem.*, **26**, 2631 (1961).
[5] P. K. Kadaba, *Tetrahedron*, **22**, 2453 (1966).
[6] P. K. Kadaba, "Paper presented at the second Mid-Atlantic Regional Meeting of the ACS", Feb. 7, 1967 in New York.
[7] P. K. Kadaba and N. F. Hanin, *J. Heterocyclic Chem.*, **4**, 301 (1967).
[8] I. L. Knunyants and Y. V. Zaifman, *Bull. Acad. Sci. U.S.S.R.*, **1967**, 711.
[9] W. L. Klipschitz and Z. Hadidian, *J. Pharmacol. Exptl. Therap.*, **81**, 84 (1944).
[10] L. J. Bellamy, "The Infrared Spectra of Complex Molecules", Methuen, London, 2nd ed. 1958.

Revue Roumaine de Chimie **26**, *3*, 477–480 (1981)

SYNTHESIS OF SOME NEW FLUOROSUBSTITUTED TRICYCLIC HETEROCYCLICS

S. B. TAMBI, R. K. JAIN and R. L. MITAL
Chemical Laboratories, University of Rajasthan,
Jaipur-302004, India

Received December, 28, 1979

3-Alkoxy-7-fluoro-2-methoxy-10-[3-(4-methyl-1-piperazinyl)-propyl]-phenothiazine (IVd) and (IVe) have been synthesized by condensation of 3-alkoxy-7-fluoro-2-methoxy phenothiazine (IVb) or (IVc) with 1-(3-chloropropyl)-4-methyl-piperazine. 7-Fluoro-2-methoxy phenothiazin-3-ol (IVe) was obtained by the reduction of 7-fluoro-2-methoxy phenothiazin-3-one (III), obtained by the condensation of zinc salt of 2-amino-5-fluoro benzenethiol (I) with 2-chloro-5-methoxy-*p*-benzoquinone (II).

The extensive importance of trifluoperazine[1,2] has aroused interest in the synthesis of some new fluoro substituted tricyclic heterocyclics. Some of the possible metabolites[3,4] of trifluoperazine have been recently synthesized. Several workers[5-7] have reported the formation of substituted phenothiazines through thionation of appropriately substituted diphenylamines and attempts have also been made to synthesize them via Smiles rearrangement.[8,9] Recently Terdic and coworkers [10] have synthesized some disubstituted phenothiazin-3-ones. Synthesis of 7-fluoro-2-methoxy phenothiazin-3-one (III) was initiated by condensation of zinc salt of 2-amino-5-fluoro benzenethiol[11] (I) and 2-chloro-5-methoxy-*p*-benzoquinone [12,13] (II).

(III) on reduction with sodium dithionite furnished the corresponding phenothiazine ; 7-fluoro-2-methoxy-phenothiazin-3-ol (IVa). Reaction of (IVa) with dimethylsulphate in acetone potassium hydroxide solution gave 7-fluoro-2,3-dimethoxy phenothiazine (IVb). 7-fluoro-3-isopropoxy-2-methoxy phenothiazine (IVc) was obtained when (IVa) reacted with 2-bromopropane in acetone alcoholic potassium hydroxide solution.

N-alkylation of (IVb) and (IVc) with 1-(3-chloropropyl)-4-methyl piperazine[14,15] in dimethylsulphoxide in the presence of NaH under nitrogen atmosphere, gave 7-fluoro-2,3-dimethoxy-10-[3-(4-methyl-1-piperazinyl)-propyl]-phenothiazine (IVd) and 7-fluoro-3-isopropoxy-2-methoxy-10-[3-(4-methyl-1-piperazinyl)-propyl] -phenothiazine (IVe).

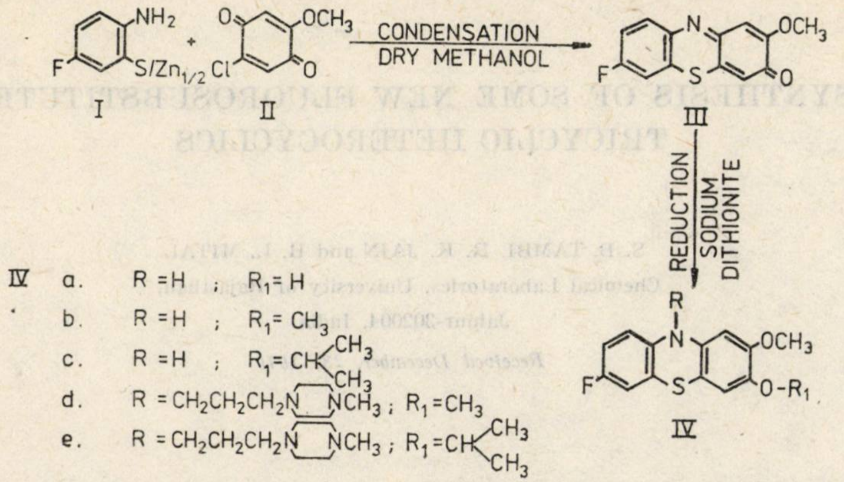

EXPERIMENTAL*

7-FLUORO-2-METHOXY PHENOTHIAZIN-3-ONE (III)

A mixture of 1.89 g. (0.011 mole) of 2-chloro-5-methoxy-*p*-benzoquinone and 1.75 g. (0.005 mole) of zinc salt of 2-amino-5-fluoro benzenethiol in dry methanol (40 ml) was stirred for one hour at room temperature and then boiled under reflux for 3 hours. After cooling, the separated product was filtered, washed with water, dried and crystallized from benzene to give 7-fluoro-2-methoxy phenothiazin-3-one, m.p. 145°C, yield 60 %, *IR*. 1645 cm^{-1}(ν(C=O)), 1610 cm^{-1} (C=N stretching) and 1255 cm^{-1}(ν(C−F)), 1235 cm^{-1} ($-OCH_3$ group).

Anal. $C_{13}H_8FNO_2S$; Calcd. N : 5.36 %, Found N : 5.33 %.

7-FLUORO-2-METHOXY PHENOTHIAZIN-3-OL (IVa)

A mixture of 1 g. (III) 1.5 g sodium dithionite, 5 ml water and 50 ml acetone was heated under reflux for 2 hours. After cooling, the mixture was poured into 200 ml cold water containing 1−2 g of sodium dithionite. The solid was extracted with ether. The ethernal extract was dried over anhydrous sodium sulphate and the solvent was evaporated in vacuo at 100°C. The product was crystallized from benzene and gave 7-fluoro-2-methoxy phenothiazin-3-ol. M.p. 178°C, yield 90 %, *IR* 3500 cm^{-1}(−OH stretching), 3325 cm^{-1} (N−H stretching) and 1255 cm^{-1}(ν(C−F)), 1275 cm^{-1} ($-OCH_3$ group).

Anal. $C_{13}H_{10}FNO_2S$; Calcd. N : 5.32 %, Found N : 5.31 %.

7-FLUORO-2,3-DIMETHOXY PHENOTHIAZINE (IVb)

To a mixture of 2.63 g (0.01 mole) of (IV-a), 0.5 g sodium dithionite, 50 ml acetone and 10 ml 10 % solution of potassium hydroxide was added 1.764 g (0.014 mole) dimethyl sulphate. The mixture was refluxed for 5 hours and the resulting green suspension was poured into 200 ml cold water. The solid was extracted with ether. The ethereal extract was dried and the solvent was evaporated in vacuo at 100°C. The product was crystallized from benzene to give 7-fluoro-2,3-dimethoxy phenothiazine. M.p. 168°C, yield 60 %, IR 3275 cm^{-1} (s) (N—H stretching), 1255 cm^{-1} (ν(C—F)) and a weak band at 1230 cm^{-1}(—OCH_3 group).

---

* All m.ps. are uncorrected.
The substances were prepared as KBr pellets for recording IR spectra.

Anal. $C_{14}H_{12}FNO_2S$; Calcd. N : 5.05 %, Found N : 5.02 %.

7-FLUORO-3-ISOPROPOXY-2-METHOXY PHENOTHIAZINE (IVc)

To a mixture of 2.63 g (0.01 mole) (IVa), 0.5 g sodium dithionite, 50 ml acetone and 10 ml 10 % ethanolic solution of potassium hydroxide was added (0.014 mole) 2-bromo-propane. The mixture as refluxed for 6 hours and then poured into 200 ml cold water. The solid was extracted with ether and worked up similarly as described above. The product was crystallized from benzene to give 7-fluoro-3-isopropoxy-2-methoxy phenothiazine. N.p 180°C, yield 60 %. IR 3270 cm^{-1}(s) (N—H stretching), 1255 cm^{-1} (s) (ν(C—F)), 1230 cm^{-1}(—OCH_3 group) and two peaks 1405 cm^{-1}, 1370 cm^{-1} (gem dimethyl group).

Anal. $C_{16}H_{16}FNO_2S$; Calcd. N : 4.59 %, Found N : 4.58 %).

7-FLUORO-2,3-DIMETHOXY-10-[3-(4-METHYL-1-PIPERAZINYL)-PROPYL]-PHENOTHIAZNE (IVd)

A suspension of NaH (20 % dispersion) 4.20 g (0.035 mole) in dimethylsulphoxide 30 ml was added (IVb) 4.709 g. (0.017 mole) in 40 ml dimethylsulphoxide. The resulting brown mixture was stirred for 2 hours at room temperature and then heated at 60—70°C for 5 hours, after adding a solution of 1-(3-chloropropyl)-4-methyl piperazine 3.53 g (0.02 mole) in 15 ml dimethylsulphoxide. The mixture was poured into ice cold water containing ammonium chloride and then extracted with ether. The ethereal extract was treated with 10 % HCl and the acid extract was basified with 10 % NaOH solution. The base so obtained was taken up in ether. The ether extract was dried over anhydrous sodium sulphate and concentrated to give a yellow oil which was converted into stable dioxalate of title compound. M.p. 196°C, yield 50 %. *IR* 1250 cm^{-1}(ν(C—F)) 1260 cm^{-1} (—OCH_3 group).

Anal. $C_{26}H_{32}FN_3O_{10}S$; Calcd. N : 7.03 %, Found N : 7.01 %.

7-FLUORO-3-ISOPROPOXY-2-METHOXY-10-[3-(4-METHYL-1-PIPERAZINYL)-PROPYL]-PHENOTHIAZINE (IVe)

The title compound was prepared similarly as (IV d) by taking 7-fluoro-3-isopropoxy-2-methoxy phenothiazine. The resulting yellow oil was converted into stable dioxalate. M.p. 207°, yield 55 %. IR 1250 cm^{-1}(ν(C—F), 1275 cm^{-1}(—OCH_3 group), and two bands at 1405 cm^{-1}, 1360 cm^{-1} (gem dimethyl group).

Anal. $C_{28}H_{36}FN_3O_{10}S$; Calcd. N : 6.72 % Found N : 6.70 %.

All the experiments were carried out in nitrogen atmosphere.

ACKNOWLEDGEMENT. The authors wish to thank Prof. J. P. Tandon, Head of the Chemistry Department, University of Rajasthan, Jaipur for providing laboratory facilities. One of the authors, (R.K.J.) is indebted to University Grants Commission, New Delhi, for awarding a Teacher fellowship.

REFERENCES

[1] P. N. Craig, E. A. Nodiff, J. J. Lafferty and G. E. Ullyot, *J. Org. Chem.*, **22**, 709 (1957).
[2] G. E. Ullyot, U. S. Patent, 3, 058, 979 ; *Chem. Abstr.*, **58**, 6841 (1963).
[3] R. L. Mital, M. Mittal, A. P. Shukla, S. Mittal and V. Laxmi *Indian J. Chem.*, **15B**, 1145 (1977).

[4] M. Mittal and R. L. Mital, *Z. Naturforsh.*, **33B**, 336 (1978).

[5] A. Bernthsen, *Ber. dtsch. chem. Ges.*, **16**, 2896 (1833).

[6] E. Knoevenagel, *J. prakt. Chem.*, **89**, 11 (1914).

[7] D. Chandra, V. N. Sharma and R. L. Mital, *Canad. J. Chem.*, **45**, 761 (1967).

[8] R. L. Mital and S. K. Jain, *Ann. Soc. Sci. Bruxelles.*, **83**, 182 (1969).

[9] R. L. Mital and S. K. Jain, *J. Chem. Soc. (C).*, **1969**, 2148.

[10] M. Terdic and I. Valter, *Liebigs Ann. Chem.*, **8**, 1285 (1978).

[11] R. L. Mital and P. C. Taunk, *Monatsh.*, **102**, 760 (1971).

[12] L. C. Raiford and J. G. Lichty, *J. Amer. Chem. Soc.*, **52**, 4576 (1930).

[13] I. S. Ioffe and A. F. Sukhina, *Zhur. obshchei, Khim.*, **23**, 295 (1953).

[14] L. P. Walls, Brit 834, 300, May 4, 1960 ; *Chem. Abstr.*, **54**, 24822 (1960).

[15] P. A. Barrett, A. G. Caldwell and L. P. Walls, *J. Chem. Soc.*, *Part II*, **1961**, 2404.

Revue Roumaine de Chimie, **26**, *3*, 481–490 (1981)

ALTERNATING TENDENCY IN COPOLYMERIZATION. VI[1]

CHAIN TRANSFER FOR COMPLEXED MONOMERS

DAN SORIN VASILESCU
Laboratory of Macromolecular Chemistry, Polytechnical Institute, Calea Victoriei 149, Bucharest, Romania

Received April 19, 1980

The homopolymerization of methyl methacrylate (MMA) in the presence of $ZnCl_2$ and CBr_4 was studied; the kinetic evidence enabled us to point out that all the steps, including initiation, propagation and chain transfer, are affected in the presence of $ZnCl_2$. The results indicate that MMA radical may be present in a complexed form with zinc chloride.

1. INTRODUCTION

The reactivity of a monomer, radical, or generally speaking of a certain substance, is a notion which reflects to a great extent the structure of the reactant. In the field of vinyl polymerization, Alfrey and Price[2] proposed the "Q-e" scheme in order to explain the reactivity of monomers and of their derived radicals.

Bamford, Jenkins and Johnston[3-6] were the first to make a quantitative approach to tackle this problem. They have developed the well-known "α-β-σ" scheme, which has as starting point the measurement of various coefficients for the rate of chain transfer reactions; indeed, knowing these values for the reaction of a radical with different substances (denoted usually as solvents), we may have a quantitative idea about the reactivity of radicals.

These coefficients can be obtained by using the "classical" Mayo equation:

$$\frac{1}{\overline{DP}} = A\frac{R_p}{[M]^2} + \sum C_X \frac{[X]}{[M]} \tag{1}$$

where:

$$A = (k_{t,k} + 2k_{t,a})/2k_p^2 \tag{2}$$

X may be the initiator, the monomer, the solvent, or even the "dead" polymer. The procedure for obtaining C_X is a straightforward graphical calculation. Since $C_X = k_{fs}/k_p$, k_{fs} may be obtained if k_p is known. For methyl methacrylate the transfer constants are given in table 1.[7]

TABLE 1

Transfer constants (C_X) for methyl methacrylate[a]

Temperature	$C_M \cdot 10^4$	$C_P \cdot 10^4$	C_I	$C_S \cdot 10^4$
50°C	0.1	<0.3	0	
60°C	0.07		0	2 700
70°C	0.2			
80°C				3 300
100°C				4 600

---

[a] C_M — transfer constant with monomer
C_P — transfer constant with the "dead" polymer
C_I — transfer constant with AIBN
C_S — transfer constant with carbon tetrabromide

As can be seen from table 1, C_P and C_I can be neglected; consequently, equation (1) becomes:

$$\frac{1}{\overline{DP}} = \frac{1}{\overline{DP}_0} + C_M + C_S \frac{[S]}{[M]} \tag{3}$$

The idea of this work is to establish to what extent the methyl methacrylate (MMA) radical exists in a complexed form. In the system MMA-$ZnCl_2$, Zubov et al.[8–12] proposed that the homopolymerization of MMA involved -MMA-$ZnCl_2$ radicals. If the radical is a complexed one, it should have a partial positive charge (as a result of electron withdrawal caused by the complexing to metal salt), as compared to the "normal" MMA radical; accordingly (taking also into account the nature of the chain transfer agent), the transfer coefficient ($k_{f,s}$) for the reaction of the complexed radical with carbon tetrabromide, should be smaller than for pure MMA. On the contrary, a similar value would indicate that the propagation would take place through uncomplexed radicals.

2. EXPERIMENTAL

Methyl methacrylate (MMA) was purified according to the usual methods and dried over calcium hydride.

Solvents were purified by distillation from appropriate drying agents.

Azobisisobutyronitrile (AIBN) was recrystallized from methanol and from chloroform.

Carbon tetrabromide was sublimed in vacuum.

The usual reagent grade $ZnCl_2$ may contain small amounts of ZnO as a result of the partial hydrolysis of $ZnCl_2$. Since the operation of sublimation is a slow process and the complex MMA-$ZnCl_2$ was required in large amounts, the following technique was used. The necessary amount of $ZnCl_2$ was introduced into a flask and dried in vacuum; a known quantity of MMA was distilled into the flask on the vacuum line. The mixture was shaken and left for decantation; the upper homogeneous layer was used as a concentrated solution of MMA-$ZnCl_2$ complex in excess of MMA. Analytical determinations were carried out in order to obtain the exact $ZnCl_2$/MMA ration.

A known volume of complex solution was dissolved in acetone and a convenient amount of this solution was titrated against a solution 0.1 M $AgNO_3$; potassium chromate was used as indicator. Dilution of the MMA-$ZnCl_2$ mixture with acetone ensured that the ternary system MMA-water-acetone was homogeneous, then allowing a sharp titration of chlorine.

The polymers (obtained by conventional methods) were submitted to viscometric measurements in dilute solutions. Number-average molecular weights were calculated for poly-MMA with the aid of the equation of Fox[13] which applies to "disproportionation" polymers :

$$[\eta] = 8.69\ 10^{-5}\overline{M}_n^{0.76} \tag{4}$$

3. RESULTS AND DISCUSSION

In order to obtain suitable molecular weights, as far as they could be predicted, several calculations were made, prior to the experiments. The concentration of AIBN influences the value of $\overline{DP}_0$ (the degree of polymerization obtained in the absence of chain transfer agent). Since

$$\overline{DP}_0 = \frac{k_p[\mathrm{M}]}{k_t^{1/2}k_d^{1/2}[\mathrm{AIBN}]^{1/2}} \tag{5}$$

we have chosen $[\mathrm{AIBN}] = 8\ 10^{-4}$ mol/l. Knowing the values k_p and k_t for MMA, k_d and efficiency of initiation for AIBN, we calculate $\overline{DP}_0$ as approximately 10^4 ; this is a measurable value. Zubov and his associates [8-12] reported that in the presence of $ZnCl_2$, the chain transfer with the complexed monomer takes place to some extent ; accordingly, $\overline{DP}_{0,z}$ (the average degree of polymerization in the presence of $ZnCl_2$, but in the absence of CBr_4) has to have a somewhat smaller value than $\overline{DP}_0$.

Another major concern was to choose the right concentrations for the chain transfer agent (CBr_4), so as to obtain measurable molecular weights. The highest CBr_4 concentration was $34\ 10^{-3}$ mol/l ; for the polymerization of uncomplexed MMA :

$$C_S[\mathrm{S}]/[\mathrm{M}] = (0.27)\ (34\ 10^{-3}\mathrm{mol/l})/(9.35\mathrm{mol/l}) = 9.82\ 10^{-4}$$

By introducing this value into eq. (3) we find $\overline{DP} = 931$ (about ten times smaller than $\overline{DP}_0$) ; this means that all the polymers should have measurable molecular weights by the viscometric technique. We had also expected identical or perhaps smaller values for the degrees of polymerization of the polymers obtained in the presence of $ZnCl_2$.

We have performed three series of experiments at different concentrations of $ZnCl_2$, to study the influence of the ratio $ZnCl_2$/MMA on the chain transfer reaction ; besides these tests, we have repeated the experiments in the absence of the complexing agent, as a direct checking of the accuracy of our work.

The initial solution of $ZnCl_2$ in MMA was mixed with suitable amounts of other solutions (AIBN in MMA, CBr_4 in MMA) and pure MMA; we have obtained twenty different samples (10 ml each) which were subjected to polymerization. The results are collected in table 2.

Since Mayo equation has a differential character,[14] we have tried to stop the polymerization reaction at small conversions. In the presence of $ZnCl_2$, the overall reaction rate increases; at the highest ratio $ZnCl_2$/MMA, the polymerization time was only five minutes. Accordingly, these results cannot be regarded as reliable for the calculation of the ratio $k_p/k_t^{0.5}$, but may be used in the calculation of C_S.

TABLE 2

The polymerization of MMA in the presence of $ZnCl_2$ and CBr_4; [AIBN] = 8.09 10^{-4} mol/l; T = 60°C

Test	$[ZnCl_2]$ / [MMA]	$[CBr_4]$ (mole/l)	Polymerization time (min.)	Yield (mg.)
1	0.0	0.0	20	132.0
2	0.0854	0.0	15	234.4
3	0.1708	0.0	10	267.0
4	0.2989	0.0	20	617.6
5	0.0	0.00426	20	163.0
6	0.0854	0.00426	15	402.5
7	0.1708	0.00426	10	381.0
8	0.2989	0.00426	5	73.2
9	0.0	0.00852	20	187.3
10	0.0854	0.00852	20	408.0
11	0.1708	0.00852	10	276.0
12	0.2989	0.00852	5	97.8
13	0.0	0.01705	20	156.0
14	0.0854	0.01705	15	331.6
15	0.1708	0.01705	20	544.0
16	0.2989	0.01705	5	104.0
17	0.0	0.03410	20	144.0
18	0.0854	0.03410	15	136.7
19	0.1708	0.03410	10	—
20	0.2989	0.03410	5	103.4

Our next set of experiments is presented in table 3. We have used a smaller concentration of AIBN (1.414 10^{-4} mol/l), in order to allow longer polymerization times for reaching the same small conversions.

A very controversial point in the literature is whether the decomposition rate of AIBN is affected[8,15] or not [16] in the presence of $ZnCl_2$.

As the experiments presented in table 3 differ from the previous ones (table 2) only by the concentration of AIBN, we have expected that a comparison of the initial polymerization rates might be worthwhile.

The polymers obtained were subjected to viscometric measurements. For each polymer sample, its intrinsic viscosity was determined by extrapolating the experimental data $(\eta_{s/c})$ as a function of concentration. The best straight line was obtained analytically by using the least square method; the intercept (infinite dilution) represents the intrinsic viscosity. The results are presented in table 4.

TABLE 3

The poylmerization of MMA in the presence of $ZnCl_2$ and CBr_4;[AIBN] = 1.414 10^{-4}mole/l; T = 60°C

Test	$\frac{[ZnCl_2]}{[MMA]}$	$[CBr_4]$ (mole/l)	Polymerization time (min.)	Yield (mg.)
21	0.0	0.00000	58	207.3
22	0.0	0.00426	58	177.6
23	0.0	0.00852	58	264.2
24	0.0	0.01705	58	220.2
25	0.0	0.03410	58	191.5
26	0.0752	0.00000	43	236.7
27	0.0752	0.00426	43	293.6
28	0.0752	0.00852	43	225.7
29	0.0752	0.01705	43	226.6
30	0.0752	0.03410	43	251.4
31	0.1504	0.00000	30	114.9
32	0.1504	0.00426	30	139.8
33	0.1504	0.00852	30	133.4
34	0.1504	0.01705	30	140.2
35	0.1504	0.03410	30	163.1
36	0.2632	0.00000	22	57.0
37	0.2632	0.00426	22	59.5
38	0.2632	0.00852	22	65.6
39	0.2632	0.01705	22	57.4
40	0.2632	0.03410	22	66.8

Our next concern has been to calculate the transfer constant C_S. We have plotted the values $1/\overline{DP}$ against the concentration of transfer agent (CBr_4). We have also used the least square method to obtain the best straight lines. The slope of these lines represents, of course, the product $C_S \frac{[S]}{[M]}$ (eq. 3), while the intercept is $1/\overline{DP}_0$. As the procedure of obtaining C_S implies a great deal of calculations, we have written two similar computer programs (one for the experiments 1—20, the other for the experiments 21—40).

TABLE 4

Intrinsic viscosities and the corresponding $1/(\overline{DP})$ values for the samples 1–40

Test	Intrinsic viscosity (dl/g)	$1/(\overline{DP}).10^4$	Test	Intrinsic viscosity (dl/g)	$1/(\overline{DP}).10^4$
1	3.2153	0.9764	21	3.9378	0.7478
2	2.7405	1.2049	22	3.1135	1.0187
3	2.2736	1.5406	23	2.2181	1.5915
4	2.4712	1.3805	24	1.6598	2.3307
5	2.6650	1.2500	25	0.8482	5.6377
6	2.0974	1.7130	26	2.9863	1.0761
7	2.0886	1.7226	27	2.1492	1.6590
8	1.1841	3.6348	28	1.8908	1.9635
9	2.0356	1.7818	29	1.3222	3.1435
10	1.5423	2.5670	30	0.8774	5.3925
11	1.7727	2.1374	31	1.7114	2.2386
12	1.1817	3.6446	32	1.6597	2.3308
13	1.1842	3.6343	33	1.4064	2.8984
14	1.2760	3.2943	34	1.3483	3.0638
15	1.2335	3.4443	35	0.9483	4.8680
16	1.0569	4.2212	36	0.9364	4.9497
17	0.7153	7.0557	37	0.8607	5.5307
18	0.8472	5.6466	38	0.9240	5.0373
19	—	—	39	0.7751	6.3476
20	0.9926	4.5842	40	0.6967	7.3043

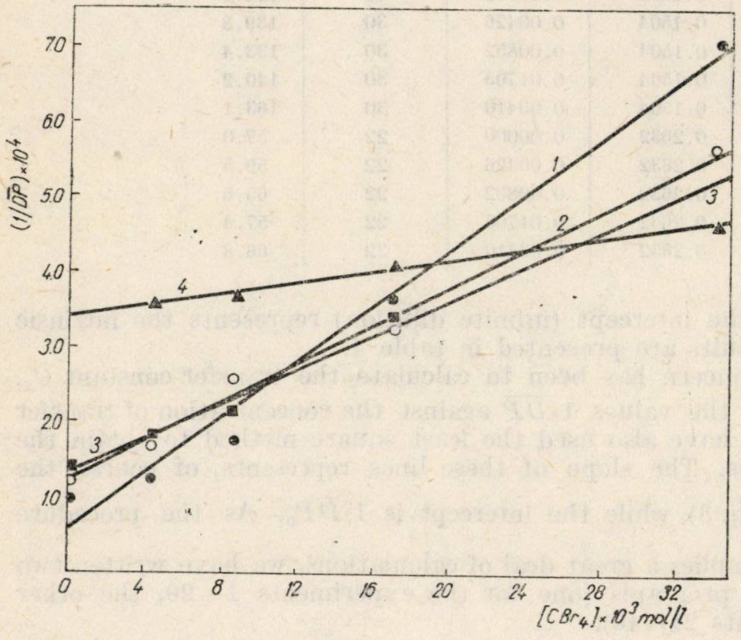

Fig. 1. – Determination of the transfer constants in the system MMA-$ZnCl_2$-CBr_4; [AIBN] = = 8.09 10^{-4} mol/l; $T = 60$°C. *1.* $ZnCl_2$/MMA = 0.0; *2.* $ZnCl_2$/MMA = 0.0854; *3.* $ZnCl_2$/MMA = = 0.1708; *4.* $ZnCl_2$/MMA = 0.2989.

The results of calculations are illustrated in figures 1 and 2; figure 1 refers to the experiments carried out with $[\text{AIBN}] = 8.09\ 10^{-4}$ mol/l (tests 1—20), while figure 2 to the experiments corresponding to a smaller concentration of AIBN ($1.414\ 10^{-4}$ mol/l). As results from table 5, the value C_{SO} (transfer constant to CBr_4 for the homopolymerization of pure MMA) is smaller than that previously reported[7]; nevertheless, this partial

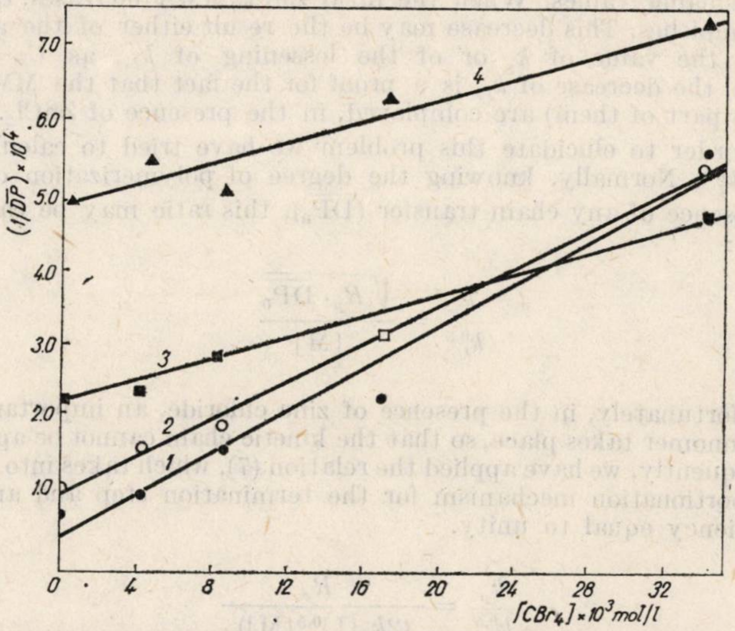

Fig. 2. — Chain transfer in the system MMA-$ZnCl_2$-CBr_4; $[\text{AIBN}] = 1.414\ 10^{-4}$ mol/l; $T = 60$°C. *1.* $ZnCl_2$/MMA = 0.0; *2.* $ZnCl_2$/MMA = 0.0752; *3.* $ZnCl_2$/MMA = 0.1504; *4.* $ZnCl_2$/MMA = 0.2632.

TABLE 5

Kinetic parameters in the system MMA-$ZnCl_2$-CBr_4

No	$\frac{[ZnCl_2]}{[MMA]}$	$[\text{AIBN}].10^4$ (mol/l)	$R_p.10^4$ (mol/l.s)	$\frac{k_p}{k_t^{1/2}}$	C_S	$\frac{k_{fs}}{k_t^{1/2}}$
1	0.0	1.414	0.6090	0.1332	0.1357	0.01808
2	0.0	8.09	1.2383	0.1133	0.1738	0.01969
3	0.0752	1.414	0.9556	0.2115	0.1154	0.02486
4	0.0854	8.09	3.2264	0.3062	0.1158	0.03547
5	0.1504	1.414	0.7831	0.1829	0.0677	0.01238
6	0.1708	8.09	4.5246	0.4452	0.1000	0.04452
7	0.2632	1.414	0.4639	0.1140	0.0584	0.00666
8	0.2982	8.09	3.5544	0.3712	0.0278	0.01033

agreement may be regarded as satisfactory since the original work by Furhman and Mesrobian [7] was performed many years ago.

The calculation of the other transfer constants (C_S) shows a tendency towards smaller values. When the ratio $ZnCl_2$/MMA increases, the value of C_S diminishes. This decrease may be the result either of the augmentation in the value of k_p or of the lessening of k_{fs}, as $C_S = k_{fs}/k_p$. Of course, the decrease of k_{fs} is a proof for the fact that the MMA radicals (or a part of them) are complexed, in the presence of $ZnCl_2$.

In order to elucidate this problem we have tried to calculate the ratio $k_p/k_t^{0.5}$. Normally, knowing the degree of polymerization obtained in the absence of any chain transfer ($\overline{DP}_0$), this ratio may be calculated as being :

$$\frac{k_p}{k_t^{0.5}} = \frac{\sqrt{R_p \cdot \overline{DP}_0}}{[M]} \tag{6}$$

Unfortunately, in the presence of zinc chloride, an important transfer to monomer takes place, so that the kinetic chain cannot be appreciated. Consequently, we have applied the relation (7), which takes into account a disproportionation mechanism for the termination step and an initiation efficiency equal to unity.

$$\frac{k_p}{k_t^{0.5}} = \frac{R_p}{(2k_d[I]^{0.5}[M])} \tag{7}$$

The results of this calculation are also presented in table 5. We have noticed a very good agreement for the value $k_p/k_t^{0.5}$, using both eq. (6) and (7), only for pure MMA ; as we have previously pointed out, eq. (6) cannot be used for the complexed MMA.

Eq. (7) contains some restrictions. R_p may be easily obtained experimentally ; the values used by us are average values from five different experiments. In order to calculate the initiation rate ($2f\,k_d[I]$) we thought that k_d ($8.45\ 10^{-6}\ s^{-1}$ at 60°) is constant, regardless of the reaction medium. Let us consider for the moment that this point of view is valid.

The data published by Bamford et al.[17,18] and subsequently by Zubov and his co-workers [15,19–21] showed that the complexing agent produces increases in the values of k_p and to a smaller extent of k_t. Taking into account that :

$$(k_p/k_t^{0.5})C_S = k_{fs}/k_t^{0.5} \tag{8}$$

this ratio ($k_{fs}/k_t^{0.5}$) was considered by us as a measure of k_{fs}, as k_t is less affected in the presence of $ZnCl_2$. Since this ratio shows an appreciable decrease it might be said that this is a proof for the existence of complexed propagating radicals of MMA. However, this conclusion is based on the calculations which implied the postulate of the constancy of k_d.

In the systems studied by us, two concentrations of initiator were used. As

$$([\mathrm{Init}]_1/[\mathrm{Init}]_2)^{0.5} = (8.09\ 10^{-4})/(1.414\ 10^{-4}) = 2.39 \tag{9}$$

is to be expected that this value would be the ratio of the polymerization rates, for two systems with the same $[\mathrm{ZnCl_2}]/[\mathrm{MMA}]$, but with different [AIBN]. Since the systems 3 and 4, 5 and 6, 7 and 8 respectively have similar concentrations of $\mathrm{ZnCl_2}$, we calculated the ratios :

$$R_{p2}/R_{p1} = 2.03\,; \qquad R_{p4}/R_{p3} = 3.37\,;$$

$$R_{p6}/R_{p5} = 5.77\,; \qquad R_{p8}/R_{p7} = 7.66$$

These values may be interpreted as the evidence for the startling fact that the decomposition rate for AIBN is affected by zinc chloride.

A first conclusion is that the use of eq. (7) becomes unreliable ; the results regarding the ratios $k_{fs}/k_t^{0.5}$ have, consequently, only a qualitative character.

In our opinion, the modification of the polymerization rate may be interpreted in two different ways.

A) Zinc chloride forms a complex with AIBN, which in turn decomposes faster than pure AIBN. Zubov et. al.[19–21] favoured this idea ; on the other hand, Funt and Pawelchak[16] have shown that in the polymerization of acrylonitrile in the presence of $\mathrm{ZnCl_2}$, the value of k_d for AIBN remains constant. The above-quoted authors[16] have used relatively small concentrations of AIBN and $\mathrm{ZnCl_2}$; in our work these concentrations were higher. Funt's results and ours may however agree, only if we consider a complex $\mathrm{ZnCl_2/AIBN} = 2/1$; in this case the importance of the concentration of $\mathrm{ZnCl_2}$ becomes evident.

B) Our experiments indicated an important transfer to the complexed monomer. As results from table 6, the values of C_M become

TABLE 6

Transfer constants with the monomer for the polymerization of MMA in the presence of $\mathrm{ZnCl_2}$ at 60°C

$\frac{[\mathrm{ZnCl_2}]}{[\mathrm{MMA}]}$	$[\mathrm{AIBN}].10^4$ (mol/l)	$C_M \cdot 10^5$
0.0752	1.414	6.10
0.1504	1.414	16.78
0.2632	1.414	45.23
0.0854	8.09	2.65
0.1708	8.09	3.75
0.2989	9.09	16.10

important when the concentration of zinc chloride in the system is high. The new formed radicals, less active, may introduce retardation phenomena, as those communicated by Bamford and Brumby[18] for the polymerization of MMA in the presence of $AlCl_3$.

This interpretation permits a logical explanation for the modifications noticed in the polymerization rates.

Conclusively, our results seem to indicate the fact that the propagating radical of MMA is complexed, but due to the fact that the system is very complicated and apparently all the stages of the polymerization process are affected in the presence of $ZnCl_2$, these conclusions cannot have a quantitative form.

REFERENCES

[1] Part V. D. S. Vasilescu, *Rev. Roumaine Chim.*, **25**, (1980).

[2] T. Alfrey and C. C. Price, *J. Polymer Sci.*, **2**, 101 (1947).

[3] C. H. Bamford, A. D. Jenkins and R. Johnston, *Trans. Faraday Soc.*, **55**, 418 (1959).

[4] C. H. Bamford and A. D. Jenkins, *J. Polymer Sci.*, **53**, 149 (1961).

[5] C. H. Bamford and A. D. Jenkins, *Trans. Faraday Soc.*, **59**, 530 (1963).

[6] C. H. Bamford and A. D. Jenkins, *J. Polymer Sci.*, *B*, **1**, 609 (1963).

[7] N. Furhman and R. B. Mesrobian, *J. Amer. Chem. Soc.*, **76**, 3281 (1954).

[8] V. P. Zubov, L. I. Valuev, V. A. Kabanov and V. A. Kargin, *J. Polymer Sci.*, *A-1*, **9**, 833 (1971).

[9] Yu. D. Semchinov, A. V. Ryabov, N. L. Khratova and Ye. N. Milchenko, *Vysokomol. Soedineniya*, *A*, **15**, 451 (1973).

[10] V. I. Zubov and V. A. Kabanov, *Vysokomol. Soedineniya*, *A*, **14**, 5 (1972).

[11] V. B. Golubev, V. P. Zubov, G. S. Georgiev, I. L. Stoyachenko and V. A. Kabanov, *J. Polymer Sci.*, *A—1*, **11**, 2463 (1973).

[12] G. S. Georgiev, A. M. Kaplan, V. P. Zubov, V. B. Golubev, I. M. Barkalov and V. A. Kabanov, *Vysokomol. Soedineniya*, *A*, **14**, 177 (1972).

[13] T. G. Fox, J. B. Kinsinger, H. F. Mason and E. M. Schuele, *Polymer*, **3**, 71 (1962).

[14] F. R. Mayo, *J. Amer. Chem. Soc.*, **65**, 2324 (1943).

[15] V. P. Zubov, M. B. Lachinov, V. B. Golubev, V. F. Kulikova, L.S. Polak, V. A. Kabanov and V. A. Kargin, *J. Polymer Sci.*, *C*, **23**, 147 (1968).

[16] B. L. Funt and S. Pawelchak, *J. Polymer Sci.*, *B*, **13**, 451 (1975).

[17] C. H. Bamford, S. Brumby and R. P. Wayne, *Nature*, **209**, 292 (1966).

[18] C. H. Bamford and S. Brumby, *Makromol. Chem.*, **174**, 159 (1970).

[19] M. B. Lachinov, V. P. Zubov and V. A. Kabanov, *Vysokomol. Soedineniya*, *B*, **12**, 4 (1970).

[20] A. A. Panasenko, V. B. Golubev, V. P. Zubov, V. A. Kabanov and V. A. Kargin, *Vysokomol. Soedineniya*, A, **12**, 865 (1970).

[21] M. B. Lachinov, B. M. Abu-El'Khaur, V. P. Zubov and V. A. Kabanov, *Vysokomol. Soedineniya*, A, **15**, 504 (1973).

Revue Roumaine de Chimie, **26**, *3*, 491–501 (1981)

EFFECT OF SURFACTANTS ON KINETICS OF REDUCTION OF V(V) IN UNIVERSAL BUFFER SOLUTIONS AT THE DROPPING MERCURY ELECTRODE

M. THARWAT, A. AWAD and F. RASHWAN
Chemistry Department, Faculty of Science, Sohag, Egypt

Received October 17, 1979

The polarographic behaviour of pentavalent vanadium at the DME is investigated in universal buffer solutions of varying pH values in the absence and presence of charged and uncharged surfactants. In the absence of SAS, the polarogram consists of two waves of unequal heights. The former is assigned to the reduction step V(V) → V(IV), whereas the latter wave is found to correspond to the reduction of V(IV) → V(II). The polarographic behaviour of V(V) in the presence of electroinactive substances indicated that both anionic ($NaDDBSO_3$) and nonionic (T.X-100) surfactants caused extensive retardation of the reduction process and rendered the reduction waves more irreversible. A cationic ($DDAClO_4$) surfactant showed either a similar or an opposite effect. The kinetic parameters of the electrode processes in the absence and presence of SAS have been determined.

INTRODUCTION

Solutions of vanadium have been frequently investigated by the polarographic method.[1-7] The reduction of $+5$ vanadium on the dropping mercury electrode in acid solutions (0.05 M H_2SO_4) produces two polarographic waves, one starting from zero, the other from -0.98 applied e.m.f. *vs*, SCE. In ammoniacal solutions containing 1 Mammonium chloride and less than 6 M ammonia, two very close waves arise in the interval -1 to -1.3 V. *vs*. SCE. With increase of ammonia concentration the first wave shifts toward more negative and the second toward more positive potentials, so that only one wave remains at concentrations above 6 M ammonia. In strongly basic solutions (0.1 M lithium hydroxide) a single wave develops, starting at about -1.7 V. *vs*. SCE. Hence, it is evident that the polarographic behaviour of $+5$ vanadium depends on pH. To elucidate the chemical mechanism of the electrode process in the presence of the different types of SAS concerning the evaluation of the kinetic parameters, a systematic polarographic investigation of V(V) in universal buffer solutions has been carried out.

EXPERIMENTAL

CHEMICALS AND SOLUTIONS

All chemicals used are of A. R. grade. A stock of 2.5×10^{-2} M V(V) solution is prepared by dissolving the appropriate quantity of ammonium metavanadate (NH_4VO_3) in bidistilled water. The amount of vanadium in the stock is determined volumetrically by a recommended procedure.[8] The surface active materials such as Triton X-100 (T.X-100), dodecylamine perchlorate ($DDAClO_4$) sodium dodecylbenzene sulphonate ($NaDDBSO_3$) are products of Rohm and Hass Co., Philadelphia. 1—3% solutions of the different surfactants are prepared by dissolving the appropriate amounts in bidistilled water. 2% Dodecylamine perchlorate solution ($DDAClO_4$) is prepared by dissolving the required quantity of dodecylamine base in the equivalent amount of perchloric acid. The pH value of the resulting solution is 6. Universal buffer solution of different pH values ranging from 2.1 to 11.8 is prepared and checked by means of pH meter of the Radiometer type-model 28, which is accurate to ±0.05 pH unit.

WORKING PROCEDURE AND APPARATUS

The experimental technique and the electrolysis cell were those previously described by Issa and Tharwat.[9]

The polarograms were recorded by a PO_4 Radiometer polarograph. The electrode characteristics for two capillaries used are :
1) $m = 1.625$ mgs^{-1}, $t = 4.8$ s.drop^{-1} and
2) $m = 1.894$ mgs^{-1}, $t = 3.9$ s. drop^{-1}
The values of both m and t were measured at open circuit and at a height of mercury reservoir of 33 cm Hg. (in 0.1 M oxygen-free KCl with respect to the drop time t).

RESULTS AND DISCUSSION

Figure 1 represents the electroreduction of V(V) at DME in universal buffer solutions of pH ranging from 2.1 to 11.8. In acidic buffer solu-

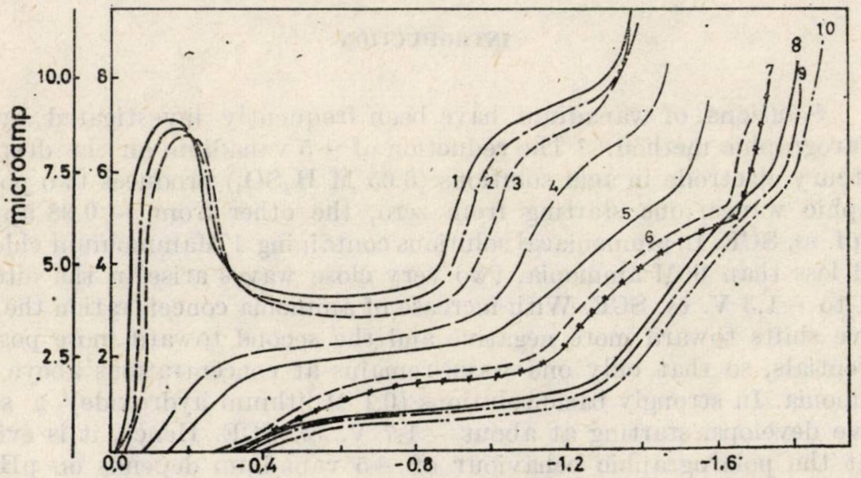

Fig. 1. — 1 mM V(V) in universal buffer solutions

Curve	1	2	3	4	5	6	7	8	9	10
pH	2.1	3.1	4.2	5.1	6.5	7.0	8.8	9.1	10.85	11.8

tions (pH 2.1 to 4.2), the polarogram consists of two waves of unequal heights and is characterized by a large maximum covering the rising portion of the first wave. In moderatly acidic and neutral buffer solutions (pH 5.1, 6.2), a slight shift of the waves to more negative potential values and disappearance of the maximum are observed. In alkaline buffer solutions (pH 9.1) and up to 11.8, the polarogram suffers more shift to negative potentials and the 1st wave is retarded whereas, the second one is enhanced.

In order to find out the mechanism of the reduction, one has to calculate the number of electrons involved in the reduction process. The value of the diffusion coefficient of VO_3^- species is known and is equal to 2.7×10^{-6} cm²/s (in 0.05 M H_2SO_4 from microcoulometric data).

Substituting for the various values of i_d, C, t, m, and D° in the Ilkovic equation, n is found equal to 3. This indicates that the reduction of the vanadate along both waves passes to the divalent state. Since the height of the first wave is about half of that of the second, one can conclude easily that the first wave is a unielectron wave and represents the reduction stage V(V) → V(IV), whereas the second one involves the uptake of extra two electrons and corresponds to the reduction step V(IV) → V(II). This view is supported by many authors.[2-7]

(i) *Behaviour at pH 2.1*

The polarograms shown in figure 2 (A, B and C) represent the behaviour in the presence of increasing amounts of each of the three SAS. The values of the kinetic parameters as calculated from the analysis of these waves are listed in table 1 (A and B).

Depending on the above conclusion, the reduction of V(V) in the absence of SAS takes place along two waves representing production of V(IV) and V(II). Analysis of the two waves reveals less and high irreversibility of reduction respectively in this medium.

The effects produced by T.X—100 and Na DDBS are quite similar and differ from those of DDA^+. The first wave is distorted by a minimum in the presence of both T.X—100 and $DDBS^-$, whereas only suppression in its current is noticed in the case of DDA^+. The strongest effects produced by T.X—100 such as minimum occurrence, vitiation and strong shift to more negative potentials are atributed to a stronger adsorbability and wider potential range of adsorption.[10] The effecs produced by DDBS- are in agreement with Frumkin's theory of electrostatic effects,[11] the reducible species being anionic, whereas the effects noticed in the case of T.X—100 are attributed to blocking of the electrode surface by an adsorbed film of the nonionic surfactant. Elimination of the second wave in the presence of DDA^+ indicates that this wave falls in the working potential range of the surfactant.

(*ii*) *Behaviour at pH 7.0*

The polarographic reduction of an mM solution of V(V) at DME in a solution of pH 7.0 is represented by double step polarogram. Thus, as concluded, the first wave represents the formation of quadrivalent vanadium whereas, the reduction along the second shows the formation of divalent element. Analysis of the two waves as cited in table 2 indicates

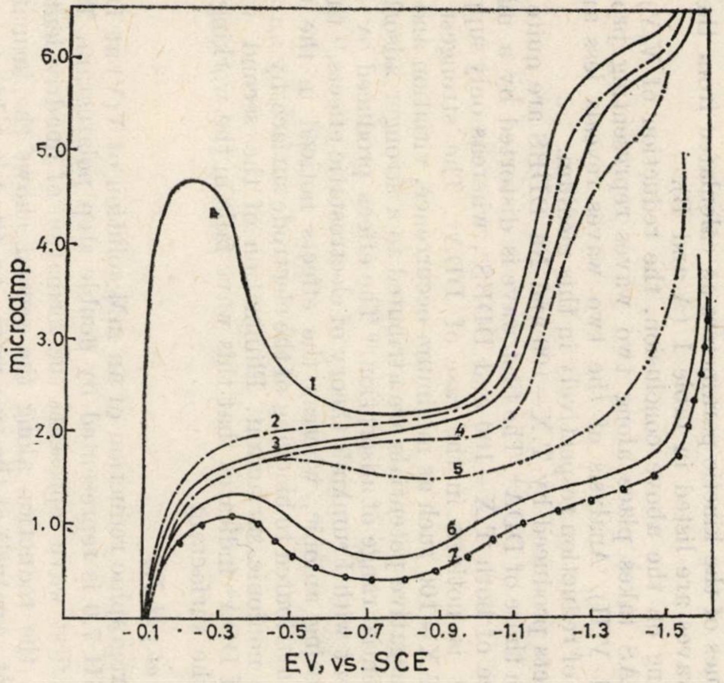

Fig. 2(A) — Effect of T.X—100 on 0.6 mM V(V) in universal buffer solution of pH 2.1.

Curve	1	2	3	4	5
SAS%	0.00	1×10^{-4}	2×10^{-4}	2.3×10^{-3}	4.3×10^{-3}
Curve	6	7			
SAS%	8.3×10^{-3}	1.23×10^{-2}			

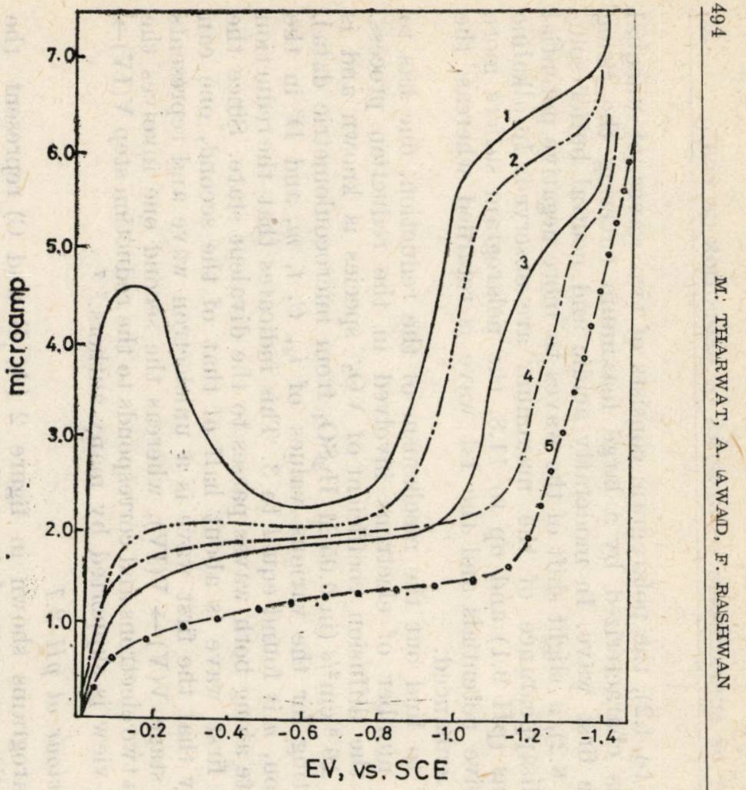

Fig. 2(B). — Effect of $DDAClO_4$ on 0.6 mM V(V) in universal buffer solution of pH 2.1.

Curve	1	2	3	4	5
SAS %	0.00	2×10^{-4}	8×10^{-4}	4.88×10^{-3}	4.54×10^{-2}

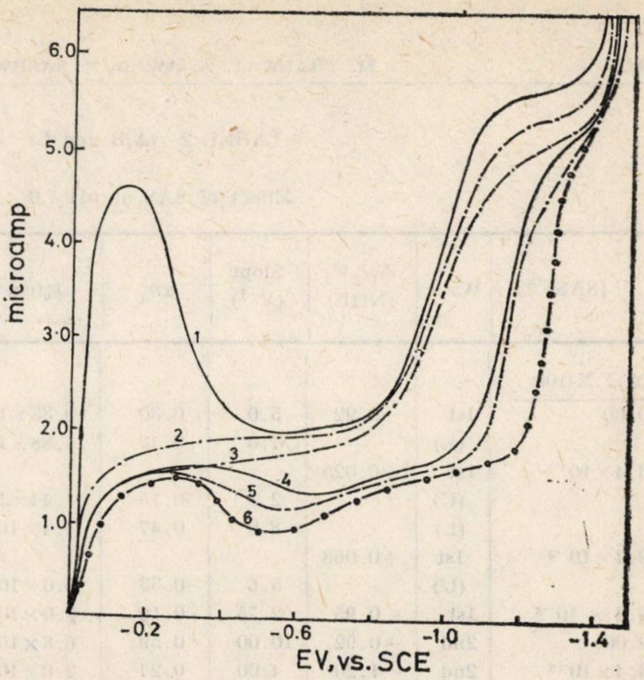

Fig. 2(C) — Effect of $NaDDBSO_3$ on 0.6 mM (V) in universal buffer solution of pH 2.1.

Curve	1	2	3	4	5	6
SAS %	0.00	1×10^{-3}	2.5×10^{-3}	8.5×10^{-3}	1.2×10^{-2}	3.2×10^{-2}

TABLE 1 *(A, B)*

Effect of SAS at pH 2.1

[SAS] %	Wave	$E_{1/2}/V$ (NHE)	Slope (V^{-1})	αn_a	k_0(cm s^{-1})	ΔG (kJ)	$k_0 D^{-1/2}$
(A) T.X-100							
0.00	1st	−0.198	10.8	0.65	1.0×10^{-5}	14.00	4.1×10^{-2}
	2nd	−0.675	8.5	0.50	2.6×10^{-9}	19.00	1.7×10^{-6}
	(L)		8.0	0.47	0.20	8.00	82.4
1×10^{-4}	1st	+0.275					
	(U)		3.64	0.22	1.3×10^{-2}	9.67	5.2
			6.4	0.38	6.73×10^{-2}	8.67	27.8
2.3×10^{-3}	1st(L)	+0.220					
			3.08	0.18	8.5×10^{-3}	9.90	3.5
1.23×10^{-2}	1st*(U)	−0.622	4.86	0.29	1.6×10^{-8}	17.80	6.6×10^{-6}
0.00	2nd	−0.673	8.00	0.47	5.2×10^{-9}	18.50	2.13×10^{-6}
	(L)		8.00	0.47	1.6×10^{-9}	19.2	6.6×10^{-7}
1×10^{-4}	2nd	−0.737					
	(U)		5.14	0.3	6.6×10^{-7}	15.5	2.7×10^{-4}
2.3×10^{-3}	2nd	−0.775	7.2	0.43	3.3×10^{-9}	18.77	1.4×10^{-6}
(B) $NaDDBSO_3$							
0.00	2nd	−0.673	8.0	0.47	5.2×10^{-9}	18.5	2.13×10^{-6}
	(L)		12.0	0.71	4.0×10^{-15}	27.0	2.10×10^{-12}
1.2×10^{-2}	2nd	−0.958					
	(U)		4.6	0.27	5.0×10^{8}	17.2	2.0×10^{-5}
	(L)		16.0	0.95	0.68	7.3	25.0
3.2×10^{-2}	1st	+0.172					
	(U)		8.0	0.47	0.03	9.2	11.0
3.2×10^{-2}	1st*	−0.583	4.0	0.24	4.4×10^{-3}	10.3	10.80

* Shifted wave. (L) Lower portion. (U) Upper portion.

TABLE 2 (A,B and C)

Effect of SAS at pH 7.0

[SAS] %	Wave	$E_1/_2 V$ (NHE)	Slope (V^{-1})	αn_a	k_0(cm s^{-1})	$\Delta G (kJ)$	$k_0 D^{0.5}$
(A)T.X-100							
0.00	1st	-0.22	5.0	0.30	9.33×10^{-5}	12.62	4.67×10^{-2}
	(L)		7.0	0.42	1.88×10^{-3}	16.40	0.8
3.4×10^{-3}	1st	$+0.025$					
	(U)		2.5	0.15	1.44×10^{-3}	10.70	0.6
	(L)		8.0	0.47	4.4×10^{-3}	10.30	1.8
9.4×10^{-3}	1st	$+0.068$					
	(U)		5.6	0.33	3.0×10^{-3}	10.50	1.24
9.4×10^{-3}	1st	-0.95	2.75	0.16	3.0×10^{-6}	14.70	1.30×10^{-3}
0.00	2nd	-0.92	10.00	0.59	6.8×10^{-13}	23.90	3.30×10^{-10}
3.4×10^{-3}	2nd	-1.20	4.00	0.24	2.0×10^{-8}	17.7	0.82×10^{-5}
(B)DDACLO$_4$							
	(L)		4.44	0.26	1.14×10^{-3}	11.12	0.047
2.0×10^{-4}	1st	-0.01					
	(U)		1.50	0.10	1.22×10^{-3}	11.10	0.50
	(L)		7.00	0.41	2.04×10^{-3}	10.80	0.84
1.2×10^{-2}	1st	$+0.03$					
	(U)		2.10	0.12	1.45×10^{-3}	10.97	0.60
	(L)		3.11	0.20	1.4×10^{-3}	11.00	0.60
1.2×10^{-2}	1st*	-0.015					
	(U)		7.20	0.43	9.8×10^{-4}	11.20	0.405
	(L)		10.00	0.59	2.2×10^{-14}	25.90	1.00×10^{-11}
1.0×10^{-3}	2nd	-1.075					
	(U)		4.50	0.27	1.7×10^{-8}	17.77	0.8×10^{-5}
	(L)		8.33	0.49	9.1×10^{-13}	23.70	4.3×10^{-10}
6.0×10^{-3}	2nd	-1.095					
	(U)		4.00	0.24	5.0×10^{-8}	17.14	2.4×10^{-5}
	(L)		7.22	0.43	2.4×10^{-12}	23.11	1.14×10^{-9}
1.2×10^{-2}	2nd	-1.205					
	(U)		2.40	0.14	1.5×10^{-6}	15.08	0.7×10^{-3}
(C)NaDDBSO$_3$							
1.2×10^{-2}	1st	$+0.079$	8.14	0.48	5.5×10^{-3}	10.20	2.3
	(L)		15.00	0.90	9.4×10^{-2}	8.46	39.0
4.0×10^{-2}	1st	$+0.125$					
	(U)		6.00	0.40	7.1×10^{-3}	10.00	2.93
4×10^{-2}	1st	$+0.960$	4.94	0.3	2.3×10^{-8}	17.60	9.5×10^{-8}
	(L)		7.50	0.44	5.3×10^{-11}	21.25	2.5×10^{-8}
1.2×10^{-2}	2nd	-0.983					
	(U)		10.0	0.59	1.9×10^{-13}	24.65	0.9×10^{-10}

a higher degree of irreversibility along the first wave ($\alpha = 0.3$) than that of the second wave ($\alpha = 0.59$). These values for the transfer coefficient, α, are obtained when αn_a is taken equal.

The polarograms shown in figures 3(A,B and C) represent the behaviour in the presence of increasing [SAS]. The effects of DDA^+ can be expressed as enhancement of reduction along the first wave, its $E_{1/2}$ is shifted to less negative potential values at higher SAS concentrations. The reducible species being anionic, the effects produced by DDA^+ cations are in accordance with Frumkin's theory.[11] The effects produced by T.X−100 show complete retardation along both waves. A similar but more profound retardation along the first wave is observed in the presence of $DDBS^-$; this is an expected result in the light of Frumkin's theory.

(iii) *Behaviour at pH 11.8*

The electroreduction of V(V) in this medium takes place along a polarogram and consists of a small first wave and a large second one. This marked decrease in i_l of the first wave indicates that reduction of V(V) is retarded in this medium. Thus, the second wave corresponds to the reduction of some hindered species of V(V) to V(IV) together with

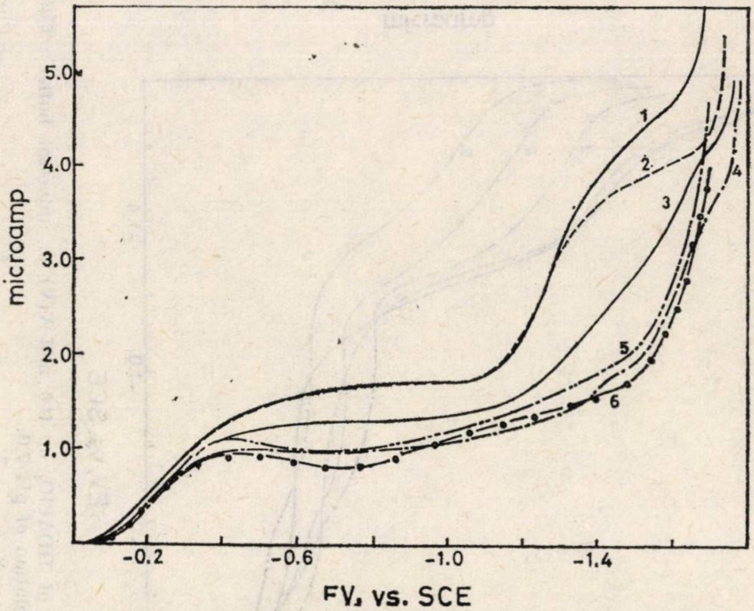

Fig. 3(A). — Effect of T.X. — 100 on 0.6 mM V(V) in universal buffer solution of pH 7.0.

Curve	1	2	3	4	5	6
SAS %	0.00	1.4×10^{-3}	3.4×10^{-3}	5.4×10^{-3}	7.4×10^{-3}	9.4×10^{-3}

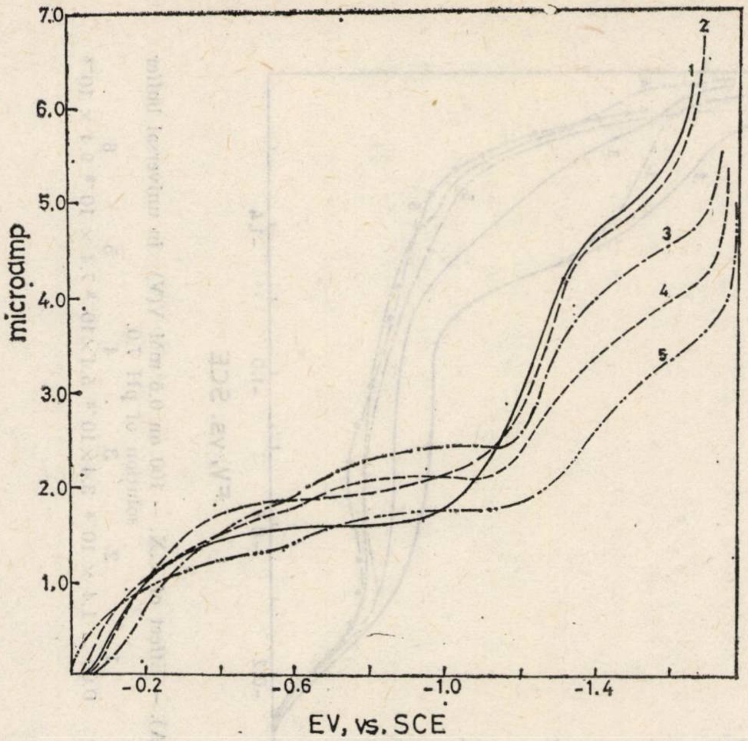

Fig. 3(B). — Effect of DDAClO$_4$ on 0.6 mM V(V) in universal buffer solution of pH 7.0.

Curve	1	2	3	4	5
SAS %	0.00	2×10^{-4}	1×10^{-3}	6×10^{-3}	1.2×10^{-2}

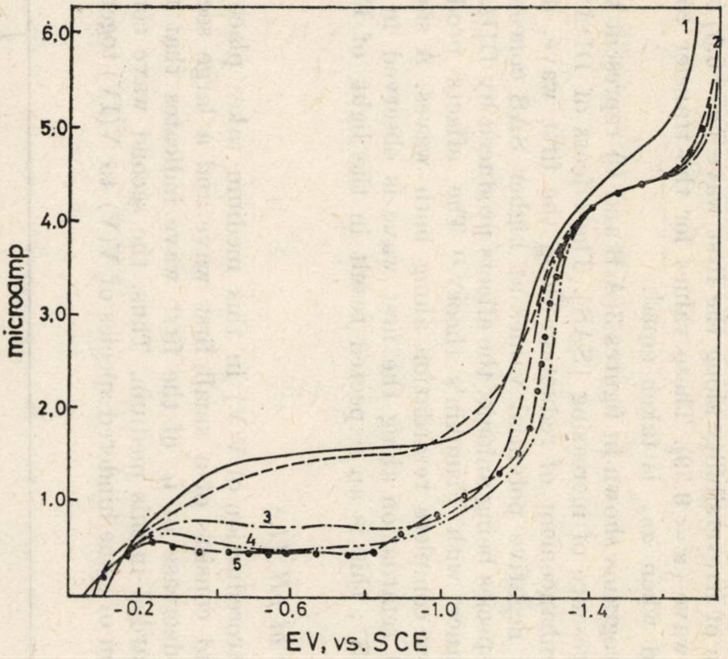

Fig. 3(C). — Effect of NaDDBSO$_3$ on 0.6 mM V(V) in universal buffer solution of pH 7.0.

Curve	1	2	3	4	5
SAS %	0.00	4×10^{-3}	1.2×10^{-2}	1.8×10^{-2}	4×10^{-2}

further reduction to the divalent state. Thus, the previously mentioned conclusion that the number of electrons amounts 3 is still valid.

Analysis of the two waves by the aid of log $i/i_a - i$ *vs.* E_{NHE} yields straight and broken lines for the 1st and 2nd waves respectively. The values obtained for the kinetics parameters are listed in table 3.

TABLE 3(A and B)

Effect of SAS (NHE) at pH 11.8

[SAS] %	Wave	$E_{1/2}/V$ (NHE)	Slope (V^{-1})	αn_a	k_0 (cm s^{-1})	ΔG (kJ)	$k_0 D^{-1/2}$
(A)T.X-100							
0.00	1st	−0.23	7.11	0.42	2.3×10^{-5}	13.45	1.35×10^{-2}
			4.00	0.42	2.3×10^{-8}	17.38	1.35×10^{-5}
0.00	2nd(L)	−1.12					
	(U)		7.77	0.46	2.0×10^{-12}	23.4	1.2×10^{-9}
	1st	+0.042	5.45	0.32	2.14×10^{-3}	10.74	0.88
2.45×10^{-3}	2nd	−1.27	3.90	0.23	7.0×10^{-8}	10.86	2.9×10^{-5}
1.3×10^{-2}	1st*	−1.033	5.53	0.33	2.6×10^{-9}	18.95	1.1×10^{-6}
(B) $NaDDBSO_3$							
3×10^{-3}	1st	−0.21	5.54	0.33	6.9×10^{-5}	12.8	4.1×10^{-2}
	2nd	−1.08	4.5	0.27	1.7×10^{-8}	17.8	7.0×10^{-6}
4.7×10^{-2}	2nd(L)	−1.33					
	(U)		6.0	0.36	1.0×10^{-11}	22.22	5.9×10^{-9}

The resulting values of the transfer coefficient α reveal the irreversibility of the reduction process occurring along the first wave ($\alpha = 0.42$); on the other hand α increases from 0.24 to 0.46 along the lower and upper portions of the second wave. Accordingly, the process of reduction takes place more irreversibly along the lower part and becomes less as the potential becomes more negative. It is also evident that the rate constants k_0 decrease with the increase of pH, while ΔG^* increases in the same direction. This is in favour of the fact that the process of reduction becomes more difficult as the pH of the solution increases.

The effects produced by increasing the concentration of the three surfactants on the electroreduction of V(V) in this medium are represented by the polarograms shown in figures 4 (A, B and C).

The results produced by DDA^+ and $DDBS^-$ ar quite similar and differ from those of T.X—100. The retarding effects produced in the presence of T.X—100 are attributed to blockage of the electrode surface by an adsorbed film of the nonionic surfactant.

The effects produced by the presence of $DDBS^-$ are restricted to the first wave; the second wave being unaffected, DDA^+ causes never effect on the reduction behaviour of V(V) in this medium.

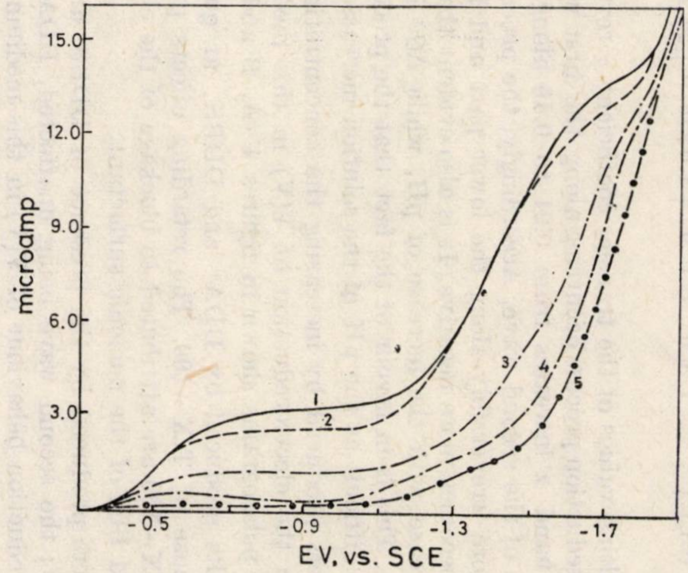

Fig. 4(A). — Effect of T.X.-100 on 3.2 mM V(V) in universal buffer solution of pH 11.8.

Curve	1	2	3	4	5
SAS%	0.00	2.5×10^{-4}	2.45×10^{-3}	5.75×10^{-3}	1.3×10^{-2}

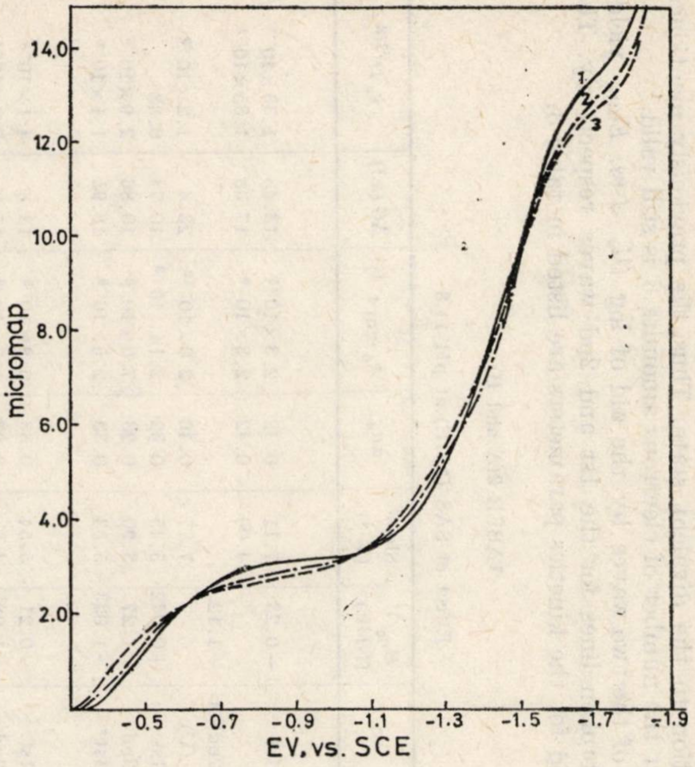

Fig. 4(B). — Effect of $DDAClO_4$ on 3.2 mM V(V) in universal buffer solution of pH 11.8.

Curve	1	2	3
SAS%	0.00	2×10^{-3}	6×10^{-3}

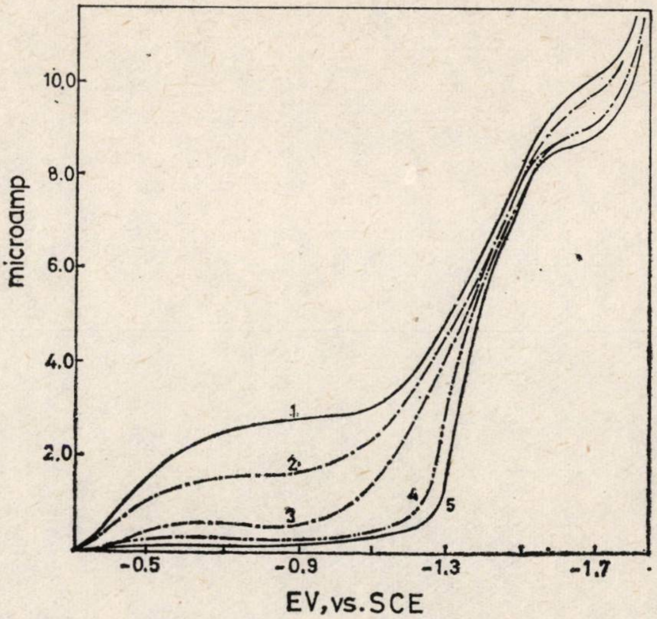

Fig. 4(C). — Effect of $NaDDBSO_3$ on 3.2 mM V(V) in universal buffer solution of pH 11.8.

Curve	1	2	3	4	5
SAS%	0.00	3×10^{-3}	7×10^{-3}	2.3×10^{-2}	4.7×10^{-2}

REFERENCES

[1] I. M. Kolthoff and J. J. Lingane, "Polarography", vol. 11, Interscience Publishers, New York, 1955, p. 447—52.

[2] S. Zeltzer, *Coll. Czech. Chem. Comm.*, **4**, 319 (1932).

[3] M. von Stackelberg, P. Klinger, W. Koch and E. Krath, *Tech. Mitt. Krupp Forschungsher*, **2**, 59 (1939).

[4] G. Thanheiser and J. Williams, *Arch. Eisenhuttenw*, **13**, 73 (1939).

[5] M. Voriskova, *Coll. Czech. Chem. Comm.*, **11**, 588 (1939).

[6] J. J. Lingane, *J. Amer. Chem. Soc.*, **67**, 182 (1945).

[7] J. J. Lingane and L. Meites, *J. Amer. Chem., Soc.*, **69**, 1021, 1882 (1947) ; **70**, 2525 (1948).

[8] A. L. Vogel, "A Text Book of Quantitative Inorganic Analysis", 2nd Edition Longman, London, 1951, p. 381.

[9] I. M. Issa and M. Tharwat, *Electrochim. Acta*, **17**, 343 (1972).

[10] I. M. Issa, M. M. Ghoneium, A. A. El-Shamy and M. Tharwat, *Electrochim. Acta*, **17**, 1251 (1972).

[11] A. N. Frumkin, *Zhur. fiz. Khim.*, **24**, 244 (1950).

Revue Roumaine de Chimie, 26, *3*, 503—505 (1981)

COMPTES RENDUS

V. PĂRĂUŞANU, M. COROBEA and G. MUSCA, "Economia hidrocarburilor" (The Economics of Hydrocarbons), vol. I. Ed. Ştiinţifică şi Enciclopedică, Bucharest, 1980, 550 p. and 10 diagrams.

Issued at a time dominated by the energy and raw material shortage the book fills a gap in chemical literature and synthesizes the points of view of well known scientists. This shortage, which turned out to be a world problem, affects oil importing as well as exporting countries, no matter what their economic, social and political system, given the ever increasing interdependence of national economies within the unity of world market. In the book it is shown that, under present circumstances, no nation, regardless of its potential and level development, can escape the direct or indirect effects of world energy crisis. All the phenomena specific to our times account for the general interest of all countries, be they large or small, in rapid and efficient actions directed towards rational utilization of existing resources and towards the discovery of new alternative energy sources. The analysis of all these reasons shows that, according to all programs of development and energy consumption, the priority is the economy of energy such as at lower energy consumption the same or even higher economic effects are obtained.

The book emphasizes the outstanding importance of research and utilization of alternative energy and raw material sources ; this is imposed by the exhaustible, nonregenerative character of primary energy classical sources i.e. crude oil, natural gas and coal. However, industrial utilization of alternative sources is still kept at low pace by the technologic potential required which still rises unsolved problems at the present level of consumer's needs. Chemical industry is among the greatest primary energy consumers in Romania and therefore its strategy of development has focused careful consideration. Utilization and reassessment of primary energy in chemical industry will influence ever stronger the rhythm and level of development of national economy since chemistry has always been a great primary energy consumer (as raw material or utilities) and yet a supplier of raw material for other industries and of commodities. The spectacular development of Romanian economy during the scientific-technical revolution in conditions of world energy and raw material crisis requires the increase of energy potential of the nation by enlargement of existing mineral raw material and energy resources, their more efficient and rational utilization.

The book divided in four parts presents technical and economic data regarding the directions of C_1-C_5 hydrocarbons higher utilization, the synthesis of substitution gases and some intermediate products of chemical industry from coal. The authors contribute to the general effort by presenting the data in literature which may be useful to researchers, designers, producers and mostly to executives who assume the difficult though important task of orienting the future development of our economy.

The first part of the book specializes in general economic considerations regarding the world production and consumption of primary energy. A review of the world energy consumption, of the evolution of primary energy resources, of the dynamics of energy consumption and its structural change, of the interdependence energy consumption — economic development of contemporary society is followed by a discussion of the development of scientific investigation and the search for new sources of primary energy. A brief outline is presented of the main nonconventional forms of primary energy which are considered as possible future suppliers of of energy as solar energy, hydrogen, nuclear energy, geothermal energy, aeolian energy, the energy of tides, the thermal energy of the ocean and the energy of water falls. The first part the books is concluded with foreknowledge about energy research and industrialization, prospects and estimates of the energy policy of our country and of chemical industry development.

The second part which deals with the economics of methane (the natural gas) provides at first a review of gas reserves and consumption the world over and of the economic characteristics of natural gas production. The economics of chemical processing of gas is emphasized ; it yields products as : methanol, formaldehyde, synthesis gas, ammonia, acetylene and derivatives. From the very beginning, the authors underline that, according to the modern concepts, the components of natural gas may be integrally utilized in technology and the economic efficiency of this utilization depends primarily on the yield of transformation of those components in useful products.

The trends of utilization of C_2-C_5 hydrocarbons in associated gases are the subject of the third part of the book. The associated gas includes all fractions of natural and refinery hydrocarbons which also contain C_1-C_5 hydrocarbons. These hydrocarbons are the main source of raw materials for the petrochemical industry and for synthesis chemistry in general. Chemical processing of these raw materials yields a wide range of polymers, resins, man-made fibres and elastomers. Inclusion in this part of C_4-C_5 fractions which result from primary processing of crude oil aims at achieving a unitary presentation of potential C_2-C_5 hydrocarbons sources and their utilization.

The final part of the book specializes in gases, hydrocarbons and substitution raw materials originating in coal. As the authors show, the extending of coal consumption to enlarge the variety of substitution products and sustain the rising rhythm of consumption of monomers, polymers, man-made fibres, synthetic rubber, fertilizers and low tonnage products requires technological and energy integration of coal chemical processing and of primary processes of nuclear energy utilization. Special attention is awarded to prospective technologies regarding coal chemical processing since our country possesses carbochemical raw materials resulted from metallurgical coke production, materials whose utilization allows further development of fine synthesis of low and medium tonnage. The book is provided with an extensive bibliography.

D. I. Marchidan

S. R. MORRISON, "The chemical Physics of surfaces", Plenum Press, New York and London 1977, 415 pages.

In the last years, surface science has been the subject of a spectacular development. More and more realistic models are advanced to account for physical and chemical properties of solid surfaces. These confer some interdisciplinary features to surface science.

In his book, S.R. Morrison presents an original synthesis of these two aspects of surface science : surface physics and surface chemistry. This is also the explanation of the book title.

The book is divided into ten chapters.

In the first one — an introduction to subject — the concepts of surface states and surface sites, their relation to chemical and physical representation of surfaces, the types of bonding of foreign species are discussed.

Section two is devoted to the analysis of space charge effects and to electrons and holes transport in solids from the bulk to the surface.

The experimental methods presented in the third chapter are divided into three groups : electrical measurements, surface spectroscopies and specific chemical techniques, according to the way and type of information obtained on the surface states.

The discussion of the adsorbate free surface — the aim of chapter 4 — is centred on the theoretical — semiclassical and quantum-models describing the clean solid surface as well as on experimental results concerning its different properties.

The next sections of the book are concerned with the behaviour of foreign species on solid surfaces and their influence on the chemical and physical properties of surfaces.

Present state of quantuum theories describing the bonding of foreign species to surfaces is shortly but clearly presented in chapter 5 together with the experimental results on some systems. The emphasis is put on describing energy levels associated with steady state.

A very interesting insight of great practical value in this field is the formation of real surfaces and the control of surface properties by using additives. Phenomena like surface activation, surface passivation and systems like metal-support and doped semiconductors are also analysed in this new chapter.

A concise description of adsorption emphasizing the models for different types of gas-solid adsorption is given in chapter 7. Chapter 8 is devoted to solid-liquid interface especially to semiconductor — electrolyte systems. The differences and similarities between solid-liquid and solid-gas systems are discussed.

In the next section the photoeffects at semiconductor surfaces — in which field author's contributions are well known for long time — are thoroughly presented.

The enlightening discussions of surface sites and their role in heterogeneous catalysis, analysis of some examples of the mechanism of catalytic reactions are the subjects of the last chapter.

The book is fluently and clearly written insisting on the basic concepts in surface science. The way in which this rich material is presented gives not only a deep view in the surface phenomena but also a method to guide a surface chemist in getting new experimental and theoretical insights in this field.

M. I. Vass and N. I. Ionescu

NOTE POUR LES AUTEURS

La Revue Roumaine de Chimie publie des articles en anglais, français, russe, allemand ou espagnol. Les auteurs sont priés d'envoyer des articles et des comptes rendus inédits.

Les manuscrits seront dactylographiés à deux intervalles. La bibliographie, les tableaux et la légende des figures seront placés après le texte.

Si l'article fait partie d'une série numérotée, le titre de la partie précédente sera indiqué dans une note au bas de la première page.

Chaque article sera précédé d'une résumé comprenant quinze lignes au maximum.

Les références bibliographiques dans le texte seront faites par des exposants sans parenthèses et paraîtront à la fin de l'ouvrage.

Les publications périodiques mentionnées dans la bibliographie seront présentées suivant les prescriptions internationales : le nom de l'auteur précédé de l'initiale du prénom, le titre du périodique abrégé conformément à « Chemical Abstracts » et souligné par une ligne, le numéro du tome indiqué par des chiffres arabes et souligné par deux lignes, suivi de la première page de l'article ; à la fin, l'année de la parution sera placée entre parenthèses. Le numéro de la revue ne sera pas indiqué, si les pages du volume sont numérotées consécutivement.

Les textes des livres ou traités incluront : le nom des auteurs, les initiales du prénom, le titre du livre entre guillements et sans être souligné, le numéro du tome précédé par l'abréviation « vol. » (ou « Bd. »), le numéro de l'édition, les éditions (the publisher), la localité de la parution du livre, l'année de la parution et la page de la référence précédée par l'abréviation «p. » (ou « S. »).

Les brevets seront indiqués comme suit : l'auteur ou la firme, le pays et le numéro du brevet, la date et la revue (Chem. Abstr.). Par ex. : M. Jones (to Union Carbide Co), Brit. Pat. 601—238, 2 Sept. 1959, *Chem Abstr.*, **54**, 12808 (1960).

Si la référence n'a pas été lue en original, on indiquera aussi la revue de références consultée.

Les diagrammes seront tracés à l'encre de Chine sur papier calque. Les tableaux et les figures (en nombre strictement nécessaire) seront numérotés par des chiffres arabes. Les courbes dans les figures seront numérotées par des chiffres arabes et leur explication sera donnée dans la légende des figures. Prière de ne pas inscrire les mêmes données dans les tableaux et dans les figures. Chaque tableau aura un titre. On indiquera dans le texte la place approximative des tableaux et des figures. Les formules chimiques seront incluses dans le texte ; en outre, elles seront transcrites sur papier calque, à l'encre de Chine.

Les auteurs sont priés d'indiquer les caractères italiques (en soulignant les lettres au crayon), ainsi que tout autre caractère spécial ; les préfixes *ortho, meta, para, cis, trans,* etc. seront soulignés pour indiquer leurs caractères italiques et ne seront jamais écrits avec des majuscules.

Aucune correction à la main ne sera admise sur le manuscrit. Les corrections seront frappées à la machine. Les lettres grecques ou autres symboles spéciaux seront insérés à la main à l'encre clairement.

Le manuscrit sera signé par l'auteur.

Le colonne-titre aura 50 lettres au maximum.

L'entière responsabilité du contenu des articles appartient aux auteurs.

Pour détails voir le n^0 1 (1981).

PRINTED IN ROMANIA

TRAVAUX PARUS AUX ÉDITIONS DE L'ACADÉMIE DE LA RÉPUBLIQUE SOCIALISTE DE ROUMANIE

ELENA CEAUŞESCU, **Polimerizarea stereospecifică a izoprenului** (La polymérisation stéréospecifique de l'isoprène), 1979, 307 p.

CR. SIMIONESCU, VALERIA GORDUZA, **Polimeri biocompatibili şi biologic activi** (Polymères biocompatible et biologiquement actifs), 1980, 497 p.

M. FLORESCU, **Metode ştiinţifice în dezvoltarea industriei chimice moderne** (Méthodes scientifiques dans le développement de l'industrie chimique moderne), 1979, 256 p.

Ş. MOLDOVEANU, A. SAVIN, **Aplicaţii în chimie ale metodelor semi-empirice de orbital moleculari** (Applications en chimie des méthodes semi-empiriques d'orbitaux moléculaires), 1980, 286 p.

A. T. BALABAN, L. GĂLĂŢEANU, G. GEORGESCU, LIGIA SIMIONESCU, **Compuşi marcaţi şi radiofarmaceutici cu aplicaţii în medicina nucleară** (Composés marqués et radiopharmaceutiques à application en médecine nucléaire), 1979, 495 p.

I. G. MURGULESCU, E. SEGAL, **Introducere în chimia fizică**, Vol. II.1. **Teoria molecular-cinetică a materiei** (Introduction à la chimie physique Vol. II 1. La théorie moleculaire-cinétique de la matière), 1979, 1003 p.

I. E. TEODORESCU, M. FITI, **Iradierea tehnologică** (L'Irradiation technologique), 1979, 216 p.

S. STERNBERG, FL. DANEŞ, **Termodinamica chimică aplicată** (La thermodynamique chimique appliquée), 1978, 400 p.

I. G. MURGULESCU, V. EM. SAHINI, **Introducere în chimia fizică**. Vol. I.2. **Structura şi proprietăţile moleculelor** (Introduction à la chimie physique, Vol. I, 2. La structure et les propriétés des molécules), 1978, 604 p.

C. DRĂGULESCU, E. PETROVICI, **Chimie structurală modernă. Chimia coordinaţiei 8** (La chimie structurale moderne. La chimie de la coordinence 8), 1977, 947 p.

D. PURDELA (sous la direction de), **Nomenclatura chimiei anorganice** (La nomenclature de la chimie inorganique), 1977, 153 p.

I. ZUGRĂVESCU, MAGDA PETROVANU, **N-Ylid chemistry**, 1977, 396 p.

D. NEGOIU, ANGEL KRIZA, **Poluanţi anorganici în aer** (Polluants inorganiques dans l'air) 1977, 220 p.

I. G. MURGULESCU, **Introducere în chimia fizică** Vol. I.1. **Atomi, molecule, legătură chimică** (Introduction à la chimie physique, 1er vol. I. Atomes, molécules, liaison chimique), 1976, 560 p.

E. P. BALTĂ, E. BALTĂ, **Introduction to the physical chemistry of the vitreous state**, coédition avec Abacus Press, 1976, 287 p.

I. I. GĂLĂŢEANU, **Radiochimia aplicată. Metode şi probleme** (La radiochimie appliquée. Méthodes et problèmes), 1976, 307 p.

CONST. V. UGLEA, **Cromatografia pe gel permeabil. Noi domenii de aplicare** (La chromatographie sur gel perméable. Nouveaux domaines d'application), 1976, 123 p.

CONST. GH. MACAROVICI, D. MACAROVICI, **Chimia oxizilor dubli şi utilizările lor** (La chimie des oxydes doubles et leur utilisation), 1975, 195 p.

ELENA CEAUŞESCU, **Research work on synthesis and characterization of macromolecular compounds. Contributions**, 1974, 251 p.

CR. SIMIONESCU, VIORICA RUSAN, V. POPA, **Chimia algelor marine** (La chimie des algues marines), 1974, 212 p., 1 pl.

I. P. Informaţia c. 2780

43 426

Lei 25.

$ 55 (pour un abonement annuel)

F 1103

REFERÁLVA

R

ACADÉMIE DE LA RÉPUBLIQUE SOCIALISTE DE ROUMANIE

REVUE ROUMAINE DE CHIMIE

TOME 26
N° 4
Avril 1981

EDITURA ACADEMIEI REPUBLICII SOCIALISTE ROMÂNIA

Rev. Roumaine Chim.

RRCHAX, 26, 4, p. 507–656 (1981), Bucarest

ACADÉMIE DE LA RÉPUBLIQUE SOCIALISTE DE ROUMANIE

COMITÉ DE RÉDACTION

Rédacteur en chef :

I. G. MURGULESCU, membre de l'Académie de la République Socialiste de Roumanie

Rédacteurs en chef adjoints :

A. T. BALABAN et V. EM. SAHINI, membres correspondants de l'Académie de la République Socialiste de Roumanie

Collège de rédaction :

EM. BRATU, ELENA CEAUȘESCU, ECATERINA CIORĂNESCU-NENITZESCU, CR. SIMIONESCU, membres de l'Académie de la République Socialiste de Roumanie ; P. SPACU, membre correspondant de l'Académie de la République Socialiste de Roumanie ; MARGARETA AVRAM, M. BANCIU, I. HAIDUC, D. I. MARCHIDAN, I. MOLDOVAN, G. NIAC et D. SĂNDULESCU

La Revue Roumaine de Chimie paraît 10 fois par an. Toute commande de l'étranger pour les travaux parus aux Editions de l'Académie de la République Socialiste de Roumanie sera adressée à ILEXIM, Departamentul Export-Import Carte (Livres)/Departamentul Export-Import Presă (Revues), P.O.B. 136—137, télex 11226, 3, str. 13 Decembrie, 79517 Bucarest, Roumanie

Les manuscrits, les livres et les revues proposés en échange ainsi que toute correspondance seront envoyés à la rédaction :

REVUE ROUMAINE DE CHIMIE

125, Calea Victoriei, 79717 Bucarest, Roumanie, téléphone 50 76 80

EDITURA ACADEMIEI REPUBLICII SOCIALISTE ROMÂNIA
125, Calea Victoriei, 79717, Bucarest, Roumanie, téléphone 50 76 80

ORSZÁGOS MŰSZAKI KÖNYVTÁR ÉS DOKUMENTÁCIÓS KÖZPONT 1983

REVUE ROUMAINE DE CHIMIE

Tome 26, N° 4 **Avril, 1981**

ELENA CEAUŞESCU, R. BORDEIANU, IRINA CERCHEZ, MARIA BĂLĂNESCU and P. GHIOCA, Kinetics of anionic polymerization of butadiene and styrene with organolithium catalysts in toluene 509–520

JOSETTE WEINBERG and V. EM. SAHINI, Xylidine isomers. V. Molecular complex spectra of iodine with xylidines 521–526

RODICA VÎLCU and A. CIOCHINĂ, Absolute measurement of thermal conductivity and thermal diffusivity of liquids by classical procedure of the transient hot-wire method . . . . 527–537 R

F. SEOANE, Temperature effect on the kinetics of the α-chimotrypsin-catalyzed hydrolysis of the ethyl ester of N-benzoyl-L-tyrosine (in Spanish) 539–543

R. DINESCU and M. V. CERCHEZ, Kinetics and reaction mechanism of chemical compounds in mixtures belonging to the $Na_2O-CaO-Al_2O_3-SiO_2-CO_2$ system (in German) . . . . 545–564 R

R. SWAMY, H. S. YATHIRAJAN and D. S. MAHADEVAPPA, Kinetics and mechanism of oxidation of phenyl allyl alcohol by sodium N-chloro-benzene sulphonamide in hydrochloric acid medium 565–574

GH. MARCU, CS. VÁRHELYI, MAGDA SOMAY and DANA AVRAMESCU, New cobalt (III) complex compounds with methylisopropyl-glyoxime (in German) 575–585

MARIA MARC and ANA UNGUREANU, Nickel (II) and manganese (II) complexes of cystine 587–591

IOAN MOŢOC and ALEXANDRU T. BALABAN, Topological indices: intercorrelations, physical meaning, correlational ability . . . . 593–600 Bo

A. ESSAWY, M. ABDALLA and A. DEEB, Some reactions with Michael adducts of bromobenzoyl acrylic acid and its amides 601–610

R. BACALOGLU, A. CHICU, ILSE BACALOGLU and L. COTARCĂ, Nucleophilic substitutions at carbonic acid derivatives. XVIII. Kinetics and mechanism of the alcoholysis of N,N,N′-trisubstituted carbonic acid chloramidines (in German) 611–621

S. H. DOSS and F. A. RASHID, Identification of two organic sultam compounds 623–627

Revue Roumaine Chim. **26**, *4*, 507–656 (1981) Bucarest

F. BADEA, ALICE MARIE GLATZ and A. C. RĂZUŞ, Ring opening in benzo[b]bicyclo [3.1.0] hexyl cations 629–637

M. ANWAR, Reactions of some 4(3H) quinazolinones 639–645

M. EL-DEEK, M.A.I. SALEM, A. A. HAMED and M. SAMAAN, Studies on pyridones. I. Synthesis and reactions of 3-acetyl-(3,4-dichlorophenyl)-2-(1H)-pyridones 647–653

BOOK REVIEWS 655–656

Revue Roumaine de Chimie, **26**, *4*, 509–520 (1981)

KINETICS OF ANIONIC POLYMERIZATION OF BUTADIENE AND STYRENE WITH ORGANOLITHIUM CATALYSTS IN TOLUENE

ELENA CEAUȘESCU, R. BORDEIANU, IRINA CERCHEZ, MARIA BĂLĂNESCU
and P. GHIOCA
Chemical Research Institute ICECHIM, 202 Splaiul Independenţei, Bucharest, Romania

Received October 7, 1980

The kinetics of anionic polymerization of butadiene and styrene initiated with *sec*-butyllithium was investigated in toluene. In both cases the propagation step was found to be first-order to monomer concentration. Fractional reaction orders to catalyst concentration were found, i.e. 0.5 for styrene and 0.3 for butadiene propagation, respectively. The activation energies are 15,200 cal.mole^{-1} for styrene and 24,400 cal. mole^{-1} for butadiene.

1. INTRODUCTION

The anionic polymerization of butadiene and styrene with organolithium catalysts in hydrocarbons is widely used for the synthesis of a range of polymers and copolymers of increasing importance such as, in the first place, polybutadiene and butadiene-styrene thermoplastic rubbers. The point can be stressed by mentioning that, at present, about one million tons of polymers are being produced annually by anionic processes in more than 20 industrial plants.[1]

However, the polymerization kinetics of butadiene and styrene by anionic mechanisms is not yet fully understood.[2,3] There is no consensus as regards the order of the propagation step on catalyst concentration (at least for the polymerization of butadiene) and the existing data on the activation energies are few and inconclusive.

In the present paper we shall present the results of our studies on the polymerization kinetics of butadiene and styrene with *sec*-butyllithium catalyst in toluene. The catalyst used was *sec*-butyllithium since its rate of initiation in hydrocarbon solvents is considerably faster than that of many other organolithium compounds.[4,5] The propagation step can thus be investigated without unwanted interference from the initiation step.

The solvent is also an important factor, determining (at constant temperature) the rate of propagation. For any given monomer the rates are higher in aromatic than in alifatic solvents, increasing in the following series :[4]

cyclohexane < *n*-hexane < benzene < toluene

Toluene is an easily available solvent, very useful for the synthesis of polybutadiene and butadiene-styrene copolymers, since it is a good solvent for polystyrene as well as for polybutadiene. In contrast to benzene or alifatic or cycloalifatic hydrocarbons, in toluene a transfer to solvent may occur consisting in a metallation of the methyl group leading to benzyllithium:

$$C_6H_5-CH_3+R-Li \rightarrow C_6H_5-CH_2-Li+R-H$$

Benzyllithium is a very active polymerization catalyst, capable of initiating a new chain. The results of the kinetic studies on the polymerization of styrene or methoxystyrenes in toluene were questioned by Fetters on account of a probable transfer to solvent.[3] However at moderate temperatures, the rate of the transfer reaction is so low ($4.7\times10^{-7} l\cdot mol^{-1}\cdot s^{-1}$ at 60°C[6]) that it can be safely neglected. Even if a small transfer is allowed for, the overall formal kinetics of the polymerization reaction remains virtually unchanged since, as already mentioned, the benzyllithium resulted from the transfer reaction is a very fast initiator.

A fairly large amount of consistent experimental data seem to indicate that the propagation rate of styrene in hydrocarbons is half-order to catalyst and first-order to monomer. A summary of the available data can be found in the excellent review by Morton and Fetters.[3] The following kinetic scheme was proposed based on the assumption that the polymerization takes place only on active unimeric chains resulting by dissociation of dimeric aggregates, the latter assumed to be inactive:[7,8]

$$(P-Li)_2 \overset{K_d}{\rightleftarrows} 2\,P-Li$$

$$P-Li+M \xrightarrow{k_p} P-Li$$

where P is a polymer chain, M is a monomer molecule, K_d is the dissociation constant of dimeric aggregates to active unimers and k_p is the actual rate constant of the propagation step. Consequently the overall polymerization rate should be given by the following equation:

$$-\frac{d[M]}{d\tau}=k_pK_d^{1/2}[(P-Li)_2]^{1/2}[M]\approx\frac{k_pK_d^{1/2}}{\sqrt{2}}[P-Li]^{1/2}[M] \qquad (1)$$

The above kinetic scheme is based on the half-order of the polymerization reaction to catalyst determined experimentally and on the association of the P—Li molecules in pairs established beyond any doubt by very precise viscometric measurements.[9,10]

Very recent kinetic studies have shown[11] that in the polymerization of styrene in the presence of ethers such as anisole, diphenylether or tetrahydrofuran, the reaction order to catalyst remains constantly one-half while the degree of association of polystyryllithium chains decreases considerably due to the coordination of the active chain-ends with the Lewis bases. This very conclusively demonstrates that a direct correlation between the degree of association and the reaction order is not justified.

Even less realistic is the kinetic scheme mentioned above when applied to the polymerization of dienes in hydrocarbons. The degree of association of polyisoprenyllithium and polybutadienyllithium chains in hydrocarbon solvents was convincingly demonstrated to be two[9] while the reaction order to catalyst, although still uncertain, was found to be in any case considerably lower than 1/2. Thus, it can be stated that at present there is no reason to establish a link between the reaction order to catalyst and the degree of association of the growing chains.[12] Consequently, the mechanisms suggested by Brown,[16, 17] and involving a direct reaction of the monomer with the associate active chains, would seem to be valid.

In the present paper we would therefore not attempt to correlate our experimental data with a kinetic scheme, restricting our discussion to a formal kinetic treatment.

In the specific case of styrene and butadiene polymerization with lithium-based catalysts in toluene, the kinetic data published in the open literature are very scarce. In Table 1 an attempt was made to summarize available information, recalculating the values of frequency factors and even sometimes the activation energies where not explicitely given from data included in the respective references. It can be seen that, especially in the case of butadiene polymerization, there are rather wide discrepancies between the kinetic parameters determined by various investigators or calculated from their data. A possible explanation lies in the fact that kinetic studies are rendered difficult by the very high purity requirements of anionic polymerization.

TABLE 1

Kinetic Parameters of the Propagation Step in the Polymerization of Styrene and Butadiene by Anionic Mechanism with Organolithium Catalysts in Toluene

Monomer	Frequency Factor	Activation Energy cal. mol^{-1}	Temperature °C	Reaction Order to monomer	Reaction Order to catalyst	Ref.
Styrene	(4.22×10^{9})*)	14000	33–47	1	(1/2)	13
	(1.02×10^{8})*)	11600	60–72	1	(1/2)	13
	(3.1×10^{9})*)	13600		1	(1/2)	14
Butadiene	(7.4×10^{9})	(15300)		1	1/3	13
	(6.35×10^{12})	19600	40–60	1	0.298	15
	(6.7×10^{14})	22500	<30	1	0.196	15

( ) Calculated from data given in reference
*) Calculated assuming a half-order to catalyst concentration.

2. EXPERIMENTAL

The polymerizations were carried out in a jacketed Pyrex glass reactor equipped with a magnetic stirrer.

The reaction mixture was thermostated by circulating distilled water from a Wobser Ultrathermostat through the reactor jacket. The temperature inside the reactor was measured with a calibrated thermocouple and continously recorded by an electronic potentiometer. The temperature was kept at the prescribed value within a ± 0.1° interval.

Butadiene (Fluka pss. grade) was purified by distillation directly from the original steel cylinder and dried by passing it in vapor phase through a tower containig activated alumina (Rhône-Poulenc). In order to remove the acetylenic impurities, gaseous butadiene was then passed through a tower filled with activated finely divided copper deposited on a carrier (BTS catalyst-BASF). The monomer was then condensed in a jacketed vial cooled with brine at −20°C. Liquid butadiene was treated with *n*-butyllithium at 0°C for the final removal of all traces of reactive impurities. Immediately before use the monomer was distilled into the solvent charged in the reactor. The amount of butadiene charged was determined gravimetrically.

Styrene (Petrochemical Works Borzeşti — polymerization grade) was distilled in vacuum at 10 torr on a Vigreux column and then treated under argon with *sec*-butyllithium until the development of a faint red color indicating the consumption of all of the reactive impurities and the formation of polystyryllithium. During the addition of *sec*-butyllithium, a vigorous stirring was maintained by bubbling purified argon throught the monomer. The purified monomer was then flash distilled again at 10 torr residual pressure immediately before use.

The solvent (toluene, Petrochemical Works Brazi, polymerization grade) was purified on a system of 3 distillation columns operated continuously. At the top of the first column most of the water contained in the solvent was removed as water-toluene binary azeotrope. In the second column the components lighter than toluene were separated and the bottom product was fed to the third column from which pure toluene was collected as distillate, the heavy components being removed from the still of the column. The last column in the series was kept under a stream of purified argon. The solvent purified as above was then percolated slowly through a tower containing activated alumina for a final drying. Before use the toluene was refluxed for one hour over molten sodium on a Vigreux column and then flash distilled.

The catalyst (*sec*-butyllithium) was synthesized from 2-chlorobutane (Merck) and a dispersion of lithium metal (Lithium Corp. of America) in hexane (Merck). Catalyst concentration (usually 0.7 M) was determined by double titration (Gilman-Haubein).

All of the preparatory operations as well as the polymerization reactions were performed under a blanket of argon purified by passing through a tower with activated alumina and BTS- catalyst (BASF) in series for the retention of moisture and traces of oxygen.

Before each polymerization reaction the reactor was repeatedly evacuated and purged with purified argon at elevated temperature. After cooling the walls of the reactor were washed with a solution of polystyryllithium in order to eliminate all the traces of reactive impurities. The solvent and monomer were then charged under argon. The temperature of the solution was adjusted to the prescribed value by circulating thermostated water through the reactor jacket. Finally, the polymerization reaction was initiated by injecting the necessary amount of catalyst through a septum into the reactor.

The progress of the reaction was followed by determining the conversion at certain time intervals. The conversions were measured gravimetrically by precipitating the polymer contained in a 20 to 30 g aliquot with methanol containing a small amount of phenyl-β-naphthylamine and drying to constant weight in vacuum at 40°C.

The polymers obtained were characterized, after completion of the reaction, by membrane osmometry (Stabin-Shell osmometer, Hallikainen) in toluene at 30°C. Number-average molecular weights ($\overline{M}_n$) thus determined were in general within ±10% of the stoichiometric (kinetic) average molecular weights ($\overline{M}_s$) given by the ratio:

$$\overline{M}_s = \frac{\text{grams of monomer}}{\text{mols of catalyst}} \tag{2}$$

When larger differences between M_n and M_s were found, the effective catalyst concentration was recalculated from $\overline{M}_s$, using eq. (2).

All of the polymerizations of styrene and some of the polymerizations of butadiene were performed isothermally, such as to keep the temperature of the mixture at the preset value with an accuracy of ± 0.2°C. In some other butadiene polymerizations the temperature was varied in steps during the same experiment. In each step the temperature was held constant but at a value different from that of the other steps. In that mode of operation, each temperature step could be considered as an independent isothermal polymerization since anionic polymerizations with organolithium catalysts in hydrocarbons proceed through living polymers and the concentration of active chain ends remains virtually constant. If at the beginning of the n-th step the fractional conversion is x_n and at the end of the same step the conversion is x_{n+1}, then the partial conversion x' within the n-th step is given by :

$$x' = \frac{x_{n+1} - x_n}{1 - x_n} \tag{3}$$

3. RESULTS AND DISCUSSION

3.1. STYRENE POLYMERIZATION

3.1.1. Reaction Order to Monomer

In figure 1 the conversion was plotted against time for two of the polymerization reactions. The linearity of the plots indicates that the polymerization of styrene is first-order to monomer concentration :

$$-\frac{d[S]}{d\tau} = k_I[S] \tag{4}$$

where [S] is styrene concentration (mol.l^{-1}), τ is time (min), and k_I is the rate constant of the first-order reaction (min^{-1}).

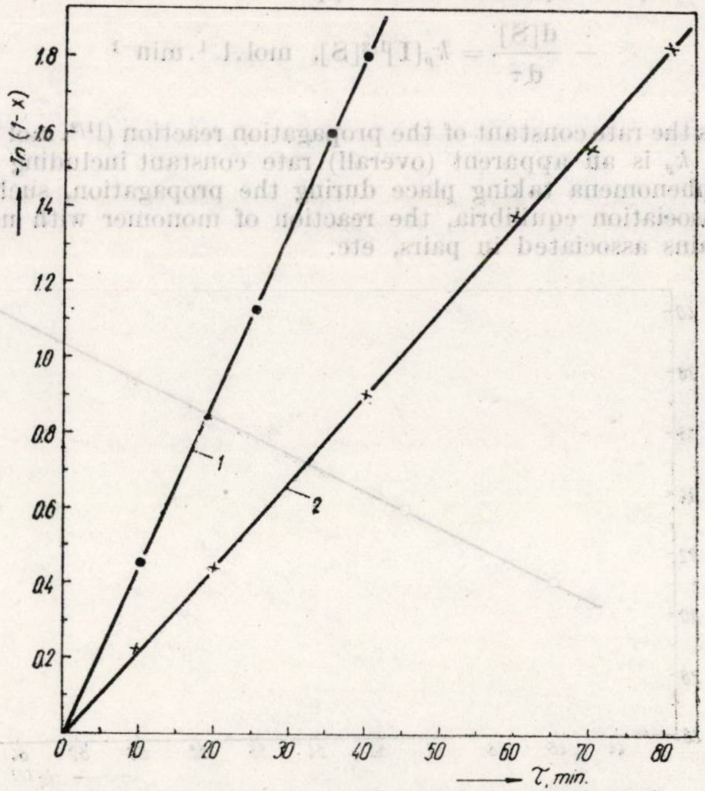

Fig. 1. — Plot of conversion vs. time in styrene polymerization 1.(●) t = 30°C, [I] = 10^{-2}M ; 2.(+) t = 30°C, [I] = 2.28×10^{-2}M.

By integrating Eq. (4) and simple transformations one gets

$$\ln(1-x) = k_{\mathrm{I}}\tau \tag{5}$$

It can be seen that the experimental points lie well on straight lines according to Eq. (5). Also, the absence of an induction period can be remarked, confirming thus the very fast initiation of the polymerization reaction achieved by using *sec*-butyllithium as catalyst.

3.1.2. Reaction Order to Catalyst

In order to determine the reaction order to catalyst concentration, a series of polymerizations were carried out at constant temperature and at the same initial monomer concentration. By plotting in a log-log diagram the rate constant of the first-order reaction (k_{I}) against catalyst concentration a straight line with the slope 0.5 was obtained (see Fig. 2). This confirms the data of other investigators who found a half-order to catalyst concentration in the anionic polymerization of styrene with organolithium catalysts.[2,3,8,11,13,18]

It follows that the rate of polymerization of styrene can adequately be described by an equation of the type:

$$-\frac{d[S]}{d\tau} = k_p[I]^{1/2}[S], \quad \mathrm{mol.l^{-1}.min^{-1}} \tag{6}$$

where k_p is the rate constant of the propagation reaction ($\mathrm{l^{1/2}.mol^{-1/2}.min^{-1}}$) Obviously k_p is an apparent (overall) rate constant including the whole range of phenomena taking place during the propagation, such as association-dissociation equilibria, the reaction of monomer with unimers or active chains associated in pairs, etc.

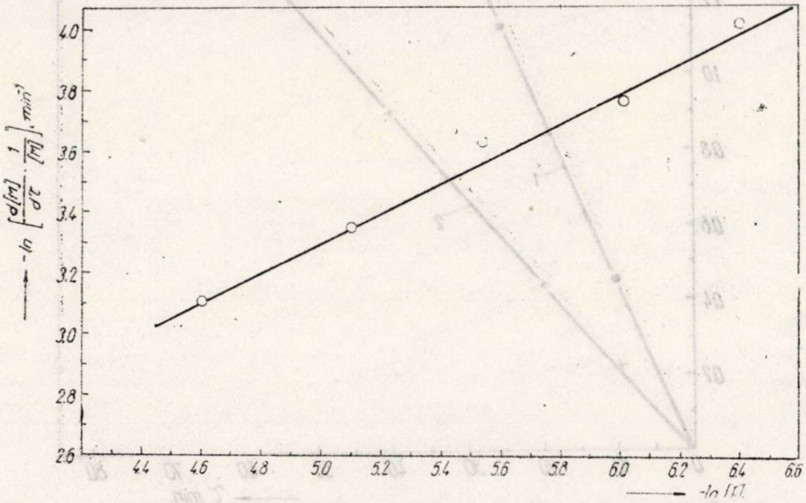

Fig. 2. — Dependence of first-order rate constant on catalyst concentration in styrene polymerization : $t = 30°\mathrm{C}$, $[S]_0 = 1.73$ M.

3.1.3. Activation Energy of the Propagation Step

The activation energy of the propagation step was determined from data gathered in polymerizations performed isothermally. By calculating for each temperature the value of the rate constant from Eq. (6) and plotting k_p against $1/T$, the activation energy, E_p, is given by the slope of the straight line assuming that the temperature effect on k_p is adequately expressed by an Arrhenius-type equation:

$$k_p = A \exp\left(-E_p/RT\right) \tag{7}$$

i.e.

$$\ln k_p = \ln A - \mathrm{E}_p/\mathrm{RT} \tag{8}$$

where A is the frequency factor and T is the absolute temperature (K) The Arrhenius plot is given in figure 3. A straight line was drawn through the experimental points by a linear least-squares method. The parameters of the line give for the activation energy the value

$$E_p = 15\,200 \ \text{cal.mol}^{-1}$$

and for the frequency factor a value

$$A = 4.071 \times 10^{10} \ \text{l}^{1/2}.\text{mol}^{-1/2}.\text{min}^{-1}$$

It can be seen that the activation energy determined in the present study has a value close to other published data (see Table 1).

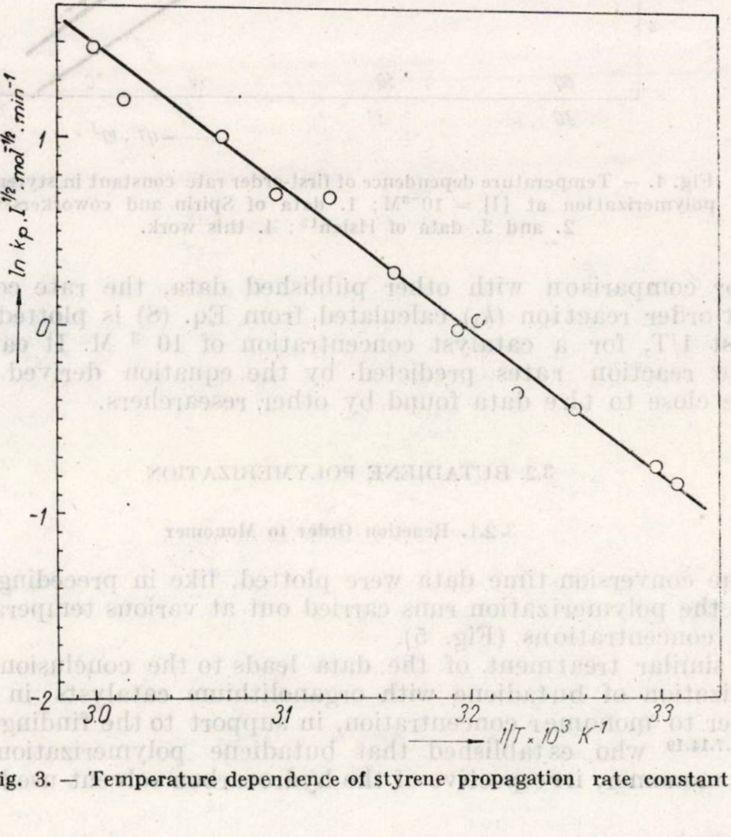

Fig. 3. — Temperature dependence of styrene propagation rate constant.

3.1.4. The Rate Equation

From the data given above, a kinetic equation may be derived, describing the overall reaction rate of styrene polymerization with organolithium catalysts in toluene, viz. the apparent rate of the propagation step :

$$-\frac{d[S]}{d\tau} = 4.071\times 10^{10}\exp(-15\,200/RT)[I]^{1/2}[S]\ \text{mol.l}^{-1}\text{min.}^{-1} \qquad (9)$$

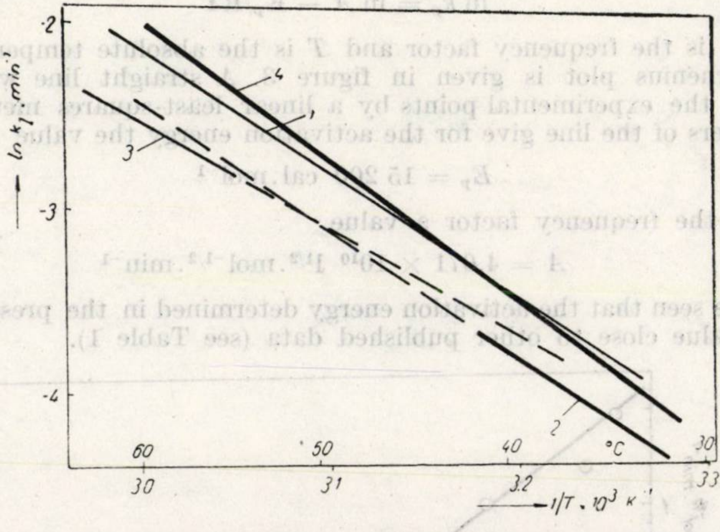

Fig. 4. — Temperature dependence of first-order rate constant in styrene polymerization at $[I] = 10^{-3}$M ; 1. data of Spirin and coworkers[14] ; 2. and 3. data of Hsieh[15] ; 4. this work.

For comparison with other published data, the rate constant of the first-order reaction (k_I) calculated from Eq. (8) is plotted in figure 4 against 1/T, for a catalyst concentration of 10^{-3} M. It can be seen that the reaction rates predicted by the equation derived from our data are close to the data found by other researchers.

3.2. BUTADIENE POLYMERIZATION

3.2.1. Reaction Order to Monomer

The conversion-time data were plotted, like in preceding case, for three of the polymerization runs carried out at various temperatures and catalyst concentrations (Fig. 5).

A similar treatment of the data leads to the conclusion that the polymerization of butadiene with organolithium catalysts in toluene is first-order to monomer concentration, in support to the findings of other authors[3,7,14,19] who established that butadiene polymerization is first-order to monomer, irrespective of the hydrocarbon solvent used.

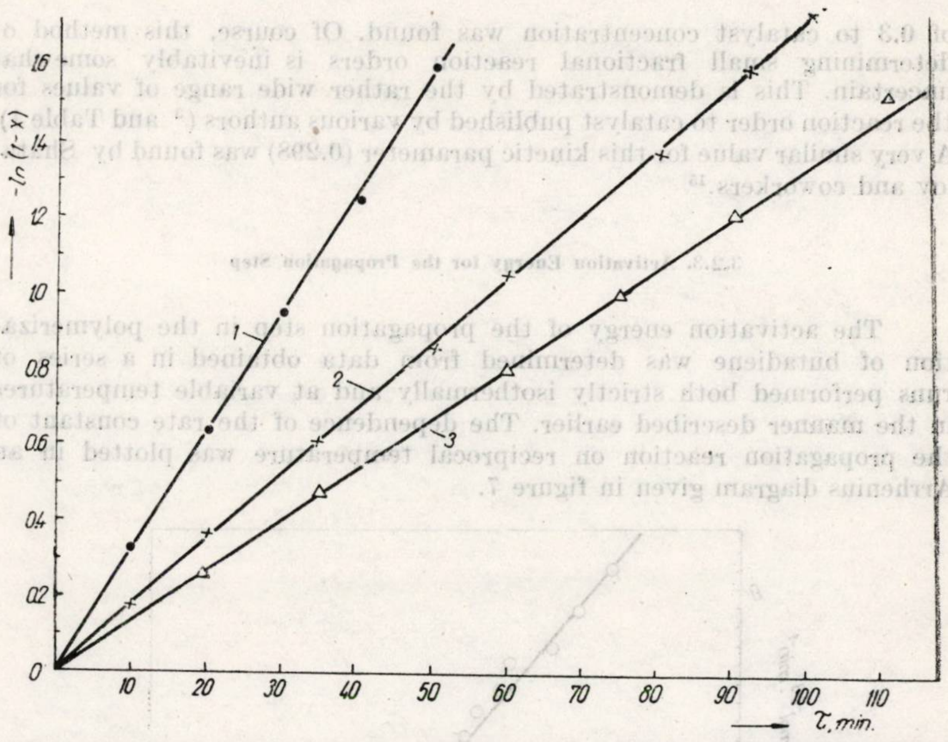

Fig. 5. — Plot of conversion vs. time in butadiene polymerization : 1.(●) $t = 50^{\circ}C$, $[I] = 1.23\times10^{-3}$ M ; 2.(+) $t = 45^{\circ}C$, $[I] = 1.36\times10^{-3}$ M ; 3.(△)$t = 45^{\circ}C$, $[I] = 0.55\times10^{-3}$M.

3.2.2. Reaction Order to Catalyst

The dependence of the rate constant of the first-order reaction(k_1) on catalyst concentration was determined in a series of runs performed at constant temperature (Fig. 6). From the slope of the line, a reaction order

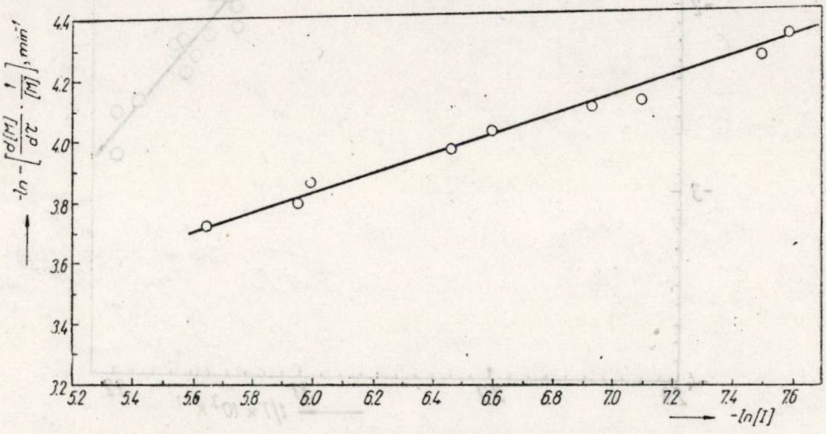

Fig. 6. — Dependence of first-order rate constant on catalyst concentration in butadiene polymerization : $t = 45^{\circ}C$, $[B]_0 = 1.64$ M.

of 0.3 to catalyst concentration was found. Of course, this method of determining small fractional reaction orders is inevitably somewhat uncertain. This is demonstrated by the rather wide range of values for the reaction order to catalyst published by various authors ([3] and Table 1). A very similar value for this kinetic parameter (0.298) was found by Shatalov and coworkers.[15]

3.2.3. Activation Energy for the Propagation Step

The activation energy of the propagation step in the polymerization of butadiene was determined from data obtained in a series of runs performed both strictly isothermally and at variable temperatures in the manner described earlier. The dependence of the rate constant of the propagation reaction on reciprocal temperature was plotted in an Arrhenius diagram given in figure 7.

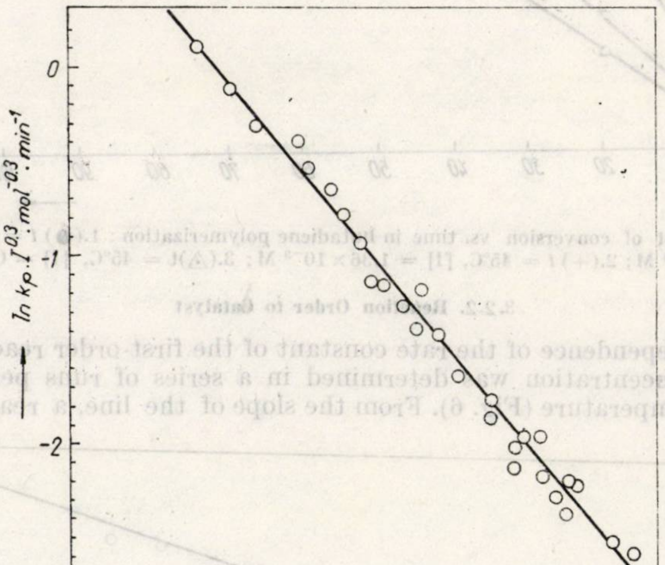

Fig. 7. — Temperature dependence of butadiene propagation rate constant.

By using a linear least squares method a straight line was drawn through the experimental points. The slope and the intercept five an activation energy

$$E_p = 24,400\ \text{cal.mol}^{-1}$$

and a frequency factor

$$A = 7,825 \times 10^{15}\ \text{l}^{0.3}.\text{mol}^{-0.3}\ \text{min}^{-1}$$

respectively.

Our value for the activation energy is somewhat higher than other published data (see Table 1). A virtually similar value (22,500 cal.mol^{-1}) was found by Shatalov and coworkers [15] for the polymerization of butadiene in toluene at temperature below 30°C.

3.2.4. The Rate Equation

From the data given in the preceding sections, an equation can be derived, describing the polymerization kinetics of butadiene in toluene with organolithium catalysts :

$$-\frac{d[B]}{d\tau} = 7.825 \times 10^{15} \exp(-24,400/RT)[I]^{0.3}[B] \qquad (10)$$

where [B] is butadiene concentration. The dependence of the rate constant of the first-order reaction (k_I) on reciprocal temperature, calculated from Eq. (9) and from data published by other authors, is given in figure 8.

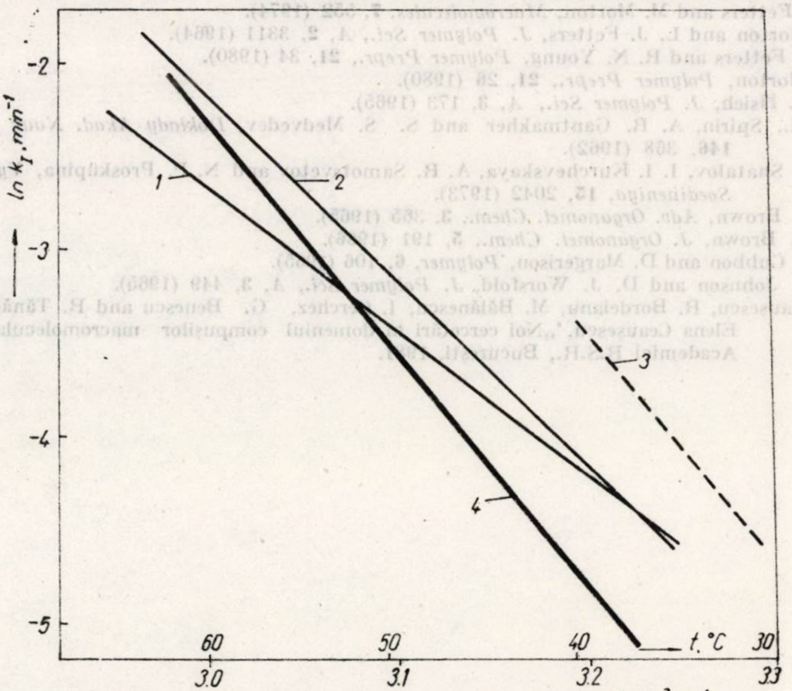

Fig. 8. — Temperature dependence of first-order rate constant in butadiene polymerization : *1.* data of Hsieh [13] ; *2.* data of Shatalov[15] ; 3. data of Shatalov[15] extrapolated from temperatures below 30°C ; *4.* this work.

At constant catalyst concentration ($[I] = 10^{-3}M$) the reaction rates predicted by various kinetic equations can thus be compared even if the reaction orders to catalyst concentration may be different. It can be seen that at lower temperatures (under 50°C) our data and hence Eq. (9) indicate lower rates of polymerization than those given by other investigators. The causes of this difference are not clear yet. However, the adequacy of our kinetic equation has also been confirmed by its use in a mathematical model of anionic copolymerization of butadiene and styrene[20] as well as by a large body of data gathered in a series of polymerization runs carried out in a pilot plant and not used in the present study.

REFERENCES

[1] H. L. Hsieh, R. C. Farrar and K. Udipi, *Polymer Prep.*, **21**, 46 (1980).

[2] M. Szwarc, "Carbanions, Living Polymers and Electron Transfer Processes", Wiley, New York, 1968.

[3] M. Morton and L. J. Fetters, *Rubber Chem. Technol.*, **48**, 359 (1975).

[4] H. L. Hsieh, *J. Polymer Sci.*, *A*, **3**, 163 (1965).

[5] C. M. Selman and H. L. Hsieh, *J. Polymer Sci*, *A*, **4**, 79 (1970).

[6] A. L. Gatzke, *J. Polymer Sci.*, *A-1*, **7**, 2281 (1969).

[7] M. Morton, E. E. Bostick and R. A. Livigni, *Rubber Plastics Age*, **42** 397 (1961).

[8] D. J. Worsfold and S. Bywater, *Canad. J. Chem.*, **38**, 1891 (1960).

[9] L. J. Fetters and M. Morton, *Macromolecules*, **7**, 552 (1974).

[10] M. Morton and L. J. Fetters, *J. Polymer Sci.*, *A*, **2**, 3311 (1964).

[11] L. J. Fetters and R. N. Young, *Polymer Prepr.*, **21**, 34 (1980).

[12] M. Morton, *Polymer Prepr.*, **21**, 26 (1980).

[13] H. L. Hsieh, *J. Polymer Sci.*, *A*, **3**, 173 (1965).

[14] Yu. L. Spirin, A. R. Gantmakher and S. S. Medvedev, *Doklady Akad. Nauk S.S.S.R.* **146**, 368 (1962).

[15] V. P. Shatalov, I. I. Kurchevskaya, A. R. Samotsvetov and N. P. Proskupina, *Vysokomol. Soedineniya*, **15**, 2042 (1973).

[16] T. L. Brown, *Adv. Organomet. Chem.*, **3**, 365 (1965).

[17] T. L. Brown, *J. Organomet. Chem.*, **5**, 191 (1966).

[18] R. C. Cubbon and D. Margerison, *Polymer*, **6**, 106 (1965).

[19] A. F. Johnson and D. J. Worsfold, *J. Polymer Sci.*, *A*, **3**, 449 (1965).

[20] E. Ceauşescu, R. Bordeianu, M. Bălănescu, I. Cerchez, G. Benescu and R. Tănăsescu, in Elena Ceauşescu, „Noi cercetări în domeniul compuşilor macromoleculari," Ed. Academiei R.S.R., Bucureşti, 1981.

Revue Roumaine de Chimie, 26 4, 521–526 (1981)

XYLIDINE ISOMERS. V[1]

MOLECULAR COMPLEX SPECTRA OF IODINE WITH XYLIDINES

JOSETTE WEINBERG* and V. EM. SAHINI**
* Centre of Physical Chemistry, Splaiul Independenței 202, Bucharest, Romania
** Physical Chemistry Laboratory, Blvd. Republicii 13, Bucharest, Romania

Received July 17, 1980

Spectrophotometric studies were carried out on 1 :1 iodine complexes of some xylidine isomers in n-heptane. Various properties of these isomers, like their dipole moment, pK_a value and HNH angle value in the ground state, are discussed in relation to the charge-transfer complexes. The lowest value of K in the iodine $-$2,6-xylidine complex is assigned to the presence of the steric effects of the two *ortho*-CH_3 groups.

Charge transfer complexes are specific associations resulting from the interaction between molecules of low ionization potential and molecules of high electron affinity.[2] They can be formed either between the reacting partners and therefore represent a true reaction intermediate or between an unreactive complexing agent and the reacting substrate, when the reactivity of the latter is modified. These catalytic effects occur under milder conditions than classical acid –base catalysis, therefore they may play a considerable role in biological and therapeutical reactions of the living organisms.[3]

The modern theory of chemical reactivity emphasizes the charge-transfer between reacting partners as an indispensable and unavoidable step in the overall reaction.[4]

The purpose of the present paper is to report the results of a spectrophotometric study on iodine complexes with some xylidine isomers, the substituent and steric effects being discussed in terms of K, ΔH and ΔS.

The equilibrium constants for the complex formation were obtained by the least-squares method, using the modified Benesi-Hildebrand equation as indicated by Tsubomura [5] :

$$C(\mathrm{D})/d = 1/C(\mathrm{I}_2)\, K \in + C(\mathrm{D})/C(\mathrm{I}_2) \in \qquad (1)$$

where : C(D) and $C(\mathrm{I}_2)$ are the concentrations of the donor and iodine in mole/l respectively ;

d is the optical density of the band ;

K the equilibrium constant, and

ϵ the molar extinction coefficient.

The plots of ln K against $1/T$ yield straight lines; ΔH and ΔS are obtained from the slope and the intercept, respectively.

EXPERIMENTAL

Xylidine isomers (Schuchardt) were purified by distillation under low pressure. Fischer certified iodine, repurified by sublimation, was kept protected from the light in a desiccator over calcium chloride. Absorption spectra were measured with a UNICAM SP 800 spectrophotometer equipped with a temperature controlled cell holder; temperature was maintained constant within ± 0.5°C by circulating water from a thermostat.

When the concentration of iodine was 3.10^{-5} M (and that of xylidine 0.03—0.1 M), no change in the absorption spectra of complex was evidenced during a 24 hours observation.

RESULTS AND DISCUSSION

Figure 1 presents the complete form of CT band of 2,6-xylidine iodine complex. The spectrum was recorded in n-heptane at a concentration of $1.85.10^{-2}$ M xylidine and 5.10^{-4}M iodine.

The concentration of iodine was tenfold that utilized for the rest of measurements.

This aimed at evidencing more clearly the band shape in the 325—350 nm range; examination of the figure shows that the band is shaped as a shoulder in the above mentioned region.

Molecular complex spectra of iodine with 2,6-xylidine at 23°C for several concentrations are shown in figure 2.

It is visible that on addition of xylidine to the solution, the free iodine at 525 nm diminishes in intensity and a strong absorption band appears at shorter wavelengths. This absorption may be attributed to the charge-transfer band of the iodine-xylidine complex.

Mulliken's works demonstrate that the iodine-aromatic compound molecular complexes exhibit a strong absorption near 300 nm; in this range neither the single aromatic compound nor single iodine absorb.[6]

At higher xylidine concentration, the intensity of free iodine band decreases, an isosbestic point observed at 490 nm proves the formation of the molecular complex of xylidine with iodine. The intensities of the strong bands decrease with the increasing of temperature and, at the same time, the free iodine band gains in intensity. This indicates that these bands are due to the complex which is in equilibrium with free components. Similar spectra were obtained for the other isomers of xylidine in complex with iodine.

Use has been made of the extinction coefficient data for two or three wavelengths in the region attributed to the complex to draw Benesi—Hildebrand plot; the equilibrium constants were then calculated by eq. (1) and are listed in table 1. Three isomers have been sorted out as the most representative of the series, namely, 2,6-; 2,3- and 3,4-xylidine.[7]

From table 1, 2,6-xylidine has the lowest value for equilibrium constant and 3,4-xylidine the highest one. In all cases, the higher the temperature, the lower the intensities of charge-transfer bands and the more intense the free iodine band.

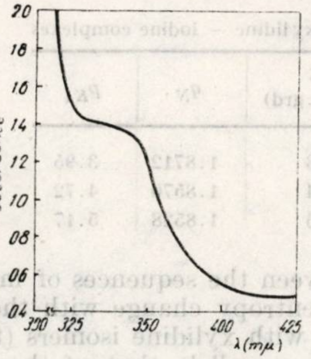

Fig. 1 — Charge transfer band of 2,6-xylidine— iodine complex in n-heptane ;

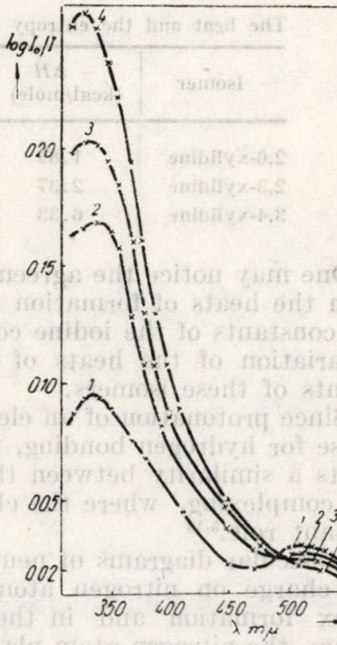

Fig. 2. — The absorption spectra of the n-heptane solutions of iodine and 2,6-xylidine at 23°C. The concentrations of 2,6-xylidine are : 0.03152 M for solution 1 ; 0.06304 M for solution 2 ; 0.0788 M for solution 3 and 0.1103 M for solution 4. The concentration of iodine 2.99×10^{-5} M.

TABLE 1

The equilibrium constants of xylidine—iodine complexes

Isomer	λ (nm)	k(ℓ/mole)			∊ (mole/ℓ.cm)		
		23°C	30°C	37°C	23°C	30°C	37°C
2,6-xylidine	330	3.74	3.40	3.07	14000	13500	14000
	350	3.74	3.42	3.00	14000	13500	14000
		Average					
		3.74	3.41	3.03			
2,3-xylidine	330	6.52	6.35	5.77	17730	14451	13441
	340	7.70	6.44	4.84	15455	14025	16667
	350	6.34	—	5.88	16667	—	12500
		Average					
		6.85	6.39	5.50			
3,4-xylidine	330	17.51	12.62	—	14286	14286	—
	350	17.47	12.27	8.33	14286	14286	14286
	370	16.67	—	9.69	14286	—	12500
		Average					
		17.22	12.45	9.18			

The heat and the entropy changes of complexes formation are listed in table 2 together with π-electron density (obtained by an SCF–MO–PPP computation[8]) and the basicity constants.[9]

TABLE 2

The heat and the entropy changes of xylidine — iodine complexes

Isomer	$-\Delta H$ (kcal/mole)	$-\Delta S$ (cal/mole.grd)	q_N	p_{K_a}
2,6-xylidine	1.89	2.03	1.8712	3.95
2,3-xylidine	2.37	3.04	1.8570	4.72
3,4-xylidine	6.33	3.76	1.8528	5.17

One may notice the agreement between the sequences of increasing of both the heats of formation and the entropy change with the equilibrium constants of the iodine complexes with xylidine isomers (table 1). The variation of the heats of formation parallels that of the basicity constants of these isomers.

Since protonation of an electron donor is considered to be the limiting case for hydrogen bonding, the relationship among ΔH, K and pK_a suggests a similarity between the mechanisms of hydrogen bonding and iodine complexing, where the charge-transfer force undoubtedly plays an important role.[5,10]

Molecular diagrams of neutral molecules point out that the π-electronic charge on nitrogen atom is the most significant factor for the complex formation and in the reactions of electrofile reactants with xylidines, the nitrogen atom plays the major role. 2,6-Xylidine, from the isomers, has the highest π-electronic density on nitrogen atom, an expectation which should be confirmed by the base strengthening (+I) effect of the two *ortho*-CH_3 groups in respect to NH_2 group. Potentially, this isomer is expected to have considerable donor strength toward iodine, but, at the same time, a larger steric strain (−S) of both *ortho*-CH_3 groups prevents the charge-transfer complex from forming and 2,6-xylidine has the lowest value of K.

In a previous paper we calculated, on the basis of a theoretical model, the values of the HNH angle between the two N–H bonds of NH_2 group versus isomerism, for xylidine molecule.[8] Table 3 presents

TABLE 3

The correlation of equilibrium constants of CT complexes with some theoretical and experimental properties

Isomer	K (ℓ/mole)	$\widehat{HNH}$	μ(D) theoret.	μ(D) exper. in C_6H_6	μ(D) exper. in CCl_4	μ(D) exper. in n-C_6H_{12}
2,6-xylidine	3.74	95°	1.67	1.62	1.63	1.62
2,3-xylidine	6.85	100°	1.58	1.51	1.55	1.45
3,4-xylidine	17.22	115°	1.28	1.31	1.19	1.17

these data together with the equilibrium constants of iodine-xylidine charge-transfer complexes at 23°C.

Examination of this table presents a correlation of the variation of this constant with the variation of the HNH angle : 2,6-xylidine with $\widehat{HNH} = 95°$, which means an almost complete destruction of the resonance between the π-electrons of the ring and the lone pair of nitrogen electrons, presents the lowest value of the equilibrium constant, due to the presence of both *ortho*-CH_3 groups. For the other isomers the variation of angle parallels that of equilibrium constant. At the same time the influence of the solvent on the dipole moment agrees with the modification of charge-transfer complexes caused by changes of isomerism.[8]

Table 4 presents the equilibrium constants together with the heats of formation for xylidine isomers and some N,N-dimethylanilines (Tsubomura's data[5]).

TABLE 4

The equilibrium constants for xylidine and N, N-dimethylanilines-iodine complexes

	2,6-xylidine	N, N-dimethyl-2, 6-xylidine
K(ℓ/mole)	3.40[a]	1.70[b]
ΔH(kcal/mole)	−1.89	−1.70
	2,3-xylidine	N,N-dimethyl-0-toluidine
K(ℓ/mole)	6.39	2.04
ΔH(kcal/mole)	−2.37	−2.30
	3,4-xylidine	N, N-dimethyl-p-toluidine
K(ℓ/mole)	12.45	24.00
ΔH(kcal/mole)	−6.33	−8.30

a) Equilibrium constants at 30°C.
b) Equilibrium constants at 33°C.

For N,N-dimethyl-2,6-xylidine, the two CH_3 groups from dimethylamino group and the two *ortho*-CH_3 groups have a considerable steric strain that prevents the charge-transfer complex from forming, the equilibrium constant and the heat of formation being very small. In comparison with this molecule, 2,6-xylidine, where the CH_3 groups are only in *ortho* position, forms with iodine a complex of a larger constant. In N-N-dimethyl-*ortho*-toluidine, where only one *ortho* position is occupied, the steric strain is smaller than in N-N-dimethyl-2,6-xylidine ; the equilibrium constant is accordingly larger, yet smaller than that of 2,3-xylidine.

In N,N-dimethyl-*para*-toluidine, where the steric strain due to the *ortho*-CH_3 group is not present, the equilibrium constant with iodine increases remarkably. This fact is due to the significant polar effects of alkyl groups on nitrogen atom and in the para position to the ring. 3,4-xylidine forms with iodine a stronger complex, but not as strong as the one formed by the N,N-dimethyl-*para*-toluidine. This behaviour has been expected as the N-alkyl group is absent in the former isomer.

REFERENCES

[1] Previous paper: V. E. Sahini, J. Weinberg and M. Vasilescu, *Rev. Roumaine Chim.*, **21**, 1121 (1976).

[2] "Molecular Association", vol. 1, Roy Foster ed., Acad. Press, London, New York, San Francisco, 1975.

[3] O. B. Nagy and J. B. Nagy, "Environmental Effects of Molecular Structure and Properties" B. Pullman ed., 1976, p. 179.

[4] "Chemical Reactivity and Reaction Paths", G. Klopman ed., Wiley-Interscience, New York 1974

[5] Tsubomura, *J. Amer. Chem. Soc.*, **82**, 40 (1960).

[6] R. S. Mulliken and W. B. Person, "Molecular Complexes", Wiley-Interscience, 1969.

[7] V. E. Sahini and J. Weinberg, *Anal. Univ. Bucuresti*, **20**, 2 (1971).

[8] V. E. Sahini and J. Weinberg, *Rev. Roumaine Chim.*, **18**, 1493 (1973).

[9] R. N. Beale, *J. Chem. Soc.*, **1954** 4494; B. M. Wepster, *Rec. Trav. chim.*, **76**, 357 (1957).

[10] T. Kubota, *J. Amer. Chem. Soc.*, **87**, 458 (1965).

Revue Roumaine de Chimie, 26, *4*, 527–537 (1981)

ABSOLUTE MEASUREMENT OF THERMAL CONDUCTIVITY AND THERMAL DIFFUSIVITY OF LIQUIDS BY CLASSICAL PROCEDURE OF THE TRANSIENT HOT-WIRE METHOD

RODICA VÎLCU* and ALIN CIOCHINĂ**

* Polytechnical Institute, Department of Physical Chemistry, Blvd. Republicii 13, Bucharest, Romania

** ICECHIM, Centre of Physical Chemistry, Spl. Independenţei No. 202, Bucharest, Romania

Received July 7, 1980

The paper briefly describes the principle of the transient hot-wire method and an improved apparatus for thermal conductivity measurements of liquids in an absolute way. Determinations consist in principle in measuring the time when the hot wire attains six preset and adjustable temperature values. The thermal conductivity is calculated from the slope of a (θ, lnt) diagram on which different pairs of these quantities have been determined with accuracy. Results on toluene and carbon tetrachloride at 303 K and 323 K are given. The accuracy is better than 2%, as estimated from both computation of phenomenological errors and comparison with the available data in literature. The thermal diffusivity is computed by extrapolating the straight line $\theta(\ln t)$ for $\theta = 0$. The accuracy is about 10% as estimated from the available data in literature.

1. INTRODUCTION

The transient hot-wire method is frequently used in determining the thermal conductivity of fluids. Accurate measurements of the transport properties are important for the experimental testing of the molecular theory of the transport properties of fluids, as well as for many heat transfer processes which occur in technology.

The thermal conductivity of liquids and liquid mixtures is an industrially important physical property. On process and plant design, especially in the field of heat transfer, the thermal conductivity is dominant in the many non-dimensional parameters used in design procedure.

The paper is devoted to a presentation of the measurements on toluene and carbon tetrachloride at 303 K and 323 K, and to the computation of the main phenomenological corrections assuming temperature independent properties of the investigated liquids.

2. THE LINE SOURCE SOLUTION

The simplest mathematical description of the non-steady-state hot-wire cell is provided by the line-source solution of the conduction equation:

$$\rho c_p \frac{\partial T}{\partial t} = \lambda\left(\frac{\partial^2 T}{\partial r^2} + \frac{1}{r}\frac{\partial T}{\partial r}\right) \tag{1}$$

where ρ, c_p, λ are respectively density, specific heat at constant presure and thermal conductivity of the fluid.[1] In this solution the fluid is considered to be unbounded and isotropic, has temperature independent properties and is initially at a uniform and constant temperature T_0. At zero time, $t = 0$, a line source of heat, of infinite length and with uniform power q per unit length, originates at $r = 0$. The temperature rise at time t referred to the initial value, is given by the equation[2]:

$$\theta(r, t) = -\frac{q}{4\pi\lambda}\left[E_i\left(-\frac{r^2}{4at}\right)\right] \tag{2}$$

where $a = \lambda/(\rho c_p)$ is the thermal diffusivity of the fluid and E_i is the exponential integral.

$$-E_i(-x) = \int_x^\infty \frac{e^{-u}}{u}\mathrm{d}u$$

$$= -\gamma - \ln x - \sum_{n=1}^{\infty} \frac{(-1)^n x^n}{n n!} \quad (|\arg x| < \pi)$$

Taking the expansion to the second term of the summation, equation (2) becomes:

$$\theta(r,t) = \frac{q}{4\pi\lambda}\left[\ln\frac{4at}{r^2 C} + \frac{r^2}{4at} + \ldots\right] \tag{3}$$

where $C = \exp\gamma$ and $\gamma = 0.5772\ldots$ is Euler's constant.

The hot-wire temperature is obtained by substituting $r = r_1$, where r_1 is the radius of the wire. Provided that $r_1^2/(4at)$ is sufficiently small within the range t_1 to t_2, we may write:

$$\theta(r_1, t_2) - \theta(r_1, t_1) \simeq \frac{q}{4\pi\lambda}\ln\frac{t_2}{t_1} \tag{4}$$

A first estimate of the thermal conductivity can be obtained from the slope of the hot-wire temperature plotted against ($\ln t$), provided that q is known. The truncation errors are negligible only if the terms to $x^2/4$ are included in eq (3). The use of equation (4) involves a lot of approximations in addition to truncation errors: those involved in reducing the full energy conservation equation to equation (1) and the idealization leading to the line-source solution.[1] The experimental conditions must be so chosen that the errors introduced by these approximations to be as small as possible.

3. WORKING EQUATION OF TRANSIENT HOT-WIRE METHOD

In the transient, hot-wire method, the thermal conductivity of the liquid is determined by observing the rate of the temperature rise of a thin platinum wire in time, after a step change in voltage has been applied,[3] thus creating in the liquid a line source of constant heat flux per unit length, q. This has the effect of producing a time increasing radial field of temperature of cylindrical symmetry throughout the liquid. After a time t_A from starting the step-pulse ($t = 0$), the product between the time and the rate of temperature rise in wire is inversely proportional to the liquid thermal conductivity, λ. For $t \geqslant t_A$, the temperature increase $\theta(r_1, t)$ of the wire of radius r_1 is described by the formula :

$$\theta(r_1, t) = \frac{q}{4\pi\lambda} \ln \frac{4\tau}{C} \tag{5}$$

where $\tau = at/r_1^2$.

The increase in temperature described by eq. (5) gives a straight line, (D), when ploting $\theta(r_1,t)$ versus ($\ln t$) and the slope p of this line is inversely proportional to the thermal conductivity. This linear logarithmic law will be observed only between times t_A and t_B, $t_A \leqslant t \leqslant t_B$, systematic deviations occurring for both short ($t < t_A$) and long ($t > t_B$) times. Time t_A depends on geometrical and physical finite constants of the wire, and t_B is the critical time for the natural convection onset and wall cell effect.

Equation (5) represents the wire temperature rise with a close approximation only for sufficiently large values of τ.

4. EXPERIMENTAL ASSEMBLY

4.1. PRINCIPLE OF OPERATION OF THE APPARATUS

The heating wire is connected to an Wheatstone bridge. The wire is calibrated like a resistance thermometer, so that the resistance $R(T,t)$ is an indication of the temperature rise, $\theta(r_1, t)$. The temperature rise can be measured by monitoring the output signal of the bridge. The time intervals are measured by means of electronic counters which are triggered by comparators. At $t = 0$ the resistances in the bridge are adjusted in such a way that the bridge is balanced (the heating current is zero). At instant $t = 0^+$, a switch is on as to send a current through the wire, the bridge is activated and, simultaneously, six electronic counters are set in operation. The heating current causes a rise in temperature of the wire and also an increase of its resistance. At the instant when the output signal of the bridge equals the preset voltage levels of comparators, the latter send a signal to stop the counters. In this manner, the time intervals can be measured from the moment $t = 0^+$ up to the times $t_1, \ldots, t_6$ when the output signal of the bridge equals the six preset voltage values of the comparators. The temperature rise of the wire between $t = 0^+$ and $t = t_i$ ($i = 1 \ldots 6$) can be determined from the bridge equation and the temperature coefficient of the wire resistance. The amount of heat produced in the wire per unit length can be calculated (by measuring the voltage across the bridge, E_p, the resistance R of the wire at $t = 0$ and the length, L, of the wire) using the relation $q = E_p^2/(4RL)$.

4.2. CELL DESCRIPTION

The measuring cell, made of Pyrex glass tube (15 mm i.d. × 17 mm o.d.), contains the investigated liquid. The transducer, made of a piece of pure platinum wire ($2r_1 \simeq 0.015$ mm, $L \simeq 150$ mm) soldered at the ends on thick copper leads, is vertically immersed into the fluid. The assembly is maintained at the constant temperature T_0 ($\pm$ 0.02 K) in a Dewar flask connected to a U — 10 type thermostat. The detailed description of the experimental assembly and working procedure will be given in a subsequent paper.[4]

5. EXPERIMENTAL RESULTS

The results obtained on toluene and carbon tetrachloride ("Reactivul" p.a. reagents) at 303 K and 323 K are reported in this paper.

This new apparatus can be used as an absolute one in four modes:

a) The thermal conductivity can be calculated with the eq. (5) from each pair of values of (θ ; t), remembering that λ occurs explicitly as well as a factor in $a = \lambda/(\rho c_p)$. Since in our version of the apparatus six such pairs are measured during each run, it is possible to deduce a lot of direct, absolute values for λ and to take an average. In this mode of evaluation, the result, λ, would contain beside the instrumental errors, uncertainties due to the errors in ρ, c_p, r_1 and q.

b) The method[5] consists in measuring the time, t, when the wire temperature reaches the preset voltage threshold of a comparator and of the slope of the curve θ (r_1, t) versus t between the moments t and $t + \mathrm{d}t$, for $\mathrm{d}t \ll t$.

c) In a third mode, one measures $\theta(r_1, t)$ at two times t_1 and t_2 within the (t_A, t_B) interval, and computes the thermal conductivity with the equation (4).

d) The last method is to fit a straight line, (Δ), by the least squares to all measured points, within the (t_A, t_B) interval, and to calculate λ from the slope $p = q/(4\pi\lambda)$ as subjected only to an uncertainty stemming from the error in q and θ.

We employ the last two methods, the fourth one being the most accurate of them all. Actually, the run is repeated five to ten times under identical conditions; the straight line (Δ) is finally drawn through 6—30 points obtained from different (θ, t) pairs.

The Tables 1 and 2 contain a representative set of the experimental data for toluene and carbon tetrachloride at 303 K, and the values for λ and "a" at 323K as computed from (Δ) line.

The error involved in assuming a heat-source of zero diameter can be estimated using a result obtained by Jaeger.[6] In the solution of eq. (1), the heat-source is considered to be of diameter $2r_1$, and to have infinite thermal conductivity. Heat is generated at a rate q per unit length of the source. The temperature rise of the wire, for large values of τ is given by the equation[1,3]:

$$\theta(r_1,t) = \frac{q}{4\pi\lambda}\left[\ln\frac{4\tau}{C} + \frac{1}{2\tau} + \left(\frac{\omega-2}{2\omega\tau}\ln\frac{4\tau}{C}\right) + \ldots\right] \tag{6}$$
$$= \frac{q}{4\pi\lambda}\left[\left(1 - \frac{\rho_1 c_1 - \rho c_p}{2\lambda t} r_1^2\right)\ln\frac{4\tau}{C} + \frac{1}{2\tau} + \ldots\right]$$

where $\omega = 2\rho c_p/(\rho_1 c_1)$ and ρ_1, c_1 are the density and respectively the specific heat of the platinum.

TABLE 1

Sample measurement on toluene

$T_0 = 302.27$ K ; $R = 88.86\Omega$; $L = 0.141$ m ; $E_p = 3.0426$ V ; $r_1 = 7.79 \times 10^{-6}$ m

θ (K)	t (s)	$10^3\delta\theta_1$ (K)	e_1 (%)	t_B (s)	r_2 (mm)	τ	e_3 (%)	$10^5 e_4$	λ_{exp} (W/(mK)) eq.(4)	λ_{exp} (W/(mK))	$10^7 a_{\mathrm{exp}}$ (m²/s) eq.(17)	$10^7 a_{\mathrm{exp}}$ (m²/s)
0.580	0.0528	3.35	−1.81	21.2	0.34	78	0.44	4.8	0.1263		0.749	
0.664	0.1080	1.86	−1.09	19.4	0.48	160	0.47	5.4	0.1298		0.878	
0.705	0.1549	1.38	−0.83	18.6	0.58	229	0.48	5.7	0.1299		0.882	
0.746	0.2232	1.01	−0.63	17.9	0.70	330	0.49	6.1	0.1293		0.856	
0.788	0.3218	0.74	−0.47	17.3	0.83	476	0.51	6.4	0.1287		0.829	
0.830	0.4652	0.54	−0.35	16.7	1.00	688	0.52	6.8		0.1315		0.961
0.820	0.4296	0.58	−0.37	16.8	0.96	635	0.52	6.7	0.1310		0.941	
0.904	0.9033	0.30	−0.20	15.8	1.40	1335	0.54	7.4	0.1331		1.070	
0.945	1.3080	0.22	−0.15	15.3	1.68	1933	0.56	7.7	0.1339		1.127	
0.986	1.9072	0.16	−0.11	14.9	2.03	2819	0.57	8.1	0.1344		1.165	
1.028	2.7909	0.11	−0.08	14.5	2.46	4125	0.58	8.4	0.1348		1.198	
1.070	4.1083	0.08	−0.06	14.1	2.98	6072	0.59	8.8				
$T_0 = 322.60$ K										0.1264		0.910

TABLE 2

Sample measurement on carbon tetrachloride

$T_0 = 302.30$ K ; $R = 88.87\Omega$; $L = 0.141$ m ; $E_p = 2.6804$ V ; $r_1 = 7.79 \times 10^{-6}$m

θ (K)	t (s)	$10^3\delta\theta_1$ (K)	e_1 (%)	t_B (s)	r_2 (mm)	τ	e_3 (%)	$10^5 e_4$	λ_{exp} (W/(mK)) eq. (4)	λ_{exp} (W/(mK))	$10^7 a_{\mathrm{exp}}$ (m²/s) eq.(17)	$10^7 a_{\mathrm{exp}}$ (m²/s)
0.659	0.1098	2.56	−1.54	17.3	0.45	138	0.52	6.8	0.0968		0.661	
0.753	0.2440	1.31	−0.84	15.8	0.67	307	0.56	7.8	0.0977		0.701	
0.800	0.3643	0.93	−0.61	15.2	0.82	459	0.57	8.3	0.0998		0.813	
0.847	0.5516	0.65	−0.44	14.7	1.01	694	0.59	8.8	0.1007		0.869	
0.895	0.8367	0.45	−0.31	14.1	1.24	1053	0.61	9.2	0.1037		1.099	
0.942	1.2824	0.31	−0.22	13.7	1.53	1615	0.62	9.8		0.1009		0.882
0.779	0.3029	1.09	−0.71	15.5	0.75	381	0.57	8.0	0.0991		0.776	
0.873	0.6861	0.54	−0.37	14.4	1.12	864	0.60	9.0	0.1022		0.984	
0.920	1.0435	0.37	−0.26	13.9	1.38	1314	0.62	9.5	0.1029		1.041	
0.967	1.6010	0.26	−0.18	13.4	1.71	2016	0.63	10.0			1.538	
1.015	2.4977	0.17	−0.12	13.0	2.14	3145	0.65	10.5	0.1075		3.247	
1.062	4.0266	0.11	−0.08	12.6	2.72	5069	0.67	11.1	0.1159			
$T_0 = 322.62$ K										0.0973		0.832

The eq. (6) shows that the actual temperature rise, $\theta(r_1, t)$, is equal to the difference between the ideal temperature increase given by the eq. (5), and a correction:

$$\delta\theta_1(r_1, t) = \frac{q}{4\pi\lambda}\,\frac{\rho_1 c_1 - \rho c_p}{2\lambda t}\, r_1^2 \ln\frac{4\tau}{C} \tag{7}$$

Adding $\delta\theta_1(r_1, t)$ to the measured $\theta(r_1, t)$ brings this point into coincidence with the straight line whose slope determines the measured thermal conductivity.[3] The correction $\delta\theta_1(r_1, t)$ is presented in the third column of Tables 1 and 2, using the physical properties of liquids as given in the literature,[7-10] and presented in Table 3. For platinum wire, $r_1 = 7.8 \times 10^{-6}$ m, and $\rho_1 = 21450$ kg/m^3 and $c_1 = 131$ J/(kg.K), as mean values[9] over 273–373 K temperature range.

TABLE 3

Physical properties of the investigated liquids

Liquid	T (K)	ρ (kg/m^3)	ref.	C_p (J/(kg.K))	ref.	λ (W/(m.K))	ref.	$10^7\,a$ (m^2/s)	$10^4\,\eta$ (N.s/m^2)	ref.	$10^3\beta$ (1/K)	ref.
Toluene	303	857,7	7	1733.6	8	0.132 0.1334* 0.128–0.136	7 8 10	0.888 0.897* 0.861–0.915	5.22	7,9	1.10	7
	323	838.9	7	1800	7	0.127 0.1283* 0.124–0.129	7 8 10	0.841 0.850* 0.821–0.854	4.20	7,9	1.15	7
CCl$_4$	303	1575.1	7,9	864.2 856.5*	7 8	0.1019 0.1031* 0.097–0.109	7 8 10	0.749 0.764* 0.717–0.810	8.43	7,9	1.25	7
	323	1536.4	7,9	867.2	8	0.0975 0.107 0.0992* 0.093–0.103	7 9 8 10	0.732 0.803 0.745* 0.700–0.773	6.51	7,9	1.28	7

* Values used in errors computation

The influence of the time t_A can be evaluated[11] from the relative error, e_1, in the slope of the straight line $\theta(r_1, t)$ versus $(\ln t)$, which is a function of τ and ω.

$$\frac{d\,\theta(r_1, t)}{d(\ln t)} = \frac{q}{4\pi\lambda}\left\{1 - \frac{1}{2\tau}\left[1 + \left(1 - \frac{\rho_1 c_1}{\rho c_p}\right)\left(\ln\frac{4\tau}{C} - 1\right)\right] + \dots\right\}$$

$$e_1 = \frac{1}{2\tau}\left[1 + \left(1 - \frac{\rho_1 c_1}{\rho c_p}\right)\left(\ln\frac{4\tau}{C} - 1\right)\right] \tag{8}$$

The calculated e_1 values are presented in the 4th column of Tables 1 and 2.

In order to prevent disturbances in the heat conduction process, the free convection must be avoided during measurements. The critical time t_B of onset of free convection can be approximately evaluated from the equation[11] :

$$\frac{g\beta r_1^3}{\nu a}\,\frac{q}{4\pi\lambda}\,\ln\frac{4at_B}{r_1^2\,C}\left(\sqrt{\frac{4at_B}{r_1^2\,C}}-1\right)^3 \leqslant 1000 \tag{9}$$

where $g = 9.81\ \text{m/s}^2$ is the acceleration of gravity, β is the thermal expansion coefficient and $\nu = \eta/\rho$ is the kinematic viscosity of the liquid.

$$t_B \leqslant 0.445\left[\left(\frac{1000\ \nu}{g\beta\theta(r_1,t)\sqrt{a}}\right)^{1/3}+\frac{r_1}{\sqrt{a}}\right]^2 \tag{10}$$

Assuming that the physical properties of the liquids are temperature independent, the values of t_B were computed with eq. (10) and listed in the 5th column of Tables 1 and 2.

The effect of a bounded medium in radial direction (wall cell effect) is negligible if $r_2^2/(4at) > 6$, where r_2 is the distance between the platinum wire and the thick copper lead supporting the lower end of the wire. The resulting r_2 values as listed in the 6th column of Tables 1 and 2 are all lower than 5 mm, the actual r_2 value of the cell.

The finite length of the wire affects the wire temperature rise in two ways. Firstly, the discontinuity in heating along the wire axis distorts the temperature field near each end. The relative error, e_2, introduced, in the slope $p = \mathrm{d}\theta\,(r_1, t)/(\mathrm{d}\ln t)$, averaged over the wire length, L, is given approximately by the relation[11] :

$$e_2 \simeq \frac{\sqrt{4at}}{L}\,\mathrm{ierfc}\,\frac{L}{\sqrt{4at}} \tag{11}$$

and increases with $at/L^2 = \tau(r_1/L)^2$. For $\tau < 3 \times 10^5$ the value of e_2 is negligible. The experimentally τ values are listed in the 7th column of Tables 1 and 2.

Secondly, the heat is lost by conduction along the wire to the connecting leads. The relative error, e_3, introduced in the slope p, due to this effect is given approximately by the relation[11] :

$$\mathrm{d}\theta(r_1,\ t)/\mathrm{d}\ (\ln\ t) = [q/(4\pi\lambda)]\ (1 - e_3)$$

$$e_3 \simeq [3r_1/(2L)]\ (\lambda_1/\lambda)^{1/2}\ [\ln\ (4\tau/C)]^{1/2} \tag{12}$$

where λ_1 is the thermal conductivity of the platinum. With $\lambda_1 = 71.5$ W/(mK), the e_3 values are listed in the 8th column of Tables 1 and 2.

In the most unfavorable case, liquid with transmissivity equal to unity, the relative error, e_4, in the slope p due to heat lost by radiation, is given approximately by the relation:

$$e_4 \simeq \frac{2r_1\ \sigma\ \varepsilon_1\ T_0^3}{\lambda} \ln \frac{4\tau}{C} \tag{13}$$

where ε_1 is the total emissivity of the wire surface, $\sigma = 5.67 \times 10^{-8}$ W/(m^{2}K^4) is the Stefan-Boltzmann constant and T_0 is the initial absolute temperature. With $\varepsilon_1 = 0.05$, the resulting values of e_4 are listed in the 9th column of Tables 1 and 2.

Our values, $\lambda_{\exp}$, calculated with the equation (4) and ρ, c_p from Table 3, are listed in the 10th column of Tables 1 and 2.

Our values, $\lambda_{\exp}$, as calculated from the slope of the straight line (Δ) fitted by least squares with all measured points in the range $0.15\ s \leqslant t \leqslant 2.79\ s$ for toluene and $0.30\ s \leqslant t \leqslant 1.60\ s$ for carbon tetrachloride, are listed in the 11th column of Tables 1 and 2.

In the point when the straight line $\theta(r_1, t)$ versus ($\ln t$) intercept the ($\ln t$) axis, we have:

$$4at_0/(r_1^2\ C) = 1 \tag{14}$$

thus:

$$a = r_1^2 C/(4t_0) \tag{15}$$

For t_i and t_j within the $t_A - t_B$ range:

$$\lambda_{ji} = \frac{q}{4\pi}\ \frac{\ln t_j - \ln t_i}{\theta(r_1,\ t_j) - \theta(r_1,\ t_i)}$$

$$\ln t_0 = \ln t_i - \frac{4\pi}{q}\, \theta(r_1,\ t_i)\lambda_{ji} \tag{16}$$

$$a = \frac{r_1^2\ C}{4\ t_i}\ \exp\left[\frac{4\pi}{q}\, \theta\ (r_1,\ t_i)\ \lambda_{ji}\right] \tag{17}$$

The experimental thermal diffusivity values, $a_{\exp}$, computed from the eq. (17) with $j = i + 1$ are listed in the 12th column of Tables 1 and 2. The experimentally thermal diffusivity values, $a_{\exp}$, as calculated with the t_0 value obtained from extrapolating the (Δ) line, are listed in the 13th column of Tables 1 and 2.

The data in Tables 1 and 2 confirm, qualitatively and partially quantitatively, the theoretical statements as follows:

a) Within the range of short times, the measured $\theta(r_1,\ t)$ values (eq. (6)) are lower than the ideal ones (eq.(5)); the $\delta\theta_1(r_1,t)$ correction decreases when the time increases. The slope calculated from the measured $\theta(r_1,\ t)$ values is steeper than the ideal one, that is the λ value is smaller than the one which one would get in the ideal case (r_1, ρ_1, c_1 equal to nil). The relative error, e_1, of the slope, presently negative (can be positive or negative depending on the τ and $\rho_1 c_1/(\rho c_p)$ values of the liquid), decreases when the time increases.

b) Because of the heat losses at the wire ends (λ_1, L finite) the measured $\theta(r_1, t)$ values are lower than the ideal ones (λ_1, L infinite) and the difference increases with time. The slope calculated from the measured $\theta(r_1, t)$ values is smaller than the ideal slope, that is the measured λ is higher than the value one would obtain in the ideal case. The relative error, e_3, of the slope increases with time.

c) In the present case, over the time interval for which the (Δ) straight line fits, the e_1 and e_3 errors being of opposite signs, they compensate each other.

d) The theoretical equations for calculating the $\delta\theta_1(r_1,t)$ correction and the heat losses at the wire ends are accurate enough. The maximum accuracy for measuring r_1 is $\pm$ 0.5μ (3.33 %), the ρ_1, c_1, λ_1, ρ, c_p, λ values are taken from literature with an accuracy of 3–10% and their selection for correction computation is subjective. This is the first reason which made us give up correcting the crude experimental results according to the undertaken estimative calculations.

e) The t_B time for the free convection onset is much longer than the maximum experimental time employed. Lengthening the experimental run duration and using the values for longer times would have eliminated the e_1 error but also would have increased the e_3 error. The calculation of the latter would have also implied the knowledge of the $\lambda_1, r_1, \rho, c_p$, and λ values. On top of that, an error e_4 of the slope would show up due to the initial temperature fluctuations. If $\mathrm{d}T_0/\mathrm{d}t$ is the time derivative value due to the initial non-steady state T_0 temperature, the slope error over the asymptotic range is:

$$e_4 = \frac{4\pi\lambda t}{q}\,\frac{\mathrm{d}T_0}{\mathrm{d}t}$$

Under the condition $e_4 < 10^{-2}$ and $t = 4s$, for toluene and carbon tetrachloride, $\mathrm{d}T_0/\mathrm{d}t < 2.8 \times 10^{-4}$ K/s.

f) The λ, ρ, c_p magnitudes necessary to calculate the corrections are tabulated for just a few single liquids and mixtures; the practical interest is to know the thermal conductivity of liquids for which this magnitude has not been measured yet.

g) The classical procedure of the transient hot-wire method implies *ab initio* a thermal conductivity determination from the slope of the $\theta(r_1, t)[\ln t]$ straight line and becomes practically useful only if it opperates with direct measurable quantities. This is the second reason for which the crude experimental data have not been corrected.

h) The relative error for the thermal diffusivity, $\delta a/a$, determined by extrapolating the (Δ) line is at least equal to $2(\delta r_1/r_1) + (\delta p/p)$, being very sensitive to the measurement accuracy of the quantities $\theta_i(r_1, t_i)$ and λ implied in the computation by means of the exponential. As $2(\delta r_1/r_1) \geqslant 7\%$, $\delta a/a \simeq 10\%$ and, in our oppinion, this is the lower limit of the error in the thermal diffusivity value thus determined.

By comparison of the data listed in Tables 1—3 it results that our absolute measurements of the thermal conductivity of liquids is accurate to 1.5% and the accuracy of the thermal diffusivity measurement is about 10%.

6. CONCLUSIONS

In concluding this study we find it necessary to emphasize some important findings regarding the *classical procedure* of the transient hot wire method:

— the thermal conductivity can be determined from pairs of points $[\theta(r_1, t), \ln t]$ within the range of linear logarithmic law given by eq. (5).

— eq. (5) represents the wire temperature rise with a close approximation only for sufficiently large values of $\tau = at/r_1^2$.

— the duration of the range governed by a linear logarithmic law is determined by the wire diameter and $\rho c_p/(\rho_1 c_1)$ ratio within the short time range and by the onset of the natural convection within the long time range.

— in order to increase the time interval for which the linear logarithmic law is obeyed with close approximation, both the wire diameter and induced power in the wire have to be as low as possible;

— establishing the validity range for the linear logarithmic law and applying the corrections imply the knowledge of the r_1, ρ_1, c_1, λ_1, ρ, c_p, λ magnitudes;

— in the case of liquids, the duration of the linear logarithmic law range is long enough to allow for a thermal conductivity determination only from the slope of the (Δ) straight line;

— the cell non-ideality, along with the physical phenomenon of heat transfer introduces some additive terms in the line source equation. The (Δ) and (D) straight lines have both the same slope but they are translated one from the other;

— the random measurement errors can be diminished by a statistical computation of the experimental data; the systematic errors do not alter the slope of the (Δ) straight line.

— the determination of thermal diffusivity is accomplished by extrapolating the (Δ) straight line, for $\theta = 0$;

— the instrumental systematic errors and failing to work within the linear logarithmic law range affect seriously the thermal diffusivity value obtained by this procedure;

— the accuracy of thus obtained thermal diffusivity value is, in our oppinion, the most severe experimental test for the measurement accuracy and it constitutes the proof of having worked within the range of linear logarithmic law.

As will be given in a subsequent paper, [12] all these *restrictive conditions* for the *classical procedure* of thermal conductivity and thermal diffusivity determination by the transient hot wire method lead to almost unexceedable difficulties in the case of *gases*, unless a wire of micron-order diameter is employed.

REFERENCES

[1] E. McLaughlin and T.F.T. Pittman, *Phyl. Trans. Roy. Soc. London*, **A 270**, 557 (1971).

[2] H. S. Carslaw and J. C. Jaeger, "Heat Conduction in Solids", Oxford Univ. Press, 1959.

[3] J. J. de Groot, T. Kestin and H. Sookiazian, *Physica*, **75**, 454 (1974).

[4] D. Serbănescu, Gh. Vasu and A. Ciochină, *Rev. Roumaine Chim.*, in press.

[5] R. Vîlcu and A. Ciochină, *Rev. Roumaine Chim.*, **25**, 1113 (1980).

[6] J. C. Jaeger, *Austral. J. Phys.*, **9**, 167 (1956).

[7] N. B. Vargaftik, "Spravochinik po teplofiziceskim svoistvam gazov i zhidkostei", Nauka, Moskva, 1972.

[8] Y. S. Touloukian, P. E. Liley and S. C. Saxena, "Thermophysical Properties of Mater", vol. 3, TPRC Data Series, Plenum Press, New York, 1970.

[9] K. Raznjevic, "Tabele şi diagrame termodinamice", Ed. Tehnică, Bucureşti, 1978.

[10] D. T. Jamieson, T. B. Irving and T. S. Tudhope, "Liquid Thermal Conductivity, a Data Survey to 1973", N.E.L., Edinburgh, 1975.

[11] A.F.O. Falcao, *Rev. Port. Quim.*, **7**, 65 (1965).

[12] R. Vîlcu and A. Ciochină, *Rev. Roumaine Chim.*, in press.

Revue Roumaine de Chimie, 26, 4, 539—543 (1981)

EFECTO DE LA TEMPERATURA SOBRE LA CINÉTICA DE LA HIDRÓLISIS DEL ESTER ETÍLICO DE LA N-BENZOIL-L-TIROSINA CATALIZADA POR α-QUIMOTRIPSINA

F. SEOANE
Seminario de Física y Química. Instituto Nacional "Juan Montes", Lugo, España

Recibido; 10 de enoro de 1980

Se ha estudiado el efecto de la temperatura sobre la cinética de la hidrólisis del éster etílico de la N-benzoil-L-tirosina catalizada por α-quimotripsina. Los parámetros de activación obtenidos están dentro del margen de valores de la energía de enlace por puente de hidrógeno, por lo que puede pensarse que el mecanismo de la reacción transcurra a través de procesos de formación y ruptura de tales enlaces. La presencia de dos zonas de diferente pendiente en las representaciones de Arrhenius y de van't Hoff indica que la α-quimotripsina puede encontrarse en dos estructuras conformacionales dependientes de la temperatura.

The effects of the temperature on the kinetics constants of the α-chymotrypsin-catalyzed hydrolysis of N-benzoyl-L-tyrosine ethyl ester are studied. The activation parameters achieved are in the range of values for bonding energy of the hydrogen bond, then we can suppose that the reaction mechanism occurs by forming and breaking of hydrogen bond processes. The appearance of two different slope fields in Arrhenius and van't Hoff plots, indicates that the α-chymotrypsin can be found in two conformational structures depending on temperature.

El comportamiento cinético de la α-quimotripsin a muestra una fuerte dependencia de la temperatura. De hecho, las constantes de Michaelis y del catalizador de las hidrólisis de ésteres catalizadas por este enzima varían con la temperatura.[1–5]

En este trabajo pretende aclararse la naturaleza de esta influencia, mediante el estudio de la reacción de hidrólisis del éster etílico de la N-benzoil-L-tirosina catalizada por α-quimotripsina.

PARTE EXPERIMENTAL

Materiales. Los reactivos éster etílico de la N-benzoil-L-tirosina (BTEE), N-trans-cinamoil-imidazol, Tris buffer y α-quimotripsina de páncreas bovino 3x cristalizada y liofilizada fueron obtenidos de la Sigma Chem. Co.; el 1,4-butanodiol y el ClK eran de Merck. Todos los reactivos eran P.A. y fueron utilizados sin ulterior purificación.

Las disoluciones de α-quimotripsina fueron preparadas en agua destilada y desionizada inmediatamente antes de cada serie de experiencias. Su normalidad fue determinada por valoración espectrofotómetrica con N-trans-cinamoil-imidazol.[6]

Los márgenes de concentración utilizados fueron : α-quimotripsina $1{,}00-1{,}40 \cdot 10^{-8}$ N y BTEE $0{,}50-2{,}50 \cdot 10^{-4}$ M.

Métodos. La reacción fue seguida por medida de la formación de aminoácido a 255 nm, según el método espectrofotómetrico diferencial de Hummel,[7] utilizando un espectrofotómetro PYE UNICAM SP 1700 provisto de portacubetas termostatado con un error de 0,01°C y unido a un AR 25 Linear Recorder. El cambio total de absorbancia resultaba ser de aproximadamente 0,01 a 0,25 unidades de absorbancia, según fuera el valor de la concentración de las disoluciones de sustrato.

Las experiencias cinéticas fueron realizadas en cubetas de cuarzo de 10 mm, conteniendo 2,50 ml de disolución de sustrato. La reacción se hacía comenzar por adición de 0,100 ml de disolución de enzima. Las velocidades iniciales fueron determinadas a partir de las tangentes en el origen de las curvas absorbancia — tiempo extrapoladas hasta el instante de la adición de la enzima.

Se realizaron experiencias a varios valores de la temperatura comprendidos entre 15 y 28°C y a fuerza iónica constante (50 M) para tres valores diferentes del pH (7,60 ; 7,84 y 8,00). El pH se mantenía constantescon regulador Tris 0,05 M y la fuerza iónica se controlaba con ClK. Todas las experiencias se repitieron al menos dos veces.

Las constantes de Michaelis y del catalizador fueron determinadas mediante la representación de los inversos de las velocidades iniciales frente a inversos de concentraciones iniciales de sustrato según el método de Lineweaver-Burk. En todos los casos se trabajó con concentración 0,40 M de 1,4-butanodiol. Se eligió este valor porque es el que conduce a valores de la constante de Michaelis del orden de los requeridos para la correcta aplicación del método antes citado.

RESULTADOS Y DISCUSIÓN

Cuando se realizaron las representaciones gráficas de Arrhenius y van't Hoff se observó que ambas satisfacían la linealidad, presentando la particularidad de que en las correspondientes a pH = 7,84 aparecían dos rectas bien definidas. Este resultato parecía sugerir que existían dos formas de α-quimotripsina dependientes de la temperatura. La idea de diferentes conformaciones dependientes de la temperature para la α-quimotripsina aparece ya en la bibliografía. Así, Kaplan y Laidler[1] la utilizan para explicar la existencia de dos líneas de diferente pendiente en la representación de Arrhenius correspondiente a la hidrólisis de ésteres metílicos de algunos aminoácidos ; además, proponen que la diferencia entre ambas formas corresponde a una desnaturalización reversible. Estas ideas fueron desarrolladas por Fersht y Requena[8] y Wedler y cols.,[9] quiénes las modificaron en el sentido de considerar que las dos formas son catalíticamente activas. Posteriormente, Adams y cols.[10-11] demonstraron la validez de la hipótesis de cambio conformacional, aunque con la modificación de considerar que la temperatura no tiene por qué alterar la estructura de la enzima, sino que es suficiente con que modifique la parte hidrófoba del centro activo.

En un estudio realizado por nosotros[12] habíamos encontrado la existencia de dos conformaciones dependientes del pH, lo que nos indujo a pensar que podía existir alguna relación entre ambos fenómenos. Por ello, se repitieron todas las experiencias a dos valores del pH, uno inferior (7,60) y otro superior (8,00) al utilizado anteriormente, de modo que en cada caso la enzima se encontrase en una sola de las formas. Se eligió el valor de pH = 8,00 porque es lo suficientemente elevado para los fines buscados, no presenta los inconvenientes que plantea el trabajo en medios fuertemente básicos (autohidrólisis, desnaturalización, etc) y, sobre todo, porque podía ser alcanzado con el mismo regulador, con lo que no se introducía ningún elemento extraño. El pH = 7,60 se eligió por motivos idénticos a los anteriores.

Las correspondientes representaciones de Arrhenius y van't Hoff se exponen en las gráficas 1 y 2, cuya interpretación realizaremos a continuación.

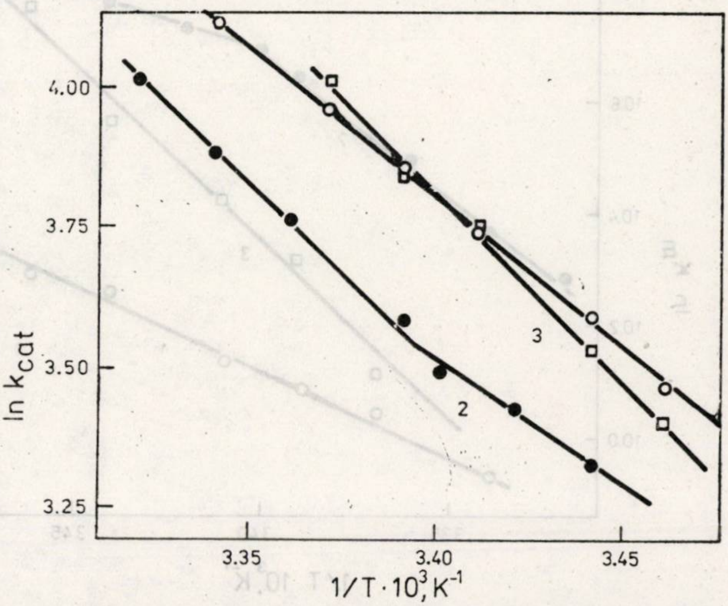

Fig. 1. — Representación del logaritmo neperiano de la constante del catalizador frente al inverso de la temperatura absoluta para los valores del pH: 1. 7,60 (○), 2. 7,84 (●) y 3. 8,00 (□).

En primer lugar centraremos la atención sobre las representaciones de Arrhenius. Lo primero que se observa es que a valores del pH altos y bajos sólo se obtiene una recta, en tanto que al pH intermedio aparecen dos, dependientes del intervalo de temperatura. Al comparar los valores de las energías de activación se obtiene que al correspondiente a pH = 7,60 (45,6 kJ/mol) es sensiblemente igual al registrado a las temperaturas inferiores a 21 °C y pH = 7,84 (44,7 kJ/mol), lo mismo le sucede al obtenido a las temperaturas superiores a 21 °C y pH = 7,84 (53,1 kJ/mol) y al correspondiente a pH = 8,00 (56,2 kJ/mol). Según acabamos de ver, los dos primeros valores son practicamente iguales y los dos últimos, también. Por tanto, puede considerarse que sólo existen dos energías de activación diferentes. Además, el que ambas sean de unos órdenes de magnitud comprendidos en el intervalo de posibles valores de las energías de formación de enlaces por puente de hidrógeno conduce a pensar que la reacción objeto de estudio transcurre a través de un mecanismo en el que procesos de formación y ruptura de tales enlaces pueden desmpeñar un papel determinante.

Resultados totalmente análogos se obtienen al considerar los valores de las entropías de activación.

En este punto pasaremos a considerar las representaciones de van't Hoff, realizadas para los valores de la constante de Michaelis. En primer lugar, puede comprobarse que a los valores extremos del pH sólo se obtiene una recta para el intervalo de temperaturas estudiado, mientras que, al intermedio, aparecen dos con diferente pendiente. Todas estas observaciones vienen a apoyar la interpretación, ya expuesta, de que a los valores extremos del pH la α-quimotripsina se encuentra en una sola forma y en el intermedio es posible que aparezcan dos formas diferentes de acuerdo con el intervalo de temperaturas.

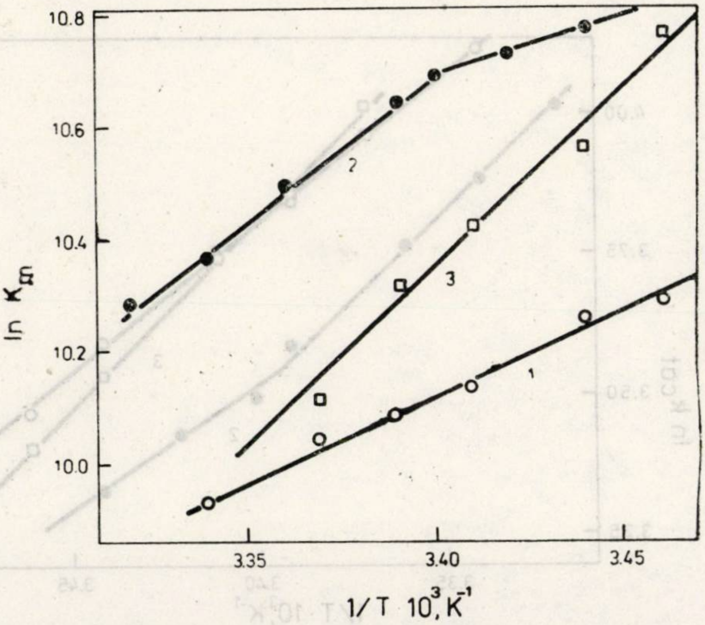

Fig. 2. — Representación del logaritmo neperiano de la constante de Michaelis frente al inverso de la temperatura absoluta para los valores del pH : 1. 7,60 (○), 2. 7,84 (●) y 3. 8,00 (□).

El valor de la entalpía obtenido a pH intermedio y a temperaturas inferiores a 21 °C (20,1 kJ/mol) es igual sensiblemente al correspondiente a pH = 7,60 (24,7 kJ/mol), lo mismo que sucede con el registrado a las temperaturas superiores a 21 °C (48,2 kJ/mol) y el de pH = 8,00 (53,6 kJ/mol). Además, el que todos estos valores sean de unos órdenes de magnitud comprendidos en el intervalo de los posibles valores de la energía de enlace por puente de hidrógeno apoya la hipótesis de que la reacción puede encontrarse condicionada por procesos de formación y ruptura de dichos enlaces.

A la luz de estos resultados cabe discutir las posibilidades de que el cambio conformacional producido por el pH sea o no igual al producido por la temperatura.

En primer lugar, si consideramos tanto los valores de las entalpías de activación como las de formación del complejo, puede pensarse que tales cambios son iguales, debido a que los pares de valores correspondientes a aquellas magnitudes obtenidos a pH = 8,00 pueden identificarse con los registrados en la región de temperaturas más altas y pH = 7,84, lo mismo que sucede con los correspondientes a pH = 7,60 y los de la región de temperaturas más bajas y pH = 7,84. También los valores de las entropías de activación apoyan esta interpretación.

En segundo lugar, como el pH = 7,84 es el correspondiente al punto isoeléctrico, puede aceptarse que en él coexisten las dos formas de α-quimotripsina dependientes de la acidez. Por esa misma razón, para cada uno de los otros valores del pH existirá solamente una de las dos formas.

En tercer lugar, el comportamiento de la reacción respecto a la temperatura es diferente según que el pH tome el valor de 7,60 ó de 8,00, como indican los diferentes valores de las entalpías y entropías de activación y de formación del complejo.

Así pues, una variación en la forma de la enzima que predomine permite interpretar el cambio de comportamiento registrado para pH = = 7,84, es decir, que el efecto de la temperatura puede consistir simplemente en ,,destacar'' una de las formas dependientes del pH que ya existen ennel medio.

Como consecuencia de todo lo anterior, es posible considerar que el cambio conformacional debido a la temperatura es el mismo que el producido por el pH.

AGRADECIMIENTOS. Quiero agradecer al Ministerio de Educación y Ciencia de España la concesión de una beca de formación de personal investigador.

BIBLIOGRAFÍA

[1] H. Kaplan y K. J. Laidler, *Canad. J. Chem.*, **45**, 547 (1967).
[2] T. H. Fife y J.B. Milstein, *Biochemistry*, **6**, 2901 (1967).
[3] R. Lumry, *J. Phys. Chem.*, **75**, 1375 (1971).
[4] J. M. Glick, *Biochim. Biophys. Acta*, **250**, 390 (1971).
[5] J. E. Baggott y H. Klapper, *Biochemistry*, **15**, 1473 (1976).
[6] G. R. Schombaum, B. Zerner y M. L. Bender, *J. Biol. Chem.*, **236**, 2390 (1961).
[7] B.C.W. Hummel, *Can. J. Biochem. and Physiol.*, **37**, 1393 (1959).
[8] A. R. Fersht y Y. Requena, *J. Mol. Biol.*, **60**, 279 (1971).
[9] F. C. Wedler, L. S. Uretsky, G. McLune y J. Cencula, *Arch. Biochem. Biophys.*, **170**, 476 (1975).
[10] P. A. Adams y E. R. Swart, *Biochem. J.*, **161**, 83 (1977).
[11] P. A. Adams, E. R. Swart y C. A. Vernon, *J. Chem. Soc. Faraday*, **172**, 397 (1976).
[12] J. M. Cachaza, J. Casado y F. Seoane, *Rev. Roumaine Chim.* (En prensa).

Revue Roumaine de Chimie, **26**, *4*. 545–564 (1981)

KINETIK UND MECHANISMEN DER REAKTION IN DEN REAKTANTENMISCHUNGEN IM SYSTEM $Na_2O-CaO-Al_2O_3-SiO_2-CO_2$

RADU DINESCU* und MIHAI V. CERCHEZ**
* Politechnisches Institut, Bukarest, Rumänien
** Forschung- und Projektierungsinstitut für Glas und Keramiktechnologien, Bukarest, Rumänien

Eingegangenam 24. April 1980

An drei representativen Mischungen der quarzreichen Seite des Systems $Na_2O-CaO-Al_2O_3-SiO_2-CO_2$ werden, bis Temperaturen von 900–1 000°C, kynetische Untersuchungen in nichtisothermen Regime durchgefürht. Die vergleichende Analyse, einerseits der bestimmten kinetischen Parametern und anderseits der Verlauf der thermischen Kurven (DTA und TG), hat die phänomenologische Charakterisierung. Die Hauptreaktionen, die bis 1.000°C in den untersuchten Mischungen stattfinden, sind ähnlich mit jenen die in den Reaktantenmischungen des Systems $Na_2O-CaO-SiO_2-CO_2$ stattfinden, mit der Erwähnung, dass Unterschiede auftreten, abhängig von der chemischen Zusammensetzung, in der Reihenfolge und Menge der sich bildenden Komponenten.

For three representative compositions belonging to the siliceous zone of the $Na_2O-CaO-Al_2O_3-SiO_2-CO_2$ system a kinetic study is undertaken, in non-isothermal working conditions, up to 900–1 000°C. The comparative analysis of the kinetic parameters and, at the same time, of the general appearance of the DTA — curve, permitted a phenomenological characterisation of the reaction mechanism for the three compositions. The main reactions taking place in the studied mixtures, up to 1 000°C, are the same as in the $Na_2O-CaO-SiO_2-CO_2$ system, existing only differences, related to the chemical compositions in the succession and quantity of the formed compounds.

Die Reaktionsmechanismen zwischen den verschiedenen Verbindungen, welche die Zusammensetzung der Rohstoffmischungen bilden während der bestimmten Wärmebehandlung, spielen eine wichtige Rolle in der Herstellung von silikatischen und oxydischen Massen mit verschiedenen Anwendungen (Kröger,[1-4] Eitel,[2] u.a.). Diese Tatsache wurde sowohl in der Keramik- und Feuerfeststoffindustrie (Solacolu, [5] Solacolu und Dinescu,[6] u.a.) als auch in der Glastechnologie, besonders zur Erzielung homogener Schmelzen bei niederen Temperaturen (Roy,[7] Dislich,[8] Malarme,[9] Bezborodov,[10] u.a.), bewiesen.

Die Kenntnis der Reaktionskinetik von Zusammensetzungen der Rohstoffmischungen erlaubt die Beurteilung und Leitung thermischer Prozesse auf physikalisch-chemischen Grundlagen sowohl bei wissenschaftlichen Versuchen als auch in der industriellen Praxis.

Die Verwendung von künstlichen Verbindungen oder natürlichen Mineralien in den industriellen Rohstoffmischungen, die alkalische oder erd-alkalische Oxyde enthalten, bewirkt bedeutende Unterschiede im Verlauf der Reaktionen, da in den polinären Zusammensetzungen oft Prozesse und Phasen von Gleichgewichtstörungen wie z.B. selbständige Schmelzvorgänge einiger der Rohstoffe vorkommen.[5,6]

Die Zunahme der Oxydeanzahl im System kompliziert die Reaktionsmechanismen, gemäss dem Phasengesetz, durch Anzahlzuwachsen der möglichen Verbindungen und Ab-oder Zunahme der Wahrscheinlichkeit des Erhaltens bestimmter Phasen welche in einigen Fällen Glas erzeugen können.

Wenn auch die Reaktionen bei thermischer Behandlung von Massen des Systems $Na_2O - CaO - SiO_2$, vom Gebiet der Zusammensetzung der Natronkalkgläser eingehend studiert sind,[1,2,10] wurden dagegen jene der quaternären entsprechend den obenerwähnten, mit Al_2O_3, noch nicht geforscht.

In den folgenden Auslegungen sind Hauptangaben aus der Fachliteratur betreffend Mechanismen und Kinetik der Reaktionen aus den studierten binären und ternären Systemen, einiger Zusammensetzungen entsprechend den üblichen Natronkalkgläser und ferner einige originelle phänomenologische Erwägungen die den Reaktionsmechanismus und Kinetik bis 900°C betreffen, auf der Basis thermogravimetrischer Forschungen für quaternäre Massen des Systems $Na_2O - CaO - Al_2O_3 - SiO_2$, dargelegt.

1. ANGABEN AUS DER FACHLITERATUR BETREFFEND MECHANISMEN UND KINETIK DER REAKTIONEN IN OXYDISCHEN SYSTEMEN DIE FÜR DIE GLAS -UND KERAMIKTECHNOLOGIE VON INTERESSE SIND

Die Literaturangaben,[1-16] insbesondere auf dem Gebiet des Glases sind auf Untersysteme gruppiert die dem quaternären System $Na_2O - CaO - Al_2O_3 - SiO_2 - CO_2$ angehören.

Die Analyse der Reaktionen in fester Phase und in Anwesenheit erster Mengen flüssiger Phase der Komponenten (Oxyde, Salze, Naturrohstoffe) der Reaktantenmischung aus den dazugehörigen Untersystemen, erlaubt die Festlegung einiger Studiumvoraussetzungen für die bis heute noch nicht eforschten Massen des Systems $Na_2O - CaO - Al_2O_3 - SiO_2$ die aus körnigen Quarz, Natrium- und Kalziumkarbonaten sowie auch Tonerde, sämtliche von kontrollierter Körnung, hergestellt wurden.

1.1. DAS SYSTEM $Na_2O - SiO_2 - CO_2$

Im System $Na_2O - SiO_2 - CO_2$ ist der ausschlaggebende Faktor der Reaktionenkinetik in fester Phase und im Vorhandensein von Schmelze die Diffusion.

Es ist bekannt, dass der Reaktionsanfang zwischen Na_2CO_3 und SiO_2 in Quarzform, nachgewiesen durch eine der empfindlichsten Druckmessmethode welche die ausgeströmten Gase der Reaktion erfasst, bei niedrigen Temperaturen von 300 –400°C stattfindet, wenn die thermische Schwingungsenergie ausreichend wird, und die Zerstörung der Bindungen zwischen den SiO_4- Tetraedern und deren Reaktion mit dem

Natriumkarbonat erlaubt. Die erste Verbindung die sich bildet ist das Metasilikat das bei höheren Temperaturen (700°C) in Disilikat übergeht[1–4,10–14,17] mittels Mechanismen deren Kinetik Diffusions kontrolliert ist. Es ist eine allgemein anerkannte Tatsache, dass die Hauptreaktionen bis 1000°C mit Bildung dieser Verbindungen ablaufen deren Zusammensetzung von den Mengen der beiden Oxyde der Rohstoffmischung und den Bedingungen der Reaktionsabwicklung abhängen. Neuere Forschungen [18] präzisieren die Bildung des $Na_2O \cdot 2SiO_2$, im System ohne aber zuesrt die Bildung des Metasilikates anzugeben. Dieselben Forschungen zeigen aber die Bildung von Metasilikat bei Temperaturen über 850°C an.

Betreffend die Methodologie der Erforschung von Bildungsreaktionen der angeführten Verbindungen, empfehlen Oldfield,[15] Wilburn und Thomasson[16], Wilburn, Thomasson und Cole,[19] Wilburn, Metcalfe und Warburton[20] und Partridge[21] die Möglichkeit, beim Studium der Reaktionen zwischen den ursprünglichen Komponenten der Rohstoffmischung bis zur Glasbildung, die differentiellen thermischen und thermogravimetrischen Analysen zu benützen. Die, durch diese Forscher durchgeführten Studien haben nur einen qualitativen, nichtkinetischen Charakter, und betreffen nur die Erkennung der Phasen die sich bei hoher Temperatur in der Reaktantenmischung bilden. Diese Studien[15–18,19–21,22] präzisieren die Tatsache, dass im System $SiO_2 - Na_2CO_3$ wichtige Reaktionen die von der Anwesenheit der flüssigen Phase bestimmt sind erst ab ungefähr 830°C anfangen. Die vorangehenden Reaktionen die sich besonders in der festen Phase abspielen sind von keiner Bedeutung.

Bezüglich der Bildung verschiedener Verbindungen wird, im Falle der Benützung von diffraktometrischen Techniken, noch die Erscheinung im binären System von einigen Linienintensitäten angezeigt die nicht erklärt werden können.[22] Es wurde durch Studium von Phasendiagramme[23,24] auch die Existens der Verbindung $3Na_2O \cdot 8SiO_2$ erkannt, welche aber bis heute in den kinetischen Forschungen nicht nachgewiesen wurde. Das es eine Verbindung mit Kieselsäuereüberschuss ist, ist es möglich, dass diese mit der vorher durch Budnicov und Matveev erkannte Verbindung gleich sein könnte, welche von diesen als $Na_2O \cdot 3SiO_2$ bezeichnet wurde.[25]

Howarth, Sykes und Turner[26–27] prüfen die Kinetik der Reaktionenentwicklung und nehmen an, dass ein Diffusionsmechanismus in den Mischungen mit dem Molarverhältnis $Na_2CO_3 : SiO_2$ von 1:1 und 1:4 vorhanden ist; es wurde die Erhöhung der Reaktionsgeschwindigkeit mit zunehmender SiO_2-Menge und der Temperatur der Mischung festgelegt (die Reaktionsgeschwindigkeit steigt am schnellsten von 650°C bis 700°C und die Reaktion in fester Phase ist bei 900°C praktisch beendet). Kröger und Mitarbeiter[13–14] bestätigen diese Festlegungen, bezüglich des Diffusionsmechanismus der Reaktionskinetik, und stellen die Erhöhung der Reaktionsgeschwindigkeit mit der Zunahme des Verhältnisses $SiO_2 : Na_2CO_3$, fest.

Auf Grund dieser Angaben kann man abschliessend sagen, dass über 700°C, im Bereich der intensiven Diffusionsprozesse im Volumen, der Gebrauch der Jander-Relation als möglich erscheint. Der klassische Ausdruck wurde aber durch Kröger und Blömer korrigiert, die die Beziehung vorschlagen:

$$[1 - \sqrt[3]{(100 - x)/100}]^2 = k \ln t \qquad (1)$$

in welcher:

x = Menge des reagierten Erzeugnisses;

t = Zeit;

k = Konstante der Reaktionsgeschwindigkeit die logarithmische Korrektur nimmt in Betracht, gemäss den Autoren, einige Änderungen gegenüber den Lehren des Tammann und Jander die den Diffusionskoeffizient und die Temperatur als unveränderlich für die Verbindungen welche in der Kontaktschichte reagieren, betrachten.[1,3-4,13-14]

Die vorgeschlagene kinetische Beziehung wurde durch Experiment auf verschiedene Zusammensetzungen von binären und ternären Messen des Systems $Na_2O - CaO - SiO_2 - CO_2$ als korekt erwiesen.

1.2. DAS SYSTEM $CaO - SiO_2 - CO_2$

Im System $CaO - SiO_2 - CO_2$ treten keine fühlbaren Reaktionen in der Bildung von Verbindungen als nur über 1000°C auf.[18,28-29,20] Die üblich erste erscheinende Verbindung ist das Dikalziumsilikat gefolgt vom Kalziummetasilikat.

Abd-Ed-Moneim, Abou-El-Azm und Moore[28] studieren die Reaktionskinetik zwischen SiO_2 und den verschiedenen Oxyden; es wird bewiesen, dass im System $CaO - SiO_2$ die Reaktionen auf fassbarer Weise über 1200°C erscheinen und dass die Reaktiongeschwindigkeiten zwischen SiO_2 und anderen Oxyden sowohl in den binäran als auch in den ternären Mischungen und der Reihenfolge: $K_2O > Li_2O > Na_2O > Na_2O > PbO > B_2O_3 > BaO > CaO > ZnO > MgO > TiO_2 > Al_2O_3 > ZrO_2$ abnehmen.

1.3. DAS SYSTEM $Al_2O_3 - SiO_2 - H_2O$

In diesem System sind besonders die Abwicklungsbedingungen der Dehydroxylierreaktionen und der Bildung von binären Verbindungen[17,30,31-34] aus tonartigen Mineralien bekannt. Sowohl durch Experiment als auch theoretisch ist auf diese Weise die Bildung des Mullits bei Temperaturen von über 1000°C eindeutig bewiesen.

1.4. DAS SYSTEM $Na_2O - CaO - CO_2$

Dieses System ist vom thermodynamischen Standpunkt unter Form von Karbonaten nachgeforscht worden, deren Diagramm des thermischen Gleichgewichts,[35,36] in welchem die Bildung der Verbindung $Na_2CO_3 \cdot CaCO_3$ und einiger festen Lösungen von doppelten Karbonaten angezeigt wird, bekannt ist.

1.5. DAS SYSTEM $Na_2O - Al_2O_3 - CO_2$

Die Verbindungen Na_5AlO_4 und $NaAlO_2$ werden bei Temperaturen unter 1000°C, nur in binären Mischungen mit über 38 % Na_2O erhalten, während $NaAl_5O_8$ und $NaAl_4O_7$, welche feuerfest sind, sich bei Temperaturen von über 1000°C bilden.[37-38] Desgleichen wurde auch das Vorkommen der Verbindung $NaAl_2O_2$[39] angezeigt.

1.6. DAS SYSTEM $CaO-Al_2O_3-CO_2$

Durch hohe Feuerfestigkeit gekennzeichnet,[35-40] ist dieses System gegenwärtig, vom kinetischen Standpunkt nicht studiert.

1.7. DAS SYSTEM $Na_2O-CaO-SiO_2-CO_2$

Die kinestischen Reaktionstudien begründet auf der Bestimmung der sich ergebenden Gasmenge, im ternären System $Na_2O-CaO-SiO_2$ die von Kröger und Marwan[1,3] durchgeführt wurden, zeigen Änderungen der Reaktiongeschwindigkeitskonstante mit chemischer Zusammensetzung in Anbetracht des Umstande, dass in den Massen der Art $Na_2O \cdot xCaO \cdot ySiO_2$ ($x=1-2{,}7$; $y=2-9{,}3$), die aus Natriumkarbonat, Kalziumkarbonat und Quarzsand erhalten, die Reaktionen sich nach einem räumlichen Diffusionsmechanismus entwickeln.

Kröger und Blömer[4] geben ein qualitatives Schema an das den Migrationsmechanismus, durch Diffusion in entgegengesetzter Richtung der Kationen, aus Mischungen mit der Zusammensetzung des gewöhnlichen Glasses, die bis zu Temperaturen entsprechend dem Reaktionsbereich in fester Phase erwärmt, wurden veranschaulicht.

Desgleichen wird betrachtet angenommen, dass die Reaktionsgeschwindigkeit, bei 700 — 900°C, in ternären Mischungen, mit den Körnunggrössen die den industriellen Glasgemengen entsprechen, von der durch das Schmelzen der Karbonate sich bildenden flüssigen Phase abhängt.

Die Hauptreaktionen bis 1000°C verlaufen mit Bildung von binären Natriumoxyd-Kieselsäureverbindungen und den ternären Natron-Kalksilikaten aus dem sauren Bereich des Systems $Na_2O-CaO-SiO_2$, was durch die erhöhten freien Bildungsenergien dieser Verbindungen bestätigt ist.

Kautz[18,22] macht im Jahre 1969 eingehende vergleichende Studien, anfangs an bibliographische, dann experimentell, an einigen Industriellen sowie Mischungen aus Laborreagenzien. Auf Grund dieser sowie der von uns oben angeführten Erfahrungen zusammenfassend, wurde die Tatsache präzisiert, dass in Übereinstimmung mit den Forschungen von Kröger und Mitarbeiter, die flüssige Phase bei 760°C auftritt. Diese Schmelze ist das Resultat der peritektischen Reaktion bei der angeführten Temperatur zwischen vorher gebildeten binären und ternären Verbindungen. Des weiteren, wird die Entwicklung der Menge flüssiger Phase durch das Schmelzen des Eutektikum des doppelten Karbonates mit seinen, an Natriumkarbonat reichen festen Lösungen, bei 790°C, sowie das Schmelzen bei 820°C des $Na_2CO_3 \cdot CaCO_3$ und bei 856°C des Na_2CO_3 erklärt.

Kautz und Stromburg[22] durch weitere eigene Laborarbeiten weisen als sicher sich bildend die Verbindungen nach $Na_2Ca(CO_3)_2$ (zwischen 500 —835°C), $2NaO \cdot CaO \cdot 3SiO_2$ (zwischen 790 —1100°C) und $Na_2O \cdot SiO_2$ welches sich ab 850°C zu bilden anfängt. Es ist merkwürdig, dass die Autoren die Bildung von $Na_2Ca(CO_3)_2$ und $Na_2O \cdot SiO_2$ in den Gemengen der Industrie nicht identifizieren, ihrer Meinung nach wegen der grossen Körnung des Dolomites.

Beim diffraktometrischen Studium erscheinen sowohl im Fall der industriellen Glasgemenge als auch bei jenen für Laborexperimente, Reflexe von verminderter Intensität welche nicht erklärt werden können. Also, können sich neben den Verbindungen $Na_2O \cdot SiO_2$, $Na_2O \cdot 2SiO_2$, $Na_2O \cdot 2CaO \cdot 3SiO_2$ und $2Na_2O \cdot CaO \cdot 3SiO_2$ auch andere Verbindungen oder feste Lösungen bilden.

Im Jahre 1971[23] wird die Verbindung $Na_2O \cdot CaO \cdot 5SiO_2$ identifiziert welche eine beständige Phase, besonders im Subsolidusbereich ist und es ist wahrscheinlich, dass diese sich auch bei der Erwärmung der Glasgemenge bildet.

1.8. DAS SYSTEM $Na_2O-Al_2O_3-SiO_2-CO_2$

Im System $Na_2O-Al_2O_3-SiO_2-CO_2$ bilden sich bis 1000°C nur Natriumsilikate was durch die grosse Reaktivität des Na_2CO_3 gegenüber den SiO_2 im Vergleich zum Al_2O_3 erklärlich ist. Desgleichen, sind Mechanismen und Reaktionskinetik im ternären System natürlicher Rohstoffe : Quarz-Kaolinit –Feldspat gut bekannt.[2,6]

1.9. DIE SYSTEME $CaO-Al_2O_3-SiO_2-CO_2$ und $Na_2O-CaO-Al_2O_3-CO_2$

Im System $CaO-Al_2O_3-SiO_2-CO_2$ treten keine erfassbaren Reaktionen der Bildung von Verbindungen als nur über 1000°C auf,[15,28–29] wo sich erst die binären basischen Verbindungen und nachher die ternären Verbindungen bilden. Die Reaktionsdauer ist gross : bis Hunderte von Stunden.

Das System $Na_2O-CaO-Al_2O_3$ [39] ist vom Standpunkt der thermischen Gleichgewichte nur teilweise erforscht worden während die Reaktionsmechanismen noch nicht studiert sind.

1.10. DAS SYSTEM $Na_2O-CaO-Al_2O_3-SiO_2-CO_2$

Dieses System ist vom Standpunkt der thermischen Gleichgewichte, in der Nähe des Bereiches des Untersystems $Al_2O_3-SiO_2$ eingehend studiert [40–43] worden und das Studium der Untersysteme die dem Glas angehört hat begonnen.[24]

★

Aus den durchgeführten Forschungen in den binären und ternären Systemen kann man schliessen, dass die Zugabe von Al_2O_3, in beschränkten Mengen zu den Massen des Systems $Na_2O-CaO-SiO_2-CO_2$, bei niederen Temperaturen, nur die Rolle eines Verdünnungsmittels hat, inaktiv vom chemischen Standpunkt, ohne die Art und Reihenfolge in der Bildung von Verbindungen des angeführten ternären Systems zu verändern.

Die vorliegende Arbeit beabsichtigt das chemische Verhalten der Tonerde in den quaternaren Natronkalkmassen mit verschieden Tonerdegehalt, zu klären. Gleichfalls wurde die Bildung und Entwicklung der flüssigen Phasen im System in Beziehung mit der Oxydzusammensetzung der Rohstoffmischungen sowie mit den physikalische-chemischen Hauptreaktionen der enstandenen Verbindungen verfolgt.

TABELLE 1

Modulare oxydische Zusammensetzung*) und die Lage**) der quaternären Massen im System $Na_2O - CaO - Al_2O_3 - SiO_2$

Massen Nr.	SiO_2	Al_2O_3	CaO	Na_2O	SiO_2 (%) / Na_2O (%)	SiO_2 (%) / Al_2O_3 (%)	Al_2O_3 (%) / Na_2O (%)	M_A	M_C	Lage	Untersystem	Gebiet vom technologischen interese
	% — Gewicht (Mole)											
1.	69,8 (23,2)	21,0 (4,2)	6,0 (2,2)	3,2 (1,0)	21,8	3,3	6,6	43,8	6,5	$F_1 = -S - 1,55A - 0,086N + 100 < 0$ $F_2 = -S - 0,43A + 1,73N + 58,9 < 0$ $F_3 = -S - A - N + 100 > 0$	I : $NAS_6 - CAS_2 - A_3S_2 - S$	Keramik
2.	60,9 (5,7)	21,3 (1,2)	6,5 (0,9)	11,2 (1,0)	5,4	2,9	1,9	83,1	3,7	$F_1 > 0$ $F_4 = A - 1,65N > 0$ $F_5 = -S - 0,23A + 1,83N + 51,75 < 0$	II : $NAS_6 - CAS_2 - CS - S$	
3.	71,7 (6,6)	10,7 (0,6)	6,7 (0,7)	11,0 (1,0)	6,5	6,7	1,0	165,4	3,8	$F_4 < 0$ $F_6 = S - 0,34A - 0,89N - 51,75 > 0$ $F_7 = S + 0,65A - 3,72N + 100 > 0$	III : $NAS_6 - NC_3S_6 - CS - S$	Glas

*) In vorherigen Arbeiten [45,46] wurden die Grundlagen eines Modulären Systems für die Charakterisierung der quaternären oxydischen Massen ausgearbeitet aus welchen in dieser Arbeit benützt werden:

$$M_A = \frac{\% CaO + \% Na_2O}{\% Al_2O_3} 100 ; \quad M_C = \frac{\% CaO}{\% Na_2O + \% CaO} 10 ;$$

**) In den gleichen Arbeiten [45,46] sind die quaternären Untersysteme analytisch, durch die Grenzwertgleichung (ebene) der ternären Untersysteme, mit Buchstabe F bezeichnet, begrenzt ; $N = Na_2O$, $C = CaO$, $A = Al_2O_3$, $S = SiO_2$.

Die Entwicklung im einzelnen der Phasenzusammensetzung unter bestimmten Wärmebehandlungsbedingungen mit den gegenwärtigen Forschungstechniken schwer zu beurteilen, wurde nur im allgemeinen verfolgt.

2. ARBEITSWEISE

2.1. EXPERIMENTELLE BESTIMMUNGEN

Die quaternären Mischungen wurden durch trocken Method unter Verwendung folgender chemische Stoffe hergestellt: Natriumkarbonat, Kalziumkarbonat, Korund, alle von proanalysi Reinheit sowie gemahlter Quarz, der aus einer inländischen Lagerstäte stammt, mit einem Gehalt von über 99,8% an SiO_2.

Die oxydische Zusammensetzung, moduläre Kennzeichnung und die Lage im quaternären System $Na_2O-CaO-Al_2O_3-SiO_2$ der untersuchten Massen sind in der Tabelle 1 angegeben. Die Körnung der dosierten Reaktanten ist in Tabelle 2 enthalten; diese wurden während einer Minute im Vibrator vom Typ Ardenne, mit einer Kugel, homogenisiert. Der Homogenisierungsgrad wurde durch übliche chemische, Methoden geprüft.

TABELLE 2 a

Granulometrische Zusammensetzung der benützten Reaktanten (%)

Körnunggrösse	Quarz		Natriumkarbonat		Kalziumkarbonat		Kalzinierte Tonerde	
	Ursprünglich	Nach 1 Minute im Homogenisiergerät	Ursprünglich	Nach 1 Minute im Homogenisiergerät	Ursprünglich	Nach 1 Minute im Homogenisiergerät	Ursprünglich	Nach 1 Minute im Homogenisiergerät
0,4 mm > Ø > 0,2 mm	25,0	18,0	92,5	53,5	25,0	22,5	—	—
0,2 mm > Ø > 0,1 mm	43,5	43,5	5,0	28,5	15,0	15,5	12,5	17,5
0,1 mm > Ø > 0,09 mm	8,5	9,0	2,5	3,5	17,5	17,5	24,0	15,0
Ø < 0,09 mm	23,0	29,5	0,0	14,5	42,5	45,0	63,5	67,5

TABELLE 2 b

Granulometrische Zusammensetzung untersuchter Reaktantenmischungen nach einer Minute Homogenisierung (%)

Körnunggrösse	Masse 1	Masse 2	Masse 3
0,4 mm > Ø > 0,2 mm	0,57	7,52	5,30
0,2 mm > Ø > 0,1 mm	30,96	33,18	35,40
0,1 mm > Ø > 0,09 mm	9,50	10,62	7,52
Ø < 0,09 mm	58,97	48,67	51,77

Thermogravimetrische Bestimmungen wurden mittels Derivatograph vom Typ OD-102/MOM-Budapest mit einer Temperatursteigung von 10°/Minute bis 1000°C durchgeführt.

Die Korrektur der Temperaturenskala, die durch die Geschwindigkeit der Erwärmung gegen höhere Temperaturen verschoben wurde, ist durch Aufstellung einer Eichkurve (Abb. 1) mit SiO_2, Kl, NaCl, und $BaCl_2$ vorgenommen worden. In den Bild 2–6 sowie im Text sind nur die registrierten Temperaturen bei Erwärmungsgeschwindigkeiten von 10°C/ Minute angegeben.

2.2. RECHNUNGSWEISE

Die kinetischen Studiermethoden der chemischen Gleichungen im isothermen und nichtisothermen Regime sind gut bekannt.[2,4,44–49] Einige der wichtigeren methodologischen Fragen wurden in unseren vorherigen Arbeiten dargelegt.[44–49]

Die kinetischen Berechnungen wurden in beiden Varianten, quasiisotherm *) und nichtisotherm durchgeführt, dieses auch zwecks Klärung und Vergleichung der beiden Untersuchungsmethoden der Kinetik die auf dynamische thermogravimetrische Angaben beruhen. Obwohl in der vorliegenden Arbeit der Umsatzgrad der Reaktion durch thermogravimetrische Bestimmungen festgelegt wurde, kann dieser auch aus thermodifferentiellen Angaben geschätz werden.[47]

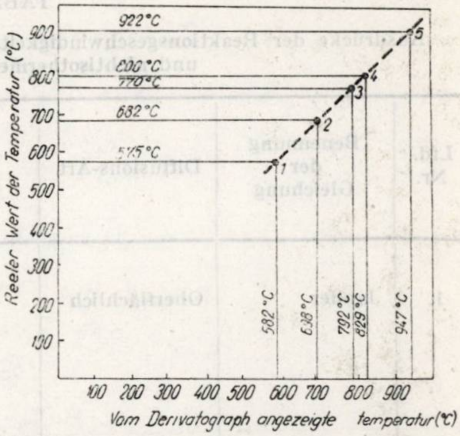

Abb. 1. — Korrektur der vom Derivatograph verzeichneten Temperaturen in Abhängigkeit der Erwärmungsgeschwindigkeit: 1. SiO_2; 2. KI; 3. KCl; 4. NaCl; 5. $BaCl_2$.

In der Tabelle 3 sind die Rechnungsbeziehungen der Reaktionskinetik die auf Diffusionsmechanismus beruht sowohl in quasiisothermen als auch in nichtisothermen Varianten angegeben. Nach der Bestimmung des Umsatzgrades wurden die Konstanten der Reaktionsgeschwindigkeit unter quasiisothermen Bedingungen sowie die Beziehungen der entsprechenden Reaktionsgeschwindigkeit für nichtisotherme Bedingungen berechnet.

Aus den graphischen Darstellungen, in Abhängigkeit vom Kehrwert der Temperatur in Absolutgraden, haben sich lineare Variationen ergeben welche die Abschätzung der Aktivierungsenergie aus der Geradenneigung erlauben.

Die Rechnungen wurden mittels eines Rechners auf Grund entsprechender Programme durchgeführt.

3. ERHALTENE ERGEBNISSE

3.1. CHEMISCHE REAKTIONEN BEI DER WÄRMEBEHANDLUNG VON MISCHUNGEN AUS REAKTANTEN

Der Vergleich thermischer Effekte der Massen 1—3, bei Erwärmung der Mischungen (Abb. 2) zeigt die Differenzierung der Masse 1 gegenüber den Proben 2 und 3. Diese Erscheinung ist in Übereinstimmung mit dem Gehalt an Natriumdioxyd und Kalziumoxyd der drei Proben u.z.w.: Mischung 1 enthält für einen Prozentsatz von 6% CaO nur 3,2% Na_2O, während die Proben 2—3 einen Gehalt an CaO von 6,5—6,7% und an Na_2O von 11,0—11,2% haben. Die Probe 1 enthält also in Überschuss $CaCO_3$ gegenüber Na_2CO_3 welcher auf der DTA-Kurve durch die Spitze des endothermen Effektes bei 920°C erkannt wird, Effekt welcher im Falle der Massen 2—3, bei welchen das Natriumkarbonat in grösserer Menge ist, abwesend ist.

Die endothermen Effekte von niedriger Temperatur (130°C) zeigen die Wassermenge der Reaktantenmischungen an, die von der kalzinierten

---

*) Ein quasiisothermischer Prozess ergibt sich als Annäherung eines dynamischen Prozess mit einer Unendlichkeit izothermer Gleichgewichte.

TABELLE 3

Ausdrücke der Reaktionsgeschwindigkeitskonstante, diffusionsgrenzend in isothermen und nichtisothermen Regime gerechnet*)

Lfd. Nr.	Benennung der Gleichung	Diffusions-Art	Ausdruck der Kinetischen Relation in isothermen Regime	Ausdruck der Kinetischen Relation in nichtisothermen Regime
1.	Jander	Oberflächlich	$\alpha^2 = 2kt$	$\log \frac{1}{T^2} \frac{\alpha^2}{2} = = \log \frac{k_0 R}{a} \left(1 - \frac{2RT}{E}\right) - \frac{E}{4{,}575\,T}$
2.	Jander	Im Volumen	$[1(1 - \alpha)^{1/3}]^2 = kt$	$\log \frac{1}{T^2} \left\{ \frac{1}{2} [1 + (1 - \alpha)^{2/3}] - - (1 - \alpha)^{1/3} \right\} = = \log \frac{k_0 R}{3aE} \left(1 - \frac{2RT}{E}\right) - \frac{E}{4{,}575\,T}$
3.	Ginstling-Brounshtein	Im Volumen	$1 - \frac{2}{3}\alpha - (1 - \alpha)^{2/3} = kt$	$\log \frac{1}{T^2} \left\{ \frac{3}{2} [1 - - (1 - \alpha)^{2/3}] - \alpha \right\} = = \log \frac{k_0 R T^2}{aE} \left(1 - \frac{2RT}{E}\right) - \frac{E}{4{,}575\,T}$
4.	Kröger	Im Volumen	$[1 - (1 - \alpha)^{1/3}]^2 = k \ln t$	

*) α — Umsatzgrad, k — Konstante der Reaktiongeschwindikeit, t — Zeit, T — Temperatur, a — Erwärmungsgeschwindikeit (dT/dt), R — Konstante den perfekten Gasen, E — Aktivierungsenergie und k_0 — Konstante.

Soda, während und nach Dosierung und Homogenisierung aufgesaugt wird.

Der schwach hervortretende endotherme Effekt von den Kurven 2 und 3 (Bild 2), bei 785 –790°C, kann nur von der DTA-Kurve nicht geklärt werden er kann sowohl dem Eutektikum $Na_2CO_3 - CaCO_3 \cdot Na_2CO_3$ (790°C) als auch der peritektischen Schmelze gemäss Gleichgewicht :

$$Na_2O \cdot 2CaO \cdot 3SiO_2 + \text{liq.} \overset{760°C}{\rightleftarrows} Na_2O \cdot 2SiO_2 + Na_2O \cdot 3CaO \cdot 6SiO_2 \quad (1)$$

zugeschrieben werden.

Folglich sind, für die Klärung des Reaktionsmechanismus der polinären Massen des Systems Na_2O—CaO —Al_2O_3 —SiO_2 noch andere Forschungsmethoden und entsprechende Auslegungen, für die genaue Hervorhebung der Reaktionen welche bei der Erwärmung der Rohstoffmischung stattfinden notwendig, so wie in den weiter folgenden, im Kapitel 3.2 dargelegt wird.

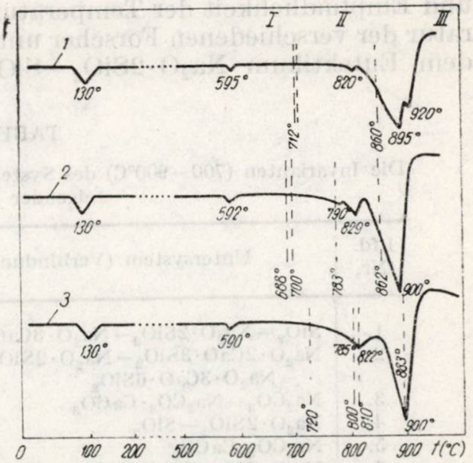

Abb. 2.—Die thermischen Effekte bis 900°C der untersuchten Mischungen des Systems $Na_2O - CaO - Al_2O_3 - SiO_2$

I — Hervortretender Anfang der Reaktion mit diffusionellen Mechanismus der Jander-Art, $Na_2CO_3(Na_2CO_3 \cdot CaCO_3) + SiO_2$ in fester Phase

II — Ursprüngliche binäre und ternäre eutektische und peritektische Schmelzen

III — Schmelze des doppelten Natrium- und Kalziumkarbonat und des Natriumkarbonats und die Reaktion der flüssigen Phase mit SiO_2.

Desgleichen ist es schwer den endothermen Effekt bei 820 –829°C, der auf sämtliche grafischen Eintragungen vorhanden ist, aus den DTA-Kurven auszulegen. In Zusammenhang damit wird bemerkt, dass auch die Fachliteratur bezüglich der durchgefürten Forschungen betreffend ternäre Massen nicht schlüssig ist[15-16,21] da Körnunggrösse der Rohstoffe

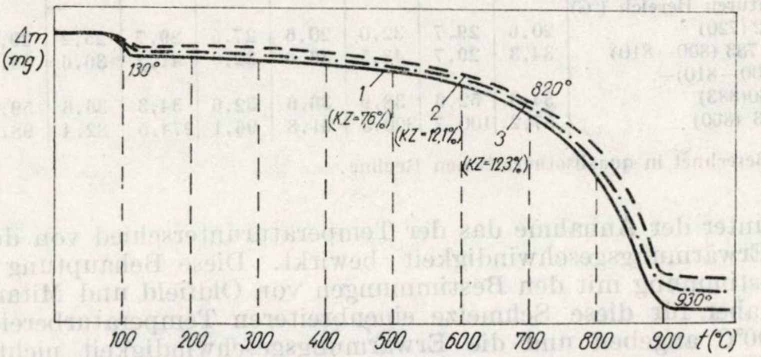

Abb. 3. — Thermogravimetrische Analysen der untersuchten Reaktantenmischungen (die Empfindlichkeit der Thermowaage ist doppelt bei Probe 1 gegenüber Proben 2 und 3) K. V. — Kalzinierverluste.

und Empfindlichkeit der Temperaturenskala der verwendeten DTA-Apparatur der verschiedenen Forscher unterschiedlich ist. Dieser Effekt könnte dem Eutektikum $Na_2O \cdot 2SiO_2 - SiO_2$ (Tabelle 4) zugeschrieben werden,

TABELLE 4

Die Invarianten (700—900°C) des Systems $Na_2O - CaO - SiO_2$ (in der Reihenfolge steigender Temperatur)

Lfd. Nr.	Untersystem (Verbindung)	Invariant	Temperatur (°C)
1.	$SiO_2 - Na_2O \cdot 2SiO_2 - Na_2O \cdot 3CaO \cdot 6SiO_2$	Eutektik	740[24]
2.	$Na_2O \cdot 2CaO \cdot 3SiO_2 - Na_2O \cdot 2SiO_2 - - Na_2O \cdot 3CaO \cdot 6SiO_2$	Peritektik	760[24]
3.	$Na_2CO_3 - Na_2CO_3 \cdot CaCO_3$	Eutektik	790[36]
4.	$Na_2O \cdot 2SiO_2 - SiO_2$	Eutektik	789[23], 790[40]
5.	$Na_2CO_3 \cdot CaCO_3$	Schmelzen	820[36]
6.	$Na_2O \cdot SiO_2 - Na_2O \cdot 2SiO_2 - - 2Na_2O \cdot CaO \cdot 3SiO_2$	Eutektik	821[24]
7.	$2Na_2O \cdot CaO \cdot 3SiO_2 - Na_2O \cdot 2CaO \cdot 3SiO_2 - - Na_2O \cdot 2SiO_2$	Peritaktik	827[24]
8.	$Na_2O \cdot SiO_2 - Na_2O \cdot 2SiO_2$	Eutektik	837[23]
9.	Na_2CO_3	Schmelzen	860[36]
10.	$Na_2O \cdot 2SiO_2$	Schmelzen	874[23]

TABELLE

Die berechneten Werte der Aktivierungsenergie (kcal/mol) in quasiisothermen

Art der Gleichung	Jander oberflächlich						Ginstling		
Thermisches Regime	Quasiisotherm			Nichtisotherm			Quasiisotherm		
Probe- Nr.	1	2	3	1	2	3	1	2	3
Temperaturen Bereich (°C)									
1. < 712 (720)	20,6	29,7	32,0	20,6	27,5	29,7	25,2	29,7	29,7
2. 712—783 (800—810)	34,3	29,7	43,5	36,6	32,0	41,2	36,6	34,3	43,5
3. 783(800—810)— — 860(883)	34,3	52,6	38,9	36,6	52,6	34,3	36,6	59,5	41,2
4. > 883 (860)	57,2	100,7	320,3	61,8	96,1	274,5	82,4	98,4	402,6

* Berechnet in quasiisothermischen Regime

wurde unter der Annahme das der Temperaturunterschied von der grösseren Erwärmungsgeschwindigkeit bewirkt. Diese Behauptung ist in Übereinstimmung mit den Bestimmungen von Oldfield und Mitarbeiter[15] welche aber für diese Schmelze einenbreiteren Temperaturbereich, von 770—800°C angeben und die Erwärmungsgeschwindigkeit nicht präzisieren. Folglich, der Schmelze des doppelten Karbonates und des Sodaüberschusses vorausgehend, erscheint die eutektische Schmelze $Na_2O \cdot 2SiO_2 - SiO_2$, auf diese Weise hebt sich, ähnlich in den ternären Systemen, die Bildung des Natriumorthosilikates hervor. Der endotherme Effekt, der der eutektischen Schmelzung von 820—829°C entspricht, wurde unsererseits, auf Grund der Ergebnisse der binären Systeme, auch in dem quaternären System identifiziert.

Die Gewichtänderung der Proben während der Wärmbehandlung zeigt Gewichtverlusteffekte in Übereinstimmung mit den thermischen Effekten, sowohl als Bereichausdehnung als auch Temperatur erlaubt aber nicht die Veranschaulichung neuerer Schlussfolgerungen betreffend Reaktionsmechanismen. Der Gewichtverlust bis 150°C kann mit den Feuchtigkeitsverlust bei den statischen Bestimmungen verglichen werden.

Wie aus dem Dargelegten zu bemerken ist, durch die thermische und thermogravimetrische Analysen, besonders aus den ersten, können einige nützliche, aber nicht gänzlich aufklärende Indikationen betreffend Reaktionsmechanismen bei Erwärmen polynärer Rohstoffe erhalten werden.

3.2. REAKTIONSKINETIK

Die Konstanten der Reaktionsgeschwindigkeiten und die Aktivierungsenergien des Diffusionsmechanismus bei Wärmebehandlung der untersuchten Mischungen sind in den Abb. 4 —6 und Tabelle 5 angegeben.

3.2.1. Kinetik und Reaktionsmechanismen der drei Rohstoffmischungen

Reaktantenmischung 1 (*Bild 4*) zeigt drei Temperaturbereiche u.z.w. den ersten bei 698°C, den zweiten bei Temperaturen zwischen 698° —837°C und den dritten bei 837°C, in welchen die betreffenden Reaktionen mit konstanter Aktivierungsnergie verlaufen. Die Werte der Aktivierungsenergien sind am niedrigsten im Vergleich mit jene der anderen Mischungen, was das Vorhandensein einiger kleineren Mengen von flüssiger Phase, in Übereinstimmung mit der chemischen Zusammensetzung (21 % Al_2O_3 und 3 % Na_2O), beim Erwärmen zeigt.

5

und nichtisothermen Regime, der untersuchten Reaktantenmischungen

-Brounshtein			Jander volumen						Kröger*		
Nichtisotherm			Quasiisotherm			Nichtisotherm			Quasiisotherm		
1	2	3	1	2	3	1	2	3	1	2	3
18,3	28,0	32,0	25,2	29,7	29,7	20,6	32,0	29,7	25,2	32,0	32,0
38,9	31,7	43,5	41,2	34,3	43,5	38,9	36,6	43,5	41,2	41,8	52,6
38,9	54,9	38,9	41,2	59,5	41,2	38,9	61,8	41,2	41,2	61,8	43,5
80,6	86,9	329,4	89,2	98,4	402,6	91,5	107,8	320,3	100,7	112,1	329,4

Diese Behauptung, von uns geprüft, zeigt die Tatsache an, dass neben der thermodynamischen Reaktivität, die aus den Angaben des thermischen Phasengleichgewicht üblich erweise bestimmt wird, auch noch eine kinetische Komponente der Reaktivität auftritt. Also, je schmelzbarer die Reaktantenmischung ist und eine grössere Menge flüssiger Phase entwickelt, entfaltet sich die interatomische Diffusion anders, während die Aktivierungsenergie, wenn eine Mischung flüssiger und fester Phase vorhanden ist, eine andere Bedeutung gegenüber dem Fall der gegenseitigen Reaktion fester kristalliner Gitter-bekommt.[50] Das Erscheinen einiger Lücken im Gitter und anderen Atomnachbarschaften (neu gebildete Verbindungen, Teile aus anderen Gittern, u.s.w) sowie einige physikalisch-chemische Phänomene wie Sinterung, u.a. beeinflussen den Wert der Aktivierungsenergie und folglich, obwohl die Diffusionserscheinungen sich erweitern (die Diffusionskonstante steigt) nimmt auch der Bedarf an Wärme für Atomverschiebung zu.

Der endotherme Effekt bei 820°C (Abb. 2) der der eutektischen Schmelze $Na_2O \cdot 2\,SiO_2 - SiO_2$ zugeschrieben wird, ist wegen der Erwärmungsgeschwindigkeit von 10°/Minute auf höhere Werte verschoben. Die Menge der durch diesen Prozess gebildeten Schmelze ist gering ohne den Wert der Aktivierungsenergie zu ändern.

Die Aktivierungsenergie steigt mit Zunahme der Temperatur und erreicht die höchsten Werte über 860°C wenn das doppelte Karbonat und das Natriumkarbonat schmelzen. Die diffusionellen Relationen können bei höheren Temperaturen von 880°—900°C nicht mehr verfolgt werden da Entwicklung von CO_2, welcher als Anzeige für die in der Mischung vorgehenden Reaktionen dient, aufhört. Bei 920°C zersetzt sich das gegen Na_2CO_3 überschüssige $CaCO_3$.

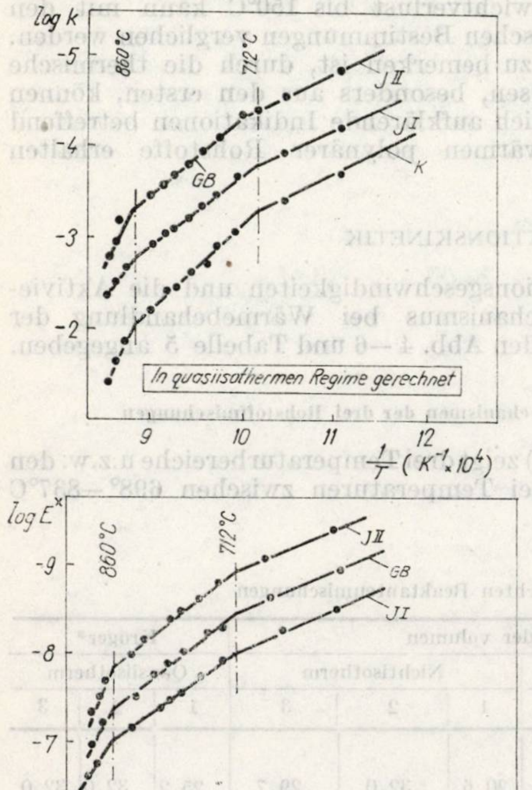

Abb. 4. — Graphische Berechnung der Reaktionskinetik bei Erwärmung der Reaktantenmischung 1
x) E — Ausdruck der kinetischen Relationen in nichtisothermen Regime
JI — Jander-Gleichung (oberflächliche Diffusion)
JII — Jander-Gleichung (volumen Diffusion)
BG — Ginstling-Brounshtein Gleichung
K — Kröger-Gleichung.

Reaktantenmischung 2 (*Abb.* 5) Mit steigender Temperatur identifiziert man vier kinetische Bereiche, der erste bei niedrigerer Temperatur von 688°C, der zweite zwischen 700 —783°C, der dritte zwischen 783 —862°C und der letzte bei Temperaturen über 862°C, zwei der Temperaturgrenzen, 862°C und 688 —700°C sind dem Wert derjenen der Masse 1 nahe. Zusätzlich erscheint der Wendepunkt bei 783°C welcher der peritektischen Reaktion (1) zugeschrieben wird, die, wie in den ternären Systemen[1,2] auch auf dem DTA zu erkennen ist. Gleichzeitig ist auch die Erscheinung der flüssigen Phase, die Bildung des Natriumorthosilikates und der doppelten, ternären Silikate zu beobachten. Die chemischen Zusammensetzungsbedingungen benachteiligen die Bildung des doppelten Karbonats in grösseren Mengen, wahrscheinlich wegen des grossen Prozentsatzes an Tonerde, welche das gegenseitige Wandern der Natrium- und Kalziumionem nicht bei Temperaturen unter 850°C erlaubt. Es bildet sich also keine bedeutende Menge von doppelten Karbonat welche selbständig schmelzen soll und die weder auf der DTA-Kurve, noch durch kinetische Auslegung des Reaktionsmechanismus identifiziert werden kann. Unter diesen Bedingungen beeinflusst der endotherme Effekt bei 829°C der eutektischen Schmelze $Na_2O \cdot 2SiO_2 - SiO_2$ zugeschrieben, den physikalisch-chemisch Haupt-mechanismun nicht (die Aktivierungsenergie bleibt konstant) im Verhältniss zu der vorherigen peritektischen Reaktion. Der Wert der Aktivierungsenergie über 862° C ist 1,08—1,76 mal grösser als jener der Masse 1, was eine grössere Reaktivität, im Sinne der Erscheinung einer grösseren Menge flüssiger Phase zeigt, im Falle dieser Zusammensetzung die den gleichen Gehalt an Al_2O_3, aber um 9% weniger SiO_2 und 3,5 mal mehr Na_2O hat.

Die Diffusionsrelationen, so wie im Fall der Mischung 1 können über 862°C aus denselben oben angeführten Gründen nicht mehr verfolgt werden.

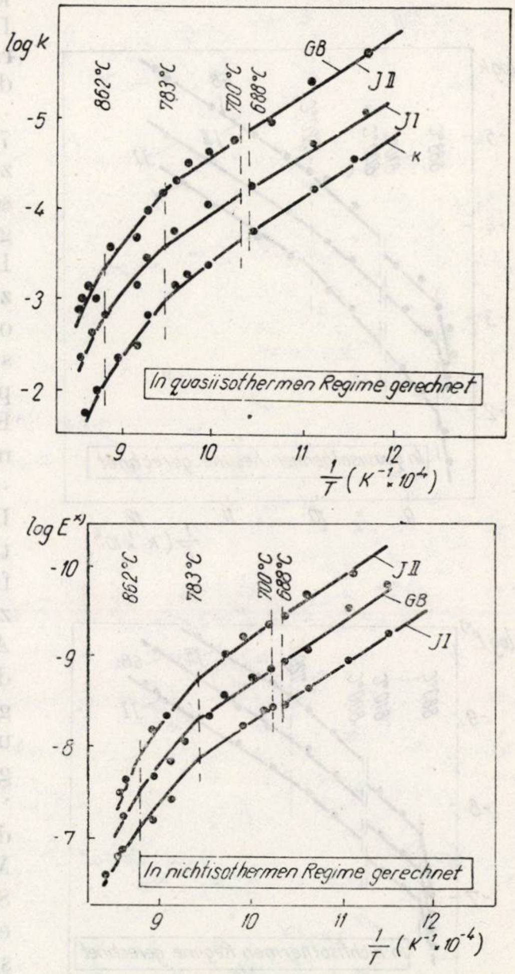

Abb. 5. — Graphische Berechnung der Reaktionskinetik bei Erwärmung der Reaktantenmischung 2

×) E — Ausdruck der kinetischen Relationen im nichtisothermen Regime

J *I* — Jander-Gleichung (oberflächliche Diffusion)

J *II* — Jander-Gleichung (volumen Diffusion)

GB — Ginstling — Brounshtein Gleichung

K — Kröger — Gleichung.

Reaktantenmischung 3 (Abb. 6) Auch in diesem Fall erscheinen desgleichen vier Bereiche von Reaktionsmechanismen, der erste bei niedrigen Temperaturen unter 720°C, dann zwischen 720 –800° (810°C), weiter zwischen 800° (810°) –883°C und zu Ende bei höheren Temperaturen als 883°C, eine dieser Temperaturgrenzen, von 800 –810°C ist nicht kontinuierlich. Die Schwelle dieser Diskontinuität (doppelten Temperaturgrenze) ist dem Schmelzpunkt der Eutektiken $Na_2CO_3 - Na_2CO_3 \cdot CaCO_3$ und $Na_2O \cdot 2SiO_2 - SiO_2$ der 790°C sehr nah.[23,24] Diese Tatsache zeigt, dass bei dieser Zusammensetzung, in welcher das Al_2O_3 gegenüber der Mischung 2 zur Hälfte gesunken ist und der Prozentsatz von SiO_2 71,6 % ist, optimale Bedingungen sind damit sich, erhöhte Mengen von doppelten Karbonat bilden. Dieses Eutektikum schmilzt gleichzeitig mit dem Eutektikum $Na_2O \cdot 2SiO_2 - SiO_2$ – was auch auf der DTA-Kurve durch den endothermen Effekt bei 822°C identifiziert wird– und diesem gleichfalls zum verschmelzen antreibt. Das Ausseben der DTA-Kurve bestätigt diesen Mechanismus –die absteigende DTA-Kurve erscheint abgerundeter – welcher sonst nicht geklärt werden kann.

Eine andere Charakteristik des Reaktionsmechanismus dieser Mischung besteht darin, dass nach 800 –810° C die Aktivierungsenergie der Reaktion ein wenig sinkt und nachher wieder zunimmt um über 883°C zwischen 3,27–5,59 mal grösser zu sein gegenüber jener der Reaktantenmischung 1, was eine erhöhte Reaktivität anzeigt und folglich ein besseres Verhalten in der Praxis, dieses infolge der ausgewählten Zusammensetzung welche sich, wahrscheinlich der Zusammensetzung eines quaternären invariablen Punkt nähert.

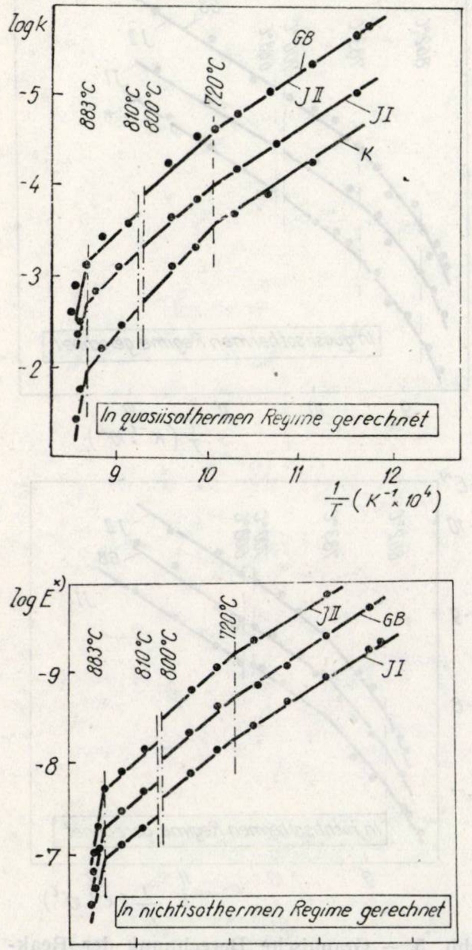

Abb. 6. – Graphische Berechnung der Reaktionskinetik bei Erwärmung der Reaktantenmischung 3

×) E – Ausdruck der kinetischen Relationen im nichtisothermen Regime

J I – Jander-Gleichung (oberflächliche Diffusion)

J II – Jander-Gleichung (Volumen-Diffusion)

GB Ginstling-Brounshtein Gleichung

K – Kröger-Gleichung.

3.2.2. Vergleichung der Reaktionkinetik von Reaktantenmischungen

Die vergleichende Prüfung der Reaktionenkinetik der Reaktantenmischungen 1—3 hebt folgende Merkmale hervor:

— Ähnlicher Verlauf beim Erwärmen, in Übereinstimmung mit Gleichartigkeit der chemischen Zusammensetzung, der Reaktionskinetik von Zusammensetzungen 2 und 3 welche aber gegenüber der Zusammensetzung 1 verschieden ist; so werden im ersten Fall vier Bereiche von Reaktionsmechanismen abgegrenzt welche mit konstanter Aktivierungsenergie ablaufen und im zweiten Fall nur drei Bereiche. Aus Tabelle 1 ist zu bemerken, dass die Massen 2 und 3 praktisch den gleichen Kalziummodul (M_c) aufweisen, der in diesem Fall geeigneter erscheint das kinetische Verhalten der Massen aus den erforschten Untersystemen zu beschreiben, gegenüber anderen Korrelationen (verschiedene andere Verhältnisse von andere zwei oxydische Verbindungen oder andere Module).

— Die Temperaturgrenzen — korrigierte Werte je nach Erwärmungsgeschwindigkeit — kann man mit unäre, binäre und ternäre invariable Punkte des oxydischen Systems, in welchen sich die Reaktantenmischug einräumt, korrelieren; der einzige kinetische Effekt welcher nur hypotetisch ausgelegt werden kann ist jener bei 688—720°C (von niedrigster Temperatur), der entweder einem unberkannten quaternären Punkt, einer Hemmung der Diffusion in reaktiver Schicht bei fester Phase, oder, einer polimorphen Umsetzung des $Na_2O \cdot 2SiO_2$ [23,24] zugeschrieben sein könnte.

— Die Temperaturbereiche in welchen die Aktivierungsenergie konstant ist sind deutlich abgegrenzt und die Anfangtemperaturen der physikalisch-chemischen Prozesse, kinetisch spezifisch, entsprechen nicht jenen der Spitzen thermodifferenzieller Effekte; diese letzteren, zeigen den Höchstpunkt der Prozessentwicklung an, der Beginn physikalisch-chemischer Haupterscheinungen liegt allgemein bei niedrigeren Temperaturen die auf den DTA nicht genau eingetragen werden können, sondern nur durch unsere Methode;

— Der Reaktionsmechanismus, gemäss welchem die chemischen Reaktionen im untersuchten quaternären System ablaufen, in welchem sich auch die Reaktantenmischungen für Glas einräumen, ist die Diffusion die gleichzeitig auf der Oberfläche und im Volumen der Mikropartikeln stattfindet. Ein ständiges Gleichgewicht ist zwischen diesen beiden Arten von Prozessen vorhanden. Es wird angenommen, dass im Temperaturbereich von 650—850°C eine Reihe von Diffusionsphänomene erscheinen, überwiegend in fester Phase, welche ihre Tätigkeit auch über 850°C fortsetzen, im Augenblick der Erscheinung von grösseren Mengen flüssiger Phase im System;

— Das Ergebnis kinetischer Bestimmungen, in nichtisothermen Regime geschätzt, im Vergleich zu denen der Forschungen im quasiisothermen Regime zeigt eine gute Übereinstimmung, mit der Erwähnung, dass die meisten Werte der Aktivierungsenergie in nichtisothermen Regime kleiner als jene im quasiisothermen Regime sind; die Bestimmungen im nichtisothermen Regime werden als representativer betrachtet da die physisch-chemische Erscheinung als ein einheitliches Ganzes beschrieben wird welches sich weiterentwickelt und nicht als eine isotherme Reaktion bei einer gewissenen Temperatur die getrennt gegenüber dem vorausgehenden oder nachkommenden Gleichgewicht betrachtet wird;

— Die besonders grosse Annäherung bis zur Übereinstimmung erscheint offenbar, im Falle der Verwendung der kinetischen Relationen im quassiisothermen Regime, für die Volumen-Diffusionsmechanismen nach Jander und Ginstling-Brounshtein; gleichzeitig erscheint noch ein Vorteil der kinetischen Rechnungsart in nichtisothermen Regime: bei Einhaltung der Identität zwischen den Ergebnissen der Aktivierungsenergiewerten erhält man eine sehr gute graphische Trennung der Darstellung beider Arten von kinetischen Relationen;

— Die Werte der Aktivierungsenergie, gemäss der Jander-Gleichung, logarithmisch von Kröger korrigiert, entfernen sich nicht viel von den mittels Jander und Ginstling-Brounshtein Relationen erhaltenen Ergebnissen; diese nur im quasiisothermen Regime berechneten Werte*) sind im allgemeinen etwas grösser gegenüber den Ergebnissen im nichtisothermen Regime, was, wie schon erwähnt, als näher der reelen Situation für den Fall der Diffusion im Volumen betrachtet wird;

— Auf den Bilderu in welchen die kinetischen Veranschaulichungen dargestellt sind, sind die Geraden mit stärkster Neigung, bei höheren Temperaturen als 880°C (Abb. 6) auf Schmelzen des nichtreaggierten doppelten Kalzium- und Natriumkarbonats und des Natriumkarbonats zurückzuführen und entspricht den graphischen Ergebnissen von Kröger und Mitarbeiter[1,3,4];

— Die Diffusion an der Oberfläche und im Innern der Mikropartikeln findet in fester Phase in Anwesenheit der ersten Mengen flüssiger Phase statt; mit Zunahme der Temperatur ist die Diffusion in festem Zustand als solche, von der Diffusion in der festen Phase in Anwesenheit der Schmelzen gefolgt und folglich steigen ohne Ausnahme die Werte der Aktivierungsenergie; bedeutende Unterschiede der Aktivierungsenergiewerte unter 860—883°C zwischen den drei Zusammensetzungen werden nicht erhalten, nur die Masse 2 benötigt etwas höhere Aktivierungsenergien, ist also in diesem Temperaturbereich schmelzbarer; dagegen, über 860—883°C nach Beginn des Schmelzens vom doppeltem Kalzium- und Natriumkarbonat sowie des überschüssigen Natriumkarbonats steigen die gesamten Aktiwierungsenergiewerte besonders viel gegenüber den vorherigen Werten, von 1,67 bis 5,59 mal, je nach der Reaktantenmischung und besonders in Korrelation mit der Zunahme des Na_2O — Prozentsatzes und Abnahme des Al_2O_3-Prozentsatzes; die bedeutenden Differenzen welche zwischen den Aktivierungsenergiewerten über 860—883°C zwischen den verschiedenen Zusammensetzungen erscheinen, in Übereinstimmung mit den praktischen Beobachtungen erlauben uns die Reaktivität der Reaktantenmischungen zu charakterisieren, beziehungsweise deren Fähigkeit leichter oder schwerer Glas zu erzeugen, zu beurteilen; also, erlaubt unsere Methode die quantitative Bestimmung welche der Zusammensetzungen von Reaktantenmischungen reaktiver, für eine optimale Schmelzung geeigneter, vom technologischen Standpunkt wirtschaftlicher sind.

---

*) Da bis zur Zeit die Differenzierung der Gleichung aus integraler Form nicht durch eine einfache Methode durchgeführt werden konnte.

4. SCHLUSSFOLGERUNGEN

4.1. Es wurde die Reaktionskinetik bei Erwärmung mit 10°C/Minute von drei repräsentativen Massen aus drei Hauptuntersystemen mit SiO_2 des quaternären Systems $Na_2O-CaO-Al_2O_3-SiO_2$ zwischen 600° und 900° C bestimmt, wobei die gleichzeitige Gültigkeit der kinetischen Relationen Jander und Ginstling-Brounshtein hervorgehoben und die Diffusion sowohl auf der Oberfläche als auch im Volumen beschrieben wurde.

4.2. Durch vergleichendes Studium wurde gegenüber der quasiisothermen Kinetik die Möglichkeit der Verwendung kinetischer Rechnungen im nichtisothermen Regime für quaternäre Mischungen des Systems $Na_2O - CaO - Al_2O_3 - SiO_2$ hervorgehoben, welche die physikalisch-chemischen Erscheinungen die im Laufe der Erwärmung stattfinden was dem tatsächlichen Vorkommen der industriellen Praxis viel näher ist.

4.3. Auf kinetischen Grundlagen (graphische Darstellungen und Berechnungen der Aktivierungsenergie) wurden die Mechanismusunterschiede physikalisch-chemischer Reaktionen bei Erwärmung der quarternären Reaktantenmischungen ausgelegt; die kinetischen Rechnungen wurden für einen Temperaturbereich von fast dreihundert Grad — Hauptreaktionsbereich der Reaktantenschmelzung vorausgehend — durchgeführt, während die Abgrenzung der Reaktionsmechanismen nach den Wendepunktgrenzen der liniären graphischen Darstellungen (kinetische Effekte) gemacht wurde. Auf diese Weise wurden Differenzen in der Bildung von Verbindungen sowie deren Mengen (die Bildung von grösseren Schmelzemengen vom doppelten Karbonat oder des ternären Peritektikum bei 760°C) was beim Schmelzen das Endbetragen beeinflusst, also die Fähigkeit der Mischung Glas zu erzeugen hervorgehoben.

4.4. Es wurde die Tatsache festgesetzt, dass Al_2O_3 in Mengen bis etwa 21 %, im quaternären System eine inerte Rolle hat, die sich bildenden Verbindungen sowie der Reaktionsmechanismus praktisch derselbe ist wie im ternären System $Na_2O-CaO-SiO_2$.

4.5. Eine quantitative Methode mit sofortiger Anwendungsmöglichkeit wurde festgesetzt, welche duch Berechnung der Aktivierungsenergie über 860 —883°C die Bestimmung der Reaktantenmischungreaktivität erlaubt, also die Möglichkeit Zusammensetzungen einiger Gläser welche bei niedrigeren Temperaturen schmelzen hervorzuheben. Es wird gezeigt, dass die kinetische Reaktivität der untersuchten quaternären Mischungen charakterisiert durch den Wert der Aktivierungsenergie — umgegekehrt zu der thermodynamischen Komponente der Reaktivität variiert. Bezogen auf den gesammten Verbrauch thermischer Energie die zur Erwärmung des Gemenges benötigt wird, erreicht die energetische kinetische Komponente beachtliche Werte.

LITETATURVERZEICHNIS

[1] C. Kröger, "Gemengereaktionen und Glasschmelze. Forschungsberichte des Wirtschafts — und Verkehrministeriums Nordrhein — Westfalen," Westdeutscher Verlag, Köln, 1956, S. 1—109.

[2] W. Eitel, "Silicate Science", vol. V, Academic Press, London, 1965, S. 33—34, 102—107, 137—181, 247; Vol. VIII, Academic Press, London, 1976, S. 3—40.

[3] C. Kröger und F. Marwan, *Glastechn. Ber.*, **28**, 51, 89, (1955).

[4] C. Kröger und J. Blömer, *Z. anorg. Chem.*, **280**, 51 (1955).

[5] S. Solacolu, "Chimia Fizică a silicaţilor tehnici", Editura Tehnică, Bucureşti, 1968, S. 431.

[6] S. Solacolu und R. Dinescu, *Bull. Soc. franç. Céram.*, **1961**, 3.

[7] R. Roy, "Proceedings of the XI-th Conference on the Silicate Industry", Vol. II, OMKDK — Technoinform, Budapest, 1973, S. 1005.

[8] H. Dislich, *Glastechn. Ber.*, **44**, 1 (1971).

[9] L. Malarme, *Glastekn. Tidskr.*, **19**, 35 (1964) ; *Glass*, **41**, 545, 569 (1964).

[10] M. A. Bezborodov, "Sintez i stroienia silicatnyh stecol", Izd. Nauca, i Technica, Minsk, 1968, S. 45—76.

[11] * * * "Elaboration du Verre. Symposium de l'Union Scientifique Continentale du Verre", Ed. Union Scientifique Continental du Verre, Madrid, 1973, S. 27—51.

[12] P. Baltă, "Tehnologia sticlei", Ed. Didactică şi Pedagogică, Bucureşti, 1966, S. 169—177.

[13] C. Kröger, *Glastechn. Ber.*, **25**, 307, 311 (1952).

[14] C. Kröger und E. Fingas, *Z. anorg. Chem.*, **213**, 12 (1933).

[15] L. F. Oldfield, "Symposium sur la fusion du verre", Ed. Union Scientifique Continental du Verre, Bruxelles, 1958, S. 383—413.

[16] F. W. Wilburn und C. V. Thomasson, *J. Soc. Glass Technol.*, **42**, 158 (1958).

[17] J. A. Aksay und J. A. Park, *J. Amer. Ceram. Soc.*, **58**, 507 (1975).

[18] K. Kautz und G. Stromburg, *Glastechn. Ber.*, **52**, 309, (1969).

[19] F. W. Wilburn, C. V. Thomasson und H. Cole, "Symposium sur la fusion du verre", Ed. Union Scientifique Continental du Verre, Bruxelles, 1958, S. 373—381.

[20] F. W. Wilburn, S. A. Metcalfe und R. S. Warburton, *Glass Technol.*, **6**, 107 (1965).

[21] S. H. Partridge, *J. Soc. Glass Technol.*, **40**, 195, 301 (1956).

[22] K. Kautz, *Glastechn. Ber.*, **42**, 244 (1959).

[23] K. A. Shahid und F. P. Glasser, *Phys. and Chem. Glasses*, **12**, 50 (1971).

[24] G. K. Moir und F. P. Glasser, *Phys. and Chem. Glasses*, **15**, 6 (1974).

[25] P. P. Budnicov und M. A. Matveev, *Doklady Akad. Nauk S.S.S.R.*, **107**, 547 (1956).

[26] J. T. Howarth, R. F. R. Sykes und W. E. S. Turner, *J. Soc. Glass. Technol.*, **18**, 290 (1935).

[27] J. T. Howarth und W. E. S. Turner, *J. Soc. Glass. Technol.*, **14**, 402 (1930).

[28] Abd-el-Moneim, Abou-el-Azm und H. Moore, *J. Soc. Glass. Technol.*, **37**, 129 (1953).

[29] R. S. Warburton und F. W. Wilburn, *Phys. and Chem. Glasses*, **4**, 91 (1963).

[30] R. F. David und S. A. Pask, *J. Amer. Ceram. Soc.*, **55**, 525 (1972).

[31] R. M. Anderson und F. W. Schneider, *J. Amer. Ceram. Soc.*, **56**, 347 (1973).

[32] G. Rehfeld und H. E. Schwiete, *Ber. dtsch. keram. Ges.*, **48**, 258 (1971).

[33] J. Grofscik, "Mullite. Its Sructure, Formation and Significance", Ed. Akademiai Kiado, Budapest, 1961, S. 103—108.

[34] V. I. Babuskin, G. M. Matveev und O. P. Mtschedlov — Petrosian, "Thermodinamica silicatov", Izd. Literaturi po Stroitelstvu, Moscova, 1965, S. 5—7, 71—76.

[35] V. A. Toropov, V. P. Barzacovici, V. I. Lapin und N. Curtzeva, "Diagramy Sostoienia Silicatnyh Sistem Spravocnic", Izd. Nauca, Moscova, 1965, S. 16—161.

[36] H. W. Billhardt, *Glastechn. Ber.*, **42**, 272 (1969).

[37] A. G. Elliot und R. A. Huggins, *J. Amer. Ceram. Soc.*, **58**, 497 (1975).

[38] S. G. Ampian, *Amer. Ceram. Soc. Bull.*, **52**, 342 (1973).

[39] L. T. Brownmiller und R. H. Bogue, *J. Res. Nat. Bur. Stand.*, **8**, 293 (1932).

[40] E. M. Levin, C. R. Robbins und H. F. Mc. Murdie, "Phase Diagrams for Ceramists", Ed. The American Ceramic Society Inc., Columbus-Ohio, 1964, S. 123, 183, 219.

[41] M. V. Cerchez, Ph. D. Thesis, 1972, Polytechnic Institute of Bucharest, S. 1—103.

[42] R. Dinescu und M. V. Cerchez, *Chimie et Industrie*, **104**, 255 (1971).

[43] R. Dinescu und M. V. Cerhez, *Silicates Industriels*, **36**, 151 (1971).

[44] W. Jander, *Z. anorg. Chem.*, **163**, 1, 31 (1927) ; **168**, 113 (1928).

[45] V. Satava und F. Skvara, *J. Amer. Ceram. Soc.*, **52**, 591 (1969).

[46] J. Robredo, "L'analyse thermique différentielle en verrerie", Ed. Commission Internationale du Verre, Bruxelles, 1967, S. 64—117.

[47] M. V. Cerchez und Mihaela Constantin, *Verras et Réfractaires*, **30**, 827 (1976).

[48] W. Wm. Wendlandt, "Thermal Methods of Analysis. Second Edition", Ed. Wiley, New-York, 1974, S. 43—49.

[49] S. Solacolu, M. V. Cerchez und E. Segal, *Rev. Roumaine Chim.*, **18**, 203 (1973).

[50] V. Boldirev und K. Meyer (Redakteurs), "Festkörperchemie", V.E.B. Deutscher Verlag fur Grundstoffindustrie, 1973, S. 54—128, 221—246.

Revue Roumaine de Chimie, 26, 4, 565–574 (1981)

KINETICS AND MECHANISM OF OXIDATION OF PHENYL ALLYL ALCOHOL BY SODIUM N-CHLORO-BENZENESULPHONAMIDE IN HYDROCHLORIC ACID MEDIUM*

R. SWAMY, H. S. YATHIRAJAN and D. S. MAHADEVAPPA **
Department of Post-graduate Studies and Research in Chemistry, University of Mysore, Manasagangotri, Mysore – 570006, India

Received January 24, 1980

The kinetics of oxidation of phenyl allyl alcohol in 50 :50 v/v ethanol-water mixture by sodium N-chloro-benzenesulphonamide or chloramine-B (CAB)in the presence of hydrochloric acid (0.08–0.25 M) has been sudied at 0°C. The reaction is first order in [CAB], shows a second order dependence on the gross concentration of HCl and is independent of [substrate]. Activation parameters are $E_a = 57.4$ kJ mole^{-1} and $\Delta S^{\neq} = -76.37$ JK^{-1}. The Arrhenius factor is 1.021×10^{9}s^{-1}. Ionic strength and addition of the reaction product (benzenesulphonamide) have negligible influence on the rate. Chloride ion catalyses the oxidation in accordance with the mixed rate law :

$$-\frac{d[CAB]}{dt} = k'[CAB]\,[H^+]^{1.4} + k''[CAB]\,[Cl^-]^{0.6}$$

When the ethanol content of reaction mixture is varied, a plot of $\log k_1$ vs. $\frac{1}{D}$, where D is the dielectric constant of the medium gives straight line with a positive slope. The proposed mechanism assumes a stepwise addition of two protons to release the precursor chlorinium ion, which on hydrolysis yields H_2OCl^+. The latter attacks the substrate in a fast step to form the reaction products, phenyl allyl aldehyde and benzenesulphonamide.

Organic haloamines are compounds containing positive halogen. These are well-known as mild oxidants and are employed as analytical reagents in the estimation of variety of reductants. The prominent member of this class is chloramine-T (Sodium N-chloro-4-methyl benzene sulphonamide, abbreviated as CAT). The other member is chloramine-B (Sodium N-chloro benzene sulphonamide, abbreviated as CAB) which has also been used as oxidant for estimating compounds. The N–Cl bond in CAT and CAB is highly polar and hence these two compounds are fairly strong electrophiles, since chlorine leaves as Cl^+ in reactions. Although oxidation mechanisms of many chloraminometric reactions have been kinetically investigated,[1, 2] almost no information is available in literature about the oxidative behaviour of CAB. It was therefore found to be of interest to investigate the mechanism of oxidation of unsaturated alcohols by CAB. The present communication reports the kinetics of oxidation of phenyl allyl alcohol by CAB in HCl medium.

---

* Presented at the Annual Convention of Chemists held at Kurukshetra, India, from 23rd to 27th September 1979.

** To whom correspondence should be addressed.

MATERIALS AND METHODS

Phenyl allyl alcohol (Naarden, b.p. 256.6) was distilled under reduced pressure. The purity of the compound was checked by phthalation with phthalic anhydride in pyridine.[3] The requisite amount of alcohol was accurately weighed and dissolved in ethanol. Chloramine-B was prepared by passing pure chlorine through benzenesulphonamide[4] dissolved in NaOH solution (4M) over a period of one hour at 70°C. The mass obtained was filtered, dried and recrystallized from water. The purity of the compound was checked by estimating the amount of active chlorine present in the compound. An aqueous solution of CAB was prepared and standardised by the iodometric method. All other reagents used were of accepted grades of purity. A concentrated solution of sodium perchlorate was used to keep the ionic strength constant.

The reaction was carried out in a glass stoppered pyrex boiling tube. Requisite amounts of phenyl allyl alcohol, HCl, $NaClO_4$ solutions and water to keep the total volume constant for all runs were taken in the tube. Required amount of ethanol was added to the mixture to keep the ethanol content constant (50%). The mixture was thermostated in an ice bath maintained at 0°C. A measured volume of CAB solution also cooled to 0°C, was added to the mixture in the boiling tube. The progress of the reaction was followed by iodometric estimation of CAB in a measured aliquot of the reaction mixture at various intervals of time.

Conductance measurements were made at room temperature (25°C) using a Philips PR 9500 conductivity bridge and a dip type conductivity cell (cell constant 0.66 cm^{-}).

Potentiometric titrations were carried out on an Elico model Li-10 pH meter.

STOICHIOMETRY

Reaction mixtures containing excess of CAB over phenyl allyl alcohol and vice versa were kept at room temperature in the presence of HCl (0.08–0.5 M) for 24 hours. The estimation of the unconsumed CAB showed that one mole of phenyl allyl alcohol consumed one mole of CAB.[5]

$$C_6H_5CH = CHCH_2OH + RNCl\,Na \longrightarrow C_2H_5CH = CHCHO + RNH_2 + NaCl$$

where R is $C_6H_5SO_2$.

The presence of phenyl allyl aldehyde among the reaction products was shown by spot tests.[6] Further, the aldehyde was isolated as its 2,4-dinitro phenyl hydrazone[7] (m.p. 253°C). The presence of benzene sulphonamide in the reaction mixture was identified by TLC technique. A mixture of petroleum ether, chloroform and n-butanol (1 :1 :0.5 v/v) was used as the solvent. with iodine as the developing reagent ($R_F = 0.88$).

RESULTS

EFFECT OF REAGENTS

The kinetics of oxidation of phenyl allyl alcohol by CAB were investigated at several initial concentrations of the reactants. When the alcohol is in large excess, plots of log [CAB] against time are found to be linear (Fig. 1) indicating first order dependence on [CAB]. The pseudo first order rate constants in CAB at different initial concentrations of the reactants are found to be independent of the substrate concentration (Table 1). Hence, the reaction is zero order with respect to alcohol.

TABLE 1

Effect of varying initial [phenyl allyl alcohol] and [chloramine-B] on rate constant

Medium : aq. ethanol (50% v/v); $[HCl] = 0.2$ M; $\mu = 0.5$ M; Temp : 0°C

$[CAB]_0$ M	$[Substrate]_0$ M	$k_1 \times 10^4$ s^{-1}
0.005	0.050	4.26
0.005	0.10	4.30
0.005	0.15	4.30
0.005	0.20	4.37
0.005	0.25	4.41
0.003	0.10	4.07
0.004	0.10	4.15
0.006	0.10	4.45
0.007	0.10	4.30
0.005*	0.10	4.22
0.005**	0.10	3.95

* In the presence of excess benzene sulphonamide.

** Ionic strength 1.0 M.

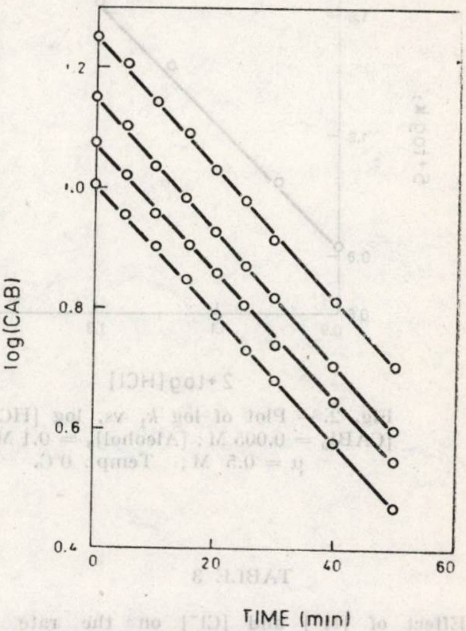

Fig. 1. — Plot of log [CAB] vs. time (min.) $[Alcohol]_0 = 0.1$ M; $[HCl]_0 = 0.2$ M; $\mu = 0.5$M; Temp : 0°C;

$[CAB]_0 =$
0.003 M (a)
0.004 M (b)
0.005 M (c)
0.006 M (d).

EFFECT OF [HCl]

The kinetics of the reaction were studied at different overall concentrations of HCl. The rate of reaction increased linearly with increase in [HCl] (Table 2). The order with respect to [HCl] was found to be two. This was also verified by plotting log k_1 *vs.* log [HCl] (Fig. 2) where the straight line obtained has a slope of two.

EFFECT OF $[H^+]$

Since chloride ion was found to catalyse the reaction $[Cl^-]$ in solution was kept constant by the addition of NaCl and $[H^+]$ was varied. The rate increased with increase in $[H^+]$ (Table 3). Plots of log k_1 vs. log $[H^+]$ gave a straight line of slope 1.39 (Fig. 3).

EFFECT OF $[Cl^-]$

Addition of sodium chloride increases the rate of reaction (Table 3) at constant $[H^+]$. A plot of log k_1 vs. log $[Cl^-]$ gave a straight line of slope 0.57 (Fig. 4).

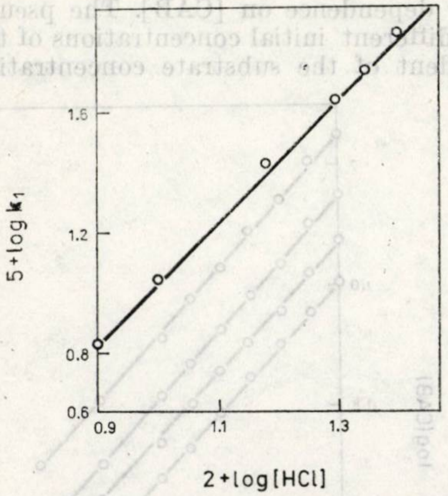

Fig. 2. — Plot of log k_1 vs. log [HCl] $[CAB]_0 = 0.005$ M ; $[Alcohol]_0 = 0.1$ M ; $\mu = 0.5$ M ; Temp : 0°C.

TABLE 2

Effect of gross [HCl] on the reaction rate $[CAB]_0 = 0.005$ M ; $[Substrate]_0 = 0.1$ M ; $\mu = 0.5$ M ; Temp : 0°C

[HCl] M	$10^4 k_1$ s^{-1}	$\frac{10^2 k_1}{[HCl]^2}$
0.080	0.61	0.96
0.100	1.08	1.08
0.150	2.69	1.18
0.200	4.30	1.08
0.225	5.37	1.06
0.250	7.22	1.15

TABLE 3

Effect of $[H^+]$ and $[Cl^-]$ on the rate $[CAB]_0 = 0.005$ M $[Substrate]_0 = 0.1$ M ; $\mu = 0.5$ M ; Temp : 0°C

$[H^+] = 0.2$ M		$[Cl^-] = 0.25$ M	
$10[Cl^-]_0$	$10^4 k_1$ s^{-1}	$10^2 [H^+]_0$	$10^4 k_1$ s^{-1}
2.25	4.95	8.0	1.96
2.60	5.41	10.0	2.28
3.00	5.90	15.0	3.99
3.50	6.43	20.0	5.89
3.80	6.79	22.5	6.99
—	—	25.0	8.32

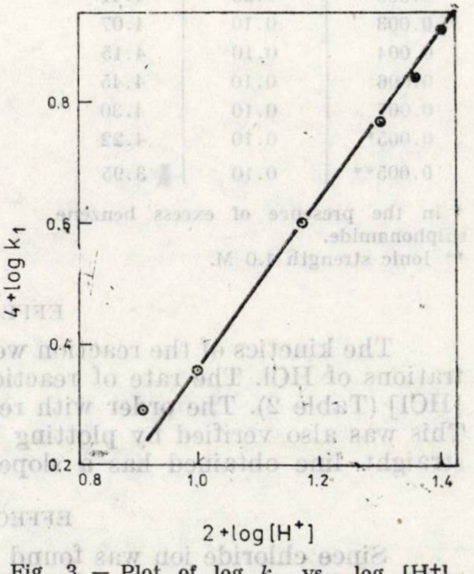

Fig. 3. — Plot of log k_1 vs. log $[H^+]$. $[CAB]_0 = 0.005$ M ; $[Alcohol]_0 = 0.1$ M ; $\mu = 0.5$ M ; $[Cl^-]_0 = 0.25$ M ; Temp : 0°C.

EFFECT OF IONIC STRENGTH

Ionic strength of the medium was varied by varying the concentration of $NaClO_4$ (0.5—1.0 M). No significant effect on the rate of reaction (Table 1) was noticed.

EFFECT OF BENZENESULPHONAMIDE

Addition of the reaction product, benzenesulphonamide (saturated solution) has no significant effect on the rate of reaction (Table 1).

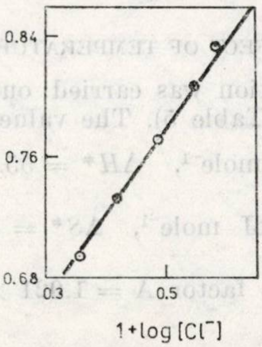

Fig. 4. — Plot of log k_1 vs. log [Cl^-]
[CAB]$_0$ = 0.005 M ; [Alcohol]$_0$ = 0.1 M ;
[H^+]$_0$ = 0.2 M ; μ = 0.5 M ; Temp : 0°C

TABLE 4

Effect of changing the solvent composition on the rate [CAB]$_0$ = 0.005 M ; [Substrate]$_0$ = = 0.1 M ; μ = 0.5M ; Temp : 0°C. [HCl]$_0$= 0.2 M

Ethanol %	$10^4\ k_1$ s^{-1}
30	3.81
40	4.00
50	4.30
60	4.56
70	4.98

EFFECT OF CHANGING SOLVENT COMPOSITION

The effect of changing solvent composition on the rate was studied by changing ethanol composition of the reaction mixture.

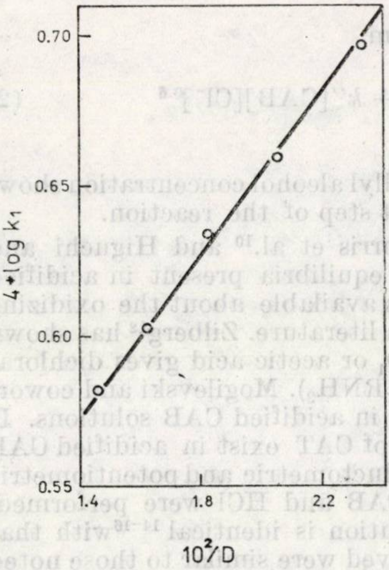

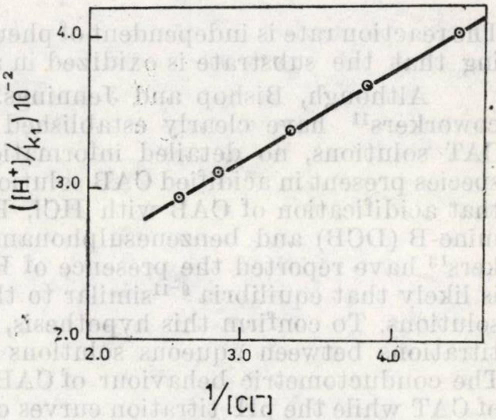

Fig. 5. — Plot of log k_1 vs. $\frac{1}{D}$

[CAB]$_0$ = 0.005 M ; [Alcohol]$_0$ = 0.1 M ;
[HCl]$_0$ = 0.2 M ; μ = 0.5 M ; Temp : 0°C.

Fig. 6. — Plot of $\frac{[H^+]}{k_1}$ against $\frac{1}{[Cl^-]}$

[CAB]$_0$ = 0.005 M ; [Alcohol]$_0$ = 0.1 M ;
[H^+]$_0$ = 0.2 M ; μ = 0.5 M ; Temp : 0°C.

The rate increased with the increase in ethanol content (Table 4). A plot of log k_1 vs. $\frac{1}{D}$ where D is the dielectric constant of the ethanol-water mixtures[8] gives a straight line (Fig. 5), with a positive slope.

EFFECT OF TEMPERATURE

The reaction was carried out at different temperatures (Table 5). The values are:

$$E_a = 57.4 \text{ kJ mole}^{-1}, \quad \Delta H^{\ddagger} = 55.05 \text{ kJ mole}^{-1},$$

$$\Delta G^{\ddagger} = 76.45 \text{ kJ mole}^{-1}, \quad \Delta S^{\ddagger} = -76.37 \text{ JK}^{-1}$$

Arrhenius factor A = 1.021×10^9 s^{-1}.

TABLE 5

Effect of varying temperature on reaction rate $[CAB]_0 = 0.005$ M; $[Substrate]_0 = 0.1$M; $[HCl] = 0.2$ M; $\mu = 0.5$ M

Temp (°K)	$10^4 k_1$ s^{-1}
273.0	4.30
277.1	5.15
279.9	8.25
282.8	10.36
285.9	13.81

DISCUSSION

It is interesting to note that the over-all rate law for the oxidation of phenyl allyl alcohol by CAB in the presence of HCl is of the form:

$$-\frac{d[CAB]}{dt} = k[CAB]\,[HCl]^2 \tag{1}$$

while the composite rate law takes the form

$$-\frac{d\,[CAB]}{dt} = k'[CAB][H^+]^{1.4} + k''[CAB][Cl^-]^{0.6} \tag{2}$$

The reaction rate is independent of phenyl allyl alcohol concentration showing that the substrate is oxidized in a fast step of the reaction.

Although, Bishop and Jennings,[9] Morris et al.[10] and Higuchi and coworkers[11] have clearly established the equilibria present in acidified CAT solutions, no detailed information is available about the oxidizing species present in acidified CAB solutions in literature. Zilberg[12] has shown that acidification of CAB with HCl, H_2SO_4 or acetic acid gives dichloramine-B (DCB) and benzenesulphonamide (RNH_2). Mogilevski and coworkers[13] have reported the presence of HOCl in acidified CAB solutions. It is likely that equilibria [9-11] similar to those of CAT exist in acidified CAB solutions. To confirm this hypothesis, conductometric and potentiometric titrations between aqueous solutions of CAB and HCl were performed. The conductometric behaviour of CAB solution is identical [14-16] with that of CAT while the pH titration curves observed were similar to those noted by Morris et al. and Mahadevappa and Rangaswamy[15] in CAT–HCl titrations. Further, pH measurements on aqueous CAB solutions showed that a 0.05 M CAB solution was a pH of 7.7 at 25°C. Using these data, the ionization constant (K) of the corresponding acid (RNHCl) is found to be 2.4×10^{-3} indicating that RNHCl is a fairly strong acid like N-chloro-p toluene sulphonamide and hence a similar set of equilibria can be expected in CAB solutions.

The possible equilibria in aqueous CAB solutions are:

$$RNCl^- + H^+ \rightleftharpoons RNHCl \qquad (3)$$

$$2\ RNHCl \rightleftharpoons RNH_2 + RNCl_2 \qquad (4)$$

$$RNCl_2 + H_2O \rightleftharpoons RNH_2 + HOCl \qquad (5)$$

$$RNHCl + H_2O \rightleftharpoons RNH_2 + HOCl \qquad (6)$$

The probable oxidizing species in acidified CAB solutions are RNHCl, $RNCl_2$ and HOCl.

If $RNCl_2$ were to be the active species, the rate law should predict a second order dependence of rate on [CAB] as seen from equation (4), which is contrary to the experimental observations. Ionic strength of the medium has no effect on the rate indicating that neutral species are involved in the rate determining step. In the case of CAT solutions, Pryde and Soper[17] have shown that the direct interaction of RNHCl with the substrate could be slow while HOCl formed by the hydrolysis of RNHCl and $RNCl_2$ would attack at a faster rate. It is likely that HOCl is the reactive species in the oxidation of phenyl allyl alcohol with CAB. This is further supported by the fact that equations (4), (5) and (6) would result in a net reaction involving the hydrolysis of the free acid RNHCl. Since the rate is independent of [alcohol], formation of the active oxidizing species would be rate determining and the disappearance of alcohol takes place by a fast reaction with HOCl. Scheme I is proposed for explaining the observed kinetics.

Scheme I

$$RNCl^- + H^+ \underset{k_{-1}}{\overset{k_1}{\rightleftharpoons}} RNHCl \text{ (i) Fast equilibrium.}$$

$$RNHCl + H^+ \xrightarrow{k_2} RNH_2 + Cl^+ \text{ (ii) Slow and rate determining.}$$

$$Cl^+ + H_2O \xrightarrow{k_3} H_2OCl^+ \text{ (iii) Fast.}$$

$$H_2OCl^+ + C_6H_5CH = CHCH_2OH \xrightarrow{k_4} C_6H_5CH=$$

$$= CHCHO + HCl + H_3O^+ \text{ (iv) Fast.}$$

The chlorinium ion is only a precursor for the protonated H_2OCl^+ which attacks the substrate in a fast step.

Applying steady state conditions or RNHCl, rate law (7) can be derived in the form,

$$-\frac{d[\mathrm{CAB}]}{dt}=\frac{k_1k_2[\mathrm{CAB}][\mathrm{H}^+]^2}{k_{-1}+k_2[\mathrm{H}^+]} \tag{7}$$

Equation (7) explains the fractional order dependence on $[\mathrm{H}^+]$ in accordance with our experimental results.

Scheme I is supported by the following facts :

i) Negligible influence of ionic strength on the rate of reaction.

ii) Addition of RNH_2 has no significant effect on the rate.

iii) The rate increases with the decrease in dielectric constant of the medium.

Amis and Jaffe have shown that

$$\log k'_D = \log k' + \frac{Ze\mu}{2.303\ kTr^2D} \tag{8}$$

where k'_D is a function of dielectric constant D, Ze is the charge on the ion, μ is the dipolemoment of the dipole, k is the Boltzmann constant, T is the absolute temperature and r is the distance of approach between the ion and dipole. Equation (8) predicts a linear relation between $\log k_1$ and $\frac{1}{D}$. The slope of the line should be negative for a reaction between a negative ion and a dipole, while a positive slope is obtained for positive ion-dipole reactions. In the present investigations, plot of $\log k_1$ vs. $\frac{1}{D}$

Scheme II

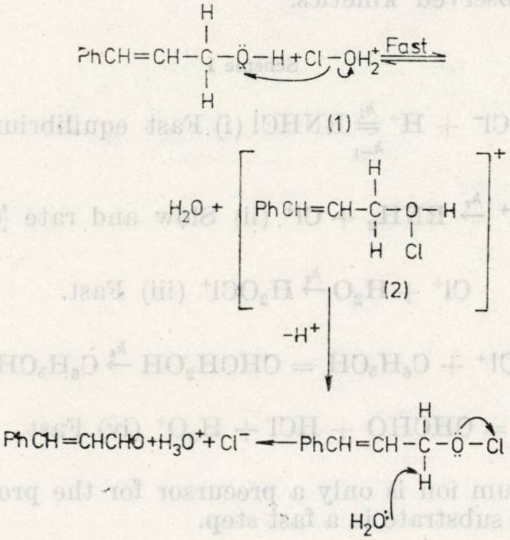

is linear with a positive slope (Cf. Fig. 5), thus supporting the participation of a positive ion and a dipole in the rate determining step (Scheme I).

iv) Stoichiometry of reaction also supports Scheme I.

A detailed mechanism of oxidation of phenyl allyl alcohol in the fast steps by CAB is given in Scheme II. An electrophilic attack by H_2OCl^+ (1) at oxygen of the primary alcohol produces a chloronium ion complex (2). The complex undergoes a proton abstraction reaction promoted by the electron cloud in the substrate leading to the formation of phenyl allyl aldehyde. The low energy of activation and the high negative entropy of activation support the formation of the highly solvated chloronium complex (2) in a fast step.

EFFECT OF CHLORIDE ION

Addition of chloride ion increases the rate of reaction and a fractional order dependence on $[Cl^-]$ is observed. Such behaviour has been noted in the Orton rearrangement[18] involving N-haloamides. Scheme III is proposed for explaining the observations.

Scheme III

$$\mathrm{RNCl^- + H^+ \underset{k_{-1}}{\overset{k_1}{\rightleftharpoons}} RNHCl} \quad \text{(i) Fast.}$$

$$\mathrm{RNHCl + Cl^- \xrightarrow{k_2} RNH^- + Cl_2} \quad \text{(ii) Slow and rate determining.}$$

$$\mathrm{Cl_2 + H_2O \xrightarrow{k_3} HOCl + H^+ + Cl^-} \quad \text{(iii) Fast.}$$

$$\mathrm{HOCl + H^+ \xrightarrow{k_4} H_2OCl^+} \quad \text{(iv) Fast.}$$

$$\mathrm{H_2OCl^+ + C_6H_5CH = CHCH_2OH \xrightarrow{k_5}}$$

$$\mathrm{\xrightarrow{k_5} C_6H_5CH = CH\,CHO + H_3O^+ + HCl} \quad \text{(v) Fast.}$$

$$\mathrm{RNH^- + H_3O^+ \xrightarrow{k_6} RNH_2 + H_2O} \quad \text{(vi) Fast.}$$

Assuming steady state conditions for RNHCl, the rate law

$$-\frac{d[\mathrm{CAB}]}{dt} = \frac{k_1 k_2 [\mathrm{CAB}][\mathrm{H^+}][\mathrm{Cl^-}]}{k_{-1} + k_2[\mathrm{Cl^-}]} \tag{9}$$

can be derived in agreement with experimental results. Equation (9) can be transformed into equations (10) and (11).

$$k_{\mathrm{I}} = \frac{k_1 k_2 [\mathrm{H^+}][\mathrm{Cl^-}]}{k_{-1} + k_2[\mathrm{Cl^-}]} \tag{10}$$

where k_I is the pseudo first order rate constant.

$$\frac{[\mathrm{H}^+]}{k_I} = \frac{k_{-1}}{k_1 k_2 [\mathrm{Cl}^-]} + \frac{1}{k_1} \tag{11}$$

$$= \frac{K}{k_2[\mathrm{Cl}^-]} + \frac{1}{k_1} \text{ where } K = \frac{k_{-1}}{k_1} \text{ is the}$$

equilibrium constant for reaction (i) in Scheme III.

A plot of $\frac{[\mathrm{H}^+]}{k_I}$ vs. $\frac{1}{[\mathrm{Cl}^-]}$ gives a straight line (Fig. 6). From the values of intercept and slope, k_1 and k_2 were calculated to be $3.9 \times \times 10^{-3}$ l.mole^{-1} s^{-1} and 4.0×10^{-3} l.mole^{-1} s^{-1} respectively.

ACKNOWLEDGEMENT. One of us (R.S) gratefully acknowledges the financial assistance from the University Grants Commission, New Delhi, India.

REFERENCES

[1] M. C. Agarwal and S. P. Mushran, *J. Phys. Chem.*, **75**, 838 (1971); *Z. phys. Chem.* (*Leipzig*), **225**, 293 (1974); *J. Chem. Soc.*, **1973**, 762.

[2] D. S. Mahadevappa and H.M.K. Naidu, *Austral. J. Chem.*, **27**, 1203 (1974); **28**, 899 (1975).

[3] A. I. Vogel, "Elementary Practical Organic Chemistry", Longmans Green, London, Part III, 1958, p. 679.

[4] A. Chrzaszczewska, *Chem. Abstr.*, **49**, 212 (1955).

[5] H. S. Yathirajan, S. Rangaswamy and D. S. Mahadevappa, *J. Indian Chem. Soc.*, **56**, 421 (1979).

[6] F. Feigl, "Spot Tests in Organic Analysis", Elsevier, Amsterdam, 5th Edn. 1956, p. 334.

[7] N. D. Cheronis, J. B. Entrikin and E. M. Hodnett, "Semimicro Qualitative Organic Analysis" Interscience, New York, 3rd Edn., 1965, p. 728.

[8] G. Akerlof, *J. Amer. Chem. Soc.*, **54**, 4125 (1932).

[9] E. Bishop and V. J. Jennings, *Talanta*, **1**, 197 (1958).

[10] J. C. Morris, J. R. Salazar and M. A. Winemann, *J. Amer. Chem. Soc.*, **70**, 2036 (1948).

[11] J. Higuchi and A. Hussain, *J. Chem. Soc.*, *B*, **1967**, 549.

[12] I. G. Zilberg, *Chem. Abstr.*, **42**, 144 (1948).

[13] M. S. Mogilevskii, V. I. Malchevskaya and E. P. Voinarovskaya, *Chem. Abstr.*, **53**, 22749 (1959).

[14] D. S. Mahadevappa and S. Rangaswamy, *Indian J. Chem.*, **11**, 811 (1973).

[15] D. S. Mahadevappa and S. Rangaswamy, *Rev. Roumaine Chim.*, **22**, 1233 (1977).

[16] R. Swamy and D. S. Mahadevappa, *Indian J. Chem.*, **14A**, 463 (1976).

[17] L. R. Pryde and F. G. Soper, *J. Chem. Soc.*, **1931**, 1510.

[18] E. S. Gould, "Mechanism and Structure in Organic Chemistry", Holt, Rinehart and Winston, New York, 1964, p. 650.

Revue Roumaine de Chimie, **26**, *4*, 575–585 (1981)

NEUE KOBALT (III)-KOMPLEXVERBINDUNGEN MIT METHYLISOPROPYLGLYOXIM

GH. MARCU, CS. VÁRHELYI, MAGDA SOMAY und DANA AVRAMESCU

Fakultät der Chemischen Technologie, „Babeş-Bolyai Universität", Cluj-Napoca, Arany János Str. Nr. 11, Rumänien

Eingegangen am 22. September 1979

Es wurden 7 neue Chelatkatione des Typs $[Co(Propox.\,H)_2\,(Amin)_2]^+$ durch direkte Synthese, bzw. durch Substitutionsreaktion erhalten. Für die Charakterisierung dieser Chelate wurden 33 neue Komplexsalze durch doppelte Umsetzungsreaktionen isoliert. Für die Lösung einiger Struktur- und thermischer Stabilitätsfragen wurden IR und UV spektroskopische Messungen und derivatographische Untersuchungen durchgeführt.

Seven new chelate cations of the type $[Co(Propox.H)_2(amine)_2]^+$ were obtained by direct synthesis and by means of a substitution reaction. For the characterization of these chelates 33 new complex salts were isolated by means of a series of double exchange reactions. Some structural and thermal stability problems were resolved and discussed by means of IR and UV spectral measurements and by derivatographic study.

EINLEITUNG

Von den sechs isomeren Hexandiondioximen hat das 3,4-Hexandiondioxim (Diäthylglyoxim) eine symmetrische Struktur. Die anderen Isomeren sind unsymmetrisch. Die meisten Hexandiondioxime wurden erhalten und durch UV-spektroskopische Untersuchungen charakterisiert.[1–4]

Die isomeren vicinalen Hexandiondioxime verhalten sich gegen Fe(II), Co(II), Ni(II), Pd(II) und Pt(II), bzw. gegen Co(III), Rh(III) und Ir(III)-Salze wie die anderen aliphatischen und alyzyklischen α-Dioxime (Bildung von Chelaten: $[M(Diox.H)_2]$, bzw. $[M(Diox.H)_2XY]$). Von koordinationschemischen Standpunkt wurden aber diese Verbindungen sehr wenig untersucht.

ERGEBNISSE UND DISKUSSION

Das 2,3-Hexandiondioxim (Methyl-isopropylglyoxim, „Propoxim") kann leicht durch Isonitrosierung und nachfolgender Oximierung des Methyl-isobutylketons erhalten werden. In unseren vorhergehenden Arbeiten[5–7] haben wir einige Komplexsäuren vom Typ $H_n[Co(Propox.H)_2X_2]$

(Propox.H = das monodeprotonierte Propoxim ($CH_3-C(=N-O..)-$ $-C(=N-OH)-CH(CH_3)_2$), X = Cl, Br, J, NO_2, SO_3, S_2O_3) beschrieben und die Kinetik der Aquotisierung der Komplexe untersucht.

In Fortsetzung dieser Arbeiten wurde die Oxydation der Kobalt(II)-salzlösungen in Anwesenheit von Propoxim und von einigen aromatischen und heterozyklischen Aminen untersucht. Es wurde beobachtet, daß das schwach alkalische Medium (pH = 10 – 12) die Bildung der Komplexbasen begünstigt.

$$2Co^{2+} + 4\,Propox.H_2 + 4\ Amin + 1/2O_2 = 2[Co(Propox.H)_2\,(Amin)_2]^+ + + H_2O + 2H^+ \qquad (1)$$

Die aromatischen Amine mit pK_b-Werten zwischen 9 und 12, wie z.B. Alkyl-, Alkoxy-aniline, Naphtylamine, usw., sind für diese Reaktion sehr geeignet.

Die Chelatkatione vom Typ $[Co(Propox.H)_2(Amin)_2]^+$ können aus wässrigen-alkoholischen Lösungen durch doppelte Umsetzungsreaktionen ausgeschieden werden. Zu diesem Zweck wurden überschüssige KJ, KBr, $NaClO_4$, KCNS, $NaBF_4$, Pikrinsäure und verschiedene Komplexsäuren des Kobalts (III) und Chroms (III) (z.B. $H[Co(DH)_2X_2]$, $NH_4[Co(NH_3)_2(NO_2)_4]$, $K_3[Cr(NCS)_6]$, $Amin.H[Cr(NCS)_4(Amin)_2]$) in wässriger oder verdünnter alkoholischer Lösung verwendet. Die Komplexsalze lösen sich im allgemeinen in Alkohol. Die besten Lösungsmitteln für die Thiocyanatochrom (III)-derivate sind Aceton, Dimethylformamid und Dimethylsulphoxid.

Die binären Komplexsalze des Typs $[Co(Propox.H)_2(Amin)_2].[Co(DH)_2X_2]$ bilden Koordinationsisomerpaare mit den entsprechenden $[Co(DH)_2\,(Amin)_2]\,[Co(Propox.H)_2X_2]$.[5-6]

Im Falle dieser Koordinationsisomere können kleine Unterschiede in den Papier- und dünnschichtchromatographischen R_F-Werten, in Löslichkeit und in der Kristallform auftreten. Analoge Erscheinung wurde bei uns bei den entsprechenden Derivaten mit Dimethylglyoxim und Nyoxim beobachtet.[8-9]

Einige neue Komplexsalze sind in den Tabellen 1 und 2 charakterisiert.

Das Propoxim reagiert auch mit Kobalt (III)-komplexsalzen mit leichter austauschbaren Liganden, wie z.B. $Na_3\,[Co(NO_2)_6$, $Na_3[Co(CO_3)_3]$, $[Co(NH_3)_6]Cl_3$, $[Co(NH_3)_5Cl]Cl_2$, usw.

Mit Hexamminsalzen geht die Substitutionsreaktion nach der Gleichung:

$$[Co(NH_3)_6]Cl_3 + 2\ Propox.H_2 = [Co(Propox.H)_2(NH_3)_2]Cl + + 2\,NH_4Cl + 2NH_3 \qquad (2)$$

Einige Derivate des $[Co(Propox.H)_2(NH_3)_2]^+$ sind auch in Tabelle 1 charakterisiert.

TABELLE 1

Neue Komplexverbindungen des Typs
$[Co(Propox.H)_2(NH_3)_2]X$ und $[Co(Propox.H)_2\ (Pyridin)_2]X$

Formel	Ausb. (%)	Charakteristik	Analyse		
				Ber.	Gef.
A. $Br.H_2O$	15	Gelbe, rhomb. Platten	Co H_2O NH_3	12,36 3,77 7,13	12,46 3,50 7,50
A. J	18	Unregelmäß. goldgelbe Krist.	Co NH_3	11,64 6,73	11,47 6,90
A. $[Co(NH_3)_2(NO_2)_4].H_2O$	30	Gelbe Würfel	Co H_2O NH_3	17,48 2,67 10,10	17,38 3,04 10,25
A. $[Co(DH)_2(NO_2)_2].H_2O$	20	Schöne, gelbe reguläre Prismen	Co H_2O NH_3	15,14 2,31 4,38	14,82 2,30 4,60
B.J	80	Aggregate aus kleinen braunen Prismen	Co J	9,35 20,13	9,30 20,33
B. $[Co(DH)_2(N_3)_2]$	50	Gelbbraune Prismen	Co N	13,45 25,56	13,33 24,90
B. $[Co(DH)_2(NO_2)_2].1,5\ H_2O$	60	Gelbe Tafeln	Co H_2O	12,93 2,94	12,68 3,03
B. $[Co(DH)_2(CN)_2]$	80	Glebbraune, kleine Prismen	Co	13,95	14,02
B. $[Co(DH)_2(NCSe)_2]$	60	Braune, dünne Platten	Co N	11,76 16,74	11,89 16,90

DH = Dimethylglyoximinrest ($C_4H_7N_2O_2$)
Propox.H = ($C_6H_{11}N_2O_2$)
A = $[Co(Propox.H)_2\ (NH_3)_2]^+$; B = $[Co(Propox.H)_2\ (Pyridin)_2]^+$

Wenn die Oxydation einer Mischung von CoX_2, Propoxim und Amin bei niedrigeren pH-Werten (in Ammoniumacetat-pufferlösung mit einem pH = 4,5) ausgeführt wird, entstehen Nichtelektrolyte :

$$2\ Co^{2+} + 4\ Propox.H_2 + 2\ Amin + 2X^- + 1/2\ O_2 =$$

$$2[Co(Propox.H)_2\ (Amin)X] + H_2O + 2H^+ \qquad (3)$$

Im Gegensatz zu den analogen Derivaten mit Dimethylglyoxim $[Co(DH)_2(Amin)X]$ und Nyoxim ($[Co(Niox.H)_2\ (Amin)X]$), welche schön kristallisierende Produkte sind, wurden die $[Co(Propox.H)_2\ (Amin)\ X]$ Nichtelektrolyte als ölartige Substanzen erhalten.

Die IR-Spektren der $[Co(Propox.H)_2\ (Amin)_2]J$ — Komplexe (Abb. 1.) zeigen die Anwesenheit von starken intramolekularen O—H..O Wasserstoffbrücken (δO—H..O 1700—1770 cm^{-1} (schw.) Das Auftreten

TABELLE 2

Neue Komplexverbindungen des Typs $[Co(Propox.H)_2(Amin)_2]X$

Formel	Ausb. (%)	Charakteristik	Analyse		
				Ber.	Gef.
C. Br	50	Braune Prismen	Co Br	8,66 11,75	8,19 11,90
C. J	60	Aggregate aus braunen Prismen	Co H_2O J	7,72 4,72 16,62	7,71 4,98 16,88
C. $[Co(DH)_2(NO_2)_2].4H_2O$	70	Gelbe mikrokrist. Masse	Co H_2O	11,19 6,84	10,85 7,03
C. $[Co(DH)_2(CN)_2].2H_2O$	75	Schöne, gelbe Prismen	Co H_2O N	12,06 3,68 17,20	11,70 4,04 17,60
D. Br	75	Gelbe Prismen	Co Br	8,28 11,23	8,38 11,50
D. J. $2H_2O$	80	Gelbbraune Prismen	Co H_2O J	7,42 4,53 15,97	7,48 4,88 16,18
D. $[Co(NH_3)_2(NO_2)_4].H_2O$	70	Gelbe mikrokrist. Masse	Co H_2O N	12,75 1,95 18,18	12,30 2,20 18,65
D. $[Co(DH)_2(NO_2)_2].2H_2O$	40	Unregelmäß. Platten	Co H_2O N	11,24 3,43 16,02	10,88 3,65 16,25
D. $[Co(DH)_2(CN)_2].3H_2O$	90	Kurze, gelbe Prismen	Co H_2O	11,48 5,26	11,62 5,60
E. J	50	Unregelmäß. braune Prismen	Co J	8,95 19,27	8,57 19,54
E. $[Co(DH)_2(CN)_2]$	40	Gelbbraune Prismen	Co	13,51	13,47
E. $[Co(DH)_2(N_3)_2].H_2O$	25	Rotbraune Plättchen	Co H_2O N	12,77 1,95 24,27	12,60 2,18 24,56
E. $[Co(DH)_2(NO_2)_2].2H_2O$	50	Dünne, gelbe Platten	Co H_2O	12,42 3,80	12,43 3,66
E. $[Co(DH)_2(NCSe)_2].5H_2O$	30	Unregelmäßige braune Prismen	Co H_2O N	10,51 8,04 15,01	10,48 8,16 15,25
F. J. H_2O	70	Gelbbraune schöne Prismen	Co H_2O J	8,00 2,44 17,23	7,89 2,68 17,52
F. NCS	75	Aggregate aus gelben unregelmäß. Krist.	Co S	9,07 4,94	9,13 5,30

Tabelle 2 (Fortsetzung)

Formel	Ausb. (%)	Charakteristik	Analyse	
			Ber.	Gef.
F. $[Co(DH)_2(CN)_2 . H_2O$	80	Kleine gelbbraune Prismen	Co 12,40 H_2O 1,89	12,32 2,15
F. $[Co(DH)_2(NCS)_2] . H_2O$	70	Dunkelbraune, unregelmäß. Krist.	Co 11,61 S 6,32 H_2O 1,77	11,50 6,60 1,98
F. $[Co(DH)_2 (NCSe)_2] . H_2O$	70	Rhomboedrische Prismen	Co 10,63 H_2O 1,62 N 15,17	10,68 1,88 15,32
G. Br. H_2O	15	Braune quadratische Krist.	Co 8,07 H_2O 2,47 Br 10,95	7,82 2,68 11,08
G. J. 2,5 H_2O	10	Rotbraune Platten	Co 7,33 H_2O 5,60 J 15,80	7,23 5,75 15,98
G. $[Co(NH_3)(NO_2)_4] . 1,5\ H_2O$	60	Rotbraune Platten	Co 12,60 H_2O 2,88	12,56 3,13
G. $[Co(DH)_2(NO_2)_2]$	50	Rotbraune Prismen	Co 11,64 N 16,60	11,76 16,10
G. $[Co(DH)_2(CN)_2]$	50	Dunkelgelbe Nadeln	Co 12,11 N 17,28	12,29 17,60

C = $[Co(Propox. H)_2$ (*p*-Cl-Anilin$)_2]^+$; D = $[Co(Propox. H)_2$(β-Naphtylamin$)_2]^+$; E = = $[Co(Propox. H)_2$ (Anilin$)_2]^+$; F = [Co (Propox. H$)_2$ (*p*-Anisidin$)_2]^+$; G = [Co(Propox. H$)_2$ α-Naphtylamin$)_2]^+$

dieser schwachen Banden ist ein direkter Beweis für die planare Konfiguration des Co(Propox. H$)_2$ — Restes, bzw. für die trans-Anordnung der $[Co(Propox. H)_2 (Amin)_2]^+$ — Komplexe.[10–11]

Für das kooridinierte Propoxim charakteristischen νC = N, $^{\nu}$(N — O) und $^{\nu}$(N — OH) Banden liegen bei 1550 — 1570 cm^{-1} (m — s), 1230 — 1235 cm^{-1} (s.s.) und 1100 — 1120 cm^{-1} (s.s.). Bei den analogen Dimethylglyoxim-Derivaten $[Co(DH)_2(Amin)_2]X$ erscheinen diese Banden bei 1240 cm^{-1} (s.s.) und 1090 cm^{-1} (s.s.). Die $^{\nu}$(C — H), $\delta(CH_3)$ und $\delta(CH_2)$-Frequenzen treten bei 2980 — 2990 cm^{-1} (m.s.), 1470 cm^{-1} (s) und (1370 — 1380 cm^{-1} (s.), durch den Koordinationseffekt nicht beeinflußt auf. Die Verschiebung der ν(C=N), ν(N — O) — Frequenzen in den Spektren der Komplexsalze gegen jene des freien, nichtkoordinierten Propoxims bestätigt den stark kovalenten Charakter der Co-Oxim-Bindungen.

Die ν(N — H) — Valenzschwingungsfrequenzen der in der inneren Koordinationssphäre gebundenen primären Amine erscheinen bei 3280 — 3300, bzw. 3070 — 3100 cm^{-1}. Die Verschiebung gegen die freien, nichtkoordinierten Amine beträgt um 200 — 250 cm^{-1} nach niederen Wellenzahlen. Die Co — N(Amin) — Bindung hat dann einen kovalenten Charakter (Tabelle 3).

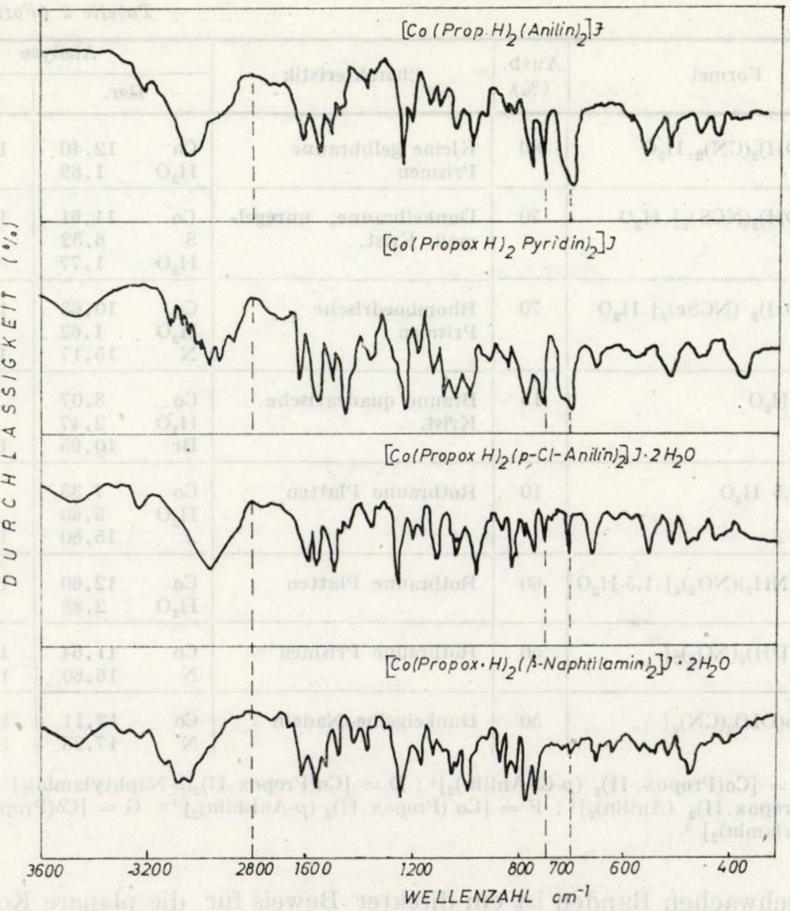

Abb. 1. — IR-Spektren einiger Komplexe des Typs: $[Co(Propox.H)_2(Amin)_2]$ J.

Die Salze der $[Co(Propox.H)_2(Amin)_2]^+$-Kationemit farblosen Anionen sind braun-gelb gefärbt. Die Absorptionsspektren zeigen 3 gut ausgeprägte Maxima. (Abb. 2 und Abb. 3.)

Die Absorptionsspektren hängen von der Natur der koordinierten Aminen ab.

Das gut ausgeprägte Band zwischen 20 und 30 kK (Tabelle 4) kann man zu einem Ladungstransferübergang: Amin→Co zuschreiben.[12], Der Vergleich der Lage dieses Bandes im Falle des Anilins und Pyridins mit der Lage, die man in den Spektren der analogen Dimethylglyoxim[13] und Benzyldioxim[14] Abkömmlinge beobachten kann, zeigt eine regelmässige Verschiebung der Wellenzahlen gegen niedrigere Werte in der Reihe DH > Propox.H > Diph.H. Die anderen Bänder haben vielleicht einen komplexen Charakter und die Überlagerung von reinen Ligand (Amin und Dioxim) — Übergänge und von Co — Ligand Ladungstransferübergänge

TABELLE 3

IR Spektraldaten einiger Komplexe des Typs $[Co(Propox.H)_2\ (Amin)_2]J$

Schwingungsfrequenz	I.	II.	III.	IV.	V.
$\nu(O-H)$	3380–3470 m		3370–3470 s	3430–3470 m	3360–3520 s
$\nu(N-H)$	3220 m	3215 m	—	3270–3310 m	3290–3310 m
	3067–2970 ss	2970–3060 ss	—	3220 m	3215–3225 m
$\nu(C-H)$	2985 m	2980 Schult	2925 ms	2980–85 ss	2980–90 ms
	2955 m	2945 Schult	2940–50 ms	2940–50 ms	2950–60 ms
$\delta(O-H-O)$	1705–1800 sch	1710–1740 sch	1725–1755 sch	1710–1770 sch	1700–1800 sch
$\delta(H_2O)$	1660 Schult	—	—	—	1660 m
$\delta(NH_2)$	1620 ss	1660 sch	—	1640 m	1640 sch
$\nu(ring)$ $\nu(C_{Ar}-C_{Ar})$	1665 ss	1600 ss	1615 s 1500 s	1600 ss	
$\nu(C=N)$	1555 s	1555 ss	1565 ss	1555 ss	1560 ss
$\delta(CH_3)$	1465 s	1480 s 1465 Schult	1460 ss	1465 sch	1465 ss
$\delta(CH_2)$	1370 ms	1370 s	1375 ms	1370 ms	1375 s
$\nu(N-OH)$	1235 ss	1235 ss	1235–1245 ss	1235 ss	1230–35 ss
$\nu(N-O\ldots)$	1115 s	1110 ms	1110 s	1105 ss	1115 ms
$\gamma(OH)$	980 s	986 s	985 s	980 ss	985 ss
$\gamma(NH_2)$	835 ss	835 m	830 s	835 ss	825 s
$\gamma(C_{Ar}-H)$	750 s	765 ss	785 ss	765 ms	780 ss
$\gamma(C_{Ar}-C_{Ar})$	725 ms	705 ss	710 ss	715 ms	755 ss
$\nu(Co-N)$	510 m	505–510 s	510–515 m	510 s	510–525 m

I. $[Co(Propox.H)_2(p\text{-}Anisidin)_2]J$; II. $[Co(Propox.H)_2(Anilin)_2]J$; III. $[Co(Propox.H)_2\ (Pyridin)_2]J$; IV. $[Co(Propox.H)_2\ (p\text{-}Cl\text{-}Anilin)_2]J.2H_2O$; V. $[Co(Propox.H)_2\ \beta\text{-}Naphtylamin)_2]\ J.2H_2O$

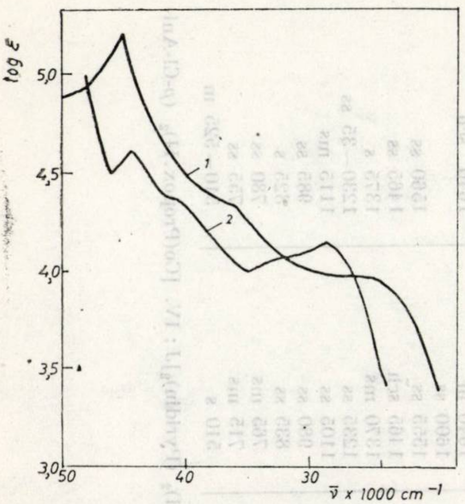

Abb. 2. — Lichtabsorption von: 1. [Co(Propox. H)$_2$ (β-Naphtylamin)$_2$] J; 2. [Co(Propox. H)$_2$ (Anilin)$_2$]J.

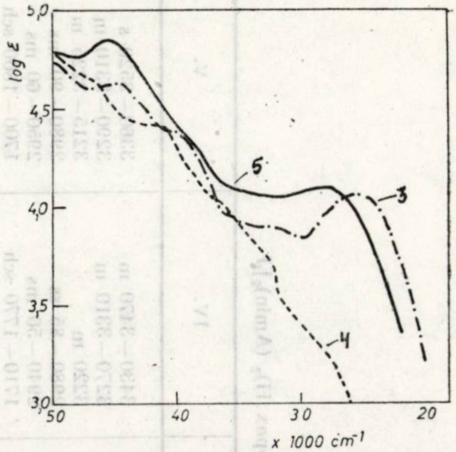

Abb. 3. — Lichtabsorption von: 3. [Co(Propox.H)$_2$ (*p*-Anisidin)$_2$]J; 4. [Co(Propox.H)$_2$ (Pyridin)$_2$] J; 5. [Co(Propox.H)$_2$ (*p*-Cl-Anilin)$_2$] J.

macht die Interpretation der Spektren sehr schwierig. Der Inflexionspunkt bei 39,5—40,5 kK entspricht vielleicht der Absorptionsbande, die nach Ablov und Filippov[15] im Falle der Dimethylglyoximinkomplexen, dem Co(DH)$_2$ Skelett zugeschrieben war.

Die thermische Stabilität einer Reihe von Komplexen des Typs [Co(Diox.H)$_2$ (Amin)$_2$]X (Diox.H$_2$ = Dimethylglyoxim oder Nyoxim) wurde thermogravimetrisch untersucht. Wenn das Anion ein Halogen oder Pseudohalogen ist, tritt in der ersten Phase der Thermolyse eine partielle Dezaminierungsreaktion auf:

$$[\mathrm{Co(Diox.H)_2(Amin)_2}]\mathrm{X} = [\mathrm{Co(Diox.H)_2(Amin)X}] + \mathrm{Amin} \qquad (4)$$

Die kinetischen Parameter dieser Reaktion wurden aus thermogravimetrischen Data berechnet.[16-18]

Die derivatographische Untersuchung der Propoximderivate zeigt, daß die thermische Stabilität der [Co(Propox.H)$_2$]Amin)$_2$] X — salze kleiner, als diejenige der Dimethylglyoximderivate, ist.

Wie aus der Abb. 4. und 5. hervorgeht, tritt kein [Co(Propox.H)$_2$ (Amin)X]-Nichtelektrolyt, als stöchiometrisches Abbauzwischenprodukt auf. Der Inflexionspunkt auf den Thermogrammen entspricht wahrscheinlich einem unbeständigen pentakoordinierten Co(Propox.H)$_2$X Derivat. Das Endprodukt der Pyrolyse um 850—900° ist Co$_3$O$_4$. Die thermodifferenziellen Kurven zeigen, daß die Aminabspaltung ein endothermer

TABELLE 4

UV Spektraldaten der Komplexe vom Typ $[Co(Propox.H)_2(Amin)_2]J$

Verbindung	ν_1	log ε_1	ν_2	log ε_2	ν_3	log ε_3	ν_4	log ε_4	ν_5	log ε_5
$[Co(Propox.H)_2-(p\text{-Anisidin})_2]J.H_2O$	25.200	4,09	32.000 i	3,90	40.500 i	4,38	44.800	4,66	47.500 1	4,59
$[Co(Propox.H)_2-(p\text{-Cl-Anilin})_2]J.2H_2O$	27.900	4,13	31.000— 33.000 i	4,06	40.500 i	4,43	45.300	4,86	48.200— 49.000 i	4,75
$[Co(Propox.H)_2-(\beta\text{-Naphtylamin})_2]J.2H_2O$	24.500	3,96	32.500 i	4,05	40.500 i	4,46	45.300	5,19	—	—
$[Co(Propox.H)_2-(Pyridin)_2]J$	27.500— 28.500 i	3,23	31.500— 32.500 i	3,68	39.500— 40.500 i	4,43	41.800	4,47	46.000	4,69
$[Co(Propox.H)_2-(Anilin)_2]J$	28.500	4,11	31.500— 32.500 i	4,01	39.500— 40.500 i	4,32	44.200	4,51	—	—

i = Inflektionspunkt

Prozeß ist. Der Zerfall der Komplexe über 200° geht aus mehreren simultanen, exothermen Redox- und Eliminierungsreaktionen hervor (Exotherme Maxima auf den DTA-Kurven).

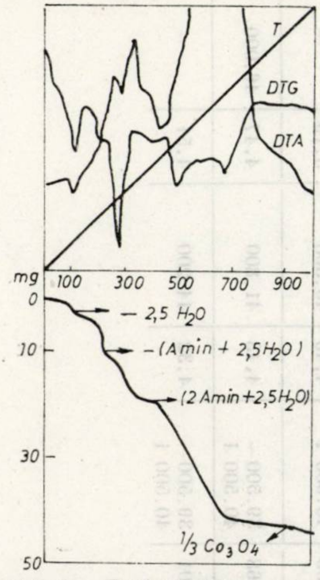

Abb. 4. — Derivatogramm von $[Co\ (Propox.\ H)_2\ (\beta\text{-Naphtylamin})_2]\ J.2,5\ H_2O$.

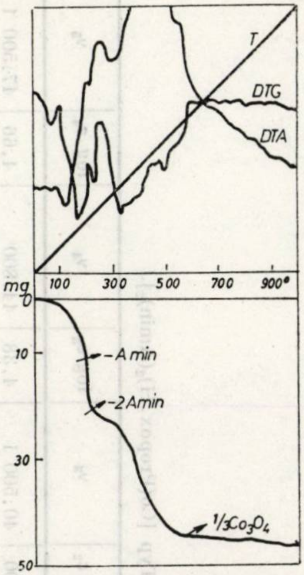

Abb. 5.— Derivatogramm von $[Co(Propox.H)_2(Anilin)_2]J$

EXPERIMENTELLER TEIL

Methyl-isopropylglyoxim. Aus Methyl-isobutylketon (Austranal) wurde durch Isonitrosierung mit gasförmigem Äthylnitrit unter Kühlung in Anwesenheit von HCl zunächst das 3-Monoxim :

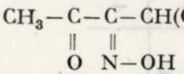

$$CH_3-\underset{\underset{\textstyle O}{\|}}{C}-\underset{\underset{\textstyle N-OH}{\|}}{C}-CH(CH_3)_2$$

erhalten (Schmp. 74°), das durch Behandeln mit überschüss. Hydroxylaminchlorhydrat in acetatgepufferter Lösung weiter in das Dioxim (Schmp. 158°) übergeführt wurde.

$[Co(Propox.H)_2\ (Amin)_2]Cl$ — Lösungen. 50 mMol $CoCl_2$ in 100 ml Wasser werden mit 100 mMol Propoxim und 150 mMol Amin in 250 ml Methanol versetzt. Die Mischung beider Lösungen wird mit einem kraften Luftstrom 6—8 Stunden lang oxydiert, von den Oxydationsnebenprodukten abfiltriert und die braunen Lösungen zur doppelten Umsetzungsreaktion verwendet.

$[Co(Propox.H)_2\ (NH_3)_2]Cl$ — Lösung. 50 mMol $[Co(NH_3)_6]Cl_3$ in 100 ml Wasser wird auf dem Wassebade mit 100 mMol Propoxim in 150 ml Methanol bis zum Aufhören der NH_3 — Entwicklung erwärmt, dann abfiltriert und die gelbe Lösung zur doppelten Umsetzungsreaktion verwendet.

Für die doppelten Umsetzungsreaktionen wurden je 10 mMol $[Co(Propox.H)_2\ (Amin)_2]$ Cl in 60—80 ml Wasser oder verd. Alkohol (1 :1) und überschüssige 10 proz-e KBr, KJ, -bzw. 2—3 proz-e $H[Co(DH)_2X_2]$, $K[Cr(NCS)_4\ (Amin)_2]$, $NH_4[Co(NH_3)_2(NO_2)_4]$ — Lösungen in Wasser oder in verd. — tem Methanol (1 :1) verwendet.

Die Lichtabsorption von $[Co(Propox.H)_2\ (Amin)_2]J$ wurde mit einem Specord (Carl Zeiss Jena)— spektrophotometer in Methanol gemessen. Die IR Spektren der obenerwähnten Substanzen wurden in KBr-Pressling untersucht.

Für die derivatographischen Messungen[19] wurde eine Probemenge von 20 mg verwendet.

LITERATURVERZEICHNIS

[1] A. Treibs und K. Hintermeier, *Chem. Ber.*, **87**, 1163 (1954).
[2] C. V. Banks und A. Anderson, *Inorg. Chem.*, **2**, 112 (1963).
[3] E. Borello und M. Colombo, *Gazz. chim. ital.*, **87**, 614 (1957).
[4] M. Millone, E. Borello und C. Ambrosio, *J. Inorg. Nuclear Chem.*, **8**, 496 (1958).
[5] Cs. Várhelyi, Z. Finta, A. Benkö und A. Binder, *Monatsh.*, **105**, 490 (1974).
[6] Cs. Várhelyi, Z. Finta, A. Benkö und Sz. Mihálycsa, *Acta Chim., Acad. Sci. Hung.*, **89**, 45 (1976).
[7] Gh. Marcu, Cs. Várhelyi, M. Somay und A. Koch, *Studia Univ. Babeş-Bolyai, Chem.*, **23**, (1), 23 (1978).
[8] A. Soó, Cs. Várhelyi und M. Bartunek, *Studia Univ. Babeş-Bolyai, Chem.*, **17**, (2), 23 (1972).
[9] A. Soó, Cs. Várhelyi und Gy. Kiss-Gálfalvi, *Studia Univ. Babeş-Bolyai, Chem.* ,**18**, (2), 47 (1975).
[10] A. Nakahara, *Bull. Chem. Soc. Japan*, **28**, 473 (1955).
[11] R. Ripan, Cs. Várhelyi und E. Hamburg, *Studia Univ. Babeş-Bolyai, Chem.*, **9**, (2), 33 (1964).
[12] C. Matsumoto, T. Kato şi K. Shimura, *Nippon Kagaku Zasshi*, **86**, 1266 (1965); *Chem. Abstr.*, **65**, 13027 (1966).
[13] J. Zsakó, J. Sata und Cs. Várhelyi, *Rev. Roumaine Chim.*, **18**, 1759 (1973).
[14] J. Zsakó, J. Sata und Cs. Várhelyi, *Studia, Univ. Babeş-Bolyai, Chem.*, **18**, (1), 37 (1973).
[15] A. V. Ablov und M. P. Filippov, *Zhur. neorg. Khim.*, **3**, 1565 (1958); **4**, 2204, 2213 (1959).
[16] J. Zsakó, E. Kékedy und Cs. Várhelyi, *J. Thermal Anal.*, **1**, 339 (1969).
[17] J. Zsakó, E. Kékedy und Cs. Várhelyi, *Rev. Roumaine Chim.*, **15**, 867 (1970).
[18] J. Zsakó, Cs. Várhelyi und E. Kékedy, *J. Inorg. Nuclear Chem.*, **32**, 2999 (1970).
[19] F. Paulik, J. Paulik und L. Erdey, *Z. analyt. Chem.*, **160**, 241 (1958).

Revue Roumaine de Chimie, **26**, *4*, 587–591 (1981)

NICKEL(II) AND MANGANESE (II) COMPLEXES OF CYSTINE

MARIA MARC and ANA UNGUREANU

Institute of Chemistry, Str. Donath, No. 65–103, 3400 Cluj-Napoca, Romania

Received July 25, 1979

Nickel (II) and manganese (II) form with cystine 1 :1 complexes which were isolated in solid state. Infrared spectra suggest coordination of carboxylic and amino groups of cystine to the metal. Diffuse reflectance spectra and magnetic moments indicate tetrahedral coordination of the two metals. The thermal decomposition of the two complexes was investigated by means of TG and TDA techniques.

Cystine complexes of transition metals have been investigated only to a limited extent. This may be due to the low solubility of the ligand and to the low stability of cystine under the conditions of complex formation.

Among the cystine complexes reported were those of copper (II),[1-6] cobalt (III),[7-8] cobalt (II),[9] and iron (II).[9]

Here we report on the nickel (II) and manganese (II) complexes of cystine which were isolated in solid state and investigated by spectroscopic (infrared and electronic), magnetochemical and thermogravimetric methods.

EXPERIMENTAL PART

PREPARATION OF COMPLEXES

NICKEL(II) CYSTINE COMPLEX

A solution containing 0.04 moles/liter cystine in sodium carbonate was treated with an equivalent amount of a 0.02 M nickel (II) chloride aqueous solution, added dropwise, under stirring and gentle heating. A blue-green precipitate was formed, which was filtered after cooling the reaction mixture, washed with a sodium carbonate solution (of pH = 8) and then with distilled water. The solid product was dried at 105°C.

In an alternative procedure, the cystine dissolved in a 1.5 M hydrochloric acid solution is treated with the equivalent amount of nickel (II) chloride, and then the pH is carefully adjusted to 8 with sodium carbonate or hydroxide. The blue-green complex is again formed in slightly alkaline mixture.

Found : Ni 18.41, C 22.87, H 3.68, N 8.70, S 19.90 %. $Ni/H_2N-CH(COO)CH_2S/_2.H_2O$ requires : Ni 18.63, C 22.87, H 3.83, N 8.89, S 20.35%

MANGANESE (II) CYSTINE COMPLEX

A solution containing 0.03 moles/liter cystine in aqueous sodium hydroxide at $pH = 8$ was treated under stirring and moderate heating with a 0.04 M aqueous solution of manganese (II) sulfate. At $pH = 8$ a beige precipitate was formed. This was washed with a dilute sodium hydroxide solution then with a large amount of water and the solid was dried at 105°C.

Found : Mn 18.94, C 24.50, H 3.50, N 9.66, S 21.60 %. $Mn/H_2N-CH(COO)\ CH_2S/_2$ requires : Mn 18.73, C 24.57, H 3.43, N 9.55, S 21.86%.

ANALYSIS AND PHYSICO-CHEMICAL STUDIES

The complexes were decomposed with a mixture of hydrochloric and perchloric acids and the metals were determined from this solution : nickel with dimethylglyoxime (gravimetrically), and manganese by oxidation with ammonium persulfate in the presence of Ag^+ ions as catalyst (colorimetrically), according to wellknown procedures. The non-metals were determined by microcombustion.

Infrared spectra were recorded in KBr pellets, with an UR−10 Carl Zeiss Jena instrument.

Diffuse reflectance spectra were recorded with a VSU-1 Carl Zeiss Jena spectrophotometer.

Magnetic moments were determined by the Gouy method.

Thermal analysis (thermogravimetric TG and differential thermal analysis DTA) was performed with the aid of an OD-2 Derivatograph.

THERMAL STABILITY

The thermogravimetric (TG) and differential thermal analysis (DTA) investigation of the two compounds showed that decomposition occurs above 300°C with exothermic effects. The data are shown in Tables 1 and 2.

The amount of oxide residues (NiO and Mn_2O_3 respectively) is in agreement with the 1 :1 metal-ligand combination ratio in both complexes.

TABLE 1

Thermal decomposition of Ni(II)-cystine complex

Temperature range (°C)	TG (% weight loss)		DTA (°C)		Supposed process
	obsd.	calcd.	*endo*	*exo*	
< 190	6.0	5.7	120		$Ni\ cys.\ H_2O \xrightarrow[-H_2O]{} Ni\ cys$
190−340	54.8	55.3		310	$Ni\ cys \xrightarrow[-NO,\ -H_2O,\ -CO_2]{+O_2} NiS+S$
360−1100	15.8	15.3		420	$S + O_2 \longrightarrow SO_2$
				520	$SNi + 2O_2 \longrightarrow NiSO_4$
			830		$NiSO_4 \xrightarrow[-SO_2]{} NiO$

Total weight loss : obsd. 76.6, calcd. 76.3 %

TABLE 2

Thermal decomposition of Mn(II)-cystine complex

Temperature range (°C)	TG (% weight loss)		DTA (°C)		Supposed process
	obsd.	calcd.	endo	exo	
150 – 360	53.7	54.0		340	$\text{Mn cys} \xrightarrow[-NO,\ -CO_2,\ -H_2O]{+O_2} MnO + 2S$
360 – 1100	20.0	20.0	940	440	$Mn + S \xrightarrow{+O_2} MnSO_4$ $S + O_2 \longrightarrow SO_2$ $MnSO_4 \xrightarrow[-SO_2]{} Mn_3O_4$

Total weight loss: obsd. 73.7, calcd. 74.0%

RESULTS AND DISCUSSION

The two complexes prepared are crystalline powders, insoluble in water, polar and nonpolar organic solvents, diluted mineral acids and bases.

Regardless of the metal-cystine ratio, only the 1:1 complexes are formed. In the preparation a slight excess of cystine was used, in order to avoid coprecipitation of the metal hydroxides.

INFRARED SPECTRA

Cystine contains three functional groups, which might participate in coordination: COO^-, NH_2 and S–S. Infrared spectroscopy was used to establish which one is involved in metal-ligand bonding. The significant infrared bands observed are listed in Table 3.

TABLE 3

Infrared spectral bands of the complexes (cm^{-1})

Compound	ν(COO⁻)			δ(N–H)		ν(N–H)	
	sym.	asym.	Δν	sym.	asym.	sym.	asym.
Cystine	1418 s	1595 s	177	1500 s	1635 s	3030 broad	
Ni-cystine complex	1415 s	1620 s	205	–	–	3290 m	3355 m 3375 m
Mn-cystine complex	1410 s	1608 s	198	–	–	3262 m 3275 m	3338 m 3350 m

The absorption bands of the carboxylic group in aminoacid ligands are readily identified and they are very sensitive to changes in the metal-ligand bond strength.[10] Due to the resonance effect, the dissociated carboxylato group shows two bands located at 1610 – 1550 cm^{-1} (ν_{asym}) and

1400 –1300 cm^{-1} (ν_{sym}). In the free amino-acids the formation of the zwitter-ion leads to the same result.[11] When the COO$^-$ group is coordinated the difference between ν_{sym} and ν_{asym} ($\Delta\nu$) increases and $\Delta\nu$ is a measure of the covalent character of the metal-oxygen bond.[11] The data shown in Table 3 confirm the coordination of the carboxylato groups, the Ni –O bond being slightly stronger than the Mn –O bond.

In aminoacids the νN – H bond stretching gives rise to a single broad band, in the range 3130 –3030 cm^{-1} [11]and the –NH_3^+ groups of the zwitter-ion produce bands in the range 1660 –1610 and 1550 –1485 cm^{-1}. In the complexes obvious changes occur : the δ(N –H) band are no more observed and the ν(N –H) are shifted to lower wave numbers due to coordination. The shift of the ν(N –H) band of complexes was compared with that of cystine lithium salt.[12]

The S –S group of cystine produces only weak bands. According to some authors[11] the 454 cm^{-1} band in cystine is due to the S – S bond vibration. Other authors[13] assigned the 540 cm^{-1} band to the same group. In the infrared spectra of the two complexes both these bands were present and the wave numbers of the stretching vibrations for solid uncomplexed cystine and cystine complexes coincide. Therefore the S –S group is not involved in metal ligand bonding.

DIFFUSE REFLECTANCE SPECTRA AND MAGNETIC MOMENTS

The nickel (II) cystine complex exhibits an absorption band at 10750 cm^{-1} ($^3A_2 \leftarrow {}^3T_1$), a broad band with two maxima at 15500 – 16800 cm^{-1} ($^3T_1(P) \leftarrow {}^3T_1$) and another absorption at 24600 cm^{-1} (charge transfer), suggesting tetrahedral coordination of the nickel atom, in agreement with literature data.[14,15]

The magnetic moment $\mu_{eff} = 3.53$ BM measured at room temperature for the cystine complex also supports the tetrahedral coordination of nickel (II).[14,16]

The diffuse reflectance spectrum of the Mn(II) cystine complex exhibits absorption bands at 17800 cm^{-1} ($^4T_{1g} \leftarrow {}^6A_{1g}$) and 23.700 cm^{-1} ($^4T_{2g} \leftarrow {}^6A_{1g}$). These values are common for tetrahedrally and octahedrally coordinated Mn(II).[15]

The magnetic moment $\mu_{eff} = 6.20$ Bohr magnetons. Such high values of the magnetic moment ($\mu_{eff} > 6.10$ Bohr magnetons are to be found only in tetracoordinated manganese (II) complexes.[16, 17]

STRUCTURE

On the basis of the data presented above some speculations on the structure of the complexes can be made. Although Dreiding models indicate the possibility of coordinating both ends of the cystine molecule to the same metal atom (thus leading to monomeric complexes) the very low solubility of the two compounds suggests a polymeric structure of the type proposed for the copper(II) cystine complex.[3]

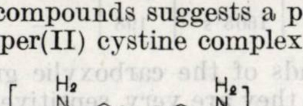

REFERENCES

[1] P. Rây and A. Badhuri, *J. Indian Chem. Soc.*, **27**, 297 (1950).
[2] H. Kahler, B. J. Lloyd and M. Eden, *J. Phys. Chem.*, **56**, 768 (1952).
[3] O. Dobozy, F. Guba and T. Mandy, *Magyar. Kém. Folyoirat*, **68**, 1 (1962).
[4] C. J. Hawkins and D. D. Perrin, *Inorg. Chem.*, **2**, 843 (1963).
[5] S. Kominami, P. Riesz, T. Akiyama and J. V. Silverton, *J. Phys. Chem.*, **80**, 203 (1967).
[6] R. J. Gale and C. A. Winkler, *Inorg. Chim. Acta*, **21**, 151 (1977).
[7] Per Saland and K. Kllos, *Nature*, **163**, 565 (1949).
[8] V. Carassiti and L. Moggi, *Ann. Chim. (Ital.)*, **50**, 602 (1960).
[9] A. Ungureanu and M. Marc, *Rev. Roumaine Chim.*, **25**, 845 (1980).
[10] N. Nakamoto, M. Marimoto and A. E. Martel, *J. Amer. Chem. Soc.*, **83**, 4528 (1961).
[11] L. J. Bellamy, "The Infra-red Spectra of Complex Molecules", London 1960, p. 174–176, 234–235, 353.
[12] J. P. Casey and R. B. Martin, *J. Amer. Chem. Soc.*, **94**, 6141 (1972).
[13] E. J. Bastian and R. B. Martin, *J. Phys. Chem.*, **77**, 1129 (1973).
[14] R. L. Carlin, "Transition Metal Chemistry", vol. 4, Arnold, London 1968, p. 244, 341–351.
[15] A. P. B. Lever, "Inorganic Electronic Spectroscopy", Elsevier, London 1968, p. 229, 341–343, 136, 292.
[16] N. M. Hughes, "The Inorganic Chemistry of Biological Progresses", Wiley, London 1974, p. 48.
[17] P. W. Selwood, "Magnetochemistry", Interscience, New York, 1956, p. 208.

Revue Roumaine de Chimie, **26**, *4*, 593–600 (1981)

TOPOLOGICAL INDICES: INTERCORRELATIONS, PHYSICAL MEANING, CORRELATIONAL ABILITY

IOAN MOȚOC[a] and ALEXANDRU T. BALABAN[b]

[a] Chemical Research Centre, Bul. Mihai Viteazul 24, 1900 Timișoara, Romania
[b] The Polytehnic, Organic Chemistry Department, Bucharest, Romania

Received October 13, 1980

Seventeen topological indices were examined in order to see if they are intercorrelated, finding that all but I_{pc} are strongly intercorrelated. Some topological indices reflect accurately van der Waals volumes, as indicated by correlations with molar refractions or densities of alkanes. Boiling point correlations with some topological indices were tested.

1. INTRODUCTION

Topological indices express in numerical form the topology of molecules. Organic molecules are usually represented by hydrogen-depleted graphs depicting only the covalent bonds between non-hydrogen atoms. For hydrocarbons the carbon skeleton is a non-labelled non-directed multigraph. The carbon skeletons of alkanes which will illustrate the present paper are represented by simple graphs without loops, multiple bonds, or cycles, i.e., by trees whose vertices have degrees 1, 2, 3 or 4.

For definitions and exemplifications of topological indices, including the corresponding bibliography, several reviews are available.[1-3] In the following, only the notation will be indicated for seventeen topological indices $T_j (j = 1, 2, \ldots, 17)$:

w = Wiener index.
Z = Hosoya index.
χ = Randić index (sometimes denoted by M_2).
M_1 = Gutman, Ruscić, Trinajstić and Wilcox's index.
N_2 = Gordon and Scantlebury's index.
Q = normalized quadratic index.[1]
B = centric index.[1]
C = normalized centric index.[1]
C' = binormalized centric index.[1]
Q' = binormalized quadratic index.[2]
I_D^E = information content on the distribution of distances.[5]
I_D^w = information content on realized distances.[5]
$\bar{I}_D^E$ = mean information content on the distribution of distances.[5]
$\bar{I}_D^w$ = mean information content on realized distances.[5]
I_{pc} = information content on polynomial coefficients.[5]
$\bar{I}_{pc}$ = mean information content on polynomial coefficients.[5]
SI = superindex, recently defined.[4]

2. INTERCORRELATION OF TOPOLOGICAL INDICES

In parametric correlations of type (1), e.g., quantitative structure-property relationships like LFER (Linear Free-Energy Relationships) and QSAR (Quantitative Structure-Activity Relationships), the viability of the model is determined by the absence of multicollinearity of predictor variables.[6, 7] The property is Q, a and b_j are constants to be determined by the least-squares method.

$$Q = a + \sum_j b_j x_j \tag{1}$$

The predictor variables $x_i, x_{i+1}, \ldots, x_{i+p}$ are multicollinear if:

$$x_i = f(x_{i+1}, \ldots, x_{i+p}) \quad p = 0,\ 1, \ldots \tag{2}$$

In practice, multicollinearity is considered to be absent when the predictor variables are pairwise orthogonal, i.e., if the regressional equations (3) have the correlation coefficient[8, 9] $r^2 \leqslant 0.40$:

$$x_i = m + n x_j, \quad i \neq j \tag{3}$$

The matrix (4) displayed in Figure 1 presents the intercorrelation coefficients for the seventeen topological indices enumerated in the Introduction. Equations (3) were calculated using the topological indices for the octane isomers.[10]

It can be observed that, with the exception of the I_{pc} index, all other topological indices intercorrelate significantly. This result indicates that the sixteen topological indices examined here (i.e., all but I_{pc}) express in different form approximately the same type of constitutional information. The values of intercorrelation coefficients presented in matrix (4) indicate that the formulation of a model (1) with two or more topological indices as predictor variables requires as a preliminary step the calculation of equation (3) for proving that the topological indices involved in the model are orthogonal. A similar condition applies to constructing superindices[4] as linear combinations of other topological indices.

3. PHYSICAL MEANING OF SOME TOPOLOGICAL INDICES

Correlations LFER or QSAR using topological indices as predictor variables are known.[2, 3, 10] However, it would be interesting to see whether some topological indices have a physical meaning.

So far no attempt was made to translate topological indices into intuitive notions, or to look for topological indices which reflect in a substantial amount an intuitive, independently measurable property of the molecule (it has been argued[5] that topological indices measure the branching of molecules and this is indeed so, but there is no independent measure for branching).

Using the values of molar refraction (MR) and of the van der Waals volume (WV, Å^3) contained in Table 1, equations (5) and (6) were calculated:

$$MR = -1.966 + 0.323\ WV^a \tag{5}$$

$$(r = 0.95,\ s = 2.01,\ F = 128.53,\ EV = 0.91)$$

$$MR = -1.455 + 0.343\ WV^b \tag{6}$$

$$(r = 0.93,\ s = 2.38,\ F = 87.84,\ EV = 0.87)$$

Figure 1. The matrix (4) displaying intercorrelation coefficients, *r*, between topological indices

	B	C	M_1	Q	C'	Q'	N_2	I_D^E	w	Z	I_D^w	I_{pc}	$\bar{I}_D^E$	$\bar{I}_D^w$	χ
B	1.00	1.00	0.90	0.90	1.00	0.90	0.90	−0.93	−0.91	−0.78	−0.91	−0.41	−0.93	0.86	0.93
C		1.00	0.90	0.90	1.00	0.90	0.90	−0.93	−0.91	−0.78	−0.91	−0.41	−0.93	0.86	0.93
M_1			1.00	1.00	0.90	1.00	1.00	−0.85	−0.85	−0.89	−0.86	−0.43	−0.85	0.76	0.18
Q				1.00	0.90	1.00	1.00	−0.85	−0.85	−0.89	−0.86	−0.43	−0.85	0.76	0.85
C'					1.00	0.90	0.90	−0.93	−0.91	−0.78	−0.91	−0.41	−0.93	0.86	0.91
Q'						1.00	1.00	−0.84	−0.85	−0.89	−0.86	−0.43	−0.85	0.75	0.31
N_2							1.00	−0.85	−0.85	−0.89	−0.86	−0.43	−0.85	0.76	0.42
I_D^E								1.00	0.98	0.56	0.98	0.21	1.00	−0.97	0.84
w									1.00	0.58	1.00	0.21	0.98	−0.98	0.81
Z										1.00	0.59	0.64	0.59	−0.45	0.99
I_D^w											1.00	0.22	0.98	−0.98	0.81
I_{pc}												1.00	0.21	−0.13	0.96
I_D^E													1.00	−0.97	0.84
I_D^w														1.00	0.54
χ															1.00

TABLE 1

Values of molecular refraction (MR) and van der Waals volume (WV)

No.	Substituent	*MR**	WV^a	WV^b
1.	CH_3	5.7	23.08	24.86
2.	CH_2Cl	10.5	41.71	38.16
3.	CH_2Br	13.4	46.40	41.08
4.	CH_2I	18.6	57.12	51.14
5.	CHF_2	5.2	31.41	26.76
6.	CF_3	5.0	34.55	27.33
7.	$CHCl_2$	15.3	55.97	46.19
8.	F	0.8	10.29	6.85
9.	Cl	5.8	24.44	18.29
10.	Br	8.7	31.01	24.03
11.	H	1.0	7.22	7.91
12.	I	14.0	41.52	34.39
13.	NO_2	6.7	26.69	20.84
14.	$C(O)CH_3$	11.2	37.87	36.15
15.	NH_2	4.4	19.40	18.29
16.	CN	5.5	23.38	20.43
17.	CH_2OH	7.2	31.12	30.71
18.	COOH	6.9	31.38	28.17
19.	OH	2.6	14.78	13.04
20.	CO_2^-	6.1	28.42	24.13
21.	$n\text{-}C_4H_9$	19.6	68.05	70.01
22.	$CH_2C(O)CH_3$	15.1	56.33	56.00
23.	CH_2OCH_3	12.1	48.09	48.32
24.	$CHBrCH_3$	18.0	61.92	57.34
25.	SCH_3	13.5	23.92	24.75
26.	CBr_3	28.8	89.04	72.83
27.	CCl_3	20.1	70.53	56.07
28.	$C(OH)(CH_3)_2$	16.4	57.98	58.27
29.	$n\text{-}C_3H_7$	15.0	53.85	53.51

* *MR* values are from ref.[14].

TABLE

Data used for calculating

No.	Alkane	*MR*	*B*	*C*	M_1	*Q*	*C′*	*Q′*	N_2	*w*
1.	$n-C_4$	20.6	8	0	10	0	0.000	0.000	2	10
2.	$i-C_4$	20.7	10	1	12	1	1.000	1.000	3	9
3.	$n-C_5$	25.3	9	0	14	0	0.000	0.000	3	20
4.	$2-Me-C_4$	25.3	13	2	16	1	0.500	0.333	4	18
5.	$2,2-Me_2-C_3$	25.3	17	4	20	3	1.000	1.000	6	16
6.	$n-C_6$	29.9	12	0	18	0	0.000	0.000	4	35
7.	$2-Me-C_5$	29.9	14	1	20	1	0.143	0.167	5	32
8.	$2,2-Me_2-C_4$	30.0	24	6	24	3	0.857	0.500	7	28
9.	$3-Et-C_5$	34.5	19	3	24	1	0.250	0.100	6	48
10.	$2,2,3-Me_3-C_4$	34.6	29	8	30	4	0.667	0.400	9	42
11.	$n-C_8$	39.1	16	0	26	0	0.000	0.000	6	84

MR values are taken from ref. [14]

where r is the correlation coefficient, s is the standard deviation, F is the Fisher statistics and EV is the explained variance.

The values WV^a and WV^b were computed using the atomic van der Waals radii from references[11] and [12], respectively, and integrating by a Monte Carlo method the envelopes of substituents; ref.[13] should be consulted for details concerning these calculations.

The values of the EV factors indicate that the steric component, i.e., the van der Waals volume, comprises approximately 90% of the molecular refraction. This result suggests that equations (7) can be used for determining if topological indices T_j, $j = 1, 2, \ldots, 17$, are proportional to van der Waals volumes.

$$MR = a + bT_j \; (j = 1, \; 2, \ldots, 17) \tag{7}$$

With the data from Table 2, the equations (7) which were obtained are systematically presented in Table 3.

This latter table indicates that I_D^w, χ, w, I_D^w and I_D^E express accurately the van der Waals volume ($r = 0.996 - 0.992$). Indices M_1, Z, I_{pc} and $\overline{I}_{pc}$ express with a resonable accuracy the van der Waals volume ($r = 0.894 - 0.846$), while for the remaining indices the van der Waals volume constitutes a minor component.

The equations (presented in Table 4) relating the density D_4^{20} of alkanes to the ratio MW/T_j, where MW is the molecular weight of the alkane, support the above interpretation.

4. CORRELATIONAL ABILITY OF SOME TOPOLOGICAL INDICES

With the data collected in Table 5, the equations relating the boiling points of alkanes (BP) to topological indices T_j were calculated.

2

equations MR *vs* T_j.

Z	I_E^D	I_D^w	I_{pc}	$\overline{I}_D^E$	$\overline{I}_D^w$	$\overline{I}_c^p$	χ	SI
5	8.7549	24.4644	6.8547	1.4591	2.4464	2.2849	1.9142	7.7356
4	6.0000	22.5293	3.2451	1.0000	2.5033	1.6226	1.7321	5.7485
8	18.4644	63.9288	11.2451	1.8464	3.1464	3.7984	2.4142	9.5667
7	15.2193	57.5489	9.6515	1.5219	3.1972	3.2172	2.2701	10.3397
5	9.7095	52.0000	7.6096	0.9710	3.2400	1.8048	2.0000	6.1376
13	32.2388	129.6506	20.9863	2.1493	3.7043	5.2466	2.9142	10.4595
11	28.6292	119.7353	14.8345	1.9086	3.7417	4.9448	2.7701	11.6413
9	22.5873	106.3413	12.1648	1.5058	3.7979	4.0549	2.5607	10.4828
20	40.9544	203.5488	34.3995	1.9502	4.2406	6.0472	3.3461	10.8434
13	32.6898	179.9479	17.0862	1.5567	4.2895	5.6954	2.9434	11.2644
34	73.0802	400.5244	61.4996	2.6100	4.7681	12.2999	3.9142	12.4735

TABLE 3

Coefficients and statistical analysis of equations (7) relating molar refraction, *MR*, to topological indices T_j

No.	T_j	a	b	r	s	F	EV
1.	B	20.001	0.566	0.641	4.511	2.790	—
2.	C	27.235	0.625	0.289	5.626	0.366	—
3.	M_1	12.163	0.848	0.894	2.627	16.028	0.778
4.	Q	27.801	0.671	0.162	5.800	0.108	—
5.	C'	30.093	−3.582	0.254	5.685	0.276	—
6.	Q'	30.544	−5.939	0.384	5.426	0.692	—
7.	N_2	18.143	2.102	0.733	3.997	4.647	—
8.	I_D^E	21.246	0.282	0.922	2.272	22.761	0.834
9.	w	20.720	0.255	0.940	2.009	30.241	0.870
10.	Z	21.697	0.593	0.881	2.778	13.898	0.752
11.	I_D^w	22.526	0.050	0.924	2.253	23.228	0.837
12.	I_{pc}	23.242	0.298	0.846	3.130	10.099	0.685
13.	I_D^E	13.657	8.928	0.732	4.004	4.618	—
14.	I_D^w	−0.401	8.159	0.996	0.525	514.588	0.991
15.	I_{pc}	20.488	1.761	0.889	2.695	15.024	0.776
16.	χ	5.995	8.661	0.961	1.621	48.562	0.915
17.	SI	7.497	2.181	0.822	3.351	8.304	0.639

($F_{0.01,\,8,\,1} = 10.56$, $F_{0.05,\,8,\,1} = 5.12$, $F_{0.10,\,8,\,1} = 3.40$)

TABLE

Data used for calculating equations

No.	Alkane	D_4^{20} g/ml	BP °C(1 atm)	Topological indices T_j			
				M_1	I_E^D	w	Z
1,	$i-C_4$	—	—	12	6.0000	9	4
2.	$n-C_5$	0.62624	36.1	14	18.4644	20	8
3.	$2-Me-C_4$	0.61967	27.9	16	15.2193	18	7
4.	$2,2-Me_2-C_3$	—	9.5	20	9.7095	16	5
5.	$n-C_6$	0.65937	68.7	18	32.2388	35	13
6.	$2-Me-C_5$	0.65315	60.2	20	28.6292	32	11
7.	$3-Me-C_5$	0.66431	63.5	20	27.3841	31	12
8.	$2,2-Me_2-C_4$	0.64916	49.7	24	22.5873	28	9
9.	$2,3-Me_2-C_4$	0.66164	57.9	22	23.4839	29	10
10.	$n-C_7$	0.68376	99.3	22	50.3644	56	21
11.	$2-Me-C_6$	0.67859	90.0	24	46.4642	52	18
12.	$2,2-Me_2-C_5$	0.67385	79.2	28	39.9740	46	14
13.	$2,3-Me_2-C_5$	0.69508	86.0	26	39.5676	46	17
14.	$2,4-Me_2-C_5$	0.67270	80.5	26	41.0774	47	15
15.	$2,2,3-Me_3-C_4$	0.69011	80.9	30	32.6898	42	13
16.	$n-C_8$	0.70252	125.7	26	73.0802	84	34
17.	$3-Me-C_7$	0.70582	119.0	28	67.0382	76	31
18.	$2,3-Me_2-C_6$	0.71214	115.6	30	61.3099	70	27
19.	$2,5-Me_2-C_6$	0.69354	109.1	30	63.3448	74	25
20.	$3,4-Me_2-C_6$	0.71923	117.7	30	58.9544	68	29
21.	$2,2,4-Me_3-C_5$	0.69192	99.9	34	54.6154	66	19
22.	$2,2,3-Me_3-C_5$	0.71602	109.9	34	52.9802	63	22

The D_4^{20} and BP values are taken from ref.[3].

TABLE 4

Coefficients and statistical analysis[a] of equation $D_4^{20} = a + b(MW/T_j)$ relating the density of alkanes to MW/T_j

No.	T_j	a	b	r	s	F	EV
1.	M_1	0.7190	−0.0105	0.356	0.0262	1.235	—
2.	I_D^E	0.7535	−0.0285	0.873	0.0137	27.346	0.750
3.	w	0.7588	−0.0354	0.915	0.0113	43.655	0.828
4.	Z	0.7566	−0.0122	0.883	0.0132	29.958	0.767
5.	I_D^w	0.7342	−0.0972	0.927	0.0106	51.608	0.851
6.	I_{pc}	0.7179	−0.0095	0.670	0.0208	6.929	0.418
7.	$\bar{I}_D^w$	−0.0857	0.0323	0.860	0.0143	24.067	0.724
8.	$\bar{I}_{pc}$	0.7663	−0.0059	0.826	0.0158	18.287	0.665
9.	χ	0.6907	−0.0004	0.020	0.0281	—	—

$(F_{0.01,18,1} = 8.29,\ F_{0.05,18,1} = 4.41,\ F_{0.1,18,1} = 3.05)$

[a] The data used for computing these equations are collected in Table 5.

5

D_4^{20} *vs.*(MW/T_j) and BP *vs.* T_j

Topological indices T_j					
I_D^w	I_{pc}	$\bar{I}_D^w$	$\bar{I}_{pc}$	χ	SI
22.5293	3.2451	2.5033	1.6226	1.7321	5.7485
62.9288	11.2451	3.1464	3.7984	2.4142	9.5667
57.5489	9.6515	3.1972	3.2172	2.2701	10.3397
52.0000	7.6096	3.2500	1.8048	2.0000	6.1376
129.6506	20.9863	3.7043	5.2466	2.9142	10.4595
119.7353	14.8345	3.7417	4.9448	2.7701	11.6413
116.5605	13.8003	3.7600	4.9501	2.8081	11.3094
106.3413	12.1648	3.7979	4.0549	2.5607	10.4828
109.8619	13.6097	3.7883	4.5366	2.6427	8.7078
233.4633	35.5096	4.1690	8.8774	3.4142	11.6638
218.1841	29.0195	4.1959	7.2549	3.2701	13.0755
195.0642	18.1417	4.2405	6.9943	3.0607	11.6988
195.5544	27.9771	4.2512	6.3645	3.1807	12.6450
203.0586	19.0936	4.2304	8.5999	3.1259	10.0423
179.9479	17.0862	4.2895	5.6954	2.9434	11.2644
400.5244	61.4996	4.7681	12.2999	3.9142	12.4735
349.9745	56.6256	4.6049	11.3251	3.8081	14.2873
324.5463	45.1150	4.6364	11.2788	3.6807	13.9967
341.2866	40.3392	4.6120	10.0848	3.6259	13.1833
316.2987	53.4727	4.6515	10.6945	3.7187	12.9456
307.1555	23.0054	4.6539	7.6685	3.4165	11.9728
294.5294	35.6474	4.6751	8.9119	3.4814	13.1891

The results are presented in Table 6.

TABLE 6

Coefficients and statistical analysis of equations BP $= a + bT_j$

No.	T_j	a	b	r	s	F	EV
1.	M_1	−26.9674	4.3121	0.752	21.195	11.708	0.543
2.	I_D^E	10.2825	1.7120	0.972	7.600	152.701	0.941
3.	w	8.3990	1.5114	0.967	8.221	129.187	0.931
4.	Z	17.7678	3.6477	0.941	10.857	70.227	0.880
5.	I_D^w	21.1483	0.2879	0.958	9.263	99.855	0.913
6.	I_{pc}	55.9854	0.6875	0.371	34.057	1.437	0.092
7.	$\bar{I}_D^w$	−165.2522	59.7076	0.957	9.320	98.513	0.912
8.	$\bar{I}_{pc}$	7.3221	10.3129	0.956	9.462	95.305	0.909
9.	χ	−105.9752	60.1621	0.994	3.544	734.737	0.987
10.	SI	−86.608	14.339	0.861	16.382	25.799	0.728

$(F_{0.01,19,1} = 8.18, F_{0.05,19,1} = 4.38, F_{0.1,19,1} = 3.00)$

The correlational ability for various topological indices T_j for this property (in the limited series under study) varies from excellent (χ, $r = 0.994$), through weak (M_1, $r = 0.752$), to insignificant (I_{pc}, $r = 0.371$)

These results, like the correlations of MR versus T_j, evidence the "compositional inhomogeneity" of topological indices. As a consequence, for a given property Q, the best suited topological index or indices for correlations of type (1) must be determined by trials.

REFERENCES

[1] A. T. Balaban, *Theor. Chim. Acta*, **53**, 355 (1979).

[2] A. T. Balaban, A. Chiriac, I. Moţoc and Z. Simon, "Steric Fit in Quantitative Structure-Activity Relations", Lecture Notes in Chemistry, vol. 15, Springer, Berlin, 1980.

[3] L. B. Kier and L. Hall, "Molecular Connectivity in Chemistry and Drug Research", Academic Press, New York, 1976.

[4] D. Bonchev, O. Mekenjan and N. Trinajstić (in press).

[5] D. Bonchev and N. Trinajstić, *J. Chem. Phys.*, **67**, 4517 (1977).

[6] R. R. Hocking, *Biometrics*, **32**, 1 (1976).

[7] R. L. Mason, *Comm. Statist.*, **4**, 277 (1975).

[8] J. G. Topliss and R. J. Costello, *J. Med. Chem.*, **15**, 1066 (1972).

[9] J. G. Topliss and R. P. Edwards, *J. Med. Chem.*, **22**, 1238 (1979).

[10] A. T. Balaban and I. Moţoc, *Math. Chem.*, **5**, 197 (1979).

[11] J. L. Weble, "Enzymes and Metabolic Inhibitors", Academic Press, New York, 1963.

[12] R. J. Boyd, *J. Phys.* B., **10**, 2283 (1977).

[13] I. Moţoc, *Arzneimittel Forsch.* (in press); I. Moţoc, O. Dragomir-Filimonescu and R. Vâlceanu, *Math. Chem.* (in press).

[14] S. H. Unger and C. Hansch, *Progr. Phys. Org. Chem.*, **12**, 91 (1976)

Revue Roumaine de Chimie, **26**, *4*, 601–610 (1981)

SOME REACTIONS WITH *MICHAEL* ADDUCTS OF BROMOBENZOYL ACRYLIC ACID AND ITS AMIDES

A. ESSAWY, M. ABDALLA and A. DEEB
Faculty of Science, Zagazig and Assiut (Aswan)
Universities, Egypt, A.R.E.

Received March 27, 1978
Revised October 20, 1980

The Michael condensation of β-*p*-bromobenzoyl acrylic acid (**1**) with benzyl methyl ketone and ethyl acetoacetate gives the adducts **2** and **4**. Chemical reactions of adducts **2** and **4** with hydrazines in alcohol and/or acetic acid, hydroxylamine hydrochloride, benzaldehyde, alcoholic potassium hydroxide and Grignard reagents were investigated. Reaction of oxime **8b** with polyphosphoric acid gives the lactam **9**. Reaction of dibromide **12** with amines and/or hydrazines gives **13a-d** and **14** respectively. Acetylation and esterification of **14** gives **18** and **15** respectively. Reactions of β-aroyl-N-arylacrylamides **17** with diethylmalonate, benzyl methyl ketone, thiourea and benzylthiourea were investigated.

Reaction of aroylacrylic acid under Michael conditions has been investigated earlier.[1,2] In the present paper we have examined the reactivity of the Michael adducts of β-*p*-bromobenzoylacrylic acid and its amides. Thus β-*p*-bromobenzoyl acrylic acid (**1**) reacted with benzyl methyl ketone in the presence of sodium methoxide to give 3-*p*-bromophenyl-5-oxo-6-phenyl-3-cyclohexene-1-carboxylic acid (**2**). (for IR spectra of Table 1). Moreover **2** was condensed with benzaldehyde under Erlenmeyer conditions (molar ratio 1 :1) in boiling acetic anhydride for 6 hrs to give the corresponding 2-benzylidene-5-oxo-6-phenyl-3-*p*-bromophenyl-3-cyclohexene-1-carboxylic acid (**3**). (IR spectra, Table 1).

Ethyl acetoacetate readily undergoes base catalyzed cycloaddition with β-*p*-bromobenzoyl acrylic acid (**1**) to give 2-ethyl hydrogen-5-*p*-bromophenyl-3-oxo-4-cyclohexene 1,2 dicarboxylate (**4**) (IR spectra, Table 1). Decarboxylation of **4** was accomplished by heating with alcoholic potassium hydroxide to give 3-*p*-bromophenyl-5-oxo-3-cyclohexene-1-carboxylic acid (**5**). The structure of **5** was established on the basis of IR spectra (Table 1) and solubility in aqueous sodium carbonate solution. Compounds **2** and **4** yielded hydrazones **6a** and **6b** and phenyl hydrazones **6c** and **6d** respectively on treatment with hydrazine hydrate and phenyl hydrazine in boiling ethanol.[3,4] Condensation of **5** with hydrazine hydrate in boiling alcohol yielded 5-oxo-3-*p*-bromophenyl-3-cyclohexene-1-carboxylic acid hydrazone (**6b**). On the other hand, the condensation of **4** with hydrazine hydrate and/or phenyl hydrazine in boiling acetic acid[3,4] gave 3,3,4,5-tetrahydro-3-oxo-6-*p*-bromophenyl-2*H*-indazole-4-carboxylic acid (**7a**) and 3,3,4,5-tetrahydro-3-oxo-2-phenyl-6-bromophenyl-2*H*-indazole-4-carboxylic acid (**7b**) respectively. The structure assignments of

TABLE 1

IR spectra of compounds 2—22

Comp.	IR absorptions : CM^{-1}					
	$\nu(CO)$	$\nu(OH)$	Carboxylic $\nu(CO)$	$\nu(C=C)$	$\nu(C=N)$	Others
2	1650	3200	1740	1600	—	
3	1620	3500	1736	1600	—	
4	1740, 1660	3230	1720	—	—	
5	1700	3260	1720	—	—	3020 : $\nu(CH_2)$
6	—	3435	1720	1600	1640	3280 : $\nu(NH)$, 2900 : $\nu(CH_2)$
7	1730	3450	1720	1620	1630	2980 : $\nu(CH_2)$
8	—	3430	1710	1620	1660	2910 : $\nu(CH_2)$
9	1730	3260	1660	1610	—	3440 : $\nu(NH)$, 2930 : $\nu(CH_2)$
10	—	3450	1700	1610	—	—
11	—	3420	1710	1600	—	—
13	1680	3470	1720	—	—	2860 : ν(tert. CH)
14	—	3300	1700	—	1610	3200 : $\nu(NH)$
16	1680	3270	1720	1610	1620	2900 : $\nu(CH)$
18	1750, 1680 1720	—	—	—	—	3520 : $\nu(NH)$, 2965 $\nu(CH)$
19	1780, 1740	3520	1715	1610	—	—
20	1700, 1680	3420	1715	1615	—	3350 : $\nu(NH)$
21	1700, 1680	—	—	1610	—	3500 : $\nu(NH)$, 2980 $\nu(CH_2)$
22	1670	—	—	1600	—	3220 : $\nu(NH)$, 1380 $\nu(C=S)$

7 were based on IR spectra (Table 1) and solubility in aqueous sodium carbonate solution. Refluxing a mixture of **2** and **4**, hydroxylamine hydrochloride, sodium acetate and alcohol afforded the formation of 3-*p*-bromophenyl-5-oxo-6-phenyl-3-cyclohexene-1-carboxylic acid oxime (**8a**) and 3-*p*-bromophenyl-5-oxo-3-cyclohexene-1-carboxylic acid oxime (**8b**) respectively (IR spectra, Table 1). Treatment of **5** with hydroxylamine hydrochloride, and sodium acetate in boiling alcohol gave the oxime derivative **8b**.

Heating **8b** with polyphosphoric acid caused it to undergo the Beckmann rearrangement, with formation of lactam **9** (IR spectra, Table 1) 3-*p*-Bromophenyl-5-oxo-6-phenyl-3-cyclohexene -1-carboxylic acid (**2**) reacted with Grignard reagents,[4] namely ethylmagnesium iodide, phenylmagnesium bromide and benzylmagnesium chloride with subsequent decomposition and hydrolysis to give **10** (IR spectra, Table 1). One possible approach to explain the formation of **10** is the assumption that one mole of the Grignard reagent is consumed in addition to the carbonyl group with the formation of the intermediate magnesium salt. The latter upon acidification is decomposed and loses water with the formation of **10**. On the other hand, treatment of **4** with phenylmagnesium bromide, ethylmagnesium iodide and methyl magnesium iodide provided **11**, (IR spectra, Table 1). In the previous reaction three moles of Grignard reagent are incorporated and the products are the tertiary alcohols **11 a**—**c**. The reaction of β-*p*-bromobenzoylacrylic acid (**1**) with bromine in chloroform gives α, B-dibromo-β-*p*-bromobenzoyl propionic acid (**12**) which on reaction with amines in absolute alcohol gives **13** (IR spectra, Table 1). Dibromo derivative **12** reacted with hydrazine hydrate in the presence of glacial acetic acid to give 3-*p*-bromophenyl pyrazole-5-carboxylic acid (**14**) (IR spectra, Table 1). Esterification of **14** with diazomethane gave methyl-3-*p*-bromophenyl pyrazole-5-carboxylate (**15**). Hydrolysis of **15** with a mixture of acetic and hydrochloric acid (1 :1) gave **14**. Acetylation of **14** with sodium acetate and acetic acid gave 1-acetyl-3-*p*-bromophenyl-pyrazole-5-carboxylic acid (**16**), (IR spectra, Table 1).

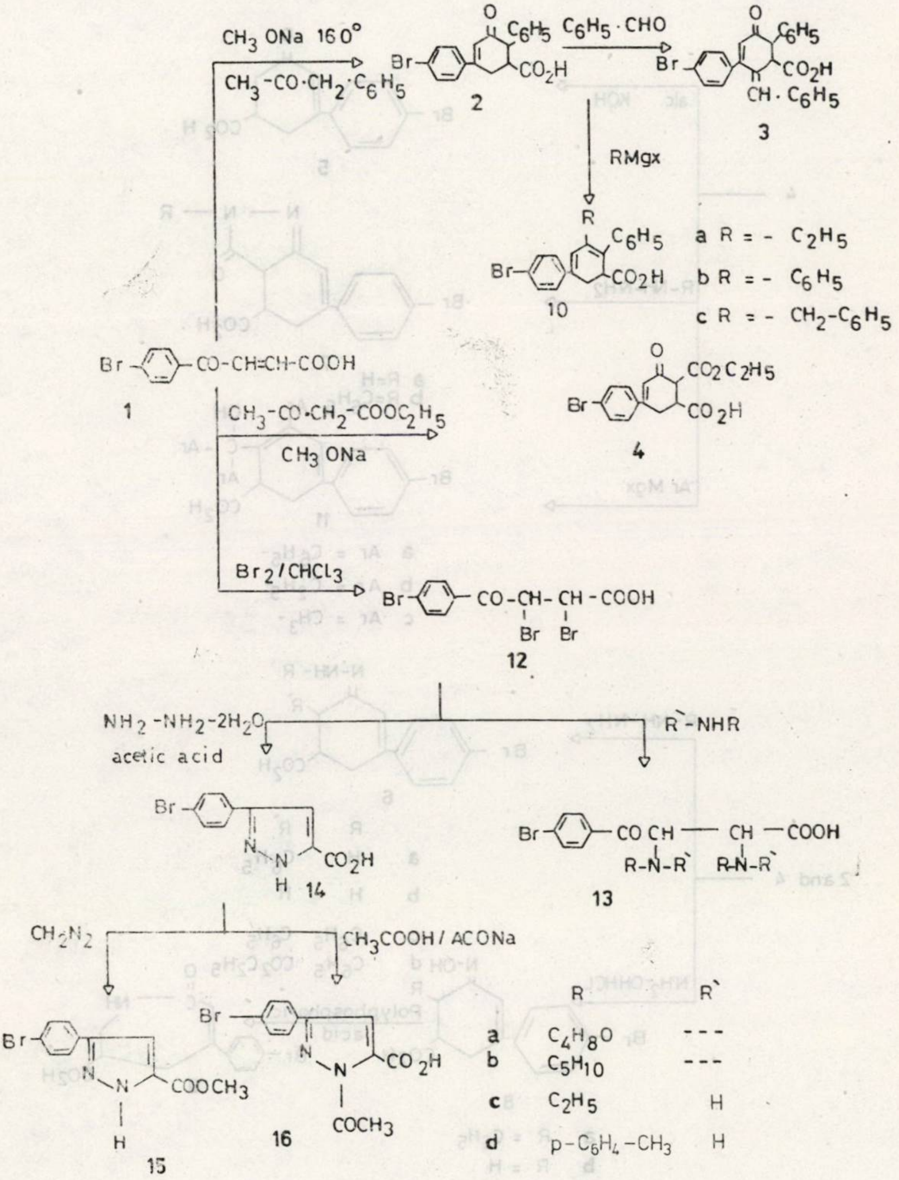

CH_3ONa 160°
$CH_3-CO\cdot CH_2\cdot C_6H_5$
$C_6H_5\cdot CHO$
2
3
RMgx
10
a R = - C_2H_5
b R = - C_6H_5
c R = - $CH_2-C_6H_5$
Br-⟨⟩-CO-CH=CH-COOH
1
$CH_3-CO\cdot CH_2-COOC_2H_5$
CH_3ONa
4
$Br_2/CHCl_3$
12
$NH_2-NH_2-2H_2O$
acetic acid
R'-NHR
14
13
CH_2N_2
CH_3COOH / AcONa
15
16
R R'
a C_4H_8O ---
b C_5H_{10} ---
c C_2H_5 H
d p-$C_6H_4-CH_3$ H

Diethyl malonate readily undergoes base catalyzed cycloaddition with β-aroyl-N-aryl-acrylamides **17** to give ethyl-3,4-dihydro-6-aryl-4-(arylcarbamoyl)-2*H* pyron-3-carboxylates (**18**). Boiling of **18a** with hydrochloric-acetic acid mixture or with 50% alcoholic potassium hydroxide solution gave 3-ethyl hydrogen 3,4-dihydro-2-oxo-6-*p*-bromophenyl-2*H*-pyran-3,4-dicarboxylate (**19**) and 3,4-dihydro-2-oxo-6-bromophenyl-2*H*-pyran-3-carboxy-4-carboxanilide (**20**) respectively. Addition of benzyl

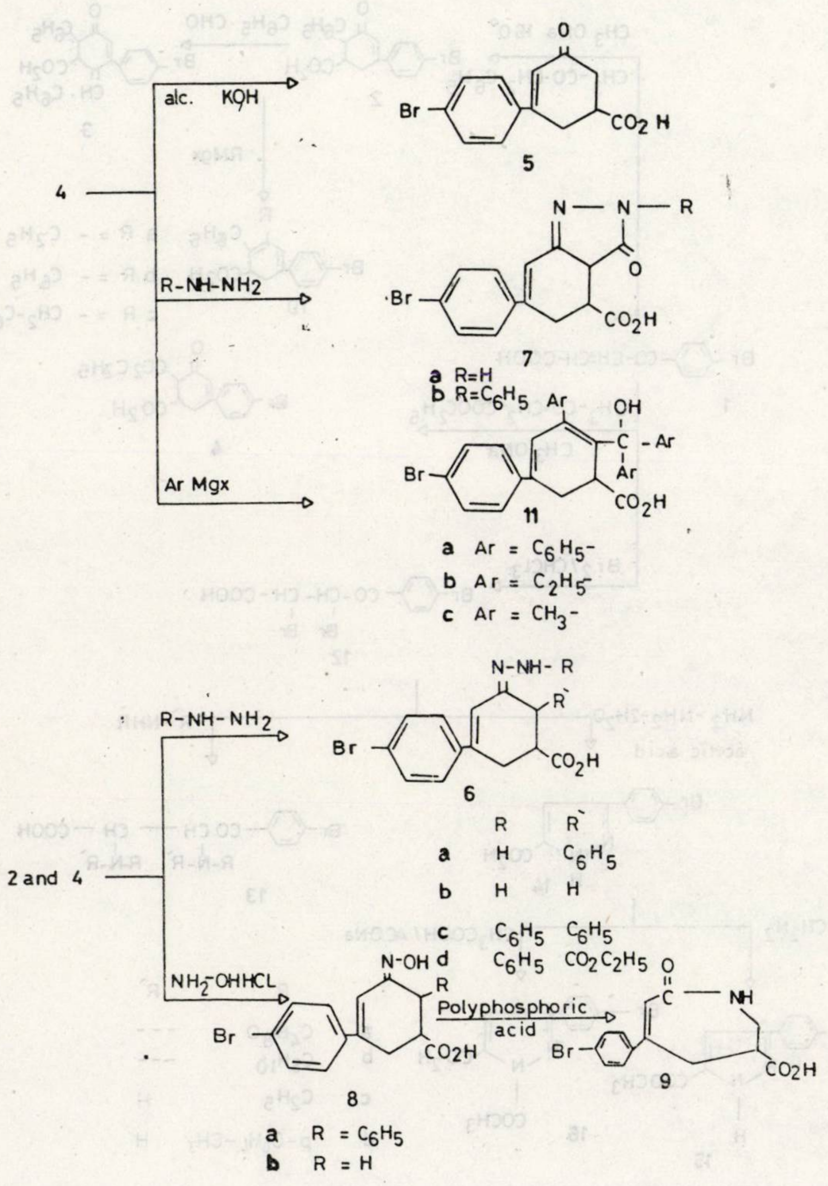
4
alc. KOH
R-NH-NH2
Ar Mgx
Br
O
CO2H
5
N — N — R
O
7
a R=H
b R=C6H5
Ar
OH
C - Ar
Ar
11
a Ar = C6H5-
b Ar = C2H5-
c Ar = CH3-
2 and 4
R-NH-NH2
N-NH- R
R`
6
R R`
a H C6H5
b H H
c C6H5 C6H5
d C6H5 CO2C2H5
NH2-OHHCL
N-OH
R
8
a R = C6H5
b R = H
Polyphosphoric acid
NH
9

methyl ketone to **17a** in the presence of sodium methoxide, was found to give the Michael adduct **21**. Thiourea reacted with the amide **17c** to give 2-thio-1-(3-P-bromobenzoyl acryloyl) urea (**22**). Similarly, benzylthiourea reacted with the amide **17b** to give 1-benzyl-2-thio-3-(3-*p*-bromobenzoyl acryloyl) urea (**23**). Heating a mixture of β-*p*-bromobenzoyl acrylyl chloride, thiourea and/or benzyl thiourea (molar ratio 1 : 2) in ether for 6 hrs afforded the products **22** and **23** respectively.

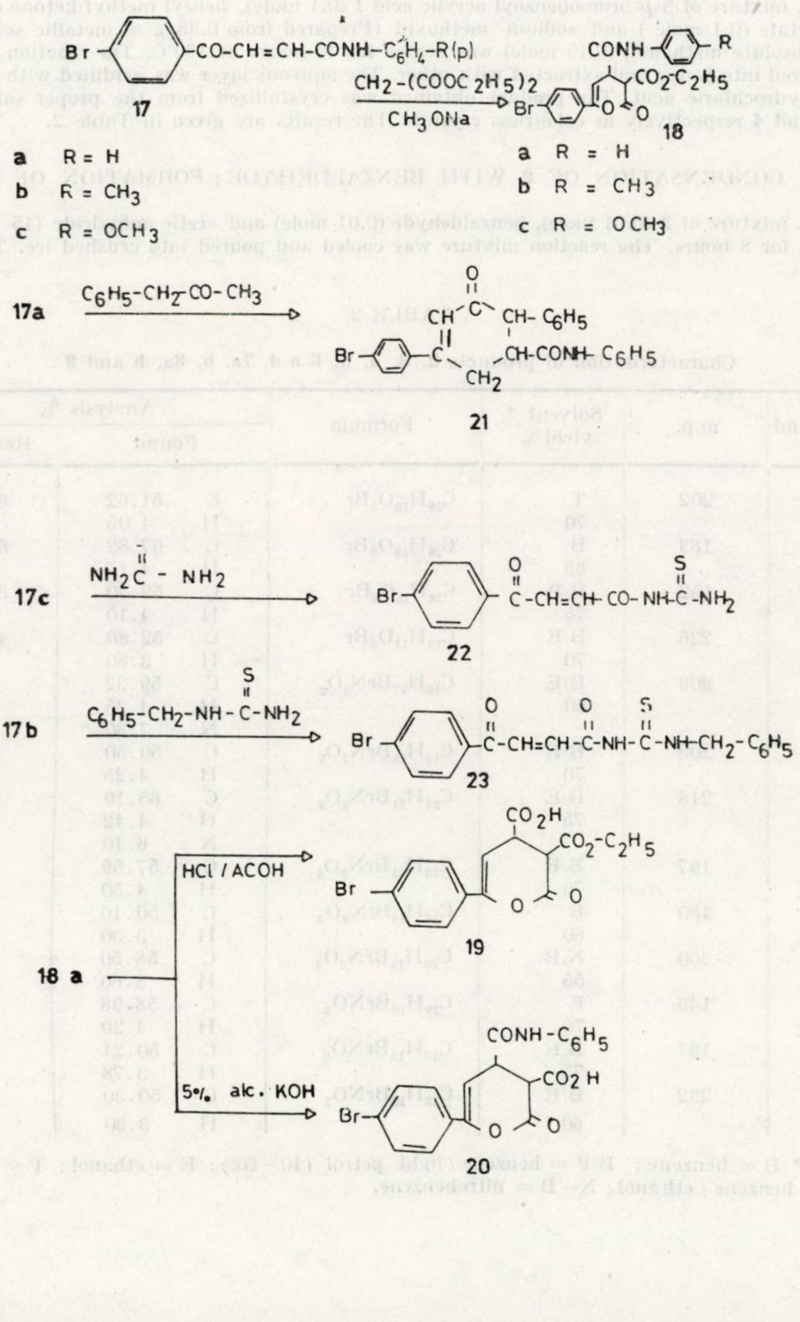
Br–C6H4–CO-CH=CH-CONH–C6H4–R(p)
17
CH2-(COOC2H5)2
CH3ONa
CONH
R
CO2C2H5
Br
O
O
18
a R = H
b R = CH3
c R = OCH3
a R = H
b R = CH3
c R = OCH3
17a
C6H5-CH2-CO-CH3
O
CH
C
CH- C6H5
Br
C
CH-CONH- C6H5
CH2
21
17c
NH2C(=S)- NH2
Br
C-CH=CH-CO-NH-C-NH2
O
S
22
17b
C6H5-CH2-NH-C-NH2
S
Br
C-CH=CH-C-NH-C-NH-CH2-C6H5
O
O
S
23
HCl / ACOH
CO2H
CO2-C2H5
Br
O
O
19
18 a
5% alc. KOH
CONH-C6H5
CO2H
Br
O
O
20

EXPERIMENTAL

The infrared absorption spectra were determined with a Unicam Sp 1200 spectrophotometer using KBr wafer technique. All melting points are uncorrected.

BASE CATALYZED CYCLOADDITION OF BENZYL METHYL KETONE AND/OR ETHYL ACETOACETATE TO β-*p*-BROMOBENZOYLACRYLIC ACID (1) : FORMATION OF 2 AND 4

A mixture of β-*p*-bromobenzoyl acrylic acid **1** (0.1 mole), benzyl methyl ketone or ethy acetoacetate (0.1 mole) and sodium methoxid (Prepared from 0.35 g of metallic sodium in 15 ml absolute methanol) (0.15 mole) was heated for 10 hours at 160°C. The reaction mixture was poured into water and extracted with ether. The aqueous layer was acidified with ice cold dilute hydrochloric acid. The product obtained was crystallized from the proper solvent to give **2** and **4** respectively as colourless crystals. The results are given in Table 2.

CONDENSATION OF 2 WITH BENZALDEHYDE ; FORMATION OF 3

A mixture of **2** (0.01 mole), benzaldehyde (0.01 mole) and acetic anhydride (15 ml) was refluxed for 8 hours. The reaction mixture was cooled and poured into crushed ice. The oily

TABLE 2

Characterisation of products **2**, **3**, **4**, **5**, **6 a-d**, **7a**, **b**, **8a**, **b** and **9**

Compound	m.p.	Solvent * yield %	Formula	Analysis % Found	Analysis % Required
2	202	T	$C_{19}H_{15}O_3Br$	C 61.62	61.45
		70		H 4 05	4.04
3	183	B	$C_{26}H_{19}O_3Br$	C 67.82	67.97
		65		H 4.17	4.13
4	152	B/P	$C_{16}H_{15}O_5Br$	C 52.50	52.31
		75		H 4.10	4.08
5	226	B/E	$C_{13}H_{11}O_3Br$	C 52.80	52.88
		70		H 3.80	3.72
6a	209	B/E	$C_{19}H_{17}BrN_2O_2$	C 59.32	59.22
		60		H 4.35	4.41
				N 7.30	7.27
6b	208	B/E	$C_{13}H_{13}BrN_2O_2$	C 50.50	50.48
		70		H 4.25	4.20
6c	218	B/E	$C_{25}H_{21}BrN_2O_2$	C 65.10	65.075
		75		H 4.42	4.55
				N 6.10	6.07
6d	197	B/E	$C_{22}H_{21}BrN_2O_4$	C 57.59	57.76
		70		H 4.50	4.59
7a	180	E	$C_{14}H_{11}BrN_2O_3$	C 50.10	50.14
		60		H 3.30	3.28
7b	>300	N.B	$C_{20}H_{15}BrN_2O_3$	C 58.50	58.39
		55		H 3.60	3.64
8a	149	E	$C_{19}H_{16}BrNO_3$	C 58.98	59.06
		70		H 4.20	4.14
8b	197	B/E	$C_{13}H_{12}BrNO_3$	C 50.21	50.32
		75		H 3.78	3.87
9	232	B/E	$C_{13}H_{12}BrNO_3$	C 50.30	50.32
		60		H 3.90	3.87

* B = benzene ; B/P = benzene / light petrol (40 − 60°) ; E = ethanol ; T = toluene ; B/E = benzene / ethanol ; N − B = nitrobenzene.

products formed were boiled with water and the solid products formed after cooling were filtered off, washed with water several times, dried and then crystallized from benzene to give **3** as yellow crystals (Table 2).

DECARBETHOXYLATION OF 4; FORMATION OF 5

Cyclohexenone derivative **4** (0.01 mole) was added to a solution containing sodium hydroxide (0.1 mole) dissolved in a mixture of 50 ml ethanol and 30 ml water. The mixture was refluxed for 5 hrs cooled and acidified with dilute hydrochloric acid. The solid obtained was crystallized from benzene/ethanol mixture to give **5** as colourless crystals (Table 2).

REACTION OF 2 AND 4 WITH HYDRAZINES; FORMATION OF 6a–d

A mixture of **2** and/or **4** (0.01 mole), hydrazine hydrate or phenyl hydrazine (0.01 mole) and ethanol (15 ml) was refluxed for 6 hrs. The solid product obtained after concentration and cooling was crystallized from a proper solvent to give **6a-d** as colourless crystals (Table 2).

CONDENSATION OF 4 WITH HYDRAZINES IN BOILING ACETIC ACID; FORMATION OF 7a AND b

A mixture of **4** (0.01 mole), hydrazine hydrate or phenyl-hydrazine (0.01 mole) and glacial acetic acid (15 ml) was refluxed for 6 hours. The solid product obtained was crystallized from the proper solvent to give **7a** and **7b** as yellow crystals (Table 2).

REACTION OF 2 AND 4 WITH HYDROXYLAMINE HYDROCHLORIDE; FORMATION OF 8a AND b

A mixture of **2** and/or **4** (0.01 mole), hydroxylamine hydrochloride (0.01 mole), sodium acetate (0.03 mole) ethanol (20 ml) and a few drops of water was refluxed for 8 hours. The solid product formed after concentration and cooling was crystallized from a proper solvent to give **8a** and **8b** as colourless crystals (Table 2).

ACTION OF POLYPHOSPHORIC ACID ON OXIME 8b; FORMATION OF LACTAM 9

The oxime **8b** (0.006 mole) was heated with stirring with polyphosphoric acid (0.6 mole) for ten min. at 130–140°C. The mixture was cooled and treated with water. The product was separated by extraction with chloroform. Recrystallization from benzene provided **9** as colourless crystals (Table 2).

REACTION OF GRIGNARD REAGENTS WITH 2 AND 4; FORMATION OF 10a-c AND 11 a-c

A dry benzene solution of **2** or **4** (0.01 mole) was added to an ethereal solution of the appropriate aryl or alkylmagnesium halide (from 0.7 g magnesium). After 3 hrs of reflux the reaction mixture was decomposed into the usual way with ice and ammoninm chloride solution and the products **10** and **11** recovered with the help of ether as oils, were triturated and crystallized from the suitable solvent as colourless crystals (Cf. Table 3).

REACTION OF β-*p*-BROMOBENZOYLACRYLIC ACID (1) WITH BROMINE; FORMATION OF 12

A solution of compound **1** (0.01 mole) in 20 ml chloroform was treated with 20 ml of 1 M solution of bromine in chloroform. During addition the solution was chilled in an ice bath and stirred. After addition, absolute ethanol was added and the solution chilled. The colourless solid precipitated was crystallized from benzene to give dibromo-α-β-bromobenzoyl propionic acid (**12**) (Table 3).

TABLE 3

Characterisation of products **10a-c**, **11a-c**, **12**, **13a-d**, **14**, **15** and **16**

Compound	m.P°	Solvent* yield %	Formula	Analysis %		
					Found	Required
10a	195	B	$C_{21}H_{19}O_2Br$	C	65.80	65.79
		40		H	4.10	4.96
10b	175	B	$C_{25}H_{19}O_2Br$	C	69.50	69.60
		50		H	4.50	4.40
10c	125	B/P	$C_{26}H_{21}O_2Br$	C	70.20	70.11
		60		H	4.67	4.71
11a	280	B	$C_{32}H_{25}O_3Br$	C	71.30	71.50
		40		H	4.70	4.65
11b	118	B/P	$C_{20}H_{25}O_3Br$	C	61.10	61.06
		45		H	6.40	6.36
11c	125	P	$C_{17}H_{19}O_3Br$	C	58.20	58.11
		35		H	5.30	5.41
12	155	B	$C_{10}H_7O_3Br_3$	C	29.00	28.91
		60		H	1.70	1.68
13a	130	B/P	$C_{18}H_{23}BrN_2O_5$	C	50.39	50.58
		40		H	5.30	5.38
13b	110	B/P	$C_{20}H_{27}BrN_2O_3$	C	56.54	56.73
		30		H	6.40	6.38
13c	90	B/P	$C_{14}H_{19}BrN_2O_3$	C	49.00	48.97
		45		H	5.49	5.53
13d	290	E	$C_{24}H_{23}BrN_2O_3$	C	61.58	61.67
		60		H	4.83	4.92
14	230	A	$C_{10}H_7BrN_2O_2$	C	44.87	44.94
		65		H	2.58	2.62
15	210	E	$C_{11}H_9BrN_2O_2$	C	47.00	46.97
		60		H	3.15	3.20
16	190	A	$C_{12}H_9BrN_2O_3$	C	46.56	46.60
		70		H	3.00	2.91

* A = acetic acid, B = benzene, E = ethanol, B/P = benzene / light petrol (40–60°), P = light petrol (60–80°).

REACTION OF 12 WITH AMINES ; FORMATION OF 13a-d

To an absolute ethanolic (50 ml) suspension of **12** (0.01 mole), morpholine, piperidine, ethylamine and/or *p*-toluidine (0.05 mole, excess) were added rapidly with stirring. The dibromide dissolved and the solution was left for 24 hrs at room temperature to give a colourlesr product which was washed with water several times then dried and crystallized from a propes solvent to give **13** (Table 3).

REACTION OF 12 WITH HYDRAZINE HYDRATE ; FORMATION OF 14

To a solution of **12** (0.01 mole) in glacial acetic acid (10 ml) hydrazine hydrate (0.02 mole) was added dropwise, then the mixture was refluxed for 8 hrs. The product obtained was crystallized from acetic acid to give **14** as colourless crystals (Table 3).

ACETYLATION OF 14 ; FORMATION OF 16

A mixture of **14** (0.01 mole), sodium acetate equivalent weight, and glacial acetic acid (15 ml) was refluxed for 6 hrs. The reaction mixture was poured into ice. The separated solid product was filtered off, washed with water several times, dried and then crystallized from acetic acid to give **16** as brown crystals. (Table 3).

ESTERIFICATION OF 14; FORMATION OF 15

To an ethereal solution of **14** (0.01 mole) an ethereal solution of diazomethane (prepared from nitrosomethylurea (0.03 mole) was added. The solution was kept for 24 hrs in a refrigerator, the solid obtained after evaporation of ether was crystallized from ethanol to give **15** as pale yellow crystals (Table 3).

SYNTHESIS OF β-*p*-BROMOBENZOYL-N-ARYL ACRYLAMIDES (17a-c)

An ethereal solution of amine (0.01 mole) was added dropwise to an ethereal solution of β(*p*-bromobenzoyl) acrylyl chloride (0.01 mole). The solid product formed crystallized from ethanol to give **17 a-c** as yellow crystals (Table 4).

BASE CATALYZED CYCLOADDITION OF DIETHYL MALONATE TO 17a-c; FORMATION OF 18 a-c

A mixture of **17 a-c** (0.1 mole), diethyl malonate (0.1 mole) and sodium methoxide (0.13 mole) was fused at 170°C for 8 hrs. The reaction mixture was poured into water then extracted with ether. The aqueous layer was acidified with ice-cold dil.HCl.

The residual oil formed was triturated with light petrol (b.p 40—60°C) The solid obtained was crystallized from ethanol to give **18 a-c** as yellow crystals (Table 4).

ACID HYDROLYSIS OF 18a; FORMATION OF 19

A solution of **18a** (0.005 mole) in glacial acetic acid (10 ml) and concentrated hydrochloric acid (10 ml) was refluxed for 4 hours. The reaction mixture was poured into ice. The solid separated was filtered off and recrystallized from benzene to give **19** as pale yellow crystals (Table 4).

TABLE 4

Characterisation of products **17a-c**, **18a-c**, **19**, **20**, **21**, **22** and **23**

Compound	m.pC°	Solvent* yield %	Formula	Analysis % Found	Analysis % Required
17a	210	E	$C_{16}H_{12}BrNO_2$	C 58.20	58.18
		65		H 3.52	3.63
17b	205	E	$C_{17}H_{14}BrNO_2$	C 59.19	59.30
		70		H 4.10	4.06
17c	190	E	$C_{17}H_{14}BrNO_3$	C 56.55	56.66
		60		H 3.89	3.88
18a	220	B/P	$C_{21}H_{18}BrNO_5$	C 56.67	56.75
		65		H 4.10	4.05
18b	300	B/P	$C_{22}H_{20}BrNO_5$	C 57.52	57.64
		55		H 4.28	4.36
18c	150	B/P	$C_{22}H_{20}BrNO_6$	C 55.59	55.69
		60		H 4.16	4.21
19	180	B	$C_{15}H_{13}O_6Br$	C 48.80	48.78
		50		H 3.50	3.52
20	200	E	$C_{19}H_{14}BrNO_5$	C 54.71	54.80
		40		H 3.40	3.36
21	230	B/P	$C_{25}H_{20}BrNO_2$	C 67.30	67.26
		50		H 4.50	4.48
22	160	B/P	$C_{11}H_9BrN_2O_2S$	C 42.20	42.17
		50		H 2.84	2.87
23	110	B/P	$C_{18}H_{15}BrN_2O_2S$	C 53.60	53.59
		60		H 3.67	3.72

* B = benzene; B/P = benzene/light petrol (40—60°), E = ethanol.

ALKALINE HYDROLYSIS OF **18a**; FORMATION OF **20**

A mixture of **18a** (0.005 mole) in ethanol (50 ml) and (5%) potassium hydroxide solution (10 ml) was refluxed for 10 hours. The cold mixture was acidified with dilute hydrochloric acid. The product was crystallized from ethanol to give **20** as colourless crystals (Table 4).

BASE CATALYZED CYCLOADDITION OF BENZYL METHYL KETONE TO **17a**; FORMATION OF **21**

A mixture of **17a** (0.1 mole), benzyl methyl ketone (0.1 mole), and sodium methoxide (0.15 mole) was fused at 180°C for 6 hours. The reaction mixture was poured into water, then extracted with ether. The aqueous layer was acidified with ice-cold dil.HCl. The solid obtained was crystallized from benzene/light petrol (40—60°) to give **21** as pale yellow crystals (Table 4).

REACTION OF **17b** AND **17d** WITH BENZYLTHIOUREA AND THIOUREA; FORMATION OF **23** AND **22**

A mixture of **17b** and/ or **17d** (0.01 mole), benzylthiourea and/or thiourea (0.02 mole) and ethanol (15 ml) was treated with 10 drops of glacial acetic acid and relufxed for 8 hrs. The solid product separated was crystallized from benzene/light petrol (40—60°) to give **22** and **23** as colourless crystals (Table 4).

PREPARATION OF AUTHENTIC SAMPLES OF **22** AND **23**

A mixture of β-*p*-bromobenzoyl acrylyl chloride (0.01 mole) (prepared from 0.01 mole of β-*p*-bromobenzoyl acrylic acid and 0.012 mole phosphorous pentachloride) thiourea and/or benzylthiourea (0.02 mole), and ether (40 ml) was refluxed on a water bath for 6 hours. The solid product obtained after evaporation of ether, was crystallized from benzene/light petrol (40—60°) to give products proved to be **22** and **23** respectively by melting point and mixed melting point determination.

REFERENCES

[1] A. Sammour, M. Abdalla, A. Essawy and M. El-Mobayed, *Egypt J. Chem.*, **19**, 911 (1976).
[2] A. Sammour, M.I.B. Selim and E. A. Soliman, *Egypt. J. Chem.*, **16**, 311 (1972).
[3] A. Sammour, M.I.B. Selim, A. Essawy and M. Elkasaby, *Egypt. J. Chem.*, **16**, 197 (1973).
[4] A. Sammour, M.I.B. Selim and Y. Abd. El-Rehim, *Egypt. J. Chem.*, **12**, 493 (1969).

Revue Roumaine de Chemie, **26**, *4*, 611–621 (1981)

NUCLEOPHILE SUBSTITUTIONEN AN KOHLENSÄUREDERIVATEN. XVIII[1]

KINETIK UND MECHANISMUS DER ALKOHOLYSE VON N,N,N'- TRISUBSTITUIERTEN KOHLENSÄURECHLORAMIDINEN

R. BACALOGLU, A. CHICU, ILSE BACALOGLU und L. COTARCĂ
Technische Hochschule „Traian Vuia“ Bocşa-Str. 6, 1900 Timişoara, Rumänien

Eingegangen am 27. März, 1980

Durch die Reaktion der N,N,N'-trisubstituierten Chlorformamidine mit Alkoholen entstehen die entsprechenden iso-Harnstoffe, die in einer raschen Etappe das Alkylradikal verlieren und in Harnstoff übergehen. Die langsame Etappe des Prozesses besteht aus der monomolekularen Chloratomionisierung, wobei ein Karbokation entsteht. Diese Etappe wurde anhand der Lösungsmittel-, elektronischen und sterischen Effekte der Substituenten und durch Zusatz von Nucleophilen und Salzen bewiesen.

The izoureas which are formed by the reaction of N, N, N'-trisubstituted chloroformamidines with alcohols split the alkyl radicals to the corresponding, N, N, N'-trisubstituted ureas. Through kinetic investigation of solvent, electronic and steric, nucleophiles and salts effects it has been shown that the monomolecular ionization to the carbocation is the slower step of the process.

Durch das Studium der Hydrolyse der N,N,N'-trisubstituierten Kohlensäurechloramidine[1,2] wurde bewiesen, daß die Anwesenheit von zwei Stickstoffatomen am Kohlenstoffatom, durch deren mesomeren elektronenstoßenden Effekt, das gebildete Karbokation durch Chloreliminierung derart stabilisiert, daß der Prozeß ausschließlich einen monomolekularen Weg einschlägt. In bestimmten Bedingungen kann sogar die Reaktion des Kations mit dem Nucleophil zur langsamen Etappe werden, wobei die Ionisierung ein rasches Vorgleichgewicht darstellt. In solchen Bedingungen ist zu erwarten, daß die N,N,N'-trisubstituierten Chlorformamidine verhältnismäßig leicht auch mit anderen Nucleophilen reagieren, wie zum Beispiel, mit den in der vorliegenden Arbeit untersuchten Alkoholen.

ERGEBNISSE UND DISKUSSION

REAKTIONSPRODUKTE

Die Reaktionen der Chlorformamidine mit Alkoholen und Phenolen sind verhältnismäßig wenig studiert worden. In der Literatur ist die Reaktion der N,N,N'-trisubstituierten Chlorformamidine mit Natriumalkoxyden in den entsprechenden Alkoholen beschrieben, wobei sich die N,N,N′-trisubstituierten O-Alkylisoharnstoffe[3,4] bilden. Durch die Reaktion des N′-Phenyl-N,N-dimethylchlorformamidins mit Phenoxyd in Dioxan[5] oder mit Phenolen in Gegenwart von tertiären Aminen[6] wurden O-Phenyl-N′-phenyl-N,N-dimethylisoharnstoffe synthetisiert:

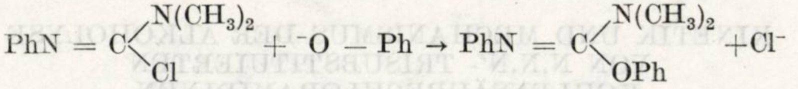

$$\mathrm{PhN}=\mathrm{C}\begin{array}{l}\diagup \mathrm{N(CH_3)_2}\\ \diagdown \mathrm{Cl}\end{array} + {}^{-}\mathrm{O}-\mathrm{Ph}\rightarrow \mathrm{PhN}=\mathrm{C}\begin{array}{l}\diagup \mathrm{N(CH_3)_2}\\ \diagdown \mathrm{OPh}\end{array} + \mathrm{Cl^-}$$

In den Bedingungen, in denen wir unsere Versuche durchgeführt haben – Alkohol-Dioxan-Gemisch in verschiedenen Proportionen-war es unmöglich die N,N,N′-trisubstituierten O-Alkylisoharnstoffe zu isolieren oder wenigstens zu identifizieren.

So wurde durch die Verfolgung der Alkoholyse der N,N,N′-Triphenylchlorformamidine in Gemischen von Methanol, *iso*-Propanol oder *tert*-Butanol-Dioxan (2/3 Volumen/Volumen) bei Temperaturen zwischen 30–80°, auf Grund der von Zeit zu Zeit registrierten IR-Spektren, als einziges Reaktionsprodukt der N,N,N′-Triphenylharnstoff gefunden. Es konnte keine einzige Bande, von noch so schwacher Intensität identifiziert werden, die einem entsprechenden O-Alkyl-N,N,N′-triphenylisoharnstoff zugeschrieben hätte werden können. Schon vom Anfang dieser Prozesse, wird gleichzeitig mit dem Verschwinden der dem N,N,N′-Triphenylchlorformamidin[7] kennzeichnenden Banden von 1680 $\mathrm{cm^{-1}}$ (ν(C=N))und 1190 $\mathrm{cm^{-1}}$ (ν(C–N)) das Erscheinen der dem N,N,N′-Triphenylharnstoff[8,9] charakteristischen Banden von 1690 $\mathrm{cm^{-1}}$ (Amid I (ν(CO)), 1520–1530 $\mathrm{cm^{-1}}$ (Amid II (δ(NH)), 1300–1315 $\mathrm{cm^{-1}}$ und 1220 $\mathrm{cm^{-1}}$ (Amid III (ν(CN)) beobachtet. Während des Prozesses bleiben mehrere den aromatischen Ringen eigene Banden (690, 750, 1490 und 1590 $\mathrm{cm^{-1}}$) an Intensität und Lage unverändert, da diese weniger empfindlich auf unwesentliche Strukturveränderungen sind. Weil Dioxan und die im Überschuß vorhandenen Alkohole eine starke Absorbtion aufweisen, konnten die Bereiche von 780–1180 $\mathrm{cm^{-1}}$, 1300–1480 $\mathrm{cm^{-1}}$ oder 2700–3600 $\mathrm{cm^{-1}}$ nicht untersucht werden.

Die durch Verdampfung des Lösungsmittels in allen Fällen der Alkoholyse von N,N,N′-Triphenylchlorformamidinen isolierten Reaktionsprodukte, bewiesen sich identisch untereinander und mit einer authentischen Probe von N,N,N′-Triphenylharnstoff, durch Schmelzpunktbestimmungen, Mischschmelzpunkte und IR-Spektren.

Um die Möglichkeit einer Reaktion mit den im System vorhandenen Wasserspuren auszuschalten, wurden alle Versuche in wasserfreiem Dioxan und Alkoholen mit besonderer Vorsicht durchgeführt.

Die IR-Spektren konnten keine Auskunft über die restlichen, ein aliphatisches Radikal enthaltende Reaktionsprodukte geben, wegen der eigenen Absorbtion des Dioxans und dem großen Überschuß an Alkohol. Um diese Produkte trotzdem verfolgen zu können, wurde ein Versuch in *n*-Butanol durchgeführt, weil in diesem Fall schwerer flüchtige Verbindungen entstehen konnten, die eventuell unter drastischen Bedingungen im System behalten werden konnten.

Es wurde N,N,N′-Triphenylchlorformamidin in *n*-Butanol, unter Rückfluß, 5 Stunden lang erwärmt, dann abgekühlt und der N,N,N′-Triphenylharnstoff filtriert (durch Schmelzpunkt und IR-Spektren gleich denen einer authentischen Probe identifiziert), und anschließend die erhaltene Lösung einer gaschromatographischen Analyse unterworfen. Außer dem Maximum des *n*-Butanols, wurden noch 5 Maxima von viel kleinerer Intensität bemerkt. Von diesen konnten die drei wichtigeren Maxima mit Hilfe einiger authentischer Präparate identifiziert werden und zwar mit di-*n*-Butyläther, *n*-Butylchlorid und *sek*-Butylchlorid. Im System konnte kein *n*-Butyl-*sek*-Butyläther entdeckt werden, weil dieser in den benützten chromatographischen Bedingungen dieselbe Retentionszeit hatte wie auch der Butanol als Lösungsmittel. Die Ausbeute an diesen Produkten konnte auf Grund der chromatographischen Analyse als 35 % für Butylchlorid, 6 % für *iso*-Butylchlorid und 6 % für di-*n*-Butyläther bestimmt werden. Die Konversion von 67 % für N,N,N′-Triphenylharnstoff wurde durch Abwägung des Produktes derselben Reaktion berechnet.

Aus den obigen Ergebnissen geht hervor, daß die durch die Reaktion der Chlorformamidine mit Alkoholen gebildeten *iso*-Harnstoffe, eine Zersetzung unter der Wirkung des in der Reaktion gebildeten Chlorwasserstoffs erleiden. Letzterer Prozeß ist höchstwahrscheinlich bimolekular und teilweise auch monomolekular für das *n*-Butylderivat, weil sich neben *n*-Butylchlorid auch *sek*-Butylchlorid bildet :

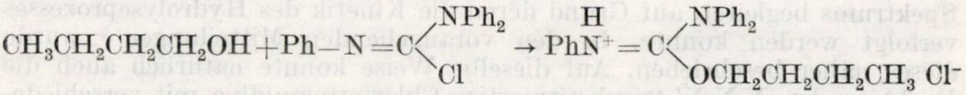

$$CH_3CH_2CH_2CH_2OH + Ph{-}N{=}C\begin{matrix}NPh_2\\ Cl\end{matrix} \rightarrow Ph\overset{H}{N}{}^{+}{=}C\begin{matrix}NPh_2\\ OCH_2CH_2CH_2CH_3\end{matrix}\ Cl^-$$

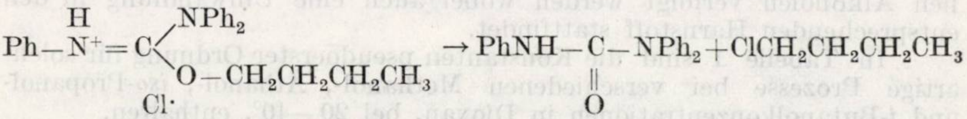

$$Ph{-}\overset{H}{N}{}^{+}{=}C\begin{matrix}NPh_2\\ O{-}CH_2CH_2CH_2CH_3\end{matrix}\ Cl^{\cdot} \rightarrow PhNH{-}\underset{\overset{\|}{O}}{C}{-}NPh_2 + ClCH_2CH_2CH_2CH_3$$

Im Falle von *iso*-Propylalkohol oder *tert*-Butylalkohol wird wahrscheinlich der monomolekulare Weg bevorzugt. Im Falle von Methylalkohol ist der bimolekulare Prozeß der einzig mögliche.

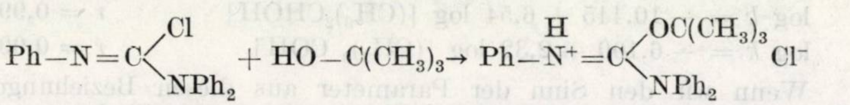

$$Ph{-}N{=}C\begin{matrix}Cl\\ NPh_2\end{matrix} + HO{-}C(CH_3)_3 \rightarrow Ph{-}\overset{H}{N}{}^{+}{=}C\begin{matrix}OC(CH_3)_3\\ NPh_2\end{matrix}\ Cl^-$$

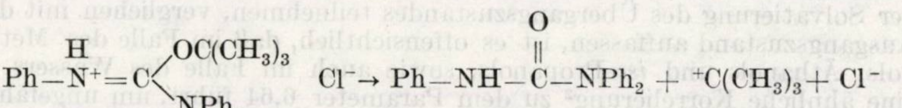

$$Ph{-}\overset{H}{N}{}^{+}{=}C\begin{matrix}OC(CH_3)_3\\ NPh_2\end{matrix}\ Cl^- \rightarrow Ph{-}NH{-}\overset{\overset{O}{\|}}{C}{-}NPh_2 + {}^{+}C(CH_3)_3 + Cl^-$$

$${}^{+}C(CH_3)_3 + Cl^- \rightarrow Cl{-}C(CH_3)_3$$

Da die entsprechenden *iso*-Harnstoffe durch IR-Spektroskopie nicht identifiziert werden konnten, ist es offensichtlich, daß ihre Zersetzung eine rasche Etappe ist. Die langsame Etappe ist die Reaktion des Chlorformamidins mit dem entsprechenden Alkohol.

Obwohl wenig studiert, ist die Alkylierung mit *iso*-Harnstoff durch bi- oder monomolekularen Mechanismus trotzdem bekannt. So hat O-Methylisoharnstoffsulfat eine alkylierende Wirkung auf das Iodidion, bei 50°C, unter Bildung von guten Ausbeuten an Methyliodid.[10] Die Karboxylsäuren können in Ester,[11] Phenole in Arylalkyläther,[12] und die Merkaptane in Alkylsulfide[13] auch in sehr guten Ausbeuten umgewandelt werden. Die Alkohole reagieren viel schwerer in solchen Bedingungen und es bildet sich Äther in kleinen Ausbeuten.[14]

Wenn die Carboxylsäuren und die Phenole,[12] mit *t*-Butyl O-isoharnstoff alkyliert werden, kann die Bildung des *t*-Butylkations, durch Isolierung von Isobuten und einiger Alkylierungsprodukte am aromatischen Ring der Phenole,[12] beziehungsweise der aromatischen Karboxylsäuren[11] bewiesen werden, wodurch der monomolekulare Mechanismus klar zum Vorschein kommt. Im Falle von mit primärem und sekundärem Alkyl am Sauerstoffatom ersetzten *iso*-Harnstoffen, wird ein bimolekularer Mechanismus vorausgesetzt.

REAKTIONSKINETIK

Die Umwandlung des N,N,N'-Triphenylchlorformamidins in N,N,N'-Triphenylharnstoff ist von einer bedeutenden Veränderung des UV-Spektrums begleitet, auf Grund deren die Kinetik des Hydrolyseprozesses verfolgt werden konnte. In den vorangehenden Mitteilungen[1,2], wurde dieses näher beschrieben. Auf dieselbe Weise konnte natürlich auch die Reaktion der N,N,N'-trisubstituierten Chlorformamidine mit verschiedenen Alkoholen verfolgt werden wobei auch eine Umwandlung in den entsprechenden Harnstoff stattfindet.

In Tabelle 1 sind die Konstanten pseudoerster Ordnung für solchartige Prozesse bei verschiedenen Methanol-, Äthanol-, *iso*-Propanol- und *t*-Butanolkonzentrationen in Dioxan, bei 20 –40°, enthalten.

Es wurden gute lineare Beziehungen durch folgende Darstellungen erhalten :

$$\log k = -9{,}830 + 7{,}40 \log [\mathrm{CH_3OH}] \qquad r = 0{,}995$$

$$\log k = -10{,}388 + 7{,}54 \log [\mathrm{CH_3CH_2OH}] \qquad r = 0{,}981$$

$$\log k = -10{,}445 + 6{,}54 \log [(\mathrm{CH_3})_2\mathrm{CHOH}] \qquad r = 0{,}999$$

$$\log k = -6{,}100 + 2{,}32 \log [(\mathrm{CH_3})_3\ \mathrm{COH}] \qquad r = 0{,}999$$

Wenn wir den Sinn der Parameter aus diesen Beziehungen als Differenz zwischen der Molekülanzahl der Hydroxylverbindungen die an der Solvatierung des Übergangszustandes teilnehmen, verglichen mit dem Ausgangszustand auffassen, ist es offensichtlich, daß im Falle des Methanols, Äthanols und *iso*-Propanols, sowie auch im Falle des Wassers, wo eine ähnliche Korrelierung[2] zu dem Parameter 6,64 führt, um ungefähr 7 Moleküle mehr am Übergangszustand teilnehmen, als im Ausgangszustand. Von hier folgt die wichtige Rolle der Solvatierung für den ganzen Prozeß. Ein wesentlicher Unterschied ist im Falle des *t*-Butanols zu verzeichnen.

TABELLE 1

Alkoholyse des Kohlensäure N,N,N′-triphenylchlorformamidins (2,0–2,7·$\cdot 10^{-4}$ Mol/kg) in Dioxan, verfolgt anhand der Extinktionsveränderungen zwischen 300–315 nm

Alkohol E_S^{15}, σ^{*15}, E_T^{16}			Konzentration Mol/kg	t °C	$k \cdot 10^3$ s^{-1}
	CH_3OH		9,57	20	2,58
0	0	55,5	10,92		6,85
			11,59		13,23
			12,57		20,33
			13,62		34,29
			14,00*		45,20
	C_2H_5OH		14,00*	20	18,00
−0,07	−0,10	51,9	15,59		43,67
			16,60		56,76
			17,29		88,54
			18,11		132,10
	$(CH_3)_2CHOH$		13,88	20	1,07
−0,47	−0,19	48,6	14,00*		1,14
			14,53		1,50
			15,25		2,01
			15,94		2,67
	$(CH_3)_3COH$		11,73	20	0,244
		43,9	12,34		0,273
			12,91		0,305**
			14,00*		0,370
			12,90	30	0,840**
			12,89	40	1,730**

* Extrapolierte Werte laut der Ghleichungen aus dem Text.

** $\Delta S^{\neq} = -20{,}5$ cal/Mol K
$\Delta H^{\neq} = 15{,}2$ kcal/Mol

Werden die k-Werte für molare Konzentrationen des Alkohols von 14 mol/kg interpoliert und wird eine lineare Beziehung mit diesen Werten und Taft-Parametern der Alkoholradikale versucht, erhält man folgende Beziehungen:

$$\log k = -0{,}057\ E_S + 7{,}77\sigma^* - 1{,}249 \qquad r = 0{,}974$$

oder

$$\log k = 7{,}48\ \sigma^* - 1{,}262 \qquad r = 0{,}974$$

Von hier folgt klar, daß der sterische Effekt des Alkylradikals verhältnismäßig unwichtig ist. Die Reaktivität wächst aber mit dem Abfallen des elektronenstoßenden Effekts dieses Radikals. Der Alkohol kann also in der langsamen Etappe nicht die Rolle des Nucleophils spielen, sondern er dient nur zur Solvatierung, welche natürlich gleichzeitig mit der Polarität des Alkohols ansteigen muß, was auch aus folgender Beziehung hervorgeht:

$$\log k = -12{,}02 + 0{,}193\ E_T \qquad r = 0{,}970$$

Wie bekannt,[16] wiederspiegelt der E_T-Parameter die Solvatierungskapazität der entsprechenden Lösungsmittelmoleküle.

In Tabelle 2 sind die Geschwindigkeitskonstanten pseudoerster Ordnung für die Reaktion der N,N,N'-trisubstituierten Chlorformamidine in Dioxan und *t*-Butanol angegeben.

TABELLE 2

Die Reaktion der N,N,N'-trisubstituierten Chlorformamidinen ($1-6\cdot10^{-4}$ Mol/kg) mit *t*-Butanol in *t*-Butanol/Dioxan (12,9 Mol/t-Butanol/kg) und die Reaktion in Gegenwart von $LiClO_4$ (11,60 Mol *t*-Butanol/kg, $0,78\cdot10^{-2}$ Mol $LiClO_4$/kg), bei 20°

Nr.	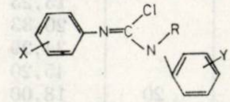 X	R	Y	a) σ	b) Σσ*	b) ΣE_S	c) λ nm	*t*-BuOH $k\cdot10^3$ s^{-1}	$LiClO_4$ $k\cdot10^3$ s^{-1}
1	H	CH_3	$4-OCH_3$	−0,27			300	0,85	15,57
2	H	CH_3	$4-CH_3$	−0,17			300	0,65	8,18
3	H	CH_3	H	0,00	0,60	−2,55	300	0,58	—
4	H	CH_3	$4-Cl$	0,23			305	0,42	2,91
5	H	CH_3	$3-Cl$	0,37			305	0,38	1,51
6	H	CH_3	$4-NO_2$	0,78			300	0,28	0,75
7	$4-CH_3$	CH_3	H	−0,17			300	0,83	13,66
8	$3-CH_3$	CH_3	H	−0,07			300	0,55	8,53
9	$4-Cl$	CH_3	H	0,23			305	0,10	0,70
10	$3-Cl$	CH_3	H	0,37			300	0,058	0,25
11	H	C_6H_5	H		1,20	−5,10	315	0,305	1,59
12	H	C_6H_5	H		0,50	−2,48	300	0,84	8,18
13	H	C_2H_5	$C_2H_5^{d)}$		−0,20	−0,14	275	5,88	464,20
14	H	$CH(CH_3)_2$	H		0,41	−2,08	275	4,06	61,42
15	H	CH_3	$2,6(CH_3)_2$				290	0,036	0,20
16	H	CH_3	$2,6(C_2H_5)_2$				285	0,045	0,25
17	$2-CH_3$	CH_3	H				300	0,24	1,08
18	$C_{10}H_7^{e)}$	CH_3	H				325	0,47	3,99

a) Hammett-Parameter
b) Nichtsummierte Taft-Parameter für die Substituenten des Amidstickstoffatoms.
c) Die Wellenlänge bei der die Geschwindigkeitskonstanten bestimmt wurden.
d) $N(C_2H_5)_2$ — Gruppe
e) 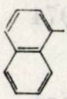 — Gruppe

Die Substituenten am Benzolring des Amidstickstoffs (Verbindungen **1**—**6**) üben einen kleinen Einfluß auf die Reaktionsgeschwindigkeit aus:

$$\log k = -0{,}44\ \sigma - 3{,}237 \qquad r = 0{,}981$$

Einen wesentlich größeren Einfluß üben die Substituenten am Benzolring des Iminstickstoffs aus (Verbindungen **3**, **5**, **7**—**10**), was aus der Hammett-Gleichung hervorgeht:

$$\log k = -2{,}29\ \sigma - 3{,}397 \qquad r = 0{,}982$$

In beiden Fällen erleichtern die elektronenstoßenden Substituenten den Prozeß, was einen klaren kationischen Charakter des zentralen Kohlenstoffatoms im Übergangszustand beweist. Der viel größere Einfluß der Substituenten am aromatischen Ring des Iminstickstoffs, kann leicht erklärt werden, anhand der direkten Konjugierung zwischen dem aromatischen Ring und dem Chlorformamidinkohlenstoff. Für die Substituenten am aromatischen Ring des Amidstickstoffs, wird der mesomere Effekt dieses Rings nur indirekt, durch das Stickstoffatom, übertragen.

Es kann eine zufriedenstellende Taft-Beziehung erhalten werden, wenn beide Substituenten vom Amidstickstoffatom in Betracht gezogen werden (Verbindungen **3**, **11**–**14**):

$$\log k = -0{,}81 \sum \sigma^* + 0{,}087 \sum E_s - 2{,}269 \qquad r = 0{,}913$$

Der elektronenstoßende Effekt begünstigt ebenfalls die Reaktion, wobei der sterische Effekt praktisch unwichtig ist.

In Gegenwart von Piperidin wächst die Reaktionsgeschwindigkeit der *t*-Butanolyse des N,N,N′-Triphenylchlorformamidins zuerst verhältnismäßig wenig an, um dann bis zu ziemlich großen Piperidinkonzentrationen (Tabelle 3) konstant zu bleiben, was die unwesentliche Rolle der Nucleophile in diesem Prozeß bestätigt.

TABELLE 3

t-Butanolyse und Aminolyse des Kohlensäure N,N,N′-triphenylchlorformamidins ($2{,}8 \cdot 10^{-4}$ Mol/kg) in Dioxan-*t*-Butanol (12,9 Mol/kg) in Gegenwart von Piperidin

$C_5H_{11}N$ Mol/kg·10^2	t °C	$k \cdot 10^3$ s^{-1}	$C_5H_{11}N$ Mol/kg·10^2	t °C	$k \cdot 10^3$ s^{-1}
0,00	20	0,305*	6,31	20	0,437***
0,043	20	0,332*	12,64	20	0,446***
0,21	20	0,355*	16,63	20	0,444**
2,13	20	0,429***	16,78	30	0,994**
4,22	20	0,429***	16,88	40	1,870**

* $k = 0{,}021\ [C_5H_{11}N] + 0{,}313 \cdot 10^{-3}$

** $\Delta H^{\neq} = 12{,}5$ kcal/Mol ; $\Delta S^{\neq} = -29{,}2$ cal/MoloK

*** $k_{\text{med}} = (0{,}437 \pm 0{,}008) . 10^{-3}\ s^{-1}$

Die Aktivierungsentropie von -20 E.A. der *t*-Butanolyse und $-29{,}2$ E.E. in Gegenwart von Piperidin spricht für einen monomolekularen Mechanismus, so wie wir auch in den vorangehenden Mitteilungen dieser Reihe[1,2] gezeigt haben, um so mehr, wenn man auch die verhältnismäßig großen Aktivierungsenthalpien (15,2 bzw. 12,5 kcal/Mol) in Betracht zieht. Wird ein besonders wirksames Nucleophil, wie z.B. Piperidin zugesetzt, bleiben die Aktivierungsparameter praktisch unverändert.

Aus allen erhaltenen Befunden kann man auf einen monomolekularen Mechanismus schließen, wobei die langsame Etappe die Ionisierung des Stickstoffs darstellt:

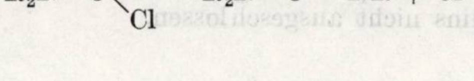

$$R_2N-C\begin{matrix}\nearrow NR\\ \searrow Cl\end{matrix} \rightarrow R_2N-\overset{+}{C}=NR + Cl^-$$

Die zweite Etappe, die Reaktion des Karbokations mit dem Alkohol, hat eine viel bedeutendere Geschwindigkeit, was durch die unwesentliche Veränderung der Globalgeschwindigkeit des Prozesses, durch Zusetzung von kräftigen Nucleophilen bestätigt wird. Laut Erwartung, werden die elektronenspendenden Substituenten diesen monomolekularen Ionisierungsprozeß begünstigen.

Wird Lithiumperchlorat zugesetzt, wächst die Reaktionsgeschwindigkeit in allen Fällen wesentlich an (Tabelle 2), was den katalytischen Effekt des Lithiums auf die Chlorioneneliminierung aus dem Chlorformamidin bestätigt.[1,2]

Interessant hervorzuheben ist die Rolle der elektronischen Effekte auf den Globalprozeß, was auch aus den Hammett- :

$$\log k = -1{,}24\sigma - 2{,}243 \; (\mathrm{N_{Amid}}, \text{ Verbindungen } \mathbf{1}-\mathbf{6}) \qquad r = 0{,}985$$

$$\log k = -3{,}20\sigma - 2{,}455 \; (\mathrm{N_{Imin}}, \text{ Verbindungen } \mathbf{7}-\mathbf{10}) \qquad r = 0{,}974$$

oder Taft-Beziehungen:

$$\log k = 1{,}38 \sum \sigma^* + 0{,}24 \sum E_s - 0{,}512 \; (\text{Verbindungen } \mathbf{11}-\mathbf{14}) \quad r = 0{,}913$$

hervorgeht.

Die größere Bedeutung der elektronischen Effekte entspricht einem Abfall der Elektronendichte am zentralen Kohlenstoffatom im Übergangszustand, der durch die Komplexierung des Chlors durch das Lithiumatom stattfindet:

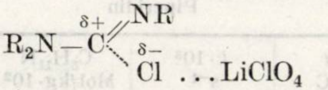

$$R_2N-\overset{\delta+}{C}(=NR)\cdots\overset{\delta-}{Cl}\ldots LiClO_4$$

Wird Lithiumchlorid zugesetzt (Tabelle 4), verändert sich die Reaktionsgeschwindigkeit praktisch nicht. Der katalytische Effekt des Lithiums ist wahrscheinlich durch die Nichtdissoziation des Lithiumchlorids im Reaktionssystem verhindert. Natürlich wird auch ein Masseneffekt der Chloridionen auf die Komplexierung des Lithiums oder die Dissoziation des Chlorformamidins nicht ausgeschlossen.

TABELLE 4

Salzeffekte (LiCl) bei der Solvolyse des N,N,N′-Triphenylchlorformamidins ($2{,}8 \cdot 10^{-4}$ Mol/kg) bei 40° in Dioxan-*n*-Butylalkohol

LiCl Mol/kg·10^2	$k \cdot 10^3$ s^{-1}	LiCl Mol/kg·10^2	$k \cdot 10^3$ s^{-1}
—	1,73*	4,60	1,85*
0,285	1,67*	5,80	1,84*
1,14	1,89*	6,85	1,98*
2,29	1,78*	8,26	1,88*
3,47	2,06*		

* $k_{med} = (1{,}85 \pm 0{,}12) \cdot 10^{-3}\ s^{-1}$

Schließlich muß noch bemerkt werden, daß die sterische Hinderung die durch die Einführung einiger Substituenten an den aromatischen Ringen (Verbindungen **15**—**18**) zustande kommt, nicht den erwarteten beschleunigenden sterischen Effekt für einen monomolekularen Ionisierungsprozeß aufweist. Die Ergebnisse sind nicht zahlreich genug, um diese Tatsache erklären zu können. Es ist möglich, daß die sterische Hinderung einen ungünstigen Einfluß auf die Kationsolvatation haben könnte und auf diese Weise die Ionisierung beungünstigt. Diese Tatsache wäre im Einklang mit den von den Stickstoffsubstituenten ausgeübten sterischen Effekten, die durch die Taft-Beziehung ausgedrückt werden, sowie auch mit dem katalytischen Effekt des Lithiumperchlorats, der auch im Falle sterisch gehinderter Moleküle nichts von seiner Wichtigkeit einbüßt. Es ist aber nicht ausgeschlossen, daß der Bindungsprozeß des Karbokations mit den Alkoholmolekülen in diesem Fall einen größeren Einfluß auf die Geschwindigkeit des Globalprozesses ausüben könnte. Durch eine beträchtliche sterische Hinderung wird der Ionisierungsprozeß langsamer und kann vergleichbare Geschwindigkeiten mit dem Bindungsprozeß aufweisen.

VERSUCHSTEIL

VERWENDETE SUBSTANZEN

Alle Chlorformamidine wurden aus den entsprechenden Harnstoffen durch Chlorierung mit Phosphorpentachlorid hergestellt, nach einem bekannten Verfahren, das zum ersten Mal für die Synthese der N,N,N′-Triphenylchlorformamidine und anderer Derivate [3,17–19] benützt wurde. Die Harnstoffe wurden ihrer seits nach einer allgemeinen Methode nach Appel,[20] durch die Reaktion der Isocyanate mit den entsprechenden Aminen hergestellt.

In der vorangehenden Mitteilung[21] werden die druchgeführten Synthesen, sowie die erhaltenen Verbindungen eingehend beschrieben.

KINETISCHES STUDIUM

Die Kinetik der Alkoholyse der N, N, N′-trisubstituierten Chlorformamidine wurde durch UV-Spektroskopie (Spektrograph UNICAM SP 8000) verfolgt. Die Methodik ist dieselbe wie schon für das kinetische Studium der Hydrolyse des N, N, N′-Triphenylchlorformamidins und der N, N, N′-trisubstituierten Chlorformamidine[1,2] beschrieben wurde. Die Geschwindigkeitskonstanten wurden für eine Kinetik erster Ordnung berechnet.

IDENTIFIZIERUNG DER REAKTIONSPRODUKTE

Zwecks Identifizierung der Reaktionsprodukte die aus der Reaktion zwischen N, N,N′-Triphenylchlorformamidin und Alkoholen hervorgehen, wurde die IR-Spektroskopie und Gaschromatographie verwendet.

A. Das Verfahren durch IR-Spektroskopie wurde in einer vorangehenden Arbeit[2] ausführlich beschrieben. Die Substratkonzentration war 0,06 Mol/kg und die Alkohol-Dioxan-Gemische waren identisch mit denen der beschriebenen Methode (2 V/3V). Um den Einfluß eventuell anwesender Wasserspuren zu vermeiden, wurden die Alkohole durch Rückflußkochen auf Calciumoxyd und Destillation wasserfrei gemacht. Die Reaktion wurde in einer thermostatierten mit Siliziumfenstern versehenen Glasküvette durchgeführt. Von Zeit zu Zeit wurden Spektren auf dem Spektrographen Specord IR 71 registriert. Während der Reaktion konnte das Verschwinden der dem N, N, N′-Triphenylchlorformamidin charakteristischen Banden von 1660 und 1190 cm^{-1}, sowie das Erscheinen der Banden des N,N,N′-Triphenylharnstoffs beobachtet werden. Nach Beendigung der Reaktion wurde das Lösungsmittel verdampft und das erhaltene Reaktionsprodukt durch Schmelzpunkt, Mischschmelzpunkt mit einem authentischen N,N,N′-Triphenylharnstoff und IR-Spektren charakterisiert (Tabelle 5).

TABELLE 5

Alkoholyseprodukte des N, N, N′-Triphenylchlorformamidins in Dioxan-Alkohol (3V/2V) bei 30° C

Alkohol	Retentionszeit Stunden	Rohes Reaktionsprodukt		Triphenylharnstoff Schmelzpunkt °C
		Schmelzpunkt °C	Mischschmelzpunkt mit Triphenylharnstoff °C	
CH_3OH	15	133–136	130–135	136–136,5
$(CH_3)_2CHOH$	24	—	—	—
$(CH_3)_3COH$	72	136–138	129–134	136–136,5

Charakteristische IR-Banden (cm^{-1}) der im Laufe der Reaktion entstandenen Produkte.

Authentischer Triphenylharnstoff (KBr)	N,N,N′-Triphenylchlorformamidin und				
	CH_3OH		$(CH_3)_2OH$	$(CH_3)_3COH$	
	Bestimmt in Dioxan	Isoliertes Produkt (KBr)	Bestimmt in Dioxan	Bestimmt in Dioxan	Isoliertes Produkt (KBr)
1670	1690	1670	1690	1690	1670
1590	1590	1590	1595	1595	1590
1510	1520	1510	1525	1520	1510
1480	1490	1480	1495	1490	1480
1430		1430			1430
1320	1300	1320	1315	1300	1330
1220	1225	1220	1215	1225	1225
1065		1070			
755	750	760	755	755	760
740		745			750
695	690	700	695	695	695
680		685		695	685

B. Zwecks einer genaueren Identifizierung aller Reaktionsprodukte des N,N,N′-Triphenylchlorformamidins mit Alkoholen wurden diese auch gaschromatographisch verfolgt : 2g Triphenylchlorformamidin und 10 ml *n*-Butanol, wurden 6 Stunden lang unter Rückfluß gekocht. Nach dem Abkühlen wurde ein weißes Produkt isoliert (1,15 g, entsprechend einer Umwandlung von 67 %), mit Schmelzpunkt : 135–136°C und mit folgenden charakteristischen IR-Banden (KBr) : 1680,1595,1525,1480, 1440, 1320, 1230, 1070, 750, 685 cm^{-1}. Das Gaschromatogramm der erhaltenen Lösung wurde mit einem Gaschromatographen Chromatron G.H. 18.3 registriert. Es wurde eine mit Karbowax 1500 10 %auf Chromosorb 60–80 mesh gefüllte Säule, im Stickstoffstrom und mit Flammenionisierungsdetektor, bei einer Säulentemperatur von 185° benützt. Weil angenommen wurde, daß sich einige Halogenderivate und Äther bilden könnten, wurden in den Chromatographen unter denselben Bedingungen auch folgende Präparate eingeführt : *n*-Butylchlorid, *sek*-Butylchlorid, di-*n*-Butyläther, *n*-Butyl-*sek*-Butyläther. Die relativen Retentionszeiten der Produkte des analysierten Gemisches, der Eichsubstanzen, sowie die Annäherungsrechnungen der Konversion im Gemisch, sind in Tabelle 6 eingetragen.

TABELLE 6

Relative Retentionen, Konzentrationen und Konversionen der Produkte der n-Butanolyse des N,N,N'-Triphenylchlorformamidins

	Relative Retention n-Butanol	In den Reaktionsprodukten bestimmte Retention	% Molar	Ausbeute (aprox.)
s-BuCl	0,39	0,33	0,40	6%
n-BuCl	0,44	0,43	2,25	35%
n-Bu-O-n-Bu	0,60	0,60	0,40	6%
n-Bu-O-s-Bu	1,00	?	?	?
BuOH	1,00	1,00		
Unbekannt I		0,70*		
Unbekannt II		0,87*		

* Nichtidentifizierte Schultern auf dem Maximum des n-Butanols.

LITERATURHINWEISE

[1] XVII. Mitt., A. Chicu und R. Bacaloglu, Rev. Roum. Chim., unter Druck.
[2] R. Bacaloglu, A. Chicu und I. Bacaloglu, *J. prakt. Chem.*, unter Druck.
[3] A. Steindorff, *Ber. dtsch. chem. Ges.*, **37**, 964 (1904).
[4] S. E. Forman, C. A. Erikson und H. Adelman, *J. Org. Chem.*, **28**, 2653 (1963).
[5] H. G. Viehe und Z. Janousek, *Angew. Chem. Int. Ed.*, **10**, 573 (1971).
[6] G. Bock, *Chem. Ber.*, **100**, 2870 (1967).
[7] T. Korodi, I. Bacaloglu und R. Bacaloglu, *Bul. şt. tehn. I. P. Timişoara*, unter Druck.
[8] G. Ostrogovich, R. Bacaloglu, A. Nemeş, E. Catalina und M. Nuţiu, *Studii şi Cercetări de Chimie, Acad. R.P.R.*, **10**, 71 (1963).
[9] Y. Mido, *Spectrochim. Acta*, **28A**, 1503 (1972).
[10] S. Weiss, *Chem-Ztg.*, *1975*, 244.
[11] E. Vowinkel, *Chem. Ber.*, **100**, 16 (1967).
[12] E. Vowinkel, *Chem. Ber.*, **99**, 1479 (1966).
[13] E. Vowinkel und C. Wolff, *Chem. Ber.*, **107**, 496 (1974).
[14] E. Däbritz, *Angew. Chem.*, **78**, 483 (1966).
[15] J. E. Leffler und E. Grünwald, „Rates and Equilibria of Organic Reactions“, J. Wiley, New York, 1963, p. 222, 228.
[16] Ch. Reichardt und K. Dimroth, *Forsch. Chem. Forsch.*, **11**, 1 (1968).
[17] H. Eilingsfeld, M. Seefelder und H. Weidinger, *Angew. Chem.*, **72**, 84 (1970).
[18] E. I. du Pont de Nemours, *Brit. Pat.* 874928 ; *Chem. Abstr.*, **56**, 9978 (1962).
[19] A. F. Hegarty, J. D. Cronin und L. F. Scott, *J. Chem. Soc. Perkin Trans.* II, *1975*, 429.
[20] R. Appel, K. Warning und K. D. Ziehn, *Chem. Ber.*, **107**, 698 (1974).
[21] A. Chicu, R. Bacaloglu und C. Csunderlik, *Bul. şt. tehn. I. P. Timişoara, Seria Chimie*, unter Druck.

Revue Roumaine de Chimie, **26**, *4*, 623–627 (1981)

IDENTIFICATION OF TWO ORGANIC SULTAM COMPOUNDS

S. H. DOSS[a] and F. A. RASHID[b]
[a]College of Medicine, Sulaimania University, Sulaimania, Iraq
[b]National Research Centre, Dokki, Cairo, Egypt

Received June 23, 1979

During the synthesis of some sultam derivatives, the elemental analysis of two resulted compounds, IV and VI, does not fit for the expected structures. With the aid of MS, N.M.R. and I.R. the exact structures of these two compounds were identified.

It has been shown that several sultam ring compounds have antitumor activity.[1] One of these is a bis-saturated compound[2] (patent applied for) and it has a marked activity against 52% tumor. This is the first report of the bis-saturated sultam ring compounds having antitumor activity; therefore it is worthwhile to extend the studies to synthetization of other such substances from this series. An attempt to synthesize several such compounds conducted to unexpected results.

Thus, when hydrazine hydrate was added to the keto-sultam 4′-(tetrahydro-2H-1,2-thiazin-2-yl) acetophenone S, S-dioxide (I)[3] to produce, 4′-(tetrahydro-2H-1,2-thiazine-2-yl) acetophenone hydrazone, S, S-dioxide (II) and subsequently, tetrahydro-2-[*p*-[N-(tetrahydro-2H-1,2-thiazin-2-yl) acetimidoyl] phenyl]-2 H-1,2-thiazine S, S, 1, 1-tetraoxide (III), compound IV was found to be the end product. Compund IV is a symmetrical azine (scheme 1) and its formation indicates that 2-moles of compound I have reacted with one-mole of hydrazine hydrate.

One possibility is that compound II was an intermediate in the formation of compound IV. However this would appear unlikely because the amount of hydrazine – hydrate used was minimal. Another likely possibility is that the synthesis is due to the delocalizing effect of the sultam ring which activates the carbonyl group (see ref. 4).

Nevertheless, such behavior was reported for the preparation of benzalazine by the condensation of benzaldehyde with hydrazine.[5]

Mass spectra showed $M^+ = 502$ which accomodate with the azine structure IV. The fragmentation pathways are shown in Scheme 2.

The peak at $m/e = 251$ could indicate a symmetrical fission at the azinic bond $= N - N =$, but could be due to the presence of a doubly charged cation i.e. $M^{++}/2$ instead of $M^+/1$. As the intensity of the peak is large we suggest that it is a mixture of both.

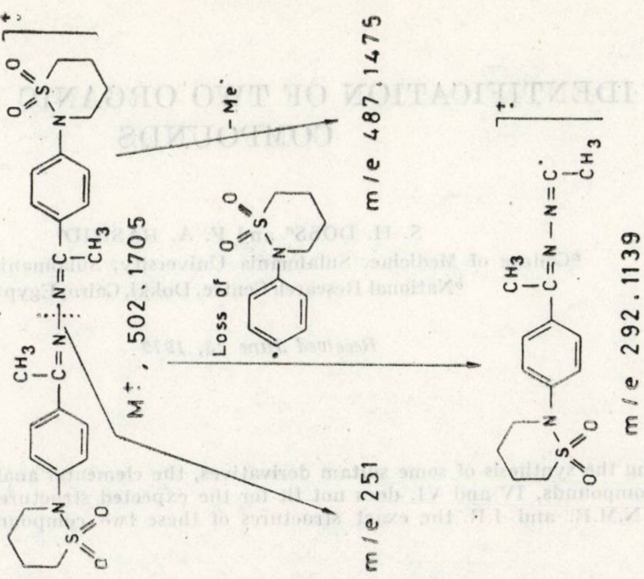
IV.
M+, 502.1705
m/e 251
Loss of
-Me
m/e 487.1475
m/e 292.1139

Scheme 2

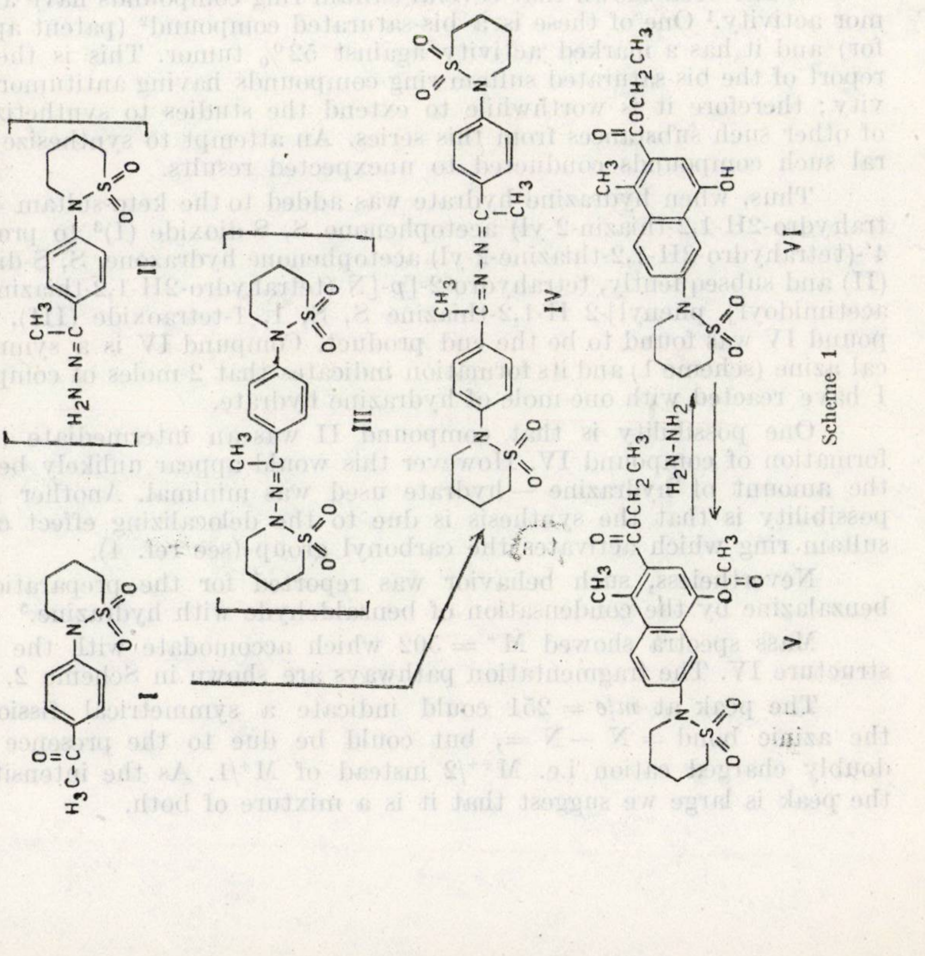
I
II
III
IV
V
VI
H2N-NH2

Scheme 1

N.M.R. spectrum of IV revealed the following bands: an ill-defined multiplet centered at δ 1.95 (4 CH_2), a singlet at δ 2.3 (2 CH_3), a triplet centered at δ 3.32 ($2CH_2-SO_2$)[6], a triplet centered at δ 3.8 (2 CH_2-N) and two doublets centered at δ 7.45 and δ 8 (8 aromatic protons).

IR spectrum of IV exhibited the following bands: at 2940 and 2860 cm^{-1} (ν (C–H) for CH_2 and CH_3) 1660 cm^{-1} (ν(C=N)); 1600 cm^{-1} (N–N), 1360 cm^{-1} (SO_2N); 1330 cm^{-1} (SO_2 asym); 1290 cm^{-1} (sultam ring),[7] 1135 cm^{-1} (SO_2 sym) and 825 cm^{-1} (two adjacent aromatic hydrogen atoms).

A further unexpected chemical reaction was detected. When hyrazine hydrate was added in excess to the naphthosultam V,[8] it was anticipated that the ester carboxylic but not the acetyl carboxyl would be attacked. Such reactions have been observed with naphthoate derivatives.[9] In fact it was shown that the opposite reaction occurred and only the acetyl carboxyl was removed, to give compound VI instead of VII. It is suggested that the presence of sultam ring is due to the behavior of compound V.[10] Also, the monomolecular phenol ester cleavage may be due to SN2 substitution on the ring. Another possible interpretation is: the C–1 carbonyl group is more receptive to nucleophilic attack and the loss of ArO^- in VIII probably represents a better leaving group than ETO^-; the latter would have to be lost in forming VII. ArO^- can be stabilised by resonance delocalisation of the negative charge as shown in scheme 3.

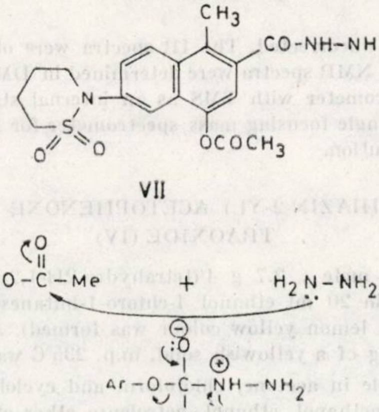

VII

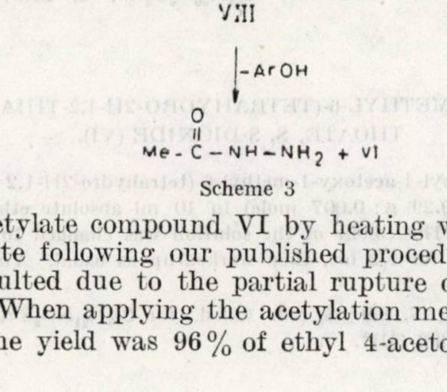

Scheme 3

Trials to acetylate compound VI by heating with acetic anhydride and sodium acetate following our published procedure gave low yield.[11] This behavior resulted due to the partial rupture of the sultam ring to soluble sulphate. When applying the acetylation method of Turner[12] and Huang-Minlon[13] the yield was 96% of ethyl 4-acetoxy-1-methyl-6-(tetrahydro-2H-1,2-thiazine 2-yl)-2-naphthoate, S, S-dioxide. When this compound mixed with V no depression in the melting point occurred also both IR spectra were superimposable. This chemical proof in addition to the physical data emphasizes the structure of product VI. The mass spectrum of compound VI showed $M^+ = 363$ which accomodates with the suggested structure. The N.M.R. spectrum exhibited a triplet centered at δ 1.35 (CH_3 neighbouring CH_2) (J=7H), two ill-defined multiples centered at δ 1.9 and δ 2.2 ($2CH_2$; sultam ring) singlet centered at δ 2.72 (CH_3-naphthaline ring) triplet centered at δ 3.35 (CH_2-SO_2)[6], a triplet centered at δ 3.8 (CH_2-N), a quartet centered at δ 4.36 (CH_2 neighbouring CH_3) and the four aromatic protons centered at δ 7.4 and δ 8.1.

The IR spectrum of VI showed the following bands which emphasize the suggested structures : 3400 cm^{-1} (OH), 2870 cm^{-1} ($\nu(CH_3)$) ; 1720 cm^{-1} (aromatic ester) ; 1460 cm^{-1} (δ CH for CH_2 and CH_3) ; 1380 cm^{-1} (δ CH for CH_3), 1310 cm^{-1} (SO_2 asym.), 1290 cm^{-1} (sultam band)[7], 1200 cm^{-1} ($COO-C_2H_5$) : 1115 cm^{-1} (SO_2 sym.) ; 880 cm^{-1} (1 aromatic hydrogen), 830 cm^{-1} (two adjacent aromatic hydrogen atoms). The stretching frequencies of $\nu(C=O)$ are interfered with SO_2 (sym and asym) bands.

EXPERIMENTAL

All melting points are uncorrected. The IR spectra were obtained on a Perkin Elmer 297 grating spectrometer ; the NMR spectra were determined in DMSO and $CDCl_3$ on a Perkin Elmer R 32 (90 MHz) spectrometer with TMS as an internal standard. Mass spectra were determined by AEI MS 12 single focusing mass spectrometer for low resolution and MS 902 double focusing for high resolution.

4′-(TETRAHYDRO-2H-1,2-THIAZIN-2-YL) ACETOPHENONE AZINE, S, S, S′, S′-TETRAOXIDE (IV)

To a solution of 0.01 mole , 2.7 g 4′(tetrahydro-2H-1,2-thiazin-2-yl) acetophenone hydrazone S,S-dioxide (II) in 20 ml ethanol 4-chloro-1-butanesulfonyl chloride (3 g) were added dropwise over 2 hrs a lemon yellow colour was formed). After filtration and crystallization from allyl alcohol 2.5 g cf a yellowish solid, m.p. 235°C was formed.

Compound IV is soluble in acetone, chloroform and cyclohexanone, sparingly soluble in benzene and insoluble in methanol, ethanol, petroleum ether, ether and water. Found : C, 57.3 ; H, 6.0 ; N, 11.1 ; S, 12.9. Calcd. for $C_{24}H_{30}N_4O_4S_2$: C, 57.37 ; H, 5.97 ; N, 11.15 ; S, 12.75%.
MS : m/E 502 $(M)^+$.

ETHYL 4-HYDROXY-1-METHYL-6-(TETRAHYDRO-2H-1,2-THIAZIN-2-YL-2-NAPHTHOATE, S, S-DIOXIDE (VI).

To a suspension of ethyl-4-acetoxy-1-methyl-6-(tetrahydro-2H-1,2 thiazin -2-yl)-2-naphthoate, S, S-dioxide (V), (0.29 g ; 0.007 mole) in 10 ml absolute ethanol, 6 ml hydrazine hydrate 80 % were added. The colour of the solution was changed to yellowish green. The whole mixture was refluxed for 1/2 hr., then worked-up as usual.[6] Yield 0.2 g of colourless crystals of VI, m.p. 170°C.

Found : 59.3 ; H, 5.7 ; N, 3.9 ; S, 8.3. Calcd. for $C_{18}H_{21}NO_5S$:C, 59.50 ; H, 5.78 ; N, 3.85 ; S, 8.81 % MS : m/e 363 $(M)^+$.

ETHYL 4-ACETOXY-1-METHYL-6-(TETRAHYDRO-2H-1,2-THIAZIN-2-YL)-2-NAPHTHOATE, S,S-DIOXIDE (V).

To a suspension of ethyl 4-hydroxy-1-methyl-6-(tetrahydro-2H-1,2-thiazin-2-yl-2-naphthoate, S,S-dioxide (VI), (0.4 g, 0.011 mole) in 8 ml acetic anhydride, 0.3 g *p*-toluenesulfonic acid monohydrate, was added. The whole mixture was stirred at room temp. for 22 hrs, then chilled in an ice bath for one hour and treated slowly with water; stirring was cotinued for 3 hours at room temp. Filtration of the acetylated product gave 0.379 g, which was crystallized from benzene, pet. ether (40—60°) into nearly colourless crystals of m.p. 135°C.

Its IR and NMR are superimposable with the authentic sample spectra.

ACKNOWLEDGEMENT. The author thanks Prof. Dr. H. Locksly, Chemistry Department, University of Salford, England, for his interest and the facilities provided.

REFERENCES

[1] S. Hayshi, H. Ueki, Y. Sako, T. Ashimura, K. Hayashi and K. Takase, *Kumamot Pharm. Bull.*, **5**, 51, 327 (1962).

[2] S. H. Doss, Unpublished results.

[3] S. H. Doss, A. B. Sakla and M. Hamed, *Org. Prep. Proced. Inter.*, **10**, 48 (1978).

[4] S. H. Doss and S. S. Dimitry, *Org. Prep. Proced. Inter.*, **9**, 299 (1977). Cf. also, S. H. Doss, *Rev. Roumaine Chim.*, **22**, 425 (1977).

[5] J. Thiele, *Liebigs Ann. Chem.*, **376**, 244 (1910); H. H. Hatt, *Org. Syn. Coll.*, **2**, 395 (1943).

[6] S. H. Doss, *Rev. Roumaine Chim.*, **17**, 905 (1972); K.-H. Albert, H. Dürr, S. H. Doss and J. P. Zahra, *Org. Mag. Res.* in press (1980).

[7] S. H. Doss, *Chem. Industry*, 961. (1971); *Acta Chem. Acad. Sci. Hung.*, **72**, 341 (1973); *Rev. Roumaine Chim.*, **17**, 1611 (1972); *Appl. Spectroscopy* **32**, 110 (1978); *Zanco*, **5**, 203 (1979).

[8] S. H. Doss and (in part) M. Hamed, *ibid.* in press (1980).

[9] A. M. El Abbady, S. H. Doss and M. S. Ahmed, *J. Drug Research Egypt*, **4**, 123 (1972).

[10] S. H. Doss, *Org. Prep. Proced. Inter.*, **9**, 27 (1977).

[11] A. M. El- Abbady, S. H. Doss, H. H. Moussa and M. Nosseir, *J. Org. Chem.*, **26**, 4871 (1961).

[12] R. B. Turner, *J. Amer. Chem. Soc.*, **74**, 4220 (1952).

[13] Huang-Minlon, E. Wilson, N. L. Wendler and M. Tishler, *J. Amer. Chem. Soc.*, **74**, 5394 (1952).

Revue Roumaine de Chimie, **26**, *4*, 629–637 (1981)

RING OPENING IN BENZO[b]BICYCLO[3.1.0]HEXYL CATIONS

F. BADEA, ALICE MARIE GLATZ and A. C. RĂZUŞ
Centre of Organic Chemistry, Spl. Independenţei 202 B, R–78100, Bucharest 12, România

Received August 20, 1980

The rearrangement of the unsubstituted and methyl substituted benzo[b]bicyclo[3.1.0] hexyl cations into the corresponding naphthalenium ions is treated considering the symmetry of the relevant MO's involved in the transformation. Contrary to the similar ring opening of bicyclo[3.1.0]hexyl cations, which is a smooth thermally process, the ring opening discussed herein proceeds photochemically or thermally, depending upon the substituents in the bicyclic system. An MO interpretation of the behaviour of these cations is given.

In the preceding communications[1,2] as well as in the following paper[3] we report that benzo [b]bicyclo[3.1.0]hex-2-en-4-yl cations **1**, generated from the corresponding alcohols **2** in acid media, rearrange into the primary alcohols **3**.

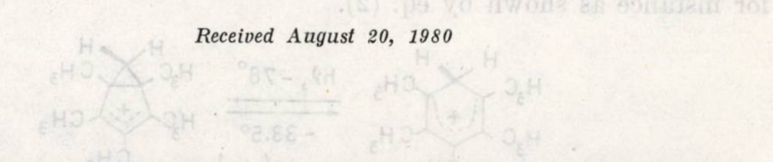

(1)

a. $R^1 = R^2 = R^3 = H$; **b.** $R^1 = R^2 = H$; $R^3 = CH_3$

c. $R^1 = CH_3$; $R^2 = R^3 = H$; $R^1 = R^3 = H$; $R^2 = CH_3$

Variable amounts of naphthalene **4** usually accompany the formation of the rearranged alcohol. However, for the parent compound **2a**, naphthalene does not exceed a few per cent of the overall reaction product, even at 300°. We have concluded from the behaviour of the parent compound[1] that the ring opening to naphthalenium ion must be symmetry-controlled and Woodward-Hoffman's rules[4] are governing the process. Indeed, when the same reaction was performed under photochemical conditions,[1] the ring opening of the unsubstituted cation **1a** afforded mainly naphthalene (about 70 %). It should be mentioned that the simple bicyclo[3.1.0]hexenyl cations, studied by Childs and Winstein,[5–7] rearrange into benzenium ions in a thermal process, although the cyclisation of the benzenium ions, in agreement with Woodwart-Hoffmann's rules, occurs photochemically. Later we have found[2,3] that methyl group substituted cations **1** rearrange to naphthalene either photochemically or thermally. The different behaviour of the substituted bicyclo[3.1.0]hexenyl cations is the subject of this paper.

1. THE REVERSIBLE CYCLISATION OF BENZENIUM IONS

Childs and Winstein[5] reported that methyl-substituted benzenium ions **5**, at —78° and UV-irradiated, generate bicyclo[3.1.0]hexyl cations, for instance as shown by eq. (2).

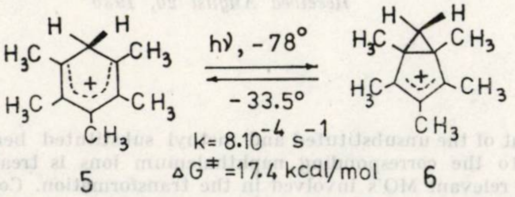

(2)

The isomerisation of **5** is a four-electron electrocyclic process and should proceed from the ground state as a conrotatory process, whereas from the excited state as a disrotatory symmetry-allowed cyclisation. As the cyclic system of the benzenium ion allows only a disrotatory movement, the process may be observed only if performed photochemically. The same theory would suggest a photochemical ring opening of the bicyclic ion **6**. However, methyl substituted ions **6** rearrange into the benzenium ions in a smooth thermal process,[6] which can be followed by the NMR technique. A barrier of about 17 kcal/mol was calculated from the determined rate constant. This barrier was considered[5] high enough for the occurrence of the symmetry-forbidden process. Nevertheless, it does not explain why the benzenium ion suffers the electrocyclic process from the excited state, while with bicyclo[3.1.0]hexenyl cation the ground state is involved. It seemed to us instructive to set up a correlation diagram (Fig. 1).

The five molecular orbitals relevant for the reversible process (2) are: in the monocyclic cation — four π orbitals (π_1, π_2, π_1^* and π_2^*) and a non-bonding orbital *n*; in the bicyclic cation — two σ-orbitals (σ and σ*), two π orbitals (π and π*) and a non-bonding orbital, *n'*. The disrotatory movement of the marginal atoms implies a common symmetry plane in order to relate the levels of similar symmetry (Fig. 1).

A level crossing results between the HOMO's and the LUMO's of the two ions, which forbids the process in the ground state. However, in order to occur in the ground state, the process would need an activation energy high enough to avoid crossing, as electron repulsion prevents the crossing of states of similar symmetry. Fig. 1 predicts an activation energy of about 0.41 β for the cyclisation and about 0.82 β for the ring opening, respectively. On the other hand, cyclisation also implies loss of conjugation energy and gain in strain energy. Therefore, the energy barrier in passing from benzenium ion to the bicyclic ion must be higher than the value predicted by the diagram. For the same reason, the energy of 0.82 β could be a better approximation for the reverse process. Indeed, from the observed activation energy[5,6] a value of about 20 kcal/mol for the parameter β can be calculated, in very good agreement with the value obtained from the resonance energies.[8] Thus, even if the cyclisation of the benzenium ion were to occur by heating above —33.5°C, the reverse process of ring opening would be more rapid and, thus, would prevent observation.

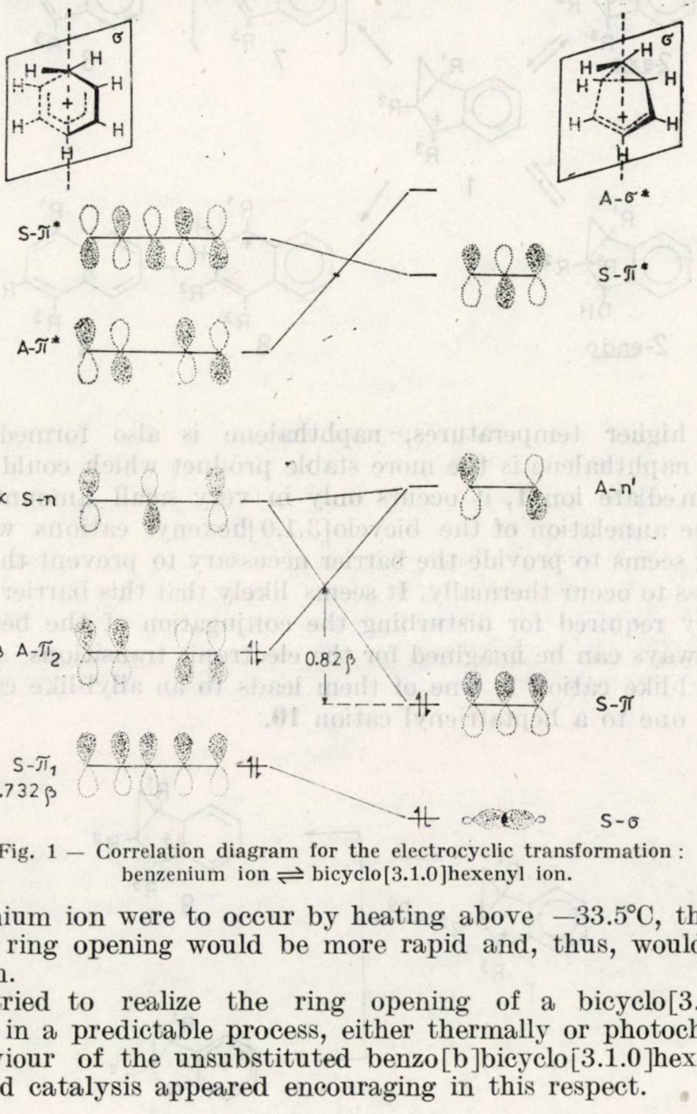

Fig. 1 — Correlation diagram for the electrocyclic transformation : benzenium ion ⇌ bicyclo[3.1.0]hexenyl ion.

We tried to realize the ring opening of a bicyclo[3.1.0]hexenyl cation in a predictable process, either thermally or photochemically. The behaviour of the unsubstituted benzo[b]bicyclo[3.1.0]hex-2-en-4-ol (**2a**) in acid catalysis appeared encouraging in this respect.

2. THE ELECTROCYCLIC TRANSFORMATION OF BENZO[b]BICYCLO[3.10.] HEXENYL CATION 1a.

Benzo[b]bicyclo[3.1.0]hex-2-en-4-ols in the presence either of Lewis acids or Brönsted acids at moderate temperatures (50 —60°C) undergo an *exo*⇌*endo* epimerisation. Above 60°C, the primary alcohol **3** is also formed.

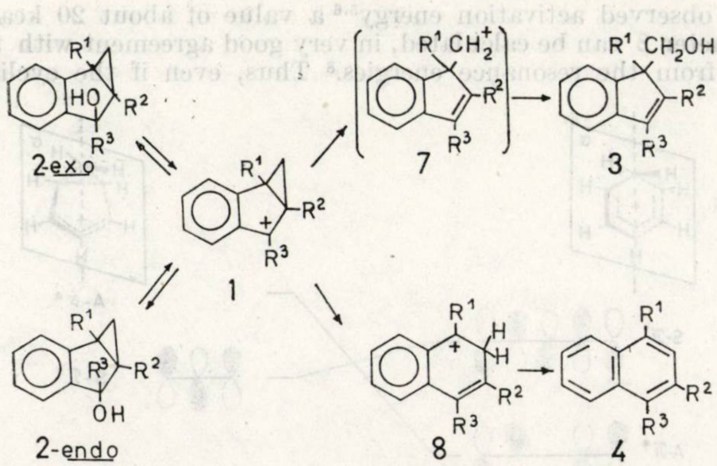
R¹
HO
R²
R³
2-exo
R¹CH₂⁺
R²
R³
7
R¹ CH₂OH
R²
R³
3
R¹
R²
+
R³
1
R¹
R³
R²
OH
2-endo
R¹
H
+
H
R²
R³
8
R¹
R²
R³
4

At higher temperatures, naphthalene is also formed. However, although naphthalene is the more stable product which could arise from the intermediate ion **1**, it occurs only in very small amounts, even at 300°C. The annelation of the bicyclo[3.1.0]hexenyl cations with a benzene ring seems to provide the barrier necessary to prevent the electrocyclic process to occur thermally. It seems likely that this barrier represents the energy required for disturbing the conjugation of the benzene ring. Two pathways can be imagined for the electronic transitions suffered by the benzyl-like cation **1**. One of them leads to an allyl-like cation **9** and the other one to a heptatrienyl cation **10**.

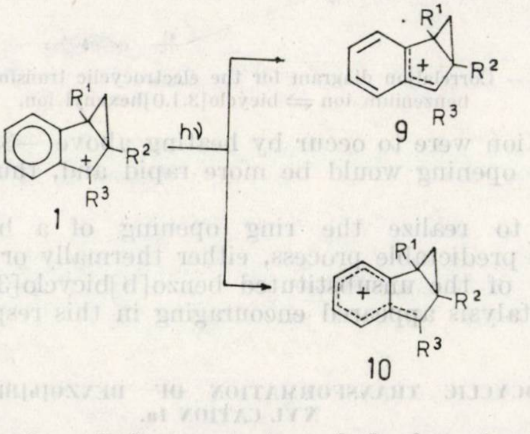
R¹
+
R²
R³
1
hν
R¹
+
R²
R³
9
R¹
+
R²
R³
10

(4

The examination of the symmetry of the lowest unoccupied orbital (LUMO) of the benzyl cation[9a] (Fig. 2) shows no analogy with a system from butadiene and an allyl cation. However, the symmetry of the non-bonding orbital of the benzyl cation is similar to the symmetry of the non-bonding orbital of the acyclic heptatrienyl cation.[9b] Moreover, the symmetry of the LUMO of the napthalenium ion **8** is the same as the symmetry of the non-bonding orbital of the nonatetraenyl cation.[9c,d] The

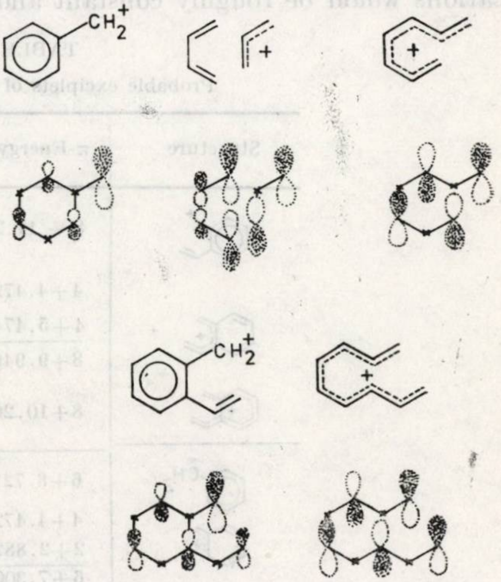

Fig. 2. — Lowest unoccupied molecular orbitals (LUMO) of : A. Benzyl cation B. Naphthalenium ion.

reversible electrocyclic transformation of naphthalenium ion **8** is thus a 1,9-cyclisation quite different the cyclisation 1,5 described by Childs and Winstein.[5-7] However, the Woodward-Hoffmann rules predict the same stereochemical progress of the reaction (5).

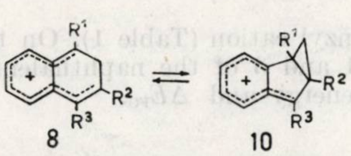

(5)

The same conclusion is borne out by the examination of table 1. The heptatrienyl cation is more stable than a butadiene molecule plus an allyl cation by 0.634β, whereas naphthalenium cation[9c] is more stable by 1.268β units than a nonatetraenyl cation.

The correlation diagram set up for the reversible transformation nonatetraenyl cation ⇌ cyclononatrienyl cation shows that the formation of the latter species needs a lower activation energy than bicyclo[3.1.0] hexenyl cation in order to undergo ring opening. However, the actual energy barrier for the electrocyclic process of the benzo[b]bicyclo[3.1.0] hexenyl cations **1** should depend upon the conjugation energy ΔE of the two ions (**1** and **8**) which is lost in the process, and upon the difference between the frontier orbitals, ΔE_{FO} of the cations, respectively. In studying substituent effects on the rate of ring opening of **1**, it is convenient to keep unchanged ΔE and ΔE_{FO} of the bicyclic ion **1a** and to vary these values for the naphthalenium ion. That can be easily brought about by substituting the hydrogen atoms of the cyclopropane ring and leaving unsubtituted all other positions. The conjugation energy resulting cations would be roughly constant and approximately equal to the conjugation energy of the benzyl cation (Table 1). On the other hand, substituents in the position 1 and 3 of the naphthalenium ion must strongly affect the conjugation energy and ΔE_{FO}.

TABLE 1

Probable exciplets of cations **1** and **8**

Structure	π-Energy[a]	ΔE[b] β-units	$\Delta\Delta E$[c] β-units
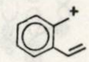	$8 + 11.204$	3.204	—
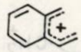	$4+4.472$ $4+5.474$ $8+9.946$	1.946	1.946
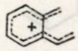	$8+10.268$	2.628	0.576
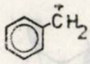	$6+8.721$	2.721	—
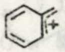	$4+4.472$ $2+2.882$ $6+7.300$	1.300	1.300
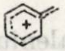	$6+8.055$	2.055	0.666

[a] Values given in reference 9. [b] Calculated from π-energy and the appropiate number of ethylene units. [c] Calculated from values of ΔE cited in this table.

3. METHYL-SUBSTITUTED BENZO[b]BICYCLO[3.1.0]HEXYL CATIONS

In comparing conjugation energies of different π-systems having different number of carbon atoms in the π-lattice we usually recur to the *resonance energy per π-electron*[10] (REPE). Table 2 gives REPE values and ΔE_{FO} for some different classes of polyenes and some polyenyl systems (cations, free radicals, anions). It can easily be seen that except for the cations, for all other systems an increase in REPE corresponds to a decrease in ΔE_{FO}. For the cation series the decrease of REPE is accompanied by the decrease of ΔE_{FO}.

Experimentally, a π system can easily be expanded by methyl substitution. However, calculation of methyl-substituted polyenes is not straightforward. Approximate methods are known[11] and we have chosen

TABLE 2

REPE values for some polyenyl systems

Number of electrons	Structure	REPE[a,b] β units	ΔE_{FO}[a] β units
2	Ethene	—	2
2	Allyl — cation	0.414	1.414
3	— free radical	0.276	1.414
4	— anion	0.207	1.414
4	Butadiene	0.118	1.236
4	Pentadienyl — cation	0.366	1.000
5	— free radical	0.293	1.000
6	— anion	0.244	1.000
6	Hexatriene	0.1647	0.890
6	Heptatrienyl — cation	0.342	0.765
7	— free radical	0.293	0.765
8	— anion	0.256	0.765
8	Octatetraene	0.190	0.694
8	Nonatetraenyl — cation	0.328	0.618
9	— free radical	0.292	0.618
10	— anion	0.263	0.618
8	Cyclooctatetraene	0.207	1.414
10	Cyclodecapentaene	0.294	1.236
6	Benzyl-cation	0.389	1.000
8	Naphthalenium cation **8**	0.356	0.726

[a] Values given in reference 9 have been used. [b] Calculated from ΔE divided by the number of π-electrons.

the heteroatomic model. According to this model a methyl-substituted polyene **11** may be approximated with a heteroatom system **12**, in which the methyl group ($X{=}CH_3$) contributes only with two electrons.

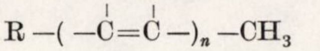

$$R-(-\overset{|}{C}=\overset{|}{C}-)_n-CH_3$$

11

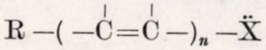

$$R-(-\overset{|}{C}=\overset{|}{C}-)_n-\ddot{X}$$

12

The conjugation energy of **12** is given by equation (6)

$$E = q_r H_X + 1/2\ \pi_{r,r} h_X^2 \tag{6}$$

where : q_r the total electron density of atom r of the carbon lattice substituted by X

h_X the heteroatomic parameter, with a recommended value between 1.4 and 3.3.[11]

$\pi_{r,r}$ the atom polarisability

The total electron density q_r in equation (6) was calculated from equation (7) :

$$q_r = \sum_j n_j c_{jr}^2 \tag{7}$$

where c_{jr} is the coefficient of the atom r in the jth MO which is occupied by n_j electrons.

Ions **1c** and **1d** correspond roughly to the heteroatomic species **13** and **14** respectively:

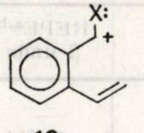

13

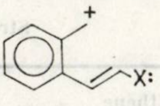

14

Using tabulated values for c_{jr}[9], resonance energies of 1.310β for **13** and 3.073β for **14**, respectively, have been calculated.

The unsubstituted naphthalenium ion as well as the benzyl cation belong to the cationic series of table 2. However, methyl-substituted cations **8** should not belong to the same series as a methyl substituent would contribute two electrons to the π system. Thus, the relationship between ΔE and ΔE_{FO} for even carbon atoms in the π system is also operative both for **13** and **14**. This means that the bicyclic ion **1c**, substituted with a methyl group in position 1 would be more prone to ring opening than is its isomer **1d**. Indeed, experimentally was found[2,3] that **1c** gives high yields of naphthalene under both photochemical and thermal conditions, whereas **1d** yields higher amounts in the irradiated experiment than in the thermal process.

A confirmation of the correctness of the above assumptions was offered by the acid rearrangement of alcohol **2b**.[2]

In that case the delocalisation energy ΔE for the naphthalenium cation should not be drastically modified. On the other hand, the delocalisation energy ΔE of the benzyl cation **1b** should be higher than for **1a**. As figure 3 suggests, a slight increase of the activation energy in ring opening should be observed. Actualy, alcohol **2b** behaves similarly with the parent compound.

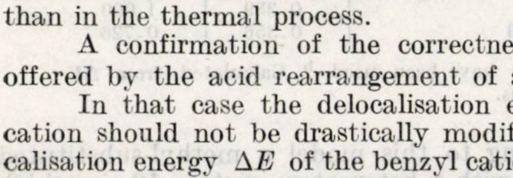

Fig. 3.—A. Interaction between the frontier orbitals in the reversible transformation naphthalenium ion ⇌ benzo[b]bicyclo[3.1.0]hexenyl cation.
B. The same interaction between involving a bicyclic component with the same ΔE_{FO} as above, but a naphthalenium ion with a smaller ΔE_{FO}.
C. The bycyclic component has a larger ΔE_{FO} than in A and B.

The behaviour of benzo[b]bicyclo[3.1.0]hexenyl cation **1a** and its methyl-substituted derivatives **1b** – **1d** supports the conclusion that the rearrangement of cations **1** is an eight-electron electrocyclic process subjected to the same selection rules[4] as a four-electron electrocyclic process. Annelation of bicyclo[3.1.0]hexenyl cations provides an energy barrier in ring opening, surmounted only by irradiation, as actually predicted by Woodward-Hoffmann's rules. However, this energy barrier may be lowered to a value allowing a thermal process by substituting positions 1 and 3 of the 2-protonated naphthalenium ion with electron-donating groups, such as methyl group. Position 1 is the most favourable position in promoting ring opening.

REFERENCES

[1] A. C. Răzuş, V. Wertheimer, F. Badea and A. M. Glatz, *Tetrahedron Letters*, **1975**, 1799.

[2] V. Wertheimer, A. M. Glatz and A. C. Răzuş, *Rev. Roumaine Chim.*, **22**, 1505 (1977).

[3] A. C. Răzuş, F. Badea, Zs. Arvay and A. M. Glatz, *Rev. Roumaine Chim.*, **26**, 000 (1981).

[4] R. B. Woodward and R. Hoffmann, "The Conservation of Orbital Symmetry", Verlag Chemie, Weinheim, 1970.

[5] R. F. Childs, M. Sakai and S. Winstein, *J. Amer. Chem. Soc.*, **90**, 7144 (1968).

[6] R. F. Childs and S. Winstein, *J. Amer. Chem. Soc.*, **90**, 7146 (1968).

[7] R. F. Childs, M. Sakai, B. D. Parrington and S. Winstein, *J. Amer. Chem. Soc.*, **96**, 6403 (1974); R. F. Childs and S. Winstein, *J. Amer. Chem. Soc.*, **96**, 6409 (1974).

[8] A. Streitwieser, Jr., "Molecular Orbital Theory for Organic Chemists", Wiley New York, 1961, chapter 9.

[9] E. Heilbronner and H. Bock, "Das HMO-Modell und seine Anwendung", III, Weinheim, 1970; a. p. 76; b. p. 25; c. p. 169; d. p. 33.

[10] B. A. Hess, Jr. and L. J. Schaad, *J. Amer. Chem. Soc.*, **95**, 3907 (1971).

[11] Reference 8, chapter 4 and 5.

Revue Roumaine de Chimie, 26, 4, 639–645 (1981)

REACTIONS OF SOME 4(3H) QUINAZOLINONES

M. ANWAR

Chemistry Department, Faculty of Science, Tanta University, Tanta, A. R. Egypt

Received March 28, 1979

Halo-compounds and amines react with 4(3H) quinazolinones (I) to give compounds II and III. 3,1(4H) Benzoxazones (V) react with some amino-compounds forming VI–IX. Compounds IIa and IIb react with aromatic aldehydes, ketones, anilides, anhydrides, and imides forming compounds X–XIV. Compound XIV reacts with aromatic amines forming compounds XV.

4(3H) Quinazolinones Ia and Ib were prepared by the recommended methods.[1-3]

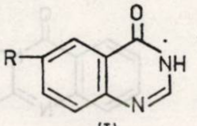

(I)

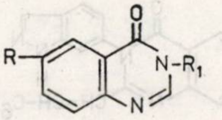

(II)

I a, R = H

b, R = NO_2

II	R	R_1
a,	H	CH_3
b	H	$COCH_3$
c,	NO_2	CH_3
d,	NO_2	C_2H_5
e,	NO_2	$COCH_3$
f,	NO_2	COC_6H_5
g,	NO_2	$SO_2-C_6H_4-CH_3(p)$

Compound I reacts with halo-compounds, namely methyliodide, bromobenzene, acetyl chloride, benzoyl chloride and *p*-toluene-sulphonyl chloride, affording the corresponding derivatives II.[4]

Quinazolinone Ib reacts with aromatic amines and phenyl-hydrazine on heating in benzene affording compounds IIIa-d. The cleavage of the quinazolone ring is similar to that described in the reaction of 2-styryl-4 (3H) quinazolinones with hydroxylamine.[5]

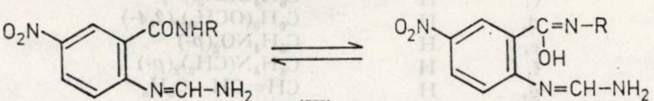

(III)

III a, R = C_6H_5 ; b, R = $C_6H_4CH_3(p)$

c, R = $C_6H_4NO_2(p)$; d, R = $NH-C_6H_5$

Cyclization of IIIa by heating at 5–10°C over its melting point yielded IV.

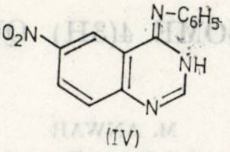

(IV)

3,1 4(H) Benzoxazones (V)[6,7] react with some amino-heterocyclic derivatives, namely 2-amino-pyridine, 2-amino-4-phenyl thiazole, 2-amino-5-methyl-4-phenyl thiazole, 6-aminoindazole and 5-aminoquinoline to form compounds VI–IX.

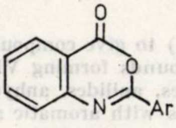

(V)

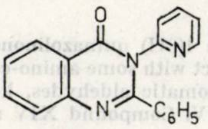

(VI)

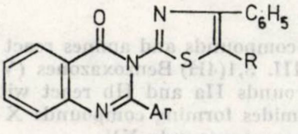

(VII)

V a, Ar = C_6H_5
b, Ar = $CH = CH-C_6H_4-OCH_3(p)$
c, Ar = $CH = CH-C_6H_4-Cl(o)$

	Ar	R
VII a,	C_6H_5	H
b,	$CH{=}CH-C_6H_4OCH_3(p)$	H
c,	$CH{=}CH-C_6H_4Cl(o)$	CH_3

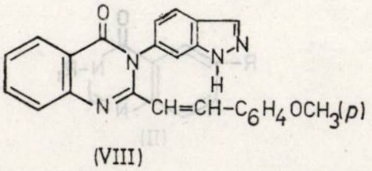

(VIII)

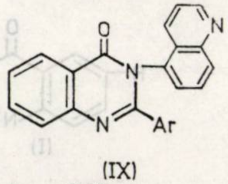

(IX)

IX a, Ar = C_6H_5
b, Ar= $CH{=}CH-C_6H_4OCH_3(p)$

A number of new 3-styryl-4(3H)quinazolinones, X – XII, were prepared by fusion of IIa with aromatic aldehydes, ketones, benzil and anilides. The reaction proceeds similar to the condensation of 2-methyl-3,1 (4H) benzoxazone with aldehydes and ketones.[7]

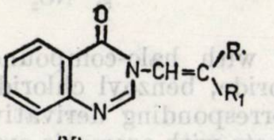

(X)

	R	R_1
X a,	H	C_6H_5
b,	H	$C_6H_4OH(o\text{-})$
c,	H	$C_6H_4OCH_3(p\text{-})$
d,	H	$C_6H_3(OCH_3)_2(2,4\text{-})$
e,	H	$C_6H_4NO_2(p\text{-})$
f,	H	$C_6H_4N(CH_3)_2(p\text{-})$
g,	H	$CH{=}CH-C_6H_5$
h,	CH_3	CH_3
i,	C_6H_5	C_6H_5
j,	C_6H_5	$C_6H_4OH(p\text{-})$
k,	C_6H_5	$C_6H_4OCH_3(p\text{-})$

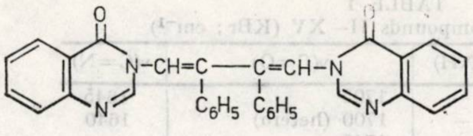

(XI)

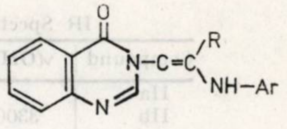

(XII)

	R	Ar
XII a,	CH_3	C_6H_5
b,	C_6H_5	C_6H_5
c,	CH_3	$C_6H_4CH_3(p\text{-})$

Similarly, IIb reacts with aromatic aldehydes forming the compounds XIIIa-d.

2-Ethyl-3,1(4H) benzoxazone was reported to condense with anhydrides and imides giving the corresponding condensation products.[8] In the present investigation the condensation of IIa with maleic, succinic and phthalic anhydrides, as well as with phthalic imides was studied. The reaction proceeds similarly, yielding compounds XIVa-e.

The condensation of XIVa-c with aromatic amines gives compounds XVa-c.

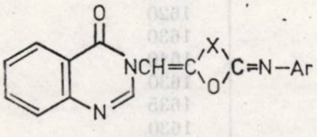

(XIII)

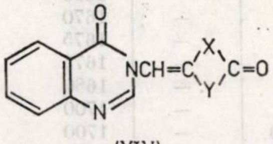

(XIV)

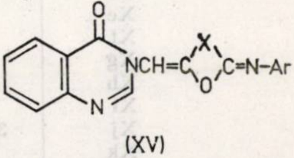

(XV)

XIII a, Ar = $C_6H_4OCH_3(p\text{-})$
b, Ar = $C_6H_4CH_3(p\text{-})$
c, Ar = $C_6H_4OH(p\text{-})$
d, Ar = $C_6H_4NO_2(p\text{-})$

	X	Y
XIV a,	$CH{=}CH$	O
b,	CH_2-CH_2	O
c,	C_6H_4	O
d,	CH_2-CH_2	NH
e,	C_6H_4	NH

	X	Ar
XV a,	$CH = CH$	C_6H_5
b,	$CH{=}CH$	$C_6H_4CH_3(p\text{-})$
c,	CH_2-CH_2	C_6H_5
d,	CH_2-CH_2	$C_6H_4CH_3(p\text{-})$
e,	C_6H_4	C_6H_5
f,	C_6H_4	$C_6H_4CH_3(p\text{-})$

The structure of the compounds newly prepared in this investigation is confirmed by elemental analysis and infrared spectral studies.

The IR spectra of the above compounds are listed in table 1.

All the compounds show the three quinazolone skeletal bands[9] in the regions of 1605 –1590 ; 1580 –1550 ; 1540 –1490 cm^{-1}.

Compounds IIb, IIe XIVb,d and e display keto-enol tautomerism. It is clear from the data obtained that the carbonyl and azo-methine groups are highly affected by the nature and position of the substituent. The presence of the nitro group in compounds IIc-g causes a blue shift in the frequencies of C=O and C=N (1660 and 1610 cm^{-1}) in comparison with that of compounds IIa,b (1705 and 1645 cm^{-1}).

TABLE 1
IR Spectra of compounds II–XV (KBr ; cm^{-1})

Compound	ν(OH)	ν(NH)	ν(C=O)	ν(C=N)
IIa	—	—	1705	1645
IIb	3300	—	1700 (hetero) 1745	1640
IIc	—	—	1660	1610
IId	—	—	1665	1610
IIe	3240	— —	1660 (hetero) 1735	1610
IIf	—	—	1665 (hetero) 1740	1615
IIg	—	—	1660	1610
IIIa	$3300-3280^{br}$		1675	1625
IIIb	$3240-3220^{br}$		1665	1625
IIIc	$3260-3240^{br}$		1660	1620
IIId	3260	3240	1665	1630
IV	—	3320	—	1635
VI	—	—	1685	1640
VIIa	—	—	1690	1645
VIIb	—	—	1690	1640
VIIc	—	—	1695	1645
VIII	—	3280	1690	1635
IXa	—	—	1680	1635
IXb	—	—	1685	1635
Xa	—	—	1680	1630
Xb	3510	—	1680	1630
Xc	—	—	1675	1640
Xd	—	—	1690	1635
Xe	—	—	1670	1620
Xf	—	—	1675	1630
Xg	—	—	1675	1640
Xh	—	—	1680	1630
Xi	—	—	1700	1635
Xj	3510	—	1700	1630
Xk	—	—	1700	1635
XI	—	—	1690	1630
XIIa	—	3300	1700	1630
XIIb	—	3250	1685	1640
XIIc	—	3260	1690	1640
XIIIa	—	—	1700 (hetero) 1750	1640
XIIIb	—	—	1700 (hetero)	1640
XIIIc	3400	—	1695 1745	1640
XIIId	—	—	1675 (hetero)	1625
XIVa	—	—	1690 (hetero) 1740 (anhydr.)	1640
XIVb	3460	—	1695 (hetero) 1735 (anhydr.)	1635
XIVc	—	—	1685 (hetero) 1730 (anhydr.)	1640
XIVd	$3500-3470^{br}$		1680 (hetero) 1740 (imide)	1620
XIVe	$3300-3270^{br}$		1700 (hetero) 1760 (imide)	1615
XVa	—	—	1720	1635
XVb	—	—	1700	1630
XVc	—	—	1660	1625
XVd	—	—	1670	1625
XVe	—	—	1665	1620

br = broad

EXPERIMENTAL

The IR spectra were recorded with a Unicam S.P. 1200 spectrophotometer using the KBr pellet technique.

All melting points are not corrected.

REACTION OF 4(3H) QUINAZOLINONES I WITH HALO-COMPOUNDS

A mixture of 4(3H) quinazolinone I (0.01 mole) and halo-compound, namely methyl iodide acetyl chloride, bromobenzene, benzoyl chloride, and *p*-toluene sulphonyl chloride (0.015 mole) was dissolved in the least amount of pyridine. The reaction mixture was refluxed for 3 hrs. and the product was poured into ice-cold water. The products were crystallized from benzene to give compounds IIb-g (yields about 80 %) (See Table 2).

REACTION OF Ib WITH AROMATIC AMINES AND PHENYLHYDRAZINE

A mixture of Ib (0.01 mole) and aromatic amine, namely aniline, *p*-toluidine, *p*-nitroaniline and/or phenylhydrazine (0.01 mole) in 50 ml benzene was refluxed for 3 hrs. After concentration and cooling, the solids obtained were recrystallized from benzene to form compounds IIIa-d (yields 80—85 %) (See Table 2).

CYCLIZATION OF IIIA

In a dry conical flask, IIIa (1g) was heated in an oil bath for 1 hr at 210°C . The product was left to cool and crystallized from benzene to give IV (yield 85 %) (See Table 2).

REACTION OF SOME HETEROCYCLIC AMINES WITH 3,1 (4H)-BENZOXAZONES

A mixture of 3,1 (4H) benzoxazone (V)[6,7] (0.01 mole), amino compound, namely : 2-amino-pyridine, 2-amino-4-phenyl thiazole, 2-amino-5-methyl-4-phenyl thiazole, 6-aminoindazole and 5-aminoquinoline (0.015 mole) and anhydrous zinc chloride (0.003 mole) was heated in

TABLE 2

Compounds II—IV

Compound	M.P. (°C)	Formula	Analysis (Calcd./Found) %		
			C	H	N
IIb	206	$C_{10}H_8N_2O_2$	63.83 63.49	4.26 4.52	14.89 15.01
IIc	227	$C_9H_7N_3O_3$	52.68 52.64	3.41 3.63	20.49 20.34
IId	213	$C_{14}H_9N_3O_3$	62.92 62.66	3.37 3.70	15.73 15.47
IIe	233	$C_{10}H_7N_3O_3$	55.30 55.01	3.23 3.48	19.35 19.23
IIf	223	$C_{15}H_9N_3O_4$	61.02 60.87	3.05 3.40	14.24 14.42
IIg	225	$C_{15}H_{11}N_3O_5S$	52.17 52.33	3.19 3.51	12.17 12.01
IIIa	202	$C_{14}H_{12}N_4O_3$	59.15 59.02	4.23 4.47	19.72 20.02
IIIb	243	$C_{15}H_{14}N_4O_3$	60.40 60.21	4.70 5.09	18.79 19.03
IIIc	257	$C_{14}H_{11}N_5O_5$	51.06 51.00	3.34 3.68	21.28 21.00
IIId	237	$C_{14}H_{13}N_5O_3$	56.19 56.07	4.34 4.70	23.41 23.23
IV	209	$C_{14}H_{10}N_4O_2$	63.16 63.22	3.76 4.12	21.05 21.00

an oil bath at 160–180°C for 3 hrs. The solid obtained on cooling was washed with dilute hydrochloric acid (5%) then filtered off and crystallized from ethanol to give the corresponding 4-quinazolones (VI–IX) (See Table 3).

TABLE 3

Compounds VI–IX

Compound	M.P. (°C)	Formula	Analysis (Calcd./Found) % C	H	N	S
VI	172	$C_{19}H_{13}N_3O$	72.38	4.13	13.33	—
			72.01	4.51	13.01	—
VIIa	196	$C_{23}H_{15}N_3OS$	72.44	3.94	11.02	8.40
			72.06	4.23	10.73	8.21
VIIb	180	$C_{26}H_{19}N_3O_2S$	71.40	4.34	9.61	7.32
			71.00	4.71	9.82	7.36
VIII	156	$C_{24}H_{18}N_4O$	73.10	4.57	14.21	—
			73.00	4.77	14.03	—
IXa	199	$C_{23}H_{15}N_3O$	79.08	4.30	12.03	—
			79.01	4.68	11.79	—
IXb	150	$C_{26}H_{19}N_3O_2$	77.04	4.69	10.37	—
			76.78	5.01	10.06	—

GENERAL METHOD FOR PREPARATION OF 4-QUINAZOLONES X–XIV

A mixture of IIa (and/or IIb), (0.01 mole), the aromatic aldehyde, ketone, benzil, anilide, anhydride or imide (0.015 mole) was heated in an oil bath at 200–220°C for 5 hrs. After cooling the product was crystallized from ethanol to give compounds X–XIV respectively. The results are given in Table 4.

REACTION OF XIVa-c WITH AROMATIC AMINES

A mixture of XIVa-c (0.01 mole) and aromatic amine, namely aniline or *p*-toluidine (0.01 mole) in 30 ml ethanol was refluxed for 5 hrs. The solid separated on cooling was crystallized from ethanol to give compounds XVa-f respectively (yields 65–75%) (See Table 4).

TABLE 4

Compounds X–XV

Compound	M.P. (°C)	Formula	Analysis (Calcd./found) % C	H	N
Xa	218	$C_{16}H_{12}N_2O$	77.42	4.84	11.29
			76.98	4.49	11.35
Xb	230	$C_{16}H_{12}N_2O_2$	72.73	4.55	10.61
			72.40	4.36	11.00
Xc	201	$C_{17}H_{14}N_2O_2$	73.38	5.04	10.07
			73.12	4.64	10.41
Xd	184	$C_{18}H_{16}N_2O_3$	70.13	5.19	9.09
			69.80	4.89	9.51
Xe	220	$C_{16}H_{11}N_3O_3$	65.53	3.75	14.33
			65.13	3.97	14.02
Xf	169	$C_{18}H_{17}N_3O$	74.23	5.84	14.43
			74.30	5.52	14.00
Xg	253	$C_{18}H_{14}N_2O$	76.80	5.60	11.20
			76.61	5.23	11.61
Xh	245	$C_{12}H_{12}N_2O$	72.00	6.00	14.00
			71.56	5.59	14.46
Xi	243	$C_{22}H_{16}N_2O$	81.48	4.94	8.64
			81.06	4.67	9.01

Table 4 (continued)

Compound	M.P. (°C)	Formula	Analysis (Calcd./Found) % C	H	N
Xj	205	$C_{22}H_{16}N_2O_2$	77.65	4.71	8.24
			77.20	4.46	8.71
Xk	195	$C_{23}H_{18}N_2O_2$	77.97	5.08	7.91
			77.48	4.62	8.36
XI	272	$C_{32}H_{22}N_4O_2$	77.73	4.45	11.34
			77.46	4.41	11.70
XIIa	238	$C_{17}H_{15}N_3O$	73.65	5.42	15.16
			73.24	5.06	14.87
XIIb	269	$C_{22}H_{17}N_3O$	77.88	5.01	12.39
			77.48	5.49	12.00
XIIc	280	$C_{18}H_{17}N_3O$	74.23	5.89	14.43
			73.88	5.52	14.01
XIIIa	205	$C_{18}H_{14}N_2O_3$	70.59	4.58	9.15
			70.36	4.58	9.01
XIIIb	211	$C_{18}H_{14}N_2O_2$	74.48	4.83	9.66
			74.52	5.31	10.05
XIIIc	239	$C_{17}H_{12}N_2O_3$	69.86	4.11	9.59
			69.67	4.50	10.01
XIIId	261	$C_{17}H_{11}N_3O_4$	63.55	3.43	13.08
			63.23	3.72	13.03
XIVa	243	$C_{13}H_8N_2O_3$	65.00	3.33	11.67
			65.03	3.70	11.22
XIVb	178	$C_{13}H_{10}N_2O_3$	64.46	4.13	11.57
			64.23	4.52	11.26
XIVc	201	$C_{17}H_{10}N_2O_3$	70.34	3.45	9.66
			70.01	3.32	10.05
XIVd	184	$C_{13}H_{11}N_3O_2$	64.73	4.56	17.43
			64.34	5.04	17.62
XIVe	210	$C_{17}H_{11}N_3O_2$	70.59	3.81	14.53
			70.64	3.64	14.29
XVa	264	$C_{19}H_{13}N_3O_2$	72.38	4.13	13.33
			72.00	4.52	13.17
XVb	242	$C_{20}H_{15}N_3O_2$	72.95	4.56	12.77
			73.01	5.01	12.29
XVc	255	$C_{19}H_{15}N_3O_2$	71.91	4.73	13.23
			71.66	5.12	13.00
XVd	237	$C_{20}H_{17}N_3O_2$	72.51	5.14	12.69
			72.36	5.18	12.26
XVe	293	$C_{23}H_{15}N_3O_2$	75.62	4.11	11·51
			75.26	4.52	11.09
XVf	281	$C_{24}H_{17}N_3O_2$	75.99	4.49	11.08
			76.21	4.82	10.86

REFERENCES

[1] S. V. Niementowski, *J. prakt. Chem.*, **51**, 564 (1895).

[2] J. F. Meyer and E. C. Wagner, *J. Org. Chem.*, **8**, 239 (1943).

[3] A. Ahmed, K. S. Narang, and J. M. Ray, *J. Indian Chem. Soc.*, **15**, 152 (1938).

[4] M. T. Bogert and G. A. Geiger, *J. Amer. Chem. Soc.*, **43**, 524 (1912).

[5] M. Anwar, M. Omara, F. I. Abdel-Hay and A. A. Saafan, Proceeding of the XIVth **Conference** Pharmaceutical Science, Cairo, Egypt, 1975, 69.

[6] D. T. Bain and R. K. Smally, *J. Chem. Soc. (C)*, **1968**, 1593.

[7] A. Sammour, M. I. Selim, and M. Anwar, *U.A.R., J. Chem.*, **14**, 197 (1971).

[8] A. Sammour, M. I. Selim, M. El-Kasaby, and M. Abdella, *Acta. Chim. Acad. Sci. Hung.*, **78**, 293 (1973).

[9] M. Anwar and S. H. Etaiw, *Rev. Roumaine Chim.*, **22**, 1217 (1977).

Revue Roumaine de Chimie, **26**, *4*, 647–653 (1981)

STUDIES ON PYRIDONES. I

SYNTHESIS AND REACTIONS OF 3-ACETYL-(3,4-DICHLOROPHENYL)-2-(1H)-PYRIDONES

M. EL-DEEK, M.A.I. SALEM, A. A. HAMED and M. SAMAAN
Chemistry Department, Faculty of Science, Ain Shams University, Cairo, Egypt

Received January 14, 1980

3-Acetylpyridones (VII) have been synthesized from the cyanopyridones (II) and methylmagnesium iodide. Compounds II were obtained from the condensation of ethyl cyanoacetate with chalcones I in the presence of ammonium acetate under Michael conditions. The same compounds VII were also obtained from the condensation of chalcones I with acetoacetamides. Condensation of VII with hydroxylamine, hydrazine and phenylhydrazine is described.

In continuation of our work on the chemistry of pyridones,[1] the present paper describes the synthesis and reactions of 3-acetyl-(3,4-dichlorophenyl)-2-(1H) pyridones. Recent work on pyridones has shown that compounds of type II are the only products obtained in the base catalysed condensation of unsaturated ketones with ethyl cyanoacetate.[2–6] However, when ethyl cyanoacetate was fused with chalcone I in the presence of ammonium acetate, it gave a mixture of three products II, III and IV. Compounds II and III were obtained as major products. The reaction is summarized in scheme I.

These products II and III are characterized both by elemental analysis and by IR measurements which showed stretching frequencies around 2220 cm^{-1}; 1660 cm^{-1} and 3350 cm^{-1} characteristic for nitrile group, carbonyl group of pyridine, and NH group respectively. The IR spectra of aminopyridines (IV) showed the stretching frequencies at 1720 cm^{-1}, at 3280 cm^{-1} and at 1610 cm^{-1} which are characteristic for the ester carbonyl group, the N–H group and C=N group respectively.[7]

The NMR spectrum of compound IIb in $CDCl_3$ shows signals (in p.p.m) at $\delta = 3.74$ (s) for (3$\underline{H}$) of $-O-CH_3$ group, $\delta = 6.43$ (s) for (1$\underline{H}$) of $-CH=$ group, $\delta = 6.87$ (s) for (1$\underline{H}$) of the $-NH-$ group and at $\delta = 7.22-7.78$ ($\underline{m}$) for 7 aromatic protons. Compound IVb in $CDCl_3$ shows the following signals (in p.p.m) at $\delta = 1.8-2.1$(t) for (3$\underline{H}$) of the CH_3- of ester group, $\delta = 2.52$ (s) for (3$\underline{H}$) of $O-CH_2$ group, $\delta = 4.8-5.2$ (q) for (2$\underline{H}$) of the $-CO-O-CH_2-$ group, $\delta = 6.38$ (s) for (1$\underline{H}$) of $-CH$ group, $\delta = 7.03$ (two *s*) for (2$\underline{H}$) of two $-NH-$ groups and at $\delta = 7.42-7.45$ (m) for 7 aromatic protons.

Further support for the structure assigned for the cyanopyridones II was brought by hydrolysis which yields the corresponding acids V. Th e hydrazides VI were also prepared from the acid chlorides.

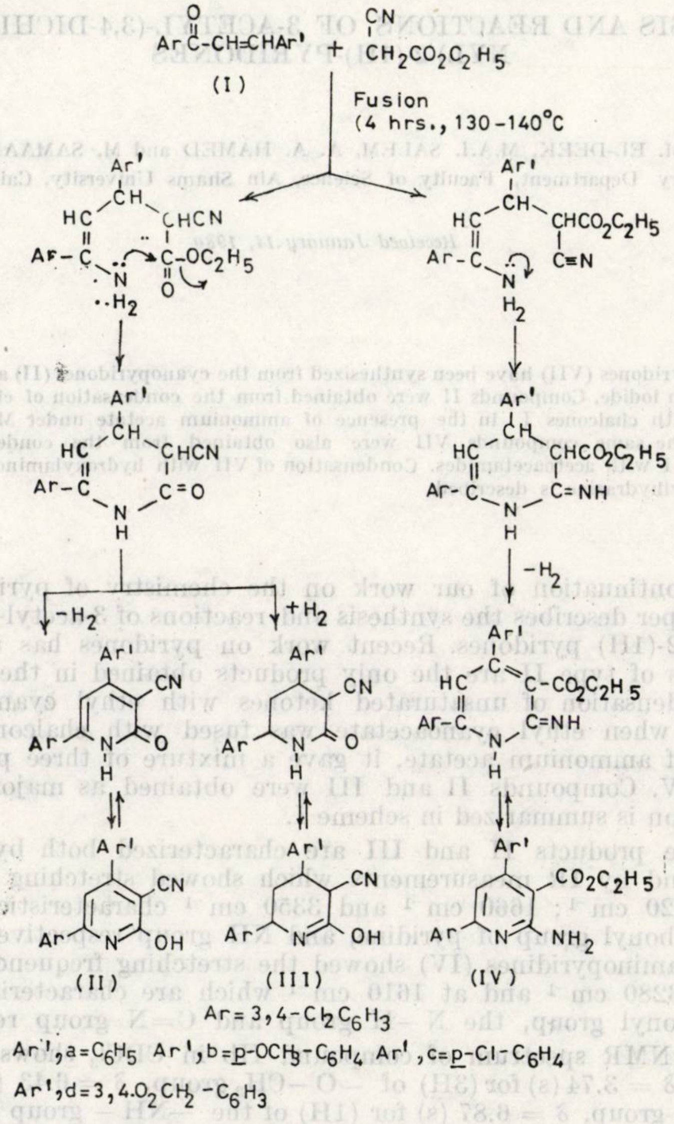
(I)
Fusion
(4 hrs., 130-140°C
-H2
+H2
-H2
(II)
(III)
(IV)
Ar= 3,4-Cl2C6H3
Ar',a=C6H5 Ar',b=p-OCH3-C6H4 Ar',c=p-Cl-C6H4
Ar',d=3,4.O2CH2-C6H3

Scheme I

To prepare the actetylpyridones VII, the key-starting cyanopyridones II were condensed with methyl magnesium iodide. Excess Grignard reagent (5 fold) was found to give the optiumum results. The acetylpyridones VII have been also prepared by condensation of acetoacetamide with chalcones I.

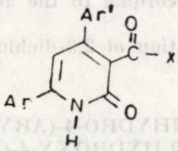

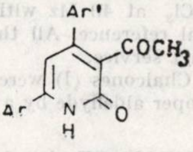

(VII)

$\mathrm{Ar} = 3{,}4-\mathrm{Cl_2}-\mathrm{C_6H_3}$

Va) $\mathrm{Ar'} = \mathrm{C_6H_5}$; $\mathrm{X} = \mathrm{OH}$
Vb) $\mathrm{Ar'} = \mathrm{C_6H_4-OCH_3}$-$p$; $\mathrm{X} = \mathrm{OH}$
Vc) $\mathrm{Ar'} = \mathrm{C_6H_3-O_2CH_2}-3{,}4$; $\mathrm{X} = \mathrm{OH}$
VIa) $\mathrm{Ar'} = \mathrm{C_6H_5}$; $\mathrm{X} = \mathrm{NH-NH_2}$
VIb) $\mathrm{Ar'} = \mathrm{C_6H_4-OCH_3}$-$p$; $\mathrm{X} = \mathrm{NH-NH_2}$
VIc) $\mathrm{Ar'} = \mathrm{C_6H_3-O_2CH_2}-3{,}4$; $\mathrm{X} = \mathrm{NH-NH_2}$

Ar'a $= \mathrm{C_6H_5}$
b $=$ p-$\mathrm{CH_3O-C_6H_4}$
c $=$ p-$\mathrm{Cl-C_6H_4}$
d $= 3{,}4$-$\mathrm{O_2CH_2C_6H_3}$

Correct analytical values support the structure assigned for product VII. The infrared spectra revealed absorption bands at 1700 —1710 and at 1650 $\mathrm{cm^{-1}}$ attributable to the acyl carbonyl group and to the carbonyl group of pyridone respectively; another band at 3040 — 3100 is attributed to the NH group.

The NMR spectrum of the representative compound VIIb in $\mathrm{CDCl_3}$ shows the following signals (in p.p.m at $\delta = 5.24$ (s) for $(3\underline{\mathrm{H}})$ of $-\mathrm{CO}-\mathrm{CH_3}$ group, $\delta = 6.43$(s) for $(1\underline{\mathrm{H}})$ of $-\mathrm{CH}=$ group, $\delta = 6.98$ (s) for $(1\underline{\mathrm{H}})$ of $-\mathrm{NH}-$ group and at $\delta = 7.35 - 7.92$ (m) for 7 aromatic protons).

In order to test whether the carbonyl of the 3-acetyl group or the amido carbonyl of the pyridone from compounds VII is the reactive centre towards carbonyl reagents, compounds II and VI were allowed to react with hydroxylamine, hydrazine, and phenylhydrazine. The fact that only oximes, hydrazones and phenylhydrazones were formed from VII indicated that the reactive carbonyl group of VII is the 3-acyl group. All the compounds VIII showed in the spectrum the following bands: 3450 $\mathrm{cm^{-1}}$, 3120 $\mathrm{cm^{-1}}$, 1660 $\mathrm{cm^{-1}}$, 1620 $\mathrm{cm^{-1}}$, attributable to ν(OH), ν(NH), ν(CO) of pyridone and ν(C=N) respectively.

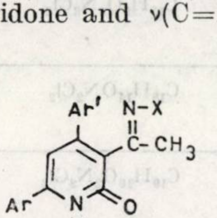

(VIII)

$\mathrm{Ar} = 3{,}4-\mathrm{Cl_2C_6H_3}$

Ar'a $=$ p-$\mathrm{CH_3O-C_6H_4}$; $\mathrm{X} = \mathrm{OH}$ d $=$ p-$\mathrm{Cl-C_6H_4}$; $\mathrm{X} = \mathrm{NH_2}$
b $=$ p-$\mathrm{Cl-C_6H_4}$; $\mathrm{X} = \mathrm{OH}$ e $=$ p-$\mathrm{CH_3O-C_6H_4}$; $\mathrm{X} = \mathrm{NHC_6H_5}$
c $=$ p-$\mathrm{CH_3O-C_6H_4}$; $\mathrm{X} = \mathrm{NH_2}$ f $=$ p-$\mathrm{Cl-C_6H_4}$; $\mathrm{X} = \mathrm{NHC_6H_5}$

EXPERIMENTAL

All the melting points are uncorrected, IR spectra were carried out using KBr pellets on a Pye Unicam SP 1200 spectrometer, and NMR spectra were determined on 5 % solutions in $CDCl_3$ at 40 Mz with a Varian Associates Model V 4300 B spectrometer using TMS as internal reference. All the compounds were named according to the advice of the Chemical Abstract service.

Chalcones (I) were prepared from the condensation of 2,3-dichloroacetophenone[8] with the proper aldehyde by a known procedure.

SYNTHESIS OF 6-(3,4-DICHLOROPHENYL)-1,2-DIHYDRO-4-(ARYL)-2-OXONICOTINO NITRILES (IIa-e), 6-(3,4-DICHLOROPHENYL)-2-HYDROXY-4-(ARYL)-NIPECOTO NITRILES (IIIa-e) AND ETHYL-2-AMINO-6-(3,4-DICHLOROPHENYL)-4-(ARYL)-NICOTINATES (IV a-e)

0.01 mole of the chalcone Ia-e was graded to 0.012 mole of ethyl cyanoacetate in a flask and to them 10 g of ammonium acetate were then added. The mixture was well swirled and then fused for 4 hrs on oil bath at 130—140°C. The mixture cooled down at room temperature and poured on water (400 ml) where an oil separated out after washing with warm water. The oil solidified and by fractional crystallization using light petrol (60—80°), ethanol and acetic acid, compounds IVa-e, IIIa-e and IIa-e were separated as yellow crystals respectively (cf. Table 1).

TABLE 1

Physical characteristics of compounds IIa-e, IIIa-e and IVa-e

Compound	m.p. (°C) yield (%)	Formula	Analysis %		
				Found	Calc.
IIa	280—281	$C_{18}H_{10}ON_2Cl_2$	C	63.82	63.33
	(55)		H	3.05	2.93
			N	7.88	8.21
IIb	274—275	$C_{19}H_{12}O_2N_2Cl_2$	C	61.82	61.45
	(60)		H	3.32	3.23
			N	7.45	7.45
IIc	289—290	$C_{18}H_9ON_2Cl_3$	C	58.05	57.52
	(62)		H	2.42	2.39
			N	7.21	7.45
IId	215—216	$C_{19}H_{10}O_3N_2Cl_2$	C	59.54	59.22
	(58)		H	2.45	2.59
			N	7.40	7.27
IIe	over 300	$C_{18}H_9O_3N_3Cl_2$	C	56.20	55.95
	(48)		H	2.22	2.33
			N	11.05	10.88
IIIa	240—241	$C_{18}H_{14}ON_2Cl_2$	C	62.40	62.60
	(38)		H	4.21	4.05
			N	8.32	8.11
IIIb	265—266	$C_{19}H_{16}O_2N_2Cl_2$	C	60.88	60.80
	(4)		H	4.42	4.26
			N	7.54	7.46
IIIc	283—284	$C_{18}H_{13}ON_2Cl_3$	C	57.22	56.91
	(38)		H	3.33	3.42
			N	7.48	7.37
d	212—213	$C_{19}H_{14}O_3N_2Cl_2$	C	58.92	58.61
	(66)		H	3.45	3.50
			N	7.02	7.19

Table 1 (continued)

Compound	m.p. (°C) yield (%)	Formula	Analysis %	Found	Calc.
IIIe	over 300	$C_{18}H_{13}O_3N_3Cl_2$	C	55.42	55.38
	(52)		H	3.50	3.33
			N	10.68	10.76
IVa	187–188	$C_{20}H_{16}O_2N_2Cl_2$	C	62.50	62.01
	(30)		H	4.05	4.13
			N	7.38	7.23
IVb	135–136	$C_{21}H_{18}O_3N_2Cl_2$	C	60.82	60.43
	(32)		H	4.40	4.31
			N	6.82	6.71
IVc	248–249	$C_{20}H_{15}O_2N_2Cl_3$	C	56.85	56.93
	(30)		H	3.48	3.55
			N	6.82	6.64
IVd	207–208	$C_{21}H_{16}O_4N_2Cl_2$	C	58.32	58.46
	(35)		H	3.82	3.71
			N	6.55	6.49
IVe	169–170	$C_{20}H_{15}O_4N_3Cl_2$	C	55.90	55.55
	(35)		H	3.28	3.47
			N	9.68	9.72

SYNTHESIS OF 6-(3,4-DICHLOROPHENYL)-1,2-DIHYDRO-4-(ARYL)-2-OXONICOTINIC ACIDS (Va-c)

0.01 mole of IIa,b and d was added to 2 g KOH dissolved in 10 ml H_2O, and the mixture was refluxed in ethanol for 4 hrs. Ethanol was then removed and the residue acidified by 1 N hydrochloric acid, then acids Va-c were separated out as colourless solids respectively (cf. Table 2).

TABLE 2

Physical characteristics of 6-(3,4-dichlorophenyl)-1,2-dihydro-4-(aryl)-2-oxonicotinic acid (Va-c) and its hydrazides (VIa-c)

Compound	m.p. (°C) yield (%)	Solvent	Formula	Analysis %	Found	Calc.
Va	261–262	Ethanol +	$C_{18}H_{11}NO_3Cl_2$	C	60.48	60.00
	(48)	benzene		H	3.03	3.05
				N	3.90	3.88
Vb	228–229	Ethanol	$C_{19}H_{11}NO_5Cl_2$	C	58.28	58.46
	(35)			H	3.45	3.33
				N	3.62	3.58
Vc	238–239	Benzene	$C_{19}H_{11}NO_5Cl_2$	C	56.61	56.43
	(48)			H	2.86	2.72
				N	3.28	3.46
VIa	183–184	Methanol	$C_{18}H_{12}N_3O_2Cl_2$	C	58.22	57.90
	(72)			H	3.40	3.21
				N	11.18	11.26
VIb	287–288	light petrol	$C_{19}H_{12}N_3O_4Cl_2$	C	56.80	56.57
	(75)	+ benzene		H	3.22	2.97
				N	10.38	10.42
VIc	266–267	acetic acid	$C_{19}H_{12}O_4N_3Cl_2$	C	54.62	54.67
	(65)			H	2.90	2.87
				N	10.15	10.07

SYNTHESIS OF 6-(3,4-DICHLOROPHENYL)-1,2-DIHYDRO-4-(ARYL)-2-OXONICOTINIC ACID HYDRAZIDES (VIa-c)

To 0.01 mole of the corresponding acid chloride (prepared via the reaction of the acids Va-c with PCl_5) 0.02 mole of hydrazine hydrate in ether was added and the mixture was stirred for 6 hrs on water bath. The precipitated hydrazides were separated out as colourless solids, then washed with warm water, dried and crystallized from the proper solvent to give VIa-c respectively (cf. Table 2).

SYNTHESIS OF 3-ACETYL-6-(3,4-DICHLOROPHENYL)-4-ARYL-2(1H)-PYRIDONES (VIIa-e)

a) To 0.01 mole of methyl Mg iodide in dry ether (60 ml) 0.01 mole of the cyanopyridones IIa-e was added and the mixture was stirred for 12 hrs on water bath. The mixture was then poured on saturated solution of ammonium chloride. A crystalline yellow material was separated which was collected and crystallized from the proper solvent to give VIIa-e respectively (cf. Table 3).

TABLE 3

Physical characteristics of 3-acetyl-6-(3,4-dichlorophenyl)-(4-aryl)-2(1H)pyridones VIIa-e and their oximes and hydrazones VIIIa-f

Compound	m.p. (°C) yield (%)	Solvent	Formula	Analysis %		
					Found	Calc.
VIIa	219–220 (82)	Benzene + light petrol (60–80°C)	$C_{19}H_{13}NO_2Cl_2$	C H N	64.02 3.78 3.80	63.68 3.63 3.91
VIIb	228–229 (76)	Toluene	$C_{20}H_{15}NO_3Cl_2$	C H N	61.26 3.90 3.82	61.85 3.86 3.60
VIIc	225–226 (80)	Ethanol + benzene	$C_{19}H_{12}NO_2Cl_3$	C H N	58.28 3.02 3.68	58.08 3.05 3.56
VIId	188–189 (74)	Benzene	$C_{20}H_{13}NO_4Cl_2$	C H N	59.82 3.34 3.60	59.70 3.23 3.48
VIIe	168–169 (72)	Methanol	$C_{19}H_{12}N_2O_4Cl_2$	C H N	56.92 3.05 6.88	56.57 2.97 6.94
VIIIa	235–236 (62)	Methanol	$C_{20}H_{16}N_2O_3Cl_2$	C H N	59.85 3.82 7.01	59.55 3.97 6.95
VIIIb	113–114 (62)	Light petrol (60–80°C)	$C_{19}H_{13}N_2O_2Cl_3$	C H N	56.20 3.22 6.98	55.95 3.19 6.87
VIIIc	209–210 (58)	Benzene	$C_{20}H_{17}N_3O_2Cl_2$	C H N	60.10 4.18 10.28	59.70 4.23 10.45
VIIId	266–267 (55)	Ethanol	$C_{19}H_{14}N_3OCl_3$	C H N	56.22 3.49 10.52	56.08 3.44 10.33
VIIIe	172–173 (52)	Ethanol + benzene	$C_{26}H_{21}N_3O_2Cl_2$	C H N	65.60 4.23 8.70	65.27 4.39 8.78
VIIIf	284–285 (60)	Methanol	$C_{25}H_{18}N_3OCl_3$	C H N	62.05 3.80 8.92	62.17 3.73 8.70

b) Refluxing chalcone I with the equivalent amount of acetoacetamide in ethanol, in the presence of gaseous hydrogen chloride gave compounds VII as sole products.

CONDENSATION OF 3-ACETYL-6-(3,4-DICHLOROPHENYL)-4-(ARYL)-2(1H)-PYRIDONES (VIIb,c) WITH CARBONYL REAGENTS; SYNTHESIS OF (VIIIa-f)

3-Acetyl-2(1H)pyridones VIIb,c were refluxed in ethanol with an equivalent amount of hydroxylamine hydrochloride in the presence of an equivalent amount of sodium acetate which was dissolved in a few drops of water, hydrazine hydrate or phenylhydrazine, the solvent was removed under vacuum and the solids VIIIa-f were crystallized from the proper solvent (cf. Table 3).

REFERENCES

[1] A. Sammour, Y. Akhnoukh and H. Jahine, *J. Chem. U.A.R.*, **13**, 421 (1970).
[2] A. Sammour, M. T. Zimaity and A. Abd El Maksoud, *J. Chem. U.A.R.*, **12**, 481 (1969).
[3] C. Barat, *J. Indian Chem. Soc.*, **8**, 699 (1931).
[4] U. Basu, *J. Indian Chem. Soc.*, **7**, 481 (1930).
[5] I. I. Abdel-Gawad, A. M. Khalil, T. Zimaity and S. Fouda, *J. Indian Chem. Soc.*, **54**, 626 (1977).
[6] A. Sakurai and H. Midorikawas, *Bull Chem. Soc. Japan*, **40**, 1680 (1967).
[7] L. J. Bellamy, "The Infrared Spectra of Complex Molecules", Second (Methun, London), page 214 (1958).
[8] A. Sammour, A. Fahmy and M. S. Abd El Moez, *J. Chem. U.A.R.*, **14**, 581 (1971).

Revue Roumaine de Chimie, 26, 4, 655–656 (1981)

COMPTES RENDUS

CR. SIMIONESCU and V. GORDUZA, "Polimeri biocompatibili și biologic activi" (Biocompatible and Bioactive Polymers), Editura Academiei, Bucharest, 1980 (480 pages), 36 lei.

The utilization of macromolecular compounds in medicine is in its infancy, but the progress achieved so far during the last decennia justifies the present comprehensive review. The first author is well known, both as director of the Institute for Macromolecular Chemistry "Petru Poni" in Jassy, and as professor, research worker, author and editor of international journals in the field of macromolecular chemistry.

The authors present a critical review of the achievements and perspectives of biocompatible and bioactive polymers. By its nature, the book is interdisciplinary, being addressed both to chemists (who find in the pages of the monograph the possibilities and rationalizations of utilizing in pharmacy and in medicine either modified natural polymers, or synthetic polymers) and to physicians, biochemists or pharmacists (who can gather from the book information on various applications of biocompatible or biologically active polymers).

Till now, the main uses of macromolecular compounds in the human medicine and pharmacy have been on one hand as grafting materials for blood vessels, as suture materials and as dental products, and on the other hand in pharmacy for therapy (either directly, e.g. as blood plasma substitutes, or as auxiliary products along with known drugs, modifying the behaviour of the latter in the living organism). An example for the last type of use is the conditioning effect of polymers on drugs in obtaining forms with a controlled rate of release of the active principles, leading for instance to "retard" drugs. There exist original Romanian contributions based on this line of thought, such as the drug "Covalitin" which uses macromolecular ion exchangers against all kinds of mineral deposits such as gallstones, kidney stones, etc.

The book presents the main categories of biomedical polymers and their applications in surgery, ophthalmology or stomatology, together with the main systems used in blood dialysis and oxygenation. After a brief introduction, the book is divided into several chapters :

- Biologically active polymers
    - Interactions between drugs and biopolymers
    - Correlations between chemical structure and biological activity
    - Types of bioactive macromolecular compounds
    - Interactions between drugs and polymers (100 pages)
    - Biopolymers and their biologically active analogues (100 pages)
    - Blood plasma macromolecular substitutes (expanders)
    - Bioactive modified natural products
    - Physiologically active synthetic polymers
- Biomedical polymers
    - Correlations between biostructures, biocompatibility and biomaterials
    - Types of biomedical polymers
    - Polymeric membranes
    - Surgical applications
    - Ophthalmological applications
    - Stomatological applications
- Perspectives of biocompatible and bioactive polymers

Each of the chapters enumerated above treats exhaustively the topic under discussion. The book is well illustrated by chemical and mathematical formulas, tables, diagrams, physico-chemical relationships. The bibliography is vast, including over 2900 literature quotations.

The book is remarkable through its specialist-level treatment (yet accessible also to those less familiar with certain topics), including problems which are collateral to the main theme, e.g. the chemical structure — biological activity correlations, methods for studying the interactions between drugs and polymers or biopolymers, the Freundlich and Langmuir relations, etc.

An English abstract of one page and the English translation of the headings of all chapters and subchapters are appended.

Two small suggestions for improvement in a future edition or in a translation are the replacement of Roman by boldface Arabic numerals for the 140 odd chemical formulas, and the inclusion of an index (the publishing house should always allocate extra editorial space for indexes in the case of such books, at the proposal of the authors).

The book is useful for a wide range of readers belonging to various professions : chemists, biochemists, biologists, physicians, pharmacists, as well as students of these professions.

A. T. Balaban

NOTE POUR LES AUTEURS

La Revue Roumaine de Chimie publie des articles en anglais, français, russe, allemand ou espagnol. Les auteurs sont priés d'envoyer des articles et des comptes rendus inédits.

Les manuscrits seront dactylographiés à double interligne. La bibliographie, les tableaux et la légende des figures seront placés après le texte.

Si l'article fait partie d'une série numérotée, le titre de la partie précédente sera indiqué dans une note au bas de la première page.

Chaque article sera précédé d'un résumé comprenant quinze lignes au maximum.

Les références bibliographiques dans le texte seront faites par des exposants sans parenthèses et paraîtront à la fin de l'ouvrage.

Les publications périodiques mentionnées dans la bibliographie seront présentées suivant les prescriptions internationales : le nom de l'auteur précédé de l'initiale du prénom, le titre du périodique abrégé conformément à « Chemical Abstracts » et souligné par une ligne, le numéro du tome indiqué par des chiffres arabes et souligné par deux lignes, suivi de la première page de l'article ; à la fin, l'année de la parution sera placée entre parenthèses. Le numéro de la revue ne sera pas indiqué si les pages du volume sont numérotées consécutivement.

Les textes des livres ou traités inclueront : le nom des auteurs, les initiales du prénom, le titre du livre entre guillemets et sans être souligné, le numéro du tome précédé par l'abréviation « vol. » (ou « Bd. »), le numéro de l'édition, les éditions (the publisher), la localité de la parution du livre, l'année de la parution et la page de la référence précédée(s) par l'abréviation « p ». (ou « S. »).

Les brevets seront indiqués comme suit : l'auteur ou la firme, le pays et le numéro du brevet, la date et la revue (Chem. Abstr.). Par ex. : M. Jones (to Union Carbide Co.), *Brit. Pat.* 601 238, (2 sept. 1959); cf. *Chem. Abstr.*, 54, 12808 (1960).

Les diagrammes seront tracés à l'encre de Chine sur papier calque. Les tableaux et les figures (en nombre strictement nécessaire) seront numérotés par des chiffres arabes. Les courbes dans les figures seront numérotées par des chiffres arabes et leur explication sera donnée dans la légende des figures. Prière de ne pas inscrire les mêmes données dans les tableaux et les figures. Chaque tableau aura un titre. On indiquera dans le texte la place approximative des tableaux et des figures. Les formules chimiques seront incluses dans le texte ; en outre, elles seront transcrites sur papier calque, à l'encre de Chine.

Les auteurs sont priés d'indiquer les caractères italiques (en soulignant les lettres au crayon), ainsi que tout autre caractère spécial ; les préfixes *ortho*, *meta*, *para*, *cis*, *trans*, etc. seront soulignés pour indiquer leurs caractères italiques et ne seront jamais écrits avec des majuscules.

Aucune correction à la main ne sera admise sur le manuscrit. Les corrections seront frappées à la machine. Les lettres grecques ou d'autres symboles spéciaux seront insérés à la main à l'encre clairement.

Le manuscrit sera signé par l'auteur.

Le colonne-titre aura 50 lettres au maximum.

L'entière responsabilité du contenu des articles appartient aux auteurs. Pour détails voir le No 1 (1981).

ORSZÁGOS MŰSZAKI KÖNYVTÁR ÉS DOKUMENTÁCIÓS KÖZPONT 1983

PRINTED IN ROMANIA

TRAVAUX PARUS AUX ÉDITIONS DE L'ACADÉMIE DE LA RÉPUBLIQUE SOCIALISTE DE ROUMANIE

ELENA CEAUŞESCU, **Polimerizarea stereospecifică a izoprenului** (La polymérisation stéréospécifique de l'isoprène), 1979, 307 p.

I.G. MURGULESCU, TATIANA ONCESCU, E. SEGAL, **Introducere în chimia fizică. II.2 Cinetică chimică şi cataliză** (Introduction à la chimie physique vol. II. 2. Cynétique chimique et catalyse), 1981, 1024 p.

V. DRĂGUŢAN, A. T. BALABAN, M. DIMONIE, **Metateza olefinelor şi polimerizarea prin deschidere de inel a cicloolefinelor** (La métathèse des oléfines et la polymérisation par ouverture annulaire des cyclooléfines) 1981, 254 p.

O. IORDACHE, **Procese polistocastice aplicate la fenomenele de transfer** (Processus polystochastiques appliqués aux phénomènes de transfert) 1981, 187 p.

CR. SIMIONESCU, VALERIA GORDUZA, **Polimeri biocompatibili şi biologic activi** (Polymères biocompatible et biologiquement actifs), 1980, 479 p.

Ş. MOLDOVEANU, A. SAVIN, **Aplicaţii în chimie ale metodelor semiempirice de orbitali moleculari** (Applications en chimie des méthodes semi-empiriques d'orbitaux moléculaires), 1980, 286 p.

M. FLORESCU, **Metode ştiinţifice în dezvoltarea industriei chimice moderne** (Méthodes scientifiques dans le développement de l'industrie chimique moderne), 1979, 256 p.

CONST. GH. MACAROVICI, **Analiza chimică cantitativă anorganică** (L'Analyse chimique quantitative inorganique), 1979, 457 p.

A. T. BALABAN, I. GĂLĂŢEANU, G. GEORGESCU, LIGIA SIMIONESCU, **Compuşi marcaţi şi radiofarmaceutici cu aplicaţii în medicina nucleară** (Composés marqués et radiopharmaceutiques à application en médecine nucléaire), 1979, 495 p.

I. G. MURGULESCU, E. SEGAL, **Introducere în chimia fizică, Vol. II. 1. Teoria molecular cinetică a materiei** (Introduction à la chimie physique. IIe vol. 1. La théorie moléculaire-cinétique de la matière), 1979, 1036 p.

I. E. TEODORESCU, MARIA FITI, **Iradierea tehnologică** (Irradiation technologique), 1979, 1979, 216 p.

S. STERNBERG, FL. DANEŞ, **Termodinamica chimică aplicată** (La thermodynamique chimique appliquée), 1978, 400 p.

I. G. MURGULESCU, V. EM. SAHINI, **Introducere în chimia fizică. Vol. 1. 2. Structura şi proprietăţile moleculelor** (Introduction à la chimie physique. Vol. I. 2 . La structure et les propriétés des molécules), 1978, 604 p.

C. DRĂGULESCU, E. PETROVICI, **Chimie structurală modernă. Chimia coordinanţei 8** (La chimie structurale moderne. La chimie de la coordinance 8), 1977, 947 p.

D. PURDELA (sous la direction de), **Nomenclatura chimiei anorganice** (La nomenclature de la chimie inorganique), 1977, 153 p.

I. ZUGRAVESCU, MAGDA PETROVANU, **N-ylid chemistry,** coédition avec McGraw-Hill 1977, 396 p.

I. G. MURGULESCU, **Introducere în chimia fizică. Vol. I. Atomi, molecule, legătură chimică** (Introduction à la Chimie Physique, Ier vol. 1. Atomes, molécules, liaison chimique), 1976, 560 p.

E. P. BALTĂ, E. BALTĂ, **Introduction to the physical chemistry of the vitreous state,** coédition avec Abacus Press, 1976, 287 p.

CONST. GH. MACAROVICI, D. MACAROVICI, **Chimia oxizilor dubli şi utilizările lor** (La chimie des oxydes doubles et leur utilisation), 1975, 195 p.

ELENA CEAUŞESCU, **Research work on synthesis and characterization of macromolecular compounds. Contributions.** 1974, 251 p.

CR. SIMIONESCU, VIORICA RUSAN, V. POPA, **Chimia algelor marine** (La chimie des algues marines), 1974, 212 p. 1 pl.

1981 NOV 26

I. P. INFORMAŢIA c. 2841

43 426

Lei 25

$ 55 (pour un abonnement annuel)

F 1103

R

ACADÉMIE DE LA RÉPUBLIQUE SOCIALISTE DE ROUMANIE

REFERÁLVA

REVUE ROUMAINE DE CHIMIE

TOME 26
N° 5
Mai 1981

EDITURA ACADEMIEI REPUBLICII SOCIALISTE ROMÂNIA

Rev. Roumaine Chim.

RRCHAX, **26**, *5*, p. 657–802(1981), Bucarest

ACADÉMIE DE LA RÉPUBLIQUE SOCIALISTE DE ROUMANIE

COMITÉ DE RÉDACTION

Rédacteur en chef:

I. G. MURGULESCU, membre de l'Académie de la République Socialiste de Roumanie

Rédacteurs en chef adjoints :

A. T. BALABAN et V. EM. SAHINI, membres correspondants de l'Académie de la République Socialiste de Roumanie

Collège de rédaction :

EM. BRATU, ELENA CEAUŞESCU, ECATERINA CIORĂNESCU-NENITZESCU, CR. SIMIONESCU, membres de l'Académie de la République Socialiste de Roumanie; P. SPACU, membre correspondant de l'Académie de la République Socialiste de Roumanie ; MARGARETA AVRAM, M. BANCIU, I. HAIDUC, D. I. MARCHIDAN, I. MOLDOVAN, G. NIAC et D. SĂNDULESCU

La Revue Roumaine de Chimie paraît 10 fois par an. Toute commande de l'étranger pour les travaux parus aux Editions de l'Académie de la République Socialiste de Roumanie sera adressée à ILEXIM, Departamentul Export-Import Carte (Livres)/Departamentul Export-Import Presă (Revues), P.O.B. 136—137, télex 11226, 3, str. 13 Decembrie, 79517 Bucarest, Roumanie

Les manuscrits, les livres et les revues proposés en échange, ainsi que toute correspondance seront envoyés à la rédaction :

REVUE ROUMAINE DE CHIMIE

125, Calea Victoriei 79717 Bucarest, Roumanie, téléphone 50 76 80

EDITURA ACADEMIEI REPUBLICII SOCIALISTE ROMÂNIA
125, Calea Victoriei, 79717 Bucarest, Roumanie, téléphone 50 76 80

ORSZÁGOS MŰSZAKI KÖNYVTÁR ÉS DOKUMENTÁCIÓS KÖZPONT 1983

REVUE ROUMAINE DE CHIMIE

Tome 26, N° 5 Mai, 1981

MARIANA CIUREANU, FELICIA CORNEA, CORNELIA CERCASOV and M. CONTINEANU, Internal rotation in charge transfer complexes 659–665

R. M. ISSA, N. T. ABDEL-GHANI, A. L. EL-ANSARY and A. F. SHOUKRY, Charge transfer complexes of some pyridine derivatives with aromatic tri- and di-nitrocompounds 667–674

R. H. SCHUSTER, Influence of medium on the solvolysis of alkyl halides. IX. Temperature dependence of linear salt effects in methanol-water ($X_{H_2O} = 0.359$) (in German) 675–680

N. I. IONESCU, P. BANYAI, MONICA CĂLDĂRARU and M. CHIRCA, The reduction of a complex molybdenum – bismuth oxide catalyst with propylene . 681–685 R

O. S. JOSYULU, J. SOBHANADRI and B. VISWANATHAN, Lattice constant and saturation magnetization of cobalt zinc ferrites and magnesium zinc ferrite 687–692

ANGELA KRIZA and MARTA NASTA, Complex compounds of zirconium (IV) with azomethine 693–698

E. A. SOLIMAN, Some reactions of 2-[3-(3,4-dichlorophenyl)-2-pyrazolin-5-yl]-4*H*-benzoxazin-4-one 699–703

J. SÁNCHEZ BALLESTEROS, F. HERNANDEZ HERNANDEZ and D. J. McPHEE, Study and transformations of the condensation products of isopropylidene-D-glyceraldehyde with active methylenes 705–715

M. A. ELKASABY and M.A.I. SALEM, Synthesis and reactions of 6,7(4′-alkyl-α-pyrano)4-alkyl coumarins 717–723

MIRCEA V. DIUDEA, Phenazathionium cations. III. The selective nucleophilic substitutions on phenazathionium cations 725–732

KONST. KOKKINOS and CHR. MARKOPOULOS, Attempts towards the synthesis of 10-methyl-9-methylene-dihydroacridine-ω-aldehyde (in German) 733–738

ALI ALI KHALAF and AHMED M.A. EL-KHAWAGA, Modern Friedel-Crafts chemistry. IX. On the cycloalkylation of aryl alkenyl ketones and other related systems 739–753

F. URSEANU, D. POPESCU, D. BRĂCĂCESCU, T. OLTEANU, Synthesis of dyes with dibenzo[*f*, *ij*] isoquinoline [2,3-b] quinazoline-5,10-dione structure 755–759

M. BURGUERA and J. L. BURGUERA, and A. TOWNSHEND, Analysis by molecular emission in cavity for the determination of nonmetals using volatilization systems (in Spanish) 761–768

Rev. Roumaine Chim. **26**, *5*, 657–802 (1981) Bucarest

A. M. DEMIAN and W. SCHMIDT, Rapid photometric determination of absorbing substances in mixtures (in German) . . . . 769—774

M. EL-DEEK, M.A.I. SALEM, A. A. HAMED and M. SAMAAN, Studies on pyridones. II. Synthesis and reactions of 6-(3,4-dichlorophenyl)-3-(substitued cinnamoyl)-4-aryl-2(1*H*)-pyridones . . . . 775—781

N. CALU and OLGA VICOL, New aspects in the spectrophotometric analysis. I. Computational equations for the dosage of some dyestuffs in mixtures 783—792

MARGARETA TOMESCU, IOANA DEMETRESCU and E. SEGAL, Study on the thermal degradation of acrylic copolymers . . . . 793—799

BOOK REVIEWS . . . . 801—802

R

BC

Revue Roumaine de Chimie, **26**, *5*, 659–665 (1981)

INTERNAL ROTATION IN CHARGE TRANSFER COMPLEXES

MARIANA CIUREANU, FELICIA CORNEA, CORNELIA CERCASOV and MIHAI CONTINEANU

The Polytechnic Institute of Bucharest, National Institute of Chemistry, Bucharest, Bd. Republicii 13, Romania

Received May 23, 1980

A nuclear magnetic resonance study of molecular complexes formed by iodine with several thiobenzoylpiperidides was carried out. The downfield shift of the signal of the *anti* αNCH_2 protons upon complex formation was explained in terms of the diamagnetic anisotropy of the thioamide group. The barrier to internal rotation around the C—N bond was found to be higher for the iodine complexes than for the corresponding donors. The increase of the barrier upon molecular complexing was shown to be dependent on the electron-withdrawing character of the substituent in the aromatic ring of the donor.

1. INTRODUCTION

Numerous attempts have been made to assess the influence of molecular complexing on the magnetic resonance spectra of various types of molecules. [1,2] Complexes formed by amides with a variety of electron acceptors have been the object of most intensive study, aiming to ascertain the effect of complex formation on the chemical shifts and rotational barriers about the C—N bond, [3–7] or to obtain rate data for the exchange processes between complexed and uncomplexed molecules [8]. Despite of this effort, similar complexes of thioamides have received very little attention up to the present. [7,9] We considered therefore of interest to investigate the effect of molecular complexing on the nuclear magnetic resonance spectra of several tertiary thioamides and to determine the rotational barriers in the complexes as compared with the free molecules.

This paper reports on a study of the effects of molecular complexing on the ^1H—NMR spectra of several thiobenzoylpiperidides, with special attention paid to the influence of the substituents in the aromatic ring of the donor. The following compounds were used as electron donors:

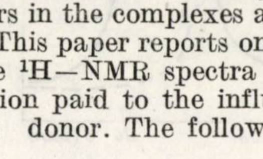

1.

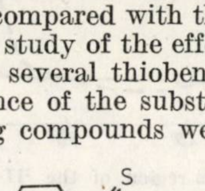

2.

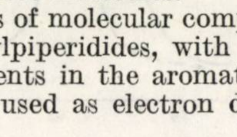

3.

These donors were chosen because of their ability to form strong charge transfer complexes with iodine, as demonstrated by infrared [10] and ultraviolet spectroscopy. [11] The latter results have unambiguously shown that iodine coordinates at the sulphur atom.

The ^1H-NMR spectra and rotational barriers around the C—N bond in the uncomplexed molecules (in *o*-dichlorbenzene as a solvent) were reported by us elsewhere. [12-13]

2. EXPERIMENTAL

The donors were prepared by the Willgerodt-Kindler method, as reported in a previous paper. [10]

Bromophorm, used as a solvent in our experiments, was kept over Na_2CO_3, dried over molecular sieves and freshly distilled before use.

The ^1H-NMR measurements were made with a Tesla BS 487 spectrometer operating at 80 MHz. The chemical shifts were measured against internal HMDSO. The precision of the chemical shifts reported was about ±0.01 p.p.m.. The temperatures of the variable temperature probe were calibrated against a thermocouple. The precision of the temperature measurements was about ± 0.5°.

3. RESULTS AND DISCUSSION

3.1. Chemical shifts

The ^1H-NMR spectra of the compounds under investigation in free and complexed form were recorded in $CHBr_3$ solution at temperatures ranging from 19 to 140°C. The assignments of the piperidide protons were made according to our previous reports. [12-13] The two resonances at about 4.30 and 3.50 p.p.m., assigned to the αNCH_2 protons which are *syn* and respectively *anti* to the C = S group, were found to be particularly sensitive to temperature and complexation effects.

Figure 1 illustrates the ^1H-NMR spectrum in the 3.3—4.4 p.p.m. region, recorded at room temperature for a solution containing thiobenzoylpiperidide and iodine in a 1 : 3 mole ratio, as compared with a solution of the same concentration of the donor. It may be seen that only one set of resonance signals is observed for the first solution, since rapid exchange averages the signals arising from the complex and of the remaining uncomplexed donor molecules.

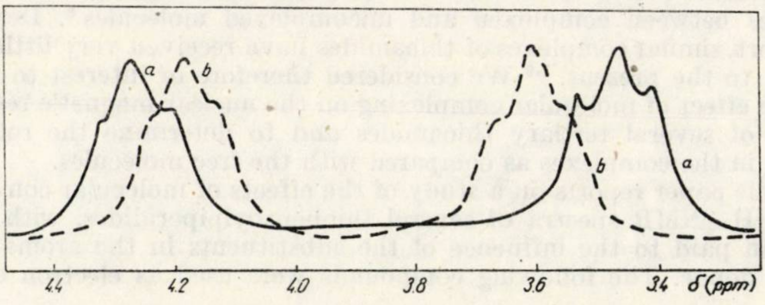

Fig. 1. — The 3.3—4.4 ppm region of the ^1H-NMR spectrum of thiobenzoylpiperidide in free (a) and complexed (b) form.

The retention of separate signals for the *syn* and *anti* αNCH_2 protons shows that iodine coordinates at the sulphur atom, since N coordination would destroy the double bond character of the C−N bond and allow free rotation around it.

In Table 1, the resonance signals of the *syn* and *anti* αNCH_2 protons are tabulated for the three complexes under investigation, as compared with those of the free molecules. For every system listed, the signal of the *anti* protons arising from complexed molecules (δ_a^c) appear at a lower field than for the free donors (δ_a). For the *syn* protons, the signal shows only a small upfield shift on molecular complexing. These shifts provide the most unambiguous measure of the effect of molecular complexing on the compounds under investigation.

TABLE 1

Chemical shifts of the αNCH_2 protons in the free and complexed donors (δ in ppm)

Donor	[donor] M kg^{-1}	[I$_2$] M kg^{-1}	Free donor			Complex			Shifts		
			δ_s	δ_a	$\Delta\delta_{sa}$	δ_s^c	δ_a^c	$\Delta\delta_{sa}^c$	$\Delta_s = \delta_s^c - \delta_s$	$\Delta_a = \delta_a^c - \delta_a$	$\Delta\delta_{sa}^c - \Delta\delta_{sa}$
1	0.039	0.125	4.24	3.53	0.71	4.19	3.69	0.50	−0.05	0.16	−0.21
2	0.042	0.109	4.26	3.48	0.78	4.18	3.60	0.58	−0.08	0.12	−0.20
3	0.042	0.135	4.26	3.45	0.81	4.26	3.60	0.66	0.0	0.15	−0.15

The magnitude of these shifts ($\Delta_s = \delta_s^c - \delta_s$ and $\Delta_a = \delta_a^c - \delta_a$) increases with the molar ratio $w = \dfrac{[acceptor]}{[donor]}$; however, for w exceeding unity, they approach a constant value *. This observation can be justified in terms of the very high formation constants of these complexes (about 10^4 at room temperature [11]) : for w larger than 1, the donor is practically entierly complexed, so that the observed shifts can be considered to be "the pure complex shift". Therefore, the data in Table 1 were obtained for a w value of about 3.

Table 1 presents also the chemical shift differences of the *syn* and *anti* protons in the complex, as compared with those of the free molecules ($\Delta\delta_{sa} = \delta_s - \delta_a$). It may be seen that both for the free and complexed molecules, $\Delta\delta_{sa}$ shows a small increase with the electron-withdrawing character of the substituent in the aromatic ring :

$$(\Delta\delta_{sa})_{pOCH_3} < (\Delta\delta_{sa})_H < (\Delta\delta_{sa})_{pNO_2}$$

For uncomplexed donors, this trend was previously rationalized in terms of an increase of the torsional angle around the C−C(S) bond, [13] resulting in an increase of the shielding of the *anti* αNCH_2 protons by the ring current; we believe that this explanation holds also for the complexed molecules.

---

* The same observation was noted in a previous communication for the *p*-chlorocinnamoylpiperidide-I$_2$ complex. [14]

Since the resonances of the *syn* and *anti* protons are shifted to opposite directions on molecular complexing, the chemical shift difference of the two signals is smaller in the complex than in the corresponding donor:

$$\Delta\delta^c_{sa} < \Delta\delta_{sa}$$

The latter observation can be rationalized in terms of the structural changes occurring on complex formation:

a) The electron transfer from the donor to the acceptor, resulting in a deshielding experienced by the protons of the former. This effect should probably produce shifts of a comparable magnitude for the *syn* and *anti* αNCH_2 protons, which is not in agreement with our observations; therefore, this effect is probably neither the only, nor the most important cause of the observed shifts.

b) The increase of the contribution of the resonance form III in the ground state of the complex (Scheme 1).

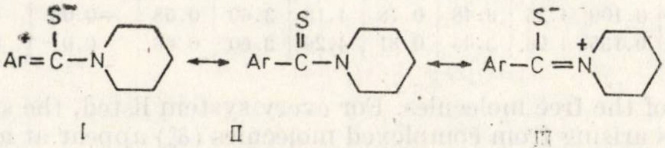

HMO calculations on a simple whole-molecule model [10] have indeed shown an increase of the p_{CN} bond order and a decrease of the p_{CS} bond order on complex formation; this conclusion is also reinforced by the frequency shifts observed in the infrared spectra upon molecular complexing (Table 2) [10].

TABLE 2

Infrared data and HMO calculations for thiobenzoylpiperidides in free and complexed form*

	C—N stretching frequency (in cm^{-1})		C—S stretching frequency (in cm^{-1})		HMO data							
	$\tilde{\nu}_{(CN)}$	$\tilde{\nu}_{(CN)}$	$\tilde{\nu}_{(CS)}$	$\tilde{\nu}_{(CS)}$	p_{CN}	p^c_{CN}	p_{CS}	p^c_{CS}	q_N	q^c_N	q_S	q^c_S
1	1491	1511	1012	977	0.4563	0.5155	0.6460	0.4121	1.8331	1.7939	1.6405	1.2539
2	1489	1526	1016	978	0.4610	0.5269	0.6592	0.4202	1.8299	1.7864	1.6236	1.2526
3	1491	1535	1014	979	0.4612	0.5332	0.6716	0.4297	1.8287	1.7801	1.5877	1.2472

* Reference [10]

The increase of the contribution of the structure III is expected to produce an increase of the anisotropy of the C—N bond, resulting in a deshielding of the *syn* and *anti* protons. (This effect is reinforced by the deshielding produced by the decrease of the electron density on nitrogen, as discussed at point a)). Another effect is a decrease of the anisotropy of the C=S bond resulting in an increased shielding of the *syn* protons. [15] The latter effect compensates the former, so that the net result will be a downfield shift of the resonance of the *anti* protons and a small up- or downfield shift for the *syn* protons.

3.2. Rotational barriers around the C−N bond

The rotational barriers to hindered rotation around the C−N bond ($\Delta G^{\neq}_{T_c}$) were determined from the coalescence temperatures (T_c) for the signals of the *syn* and *anti* protons and the $\Delta\delta_{sa}$ values determined at low temperatures [15].

$$\Delta G^{\neq}_{T_c} = 4.573\, T_c \left(9.972 + \log \frac{T_c}{\Delta\delta_{sa}}\right)$$

with $\Delta\delta_{sa}$ in Hz and $\Delta G^{\neq}_{T_c}$ in kcal/mole.

The coalescence temperatures T_c and the values $\Delta G^{\neq}_{T_c}$ are presented in Table 3 for the free and complexed molecules in bromophorm. The increase of the rotational barrier of the complex relative to the free donor $\Delta\Delta G^{\neq}_{T_c}$ is also presented.

It should be noted that the coalescence temperatures for the complex solutions increase with the concentration of the acceptor, but for *w* exceeding unity, they approach to a constant value. Therefore, the data presented in Table 3 were obtained for the same concentrations as shown in Table 1.

Certain conclusions emerge from the results presented in Table 3.

a) Introduction of an electron-releasing substituent (OCH_3) in the *para* position of thiobenzoylpiperidide lowers the barrier, whereas an electron-withdrawing substituent (NO_2) raises the barrier. This effect was previously noted for a larger series of thiobenzoylpiperidides in a different solvent -*o*-dichlorobenzene. [12] The trend can be explained in terms of the electronic effects of the substituents: an electron-releasing substituent increases the conjugation of the thiocarbonyl group with the aromatic

TABLE 3

Coalescence temperatures and rotational barriers for thiobenzoylpiperidides in free and complexed form

Donor	Free donor		Complex		$\Delta\Delta G^{\neq}_{T_c}$
	T_c(K)	$\Delta G^{\neq}_{T_c}$(kcal/mole)	T_c(K)	$\Delta G^{\neq}_{T_c}$ (kcal/mole)	(kcal/mole)
1	337.6	16.60	372.1	18.63	2.03
2	365.4	17.95	389.2	19.43	1.48
3	377.1	18.53	397.1	19.71	1.18

ring, resulting in a stabilization of the ground and transition state for the rotational process. The delocalization energy gain is larger in the transition state than in the ground state, since in the transition state the cross-conjugation with the N lone pair electrons is absent [16,17].

b) The same trend was also noted for the series of complexes under investigation : the highest barrier was observed for the *p*-nitrothiobenzoylpiperidide-I_2 complex and the smallest for the complex formed by the *p*-methoxy derivative. It may be inferred that the same explanation should hold for the substituent effects in the series of complexes, as for the free donors ; substituent effects are more important in the transition than in the ground state of the complex.

c) For all the compounds studied, the barrier raises on complex formation. This observation supports the conclusion drawn from infrared measurements, that the coordination site for iodine is the sulphur atom ; N coordination would destroy the double bond character of the C–N bond and therefore would lower the barrier. On complex formation the ground and transition state are stabilized ; in view of the increase of the barrier observed, we may conclude that this effect should be less important for the transition state than for the ground state. It may be inferred that the rotational barrier height in the complex is raised relative to the free donor because of the preferential stabilization of the ground state.

d) The increase of the rotational barrier in the complex relative to the free donor $\Delta\Delta G^{\neq}_{T_c}$ is larger when the electron-releasing character of the ring substituent is higher. In view of this result, we may conclude that the difference in the stabilization energy gain in the ground and in the transition state (ΔE_{ot}) should have the following trend :

$$(\Delta E_{ot})_{p\mathrm{OCH_3}} > (\Delta E_{ot})_{\mathrm{H}} > (\Delta E_{ot})_{p\mathrm{NO_2}}$$

This trend could be accounted for in terms of the stabilization energy of the complex in the ground state : the latter should be larger if the donor contains an electron-releasing substituent. This ideea is supported by the larger donor ability of the *p*-methoxy derivative, as predicted on the basis of the larger electron density on the sulphur atom (Table 2).

4. CONCLUSIONS

Chemical shift determinations for the αNCH_2 protons in the charge transfer complexes formed by substituted thiobenzoylpiperidides support infrared results concerning the iodine coordination at the sulphur atom. The observed complex shifts can be justified in terms of the anisotropy changes for the thioamide group, produced as a consequence of the increased contribution of the polar structure III.

Barrier height determinations reveal that the substituent effects affect mainly the transition state, whereas complex formation affects mainly the ground state for rotational process.

REFERENCES

[1] R. Foster and C. A. Fyfe, in "Progress in Nuclear Magnetic Resonance Spectroscopy", Pergamon Press, Oxford, Chap. 1, 1969.

[2] M. Ciureanu, and M. Contineanu, *Adv. Molec. Relax. Inter. Proc.*, **15**, 135 (1979).

[3] A.J. Carty, *Canad. J. Chem.*, **44**, 1881 (1966).

[4] S. J. Kuhn and J. S. Mc Intre, *Canad. J. Chem.*, **43**, 375 (1965).

[5] G. Matsubayash iand T. Tanaka, *Org. Magn. Reson.*, **2**, 219 (1970).

[6] E. S. Gore, G. Blears and S. S. Danyluk, *Canad. J. Chem.*, **43**, 2135 (1965).

[7] T. H. Siddal III, E. L. Pye and W. E. Stewart, *J. Phys. Chem.*, **74**, 595 (1970).

[8] A. Fratiello, D. P. Miller and P. Schuster, *Mol. Phys.*, **12**, 111 (1967).

[9] F. M. Menger and G. Saito, *J. Org. Chem.*, **40**, 2003 (1975).

[10] F. Cornea, C. Cercasov and M. Ciureanu, *Spectrochim. Acta*, in press.

[11] F. Cornea, C. Fulea and S. Moldoveanu, *Rev. Roumaine Chim.*, **19**, 429 (1970).

[12] C. Piccini-Leopardi, O. Fabre, D. Zimmermann, J. Reisse, F. Cornea and C. Fulea, *Canad. J. Chem.*, **55**, 2649 (1977).

[13] M. Ciureanu, C. Cercasov, F. Cornea and M. Contineanu, *Rev. Chim.*, București, in press.

[14] M. Ciureanu, C. Cercasov, F. Cornea and M. Contineanu, in press. Org. Magn. Res.

[15] W. E. Stewart and T. H. Siddall III, *Chem. Rev.*, **70**, 517 (1970).

[16] J. Sandstrom *J. Phys. Chem.*, **71**, 2318 (1961).

[17] L. M. Jackman, in "Dynamic Nuclear Magnetic Resonance Spectroscopy", Ed. L. M. Jackman and F. A. Cotton, Academic Press, New York, 1975.

Revue Roumaine de Chimie, **26**, *5*, 667–674, (1981)

CHARGE TRANSFER COMPLEXES OF SOME PYRIDINE DERIVATIVES WITH AROMATIC TRI- AND DI-NITRO-COMPOUNDS

R.M. ISSA, N. T. ABDEL-GHANI, A. L. EL-ANSARY and A. F. SHOUKRY
Chemistry Department, Faculty of Science, Cairo University, Cairo, Egypt

Received June 29, 1979
Revised December 2, 1980

Molecular complexes of ten pyridine derivatives with some tri- and di-nitro aromatic compounds are prepared and studied by infrared spectroscopy. The bonding between the donor and acceptor molecules in the molecular complex, which may involve $\pi-\pi^*$ and $n-\pi^*$ interactions or proton transfer, is found to depend on the structure of both donor and acceptor molecules. The spectral characterisation of the type of bonding is pointed out.

INTRODUCTION

Molecular complexes of the charge transfer (C.T.) type have become of interest in the last few decades. Though many investigations have been carried out using absorption spectrophotometry in solution, yet few studies dealt with solid complexes. The reaction of aniline derivatives or azo-aromatic compounds with electron acceptors was found to occur through π-electron interaction in the case of π-acceptors [1] or n-electron transfer [2–4] with molecular iodine. In some cases both types of electron transfer can take place if the π-acceptor contains a strong acceptor substituent (e.g. NO_2 group). [5–7]

C.T. complexes of pyridines with trinitrobenzene were of interest regarding the type of bonding in these compounds and their stability. [7] These studies were carried out in CCl_4 or $CHCl_3$ solutions using NMR measurements. C.T. complexes of pyridine and few of its derivatives with picric acid were included in the investigation carried out by Kross and Fassel [8].

In the present work, the C.T. complexes of pyridine and nine of its derivatives with six trininitro- and dinitrobenzenes are prepared. The type of bonding in these C.T. complexes is investigated in the solid state using infrared spectroscopy.

EXPERIMENTAL

The chemicals used in the present investigation were BDH pure laboratory grade chemicals. Few pyridine derivatives were obtained from T. Schuchardt (München).

The donor molecules have the general formula,

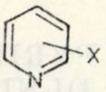

where X = H (a), 2−Cl (b), 2−Br (c), 3−Br (d), $2-CH_2-Ph$ (e),
$3-CH_2-Ph$ (f), $3-COCH_3$, (g), $2-NH_2$ (h),
$3-NH_2$ (i), $4-NH_2$ (j).

The acceptors used were picryl chloride (**1**), picric acid (**2**), 3,5-dinitrosalicylic acid (**3**), 3,5-dinitrobenzoic acid (**4**), 2,4-dinitrophenol (**5**) and picramic acid (6-amino, 2,4-dinitrophenol) (**6**).

The preparation of the solid complexes and KBr discs for recording the IR-spectra were the same as given before. [6] The IR spectra were recorded on a Unicam SP 1000 infrared spectrophotometer.

RESULTS AND DISCUSSION

These compounds, based on the type of molecular complex formed with the various acceptors used, can be classified into two main groups.

1. Complexes with intermolecular charge transfer only

This type of C.T. complexes is formed between acceptors **1**, **5** or **6** with all donors as well as between acceptors **2**, **3** or **4** with donors a, b, c, d and g. The acceptors in this case are unable to undergo interaction of the acid-base type with the donors, hence only one type of molecular compounds is formed. The formation of the molecular complex takes place mainly through charge transfer of different types. The acceptors used can behave mainly as π-acceptors [6,7] and also the NO_2-groups may function as acceptors for *n*-electrons. [6,8] The main spectral shifts on complex formation are :

(a) The ν (CH) bands of the acceptors shift to lower wavenumbers while those of the donors display the opposite behaviour. This denotes an increased π-electron density on the acceptor molecule and its decrease on the donor one. This results from the intermolecular charge transfer of the π-π* type.

(b) The ν (OH) bands of **5** and **6** as well as the ν (NH_2) bands of **6** are shifted to lower wavenumbers. This results from the increased π-electron density on the acceptor molecules which favours a stronger intramolecular hydrogen bonding in the C.T. complex.

(c) The asym. NO_2-bands display shifts differing both in their direction and magnitude. The smaller wavenumber band shifts to lower values as a result of the increased polarisation of the NO_2-group in the C.T. complex due to π-π* interaction [6,8] and increased strength of the intramolecular hydrogen bonding on complex formation in the case of acceptors (**5**) and (**6**). The higher NO_2-band shows a different behaviour : it shifts either to lower wavenumber, retains its position or is displaced to higher values. The shift to lower wavenumber values is in accordance with the increased polarisation of the NO_2-group, while the shift to higher wavenumber values denotes the occurrence of an interaction involving *n*-π* transition. This latter one involves the transfer of an *n*-electron from the heterocyclic nitrogen atom to the lowest vacant π-level on one

TABLE 1

Important bands in the IR spectra of molecular complexes with acceptors **1**,**5** and **6**

Donor	Colour	M.p.°C	ν(OH)	NO_2-asym.	NO_2-sym.	ν(CH) acceptor
	Complexes with picryl chloride **(1)**					
	Bands of free acceptor			1553, 1540	1348	788
a	greenish-yellow	209		1552, 1535	1352, 1340	785
b	pale-yellow	79		1553, 1533	1348, 1335	783
c	yellow	107		1555, 1530	1350, 1330	770
d	brown-yellow	71		1560, 1535	1350, 1335	782
g	light-brown	81		1500, 1525	1345, 1330	779
h	orange-brown	93		1555, 1535	1350, 1335	776
i	orange-yellow	107		1555, 1538	1355, 1340	782
j	red	115		1560, 1535	1355, 1338	781
	Complexes with 2,4-dinitrophenol **(5)**					
	Bands of free acceptor		3280	1540, 1520*	1350	928, 825
a	yellow	109	3270	1530, 1515	1345, 1335	922, 820
b	brown	115	3260	1533, 1512	1345, 1335	915, 818
c	yellowish-brown	116	3265	1530, 1515	1345, 1333	918, 815*
d	brown	109	3260	1535, 1515	1345, 1335	917, 820
f	pale-brown	69	3250	1530, 1515	1345, 1338	920, 819
g	orange-brown	111	3260	1540, 1515	1348, 1335	917, 818
h	greenish-yellow	152	3270	1540, 1515	1335, 1325	921, 821
i	orange	146	3260	1535, 1520	1345, 1330	920, 819
j	greenish-yellow	166	3270	1545, 1520	1345, 1335	922, —
	Complexes with picramic acid **(6)**					
	Bands of free acceptor		3270	1555, 1540	1340	820, 810
a	brown	158	3250	1560, 1537	1352, 1335	815, 795
b	conc. brown	169	3250	1555, 1525	1350. 1335	817, 805
c	brown	172	3250	1550. 1535	1345, 1335	818, 800*
d	reddish-brown	161	3240	1553, 1530	1350, 1337	817, 806
f	dark-brown	82	3260	1545, 1535	1340, 1332	—, 800
g	brown	115	3260	1558, 1540	1355	—, 800
h	dark-brown	201	3260	1555, 1535	1320	820, 800
i	dark-green	213	3260	1560, 1535	1330	817, —
j	dark-green	214	3250	1560, 1530	1320	815,* 800

* Shoulder.

TABLE 2

Important bands in the IR spectra of molecular complexes with acceptors **2**, **3**, and **4**

Donor	Colour	M.p.°C	ν(OH)	ν(C=O)	(NO_2^2-asym.)	(NO_2-sym.)	ν(CH)
	Complexes with picric acid **(2)**						
	Bands of free acceptor	3110	—		1555, 1540, 1530	1350	784
a	yellow	163	3100		1565, 1550, 1525	1360, 1345	782
b	yellow	103	3090		1560, 1540, 1525	1360, 1343	782
c	brownish-yellow	102	3070		1555, 1535, 1525	1340	781
d	brownish-yellow	154	3990		1545, 1535, 1528	1345, 1340	781
e	yellow	135	3100		1565, 1545, 1527	1345	775
f	yellowish-brown	138	—		1555, 1545, —	1345	780
g	pale yellow	130	3070		1555, 1540, 1525	1355, 1342	779
h	pale yellow	208	—		1560, 1540, —	1340	—
i	pale yellow	198	—		1560, 1545, —	1335	—
j	yellow	211	—		1557, 1538, —	1335	782
	Complexes with 3,5-dinitrosalycilic acid **(3)**						
	Bands of free acceptor		3570 3470, 3100		1540, 1530	1349	925, 825
a	pale-yellow	150	3420, 3990	1690	1537, 1525	1352, 1335	922, 813
b	pale-brown	115	3430, 3080	1685	1545, 1525	1355, 1340	918, 818
c	brown	116	3400, 3030	1690	1548, 1530	1355, 1384	917, 812

d	pale-yellow	156	3400, 3070	1695	1535, 1515	1384, 1325	922, 818
e	pale-yellow	109	3420, 3090	1690	1535, 1525	1345, 1338	918, 815
f	pale-yellow	158	3380, —	1710	1535, 1530	1345, 1325	920, 810
g	pale-yellow	132	3380, 3080	1710	1535, 1530	1348, 1325	910, —
h	pale-yellow	106	3450, —	1690	1535, 1528	1348, 1330	—, 812
i	pale-yellow	164	3440, —	1705	1538, 1530	1350, 1330	920, 813
j	pale-yellow	149	3450, —	1670	1535, 1529	1352, 1330	920, 811

Complexes with 3,5-dinitrobenzoic acid (4)

	Bands of free acceptor		3190		1555, 1540	1350	923, 808, 727
a	white	173	3290	1700	1545, 1535	1345	920, 798, —
b	white	201	3250	1705	1548, 1535	1348	922, 805, 722
c	brown	136	3380	1700	1545, 1530	1344	918, 803, 725
d	white	96	3340	1710	1550, 1535	1345	920, —, 722
e	white	125	3260	1710	1545, 1530	1345	915, 803, 725
f	white	102	3350*	1690	1550, 1535	1345	920, 805, 723
g	white	206	3400	1670	1550, 1540	1347	920, 803, 725
h	yellowish-white	148	3410	1690	1550, 1538	1345	918, —, 720
i	white	110	3380	1675	1545, 1537	1347	920, 800, 723

(S) : Salt,* : shoulder

NO_2-group of the acceptor molecule. Though the shift of the higher asym. NO_2-band is not very regular, yet it can be stated that the shift to higher values takes place with pyridines having donor substituents while the displacement to lower values occurs with pyridines having acceptor substituents. Thus it is apparent that n-π^* donation increases with donor substituents i.e. as the *n*-ionisation potential decreases. As a matter of fact, donor molecules having both π- and *n*-electrons can interact with acceptor molecules through π-π^* and n-π^* bonding. However, the contribution of n-π^* transition depends on the structure of both donor and acceptor molecules. For the acceptors under investigation this seems to be the case. The π-π^* interaction causes a shift of the NO_2-bands to lower wavenumbers while n-π^* leads to an opposite shift. The observed shift would be the resultant of both effects. If the π-π^* interaction is of lower energy compared to the n-π^* transition, which is the case with pyridines having an acceptor substituent, the result is a shift to lower wavenumbers. If the n-π^* energy is low enough to overcome the π-π^* polarising influence, the band shifts to higher values. If both effects compensate each other, the band retains its position.

The effect of n-π^* interaction is quite apparent with the strong acceptor **(1)** while it is of low contribution in the case of **(6)**. Generally, the effect of n-π^* interaction decreases as the number of acceptor groups on the molecule decreases or as the number of donor groups increases i.e. in the order, **(1)** > **(5)** > **(6)**.

This is the order of the decreased electron affinity of the acceptor molecule, which is in accordance with the relations governing the energy of C.T. interactions [9].

$$E_{C.T.} = I_P - (E_f + C)$$

in which, I_P = ionisation potential of donor molecule,
E_f = electron affinity of the acceptor centre,
C = coulombic force between the electron transfered and the positive hole left behind.

This relation though utilised in a quantitative manner in the case of UV-vis absorption spectra, [9] yet with IR-spectra it is difficult to carry out such quantitative treatment due to small shifts observed in this case.

(d) The sym. NO_2 bands appear in the spectra of the free acceptors as a single broad band but in the spectra of the molecular complexes they appear mostly resolved into two peaks. The shift of these bands is almost in accordance with that of the asym. NO_2-bands.

(e) The $\nu(NH_2)$ bands of donor (h, i, j) containing the NH_2-group display an apparent shift to higher wavenumbers. This results from the decreased charge density on the donor molecule which results from both the π-π^* interactions. With these donors, the n-π^* interaction is quite apparent as compared to other donors. This leads to the opinion that the n-π^* interaction with these donor molecules might involve *n*-electron from the NH_2-group rather than from the heterocyclic nitrogen atom. This is based on the higher basicity of the NH_2-group than the heterocyclic nitrogen atom. [10]

For complexes with acceptor **4**, the ν(OH) band of the acceptor shifts largely to higher values but does not attain the position of the free OH-group. The shift of the ν(OH) band to higher values is due to the destruction of the intermolecular hydrogen bond involving the COOH group. The lower value of the ν(OH) band than that of the free OH-groups is due to the increased charge density on the acceptor molecule and the possible existence of a weak intermolecular hydrogen bonding between the donor and acceptor molecules in the C.T. complex.

2. Complexes with intermolecular proton and charge transfer

This type of C.T. complexes is formed between donors h, i and j with acceptors **2**, **3** and **4** as well as donor f with acceptors **2** and **3**.

In this case the NH_2 group behaves as basic compounds towards the acidic acceptors. The reaction involves besides intermolecular charge migration, the transfer of a proton from the phenolic group of **2** and **3** or from the carboxylic group of **4**. The spectral changes due to complex formation are;

(a) The ν(CH) bands of the acceptors shift to lower wavenumbers while those of the donors are shifted to higher values indicating a π-π* interaction between the rings of the two molecules

(b) The ν(OH) bands of the phenolic groups of **2** and **3** at 3110 and 3100 cm^{-1} respectively as well as the $\nu(NH_2)$ bands of donors h, i and j within the 3450—3300 cm^{-1} range are no more apparent in the spectra of the molecular complexes. Instead of these, a group of intense bands is observed within 3000—2400 cm^{-1}. These bands correspond to the stretching vibration of the $-\overset{+}{N}H_3$ ion. [11-12] With acceptor **4**, the spectra display the bands characteristic of the $-\overset{+}{N}H_3$ in addition to weak $\nu(NH_2)$ bands. This behaviour indicates that the reaction of acceptor **4** with aminopyridines leads to a mixture of the two types of molecular complexes. These spectral changes indicate the transfer of a proton from the phenolic group in the case of acceptors **2** and **3** or from the carboxylic group of **5** to the amino group of the donor molecules h, i or j. The intermolecular interaction could be represented as follows

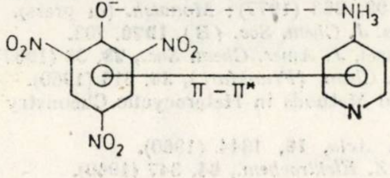

(c) The separated C=O bands of **3** are converted into a single band denoting the disappearance of the rotational isomerism, occurring in the free acceptor, on complex formation. The C=O band of acceptor **4** is slightly shifted to lower wavenumbers and displays a relatively low intensity in comparison with molecular complexes with other donors. This denotes that the carboxylic group has been partly involved in the complex formation through proton transfer to the NH_2 group of the donor molecule.

(d) The asym. and sym. NO_2-bands shift to lower values as compared to those of the free acceptor as a result of the increased polarisation of the NO_2-groups. The asym. NO_2-bands corresponding to the NO_2-groups involved in intra- or inter-molecular hydrogen bonding display either a shift to lower or to higher wavenumber values. The shift is the resultant of the increased frequency due to the destruction of the hydrogen bond and its decrease resulting from increased polarisation of the NO_2-group as a sequence of the π-π^* charge transfer. Generally, the difference in the frequency of the two asym. NO_2-bands becomes lower in the spectra of the molecular complexes. In the case of acceptor **2**, the number of asym. NO_2-bands decreases, this is the general behaviour for molecular complexes involving the proton transfer.

With donor f, the behaviour is somewhat peculiar. This donor forms molecular complexes involving π-π^* and n-π^* with acceptor **4** while with acceptors **2** and **3** it forms compounds involving proton transfer. This behaviour indicates that the basic character of this would be somewhat higher than pyridine due to the presence ot the weak donating C_6H_5-CH_2 group at position 3. When this group is present at position 2, the donor becomes incapable of accepting the proton. This may be due to the steric effect of the bulky substituent in the neighbourhood of the heterocyclic nitrogen.

Since the NH_2 group of donors h, i and j is the centre acting as the proton acceptor it should exhibit a higher basicity than the N-atom of the pyridine nucleus. This supports the assumption given above that the NH_2-group would be the origin of the n-π^* charge transfer rather than the heterocyclic nitrogen.

REFERENCES

[1] H. Tsumboura, *J. Amer. Chem. Soc.*, **82**, 40 (1960).
[2] R. S. Mulikan et al., *J. Amer. Chem. Soc.*, **76**, 3869 (1954), **81**, 823 (1959); **91**, 1237 (1969).
[3] H. D. Bist and W. B. Person, *J. Phys. Chem.*, **71**, 2750 (1967).
[4] D. K. Kearns, P. Gardner and J. Carmody, *J. Phys. Chem.*, **71**, 931 (1969).
[5] B. B. Wayland and R. S. Drago, *J. Amer. Chem. Soc.*, **86**, 5240 (1964).
[6] R. M. Issa et al., *Z. phys. Chem. (Leipzig)*, **253**, 96 (1973); *Acta Chim. Acad. Sci. Hung.*, **88**, 341 (1976) **92**, 263 (1977); *Monatsh.* (in press).
[7] R. Foster and J. W. Morris, *J. Chem. Soc. (B)*, **1970**, 703.
[8] R. D. Kross and V. A. Fassel, *J. Amer. Chem. Soc.*, **79**, 38 (1957).
[9] G. Briegleb et. al., *Z. phys. Chem. (Frankfurt)*, **30**, 316 (1960).
[10] A. R. Katritzky, "Physical Methods in Heterocyclic Chemistry", Vol. 1, Academic Press, London, 1963.
[11] J. Bellanato, *Spectrochim. Acta*, **16**, 1344 (1960).
[12] G. Briegleb and H. Delle, *Z. Elektrochem.*, **64**, 347 (1960).

Revue Roumaine de Chimie, 26, 5, 675–680 (1981)

MEDIUMEINFLÜSSE BEI DER SOLVOLYSE VON ALKYLHALOGENIDEN. IX. [1]

TEMPERATURABHÄNGIGKEIT LINEARER SALZEFFEKTE IN METHANOL-WASSER ($X_{H_2O} = 0{,}359$)

R. H. SCHUSTER
Zentrum für physikalische Chemie, ICECHIM, Bukarest, Romania
Splaiul Independenţei, 202

Eingegangen am 13. Mai 1980

Der Einfluss der Temperatur auf den „normalen" Salzeffekt von NaCl wurde bei der Hydrolyse von t-Butylchlorid in Methanol-Wasser Gemisch mit X_{H_2O}= 0,359 im Temperaturbereich 293,4–308,2 K untersucht. Anhand eines statistischen Modells wurde der Temperaturanstieg des *b*-Parameters der Winstein'schen Gleichung diskutiert.

The temperature influence on „normal" salt effect of NaCl was studied in the case of hydrolysis of t-butylchloride in the methanol-water mixture with $X_{H_2O} = 0.359$ at a temperature range 293.4–308.2 K. Temperature dependence of *b*-parameter in Winsteins' equation was discussed using a statistical model.

Bekanntlich ruft die Zugabe eines Elektrolyten in einem Medium durch die Solvatation der Ionen, Änderungen hervor, die den Ablauf einer Reaktion wesentlich beeinflussen. Für die Salzeffekte die in wässerigen Lösungen auftreten liegt bislang keine hinreichende Interpretation vor. [2–5] Es kann jedoch die Winstein'sche Gleichung

$$k = k_0(1 + b[\mathrm{MX}]) \qquad (1)$$

mit gutem Erfolg angewandt werden, um den Salzeffekt zu beschreiben. In dieser Gleichung sind k und k_0 die Reaktionsgeschwindigkeitskonstante (RGK) in Gegenwart und bzw. Abwesenheit eines zugegebenen Elektrolyten, b ein von der Natur des Elektrolyten abhängiger Parameter und [MX] die Molkonzentration des Elektrolyten.

Bei ionogenen Reaktionen kann der lineare Anstieg der RGK [1] mit der durch den Elektrolyten bewirkten Verminderung der Solvatation des Übergangszustandes in Verbindung gebracht werden. Die Temperaturabhängigkeit der Salzeffekte fand jedoch wenig Beachtung. Eine theoretische Behandlung dieser Temperaturabhängigkeit kann beim heutigen Stand der Kenntnisse schwerlich mehr als qualitative Aspeckte hervorheben. Es ist jedoch interessant zu untersuchen ob sich ein gewisser Trend der RGK in Abhängigkeit von Salzkonzentration und Temperatur abzeichnet. Daher wurde in der vorliegenden Arbeit die Temperaturabhängigkeit der *b*-Parameter der Gleichung (1) bei der Hydrolyse von *t*-Butylchlorid (*t*-BuCl) in Gegenwart von NaCl im System Methanol – Wasser ($X_{H_2O} = 0,359$) untersucht.

EXPERIMENTELLES

Die benötigten Lösungen wurden gravimetrisch aus Leitfähigkeitswasser, trockenem Methanol und umkristallisiertem NaCl hergestellt.

Die kinetischen Messungen wurden mit der in einer vorangegangenen Arbeit [1] beschriebenen Extraktionsmethode durchgeführt. Die Gegenwart von Methanol im System beeinträchtigt die Resultate insoweit, dass grösser Standardfehler der RGK als in reinem Wasser erhalten wurden.

ERGEBNISSE UND DISKUSSION

In der vorliegenden Arbeit wurde der von NaCl hervorgerufene „normale“ Salzeffekt auf die Hydrolyse von *t*-BuCl in Methanol – Wasser ($X_{H_2O} = 0,359$) im Temperaturbereich 293,4 – 308,2 K untersucht. Die erhaltenen kinetischen Messergebnisse (mit den Standardfehlern σ) sind in Tabelle 1 angeführt.

TABELLE 1

Reaktionsgeschwindigkeitskonstanten bei der Solvolyse von *t*-BuCl in Methanol-Wasser ($X_{H_2O} = 0,359$) bei verschiedenen NaCl Konzentrationen [MX] und Temperaturen $k \times 10^5$ (s^{-1})

MX Mol. 1^{-1}	293,46 K	298,06 K	303,66 K	308,26 K
0,000	1,23	2,28	4,69	8,26
0,033	1,25	2,30	4,78	8,43
0,051	1,26	2,35	4,84	8,54
0,098	1,28	2,37	4,92	8,76
0,175	1,32	2,49	5,16	9,21
0,223	1,35	2,50	5,29	9,42
0,288	1,39	2,59	5,45	9,69
0,352	1,42	2,64	5,62	10,10
0,438	1,46	2,83	5,82	10,6
0,510	1,49	2,85	6,09	10,9

Wie erwartet steigen die RGK Werte in Abhängigkeit der Molkonzentration des zugeführten Elektrolyten an. Nach Ingold [4] ist, aufgrund theoretischer Erwägungen, der Logarithmus der RGK eine lineare Funktion der Molkonzentration eines einwertigen Elektrolyten, während von Winstein, [5] aufgrund experimenteller Ergebnisse eine lineare Abhängigkeit der RGK von der Molkonzentration angegeben wurde. Um bei konstanter Temperatur die analytische Form dieser Abhängigkeit der RGK von der Mokonzentration des zugegebenen Elektrolyten zu charakterisieren sind in Abbildung 1 ln k (Kurve a) und k (Kurve b) in Abhängigkeit von der NaCl—Molkonzentration dargestellt.

Wie aus Abb. 1 ersichtlich, besteht eine hinreichend gute lineare Abhängigkeit im Falle von Kurve b wodurch im folgenden die Anwendung von Gleichung (1) zur Darstellung des Salzeffektes gerechtfertigt ist. Werden nun die RGK Werte (Tabelle 1) in Abhängigkeit der Molkonzentration von NaCl dargestellt (Abbildung 2) und so ergibt sich für die Koeffizienten der Gleichung (1) folgendes Bild:

$$k_{293.4} = 1{,}228 \cdot 10^{-5}(1 + 0{,}429\,[\mathrm{NaCl}]) \tag{2}$$

$$k_{297.9} = 2{,}269 \cdot 10^{-5}(1 + 0{,}508\,[\mathrm{NaCl}]) \tag{3}$$

$$k_{303.6} = 4{,}686 \cdot 10^{-5}(1 + 0{,}571\,[\mathrm{NaCl}]) \tag{4}$$

$$k_{308.2} = 8{,}260 \cdot 10^{-5}(1 + 0{,}631\,[\mathrm{NaCl}]) \tag{5}$$

Es ist bemerkenswert, dass die b-Parameter der Gleichung (1)mit der Temperatur ansteigen. Dieser Anstieg ist an sich ungewöhnlich, da bei Solvolysen von Alkylhalogeniden oder Sulphonsäuereestern in Eisessig des öfteren ein Abfall der b-Parameter in Abhängigkeit der Temperatur beobachtet wurde. Somit ist nicht nur der Wert des b-Parameters, sondern auch eine Temperaturabhängigkeit von dem Lösungsmittel abhängig. Folgende Gleichung gibt die Temperaturabhängigkeit des b-Parameters auf 1,5% genau wieder:

$$b = -0{,}348 + 0{,}013348\;T \tag{6}$$

Eine Erklärung dieses überraschenden Ergebnisses kann aufgrund eines statistischen Modells gegeben werden, wenn angenommen wird, dass der Übergangszustand der ionogenene Hydrolyse ein Ionenpaar ist und der zugegebene Elektrolyt grösstenteils als Ionenpaar vorliegt, was bei kleinen Wasserkonzentrationen zutreffen könnte.

Gemäss dem Brönsted'schen Geschwindigkeitsgesetz steigt die RGK in Gegenwart des zugegebenen Elektrolyten an, da dieser ein Abfallen des Aktivitätskoeffizienten des dipolaren Übergangszustandes bewirkt. Theoretische Behandlungen dieses Problems vernachlässigen meist den Einfluss des zugegebenen Elektrolyten auf den weniger polaren Grundzustand, da der Einfluss mit dem Dipolmoment stark anwächst. Es lässt sich zeigen, [6] dass der Aktivitätskoeffizient des Übergangszustandes als Virialserie von Potenzen der Elektrolytkonzentration dargestellt werden kann. Verwendet man ein statistisches Modell in dem nur der zweite Virialkoeffizient berücksichtigt ist, erhält man für den Aktivitätskoeffizienten des Übergangszustandes:

$$-\ln \gamma_{\neq} = \sum_{i=1}^{n} B_{\neq i}\,\rho_i \tag{7}$$

wo ρ_i die Dichtezahl des Elektrolyten i ist und $B_{\neq i}$ eine Funktiorn der Wechselwirkungsenergie der Dipole des Übergangszustandes und der

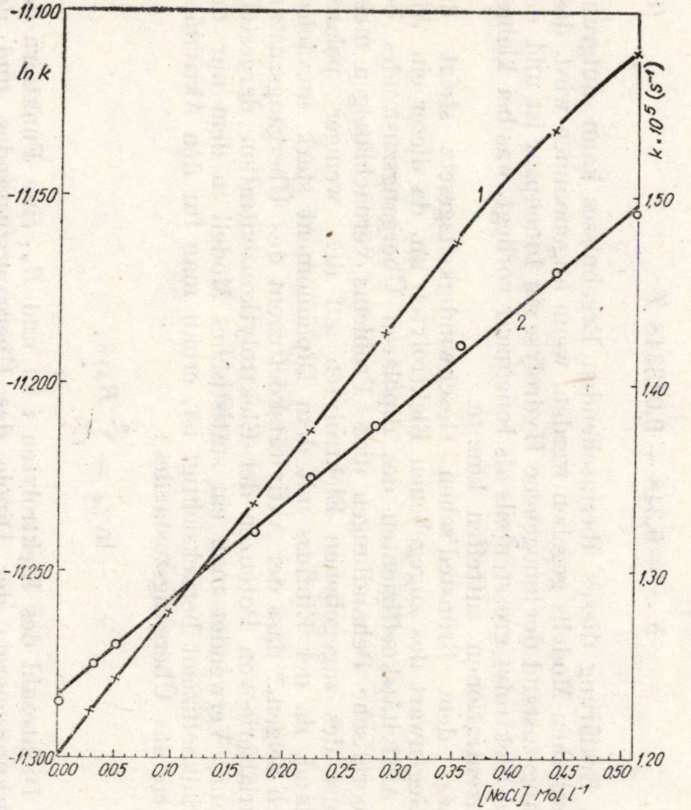

Abb. 1. — Zwei analytischen Formen des Anwachsens der RGK Werte in Abhängigkeit der Konzentration des zugegebenen Elektrolyten bei 293.46 K. Kurve 1 stellt $\ln k = f\,[\mathrm{NaCl}]$ und Kurve $2 = f\,[\mathrm{NaCl}]$ dar.

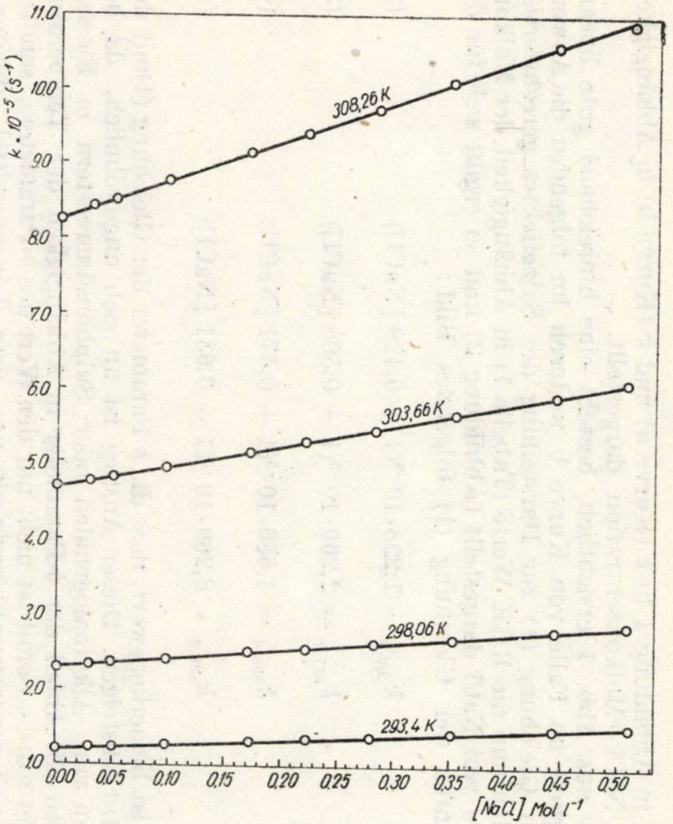

Abb. 2. — Anwachsen der RGK Werte in Abhängigkeit des zugegebenen Elektrolyten

$m_1, m_2 \ldots m_i$ zugegebenen Elektrolyten ist. Diese Wechselwirkung kann durch den vereinfachten Ausdruck:

$$B_{\neq s} = \frac{4}{3} \pi r_0^3 \sum_{n=1}^{\infty} C_n x^{2n} \tag{8}$$

dargestellt werden, wenn C und x durch folgende Ausdrücke definiert werden:

$$C = \frac{1}{(2n+1)!\,(2n-1)} \sum_{m=0}^{n} \frac{n!}{m!\,(n-m)!} \cdot \frac{3^m}{2m+1} \tag{9}$$

$$x = \frac{\mu_i\, \mu_{\neq}}{D k T r_0^3} \tag{10}$$

wo n die Anzahl der Elektrolytmoleküle der Art m in einem Cluster, der den Übergangszustand umgibt, darstellt; μ_i und $\mu_{\neq}$ die Dipolmomente des Elektrolyten i bzw des Übergangszustandes sind, während D die makroskopische Dielektrizitätskonstante und r_0 den kleinsten Abstand zwischen den punktförmigen angenommenen Dipolen bedeutet. Mit einigen Annäherungen kann der b-Parameter aus Gleichung (1) mit Hilfe des obigen Modells wie folgt ausgedrückt werden [8]:

$$b = B_{\neq s}\, \mathrm{N}/1000 \tag{11}$$

wo N die Avogadro'sche Zahl ist. Gleichung (11) ermöglicht qualitative Aussagen über die Temperaturabhängigkeit des b-Parameters, die laut Gleichung (10) unter anderen Faktoren auch vom Produkt DT bestimmt wird. Im Fall des von uns untersuchten Systems fällt die Dielektrizitätskonstante mit ansteigender Temperatur ab und es gilt ausserdem $\mathrm{d}(DT)/\mathrm{d}T = 0$. Dadurch erhält $B_{\neq s}$ höhere Werte mit ansteigender Temperatur, was zumindest teilweise die von uns gefundene Temperaturabhängigkeit der b-Parameter in Methanol-Wasser ($X_{H_2O} = 0{,}359$) erklärt.

Die Temperaturabhängigkeit der b-Parameter bewirkt eine Änderung der Arrhenius-Aktivierungsenergie mit der Salzkonzentration die in Tabelle 2 angeführt ist.

Der durch die Salzkonzentration bedingte Anstieg der Arrhenius-Aktivierungsenergie kann durch folgende Gleichungen angenähert werden:

$$E_{A(295{,}76\ \mathrm{K})} = 23220 + 2406\ [\mathrm{NaCl}] \tag{12}$$

$$E_{A(300{,}86\ \mathrm{K})} = 23290 + 1608\ [\mathrm{NaCl}] \tag{13}$$

$$E_{A(305{,}96\ \mathrm{K})} = 22940 + 1891\ [\mathrm{NaCl}] \tag{14}$$

Durch die Elektrolytzugabe kommen wahrscheinlich zahlreiche und schwer zu erfassende Wechselwirkungen zwischen Ionen, Ionenpaaren, Lösungsmittel — und Reaktantenmolekülen zustande, die sowohl die Solvatationsverhältnisse des Übergangszustandes als auch die, im angeführten Modell[6] vernachlässigten, Solvatationsverhältnisse des Grundzustandes hinreichend verändern um den beobachteten Effekt hervorzurufen. Es ist möglich, dass eine kompetitive Solvatation des Elektrolyten und der Ionenpaare des Übergangszustandes bei ansteigender Temperatur und Elektrolytkonzentration zugunsten der Solvatation des Elektrolyten entschieden wird. Dabei müsste die Solvatation des Übergangszustandes verringert werden letztlich bei Elektrolytzugabe ein Anwachsen der Aktivierungsenergie zur Folge hat.

TABELLE 2

Aktivierungsenergien in (cal. mol^{-1}) Abhängigkeit der Elektrolytkonzentration ([MX]) fur drei Temperaturen

MX $Mol.l^{-1}$	$E_{(295,76\ K)}$	$E_{(300,86\ K)}$	$E_{(305,96\ K)}$
0,000	23310	23150	22880
0,033	23030	23486	22930
0,051	23540	23190	22950
0,098	23270	23450	23320
0,175	24550	23390	23420
0,223	23270	24060	23320
0,288	23780	23880	23260
0,352	23420	24260	23700
0,438	24740	23150	24230
0,510	24500	24380	23530

LITERATURHINWEISE

[1] R. H. Schuster, *Rev. Roumaine Chim.* (in Druck).

[2] L. P. Hammett, ,,Physical Organic Chemistry" 2 ed. McGraw Hill, New York 1970, Kap. 7, S. 187–219.

[3] F. Badea, ,,Mecanisme de reacţie in chimia organică", Ed. ştiinţifică, Bucureşti 1973, cap. 3.

[4] L. C. Bateman, M. G. Church, E. D. Hughes, C. K. Ingold und N. A. Taher, *J. Chem. Soc.*, **1940**, 979.

[5] A. Fainberg und S. Winstein, *J. Amer. Chem. Soc.*, **78**, 2763, 2767, 2780 (1956).

[6] C. L. Perrin und J. Pressing, *J. Amer. Chem. Soc.*, **93**, 5705 (1971).

Revue Roumaine de Chimie 26, 5, 681–686 (1981)

THE REDUCTION OF A COMPLEX MOLYBDENUM–BISMUTH OXIDE CATALYST WITH PROPYLENE

N. I. IONESCU, P. BANYAI, MONICA CĂLDĂRARU and M. CHIRCA
Center of Physical Chemistry, Splaiul Independenţei 102, Bucharest, Romania

Received June 21, 1980

The reduction of complex molybdenum–bismuth oxide catalyst by propylene has been studied by a microgravimetric method. The experimental results show that the interaction of propylene with the catalyst starts at 240°C, the effect being much enhanced at 300–310°C. Two different kinds of interactions can be assigned to these experimental facts.

The Mars-van Krevelen type of mechanism [1] in the selective oxidation of olefines on the molybdenum–bismuth oxide catalyst is now a well accepted one. The reduction of the oxide catalyst with the olefine, as an important step of this mechanism, is not yet well known.

The aim of this work is to continue our studies [2-5] on the selective oxidation of propylene to acrolein following the reduction with propylene of a complex molybdenum–bismuth oxide catalyst, by a microgravimetric method.

EXPERIMENTAL

The microgravimetric measurements of the catalyst sample under propylene reduction were performed with a vacuum Sartorius 4102 microbalance, attached to a vacuum line.

To avoid thermodiffusion, the two microbalance quartz tubes and their ovens were symmetrically arranged.

Precautions were taken to eliminate the electrostatic charges on the quarz tubes of the balance.

The sample in an amount of 100 mg was a complex Mo–Bi oxide catalyst (containing P, Ni, Fe and Zn) with Bi :Mo :Ni :Fe atomic ratio as 1 :5 :0,75 :1 ; the catalyst was prepared by co-precipitation on 25 % silica. Propylene of 99.5% purity was used, between 220 and 450 °C.

Before each experiment the sample was outgassed (10^{-3} – 10^{-4} torr) at 450°C for several hours.

After every reducing experiment the sample was re-oxidized in oxygen, at 400°C, when its weight regained its initial value.

RESULTS AND DISCUSSIONS

At temperatures under 310°C, for different propylene pressures, the behaviour of the sample is almost identical. The reaction reaches its equilibrium after few minutes. At these temperatures the interaction of the propylene with the catalyst is weak, a fact already established by electrical conductance and catalytic activity measurements.[2,3,6]

At temperatures higher than 310°C an important and fast loss of weight is followed by an almost equilibrium state, characterized by very small changes in weight. A typical example is given in figure 1.

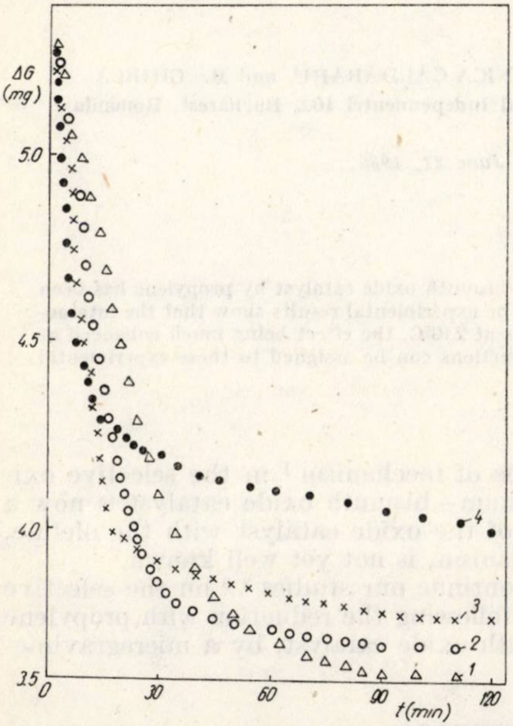

Fig. 1. — The variation of the weight of the sample for different propylene pressures. $T = 370°C$; $1 = 23$ torr; $2 = 50$ torr; $3 = 85$ torr; $4 = 120$ torr.

As the propylene pressure is lower the loss of weight of the catalyst is higher.

Tentatively, we could explain these by the following:

The loss of the weight of the sample during reduction with propylene could be the result of two opposite processes: the reduction of the catalyst and the adsorption on its surface, accompanied by a loss and a rise of weight, respectively.

An additional supposition is made that the propylene adsorption on the surface is irreversible at this temperature, and it occurs only on the reduced surface sites.

At the beginning of the experiments the propylene is reversibly adsorbed on the sample. Due to reduction, a part of surface becomes free and irreversible adsorption takes place on it, so that:

$$v_{\text{red}} = k_{\text{red}}\,\theta_{\text{rev}} \qquad (1)$$

$$v_{\text{ads}} = k_{\text{ads}}\,p_{C_3H_6}(1 - \theta_{\text{rev}}) \qquad (2)$$

where v_{red} and v_{ads} are the rate of reduction and respectively the rate of adsorption, k_{red} and k_{ads} are the rate constants of reduction and adsorption, $p_{C_3H_6}$ is the propylene pressure and θ_{rev} is the fraction of the surface which is reversibly covered with propylene.

The total rate v will be

$$v = \frac{\Delta G_{\text{red}}}{t} - \frac{\Delta G_{\text{ads}}}{t} = v_{\text{red}} - v_{\text{ads}} = k_{\text{red}}\,\theta_{\text{rev}} -$$

$$- k_{\text{ads}}\,p_{C_3H_6}(1 - \theta_{\text{rev}}) = A - B\,p_{C_3H_6} \qquad (3)$$

where $A = k_{\text{red}}\,\theta_{\text{rev}}$ and $B = k_{\text{ads}}(1 - \theta_{\text{rev}})$. As in figure 2, at the end of the reaction the rate is linearly dependent on the pressure, with a negative slope.

At the same time the obtained results cannot be explained using simple time dependencies.

Finding the rate equation which completely describes the kinetic behaviour of the catalyst reduction is a very difficult task. Some researchers [7,8] have found mathematical equations for the different parts of the reduction curve. Others [2] have tried to fit the experimental behaviour into a unic mathematical relation, but the result was a complicated multiparameters equation.

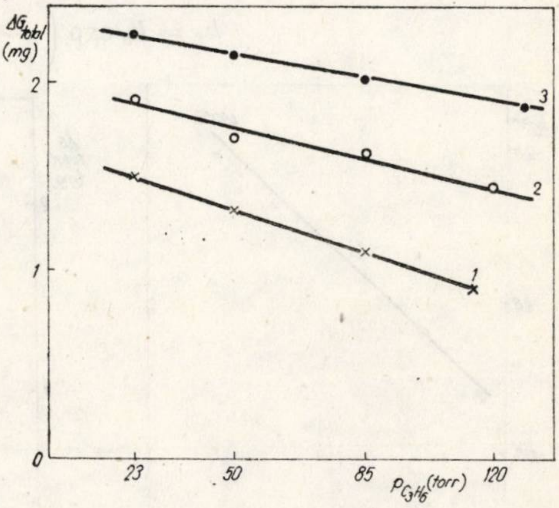

Fig. 2. — The variation of the weight ΔG at the end of reaction with propylene pressure. *1* = 350°C ; *2* = 370°C ; 3 = 390°C.

For evaluating the kinetic parameters, a different way has been used here. As the continuous loss of weight occurs in isothermal and isobaric conditions, the following equation could account for the reduced amount dG of the catalyst sample, when the reaction products are totally removed :

$$-\,\mathrm{d}G = k_T\, A(t)\, p^{\mathrm{n}}_{\mathrm{C_3H_6}}\, \mathrm{d}t \qquad (4)$$

where k_T is the rate constant of the reaction, $A(t)$ is the surface of the sample at the t moment, $p_{\mathrm{C_3H_6}}$ is the propylene pressure and n is the reaction order in respect to propylene. If one admits the extension in this case of the findings from ZnO, [10,11] that the surface (for samples heavier than 36 mg) is not changed during the reduction, to our case then, by integrating the equation (4) with the initial condition $t = 0, G = G_0$, one obtains :

$$G_0 - G_t = k_T\, A p^{\mathrm{n}}_{\mathrm{C_3H_6}}\, t \qquad (5)$$

For the reaction rate on the surface unit v, one gets :

$$v = \frac{1}{A}\,\frac{\mathrm{d}(G_0 - G_t)}{\mathrm{d}t} = k_T\, p^{\mathrm{n}}_{\mathrm{C_3H_6}} \qquad (6)$$

The relationship (6) allows the evaluation of the kinetic parameters n and k_T as follows :

$$n \log p = \log v - \log k_T \tag{7}$$

The n and k_T values can be determined as the slope, respectively the intercept of the graphical dependence log v versus log p.

As

$$k_T = k_0 \exp\left(-\frac{E}{RT}\right) \tag{8}$$

using an Arrhenius dependence between log v and $1/T$, the activation energy of the reduction can be obtained. Figure 3 and table 1 show the evaluation of the reaction order n at 400°C and its dependence on temperature respectively.

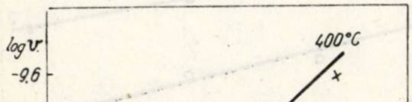

Fig. 3. — The determination of the reaction order n.

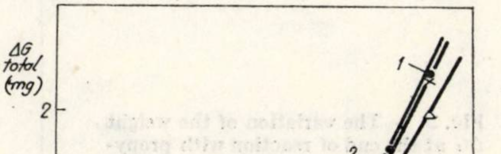

Fig. 4. — The loss of the weight of the sample at the equilibrium state versus temperature for different propylene pressures. *1* = 23 torr ; *2* = 50 torr ; *3* = 120 torr.

TABLE 1

The temperature dependence of the reaction order n

Temperature °C	n
380	0,54
400	0,39
420	0,39

The activation energy of the reduction for the studied catalyst has been found to be 82.5 kJ/mol.

The loss of the weight at equilibrium versus temperature for different propylene pressures is given in figure 4. There are two kinds of straight lines (suggesting two possibilities of propylene-catalyst interaction[6]) ; one of them intercepts x axis in the range 300—310°C, the same range of temperature where the conversion and conductance measurements are significantly changed.[2,3] The second interception of the temperature axis in the range 240—250°C could be an indication for antoher type of interaction (or beginning of it) between the propylene and the catalyst.

Related to the last supposition the change in the weight of the sample (at 23 torr propylene pressure, when, as it appears from Figure 1, the highest effect was observed) was followed versus time at different temperatures (Figure 5).

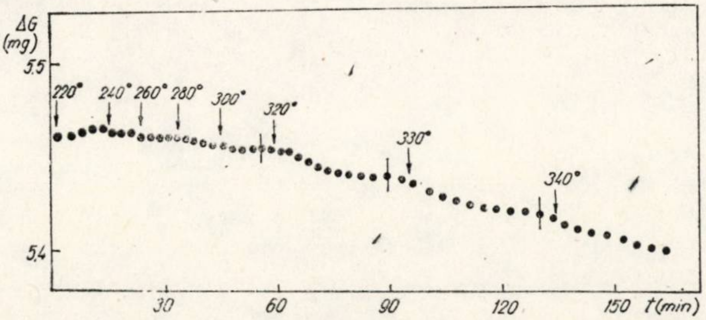

Fig. 5.—The change of the weight of the sample at different temperatures.

In this experiment, the temperature was consecutively increased each time after the weight remained constant. In figure 5 the lines indicate the moment when the temperature was risen, while the arrows indicate the moments when the weight remained constant. The behaviour of the catalyst, as indicated in figure 5, shows that at 240—260°C it is a significant loss of the weight of the sample, as an evidence for the beginning of its interaction with the propylene; below these temperatures the loss of the weight could be due to the outgassing of the sample (the loss of water).

The second jump of the weight is around 310°C, at this temperature the changes in conductance and conversions have been noticed too. [2]

In conclusion our experiments suggest that the propylene starts to interact with the catalyst at 240°C, its effect being much enhanced at 300—310°C.

Two different kinds of interactions can be assigned to these experimental facts. The studies of these interactions are in progress.

REFERENCES

[1] P. Mars and D. W. van Krevelen, *Chem. Eng. Sci., Suppl.*, **3**, 41 (1954).
[2] N. I. Ionescu and M. Căldăraru, *Reac. Kin. Catal. Lett.*, **8**, 477 (1978).
[3] N. I. Ionescu, M. Căldăraru and P. Banyai, "Proc. 4th International Symposium Heterogeneous Catalysis, Varna, 1979", Publishing House of the Bulgarian Academy of Sciences, Sofia, 1979, vol 1, p. 229.
[4] R. Mănăilă, N. I. Ionescu, M. Căldăraru, S. Serban, A. Belea, A. Weidenbecher and A. Rusu, "Proc. 4th International Symposium Heterogeneous Catalysis, Varna, 1979", Publishing House of the Bulgarian Academy of Sciences, Sofia, 1979, vol. 1, p. 223.
[5] R. Mănăilă, N. I. Ionescu and M. Căldăraru, *Z. anorg. Chem.*, **466**, 221 (1980).
[6] M. Căldăraru, P. Banyai and N. I. Ionescu, *Rev. Roumaine Chim.*, (in print).
[7] A. Yamaguchi and Y. Moriyama, *J. Jap. Inst. Metals*, **28**, 692 (1964).
[8] A. Yamaguchi and Y. Moryama, *J. Jap. Inst. Metals*, **29**, 831 (1965).
[9] R. Frety, L. Tournayan and H. Charcosset, *Ann. Chim. (France)*, **9**, 341 (1974).
[10] M. Grunze, W. Hirschwald and S. Krebs, *Z. phys. Chem. (Frankfurt)*, **102**, 57 (1976).
[11] W. Hirschwald and D. Noack, *Z. phys. Chem. (Frankfurt)*, **77**, 1 (1972).

Related to the last supposition the change in the weight of the sample (at 23 torr propylene pressure, when, as it appears from Figure 1, the highest effect was observed) was followed versus time at different temperatures (Figure 5).

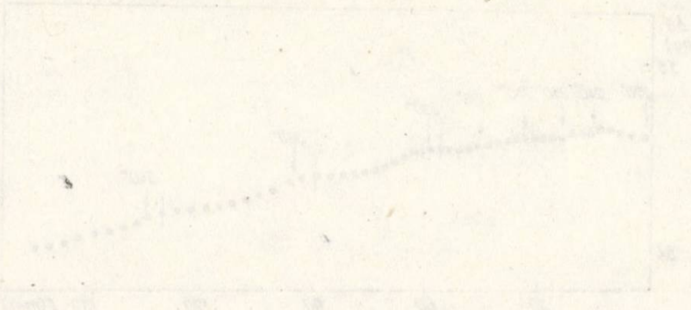

Fig. 5. The change of the weight of the sample at different temperatures

In this experiment, the temperature was consecutively increased each time after the weight remained constant. In Figure 5 the lines indicate the moment when the temperature was risen, while the arrows indicate the moments when the weight remained constant. The behaviour of the catalyst, as indicated in Figure 5, shows that at 240–260°C it is a significant loss of the weight of the sample, as an evidence for the beginning of its interaction with the propylene; below these temperatures the loss of the weight could be due to the outgassing of the sample (the loss of water).

The second jump of the weight is around 310°C; at this temperature the changes in conductance and conversions have been noticed too.

In conclusion our experiments suggest that the propylene starts to interact with the catalyst at 240°C, its effect being much enhanced at 300–310°C.

Two different kinds of interactions can be assigned to these experimental facts. The studies of these interactions are in progress.

REFERENCES

[1] P. Mars and D. W. van Krevelen, Chem. Eng. Sci. Suppl. 3, 41 (1954).
[2] N. I. Ionescu and M. Caldararu, Rev. Roum. Chim. 3, 477 (1978).
[3] N. I. Ionescu, M. Caldararu and P. Hangyal, "Proc. 4th International Symposium Heterogeneous Catalysis, Varna, 1979", Publishing House of the Bulgarian Academy of Sciences, Sofia, 1979, vol. 1, p. 229.
[4] R. Mandru, N. I. Ionescu, M. Caldararu, S. Serban, A. Belea, A. Weidenbecher and A. Rusu, "Proc. 4th International Symposium Heterogeneous Catalysis, Varna, 1979", Publishing House of the Bulgarian Academy of Sciences, Sofia, 1979, vol. 1, 223.
[5] R. Mandru, N. I. Ionescu and M. Caldararu, Z. anorg. Chem. 466, 221 (1980).
[6] M. Caldararu, P. Hangyal and N. I. Ionescu, Rev. Roumaine Chim. (in print).
[7] A. Yamaguchi and Y. Moriyama, J. Jap. Inst. Metals, 28, 592 (1964).
[8] A. Yamaguchi and Y. Moriyama, J. Jap. Inst. Metals 29, 834 (1965).
[9] R. Frety, L. Tournayan and H. Charcosset, Ann. Chim. (France), 9, 341 (1974).
[10] M. Grunze, W. Hirschwald and S. Krebs, Z. phys. Chem. (Frankfurt) 102, 57 (1976).
[11] W. Hirschwald and D. Stanek, Z. phys. Chem. (Frankfurt), 77, 1 (1972).

Revue Roumaine de Chimie, 26, 5, 687–692 (1981)

LATTICE CONSTANT AND SATURATION MAGNETIZATION OF COBALT ZINC FERRITES AND MAGNESIUM ZINC FERRITE

O. S. JOSYULU[a], J.SOBHANADRI[a] and B. VISWANATHAN[b]
[a]Department of Physics
[b]Department of Chemistry, Indian Institute of Technology Madras–600 036, India

Received February 4, 1980

In the present paper the preparation, chemical composition, and magnetic susceptibility of $Co_{1-x}Zn_xFe_2O_4$ (x=0.86, 0.68, 0.51, 0.26) and $Mg_{0.25}Zn_{0.75}Fe_2O_4$ were presented. X-ray diffraction spectrum was taken using CoKα radiation to calculate the lattice constant and the density of these ferrites. Single phase existence of the ferrite was established from the absence of any other extra lines in the diffraction spectrum even to the maximum intensity radiation. Susceptibility measurements were taken using Faraday balance in the field range (1340 G – 8000 G) and in the temperature range (100 K – 300 K). Magnetic moments were calculated and plotted. In the case of $Co_{1-x}Zn_x$ Fe_2O_4 when x is less than 0.5, the magnetic moment increases. When x is greater than 0.5, this starts decreasing and when x reaches 1.0, the magnetic moment reaches a value 0.0. This deviation above x = 0.5 is attributed to the non-collinear spin structure.

INTRODUCTION

Ferrites find intensive applications at microwave frequencies. The usefulness of ferrites is influenced by the physical and chemical properties of the material, which again depends on several factors including the method of preparation. The microstructure which is influenced by the firing time and temperature, the gain structure and the rate of cooling during heat treatment considerably influences the properties. The chemical composition along with the valency of the cations and the oxygen anions present is considered to be an important aspect of the material.

Zinc ferrite ($ZnFe_2O_4$) is a normal ferrite, whereas cobalt ferrite ($CoFe_2O_4$) is an inverse ferrite. Therefore the mixed ferrite $Zn_xCo_{1-x}Fe_2O_4$ (x = 0.0 to 1.0) is an interesting ferrite to study its properties. In the present paper, the chemical composition, the method of preparation and the saturation magnetic moments of $Zn_xCo_{1-x}Fe_2O_4$ (x = 0.86, 0.68, 0.51, 0.26) and $Mg_{0.25}$ $Zn_{0.75}$ Fe_2O_4 are presented.

EXPERIMENTAL

The ferrites were prepared by the conventional double stage sintering process. CoO, ZnO, Fe_2O_3 were mixed together in stoichiometric proportions and preheated in air at 900°C for several hours. The resulting powder was sintered at 1250°C in air for about 9 hours and furnace cooled.

An atomic absorption type Carl-Zeiss spectrometer was used to analyze the major elements. 0.05 g of ferrite material was dissolved in 10 cc of HCl acid. The percentage of elements in the solution of the ferrites was obtained in comparison with the standard solution of the respective elements.

Mass spectrum analysis was also carried out to estimate the major elements as well as minor elements in the sample. The minor elements were found to be less than 1% with respect to iron as 100%.

Using a Faraday balance, the magnetic moment was calculated from the susceptibility measurements. The lattice constants were calculated from the X-ray diffractogram using Co-Kα radiation.

RESULTS

The chemical analysis is done to find the proportions of the elements, considering the comparison to be stoichiometric with respect to oxygen. The mass spectral data are analysed on the basis that iron is 100%. The chemical formulae derived from analysis are found to be in good agreement with the mass spectral data. The chemical formulae together with molecular weights are shown in Table 1.

TABLE 1

Parameters obtained from X-ray analysis and susceptibility measurements

Sample	Chemical formula	Molecular weight	Lattice constant a (Å)	Density g/ml	Magnetic moment (μ B)
CO−1	$Co_{0.14}\ Zn_{0.86}\ Fe_2O_4$	240.1684	8.483	5.32	1.32
CO−2	$Co_{0.32}\ Zn_{0.68}\ Fe_2O_4$	239.0092	8.425	5.31	3.93
CO−3	$Co_{0.49}\ Zn_{0.51}\ Fe_2O_4$	237.9144	8.415	5.303	6.050
CO−4	$Co_{0.74}\ Zn_{0.26}\ Fe_2O_4$	236.3044	8.401	5.294	5.62
MgZn	$Mg_{0.25}\ Zn_{0.75}\ Fe_2O_4$	230,805	8,425	5.127	4.25
	Barium Ferrite				

X-ray diffractogram was recorded to calculate the lattice constant and to establish the existence of single phase of the material. In all Co-Zn ferrites and MgZn ferrite, (3,1,1) line is found to be the most intense one. The relative intensities of the various peaks are calculated. The lattice constant together with the density calculated are also given in Table 1. The variation of lattice constant with zinc concentration is shown in

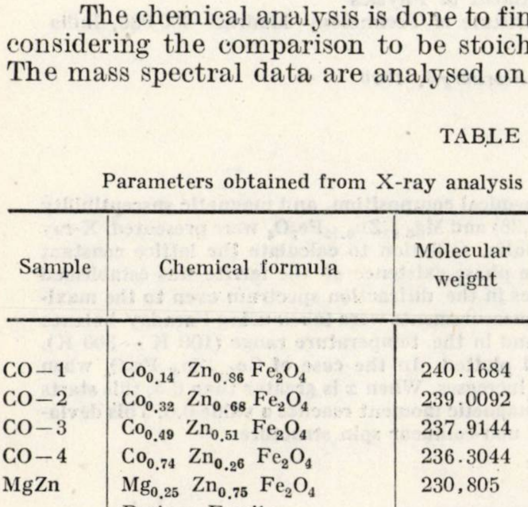

Fig. 1. — Variation of the lattice constant of $Co_{1-x}Zn_xFe_2O_4$ with zinc concentration.

figure 1, which reveals a linear variation with composition. The end values for $ZnFe_2O_4$ and $CoFe_2O_4$ are taken from ASTM tables.

The susceptibility measurements are carried out with a Faraday balance. The susceptibility at room temperature is calculated at various magnetic fields (upto 8000 G) and the magnetization values are calculated. The plots between magnetization and magnetic field are shown in figure 2. A saturation value is reached at high magnetic fields. As the zinc concentration is reducing, the saturation is obtained at higher magnetic fields. When zinc concentration is more than 0.5, the saturation is obtained at lower magnetic fields.

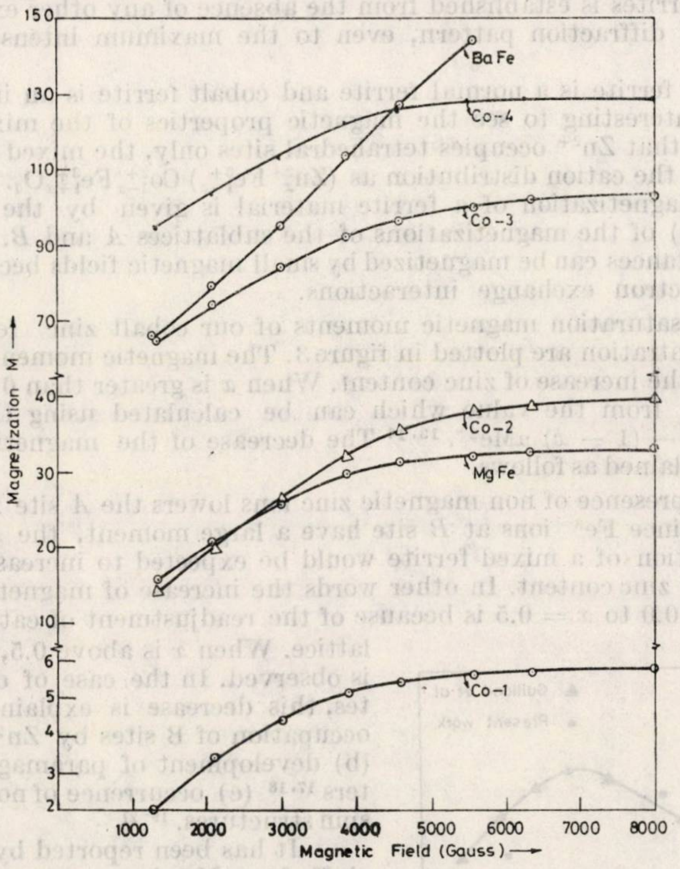

Fig. 2. — Variation of the magnetization of $Co_{1-x}Zn_xFe_2O_4$, $Mg_{0.25}Zn_{0.75}Fe_2O_4$ and barium ferrite with the magnetic field.

DISCUSSION

The lattice constants of the mixed cobalt zinc ferrites are in good agreement with the values obtained from the interpolation of the $CoFe_2O_4$, $ZnFe_2O_4$ values taken from ASTM tables [1] and shown in figure 1. However there are considerable deviations in the lattice constants reported in the literature for cobalt ferrite, zinc ferrite and magnesium ferrite. For zinc ferrite the lattice constant varies from 8.44 Å to 8.416 Å, [2-9] while for cobalt and magnesium ferrites, it varies from 8.36 Å to 8.399 Å [3,5,9,10] and from 8.375 Å to 8.36 Å [11,12] respectively. The single phase nature of these ferrites is established from the absence of any other extra line in the X-ray diffraction pattern, even to the maximum intensity diffraction.

Zinc ferrite is a normal ferrite and cobalt ferrite is an inverse one. So it is interesting to see the magnetic properties of the mixed ferrite. Assuming that Zn^{2+} occupies tetrahedral sites only, the mixed cobalt zinc ferrite has the cation distribution as $(Zn^{2+}_x Fe^{3+}_{1-x})\ Co^{2+}_{1-x} Fe^{3+}_{1+x} O_4$. The spontaneous magnetization of a ferrite material is given by the difference $(M_A - M_B)$ of the magnetizations of the sublattices A and B. Ferromagnetic substances can be magnetized by small magnetic fields because of the strong electron exchange interactions.

The saturation magnetic moments of our cobalt zinc ferrites with zinc concentration are plotted in figure 3. The magnetic moment is increasing with the increase of zinc content. When x is greater than 0.5, it starts decreasing from the value which can be calculated using the relation $M_S = 10x - (1 - x)\ \mu Me^{2+}$. [13,14] The decrease of the magnetic moment can be explained as follows.

The presence of non magnetic zinc ions lowers the A site magnetization and since Fe^{3+} ions at B site have a large moment, the saturation magnetization of a mixed ferrite would be expected to increase with the increase of zinc content. In other words the increase of magnetic moment when $x = 0.0$ to $x = 0.5$ is because of the readjustment of cations in the lattice. When x is above 0.5, a decrease is observed. In the case of other ferrites, this decrease is explained by (a) occupation of B sites by Zn^{2+} ions [15,16] (b) development of paramagnetic clusters [17,18] (c) occurrence of non-collinear spin structures. [19-21]

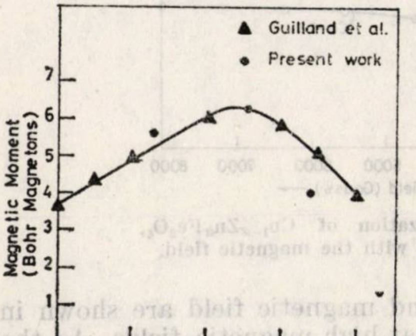

Fig. 3. — Variation of the magnetic moments (in Bohr Magnetons) of $Co_{1-x}Zn_xFe_2O_4$ with zinc concentration.

It has been reported by Petitt et al. [22] from Mossbauer experiments on $Co_{1-x}Zn_xFe_2O_4$ that for $0.4 < x < 1.0$, with the field aligned parallel to the direction of magnetization, the effective field at A site increases and that at B site decreases indicating ferrimagnetic ordering with moments of iron ions at B sites larger than at A sites. Nowik [23,24] also explained the results obtained by Gorter et al. by a single statistical local molecular field model. He also reported for some garnets that when substitution is in octahedral site, canting occurs in tetrahedral site and vice versa. But canting is less in octahedral site when the substitution is in tetrahedral site.

In our system, generally Zn^{2+} prefers the tetrahedral site. So the presence of Zn^{2+} in octahedral site is negligible. As the zinc concentration increases, the substitution at the tetrahedral site increases and the occurrence of non-collinear spin structures — canting — is less. This might be a major factor in reducing the saturation moments above $x = 0.5$ in our system. To understand this further, one has to study the temperature variation of Mossbauer effect which is now under progress.

The magnetic moments of our system at room temperature are in good agreement with the values reported by Guillaud and others.[15, 25, 26] The difference in the value is due to the preparation techniques, grain size and the distribution of cations.[27]

The temperature variation from 100 K to 295 K of the susceptibility at the lowest and the highest concentration of cobalt at the lowest field (1340 G) is shown in figure 4. It is obvious from figure 4 that the Neel temperature cannot be obtained from this temperature range variation, and also it is obvious that Neel temperature is above 300 K for the highest concentration of cobalt. It is reported that above 9 K, $ZnFe_2O_4$ is antiferromagnetic. So a detailed study of the temperature variation from 8 K to 700 K will give the Neel temperature and, the curie points if they are there.

ACKNOWLEDGEMENTS. **One of the authors (O.S.J) gratefully acknowledges the C.S.I.R. (India) for awarding the fellowship.**

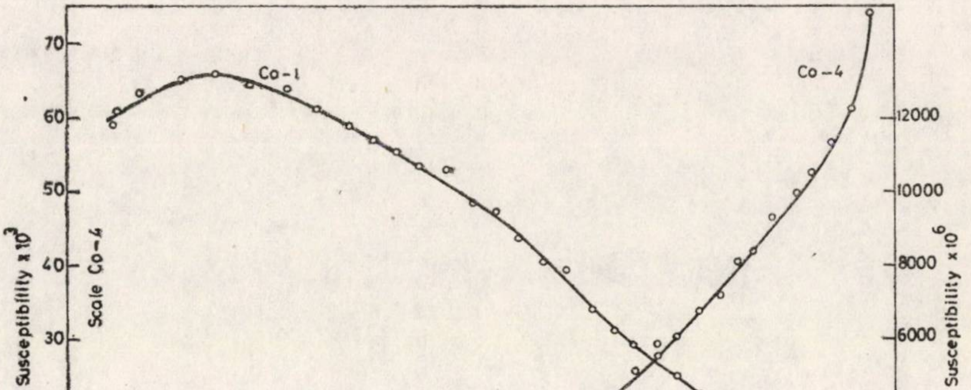

Fig. 4. — Temperature dependence of the susceptibility of Co—1 and Co—4.

REFERENCES

[1] Fink (Six-Entry) Inorganic Index to Powder Diffraction File (1971).
[2] J. M. Hestings and L. M. Corliss, *Rev. Mod Phys.*, **25**, 114 (1953).
[3] E. J. W. Verwey and E. L. Heilmann, *J. Chem. Phys.*, **15**, 174 (1947).
[4] C. Guillaud, *J. Phys. Rad.*, **12**, 239 (1951).
[5] E. W. Gorter, *Phillips, Res. Rep.*, **2**, 321 (1954).
[6] G. Blasse, *Phillips, Res. Rep. Suppl.*, **3** (1964).
[7] G. Blasse, *Phillips, Res. Rept.*, **18**, 383 (1966).
[8] G. Blasse, *J. Phys. Chem. Solids*, **27**, 383 (1966).
[9] F. K. Lotgering, *Phillips. Res. Rept.*, **11**, 190, 337 (1956).
[10] E. Prince and R. G. Treuting, *Acta. Cryst.*, **9**, 1025 (1956).
[11] L. M. Corliss, J. M. Hestings, F. G. Brockman, *Phys. Rev.*, **90**, 1013 (1953).
[12] G. E. Bacon and F. F. Roberts, *Acta. Cryst.*, **6**, 57 (1953).
[13] E. W. Gorter, *Phillips. Res. Reports.*, **9**, 321 (1954).
[14] L. Neel, *Compt. rend.*, **230**, 375 (1950).
[15] G. Guillaud and H. Creveaux, *Compt. rend.*, **230**, 1458 (1950).
[16] E. W. Gortern, *Phillips. Res. Rept.*, **9**, 1 (1954).
[17] Y. Ishikawa, *J. Phys. Soc. Japan*, **17**, 1877 (1962).
[18] M. A. Gilleo, *J. Phys. Chem. Solids*, **13**, 33 (1960).
[19] Y. Yafet and C. Kittel, *Phys. Rev.*, **87**, 290 (1952).
[20] D. H. Lyons, T. A. Kalpan, K. Dwight and N. Menyuk, *Phys. Rev.*, **126**, 540 (1962).
[21] A. Rosencwaig, *Canad. J. Phys.*, **48**, 2857 (1970).
[22] G. A. Petitt and D. W Forester, *Bull. Amer. Phys. Soc.* **15**, 207 (1970).
[23] I. Nowik, *J. Appl. Phys.*, **40**, 872 (1969).
[24] I. Nowik, *J. Appl. Phys.*, **40**, 5184 (1969).
[25] J. Smit and H.P.J. Wijn, 'Ferrites', Phillips Technical Library, 1959.
[26] R. Pautheut, *Ann. Phys. Paris.*, **7**, 710 (1952).
[27] E.J.W. Verway, F. DoBoer and J. H. Van Santen, *J. Chem. Phys.*, **16**, 1091 (1948).

Revue Roumaine de Chimie, 26, 5, 693–698 (1981)

COMPLEX COMPOUNDS OF ZIRCONIUM (IV) WITH AZOMETHINE

ANGELA KRIZA[a] and MARTA NASTA[b]

[a] The Polytechnic Institute of Bucharest, Faculty of Chemical Technology, Splaiul Independenţei 202, Bucharest, Romania

[b] I.C.D., Blvd. Ion Şulea 264, Bucharest, Romania

Received November 4, 1976
Revised June 26, 1980

Six new compounds of tetravalent zirconium with bi- and tridentate azomethine ligands of the ZrOCl(SB) and $ZrO(SB)_2$ type were obtained. Synthesis of the compounds was obtained directly by zirconium oxychloride reaction with Schiff bases, or by Template reaction. The IR spectra were determined in order to establish the nature of the bonds in the complexes derived from zirconium oxychloride.

There are few works in the specialty literature referring to tetravalent zirconium complexes.

Kogan, Sokolov and Osipov synthetized [1] complex compounds of zirconium tetrachloride with benzalaniline, 2-metoxy-benzalaniline, salicylal-*p*-toluidine and salicylal-*p*-nitroaniline of the $ZrCl_4 \cdot 2SBH$ form. Orlova, Garnovski, Osipov and Kukushkina [2] studied the interaction between a wide range of benzal-*o*-aminophenols and zirconium tetrachloride, also obtaining molecular complexes with a donor-acceptor type of bond between azomethine nitrogen and zirconium atom. In 1974 Biradar, Locker and Kulkarni [3] prepared several molecular complexes of zirconyl chloride with Schiff bases derived from salicylaldehyde and aromatic amines.

As far as the chelate compounds of zirconium (IV) are concerned, Pfeiffer and Phitzner [4] studied the complex compounds of zirconium oxychloride with bis-salicylalbenzidine and bis-*p*-methoxysalicylal benzidine and with Schiff bases derivatives, without hydroxy groups in the "*ortho*" position in terms of the carbonyl function.

Macarovici, Perţe and Moţiu [5] obtained internal complexes, starting with zirconyl chloride and bis-acetylacetone ethylenediamine.

A detailed study on the reaction between zirconium isopropoxide and Schiff bases, derived from salicylaldehyde and hydroxyalkylamine, [6] led to the identification of some monomer and polymer chelates. IR spectra lend support to these structures. Subsequently, [7–10] the zirconium oxypropoxide complexes with bi- and trifunctional Schiff bases were obtained.

Other works were published on zirconium chelates with salicylaldoxime and with N, N'bis-(2-hydroxy-naphthilidene)-hexamethyldiamine. [11]

The present paper reports on the results obtained in the synthesis of some new complex zirconium (IV) compounds with bi-and tridentate azomethine ligands starting from hydrated zirconium oxychloride $ZrOCl_2 \cdot 8H_2O$. Two methods were applied for the synthesis of complex zirconium (IV) compounds with Schiff bases: the direct reaction between $ZrOCl_2 \cdot 8H_2O$ and aromatic Schiff bases and the Template reaction. The former led to the formation of two types of compounds, in terms of the azomethine ligand used.

The direct reaction of zirconium oxychloride with aromatic Schiff bases (Table 1) in 1 : 1 or 1 : 2 ratio gave compounds for which the elementary analysis indicated formula $ZrOCl_x(SB)_{2-x}$ (where $x = 0$ or 1). The compounds appear as brightly coloured powders, soluble in alcohol and insoluble in non-polar solvents, except for the compound with salicylal-aminophenol which is only slightly soluble in alcohol and ether and soluble in benzene, carbon tetrachloride, chloroform. Compounds of the ZrOCl(SB) type are less stable in the atmosphere than the $ZrO(SB)_2$ compounds.

Using the second method of synthesis, compounds of the ZrOCl(SB) type were obtained, in which the Schiff base is salicylal-α-aminophenol and salicylal-*m*-toluidine. It is of interest to note that $ZrO(SAPh)_2$ could not be obtained by the Template reaction. Even when the $ZrOCl_2$:SA : APh ratio was = 1 : 2 : 2 where SA = salicylaldehyde; APh = α aminophenol), the same $ZrOCl_2(SAPh)$ compound was obtained.

The analytical data of the compounds obtained are shown in table 2.

The data of the elementary analysis, as well as the way in which the reaction takes place, suggest a chelate structure for the zirconium oxychloride compounds with aromatic Schiff bases of the $ZrOCl_x(SB)_{2-x}$ form (where $x = 0$ or 1).

In order to determine the way in which the Schiff base binds to the metallic atom, the IR spectra of salicylamines and their compounds with zirconium oxychloride were studied.

Valuable information on the nature of the bond between zirconium and the Schiff base was obtained by comparing the frequency of the azomethine and phenoxy groups in the spectra of the compounds and of the ligands. Table 3 gives the comparative vibration frequencies ν(Ph—O) and ν(C=N) in the spectra of the complexes and of the Schiff bases.

In the specialty literature [12] it is shown that in the case of the chelate compounds formed of azomethine ligands with different metallic atoms, the IR spectra present a decrease of ν(C=N) as compared to the ligand spectra, coupled with an increase of ν(Ph—O).

In the case of the synthesized complexes, irrespective of the way in which they are obtained, an increase of ν(Ph—O) is observed in their spectra, as compared to those of the ligands, and a concomitant decrease of ν(C=N) (Table 3).

In the IR spectrum of salicylal-α-aminophenol, i.e. 3 440 cm^{-1} the band characteristic of the free hydroxyl appears. In the vibration spectra of the Schiff bases, derived from salicylaldehyde and *o*- and *m*-toluidine, the absence of the *o*-anisidine and α-aminopyridine band in the 3 200—3 600 cm^{-1} range, characteristic of free hydroxyl, was noted. In the

TABLE 1

Schiff bases

No.	Schiff basis	Notation	Aspect	m.p.or b.p. C/mm Hg	N% calcd.	N% found
1	salicylal-*o*-toluidine	SOT	orange solid	49.5	6.63	6.58
2	salicylal-*m*-toluidine	SMT	yellow liquid (solid)	110/6	6.63	6.60
3	salicylal-*o*-anisidine	SOA	orange solid	59.5	6.12	6.10
4	salicylal-α-aminophenol	SAPh	brick-red solid	184—185	6.17	6.62
5	salicylal-α-aminopyridine	SAPy	orange solid	—	14.14	14.02

TABLE 2

Analytical data on the compounds of the $ZrOCl_x(SB)_{2-x}$ type (where $x = 0$ or 1)

No.	Compound	Colour	Zr%		Cl%		N%		H%		C%	
			calcd.	found	calcd.	found	calcd.	found	calcd.	found	calcd.	found
1	ZrOCl(SOT)	green	25.80	24.57	10.06	10.28	3.96	3.91	3.40	2.99	47.62	47.12
2	ZrOCl(SOA)	dark green	24.73	24.32	9.65	9.23	3.79	3.67			45.29	44.98
3	ZrOCl(SMT)	mustard-yellow	25.80	26.06	10.06	10.15	3.96	3.88	3.40	2.85	47.62	47.85
4	ZrO(SAPh)	orange-yellow	25.71	25.45	—	—	3.94	4.05	2.81	2.98	43.98	44.10
5	$ZrO(SAPh)_2$	orange	17.15	17.28	—	—	5.27	5.40	3.77	3.98	58.73	59.00
6	$ZrO(SAPy)_2$	light brown	18.20	18.02	—	—	5.58	5.42	—	—	57.48	56.99

vibration spectra of the aromatic Schiff bases in the 2 800–3 200 cm^{-1} range, a broad band with a hazy contour appears which, according to the published data [13], corresponds to the valence vibration of the hydroxyl groups chelated by a strong hydrogen bond between nitrogen of the azomethine group and hydrogen of the hydroxyl group. Indeed, within this range, such bonds appear in the vibration spectra of the synthetized Schiff bases used in the present work.

TABLE 3

IR spectra of the compounds and ligands

No.	COMPOUND	$\nu(C=N)$ (cm^{-1})			$\nu(Ph-O)$ (cm^{-1})		
		Ligand	Compound	$\Delta\nu$	Ligand	Compound	$\Delta\nu$
1	ZrOCl(SOT)	1630	1610	−20	1290	1310	+20
2	ZrOCl(SOA)	1630	1615	−15	1290	1310	+20
3	ZrOCl(SMT)	1629	1610	−19	1295	1305	+10
4	ZrOCl(SAPh)	1637	1610	−27	1280	1305	+25
5	$ZrO(SAPh)_2$	1637	1612	−25	1280	1300	+20
6	$ZrO(SAPy)_2$	1620	1670	+50	1285	1310	+25

In the vibration spectra of the compounds with salicylal-*o*-toluidine, *m*-toluidine, *o*-anisidine and aminopyridine in the 3 200–3 600 cm^{-1} range, the free hydroxyl band cannot be observed, an additional argument lending support to the formation of the Ph–O–Zr bond. In the IR spectra of the compounds with salicylal-α-aminophenol there appears at about 3 500 cm^{-1}, a broad band corresponding to the free hydroxyl on the aminophenol nucleus not involved in the bond with zirconium.

On the basis of the spectrum data, a structure of chelate complexes with a tetracoordinated zirconium atoms (I) can be attributed to compounds of the ZrOCl(SB) type. For the $ZrO(SAPh)_2$ compound, the structure of a chelate complex implies coordination 5 for the zirconium atom (II).

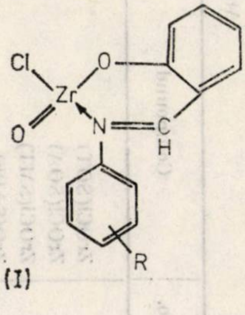

(I)

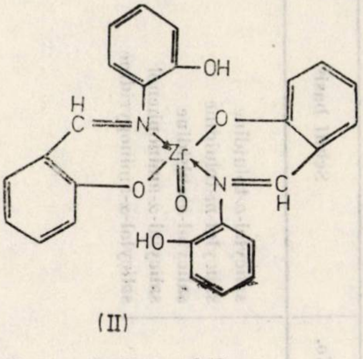

(II)

$R = o-CH_3,\ m-CH_3,\ o-OCH_3,\ o-OH.$

As concerns the $ZrO(SAPy)_2$ compound, two formulas can be proposed: with a penta-and with a heptaccordinated zirconium atom (III and IV).

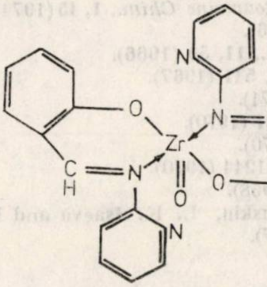

(III)

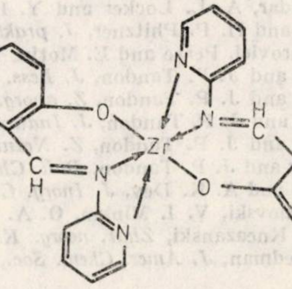

(IV)

In the IR spectra of this compound, ν(Ph—O) shifts by 25 cm^{-1} towards values higher than in the ligand spectrum, indicating the existence of a Zr—O—Ph bond. In contrast to all the other complexes studied, it presents in the IR spectrum a marked increase of ν(C=N) and also a shift towards higher values of the frequency characteristic of the pyridin cycle from 1 580 cm^{-1} to 1 598 cm^{-1}. This, in keeping with the data of Garnovski et al., [12] pleads for the implication of pyridin nitrogen in the formation of the $ZrO(SAPy)_2$ complex.

EXPERIMENTAL

Amines of p.a. purity and salicylic aldehyde purified by distillation, were used for the synthesis of Schiff bases. All the solvents used for the synthesis of the Schiff bases and of the complexes were previously purified and anhydrized.

The aromatic Schiff bases were obtained by mixing 0.1 mol. salicylic aldehyde with 0.1 mol. aromatic anhydride amine in anhydric ethyl alcohol. The mixture was refluxed over a water bath for about 3—4 hours. After partial elimination of the solvent, brightly coloured crystals appeared, which were filtered and purified by recrystallization from ethyl alcohol for SOA, ethanol-water mixture for SAPh and n-butanol for SAPy. Salicylal-*o*-toluidine presents a particular behaviour. After elimination of the reaction medium, a yellow-orange fluid was distilled at 110°C and 6 mm Hg; a slight cooling transformed it into a dark-yellow solid, soluble in the usual organic solvents.

Reaction between $ZrOCl_2 \cdot 8H_2O$ and aromatic Schiff bases. 0.01 mol $ZrOCl_2 \cdot 8H_2O$ were mixed in methyl alcohol with 0.01 or 0.02 mol Schiff bases in ethyl ether. After reflux and removal of the solvent, ethyl ether was added. The different coloured compounds obtained were dried for long intervals in a vacuum desiccator, obtaining solids with a microcrystalline aspect.

The Template reactions were used in order to obtain ZrOCl (SMTo) and ZrOCl(SAPh) compounds. A methanol solution of zirconium oxychloride was mixed with a methanol or ether solution of salicylic aldehyde. The mixture was yellow. Amine was then added to the solution, so as to maintain the 1 :1 :1 ratio between zirconium oxychloride, salicylic aldehyde and aromatic amine. In the case of ZrOCl (SMTo), the reaction medium was ether and in that of ZrOCl(SAPh) the reaction medium was ethyl alcohol. The mixture was refluxed for 1—2 hours in order to reduce the excess solvent. A precipitate was obtained that was filtered under nitrogen and washed with anhydrous ether. A new quantity of the compound could be recovered from the filtrate by adding ethyl ether.

REFERENCES

[1] V. A. Kogan, V. S. Sokolov and O.A. Osipov, *Zhur. neorg. Khim.*, **13**, 2314 (1968).

[2] L. V. Orlova, A. G. Garnovski, O. A. Osipov and I. I. Kukushkina, *Zhur. Obshch. Khim.*, **38**, 1850 (1968).

[3] N. S. Biradar, A. L. Locker and Y. H. Kulkarni, *Rev. Roumaine Chim.*, **1**, 45 (1974).

[4] O. Pfeiffer and H. P. Phitzner, *J. prakt. Chem.*, **5**, 243 (1936).

[5] C. G. Macarovici, Perţe and E. Moţiu, *Rev. Roumaine Chim.*, **11**, 59 (1966).

[6] P. Prashar and J. P. Tandon, *J. Less. Common Metals*, **13**, 541 (1967).

[7] P. Prashar and J. P. Tandon, *Z. anorg. Chem.*, **383**, 81 (1971).

[8] P. Prashar and J. P. Tandon, *J. Indian Chem. Soc.*, **47**, 1081 (1970).

[9] P. Prashar and J. P. Tandon, *Z. Naturforsch.*, **256**, 32 (1970).

[10] P. Prashar and J. P. Tandon, *Bull. Chem. Soc. Japan*, **43**, 1244 (1970).

[11] S. Mandal and A. K. Dey, *J. Inorg. Chem.*, **35**, *12*, 221 (1968).

[12] A. D. Garnovski, V. I. Minkin, O. A. Osipov, V. T. Paniuskin, L. K. Isaeva and M. Kneazanski, *Zhur. neorg. Khim.*, **12**, 2443 (1967).

[13] H. H. Freedman, *J. Amer. Chem. Soc.*, **83**, 2900 (1961).

Revue Roumaine de Chimie, **26**, *5*, 699—703 (1981)

SOME REACTIONS OF 2-[3-(3,4-DICHLOROPHENYL)-2-PYRAZOLIN-5-YL]-4*H*-BENZOXAZIN-4-ONE

E.A. SOLIMAN
Faculty of Science, Ain Shams University, Cairo, Egypt

Received February 28, 1980

2-[3-(3,4-Dichlorophenyl)-2-pyrazolin-5-yl]-4*H*-3,1-benzoxazin-4-one (II) reacts with acetyl chloride, benzoyl chloride, secondary amines as morpholine and piperidine, nitrous acid and bromine to give the corresponding pyrazolines derivatives (III, VI and VII). Fusion of II with aliphatic amines gives the corresponding quinazoline derivative (V), while condensation of (I) with hydroxylamine hydrochloride gives N-phenylpyrazoline VIIIa and isoxazoline derivatives VIIIb respectively.

Recently,[1,2] it has been reported that, 2-[2-(3,4-dichlorophenylvinyl)]-4*H*-3,1-benzoxazin-4-one (I) easily reacts with hydrazine hydrate in boiling ethanol to give 2-[3-(3,4-dichlorophenyl)-2-pyrazolin-5-yl]-4*H*-benzoxazin-4-one (II). The aim of this work is to study the reactivity of the pyrazoline and benzoxazinone ring formed in this reaction.

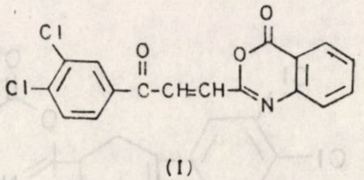

(I)

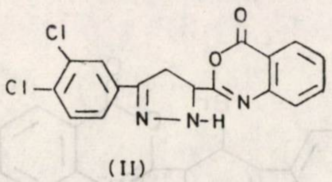

(II)

Acetylation or benzoylation of II using acetyl chloride or benzoyl chloride gives the corresponding 1-acetyl and 1-benzoyl-3-(3,4-dichlorophenyl)-5-(4-oxo-4*H*-3,1-benzoxazin-2-yl)-2-pyrazoline (IIIa and b) respectively.

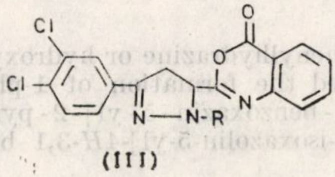

(III)

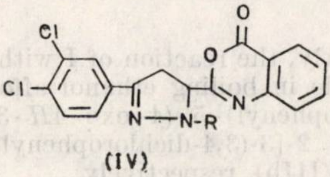

(IV)

IIIa, R = $COCH_3$
b, R = COC_6H_5

IVa, R = NC_4H_8O
b, R = NC_5H_{10}

As a point of interest, cyanoethylation of pyrazoline is not unusual. [3] Thus, treatment of ethanolic solution of pyrazoline II with secondary amines, namely morpholine or piperidine afforded the formation of N-Mannich bases, 2-[3-(3,4-dichlorophenyl)-1-(morpholinomethyl and or piperidinomethyl)-2-pyrazolin-5-yl]-4*H*-3,1-benzoxazin-4-ones (IVa and b) respectively.

On the other hand, the fusion of II with primary amines, namely methylamine, *n*-butylamine, benzylamine or *p*-anisidine at 200°C afforded the formation of 3-methyl, 3-*n*-butyl, 3-benzyl and 3-*p*-anisyl-2-[3-(3,4-dichlorophenyl)-2-pyrazolin-5-yl]-4(3*H*)-quinozolinones (Va-d) respectively.

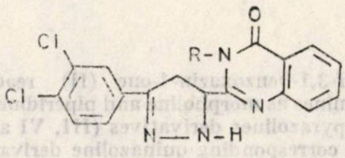

(V)

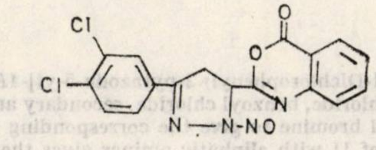

(VI)

a, R = CH_3
b, R = C_4H_9 (*n*)
c, R = $CH_2C_6H_5$
d, R = $C_4H_6OCH_3$ (*p*)

Nitrosation of II afforded the formation of 2-[3-(3,4-dichlorophenyl)-1-nitroso-3-pyrazolin-5-yl]-4*H*-3,1-benzoxazin-4-one (VI).

Bromination of (II) using bromine in chloroform afforded the formation of 2-[4-bromo-3-(3,4-dichlorophenyl)-2-pyrazolin-5-yl]-4*H*-3,1-benzoxazin-4-one (VII).

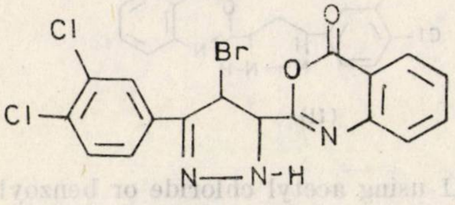

(VII)

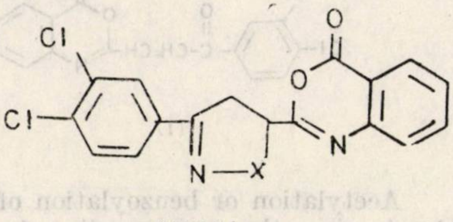

(VIII)

a, X = $N-C_6H_5$
b, X = 0

Similarly, the reaction of I with phenylhydrazine or hydroxylamine hydrochloride in boiling ethanol afforded the formation of 1-phenyl-3-(3,4-dichlorophenyl)-5-(4-oxo-4*H*-3,1-benzoxazin-5-yl]-2-pyrazoline (VIIIa) and 2-[3-(3,4-dichlorophenyl)-2-isoxazolin-5-yl]-4*H*-3,1-benzoxazin-4-one (VIIIb) respectively.

In tables I and II some spectral characteristics of the new compounds are presented.

TABLE 1

Infrared spectra of new compounds (KBr ; cm^{-1})

Compd.	Groups/absorption band				
II	$-C=N$ 1685,1690	$-NH$ 3380	$-C=O$ 1720	$-C=C-$ 1610	
IIIa	$C=N$ 1680	$C=O$ 1700,1720	$C=C$ 1620	CH_2 2890	
IVb	$-C=N$ 1685	$C=O$ 1715	CH_2 2960,2840	$C=C$ 1610	CH_2 2860
Va	$C=N$ 1680	$C=O$ 1715	$-NH$ 3420	$C=C$ 1620	CH_2 2940
Vc	$C=N$ 1695,1685	$C=O$ 1720	$-NH$ 1680	CH_2 2920,2940	$C=C$ 1610
VI	$C=N$ 1690	$C=O$ 1710	$C=C$ 1610	CH_2 2900	
VII	$C=N$ 1695	$C=O$ 1720	$-NH$ 3440	$C=C$ 1620	
VIIIa	$C=N$ 1680	$C=O$ 1720	$-CH_2-$ 2930	$C=C$ 1600	

TABLE 2

^{1}H$-$NMR Spectra of compounds IV, V, VII and VIII

Compd.	ppm	No. of protons	Attribution
IVb	signals at 8.2 ;8.1 ; 7.8 ; 7.5 ; 7.2 signal at 4.2 ; 4.1 signal at 3.3	7 H 4 H 10 H	aromatic protons CH_2 piperidine ring
Va	signals at 7.8 ; 7.3 ; 7.1 ; 6.8 ; 6.6 signal at 4.8 signal at 3.4	7 H 1 H 3 H	aromatic protons NH CH_3
VII	multiplet centred at 7.3 signal at 4.7 signal at 2.3	7 H 1 H 1 H	aromatic protons NH CH
VIII	multiplet at 6.6$-$7.4 signal at 2.4	12 H 2 H	aromatic protons CH_2

TABLE 3

The pyrazoline, quinazolinone and isoxazoline derivatives II–VII

Compd.	m.p. (°C) yield (%)	Colour	Solvent of crystn. *	Formula	Analysis %		
						Found	Requd.
IIIa	145	Colourless	A	$C_{19}H_{12}N_3O_3Cl_2$	C	56.22	56.85
	(80)				H	2.75	2.99
					N	10.20	10.47
					Cl	17.37	17.70
IIIb	221	Colourless	B	$C_{24}H_{14}N_3O_4Cl_2$	C	59.80	60.12
	(70)				H	2.77	2.92
					N	8.24	8.76
					Cl	14.50	14.82
IVa	162	Colourless	E	$C_{22}H_{19}N_4O_3Cl_2$	C	56.82	57.64
	(85)				H	3.95	4.14
					N	11.74	12.22
IVb	198	Colourless	E	$C_{23}H_{21}N_4O_2Cl_2$	C	60.40	60.52
	(60)				H	4.25	4.60
					N	11.98	12.28
Va	138	Colourless	B	$C_{18}H_{13}N_4OCl_2$	C	57.16	58.06
	(75)				H	3.50	3.49
					N	14.56	15.05
					Cl	18.82	19.08
Vb	216	Colourless	E	$C_{21}H_{19}N_4OCl_2$	C	60.11	60.86
	(90)				H	4.32	4.58
					N	13.04	13.52
Vc	158	Yellow	E	$C_{24}H_{17}N_4OCl_2$	C	58.40	59.01
	(60)				H	2.99	3.48
					N	11.34	11.47
Vd	191	Yellow	B	$C_{24}H_{17}N_4O_2Cl_2$	C	57.66	58.29
	(40)				H	2.95	3.44
					N	10.86	11.33
VI	187	Colourless	B/E	$C_{17}H_9N_4O_3Cl_2$	C	52.15	52.57
	(65)				H	2.24	2.31
					N	13.74	14.43
VII	167	Colourless	E	$C_{17}H_9N_3O_2Cl_2Br$	C	46.00	46.52
	(60)				H	1.97	2.05
					N	9.22	9.58
					Br	17.90	18.56
VIIIa	201	Yellow	B	$C_{23}H_{15}N_3O_2Cl_2$	C	62.67	63.30
	(75)				H	3.00	3.44
					N	9.15	9.63
					Cl	15.60	16.28
VIIIb	161	Colourless	E	$C_{17}H_9N_2O_3Cl_2$	C	56.40	56.66
	(70)				H	2.22	2.50
					N	7.51	7.77

* A = Acetic acid, B = Benzene, E = Ethanol.

EXPERIMENTAL

The infrared absorption spectra were determined with an Unicam SP 1200 Spectrophotometer using KBe Wafer technique. All melting points are not corrected. The ^{1}H–NMR spectra were determined with a VN S–60 T spectrometer.

Reaction of II with acetyl chloride and benzoyl chloride; Formation of IIIa and b

A solution of pyrazoline II (0.01 mole) in 20 ml of acetyl or benzoyl chloride was refluxed over a steam bath for 4 hrs, then poured into cold water. The solid product obtained was crystallized from a proper solvent to give the corresponding acetyl and benzoyl derivatives IIIa and IIIb respectively (cf. Table 3).

Reaction of II with secondary amines; Formation of Mannich-bases IVa and b

A mixture of II (0.01 mole), morpholine or piperidine (0.01 mole) and 20 ml ethanol was refluxed for 6 hrs. The solid product obtained after evaporation of most of the solvent and cooling was crystallized from ethanol to give the corresponding N-Mannich bases IVa and IVb respectively (cf. Table 3).

Fusion of II with primary amines; Formation of quinazolinones Va-d

A mixture of II (0.01 mole) and primary amines, namely : methyl amine, *n*-butyl amine, benzyl amine and/or *p*-anisidine (0.01 mole) was heated in an oil bath at 200°C for 10 hrs. The oily product obtained was triturated with light petrol (b. p. 80–100°C) to give a solid compound which was crystallized from a proper solvent to give the corresponding quinazolinones derivatives Va-d respectively (cf. Table 3).

Nitrosation of II; Formation of VI

A solution of pyrazoline II (0.01 mole) in hydrochloric acid (10 ml) was heated with a solution of sodium nitrite (0.03 mole) in water (3 ml). The reaction mixture was heated on a water bath for one hr., the solution was then poured into ice and the solid separated was crystallized from a mixture of benzene and ethanol to give the corresponding N-nitrose derivative VI as pale yellow crystals (cf. Table 3).

Bromination of II; Formation of VII

A solution of pyrazoline II (0.01 mole) in chloroform (20 ml) was treated with a solution of bromine (0.03 mole) in chloroform (20 ml). The solid product obtained after complete addition of bromine and evaporation of the chloroform was crystallized from benzene to give the bromopyrazoline derivative VII (cf. Table 3).

Condensation of I with phenylhydrazine and hydroxylamine hydrochloride; Formation of VIIIa and b

A solution of I (0.01 mole), phenylhydrazine or hydroxylamine hydrochloride (0.01 mole) and ethanol (20 ml) was refluxed for 6 hrs. The solid product obtained after evaporation of most of the solvent was crystallized from a proper solvent to give the corresponding N-phenylpyrazoline and isoxazoline derivatives VIIIa and VIIIb respectively (cf. Table 3).

REFERENCES

[1] E. A. Soliman and G. Hosni, *Indian J. of Chem.*, **16 B**, 884 (1978).

[2] E. A. Soliman, *Rev. Roumaine Chim.*, **23**, 1597 (1978).

[3] A. A. Afify, G. Hosni and S. Shafiek, *Rev. Roumaine Chim.*, **23**, 1541 (1978).

Revue Roumaine de Chimie, 26, 5, 705—715 (1981)

STUDY AND TRANSFORMATIONS OF THE CONDENSATION PRODUCTS OF ISOPROPYLIDENE-D-GLYCERALDEHYDE WITH ACTIVE METHYLENES

J. SÁNCHEZ BALLESTEROS, F. HERNANDEZ HERNANDEZ and D. J. McPHEE
Department of Organic Chemistry, Faculty of Sciences, University of Málaga, Spain

Received February 20, 1980

The reaction of 2,3-O-isopropylidene-D-glyceraldehyde(I) with active methylenes, in the presence of basic catalysts, affords mixtures of unsaturated isomers : one with α, β unsaturated structure (III), another with β, γ unsaturated structure (IV). When the methylene compounds are keto derivatives, as well as the condensation products III and IV, a third enolic isomer (V) appears, and may be isolated pure when the reaction between I and the ketonic methylene is catalysed by triethanolamine or when III and IV are treated with triethylamine or with a partially neutralised cationic resin. Acid catalysis of V, in aprotic conditions, leads quantitatively to ketospiro structures (VIII), as a result of an intramolecular cyclisation. By prolonged treatment of VIII with acid in aprotic conditions, dispiro structures (IX) are obtained. Hydrolytic cleavage of VIII affords γ-diketones (XII and XIII), which in the presence of Lewis acids easily cyclise to give furanic structures.

INTRODUCTION AND DISCUSSION

The reaction of 2,3-0-isopropylidene-D-glyceraldehyde (I) with active methylenes in the absence of catalysts leads, by addition of the methylene to the carbonyl group of the sugar, to hydroxylated addition products.[1,2] When the reaction takes place in the presence of basic catalysts (pyridine, piperidine or diethylamine) unsaturated products are obtained, which may also be prepared by crotonisation of the previously mentioned addition products. Three types of unsaturated isomers have been described in the condensation reactions of I with active methylene compounds: those corresponding to structures III, IV and V, although the abundance of the different isomers in these mixtures depends on the methylene employed and the conditions in which the reaction is effected.

Thus, in the reactions of I with malondiamide (IIg) and cyanoacetamide (IIe) a sole condensation product is isolated, whose analytical and spectroscopic data indicate an α, β unsaturated amide structure (IIIg and IIIe respectively). Similarly, the condensation of I with freshly prepared acetoacetic acid (IId) affords, via a decarboxylative elimination reaction, an α, β unsaturated ketone (VIh). On the other hand, in the condensation of I with the ethyl cyanoacetate (IIf) a sole condesation product is isolated, corresponding in this case to a β, γ unsaturated ester nitrile (IVf).

When one of the methylene groups is a ketonic group, a greater variety of condensation products is observed : in the reaction of I with

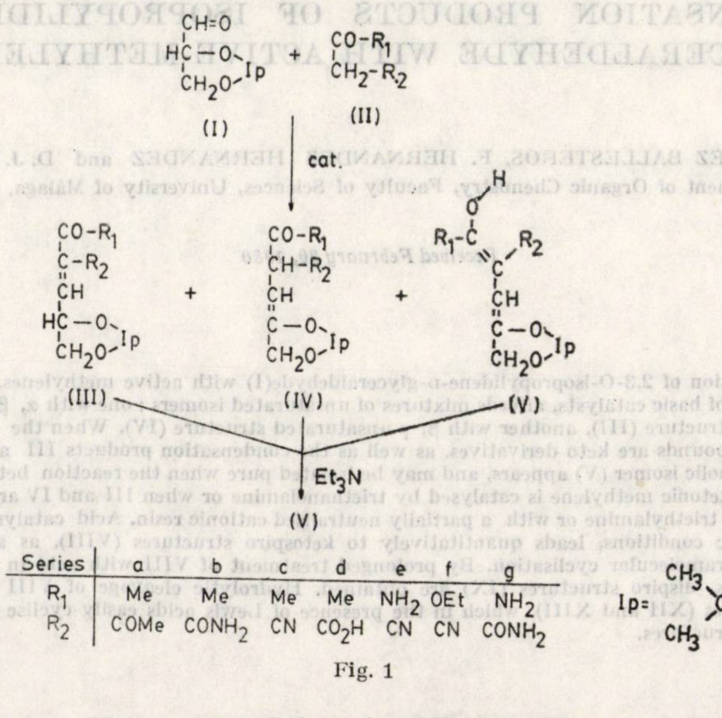
CH=O
HC—O
CH₂O
Ip
+
CO-R₁
CH₂-R₂
(I)
(II)
cat.
CO-R₁
C-R₂
CH
HC—O
CH₂O
Ip
(III)
+
CO-R₁
CH-R₂
CH
C—O
CH₂O
Ip
(IV)
+
H
O
R₁-C
R₂
C
CH
C—O
CH₂O
Ip
(V)
Et₃N
(V)
Series a b c d e f g
R₁ Me Me Me Me NH₂ OEt NH₂
R₂ COMe CONH₂ CN CO₂H CN CN CONH₂
Ip=
CH₃
C
CH₃

Fig. 1

acetylacetone (IIa), catalysed by piperidine, a mixture of isomers IIIa and Va was found, in 1 :1 proportion. Refluxing this mixture with triethylamine or treating it with a partially neutralised cationic resin affords isomerization of IIIa to Va. When acetylacetamide (IIb) or acetylacetonitrile (IIc) are used as methylenes in the reaction with I, catalysed by piperidine or diethylamine, a mixture of three unsaturated isomers III, IV and V is obtained. In both cases treatment of these mixtures with triethylamine produces isomerization of III and IV to V. In the reaction of I with IIa, IIb or IIc, when triethanolamine is used as catalyst, a sole condensation product, which corresponds to the enolic isomer V, is isolated. The signals of vinyl protons [δ 6.6(d,^{3}J 6Hz) for the α, β unsaturated product IIIa ; 5.3 (t, ^{4}J 1.2 Hz) for the enolic isomer Va and 5.1 (dt, ^{3}J 12 ; ^{4}J 1.2 Hz) for the β, γ-unsaturated product IVf] were important in the interpretation of the ^{1}H—NMR spectra of mixtures.

It is worth mentioning that in the reaction of I with IId the *trans* configuration of the condensation product VIh has been determined. For this purpose we proceeded to degrade VIh to fumaric acid (X).

Haloform reaction of VIh affords the acid VIk, which may also be prepared by alkaline hydrolysis of IIIe or IIIg, or directly by condensation of I with malonic acid. Treatment of VIk with aqueous acetic acid gives *trans*-4,5-dihydroxypenten-2-oic acid (VIIk) via hydrolysis of the acetal group. This acid may also be prepared from VIh using a different route: acid hydrolysis to give VIIh and afterwards a haloform reaction to afford VIIk. Treatment of VIIk with lead tetraacetate yields *trans*-butenal-oic acid (IX), which in turn forms a crystalline semicarbazone with semicarbazide hydrochloride. Subsequent oxidation of IX with humid silver oxide leads to fumaric acid (X).

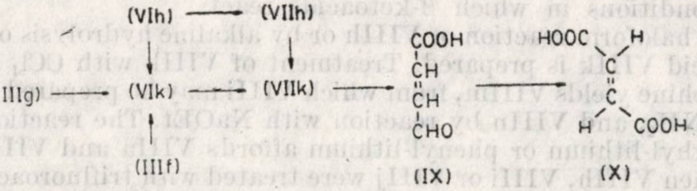

Fig. 2

By acid catalysis of V, substance VIII is obtained. The formation of VIII involves a process subsequent to the Knoevenagel reaction. From the type of catalysis and structural change, the formation of VIII can be considered to involve an intramolecular addition to a vinyl ether. The participation of the electron-releasing oxygen atom may be the reason why this type of compound is not a product of a normal Knoevenagel reaction. The structure of VIII is indicated by spectroscopic data: the two diastereotopic hydrogens in the dioxolane ring appear as AB systems in the ^{1}H—NMR spectra (in $CDCl_3$ or CCl_4), but those in the dihydrofuran moiety are accidentally equivalent and long-range coupled to Me-2. The diastereotopic character could be clearly observed in benzene solution. In the IR spectra only a carbonyl stretching band was observed for VIIIh and VIIIi and none for VIIIj. Other proof that supports the proposed struc-

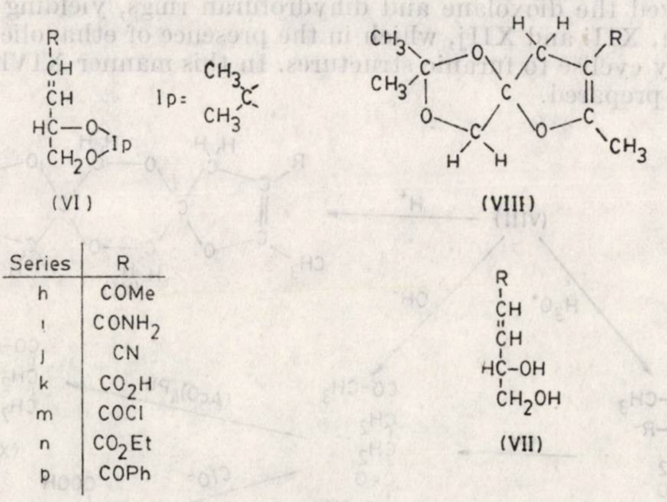

Series	R
h	COMe
i	$CONH_2$
j	CN
k	CO_2H
m	COCl
n	CO_2Et
p	COPh

Fig. 3

ture is the negative enol assay of VIIIh and VIIIi, the negative haloform assay of VIIIi and and VIIIj, the formation of one monosemicarbazone from VIIIh and none from VIIIi and VIIIj, the oxidation of methyl ketone in VIIIh, the basic hydrolysis of carbamide and nitrile groups in VIIIi and VIIIj respectively, to yield an acid which did not decarboxylate under conditions in which β-ketoacids react.

By haloform reaction of VIIIh or by alkaline hydrolysis of VIIIi and VIIIj, acid VIIIk is prepared. Treatment of VIIIk with CCl_4 and triphenylphosphine yields VIIIm, from which VIIIi may be prepared by reaction with $NaNH_2$, and VIIIn by reaction with NaOEt. The reaction of VIIIk with methyl-lithium or phenyl-lithium affords VIIIa and VIIIp respectively. When VIIIh, VIIIi or VIIIj were treated with trifluoroacetic acid or boron trifluoride in an aprotic solvent under more drastic conditions, acetone was removed and a new type of product was formed, for which spectroscopic data indicated the structures XIh, XIi and XIj respectively. The ^1H-NMR spectra were also similar to those of VIII, except for the signals of the CMe_2 group, which in the spectra of XI have disappeared. An X-ray crystal structure determination indicates that the products have a centrosymmetrical *trans* configuration, in accordance with the fragmentations given by their mass spectra.

Acid hydrolysis of VIIIh, VIIIi and VIIIj, in mild conditions, partially cleaved the dioxolane and dihydrofuran rings, yielding the γ-diketones XIIh, XIIi and XIIj, which in the presence of ethanolic or aqueous $ZnCl_2$ easily cyclise to furanic structures. In this manner XIVh, XIVi and XIVj are prepared.

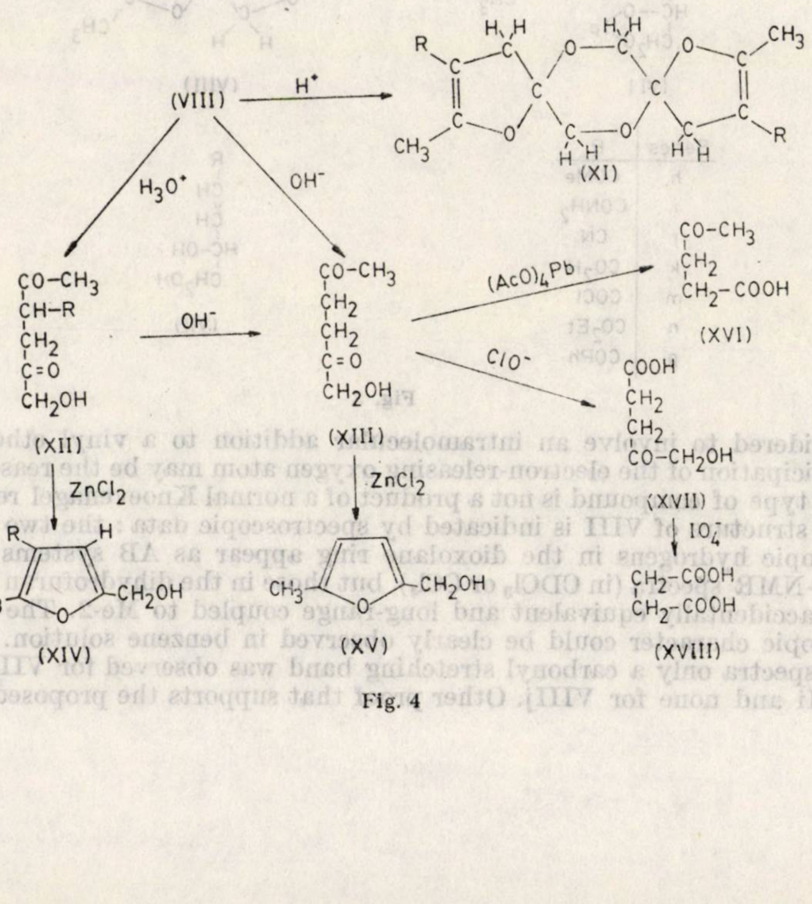

Fig. 4

Alkaline hydrolysis, under reflux, of VIIIh, VIIIi, VIIIj and VIIIk partially cleaved the dihydrofuran and dioxolane rings to afford 1-hydroxyhexane-2,5-dione (XIII), which may also be prepared from VIIIi and VIIIk by acid hydrolysis at 100°C. When acid hydrolysis of VIIIk is effected with aqueous $ZnCl_2$ then 5-hydroxymethyl-2 methyl-furan (XV) is obtained. The same product is prepared in better yield from XIII in the same conditions. $Pb(OAc)_4$-oxidation of XIII yielded levulinic acid, while its haloform reaction gave XVII, which in turn afforded succinic acid by periodate oxidation.

EXPERIMENTAL

General Methods

Melting points are uncorrected. IR spectra (KBr disks) were obtained with a Beckman Aculab IV or a Perkin-Elmer mod. 121 spectrometer. ^{1}H-NMR spectra were recorded for CCl_4 solutions (internal TMS) with a Perkin-Elmer-Hitachi R-20B or a Perkin-Elmer R-24B spectrometer. Chemical shifts (first order) are given on the δ scale and first-order couplings in Hz. Concentration of solutions was performed under diminished pressure at temperatures under 40°C using a rotary evaporator.

2,3-O-Isopropylidene-D-glyceraldehyde (I). — Prepared as in [3]. *Acetylacetamide (IIb).* — Prepared as in [4]. *Acetylacetonitrile (IIc).* — Prepared as in [5]. *Acetoacetic acid (IId).* — Prepared as in [6].

Condensation of I with acetylacetone (IIa). — When 15.5 g of I, 12 g of IIa, 6 drops of piperidine and 180 ml of ether were mixed, the temperature rose to 50°C. The mixture was kept in the dark for 12 hrs, then distilled to yield 22 g of a mixture of isomers IIIa and Va (55%), b. p. 96–97°C/0.1 Torr. NMR indicated an almost equimolar mixture of isomers which had $\bar{\nu}_{max}^{film}$ 3450, 2980, 2925, 2860, 1692, 1670, 1665, 1610–1580, 1450, 1410, 1370, 1350, 1315, 1255, 1205, 1150, 1115, 1050 and 885 cm^{-1}. ^{1}H–NMR data : i) α, β *unsaturated isomer IIIa* : δ 6.6(d,1H,J 6Hz, = CH), 4.58 (d, 2H, J 6Hz, dioxolane CH_2), 4.5–3.5 (m, unresolved), 2.32 (s, 3H, Ac), 2.16 (s, 3H, Ac) and 1.3 (6H, CMe_2) ; ii) *enolic isomer Va* : δ 13.6 (s, 1H,OH), 5.3 (t, 1H, J 1.2Hz, = CH), 4.3 (d,2H, J 1.2Hz, dioxolane CH_2), 2.08 (s, 3H, Ac), 2.04 (s, 3H, enol Me) and 1.4(6H, CMe_2). Irradiation showed coupling between the signals at 5.3 and 4.3. Anal. calc. for $C_{11}H_{16}O_4$: C, 62.26 ; H, 7.54. Found : C, 61.98 ; H, 7.41%. The previous condensation was repeated using triethanolamine as solvent and catalyst (35 ml per mole of aldehyde), yielding Va directly.

Isomerization of IIIa to Va. — a) *using triethylamine* : To a solution of 6 g of III a and Va in 18 ml of carbon tetrachloride, 3 ml of triethylamine was added and the mixture was kept under reflux for 3 hrs. Solvent was eliminated and the residue distilled to yield 5.7 g of Va, b. p. 100–101°C/0.2 Torr ; b) *using cationic resin* : 20 g of Lewatit S-100 resin was partially neutralised by stirring for 3 days with aqueous sodium hydroxide (20–40 mequiv.) and then dried over calcium chloride. A solution of 8 g of the mixture of IIIa and Va in 40 ml of carbon tetrachloride was shaken with 16 g of the neutralised resin until the NMR signals of IIIa disappeared. The catalyst was then removed and the filtrate was concentrated under diminished pressure to give Va, which gave a positive enol test with ferric chloride and had $\bar{\nu}_{max}^{film}$ 3450, 2980, 2930, 2880, 1680, 1620, 1600, 1450, 1420, 1370, 1240, 1210, 1180, 1150, 1120 and 1060 cm^{-1}.

DL-*8-Acetyl-2,2,7-trimethyl-1,3,6-trioxaspiro (4,4) non-7-ene (VIIIh).* — A solution of 8 g of Va and 0.5 ml of trifluoroacetic acid in 40 ml of CCl_4 was heated at 40°C for 8 hrs then neutralised by shaking with saturated aqueous sodium hydrogen carbonate, dried (Na_2SO_4) and concentrated. The residue was distilled, affording 3.6 g of VIIIh (45%), b.p. 71–73°C/0.5 Torr (negative enol test). λ_{max}^{EtOH} 271nm (ε 1.04 × 10^5). $\bar{\nu}_{max}^{film}$ 2980, 2920, 2860, 1670, 1625–1595, 1450, 1433, 1418, 1380, 1365, 1270, 1230, 1218, 1145, 1080, 1060, 1040, 965, 890, 840, 795 and 750 cm^{-1}. ^{1}H-NMR data (CCl_4) : δ 4.18 and 3.88 (2d, 2H, J 9Hz, dioxolane CH_2), 3.0 (q, 2H, J 1.8Hz, dihydrofuran CH_2), 2.25 (t, 3H, J 1. 8Hz, Me), 2.1 (s, 3H, Ac), 1.5 and 1.4 (2s, 6H, CMe_2). Mass spectrum : m/e 212(M*), 197 (M-Me), 169 (M-Ac), 154 (M-$COMe_2$), 139 (154-Me), 137 (154-OH), 123(154-CH_2OH), 111(154-Ac), 95(154-$COCH_2OH$) and 43 (Ac).

Anal. calc. for $C_{11}H_{16}O_4$: C, 62.66 ; H, 7.54. Found : C, 62.42 ; H,75 %. The semicarbazone of VIIIh (78 %) had m.p. 255—256°C (from ethanol-water 1 :1). Anal. calc. for $C_{12}H_{19}N_3O_4$:C, 53.53 ; H, 7.06 ; N, 5.61. Found : C, 53.60 ; H, 6.98 ; N, 5.60 %.

Trans-3,11-diacetyl-2,10-dimethyl-1,6,9,13-tetraoxadispiro (4,2,4,2) tetradeca-2,10-diene (XIh). — A solution of 4 g of VIIIh in 40 ml of 10 % trifluoroacetic acid in CCl_4 was heated at 90°C for 12 hrs. The solid formed was collected and recrystallised from CCl_4 to yield 1.7 g of XIh (46 %), m.p. 119—120°C. $\lambda_{max}^{CHCl^3}$ 268 nm (ε 2×10^4). $\bar{\nu}_{max}^{KBr}$ 2978, 2930, 1730, 1665, 1620, 1450, 1430, 1375, 1250, 1210, 1155, 1115 and 1060 cm^{-1}. ^{1}H-NMR data ($CDCl_3$) : δ4.21 and 3.71 (2d, 4H, J 12Hz, H-7,14), 2.8 (q,4H, J 1.6Hz, H-4,12), 2.27 (t, 6H, J 1. 6Hz, 2Me) and 2.2 (s, 6H, 2Ac). Mass spectrum : m/e 308 (M*), 293 (M-Me), 265(M-Ac), 153 (M-$C_8H_9O_2$—H_2O), 138 ($C_8H_{10}O_2$), 43 (Ac, 100 %) and (15 Me). Anal. calc. for $C_{16}H_{20}O_6$: C, 56.47 ; H, 5.88. Found : C, 56.31 ; H, 6.02 %.

Condensation of I with IIb. — To a solution of 21 g of I and 16.95 g of IIb in 20 ml of pyridine 6 drops of piperidine were added. Evolution of heat was observed. The solution was kept in darkness for 12 hrs then heated at 100°C for 30 min. before being concentrated from dioxane to yield 18 g (52 %) of a product with m.p. 82—85°C, that appeared to be a mixture of the following isomers : $\bar{\nu}_{max}^{KBr}$ (mixture) 3450, 3380, 3320, 2980, 2910, 2870, 1700, 1670, 1665, 1620—1590, 1450, 1420, 1380, 1355, 1318, 1260, 1230, 1200, 1119, 1060 and 885 cm^{-1}. ^{1}H-NMR data ($CDCl_3$) : i) α, β *unsaturated ketoamide IIIb* : δ 6.8 (d, 1H, J 6Hz, = CH), 5.46 (broad, exchangeable with D_2O, 2H, NH_2), 4.62 (d, 2H, J 6Hz, dioxolane CH_2), 4.55—3.5 (m, unresolved), 2.30 (s, 3H, Ac), 1.58 and 1.43 (2s, 6H, CMe_2) ; ii) β, γ *unsaturated ketoamide IVb* : δ 5.46 (broad, exchangeable with D_2O, 2H, NH_2), 5.2—4.7 (m,1 H, vinyl ether = CH), 4.49 (d, 2H, J 2Hz, dioxolane CH_2), 2.15 (s, 3H, Ac), 1.55 and 1.45 (2s, 6H, CMe_2) ; iii) *enol Vb* : its signals were those of the pure sample described below. Anal. (of the mixture of isomers). Calc. for $C_{10}H_{15}O_4N$: C, 56.34 ; H, 7.04 ; N, 6.57. Found : C, 56.61 ; H, 7.21 ; N, 6.82 %.

Isomerization of IIIb and IVb to Vb. — a) *using triethanolamine* : The previous condensation was repeated using triethanolamine as solvent and catalyst (35 ml per mole of aldehyde). A solid, which washed with cold dioxane and dried has a m.p. 85—87°C was obtained. It gave a positive enol test with ferric chloride and had $\bar{\nu}_{max}^{KBr}$ 3450, 3380, 3320, 2980, 2910, 2870, 1685, 1625, 1600, 1450, 1420, 1380, 1260, 1200, 1183, 1120 and 1060 cm^{-1}. ^{1}H-NMR data ($CDCl_3$) : δ 13.0 (s, 1H, OH), 5.46 (broad, exchangeable with D_2O, 2H, NH_2), 5.32 (t, 1H, J 1.2Hz, = CH), 4.33 (d, 2H, J 1.2 Hz, dioxolane CH_2), 2.12 (s, 3H, enol Me), 1.55 and 1.45 (2s, 6H, CMe_2). Irradiation showed coupling between the signals at 5.32 and 4.33 b) *using triethylamine* : To a solution of 5 g, the mixture of IIIb, IVb and Vb in 25 ml of CCl_4 2.8 ml of triethylamine was added and the mixture was refluxed for 3 hrs. The solvent was then eliminated, leaving a solid which was washed with dioxane and dried. Its analytical data coincide with those of Vb.

DL-8-Carbamyl-2,2,7-trimethyl-1,3,6-trioxaspiro (4,4) non-7-ene(VIIIi). — A solution of 9 g of Vb and 6 ml of acetic acid in 54 ml of CCl_4 was refluxed for 1 hr then neutralised by shaking with saturated aqueous sodium hydrogen carbonate, dried (Na_2SO_4) and concentrated. The residue washed with cold water and recrystallised from ethanol-water yielded 6.75 g (75 %) of VIIIi, m.p. 161—162°C. λ_{max}^{EtOH} 246 nm (ε 1.1×10^4). $\bar{\nu}_{max}^{KBr}$ 3415, 3170, 2980, 2940, 1655, 1590, 1445, 1370, 1320, 1280, 1255, 1212, 1160, 1115, 1085, 1060, 1025, 960, 895, 840 and 760 cm^{-1}. ^{1}H-NMR data ($CDCl_3$) : δ 5.37 (broad, exchangeable with D_2O, 2H, NH_2), 4.31 and 3.97 (2d, 2H, J 8.5Hz, dioxolane CH_2), 3.0 (q, 2H, J 1.8Hz, dihydrofuran CH_2), 2.27 (t, 3H, J 1.8Hz, Me), 1.56 and 1.44 (2s, 6H, CMe_2). Mass spectrum : m/e 213 (M*), 198 (M-Me), 170 (M-Ac), 169 (M-$CONH_2$), 155 (M-$COMe_2$), 144 (155-Me), 112(155-Ac), 111(155-$CONH_2$), 44($CONH_2$), 43(Ac) and 15 (Me). Anal. calc. for $C_{10}H_{15}NO_4$: C, 56.34 ; H, 7.04 ; N, 6.57. Found : C, 56.27 ; H, 6.83 ; N, 6.57 %.

Trans-3,11-dicarbamyl-2,10-dimethyl-1,6,9,13-tetraoxadispiro (4, 2, 4, 2) tetradeca-2,10-diene (XIi). — Following a method similar to that described above for XIh, 6 g of VIIIi were converted into 2.9 g of XIi (47 %), m.p. 172—173. $\lambda_{max}^{CHCl_3}$ 246 nm (ε 1.9×10^4). $\bar{\nu}_{max}^{KBr}$ 3420, 3200, 2990, 2930, 1675, 1650, 1440, 1415, 1380, 1245, 1200, 1160, 1100, 1050 and 860 cm^{-1}. ^{1}H-NMR data ($CDCl_3$) :δ 5.45 (broad, 4H, 2NH_2), 4.25 and 3.75 (2d, 4H, J 12. 2Hz, H-7, 14), 2.9 (q, 4H, J 1.8Hz, H-4,12) and 2.31 (t, 6H, J 1.8Hz, 2Me). Mass spectrum : m/e 310 (M*), 295 (M-Me), 266 (M-$CONH_2$), 154 (M-$C_7H_3O_2N$—H_2O), 139($C_7H_9O_2N$), 138($C_7H_8O_2N$), 44($CONH_2$) and 43(Ac). Anal. calc for $C_{14}H_{18}O_6N_2$: C, 54.19 ; H, 5.81 ; N, 9.03. Found : C, 54.31 ; H, 6.02 ; N, 8.92 %.

Reaction of I with acetylacetonitrile (IIc). — This reaction was accomplished as described above for IIb, starting from 18 g of I, 11.8 g of IIc, 6 drops of piperidine and 120 ml of toluene to give 18.6 g of a mixture of isomers IIIc, IVc, and Vc (65 %), b.p. 90—92°C/0.1 Torr. Positive, enol test with ferric chloride. $\bar{\nu}_{max}^{film}$ 3450, 2990, 2920, 2870, 2870, 2360, 1690, 1670, 1630—1580, 1550, 1500, 1480, 1440, 1380, 1320, 1250, 1200, 1160, 1105, 1080, 980 and 850 cm^{-1}. ^{1}H-NMR data ($CDCl_3$) : i) α, β *unsaturated isomer IIIc* : δ 6.72 (d, 1H, J 6Hz, =CH), 4.6—4.45 (m, 2H, dioxolane CH_2), 4.5—3.3 (m, unresolved), 2.33 (s, 3H, Ac), 1.52 and 1.43 (2s, 6H, CMe_2) ii) β, γ *unsaturated isomer IVc* : δ 5.1—4.8 (m, 1H, vinyl ether = CH), 4.6—4.45 (m, 2H, dioxolane CH_2), 2.20 (s, 3H, Ac), 1.48 and 1.42 (2s, 6H, CMe_2). iii) *enol isomer Vc* : δ 12.0 (s, 1H, OH), 5. 28 (t, 1H, J 1.4Hz, =CH), 4.27 (d, 2H, J 1.4Hz, dioxolane CH_2), 2.02 (s,3H, enol Me), 1.48 and 1.42 (2s, 6H, CMe_2). Anal. calc. for $C_{10}H_{13}O_3N$: C, 61.54 ; H, 6.67 ; N, 7.18. Found : C, 61.81 : H, 6.75 ; N, 7.32 %.

DL-*8-Cyano-2,2,7-trimethyl-1,3,6-trioxaspiro (4,4) non-7-ene (VIIIj).* — a) *from Vc* : A solution of 7 g of the mixture of IIIc, IVc and Vc in 40 ml of CCl_4 was shaken with 14 g of the neutralised resin for 30 hrs at 40°C. The catalyst was removed and to the filtrate 0.5 ml of trifluoroacetic acid were added and the mixture was heated at 80°C for 2 hrs, then neutralised by shaking with saturated aqueous sodium hydrogen carbonate, dried (Na_2SO_4) and concentrated. The residue was distilled to afford 4.2 g of VIIIj (60 %), b. p. 100—102°C/0.3 Torr. $\bar{\nu}_{max}^{film}$ 2990, 2910, 2250, 1620—1580, 1460, 1430, 1380, 1290, 1200, 1160, 1100, 940, 890, 820, 780 and 750 cm^{-1}. ^{1}H-NMR data ($CDCl_3$) : δ 4.30 and 3.90 (2d, 2H, J 9.5Hz, dioxolane CH_2), 3.15 (q, 2H, J 1.8Hz, dihydrofuran CH_2), 2.3 (t, 3H, J 1.8 Hz, Me), 1.55 and 1.45 (2s, 6H, CMe_2). Mass spectrum : m/e 195(M*), 180 (M-Me), 169(M-CN), 152(M-Ac), 137(M-$COMe_2$), 122(137-Me), 120(137-OH), 111(137-CN), 106(137-CH_2OH), 94(137-Ac), 78(137-$COCH_2OH$), 59($COCH_2OH$), 55(CH_2=CHCO), 43(Ac, 100 %), 31(CH_2OH) and 26(CN). Anal. calc. for $C_{10}H_{13}O_3N$: C, 61.54 ; H, 6.66 ; N, 7.18. Found : C, 61.55 ; H, 6.87 ; N, 7.23 %.

b) *from VIIIi* : To a hot solution of 3 g of VIIIi in 40 ml of toluene 2.15 g of P_2O_5 were added, the mixture was heated at 70°C for 1 hr, extracted with ether (3 × 50 ml), dried (Na_2SO_4) and concentrated under diminished pressure. The residue was distilled to afford 1 g of VIIIj) (36 %), b.p. 106—108°C/0.5 Torr, m.p. 42°C.

Trans-3,11-dinitrile-2,10-dimethyl,1-6,9,13-tetraoxadispiro (4,2,4,2) tetradeca-2,10-diene (XIj). — Using a method similar to that described above for VIIIa, 3.68 g of VIIIj were converted into 1.38 g of VIIIj (42 %), m.p. 131-132°C (from dioxane). $\bar{\nu}_{max}^{KBr}$ 2990, 2915, 2210, 1620, 1600, 1575, 1500, 1470, 1440, 1360, 1300, 1270, 1200, 1150, 1110, 940 and 780 cm^{-1}. ^{1}H-NMR data ($CDCl_3$) : δ 4.35 and 3.80 (2d, 4H, J 12 Hz, H-7,14), 2.88 (q, 4H, J. 1.7 Hz, H-4,12), and 2.35 (t, 6H, J 1.7 Hz, 2Me). Mass spectrum : m/e 274 (M*), 259 (M-Me), 248(M-CN), 231(M-Ac), 136(M-C_7H_6NO-H_2O), 121(C_7H_7ON), 43(Ac) and 26(CN). Anal. calc. for $C_{14}H_{14}O_4N_2$: C, 61.31 ; H, 5.11 ; N, 10.22. Found : C, 61.07 ; H, 4.96 ; N, 9.98 %.

DL*-8-Carboxy-2-2,7-trimethyl-1,3,6-trioxaspiro (4,4) non-7-ene (VIIIk).* — a) *by hydrolysis of VIIIi* : A solution of 0.84 g of potassium hydroxide in 8 ml of water was added to a solution of 2.42 g of VIIIi in 5 ml of ethanol. After stirring for 2 hrs the mixture was stored for 64 hrs then extracted with ether (3 × 20 ml). The aqueous layer was acidified (Congo Red) with 10 % hydrochloric acid and the solid formed was collected, washed with cold water and recrystallised from water to give 1.53 g of VIIIk (63 %), m.p. 116—118°C. λ_{max}^{EtOH} 224 nm (ε 1.47 × 10^4). $\bar{\nu}_{max}^{KBr}$ 3400—2560 (broad), 2980, 2910, 1670, 1430, 1370, 1340, 1305, 1270, 1225, 1150, 1105, 1085, 1060, 970, 920, 890 and 840 cm^{-1}. ^{1}H-NMR data ($CDCl_3$) : δ 10.5—9.0 (bs, 1H, CO_2H), 4.27 and 3.95(2d, 2H, J 1OHz, dioxolane CH_2), 3.02 (q, 2H, J 2Hz, dihydrofuran CH_2), 2.23 (t, 3H, J 2Hz, Me), 1.52 and 1.40 (2d, 6H, CMe_2). Mass spectrum : m/e 214 (M*), 199(M-Me), 156(M-$COMe_2$), 141(156-Me), 139(156-OH), 125(156-CH_2OH), 113(156-Ac), 112(156-CO_2), 111(156-CO_2H), 97(156-$COCH_2OH$, 156-CO_2-Me), 95(156-CO_2—OH), 81(156—CO_2—CH_2OH), 69(156—CO_2—Ac), 59($COCH_2OH$), 58($COMe_2$), 55(CH_2=CHCO), 45(CO_2H, 100 %), 44(CO_2), 39(C_3H_3), 31(CH_2OH) and 17(OH). b) *by hydrolysis of VIIIj* : The procedure that followed was identical to that indicated above in a), with the difference that once the 64 hrs of storage elapsed, the mixture was heated for 30 min at 50°C. Yield : 52 %. c) by *haloform reaction of VIIIh* : A solution of 8 g of calcium hypochlorite in 50 ml of warm 60 % aqueous methanol was treated with 7 g of anhydrous potassium carbonate and a solution of 2.25 g of potassium hydroxide in 25 ml of the same aqueous methanol. After stirring for 5 min the mixture was cooled and filtered. The solid residue was washed with cold methanol (ice bath). To the combined filtrates a solution of 2.25 g of VIIIh in 25 ml of methanol was added dropwise with stirring. The stirring was maintained for 6 hrs then a solution of

2.25 g of sodium hydrogen sulphite dissolved in the minium possible quantity of water was added. The mixture was acidified (10 % hydrochloric acid) and the solid that separated was recrystallised from water to give 1 g (22 %) of VIIIk.

DL -*8-Chloroformyl-2,2,7-trimethyl-1,3,6-trioxaspiro (4,4) non-7-ene (VIIIm).* — A mixture of 17 g of VIIIk, 100 ml of CCl_4 and 20 g of triphenylphosphine was refluxed for 4 hrs, cooled to 0°C, filtered and concentrated to dryness. The residue was extracted with light petroleum (3 × 100 ml), the combined extracts were concentrated and the residue distilled to yield 10.64 g of VIIIm (61 %), b.p. 87—89°C/0.1 Torr. It descomposes under light. $\bar{\nu}^{film}_{max}$ 2980 2920, 1755, 1700, 1630, 1430, 1405, 1360, 1335, 1260 1200, 1115, 1040, 950, 880, 775 and 740 cm^{-1}. ^1H-NMR data (CCl_4) : δ 4.29 and 3.98 (2d, 2H, J 9.6Hz, dioxolane CH_2), 3.25 (q. 2H, J 1.5Hz, dihydrofuran CH_2), 2.23 (t,3H, J 1.5Hz, Me), 1.51 and 1.41 (2s, 6H, 6H, CMe_2),

DL -*8-Ethoxycarbonyl-2-2,7-trimethyl-1,3,6-trioxaspiro (4,4) non-7-ene (VIIIn).* — A solution containing 3 g of VIIIm was dissolved in light petroleum and stirred with 3 g of a suspension of sodium ethoxide in ethanol (1 :1) for 3 hrs under anhydrous conditions, then refluxed for 1 hr ; 10 ml of water were added and the solution was extracted with ether (3 × 15 ml), dried ($CuSO_4$), concentrated and distilled, giving 2.12 g of VIIIn (68 %), b.p. 96—98°C/0.2 Torr. λ^{EtOH}_{max} 248 nm (ε 1.12×10^4). $\bar{\nu}^{film}_{max}$ 2985, 2920, 2858, 1695, 1680, 1668, 1648, 1630, 1555, 1465, 1445, 1395, 1370, 1330, 1290, 1250, 1100, 1050, 960 and 890 cm^{-1}. ^1H-NMR data (CCl_4) : δ 4.23 and 3.90 (2d, 2H, J 9.6Hz, dioxolane CH_2), 2.97 (q, 2H, J 2Hz, dihydrofuran CH_2), 2.22 (t, 3H, J 2Hz, Me), 1.48 and 1.43 (2s, 6H, CMe_2), 1.26 (t, 3H, J 8Hz) and 4.15 (q, 2H, J 8Hz) both corresponding to the OEt group ; (C_6H_6) : δ 4.06 and 3.61 (2d, 2H, J 10 Hz, CH_2), 4.11 (q, 2H, J 7Hz) and 1.05 (t, 3H, J 7Hz) both corresponding to the OEt group, 3.09 (dq, 1H, J 2.5 and 16Hz) and 2.77 (dq, 1H, J 2,5 and 16Hz) both corresponding to the diastereotopic protons in the dihydrofuran CH_2 group, 2.18 (t, 3H, J 2.5Hz, Me), 1.52 and 1.29 (2s, 6H, CMe_2). Mass spectrum : m/e 242 (M*), 227 (M-Me), 199(M-Ac), 184 (M-$COMe_2$), 169(M-CO_2Et), 153(184-CH_2OH), 141(184-Ac), 111(184-CO_2Et), 73(CO_2Et), 43 (Ac,100 %) and 15(Me). Anal. calc. for $C_{12}H_{18}O_5$:C, 59.50 ; H, 7.43. Found : C, 59.20 ; H, 7.23 %.

Treatment of 1.4 g of VIIIn with 5 ml of aqueous potassium hydroxide, as described above for VIIIi, and recrystallisation of the product from water, afforded 0.8 g of VIIIk (64 %), m.p. 116—118°C.

When instead sodium ethoxide, sodamide in toluene (1 :1) was used in the reaction with VIIIm, the compound VIIIb was prepared in 51 % yield, m.p. 160—161°C.

DL-*8-Benzoyl-2,2,7-trimethyl-1,3,6-trioxaspiro (4,4) non-7-ene (VIIIp).* — To a solution of 2.6 g of VIIIk in 12 ml of dry dimethoxyethane a solution of 1 g of phenyl-lithium in 10 ml of ether was added dropwise with stirring under 5°C. Stirring was maintained for 3 hrs at room temperature, 15 ml of aqueous 30 % ammonium chloride were added and the suspension was extracted with ether (3 × 60 ml). The extracts were dried ($CuSo_4$) and concentrated and the residue distilled to yield 0.97 g of VIIIp, b.p. 120°/0.2 Torr. $\lambda^{CHCl_3}_{max}$ 316 nm (ε 2.8×10^4) · ν^{film}_{max} 3040, 2920, 2900, 2840, 1635, 1620, 1580, 1540, 1440, 1350, 1280, 1210, 1130, 1070, 950, 765 and 730 cm^{-1}. ^1H-NMR data ($CDCl_3$) : δ 7.45 (m, 5H, Ph), 4.3 and 3.99 (2d, 2H, J 9Hz, dioxolane CH_2), 3.20 (q, 2H, J 1.2Hz, dihydrofuran CH_2), 1.90 (t, 3H, J1.2 Hz, Me), 1.58 and 1.45 (2s, 6H, CMe_2). Mass spectrum : m/e 274 (M*), 259 (M-Me), 231 (M-Ac), 216 (M-$COMe_2$), 201 (216-Me), 197 (M-Ph), 185 (216-CH_2OH), 169(M—COPh), 139(216-Ph), 111(216-COPh), 105(COPh, 100 %), 77(Ph) and 15(Me). Anal. calc. for $C_{16}H_{18}O_4$: C, 70.07 ; H, 6.57. Found : C, 69.90 ; H, 6.42 %.

When methyl-lithium is used instead of phenyl-lithium, VIIIh is obtained in 49 % yield.

4-Acetyl-1-hydroxy-hexane-2,5-dione (XIIh). — A solution of 15 g of VIIIh in 80 ml of acetic acid-water (1 :1) was heated at 80°C for 1 hr. After removal of the solvent under diminished pressure, the residue was distilled, yielding 6.7 g of XIIh (55 %), b.p. 91—93°C/0.5 Torr, m.p. 54°C. $\bar{\nu}^{film}_{max}$ 3500, 2990, 2910, 2870, 1720, 1690, 1420, 1400, 1375, 1340, 1270, 1165, 1080, 1000, 980 and 940 cm^{-1}. ^1H-NMR data ($CDCl_3$) : δ 12.6 (s, 1H, OH), 4.25 (bs, 2H, H—1), 3.33 (broad, exchangeable with D_2O, 1H, OH), 2.80 (m, 2H, H-3), 2.12 (s, 3H, Ac) and 2.06 (s, 3H, enol Me). Mass spectrum : m/e 172 (M*), 157 (M-Me), 155(M-OH), 141 (M-CH_2OH), 129(M-Ac), 113(M—$COCH_2OH$), 99(M—CH_2COCH_2OH), 73(CH_2COCH_2OH), 59($COCH_2OH$), 43(Ac, 100 %) and 31(CH_2OH). Anal. calc. for $C_8H_{12}O_4$: C, 55.81 ; H, 6.98. Found : C, 56.06 ; H, 7.11 %.

3-Acetyl-5-hydroxymethyl-2-methyl-furan (XIVh). — A solution of 3 g of XIIh, 3 g of $ZnCl_2$ and 60 ml of ethanol-water (1 :1) was heated at 90°C for 1 hr. Ether (3 × 50 ml) was added and the organic layer was dried ($CuSO_4$) and concentrated under diminished pressure. The residue was distilled to afford 1.96 g of XIVh (67%), b.p. 67–70°C/0.1 Torr. The analytical and spectroscopic data of this substance are given in [2].

4-Carbamoyl-1-hydroxy-hexane-2,5-dione (XIIIi). — Using a method similar to that described above for XIIh, but heating the reaction mixture at 45°C for 1 hr, VIIIi was converted into XIIi in a 51% yield, m.p. 79–80°C. $\tilde{\nu}_{max}^{KBr}$ 3400, 3115, 2980, 2920, 1680, 1660, 1580, 1440, 1380, 1300, 1260, 1210, 1150, 1100, 1040, 960 and 830 cm^{-1}. ^1H-NMR data ($CDCl_3$) : δ 5.55 (broad, exchangeable with D_2O, 2H, NH_2), 4.25 (b, 2H, H–1), 3.38 (b, 1H, exchangeable with D_2O, OH), 2.80–2.68 (m, 3H, H-3,4) and 2.20 (s, 3H, H-6). Mass spectrum : m/e 173 (M^*), 158(M-Me), 157($M-NM_2$), 142($M-CH_2OH$), 130 (M–Ac), 129($M-CONH_2$), 114($M-COCH_2OH$), 73($M-C_4H_6O_2N$), 59 ($COCH_2OH$), 44($CONH_2$), 43(Ac, 100%), 31(CH_2OH), 17(OH) and 16(NH_2). Anal. calc. for $C_7H_{11}O_4$ N : C, 48.55 ; H, 6.36 ; N, 8.09. Found : C, 48.71 ; H, 6.08 ; N, 8.76%.

3-Carbamoyl-5-hydroxymethyl-2-methyl-furan (XIVi). — Using a method similar to that described above for XIVh, XIIi is converted into XIVi in 45% yield. The analytical and spectroscopic data of this substance are given in[2].

1-Hydroxyhexane-2,5-dione (XIII). — a) *by hydrolysis of VIIIi* : A suspension of 2.39 g of VIIIi in 10 ml of 10% aqueous sodium hydroxide was heated at 100°C for 1 hr. Ether was added (3×10 ml) and the aqueous layer was acidified with dilute hydrochloric acid and the product was extracted with ether (3×50 ml). The combined extracts were dried ($CuSO_4$) and concentrated under diminished pressure then the residue was fractionated, affording 1 g of XIII (60%), b.p. 82–85°C/0.5 Torr, m.p. 51°C. $\tilde{\nu}_{max}^{film}$ 3460, 2980, 2900, 1710, 1695, 1405, 1385, 1350, 1150, 1060, 1000, 970 and 940 cm^{-1}. ^1H-NMR data ($CDCl_3$) :δ 4.25 (bs, 2H, H–1), 3.25 (b, exchangeable with D_2O, 1H, OH), 2.70(m, 4H, H–3,4) and 2.18 (s, 3H, H–6). Mass spectrum : m/e 130 (M^*), 113(M–OH), 99($M-CH_2OH$), 87(M–Ac), 73($M-CH_2COMe$),71($M-COCH_2OH$), 59($COCH_2OH$), 57(CH_2COMe), 43(Ac), 31(CH_2OH) and 17(OH). Anal. calc. for $C_6H_{10}O_3$: C, 55.38 ; H, 7.69. Found : C, 55.57 ; H, 7.78%. b) *by alkaline hydrolysis of VIIIj, VIIIk or XIIi* : using a method similar to that described above in a), XIII was prepared from VIIIj, VIIIi or XIIi in 54 ; 68 and 71% yield respectively. c) *by acid hydrolysis of VIIIk* : using a method similar to that described above for XIIh, the compound XIII was prepared from VIIIk in 67% yield. d) *by haloform reaction of XIIh* : a solution of 5.5 g of XIIh in 10 ml of ethanol was added, with stirring, to a solution of I_2-KI, prepared dissolving 20 g of KI and 10 g of I_2 in water until the iodine colouring was permanent. Stirring was continued until a yellow precipitate of iodoform was observed. It was separated by filtration, extracted with ether (3×40 ml), dried ($CuSO_4$), filtered and the solvent eliminated under diminished pressure, giving 2.4 g of XIII (58%), b. p. 83–85°C/0.5 Torr. Treatment of 2 g of XIII with 4.30 g of sodium periodate (80% purity) in 15 ml of water, with stirring, for 20 min, after adition of 1 g of sodium hydrogen carbonate and separating the possible residuum of unreacted XIII, extracting with diethyl ether and acidifying (Congo Red) with 10% HCl, extracting again with diethyl ether (4×20 ml), drying the extracts (Na_2SO_4), filtering and eliminating the solvent yields, by distillation, 0.8 g (45%) of a product with b.p. 137–139°C/10 Torr, analytically and spectroscopically identical to authentic sample of levulinic acid.

5-Hydroxy-4-oxo-hexanoic acid (XVII). — Using a method similar to that described above for preparation of XIII from XIIh, but refluxing for 1 hr, XIIh and XIII were converted into XVII (47 and 53% yields respectively), b.p. 151–153°C/10 Torr. $\tilde{\nu}_{max}^{film}$ 3450–2500 (broad), 1715, 1690, 1440, 1330, 1280, 1200, 1115, 1050, 860 and 780 cm^{-1}. ^1H-NMR data ($CDCl_3$) : δ 11.5(b, 1H, CO_2H), 4.31 (bs, 2H, H–1), 3.32 (b, 1H, OH) and 2.85 (m, 4H, H–3,4). Anal. calc. for $C_5H_8O_4$: C, 45.45 ; H, 6.06. Found : C, 45.31 ; H, 5.89%.

Treatment of XVII with sodium periodate in water, as indicated in the preparation of levulinic acid from XIII, affords succinic acid (43%).

Condensation of I with IId (VIh). — A mixture of 29 g of I, 22.50 g of IId, 6 drops of piperidine and 200 ml of toluene was stirred for 12 hrs at room temperature (descarboxylation is observed). After heating at 80°C (1 hr) the toluene layer was separated and concentrated under diminished pressure. The residue was distilled to afford 25.64 g of 5,6-O-isopropylidene-2-oxo–3-hexene (VIh, 68%), b. p. 83–85°C/18 Torr. λ_{max}^{MeOH} 221 nm (ε 9.07×10^3). ν_{max}^{film} 2990, 2920, 2880, 1660, 1620, 1590, 1570, 1420, 1380, 1250, 1200, 1140, 1060 and 940 cm^{-1}. ^1H-NMR data (CCl_4) :δ 6.7 (dd, J 2 and 11Hz, 1H, H–3), 6.25 (dd, J 11 and 8Hz, 1H, H–4), 4.6 (m, 1H, H–2), 4.3 and 3.6(2dd, J 6Hz, 2H, dioxolane CH_2), 2.3 (s, 3H, Me), 1.5 and 1.4 (2s, 6H, CMe_2). Anal. calc. for $C_9H_{14}O_3$:C, 63.53 ; H, 8.23. Found : C, 63.47 ; H, 8.46 %.

Treatment of VIh with I_2-KI reagent leads, with 61 % yield, to *trans*-4,5-isopropylidenedioxypent-2-enoic acid (VIk), b.p. 130°C/0.1 Torr. $\bar{\nu}_{\max}^{\text{film}}$ 3500–2500 (broad), 2970, 2900, 2870, 1720, 1610–1580, 1430, 1360, 1280, 1210, 1120, 1040, 960 and 760 cm^{-1}. ^{1}H–NMR data (CCl_4) : δ 11.0(b, 1H, CO_2H), 6.9(dd, J 2 and 12 Hz, 1H, H–3), 6.1 (dd, J 12 and 9Hz, 1H, H–4), 4.7 (m, 1H, H–2), 4.2 and 3.7(2dd, J 7Hz, 2H, dioxolane CH_2), 1.45 and 1.35 (2s, 6H, CMe_2). Anal. calc. for $C_8H_{12}O_4$: C, 55.81 ; 6.97. Found : C, 55.61 ; H, 7.22 %.

Trans-5,6-dihydroxypent-3-en-2-one (VIIh). — A solution of 2 g of VIh in 20 ml of acetic acid-water (1 :1) was heated at 80°C for 1 hr. After removal of the solvent under diminished pressure, the residue was distilled, yielding 0.76 g of VIIh (72 %), b.p. 52°C/15 Torr $\bar{\nu}_{\max}^{\text{film}}$ 3500, 2990, 2910, 1710, 1630, 1430, 1380, 1250, 1120, 1080, 1050, 980 and 870 cm^{-1}. ^{1}H-NMR data (D_2O) : δ 6.97 (dd, J 14 and 6Hz, 1H, H–4), 6.26 (dd, J 16 and 1.7Hz, 1H, H–3), 4.45 (m, 1H, H–5), 3.65 (dd, J 7 and 5Hz, 2H, H–6), 2.36 (s, 3H, Ac). Mass spectrum : m/e 130 (M*), 115(M-Me), 113(M–OH), 112(M–H_2O), 99(M–CH_2OH), 98(99–H), 87(M-Ac), 70(98-CO), 55(70-Me), 43(Ac) and 28(C_2H_4). Anal. calc. for $C_6H_{10}O_3$: C, 55.38 ; H, 7.69. Found : C, 55.60 ; H, 7.47 %.

Condensation of I with IIe (IIIe). — A mixture of 10 g of I, 6.5 g of IIe, 5 drops of piperidine and 10 ml of pyridine was stirred for 12 hrs at room temperature and then refluxed for 30 min. before the solvent was removed. The residue, washed with cold CCl_4 and recrystallised from ethanol-hexane yielded 9 g (63 %) of IIIe, m.p. 139–141°C. $\bar{\nu}_{\max}^{\text{KBr}}$ 3400–3050, 2990, 2960, 2240, 1700, 1650, 1620, 1470, 1450, 1380, 1310, 1250, 1210, 1150, 1100–1050, 1000, 990, 920, 850, 790, 730 and 690 cm^{-1}. ^{1}H-NMR data ($CDCl_3$) :δ 6.70 (d,J 7Hz, 1H, = CH), 5.60 (broad, exchangeable with D_2O, 2H, NH_2), 4.61 (d, J 7Hz, 2H, dioxolane CH_2), 4.56 (m, 1H, H-4) and 1.50(s, 6H, CMe_2). Anal. calc. for $C_9H_{12}O_3N_2$: C, 55.10 ; H, 6.12 ; N, 14.28. Found : C, 55.39 ; H, 6.31 ; 14.41 %.

Alkaline hydrolysis of IIIe, in the same conditions described for XIII, affords VIk (42 %), b. p. 128–130°C/0.1 Torr.

Condensation of I with IIf (IVf). — As in the above-mentioned piperidine catalysed reactions, equimolar proportions of I and IIf were used, but only ethyl-2-cyano-4,5-isopropylidenedioxypent-3-enoate (IVf), (29 g, 60 %) was isolated, b.p. 110–112°C/0.5 Torr. When diethylamine was used as catalyst, the yield was only 50 %. $\bar{\nu}_{\max}^{\text{film}}$ 2990, 2970, 2230, 1760, 1710, 1470, 1390, 1330, 1270, 1230, 1170, 1140, 1070, 1040, 980, 950, 855, 810 and 780 cm^{-1}. ^{1}H-NMR data (CCl_4) : δ 4.70 (m, 1H, vinyl ether =CH), 4.55–4.42 (m, 3H), 4.28 (q, J 8.5 Hz, 2H, $OC\underline{H}_2\ CH_3$), 1.60 (s, 6H, CMe_2) and 1.45 (t,J 8.5Hz, 3H, $OCH_2C\underline{H}_3$). Mass spectrum : m/e 225 (M*), 199(M–CN), 180(M-OEt), 167(M-$COMe_2$), 152 (M–CO_2Et), 136(167–CH_2OH), 73(CO_2Et), 45(OEt) and 26(CN). Anal. calc. for $C_{11}H_{15}\ O_4N$: C, 58.67 ; H, 6.67 ; N, 6.22. Found : C, 58.43 H, 6.73 ; N, 6.08 %.

Condensation of I with IIg (IIIg). — When 11 g of I, 5.58 g of IIg and 8 drops of diethylamine are mixed, a rise in the temperature of the mixture to 60°C is observed. The mixture was kept in the dark for 12 hrs, concentrated at 80°C/1 Torr and the residue washed with cold CCl_4 and recrystallised from ethanol-petroleum ether to give 12.8 g of IIIg (85 %), m.p. 90–92°C. $\bar{\nu}_{\max}^{\text{KBr}}$ 3400, 3180, 2980, 2915, 2870, 1680, 1670, 1630–1580, 1430, 1380, 1360, 1240, 1210, 1160, 1110, 1050, 950, 910, 850 and 710 cm^{-1}. ^{1}H–NMR data ($CDCl_3$) : δ 6.63 (d, J 6Hz, 1H, = CH), 5.70 (b, 4H, $2NH_2$), 4.65 (d,J 6Hz, 2H, dioxolane CH_2), 4.55 (m, 1H, H–4) and 1.48 (s, 6H, CMe_2). Anal. calc. for $C_9H_{14}O_4N_2$: C, 50.47 ; H, 6.54 ; N, 13.08. Found ; C, 50.21 ; H, 6.42 ; N, 13.08 %.

When a solution of 4 g of IIIg in 10 ml of ethanol and 10 ml of 10 % aqueous sodium hydroxide is heated at 70°C for 1 hr, ethyl acetate (3×50 ml) added and the aqueous layer is neutralised with dilute hydrochloric acid, decarboxylation is observed. The product is extracted with more ethyl acetate (3× 60 ml), the extracts are dried (Na_2SO_4) and concentrated under diminished pressure. The residue, distilled, gives 2.08 of VIk (65 %), b.p. 128–130°C/0.1 Torr.

Trans-4,5-dihydroxypent-2-enoic acid (VIIk). — a) *by acid hydrolysis of VIk* : Using a method similar to that described above for XIIh, the compound VIIk was prepared from VIk in 68 % yield, m.p. 117–119°C (from ethyl acetate). $\bar{\nu}_{\max}^{\text{KBr}}$ 3400–2600 (broad), 1800, 1690, 1650, 1460, 1405, 1345, 1280, 1230, 1125, 1070, 990, 930, 860 and 750 cm^{-1}. ^{1}H-NMR data ($CDCl_3$) : δ 12.0 (b, 1H, CO_2H), 7.0(dd, J 15 and 7Hz, 1H, H–3), 6.1(dd, J 16 and 1.8Hz, 1H, H-2), 4.50 (m, 1H, H–4) and 3.68 (dd, J 8 and 6Hz, 2H, H–5). Anal. calc. for $C_5H_8O_4$:C, 45.45 ; H, 6.09. Found : C, 45.60 ; H, 5.88 %. b) *by haloform reaction from VIIh* : Using a method similar to that described above for preparation of XIII from XIIh, VIIk was prepared from VIIh in 38 % yield.

Trans-butenaldehyde-oic acid (IX). — A solution of 4 g of VIIk in 10 ml water was treated with 7 g of $NaIO_4$ in 50 ml of water at room temperature during 3 hrs, ether (3 × 50ml) was added, the organic layer was dried (Na_2SO_4) and the solvent eliminated, thus obtaining 2.68 g of IX (from ether-petroleum ether) (89 %). $\bar{\nu}_{max}^{KBr}$ 3040—2800 (broad), 2700, 2200, 1860, 1670, 1560, 1420, 1380, 1300, 1270, 1210, 1160, 1020, 940, 835 and 690 cm^{-1}. ^1H-NMR data ($CDCl_3$) : δ 12.0 (broad, 1H, CO_2H), 9.74(d, J 12Hz, CHO), 7.15 (dd, J 16 and 7Hz, 1H, H—2) and 6.2 (d, J 7Hz, 1H, H—3). Anal. calc. for $C_4H_4O_3$:C, 48.O ; H, 4.02. Found : C, 47.79 ; H, 4.12 %. This substance forms a semicarbazide hydrochloride in 79 % yield ; m.p. 258—259°C (from water). Anal. calc. for $C_5H_7O_3N_3$: C, 38.21 ; H, 4.48 ; N, 26.73. Found : C, 38.34 ; H, 4.25 ; N, 26.71 %.

Treatment of 1.5 g of IX with a mixture of 4.5 g of $AgNO_3$, 1.5 g of NaOH and 50 ml of water, with stirring, for 3 hrs leads to 1.16 g of fumaric acid (67 %).

REFERENCES

[1] J. Sánchez Ballesteros, I. Mugaburu Lacabrera and F. Hernandez Hernandez, *Carboh. Res.* UK 1974, in press.

[2] J. Sánchez Ballesteros, D. J. McPhee and F. Hernandez Hernandez, *Rev. Roumaine Chim.*, in press.

[3] H.O.L.Fischer and E. Baer, *Helv. Chim. Acta*, **17**, 622 (1934).

[4] L. Claisen and K. Meyer, *Ber. Oltrch. Chem. Ges.*, **35**, 583 (1902).

[5] K. Kumasa Sato and T. Amakasu, *J. Org. Chem.*, **33**, 2449 (1968).

[6] C. Robert and J. Kreuger, *J. Chem. Soc.*, **1952**, 5536.

Revue Roumaine de Chimie, **26**, *5*, 717—723 (1981)

SYNTHESIS AND REACTIONS OF 6,7(4′-ALKYL-α-PYRANO)4-ALKYL COUMARINS

M.A. ELKASABY and M.A.I. SALEM

Chemistry Department, Faculty of Science, Ain Shams University, Cairo, Egypt A.R.E.

Received February 29, 1980

6,7(4′-Alkyl-α-pyrano)4-alkyl coumarins I were obtained by reaction of polyhydroxyphenols with a β-ketoester in TFA or with ethyl phenyl propiolate in the presence of $ZnCl_2$. Compounds II were prepared by condensation of Ia—c with aldehydes. The Diels Alder reaction of II with maleic anhydride and N-aryl maleimides has been investigated.

The present work deals with the synthesis of 6,7(4′-alkyl-α-pyrano)-4-alkyl coumarins Ia—f. The reaction of polyhydroxyphenols, namely: resorcinol, pyrogallol and gallic acid with a β-ketoester such as: ethyl acetoacetate or ethyl benzoylacetate in the presence of trifluoroacetic acid gives Ia—f.

6,7(4′-Phenyl-α-pyrano)-4-phenyl coumarin derivatives Id—f were also obtained by the reaction of polyhydroxyphenols (resorcinol, pyrogallol, and gallic acid) with ethyl phenylpropiolate.

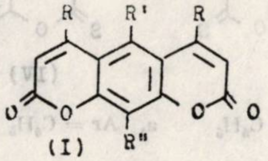

(I)

	R	R′	R″		R	R′	R″
a,	CH_3	H	H	d,	C_6H_5	H	H
b,	CH_3	H	OH	e,	C_6H_5	H	OH
c,	CH_3	COOH	OH	f,	C_6H_5	COOH	OH

The IR spectra of compounds I showed absorption bands attributable to ν(C=O) of unsaturated δ-lactones, ν(C=O) of acids and ν(OH) at 1730—1710 cm^{-1} and 3300—2720 cm^{-1} respectively.[1,2]

Compounds Ia—c, being typical compounds with active methyl group, condense with aldehydes, namely: benzaldehyde, anisaldehyde, piperonal, *p*-nitrobenzaldehyde or furfural, leading to the formation of 6,7(4′-styryl or furfurylidene-α-pyrano)-4-styryl or furfurylidene coumarins IIa—f [Di (4′-styryl or furfurylidene pyrano)-benzene].

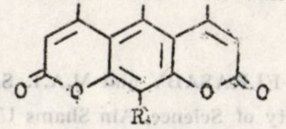

(II)

	R	R″	R′		R	R″	R′
a,	C_6H_5	H	H	g,	$3,4\text{-}CH_2O_2 - C_6H_3$	H	H
b,	C_6H_5	H	OH	h,	$3,4\text{-}CH_2O_2 - C_6H_3$	H	OH
c,	C_6H_5	COOH	OH	i,	$3,4\text{-}CH_2O_2 - C_6H_3$	COOH	OH
d,	$p\text{-}CH_3O - C_6H_4$	H	H	j,	C_4H_3O	H	H
e,	$p\text{-}CH_3O - C_6H_4$	H	OH	k,	C_4H_3O	H	OH
f,	$p\text{-}CH_3O - C_6H_4$	COOH	OH	l,	C_4H_3O	COOH	OH

The IR spectra of compounds II showed well defined absorption bands at 1720—1710 cm^{-1} (due to ν(C=O) of unsaturated δ-lactone), at 1700 cm^{-1} (due to ν(C=O) of carboxylic acid), at 1610—1600 cm^{-1} (due to ν(C=C)) and at 3300—2600 cm^{-1} (a broad band due to ν(OH)).

Compounds Ia and Id were allowed to react with phosphorous pentasulphide and gave the thione derivative IIIa and IIIb.

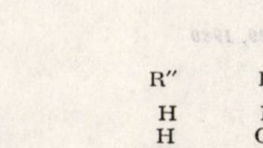

(III)

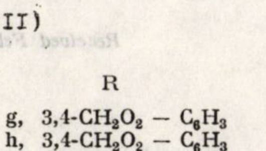

(IV)

a, R = CH_3 b, R = C_6H_5 a, Ar = C_6H_5 b, $p\text{-}CH_3-O-C_6H_4$

The thione compound IIIa, when allowed to react with benzaldehyde or anisaldehyde, gave dark olive green crystalline solids IVa and IVb respectively.

The thiocoumarins IVa and IVb were also obtained by heating IIa and IId under reflux with phosphorous pentasulphide. The IR spectra of compounds III and IV showed well defined bands at 1370—1350 cm^{-1} attributable to ν(C=S) and at 1600—1610 cm^{-1} attributable to ν(C=C).

The di(4′-styrylpyrano) benzenes II have been subjected to a Diels-Alder reaction. [3] The dienophiles used were maleic anhydride, N-phenyl and N-*p*-tolylmaleimide. The reaction affords the Diels Alder adducts Va—j.

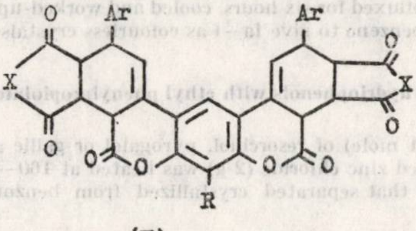

(V)

	Ar	R	X		Ar	R	X
a,	C_6H_5	H	O	f,	p-$C_6H_4-OCH_3$	H	O
b,	C_6H_5	H	C_6H_5-N	g,	p-$CH_3-O-C_6H_4$	H	C_6H_5-N
c,	C_6H_5	H	p-$CH_2-C_6H_4N$	h,	p-$CH_3-O-C_6H_4$	H	p-$CH_3-C_6H_4N$
d,	C_6H_5	OH	O	i,	p-$CH_3-O-C_6H_4$	OH	O
e,	C_6H_5	OH	C_6H_5-N	j,	p-$CH_3-O-C_6H_4$	OH	C_6H_5-N

The structures of the adducts V were proved:

(a) Chemically, via hydrolysis of Va and Vf to the acids VIa and VIb, which were identical with that obtained authentically via the Diesl-Alder reaction of IIa and IIb with maleic acid as dienophile.

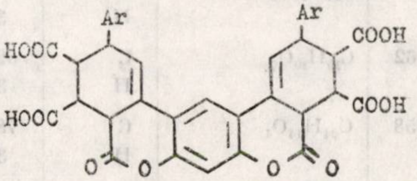

(VI)

a, Ar = C_6H_5 b, Ar = p-$CH_3-O-C_6H_4$

The IR spectra of the acids VI showed bands at 1700—1690 cm^{-1} (for ν(C=O) of carboxylic acid); at 1750 cm^{-1} (for ν(C=O) of δ-lactone); at 3050—2950 cm^{-1} (as a broad band for ν(OH)) and a band at 3060 cm^{-1} (dimeric OH).

(b) Spectroscopically, the infrared spectra of V showed bands attributable to ν(C=O) of anhydride (doublet at 1840 and 1760 cm^{-1}), ν(C=O) of imide (doublet at 1720 and 1700 cm^{-1}), ν(C=O) of δ-lactone at 1740—1720 cm^{-1} and ν(OH) group at 3300—2900 cm^{-1}.

EXPERIMENTAL

The infrared absorption spectra were determined with a Perkin Elmer infracord Model 577 and an Unicam SP. 1200 spectrometer using KBr wafer technique. Melting points are not corrected.

6,7(4'-Alkyl-α-pyrano)-4-alkylcoumarins Ia—f

A mixture of (0.01 mole) of polyhydroxyphenol, namely : resorcinol, pyrogallol or gallic acid and (0.02 mole) of β-ketoester, namely : ethyl acetoacetate or ethyl benzoylacetate in 25 ml trifluoroacetic acid was refluxed for six hours, cooled and worked-up. The solid obtained was crystallized from ethanol or benzene to give Ia—f as colourless crystals (yield 60—70 %, cf. table 1).

Reaction of polyhydriophenols with ethyl phenylpropiolate. Formation of Id—f

A mixture of (0.01 mole) of resorcinol, pyrogalol or gallic acid and (0.02 mole) of ethyl phenylpropiolate and fused zinc chloride (2 g) was heated at 160—170°C for six hours and poured into water. The solid that separated crystallized from benzone or ethanol to give Id—f (cf. Table 1).

TABLE 1

6,7(4'-Alkyl-α-pyrano)-4-alkylcoumarin derivatives (I) and
6,7(4'-methyl or phenyl-α-thiopyrano)-4-methyl- or phenyl-thiocoumarins (III)

Compounds	m.p. °C	Formula	Analysis %		
				Calcd.	Found
Ia	186	$C_{14}H_{10}O_4$	C	69.42	69.60
			H	4.13	4.14
Ib	203	$C_{14}H_{10}O_5$	C	65.12	65.00
			H	3.83	3.88
Ic	262	$C_{15}H_{10}O_7$	C	59.60	59.50
			H	3.31	3.30
Id	258	$C_{24}H_{14}O_4$	C	78.68	78.80
			H	3.82	3.64
Ie	286	$C_{24}H_{14}O_5$	C	75.39	75.50
			H	3.66	3.64
If	>300	$C_{25}H_{14}O_7$	C	70.42	70.61
			H	3.28	3.27
IIIa	228	$C_{14}H_{10}O_2S_2$	C	61.31	61.20
			H	3.65	3.64
IIIb	239	$C_{24}H_{14}O_2S_2$	C	72.36	72.21
			H	3.52	3.50

6,7(4'-Styryl or furfurylidene-α-pyrano)-4-styryl or furfurylidenecoumarins (IIa—1).

To a solution of Ia—c (0.01 mole) in 10 ml absolute ethanol, 15 ml of alcoholic solution of sodium ethoxide (prepared from 0.5 sodium metal and absolute ethanol at room temperature) was added. A solution of the aldehyde, namely : benzaldehyde, anisaldehyde, piperonal or furfural (0.02 mole) in 10 ml absolute ethanol was added ; the colourless solution immediately turned to yellow, colour which was then changed to intense red. The reaction mixtures were left to stand overnight at room temperature. The preciptated solid was filtered off, washed with H_2O and crystallized from a proper solvent to give IIa—1 as yellow crystals (yield 70—80 %, cf. Table 2).

TABLE 2

Di(4'-styryl or furfurylidenepyrano) benzene (II) and Di(4'-styrylthiopyrano)benzene (IV)

Compound	Solvent of cryst n*	m.p. °C	Formula		Analysis %	
					Calcd.	Found
IIa	B	167	$C_{28}H_{18}O_4$	C	80.38	80.12
				H	4.30	4.30
IIb	B	172	$C_{28}H_{18}O_5$	C	77.41	77.60
				H	4.14	4.15
IIc	B	194	$C_{29}H_{18}O_7$	C	72.80	72.96
				H	3.76	3.75
IId	E	159	$C_{30}H_{22}O_6$	C	75.31	75.20
				H	4.60	4.60
IIe	B	182	$C_{30}H_{22}O_7$	C	72.87	72.70
				H	4.45	4.46
IIf	E	178	$C_{31}H_{22}O_9$	C	69.14	69.30
				H	4.08	4.07
IIg	B−E	148	$C_{30}H_{18}O_8$	C	71.14	71.30
				H	3.56	3.57
IIh	B−E	165	$C_{30}H_{18}O_9$	C	68.96	69.24
				H	3.45	3.46
IIi	B−E	198	$C_{31}H_{18}O_{11}$	C	65.72	65.90
				H	3.18	3.17
IIj	B−P	201	$C_{24}H_{14}O_6$	C	72.36	72.50
				H	3.52	3.52
IIk	B	228	$C_{24}H_{14}O_7$	C	69.56	69.70
				H	3.38	3.39
IIl	B	>300	$C_{25}H_{14}O_9$	C	65.50	65.33
				H	3.06	3.06
IVa	E−H_2O	202	$C_{28}H_{18}O_2S_2$	C	74.66	74.80
				H	4.00	4.00
IVb	E−H_2O	213	$C_{30}H_{22}O_4S_2$	C	70.58	70.70
				H	4.31	4.30

* B = Benzene, E = Ethanol, P = Light petrol (b.p. 60−80).

6,7(4'-methyl or phenyl α-thiopyrano)-4-methyl or phenyl thiocoumarins IIIa and b

To a solution of Ia or Ib (0.005 mole) in 30 ml dry benzene, 2 g of freshly purified phosphorous pentasulphide was added. The reaction mixture was heated under reflux for four hours then filtered. The residue was repeatedly extracted with benzene. The combined filtrate and benzene extract was evaporated to dryness. The solid obtained was crystallized from methanol giving IIIa and IIIb respectively as violet needles (yield 70 %, cf. Table 1).

6,7(4'-styryl-α-thiopyrano)-4-styryl-thiocoumarins IVa and IVb

Method A :

To a solution of IIIa (1.37 g ; 0.05 mole) in 10 ml absolute ethanol, sodium ethoxide solution (prepared from 0.26 g sodium metal in 10 ml absolute ethanol) was added. A solution of (0.01 mole) of benzaldehyde or anisaldehyde in 10 ml absolute ethanol was added and the reaction mixture was left at room temperature for four hours. A green crystalline solid was separated. The products were filtered and recrystallized from dil. ethanol (cf. Table 2).

Method B :

To a solution of IIa and IId (0.001 mole) in 20 ml benzene, 2 g of freshly purified P_2S_5 were added. The reaction mixture was heated under reflux for four hrs., then filtered while hot. The residue was repeatedly extracted with benzene. The combined filtrates and benzene extract were evaporated to dryness and the solid obtained was crystallized from dil. ethanol. The mixed melting points of the products with those obtained by procedure A were not depressed.

Diels Alder reaction with II. Formation of Va – j

A mixture of IIa, b, d and e (0.003 mole), maleic anhydride, N-phenyl or N-*p*-tolylmaleimide (0.03 mole) and dry xylene (30 ml) was heated under reflux for 4 hrs. The colourless solids that separated after concentration and cooling were the adducts Va – j (yield 50 – 60 % ; cf. Table 3).

TABLE 3

Diels Alder adducts V and acids VI

Compound	Solvent of crystn*	m.p. °C	Formula	Analysis %		
					Calcd.	Found
Va	T	196	$C_{36}H_{22}O_{10}$	C	70.35	70.50
				H	3.58	3.59
Vb	X	231	$C_{48}H_{32}N_2O_8$	C	78.69	78.90
				H	4.37	4.36
				N	3.82	3.80
Vc	X	252	$C_{50}H_{36}N_2O_8$	C	78.94	78.80
				H	4.73	4.74
				N	3.68	3.69
Vd	Ac	220	$C_{36}H_{22}O_{11}$	C	68.57	68.80
				H	3.49	3.50
Ve	Ac	276	$C_{48}H_{32}N_2O_9$	C	73.84	74.00
				H	4.10	4.10
				N	3.55	3.54
Vf	T	186	$C_{38}H_{26}P_{12}$	C	67.65	67.80
				H	3.85	3.86
Vg	T	212	$C_{50}H_{36}N_2O_{10}$	C	72.81	72.68
				H	4.36	3.36
				N	3.40	3.42

Table 3 (continued)

Compound	Solvent of cryst*n**	m.p. °C	Formula	Analysis %		
					Calcd.	Found
Vh	T	235	$C_{52}H_{40}N_2O_{10}$	C	73.24	73.50
				H	4.69	4.71
				N	3.28	3.27
Vi	Ac	>300	$C_{38}H_{26}O_{13}$	C	66.08	66.18
				H	3.76	3.76
Vj	Ac	>300	$C_{50}H_{36}N_2O_{11}$	C	71.42	71.60
				H	4.28	4.29
				N	3.33	3.33
VIa	X	>300	$C_{36}H_{26}O_{12}$	C	66.46	66.60
				H	4.00	4.00
VIb	X	>300	$C_{38}H_{30}O_{14}$	C	64.22	64.00
				H	4.22	4.21

---

* Toluene X = Xylene Ac = Acetic acid.

Hydrolysis of Diels Alder adducts : Formation of VI

A mixture of Va and Vf (0.006 mole) and 20 ml of alcoholic KOH solution (10 %) was heated under reflux for two hours. The solution was acidified, and the precipitated solids were crystallized from xylene as colourless crystals (yield about 60 %, cf. Table 1).

Authentic sample of VI

Compounds IIa and IIc were allowed to undergo Diels Alder reaction with maleic acid by the procedure described before ; the products gave, after crystallization, the same acids VIa and b identified by m.p. and mixed m.p. determination and comparison of their IR spectra.

REFERENCES

[1] L. J. Bellamy, "The Infrared Spectra of Complex Molecules" Methuen, London, 1968.
[2] R. Silverstein and G. Bassler, "Spectrometric Identification of Organic Compounds", Wiley, New York, 1967.
[3] I. Adams, *J. Amer. Chem. Soc.*, **65**, 356 (1943).

Revue Roumaine de Chimie, 26, 5, 725–732 (1981)

PHENAZATHIONIUM CATIONS. III[1].

THE SELECTIVE NUCLEOPHILIC SUBSTITUTIONS ON PHENAZATHIONIUM CATIONS

MIRCEA V. DIUDEA
Drug Factory "Terapia", Cluj-Napoca, 124, Fabricii Str. Romania

Received December 23, 1979

The selective nucleophilic substitutions in positions 3 and 1 of phenazathionium cations, generated by disproportionation of phenothiazinyl cation-radicals from their complexes with $CuCl_2$ are reported. Thus, 3-chlorophenothiazine (2), 3-nitrophenothiazine (3), 1,3,7-trichlorophenothiazine (4), 1,3,7-trinitrophenothiazine (5) and 1-nitro-3,7-dichlorophenothiazine (6) were obtained. The selective nitration reaction of the phenothiazine dimers (10,10′; 1,10′ and 3,10′) is also reported, demonstrating the intermediacy of dimer — $CuCl_2$ complexes and disproportionation of dication-diradicals, as mechanistic aspects. A series of nitro-dimers (new substances) was thus obtained.

1. INTRODUCTION

In the previous papers of this series, [1,2] (concerning kinetically and thermodynamically controlled nucleophilic substitution on phenazathionium cations) we stated that due to the dual behaviour of these cations, either S-derivatives (products of kinetic control) or C-derivatives (products of thermodynamic control) are formed, and that the positions 1(9) of the phenothiazine ring (usually unaffected by nucleophilic substitution) become accessible under thermodynamically controlled conditions. We inferred also [1,2] that the concentrations of the active species, phenazathionium cations and nucleophilic agents (by the intermediacy of the mass law), and the nucleophilicity of nucleophiles play a decisive role in the achievement of the thermodynamic control in the processes occurring in phenothiazine—oxidant—nucleophile systems along with the influence of well-known parameters (pH, temperature, reaction time, solvent). The formation of polysubstituted derivatives, even under such conditions in which monosubstitution should be expected, points towards the T^+ cation destabilization by a symmetrical substitution as well as to the excess of oxidant.

In the systems with less acidic pH and without other oxidizing agents, the phenothiazinyl cation-radicals disproportionate [3] to phenothiazines and phenazathionium cations. When disproportionation takes place in the presence of nucleophiles, these will attack the positions with high positive charge density of the resulted phenazathionium cations, leading to either C-derivatives [4] or S-derivatives [5-11] depending on the nature of the radical species and of nucleophile as well as on circumstances related to the medium. In all cases the monosubstitution is reached and the disproportionation (involving the absence of any oxidant) becomes the key-condition of the monosubstitution.

In experimental work the perchlorates of cation-radicals were most extensively used.[4–8,11]

The "reductive halogenation"[12] is another case of a reaction which, for the same reasons, leads to monosubstitution. Monosubstitution on phenazathionium cation T^+ generated *in situ* by means of $FeCl_3$ in alcoholic buffered medium was also reported.[13,14]

2. RESULTS AND DISCUSSION

2.1. Monosubstitution

We developed the monosubstitution on phenothiazine ring by using the tetrachlorocuprate (II) of phenothiazinyl cation-radical (**1**) (see [15,16]) in polar solvents (DMF, acetone, ethanol), as shown in Scheme 1.

Scheme 1

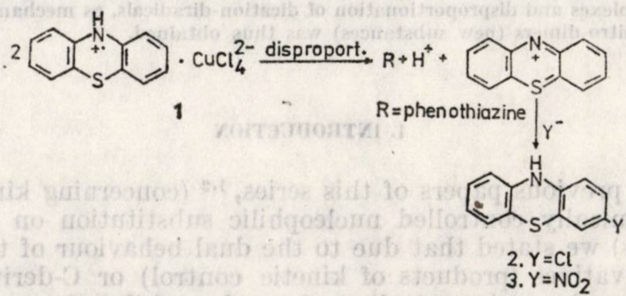

The nucleophile Y^- can be Cl^-, from the complex anion $Cu^{II}Cl_4^{2-}$ (the reaction occurs just by stirring **1** in warm DMF, without other reagent), or NO_2^- (from $NaNO_2$). In each case, the presence in the reaction mixture of phenothiazine (proving the disproportionation of cation-radical contained in **1**, as a central mechanistic aspect) was established. These reactions compete, both in yield and simplicity, with the monosubstitution reactions starting from the cation-radical perchlorates.[4]

The systems phenothiazine—$CuCl_2$—nucleophile follow a similar route, the intermediacy of the type **1** complexes being proved by the achievement of monosubstitution. Thus, the 3,7-disubstituted phenothiazines, in the presence of $CuCl_2$, in DMF, undergo the selective attack of some nucleophiles Y^- (Cl^-, NO_2^-) in position 1 (the reaction conditions being those of thermodynamic control). The 1,3,7-trisubstituted phenothiazines are obtained (see Scheme 2), the redox potential of the starting phenothiazine, as well as the nucleophilicity of the reagent directly influencing the reaction yields.

The ^1H-NMR spectra of such derivatives show an AX proton system, strongly deshielded (δ between 7 and 9 ppm), and an ABX system, at a somewhat higher field,[16] supporting the 1,3,7-trisubstituted phenothiazine structures. The existence of the nitro group in position 1 has also been demonstrated by its participation, under electron impact, in a McLafferty-type rearrangement.[16]

Scheme 2

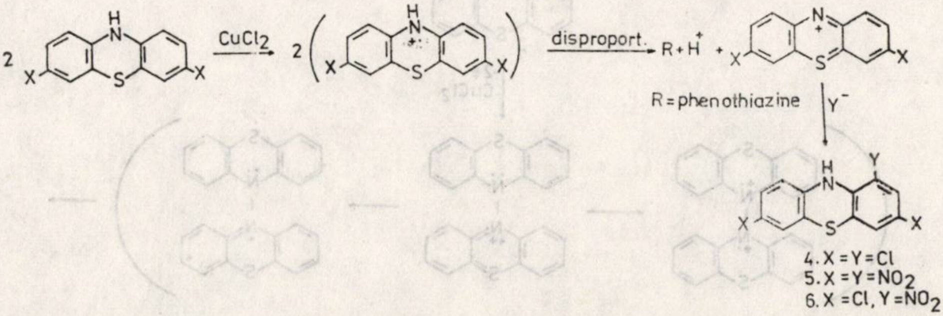

The reactions herein presented are the first selective nucleophilic substitutions in position 1 of the phenothiazine ring, reported in the literature.

2.2. Nitrodimers

Copper chloride oxidizes the phenothiazine dimers to dication-diradicals (either *in situ* or as solid salts, by analogy with **1**), which disproportionate intramolecularly, the resulting dimeric dication being subjected to the attack of a nucleophile Y^- (e.g. NO_2^- from $NaNO_2$).[16]

We performed the nitration of 10,10′-diphenothiazine **(7)** starting from both **7** and 10,10′-diphenothiazinyl tetrachlorocuprate (II) **(8)** (similar to complex **1**), thus demonstrating the intermediacy of the complexes

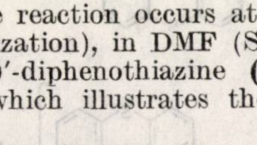

8

of diradicals with Cu. The reaction occurs at room temperature (or by gentle heating, for solubilization), in DMF (Scheme 3).

Besides 3-nitro-10,10′-diphenothiazine **(9)**, we have also found 3,7-dinitrophenothiazine, which illustrates the thermolability of N—N bonds in **7**.

We also carried out the nitration of 1,10′-diphenothiazine **(10)** by *in situ* generation of type **1** radicalic salt, in DMF, at room temperature (Scheme 4). From the reaction mixture we isolated a mononitroderivative **(11)** and traces of a dinitro-derivative **(12)**, as expected for a reaction taking place in the presence of a moderate excess of $CuCl_2$ and $NaNO_2$.

Scheme 3

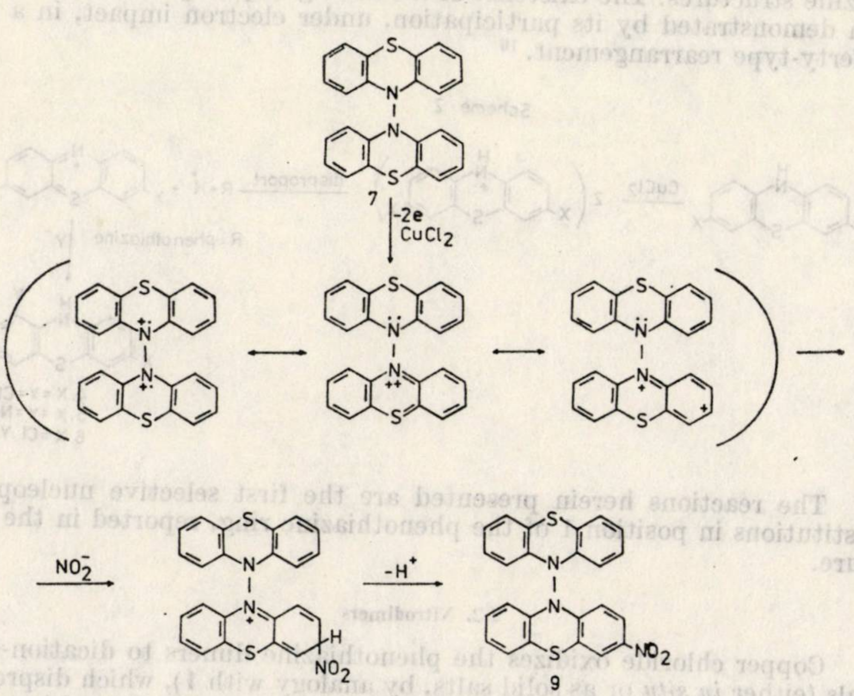
7
-2e
CuCl2
NO2-
-H+
NO2
H
9

Scheme 4

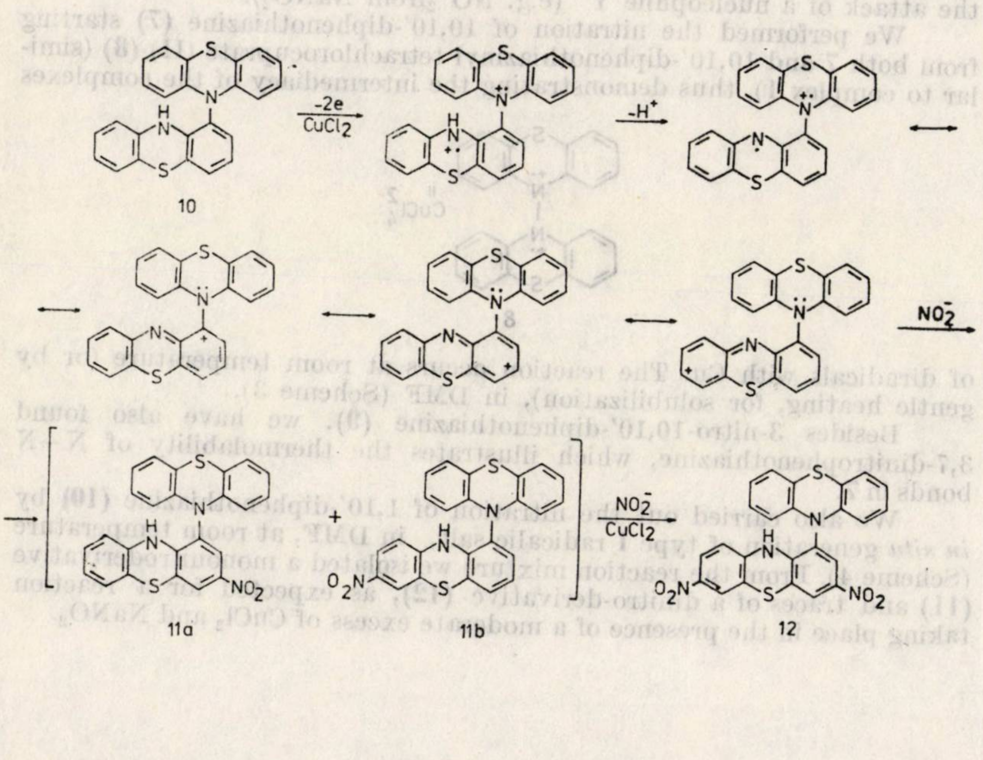
10
-2e
CuCl2
-H+
NO2-
11a
11b
NO2-
CuCl2
12

The mononitro-derivative **11** consists of a 1 : 1 mixture of two isomers. The elemental analysis pointed out only one nitro group in the molecule, and by subjecting **11** to repeated column chromatography on alumina, we succeeded in isolating the two isomers, probably **11a** and **11b** (characterized by m.p., TLC and IR). However, no attempt was made to assign firmly the above structures (3-nitro-1,10′-diphenothiazine **11a** and 7-nitro-1,10′-diphenothiazine **11b**) to the two isomers, because of lack of substance. The treatment of the mixture of mononitroderivatives **11** with $CuCl_2$ and $NaNO_2$ led to a single dinitro-derivative **12**, the ^1H-NMR spectrum of which shows an AX proton system, supporting a 1,3,7-trisubstituted phenothiazine structure.[16] Under electron impact a peak appears at $m/e = 198$, $I\% = 10.00$, suggesting an unsubstituted phenothiazine ring.[16] The formation of the specific deep-blue colour of *aci-nitro* forms in alkaline media, as well as of a single dinitro-derivative **(12)**, demonstrates that only one phenothiazine ring, the 1-substituted ring was subjected to the attack of the nucleophile NO_2^- in the formation of **11** and **12**(10-substituted-nitro-derivatives can not produce *aci-nitro* derivatives[12]). A similar result was reported in the phenoxazine class.[17]

We carried out the nitration of 3,10′-diphenothiazine starting just from the dimeric cation G^+ (*green product*) isolated,[15,16] as a solid complex salt, the G^+-dichlorocuprate (I), **13** (Scheme 5).

The resulting mononitro-dimer **14** forms *aci-nitro* colour demonstrating that the 10-substituted phenothiazine ring remained unsubstituted. The isolation,[16,18] of a dimeric phenothiazone substituted in the same positions as **14**, as well as of an analogous compound in the phenoxazine class,[17,19] underscores the possibility of the nucleophilic substitution in position 7 of the 3-substituted phenothiazine ring.

Scheme 5

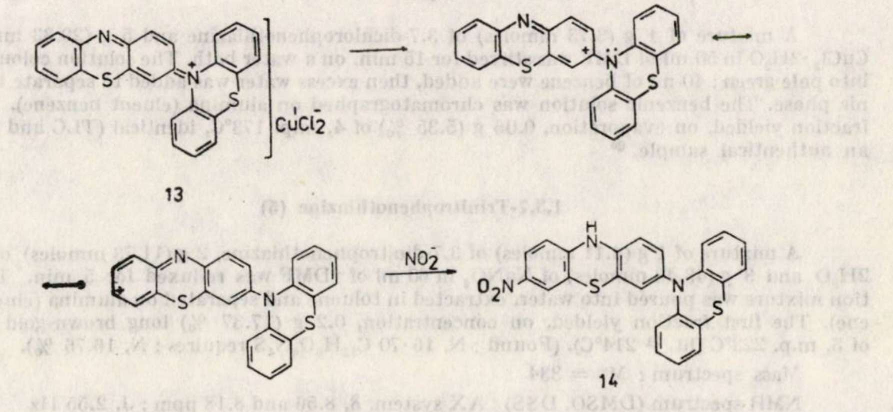

The dimers used as starting material in these reactions were prepared by original methods.[16] The above discussed nitro-dimers are new substances.

The herewith reported facts demonstrate that the copper (II) halides can act in the phenothiazine chemistry both as oxidizing agents and as halogenating reagents, thereby providing means for selective radicalic [20] as well as nucleophilic substitution reactions, which can be carried out under mild conditions with good preparative efficiency.

EXPERIMENTAL

Melting points are uncorrected. Elemental analyses were performed in the Analytical Laboratory of the Institute of Chemistry, Cluj-Napoca. IR spectra were recorded in KBr pellets on a double-beam UR—10 Carl Zeiss Jena spectrophotometer, mass-spectra were recorded on a MAT-Atlas 311 (Bremen) and ^1H—NMR spectra on a WP—60 Bruker pulse-Fourier-transform spectrophotometer.

3-Chlorophenothiazine (2)

A suspension of 1 (8 g, 13.25 mmoles) in 100 ml of DMF was stirred for 30 min. at 40 to 50°C. The green solution turned dark-brown; the reaction mass was poured into water and filtered. The precipitate thus formed was extracted in toluene and chromatographed on alumina column (eluent toluene). The first fraction yielded, on concentration, 2 g (65.01 %) of white-green plates of **2**, m.p. 202°C (lit.[4] 202°C) (Found : Cl, 15.24 ; $C_{12}H_8ClNS$ requires : Cl, 15.12 %).

3-Nitrophenothiazine (3)

A suspension of **1** (1 g, 1.66 mmoles) in 100 ml of acetone was treated with 5 g (72.47 mmoles) of $NaNO_2$ under stirring for 15 min. at room temperature. The brown solution was filtered and diluted with excess water, the violet-brown precipitate was filtered off, dried and washed with 40 to 50 ml of warm benzene (in order to remove the accompanying phenothiazine). The precipitate was then extracted with acetone and the solution evaporated to dryness. On recrystallisation from aniline, 0.29 g (72.5 %) of dark-violet powder of **3**, m.p. 211°C (lit. [13] 212°C) was obtained. (Found : N, 11.94 : $C_{12}H_8O_2N_2S$ requires : N, 11.76 %).

1,3,7-Trichlorophenothiazine (4)

A mixture of 1 g (3.73 mmoles) of 3,7-dichlorophenothiazine and 5 g (29.33 mmoles) of $CuCl_2 \cdot 2H_2O$ in 50 ml of DMF was stirred for 15 min. on a water bath. The solution colour turned into pale green ; 40 ml of benzene were added, then excess water was added to separate the organic phase. The benzenic solution was chromatographed on alumina (eluent benzene). The first fraction yielded, on evaporation, 0.06 g (5.35 %) of **4**, m.p. 173°C, identical (TLC and IR) with an authentical sample. [20]

1,3,7-Trinitrophenothiazine (5)

A mixture of 1 g (4.11 mmoles) of 3,7-dinitrophenothiazine, 2 g (11.73 mmoles) of $CuCl_2 \cdot 2H_2O$ and 3 g (43.48 mmoles) of $NaNO_2$ in 60 ml of DMF was refluxed for 5 min. The reaction mixture was poured into water, extracted in toluene and separated on alumina (eluent toluene). The first fraction yielded, on concentration, 0.2 g (17.37 %) long brown-gold crystals of **5**, m.p. 223°C (lit. [21] 214°C). (Found : N, 16 ·70 $C_{12}H_6O_6N_4S$ requires : N, 16.76 %).

Mass spectrum : $M^+ = 334$

NMR spectrum (DMSO, DSS) : AX system, δ, 8.56 and 8.18 ppm ; J, 2.55 Hz

IR spectrum (cm^{-1}) : 1335, 1505, 3280.

1-Nitro-3,7-dichlorophenothiazine (6)

A mixture of 1 g (3.73 mmoles) of 3,7-dichlorophenothiazine, 1.25 g (7.33 mmoles) of $CuCl_2 \cdot 2H_2O$ (molar ratio 1 :2) and 3 g (43.48 mmoles) of $NaNO_2$ (molar ratio 1 :10) in 50 ml of DMF, was stirred for 15 min. at room temperature. The reaction mixture was poured into water, filtered, the precipitate dried, extracted in benzene and chromatographed on alumina (eluent benzene). The first fraction yielded, on concentration, 0.15 g (12.8 %) long brown-indigo crystals of **6**, m.p. 203°C (lit. [22] 203°C). (Found : N, 9.15 ; $C_{12}H_6Cl_2O_2N_2S$ requires : N, 8.94 %).

Mass spectrum : $M^+ = 312$

MR spectrum ($CDCl_3$, TMS) : AX system, δ, 7.91 and 7.15 ppm ; J, 2.33 Hz

IR spectrum (cm^{-1}) : ν(NH), 3275.

3-Nitro-10,10′-diphenothiazine (9)

Procedure a). A solution of 0.8 g (2.02 mmoles) of **7** in 50 ml of benzene and 50 ml of DMF was treated under stirring for 30 min. with 3 g (17.59 mmoles) of $CuCl_2 \cdot 2H_2O$ and 8 g (115.95 mmoles) of $NaNO_2$. The brown-green solution was filtered and diluted with excess water to separate the organic phase. The benzenic solution was diluted with excess acetone, the precipitate filtered off, extracted in benzene and chromatographed on alumina (eluent benzene). The first fraction yielded on evaporation, 0.2 g (23.59 %) of brown powder of **9** (resinification over 310°C).

Mass spectrum : $M^+ = 441$.

Procedure b). A suspension of 0.6 g (0.99 mmoles) of **8** and 3 g (43.48 mmoles) of $NaNO_2$ in 100 ml of DMF and 50 ml of benzene was stirred for 10 min. at 30 to 40°C, then 30 min. at room temperature. The resulting brown solution was diluted with excess water and the benzenic phase separated, then chromatographed on alumina (eluent benzene). The first fraction yielded on evaporation, 0.1 g (24.81 %) of brown powder of **9**, identical (TLC and IR) with the product obtained above (procedure a).

3(7)-Nitro-1,10′-diphenothiazine (11)

A suspension of 0.5 g (1.26 mmoles) of **10** in 20 ml of DMF was treated under stirring for 20 min. with 2.2 g (12.90 mmoles) of $CuCl_2 \cdot 2H_2O$, then 4 g (57.97 mmoles) of $NaNO_2$ were added during 1 min. The brown-red reaction mixture was poured into water, the precipitate filtered off, extracted in acetone and again poured into water. The precipitate was filtered off, dried and chromatographed on alumina (eluent benzene). The first fraction yielded, on concentration, 0.38 g (69.01 %) of 1 :1 isomeric mixture of **11**, m.p. 203°C. (Found : N, 9.29 ; $C_{24}H_{15}O_2N_3S_2$ requires : N, 9.52 %).

The subsequent separation of the isomeric mixture (eluent ligroine) showed the presence of two mononitrated isomers : one, m.p. 227 to 228°C, IR spectrum (cm^{-1}) : 775–1100, 1178, 1242 $>$ 1270, 1318–1332, 1470–1486–1510, 1531, 1573, 1605, 3350–3380, and another, m.p. 216 to 216°C, IR spectrum : 775, 1141, 1241 $<$ 1270, 1310–1328, 1470–1502, 1525, 1577, 1603, and 3340 – broad, probably representing the 3- and 7-mononitroderivatives **11** a and **11**b.

3,7-Dinitro-1,10′-diphenothiazine (12)

A mixture of 0.2 g (0.45 mmoles) of **11** and 2 g (11.73 mmoles) of $CuCl_2 \cdot 2H_2O$ in 50 ml of DMF was stirred for 2 to 3 min., then 4 g (57.97 mmoles) of $NaNO_2$ were added and stirred for 10 min. The reaction mixture was poured into water, the precipitate filtered off, purified by extraction in acetone and reprecipitation with water, then filtered off, dried and chromatographed on alumina (eluent benzene). The first fraction yielded, on concentration, 0.185 g (83.9 %) coral-red crystals of **12**, m.p. 296 to 297°C.

Mass spectrum : $M^+ = 486$

NMR spectrum ($CDCl_3$, TMS) : AX system, δ, 8.35 and 7.97 ppm ; J, 2.50 Hz.

7-Nitro-3,10′-diphenothiazine (14)

A suspension of 1 g (1.88 mmoles) of **13** in 100 ml of acetone, was stirred for 15 min. with 5 g (72.47 mmoles) of $NaNO_2$ at room temperature. The solution turned from green into brown, then was filtered and poured into water. The precipitate was filtered off, dried, extracted in benzene and filtered through a small amount of alumina. The filtrate yielded, on concentration, a violet product. On recrystallization from benzene, 0.26 (31.32 %) of dark-violet crystals of **14**, m.p. 135 to 137°C were obtained (Found : N, 9.48 ; $C_{24}H_{15}O_2N_3S_2$ requires : N, 9.52 %).

REFERENCES

[1] Part. II I.A. Silberg and M. V. Diudea, *Rev. Roumaine Chim.*, **25**, 1239(1980).
[2] I. A Silberg and M. V. Diudea, *Rev. Roumaine Chim.*, **25**, 1229(1980).
[3] P. Hanson and R.O.C. Norman, *J. Chem. Soc. Perkin Trans. II*, 264 (1973).
[4] H. J. Shine, J. J. Silber, J. R. Burssey and T. Okujama, *J. Org. Chem*, **37**, 2691(1972).
[5] H. J. Shine and K. Kiongtae, *Tetrahedron Lett.*, 99 (1974).
[6] K. Bandlish-Baldev, A. G. Padilla and H. J. Shine, *J. Org. Chem.*, **40**, 2590 (1975).
[7] J. F. Evans, J. R. Lenhard and H. N. Blount, *J. Org. Chem.*, **42**, 983 (1977).
[8] A. G. Padilla, K. Bandlish-Baldev and H. J. Shine, *J. Org. Chem.*, **42**, 1833 (1977).
[9] E. F. Perozzi and J. C. Martin, *J. Org. Chem.*, **42**, 3222 (1977).
[10] J. J. Shah, *J. Tenn. Acad. Sci.*, **52**, 19 (1977) ; *Chem. Abstr.*, **86**, 129972 (1977).
[11] K. Bandlish-Bandlev, W. R. Porter Jr. and H. J. Shine, *J. Phys. Chem.*, **82**, 1168 (1978).
[12] C. Bodea and I. A. Silberg, *Adv. Heterocycl. Chem.*, **9**, 322 (1968) (A. R. Katritzky and A. J. Boulton, ed.) Academic Press, New York.
[13] J. Daneke and W. H. Wantzlik, *Liebigs Ann. Chem.*, **740**, 52 (1970).
[14] W. H. Wantzlik and J. Daneke, Ger. Offen 2, 047, 078 ; *Chem. Abstr.*, **77**, 19661 (1972).
[15] I. A. Silberg and M. V. Diudea, *J. prakt. Chem.*, in press.
[16] M. V. Diudea, Ph. D. Dissertation, Institute of Chemistry, Cluj-Napoca, 1979.
[17] H. Musso, *Chem. Ber.*, **92**, 2873 (1959).
[18] Y. Tsujino, K. Nishikida and T. Naito, *Nippon Kagaku Zasshi*, **91**, 1080 (1970) ; Chem. Abstr., **74**, 125598 (1971).
[19] H. Musso, *Chem. Ber.*, **92**, 2862 (1959).
[20] I. A. Silberg, V. Fărcășan and M. V. Diudea, *J. prakt. Chem.*, **318**, 353 (1976).
[21] F. Kehrmann and F. Ringer, *Ber. dtsch. chem. Ges.*, **46**, 3014 (1913).
[22] R. L. Mital and S. K. Jain, *Ann. Soc. Sci. Bruxelles, ser. 1*, **83**, 182 (1968) ; *Chem. Abstr.*, **71**, 49874 (1969).

Revue Roumaine de Chimie, 26, 5, 733–738 (1981)

VERSUCHE ZUR DARSTELLUNG DES 10-METHYL-9-METHYLENDIHYDROACRIDIN-ω-ALDEHYDS

KONST. KOKKINOS und CHR. MARKOPOULOS
Fachbereich Organische Chemie
N.R.C. „Demokritos" Aghia Paraskevi-Attikis
Athen – Griechenland

Eingegangen am 28. Februar 1980

Aus 9,10-Dimethylacridiniumsalz und eines Überschußes von Orthoameisensäureester wird das 10-Methyl-9-methylendihydroacridin-ω-aldehyd-perchlorat, und daraus der freie Aldehyd erhalten.

9,10-Dimethylacridinium salt reacts with an excess of orthoformic ester yielding 10-methyl-9-methylene-dihydroacridine-ω-aldehyde perchlorate, from which the free aldehyde is obtained.

Wie König [1] zeigte, bilden sich bei der Einwirkung von Orthoameisenester auf sogenannte 2-oder-4-Methyl-cycloammoniumsalze in meist glatter Reaktion symmetrische Trimethincyanine.

Stöchiometrisch läßt sich die Bildung der Trimethine wiedergeben durch die Gleichung (II).

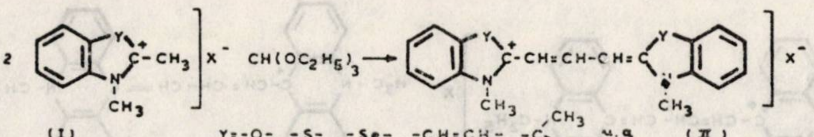

Die Kondensation wird in Essigsäureanhydrid oder in einem Gemisch von Essigsäure-anhydrid und Pyridin durchgefürt. Es liegt daher am Schluß kein freier Alkohol vor, sondern Essigester.

Die Farbstoffbildung selbst verläuft in zwei Stufen.

Zuerst kondensiert der Orthoameisensäureester mit einem Mol Methylcarbeniumsalz zum Acetalsalz eines sogenannten „ω-Aldehydes" (III) nämlich zu (V).

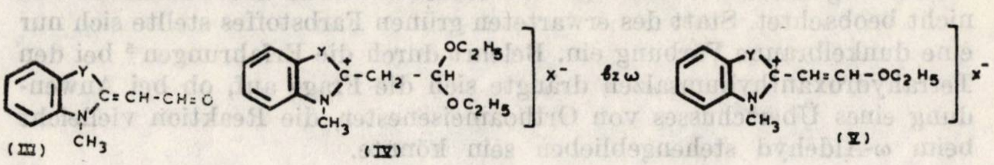

Das Salz kondensiert weiter unter Alkoholabspaltung mit dem zweiten Molekül Carbeniumsalz (II).

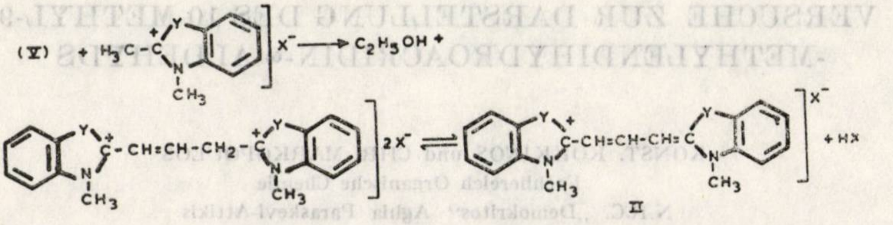

Das Gleichgewicht zwischen Dicarbeniumsalz und Monocarbeniumsalz und Säure liegt weitgehend auf der rechten Seite. Die Säureabspaltung erfolgt unter dem Einfluss der beiden acidifizierenden Carbenium-C und einer Doppelbildung sehr leicht. [2]

Beide Reaktionsstufen, die Bildung des ω-Aldehyds bzw. seines Acetalsalzes und die Bildung des Trimethins folgen so rasch aufeinander, daß es zu schwer gelang aus einem „Methylcycloammonium Salz" mit Orthoameisensäureester ein ω-Aldehyd darzustellen. Diese ω-Aldehyde sind aber sehr wichtig, denn sie eignen sich zur Darstellung einer großen Zahl interessanter Substanzen von denen viele brauchbare photographische Sensibilisatoren sind. In dieser Hinsicht sind die wichtigsten Verbindungsgruppen die unsymmetrischen Trimethine, die Marocyanine, und die Kondensationsprodukte mit primären aromatischen Aminen, vor allem den *p*-Diaminen. In Jahre 1937 versuchte WIZINGER [3] aus 9,10-Dimethylacridiniumsalz und Orthoameisensäureester das dem Bis-4-(1-äthylchinolin)-trimethincyanin (Lepidincarbocyanin) (VI) analoge Bis-9-(10-methylacridin)-trimethincyanin (VII) zu synthetisieren.

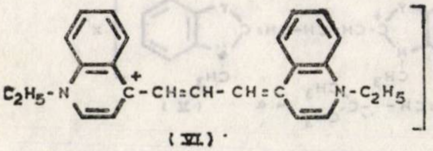

(VI)

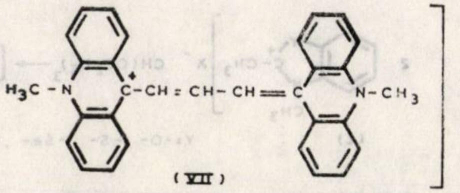

(VII)

In Jahre 1920 kam VI unter dem Namen „Kryptocyanin" in Amerika und einige Jahre später in Deutschland als „Rubrocyanin" in den Handel. [4] Die alkoholische Lösung ist blaugrün und zeigt ein Absorptionsmaximum bei 710 nm. Das Sensibilisierungsmaximum liegt bei 730 nm. Der Farbstoff war der erste Sensibilisator für das nahe Ultrarot. Bei einer größeren Anzahl von Vorversuchen wurde das Trimethin VII nicht beobachtet. Statt des erwarteten grünen Farbstoffes stellte sich nur eine dunkelbraune Färbung ein. Belehrt durch die Erfahrungen [5] bei den Tetrahydroxanthyliumsalzen drängte sich die Frage auf, ob bei Anwendung eines Überschusses von Orthoameisenester, die Reaktion vielleicht beim ω-Aldehyd stehengeblieben sein könnte.

Zunächst handelt es sich darum das 9,10-Dimethyl-acridiniumsalz darzustellen. Das für die Synthese dieser Farbsalze benötigte Dimethylacridiniumsalz kann auf zwei Wegen erhalten werden. Ein Verfahren besteht in der Einwirkung von Methylmagnesiumbromid auf N-Methylacridon.[6] Diese Methode hat den Nachteil, daß nur in Ansätzen von wenigen Gramms gearbeitet werden kann und Ausbeuten von höchstens 40 % erhalten werden. Der zweite Weg führt über das 9-Methyl-acridin. Die Arbeiten nach den Vorschriften[7] durch Erhitzen von Diphenylamin mit Eisessig und Chlorzink, sowie nach den Vorschriften[8-9] gestalteten sich nicht gerade erfreulich. Schließlich erhält man das reine 9-Methylacridin vom F 117 –118° aber in schlechter Ausbeute.

In der Hoffnung eine bessere Ausbeute zu erhalten, änderten wir das Verfahren ab. Statt vom Diphenylamin gingen wir vom Acetyldiphenylamin[10] aus. Die besten Ergebnisse wurden erhalten bei Anwendung eines Verhältnisses vom Acetyldiphenylamin : Eisessig : Chlorzink = 1 : 1 : 2. Die Ausbeute ist beachtlich größer, nämlich 6 g reines Methylacridin aus 30 g Acetyldiphenylamin.Die Überführung des 9-Methylacridins in das 9,10-Dimethyl-acridiniumperchlorat geht dann einfach vor sich. Beim Erwärmen von 9-Methylacridin mit Dimethylsulfat in benzolischer Lösung fällt das 9,10-Dimethylacridinium-methylsulfat aus. Dieses wird in Wasser gelöst und 20 % ige Na-perchloratlösung zugegeben. Das 9,10-Dimethylacridiniumperchlorat bildet gelbe Kristalle, von F = 230° (Zers). Die Lösungen in Wasser, Alkohol, oder Eisessig (geringe Löslichkeit) zeigen starke grüne Fluoreszenz. Der Mechanismus der Reaktion ist nicht restlos aufgeklärt. Wahrscheinlich findet zunächst eine Umlagerung im Sinne einer Fries'schen Verschiebung statt, worauf sich dann der Ringschluß unter Wasserabspaltung vollzieht (X).

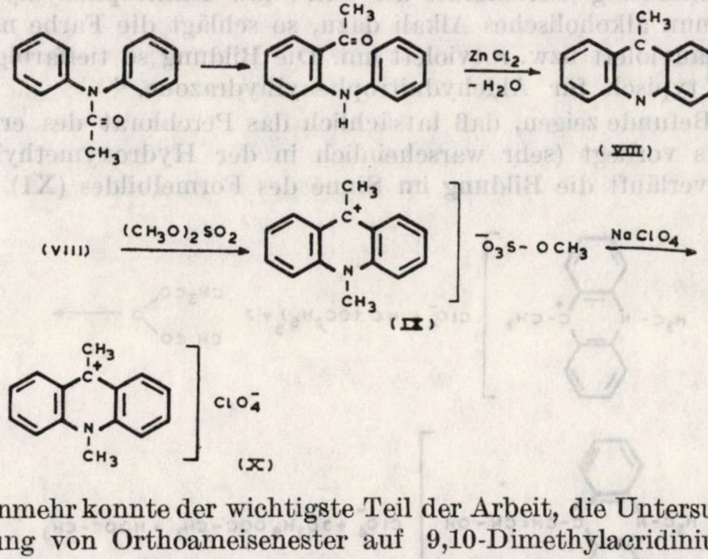

Nunmehr konnte der wichtigste Teil der Arbeit, die Untersuchung der Einwirkung von Orthoameisenester auf 9,10-Dimethylacridiniumsalze in Angriff genommen werden. Es wurden zunächst Vorversuche mit 9,10-Dimethylacridinium-methylsulfat (IX) und-perchlorat (X) unternommen. Das Erhitzen des Methylsulfats (IX) mit Orthoameisensäureäthylester in Essigsäureanhydrid ergab dunkelbraune Lösungen; die Reaktion blieb also anscheinend beim ω-Aldehyd stehen, doch schied sich das Reaktionsprodukt nicht aus. Das Perchlorat (X) dagegen, ging beim Erhitzen mit Essigsäureanhydrid und Orthoameisenester zunächst mit hellgelber Farbe in Lösung, dann trat rasch Kondensation unter Dunkelbraunfärbung ein, und bei Kühlung schied sich ein gelbbraunes kristallines Pulver aus (Grünfärbung, d. h. Trimethin-bildung was nicht zu beobachten). Aus 2 Teile Dimethylacridiniumperchlorat, 20 Teile Essigsäureanhydrid und 3 Teile Orthoameisensäureester, wurden rund 70% des Kondensationsproduktes erhalten. Wie schon das Verpuffen beim Erhitzen zeigt, ist das Produkt ein Perchlorat.

Schon aus einer Reihe von Vorversuchen ergab sich, das die neue Verbindung das Perchlorat des vermuteten ω-Aldehyds ist.

Die alkoholische Lösung wird in der Kälte langsam, rasch beim Erwärmen durch fuchsinschweflige Säure intensiv schön violettrot. Beim Erwärmen der alkoholischen Suspension des Perchlorats mit einer Lösung von Salzsäurem Hydroxylamin entsteht eine intensive braunorangefarbene Lösung des Perchlorats des Oxims; auf Zusatz von alkoholischem Alkali wird daraus das rein orangegelbe Oxim erhalten. Mit Phenylhydrazin bildet sich sehr rasch das Perchlorat des Phenylhydrazones (sehr intensiv organgegelb, in dicker schicht gelb-braun), und daraus mit alkoholischem NaOH das schön orangefarbene freie Phenylhydrazon.

Mit *p*-Nitrophenyl-hydrazin und 2,4-Dinitrophenylhydrazin tritt beim Erwärmen in Alkohol ebenfalls rasch eine Reaktion ein, unter intensiver Braunfärbung (Perchlorate des Nitro-bzw Dinitrophenylhydrazins): gibt man nun alkoholisches Alkali dazu, so schlägt die Farbe nach sehr intensiv blauviolett bzw. rotviolett um. Die Bildung so tieffarbiger Alkalisalze ist typisch für Aldehydnitrophenylhydrazone.[11]

Die Befunde zeigen, daß tatsächlich das Perchlorat des erwarteten ω-Aldehyds vorliegt (sehr warscheinlich in der Hydroxymethylenform). Demnach verläuft die Bildung im Sinne des Formelbildes (XI).

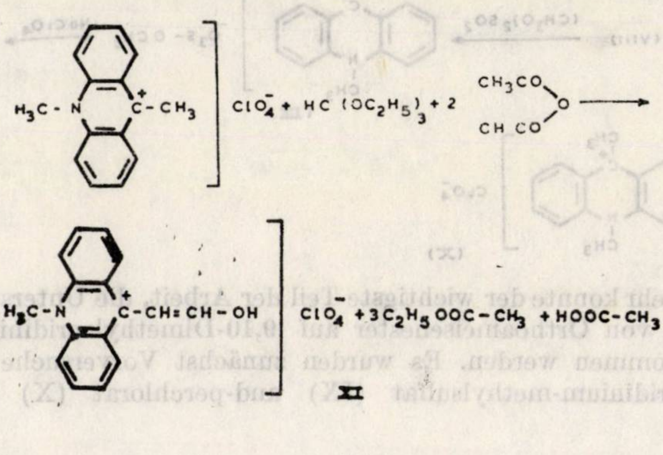

XI

Es muß angenommen werden, daß sich primär der Äthoxymethylenkörper XII bildet der aber rasch aufgespalten wird.

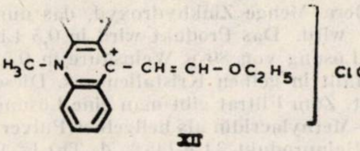

XII

Die leichte Aufspaltbarkeit zum Hydromethylenkörper erklärt sich aus dem azidifizierten Einfluß des α-C-Atoms [12] welches dem Carbeniumzustand noch ziemlich nahe steht, d.h. einen beachtlichen Elektronenhunger besitzt und dadurch der Methoxygruppe den Charakter eines Esters einer starken Säure verleiht. Die Reaktion entspricht der sehr leicht vor sich gehenden Umwandlung von Äthoxymethylenacetessigester in Hydroxymethylenacetessigester (XIII).

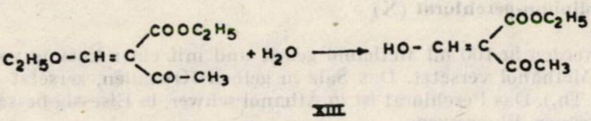

XIII

Trägt man das Perchlorat in alkoholische Natronlauge ein, und erwärmt es bis sich alles gelöst hat, so bildet sich unter Säureabspaltung der freie Aldehyd, der sich dann durch Wasserzusatz ausfällen läßt. Durch umkristallisieren aus Petroläther kann er die Form eines rotbraunen Pulvers von F⁰C 117 –119 (Zers) erhalten. Er ist unlöslich in Wasser, aber leicht löslich in den üblichen organischen Lösungsmitteln (XIV).

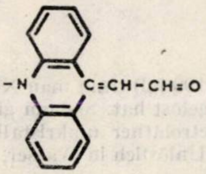

(XIV)

EXPERIMENTELLER TEIL

Acetyldiphenylamin[8]

150 g Diphenylamin werden in 120 g Acetanhydrid gelöst und 4 Std. auf dem Wasserbad erwärmt. Engt man die Lösung am Vakuum auf 1/3 des ursprünglichen Volumens ein, und läßt über Nacht stehen. Abfitriert, und mit Äthanol und Äther gewaschen. Ausbeute 120 g. Durch Versetzen der Mutterlauge mit Äther lassen sich weitere 20 g gewinnen. Gesamtausbeute 140 g (75 % d. Th.).

9-Methylacridin (VIII)

Es werden 80 g (0,38 Mol) Acetyldiphenylamin, 85 ml Eisessig und 160 g wasserfreiers Zinkchlorid während 30 Std. auf 220–230° erhitzt. Die heiße Schmelze wird in dünnem Strahl und starkem Rühren in eine siedende Lösung von 25 ml konz. Schwefelsäure in 700 ml Wasser gegossen. Die teerige Masse wird noch eine Stde ausgekocht. Die gelbe Lösung gießt man noch siedend heiß durch ein Faltenfilter, während der Rückstand mit je der gleichen Menge verd. Schwefelsäure-wie-oben angegeben-noch 5 mal ausgekocht wird. Die Filtrate werden mit konz. Ammoniak versetzt, bis ein gelber, flockiger Niederschlag ausfällt, und nutscht dann ab. Der Niederschlag erhält noch größere Menge Zinkhydroxyd, das durch mehrmaliges Auswaschen mit konz. Ammoniak entfernt wird. Das Produkt wird in 0,5 Liter Äthanol unter Erwärmen gelöst, und mit einer heißen Lösung von 80 g Weinsäure in 0,5 Liter Äthanol versetzt. Das Tartrat des 9-Methylacridins fällt in gelben Kristallen aus. Dieses wird in ca 5 l siedendem Wasser gelöst und heiß filtriert. Zum Filtrat gibt man eine Lösung von 60 g Soda (Wasserfrei) in 200 ml Wasser, wobei das 9-Methylacridin als hellgelbes Pulver ausfällt. Es wird aus Aceton umkristallisiert. Ausbeute an Reinprodukt 34 g (45% d. Th) F° 119–120°C.

9,10-Dimethylacridinium-methylsulfat (IX)

7,8 g (VIII) werden in 30 ml Benzol unter Erwärmen gelöst. Man gibt eine Lösung von 6,5 g oder 5 ml Dimethylsulfat in 10 ml Benzol und erhitzt während 4 Stdn am Rückfluß. Aus Methanol umkristallisiert. Ausbeute 9,0 g Dimethylacridiniummethylsulfat, in gelben Nadeln, die sich bei 215°C zersetzen. Aus der Mutterlauge lassen sich weitere 1 g gewinnen. Gesamtausbeute 10,5 g (80% d. Th.); starke grüne Fluoreszenz in Eisessig und Konz. Schwefelsäure.

9,10-Dimethylacridinium-perchlorat (X)

5 g (IX) werden in 100 ml Methanol gelöst und mit einer Lösung von 2 g Natriumperchlorat in 15 ml Methanol versetzt. Das Salz in gelben Kristallen, zersetzt sich bei 235°. Ausbeute 4 g (90% d. Th.). Das Perchlorat ist in Äthanol schwer, in Eisessig besser löslich mit gelber Farbe und gelbgrüner Fluoreszenz.

10-Methyl-9-methylen-dihydroacridin-ω-aldehyd-perchlorat (XI)

Zu 20 g (X) gibt man 200 ml Essigsäureanhydrid sowie 300 ml Orthoameisensäureester und kocht 1/2 Stde am Rückfluß. Gelbbraunes kristallines Pulver. Ausbeute 14,8 g (70%d. Th.). Unlöslich in Wasser, Äther, und Benzol, etwas löslich in Alkohol und Eisessig mit gelber Farbe und grüner Fluoreszenz. Leicht löslich in konz. Schwefelsäure mit braungelber Farbe und starker grüner Fluoreszenz.

Freier Aldehyd (XIV)

In alkoholische Natronlauge (100 ml) trägt man XI 10 g ein, und erwärmt, bis sich unter Abspaltung der Perchlorsäure alles gelöst hat. Sodann gießt man die Lösung in Wasser, wobei der freie Aldehyd ausfällt. Aus Petroläther umkristallisiert. Rotbraunes Pulver F 117/119° (Zers). Ausbeute 6,8 g (68% d. Th.) Unlöslich in Wasser, gut löslich in den üblichen organischen Lösungsmitteln.
Analyse : $C_{16}H_{3}ON$ (225,15) Ber. C 81,72 ; H 5,53 ; N 5,95 ; Gef C 81,02 ; H 5,63 N 6,34 %.

LITERATURHINWEISE

[1] W. König, *Ber. dtsch. Chem. Ges.*, **55**, 3293 (1922) ; D.R.P. 41048.
[2] R. Wizinger, *J. prakt. Chem.*, **154**, 1 (1939) ; *ibid.*, **154**, 129 (1941) ; D.R.P. 639910 (1930).
[3] R. Wizinger, (1970), (Privatmitteilung).
[4] Agfa-Veröffentlichungen Bd. VI S. 5.
[5] R. Wizinger (Privatmitteilung).
[6] R. Wizinger (Privatmitteilung).
[7] O. Fischer und E. Besthorn, *Ber. dtsch. Chem. Ges.*, **16**, 74 (1883).
[8] A. Bernthsen, *Liebigs Ann. Chem.*, **224**, 34 (1884).
[9] W. König, *Ber. dtsch. Chem. Ges.*, **32**, 3604 (1909).
[10] A. Claus, *Ber. dtsch. Chem. Ges.*, **14**, 2366 (1881).
[11] E. Bamberger und F. Hyde, *Ber. dtsch. Chem. Ges.*, **32**, 1807 (1899).
[12] R. Wizinger, *J. prakt. Chem.*, **157**, 129 (1941).

Revue Roumaine de Chimie, **26**, *5*, 739–753 (1981)

MODERN *FRIEDEL-CRAFTS* CHEMISTRY. IX.[1]

ON THE CYCLOALKYLATION OF ARYL ALKENYL KETONES AND OTHER RELATED SYSTEMS

ALI ALI KHALAF and AHMED M.A. EL-KHAWAGA

Department of Chemistry, Assiut University, Assiut,
Arab Republic of Egypt

Received October 30, 1979

Some aryl alkenyl ketones and other related compounds were prepared and subjected to the action of Friedel-Crafts catalysts. The failure of these ketones to cyclise under the employed conditions demonstrated that ring closure is supressed due to the deactivating carbonyl group placed in conjugation with the aromatic nucleus. Thus, in line with other electrophilic substitution reactions, nucleophilicity of the aromatic nucleus upon which the attack occurs plays a determining role in Friedel-Crafts cyclisations. Accordingly, the present results call for the reinvestigation of the numerous earlier data claiming facile closures of such carbonyl-deactivated systems. A mechanism for the reaction of unsaturated acid chlorides with arenes and $AlCl_3$ is also suggested.

INTRODUCTION

Examination of the literature results and discussions [1a] on the Friedel-Crafts cycloalkylations of alkenyl ketones [2–29] and the related hydroxyalkyl [11,30,31] and haloalkyl [4, 23, 32–47] aryl ketones reveals considerable discrepancies. For example, α, β-unsaturated ketones of general formula **1** have been claimed to undergo facile five-membered ring closures to 1-indanones of general formula **2** upon treatment with acid catalysts (eq. 1). [2–6,8,9,11–15,17–20,22–27]

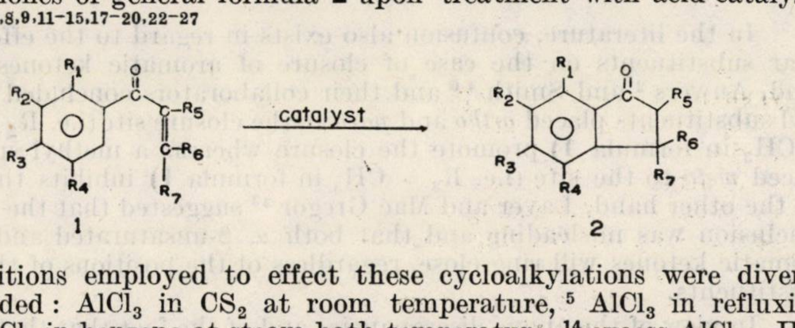

1 **2** (1)

The conditions employed to effect these cycloalkylations were diverse and included: $AlCl_3$ in CS_2 at room temperature, [5] $AlCl_3$ in refluxing CS_2, [5,8] $AlCl_3$ in benzene at steam bath temperature, [14] excess $AlCl_3-HCl$ in refluxing CS_2, [4,13] $H_3PO_4-HCOOH$ [18,26] and $AlCl_3-NaCl$ at 100°C to 180°C. [15,17,20,27]

Added to these direct closures, α,β-unsaturated aromatic ketones have also been proposed as reaction intermediates in the acid catalysed formation of 1-indanones from aryl α-bromoalkyl ketones (**3**, eq. 2), [2,23] α-alkyl-β-hydroxypropiophenones (**4**, eq. 3) [11,30,31] and arene-α, β-unsaturated acid chloride mixtures (eq. 4). [4,8,9,14,25]

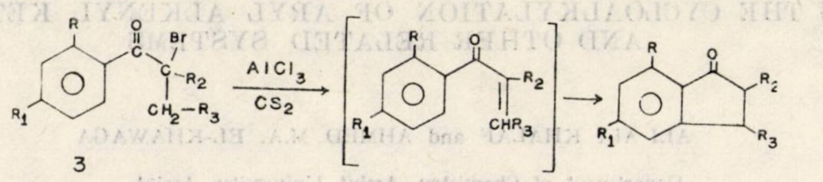

(2)

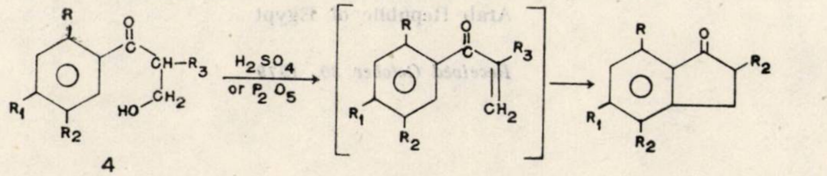

(3)

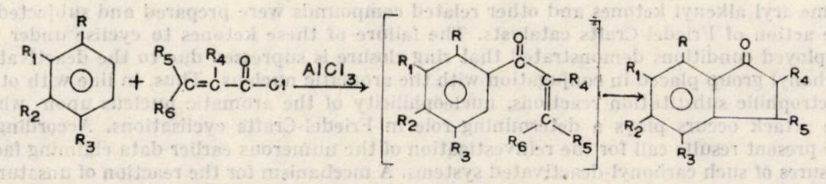

(4)

In contrast with the preceding claims, Colonge and Grimaud [12] reported that unsaturated aromatic ketones of the general formula **5** failed to cyclise to 1-tetralones upon treatment with acid catalysts (eq. 5).

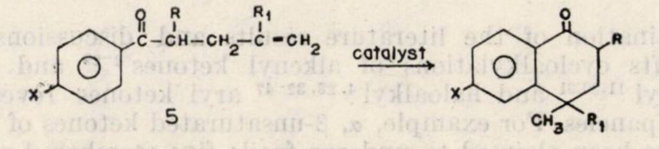

$X = Cl, CH_3 : R = CH_3 ; R_1 = H, CH_3$

In the literature, confusion also exists in regard to the effect of nuclear substituents on the ease of closure of aromatic ketones. On one hand, Auwers [2] and Smith [4,6] and their collaborators concluded that methyl substituents placed *ortho* and *para* to the closure site (i.e. R_2 and $R_4 = CH_3$ in formula **1**) promote the closure whereas a methyl substituent placed *meta* to the site (i.e. $R_3 = CH_3$ in formula **1**) inhibits the closure. On the other hand, Layer and Mac Gregor [23] suggested that the preceding conclusion was misleading and that both α, β-unsaturated and α-bromo aromatic ketones will ring close, regardless of the positions of the nuclear substituents.

In view of the above discrepancies and of the fact that the reactivity of aromatic carbonyl compounds towards electrophilic reagents (e.g. alkylating and acylating agents) is considerably low, [39,41,48–51] we felt that an up-to-date tackling of this interesting problem is both important and timely. As a first step in this direction, we now describe the synthesis of some unsaturated aromatic ketones together with the results of their attempted closure under a variety of Friedel-Crafts conditions. These results are compared to those from earlier studies and discussed in terms of our recent findings about ring closure reactions.[41,52-60] In an effort to confirm our present views about the cyclisation behaviour of the investigated aromatic ketones, we have also examined the reaction of benzene with succinyl chloride under similar Friedel-Crafts conditions.

RESULTS

Synthesis of required materials

The required cycloalkylation substrates and the expected cycloalkylation products were synthesised by application, extension or adaptation of established procedures. Thus, benzalacetophenone **(7a)**, *p*-methoxybenzalacetophenone **(7b)** and isobutylideneacetophenone **(7c)** were obtained by the base-catalysed condensation of acetophenone with benzaldehyde **(6a)**,[61] *p*-methoxybenzaldehyde **(6b)**[62] and isobutyraldehyde **(6c)**,[63] respectively (eq. 6); ethylideneacetophenone (**9**, eq. 7) and isopropylideneacetophenone (**11**, eq. 8) were obtained from crotonyl chloride **(8)** and β, β-dimethylacrylyl chloride **(10)**, respectively (in pure form through coupling with diphenylcadmium) but mixed mainly with 3-methylindanone and 3,3-dimethylindanone,[2,8,9,64] respectively, through reactions with benzene and $AlCl_3$. Benzyl styryl ketone (**13**, eq. 9), β-phenylethyl-β-styryl ketone (**15**, eq. 10) and β,β-distyryl ketone (**16** eq. 11) were prepared by the sodium hydroxide catalysed condensation of benzaldehyde with phenylacetone **(12)**[28,64] benzylacetone **(14)**[65] and acetone,[66] respectively; β-(3,4-dimethylbenzoyl) acrylic acid **(17)** was prepared by the interaction of maleic anhydride with *p*-xylene and $AlCl_3$ (eq. 12)[15]; 2-benzoyl-1-propanol **(18)** was obtained by the sodium carbonate catalysed condensation of propiophenone with paraformaldehyde[30] (eq. 13); 3-methylindanone **(20)**[9] and 3,3-dimethyl-indanone **(22)** were obtained from acid chlorides **19** and **21** by the steps outlined in equations 14[67] and 15[68], respectively.

$$\underset{6}{RCHO + CH_3-CO-Ph} \xrightarrow[aq.\,C_2H_5OH]{NaOH} \underset{7}{R-CH=CH-CO-Ph} \qquad (6)$$

a, R = phenyl
b, R = p-methoxyphenyl
c, R = isopropyl

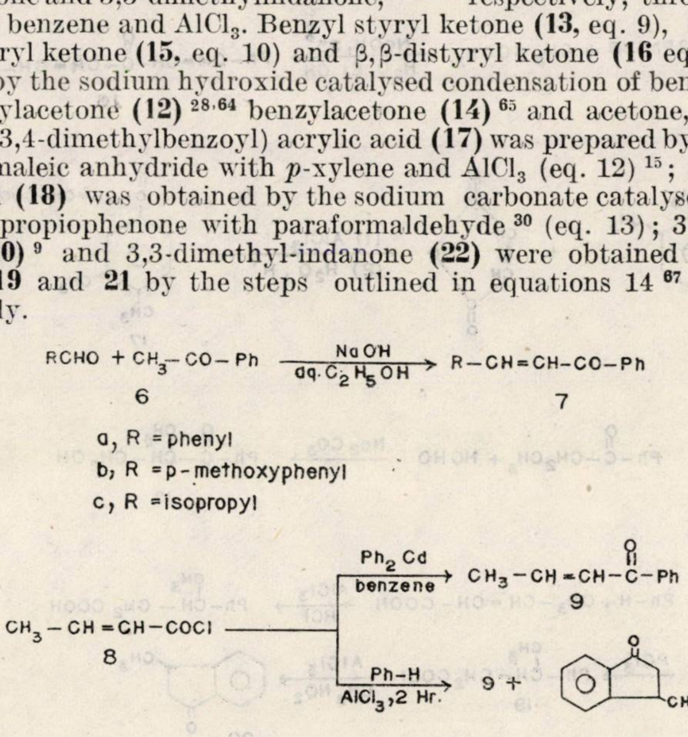

(7)

20

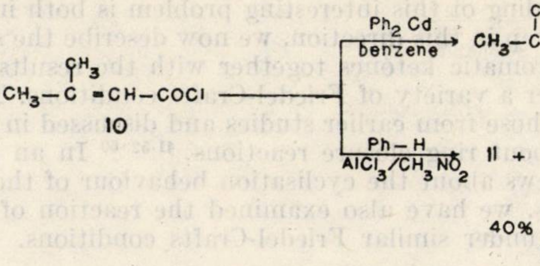
Ph2 Cd
benzene
CH3–C=CH–C(O)–Ph
11
CH3–C(CH3)=CH–COCl
10
Ph–H
AlCl3/CH3NO2
11 +
CH3
CH3
40%
60%
22

(8)

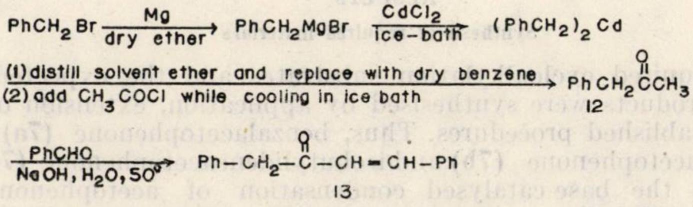

$$PhCH_2Br \xrightarrow[\text{dry ether}]{Mg} PhCH_2MgBr \xrightarrow[\text{ice-bath}]{CdCl_2} (PhCH_2)_2Cd$$

$$\xrightarrow[\text{(2) add } CH_3COCl \text{ while cooling in ice bath}]{\text{(1) distill solvent ether and replace with dry benzene}} \underset{12}{PhCH_2\overset{O}{\overset{\|}{C}}CH_3}$$

(9)

$$\xrightarrow[NaOH,\ H_2O,\ 50^{\circ}]{PhCHO} \underset{13}{Ph-CH_2-\overset{O}{\overset{\|}{C}}-CH=CH-Ph}$$

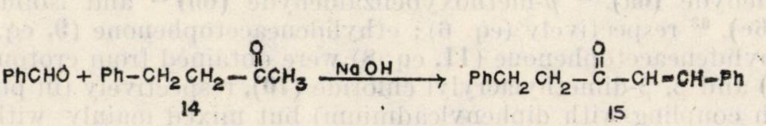

$$PhCHO + \underset{14}{Ph-CH_2CH_2-\overset{O}{\overset{\|}{C}}CH_3} \xrightarrow{NaOH} \underset{15}{PhCH_2CH_2-\overset{O}{\overset{\|}{C}}-CH=CH-Ph}$$

(10)

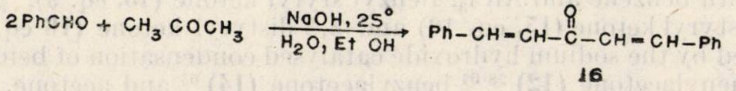

$$2\,PhCHO + CH_3COCH_3 \xrightarrow[H_2O,\ Et\ OH]{NaOH,\ 25^{\circ}} \underset{16}{Ph-CH=CH-\overset{O}{\overset{\|}{C}}-CH=CH-Ph}$$

(11)

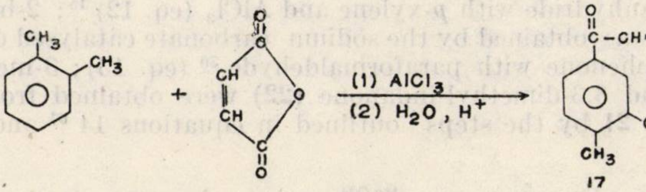
CH3
CH3
+
CH
CH
O
O
O
(1) AlCl3
(2) H2O, H+
C–CH=CH–COOH
O
CH3
CH3

17

(12)

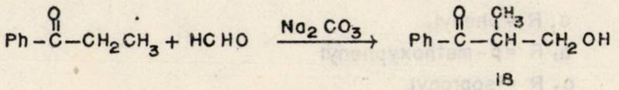

$$Ph-\overset{O}{\overset{\|}{C}}-CH_2CH_3 + HCHO \xrightarrow{Na_2CO_3} \underset{18}{Ph-\overset{O}{\overset{\|}{C}}-\overset{CH_3}{\overset{|}{CH}}-CH_2OH}$$

(13)

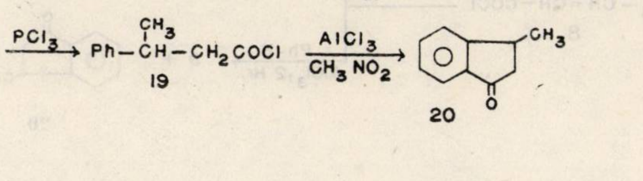
Ph–H + CH3–CH=CH–COOH
AlCl3
HCl
Ph–CH(CH3)–CH2COOH
PCl3
Ph–CH(CH3)–CH2COCl
19
AlCl3
CH3NO2
CH3
O

20

(14)

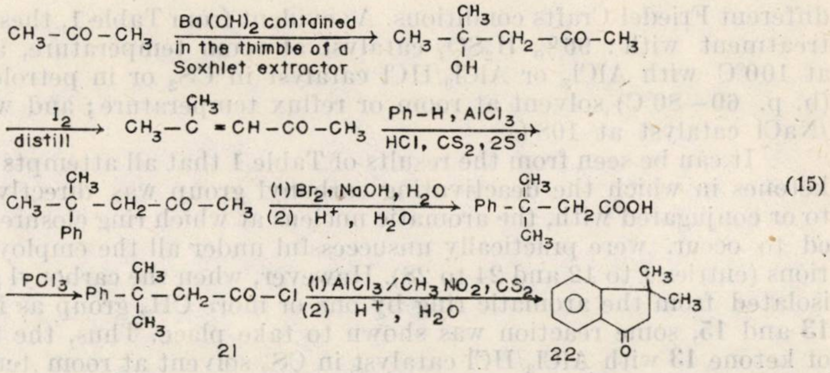
Ba(OH)₂ contained in the thimble of a Soxhlet extractor
I₂ distill
Ph-H, AlCl₃ HCl, CS₂, 25°
(1) Br₂, NaOH, H₂O (2) H⁺, H₂O
(15)
PCl₃
(1) AlCl₃/CH₃NO₂, CS₂ (2) H⁺, H₂O
21
22

Cyclisation results

In this work, several trials were carried out to effect the Friedel-Crafts cyclisation of compounds **7**, **9**, **11**, **13**, **15**, **16**, **17** and **18**. The results of these experiments are compiled in Table 1.

Comparing the results of this work with those reported by earlier workers we would like to point out the following :

(1) In contrast to earlier claims about the $AlCl_3$-catalysed closure of ethylideneacetophenone [8] **(9)** and isopropylideneacetophenone **(11)** to 3-methylindanone and 3,3-dimethylindanone, respectively, we failed to effect this closure in the presence of the same catalyst.

(2) In the literature, [15] β-(3,5-dimethylbenzoyl) acrylic acid **(17)** was reported to yield 87% of 3-carboxy-4,7-dimethyl-1-indanone on treatment with $AlCl_3/NaCl$ catalyst at 135°C for one hour. In our hands, treatment of compound **17** (entry 25) with similar amounts of catalyst but at 100°C for two hours gave a solid mass from which 40% of the starting material was recovered ; none of the previously reported product could be detected, however.

(3) The primary alcohol 2-benzoyl-1-propanol **(18)** was reported by Fuson [30] and by Colonge and Weinstein [31] to give 67% and 81% yields respectively, of 2-methyl-1-indanone on treatment with concentrated H_2SO_4. In this work, we repeated the reactions of ketoalcohol **18** under the reported conditions (entries 26 and 27) but instead of 2-methyl-1-indanone we obtained a sulphur-containing resinous material of unidentified nature. Moreover, we conducted a third experiment (entry 28) in which the alcohol and the catalyst were heated on a boiling water bath for three hours but again the result was similar to those of the other two experiments.

DISCUSSION OF RESULTS

As indicated before, this work was primarily adressed to investigate the effect of the electron-attracting carbonyl group on the ease of Friedel-Crafts cyclisations of α, β-unsaturated aromatic ketones and other related systems. Accordingly, the unsaturated ketones **7**, **9**, **11**, **13**, **15** and **16**, the keto-acid **17**, and the hydroxy ketone **18** were subjected to one or more different Friedel-Crafts conditions. As evident from Table 1, these included treatment with: 96% H_2SO_4 catalyst at room temperature, at 70°C or at 100°C with $AlCl_3$ or $AlCl_3/HCl$ catalyst in CS_2 or in petroleum ether (b. p. 60–80°C) solvent at room or reflux temperature; and with $AlCl_3/$ $/NaCl$ catalyst at 108°C.

It can be seen from the results of Table 1 that all attempts to cyclise ketones in which the deactivating carbonyl group was directly attached to or conjugated with, the aromatic nucleus at which ring closure is expected to occur, were practically unsuccessful under all the employed conditions (entries 1 to 12 and 24 to 28). However, when the carbonyl group was isolated from the aromatic ring by one or more CH_2 group as in ketones **13** and **15**, some reaction was shown to take place. Thus, the treatment ot ketone **13** with $AlCl_3/HCl$ catalyst in CS_2 solvent at room temperature (entry 22) gave 40% of the cyclisation product 4-phenyl-2-tetralone (eq. 16).

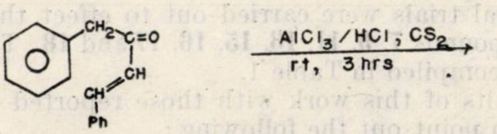

(40% yield) (16)

Again, treatment of ketone **15** (entry 23) produced a complex mixture containing some ot the hydride transfer product dibenzylacetone. In line with our previous report about the cyclisation of 1,5-diphenyl-1-pentanol [55] it is belived that this complex mixture might also contain some of the cyclisation product 5-phenyl-3-benzosuberone (**23**, eq. 17).

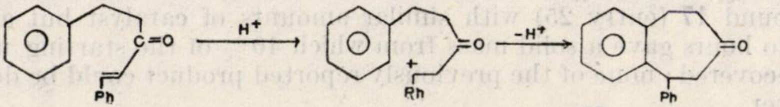

(17)

15 23

In rationalising the results of this work we suggest that the lack of ring closure of ketones **7a**, **7b**, **7c**, **11** and **16** is mainly due to the deactivating effect exerted on the aromatic nucleus by the adjacent carbonyl group. This is evident from the finding that, in the absence of this carbonyl effect, facile closures to tetralins are achieved through primary, secondary and tertiary carbonium ion intermediates and to indans through benzylic secondary and tertiary carbonium ion intermediates. [41,52-60] As to ketones **9**, **17** and **18** we suggest that the failure to cyclise them under the employed conditions is due not only to carbonyl deactivation but also to the expected involvement of primary (as in ketone **18**) and of ordinary secondary (as in ketones **9** and **17**) carbonium ion in closures to a five-membered ring. Recently, Khalaf and Roberts [41,52-60] have established that primary and ordinary secondary carbonium ion intermediates generated directly or *via* rearrangement from arylalkanols and arylhaloalkanes under Friedel-Crafts conditions are incapable of closing to indans.

The failure to cyclise dibenzylideneacetone (**16**) under the conditions employed in entry 24 is also in good accord with our conclusions.

The carbonyl group in this ketone, though not directly attached to the aromatic nucleus, is still in conjugation with it and its deactivating effect can be transmitted to the nucleus especially upon coordination with the acidic catalyst (eq. 18).

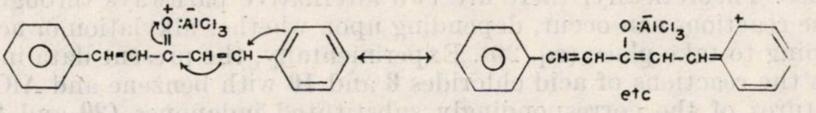

(18)

Aside from the foregoing cases, carbonyl retardation to ring closure has also been manifested during other related reactions. In this work, treatment of mixture of benzene and succinyl chloride with aluminium chloride followed by the usual hydrolysis gave β-benzoylpropionic acid **(25)** as the end product. Alternatively, distillation of the reaction mixture prior to hydrolysis gave β-benzoylpropionyl chloride **(24)** as the end product [69] (eq. 19).

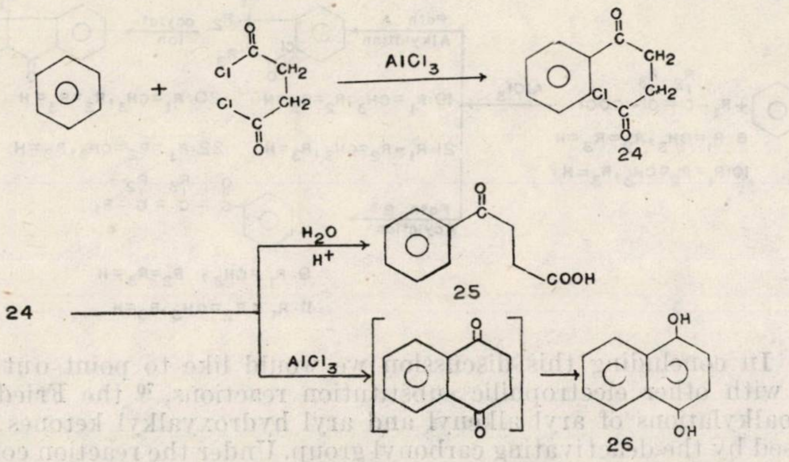

(19)

The failure of β-benzoylpropionyl chloride **(24)** to undergo intramolecular cyclisation to 1,4-naphthalenediol **(26)** under the employed conditions is undoubtedly due to deactivation of the aromatic nucleus by the adjacent carbonyl group.

In the literature, retardation of ring closure by carbonyl deactivation was again experimented during the $AlCl_3$-catalysed cyclisation of halophenones [39] (e.g. γ-chlorobutyrophenone **27**), [41] *p*-(haloalkyl)acetophenones [39] (e.g. 1-chloro-4-*p*-acetylphenylbutane, **28** [44] and β-aroylacrylic-acids (e. g. β-2,5-dimethylbenzoylacrylic acid, **29**). [15,17,19,27] As can be seen in the cited references, closure of compounds such as **27**, **28** and **29**

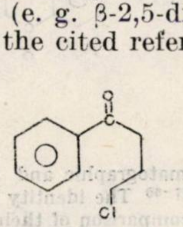
27

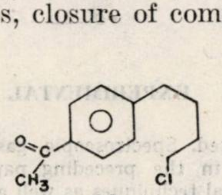
28

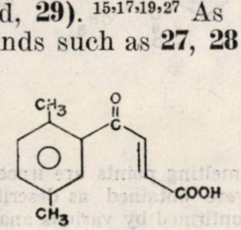
29

could only be effected under strenuous conditions involving heating with excess $AlCl_3-NaCl$ catalyst at temperatures higher than 100°C.

It is of interest to point out that the results of this work threw some light upon the mechanism of reaction of unsaturated acid chlorides with arenes. Theoretically, there are two alternative pathways through which these reactions can occur, depending upon whether alkylation or acylation is going to take place (eq. 20). Experimentally, the present data indicated that the reactions of acid chlorides **8** and **10** with benzene and $AlCl_3$ gave mixtures of the correspondingly substituted indanones (**20** and **22**, respectively) and unsaturated ketones (**9** and **11**, respectively) (see eqs. 7 and 8). The data also indicated that indanones **20** and **22** could be formed from chlorides **19** and **21** but not from unsaturated ketones **9** and **11** upon treatment with $AlCl_3$. Judging from these findings, one can assign path A for the formation of indanones and the competing path B for the formation of unsaturated ketones (eq. 20).

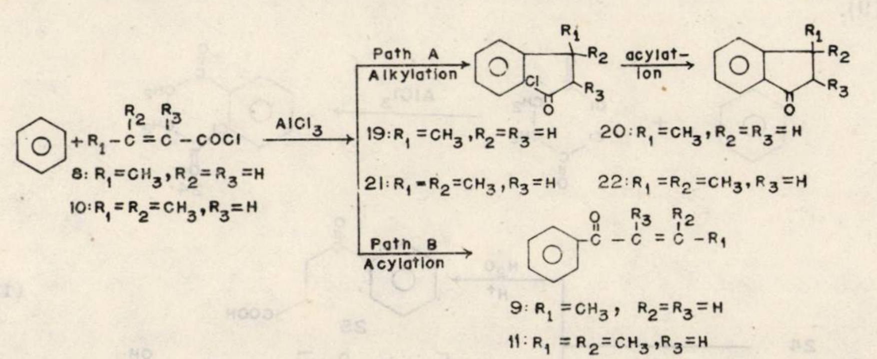

R2 R3
+ R1 – C = C – COCl
8: R1=CH3, R2=R3=H
10: R1=R2=CH3, R3=H
AlCl3
Path A
Alkylation
R1
R2
Cl
R3
O
acylation
R1
R2
R3
O
19: R1=CH3, R2=R3=H
20: R1=CH3, R2=R3=H
21: R1=R2=CH3, R3=H
22: R1=R2=CH3, R3=H
Path B
Acylation
O R3 R2
C – C = C – R1
9: R1=CH3, R2=R3=H
11: R1=R2=CH3, R3=H

(20)

In concluding this discussion we would like to point out that, in line with other electrophilic substitution reactions,[70] the Friedel-Crafts cycloalkylations of aryl alkenyl and aryl hydroxyalkyl ketones are suppressed by the deactivating carbonyl group. Under the reaction conditions, this suppression is greatly enhanced not only by coordination of the carbonyl group with the acid catalyst ($C = \overset{+}{\ddot{O}}:H$ or $C = \overset{+}{\ddot{O}} : \overset{-}{AlCl_3}$) but also by the possible formation of a stable oxonium ion similar to those detected by Pines and Douglas[44] during the cycloalkylation of the related ω-halophenones (eq. 21).

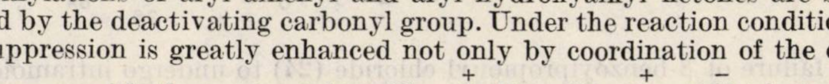

F
Cl
C
O
CH3
AlCl3
100
F
+O
AlCl3
F
Cl
C
O

(21)

EXPERIMENTAL

All melting points are uncorrected. Spectroscopic, gas chromatographic and elemental analyses were obtained as described in the preceding papers.[57-60] The identity of materials was confirmed by various analytical techniques as well as by comparison of their physical constants with those reported by other workers.

Synthesis of required materials

Of the required materials, benzalacetophenone **(7a)**,[61] *p*-methoxybenzalacetophenone **(7b)**, [62] isobutylideneacetophenone **(7c)**, [63] benzyl β-styryl ketone **(13)**, [28,64] β-phenylethyl-β-styryl ketone **(15)** [65] β-distyryl ketone **(16)**[66] β-(3,4-dimethylbenzoyl) acrylic acid **(17)**, [15] 2-benzoyl-1-propanol **(18)**,[30] 3-methylindanone **(20)**[9,67] and 3,3-dimethylindanone **(22)** [68] were prepared by the reaction sequences summarised schematically in the results section following essentially the procedures outlined in the cited references. Succinyl chloride was prepared through-the interaction of succinic anhydride with thionyl chloride in the presence of $ZnCl_2$.

Cyclisation procedures

The procedures employed in this study to examine the cyclisation behaviour of the ketonic substrates **7, 9, 11, 13, 15, 16,17** and **18** are outlined below. The results obtained are summarised in table 1.

Attempted cyclisation of unsaturated ketones **7** *and* **16.** Three general procedures (A, B and C) were attempted.

Procedure A. In this procedure, a 100 ml, three-necked flask was equipped with a reflux condenser protected by a calcium chloride tube, a thermometer, a pressure-equalising dropping funnel and a magnetic stirring bar. The flask was charged with the required amount of ketone followed by addition of the required amount of 96% H_2SO_4 through the dropping funnel over a period of 5 minutes. After addition, the reaction mixture was stirred at the desired temperature for 3 hrs. during which it became dark in colour and at the end of which it was decomposed by pouring onto ice. The precipitated solid was filtered off, washed with water, air dried, recrystallised from the proper solvent and identified.

Procedure B. The apparatus was similar to that used in procedure A except that the thermometer was replaced by a gas disperser. In the flask, there were introduced the required amount of $AlCl_3$ and half of the total amount of solvent (CS_2 or petroleum ether, b.p. 60—80°C). The required amount of ketone dissolved in the second half of solvent was then introduced into the reaction flask over a period of 15 minutes. The resulting mixture was stirred at the desired temperature for 3 hrs. and decomposed by pouring it over a mixture of ice and conc. HCl. The precipitated solid was filtered off, washed with water, air dried, recrystallised from the proper solvent and identified.

Procedure C. The apparatus and steps were essentially similar to those used in procedure B with the exception that a slow stream of dry HCl gas was allowed to pass through the reaction mixture during the reaction time.

Attempted cyclisation of ketones **7c, 9** *and* **11** :

The attempted procedures were that of Plattner and co-workers [9] in the cases of isobutylideneacetophenone **(7c)** and ethylideneacetophenone **(9)** and that of Smith and Prichard [4] in the case of isopropylideneacetophenone **(11)**. In all of the three cases, the products obtained were shown by infrared and glpc analysis as well as by m.p. and m.m.p. determinations of 2,4-dinitrophenylhydrazone derivatives to be the recovered starting materials (80—87 %).

Cyclisation of benzyl β-styryl ketone **(13)** :

The procedure of Fine and Stern [71] was essentially followed with the exception that dry HCl gas was bubbled through the reaction mixture during the reaction. Distillation of the crude mixture under vacuum gave 40% yield of colourless 4-phenyl-2-tetralone : b.p. 210°C at 2 mm. ; IR (thin film) showed bands at 1720 cm^{-1} for nonconjugated C=O, at 1500 cm^{-1} and 1460 cm^{-1} for benzenoid structure and between 790—740 cm^{-1} and 718 cm^{-1} for mono- and disubstituted benzene rings ; Oxime-white needles m.p. 93°C from aqueous ethanol.

Attempted cyclisation of β-phenylethyl β-styryl ketone **(15)** :

The procedure followed was a duplication of that of Fine and Stern [71] with the exception that dry HCl gas was bubbled through the reaction mixture during the reaction. In this experiment 1.18 g (0.005 mole) of ketone, 1.59 g (0.01 mole) of anhydrous $AlCl_3$ and 100 ml of dry CS_2 were used. Decomposition and extraction gave 0.8 g of crude viscous material. Attempted distillation of 0.5 g of the crude product under vacuum gave no distillable material ; instead the material polymerised in the distilling flask. However, T.L.C. analysis of this crude mixture on silica gel using a mixture of benzene and petroleum ether (b.p. 40—60°C) in a volume ratio of 1 : 9 as eluent revealed it to be a mixture of dibenzylacetone and recovered starting material.

TABLE 1

Conditions and results of treatment of ketones **7**, **9**, **11**, **13**, **15**, **16**, **17** and **18** with Friedel-Crafts catalysts

Entry	Starting ketone			Procedure	Catalyst (amount)	Total solvent (ml)	Temperature *	Product (% yield)
	Formula	No.	Amount					
1	Ph−CH=CH−CO−Ph	**7a**	(2.08 g ; 0.01 mole)	A	96% H_2SO_4 (2 g)	None	rt	96% recovered
2	Ph−CH=CH−CO−Ph	**7a**	(2.08 g ; 0.01 mole)	A	96% H_2SO_4 (10 g)	None	rt	96% recovered
3	Ph−CH=CH−CO−Ph	**7a**	(2.08 g ; 0.01 mole)	A	69% H_2SO_4 (10 g)	None	70	91% recovered
4	Ph−CH=CH−CO−Ph	**7a**	(2.08 g ; 0.01 mole)	B	$AlCl_3$ (1.6 g ; 0.012 mole)	CS_2 (20)	rt	19% recovered
5	Ph−CH=CH−CO−Ph	**7a**	(2.08 g ; 0.01 mole)	B	$AlCl_3$ (1.6 g ; 0.012 mole)	CS_2 (20)	reflux	86% recovered
6	Ph−CH=CH−CO−Ph	**7a**	(2.08 g ; 0.01 mole)	B	$AlCl_3$ (1.6 g ; 0.012 mole)	PE (20)	rt	86% recovered
7	Ph−CH=CH−CO−Ph	**7a**	(2.08 g ; 0.01 mole)	B	$AlCl_3$ (1.6 g ; 0.012 mole)	PE (20)	reflux	87% recovered
8	Ph−CH=CH−CO−Ph	**7a**	(1.5 g ; 0.072 mole)	C	$AlCl_3$ (1.5 g) (0.011 mole) HCl	CS_2 (20)	rt	86% recovered
9	Ph−CH=CH−CO−Ph	**7b**	(1.5 g ; 0.0072 mole)	C	$AlCl_3$(1.5 g) (0.011 mole) HCl	CS_2 (20)	reflux	81% recovered

10	p-$CH_3O(C_6H_4CH=CH-$ $COPh)$	**7b**	(2.38 g ; 0.01 mole)	A	90% H_2SO_4 (2 g)	None	rt	96% recovered
11	p-$CH_3O(C_6H_4CH=CH-$ $COPh$	**7b**	(2.38 g ; 0.01 mole)	A	96% H_2SO_4 (10 g)	None	rt	96% recovered
12	p-$CH_3O(C_6H_4CH=CH-$ $COPh$	**7b**	(2.38 g ; 0.01 mole)	A	96% H_2SO_4 (10 g)	None	70°	88% recovered
13	p-$CH_3O(C_6H_4CH=CH-$ $COPh$	**7b**	(2.38 g ; 0.01 mole)	B	$AlCl_3$(1.6 g) 0.12 mole	CS_2 (20)	rt	86% recovered
14	p-$CH_3O(C_5H_4CH=CH-$ $COPh$	**7b**	(2.38 g ; 0.01 mole)	B	$AlCl_3$(1.6 g) 0.12 mole	CS_2 (20)	reflux	87% recovered
15	p-$CH_3O(C_6H_4CH=CH-$ $COPh$	**7b**	(2.38 g ; 0.01 mole)	B	$AlCl_3$(1.6 g) 0.12 mole	PE (20)	rt	87% recovered
16	p-$CH_3O(C_6H_4CH=CH-$ $COPh$	**7b**	(2.3 g ; 0.01 mole)	B	$AlCl_3$(1.6 g) 0.12 mole	PE (20)	reflux	86% recovered
17	p-$CH_3O(C_6H_4CH=CH-$ $COPh$	**7b**	(2.38 g ; 0.01 mole)	C	$AlCl_3$(1.5 g, 0.011 mole) HCl	CS_2 (20)	rt	91% recovered
18	p-$CH_3O(C_6H_4CH=CH-$ $COPh$	**7b**	(2.38 g ; 0.01 mole)	C	$AlCl_3$(1.5 g, 0.011 mole) HCl	CS_2 (20)	reflux	84% recovered
19	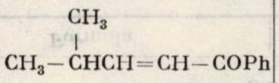 $CH_3-\overset{\overset{CH_3}{\mid}}{C}HCH=CH-COPh$	**7c**	(1.74 g, 0.01 mole)	C^b	$AlCl_3$(1.58 g, 0.011 mole) HCl	CS_2 (50)	rt	80% recovered
20	$CH_3CH=CHCOPh$	**9**	(1.46 g, 0.01 mole)	C^b	$AlCl_3$(1.59 g, 0.0 1 mole)	CS (50)	rt	82% recovered

Table 1 (continued)

Entry	Starting ketone			Procedure	Catalyst (amount)	Total solvent (ml)	Temperature	Product (% yield)
	Formula	No.	Amount					
21	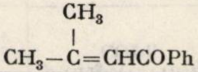 $CH_3-\overset{CH_3}{\overset{\vert}{C}}=CHCOPh$	**11**	(1.6 g, 0.01 mole)	C[b]	$AlCl_3$, 1.59 g, 0.011 mole) HCl	CS (50)	rt	87% recovered
22	$Ph-CH=CH-COCH_2Ph$	**13**	(1.11 g, 0.005 mole)	C	$AlCl_3$(1.59 g/ 0.011 mole)/HCl	CS_2 (50)	rt	40% 4-phenyl-2-tetralone
23	$Ph-CH=CH-CO-$ $-CH_2CH_2Ph$	**15**	(1.18 g, 0.005 mole)	C[b]	$AlCl_3$(1.59 g/ 0.011 mole)/ HCl	CS_2 (50)	rt	80% of viscous crude mixture containing some dibenzylacetone and unchanged starting material
24	$Ph-CH=CH-CO-CH=$ $=CHPh$	**16**	(1.18 g, 0.005 mole)	C	$AlCl_3$(1.59 g; 0.011 mole)/HCl	CS (100)	rt	75% recovered
25	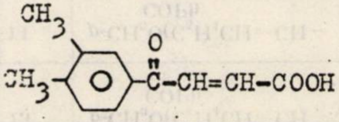	**17**	(1.01 g, 0.005 mole)	Ref. [15]	$AlCl_3$ (10g; 0.073 mole) NaCl (1 g; 0.02 mole)	None	100	40% recovered + 30% black resin
26	$Ph-CO-CH(CH_3)CH_2OH$	**18**	(10 g, 0.061 mole)	Ref. [11]	96% H_2SO_4 (20 ml)	None	0°	86% (sulfur-containing black resin).
27	$Ph-CO-CH(CH_3)CH_2OH$	**18**	(2 g, 0.012 mole)	See exptal.	96% H_2SO_4 (18.4 ml)	None	boiling water bath temp.	90% (same as above)
28	$Ph-CO-CH(CH_3)CH_2OH$	**18**	(10 g, 0.061 mole)	Ref. [31]	96% H_2SO_4 (30 ml)	None	below 45	91% (same as above)

[*a] Except for entry 25 where reaction time was 2 hrs, all other reactions were carried out for 3 hrs.

[b] See experimental for additional informations.

rt = room temperature.

Attempted cyclisation of β-(3,4-dimethylbenzoyl) acrylic acid **(17)** :

The procedure used was a repetition of that employed previously by Baddeley and co-workers.[15] Fractional crystallisation of the crude material (obtained from 1.0 g of starting acid), from benzene-petroleum ether (b.p. 40—60°C) gave 0.4 g (40% yield) of recovered starting acid (m.p. and m.m.p.) and 0.3 g of a black polymer which did not melt up to 360°C.

Attempted cyclisation of 2-benzoyl-1-propanol **(18)** :

The reaction was carried out in three different ways. The procedures used in entries 26 and 27 were repetitions of those used previously by Burckhalter and Fuson[11] and by Colonge and Weinstein[31] respectively. The procedure of entry 28 was different in that the stirred reaction mixture consisting of 2 g of benzoylpropanol **(18)** and 10 g of conc. H_2SO_4 was heated on a boiling water bath for three hours. In all of the three experiments, the products separated after dilution with water consisted of a black sulphur-containing resinous material of unknown structure. This material did not melt up to 360°C and was insoluble in petroleum ether, methanol, ethanol, ether, benzene, acetone and conc. hydrochloric acid.

Reaction of succinyl chloride with benzene and $AlCl_3$:

In a 500 ml, three-necked flask equipped with a reflux condenser protected with a calcium chloride tube, a mercury sealed mechanical stirrer and a pressure-equalising dropping funnel, 7.8 g (0.1 mole) of dry benzene and 31.92 g (0.24 mole) of anhydrous $AlCl_3$ were introduced. To this mixture, 15 g (0.1 mole) of succinyl chloride were added dropwise via the funnel over a period of 30 minutes. After addition, the reaction mixture which became very difficult to stir, was left for another 30 minutes and decomposed with a mixture of 200 g ice and 50 ml of conc. hydrochloric acid. The organic layer was separated and the aqueous layer was extracted with three 200 ml-portions of ether. The combined organic layers were washed repeatedly with sodium carbonate solution and dried over anhydrous magnesium sulphate. Acidification of the carbonate extract with conc. hydrochloric acid precipitated a solid which was filtered off, washed with water and recrystallised from petroleum ether (b.p. 40—60°C) in the form of colourless needles. This solid weighed 11.9 g and was found, by m.p. and m.m.p. determinations as well as by IR analysis to be β-benzoylpropionic acid.

Evaporation of the organic layer left about 1.0 g of a white solid which was recrystallised from ethanol in the form of white needles which melted at 92°C. It also dissolved in aqueous sodium hydroxide giving a pink coloured solution and showed a carbonyl band in the infrared spectrum at 1715 cm^{-1}. The structure of this compound was not fully determined.

REFERENCES

[1] Part VIII. : See ref. [60]

[1a] For reviews see : R. C. Barclay in "Friedel-Crafts and Related Reactions", G. A. Olah, Ed. Interscience Publishers, New York, 1972, Vol. II, Chapter XXII, pp. 785—813, 826—827 ; G. A. Olah, "Friedel-Crafts Chemistry", lst ed., Wiley, New York, 1973, pp. 104, 114—115, 435—439.

[2] K. Von Auwers and E. Risse, *Liebigs Ann., Chem.*, **502**, 282 (1933).

[3] A. Cohen and J. W. Cook, *J. Chem. Soc.*, **1935**, 1570.

[4] L. I. Smith and W. W. Prichard, *J. Amer. Chem. Soc.*, **62**, 772 (1940).

[5] C. F. Koelsch and J. A. Anthes, *J. Org. Chem.*, **6**, 558 (1941).

[6] L. I. Smith and L. J. Spillane, *J. Amer. Chem. Soc.*, **65**, 202 (1943).

[7] C. D. Gutsche and W. S. Johnson, *J. Amer. Chem. Soc.*, **68**, 2239 (1946).

[8] J. Colonge and J. Chambion, *Bull. Soc. chim. France*, **1947**, 999.

[9] P. A. Plattner, A. Furst, and K. Jirasek, *Helv. Chim. Acta*, **30**, 1320 (1947) ; *Chem. Abstr.*, **42**, 1256 (1948).

[10] J. Colonge and J. Chambion, *Compt. rend.*, **224**, 128 (1947).

[11] J. H. Burckhalter and R. C. Fuson, *J. Amer. Chem. Soc.*, **70**, 4184 (1948).

[12] J. Colonge and E. Grimaud, *Bull. Soc. chim. France*, **1951**, 857.

[13] L. I. Smith and P. N. Gordon, *J. Amer. Chem. Soc.*, **73**, 3747 (1951).

[14] W. Baker and P. G. Jones, *J. Chem. Soc.*, **1951**, 787.

[15] G. Baddeley, G. Holt and S. M. Maker, *J. Chem. Soc.*, **1952**, 3289.

[16] W. S. Johnson, D. K. Banerjee, W. P. Schneider, C. D. Gutsche, W. E. Shelberg. and L. J. Chinn, *J. Amer. Chem. Soc.*, **74**, 2832 (1952).

[17] G. Baddeley, G. Holt, S. M. Makar, and M. G. Ivinson, *J. Chem. Soc.*, **1952**, 3605.

[18] E. A. Braude and W. F. Forhes, *J. Chem. Soc.*, **1953**, 2208.

[19] G. Baddeley, S. M. Makar, and M. G. Ivinson. *J. Chem. Soc.*, **1953**, 3969.

[20] G. Baddeley and R. Williamson, *J. Chem. Soc.*, **1953**, 2120.

[21] H. Khastgir, S. M. Mukherji, and B. K. Bhattacharyya, *J. Indian Chem. Soc.*, **31**, 351 (1954).

[22] W. E. Parham, E. L.Wheeler, and R. M. Dodson, *J. Amer. Chem. Soc.* **77**, 1166 (1956).

[23] R. W. Layer and L. R. MacGregor, *J. Org. Chem.*, **21**, 1120 (1956).

[24] E. D. Bergmann, *Bull. Res. Council Israel*, **5A**, 150 (1956) ; *Chem. Abstr.*, **50**, 15493 (1956).

[25] R. M. Granger, Corbier, J. Vinas, and P. Nau, *Compt. rend.*, **244**, 1048 (1957).

[26] E. D. Bergmann and R. Ikan, *J. Amer. Chem. Soc.*, **83**, 5803 (1958).

[27] S. M. Mahar, H. F. Bassilios, and A. Y. Salem, *J. Chem. Soc.*, **1958**, 2437.

[28] (a) H. Gilman and J. F. Nelson, *Rec. Trav. chim.*, **55**, 518 (1936) ; (b) S. A. Fine and R.L. Stern, *J. Org. Chem.*, **32**, 4132 (1967).

[29] L.R.C. Barelay, K. L. Adams, H. M. Foote, E. C. Sanford and R. H. Young, *Canad. J. Chem.*, **48**, 2763 (1970),
[a] H.O. House, V. Paragamian, R. S. Ro and D. J. Wluka, *J. Amer. Chem. Soc.*, **82**, 1457 (1960) and other references cited therein.
[b] A. Sammour and M. Elkasaby, *U.A.R.J. Chem.*, **13**, 409 (1970).

[30] R. C. Fuson, W. E. Ross and G. H. Mckeever, *J. Amer. Chem. Soc.*, **60**, 2935 (1938).

[31] J. Colonge and G. Weinstein, *Bull. Soc. chim. France*, 462 (1952) ; *Chem. Abstr.*, **47**, 3287 (1953).

[32] N. Kishner, *J. Russ. Phys. Chem. Soc.*, **46**, 1411 (1914).

[33] F. Mayer and P. Maller, *Ber. dtsch. Chem. Ges.*, **60B**, 2278 (1927) ; *Chem. Abstr.*, **22**, 417 (1928).

[34] F. Mayer, K. Billing, K. Horst and K. Schirmacher, *U.S. Patent* 1754631 (1930) ; *Chem. Abstr.*, **24**, 2469 (1930).

[35] F. Mayer, German Patent 513204 (1926) ; *Chem. Abstr.*, **25**, 1260 (1931).

[36] F. Mayer, German Patent 515110 (1927) ; *Chem. Abstr.*, **25**, 1841 (1931).

[37] K. Von Auwers and E. Risse, *Liebigs Ann. Chem*, **502**, 282 (1933).

[38] R. T. Arnold and E. Rondestvedt, *J. Amer. Chem. Soc.*, **67**, 1265 (1945).

[39] G. Baddeley and R. Williamson, *J. Chem. Soc.*, **1956**, 4647.

[40] J. H. Burckhalter and J. R. Campbell, *J. Org. Chem.*, **26**, 4232 (1961).

[41] A. A. Khalaf and R. M. Roberts, *J. Org. Chem.*, **31**, 89 (1966).

[42] W. F. Erman and H. C. Kreschmar, *J. Org. Chem.*, **33**, 1545 (1968).

[43] H. Martens and G. Hoornaert, *Tetrahedrom Letters*, **1970**, 1821.

[44] S. H. Pines and A. W. Douglas, *Tetrahedron Letters*, **1976**, 1955.

[45] R. J. Murray and N. H. Cromwell, *J. Org. Chem.*, **41**, 3540 (1976).

[46] R. T. Hart and R. F. Teble, *J. Amer. Chem. Soc.*, **72**, 3286 (1950).

[47] E. M. McMahon, J. N. Roper, Jr., W. P. Utermohlen, Jr., R. H. Hasek, R. C. Harris and J. H. Brant, *J. Amer. Chem. Soc.*, **70**, 2971 (1948).

[48] P. H. Gore and J. A. Hoskins, *J. Chem. Soc.*, C., **1970**, 517.

[49] R. T. Morrison and R. N. Boyd, "Organic Chemistry", Allyn and Bacon, Inc., Boston, 2nd ed., six printing, 1969, pp. 379—380.

[50] P. H. Gore in "The Chemistry of Acyl Halides", S. Patai Ed., Interscience Publishers, New York, 1972, Chapter 5, pp. 138—141, 157—168 and references therein.

[51] J. March, "Advanced Organic Chemistry : Reactions, Mechanisms and Structure", McGraw-Hill, New York, 1968, pp. 406—415 and references therein.

[52] A. A. Khalaf and R. M. Roberts, *J. Org. Chem.*, **34**, 3571 (1969).

[53] A. A. Khalaf and R. M. Roberts, *J. Org. Chem.*, **36**, 1040 (1971).

[54] R. M. Roberts, G. P. Anderson, Jr., A. A. Khalaf and Chow-Eng Low, *J. Org. Chem.*, **36**, 3342 (1971).

[55] A. A. Khalaf and R. M. Roberts, *J. Org. Chem.*, **37**, 4227 (1972).

[56] A. A. Khalaf and R. M. Roberts, *J. Org. Chem.*, **38**, 1388 (1973).

[57] A. A. Khalaf, *Indian J. Chem.*, **12**, 476 (1974).

[58] A. A. Khalaf, *Rev. Roumaine Chim.*, **18**, 297 (1973).

[59] A. A. Khalaf, *Rev. Roumaine Chim.*, **19**, 1361 (1974).

[60] A. A. Khalaf, *Rev. Roumaine Chim.*, **19**, 1373 (1974).

[61] E. P. Kohler and H. M. Chadwell, *Org. Syn. Coll. Vol.*, **1**, 78 (1944).

[62] [a] F. J. Pond and A. S. Schoffstall, *J. Amer. Chem. Soc.*, **22**, 666 (1900) ; [b] W. Davey and D. J. Tivey, *J. Chem. Soc.*, **1958**, 1230. [c] D. N. Dhar, *J. Indian Chem. Soc.*, **37**, 799 (1960).

[63] [a] H. Thoms and H. Kahre, *Arch. Pharm.*, **263**, 241 (1925) ; *Chem. Abstr.*, **19**, 2474 (1925) ; [b] K. Kulka, R. J. Eiserle, J. A. Rogers and F. W. Richter, *J. Org., Chem.*, **25**, 270 (1960) ; [c] R. Anet, *J. Org. Chem.*, **26**, 246 (1961).

[64] [a] G. Goldschmiedt and G. Knopfer, *Monatsh.*, **18**, 437 (1897) ; [b] P. L. Southwick, L. A. Pursglove and P. Numerof, *J. Amer. Chem. Soc.*, **72**, 1604 (1950).

[65] [a] C. Harries, *Liebigs Ann., Chem.*, **330**, 233, 257 (1904) ; [b] C. M. Cark and J.D.A. Johnson, *J. Chem. Soc.*, **1962**, 126.

[66] C. R. Conard and M. A. Dollivery, *Org., Syn., Coll. Vol.*, **2**, 167 (1943).

[67] [a] V. N. Ipatieff, H. Pines and R. C. Olberg, *J. Amer. Chem. Soc.*, **70**, 2123 (1948) ; [b] J. von Brawn and G. Kirschbaum, *Ber. dtsch. Chem. Ges.*, **46**, 3041 (1913) ; *Chem. Abstr.*, **8**, 123 (1914) ; [c] C.S. Marvel, J. Dec., H. G. Cooke, Jr. and J.C. Cowan, *J. Amer. Chem. Soc.*, **62**, 3499 (1941).

[68] [a] J. B. Conant and N. Tuttle, *Org. Syn., Coll. Vol.*, **1**, 199 (1941) ; [b] J.B. Conant and N. Tuttle, *Org. Syn., Coll. Vol.*, **1**, 345 (1941) ; [c] H. Alfred, *J. Amer. Chem. Soc.*, **51**, 2542 (1929) ; [d] J. Colonge and L. Pichat, *Bull. Soc. chim. France*, **16**, 180 (1949) ; [e] K. von Auwers, *Ber. dtsch. chem. Ges.*, **54**, 994, 995 (1912) ; [f] C. F. Koelsch and C. D. Le Claire, *J. Org. Chem.*, **6**, 516 (1941).

[69] For reviews see :
[a] L. Stock, "Aromatic Substitution Reactions", Prentice-Hall, Englewood Cliffs, New Jersey, 1968 ; [b] R.O.C. Norman and R. Taycor, "Electrophilic Substitution in Benzenoid Compounds", Elsevier, Amsterdam, 1965 ; [c] E. Berliner, *Progr. Phys. Org. Chem.*, **2**, 253 (1964) ; [d] L. M. Stock and H. C. Brown, *Adv. Phys. Org. Chem.*, **1**, 35 (1963) ; [e] P.B.D. de la Mare, *Acc. Chem. Res.*, **7**, 361 (1974) ; [f] J. G. Hoggett, R. B. Moodie, J. R. Penton and K. Schofield, "Nitration and Aromatic Reactivity", Cambridge University Press, London, 1971.

[70] [a] L. F. Fieser and E. L. Martin, *Org. Syn. Coll. Vol.*, **2**, 560 (1943) ; [b] P. Ruggli and A. Maeder, *Helv . Chim. Acta*, **26**, 1486 (1943).

[71] S. A. Fine and R. L. Stern, *J. Org. Chem.*, **32**, 4132 (1967).

Revue Roumaine de Chimie, **26**, *5*, 755–759 (1981)

SYNTHESES OF DYES WITH DIBENZO [*f,ij*] ISOQUINOLINE [2,3-*b*] QUINAZOLINE-5,10-DIONE STRUCTURE

F. URSEANU 1), D. POPESCU 2), D. BRĂCĂCESCU 2), T. OLTEANU 1)

1) Laboratory of Chemistry and Technology of Aromatic Intermediates and Dyes, Polytechnic Institute, Bucharest, Calea Victoriei, nr. 149, Romania

2) Textile Research Institute, Bucharest, Lucreţiu Pătrăşcanu Street, nr. 3A, Romania

Received December 22, 1979

Syntheses of the two new disperse dyes and a new cationic dye with dibenzo [*f,ij*] isoquinoline [2,3-b] quinazoline-5,10-dione structure are described.

1. INTRODUCTION

In two previous papers the experimental results concerning the obtaining of new disperse dyes[1] and a new cationic dye[2] with dibenzo [*f*, *ij*] isoquinoline [2,3-b]quinazoline-5,10-dione structure were presented.

In the present work we report on the syntheses carried out in order to prepare two new disperse dyes (I and II) and a new cationic dye (III), having a similar structure:

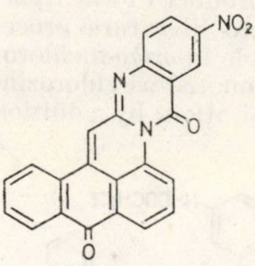

I

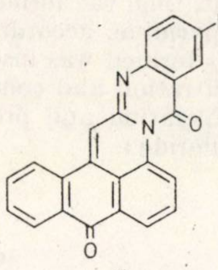

II

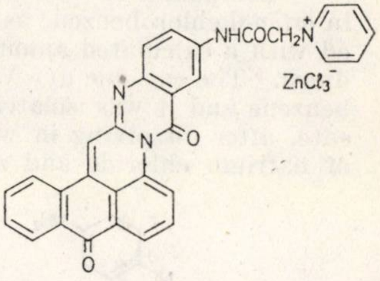

III

2. SYNTHESIS OF THE DISPERSE DYES I AND II

Compound I was synthesized according to a known literature method,[3] namely the reaction of 1-aminoanthraquinone (IV) with 5-nitroanthranilic acid (V) in the presence of a dehydrating agent, such as a mixture of acetic anhydride and anhydrous zinc chloride:

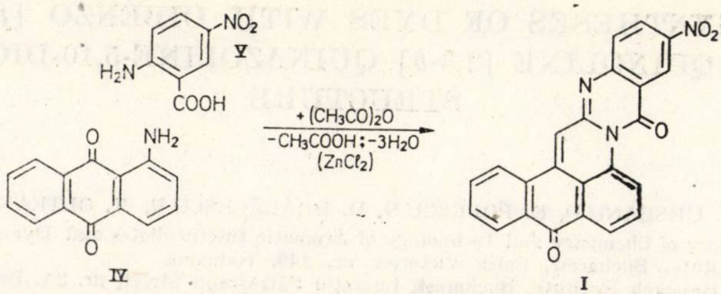
NO2
V
H2N
COOH
O
NH2
O
IV
+ (CH3CO)2O
-CH3COOH; -3H2O
(ZnCl2)
NO2
N
N
O
O
I

Compound II was obtained from the product I by the reduction of the nitro group with aqueous solution of sodium sulphide in N, N-dimethylformamide as solvent, according to literature procedure [4]:

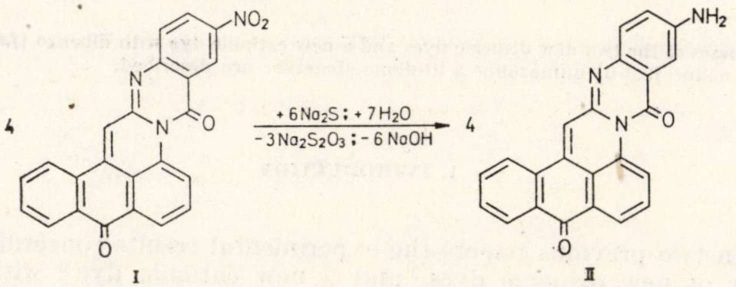
4
NO2
N
N
O
O
I
+ 6Na2S; + 7H2O
- 3Na2S2O3; - 6NaOH
4
NH2
N
N
O
O
II

3. SYNTHESIS OF THE CATIONIC DYE III

Compound II was acylated by heating with chloroacetyl chloride in *ortho*-dichlorobenzene as solvent, then the formed product VI was treated with a calculated amount of pyridine, according to literature procedures. [5] The cationic dye VII thus formed was insoluble in *ortho*-dichlorobenzene and it was isolated by filtration and conditionated as chlorozincate, after dissolving in water, filtration and precipitation, by addition of natrium chloride and zinc chloride:

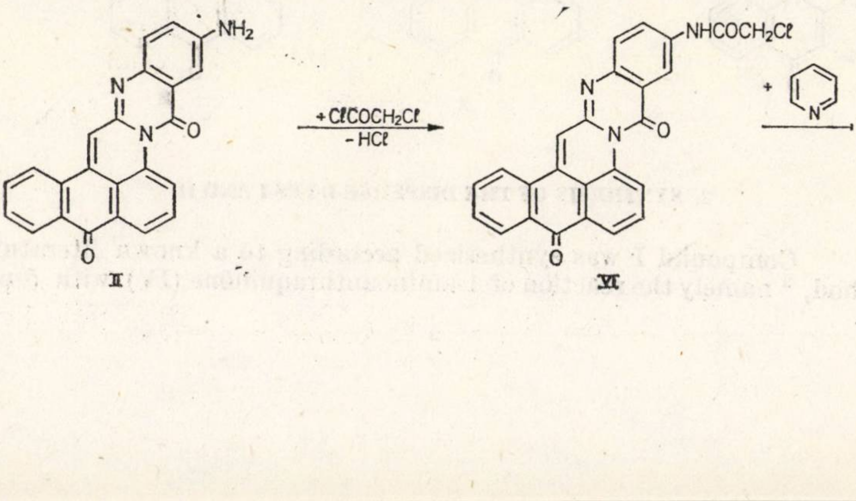
NH2
N
N
O
O
II
+ ClCOCH2Cl
- HCl
NHCOCH2Cl
N
N
O
O
VI
+
N

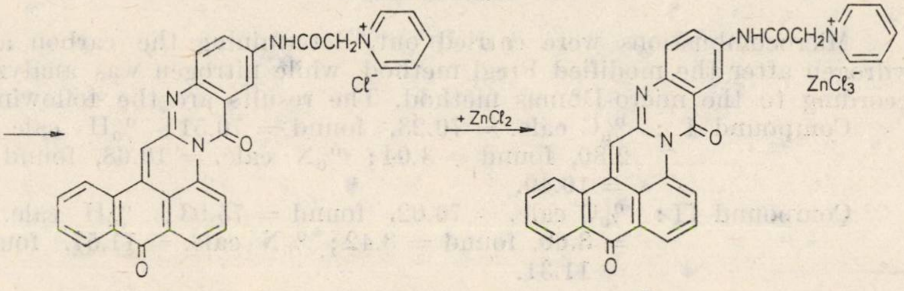

VII III

4. EXPERIMENTAL

4.1. A mixture of 8.92 g (0.04 mol) of 1-aminoanthraquinone and 60 ml acetic anhydride is heated at 100°C for 20 minutes with removal of the acetic acid formed during the acylation, under a slight vacuum. Then, the temperature is decreased at 80—90°C and 8 g (0.044 mol) of 5-nitroanthranilic acid and 10 g of anhydrous zinc chloride are added. The mixture is heated at 110—120°C for two hours, with the continuous distillation of the acetic acid formed ; the reaction mass colour turns gradually from red to greenish-yellow.

Finally, when the reaction ends, the mixture is cooled to 20°C, filtered, and the precipitate is washed with 50 ml of acetic acid. Then, the precipitate is introduced into 250 ml of 10% CH_3COONa solution and heated at 70—80°C to be neutralized ; the suspension is filtered and the precipitate is washed with 200 ml of water (in portions) and dried at 80°C, yielding 12.5 g of product I (79.5% yield).

4.2. 7.86 g (0.02 mol) of compound I are dissolved in 120 ml of N.N-dimethylformamide at 80—90°C. To the resulted solution a warm solution (80°C) of 7 g $Na_2S \cdot 7H_2O$ in 10 ml water is added dropwise for 30 minutes. The reaction is completed by heating at 95—98°C for three hours ; the colour of the reaction mass turns gradually from yellow to reddish-brown. Finally, the reaction mass is cooled to 20°C and 120 ml of water are added ; the mixture is neutralized with concentrated HCl to pH=7, the formed precipitate is filtered, washed with 150 ml of water and dried at 70—80°C, yielding 6.5 g of product II (89.5 yield).

4.3 Compound II (3.63 g ; 0.01 mol) is dissolved in 70 ml of *ortho*-dichlorobenzene at 175°C ; 10 ml of *ortho*-dichlorobenzene are distilled from the formed solution in order to remove any water traces, then 1 ml (1.5 g ; 0.013 mol) of chloroacetyl chloride are added at 90°C. The reaction is completed by heating at 170—175°C for 30 minutes. The reaction mass is cooled at 100°C, 1.3 ml (1.27 g ; 0.016 mol) of pyridine are added and the mixture is heated at 130—140°C for 30 minutes. The formed precipitate is filtered at 20°C, washed with 30 ml of benzene and dried at 40°C. The product thus obtained is introduced into 100 ml of hot water (80°C), 5 ml of acetic acid are added, the mixture is heated at 90—95°C for 10 minutes and filtered ; a small quantity of insoluble residue remains on the filter. The filtrate is treated with natrium chloride and zinc chloride for the precipitation of the cationic dye as chlorozincate (III), which is filtered, washed with 25 g of solution 20% NaCl, and dried at 40—50°C ; 7 g of product (III as salt) are thus obtained (90% yield).

5. ANALYSES

The analysed compounds were previously purified. Compounds I and II were recrystallized from *ortho*-dichlorobenzene, while the cationic dye III was purified by dissolving in absolute methanol, filtration and precipitation with ether. The melting point of the compound II is 343°C. Compound I decomposes over 350°C. The purified compounds were subjected to elemental, spectral and tinctorial analyses.

5.1. Elemental analysis

Microcombustions were carried out, determining the carbon and hydrogen after the modified Pregl method, while nitrogen was analyzed according to the micro-Dumas method. The results are the following:

Compound I : %C calc. = 70.23, found = 70.51; %H calc. = 2.80, found = 3.04; %N calc. = 10.68, found = 10.40.

Compound II: %C calc. = 76.02, found = 75.93; %H calc. = 3.60, found = 3.42; %N calc. = 11.57, found = 11.31.

5.2. Spectral analysis

Infrared, ultraviolet and visible spectra of the products were recorded.

IR spectra were recorded using a BECKMAN IR 4260 Research Infrared Spectrophotometer, in KBr pellet.

Characteristic vibration frequencies ν [cm^{-1}]:

Compound I: 698 m; 785 m; 845 m; 1070 w; 1310 s; 1340 vs; 1515 vs; 1610 s; 1665 s and 3100 w

Compound II: 698 m; 778 s; 835 m; 1310 vs; 1610 s; 1660 vs; 1685 s; 3350 vs and 3430 s

Compound III: 705 m; 805 m; 1310 m; 1488 vs; 1585 s; 1630 vs; 1690 m; 2850 w; 2920 w; 2980 w and 3440 s

(w = weak; m = medium; s = strong; vs = very strong).

Ultraviolet and visible spectra were determined with a "Specord UV–VIS" apparatus. The determinations were carried out in N,N-dimethylformamide and the extinction coefficients ε_{max} were calculated.

The characteristic absorption maxima λ_{max} and lg ε_{max} are presented in table 1.

TABLE 1

Absorption maxima in ultraviolet and visible region

Compound	λ_{max} [nm]	lg ε_{max}
I	340	4.268
	354	4.132
	411	4.180
	443	4.259
	454 sh	4.166
II	298	4.337
	357	4.196
	516	4.145
	544	4.139
III	333	4.221
	454	4.057

sh = shoulder

5.3. Tinctorial analysis

Compounds I and II were used as disperse dyes for "Terom" polyester fibres, and compound III was used to dye polyacrylonitrile fibres (as cationic dye). The results obtained with dyed samples are presented in table 2.

TABLE 2

Determinations with dyed fibres

Compound	Dyed fibres	Colour	Fastness						
						Perspiration		Rubbing	
			Light	Cold water	Washing at 40°C	acid pH = 5.5	alkaline pH = 8.4	dried	wet
I	PE	Greenish-yellow 1 (Bright)	7	5/5/5/	5/5/5/	5/5/5	5/5/5	4	4–5
II	PE	Yellowish-red 7 (Bright)	6	5/4–5/4	5/4–5/4	5/4/4	5/4/4	4	4
III	PNA	Yellowish-orange 4	5–6	5/5/4–5	5/5/5	5/5/5	5/5/5	4–5	4–5

PE = polyester fibres
PNA = polyacrylonitrile fibres

The dyeings obtained are characterized by very good fastness properties, especially by fastness to light and washing. Dyes I and II have a strong brilliance of shade. The colours were defined according to C. I. Hue Chart.[5] A good agreement is observed between the seen colours and the values of the absorption maxima.[6]

REFERENCES

[1] F. Urseanu, *Rev. Roumaine Chim.*, **20**, 107 (1975).

[2] F. Urseanu and C. Drăghici, *Rev. Roumaine Chim.*, **23**, 1471 (1978).

[3] R. Lesser and G. Gad, Ger. Pat. 536–448, March 5, 1930; *Chem. Abstra.*, **26**, 1452 (1932).

[4] F. Urseanu, C. Drăghici and V. Olteanu, *Rev. Roumaine Chim.*, **19**, 1751 (1974).

[5] C. I. Hue "Indication Chart, American Association of Textile Chemists and Colourists", Lowell Institute, Lowell Massachusetts, USA.

[6] C. D. Nenițescu, "Chimie Organică", vol. 2, ed. 7, Ed. didactică și pedagogică, Bucharest, 1974, p. 529.

Revue Roumaine de Chimie, 26, 5, 761–768 (1981)

EL ANÁLISIS POR EMISIÓN MOLECULAR EN CAVIDAD PARA LA DETERMINACIÓN DE NO-METALES USANDO SISTEMAS DE VOLATILIZACIÓN

M. BURGUERA y J. L. BURGUERA
Universidad de Los Andes, Facultad de Ciencias,
Departamento de Química, Mérida, Venezuela.

A. TOWNSHEND
University of Birmingham, Department of Chemistry
P.O. Box 363, Edgbaston, Birmingham, B15 2TT, England.

Recibido : el 20 de Febrero de 1980

El análisis por emisión molecular en cavidas (MECA) es una técnica en llama la cual generalmente analiza no-metales y metaloides. Este artículo de revisión describe los sistemas de volatilización usados junto con MECA dando, a su vez detalles sobre las reacciones utilizadas para convertir la muestra en un compuesto volátil. Las sensitividades logradas y las posibles especies emitentes son descritas.

Molecular Emission Cavity Analysis (MECA) is an analytical flame technique which generally analyses non-metals and metalloids. This paper is reviewing the volatilization systems used in conjunction with MECA giving some details on the reactions used to convert the analyte in a volatile compound. The sensitivities achieved and the possible emitting species are given.

INTRODUCCION

El análisis por emisión molecular en cavidad conocido como MECA[1-3] está basado en la generación de moléculas simples tales como S_2, HPO, BO_2, etc., en una llama de hidrógeno, seguido por la medición de la intensidad de emisión a una cierta longitud de onda. Para el análisis de elementos cuyas lineas de rosonancia están en ultravioleta lejano, los métodos de llama convencionales basados en espectros atómicos, emplean fuentes poderosas de excitación y monocromadores de alta resolución. Las moléculas formadas por muchos de estos elementos en la llama MECA emiten bandas anchas en la región visible ó ultravioleta cercano. Por eso, en la práctica, se encontró que MECA es una técnica complementaria a la de absorción atómica.

En MECA se han desarrollado concurrentemente dos métodos que difieren en la manera de introducir la muestra para el análisis en la cavidad :

a) Método convencional, que consiste en inyectar las muestras líquidas en una pequeña cavidad (5 mm en diámetro con una capacidad máxima de 45 ul) situada en la llama de hidrógeno, frente al detector.

b) Método de vaporización que usa una reacción química selectiva para isolar el elemento en estudio en forma de vapor y la medición de la emisión que se forma cuando sus vapores llegan a la cavidad.

Este artículo se propone describir el sistema de volatilización presentando las reacciones y dispositivos de volatilización usados desde que se inició la técnica hasta el presente.

INSTRUMENTACION

Los aparatos ompleados en el análisis por emisión molecular en cavidad han sido descritos en varias oportunidades. [1,3] Generalmente son espectrofotómetros comerciales de emisión ó espectrofotómetros de absorción atómica, modificados. La parte más importante del aparato es el soporte de la cavidad que permite el movimiento de ésta al frente del detector.

En el sistema de volatilización, la cavidad está conectada a un reactor en el cual la muestra se volatiliza directamente ó se transforma en un compuesto volátil a través de una reacción química. La reacción escogida debe cumplir ciertas condiciones: ser selectiva, eficiente y producir compuestos estables.

Los dispositivos de volatilización (Figura 1) consisten en un reactor cerrado donde se deposita la muestra y en el cual se inyecta el reactivo necesario para generar el gas. Un sistema eléctrico para calentar el reactor y un agitador magnético hacen que la reacción sea rápida y homogénea. Una corriente de nitrógeno ó helio, lleva el gas formado a la cavidad.

En el caso que dos ó más elementos forman compuestos volátiles en las mismas condiciones experimentales (i.e., arsénico, selenio y estaño forman hidruros cuando sus diferentes compuestos se reducen con borohidruro de sodio en medio ácido [4]), MECA pierde selectividad. El uso de una columna cromatográfica ó una trampa fria entre el reactor y la cavidad, elimina este problema. En la Figura 1 se dá el esquema de un dispositivo de volatilización.

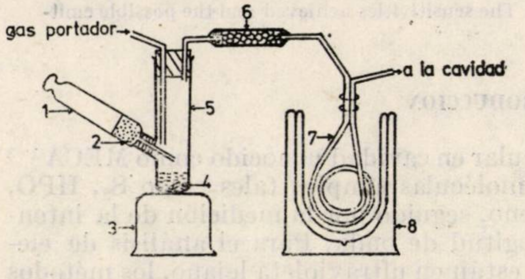

Fig. 1. — Sistema de volatilización: *1* — Jeringa; *2* — muestra; *3* — agitador magnético; *4* — reactivo; *5* — reactor; *6* — tubo absorbente de humedad; *7* — tubo de teflón que se usa como trampa fria ó comocolumna cromatográfica; *8* — termos u horno cromatográfico.

La cavidad, siendo permanentemente situada en la llama se pone incandescente y se deteriora, por eso tiene un dispositivo simple de enfriamiento, así como se ve en la Figure 2. Para cietros elementos, como nitrógeno, arsénico, boro, silicio, etc. las especies moleculares emitentes se forman en la cavidad sólo en la presencia de una pequeña corriente de oxígeno. Por lo tanto, además del tubo que la conecta con el reactor, la cavidad tiene otro tubo lateral que la conecta con la bombona de oxígeno (Figura 2).

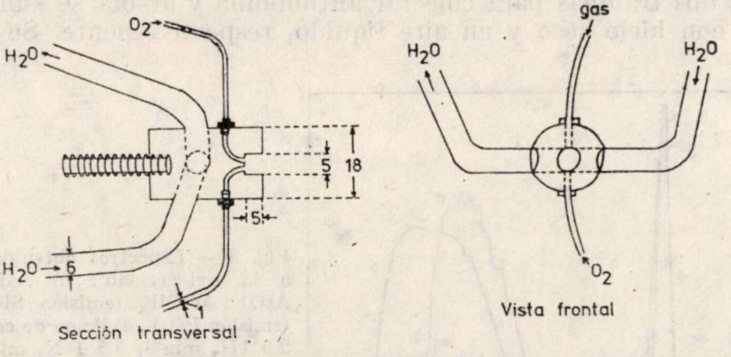

Fig. 2. — Oxi-cavidad de duraluminio con sistema de enfriamiento (Dimensiones en mm).

DETERMINACION DE DIFERENTES ELEMENTOS

A continuación se describirán las reacciones empleadas y los resultados para cada elemento estudiado.

Boro. — El primer elemento determinado usando un sistema de volatilización fué el boro, después de convertirlo en borato de metilo. [5] El gas se obtuvo al calentar una solución de ácido bórico con una mezcla de metanol y ácido sulfúrico concentrado (5 :1), a 80°C. La emisión BO_2 que se forma en presencia de oxígeno en la cavidad, se midió a 518 nm (Ver espectro BO en Figura 3). Aunque el procedimiento es libre de otras interferencias, el exceso de metanol produce una emisión azul persistente (CH) que no permite detectar cantidades de boro menores de 2 μg. Este efecto se redujo considerablemente colocando una trampa fria (hielo seco en una mezcla de cloroformo y tetracloruro de carbone) entre el reactor y la cavidad (Figura 1). [6] El limite de detección, fué 0.04 ppm (20 ng en 2 ml de muestra) y el gráfico de calibración fué linear entre 0.05 μg y 30 ug de boro. El método se aplicó al análisis de aceros con muy altas (15%) ó muy bajas (0.0001%) concentraciones de boro.

Haciendo reaccionar diferentes compuestos de boro con ácido sulfúrico concentrado en exceso de fluoruro, se obtiene el trifluoruro de boro que también produce la emisión BO_2 a 518 um. [6] El desarrollo de un procedimiento para la determinación de boro como su fluoruro, bajo condiciones óptimas podría proporcionar alta sensitividad.

Arsenico, antimonio y estaño. — La inyección directa de soluciones de estos elementos en una oxi-cavidad situada en una llama de hidrógeno produce una banda ancha entre 330—550 nm [5] atribuída a los respectivos óxidos (ver por ejemplo el espectro AsO en Fig. 3). Emisiones más intensas se obtienen si estos elementos se introduen en la cavidad como sus hidruros preparados por reducción con borohidruro de sodio en medio ácido. [7,8] El rango de linearidad fué 0.4—5 μg para arsénico y casi el doble para antimonio.

Arsénico, antimonio y estaño interfieren mutuamente, por eso se han hecho intentos de separarlos en base a la diferencia que hay entre sus puntos de ebullición (−55°C para arsina y −17.1°C para antimonina). Por ejemplo, dos trampas para colectar antimonina y arsina se sumergen en acetona con hielo seco y en aire líquido, respectivamente. Se encontró que el procedimiento no es práctico porque la primera trampa retiene solo parcialmente la antimonina. Una separación muy eficiente se obtuvo usando una columna cromatográfica entre el reactor y la cavidad. El hidruro de estaño que se genera bajo las mismas condiciones experimentales, también se separó (Figura 4). El hidrógeno que se produce durante el proceso de reducción aumenta considerablemente la emisión de fondo. Usando la columna cromatográfica, el hidrógeno sale antes que los hidruros, por lo tanto no afecta las medidas de emisión y se puede llegar a sensitividades de 0.2 µg, 0,7 µg y 0.75 µg para arsénico, antimonio y estaño, respectivamente.

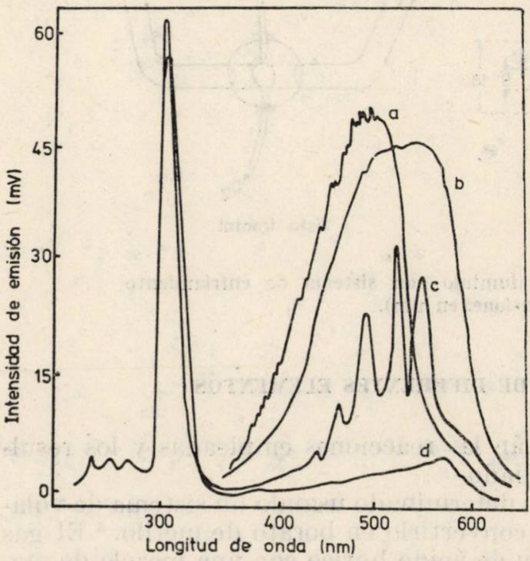

Fig. 3. — Espectros obtenidos al llevar a la oxi-cavidad: *a*) AsF_3 (emisión AsO); *b*) SiF_4 (emisión SiO); *c*) BF_3 (emisión BO_2); *d*) llama de composición: 2.0 1 H_2 min^{-1}, 5.5 1 N_2 min^{-1}; 110 ml O_2 min^{-1}; 30 ml N_2 min^{-1} como gas portador; temperatura del reactor = = 180°C; apertura del monocromador = = 0.15 nm.

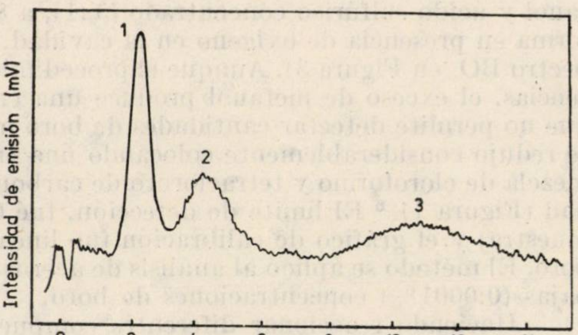

Fig. 4. — Separación cromatográfica de los hidruros: *1* — arsénico (10 µg As); *2* — antimonio (25 µg Sb); *3* — estaño (25 µg Sn), usando una columna de Teflón llena con goma de silicón en porapak Q.

Optimizando las condiciones experimentales para la generación de hidruro de estaño, so logró un límite de detección de *ca* 80 ng de Sn(II) en 1 ml de solución,[9] sin usar la columna cromatográfica.

El efecto negativo de varios metales en la generación de hidruros fué eliminado al preparar soluciones estandar 0.01 M en EDTA.[10]

Selenio y telurio. — La reacción entre soluciones de selenio (IV) y telurio (IV), 2N en ácido clorhídrico, con borohidruro de sodio, produce los respectivos hidruros. En la cavidad MECA, los hidruros producen varias bandas de emisión con el máximo a 411 nm para SeH_2 y 500 nm para TeH_2.[8] El límite de detección fué 0.1 ppm para selenio y telurio (ver Tabla 1). Usando soluciones de selenio (VI), no se ha obtenido emisión apreciable, por eso fué necesario reducir Se (VI) a Se(IV).

TABLA 1

Aplicaciones del sistema de volatilización

Elemento	Reactivo	Gas formado	Especie emitente	λmax (nm)	Detección límite (ppm)	Ref.
Arsénico	$NaBH_4$	AsH_3	AsO	400	0.2	4,5,10
Boro	$H_2SO_4+CH_3OH$	$(CH_3)_3BO_3$	BO_2	518	0.04	5,6
Nitrógeno	$NH_4^+ + NaOH+$ aleación Devarda	NH_3	NO−O	500	1.0	12
	$NO_2^- + I^-$	NO	NO−O	500	1.0	9
Antimonio	$NaBH_4$	SbH_3	SbO	355	1.0	4,8
Selenio	$NaBH_4$	SeH_2	Se_2	413	0.1	8
Telurio	$NaBH_4$	TeH_2	Te_2	500	0.1	8
Estaño	$NaBH_4$	SnH_4	SnO	485	0.2	4, 5, 9
Azufre	$SO_4^{2-} + Sn/H_3PO_4$	H_2S	S_2	384	0.01	19
	$SO_3^{2-} + HCl$ (caliente) ó H_3PO_4	SO_2	S_2	384	0.02	18

Un estudio de las interferencias demostró que hay muchos elementos que disminuye la intensidad de emisión del selenio. Algunos metales, (Pb Bi, Cu) son reducidos por el borohidruro de sodio y forman suspensiones oscuras en el reactor.

Arsénico, antimonio, estaño, talio y los iones sulfuro y sulfito, se convierten en hidruros volátiles bajo las condiciones de preparación del SeH_2. Algunas de las interferencias han sido fácilmente eliminadas — el sulfuro se oxida con peróxido de hidrógeno a sulfato, que no interfiere. El efecto del arsénico y antimonio se liminó generando selectivamente arsina y antimonina a partir de soluciones 0.1 M en ácido clorhídrico, condiciones en las cuales SeH_2 no se forma. Después de aeriar el sistema se aumenta la acidez de la solución en el reactor y se mide la emisión que da el SeH_2 sólo.

Silicio. — La inyección de soluciones acuosas de compuestos inorgánicos de silicio en la cavidad MECA no producen ninguna emisión, posiblemente porque la energía de la llama usada es muy baja para promover excitación. Introducción de compuestos más volátiles (i. e. $SiCl_4$, SiF_4, $CH[Si(CH_3)_3]_2$, etc.) en la oxi-cavidad, produjo una banda ancha entre 540 y 620 nm, atribuida a la especie SiO [6,11] (ver espectro SiO en Figura 3). Basado en esta emisión se desarrolló un procedimiento para el análisis de silicio, generando tetrafluoruro de silicio en un reactor de Teflón. A una mezcla de un silicato en exceso de fluoruro y cloruro se le inyecta 1.0 ml de ácido sulfúrico concentrado y se calienta a 135°C en un baño de aceite. El gas formado es llevado a la cavidad y la emisión se mide a 540 nm. El límite de detección fué 0.5 μg silicio en 0.2 ml de solución. El procedimiento se aplicó satisfactoriamente a la determinanción de silicio en minerales de hierro y en rocas fosfáticas. Los únicos interferentes serios fueron el arsénico y el boro que forman fluoruros bajo las mismas condiciones experimentales.

Para aumentar la sensitividad y evitar el manejo del aceite caliente, mezclas acuosas de silicato y fluoruro (0.2 ml) se evaporan al seco directamente en los reactores. Después de agregar ácido sulfúrico concentrado, los reactores se calientan eléctricamente hasta 180°C durante 5 minutos. Un pequeño flujo de nitrógeno lleva el gas formado a la oxi-cavidad de aluminio con sistema de enfriamiento situada en la llama (Figura 2). El límite de detección fué en este caso 0.3 ug de silicio y la mayoria de las interferencias eliminadas debido a la evaporación al seco y a la ausencia de cloruro.

Nitrogeno. — Algunos compuestos de nitrógeno han sido estudiados en el sistema de volatilización, después de convertirlos en óxidos de nitrógeno [9] ó amoníaco. [12] Los gases llevados a la cavidad producen también una banda ancha entre 330 y 700 nm, con el máximo alrededor de 500 nm; la especie emitente es, posiblemente el continuo NO—O. [13]

Los nitratos se reducen en presencia de manganeso (IV) en medio alcalino, a nitritos, que al reaccionar con ioduro en medio ácido se convierten en monóxido de nitrógeno. La reacción ocurre en 60—80 segundos a 84°C. Los límites de detección fueron 1 ng y 2 ng de nitrógeno para nitritos y nitratos, respectivamente.

Basado en la misma emisión, se desarrolló un método para la determinación de iones amonio, [12] convirtiendo la muestra en amoníaco al hacerla reaccionar con hidróxido de sodio. Se encontró que el procedimiento no es afectado por otros iones nitrógeno y que el límite de detección es 1 ppm. El método se aplicó a la determinación de nitrógeno amoniacal en fertilizantes, agua de rio y afluentes industriales.

Si en la oxi-cavidad se introducen compuestos de nitrógeno que contienen carbono, además del continuo NO—O se generan las emisiones NO, NH y CN pero sus intensidades dependen de la naturaleza del compuesto.[14] En cambio, los compuestos de nitrógeno que contienen azufre producen la emisión S_2 en ausencia de oxígeno y en la oxi-cavidad se promueven las especies CH y NO—O. [14]

Halogenos. — Para la determinación de halogenos (excepto fluoruro) se está dosarrollando un método que consiste en convertir la muestra en los ácidos correspondientes (HX, $X = Cl, Br, I$) y medición de la intensidad de emisión que se produce cuando los gases llegan a una cavidad cubierta con indio (se forma InX) ó con estaño (se forma SnX). [15]

El iodo se obtuvo también en un sistema de volatilización a partir de una solución ácida de ioduro en presencia de dicromato. La emisión InI se puede medir a 410 nm, pero el método necesita desarrollo.

El fluoruro se determinó indirectamente usando el procedimiento descrito para silicio [16] con la única modificación que se usó un pequeño exceso de silicio. El límite de detección fué 5 μg de fluoruro en 0.2 ml de solución. Un estudio de las interferencias demostró que todos los ácidos (nítrico, sulfúrico, fosfórico y clorhídrico) agregados a los reactores antes de evaporar al seco, disminuyen la emisión posiblemente debido a la evolución de ácido fluorhídrico. Esta interferencia se eliminó al ajustar el pH de las soluciones iniciales a $\geqslant 7$. Los iones amonio que normalmente producen la emisión $NO-O$ no interfieren, puesto que cuando se efectúa la evaporación al seco de la solución alcalina, todo el amonio se elimina como amoníaco antes de hacer las mediciones. Arsénico y boro refueron los únicos interferentes serios. Sus efectos se puden disminuir considerablemente al medir la intensidad de emisión a 580 nm y usando una apertura del monocromador de solo 0.2 nm = 13 nm.

El procedimiento para la determinanción indirecta de fluoruro se aplicó al análisis de agua y cremas dentales y los resultados obtenidos se compararon con aquellos obtenidos por el método espectrofotométrico del azul de alizarina. [17]

Debido a que el arsénico y el boro forman fluoruros bajo las condiciones en que se prepara el tetrafluoruro de silicio, se pueden usar en vez de silicio para la determinanción indirecta de fluoruro. Los límites de detección fueron 1.6 μg y 10 μg de fluoruro para los trifluoruros de arsénico y boro, respectivamente.

Azufre. — Los compuestos de azufre se convierten en dióxido de azufre [18] ó sulfuro de hidrógeno [8,19] en un sistema de volatilización.

Dióxido de azufre [18] se genera de soluciones ácidas. Se desarrolló un método para la determinanción de sulfito en bebidas suaves, usando ácido fosfórico, llegando a un límite de detección de 25 ng de SO_2.

El sulfuro de hidrógeno [8] se genera inyectando una solución de sulfuro en un reactor que contiene ácido clorhídrico 3—8 M. El gas es llevado a la cavidad y la emisión resultante se mide a 384 nm. El límite de detección para sulfuro fué 40 ng ó 10 ng de azufre, cuando se inyecta 1 μl ó 50 μl de muestra, respectivamente. El procedimiento se mejoró al usar un reactivo especial para generar el sulfuro de hidrógeno. [19] El reactivo se preparó calentando estaño metálico en ácido fosfórico anhidro. Si se inyecta un compuesto de azufre en un reactor que contiene el reactivo, y se calienta a 200°C, se genera rápidamente H_2S. El límite de detección es *ca* 1 ng de azufre en $\leqslant 1$ ml de solución.

En la Tabla 1 se dan algunas características, y los mejores límites de detección obtenidos para los no-metales determinados usando sistemas de volatilización.

CONCLUSION

El uso de un sistema de volatilización conjuntamente con MECA, es, en muchos casos, una fuente adicional de sensitividad y selectividad si se escoge la reacción acertada.

Dedicándose a determinar específicamente no-metales y metaloides, MECA es una técnica complementaria a la espectrometría atómica, teniendo las ventajas de las demás técnicas que usan llamas frias : baja emisión de fondo a longitudes de ondas cortas, capacidad de generar emisiones quimioluminescentes y mínimas interferencias por ionización debido a la baja temperatura de la llama.

La abilidad de generar óxidos emitentes que producen bandas anchas de emisión sobre una gran porción de la región visible (Figura 3), hizo posible la determinación simultánea de dos o más elementos a la misma longitud de onda después de separación cromatográfica.[8] Esto condujo la investigacion hacia el desarrollo de MECA como multidetector cromatográfico.[20]

Aunque MECA tiene un amplio campo de aplicaciones, le queda todavía un gran potencial para ser desarrollado en un futuro inmediato.

REFERENCIAS

[1] R. Belcher, S. L. Bogdanski y A. Townshend, *Analyt. Chim. Acta*, **67**, 1 (1973) ; U. S. Pat. 3, 871, 768, Marzo 18, 1975.

[2] R. Belcher, S. L. Bogdanski y A. Townshend, *Rev. Chim. (Bucureşti)*, **26**, 59 (1975).

[3] M. Burguera, A. Townshend y S. L. Bogdanski, *Crit. Rev. Analyt. Chem.*, en prensa, 1980.

[4] R. Belcher, S. L. Bogdanski, E. Henden y A. Townshend, *Analyt. Chim. Acta*, **92**, 33 (1977).

[5] R. Belcher, S. L. Bogdanski S. A. Ghonaim y A. Townshend, *Analyt. Chim. Acta*, **72**, 183 (1974).

[6] M. Burguera, Tesis de Doctorado, Universidad de Birmingham, Inglaterra, 1979.

[7] R. S. Braman, L. L. Yusten y C. C. Foreback, *Analyt. Chem.*, **44**, 2195 (1972).

[8] E. Henden, Tesis de Doctorado, Universidad de Birmingham, Inglaterra, 1976.

[9] I. Z. Al-Zamil, Tesis de Doctorado, Universidad de Birmingham, Inglaterra, 1978.

[10] R. Belcher, S. L. Bogdanski, E. Henden y A. Townshend, *Analyst*, **100**, 522 (1975).

[11] M. Burguera, en „Molecular Emission Cavity Analysis", S. L. Bogdanski, D. A. Stiles y A. Townshend (Eds.), M. Dekker, New York, 1980.

[12] R. Belcher, S. L. Bogdanski, A. C. Calokerinos y A. Townshend, *Analyst*, **102**, 220 (1977).

[13] R. W. B. Pearse y A. G. Gaydon, „The Identification of Molecular Spectra", 4th Ed., Chapman and Hall, London, 1974.

[14] A. C. Calokerinos, Tesis de Doctorado, Universidad de Birmingham, Inglaterra, 1978.

[15] N. Puretza, trabajo no publicado.

[16] M. Burguera y A. Townshend, *Analyt. Chim. Acta*, en prensa, 1980.

[17] M. A. Leonard y G. T. Murray, *Analyst*, **99**, 645 (1974).

[18] S. L. Bogdanski, A. Townshend y B. Yenigül, *Analyt. Chim. Acta*, en prensa, 1980.

[19] S. L. Bogdanski, I. M. Shakir, W. I. Stephen y A. Townshend, *Analyst*, **104**, 886 (1979).

[20] R. Belcher, S. L. Bogdanski, M. Burguera, E. Henden y A. Townshend, *Analyt. Chim. Acta*, **100**, 525 (1978).

Revue Roumaine de Chimie, 26, 5, 769—774 (1981)

PHOTOMETRISCHE SCHNELLBESTIMMUNG ABSORBIERENDER VERBINDUNGEN IN GEMISCHEN

A. M. DEMIAN und W. SCHMIDT
Centrul de Chimie, Timişoara, b-dul M. Viteazul 24, Rumänien

Eingegangen am 20. Mai 1980

Aus den Absorptionsspektren der Lösungen von zwei oder drei Verbindungen können mit Hilfe eines gegebenen Programms die Absorptionsspektren der Gemische beliebiger Zusammensetzung berechnet werden. Durch Vergleich der Spektren werden bestimmte quantitative Beziehungen (z. B. Verhältnis der Extinktionen bei zwei Wellenlängen, Lage von Maxima oder Minima, usw.) ausgewählt, die es ermöglichen aus der Absorptionskurve die Zusammensetzung eines beliebigen Gemisches unter Verwendung der berechneten Spektren als Eichkurven zu ermitteln.

From the absorption spectra of the solutions of two or three substances the absorption spectra of mixtures of any composition may be computed by the aid of a given program. By comparison of the spectra, quantitative relations (e.g. rate of the absorbances at two wavelengths, position of maxima and minima) are selected which allow the calculation of the composition on any mixture from the absorption spectra, based on computed calibration curves.

Es ist bekannt, dass die Konzentration von zwei, aber auch von mehreren Komponenten in Lösungen mit Hilfe spektrophotometrischer Daten bestimmt werden können, wenn die spezifischen oder molaren Extinktionskoeffizienten der reinen Komponenten für die entsprechenden Wellenlängen gegeben sind. Die Werte für die Extinktionskoeffizienten und die für die gemessene Gesamtextinktion des Gemisches bei zwei oder mehreren Wellenlängen werden in ein System von zwei oder mehreren Unbekannten eingesetzt. Die Lösung des Gleichungssystems ergibt die gesuchten Werte für die Konzentrationen. Dabei wird die Gültigkeit des Gesetzes von Bouguer-Lambert-Beer und die Additivität der Absorptionen der Einzelkomponenten vorausgesetzt. [1]

Die Lösung solcher Gleichungssysteme erfordert bedeutenden Rechenaufwand und ist oft wegen der Ungenauigkeit der photometrischen Messungen nicht möglich (z. B. negative Konzentrationen als Ergebnis), besonders wenn eine oder mehrere Komponenten in kleinen Konzentrationen neben einer Hauptkomponente in grosser Konzentration vorliegen. Daher wurde versucht, andere Möglichkeiten zur analytischen Auswertung der Absorptionskurven zu erschliessen. Als Voraussetzung dafür wurde die Möglichkeit ausgewertet, aus den Absorptionskurven der reinen Komponenten die Absorptionskurven von Gemischen verschiedener Zusammensetzung zu berechnen.

Zu diesem Zweck wurde ein Programm erstellt, dass die Gesamtextinktionen eines Gemisches von zwei oder drei Komponenten in Lösung berechnet. Im Programm werden die folgenden Rechengrössen verwendet:

$$A = \frac{C_A}{C_A + C_B + C_C} \qquad B = \frac{C_B}{C_A + C_B + C_C}$$

$$C = \frac{C_C}{C_A + C_B + C_C}$$

zwischen welchen die Beziehung $A + B + C = 1$ besteht.

Hier bedeuten:

C_A, C_B, C_C — Konzentration der Komponenten in g/L oder mol/L
In diesem Fall ist

$$C_A = \frac{A}{1 - A}(C_B + C_C) \tag{1}$$

Wenn $Q = \dfrac{C_B}{C_B + C_C}$ definiert wird, so folgt:

$$C_C = \frac{Q}{1 - Q} C_B \tag{2}$$

$$C_A = \frac{A}{1 - A}\left(C_B + \frac{Q}{1 - Q} C_B\right) = \frac{A}{(1 - A)(1 - Q)} C_B \tag{3}$$

Durch Umformung der oben genannten Beziehungen gelangt man zu einem Ausdruck für die Berechnung der Extinktion bei einer bestimmten Frequenz (oder Wellenlänge), wenn Additivität der Absorption für alle drei Komponenten vorausgesetzt wird:

$$^{\lambda}E = [^{\lambda}\varepsilon_A \cdot A/(1 - A)(1 - Q) + {}^{\lambda}\varepsilon_B + {}^{\lambda}\varepsilon_C \cdot Q/(1 - Q)] . C_B . d \tag{4}$$

wo

$^{\lambda}E$ — Gesamtextinktion des Gemisches bei der Wellenlänge λ

$^{\lambda}\varepsilon_A$, $^{\lambda}\varepsilon_B$, $^{\lambda}\varepsilon_C$ — spezifische (oder molare) Extinktionskoeffizienten

d — Dicke der Flüssigkeitsschicht, in cm bedeuten.

Mit Hilfe des Ausdrucks (4) kann die Gesamtextinktion E für jede Wellenlänge und jede Zusammensetzung des Gemisches berechnet werden. Voraussetzung dafür sind Daten, die bei der Bestimmung der Absorptionskurven $\varepsilon_i = f(\nu)$ für jede Komponente erhalten werden. Bei der Berechnung der Absorptionskurven der Gemische wird eine entsprechende Anfangskonzentration für eine der Komponenten gewählt (Hauptkomponente). Im Falle des vorliegenden Programms ist die Konzentration der Hauptkomponente C_B, während die Grössen A und Q mit den Inkrementen DA und DQ geändert werden. Mit diesen Werten wird E für verschiedene Wellenlängen berechnet, d.h. für eine genügend grosse Anzahl von

Wellenlängen, so dass die charakteristischen Elemente der Absorptionskurve (Maxima, Minima) für alle Gemische erfasst werden können.

Das Ablaufschema des Programms wird in Abb. 1 dargestellt. Das Programm wurde auf einem Rechner Felix C—256 angewendet. Als kon-

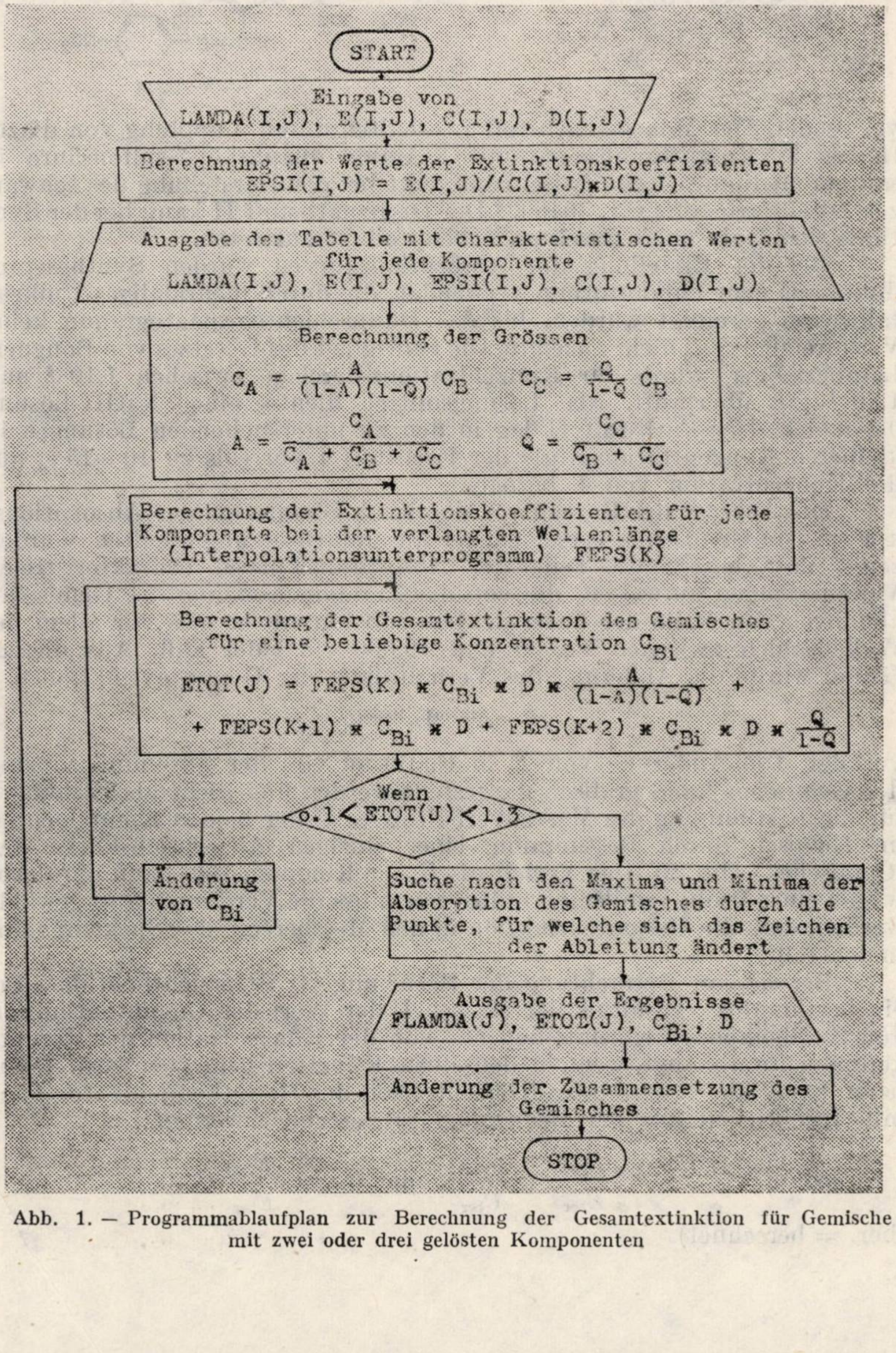
START
Eingabe von
LAMDA(I,J), E(I,J), C(I,J), D(I,J)
Berechnung der Werte der Extinktionskoeffizienten
EPSI(I,J) = E(I,J)/(C(I,J)*D(I,J)
Ausgabe der Tabelle mit charakteristischen Werten
für jede Komponente
LAMDA(I,J), E(I,J), EPSI(I,J), C(I,J), D(I,J)
Berechnung der Grössen
$C_A = \frac{A}{(1-A)(1-Q)} C_B$
$C_C = \frac{Q}{1-Q} C_B$
$A = \frac{C_A}{C_A + C_B + C_C}$
$Q = \frac{C_C}{C_B + C_C}$
Berechnung der Extinktionskoeffizienten für jede
Komponente bei der verlangten Wellenlänge
(Interpolationsunterprogramm) FEPS(K)
Berechnung der Gesamtextinktion des Gemisches
für eine beliebige Konzentration C_{Bi}
$ETOT(J) = FEPS(K) * C_{Bi} * D * \frac{A}{(1-A)(1-Q)} +$
$+ FEPS(K+1) * C_{Bi} * D + FEPS(K+2) * C_{Bi} * D * \frac{Q}{1-Q}$
Wenn
$0.1 < ETOT(J) < 1.3$
Änderung
von C_{Bi}
Suche nach den Maxima und Minima der
Absorption des Gemisches durch die
Punkte, für welche sich das Zeichen
der Ableitung ändert
Ausgabe der Ergebnisse
FLAMDA(J), ETOT(J), C_{Bi}, D
Änderung der Zusammensetzung des
Gemisches
STOP

Abb. 1. — Programmablaufplan zur Berechnung der Gesamtextinktion für Gemische mit zwei oder drei gelösten Komponenten

kretes Beispiel wurden Gemische von zwei Azofarbstoffen der Struktur

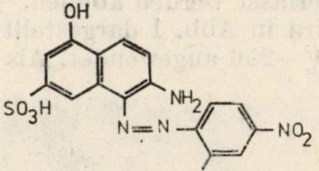

I.

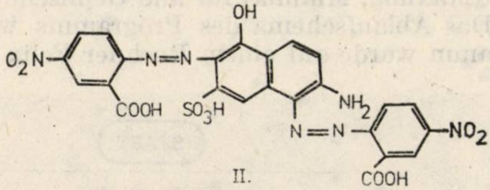

II.

verwendet. Der Monoazofarbstoff I, erhalten durch Kupplung von diazotierter 5-Nitroanthranilsäure mit 2-Amino-5-naphthol-7-sulfonsäure in saurem Medium, ist ein Zwischenprodukt bei der Herstellung des schwarzen Direktfarbstoffs C.I. 30400. [2] Der Disazofarbstoff II kann bei der Synthese von I als unerwünschtes Nebenprodukt auftreten.

Bei der Erstellung der Absorptionskurven wurden Syntheseprodukte aus dem Laboratorium verwendet, die durch mehrmaliges Umkristallisieren gereinigt wurden, bis das Dünnschichtchromatogramm keine Verunreinigungen mehr anzeigte. Die Gültigkeit des Gesetzes von Bouguer-Lambert-Beer wurde für Konzentrations-bereiche zwischen 1.10^{-4} und 1.10^{-1} g/L überprüft. Als Lösungsmittel diente eine NaOH-Lösung 0,1 mol/L. Der Farbstoff II lag in den zu untersuchenden Lösungen in kleineren Konzentrationen als der Farbstoff I vor (bis zu 10 –15 % auf die Konzentration von I bezogen).

Die Analyse der Ergebnisse, die durch Simulation der Absorptionskurven von Gemischen verschiedener Zusammensetzung erhalten wurden zeigt, dass bestimmte Teile der Absorptionskurven charakteristische Veränderungen aufweisen, die von der Zusammensetzung des Gemisches abhängen. Im Falle der untersuchten Substanzen ist dies vor allem bei Wellenzahlen zwischen 18.000 und 19.000 cm^{-1} der Fall. Aus diesem Grund wurde die Änderung des Verhältnisses der Gesamtextinktionen

$$R = {}^{19000}\mathrm{E}/{}^{18000}\mathrm{E}$$

verfolgt. Die Änderung von R in Funktion von der Zusammensetzung des Gemisches kann grafisch dargestellt werden und dient als Eichkurve für die Bestimmung des Massenverhältnisses U der beiden Komponenten im Gemisch durch Bestimmung einer einzigen Absorptionskurve des Gemisches (Abb. 2). Das Verhältnis U der Komponenten kann ohne Abwägen einer Probe ermittelt werden, nur muss die Verdünnung so gewählt werden, dass die Gesamtextinktion in den Messberecih des Spektrophotometers fällt.

Bei näherer Betrachtung der Beziehung (4) ist ersichtlich, dass für ein bestimmtes Verhältnis der Massen U der Wert der Gesamtextinktion von Zweikomponentengemischen nur von der Konzentration der Hauptkomponente abhängt, wenn in denselben Küvetten gemessen wird. Demnach kann die tatsächliche Konzentration der Hauptkomponente (C_{real}) mit Leichtigkeit aus der Beziehung (5) berechnet werden:

$$(5) \qquad \frac{E_{\text{real}}}{E_{\text{ber}}} = \frac{C_{\text{real}}}{C_{\text{ber}}}, \text{ oder } C_{\text{real}} = \frac{E_{\text{real}}}{E_{\text{ber}}} C_{\text{ber}}.$$

(ber. = berechnet)

Dadurch wird die spektrophotometrische Bestimmung eines Gemisches der beiden Farbstoffe bei Verwendung von Eichkurven, erhalten durch Simulation mit Hilfe eines Rechners, besonders einfach und erfordert folgende Operationen:

a) Herstellen einer Lösung des Gemisches in einem entsprechenden Lösungsmittel

b) Verdünnen der Lösung, so dass die Gesamtextinktion in den Messbereich des Gerätes fällt, wobei der Verdünnungsgrad notiert wird

c) Aufnahme der Absorptionskurve der Lösung

d) Berechnung des Wertes ${}^{19000}E/{}^{18000}E$ und Ablesen des Wertes A aus der Eichkurve in Abb. 2.

e) Berechnen der realen Konzentration der Hauptkomponente aus den Werten E_{real} und E_{ber} für das Verhälthis A und der Konzentration der anderen Komponente mit Hilfe von (3), des im Falle von Zweikomponentengemischen die Form

$$C_A = \frac{A}{1-A} C_B$$

annimmt.

TABELLE 1

Disazofarbstoff II im Gemisch der Farbstoffe I und II (% oder 100 × A)

Lösung mit bekanntem Gehalt	Ergebnis der Messung
2,7	3,1
2,7	1,5
4,2	3,5
5,6	7,7
5,6	7,6
7,2	8,5
8,7	12,3
8,7	10,5
10,4	12,4

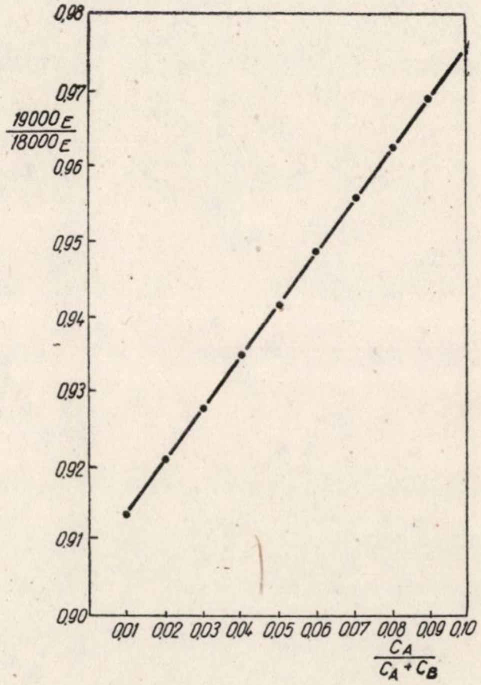

Abb. 2. – Disazofarbstoff im Gemisch der Farbstoffe I und II.

Die Operationen b – e dauern nicht mehr als 10 Minuten. Die Zeit für das Lösen der Probe (Operation a) hängt von der Form ab, in welcher das Gemisch für die Analyse vorliegt.

In Tabelle 1 werden die Ergebnisse der Bestimmung von kleinen Mengen II in I (bis zu 10 – 15% der Gesamtmenge) für verschiedene

Gemische bekannter Zusammensetzung angegeben. Die Ergebnisse sind für die Anforderungen einer technischen Betriebskontrolle zufriedenstellend, vor allem wenn in Betracht gezogen wird, wie schnell das Ergebnis vorliegt und dass die übliche dünnschichtchromatografische Analyse auch keine genaueren Angaben liefert.

LITERATURHINWEISE

[1] G. Kortüm, „Kolorimetrie, Photometrie und Spektrometrie", 3. Aufl., Springer Verlag, Berlin, 1955, S. 23 ; I. Pogany, M. Banciu, „Metode fizice în chimia organică", Editura Ştiinţifică, Bucureşti 1972, S. 160.

[2] „Colour Index", Bd. 4, 3rd edition, The Society of Dyers and Colourists, Bradford, 1971, S. 4290 ; Schw. P. 250.815 (Geigy).

Revue Roumaine de Chimie, **26**, *5*, 775–781 (1981)

STUDIES ON PYRIDONES. II[1]

SYNTHESIS AND REACTIONS OF 6-(3,4-DICHLOROPHENYL)-3-(SUBSTITUTED CINNAMOYL)-4-ARYL-2(1*H*)-PYRIDONES

M. EL-DEEK, M.A.I. SALEM, A.A. HAMED and M. SAMAAN
Chemistry Department, Ain Shams University, Abbassia, Cairo,Egypt

Received January 14, 1980

Some 3-cinnamoylpyridones (II) have been synthesized by condensation of 3-acetylpyridones (I) with different aromatic aldehydes. The cinnamoylpyridones (II) have been brominated and the dibromo derivatives (V) have been subsequently treated with hydroxylamine, hydrazine or phenylhydrazine to yield isoxazoles and pyrazoles (VI). The cyclic Michael adducts (III) of (II) with cyclohexanone have been described. The adducts (III) have been converted with benzylamine to the quinolines (IV).

The promising usefulness of chalcones and their analogues as bactericides, [1-6] germicides, [7-12] cardiovascular sedative [13] and fertility [14] agents have been reported.

These observations have encouraged the authors to synthesize the heterocyclic chalcones (II) in which the phenyl ring is replaced by the heterocyclic pyridone ring, in the hope that structural variations will bring the corresponding modification in the properties of chalcones, which would, in turn, influence the biological activity.

In a previous paper [15] we described the synthesis of 3-acetyl-(3,4-dichlorophenyl)-2-(1*H*)-pyridones (I). The present paper deals with some reactions of the chalcones prepared from (1).

The condensation of the 3-acetylpyridones (I) with benzaldehydes in ethanol in the presence of potassium hydroxide gave a mixture of *cis*- and *trans*-3-cinnamoylpyridones (II). The infrared spectra of 3-cinnamoylpyridones (II) showed absorption bands attributable to C=O (cyclic amide) at 1670 cm^{-1}, C=O (aroyl) at 1630 cm^{-1}, the C=N group at 1625 cm^{-1}, and the C=C group at 1600 cm^{-1}. The OH group appeared at 3380 cm^{-1}.

The ^{1}H–NMR spectrum of the representative compound IIa showed ethylenic protons at δ 6.46 ppm (doublet), the aromatic proton of the pyridone ring appeared at 6.48 ppm (singlet) while the NH proton appeared as a broad peak at 6.74 ppm (singlet). The 13 aromatic protons appeared as a multiplet at 7.15–8.2 ppm.

In order to study the chemical behaviour of cinnamoylpyridones (II), the following reactions were investigated and discussed below :

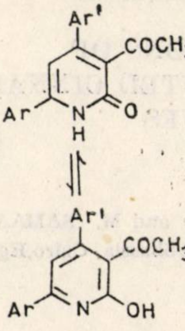

(I)

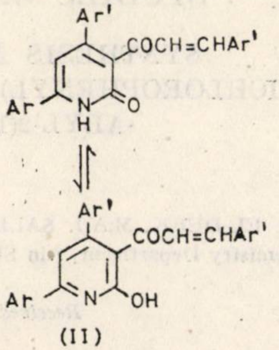

(II)

Ar = 3,4-$Cl_2C_6H_3$-

II	Ar′	Ar″		Ar′	Ar″
a	C_6H_5	C_6H_5	d	p-$CH_3OC_6H_4$	p-$CH_3OC_6H_4$
b	C_6H_5	p-$CH_3OC_6H_4$	e	p-ClC_6H_4	C_6H_5
c	p-$CH_3OC_6H_4$	C_6H_5	f	p-ClC_6H_4	p-$CH_3OC_6H_4$
			g	3,4(O_2CH_2)C_6H_3	C_6H_5

1 – *Formation of Michael adducts with cyclohexanone*

The cyclic Michael adducts (III) were prepared by heating the cinnamoylpyridones (II) with cyclohexanone in the presence of potassium hydroxide as a base.

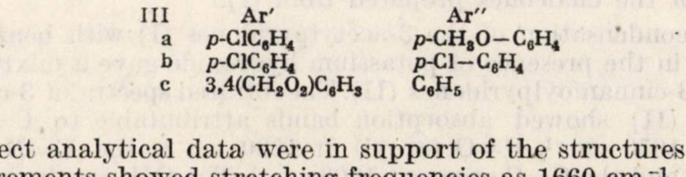

(III)

Ar = 3,4-$Cl_2C_6H_3$

III	Ar′	Ar″
a	p-ClC_6H_4	p-CH_3O-C_6H_4
b	p-ClC_6H_4	p-Cl-C_6H_4
c	3,4(CH_2O_2)C_6H_3	C_6H_5

Correct analytical data were in support of the structures (III). The IR measurements showed stretching frequencies as 1660 cm^{-1}, 1630 cm^{-1}, 3030 cm^{-1}, and 3420 cm^{-1} characteristic for CO (cyclic amide), C=N, NH and the OH group respectively. The ^1H-NMR spectrum ot the representitive compound (IIIb) showed the 8 methylene protons as a multiplet at δ 2.65 ppm, the -CH proton on the pyran ring as a doublet at 4.22 ppm. The aromatic proton of the pyridone ring appears at 6.34 ppm as a singlet while the NH proton appears as a broad peak at 6.72 ppm, the ethylenic proton of pyran ring at 6.48–6.50 ppm as a doublet and the 11 aromatic protons as a multiplet at 7.22–8.05 ppm.

The structure of the above pyranes III has been confirmed by converting them into the quinolines (IV) by reaction with benzylamine in boiling ethanol.

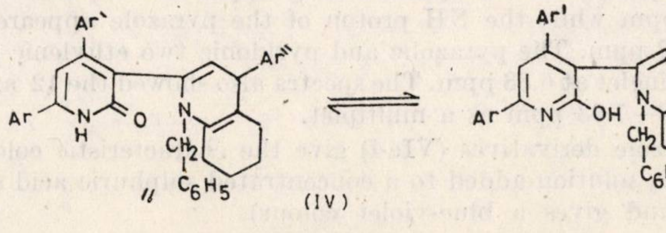

(IV)

$Ar = 3,4-Cl_2C_6H_3$, $Ar' = p-Cl-C_6H_4$
Ar'' a = $p-CH_3OC_6H_4$
b = $p-ClC_6H_4$

2 — *Bromination*

cis and *trans* Chalcones (II) reacted readily with bromine in acetic acid to give the same dibromo derivatives (V) which are characterized both by elemental analysis and by IR measurements. The infrared spectra showed well-defined absorption bands attributable to the carbonyl group at 1660 cm^{-1} (cyclic amide) and at 1640 cm^{-1} (aroyl), as well as the hydroxyl group at 3450 cm^{-1} with the concomitant disappearance of the C=C stretching vibration which appeared in the IR spectra of the cinnamoylpyridones (II).

When the dibromides (V) were allowed to react with hydroxylamine, hydrazine or phenylhydrazine in ethanol, the corresponding oximes and hydrazones were obtained, but they rearrange and dehydrobrominate immediately to give the isomeric isoxazoles and pyrazoles (VI). This result is in accord with a previous study. [16]

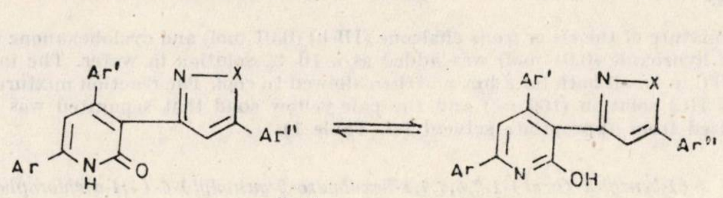

(VI)

$Ar = 3,4-Cl_2C_6H_3$
$Ar'' = p-CH_3OC_6H_4$

VI	Ar'	X		Ar'	X
a	C_6H_5	O	d	$p-CH_3OC_6H_4$	NH
b	$p-CH_3OC_6H_4$	O	e	C_6H_5	NC_6H_5
c	C_6H_5	NH	f	$p-CH_3OC_6H_4$	NC_6H_5

Correct analytical values are in support of the structure assigned for (VI). Besides, the infrared spectra of (VIa,b) revealed absorption bands at 3450 cm^{-1}, 3100 cm^{-1}, 1670 cm^{-1} and 1640 cm^{-1}, attributable to the OH, NH, CO (cyclic amide) and C=N stretching vibrations respectively. The IR spectra of the pyrazoles (VIc-f) showed absorption bands due to the carbonyl (cyclic amide), at 1665 cm^{-1}, the C=N group at 1640 cm^{-1} and the OH at 3400 cm^{-1}. The ^{1}H—NMR of the representative compound (VIc) showed a singlet at δ 3.85 ppm due to the methoxy protons; the NH proton of the pyridone ring appeared as a broad singlet peak at 6.78 ppm while the NH proton of the pyrazole appeared as a singlet at 11.92 ppm. The pyrazolic and pyridonic two ethylenic protons appeared as a singlet at 6.38 ppm. The spectra also showed the 12 aromatic protons at 7.18—7.93 ppm as a multiplet.

The pyrazole derivatives (VIc-f) give the characteristic colour test (a drop of $FeCl_3$ solution added to a concentrated sulphuric acid solution of the compound gives a blue-violet colour).

EXPERIMENTAL

Melting points are uncorrected. IR spectra were carried out on Pye Unicam SP 1200 spectrometer as KBr pellets, ^{1}H—NMR spectra were determined in $CDCl_3$ with Varian Model V 4300 B spectrometer using tetramethylsilane as internal reference. All the compounds were named according to the advice of Chemical Abstract Service.

Synthesis of 6-(3,4-Dichlorophenyl)-3-(p-substituted cinnamoyl)-4-(aryl)-2-(1H)-pyridones (IIa-h).

To a solution of acetylpyridone (I) (0.01 mol) in alcoholic potassium hydroxide, appropriate aldehydes were added (0.01 mol) and the reaction mixture was stirred overnight at room temperature. The solid obtained upon dilution of the reaction mixture with dilute HCl was filtered off and by fractional crystallization *cis* and *trans* isomers were separated as yellow solids (cf. Table 1).

Synthesis of 6-(3,4-Dichlorophenyl)-4-(aryl)-3-(5,6,7,8-tetrahydro-4-(aryl)-2H-1-benzopyran-2--yl)-2(1H)-pyridones (IIIa-c).

To a mixture of the *cis* or *trans* chalcone (IIf-h) (0.01 mol) and cyclohexanone (0.015 mol) of potassium hydroxide (0.01 mol) was added as a 10 % solution in water. The mixture was heated at 170°C in an oil bath for 8 hrs, and then allowed to cool. The reaction mixture was diluted with 1N HCl solution (100 ml) and the pale-yellow solid that separated was filtered off and crystallized from appropriate solvent (cf. Table 1).

Synthesis of 3-(1-benzyl-4-(aryl)-1,2,5,6,7,8-hexahydro-2-quinolyl)-6-(3,4-dichlorophenyl)-4-(p-chlorophenyl)-2(1H)-pyridones (IVa, b).

A mixture of pyrano (IIIa, c) (0.01 mol) and benzylamine (0.01 mol) in ethanol (30 ml) was refluxed for 4 hrs, then allowed to cool. The colourless solid which separated after concentration was filtered and crystallized from suitable solvent (cf. Table 1).

Synthesis of 3-(α,β-Dibromo-p-alkylhydrocinnamoyl)-6-(3,4-dichlorophenyl)-4-(aryl)-2(1H)-pyridones (Va-d).

To (0.01 mol) of *cis* or *trans* chalcone (IIa-d) in acetic acid (40 ml), bromine (0.02 mol) in acetic acid (20 ml) was added dropwise (4 hrs) with continuous stirring. The reaction mixture was heated on a water-bath (1 hr) then left at room temperature. The precipitated dibromo derivative was collected as dainty yellow solid and crystallized from suitable solvent (cf. Table 2).

TABLE 1

Physical characteristics of compounds IIa-h, IIIa-c and IVa, b

Compound	m.p.°C yield (%)	Solvent	Formula	Analysis %		
					Found	Calcd.
IIa	181–2	Methanol	$C_{26}H_{17}NO_2Cl_2$	C	69.62	69.96
	(30)			H	3.88	3.81
				N	3.20	3.14
IIa′	243–4	Acetic acid	$C_{26}H_{17}NO_2Cl_2$	C	70.24	69.96
	(58)			H	4.01	3.81
				N	3.24	3.14
IIb	194–5	Benzene +	$C_{27}H_{19}NO_3Cl_2$	C	68.48	68.06
	(32)	toluene		H	4.11	3.99
				N	3.05	2.94
IIb′	206–7	Benzene	$C_{27}H_{19}NO_3Cl_2$	C	68.32	68.06
	(55)			H	4.08	3.99
				N	2.80	2.94
IIc	207–8	Acetic acid	$C_{27}H_{19}NO_3Cl_2$	C	68.26	68.06
	(25)			H	3.82	3.99
				N	2.90	2.94
IIc′	228–9	Toluene	$C_{27}H_{19}NO_3Cl_2$	C	68.29	68.06
	(65)			H	4.14	3.99
				N	3.08	2.94
IId	187–8	Toluene +	$C_{28}H_{21}NO_4Cl_2$	C	66.80	66.40
	(38)	light petrol		H	4.25	4.15
		(60–80°C)		N	2.80	2.77
IId′	214–5	Toluene	$C_{28}H_{21}NO_4Cl_2$	C	66.24	66.40
	(55)			H	4.38	4.15
				H	2.92	2.77
IIe	238–9	Benzene	$C_{26}H_{16}NO_2Cl_3$	C	64.59	64.93
	(32)			H	3.52	3.33
				N	3.05	2.91
IIe′	288–9	Toluene	$C_{26}H_{16}NO_2Cl_3$	C	65.10	64.93
	(60)			H	3.15	3.33
				N	3.12	2.91
IIf	225–6	Benzene	$C_{27}H_{18}NO_3Cl_3$	C	63.84	63.46
	(37)			H	3.32	3.53
				N	2.82	2.74
IIf′	256–7	Toluene +	$C_{27}H_{18}NO_3Cl_3$	C	63.35	63.46
	(58)	benzene		H	3.42	3.53
				N	2.98	2.74
IIg	217–8	Benzene	$C_{27}H_{17}NO_4Cl_2$	C	66.40	66.12
	(35)			H	3.78	3.47
				N	3.12	2.86
IIg′	235–6	Acetic	$C_{27}H_{17}NO_4Cl_2$	C	66.38	66.12
	(62)	acid		H	3.70	3.47
				N	2.78	2.86

Table 1 (continued)

Compound	m.p.°C Yield %	Solvent	Formula	Analysis %		
					Found	Calcd.
IIh	260–1	Benzene	$C_{26}H_{15}NO_2Cl_4$	C	60.90	60.58
	(35)			H	2.85	2.91
				N	2.88	2.72
IIh′	294–5	Ethanol	$C_{26}H_{15}NO_2Cl_4$	C	60.39	60.58
	(60)			H	3.12	2.91
				N	2.80	2.72
IIIa	268–9	Benzene	$C_{33}H_{26}NO_3Cl_3$	C	67.20	67.06
	(65)			H	4.55	4.40
				N	2.42	2.37
IIIb	201–2	Ethanol	$C_{33}H_{25}NO_4Cl_2$	C	69.52	69.47
	(60)			H	4.44	4.38
				N	2.52	2.46
IIIc	243–4	Benzene+ light petrol (60–80°C)	$C_{32}H_{23}NO_2Cl_4$	C	64.68	64.53
	(65)			H	3.90	3.86
				N	2.48	2.35
IVa	251–2	Benzene	$C_{40}H_{33}N_2O_2Cl_3$	C	70.82	70.64
	(45)			H	4.66	4.57
				N	4.30	4.12
IVb	223–4	Toluene	$C_{39}H_{30}N_2OCl_4$	C	53.68	53.80
	(55)			H	4.49	4.39
				N	4.20	4.09

TABLE 2

Physical characteristics of compounds Va-d, VIa-f

Compound	m.p.°C Yield %	Solvent	Formula	Analysis %		
					Found	Calcd.
Va	157–8	Methanol	$C_{26}H_{17}NO_2Cl_2Br_2$	C	51.55	51.48
	(85)			H	2.98	2.81
				N	2.40	2.31
Vb	183–4	Benzene	$C_{27}H_{19}NO_3Cl_2Br_2$	C	51.21	50.94
	(92)			H	3.02	2.99
				N	2.38	2.20
Vc	196–7	Benzene	$C_{27}H_{19}NO_3Cl_2Br_2$	C	51.30	50.94
	(82)			H	2.95	2.99
				N	2.32	2.20
Vd	191–2	Benzene+	$C_{28}H_{21}NO_4Cl_2Br_2$	C	50.65	50.45
	(85)			H	3.25	3.15
				N	2.28	2.10
VIa	245–6	Methanol	$C_{27}H_{18}N_2O_3Cl_2$	C	66.40	66.26
	(70)			H	3.70	3.68
				N	5.88	5.73

Table 2 (continued)

Compound	m.p.°C Yield %	Solvent	Formula	Analysis %		
					Found	Calcd.
VIb	268–9 (72)	Benzene	$C_{28}H_{20}N_2O_4Cl_2$	C H N	64.82 3.94 5.60	64.74 3.85 5.39
VIc	213–4 (65)	Ethanol	$C_{27}H_{19}N_3O_2Cl_2$	C H N	66.48 3.68 8.76	66.39 3.89 8.60
VId	264–5 (60)	Benzene	$C_{28}H_{21}N_3O_3Cl_2$	C H N	64.94 4.20 8.28	64.86 4.05 8.11
VIe	208–9 (55)	Benzene+	$C_{33}H_{23}N_3O_2Cl_2$	C H N	70.40 4.22 7.58	70.21 4.08 7.45
VIf	235–6 (60)	Toluene+ light petrol (60–80°C)	$C_{34}H_{25}N_3O_3Cl_2$	C H N	68.90 4.18 7.12	68.69 4.21 7.07

Synthesis of 6-(3,4-Dichlorophenyl-4-(aryl)-3|5-(aryl)-isoxazole-3-yl|-2(1H)pyridones (VIa,b), and synthesis of 6-(3,4-dichlorophenyl)-4-(aryl)-3-(5-(aryl)-pyrazole-3-yl |-2(1H)pyridones (VIc-f).

A mixture of the chalcone dibromide (Vb,d) (0.01 mol), hydroxylamine hydrochloride (0.01 mol) and sodium acetate (0.01 mol) in ethanol (50 ml) was refluxed for 8 hrs. The reaction mixture was cooled and the precipitated pale yellow solid was collected by filtration. Recrystallization of the product from suitable solvent gave the isoxazoles (VIa, b). The pyrazole derivatives were (VIc-f) similarly prepared by heating hydrazine hydrate or phenylhydrazine with chalcone dibromide in boiling ethanol (cf. Table 2).

REFERENCES

[1] M. El-Deek, M.A.I. Salem, A.A. Hamed and M. Samaan, *Rev. Roumaine Chim.* (1981).
[2] A. Sammour, M. El-Kassaby, M.A. Hassan and M.A.I. Salem, *Egyptian J. of Chem.*, **20**, 2 (1977).
[3] S. S. Misra and Bhola Nath, *Indian J. App. Chem.*, **34**, 200 (1971).
[4] S. S. Misra and J. B. Lal, *Proc. Nat. Acad. Sci. Chim.*, **40**, 296 (1970).
[5] H. P. Bun-Hoi and N. D. Xuong, *Bull. Soc. chim. France*, **1956**, 1646.
[6] S. C. Kushwaha, S. S. Misra and J. B. Lal, *Proc. Nat. Acad. Sci.*, **40**, 301 (1970).
[7] S. S. Misra, A. Labdev, *J. Sci. Tech. (India)*, **8**, 152 (1971).
[8] S. C. Kushwaha and J. B. Lal, *Indian J. Chem.*, **5**, 82 (1967).
[9] W. S. Ceiger and J. E. Conn., *J. Amer. Chem. Soc.*, **67**, 112 (1945).
[10] S. S. Misra, *Indian J. App. Chem.*, **34**, 211 (1971).
[11] S. S. Misra and S. Dinkar, *J. Indian Chem. Soc.*, **40**, 637 (1972).
[12] S. S. Misra, *J. Indian Chem. Soc.*, **51**, 909 (1974).
[13] S. S. Misra, and S. Dinkar, *J. Indian Chem. Soc.*, **52**, 556 (1975).
[14] S. S. Misra and S. C. Kushwaha, *J. Indian Chem. Soc.*, **52**, 564 (1975).
[15] K. K. Hsu and F. G. Chen, *Tiwan K'Hsueh*, **27**, 236 (1973).
[16] C. W. Wilson and D. E. Floyd, *J. Pharmacol, Expell. Therap.*, **49**, 399 (1949).

Revue Roumaine de Chimie, **26**, *5*, 783–792 (1981)

NEW ASPECTS IN THE SPECTROPHOTOMETRIC ANALYSIS. I.

COMPUTATIONAL EQUATIONS FOR THE DOSAGE OF SOME DYESTUFFS IN MIXTURES

N. CALU and OLGA VICOL
The Polytechnic Institute "Gh. Asachi"
Splai Bahlui, 71 Iassy, Romania

Received February 16, 1978
Revised May 6, 1980

When graphically plotting the function $A/d = f(c)$ for different substances, lines or curves passing through the origin are obtained, as they obey or not the Lambert-Beer law. Quite often, in some concentration ranges the curves confound themselves with lines (characterized by tgα and n) departing from the origin. The solving agent together with other substances as well as pH of the solution can provide a better linearity between A and c. This is the behaviour of some antraquinone dyestuffs used in this work. A set of equations in tgα and n has been elaborated in this paper for the concentration calculations by the simultaneous or separate dosage of the substances displaying a linear relationship between A and c but with $n \neq 0$.

INTRODUCTION

The quantitative analysis by light absorption spectrophotometry is sensitive, rapid and fairly accurate.[1-3]

This method shows limitations, as mentioned, for the simultaneous dosage of the substances in the mixtures.

In such a case the determination and implicitly the calculation of the concentration is done by using a set of algebraic equations based upon the Lambert-Beer law.[4-7]

$$A = \lg \frac{I_0}{I} = dK\,c \tag{1}$$

and

$$A' = d \sum_i K_i c_i \tag{2}$$

where:

A = the absorbance of the solution containing only one substance;
A' = the total absorbance equaling the sum of absorbances of the different substances contained in a solution;
I_0 = the intensity of the incident beam of light (monochromatic);
I = the intensity of the emergent beam of light;
d = the thickness of the solution layer;

K = a proportionality constant called molar absorption coefficient or specific absorption coefficient if the concentration of the solution is expressed in moles/l or g/l, respectively;
c = the concentration of the solution in moles/l or g/l.

But if there is a deviation from this law of the light absorption produced by the substances to be determined, the calculation equations become impractical.

These limitations are often overcome by extending the calculation equations to the cases where the variation of the substances absorbance, as a function of their concentration, is described not only by a straight line passing through the origin, as the Lambert-Beer law requests, but also by a certain line. Such equations are to be established in the present work.

A. COMPUTATIONAL EQUATIONS AS GIVEN IN THE LITERATURE FOR THE SPECTROPHOTOMETRIC DOSAGE OF SUBSTANCES

Generally, the concentration calculations by the substance dosage on the spectrophotometric way, as given in the literature, are based on the equations (1) and (2) expressing the Lambert-Beer law.

If a substance from the solution does not follow the equation (1), its dosage is done by the use of a standard curve.

By the simultaneous dosage of more than one substance from a solution, more laborious calculations are dealt with. In such a case equation (2) has to be respected as the set of equations is established on its basis. The set contains a number of equations equaling the number of components of the solution. The equations are etablished for an equal number of values of the total absorbance, for certain wave-lengths suitably chosen, as the difference between the proportionality coefficients of the substances to be determined should be as high as possible.

Thus, for a two-component solution, the following set of equations is valid,

$$\begin{aligned} A' &= K_{1\lambda'}x + K_{2\lambda'}y \\ A'' &= K_{1\lambda''}x + K_{2\lambda''}y \end{aligned} \tag{3}$$

where:

A' and A'' = the total absorbances of the two-component solution determined for the wavelengths λ' and λ'', respectively;
$K_{1\lambda'}$ and $K_{2\lambda'}$ = the proportionality constants of the substance 1 at λ' and λ'' respectively;
$K_{2\lambda'}$ and $K_{2\lambda''}$ = the proportionality constants of the substance 2 at λ' and λ'' respectively;
x and y = the concentrations of the substances 1 and 2 respectively;

$$d = 1 \text{ cm}$$

The deviations from the Lambert-Beer law can be produced by the interactions between the molecules of the substances to be determined, by chemical equilibrium shift at dilution of the solution, a.s.o.

Thus, the spectrophotometric behaviour of the substances in the actual working conditions, the nature and content of the solution, etc. have to be known.

Besides the determination of the absorption coefficient K, it is also necessary to plot the absorbance as a function of the concentration of the substances. The lines, as resulted from plots, by their parameters tg α and n avoid the spectrophotometric characterization of the substances – as it will be proceeded in the next sections.

B. THE EXTENSION OF THE CALCULATION EQUATIONS TO THE DOSAGE OF THE SUBSTANCES WHOSE $A-c$ RELATION IS REPRESENTED BY A CERTAIN LINE

A graphical plot of the function

$$\frac{A}{d} = f(c) \qquad (4)$$

for various substances will result in the lines or curves shown in figure 1.

If a and c are directly proportional to each other according to the equation :

$$y = m\,x \qquad (5)$$

representing a straight line passing through the origin, (line 1 in Figure 1), the respective substance obeys the Lambert-Beer law.

If representing A as a function of c the dotted curve 2 in Figure 1 results, and the respective substance does not obey the above-mentioned law. Furthermore, for certain concentration ranges, the dotted curve 2 and the straight line 2′ (ab) are colinear and are described by the equation :

$$y = mx + n \qquad (6)$$

which represents a certain line, not passing through the origin.

This is the behaviour of a series of compounds (including the Hg(II)-dithisone complex), and some antraquinone dyestuffs in the reduced state (by themselves or in a mixture), as studied by us.

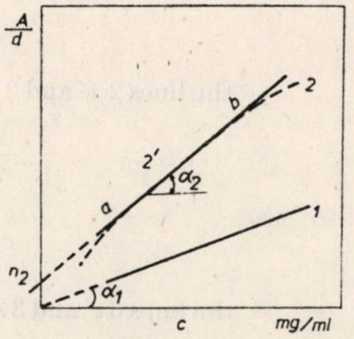

Fig. 1. – Possible line or curve when representing graphically the function (4) for various substances. In the *ab* range curve 2 shows a linear partion. The slope of the line 1 or tg α respectively can be indentified with the absorption coefficient K_1 of the substances.

This behaviour of the substance as represented by a certain line (not passing through the origin) denoting a linear relation between A and c is briefly termed n-Beer, where n suggests a line with $n \neq 0$.

We consider that by the spectrophotometric dosage of the substances this phenomenon has to be taken into account.

In the analytical practice, the case of drawing the $A = f(c)$ line appears quite often but it is never checked if it passes through the origin. That is why such a line can be used as a reference line, but it fails to characterize the substance to be dosed by concentration calculations involving equation (1) or (2).

Taking all these into account we can suggest a set of equations for calculating the concentrations in the spectrophotometric dosage of the substances showing an n-Beer behaviour.

This is an extension of the computational equations to every substance characterized by a linear relationship between A and c.

A fact deserving special emphasis is that the simultaneous dosage is based upon concentration calculations and does not involve reference lines.

For this purpose each substance and implicitly its corresponding $A = f(c)$ line, called a test-line, are characterized by the line slope (tg α) and its y — axis intercept (n), which are base parameters in the concentration calculations.

Thus, the various lines in figure 2 and the possible cases of spectrophotometric behaviour of the substances respectively, imply the following calculation equations of the concentrations :

— the lines $1\lambda'$ and $1\lambda''$,

$$\frac{A_1}{d} = \operatorname{tg} \alpha_1 \cdot c,$$

$$c = \frac{A_1}{d} \cdot \frac{1}{\operatorname{tg} \alpha_1} \tag{7}$$

— the lines $2\lambda'$ and $2\lambda''$,

$$\frac{A_2}{d} - n_2 = \operatorname{tg}\alpha_2 \cdot c;$$

$$c = \left(\frac{A_2}{d} - n_2\right) \cdot \frac{1}{\operatorname{tg} \alpha_2} \tag{8}$$

— the lines $3\lambda'$ and $3\lambda''$,

$$\frac{A_3}{d} + n_3{}^* = \operatorname{tg}\alpha_3 \cdot c;$$

$$c = \left(\frac{A_3}{d} + n_3\right) \cdot \frac{1}{\operatorname{tg} \alpha_3} \tag{9}$$

Equations (7)—(9) are essential when establishing the set of equations for the concentration calculations in the case of the simultaneous dosage of the substances.

---

* Absolute value.

Such an equation can be obtained considering the total absorbance of the substances in a solution at a certain wavelength. Thus, if two substances whose absorbances as a function of concentration vary as described

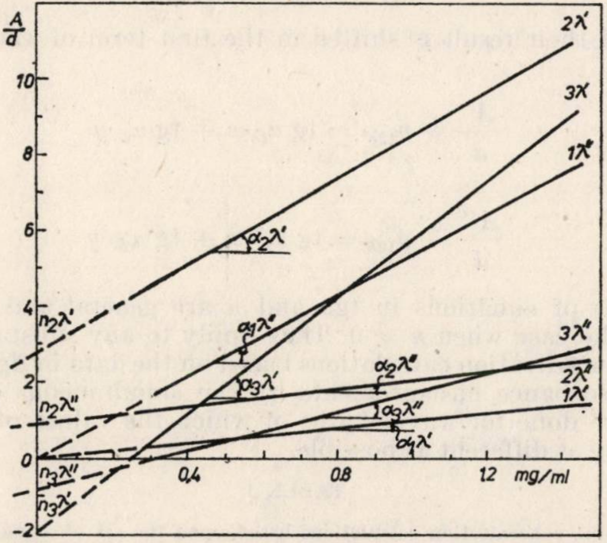

Fig. 2. — The lines possible to appear by graphic representation of the function (4). Each line is assigned to a substance designated by 1, 2, 3 and each substance tested for two wavelengths λ' and λ''. The parameters of the lines as well as the specific absorption coefficients of the three substances have the values :

1. $1\lambda'$; $n_{1\lambda'} = 0$; $\text{tg}\ \alpha_{1\lambda'} = 1.01$; $K_{1\lambda'} = 1.01$
$1\lambda''$; $n_{1\lambda''} = 0$; $\text{tg}\ \alpha_{1\lambda''} = 5.38$; $K_{1\lambda''} = 5.38$
2. $2\lambda'$; $n_{2\lambda'} = 2.77$; $\text{tg}\ \alpha_{2\lambda'} = 5.77$; $K_{2\lambda'} = 8.34$
$2\lambda''$; $n_{2\lambda''} = 0.88$; $\text{tg}\ \alpha_{2\lambda''} = 1.16$; $K_{2\lambda''} = 2.04$
3. $3\lambda'$; $n_{3\lambda'} = -1.96$; $\text{tg}\ \alpha_{3\lambda'} = 7.75$; $K_{3\lambda'} = 5.79$
$3\lambda''$; $n_{3\lambda''} = -0.83$; $\text{tg}\ \alpha_{3\lambda''} = 2.55$; $K_{3\lambda''} = 1.72$

by the lines $1\lambda'$ and $2\lambda'$, for λ', figure 2, their total absorbance is given by the equation,

$$\frac{A'}{d} = \text{tg}\ \alpha_{1\lambda'} x + \text{tg}\ \alpha_{2\lambda'} y + n_{2\lambda'} \tag{10}$$

where x and y are the concentrations of the two substances in the solution.

Generally, for two substances designed by 1 and 2 having testlines characterized by the parameters tg α and n, the following set of equations can be established :

$$\frac{A'}{d} = \text{tg}\ \alpha_{1\lambda'} x \pm n_{1\lambda'} + \text{tg}\ \alpha_{2\lambda'} y \pm n_{2\lambda'} \tag{11}$$

$$\frac{A''}{d} = \text{tg}\ \alpha_{1\lambda''} x \pm n_{1\lambda} + \text{tg}\ \alpha_{2\lambda''} y \pm n_{2\lambda''}$$

where the $+$ sign stands for $n > 0$ and the sign $-$ stands for $n < 0$.

If the summations :

$$\pm n_{1\lambda} \pm n_{2\lambda'} = \pm n_{12\lambda}$$

$$\pm n_{1\lambda''} \pm n_{2\lambda''} = \pm n_{12\lambda'}$$

are made and their result is shifted in the first term of these equations, it results :

$$\begin{aligned} \frac{A'}{d} \mp n_{12\lambda'} &= \operatorname{tg} \alpha_{1\lambda'} x + \operatorname{tg} \alpha_{2\lambda'} y \\ \frac{A''}{d} \mp n_{12\lambda} &= \operatorname{tg} \alpha_{1\lambda''} x + \operatorname{tg} \alpha_{2\lambda''} y \end{aligned} \tag{12}$$

The sets of equations in tgα and n are general and they include those in K, the case when $n = 0$. They apply to any substance, as certified by the concentration calculations based on the data in figure 2, table 1.

The absorbance measurements by the simultaneous dosage of the substances are done for wavelengths of which the values of the testlines parameters are as different as possible.

TABLE 1

The results of some concentration calculations based upon the set of equations (3) and (12) as well as on the data in figure 2

Substances used in the mixture	$\frac{\Sigma_i \frac{A_i}{d}}{\lambda' \lambda''}$		Equations set used for the calculations	Amount of the substance mg/ml					
				Theoretical value		Calculation value		e%	
	$\left(\frac{A'}{d}\right)$	$\left(\frac{A''}{d}\right)$		1	2	1	2	1	2
1 and 2	8.21	6.13	3(K)	0.800	0.800	0.815	0.865	+1.87	+8.12
			12 (tgα and n)			0.804	0.802	+0.50	+0.25
	8.02	5.05	12 (tgα and n)	0.600	0.800	0.599	0.805	−0.17	+0.62
1 and 3	5.05	5.52	(3K)	0.800	0.800	0.792	0.734	−1.00	−8.25
			12 (tgα and n)			0.802	0.800	+0.25	0.00
	4.86	4.44	12 (tgα and n)	0.600	0.800	0.598	0.802	−0.33	+0.25
				2	3	2	3	2	3
2 and 3	10.47	2.80	(12 tgα and n)	0.600	0.800	0.581	0.814	−3.17	+1.75

a) The total absorbance at λ' and λ'' is obtained by summing the absorbances of the constituents, as read on the lines in figure 2, according to the theoretical amounts of substances considered in the calculations.

C. THE CORRELATION BETWEEN THE CHARACTERISTIC PARAMETERS OF A SUBSTANCE K, tg α AND n

Between the proportionality coefficient, K, the line slope, tg α and the y – axis intercept n characteristic to a substance, as shown in figure 3, the following relationships are established:

— when $n = 0$, $\mathrm{tg}\alpha = K$ (13)

— when $n \neq 0$, $\mathrm{tg}\alpha = K \pm n$** (14)

— Thus, for $n > 0$

$$\mathrm{tg}\alpha_2 = K_2 - n_2 \tag{15}$$

where

$$\frac{A_2}{d} - n_2 = (K_2 - n_2)\,c$$

or

$$\frac{A_2}{d} = K_2c - n_2c + n_2 = K_2c + n_2(1 - c) \tag{16}$$

From equation (16) and figure (4) where the relation

$$n(1 - c) = f(c) \tag{17}$$

was graphically represented, it results that the more different c from 1 and the bigger n in absolute value the more important the deviation from the equation (1) – expressing the Lambert-Beer law.

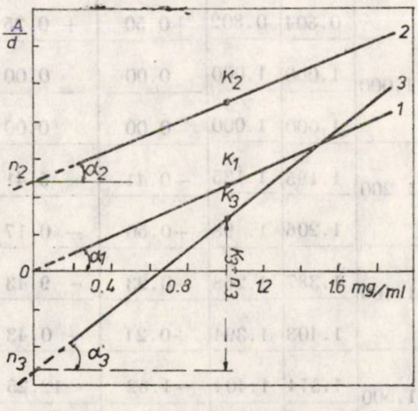

Fig. 3. — The correlation between the specific proportionality coefficient (K), the slope (tgα) and the y-axis intercept (n), characteristic of a substance for different cases (1–3).

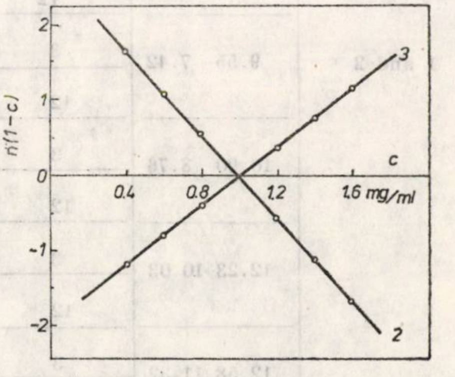

Fig. 4. — Possible lines when representing graphically the n-term of the equations having the form (16) as a function of concentration.
2. $n_2 = 2.77$ 3. $n_3 = -1.96$

If the concentration of a substance in the solution is accidentally 1g/l(value for which the specific proportionality coefficient was ascertained) the n-term disappears and equation (16) becomes identical with equation (1). In fact this is the only case where the set of equations (3), as

---

** Absolute value

given by the literature, would provide reliable results in the dosing of the substances in mixtures, should the Lambert-Beer law be not checked by lines passing through the origin (Table 2).

TABLE 2

The results of some concentration calculations based upon the set of equations (3) and (12), as well as on the data in figure 2

Substances used in the mixture	$\Sigma_i \frac{A_i}{d}$ λ′ λ″		Equation set used for the calculations	Amount of substance mg/ml					
				Theoretical value		Calculated value		e %	
	$\left(\frac{A'}{d}\right)$	$\left(\frac{A''}{d}\right)$		1	2	1	2	1	2
1 and 2	5.48	3.50	3	0.400	0.400	0.429	0.591	+7.25	+47.75
			12			0.398	0.400	−0.50	0.00
	6.85	4.82	3	0.600	0.600	0.618	0.729	+3.00	+21.50
			12			0.600	0.602	0.00	+ 0.33
	8.21	6.13	3	0.800	0.800	0.815	0.865	+1.87	+ 8.12
			12			0.804	0.802	+0.50	+ 0.25
	9.55	7.42	3	1.000	1.000	1.000	1.000	0.00	0.00
			12			1.000	1.000	0.00	0.00
	10.90	8.76	3	1.200	1.200	1.195	1.135	−0.41	− 5.41
			12			1.206	1. 98	+0.50	− 0.17
	12.23	10.03	3	1.400	1.400	1.387	1.268	−0.93	− 9.43
			12			1.403	1.394	+0.21	− 0.43
	12.58	11.32	3	1.600	1.500	1.574	1.404	−1.62	−12.25
			12			1.597	1.594	−0.19	− 0.38

Based upon equation (14), the equation set (11) can be expressed as a function of K and n as follows,

$$\begin{aligned} \frac{A'}{d} &= (K_{1\lambda'} \mp n_{1\lambda'})x \pm n_{1\lambda'} + (K_{2\lambda'} \mp n_{2\lambda'})y \pm n_{2\lambda'} \\ \frac{A''}{d} &= (K_{1\lambda''} \mp n_{1\lambda''})x \pm n_{1\lambda''} + (K_{2\lambda''} \mp n_{2\lambda''})\,y \pm n_{2\lambda''} \end{aligned} \quad (11)$$

where the n — terms in the brackets have the — sign for $n > 0$ and the + sign for $n < 0$; the other terms have the signs specified in equation (11).

The set of equations (11′) identifies itself with the set (11) in the concentration calculations.

Such sets of equations can be established for the simultaneous dosage of more than 2 substances in a solution.

D. ON THE SPECTROPHOTOMETRIC DOSAGE

When dosing the substances it is necessary that the test-lines should be obtained in the analysis conditions.

Usually, in the case of simultaneous dosage of two substances in a mixture, a common range of concentration showing a linear relationship between A and c is determined for the standard solutions and the characteristic parameters of the test-lines defined.

If $n_{12} \neq 0$ this is an/n-Beer case and the analysis calculations are performed using equations (12), valid for the concentration range where the test-lines were drown.

There are a few aspects of interest connected with the simultaneously dosed substances such as : their nature, if they show a weak or strong interaction in solution, or are frequently found and others.

In this regard one must consider the fact that these dosages are necessary when the substances to be mixed show common absorption spectra, that is there is no wavelength in their spectrum, where only one of the components should display a considerable absorption.

It is evident that the substances displaying common absorption spectra can be similar from the chemical point of view. In the practice such substances in mixtures are often found. This is the case of some textile dyestuffs, isomers resulting from the synthesis of some substances, and others.

As these substances are chemically alike, the eventual interactions between their molecules are expected to be rather weak, of the Van der Waals type. These interactions diminish when diluting the solution or raising the temperature. Again, the nature of the solving agent, the pH of the solution, as well as the presence of some substances can influence even the stronger molecula interactions. For instance, the interaction between the molecules of some dyestuffs can be cancelled by adding pyridine.

Thus, the solving agent together with the adequate substances can determine the interaction with each separate substance in the mixture. When it is in excess, the solving agent together with the adequate substances prevent the interactions and provide a linear relationship between A and c for the substances to be dosed.

As an example we present a few data which were obtained for two anthraquinone dyestuffs in reduced form in basic medium, table 3.

TABLE 3

The test-line parameters of some dyestuffs

Dyestuff	Concentration g/ml	λ_{nm}	n	tg α
B C votblue	$0.5-5.0.10^{-5}$	650	0.020	$0.77.10^{4}$
Vot navyblue	$0.5-5.0.10^{-5}$	650	0.003	$3.54.10^{4}$

It results from table 3 that the two anthraquione dyestuffs show test-lines presenting departures from the origin. Especially the value $n = 0.02$ (A/d) cannot be neglected. Such a value lies still in the optimum absorbance range as used in the spectrophotometry.

The dosing of these dyestuffs in the mixture can be made using equations (12).

CONCLUSIONS

The cause of some deviations from the absorbance additivity of some substances in solution can be the interaction of the molecules pertaining to the respective substances. Such interactions can be reduced by interaction of the solving agent with adequate substances, pH of the solution, dilution, a.s.o. This is the behaviour of some anthraquinone dyestuffs as mentioned in this work.

In basic medium and reduced form these dyestuffs show a linear relationship between A and c but their test-lines departure from the origin. This is what we call an/n-Beer behaviour.

When dosing such substances or their mixtures a set of computational equations in tg α and n established in this work is used.

REFERENCES

[1] G. Kortüm, *Angew. Chem.*, **50**, 193 (1937).

[2] M. J. Vanderbilt, J. Forsith and A. Garrett, *Ind. Eng. Chem. Analyt. Ed.*, **17**, 235 (1945).

[3] O. W. Caster, *Analyt. Chem.*, **23**, 1229 (1951).

[4] I. M. Kolthoff and E. B. Sandell, "Textbook of Quantitative Analysis", Interscience Publishers, third Edition, 1956, pag. 613.

[5] I. M. Kolthoff and E. B. Sandell, *Ibid.*

[6] J. Beer, *Ann. Physik*, **86**, 78 (1852).

[7] F. Bernard, *Ann. Chim. Phys.*, **35**, 385 (1852).

Revue Roumaine de Chimie, **26**, *5*, 793–799 (1981)

STUDY ON THE THERMAL DEGRADATION OF ACRYLIC COPOLYMERS

MARGARETA TOMESCU, IOANA DEMETRESCU and E. SEGAL
National Institute of Chemistry, Chair of Physical
Chemistry and Electrochemical Technology Bucharest, Romania

Received June 26, 1980

The thermal degradation of the following copolymers prepared by radical polymerization : acrylonitrile-butyl acrylate-vinylidene chloride, acrylonitrile-butyl acrylate-vinylidene chloride-styrene, and acrylonitrile-methacrylic acid-vinylidene chloride-styrene was investigated. The techniques of thermogravimetry and differential thermal analysis were used. The IR spectra of degraded copolymers are discussed.

INTRODUCTION

There are numerous papers[1-5] devoted to the influence of comonomers on the exothermic oligomerization of nitrile groups, characteristic of acrylonitrile homopolymers.[6,7]

Acrylate and methacrylate comonomers[3,4] have a diluent effect on the exothermic reaction without inhibiting or initiating the nitrile rearrangements. Acid comonomers[3] have a strong initiating effect on the exothermic reaction. Chlorinated comonomers as vinylidene chloride[4] reduce the intensity of the exothermic reaction, but do not effectively block the reaction. Styrene and other comonomers of this type have a marked inhibiting effect on the nitrile reaction.

The present paper describes the effect of comonomers on the thermal degradation of polyacrylonitrile in the systems : acrylonitrile (AN)-butylacrylate (BA)-vinylidene chloride (CV), acrylonitrile-butylacrylate-vinylidene chloride-styrene (S) and acrylonitrile-methacrylic acid (AM)-vinylidene chloride-styrene.

The results concerning copolymers synthesis, compositional distribution, spectral characterization and some potential industrial applications are given elsewhere.[8-12]

EXPERIMENTAL

Copolymers

The copolymers and polyacrylonitrile (PAN) used were prepared in solution at 60°C using 0.1 % azoizobutyronitrile. Polymerizations were carried out in an inert atmosphere. The copolymer composition was determined by nitrogen, chlorine and analysis of carboxylic groups, using the micro Kjeldhal, Schöniger and potentiometric titration methods, respectively.

Copolymer compositions are summarized in table 1.

TABLE 1

Composition data of Copolymers

Copolymer code	Composition, % — weight			
	AN	BA or AM	CV	S
AN— BA—CV	70.29	26.91	2.80	—
AN— BA—CV—S	18.39	43.31	25.00	13.30
AN— AM—CV—S	53.80	13.56	10.50	22.14

Thermal analysis

A derivatograph MOM-Budapest type Paulik-Paulik-Erdely was used. In both DTA and TG analysis the samples were heated at 10°/min in argon flow and in the air.

Infra-red spectra

A UR—10 Karl Zeiss Jena spectrophotometer (range 400—5000 cm^{-1}) and a Unicam SP 1000 IR spectrophotometer (range 625—3800 cm^{-1}) were used.

RESULTS AND DISCUSSION

DTA and TG results concerning copolymers and PNA in the air and in argon flow are presented in figures 1—4. The IR spectral changes of the degraded copolymers are illustrated by figure 5.

Polyacrylonitrile

The DTA curve (fig. 1) obtained for PAN in the air is consistent with that observed in references[1,2] showing a strong and sharp exotherm which peaks at 340°C. The sharp exothermic reaction is an important feature of PAN pyrolysis, caused by nitrile group oligomerization.[13]

TG curves clearly show the two stages of the oxidative degradation. The fast weight loss of 20 percent in the temperature range of the exotherm may be explained by chain scission which occurs concurrently. The second stage degradation is clearly oxidative.

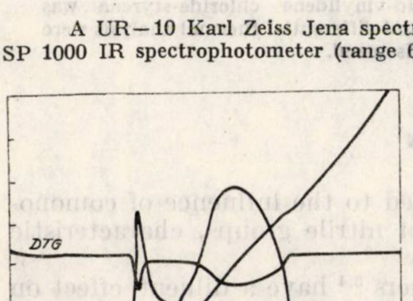

Fig. 1. — DTA, TG and DTG curves for polyacrylonitrile in the air.

AN – BA – CV – copolymer

The thermal behaviour of degraded copolymers is clearly different from that of PAN.

The DTA curve in the air (Fig. 2) shows a reduced exothermicity associated with nitrile rearrangement from AN sequences in the copolymer. The curve is still sharp, although it is less intense and broader than that of PAN.

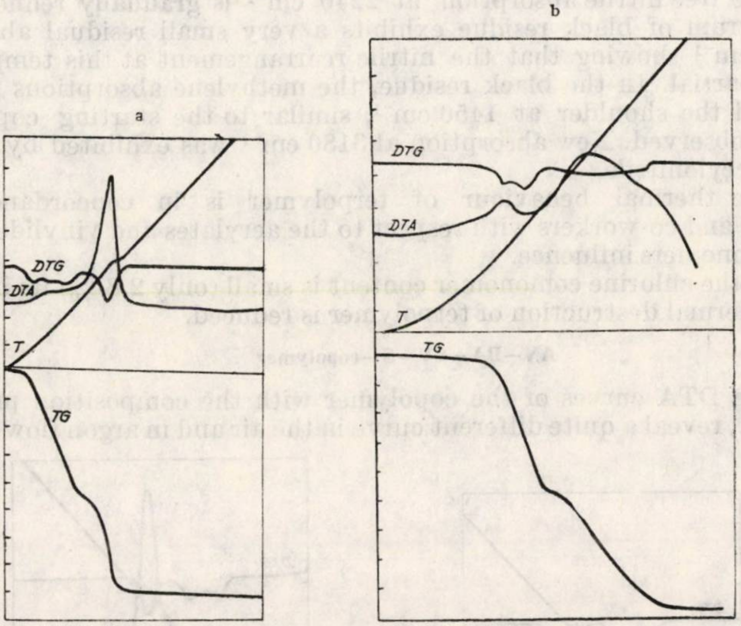

Fig. 2. – DTA, TG and DTG curves for acrylonitrile-butyl acrylovinylidene chloride copolymer : (a) under argon ; (b) in the air.

The temperature at which the exothermic effect occurs, is the same as in PAN, so that there is no marked retarding or initiating effect on the acrylonitrile cyclization.

The exothermic effect associated with nitrile groups reaction is followed by a very small exothermic one. During the early stage of pyrolysis the exotherm is affected by concurrent processes, the most important being the chain scission. The dehydrochlorination of some units of vinylidene chloride occurs too.

The DTA curve in argon flow reveals a broader and less pronounced exothermic peak at the same temperature as in PAN. The difference between the curves obtained in argon and air, can be assigned to the easier volatilization of the chain fragments and to the decomposition of acrylate taking place in argon flow.

The TG curve indicates a stable copolymer up to 240°C.

Infrared spectra of heating copolymers in the air up to 200°C and 320°C respectively show the following changes.

The spectrum of the pale yellow heated copolymer at 200°C shows the complete disappearance of the chlorine absorption, which accounts for the dehydrochlorination of vinylidene chloride units at lower temperatures.

The original acrylate carbonyl absorption at 1740 and 1705 cm^{-1} and the original C—O—R absorption at 1260 cm^{-1} disappears completely in the spectrum of the black residue at 320°C. It is concluded that the acrylate comonomers are decomposed by similar reactions as proposed in the literature [2,14,15] for polybutyl acrylate and their copolymers.

The free nitrile absorption at 2240 cm^{-1} is gradually reduced. The IR spectrum of black residue exhibits a very small residual absorption at 2240 cm^{-1} showing that the nitrile rearrangement at this temperature is only partial. In the black residue, the methylene absorptions at 2940, 2880 and the shoulder at 1450 cm^{-1}, similar to the starting copolymer, are also observed. New absorption at 3180 cm^{-1} was exhibited by degraded polyacrylonitrile.

The thermal behaviour of terpolymer is in concordance with Grassie's and co-workers with respect to the acrylates and vinylidene chloride comonomers influence.

As the chlorine comonomer content is small (only 2.8 %) its influence on the thermal destruction of terpolymer is reduced.

AN—BA—CV—S—copolymer

The DTA curves of the copolymer with the composition presented in table 1, reveal a quite different curve in the air and in argon flow (Fig. 3).

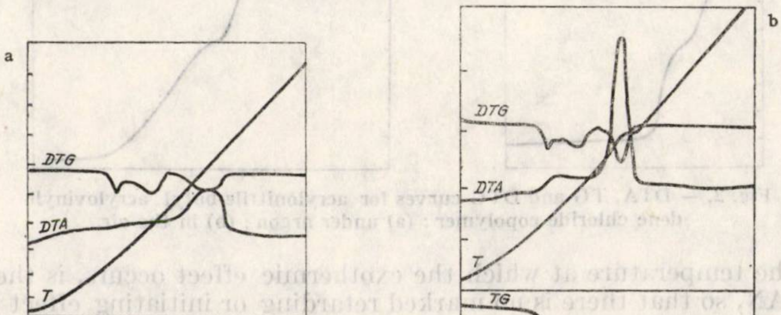

Fig. 3. — DTA, TG and DTG curves for acrylonitrile-butyl acrylatevinylidene chloride-styrene copolymer : (a) under argon ; (b) in the air.

The DTA curve obtained in the air shows a broad and complex exothermic peak with two distinct maxima at 310 and 380°C, preceded by a small endothermic one. The shape of the DTA curve suggests the numerous reactions taking place concurrently during the early stage of decomposition. In argon flow the exothermic reaction is covered by the endothermic dehydrochlorination of CV units, by the depolymerization of styrene units, and also by the acrylate chain scission processes.

All these processes take place more intensely than in the air.

The DTA curve in argon flow does not exhibit sharp peaks. The TG behaviour is similar in the both atmospheres, in argon flow and in the air. Up to 240°C, the copolymer is completely stable. The TG curveshows two decomposition stages quite clearly defined. In the first stage, up to 470°C, the copolymer is almost destroyed. The IR spectrum of the black residue of 20 minutes heated copolymer at 320°C is almost identical with that of the pure spectral carbon. Slight metylene absorptions at 2935, 2875 and 1460 cm^{-1} remain. There are also some slight new absorption peaks at 3270, 3340 and 1650 cm^{-1}.

The N – H bands, about 3200 cm^{-1}, have been explained by Grassie and co-workers [16] by an α iminonitrilic structure or by a corresponding tautomeric form, which can be produced during degradation of AN units.

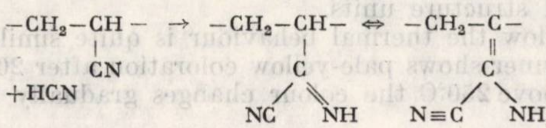

$$\underset{+HCN}{-CH_2-\underset{\underset{CN}{|}}{CH}-} \rightarrow -CH_2-\underset{\underset{NC\quad NH}{\underset{/\;\;\backslash\backslash}{\overset{|}{C}}}}{CH}- \Leftrightarrow -CH_2-\underset{\underset{N\equiv C\quad NH_2}{\underset{/\;\;\backslash}{\overset{||}{C}}}}{C}-$$

The broad 1650 cm^{-1} band is going to support such a structure. In fact this polymer contains 25 percent CV, so partially the 1650 cm^{-1} band can be done also by isolated C=C structure.

AN – AM – CV – S copolymer

The thermal analysis data for examined copolymer in the air and in argon flow are shown in figure 4.

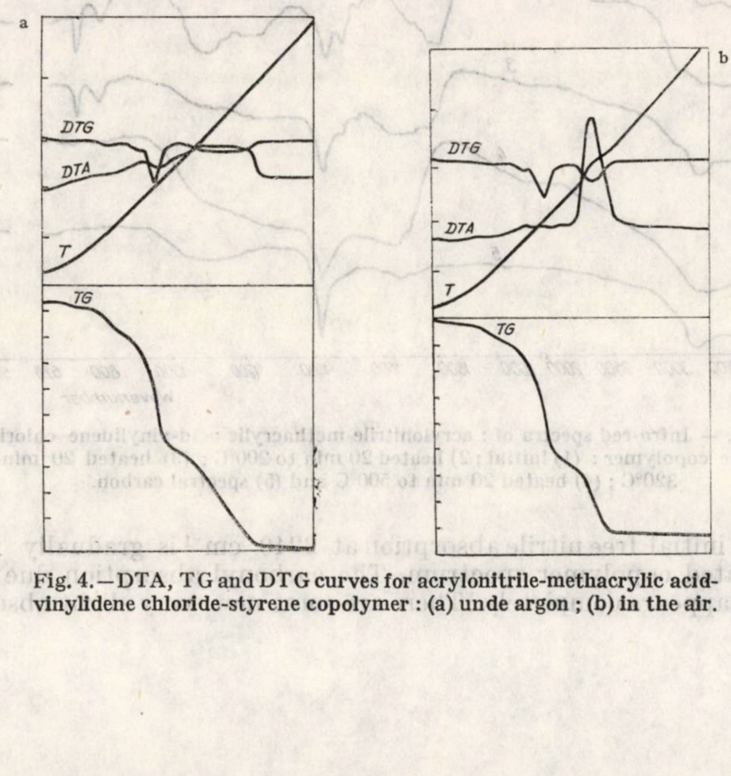

Fig. 4. – DTA, TG and DTG curves for acrylonitrile-methacrylic acid-vinylidene chloride-styrene copolymer : (a) unde argon ; (b) in the air.

The data curve in the air shows many small peaks. The exotherm at about 320°C, associated with a little weight loss is probable due to the nitrile group oligomerization. The exotherm is affected by a concurrent endothermic reaction with it, corresponding to CV units dehydrochlorination.

The small weight loss in the region of the exothermic reaction suggested that the initial chain fragmentation occurred in copolymer to a smaller extent than in pure polyacrylonitrile.

It is possible that across-linking reactions by HCl inter-molecular elimination from chlorine groups and by H_2O intermolecular elimination from acidic groups may oppose the formation of the chain fragments. This observation is in agreement with Grassie and co-workers with respect to the thermal degradation of pure polymethacrylic acid [16] and of acrylonitrile copolymers. [3,4] The shape of the DTA curve in region 360–490°C associated with an important loss of weight is the sum of exothermic and endothermic processes : comonomers chain scission and some decomposition of the acid structure units.

In argon flow the thermal behaviour is quite similar.

The copolymer shows pale-yellow coloration after 20 minutes pyrolisis at 200°C. Above 250°C the colour changes gradually from brown to black.

Changes in IR spectra of heated copolymers are shown in figure 5, in comparison with original copolymer spectrum and pure carbon spectrum.

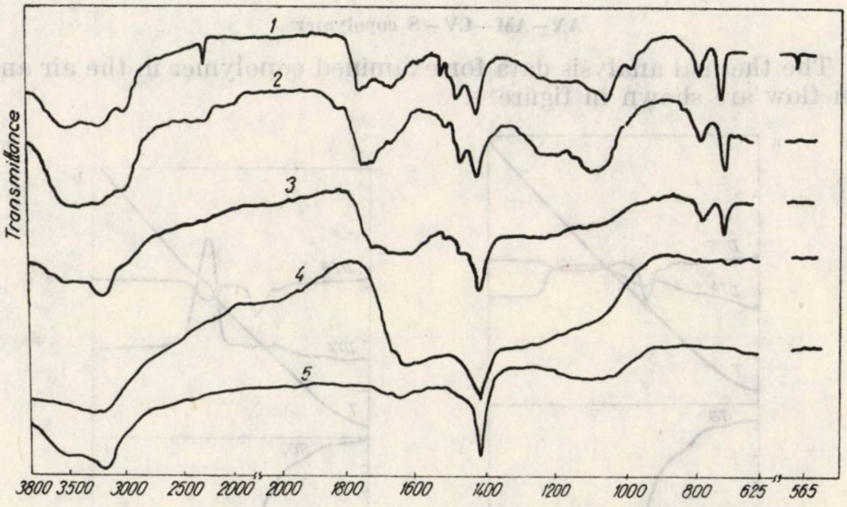

Fig. 5. — Infra-red spectra of : acrylonitrile-methacrylic acid-vinylidene chloride-styrene copolymer : (1) initial ; 2) heated 20 min to 200°C ; (3) heated 20 min to 320°C ; (4) heated 20 min to 500°C and (5) spectral carbon.

The initial free nitrile absorption at 2240 cm^{-1} is gradually reduced in the heated copolymer spectrum. The carbonyl absorption due to acid groups disappears completely. There are some new, very slight absorptions at 1800 and 1830 cm^{-1}. This can be a suggestion that a transient intermolecular anhydride species similar to that reported in the literature [3] is formed during degradation. The free acid band due to AN sequences at 3480 cm^{-1} does not appear in the spectrum of heated copolymer at 200°C.

The chlorine absorption due to CV units dissapears in the spectrum of the heated copolymer at 200°C.

An interesting feature here is the absorption at 710 and 770 cm^{-1} assigned to C—H vibrations in phenyl rings still remaining in the spectrum of the residue at 320°C and even in residue at 500°C. Also CH_2 bands at 2940, 2880 and 1460 cm^{-1} persist in all studied spectra.

CONCLUSIONS

1. Thermogravimetry and differential thermal analysis were used in order to investigate the following copolymers :

AN—BA—CV, AN—BA—CV—S, and AN—AM—CV—S.

2. Thermal analysis data are in agreement with spectra of heated copolymers at various temperatures.

3. Comonomers effects on thermal degradation are discussed, with special emphasis on oligomerization of nitrile groups.

REFERENCES

[1] N. Grassie and J. N. Hay, *J. Polymer Sci.*, **56**, 189 (1962).
[2] N. Grassie and R. Mc. Guchan, *Europ. Polym. J.*, **8**, 865 (1972).
[3] N. Grassie and R. Mc. Guchan, *Europ. Polym. J.*, **8**, 257 (1972).
[4] N. Grassie and R. Mc. Guchan, *Europ. Polym. J*, **9**, 507 (1973).
[5] N. Grassie and R. Mc. Guchan, *Europ. Polym. J.*, **9**, 113 (1973).
[6] N. Grassie and R. Mc. Guchan, *Europ. Polym. J.*, **6**, 1277 (1970).
[7] N. Grassie and R. Mc. Guchan, *Europ. Polym. J.*, **7**, 1091 (1971).
[8] M. Tomescu, V. Părăuşanu and M. Georgescu, S. Creţu, I. Hogea, D. Mihăiţă, E. Rizescu, RSR Patent 59667, 10 ian. 1975.
[9] M. Tomescu, V. Părăuşanu, M. Georgescu, S. Creţu, I. Hogea, D. Mihăiţă and E. Rizescu, R.S.R. Patent 59668, 10 ian. 1975.
[10] M. Tomescu and Cr. Simionescu, *Makromol. Chem.*, **177**, 3221 (1976).
[11] M. Tomescu, I. Demetrescu and D. Oancea, *Rev. Roumaine de Chim.*, **22**, 1267 (1977).
[12] M. Tomescu, *Rev. Roumaine de Chim.*, in press.
[13] L. Reich, *Macromol. Rev.*, **3**, 49 (1968).
[14] N. Grassie, J. G. Speakman and T. I. Davis, *J. Polymer Sci.*, **A— 7, 9**, 931 (1971).
[15] N. Grassie and J. D. Fortune, *Makromol. Chem.*, **169**, 117 (1973).
[16] D. M. Grant and N. Grassie, *Polymer*, **1**, 125 (1960).
[17] W. J. Burlant and J. L. Parsons, *J. Polym., Sci.*, **22**, 249 (1956).

COMPTES RENDUS

"Topics in Current Chemistry. Volume 91. Syntheses of Natural Products", Springer Verlag, Berlin, Heidelberg, New York, 1980, 118 pages.

The present volume contains three contributions concerning some particular aspects of natural products and the Author Index for volumes 50–91 of the series.

The first chapter : "Reagents for natural product synthesis based on the Ph_2PO and PhS groups" (27 pages, 90 references) is written by Stuart G. Warren. The article describes mainly the author's works which realise – with the aid of compounds containing PhS and Ph_2SO groups – regiospecific reagents for synthons as well as different special syntheses of natural products. The main headings are : regiospecific allyl synthons ; acyl anion equivalents for 1,2-alkylative carbonyl transpositions ; specific enol equivalents ; reagents for the synthesis of 1,4-dicarbonyl compounds and enones ; homoenolate equivalents ; reagents for the synthon $^-C{=}C{-}CO$ and phenylthiobutadienes for Diels-Alder reaction.

Some useful comparisons between the interesting author's results using the versatile PhS and Ph_2SO derivatives and different alternative syntheses are made.

The second chapter : "Applications of Palladium-Catalysed or Promoted Reactions to Natural Product Syntheses" (45 pages, 101 references) is written by Jiro Tsuji, a well-known authority in this domain. In the first part of the paper the stoichiometric oxidative reactions with Pd^{2+} compounds are presented, namely : Wacker-type oxidative reactions of olefins with nucleophiles, reactions of π-allylpalladium complexes with nucleophiles, reactions based on chelation and transmetallation of organomercury compounds.

The second part of the review describes catalytic reactions with Pd, e.g : telomerization of conjugated dienes, reactions of allylic or alkenyl esters and ethers and of organic halides. Numerous interesting recent examples of natural product syntheses, e.g. citronellol, oestrone, isoflavanone, prostaglandines, nortestosterone, pheromones etc. are presented in a short but attractive way.

The last chapter : "Aflatoxin Chemistry and Syntheses" (36 pages, 188 references) is written by Paul Francis Schulda.

After a short introduction underlining the extremely high toxicity and carcinogenicity of the aflatoxins (the mycotoxins produced during spoiling of various foodstuffs by *Aspergillus* molds) the isolation and structural elucidation of different aflatoxins (compounds generally containing a cyclopentenone /2,3-c/ coumarin skeleton fused with a bis-furane ring) are discussed. Numerous details (e.g. spectral data) are given.

The second part of the review describes synthetic approaches to mycotoxins (most of them applying different variations of von Pechmann coumarin synthesis) and underlines the "truly excellent synthetic efforts of both G. Büchi and J. C. Roberts."

We recommend this book to all organic chemists interested in natural product synthesis.

M. Banciu

CANDIN LITEANU and ION RÎCĂ : ***"Teoria şi metodologia statistică a analizei urmelor"* (Statistical Theory and Methodology of Trace Analysis), Editura "Scrisul românesc", Craiova, 1979,422 p.**

The book appeared in the nowadays spectacular development of modern analytical chemistry. The revolution in science and technology,present in all fields of activity, necessitates both in the fundamental and applied chemical research, new processing methods for the determination, as traces, of components in very low concentration. Due to the complexity of the contemporary science and technology, the trace analysis represents the most important part of the analytical chemistry, its applicability in numerous domains being conditioned by the production of chemical reagents of high purity. The improvement of the procedures used for determining the components as traces, was possible only by the present knowledge both in the domain of component detection from the material to be analysed and in the exact evaluation of its content.

The authors, already known by their works published in the country and abroad, have taken into account these needs of the analytical chemistry. They have elaborated a statistical theory and methodology of trace analysis in a book which represents the first of this kind in Romania. This special field is of very high importance and perspective in our epock when the estimation of the purity degree for a lot of materials (such as semiconductors), the determination of the environmental pollution degree or studies in cosmic geology constitue a necessity and also a premise for a correct understanding with practical consequences.

The book is divided into chapters, the reader being logically and gradually acquainted with the modern methodology by means of a rigorous, qualitative and quantitative scientific description.

The first chapter deals with the analytical problems connected with the determination of very low amounts which make necessary the use of a mathematical statistical methodology for the exact evaluation of the components as traces. The second chapter contains aspects concerning the repartition of the stochastic variables and the proof of the statistical hypotheses and the modality of their use in analytical chemistry. The third chapter is devoted to the informational processing of the analytical results, in order to define the qualitative features of the analytical systems of measurement. The following two chapters study the stability of the analytical sytems and the calibration problem particularly important for microanalysis. The sixth chapter largely debates the possibility of finding the maximum efficiency of the chemical information from experimental data, using the theory of the signal detection. The subsequent chapter refers to the estimation of the detection limit for widely used techniques applied in trace analysis : radiometric, spectral methods, chromatography. The eighth chapter shows the implications of determination limit of an analytical method and the risk level in the nonhomogeneity evaluation of a sample. The last chapter develops aspects regarding the optimization of the analytical conditions and instrumentation, as well as aspects concerning the analytical measurements processing through mathematical and statistical treatement, in order to improve the signal-noise ratio.

As may be observed from this succint description, the book aims at improving the qualitative performance of the analytical systems by the development of the methods of processing and data estimation.

The book is an original work, as it entails a new spirit in result interpretation of chemical analysis and represents a judicious combination of a vast documentary material with the authors' own researches.

Due to the problems tackled and their rigorous treatement, this work appeals to a wide range of specialists dealing with analytical chemistry, as well as to students in chemistry and it is a precious tool in top-level solving of some practical problems.

Elena Jercan

NOTE POUR LES AUTEURS

La Revue Roumanie de Chimie publie des articles en anglais, français, russe, allemand ou espagnol. Les auteurs sont priés d'envoyer des articles et de comptes rendus inédits.

Les manuscrits seront dactylographiés à deux intervalles. La bibliographie, les tableaux et la légende des figures seront placés après le texte.

Si l'article fait partie d'une série numérotée, le titre de la partie précédente sera indiqué dans une note au bas de la première page.

Chaque article sera précédé d'un résumé comprenant quinze lignes au maximum.

Les références bibliographiques dans le texte seront faites par des exposants sans parenthèses et paraîtront à la fin de l'ouvrage.

Les publications périodiques mentionées dans la bibliographie seront présentées suivant les prescriptions internationales ; le nom de l'auteur précédé de l'initiale du prénom, le titre du périodique abrégé conformément à « Chemical Abstracts» et souligné par une ligne, le numéro du tome indiqué par des chiffres arabes et souligné par deux lignes, suivi de la première page de l'article : à la fin, l'année de la parution sera placée entre parenthèses. Le numéro de la revue ne sera pas indiqué, si les pages du volume sont numérotées consécutivement.

Les textes des livres ou traités inclueront : les noms des auteurs, les initiales du prénom, le titre du livre entre guillemets et sans être souligné, le numéro du tome précédé par l'abréviation « vol. » (ou « Bd. »), le numéro de l'édition, les éditions (the publisher), la localité de la parution du livre, l'année de la parution et la page de la référence précédée(s) par l'abréviation « p » (ou « S »).

Les brevets seront indiqués comme suit : l'auteur ou la firme, le pays et le numéro du brevet, la date et la revue (Chem. Abstr.) Par ex. : M. Jones (to Union Carbide Co.), Brit. Pat. 601 238, 2 Sept. 1959; cf. *Chem. Abstr.*, **54**, 12808 (1960).

Les diagrammes seront tracés à l'encre de Chine sur papier calque. Les tableaux et les figures (en nombre strictement nécessaire) seront numérotés par des chiffres arabes. Les courbes dans les figures seront numérotées par des chiffres arabes et leur explication sera donnée dans la légende des figures. Prière de ne pas inscrire les mêmes données dans les tableaux et les figures. Chaque tableau aura un titre. On indiquera dans le texte la place approximative des tableaux et des figures. Les formules chimiques seront incluses dans le texte : en outre, elle seront transcrites sur papier calque, à l'encre de Chine.

Les auteurs sont priés d'indiquer les caractères italiques (en soulignant les lettres au crayon), ainsi que tout autre caractère spécial : les préfixes *ortho, meta, para, cis, trans*, etc. seront soulignés pour leurs caractères italiques, et ne seront jamais écrits avec des majuscules.

Aucune correction à la main ne sera admise sur le manuscrit. Les corrections seront frappés à la machine. Les lettres grecques ou autres symboles spéciaux seront insérés à la main à l'encre clairement.

Le manuscrit sera signé par l'auteur.

Le colonne-titre aura 50 lettres au maximum.

L'entière responsabilité du contenu des articles appartient aux auteurs.

Sur demande on peut obtenir un note plus complète.

PRINTED IN ROMANIA

ORSZ. MŰSZAKI DOKUMENTÁCIÓS KÖZP. 1883

TRAVAUX PARUS AUX ÉDITIONS DE L'ACADÉMIE DE LA RÉPUBLIQUE SOCIALISTE DE ROUMANIE

ELENA CEAUŞESCU, **Polimerizarea stereospecifică a izoprenului** (La polymérisation stéréospécifique de l'isoprène), 1979, 307 p.

I. G. MURGULESCU, TATIANA ONCESCU, E. SEGAL, **Introducere în chimia fizică, II. 2 Cinetică chimică şi cataliză** (Introduction à la chimie physique IIe vol. 2. Cinétique chimique et catalyse), 1981, 1024 p.

V. DRĂGUŢAN, A. T. BALABAN, M. DIMONIE, **Metateza olefinelor şi polimerizarea prin deschidere de inel a cicloolefinelor** (La métathèse des oléfines et la polymérisation par ouverture annulaire des cyclooléfines) 1981, 254 p.

O. IORDACHE, **Procese polistocastice aplicate la fenomenele de transfer** (Processus polystochastiques appliqués aux phenomènes de transfert) 1981, 187 p.

CR. SIMIONESCU, VALERIA GORDUZA, **Polimeri biocompatibili şi biologic activi** (Polymères biocompatibles et biologiquement actifs), 1980, 497 p.

M. FLORESCU, **Metode ştiinţifice în dezvoltarea industriei chimice moderne** (Méthodes scientifiques dans le développement de l'industrie chimique moderne), 1979, 256 p.

Ş. MOLDOVEANU, A. SAVIN, **Aplicaţii în chimie ale metodelor semiempirice de orbitali moleculari** (Applications en chimie des méthodes semi-empiriques d'orbitaux moléculaires), 1980, 286 p.

CONST. GH. MACAROVICI, **Analiza chimică cantitativă anorganică** (L'Analyse chimique quantitative inorganique), 1979, 457 p.

A. T. BALABAN, I. GĂLĂŢEANU, G. GEORGESCU, LIGIA SIMIONESCU, **Compuşi marcaţi şi radiofarmaceutici cu aplicaţii în medicina nucleară** (Composés marqués et radiopharmaceutiques à application en médecine nucléaire), 1979, 495 p.

I. G. MURGULESCU, E. SEGAL, **Introducere în chimia fizică**, vol. II. 1. **Teoria molecular cinetică a materiei** (Introduction à la chimie physique. IIe vol. 1. La théorie moléculaire-cinétique de la matière), 1979, 1036 p.

I. E. TEODORESCU, MARIA FITI, **Iradierea tehnologică** (L'irradiation technologique), 1979, 216 p.

S. STERNBERG, FL. DANEŞ, **Termodinamica chimică aplicată** (La thermodynamique chimique appliquée), 1978, 400 p.

I. G. MURGULESCU, V. EM. SAHINI, **Introducere în chimia fizică**. Vol. 1. 2. **Structura şi proprietăţile moleculelor** (Introduction à la chimie physique. Ier vol. 2. La structure et les propriétés des molécules), 1978, 604 p.

C. DRĂGULESCU, E. PETROVICI, **Chimie structurală modernă. Chimia coordinanţei 8** (La chimie structurale moderne. La chimie de la coordinance 8), 1977, 947 p.

D. PURDELA (sous la direction de), **Nomenclatura chimiei anorganice** (La nomenclature de la chimie inorganique), 1977, 153 p.

I. ZUGRĂVESCU, MAGDA PETROVANU, **N-ylid chemistry**, coédition avec McGraw-Hill, 1977, 396 p.

I. G. MURGULESCU, **Introducere în chimia fizică**. Vol. I. 1. **Atomi, molecule, legătură chimică** Introduction à la chimie physique, Ier vol. 1. Atomes, molécules, liaison chimique), 1976, 560 p.

I. GĂLĂŢEANU, **Radiochimia aplicată. Metode şi probleme** (La radiochimie appliquée, Méthodes et problèmes), 1976, 307 p.

CONST. GH. MACAROVICI, D. MACAROVICI, **Chimia oxizilor dubli şi utilizările lor** (La chimie des oxydes doubles et leur utilisation), 1975, 195 p.

ELENA CEAUŞESCU, **Research work on synthesis and characterization of macromolecular compounds. Contributions**. 1974, 251 p.

CR. SIMIONESCU, VIOREL RUSAN, V. POPA, **Chimia algelor marine** (La chimie des algues marines), 1974, 212 p. 1 pl.

I. P. „INFORMAŢIA", c. 1049

43 426

Lei 25.—

$ 55 (price per year)

F 1103

REFERÁLVA

ACADÉMIE DE LA RÉPUBLIQUE SOCIALISTE DE ROUMANIE

R

REVUE ROUMAINE DE CHIMIE

TOME 26
N° 6
Juin 1981

EDITURA ACADEMIEI REPUBLICII SOCIALISTE ROMÂNIA

Rev. Roumaine Chim.

RRCHAX, **26**, *6*, p. 803–924 (1981), Bucarest

ACADÉMIE DE LA RÉPUBLIQUE SOCIALISTE DE ROUMANIE

COMITÉ DE RÉDACTION

Rédacteur en chef :

I. G. MURGULESCU, membre de l'Académie de la République Socialiste de Roumanie

Rédacteurs en chef adjoints :

A. T. BALABAN et V. EM. SAHINI, membres correspondants de l'Académie de la République Socialiste de Roumanie

Collège de rédaction :

EM. BRATU, ELENA CEAUŞESCU, ECATERINA CIORĂNESCU-NENITZESCU, CR. SIMIONESCU, membres de l'Académie de la République Socialiste de Roumanie ; P. SPACU, membre correspondant de l'Académie de la République Socialiste de Roumanie ; MARGARETA AVRAM, M. BANCIU, I. HAIDUC, D. I. MARCHIDAN, I. MOLDOVAN, G. NIAC et D. SĂNDULESCU

La Revue Roumaine de Chimie parait 10 fois par an. Toute commande de l'étranger pour les travaux parus aux Editions de l'Académie de la République Socialiste de Roumanie sera adressée à ILEXIM, — Departamentul Export-Import Carte (Livres)/Departamentul Export-Import Presă (Revues) P.O.B. 136—137, télex 11226, 3, str. 13 Decembrie, 79517 Bucarest, Roumanie

Les manuscrits, les livres et les revues proposés en échange, ainsi que toute correspondance seront envoyés à la rédaction :

REVUE ROUMAINE DE CHIMIE

Calea Victoriei, 125, 79717 Bucarest, Roumanie, téléphone 50 76 80

EDITURA ACADEMIEI REPUBLICII SOCIALISTE ROMÂNIA
125, Calea Victoriei, 79717 Bucarest, Roumanie, téléphone 50 76 80

REVUE ROUMAINE DE CHIMIE

ORSZÁGOS MŰSZAKI KÖNYVTÁR ÉS DOKUMENTÁCIÓS KÖZPONT 1883

Tome 26, N° 6 Juin, 1981

VICTOR DAVID and ŞERBAN MOLDOVEANU, The long-range interaction of two molecules in the presence of a *Kirkwood* perturbational field 805–809

N. D. TOTIR, Kinetic studies of electrode processes using the method of half-lives . . . . 811–813 R Bc

N. I. IONESCU, Concerning a recently proposed equation for the adsorption of gases on solids 815–817

R. H. SCHUSTER, N. I. IONESCU, D. OANCEA, D. POPESCU and V. GOŞA, The explosive combustion of propylene. II. Flame speed determination in tubes by photographic methods 819–827

MAURICE ABRAHAM, The activity of one salt at high concentrations in pure water (in French) 829–835

MONICA CĂLDĂRARU, P. BANYAI and N. I. IONESCU, Electrical conductivity of a complex bismuth–molybdenum catalyst in the reaction of propylene oxidation 837–842

N. PETRESCU and LUCIA GANOVICI, Self-diffusion of tellurium in the liquid Pb–Te eutectic alloy . . . . 843–850 Bc R

RODICA VĂŢULESCU, T. BUDIU and GH. MARCU, Heteropolytungstates with Ti(IV) and Ni(II). I. The formation of two new heteropolyanions with Ti(IV) and Ni(II) in solution 851–855

A. SYAMAL and B. K. GUPTA, New dioxouranium (VI) complexes with bidentate ON donor Schiff bases derived from salicylaldehyde or substituted salicylaldehyde and benzoylhydrazide 857–860

ELENA BĂLĂ, MARIANA S. IONESCU and. C. STOICESCU, Copper (II) complexes of threonine and allothreonine 861–866

J. M. CAMPELO, D. LUNA and M. MARINAS, Liquid-phase reduction of cyclohexene in the presence of new systems of supported nickel catalysts (in Spanish) 867–873

R. K. PANDE, R. SHARMA and B. C. JOSHI, A novel route for the synthesis of keto-benzoic acid derivatives, auxin transport inhibitors . . . . 875–878 R

FLORENTINA GEORGESCU, F. CHIRALEU, E. GEORGESCU and I. ZUGRĂVESCU, Pyridinium-ylids. II. The reactions of some carbanion–monosubstituted 4-phenylpyridinium-ylids with activated acetylenes (in French) 879–885

Revue Roumaine Chim. 26, 6, 803–924 (1981) Bucarest

MIRCEA V. DIUDEA, Phenazathionium cations. IV. Demonstration on the structure of 1,3,7-trisubstituted derivatives of phenothiazine by mass spectrometry and ^1H-NMR 887–898
J. SÁNCHEZ BALLESTEROS, D. J. McPHEE and F. HERNANDEZ HERNANDEZ, Preparation of polyfunctional furanic derivatives from trioses 899–907
CANDIN LITEANU and IOANA ILEANA PANOVICI, Frequentometric detection in different stability conditions of IR analytic systems 909–916
P. P. SINHA, R. S. CHAWLA, S. K. SINDHWANI and FASIHUDDIN KAMIL, Thiovioluric acid as an analytical reagent. Spectrophotometric and complexometric determination of copper (II) 917–923

Revue Roumaine de Chimie, 26, 6, 805–809 (1981)

THE LONG-RANGE INTERACTION OF TWO MOLECULES IN THE PRESENCE OF A *KIRKWOOD* PERTURBATIONAL FIELD

VICTOR DAVID and ŞERBAN MOLDOVEANU
The Polytechnic, Faculty of Chemical Technology, Splaiul Independenţei 202,
Bucharest, România

Received October 18, 1980

The general equation and its physical meaning are established for the perturbation potentials of two interacting molecules in the presence of a perturbational field produced by the surrounding continuum and homogeneous medium. This equation is explicited for some simple cases.

INTRODUCTION

Between two identical collections of charges (that is two identical molecules imagined as such collections of charges) occur well-known long-range electric forces and the following interacting potential energy: [1,2]

$$U = \hat{\mathbf{V}}\hat{\mathbf{V}}\mathbf{R}^{-1} = \sum_{\nu=0}^{\infty} \sum_{\mu=0}^{\infty} \hat{\mathbf{T}}_{\nu}\hat{\mathbf{T}}_{\mu}\mathbf{R}^{-1} \qquad (1)$$

where $\mathbf{R}$ is the distance between their mass centers.

THEORY

This paper deals with the theoretical thoroughgoing study of the form of the potential operators $\hat{\mathbf{V}}$ in the case of interacting molecules embedded in a perturbational Kirkwood field.

The reaction Kirkwood field is a perturbational field represented as a row-vector with an infinite number of components:

$$\mathbf{G} \equiv [\mathbf{G}_q\mathbf{G}_p\mathbf{G}_Q\mathbf{G}_O \ldots] \qquad (2)$$

$\mathbf{G}_q$, $\mathbf{G}_p$, $\mathbf{G}_Q$, $\mathbf{G}_O$,... are the monopole, dipole, quadrupole, octupole, ..., components.

Molecule i assimilated to a charge collection, produces an electric field $\mathbf{V}$ perturbated by $\mathbf{G}$. It can be represented as a column-vector with an infinite number of components :

$$\mathbf{V}^i = \hat{\mathbf{V}}_i \mathbf{R}^{-1} \equiv \begin{bmatrix} \mathbf{M}_q \\ \mathbf{M}_p \\ \mathbf{M}_Q \\ \mathbf{M}_O \\ \vdots \end{bmatrix} \tag{3}$$

$\mathbf{M}$'s being the pole electric moments of the charge distribution.

The action of the field $\mathbf{G}$ on the molecule i can be represented as a product between $\mathbf{G}$ and $\mathbf{V}$ matrices. Thus :

$$[\mathbf{G}_q \mathbf{G}_p \mathbf{G}_Q \mathbf{G}_O \ldots] \begin{bmatrix} \mathbf{M}_q \\ \mathbf{M}_p \\ \mathbf{M}_Q \\ \mathbf{M}_O \\ \vdots \end{bmatrix} = \begin{bmatrix} \mathbf{G}_q\mathbf{M}_q & \mathbf{G}_p\mathbf{M}_q & \mathbf{G}_Q\mathbf{M}_q & \mathbf{G}_O\mathbf{M}_q & \ldots \\ \mathbf{G}_q\mathbf{M}_p & \mathbf{G}_p\mathbf{M}_p & \mathbf{G}_Q\mathbf{M}_p & \mathbf{G}_O\mathbf{M}_p & \ldots \\ \mathbf{G}_q\mathbf{M}_Q & \mathbf{G}_p\mathbf{M}_Q & \mathbf{G}_Q\mathbf{M}_Q & \mathbf{G}_O\mathbf{M}_Q & \ldots \\ \mathbf{G}_q\mathbf{M}_O & \mathbf{G}_p\mathbf{M}_O & \mathbf{G}_Q\mathbf{M}_O & \mathbf{G}_O\mathbf{M}_O & \ldots \\ \vdots & \vdots & \vdots & \vdots & \ddots \end{bmatrix} \tag{4}$$

Here the product $\mathbf{G}_\nu \mathbf{M}_\mu$ ($\nu, \mu = q, p, Q, O, \ldots$) shows the action of ν-th pole of the perturbational field on the μ-th pole of the molecule. The perturbation may be generally expressed by the perturbation operator $\hat{\mathbf{A}}^\nu_\mu$ whose matrix representation is given by

$$\underset{\text{(I)}}{\begin{bmatrix} \mathbf{G}_q\mathbf{M}_q & \mathbf{G}_p\mathbf{M}_q & \mathbf{G}_Q\mathbf{M}_q & \mathbf{G}_O\mathbf{M}_q & \ldots \\ \mathbf{G}_q\mathbf{M}_p & \mathbf{G}_p\mathbf{M}_p & \mathbf{G}_Q\mathbf{M}_p & \mathbf{G}_O\mathbf{M}_p & \ldots \\ \mathbf{G}_q\mathbf{M}_Q & \mathbf{G}_p\mathbf{M}_Q & \mathbf{G}_Q\mathbf{M}_Q & \mathbf{G}_O\mathbf{M}_Q & \ldots \\ \mathbf{G}_q\mathbf{M}_O & \mathbf{G}_p\mathbf{M}_O & \mathbf{G}_Q\mathbf{M}_O & \mathbf{G}_O\mathbf{M}_O & \ldots \\ \vdots & \vdots & \vdots & \vdots & \ddots \end{bmatrix}} \longrightarrow \underset{\text{(II)}}{\begin{bmatrix} \hat{\mathbf{A}}^q_q & \hat{\mathbf{A}}^p_q & \hat{\mathbf{A}}^Q_q & \hat{\mathbf{A}}^O_q & \ldots \\ \hat{\mathbf{A}}^q_p & \hat{\mathbf{A}}^p_p & \hat{\mathbf{A}}^Q_p & \hat{\mathbf{A}}^O_p & \ldots \\ \hat{\mathbf{A}}^q_Q & \hat{\mathbf{A}}^p_Q & \hat{\mathbf{A}}^Q_Q & \hat{\mathbf{A}}^O_Q & \ldots \\ \hat{\mathbf{A}}^q_O & \hat{\mathbf{A}}^p_O & \hat{\mathbf{A}}^Q_O & \hat{\mathbf{A}}^O_O & \ldots \\ \vdots & \vdots & \vdots & \vdots & \ddots \end{bmatrix}} \tag{5}$$

Matrix (I) indicates the perturbing action of $\mathbf{G}$ on $\mathbf{V}$ and the matrix (II) is the matrix of the perturbation operator $\hat{\mathbf{A}}^\nu_\mu$. Each line in (II) represents the components of the perturbation operator of a pole by all the components of the perturbational field $\mathbf{G}$. For example, $\hat{\mathbf{A}}^q_O$ is the perturbation operator of the electric octupole moment of the molecule by the monopole of the external perturbational field.

It results from (1) that the potential interacting energy between the ν-th pole of the first molecule and the μ-th pole of the second molecule is :

$$U_{\nu\mu} = \hat{\mathbf{T}}_\nu \hat{\mathbf{T}}_\mu \mathbf{R}^{-1}. \tag{6}$$

In the presence of the perturbational field, it becomes :[2]

$$U'_{\nu\mu} = \frac{1}{2}\,[(\hat{\mathbf{T}}_\nu + \hat{\mathbf{A}}_\nu)(\hat{\mathbf{T}}_\mu + \hat{\mathbf{A}}_\mu) + (\hat{\mathbf{T}}_\mu + \hat{\mathbf{A}}_\mu)(\hat{\mathbf{T}}_\nu + \hat{\mathbf{A}}_\nu)]\mathbf{R}^{-1} \qquad (7)$$

$\hat{\mathbf{T}}_\nu$ is the potential operator of the ν-th pole represented as the matrix $[\hat{\mathbf{T}}_{\rho_1\rho_2\ldots\rho_\nu}]$, $\rho_k = 1, 2, 3$;
$\hat{\mathbf{T}}_\nu\hat{\mathbf{T}}_\mu$ — potential energy operator of the interaction $\nu - \mu$;
$\hat{\mathbf{A}}_\nu$ — perturbation operator of the potential of ν-th pole. Details concerning these quantities may be found elsewhere.[2]

Because the perturbation potentials were introduced additively, the significance of the terms $\hat{\mathbf{T}}_\nu\hat{\mathbf{A}}_\mu$, $\hat{\mathbf{A}}_\nu\hat{\mathbf{T}}_\mu$, $\hat{\mathbf{A}}_\nu\hat{\mathbf{A}}_\mu$, $\hat{\mathbf{A}}_\mu\hat{\mathbf{A}}_\nu$ is as follows : $\hat{\mathbf{T}}_\nu\hat{\mathbf{A}}_\mu$ represents the potential energy operator of the interaction between the pole ν of the first molecule and the variation of the pole μ of the second molecule due to the external field of the surrounding medium, etc.

We shall try, in the following, to obtain an explicit expression for the $\hat{\mathbf{A}}^\nu_\mu$ operator.

In a previous paper,[2] a general differential equation which binds these operators was given :

$$\begin{gathered}(\hat{\mathbf{T}}_\nu\hat{\mathbf{A}}_\mu + \hat{\mathbf{A}}_\nu\hat{\mathbf{T}}_\mu + \hat{\mathbf{A}}_\nu\hat{\mathbf{A}}_\mu + \mathbf{R}\mathbf{G}_\mu)\mathbf{R}^{-1} = 0, \\ \mu = 0, 1, 2, \ldots, \infty, \\ \nu = 0, 1, 2, \ldots, \infty. \end{gathered} \qquad (8)$$

For simplicity, let's write down the left member of this equation :

$$\mathbf{S}_{\nu\mu} = 0 \qquad (9)$$

Equation (9) allows us to determine the perturbation operators $\hat{\mathbf{A}}_\nu$ of a molecule in the presence of the perturbational action of the μ-th pole of an external field.

Equation : $\mathbf{S}_{\mu\mu} = 0$ indicates the perturbation ot the pole μ in the interaction with the same pole of the second molecule by the pole of the field $\mathbf{G}_\mu$ and thus, it allows us to determine the $\hat{\mathbf{A}}^\mu_\mu$ from matrix II (formula 5).

Equation : $\mathbf{S}_{\nu\mu} = 0$ ($\nu \neq \mu$) indicates the perturbation of the poles ν and μ of the two interacting molecules by the pole of the field $\mathbf{G}_\mu$, that is $\hat{\mathbf{A}}^\mu_\nu$ and $\hat{\mathbf{A}}^\mu_\mu$. Knowing $\hat{\mathbf{A}}^\mu_\mu$ from the precedent equation one may determine $\hat{\mathbf{A}}^\mu_\nu$ from $\mathbf{S}_{\nu\mu} = 0$.

Equation $\mathbf{S}_{\mu\nu} = 0$ ($\mu \neq \nu$) indicates the perturbation of the poles ν and μ of the two interacting molecules by $\mathbf{G}_\nu$. The quantities $\hat{\mathbf{A}}^\nu_\nu$ and $\hat{\mathbf{A}}^\nu_\mu$ can be thus found. Knowing $\hat{\mathbf{A}}^\nu_\nu$ from the equation $\mathbf{S}_{\nu\nu} = 0$, we determine $\hat{\mathbf{A}}^\nu_\mu$.

Equation (8) must be therefore written in a more general form:

$$(\hat{\mathbf{T}}_\nu \hat{\mathbf{A}}^\mu_\mu + \hat{\mathbf{A}}^\mu_\nu \hat{\mathbf{T}}_\mu + \hat{\mathbf{A}}^\mu_\nu \hat{\mathbf{A}}^\mu_\mu + \mathbf{R}\mathbf{G}_\mu)\mathbf{R}^{-1} = 0. \tag{10}$$

Operator $\hat{\mathbf{A}}^\mu_\nu$ from the equation (10) was suggested [2] to be of the form:

$$\hat{\mathbf{A}}^\mu_\nu = \frac{1}{\nu!} \sum_{\rho_1=1}^{3} \sum_{\rho_2}^{3} \cdots \sum_{\rho_\nu}^{3} \boldsymbol{\alpha}^\mu_{\rho_1\rho_2\ldots\rho_\nu} \partial^\nu_{X_{\rho_\nu}} \tag{11}$$

Where:

$$\partial_{X_{\rho_\nu}} \equiv \frac{\partial^\nu}{\partial X_{\rho_1} \partial X_{\rho_2} \ldots \partial X_{\rho_\nu}}. \tag{12}$$

To solve the operator equation (10), it means to determine the functions $\boldsymbol{\alpha}$. According to the present interpretation, the expression (10) given explicitly elsewhere,[2] becomes:

$$\sum_{\rho_1\ldots\rho_\nu}^{3} \sum_{\rho'_1\ldots\rho'_\mu}^{3} \left\{ \sum_{b=0}^{\nu} [C_\nu^{\nu-b}(\mathbf{M}_{\rho_1\rho_2\ldots\rho_\nu} + \boldsymbol{\alpha}^\mu_{\rho_1\rho_2\ldots\rho_\nu}) \partial^{\nu-b} \boldsymbol{\alpha}^\mu_{\rho'_1\rho'_2\ldots\rho'_\mu} \cdot \partial^{\mu+b}] + \right.$$

$$\left. + \boldsymbol{\alpha}^\mu_{\rho_1\rho_2\ldots\rho_\nu} \mathbf{M}_{\rho'_1\rho'_2\ldots\rho'_\mu} \partial^{\nu+\mu} + \nu!\,\mu!\,\mathbf{R}\mathbf{G}_\mu \right\} \mathbf{R}^{-1} = 0 \tag{13}$$

$$\nu,\ \mu = 0,\ 1,\ 2,\ \ldots\ \infty$$

For $\nu = 0$, $\mu = 0$ from (13) one obtains:

$$\hat{\mathbf{A}}^q_q = \alpha^0_0 = -q \pm \sqrt{q^2 - RG_0}. \tag{14}$$

The quantity G_0 as derived from Kirkewood's model is [3]:

$$G_0 = \frac{(1-\varepsilon)q^2}{2\varepsilon a}, \tag{15}$$

where ε is the dielectric constant of the surrounding continuum and homogeneous medium, q — the net charge of the system formed by the two interacting ions:

$$q = |q_1| + |q_2| \tag{16}$$

q_1, q_2 are the net charges of the first and second ion respectively, a is the radius of the cavity of an ion.
One obtains:

$$\hat{\mathbf{A}}^q_q = -q\left(1 \pm \sqrt{1 - \frac{R(1-\varepsilon)}{2\varepsilon a}}\right). \tag{17}$$

For $R \geqslant 2a$, $\varepsilon > 1$, it results :

$$1 - \frac{R(1 - \varepsilon)}{2\varepsilon a} > 0 \tag{18}$$

for any value of the radius R.
For $\nu = 1$, $\mu = 0$ from (13) one obtains :

$$\sum_{\rho_1=1}^{3} [(M_{\rho_1} + \alpha^0_{\rho_1})(R^{-1}\partial_{X_{\rho_1}}\alpha^0_0 + \alpha^0_0\partial_{X_{\rho_1}}R^{-1}) + \alpha^0_{\rho_1}M_0\partial_{X_{\rho_1}}R^{-1} + G_0] = 0 \tag{19}$$

If we denote $X_{\rho_1} = X$, $X_{\rho_2} = Y$, $X_{\rho_3} = Z$, α^0_X, α^0_Y and α^0_Z result. If these quantities are now introduced into (11), one obtains the following expressions :

$$\hat{\mathbf{A}}^q_{p_X} = \pm \frac{G_0 + p_X \dfrac{\partial}{\partial X}(\hat{A}^q_q R^{-1})}{\dfrac{\partial}{\partial X}\left(R^{-1}\sqrt{1 - \dfrac{RG_0}{q^2}}\right)} \cdot \frac{\partial}{\partial X}$$

$$\hat{\mathbf{A}}^q_{p_Y} = \pm \frac{G_0 + p_Y \dfrac{\partial}{\partial Y}(\hat{A}^q_q R^{-1})}{\dfrac{\partial}{\partial Y}\left(R^{-1}\sqrt{1 - \dfrac{RG_0}{q^2}}\right)} \cdot \frac{\partial}{\partial Y}$$

$$\hat{\mathbf{A}}^q_{p_Z} = \pm \frac{G_0 + p_Z \dfrac{\partial}{\partial Z}(\hat{A}^q_q R^{-1})}{\dfrac{\partial}{\partial Z}\left(R^{-1}\sqrt{1 - \dfrac{RG_0}{q^2}}\right)} \cdot \frac{\partial}{\partial Z} \tag{20}$$

The same procedure can be followed for other values of ν and μ in order to obtain explicit expressions for the $\hat{\mathbf{A}}$ operators.

ACKNOWLEDGEMENTS. We are indebted to Dr. Simona Bădilescu and Dr. Ilie Bădilescu for the many valuable discussions. We also thank Dr. Costinel Lepădatu for his suggestions.

REFERENCES

[1] H. Margeanu and N. R. Kestner, "Theory of Intermolecular Forces", Pergamon Press, 1971, p. 15.
[2] V. David and Ş. Moldoveanu, *Rev. Roumaine Chim.* **26**, 333 (1981).
[3] D. L. Beveridge and G. W. Schnuelle, *J. Phys. Chem.*, **79**, 2062 (1975).

Revue Roumaine de Chimie, **26**, *6*, 811–813 (1981)

KINETIC STUDIES OF ELECTRODE PROCESSES USING THE METHOD OF HALF-LIVES

N. D. TOTIR
Centre of Physical Chemistry, Splaiul Independenţei 202, Bucharest 77208, Romania

Received September 29, 1980

The procedure of applying the method of half-lives to kinetic studies of electrode processes is described.

The method of half-lives has been applied successfully in chemical kinetics and radiochemistry till now. There is no indication in the literature of applying this method in electrochemical kinetics. In a short communication,[1] the possibility of using the method of half-lives for kinetic studies of electrode processes was noticed.

This paper describes the procedure of applying the method of half-lives to electrochemical kinetics.

It is well known from chemical kinetics that for a first-order reactions written as

$$aA + bB + \ldots \rightarrow \text{products} \tag{1}$$

at a time $t = t_{1/2}$, where $t_{1/2}$ is the half-life of the reaction, the following relation holds

$$t_{1/2} = \frac{\ln 2}{K_A}. \tag{2}$$

For an electrochemical reaction which takes place according to relation (1), regardless of the current controlling factor, the current density is given by Faraday's law

$$i_t = nF\left(\frac{\mathrm{d}N}{\mathrm{d}t}\right) \tag{3}$$

where n is the number of electrons transferred in the electrode process, F is Faraday's constant and $\mathrm{d}N/\mathrm{d}t$ is the number of mole of substance reaching the electrode in unit time.

In certain experimental conditions $\mathrm{d}N/\mathrm{d}t$ is the same to the bulk of the solution as at the electrode surface and therefore eq. (3) becomes

$$i_t = -nFV\left(\frac{\mathrm{d}C_A}{\mathrm{d}t}\right) \tag{4}$$

where V is the total volume of the solution and C_A is the concentration of species A being consumed. It has been introduced the minus sign because $\mathrm{d}C_A/\mathrm{d}t$ is a negative quantity.

According to Butler-Volmer relation the current is given also by the following equation

$$i_t = i_0[\mathrm{e}^{(1-\beta)\eta F/RT} - \mathrm{e}^{-\beta\eta F/RT}]. \qquad (5)$$

Combining equation (4) with equation (5) we obtain

$$\frac{\mathrm{d}C_A}{\mathrm{d}t} = -\frac{i_0}{nFV}[\mathrm{e}^{(1-\beta)\eta F/RT} - \mathrm{e}^{-\beta\eta F/RT}]. \qquad (6)$$

Inserting the expression for the equilibrium exchange-current density i_0

$$i_0 = nFK_sC_A\,\mathrm{e}^{-\beta\Delta\Phi_\mathrm{e}F/RT} \qquad (7)$$

in equation (6) results

$$\frac{\mathrm{d}C_A}{\mathrm{d}t} = -\frac{K_sC_A\,\mathrm{e}^{-\beta\Delta\Phi_\mathrm{e}F/RT}}{V}[\mathrm{e}^{(1-\beta)\eta F/RT} - \mathrm{e}^{-\beta\eta F/RT}]. \qquad (8)$$

When $V = 1$ we may write

$$\frac{\mathrm{d}C_A}{C_A} = -K_s\mathrm{e}^{-\beta\Delta\Phi_\mathrm{e}F/RT}[\mathrm{e}^{(1-\beta)\eta F/RT} - \mathrm{e}^{-\beta\eta F/RT}]\,\mathrm{d}t \qquad (9)$$

or

$$\ln C_A = -K_s\,\mathrm{e}^{-\beta\Delta\Phi_\mathrm{e}F/RT}[\mathrm{e}^{(1-\beta)\eta F/RT} - \mathrm{e}^{-\beta\eta F/RT}]t + cst \qquad (10)$$

If $t = 0$, $\ln C_{A_0} = cst$, and we get

$$\ln\frac{C_A}{C_{A_0}} = -K_s\,\mathrm{e}^{-\beta\Delta\Phi_\mathrm{e}F/RT}[\mathrm{e}^{(1-\beta)\eta F/RT} - \mathrm{e}^{-\beta\eta F/RT}]t. \qquad (11)$$

When $t = t_{1/2}$, $C_A = C_{A_0}/2$ and theretore

$$t_{1/2} = \frac{\ln 2}{K_s\,\mathrm{e}^{-\beta\Delta\Phi_\mathrm{e}F/RT}[\mathrm{e}^{(1-\beta)\eta F/RT} - \mathrm{e}^{-\beta\eta F/RT}]} \qquad (12)$$

or

$$K_s = \frac{\ln 2}{t_{1/2}\,\mathrm{e}^{-\beta\Delta\Phi_\mathrm{e}F/RT}[\mathrm{e}^{(1-\beta)\eta F/RT} - \mathrm{e}^{-\beta\eta F/RT}]}. \qquad (13)$$

Considering that

$$\eta = \Delta\Phi - \Delta\Phi_\mathrm{e} \qquad (14)$$

thus equation (13) becomes

$$K_s = \frac{\ln 2}{\left[e^{(1-\beta)\Delta\Phi F/RT}\, e^{-\Delta\Phi_e F/RT} - e^{-\beta\Delta\Phi F/RT}\right] t_{1/2}} \cdot \tag{15}$$

By retaining only the first two terms of each exponential term we get after expansion

$$K_s = \frac{\ln 2}{\left\{\left[1 + \frac{(1-\beta)\Delta\Phi F}{RT}\right]\left[1 - \frac{\Delta\Phi_e F}{RT}\right] - \left[1 - \frac{\beta\Delta\Phi F}{RT}\right]\right\} t_{1/2}} \cdot \tag{16}$$

Finally, by neglecting the term

$$\frac{(1-\beta)\Delta\Phi F}{RT} \cdot \frac{\Delta\Phi_e F}{RT}$$

the following equation results

$$K_s = \frac{\ln 2}{\frac{F}{RT}(\Delta\Phi - \Delta\Phi_e) t_{1/2}} \tag{17}$$

or

$$K_s = \frac{RT}{F} \cdot \frac{\ln 2}{\eta t_{1/2}} \tag{18}$$

which gives the rate constant of a first order electro-chemical reaction provided that half-lives is determined by chemical analysis during controlled potential electrolysis.

REFERENCES

[1] N. D. Totir, *Rev. Chim.* (Bucureşti), **31**, 492 (1980).

Revue Roumaine de Chimie, **26**, *6*, 815–817 (1981)

CONCERNING A RECENTLY PROPOSED EQUATION FOR THE ADSORPTION OF GASES ON SOLIDS

N. I. IONESCU
Center of Physical Chemistry, Splaiul Independenţei 202, Bucharest, Romania

Received August 20, 1980

The equation proposed by Ritchie[1] for the adsorption of gases on solids has a common starting point with the logarithmic law and was described before by Suhrmann-Wedler and Murgulescu-Ionescu.

Recently Ritchie has shown [1] that the kinetics of adsorption of gases on solids, usually described by the logarithmic law, can be very well fitted by the equation :

$$\frac{q_\infty}{q_\infty - q} = Ct + 1 \tag{1}$$

where q_∞ and q are the amounts adsorbed at infinity and at time t respectively and C a constant. The simple model used [1] for the explanation of this law was based on the assumptions that n surface sites are occupied by a chemisorbed molecule and that the rate of adsorption depends solely on the fraction of unoccupied site at any time. When $n = 2$, the model leads to equation (1).

In the present paper we discuss some new aspects connected with this equation.

RESULTS AND DISCUSSIONS

Let us consider the adsorption as a probabilistic discontinous process, which progresses in discrete steps in a background of fluctuations. Each forward step is assumed to decrease the probability $p(t)$ of a further step occurring, by an amount which is proportional [2] to the probability at time t. In this case, the decreasing rate of the probability will be :

$$-\frac{\mathrm{d}p}{\mathrm{d}t} = k_1 p \cdot k_2 p = \alpha p^2 \tag{2}$$

where α is a general constant.

In the case of adsorption p has the physical signification of the number of unoccupied sites. [2]

Let now consider n_s as the number of unoccupied sites of the surface and n_a the number of adsorbed molecules at the t moment.

With this notation, equation (2) becomes :

$$-\frac{\mathrm{d}n_s}{\mathrm{d}t} = \alpha n_s^2 \qquad (3)$$

In order to justify the logarithmic law, many models have been proposed ;[3] in all cases, by neglecting desorption, the validity of the conventional kinetic formulation for a gas in contact with a set of unoccupied sites was assumed.[4]

The models concerning n_s simply assume that the expression

$$n_s = \text{const. exp}\,(-\beta n_a) \qquad (4)$$

is satisfied rather than the usual conservative relation

$$n_s = n_\infty - n_a \qquad (5)$$

where n_∞ is the highest number of sites which can be covered at equilibrium.

Now, using in equation (3) the relationship (4) for n_s one obtains

$$\frac{\mathrm{d}n_a}{\mathrm{d}t} = D\,\exp\,(-\beta n_a) \qquad (6)$$

where D is a constant, which is the differential form of the logarithmic law.

If instead of relation (4), the expression (5) is used in equation (3), then

$$\frac{\mathrm{d}n_a}{\mathrm{d}t} = C\left(1 - \frac{n_a}{n_\infty}\right)^2 \qquad (7)$$

where C is a constant. By integrating this equation with the initial conditions $t = 0$, $n_a = 0$, the following results :

$$\frac{n_\infty}{n_\infty - n_a} = \gamma t + 1 \qquad (8)$$

where γ includes all constants. Equation (8) is nothing else than equation (1) calculated by Ritchie. Both formulas (6) and (8) have a common starting point.

It must be mentioned that equation (8) was firstly described in 1957 by Suhrmann and Wedler [5] for the variation of the electrical resistance of sintered thin metallic films due to gas chemisorption, being written as follows :

$$\frac{1}{\Delta R_\infty - \Delta R} = \frac{A}{\Delta R_\infty}\,t + \frac{1}{\Delta R_\infty} \qquad (9)$$

where ΔR_∞ is the resistance variation at equilibrium, ΔR the resistance variation at the t moment and A a constant.

In 1967 Murgulescu and Ionescu obtained,[6] in another way, equation (8) which has been applied to the kinetics of electrical resistance variation of thin unsintered silver films due to oxygen chemisorption.

Later, the same authors deduced [7] a formula which implied both cases treated by Ritchie [1] with $n = 2$ and $n = 1$, respectively.

The kinetic process of the electrical resistance variation of sintered thin copper [7] and silver [8] films due to oxygen chemisorption verifies, with the same probability, the Suhrmann-Wedler equation and the logarithmic law. [9] When two straight lines with different slopes were obtained in a logarithmic plot, then, by applying Suhrmann-Wedler's equation, two intersecting straight lines were also obtained.[9] When the results do not obey the logarithmic law, they do not verify [10] equations (8) too.

REFERENCES

[1] A. G. Ritchie, *J.C.S. Faraday I*, **73**, 1650 (1977).
[2] P. T. Landsberg, *J. Appl. Phys.*, **33**, 2251 (1962).
[3] C. Aharoni and F. C. Tompkins, *Adv. Catalysis*, **21**, 1 (1970).
[4] A. M. Peers, *J. Catalysis*, **4**, 672 (1965).
[5] R. Suhrmann and G. Wedler, *Z. phys. Chem. (Frankfurt)*, **10**, 84 (1957).
[6] I. G. Murgulescu and N. I. Ionescu, *Rev. Roumaine Chim.*, **12**, 1395 (1967).
[7] I. G. Murgulescu and N. I. Ionescu, *Rev. Roumaine Chim.*, **13**, 1533 (1968).
[8] I. G. Murgulescu and N. I. Ionescu, *Rev. Roumaine Chim.*, **11**, 1035 (1966).
[9] N. I. Ionescu, *Rev. Roumaine Chim.*, **14**, 869 (1969).
[10] N. I. Ionescu, Thesis, University Bucharest, 1969.

Revue Roumaine de Chimie, 26, 6, 819–827 (1981)

THE EXPLOSIVE COMBUSTION OF PROPYLENE. II.[1]

FLAME SPEED DETERMINATION IN TUBES BY PHOTOGRAPHIC METHODS

R. H. SCHUSTER, * N. I. IONESCU, * D. OANCEA, ** D. POPESCU * and V. GOŞA *

* Center of Physical Chemistry, Bucharest, Spl. Independenţei 202, Romania
** Department of Physical Chemistry and Electrochemical Technology of the Polytechnic Institute, Bucharest, Bd. Republicii 13, Romania

Received June 21, 1980

The explosive combustion of propylene in air, at subatmospheric initial pressures, was studied using the flame pictures and the continuous record of the flame motion on a rotating drum. By means of these methods, the flame velocities in mixtures with various propylene concentrations have been determined.

The photographic recording of the flame propagation is very useful in the study of explosive combustions of gaseous mixtures. Two photographic methods are very often used : (a) successive snapshots taken through a rotating disk [2] and (b) continuous recording of the flame propagation with the aid of a rotative drum on which a sensitive photographic film has been mounted.[3,4] As the propylene—air system was not studied from this point of view, we used these two methods as an alternative approach for the characterisation of its explosive combustion.

EXPERIMENTAL

The explosive combustions have been performed in an installation previously described.[1] The explosion cell consisted of a Pyrex glass tube ($\varnothing = 35$ mm ; L = 1 m). The initiation source was an electric spark obtained by the discharge of an induction coil between two stainless steel electrodes, mounted at the cell bottom. On the top-polished edge of the cell, a hard rubber disk was placed, so that the explosion cell could be opened when the pressure exceeded the normal pressure.

The upwards-moving flame was monitored by :

a) successive snapshots taken through the slits of a disk rotating at a known velocity before the objective of a camera ;

b) continuous record of the flame progress on a film fixed on a drum, rotating at a known speed.

The experimental devices were built according to literature description.[5] The instantaneous shots of the flame front were taken through a disk ($\varnothing = 400$ mm) having one or two slits cut as circle sectors $\left(\text{opening } \frac{\pi}{24} \cdots \frac{\pi}{6}\right)$. The disk was rotating at a variable speed (200—1150 r.p.m.). Several dark marks were uniformly laid on the explosion cell at distances of

50 or 100 mm. These marks allow the exact identification of the flame position as compared to the initiation source, as well as the calculation of the object to image ratio. In the continuous recording of the flame progress, the flame image was casted on a film mounted on the external side of a drum ($\varnothing = 142$ mm, $h = 62$ mm) rotating with variable speed of 50—300 r.p.m. Knowing the linear velocity of the film (v_1), the angle α of inclination which the path of the flame front forms at any point with the direction of the film movement and the object to image ratio (f), the velocity of flame propagation (v_f) can be calculated by the following relation :

$$v_f = f\, v_1 \operatorname{tg} \alpha \tag{1}$$

Reagents : Propylene of 99.4 % purity was used. Air was dried by means of several columns filled with H_2SO_4 (c), KOH (gr), P_2O_5 on glass wool and molecular sieves of 5 Å. The propylene — air mixtures were prepared by the partial pressures method, using the installation previously described.[1]

RESULTS AND DISCUSSION

During the explosive combustion of a gaseous mixture, the flame propagation has specific features, depending upon the volume and geometry of the explosion vessel.[6] If the explosion takes place in a long tube, the walls do not allow a uniform thermal expansion of the burned gas and therefore, the currents caused by the gas expansion in a closed cell reach much higher velocities than in an open vessel.

The experiments described in this paper deal with combustion waves propagating in tubes which are closed by a hard disk at the top, within two initial pressure ranges :

a) initial pressures for which the maximum explosion pressure (P_{max}) is lower than the atmospheric pressure, so that the explosion takes place in a closed cell.

b) initial pressures for which, at the same mixture composition, the explosion pressure exceeds the atmospheric pressure and starting from that time, the explosion takes place in an open cell.

The experiments have been performed using several propylene—air mixtures, whose composition (4.35 ; 4.65 and 4,75 % propylene) was close to the stoichiometric composition.

The combustion wave propagation in a closed tube

The study of propylene explosive combustion in a closed tube revealed some interesting aspects. Considering an explosion initiated by a spark produced near the cell bottom, the combustion wave has a spherical symmetry in the first moments after the initiation. After the impact with the tube walls, the wave front becomes flat. The flame profiles situated at the lower part in figure 1.a and 1.b support this idea, which was already suggested by other authors.[7]

Usually, the front profile has a complicated internal structure caused by the compressed fresh gas flowing toward it. As a consequence, whole portions of unburned gas can get behind the flame front, where they then burn. This fact can be observed within the flame front situated at the lower part in figure 1.a, where the shining streaks moving in the opposite direction as compared to the flame front indicate the turbulent flow of the unburned gas streaming towards the burned gas. This turbulence results in an increasing burning surface, which causes an acceleration of the flame and a stronger distortion of the flame front. After a short acceleration period, as the combustion wave is getting closer to the upper part of the explosion tube, it is decelerated. This fact can be seen at the upper part in figures 1.a and 1.b, as the flame front images are getting closer and closer.

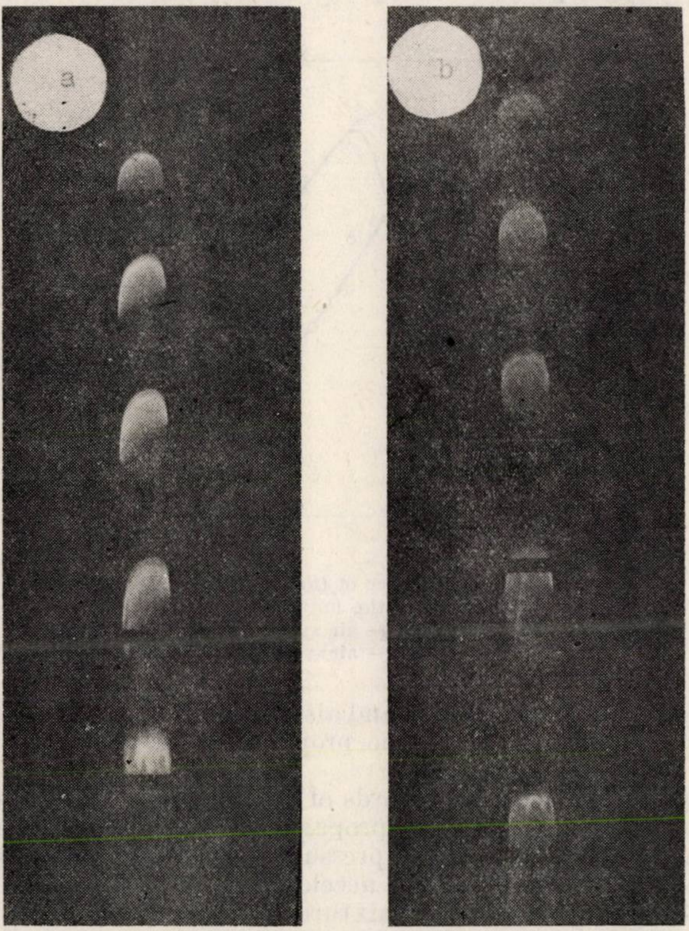

Fig. 1. — Flame profiles obtained by the method of instantaneous shots. Distance between the dark marks : 10 cm.
a) 2.50 % propylene — air system, at $P_0 = 6.66 \cdot 10^4$ Pa. Exposure time = 0.0083 s ; time between two successive exposures = 0.041 s.
b) 4.75 % propylene — air system, at $P_0 = 2.66 \cdot 10^4$ Pa. Exposure time = 0.0045 s ; time between two successive exposures = 0.011 s.

The diagrams shown in figure 2 depict the changes of the flame front velocity in a closed tube, measured by the method of instantaneous photographic shots. It can be observed a strong flame acceleration in the lower part of the tube, where the flame speed increases when the initial mixture pressure and the propylene concentration increase. In the performed experiments, a steady-state of the flame propagation was not observed. After the first acceleration mentioned above, the combustion wave is slowing down in the upper part of the explosion tube; this observation is consistent with other literature data[3,8] and also with other results obtained from pressure measurements during the propylene — air explosions in closed vessels.[9]

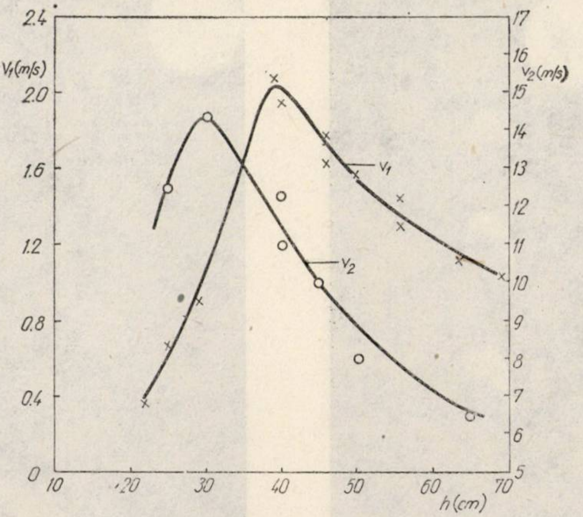

Fig. 2. — The dependence of the flame speed on the distance from the initiation source.
(v_1) — 2.50 % propylene — air system, at $P_0 = 6.0 \cdot 10^4$ Pa.
(v_2) — 4.75 % propylene — air system, at $P_0 = 2.66 \cdot 10^4$ Pa.

Using the photographic records of the flame with the aid of a rotating drum, the combustion wave propagation in the explosion tube could be observed in detail. Within the pressure range $(4.0 \ldots 6.7) \cdot 10^4$ Pa, the explosion starts by a strong flame acceleration, until the speed is 60 cm/s (for the 4.35% propylene — air mixture, at $P_0 = 6.7 \cdot 10^4$ Pa). After the first third of the tube, the flame propagation is hampered and the flame performs some oscillations, which can be observed in figures 3 and 4. The appearance of such oscillations during the flame propagation was usually observed in systems supporting slowly moving combustion waves.[8,10,11] This type of perturbations was observed in all our experiments and seems to be responsible for the flame slowing-down. The diagram of the flame velocities versus the distance h from the initiation source shows clearly the decrease of the flame speed caused by these oscillations, irrespective of the initial mixture pressure — figure 5. At the same time, it is seen that the oscillations appearance is faster as the initial pressure and the initial flame velocity have greater values, in good agreement with an earlier observation.[12] In a closed container in which a flame is progressing, initially accelerated, a weak gas oscillation is stimulated. The reaction velocity is always increased if a densification passes the reaction zone; the

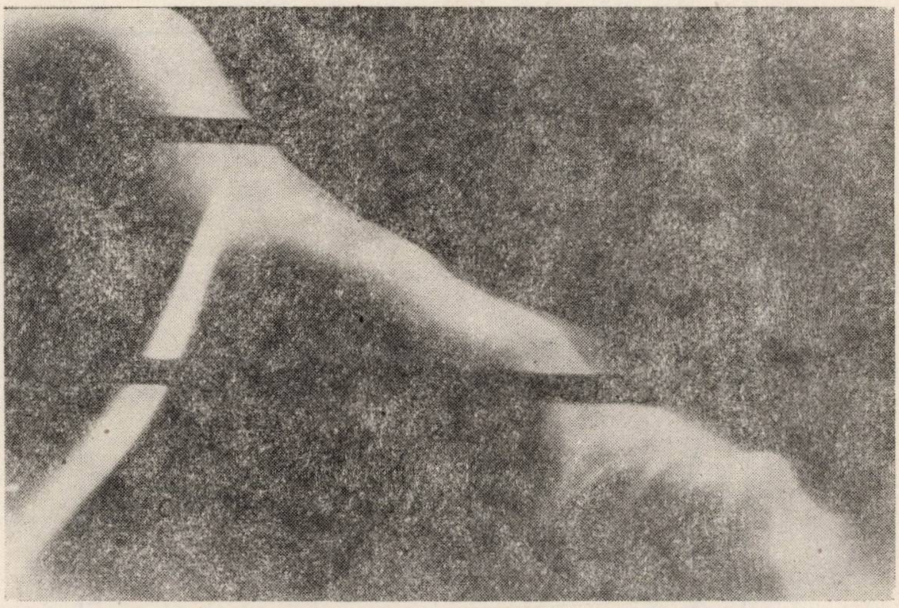

Fig. 3. — Photographic record of the flame propagation on a rotative drum in the 4.35 % propylene — air system, at $P_0 = 4.66 \cdot 10^4$ Pa ; distance between the dark marks = 10 cm.

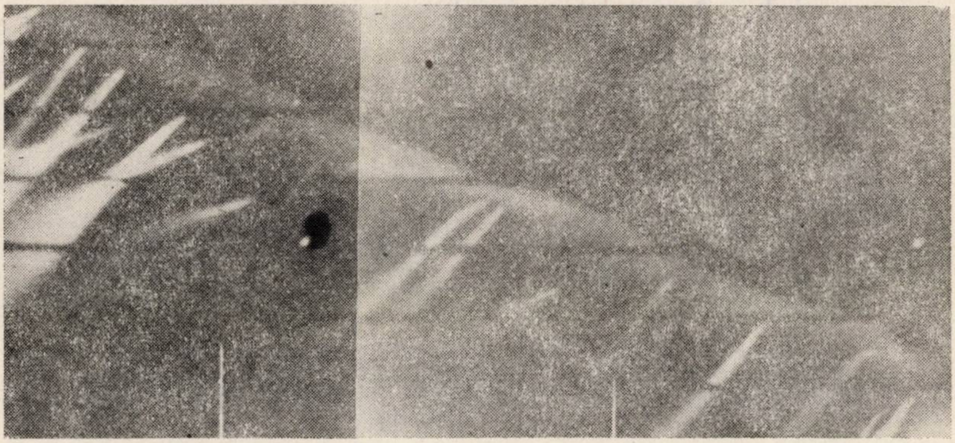

Fig. 4.—Photographic record of the flame propagation on a rotative drum in the 4.35 % propylene — air system, at $P_0 = 6.66 \cdot 10^4$ Pa ; distance between the dark marks = 5 cm.

reverse is true for the troughs of the wave. It would not be implausible that just such a process took place in slow-burning systems, where the wave often passes across the flame front.[12]

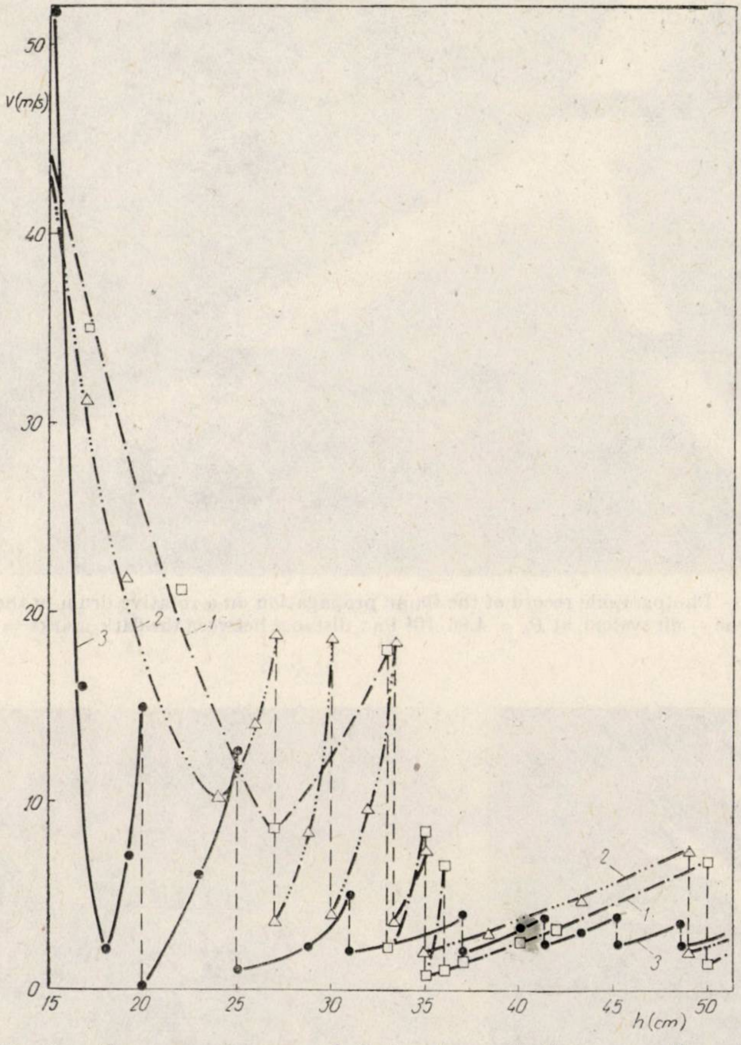

Fig. 5. — Flame speeds measured during the oscillating propagation of the flame in a closed tube, at various distances *h* from the initiation source ; 4.35 % propylene — air system (*1*) $P_0 = 4.66 \cdot 10^4$ Pa ; (*2*) $P_0 = 5.33 \cdot 10^4$ Pa ; (*3*) $P_0 = 6.66 \cdot 10^4$ Pa.

During the flame propagation, another important aspect is the cooling of the burned gas, which is promoted by the gas oscillations, contributing then to the overall slowing-down of the flame propagation.

Another phenomenon which can be observed in the successive snapshots of the flames consists in the shining streaks, which start behind the flame front and propagate in the opposite direction — figures 3.4. It was suggested that the fresh gas, which is streaming towards the burned gas, can also get behind the flame front, where it can burn, producing then the shining streaks. In figure 4, the shining streaks appear with a good periodicity and are of three different kinds, according to their mean speed : 9.20 ; 5.60 and 3.70 m/s. Generally, the descendent wave appears when the flame speed reaches a maximum value during its oscillations.

In the second third of the tube, the wave propagation is perturbed only by weak oscillations, which can be neglected. The propagation speeds obtained in this case are shown in table 1.

TABLE 1

Flame speeds measured in the second third of the explosion tube, for propylene—air mixtures, at various initial pressures

$[C_3H_6]$ (vol %)	$P_0 \cdot 10^{-4}$ (Pa)	v (m/s)
4.35	4.66	2.90
	5.33	2.95
	6.66	3.30
4.75	4.00	8.1
	4.66	9.1
	5.33	10.9

It must be observed that the evolution of the combustion is the same in all these cases, but the speed values change to a great extent even when the experimental conditions are rigorously maintained constant. A good reproducibility in flame speed measurements depends on the experimental conditions[13,14]; according to some authors,[15] even under the same experimental conditions, the flame propagation can have different speeds. At the same time, in several experiments performed under the same conditions, the shining streaks do not appear with the same frequency as in the explosion shown in figure 4.

The combustion wave propagation in an open tube

The explosions of the 4.75% propylene — air mixture taking place at initial pressures higher than $5.33 \cdot 10^4$ Pa, blow up the closing disk of the explosion tube with an increasing speed, as the initial pressure is closer to the atmospheric pressure. In this case, the characteristics of the propagation process change ; the main feature of the explosion is a stronger acceleration of the wave as compared to the explosion in closed tubes, accompanied by a loud deep sound and an intense yellow light emission. These direct observations are completed by instantaneous shots. Even at the shortest exposure time, the photographs do not present any more a succession of flame profiles, but a single bright image of the front flame and some shining streaks produced by the reflected waves. As it is seen in figures 6.a and 6.b, the flame profile is split in two parts because of the fresh gas penetration behind the flame front into the burned hot gas. In this place, the fresh gas burns, forming the descendent waves. The sooner the explosion tube opens (at higher initial pressures), the stronger is the turbulence which causes the changes of the propagation phenomenon. For instance, in figure 6.a (explosion in a closed tube), the flame profile is flat and a single shining streak goes through the burned gas ; in figure 6.b (explosion in an open tube), at the same distance from the initiation source, the phenomenon is much more complex. A significant number of shining streaks pass across the flame front and moreover, the gas turbulence results in two descendent waves. A good image of such a wave is shown in figure 6.c. When the flame spreads above the open end of the explosion tube, a last descendent wave propagates, with a high speed, in the burned gas. At the lower part of the tube, an earlier descendent (reflected) wave can be seen, which is reached by a subsequent wave. In this case, the flame speed is much higher than in a closed tube, as it can be seen from tables 1 and 2, comparing the experiments performed at $P_0 = 5.5\cdot10^4$ Pa (when the combustion wave opened the explosion tube) and $P_0 = 5.33\cdot10^4$ Pa (when the explosion occurred in a closed tube). The further rise of the initial pressure results in a significant increase of the flame velocity (at the same distance from the initiation source).

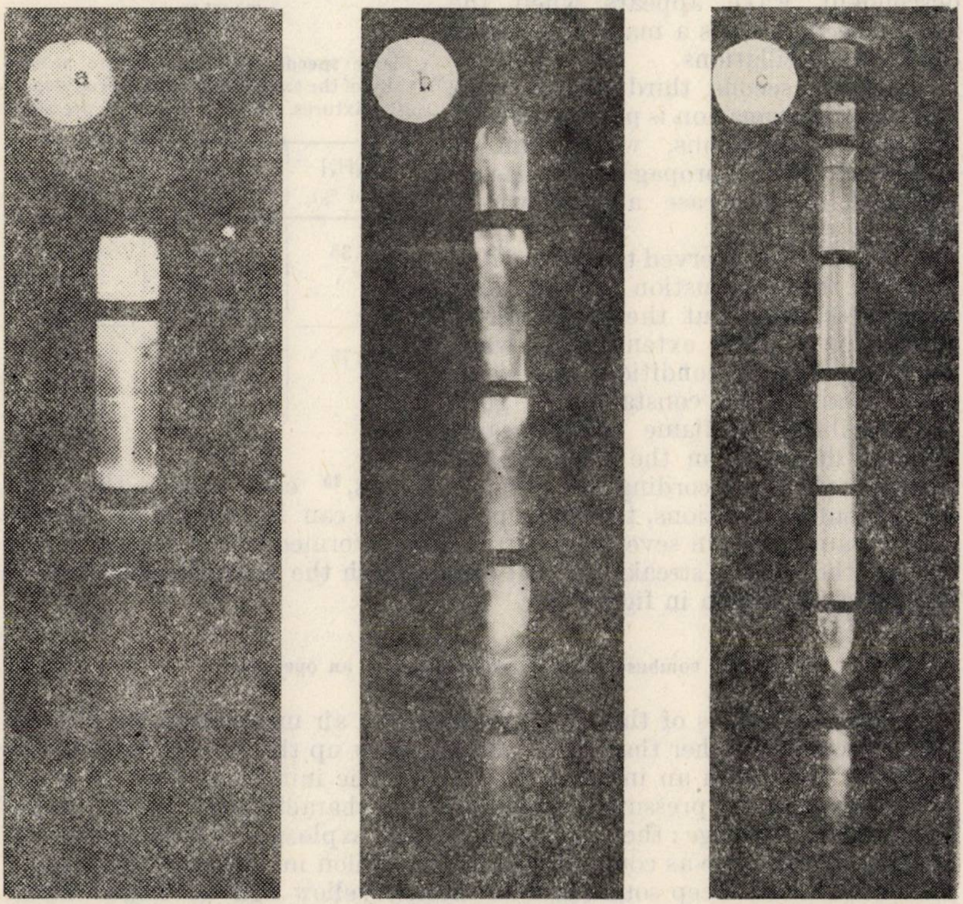

Fig. 6. — Flame front images obtained by the method of instantaneous shots in the propylene—air system (4.75 % C_3H_6). Distance between the dark marks = 10 cm. Exposure time = 0.0022 s. (a) $P_0 = 5.33\cdot10^4$ Pa ; (b) and (c) $P_0 = 6.66\cdot10^4$ Pa.

One can conclude that the photographic recording of the flame propagation, as well as pressure measurements made during the explosions in closed vessels, are very useful for the qualitative and quantitative description of the phenomena which occur during the evolution of the explosive combustion of gaseous mixtures. If the explosion propagates in a closed tube, the combustion wave is continuously slowed down, as the wave is approaching the end of the tube. When the explosion takes place in an open tube, the burned gas expansion towards the open end results in a strong turbulence, which causes a continuous flame acceleration.

TABLE 2

Flame speeds measured in open tubes, at various distances from the initiation source, for the 4.75 % propylene – air system

$P_0 \cdot 10^{-4}$ (Pa)	Distance from the initiation source (cm)	v (m/s)
5.50	27	60
	38	87
	59	116
	65	132
6.66	25	190
	27	197
	35	256

REFERENCES

[1] D. Popescu, V. Goşa, R. H. Schuster, N. I. Ionescu and D. Oancea, *Rev. Roumaine Chim.*, **26**, 197 (1981).
[2] C. Ellis and W. A. Kirkby, "Flame", Methuen, London, 1936.
[3] E. Mallard and H. Le Châtelier, *Ann. Mines*, **4**, 274 (1883).
[4] W. Payman and R. Wheeler, *J. Chem. Soc.*, **1932**, 1251.
[5] W. Jost, "Explosions- und Verbrennungsvorgänge in Gasen", Springer Verlag, Berlin, 1939, p. 90–91.
[6] H. G. Wagner, *Chemie-Ing. Techn.*, **47**, 223 (1975).
[7] C. Ellis, *Fuel*, **7**, 502 ; 526 (1928).
[8] W. A. Bone and R. P. Fraser, *Phil. Trans. Roy. Soc. London*, **228**, 28 (1928).
[9] N. I. Ionescu, D. Oancea, D. Popescu, V. Goşa and R. H. Schuster, in preparation.
[10] R. V. Oettingen and F. Gernet, *Ann. Phys. u. Chem.*, **33**, 63 (1935).
[11] B. Lewis and G. von Elbe, *J. Chem. Phys.*, **3**, 63 (1935).
[12] W. Jost, "Explosions- und Verbrennumgsvorgänge in Gasen", Springer Verlag, Berlin, 1939, p. 141–142.
[13] W. Payman and R. Wheeler, *J. Chem. Soc.*, **1923**, 1251.
[14] W. Payman and R. Wheeler, *J. Chem. Soc.*, **1932**, 1835.
[15] W. A. Bone, R. P. Fraser and D. A. Winter, *Proc. Roy. Soc. (London)*, **A 114**, 402 (1927).

Revue Roumaine de Chimie, **26**, *6*, 829–835 (1981)

L'ACTIVITÉ D'UN SEL À HAUTES CONCENTRATIONS DANS L'EAU PURE

MAURICE ABRAHAM
Département de Chimie, Université de Montréal, Case postale 6210, Succursale A,
Montréal, Québec, Canada H3C 3V1

Reçu le 4 mars 1980

L'équation suivante est obtenue qui donne l'activité a_s d'un sel dans un mélange binaire contenant de l'eau et ce sel, valable probablement pour des fractions molaires de sel plus grandes que 0.5

$$\frac{\lambda(1-x_s)}{x_s(1-\lambda)} = \frac{r}{c} + \frac{r(c-1)}{c}\lambda$$

avec

$$\lambda = a_s^{\frac{1}{r}}$$

r et c sont les constantes B.E.T. habituelles apparaissant dans l'équation Stokes-Robinson. On discute comment ces équations, et le fait que les constantes B.E.T. suivent certaines règles simples d'additivité pour certains systèmes contenant plus d'un sel pourraient conduire à quelques progrès dans le traitement thermodynamique de solutions aqueuses très concentrées d'un sel. Les règles d'additivité sont attribuées à la dissociation des sels en ions et à la prédominance d'interactions à courte distance.

The following equation is derived, giving the activity a_s of a salt in a binary mixture containing water and one salt, probably valid for salt mole fractions $x_s > 0.5$

$$\frac{\lambda(1-x_s)}{x_s(1-\lambda)} = \frac{r}{c} + \frac{r(c-1)}{c}\lambda$$

where

$$\lambda = a_s^{\frac{1}{r}}$$

r and c are the usual B.E.T. constants appearing in the Stokes-Robinson equation. It is discussed how these equations and the conformity of the B.E.T. constants of some systems containing more than one salt to simple additivity rules, could lead to some progress in the thermodynamic treatment of very concentrated aqueous solutions of one salt. The additivity rules are attributed to the ionic dissociation of salts and the predominance of short range interactions.

INTRODUCTION

Les propriétés thermodynamiques des solutions aqueuses concentrées d'électrolytes ont été moins étudiées que les solutions diluées, aussi bien sur le plan expérimental que sur le plan théorique. Une raison peut être trouvée dans l'existence des limites de solubilité et la nécessité d'augmenter la température pour les repousser. Mais une autre raison vraisemblablement de grande importance est la difficulté d'étendre aux solutions concentrées les concepts issus des travaux sur les solutions diluées.

Peu à peu l'idée s'est quelque peu imposée que davantage de progrès dans la compréhension des solutions concentrées d'électrolytes pourrait provenir de l'étude des sels fondus considérés comme le cas extrême des solutions très concentrées. Dans la perspective où les sels fondus et les solutions aqueuses très concentrées soulèvent des problèmes communs, [1-12] des études de pressions de vapeur de ces dernières solutions ont conduit à quelques résultats intéressants concernant des systèmes contenant des nitrates et chlorures alcalins et alcalino-terreux.[2,13-18] Il est apparu dans ces études que le modèle B.E.T.[19] peut fournir une base théorique de discussion par l'intermédiaire de l'équation de Stokes et Robinson [20] qui en dérive. Celle-ci donne l'activité de l'eau. Or il peut être utile pour la suite des recherches de disposer d'une équation donnant l'activité d'un sel sur la base du même modèle, même si le résultat se trouve pour l'instant limité à des systèmes binaires aqueux ne contenant qu'un seul sel.

CALCUL ET DISCUSSION

Posons,

a_s : activité du sel

x_s : fraction molaire du sel

N_s : nombre de moles de sel

m : nombre de sites d'adsorption disponibles dans le sel fondu

r : rapport molaire des sites au sel

n_0 : nombre total de molécules d'eau

n : nombre de molécules d'eau adsorbées sur les sites disponibles dans le sel fondu

E : énergie d'adsorption d'une molécule d'eau sur un site

E_L : énergie de liquéfaction relative à une molécule d'eau

A : nombre d'Avogadro

k : constante de Boltzmann

Les paramètres m et r sont reliés par les expressions

$$m = n_s r \quad \text{et} \quad n_s = N_s A$$

D'après le modèle B.E.T. [19-21] l'entropie de mélange du sel fondu et de l'eau peut s'exprimer par

$$[1] \qquad \Delta S = k \ln W.$$

avec

$$[2] \qquad W = \frac{m!}{n!(m-n)!} \times \frac{(n_0-1)!}{[(n_0-1)-(n-1)]!(n-1)!}$$

Comme n et n_0 sont des grands nombres, [2] peut d'écrire :

$$[3] \qquad W = \frac{m!}{n!(m-n)!} \times \frac{n_0!}{(n_0-n)!n!}$$

En appliquant l'approximation de Stirling suivante :

$$\ln x! = x \ln x - x$$

la relation [3] devient

$$\ln W = m \ln m + n_0 \ln n_0 - 2n \ln n - (m - n) \ln (m - n) - \\ - (n_0 - n) \ln (n_0 - n) \tag{4}$$

Par ailleurs l'enthalpie de mélange du sel et de l'eau s'exprime par

$$\Delta H = n(E - E_L) = n\Delta E \tag{5}$$

Et l'enthalpie libre de mélange est donnée par

$$\Delta G = \Delta H - T\Delta S$$

qui, compte tenu de [5] et [1] s'exprime par

$$\Delta G = n\Delta E - kT \ln W \tag{6}$$

A l'équilibre thermodynamique, n doit être tel que :

$$\frac{\partial G}{\partial n} = 0$$

ou

$$\Delta E - kT \frac{\partial \ln W}{\partial n} = 0 \tag{7}$$

D'après [4],

$$\frac{\partial \ln W}{\partial n} = \ln \frac{(m - n)(n_0 - n)}{n^2} \tag{8}$$

Avec [8], [7] devient :

$$\frac{n^2}{(m - n)(n_0 - n)} = \exp\left(-\frac{\Delta E}{kT}\right) = c \tag{9}$$

En introduisant la relation [9] dans la relation [4], celle-ci donne :

$$\ln W = m \ln \frac{m}{m - n} + n_0 \ln \frac{n_0}{n_0 - n} + \frac{n\Delta E}{kT} \tag{10}$$

Les relations [6] et [10] permettent alors d'exprimer l'enthalpie libre de mélange par :

$$\Delta G = kT \left(m \ln \frac{m - n}{m} + n_0 \ln \frac{n_0 - n}{n_0} \right) \tag{11}$$

Jusqu'ici le déroulement des calculs est proche de celui suivi par Hill [21] pour démontrer l'équation B.E.T. par la thermodynamique statistique. Cependant le formalisme employé ici est différent et simplifié.

L'expression [11] permet de retrouver directement l'équation de Stokes et Robinson[20] en dérivant ΔG par rapport à n_0. Si [11] donne ainsi accès à l'activité de l'eau, on doit s'attendre à ce que l'activité du sel soit aussi calculable à partir du même point de départ.

Ainsi l'activité a_s du sel est donnée par [12]

$$kT \ln a_s = \frac{\partial \Delta G}{\partial n_s} \tag{12}$$

D'après [11] et [12] :

$$\ln a_s = \frac{\partial}{\partial n_s}\left[m \ln \frac{m-n}{m} + n_0 \ln \frac{n_0 - n}{n_0} \right] \tag{13}$$

Comme $m = n_s r$, on a aussi

$$\ln a_s = \frac{\partial}{\partial n_s}\left[n_s r \ln \frac{n_s r - n}{n_s r} + n_0 \ln \frac{n_0 - n}{n_0} \right] \tag{14}$$

Tous calculs faits, [14] se transforme en :

$$\ln a_s = r \ln \frac{n_s r - n}{n_s r} + \frac{rn}{n_s r - n} - \left[\frac{rn_s}{rn_s - n} + \frac{n_0}{n_0 - n} \right] \frac{\partial n}{\partial n_s} \tag{15}$$

Par ailleurs l'équation [9] peut s'écrire

$$n^2\left(\frac{1}{c} - 1\right) + mn = n_0(m - n) \tag{16}$$

d'où

$$\frac{\partial n}{\partial n_s} = \frac{r(n_0 - n)}{2n\left(\frac{1}{c} - 1\right) + m + n_0} \tag{17}$$

En tirant de [16] une expression de $\left(\frac{1}{c} - 1\right)$ et l'introduisant dans [17] on obtient

$$\frac{\partial n}{\partial n_s} = \frac{rn(n_0 - n)}{2n_0 m - n_0 n - mn} \tag{18}$$

Ensuite de [15] et [18] on trouve

$$\ln a_s = r \ln \frac{n_s r - n}{n_s r} \tag{19}$$

D'où

[20] $$\frac{n_s r - n}{n_s r} = a_s^{\frac{1}{r}}$$

Posons :

[21] $$a_s^{\frac{1}{r}} = \lambda$$

Alors [20] et [21] donnent :

[22] $$n_s r - n = n_s r \lambda \quad \text{et}$$

[23] $$n = n_s r (1 - \lambda)$$

En introduisant [22] et [23] dans [9] on obtient :

[24] $$(1 - \lambda)^2 = c\lambda \left[\frac{n_0}{n_s r} - (1 - \lambda) \right]$$

Par définition de la fraction molaire du sel x_s on a :

[25] $$\frac{n_0}{n_s} = \frac{1 - x_s}{x_s}$$

Finalement, [25] et [24] donnent :

[26] $$\frac{\lambda(1 - x_s)}{x_s(1 - \lambda)} = \frac{r}{c} + \frac{r(c - 1)}{c} \lambda$$

avec λ lié à l'activité du sel a_s par $\lambda = a_s^{\frac{1}{r}}$

L'équation [26] présente une certaine analogie de forme avec l'équation de Stokes et Robinson [20] laquelle s'écrit :

[27] $$\frac{a_e(1 - x_e)}{x_e(1 - a_e)} = \frac{1}{cr} + \frac{(c - 1)}{cr} a_e$$

avec les mêmes significations s'attachant aux paramètres c et r, mais ici a_e étant l'activité de l'eau et x_e sa fraction molaire. On passe de [27] à [26] en changeant r en $\frac{1}{r}$, a_e en $a_s^{\frac{1}{r}}$ et x_e en x_s.

Dans le cas où les propriétés d'un sel seraient telles que $r = 1$ l'équation [26] aurait la même forme que celle de Stokes et Robinson. [20]

L'équation [26] ne donne évidemment que l'activité du sel dans un système binaire (sel + eau). Par contre, l'intervalle de concentration pourrait être compris entre 0,5 et 1 puisque le modèle B.E.T. semble vérifié dans cet intervalle d'après des études récentes.[2,13-18]

Pour appliquer l'équation [26] il faut déterminer c et r caractéristiques d'un sel. Ceci doit être réalisé en principe par le tracé de l'isotherme B.E.T. Or cette opération n'est pas toujours expérimentalement possible pour des sels purs, à cause des limites de solubilité, des points de fusion trop élevés, des pressions de vapeur grandes et augmentant rapidement avec la température. Il se pourrait que ces difficultés puissent être contournées, dans certains cas tout au moins, s'il se confirme que les constantes B.E.T. suivent des règles d'additivité observées lors d'études de solutions contenant plusieurs nitrates.[14,16-18]

Une propriété d'additivité du paramètre B.E.T. r a été constatée, qui s'exprime par la relation

$$r = r_0 + (r_1 - r_0)x_1 \tag{28}$$

r_0 : constante relative à un seul fondu ou mélange de sels fondus d'une composition donnée.
r_1 : constante relative à un autre sel fondu ajouté.
x_1 : fraction molaire du sel fondu ajouté, dans le mélange de sels fondus.

De même, une propriété d'additivité du produit des paramètres B.E.T. «rE» a été aussi constatée, qui s'exprime par

$$rE = r_0E_0 + (r_1E_1 - r_0E_0)x_1 \tag{29}$$

[28] transforme alors la relation [29] en

$$r\Delta E = r_0\Delta E_0 + (r_1\Delta E_1 - r_0\Delta E_0)x_1 \tag{30}$$

avec

$$\Delta E_0 = E_0 - E_L$$
$$\Delta E_1 = E_1 - E_L$$

E_0 et E_1 étant définis comme r_0 et r_1.

Les propriétés exprimées par les relations [28] et [30] sont compatibles avec plusieurs caractères que l'on reconnaît souvent aux sels fondus.[1-12] Ces propriétés pourraient, en effet, être les conséquences d'une dissociation totale en ions, de la conservation de ces entités ioniques quand on passe des sels purs à leurs mélanges, et de la prédominance des interactions à courte distance dans le phénomène d'adsorption de l'eau. Lorsque des molécules d'eau viennent s'insérer entre un cation et ses plus proches voisins qui sont des anions, r et E dépendent en premier lieu de la nature de ce cation et de ses plus proches voisins anioniques. Les cations voisins plus éloignés influenceraient relativement peu r et E. Autrement dit, les caractéristiques configurationnelles reflétées par r et les caractéristiques énergétiques reflétées par E, seraient surtout imposées par l'environnement local. Si on substitue un cation M_1 à un cation M_0, on change localement r_0 en r_1 et E_0 en E_1. La conservation des entités ioniques fait que dans les mélanges les valeurs de r_0, r_1, E_0 et E_1 sont proches de leurs valeurs dans les sels purs. On mesure alors avec un mélange une moyenne de r_0 et r_1, et une moyenne de r_0E_0 et r_1E_1.

Par contre, on s'attendrait à ce que ces lois simple d'additivité n'apparaissent par quand les mélanges sont accompagnés de réactions chimiques et de la formation de complexes.

BIBLIOGRAPHIE

[1] J. Braunstein, Chapitre 4 dans «Ionic Interactions : From Dilute Solutions to Fused Salts », Vol. I. Edité par D. S. Petrucci, Academic Press, New York, 1971.

[2] H. Braunstein et J. Braunstein, *J. Chem. Thermodyn.*, **3**, 419 (1971).

[3] Y. K. Delimarskii et B. F. Markov, « Electrochemistry of Fused Salts », Sigma Press, Washington, 1961.

[4] G. Charlot et B. Tremillon, «Les réactions chimiques dans les solvants et les sels fondus », Gauthier-Villars Editeurs, Paris, 1963.

[5] M. Blander, « Molten Salts Chemistry », Interscience Publishers, New York, 1964.

[6] J. Lumsden, « Thermodynamics of Molten Salts Mixtures », Academic Press, New York, London, 1966.

[7] G. J. Janz, « Molten Salts Handbook », Academic Press, New York, 1967.

[8] M. Rolin, «L'électrochimie dans les sels fondus », dans « Introduction aux méthodes életrochimiques », Coordonnateur : J. Robin, Masson et Cie Editeurs, Paris, 1967.

[9] H. Bloom, « The Chemistry of Molten Salts », W. A. Benjamin Inc., New York, Amsterdam, 1967.

[10] G. Morand et J. Hladik, « Electrochimie des sels fondus », Masson et Cie Editeurs, Paris, 1969.

[11] G. E. Blomgren, Chapitre 10 dans « Physical Chemistry, An advanced Treatise », Vol 1 × B. Edité par H. Eyring, Academic Press, New York, London, 1970.

[12] J. Braunstein, G. Mamantov et G. P. Smith, « Advances in Molten Salt Chemistry », Plenum Press, New York, 1971.

[13] M. C. Trudelle, M. Abraham et J. Sangster. *Canad.* J. *Chem.*, **55**, 1713 (1977).

[14] J. Sangster, M. C . Abraham et M. Abraham. *Canad. J. Chem.*, **56**, 348 (1978).

[15] M. C. Abraham, M. Abraham et J. Sangster. *Canad. J. Chem.*, **56**, 635 (1978).

[16] M. C. Abraham, M. Abraham et J. Sangster. *J. Chim. Phys.*, **76**, 125 (1979).

[17] J. Sangster, M. C. Abraham et M. Abraham. *J. Chem. Thermodyn.*, **11**, 619 (1979).

[18] M. C. Abraham, M. Abraham et J. Sangster, *J. Sol. Chem.*, **8**, 647 (1979).

[19] S. Brunauer, P. M. Emmet et E. Teller. *J. Amer. Chem. Soc.*, **60**, 309 (1938).

[20] R. H. Stokes et R. A. Robinson, *J. Amer. Chem. Soc.*, **70**, 1870 (1948).

[21] T. L. Hill, *J. Chem. Phys.*, **14**, 263 (1946).

Revue Roumaine de Chimie, 26, 6, 837–842 (1981)

ELECTRICAL CONDUCTIVITY OF A COMPLEX BISMUTH–MOLYBDENUM CATALYST IN THE REACTION OF PROPYLENE OXIDATION

MONICA CĂLDĂRARU, P. BANYAI and N. I. IONESCU
Center of Physical Chemistry, Spl. Independenţei 202, Bucharest, Romania

Received December 10, 1980

The simultaneous determination of electrical conductance and of activity of a complex bismuth – molybdenum catalyst in the reaction of propylene oxidation showed a sharp change of these properties around 583 K. The kinetic parameters showed a unitary reaction order in respect to the propylene partial pressure and an overall activation energy of 46.4 kJ/mol.

Important information on the mechanism of catalytic reactions can be obtained by electrical conductivity measurements. Correlated with kinetic and catalytic activity data, they are very useful for the understanding of catalysis on oxides.

In the most usual case, the sample is a polycrystalline specimen ; in this case, difficulties appear in the interpretation of the results obtained by d.c. measurements, as the total resistance is a complicated function of grain and contact resistances.

Using a.c. measurements, under certain frequency ranges, is possible to obtain the simplification of the used relations ; under certain specific conditions, even a separation between characteristics of the surface and "bulk" material can be made.[1,2]

In this paper we report a.c. conductivity measurements on a complex bismuth – molybdenum oxide catalyst during the selective oxidation of propylene to acrolein, as a continuation of our earlier results in this field.[3-6]

EXPERIMENTAL

The experiments were run at atmospheric pressure in a single pass integral flow reactor which allows the determination of the electrical conductance and catalytic activity simultaneously.[3] The electrodes were two coaxial nickel cylinders ($\varnothing = 8$ and 22 mm). The catalyst grains filled the space between the electrodes.

The mixing of the reaction gases occurs at the bottom of the reactor, which was heated in a molten salts bath. The temperature range was between 533 and 673 K, monitored with a chromel-alumel thermocouple inserted in the middle of the catalyst bed.

The propylene was 99.7% pure.

A complex molybdenum–bismuth oxide catalyst of general formula $Ni_{1.8}Fe_{2.4}Bi_{2.3}Zn_{0.6}P_{0.6}Mo_{12}O_x$ prepared by coprecipitation and supported on 25% SiO_2 was used.

The kinetic measurements have been done by following the propylene conversion in the temperature range 573–653 K, using propylene-air mixtures as 1 : 8, 1 : 10, 1 : 12, 1 : 15.

The product distribution was determined by an in-line Pye series 104 gas chromatograph, using two parallel 1.5 m columns (Porapak Q and molecular sieves) and a thermal conductivity detector.

The a.c. conductance measurements were performed with a Tesla semiautomatic precision bridge BM 484 with a frequency of 1592 Hz.

RESULTS AND DISCUSSIONS

The preliminary measurements showed that important changes of conductance occur during the experiments, and these changes are sensitive to the reaction conditions.

The overall behaviour of the sample indicated an n-type semiconduction.

The uncertain geometry of the grains made it pointless to calculate the specific conductances; in our case the obtained information refer to the overall changes of the conductance in different reaction conditions.

a) Kinetic measurements

The measurements of the catalytic activity showed (Figure 1) a sharp increase of the conversion (by a factor of 2 or 3) at 573 K. At 648 K, the propylene conversion was lower for the reaction mixtures with higher propylene contents (Figure 1).

The selectivity for acrolein is higher when the reaction mixture contains more propylene; in this case the selectivity for the total oxidation products is lower (Table 1).

From the kinetic measurements, a unitary reaction order in respect to the propylene partial pressure was established; the comparison of the experimental conversion plots with the theoretical one indicated a unitary overall reaction order.

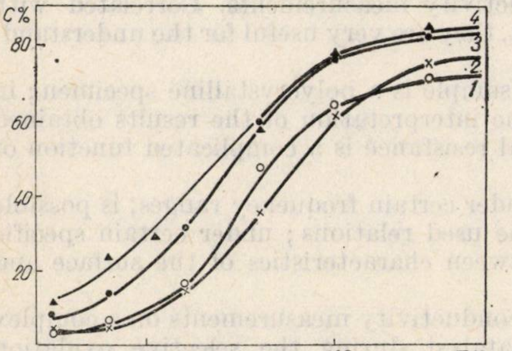

Fig. 1. – The temperature variation of the propylene conversion for different mixtures propylene : air 1 : 8 (curve *1*); 1 : 10 (curve *2*); 1 : 12 (curve *3*); 1 : 15 (curve *4*).

The calculated overall activation energy from an Arrhenius plot in the temperature range 573–653 K is 46.4 kJ/mol.

b) Electrical conductance measurements

In figure 2 the dependence of conductance G, $\ln G = f(1/T)$ is presented for several runs in which air or argon flow on the catalyst in its normal oxidised state, or in the reduced state. One experiment was done

TABLE 1

The propylene conversion and selectivities for the principal products (acrolein and $CO + CO_2$) in the propylene oxidation on the $Ni_{1.8}Fe_{2.4}Bi_{2.3}Zn_{0.6}P_{0.6}Mo_{12}O_x$ catalyst, using propylene : air mixture as 1 : 8, 1 : 10, 1 : 15, $\tau \sim$ 4s.

C_3H_6 : air mixture	T K	Conversion %	Selectivity for $CH_2{=}CHCHO$ %	Selectivity for $CO + CO_2$ %
1 : 8	548	3.0	68.6	22.2
	563	5.7	72.7	19.7
	583	16.1	71.8	22.8
	603	47.1	71.5	17.5
	623	63.1	68.1	17.4
	648	71.4	61.5	19.4
1 : 10	548	3.4	64.7	18.4
	563	3.9	65.6	21.6
	583	14.8	71.3	21.4
	603	34.9	70.8	19.2
	623	61.4	69.8	22.2
	648	75.6	61.4	25.1
1 : 15	548	10.7	62.6	22.4
	563	23.4	61.6	19.7
	583	51.3	65.3	23.5
	603	57.2	62.2	25.7
	623	77.8	56.0	31.4
	648	85.2	47.5	37.5

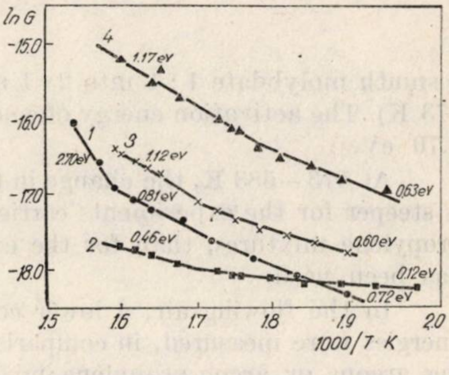

Fig. 2. — $\ln G = f(1/T)$ for the catalyst sample in no-flowing argon (curve *1*, reference sample), flowing air (*2*), flowing argon (*3*) flowing argon after sample reduction with propylene (*4*).

measuring the electrical conductivity in no-flowing argon atmosphere (Figure 2-reference sample).

The dependences $\ln G = f(1/T)$ for different mixtures of propylene-argon and propylene-air (usual reaction mixture) are shown in figure 3, respectively figure 4.

In all experiments, the dependence of the conductance on the temperature presents a change of the slope at 573—583 K, its value being related to the type of the flowing gas used. In expriments with no-flowing argon, an extra change of the slope occurs at 623 K; this could be associated with the transition from the extrinsic conduction range in the low temperature range, to the non-extrinsic one to the higher temperature. Another explanation could be a phase transition in this temperature range (Kumar and Ruckenstein [7] have evidenced a transition of thin films of bismuth molybdate 1 : 1 into 2 : 1 and MoO_2 at low pressures and 623 – 673 K). The activation energy of conduction rises in this case from 0.81 to 2.70 eV.

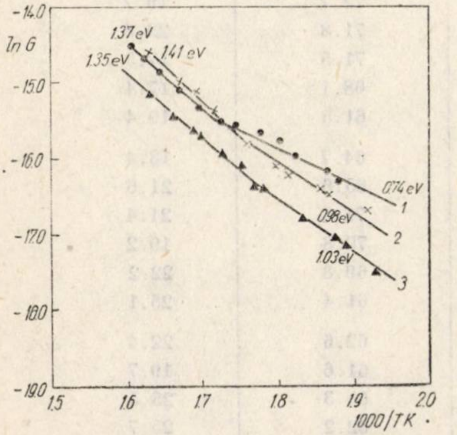

Fig. 3. — ln $G = f(1/T)$, for the catalyst sample in flowing propylene : argon mixtures 1 : 1.85 (*1*); 1 : 1.44 (*2*); 1 : 1 (*3*).

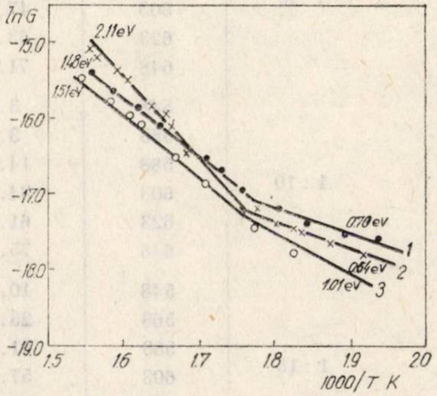

Fig. 4. — ln $G = f(1/T)$ for the catalyst sample in flowing propylene : air mixtures, 1 : 10 (1); 1 : 8 (2); 1 : 15 (3).

At 573 – 583 K, the change in the slope of the electrical conductance is steeper for the experiments carried out in flowing air, argon, or argon-propylene mixtures, than for the experiment in which no-flowing argon has been used.

In the flowing air, a lower conductance and also lower activation energies were measured, in comparison with the experiments done in flowing argon, or argon-propylene mixture, probably due to the saturation of the surface with oxygen, acting as an acceptor species.

It is of particular interest that in experiments performed with propylene – air mixture (Figure 4) the values of conductance were almost in the same order of magnitude as those of the experiments which used propylene – argon mixture. Considering the mechanism of the reaction as a redox type one, these findings support the idea that in the stationary work conditions the catalyst acts in a partially reduced state.[8]

c) General discussion

The interpretation of the conductance Arrhenius plots is not so simple.

For a polycrystalline n-type semiconductor, the electrical conductivity σ is well described by the equation

$$\sigma = [e']\mu_n q \qquad (1)$$

where $[e']$ is the concentration of the conduction electrons in the solid, μ_n is their mobility and q is the electron charge.

For small temperature modifications (no more than 100 K), the electrical conductivity can be satisfactory written as

$$\sigma = \text{const}\ [e'] \qquad (2)$$

because the temperature dependence of the $[e']$ is an exponential one, and is much important than the change of the mobility μ_n in this temperature range.[9]

That means that the electrical conductivity σ is strongly dependent on the nonstoichiometry of the sample, the factor $[e']$ being directly related to the concentration of the defects in the solid sample.

In our case, the electrical conductivity of the catalyst indicates an overall n-type semiconduction. As known, an important role for the n-type electrical conductivity is played by anionic vacances as well as by interstitial cations (with or without valence changes); both kind of defects are finally correlated with the concentration of the conduction electrons. Besides their original formation, these defects can appear during the catalytic reaction too, as follows:

$$\text{propylene} + \text{catalyst} \longrightarrow \text{products} + \text{catalyst} - |\text{O}|^{\bullet} + e' \qquad (3)$$

where catalyst $- |\text{O}|^{\bullet}$ represents an anionic vacance.

In the measurements conditions it is possible that these two kind of defects are differently activated by the temperature; the change of the slope of the conductivity plot at 573–583 K might be explained on the basis of this behaviour.

Experiments in no-flowing argon showed a slow rise of the conductance when the temperature is risen. In flowing argon, due to the mechanical removal of the oxygen adsorbed on the surface, the rise of the conductance is faster, and much faster is this process when the flowing gas contains propylene.

Under 573–583 K, the propylene influence is stronger when the flowing gas is more concentrated with propylene. Above this temperature, no difference in the activation energy of the conductance for different propylene – argon mixtures was evidenced.

This findings suggest that the slope change of the plot of conductance around 573–583 K could be due to the change of the stability (or the type) of the oxygen surface species around this temperature. The sharp increase of the conversion, which other researchers have evidenced too,[10] in the 2-butene oxidation of Fe_2O_3–MoO_3 catalyst, supports this supposition.

Further experiments are in progress.

REFERENCES

[1] T. J. Gray in "Experimental Methods in Catalytic Research", R. B. Anderson, editor, Academic Press, New York, 1968, cap. 7. p. 286.

[2] A. Bielanski, M. Najbar and M. Szimonska-Stachura. *Bull. Pol. Acad. Sci. Ser. Sci. Chim.*, **26**, 249 (1978).

[3] N. I. Ionescu and M. Căldăraru, *Reac. Kin. Catal. Lett.*, **8**, 477 (1978).

[4] N. I. Ionescu, M. Căldăraru and P. Banyai, "Proc. 4th International Symposium Heterogeneous Catalysis, Varna, 1979", D. Shopov, A. Andreev, A. Palazov, L. Petrov, editors, Publishing House of the Bulgarian Academy of Sciences, Sofia, 1979, vol. 1, p. 229.

[5] R. Mănăilă, N. I. Ionescu and M. Căldăraru, *Z. anorg. Chem.*, **466**, 221 (1980).

[6] N. I. Ionescu, P. Banyai, M. Căldăraru and M. Chirca, *Rev. Roumaine Chim.*, **26**, 681 (1981).

[7] J. Kumar and E. Ruckenstein, *J. Solid State Chem.*, **31**, 41 (1980).

[8] J. M. Peacock, A. J. Parker, P. G. Ashmore and J. A. Hockey, *J. Catalysis*, **15**, 397 (1969).

[9] J. M. Hermann, *J. Chim. Phys.*, **73**, 474 (1976).

[10] I. Pasquon, F. Trifiro and G. Caputo, *Chimica e Industria*, **55**, 168 (1973).

Revue Roumaine de Chimie, 26, *6*, 843–850 (1981)

SELF-DIFFUSION OF TELLURIUM IN THE LIQUID Pb–Te EUTECTIC ALLOY

N. PETRESCU* and LUCIA GANOVICI**

* Department of Metallurgy, The Polytechnic, Spl. Independenţei 313, Bucharest, Romania

** Centre of Physical Chemistry, Spl. Independenţei 202, Bucharest, Romania

Received June 18, 1980

The paper gives the results of the experimental determinations of the self-diffusion coefficients of tellurium in the liquid eutectic Pb–Te alloy in the temperature range 475–600°C. The determinations have been made by two methods: the capillary–reservoir method and the plane source method using the radioactive labelling of tellurium. The experimental results on diffusion are discussed in terms of the thermally activated states theory in connection with the viscosity data in the molten Pb–Te alloys. The higher values of the diffusion coefficients in the molten Pb–Te eutectic in comparison with the self-diffusion coefficients in the liquid components (Te or Pb) are consistent with the viscosity minimum at the eutectic composition. The second way of interpreting the experimental data on the self-diffusion of tellurium in the molten Pb–Te eutectic alloy refers to the small fluctuations theory of the liquid; this interpretation allowed the calculation of the maximum distance for diffusive atomic displacement, which proved to be an order of magnitude lower than the interatomic distance in the melt.

The mass transport properties in the liquid Pb–Te alloys have been studied on the whole composition range by viscosity measurements. The viscosity isotherms [1] have made evident some singular points, namely a maximum at the composition of the equiatomic PbTe compound and a minimum at the composition of the Te – PbTe eutectic. The point of the maximum in the viscosity isotherm has been ascribed to the strong interatomic forces in the PbTe compound; these strong interatomic forces are also manifested in the far higher melting point of the compound in comparison with the melting point of the component elements.

The study of the isotherms of the electrical conductivity in the Pb – Te melts,[1] has also put in evidence a minimum at the composition of the PbTe compound, but no peculiarities at the eutectic composition. This is not surprising because the electrical conductivity isotherms have been obtained in a highly overheated eutectic melt, at 924°C, far above the eutectic point (405°C).

To our knowledge the self-diffusion in the Pb–Te melts has not been studied as yet. In this paper we present our results on the self-diffusion of tellurium in the molten eutectic alloy 14.5 at. % Pb – 85.5 at. % Te, in a temperature range from 600 to 475°C. The interest for such determinations is twofold. From a theoretical point of view, self-diffusion determinations result in a better understanding of the structure and properties of the melt. From a practical point of view, the liquid eutectic alloy is a useful solvent for growing single crystals of PbTe compound from easy melting melts.

The growth of a compound from the melts having a composition different from the stoichiometric composition of the compound is a diffusion controlled process ; for this reason the diffusion coefficients in the melt are very important for the calculation of the growth rate. The PbTe compound is especially apt to be grown from nonstoichiometric melts for at least two reasons. First, it has a high melting point (917°C) which makes very difficult its synthesis at the stoichiometric composition, on account of the high volatility of tellurium at such temperatures ; close control of the tellurium partial vapour pression is needed in these conditions. On the second hand, recent studies [2] show a narrow solid state solubility around the stoichiometric composition of the PbTe compound (maximum 0.006 at. % Pb or 0.013 at. % Te) ; this makes the composition of the compound uncertain when synthesised from the component elements. Thus, the growing of the compound from tellurium rich solutions has two advantages : a lower temperature is needed and a more accurate stoichiometry is achieved.

The practical interest of the PbTe compound lies in its semiconducting properties, especially its remarkable thermoelectric power which preserves its high values at high temperatures. The accuracy of the stoichiometry of the compound is highly important in this respect, because a slight exces of Te or Pb results in drastic modifications of the properties, namely a change of sign of the thermoelectric power and a change of electrical conductivity from -p type to -n type.

EXPERIMENTAL METHOD

The eutectic alloy has been prepared from metals of high purity (99.999 %) by melting them in a sealed quartz ampoule under inert gas pressure. After omogenisation the melt was quickly solidified to ensure a fine structure of the eutectic.

The diffusion runs have been carried out by two experimental methods : the capillary-reservoir method described in a previous work [3] and the plane source method. The diffusion has taken place in capillary columns of 0.8 to 1 mm diameter bored through spectrally pure graphite rods ; the length of the capillary was 21—22 mm for the capillary-reservoir method and 30—40 mm for the plane source method. The diffusion has been surveyed by labelling with radioactive tellurium. In the capillary-reservoir method the alloy in the reservoir has been labelled, but in the plane source method the radioactive tracer has been incorporated into a tiny amount of alloy introduced at the bottom of the capillary.

The diffusion samples for the capillary-reservoir method have been obtained by introducing liquid eutectic alloy in the vaccum evacuated capillary under inert gas pressure.

The diffusion samples for the plane source method have been obtained by introducing the radioactive source in the capillary bore and then introducing a cylinder of solid eutectic alloy fitted to the capillary inner diameter ; this cylinder has been cast separately. The radioactive source consisted of a little amount of eutectic alloy prepared from radioactive tellurium, shaped to a disk of 1 mm height and a diameter equal to the inner diameter of the capillary. The length of the capillary diffusion samples can be considered semi-infinite in comparison with the plane source. The contact surface between the radioactive alloy disk and nonradioactive alloy column in the capillary has been made perfectly clean and flat by a careful polishing. The contact between the radioactive disk and the nonradioactive column has been ensured by melting them in the capillary under inert atmosphere.

The time of diffusion was chosen so that the radioactive tracer could not reach the opposite end of the capillary. Considering that the entire amount of the diffusion substance is located in the plane $x = 0$ at the initial moment $t = t_0$, the solution of Fick's second law, for the diffusion in a semi-infinite cylinder of unit cross-area, is given by equation :

$$C(x,\ t) = \frac{S}{\sqrt{\pi D t}} \exp \cdot \left(- \frac{x^2}{4Dt} \right) \tag{1}$$

Equation (1) gives the concentration distribution of the diffusing atomic species along the sample length for every time $t > t_0$.

To derive the diffusion coefficients from eq. (1) one has to build in coordinates $\ln C$ versus x^2, the straight lines corresponding to eq. (2) :

$$\ln C(x,\ t) = \text{const.} - \frac{x^2}{4Dt} \tag{2}$$

where $C(x, t)$ is the concentration of the radioactive element, proportional to the counting rate, and x is the distance from the interface of diffusion to the plane where the concentration has been actually measured. The slope M of these straight lines can be derived from a statistical treatment of the experimental data ; from the value of the slope one gets directly the value of the diffusion coefficient D, using the expression $D = \frac{1}{4\,Mt} \cdot$

The profile of the radioactive tracer concentration along the capillary after diffusion has been obtained by measuring the radioactivity of successive layers 1 mm height ; each layer has been drawn from the sample by polishing on a circle shaped metallographic paper of 30 mm diameter whose radioactivity has subsequently been measured in standard conditions.

We have carried out the first diffusivity determinations by the capillary-reservoir method. From radioactivity measurements of the whole diffusion sample (integral measurements [3]), we have derived the self-diffusion coefficient of tellurium. The values of the diffusion coefficient at the same temperature derived from different diffusion samples were self-consistent. For instance, from two different samples at 550°C we have got for the self-diffusion coefficient of tellurium the values : $6.20 \cdot 10^{-5} \mathrm{cm^2 s^{-1}}$ and $6.64 \cdot 10^{-5}\ \mathrm{cm^2 s^{-1}}$. But sometimes the values were divergent especially on account of overestimated values. In order to get an image on the possible sources of error in these determinations, we have resorted to the analysis of the penetration curves.[3] To this purpose we have made radioactivity measurements on successive layers of the diffusion sample by polishing it at different depths.

A penetration curve has to satisfy eq. (3) in every of its points. Eq. (3) results from Fick's second law by integrating it for the initial and limit conditions existing in the experimental system :

$$\frac{C(x,\ t)}{C_0} = 1 - \frac{4}{\pi} \sum_{x=0}^{\infty} \frac{1}{(2n+1)} \sin \cdot \frac{(2n+1)\pi}{2} \frac{x}{\ell} \exp \left(- \frac{(2n+1)^2 \pi^2}{4} \frac{Dt}{\ell^2} \right) \tag{3}$$

In eq. (3), C_0 is the radioactivity concentration in the reservoir, $C(x, t)$ is the radioactivity concentration in the sample after a diffusion time t, at a distance x from the open end of the capillary of the length ℓ. To make easier the computations we have tabulated eq. (3) versus two parameters, namely $\delta = x/\ell$ and $\theta = Dt/\ell^2$. By using a computer for the tabulation, we have obtained tables for a large number of the above mentioned parameters. These tables have given us the possibility to analyse any penetration curve resulting from an experimental diffusion run, and to derive at the same time the value of the diffusion coefficient. Only those diffusion samples have been considered successful for which the concentration profile along the capillary agreed with a diffusion curve. The diffusion samples which resulted in abnormally high values of the diffusion coefficient, when analysed by the sectioning method, produced penetration curves which differed markedly from the theoretical exponential diffusion curves. In these anomalous samples the process seemed to correspond to a displacement of the diffusion interface from the open end of the capillary, at a certain depth inside the capillary length (Fig. 1).

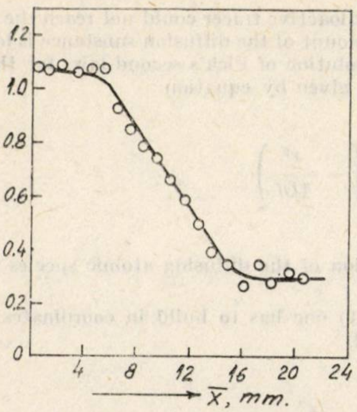

Fig. 1. — End effect in a diffusion sample.

Such a phenomenon could be ascribed either to a convection process at the top of the capillary, or to the breaking of the liquid capillary column and replacing the disrupted upper part of the non-radioactive capillary column, by radioactive alloy from the reservoir.

Because such sources of errors were of more frequent occurrence with the Pb—Te alloys than with other liquid alloys we have studied, we decided to resort to a second method for the determination of the self-diffusion coefficients, namely the plane source method. This method, checked in some of our previous works, [4] has resulted in highly reproductible data. By using this method we have obtained a good reproductibility of the diffusion results for the liquid Pb—Te alloy, as one can see from the penetration curves given in Fig. 2 a. In Fig. 2 b the experimental results are plotted in terms of eq. (2) which leads to a linearisation of the penetration curves.

The straight lines in Fig. 2 (b) are almost parallel and correspondingly the diffusion coefficients represented by their slopes have almost identical values, namely $D_1 = 5.52\ 10^{-5}\mathrm{cm}^2\mathrm{s}^{-1}$ and $D_2 = 5.56\ 10^{-5}\mathrm{cm}^2\mathrm{s}^{-1}$.

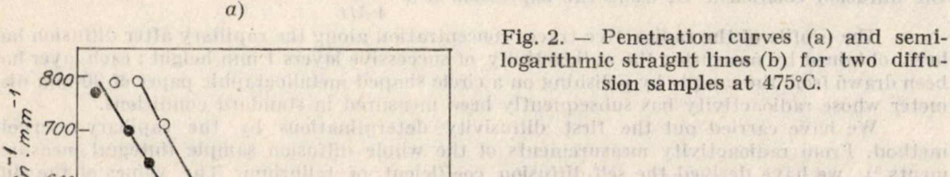

Fig. 2. — Penetration curves (a) and semilogarithmic straight lines (b) for two diffusion samples at 475°C.

RESULTS AND DISCUSSION

In table 1 we give the values of the self-diffusion coefficients of tellurium in the molten Pb-Te eutectic alloy that we have derived from the diffusion runs in the temperature range 475—600°C, carried out both by the capillary-reservoir method and by the plane source method.

The experimental data are discussed in terms of the thermally activated states theory and in terms of the small density fluctuations theory for liquids.

TABLE 1

Experimental data on self-diffusion of tellurium in liquid Pb—Te eutectic alloy

Temperature °C	Experimental method	$D \cdot 10^5$ $\mathrm{cm^2 s^{-1}}$	$(\bar{D} \pm \sigma_{\bar{D}}) \cdot 10^5$ $\mathrm{cm^2 s^{-1}}$
475	plane source	5.52	5.54±0.02
475	,, ,,	5.56	
500	plane source	5.15	
500	,, ,,	5.47	5.56±0.26
500	,, ,,	6.05	
525	capillary-reservoir	6.19	
525	plane source	5.75	6.01±0.13
525	,, ,,	6.10	
550	capillary-reservoir	6.20	6.42±0.22
550	,,	6.64	
575	capillary-reservoir	7.02	
575	,,	7.22	6.83±0.30
575	,,	6.24	
600	plane source	6.90	
600	,, ,,	7.91	7.41±0.50

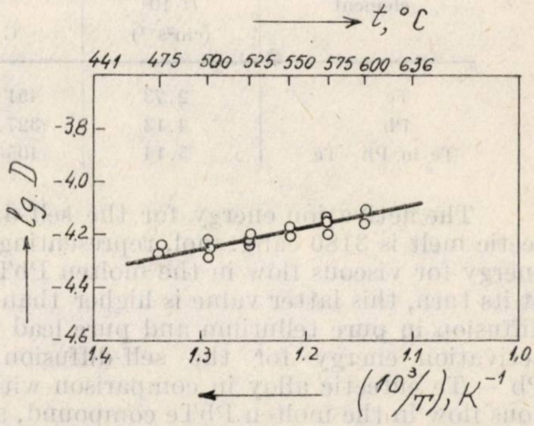

Fig. 3. — Semilogarithmic representation of the experimental diffusion data versus the reciprocal of the absolute temperature.

A theoretical exponential temperature dependence of the diffusivity is derived if one admits a diffusion mechanism by means of thermally activated atomic jumps of length equal to the interatomic distances. To verify the adequacy of this mechanism we have plotted in figure 3 our diffusion data in semilogarithmic representation versus the reciprocal of the absolute temperature. In such a plot, the exponential Arrhenius equation becomes a straight line, whose slope and intercept allow the calculation of the activation energy for diffusion and the frequency factor.

A statistical treatment of the experimental data allowed us to derive the equation of the straight line in figure 3 representing the Arrhenius equation for the temperature variation of the self-diffusion of tellurium in the molten Pb — Te eutectic alloy :

$$D = (4.52 \pm 1.37)\, 10^{-4} \exp\,(-3180 \pm 480)/RT \qquad (4)$$

Our results on the diffusion in the molten Pb — Te eutectic alloy agree with the conclusions of the viscosity studies in liquid Pb—Te alloys. On the viscosity isotherms a sharp peak is manifest at stoichiometric composition of the equiatomic PbTe compound.[1] This peak can be ascribed to the formation of some "molecular groups" with the composition PbTe, or to a short range order in the molten compound. At the eutectic composition, the viscosity minimum suggests that the molecular groups are destroyed and thus one can infer that the diffusion coefficient should increase in the eutectic melt. In fact, the values of the self-diffusion coeficient of tellurium at the eutectic composition, obtained experimentally in the present work, are higher than the self-diffusion coefficients in pure liquid tellurium [5] or in pure liquid lead,[6] as one can see in table 2.

TABLE 2

Self-diffusion data of tellurium in molten Pb—Te eutectic alloy in comparison with self-diffusion in pure liquid tellurium and lead

Diffusing element	Self-diffusion coeff. at 450°C, $D \cdot 10^5$ (cm^2s^{-1})	Melting point °C	Activation energy of diffusion $cal(g \cdot mol)^{-1}$	Frequency factor $D_0 \cdot 10^4$ (cm^2s^{-1})
Te	2.73	451	5550	12.9
Pb	4.13	327.5	4450	9.15
Te in Pb—Te	5.14	405	3180	4.52

The activation energy for the self-diffusion of tellurium in the eutectic melt is 3180 cal/g. mol, representing less than half of the activation energy for viscous flow in the molten PbTe compound (6850 cal/g.mol[1]); at its turn, this latter value is higher than the activation energy for self-diffusion in pure tellurium and pure lead (Table 2). The low value of the activation energy for the self-diffusion of tellurium in the molten Pb — Te eutectic alloy in comparison with the activation energy for viscous flow in the molten PbTe compound, argues for the dissociation of the molecular groups with the composition PbTe.

A second line of using the experimental diffusion data for obtaining information about the structure of the melt is feasible in the framework of the small fluctuations theory. In this line, we have used the data about the self-diffusion of tellurium in the molten Pb—Te eutectic alloy to check up the diffusion model which presumes that the atomic diffusion shifts are a consequence of small density fluctuations in the melt.[7-9]

This assumption results in the following expression[10] for the temperature dependence of the diffusion coefficient :

$$D = -1.72\ 10^{24}\ ZX_0^4K + 2.08\ 10^9\ ZX_0^2T \tag{5}$$

where Z is the coordination number in the melt, X_0 is the maximum distance of diffusive jump, (Å) and K is the force constant of the interatomic bond. The linear relationship between the diffusion coefficient and temperature assumed in eq. (5), is well verified by our experimental data on the self-diffusion of tellurium in the molten Pb—Te eutectic alloy (Fig. 4).

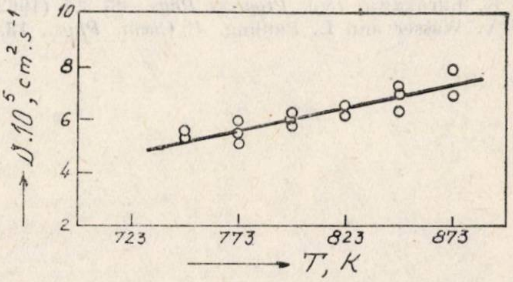

Fig. 4. — Temperature dependence of the self-diffusion coefficients of telurium in the liquid eutectic Pb—Te, in terms of the small fluctuations theory.

The analytical expression of the straight line in figure 4 derived by statistical treatment of the experimental data is :

$$D = -6.43\ 10^{-5} + 0.016\ 10^{-5}\ T \tag{6}$$

By identifying the coefficients in equations (5) and (6) we have obtained a value for the maximum distance of diffusion jump $X_0 = 0.354$ Å. This value is about one tenth of the interatomic distance[11] in the liquid alloy, thus pleading for the small fluctuations mechanism of diffusion (Table 3). In these computations we have adopted a value $Z = 6$ which corresponds to the coordination number in liquid tellurium.[11]

TABLE 3

Structural data of liquid Pb—Te eutectic alloy obtained from experimental diffusion data

Z	X_0 (Å)	$\bar{d}_{\text{liquid}} = \frac{1}{2}(\bar{d}_{\text{Pb}} + \bar{d}_{\text{Te}})$ (Å)	$\frac{X_0}{\bar{d}}$	$K\ 10^{-4}$ dyn.cm^{-1}	
				From diff. data	Experimental
6	0.354	3.15	0.112	3.94	3.71

The data in table 3 point also to a good agreement between the force constant of the interatomic bond derived from our experimental data on diffusion and the value derived from compressibility data.[12]

REFERENCES

[1] V. M. Glazov, S. M. Cijevskaia and N. V. Glagoleva, "Zhidkie poluprovodniki", Izd. Nauka, Moskwa, 1967, p. 141, 199.

[2] M. P. Gomez, D. A. Stevenson, and R. A. Huggins, *J. Chem. Phys. Solids*, **32**, 335 (1971).

[3] N. Petrescu and L. Ganovici, *Rev. Roumaine Chim.*, **26**, (1981).

[4] N. Petrescu and L. Ganovici, *Rev. Roumaine Chim.*, **21**, 1293 (1976).

[5] E. Nicoloiu, L. Ganovici, and I. Ganovici, *Rev. Roumaine Chim.*, **15**, 1713 (1970).

[6] S. J. Rothman and L. D. Hall, *Trans. A.I.M.E.*, **206**, 199 (1956).

[7] R. A. Swalin, *Acta Met.*, **7**, 736 (1959).

[8] M. Petrescu, *Rev. Roumaine Chim.*, **13**, 687 (1968).

[9] R. J. Reynik, *Appl. Phys. Letters*, **9**, 239 (1966).

[10] R. J. Reynik, *Trans. Met. Soc. A.I.M.E.*, **245**, 75 (1969).

[11] K. Furukawa, *Rep. Progress Phys.*, **25** 395 (1962).

[12] Y. Wasser and L. Pauling, *J. Chem. Phys.*, **18**, 747 (1950).

Revue Roumaine de Chimie, 26, 6, 851–855 (1981)

HETEROPOLYTUNGSTATES WITH Ti(IV) AND Ni(II). I.

THE FORMATION OF TWO NEW HETEROPOLYANIONS WITH Ti(IV) AND Ni(II) IN SOLUTION

RODICA VĂŢULESCU, T. BUDIU and GH. MARCU
Institute of Chemistry, 65–103, Str. Donath, Cluj-Napoca, Romania

Received July 2, 1980

The present work summarizes a part of our series of investigations on two new heteropolyanions, namely, heteropolytungstates with Ti(IV) and Ni(II), one of them belonging to the 2 : 11 series, the other to the 2 : 5 series. In this first note we present the conditions of formation of the two compounds as a function of pH, temperature and time, by using the spectrophotometric technique.

INTRODUCTION

The class of heteropolyelectrolytes has been enriched in the last two decades by the appearance of new types of heteropolytungstates having two heteroatoms in the polytungstate anion, namely, the 2 : 11 series, well-known and intensely studied in the literature, and the 2 : 5 series, less represented and therefore yet insufficiently characterized.

The studies referring to the 2 : 11 series were started in 1956 by Baker and co-workers ;[1] afterwards, many authors showed that the ions of the transition metals, M^{m+}, were added to the lacunary structures of the type $[X^{x+}W_{11}O_{39}]^{(12-x)-}$ in order to form mixed heteropolyanions $[X^{x+}M^{m+}W_{11}O_{39}]^{(12-m-x)-}$.[2-8] Following the numerous physico-chemical studies on the heteropolytungstates belonging to this series, a general formula of the type $[Y^{y-}M^{m+}O_5X^{x+}O_4W_{11}O_{30}]^{(12-m-x-y)-}$ was assigned to them,[9] where Y stands for a monodentate ligand which occupies an isolated coordinative position of M^{m+}.

Referring to the 2 : 5 series, there are still few data in the literature because, for the time being, only a small number of representatives with molybdenum [10-12] and tungsten are known.[13-16]

If two metallic ions are simultaneously present in the system in which the formation of the tungstate polyanions takes place, then depending on the conditions and on the ability of those ions to generate complexes, either a mixture of heteropolyspecies, or heteropolycompounds containing two metallic ions in the same complex-anion are being formed.

EXPERIMENTAL

a) First of all, we have to explain the formation conditions of the two complexes investigated by us ; they will be noted, for the sake of brevity, as $NiTiW_{11}$ and $NiTiW_5$ respectively.

Because, in general, the pH plays the most important role in the formation of the heteropolycompounds, the influence of this parameter was the first to be studied. This influence was correlated with the optimum time of reaction for the formation of the complexes and with the temperature. The obtained heteropolytungstates being coloured compounds, the photocolorimetric method was chosen as an investigation technique for the study of their formation conditions.

In fact, nine samples were made by solving about 5 g of $Na_2WO_4 \cdot 2H_2O$ in 25 ml of water (C = 0.6 M), and were treated, at the room temperature, with a solution which contains 0.5 ml $TiCl_4$ (T = 0.1278 g Ti/ml) and 0.4 g $Ni(NO_3)_2$ in 20 ml water (in this way the elements were added in a stoichiometric ratio of 1 : 1 : 11). Immediately after mixing, the pH of the samples was corrected to the values 4 ; 4.5 ; 5 ; 5.5 ; 6 ; 6.5 ; 7 ; 7.5 and 8 respectively, with acetic acid. They were heated at 60°C, when the initially formed hydroxides precipitate was solved, and then the resulting solutions were boiled. At established intervals of time (between 30 minutes and 7 1/2 hours) the samples were cooled, brought to 25 ml in volumetric flasks, and were colorimetred by means of colorimeter of the FEK-56 type, filter 4 ($\lambda \simeq 440$ nm). During the whole series of the experiments the pH of the samples was kept at the above mentioned values.

b) In order to prove the formation of the complex $NiTiW_{11}$, a solution was prepared, containing TiW_{11}-anion by solving 25 g $Na_2WO_4 \cdot 2H_2O$ in 125 ml water (C=0.6 M) to which 2.6 ml $TiCl_4$ (T = 0.1278 g Ti/ml), diluted beforehand in 50 ml water were added at room temperature. The pH was corrected to 5 with acetic acid and the solution was slightly warmed, until it became clear, due to the formation of a heteropolyanion with titanium and tungsten (because otherwise under these working conditions — pH = 5 and heating — the titanium would be completely hydrolyzed). After cooling, the solution was brought to a volumetric flask of 200 ml and 25 ml aliquotes were taken, to which a solution of $Ni(NO_3)_2$ (T = 0.01094 gNi/ml) was added, so that the molar ratio Ni/Ti was 0.25 : 1 ; 0.5 : 1 ; 0.75 : 1 ; 1 : 1 . . . 2 : 1.

In order to obtain the second complex, a solution of $TiW_5$was prepared in the same way from 11.5 g $Na_2WO_4 \cdot 2H_2O$, solved in 125 ml water (C $\simeq$0.3 M) and 2.6 ml $TiCl_4$ (T = 0.1278 g Ti/ml), diluted to 50 ml with water. Then, the pH was corrected to the value 7.5 and the solution was heated, proceeding as shown for the formation of the complex $NiTiW_{11}$.

In both cases, after adding the Ni^{2+} ions in the above-mentioned ratios, the samples were boiled, according to the optimum time of formation for two complexes, established in the first part of this study.

RESULTS AND DISCUSSIONS

The results of the experimental data referring to the conditions of formation of the two complexes under discussion are shown in figure 1. (for the sake of clarity, the curves are presented in two diagrams).

From the aspect of the recorded curves the conclusion is drawn that in the investigated system, Ni : Ti : W, two compounds are formed, at two distinct values of pH, and it is found that the reaction time has a great influence on their yield of formation.

One of the complexes is formed in the domain of pH = 4.5—6.0, but the optimum pH (according to the maximum absorption) is around the value 5.

The second complex results in a narrow domain of pH (as it can be seen in figure 1), namely the optimum pH of formation is around 7.5.

It has been experimentally observed that the syntheses of the two complexes must be carried out in warm solutions ; at room temperature and at the pH values which we mentioned before, the titanium in both cases, as well as nickel in the second case, (A = 0), are completely hydro-

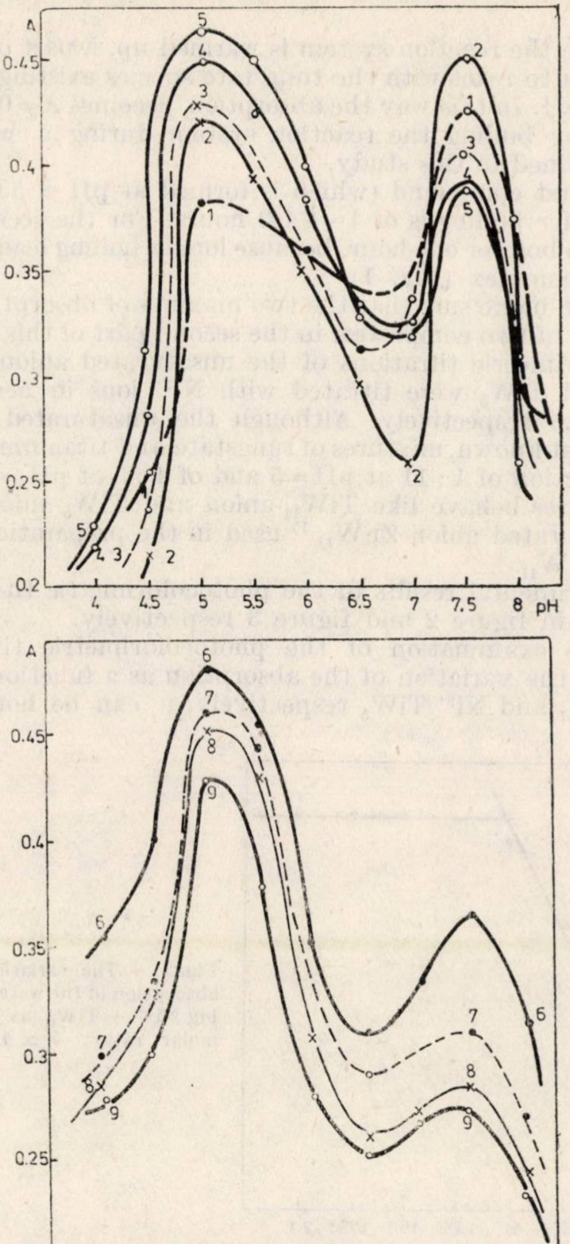

Fig. 1. — The variation of the optical absorption of the ion mixtures containing Ti^{4+}, Ni^{2+} and W^{6+} in water solutions, molar ratio 1 : 1 : 11, as a function of pH and time : *1*) boiling time = 1/2 hour ; *2*) an hour ; *3*) 1 1/2 hours ; *4*) 2 1/2 hours ; *5*) 3 1/2 hours ; *6*) 4 1/2 hours ; *7*) 5 1/2 hours ; *8*) 6 1/2 hours ; *9*) 7 1/2 hours., $\lambda \simeq 440$ nm ; 1 = 1 cm.

lyzed. But while the reaction system is warmed up, a part of the titanium and nickel begin to react with the tungstate species existing in solution at the respective pH. In this way the absorption becomes $A \neq 0$ and it reaches its maximum by boiling the reaction system during a well-established time, as determined in this study.

For the first compound (which is formed at pH $\simeq$ 5.0) the best reaction time under boiling is of 4—4 1/2 hours. For the second compound it is sufficient to boil for one hour, because longer boiling leads to the degradation of the complex (Fig. 1).

In order to make sure that the two maxima of absorption correspond to the existence of two complexes, in the second part of this study, in solution, photocolorimetric titrations of the unsaturated anions were carried out; TiW_{11} and TiW_5 were titrated with Ni^{2+} ions in acetic buffer at pH = 5 and 7.5 respectively. Although the unsaturated anions TiW_{11} and TiW_5 are not known, mixtures of tungstate and titanium ions were prepared in proportion of 1 : 11 at pH=5 and of 1 : 5 at pH=7.5 respectively. These mixtures behave like TiW_{11}-anion and TiW_5-anion, by analogy with the unsaturated anion ZnW_{11} [17] used in the preparation of the complexes $Zn^{2+}M^{m+}W_{11}$.

The experimental results of the photocolorimetric titrations carried out are shown in figure 2 and figure 3 respectively.

From the examination of the photocolorimetric titration curves which describe the variation of the absorption as a function of the molar ratio Ni^{2+}/TiW_{11} and Ni^{2+}/TiW_5 respectively, it can be noted that these consist of two straight lines which cross at the value of the molar ratio = 1 : 1 in each case. This fact confirms a simple process of formation of two distinct heteropolytungstates.

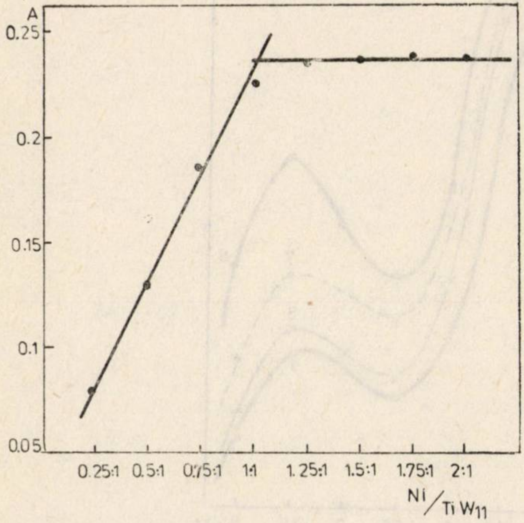

Fig. 2. — The variation of the optical absorption of the water mixtures containing $Ni^{2+} + TiW_{11}$ as a function of the molar ratio; $\lambda \simeq 440$ nm; 1=1 cm.

The newly obtained complexes, the formation of which was presented here, were studied both in solution and in the solid state, in order to formulate them and to characterize these compounds more completely.

In the following notes of this series we shall present the synthesis and analysis of such complexes, the determination of the basicity, proofs for the presence of the two heteroatoms (Ti and Ni) in the complex anion, absorption spectra in UV and visible, the behaviour towards the H^+ and OH^- ions, structure determinations by X-ray diffraction (the powder method), as well as the thermal behaviour and the infrared absorption spectra of the two new heteropolyanions.

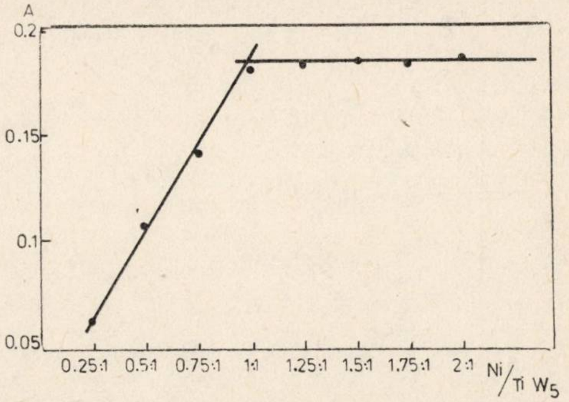

Fig. 3. — The variation of the optical absorption of the water mixtures containing Ni^{2+} + TiW_5 as a function of the molar ratio; $\lambda \simeq 440$ nm ; $1 = 1$ cm

REFERENCES

[1] L. C. W. Baker and Th. P. Mc. Cutcheon, *J. Amer. Chem. Soc.*, **78**, 4503 (1956).
[2] T. J. R. Weakley and S. A. Malik, *J. Inorg. Nuclear Chem.*, **29**, 2935 (1967).
[3] C. M. Tourne and G. Tourne, *Bull. Soc. chim. France*, **4**, 1124 (1969).
[4] O. W. Rollins, *J. Inorg. Nuclear Chem.*, **33**, 75 (1971).
[5] R. Ripan, A. Duca, M. Puşcaşiu and D. Stănescu, "Proceedings XXth I.U.P.A.C. D26", Moscow 1965, p. 68.
[6] R. Ripan, A. Duca, S. Stănescu and M. Puşcaşiu, *Z. anorg. Chem.*, **347**, 333 (1966).
[7] Gh. Marcu, M. Rusu and L. Ochişel, *Rev. Roumaine Chim.*, **22**, 849 (1977).
[8] C. M. Tourne and G. Tourne, *Rev. Chim. Miner.*, **14**, 83 (1977).
[9] L. C. W. Baker and J. S. Figgis, *J. Amer. Chem. Soc.*, **92**, 3794 (1970).
[10] P. Souchay, M. Cadiot and C. Volfovsky, *Compt. rend.*, **269**, 826 (1969).
[11] R. Strandberg, *Acta Chem. Scand.*, **27**, 1004 (1973).
[12] J. Fischer, L. Ricard, and P. Toledano, *J.C.S. Dalton*, **9**, 941 (1974).
[13] M. Michelon and G. Hervé, *Compt. rend.*, **274**, 209 (1972).
[14] B. Schoenfeld, W. Baehr, B. Buss and O. Glemser, *Z. Naturforsch.*, **30B**, 831 (1975).
[15] A. Rosenheim and A. Wolff, *Z. anorg. Chem.*, **193**, 47 (1930).
[16] S. Prasad and R. Swarup, *J. Inorg. Nuclear Chem.*, **30**, 1337 (1968).
[17] C. M. Tourne, G. Tourne, S. A. Malik and T. J. R. Weakley, *J. Inorg. Nuclear Chem.*, **32**, 3875 (1970).

Revue Roumaine de Chimie, **26**, *6*, 857–860 (1981)

NEW DIOXOURANIUM (VI) COMPLEXES WITH BIDENTATE ON DONOR SCHIFF BASES DERIVED FROM SALICYLALDEHYDE OR SUBSTITUTED SALICYLALDEHYDE AND BENZOYLHYDRAZIDE

A. SYAMAL and B. K. GUPTA

Department of Applied Sciences and Humanities, Kurukshetra University, Kurukshetra 132119, Haryana and Department of Chemistry, Regional Engineering College, Kurukshetra 132119, Haryana, India

Received June 12, 1980

New dioxouranium (VI) complexes of the type $UO_2(LH)_2$ (where LH_2 = the Schiff base derived from salicylaldehyde, 5-chlorosalicylaldehyde, 5-bromosalicylaldehyde, 5-nitrosalicylaldehyde, 5-methoxysalicylaldehyde, 3,5-dichlorosalicylaldehyde, 3-ethoxysalicylaldehyde, 2-hydroxy-1-naphthaldehyde and benzoylhydrazide) have been synthesized and characterized on the basis of elemental analysis, electrical conductance, molecular weight, infrared and electronic spectra, and magnetic susceptibility measurements. In complexes the Schiff bases behave as monobasic, ON donor bidentate ligands. The complexes are non-electrolytes, monomers, diamagnetic and possess octahedral structure.

INTRODUCTION

In recent years there has been considerable research interest [1-4] on the Schiff base complexes of oxometal cations like VO^{2+}, MoO_2^2 and UO_2^{2+}. The strongly bound oxygens of the oxometal entity remain intact during chemical reactions and produce absorption bands beyond those normally available to transition metal complexes. As relatively a few dioxouranium (VI) complexes with Schiff bases are known, [5] we report in this paper the synthesis of new dioxouranium (VI) complexes of the Schiff bases (**I**) derived from salicylaldehyde or substituted salicylaldehyde and bezoylhydrazide.

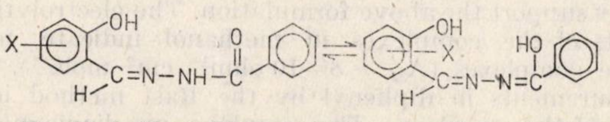

I. X = H, 5-chloro, 5-bromo, 5-nitro, 5-methoxy, 5-ethoxy, 3-ethoxy, 5,6-benzo, 3,5-dichloro.

The complexes have been characterized on the basis of elemental analysis, infrared and electronic spectra, electrical conductance, molecular weight and magnetic susceptibility measurements.

EXPERIMENTAL

Materials

Reagent grade salicylaldehyde was purchased from Sarabhai M. Chemical Co. 5-Chlorosalicylaldehyde and benzoylhydrazide were prepared according to the procedures reported in the literature.[6,7] 5-Methoxysalicylaldehyde, 3-ethoxysalicylaldehyde and 5-bromosalicylaldehyde were obtained from Aldrich Chemical Co. (U.S.A.). 5-Nitrosalicylaldehyde, 3,5-dichlorosalicylaldehyde were purchased from Eastman Kodak Co. (U.S.A.). 3-Methoxysalicylaldehyde and 2-hydroxy-1-naphthaldehyde were the products of Fluka A. G. (Switzerland). Uranyl nitrate hexahydrate was purchased from BDH Chemicals Ltd. (England).

Physical Measurements

The metal content in the complex was analysed by destroying the organic moiety by concentrated nitric acid followed by calcination in an electrical oven and weighing as U_3O_8. The nitrogen analysis was done microanalytically. The conductance measurements were done in methanol with the help of a Toshniwal Conductivity bridge (Model CL 01—02A) and a dip type cell calibrated with aqueous KCl solutions. The infrared spectra were recorded in KBr discs using a Perkin Elmer — 257 infrared spectrophotometer calibrated with polystyrene. The molecular weight measurements of the compounds were performed by the Rast method [8] using diphenyl as the solvent.

General method of synthesis of Schiff bases

Benzoylhydrazide (1.36 g, 0.01 mole) was dissolved in 50 ml of 95% ethanol. To this salicylaldehyde (1.25 g, 0.01 mole) or substituted salicylaldehyde (0.01 mole) was added in 95% ethanol (50—70 ml). The mixture was refluxed on a water bath for one h. The partial removal of solvent on a water bath followed by cooling produced colourless crystalline product which was suction filtered, washed with cold ethanol and dried under vacuum. Yield = 80%.

General method of synthesis of dioxouranium (VI) complexes

A methanolic solution of the uranyl nitrate hexahydrate (0.50 g, 0.001 mole in 10 ml) was added to the Schiff base solution (0.002 mole in 10—15 ml). The solution was refluxed for 2 hrs on a water bath. The solid compound was obtained after partial evaporation under a fan. This was suction filtered, washed with methanol and dried under vacuum. Yield = 70% The analytical data are given in table 1.

RESULTS AND DISCUSSION

The reaction of methanolic solutions of uranyl nitrate hexahydrate and the Schiff bases (I) in 1 : 2 ratio under reflux condition produces complexes of the type UO_2 $(LH)_2$ (where LH_2 = bidentate Schiff base). The complexes are reddish orange or brown in colour. The analytical data of the complexes support the above formulation. The electrolytic conductance measurements of the complexes in methanol indicate non-electrolytic nature of the complexes ($\Lambda_M = 8-10$ ohm^{1-} cm^2 $mole^{-1}$). The molecular weight measurements in diphenyl by the Rast method indicate monomeric nature of the complexes. The complexes are diamagnetic as required for a $5f^{\circ}$ system. They are six coordinated and octahedral.

The infrared spectral data of the complexes are presented in table 1. A strong band at 860—960 cm^{-1} range is assigned to the asymmetric stretching frequency of the dioxouranium ion.[9] The force constant (f) for this vibration has been calculated by following Jones' method [11] which is in

TABLE 1

Analysis, molecular weight and IR spectral data of dioxouranium (VI) complexes of Schiff bases [a]

Complex	Stoichiometry	M.W. Found (Calcd.)	Found (Calcd.)		$\nu_{as}(O=U=O)$	f_{UO} mdynes/A°	R_{UO} A°	$\nu_s(O=U=O)$
			%U	%N				
$UO_2(sal\text{-}BZH)_2$	$C_{28}H_{20}O_6N_4U$	751 (746)	30.98 (31.90)	7.73 (7.51)	895	6.72	1.73	800
$UO_2(5\text{-}Cl\text{-}sal\text{-}BZH)_2$	$C_{28}H_{18}O_6N_4Cl_2U$	825 (815)	28.38 (29.20)	6.99 (6.87)	895	6.72	1.73	820
$UO_2(5\text{-}Br\text{-}sal\text{-}BZH)_2$	$C_{28}H_{18}O_6N_4Br_2U$	935 (904)	25.22 (26.32)	6.01 (6.19)	915	7.02	1.74	805
$UO_2(5\text{-}NO_2\text{-}sal\text{-}BZH)_2$	$C_{28}H_{18}O_{10}N_6U$	832 (836)	27.29 (28.46)	6.98 (6.69)	895	6.72	1.73	800
$UO_2(3\text{-}MeO\text{-}sal\text{-}BZH)_2$	$C_{30}H_{24}O_8N_4U$	827 (806)	28.17 (29.52)	7.19 (6.94)	880	6.49	1.71	825
$UO_2(5\text{-}MeO\text{-}sal\text{-}BZH)_2$	$C_{30}H_{24}O_8N_4U$	830 (806)	28.98 (29.52)	7.32 (6.94)	890	6.58	1.72	790
$UO_2(3\text{-}EtO\text{-}sal\text{-}BZH)_2$	$C_{32}H_{28}O_8N_4U$	814 (834)	28.17 (28.53)	6.50 (6.71)	900	6.73	1.73	815
$UO_2(HO\text{-}BZH)_2$	$C_{36}H_{24}O_6N_4U$	853 (846)	28.16 (28.13)	6.46 (6.62)	890	6.58	1.72	800
$UO_2(3{,}5\text{-}Cl_2\text{-}sal\text{-}BZH)_2$	$C_{28}H_{16}O_6N_4Cl_4U$	899 (884)	27.16 (26.92)	6.67 (6.33)	895	6.72	1.73	790

Abbreviation sal = salicylaldehyde, 5-Cl-sal = 5-chlorosalicylaldehyde, 5-Br-sal = 5-bromosalicylaldehyde, 5-NO_2-sal = 5-nitrosalicylaldehyde, 5-MeO-sal = 5-methoxysalicylaldehye, 3-MeO-sal = 3-methoxysalicylaldehyde, 3-EtO-sal = 3-ethoxysalicylaldehyde, 3,5-Cl_2-sal = 3,5-dichlorosalicylaldehyde, HO = 2-hydroxy-1-naphthaldehyde and BZH = benzoylhydrazide.

the range 6.5—7.0 m dynes/A°, and this agrees well with the reported values of force constant of dioxouranium (VI) complexes.[10] The U—O bond distance as calculated using the relation[12] $R_{U-O} = 1.80\, f^{-1/3} + 1.17$ is $\sim$ $\sim$ 1.73 A°, which is in the usual range (1.60—1.92 A°) observed for many dioxouranium (IV) complexes.[13] The symmetrical stretching frequency of the dioxouranium ion has been observed in the region 790—825 cm^{-1}.[4]

The Schiff bases (I) exhibit a medium intense broad band in the region 3200—3400 cm^{-1} which is assigned to the hydrogen bonded ν(OH) stretch and ν(NH) stretch. The complexes exhibit a band in the region 3300—3400 cm^{-1} which is assigned to the uncoordinated ν(OH) (phenolic) stretch. The ligands exhibit a band in the region 1635—1670 cm^{-1} and this is assigned to the ν(C = O) stretch. In the complexes the absence of a band in the region 1620—1670 cm^{-1} indicates the destruction of C = O group due to enolisation. As a result, the conjugated C=N—N=C group is produced and a strong band in the region 1590 — 1605 cm^{-1} is assigned to this vibration. The ν(C = N) stretch of the ligands (1600 — 1610 cm^{-1}) shifts to lower frequency (5 — 15 cm^{-1}) indicating nitrogen coordination of azomethine moiety. The ν(C—O) (alcoholic) stretch of the ligands (1185 — 1245 cm^{-1}) shifts to higher frequency by 15 — 30 cm^{-1} indicating alcoholic oxygen coordination in the complexes. Thus the ligands are behaving as monobasic, bidentate ON donor ligands and the uranium (VI) complexes are octahedrally coordinated to the ligands and two oxygen atoms.

ACKNOWLEDGEMENT. The authors are grateful to the Council of Scientific and Industrial Research, New Delhi 110001 for financial support of this work.

REFERENCES

[1] J. Selbin, *Chem. Rev.*, **65**, 153 (1965); *Coord. Chem. Rev.*, **1**, 293 (1966).

[2] A. Syamal, *Coord. Chem. Rev.*, **16**, 309 (1975).

[3] P. C. H. Mitchel, *Coord. Chem. Rev.*, **1**, 315 (1966).

[4] R. L. Belford and G. Belford, *J. Phys. Chem.*, **34**, 1330 (1961); S. P. McGlynn, J. K. Smith and W. C. Neely, *J. Chem. Phys.*, **35**, 105 (1961).

[5] A. T. T. Hsieh, R. M. Sheahan and B. O. West, *Austral. J. Chem.*, **28**, 885 (1975).

[6] F. J. Welcher, "Organic Analytical Reagents", Van Nostrand, New York, vol. 3, 1947, p. 254.

[7] L. Gatterman and H. Wieland, "Laboratory Methods of Organic Chemistry", Macmillan, London, 1963, p. 153.

[8] F. G. Mann and B. C. Saunders, "Practical Organic Chemistry", Longmans, 1961, p. 435.

[9] A. E. Comyns, B. M. Gatehouse and E. Wait, *J. Chem. Soc.*, **1958**, 4655.

[10] A. Syamal and O. P. Singhal, *Transition Met. Chem.*, **4**, 179 (1979).

[11] L. H. Jones, *Spectrochim. Acta*, **10**, 395 (1958); **11**, 409 (1959).

[12] S. P. (McGlynn, J. K. Smith and W. C. Neely, *J. Chem. Phys.*, **35**, 105 (1961).

[13] W. H. Zachariasen, *Acta Crystallogr.*, **8**, 847 (1954); I. I. Chernyaev, "Complex Compounds of Uranium", Translated by L. Mandal, Israel Program for Scientific Translations, 1966.

Revue Roumaine de Chimie, **26**, *6*, 861–866 (1981)

COPPER(II) COMPLEXES OF THREONINE AND ALLOTHREONINE

ELENA BĂLĂ, MARIANA S. IONESCU and C. STOICESCU
Institute of Chemical and Pharmaceutical Research, Bucharest, Romania

Received October 10, 1980

The structure of threonine and allothreonine copper(II) complexes formed by condensation of bis(glycinato)copper(II) with acetaldehyde is discussed. A bis(2,5-dimethyloxazolidine-4-carboxylato)copper(II) dihydrate structure is suggested, based on electronic, IR and thermogravimetric data.

In 1957, Okawa and Akabori[1] devised a new, rather stereospecific method for the synthesis of D,L-threonine via the base-catalyzed aldol condensation of bis(glycinato)copper(II) (gly_2Cu) with acetaldehyde. A mixture of threonine and allothreonine copper(II) complexes results from the reaction. Elemental analysis of the complexes accounts for an empirical formula $C_{12}H_{24}CuN_2O_8$, containing two more molecules of acetaldehyde, as expected. The real structure of these complexes is controversial. Moreover, most researchers have studied and suggested various formulations for the threonine copper complex only. No data on the structure of the allothreonine copper complex are available in literature. The following three formulae have been suggested for the threonine copper(II) complex resulted from the condensation reaction :

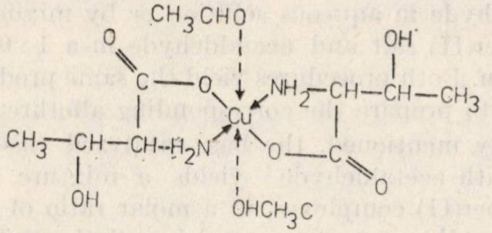

Belikov[2]

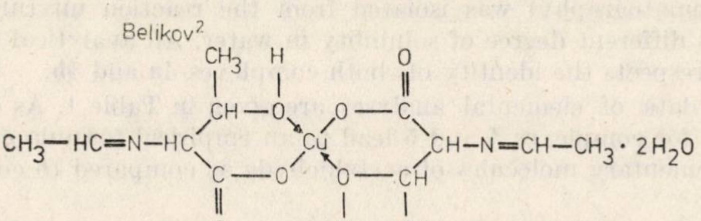

II.

Sato[3]

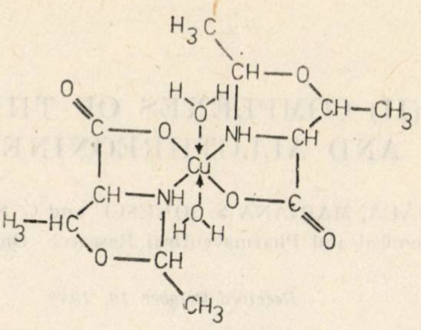

III.

Maldonado[4]

Therefore, we further investigated the structure of threonine and allothreonine copper(II) complexes in order to get more information for the stereoselective feature of the condensation reaction mechanism.

RESULTS AND DISCUSSION

Bis(glycinato)copper (**1**), bis(threoninato)copper (**2**) and bis(allothreoninato)copper (**3**) were prepared from the Na salts of the corresponding amino acids and a copper(II) salt (carbonate or sulphate) in concentrated aqueous solution.[5] The acetaldehyde containing copper complex of threonine (**4a**) was prepared either by treating bis(threoninato)copper (II) with acetaldehyde in aqueous solution or by mixing sodium threoninate with a copper(II) salt and acetaldehyde in a 1 : 0.5 : 1 molar ratio in aqueous solution. Both procedures yield the same product (**4a**). A similar method was used to prepare the corresponding allothreonine complex (**5**).

As previously mentioned, the base-catalyzed reaction of bis(glycinato)copper(II) with acetaldehyde[1] yields a mixture of threonine and allothreonine copper(II) complexes, in a molar ratio of about 2.5/1. The threonine complex (**4b**), uncontaminated by allothreonine (as checked by paper chromatography) was isolated from the reaction mixture on the basis of its different degree of solubility in water. All analytical data proved in all respects the identity of both complexes **4a** and **4b**.

The data of elemental analyses are given in Table 1. As expected, the results for complexes **4** and **5** lead to an empirical formula containing two supplementary molecules of acetaldehyde as compared to compounds **2** and **3**.

Although the K. Fischer's water determination is not highly accurate, the results (shown in Table 1) clearly indicate the presence of two molecules of hydration water in complexes **4** and **5**. More evidence was provided by thermogravimetry. The thermograms of both complexes **4**

TABLE 1

Elemental analyses and conductivity data of copper(II) complexes

Complex	Formula	C % calc. found	H % calc. found	N % calc. found	Cu % calc. found	O % calc. found	H_2O % calc. found	$\Omega 10^2$ cm^2
(1)	$C_4H_{10}CuN_2O_5$	20.91	4.35	12.20	27.66	34.85	7.48	1.48
		20.57	4.41	12.44	27.84	34.74	*)	
(2)	$C_8H_{16}CuN_2O_6$	32.05	5.34	9.35	21.20	32.05	—	1.84
		32.40	5.40	9.18	21.28	31.74		
(3)	$C_8H_{16}CuN_2O_6$	32.05	5.34	9.35	21.20	32.05	—	1.08
		32.09	5.35	9.35	21.23	31.98		
	$C_{12}H_{24}CuN_2O_8$	37.16	6.19	7.22	16.39	33.03	9.29	
(4a)		37.50	5.95	7.29	16.56	32.70	11.44	0.96
(4b)		36.52	6.30	7.20	16.91	33.07	7.72	1.18
(5)	$C_{12}H_{24}CuN_2O_8$	37.16	6.19	7.22	16.39	33.03	9.29	0.80
		37.10	5.90	7.19	16.59	33.19	11.23	

---

*) Bis(glycinato)copper(II) is insoluble in most organic solvents and water determination could not be carried out.

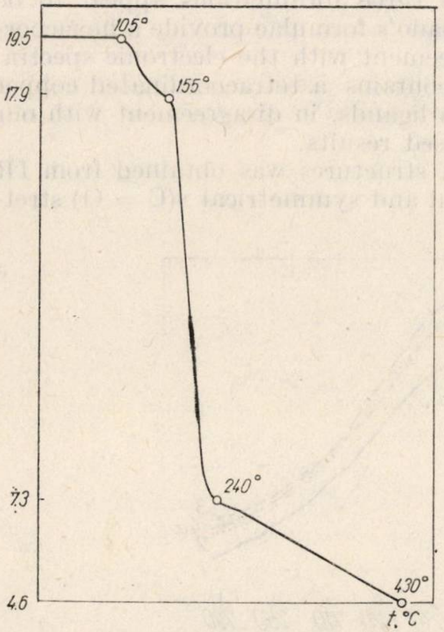

Fig. 1. — Weight loss vs. temperature for complex 4. (Complex 5 shows a similar pattern).

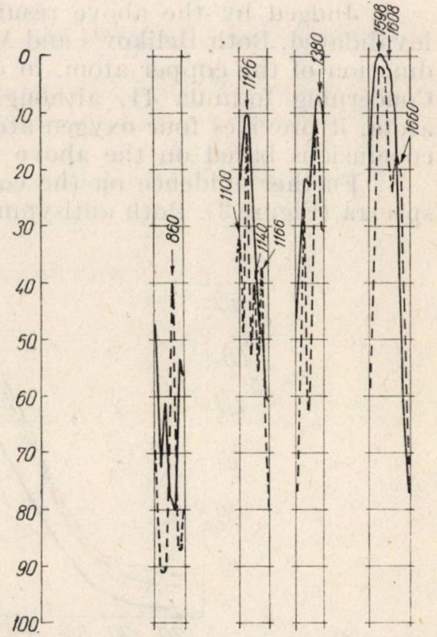

Fig. 3. — IR spectra of complexes 2 (full-line) and 4 (dotted-line).

and **5** (Figure 1) have a similar pattern, showing the loss of two molecules of water at about 100—110°C. These findings invalidate Belikov's formula (I) which contains no hydration water.

Table 1 also contains the conductivities of compounds (**1**)—(**5**) determined in aqueous solution. They have very low values providing, as expected, the non-ionic structure of the copper(II) complexes.

In the visible spectra of the complexes, a single broad band is observed at 610—615 nm, with molar extinction coefficients of about 50—55 $cm^{-1} \cdot mol^{-1} \cdot l$ (Figure 2). Such behaviour corresponds to a square planar structure of a tetracoordinated copper atom. Both the position of the absorption bands and their molar extinction coefficients remain unchanged for complexes (**2**)—(**5**), which means that copper coordination in threonine and allothreonine complexes is identical. Moreover, the acetaldehyde containing complexes (**4**) and (**5**) and the bis(threoninato)copper (II) (**2**) and bis(allothreoninato)copper(II) (**3**) have the same absorption maxima and extinction coefficients. Once more we concluded that acetaldehyde is attached in such a way as to maintain the copper coordination unchanged. The constant wavelength of the absorption maxima of all compounds (**1**)—(**5**) also proves that no change of ligands took place by reaction of bis(threoninato)copper(II) and bis(allothreoninato)copper(II), respectively, with acetaldehyde. The ligands must remain the same as in bis(glycinato)copper(II). This conclusion is also supported by comparing with the $Cu(H_2O)_4^{++}$ ion in which the central copper ion is surrounded by four oxygen atoms (as in structure II) and shows an absorption maximum at 635 nm.

Judged by the above results, all three formulations appear to be invalidated. Both Belikov's and Maldonado's formulae provide a hexacoordination of the copper atom, in disagreement with the electronic spectra. Concerning formula II, although it contains a tetracoordinated copper atom, it provides four oxygen atoms as ligands, in disagreement with our conclusions based on the above discussed results.

Further evidence on the complex structures was obtained from IR spectra (Figure 3). Both antisymmetrical and symmetrical $\nu(C=O)$ stret-

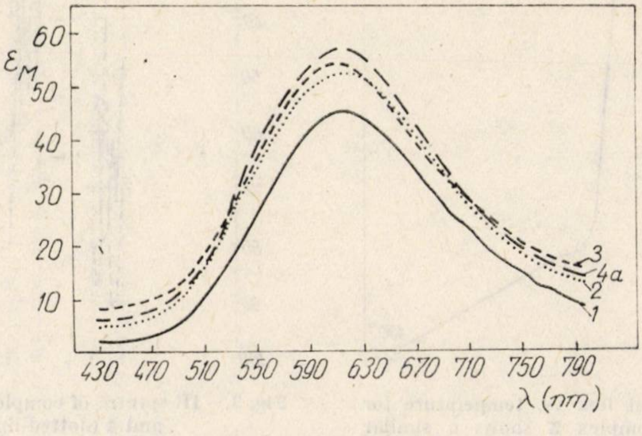

Fig. 2.— Visible spectra of complexes 1—5.

ching vibrations of the carbonyl group at 1598 and 1380 cm^{-1} are present in the spectra of compounds (**2**) — (**5**). The 1598 cm^{-1} band shows a shoulder at 1608 cm^{-1} attributed to a δ(NH) deformation vibration. Complexes (**4**) and (**5**) show no band in the 1700 cm^{-1} region corresponding to a ν(C=O) stretching vibration of acetaldehyde. This result again invalidates structure I.

Within the 1200—1100 cm^{-1} region, complexes (**2**) and (**3**) show a single band at 1126 cm^{-1} attributed to a ρ_t (NH) vibration.[6] On the other hand, complexes (**4**) and (**5**) show four bands in this same region, namely, apart from the above-mentioned 1126 band, three more absorption maxima at 1166, 1140 and 1100 cm^{-1}. According to Bergman,[7] those triple bands are characteristic for an oxazolidine ring. The oxazolidinic structure is strengthened by the occurrence of a new band in the IR spectra ot complexes (**4**) and (**5**) at 860 cm^{-1}, attributed by Habermehl[8] to a ring pulsation vibration of the five-membered heterocycles. This band is present only in the spectra of complexes (**4**) and (**5**) and does not appear in the spectra of complexes (**2**) and (**3**).

The infrared spectra of complexes (**4**) and (**5**) show a medium intensity band at about 1660 cm^{-1} which is attributed to a bending mode of lattice water.[9] The same band is found in the spectrum of bis(glycinato) copper(II) (**1**) containing one molecule of hydration water, as well as in the spectrum of a hydrated bis(threoninato)copper(II) containing 4.5 molecules of hydration water, prepared according to.[5] The presence of such a band in the spectra of hydrated complexes allows us to assign this vibration mode to lattice water and not to a C = N bond as resulting from an oxazolidine ⇄ Schiff base equilibrium.

Thus, IR data confirm an oxazolidine structure of the complexes, as in formula III, but both IR and visible data are not concordant with the coordination of two water molecules on the copper atom.

Based on the above data, we suggest that the structure of both threonine (**4**) and allothreonine (**5**) complexes as resulted from the condensation of bis(glycinato)copper(II) with acetaldehyde is a bis-oxazolidine formula with a tetracoordinated copper atom, a trans configuration and also contains two molecules of hydration water (formulae IV and V).

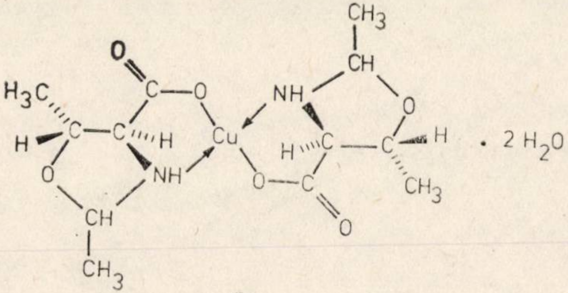

IV.

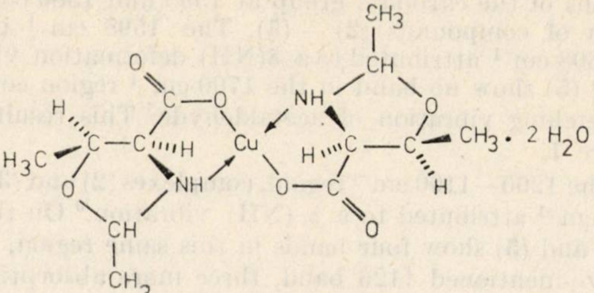

V.

EXPERIMENTAL

The visible spectra were recorded in water solution with a PMQ-KM-3 Opton Spectrophotometer. The IR spectra were recorded as KBr pellets with a UR—20 Carl Zeiss Jena Spectrophotometer. The thermogravimetric analyses were performed in air atmosphere at a 12.4°/min heating rate with a MOM-Budapest thermobalance.

REFERENCES

[1] K. Okawa and S. Akabori, *Bull. Chem. Soc. Japan*, **30**, 937 (1957).

[2] V. M. Belikov, N. I. Kuznetsova and E. N. Safonova, *Khim. prir. Soedinenya*, **3**, 31 (1967).

[3] Y. Sato, T. Takahashi, S. Imado and N. Sugimoto, *Yakugaku Zasshi*, **81**, 819 (1961); *Chem. Abstr.*, **55**, 24582 (1961).

[4] P. Maldonado, C. Richaud, J. P. Aune and J. Metzger, *Bull. Soc. chim. France*, **1971**, 2933.

[5] L. F. Chapurina, A. V. Ablov, I. A. Dyakon and S. V. Donu, *Zhur. neorg. Khim.*, **21**, 158 (1976).

[6] K. Nakamoto and P. J. McCarthy, "Spectroscopy and Structure of Metal Chelate Compounds", Wiley, New York, 1968, p. 270.

[7] E. D. Bergman, E. Zimkin and S. Pinchas, *Rec. Trav. chim.*, **71**, 168 (1952).

[8] G. Habermehl, *Chem. Ber.*, **96**, 2029 (1963).

[9] K. Nakamoto, "Infrared Spectra of Inorganic and Coordination Compounds", Wiley, New York, 1966, p. 214.

Revue Roumaine de Chimie, 26, *6*, 867–873 (1981)

REDUCCION DE CICLOHEXENO, EN FASE LIQUIDA, CON NUEVOS SISTEMAS DE NIQUEL SOPORTADO

J. M. CAMPELO, D. LUNA y J. M. MARINAS
Departamento de Química Orgánica de la Facultad de Ciencias de la Universidad de Córdoba,
Córdoba, España

Recibido: el 14 de Abril de 1980

En el presente trabajo se estudia el comportamiento del niquel soportado (al 5, 10 y 20%) sobre $AlPO_4$, $AlPO_4-Al_2O_3$ y $AlPO_4-SiO_2$, como catalizador de reducción de ciclohexeno con hidrógeno a 298 K y 4 atmósferas, en sistema tipo Parr. La actividad catalítica crece con el contenido de niquel, pero permanece constante para un determinado soporte y contenido en metal, a pesar de que el área metálica varíe. El proceso de reducción del ciclohexeno sigue una cinética de orden cero respecto a la concentración de olefina y la presión de hidrógeno, en nuestras condiciones de operación.

The catalytic behaviour of nickel supported on $AlPO_4$, $AlPO_4-Al_2O_3$, and $AlPO_4-SiO_2$ at three different metal loadings (5, 10, and 20%) in the reduction of cyclohexene with hydrogen at 298 K and 4 atm in a Parr-type system is studied. The catalytic activity increases as the content in nickel dies, but it remains constant for a given support and nickel content despite the change in the metallic surface area. The reduction process follows a zero-order kinetics as respects the concentration of olefin and hydrogen pressure.

INTRODUCCION

El niquel depositado sobre diferentes soportes (alúmina, sílice, zeolitas, etc) ha sido utilizado como catalizador de diferentes procesos de hidrogenación y deshidrogenación. Circunscribiéndonos a los primeros, la reducción del ciclohexeno ha sido elegido como "proceso test" a la hora de optimizar nuestros catalizadores de reducción.

En publicaciones precedentes, hemos puesto de manifiesto la utilidad de los ortofosfatos de aluminio y sistemas $AlPO_4 - Al_2O_3$ y $AlPO_4 - SiO_2$ como catalizadores de diferentes procesos orgánicos. En la actualidad estamos aplicando estos sistemas como soportes de diversos metales (Ni, Pd, Pt y Rh) con el fin de obtener posibles catalizadores de contacto aplicables a procesos orgánicos de reducción.

En el presente trabajo damos cuenta de los resultados obtenidos con niquel depositado, a diferentes concentraciones, sobre los sistemas anteriores, en el proceso de hidrogenación del ciclohexeno. La reacción se ha efectuado en un sistema de reactores tipo "Parr", a baja presión (inferior a 5 atmósferas) y temperatura (298 K), lo que previene otras reacciones secundárias especialmente de isomerización de esqueleto.

PARTE EXPERIMENTAL

Soportes utilizados

Se han utilizado tres tipos de soportes, cuya síntesis ha sido descrita con anterioridad. El denominado B[1] es un ortofosfato de aluminio puro gelificado en óxido de etileno. El C[1] está formado por un sistema $AlPO_4-Al_2O_3$ (75 : 25 %, en peso). El E[2] está constituido por $AlPO_4-SiO_2$ (20 : 80 %, en peso). Todos ellos han sido tamizados entre 70—230 mesh.

Sus propiedades fisicoquímicas aparecen en la Tabla 1. La superficie específica (S_{esp}), volumen total de poros (V_p) y radio medio de poro ($\bar{r}$) han sido determinados a partir de la rama de desorción de la isoterma de nitrógeno, a la temperatura de nitrógeno líquido. Para las medidas de acidez se ha utilizado un procedimiento espectrofotométrico[3] basado en la cantidad de piridina ó 2,6-ditercbutil-4-metilpiridina (DTBMP) para formar una monocapa sobre et sólido.

TABLA 1

Propiedades texturales y de acidez de los soportes

Soporte	Acidez (μ mol·g^{-1}) frente		S_{esp} ($m^2.g^{-1}$)	V_p (mls.g^{-1})	$\bar{r}$ (A)
	Piridina	DTBMP			
E	350	15	327	0,46	30
B	470	90	256	0,50	40 y 120
C	300	50	263	0,53	30

Sistemas metal-soporte

Los sistemas niquel-soporte se han preparado por impregnación de 10 g de soporte con 20 ml de disolución de $(NO_3)_2Ni.6H_2O$ de concentración adecuada para la obtención del porcentaje de metal deseado. El disolvente se elimina a rotavapor y el soporte impregnado se deseca en estufa a 380—390 K durante 24 horas. A partir del mismo se obtienen dos sistemas diferentes, uno reducido en corriente de hidrógeno (100 ml.min^{-1}) a una temperatura de 673 K durante 4, 5 ó 6 horas según se trate del soporte E, B y C, respectivamente, y otro calcinado previamente a 573 K durante 2 horas, reduciéndole en las mismas condiciones anteriores. El análisis de niquel se efectúa por absorción atómica.

Las medidas de dispersión metálica se han efectuado por difracción de rayos X, siguiendo el procedimiento de "semianchura de la banda", de Scherrer.[4-6] El procedimiento es válido, en principio, para tamaños medios de cristales metálicos entre 30—500 A. Todos los valores de nuestros sistemas, quedan dentro de este intervalo, habiéndose comprobado por quimisorción de hidrógeno que en los valores más alto y más bajo de nuestras series, hay concordancia entre la técnica de rayos X y la de adsorción de hidrógeno.

En lo que se refiere a la nomenclatura de los sistemas metálicos, consta de una letra que indica el soporte de que se trate, seguida de un subíndice que hace referencia al % de metal. Finalmente los caracteres C ó NC hacen referencia, respectivamente a que hayan sido sometidos a un proceso de calcinación o no, antes de sufrir la reducción con hidrógeno.

Dispositivo y Metodología experimental

Los procesos de hidrogenación se han efectuado en un hidrogenador de baja presión (hasta 6 atms) de la Firma "Gerhardt", provisto de velocidad de agitación y calefacción regulables. La botella de reacción es de 500 mls, habiéndose intercalado un manómetro (que permite apreciar fluctuaciones de presión de 0,05 atms) entre el tanque de hidrógeno y dicha botella. Esta va introducida en un baño de agua cuya temperatura es regulable con una precisión de ±1 K. Todas las experiencias se han efectuado con 50 ml de disolución metanólica de ciclohexeno 1M, utilizando $0{,}5.10^{-3}$ átomo-gramos de niquel (0,1467 g de catalizador de Ni al 20 %, el doble de. peso al 10 %, y el cuádruple al 5 %).

Previamente se han controlado los procesos de difusión, habiéndose observado que, a partir de 200 sacudidas.min^{-1}, en la agitación del reactor, el rendimiento permanece constante. En todas las experiencias se opera a 300 sacudidas.min^{-1}.

Todos los reactivos utilizados son de la Firma Merck, calidad purísima.

Antes de cada experiencia se activa el catalizador de la siguiente forma : en un reactor de flujo, en vidrio Pyrex, se hace pasar una corriente de hidrógeno purísimo con un flujo de 100 ml.min^{-1}, a 673 K. Se deja enfriar a la temperatura ambiente manteniendo el flujo de H_2 (15 minutos), introduciéndolo seguídamente en la botella de reacción. Tras extraer el aire de ésta mediante vacío, se introduce el hidrógeno a la presión deseada. El trascurso de la reacción se sigue por la disminución de la presión de hidrógeno con el tiempo, obteniéndose curvas como las que aparecen en la figura 1.

Las velocidades iniciales de reacción se obtienen por el procedimiento convencional de las pendientes.

El análisis de los productos de reacción se efectúa por cromatografía de gases, utilizando un cromatógrafo de gases "Hewlett Packard" modelo 5830, provisto de una columna de polifeniléter sobre Chromosorb G AW-DMCS de 2m de longitud y 1/8 de pulgada. En las condiciones de nuestras experiencias únicamente se ha obtenido ciclohexano como producto de reducción del ciclohexeno.

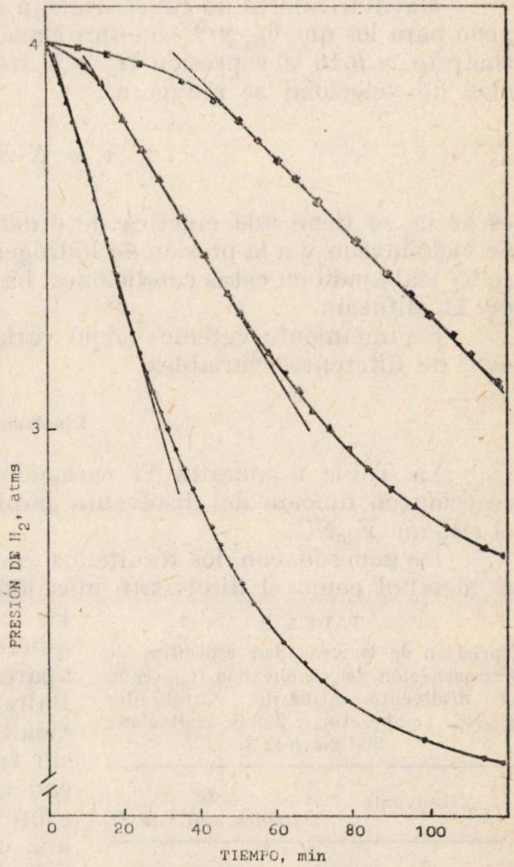

Fig. 1. — Variación de la presión de hidrógeno con el tiempo para los sistemas $E_{20}NC$ (●), $B_{20}NC$(▲) y $C_{20}NC$ (■).

RESULTADOS EXPERIMENTALES

La cinética de la hidrogenación catalítica de cicloalquenos a los correspondientes ciacloalcanos ha sido estudiada ampliamente por Price [7] operando en fase líquida en un sistema de semiflujo, y por Hussey [8] en fase líquida en reactor a presión atmosférica. A partir de estas investigaciones, Baltzy [9] ha efectuado la reducción de ciclohexeno y otras olefinas con hidrógeno, en reactores a baja presión, del tipo utilizado por nosotros. Este autor propone la ecuación cinética siguiente :

$$v(\text{moles.min}^{-1}) = \Delta \cdot K \cdot w \cdot \theta_{H_2} \cdot \theta_S$$

siempre que los fenómenos de difusión y transporte no controlen el proceso.

Δ es una constante que tiene en cuenta la solubilidad del H_2 en el disolvente utilizado, la viscosidad y tensión superficial del mismo y la eficacia de la mezcla de reacción.

w representa el peso de catalizador o el área superficial metálica del mismo.

K es la constante real de la hidrogenación y θ_{H_2} y θ_S son los términos correspondientes a la adsorción del hidrógeno y del sustrato, respectivamente, sobre el catalizador sólido.

Existen valores de concentración del sustrato y de presión de hidrógeno para los que θ_{H_2} y θ_S son aproximadamente la unidad (concentración sustrato $> 0{,}16$ M y presión $H_2 \geqslant 3$ atms). En estas condiciones, la ecuación de velocidad se reduce a:

$$v = \Delta \cdot K \cdot w$$

es decir, se tiene una cinética de orden cero respecto a la concentración de ciclohexeno y a la presión de hidrógeno. En todas nuestras experiencias se ha trabajado en estas condiciones, habiéndose comprobado el no control de la difusión.

Seguídamente veremos cómo varía la velocidad de reacción en función de diferentes variables.

Disolventes

La Tabla 2 muestra la variación de la velocidad específica de la reacción en función del disolvente empleado, utilizando como catalizador el sistema $E_{20}NC$.

De acuerdo con los resultados que muestra la Tabla 2 se ha elegido el metanol como el disolvente más idóneo, habiéndose efectuado con él las restantes experiencias. Esto nos quiere decir que la constante Δ que aparece en la expresión cinética de Baltzy, es un factor decisivo en la velocidad específica de reacción. Gouzo[10] sin embargo, al hidrogenar ciclohexeno con catalizadores de paladio soportado sobre sílice o alúmina, no encuentra una influencia apreciable de Δ sobre la velocidad de reacción. Este hecho puede ser debido a que si bien en sus experiencias $\theta_S \simeq 1$, el valor de θ_{H_2} es, aproximadamente, 1,5 lo que puede "compensar" el peso que la constante Δ puede ejercer en la expresión cinética.

TABLA 2

Variación de la velocidad específica de hidrogenación del ciclohexeno (r_0), según el disolvente utilizado. Catalizador $E_{20}NC$. Temperatura : 298 K. Agitación : 300 sac.min^{-1}.

Disolvente	r_0 (moles.min^{-1}.m^{-2})
Metanol	0,223
Etanol	0,114
Isopropanol	0,004
Acetato de etilo	0,003
Ciclohexano	0,182
n-Hexano	0,119

Velocidades específicas de reacción, utilizando como catalizadores los diferentes sistemas metálicos soportados

En la Table 3 aparecen las actividades catalíticas de los diferentes sistemas metálicos de niquel, utilizados como catalizadores, en la hidrogenación de ciclohexeno. La actividad se expresa como velocidad específica de conversión de ciclohexeno a ciclohexano (moles convertidos. min$^{-1}\cdot$m^{-2} de niquel). En la misma Tabla aparece la superficie específica metálica de cada sistema ($m^2 \cdot g^{-1}$ de niquel), el diámetro medio de los cristales metálicos, $D(A)$. La superficie específica metálica se obtiene mediante la expresión :

$$S = \frac{6\,m}{\rho D}$$

donde : m, es la masa de metal disperso y ρ es la densidad del metal.

TABLA 3

Actividad catalítica específica (r_0, moles de ciclohexeno convertidos$\cdot min^{-1} \cdot m^{-2}$ de Ni) de los diferentes sistemas de niquel, en la hidrogenación de ciclohexeno.

Sistema	D (A)	S_{esp}met ($m^2.g^{-1}$)	r ($mol.min^{-1}$)	r_0 ($mol.min^{-1}.m^{-2}$Ni)
E_5NC	31	218	0,413	0,064
E_5C	91	74	0,131	0,060
E_{10}NC	47	142	0,748	0,180
E_{10}C	65	104	0,544	0,178
E_{20}NC	57	118	0,773	0,223
E_{20}C	80	84	0,538	0,219
B_5NC	43	156	0,175	0,038
B_5C	58	116	0,135	0,039
B_{10}NC	79	86	0,181	0,072
B_{10}C	131	51	0,105	0,070
B_{20}NC	75	90	0,436	0,165
B_{20}C	122	55	0,272	0,167
C_5NC	49	138	0,240	0,059
C_5C	89	76	0,125	0,056
C_{10}NC	53	128	0,241	0,064
C_{10}C	97	70	0,133	0,065
C_{20}NC	58	116	0,275	0,081
C_{20}C	93	63	0,177	0,095
E_{20}C*	81	74	0,489	0,226

* muestra preparada idénticamente que E_{20}C, pero a partir de un precursor diferente.

Todas las experiencias están realizadas a 298 ± 1°K ; presión inicial de hidrógeno, 4 atms. ; agitación 300 sacudidas. min^{-1}.

De los datos consignados en la Tabla 3, se deduce que la actividad catalítica del niquel soportado sobre los soportes E, B y C decrece al disminuir el contenido en metal. Generalmente la variación en la actividad catalítica específica de un metal soportado es debida al diferente tamaño de las partículas metálicas o a la existencia de algún tipo de interacción metal-soporte. Como puede observarse en la Tabla 3 el tamaño de las partículas no afecta a la actividad catalítica de los sistemas, ya que para un sistema con proporción fija de metal (calcinado y sin calcinar) el diámetro medio de los cristales metálicos es diferente y, sin embargo, la actividad catalítica es idéntica, dentro del error experimental. Estos procesos han sido denominados "fáciles" por Boudart.[11] Otros autores como Gouzo[10] llegan a la misma conclusión trabajando con diferentes metales y soportes.

Parece pues que, en nuestro caso, la disminución en la actividad catalítica del sistema con el tanto por ciento de niquel, debe atribuirse a algún tipo de interacción metal-soporte, hecho comprobado por otros investigadores [12-14] operando con diferentes metales soportados, y al que se han dado diferentes interpretaciones. En nuestro caso la técnica de difracción de rayos X no ha puesto de manifiesto la aparición de especies químicas nuevas : aluminatos, fosfatos o silicatos de niquel. Por otra parte, la acidez del soporte no parece influir de forma clara en la actividad catalítica de nuestros sistemas, en contradicción con lo encontrado por Richardson [15] operando con otros sistemas metálicos.

Influencia de la temperatura en la velocidad específica de la reducción del ciclohexeno

La influencia de la temperatura se ha calculado, únicamente, en el caso del niquel soportado al 20%. En la Tabla 4 aparecen los resultados obtenidos operando entre 298 y 333 K.

TABLA 4

Efecto de la temperatura en la velocidad específica (r_0) de reducción del ciclohexeno. Presión inicial : 4 atms

Sistema	T (K)	r_0 (mol.min^{-1}.m^{-2} Ni)
$E_{20}NC$	298	0,285
$E_{20}NC$	308	0,352
$E_{20}NC$	313	0,380
$E_{20}NC$	321	0,474
$E_{20}NC$	330	0,528
$B_{20}NC$	298	0,168
$B_{20}NC$	308	0,236
$B_{20}NC$	319	0,285
$B_{20}NC$	333	0,621
$C_{20}NC$	298	0,081
$C_{20}NC$	308	0,094
$C_{20}NC$	319	0,193
$C_{20}NC$	329	0,241

TABLA 5

Valores de las energías de activación aparente (E'_A) y de la constante de Arrhenius (Δ'), en el proceso de hidrogenación de ciclohexeno, utilizando como catalizadores diferentes sistemas de niquel soportado.

Sistema	E'_A (kj.mol^{-1})	Δ' (mol.min^{-1}.m^{-2} Ni)
$E_{20}NC$	22,9	2,5
$B_{20}NC$	29,2	20,7
$C_{20}NC$	32,0	30,1

Energías de activación

En la Tabla 5 se muestran los valores encontrados para la energía de activación aparente y la constante Δ', a 298 K (utilizando la expresión de Arrhenius) en el proceso de hidrogenación de ciclohexeno utilizando como catalizadores los sistemas con niquel al 20%.

Los valores obtenidos en las energías de activación aparentes son del mismo orden de magnitud que los encontrados por Hussey [8] y Gouzo [10] en la hidrogenación del ciclohexeno utilizando como catalizadores $Pt-Al_2O_3$ y $Pd-Al_2O_3$, tanto en fase líquida como gaseosa.

A la vista de los resultados obtenidos, podemos concluir que los sistemas formados por niquel soportado sobre $AlPO_4$ y sistemas $AlPO_4$ —

Al_2O_3 y $AlPO_4-SiO_2$ parecen ser catalizadores muy eficientes en los procesos de hidrogenación de olefinas a baja temperatura y presión de hidrógeno.

BIBLIOGRAFIA

[1] J. M. Campelo, Tesis Doctoral, Facultad de Química Universidad Complutense Madrid, 1977.

[2] C. Jimenez, Tesis Doctoral, Facultad de Química, Universidad Complutense, Madrid, 1977.

[3] J. M. Marinas, J. M. Campelo, C. Jimenez, M. A. Aramendia, V. Borau y D. Luna, Trabajo presentado al VII Simposio Iberoamericano de Catálisis, La Plata (Argentina), 1980.

[4] P. Scherrer, *Nachrechten*, **2**, 98 (1919).

[5] H. P. Klug y L. E. Alexander, "X-ray Difraction Procedures" Wiley, New York, 1976.

[6] R. L. Moss, "Experimental Methods in Catalytic Research" (R. B. Anderson y P. T. Dawson Ed.) Vol. 2, Academic Press, New York, 1976.

[7] R. H. Price y D. B. Schiewetz, *Ind. Eng. Chem.*, **49**, 807 (1957).

[8] A. S. Hussey, G. B. Hendes, C. P. Navack y R. H. Baker, *J. Org. Chem.*, **33**, 610 (1968).

[9] R. Baltzly, *J. Org. Chem.*, **41**, 920 (1976).

[10] E. E. Gouzo, *J. Catalysis*, **52**, 462 (1978).

[11] M. Boudart, *Adv. in Catalysis, Relat. Sub.*, **20**, 153 (1969).

[12] F. Solymon, *Catalysis Reviews*, **1**, 233 (1968).

[13] P. W. Selwood, *Adv. in Catalysis*, **3**, 27 (1951).

[14] G. T. Rymer, J. M. Bridges y J. R. Tomlinson, *J. Phys. Chem.*, **65**, 2152 (1961).

[15] J. T. Richardson, *J. Catalysis*, **21**, 122 (1971).

Revue Roumaine de Chimie, 26, 6, 875–878 (1981)

A NOVEL ROUTE FOR THE SYNTHESIS OF KETO-BENZOIC ACID DERIVATIVES, AUXIN TRANSPORT INHIBITORS

R. K. PANDE, R. SHARMA and B. C. JOSHI *
Chemical Laboratories, University of Rajasthan, Jaipur, India

Received April 24, 1980

A novel route for the synthesis of keto-benzoic acids (or its derivatives) known as auxin transport inhibitors, is described by reaction of aryl-magnesium halides with N-alkyl phthalimides followed by subsequent hydrolysis.

Some keto-benzoic acid derivatives have been reported as auxin transport inhibitors in plants [1] and a few have also been isolated from the species of *Phaseolus* and *Raphanus*.[2] These compounds have earlier been

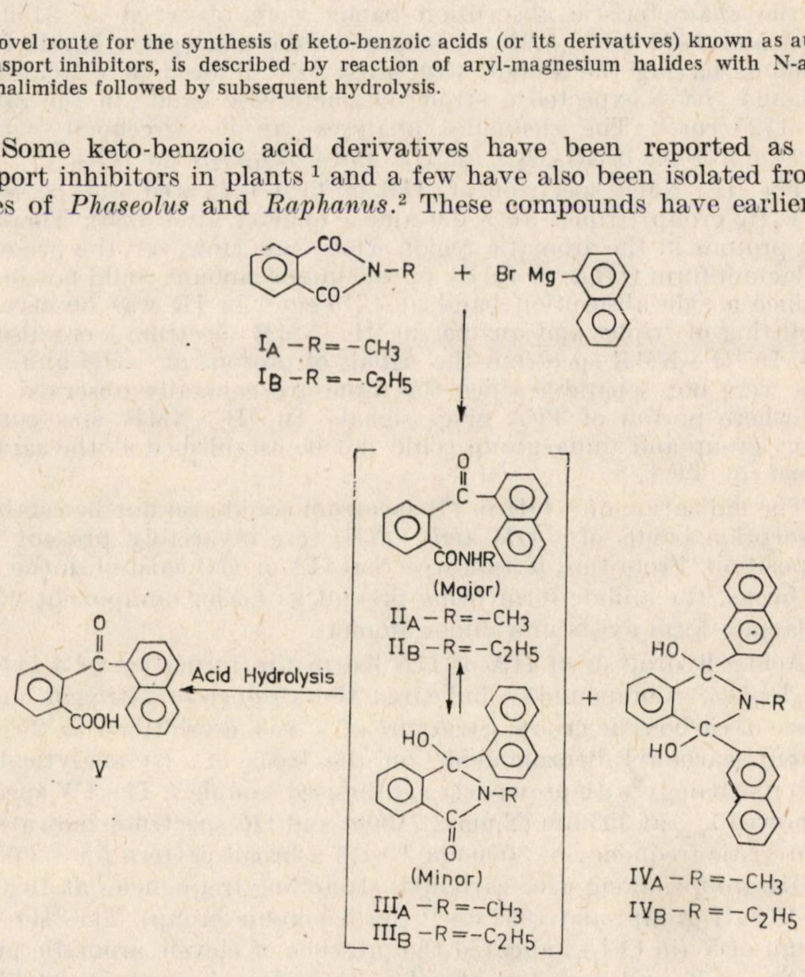
N-R
+ Br Mg
$I_A - R = -CH_3$
$I_B - R = -C_2H_5$
CONHR
(Major)
$II_A - R = -CH_3$
$II_B - R = -C_2H_5$
COOH
V
Acid Hydrolysis
HO
N-R
(Minor)
$III_A - R = -CH_3$
$III_B - R = -C_2H_5$
+
HO
N-R
HO
$IV_A - R = -CH_3$
$IV_B - R = -C_2H_5$

---

* Correspondence author

prepared in lower yields only by the interaction of phthalic anhydride derivatives with alkyl or aryl organo-cadmium compounds.[3]

In the interaction of α-naphthyl-magnesium bromide with N-alkylphthalimides (IA. $-N-CH_3$; IB. $-N-C_2H_5$) two products were mostly obtained. One of these products was identified as 2-(1-naphthalenyl carbonyl)-N-alkyl-benzanilide (IIA. $-N-CH_3$, IIB. $-N-C_2H_5$) and the other as 3,5-dihydroxy-3,5-dinaphthyl-N-alkyl phthalimidines (IVA, or IVB). Compounds IIA or IIB on acid hydrolysis led to the formation of keto-acid V, whose structure was established.

Earlier workers [4-7] indicated the presence of ring-chain tautomerism in the compounds obtained by the interaction of aryl or aralkyl magnesium halide with N-alkyl phthalimides. In the present study when α-naphthyl magnesium bromide reacted with N-methyl (IA) or N-ethyl (IB) phthalimides, products IIA or IIB were identified in the anilide forms since the characteristic absorption bands were observed at 3150 cm^{-1} (3.17 μ) and 1680 cm^{-1} (5.95 μ), (characteristic absorption bands for the compounds having the anilide structure). Had it been in δ-lactam form one should have expected a strong characteristic band in the range of 1712 – 1725 cm^{-1}. The elemental analyses are in agreement with the theoretical values ($C_{19}H_{15}O_2N$ for IIA and $C_{20}H_{17}O_2N$ for IIB).

The ^1H–NMR spectrum of IIB in TFA indicated the presence of $-N-C_2H_5$ group (triplet at δ 0.9 and a quartet at δ 3.85). There were eleven protons in the aromatic region δ 6.6 – 8.6. However, the presence of the δ-lactam form (IIIA or IIIB) in the minor amount could not be ruled out, since a side absorption band at 1715 cm^{-1} in IR was observed and the splitting of triplet and quartet in ^1H–NMR spectrum were also noticeable. In ^1H–NMR spectrum the signals of protons of –OH and $-NH_2$ groups were not separable since the same are generally observed in the range where proton of TFA gives signals. In ^1H–NMR spectrum the hydroxy group and amino group could not be established as the same was obtained in TFA.

The indication of –OH in IR spectrum could also not be established as absorption bands of –OH and –NH were invariably present in the same position. From this, it appeared that IIA or IIB existed in the tautomeric forms, the anilide form being present as major component whereas the δ-lactam form exists in a minor amount.

Acidic hydrolysis of IIA or IIB led to the formation of a keto-acid (V, $C_{18}H_{12}O_3$). Compound V indicated the absence of nitrogen, and the presence of carboxylic group. Structure of V was established as 2-(-naphthalenenyl-carbonyl)-benzoic acid [3] on the basis of: (i) analytical data and (ii) its analogy with previously synthesised sample [3]. The UV spectrum of V showed λ_{max} at 323 nm (Σ max. 74000) and IR spectrum indicated the characteristic frequency of 3050 cm^{-1} with a broad pattern for –OH and –COOH groups, along with carbonyl stretching frequencies at 1680 cm^{-1} (for –COOH group) and 1662 cm^{-1} (for a ketonic group). The ^1H–NMR spectrum of V (in CCl_4) indicated the presence of eleven aromatic protons at δ 7.28 – 8.00 and a proton attached to carboxyl group at δ 9.65 as a singlet. All these observations confirmed the assigned structure to V.

EXPERIMENTAL

All the m.p.'s are uncorrected. IR spectra were recorded on a Perkin Elmer Infracord in KBr phase. ^1H-NMR spectra were recorded on a Perkin Elmer R 12B spectrometer using TMS as internal standard.

Reactions of α-naphthyl magnesium bromide with N-methyl phthalimide (IA)

N-Methyl phthalimide (IA, 8.05 g., 0.05 M) was taken in dry ether (100 ml) in a three necked flask fitted with a mercury sealed stirrer, condenser and dropping funnel. An ethereal solution of α-naphthylmagnesium bromide (α-bromonaphthalene 31.05 g, 0.15 M : magnesium 3.60 g, 0.15 M and ether 200 ml) was added. The reaction mixture was stirred vigorously at 10–15°C for 2 hrs and then at 30–40°C for 3 hrs. The reaction mixture was then poured on crushed ice containing NH_4Cl and NH_4OH. It was then extracted with chloroform. After drying (over anhydrous Na_2SO_4), the solvent was distilled off and the crude product so obtained was boiled with benzene, a part was crystallized from alcohol to a white product, IIA (m.p. 220°C, 8.67g, 60%). The benzene soluble portion gave a yellow product which was crystallized from acetone-petroleum ether mixture (IVA m.p. 240°C, 5.21 g, 25%).

Similarly, N-ethyl-phthalimide (IB) (8.75 g, 0.05M) was treated with α-naphthyl-magnesium bromide (0.15 M) and the products IIB (m.p. 178°C, 7.57 g, 50%) and IVB (m.p. 203°C, 4.31 g, 20%) were isolated.

Synthesis of 2-(-naphthalenyl carbonyl)-benzoic acid – V

Compound IIA (5.78 g, 0.02 M) was refluxed for 4 hrs with 2N–HCl (25 ml.). The reaction mixture was then poured on crushed ice and basified with NH_4OH. It was extracted with ether. Removal of the solvent afforded a white solid (V) which was crystallized from acetone-ether (4.90 g, 88%, m.p. 170°C, lit. 173°C)[3].

On similar lines, hydrolysis of IIB with 2N–HCl yielded the same product V (m.p. 170°C, 80%). The analytical and spectral data of all these compounds are summarised in table 1.

TABLE 1

Analytical and spectral data of compounds II, III, and V

Compound number	Molecular formula	M.P. °C	% Analysis Calcd. (Found) C	H	N	IR data νcm^{-1}	UV data λ max·nm
IIA	$C_{19}H_{15}O_2N$	220	78.20 (78.38)	5.19 (5.06)	4.84 (4.96)	3150, 1680	–
IIB	$C_{20}H_{17}O_2N$	178	79.30 (79.01)	5.61 (5.48)	4.62 (4.52)	3155, 1680	–
IVA	$C_{29}H_{23}O_2N$	240	83.42 (83.18)	5.51 (5.48)	3.30 (3.16)	3440, 1350	–
IVB	$C_{30}H_{25}O_2N$	203	83.52 (83.38)	5.80 (5.68)	3.20 (3.08)	3455, 1365	–
V	$C_{18}H_{12}O_3$	170	78.26 (78.14)	5.55 (5.48)	–	3050, 1680 1662	323 (Σ max. 74000)

ACKNOWLEDGEMENT. The authors thank the Head of the Chemistry Department, University of Rajasthan, Jaipur, for providing necessary facilities and ICMR authorities for financial assistance.

REFERENCES

[1] G. F. Katekar and A. E. Geissler, *Plant Physiol.*, **60**, 826 (1973).
[2] P. L. De Benneville, *J. Org. Chem*, **6**, 462 (1941).
[3] P. W. Daniel and J. P. Crane, *J. Org.. Chem.*, **38**, 3375 (1973).
[4] F. Iachs and A. Ludwig, *Chem. Ber.*, **37**, 385 (1964).
[5] C. Beis, *Compt. rend.*, **143**, 430 (1966).
[6] H. Bauer, *Ber. dtsch. chem. Ges.*, **38**, 241 (1905).
[7] A. M. Aslam and G.E.M. Younes, *Egypt. J. Chem.*, **16**, 1 (1973).

Revue Roumaine de Chimie, 26, 6, 879–885 (1981)

PYRIDINIUM-YLURES. II[1]

LES RÉACTIONS DE QUELQUES 4-PHÉNYLPYRIDINIUM-YLURES CARBANION-MONOSUBSTITUÉS AVEC DES ACÉTYLÈNES ACTIVES

FLORENTINA GEORGESCU[a], FILIP CHIRALEU[b], EMILIAN GEORGESCU[a]
et ION ZUGRĂVESCU[c]

[a] Centre de Recherches, 1, str. Uzinei, Rm. Vîlcea, Roumanie
[b] Centre de Chimie Organique, Bucarest
[c] Institut Polytechnique, Jassy, Roumanie

Reçu le 20 août 1980

On a étudié les réactions de cycloaddition 3 + 2 dipolaires de quelques 4-phénylpyrimidinium-ylures carbanion-monosubstitués avec le diméthylacétylendicarboxylate et le propyolate d'éthyle. On a mis en évidence l'existence d'un équilibre entre les 4-phénylpyrimidinium-benzoylméthylures (**2 a—d**) et les dimères dipyrimido-pyraziniques (**3 a—d**) dans des solvants organiques polaires et sous l'action de l'agent dipolarophile.

There have been investigated the 3 + 2 dipolar cycloaddition reactions of some carbanion-monosubstituted 4-phenylpyrimidinium-ylids with methylacetylendicarboxylate and ethylpropyolate. Using polar organic solvents and under the influence of a dipolarophil reagent an equilibrium occurs, between the 4-phenylpyrimidinium derivatives **2 a—d** and the dipyrimido-pyrasine dimers **3 a—d**.

Dans un travail précédent[1], on a présenté les synthèses des sels quaternaires de 4-phénylpyrimidinium (**1 a—e**) qui, par déhydrohalogénation en milieu alcalin, donnent naissance aux 4-phénylpyrimidinium-ylures carbanion-monosubstitués (**2 a—e**).

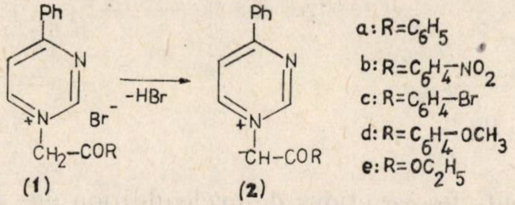

Le 4-phénylpyrimidinium-1-(*p*-nitrobenzoyl) méthylure (**2 b**) et le 4-phénylpyrimidinium-1-(*p*-brombenzoyl) méthylure (**2 c**) ont été isolés comme des produits avec des propriétés physiques distinctes.

Les 4-phénylpyrimidinium-1-benzoylméthylures (**2 a**) et (**2 d**) moins stables se transforment en produits d'inactivation possédant la structure des dimères dipyrimido-pyraziniques (**3 a**) et (**3 d**). Les 4-phénylpyrimidinium-benzoylméthylures stables (**2 b**) et (**2 c**) subissent le même processus d'inactivation par conservation prolongée ou par le chauffage des solutions de sels quaternaires respectifs, en milieu alcalin, conduisant aux dimères dipyrimidopyraziniques (**3 b**) et (**3 c**).

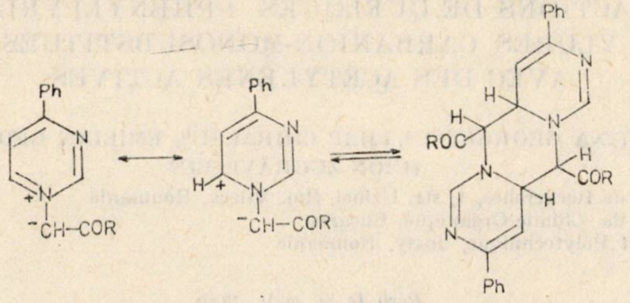

(**2**a-d) (**3**a-d)

Le caractère dipolaire des ylures est, en général, mis en évidence [2] par la participation directe aux réactions de cycloadditon 3 + 2 dipolaires avec des acétylènes activés ou des oléfines activées. Cependant, dans la littérature on trouve peu d'indications [3] concernant les réactions de cycloaddition 3 + 2 dipolaires des pyrimidinium-ylures.

Poursuivant les investigations concernant la synthèse et la réactivité des 4-phénylpyrimidinium-ylures nous avons étudié les réactions de ces composés avec des acétylènes activés.

Les 4-phénylpyrimidinium-ylures **2 a—e** ont les positions 2 et 6 du cycle pyrimidinique avec déficit d'électrons. Il existe donc la possibilité d'obtenir deux cycloadducts au cours des réactions de cycloaddition avec des acetylènes activés : des dérivés pyrrolo [1,2-a] pyrimidiniques (**4**) et des dérivés pyrrolo [1,2-c] pyrimidiniques (**5**).

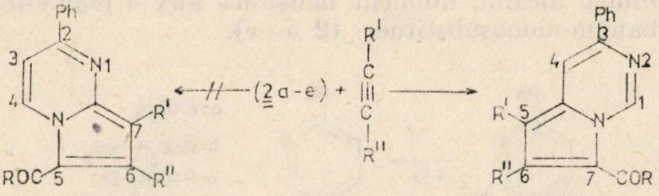

(**4**) (**5**)

Pratiquement, les réactions de cycloaddition des 4-phénylpyrimidinium-ylures carbanion-monosubstitués avec des acétylènes activés ont conduit à la formation d'un seul type de cycloadduct.

Ainsi, par le traitement de 4-phénylpyrimidinium-ylures **2 a—e** avec des diméthylacéthylendicarboxylate, respectivement le propyolate d'éthyle, on a obtenu directement les dérivés pyrrolo/1,2 —c/pyrimidiniques **7 a —e**, resp. **8 a —e**.

Le mécanisme réactionnel implique la formation des cycloadducts intermédiaires de type **6**, qui subit un processus d'aromatisation spontané, conduisant aux cycloadducts **7 a—e**, resp. **8 a—e**.

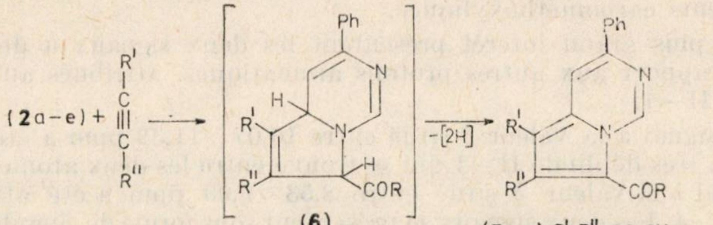

(6)

(7a–e): $R'=R''=CO_2CH_3$

(8a–e): $R'=CO_2C_2H_5$, $R''=H$

Les réactions ont été effectuées par le traitement des ylures (**2 a—e**) avec le diméthyleacétylènedicarboxylate, resp. le propyolate d'éthyle en milieu de diméthylformamide ou d'acétonitrile à reflux. Les 4-phénylpyrimidinium-ylures moins stables **2 a**, **2 d** et **2 e**, ont été introduits en réaction immédiatement après la séparation, sans purification préalable, dans le but d'éviter le processus de dimérisation.

Concomitamment, ces réactions ont été effectuées avec les 4-phénylpyrimidinium-ylures formées « in situ ». Ainsi, les sels quaternaires **1 a—e** dans l'acétonitrile ou le diméthylformamide ont été traités avec le diméthylacétylendicarboxylate, respectivement le propyolate d'éthyle, en présence de triéthylamine.

Dans ces deux variantes expérimentales les rendements sont assez faibles dû à la grande réactivité des ylures qui détermine l'apparition des réactions secondaires.

C'est pourquoi dans le cas des réactions effectuées « in situ » on a étudié la possibilité de remplacer la triéthylamine par un accepteur d'acide plus faible. Ainsi la vitesse de formation de l'ylure du sel quaternaire sera plus faible et l'ylure sera consommée pendant la réaction avec la dipolarophile à mesure qu'il se forme.

Pendant les expérimentations on a établi que les accepteurs d'acide les plus convenables pour ces cas sont les époxydes. Des raisons expérimentales nous ont déterminé de choisir le propylène oxyde comme accepteur d'acide et solvant dans ces réactions. Les rendements et la pureté des cycloadducts obtenus confèrent une valeur synthétique à cette méthode de préparation des pyrrolo [1,2-c] pyrimidines.

La structure pyrrolo/1,2-c/pyrimidinique, attribuée aux produits de cycloaddition, a été prouvée par les analyses chimiques et par les spectres IR et RMN.

Ainsi, dans les spectres IR des cycloadducts **7 a—e** on remarque les deux bandes d'absorption correspondant aux groupements carbonyle estériques à 1730—1745 cm^{-1} et 1700—1715 cm^{-1} et la bande d'absorption caractéristique au groupement carbonyle cétonique à 1610—1630 cm^{-1}.

Par la position et la forme des signaux les spectres RMN confirment les structures proposées. Ainsi, les spectres des cycloadducts **7 a**—**e** présentent deux signaux sous forme de singulets à des valeurs δ situées entre 3,40—3,60 ppm et respectivement 3,92—4,18 ppm, correspondant aux groupements carbométhoxyliques.

Un plus grand intérêt présentent les deux signaux à des champs bas par rapport aux autres protons aromatiques, attribués aux protons H—4 et H—1.

Le signal à la valeur δ situé entre 10,07—11,39 ppm a été attribué au proton très déblindé H—1 qui se trouve entre les deux atomes d'azote, et le signal à la valeur δ situé entre 8,53—9,00 ppm a été attribué au proton H—4. Les deux signaux se présentent sous forme de singulets élargis ou sous forme de doublets avec les constantes de couplage $\leqslant$ 1,5 Hz. Les petites valeurs des constantes de couplage montrent que c'est la position 6 des ylures **2** qui est engagée dans l'addition.

Dans les spectres RMN des dérivés pyrrolo [1,2-a] pyrimidiniques **(4)**, les deux protons aromatiques des positions 3 et 4 devront produire un système AB à constante de couplage $J_{3,4} = 7-8$ Hz dès qu'il y a des déplacements correspondant aux valeurs plus hautes du champ.

Les spectres RMN des cycloadducts **8 a**—**e** confirment les structures attribuées à ces produits.

Ainsi, dans les spectres RMN des cycloadducts **8 a**—**e** les signaux des protons méthyléniques du groupement carbéthoxylique ont un déplacement chimique normal (δ entre 4,36 et 4,65 ppm) pour un ester éthylique non substitué en position β.[4] Le groupement carbéthoxylique occupe donc la position 5 dans les cycloadducts **8 a**—**e**, n'étant pas blindé par le groupement benzoyle de la position 7, ce qui prouve que l'addition a lieu dans le sens favorisé par les facteurs électroniques.

Les signaux des protons H—4 et H—1 apparaissent sous forme de deux doublets avec les constantes de couplage $\leqslant$ 1,5 Hz, à des valeurs δ situées entre 8,36—8,87 ppm, resp. δ entre 9,00—11,52 ppm.

Malgré le fait que le processus de dimérisation des 4-phénylpyrimidinium-benzoylméthylures **(2 a)** et **(2 d)** commence immédiatement après la séparation, dans les réactions de cycloaddition de ces ylures avec le diméthylacétylènedicarboxylate et respectivement le propyolate d'éthyle, dans l'acétonitrile ou dans le diméthylformamide, on a obtenu des produits normaux de cycloaddition.

Ces résultats nous ont suggéré l'idée que, dans les conditions expérimentales utilisées, la réaction de dimérisation est réversible. Un phénomène similaire a été signalé par Kröhnke et collab.[5] dans la série des isoquinolinium-ylures.

L'existence de l'équilibre entre les dimères dipyrimido-pyraziniques **3 a**—**d** et les 4-phényl-pyrimidinium-ylures **2 a**—**d** a été démontrée expérimentalement par l'isolement des cycloadducts **7 a**—**d**, respectivement **8 a**—**d**, dans les réactions des dimères **3 a**—**d** isolés avec le diméthylacétylèndicarboxylate, respectivement le propyolate d'éthyle, dans l'acétonitrile ou dans le diméthylformamide. Dans le benzène la réaction n'a pas lieu; on obtient les dimères non transformés.

Ces données mettent en évidence l'existence d'un équilibre ylure-dimère en solvants organiques polaires et sous l'action de l'agent dipolarophile, la polarité du solvant tenant un rôle important.

PARTIE EXPÉRIMENTALE

Les sels quaternaires **1 a—e**. les 4-phénylpyrimidinium-ylures **2 a—e** et les dimères dipyrimidopyraziniques **3 a—e** ont été obtenus d'après les procédés décrits antérieurement.[1]

Les points de fusion ne sont pas corrigés. Les spectres RMN ont été enregistrés sur un spectromètre VARIAN A—60A et les spectres IR sur un spectromètre UR-20. C. Zeiss.

Les dérivés pyrrolo/1,2-c/pyrimidiniques (**7 a—e**) et (**8 a—e**) ont été obtenus d'après les procédées généraux suivants :

a) A une suspension de 10 mmoles de 4-phénylpyrimidinium-ylure (**2 a—e**) dans 50 ml d'acétonitrile ou de diméthylformamide, on ajoute 11 mmoles (1,35 ml) de diméthylacétylendecarboxylate, ou 11 mmoles (1,25 ml) de propyolate d'éthyle. Le mélange réactionnel est porté à reflux pendant 8 heures. On chasse sous vide la plupart du solvant. Après refroidissement on filtre et on recristallise le produit obtenu.

b) A une suspension de 10 mmoles de sel quaternaire (**1 a—e**) dans 50 ml d'acétonitrile ou de diméthyleformamide, on ajoute 11 mmoles (1,35 ml) de diméthylacétylendicarboxylate ou 11 mmoles (1,25 ml) de propyolate d'éthyle. On ajoute, sous agitation, 11 mmoles (1,5 ml) de triéthylamine. On agite le mélange 15h à la température ambiante, ou le mélange est porté à reflux pendant 8 heures. On évapore une partie du solvant sous pression réduite. Après le refroidissement le produit obtenu est filtré et lavé à l'eau sur le filtre pour chasser le bromhydrate de la triéthylamine. Le produit obtenu est recristallisé.

c) A une suspension de 10 mmoles de sel quaternaire (**1 a—e**) dans 50 ml de propylène oxyde, on ajoute 11 mmoles (1,35 ml) de diméthylacétylendicarboxylate ou 11 mmoles (1,25 ml) de propyolate d'éthyle et on agite 12—16 heures à la température ambiante. On chasse une partie du solvant sous vide. Après refroidissement le produit obtenu est filtré et lavé sur le filtre à l'éther éthylique.

3-Phényl-5,6-dicarbométhoxy-7-benzoyle-pyrrolo /1,2-c/-pyrimidine (*7a*) : cristaux aciculaires blancs à $P_f = 259-261°$ (dans du chloroforme) ; rend. 20%(a), 25%(b), 45%(c). Analyse : $C_{24}H_{18}N_2O_5$: *calculé* : C 69,56 ; H 4,34 ; N 6,76% *trouvé* : C 69,03 ; H 4,12 ; N 6,51%.

Spectre IR (KBr) : 1730 cm^{-1} et 1700 cm^{-1} ($\nu(C = O)$ estérique) ; 1620 cm^{-1} ($\nu(C = O)$ cétonique).

Spectre RMN (CF_3COOH, δ, ppm) : 3,62 et 4.18 (2 s, 6 H, 2 CH_3 des deux groupements carbométhoxy) 7,60—8,16 (m, 10 H, les protons phényliques), 9,00 (s.e, 1 H, H—4) ; 11,39 (s.e., 1 H, H—1).

3-Phényl-5,6-dicarbométhoxy-7-(p-nitrobenzoyle)-pyrrolo /1,2-c/pyrimidine (*7b*) : cristaux aciculaires jaunes, $P_f = 239-240°$ (trichloréthylène) ; rend. : 32% (a) ; 30% (b), 55% (c). Analyse : $C_{25}H_{17}N_3O_7$: *calculé* : C 62,74, H 3,70, N 9,15% *trouvé* : C 62,90 ; H 3,96 ; N 9,20%.

Spectre IR (KBr) : 1738 cm^{-1} et 1715 cm^{-1} ($\nu(C = O)$ estérique) ; 1635 cm^{-1} ($\nu(C = O)$ cétonique).

Spectre RMN ($CDCl_3$, δ, ppm) : 3,40 et 3,93 (2s, 6 H, 2 CH_3 des groupements carbométhoxy) ; 6,81—7,70 (m, 3 H, H—3′, H—4′ et H—5′ du groupement phényle de la position 3), 7,88 et 8,38 (système A_2B_2, 4H, les protons du groupement benzoyle), 8,13—8,33 (m, 2 H, H—2′ et H—6′ du groupement phényl de la position 3), 8,65 (d, 1 H, H—4). 10,48 (d, 1 H, H—1, $J_{1,4} = 1,0$ Hz).

3-Phényl-5,6-dicarbométhoxy-7-(p-bromobenzoyle) pyrrolo/1,2-c/pyrimidine (*7c*) : cristaux aciculaires jaunes ; $P_f = 201-202°$ (dans du chloroforme) ; rend.: 30%(a), 28%(b), 50%(c). Analyse $C_{24}H_{17}N_2O_5Br$: *calculé* : C 58,41 ; H 3,44 ; N 5,76% ; *trouvé* : C 58,17 ; H 3,52 ; N 6,01%.

Spectre IR (KBr) : 1730 cm^{-1} et 1700 cm^{-1} ($\nu(C = O)$ estérique) ; 1620 cm^{-1} ($\nu(C = O)$ cétonique).

Spectre RMN ($CDCl_3$, δ, ppm) : 3,42 et 3,92 (2 s, 6 H, 2 CH_3 des groupements carbométhoxy), 7,35—7,65 (m, 3H, H—3′, H—4′ et H—5′ du groupement phényl de la position 3), 7,60 (s, 4 H, les protons du groupement benzoyle), 8,00—8,25 (m, 2H, H—2,′ și H—6′ du groupement phényl de la position 3) 8,60 (d, 1 H, H—4), 10,27 (d, 1 H, H—1, $J_{1,4} = 1,5$ Hz).

3-Phényl-5,6-dicarbométhoxy-7-(p-méthoxybenzoyle) pyrrolo/1,2-c/pyrimidine (*7d*) : cristaux aciculaires blancs ; p.f. = 152—154° (dans du chloroforme/éther) ; rend. : 20% (a), 22% (b), 42% (c). Analyse : $C_{25}H_{20}N_2O_6$: *calculé* : C 67,56, H 4,50, N 6,30% Trouvé : C 67,73, H 4,97, N 6,43%

Spectre IR(KBr) : 1735 cm^{-1} et 1705 cm^{-1} ($\nu(C = O)$ estérique) ; 1620 cm^{-1} ($\nu(C = O)$ cétonique).

Spectre RMN ($CDCl_3$, δ, ppm) : 3,44 et 3,92 (2s, 6H, 2 CH_3 des groupements carbométhoxy), 3,88 (s, 3 H, CH_3 du groupement OCH_3), 6,95 (d, 2 H, H—3′ et H—5′ du groupement benzoyle), 7,36—7,53 (m, 3 H, H—3′, H—4′ et H—5′ du groupement phényl de la position 3) 7,75 (d, 2H, H—2′ et H—6′ du groupement benzoyle), 8,00—8,20 (m, 2 H, H—2′, et H—6′ du groupement phényl de la position 3) 8,53 (d, 1 H, H—4), 10,07 (d, 1 H, H—1, $J_{1,4}$= 1,5 Hz).

3-Phényl-5,6-dicarbométhoxy-7-carbétoxy-pyrrolo/1,2-c/pyrimidine (*7 e*) : cristaux aciculaires blancs ; P_f = 174—176° (dans du méthanol) ; rend. 25 % (a), 25 (b), 40 % (c). Analyse $C_{20}H_{20}N_2O_6$: *Calculé* : C 62,82, H 4,71, N 7,32 % *Trouvé* : C 63,13, H 5,01, N 7,41 %.

Spectre IR (KBr) : 1753 cm^{-1}, 1715 cm^{-1} et 1705 cm^{-1} (ν(C=O) estérique).

Spectre RMN (CF_3COOH, δ, ppm) : 1,41 (tr., 3 H, CH_3 du groupement éthyle estérique), 4,00 et 4,08 (2 s, 6 H, 2CH_3 des groupements carbométhoxy) 4,46 (q, 4 H, CH_2 du groupement éthyle estérique) 7,46—7,68 (m, 3H, H—3′, H—4′ et H—5′ du groupement phényl de la position 3), 8,11—8,33 (m, 2 H, H—2′ et H—6′ du groupement phényl de la position 3), 8,59 (d, 1 H, H—4) 10,28 (d, 1 H, H—1, $J_{1,4}$ = 1,2 Hz).

3-Phényl-5-carbéthoxy-7-benzoylpyrrolo/1,2-c/pyrimidine (*8 a*) cristaux aciculaires blancs ; P_f = 161—163° (dans du chloroforme) ; rend : 20,4 % (a), 18 % (b), 50 % (c). Analyse : $C_{23}H_{18}N_2O_3$: *Calculé* : C 74,59, H 4,86, N 7,56 % *Trouvé* : C 73,98, H 5,01, N 7,06 %

Spectre IR (KBr) : 1695 cm^{-1} (ν(C=O) estérique) ; 1625 cm^{-1} (ν(C=O) cétonique).

Spectre RMN (CF_3COOH, δ, ppm) : 1,58 (tr. 3 H, CH_3 du groupement éthyle estérique), 4,65 (q, 2H, CH_2 du groupement éthyle estérique), 7,48—8,11 (m, 11 H, les protons des groupements phényl de la position 3 et benzoyle de la position 7), 8,51(s, 1 H, H—4), 8,97 (s, 1 H, H—1).

3-Phényl-5-carbéthoxy-7-(*p-nitrobenzoyl*) *pyrrolo/1,2—c/pyrimidine* (*8 b*) : cristaux jaunes ; P_f = 229—231° (dans du chloroforme) ; rend. 39,7 % (a), 38 % (b), 52 % (d). Analyse $C_{23}H_{17}N_2O_5$: *Calculé* :C 66.5, H 4,09, N 10,12 % *Trouvé* : C 65,91, H 4,09, N 10,02 %.

Spectre IR (KBr) : 1705 cm^{-1} (ν(C=O) estérique), 1628 cm^{-1} (ν(C=O) cétonique).

Spectre RMN ($CDCl_3$, δ, ppm) : 1,46 (tr., 3H, CH_3 du groupement éthyle estérique), 4,50 (q, 2H, CH_2 du groupement éthyle estérique) 7,53—7,70 (m, 3H, H—3′, H—4′ et H—5′, du groupement phényl de la position 3), 7,85 (s, 1 H, H—6), 8,11—8,61 (m, 6 H, les protons aromatiques) 8, 75 (d, 1H , H—4), 10,67 (d, 1 H, H—1, $J_{1,4}$=1,5 Hz).

3-Phényl-5-carbéthoxy-7-(*p-brombenzoyl*) *pyrrolo/1,2-c/pyrimidine* (*8c*) : cristaux aciculaires jaunes ; P_f = 200—202° (dans du chloroforme) ; rend. : 37,2 % (a), 35 (b), 50 % (c). Analyse : $C_{23}H_{17}N_2O_2Br$: *Calculé* : C 61,47, H 3,78, N 6,23 % Trouvé : C 60,98, H 3,68, N 6,12 %.

Spectre IR (KBr) : 1697 cm^{-1} (ν(C=O) estérique) ; 1620 cm^{-1} (ν(C=O) cétonique).

Spectre RMN ($CHCl_3$ + CF_3COOH, δ, ppm) : 1,53 (tr, 3 H, CH_3 du groupement éthyle estérique) 4,61 (q, 2 H, CH_2 du groupement éthyle estérique) 7,62—8,14 (m, 9 H, les protons aromatiques). 8,37 (s, 1 H, H—6) 8,87 (s.é, 1 H, H—4) 11,52 (s.é., 1 H, H—1).

3-Phényl-5-carbétoxy-7-(*p-méthoxybenzoyl*)*-pyrrolo/1,2-c/pyrimidine* (*8 d*) : cristaux aciculaires blancs ; P_f = 169—171° (dans du chloroforme/éther) ; rend. : 17,5 % (a), 5,3 % (b), 38 % (c) Analyse : $C_{24}H_{20}N_2O_4$: *Calculé* : C 72,00, H 5,00, N 7,00 % *Trouvé* : C 71,86, H 4,78, N 6,97 %.

Spectre IR (KBr) : 1695 cm^{-1} (ν(C=O) estérique) ; 1605 cm^{-1} (ν(C=O) cétonique).

Spectre RMN ($CDCl_3$ + CF_3COOH, δ, ppm) : 1,50 (tr., 3 H, CH_3 du groupement OCH_3) ; 4,55 (q, 2 H, CH_2 du groupement éthyle estérique), 7,10 (d, 2 H, H—2′ et H—6′ du groupement benzoyle), 7,50—8,03 (m, 7 H, les protons aromatiques), 8,23 (s, 1 H, H—6), 8,73 (d, 1 H, H—4) ; 11,38 (d, 1 H, H—1 ($J_{1,4}$ = 1,5 Hz).

3-Phényl-5,7-dicarbéthoxy-pyrrolo/1,2-c/pyrimidine (*8 e*) : cristaux blancs ; P_f = 129—131° (dans du méthanol) ; rend. 25 %.(a, 25 % (b), 47 % (c). Analyse $C_{19}H_{18}N_2O_4$: *Calculé* : C 67,45, H 5,32, N 8,28 % *Trouvé* : C 67,54, H 5,43, N 8.20 %.

Spectre IR (KBr) : 1695 (ν(C=O) estérique).

Spectre RMN ($CDCl_3$, δ, ppm) : 1,41 (tr. 6 H, 2 CH_3 des groupements éthyle estérique), 4,36 (q, 4 H, 2 CH_3 des groupements éthyle estérique) 7,26—8,14 (m, 3 H, H—3′, H—4′ et H—5′ du, groupement phényl de la position 3)7,80 (s,1 H, H—6), 7,95—8,25 (m, 2H, H—2′ et H—6′ du groupement phényl de la position 3) 8,36 (d, 1 H, H—4), 10,10 (d, 1 H, H—1, $J_{1,4}$=1,5 Hz).

Réaction des dimères (3 a—d) avec le diméthylacétylendicarboxylate, respectivement le propyolate d'éthyle.

A une solution de 10 mmoles dimères **(3 a – d)** dans 50 – 100 cm^3 d'acétonitrile ou de diméthylformamide on ajoute 22 mmoles de diméthylacétylendicarboxylate ou 22 mmoles de propyolate d'éthyle. Le mélange est chauffé à reflux pendant 24 heures. On évapore une partie du solvant. On abandonne au réfrigérateur pendant 2 heures et on filtre le produit formé.

Les produits obtenus ont les points de fusion, les analyses chimiques et spectrales identiques avec les même caractéristiques des cycloadducts **(7 a – d)**, respectivement **(8 a – d)** ; les rendements sont similaires à ceux de la méthode a.

RÉFÉRENCES

[1] I. Zugrăvescu, F. Georgescu, F. Chiraleu, P. Filip et E. I. Georgescu, *Rev. Chim. (București)*, **31**, 11 (1980).
[2] I. Zugrăvescu et M. Petrovanu, « Chimie N-ilidelor », Ed. Academiei, București, 1974.
[3] J. Kobayashi, T. Kutsuma et. K. Murinaga, *Chem. Pharm Bull.*, **19**, 2106 (1971).
[4] L. M. Jackman et S. Sternhell, « Application of Nuclear Magnetic Resonance Spectroscopy in Organic Chemistry », ed. II, Pergamon Press, Oxford, 1979, p. 314.
[5] H. Ahlbrecht, J. Fröhlich, U. Habermaltz et F. Kröhnke, *Tetrahedron Letters*, **1967**, 3649.

Revue Roumaine de Chimie, 26, 6, 887–898 (1981)

PHENAZATHIONIUM CATIONS. IV[1]

DEMONSTRATION ON THE STRUCTURE OF 1,3,7-TRISUBSTITUTED DERIVATIVES OF PHENOTHIAZINE BY MASS SPECTROMETRY AND ^1H-NMR

MIRCEA V. DIUDEA
Drug Factory "Terapia", 3400 Cluj-Napoca, 124, Fabricii Str., Romania

Received April 14, 1980

The structure of the following 1,3,7-trisubstituted phenothiazine derivatives : 1,3,7-trinitrophenothiazine (I, $X = NO_2$; $R = NO_2$), 1-nitro-3,7-dichlorphenothiazine (I, $X = Cl$; $R = NO_2$) and 3,7-dinitro-1-10′-diphenothiazine (I, $X = NO_2$; R = phenothiazin-10-yl) is demonstrated by mass spectrometry and ^1H-NMR. The participation of NO_2 group from position 1 ($R = NO_2$) to a McLafferty type rearrangement as information carrier and the great stability of phenothiazine nucleus towards electronic impact are to be mentioned. The peak $m/e = 198$ from the spectrum of the nitrodimer (I, $X = NO_2$, R = phenothiazin-10-yl) demonstrates that the 10-substituted phenothiazine nucleus does not participate in the nucleophilic substitution. ^1H-NMR spectrometry shows two protonic systems on the 1,3,7-trisubstituted phenothiazine nucleus, AX and ABX respectively, the spectra simulated on the base of experimental parameters coming to confirm the structure proposed.

In a previous paper[1] we reported the selective nucleophilic substitution on the phenothiazine nucleus, through phenazathionium cations generated by disproportioning phenothiazinyl cation-radicals from their complexes formed with $CuCl_2$. In the afore-mentioned paper we stated that under the circumstances of thermodynamic control upon the reaction, positions 3 and 1 are selectively substituted thus forming 3-mono-derivatives and 1,3,7-phenothiazin-triderivatives respectively.

This paper deals with the demonstration of the structure of some 1,3,7-trisubstituted phenothiazines, by splitting under electronic impact and by ^1H-NMR.[2]

EXPERIMENTAL

The mass spectra were recorded on a MAT-ATLAS, 311 (Bremen) spectrometer. Tables 1 and 2 show the relative intensities and the corresponding species to the main peaks, supporting structure I.

The ^1H-NMR spectra were recorded on a Brüker-WP-60 spectrometer. Figs 1, 2 and 5 show the ^1H-NMR spectra of structure I recorded with DMSO (I, $X = NO_2$; $R = NO_2$) and $CDCl_3$ (I, $X = Cl$; $R = NO_2$; I, $X = NO_2$; R = phenothiazin-10-yl) as solvents, with internal standards DSS and TMS respectively.

RESULTS AND DISCUSSION

1. *Mass spectrometry of 1,3,7-trisubstituted phenothiazines.* The characteristic structural component of structure I (R = NO_2) is NO_2 group from position 1 which takes part, under electronic impact, in a McLafferty type rearrangement [3,4] their mass spectra showing an M^+-17 peak. The scheme of this rearrangement implies a cyclic electron transfer (of six centers)[3,5]

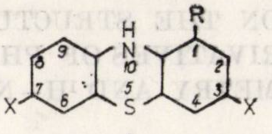

I

X = NO_2 R = NO_2
X = Cl R = NO_2
X = NO_2 R = phenothiazin-10-yl

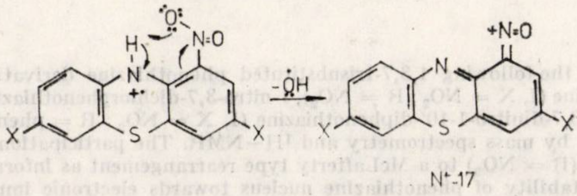

The fulfilment of the delocalization implies a closed coplanarity of the six atoms involved in the cyclic transfer. This stereo-electronic requirement suggests that the molecule adopted an *H-intra* configuration [3] (O—H length 1.8 Å), in which the doublet of nitrogen takes part in the extended conjugation.[6]

The relative intensity of the M^+-17 peak, lower for I(X = NO_2; R = NO_2 — I% = 3.051) than for I(X = Cl; R = NO_2 — I% = 53.931) could be explained by the decreased electronic density at heterocyclic nitrogen,[7] caused by the strongly attractive NO_2 groups from position *para* (3,7); this fact could render rather difficult the electronic cyclic transfer.

The stabilisation of phenothiazine nucleus by NO_2 groups comes out from the relatively low intensity (I, X = NO_2; R = NO_2 — I% < 30) of the peaks shown by the resulting fragments.

The NO_2 groups partially isomerize to *nitroso* [2] form, losing the NO_2 group (peak M^+-30).

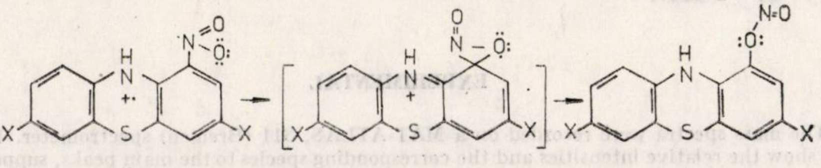

Trinitrophenothiazine (I, X = NO_2, R = NO_2) shows this characteristic for all the three NO_2 groups (peaks M^+-30; M^+-76; M^+-122 and relative intensities between 2 and 4 p.c. See Table 1).

TABLE 1

Relative intensities and corresponding species to the main peaks for I, $R=NO_2$, $X=NO_2$ or Cl

$R = NO_2$ Substituent X	m/e	$M^+ - n$	I(%)	Species 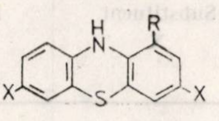
$X = NO_2$	334	M^+	100.000	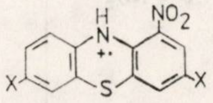
$X = Cl$	321		100.000	
$X = NO_2$	317	$M^+ - 17$	3.051	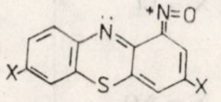
$X = Cl$	295		53.931	
$X = NO_2$	304	$M^+ - 30$	4.661	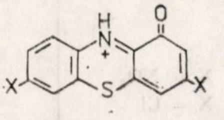
$X = Cl$	282		3.448	
$X = NO_2$	288	$M^+ - 46$	24.576	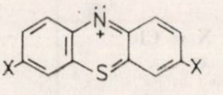
$X = Cl$	266		35.517	
$X = NO_2$	287	$M^+ - 47$	10.168	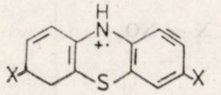
$X = Cl$	265		91.586	
$X = NO_2$	258	$M^+ - 76$	1.695	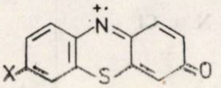
—	—		—	
$X = NO_2$	242	$M^+ - 92$	27.966	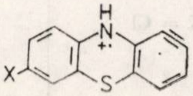
$X = Cl$	231	$M^+ - 81$	24.552	
$X = NO_2$	241	$M^+ - 93$	22.881	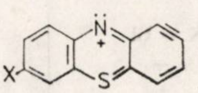
$X = Cl$	230	$M^+ - 82$	90.334	

Table 1 (continued)

R = NO_2 Substituent X	m/e	$M^+ - n$	I(%)	Species 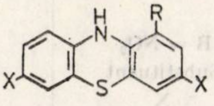
X = NO_2 —	212 —	$M^+ - 122$ —	4.237	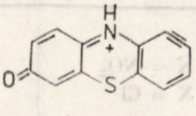
X = NO_2 X = Cl	196 196	$M^+ - 138$ $M^+ - 116$	25.424 19.855	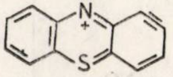
X = NO_2 X = Cl	195 195	$M^+ - 139$ $M^+ - 117$	17.796 15.724	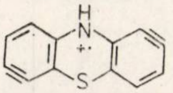
X = NO_2 X = Cl	164 164	$M^+ - 170$ $M^+ - 148$	1.661 1.724	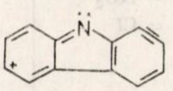
X = Cl —	156 —	$M^+/2$ —	8.069 —	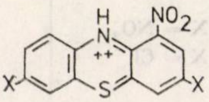
X = NO_2 —	152 —	$(M^+ - 30)/2$ —	7.627 —	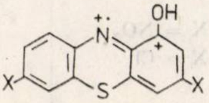
X = Cl —	133 —	$(M^+ - 46)/2$ —	9.379 —	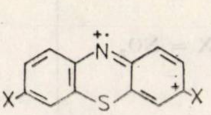
X = Cl —	115.5	$(M^+ - 81)/2$	13.103	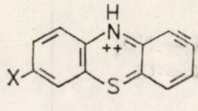
X = Cl —	97.5 —	$(M^+ - 117)/2$ —	7.720 —	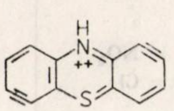

The M^+-46 peak corresponds to the loss of a NO_2 group ; three peaks corresponding to the loss of the three NO_2 groups were scored for triphenothiazine **I** ($X = NO_2$; $R = NO_2$), as follows : M^+-46 ; M^+-92 and M^+-138.

The *nitroso* form is also responsible for the M^+-47 peak corresponding to the loss of HNO_2 group[3].

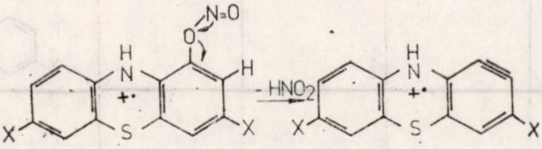

Relatively lower intensities were scored for trinitrophenothiazine **I** ($X = NO_2$; $R = NO_2$) (peaks M^+-47, M^+-93 and M^+-139) than for **I** ($X = Cl$; $R = NO_2$) (see Table 1) the explanation being similar to that for peak M^+-17.

Loss of the heterocyclic sulphur is difficult due to the presence of the electron-attractive substituents which highly delocalize the charge.

Only after losing the substituents the last removal of sulphur is accomplished (peak $m/e = 164$; $I\%$ about 1), fact that comes to demonstrate once more the stability of phenothiazine nucleus and the way of its stabilizing by electron-attractive substituents (see [3,9]).

The essentially identical splittings of the two substances $I(X = NO_2$, C ; $R = NO_2)$ are noted, with the appearance of the same ionic species. Greater differences are observed concerning the double-charged ionic species.

3,7-Dinitro-1,10′-diphenothiazine **I** ($X = NO_2$; $R =$ phenothiazin-10-yl) behaves in an analogous way under electronic impact. From the partial analysis of the mass spectrum of 1,10′-diphenothiazine dinitro-derivative (by comparison with the spectrum of the unsubstituted 1,10′-dimer **I**, $X = H$, $R =$ phenothiazin-10-yl) we concluded that the phenothiazinic nucleus linked in position 10 (marked by R) was not substituted during nucleophilic reaction of nitration [1,2] (see peak M^+-288, $m/e = 198$, $I\% = 10.000$, Table 2).

As concerns the nitro-dimer, splitting of the two NO_2 groups linked by the trisubstituted phenothiazine nucleus (M^+-46, M^+-92) is noted.

In the case of 1,10′-diphenothiazines the loss of heteroatomic sulphur occurs simultaneously with the loss of one proton ($-m/e = 33$), possibility coming out probably from the intervention of some extended *ortho*-quinoid structures.

In all the cases the molecular peaks are base peaks, the high stability of phenothiazine nucleus being once more proved.

2. *^1H-NMR spectrometry of 1,3,7-trisubstituted phenothiazines.* Trisubstituted phenothiazines of type **I** have five protons on their nuclei grouped in two systems : AX – protons on the disubstituted phenylic ring, and ABX – protons on the monosubstituted one (Figs 1 and 2).

TABLE 2

Relative intensities and corresponding species to the main peaks for I, R = phenothiazin-10-yl; X = NO_2 or H

Substituent X	*m/e*	$M^+ - n$	I(%)	Species 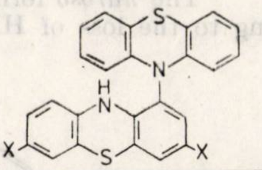
X = NO_2 X = H	486 396	M^+ M^+	100.000 100.000	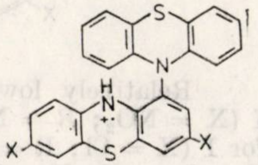
X = NO_2	470	M^+-16	0.923	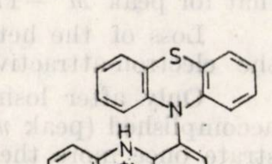
X = NO_2	456	M^+-30	2.384	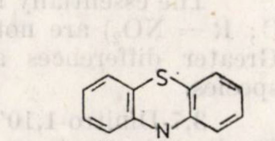
X = NO_2 X = H	453 363	M^+-33 M^+-33	3.461 18.260	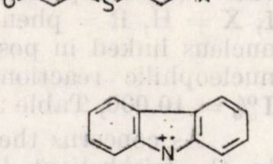
X = NO_2	440	M^+-46	8.692	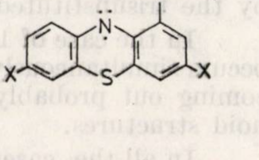

Table 2 (continued)

Substituent X	m/e	$M^+ - n$	I(%)	Species 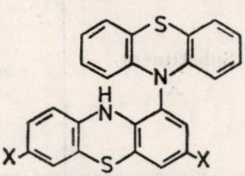
X = NO_2	423	M^+-53	0.538	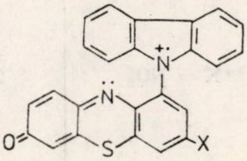
X = NO_2	407	M^+-79	9.538	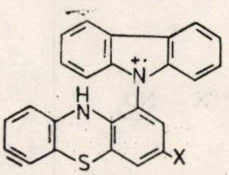
X = NO_2	394	M^+-92	9.538	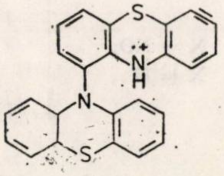
X = NO_2	377	M^+-109	1.615	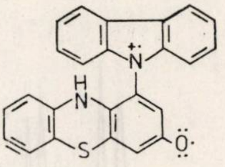
X = NO_2	361	M^+-125	9.000	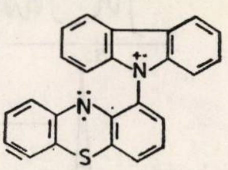
X = NO_2	329	M^+-157	1.384	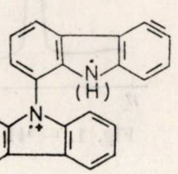
X = H	330	M^+-66	15.380	

Table 2 (continued)

Substituent X	m/e	$M^+ - n$	I(%)	Species 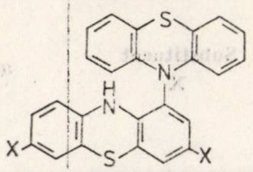
++X = NO$_2$	243	$M^+/2$	3.692	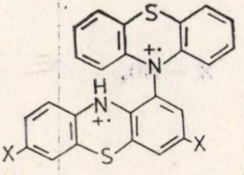
++X = NO$_2$	220	$(M^+-46)/2$	2.000	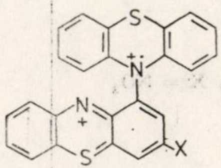
X = NO$_2$ X = H	198 198	M^+-288 M^+-198	10.000 36.530	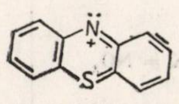

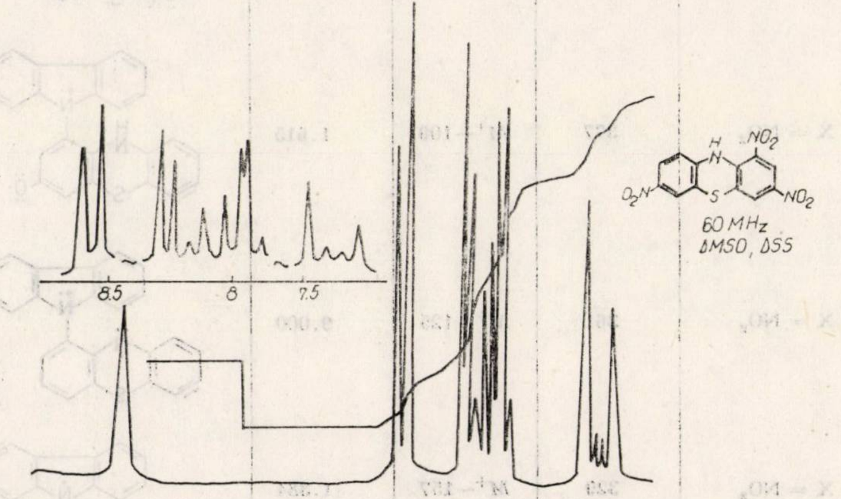

Fig. 1. — ^{1}H—NMR spectrum of 1,3,7-trinitrophenothiazine (I, X = NO$_2$; R=NO$_2$) in DMSO, DSS.

AX-type protons give signals in the low field region (δ of about 8–9 ppm for I, $X = NO_2$; $R = NO_2$ and of about 7–8 ppm for I, $X = Cl$; $R = NO_2$) showing a strong deshielding caused by the attractive substituents [10] on phenylic protons.

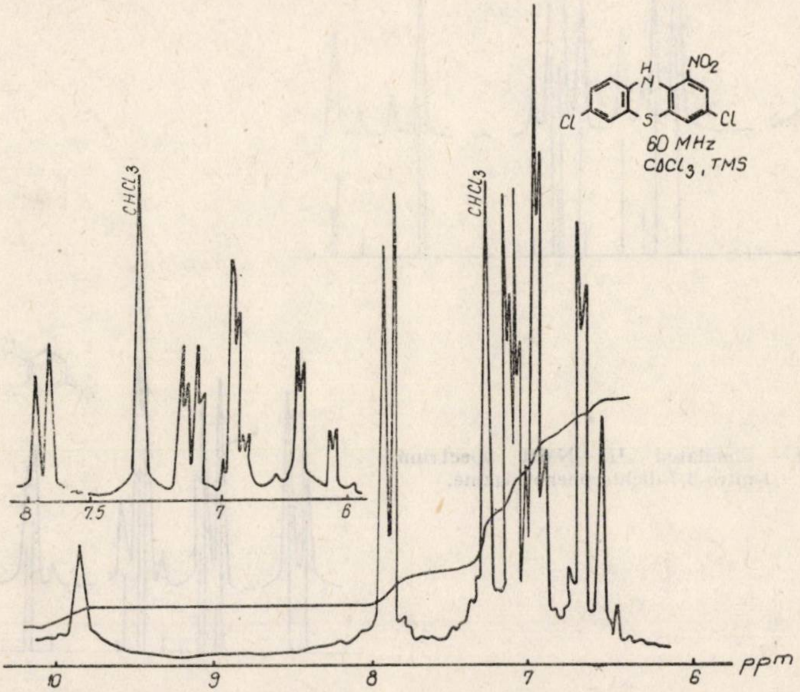

Fig. 2. – ^1H-NMR spectrum of 1-nitro-3,7-dichlorphenothiazine (I, $X = Cl$; $R = NO_2$) in $CDCl_3$, TMS.

ABX protonic system gets into resonance in somewhat higher fields and has four lines in the X-area for I, $X = NO_2$; $R = NO_2$ and six lines for I, $X = Cl$; $R = NO_2$ (see[11]).

The signal of the iminic proton is a singlet (10.40 ppm for I, $X = NO_2$; $R = NO_2$ and 9.74 ppm for I, $X = Cl$; $R = NO_2$).

The strong deshielding of the iminic proton (rendered evident by the signal shifting on the left) is related to the participation of the NO_2 groups, highly attractive to the extended conjugation (see[7]) and suggests the approximate position of the proton in the median plan of the π-electronic system, that means *H-intra* configuration, position also suggested by the participation of the NO_2 group from position 1 to the McLafferty rearrangement (see above).

The spectra (Figs 3 and 4) simulated according to the experimental figures [2,11] tally with the experimental spectra, coming to support structure I.

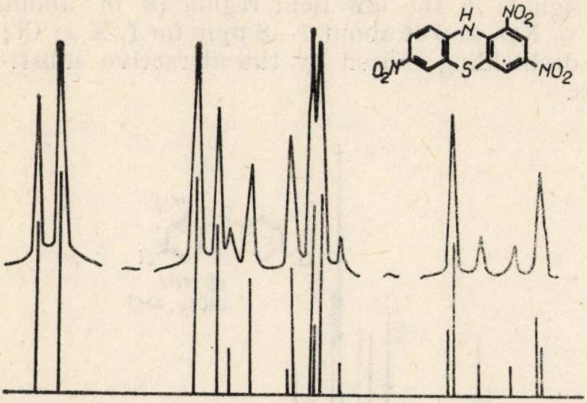

Fig. 3. – Simulated ^{1}H–NMR spectrum for 1,3,7-trinitrophenothiazine.

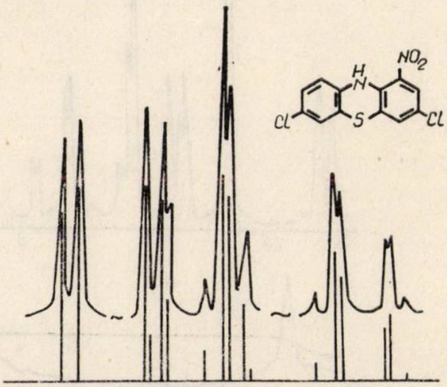

Fig. 4. – Simulated ^{1}H–NMR spectrum for 1-nitro-3,7-dichlorphenothiazine.

Table 3 shows the figures used for simulating the spectra from Figs 3 and 4.

^{1}H–NMR spectrum of the nitro-dimer I ($X = NO_2$; R=phenothiazin-10-yl (Fig. 5) shows an AX protonic system, deshielded (δ between 7.9 and 8.5 ppm), on the disubstituted phenylic ring. Due to the great number of protons on the unsubstituted phenothiazine nucleus (relatively similar as chemical ambiance) and to the overlapping of their signals over ABX signals, the above mentioned spectrum is very difficult to analyse rigorously.

Spectral data and the chemical ones support quite positively the structure proposed.

In conclusion, the 1,3,7-trisubstituted phenothiazines of structure I show characteristic structural features easily rendered evident by mass spectrometry and ^{1}H–NMR.

Structure I is confirmed by physico-chemical behaviour of the discussed compounds.

The demonstration on the structure that we have presented in this paper is for the first time reported within literature now.

ACKNOWLEDGEMENT to Dr. Ioan A. Silberg of the Chemistry Institute Cluj-Napoca for his encouragement and assistance in achieving and interpreting the ^{1}H–NMR spectra.

TABLE 3

Parameters used for simulating ^{1}H−NMR spectra for I, R = NO_2 ; X = NO_2 or Cl

R = NO_2 X	Chemical shifts (Hz)		Coupling constants (Hz)	
X = NO_2	V_1	513.79	$J_{1,2}$	2.55
	V_2	491.12	$J_{1,3}$	0
	V_3	481.98	$J_{1,4}$	0
	V_4	480.37	$J_{1,5}$	0
	V_5	442.11	$J_{2,3}$	0
			$J_{2,4}$	0
			$J_{2,5}$	0
			$J_{3,4}$	2.50
			$J_{3,5}$	8.93
			$J_{4,5}$	0.61
X = Cl	V_1	475.186	$J_{1,2}$	2.3368
	V_2	429.148	$J_{1,3}$	0
	V_3	423.598	$J_{1,4}$	0
	V_4	418.340	$J_{1,5}$	0
	V_5	399.971	$J_{2,3}$	0
			$J_{2,4}$	0
			$J_{2,5}$	0
			$J_{3,4}$	2.5052
			$J_{3,5}$	8.2967
			$J_{4,5}$	0.0080

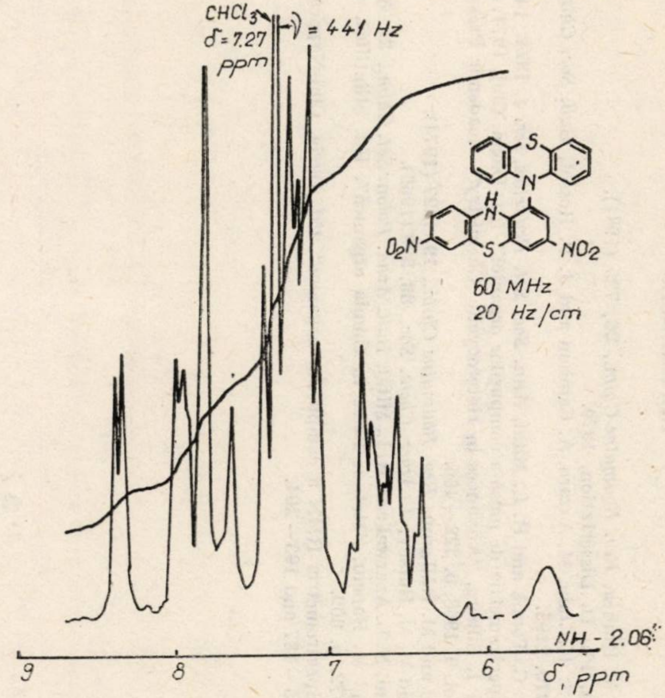

Fig. 5. — ^{1}H−NMR spectrum of 3,7-dinitro-1-10′-diphenothiazine (I, X = NO_2 ; R = phenothiazin-10-yl) in $CDCl_3$, TMS.

REFERENCES

[1] Part. III : M. V. Diudea, *Rev. Roumaine Chim.*, **26**, 725 (1981).
[2] M. V. Diudea, Ph. D. Dissertation, 1979.
[3] L. R. Mital, S. K. Jain, M. Azzaro, A. Cambon and J. P. Rosset, *Bull. Soc. Chim. France*, **1970**, 2195.
[4] S. K. Jain, P. C. Tounk and R. L. Mital, *Ann. Soc. Sci. Bruxelles, ser. 1*, **1974**, 149.
[5] I. Oprean, "Spectrometria de masă a compuşilor organici", Ed. Dacia, Cluj, 1974, p. 84.
[6] C. Bodea and I. Silberg, "Advances in Heterocyclic Chemistry", Academic Press, London Vol. 9, 1968, p. 322–466.
[7] M. Hillebrand and M. Răileanu, *Rev. Roumaine Chim.*, **19**, 1227 (1974).
[8] McLafferty and M. M. Bursey, *J. Amer. Chem. Soc.*, **88**, 529 (1966).
[9] M. D. Sadhnani, N. L. Agarwal and R. L. Mital, *Bull. Acad. Polon. Sci. Chim.*, **21**, 873 (1973).
[10] I. Pogany and M. Banciu, "Metode fizice în chimia organică", Ed. Ştiinţifică, Bucureşti, 1972, p. 309.
[11] I. Silberg, "Spectrometria RMN a compuşilor organici", Ed. Dacia, Cluj-Napoca, 1978, p. 185 – 187 and 193 – 204.

Revue Roumaine de Chimie, **26**, *6*, 899—907 (1981)

PREPARATION OF POLYFUNCTIONAL FURANIC DERIVATIVES FROM TRIOSES

J. SÁNCHEZ BALLESTEROS, D. J. McPHEE and F. HERNANDEZ HERNANDEZ
Department of Organic Chemistry, Faculty of Sciences, University of Málaga, Spain

Received February 20, 1980

The reaction of trioses with active methylenes, in the absence of catalysts, affords, with quantitative yields, hydroxylated addition products (IV or V). Treatment of these addition products with a Lewis acid, in ethanolic or aqueous solution, yields furanic structures (VI). The same structures may be also reached by treatment with Lewis acid of the mixtures of crotonized products obtained when the reaction is catalysed with bases and 2,3-O-isopropylidene-D-glyceraldehyde is used as triose. Treatment of the condensation products with dilute acids affords, after hydrolysis of the acetal group, α, β unsaturated carbonylic compounds (X) from which furanic derivatives may be prepared by cyclisation in acid media. The hydroxymethyl group in the α position of these furanic derivatives (VI) is highly reactive and has characteristics of a benzylic type alcohol that justify the easy substitution of the hydroxyl group by methoxyl groups in a nucleophilic substitution process, or its substitution by halogen atoms.

INTRODUCTION

The first studies of preparations of furanic derivatives from the products of reactions between sugars and active methylene compounds are due to Garcia Gonzalez and col.,[1-3] who studied the preparation of furanic derivatives from hexoses or pentoses and ethyl acetoacetate or acetylacetone. In every case the synthesis of these furanic substances is effected from the product resulting from the addition of the methylene to the carbonyl group of the sugar, without being isolated, by cyclisation in acid medium. The purpose of this work is double : firstly, to augment the number of preparations of furanic derivatives thanks to the use of trioses and different other types of active methylenes, and secondly, to offer an alternative for synthesis of furanic derivatives from the unsaturated products obtained in the above mentioned condensation reactions.

RESULTS AND DISCUSSION

Firstly we have studied the preparation of furanic derivatives (VI) from the hydroxylated addition products obtained in the reactions of D-glyceraldehyde (III) or 2,3-O-isopropylidene-D-glyceraldehyde (II) with the following active methylenes : methyl acetoacetate (Ia), acetylacetone (Ib), acetylacetamide (Ic), acetylacetonitrile (Id), methyl benzoylacetate (If), bezoylacetone (Ig), dibenzylmethane (Ii) and bezoylacetonitrile (Ik).

In previous papers [4-6] the reactions of II with some active methylenes have been studied, showing that when the reaction is effected in the absence of basic catalysts, it occurs via the addition of the methylene to the carbonyl group of the aldehyde-sugar to give hydroxylated adducts (IV), which may be dehydrated, in the presence of basic catalysts, to give complex mixtures of unsaturated isomers VII, VIII and IX (Figure 2). These mixtures may also be prepared when the reaction between I and II is catalysed by bases.[7] In this manner, when in the addition reaction we employ II as the aldehydo-sugar, the addition products IVa, IVb, IVc, IVd, IVf, IVg, IVi and IVk respectively are easily obtained. In a similar manner the corresponding adducts V are obtained when III is used in place of II. These adducts V may be prepared from IV by treatment with dilute aqueous acid, via hydrolysis of the acetal group (Fig. 1).

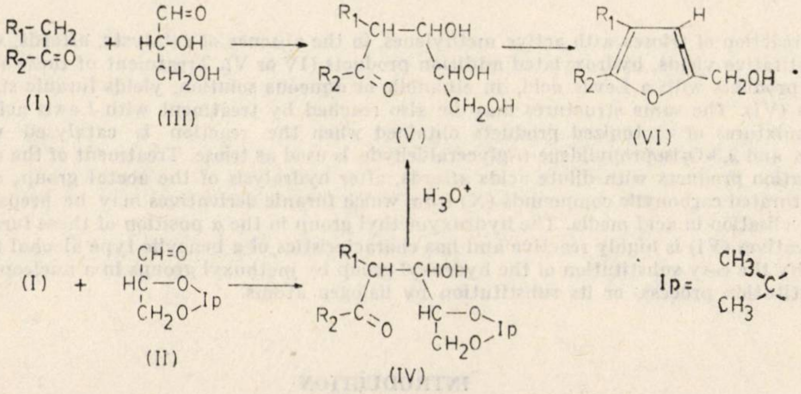

Treatment of the adducts IV or V with aqueous or ethanolic $ZnCl_2$ or treatment of the mixtures of crotonized products, affords, with good yields, polyfunctional furanic derivatives (VI). It is interesting to note that when the acidic hydrolysis of the mixtures of unsaturated isomers VII, VIII and IX is effected with 50% acetic acid a sole type of reaction product is isolated, that corresponding to the dihydroxylated structure (X). The existence of a double bond in α, β position regarding the carbonyl in these structures indicates that either only the product of hydrolysis of VII has been isolated or in this reaction a prototropy of the β, γ unsatured structures has occurred to give the α, β unsaturated isomer (VI). In the preparation of VIc, VId and VIk precaution must be taken to effect the acidic treatment at temperatures under 60°C, avoiding thus the hydrolysis of the nitrogenated group in the adducts or from the unsaturated starting products. In the case of the reaction of Ig with II, the posterior cyclisation in acidic medium of the reaction products, with or without catalyst, leads to two furanic substances, VIg and VIh, depending on which carbonyl group present in the molecule participates. The chemical transformations or the substituents in α and β in the furanic compounds prepared have also been studied. Treatment with aqueous alkali of furanic derivatives VIa, VIc and VId affords, by hydrolysis of the respective ester, amide and nitrile groups, the furanic acid VIe. Similarly, by alkaline hydrolysis of VIf, VIk and VIm respectively, VIn is prepared. Compounds VIe and VIn may also be prepared by haloform reaction of VIb and VIh respectively. Alkaline hydrolysis with 12% H_2O_2 of VId and VIk affords, with acceptable

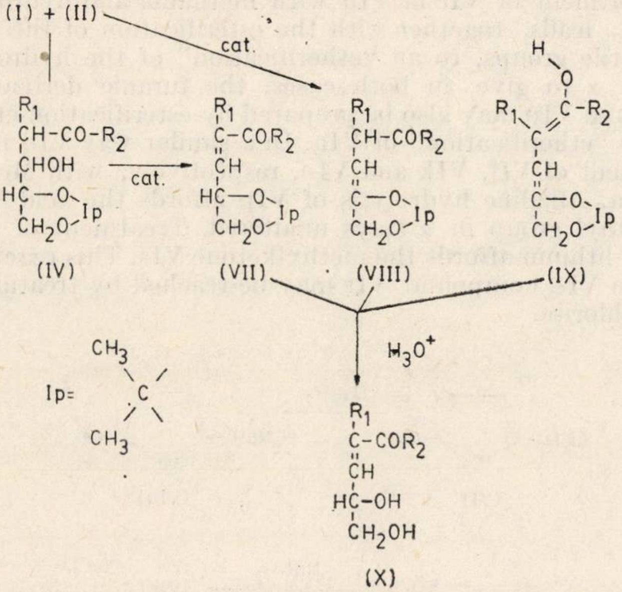
(I) + (II)
cat.
cat.
(IV)
(VII)
(VIII)
(IX)
H_3O^+
Ip=
(X)

Series	R_1	R_2
a	CO_2Me	Me
b	COMe	Me
c	$CONH_2$	Me
d	CN	Me
e	CO_2H	Me
f	CO_2Me	Ph
g	COPh	Me
h	COMe	Ph
i	COPh	Me
j	COPh	Ph
k	CN	Ph
m	$CONH_2$	Ph
n	CO_2H	Ph

yields, the furanic carbamides VIc and VIm respectively. This reaction is reversible since treatment of VIc with P_2O_5 causes dehydration of the carbamido group in β′ to give VId.

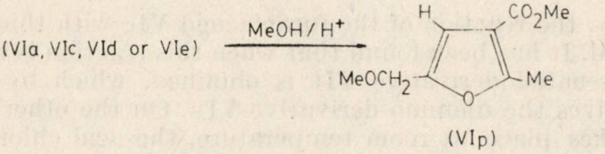
(VIa, VIc, VId or VIe)
MeOH/H⁺
(VIp)

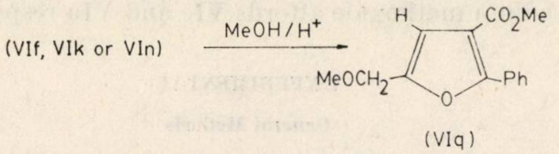
(VIf, VIk or VIn)
MeOH/H⁺
(VIq)

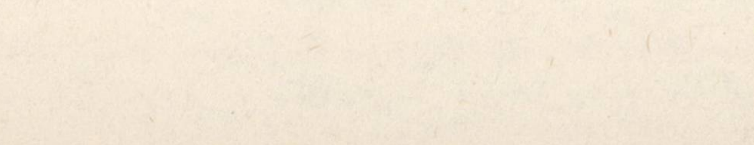
(VIp)
OH⁻
MeLi
ClO⁻
(VIr)
(VIs)

The great reactivity of the hydroxyl of the hydroxymethyl group in α has been noted. This group has characteristics of a benzylic type alcohol that justify its easy substitution by methoxyl groups in a nucleophilic substitution process when esterification reactions of VIc, VId and VIe are accomplished. Treatment of VIc or VId with methanol and hydrogen chloride, under reflux, leads, together with the esterification of the respective amide and nitrile groups, to an "etherification" of the hydroxymethyl substituent in α to give, in both cases, the furanic derivative VIp. The same compound VIp may also be prepared by esterification-etherification of VIe or by "etherification" of VIa. In a similar way VIq may be prepared by treatment of VIf, VIk and VIn, respectively, with MeOH in aprotic acidic media. Alkaline hydrolysis of VIp affords the acid VIr, while the methoxymethyl group in α stays unaltered. Treatment of this substance with methyl-lithium affords the methylketone VIs. This reaction is reversible, since from VIs, compound VIr may be reached by treatment with potassium hipochlorite.

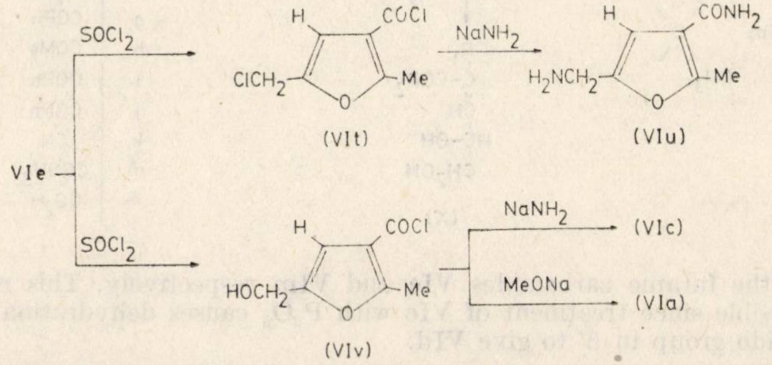

Lastly, the reaction of the furanic acid VIe with thionyl chloride has been studied. It has been found that when this reaction is effected at reflux the dihalogenated derivative VIt is obtained, which by treatment with sodamide gives the diamino derivative VIn. On the other hand, when the reaction takes place at room temperature, the acid chloride VIv is prepared. In this substance, substitution of the hydroxyl of the hydroxymethyl group by the halogen has not been accomplished. Treatment of VIv with sodamide or sodium methoxide affords VIc and VIa respectively.

EXPERIMENTAL

General Methods

Melting points are uncorrected. IR spectra (KBr disks or films) were obtained with a Beckman Aculab IV or a Perkin-Elmer mod. 121 spectrometer. ^1H-NMR. spectra were recorded for CCl_4 or $CDCl_3$ solutions (internal TMS) with a Perkin-Elmer-Hitachi 2-20B or a Perkin-Elmer-Hitachi R-24B spectrometer. Chemical shifts (first order) are given on the δ scale and first-order couplings in Hz. Concentration of solutions was performed under diminished pressure at less than 40°C using a rotary evaporator.

D-Glyceraldehyde (III), 2,3-O-isopropylidene-D-glyceraldehyde (II), acetylacetamide (Ic), acetylacetonitrile (Id), methyl benzoylacetate (If) and *benzoylacetonitrile (Ik)* were prepared following the instruction given in [8–13] respectively.

Reactions between I and II in the absence of catalysts. This reaction has been effected, in all cases, at room temperature, directly mixing, in equimolar proportion, I with II, for Ia, Ib and If, or dissolving I in ethyl ether and adding II in equimolar proportion for Ic, Id, Ig, Ij and Ik. The reaction was exothermic in every case. All the reactions were followed by NMR spectroscopy observing the disappearance of the initial products. After allowing the solution to stand for 12 hrs, the solvent was eliminated in the cases in which ethyl ether was used and the addition products were studied spectroscopically, with the following results :

1) *4,5-isopropylidene derivative of the methyl ester of 2-acetyl-3,4,5-trihydroxypentanoic acid* (IVa) : $\bar{\nu}_{max}^{film}$ 3490, 2990, 2945, 2890, 1730, 1720, 1650–1630, 1440, 1370, 1250, 1215, 1150 and 1015 cm^{-1}. ^{1}H–NMR data : δ 4.40–3.30 (m, 9H), 2.20 (s, 3H, Ac), 1.30 and 1.24 (2s, 6H, CMe_2).

2) *5,6-isopropylidene derivative of 3-acetyl.–4,5,6-trihydroxy-hexan-2-one (IVb).* $\bar{\nu}_{max}^{film}$ 3450, 2980, 2915, 2870, 1720, 1615, 1410, 1365, 1240, 1210, 1150 and 1060 cm^{-1}. ^{1}H–NMR data : δ 3.94 (broad, 6H, unresolved), 2.20 (s, 3H, Ac), 2.0 (s, 3H, enol), 1.33 and 1.27 (2s, 6H, CMe_2).

3) *4,5-isopropylidene derivative of the carbamide of 2-acetyl-3,4,5-trihydroxy-pentanoic acid (IVc).* m.p. 58–59°C. $\bar{\nu}_{max}^{KBr}$ 3445, 3200, 2990, 2925, 2890, 1700, 1680, 1520, 1445, 1370, 1300, 1240, 1205, 1130, 1030 and 840 cm^{-1}. ^{1}H–NMR data ($CDCl_3$) : δ 5.35 (broad, 2H, NH_2), 4.40–3.45 (m, 6H), 2.25 (s, 3H, Ac), 1.34 and 1.25 (2s, 6H, CMe_2).

4) *4,5-isopropylidene derivative of the nitrile of 2-acetyl-3,4,5-trihydroxypentanoic acid (IVd).* m.p. 35–36°C. $\bar{\nu}_{max}^{KBr}$ 2990, 2940, 2885, 2200, 1710, 1610, 1440, 1380, 1250, 1200, 1161, 1030 and 850 cm^{-1}. ^{1}H–NMR data ($CDCl_3$) : δ 4.45–3.30 (m, 6H), 2.22 (s, 3H, Ac), 1.40. and 1.30 (2s, 6H, CMe_2).

5) *4,5-isopropylidene derivative of the methyl ester of 2-benzoyl-3,4,5-trihydroxypentanoic acid (IVf).* $\bar{\nu}_{max}^{film}$ 3450, 3070, 2985, 2920, 2890, 1730, 1645, 1590, 1550, 1490, 1420, 1400, 1350, 1200, 1140, 1050, 1000, 825 and 750 cm^{-1}. ^{1}H–NMR data : δ 7.30 (m, 5H, Ph), 4.50–3.50 (m, 9H), 1.30 and 1.21 (2s, 6H, CMe_2).

6) *5,6-isopropylidene derivative of 3-benzoyl-4,5,6-trihydroxy-hexan-2-one (IVg).* m.p. 31–32°C. $\bar{\nu}_{max}^{KBr}$ 3445, 3050, 2985, 2920, 2880, 1715, 1660 1640, 1580, 1560, 1500, 1440, 1405, 1360, 1345, 1200, 1145, 1050, 1010, 830 and 750 cm^{-1}. ^{1}H–NMR data ($CDCl_3$) : δ 8.0–7.20 (m, 5H, Ph), 3.92 (broad, 6H). 2.10 (s, 3H, Ac), 1.40 and 1.20 (2s, 6H, CMe_2).

7) *3,4-isopropylidene derivative of (1-benzoyl-2,3,4-trihydroxybutyl)-phenylketone (IVj).* m.p. 39–40°C. $\bar{\nu}_{max}^{KBr}$ 3445, 3060, 2985, 2925, 2885, 1715, 1700, 1650, 1590, 1580, 1555, 1480, 1420, 1350, 1200, 1135, 1100, 1020, 850 and 760 cm^{-1}. ^{1}H–NMR data ($CDCl_3$) : δ 8.10–7.30 (m, 10H, 2Ph), 3.90 (broad, 6H), 1.37 and 1.20 (2s, 6H, CMe_2).

8) *4,5-isopropylidene derivative of the nitrile of 2-benzoyl-3,4,5-trihydroxy-pentanoic acid (IVk).* m.p. 42–43°C. $\bar{\nu}_{max}^{KBr}$ 3450, 3060, 2985, 2920, 2870, 2210, 1710, 1630–1580, 1525, 1450, 1380, 1250, 1210, 1150, 1060, 980, 810 and 750 cm^{-1}. ^{1}H–NMR data ($CDCl_3$) : δ8.0 (m, 5H, Ph), 3.85–4.90 (m, 6H), 1.30 and 1.20 (2s, 6H, CMe_2).

5-*Hydroxymethyl-3-methoxycarbonyl-2-methyl-furan (VIa).* a) *from Ia and III* : A solution of 11.6 g of Ia and 9.0 g of III in 140 ml of ethanol is added to a solution of 18 g $ZnCl_2$ in 100 ml of water-ethanol (3 : 1) and the mixture is heated at 50°C to complete homogeneization. Then 300 ml of ethyl acetate are added and the organic layer is washed successively with water (2 × 100 ml) and saturated $NaHCO_3$ solution (100 ml), dried ($CuSO_4$) and concentrated. Distillation of the residue affords 13.95 g (82 %) of VIa, b.p. 94–95°C/0.1 Torr. $\bar{\nu}_{max}^{film}$ 3420, 2970, 2920, 2900, 2840, 1680, 1670, 1585, 1550, 1430, 1420, 1375, 1345, 1275, 1205, 1115, 1070, 1000, 950, 900, 800, 750 and 660 cm^{-1}. ^{1}H–NMR data (CCl_4) : δ6.32 (s, 1H, H–4), 4.38 (s, 2H, CH_2OH), 3.70 (s, 3H, OMe) and 2.50 (s, 3H, Ac). Mass spectrum : m/e 170 (M), 155 (M–Me), 153 (M–OH), 139 (M–CH_2OH), 127 (M–Ac), 111 (M–CO_2Me, M–$COCH_2OH$), 59 (CO_2Me), 43 (COMe, 100 %) and 31 (CH_2OH or OMe). Anal. Calc. for $C_8H_{10}O_4$: C, 56.52 ; H, 6.54 . Found : C, 56.43 ; H, 6.32 %. b) *from IV a* : A solution of 9.5 g of IVa, 150 ml of ethanol, 150 ml of acetic acid, 100 ml of water and 5 drops of hydrochloric acid is heated at 80°C for 30 hrs and from this point is treated as indicated in a). In this manner 5.1 g of VIa are obtained (77 %). c) *from the products of condensation of Ia with III* : A solution of 5.7 g of the mixture of isomers VIIa, VIIIa and IXa, prepared as shown in,[4] in 60 ml of ethanol is added to another solution of 5.2 g of $ZnCl_2$ in 60 ml of water-ethanol (3 : 1) and the mixture is heated at 80°C for 2 hrs. From this point the mixture is treated as in a), yielding 2.80 g (66 %) of VIa.

3-Acetyl-5-hydroxymethyl-2-methyl-furan (VIb). a) *from Ib and III* : Starting from 10 g of Ib, 9 g of III and 19 g of $ZnCl_2$ in 200 ml of water-ethanol (1 : 1) and following a procedure identical to that indicated above for preparation of VIa from Ia and III, 16.24 g (84 %) of IVb are prepared ; b.p. 68—70°C/0.1 Torr. $\bar{\nu}_{max}^{film}$ 3450, 2980, 2900, 1740, 1721, 1630, 1545, 1390, 1335, 1200, 1160, 1130, 1050 and 1030 cm^{-1}. ^{1}H—NMR data (CCl_4) : δ 6.51 (s, 1H, H—4), 4.55 (s, 2H, CH_2OH), 2.57 (s, 3H, Ac) and 2.39 (s, 3H, Me). Mass spectrum : m/e 154 (M), 139 (M—Me), 123 (M—CH_2OH), 111 (M—Ac), 95 (M—$COCH_2OH$), 59($COCH_2OH$), 43 (Ac, 100 %) 31 (CH_2OH) and 15(Me). Anal. Calc. for $C_8H_{10}O_3$: C, 62.33 ; H, 6.53. Found : C, 62.49 ; H, 6.50 %. b) *from IVb* : A mixture of 9.5 g of IVb, 9.5 g of $ZnCl_2$ and 120 ml of water-ehanol (1 : 1) is used, heating at 80°C for 2 hrs. Thus 5.54 g (72 %) of IVb are prepared. c) *from the products of condensation of Ib with II* : When 8.1 g of the mixture of unsaturated isomers VIIb and IXb, prepared as indicated in [7] are employed in place of IVb, in the same conditions indicated in (b), a yield of 4.23 g (55 %) of VIb is obtained.

3-Carbamido-5-hydroxymethyl-2-methyl-furan (VIc). a) *from Ic and III* : A solution of 9 g of $ZnCl_2$ in 90 ml of water-ethanol (1 : 1) is added to a mixture of 5.05 g of Ic and 4.5 g of III and heated at 50°C for 1 hr. The solution is extracted with ethyl acetate (3 × 60 ml) and the organic layer is successively washed with water (60 ml) and saturated $NaHCO_3$ solution (30 ml), dried (Na_2SO_4) and concentrated. The residue is recrystallised from water-ethanol (1 : 1) to afford 5.19 g (67 %) of VIc ; m.p. 177—178°C. $\bar{\nu}_{max}^{KBr}$ 3500, 3300, 3070, 2990, 2920, 1670, 1540, 1510, 1420, 1400, 1370, 1300, 1220, 1100, 1070 and 750 cm^{-1}. ^{1}H—NMR data ($CDCl_3$) : δ 6.45 (s, 1H, H—4), 5.5 (broad, 2H, NH_2), 4. 56(s, 2H, CH_2OH), 2.56 (s, 3H, Me) Mass spectrum : m/e 155 (M), 140 (M—Me), 139 (M—NH_2), 138 (M—OH), 124 (M—CH_2OH), 112 (M—Ac), 111(M—$CONH_2$), 59($COCH_2OH$), 44($CONH_2$, 100 %), 43 (Ac), 31 (CH_2OH) and 16 (NH_2). Anal. Calc. for $C_7H_9O_3N$: C, 54.19 ; H, 5.80 ; N, 9.03. Found : C, 54.37 ; H, 5.89 ; N, 9.03 %. b) *from IVc* : To a solution of 11.55 g of IVc in 120 ml of ethanol 10 g of $ZnCl_2$ in 80 ml of ethanol are added and the mixture is heated at 58°C until completely homogeneous. From this point it is treated as indicated previously. 4.49 g (58 %) of VIc are obtained. c) *from the products of condensation of Ic with II* : When in place of IVc a mixture of VIIc, VIIIc and IXc, prepared as indicated in [7] is used, VIc is prepared with a 52 % yield. d) *from VId* : To a mixture of 4.55 g of VId, 40 ml of ethanol and 40 ml of 1N NaOH solution, 40 ml of 10 %H_2O_2 are added dropwise with stirring, taking precaution to ensure that the temperature of reaction does not surpass 10°C. Once the addition is completed the mixture is heated at 50°C for 30 min. and 70 ml of ice-water (1 : 1) to afford 2.53 g (49 %) of a product spectroscopically identical to VIc.

3-Cyano-5-hydroxymethyl-2-methyl-furan (VId). a) *from Id and III* : Following the procedure described above for VIc from Ic, 5.53 g of Id, 6 g of III, 11 g of $ZnCl_2$ and 120 ml of ethanol-water (1 : 1) were used to prepare 6.48 g of VId (71 %) ; m.p. (recrystallised from CCl_4) 122—123°C. $\bar{\nu}_{max}^{KBr}$ 3500, 3030, 2970, 2900, 2880, 2200, 1600, 1560, 1520, 1430, 1330, 1220, 1130, 1070, 980 and 780 cm^{-1}. ^{1}H—NMR data ($CDCl_3$) : δ 6.60 (s, 1H, H—4), 4.55 (s, 2H, CH_2OH), 2.50 (s, 3H, Me). Mass Spectrum : m/e 137 (M), 122 (M—Me), 120 (M—OH), 111 (M—CN), 106 (M—CH_2OH), 94 (M—Ac), 59 ($COCH_2OH$), 43 (Ac, 100 %), 31 (CH_2OH), 26(CN), 17(OH) and 15 (Me). Anal. Calc. for $C_7H_7O_2N$: C, 61.31 ; H, 5.10 ; N, 10.21. Found : C, 51.56 ; H, 4.82 ; N, 10.38 %. b) *from IVd* : Following the procedure indicated for preparation of VIc from IVc, using 6.92 g of IVd, 6.20 g of $ZnCl_2$ and 60 ml of ethanol, 4.35 g of VId (55 %) were prepared. c) *from VIc* : 5.40 g of P_2O_5 are added to a suspension of 5.40 g of VIc in 54 ml of toluene (dry). The mixture is heated at 60°C, with stirring, for 1 hr and left to cool. Once cooled it is extracted with ethyl ether (3 × 50 ml). The combined extracts are washed successively with water and saturated $NaHCO_3$ solution, dried over $CuSO_4$ and concentrated to dryness. The residue, recrystallised from CCl_4 affords 1.87 g (39 %) of a product spectroscopically identical to VId.

5-Hydroxymethyl-2-methyl-furan-3-carboxylic acid (VIe). a) *from VIa* : 4 g of VIa (0.023 moles) are dissolved in 40 ml of 10 % NaOH (ethanol-water, 1 : 1) and heated at 100°C for 1 hr. The solution is concentrated to dryness and the residuum is dissolved in 30 ml of water, acidified (Congo Red) with 12 % HCl and extracted with ethyl ether (3 × 30 ml). The extracts are dried over $CuSO_4$, the solvent is eliminated and the resulting residue is recrystallised from water, yielding 2.60 g (71 %) of VIe ; m.p. 153—154°C. $\bar{\nu}_{max}^{KBr}$ 3500—2500, 2990, 2910, 2880, 1690, 1630, 1590, 1550, 1440, 1370, 1300, 1230, 1140, 1080 and 760 cm^{-1}. ^{1}H—NMR data ($CDCl_3$) : δ 11 (broad, 1H, CO_2H), 6,65 (s, 1H, H—4), 4.60 (s, 2H, CH_2OH), 2.55 (s, 3H, Me). Mass spectrum : m/e 156 (M), 141 (M—Me), 139 (M—OH), 125 (M—CH_2OH), 113 (M—Ac), 112 (M—CO_2), 111 (M—CO_2H), 59 ($COCH_2OH$), 45 (CO_2H, 100 %), 43(Ac), 31 (CH_2OH), 17(OH) and 15 (Me). Anal. Calc. for $C_7H_8O_4$: C, 53.84 ; H, 5.12. Found : C, 53.86 ; H, 5.10 %. b) *from VIb* : A solution of calcium hypochlorite (6 g) in 40 ml of warm 60 % aqueous methanol is treated with 5g of anhydrous potassium carbonate and a solution of 1.8 g of potassium hydroxide in 20 ml of the same aqueous methanol. After stirring for 5 min the mixture is cooled and filtered, the solid residue being washed with 10 ml of cold methanol. To the filtrate a solution of 3.3 g of VIb in 20 ml of methanol is added, with cooling (ice bath), and the stirring is maintained for 5 hrs. A solution of sodium hydrogen sulphite (2g) in water is added, followed by acidification (10% hydrochloric acid). The solid that separates is recrystallised from water to give 2.74 g (82%) of VIe. c) *from VIc* : Following a procedure similar to that indicated above in a), but using VIc in place of Via, VIe is prepared with 63% yield. d) *from VId* : VIe is prepared in 50% yield following the procedure indicated in a), but employing VId in place of VIa.

2-Methyl-3-methoxycarbonyl-5-methoxymethyl-furan (VIp). a) *from VIe* : A current of dry hydrogen chloride is passed through a solution of 7.8 g (0,05 moles) of VIe in 78 ml of methanol for 2 hrs. The mixture is refluxed for 1 hr, concentrated and the residue poured into 50 ml of water and extracted with ethyl ether (3 × 50 ml). The reunited extracts are washed successively with water and saturated $NaHCO_3$ solution, dried over Na_2SO_4 and concentrated. The residue is distilled, affording 7 g (76%) of VIp ; b.p. 78–80°C/0.1 Torr. $\bar{\nu}_{max}^{film}$ 2980, 2920, 1700, 1610, 1570, 1520, 1430, 1420, 1370, 1310, 1220, 1180, 1100, 1050 and 760 cm^{1-}.^{1}H–NMR data(CCl_4) : δ 6.32 (s, 1H, H–4), 4.25 (s, 2H, CH_2OR), 3.70 (s, 3H, CO_2Me), 3.30 (s, 3H, OMe), 2.43 (s,3H, Me). Mass spectrum : m/e 184 (M), 169 (M-Me), 153 (M–OMe), 141 (M–Ac), 139 (M–CH_2OMe), 125 (M–CO_2Me), 59(CO_2Me), 45 (CH_2OMe), 43(Ac, 100%), 31 (OMe) and 15 (Me).Anal. Calc. for $C_9H_{12}O_4$; C, 58.69 ; H, 6.52. Found : C, 58.85 ; H, 6.48%. b) *from VIa, VIc* or *VId* :When VIa, VIc or VId are employed in place of VIe, VIp is prepared with 80, 58 and 51% yields respectively.

2-Methyl-5-methoxymethyl-furan-3-carboxylic acid (VIr). This substance is prepared following the procedure indicated above for preparation of VIe from VIa, employing 6 g of VIp and 50 ml of 12% NaOH. In this manner, 4.65 g (84%) of a solid which is recrystallised from water are obtained ; m.p. 131–132°C. $\bar{\nu}_{max}^{KBr}$ 3600–2450, 2980, 2900, 1680, 1600, 1575, 1540, 1440, 1380, 1310, 1260, 1210, 1120, 1030 and 760 cm^{-1}. ^{1}H–NMR data ($CDCl_3$) : δ 11.3 (broad, 1H, CO_2H), 6.44 (s, 1H, H–4), 4.27 (s, 2H, CH_2OR), 3.30 (s, 3H, OMe) and 2.55 (s, 3H, Me).Mass spectrum : m/e 170 (M), 155(M–Me), 139 (M–OMe), 127 (M–Ac), 126 (M–CO_2), 125 (M–CO_2H, M–CH_2OMe), 97 (M–$COCH_2OMe$), 73 ($COCH_2$ OMe), 45 (CO_2H or CH_2OMe, 100%), 44(CO_2), 43(Ac), 31(OMe) and 15 (Me). Anal. Calc. for $C_8H_{10}O_4$: C, 56.47 ;H, 5.88. Found :.C, 56.70 ; H, 5.87%.

3-Acetyl-2-methyl-5-methoxymethyl-furan (VIs). A solution of 0.75 g of methyl-lithium in 10 ml of ether is added dropwise, with stirring, at less than 5°C, to a solution of 2.5 g of VIr in 15 ml of dry dimethoxyethane. The stirring is maintained for 4 hrs at room temperature, then 30% aqueous ammonium chloride (15 ml) is added and the suspension is extracted with ether (3 × 50 ml). The extracts are dried ($CuSO_4$) and concentrated. The residue is distilled to yield 1.25 g (50%) of VIs ; b.p. 67–70°C/0.1 Torr. $\bar{\nu}_{max}^{film}$ 2990, 2925, 2890, 1680, 1620, 1600, 1570, 1440, 1400, 1380, 1300, 1220, 1160, 1090, 900 and 750 cm^{-1}. ^{1}H–NMR data (CCl_4) : δ 6.48 (s, 1H, H–4), 4.25 (s, 2H, CH_2OR), 3.30 (s, 3H, OMe), 2.57 (s, 3H, OMe), 2.30 (s, 3H, OMe). Mass spectrum : m/e 168 (M), 153 (M–Me), 137 (M–OMe), 125 (M–Ac), 123 (M–CH_2 OMe), 95 (M–$COCH_2OMe$), 73 ($COCH_2$ OMe), 45 (CH_2OMe), 43 (Ac, 100%), 31 (OMe) and 15 (Me). Anal. Calc. for $C_9H_{12}O_3$: C, 64.28 ; H, 7.14. Found : C, 64.10 ; H, 7.23%.

By haloform reaction, as indicated above in the preparation of VIe from VIb, VIr is prepared with 48% yield.

2-Phenyl-5-hydroxymethyl-3-methoxycarbonyl-furan (VIf). a) *from If and III* : Following the procedure described above for preparation of VIa from Ia, using 17.8 g of If, 9 g of III and 25 g of $ZnCl_2$ in 180 ml of ethanol-water (1 : 1), 17.86 g (77%) of VIf are prepared ; b.p. 147–148°C/0.3 Torr. $\bar{\nu}_{max}^{film}$ 3500, 3070, 2990, 2920, 2890, 1720, 1650, 1610, 1580, 1555, 1500, 1430, 1385, 1310, 1230, 1160, 1110, 1040, 920, 830, 760 and 670 cm^{-1}.^{1}H–NMR data (CCl_4) : δ 7.80–7.40 (m, 5H, Ph), 6.45 (s, 1H, H–4), 4.30 (s, 2H, CH_2OH), 3.65 (s, 3H, OMe). Mass spectrum : m/e 232 (M), 215 (M–OH), 201 (M–OMe), 173 (M–$COCH_2OH$, M–CO_2Me), 155 (M–COPh), 105 (COPh, 100%), 77 (Ph), 59(CO_2Me, $COCH_2OH$) and 31 (CH_2OH, OMe). Anal. Calc. for $C_{13}H_{12}O_4$: C, 67.24 ; H, 5.17. Found : C, 67,25 ; H, 5.01%. b) *from IVf* : Following the procedure described for preparation of VIa from IVa, 3.15 g (68%) of VIf are prepared using 6.16 g of IVf, 120 ml of acetic acid, 80 ml of water and 5 drops of HCl. c) *from the product of condensation of If with II* : 8 drops of piperidine are added to a solution of 9.9 g of If and 7.20 g of II in 80 ml of toluene. The mixture is left standing in darkness for 12 hrs, the water formed is decanted and the mixture is heated for 30 min at 80°C. The solvent is eliminated and the residue is dissolved in 50 ml of ethanol and mixed with 15 g of $ZnCl_2$ in 90 ml of ethanol-water (1 : 2). After heating for 1 hr at 80°C, the solution is extracted with water and saturated $NaHCO_3$ solution, dried over $CuSO_4$. The solvent is eliminated and the residue distilled to afford 6.8 g of VIf.

3-Acetyl-2-phenyl-5-hydroxymethyl-furan (VIh) and 3-benzoyl-5-hydroxymethyl-2-methyl-furan (VIi). Following the procedure indicated for VIa, employing 22.5 g of IVh and 20 g of $ZnCl_2$ in 150 ml of ethanol, 6.4 g of a substance of b.p. 95–96°C/0.1 Torr (VIh) and 14.1 g of a substance of b.p. 135–137°C/O.1 Torr (VIi) are obtained. *VIh*: $\bar{\nu}_{max}^{film}$ 3400, 3030, 2985, 2910, 2890, 1680, 1600, 1580, 1550, 1420, 1380, 1650, 1290, 1220, 1080, 850 and 760 cm^{-1}. ^1H–NMR data ($CDCl_3$) : δ 7.8–7.4 (m, 5H, Ph), 6.22 (s, 1H, H–4), 4.50 (s, 2H, CH_2OH) 2.48 (s, 3H,Me). Anal. Calc . for $C_{13}H_{12}O_3$: C, 72.22 ; H, 5.55. Found : C, 72.51 ; H, 5.65 %. This substance gives a positive haloform assay. *VIi* : $\bar{\nu}_{max}^{film}$ 3450, 3060, 2980, 2900, 2880, 1700, 1640, 1610, 1585, 1560, 1440, 1380, 1310, 1260, 1210, 1150, 1070, 830 and 760 cm^{-1}.^1H–NMR data ($CDCl_3$) : δ 8.3–7.9 (m, 5H, Ph), 6.30 (s, 1H, H–4), 4.30 (s, 2H, CH_2OH) and 2.25 (s, 3H, Me). Anal. Calc. for $C_{13}H_{12}O_3$: C, 72.22 ; H, 5.55. Found : C, 71.98 ; H, 5.72 %. This substance gives a negative haloform assay.

3-Cyano-2-phenyl-5-hydroxymethyl-furan (VIk). a) *from Ik and III* : Following the procedure indicated for VId, but employing 11.15 g of Ik, 6.92 g of III and 15 g of $ZnCl_2$ in 140 ml of ethanol-water (1 : 1), 9.33 g (61 %) of VIk are obtained ; m.p. 127–128°C (recrystallised from dioxane). $\bar{\nu}_{max}^{KBr}$ 3500, 3050, 2930, 2890, 2200, 1640, 1610, 1580, 1540, 1430, 1300, 1240, 1220, 1100, 1070 and 780 cm^{-1}.^{-1}H–NMR data ($CDCl_3$) : δ 8.0–7.5 (m, 5H, Ph), 6.3 (s, 1H, H–4), 4.45 (s, 2H, CH_2OH). Mass spectrum : m/e 199 (M), 182 (M–OH), 173 (M–CN), 168 (M–CH_2OH), 122 (M–Ph), 105 (COPh, 100 %), 94 (M–COPh), 77 (Ph), 59 ($COCH_2OH$), 31 (CH_2OH), 26 (CN) and 17(OH). Anal. Calc. for $C_{12}H_9O_2N$: C, 72.36 ; H, 4.52 ; N, 7.03. Found : C, 72.51 ; H, 4.44 ; N, 7.21 %. b) *from IVk* : Then IVk is employed VIk is prepared in 56 % yield.

3-Carbamido-2-phenyl-5-hydroxymethyl-furan (VIm). This substance is prepared as indicated for VIc, section d). Employing VIk, VIm is obtained in 51 % yield. It is recrystallised from ethanol-water (3 : 2) ; m.p. 147–148°C. $\bar{\nu}_{max}^{KBr}$ 3500, 3250, 3060, 2900, 1685, 1640, 1615, 1585, 1570, 1440, 1340, 1280, 1210, 1140, 1080, 1010, 970, 790 and 750 cm^{-1}. ^1H–NMR data ($CDCl_3$) : δ 7.7 (m, 5H, Ph), 6.38 (s, 1H, H–4) ; 5.42 (broad, exchangeable with D_2O, 2H, NH_2), 4.51 (s, 2H, CH_2OH). Mass spectrum : m/e 217 (M), 201 (M–NH_2), 200 (M–OH), 186 (M–CH_2OH), 173 (M–$CONH_2$), 140 (M–Ph), 112 (M–COPh), 105 (COPh, 100 %), 77 (Ph), 59 ($COCH_2OH$), 44 ($CONH_2$), 31 (CH_2OH), 17 (OH) and 16(NH_2). Anal. Calc. for $C_{12}H_{11}O_3N$: C, 66.36 ; H, 5.07 ; N, 6.45. Found : C, 66.51 ; H, 4.89 ; N, 6.62 %.

2-Phenyl-5-hydroxymethyl-furan-3-carboxylic acid (VIn). This compound is prepared as indicated in the synthesis of VIe from VIa. When VIf is employed VIn is obtained in 82 % yield. When VIk or VIm are used, the yields are 67 and 56 % respectively ; m.p. 158–160°C. $\bar{\nu}_{max}^{KBr}$ 3500–2400, 3040, 2970, 1670, 1580, 1530, 1500, 1420, 1310, 1250, 1200, 1120, 1080, 960 and 760 cm^{-1}.^1H–NMR data ($CDCl_3$) : δ 11.2 (broad, 1 H, CO_2H), 8.2–7.8 (m, 5H, Ph), 6.40 (s, 1H, H–4), 4.5 (s, 2H, CH_2OH). Mass spectrum : m/e 218 (M), 201 (M–OH), 187(M–CH_2OH), 174 (M–CO_2) 173 (M–CO_2H), 159 (M–$COCH_2OH$), 141 (M–Ph), 113 (M–COPh), 105 (COPh), 77(Ph), 59 ($COCH_2OH$), 45(CO_2H, 100 %), 44 (CO_2), 31(CH_2OH) and 17(OH). Anal. Calc. for $C_{12}H_{10}O_4$: C, 66.05 ; H, 4.58. Found : C, 65.80 ; H, 4.61 %.

2-Phenyl-3-methoxycarbonyl-5-methoxymethyl-furan (VIq).—a) *from VIn* : Following the instruction given for preparation of VIp from VIe, employing 6.6 g of VIn, 5.73 g (76 %) of VIq are prepared ; b.p. 140–142°C/0.2 Torr. $\bar{\nu}_{max}^{film}$ 3070, 2990, 2930, 2890, 1715, 1610, 1580, 1555, 1440, 1375, 1300, 1220, 1115, 1080, 940, 840 and 770 cm^{-1}.^1H–NMR data (CCl_4) : δ 7.75–7.45 (m, 5H, Ph), 6.41 (s, 1H, H–4), 4.32 (s, 2H, CH_2OR), 3.65 (s, 3H, CO_2 Me), 3.2 (s, 3H, OMe). Mass spectrum : m/e 246 (M), 215 (M–OMe), 201 (M–CH_2OMe), 187 (M–CO_2Me), 173 (M–$COCH_2OMe$), 167 (M–Ph), 141 (M–COPh), 105 (COPh, 100 %), 77 (PH), 73 ($COCH_2$ OMe), 59 (CO_2Me) and 45 (CH_2OMe). Anal. Calc. for $C_{14}H_{14}$ O_3 : C, 73.04 ; H, 6.08. Found : C, 72.86 ; H, 6.37 %. b) *from VIf or VIk* : When VIf or VIk are employed VIq is prepared with 82 and 61 % respectively.

3-Chlorocarbonyl-5-chloromethyl-2-methyl-furan (VIt). 9 g of VIe are refluxed for 1 hr with 30 ml of $SOCl_2$; the SCl_2 is eliminated and the residue is distilled, affording 6 g (42 %) of VIt ; b.p. 82–84°C/0.3 Torr. It decomposes under light. $\bar{\nu}_{max}^{film}$ 2910, 1710, 1620, 1590, 1555, 1490, 1430, 1245, 1210, 1170, 1080, 970, 850 and 760 cm^{-1}.^{1} H–NMR data (CCl_4) : δ 6.7 (s, 1H, H–4), 4.45 (s, 2H, CH_2Cl), 2.55 (s, 3H, Me).

5-Aminomethyl-3-carbamido-2-methyl-furan (VIn). A suspension of 2.5 g of $NaNH_2$ (50 %) in toluene is added to a solution of 4 g of VIt in 40 ml of petroleum ether and heated at 80° C for 1 hr. The mixture is cooled to 5°C and then a solution of 1.2 g of NH_4Cl in 5 ml of water is slowly added, and then 15 ml of water are added, causing the appearence of a precipitate that is collected by filtration and recrystallised from ethanol-water (1 : 1) giving

1.87 g (46 %) of VIn ; m.p. 161–163°C. $\bar{\nu}_{max}^{KBr}$ 3500, 3250, 2990, 2925, 2880, 1685, 1640, 1600, 1570, 1440, 1400, 1380, 1330, 1280, 1220, 1150, 990, 800 and 750 cm^{-1}.^{1}H–NMR data (DMS) : δ 6.30 (s, 1H, H–4), 5.54 (broad, 2H, $CONH_2$), 4.85 (b, 2H, NH_2), 4.10 (t, J 6Hz, 2H, CH_2O) and 2.4 (s, 3H, Me). Mass spectrum : m/e 154 (M), 139 (M–Me), 138 (M–NH_2), 124 (M–CH_2NH_2), 111 (M–Ac), 110 (M–$CONH_2$), 96 (M–$COCH_2$ NH_2), 58 ($COCH_2NH_2$), 44 ($CONH_2$, 100 %), 43 (Ac), 16(NH_2) and 15 (Me). Anal. Calc. for $C_7H_{10}O_2N_2$: C, 54.54 ; H, 6.49 ; N, 18.18. found : C, 54.25 ; H, 6.52 ; N. 18.20 %.

3-Chlorocarbonyl-5-hydroxymethyl-2-metyhl-furan (VIv). This substance is prepared as indicated for VIt, with the difference that in this case the initial mixture is not heated and is stirred for 90 min. VIv is thus prepared in 50 % yield ; b.p. 91–92°C/0.3 Torr. It decomposes under light. $\bar{\nu}_{max}^{film}$ 3450, 2990, 2920, 2850, 1720, 1640, 1600, 1565, 1440, 1380, 1310, 1230, 1190, 1120, 1075, 950 and 760 cm^{-1}.^{1}H–NMR data (CCl_4) : δ 6.65 (s, 1H, H–4), 435 (s, 2H, CH_2OH), 2.60 (s, 3H, Me).

When treated with sodamide (in equimolar ratio), as indicated for VIn, VIc is prepared in 53 % yield. When treated with sodium methoxide (in equimolar ratio) in ethanol, after heating for 1 hr at 80°C, it affords VIa in 58 % yield.

Methyl ester of 2-acetyl-5,6-dihydroxy-hexen-2-oic acid (Xa). 6 g of the mixture of VIIa, VIIIa and IXa, prepared as instructed in,[7] is dissolved in 18 ml of ethanol and 18 ml of 50 % acetic acid. The mixture is heated at 55°C for 2 hrs, the solvent is eliminated to afford by distillation 4.1 g (83 %) of Xa ; b.p. 79–81°C/0.5 Torr. $\bar{\nu}_{max}^{film}$ 3500, 2990, 2910, 2880, 1700, 1600, 1570, 1510, 1440, 1380, 1320, 1270, 1200,1140, 1060, 980 and 840 cm^{-1}.$^{-1}$H–NMR data ($CDCl_3$) : δ 6.75 (d, J 10 Hz, 1H, H–3), 4.80 (broad, 4H, CH_2 OH and OH), 3.72 (s, 3H, OMe), 3.60 (m, 1H, H–5) and 2.25 (s, 3H, Ac). Mass spectrum : m/e 188(M), 171 (M–OH), 157 (M–OMe), 145 (M–Ac), 129 (M–CO_2Me), 59 (CO_2Me), 43 (COMe, 100 %), 31 (OMe) and 17 (OH) Anal. Calc. for $C_8H_{12}O_5$: C, 51.06 ; H, 6.38. Found : C, 51.22 ; H, 6.19 %.

Treatment of 2 g of Xa with 2 g of $ZnCl_2$ in 20 ml of ethanol-water (1 : 1) affords 1.2 g (66 %) of VIa.

Nitrile of 2-acetyl-5,6-dihydroxy-hexen-2-oic acid (Xd). This compound is prepared as indicated for Xa employing 6g of VId, VIIId and IXd and 15 ml of 50 % acetic acid. Thus 2.23 g (51 %) of Xd are prepared ; b.p. 75–76°C/0.5 Torr. $\bar{\nu}_{max}^{film}$ 4450, 2990, 2910, 2850, 2210, 1710, 1605, 1550, 1490, 1440, 1380, 1290, 1220, 1120, 1000 and 850 cm^{-1}. ^{1}H–NMR data ($CDCl_3$) : δ 6.70 (d, J 11 Hz, 1H, H–3), 4.70 (b, 4H, CH_2OH and OH), 3.68 (m, 1H, H–5), 2.22 (s, 3H, Ac). Mass spectrum : m/e 155 (M), 140 (M–Me), 138 (M–OH), 129 (M–CN), 124 (M–CH_2OH), 112 (M–Ac), 43 (Ac, 100 %), 31 (CH_2OH), 26(CN) and 17(OH). Anal. Calc. for $C_7H_9O_3N$: C, 54.19 ; H, 5.81 ; N, 9.03. Found : C, 54.31 ; H, 5.60 ; N, 8.92 %.

Treatment of Xd with 30 % ethanolic $ZnCl_2$ solution (in molar ratio) at 50°C for 1 hr affords VId in 42 % yield.

REFERENCES

[1] F. Garcia Gonzalez, *Adv. Carbohyd. Chem.*, **11**, 111 (1956).

[2] G. Garcia Gonzales and A. Gomez Sánchez, *Adv. Carbohyd. Chem.*, **20**, 303 (1975).

[3] F. Garcia Gonzalez and F. J. López Aparicio, *Anal. Real Soc. Esp. Fis. Quim.*, **41**, 846 (1945).

[4] F. J. López Aparicio, F. J. López Herrera and J. Sánchez Ballesteros, *Carboh. Res.*, **69**, 55 (1979).

[5] J. Sánchez Ballesteros, I. Mugaburu Lacabrera and F. Hernandez Hernandez, *Carboh. Res.*, UK 1974, in press.

[6] J. Sánchez Ballesteros, F. Hernandez Hernandez, L. Ayala Montoro and J. Laguna Garcia, *Anal. Real Soc. Esp. Fis. Quim.*, 253/79 in press.

[7] J. Sánchez Ballesteros, F. Hernandez Hernandez and D. J. McPhee, *Rev. Roumaine Chim.*, **26**, 705 (1981).

[8] E. Baer and H.O.L. Fischer, *J. Amer. Chem. Soc.*, **61**, 761 (1939).

[9] H. O. L. Fischer and E. Baer, *Helv. Chim. Acta*, **17**, 622 (1934).

[10] L. Claisen and K. Meyer, *Ber. dtsch. Chem. Gess.*, **35**, 583 (1902).

[11] K. Kumasa Sato and T. Amakasu ; *J. Org. Chem.*, **33**, 2449 (1968).

[12] Y. F. Chi and Y. M. Lee, *Trans. Science. Soc. China*, **8**, 87 (1934).

[13] R. Eby and C.R. Hauser, *J. Amer. Chem. Soc.*, **79**, 723 (1957).

Revue Roumaine de Chimie, **26**, *6*, 909–916 (1981)

FREQUENTOMETRIC DETECTION IN DIFFERENT STABILITY CONDITIONS OF IR ANALYTIC SYSTEMS

CANDIN LITEANU* and IOANA ILEANA PANOVICI **

* Department of Chemical Technology, University of Cluj-Napoca, str. Arany Janos 11, Cluj-Napoca, Romania

** Technological Research and Design Institute for Refineries and Petrochemical Plants, Bd. Republicii 291, Ploiești, Romania

Received 31 October 1980

The functional instability of infrared spectrometers can result in serious errors of analysis. To appreciate the stability of IR analytic systems, the serial correlation and χ^2 criterion linked with the method of mean square of successive differences were used. This work shows how the instability of an IR analytic system influences the frequentometric estimation of detection limit, by detection of N-methyl-2-pyrrolidone in styrene in different conditions of stability.

I. INTRODUCTION

A basic problem connected to any analytical determination is that of stability of the analytic system i.e. parametric stability of the transfer function $y = f(c)$. Both the estimation of the detection limit and the determinations using calibration curves raise the same problem.

When the analytic system is stable the values of analytic signal y belong to a real n-dimensional region

$$y \in Y \subset R^n$$

When the analytic system is unstable the analytic signal becomes time-dependent $y(t) = \{y_q, t\}$ so that set Y has one more dimension

$$y \in Y \subset R^{n+1}$$

Whenever the analytical signal is time-dependent one says that it belongs to a "phase space", R^{n+1}, a space having time among its dimensions. To check the stability of an analytic system means to verify if analytic signal is or is not time-dependent. The time dependence may be seen as an influence of the time on transfer function parameters. This influence can not be ignored because if it exists it can introduce important errors when the signal is transformed in values of concentration.

A stable analytic system determines random variations of the values in a sequence of data. The instability of an analytic system leads to extreme variations, to periodic fluctuations or to discontinuity, makes the data drift. These phenomena may appear simultaneously.

There are many tests used to verify the stability of an analytic system but the most useful are the quantitative ones e.g. χ^2,[1] the method of mean square of successive differences (MSSD)[2-5] and serial correlation.[2,6,7]

A special attention must be paid to analytic system stability when the frequentometric method is used because it influences the detection limit.

The randomness of any signal always results in a superposition of analytic signal fluctuations and the noise. This is the reason to associate to detection decision, i.e. to correlation between the analytic signal and the presence of a given component, a probability of correctness and another one of falseness.

If the concentration is c one can write :

$$p = n_+/n = f(c),\ n \to \infty \Rightarrow p \to 1 \tag{1}$$

This relation can be considered a transfer function defined on concentration set and valued in the interval [0,1] of positive sample probability i.e. the probability to accept the hypothesis $H_1 : y > y_0$.[8-10]

To define and estimate the detection limit a two-step statistical model (see Fig. 1) and Neyman-Pearson test were used.[14,15] The detection i.e. verification of hypothesis $H_1 : y > y_k$ is based on decision level [13,14] or detection level y_k[15,16] to which a probability to be correct P_{11} and another probability to be wrong P_{10} are associated.

If the analytic signal is normally distributed then

$$P_{10} = \int_{y_k}^{\infty} p(y_0)\,\mathrm{d}y_0 \tag{2}$$

and the variable y_0 of $\bar{y}_0$ mean and $\sigma_{y_0}^2$ variance can be related to a zero mean and unit variance normal variable $z_k = |y_k - \bar{y}_0|/\sigma_{y_0}$:

$$y_k = \bar{y}_0 + z_k\sigma_{y_0} \tag{3}$$

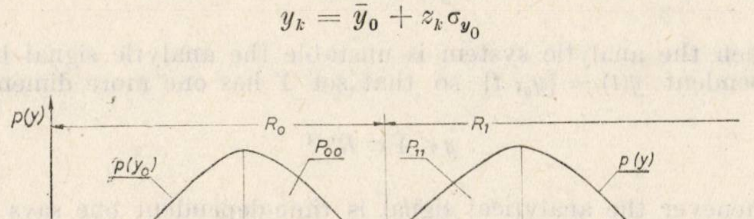

Fig. 1. — Two-step statistical model for defining the detection limit. [13]

The standard variable z_k and the probability P_{10} are related through Laplace function $\Phi(z_k) = 0.5 - P_{10}$.[17]

When the number of samples is small the equation (1) becomes

$$n_+/n = F_n(c) = f(c) = P_{11} \tag{4}$$

where P_{11} is the probability of a correct detection so that using the two-step model (Fig. 1) we obtain:

$$P_{11} = F_n(c) = \int_{y_k}^{\infty} p(y)\, d(y) = 0.5 + \Phi(z) = f(c) \tag{5}$$

there we have $\Phi(z) = 0.5 - F_n(c)$ whenever $F_n(c) < 0.5$ and $\Phi(z) = 0.5 + F_n(c)$ whenever $F_n(c) > 0.5$.

Equation (5) results in

$$z = f(c) \tag{6}$$

and the transfer function (1) will have the form

$$z = \frac{c - \bar{c}}{\sigma_y} = a + b\,c \tag{7}$$

The values of the analytic signal z can be obtained using equation (4) where n_+ samples from all n measured indicate $y > y_k$ [11,13]

If the probability of a correct detection is P_{11}, using equation (5) and the corresponding value of Laplace function one obtains the value of standard variable z_a and from equation (7) we have the detection limit $\bar{c}_d$.

The instability of an IR analytic system may influence the detection limit value through parameters $\bar{y}_0$ and s_{y_0} which determine that value. To appreciate the changes in the two parameters the use of statistical criteria is needed. The criterion t (Student) is adequate to verify $\bar{y}_0$ and the criterion F is good for $s_{y_0}^2$.

Finally the hypothesis $H_1 : (\bar{c}_d)_{\text{stable}} \neq (\bar{c}_d)_{\text{unstable}}$ was verified by the comparison of the two calibration lines, obtained in different conditions of stability.[18]

How the instability of an IR analytic system influences the frequentometric evaluation of detection limit is illustrated by detection of N-methyl-2-pyrrolidone in styrene in different conditions of stability.

II. EXPERIMENTAL

1) *Apparatus*: IR absorption spectrophotometer UR-10 with recorder and integrator; NaCl prism; cell with layer width of 0.200 cm and NaCl windows.

2) *Working conditions*: frequency 1682 cm^{-1} fixed, solvent CCl_4, slit 4, recorder sensibility 2, integration time 12 seconds. In standard conditions the gain was 6 and an attenuator was used. In modified conditions the gain was 5 and no attenuator was used.

3) *Determination of IR analytic system stability*

A standard sample of N-methyl-2-pyrrolidone and styrene in CCl_4 having a concentration of 0.377 mg% N-methyl-2-pyrrolidone was prepared. The standard sample was recorded 20 times in both standard and modified working conditions.

To appreciate the stability of IR analytic system the serial correlation and χ^2 criterion linked with MSSD were used.

By serial correlation of the 20 values obtained in standard conditions we have found a correlation coefficient $R_1 = -0.109$ and because $R_{1(0.975)} = -0.399 < R_{1(\exp)} = -0.109 < 0.299 = R_{1(0.025)}$, we concluded that the system is stable.

The same serial correlation method applied to the other 20 values obtained in modified conditions leads to $R_1 = 0.450$. This time the system is unstable because $R_{1(\exp)} = 0.450 > 0.432 = R_{1(0.005)}$.

To establish what kind of instability occurs in this second case MSSD and χ^2 criterion have been applied. The data have $\chi^2_{\exp} = 41.67$, $\eta_s = 0.83$ and $\eta_y = 1.82$. From tables we obtained $\chi^2_{(0.995;19)} = 38.58$, $\eta_{0.99} = 1.04$, $\eta_{0.95} = 1.30$ and $\eta_{0.05} = 2.70$. The following statements are now true : $\chi^2_{\exp}$ is significant because $41.67 > 38.58$; η_s is small but significant because $0.83 < 1.04$; η_y is not significant because $1.30 < 1.82 < 2.70$.

The comparison between calculated and tabulated values leads to conclusion that the instability exists and is a drift.

4) *Drawing calibration curves*

a) Stable system.

To establish the detection level y_k, the noise was recorded 20 times. The values obtained gave $\bar{y}_0 = 3453$ and $s_{y_0} = 79.2$. If we admit a probability of false detection $P_{10} = 0.025$ ($z_k = 1.96$) then from equation (3) we obtain $y_k = 3608$.

A number of 7 standard samples of N-methyl-2-pyrrolidone and styrene in carbon tetrachloride, concentrations between 0.150 and 0.701 mg%, were prepared and each of them was recorded 20 times. An n_+ for each concentration was established so that a set of pair concentrations — positive sample probability, $P(y > y_k) = n_+/n = F_n(c)$, were obtained (see Table 1).

TABLE 1

Data obtained on a stable analytic system

No.	Conc. mg%	n	n_+	$F_n(c)$	$\Phi(z)$	z
1	0.701	20	19	0.95	0.45	1.645
2	0.535	20	16	0.80	0.30	0.842
3	0.490	20	14	0.70	0.20	0.524
4	0.377	20	10	0.50	0.00	0.000
5	0.320	20	8	0.40	0.10	−0.253
6	0.231	20	5	0.25	0.25	−0.675
7	0.150	20	3	0.15	0.35	−1.037

The linearization of the curve $F_n(c) = f(c)$ followed using Laplace function and equation (7). Through the points (z_i, c_i) a least square straight line, the calibration line, was drawn (see Fig. 2). The equation of calibration line is

$$z = -1.814 + 4.899\, c \tag{8}$$

The confidence strip attached to function (8), at $P = 0.95$, is bounded by two hyperbolic arcs :

$$z = z_i \pm 0.085\sqrt{0.215 + 7(c_i - 0.400)^2} \tag{9}$$

b) Unstable system.

The same standard samples except the lowest concentration one were used. The noise had the parameters $\bar{y}_0 = 3384$ and $s_{y_0} = 75.6$ so that at $P_{10} = 0.025$ the detection level was $y_k = 3532$.

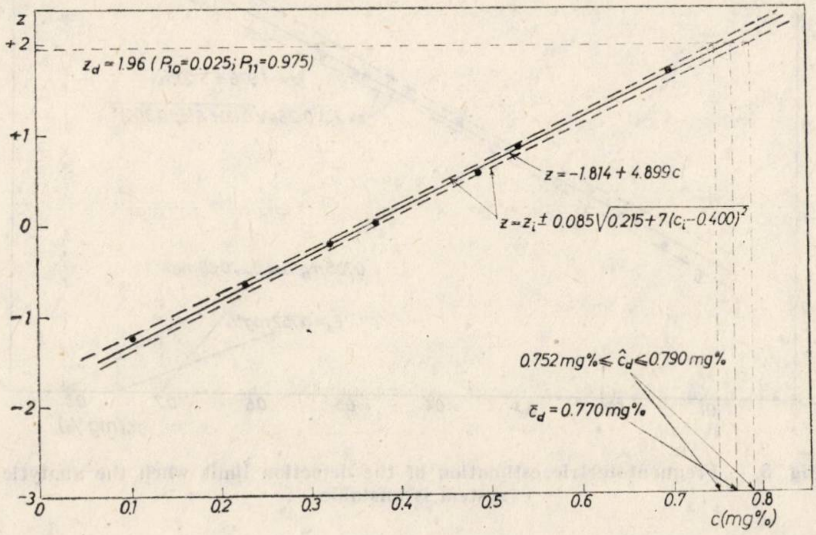

Fig. 2. — Frequentometric estimation of the detection limit when the analytic system is stable.

In table 2 the data and the calculation results are given.

TABLE 2

Data obtained on an instable analytic system

No.	Conc. mg %	n	n_+	$F_n(c)$	$\Phi(z)$	z
1	0.535	20	16	0.80	0.30	0.842
2	0.490	20	14	0.70	0.20	0.524
3	0.377	20	10	0.50	0.00	0.000
4	0.320	20	8	0.40	0.10	−0.254
5	0.231	20	5	0.25	0.25	−0.675
6	0.150	20	2	0.10	0.40	−1.282

The calibration line equation for the drifting data is

$$z = -1.976 + 5.235\,c \tag{10}$$

and the attached confidence strip at $P = 0.95$ is also bounded by two hyperbolic arcs (see Fig. 3) having the equation :

$$z = z_i \pm 0.264\sqrt{0.110 + 6(c_i - 0.350)^2} \tag{11}$$

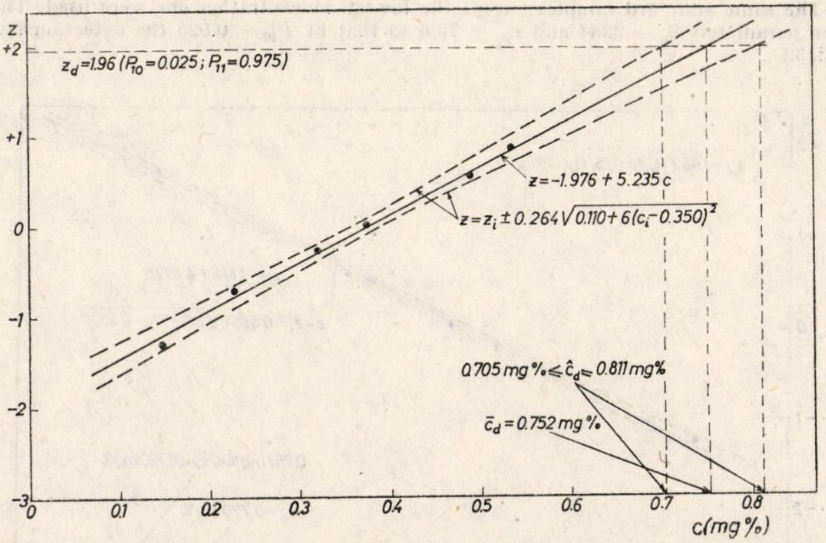

Fig. 3. — Frequentometric estimation of the detection limit when the analytic system is unstable.

III. RESULTS AND DISCUSSIONS

a) Stable system.

To estimate the detection limit $\bar{c}_d$, the real detection probability $P_{11} = 0.975$ was considered so that $z_d = 1.96$. Substituting this value in equation (8) a value of $(\bar{c}_d)_{\text{stable}} = 0.770$ mg% was found and from equation (9) the confidence interval $0.752\ \text{mg}\% \leqslant (\hat{c}_d)_{\text{stable}} \leqslant 0.790\ \text{mg}\%$ was determined.

b) Unstable system.

Choosing the same real detection probability $P_{11} = 0.975$ ($z_d = 1.96$) from equation (10) a detection limit $(\bar{c}_d)_{\text{unstable}} = 0.752$ mg% was determined. The confidence interval of the detection limit is $0.705\ \text{mg}\% \leqslant (\hat{c}_d)_{\text{unstable}} \leqslant 0.811\ \text{mg}\%$.

c) Testing hypothesis $H_1 : (\bar{c}_d)_{\text{stable}} \neq (\bar{c}_d)_{\text{unstable}}$

The value of $\bar{c}_d$ can be estimated using either equation (8) or equation (10) at the same probability $P_{11} = 0.975$ ($z_d = 1.96$). To verify if the two values of $\bar{c}_d$ are really different we must compare the two calibration lines. If the two empirical lines estimate the same theoretical line then the alternate hypothesis $H_0 : (\bar{c}_d)_{\text{stable}} = (\bar{c}_d)_{\text{unstable}}$ is accepted.

To test the two regression lines we have to compare their slopes $b_1 = 4.899$ and $b_2 = 5.235$ and the two values of the theoretical line slope, $\bar{b}$ and $\hat{b}$, calculated using b_1 and b_2 and the variation between systems.

To test the hypothesis $H_0 : b_1 = b_2$, the two slopes unsignificantly different, a variable t (Student) with $n_1 + n_2 - 4$ degrees of freedom is used but before this the identity of the two variances estimated by $s^2_{\text{stable}} = 0.001648$ and $s^2_{\text{unstable}} = 0.005893$ must be tested. Using the F criterion we obtain $F = 3.58 < 5.19 = F_{(0.95;4,5)}$ so that the two variances do not differ. It was calculated the weighed variance estimated by $\bar{s}^2 = 0.003535 = (0.005893 \times 4 + 0.001648 \times 5)/(5 + 4)$.

The value of s_T was introduced in equation (12):

$$t = \frac{b_1 - b_2}{\bar{s}\sqrt{\dfrac{1}{\Sigma(c_{i1} - \bar{c}_1)^2} + \dfrac{1}{\Sigma(c_{i2} - \bar{c}_2)^2}}} \qquad (12)$$

and we obtained $t = 1.52 < 2.26 = t_{(0.95;9)}$ which confirms the equality of the slopes of the two theoretical lines estimated by empirical lines (8) and (10). The two lines will coincide when the weighed average $\bar{b}$ of the two empirical slopes will not differ significantly from slope $\hat{b}$ of the line passing through the points $(\bar{c}_1, \bar{y}_1)$ and $(\bar{c}_2, \bar{y}_2)$.

The $\bar{b}$ and $\hat{b}$ values were obtained using the following equations

$$\bar{b} = \frac{b_1 \Sigma(c_{i1} - \bar{c}_1)^2 + b_2 \Sigma(c_{i2} - \bar{c}_2)^2}{\Sigma(c_{i1} - \bar{c}_1)^2 + \Sigma(c_{i2} - \bar{c}_2)^2} \qquad (13)$$

$$\hat{b} = \frac{\bar{z}_{\text{stable}} - \bar{z}_{\text{unstable}}}{\bar{c}_{\text{stable}} - \bar{c}_{\text{unstable}}} \qquad (14)$$

and the calculation gave $\bar{b} = 5.013$ and $\hat{b} = 5.800$. To verify the equality of the two slopes a t variable with $n_1 + n_2 - 3$ degrees of freedom was used:

$$t = \frac{\bar{b} - \hat{b}}{s_G \sqrt{\dfrac{1}{\Sigma(c_{i1} - \bar{c}_1)^2 + \Sigma(c_{i2} - \bar{c}_2)^2} + \dfrac{1}{(\bar{c}_1 - \bar{c}_2)^2}\left(\dfrac{1}{n_1} + \dfrac{1}{n_2}\right)}} \qquad (15)$$

where

$$s_G^2 = \frac{(n_1 - 2)s^2_{\text{stable}} + (n_2 - 2)s^2_{\text{unstable}} + \dfrac{(b_1 - b_2)^2}{\dfrac{1}{\Sigma\,(c_{i1} - \bar{c}_1)^2} + \dfrac{1}{\Sigma\,(c_{i2} - \bar{c}_2)^2}}}{n_1 + n_2 - 3} \qquad (16)$$

is a new estimation of general variance σ^2.

The value $t = 1.11 < 2.23 = t_{(0.95;10)}$ indicates the insignificance of the difference between $\bar{b}$ and $\hat{b}$.

Looking once more to the tests already carried out, the conclusion is that the two regression lines (8) and (10) estimate the same theoretical regression line. So the hypothesis $H_0 : (\bar{c}_d)_{\text{stable}} = (\bar{c}_d)_{\text{unstable}}$ is confirmed

To appreciate the changes in the parameters $\bar{y}_0$ and s_{y_0} the criterion t (Student) and the criterion F were used. The criterion t makes evident the significant difference between $(\bar{y}_0)_{\text{stable}}$ and $(\bar{y}_0)_{\text{unstable}}$ because $t = 2.81 > > 2.02 = t_{(0.95;38)}$. The two variances estimated by $(s^2_{y_0})_{\text{stable}}$ and $(s^2_{y_0})_{\text{unstable}}$ are not significantly different because $F = 1.09 < 2.17 = F_{(0.95;19,19)}$.

The criterion t applied to detection levels leads to $t = 3.01 > 2.02 = = t_{(0.95;\,38)}$, so that the two values are significantly different.

Examining tables 1 and 2 we observe that $F_n(c) = n_+/n$ has the same values in both situations, except the last one where the effect of drift becomes sensible. Thus the drift determined a proportional change of the analytic signal comparing to noise i.e. the ratio of analytic signal to detection level maintained approximatively the same, no matter that $\bar{y}_0$ and y_k have lower values when the analytic system is unstable.

IV. CONCLUSIONS

The detection limit in different conditions of analytic system stability was estimated by frequentometric method.

An analysis of the results shows that the number n_+ of positive detection samples is the same in different conditions of stability except for the lowest concentration $c = 0.150$ mg%. This error appears to be normal because it occurs toward the inferior section of calibration curve.

To verify the hypothesis concerning the equality of the two $\bar{c}_d$ values, two regression lines were compared by t criterion. The two empirical regression lines were found to be estimates of the same theoretical line. This is a solid reason to accept the hypothesis of equality of the two $\bar{c}_d$'s. In other words the drift presence in analytic system does not influence on detection limit established by frequentometric method.

However the drift brings about a significant difference between the $\bar{y}_0$'s and also between y_k's. But despite these differences the drift has determined a proportional change of analytic signal compared with detection limit i.e. the number of positive detection samples holds at the same concentration.

We can conclude that, when the detection limit is estimated by frequentometric method, the drift modifies the values $\bar{y}_0$ and y_k but does not influence the detection limit $\bar{c}_d$.

REFERENCES

[1] I. Miller and J. E. Freund, "Probability and Statistics for Engineers", Prentice- Hall, Englewood Cliffs, New York, 1965.

[2] C. A. Bennett and N. L. Franklin, "Statistical Analysis in Chemistry and the Chemical Industry", Wiley, New York, 1954, p. 626.

[3] H. R. Bellinson, J. von Neumann, R. H. Kent and B. L. Hart, "The Mean Square Successive Difference", *Annals Math. Stat.*, **12**, 153 (1941).

[4] B. W. Lindgren, "Statistical Theory", Macmillan, New York, 1963, p. 330.

[5] K. A. Hooton and M. L. Parsons, *Analyt. Chem.*, **45**, 2218 (1973).

[6] R. L. Anderson, *Annals Math. Stat.*, **13**, 1 (1942).

[7] C. Liteanu and I. I. Panovici, *Talanta*, **24**, 196 (1977).

[8] C. Liteanu and I. Florea, *Mikrochim. Acta*, **1966**, 983.

[9] C. Liteanu and R. Alexandru, *Mikrochim. Acta*, **1968**, 639.

[10] C. Liteanu, *Mikrochim. Acta*, **1970**, 715.

[11] J. Neyman and E. Pearson, *Phil. Trans. Roy. Soc.*, **231**, 289 (1933).

[12] C. H. Helstrom, "Statistical Theory of Signals Detection", Pergamon Press, Oxford, 1960, p. 68.

[13] C. Liteanu and I. Rîcă, *Mikrochim. Acta*, **1973**, 745.

[14] L. A. Currie, *Analyt. Chem.*, **40**, 586 (1968).

[15] C. Liteanu and I. Rîcă, *Mikrochim. Acta*, **1975**, 311.

[16] C. Liteanu and I. Rîcă, *Pure Appl. Chem.*, **44**, 535 (1975).

[17] C. Liteanu and I. Rîcă, "Statistical Theory and Methodology of Trace Analysis", E. Horwood, Chichester, 1980, p. 427.

[18] N. Rancu and L. Tövissi, "Statistica matematică cu aplicaţii în producţie", Editura Academiei, Bucureşti, 1963, p. 654.

Revue Roumaine de Chimie, 26, *6*, 917—923 (1981)

THIOVIOLURIC ACID AS AN ANALYTICAL REAGENT

SPECTROPHOTOMETRIC AND COMPLEXOMETRIC DETERMINATION OF COPPER(II)

P. P. SINHA, R. S. CHAWLA *, S. K. SINDHWANI and FASIHUDDIN KAMIL
Department of Chemistry, University of Delhi, Delhi—110007 India

Received May 6, 1980

Aqueous solution of thiovioluric acid (HTVA) forms a chocolate-yellow coloured complex with copper (II). The appearance of turbidity after some time, has been overcome by the addition of ethanol. The determination of 10.2 to 38.1 μg of copper may be carried out over the pH range 4.5—7.5. The sensitivity of the method at 395 nm is 0.0078 $\mu g/cm^2$. Copper and HTVA combine in the ratio of 1 : 1. In the complexometric determination of copper (II) with HTVA, the colour changes from yellow to light blue. The useful pH range is from 2.3 to 3.3. For accurate determination of copper (II) the optimum amount should be from 0.63 to 8.89 mg Cu/5 ml. The selectivity of the methods has also been investigated.

INTRODUCTION

Thiovioluric acid (HTVA) has already been employed for the gravimetric determination of palladium [1] and spectrophotometric determinations of ruthenium [2] and cobalt.[3] Stability constants of some bivalent metal complexes with thiovioluric acid have also been reported earlier.[4] In the present communication, attempts have been made to utilise the reagent for the spectrophotometric and complexometric determination of copper (II).

Cuproine,[5] neocuproine[6] and bathocuproine[7] are most selective reagents for the spectrophotometric determination of copper as they do not react with other metals. Diethyldithiocarbamate [8] has been used with success and large amounts of Al(III), As(III), Fe(III), Zn(II), Ni(II) and Co(II) do not interfere. 2.2′-Biquinoline [9] is quite a selective reagent for copper and its sensitivity is fairly good (0.010 μg). Dithizone [10] is one of the most popular organic reagents for the spectrophotometric determination of copper. It has the advantage of very high sensitivity and mineral acid reaction medium. It can be used to determine copper directly in the presence of nickel and cobalt. The strong colour of dithizone and the mediocre stability of its solutions are disadvantages.

---

* Present address : Department of Chemistry, Ramjas College, University of Delhi, Delhi-110007

Thiovioluric acid is not specific like cuproine, neocuproine and bathocuproine because it gives colour reactions with other metal ions. Though HTVA is not so sensitive as dithizone, it has a light yellow colour and is stable in solutions. Moderate quantities of silver (I) and mercury (II) are tolerated but they interfere in dithio-oxamide method.[11] No protective colloid is used as in the case of dithio-oxamide. Lead and zinc do not interfere in the case of thiovioluric acid but these have been found to interfere in the case of bicyclohexanoneoxalyldihydrazone.[12] It is more sensitive (sensitivity = 0.0078 μg cm^2) than 2,2′-biquinoline and compares favourably with other methods mentioned above.

In the titrimetric determination of copper, murexide [13] does not involve any difficulty if care is taken to avoid very high concentration of ammonia and ammonium ions. It has been observed that high concentrations of ammonia decompose the copper – murexide complex and copper tetramine complex is formed. PAN[14] and PAR [15,16] as indicators in the determination of copper has the disadvantage that the titrations have to be carried out in hot solution. Copper (II) can be estimated by back titration with manganese sulphate solution using eriochrome black T as indicator.[17] The method has the disadvantage that pH of the solution has to be controlled very carefully and moreover, the end point is not very sharp.

In the present work, HTVA has been used for the estimation of copper (II) with EDTA. Accurate results are obtained if the amount of copper present is 0.63 to 8.89 mg/5 ml. The method works at room temperature and therefore, no heating is required as is the case with PAN and PAR. In addition, the colour change at the end point is easily detectable. HTVA is favourably comparable with other recently reported indicators.

EXPERIMENTAL

Reagents and equipment

A stock solution of copper (II) was prepared by dissolving AnalaR, B.D.H., sample of cupric sulphate pentahydrate in double distilled water. The solution was further standardised gravimetrically by thiocyanate method.

The solution of thiovioluric acid was prepared in double distilled water.

A Unicam, SP600, Spectrophotometer was used for absorbance measurements and an ECIL Expanded Scale pH meter, PH 821 A, was employed for measurements of pH.

Precalibrated pipettes, burette and measuring flasks (Pyrex or corning make) were used for volume measurements.

Procedure for spectrophotometric determination

To the sample solution containing 10.2–38.1 μg of copper, add thirty times molar excess of aqueous solution of thiovioluric acid and transfer the solution to 25 ml volumetric flask. Adjust the pH in the range 4.5–7.5 with acetate buffer (above pH 6.0, sodium hydroxide may be used) and add 6 ml of ethanol. Dilute the solution up to the mark with double distilled water and measure the absorbance at 395 nm against the corresponding reagent blank prepared under identical conditions. Calculate the amount of copper from the calibration curve.

Procedure for complexometric determination

Take a suitable aliquot of sample solution containing 0.63 to 8.89 mg of copper (II) and add five drops of 0.25 % ethanolic solution of thiovioluric acid indicator. Adjust the pH to 3.0 with sodium acetate – acetic acid buffer and titrate the mixture against standard EDTA solution taken in a microburette. Note the end point when the colour of the solution changes from yellow to light blue.

RESULTS AND DISCUSSION

a) Spectrophotometric determination of copper (II)

When an aqueous solution of thiovioluric acid is added to a solution of copper (II), a chocolate-yellow colour is produced immediately, accompanied by a slight turbidity after some time. The appearance of turbidity has been overcome by the addition of ethanol. A series of solutions containing a fixed amount of metal ion (1 ml of 1×10^{-3} M) and a large excess of the reagent (3 ml of 1×10^{-2} M) were prepared. 6 ml of ethanol were added in each case, pH's were adjusted at different levels and the volume was made up to 25 ml. The absorbances of these solutions were recorded at different wavelengths against the corresponding reagent blanks, prepared under similar conditions. It has been found that the system exhibits maximum absorbance at 395 nm at all pH's and this wavelength was selected for subsequent studies. The absorption characteristics at different pH's being similar, it is concluded that only one complex is formed under the conditions. A plot of pH vs. absorbance showed that the constant absorbance is exhibited in the pH range 4.5—7.5. Subsequent studies have been carried out at pH 6.0. Since the complex precipitated out on addition of the reagent, the effect of various polar solvents was investigated. It was found that ethanol, methanol and acetone were all equally effective. However, ethanol was added in subsequent studies; adding a small amount of EtOH caused the removal of turbidity. It was found that up to 50% (V/V) of ethanol caused no change in absorbance; above this limit a slight decrease in absorbance was observed. In subsequent work, ethanol concentration was maintained at 25% (V/V). The minimum amount of reagent required for full colour development was determined by measuring absorbances of a number of solutions, containing a fixed amount of copper and varying amounts of the reagent against the corresponding reagent blanks at 395 nm. The absorbance values plotted against the moles of ligand showed that the absorbance became maximum when 20 times molar excess of the reagent was present. During subsequent studies, 30 times molar excess of the reagent was added. Solutions of the complex have been found to exhibit constant absorbance up to 8 hours after which a slight turbidity appears. The system obeys Beer's law up to 4.07 ppm of copper and the optimum range for accurate determination of the metal is 1.02 to 3.81 ppm. The sensitivity of the reaction is 0.0078 μg Cu/cm^2 for $\log I_0/I = 0.001$ at 395 nm and the corresponding molar absorptivity is 8086. The combining ratio of copper and thiovioluric acid in the complex was determined by Job's method of continuous variations [18,19] at different pH values. The maximum occurring at 0.5 mole fraction of copper(II) indicated that copper(II) and thiovioluric acid combine in the ratio of 1 : 1. The composition was found to be the same at all pH values. Seven samples each containing the same amount of copper (0.5 ml of 1×10^{-3} M) in a total volume of 12.5 ml gave an average relative deviation of $\pm 0.31\%$ and standard deviation at 0.0036.

Effect of foreign ions

The effect of foreign ions was studied in the determination of 2.54 ppm of copper and it was possible to avoid the interferences in some cases. Interference due to nickel has been avoided by the use of tartrate as masking agent. Palladium (II) gave precipitates and its interference was removed by adding excess of the reagent and measuring the absorbance of the supernatant solution after centrifugation. The tolerance limit of zinc is also increased by making use of tartrate as masking agent. Iodide, thiosulphate, thiocyanate and some of the eighth group metals interfere. The amounts (in ppm) of various ions which do not interfere in the determination are given below in parentheses :

Cl^-, SO_3^{2-} or SO_4^{2-} (1000), Br^-, PO_4^{3-}, NO_3^-, ClO_3^- or tartrate (500) ; NO_2^- (600), BO_3^{3-} (50), Ca(II), Ba(II), Sr(II) or Mg(II) (50), Ag(I) (5), Pb(II) (10), Zn(II) (15), Cd(II) (30), Al(III) (25), V(V) (50), Mo(VI) (10), Be(II) (25), Th(IV) or Ti(IV) (50), Zr(IV) (10), Au(III) (5), Mn(II) (200), Sb(III) (400), Sn(II) (5), W(VI) (100), Hg(II) (10), Bi(III) (100), Ir(III) (5), Pd(II) (2.5), Tl(I) (120), As(III) (200), U(VI) (50), Nb(V) (20), Ta(V) (20), Ni(II) (15) and Zn(II) (100).

b) Complexometric determination of copper(II)

The utility of thiovioluric acid as an indicator for the complexometric determination of copper (II) has been studied in detail. In order to investigate the effect of hydrogen ion concentration, a series of solutions containing the same amount of copper (II) were buffered to different pH values with sodium acetate — acetic acid buffers. Five drops of indicator were added to each solution and a yellow coloured complex was formed. These solutions were titrated against standard EDTA solution, taken in a microburette till the yellow colour changed to light blue. The order of colour change was found to be from yellow to light green and finally to light blue at the end point. The observations are given in table 1.

TABLE 1

Amount of copper (II) taken = 2.542 mg
Strength of EDTA used = 0.02 M

pH of the solution	Amount of Cu(II) found (mg)	% Error
1.5	2.287	−10.03
2.0	2.465	− 3.03
2.3	2.542	0.00
2.5	2.542	0.00
2.9	2.542	0.00
3.1	2.542	0.00
3.3	2.542	0.00
3.5	2.618	+ 2.99
4.0	2.719	+ 6.98

It is clear from the table that for accurate determination of the pH range is 2.3 to 3.3. In subsequent studies, pH 3.0 was maintained. The optimum concentration of the indicator required for the determination of copper (II) has been investigated. Titrations were carried out with different amounts of the indicator and it was observed that 3 to 5 drops of 0.25% solution of the indicator were sufficient to cause a sharp change at the end point. In subsequent work, five drops of 0.25% indicator were added. Titrations at various temperatures, ranging from 5° to 90° C were performed. From the data it was observed that for accurate determination, the temperature should be in the range of 10° to 40°C, below and above which erratic results are obtained. Below 10°C, the end point is reached very slowly. At temperatures greater than 40°C, the results are low. However, the titrations were successfully performed at room temperature (30 ± 5°C). The limiting amounts of copper (II) which can be accurately estimated, have been investigated. Solutions containing different amounts of copper (II) were titrated against standard solution of EDTA of a suitable strength. The results of this study are given in table 2. The table shows that for accurate determination (within ±0.5% error) and sharp end point, the optimum amount of copper (II) should be 0.63 to 8.89 mg/5 ml. In order to check the precision of the method, eight identical solutions of copper (II), each containing 2.542 mg of copper were taken and titrated according to the recommended procedure. The results are given in table 3.

TABLE 2

Titrable amounts of copper (II) for accurate determination

Amount of Cu(II) taken (mg)	Strength of EDTA used (molar)	Amount of Cu(II) found (mg)	% Error	Remarks
25.416	1×10^{-1}	24.145	−5.0	Green colour which changed to blue at the end point. Change was not sharp
12.708	5×10^{-2}	12.454	−1.99	
8.895	5×10^{-2}	8.852	−0.48	
6.354	5×10^{-2}	6.372	+0.28	
2.541	1×10^{-2}	2.549	+0.31	
0.6354	5×10^{-2}	0.6338	−0.25	
0.2541	1×10^{-3}	0.2520	−0.82	
0.0635	5×10^{-4}	0.0641	+0.94	Light yellow colour, end point is not sharp

Effect of diverse ions

To investigate the selectivity of the method, titrations were performed in the presence of diverse ions. The amounts (in ppm) of various ions which did not interfere in the determination of 2.542 mg of Cu(II) are given below in parentheses :

NO_3^- (700), $C_2O_4^{2-}$ (100), citrate (500), tartrate (370), PO_4^{3-} (650), SO_4^{2-} (2500), F^- (400), Cl^- (500), Br^- (1200), Hg(II) (50), U(VI) (25), Ba(II) (30) and Mg (II) (150).

TABLE 3

Strength of EDTA used = 0.02 M

Amount of Cu(II) found (mg) x	Deviation from average $(x - \bar{x})$	Square of deviation $(x - \bar{x})^2$
2.542	−0.001	1.00×10^{-6}
2.542	−0.001	1.00×10^{-6}
2.567	+0.024	5.76×10^{-4}
2.542	−0.001	1.00×10^{-6}
2.516	−0.027	7.29×10^{-4}
2.554	−0.011	1.21×10^{-4}
2.542	−0.001	1.00×10^{-6}
2.542	−0.001	1.00×10^{-6}

Average value, $\bar{x} = 2.543$

Standard deviation $= [\Sigma (x - \bar{x})^2/n - 1]^{\frac{1}{2}} = 0.0142$

Relative average deviation $= \pm 0.31\%$

Coefficient of variation $= 0.55\%$

The following cations were masked by the anions mentioned against each :

V(IV) (50, SCN^-), Mn(II) (75, cit), Pd(II) (20, tar), Ce(IV) (65, tar), Zr(IV) (20, F^-) and Pb(II) (600, SO_4^{2-}). Attempts to mask Fe(II), Co(II), Ni(II) and Zn(II) were, however, unsuccessful.

CONCLUSION

Thiovioluric acid (HTVA) has been successfully employed as a reagent for the spectrophotometric determination and as an indicator for the complexometric estimation of copper (II) with EDTA. Optimum conditions for accurate determination have been explored and attempts have been made to determine the metal in the presence of diverse ions.

ACKNOWLEDGEMENT. The authors (P.P.S. & F.K.) are thankful to the University Grants Commission and the Council of Scientific and Industrial Research, New Delhi, respectively, for financial assistance.

REFERENCES

[1] R. S. Chawla and R. P. Singh, *Talanta*, **16**, 119 (1969).
[2] R. S. Chawla and R. P. Singh, *Mikrochim. Acta*, 496 (1972).
[3] R. S. Chawla and R. P. Singh, *Mikrochim. Acta*, 332 (1970).
[4] R. S. Chawla and R. P. Singh, *Microchem. J.*, **18**, 646 (1973).
[5] Hoste, *Anal. Chim. Acta*, **4**, 23 (1950).
[6] G. F. Smith and W. H. Mc Curdy, Jr., *Analyt. Chem.*, **24**, 371, (1952).
[7] G. F. Smith and D. H. Wilkins, *Analyt. Chem.*, **25**, 510 (1953).
[8] Sesiti Ikeda and Hirshi Negai, *Japan Analyst*, **7**, 76 (1958).
[9] C. E. A. Shanahan and R. H. Senkins, *Analyst*, **86**, 166 (1961).
[10] P. D. Kartz, I. Jay and A. Feldman, *Analyst. Chem.*, **20**, 524 (1952).
[11] A. Paul, *Analyt. Chem.*, **35**, 2119 (1963).
[12] E. B. Sandell and Hiroshi Onishi, "Photometric Determination of Traces of Metals", Interscience Publishers. New York, 1978, p. 360.
[13] G. Schwarzenbach, "Komplexon Methoden", Siegfried, Zofingen, 1948.
[14] I. A. Crisan and A. S. Matei, *Rev. Roumaine Chim.*, **13**, 1347 (1968).
[15] P. Wehber, *Z. anal. Chem.*, **166**, 186 (1959).
[16] M. Hnilickova and L. Sommer, *Coll. Czech. Chem. Comm.*, **26**, 2189 (1961).
[17] W. Biedermann and G. Schwarzenbach, *Chimia (Basel)*, **2**, 56 (1948).
[18] P. Job, Liebig. *Ann. Chem.*, **9**, 113 (1928).
[19] H. Irving and T. B. Pierce, *J. Chem. Soc.*, **1959**, 2565.

ORSZÁGOS MŰSZAKI KÖNYVTÁR ÉS DOKUMENTÁCIÓS KÖZPONT

NOTE POUR LES AUTEURS

La Revue Roumaine de Chimie publie des articles en anglais , français, russe, allemand ou espagnol. Les auteurs sont priés d'envoyer des articles et des comptes rendus inédits.

Les manuscrits seront dactylographiés à deux intervalles. La bibliographie, les tableaux et la légende des figures seront placés après le texte.

Si l'article fait partie d'une série numérotée, le titre de la partie précédente sera indiqué dans une note au bas de la première page.

Chaque article sera précédé d'un résumé comprenant quinze lignes au maximum.

Les références bibliographiques dans le texte seront faites par des exposants sans parenthèses et paraîtront à la fin de l'ouvrage.

Les publications périodiques mentionnées dans la bibliographie seront présentées suivant les prescriptions internationales : le nom de l'auteur précédé de l'initiale du prénom, le titre du périodique abrégé conformément à « Chemical Abstracts » et souligné par une ligne, le numéro du tome indiqué par des chiffres arabes et souligné par deux lignes, suivi de la première page de l'article ; à la fin, l'année de la parution sera placée entre parenthèses. Le numéro de la revue ne sera pas indiqué, si les pages du volume sont numérotées consécutivement.

Les textes des livres ou traités inclueront : le nom des auteurs, les initiales du prénom, le titre du livre entre guillemets et sans être souligné, le numéro du tome précédé par l'abréviation « vol. » (ou « Bd. »), le numéro de l'édition, les éditions (the publisher), la localité de la parution du livre, l'année de la parution et la page de la référence précédée(s) par l'abréviation « p ». (ou « S. »).

Les brevets seront indiqués comme suit : l'auteur ou la firme, le pays et le numéro du brevet , la date et la revue (Chem. Abstr.). Par ex. : M. Jones (to Union Carbide Co), *Brit. Pat.* 601 238, 2 Sept, 1959, *Chem Abstr.*, **54**, 12808 (1960).

Les diagrammes seront tracés à l'encre de Chine sur papier calque. Les tableaux et les figures (en nombre strictement nécessaire) seront numérotés par des chiffres arabes. Les courbes dans les figures seront numérotés par des chiffres arabes et leur explication sera donnée dans la légende des figures. Prière de ne pas inscrire les mêmes données dans les tableaux et les figures. Chaque tableau aura un titre. On indiquera dans le texte la place approximative des tableaux et des figures. Les formules chimiques seront incluses dans le texte; en outre elles seront transcrites sur papier calque, à l'encre de Chine.

Les auteurs sont priés d'indiquer les caractères italiques (en soulignant les lettres au crayon), ainsi que tout autre caractère spécial ; les préfixes *ortho*, *meta*, *para*, *cis*, *trans*, etc. seront soulignés pour indiquer leurs caractères italiques et ne seront jamais écrits avec des majuscules.

Aucune correction à la main ne sera admise sur le manuscrit. Les corrections seront frappées à la machine. Les lettres grecques ou autres symboles spéciaux seront insérés à la main à l'encre clairement.

Le manuscrit sera signé par l'auteur.

Le colonne-titre aura 50 lettres au maximum.

L'entière responsabilité du contenu des articles appartient aux auteurs.

Sur demande on peut obtenir un note plus complète.

PRINTED IN ROMANIA

TRAVAUX PARUS AUX ÉDITIONS DE L'ACADÉMIE DE LA RÉPUBLIQUE SOCIALISTE DE ROUMANIE

ELENA CEAUŞESCU, **Polimerizarea stereospecifică a izoprenului** (La polymérisation stéréospécifique de l'isoprène), 1979, 307 p.

I. G. MURGULESCU, TATIANA ONCESCU, E. SEGAL, **Introducere în chimia fizică, vol. II. 2. Cinetică chimică şi cataliză** (Introduction à la Chimie physique. IIe vol. 2, Cinetique chimique et catalyse), 1981, 1024 p.

V. DRĂGUŢAN, A. T. BALABAN, M. DIMONIE, **Metateza olefinelor şi polimerizarea prin deschidere de inel a cicloolefinelor** (La métathèse des oléfines et la polymérisation par ouverture annulaire des cyclooléfines), 1981, 254 p.

OCTAVIAN IORDACHE, **Procese polistocastice aplicate la fenomenele de transfer** (Processus polystochastiques appliqués aux phénomènes de transfert) 1981, 186 p.

CR. SIMIONESCU, VALERIA GORDUZA, **Polimeri biocompatibili şi biologic activi** (Polymères biocompatibles et biologiquement actifs), 1980, 479 p.

Ş. MOLDOVEANU, A. SAVIN, **Aplicaţii în chimie ale metodelor semiempirice de orbitali moleculari** (Applications en chimie des méthodes semi-empiriques d'orbitaux moléculaires), 1980, 286 p.

M. FLORESCU, **Metode ştiinţifice în dezvoltarea industriei chimice moderne** (Méthodes scientifiques dans le développement de l'industrie chimique moderne), 1979, 256 p.

CONST. GH. MACAROVICI, **Analiza chimică cantitativă anorganică** (L'Analyse chimique quantitative inorganique), 1979, 457 p.

A. T. BALABAN, I. GĂLĂŢEANU, G. GEORGESCU, LIGIA SIMIONESCU, **Compuşi marcaţi şi radiofarmaceutici cu aplicaţii în medicina nucleară** (Composés marqués et radiopharmaceutiques à application en médecine nucléaire), 1979, 495 p.

I. G. MURGULESCU, E. SEGAL, **Introducere în chimia fizică, vol. II. 1. Teoria molecular cinetică a materiei** (Introduction à la Chimie physique. IIe vol. 1. La théorie moléculaire-cinétique de la matière), 1979, 1036 p.

I. E. TEODORESCU, MARIA FITI, **Iradierea tehnologică** (L'Irradiation technologique), 1979, 216 p.

S. STERNBERG, FL. DANEŞ, **Termodinamica chimică aplicată** (La thermodynamique chimique appliquée), 1978, 400 p.

I. G. MURGULESCU, V. EM. SAHINI, **Introducere în chimia fizică. Vol. I. 2. Structura şi proprietăţile moleculelor** (Introduction à la chimie physique. Ier vol. 2. La structure et les propriétés des molécules), 1978, 604 p.

C. DRĂGULESCU, E. PETROVICI, **Chimie structurală modernă. Chimia coordinanţei 8** (La chimie structurale moderne. La chimie de la coordinence 8), 1977, 947 p.

D. PURDELA (sous la direction de), **Nomenclatura chimiei anorganice** (La nomenclature de la chimie inorganique), 1977, 153 p.

I. ZUGRĂVESCU, MAGDA PETROVANU, **N-ylid chemistry**, coédition avec McGraw-Hill, International Book Company, U.S.A., 1977, 396 p.

I. G. MURGULESCU, **Introducere în chimia fizică. Vol. I. Atomi, molecule, legătură chimică** (Introduction à la chimie physique, Ier vol. 1. Atomes, molécules, liaison chimique), 1976, 560 p.

E. P. BALTĂ, E. BALTĂ, **Introduction to the physical chemistry of the vitreous state**, coédition avec Abacus Press, 1976, 287 p.

CONST. GH. MACAROVICI, D. MACAROVICI, **Chimia oxizilor dubli şi utilizările lor** (La chimie des oxydes doubles et leur utilisation), 1975, 195 p.

ELENA CEAUŞESCU, **Research work on synthesis and characterization of macromolecular compounds. Contributions**, 1974, 251 p.

CR. SIMIONESCU, VIORICA RUSAN, V. POPA, **Chimia algelor marine** (La chimie des algues marines), 1974, 212 p., 1 pl.

I. P. INFORMAŢIA c. 1136

43426

Lei 25.—

\$ 5^{5} (price per year)

F 1103

ACADÉMIE DE LA RÉPUBLIQUE SOCIALISTE DE ROUMANIE

REFERÁLVA

R

REVUE ROUMAINE DE CHIMIE

TOME 26
N° 7
Juillet 1981

EDITURA ACADEMIEI REPUBLICII SOCIALISTE ROMÂNIA

Rev. Roumaine Chim.

RRCHAX, 26, 7, p. 925–1042 (1981), Bucarest

ACADÉMIE DE LA RÉPUBLIQUE SOCIALISTE DE ROUMANIE

COMITÉ DE RÉDACTION

Rédacteur en chef:

I. G. MURGULESCU, membre de l'Académie de la République Socialiste de Roumanie

Rédacteurs en chef adjoints:

A. T. BALABAN et **V. EM. SAHINI**, membres correspondants de l'Académie de la République Socialiste de Roumanie

Collège de rédaction:

EM. BRATU, ELENA CEAUŞESCU, ECATERINA CIORĂNESCU-NENITZESCU, CR. SIMIONESCU, membres de l'Académie de la République Socialiste de Roumanie; P. SPACU, membre correspondant de l'Académie de la République Socialiste de Roumanie: MARGARETA AVRAM, M. BANCIU, I. HAIDUC, D. I. MARCHIDAN, I. MOLDOVAN, G. NIAC et D. SĂNDULESCU

La Revue Roumaine de Chimie paraît 10 fois par an. Toute commande de l'étranger pour les travaux parus aux Editions de l'Académie de la République Socialiste de Roumanie sera adressée à ILEXIM, Departamentul Export-Import Carte (Livres)/Departamentul Export-Import Presă (Revues), P.O.B. 136–137, télex 11226, 3, str. 13 Decembrie, 79517 Bucarest 12, Roumanie

Les manuscrits, les livres et les revues proposés en échange ainsi que toute correspondance seront envoyés à la rédaction:

REVUE ROUMAINE DE CHIMIE

125, Calea Victoriei, 79717 Bucarest, Roumanie, téléphone 50 76 80

EDITURA ACADEMIEI REPUBLICII SOCIALISTE ROMÂNIA
125, Calea Victoriei 79717, Bucarest, Roumanie, téléphone 50 76 80

ORSZÁGOS MŰSZAKI KÖNYVTÁR ÉS DOKUMENTÁCIÓS KÖZPONT 1982

REVUE ROUMAINE DE CHIMIE

Tome 26, N° 7 Juillet, 1981

DOMNINA POPESCU, V. GOŞA, R. H. SCHUSTER, N. I. IONESCU and D. OANCEA, The explosive combustion of propylene. I. The explosion limits of propylene in air . . . . 927–931 R

D. OANCEA, DOMNINA POPESCU, V. GOŞA, R. H. SCHUSTER, N. I. IONESCU and FELICIA CÎRJALIU, Overall activation energy of explosive combustion of methane–air mixtures . . . . 933–937 R

S. P. SRIVASTAVA, ANIL KUMAR and V. K. GUPTA, Kinetics and mechanism of Ag(I) catalysed oxidation of hexane-1,6-diol by peroxydisulphate ion 939–946

FLORIN-EMILIAN DANEŞ and DAN GEANĂ, Computation of chemical equilibrium of methanol synthesis using state equations of gases at high pressure (in French) . . . . 947–954 Bc

CLEOPATRA CALU, N. CALU and ANA ONU, Ion exchange in the system Na_2WO_4 (solution) – Amberlite IR 120(H^+). II. Polytungstic acid T (in French) 955–960

MAMDOUH S. MASOUD, M. M. OSMAN and H. A. EL-NAGGAR, Studies on osmium–quinisatine oxime reaction 961–965

ANA NIMARA, ECATERINA PRINCZ and AGNETA BALINT, Bismuth(III)–ethylenediaminetetraacetic acid complexes. III. Exchange reaction of Bi(III) from BiEDTA with Fe(III) 967–970

RODICA VĂŢULESCU, T. BUDIU and GH. MARCU, Heteropolytungstates with Ti(IV) and Ni(II). II. The synthesis and basicity of heteropolyanions $[H_2ONiTiW_{11}O_{39}]^{6-}$ and $[H_2ONiTiW_5O_{20}]^{4-}$ 971–977

M. HASSAN, A. R. O. ABDEL NOUR, A. M. SATTI and I. A. WAKEEL, Studies of the reactions of aryl propene oxides in basic media. II. Reactions of some *o*-substituted epoxides compared to *p*- and *m*-substituted analogues 979–983

S. MATEI, JANA RUSSU and PETRONELA COLŢEA, The synthesis and the electronic spectra of some *trans*-α-cyano-2-styrylbenzimidazoles 985–992

M. ANWAR and F. I. ABDEL-HAY, Reactions of 1-phenyl-3,5-pyrazolidinedione 993–999

C. I. CHIRIAC, A convenient new method for synthesis of aromatic amides under mild conditions 1001–1004

M. S. K. YOUSSEF, Cyclocondensation of mercaptoacetic acid with thienylidene anils 1005–1009

Rev. Roumaine Chim. **26**, 7, 925–1042 (1981), Bucarest

C. P. SINGH, RENU JAIN and A.C. OJHA, Synthesis of N^1-(substituted phenyl)-3-methyl-4-(substituted phenylazo)-2-pyrazolin-5-one 1011–1017

LUMINIȚA VLĂDESCU and CLAUDIA DOINA MARIA POP, Utilization of Ferron in separation and concentration of iron with ion exchange resins 1019–1024

A. AWAD, F. EL-CHEIKH and A. ABD EL-GABER, Adsorption effects of some natural and synthetic macromolecules at charged interfaces 1025–1032

SUDHA CALLA, S. P. MATHUR, R. S. THAKUR and C. S. BHANDARI, Direct photometric determination of cerium(IV) with 3-phenylazohydroxylamine 1033–1034

JOSÉ GAYOSO and OURIDA OUAMERALI, A new aromaticity index based on the exaltation of diamagnetic susceptibility (in French) 1035–1040

BOOK REVIEWS 1041–1042

R

Revue Roumaine de Chimie, 26, 7, 927–931 (1981)

THE EXPLOSIVE COMBUSTION OF PROPYLENE. I.

THE EXPLOSION LIMITS OF PROPYLENE IN AIR

DOMNINA POPESCU,* V. GOŞA,* R. H. SCHUSTER,* N. I. IONESCU *
and D. OANCEA **

* Center of Physical Chemistry, Spl. Independenţei no. 202, Bucharest, Romania

** The Polytechnic, Department of Physical Chemistry and Electrochemical Technology, Bd. Republicii no. 13, Bucharest, Romania

Received May 5, 1980

The explosion limits and minimum explosion pressures of the propylene–air and propylene–oxygen systems have been determined using a hot wire, a fusing wire or an electric spark as initiation source. With the hot wire as initiation source, the flammability range consisted of several lobes, characterised by the flame colour and propagation pattern.

The study of propylene–air or propylene–oxygen explosions implies, as a first step, the measurement of the pressure–concentration explosion limits. The experiments described in this paper have been performed at room temperature and subatmospheric initial pressures, using different initiation sources : a hot wire, a fusing wire or an electric inductive spark.

EXPERIMENTAL

The explosion limits measurement for the propylene–comburant mixtures was carried out by means of an installation previously described.[1] The explosion cell, having a diameter of 3.5 cm and a volume of 100 cm^3, was made of glass. The following initiation sources have been used :

a) a platinum wire (Ø = 0.1 mm ; L = 50 mm), heated by applying a 7 V d.c. voltage ;

b) a nichrom wire (Ø = 0.1 mm ; L = 25 mm), fused by applying 100 V or 200 V a.c. voltage ;

c) an electric spark obtained by the discharge of an induction coil between two stainless steel electrodes, having a plane surface of 4.5 mm^2 area.

Reagents : Propylene, 99.4 % purity, checked by gas-chromatography, was purchased from the Petrochemical Factory Piteşti. Oxygen (99.6 % purity) and air were dried by means of several columns filled with $CaCl_2$, P_2O_5 on glass wool and molecular sieves.

RESULTS AND DISCUSSIONS

The flammability range of propylene in air, indicating the minimum explosion pressures (MEP) obtained by hot wire initiation against propylene concentration, is given in Figure 1.

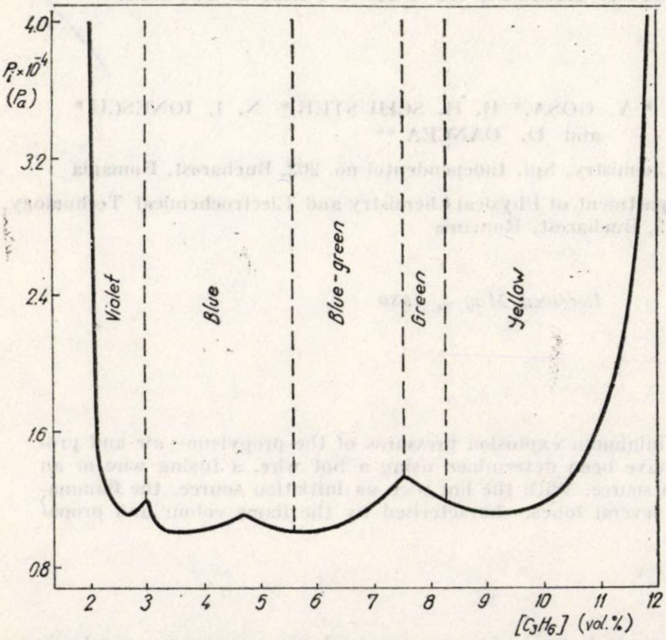

Fig. 1. — Explosion limits of propylene in air; initiation by hot platinum wire.

For each run, the flame appearance and propagation within the explosion cell was considered as an explosion.

At the extremities of the flammability range, small changes of the propylene concentration resulted in steep changes of the MEP's values, indicating by extrapolation to normal pressure, the explosion limits of propylene in air : 2 and 12% respectively. The lowest value of the MEP between these limits is 1.10^4 Pa and corresponds to the mixture containing 5.7% propylene, value close to the stoichiometric concentration calculated for the complete oxidation.

The curve in Figure 1 has a characteristic multilobar shape, already observed in the case of other hydrocarbon—air explosions.[2-6] The form of the flame front and its propagation speed are different for the domains delimited by these lobes. In mixtures corresponding to the first three lobes, the flame propagates with a high speed, both upwards and downwards, The colour of these flames changes slowly from violet to light blue and finally to green, indicating a gradual change of the reaction intermediates as well as the change of the reaction mechanism, while the hydrocarbon to comburant ratio changes.[5] In the last lobe (7.5—12% propylene), the slow moving yellow flames propagate only upwards. As the propylene concentration increases, exceeding 9%, the propylene pyrolysis to carbon black becomes more and more important.

The flammability range of propylene—air mixtures determined by fusing wire initiation is shown in Figure 2.

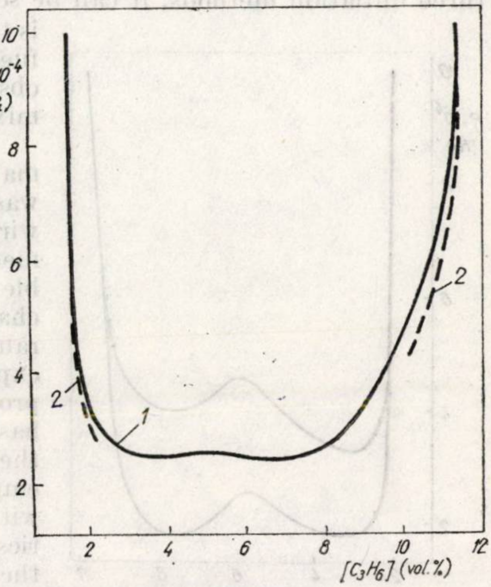

Fig. 2. — Explosion limits of propylene in air; initiation by exploding wire. 1) applied voltage: 100 V a.c. 2) applied voltage: 200 V a.c.

When a higher voltage of 200 V a.c. is applied across the wire, the MEP's values are lowered (curve *2* as compared to curve *1*) resulting in a more efficient initiation of the explosion. The extrapolation of both *1* and *2* curves to normal pressure indicates again the explosion limits (1.4 and 11.6% propylene) in the case of the fusing wire initiation.

Taking into account the intense light emission due to the wire fusing, we could no more observe the flame colour in the different domains of the flammability range and furthermore, we could not use the previous criterion for detecting the explosion. In this case, only the systems for which the maximum pressure reached during the explosion exceeded the normal pressure were considered to be explosive. According to this, the lowest value of the MEP obtained in the case of fusing wire initiation is $2.4 \cdot 10^4$ Pa.

The flammability range of propylene in air obtained by the electric spark initiation is shown in Figure 3 (curve *1*), indicating the concentrations of 2% and 9.9% propylene as the explosion limits at normal pressure, in good agreement with the data reported by Gaube [7] (2—10.1% propylene). On the same diagram, curve *2* shows comparatively the flammability range of propylene—air mixtures ignited by the same inductive electric spark, established according to the same criterion as in the case of the fusing wire initiation. Irrespective of the criterion used, the explosion limits determined from curve *1* or *2* in Figure 3 are the same, only the MEP's values change from $1.6 \cdot 10^4$ Pa (curve *1*) to $3.2 \cdot 10^4$ Pa (curve *2*).

Comparing the explosion limits of propylene in air obtained by these three initiation methods, it can be seen that the inductive electric spark is the least efficient, especially for the fuel-rich mixtures. This was already observed in the case of ethylene — air mixtures.[3]

The investigation of the flammability range of proyplene in oxygen was carried out using a hot platinum wire as an initiation source, as this method is proved to be the most suitable for the observation of the flame characteristics in a large concentration range. In Figure 4 the minimum explosion pressures are plotted against propylene concentration; this curve has also a multilobar shape. Similar to the propylene—air system, the ranges emphasized in Figure 4 are different with respect to the flame characteristics. The same colour sequence as in the case of propylene—air mixtures was observed, probably determined by the appearance of the same reactive intermediates, whose nature is independent of the presence of nitrogen in the mixture.

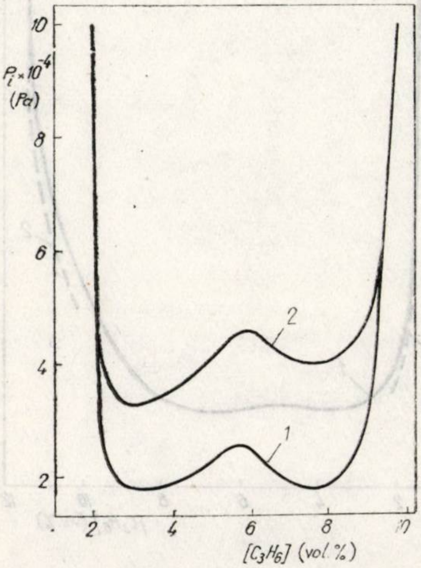

Fig. 3. — Explosion limits of propylene in air; initiation by electric spark; (1) and (2) — see the text.

Similar to other hydrocarbon—oxygen mixtures,[8] the dilution by nitrogen does not change the lower explosion limit (2% propylene). Comparatively, the propylene—oxygen mixtures whose concentration exceeds the stoichiometric concentration ("fuel-rich" mixtures) sustain, in a much greater extent than the propylene—air mixtures, the propylene decomposition by pyrolysis. The large amounts of carbon black generated in the propylene—oxygen mixtures having more than 35% propylene hamper the visual observation of explosion, so that the measurement of the upper explosion limit of this system was not possible.

The narrow flammability range of propylene—air system as compared to propylene—oxygen system shows the inhibitory effect of nitrogen; the same conclusion is supported by the comparison of the lowest values for MEP in these systems: $0.24 \cdot 10^4$ Pa (propylene—oxygen) and 1.10^4 Pa (propylene—air).

As a result of our experiments, the values of the explosion limits and minimum explosion pressures for propylene—air and propylene—

oxygen mixtures, using a hot wire, a fusing wire or an electric spark as an initiation source, have been determined.

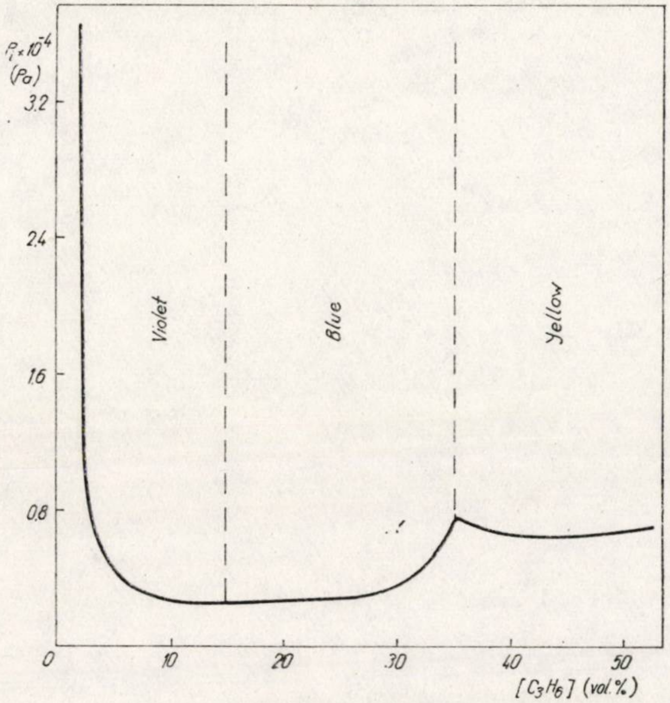

Fig. 4. – Explosion limits of propylene in oxygen ; initiation by hot platinum wire.

REFERENCES

[1] R. H. Schuster, N. I. Ionescu, D. Popescu and D. Oancea, *Rev. Roumaine Chim.*, **24**, 531 (1979).

[2] J. T. Di Piazza and M. Gerstein, *Ind. Eng. Chem.*, **43**, 2721 (1951).

[3] D. Oancea, D. Popescu, V. Goşa, R. H. Schuster and N.I. Ionescu, *Bul. Inst. Politehnic Bucureşti, Seria Chimie-Metalurgie*, **42**, 41 (1980).

[4] D. Popescu, V. Goşa, R. H. Schuster, N. I. Ionescu and D. Oancea, *Rev. Roumaine Chim.*, (in press).

[5] V. Goşa, R. H. Schuster, N. I. Ionescu, D. Oancea and D. Popescu, *Rev. Roumaine Chim.*, (in print).

[6] N. I. Ionescu, D. Oancea, D. Popescu, V. Goşa and R. H. Schuster, *Z. phys. Chem. (Leipzig)*, (in press).

[7] J. Gaube, H. Grosse-Wortmann and K. H. Simmrock, *Chem. Ing. Tech.*, **40**, 660 (1968).

[8] W. Jost, "Explosion and Combustion Processes in Gases", 1st Edition, McGraw-Hill, New York, 1946.

Revue Roumaine de Chimie, 26, 7, 933–937 (1981)

OVERALL ACTIVATION ENERGY OF EXPLOSIVE COMBUSTION OF METHANE–AIR MIXTURES

D. OANCEA *, DOMNINA POPESCU **, V. GOŞA **, R. H. SCHUSTER **,
N. I. IONESCU** and FELICIA CÎRJALIU*

* The Polytechnic, Department of Physical Chemistry and Electrochemical Technology
Bd. Republicii 13, Bucharest, Romania

** Center of Physical Chemistry, Spl. Independenţei no. 202, Bucharest, Romania

Received June 12, 1980

Overall activation energies of explosive combustion of some methane–air mixtures were measured using the initiation source temperature dependence upon the initial pressure of the explosive mixture. With a heated platinum filament as initiation source, the calculated activation energies are in very good agreement with the literature values, obtained by different methods.

Among the various parameters determining the stability of an explosive mixture, the overall activation energy of the preexplosive combustion is of a particular value. Its significance is generally complex, depending on the actual reaction mechanism of combustion. Besides the classical method using the reaction rate dependence upon the temperature in quasi-isothermal preexplosive conditions for the measurement of the overall activation energy, a number of specific methods has also been worked out. The most important are those using either the autoignition pressure or induction period dependence upon the autoignition temperature, or the measurement of the combustion velocity at different initial temperatures (preheating method) or at different initial compositions by dilution with an inert gas (dilution method).[1,2]

In several previous papers[3-6] we have studied the explosive behaviour of some gaseous mixtures using heated filaments as initiation sources. The experimental method allowed the measurement of the filament resistance during the heating period and the calculation of its temperature by means of a calibration curve. It has been found that the filament temperature before explosion was a monotonous function of the initial pressure of the mixture, allowing the calculation of an overall activation energy. Some methane–air mixtures within the explosive range were investigated and the results were compared with the literature data.

EXPERIMENTAL

Methane was of 99.8 % purity (checked by gas chromatography). The different explosive mixtures were prepared on the basis of partial pressure measurements. The explosion cell was a steel cylindrical vessel with an inner diameter, Ø = 4.7 cm, and a height, h = 9.7 cm..

The explosion was initiated by a heated platinum filament situated in the middle of the cell. The filament was made of a platinum wire with Ø = 0.1 mm and a length, l = 15 cm, evenly winded around a rod with Ø = 0.5 cm, and was heated electrically using a d.c. stabilised power supply. Oscillographic recordings of the current through the circuit (measured as the potential across a standard resistor connected in the circuit) during the heating period allow the calculation of the filament resistance. Using a calibration curve (resistance of platinum wire against temperature) the average filament temperature at any time during the heating period can be found. When the explosion starts, a sudden rise of the filament temperature (and resistance) occurs due to the heat delivered by the exothermic combustion reaction. It is thus possible to establish the average temperature of the filament just before the explosion started. The sensitivity of the electrical measurements was increased by compensating the initial potential across the standard resistor (with the filament at room temperature) with a potential taken from a supplementary d.c. stabilised power supply.

RESULTS AND DISCUSSION

The relative variation, $\Delta E/\Delta E_{\max}$, of the potential across the standard resistor during the heating period as well as the calculated curve showing the corresponding temperature change of filament for a 9.48% methane–air mixture at an initial pressure $P_i = 2.08 \times 10^4$ Pa are given in Figure 1. The variation of the mean filament temperature (curve *2*) exhibits a jump indicating the outset of the explosion. It can be seen that the filament temperature is larger in the explosive mixture than in air at the same pressure (curve *2'*) due to the exotermic methane combustion on the platinum wire which becomes perceptible at lower temperatures (in this case around 700°C). The exothermic contribution of the combustion on the filament can also be observed on the curves $\Delta E/\Delta E_{\max}$ versus time for the explosive mixture (curve *1*) and air at the same pressure (curve *1'*).

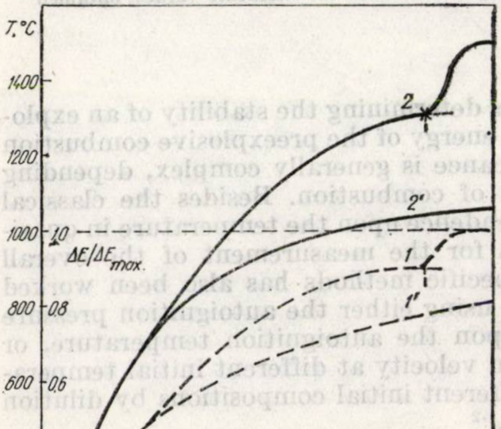

Fig. 1. — The experimental variation of the potential across the standard resistor within the heatind period (curves *1*, *1'*) and calculated mean filament temperatures (curves *2*, *2'*) for a 9.48% CH_3–air mixture at $P_i = 2.08 \times 10^4$ Pa).

The corresponding curves ΔE vs. time of methane – air mixtures of different compositions at different initial pressures P_i were recorded. From these curves the initiation source temperatures at the outset of the explosion were calculated. The investigated mixtures were of the following compositions : 9.48 % CH_4, close to the stoichiometric mixture, 5.25 % CH_4, close to the lower explosion limit, and 7.00 % CH_4, in the middle of this range. The results are given in table 1.

TABLE 1

Critical temperatures of the filament T_s(K) at different initial pressures P_i(Pa), for different methane—air mixtures

% CH_4					
5.25		7.00		9.48	
$P_i \times 10^{-4}$	$T_s \times 10^{-3}$	$P_i \times 10^{-4}$	$T_s \times 10^{-3}$	$P_i \times 10^{-4}$	$T_s \times 10^{-3}$
6.43	1.233	5.92	1.084	5.85	1.241
4.67	1.235	5.39	1.104	5.45	1.295
3.05	1.299	4.85	1.121	4.97	1.380
2.53	1.322	3.75	1.186	4.65	1.390
2.03	1.344	3.17	1.213	3.96	1.429
		2.49	1.216	3.44	1.442
		2.15	1.236	2.40	1.492
				2.08	1.602

Besides the measurement of the critical source temperature, the recorded curves can be used to calculate the critical energy of the initiation source :

$$Q_{cr} = \int_0^{\tau_{cr}} \frac{E_f^2}{R_f} \cdot d\tau \tag{1}$$

taking into account the change of the filament resistance during the heating period $(0 - \tau_{cr})$.

As the filament has a large thermal inertia, working as a source with slow heat dissipation, it is not the absolute value of the critical energy which is significant, but its change with the initial pressure in the explosion cell. Calculated critical energy (by graphical integration) increases monotonously as the initial pressure decreases, following a hyperbolic law with the minimum explosion pressure as asymptote. This behaviour is illustrated in Figure 2 for 7.00 % CH_4—air mixture.

An analysis of the results given in table 1 indicates that the critical source temperature is a monotonous function of the initial pressure in the explosion cell. It must be emphasized that the heat transferred from the filament to the surrounding gas produces a pressure increase. Under the specified conditions, this increase was at the most 5 % and it was neglected in the subsequent treatment of the experimental data.

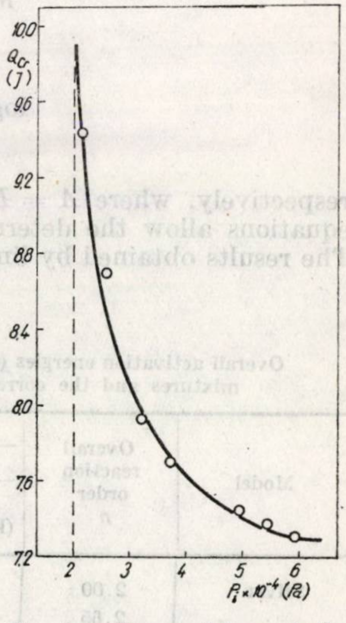

Fig. 2. — The variation of the critical energy of the ignition source vs. initial pressure of the explosive mixture (7.00 % CH_4—air).

The critical temperature—initial pressure data were analysed on the basis of the thermal theories of ignition initiated by hot bodies. The relationships obtained by Silver [7] and Khitrin [8] can be put respectively in the following forms:

$$\Delta T = a \cdot v_s \tag{2}$$

$$(\Delta T)^2 = b \cdot T_s^2 \cdot v_s \tag{3}$$

where $\Delta T = T_s - T_i$ is the difference between source temperature T_s and surrounding (initial) temperature T_i (in K), v_s is the rate of the combustion reaction in the neighbourhood of the initiation source, and a and b are constants.

If n_1 and n_2 are the partial reaction orders with respect to CH_4 and O_2, respectively, and n the overall reaction order, v_s becomes:

$$v_s = k \cdot \frac{P_i^n}{T_i^n} e^{-E/RT_s} \tag{4}$$

Introducing eq. (4) into (2) and (3), and taking the logarithm, the following results:

$$\log \frac{P_i}{(\Delta T)^{1/n}} = \frac{A}{T_s} + B \tag{5}$$

$$\log \frac{P_i}{(\Delta T / T_s)^{2/n}} = \frac{A}{T_s} + B' \tag{6}$$

respectively, where $A = E/2.303\,nR$, and B, B' are constants. These equations allow the determination of the overall activation energy E. The results obtained by linear regression are given in table 2.

TABLE 2

Overall activation energies (kJ/mol) of the explosive combustion of methane—air mixtures and the correlation coefficients r of the equations (5) and (6)

Model	Overall reaction order n	CH_4% 5.25 E (kJ/mol)	5.25 r	7.00 E (kJ/mol)	7.00 r	9.48 E (kJ/mol)	9.48 r
Silver	2.00	257	0.98	149	0.97	118	0.94
	2.65	336	0.98	194	0.97	152	0.94
Khitrin	2.00	250	0.98	143	0.96	109	0.93
	2.65	340	0.98	188	0.96	143	0.93

The calculation of the activation energy from the above equations assumes the knowledge of the overall reaction order which is not measurable in these experiments. We considered two values, namely $n = 2.00$ and $n = 2.65$, the latter being the average value found in the literature for the homogeneous combustion within the same concentration range.[9-11]

The activation energy has the lowest value for the stoichiometric mixture and the highest value near to the lower explosion limit. The noticeable increase of the activation energy toward the lower explosion limit suggests a change in the combustion mechanism implying both the overall activation energy and reaction order, the last parameter being considered constant in our calculations within $5.25-9.48\%$ CH_4—air range.

On the other hand, there is a very good agreement between the overall activation energy for the stoichiometric mixture measured by this procedure and the corresponding literature data obtained by different methods ($E = 155$ kJ/mol),[1] although only the simple thermal model of ignition has been used.

One can conclude that, as a result of our experiments, the overall activation energies of explosive combustion of some methane—air mixtures have been obtained using the change in the critical temperature of the initiation source as a function of the initial pressure of the explosive mixtures.

REFERENCES

[1] A. Van Tiggelen, J. C. Balaceanu, J. Burger, G. de Soete, L. Sajus, B. Salé et P. J. Van Tiggelen, "Oxidations et Combustions", vol. 1, Ed. Technip, Paris, 1968, Chap. VI.

[2] W. Jost, "Explosion and Combustion Processes in Gases", 1st Edition, McGraw-Hill, New York, 1946, Chap. 1.

[3] R. H. Schuster, N. I. Ionescu, D. Popescu and D. Oancea, *Rev. Roumaine Chim.*, **24**, 531 (1979).

[4] D. Oancea, D. Popescu, V. Goşa, R. H. Schuster and N. I. Ionescu, *Bul. Inst. Politehnic Bucureşti, Seria Chimie-Metalurgie*, **42**, 41 (1980).

[5] D. Popescu, V. Goşa, R. H. Schuster, N. I. Ionescu and D. Oancea, *Rev. Roumaine Chim.* (in press).

[6] N. I. Ionescu, D. Oancea, D. Popescu, V. Goşa and R. H. Schuster, *Z. phys. Chem. (Leipzig)* **26**, 927 (1981).

[7] R. S. Silver, *Phil. Mag.*, **23**, 633 (1937).

[8] L. N. Khitrin and S. A. Goldenberg, "Sixth International Symposium on Combustion", 1957, Reinhold, New York, p. 545.

[9] I. Iosif, D. P. Lazăr and I. A. Schneider, *Internat. J. Chem. Kin.*, **3**, 15 (1971).

[10] D. E. Hoare and A. D. Walsh, "Fifth International Symposium on Combustion", 1955, Reinhold, New York, p. 467.

[11] M. Wanpéé and F. Girard, *ibid.*, p. 484.

Revue Roumaine de Chimie, **26**, 7, 939–946 (1981)

KINETICS AND MECHANISM OF Ag (I) CATALYSED OXIDATION OF HEXANE-1,6-DIOL BY PEROXYDISULPHATE ION

S. P. SRIVASTAVA, ANIL KUMAR and V. K. GUPTA
Department of Chemistry, University of Roorkee,
Roorkee – 247672, India

Received March 22, 1980

Kinetic study of Ag(I) catalysed oxidation of hexane-1,6-diol by $S_2O_8^{2-}$ reveals that this reaction, unlike other reactions of this class, does not follow simple first order kinetics and is attended, with nearly half order inhibition, by the product of oxidation in the later stages of the reaction. The specific rate is a function of the initial concentration of substrate and $S_2O_8^{-2}$. Under the kinetic control conditions the product of oxidation is 6-hydroxyhexanal, but on distilling the reaction mixture under reduced pressure, formaldehyde, valeraldehyde and 6-hydroxyhexanal are formed. The negative salt effect is of primary exponential type. Activation parameters have been determined. A suitable mechanism has been proposed to account for all these observations and a corresponding rate law derived.

INTRODUCTION

In a previous study on the oxidation of ethane-1,2-diol [1] and propane-1,3-diol [2] by peroxydisulphate ion in the presence of Ag(I) as catalyst, it has been reported that the reactions follow a simple first order kinetics but show a reverse dependence of rate constant on ethylene glycol concentration and near independence of propane-1,3-diol concentration, and that the products of oxidation are formed by C – C bond cleavage. However, our study of Ag(I) catalysed oxidation of hexane-1,6-diol by $S_2O_8^{2-}$, as reported in this paper, revealed that the reaction does not follow a simple first order kinetics and the products of oxidation are not formed by C – C bond cleavage. A suitable mechanism to account for all these observations has been proposed.

EXPERIMENTAL

Hexane-1,6-diol, Koch Light Laboratories Ltd ; $K_2S_2O_8$, G.R., E. Merck (after recrystallisation), and all other chemicals of analytical grade were used.

The progress of the reaction was followed by estimating the unreacted $K_2S_2O_8$ iodometrically by the method of Szabo, Csanyi and Galiba [3] as modified by Khulbe and Srivastava [4].

The IR spectra were recorded on a Beckman IR-20, infrared spectrophotometer, NMR on a Varian A60D spectrometer and a gas chromatographic separation was carried out on an AIMIL gas chromatograph.

RESULTS

In order to evaluate the overall order of the reaction, the kinetics was studied at equimolar concentration of the reactants ; the first order plot has been depicted in figure 1(a). An examination of figure 1(a) reveals that the first order specific rate is nearly constant for few minutes at the beginning and then begins to decrease, suggesting either of the two possibilities : the reaction may be of a higher order than unity or it may be a case of consecutive reaction.

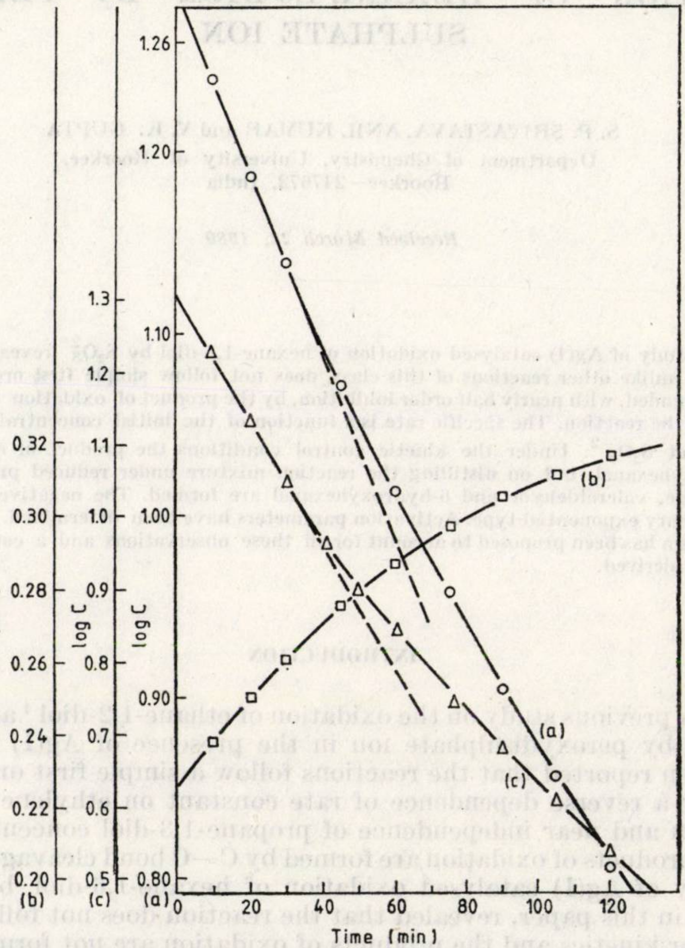

Fig. 1(a). — First order plot at equimolar concentration of the reactants. Temp. 40°C. [Hexane-1,6-diol] = 2.0 × 10^{-2}M ; [$K_2S_2O_8$] = 2.0 × 10^{-2}M ; [$AgNO_3$] = 1.0 × 10^{-3}M ; (b). — 3/2 Order Plot. Temp. 40°C. [Hexane-1,6-diol] = 2.0 × 10^{-2}M ; [$K_2S_2O_8$] = = 2.0 × 10^{-2}M ; [$AgNO_3$] = 1.0 × 10^{-3}M ; (c). — First order plot at higher concentration of substrate. Temp. 40°C. [Hexane-1,6-diol] = 15.0 × 10^{-2}M ; [$K_2S_2O_8$] = 2.0 × 10^{-2}M ; [$AgNO_3$] = = 1.0 × 10^{-3}M.

The orders in respect to $K_2S_2O_8$ and substrate were found to be unity and 0.25 by Van't Hoff's method, depicted graphically in Figure 2(a) and 2(b). However, the order in respect to substrate, as determined by fractional change method, gave varying values ranging from +0.51 to −0.48. From these data it may be concluded that the overall order of the reaction is 3/2. To verify this, a plot of $(a - x)^{-1/2}$ *vs* time was drawn (Fig. 1(b)) which did not give a linear curve, thus ruling out the possibility of the reaction to be of the 3/2 order. The first order kinetic plot at $7\frac{1}{2}$ times concentration of the substrate to oxidant (Fig. 1(c)) gave a non-linear curve which eliminated the possibility of the existence of two first order consecutive reactions. Hence, the only cause for the reaction to be slow in the later stages seems to be the presence of inhibition by the product. The presence of inhibition by the product is also indicated by the difference in value of the order in respect of concentration and in respect of time [5] (which comes out to be 2.20 with respect to time, Fig. 2(c)). Inhibition by the product was found to follow very nearly half order in the later stages of the reaction. The values of rate constants, assuming half order inhibition ($k_{1/2}$), first order inhibition (k_1) and without inhibition (k) at equimolar concentration of the two reactants at different intervals of time are recorded in table 1. The values of $k_{1/2}$ were found to be nearly constant in the later stages of the reaction. However, the increasing rate constant values in the initial stages of the reaction suggest that the inhibition by the product for this stage is negligible and hence this part can

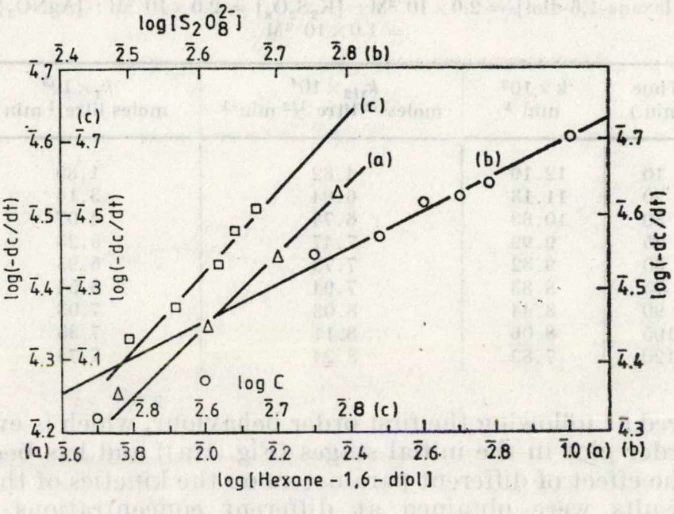

Fig. 2(a). — The reaction order with respect to hexane-1,6-diol; (b). — The reaction order with respect to hexane-1,6-diol; (c). — $\text{Log}\left(-\frac{dc}{dt}\right)$ vs. log c plot at different time intervals. Temp. 40°C.
[Hexane-1, 6-diol] = 1.0×10^{-2} M; $[K_2S_2O_8] = 5.0 \times 10^{-2}$ M; $[AgNO_3] = 1.0 \times 10^{-3}$M.

TABLE 1

First order rate constant for uninhibited, half order and first order inhibited reaction

Temp. 40°C

[Hexane-1,6-diol] = 2.0×10^{-2}M ; [$K_2S_2O_8$] = 2.0×10^{-2}M ; [$AgNO_3$] = $= 1.0 \times 10^{-3}$M

Time (min.)	$k \times 10^3$ min^{-1}	$k_{1/2} \times 10^4$ $moles^{1/2}\ litre^{-1/2}\ min^{-1}$	$k_1 \times 10^5$ $moles\ litre^{-1}\ min^{-1}$
10	12.19	4.82	1.85
20	11.13	6.04	3.14
30	10.63	6.74	4.07
45	9.99	7.47	5.23
60	9.32	7.73	5.95
75	8.83	7.94	6.54
90	8.44	8.08	7.03
105	8.06	8.11	7.35
120	7.82	8.24	7.74

be considered as following the first order behaviour, which is evident from the first order plot in the initial stages (Fig. 1(a)) and has been used for studying the effect of different parameters on the kinetics of this reaction. Similar results were obtained at different concentrations of the two reactants.

EFFECT OF THE CONCENTRATION OF PEROXYDISULPHATE ION AND HEXANE-1,6-DIOL

The first order specific rate is, however, found to be dependent on the initial concentration of $S_2O_8^{2-}$ as well as on that of hexane-1,6-diol (Tables 2 and 3). Similar dependence on the concentration of substrate has been reported by Levitt and Malinowski [6] in the oxidation of isopropyl alcohol by $S_2O_8^{2-}$ and on the concentration of $S_2O_8^{2-}$ in the case of ethylene glycol [1] and pinacol. [7] Since these kinetic runs were made at constant ionic strength and constant K^+ ion concentration, the possible reason for this dependence of rate constant on the initial concentration of the reactants may be the presence of trace impurities present even in the analytical grade

TABLE 2

Effect of the concentration of $S_2O_8^{2-}$

Temp. 40°C

[Hexane-1,6-diol] = 1.0×10^{-2}M ; [$AgNO_3$] = 1.0×10^{-3}M

[$K_2S_2O_8$] × 10^2M	3.0	4.0	5.0	6.0
[K_2SO_4] × 10^2M	7.0	6.0	5.0	4.0
$k \times 10^3 min^{-1}$	5.94	5.60	5.26	4.75

TABLE 3

Effect of the concentration of hexane-1,6-diol

Temp. 40°C

$[K_2S_2O_8] = 2.0 \times 10^{-2}M$, $[AgNO_3] = 1.0 \times 10^{-3}M$

[Hexane-1,6-diol] $\times 10^2M$	1.0	2.0	3.0	4.0	5.0	6.0	10.0	15.0
$k \times 10^3$	7.47	9.61	10.82	11.92	13.46	14.62	17.45	18.58

chemicals.[8] This fact together with the inhibition by allyl acetate suggests that the reaction follows a radical chain mechanism.

The salt effect has been observed to be negative and of primary exponential type.

ACTIVATION PARAMETERS

In order to evaluate various thermodynamic parameters, the reaction was studied at different temperatures ranging from 308 to 323°A. The energy of activation, frequency factor, entropy of activation, free energy of activation and enthalpy of activation were found to be 13.9 ± 0.3 kcal/mole, $6.52 \pm 0.03 \times 10^8$ litres/mole/s, 19.70 ± 0.15 kcal/mole and 13.30 ± 0.02 kcal/mole respectively.

ISOLATION AND CHARACTERISATION OF THE PRODUCTS

The product of oxidation, isolated under kinetic control condition and by the distillation of the reaction mixture under reduced pressure, was found to be an aldehyde (with Schiff's reagent).

Chromotropic acid test for formaldehyde in the reaction mixture was found to be negative at different intervals of time, implying that under these conditions C—C bond cleavage does not take place. 2,4-DNP derivative of the product obtained by the distillation of the reaction mixture under reduced pressure gave three spots on silicagel G tlc plate, which corresponded to the three peaks in the gas chromatographic run of the ethereal extract giving the mean retention time 3.6′, 5.3′ and 10.7′. The peak at 3.6′ corresponded to formaldehyde run under similar conditions (sample size 5 μl, column Carbowax-4000), temp. 118°C, injection temp. 100°C, carrier gas used — N_2 at a pressure of 8 PSI). The three probable products may be 6-hydroxyhexanal, formaldehyde and valeraldehyde. The formation of formaldehyde was also confirmed with the help of chromotropic acid. The three products (as their 2,4-DNP derivatives) were separated by preparative tlc, and the two fractions besides that of formaldehyde were eluted with chloroform. Only one of them could be obtained in sufficient amount for further characterization. The derivative thus collected was subjected to the following spectral studies.

IR SPECTRUM

The observation of a sharp peak at 3280 cm^{-1} due to —NH stretching, a broad band at 3600—3200 cm^{-1} due to —OH stretching and a broad band due to the saturated methylene groups (unresolved) ranging from

2960 to 2830 cm^{-1} suggested that the possible structure of the 2,4-DNP derivative may be X (chart I).

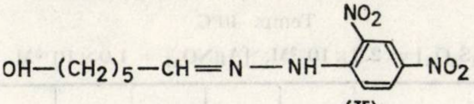

(X)

^{1}H-NMR SPECTRUM

In ^{1}H-NMR spectrum a high field triplet equivalent to two protons was observed at δ 4.2 ppm (J = 5.0 Hz) corresponding to $-CH_2$ protons adjacent to $-OH$ group. From the examination of the above structure (X), it can be predicted that the second, the third and the fourth methylene group protons should show a quintet each and the fifth methylene group should show a quartet. However, in our spectrum, unresolved peaks equivalent to two protons at δ 2.6 ppm., δ 2.02 ppm. (J = 6.0 Hz) and unresolved peaks equivalent to four protons at δ0.975 ppm (J = 5.0 Hz) were observed. A broad peak at δ 6.30 ppm due to $-OH$ group was observed and $-$ CH proton showed a triplet due to the adjacent methylene group at δ 8.3 ppm (J = 3.0 Hz). The total number of protons observed were sixteen supporting the structure X.

Thus, the product of Ag(I) catalysed oxidation of hexane-1,6-diol under kinetic condition is only 6-hydroxyhexanal while on distillation under reduced pressure the products are 6-hydroxyhexanal (main product) and formaldehyde and valeraldehyde (minor products).

THEORETICAL INTERPRETATION OF THE PRODUCT FORMED

The formation of a dialdehydic product is much more probable than a hydroxyaldehyde as both $-CH_2OH$ groups can undergo oxidation. However, this can be prevented only if it exists in the form of an oxide structure as observed by Hurd and Saunders [9] in the case of ω-hydroxyaldehydes in their UV absorption spectral studies. However, if this is true then the product should not give the normal reactions of an aldehyde, e.g., with Schiff's reagent. To verify it the total amount of aldehyde was estimated spectrophotometrically at different intervals of time at pH 2.7 and λ_{max} = 560 nm [10] and simultaneously the amount of $K_2S_2O_8$ consumed was estimated. These values are recorded in table 4.

TABLE 4

Estimation of the total aldehyde formed in comparison with peroxydisulphate used at the same time intervals

Temp. 40°C

[Hexane-1,6-diol] = 1.0×10^{-2}E ;

[$K_2S_2O_8$] = 2.0×10^{-2}M ; [$AgNO_3$] = 1.0×10^{-3}M

pH = 2.7, λ_{max} = 560 nm

Time (min)	Concentration of the total aldehyde formed in molarity $\times 10^3$	$K_2S_2O_8$ used in molarity $\times 10^{+3}$
15.0	0.55	5.50
30.0	0.72	8.90
45.0	0.83	11.00
60.0	0.83	13.00
93.5	0.83	16.00
120.0	0.80	17.7
150.0	0.76	18.6

A perusal of the data of table 4 shows that the amount of aldehyde formed as given by Schiff's reagent is rather negligible in comparison to the peroxydisulphate used. This suggests that the oxidation product in this case is hydroxyaldehyde which exists mainly in the form of an oxide structure as depicted in chart II.

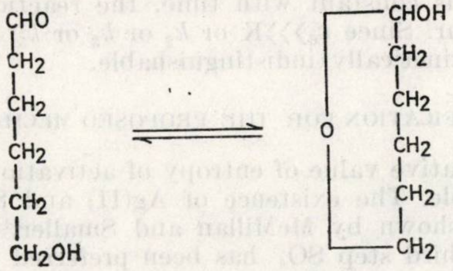

This behaviour is similar to that of glucose[11] which also fails to give colour with Schiff's reagent and was explained by Tollens[12] on the assumption of a butylene oxide structure. However, the instability of the oxide structure and cleavage of C—C bond, when the product was isolated by distillation under reduced pressure, can be explained on the basis of I strain suggested by Brown, Fletcher and Johannesen.[13]

DISCUSSION

Taking into consideration all the above kinetic results obtained and the previous studies on the redox reactions of $S_2O_8^{2-}$, the following general mechanism seems possible :

$$\mathrm{Ag(I)} + \mathrm{S_2O_8^{2-}} \underset{k_{-1}}{\overset{k_1}{\rightleftharpoons}} \mathrm{AgS_2O_8^-}\ ;\ K = \frac{k_1}{k_{-1}} \tag{1}$$

$$\mathrm{AgS_2O_8^-} \xrightarrow{k_2} \mathrm{Ag(II)} + \mathrm{SO_4^{\cdot-}} + \mathrm{SO_4^{2-}} \tag{2}$$

$$\mathrm{S} + \mathrm{SO_4^{\cdot-}} \xrightarrow{k_3} \mathrm{R} + \mathrm{HSO_4^-} \tag{3}$$

$$\mathrm{S} + \mathrm{Ag(II)} \xrightarrow{k_4} \mathrm{R} + \mathrm{Ag(I)} + \mathrm{H^+} \tag{4}$$

$$\mathrm{R} + \mathrm{S_2O_8^{2-}} \xrightarrow{k_5} \mathrm{P} + \mathrm{HSO_4^-} + \mathrm{SO_4^{\cdot-}} \tag{5}$$

$$\mathrm{R} + \mathrm{SO_4^{\cdot-}} \xrightarrow{k_6} \mathrm{P} + \mathrm{HSO_4^-} \tag{6}$$

Applying the steady state treatment to the radicals Ag^{2+}, $SO_4^{\cdot-}$ and R the following rate law is obtained for the consumption of peroxydisulphate ion with time.

$$-\frac{\mathrm{d}}{\mathrm{d}t}[\mathrm{S_2O_8^{2-}}] = k_2K[\mathrm{Ag^+}][\mathrm{S_2O_8^{2-}}] + \left(\frac{Kk_2k_3k_5}{k_6}\right)^{1/2} [\mathrm{S}]^{1/2}[\mathrm{Ag^+}]^{1/2}[\mathrm{S_2O_8^{2-}}] \tag{7}$$

where S stands for $OH-(CH_2)_6-OH$, R for $OH-(CH_2)_6-\dot{O}$ and P for $OH-(CH_2)_5-CHO$.

Equation (7) represents the rate of consumption of peroxydisulphate ion with time and represents the main kinetic features observed in the oxidation study of hexane-1,6-diol. Since the concentration of Ag(I) (being a catalyst) is constant with time, the reaction shows a kinetic first order behaviour. Since $k_6 \rangle\rangle\rangle K$ or k_2 or k_3 or k_5, the second term is rather small and kinetically indistinguishable.

JUSTIFICATION FOR THE PROPOSED MECHANISM

The large negative value of entropy of activation suggests the first step to be reversible. The existence of Ag(II) and $SO_4^{\dot{-}}$ in such redox systems has been shown by McMillan and Smaller,[14] and Chawla and Richard.[15] In the third step $SO_4^{\dot{-}}$ has been preferred to $\dot{O}H$ (formed by the hydrolysis of $SO_4^{\dot{-}}$) for abstracting hydrogen from the substrate as Norman et al.[16] and Gilbert et al.[17] in their ESR studies, have shown that $SO_4^{\dot{-}}$ has a greater tendency to bring about oxidation than $\dot{O}H$ by one electron transfer. The same view has been expressed by Chawla and Richard.[15] The existence of the radical R, however, could not be directly verified by ESR studies but the fractional order with respect to substrate,[18,19] the dependence of rate constant on initial concentration of reactants and the inhibition by allyl acetate are a proof for the operation of a free radical mechanism.

ACKNOWLEDGEMENT. The financial assistance of the Council for Scientific and Industrial Research, New Delhi, India is gratefully acknowledged.

REFERENCES

[1] M. M. Khan and S. P. Srivastava, *J. Indian Chem. Soc.*, **46**, 574 (1969).
[2] G. D. Menghani and G. V. Bakore, *Curr. Sci. (India).*, **37**, 641 (1968).
[3] Z. C. Szabo, L. Csanyi and H. Galiba, *Z. analyt. Chem.*, **135**, 269 (1952).
[4] K. C. Khulbe and S. P. Srivastava, *Agra Univ. J. Res. (Sci.)*, **9**, 177 (1960); **14**, 85 (1965).
[5] K. J. Laidler, "Chemical Kinetics", McGraw-Hill, New York, 1950, p. 18.
[6] E. R. Malinowski and L. S. Levitt, *J. Amer. Chem. Soc.*, **80**, 5334 (1958).
[7] G. V. Bakore and G. D. Menghani, *Bull. Chem. Soc. Japan*, **41**, 2574 (1968).
[8] S. P. Srivastava, S. K. Singhal and R. G. Sharma, *Indian J. Chem.*, **12**, 684 (1974).
[9] C. D. Hurd and W. H. Saunders Jr., *J. Amer. Chem. Soc.*, **74**, 5324 (1952).
[10] J. Mitchell Jr., I. M. Kolthoff, E. S. Prosakauer and A. Weissberger, "Organic Analysis", Interscience Publishers, New York, Vol. I, 1961. pp. 286–7.
[11] L. F. Fieser and M. Fieser, "Organic Chemistry", Asia Publishing House, New Delhi, 1970, p. 361.
[12] B. Tollens, Ph. D. Thesis, Göttingen, **1918**, 1841.
[13] H. C. Brown, R. S. Fletcher and R. B. Johannesen, *J. Amer. Chem. Soc.*, **73**, 212 (1951).
[14] J. A. McMillan and B. Smaller, *J. Chem. Phys.*, **35**, 1698 (1961).
[15] O. P. Chawla and W. F. Richard, *J. Phys. Chem.*, **79**, 2693 (1975).
[16] R. O. C. Norman, P. M. Storey and P. R. West, *J. Chem. Soc.*, **B.** 1970, 1087.
[17] B. G. Gilbert, J. P. Larkin and R. O. G. Norman, *J. Chem. Soc. Perkin Trans.*, **2**, 1272 (1972).
[18] F. S. Dainton, "Chain Reactions", Methuen, London, 1956.
[19] W. C. Vasudeva, M. I. Taha and S. Wasif, *J. Inorg. Nuclear Chem.*, **34**, 3159 (1972).

Revue Roumaine de Chimie, 26, 7, 947–954 (1981)

CALCUL DE L'ÉQUILIBRE CHIMIQUE À LA SYNTHÈSE DU MÉTHANOL PAR LES ÉQUATIONS D'ÉTAT DES GAZ HAUTEMENT COMPRIMÉS

FLORIN-EMILIAN DANEŞ et DAN GEANĂ
Chaire de Chimie Physique, INC, Institut Polytechnique de Bucarest, Roumanie
Boîte Postale, 78126, str. Polizu Gh., 1

Reçu le 15 mars 1980

La composition expérimentale d'équilibre est comparée aux résultats de 7 procédés de calcul thermodynamique à la synthèse du méthanol. La plus précise (la déviation standard du logarithme neperien de la constante d'équilibre en pressions partielles est $\sigma = 0{,}15$) pour 0–200 atm est une équation d'état de Himpan modifiée (HL), quoiqu'on ait utilisé la règle de Lewis & Randall (coefficient de fugacité γ en mélange égal à celui du gaz pur), tandis que pour 0–400 atm l'équation de Redlich & Kwong aux γ dépendant de la composition X s'avère la meilleure avec $\sigma = 0{,}3$, précision non améliorée par l'introduction des interactions des paires des constituants. En introduisant la dépendance $\gamma(X)$ dans la HL, la précision s'accroît : $\sigma = 0{,}08$ pour 0–400 atm.

The experimental equilibrium composition of methanol synthesis is compared with the results of 7 thermodynamic calculation procedures. The most accurate in the pressure range 0–200 atm (standard deviation of the logarithm of the equilibrium constant, ln K_p, $\sigma = 0.15$) is a modified Himpan equation of state (HL), used in relation with Lewis and Randall rule. In the pressure range 0–400 atm, Redlich-Kwong-Soave equation with composition dependent fugacity is the best one ($\sigma = 0.3$). Its accuracy is not better if the interaction constants are also considered in the mixture rules. By introducing a composition dependent fugacity in HL equation the accuracy increases : $\sigma = 0.08$ for the range 0–400 atm.

PROBLÈME DE L'ÉQUILIBRE CHIMIQUE À HAUTE PRESSION

Il y a plusieurs techniques vérifiées [1,2] pour obtenir par ordinateur à 0,1 % près la composition d'équilibre, dans les systèmes gazeux à réactions chimiques sous basse pression. Ces méthodes sont par contre défaillantes à hautes pressions,[3] faute de valeurs convenables des coefficients de fugacité γ_i, qui mesurent la déviation du potentiel chimique du constituant i du mélange gazeux par rapport au comportement idéal. L'équation viriale d'état, dont les prévisions à pressions modérées (0–30 atm) sont acceptables,[4] devient inapplicable à de centaines d'atmosphères des synthèses industrielles du méthanol ou de l'ammoniac, de l'hydrogénation des aromatiques ou de l'hydratation de l'éthylène. Le problème énoncé comporte trois étapes :

(I) choix d'une équation d'état des gaz purs *,

(II) adaptation de l'équation de (I) aux gaz en mélange et

(III) insertion des valeurs γ_i obtenues en (II) dans l'algorithme de calcul de la composition d'équilibre.

Dans cet article on propose des solutions pour (I), (II) et (III), testées aux compositions expérimentales d'équilibre de la synthèse du méthanol

$$CO + 2H_2 = CH_3\,OH \tag{I}$$

MÉTHODES DE CALCUL

ÉQUATIONS D'ÉTAT-GAZ PURS

Il n'y a pas beaucoup d'équations qui satisfassent aux exigences du calcul par ordinateur — généralité, fidélité, accessibilité et analyticité.[6] Ici on en emploie deux : celle de Redlich et Kwong,[7] dans la version de Soave,[8] très utilisée pour l'équilibre liquide-vapeur et même [9] pour l'équilibre chimique, ainsi qu'une modification propre (but : y inclure les gaz quantiques H_2, He) [5] d'une équation de Himpan.[10]

L'équation de Redlich, Kwong et Soave, $P = RT/(V - b_R) - a_R/V(V + b_R)$, mène pour φ_i — le coefficient de fugacité du gaz pur i — à

$$\ln \varphi_i = (z_i - 1) - \ln (z_i - B_i) - A_i^2 B_i^{-1} \cdot \ln (1 + B_i/z_i) \tag{1}$$

où z_i (facteur de compressibilité, $z_i = PV_i/RT$, V_i étant le volume molaire) est la plus grande des racines Z_i de l'équation

$$Z_i^3 - Z_i^2 + (A_i - B_i - B_i^2)\,Z_i - A_i\,B_i = 0,$$

$$A_i = [P_{r,i}/(2^{1/3} - 1)]^{1/2} \cdot [1 + (1 - \sqrt{T_{r,i}})(0{,}48 + 1{,}574\,\omega_i - 0{,}176\,\omega_i^2)]/3T_{r.i} \tag{2}$$

$$B_i = (2^{1/3} - 1)P_{r.i}/3T_{r.i} \tag{3}$$

Ici $P_{r,i}$, $T_{r.i}$ sont les grandeurs d'état réduites par division aux paramètres critiques du gaz i : $P_{r.i} = P/P_{c.i}$ et $T_{r.i} = T/T_{c.i}$, tandis que ω_i — facteur acentrique du gaz i après Pitzer[11] est à obtenir des tensions de vapeur ou de $\omega_i = 0{,}2033\ \alpha_{c.i} - 1{,}181$, le paramètre de Riedel $\alpha_{c.i}$ pour le gaz i[12] étant calculable de sa température d'ébullition $T_{e.i}$ par $\alpha_{c.i} = 0{,}9076\,[1 + (\ln P_{c.i})\,T_{e.i}/(T_{c.i} - T_{e.i})]$.

---

* Même une équation si complexe que celle de Beattie et Bridgman put donner à la synthèse du méthanol (300°, 200 atm) des résultats si éloignés de la réalité que les 98% de méthanol calculé par Lachakov,[5] face aux 54% expérimentaux, ce qui revient à une erreur 10 du $\ln K_p$!

En partant de l'équation Himpan, $P = RT(V - b_H)^{-1} - a_H T^{-1} \cdot (V^2 + c_H V + d_H)^{-1}$, le résultat sera :

$$\ln \varphi_i = (u_i + z'_{c,i})\, P_{r,i}/T_{r,i} - 1 + J_i H_i/T^2_{r,i} - \ln[(u_i + K_i)\, P_{r,i}/T_{r,i}] \quad (4)$$

u_i étant la plus grande des racines U_i de l'équation $[(U_i + N_i)^2 + M_i] \cdot [P_{r,i} - T_{r,i}/(U_i - L_i)] + J_i/T_{r,i} = 0$, tandis que L_i, N_i, J_i, M_i ont la signification $L_i = 2/(\alpha_{c,i} + 1)$, $N_i = L_i(\alpha_{c,i} - 1)/4$, $J_i = 8\, N_i^3$, $M_i = J_i(7 - \alpha_{c,i})/(\alpha_{c,i} - 1)$, K_i dépend du signe de M_i :

$$M_i < 0 \rightarrow K_i = (2G_i)^{-1} \ln[(u_i + N_i + G_i)/(u_i + N_i - G_i)]$$

$$M_i = 0 \rightarrow K_i = 1/(u_i + N_i)$$

$$M_i > 0 \rightarrow K_i = G_i^{-1} \operatorname{arctg}[G_i/(u_i + N_i)]$$

où $G_i = \sqrt{|M_i|}$ et $z'_{c,i}$ est la modification de [6] du facteur critique de compression $z_{c,i} = P_{c,i} V_{c,i}/RT_{c,i}$ du gaz i, c'est-à-dire :

$$T_{r,i} \leqslant 1 \rightarrow z'_{c,i} = z_{c,i}$$

$$T_{r,i} > 1 \rightarrow z'_{c,i} = z_{c,i}[(2{,}1 + 0{,}1\alpha_{c,i})\, z_{c,i}^{-1}(1 + \alpha_{c,i})^{-1}]^{1/T_{r,i}}.$$

COEFFICIENTS DE FUGACITÉ DES GAZ EN MÉLANGE

Un procédé simple recourt à la règle de Lewis et Randall qui, partant de la loi d'Amagat sur l'additivité des volumes à P et T constantes, aboutit à l'égalité des coefficients de fugacité du constituant i dans une mixture (γ_i) et du même gaz en état pur (φ_i) :

$$\gamma_i = \varphi_i(P,\ T \text{ constantes}) \quad (5)$$

Pour l'équation RKS il y a des « règles de mélange » empiriques, qui expriment P_c, T_c et ω de la mixture gazeuse en fonction des paramètres analogues des constituants individuels. Une méthode plus élaborée tient aussi compte des interactions des composants, la constante $k_{i,j}$ de l'interaction entre les constituants i et j étant par exemple : [13]

$$k_{i,j} = 1 - 128[(V_{c,i}/V_{c,j})^{1/6} + (V_{c,j}/V_{c,i})^{1/6}]^{-6}[(I_i/I_j)^{1/2} + (I_j/I_i)^{1/2}]^{-1} \quad (6)$$

où I_i est le potentiel d'ionisation du constituant i. Les valeurs I selon Vedeneev [14] sont présentées au tableau 1, ainsi que les autres paramètres des principaux constituants. Les données PVT obtenues dans les mélanges binaires ($i + j$) permettent d'obtenir des valeurs plus exactes pour les $k_{i,j}$, mais elles sont rarement disponibles. Pour les trois paires de constituants principaux, les k de (6) sont : 0,014 (CH_3OH/CO) ; 0,047 (CH_3OH/H_2) et 0,012 (CO/H_2), tandis que d'après Heidemann [15] les densités des mixtures CO/H_2 mènent à k (CO/H_2) = 0,100.

TABLEAU 1

Constantes de matériel

Composé	T_c K	P_c atm	1000 V_c 1/mole	α_c	ω	I V
CH_3OH	513,0	79,0	119,5	8,557	0,557	10,88
CO	132,9	34,5	91,5	5,955	0,047	14,01
H_2	33,25	12,8	63,7	3,454	−0,098	15,43

Les fugacités résultent de la relation

$$\ln \gamma_i = (B_i/E)(f-1) - \ln (f-E) + (DB_i/E^2 - 2C_i/E) \cdot \ln (l + E/f) \quad (7)$$

où A_i, B_i proviennent de (2,3), f est la plus grande racine F de l'équation

$$F^3 - F^2 + (D - E - E^2)F - DE = 0$$

tandis que $E = \sum_i B_i x_i$, x_i étant la fraction molaire du constituant i,

$$D = \sum_i A_i x_i \quad (8a)$$

$$C_i = A_i \sum_j A_j x_j (1 - k_{i,j}) \quad (8b)$$

En négligeant les interactions, $k_{i,j} = 0$ et (8*a*, *b*) se réduisent à

$$D = (\sum_i A_i x_i)^2 \quad (9)$$

Il n'y a pas de règles de mélange pour l'équation Himpan, mais on peut y introduire une correction expérimentale K_c de la constante d'équilibre en pressions partielles

$$K_p(\mathrm{HC}) = K_p(\mathrm{HL}) \cdot K_C \quad (10)$$

$K_p(\mathrm{HL})$ étant la valeur du produit $K_p = P(CH_3OH) \cdot P^{-1}(CO) \cdot P^{-2}(H_2)$ obtenu de l'équation d'état Himpan modifiée, combinée avec la règle de Lewis et Randall (relations (4) et (5)), $K_p(\mathrm{HC})$ – la valeur « corrigée » du même produit et K_C – le facteur de correction $K_C = \varphi(CH_3OH)\,\gamma(CO)\,\gamma^2(H_2)/\gamma(CH_3OH)\,\varphi(CO)\,\varphi^2(H_2)$ ou φ_i et γ_i sont les valeurs expérimentales de Kazarnovskii.[16]

Pour le mélange idéal des gaz parfaits

$$\gamma_i = 1 \quad (11)$$

INSERTION DANS LE PROGRAMME DE CALCUL DE LA COMPOSITION

Les compositions d'équilibre ont été calculées selon sept versions pour les γ_i (entre parenthèses sont indiquées les relations utilisées) :

ID (11) – modèle idéal ;

RL (1,5) – équation d'état RKS, combinée à la règle de Lewis et Randall ;

HL (4,5) — équation de Himpan modifiée et règle de L. et R. ;
RC (9,7) — équation RKS à γ_i dépendantes de la composition (mais sans interaction) ;
RI (6, 8, 7) — équation RKS à γ_i dépendantes de la composition et des interactions calculées.
RE — comme RI, mais à interaction expérimentale pour H_2/CO (les autres interactions sont calculées de la relation (6)).
HC (4, 5, 10) — comme HL, mais à correction ultérieure de la constante d'équilibre.

Le programme utilisé, conçu pour le caz idéal, minimise l'enthalpie libre totale G du mélange gazeux, réduite par RT :

$$G/RT = \sum_{i=i}^{N} n_i \left(g_i + \ln n_i - \ln \sum_{i=1}^{N} n_i \right) = \min \tag{12}$$

en introduisant par des multiplicateurs Lagrange les restrictions

$$b_j - \sum_{i=1}^{N} n_i a_{i,\,j} = 0, \; \forall j \in [1, \; M]$$

des bilans atomiques et avec les restrictions inégalités $n_i > 0$, $\forall i \in [1, N]$, N, M étant les nombres de constituants et d'éléments chimiques. Les n_i (quantité de constituant i, en moles) sont les variables, tandis que — puisque le système thermodynamique est fermé, isotherme et isobarique — a_{ij} (nombre des atomes type j dans la molécule type i), b_j (quantité de l'élément j, en atome-grammes) et g_i sont des paramètres constants. La signification de g_i est

$$g_i = (\Delta^f G_i^0 / RT) + \ln P \tag{13}$$

où $\Delta^f G_i^0$ est l'enthalpie libre standard de la formation du constituant i à la température T. Après avoir obtenu n_i, on calcule la composition par : $x_i = n_i / \sum_{i=1}^{N} n_i$.

Notre procédé d'insertion remplace (13) par

$$g_i = (\Delta^f G_i^0 / RT) + \ln (P \gamma_i) \tag{14}$$

traitant néanmoins g_i comme des constantes dans la minimisation (12). Si les γ_i dépendent de la composition (modèles RC, RI, RE), l'itération devient nécessaire. Dans chaque cycle :
I on obtient γ_i pour le modèle respectif des valeurs x_i du cycle précédent (pour le premier cycle, on met $\gamma = 1$)
II on calcule g_i par (14), avec les γ de I
III on substitue les g en (12) et on minimise G, ce qui donnera les n_i et ensuite des nouveaux x_i, qu'on utilisera au cycle suivant.

Les cycles cessent quand les γ du dernier cycle ($\gamma^{(k)}$) et de l'avant-dernier ($\gamma^{(k-1)}$) sont assez proches : $|\ln [\gamma_i^{(k)} / \gamma_i^{(k-1)}]| < \varepsilon_\gamma$, $\forall i \in [1, N]$.

Pour $\varepsilon_\gamma = 0{,}001$, on a obtenu dans le système testé $k = 6$ (maximum) et $k = 3$ (moyenne).

VÉRIFICATION EXPÉRIMENTALE

Les résultats des calculs de la composition d'équilibre pour la synthèse du méthanol à 300 et 350° sous 100, 200, 300 et 350 atm, en partant des mélanges $CO:H_2$ stœchiométriques ou légèrement impurifiés (à CO_2, H_2O) sont confrontés aux données expérimentales de Kazarnovskii[16], qui sont les seules assez exactes (à cause de la détermination indépendante des fugacités) pour permettre un test précis des procédés de calcul. Les autres résultats expérimentaux disponibles, présentés au tableau 2, portent seulement pour $P < 200$ atm, sont très dispersés et visiblement contradictoires. Pour ces raisons, un essai de Peter et Wenzel,[9] qui ont essayé de simuler (modèle RC) les résultats expérimentaux au catalyseur Cu/Zn/O (marqués « b » au tableau 2) n'a pas réussi : la déviation standard du ln K_p de ses résultats atteint 0,9 (valeurs K_p calculées en moyenne 2,5 fois plus grandes que les expérimentales).

TABLEAU 2

Données expérimentales de l'équilibre $CO + 2H_2 = CH_3OH$

t, °	250	258,5	274	289	298	300	300
P, atm	100	176	176	103	175	100	100
$x\ (CH_3OH) \cdot 1000$	691	717	561	182	424	383	263
$-\ 100 \ln K_p$	415	498	654	846	762	681	772
Observations	*a, c*[17]	*a, b*[20]	*a, b*[20]	*a, b*[21]	*a, b*[20]	*a, c*[17]	*d*[16]
t, °	300	300	300	320	338	350	350
P, atm	200	300	400	100	103	100	100
$x\ (CH_3OH) \cdot 1000$	540	755	811	50	38	136	82
$-\ 100 \ln K_p$	697	556	502	1014	1051	886	955
Observations	*d*[16]	*d*[16]	*d*[16]	*a, b*[21]	*a, b*[21]	*a, c*[17]	*d*[16]
t, °	350	350	350	350	400	400	400
P, atm	200	200	300	350	100	180	200
$x\ (CH_3OH) \cdot 1000$	201	240	404	483	32	76	80
$-\ 100 \ln K_p$	962	929	885	855	1064	1046	1096
Observations	*a, c*[18]	*d*[16]	*d*[16]	*d*[16]	*a, c*[17]	*a, c*[19]	*a, c*[18]

a — Analyse chimique après passage sur le catalyseur ; *b* — Catalyseur Cu/Zn/O ; *c* — Catalyseur Cr/Zn/O ; *d* — Fugacités calculées des données PVT des mélanges.

En dehors des constituants majeurs CH_3OH, CO et H_2 on a pris encore en considération CH_2O, $HCOOCH_3$, HCOOH, H_2O et CO_2 (les trois derniers, à rapport $C/O < 1/2$, seulement pour des mélanges initiaux impurifiés) mais la teneur totale des constituants mineurs s'est avérée toujours inférieure à 0,05%, de manière qu'un seul paramètre suffit pour définir la composition d'équilibre. Le plus convenable paramètre est la constante d'équilibre en pressions partielles, K_p, de la réaction (I), liée à la constante thermodynamique d'équilibre, $K_f = f(CH_3OH)/f\ (H_2)\ f\,(CO)$ par la relation

$$K_f = K_p K_\gamma$$

où $K_\gamma = \gamma(CH_3OH)/\gamma^2(H_2)\cdot\gamma(CO)$. Les K_f employées ici, obtenues des données thermodynamiques [22,23] usuelles (S^0_{298}, $\Delta^f H^0_{298}$ et $C^0_p(T)$ des trois constituants) sont $2{,}569\cdot10^{-4}$ atm^{-2} et $4{,}886\cdot10^{-5}$ atm^{-2} à 300°, respectivement à 350°. Les K_p sont obtenues de la valeur X expérimentale où calculée par la relation $K_p = 6{,}75\ X(1-X)^{-3}P^{-2}$, X étant la fraction molaire du méthanol, tandis que $x\ (CO) = (1-X)/3 = x(H_2)/2$. Le rapport K_γ des coefficients de fugacité représente la déviation du système réel de réaction par rapport au système idéal.

Les déviations des différents modèles par rapport aux expérimentations sont définies par la grandeur D

$$D = -100\ (\ln K_{p,k} - \ln K_p^{\exp})$$

où $K_{p,k}$ est la valeur calculée au modèle k et $K_p^{\exp}$ – la valeur expérimentale pour les mêmes P et T. Les déviations des sept modèles sont présentées dans le tableau 3.

TABLEAU 3

Précision des modèles de calcul

Valeurs de $D = -100 \ln K_p\,(\text{modèle})/K_p\,(\text{expér.})$

t °C	P atm	D, modèle :						
		ID	RL	RC	RI	RE	HL	HC
300	100	55	13	31	31	28	1	0
300	200	129	47	26	23	15	26	0
300	300	271	159	−6	−9	−26	130	11
300	350	339	206	−14	−18	−32	183	−12
350	100	38	8	29	29		−3	−1
350	200	64	5	34	33		−15	10
350	300	118	36	45	43		8	3
350	350	144	63	48	41		22	−11
Déviation standard	0–200 atm	79	25	30	29		15	6
	0–400 atm	176	97	33	30		81	8

L'écart D est assez important pour tous les modèles et change d'ailleurs avec la température et avec la pression. Une caractéristique globale est la déviation quadratique moyenne, D' pour 0–200 atm et D'' pour 0–400 atm :

$$D' = 4^{-0.5}\ (D^2_{11} + D^1_{12} + D^2_{21} + D^2_{22})^{0.5}$$

$$D'' = 8^{-0.5}\ (D^2_{11} + D^2_{12} + D^2_{21} + D^2_{22} + D^2_{31} + D^2_{32} + D^2_{41} + D^2_{42})^{0.5}$$

où i dans D_{ij} indique la pression ($i = 1, 2, 3$ et 4 pour 100, 200, 300 et 350 atm) et j marque la température ($j = 1$ à $t = 300°$ et $j = 2$ à 350°). Les valeurs D', D'' des modèles sont également présentées au tableau 3.

DISCUSSION

Le modèle idéal ID est le plus imprécis, dans tous les cas.

Parmi les cinq modèles suivants – modèles à gaz réels, entièrement obtenus des grandeurs thermodynamiques par les algorithmes décrits

plus haut — la situation diffère selon le domaine des pressions, nommément :
I à 0—200 atm, la précision du modèle HL (0,15) dépasse de loin celle des quatre modèles RKS, dont les précisions sont assez proches — à peu près 0,3 pour RL, RC, RI et RE.
II à 0—400 atm, les modèles RKS avec dépendance $\gamma(x)$, c'est-à-dire RC et RI, sont bien plus précis ($D'' = 0{,}3$) que les modèles RL, HL à la règle Lewis-Randall ($D'' = 1$, respectivement 0,8).

Le modèle Himpan corrigé aux K expérimentales (HC) est toujours supérieur à tous les autres : D', $D'' < 0{,}1$ (correspondant à 6—8% déviation standard de K_p), seulement les règles de mélange pour cette équation d'état sont encore à trouver.

CONCLUSIONS

L'exactitude des calculs de l'équilibre chimique en gaz comprimés dépend surtout de trois facteurs : *A* — choix de l'équation d'état des gaz purs ; *B* — règles de mélange pour la dépendance fugacités/composition ; *C* — introduction des effets d'interaction entre les constituants du mélange.

A pressions modérées (0—200 atm) le plus important est le facteur *A*, tandis qu'à pressions élevées (200—400 atm) le facteur *B* devient primordial. Le facteur *C* joue dans les deux cas un rôle subordonné.

BIBLIOGRAPHIE

[1] F. van Zeggeren et S. Storey, « The Computation of Chemical Equilibria », Cambridge University Press, Cambridge, 1970.

[2] N. F. Stepanov, M. E. Erlykina et G. G. Filippov, « Metody lineynoy algebry v fizitcheskoy khimii », Izd. Moskovskoy Universiteta, Moscu, 1976 p. 190—221.

[3] M. Gonikberg, « L'équilibre chimique et les vitesses de réactions sous hautes pressions » éd. Mir, Moscou, 1974, p.13—48.

[4] D.Geană et F.-E. Daneș, *Bul. Inst. Politeh. București, ser. Chim.-Metalurg.*, **40** (3), 31 (1978).

[5] L. M. Lachakov, *Zhur. fiz. khim*, **13**, 1102 (1939).

[6] F.-E. Daneș et D. Geană, *Bul. Inst. Politeh. București, ser. Chim.-Metalurg.*, **41** (4), 67 (1979).

[7] O. Redlich et J. Kwong, *Chem. Rev.*, **44**, 233 (1949).

[8] G. Soave, *Chem. Eng. Sci.*, **27**, 1197 (1972).

[9] S. Peter et H. Wenzel, *Chem. Ing. Tech.*, **45**, 573 (1973).

[10] J. Himpan, *Monatsh.*, **86**, 289 (1955).

[11] K. S. Pitzer et G. O. Hultgren, *J. Amer. Chem. Soc.*, **77**, 3433 (1955).

[12] L. Riedel, *Chem. Ing. Tech.*, **26**, 83 (1954).

[13] F. Gothard, « Echilibre lichid-vapori », Ed. Academiei, București, 1975, p. 43.

[14] V. I. Vedeneev, « Energii razryva khimitcheskikh svyazey, potentsialy ionizatsii i srodstva h elektronu », éd. Akad. Nauk S.S.S.R., Moscova, 1962, p. 165, 188 et 191.

[15] R. A. Heidemann, Communication au Symposium « Thermodynamique des systèmes aqueux et applications industrielles », Calgary, Octobre 1979.

[16] Ya. S. Kazarnovskiy, D. B. Kazarnovskaya et I. P. Sidorov, *Khim. Prom.*, **1963**, 426.

[17] M. Eguchi, *Trans. Chem. Eng., Congr. World Power Conf.*, **3**, 509 (1937).

[18] W. Lewis et P. Frolich, *Ind. Eng. Chem.*, **20**, 285 (1928).

[19] R. Brown et A. Galloway, *Ind. Eng. Chem.*, **20**, 960 (1928).

[20] F. von Wettberg et B. Dodge, *Ind. Eng. Chem.*, **22**, 1040 (1930).

[21] D. Newitt, B. Byrne et H. Strong, *Proc. Roy. Soc. (London)*, **A123**, 236 (1928).

[22] A. S. Kazanskaya et V. A. Skoblo, « Rastchety khimitcheskikh ravnovesiy », izd. Vysshaya Shkola, Moscou, 1974, p. 224.

[23] « Manualul Inginerului Chimist », vol. 2, Ed. tehnică, București, 1952, p. 1248.

Revue Roumaine de Chimie, **26**, 7, 955–960 (1981)

ÉCHANGE IONIQUE DANS LE SYSTÈME Na_2WO_4 (SOLUTION) – AMBERLITE IR 120 (H^+). II

ACIDE POLYWOLFRAMIQUE *T*

CLEOPATRA CALU, N. CALU et ANA ONU
Faculté de Technologie Chimique
Institut Polytechnique « Gh. Asachi », Jassy

Reçu le 23 Juin 1979

Par l'échange ionique dans le système Na_2WO_4 (solution) – Amberlite IR 120 (H^+) aux concentrations $1.10^{-1}-1.10^{-2}$ moles/lNa_2WO_4 ainsi qu'en dehors de ces limites et pH 2–3, il se forme intermédiairement un composé polywolframique avec un grand degré de condensation appelé par nous acide polywolframique T. Ce composé présente une masse ionique de l'ordre de 10^5 u.a.m. Dans les solutions aqueuses il se transforme directement ou par l'intermédiaire d'autres espèces dans l'acide métawolframique. L'acide polywolframique T représente l'espèce polywolframique avec le plus grand déplacement batochrome de la bande d'absorption en U.V., de la série des composés polywolframiques.

By an ion-exchange process in Na_2WO_4 (solution) – Amberlite IR 120 (H^+) system, at concentration of about $1.10^{-1}-1.10^{-2}$ mole $\cdot l^{-1}Na_2WO_4$ and pH 2-3, a polytungstic compound with a high degree of condensation forms intermediarily. The compound, named by us Polytungstic T Acid has an ionic mass of about 10^5 a m u. In aqueous solutions it converts straightly or by means of other species into metatungstic acid. In the polytungstic compounds, the Polytungstic T Acid exhibits the largest bathochrome shift of the UV absorption band.

INTRODUCTION

L'échange ionique successif par étapes, par la méthode statique dans le système Na_2WO_4 (solution)-Amberlite IR 120(H^+) conduit à une série de sels et acides polywolframiques. [1] Une partie de ces espèces polywolframiques a été identifiée par comparaison avec des solutions polywolframiques standard et tenant compte des données de la littérature [1,2] (fig. 1).

A côté de plusieurs analogies il existe, à ce qu'il paraît, des différences en ce qui concerne la nature des espèces polywolframiques qui résultent de l'échange ionique, par rapport à celles qui résultent lorsqu'on acidifie les wolframates avec des acides minéraux forts. La combinaison appelée par nos travaux [1] acide polywolframique T (transitoire) par exemple, correspondrait à l'espèce connue dans la littérature comme le polywolframate Y, [2,3] sur la base du pH de la solution dans laquelle il apparaît ou les spectres d'absorption en UV. Cependant, la masse ionique de l'acide polywolframique T est beaucoup plus grande que celle du polywolframate Y qui, d'après les auteurs mentionnés [2,3] serait un dodécawolframate. En raison de ces différences, l'acide polywolframique T est considéré comme une espèce différente, et c'est ce qu'on démontre dans le cadre de ce travail.

RÉSULTATS ET DISCUSSIONS

A. OBTENTION DE L'ACIDE POLYWOLFRAMIQUE T

L'acide polywolframique T (W_T) apparaît comme une espèce transitoire dans les solutions fraîchement obtenues par échange ionique intégral dans le système Na_2WO_4 (solution)-Amberlite IR 120(H^+) à des pH $\cong 2-3$ et des concentrations entre $1 \cdot 10^{-1}$ et $1 \cdot 10^{-2}$ moles/l Na_2WO_4 et aussi en dehors de ces limites (fig. 1).

On peut le séparer à l'état solide après la réalisation de l'échange ionique intégral en solution de ~ 1 mole/l Na_2WO_4. Il faut concentrer la solution au bain-marie jusqu'à la consistance d'un aglutinat qu'on passe dans un exsiccateur à vide sur de l'acide sulfurique concentré. De cette manière, on obtient une masse vitreuse, transparente d'acide polywolframique T.

On sépare l'anion de l'acide polywolframique *T* (mélangé à d'autres combinaisons polywolframiques) en le précipitant avec des ions Ba^{2+}, étant donné que le métawolframate de baryum est beaucoup plus soluble dans l'eau. Ainsi, dans le filtrat qui résulte de la séparation des combinaisons bariques (difficilement solubles) seul l'acide métawolframique est présent — identifié par sa bande d'absorption à λ_{max} 258 nm (fig. 2). En dissolvant ensuite les combinaisons wolframiques difficilement solubles par agitation avec la résine Amberlite IR 120(H^+), on ne retrouve plus l'acide polywolframique T dans la solution ; il se transforme pendant la précipitation et la dissolution (fig. 2).

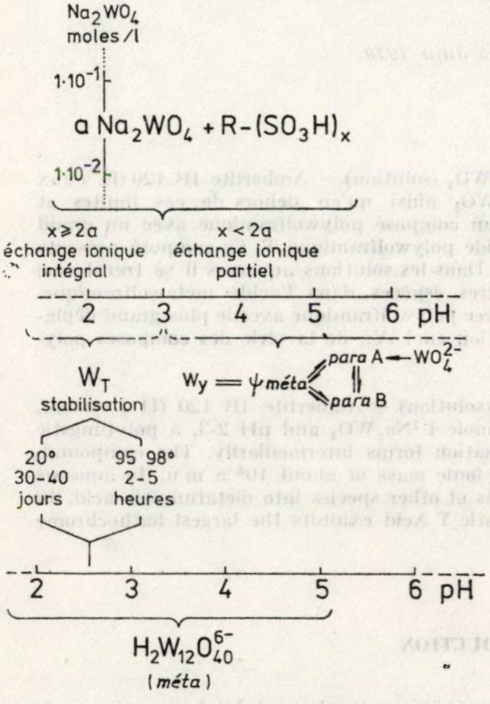

Fig. 1. — Schéma des processus de formation et de stabilisation des combinaisons polywolframiques dans le système Na_2WO_4 (solution) — Amberlite IR 120 (H^+)*.

B. CORRÉLATION DE L'ACIDE POLYWOLFRAMIQUE T AVEC L'ACIDE MÉTAWOLFRAMIQUE

L'acide polywolframique T apparaît transitoirement dans le système ci-mentionné et passe, dans les conditions d'un échange ionique intégral, à pH $\sim 2-3$ et solutions de wolframates pures, directement ou par l'intermédiaire d'autres espèces, dans l'acide métawolframique [1] (fig. 1).

---

* On note avec $R-(SO_3H)_x$ la résine Amberlite IR 120(H^+).

C. DONNÉES SUR LA CONSTITUTION ET LES PROPRIÉTÉS DE L'ACIDE POLYWOLFRAMIQUE T

A l'état solide, l'acide polywolframique T présente l'aspect d'une masse vitreuse, incolore et amorphe du point de vue röntgénographique. Introduit dans l'eau, il prend l'aspect d'une gomme qui adhère aux parois de verre mais qui se dissout complètement. La solution est incolore.

Si à l'état solide, l'acide polywolframique T demeure inchangé pendant longtemps, en solution il se décompose en temps, passant dans des combinaisons plus stables, comme l'acide métawolframique et l'acide wolframique qui se sépare sous forme de précipité jaune.[1]

L'acide polywolframique T a un caractère oxydant fortement marqué que les autres espèces polywolframiques. Sa masse ionique est beaucoup plus grande que celle des dodécawolframates, fait prouvé par les valeurs déterminées par la méthode de la diffusion de la lumière.

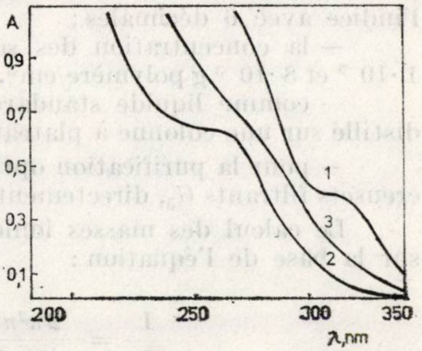

Fig. 2. — Spectres d'absorption en UV enregistrés à quelques espèces polywolframiques, séparées avec des ions Ba^{2+}. *1.* La bande d'absorption de l'acide polywolframique T avec $\lambda_{max} = 322$ nm $c_{WO_3}{}^{**} = 5.10^{-2}$ moles/l ; pH = 2,40. *2.* Solution représentant le filtrat dans la séparation des combinaisons polywolframiques difficilement solubles avec l'ion Ba^{2+}. La bande à $\lambda_{max} = 258$ nm atteste la présence dans le filtrat de l'acide métawolframique. *3.* Solution obtenue en dissolvant les combinaisons polywolframiques difficilement solubles avec le baryum par agitation avec la résine Amberlite IR 120(H^+). Cuve = 1cm³.

C1. Déterminations des masses ioniques par la méthode de la diffusion de la lumière

Il existe beaucoup de travaux concernant le degré de condensation, respectivement les masses des ions polywolframiques, parmi lesquels nous citons.[2-7]

On explique la non-concordance des valeurs des masses ioniques des ions polywolframiques, surtout pour les espèces moins stables, par la différence des méthodes ou des conditions de travail : le pH, la concentration des solutions, la température et autres.

Dans la présente étude, on a employé pour la détermination des masses ioniques des combinaisons du système Na_2WO_4 (solution) — Amberlite IR 120(H^+), la méthode basée sur la diffusion de la lumière. Cette méthode, moins influencée par la polydispersion du système, est indiquée par les solutions qui contiennent des espèces polywolframiques non homogènes du point de vue des masses ioniques.

** La concentration des solutions contenant des acides et des sels polywolframiques s'exprime par moles/l WO_3. Cette concentration est celle à laquelle l'échange ionique a eu lieu. Pour les déterminations spectrophotométriques, les solutions ont été diluées à 2.10^{-4} moles/l WO_3. Les bandes d'absorption subissent des modifications avec le temps à cause des transformations des espèces polywolframiques.

Les conditions dans lesquelles ont été effectuées les déterminations de la diffusion de la lumière :

— on a utilisé un photogoniodiffusiomètre de type SOFICA à $\lambda = 5461$ A°, en lumière non polarisée et à des angles de diffusion variant de 30° à 150°;

— l'incrément de l'indice de réfraction, dn/dc, a été déterminé avec un réfractomètre d'immersion qui a permis d'établir les valeurs de l'indice avec 6 décimales ;

— la concentration des solutions employées a été comprise entre $1 \cdot 10^{-3}$ et $8 \cdot 10^{-3}$ g polymère/cm³, en diluant les solutions plus concentrées ;

— comme liquide standard on a employé le benzène fraichement distillé sur une colonne à plateaux ;

— pour la purification optique, les solutions ont été filtrées par des creusets filtrants G_5, directement dans la cuve de mesure.

Le calcul des masses ioniques gravimétriques, $\bar{M}_W$, a été effectué sur la base de l'équation :

$$\frac{1}{\bar{M}_W} = \frac{2\pi^2 n^2}{\lambda_0^4 N_A R_B} = \left(\frac{\mathrm{d}n}{\mathrm{d}c}\right)^2 I_B \left[\frac{c}{I}\right]_{\substack{\theta=0\\ c=0}}$$

où

n — indice de réfraction du solvant (l'eau) ;

λ_0 — longueur d'onde dans le vide de la radiation utilisée ;

N_A — nombre d'Avogadro ;

R_B — constante de Rayleigh du benzène ($16{,}3 \cdot 10^{-6}$) ;

I_B — intensité de la lumière diffusée par le benzène ;

$\left[\frac{c}{I}\right]_{\substack{\theta=0\\ c=0}}$ — valeur du rapport de la concentration et de l'intensité de la lumière diffusée, à angle et concentration nuls, trouvées dans la représentation graphique de Zimm.[8]

D'après les déterminations des masses ioniques ainsi effectuées sur les espèces polywolframiques du système déjà mentionné, on fait ces constatations :

— pour la solution standard de l'acide métawolframique on n'obtient pas de données mesurables pour pouvoir calculer la masse ionique ; cela est dû au fait que l'anion métawolframique a la masse de 2848 u.a.m. et ne s'inscrit pas entre les limites d'application de la méthode par la diffusion de la lumière, qui sont de $10^4 - 10^7$ u.a.m.

— pour les solutions fraîchement préparées avec des espèces polywolframiques de concentrations $1 \cdot 10^{-2} - 1$ mole/l WO_3 et pH $\sim 2{,}5$, obtenues par échange ionique ou par dissolution des cristaux, on a trouvé des masses ioniques de l'ordre 10^5 u.a.m. et même plus grandes ;

— si les solutions étaient plus diluées, on trouvait des valeurs plus faibles que les valeurs déjà mentionnées ;

— si les solutions étaient obtenues par échange ionique partiel, à pH ~ 5, les données indiquaient des masses approximatives de 10^4 u.a.m.

En dehors du pH et des concentrations des solutions, les masses ioniques des espèces polywolframiques dépendent aussi de la manière dont l'échange a été effectué, du rythme maintenu dans l'introduction de la résine, de la température du travail, etc.

C.2. Chromatographie sur papier

Les espèces polywolframiques à masses ioniques et charges différentes se prêtent à la séparation chromatographique sur papier. C'est pourquoi on a examiné par chromatographie les espèces polywolframiques des solutions contenant les acides métawolframique et polywolframique T. Les spots des produits purs séparés ont été élués et dans les solutions respectives on a identifié par spectrophotométrie les acides ci-mentionnés (fig. 3).

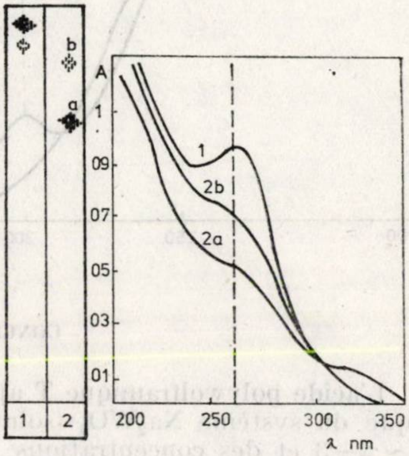

Fig. 3. — Comportement de quelques espèces polywolframiques à la chromatographie sur papier dans les conditions : — chromatographie ascendante dans l'eau ; — papier Whatman n°3 ; — les spots des différentes espèces polywolframiques ont été mis en évidence par irradiation U.V. 1. Solution à acide métawolframique : $R_f = 0{,}95$ et $\lambda_{max} = 258$ nm. 2. Solution à acide polywolframique T : *a*. espèce à $R_f = 0{,}70$ et $\lambda_{max} = 322$ nm, correspondant à l'acide polywolframique T ; *b*. espèce contenant des restes, à $R_f = 0{,}86$ nm et une inflexion dans la position de $\lambda_{max} = 258$ nm, marquant la tendance de l'acide polywolframique T de se transformer en acide métawolframique.

A la chromatographie sur papier en milieu aqueux, l'acide polywolframique T a un $R_f = 0{,}70$ qui est sensiblement plus petit que celui de l'acide métawolframique, $R_f = 0{,}97$. Cela est en accord avec les masses ioniques des deux composés — l'acide polywolframique T ayant la masse ionique plus grande.

C.3. Déplacement batochrome des bandes d'absorption dans la série des combinaisons polywolframiques

En général, le processus de condensation des ions WO_4^{2-} en espèces polywolframiques diverses est accompagné par un déplacement des bandes d'absorption vers le rouge — effet batochromique.[9]

Il est à remarquer que l'acide polywolframique T a la bande d'absorption caractéristique à $\lambda_{max} = 322$ nm., c'est-à-dire avec le plus grand déplacement batochromique et de 64 nm plus grande que la bande d'absorption caractéristique de l'acide métawolframique (fig. 4).

L'acide polywolframique T est aussi l'espèce polywolframique la plus oxydante. Ces propriétés sont une conséquence, probablement, de la structure de l'acide polywolframique T : c'est une combinaison à degré élevé de condensation et à structure moins compacte que celles de formes 12 (iso- ou hétéro-) à développement presque linéaire, à conjugaison éventuelle $p - \pi$ par l'oxygène des ponts.

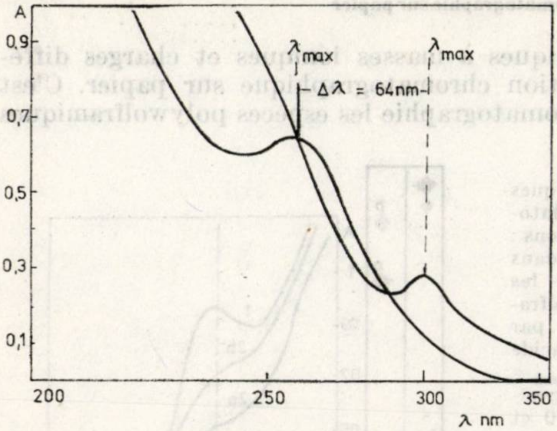

Fig. 4. — Déplacement batochrome Δλ des acides métawolframique et polywolframique T. *1.* Acide métawolframique : $\lambda_{max} = 258$ nm. *2.* Acide polywolframique T : $\lambda_{max} = 322$ nm. $C_{WO_3} = 6.10^{-2}$ moles/l ** ; cuve = 1 cm³.

CONCLUSIONS

L'acide polywolframique T apparaît transitoirement dans l'échange ionique du système Na_2WO_4 (solution)—Amberlite IR 120 (H^+), à des pH ~ 2—3 et des concentrations $1 \cdot 10^{-1}—1 \cdot 10^{-2}$ moles/l Na_2WO_4, ainsi qu'en dehors de ces limites. Il présente un grand degré de condensation. Sa masse ionique est de l'ordre de 10^5 u.a.m.

L'acide polywolframique T représente l'espèce polywolframique avec le déplacement batochrome de la bande d'absorption en UV, le plus grand de tous les acides de la série polywolframiques.

BIBLIOGRAPHIE

C. Calu et N. Calu, *Bul. Inst. Politeh. Iași* (sous presse).
[2] O. Glemser, W. Holznagel, W. Hotje et E. Schwarzmann, *Z. Naturforsch.*, **20 b**, 725 (1965).
[3] M. Boyer et P. Souchay, *Rev. Chim. Min.*, **8**, 591 (1971).
[4] G. Jander et F. Exner, *Z. phys. Chem.*, **187**, 211 (1940) ; **190**, 195 (1941).
[5] J. B. Donald et Y. Tyre, *J. Amer. Chem. Soc.*, **79**, 3355 (1957).
[6] J. Sasaki, *Acta Chem. Scand.*, **15**, 175 (1961).
[7] V. I. Spitsyn et G. N. Pirogova, **Zur. neorg. Khim.**, **2**, 2102 (1957).
[8] B. Zimm, *J. Chem. Phys.*, **16**, 1093 (1948) ; H. Fujita, *Polymer J.*, **1**, 537 (1970).
[9] G. Jander et F. Jahr. *Kolloid Z.*, **41**, 1 (1934).

Revue Roumaine de Chimie, **26**, 7, 961–965 (1981)

STUDIES ON OSMIUM-QUINISATINE OXIME REACTION

MAMDOUH S. MASOUD*, M. M. OSMAN and H. A. EL-NAGGAR
Faculty of Science, Chemistry Department, Alexandria, Egypt

Received October 5, 1979

The interaction of osmium (VIII) with quinisatine oxime was investigated spectrophotometrically. The ligand exists in the oxime structure rather than the nitrosophenol form. 1 : 3-Complex species was traced to exist with an average pK value of 4.12 ± 0.04 at 25 ± 0.1°C.

The oximes are well known chelating agents and most of them exist in equilibrium with the nitroso tautomer.[1-3] In our laboratory, the interaction of some transition metals with different nitroso compounds was done.[4-10] The chelation is due to the presence of two strong electron donors: nitrogen and oxygen. The nature of the linkage with the metal ion depends upon the dissociation of the oxime proton. In view of the great potentialities of the oximes as analytical reagents, it is desirable to study the physicochemical aspects of complexation between osmium and quinisatine oxime.

EXPERIMENTAL

The ligand (m.p. 109°) was prepared [11] from acidified 2-amino-4-hydroxyquinoline in the presence of $NaNO_2$ at O°C. The compound was recrystallized from aqueous acetic acid. Standard 250 ml Os (VIII) solution in 0.02N NaOH solution was prepared from 0.1 g ampoule of osmic acid (OsO_4). The solution was standardized iodometrically.[12] Spectrophotometric measurements were made on a Unicam SP-800 recording spectrophotometer using 1 cm path length matched cells. The infrared spectra were obtained using the KBr disc method on a Unicam SP-200 recording spectrophotometer calibrated with polystyrene. The pH values were measured on a Radiometer 28.

RESULTS AND DISCUSSION

Very few ligands containing both an aromatic nitrogen heterocycle and an oxime nitrogen at the α-position have been studied. The prepared orange solid ligand is slightly soluble in ethanol but completely soluble in dimethyl–formamide. The low solubility of the ligand in alcohol could be attributed to the formation of some sorts of intramolecular hydrogen bonding. The most probable structures of the ligand are illustrated in the following:

---

* Correspondence author.

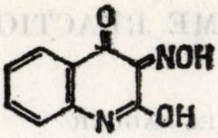

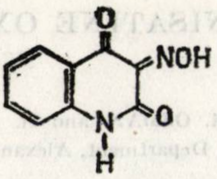

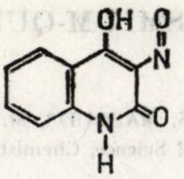

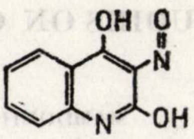

The important IR spectral bands of a KBr sample and their assignments are as follows: 3300–2700 cm^{-1} (Strong inter- or intramolecular H-bonding involving N–OH group); 3250 : ν(N–H); 3050 : ν(N–H); 2700 : ν(C–H); 1750 : ν(NOH); 1690 : ν(C=NOH); 1610 : ν($C=NO^-$); 1000 cm^{-1} : ν(N–O). The aliphatic and aromatic oximes exhibit absorptions at 3300–3100 cm^{-1} and at 1690–1620 cm^{-1} and near 939 cm^{-1}, which were assigned to bonded –OH, –C=N and N–O stretching frequencies respectively.[13] The IR spectrum of the ligand show multiple bands in the region 3300–2700 cm^{-1} indicating strong hydrogen bond involving the – NOH group in the ligand under investigation. Further down, there is a coincidence with C–H stretching vibrations. The –OH stretching vibrations of several oximes involving intramolecular or intermolecular hydrogen bonding are found to occur in 3250–2350 cm^{-1} region.[14] A salient feature of the spectra of the ligand is a strong and a sharp band at 1690 cm^{-1} which has been assigned to –OH deformation vibration of the –NOH group. The vibration of the C=N group possibly arises due to a high degree of conjugation in the ligand. The above assignment is further based on the findings of several earlier workers at different oximes such as 2-pyridine aldoxime and dimethylglyoxime.[15] The two bands traced at 3250 cm^{-1} and 3050 cm^{-1} point out the existence of –NH stretching vibration. The data depict that the compound predominates in the keto-oxime structure than in the nitrosophenolic one. The oxime group is amphiprotic, the oxime nitrogen is weakly basic[16] ($pK^{+}_{NHOH} \leqslant 2$) and the hydroxyl group is weakly acidic.[17] Proton ionization from the ligand slightly increased the basicity of the oxime nitrogen.[18] However, the presence of the metal ion leads to a complex formation that is stabilised by an increase in acidity of the oxime group.[19] A mixed solution of 3×10^{-5}M Os(VIII) and 3.6×10^{-4}M ligand showed a maximum complexation at pH 7, with $\lambda_{max} = 515$ nm. The pH of the complex solution at equilibrium is higher than the acid added. This fact could be attributed to the depression in the electropositivity of the aqueous solution, assuming the increase of the oxime tautomer to take part in the complexation for completion of the reaction. In strong alkaline solution (pH $\geqslant$ 12) there is no variation between the initial and the equilibrium pH. The solutions employed being very dilute, the probability of the existence of polynuclear species under experimental conditions was not expected to be significantly high. The molar ratio method[20] at pH 7 verified the existence of 1 : 3 species, probably in the formula $Os(HL^-)_3 . S$ (where L and S stand for the ligand and the solvent respectively). The spectra of the purple osmium–quinisatine oxime shows a regular blue shift as the pH increases suggesting that the osminate anion $OsO_4(OH)_2^{-2}$ took part in the complexation of these experimental conditions. The acid strength of a group from a ligand is increased when the ligand is coordinated to a metal through resonance stabilization of the oxime conjugate base ($=N-\bar{O}$).[21,22] A remarkable feature for the obtained electronic spectra of the ligand in the visible region (Fig. 1) is the presence

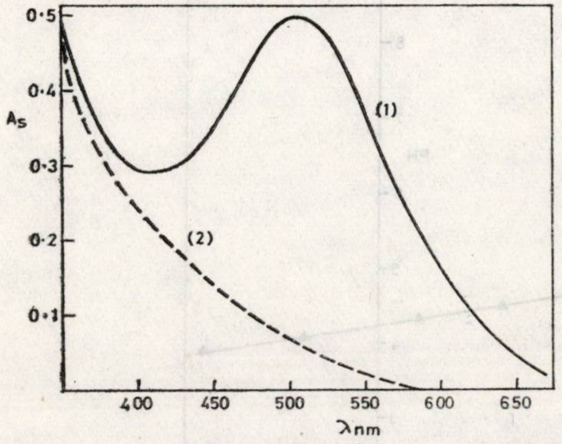

Fig. 1. — Absorption spectra of 3×10^{-5}M-Quinistaine oxime in (1) Methanol-DMF media ; (2) HCl media.

of a tail near 400 nm. This is due to the presence of a spectral band of the charge transfer type. The high molecular extinction coefficient of the compound under investigation is related to the existence of a $\pi - \pi^*$ transition. The disappearance of the maximal bands in acidic media could be attributed to the protonation of the compound with the assumption of the existence of n-π^* transition.[6] The pH increase leads to the formation of some sorts of anionic species. One step for neutralisation is apparent, indicating that the compound under investigation behaves as a monobasic acid. The variation in intensity of the electronic spectral bands at different pH values provides a mean for calculating the pH values. Using the data in the A_s-pH curve, the Colleter method [23] was applied.

$$K = \frac{[H^+]_2 - M[H^+]_3}{M-1}$$

where,

$$M = \frac{(A_s)_3 - (A_s)_1}{(A_s)_2 - (A_s)_1} \cdot \frac{[H^+]_1 - [H^+]_2}{[H^+]_1 - [H^+]_3}$$

$(A_s)_1$, $(A_s)_2$ and $(A_s)_3$ are the corresponding absorbances at their successive pH values ($pH_1 < pH_2 < pH_3$).

The average pH value obtained by this method is 4.12 ± 0.04. The limiting absorption method [4-7,9,10] gives

$$\log \frac{(A_s)_{max.} - A_s}{A_s - (A_s)_{min.}} + pH = pK$$

and plotting the logarithmic absorbance ratio at different pH's yields a straight line (Fig. 2). The slope depicts that the reaction proceeds through the liberation of 3 protons, supporting that : i) the ligand behaves as a monobasic acid, alternatively ; ii) the formation of 1 : 3 species is traced.

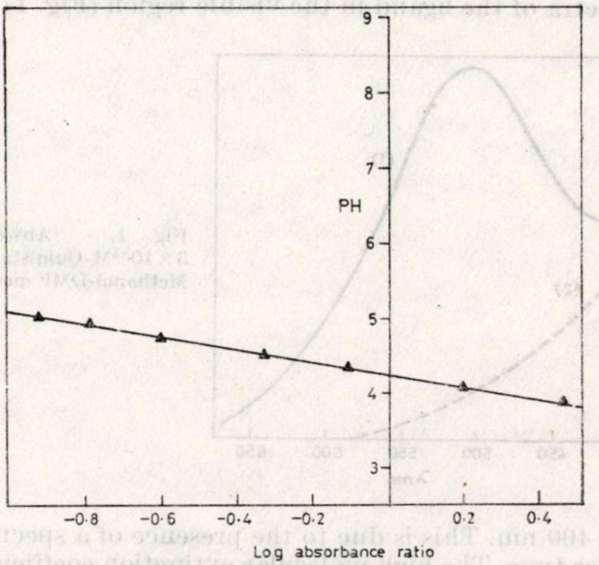

Fig. 2. — Log As — pH relationship.

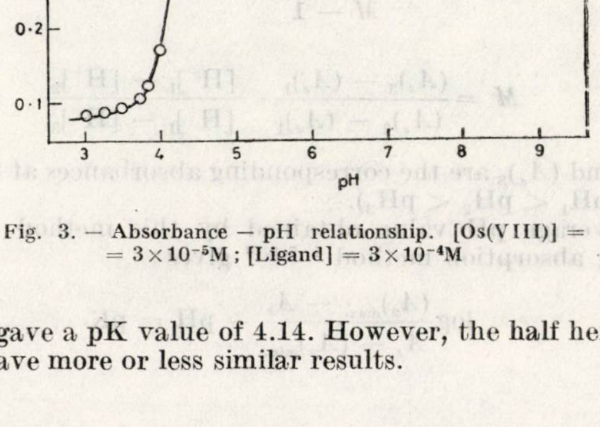

Fig. 3. — Absorbance — pH relationship. [Os(VIII)] = = 3×10^{-5}M ; [Ligand] = 3×10^{-4}M

The intercept gave a pK value of 4.14. However, the half height [24] of the A_s-pH curve gave more or less similar results.

REFERENCES

[1] R. Belcher, S. A. Ghonaim and A. Townshend, *Talanta*, **21**, 191 (1974).

[2] P. K. Bari and K. Majuwdar, *Indian J. Chem.*, **14A**, 916 (1976).

[3] D. P. Ingle and D. D. Khadikar, *Indian J. Chem.*, **14A**, 596 (1976).

[4] R. M. Issa, M. S. Masoud and S. E. Zayan, *J. Chem. UAR*, **12**, 309 (1969).

[5] S. E. Zayan, N. Ibrahim and M. S. Masoud, *Bull. Faculty of Science, Alexandria, Egypt*, **XI**, 185 (1971).

[6] M. S. Masoud, A. M. Khalil and I.I. Abdelgawad, *Indian J. Chem.*, **15(A)**, 468 (1977).

[7] M. S. Masoud, T. M. Salem and M. M. Elessawi, *Monatsh.* **109**, 221 (1978).

[8] M. S. Masoud, M. M. Osman and H. El-Naggar, *Z. analyt. Chem.* **289**, 207 (1978).

[9] M. S. Masoud, T.M. Salem and M. M. Elessawi, *J. Chem. Eng. Data* **23**, 12 (1978).

[10] M. S. Masoud and S. A. Ghonaim, *Polish J. Chem.*, **54**, 651 (1980).

[11] G. H. Ayres and T. C. Briggs, *Analyt. Chim. Acta*, **26**, 340 (1962).

[12] R. Belcher, A. Notton and A. McDonald, "Quantitative Inorganic Analysis", London, 1972.

[13] I. F. Brown, *J. Amer. Chem. Soc.*, **77**, 6431 (1965).

[14] S. Satapathy and B. Sahoo, *J. Inorg. Nuclear Chem.*, **32**, 2223 (1970); *33*, 1313 (1971).

[15] R. A. Krause, N. P. Colthup and D. H. Busch, *J. Phys. Chem.*, **65**, 221 (1961).

[16] R. G. Charles and H. Freiser, *Analyt. Chim. Acta*, **11**, 10 (1954).

[17] H. Irving, H. Rossotti and G. Harris, *Analyst*, **80**, 83 (1955).

[18] C. H. Liu and C. F. Liu, *J. Amer. Chem. Soc.*, **83**, 4169 (1961).

[19] J. H. Fraser, G. R. Hedwig, H. K. Powell and W. T. Robinson, *Austral. J. Chem.*, **25**, 747 (1972).

[20] G. N. Yoe and C. A. Jones, *Ind. Eng. Chem.*, **16**, 111 (1944).

[21] K. Lal, J. Singh and S. Gupta, *J. Inorg. Nuclear. Chem.*, **40**, 359 (1978).

[22] P. R. Murty and V. R. Rao, *Curr. Sci.*, **36**, 233 (1967).

[23] J. C. Colleter, *Ann. Chim.* (France), **5**, 415 (1960).

[24] R. A. Patrick and G. Svehla, *Analyt. Chim. Acta*, **88**, 363 (1977).

Revue Roumaine de Chimie, 26, 7, 967–970 (1981)

BISMUTH (III) — ETHYLENEDIAMINETETRAACETIC ACID COMPLEXES. III[1,2]

EXCHANGE REACTION OF Bi(III) FROM BiEDTA WITH Fe(III)

ANA NIMARĂ, ECATERINA PRINCZ and AGNETA BALINT
Chemical Research Center, Bd. Mihai Viteazul 24, Timişoara, Romania

Received November 16, 1977
Revised January 19, 1981

The kinetic study of the exchange reaction between BiEDTA complex and Fe(III) at a constant ionic strength of 0.1, over the concentration range of $1\times10^{-3}-6\times10^{-3}$ mole of each reactant and 1.50–2.30 pH range was carried out both spectrophotometrically and radiometrically. The rate was expressed by the equation :

$$R = k_1[\mathrm{BiEDTA}] + k_2\,[\mathrm{BiEDTA}][\mathrm{Fe}]$$

with $k_1 = 1.7\times10^{-3}$ min^{-1} and $k_2 = 0.6$ l·mole^{-1} min^{-1}, at 25°. Arrhenius activation energies corresponding to k_1 and k_2, evaluated by measurements at 25–80°, were found to be 11.6 kcal/mole and 3.2 kcal/mole, respectively. The exchange reaction proceeds both by a dissociative mechanism and a bimolecular direct collision process between Fe^{3+} ion and BiEDTA complex.

The study of the exchange reaction of the central ion from a complex is of particular interest for the comparison of the nature and stability of metal-ligand bonds. Although there is no simple correlation between the bond type and the exchange rate, the knowledge of the exchange mechanism, and particularly of the values of the activation energy, may provide some information concerning the nature of chemical bonds in complexes.[3,4]

It is known that EDTA forms very stable complexes both with Bi(III) and with Fe(III).[5,6] At the same time, both cations show at pH > 1, a pronounced tendency towards hydrolysis,[7,8] and those ions that hydrolyse form slowly complexes with EDTA.[9] Previous researches showed that the complexation reaction of the hydrolysed bismuth with EDTA occurs with the initial formation of some outer sphere complexes, which gradually change at different rates into inner sphere complexes. The existence of such complexes would accelerate the exchange process with Fe(III).

The present work followed up the exchange reaction of the bismuth ion from the BiEDTA complex with Fe(III), in order to determine the nature of the complex species that participate in the exchange process.

EXPERIMENTAL

MATERIALS

The bismuth and iron perchlorates were obtained by dissolving the corresponding oxides in $HClO_4$ 35 %. The iron perchlorate tagged with $^{55+59}Fe$ was obtained in a similar way. The bismuth and iron concentrations were determined by classical methods. The di-sodium salt of EDTA was reagent grade. The sodium perchlorate was of Merck purity.

PROCEDURE

The exchange rates were measured in the absence of a buffer solution (in order to avoid the supplementary complexation reactions) at a constant ionic strength of 0.1($NaClO_4$). The absorbance increase in time of the FeEDTA complex was recorded spectrophotometrically at $\lambda = 310-325$ nm, in a thermostated cell, with a Unicam SP-800 spectrophotometer. The exchange process was radiometrically studied by mixing the reactant solutions, thermostating the mixture at the needed temperature, following up the activity increase of the FeEDTA complex in time, after the precipitation with NaOH and separation of the unbound Fe^{3+} in the complex. From this solution, 20 ml were taken for activity measuring, using an electronic counter "Vakutronik VAM–16 D" with VAZ 410 G.M. tubes.

RESULTS AND DISCUSSION

The reaction system could be expressed by the equation :

$$\text{BiEDTA} + \text{Fe} \rightleftharpoons \text{FeEDTA} + \text{Bi} \qquad (1)$$

where BiEDTA and FeEDTA represent the amount of all the protonated, unprotonated and hydrolysed complexes existing in the solution. The exchange reaction rate was calculated from the absorbance, respectively from the activity values of the solution by means of the known methods.[10,11] The exchange reaction was studied at different concentrations of BiEDTA and Fe, comprised between 1×10^{-3} and 6×10^{-3} mole, in the 1.50–2.30 pH range.

The exchange reaction was observed to be of the first order with respect to the chelate concentration, of a partial order with respect to the concentration of Fe^{3+}, and independent of the concentration of hydrogen ions (figures 1 and 2).

The experimental data were found to fit a rate law of the form :

$$R\ \text{mole}\ \text{min}^{-1} = k_1[\text{BiEDTA}] + k_2[\text{BiEDTA}][\text{Fe}] \qquad (2)$$

The rate constants were evaluated by a graphical method plotting $R/[\text{BiEDTA}]$ against Fe (figure 3), and their values at 25° are as follows :

$$k_1 = 1.7 \times 10^{-3}\ \text{min}^{-1};\ k_2 = 0.6\ 1\ \text{mole}^{-1}\text{min}^{-1}$$

A comparison between the experimentally measured rate and the rate calculated from equation (2) using the above rate constants shows a good agreement. In figures 1 and 2 the solid lines have been calculated from equation (2).

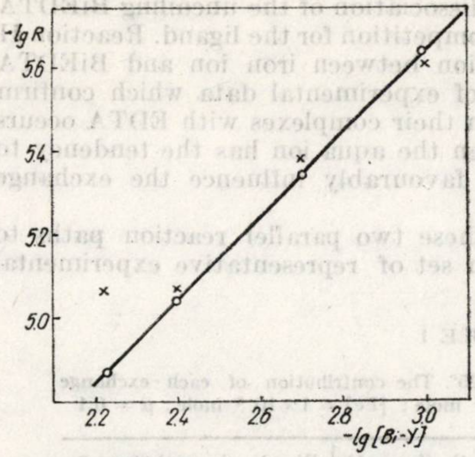

Fig. 1. — Variation of BiEDTA — Fe exchange rate with Fe(III) ion concentration; [BiEDTA] = 1×10^{-3} mole: ○ spectrophotometric values; × radiometric values.

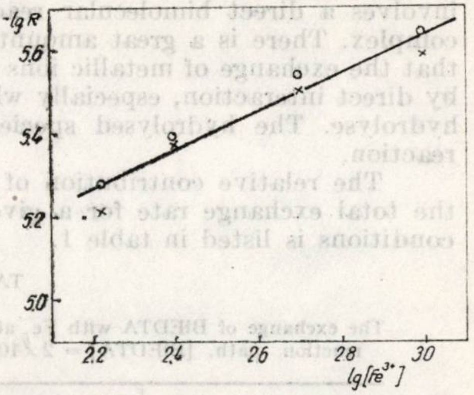

Fig. 2. — Variation of BiEDTA — Fe exchange rate with BiEDTA concentration; [Fe^{3+}] = 1×10^{-3} mole: ○ spectrophotometric values; × radiometric values.

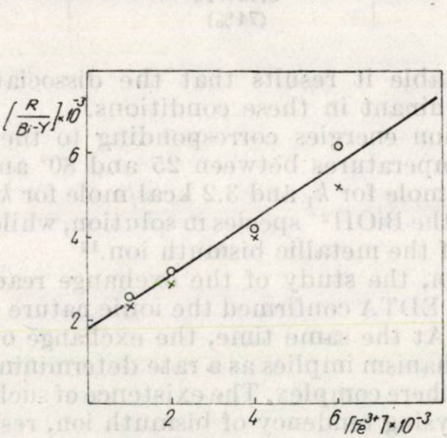

Fig. 3. — Determination of the rate constants k_1 and k_2 for the BiEDTA — Fe exchange rate: ○ spectrophotometric values; × radiometric values.

The two terms of the rate equation (2) are consistent with the following parallel reaction paths:

$$\text{BiOHEDTA} \underset{}{\overset{k_1}{\rightleftharpoons}} \text{BiOH} + \text{EDTA} \qquad \text{I}$$

$$\text{EDTA} + \text{Fe} \xrightarrow{\text{rapidly}} \text{FeEDTA}$$

$$\text{BiEDTA} + \text{Fe} \underset{H_2O}{\overset{k_2}{\rightleftharpoons}} \text{FeEDTA} + \text{BiOH} \qquad \text{II}$$

Reaction I would involve the dissociation of the uncoiling BiEDTA complex followed by the metal ions competition for the ligand. Reaction II involves a direct bimolecular reaction between iron ion and BiEDTA complex. There is a great amount of experimental data which confirm that the exchange of metallic ions in their complexes with EDTA occurs by direct interaction, especially when the aqua ion has the tendency to hydrolyse. The hydrolysed species favourably influence the exchange reaction.

The relative contribution of these two parallel reaction paths to the total exchange rate for a given set of representative experimental conditions is listed in table 1.

TABLE 1

The exchange of BiEDTA with Fe at 25°. The contribution of each exchange reaction path. [BiEDTA] = 2×10^{-3} mole ; [Fe] = 1×10^{-3} mole ; $\mu = 0.1$

Total reaction rate mole/l per sec	Dissociation path (term 1) mole/l per sec	Bimolecular path (term 2) mole/l per sec
4.57×10^{-6} (100 %)	3.40×10^{-6} (74 %)	1.17×10^{-6} (26 %)

From this table it results that the dissociation of the BiEDTA complex is predominant in these conditions.

The activation energies corresponding to the rate constants were determined at temperatures between 25 and 80° and have the following values : 11.6 kcal/mole for k_1 and 3.2 kcal/mole for k_2. The 11.6 kcal/mole value is typical of the $BiOH^{2+}$ species in solution, while that of 3.2 kcal/mole is characteristic of the metallic bismuth ion.[12]

In conclusion, the study of the exchange reaction of metallic ions in complexes with EDTA confirmed the ionic nature of the chemical bonds in these chelates. At the same time, the exchange occurring according to a dissociative mechanism implies as a rate determining step the decomposition of the outer sphere complex. The existence of such a complex is possible due to the hydrolysing tendency of bismuth ion, respectively to the competition for the two ligands OH and EDTA.

REFERENCES

[1] C. Drăgulescu, A. Nimară and I. Julean, *Rev. Roumaine Chim.*, **21**, 853 (1976).
[2] C. Drăgulescu, A. Nimară, E. Princz, A. Balint and I. Julean, *Rev. Roumaine Chim.*, **21**, 1171 (1976).
[3] M. Haissinsky and C. Dandel, *Bull. Soc. chim. France*, **1947**, 552.
[4] D. R. Stranks and R. G. Wilkins, *Chem. Rev.*, **57**, 743 (1957).
[5] B. G. Sochevanov and G. A. Volkova, *Zhur. neorg. Khim.*, **1**, 118 (1969).
[6] S. S. Jones and F. A. Long, *J. Phys. Chem.*, **56**, 25 (1952).
[7] A. Olin, *Acta Chem. Scand.*, **13**, 1791 (1959).
[8] R. M. Milburn and W. C. Vosburgh, *J. Amer. Chem. Soc.*, **77**, 1352 (1955).
[9] D. W. Margerum, *J. Phys. Chem.*, **63**, 336 (1959).
[10] H. A. McKay, *Nature*, **142**, 997 (1938).
[11] R. E. Jervis and S. S. Krishnan, *J. Inorg. Nuclear Chem.*, **29**, 97 (1967).
[12] C. Drăgulescu, A. Nimară and I. Julean, *Rev. Roumaine Chim.*, **18**, 583 (1973).

Revue Roumaine de Chimie, 26, 7, 971–977 (1981)

HETEROPOLYTUNGSTATES WITH Ti (IV) AND Ni (II). II[1]

THE SYNTHESIS AND BASICITY OF HETEROPOLYANIONS $[H_2ONiTiW_{11}O_{39}]^{6-}$ and $[H_2ONiTiW_5O_{20}]^{4-}$

RODICA VĂŢULESCU, T. BUDIU and GH. MARCU
Institute of Chemistry, 65–103, Str. Donath, Cluj-Napoca, Romania

Received September 30, 1980

The present work deals with the synthesis, analysis and determination of the basicity of heteropolyanions $[H_2ONiTiW_{11}O_{39}]^{6-}$ (I) and $[H_2ONiTiW_5O_{20}]^{4-}$ (II), as well as with the preparation of their Na^+, K^+, NH_4^+, Tl^+, Ba^{2+} and guanidinium salts.

INTRODUCTION

This note is a continuation of our studies[1] on the formation conditions of two new heteropolyanions: $[H_2ONiTiW_{11}O_{39}]^{6-}$ and $[H_2ONiTiW_5O_{20}]^{4-}$. These belong to two distinct classes of compounds: the former to the 2 :11 series, and the latter to the 2 :5 series, both characterized by the fact that they have two heteroatoms in the anions.

It is now unanimously accepted that the compounds of the 2 :11 heteropolytungstates series are formed by addition of the transition metal ions, M^{m+}, to the lacunary structures of the type $[X^{x+}W_{11}O_{39}]^{(12-x)-}$, in order to form mixed heteropolyanions $[X^{x+}M^{m+}W_{11}O_{39}]^{(12-m-x)-}$.[2-6]

In the case of heteropolyanion II, belonging to the 2 :5 series, we previously showed[1] that it is formed as a result of an addition reaction of the same type as the one occurring in the case of the 2 :11 series, having a lacunary structure, according to Michelon and Herve.[7]

The heteropolyanions of the type 2 :11 being now a well characterized class of heteropolycombinations with many representatives, and taking into account the fact that many elements can function as heteroatoms X and M, it was attempted in the literature to give general synthesis procedures,[2,3,8] which can be systematized as follows:

a) One group of such procedures has as a first step the preparation of the potassium salt of unsaturated anions XW_{11} (X = P, Si, Ge, B), from solutions containing the element X and potassium tungstate in molar ratio 1 :11 at pH = 6.3,[3,8] followed by the addition of a solution which contains the second transition element M.

b) According to another method, conditions are used in which the 1 :12 anions undergo a partial degradation to an unsaturated 1 :11 (XW_{11}) compound, which is then treated with the solution of the element M^{m+}.[2,3,8]

c) Finally, a third method starts with the alkali tungstate whose pH was corrected to the value of ≃ 6.3, followed by the addition of the element

X, sometimes in a higher quantity than the stoichiometry of the reaction asks for. The resulting solution is then slowly added to the solution of the cation M^{m+}.[8]

The most advantageous of the above three methods is the degradation method, because it results in complexes of a higher purity, but its applicability is limited only to the representatives of the 1:12 series which undergo a partial degradation as a function of the pH. The anions of the type XMW_{11}, where X = B, Zn,[8] cannot be obtained by the degradation method.

However, none of these general procedures can be used to obtain anions $[H_2ONiTiW_{11}O_{39}]^{6-}$ (I) and $[H_2ONiTiW_5O_{20}]^{4-}$ (II) (where $X = Ti^{4+}$ and $M = Ni^{2+}$), and we had to work out other synthetical methods in order to prepare them.

Thus, taking into consideration the results of our previous studies [1] dwelling on the formation conditions of these anions as a function of pH, temperature and time, correlated with the data existing in the literature on the various syntheses of heteropolytungstates,[3,7-11] we prepared first the sodium salts of anions I and II in solution. Other salts were synthetized and isolated afterwards from these solutions.

According to the spectrophotometric titration,[1] after the preparation of the unsaturated anions TiW_{11} at pH = 5 and TiW_5 at pH = 7.5, in solution, heteropolyanions $[H_2ONiTiW_{11}O_{39}]^{6-}$ and $[H_2ONiTiW_5O_{20}]^{4-}$ are formed by addition of the Ni^{2+} ions to the above mentioned unsaturated anions, in the stoichiometric ratio of 1:1.

However, it was experimentally observed that the synthesis is better achieved when a slightly different procedure is used. Thus, a mixture of Ni^{2+} and Ti^{4+} ions is added to the solution of sodium tungstate, at room temperature. Then the pH is corrected to the value necessary to form the complex, so that the anion TiW_{11} (or TiW_5), generated in the system, should react immediately with the Ni^{2+} ions already present in the solution; this procedure is different from those reported in the literature, where the pH is corrected first, and only afterwards the metallic ions, M^{m+}, are added.[3,8]

In the case of the second heteropolyanion with Ti(IV) and Ni(II), although the study of its formation indicated that the reaction takes place with stoichiometric amounts of reactants, in order to obtain better synthesis yields it is necessary to use an excess of Na_2WO_4 and to work in more diluted solutions than for anion I. It was also observed in both cases that it is better to work on relatively small quantities of substances (15–20 g $Na_2WO_4 . 2H_2O$), repeating the experiment if larger amounts are needed.

On the basis of the above considerations, the synthesis procedure described in the experimental part was arrived at.

EXPERIMENTAL

ANION $[H_2ONiTiW_{11}O_{39}]^{6-}$

Sodium salt. A solution of 20 g $Na_2WO_4 . 2H_2O$ in 100 ml water (C = 0.6 M) was treated at room temperature with a solution containing 2.08 ml $TiCl_4$ (T = 0.1278 g Ti/ml) and 1.6 g $Ni(NO_3)_2$ in 80 ml water (molar mixture 1 : 1 : 11). From the very beginning the metallic hydroxides were formed ; but correcting the pH to the value of $\simeq 5.0$ with acetic acid and stirring the mixture continuously at 70°C, it cleared up after 15—20 minutes. The solution was refluxed while stirring for about $4-4^1/_2$ hours, taking care that the pH be maintained at the value of $\simeq 5$ over the whole synthesis process.

This yellowish-green solution contains the sodium salt of heteropolyanion I, which is extremely soluble and does not crystallize, but when allowed to stand for a while it solidifies, forming a glass-like mass.

From the solution of the sodium salt of anion I were prepared, by exchange, the less soluble potassium and ammonium salts as well as the poorly soluble salts of Tl^+, Ba^{2+} and guanidinium ions.

Potassium salt. An excess of 38 % KCl solution was added to a hot solution of the sodium salt of anion I. At the beginning, by cooling, a white precipitate was separated (potassium isopolytungstate), which was removed by filtration. From the yellowish-green filtrate the potassium salt of anion $[H_2ONiTiW_{11}O_{39}]^{6-}$ crystallized at room temperature ; it was then purified by repeated crystallizations from water.

Ammonium salt. It was obtained in the same way by using a 50 % solution of NH_4CH_3COO, in excess.

A $\simeq 35$ % yield was obtained in both syntheses.

Barium salt. The hot solution of the potassium salt of anion I was treated with a solution containing $BaCl_2$ until complete precipitation, followed by filtration of the warm reaction mixture. The white-yellowish poorly soluble barium salt was washed several times on the filter with warm water and dried at room temperature.

The thallium salt (white-yellowish poorly soluble precipitate) was similarly prepared by using $TlCH_3COO$ solutions.

The guanidinium salt (yellowish-green poorly soluble precipitate) was similarly prepared by using an excess of a 40 % solution of guanidinium hydrochloride at pH = 5.

ANION $[H_2ONiTiW_5O_{20}]^{4-}$

Sodium salt. A solution containing 2.08 ml $TiCl_4$ (T = 0.1278 g Ti/ml) and 1.6 g $Ni(NO_3)_2$ in 100 ml water (equimolar mixture Ni :Ti) was added at room temperature, under continua stirring, to 100 ml of a 15 % (C = 0.45 M) solution of $Na_2WO_4 . 2H_2O$. The pH of the synthesis mixture was corrected first to $\simeq 6.5$ with acetic acid and the mixture was heated at 60—70°C for about 30 minutes.

The clear solution thus obtained was treated with 10 % Na_2CO_3 to bring the pH to the value of 7.5. Then it was refluxed for one hour, taking care that all this time the pH be maintained rigorously at the value of 7.5. Thus, the yield of the synthesis amounts to 15—20 %, whereas when the adjustment of the pH is made directly at 7.5 without passing through the intermediary phases of heating at pH = 6.5, the yield is smaller ($\simeq 10$ %).

The solution was then allowed to stand for 24 hours, during which time sodium isopolytungstate and a crystalline blue compound separated, the latter being almost insoluble. The filtration yielded a green solution containing the sodium salt of anion II. This salt, easily soluble in water, but less soluble than the sodium salt of anion I, is separated from the solution by crystallization at room temperature. Its purification was carried out by repeated crystallizations from water.

The potassium, ammonium, thallium and barium salts of anion II were prepared in the same way as described before in the case of the salts of anion I, but at pH = 7.2—7.5.

The potassium and ammonium salts of anion $[H_2ONiTiW_5O_{20}]^{4-}$ are crystalline, soluble in water, of a light green colour, while the thallium, barium and guanidinium salts are almost insoluble in water.

The guanidinium salt of anion II was obtained at pH = 5 like in the case of anion I (at a higher pH the guanidinium itself precipitates), but the pH of the solution was only adjusted before precipitation.

ANALYSIS

The chemical analysis of the above mentioned salts was carried out by using known chemical and physico-chemical methods. We started by decomposing the heteropolycompounds under discussion in alkaline medium under boiling, when the precipitation of the Ti^{4+} and Ni^{2+} ions takes place and tungsten remains in solution in the form of soluble WO_4^{2-}. After filtration nickel and titanium were solved in warm 2M H_2SO_4 and, on suitable aliquots, Ti^{4+} was determined colorimetrically with H_2O_2, and Ni^{2+} was assayed complexometrically.

We found out that the two ions (Ni^{2+} and Ti^{4+}) can be determined, in each other's presence, by the mentioned methods but in the case of nickel determination, in order to have a clear-cut colour change, the Ti^{4+} ions were complexed beforehand with sodium tartrate.

Tungsten was determined gravimetrically as WO_3, potassium and sodium flame-photometrically and ammonium by the micro-Kjeldahl method.

Thallium and barium were determined gravimetrically as iodide and sulfate, respectively.

The guanidinium cation was determined by elemental microanalysis (C, N, H).

The crystallization water was determined thermogravimetrically for the potassium, sodium and ammonium salts of anions $[H_2ONiTiW_{11}O_{39}]^{6-}$ and $[H_2ONiTiW_5O_{20}]^{4-}$. For the thallium, barium and ammonium salts of the two heteropolyanions the crystallization water was determined from the weight decrease recorded after heating them for one hour, in the oven, at 200°C.

The results of the chemical analyses are presented in table 1.

BASICITY

In order to determine the basicity of anions I and II, besides the data furnished by the chemical analyses of the insoluble salts (those of Tl^+, Ba^{2+} and guanidinium) we carried out conductometric titrations of the solutions of potassium and ammonium salts of anion I and of the sodium salt of anion II with solutions of thallium acetate.

For the potassium salt of anion I 10 ml complex solution (T = 0.002537 g W/ml) of pH $\simeq$ 5 were titrated with a 5.10^{-2}M solution of $TlCH_3COO$ (T = 0.01001 g Tl/ml). The measurements were made with a Radelkis type OK-102 conductometer.

The titration curve of the potassium salt of anion I is represented in figure 1. It is observed that the inflection point (E) corresponds to a consumption of 1.5 ml $TlCH_3COO$, indicating a stoichiometric ratio of 5.85 Tl^+ :11 W, that is, this salt has a basicity of 6.

In the case of the ammonium salt of anion I we worked in the same way, on samples of 10 ml complex solution (T = 0.002388 g W/ml), which were titrated with a solution of $TlCH_3COO$ (T = 0.01001 g Tl/ml).

For the NH_4^+ salt of anion I, the same as for the potassium salt, we obtained a graphical representation of conductivity as a function of the consumption of $TlCH_3COO$ in the form of two straight lines which cross at the point corresponding to E = 1.48 ml $TlCH_3COO$. This gives the ratio Tl :W = 6.13 :11, so that in the case of the ammonium salt of anion I practically the same basicity was obtained as for the potassium salt.

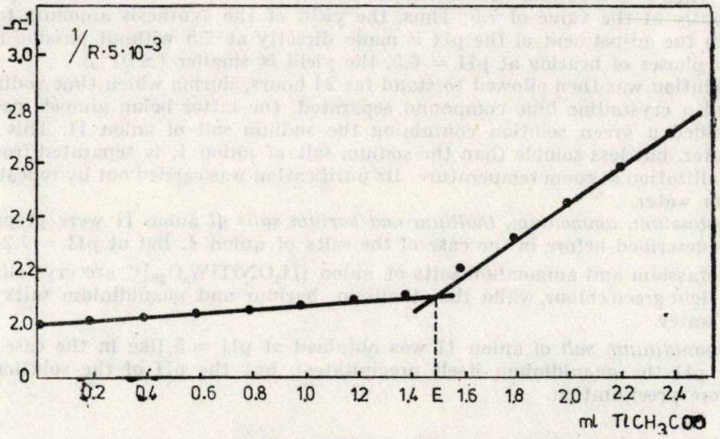

Fig. 1. — The conductometric titration of the solution of $K_6[H_2ONiTiW_{11}O_{39}]$ (T = 0.002537 g W/ml) with a solution of $TlCH_3COO$ (T = 0.01001 g Tl/ml).

For the determination of the conductometric basicity of anion II we used samples of 5 ml sodium salt solution (of complex II) (T = 0.002629 g W/ml), pH $\simeq$ 7.2, which were diluted afterwards with an equal volume of water and were titrated in the same way as before with a solution of $TlCH_3COO$. The results of this titration are illustrated in figure 2.

TABLE 1

Chemical analysis of the salts of heteropolyanions $[H_2ONiTiW_{11}O_{39}]^{6-}$ (I) and $[H_2ONiTiW_5O_{20}]^{4-}$ (II)

Compound		%									
		W	Ti	Ni	H_2O cryst.	K^+	NH_4^+	Na^+	Tl^+	Ba^{2+}	$[CN_3H_6]^+$
$K_6[H_2ONiTiW_{11}O_{39}] \cdot 13H_2O$	Calcd.	62.4	1.478	1.81	7.23	7.24					
	Found.	62.05	1.45	1.74	7.195	7.35					
$(NH_4)_6[H_2ONiTiW_{11}O_{39}] \cdot 11,5H_2O$	Calcd.	65.48	1.55	1.90	6.7		3.497				
	Found	66.06	1.53	1.93	6.75		3.5				
$Tl_6[H_2ONiTiW_{11}O_{39}] \cdot 3H_2O$	Calcd.	49.69	1.177	1.44	1.77				30.13		
	Found	49.45	1.15	1.43	1.87				29.2		
$Ba_3[H_2ONiTiW_{11}O_{39}] \cdot 6H_2O$	Calcd.	61.11	1.447	1.77	3.8					12.45	
	Found	60.82	1.42	1.79	3.76					12.72	
$(CN_3H_6)_6[H_2ONiTiW_{11}O_{39}] \cdot 4H_2O$	Calcd.	62.78	1.487	1.82	2.8						11.17
	Found	62.44	1.46	1.73	2.86						11.12
$Na_4[H_2ONiTiW_5O_{20}] \cdot 9H_2O$	Calcd.	56.81	2.96	3.62	10.01			5.68			
	Found	56.76	2.90	3.63	9.99			5.79			
$K_4[H_2ONiTiW_5O_{20}] \cdot 10H_2O$	Calcd.	54.06	2.817	3.45	10.58	9.17					
	Found	54.18	2.72	3.33	10.60	9.30					
$(NH_4)_4[H_2ONiTiW_5O_{20}] \cdot 9H_2O$	Calcd.	57.51	2.99	3.67	10.13		4.50				
	Found	57.32	2.90	3.55	10.08		4.62				
$Tl_4[H_2ONiTiW_5O_{20}] \cdot 2H_2O$	Calcd.	41.13	2.14	2.63	2.41				36.50		
	Found	41.20	2.10	2.60	2.30				35.80		
$Ba_2[H_2ONiTiW_5O_{20}] \cdot 2,5H_2O$	Calcd.	54.07	2.80	3.43	4.21					16.10	
	Found	54.60	2.74	3.45	3.91					16.70	
$(CN_3H_6)_4[H_2ONiTiW_5O_{20}] \cdot 3H_2O$	Calcd.	54.85	2.86	3.50	4.29						14.30
	Found	54.57	2.75	3.44	4.13						13.90

It is observed that in this case the inflection point E, which marks the total replacement of the natrium ions by thallium ions, was obtained at a consumption corresponding to a stoichiometric ratio of 4.18 Tl :5 W, that is basicity 4.

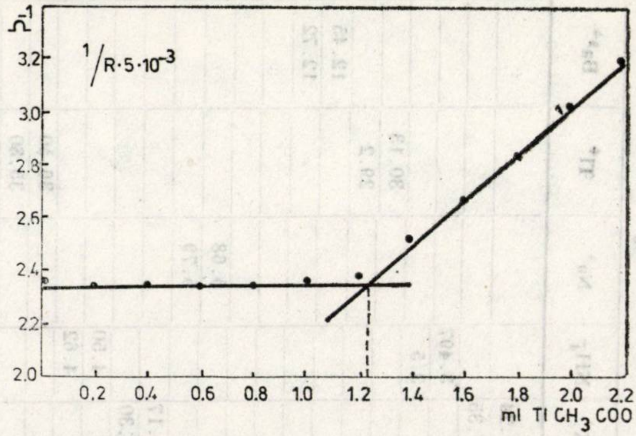

Fig. 2. — The conductometric titration of the solution of $Na_4[H_2ONiTiW_5O_{20}]$ (T = 0.002629 g W/ml) with a solution of $TlCH_3COO$ (T = 0.01001 g Tl/ml).

RESULTS AND DISCUSSION

By the synthesis and analysis of the K^+, NH_4^+, Na^+, Tl^+, Ba^{2+} and guanidinium salts of anions $[H_2ONiTiW_{11}O_{39}]^{6-}$ and $[H_2ONiTiW_5O_{20}]^{4-}$ it was proved that it is possible to isolate stable salts of these anions.

Taking into consideration the results of our previous study,[1] as well as those mentioned above referring to the chemical analysis and the basicity of the two new compounds, we formulated them as follows: I : $[H_2NiO_6TiO_4W_{11}O_{30}]^{6-}$ or $[H_2ONiTiW_{11}O_{39}]^{6-}$ in agreement with Baker and Figgis,[12] and II : $[H_2ONiTiW_5O_{20}]^{4-}$ in agreement with Michelon and Herve.[7]

As will be shown in a future note, heteropolyanion I has a modified "Keggin" structure. This necessarily implies the existence of two protons in the complex anion, required by the compensation of two supplementary negative charges. These appear as a consequence of the replacement in the conventional "Keggin" structure of a tungsten atom with a nickel one. Indeed, if it were not so, then according to the structural principles which ensure the valency and coordinative saturation of the tungsten-oxygen frame of "Keggin" heteropolytungstates, heteropolyanion I would have basicity 8. But according to the chemical analyses and the determination of basicity, it was found that the charge of anion I is 6, in agreement with Baker et al's theoretical prediction [13] referring to the necessary presence of two protons in the anions, which may occur in the form of a molecule of constitutional water.

Afterwards, it was shown [12,14] that the molecule of constitutional water can be replaced by other neutral or anionic ligands.

The direct proof of the presence of a molecule of constitutional water in heteropolyanions I and II, as formulated previously, was brought by thermogravimetric studies and by IR absorption spectra recorded at different temperatures, and will be presented in a further note.

REFERENCES

[1] R. Vățulescu, T. Budiu and Gh. Marcu, *Rev. Roumaine Chim.*, **26**, 851 (1981).
[2] T. J. R. Weakley and S. A. Malik, *J. Inorg. Nuclear Chem.*, **29**, 2935 (1967).
[3] C. M. Tourne and G. Tourne, *Bull. Soc. chim. France*, **4**, 1124 (1969).
[4] O. W. Rollins, *J. Inorg. Nuclear Chem.*, **33**, 75 (1971).
[5] Gh. Marcu, M. Rusu and L. Ochișel, *Rev. Roumaine Chim.*, **22**, 849 (1977).
[6] C. M. Tourne and G. Tourne, *Rev. Chim. Miner.*, **14**, 83 (1977).
[7] Monique Michelon and G. Herve, *Compt. rend.*, **274**, 209 (1972).
[8] C. M. Tourne, G. Tourne, S. A. Malik and T. J. R. Weakley, *J. Inorg. Nuclear Chem.*, **32**, 3875 (1970).
[9] R. Ripan, A. Duca, D. Stănescu and M. Pușcașiu, *Z. anorg. Chem.*, **347**, 333 (1966).
[10] C. M. Tourne and G. Tourne, *Compt. rend.*, **266**, 702 (1968).
[11] C. M. Tourne and G. Tourne, *Compt. rend.*, **266**, 1363 (1968).
[12] L. C. W. Baker and J. S. Figgis, *J. Amer. Chem. Soc.*, **92**, 3794 (1970).
[13] L. C. W. Baker, V. Simmons-Baker, K. Eriks, M. T. Pope, M. Shibata, O. W. Rollins, J. H. Fang and L. L. Koh, *J. Amer. Chem. Soc.*, **88**, 2329 (1966).
[14] T. J. R. Weakley, *J. Chem. Soc. Dalton Trans.*, **3**, 341 (1973).

Revue Roumaine de Chimie, **26**, 7, 979–983 (1981)

STUDIES OF THE REACTIONS OF ARYL PROPENE OXIDES IN BASIC MEDIA. II[1].*

REACTIONS OF SOME *o*-SUBSTITUTED EPOXIDES COMPARED TO *p*- AND *m*-SUBSTITUTED ANALOGUES

M. HASSAN, A. R. O. ABDEL NOUR, A. M. SATTI and I. A. WAKEEL
Chemistry Department, University of Khartoum, P.O. Box 321, Khartoum, Sudan

Received October 16, 1978
Revised February 10, 1981

The reaction of aryl propene oxides, with different single substituents at *para*-, *meta*-, or *ortho*-positions, with excess potassium tert-butoxide in tert-butanol, was investigated kinetically at 60°C. The observed rates of these reactions were found to follow first order kinetics.

The order of reactivity was found to follow the sequence :

$$p\text{-NO}_2 > o\text{-Cl} > m\text{-F} > m\text{-Br} > p\text{-Br} > m\text{-OCH}_3 > o\text{-CH}_3 >$$

$$> p\text{-CH(CH}_3)_2 > o\text{-OCH}_3$$

which is consistent with the polar effect of the substituents, a pattern previously established by the same authors.[1]

A Hammett plot of the relative rates of reactions versus σ-values rendered a straight line with a ρ value of $+2.14$, in accordance with the determined sequence of reactivity.

The postulated mechanism of the reactions is a concerted one, involving a proton—abstraction from the carbon atom α to the benzene ring producing a carbanion, followed by the epoxide ring-opening to give the corresponding cinnamyl alcohol. This mechanism is similar to that established for the isomerisation of aryl propenes under similar basic conditions.[2]

In product analysis, the unsubstituted compound produced cinnamyl alcohol in very high yield ($\sim 80\%$).

Like three-membered rings generally, the oxirane ring system is highly strained and opens readily. Ring opening is especially facile in the presence of acids,[3] the product being a 1,2-diol.

The acid-catalyzed reaction is essentially a carbonium ion reaction, and tends to occur at the ring carbon atom that would produce the more stable carbonium ion; i.e. the reaction with solvent occurs at the more highly substituted ring carbon atom.

---

* Paper to appear also in *Libyan J. Sci.*

Ring opening can also be accomplished with a base in an S_N2 displacement reaction :

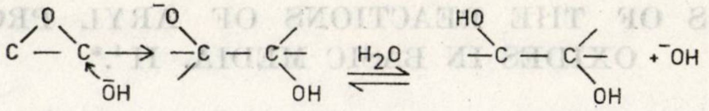

As in other S_N2 reactions, it is subject to steric influences, and the reaction occurs at the less hindered carbon atom.

In certain cases, a strong base may induce the formation of allylic products from epoxides. Cope and co-workers[4] have shown that *cis*- and *trans*-4-octene oxides with lithium diethylamide, gave trans-5-octen-4-ol, mainly by removal of a proton from α-carbon atom to the oxirane ring, rather than by removal of a proton on the ring generating a carbene intermediate.

When unsymmetrical open-chain epoxides are involved, proton-abstraction occurs readily from the least substituted carbon, with large factors separating primary from secondary from tertiary proton abstraction.[5] Thus, of the two possible isomers, 2-pentene oxide reacts to give 1-penten-3-ol and 2-methyl-3-heptene oxide gives 2-methyl-4-hepten-3-ol exclusively, both being the allylic alcohol products formed by abstraction of a proton from a primary carbon (as preferred to secondary), and from a secondary carbon (as preferred to a tertiary), respectively.

EXPERIMENTAL

PREPARATION AND PURIFICATION OF MATERIALS

Aryl propene oxides were prepared in two steps :

Firstly : The aryl propene was prepared in a Grignard reaction in dry ether by coupling substituted phenyl magnesium bromides with allyl bromide in accordance with Martin and Gleicher's method.[6]

Secondly : The olefin was epoxidized in chloroform solution by using perbenzoid acid.[7] *m*-Methoxyphenylpropene oxide was prepared in 40% yield by this method, had b.p· 68°/0.1 mm Hg, n_D^{25} 1.5279 : IR maxima (wave number) : 780 (s), 840 (m), 920 (w), 1265 (s) ;

Found : C, 72.87% ; H, 7.49% ; $C_{10}H_{12}O_2$ requires : C, 73.17% ; H, 7.32%. *o*-Methylphenyl propene oxide (59% yield), b.p. 41.5° at 0.45 mm Hg ; n_D^{25} 1.5299 ; IR maxima : 745 (s), 825 (s), 935 (m), 970 (m), 1260 (m) ; Found : C, 81.02% ; H. 8.20% ; $C_{10}H_{12}O$ requires : C, 81.08%, H, 8.11%. *o*-Methoxy phenyl propene oxide (62% yield) ; b.p. 80–81° at 0.1 mm Hg ; $n_D^{24.5}$ 1.5300 ; IR maxima : 755 (s), 825 (s), 845 (s), 935 (m), 1245 (s) ;

Found : C, 72.57% ; H, 7.47% ; $C_{10}H_{12}O_2$ requires :

C, 73.17% ; H, 7.32%. *o*-Chlorophenylpropene oxide : (56%) ; b.p. 70–72° at 0.1 mm Hg ; $n_D^{26.5}$ 1.5505 ; IR maxima : 755 (s), 825 (s), 850 (s), 935 (m), 1260 (m) ; Found : C, 63.96% ; H, 5.37% ; Cl, 20.83% ; C_9H_9ClO requires : C, 64.09% ; H, 5.34% : Cl, 21.04%. *m*-Fluorophenylpropene oxide : (57%) ; b.p. 47° at 0.02 mm Hg ; $n_D^{25.5}$ 1.5005 ; IR maxima : 785 (s), 845 (s), 940 (m) 1250 (s) ;

Found : C, 70.94% ; H, 6.07% ; C_9H_9FO requires : C, 71.05% ; H, 5.92%. *p*-Bromophenylpropene oxide : (49%) ; b.p. 100–104° at 0.35 mm Hg. n_D^{26} 1.5749 ; IR maxima : 800 (s), 835 (s), 935 (m), 1260 (m) ; Found : C, 49.08% ; H, 4.27% ; C_9H_9BrO requires : C, 50.70% ;

H, 4.22%. *p*-Isopropyl—phenyl propene oxide : (72%); b.p. 89—90° at 0.15 mm Hg., n_D^{25} 1.5115 ; IR maxima : 765 (s), 835 (s), 1260 (m) ; Found : C, 80.86% ; H, 9.05% ; $C_{12}H_{16}O$ requires : C, 81.81%; H, 9.09%. *m*-Bromo phenyl propene oxide : (54%); b.p. 66° at 0.1 mm Hg.; n_D^{26} 1.5835 ; IR maxima 780 (s), 835 (m), 855 (m), 940 (w), 1260 (m); Found : C, 50.20%; H, 4.92% : C_9H_9BrO requires : C, 50.70% ; H, 4.22%. *p*-Nitro phenyl propene oxide (epoxidized by peracetic acid in chloroform ; and the nitro compound itself being prepared by the nitration of phenyl propene) ; [8] b.p. 109—111° at 1 mm Hg ; Found : C, 60.21% ; H, 4.98% ; N, 7.88% ; Calculated for $C_9H_9NO_3$: C, 60.13% ; H, 5.20% ; N, 7.98%.

Stock solutions of epoxides were made by taking a weighed amount of epoxide in a certain volume of purified t-butanol.[9] A stock solution of potassium tert-butoxide was similarly prepared by dissolving a weighed amount of potassium metal in a known volume of alcohol, and standardizing it by titration against hydrochloric acid using phenolphthalein as indicator.

KINETIC RUNS :

The final concentration in the reaction mixture was adjusted so that the epoxide was in the order of 8×10^{-3}M, and the butoxide was in the order of 9×10^{-2}M, i.e. pseudo-first order conditions.

The two solutions were then thermostated at 60°C for enough time before being mixed in a two-necked flask fitted with a condenser and a guard tube of silica gel. At convenient time intervals, aliquots of reaction solution were pipetted out and quenched by diluting with ethanol in volumetric flasks to give a final concentration of 10^{-6}M.

Solutions were then run in a Unicam SP 800 spectrophotometer using 1—cm wide silica cells and ethanol in reference cell. The absorbance of these solutions at a wavelength in the region of 250 nm gave values of A_t (absorbance at time *t*). Using first-order relationship :

$$kt = 2.303 \log_{10} \frac{A_\infty}{A_\infty - A_t}$$

a plot of $\log_{10} A_\infty / A_\infty - A_t$ versus time rendered a straight line, which was utilised to calculate *k* by using :

$$k = \text{slope} \times 2.303$$

Table 1 includes *k* values for different epoxides :

TABLE 1

Rate constants of different substituted aryl propenes

Substituent "X"	k ; s^{-1}	Substituent "X"	k ; s^{-1}
p-NO_2	1.94×10^{-3}	*m*-OCH_3	4.289×10^{-5}
o-Cl	5.030×10^{-4}	*m*-CH_3	3.159×10^{-5}
m-Cl	4.354×10^{-4}	*p*-CH_3	3.096×10^{-5}
p-Cl	2.230×10^{-4}	*o*-CH_3	2.612×10^{-5}
m-F	1.813×10^{-4}	*p*-$CH(CH_3)_2$	1.8999×10^{-5}
m-Br	1.656×10^{-4}	*p*-$C(CH_3)_3$	1.590×10^{-5}
H	8.770×10^{-5}	*p*-OCH_3	7.117×10^{-6}
p-Br	8.224×10^{-5}	*o*-OCH_3	1.864×10^{-6}
p-F	5.782×10^{-5}		

Rate constants for *m*-fluoro-substituent with ;

i) K^+-isopropoxide 1.010×10^{-4}

ii) KOEt 6.525×10^{-6}

DISCUSSION

KINETICS AND MECHANISM :

The reaction was found to follow pseudo-first order kinetics as shown by the constancy of the rate coefficients through the course of a single run.

The reaction in question is postulated to follow the same mechanism as given before :[1]

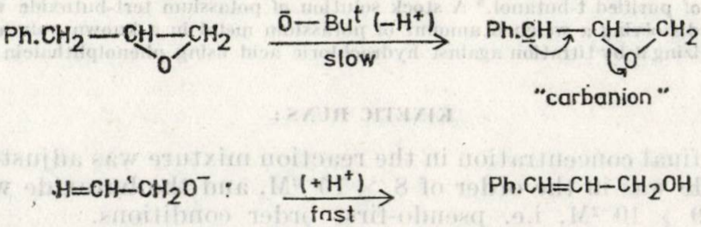

This is a two-stage concerted mechanism, where the production of the allylic alcohol is preceded by proton abstraction from the carbon atom α to the oxirane ring. The carbanion thus produced, rearranges to the products.

Evidence in support of this mechanism is three-fold :

(i) Failure of 3-methyl-3-phenyl-1,2-epoxybutane to eliminate allylic product under similar conditions instead of a hydroxyether was identified.

(ii) *Cis*- and *trans*-octene oxide-4,5-D$_2$ reacted exclusively by a similar carbanion mechanism as follows :[4]

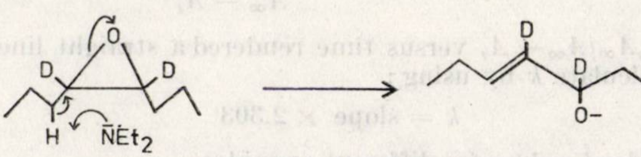

The similarity between the two reagents (NEt$_2^-$ and Ō—tBu) is evident.

(iii) Further evidence was obtained from the reaction of *m*-fluoro-3-phenyl-1,2-epoxypropane with different bases, i.e., $^-$O—tBu, $^-$O—ih and $^-$O—Et at 60°C (see Table 1).

The rate of the reaction was found to increase with the strength of the base.

SUBSTITUENT EFFECTS :

The following order of reactivity was observed for this reaction :

p-NO$_2$ $>$ o-Cl $>$ m-Cl $>$ p-Cl $>$ m-F $>$ m-Br $>$ H $>$ p-Br $>$ p-F $>$
m-OCH$_3$ $>$ m-CH$_3$ $>$ p-CH$_3$ $>$ o-CH$_3$ $>$ p-iso-pr. $>$ p-t-Bu $>$ p-OCH$_3$
m-F $>$ o-OCH$_3$

in which, the electrical effects, i.e. inductive and mesomeric, seem to influence the rate to a great extent. As a general theme, those groups which have − I effect facilitate the reaction as compared with those having +I effect (example, the halogens as compared to alkyls and methoxy.). Those which possess −T effect, as well as −I effect (as in the case of $-NO_2$ substituted), greatly increase the rate; but the rate is not necessarily decreased by virtue of the +T effect (as with the halogens). Shoppee[10] reached a similar conclusion in isomerisation of triad systems.

TABLE 2

Sigma values and log k/k_0 calculated for individual compounds

Substituent	σ-values	log k/k_0
m-Cl	+0.373	0.6955
p-Cl	+0.227	0.4053
H	0.000	0.0000
p-F	+0.062	−0.1809
m-CH_3	−0.069	−0.4434
p-CH_3	−0.170	−0.4522
p-t.Bu.	−0.197	−0.7416
p-OCH_3	−0.268	−1.0907
m-F	+0.337	0.3154
m-Br	+0.391	0.2749
p-Br	+0.232	−0.0280
p-$CH(CH_3)_2$	−0.151	−0.6643
m-OCH_3	+0.115	−0.3106
p-NO_2	+0.78	1.3448

The case of the three methoxy-substituted compounds can be taken as an evidence that −I effect only is operative whereas +T is not; and that the *ortho*-substituent is the lowest probably because of 'steric effect'.

Quantitatively, one can use the Hammett equation,

$$\log k/k_0 = p\sigma$$

to plot log k/k_0 against σ-values of the different substituents to be able to evaluate p of the reaction – which is equal to the slope of the curve (Table 2).

A value of $p = +2.14$ has been obtained, which indicates that the reaction is facilitated by electron-withdrawing groups and retarded by electron-repelling ones.

REFERENCES

[1] M. Hassan, A. R. O. Abdel Nour and A. M. Satti, *Rev. Roumaine Chim.*, **23**, 747 (1978).
[2] A. R. O. Abdel Nour and M. Hassan, *J. Chem. Soc. B*, **1970**, 1628.
[3] A. Streitwieser, Jr. and C. H. Heathcock, "Introduction to Organic Chemistry".
[4] A. C. Cope and J. K. Heeren, *J. Amer. Chem. Soc.*, **87**, 3125 (1965).
[5] B. Rickborn and R. P. Thummel, *J. Org. Chem.*, **34**, 3583 (1969).
[6] M. M. Martin and G. H. Gleicher, *J. Amer. Chem. Soc.*, **86**, 233 (1964).
[7] D. Swern, "Organic Reactions", vol. 7, Wiley, New York, 1953, p. 378.
[8] C. D. Hurd and W. W. Jenkins, *J. Org. Chem.*, **22**, 1418 (1957).
[9] A. I. Vogel, "Textbook of Practical Organic Chemistry", 3rd. Edition, Longmans, London, 1956.
[10] C. W. Shoppee, *J. Chem. Soc.*, **1930**, 968.

Revue Roumaine de Chimie, 26, 7, 985–992 (1981)

THE SYNTHESIS AND THE ELECTRONIC SPECTRA OF SOME *trans*-α-CYANO-2-STYRYLBENZIMIDAZOLES

S. MATEI, JANA RUSSU and PETRONELA COLTEA

Chemical-Pharmaceutical Research Institute,
Str. Fabricii 126, Cluj-Napoca, Romania

Received July 9, 1980

The *trans*-derivatives of substituted α-cyano-2-styrylbenzimidazoles possessing bacteriostatic and bactericidal properties were synthetized. The electronic spectra and the ionization constants of these *trans*-derivatives were determined. A correlation was established between the spectral parameters and the substituent effect in the phenyl ring.

The methylene group in 2-acetonitrilebenzimidazole has an acid character owing to the electron acceptor influence of the –CN and benzimidazole groups, and consequently it is able to give Knoevenagel type reactions.

The condensation of 2-acetonitrilebenzimidazole with benzaldehyde and *p*-nitrobenzaldehyde gave derivatives having a tuberculostatic activity.[1] The condensation with alkylaminobenzaldehyde gave dispersion dyes.[2,3] The condensations were performed with basic catalysts.

In the present paper we intend to enlarge the range of these compounds with potential bactericidal and bacteriostatic activity. We also intend to give the spectral parameters in visible and ultraviolet and to establish a correlation between the spectral parameters and the substitution effect in the phenyl ring. No references concerning these data were found in the literature. The studied compounds have the general formula:

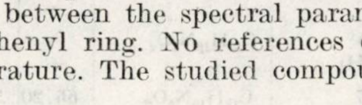

where I $R=H$
II $R=p\text{-}OH$
III $R=m\text{-}OH$
IV $R=p\text{-}OCH_3$
V $R=m\text{-}OCH_3$
VI $R=o\text{-}OCH_3$
VII $R=p\text{-}NO_2$
VIII $R=m\text{-}NO_2$
IX $R=o\text{-}NO_2$
X $R=p\text{-}Cl$
XI $R=m\text{-}Cl$
XII $R=o\text{-}Cl$
XIII $R=p\text{-}N(CH_3)_2$

EXPERIMENTAL PART

Melting points were determined on a Boetius hot stage microscope. The infrared spectra were recorded in KBr pellets on a Specord IR 75 Carl Zeiss spectrophotometer.

The ultraviolet and visible spectra were recorded by means of a VSU – 1, Carl Zeiss Jena spectrophotometer, between 240 and 500 nm. The solvents were methanol, methanol-acid, methanol-base with constant ionic strengths. The solutions ($10^{-4}-10^{-5}$M) were prepared in the dark before use. pK values were calculated according to Grimison et al.[4]

2-Acetonitrilebenzimidazole was synthetized according to Ralf et al.[5]

The *trans*-α-cyano-2-styrylbenzimidazoles were prepared according to the following method : 0.01 mole benzaldehyde derivative was added to 0.01 mole acetonitrilebenzimidazole in 20 ml glac. acetic acid, and the mixture was boiled under reflux for 15–20 minutes. The mixture was cooled, the formed precipitate was filtered off and washed with AcOH and H_2O. Compounds I, IV, V, VI were obtained by pouring the reaction mixture in ice-water. The cyanostyrylbenzimidazole derivatives were crystallized from the given solvents. The yields, elemental analysis and IR spectra are given in table 1.

TABLE 1

Physical constants of *trans*-α-cyano-2-styrylbenzimidazoles

Deriv.	Yield %	M.p. °C (solv.) *	Formula	Calculated/Found			IR spectra cm^{-1}	
				C%	H%	N%	NH	C≡N
I	95.0	219–21[a] (EtOH)	$C_{16}H_{11}N_3$	78.30 78.28	4.47 4.96	17.13 17.53	3260	2275
II	90.0	328–32 (EtOH)	$C_{16}H_{11}N_3O$	73.54 73.02	4.24 4.59	16.08 16.50	3250	2250
III	81.5	313–15 (DMF–AN)	$C_{16}H_{11}N_3O$	73.54 74.04	4.24 4.31	16.08 16.07	3250	2250
IV	86.0	219–20 (EtOH)	$C_{17}H_{13}N_3O$	74.16 73.80	4.76 5.08	15.26 15.21	3270	2250
V	71.5	219–20 (EtOH)	$C_{17}H_{13}N_3O$	74.16 73.99	4.78 4.38	15.26 15.21	3250	2255
VI	85.5	241–43 (EtOH)	$C_{17}H_{13}N_3O$	74.16 74.03	4.76 5.19	15.26 15.78	3400	2245
VII	89.9	320–21[b] (A)	$C_{16}H_{10}N_4O_2$	— —	— —	— —	3255	2275
VIII	88.5	262–64[c] (EtOH)	$C_{16}H_{10}N_4O_2$	— —	— —	— —	3325	2260
IX	89.0	195–97 (AcOH)	$C_{16}H_{10}N_4O_2$	66.20 66.04	3.47 3.06	19.30 19.46	3275	2275
X	87.7	252–54 (EtOH)	$C_{16}H_{10}ClN_3$	68.69 68.57	3.60 4.09	14.66 14.84	3290	2260
XI	84.5	245–47[d] (EtOH)	$C_{16}H_{10}ClN_3$	— —	— —	— —	3260	2270
XII	87.7	233–34 (AcOH)	$C_{16}H_{10}ClN_3$	68.69 68.72	3.60 3.23	14.66 14.90	3275	2280
XIII	98.0	314–15[e] (D)	$C_{18}H_{16}N_4$	— —	— —	— —	3250	2260

---

* A = acetone, AN = acetonitrile, AcOH = acetic acid, D = dioxane, DMF = dimethylformamide, EtOH = ethanol.

[a] 220–21, [b] 320–21, [c] 263–65, [d] 234–36, [e] 313–14.

RESULTS AND DISCUSSION

The electronic spectra were studied, taking into account the structural resemblance as well as the presence of the characteristic bands of stilbene derivatives. Table 2 shows the maxima in methanolic solution for *cis*- and *trans*-stilbene,[6] *trans*-α-cyanostilbene [7] and *trans*-α-cyanostilbazole,[8] as compared with compound I.

TABLE 2

Electronic spectra of stilbene and some of its derivatives

Derivative	$\lambda_{1\,max}$ nm	$\varepsilon_{1\,max}$ $1\cdot mol^{-1}cm^{-1}$	$\lambda_{2\,max}$ nm	$\varepsilon_{2\,max}$ $1\cdot mol^{-1}cm^{-1}$	Ref.
cis-stilbene	225	22200	285	10000	6
trans-stilbene	228	16200	311	25600	6
cis-α-cyanostilbene	224	22900	295	16590	7
trans-α-cyanostilbene	227	18620	312	25703	7
trans-α-cyano-3-stilbestrole	224	10800	310	23900	8
trans-α-cyano-2-styrylbenzimidazole	228	16200	346	23570	

A, B and C bands which appear in the electronic spectrum of unsubstituted *trans*-stilbene were assigned by Beveridge as a result of LCAO-MO-SCF-CI-PPP calculation.[9]

The spectral data of our synthetized compounds are given in table 3.

TABLE 3

Electronic spectra of *trans*-α-cyano-2-styrylbenzimidazoles in methanol

Derivative	B band		A band	
	λ_{max} nm	ε_{max} $1.mol^{-1}cm^{-1}$	λ_{max} nm	ε_{max} $1.mol^{-1}cm^{-1}$
I	280	9900	346	23500
II	235	11600	370	36000
III	—	—	350	22500
IV	235	11950	370	36800
V	—	—	350	24670
VI	285	6770	364	20540
VII	280	11600	370	24000
VIII	260	15800	350	28100
IX	275	11000	340	16100
X	285	8810	335	27240
XI	275	7660	350	24900
XII	280	7270	346	23100
XIII	310	5560	430	48800

The lower wavelength band, called B band is present in all the derivatives between 235 and 280 nm, but sometimes it is not enough outlined and appears as a shoulder. The band was assigned to the $\pi-\pi^*$ transition of the entire conjugated system ($1L_a \leftarrow {}^1A$) benzimidazolestyryl. The band is not present in the spectra of acetonitrilebenzimidazole and shows small shifts if the solvent polarity is changed (Figure 1*a* and *b*). The second band, A (340–430 nm) was assigned to an intramolecular charge transfer (CT). This transfer involves the highest occupied orbital of one part of the molecule (the phenyl ring) which acts as an electron donor, and the lower unoccupied orbital of another part of the molecule (the benzimidazole ring) acting as an electron acceptor. This simplified treatment permitted calculation of excitation energies and intensities in a very satisfactory approximation.[10,11]

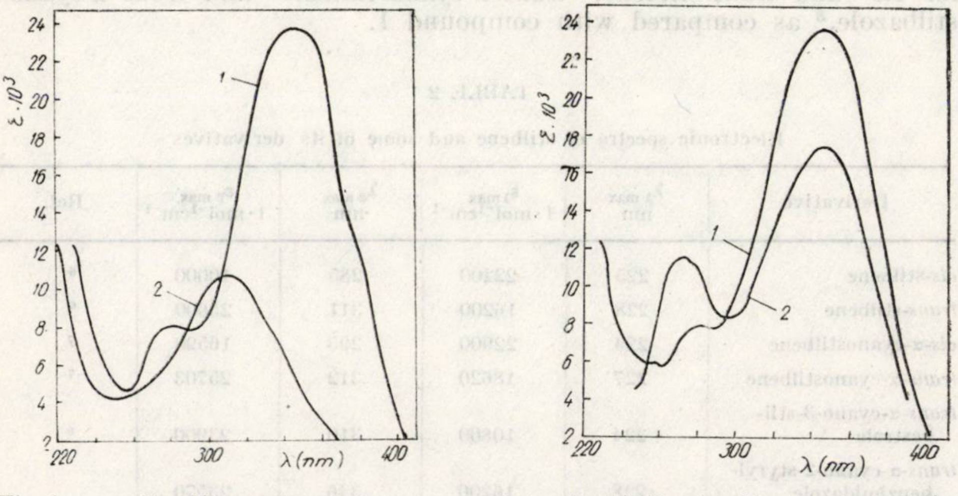

Fig. 1. — *a*, The UV spectra of *trans*-α-cyano-2-styrylbenzimidazole (*1*) and acetonitrilebenzimidazole (*2*); *b*, the UV spectra of I in methanol (*1*) and hexane (*2*).

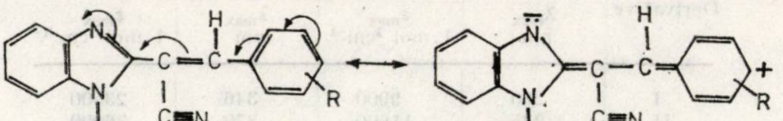

We apply the relation:

$$E_{CT} = I - E_A - E_C \tag{1}$$

where

I = ionization potential of the donor centre
E_A = electron affinity of the acceptor centre

E_C = Coulomb interaction between the migrating charge and the positive pole left behind on the aromatic nucleus

E_{CT} = energy of the intramolecular charge transfer; it is found for the unsubstituted compound I, when the donor centre is the styryl system with $I = 8.54$ eV, the acceptor centre is the C=N group of the benzimidazole ring with $E = 0.4$ eV,[12] $E_C = 5.26$ eV calculated for the benzene ring,[13,14] hence $E_{CT} = 3.61$ eV.

The experimental data were determined from λ_{max}:

$$E_{CT} = \nu h \qquad (2)$$

Substitution in eq. 2 results in:

$$E_{CT} = \frac{10^7}{3.46} \cdot \frac{1.2398}{10^4} = 3.58 \text{ eV}$$

The charge transfer type of A band may be thus confirmed by calculation.

The shift to red observed with increasing solvent polarity (Figure 1 *b*) supports the charge transfer nature of this band.[15] The spectral parameters of A band were calculated and are listed in table 4.

TABLE 4

Spectral parameters of A band

Deriv.	λ_{max} (nm)	Intensity of absorption: ε_{max} $(1.mol^{-1}cm^{-1})$	Intensity of absorption: $A \cdot 10^{-8}$ $(1.mol^{-1}cm^{-2})$	f_{exp}	Line width: $\frac{f_{exp} \cdot 10^7}{\varepsilon_{max}}$	Line width: $\Delta\nu_{1/2} \cdot 10^{-14}$ (cm^{-1})
I	346	23570	1.53	0.661	280	268
II	370	36022	2.24	0.971	266	277
III	350	22920	1.71	0.738	322	319
IV	370	36800	2.32	1.000	271	194
V	350	24600	1.39	0.596	242	211
VI	346	20537	1.39	0.596	290	215
VII	370	24037	2.00	0.860	359	304
VIII	350	23076	1.86	0.804	348	366
IX	340	16109	1.41	0.608	377	300
X	350	27244	1.97	0.852	312	230
XI	350	24865	1.86	0.807	322	350
XII	346	23045	1.80	0.776	337	330
XIII	430	48815	3.46	1.490	31	35

ε_{max} = the molar extinction coefficient.

A_{max} = the molar integrated extinction coefficient or the integrated absorption intensity.

f_{exp} = the oscillator strength.

$\Delta\nu_{1/2}$ = the frequency difference between the absorption maximum and the point corresponding to the $1/2\varepsilon_{max}$ towards the greater wavelengths.

$\frac{f_{exp}}{\varepsilon_{max}}$ = the ratio of the oscillator strength and the molar extinction.

It emerges clearly from this table that substitution in the phenyl ring yields shifts and intensity changes, depending on the substituent type and its position. A band is gradually shifted towards the red region of the spectrum as the donor character of the substituents in the *para*-position of the phenyl ring increases. This fact confirms the CT nature of this band. The sequence of this shift is known : $N(CH_3)_2 > OH = OCH_3 > Cl > H$. In the case of *meta*-derivatives no shifts of the A band maxima are observed, and the intensity of the bands differ slightly from that of the unsubstituted derivatives ; the inductive effect does not appear in this case. The *ortho*-derivatives show hypsochromic shifts as compared with the unsubstituted derivative I, in a sequence which may be explained by a deviation from the molecular coplanarity. Using the equation[16] :

$$\cos^2\theta = \varepsilon/\varepsilon' \tag{3}$$

where

θ = the twist angle
ε = the molar extinction coefficient of the partially twisted compound
ε' = the value corresponding to the homologous compound having no *ortho*-substituent and hence assumed to be planar ($\theta = 0°$)

we obtain : *ortho*-Cl : 8°30′ ; *ortho*-OCH_3 : 21° ; *ortho*-NO_2 = 35°0′.

The zwitter-ionic character of the benzimidazole ring is known.[17] It may exist in three possible forms :

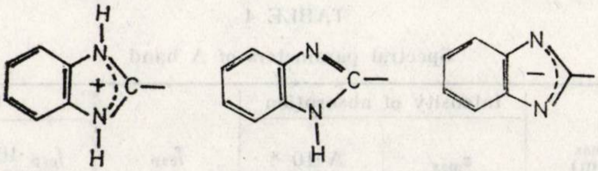

We studied the spectra of these forms in acid and basic media (Table 5)

TABLE 5

A band shifts depending on solvent as compared with aqueous-methanolic solutions with the same ionic strength

Derivative	HCl		NaOH	
	Δλ nm	Δε 1.mol^{-1}cm^{-1}	Δλ nm	Δε . mol^{-1}cm^{-1}
I	4	2771	24	−2919
II	20	2759	40	−1535
III	0	3389	20	−1054
IV	16	3779	4	−6395
V	4	−704	25	−1970
VI	21	−7626	10	−2147
VII	−14	2554	45	−14581
VIII	−10	1684	30	−3686
IX	−10	2410	0	−4847
X	0	1773	26	−4699
XI	0	2993	20	−4672
XII	0	1269	15	−4025
XIII	60	202	−5	−4065

The comparative shifts and intensity changes observed on passing from an acid to a basic medium are given in figure 2 for derivative I and in table 5 for the other derivatives.

The absorption-pH curves at various pH values are typical dissociation curves. In acid media bathochromic and hypsochromic shifts are generally observed for *para*-substituents which are electron donors. A quinonic type structure may be postulated :

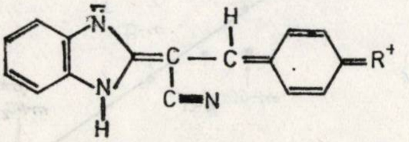

The visible shift and the increase of the maxima have the following sequence : $Cl < OCH_3 \leqslant OH < N(CH_3)_2$. The highest bathochromic shift for the *para*-$N(CH_3)_2$-derivative and the slightest variation of the band strength as compared with the other parts in *para*-substituted derivatives, confirm the existence of the quinonic form in these media (the quinonic form is also present, probably in equilibrium, in nonpolar solvents ; the shift becomes more visible for OH and $N(CH_3)_2$ substituents which may acquire a quinonic structure). For the p-NO_2 substitution the shift of the band has a reverse direction (—E).

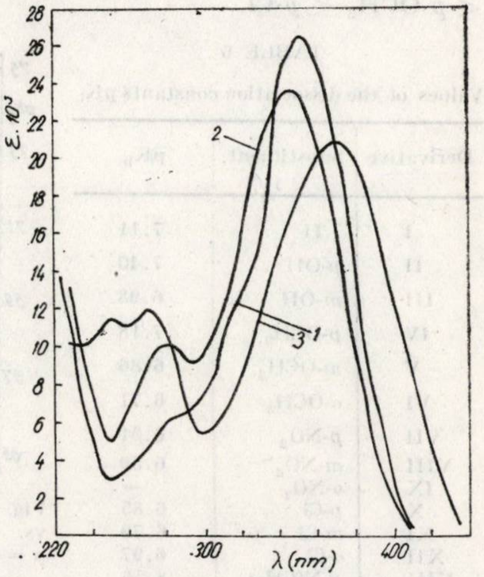

Fig. 2. — The band shifts and the intensity changes observed in acid and basic media, for derivative I : *1*, the spectrum in 1 n HCl in aqueous methanol ; *2*, the spectrum in aqueous methanol ; *3*, the spectrum in 1 n NaOH in aqueous methanol.

The *meta*-derivatives have slighter intensity variations without shifts of the maxima as compared with the spectra in hexane and methanol. As expected, in basic media the bathochromic shift, accompanied by a decrease in the band intensity as compared to nonpolar solvents has the following sequence : $NO_2 < OH < Cl < H < OCH_3 < N(CH_3)_2$. The band shifts and the absorptivity changes are given in acid and basic buffers and methanolic solutions with the same water content and ionic strength (Table 5).

The dissociation constants in acid media pK_b were calculated (Table 6). These values give a linear relationship with the σ-Hammet constant, as shown in figure 3.

Derivatives with a similar structure were tested,[1] which exhibited good tuberculostatic effects. Our compounds have a negligible tuberculostatic activity, but appreciable bacteriostatic and bactericidal properties.

The tests performed on Gram-positive (*E. coli*) and Gram-negative (*S. oxfordii* and *B. pyocyaneus*) organisms showed that the *para*-derivatives have the highest activities, following the sequence : $H < (N(CH_3)_2 < p\text{-}NO_2 <$ $< p\text{-}OCH_3 < p\text{-}Cl$.

TABLE 6

Values of the dissociation constants pK_b

Derivative	Substituent	pK_b
I	H	7.11
II	*p*-OH	7.40
III	*m*-OH	6.98
IV	*p*-OCH_3	7.18
V	*m*-OCH_3	6.86
VI	*o*-OCH_3	6.71
VII	*p*-NO_2	6.51
VIII	*m*-NO_2	6.59
IX	*o*-NO_2	—
X	*p*-Cl	6.85
XI	*m*-Cl	6.79
XII	*o*-Cl	6.97
XIII	*p*-$N(CH_3)_2$	8.56

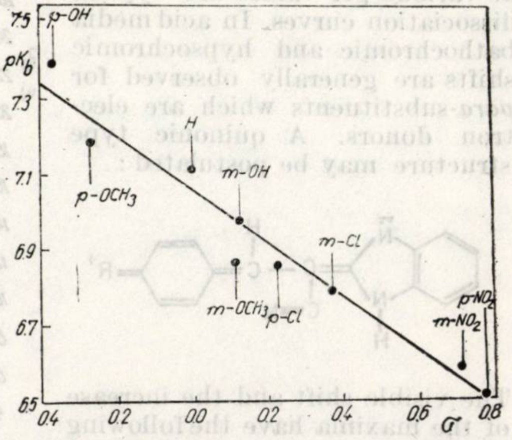

Fig. 3. — The plot of dissociation constant pK_b vs. Hammett constant : $r = 0.98$; $s = 0.057$; $\rho = 0.706$ (substituent constants tabulated by McDaniel and Brown[18] were used).

ACKNOWLEDGEMENT. We thank prof. Dr. V. Fărcășanu for the helpful discussions and Dr. V. Cristea for the bacteriological testing of our compounds.

REFERENCES

[1] J. Sawlewicz, B. Milczarska and W. Manowska, *Pol. J. Pharmacol. Pharm.*, **27,** 187 (1975).
[2] Y. Eiji, Japan Pat., 7,329,517 (September 12, 1973) ; *Chem. Abstr.*, **80,** 146971 (1974).
[3] A. Fujita, J. Armoto, Sh. Minami and H. Takamatsu, *Yakugaka Zasshi*, **86,** 427 (1966) ; *Chem. Abstr.*, **65,** 3870 (1966).
[4] A. Grimison, J. H. Ridd and B. V. Smith, *J. Chem. Soc.*, **1960,** 1353.
[5] L. Ralf, A. B. Copeland and H. R. Day, *J. Amer. Chem. Soc.*, **65,** 1074 (1943).
[6] H. Suzuki, *Bull. Chem. Soc. Japan*, **33,** 381 (1960).
[7] J. F. Codington and E. Mosseting, *J. Org. Chem.*, **17,** 1034 (1952).
[8] F. H. Clarke, G. A. Fecock, G. B. Silverman and G. M. Watnick, *J. Org. Chem.*, **27,** 535 (1962).
[9] J. E. Beveridge, *Diss. Abstr.*, **26,** 3644 (1966).
[10] H. H. Jafféa and M. Orchin, "Theory and Applications of Ultraviolet Spectroscopy", Johns Wiley and Sons, 2nd ed., New York, U.S.A., 1964.
[11] S. Nagakura and J. Tanaka, *J. Chem. Phys.*, **22,** 326 (1954).
[12] C. A. Coulson, "Valence", Oxford University Press, 2nd ed., 1969, p. 140.
[13] K. Watanabe, *J. Chem. Phys.*, **26,** 542 (1957).
[14] R. G. West, "Handbook of Chemistry and Physics", The Chemical Rubber Company, 30th ed., Ohio, U.S.A., 1969, p. 86.
[15] A. A. Khalaf, S. H. Etaiw, R. M. Issa and A. K. El-Shafei, *Rev. Roumaine Chim.*, **22,** 1251 (1977).
[16] H. H. Jaffé, *Chem. Rev.*, **53,** 191 (1953).
[17] H. Walba, D. L. Stigall and S. M. Coults, *J. Org. Chem.*, **32,** 1954 (1967).
[18] D. H. McDaniel and H. C. Brown, *J. Org. Chem.*, **23,** 420 (1958).

Revue Roumaine de Chimie, 26 7, 993–999 (1981)

REACTIONS OF 1-PHENYL-3,5-PYRAZOLIDINEDIONE

M. ANWAR and F. I. ABDEL-HAY
Chemistry Department, Faculty of Science, Tanta University, Tanta, A. R. Egypt

Received April 10, 1980

1-Phenyl-3,5-pyrazolidinedione (I) reacted with urea, amides, anhydrides and maleimides forming compounds II–V. Compounds IV reacted with aniline and phenylhydrazine forming compounds VI. Compound I reacted also with rhodanine forming VII, which condenses with aromatic aldehydes affording VIII.

3,5-Pyrazolidinedione derivatives have occupied a very prominent place in medicinal chemistry. 1-Phenyl-3,5-pyrazolidinedione was found to have antipyretic,[1] analgesic,[2] antiinflammatory [3] properties and to be active in rheumatoid arthritis.[2]

3,5-Pyrazolidinediones are typical compounds containing active methylene group. Their condensation with aldehydes and ketones,[4, 5] diazotizations and couplings with amines giving dyes used for plastics,[6] condensations with salicylic acid hydrazide [7] and with alkyl halides [8] have been already reported.

In the present investigation the reactivity of the methylene group was extended for some selected compounds containing the carbonyl group. Compound I reacted with urea and amides, namely formamide, acetamide and acetanilide forming compounds IIa–d.

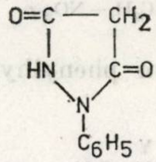

(I)

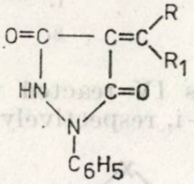

(II)

	R	R_1
a,	NH_2	NH_2
b,	H	NH_2
c,	CH_3	NH_2
d,	CH_3	NHC_6H_5

Compound IIc reacted with aromatic aldehydes, namely benzaldehyde, *p*-chlorobenzaldehyde and *p*-nitrobenzaldehyde forming compounds IIIa—c.

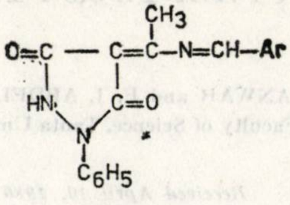

(III)

a, Ar= C_6H_5

b, Ar = C_6H_4-CL-*p*

c, Ar = $C_6H_4-NO_2$-*p*

Compound I reacted also with some anhydrides, namely, phthalic, maleic and succinic anhydrides and with some maleimides, namely phenyl maleimide, *p*-tolyl, *p*-anisyl and *p*-nitrophenylmaleimides, affording the normal condensation products IVa—g.

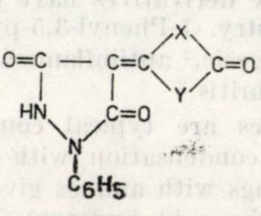

(IV)

	X	Y
a,	*o*-C_6H_4	O
b,	CH=CH	O
c,	CH_2-CH_2	O
d,	CH=CH	N–C_6H_5
e,	CH=CH	N–$C_6H_4-CH_3$-*p*
f,	CH=CH	N–$C_6H_4-OCH_3$-*p*
g,	CH=CH	N–$C_6H_4-NO_2$-*p*

Compounds IV reacted with aniline or phenylhydrazine forming compounds Va—i, respectively.

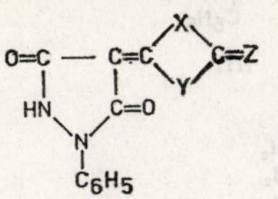

(V)

	X	Y	Z
a,	CH=CH	N–C_6H_5	N–C_6H_5
b,	CH=CH	N–$C_6H_4-CH_3$-*p*	N–C_6H_5
c,	CH=CH	O	N–C_6H_5
d,	C_6H_4	O	N–C_6H_5
e,	CH=CH	N–C_6H_5	NNH–C_6H_5
f,	CH=CH	N–$C_6H_4-CH_3$-*p*	NNH–C_6H_5
g,	CH=CH	O	NNH–C_6H_5
h,	C_6H_4	O	NNH–C_6H_5
i,	CH_2-CH_2	N–C_6H_5	NNH–C_6H_5

Acetylation of compounds IVa, b afforded the corresponding esters VIa, b similar to that obtained with 1-phenyl-3,5-pyrazolidinedione on benzoylation.[9]

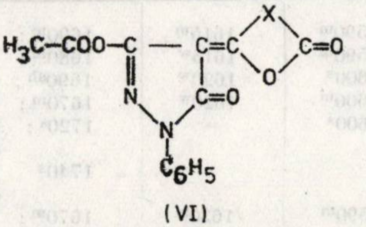

(VI)

a, $X=C_6H_4$, b, $X = CH=CH$

Compound I reacted also with rhodamine forming compound VII which also contains active methylene group. Compound VII reacted with aromatic aldehyde forming VIIIa, b.

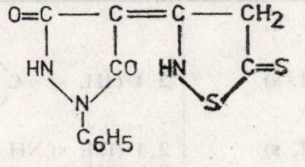

(VII)

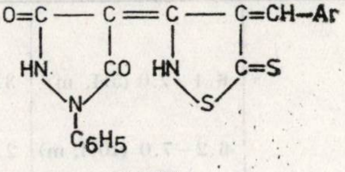

(VIII)

a, $Ar = C_6H_5$
b, $Ar = C_6H_4-Cl$-*p*

The given structures for the products were verified both by infrared and nuclear magnetic resonance spectroscopy (cf. Tables 1 and 2).

TABLE 1

IR spectra of compounds II–VIII (KBr cm^{-1}) *

Compound	Phenyl	ν(C=N)	ν(C=O)	ν(NH)
IIa	1590^{s}	1630^{m}	1660^{s} ; 1690^{s}	3500^{sb}
IIb	1595^{m}	1630^{w}	1710^{s} ; 1730^{s}	3500^{sb}
IId	1600^{m}	1620^{m}	1655^{s} ; 1680^{m}	3380^{sb}
IIIa	1600^{m}	1630^{m}	1670^{s} ; 1695^{s}	3400^{s}
IVa	1590^{s}	1630^{m}	1660^{s} ; 1690^{s}	3460^{sb}
IVb	1590^{s}	1620^{sh}	1665^{m} ; 1680^{m} 1760 (anhydride)	3480^{sb}
IVe	1590^{m}	1630^{w}	1710^{s} ; 1740^{s}	3420^{mb}
IVf	1600^{sh}	1610^{w}	1705^{s} ; 1735^{s} 1795^{m} (maleimide)	3500^{sb}
Va	1595^{s}	1610^{sh}	1710^{s} ; 1735^{s}	3400^{mb}
Vb	1600^{s}	1615^{sh}	1680^{s} ; 1720^{s}	3420^{mb}
Vc	1600^{s}	1625^{w}	1690^{sh} ; 1720^{vs}	3500^{sb}

* s = strong ; m = medium ; w = weak ; sh = shoulder ; b = broad

TABLE 1 (continued)

Compound	Phenyl	ν(C=N)	ν(C=O)	ν(NH)
Ve	1590^{m}	1615^{m}	1690^{m} ; 1760^{vs}	3480^{sb}
Vf	1590^{m}	1615^{w}	1680^{m} ; 1730^{s}	3400^{mb}
Vg	1600^{s}	1620^{w}	1690^{sh} ; 1740^{vs}	3460^{sb}
Vh	1600^{m}	1620^{w}	1670^{m} ; 1720^{m}	3480^{sb}
VIa	1600^{s}	—	1720^{s} ; 1820^{vs} (ester) 1740^{s} (anhydride)	—
VII	1590^{m}	1630^{m}	1670^{m} ; 1740^{s}	3500^{sb}

TABLE 2

The $^{1}H-NMR$ spectral data for compounds II—VII *, **

Compound	Phenyl⁽¹⁾	NH (pyrazol.)	4-position
IIa	6.4—7.0 (5H, m)	3.6 (1H, s)	2.4 (4H, s) $=\mathrm{C}\begin{array}{l}\diagup \mathrm{NH_2}\\ \diagdown \mathrm{NH_2}\end{array}$
IId	6.2—7.0 (10H, m)	2.8 (1H, s)	2.4 (1H, s) NH 3.5 (3H, s) $=C-CH_3$
IIIa	6.4—7.0 (10H, m)	2.4 (1H, s)	3.4 (3H, s) $=C-CH_3$ 6.0 (1H, s) $N=CH-$
IVa	6.4—7 (9H, m)	2.4 (1H, s)	—
IVb	6.4—7.0 (5H, m)	3.0 (1H, s)	6.1 (2H, s) $-CH=CH-$
IVe	6.1—6.8 (9H, m)	2.4 (1H, s)	3.1 (3H, s) CH_3-aromatic
IVf	6.2—6.8 (9H, m)	2.4 (1H, s)	5.9 (2H, s) $-CH=CH-$
Vb	6.2—7.0 (14H, m)	2.3 (1H, s)	3.0 (3H, s) CH_3-aromatic
VIa (2)	6.4—7.0 (9H, m)	—	—
VII	6.2—7.0 (10H, m)	2.4((2H, sb)(3)	4.3 (2H, s) $C-CH_2-C=S$

---

* Chemical shifts were determined as δ ppm (TMS).

** s = singlet ; m = multiplet ; b = broad.

(1) aromatic protons of 1- and 4-positions if any.

(2) VIa shows a signal at $\delta = 3.0$ corresponding to 3H (CH_3-COO).

(3) Pyrazolidine and rhodanine NH protons.

The IR spectra of compounds under investigation show two carbonyl bands for the pyrazolidine ring. The first carbonyl band appears at lower frequencies due to keto-enol tautomerism.[10]

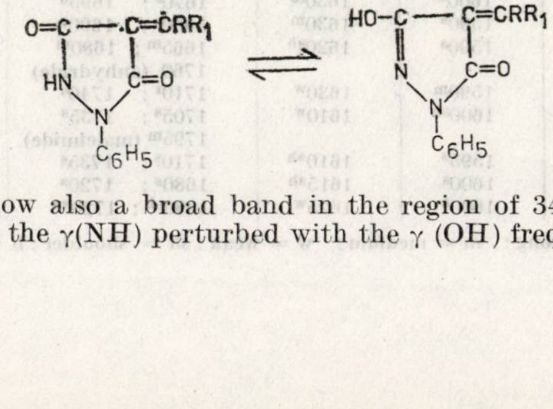

The spectra show also a broad band in the region of 3400—3500 cm⁻¹, attributable to the γ(NH) perturbed with the γ (OH) frequencies.

EXPERIMENTAL

The IR spectra were recorded with a UNICAM S.P. 1200 spectrophotometer. The KBr pellet technique was used.

The ^1H-NMR spectra were recorded at 60 MHz on a Varian A-60 spectrometer.

All melting points are uncorrected.

ACTION OF UREA AND AMIDES ON I

1-Phenyl-3,5-pyrazolidinedione[11] (1.8 g ; 0.01 mole) and urea and/or amide (0.01 mole) in 50 ml butyl alcohol were refluxed for 12 hrs using 2 drops of pyridine as catalyst. The reaction mixture was concentrated and cooled to give IIa–d, which were recrystallized from ethanol. Yields 80–85 %. The results are listed in table 3.

TABLE 3

Condensation products of 1-phenyl-3,5-pyrazolidinediones with urea and amides

Compound	m.p. (°C)	Formula	Analysis % (Found/Calcd.)		
			C	H	N
IIa	over 300	$C_{10}H_{10}N_4O_2$	54.89 55.05	4.73 4.59	25.47 25.69
IIb	261 (decomp)	$C_{10}H_9N_3O_2$	58.83 59.11	4.79 4.43	20.52 20.69
IIc	234	$C_{11}H_{11}N_3O_2$	56.51 56.41	5.13 4.70	17.79 17.95
IId	over 300	$C_{17}H_{15}N_3O_2$	69.51 69.62	5.07 5.12	14.42 14.33
IIIa	274	$C_{18}H_{15}N_3O_2$	70.62 70.82	4.99 4.92	13.81 13.77
IIIb	282	$C_{18}H_{14}ClN_3O_2$	63.24 63.62	4.50 4.12	12.46 12.37
IIIc	over 300	$C_{18}H_{14}N_4O_4$	61.31 61.71	4.33 4.00	16.02 16.00

ACTION OF AROMATIC ALDEHYDES ON II

A mixture of IIc (2.18 g; 0.01 mole) and aromatic aldehyde (0.015 mole) with 2 drops of piperidine in 50 ml ethanol was heated for 6 hrs. The reaction mixture was concentrated and cooled, the solid formed was recrystallised from ethanol to give IIIa–c in almost quantitative yield. The results are listed in table 3.

ACTION OF ANHYDRIDES AND MALEIMIDES ON I

A mixture of I (1.8 g ; 0.01 mole) and anhydride (0.01 mole) and/or maleimide (0.01 mole) was heated in an oil-bath for 5 hrs. The solid obtained was crystallised from ethanol, to give IVa–g in 80–90 % yields. The results are given in table 4.

ACTION OF ANILINE AND PHENYLHYDRAZINE ON IV

A mixture of IV (0.01 mole) and aniline (0.93 g ; 0.01 mole) and/or phenylhydrazine (1.08 g ; 0.01 mole) was heated in an oil bath for 5 hrs. The solid obtained was crystallized from ethanol to give compounds Va–i in 85–95 % yields. The results are listed in table 5.

TABLE 4

Condensation products of 1-phenyl-3,5-pyrazolidinediones with anhydrides and maleimides

Compound	m.p. (°C)	Formula	Analysis % (Found/Calcd.)		
			C	H	N
IVa	255	$C_{17}H_{10}N_2O_4$	66.34	3.52	8.93
	(decomp)		66.66	3.27	8.15
IVb	274	$C_{13}H_8N_2O_4$	60.61	3.44	10.72
			60.94	3.13	10.94
IVc	249	$C_{13}H_{10}N_2O_4$	60.11	4.09	10.71
			60.47	3.88	10.85
IVd	232	$C_{19}H_{13}N_3O_3$	68.93	4.24	12.56
			68.88	3.93	12.69
IVe	230	$C_{20}H_{15}N_3O_3$	69.27	4.59	12.00
			69.56	4.35	12.17
IVf	206	$C_{20}H_{15}N_3O_4$	66.19	4.32	11.60
			66.48	4.16	11.63
IVg	281	$C_{19}H_{12}N_4O_5$	60.30	3.51	14.82
			60.64	3.19	14.89

TABLE 5

Compounds V and VI

Compound	m.p. (°C)	Formula	Analysis % (Found/Calcd.)		
			C	H	N
Va	248	$C_{25}H_{18}N_4O_2$	73.61	4.73	13.89
	(decomp)		73.43	4.43	13.79
Vb	283	$C_{26}H_{20}N_4O_2$	74.01	5.03	13.17
			74.29	4.76	13.33
Vc	258	$C_{19}H_{13}N_3O_3$	68.61	4.30	12.62
			68.88	3.93	12.69
Vd	267	$C_{23}H_{15}N_3O_3$	72.31	4.13	11.09
			72.44	3.94	11.02
Ve	260	$C_{25}H_{19}N_5O_2$	71.01	4.73	16.43
	(decomp)		71.26	4.51	16.63
Vf	210	$C_{26}H_{21}N_5O_2$	71.51	5.10	16.03
	(decomp)		71.72	4.83	16.09
Vg	223	$C_{19}H_{14}N_4O_3$	65.92	4.24	16.06
			65.90	4.05	16.18
Vh	271	$C_{23}H_{16}N_4O_3$	69.51	4.40	14.00
			69.51	4.04	14.14
Vi	209	$C_{25}H_{21}N_5O_2$	70.71	5.03	16.30
			70.92	4.96	16.55
VIa	181	$C_{19}H_{12}N_2O_5$	65.30	3.80	8.01
			65.51	3.45	8.05
VIb	179	$C_{15}H_{10}N_2O_5$	60.51	3.52	9.47
			60.40	3.36	9.40

ACETYLATION OF IV a AND b

Compounds IVa and b (0.01 mole) and acetyl chloride (1.1 g; 0.01 mole) in 50 ml dry benzene were heated under reflux for 2 hrs. The reaction mixture was concentrated, cooled and the solid obtained was recrystallized from benzene or ethanol to give compounds VIa and b. The yields are almost quantitative. The results are listed in table 5.

ACTION OF RHODANINE ON I

A mixture of I (1.8 g; 0.01 mole) and rhodanine (1.3 g; 0.01 mole) was heated in an oil bath for 5 hrs. The solid obtained was crystallized from acetic acid to give VII in 80% yield. The physical data are given in table 6.

TABLE 6

Condensation products of 1-phenyl-3,5-pyrazolidinedione with rhodanine

Compound	m.p. (°C)	Formula	Analysis % (Found/Calcd.)			
			C	H	N	S
VII	over 300	$C_{12}H_9N_3O_2S_2$	49.51 49.48	3.34 3.09	14.20 14.43	21.73 21.99
VIIIa	292	$C_{19}H_{13}N_3O_2S_2$	60.02 60.16	3.68 3.43	10.89 11.08	16.76 16.89
VIIIb	301	$C_{19}H_{12}ClN_3O_2S_2$	55.07 55.14	3.34 2.90	10.01 10.16	15.43 15.48

ACTION OF AROMATIC ALDEHYDES ON VII

A mixture of VII (2.9 g; 0.01 mole) and aromatic aldehyde (0.01 mole), 2 drops of piperidine in 50 ml ethanol was heated under reflux for 6 hrs. The reaction mixture was concentrated and cooled, the solid obtained was recrystallised from ethanol to give compounds VIIIa—b in about 85% yield. The physical data are given in table 6.

REFERENCES

[1] S. Tawab, A. Moustafa and M. Kira, *Nature*, **186**, 165 (1960).

[2] L. Geodman and A. Gilman, "The Pharmacological Bases of Therapeutics", The MacMillan Co., New York, 2nd Ed., 1958, p. 322.

[3] E. Bavin, D. Drain, D. Seymour and P. Waterhouse, *J. Pharm. and Pharmacol.*, **7**, 1022 (1955).

[4] T. Tsumoki, *Bull.Chem. Soc. Japan*, **6**, I (1931); **7**, 45 (1932).

[5] A. Moustafa, A. Sammour, M. Kira, M. K. Hilmy, M. Anwar and N. N. Nakhla, *Arch Pharm.* **298** (8), 516 (1965).

[6] W. Porter and W. Wehrli, *Belg.* 616, 190 Apr. 30 (1962), Swiss Appl. Apr. 14, 1961; 12pp; *Chem. Abstr.*, **58**, 1466 (1963).

[7] J. Meyer and O. Nemecek, *Czech.*, 106, 252, Jan. 15 (1963).

[8] J. Buchi, J. Amman, R. Lieberherr and E. Eichenberger, *Helv. Chim. Acta*, **36**, 75 (1953).

[9] Beilstein, "Handbuch der Organischen Chemie", Vol. **24**, Springer, Berlin, 1936, p. 242.

[10] P. Gagnon, K. Savard, R. Gaudry and E. Richardson, *Can. J. Research*, **25 B**, 25 (1947).

[11] T. Tsumacl, *Bull. Chem. Soc., Japan*; H. R. Ruhkorff, *Ber. dtsch. Chem. Ges.*, **73**, 820 (1940).

Revue Roumaine de Chimie, 26, 7, 1001–1004 (1981)

A CONVENIENT NEW METHOD FOR SYNTHESIS OF AROMATIC AMIDES UNDER MILD CONDITIONS

C. I. CHIRIAC
"P. Poni" Institute of Macromolecular Chemistry, Aleea Grigore Ghica Vodă, 41A
Iași, Romania

Received July 28, 1980

Various aromatic amides in good yields are prepared by a direct condensation between diacylphenylphosphites obtained *in situ* and aromatic amines, under mild conditions.

In a previous paper,[1] we showed that triacylphosphites prepared *in situ* from acids and phosphorus trichloride, can react with amines, affording the corresponding amides.

Because only two acyl groups of the triacylphosphites can react in the conditions of this reaction, we investigated other reactive compounds, which avoid this disadvantage.

RESULTS AND DISCUSSION

It is known that aryldialkylphosphites (prepared from phenyldichlorophosphite) can be employed for the synthesis of polynucleotides.[2]

During our investigations of amides syntheses under mild reaction conditions, we have found that the diacylphenylphosphites (reactive compounds), prepared from aromatic acids and phenyldichlorophosphite, can be used for the synthesis of amides, in high yields.

These compounds have only two reactive groups, but both can participate in the reaction with the aromatic amines.

In order to simplify this method of synthesis, we prepared diacylphenylphosphites *in situ* by the treatment of aromatic acids with phenyldichlorophosphite in pyridine at 0–20°C.

Diacylphenylphosphites can be considered as mixed anhydrides of phenylphosphorus acid with aromatic acids, and for this reason, they can manifest high reactivity.

The reactivity of the diacylphenylphosphites with aromatic amines (nucleophile reagents) has not been investigated. Our investigations have shown that these compounds manifest high reactivity with amines.

In this way, we have prepared a series of diacylphenylphosphites in pyridine, used as solvent and acceptor for hydrochloric acid. These diacylphenylphosphites prepared *in situ* reacted with aromatic amines, affording the corresponding amides in high yields.

For the verification of this reaction, we prepared pure dibenzoylphenylphosphite from phenyldichlorophosphite and Na-salt of benzoic acid in benzene or with benzoic acid in benzene and pyridine as acceptor for hydrochloric acid. This compound reacts with aromatic amines in solution of pyridine, in the same conditions as the compound prepared *in situ*. The purity and the yields of the amides obtained from dibenzoylphenylphosphite prepared *in situ* were similar to those of amides obtained from pure dibenzoylphenylphosphite.

Therefore, it is not necessary to isolate these reactive compounds, because pyridine hydrochloride (by-product) does not affect the reaction, like in other cases.[1,3]

Tertiary amines play an important role in the reaction. We tried many tertiary amines, but the pyridine was found to be the most suitable base which served also as reaction medium.

By treatment of a solution of diacylphenylphosphite (1 mole), obtained *in situ* in pyridine, with an aromatic amine (2 moles) at room temperature (four hours), the yield is low. After four hours, at reflux (110—120°C), the desired product results in good yield.

As a result of these investigations, we propose the following mechanism of reaction:

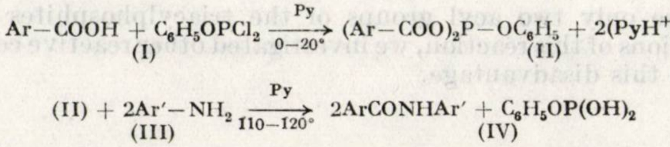

$$2\ \mathrm{Ar{-}COOH} + \underset{(\mathrm{I})}{C_6H_5OPCl_2} \xrightarrow[0-20^\circ]{\mathrm{Py}} \underset{(\mathrm{II})}{(\mathrm{Ar{-}COO})_2P{-}OC_6H_5} + 2(\mathrm{PyH^+Cl^-})$$

$$(\mathrm{II}) + \underset{(\mathrm{III})}{2\mathrm{Ar'{-}NH_2}} \xrightarrow[110-120^\circ]{\mathrm{Py}} 2\mathrm{ArCONHAr'} + \underset{(\mathrm{IV})}{C_6H_5OP(OH)_2}$$

In this reaction, similar to other cases,[4,5] $C_6H_5OP(OH)_2$ and PyH^+Cl^- result as by-products.

We supposed, similar as in other cases,[4,6,7] that this reaction involves a four-centre transition state (V).

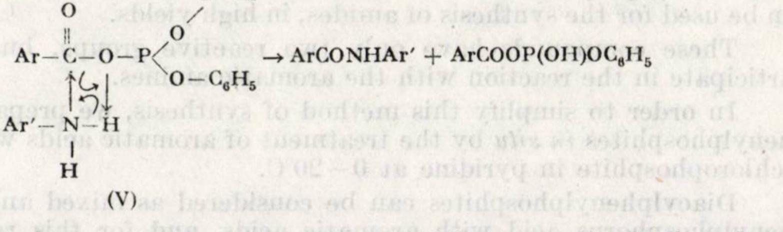

(V)

The mechanism of the reaction, on which the method is based, will be extensively discussed in a separate communication.

In a typical procedure, to a solution of 2 moles I in dried pyridine cooled to 0°, 1 mole phenyldichlorophosphites and then 2 moles III were added very slowly, under stirring (the reaction is very exothermic).

The reaction requires a large excess of pyridine for a good stirring because PyH^+Cl^- precipitates during the reaction at 0—20°C; then, by treatment with III and heating (at reflux), the solution becomes clear. Table 1 shows the amides obtained in this way.

TABLE 1

Aromatic amides obtained from diacylphenylphosphites prepared *in situ*

Acid	Amine	Amides[a] Yield[b] %	M.p.[c] °C	Reported m.p.[d] °C
Benzoic	Aniline	97	161—162	161—162
—"—	*p*-Toluidine	98	157—158	157—158
—"—	*p*-Nitroaniline	85	195—197	196—197
—"—	*p*-Chloroaniline	93	186—187	185—187
—"—	2-Naphthylamine	83	156—158	157—158
p-Toluic	Aniline	96	143—145	144—145
—"—	*p*-Toluidine	99	158—160	159—160
"—	1-Naphthylamine	85	172—174	173—174
p-Chlorobenzoic	Aniline	90	193—194	193—194
	p-Nitroaniline	80	205—207	206—207
	p-Toluidine	93	215—216	214—216

[a] The products were identified by comparison of m.p. and I.R. spectra with those of authentic samples.

[b] Yields determined by isolation of the crude products.

[c] Melting points are given as an indication of purity.

[d] From "Beilsteins Handbuch der organischen Chemie".

The large majority of the obtained amides melted, before recrystallisation, within two degrees of melting points reported in the literature and the yields ranged from 80 to 96% (table 1).

By this new direct synthesis we obtained aromatic amides in high yields, which are difficult to obtain by the heating of aromatic amines with aromatic acids.

EXPERIMENTAL

1. DIBENZOYLPHENYLPHOSPHITE

Method a

To a stirred cooled suspension of 15 g (0.1 moles) of dried Na-salt of benzoic acid in 50 ml dried benzene, a solution of 3.5 ml (0.025 moles) of phenyldichlorophosphite [8] in 10 ml dried benzene was added very slowly (1 hour). Then the mixture was stirred for 1 h at room temperature, and 2 hours at 35—40°C. The obtained solution after centrifugation and decantation is evaporated under vacuum. The obtained precipitate was washed three times with 40—50 ml dried petroleum ether by decantation and dried under vacuum, giving 8 g dibenzoylphenylphosphite, a very hygroscopic solid with a m.p. 59—61°. Yield 87% (calculated on phenyldichlorophosphite employed).

Anal. Calculated for $C_{20}H_{15}PO_5$; C, 65.57 ; H, 4.10 ; P, 8.46%. Found : C, 64.84 ; H, 4.49 ; P, 8.22%

Method b

Over a solution of benzoic acid (6.1 g, 0.05 moles) in dried benzene (40 ml) and dried pyridine (4 ml, 0.05 moles) a solution of phenyldichlorophosphite (3.5 ml, 0.025 moles) in 10 ml dried benzene was added under stirring and cooling. After stirring for 1—2 hours at room temperature, the obtained solution was worked-up as above. The resulted product is similar with the product obtained by the method a.

2. BENZANILIDE FROM PURE DIBENZOYLPHENYLPHOSPHITE

A solution of dibenzoylphenylphosphite (3.66 g, 0.01 moles) and aniline (2.048 g, 0.02 moles + excess 10%) in dried pyridine (20 ml), was heated at reflux (110—120°C), for four hours. Then the solution was poured into a large volume of water and ice (150—200 ml), under stirring. The white benzanilide was collected by filtration, washed with 20 ml 5% NaOH, 20 ml 5% HCl, three times with 15—20 ml H_2O and dried. The resulted product has a m.p. 160—162°C (mixed m.p. with pure benzanilide undepressed) ; yield 95%.

3. BENZANILIDE FROM DIBENZOYLPHENYLPHOSPHITE PREPARED *in situ*

To a stirred solution of benzoic acid (2.44 g, 0.02 moles) in dried pyridine (15 ml) cooled to 0°C, 1.4 ml (0.01 moles) of phenyldichlorophosphite in 5 ml dried C_6H_6 were added very slowly when PyH^+Cl^- (m.p. 80—82°C) precipitated. The mixture was stirred for 1—2 hours at room temperature. Then aniline (2.048 g ; 0.02 moles + 10% excess was added under stirring. The final mixture was heated for 4 hours at 110—120°C. Then the solution was worked-up as above. Benzanilide (3.8 g) was obtained with m.p. 161—162°C (mixed m.p. with pure benzanilide undepressed) ; yield 97%. Anal. Calculated for $C_{13}H_{11}NO$; C, 79.18 ; H, 5.58 ; N, 7.10%. Found : C, 79.51 ; H, 5.23 ; N, 7.38%.

In similar conditions, the other amides presented in Table 1 were obtained.

REFERENCES

[1] C. I. Chiriac, *Rev. Roumaine Chim.*, **24**, 609 (1979).
[2] R. L. Letsinger, J. L. Finnan and W. B. Lungsford, *J. Amer. Chem. Soc.*, **97**, 3278 (1975).
[3] C. I. Chiriac and J. K. Stille, *Macromolecules*, **10**, 710 (1977).
[4] B. Iselin and W. Rittel, *Helv. Chim. Acta*, **40**, 373 (1957).
[5] N. Yamazaki, *Tetrahedron Letters*, **49**, 5047 (1972).
[6] W. Gerrard and J. A. Cade, *J. Chem. Soc.*, **1954**, 2034.
[7] H. O. Becker and K. F. Funk, *J. prakt. Chem.*, **14**, 55 (1961).
[8] H. Tolkmith, *J. Org. Chem.*, **23**, 1682 (1958).

Revue Roumaine de Chimie, **26**, 7, 1005–1009 (1981)

CYCLOCONDENSATION OF MERCAPTOACETIC ACID WITH THIENYLIDENE ANILS

M. S. K. YOUSSEF
Chemistry Department, Faculty of Science, Assiut University, Assiut, Egypt

Received April 24, 1980

Thiophene-2-carboxaldehyde or its 5-bromo derivative **(1)** have been condensed with hydrazine, phenylhydrazine, semicarbazide, thiosemicarbazide and isatylidene-3-hydrazone giving the corresponding thienylidene azomethines **(2–10)**. Cyclocondensation of mercaptoacetic acid with azomethines yielded thienylthiazolidin-4-ones **(11–19)** respectively, in poor yields. The biological activities of the prepared compounds were screened against some strains of bacteria.

Previously we have discussed [1] the cyclocondensation reaction of chloroacetyl chloride and/or thioglycolic acid with different substituted heterocyclic anils. The present work is a sort of extension aiming to cover other classes of amines with the hope that the prepared compounds would possess interesting pharmacological activity. Thus, thiophene-2-carboxaldehyde (or its 5-bromo derivative) was condensed readily in absolute ethanol in the presence of piperidine as a catalyst, with hydrazine, phenylhydrazine, semicarbazide, thiosemicarbazide and isatylidene-3-hydrazone giving the corresponding thienylidene hydrazone **(2a, b)**, phenylhydrazone **(3a, b)**, semicarbazone **(4a, b)**, thiosemicarbazone **(5a, b)** and unsymmetric azines **(6a, b)**, respectively.

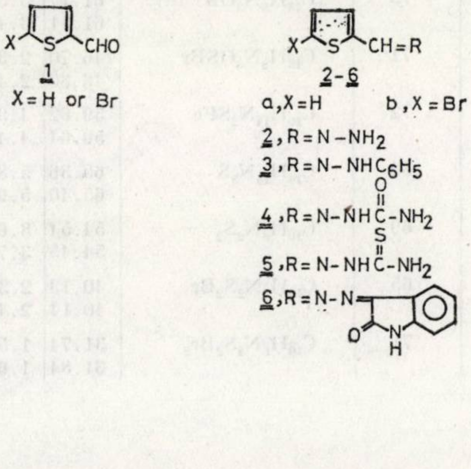

On the other hand, thienylidene-2-hydrazone(**2**) undergoes facile condensation with different aldehydes giving mixed azines (**7**—**10**), respectively.

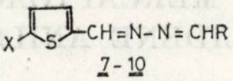

7-10

7, X=H; R=C_5H_5-Fe-C_5H_5 (ferrocenyl)
8, X=H; R=p-N$(CH_3)_2$ C_6H_4
9, X=H; R=C_4H_3S (thienyl) or/ and C_4H_2SBr (5-bromothienyl)
10, X=Br; R=C_4H_2SBr (5-bromothienyl)

The structures of compounds **2**—**10** were established from the combination of the microanalytical data (cf. Table 1) and the IR spectroscopy. The IR spectra of the compounds **2**—**10** showed a sharp absorption band

TABLE 1
Thienylidene azomethines **2**—**10**

Compd. No.	MP °C	Yield %	Molecular formula	Analysis (Calcd./Found) % C	H	N	S	Br
2 a	75—76	70	$C_5H_6N_2S$	47.61 47.59	4.76 4.80	22.22 22.14	25.39 25.19	— —
2 b	60—61	73	$C_5H_5N_2SBr$	29.26 29.30	2.43 2.50	13.65 13.76	15.60 15.66	39.02 39.05
3 a	138—139	68	$C_{11}H_{10}N_2S$	65.34 65.41	4.95 5.00	13.86 14.01	15.84 15.90	—
3 b	114—115	69	$C_{11}H_9N_2SBr$	46.97 47.00	3.20 3.22	9.96 10.01	11.38 11.40	28.46 28.66
4 a	230—231	75	$C_6H_7N_3OS$	42.60 42.70	4.14 4.15	24.85 25.60	18.93 19.08	— —
4 b	188—189	70	$C_6H_6N_3OSBr$	29.03 29.09	2.41 2.51	16.93 17.01	12.90 13.00	32.25 32.33
5 a	195—196	65	$C_6H_7N_3S_2$	30.91 31.01	3.78 4.01	22.70 22.77	34.59 34.60	— —
5 b	161—162	64	$C_6H_6N_3S_2Br$	27.27 27.31	2.27 2.30	15.90 14.01	24.24 24.30	30.30 30.40
6 a	180—182	73	$C_{13}H_9N_3OS$	61.17 61.11	3.52 3.49	16.47 16.42	12.54 12.50	— —
6 b	275—276	71	$C_{13}H_8N_3OSBr$	46.70 46.80	2.39 2.40	12.57 12.66	9.58 9.60	23.59 23.69
7 a	95—96	72	$C_{16}H_{14}N_2SFe$	59.62 59.64	4.34 4.44	8.69 8.59	9.93 10.00	— —
8 a	156—157	62	$C_{14}H_{15}N_3S$	65.36 65.40	5.83 5.90	16.34 16.40	12.45 12.46	— —
9 a	158—159	69	$C_{10}H_8N_2S_2$	54.54 54.45	3.63 3.73	12.72 12.66	29.09 29.11	— —
9 b	102—103	65	$C_{10}H_7N_2S_2Br$	40.13 40.14	2.34 2.40	9.36 9.41	21.40 21.50	26.75 26.77
10	167—168	71	$C_{10}H_6N_2S_2Br_2$	31.74 31.84	1.58 1.66	7.40 7.51	16.93 16.97	42.32 42.41

at 1640–1620 cm^{-1} for C=N group and a band near 3400 cm^{-1}: $\nu(NH_2)$ for compound **2**. Compound **7a** showed beside the forgoing absorption band, another band at 1100–1000 cm^{-1} (unsubstituted cyclopentadienyl ring in ferrocene [2]).

The cyclocondensation reaction of mercaptoacetic acid with thienylidene anils **(2–10)** proceeded smoothly in dry benzene with a reflux system using a water separator apparatus for ~20 hrs, giving the corresponding substituted thiazolidinones and bisthiazolidinones **(11–19)** in poor yields.

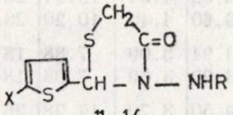

11–14

a, X = H

b, X = Br

11, R = H

12, R = C_6H_5

13, R = $\overset{O}{\overset{\|}{C}}-NH_2$

14, R = $\overset{S}{\overset{\|}{C}}-NH_2$

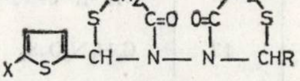

15–19

15, X = H and/or Br ; R = isatyl residue

16, X = H; R = $C_5H_5-Fe-C_5H_5$. (ferrocenyl)

17, X = H; R = p-N $(CH_3)_2$ C_6H_4

18, X = H; R = C_4H_3S (thienyl) and/or C_4H_2S Br (5-bromothienyl)

19, X = Br; R = C_4H_2S Br (5-bromothienyl)

The structures of the substituted thiazolidinones **11–19** have been proved from the elemental analysis (cf. Table 2) and IR spectral data. The IR spectra of all these compounds showed a well defined absorption band at 1700–1690 cm^{-1}, attributed to $\nu(C=O)$ group of thiazolidinones and the absence of a band corresponding to $\nu(C=N)$[2].

ANTIMICROBIAL ACTIVITIES

The antimicrobial activities of the prepared compounds against a variety of microbes were determined *. These microorganisms include Gram-positive and Gram-negative bacteria. The bacteria used were: *Bacillus subtilis*, *Staphylococcus aureus*, *Escherichia coli* and *Pseudomonas aerunginosa*. Three different concentrations of each compound were prepared in ethyleneglycol (0.5 mg/ml, 1 mg/ml and 2 mg/ml) and tested by the paper disc technique.[3]

The results showed that the inhibition effect of the prepared compounds against the tested microbes, ranges from weak to strong. Compounds **2a, 6a, 7a, 9a, 11a, 15a** were the strongest inhibitors, particularly against *Bacillus subtilis* from the Gram-positive bacteria and against *Pseudomonas aeruginosa* from the Gram-negative bacteria.

---

* Testing of biological activities was carried out in the Botanic Department, Faculty of Science, Assiut University.

TABLE 2

Thienylthiazolidin-4-ones **11 – 19**

Compd. No.	MP °C	Yield %	Molecular formula	Analysis (Cald./Found) % C	H	N	S	Br
11 a	169 – 170	20	$C_7H_8N_2OS_2$	42.00 42.01	4.00 4.01	14.00 14.02	32.00 32.03	— —
11 b	142 – 143	11	$C_7H_7N_2OS_2Br$	30.10 30.13	2.50 2.66	10.03 10.04	22.93 22.97	28.67 28.99
12 a	127 – 128	10	$C_{13}H_{12}N_2OS_2$	56.52 56.60	4.34 4.40	10.14 10.20	23.18 23.19	— —
12 b	98 – 99	12	$C_{13}H_{11}N_2OS_2Br$	43.94 43.90	3.09 3.09	7.88 7.98	18.02 18.10	22.53 22.53
13 a	234 – 235	13	$C_8H_9N_3O_2S_2$	39.50 39.60	3.70 3.80	17.28 17.30	26.33 26.43	— —
13 b	122 – 123	22	$C_8H_8N_3O_2S_2Br$	29.81 29.82	2.48 2.58	13.04 13.04	19.87 19.90	24.84 24.94
14 a	188 – 190	14	$C_8H_9N_3OS_3$	37.06 37.06	3.47 3.50	16.21 16.30	37.06 37.16	— —
14 b	179 – 180	15	$C_8H_8N_3OS_3Br$	28.40 28.50	2.36 2.40	12.42 12.50	28.40 28.50	23.66 23.70
15 a	191 – 192	18	$C_{17}H_{13}N_3O_3S_3$	50.62 50.66	3.22 3.33	10.42 10.44	23.82 23.83	— —
15 b	116 – 117	16	$C_{17}H_{12}N_3O_3S_3Br$	42.32 42.33	2.48 2.58	8.71 8.80	19.91 19.92	16.59 16.99
16 a	112 – 113	12	$C_{20}H_{18}N_2O_2S_3Fe$	51.06 51.07	3.82 3.85	5.95 5.96	20.42 20.55	— —
17 a	134 – 135	13	$C_{18}H_{19}N_3O_2S_3$	53.33 53.44	4.69 4.66	10.37 10.47	23.70 23.72	— —
18 a	147 – 148	22	$C_{14}H_{12}N_2O_2S_4$	45.65 45.66	3.26 3.33	7.60 7.66	34.78 34.77	— —
18 b	151 – 152	16	$C_{14}H_{11}N_2O_2S_4Br$	37.58 37.66	2.46 2.56	6.26 6.30	28.63 28.65	17.89 17.99
19	141 – 142	17	$C_{14}H_{10}N_2O_2S_4Br_2$	31.93 32.00	1.90 2.01	5.32 5.40	24.33 24.34	30.41 30.44

EXPERIMENTAL

The infrared absorption spectra were recorded on a Unicam SP 200 G spectrophotometer using KBr wafer technique. All melting points were uncorrected.

Thienylidene azomethines **(2 – 10) :**

a) Equimolecular amounts of thiophene-2-carboxaldehyde (or its 5-bromo analogue) and the corresponding amines were refluxed in dry alcohol in the presence of piperidine for 5 hrs. The reaction mixture was concentrated and cooled. The precipitated product was filtered, washed and crystallized from alcohol.

b) Equimolecular amounts of thienylidene-2-hydrazone and aldehyde were refluxed under the same conditions as above and the mixed azines resulted. The results are listed in Table 1.

Substituted thienylthiazolidinones **(11–19)**

A mixture of 0.02 mole of thienylidenes **2–10** and 0.02 mole of thioglycolic acid (in the case of mixed azines its quantity was doubled) in 100 ml dry benzene was refluxed for 20 hrs. The solvent was removed under reduced pressure. The residue thus obtained was dissolved in ether and seeded. In some cases the thiazolidinones separated directly from the benzene solution. The results are given in Table 2.

REFERENCES

[1] M. S. K. Youssef and Kh. M. Hassan, *Rev. Roumaine Chim.* (Accepted for publication).
[2] L. J. Bellamy, "The Infrared Spectra of Complex Molecules", Methuen, London, 1958.
[3] K. A. Oster and M. J. Golden, *J. Amer. Pharm. Assoc. Sci.*, **36**, 283 (1947).

Revue Roumaine de Chimie, 26, 7, 1011–1017 (1981)

SYNTHESIS OF N^1-(SUBSTITUTED PHENYL)-3-METHYL-4-(SUBSTITUTED PHENYLAZO)-2-PYRAZOLIN-5-ONE

C. P. SINGH*, RENU JAIN and A. C. OJHA
Chemical Laboratories, Sahu Jain College, Najibabad-246763, U.P. India

Received January 21, 1980

Several new N^1-(substituted phenyl)-3-methyl-4-(substituted phenylazo)-2-pyrazolin-5-ones and their derivatives have been synthesised by refluxing substituted phenylazo ethyl-3-oxobutyrates with substituted phenyl hydrazines, using glacial acetic acid as condensing agent. The Rf values, chemical analyses, IR and NMR spectra are given.

INTRODUCTION

The synthesis of 2-pyrazolin-5-ones, has been extensively studied with view of a prodigious range of activity. Recently, a large number of pharmaceutical applications of 2-pyrazolin-5-ones e.g. germicides,[1] antimicrobial agents,[2] antiactinics,[3] antidiuretics,[4] analgesics and antipyretics,[5] antifungals [6] and antirheumatics [7] besides their use in influenza [8] have been reported. β-Keto esters like β-diketones [9] react with aryl diazonium chlorides to yield arylazo derivatives [10,11] which, on condensation with carbonyl reagents, furnished 2-pyrazolin-5-ones.[12,13]

Ethyl-3-oxobutyrate was coupled with diazotised sulpha substituted/substituted phenyl amines to give sulpha substituted/substituted phenylazo ethyl-3-oxobutyrate. These, on reaction with different carbonyl reagents, furnished N^1-(substituted phenyl)-β-methyl-4-(substituted phenylazo)-2-pyrazolin-5-ones. It was considered of interest to synthesise some compounds having a sulpha substituted/substituted phenyl moiety attached to 4-position through an azo linkage in 2-pyrazolin-5-one ring and to study their biological activity.

The present communication reports on the synthesis of sulpha substituted/substituted phenylazo derivatives of ethyl-3-oxobutyrate of type(I) which have been prepared by coupling the β-keto esters with diazotised sulpha substituted/substituted phenyl amines. Compounds I react with different carbonyl reagents, namely : 2-chlorophenyl-, 4-chlorophenyl-, 2-chloro-4-nitrophenyl-, 4-bromophenyl-, 1-naphthyl-, 2-sulphanilamidophenyl-, N^1-2-guanyl sulphanilamidophenyl-, N^1-2-pyrimidyl sulphanilamidophenyl-, N^1-2-(4,6-dimethyl pyrimidyl) sulphanilamidophenyl-, 2,3-dimethyl-1-phenyl pyrazolone-, 4-carboxylphenyl-, 4-methylphenyl-, 2-nitrophenyl and 4-nitrophenylhydrazines, furnishing the corresponding N^1-(substituted phenyl)-3-methyl-4-(substituted phenylazo)-2-pyrazolin-5-ones of the type II.

---

* Correspondence author.

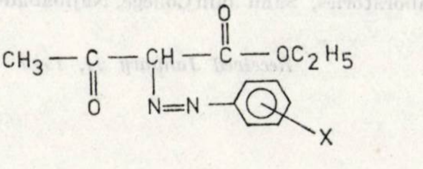

(I)

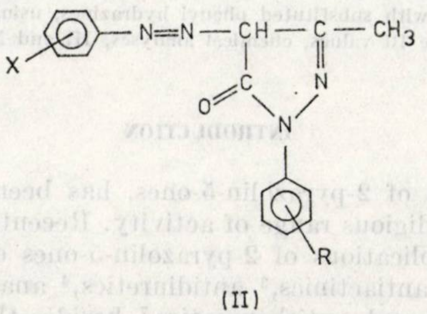

(II)

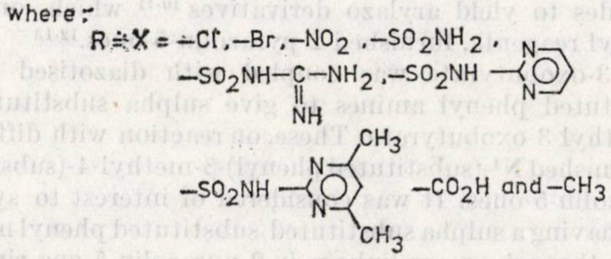

The homogeneity and purity of the compounds were checked through TLC and their structure was proved by independent synthesis and elemental analysis. Rf values were recorded in acetone/dimethyl formamide mixture (2 :1) as solvent. In each case only one spot was observed showing the formation of a single product. The compounds were analysed for nitrogen and the results were found in agreement, within the limits of the possible experimental error, with the calculated values.

EXPERIMENTAL

All the chemicals used are either BDH of E. Merck grade. The substituted sulphanilamides[14-17] and substituted phenyl hydrazines[18] required for our work were prepared by standard methods and the melting points were taken in open capillaries.

SYNTHESIS OF SUBSTITUTED PHENYLAZO-ETHYL-3-OXOBUTYRATES

To an ice cold solution of ethyl-3-oxobutyrate (4.5 mmoles) in ethanol containing sodium acetate (15.0 g), a diazotised solution of substituted phenyl amine (4.5 mmoles) was gradually added with stirring and cooling. The reaction mixture was further stirred for ten minutes and the coloured azo compound precipitated by addition of ice cold water. It was filtered, washed well with water and dried. The pure azo compound was recrystallised from ethanol/acetic acid.

Adopting this procedure, a number of substituted phenylazo ethyl-3-oxobutyrates (I) have been synthesised and their characteristics are recorded in table 1.

SYNTHESIS OF N^1-(SUBSTITUTED PHENYL)-3-METHYL-4-(Z)-2-PYRAZOLIN-5-ONE

A solution of substituted phenylazo ethyl-3-oxobutyrate (2.4 mmoles) was refluxed on water bath for 4 hrs and left overnight. The coloured compound which separated out was filtered off, washed well with water, dried and recrystallised from glacial acetic acid/dimethyl formamide/acetone.

Adopting this procedure, a number of substituted 2-pyrazolin-5-ones (II) have been synthesised and their characteristics are recorded in Table 2.

IR SPECTRA

IR spectra in KBr were recorded on a Perkin Elmer grating spectrophotometer. The spectra had characteristic peaks at 790 cm^{-1} (aromatic ring), 1575 cm^{-1} ($-N{=}N-$), 1695 cm^{-1} ($>C{=}O$) cyclic, 1280 cm^{-1} ($>C{=}N$) and 1562 cm^{-1} (heterocyclic five membered 2-pyrazolin-5-one ring). IR spectra of some compounds with characteristic bands are recorded in table 3.

NMR SPECTRA

The structures of substituted 2-pyrazolin-5-ones were also confirmed by NMR spectra.

N^1-(4-METHYL PHENYL)-3-METHYL-4-(4-METHYL PHENYLAZO) 2-PYRAZOLIN-5-ONE

^{1}H$-$NMR(CDCl$_3$), δ ppm : 2.03 (s, 3H, C_1-CH_3) ; 2.43 (s, 3H, $Ar-CH_3$ to $N{=}N$) ; 2.54 (s, 3H, $Ar-$**CH**$_3$ to N^1) ; 6.83$-$7.04 (m, 3H, Ar**H**, *m* and *p* to $N{=}N$) ; 7.13$-$7.3 (m, 1, Ar**H**, *o* to $N{=}N$) ; 7.34 (dd, 2, Ar**H** *m* to N^1, J$=$8 and 3 Hz) ; 7.78 (dd, 2, Ar**H**, *o* to N^1 J$=$8 and Hz).

^{1}H$-$NMR spectra of some other new compounds are recorded in table 4.

ACKNOWLEDGEMENTS. The authors wish to express their cordial thanks to Prof. M. K. Jain (Principal), Sahu Jain College, Najibabad, for providing laboratory facilities and to Dr. Shyam Singh, Scientist, CDRI, Lucknow, for recording IR and NMR spectra and for performing chemical analyses.

The authors wish also to express their gratefulness to CSIR, New Delhi, for financial assistance.

TABLE 1

Characteristics of substituted phenyl azo-ethyl-3-oxobutyrates (I)

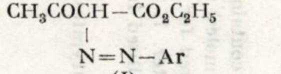

$$\underset{\displaystyle N=N-Ar}{CH_3CO\overset{}{C}H}-CO_2C_2H_5$$

(I)

Ar=	MP °C	Yield %	Colour *	Mol. formula	% of nitrogen		% of halogen/sulphur		R_f value
					Found	Calcd.	Found	Calcd.	
2-Chlorophenyl	77	65	PY	$C_{12}H_{13}O_3Cl$	10.33	10.44	13.05	13.06	0.8125
3-Chlorophenyl	78	70	SDY	$C_{12}H_{13}N_2O_3Cl$	10.31	10.44	13.09	13.06	0.7115
4-Chlorophenyl	75	80	SYF	$C_{12}H_{13}N_2O_3Cl$	10.33	10.44	13.08	13.06	0.7419
2-Chloro-4-nitrophenyl	104	73	DEY	$C_{12}H_{12}N_3O_5Cl$	13.44	13.39	11.17	11.18	0.8645
4-Bromophenyl	73	68	LPY	$C_{12}H_{13}N_2O_3Br$	8.89	8.94	25.49	25.55	0.8466
1-Naphthyl	58	60	DIB	$C_{16}H_{16}N_2O_3$	9.79	9.85	—	—	0.8865
2-Sulphanilamido phenyl	126	80	SYF	$C_{12}H_{15}N_3O_5S$	12.38	13.41	10.26	10.22	0.9597
N¹-2-guanyl sulphanilamido phenyl	146	75	PY	$C_{13}H_{17}N_5O_5S$	19.69	19.71	9.03	9.01	0.7872
N¹-2-Pyrimidyl sulphanilamido phenyl	135	65	SPY	$C_{16}H_{17}N_5O_5S$	17.86	17.90	8.16	8.18	0.8378
N¹-2(4,6-dimethyl)-pyrimidyl sulphanilamido phenyl	140	68	PY	$C_{18}H_{21}N_5O_5S$	16.65	16.70	7.64	7.63	0.8164
2,3-Dimethyl-1-phenyl pyrazolone	172	80	SDYF	$C_{17}H_{20}N_4O_4$	16.24	16.27	—	—	0.8383
4-Carboxyl phenyl	197	70	PY	$C_{13}H_{14}N_2O_5$	10.09	10.07	—	—	0.6573
4-Methylphenyl	61	85	SYF	$C_{13}H_{16}N_2O_3$	11.31	11.29	—	—	0.8518
2-Nitrophenyl	90	74	SPYN	$C_{12}H_{13}N_3O_5$	15.04	15.05	—	—	0.9303
4-Nitrophenyl	127	76	IY	$C_{12}H_{13}N_3O_5$	15.03	15.05	—	—	0.9013

* P = Pale, Y = Yellow, S = Shining, D = Dark, Dl = Dull, L = Light, B = Brown, F = Flake, N = Needles, G = Golden and Dy = Dirty.

TABLE 2

Characteristics of N^1-(R)-3-methyl-4-(Z)-azo-2-pyrazolin-5-ones (II)

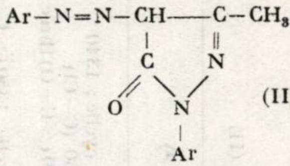

(II)

R=X=Ar	MP °C	Yield %	Colour *	Mol. formula	% of nitrogen		% of halogen/sulphur		R_f values
					Found	Calcd.	Found	Calcd.	
2-Chlorophenyl	95	75	SBF	$C_{16}H_{12}O_4OCl_2$	16.12	16.13	20.48	20.46	0.8456
3-Chlorophenyl	124	80	SON	$C_{16}H_{12}N_4OCl_2$	16.09	16.13	20.45	20.46	0.9732
4-Chlorophenyl	230	78	O	$C_{16}H_{12}N_4OCl_2$	16.14	16.13	20.45	20.46	0.9390
2-Chloro-4-nitrophenyl	247	65	LY	$C_{16}H_{10}N_6O_5Cl_2$	19.24	19.26	16.23	16.24	0.9714
4-Bromophenyl	222	75	Y	$C_{16}H_{12}N_4OBr_2$	12.78	12.84	36.66	36.69	0.8758
1-Naphthyl	250	70	DB	$C_{24}H_{18}N_4O$	14.79	14.81	—	—	0.9666
2-Sulphanilamido phenyl	265	85	SOF	$C_{16}H_{16}N_6O_5S_2$	19.28	19.26	14.66	14.67	0.8066
N^1-2-guanyl sulphanilamido phenyl	303	68	LY	$C_{18}H_{20}N_{10}O_5S_2$	26.89	26.92	12.29	12.30	0.8465
N^1-2-Pyrimidyl sulphanilamido phenyl	290	74	DO	$C_{24}H_{20}N_{10}O_5S_2$	23.59	23.64	10.80	10.81	0.7785
N^1-2(4,6-dimethyl) pyrimidyl sulphanilamido phenyl	295	70	DY	$C_{28}H_{28}N_{10}O_5S_2$	21.58	21.60	9.88	9.87	0.7885
2,3-Dimethyl-1-phenyl-pyrazolone	168	80	GDY	$C_{26}H_{26}N_8O_3$	29.12	29.13	—	—	0.7701
4-Carboxyphenyl	200	85	DY	$C_{18}H_{14}N_4O_5$	15.32	15.30	—	—	0.9251
4-Methylphenyl	210	90	SRF	$C_{18}H_{18}N_4O$	18.29	18.30	—	—	0.8051
2-Nitrophenyl	198	72	SRF	$C_{16}H_{12}N_6O_5$	22.81	22.82	—	—	0.8888
4-Nitrophenyl	300	78	Y	$C_{16}H_{12}N_6O_5$	22.80	22.82	—	—	0.9333

* F = Flake, S = Shining, B = Brown, O = Orange, Y = Yellow, D = Dark, N = Needles, L = Light, G = Golden and R = Red.

TABLE 3

IR spectra of N^1-(R)-3-methyl-4-(Z) azo-2-pyrazolin-5-ones (II)

R=X=Ar	Characteristic bands (cm^{-1})
2-Chloro-4-nitrophenyl	IR(KBr) : 1570 (N=N) ; 1680 (>C=O) cyclic ; 1340 (>C=N) ; 1520 ($C-NO_2$) ; 730 (C−Cl).
2,3-Dimethyl-1-phenyl-pyrazolone	IR (KBr) : 1585 (N=N) ; 1660, 1620, 1690 (>C=O) three ; 1360 (>C=N).
2-Nitrophenyl	IR(KBr) : 1577 (N=N) ; 1640 (>C=O) cyclic ; 1350 (>C=N) ; 1540 ($C-NO_2$).
4-Chlorophenyl	IR(KBr) : 1580 (N=N) ; 1680 (>C=O) cyclic ; 1330 (>C=N) ; 760 (C=Cl).
2-Sulphanilamidophenyl	IR(KBr) : 1575 (N=N) ; 1675 (>C=O) ; 1290 (>C=N) ; 3300 (−NH) SO_2NH_2.

TABLE 4

^{1}H-NMR spectra of N^1-(R)-3-methyl-4-(Z) azo-2-pyrazolin-5-ones (II)

R=X=Ar	Characteristic signals ($CDCl_3$; δ ppm)
4-Nitrophenyl	2.48(s, 3, $C_1-C\mathbf{H}_3$) ; 2.56 (s, 1, C**H**) ; 7.16 (bs, 4, Ar**H**, *ortho* and *meta* to NO_2) ; 7.39 (s, 4, ArH, *ortho* and *meta* to NO_2).
2-Carboxyphenyl	2.30 (s, 3, $C_1-C\mathbf{H}_3$) ; 2.50 (s, 1, C**H**) ; 2.42 (s, 3, $-ArC\mathbf{H}_3$) ; 7.12−7.47 (m, 4, −N=N− 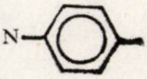 CO_2H) ; 7.74 (s, *ortho* and *meta* to CO_2H) ; 10.70−10.85 (s, 2,$2CO_2\mathbf{H}$).
4-Bromophenyl	2.12 (s, 3, $C_1-C\mathbf{H}_3$) ; 2.52 (s, 1, C**H**) ; 7.26−7.52 (m, 4, −N=N 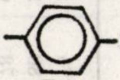 Br) ; 8.20 (s, 4, *ortho* and *meta* to Br)

REFERENCES

[1] A. R. Surrey, *J. Amer. Chem. Soc.*, **71**, 3105 (1949).

[2] P. N. Bharagava and M. R. Chauresia, *Indian J. Pharm.*, **30**, 125 (1968).

[3] M. I. Quiroga and P. H. Magnin, *Excerpta Med., Sect. XIII*, **8**, 135 (1954) ; *Chem. Abstr.*, **49**, 13593 (1955).

[4] V. Pacovsky and V. Holecek, *Casopis Lekaru Ceskych*, **95**, 300 (1956) ; *Chem. Abstr.*, **50**, 7306 (1956).

[5] J. Maj, E. Przegalinski and H. Szurska, *Diss. Pharm. Pharmacol.*, **18**, 345 (1966) ; *Chem, Abstr.*, **65**, 1444 (1967).

[6] Y. Usui and Matsmura, *Yakugaku Zasshi.*, **87**, 38 (1967).

[7] O. Danek and S. Nouzova, *Coll. Czech. Chem. Comm.*, **33**, 425 (1968).

[8] G. S. Saharia and H. R. Sharma, *J. Indian Chem. Soc.*, **2**, 354 (1974).

[9] G. S. Saharia and H. R. Sharma, *Def. Sci. J.*, **22**, 135, 139 (1972).

[10] F. D. Chattaway and D. R. Ashworth, *J. Chem. Soc.*, **475**, 1143 (1933); **476**, 1985 (1934).

[11] A. C. Ojha and C. P. Singh, *J. Indian Chem. Soc.*, **56**, 1233 (1979).

[12] H. G. Garg and C. Prakash, *J. Med. Chem.*, **14**, 175 (1971).

[13] H. G. Garg and C. Prakash, *J. Pharm. Sci.*, **60**, 323 (1971).

[14] W. Schindler, *Z. Chem.*, **5**, 382 (1965); *Chem. Abstr.*, **64**, 3517 (1966).

[15] G. L. Webster and L. D. Powers, *J. Amer. Chem. Soc.*, **60**, 1533 (1938).

[16] H. Bauer, *J. Amer. Chem. Soc.*, **61**, 613 (1939).

[17] R. O. Roblin, Jr., J. H. Williams, P. S. Winnek and J. P. English, *J. Amer. Chem. Soc.*, **62**, 1999 (1940).

[18] J. B. Cohen, "Practical Organic Chemistry", Macmillian, London, 1949, p. 190–9.

Revue Roumaine de Chimie, **26**, 7, 1019–1024 (1981)

UTILIZATION OF FERRON IN SEPARATION AND CONCENTRATION OF IRON WITH ION EXCHANGE RESINS

LUMINIȚA VLĂDESCU and CLAUDIA DOINA MARIA POP

National Institute of Chemistry, Laboratory of Analytical Chemistry, Splaiul Independenței 202, Bucharest, Romania

Received September 13, 1980

A combined spectrophotometric — ion exchange method for the quantitative determination of iron is proposed. Ferron is used both as complexing agent which allows the ion exchange separation of other elements and as colour reagent for iron.

Iron is present in various amounts in many industrial or natural products. Its accurate quantitative determination is an important step in establishing the quality of raw materials and products.

From among iron quantitative determination procedures, the best results are yielded by spectrophotometric technique which employs 7-iodo-8-hydroxyquinoline-5-sulphonic acid (Ferron)[1] as colour agent. The method is very sensitive and allows the determination of Fe^{3+} amounts in the presence of many elements : Li, Na, K, Rb, Cs, Ag, Au, Ca, Sr, Ba, Be, Mg, Zn, Cd, V, Cr, Mo, U, Fe(II) Co, Ni. However, in the presence of titanium, erroneous results are obtained.

The paper presents the utilization of this selective and sensitive technique to determine iron in titanium compounds, after the ion exchange separation. Ferron is used both as complexing agent which allows the ion exchange separation and as colour reagent for iron.

Iron (III) forms, in the presence of Ferron, three metal — ligand complex combinations of 1 :1, 1 :2, and 1 :3 content. In the presence of reagent excess, at pH = 5, the higher complex is formed.[2]

EXPERIMENTAL

REAGENT AND EQUIPMENT

— Solutions of known titrum of Fe^{3+}, TiO^{2+}, Cr^{3+}, CrO_4^- ;
— 10^{-3}—10^{-2}M Ferron aqueous solutions ;
— 30 % H_2O_2, 20 % H_2SO_4, 0.5M, 1M, 4M HCl solutions ;
— Amberlite IRA — 400 strongly basic anion exchanger ;
— Amberlite IR — 120 strongly acid cation exchanger ;
— SPECORD UV— VIS and SPEKOL spectrophotometers.

The quantitative determination of ions was made by spectrophotometric method, in the presence of Ferron [1] in the case of iron, with H_2O_2—H_2SO_4 or ascorbic acid for titanium [3] and as chromate in the case of chromium.[4]

The ionic exchange took place in glass columns 15 cm long, 1 cm in diameter, provided with stop cocks at the bottom and funnel with ground joint at the top. Five grammes of cation or anion exchanger were transferred into each column, purified and activated in ionic H^+ form and washed with distilled water up to negative Cl^- test.

RESULTS AND DISCUSSION

To establish the optimum working conditions, the influence of Ferron concentration, of resin ionic form and of pH upon the behaviour at ion exchange of Fe(III) was studied.

TABLE 1

Influence of Ferron concentration, of resin ionic form and of pH upon the ion exchange behaviour of Fe(III)

Resin		Ferron			Fe(III)		
						Determined	
Type	Ionic form	Conc. M	Volume cm^3	pH	In sample mg	in resin mg	In solution mg
Amberlite IR-120	H^+	5×10^{-3}	50	5	0.280	—	0.278
					0.560	—	0.559
	H^+	10^{-3}	50	5	0.014	—	0.012
			25	5	0.028	—	0.026
	H^+	10^{-3}	50	4	0.028	—	0.030
				2.5	0.028	0.012	0.017
				1.5	0.056	0.046	0.009
	Na^+	10^{-3}	50	5	0.028	—	0.028
				2.5	0.028	—	0.026
				1.5	0.028	0.008	0.021
	Na^+	10^{-3}	3	5	0.028	—	0.028
Amberlite IRA-400	Cl^-	10^{-3}	20	5	0.028	0.028	—
	Cl^-	10^{-3}	2	5	0.028	0.028	—

Table 1 shows that the whole Fe (III) amount is found in the effluent when H^+ form Amberlite IR — 120 is employed and Ferron solutions of various concentrations act as complexing agent and eluent at $pH = 5$. At lower pH's (2.5 and 1.5) iron is partially retained by the resin. This behaviour is accounted for by the fact that the acid medium favours formation of 1 :2 and 1 :1 lower complexes, respectively, which, as cations, are retained by cationite.

When cationite is employed as Na^+ form at lower pH's, of 1.5 and 2.5, nearly the whole Fe(III) amount is found in the effluent after passing the complex with Ferron through the resin. This is explained by the replacement of protons in solution with Na^+ from resin so that the solution, after passing through cationite, has a pH of 5 favourable to higher negative complex formation, which is excluded by cationite.

The data obtained also show that Ferron must not necessarily be employed as eluent agent as well. The amount of Ferron employed has only to ensure formation of 1:3 complex which is negative and passes through the cationite on simple washing with H_2O and can thus be spectrophotometrically determined in the effluent.

The behaviour of Fe(III) at anionic exchange in the presence of Ferron as complexing agent was also studied ; use has been made of Amberlite IRA-400 as Cl^- form. The iron—Ferron 1 : 3 complex is retained in anionite at pH = 5 and is then eluted with 0.5M HCl solution and determined by spectrophotometry.

The ion exchange behaviour of titanium (IV) and chromium (VI) was studied in the same conditions ; the results are shown in table 2. Chromium (VI) is not retained by cationite but it does not interfere in determination of Fe(III) with Ferron. It is retained by anionite and then eluted with H_2SO_4 1 M solutions after all iron has left the resin.

The study by molecular absorption spectra of titanium (IV) ion exchange behaviour in the presence of Ferron as complexing agent has evidenced the formation of a 1 : 2 Ti— Ferron complex which is retained by cationite where from it is eluted with HCl 1 M solution and escapes unretained by anionite.

Further, the influence of working procedure upon the cation exchange behaviour of iron (III) and titanium (IV) was studied ; the results are given in table 3.

There are two alternatives : either the amount of Ferron required by complex formation at pH = 5 is added to the solution to be analyzed and the solution is passed through the cationite. While the 1 : 3 Fe— Ferron complex is anionic and therefore not retained, it is eluted with water and determined by spectrophotometry in effluent ; titanium is retained as Ti —Ferron 1 : 2 complex and then eluted by HCl 1 M solution (Table 3a) ; or the cations are fixed into the resin and then eluted with Ferron. In this case part of iron stays fixed on cationite and cannot be eluted (Table 3b). Therefore, utilization of the first alternative is recommended.

These results allow to conclude that the separation of Fe(III) from Ti(IV) is possible although the latter interferes in determination ; use is made of ion exchange resins. The elution curves obtained for separation of iron from titanium in a synthetic mixture are given in figure 1.

The procedure of cationic exchange advanced here was then applied to synthetic mixtures of Fe(III), Ti(IV) and Cr(VI) of various compositions. The results are listed in table 4 and show a good agreement of the amount of eluted iron with that determined after separation.

Since 1 : 3 Fe — Ferron complex is anionic and therefore retained by anionite, the conditions of its elution were investigated. Table 5 shows that the optimal concentration of HCl required by elution of the complex fixed in anionite is 0.5 M.

The distinct anion exchange behaviour of Fe(III) and Ti(IV) has allowed the sepa-

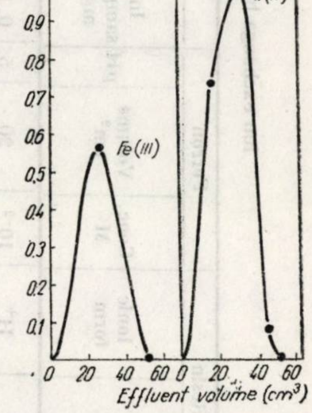

Fig. 1. — Elution curves of a cation exchange separation Fe(III)—Ti(IV).

TABLE 2

Ion exchange behaviour of Ti(IV) and Cr(VI) in the presence of Ferron

Resin		Ferron			Ti (IV)					Cr (VI)				
						Determined		Eluent			Determined		Eluent	
Type	Ionic form	Conc. M	Volume cm³	pH	In sample mg	in resin mg	in solution mg		conc. M	In sample mg	in resin mg	in solution mg		conc. M
Amberlite IR-120	H^+	10^{-2}	20	5	0.192	0.190	—	HCl	1	0.260	—	0.259	H_2O	
	K^+	10^{-3}	3	5	0.436	0.434	—	HCl	1					
Amberlite IRA-400	Cl^-	10^{-3}	20	5	0.436	—	0.437	H_2O		0.520	0.518	—	H_2SO_4	1

TABLE 3

Influence of working procedure upon the cation exchange behaviour of Fe(III) and Ti(IV)

Working procedure	Fe(III)			Ti (IV)		
		Determined			Determined	
	In sample mg	in resin mg	in solution mg	In sample mg	in resin mg	in solution mg
a	0.056	—	0.054	0.434	0.433	—
b	0.056	0.010	0.047	0.434	0.432	—

TABLE 4

Results of the separation of synthetic mixtures of Fe(III)—Ti(IV)—Cr(VI) with cation exchange resins

Fe (III)			Ti (IV)		Cr (VI)	
	Determined					
In sample mg	after separation mg	without separation mg	In sample mg	Determined after separation mg	In sample mg	Determined after separation mg
0.022	0.022	0.018	0.043	0.042	—	—
0.110	0.112	0.043	0.043	0.044	0.056	0.056
0.022	0.020	0.010	0.434	0.0433	0.056	0.054
0.022	0.023		4.340	4.341	0.560	0.560

ration of iron from binary mixtures. The elution curves are shown in figure 2. Ti(IV) is retaind by anionite, eluted with H_2O while iron complex is retained and eluted with 0.5 M HCl.

TABLE 5

Establishment of the elution conditions of iron (III) retained in an anion exchange resin in the presence of Ferron

Eluent			Fe (III)	
	Conc. M	Volume cm^3	In sample mg	Eluted mg
HCl	0.5	140	0.028	0.026
	0.1	200	0.028	—

The procedure was applied to Fe — — Ti — Cr synthetic mixtures. The results of separation of some mixtures are shown in table 6.

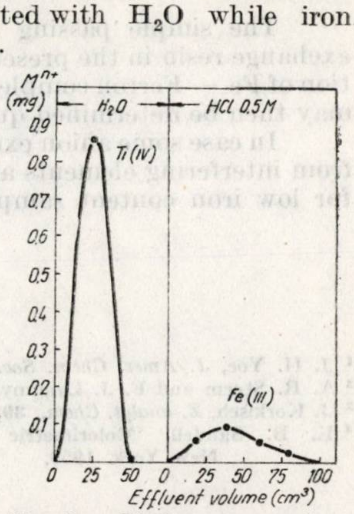

Fig. 2. — Elution curves of an anion exchange separation Fe(III)—Ti(IV).

TABLE 6

Results of the separation of synthetic mixtures of Fe(III)—Ti(IV)—Cr(VI) with anion exchange resins

Fe (III)		Ti (IV)		Cr (VI)	
In sample mg	Determined mg	In sample mg	Determined mg	In sample mg	Determined mg
0.179	0.179	0.645	0.643	—	—
0.052	0.050	0.017	0.016	—	—
0.052	0.050	4.340	4.338	0.560	0.558

The methods advanced here were also applied to solutions obtained by disaggregation with potassium pyrosulphate of some synthetic rutile samples. The results are given in table 7.

TABLE 7

Results of the determination of iron in rutile samples

Rutile sample		Content %	
no.	g	Fe	Fe_2O_3
1	0.5243	4.6 4.4	6.7 6.4
2	0.5002	3.1 3·4	4.4 4.8

CONCLUSIONS

The simple passing of solution to be analyzed through a cation exchange resin in the presence of Ferron excess at a pH = 5 yields a solution of Fe — Ferron complex free of interfering elements in which iron (III) may then be determined quantitatively by spectrophotometry.

In case some anion exchange resin is employed, iron is both separated from interfering elements and concentrated. This method is recommended for low iron content samples.

REFERENCES

[1] J. H. Yoe, *J. Amer. Chem. Soc.*, **54**, 4139 (1932).

[2] A. R. Storm and F. J. Langmyhr, *Acta Chem. Scand.*, **15**, 1765 (1961).

[3] J. Korkisch, *Z. analyt. Chem.*, **39**, 178 (1960).

[4] E. B. Sandell, "Colorimetric Determination of Traces of Metals", Wiley Interscience, New York, 1959.

Revue Roumaine de Chimie, **26**, 7, 1025–1032 (1981)

ADSORPTION EFFECTS OF SOME NATURAL AND SYNTHETIC MACROMOLECULES AT CHARGED INTERFACES

A. AWAD, F. EL-CHEIKH and A. ABD EL-GABER
Faculty of Science, Chemistry Dep., Assiut Sohag, Egypt

Received August 17, 1979

A systematic study on the adsorption effects of some natural and synthetic macromolecules has been carried out using the throwing power method and the technique of suppression of the polarographic maxima. The effects of adsorption of the macromolecules on the throwing power were investigated by the dependence of the current distribution on the concentration of the macromolecules and the variation of the polarizability. The experimental adsorption isotherms obtained from the polarographic results are found to obey Langmuir type. It was concluded that the concentration of the surfactants at which the relative coverage approaches unity depends on the type of macromolecules.

INTRODUCTION

The ability of an electrolytic bath to assume uniform distribution of the deposited metal on the cathode surface is called "the throwing power".[1] Special cells were suggested by many authors to study the property of current distribution. Some colloids and surfactants improve the throwing power of electrolytes much more than others. These colloids and surfactants were known to form adsorption *meta*-colloid complexes.[2] According to many other authors, the physical adsorption is responsible for the effect of the surfactants on the throwing power. This fact may be explained by the different values of the polarizability $\frac{dE}{di}$. The higher the increase of polarization with current, the better the distribution of current.[3] The numerous and different works conducted on the throwing power reveal that the secondary current distribution is controlled mainly by conductivity, polarizability and current efficiency behaviour.[4]

The occurrence of the polarographic maxima is related generally to the existence of a considerable surface tension on the mercury surface of the dropping electrode.[5] However the adsorption of surfactants on liquid—liquid interface is known to decrease markedly the surface tension forces, which leads to the suppression of the polarographic maxima.

Thus, the present work deals with the effect of some anionic and nonionic macromolecules on the maximum of the polarographic reduction waves of pentavalent vanadium at pH 2.3. However V (V) was selected for this study, since its polarographic reduction wave in acid region is characterized by a clear positive maximum.[6]

EXPERIMENTAL

MATERIAL AND SOLUTIONS

The studied substances are products of BASF and HOECHST. Ammonium metavanadate and all other chemicals used in this investigation are of analytical grade.

2.5×10^{-2}M stock solution of vanadium (V) was prepared by dissolving the appropriate amount of ammonium *meta*-vanadate in bidistilled water. This solution was rendered acidic by the addition of sulphuric acid to prevent hydrolysis. However, the concentration of V (V) in this solution was checked by recommended procedure.[7] Universal buffer solution of pH 2.3 was prepared as mentioned by Britton.[8]

0.02 g/100 ml bidistilled water solution of tensioactive substances was prepared for polarographic measurements. On the other hand, solutions of each of the tensioactive substances used for throwing power measurements were prepared by dissolving 0.5, 1, 2 and 5 g of each of these substances in one litre of bidistilled water.

WORKING PROCEDURE

i — *Throwing power measurements*

For the throwing power measurements, the partial currents i_n, i_f passing through two identical cathodes (C_n, C_f) connected in parallel at different distances from the anode (a) are measured (Fig. 1); the secondary distribution of the current is thus given by :

$$\text{Secondary current distribution} = \frac{i_f}{i_n} \times \times 100 \quad . \; . \; . \; . \; . \; . \; . \; . \; . \; . \; . \; (1)$$

where i_n and i_f are the partial currents on the near and far cathodes respectively. In each experiment, the anode and cathodes were pretreated chemically. The copper bath was made by dissolving 125g of copper sulphate in one litre bidistilled water containing 112 ml concentrated H_2SO_4.

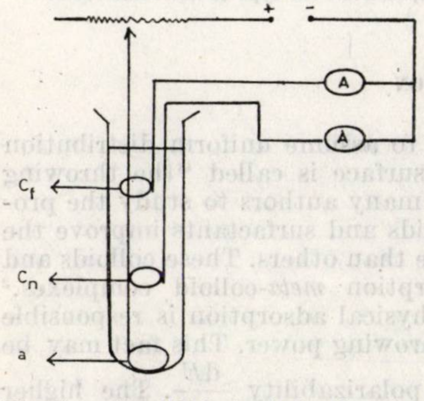

Fig 1. — Simplified circuit for throwing power measurements; C_n, C_f are the near and far cathodes a is the anode

ii — *Polarographic measurements*

The polarograms were recorded by Tacusse polarograph using a dropping Hg electrode with $m = 2.307$ mg/s and $t = 3.9$ s at a height, h, of 39 cm Hg. All measurements were performed at 25°C. The solution was dearcated by passing through it a stream of pure nitrogen for 30minutes. The nitrogen was previously purified according to the method described before.[9]

RESULTS AND DISCUSSION

THROWING POWER RESULTS

The results of the secondary current distribution are reported in table 1. From these results it is obvious that the current distribution is improved to a certain extent by the addition of macromolecules. The measurements of the throwing power at different applied currents shows greater effect at lower currents than that at higher values. This difference in

TABLE 1

The partial currents on near and far cathodes (i_n and i_f) at low and high values of current (i_1 and i_h respect.) for the different concentrations of macromolecules

Concn. $g \cdot L^{-1}$		Polyvinylalcohol (88)		Polyvinylalcohol (98)		Sod. polyacrylate (I)		Sod. polyacrylate (II)		Sod. polyacrylate (III)	
		i_n	i_f	i_n	i_f	i_n	i_f	i_n	i_f	i_n	i_f
0.0	i_1	11.0	6.75	11.0	6.75	11.0	6.75	11.0	6.75	11.0	6.75
	i_h	21.0	13.0	21.0	13.0	21.0	13.0	21.0	13.0	21.0	13.0
0.5	i_1	10.5	7.75	10.0	7.50	10.7	6.90	10.7	7.00	11.2	6.70
	i_h	20.7	14.0	20.2	13.7	20.2	13.3	20.2	13.4	20.5	13.4
1.0	i_1	10.5	7.60	10.3	7.60	10.3	7.25	10.5	7.15	10.6	7.20
	i_h	20.5	13.7	20.2	13.7	20.0	13.5	20.2	13.3	20.3	13.4
2.0	i_1	10.6	7.50	10.3	7.60	10.5	7.10	10.6	7.10	10.6	7.20
	i_h	20.7	13.7	20.5	13.5	20.1	20.1	13.4	20.2	20.1	13.2
5.0	i_1	10.6	7.60	10.3	7.20	10.4	7.25	10.7	7.00	10.2	7.20
	i_h	20.7	13.7	20.2	13.2	20.2	13.2	20.3	13.1	20.2	12.9

Concn. $g \cdot L^{-1}$		Sod. lauryl sulphate		Sod. dodecyl sulphate		Sod. dodecylbenzene sulphonate		Diammonium salt of the vinylisobutyl (ether) maleic acid		Animal glue		Gelatine	
		i_n	i_f	i_n	i_f	i_n	i_f	i_n	i_f	i_n	i_f	i_n	i_f
0.0	i_1	11.0	6.75	11.0	6.75	11.0	6.75	11.0	6.75	11.0	6.75	11.0	6.75
	i_h	21.0	13.0	21.0	13.0	21.0	13.0	21.0	13.0	21.0	13.0	21.0	13.0
0.5	i_1	11.1	6.80	10.8	6.80	10.7	7.00	10.9	7.00	10.2	7.40	10.2	7.50
	i_h	21.4	14.0	21.7	13.1	20.3	13.2	21.2	13.2	20.1	13.7	20.1	13.9
1.0	i_1	11.0	6.80	10.8	6.80	10.6	7.00	11.1	6.75	10.3	7.30	10.2	7.50
	i_h	21.2	14.0	21.8	12.8	20.2	13.2	21.2	12.8	20.1	13.7	20.2	13.9
2.0	i_1	11.0	6.90	10.8	6.80	10.5	7.00	7.00	11.1	6.75	10.3	10.2	7.50
	i_h	21.3	13.9	21.7	12.7	20.2	13.2	21.2	12.9	20.1	13.7	20.2	13.8
5.0	i_1	11.0	7.00	—	—	10.3	7.10	11.1	6.75	10.3	7.3	10.3	7.40
	i_h	21.2	13.8	—	—	20.2	13.0	21.2	12.9	20.1	1.7	20.2	13.7

behaviour may be recalled to the variation in the polarizability $\frac{dE}{di}$ at different current values.[10] It is known that, at higher currents, polarizability is lower, while at lower currents, polarizability is higher. Furthermore, the increase in the concentration of macromolecules is generally accompanied by a parallel improvement in the secondary current distribution. In this distribution where two rings of copper are used as cathodes (Fig. 1), the force lines are more or less parallel and the distribution of current is thus characteristic for the adsorption effects of the studied macromolecules and associated colloids on the polarizability. The primary distribution of current calculated for the geometrical dimensions of the cell is found to be : $i_n : i_f = 60 : 40$. The secondary distribution of current measured in the absence of any additive is found to differ slightly from the primary distribution. This fact confirms the considerable effect of the cell geometry on the distribution of force lines.

POLAROGRAPHIC RESULTS

The effects produced by the addition of successive amounts of each of the additives on the polarographic reduction waves of 1 m M V (V) at pH 2.3 were recorded. Some representative polarograms are shown in figure 2 (I—V) A.

To follow quantitatively the adsorption effects of the surface active macromolecules on the elimination of a maximum, the degree of coverage at a given concentration of the additive was determined and the degree of coverage θ was evaluated with the relation :

$$\theta = \frac{h^0 - h}{h^0}$$

where h^0 and h are the heights of the maximum in the absence and presence of macromolecules respectively.

Increasing the concentration of macromolecules, the height of the maximum decreases whereby it could be completely suppressed without bringing about any effect on the limiting current. It has been found that the elimination of the maximum depends on the type and concentration of the additives. Furthermore, the degree of coverage dependence on the concentration of macromolecules illustrates an isotherm which fits well the Langmuir adsorption. A straight line is displayed at lower concentration which possesses a constant value of θ (around unity) on increasing the surfactant concentration (Fig. 2 (I—V) B).

The concentration of the surfactant, at which θ approaches unity, differs for different tensioactive substances.

In the presence of low concentrations of gelatine and animal glue amounting to 9×10^{-5} g/100 ml, the maximum is eliminated and the first wave possesses a horizontal plateau. Thus 9×10^{-5} g/100 ml of either gelatine or animal glue is sufficient for complete coverage (i.e. $\theta = 1.0$), whereas, 1.8×10^{-4} g/100 ml of polyvinyl alcohols, is required for such coverage. These results can be attributed to the mechanical blocking of the electrode surface, depending on both the molecular weight and the chain

Fig. 2. — (A) Polarogram for 1 mM V (V) in 20 ml universal buffer solution of **pH** 2.3 with different additives. (B) Isothermic curve representing the relation between the degree of coverage and percentage for the additive.

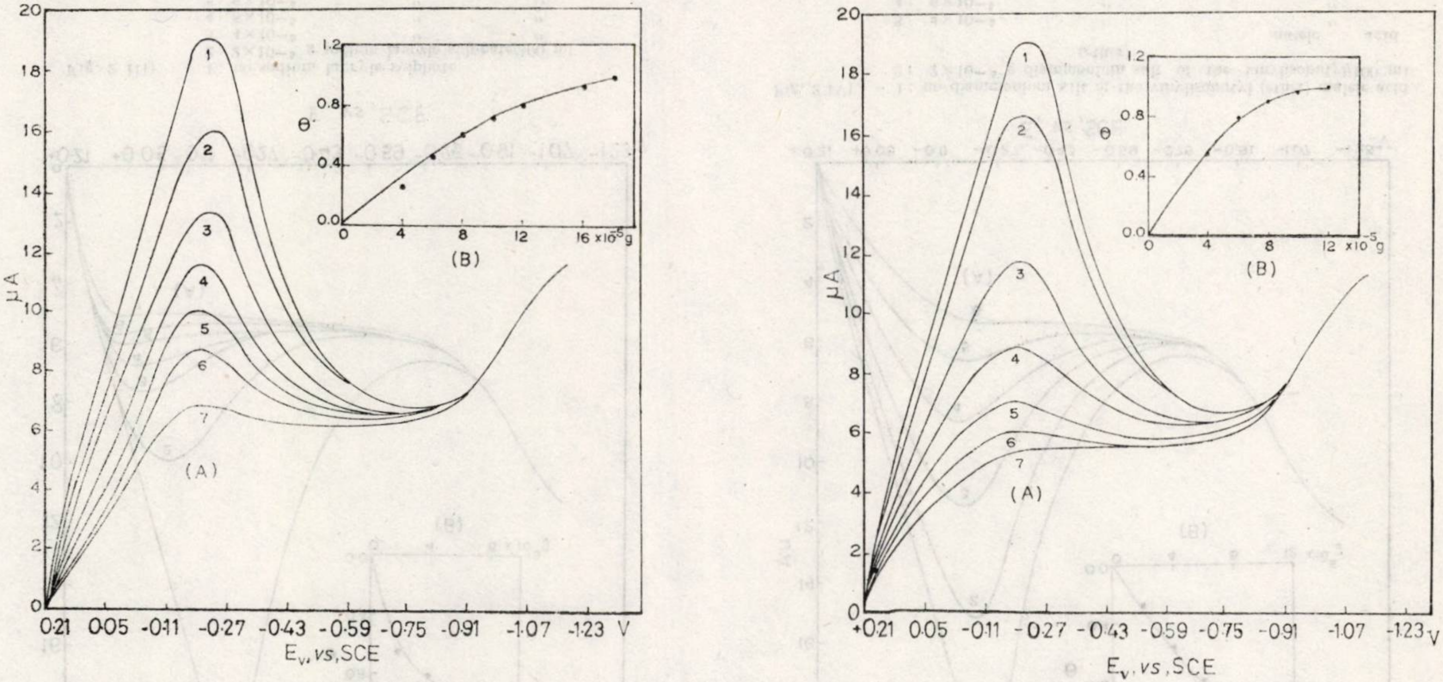

Fig. 2 I). — 1 : no polyvinylalcohol (88)
2 : 4×10^{-5} g polyvinylalcohol/100 ml water
3 : 6×10^{-5} ,, ,,
4 : 8×10^{-5} ,, ,,
5 : 10×10^{-5} ,, ,,
6 : 12×10^{-5} ,, ,,
7 : 16×10^{-5} ,, ,,

Fig. 2 II). — 1 : no sodium polyacrylate (1)
2 : 2×10^{-5} g sodium polyacrylate (1)/100 ml
3 : 4×10^{-5} ,, ,,
4 : 6×10^{-5} ,, ,,
5 : 8×10^{-5} ,, ,,
6 : 10×10^{-5} ,, ,,

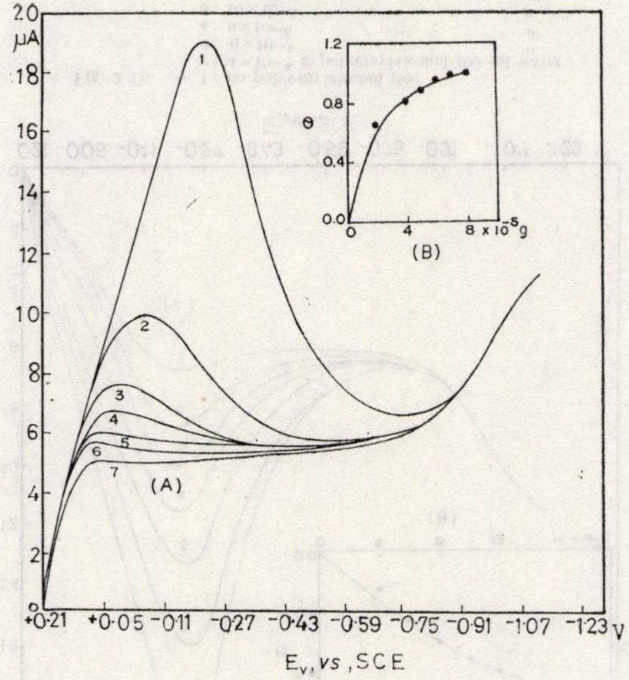

Fig. 2 III). — 1 : no sodium lauryle sulphate
2 : 2×10^{-5} g sodium lauryle sulphate/100 ml
3 : 4×10^{-5} " "
4 : 5×10^{-5} " "
5 : 6×10^{-5} " "
6 : 7×10^{-5} " "
7 : 8×10^{-5} " "

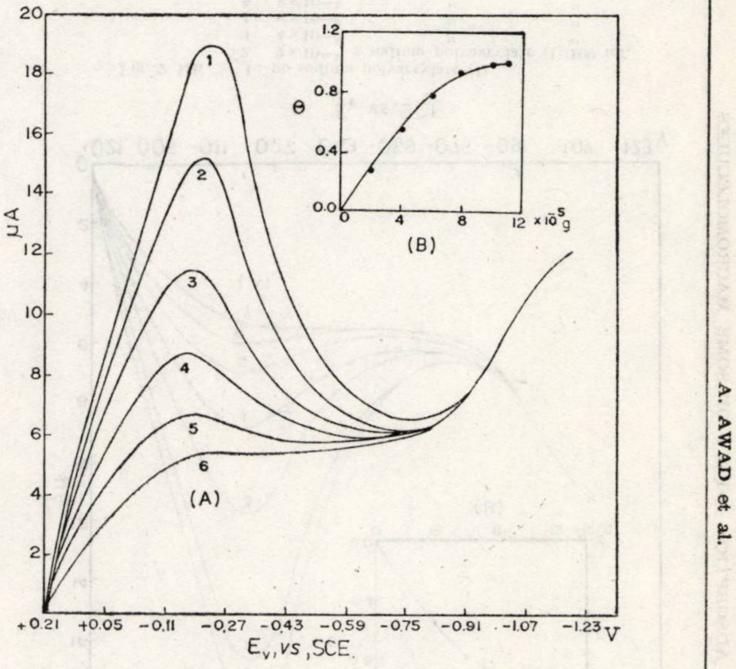

Fig. 2 IV). — 1 : no diammonium salt of the vinylisobutyl (ether) maleic acid
2 : 2×10^{-5} g diammonium salt of the vinylisobutyl/100 ml (ether) maleic acid
3 : 4×10^{-5} " "
4 : 6×10^{-5} " "
5 : 8×10^{-5} " "
6 : 10×10^{-5} " "

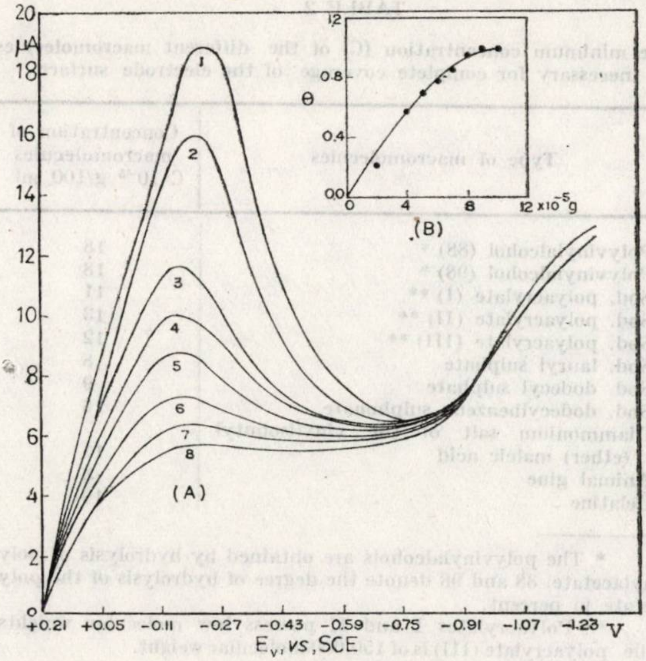

Fig. 2 V). — 1 : no polyvinylalcohol (98)
2 : 2×10^{-5} g polyvinylalcohol (98)/100 ml
3 : 4×10^{-5} " "
4 : 5×10^{-5} " "
5 : 6×10^{-5} " "
6 : 7×10^{-5} " "
7 : 8×10^{-5} " "
8 : 9×10^{-5} " "

length of each surfactant. This may be due to the nonionic character of such surfactants.

In the presence of anionic surfactants such as sodium polyacrylates, diammonium salt of the vinylisobutyl (ether) maleic acid, sodium lauryl sulphate, sodium dodecyl sulphate, and sodium dodecylbenzene sulphonate, the minimum concentration necessary for complete coverage is also shown in table 2. The careful examination of the results listed in this table reveals that the concentration of the necessary substance for complete suppression of the maximum increases in the following order :

Sod. lauryl sulphate < Sod. dodecyl sulphate < diammonium salt of the vinylisobutyl (ether) maleic acid < Sod. polyacrylates < Sod. dodecylbenzene sulphonate.

Despite of the fact that the polyacrylates and the diammonium salt of vinylisobutyl (ether) maleic acid, possess longer chains and higher molecular weights than those of the sod. dodecyl salts, the suppression of the maximum is more pronounced in the presence of the latter substances than in the presence of the former ones.

TABLE 2

The minimum concentration (C) of the different macromolecules necessary for complete coverage of the electrode surface

Type of macromolecules	Concentration of macromolecules C 10^{-5} g/100 ml
Polyvinylalcohol (88) *	18
Polyvinylalcohol (98) *	18
Sod. polyacrylate (I) **	11
Sod. polyacrylate (II) **	13
Sod. polyacrylate (III) **	12
Sod. lauryl sulphate	8
Sod. dodecyl sulphate	9
Sod. dodecylbenzene sulphonate	16
Diammonium salt of the vinylisobutyl (ether) maleic acid	11
Animal glue	8
Gelatine	10

---

* The polyvinylalcohols are obtained by hydrolysis of polyvinylacetate. 88 and 98 denote the degree of hydrolysis of the polyacetate in percent.

** Polyacrylates I and II possess low molecular weights, while polyacrylate (III) is of 150,000 molecular weight.

REFERENCES

[1] V. I. Lainer and N. T. Kunryavtsev, "Principles of Electroplating", (Russ.) Metallurgiezdat, Moscow, 1953.

[2] A. I. Levin, "Trudy po Poverknosti Aktivinykh Veshchestr", Vilnius (Russ.), 1957, P. II.

[3] A. T. Vagramyan, "Methods of Research in Electroplating", (Russ.) Ezd, Acad. Nauk. Moscow, 1961.

[4] G. A. Nachinov, "Polarizability and Force Line Distribution in Electrolytes", Moscow, 1971.

[5] J. Heyrovsky and J. Kuta, "Principles of Polarography", Academic Press., New York, 1966, p. 287 and 424.

[6] M. Tharwat and A. Awad, *Rev. Roumaine Chim.* in press.

[7] A. L. Vogel, "Text Book of Quantitative Inorganic Analysis", Longman, London Third edition, 1961.

[8] H. T. S. Britton, "Hydrogen Ion" 4th edition, Chapman and Hall, 1952.

[9] M. Tharwat, M. Sc. Thesis Assiut 1964.

[10] L. I. Kadaner, "Distribution of Galvanic Coating's", Izd. Kharkov. Univ., 1961.

Revue Roumaine de Chimie, 26, 7, 1033–1034 (1981)

DIRECT PHOTOMETRIC DETERMINATION OF CERIUM (IV) WITH 3-PHENYLAZOHYDROXYLAMINE

SUDHA CALLA, S. P. MATHUR, R. S. THAKUR and C. S. BHANDARI
Department of Chemistry, University of Rajasthan Jaipur, India

Received June 17, 1980

3-Phenylazohydroxylamine forms a 1 :2 (metal : ligand) brown complex with cerium (IV). This complex has maximum absorption at 485 nm with a molar absorptivity of 1.85×10^4/mole^{-1} cm^{-1}. Beer's law is obeyed over the concentration range 3.5×10^{-6}– 3.5×10^{-5}M. The effect of diverse ions is described.

3-Phenylazohydroxylamine acts as a non-selective ligand towards cerium (IV). The complexation between this reagent and cerium (IV) is attributed to the presence of oxime and azo groups. The suitability of this reagent for direct spectrophotometric determination of cerium in the presence of other lanthanides offers advantages over the other reagents.[1-3]

EXPERIMENTAL

3-Phenylazohydroxylamine was prepared by coupling hydroxylamine hydrochloride (3.6 gm) with benzene diazonium cloride (prepared by diazotisation of 9.3 ml aniline) at 0.5°C. The product 3-phenylazohydroxylamine hydrochloride thus obtained is neutralized with sodium carbonate to get the desired compound. It was then recrystallized with acqueous ethanol. 0.5% reagent solution was prepared in 70% ethanol.

A solution of cerium was prepared in 0.5M sulphuric acid and standardized with arsenic (III) solution.[4]

All chemicals used were of reagent grade.

Procedure : An aliquot of cerium solution (pH about 5.5) is taken in a 25 ml standard flask. 5 ml of reagent solution are added and the mixture is shaken. After 10 minutes, 2.5 ml of 8 M hydrochloric acid are added and the solution is diluted to volume with water. The absorbance is measured against an ethanol bank at 485 nm. The amount of cerium present is read on a calibration curve.

RESULTS AND DISCUSSION

In 70% ethanol–aqueous solution, 3-phenylazohydroxylamine reacts with cerium (IV) to form a highly coloured brown complex having the maximum absorbance at 485 nm. The Job [5] and slope-ratio methods [6] indicate that the complex has a metal to ligand ratio 1 : 2. The rate of complex formation increases linearly with ligand concentration and pH. The apparent pH of the system is about 5.5 before the acidification.

The cerium complex is found to be kinetically inert towards hydrogen ions. No dissociation of the complex so formed is observed in the hydrogen ion concentration range of 2.5×10^{-8} to 4.0M. The complex has the maximum absorbance at 485 nm and molar absorptivity of $1.85 \times 10^{-4\%}$ mole^{-1} cm^{-1}. Beer's law is obeyed over a cerium concentration range of $3.5 \times \times 10^{-6}-3.5 \times 10^{-5}$M.

The effect of diverse ions on the cerium reagent complex has been investigated. The following amounts (μg/ml) of foreign ions were found to give less than 10% error in the determination of 5 μg/ml of Ce (IV)La(III), 2500, Pr(III), 2500, Nd(III), 3000, Gd(III), 3000, Dy(III), 3000, Ho(III), 3000, yb(III), 3500, Y(III), 3500, Tb(III), 3000, Ir(III) 8, Pt(IV) 7, Th(IV) 725, Zr(IV) 890, U(VI) 2800, As(V), 3500, cloride 7000, bromide 9500, fluoride 8000, sulphate 6570, acetate 7250, phosphate 8525, nitrate 7280. It can be inferred that many diverse ions especially lanthanides do not interfere in the determination of Ce(IV) in the presence of large quantities of lanthanides without making use of any masking agent. The sensitivity of the proposed method is more than that of a large number of reagents used for the determination of Ce(IV).[1-3]

ACKNOWLEDGEMENT. Thanks are due to Prof. J. P. Tondon, Head, Department of Chemistry for the facilities provided.

REFERENCES

1. N. Iordonov and K. Daiev, *Zhur. anal. Khim.*, **22**, 1514, 443 (1960).
2. V. P. Khivopistsev and V. V. Perkacheva *Zhur. anal. Khim*, **25**, 104 (1963).
3. G. Somadevamma and M. S. Sarma, *Talanta*, **14**, 861 (1967).
4. A. I. Vogal "A Text Book of Quantitative Inorganic Analysis", Elbs and Longmans, London, 1968, p. 318–319.]
5. P. Job, *Ann. Chim. (France)*, **9**, 113 (1928).
6. A. E. Harvey, and D. M. Manning, *J. Amer. Chem. Soc.*, **72**, 4488 (1950).

Revue Roumaine de Chimie, 26, 7, 1035–1040 (1981)

UN NOUVEL INDICE D'AROMATICITÉ BASÉ SUR L'EXALTATION DE SUSCEPTIBILITÉ DIAMAGNÉTIQUE

JOSÉ GAYOSO et OURIDA OUAMERALI
Laboratoire de Chimie Quantique, Institut de Chimie,
Université des Sciences et de la Technologie Houari Boumediene
(USTHB), B.P. nº 9, Dar El Beïda, Alger, Algérie

Reçu le 20 août 1980

Nous montrons qu'il est possible d'obtenir, à partir de l'exaltation de susceptibilité diamagnétique, un nouvel indice d'aromaticité, équivalent, en principe, à l'énergie spécifique de résonance. La définition de cet indice est la suivante : $\rho = K(n\Lambda/S^2)$, Λ étant l'exaltation diamagnétique, n le nombre d'électrons π, S la surface de l'ensemble des cycles du composé conjugué considéré et K une constante.

We have shown that it is possible to obtain, from the diamagnetic susceptibility exaltation, a new index of aromaticity which is, in principle, equivalent to the specific resonance energy. This index can be defined by the following formula : $\rho = K(n\Lambda/S^2)$ where Λ is the diamagnetic exaltation, n the number of π electrons, S the surface area formed by the rings of the conjugated compound, and K a constant coefficient.

I. INTRODUCTION ET ÉTAT DE LA QUESTION

L'exaltation de susceptibilité diamagnétique moyenne, introduite par Pacault, [1] en 1946, peut être considérée comme un analogue magnétique de l'énergie de résonance. L'exaltation, Λ, d'un composé est égale à la différence entre la susceptibilité moyenne χ mesurée et la susceptibilité χ_L qui serait celle du composé considéré si la structure de celui-ci était représentable au moyen d'une formule développée à liaisons strictement localisées, ($\Lambda = \chi - \chi_L$). La détermination de χ_L nécessite l'emploi d'une systématique additive. Deux grandes systématiques sont, actuellement, disponibles, celle de Pascal [2], révisée par Pacault et Hoarau [3] et celle de Haberditzl. [4] Dauben, Wilson et Laity [5] ont montré, récemment, que l'exaltation diamagnétique constitue un bon critère qualitatif d'aromaticité. Cette exaltation est, en effet, élevée pour les molécules benzénoïdes, faible pour les composés à caractère polyénique, et elle change de signe lorsqu'on passe d'une molécule aromatique comme le naphtalène à un composé antiaromatique comme l'heptalène. La détermination, empirique ou théorique, de l'exaltation permet donc de ranger un composé conjugué donné dans une des trois classes d'aromaticité, ce qui signifie qu'elle permet de dire si ce composé est aromatique, non aromatique ou antiaromatique.

Par contre, l'exaltation diamagnétique ne permet pas de comparer quantitativement deux molécules d'une même classe d'aromaticité. Tous les polyacènes ont, par exemple, des exaltations diamagnétiques supérieures à celles du benzène et la situation reste la même si l'exaltation est divisée par le nombre d'électrons π.

L'indice d'aromaticité le plus ancien est l'énergie spécifique de résonance, ou énergie de résonance par électron π.[6,7a] D'autres indices quantitatifs ont cependant été proposés. Celui de Labarre [8,9] est basé sur le gradient des charges des cycles ; celui de Julg et François [10] sur l'écart quadratique moyen des longueurs de liaison périphériques du système conjugué et celui de Kemula et Krygowski [11] sur l'écart moyen absolu des ordres de liaison π. Julg [12] a également défini un indice d'aromaticité traduisant, à la fois, le gradient des charges et la plus ou moins grande égalisation des longueurs de liaison. Parmi les divers travaux consacrés aux critères quantitatifs d'aromaticité [13-19] on peut signaler l'indice établi par Kruszewski et Krygowski, [14] qui est basé sur l'énergie mise en jeu lors d'une réaction d'addition sur un système conjugué et ceux proposés par Jongh et Wynberg [18] et par Balaban et coll.[19] qui sont basés sur l'effet des courants de cycle en RMN. On doit citer enfin, parmi diverses publications consacrées entièrement ou partiellement aux questions d'aromaticité,[20-26] les travaux récents de Haddon.[20-22] Cet auteur[20-21] a développé un modèle théorique des courants de cycle, basé sur la loi de Biot et Savart. Dans le cadre de ce modèle, il a pu rationaliser la relation existant entre les courants de cycle et les déplacements chimiques de RMN des Annulènes obéissant à la règle $4n+2$ de Hückel. Par ailleurs, tout récemment Haddon [22] a réussi à établir une relation entre l'énergie de résonance et l'intensité des courants de cycle, telle qu'elle est définie dans la théorie de Hückel—London—Mc Weeny.[27-28]

A notre connaissance, aucun indice quantitatif d'aromaticité, basé sur l'exaltation diamagnétique, n'a encore été défini. Nous proposons un tel indice dans cet article.

II. DÉFINITION D'UN INDICE D'AROMATICITÉ BASÉ SUR L'EXALTATION DIAMAGNÉTIQUE

Considérons un cyclopolyène régulier formé par n carbones hybridés en sp^2 et plongé dans un champ magnétique H, statique, homogène et perpendiculaire au plan moléculaire. Les énergies e_K associées aux OM π d'un tel système sont, dans le cadre de la théorie de London [27-7b] données par la formule analytique,

$$e_k = \alpha + 2\beta \cos\left(\frac{2k\pi}{n} + \frac{\omega}{n} \mathrm{H}\right); \quad \omega = \frac{2\pi e}{hc} S \tag{1a}$$

$$k = 0, \pm 1, \pm 2 \ldots \begin{cases} \pm \dfrac{n-1}{2}, \text{ si } n \text{ est impair} \\[2ex] \pm \dfrac{n}{2}, \text{ si } n \text{ est pair} \end{cases} \tag{1b}$$

dans laquelle α et β représentent les intégrales coulombiennes et de résonance standard de la méthode de Hückel et S la surface du cycle du cyclopolyène considéré ; e, h et c désignant, respectivement, la valeur absolue de la charge de l'électron, la constante de Planck et la vitesse de la lumière. *Nous admettrons que, conformément au modèle proposé par Platt*[29] *un hydrocarbure conjugué quelconque peut, en première approximation, être représenté par un tel cyclopolyène.* Dans le cadre de la méthode de Hückel-London[27] cela revient à supprimer les liaisons entre carbones tertiaires. Le naphtalène sera, dans ces conditions, représenté par le système conjugué du cyclodécapentaène, et le pentalène par celui du cyclooctatétraène, supposé plan et parfaitement régulier. Le modèle est, bien sûr, approché, mais les conclusions auxquelles il conduit n'en sont pas moins qualitativement correctes. L'énergie E_π du système conjugué s'obtient immédiatement, à partir de (1a) :

$$E_\pi = \text{n}\alpha + \beta \sum_{k=1}^{m} 2\nu_k \cos\left(\frac{2k\pi}{n} + \frac{\omega}{n}\text{H}\right) = \text{n}\alpha + M_\pi(\text{H})\beta \qquad (2)$$

Dans la relation (2) m désigne le nombre d'OMΠ occupées, dans l'état fondamental et ν_k le nombre d'électrons situés sur la kième orbitale. La susceptibilité χ_π^c de London[27] (ou susceptibilité de cycle) s'obtient en dérivant deux fois E_π par rapport à H, puis en annulant H dans l'expression ainsi obtenue.

L'exaltation diamagnétique Λ est égale au tiers de cette susceptibilité de cycle ($\Lambda = \chi_\pi^c/3$) :

$$\chi_\pi^c = -\left(\frac{\partial^2 E_\pi}{\partial H^2}\right)_0 \rightarrow \chi_\pi^c = \left(\frac{\omega}{n}\right)^2 \cdot M_\pi^0 \beta \; ; \; \chi_\pi^c = 3\Lambda \qquad (3)$$

Dans le cadre de la méthode de Hückel l'énergie spécifique de résonance E_r^s est donnée par la formule classique[6-7]

$$E_R^S = \left(\frac{M_\pi^0}{n} - 1\right)\beta \qquad (4)$$

en éliminant M_π^0 entre (3) et (4) et en tenant compte de la définition de ω donnée en (1a), on obtient la relation :

$$E_R^S = \left(\frac{\sqrt{3}hc}{2\pi\text{e}}\right)^2 \cdot \frac{n\Lambda}{S^2} - \beta \qquad (5)$$

il est donc clair que la quantité

$$\rho = K \frac{n\Lambda}{S^2} \qquad K = 31{,}546 \qquad (6)$$

constitue un indice d'aromaticité, équivalent, en principe, à l'énergie spécifique de résonance, puisque E_R^S est une fonction linéaire de ρ. La constante K a été fixée en égalant à cent l'indice ρ du benzène, et en prenant pour l'exaltation Λ de cette molécule la valeur 13,7 (en unités -10^{-6} uemcgs) fournie par la systématique de Haberditzl.[4] Remarquons que les formules (3), (4) et (5) restent approximativement valables dans le cas des hétérocycles conjugués. La présence de l'hétéroatome introduit simplement une perturbation dans le modèle de Platt.[29] *L'applicabilité de l'indice diamagnétique d'aromaticité, défini en* (6), *devrait donc être tout à fait générale.*

III. DÉTERMINATION DE L'INDICE DIAMAGNÉTIQUE D'AROMATICITÉ DE QUELQUES COMPOSÉS CONJUGUÉS

Le tableau, joint à ce texte, rassemble les indices, ρ, obtenus à partir des exaltations fournies par la systématique de Haberditzl.[4-5] Les géométries ont été idéalisées au moyen de polygones réguliers de 1,4 Å de côté. Nous avons vérifié que cette approximation est, pratiquement, sans effet sur les valeurs des surfaces et des indices ρ.

TABLEAU 1

Indice diamagnétique d'aromaticité ($\rho = Kn\Lambda/S^2$) de quelques composés conjugués

Benzène	100	Azulène	85	Pyridine	98
Naphtalène	93	Fulvène	18	Quinoléine	91
Anthracène	92	Acénaphtylène	50	Coumarine	63
Phénanthrène	87	Acépléiadylène	67	Xanthone	49
Styrène	92	Acépléiadiène	43	Tropone	19
Biphényle	96	Tropylium	63	Pyrrole	89
Biphénylène	36	Heptafulvalène	04	Furanne	73
^{16}-annulène	-06	Heptalène	-11	Borazole	50

Il est clair, à l'examen de ce tableau que *l'indice diamagnétique d'aromaticité, proposé dans ce mémoire, permet d'établir pour les 24 Composés considérés une échelle d'aromaticité tout à fait raisonnable et apparemment exempte de contradictions.* Le pyrrole et le furanne méritent quelques commentaires. Les exaltations de ces deux composés sont, selon la systématique de Haberditzl,[4-5] respectivement égales à 10,2 et 8,9 (en unités -10^{-6}uem cgs).

Ces valeurs correspondent à des indices ρ de 170 et 148 qui sont tout à fait inacceptables puisqu'ils attribuent au pyrrole et au furanne des aromaticités de beaucoup supérieures à celles du benzène. La situation n'est pas meilleure lorsqu'on emploie la systématique de Pascal.[2-3] Les exaltations du benzène, du pyrrole et du furanne sont alors, respectivement égales à 17,6, 14,3 et 14,5 ce qui donne pour ces trois molécules des indices d'aromaticité de 100, 186 et 188. Au cours de divers travaux, réalisés dans notre laboratoire,[30-32] nous avons pu montrer que la méthode SCF$-\pi$ de Pople [33] et la technique des perturbations couplées de Hartree-Fock [34] conduisent, généralement, à des exaltations théoriques en bon accord avec les valeurs empiriques. Or cette méthode fournit pour le pyrrole et le furanne des exaltations de beaucoup inférieures à celles de la systématique de Haberditzl. On obtient, en effet, après avoir ramené à 13,7 (au lieu de 11,6) l'exaltation théorique du benzène, les valeurs 5,3 et 4,4 pour les exaltations de ces deux molécules. Ces valeurs nous paraissent beaucoup plus crédibles que celles de Haberditzl, nous les avons donc utilisées pour le calcul des indices diamagnétiques d'aromaticité du Pyrrole et du Furanne. *L'application de l'indice diamagnétique d'aromaticité au Pyrrole et au Furanne nous conduit donc à suggérer la nécessité d'une révision des systématiques de Haberditzl et de Pascal, dans le cas des hétérocycles conjugués à cinq membres.* Dauben, Wilson et Laity[5] avaient déjà émis des doutes quant à la validité de la systématique de Haberditzl pour ce type de composés.

IV. CONCLUSIONS

L'intérêt de ce travail réside, d'une part, dans la définition d'un nouvel indice d'aromaticité, basé sur l'exaltation de susceptibilité moyenne, mais *il réside aussi, selon nous, dans la démarche suivie pour établir cet indice.* Cette démarche tend à unifier les diverses formulations théoriques du concept d'aromaticité. Elle consisterait à déduire tous les indices d'aromaticité de l'énergie de résonance, considérée comme le critère fondamental. On éviterait ainsi la profusion d'indices plus ou moins compatibles et les nombreuses contradictions existant, actuellement entre les diverses échelles d'aromaticité.

REMERCIEMENTS. Ce travail a été réalisé dans le cadre du contrat O.N.R.S. (Organisme National Algérien de la Recherche Scientifique) 78 AA 03 05. Nous remercions l'O.N.R.S. pour son soutien financier. Nous remercions aussi, le rapporteur de cet article pour les remarques judicieuses qu'il a bien voulu nous faire.

BIBLIOGRAPHIE

[1] A. Pacault, *Ann. Chim. (France), Ser. XII*, **1946,** 527 ; *Rev. Sci.*, **86,** 38 (1948).

[2] P. Pascal, *Ann. Chim. Phys.*, **19,** 5 (1910) ; **25,** 289 (1912) : **29,** 218 (1913).

[3] P. Pascal, A. Pacault et J. Hoarau, *Compt. rend.*, **233,** 1078 (1951).

[4] W. Haberditzl, *Angew. Chem. Intern. Ed. Engl.*, **5,** 288 (1966).

[5] H. J. Dauben, J. D. Wilson et J. L. Laity, *Org. Chem.*, **16,** 167 (1971).

[6] A. Streitwieser, "*Molecular Orbital Theory for Organic Chemists*", Wiley, New-York, 1961, p. 237 à 255.

[7] B. Pullman et A. Pullman, « *Les Théories Electroniques de la Chimie Organique* », Masson, Paris, 1952, a : p. 216 à 245, b : p. 527 à 550.

[8] J. F. Labarre et F. Crasnier, *J. Chim. phys.*, **64,** 1664 (1967).

[9] J. F. Labarre, *Bull. Soc. chim. France*, **7,** 2463 (1970).

[10] A. Julg et P. François, *Theor. Chim. Acta*, **7,** 249 (1967).

[11] W. Kemula et T. M. Krygowski, *Tetrahedron Letters*, **49,** 5135 (1968).

[12] A. Julg dans "*Aromaticity, Pseudoaromaticity, Anti-aromaticity*". E. D. Bergman et B. Pullman (eds). The Jerusalem symposia vol. III, The Israel Academy of Sciences and humanities, Jerusalem, 1971, p. 383 à 385.

[13] O. E. Polansky et G. Derflinger, *Inter. J. Quant. Chem.*, **1,** 379 (1967).

[14] J. Kruszewski et T. M. Krygowski, *Tetrahedron Letters*, **1970,** 319.

[15] J. Kruszewski et T. M. Krugowski, *Bull. Acad. Polon. Sci., Sér. Sci. Chim.*, **20,** 907 (1972) ; **20,** 999 (1972).

[16] J. Kruszewski, *Soc. Sci. Lodz. Acta Chimica*, **16,** 77 (1971).

[17] W. D. Hobey, *Tetrahedron Letters*, **23,** 2067 (1973).

[18] H. A. P. de Jongh et H. Wynberg, *Tetrahedron*, **21**, 515 (1965).

[19] A. T. Balaban, A. Dinculescu, H. N. Koutrakis et F. Chiraleu, *Tetrahedron Letters*, **1979**, 437.

[20] R. C. Haddon, V. R. Haddon et L. Jackman, *Fortschr. Chem. Forsch.*, **16**, 103 (1971).

[21] R. C. Haddon, *Tetrahedron*, **28**, 3613, 3635 (1972).

[22] R. C. Haddon, *J. Amer. Chem. Soc.*, **101**, 1722 (1979).

[23] C. W. Haigh et R. B. Mallion, *Progress in NMR. Spectroscopy*, **13**, 303 (1979).

[24] A. T. Balaban, *Pure Appl. Chem.*, **52**, 1409 (1980).

[25] J. Aihara, *Bull. Chem. Soc. Japan*, **53**, 1163 (1980).

[26] J. Aihara, *The Theory of Aromatic Stabilization* (A Source Book 1974 – 1979), Department of Chemistry, Hokkaïdo University, 1979.

[27] F. London, *J. Phys. et le Radium*, **8**, 397 (1937).

[28] R. Mc Weeny, *Mol. Phys.*, **1**, 311 (1958).

[29] J. R. Platt, *J. Chem. Phys.*, **17**, 484 (1949).

[30] J. Gayoso et coll., à paraître.

[31] A. Boucekkine, *Thèse d'Etat*, Alger (1977).

[32] O. Ouamerali, *Thèse de* $3^{\text{ème}}$ *Cycle*, Alger (1979).

[33] J. A. Pople, *Trans. Faraday Soc.*, **49**, 1375 (1953).

[34] R. M. Stevens, R. M. Pitzer et W. N. Lipscomb, *J. Chem. Phys.*, **38**, 550 (1963).

COMPTES RENDUS

"Structure and Bonding", Volume 36, Springer-Verlag, Berlin, Heidelberg, New York, 1979, 180 p.

"Inorganic Chemistry and Spectroscopy", the volume 36 of the series "Structure and Bonding", contains three article reviews, differing in point of length and subject range.

The first article review, "The resonance Raman Effect. Review of the theory and applications in inorganic chemistry" by R. J. H. Clark and B. Stewart has 80 pages. A short introduction (2 p.) emphasizes the current importance of this method. Even though the Raman spectroscopy was between 1940 and 1960 almost completely substituted by the IR spectroscopy, after 1960 its importance has grown, due to new technical facilities, among them the use of the laser. The first part of the article review summarizes, on 43 pages, in a highly qualified manner, the theory of the Raman resonance effect. A short description (3 p.) of the most modern experimental techniques in this field follows. The last part of the work presents an exhaustive synthesis (30 p.) of the most recent experimental results obtained with the Raman spectroscopy, especially the study of different inorganic systems. The work contains 110 bibliographic quotations, many of them appeared in 1978.

The second article review is "Structure and bonding with alkali metal suboxides", by A. Simon (47 p.). The studies made in the last 10 years on these suboxides have shown that they represent a very unique class of compounds. In a simplified manner, their structural chemistry represents the opposite of that of the transition metal compounds with a high metal content. The last ones (for example the cluster-type compounds of the groups V–VII B elements) show strong directional and thus rigid metal-metal bonds, dominating the crystal structures. In contrast to that, the bonding between alkali metal atoms in the alkali metal suboxides is non-directional and "soft". The structural chemistry of the metal-rich alkali metal oxides is dominated by the strong heteroatom interaction. The article review (47 p.) deals with the structure of the alkali metal suboxides (15 p.), the chemical bonding in the stable suboxides (7 p.) and the electronic properties (electric resistivity of the stable compounds and of the metastable phases, the color and the photoelectron spectroscopy) of the alkali metal suboxides (17 p.). The work contains 89 bibliographic quotations.

The last work is "The electronic structure of cobalt (II) complexes with Schiff bases and related ligands", by Cl. Daul, C. W. Schläpfer and A. von Zelewsky (42 p.). It fulfils the conditions of a review article since it contains the analysis of numerous original papers (76 bibliographic quotations). It also fulfils the features of an original work because it contains a lot of new data which have not been published yet (many of them of Cl. Daul and C. W. Schläpfer). Some of the new results come from the Ph. D. thesis of Cl. Daul, from the University of Fribourg, 1974. The article review considers, from experimental and theoretical point of view, the electronic structure of the low-spin Co(II) complexes with tetradentate organic ligands, from the class of the Schiff bases. These complexes show a ligand field of approximately planar symmetry (C_{2v} point group). The most numerous experimental data used in this work regard the EPR spectroscopy. The theoretical treatment of the results is based on different MO calculations. The theoretical methods used to calculate the state energies are compared. A special subchapter (5 p.) is devoted to the theoretical interpretation of the EPR parameters. The EPR spectra are explained in the frame of a model which takes into account four excited electronic states, namely two doublets and two quartets. These excited states are closely placed to the ground state. Other experimental results are more difficult to be interpreted than the EPR spectra, but generally they agree with the proposed model for the energy states. The work contains, at the end, a detailed appendix (10 p.) which systematizes the spectral and magnetic properties of the low-spin Co(II) complexes with Schiff bases and related ligands.

The whole volume is of interest for the physicists and chemists which are studying the modern aspects of the structure and chemical bonding.

A. C. Banciu

M. NÓGRÁDI, "Stereochemistry. Basic concepts and applications", Akadémiai Kiadó, Budapest, 1981, 283 pp.

During the period 1950–1980 stereochemistry achieved a tremendous growth in many directions. Among them the conformational analysis, stereocotrollable synthesis of chiral molecules and stereospecificity of thermal and photochemical pericyclic transformations should be mentioned. Since then the possibility was created to render profitable the structure of molecules at three levels : constitution, configuration and conformation. At the same time these achievements were accorded with stereochemical concepts and nomenclature which allow the description of molecules and intermolecular reactions in precise and unambiguous terms. There were excellent proposals of Cahn, Ingold and Prelog to specify molecular chirality and of Prelog for the description of stereochemical entities in topological terms. The availability of modern instrumentation, for example chiroptical methods, automated X-ray methods for the study of the geometry of molecules in the solid state or nuclear magnetic resonance for the study of the temperature dependence of the conformational behaviour of molecules in solution, has also an important influence on the growth of stereochemistry.

The aim of the book is to present stereochemistry concepts from the skeleton to the deepest form for graduates or for chemists whose primary concern is not stereochemistry but who wish to be informed on its most important developments. In the first part of the book the static phenomena, that is configuration and conformation, including the methods for their determinations are discussed. The second part contains dynamic stereochemistry, including the kinetics of conformational changes with a thorough treatment of the main types of conformational motion. The last part of the book is concerned with some selected subjects regarding applied stereochemistry in which examples of the principles discussed in the first two parts are presented.

Writing this book in 1980, the author had a somehow easier task since, after an explosive development of concepts and methodology during 1960–1970 and of instrumental techniques and notations during the last ten years, the peace has now settled. Taking that stage into account the principles rather than the up-to-date information concerning some specific problems or practical details have been emphasized. In keeping with all these, the stereochemistry of natural products and its application to the reaction mechanisms have been treated only as examples to the basic concepts.

The topic of the static stereochemistry is discussed in the first chapter including the fundamental concepts on configuration and conformation and their complementarity, referring especially to the carbon compounds. Molecular geometry, symmetry and chirality make up the content of the first part of the chapter in which molecules with one chiral centre are studied. Molecules containing more than one centre of asymmetry, the determination of the absolute and relative configuration, different principles relating to the separation of enantiomers are described in some details. The conformation of cyclic and non cyclic carbon compounds closes this chapter.

The methods of dynamic stereochemistry (especially dynamic NMR spectroscopy) the kinetics of configurational and conformational change, hindered rotation, conformational equilibria in ring systems are the main subjects of chapter two.

The last chapter presents some topics of applied stereochemistry such as : reactivity and molecular symmetry, the stereochemistry of polymers, of inorganic complexes and of enzymic processes. It is to be noted that the stereochemistry of pericyclic reactions linked with the principle of the conservation of orbital symmetry was also treated in this chapter.

The book is intended for postgraduate students, chemists and chemical engineers or for researchers as a primary information source for all those dealing with fundamental concepts of stereochemistry, indispensable in both practical and theoretical problems of chemistry. A lot of excellent references of books, reviews and original papers were cited to enable the reader to obtain more information and details about the desired subjects. Some minor printing mistakes would not influence the use of the book.

Dr. M. Nógrádi, an active researcher in the field of stereochemistry, has accumulated a large knowledge and rendered it in a very concise and attractive form. This very interesting and highly useful book would surely find its place in all organic laboratories and libraries.

Flavian Cuiban

NOTE POUR LES AUTEURS

La Revue Roumaine de Chimie publie des articles en anglais, français, russe, allemand ou espagnol. Les auteurs sont priés d'envoyer des articles et des comptes rendus inédits.

Les manuscrits seront dactylographiés à double interligne. La bibliographie, les tableaux et la légende des figures seront placés après le texte.

Si l'article fait partie d'une série numérotée, le titre de la partie précédente sera indiqué dans une note au bas de la première page.

Chaque article sera précédé d'un résumé comprenant quinze lignes au maximum.

Les références bibliographiques dans le texte seront faites par des exposants sans parenthèses et paraîtront à la fin de l'ouvrage.

Les publications périodiques mentionnées dans la bibliographie seront présentées suivant les prescriptions internationales : le nom de l'auteur précédé de l'initiale du prénom, le titre du périodique abrégé conformément à « Chemical Abstracts » et souligné par une ligne, le numéro du tome indiqué par des chiffres arabes et souligné par deux lignes, suivi de la première page de l'article : à la fin, l'année de la parution sera placée entre parenthèses. Le numéro de la revue ne sera pas indiqué si les pages du volume sont numérotées consécutivement.

Les textes des livres ou traités inclueront : le nom des auteurs, les initiales du prénom, le titre du livre entre guillements et sans être souligné, le numéro du tome précédé par l'abréviation « vol. » (ou « Bd »), le numéro de l'édition, les éditions (the publisher), la localité de la parution du livre, l'année de la parution et la page de la référence précédée par l'abréviation « p » (ou « S »).

Les brevets seront indiqués comme suit : l'auteur ou la firme, le pays et le numéro du brevet, la date et la revue (Chem. Abstr.). Par ex. : M. Jones (to Union Carbide Co), *Brit. Pat.* 601 238 (2 Sept. 1959), cf. *Chem. Abstr.*, **54**, 12808 (1960).

Les diagrammes seront tracés à l'encre de Chine sur papier calque. Les tableaux et les figures (en nombre strictement nécessaire), ainsi que les courbes dans les figures, seront numérotés par des chiffres arabes. Leur explication sera donnée dans la légende des figures. Prière de ne pas inscrire les mêmes données dans les tableaux et les figures. Chaque tableau aura un titre. On indiquera dans le texte la place approximative des tableaux et des figures. Les formules chimiques seront incluses dans le texte ; en outre, elles seront transcrites sur papier calque, à l'encre de Chine.

Les auteurs sont priés d'indiquer les caractères italiques (en soulignant les lettres au crayon), ainsi que tout autre caractère spécial : le préfixe : *ortho*, *meta*, *para*, *cis*, *trans*, etc. seront soulignés pour indiquer leurs caractères italiques et ne seront jamais écrits avec des majuscules.

Aucune correction à la main ne sera admise sur le manuscrit. Les corrections seront frappées à la machine. Les lettres grecques ou autres symboles spéciaux seront insérés à la main à l'encre clairement.

Le manuscrit sera signé par l'auteur.

Le colonne-titre aura 50 lettres au maximum.

L'entière responsabilité du contenu des articles appartient aux auteurs.

Sur demande on peut obtenir un note plus compléte.

PRINTED IN ROMANIA

ORSZÁGOS MŰSZAKI KÖNYVTÁR ÉS DOKUMENTÁCIÓS KÖZPONT 1983

1982 JAN 1 4

TRAVAUX PARUS AUX ÉDITIONS DE L'ACADÉMIE DE LA RÉPUBLIQUE SOCIALISTE DE ROUMANIE

ELENA CEAUŞESCU, **Polimerizarea stereospecifică a izoprenului** (La polymérisation stéréospecifique de l'isoprene), 1979, 307 p.

I. G. MURGULESCU, TATIANA ONCESCU et E. SEGAL, **Introducere în chimia fizică. Vol. II.2. Cinetică chimică şi cataliză** (Introduction à chimie physique. IIe Vol. 2. Cynétique chimique et catalyse), 1981, 1024 p.

V. DRĂGUŢAN, A. T. BALABAN, M. DIMONIE, **Metateza olefinelor şi polimerizarea prin deschidere de inel a cicloolefinelor** (La métathése des oléfines et la polymérisation par ouverture annulaire des cyclo-oléfines), 1981, 254 p.

O. IORDACHE, **Procese polistocastice aplicate la fenomenele de transfer** (Processus polystochastiques appliqués aux phénomènes de transfert), 1981, 187 p.

CR. SIMIONESCU, VALERIA GORDUZA, **Polimeri biocompatibili şi biologic activi** (Polymères biocompatibles et biologiquement actifs), 1980, 497 p.

Ş. MOLDOVEANU, A. SAVIN, **Aplicaţii în chimie ale metodelor semiempirice de orbitali moleculari** (Applications en chimie des méthodes semi-empiriques d'orbitaux moléculaire), 1980, 286 p.

M. FLORESCU, **Metode ştiinţifice în dezvoltarea industriei chimice moderne** (Méthodes scientifiques dans le développement de l'industrie chimique moderne), 1979, 256 p.

A. T. BALABAN, I. GALĂŢEANU, G. GEORGESCU, LIGIA SIMIONESCU, **Compuşi marcaţi şi radiofarmaceutici cu aplicaţii în medicina nucleară** (Composés marqués et radiopharmaceutiques à application en médecine nucléaire), 1979, 495 p.

CONST. GH. MACAROVICI, **Analiza chimică cantitativă anorganică** (L'Analyse chimique quantitative inorganique), 1979, 457 p.

I. G. MURGULESCU, E. SEGAL, **Introducere în chimia fizică, vol. II.1. Teoria molecular cinetică a materiei** (Introduction à la chimie physique, IIe vol. 1. La théorie moléculaire-cinétique de la matière), 1979, 1036 p.

I. E. TEODORESCU, MARIA FITI, **Iradierea tehnologică** (Irradiation technologique), 1979, 216 p.

S. STERNBERG, FL. DANEŞ, **Termodinamica chimică aplicată** (La thermodynamique chimique appliquée), 1978, 400 p.

I. G. MURGULESCU, V. EM. SAHINI, **Introducere în chimia fizică, Vol. I.2. Structura şi proprietăţile moleculelor** (Introduction à la chimie physique. Ier vol. 2. La structure et les propriétés des molécules), 1978, 604 p.

C. DRĂGULESCU, E. PETROVICI, **Chimie structurală modernă. Chimia coordinanţei 8** (La chimie structurale moderne. La chimie de la coordinence 8), 1977, 947 p.

D. PURDELA (sous la direction de), **Nomenclatura chimiei anorganice** (La nomenclature de la chimie inorganique), 1977, 153 p.

I. ZUGRAVESCU, MAGDA PETROVANU, **N-ylid chemistry**, coédition avec McGraw Hill International Book Company, U.S.A., 1977, 396 p.

D. NEGOIU, ANGELA KRIZA, Poluanţi anorganici în aer (Polluants inorganiques dans l'air), 1977, 220 p.

I. G. MURGULESCU, **Introducere în chimia fizică.** Vol. **I.1. Atomi, molecule, legătură chimică** (Introduction à la chimie physique, Ier vol. 1. Atomes, molécules, liaison chimique), 1976, 560 p.

I. GALĂŢEANU, **Radiochimia aplicată. Metode şi probleme** (La radiochimie appliquée. Méthodes et problèmes), 1976, 307 p.

CONST. GH. MACAROVICI, D. MACAROVICI, **Chimia oxizilor dubli şi utilizările lor** (La chimie des oxydes doubles et leur utilisation), 1975, 195 p.

ELENA CEAUŞESCU, **Research work on synthesis and characterization of macromolecular compounds. Contributions**, 1974, 251 p.

CR. SIMIONESCU, VIORICA RUSAN, V. POPA, **Chimia algelor marine** (La chimie des algues marines), 1974, 212 p., 1 pl.

I. P. INFORMAŢIA cd. 1216

43 426

Lei 25.
$ 55 (price per year)

F1103

REFERÁLVA

ACADÉMIE DE LA RÉPUBLIQUE SOCIALISTE DE ROUMANIE

R

REVUE ROUMAINE DE CHIMIE

TOME 26

N° 8

Août 1981

EDITURA ACADEMIEI REPUBLICII SOCIALISTE ROMÂNIA

Rev. Roumaine Chim.

RRCHAX, 26, *8*, p. 1043–1196(1981), Bucarest

ACADÉMIE DE LA RÉPUBLIQUE SOCIALISTE DE ROUMANIE

COMITÉ DE RÉDACTION

Rédacteur en chef:

I. G. MURGULESCU, membre de l'Académie de la République Socialiste de Roumanie

Rédacteurs en chef adjoints:

A. T. BALABAN et V. EM. SAHINI, membres correspondants de l'Académie de la République Socialiste de Roumanie

Collège de rédaction:

EM. BRATU, ELENA CEAUŞESCU, ECATERINA CIORĂNESCU-NENITZESCU, CR. SIMIONESCU, membres de l'Académie de la République Socialiste de Roumanie ; P. SPACU, membre correspondant de l'Académie de la République Socialiste de Roumanie ; MARGARETA AVRAM, M. BANCIU, I. HAIDUC, D. I. MARCHIDAN, I. MOLDOVAN, G. NIAC et D. SĂNDULESCU

La Revue Roumaine de Chimie paraît 10 fois par an. Toute commande de l'étranger pour les travaux parus aux Editions de l'Académie de la République Socialiste de Roumanie sera adressée à ILEXIM, Departamentul Export-Import Carte (Livres)/Departamentul Export-Import Presă (Revues), P.O.B. 136—137, télex 11226, 3, str. 13 Decembrie, 79517 Bucarest, Roumanie

Les manuscrits, les livres et les revues proposés en échange, ainsi que toute correspondance seront envoyés à la rédaction :

REVUE ROUMAINE DE CHIMIE

125, Calea Victoriei, 79717 Bucarest, Roumanie, téléphone 50 76 80

EDITURA ACADEMIEI REPUBLICII SOCIALISTE ROMÂNIA

125, Calea Victoriei, 79717 Bucarest, Roumanie, téléphone 50 76 80

REVUE ROUMAINE DE CHIMIE

Tome 26, N° 8 **Août, 1981**

THE SECOND NATIONAL CONGRESS OF CHEMISTRY 1045–1046

D. ŞERBĂNESCU, GH. VASU, RODICA VÎLCU and A. CIOCHINĂ, **Transient hot wire thermal conductivimeter for absolute measurements in fluids** . . . . 1047–1062 R

MARIA ZAHARESCU and ANA BRĂILEANU, The formation mechanism of the compounds in the $MgO-V_2O_5$ system 1063–1070

R. P. PANDEY and TARA UPRETI, Extension and comparison of collision factor theory and free length theory in liquid ternary mixtures 1071–1076

G. STEINBRECHER, P. ROTARU, L. SALIU, O. BUNESCU, N. MUREŞAN and I. BUCUR, Method for determining effective diffusion coefficient of gases in catalyst pellets . . . . 1077–1083 R

FLORIAN DOMKA et MAREK LANIECKI, Influence of alkali metal oxides on the formation of a ferro-chromic catalyst for conversion of carbon monoxide by steam (in French) 1085–1090

R. H. SCHUSTER, Influence of the medium in the solvolysis of alkyl halides. VIII. Salt effects in the hydrolysis of *t*-butyl chloride (in German) 1091–1096

MARIA BREZEANU, IOANA JITARU and MAGDALENA DINCULESCU, Co(III) complex compounds with 3-amino-1-propanol and dimethylglyoxime 1097–1105

S. P. S. JADON, Kinetics of self-decomposition of tin(IV) peroxydichromate . . 1107–1110

R. D. JAIMAN, SUDHA CALLA, S. P. MATHUR and R. S. THAKUR, Spectrophotometric investigations of iron(III)-N-acetyl-N-m-tolylhydroxylamine-complexes 1111–1113

M. BANCIU, PHAN LE THUY, M. ELIAN, C. DRĂGHICI and ECATERINA CIORĂNESCU, A rearrangement of dibenzo[*c*, *e*]tricyclo[5.3.0.0^{2,10}]deca-3,5-dien-9-ol into triphenylene derivatives 1115–1125

M. ANWAR, F. I. ABDEL-HAY, A. A. El-BARBARY and M. El-BORAI, Reactions of some 5-aryl-2-thiono-1,3,4-thiadiazoles 1127–1134

ILSE BACALOGLU, TRUONG THE KY, HANS-HORST GLATT, CARMEN BOERIU, RADU BACALOGLU and DIETER MARTIN, Structure and reactivity of hetero-substituted nitriles. XXIII. Kinetics and mechanism of the formation of 2-aminobenzoxazole from *o*-aminophenol and phenylcyanate (in German) 1135–1139

A. ESSAWY, M. El-GARBY YOUNES and A. Z. M. HEIKAL, Synthesis and some reactions of 3-cyano-4-phenyl-6-[1′(2′-methoxynaphthalenyl)]-2-pyridone 1141–1148

Rev. Roumaine Chim. **26**, *8*, p. 1043–1196 (1981), Bucarest

M. IOVU and ELENA BĂDĂU, Novel aromatic thioethers (in French) . . . 1149–1159

M. El-KADI, M. A. El-HASHASH and M. A. SAYED, Action of hydrazines, amines and thiourea upon β(4-chloro-3-methyl)-benzoylacrylic acid . . . 1161–1167

GH. SURPĂŢEANU, M. CONSTANTINESCU, C. LUCHIAN, M. PETROVANU, I. ZUGRĂVESCU and A. LABLACHE-COMBIER, Theoretical study on the regioselectivity in the 1,3-dipolar cycloadditions of pyridinium-ylides to Z-substituted alkenes 1169–1176

GH. CONSTANTINESCU and CECILIA CONSTANTINESCU, Reactivity of substituted malachite green in the reaction with the tetrachloroauric anion (in French) . . . . 1177–1184 Bc

GH. HUBCA, CR. OPRESCU, MARGARETA TOMESCU and M. DIMONIE, Synthesis and polymerization of polyethylene glycol dimethacrylates. I. Study of synthesis process of polyethylene glycol dimethacrylates . . . 1185–1193

BOOK REVIEW 1195–1196

THE SECOND NATIONAL CONGRESS OF CHEMISTRY

The Second National Congress of Chemistry will take place in Bucharest between 7 and 10 September 1981. It will beorganized by the National Council of Science and Technology, the Department for Chemical Industry and the Central Institute of Chemistry, under the auspices of UNESCO.

The First National Congress of Chemistry was held in Bucharest in September 1978.Like the first one, the Second Congress will mark the continuation of the remarkable scientific research work in the field of chemistry. It is also meant to be a scientific event with international participation.

Following the European congresses of chemistry housed by Romania between the two World Wars, the Academy of the Socialist Republic of Romania organized three national conferences on chemistry (1962, 1964, 1966), and then five conferences on physical chemistry (1968, 1970, 1972, 1974, 1976), all with international participation.

Nowadays chemistry is faced with some of the most complex and important problems. Among the priorities, we should consider the raw materials for industry, the complex questions of improving the production efficiency, the optimization of energy consumption, the recovery and reuse of waste materials, the purification of water and the protection of the environment. At the beginning of this ninth decade of our century, which also means the starting point of a new Five-year-plan in Romania's development, Romanian scientific research activity in chemistry is called to work out the answers to these questions which our epoch is confronted with.

The main topics of the Congress are reflected in the titles of the scientific sections : polymers, organic chemistry, carbochemistry, petrochemistry ; inorganic chemistry and non-ferrous metals ; catalysis and catalysts ; chemical engineering ; physical chemistry and analytical chemistry ; chemical and biochemical energetics ; recovery and reuse of waste materials and of chemical products. All these topics constitute a proof of the deep concern for the above-mentioned problems.

The Second National Congress of Chemistry will be a welcome opportunity to review the results of the chemical research activity carried out in our country up to the present. It will also enable the integration of these results with the achievements of other countries and will offer a good ground for a fruitful exchange of opinions and analysis of the most up-to-date successes in chemistry.

Revue Roumaine de Chimie, **26**, *8*, 1047—1062 (1981)

TRANSIENT HOT WIRE THERMAL CONDUCTIVIMETER FOR ABSOLUTE MEASUREMENTS IN FLUIDS

D. ŞERBĂNESCU *, GH. VASU **, RODICA VÎLCU ***
and A. CIOCHINĂ **

* ICRET, Enterprise for Construction and Repair of Telecommunication Equipments, str. Izvor 112, Bucharest, Romania

** ICECHIM, Centre of Physical Chemistry, str. Independenţei 202, Bucharest, Romania

*** The National Institute of Chemistry, Dept. of Physical Chemistry and Electrochemical Technology, Bd. Republicii 13, Bucharest, Romania

Received January 16, 1981

This contribution presents a new apparatus for absolute measurements of thermal conductivity and thermal diffusivity of fluids (gases and liquids) by classical procedure of the transient hot wire method. The experimental set-up, block diagram and principle of operation, the main technical data of the component units and the working mode are described. Measurements on liquid n-heptane at 302 K and 323 K show that the accuracy is better than 2% in the case of thermal conductivity values and 2—10% in the case of thermal diffusivity ones.

1. INTRODUCTION

The transient methods of thermal conductivity measurements of fluids have many advantages over the steady state ones.[1,2] In principle, the transient hot wire method consists in measuring the temperature rise $\theta(r_1, t)$, as a function of time, t, for a metallic wire of r_1 radius, heated with a step pulse of constant power; the wire, vertically immersed in the fluid, acts as electric heater and thermoresistance. The subsequent discussion will be restricted to the classical procedure of the method, i.e. the hot wire will be approximated as a linear source of heat.

The technical difficulty of the method, an as accurate as possible measurement of the pairs of (θ, t) values, has been solved by using several modern procedures of fast recording. [3-11]

As results from the theory of the method, [2,4,5,8,9,12] correct results are obtained only when the following conditions are fulfilled: wire diameter as small as possible, long wire and the experiment duration shorter than a critical value. That means that the measurements have to be run at times t so that $t_A \leqslant t \leqslant t_B$, where t_A is determined by the thermal inertia of the wire and t_B by the onset of the natural convection.

In the most cases, the heating wire is of platinum. Wires of $0.006 \div 0.1$ mm diameters were employed for measurements on liquids, [3,4,6-8,10,11,13] and $0.0013 \div 0.005$ mm (Wollaston wire) diameters for gases [5,9]. As a function of wire diameter and its temperature rise (determined by the applied electrical power), the measurement duration in liquids is approximately located within $0.1 \div 10$ s range. For gases, if wire diameter is of the order of microns, the $(t_A \div t_B)$ range is approximately located between $0.04 \div 1$ s; when r_1 is greater, a critical situation occurs, that is $t_A > t_B$ and the classical procedure of the method is no longer suitable.

This restrictive condition, the choice of wire diameter, represents the main difficulty of principle of the classical procedure of the method.

The very thin metallic wires (Wollaston wires), beside the high cost, the difficulties in making the transducer and in measuring the diameter, can lead to systematic negative errors in thermal conductivity and thermal diffusivity values due to the pronounced non-uniformities of the diameter; [4,9,12] because of their brittleness it proves difficult to make a long transducer and the end effects become important. [8,12] In gases, the wire diameter being of the order of microns, its electrical resistance is of some thousands of ohms; [5,9] in liquids, the wire diameter can be greater and the wire electrical resistance has a value ranging from a few ohms up to tens of ohms. Therefore, in order to make measurements on gases and liquids, distinct transducers and apparatus have to be employed. The electrical resistance of Wollaston wires being high, the elimination of A.C. noise overlapping the D.C. signal becomes difficult. The errors in measuring r_1, $\theta(r_1, t)$ and t quantities, transferred to the thermal diffusivity value by means of an exponential, become high.

These are probably the reasons why this classical procedure of the method gave good results when measuring thermal conductivity of fluids, but has not been employed for thermal diffusivity measurements. Our opinion is that the accuracy of the values thus obtained of the thermal diffusivity constitutes the most objective and severe test for the accuracy of the experimental set up and for the correct location within the (t_A, t_B) range.

Since we could not purchase Wollaston wires, but only platinum ones of 0.015 mm diameter (Heraeus-Degussa) and because using platinum wires of greater diameter than 0.03 mm would eliminate the difficulties of purchasing and making of the transducer, we have proposed the following goals:

— achievement of an apparatus for measuring thermal conductivity and thermal diffusivity of fluids by classical procedure of the transient hot wire method;

— the apparatus to allow for absolute, relative and differential measurements on gases and electrically non-conductive and conductive liquids.

— working out a computation method for the absolute and simultaneous determination of thermal conductivity, λ, thermal diffusivity, $a = \lambda/(\rho c_p)$, and volumetric specific heat, $\rho c_p = \lambda/a$, of fluids, no matter the wire diameter;

— working out an experimental procedure of absolute and simultaneous measurement of the λ, a and (ρc_p) quantities, with the same apparatus and transducer, during the same experimental run, on gases and electrically non-conductive and conductive liquids.

The purpose of this work is more restricted. We shall give here only the description of the apparatus and the experimental set up for absolute measurements of the thermal conductivity and thermal diffusivity of fluids by the classical procedure of the transient hot wire method, applied on electrically non-conductive organic liquids. The temperature and pressure ranges are determined by the materials used for the cell and by the auxiliary thermostating and pressurizing units. Performances will be discussed only within the linear heat source treatment.

2. BASICS OF METHOD

The transient hot wire apparatus determines the thermal conductivity of fluid by measuring the temperature rising rate as a function of time of a metallic wire vertically immersed into the fluid. The wire, electrically heated by a step pulse of constant voltage, simulates a linear source of heat, [2] with a constant heat flow per unit length, q, and develops within the fluid a temperature field which increases radially in time and is axially symmetrical.

After a certain time, t_A, from the heat turning on ($t = 0^+$), the temperature rise $\theta(r_1, t)$ for a wire of radius r_1, at $r = r_1$ and time t, against the initial T_0 temperature of the cell at $t = 0^-$, is given by the relation : [2]

$$\theta(r_1, t) = \frac{q}{4\pi\lambda} \ln \frac{4at}{r_1^2 C} \qquad (1)$$

where $C = \exp \gamma$ and $\gamma = 0.5772$ is Euler's constant.

In the θ ($\ln t$) plot, equation (1) represents a straight line with a slope conversely proportional to the thermal conductivity. The linear logarithmic law is obeyed only for $t \geqslant t_A$, because it contains approximations for reducing the complete equation of the energy conservation and for idealising the wire behavior to an infinite linear source of heat. [8] Therefore, equation (1) is valid only for high enough $\tau = at/r_1^2$ values. This condition has to be fulfilled experimentally and it can be achieved by increasing t (duration of the experimental run) and diminishing the wire diameter. The t values are limited at $t \leqslant t_B$ (long times) by the onset of natural convection, [4,8,9] or/and by the radial limitation of the fluid (cell wall effect) [8,9] and heat losses at the wire ends; [12] towards the short times, the t values are limited at $t \geqslant t_A$ by the thermal inertia of the wire. [4,5,8,9,12] The onset of natural convection is determined by the fluid physical properties and θ (r_1, t) values; the thermal inertia of the wire as well as the heat losses at its ends are determined by the finite physical properties and geometrical dimensions of the wire. In order to achieve high τ values, wires of as small as possible diameter must be used.

The classical procedure of the method is based on the validity of the equation (1):

— thermal conductivity, $\lambda^{(0)}$, is calculated from the slope of (Δ) straight line fitted by the least square method with the experimental pairs $[\theta(r_1, t), \ln t]$, within the linear range of $\theta(\ln t)$ curve, i.e. $t_A \leqslant t \leqslant t_B$.

— thermal diffusivity, $a^{(0)}$, is determined by extrapolating the (Δ) straight line; the computation formula implies the r_1 and t_0 values, the latter being the intercept of (Δ) straight line to the ($\ln t$) axis.

The index $^{(0)}$ means that λ and a values were obtained by classical procedure of the method.

3. EXPERIMENTAL ASSEMBLY

The experimental set up consists of: measurement cell, thermostat, vacuum unit, thermal conductivimeter and electrical measurement apparatus.

3.1. MEASUREMENT CELL

A glass-made cell was employed. The inner diameter of the cell, $2r_2$, is $6 - 10$ mm for liquids and $40-60$ mm for gases. The transducer consists of a pure platinum wire (Heraeus Degussa) of a $2r_1 \simeq 0.015$ mm diameter and $L = 0.15 \div 0.30$ m length, soldered at the ends to thick copper leads. The transducer is vertically immersed in the fluid contained in the cylindrical cell. The whole assembly is immersed in the thermostating vessel.

3.2. THERMOSTATING AND VACUUM UNITS

Both units were described in a previous paper. [14]

3.3. THERMAL CONDUCTIVIMETER

3.3.1. Block diagram and operation principle

The apparatus is made up of the following main units: Wheatstone bridge; bridge power supply; instrumentation amplifier; A.C. selective amplifier; assembly of seven comparators; time-interval measuring unit; auxiliary power supplies of the units. Figure 1 shows the block diagram of the apparatus.

The platinum wire is calibrated as a thermoresistance, that is the electrical resistance variation is a measure for the temperature rise, $\theta(r_1, t)$, and it is measured on Wheatstone bridge. At $t = 0^-$ and T_0 the bridge is either balanced or a known resistive unbalance is imposed; the heating current is nil. At $t = 0^+$, a step pulse of D.C. constant voltage, E_p, is applied on the bridge input. The bridge is activated and, simultaneously, seven electronic timers are released. By Joule heating, the current on the bridge brings about a temperature rise, that is an increase in the wire electrical resistance. At the very moment when the (amplified) bridge output signal becomes successively equal to seven preset voltage levels of the comparators, each of the comparators triggers a stopping signal to the corresponding timer. Thus, the time intervals are measured from the $t = 0^+$ (START of the timers) till t_i instants ($i = 1, \ldots, 7$) (successive STOP of the timers). The wire temperature rise between $t = 0^+$ and

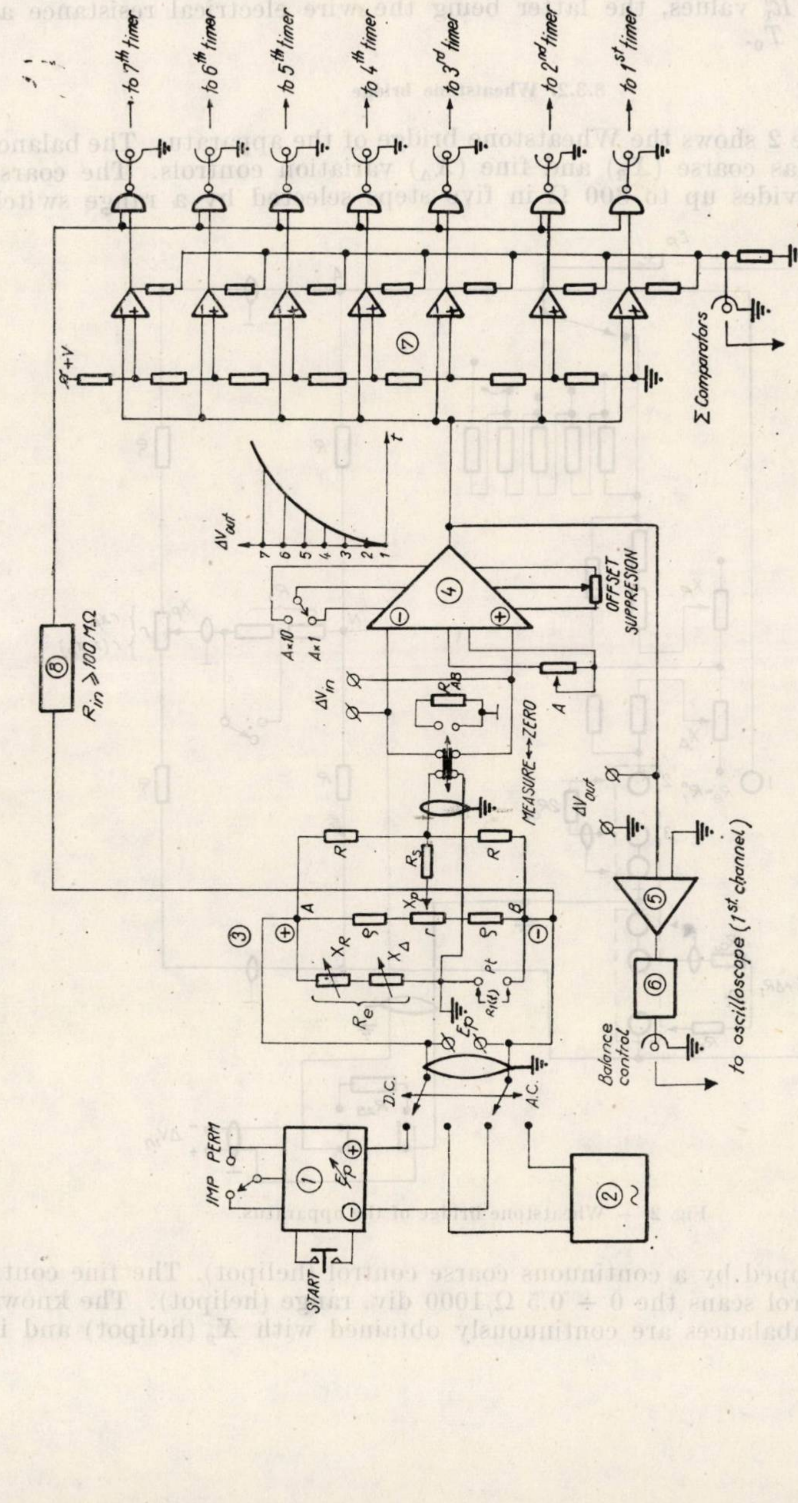
to 7th timer
to 6th timer
to 5th timer
to 4th timer
to 3rd timer
to 2nd timer
to 1st timer
+V
⑦
Σ Comparators
to oscilloscope (2nd channel)
ΔV_{out}
7
6
5
4
3
2
1
t
⑧
$R_{in} \geq 100\,M\Omega$
A×10
A×1
④
OFFSET SUPPRESION
ΔV_{in}
R_{AB}
A
MEASURE↔ZERO
ΔV_{out}
③
R
R
R_S
X_p
ρ
ρ
r
A
B
X_R
X_Δ
R_e
Pt
R(t)
E_P
⑤
⑥
to oscilloscope (1st channel)
Balance control
D.C.
A.C.
IMP
PERM
①
E_P
START
②
~

Fig. 1. — Block diagram of the apparatus: *1* — D.C. power supply of the bridge; *2* — A.C. power supply of the bridge; *3* — Wheatstone bridge; *4* — instrumentation D.C. amplifier; *5* — A.C. selective amplifier; *6* — low-pass filter; *7* — comparators; *8* — timers inhibition.

$t = t_i$ moments can be calculated from the bridge equation and temperature coefficient, α, of the wire electrical resistance. The amount of heat, q, produced on the wire unit length is calculated from the measurable E_p, L and R_1^0 values, the latter being the wire electrical resistance at $t = 0^-$ and T_0.

3.3.2. Wheatstone bridge

Figure 2 shows the Wheatstone bridge of the apparatus. The balancing arm has coarse (X_R) and fine (X_Δ) variation controls. The coarse control provides up to 300 Ω in five steps selected by a range switch and overlapped by a continuous coarse control (helipot). The fine continuous control scans the $0 \div 0.5$ Ω/1000 div. range (helipot). The known resistive unbalances are continuously obtained with X_p (helipot) and in

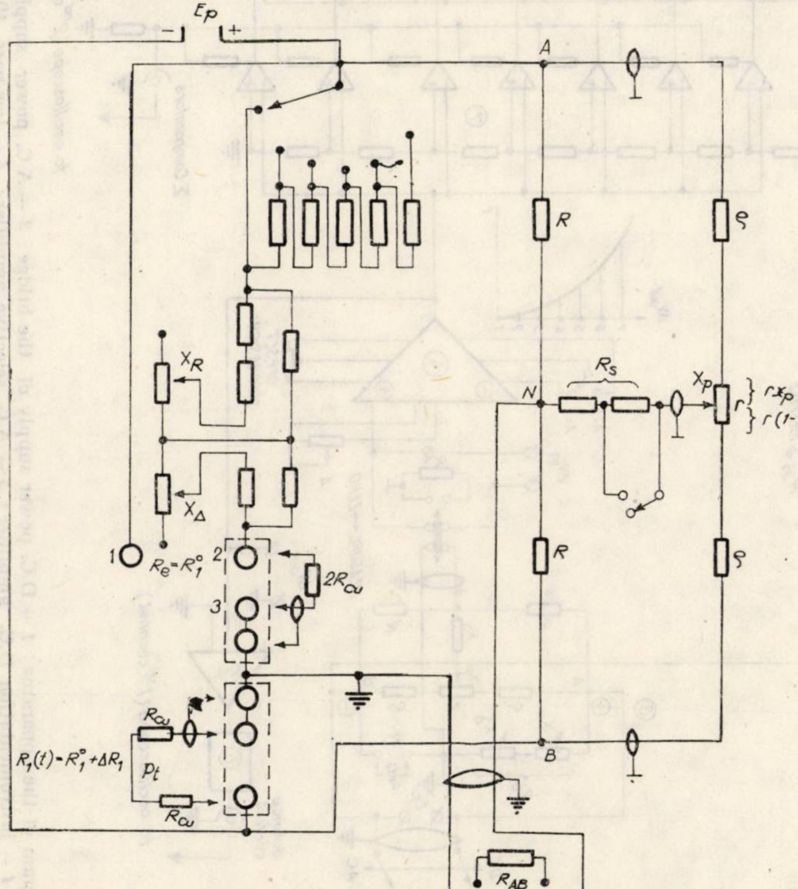

Fig. 2. — Wheatstone bridge of the apparatus.

steps by shorting the R_s resistances. The arms, containing the X_p helipot, are equal.

At $t = 0^-$, the bridge is A.C. balanced. The choice of frequency of bridge A.C. power supply is important. A high frequency provides for a better balance which can yet be altered by the reactive behavior of the cell (inductive thin wire). A value $f \simeq 16$ Hz was chosen as well as an A.C. selective amplifier with a 3 dB band at approximately 1 Hz. To pursue the balancing and suppression of D.C. amplifier offset of the bridge, an oscilloscope connected to the A.C. selective amplifier output is employed. The A.C. selective amplifier, in cascade with the bridge instrumentation amplifier, permits the passing of the D.C. signal without supplementary gain. The second channel of the oscilloscope is connected to the "Σ comparators" terminal; since, by construction, the first comparator acts on zero output voltage of the bridge D.C. amplifier, the offset of the D.C. amplifier can be suppressed accurately and the inherent noise can start symmetrically the first comparator. At the same time with the offset suppression, the drift caused by thermal emf's in the measurement chain is cancelled. This procedure can be used to buckout constant offset voltages and ensures a double check of the bridge balance at $t = 0^-$.

The electrical resistance of the connecting leads, R_{cu}, can be experimentally eliminated: on the balancing arm, terminals 2 and 3 are shorted with copper leads of the same length and diameter as those of the transducer and the balancing arm resistance R_e is measured between terminals 1 and 2 (Fig. 2).

3.3.3. Bridge power supply

Technical data: D.C. and A.C. power supply; both floating; $E_p(\text{A.C.}) \leqslant 30\ \text{mV}_{ef}$ and internally adjustable; $f \simeq 16$ Hz; harmonics content: $< 5\%$; $E_p(\text{D.C.}) = 2 \div 12$ V and continuously adjustable (helipot); $I_{max} = 200 \pm 20$ mA (D.C.), short-circuit protected at this value; drift: $< 0.1\%/\text{h}$ after 15 min. of warm-up time; rise time of the step pulse: $\sim 5\ \mu\text{s}$; $R_{in} < 0.05\ \Omega$; pulse duration: $\sim 3\text{s}$ ("IMP") and infinite ("PERM").

3.3.4. Bridge instrumentation amplifier

Technical data: true instrumentation amplifier with precision integrated μA 725 op-amp; the gain ($A = 100 \div 1000$ and $1000 \div 10000$) is continuously adjustable for each range; input tempco: $< 1\ \mu\text{V/deg}$; voltage offset: < 0.5 mV with fine suppression circuit; current offset: < 20 nA; input wide band noise: $< 5\ \mu\text{V}_{ef}$; maximum output signal: ± 12 V; rising time for 10 V output slope: $< 30\ \mu\text{s}$; c.m.r.r. in D.C.: > 100 dB; c.m.r.r. at 1000 Hz: > 40 dB; recovery from saturation: < 10 ms; overrise of the transient response: $< 2\%$.

3.3.5. Comparators

Technical data: the set up contains seven comparators made with μA 741 components; voltage thresholds are distributed between 0 and 12 V (adjustable from inside); first comparator acts for zero voltage at the bridge instrumentation amplifier output; windows width: < 0.2 mV; response time (including the output transistors): $\leqslant 2$ μs; thresholds temperature drift: < 0.2 mV/deg.

3.3.6. Measuring unit for time intervals

As an original feature of principle, this block is thus made that the timers work continuously and every time the output voltage of the bridge D.C. amplifier reaches a value below the preset thresholds of the comparators. An averaging is thus made over the time intervals when comparator window is crossed by the signal statistically uniformly overlapped by the inherent superimposed A.C. noise. The accuracy of this method is improved, given the situation of procedure when the timer is stopped at the first entry into the comparator window of the signal with noise.

3.4. AUXILIARY MEASUREMENT APPARATUS

The following auxiliary electrical apparatuses are used:

— E 0202 (IEMI) electronic counters as digital timers.

— DANA 5900 digital multimeter used for measuring E_p(D.C.) (accuracy: $\pm 0.001\%$ of full scale; resolution: 0.001% of range; $R_{\text{in}} > 10^4$ MΩ) and balancing arm electrical resistance (accuracy: $\pm$ (0.002 % of reading + + 0.001 % of full scale); resolution: 0.001 % of range).

— E 0103 (IEMI) laboratory oscilloscope for monitoring the bridge balancing (maximum sensitivity: 20 mV/cm) and determining the comparator thresholds.

4. BRIDGE EQUATION

4.1. ONE – WIRE BRIDGE

With the quotations in Fig. 2 the following results:

$$\Delta V = (U_1 - U_2)|_{x_p} = \frac{E_p}{2}\left[\frac{\Delta R_1}{2R_1^0 + \Delta R_1} + \frac{C(1 - 2x_p)}{B - r^2(1 - 2x_p)^2}\right] \tag{2}$$

where $C = 2\,R\,r$ and $B = (2\rho + r)(4R_s + 2R + 2\rho + r)$

The comparator acts when:

$$(U_1 - U_2)|_{x_p} = (U_1 - U_2)|_{x_p = x_i}$$

Therefore:

$$\frac{\Delta R_1}{2R_1^0 + \Delta R_1} + \frac{C(1 - 2x_p)}{B - r^2(1 - 2x_p)^2} = \frac{C(1 - 2x_i)}{B - r^2\,(1 - 2x_i)^2}$$

For $x_p = 0.5000$ one has:

$$f(x_i) = \frac{\Delta R_1}{2R_1^0 + \Delta R_1} = \frac{C(1 - 2x_i)}{B - r^2(1 - 2x_i)^2} \tag{3}$$

For $x_p \neq 0.5$, that is $0 < x_p < 1$, one obtains:

$$f(x_p, x_i) = \frac{\Delta R_1}{2R_1^0 + \Delta R_1} = \frac{C(1-2x_i)}{B - r^2(1-2x_i)^2} - \frac{C(1-2x_p)}{B - r^2(1-2x_p)^2} \tag{4}$$

Since:

$$\frac{\Delta R_1}{R_1^0} = 2\,\frac{f(x_p, x_i)}{1 - f(x_p, x_i)} = \alpha_{T_0}\theta(x_p, x_i) = \alpha_{T_0}\theta(r_1, t_i)$$

it results:

$$\theta(r_1, t_i) = \frac{2}{\alpha_{T_0}}\,\frac{f(x_p, x_i)}{1 - f(x_p, x_i)}\,. \tag{5}$$

4.2. TWO-WIRE BRIDGE FOR END EFFECT ELIMINATION

Due to the end effects (heat losses and temperature field deformation at the wire ends), only the middle part of the hot wire behaves as a linear heat source. This fact can be eliminated by connecting, to the balancing arm of the bridge, a second wire which is identical, except the length, with the first one, both being immersed in the same fluid (Fig. 3).

The bridge became sensitive to the resistance differences, $R(t) = R_1(t) - R_2(t)$, of the two wires and behaved as it would contain a part, $L = L_1 - L_2$, of a linear source of heat of infinite length.

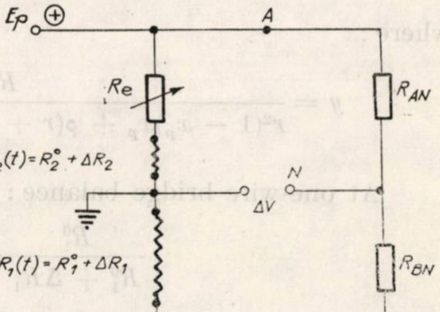
Ep ⊕
A
Re
R_{AN}
$R_2(t) = R_2^\circ + \Delta R_2$
N
ΔV
$R_1(t) = R_1^\circ + \Delta R_1$
R_{BN}
⊖
B

Fig. 3. — Two-wire bridge.

At $t = 0^-$, the bridge is balanced for $x_p = 0.5000$, thus $R_1^0 = R_2^0 + R_e$ because $R_{AN} = R_{BN}$.

$$\Delta R_1 = R_1(t) - R_1^0; \quad \Delta R_2 = R_2(t) - R_2^0$$

$$R_1^0 = \frac{\rho_{el}}{s} L_1; \quad R_2^0 = \frac{\rho_{el}}{s} L_2; \quad L_2 < L_1$$

For small temperature rises:

$$R_1(t) = R_1^0[1 + \alpha_{T_0}\theta(r_1, t)]$$
$$R_2(t) = R_2^0[1 + \alpha_{T_0}\theta(r_1, t)]$$

Since both wires are made of the same material, have the same diameter and the temperature rises are identical ($q_1 = q_2$ and the same λ), it follows that $\Delta R_2/\Delta R_1 = L_2/L_1$. With $u = 1 - (L_2/L_1)$ and $v = 1 + (L_2/L_1)$, finally one obtains :

$$\frac{\Delta R_1}{R_1^0} = 2\,\frac{f(x_p, x_i)}{v\left[\dfrac{u}{v} - f(x_p, x_i)\right]} \tag{6}$$

$$\theta(r_1, t_i) = \frac{2}{\alpha_{T_0}}\,\frac{f(x_p, x_i)}{v\left[\dfrac{u}{v} - f(x_p, x_i)\right]} \tag{7}$$

4.3. CALCULATION OF THE PRESET RESISTIVE UNBALANCE

Using the star-triangle transformation relations for the righthand half of the bridge, one obtains :

$$\frac{R_{\mathrm{AN}}}{R_{\mathrm{BN}}} = 1 + y$$

where :

$$y = \frac{Rr(1 - 2x_p)}{r^2(1 - x_p)x_p + \rho(r + \rho) + R(rx_p + \rho) + R_s(r + 2\rho)} \tag{8}$$

At one-wire bridge balance :

$$\begin{aligned} \frac{R_1^0}{R_1^0 + \Delta R_1} &= \frac{R_{\mathrm{AN}}}{R_{\mathrm{BN}}} = 1 + y \\ \Delta R_1 &= -R_1^0\,\frac{y}{1 + y} = \alpha_{T_0}\theta(r_1, t) \end{aligned} \tag{9}$$

At two-wire bridge balance :

$$\frac{R_2^0 + \Delta R_2 + R_e}{R_1^0 + \Delta R_1} = \frac{R_{\mathrm{AN}}}{R_{\mathrm{BN}}} = 1 + y$$

Since $R_1^0 = R_2^0 + R_e$ at $t = 0^-$ and $x_p = 0.5000$, it results :

$$\Delta R_1 = -R_1^0\,\frac{y}{u + y} = \alpha_{T_0}\theta(r_1, t) \tag{10}$$

4.4. SELECTION CRITERIA FOR THE WIRE MATERIAL

The physical properties of the wire (specific heat, c_1, density, ρ_1, thermal conductivity, λ_1, electrical resistivity, ρ_{el}, temperature coefficient of the electrical resistance, α) which are implied in computation, differ more for the metals (or their alloys) used in thin wires drawing [4] (Table 1).

TABLE 1

Physical properties of some metals used in drawn thin wire [4]

Metal	$10^{-6}(\rho_1 c_1)$ (J/(m^{3}K))	λ_1 (W/(mK))	$10^6(\rho_{el}/\alpha)$ (Ωm K)
Al	2.35	202	7.2
Ag	2.48	418	4.2
Cu	3.34	407	4.2
Ni	3.26	61	19
Au	2.48	290	7
W	2.62	178	13
Pt	2.85	70	29

As far as thermal properties are concerned, the $(\rho_1 c_1)$ and λ_1 values have to be minimal, in order to lower the thermal inertia of the wire and the heat losses at wire ends as well.

The electrical properties are important when measuring the output voltage, ΔV, of the bridge powered with the E_p constant voltage. For one-wire bridge:

$$\frac{\Delta R_1}{R_1^0} = \alpha_{T_0}\theta(r_1, t) = \alpha_{T_0}\frac{1}{4\pi\lambda}\, q \ln\frac{4at}{r_1^2 C}$$

$$q = \frac{E_p^2}{4 R_1^0 L} = E_p^2 \frac{1}{16\lambda}\,\frac{\alpha_{T_0}}{\rho_{el}}\left(\frac{r_1}{L}\right)^2 \ln\frac{4at}{r_1^2 C}$$

$$\Delta R_1 = \frac{E_p^2\,\alpha_{T_0}}{16\pi\, L\lambda} \ln\frac{4at}{r_1^2 C}$$

The maximum value for E_p is:

$$E_p = \left[\frac{16\,\Delta R_1}{R_1^0 \ln\dfrac{4at}{r_1^2 C}}\right]^{1/2} \lambda^{1/2}\left(\frac{\rho_{el}}{\alpha_{T_0}}\right)^{1/2}\left(\frac{L}{r_1}\right) \tag{11}$$

and for ΔV:

$$\Delta V \simeq \frac{E_p}{4}\,\frac{\Delta R_1}{R_1^0} = \left[\frac{1}{\ln\dfrac{4at}{r_1^2 C}}\right]^{1/2}\left(\frac{\Delta R_1}{R_1^0}\right)^{3/2} \lambda^{1/2}\left(\frac{\rho_{el}}{\alpha_{T_0}}\right)^{1/2}\left(\frac{L}{r_1}\right) \tag{12}$$

A metal with maximum (ρ_{el}/α_{T_0}) and L, and minimum r_1 is recommended, the last two conditions being in accordance with the theoretical claims ($L \to \infty$, $r_1 \to 0$) of the method theory.

5. ORIGINAL FEATURES OF THE APPARATUS

The apparatus has some original particularities of principle :

— At $t = 0^-$, the bridge is in an accurately determined electrical state (either balanced or with a known resistive unbalance).

— The bridge at $t = 0^-$ is A.C. balanced; this method is very accurate (narrow band amplification) and the heating of the wire is negligible.

— The bridge allows for anticipatively imposing the resistive unbalance, continuously adjustable and accurately determined from the bridge equation, in order to explore the $\theta(t)$ curve over a wide range of θ and t values.

— The bridge equation is independent of the absolute value of the transducer electrical resistance; a static simulation of the whole proceeding of the wire transient behavior becomes thus possible.

— The bridge permits the determination of the absolute value of the wire electrical resistance at $t = 0^-$, by measuring the electrical resistance of the balancing arm.

— The electrical resistance of the wire connection leads is experimentally eliminated.

— The bridge allows for connecting two transducers for eliminating the end effects of the wire and for differential measurements.

— The voltage step pulse for transducer heating is supplied by a fast-response D.C. power supply; the pulse has a fast rise front without overrises, is accurate, precise and measurable, and the voltage is continuously adjustable.

— The bridge instrumentation amplifier which determines the accuracy and precision of the results has low input noise; the offset can be suppressed; the gain is very stable, adjustable and its value is not involved into calculations. For an undistorsioned rendering of the transient signal, a compromise has been made between the amplifier band width and the noise (a relatively wide band amplifier has been chosen).

— In order to record the $\theta(t)$ curve, seven (θ, t) pairs of points are measured on the transient signal, during each pulse.

— The comparators trigger the stopping of timers when the amplified signal of the bridge crosses their narrow windows, of stable but adjustable levels.

— The determinations are absolute as all quantities implied into calculation are measurable.

6. WORKING MODE AND CLASSICAL PROCEDURE OF COMPUTATION

— The measurement cell, containing the fluid and transducer, is thermostated at constant T_0 temperature.

— The bridge is A.C. balanced, with $x_p = 0.5000$ (neutral position).

— Successive pulses are released and sets of (x_p, t) values are obtained for preset E_p(D.C.) and A(gain) values.

— The transducer is replaced with a fixed resistance (of any value from within the balancing arm variation range) and the bridge is A.C. balanced with $x_p = 0.5000$. Maintaining the same E_p(D.C.) and A values, as during the experiment, a pulse of infinite duration is released. From X_p the bridge is now unbalanced and the x_i values of X_p vernier when the comparators act (monitored on the oscilloscope) are taken down.

— The E_p(D.C.) and $R_1^0 = R_e$ resistance of the balancing arm are measured.

— Specific electrical power, q, is :

$$q = \frac{E_p^2}{4 R_1^0 L} \tag{13}$$

— The experimental temperature rises are calculated :

$$\theta_i = \frac{2}{\alpha_{T_0}} \frac{f(x_p, x_i)}{1 - f(x_p, x_i)} \tag{14}$$

— The reduced quantities, Φ_i, are computed :

$$\Phi_i = \frac{4\pi}{q} \theta_i \tag{15}$$

— The $\Phi_i(\ln t_i)$ curve is graphically plotted and Φ and t values are chosen from the *linear part*, limited by (Φ_A, t_A) and (Φ_B, t_B) values.

— The slope and intercept to $(\ln t)$ axis of the $\Phi(\ln t)$ curve are calculated by the least square method with pairs of $(\Phi, \ln t)$ points from the linear logarithmic law range, or with individual pairs. For example, when (Φ_1, t_1) and (Φ_2, t_2) with $t_2 > t_1$ one gets :

$$\lambda^{(0)} = \frac{\ln t_2 - \ln t_1}{\Phi_2 - \Phi_1} \tag{16}$$

$$a^{(0)} = r_1^2 C/(4t_0) \tag{17}$$

$$\ln t_0 = \ln t_1 - \Phi_1 \lambda^{(0)} \tag{18}$$

$$a^{(0)} = \frac{r_1^2 C}{4t_1} \exp(\Phi_1 \lambda^{(0)}) \tag{19}$$

where $C = 1{,}781$.

7. EXPERIMENTAL DATA

The experimental data are listed in tables 2 and 3 for liquid n-heptane (VEB Laboratorchemie p.a. reagent grade) at 302.3 K and 322.6 K. The $\lambda^{(0)}$ and $a^{(0)}$ values calculated with the relations (16)–(19) from subsequent $(\Phi_i, \ln t_i)$ pairs are presented respectively in the 5th and 6th columns of the tables. The thermal conductivity as calculated from the $\Phi(\ln t)$ straight line slope fitted by the least square method with the first five $(\Phi_i, \ln t_i)$ experimental points, together with thermal diffusivity calculated with relation (17), where t_0 is the intercept of the $\Phi(\ln t)$ straight line to the abscissa, are given in the two columns 7 of the tables.

The physical properties available in literature [15,16] for liquid n-heptane, are presented in table 4.

From the computation performed with the complete equation of the Φ $(\ln t)$ curve, the one which gives the influence of the wire non-ideality at short times, [12,13] it results that the employed minimum experimental time introduces a relative error lower than 1% in the Φ $(\ln t)$ straight line slope, error which decreases beneath 0.2% for $t = 1$ s. Measurements carried out at times longer than 1 s pointed out a pronounced and progressive decrease in $\Phi(\ln t)$ straight line slope, due probably to the individual or combined intervention of natural convection, heat losses at wire ends, influence of the cell wall and temperature shift of the cell wall. The cell used for these determinations has $2r_2 = 10$ mm, but the distance between the wire and the thick copper conductors sustaining the lower end of the wire is of 1.5 mm. Influence of the cell wall seems probable, according to the $r_2^2/(4at) > 6$ criterion. This effect can be cancelled by enlarging the cell diameter to the prejudice of thermostating accuracy and duration for reaching the steady-state thermal regime within the cell at $t = 0^-$. Besides all these, determinations perform-

TABLE 2

Sample measurement in liquid n-heptane

$$f = 1.99681\cdot 10^{-3}\frac{2x_i - 1}{1 - 1.838566\cdot 10^{-3}(2x_i - 1)^2}\ ;\ x_p = 0.500\ ;\ T_0 = 302.3\text{K}\ ;$$

$$\alpha = 3.337\cdot 10^{-3}\,(^\circ\text{C})^{-1}\ ;\ R = 88.93\,\Omega\ ;\ L = 0.141\ \text{m}\ ;\ E_p = 2.8143\ \text{V}.$$

x_i	θ (°C)	Φ (m°C/W)	t (s)	$\lambda^{(0)}$ (W/(mK))	$10^8 a^{(0)}$ (m²/s)	$\Phi = \alpha + \beta(\ln t)$
1	2	3	4	5	6	7
0.7615	0.627	49.885	0.14599	0.1206	7.403	$\beta = 8.0768$ $\lambda^{(0)} = 0.1238$
0.7989	0.717	57.037	0.34580	0.1237	8.866	$\alpha = 65.5267$
0.8172	0.761	60.538	0.53328	0.1252	9.701	$t_0 = \exp\left(-\frac{\alpha}{\beta}\right) = 2.9962\cdot 10^{-4}$s
0.8362	0.806	64.175	0.84090	0.1297	12.94	$r_1 = 7.7\cdot 10^{-6}$ m $a^{(0)} = 8.81\cdot 10^{-8}$
0.8550	0.852	67.775	1.34136	0.1374	21.78	
0.8735	0.896	71.320	2.18307			

Interpolated reference data from literature at $T = 302.3$ K (see table 4) :
$\lambda = 0.1262$ W/(mK) ; $a = 8.25\cdot 10^{-8}$ m²/s.

ed at long times are affected by systematic errors due to the heat losses at wire ends and the risk of natural convection set increases proportionally in time.

TABLE 3

Sample measurement in liquid n-heptane

$$f = 1.99681\cdot 10^{-3}\left[\frac{2x_i - 1}{1 - 1.838566\cdot 10^{-3}\,(2x_i - 1)^2}\right];\ x_p = 0.500\ ;\ T_0 = 322.6\text{K}\ ;$$

$$\alpha = 3.125\cdot 10^{-3}\,(^\circ\text{C})^{-1};\quad R = 94.92\ \Omega\ ;\ L = 0.141\ \text{m}\ ;\ E_p = 2.9558\ \text{V}.$$

x_i	θ (°C)	Φ (m°C/W)	t (s)	$\lambda^{(0)}$ (W/(mK))	$10^8 a^{(0)}$ (m²/s)	$\Phi = \alpha + \beta(\ln t)$	
1	2	3	4	5	6	7	
0.7491	0.638	49.096	0.10617	0.1151	7.075	$\beta = 8.5374$	$\lambda^{(0)} = 0.1171$
0.7846	0.729	56.109	0.23798	0.1180	8.344	$\alpha = 68.3060$	
0.8020	0.773	59.548	0.35714	0.1159	7.351	$t_0 = 3.3517\cdot 10^{-4}$s	
0.8200	0.820	63.107	0.53950	0.1227	11.30	$r_1 = 7.7\cdot 10^{-6}$m	$a^{(0)} = 7.88\cdot 10^{-8}$
0.8376	0.865	66.588	0.82707	0.1294	17.58		
0.8552	0.910	70.071	1.29776				

Interpolated reference data from literature at $T = 322.6$ K (see Table 4):

$$\lambda = 0.1206\ \text{W/(mK)}\ ;\ a = 7.88\cdot 10^{-8}\ \text{m}^2/\text{s}.$$

It is obvious, from the apparatus description, that it measures in principle the times when the hot wire reaches some preset temperature values.

The absolute error for experimental Φ_i quantities is given by both random and systematic instrumental errors in measuring bridge resistances R, r, ρ, R_s, R_e, thresholds x_i of comparators, E_p (d.c.) for bridge powering, temperature coefficient, α, of the wire electrical resistance and wire length, L.

TABLE 4

Physical properties of liquid n-heptane

Reference [15]			Reference [16]				
T (K)	λ (W/(mK))	c_p (J/(kg K))	T (K)	λ (W/(mK))	c_p (J/(kg K))	ρ (kg/m³)	a (m²/s)
300	0.1265	2250	293.2	0.129	2226	683.6	
310	0.1242	2287	303.2		2263	675.1	
320	0.1219	2327	313.2	0.123	2301	666.5	
330	0.1196	2367	323.2		2340	657.9	
			333.2	0.118	2390	649.1	
302.3	0.1260*	2259	302.3	0.1262*	2260*	675.8*	$8.25\cdot 10^{-8}$*
322.6	0.1213*	2337	322.6	0.1206*	2338*	658.3*	$7.88\cdot 10^{-8}$*

* linear interpolated values

The absolute error for experimental t_i quantities is given by : — random and systematic instrumental errors : bridge balance at $t = 0^-$, distorsion and delay of wire transient signal due to the bridge-amplifier-comparators-timers assembly, rising time and precision of E_p (d.c.), parasite voltages ; — random and systematic phenomenological errors : temperature fluctuations within the cell during the measurement, non-steady state thermal regime at $t = 0^-$; — systematic phenomenological errors : failing to place within the linear logarithmic law towards short times and natural convection, cell wall effect, heat losses through the wire ends towards long times.

From both statistical analysis of the measurements and study of apparatus behavior it results that (Φ_i, t_i) values are measured with an accuracy better than 1%. An error of 1% in $(\lambda\Phi)$ product becomes of 6 to 10% due to the exponential equation. The measurement error for the wire diameter being of minimum 3.3% ($15 \pm 0.5\ \mu$), the error in $a^{(0)}$ is at least 6 to 17%.

Comparing the obtained experimental results with the recommended values in literature, it results that using the classical procedure of the transient hot wire method one can measure with our apparatus thermal conductivity of liquids with an accuracy better than 2% and thermal diffusivity of liquids with an accuracy of 2 to 10%.

REFERENCES

[1] "Thermal Conductivity", R. P. Tye ed., vol. II, Academic Press, London, 1969.
[2] H. S. Carslaw and J. C. Jaeger, "Conduction of Heat in Solids", Oxford Univ. Press, London, 1959.
[3] R. Bessouat, H. Chavanel and S. Elberg, *J.Physique*, **26**, 1 (1965).
[4] P. Salé, Theses, Univ., Paris, 1967.
[5] J. W. Haarman, Dissertation, Techn. Univ. Delft, 1969.
[6] A. G. Turnbull, *J. Chem. Eng. Data*, **16**, 79 (1971).
[7] P. S. Davis, F. Theeuwes, R. J. Bearman and R. P. Gordon, *J. Chem. Phys.*, **55**, 4776 (1971).
[8] E. Mc Laughlin and J. F. T. Pittman, *Phil. Trans. Roy. Soc. London*, **270**, 557 (1971).
[9] J. J. de Groot, J. Kestin and H. Sookiazian, *Physica*, **75**, 454 (1974).
[10] P. Andersoon and G. Backstrom, *Rev. Sci. Instrum.*, **47**, 205 (1976).
[11] R. Vîlcu and A. Ciochină, *Rev. Roumaine Chim.*, **25**, 1113 (1980).
[12] A. F. O. Falcao, *Rev. Port. Quim.*, **7**, 65 (1965).
[13] A. F. O. Falcao, *Rev. Port. Quim.*, **9**, 139 (1967).
[14] R. Vîlcu and A. Ciochină, *Rev. Roumaine Chim.*, **26** (1981), in press.
[15] Y. S. Touloukian, P. E. Liley and S. C. Saxena, "Thermophysical Properties of Matter", vol. 3, TPRC Data Series, Plenum Press, New York, 1970.
[16] N. B. Vargaftik, "Spravochnik po teplofizicheskim svoistvam gazov i zhidkostei", Nauka, Moscova, 1972.

Revue Roumaine de chimie, **26**, *8*, 1063–1070 (1981)

THE FORMATION MECHANISM OF THE COMPOUNDS IN THE $MgO-V_2O_5$ SYSTEM

MARIA ZAHARESCU and ANA BRĂILEANU
ICECHIM, Center of Physical Chemistry, Spl. Independenţei 202, Bucharest, Romania

Received August 16, 1980

The formation of vanadates in the $MgO-V_2O_5$ system by solid phase reactions and in the presence of the liquid phase was studied. The experimental data support the idea of magnesium metavanadate formation. The formation mechanism of meta-, pyro- and orthovanadate under nonisothermal conditions was established.

1. INTRODUCTION

The phase equilibria and compound formation mechanisms in the $MgO-V_2O_5$ system have been described in many papers.

The $MgO-V_2O_5$ system is of a particular interest both from a scientific and a technological viewpoint. Research done in this system offers the theoretical grounds for the preparation of mixed vanadium catalysts and for understanding the problems of magnesite refractories corrosion by V_2O_5-containing liquid fuels.

The results published so far on the matter are summarized in table 1. The literature data shown in table 1 are in severe disagreement. The formation of $MgO \cdot 2V_2O_5$ and $7MgO \cdot 3V_2O_5$ claimed by some authors was flatly rejected by others. The most controversial issue remained the existence of the high V_2O_5-content compound, whose formula is, according to recent studies, either $MgO \cdot V_2O_5$ or $3MgO \cdot 2V_2O_5$. The establishing of exact formula of this compound entails difficulties related to its very low formation rate in solid phase. Clark[7] mentions that the reaction is not complete even after 14 days of thermal treatment at temperatures within 500 – 600°C range.

The present paper attempts to determine the composition of this compound, as well as the formation mechanism of all compounds in the system, under nonisothermal conditions.

2. EXPERIMENTAL

Merck reagent grade MgO, $MgCO_3$ and V_2O_5 starting materials, with grain size below 60 μm, have been used.

Mixtures were prepared either by a dry method, consisting of weighing oxides according to desired molar ratio, followed by manual homogenization, or by a wet method, *i.e.* homo-

genization of $MgCO_3$ with V_2O_5 in water. In the latter case, V_2O_5 in the presence of water yields vanadic acid which reacts with $MgCO_3$, decomposing it with formation of hydrated products which are homogeneous at molecular scale.

Thermal behaviour was studied by DTA, by using an OD-102 Paulik-Paulik-Erdey Derivatograph, with 10°/minute heating rate, up to 1000°C. All experiments were carried out in air, in quartz crucibles.

TABLE 1

Compounds reported in the $MgO-V_2O_5$ system

Compound	Melting point	Observations
$MgO \cdot 2V_2O_5$	i 710°C[1]	Formation was not confirmed by[2-11]
$MgO \cdot V_2O_5$	i 760°C[2,3] i 756°C[4] i 762°C[5] i 765°C[6] i 763°C[7]	Polymorphic transformation[7] : $\alpha \xrightarrow{567°C} \beta$ Formation was confirmed by[8,9]
$3MgO \cdot 2V_2O_5$	810°C[10] i 1091 C[1] i 760°C[11]	Polymorphic transformation[11] : 576°C Formation was not confirmed by[4,7,8,9]
$2MgO \cdot V_2O_5$	i 950°C[3] c 1128°C[5] i 1093°C[4] i 1132°C[11]	Polymorphic transformations[4] : $\beta \xrightarrow{738°C} \alpha \xrightarrow{917°C} \alpha$ Polymorphic transformation[11] : 912°C Polymorphic transformation[6] : $\alpha \xrightarrow{917°C} \beta$ Polymorphic transformations[7] : $\alpha \xrightarrow{707-717°C} \beta \xrightarrow{911°C} \gamma$ Formation was confirmed by[7,8]
$7MgO \cdot 3V_2O_5$	i 1162°C[1]	Formation was not confirmed by[2-11]
$3MgO \cdot V_2O_5$	i 1165°C[2] c 1210°C[5] i 1159°C[4] i 1212°C[11]	Formation was confirmed by[3, 6-9]

Note

i — incongruent melting

c — congruent melting

Phase analysis of reaction products was carried out by a TUR M-62 diffractometer with copper anticathode, using the $Cu_{K\alpha}$ radiation with Ni filter ; the goniometer angular speed was 0.5 degrees per minute ; the working voltage was 40 kV and the current 35 mA ; the chart paper transport speed was 600 mm per hour.

3. RESULTS AND DISCUSSION

3.1. MAGNESIUM VANADATE FORMATION

3.1.1. Dry method mixtures

The results of thermal analysis performed on mixtures of $MgO : V_2O_5$ at mole ratios of 1 : 1 and 3 : 2, obtained by the dry method are shown in figure 1. In both cases the same thermal effects are present : an exothermal one at 540°C and 3 endothermal ones at 650, 755 and 900°C, respectively.

Curve 3 corresponds to the eutectic composition in the $MgO-V_2O_5$ system.

A comparison of endothermal effect temperatures with the phase equilibria diagram (according to Wollast and Tazairt[4]) shows that the former are close to the invariant points of the diagram, *i.e.* the eutectic, at 639°C, the incongruent melting point of magnesium metavanadate ($MgO \cdot V_2O_5$) with formation of magnesium pyrovanadate ($2MgO \cdot V_2O_5$), at 756°C, and its polymorphic transformation temperature, at 912°C, respectively.

The X-ray diffraction lines for the samples of $MgO : V_2O_5$, at mole ratios of 1 :1 and 3 :2, thermally treated at 700°C, are shown in table 2.

For the 1 : 1 mixture the X-ray diagram shows the lines of magnesium metavanadate ($MgO \cdot V_2O_5$) and some of the strongest lines of unreacted V_2O_5. This confirms the previous data regarding the slow formation rate of magnesium metavanadate.[7]

For the 3 : 2 mixture besides the magnesium metavanadate diffraction lines, the pyrovanadate ($2MgO \cdot V_2O_5$) lines are seen, confirming the hypothesis according to which this composition is not a pure compound, but a mixture of metavanadate and pyrovanadate.

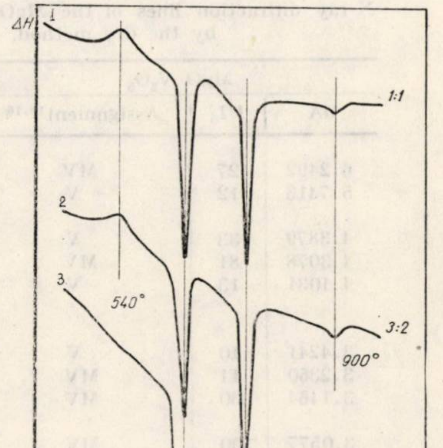

Fig. 1. — DTA curves of the dry method $MgO : V_2O_5$ mixtures at mole ratios of 1 :1 and 3 : 2.

These results, obtained with mixtures prepared by dry methods suggest the following mechanism of formation and thermal behaviour of magnesium metavanadate under nonisothermal conditions : at 540°C the solid phase reaction of $MgO \cdot V_2O_5$ formation occurs and it is not complete. On further temperature increase, at 650°C starts the melting of eutectic mixture of V_2O_5 and $MgO \cdot V_2O_5$ resulted from the reaction at 540°C. At the same time, the formation reaction of magnesium metavanadate continues with participation of the liquid phase.

The formed metavanadate melts incongruently at 755°C with formation of magnesium pyrovanadate, which further undergoes the polymorphic transformation β → γ mentioned in the literature to occur at 911°C.

The presence of V_2O_5 in the sample thermally treated at temperatures higher than the eutectic, proves that the reaction of magnesium metavanadate formation in nonisothermal conditions is not complete, even in the presence of the liquid phase.

The $MgO \cdot V_2O_5$ formation was also confirmed by the analysis of the mixtures prepared by the wet method.

TABLE 2

X-ray diffraction lines of the $MgO \cdot V_2O_5$ and $3MgO \cdot 2V_2O_5$ samples prepared by the dry method, thermally treated at 700°C

$MgO \cdot V_2O_5$			$3MgO \cdot 2V_2O_5$		
dÅ	I/I_0	Assignment[13,16]	dÅ	I/I_0	Assignment[13,14]
6.2492	27	MV	6.2317	36	MV
5.7413	12	V			
			4.7816	17	2MV
4.3879	33	V			
4.3078	81	MV	4.2996	27	MV
4.1031	13	V			
			3.7230	24	2MV
			3.5254	21	2MV
3.4241	10	V			
3.2360	11	MV	3.2291	47	MV, 2MV
3.1464	30	MV	3.1334	55	MV
			3.1099	33	2MV
3.0577	100	MV	3.0455	100	MV
			2.9005	30	2MV
2.8840	13	V			
2.7608	6	V	2.7641	16	2MV
2.7200	20	MV	2.7184	32	MV
			2.6773	13	2MV
			2.5700	23	2MV
			2.4582	15	2MV
			2.3852	17	2MV
2.3097	10	MV	2.3052	15	MV
			2.2402	15	2MV
2.1943	21	MV	2.1932	18	MV
2.1740	12	MV			
2.1562	9	MV			
			2.1016	13	2MV
2.0831	10	MV	2.0886	12	MV
1.8863	7	MV	1.8885	17	MV
1.8768	6	MV	1.8746	17	MV, 2MV
			1.7917	13	2MV
1.7421	6	MV	1.7421	19	MV
			1.6142	10	2MV
1.5303	12	MV	1.5266	13	MV
1.5051	8	V			

Note : MV = $MgO \cdot V_2O_5$; 2MV = $2MgO \cdot V_2O_5$; 3MV = $3MgO \cdot V_2O_5$; V = V_2O_5

3.1.2. Wet method mixtures

The DTA curves are shown in figure 2. Three endothermal effects are identified for the initial mixture of molar ratio 1 : 1. The effect at 360°C is assigned to the dehydration of the reaction product obtained by a wet method, with formation of $MgO \cdot V_2O_5$. The effects at 755°C and 900°C have the significance discussed above.

X-ray diffraction pattern of the sample thermally treated at 600°C exhibits only the lines of magnesium metavanadate. This confirms the compound formation at the temperature of dehydration effect (Table 3).

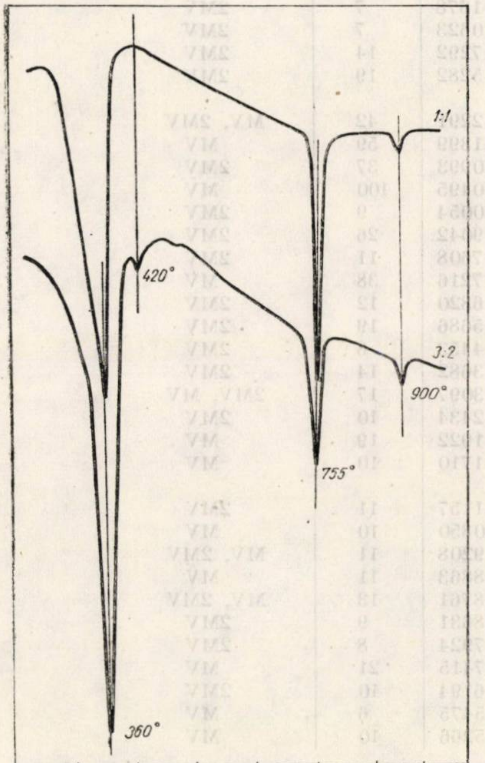

Fig. 2. — DTA curves of the wet method $MgO : V_2O_5$ mixtures at mole ratios of 1 : 1 and 3 : 2.

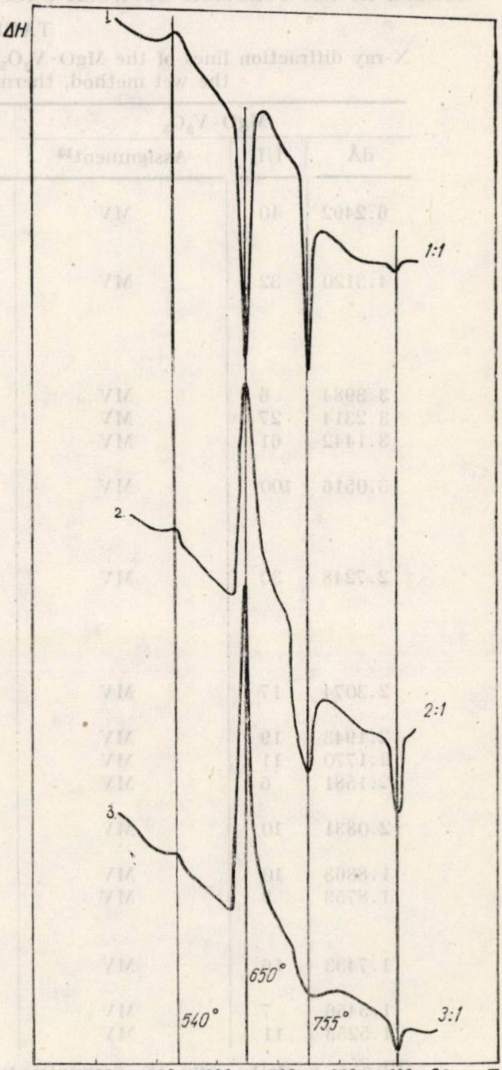

Fig. 3. — DTA curves of the starting mixtures corresponding to the 1—$MgO \cdot V_2O_5$, 2—$2MgO \cdot V_2O_5$ and 3—$3MgO \cdot V_2O_5$ formation.

The DTA curve of the 3 : 2 ratio mixture differs from the 1 : 1 one by the presence of an additional endothermal effect at 420°C which is accompanied by a weight loss. This effect can be assigned to the dehydration of $Mg(OH)_2$ formed during the wet phase reaction, [12] which is, therefore, in excess to the stoichiometric ratio corresponding to magnesium metavanadate.

The X-ray diffraction pattern of the sample thermally treated at 600°C, exhibits, besides the $MgO \cdot V_2O_5$ lines, the lines of $2MgO \cdot V_2O_5$ formed in the reaction between excess MgO and $MgO \cdot V_2O_5$.

TABLE 3

X-ray diffraction lines of the $MgO \cdot V_2O_5$ and $3\ MgO \cdot 2V_2O_5$ samples prepared by the wet method, thermally treated at 600°C

$MgO \cdot V_2O_5$			$3MgO \cdot V_2O_5$		
dÅ	I/I_0	Assignment[13]	dÅ	I/I_0	Assignment[13, 14]
6.2492	40	MV	6.2405	35	MV
			4.7918	15	2MV
			4.6523	8	2MV
4.3120	32	MV	4.2996	31	MV
			4.1678	7	2MV
			4.0623	7	2MV
			3.7292	14	2MV
			3.5282	19	2MV
3.3984	6	MV			
3.2314	27	MV	3.2291	42	MV, 2MV
3.1442	61	MV	3.1399	59	MV
			3.0993	37	2MV
3.0516	100	MV	3.0495	100	MV
			3.0054	9	2MV
			2.9042	26	2MV
			2.7608	11	2MV
2.7248	30	MV	2.7216	38	MV
			2.6820	12	2MV
			2.5686	19	2MV
			2.4453	8	2MV
			2.3682	14	2MV
2.3074	17	MV	2.3097	17	2MV, MV
			2.2434	10	2MV
2.1943	19	MV	2.1922	19	MV
2.1770	11	MV	2.1710	10	MV
2.1581	6	MV			
			2.1157	11	2MV
2.0831	10	MV	2.0850	10	MV
			1.9208	11	MV, 2MV
1.8863	10	MV	1.8863	11	MV
1.8753	9	MV	1.8761	13	MV, 2MV
			1.8631	9	2MV
			1.7924	8	2MV
1.7433	16	MV	1.7415	21	MV
			1.6194	10	2MV
1.5456	7	MV	1.5475	6	MV
1.5253	11	MV	1.5266	10	MV

These results are in agreement with Matveevicheva's data[8]; she worked on vanadyl oxalate and $MgCl_2$ solutions or on vanadyl chloride and $MgCl_2$ solutions and established the complete formation of magnesium metavanadate, by thermal treatment at 400°C.

3.2. THE FORMATION OF $2MgO \cdot V_2O_5$ AND $3MgO \cdot V_2O_5$

On the basis of the previous studies,[2-9] the presence of magnesium pyrovanadate ($2MgO \cdot V_2O_5$) and magnesium orthovanadate ($3MgO \cdot V_2O_5$), besides magnesium metavanadate ($MgO \cdot V_2O_5$), in the $MgO-V_2O_5$ system has been established.

Figure 3 shows the DTA curves of initial mixtures corresponding to well defined compound formation in the system. It is obvious that in all cases the recorded thermal effects occur at the same temperatures, yet they differ with respect to amplitude and significance. For the MgO : V_2O_5 1 : 1 mixture (curve 1) the significance of the effects is the same as that discussed above. For the MgO : V_2O_5 2 : 1 mixture (curve 2) the effect at 650°C becomes exothermal; the effect at 755°C, corresponding to the incongruent melting and to the transformation of metavanadate into pyrovanadate, is smaller than in the case of curve 1; the effect of the polymorphic transformation $\beta \rightarrow \gamma$ at 900°C is greater as compared to curve 1.

TABLE 4

X-ray diffraction lines of the $2MgO \cdot V_2O_5$ and $3MgO \cdot V_2O_5$ samples, thermally treated at 700°C

$2MgO \cdot V_2O_5$			$3MgO \cdot V_2O_5$		
dÅ	I/I_0	Assignment[13, 14]	dÅ	I/I_0	Assignment[14, 15]
6.2143	24	MV			
4.7969	56	2MV	4.8176	51	2MV
			4.6668	13	2MV
			4.5253	19	3MV
4.3120	24	MV			
4.2267	10	MV	4.2466	17	2MV, MV
4.1562	16	2MV	4.1678	17	2MV
4.0659	20	2MV	4.0659	17	2MV
3.8306	14	2MV			
3.7292	50	2MV	3.7261	47	2MV
3.5227	72	2MV	3.5309	64	2MV
			3.3606	11	3MV, MV
			3.2804	53	3MV
3.2337	62	2MV, MV	3.2406	53	2MV, MV
			3.1399	11	MV
3.1184	100	2MV, MV	3.1184	100	2MV, MV
3.0455	44	MV			
			3.0353	89	2MV, MV
3.0193	96	2MV			
			3.0093	57	3MV
2.9434	18	2MV	2.9529	15	2MV
2.9097	94	2MV	2.9116	68	2MV
			2.8500	26	3MV
2.7525	30	2MV	2.7625	32	2MV
2.6742	38	2MV	2.6773	34	2MV
2.5643	64	2MV	2.5743	57	2MV
			2.5459	81	3MV, 2MV
2.4925	14	2MV	2.4899	38	3MV, 2MV
2.4518	38	2MV	2.4582	36	3MV, 2MV
2.4274	26	2MV	2.4274	21	2MV
2.3779	40	2MV	2.3779	32	2MV
2.3480	16	2MV	2.3539	19	3MV, 2MV
2.3166	18	2MV	2.3269	17	2MV
2.2359	34	2MV	2.2413	29	2MV
2.1176	14	2MV	2.1242	21	2MV
2.0923	22	MV	2.0741	32	MV
1.9163	16	2MV			
1.8790	26	MV, 2MV	1.8681	17	3MV, 2MV

By corroborating these data with X-ray analysis (Table 4), it was established that in this case, at 540°C a small amount of metavanadate is also formed, which forms an eutectic mixture with the unreacted V_2O_5, that begins to melt at 650°C. At the same time, in the presence of liquid phase, the intensely exothermal reaction of $2MgO \cdot V_2O_5$ takes place, which changes the sign of the melting effect. At 755°C, $MgO \cdot V_2O_5$ formed in the first stage melts incongruently, resulting in $2MgO \cdot V_2O_5$. At 900°C the polymorphic transformation of magnesium pyrovanadate takes place.

For the $MgO : V_2O_5$ 3 : 1 mixture, the shape of the DTA curve is similar to the one of the 2 : 1 mixture; the only difference is in the size of these effects (curve 3). X-ray diffraction analysis confirms that in this case, at the eutectic temperature (650°C), a mixture of $2MgO \cdot V_2O_5$ and $3MgO \cdot V_2O_5$ is formed. Further, the metavanadate formed in the first stage undergoes the above discussed transformations.

Comparing the DTA curves of the mixtures corresponding to the formation of the three compounds, one can see that, regardless of starting molar ratio, in the first step magnesium metavanadate is formed. Magnesium pyrovanadate and orthovanadate are formed in the presence of the liquid phase appearing at the eutectic temperature of the $V_2O_5-MgO \cdot V_2O_5$ subsystem.

The formation heats of the compounds cannot be calculated from DTA data because the magnesium metavanadate formation reaction is not complete and the formation effects of the other two compounds are overlapped.

4. CONCLUSIONS

— The formation of magnesium metavanadate in the system is supported by experimental data presented here;

— The formation mechanism of magnesium meta-, pyro- and orthovanadate under nonisothermal conditions was established; regardless of the stoichiometric ratio of initial mixture, the metavanadate is the first reaction product, which in the presence of a MgO excess forms pyro- and orthovanadate.

REFERENCES

[1] H. Lehman, S. Kienow and P. Artelt, *Tonind.-Ztg. Keram. Rundschau*, **88**, 153 (1964).
[2] R. Kohlmühler and J. Perraud, *Bull. Soc. chim. France*, 3, 642 (1964).
[3] S. Solacolu, R. Dinescu and M. Zaharescu, *Rev. Roumaine Chim.*, **16**, 351 (1971).
[4] R. Wollast and A. Tazairt, *Silicates Ind.*, **34**, 37 (1969).
[5] J. Pollard, *Sci. Tech. Aerospace Rept.*, **3**, 1095 (1965).
[6] G. M. Clark and A. N. Pick, *J. Thermal Anal.*, **7**, 289 (1975).
[7] G. M. Clark and R. Morley, *J. Sol. State Chem.*, **16**, 429 (1976).
[8] V. A. Matveevicheva, *Zhur. fiz. Khim.*, **43**, 263 (1969).
[9] E. Pollert, *Silikaty*, **17**, 337 (1973).
[10] B. W. King and L. L. Suber, *J. Amer. Ceram. Soc.*, **38**, 306 (1955).
[11] E. I. Speranskaya, *Izv. Akad. Nauk S.S.S.R., Neorg. Mater.*, **7**, 1804 (1971).
[12] C. Duval, "Inorganic Thermogravimetric Analysis", Second Edition, Elsevier Publishing Co., Amsterdam, 1953, p. 214.
[13] "Inorganic Index to the Powder Diffraction File", A.S.T.M., Philadelphia, 1967, 23—1233.
[14] "Inorganic Index to the Powder Diffraction File", A.S.T.M., Philadelphia, 1967, 23—1235.
[15] "Inorganic Index to the Powder Diffraction File", A.S.T.M., Philadelphia, 1967, 19—779.
[16] "Inorganic Index to the Powder Diffraction File", A.S.T.M., Philadephia, 1967, 9—387.

Revue Roumaine de chimie, **26**, *8*, 1071–1076 (1981)

EXTENSION AND COMPARISON OF COLLISION FACTOR THEORY AND FREE LENGTH THEORY IN LIQUID TERNARY MIXTURES

R. P. PANDEY and TARA UPRETI
Department of Chemistry, University of Allahabad, Allahabad, India

Received June 12, 1980

An attempt has been made to extend collision factor theory due to Schaaffs and free length theory so as to enable one to calculate ultrasonic velocity in liquid ternary mixtures. The mixtures under investigation are benzene—cyclohexane—methanol, benzene—cyclohexane—ethanol at 25°C and cyclohexane—acetone—ethanol, cyclohexane—acetone—butanol, benzene—cyclohexane—butanol, benzene—acetone—chloroform and cyclohexane—benzene—carbontetrachloride at 30°C. The relative merits of both theories have been compared. It has been found that, in general, both theories agree with the experimental values reasonably well but probably collision factor theory is to be preferred.

INTRODUCTION

The previous attempts [1-9] to evaluate sound velocity in liquid mixture are limited to binary systems only. The present investigation deals with the extension and comparison of collision factor theory [3,4] and the free length theory [5,6] in liquid ternary mixtures : benzene—cyclohexane—methanol, benzene—cyclohexane—ethanol, cyclohexane—acetone—ethanol, cyclohexane—acetone—butanol, benzene—cyclohexane—butanol, cyclohexane—benzene—carbon tetrachloride and benzene—acetone—chloroform. The required experimental data were taken from the literature. [10]

THEORETICAL

In order to explain the ultrasonic velocity in pure liquids and liquid mixtures, Jacobson [5,6] introduced the concept of intermolecular free length, i.e. distance between surface of two molecules defined by the relation

$$L = \frac{2V_a}{Y}, \tag{1}$$

where $V_a = V_T - V_0$ gives the available volume per mole and $Y = (36\,\pi N V_0^2)^{1/3}$, the surface area per mole calculated under the assumption of spherical molecules by estimating their radius from the volume at absolute zero. Here N is the Avogadro number. Sound velocity has been calculated using Jacobson's [5,6] formula

$$C_{\text{mix}} L_{\text{mix}}\, \rho_{\text{mix}}^{1/2} = K, \tag{2}$$

where K is a temperature-dependent constant, whose values are given by Jacobson between 0 to 50°C. C_{mix} and ρ_{mix} are sound velocity and density of mixture, respectively, and L_{mix} is the free-length in the mixture. Free length (L) for pure liquids have been calculated using the relation

$$L = \frac{K}{C_{\text{expt}}\, \rho_{\text{expt}}}, \tag{3}$$

where C_{expt} and ρ_{expt} are experimentally determined sound velocity and density, respectively.

The surface areas, per mole, for the pure components have been calculated after obtaining the value of L and making use of relation (1). L_{mix} has been calculated using the relation

$$L_{\text{mix}} = \frac{2[V_m - (x_1 V_0^1 + x_2 V_0^2 + x_3 V_0^3)]}{x_1 Y_1 + x_2 Y_2 + x_3 Y_3}, \tag{4}$$

where the x's and V_0's represent mole fractions and volumes at absolute zero, respectively. V_m stands for molar volume of the mixture. Y_1, Y_2 and Y_3, obtained from eqn. (1), were employed in the above expression. The subscripts 1, 2 and 3 stand for the component liquids of the ternary mixtures. The V_0's were evaluated using the expression

$$V_0 = V_T(1 - T/T_C)\, 0.3, \tag{5}$$

where V_T and T_C are the molar volume at temperature T and the critical temperature, respectively.

On the basis of collision factor theory (C.F.T.), Schaaffs [4] developed the following relation for the sound velocity (C) in pure liquids.

$$C = C_\infty S \Upsilon_f = C_\infty S \frac{B}{V_M}, \tag{6}$$

where $C_\infty = 1600$ m/s, S is the collision factor, Υ_f denotes the space filling factor, B is the actual volume of the molecule per mole and v_m is the molar volume. Nutsch-Kuhnkies [3] extended this concept to the binary mixtures as follows :

$$C_{\text{mix}} = C_\infty S_{\text{mix}}\, \Upsilon_{f_{\text{mix}}}. \tag{7}$$

In case of ternary mixtures this may be written as

$$C_{\text{mix}} = C_{\infty}[x_1S_1 + x_2S_2 + x_3S_3]\frac{(x_1B_1 + x_2B_2 + x_3B_3)}{V_{\text{mix}}}. \tag{8}$$

The subscripts 1, 2 and 3 represent the components 1, 2 and 3, respectively.

The actual volume of the molecule per mole for the pure components denoted by B_1, B_2 and B_3 have been calculated using the equation

$$B = \frac{4\pi}{3}\gamma_m^3 N, \tag{9}$$

where N is the Avogadro number and γ_m is the molecular radius. The average value of γ_m obtained from the semi-empirical formula due to Schaaff's eqn. (10) and the expression derived by Gopala Rao and Venkataseshaiah[11] eqn. (11) have been employed in eqn. (9).

$$\gamma^m_{(\text{Schaaffs})} = \sqrt[3]{\frac{3}{16\pi N}V\left[1 - \frac{\gamma RT}{MC^2}\left\{\sqrt{1 + \frac{1}{3}\frac{MC^2}{\gamma RT}} - 1\right\}\right]} \tag{10}$$

$$\gamma^m_{(\text{Gopala Rao et al.})} = \sqrt[3]{\frac{3}{16\pi N}V\left[1 - \frac{\gamma RT}{MC^2}\left\{\sqrt{1 + \frac{MC^2}{\gamma RT}} - 1\right\}\right]}, \tag{11}$$

where all the symbols have their usual notations.

RESULTS AND DISCUSSION

The theoretical values of sound velocity for the ternary mixtures under investigation have been presented along with experimental values (figs. 1 to 4). In general, the theoretical values calculated on the basis of both theories are in reasonable agreement with the experimental values. Basically, in free length theory (F.L.T.), free lengths have been calculated for pure components from the experimentally determined sound velocity and density values. These free length values are used in turn to determine surface areas (Y's) of molecules of the pure components. Similarly, in the collision factor theory (C.F.T.), the collision factors (S's) for the pure components are evaluated from the experimentally determined sound velocity values. This means that surface areas (Y's) in F.L.T. and the collision factors (S's) in C.F.T. are adjusted for the pure components. These values, adjusted for the pure components, have been used to evaluate theoretical values of sound velocity at different concentrations for the corresponding ternary mixtures, using the appropriate equation. The ternary mixtures under present investigation may be divided into three categories.

(i) Nonpolar — Nonpolar — polar
(ii) Nonpolar — polar — polar
(iii) Nonpolar — Nonpolar — Nonpolar.

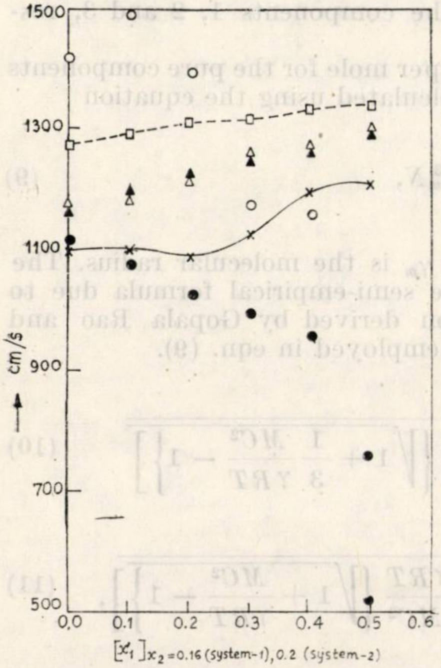

Fig. 1. — Sound velocity *vs* mole fraction curve for the systems,
(i) Benzene—cyclohexane—methanol (298 K)
(ii) Benzene—cyclohexane—ethanol (298 K)
(i) ● C.F.T.; ⊙ F.L.T.; × Expt.;
(ii) ▲ C.F.T.; △ F.L.T.; □ Expt.

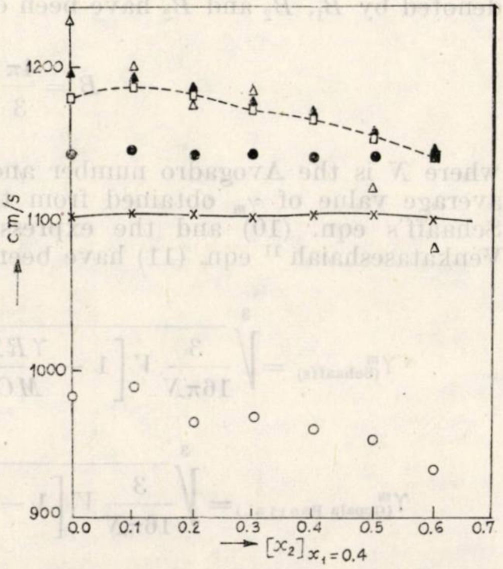

Fig. 2. — Sound velocity *vs* mole fraction for the systems,
(i) Cyclohexane—acetone—ethanol (303 K)
(ii) Cyclohexane—acetone—butanol (303 K)
(i) ● C.F.T.; ⊙ F.L.T.; × Expt.; (ii) ▲ C.F.T.; △ F.L.T.; □ Expt.

The mixtures of methanol, ethanol and butanol with benzene and cyclohexane belong to category (i), i.e. nonpolar — nonpolar — polar. An examination of figs. 1 & 2 shows that in case of the system benzene—cyclohexane—methanol, C.F.T. values deviate from 1.8 to 36.2 percent, whereas F.L.T. values show deviations around 3.2 to 55.8 percent. In case of the systems benzene—cyclohexane—ethanol and benzene—cyclohexane—butanol, C.F.T. values deviate around 4.2 to 7.9 and 7.2 to 15.4 percent respectively, whereas deviations shown by F.L.T. values range between 2.8 to 8.0 and 1.4 to 16.6 percent, respectively. Thus, C.F.T. has a sharp edge over F.L.T. in these systems. Largest deviation between theoretical and experimental values in system (i) may be attributed to the highly polar nature of methanol. As polarity decreases with increase of $-CH_2$-unit in alcoholic series, deviation shown by both theories is decreased. The systems cyclohexane—acetone—ethanol and cyclohexane—acetone—butanol belong to category (ii). An inspection of fig. 3 reveals that C.F.T. values deviate from 0.6 to 0.86 percent, whereas F.L.T. values deviate around 14.9 to 17.2 percent in case of the former system, whereas C.F.T. values deviate around 0.16 to 5.2 percent and F.L.T. values show a deviation no more than 0.17 percent in case of the latter system. Thus, C.F.T. has a sharp edge over F.L.T. in case of cyclohexane—acetone—ethanol system, whilst in case of the cyclohexane—acetone—butanol system, F.L.T. values are in better agreement with experimental sound velocity values. The system benzene—acetone—chloroform belongs to category (ii), whereas the system cyclohexane—benzene—carbon tetrachloride comes under category (iii). An examination of fig. 4 shows that C.F.T. values show a deviation of 1.03 to 1.89 percent, whereas F.L.T. values deviate around 1.54 to 5.27 percent in case of the system benzene—acetone—chloroform. In case of the system cyclohexane—benzene—carbon tetrachloride, C.F.T. values deviate around −11.5 to +0.72 percent, whereas F.L.T. values show a deviation of 10.9 to 14.9 percent.

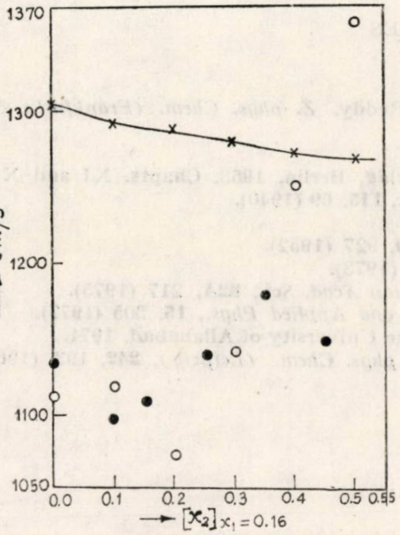

Fig. 3. — Sound velocity *vs* mole fraction for the system
(i) Benzene—Cyclohexane—butanol (298K) : ● C.F.T. ; ⊙ F.L.T. ; × Expt.

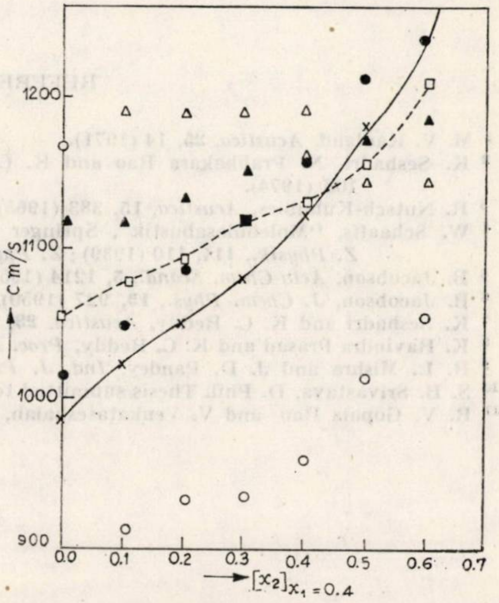

Fig. 4. — Sound velocity *vs* mole fraction for the systems,
(i) Cyclohexane— benzene — carbon tetrachloride (303K) :
● C.F.T. ; ⊙ F.L.T. ; × Expt.
(ii) Benzene—acetone—chloroform (303K) :
▲ C.F.T. ; △ F.L.T. ; □ Expt.

From the above discussion, it can be concluded that, in general, both theories agree with the experimental values reasonably well but probably the collision factor theory is to be preferred. This is due to the fact that in C.F.T., the molecules are treated as a real-non-elastic substance, whereas in the theory of free length they are supposed to be rigid spheres.

ACKNOWLEDGEMENT. One of the authors (R.P.P.) wishes to thank the U.G.C. New Delhi for financial assistance.

REFERENCES

[1] M. V. Kaulgud, *Acustica*, **25**, 14 (1971).

[2] K. Seshadri, N. Prabhakara Rao and K. C. Reddy, *Z. phys. Chem. (Frankfurt)*, **89**, 108 (1974).

[3] R. Nutsch-Kuhnbies, *Acustica*, **15**, 383 (1965).

[4] W. Schaaffs, "Molebulasabustik", Springer Verlag, Berlin, 1963, Chapts. XI and XII; *Z. Physik.*, **114**, 110 (1939); *Z. Physik*, **115**, 69 (1940).

[5] B. Jacobson, *Acta Chem. Scand.*, **5**, 1214 (1951).

[6] B. Jacobson, *J. Chem. Phys.*, **19**, 927 (1950), **20**, 927 (1952).

[7] K. Seshadri and K. C. Reddy, *Acustica*, **29**, 59 (1973).

[8] K. Ravindra Prasad and K. C. Reddy, *Proc. Indian Acad. Sci.*, **82A**, 217 (1975).

[9] R. L. Mishra and J. D. Pandey, *Ind. J. Pure and Applied Phys.*, **15**, 505 (1977).

[10] S. B. Srivastava, D. Phil. Thesis submitted to the University of Allahabad, 1971.

[11] R. V. Gopala Rao and V. Venkataseshaiah, *Z. phys. Chem. (Leipzig)*, **242**, 193 (1969).

Revue Roumaine de Chimie, **26**, *8*. 1077–1083 (1981)

METHOD FOR DETERMINING EFFECTIVE DIFFUSION COEFFICIENT OF GASES IN CATALYST PELLETS

G. STEINBRECHER, P. ROTARU, L. SALIU, O. BUNESCU,
N. MUREŞAN and I. BUCUR
University of Craiova, Department of Physics — Str. A. I. Cuza No. 13, 1 100 — Craiova,
Romania

Received November 4, 1980

A new method for determining the effective diffusion coefficient in catalyst pellets in stationary conditions is presented. The value of the effective diffusion coefficient is obtained as a function of the value of a system with known diffusion properties. The method is accurate, requires a single concentration measurement and can be applied on a large range of values of effective diffusion coefficients ; besides, the processing of the data is simple.

1. INTRODUCTION

Among the phenomena of substance transport in heterogeneous catalysis, the diffusion in porous catalyst plays a prominent part and is frequently referred to as internal diffusion. Although the diffusion mechanism in porous materials is rather complex at microscopic level of the substance transport in pores, the diffusion process can be described phenomenologically quite accurately by means of the effective diffusion coefficient. This coefficient includes the most important diffusion properties of the catalyst, its values giving direct information about the rate of the diffuse substance transport (i.e. the transport by molecular random movement) in the porous catalytic medium. The substance transport may be achieved by convection in the catalyst pellets as well, but, most often diffusion is predominant.

In principle, the determination of the effective diffusion coefficients in porous media is done by means of the solutions of the diffusion equations in pores, [1–8] in installations simulating the boundary and transport conditions, conditions established by concentration measurements, adsorption or fixing and desorption. In the previous works, various methods for determining the effective diffusion coefficient both in non-stationary and stationary regime, in the absence or presence of the chemical reaction were described. On the other hand there are a lot of methods of analysis : gaschromatography, infrared spectrometry, chemical analysis, etc. [9–13]

Based on an original idea, the purpose of this work is to give a method for determining the effective diffusion coefficient in porous catalyst pellets. The analysis of the gases is made on an infrared spectrometer.

2. PRINCIPLE OF METHOD

The effective diffusion coefficient in the catalyst pellet appears in the diffusion equation as a factor of proportionality between the substance current through the pellet, *j*, and the concentration gradient $\frac{\mathrm{d}C}{\mathrm{d}x}$. It is assumed that in the porous medium the concentration varies only along one direction (Ox), having the same value in a plane perpendicular to this direction, the gradient being expressed locally by the concentration derivative as against x. This nonvanishing concentration gradient generates an irreversible substance transport from the regions with large concentration values to the regions with lower concentration values. Thus, the system has the tendency of levelling the concentration, this process being one of the aspects of the thermodynamic equilibrium.

If the fields of temperatures and pressures in the pellet are homogenous, the transport of the substance through the pellet is carried only by repeated mutual molecular collisions and with the pore walls, i.e. by internal diffusion.

In steady state, the substance transport is thus carried out that, in a given point, the concentration remains constant in time, although it acquires different values in various points. For a stationary linear distribution of the concentrations, the gradient may be written as

$$\frac{C_N - C_M}{x_N - x_M} \tag{1}$$

where $x_N - x_M$ is the distance between two perpendicular planes on Ox, the planes also containing the points M and N.

Under these conditions, the substance current is :

$$j = -D \cdot \frac{C_N - C_M}{x_N - x_M} \tag{2}$$

while the substance flow through a pellet with cross-section S is jS.

According to Eq. (2), the calculation of the effective diffusion coefficient implies the determination of two values of the concentration as well as of the flow through the catalyst pellet.

The method suggested in the present work, enables the determination of the effective diffusion coefficient, direct evaluation of the substance flow being unnecessary. The method is stationary and makes use of a new principle in order to diminish the number of concentration determinations required by other methods described in the literature. [14–17] Our method implies a single determination after reaching the steady state. The principle scheme of the measurement cell is shown in figure 1.

Through pipeline *A*, the gas **X**, whose diffusion through pellets is studied, is introduced, through pipeline *B* another gas Y is introduced (we shall refer to it as the reference gas) which does not present absorption in infrared at the frequencies characteristic to gas X. The flow rate of the gas Y introduced through the pipeline *B* is sufficiently high compared to the quantity that can diffuse through capillary *2* and pellet *1*. Thus, the concentrations in chambers *a* and *c* are practically 0% (100%) and 100% (0%) for the gas Y (X).

The pressures in the chambers *a*, *b* and *c* are rigorously equal in order to prevent the transport of the substance by convection. The work pressure and temperature are the normal pressure and temperature of the medium. It is advisable that in the chamber *b* a stirrer for the gas — *3* should be introduced. The composition of the gas mixture from the chamber *b* is determined with an analyser — *4*.

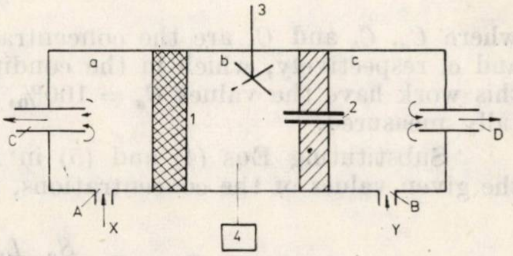

Fig. 1. — Scheme of principle of the measuring cell for the effective diffusion coefficients of the catalyst pellets. *A*, *B* — gases inlets ; *C*, *D* — gases outlets ; *a*, *b*, *c* — gas chambers ; *1* — catalyst pellet ; *2* — capillary ; *3* — gas stirrer ; *4* — analyser.

Gas X diffuses through the catalyst pellet, from chamber *a* into chamber *b*, and from there, through the capillary, into chamber *c*. Gas Y diffuses from chamber *c* into chamber *b* (through the capillary) and, then, from *b* into *a* (through the pellet).

The following symbols are employed :

S_1 — the area of the cross-section in the catalyst pellet ;
L_1 — the thickness of the catalyst pellet ;
D_1 — the effective diffusion coefficient of the gas X in the catalyst pellet ;
j_1 — the current of gas X through the pellet, in perpendicular direction on it, from chamber *a* to chamber *b* under steady state conditions ;
S_2 — the area of the cross-section in the capillary ;
D_2 — the diffusion coefficient of gas X into gas Y, obtained from constant tables ;
L_2 — the length of the capillary ;
j_2 — the current of gas X through the capillary longitudinal direction, from the chamber *b* to chamber *c*, under steady state conditions.

In steady state (when the concentration in chamber *b* becomes constant) the magnitude of the gas X flow, diffused through the pellet (from chamber *a* into chamber *b*) is equal to the magnitude of the gas X flow through the capillary (from chamber *b* into chamber *c*) :

$$j_1 S_1 = j_2 S_2 \tag{3}$$

where, according to Eq. (2), the currents have the forms :

$$j_1 = D_1 \cdot \frac{C_a - C_b}{L_1} \tag{4}$$

$$j_2 = D_2 \cdot \frac{C_b - C_c}{L_2} \tag{5}$$

where C_a, C_b and C_c are the concentrations of gas X in chambers *a*, *b* and *c*, respectively, which in the conditions of the method presented in this work have the values $C_a = 100\%$, $C_c = 0\%$ while C_b is experimentally measured.

Substituting Eqs (4) and (5) in Eq. (3) and taking into account the given values of the concentrations, we finally get to :

$$D_1 = D_2 \cdot \frac{S_2}{S_1} \cdot \frac{L_1}{L_2} \cdot \frac{C_b}{1 - C_b} \tag{6}$$

Eq. (6) represents the final formula for the calculation of the unknown effective diffusion coefficient of a gas through a porous catalyst pellet, when the dimensions of the pellet and of the capillary, the diffusion coefficient of the gas X into the gas Y are known and the concentration of the gas X in chamber *b* under stationary conditions is measured.

By means of infrared spectrometry as method of analysis of the gas composition, the concentration of the gas X in the gas Y from chamber *b* may be written as :

$$C_b = \frac{\lg \frac{T_Y}{T}}{\lg \frac{T_Y}{T_X}} \tag{7}$$

where T_X, T_Y are the transmittances of the pure gases X and Y, and T is the transmittance of gas X of concentration C_b, in the mixture with gas Y. The experimental conditions must be chosen in such a way that T_X and T_Y should be as close as possible to 0% and 100%, respectively, in order to assure the accuracy of the measurements.

In this case, Eq. (6) becomes :

$$D_1 = D_2 \cdot \frac{d_2^2}{d_1^2} \cdot \frac{L_1}{L_2} \cdot \frac{\lg \frac{T_Y}{T}}{\lg \frac{T}{T_X}} \tag{8}$$

where d_1 and d_2 represent the diameters of the catalyst pellet and of the capillary, respectively.

3. CONCEPTION AND PRESENTATION OF THE INSTALLATION

The installation was destined for the determination of the effective diffusion coefficient, on a large scale of sizes of the cylindrical or noncylindrical catalyst pellets with plane-parallel faces, with the area of the section ranging from 0.2 to 2.00 cm^2 and the height from 0.2 to 2.00 cm, as a function of the known diffusion coefficient of another porous system. As for the system with known diffusion coefficient we have chosen a capillary pipeline (slow diffusion system for which the solutions of the diffusion equations are known) of a radius and length conveniently chosen.

The installation is to satisfy the following conditions :

— it must work in a perfectly stationary regime ;

— by modifying the dimensions of the capillary a very large range of the effective diffusion coefficients for different catalysts under study must be covered, when C_b as well is approximately 50%.

— the pure gas flows carrying the diffused gases on the capillary must be sufficiently high so that the concentrations on both surfaces may be of about 100% for each of the two gases.

It is not very important to consider the diffusion in the space between the catalyst pellet and the capillary because as may be demonstrated, the error introduced by its neglection is below 1% provided the dimensions of this space are much larger than the diameter of the capillary.

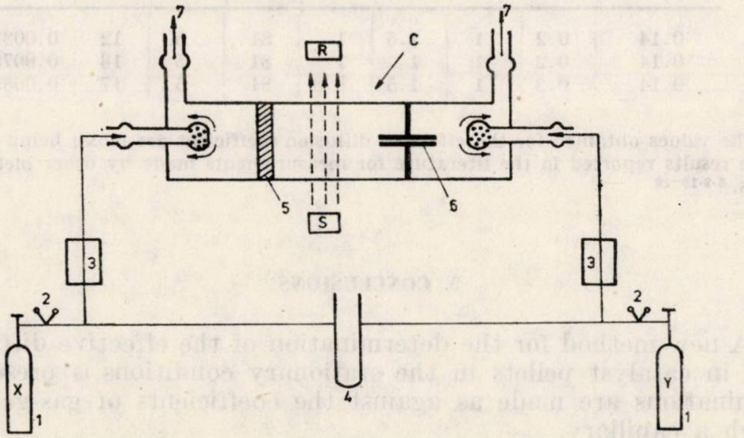

Fig. 2. — Installation for determining the effective diffusion coefficient in the catalyst pellets. *1* — gas bottle ; *2* — pressure reducer with manometer ; *3* — capillary ; *4* — control of the pressure equalization ; *5* — catalyst pellet ; *6* — capillary ; *7* — gas outlet ; *C* — diffusion cell ; *S* — infrared radiation source ; *R* — infrared radiation receiver.

In this work the authors suggest an instalation (Fig. 2) for the measurement of the effective diffusion coefficients, an installation satisfying all the former principles and requirements. The equalization of the gas supply pressures is achieved by means of the system of reducers — *2*, the capillaries — *3* and the differential manometer — *4*. The capillaries

— *3* are of similar lengths and radia, while the differential manometer — *4* consists of a U-shaped glass pipe filled with very fluid unsicative oil, with a very small vapour tension.

4. EXPERIMENTAL

Measurements of the effective diffusion coefficient on high temperature shift conversion catalyst were made in order to verify the suggested method. The pure gases used in measurements were : $X = CO_2$, $Y = N_2$. The choice of these two gases was also due to the fact that carbon dioxide displays a strong band at $\overline{\nu} = 2\,315\ cm^{-1}$, its absorption in infrared remaining unaffected by the presence of nitrogen, the latter displaying no absorption bands in the given frequency interval (its transmittance is 100%). The apparatus used for the gas analysis is of the Specord 71 IR type and enables transmittance measurements in the interval $\overline{\nu} = 4\,600 - 650\ cm^{-1}$.

The results of the measurements of the effective diffusion coefficient on three catalyst pellets are shown in table 1.

TABLE 1

Experimental measurements

D_2 (cm^2s^{-1})	d_2 (cm)	d_1 (cm)	L_2 (cm)	L_1 (cm)	T_{N_2} (%)	T_{CO_2} (%)	T (%)	D_1 (cm^2s^{-1})
0.14	0.2	1	1.5	1	81	5	12	0.00814
0.14	0.2	1	1	1	81	5	16	0.00781
0.14	0.3	1	1.5	0.8	81	5	17	0.00857

The values obtained for the effective diffusion coefficient are close, being in agreement with the results reported in the literature for measurements made by other methods on like catalysts.[3,9,16–20]

5. CONCLUSIONS

A new method for the determination of the effective diffusion coefficient in catalyst pellets in the stationary conditions is presented ; the determinations are made as against the coefficients of gas-gas diffusion through a capillary.

Compared to the methods currently employed, the method described in this work may present certain advantages :

— for the estimation of the effective diffusion coefficient it is not necessary to evaluate the substance flow in the catalyst pellet ;

— the measurements are reduced to a single concentration determination ;

— the accuracy in the determinations of the gas concentrations (pure gases), of the geometrical dimensions and of the diffusion coefficient of the reference system, as well as the accuracy in the determination of the concentration in the central chamber of the diffusion cell, imply a high precision in the determination of the diffusion coefficient in the catalyst pellet ;

— by the adaptation of the reference system, accurate determinations of the effective diffusion coefficient values in a very large range (3—4 orders of magnitude) can be obtained.

— the stationary method eliminates the influence of certain secondary processes accompanying the diffusion (gas adsorption and desorption, especially under reaction conditions);

— the special processing of the catalyst pellets required in the non-stationary methods for the elimination of systematic errors is avoided;

— the very complicated computation techniques used in the methods based on the analysis of the concentration impulses are also avoided.[18-21]

REFERENCES

[1] W. E. Lewis and J. D. Paynter, *Chem. Eng. Sci.*, **26**, 1357 (1971).
[2] A. Varma and N. R. Amundson, *Chem. Eng. Sci.*, **28**, 91 (1973).
[3] J. R. Balder and E. E. Petersen, *J. Catal.*, **11**, 195 (1968).
[4] J. R. Balder and E. E. Petersen, *J. Catal.*, **11**, 202 (1968).
[5] W. Goldstein and J. J. Carberry, *J. Catal.*, **28**, 33 (1973).
[6] J. J. Carberry and A. A. Kulkarni, *J. Catal.*, **31**, 41 (1973).
[7] L. L. Hegedus and E. E. Petersen, *Catal. Rev.-Sci. Eng.*, **9**, 245 (1974).
[8] L. L. Hegedus and E. E. Petersen, *Ind. Eng. Chem. Fundamentals*, **11**, 579 (1972).
[9] V. A. Kirillov, Yu. S. Matros, V. A. Kuzin and M. G. Slinko, *Kinetika i Kataliz*, **12**, 219 (1971).
[10] J. J. Carberry, *Chimica e Industria*, **51**, 951 (1969).
[11] H. W. Haynes and P. N. Sarma, *AIChE Journal*, **19**, 1043 (1973).
[12] Y. H. Ma and T. Y. Lee, *AIChE Journal*, **22**, 147 (1976).
[13] K. C. Pratt and W. A. Wakeham, *Chem. Eng. Sci.*, **30**, 444 (1975).
[14] F. Balfantz and D. Gelbin, *Inj. — Fiz. Zhur.*, **25**, 708 (1973).
[15] L. L. Hegedus and E. E. Petersen, *Chem. Eng. Sci.*, **28**, 69 (1973).
[16] L. L. Hegedus and E. E. Petersen, *Chem. Eng. Sci.*, **28**, 345 (1973).
[17] F. A. Feizhanov and M. I. Kolesnikov, *Zhur. priklad. Khim.*, **45**, 2452 (1972).
[18] M. Suzuki and J. M. Smith, *AIChE Journal*, **18**, 326 (1972).
[19] H. Omata and L. F. Brown, *AIChE Journal*, **18**, 967 (1972).
[20] M. T. Rusov, M. G. Slinko, O. A. Stretssov, O. A. Malinovskaia, V. S. Beskov and A. I. Loza, *Teor. Osn. Khim. Technol.*, **5**, 382 (1971).
[21] Y. Murakami, T. Hattori and T. Hattori, *J. Catal.*, **10**, 123 (1968).

Revue Roumaine de Chimie, 26, 8, 1085–1089 (1981)

INFLUENCE DES OXYDES DE MÉTAUX ALCALINS SUR LA FORMATION D'UN CATALYSEUR FERRO-CHROMIQUE ACTIF DANS LA CONVERSION DE MONOXYDE DE CARBONE PAR LA VAPEUR D'EAU

FLORIAN DOMKA et MAREK LANIECKI
Laboratoire de Cinétique et de Catalyse
Institut de Chimie UAM, 60–780 Poznań. (Pologne)

Reçu le 13 septembre 1980

The influence of alkalo metal oxides on the activity of iron-chromium oxide catalysts for CO shift conversion was studied. It has been found, on the ground of the results obtained for two series of catalyst samples, that alkali metal oxides cause a decrease in surface area of catalysts and an increase in their catalytic activity.

On a étudié l'influence des oxydes alcalins sur l'activité des catalyseurs ferro-chromiques dans la conversion de CO par la vapeur d'eau. On a constaté, à l'exemple de deux séries de préparations, que les oxydes alcalins provoquent la diminution de la surface spécifique des catalyseurs et en même temps l'accroissement de leur activité catalytique.

Dans nos travaux antérieurs [1-3] nous avons décrit une nouvelle façon d'obtention du catalyseur ferro-chromique utilisé dans la conversion de CO par la vapeur d'eau dans le domaine des températures élevées et nous avons essayé d'expliquer le rôle de Cr_2O_3 [4]. Notre attention a porté sur l'influence du procédé de préparation et du matériel initial dans la synthèse de la phase active du catalyseur. En plusieurs cas ces propriétés dépendent de la nature de l'espace interfacial et de la présence des différents promoteurs [5,6].

Nous voudrions, dans le présent travail, porter une attention particulière sur l'influence des oxydes alcalins sur la valeur de surfaces et sur les propriétés catalytiques de deux catalyseurs ferro-chromiques qui diffèrent par la façon d'obtention.

PARTIE EXPÉRIMENTALE

Les catalyseurs ont été obtenus à partir d'iso-*ortho*-hydroxyde de fer [7] et de γ-FeOOH [8] en considérant leurs propriétés catalytiques optimales. On met l'oxyde de chrome sur les hydroxydes de fer secs par une méthode d'imprégration. Deux séries de catalyseurs ont été obtenues. La première à été obtenue à partir de γ-FeOOH et de Cr_2O_3 (2 % en poids par rapport à Fe_2O_3) et la deuxième à partir d'iso-*ortho*-hydroxyde de fer imprégné par Cr_2O_3 (8 % en poids) [9]. Les catalyseurs activés par les oxydes alcalins ont été obtenus de la façon suivante : dans le mélange de l'hydroxyde de fer et de chrome on ajoutait une certaine quantité d'hydroxyde d'un métal alcalin. Ces préparations ont été séchées à 50°C pendant 24 heures. Ensuite on a broyé et fait passer au tamis (le diamètre de la maille = 0,12 mm).

Enfin on a activé pendant 3 heures dans un courant d'air à 400°. On a obtenu les catalyseurs contenant les hydroxydes de métaux alcalins dans les quantités 0,5 ; 1 ; 2 ; et 4 % de moles en comptant sur le $Me^{I}O$. L'activité catalytique a été exprimée par le taux de conversion de CO après 3 heures. La réaction de conversion a été réalisée par la méthode dynamique — sens pression [1,2] avec le rapport molaire ; vapeur d'eau/oxyde de carbone égal à 2,5. Le débit du mélange réactionnel a été fixé à 1500 cm^3/h. La température de la réaction, dans tous les cas, a été de 350°C. Les produits de la réaction ont été analysés par la méthode chromatographique. Le schéma de l'appareillage a été présenté dans un travail antérieur [1,2].

La surface spécifique a été déterminée par la méthode de la désorption thermique d'argone [10]. Les catalyseurs de la série γ-FeOOH ont été désignés par G — ensuite on a pris en considération la teneur en % de Cr_2O_3 et la teneur en % de l'oxyde alcalin. Les catalyseurs de la série iso-*ortho*- ont été désignés de la même façon en commençant par la lettre I.

RÉSULTATS ET DISCUSSION

Dans le tableau 1 sont présentées les propriétés catalytiques dans la réaction de conversion de CO par la vapeur d'eau et les valeurs de la surface spécifique.

TABLEAU 1

Taux de conversion, surface spécifique et activité spécifique des catalyseurs ferro-chromiques de la série γ-FeOOH promus par les oxydes alcalins

Symbole du catalyseur	Taux de conversion %	Activité spécifique avant/ après la réd. la réd. $cm^3/h\ m^2$	Surface spécifique avant/ après la réd. la réd. m^2/g
G−0	16,78	6,44	78,25
G−2	17,36	5,54	94,04
G−2−0,5−Li	24,60	7,68	96,05
G−2−1−Li	20,06	6,80	88,49
G−2−2−Li	8,08	2,77	87,45
G−2−4−Li	6,21	2,38	78,10
G−2−0,5−Na	40,88	12,69	96,67
G−2−1−Na	22,24	6,89	96,78
G−2−2−Na	35,26	13.73	77,05
G−2−4−Na	39,10	18,74	62,61
G−2−0,5−K	40,57	13.76	88,48
G−2−1−K	40.04	14,59	82,35
G−2−2−K	70,89	25.08 / 36,63	84,78 / 58,06
G−2−4−K	64,87	27,05	71,94
G−2−0,5−Rb	42,73	14,76	86,86
G−2−1−Rb	50,22	18,11	83,19
G−2−2−Rb	67,96	24,04	84,83
G−2−4−Rb	68,23	26.85 / 23,69	76,22 / 86,40
G−2−0,5−Cs	40,57	13,57	89,70
G−2−1−Cs	51,58	17,44	88,73
G−2−2−Cs	57,73	20,02	86,52
G−2−4−Cs	65,56	21,32	92,27

D'après le tableau, il apparaît que l'addition d'un oxyde alcalin change visiblement l'activité catalytique (colonne 1). Dans le cas des catalyseurs de la série γ-FeOOH l'oxyde de lithium dans des petites quantités (0,5 ; 1% mole) provoque une augmentation insensible du taux de conversion.

Si les concentrations de cet oxyde sont plus grandes on observe une diminution de l'activité par rapport au catalyseur respectif (G—2).

TABLEAU 2

Taux de conversion, surface spécifique et activité spécifique des catalyseurs ferro-chromiques de la série iso-*ortho*-Fe/OH/$_3$ promus par les oxydes alcalins

Symbole du catalyseur	Taux de conversion %	Activité spécifique avant/ après la réd. la red. $cm^3/h\ m^2$	Surface spécifique avant/ après la réd. la réd. m^2/g
I—O	27,88	13,38	62,53
I—8	46,03	9,02	153,10
I—8—1—Li	51,11	14,69	104,34
I—8—0,5—Li	46,27	10,17	136,43
I—8—2—Li	51,83	12,95	120,06
I—8—4—Li	42,50	13,81	92,34
I—8—0,5—Na	52,10	11,25	138,90
I—8—1—Na	62,74	14,87	126,58
I—8—2—Na	60,38	15,26	118,71
I—8—4—Na	60,00	17,99	100,06
I—8—0,5—K	62,70	12,31	152,82
I—8—1—K	75,48	16,49	137,28
I—8—2—K	68,86	14,51	142,35
I—8—4—K	75,62	20,36	111,41
I—8—0,5—Rb	56,55	11,94	142,07
I—8—1—Rb	60,98	12,49	146,41
I—8—2—Rb	67,86	16,11	126,40
I—8—4—Rb	77,76	19,02 / 27,00	122,65 / 122,10
I—8—0,5—Cs	53,76	11,68	138,09
I—8—1—Cs	59,73	13,68	131,01
I—8—2—Cs	85,69	21,19 / 17,39	121,34 / 147 / 80
I—8—4—Cs	80,35	19,14	125,94

Les autres promoteurs favorisent un accroissement considérable de l'activité. L'activité des catalyseurs contenant les oxydes de potassium, de rubidium et de césium augmente presque trois fois par rapport au catalyseur G—2. La préparation la plus active de cette série est le catalyseur qui contient 2% de mode de K_2O. Dans ce cas le taux de conversion atteint 70%.

Analogiquement comme dans le cas précédent, l'oxyde de lithium ajouté aux catalyseurs de la série iso-*ortho* favorise un accroissement du taux de conversion si sa concentration est de 1%, tandis que 4% de mole provoque son abaissement.

Les catalyseurs promus par K_2O, Rb_2O, Cs_2O, de même que dans la série γ-FeOOH, se caractérisent par une activité accrue.

Le meilleur catalyseur est un composé qui contient 2% mole de Cs_2O (I—8—2—Cs). Les catalyseurs contenant Na_2O sont moins actifs que ceux avec K_2O, Rb_2O et Cs_2O.

L'oxyde alcalin ajouté à un catalyseur ferro-chromique permet un accroissement de la conversion, excepté l'oxyde de lithium qui agit d'une façon inactivante. Mais cette activité catalytique n'est pas en relation directe avec la valeur de la surface spécifique et avec les transformations de la texture poreuse.

Dans tous les cas (voir le tableau), au fur et à mesure qu'augmente le % de l'oxyde alcalin, la valeur de la surface spécifique diminue.

Comme exception on peut citer les catalyseurs suivants :

G—2—2—K, G—2—4—Cs, I—8—2—K et I—8—4—Cs.

Il est intéressant de constater que dans les cas des préparations promues l'activité spécifique (colonne 2) est plus grande que celle des préparations respectives. Ceci est en relation avec le nombre plus grand de centres actifs à la surface des catalyseurs. Cette augmentation peut être provoquée par la formation, entre l'oxyde de fer et l'oxyde alcalin, d'un composé type ferrite alcalin (Me FeO_2) [11], ou peut être conditionnée par le changement de propriétés acides à la surface du catalyseur ferro-chromique. Il s'agit ici d'un échange ionique entre les groupes acides OH à la surface de catalyseurs et les cations du métal alcalin. La formation de l'espace interfacial entre les composants du catalyseur peut avoir une certaine importance [2].

L'identification diffractométrique ne conduit pas à la découverte d'une nouvelle phase. Toutefois on ne peut pas exclure la formation des chromates ou de $MeFeO_2$ dans une atmosphère de substances régissantes. Dans cette atmosphère fortement réductrice on ne peut pas trouvér des ions de chrome à un plus grand degré d'oxydation [12].

La réaction de conversion de l'oxyde de carbone par la vapeur d'eau est une réaction du type redox. Mais, d'après nos études, on ne peut pas exclure un certain caractère acide-basique. Dans les travaux de Boehma [13] concernant les propriétés acides des oxydes de métaux à des surfaces hydrolysées, nous trouvons la confirmation de l'existence des propriétés acides de l'oxyde de fer et de chrome.

Dans nos travaux ultérieurs, consacrés à l'étude de la nature des centres actifs des catalyseurs ferro-chromiques dans la conversion de CO par la vapeur d'eau, nous allons expliquer le rôle d'activation des oxydes alcalins.

Les auteurs voudraient bien remercier Mme Danuta Gabryszewska pour sa participation à la partie expérimentale du présent travail.

BIBLIOGRAPHIE

[1] F. Domka et M. Laniecki, « Some Aspects of Physical Inorganic Chemistry », Proceeding of the Frist Regional Symposium, Polish Academy of Science, Poznań, 1976, p. 207.

[2] F. Domka, M. Laniecki et Z. Ruszkowski, *React. Kinet. Catal. Lett.*, **3**, 261 (1975).

[3] F. Domka et M. Laniecki, *Surface Technology*, **7**, 217 (1978).

[4] F. Domka et M. Laniecki, *Z. anorg. Chem.*, **435**, 273 (1977).

[5] F. Domka et M. Laniecki, *Cahiers scientifiques de l'Université A. Mickiewicz, Chemia, Poznań*, **17**, 13 (1975).

[6] F. Domka, Z. Duzik et M. Gasiorek, *React. Kinet. Catal. Lett.*, **2**, 171 (1975).

[7] F. Domka et M. Laniecki, *Surface Technology*, **5**, 303 (1977).

[8] A. Krause, Patent PRL, 34471 (1951).

[9] M. Laniecki, Thesis, A. Mickiewicz University, 1977.

[10] F. N. Nelsen et F. T. Eggertsen, *Analyt. Chem.*, **30**, 1387 (1958).

[11] P. K. Gaur, R. M. Cursetji, G. Sengupta, H. S. Ahluwalia et N. B. Bhattacharyya, *Technology (India)*, **10**, 204 (1973)

[12] M. P. McDaniel et R. L. Burwell Jr., *J. Catalysis*, **36**, 394 (1975) .

[13] H. P. Boehm, *Discuss. Faraday Soc.*, **52**, 264 (1971).

Revue Roumaine de Chimie, **26**, *8*, 1091–1096 (1981)

MEDIUMEINFLÜSSE BEI DER SOLVOLYSE VON ALKYLHALOGENIDEN. VIII[1] SALZEFFEKTE BEI DER HYDROLYSE VON *t*-BUTYLCHLORID

R. H. SCHUSTER

Zentrum für physikalische Chemie, Splaiul Independenţei 202, Bukarest

Eingegangen am 23. Januar 1980

Für die Hydrolyse von *t*-Butylchlorid wurde der durch KNO_3, KCl und KBr bewirkte Salzeffekt bei 293,16 K untersucht. Die Ergebnisse beschreiben eine lineare Abhängigkeit der Reaktionsgeschwindigkeitskonstanten von der Molkonzentration des zugegebenen Elektrolyten. Die Neigungen der erhaltenen Geraden werden in Abhängigkeit der Natur des Elektrolyten diskutiert.

Salt effects induced by added KNO_3, KCl and KBr for the hydrolysis of *t*-butylchloride at 293,16 K were investigated. The results describe a linear dependence of reaction rates on the mole concentration of added electrolyte. The slopes of the lines are discussed as a function of the nature of electrolyte.

Das Interesse am Einfluß von Elektrolytzugaben auf die Reaktionsgeschwindigkeitskonstanten besteht schon seit Jahren [2,3] während denen eine beachtliche Anzahl von Arbeiten durchgeführt wurden, die die Natur dieses Effektes zu klären versucht haben, ohne daß sich aber eine sichere Deutung abzeichnen konnte.

So ist bei der Hydrolyse von Alkylhalogeniden ein Anstieg der Reaktionsgeschwindigkeitskonstanten während der Reaktion zu verzeichnen, der außerhalb der Fehlergrenze liegt und meist einem Salzeffekt zugeschrieben werden kann. Auch wird die ionogene Hydrolyse von Alkylderivaten durch die während der Reaktion gebildeten Elektrolyten beeinflußt.

Der Salzeffekt wurde vor allem in nichtwässerigen Lösungen wie wasserfreie Essigsäuere [3] oder in binären wässerigen Gemischen mit geringem Wassergehalt untersucht.

Da wir aber in einer Reihe von Arbeiten über die Hydrolyse von Alkylhalogeniden [4,5] auch in reinem Wasser einen Anstieg der Reaktionsgeschwindigkeitskonstanten während der Reaktion beobachten konnten, haben wir uns in der vorliegenden Mitteilung mit dem Einfluß von ein-einwertigen Salzen KNO_3, KCl und KBr auf die Hydrolyse von *t*-Butylchlorid (*t*-BuCl) in reinem Wasser befaßt.

EXPERIMENTELLES

Frisch destilliertes *t*-BuCl (BDH) ($K_p = 51{,}0°$, $n_D^{20} = 1{,}3903$) wurde in wasserfreiem Aceton zu einer Standardlösung gelöst. Wasser, für Leitfähigkeitsmessungen, wurde beim Durchleiten von destilliertem Wasser über eine Ionenaustauschersäule (1000 mm × 40 mm) mit einer Geschwindigkeit von 100 ml.Min^{-1} erhalten.

KNO_3, KCl, KBr p.a. (Merck) wurden nicht zusätzlich gereinigt. Die kinetischen Messungen sind nach zwei verschiedenen Methoden ausgeführt worden.

a) Extraktion mit kaltem Chloroform des nichtreagierten *t*-BuCl aus Proben, die zu gegebenen Zeitpunkten der Meßzelle entnommen wurden und Titrieren der entstandenen Salzsäuere in Gegenwart von Bromthymolbau.

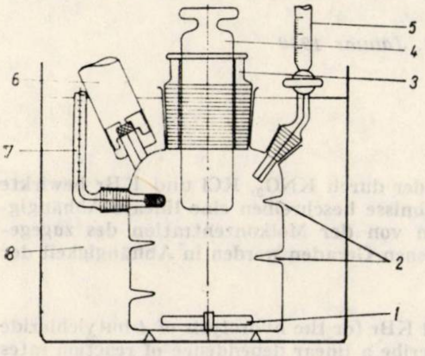

Abb. 1. — Schematische Darstellung der Meßzelle : (1) magnetischer Rührer ; (2) — Dornen in der Zellwand ; (3) Glaspfropfen ; (4) — Zylindrischer Glaskolben ; (5) — Mikrobürette ; (6) — Injektionsstutzen ; (7) — Thermometer ; (8) — Thermostat.

b) Schrittweise Neutralisation eines vorgegebenen Volumes einer NaOH Lösung bestimmter Konzentration durch die entstandene Salzsäuere in Gegenwart von Bromthymolblau und Messen des Zeitpunktes bei dem der Farbumschlag erfolgt.

In beiden Fällen wurde die in Abbildung 1 dargestellte Meßzelle verwendet.

Ein mit zentralem Ring versehener magnetischen Rührer (1) gewährleistet eine gute Durchmischung der Flüssigkeit und die in der Wand der Meßzelle befindlichen Schikanen (2) bewirkten eine Turbulenz um die Vermischzeit der Reaktanten möglichst herabzusetzen. Um eine Verflüchtigung des *t*-BuCl zu vermeiden wurde die Zelle voll angefüllt und das überschüssige Wasser beim Aufsetzen des Glaspfropfens (3) herausgedrückt. Bei der Extraktionsmethode wurde der Glaspfropfen (3) so eingesetzt, daß der zylindrische Glaskolben (4) (20 ml Volumen) sich in möglichst hochgestellter, oder bei der schrittweisen Titration in möglichst tiefgestellter Position befand. Für die schrittweise Titration wird an die Meßzelle eine Mikrobürette (5) angeschlossen wogegen bei der Extraktionsmethode die betreffende Öffnung durch einen Pfropfen geschlossen war. Die Meßzelle wurde vor jedem Versuch etwa 40 Minuten in einem Thermostatenbad auf 293,16 ± 0,02 K gebracht bei der die Reaktionsgeschwindigkeitskonstante (RGK) noch nicht zu hoch ist, so daß die Anwendung der Extraktionsmethode gestattet ist.

Durch den Injektionsstutzen (6) wurde mittels einer Hamiltonspritze 0,05—0,1 ml die die *t*-BuCl Standardlösung eingespritzt. Bei der Extraktionsmethode wurden zu bestimmten Zeitpunkten genau gemessene Proben in eine mit kaltem Chloroform halbgefüllte Spritze (2 ml) aufgezogen und anschließend schnell in einen Mikrotrenntrichter gelehrt. Nach Extraktion der organischen Phase, wurde die entstandene Säuere in der wässerigen Phase gegen Bromthymolblau titriert.

Bei der schrittweisen Titration wurde in Gegenwart desselben Indikators die Zeit ermittelt die nötig war um vorgegebene Mengen von KOH durch die entstehende Salzsäuere zu neutralisieren. Selbstverständlich ist zuerst festgestellt worden, daß die RGK von der HO^- Ionenkonzentration wenig beeinflußt wird.

Die erhaltenen Ergebnisse liegen bei der Extraktionsmethode etwas höher (etwa 2,5 %) als bei der schrittweisen Titration, besitzen aber auch einen weitaus größeren Streuungsbereich (± 2,2 % gegen 1,2 % bei der schrittweisen Titration). Allgemein liegen diese RGK Werte jedoch tiefer als die durch Leitfähigkeitsmessungen erhaltenen Werte.[4]

ERGEBNISSE UND DISKUSSION

Der Einfluß der Elektrolyten KNO_3, KCl und KBr auf die Hydrolyse von *t*-BuCl in reinem Wasser wurde für alle drei verwendeten Salze für gleiche Molkonzentrationen im Bereich 0—0,6 $Mol.l^{-1}$ bei 293,16 K untersucht. Wie aus Tabelle 1 ersichtlich, ist eindeutig ein Anstieg der RGK-Werte unter dem Einfluß der zugegebenen Elektrolyten zu erkennen, wobei jedoch auch die Natur desselben eine Rolle spielt.

TABELLE 1

Abhängigkeit der RKG Werte von *t*-BuCl von der Konzentration des zugegebenen Elektrolyten

MX Mol. l^{-1}	KNO_3		KCl		KBr	
	k (s^{-1})	k_0 (s^{-1})	k (s^{-1})	k_0 (s^{-1})	k (s^{-1})	k_0 (s^{-1})
0,00	0,01473	0,00013	0,01473	0,00013	0,01473	0,00013
0,05	0,01488	0,00011	0,01492	0,00013	0,01542	0,00011
0,10	0,01506	0,00012	0,01515	0,00011	0,01598	0,00011
0,20	0,01523	0,00016	0,01561	0,00009	0,01710	0,00008
0,25	0,01560	0,00009	0,01583	0,00008	0,01759	0,00008
0,30	0,01580	0,00011	0,01606	0,00011	0,01823	0,00007
0,40	0,01616	0,00009	0,01652	0,00004	0,01941	0,00009
0,45	0,01635	0,00011	0,01674	0,00009	0,01994	0,00006
0,50	0,01651	0,00008	0,01697	0,00011	0,02056	0,00007
0,60	0,01688	0,00008	0,01742	0,00007	0,02169	0,00009

So ist bei einem maximalen Zusatz von 0,6 $Mol.l^{-1}$ Elektrolyt, der Wert der RGK bei KNO_3 um 15%, bei KCl um 19%, und bei KBr um 47% größer als der Vergleichswert in reinem Wasser. Es sei immerhin darauf hingewiesen, daß diese Salzeffekte im Vergleich zu denen bei der Solvolyse in weniger polaren Medien als Wasser, wie z.B. binäre wässerige Gemische [5,6] oder in wasserfreier Essigsäuere erhaltenen [7-9] viel kleiner sind.

Der Salzeffekt wurde in polaren Lösungsmitteln aufgrund einiger möglichen Erscheinungen erklärt, wie: elektrostatische und Ionen-Atmosphäre Stabilisation, [8] „Lösungsmitteltrocknung" durch Elektrolyten, spezifische vom Elektrolyten induzierte Effekte usw.

Theoretische Erwägungen führten zu der Gleichung: [8]

$$\log k_A = \log k_0 + \frac{0{,}912 \cdot 10^{16}}{D^2\, T^2}\, \sigma\mu \qquad (1)$$

wo k_0 die RGK bei Salzabwesenheit, σ eine experimentelle Konstante ist und das Dipolmoment des Übergangszustandes darstellen soll, μ die Ionenstärke des Mediums, D die Dielektrizitätkonstante des Lösungsmittels und T die Temperatur sind.

Andererseits führten eine Reihe von Arbeiten in Lösungsmitteln, wie Eisessig, zu der empirischen Gleichung: [3]

$$k_A = k_0(1 + b\,[MY]) \qquad (2)$$

wo b ein empirischer Parameter ist der vom Lösungsmittel, Reaktanten, dem zugegebenen Salz und der Temperatur abhängt und [MY] die Molkonzentration des Elektrolyten bedeutet.

Unsere Meßergebnisse zeigen nun, wie aus Abbildung 2 eindeutig hervorgeht, daß die Linearität für Gleichung (1) nicht besteht (Kurve *a*, Abbildung 2) während für Gleichung (2) eine fast einwandfreie lineare Abhängigkeit besteht (Kurve *b*, Abbildung 2). Um eine Linearität nach Gleichung (1) aufzuweisen, müßte der Parameter σ einen Extremwert in etwa der Mitte des untersuchten Konzentrationbereiches des zugegebenen Elektrolyten durchlaufen, was zumindest physikalisch wenig sinnvoll scheint.

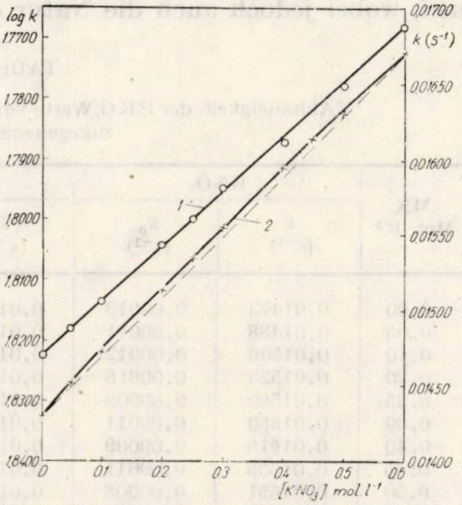

Abb. 2. — Anwachsen der RGK Werte in Abhängigkeit des zugegebenen Elektrolyten (KNO_3) nach Gleichung (1) (Kurve *a*) und nach Gleichung (2) (Kurve *b*) dargestellt.

Mann kann daher mit einiger Sicherheit behaupten, daß die untersuchten Elektrolyten während der Hydrolyse von *t*-BuCl in reinem Wasser einen „normalen" Salzeffekt bewirken, der nach folgenden Gleichungen beschrieben werden kann:

$$k = k_0\,(1 + 0{,}248\,[KNO_3]) \tag{3}$$

$$k = k_0\,(1 + 0{,}309\,[KCl]) \tag{4}$$

$$k = k_0\,(1 + 0{,}744\,[KBr]) \tag{5}$$

Die Winsteinsche Gleichung (2) erweist sich nicht nur wegen der experimentell bestätigten Linearität der RGK-Werte als nützlich sondern auch dadurch daß sich die Natur des Elektrolyten in der Neigung der erhaltenen Geraden widerspiegelt. Allgemein sind diese b Werte der Geraden mindestens um eine Größenordnung kleiner als die bei der Acetolyse gemessenen.[9,10] Dieser Befund kann darauf zurückgeführt werden, daß in Wasser die vorhandenen Ionen solvatisiert sind und infolge der hohen Dielektrizitätskonstante keine elektrostatischen Wechselwirkungen mehr auf große Distanz ausüben, wie in weniger polaren Medien. Der Einfluß der vorhandenen Ionen wird daher bei gleicher Molkonzentration allgemein geringer in Wasser oder hochwässerigen Gemischen sein.

Die Tatsache, daß *t*-BuCl in Gegenwart von KCl einen „normalen" Salzeffekt aufweist, könnte durch die hohe freie Energie des sich im Übergangszustand bildenden Karbokations bewirkt sein, die eine geringe Stabilität und hohe Reaktivität desselben bedingt. Diese Annahme ist auch mit dem Brönstedschen Geschwindigkeitsgesetz im Einklang. Somit ist es wahrscheinlicher, daß das gebildete *t*-Bu^+ Kation mit einem der benachbarten Wassermoleküle reagiert um den entsprechenden Alkohol zu bilden, als daß ein fremdes außenstehendes Cl^- Ion teilweise seine Solvatationshülle durchbricht, um zu einem Ionenpaar zurückzuführen, gemäß des von Winstein vorgeschlagenen Reaktionsschemas: [6]

$$\begin{tikzcd}
RX \arrow[r, shift left] & R^+X^- \arrow[l, shift left] \arrow[r, shift left] \arrow[d, "\text{Solv.}"] & R^+ + X^- \arrow[l, shift left] \arrow[d, "\text{Solv.}"] \\
& {} & {}
\end{tikzcd} \qquad (I)$$

Der vergleichsweise höhere Anstieg der RGK in Gegenwart von Cl^- Ionen gegenüber NO_3^-, könnte unter anderem auch auf den Unterschied der Solvatationsverhältnisse der beiden Ionen schließen lassen. Das NO_3^- Ion ist bekanntlich weder strukturbildend noch abbauend und daher schwach solvatisiert. Sein großer Ionenradius verringert den elektrostatischen Einfluß auf den ionisierenden Reaktanten *t*-BuCl, so daß der Salzeffekt für dieses Ion die kleinsten *b* Werte aufweisen müßte. Dagegen hat das Cl^- Ion, welches wegen des geringen Ionenradius eine größere Ladungskonzentration besitzt, wahrscheinlich auch durch die starke Solvatationshülle einen stärkeren ionisierenden Einfluß auf das Reaktionszentrum, das von dem voluminösen K^+ Kation assistiert wird. Dieser Effekt könnte wahrscheinlich auch noch dadurch verstärkt sein, daß infolge der stärkeren Cl^- Solvatation, im Mittel, weniger freie Wassermoleküle den Reaktanten *t*-BuCl im Ausgangszustand solvatisieren können oder anders ausgedrückt, daß eine größere Energie zur Solvatation des Reaktanten aufgebracht werden muß. Dadurch dürfte der Grundzustand bei KCl-Zusätzen weniger solvatisiert sein als bei KNO_3 Zusätzen was eine Erniedrigung der Aktivierungsenergie zurfolge hätte, die die geringen jedoch spezifischen RGK Unterschiede im Falle von NO_3^- und Cl^- Ionen erklären könnte.

Die höchsten *b* Werte wurden in Gegenwart von KBr verzeichnet. Teilweise kann dieser Befund aufgrund des winsteinschen Schemas:

$$\begin{tikzcd}
RX \arrow[r, shift left] & R^+X^- \arrow[l, shift left] \arrow[r, shift left, "\text{Solv.}"] \arrow[d, shift right] & R^+ + X^- \arrow[l, shift left] \arrow[r, "\text{Solv.}"] & {} \\
RY \arrow[r, shift left] & R^+Y^- \arrow[l, shift left] \arrow[u, shift right, "M^+Y^-"'] \arrow[r, shift left] \arrow[d, "\text{Solv.}"] & R^+ + Y^- \arrow[l, shift left] \arrow[r, "\text{Solv.}"] & {} \\
& {} & &
\end{tikzcd} \qquad (II)$$

erklärt werden, demzufolge ein Anionenaustausch beim Ionenpaar t-Bu$^+$Cl$^-$ das Auftreten in kleinen Konzentrationen des Ionenpaares t-Bu$^+$Br$^-$ bewirken kann, was zu einer globalen Geschwindigkeitserhöhung führen konnte. Wenn man in Betracht zieht, daß t-BuBr etwa 10^5 mal schneller als t-BuCl reagiert, [4,5] so dürfte auch ein nur sehr kleiner Anteil an dem obengennanten Anionenaustausche genügen, um die gefundene RGK Erhöhung im Falle von KBr zu erklären.

LITERATURHINWEISE

[1] Mitt. VII: R. H. Schuster, A. Nicolau und I. A. Schneider, *Z. Chem.*, **20**, 63 (1980).

[2] L. P. Hammett „Physical Oraganic Chemistry", Mc Graw-Hill, New York, 1970, cap. 7, 187–219.

[3] F. Badea, „Mecanisme de reacţie în chimia organică", Ed. Ştiinţifică, Bucureşti, 1973, cap. 3, p. 155–165.

[4] E. L. Allred und S. Winstein, *J. Amer. Chem. Soc.*, **89**, 4012 (1967).

[5] R. H. Schuster, A. Nicolau, *Rev. Roumaine Chim.*, **25**, 1069 (1980).

[6] R. H. Schuster, A. Nicolau und I. A. Schneider, *Z. phys. Chem. (Leipzig)*, im Druck.

[7] R. H. Schuster, A. Nicolau und I. A. Schneider, *Z. Chem.*, **20**, 24 (1980).

[8] L. C. Bateman, M. G. Church, E. D. Hughes, C. K. Ingold und N. A. Taher, *J. Chem. Soc.*, **1940**, 979.

[9] A. H. Fainberg und S. Winstein, *J. Amer. Chem. Soc.*, **78**, 2763, 2767, 2780 (1956).

[10] A. H. Fainberg und S. Winstein, *J. Amer. Chem. Soc.*, **78**, 2777 (1956).

Revue Roumaine de Chimie, 26, 8, 1097–1105 (1981)

Co(III) COMPLEX COMPOUNDS WITH 3-AMINO-1-PROPANOL AND DIMETHYLGLYOXIME

MARIA BREZEANU, IOANA JITARU and MAGDALENA DINCULESCU
National Institute of Chemistry, Department of Chemistry, Laboratory of Inorganic Chemistry, 3–5 Polizu str., Bucharest, Romania

Received February 11, 1980

The present paper reports on the results obtained in the synthesis and characterization of Co(III) complex compounds with 3-amino-1-propanol and dimethylglyoxime, belonging to the following three general types : $[CoX(DH)_2(AOH)]$ (X = Cl, Br, I, CNS) ; $[Co(DH)_2(AOH)_2]X$ (X = Cl, Br, I, CNS) and $[Co(DH)_2(AOH)_2]\ [CoX_2(DH)_2]$ (X = Cl, Br, I, CNS) where $AOH = H_2N-(CH_2)_3-OH$ and $DH = MeC(NOH)C(NO)^-Me$. The most probable stereochemistry of the compounds was determined on the basis of elemental analysis, molecular electric conductivity measurements, electronic and vibrational spectra ; the coordination of aminoalcohol by nitrogen of the amino group was also established.

The previous papers [1,2] reported on the results obtained in the study of some mono and polynuclear complex compounds of Co(II) and Co(III) in which 3-amino-1-propanol acts both as neutral and anionic ligand, i.e. mono or bidentate ligand.

Several types of complex compounds containing ethylenediamine and 3-amino-1-propanol as ligands have also been described. [3]

The present paper concerns the results obtained in the synthesis and characterization of Co(III) complex compounds which contain concomitantly two different ligands : 3-amino-1-propanol and dimethylglyoxime.

The literature mentions several Co(III) complex compounds with mixed ligands as dimethylglyoxime and 2-amino-1-ethanol. [4]

The compounds obtained in this work can be included in the following general types :

I. $[CoX(DH)_2(AOH)]$ (X = Cl, Br, I, CNS)
II. $[Co(DH)_2(AOH)_2]X$ (X = Cl, Br, I, CNS)
III. $[Co(DH)(AOH)_2]\ [CoX_2(DH)_2]$ (X = Cl, Br, I, CNS), where $DH = MeC(NOH)C(NO)^-Me$ and $AOH = H_2N-(CH_2)_3-OH$.

These compounds were characterized by elemental analysis, molecular electric conductivity measurements, electronic and vibrational spectra.

RESULTS AND DISCUSSION

In order to obtain different types of Co(III) complex compounds containing dimethylglyoxime and 3-amino-1-propanol, the synthesis of these compounds was performed varying the ratio of the components, the solvent, and the cobalt salt anion nature.

The conditions under which the compounds were synthesized are schematically represented in figure 1. As may be seen :

— different compounds are obtained on changing the ratio of the reactants ; so at a $CoX_2 : DH_2 : AOH = 1 : 2 : 1$ molar ratio, type I compounds are obtained whereas at a 1 : 2 : 4 molar ratio, type II compounds result ;

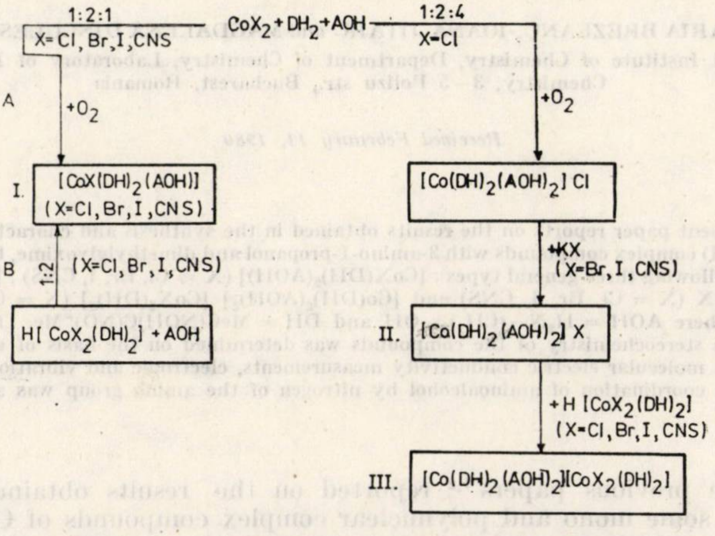
1:2:1
X=Cl, Br, I, CNS
CoX2+DH2+AOH
1:2:4
X=Cl
A
+O2
+O2
I.
[CoX(DH)2(AOH)]
(X=Cl, Br, I, CNS)
[Co(DH)2(AOH)2] Cl
B
(X=Cl, Br, I, CNS)
+KX
(X=Br, I, CNS)
H[CoX2(DH)2] + AOH
II.
[Co(DH)2(AOH)2] X
+H [CoX2(DH)2]
(X=Cl, Br, I, CNS)
III.
[Co(DH)2(AOH)2][CoX2(DH)2]

Fig. 1. — Types of obtained compounds and their conditions of synthesis.

— compounds of type I, $[CoX(DH)_2(AOH)]$ were obtained by two different methods : method (A) which is a direct one (the reaction of Co(II) salts, dimethylglyoxime and 3-amino-1-propanol and Co(II) oxidation to Co(III) with oxygen from the air) and method (B) which is based — under well established conditions — on the reaction of 3-amino-1-propanol with $H[CoX_2(DH)_2]$ compounds (the latter compounds being synthesized by Ablov's method) ;[5,6]

— compounds of type II, $[Co(DH)_2(AOH)_2]X$ were obtained from chloride $[Co(DH)_2(AOH)_2]Cl$ by double exchange reactions with potassium halides or pseudohalides ;

— in the reaction of $H[CoX_2(DH)_2]$ and $[Co(DH)_2(AOH)_2]X$, type III compounds, $[Co(DH)_2(AOH)_2]$ $[CoX_2(DH)_2]$ were obtained.

The most probable structure assumed for the obtained complex compounds is based on the correlation of electric conductivity data, electronic and vibrational spectra presented below.

MOLECULAR ELECTRIC CONDUCTIVITY DETERMINATIONS

The formulation assigned to the studied complex compounds (the nature of their ionic dissociation) was confirmed by the determination of their molar electric conductivity in D.M.F solution.

The obtained data (Table 1) show that the type I compounds are nonelectrolytes and types II and III are electrolytes 1 : 1.

TABLE 1

Molar electric conductivity* of the obtained compounds

Compound	Molar electric conductivity ($\Omega^{-1}cm^2mol^{-1}$)	Type of electrolyte
$[CoCl(DH)_2(AOH)]$	20.40	nonelectrolyte
$[CoBr(DH)_2(AOH)]$	15.70	nonelectrolyte
$[CoI(DH)_2(AOH)]$	20.25	nonelectrolyte
$[Co(SCN)(DH)_2(AOH)]$	18.30	nonelectrolyte
$[Co(DH)_2(AOH)_2]Cl$	75.51	1 : 1
$[Co(DH)_2(AOH)_2]Br$	69.35	1 : 1
$[Co(DH)_2(AOH)_2]I$	70.15	1 : 1
$[Co(DH)_2(AOH)_2]CNS$	73.10	1 : 1
$[Co(DH)_2(AOH)_2][CoCl_2(DH)_2]$	69.80	1 : 1
$[Co(DH)_2(AOH)_2][CoBr_2(DH)_2]$	72.25	1 : 1
$[Co(DH)_2(AOH)_2][CoI_2(DH)_2]$	70.10	1 : 1
$[Co(DH)_2(AOH)_2][Co(SCN)_2(DH)_2]$	75.35	1 : 1

* 10^{-3} M DMF solutions ; t = 25°.

ELECTRONIC SPECTRA

In order to establish the most probable stereochemistry of the compounds studied, their electronic reflectance spectra were recorded. These spectra were compared to those of some similar Co(III) compounds known in the literature and having a well-established structure.

Analysis of the electronic reflectance spectra, as shown in figures 2 and 3, reveals that the most probable structure of all the studied compounds is the octahedral, low spin one. [7]

Figure 2 shows the electronic reflectance spectra of type I compounds, $[Co(DH)_2(AOH)X]$ (X = Cl, Br, I, CNS) as well as the electronic spectra of compound 1,6 $[CoCl(DH)_2NH_3]$ known in the literature. [8] Study of the figure shows :

— closely resembling spectra of type I compounds and their similitude to the spectrum of compound 1,6 $[CoCl(DH)_2NH_3]$, suggesting that the $[CoX(DH)_2(AOH)]$ (X = Cl, Br, I, CNS) compounds, also have a *trans* configuration ;

— at short wavelengths the intense bands are probably $M \leftarrow X$ charge transfer bands ;

— shift of the charge transfer bands, towards longer wavelengths, from the chloroderivative to the iododerivative namely from 235 nm (42 550 cm^{-1}) and 250 nm (40 000 cm^{-1}), respectively in the chloroderivative, to 250 nm (40 000 cm^{-1}) and 320 nm (31 250 cm^{-1}) respectively in the bromoderivative and 250 nm (40 000 cm^{-1}) and 380 nm (26 100 cm^{-1}) respectively in the iododerivative is based on the corresponding increase in the reduction powder of the halogen ligand (from chloride to iodide) ; [9]

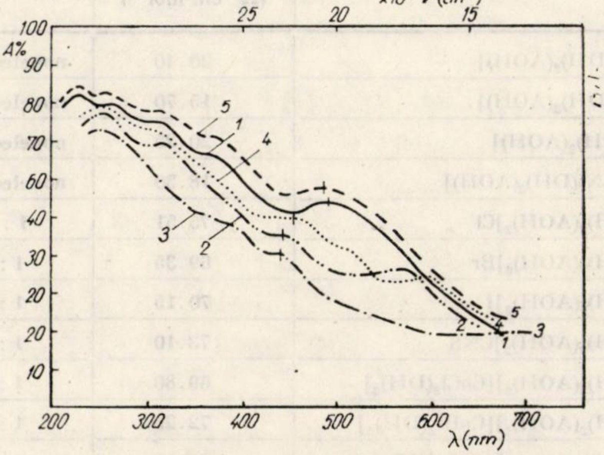

Fig. 2. — Electronic reflectancespectra of compounds : 1. [CoCl(DH)$_2$(AOH)] ; 2. [CoBr(DH)$_2$(AOH)] ; 3. [CoI(DH)$_2$(AOH)] ; 4. [Co(SCN)(DH)$_2$(AOH)] ; 5. 1,6 [CoCl(DH)$_2$(NH$_3$)].

— d-d bands which appear as shoulders (overlapped by intense charge transfer bands) in the spectra of these compounds could be ascribed as follows :

— the shoulder at 340 nm (29 400 cm^{-1}) in chlorocomplex spectrum, the absorption maximum at 445 nm (23 000 cm^{-1}) in bromocomplex spectrum and the shoulders at 445 nm (23 000 cm^{-1}) and 475 nm (21 000 cm^{-1}) respectively in the iodocomplex and thiocyanocomplex spectra probably belong to $^1T_{1g} \leftarrow {^1A_{1g}}$ transition ; the shoulder at 480 nm (20 800 cm^{-1}) in the chlorocomplex spectrum, the maximum at 565 nm (17 700 cm^{-1}) in the bromoderivative spectrum as well as the shoulder at 600 nm (16 660 cm^{-1}) in the thiocyanocomplex spectrum probably belong to the $^1T_{2g} \leftarrow {^1A_{1g}}$ transition ;

— the shift of these absorption bands towards longer wavelengths on going from the chlorocomplex to the iodocomplex and thiocyanatocomplex is due to the positions of the halogen and pseudohalogen ligands in Tsuchida's spectrochemical series. [10]

Figure 3 shows the reflectance spectra of the type II compounds, [Co(DH)$_2$(AOH)$_2$]X (X = Cl, Br, I, CNS) and of the compound 1,6 [Co(DH)$_2$(NH$_3$)$_2$] Cl, known from the literature. [8]

Analysis of these spectra shows that :

— independently of the X anions nature, all type II compounds give similar spectra (for the sake of simplification only the chloro and bromoderivative spectra are given); these spectra are very similar to the 1,6 $[Co(DH)_2(NH_3)_2]Cl$ compound spectrum ; this might be interpreted, on the one hand, as indicating the same (*trans*) configuration for all the studied compounds and, on the other hand as showing that 3-amino-1-propanol is coordinated only by amino nitrogen ;

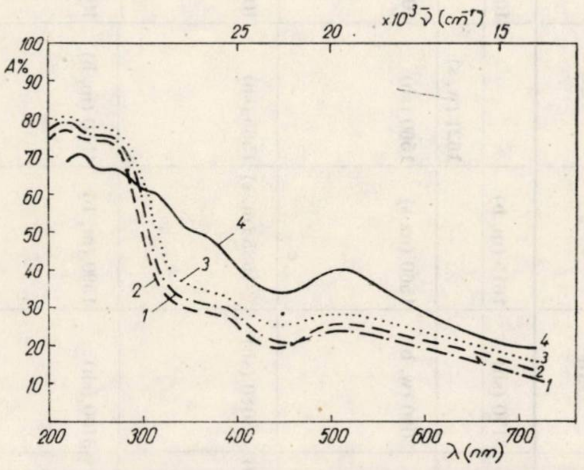

Fig. 3. — Electronic reflectance spectra of compounds : 1. $[Co(DH)_2(AOH)_2]Cl$; 2. $[Co(DH)_2(AOH)_2]Br$; 3. 1,6 $[Co(DH)_2(NH_3)_2]Cl$; 4. $[Co(DH)_2(AOH)_2][CoCl(DH)_2(AOH)]$.

— in the spectra of these compounds, the intense charge transfer bands in the nearly ultraviolet range overlap the weak d-d bands.

The electronic spectra of type III compounds (Fig. 3, curve 4) are very similar to the spectra of the two types of the compounds described.

VIBRATIONAL SPECTRA

The infrared spectra of the compounds obtained provide additional data recording the stereochemistry of these compounds, especially the coordination manner of the 3-amino-1-propanol ligand (neutral molecule or anion, mono or bidentate ligand). From this point of view, of interest are the range of O-H (ν_{OH}), C-O (ν_{CO}) and N-H (ν_{asNH} and ν_{sNH}) stretching vibrations of the 3-amino-1-propanol ligand and on the other hand, the range of O-H (ν_{OH}), C≡N (ν_{CN}) and N-O (ν_{NO}) stretching vibrations of the dimethylglyoxime ligand.

For a more correct determination of the infrared spectra of complex compounds studied we also recorded the free ligand spectra (3-amino-1-propanol and dimethylglyoxime) and compared them with published data.[11]

TABLE 2

IR frequencies of some obtained complex compounds and their probable assignments

Compound	ν_{OH}	ν_{asNH}	ν_{sNH}	δ_{NH_2}	$\nu_{C\equiv N}$	ν_{C-O}	ν_{NO}
AOH	3450(s, b)	3290 (s, b)	3170 (sh)	1615 (m, b)	—	1055 (s, s)	—
DH_2	3215 (m, b)	—	—	—	1621 (w, s)	—	970 (m, s)
$[CoCl(DH)_2(AOH)]$	3450 (m, b) (AOH) 3210 (m, b) (DH, free OH groups) 2350 (w, b) (DH, hydrogen bonds) 1780 (m, b) (DH, δ_{OH})	3170 (m, b)	3090 (w, b)	1560 (m, s) *c*	1560 (sh)	1055 (s, s)	925 (m, s)
$[Co(DH)_2(AOH)_2]$	3450 (m, b) (AOH) 3215 (m, b) (DH, free OH groups) 2360 (w, b) (DH, hydrogen bonds) 1785 (m, b) (DH, δ_{OH})	3180 (m, b)	3080 (sh)	1585 (m, s)	1565 (sh)	1055 (s, s)	930 (m, s)
$[Co(DH)_2(AOH)_2][CoX_2(DH)_2]$	3450 (w, b) (AOH) 3210 (m, b) (DH, free OH groups) 2355 (m, b) (DH, hydrogen bonds) 1780 (m, b) (DH, δ_{OH})	3200 (m, b)	3100 (sh)	1590 (m, b)	1550 (m, b)	1055 (m, s)	910 (m, s)

s -- strong, m — medium, w — weak, b — broad band; **sh** — shoulder;
AOH = $H_2N-(CH_2)_3-OH$; DH = $MeC(NOH)C(NO)^{-}Me$.

In 3-amino-1-propanol spectrum the stretching vibration frequency O—H (ν_{OH}) appears at approximately 3450 cm^{-1}; as compared to the stretching vibrations frequency, ν_{OH}, in primary alcohols (3650—3590 cm^{-1}) inter and intramolecular hydrogen bonds appear in the presence of 3-amino-1-propanol.[12]

Table 2 shows the infrared frequencies characteristic of the complex compounds studied and their probable assignments.

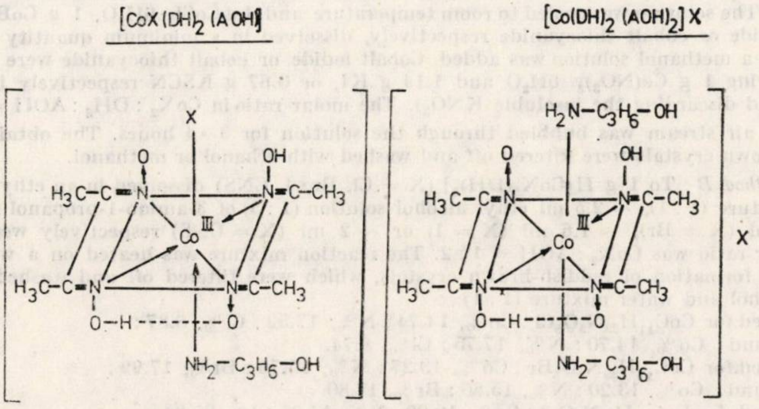

I. II.

Fig. 4. — Probable structure of type I and II complex compounds.

A study of the data included in this table suggests the following:

— in the spectra of all studied complex compounds, ν_{OH} stretching vibration, appears in the same range as the free ligand, at 3450 cm^{-1}, whereas the frequencies of the amino group (ν_{asNH}, ν_{sNH} and δ_{NH_2}) shift towards lower values relative to the free ligand, pointing to the presence of 3-amino-1-propanol as neutral, monodentate ligand coordinated only by the amino group;

— shift of the C≡N (ν_{CN}) and N—O (ν_{NO}) stretching frequency towards lower values can be interpreted as a proof of the coordination of dimethylglyoxime to the central Co(III) ion;

— presence in the spectra of the complex compounds both of the free OH characteristic bands (3210 cm^{-1}) of dimethylglyoxime and of the characteristic bands of the bound OH groups (by hydrogen bonds, 2350 cm^{-1}) attests to the *trans* octahedral configuration proposed for these compounds. In this configuration the two dimethylglyoxime molecules are to be found in the basic plane of the square pyramid (and thus may form intramolecular bonds of the hydrogen bond type); this is also based on the indication in the literature referring to other Co(III) complex compounds with dimethylglyoxime.[13-17]

Figure 4 gives the probable formulation of complex compounds of types I and II.

EXPERIMENTAL

I. SYNTHESIS AND ANALYSIS OF COMPLEXES

1. $[CoX(DH)_2(AOH)]$ $(X = Cl, Br, I, CNS)$. **The complex compounds of this type were obtained by two methods :**

Method A : 0.97 g dimethylglyoxime (X = Cl), 0.70 g (X = Br), 1.25 g (X = I) and 1.33 g (X = CNS) respectively were dissolved on a warm water bath in a minimum quantity of ethyl alcohol (X = Cl, Br) or methyl alcohol (X = I, CNS) containing ~ 0.32 ml 3-amino-1-propanol (X = Cl), ~ 0.23 ml (X = Br), ~ 0.40 ml (X = I) or ~ 0.43 ml (X = CNS) respectively. The solution was cooled to room temperature and 1 g $CoCl_2 \cdot 6H_2O$, 1 g $CoBr_2 \cdot 6H_2O$, cobalt iodide or cobalt thiocyanide respectively, dissolved in a minimum quantity of ethyl alcohol or a methanol solution was added. Cobalt iodide or cobalt thiocyanide were obtained by dissolving 1 g $Co(NO_3)_2$ $6H_2O$ and 1.14 g KI, or 0.67 g KSCN respectively in methyl alcohol and discarding the insoluble KNO_3). The molar ratio in $CoX_2 : DH_2 : AOH = 1 : 2 : 1$.

An air stream was bubbled through the solution for 3–4 hours. The obtained dark reddish-brown crystals were filtered off and washed with ethanol or methanol.

Method B : To 1 g $H[CoX_2(DH)_2]$ (X = Cl, Br, I, CNS) dissolved in an ethyl alcohol-water mixture (1 : 1), ~ 2.5 ml ethyl alcohol solution (1 : 5) of 3-amino-1-propanol (X = Cl), or ~ 2 ml (X = Br), ~ 1.6 ml (X = I) or ~ 2 ml (X = CNS) respectively were added. The molar ratio was $CoX_2 : AOH = 1 : 2$. The reaction mixture was heated on a water bath up to the formation of reddish-brown crystals, which were filtered off and washed with an ethyl alcohol and water mixture (1 : 1).

Calcd.for $CoC_{11}H_{23}N_5O_5Cl$: Co %, 14.74 ; N %, 17.52 ; Cl %, 8.87 ;
Found : Co %, 14.70 ; N %, 17.75 ; Cl %, 8.74.
Calcd.for $CoC_{11}H_{23}N_5O_5Br$: Co %, 13.27 ; N %, 15.76 ; Br %, 17.99 ;
Found : Co %, 13.20 ; N %, 15.60 ; Br %, 17.80.
Calcd. for $CoC_{11}H_{23}N_5O_5I$: Co %, 12.00 ; N %, 14.25 ; I %, 25.84 ;
Found : Co %, 12.15 ; N %, 14.10 ; I %, 25.75.
Calcd. for $CoC_{11}H_{23}N_5O_5(CNS)$: Co %, 13.95 ; N %, 19.89 ; CNS %, 13.74 ;
Found : Co %, 13.80 ; N %, 19.95 ; CNS %, 13.80.

2. $[Co(DH)_2(AOH)_2]X$ $(X = Cl, Br, I, CNS)$ The chloride of the series was obtained as follows : 0.97 g dimethylglyoxime was dissolved on a hot bath in a minimum quantity of ethyl alcohol containing 1.26 ml 3-amino-1-propanol. The solution was cooled to room temperature and 1 g $CoCl_2 \cdot 6H_2O$ (molar ratio $CoCl_2 : DH_2 : AOH = 1 : 2 : 4$) added. Air was bubbled 3–4 hours through the solution thus prepared.

The obtained dark red compound was filtered off and washed with ethyl alcohol, then purified by recrystallization from water.

The same product can be also obtained at a molar ratio $CoCl_2 : DH_2 : AOH = 1 : 2 : 4$.

Calcd. for $CoC_{14}H_{32}N_6O_6Cl$: Co %, 12.42 ; N %, 17.69 ; Cl %, 7.47 ;
Found : Co %, 12.56 ; N %, 17.35 ; Cl %, 7.20.

Bromide, iodide or thiocyanide were obtained by double exchange reactions. To a concentrated aqueous solution was added a saturated solution of KBr, KI or KSCN. The red crystals obtained were filtered off and washed with a solution of water and alcohol (1 : 1).

Calcd. for $CoC_{14}H_{32}N_6O_6Br$: Co %, 11.35 ; N %, 15.39 ; Br %, 16.18 ;
Found : Co %, 11.35 ; N %, 15.30 ; Br %, 16.10.
Calcd. for $CoC_{14}H_{32}N_6O_6I$: Co %, 10.41 ; N %, 14.84 ; I %, 22.42 ;
Found : Co %, 10.27 ; N %, 14.70 ; I %, 22.47.
Calcd. for : $CoC_{14}H_{32}N_6O_6(CNS)$: Co %, 11.85 ; N %, 19.71 ; SCN %, 11.66 ;
Found : Co %, 11.75 ; N %, 19.51 ; SCN %, 11.80.

3. $[Co(DH_2)(AOH)_2]$ $[CoX_2(DH)_2]$ $(X = Cl, Br, I, CNS)$. To a concentrated aqueous solution containing 1 g $[Co(DH)_2(AOH)_2]$ X (*X* = Cl, Br, I, CNS) was added a 1 : 1 solution of water and ethyl alcohol containing $H[CoX_2(DH)_2]$ (0.76 g for X = Cl, 0.86 g for X = Br, 0.96 for X = I and 0.82 g for X = CNS). The crystals obtained were filtered off and washed with ethyl alcohol.

Calcd. for $Co_2C_{22}H_{48}N_{10}O_{10}Cl_2$: Co %, 14.74 ; N %, 17.52 ; Cl %, 8.87 ;
Found : Co %, 14.50 ; N %, 17.32 ; Cl %, 8.45.
Calcd. for $Co_2C_{22}H_{48}N_{10}O_{10}Br_2$: Co %, 13.37 ; N %, 15.76 ; Br %, 17.99 ;
Found : Co %, 13.50 ; N %, 15.65 ; Br %, 17.75.
Calcd. for $Co_2C_{22}H_{48}N_{10}O_{10}I_2$: Co %, 12.00 ; N %, 14.25 ; I %, 25.84 ;

Found : Co%, 11.80 ; N%, 14.10 ; I%, 25.80.
Calcd. for : $Co_2C_{22}H_{48}N_{10}O_{10}(CNS)_2$: Co%, 13.95 ; N%, 19.89 ; SCN%, 13.74
Found : Co%, 13.80 ; N%, 19.75 ; SCN%, 13.65.

II. MOLAR CONDUCTIVITY MEASUREMENTS

The molar conductivity measurements were performed on a Radelkis conductometer with a cell constant K = 0.92. The measurements have been made in 10^{-3}M DMF solutions, at a temperature of 25°C.

The assignment of the electrolyte type was made according to the indication given in the literature referring to the methods of establishing the electrolyte type in DMF solutions.[18]

III. ELECTRONIC SPECTRA

The reflectance spectra have been recorded at room temperature using a C. Zeiss Jena VSU 1 spectrophotometer and magnesium oxide as reference material.

IV. VIBRATIONAL SPECTRA

I.R. spectra have been obtained by means of a Perkin Elmer spectrophotometer using a potassium bromide disk.

REFERENCES

[1] I. Jitaru and M. Brezeanu, *Rev. Roumaine Chim.*, **23**, 559 (1978).
[2] M. Brezeanu and I. Jitaru, *Rev. Roumaine Chim.*, **24**, 967 (1979).
[3] I. Jitaru, M Dinculescu and C. Ruva, *Rev. Roumaine Chim.*, (in press).
[4] V. N. Evreev, V. A. Golubov and S. V. Murashko, *Zhur. neorg. Khim.* **16**, 716 (1971).
[5] A. V. Ablov and I. M. Samushi, *Zhur neorg. Khim.*, **3**, 1818 (1958).
[6] A. V. Ablov and M. P. Filippov, *Zhur. neorg. Khim.*, **4**, 2204 (1959).
[7] A. B. P. Lever, "Inorganic Electronic Spectroscopy", Academic Press, New York, 1968, p. 309.
[8] A. Nakahara, J. Fujita and R. Tsuchuda, *Bull. Chem. Soc. Japan.*, **28**, 473 (1955).
[9] A. B. P. Lever, "Inorganic Electronic Spectroscopy", Academic Press, New York, 1968, p. 153
[10] M. Brezeanu and P. Spacu, "Coordination Compounds Chemistry", Editura Didactică și Pedagogică, Bucharest, 1974, p. 155.
[11] M. Avram and D. Mateescu, "Infrared Spectroscopy", Editura Tehnică Bucharest, 1965, p. 395.
[12] L. J. Bellamy, "Infrared Spectra of Complex Molecules", Academic Press, New York, 1958, p. 108.
[13] K. Nakamoto, "Infrared Spectra of Inorganic Coordination Compounds", Academic Press, New York, 1963, p. 230.
[14] J. Fujita, A. Nakahova and R. Tsuchida, *J. Chem. Phys.*, **23**, 1541 (1955).
[15] R. D. Gillard and G. Wilkinson, *J. Chem. Soc.*, **1963**, 6041.
[16] R. Blinc and D. Hadzi, *J. Chem. Soc.*, **1958**, 4536.
[17] R. Blinc and D. Hadzi, *Spectrochim. Acta*, **16**, 853 (1960).
[18] J. V. Quagliano, J. Fujita, D. J. Phillips and S. Y. Tyree, *J. Amer. Chem. Soc.*, **83**, 3370 (1961).

Revue roumaine de chimie, 26, 8, 1107–1109 (1981)

KINETICS OF SELF-DECOMPOSITION OF TIN(IV) PEROXYDICHROMATE

S. P. S. JADON
Department of Chemistry, S. V. College, Aligarh, India

Received September 13, 1978
Revised March 2, 1981

Rate coefficients and Arrhenius parameters were calculated for the tin(IV) peroxydichromate during its kinetic studies. On the basis of the evidences gathered, it has been found that decomposition process of tin(IV) peroxydichromate is slow, measurable, exothermic and of first order with the formation of tin(IV) dichromate.

Gandnigar [1] studied the formation and decomposition of blue peroxychromate. He found that both reactions were independent of hydrogen peroxide concentration and of the first order. Rai and Prakash [2] also confirmed the first order decomposition of chromium(III) peroxydichromate. Awasthy [3] studied the self-decomposition of chromium(III) peroxydichromate prepared with adipic acid and supported Rai's view.

EXPERIMENTAL

Tin(IV) peroxydichromate was prepared as described earlier [4] by using Analar chemicals. Dry and free from hydrogen peroxide, tin(IV) peroxydichromate (100 ml.) in an Erlenmeyer flask was kept in thermostat at a particular temperature. When, tin(IV) peroxydichromate attained the temperature of the thermostate, the stop watch was started and simultaneously a definite volume (5 ml.) of tin(IV) peroxydichromate was withdrawn and titrated iodometrically against N/100 sodium thiosulphate solution, taking the time as zero. At this time the concentration of tin(IV) peroxydichromate was assumed as initial concentration (a). After a fixed time (7.5 min) the undecomposed tin(IV) peroxydichromate was again withdrawn and titrated similarly. Since the decomposition of tin(IV) peroxydichromate (x) would proceed continuously, the quantity of tin(IV) peroxydichromate remained undecomposed (a-x) was determined with time intervals as mentioned above.

The decomposed product was yellow in colour. This decomposed product was analysed qualitatively and quantitatively (volumetrically) and was found to be tin(IV) dichromate. In a similar manner the kinetic studies of tin(IV) peroxydichromate were done by taking 10°C temperature difference.

Rate constants and Arrhenius factors were calculated on the basis of available literature. [5]

RESULTS and DISCUSSION

The presence of $Cr_2O_{10}^{-2}$ ion in tin(IV) peroxydichromate has been confirmed and assigned by the formula $Sn(Cr_2O_{10})$ (loc. cit). During the kinetic studies of tin(IV) peroxydichromate, the rate constants, calculated, for the first order process, are found constant at a particular temperature, and graph of $\log_{10}k$ versus 1/T (Tables 1 and 2) is found to be a straight line, suggesting that the decomposition of tin (IV) peroxydichromate is a first order process. This idea is also supported by temperature coefficient $(k_t + 10/k_t)$ which lies within the range $2 \sim 3$.

TABLE 1

Rate coefficients for tin (IV) peroxydichromate during its self-decomposition

Time (min.)	Rate coefficients ($k \times 10^{-3}$) at different temperatures		
	6°C	16°C	26°C
0.0	—	—	—
7.5	4.293	11.380	23.840
15.0	4.355	10.630	20.380
22.5	5.230	9.734	21.170
30.0	5.135	10.140	26.290
37.5	5.089	9.955	25.690
45.0	5.133	11.130	26.100
52.0	5.180	10.510	26.700
60.0	4.880	11.820	decomposed
67.5	4.884	decomposed	
75.0	5.091		
82.5	5.443		
90.0	decomposed		
97.5			
105 0			
	Mean $k = 4.97 \times 10^{-3}$ min^{-1}	Mean $k = 10.66 \times 10^{-3}$ min^{-1}	Mean $k = 24.30 \times 10^{-3}$ min^{-1}

Further Arrhenius parameters (Table 3) ΔE, ΔF, 'A', ΔS, and ΔH were also calculated. The value of ΔE increases with the rise of temperature. It means that the decomposition rate increases with the rise of temperature. The low values of ΔE, ΔF and A show that the decomposition reaction is measurable, while the negative values of ΔS and ΔH confirme that the decomposition of tin (IV) peroxydichromate is slow and exothermic respectively.

TABLE 2

Self-decomposition of tin (IV) peroxydichromate

S. No.	1/T	$1/T \times 10^3$	Mean $k \times 10^{-3}$ (min^{-1})	$3 + \log_{10}$ (Mean $k \times 10^3$)
1.	1/279	3.5842	4.9739	0.6967
2.	1/289	3.4602	10.6620	1.0278
3.	1/299	3.3445	24.3002	1.3838

TABLE 3

Arrhenius parameters for the self-decomposition of tin (IV) peroxydichromate

S. No.	ΔE (kcal. mol^{-1})	ΔF (kcal mol^{-1})	$A(s^{-1})$	$-\Delta S$ (e.u.)	$-\Delta H$ (kcal. mol^{-1})
1.	12.2141	2.610	1.83×10^{-7}	26.5730	5.0696
2.	14.1456	2.210	5.264×10^{-8}	19.6799	3.6743

Hence the mechanism of self decomposition of tin (IV) peroxydichromate into tin (IV) dichromate may be expressed as :

$$Sn(Cr_2O_{10})_2 \xrightarrow{\text{slow}} Sn(Cr_2O_7)_2 + 3O_2$$

REFERENCES

[1] F. Gandnigar, *Z. Phys. Chem. (Leipzig)*, **63A**, 206 (1956).

[2] R. C. Rai and S. Prakash, *Z. anorg, Chem.*, **24**, 275 (1954).

[3] S. K. Awasthy, Ph. D. Thesis, Saugar University, Saugar (1968).

[4] S. P. S. Jadon and D. S. Rathor, *J. Indian Chem. Soc.*, **53**, 527 (1976).

[5] S. Glasston, "A Text Book of Physical Chemistry", Macmillian, St. Martin's Press, New York, 1960, p. 1043—1190.

Revue Roumaine de chimie, **26**, *8*, 1111–1113 (1981)

SPECTROPHOTOMETRIC INVESTIGATIONS OF IRON (III)-N-ACETYL-N-m-TOLYLHYDROXYLAMINE-COMPLEXES

R. D. JAIMAN, SUDHA CALLA, S. P. MATHUR and R. S. THAKUR
Department of Chemistry, University of Rajasthan, Jaipur, India

Received June 26, 1980

The violet coloured complexes of Fe(III) and N-acetyl-N-tolylhydroxylamine are extractable into chloroform. The spectrophotometric studies have shown that 1 : 2 and 1 : 3 (metal : ligand) complexes predominate at different acidities. The values of stability constants, stepwise and overall, have been calculated following the extended Leden, Yatsimirskii and Harvey-Manning methods. The analytical suitability of the reagent for the microdetermination of iron has also been investigated.

INTRODUCTION

The analytical applications of N-substituted hydroxylamines have been extensively studied in our laboratories.[1-9] The present communication deals with the spectrophotometric studies of iron(III) complexes of N-acetyl-N-m-tolylydroxyl-amine (ATHA) at different acidities. The investigations have established the existence of 1 : 2 and 1 : 3 (metal : ligand) complexes depending on the pH. The analytical suitability of the reagent for microdetermination of iron has also been investigated.

EXPERIMENTAL

The reagent ATHA was prepared by following the method of Gupta and Sogani[10] The purity of the compound was established by usual methods.

A standard solution of iron(III) was prepared from pure iron wire (E. Merck). The solution was standardised gravimetrically.

All chemicals used were of analaR grade. A Beckmann model DU Quartz Spectrophotometer was used for the measurement of absorbance and a combridge bench type pH meter for pH measurements.

PROCEDURE

An aliquot of iron(III) solution, containing 10—80 μg of iron was taken in a 100 ml separatory funnel and its pH adjusted to the desired value. The reagent solution (0.1 % ATHA) in chloroform was then added and the mixture shaken thoroughly for 10 minutes. The violet colored non-aqueous layer was collected in a small beaker. The extraction was repeated with 5 ml portions of chloroform. The combined extract was diluted to 25 ml with chloroform and its absorption was measured at 410 and 430 nm.

RESULTS and DISCUSSION

All absorption measurements were taken against the reagent blank at 410 and 430 nm. The extraction with 5 ml of reagent was adequate for quantitative extraction with 2.5 N HCl. Measurements of absorbance of different sets of complementary solutions were carried out at 410 and 430 nm. Show that 1 : 2 and 1 : 3 (metal : ligand) complexes predominate in the acidity ranges of 1 – 3 NHCl and 3.5 – 5 NHCl respectively. The system obeys Beer's law over the concentration range 1 – 8 ppm with 2.5 N HCl. The optimum concentration range evaluated from Ringbom's curves were found to be 2.5 – 6 ppm at 2.5 N HCl. The molar absorptivity of the complexes calculated from Beer's law at 2.5 N HCl (410 nm) is $(1.6 \pm 0.02 \times 10\ \text{mole}^{-1}/\text{cm}^{-1})$. The sensitivity according to Sandell is 0.032 μg with 2.5 N HCl.

Moderate amounts of ions commonly associated with iron did not interfere with the estimation. U(VI), V(V), Ti(IV), Hg(II), Cu(II), Ni(II) and Bi(III) interfere in the estimation. The reagent can therefore be used for microdetermination of Fe(II). The formation constants values for 1 : 2 and 1 : 3 metal ligand complexes have been computed by the method of Leden[11], Yatsimirskii[12] and Harvey-Manning[13]. They are in close agreement to each other. The values of K_1 and K_2 being very close to each other, indicate that a simultaneous equilibrium exists in the system. The stability values are given in table 1. However, these data alone cannot definitely decide the nature of bonding and the structure of the complex.

TABLE 1

Stepwise stability constants of iron (III) complexes at 30 ± 0.5°C

Method	For 1 : 2 (metal : ligand)			For 1 : 3 (metal :ligand)			
	$\log K_1$	$\log K_2$	$\log\beta_2$	$\log K_1$	$\log K_2$	$\log K_3$	$\log\beta_3$
Leden's	6.45	6.12	12.57	6.57	6.23	4.18	16.98
Yatsimirskii's	6.36	5.98	12.34	6.41	6.17	4.27	16.85
Harvey-Manning's	—	—	12.18	—	—	—	17.04

ACKNOWLEDGEMENT. Thanks are due to Prof. J. P. Tondon, Head of Chemistry Department, University of Rajasthan, Jaipur, India for the facilities provided and U.G.C. of India for the award of financial assistance.

REFERENCES

[1] S. P. Mathur and M. R. Bhandari, *Chem. Ind. (London)*, **1975**, 572.

[2] S. P. Mathur R. S. Thakur, C. S. Bhandari and N. C. Sogani, *Chem. Analit.*, **23**, 1029 (1978)

[3] S. P. Mathur, R. S. Thakur, C. S. Bhandari and N. C. Sogani, *J. Macro. Sci. Chem.*, **A12**, 1065 (1978).

[4] S. P. Mathur, R. S. Thakur, C. S. Bhandari and N. C. Sogani, *Anales real Soc. españ. Fis. Quim.*, **74**, 673 (1978).

[5] S. P. Mathur, C. S. Bhandari and N. C. Sogani, *Bull. Inst. Chem. Acad. Sinica.*, **25**, 85, (1978).

[6] S. P. Mathur, R. S. Thakur, C. S. Bhandari and N. C. Sognai, *Talanta*, **25**, 592 (1978).

[7] S. P. Mathur, C. S. Bhandari and N. C. Sogani, *Rev. Latinoamer. quim.*, **7**, 63 (1976).

[8] S. P. Mathur, R. S. Thakur and C. S. Bhandari, *Afinidad*, **36**, 499 (1979).

[9] S. P. Mathur and M. R. Bhandari, *Ind. J. Technol.*, **14**, 359 (1976).

[10] H. K. L. Gupta and N. C. Sogani, *J. Indian Chem. Soc.*, **37**, 769 (1960).

[11] I. Leden, *Z. Phys. Chem.*, **188**, 160 (1941).

[12] K. B. Yatsmirskii and T. I. Fedorova, *Zhur. neorg. Khim*, **1**, 2310 (1956).

[13] A. E. Harvey and D. L. Manning, *J. Amer. Chem. Soc.* **74**, 4744 (1952).

Revue Roumaine de Chimie, **26**, *8*, 1115–1125 (1981)

A REARRANGEMENT OF DIBENZO[*c*, *e*] TRICYCLO $[5.3.0.0^{2,10}]$ DECA-3,5-DIEN-9-OL INTO TRIPHENYLENE DERIVATIVES*

M. BANCIU[a)], PHAN LE THUY[a)], M. ELIAN[b)], C. DRĂGHICI[b)]
and ECATERINA CIORĂNESCU[a, b)]
a) Laboratory of Organic Chemistry — TCH ; Polytechnic Institute ; 76206, Bucharest 16, Romania
b) Center of Organic Chemistry — ICECHIM ; Bucharest

Received February 26, 1981

A six-step synthesis of dibenzo[*c*, *e*]tricyclo$[5.3.0.0^{2,10}]$ deca-3,5-dien-9-ol (**5**) starting from the known 5*H*-dibenzo[*a*, *c*]-cyclohepten-5-one (**8**) is described. Reaction of **5** with *p*-toluene-sulfonic acid in benzene proceeds regioselectively and stereoselectively affording the homoallylic tosylate **11**, which is further converted into triphenylene (**10**). The mechanism of this rearrangement is discussed.

INTRODUCTION

In a previous paper [1] we described the solvolytic rearrangements accompanying the acetolysis of tosylate **1**, which proceed by cyclopropyl- and not by phenyl-participation, giving rise to acetates **2** and **3**.

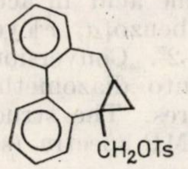

1

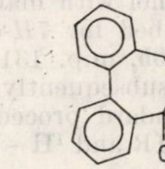

2

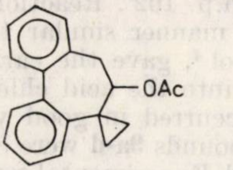

3

The investigation of the related, more complex systems **4** and **5**, seemed attractive in connection with the possible skeletal rearrangements.

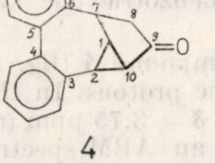

4

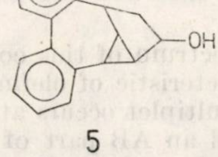

5

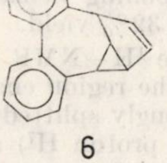

6

---

* Presented in part at the National Congress of Chemistry, Bucharest, 11—14 September, 1978.

On the other hand, we considered the compounds **4** and **5** as interesting precursors of a new dibenzo$(CH)_{10}$ valence isomer **6**.

In this paper the rearrangement which occurs on acidic treatment of the alcohol **5** is described. The results concerning the synthesis of **6** starting from derivatives **4** or **5** will be presented elsewhere.

SYNTHESIS

The synthesis of dibenzo[*c*, *e*]tricyclo[5.3.0.0.^{2,10}] deca-3,5-dien-9-one (**4**) utilized as starting material the unsaturated ketone **8** obtained by a slightly modified procedure of Cook *et al.* [2] for SeO_2 oxidation of 5*H*-dibenzo[*a*, *c*]cycloheptene (**7**).[3]

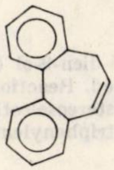

7

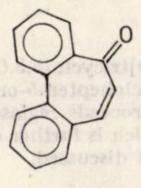

8

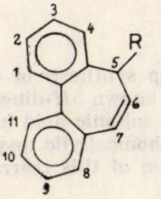

9

a ; R=OH **c**; $R=CH_2COCl$
b ; $R=CH_2COOH$ **d** ; $R=CH_2COCHN_2$

The reduction of ketone **8** with $LiAlH_4$ afforded the allyl alcohol **9a**, m.p. 102°. Reaction of this alcohol with malonic acid in acetic acid, in a manner similar to that described for 7*H*-dibenzo[*a*, *e*]cycloheptene-7-ol [4], gave the carboxylic acid **9b**, m.p. 131–2°. Conversion of this acid into the acid chloride **9c** and subsequently into diazomethylketone **9d** occurred in good yields by standard procedures. The structures of compounds **9a-d** were confirmed by IR and ^1H-NMR spectra (see Table 1 and Experimental part).

In the ^1H-NMR spectra of **9b**, **9c** and **9d** the protons H^5, H^6 and CH_2 present very broad and unstructured signals. The ^1H-NMR spectrum of the acid **9b** proved to be temperature-dependent due to the hindered rotation of the $-CH_2X$ group and/or slow ring inversion. Actually, Dreiding stereomodels of **9b** indicate important hindrances of the rotation of $-CH_2X$ group in both possible conformations.

Descomposition of the diazoketone **9d** in the presence of cooper bronze in boiling benzene afforded the dibenzotricyclic ketone **4**, m.p. 143–5°, in 32% yield.

In the ^1H-NMR spectrum of this compound **4** (fig. 1), no signals appear in the region characteristic of olefinic protons. In the same spectrum a strongly splitted multiplet occurs at $\delta = 3.75$ ppm (corresponding to benzylic proton H^7) and an AB part of an ABM spectrum is visible at $\delta = 1.3-2.6$ ppm with $J_{AB} = 19.5$ Hz (corresponding to two protons attached to C^8). Two multiplets centered at $\delta = 2.2$ and 2.9 ppm corresponding to three protons are most probably due to cyclopropanic protons.

TABLE 1

Some spectral characteristics of compounds **7**[3] and **9a**–**9d**

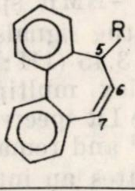

		^{1}H−NMR (CCl_4 or $CDCl_3$) : δ(ppm) and J (Hz)						IR (cm^{-1})
Com-pound	R =	H^6	H^7	H_{arom}	Other signals	$J_{6,7}$	$J_{5,6}$	
7	H	6.09	6.47	7.0–7.7	2.92($2H^5$)	10	6.5	
9a	OH	6.17	6.55	7.3–8.0	4.83(H^5) 2.98(OH)	11	4.5	3629 (ν_{OH})
9b	CH_2COOH	6.05*	6.60	7.2–7.8	3.0*(H^5 ; CH_2) 11.2(CO_2H)	10	—	1710 (ν_{CO}) 2400–3300(ν_{OH})
9c	CH_2COCl	5.9*	6.47	7.0–7.7	3.2*(H^5 ; CH_2)	10	—	1799 (ν_{CO})
9d	CH_2COCHN_2	6.05*	6.60	7.2–7.9	2.8*(H^5 ; CH_2)	10	—	1380 1670 (ν_{CO}) 2110 (ν_{N_2})

* broad signals

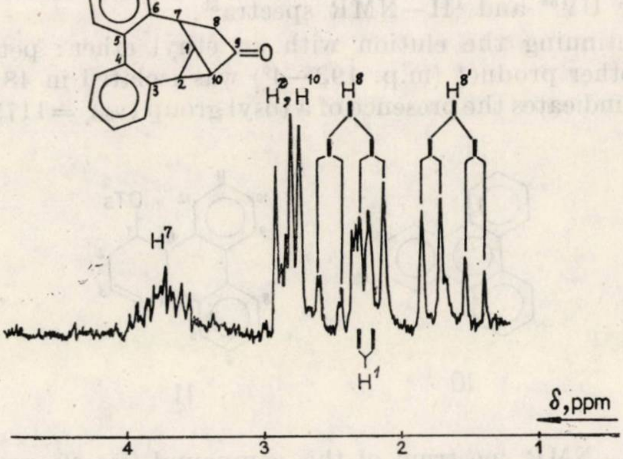

Fig. 1.—^{1}H-NMR spectrum of the ketone **4** (only aliphatic part).

Experiences performed in the presence of $Eu(DPM)_3$ as shift reagent evidenced the protons in the proximity of the carbonyl group, which showed great molar induced shifts (H^8 — 11.035 ; $H^{8'}$ — 10.86 and H^{10} — 9.52). The remaining aliphatic protons were sensibly less influenced by the shift reagent (molar induced shifts H^1 ; H^2 — 3.81 and H^7 — 4.15).

The ^1H-NMR spectrum brings sufficient information in favour of structure **4**, in addition to the IR data ($\nu_{CO} = 1729\ cm^{-1}$).

The $LiAlH_4$ reduction of the ketone **4** affords in quantitative yield the alcohol **5**, m.p. 98–100°, as a unitary product. The ^1H-NMR spectrum of this compound indicates, besides the signals of aromatic protons, two multiplets at $\delta = 3.45$ (1H; H^7) and 4.55 ppm (1H; H^9) and a complex multiplet between 0.9–2.5 ppm (5H + OH). In the IR spectrum the OH stretching band occurs at 3590 cm^{-1} and remains unchanged on dilution. This value indicates an intramolecular hydrogen bond with one of the aromatic rings, possible only in configuration **5a**.

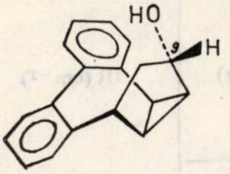

5a

RESULTS AND DISCUSSION

Attempts to obtain the tosylate of the alcohol **5** by treatment with *p*-toluenesulfochloride in pyridine failed. Consequently, another method for generation of carbocations was used, namely the treatment of the alcohol **5** with a sulfonic acid.

On refluxing the alcohol **5** with *p*-toluenesulfonic acid in benzene for three hours a crude product resulted which was chromatographed on a neutral alumina column. On elution with petroleum ether, triphenylene (**10**), m.p. 195°, was obtained in 15% yield and identified through its characteristic UV[5a] and ^1H-NMR spectra[5b].

On continuing the elution with an ethyl ether : petroleum ether mixture, another product (m.p. 193–4°) was isolated in 48% yield. The IR spectrum indicates the presence of a tosyl group (ν_{SO_2} =1175, 1351 cm^{-1})

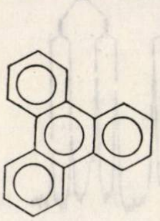

10

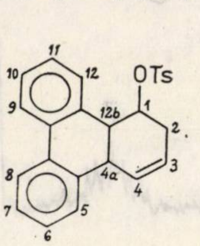

11

The ^1H-NMR spectrum of this compound (fig. 2) presents signals at $\delta = 6.7-7.6$ (m; 12H; aromatic H); 5.6–6.3 (m; 2H; olefinic H); 4.25 (m; 8 lines; 1H); 3.65 (triplet; 1H); 2.95 (m; 4 lines; 1H); 2.3–2.9 (m; 2H) and 2.38 ppm (s, 3H; CH_3). Decoupling experiments permitted the establishment of the coupling scheme which, besides the IR data and elemental analysis, indicated the structure of 1-tosyloxy-1,2,4a,12b-tetrahydrotriphenylene (**11**).

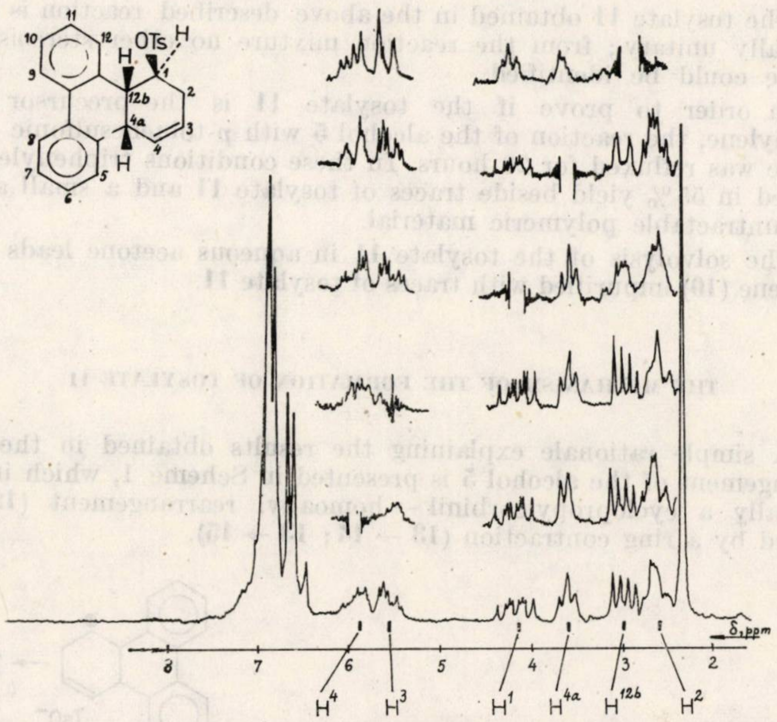

Fig. 2. — ^{1}H-NMR spectrum of the tosylate **11** (with decoupling experiments).

Four stereoisomers **11a-d** correspond to formula **11** :

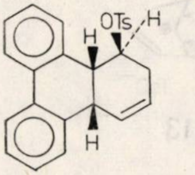

11a

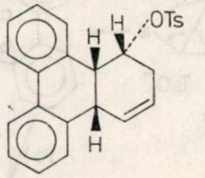

11b

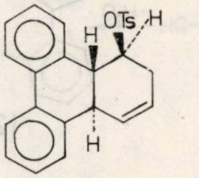

11c

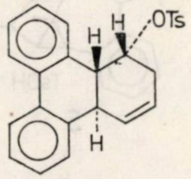

11d

The analysis of coupling constants (presented in formula **11e**) indicates the configuration **11a** for the tosylate obtained on acidic treatment of the alcohol **5**.
This assignment is based mainly on : a) the magnitude of the coupling constant $J_{4a,\,12b} = 5.5$ Hz which indicates a *cis* fusion of tetrahydronaphthalenic ring and b) the large value of the coupling constant between H^1 and H^{12b} ($J = 11$ Hz) which agrees well with a *trans* relationship of these protons.

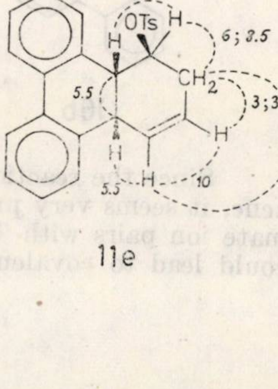

11e

The tosylate **11** obtained in the above described reaction is stereochemically unitary; from the reaction mixture no other stereoisomeric tosylate could be identified.

In order to prove if the tosylate **11** is the precursor of the triphenylene, the reaction of the alcohol **5** with *p*-toluenesulfonic acid in benzene was refluxed for 20 hours. In these conditions triphenylene was obtained in 55% yield beside traces of tosylate **11** and a small amount of an untractable polymeric material.

The solvolysis of the tosylate **11** in aqueous acetone leads to triphenylene (**10**) impurified with traces of tosylate **11**.

THE MECHANISM OF THE FORMATION OF TOSYLATE 11

A simple rationale explaining the results obtained in the acidic rearrangement of the alcohol **5** is presented in Scheme 1, which includes essentially a cyclopropylcarbinil → homoallyl rearrangement (**12** → **13**) followed by a ring contraction (**13** → **14**; **13** → **15**).

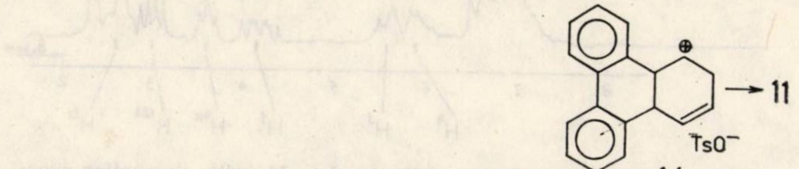

Since the reaction is performed with *p*-toluenesulfonic acid in benzene, it seems very probable that the ionic species **12**—**15** occur as intimate ion pairs with TsO⁻ anions; the internal return in such ion pairs could lead to covalent tosylates.

The ion **13** (or the corresponding covalent tosylate, *vide infra*) could follow two reaction paths (denoted by *a* and *b*) due to migration of the non-equivalent aryl groups and leading to the ion **14** and the homoallylic tosylate **11** or to the ion **15** and the allylic tosylates **16a, b**.

As it has been mentioned above, from the reaction only the homoallylic tosylate **11** with a determined configuration was obtained. It seems that *the reaction proceeds regioselectively and stereoselectively.*

In order to explain the above facts three hypotheses could be considered, namely:

1) The reaction proceeds exclusively through the path *a*.

2) The conversions **13** → **11** and **13** → **16** are reversible reactions. The allylic tosylates **16 a, b** are very easy ionisable compounds and the whole system is displaced towards the most stable covalent product, the tosylate **11** (the single isolable product).

3) The path *b* is masked by secondary reactions, e.g. triphenylene formation from **15**, or polymerisations.

At present, it cannot be determined clearly which of the above hypotheses correspond to reality, although we attempt below a rationalisation for the preference of hypothesis 1.

The examination of stereomodels corresponding to ion **13** (**17**) or to the corresponding covalent tosylate **18** does not reveal a special reason for a preferred attack of one aromatic ring to the electron defficient center (path **a** or **b**). Nevertheless, the formation of only one from the two possible phenonium ions could be determined by small conformational preferences which cannot be evaluated from molecular models.

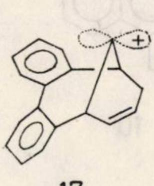

17

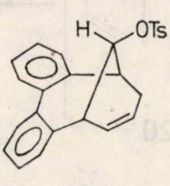

18

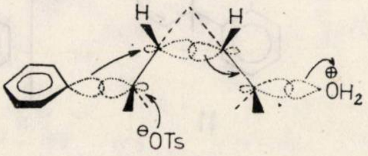

19

It must be stressed that the phenyl migration in the tosylate **18** (corresponding to path **a**) through a phenonium ion, accompanied by the attack of the TsO⁻ group from the back-side, affords the tosylate **11a** with the observed configuration at reaction product.

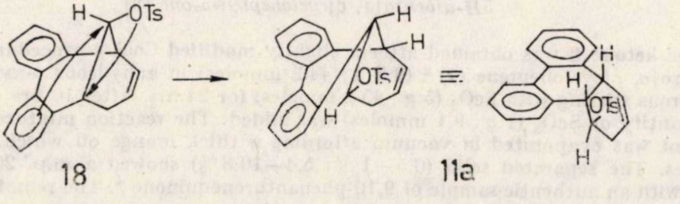

18 11a

It is interesting to remark that the examination of the stereomodel of the alcohol **5** suggests the possibility of a reaction path in which the phenyl migration, the opening of the cyclopropanic ring and the water elimination occur concertedly:

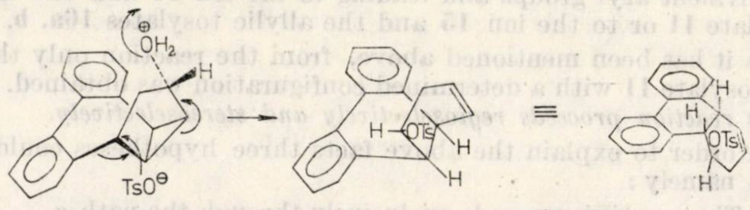

5 11a

In the alcohol **5** only one aromatic ring (that which is included in the path *a*) is favourably situated to assist the opening of cyclopropanic ring, as suggested by formula **19**, and this reaction affords the tosylate **11** with a correct configuration.

Triphenylene (**10**), the product of final conversion of the alcohol **5** in acidic catalysis, was obtained on increasing the reaction time. As it was proved through the control experiment mentioned above, triphenylene results from the tosylate **11** formed in the first stage, through an elimination reaction.

As an intermediate, dihydrotriphenylene (**20**), a dibenzo$(CH)_{10}$ hydrocarbon with a strong tendency to aromatisation is probably formed.

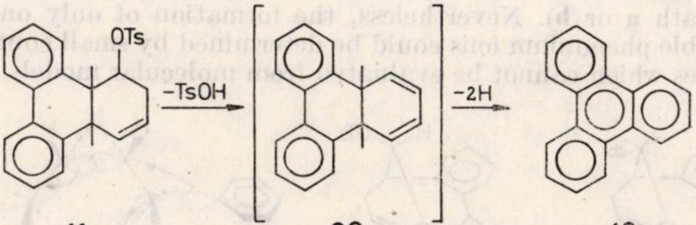

11 20 10

EXPERIMENTAL

Melting points are uncorrected. IR spectra were recorded with a double beam UR-20 Carl Zeiss Jena spectrophotometer. NMR spectra were obtained on a Varian A-60A spectrometer using TMS as internal standard.

5*H-dibenzo*[a, c]*cyclohepten-5-one* (**8**)

The ketone **8** was obtained after a slightly modified Cook's procedure [2]. A solution of 5*H*-dibenzo[*a, c*]cycloheptene (**7**) [3] (8.5 g ; 44.2 mmoles) in anhydrous *o*-xylene was refluxed with vigorous stirring with SeO_2 (5 g ; 45.2 mmoles) for 24 hrs. After 10 hrs of reflux an additional quantity of SeO_2 (1 g ; 9.1 mmoles) was added. The reaction mixture was filtered and the solvent was evaporated in vacuum affording a thick orange oil which on cooling partly crystallizes. The separated solid (0.5—1 g ; 5.4—10.8%) showed a m.p. 201—204° and was identical with an authentic sample of 9,10-phenanthrenequinone *. The remaining oil was chromatographed on neutral Al_2O_3. On elution with petroleum ether small quantities of unreacted dibenzocycloheptene were sometimes obtained (0.3–0.6 g ; 3.5–7%). On elution with 9 : 1 mixtures of petroleum ether : ethyl ether a viscous yellow oil was obtained (1 g) which was not further investigated. On elution with 7.5 : 2.5 mixtures of petroleum ether : ethyl ether the ketone **8** (yellow crystals) was obtained (4.7 g ; 52%). The final elution with ethyl ether afforded new small quantities (0.2–0.3 g) of 9.10-phenanthrenequinone.

---

* The formation of 9,10-phenanthrenequinone in oxidations of dibenzo[*a, c*]cycloheptene derivatives was mentioned by J. W. Cook, *J. Chem. Soc.*, **1950**, 140.

The ketone **8** recrystallised from ethanol, showed a m.p. 82–3° (lit. [2] 83–84°).

IR-spectrum (CS_2 ; CCl_4 ; cm^{-1}) : 732vs, 753vs, 766vs, 791s, 1485m, 1600s, 1659vs, 3025m and 3069m.

^1H-NMR-spectrum($CDCl_3$, δ ppm) : 6.67 (d ; J = 12 Hz ; 1H ; H^6) ; 7.35 (d ; J = 12 Hz ; 1H ; H^7) ; 7.4–8.2 (m ; 8H ; H_{arom}).

5*H-dibenzo*[a, c]*cyclohepten-5-ol* (**9a**)

Over a stirred suspension of $LiAlH_4$ (3.7 g ; 97.5 mmoles) in 50 ml anhydrous ether a solution of ketone **8** (14 g ; 68 mmoles) in 350 ml anhydrous ether was dropped during 1 hr. The reaction mixture was refluxed 5 hrs, then left overnight. The usual work-up affords the solid *alcohol* **9a** (14 g ; 98%), m.p. 102° (cyclohexane) ; Found : C, 86.96 ; H, 6.03, $C_{15}H_{12}O$ requires : C, 86.51 ; H, 5.81%.

IR spectrum (CS_2 ; CCl_4 ; cm^{-1}) : 734m, 756vs, 775s, 784m, 1061m, 1486w, 2855vw, 2926vw, 3030w, 3068w and 3629m.

^1H-NMR spectrum (CCl_4 ; δ ppm) : 2 : 98 (s ; 1H ; OH) ; 4.83 (m ; 1H ; H^5) ; 6.17 (dd ; $J_{6,7} = 11$, $J_{6.5} = 4.5$ Hz ; 1H ; H^6) ; 6.55 (dd ; $J_{7,6} = 11$; $J_{7.5} = 2$ Hz ; 1H ; H^7) ; 7.3–8.0 (m ; 8H ; H_{arom}).

5*H-dibenzo*[a, c]*cycloheptene-5-yl-acetic acid* (**9b**)

A solution of alcohol **9a** (14 g ; 67 mmoles) and malonic acid (12.5 g ; 120 mmoles) in 300 ml anhydrous acetic acid was refluxed for 28 hrs. Most of the acetic acid was removed in vacuum and the residue was poured into water (250 ml). The mixture was ether-extracted, washed three times with water, dried and evaporated. The residue was recrystallized from CCl_4 affording a first crop of acid **9b** (7.5 g ; 44.7%) m.p. 125°. The mother liquids were evaporated and extracted with 15% NaOH solution at 75°. After cooling, the organic components were extracted with ether and the aqueous layer was acidified with conc. HCl affording the second crop of acid **9b** (4.5 g ; 21.8%) m.p. 110–122°.

The acid **9b**, m.p. 131–2° (after three recrystallizations from CCl_4) ; Found : C, 81.49 ; H, 5.57. $C_{17}H_{14}O_2$ requires : C, 81.60 ; H, 5.63%.

IR spectrum (CS_2 ; CCl_4 ; cm^{-1}) : 734s, 755vs, 781s, 786s, 936m, 1412m, 1438m, 1489m, 1710vs, and 2400–3300 large.

^1H-NMR spectrum ($CDCl_3$; δ ppm) : 2.5–4.1 (m ; 3H ; -CH–CH_2-) ; 6.05 (m ; 1H ; H^6) ; 6.60 (d ; J = 10 Hz ; 1H ; H^7) ; 7.2–7.8 (m ; 8H ; H_{arom}) ; 11.2 (s ; 1H ; COOH).

5*H-dibenzo*[a, c]*cyclohepten-5-yl-acetylchloride* (**9c**)

Over a solution of acid **9b** (7.5 g ; 30 mmoles) in 75 ml anhydrous benzene, thionyl chloride (5 ml ; 8.2 g ; 68 mmoles) was dropped ; the mixture was refluxed for 3 hrs then left overnight. The reaction mixture was evaporated in vacuum, the residue was shaked with two portions of 30 ml petroleum ether which was subsequently evaporated. The oily brown residue (7.5 g ; 93%) could not be crystallized.

The acid chloride **9c** viscous oil.

IR spectrum (CS_2 ; CCl_4 ; cm^{-1} : 736s, 756vs, 758s, 772s, 788s, 1436m, 1446m, 1487m, 1799vs, 2926w, 3027m and 3066m.

^1H-NMR spectrum (CCl_4 ; δ ppm) : 2.5–4.0 (m ; 3H ; -CH–CH_2-) ; 5.9 (m ; 1H ; H^6) ; 6·47 (d ; J = 10 Hz ; 1H ; H^7) ; 7.0–7.7 (m ; 8H ; H_{arom}).

5*H-dibenzo*[a, c]*cyclohepten-5-yl-methyl-diazomethylketone* (**9b**)

Over a cooled stirred solution of acid chloride **9c** (7.5 g ; 27.8 mmoles) in 150 ml anhydrous ether, triethylamine (2.8 g ; 27.8 mmoles) was added, then an ethereal solution (150 ml) of diazomethane (from 15 g nitrosomethylureea) was dropped during 1.5 hrs. The reaction

mixture was stirred at 0° for 6 hrs, then left overnight at room temperature. After filtration and evaporation of the solvent, the crude *diazoketone* 9d was obtained (7.5 g ; 97 %) as a thick yellow oil.

IR spectrum **(CCl_4 ; cm^{-1}) ; 1350s, 1380vs, 1670vs, and 2110vs.**

^1H-NMR spectrum **($CDCl_3$; δ ppm) : 2.4–4.1 (m ; 3H ; -CH–CH_2-) ; 5.0 (large singlet ; 1H ; CHCO) ; 6.05 (m ; 1H ; H^6) ; 6.60 (d ; J = 10 Hz ; 1H ; H^7) ; 7.2–7.9 (m ; 8H ; H_{arom}).**

Dibenzo[c, e]*tricyclo*[5.3.0.0^{2,10}]*deca-3,5-dien-9-one* (**4**)

Over a stirred solution of diazoketone **9d** (7.5 g ; 27.2 mmoles) in 350 ml anhydrous benzene cooper bronze (3 g) was added in small portions during 3 hrs, heating at the same time the reaction to reflux. After two additional hours of reflux (evolution of N_2 ceased) the reaction mixture was left overnight, then filtered and evaporated in vacuum. The oily residue was chromatographed on neutral Al_2O_3. On elution with 8 : 2 mixture of petroleum ether : ethyl ether, an oily product was obtained (0.7 g ; 10.5 %) (IR : 1665, 1801 cm^{-1}) which was not further investigated. On elution with 7 : 3 mixture of petroleum ether : ethyl ether the crude ketone **4** was obtained (2.15 g ; 32 %) ; then on elution with 1 : 1 mixture of petroleum ether : ethyl ether, another oily product (0.5 g ; 7.5 %) (IR : 1750 ; 1780 cm^{-1}) was obtained which was not further investigated.

The ketone **4**, m.p. 143–5° (ethanol). Found : C, 87.78 ; H, 5.83. $C_{18}H_{14}O$ requires : C, 87.77 ; H, 5.73 %.

IR spectrum (CS_2 ; CCl_4 ; cm^{-1}) : 728m, 750s, 756s, 768m, 1454m, 1488m, 1729vs, 2918w, 2937w, 3028w and 3071m.

^1H-NMR spectrum ($CDCl_3$; δ ppm) : 1.53 (dd ; $J_{8,8'}$=19.5 ; $J_{8',7}$= 9 Hz ; 1H ; $H^{8'}$) ; 2.2 (m ; 1H ; H^1) ; 2.28 (dd ; $J_{8,8'}$ = 19.5 ; $J_{8,7}$ = 11 Hz ; 1H ; H^8) ; 2.6–2.9 (m ; 2H ; $H^{10,2}$) ; 3.75 (m ; 1H ; H^7) ; 7.0–7.7 (m ; 8H ; H_{arom}).

Dibenzo[c, e]*tricyclo*[5.3.0.0^{2,10}]*deca-3,5-dien-9-ol* (**5**)

Over a stirred suspension of $LiAlH_4$ (0.2 g ; 5.25 mmoles) in 20 ml anhydrous ether a solution of ketone **4** (0.5 g ; 2.1 mmoles) in 100 ml anhydrous ether was dropped. After three hours of reflux the reaction mixture was left overnight then worked-up in the usual manner, affording *the alcohol* **5** (0.5 g ; 98 %), m.p. 98–100° (cyclohexane).

IR spectrum (CS_2 ; CCl_4 ; cm^{-1}) : 739m, 755s, 779m, 1052m, 1061m, 1445w, 1487w, 2954w, 2971w, 3031w, 3068w and 3590w.

^1H-NMR spectrum (CCl_4 : δ ppm) 0.9–2.5 (m ; 6H, $H^{8,8;\,1,2,10}$, OH) ; 3.45 (m ; 1H ; H^7) ; 4.55 (m ; 1H ; H^9) ; 7.0–7.7 (m ; 8H ; H_{arom}).

Reaction of the alcohol **5** *with p-toluenesulfonic acid*

A mixture of the alcohol **5** (0.25 g ; 1 mmole) and *p*-toluenesulfonic acid (0.25 g ; 1.31 mmoles) in 75 ml anhydrous benzene was heated at 80° for three hrs. The reaction mixture was cooled, washed with water, dried and evaporated in vacuum. The oily brown residue (0.3 g) was chromatographed on a short neutral alumina column. On elution with petroleum ether (b.p. 30–40°) a yellowish-white solid was obtained (0.075 g) whose NMR spectrum indicate the presence of triphenylene (**10**) slightly impurified with a saturated product which was not further investigated. On elution with 1 : 1 petroleum ether : ethyl ether mixture the tosylate **11** was obtained as white crystals (0.170 g ; 43 %).

1-Tosyloxy-1,2,4a,12b-tetrahydrotriphenylene (**11**) m.p. 193–4° (ethanol). Found : C, 75.43 ; H, 6.00 ; S, 7.48. $C_{25}H_{22}SO_3$ requires : C, 74.60 ; H, 5.51 ; S, 7.92 %.

IR spectrum (KBr ; cm^{-1}) : 737s, 746m, 759s, 774s, 867s, 1175s, 1351s, 1594w, 2838w, 2928w, 3021w, 3040w and 3068w.

^1H-NMR spectrum ($CDCl_3$; δ ppm) : 2.38 (s ; 3H ; CH_3) ; 2.3–2.9 (m ; 2H ; H^2) ; 2.95 (dd ; $J_{12b,4a}$ = 5.5 ; $J_{12b,1}$= 11 Hz ; 1H ; H^{12b}) ; 3.65 (t ; $J_{4a,12b}$=$J_{4,4a}$=5.5 Hz ; 1H ; H^{4a}) ; 4.25 (m ; $J_{1,2}$ = 8.5 ; $J_{1,2}$ = 6 ; $J_{1,12b}$= 11 Hz ; 1H ; H^1) ; 5.60–6.30 (m ; 2H ; $H^{3,4}$) ; 6.7–7.6 (m ; 12H ; H_{arom}).

Some polymeric material was retained in the alumina column as a brown zone.

If the reaction time in the above reaction is increased to 20 hrs only traces of tosylate **11** could be identified in the products, whereas triphenylene was obtained in 55 % yield. Some brown polymeric material also remains in the chromatographic column as an insoluble zone.

Solvolysis of tosylate **11**

A solution of tosylate **11** (0.1 g ; 0.25 mmoles) in 70 ml 90% aqueous acetone was heated at 80° for 6 hrs. The reaction mixture was poured into water, then ether extracted. The organic layer was washed with water, dried and evaporated in vacuum affording a brown oily solid (0.05 g ; 88%) consisting (^{1}H-NMR) of triphenylene (**10**) contaminated with traces of unreacted **11**.

REFERENCES

[1] E. Dragu, M. Banciu, C. Drăghici and E. Ciorănescu, *Rev. Roumaine Chim.*, **21**, 1497 (1976).

[2] J. W. Cook, F. T. Dickson and J. D. Loudon, *J. Chem. Soc.*, **1974**, 746.

[3] H. Lettrè, *Angew. Chem.*, **59**, 219 (1947) ; J. Kenner and E. G. Turner, *J. Chem. Soc.*, **1911**, 2101.

[4] C. van der Stelt, A. Haasjes, H. M. Tersteege and W. T. Nauta, *Rec. Trav. chim.*, **84**, 1466 (1965).

[5] a) E. Clar and L. Lombardi, *Ber. dtsch. chem. Ges.*, **65**, 1414 (1932) ; b) J. A. Pople, W. G. Schneider and H. J. Bernstein, "High Resolution Nuclear Magnetic Resonance", Mc Graw-Hill, New York, 1959, p. 249.

Revue Roumaine de Chimie, 26, 8, 1127 — 1134 (1981)

REACTIONS OF SOME 5-ARYL-2-THIONO-1,3,4-THIADIAZOLES

M. ANWAR, F. I. ABDEL-HAY, A. A. El-BARBARY and M. El-BORAI
Chemistry Department, Faculty of Science, Tanta University, Tanta, A. R. Egypt

Received May 29, 1980

The reaction of 5-aryl-2-thiono-1,3,4-thiadiazole (I) with hydrazines and amines led to ring cleavage with the formation of compounds III and VII.

Compounds I react normally with the halo-derivatives forming disubstituted 1,3,4-thiadiazoles (VIII).

The behaviour of compounds I in the Mannich reaction has been also investigated. The structure of the newly synthesized compounds was confirmed by ultraviolet, infrared, nuclear magnetic resonance and mass spectral studies.

5-Aryl-2-thiono-1,3,4-thiadiazoles possess depressing effect on the central nervous system and have sedative effect. [1-3] They are also useful as intermediates in pharmaceutical industry. [4]

5-Aryl-2-thiono-1,3,4-oxadiazoles were reported to react with hydrazines forming 3-thiono-1,2,4-triazoles (II). [5,6]

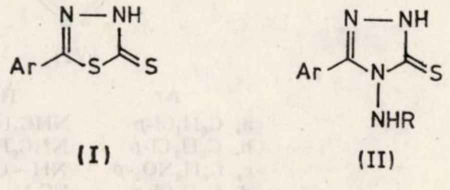

a, Ar = C_6H_4Cl-*p*
b, Ar = $C_6H_4NO_2$-*p*

In the present investigation it was found that the reaction of 5-aryl-2-thiono-1,3,4-thiadiazoles (I) with hydrazines, namely hydrazine hydrate and phenylhydrazine takes another course and the open structure compounds (IIIa-c) were obtained, respectively.

Cyclization of IIIc by heating to 5—10° C over its melting point afforded 3-*p*-nitrophenyl-2-phenyl-6-thiono-1,2,4,5-tetrazine (IV).

The structure of compounds III and IV was established by correct analytical data, infrared, ultraviolet and nuclear magnetic resonance spectral studies.

The infrared spectra of compounds III and IV show the stretching frequencies attributable to C = S in the region 1350 – 1335 cm^{-1}, and to NH in the region 3400 – 3340 cm^{-1}.

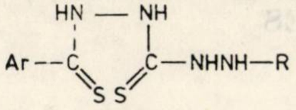

(III)

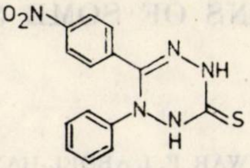

(IV)

	Ar	R
a.	C_6H_4Cl-*p*	H
b,	C_6H_4Cl-*p*	C_6H_5
c,	$C_6H_4NO_2$-*p*	H

The ultraviolet absorption spectra of compounds III show four main absorption zones in the regions : 230 – 225 nm, 260 – 255 nm, 285 – 270 nm and 410 – 340 nm.

The ^1H-NMR spectrum of compound IIIc shows the following pattern : a broad band at $\delta = 6.1$ ppm. corresponding to 5H ($NHNH_2$ and NH–NH), a doublet of doublets at $\delta = 7.8-8.6$ ppm., corresponding to 4H aromatic. The ^1H-NMR spectrum of compound IV shows the following signals : a singlet at $\delta = 5.2$ ppm. corresponding to 2H (NH—CS–NH), a multiplet at $\delta = 7.6 - 8.5$ ppm. corresponding to 9H aromatic.

2-Oxo-1,3,4-oxadiazoles were reported to undergo ring opening when subjected to the action of amines, yielding keto compounds V. [7,8] The reaction of I with some selected amines was found to proceed similarly, yielding compounds (VIa – g) respectively.

R–CONHNH–CONH–R′
(V)

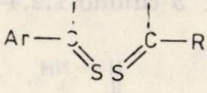

(VI)

	Ar	R
a,	C_6H_4Cl-*p*	$NHC_6H_4CH_3$-*p*
b,	C_6H_4Cl-*p*	$NHC_6H_4OCH_3$-*p*
c,	$C_6H_4NO_2$-*p*	NH–OH
d,	C_6H_4Cl-*p*	NC_5H_{10}
e,	C_6H_4Cl-*p*	NC_4H_8O
f,	$C_6H_4NO_2$-*p*	NC_5H_{10}
g,	$C_6H_4NO_2$-*p*	NC_4H_8O

The infrared spectra of compounds VI show the stretching frequencies attributable to C = S in the region 1350 – 1310 cm^{-1} and for NH in the region 3400 – 3320 cm^{-1}.

The ultraviolet absorption spectra show three main absorption zones in the regions, 230 – 210 nm, 265 – 255 nm, and 410 – 350 nm. A remarkable red shift is observed in the third zone in the spectra of compounds VIc, f, g due to the presence of the nitro group.

The ^1H-NMR spectral data for compounds (VId, e, f) are depicted in table 1.

TABLE 1

The ^1H-NMR-spectral data of compounds VI *,**

Compound	Ar	R	NH–NH
VId	7.6 – 8.2 (4H, dd)	2.1 (6H, s) ; 3.5 (4H, d) 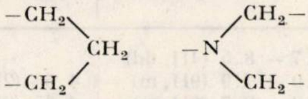 (piperidyl)	6.55 (2H, s)
VIe	7.3 – 7.9 (4H, dd)	3.15 (4H, q) ; 3.8 (4H, q) 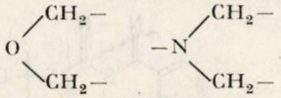 (morphyl)	6.6 (2H, s)
VIf	7.9 – 8.6 (4H, dd)	3.4 (4H, s) ; 3.8 (4H, d) 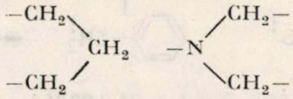	7.0 (2H, s)

* Chemical shifts were determined as δ ppm in DMSO.

** s = singlet ; d = doublet ; q = quartet ; m = multiplet

Compound I reacts with some halo-compounds, namely: methyl iodide, benzyl chloride, benzene sulphonyl chloride and 3,4-dimethylbenzene sulphonyl chloride, forming the 2,5-disubstituted 1,3,4-thiadiazoles (VIIa – f), respectively.

Oxidation of VIIc with potassium permanganate in acetic acid medium afforded the corresponding sulphone VIII similar to that obtained by the Madhavan and Srinivasan. [9]

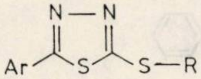

(VII)

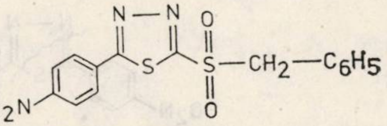

(VIII)

	Ar	R
a,	C_6H_4Cl-*p*	CH_3
b,	C_6H_4Cl-*p*	$CH_2-C_6H_5$
c,	$C_6H_4NO_2$-*p*	$CH_2-C_6H_5$
d,	C_6H_4Cl-*p*	$SO_2-C_6H_5$
e,	$C_6H_4NO_2$-*p*	$SO_2-C_6H_5$
f,	$C_6H_4NO_2$-*p*	$SO_2-C_6H_4(CH_3)_2$3,4

The infrared spectra of compounds VII show the stretching frequencies attributable to the C–S–C (2-position) in the region 720 – – 695 cm^{-1}. Compound VIII shows instead the stretching frequencies attributable to ν SO_2 in the region 1345 and 1160 cm^{-1}.

The ultraviolet absorption spectra of compounds VII show the principal absorption band characteristic of the 2-substituted 1,3,4-thiadiazoles [10,11] in the region 335 – 310 nm.

The ^{1}H-NMR spectral data for compounds VII are listed in table 2.

TABLE 2

The ^{1}H$-$NMR spectral data for compounds VII

Compound	Phenyl	S$-$CH$_2-$	S$-$CH$_3$
VIIa	7.7 $-$ 8.5 (4H, dd)	—	3.3 (3H, s)
VIIb	7.0 $-$ 7.9 (9H, m)	4.6 (2H, s)	—
VIIc	7.2 $-$ 8.7 (9H, m)	4.65 (2H, s)	—

The mass fragmentation of compounds VII b, c is also given :

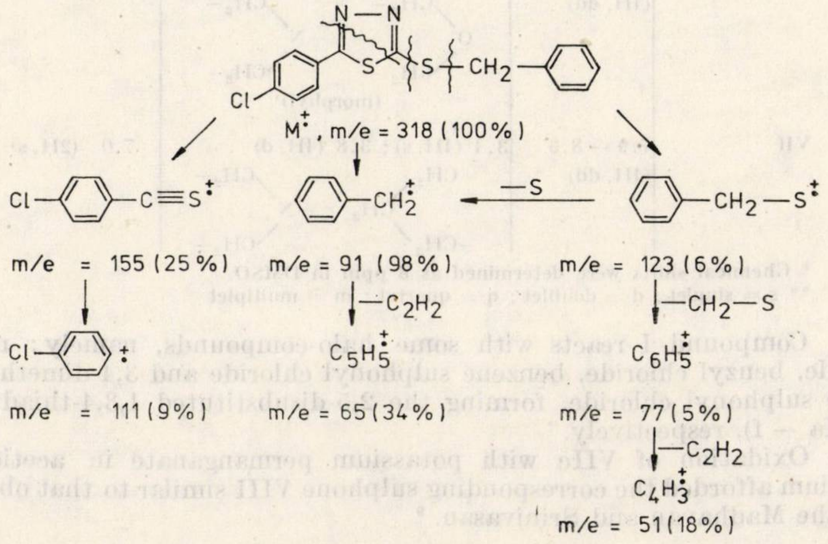
N—N
S
S
CH2
Cl
M+•, m/e = 318 (100%)
Cl—C≡S+•
m/e = 155 (25%)
CH2+•
m/e = 91 (98%)
—S
CH2—S+•
m/e = 123 (6%)
Cl
m/e = 111 (9%)
—C2H2
C5H5+•
m/e = 65 (34%)
—CH2—S
C6H5+•
m/e = 77 (5%)
—C2H2
C4H3+•
m/e = 51 (18%)

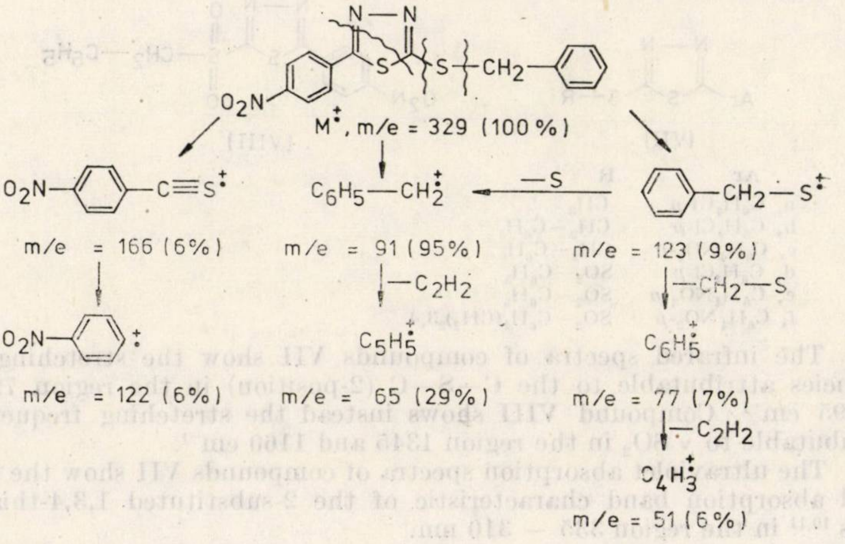
N—N
S
S
CH2
O2N
M+•, m/e = 329 (100%)
O2N—C≡S+•
m/e = 166 (6%)
C6H5—CH2+•
m/e = 91 (95%)
—S
CH2—S+•
m/e = 123 (9%)
O2N
m/e = 122 (6%)
—C2H2
C5H5+•
m/e = 65 (29%)
—CH2—S
C6H5+•
m/e = 77 (7%)
—C2H2
C4H3+•
m/e = 51 (6%)

The syntheses of Mannich bases derived from 1,3,4-thiadiazoles were also tried. Compounds I react with morpholine in the presence of formaldehyde to give compounds IXa, b, respectively.

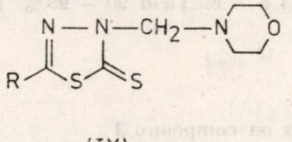

(IX)

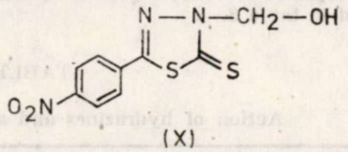

(X)

a, R = C_6H_4Cl-*p*
b, R = $C_6H_4NO_2$-*p*

Hydrolysis of IXb with dilute hydrochloric acid afforded X. The latter compound can also be obtained from the reaction of Ib with formaldehyde in ethanol. Moreover, IXb was obtained by the reaction of X with morpholine, similar to the reaction given by Radha and Srinivasan.[12]

The infrared spectra of compounds IX show stretching frequencies attributable to C = S at 1360 cm^{-1} (IXb) and at 1300 cm^{-1}(a).

The mass fragmentation of IXa shows a proof for the position of attack on the N−3 position.

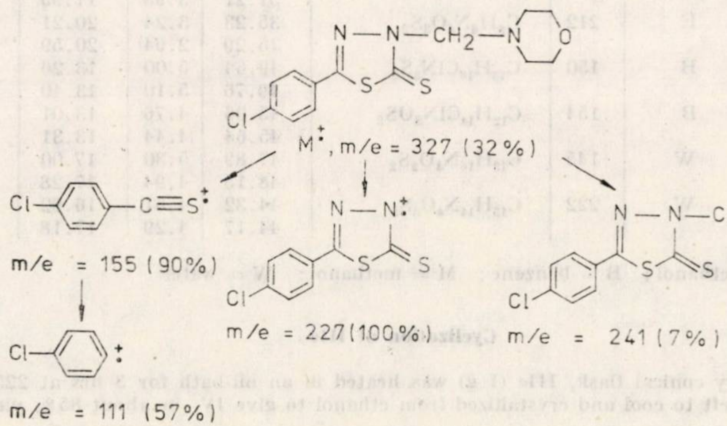

EXPERIMENTAL

The IR spectra were recorded on a UNICAM S.P. 1200 spectrophotometer. The KB_r pellet technique was used.

The absorption spectra in the UV region using ethanol as solvent were recorded on a UNICAM S.P. 800 spectrophotometer.

The ^1H-NMR spectra were recorded at 60 MHz on a Varian A-60 spectrophotometer using DMSO as solvent and TMS as reference.

Mass spectra were recorded on a V.C. Micromass 7070 F spectrometer operating at 70eV using direct inlet.

All melting poins are uncorrected.

Action of hydrazines on 5-aryl-2-thiono-1,3,4-thiadiazoles

5-Aryl-2-thiono-1,3,4-thiadiazoles [13–16] (I ; 0.01 mole) and hydrazine hydrate and/or phenylhydrazine (0.01 mole) in 50 ml dioxane were heated under reflux for 3 hrs. The reaction mixture was concentrated, cooled and filtered. The solid obtained was recrystallized from the appropriate solvent to give compounds III a — c. Yield 90 — 95 %. The physical data are listed in table 3.

TABLE 3

Action of hydrazines and amines on compound I

Compound	Solvent of cryst *	m.p. (°C)	Formula	Analysis % Found/Calcd.			
				C	H	N	S
IIIa	E	250	$C_8H_9ClN_4S_2$	36.85 36.85	3.95 3.45	21.20 21.50	24.20 24.57
IIIb	B	220	$C_{14}H_{13}ClN_4S_2$	50.13 49.93	4.24 3.96	16.37 16.64	19.00 19.02
IIIc	E	205	$C_8H_9N_5O_2S_2$	35.64 35.42	3.52 3.32	25.71 25.83	23.23 23.62
IV	E	218	$C_{14}H_{11}N_5O_2S$	53.41 53.67	3.82 3.51	22.80 22.36	10.05 10.22
VIa	B	202	$C_{15}H_{14}ClN_3S_2$	53.42 53.65	4.33 4.17	12.17 12.52	18.87 19.08
VIb	B	195	$C_{15}H_{14}ClN_3OS_2$	50.89 51.21	4.31 3.98	11.76 11.95	18.03 18.21
VIc	E	212	$C_8H_8N_4O_3S_2$	35.23 35.29	3.24 2.94	20.21 20.59	23.37 23.53
VId	B	150	$C_{13}H_{16}ClN_3S_2$	49.64 49.76	5.00 5.10	13.26 13.40	20.07 20.42
VIe	B	154	$C_{12}H_{14}ClN_3OS_2$	45.36 45.64	4.76 4.44	13.01 13.31	20.04 20.29
VIf	W	145	$C_{13}H_{16}N_4O_2S_2$	47.89 48.15	5.30 4.94	17.00 17.28	19.62 19.43
VIg	W	222	$C_{12}H_{14}N_4O_3S_2$	44.32 44.17	4.61 4.29	16.92 17.18	19.43 19.63

* E = ethanol ; B = benzene ; M = methanol ; W = water

Cyclization of IIIc

In a dry conical flask, IIIc (1 g) was heated in an oil-bath for 3 hrs at 225°C. The product was left to cool and crystallized from ethanol to give IV, in about 85 % yield. (See Table 3).

Action of amines on I

5-Aryl-2-thiono-1,3,4-thiadiazoles (I ; 0.01 mole) and amines, namely : *p*-toluidine, *p*-anisidine, hydroxylamine hydrochloride, piperidine and/or morpholine (0.01 mole) in 50 ml absolute ethanol were heated under reflux for 3 hrs. The reaction mixture was concentrated, cooled and filtered. The solid obtained was recrystallized from the appropriate solvent to give compounds VIa — g in 80 — 90 % yield. The physical data are given in table 3.

Action of halo-compounds on I

Compounds I (0.01 mole) and halo-compound, namely methyl iodide, benzyl chloride, benzene sulphonyl chloride and/or 3,4-dimethylbenzene sulphonyl chloride were heated under reflux for 1 hr. The reaction mixture was concentrated, cooled and the solid obtained was recrystallized from the appropriate solvent to give the compounds VIIa – f in almost quantitative yield. The results are given in table 4.

TABLE 4

Action of halo-compounds on compound I

Compound	Solvent of cryst *	m.p. (°C)	Formula	Analysis % (Found/ Calcd.) C	H	N	S
VIIa	W	118	$C_9H_7ClN_2S_2$	44.32 44.54	3.17 2.89	11.50 11.55	26.01 26.49
VIIb	E	130	$C_{15}H_{11}ClN_2S_2$	56.32 56.51	3.71 3.45	9.04 8.79	19.87 20.09
VIIc	E	173	$C_{15}H_{11}N_3O_2S_2$	54.52 54.71	3.64 3.34	12.72 12.77	19.32 19.45
VIId	M	195	$C_{14}H_9N_2O_2S_3$	45.32 45.59	2.83 2.44	7.79 7.60	26.00 26.05
VIIe	E	164	$C_{14}H_9N_3O_4S_3$	44.21 44.33	2.74 2.37	11.00 11.08	25.03 25.33
VIIf	E	214	$C_{16}H_{13}N_3O_4S_3$	46.82 46.99	3.51 3.19	10.11 10.32	23.32 23.59
VIII	B	200 de- comp	$C_{15}H_{11}N_3O_4S_2$	49.52 49.86	3.41 3.05	11.33 11.63	17.70 17.73

* W = water ; B = benzene ; E = ethanol ; M = methanol

Oxidation of VIIc with potassium permanganate

Potassium permanganate solution (0.46 g ; 3 mole) in the least amount of water was added gradually to a solution of VIIc (1 g ; 0.05 mole) in acetic acid (50 ml). The reaction mixture was heated on a water-bath for 30 minutes, concentrated and cooled. The reaction mixture was poured in ice cold water, the formed precipitate was filtered off and recrystallized from ethanol to give compound VIII in 85 % yield (cf. Table 4).

Synthesis of IX

Formaldehyde (1.0 ml, 40 % solution) was added to I (0.01 mole) in 30 ml absolute ethanol, the reaction mixture was heated until the solution became clear, then dry morpholine (0.15 mole ; 1.3 g) in 30 ml absolute ethanol was added. The reaction mixture was stirred for 3 hrs. at room temperature, the solvent was evaporated till dryness and the solid obtained was recrystallized from ethanol to give compounds IXa, b in about 60 % yield. (See Table 5).

Synthesis of X

Compound (Ib ; 0.01 mole) and formaldehyde (0.03 mole ; 0.9 g) in 50 ml absolute ethanol were heated under reflux for 1 hr. The reaction mixture was concentrated and cooled. The solid obtained was recrystallized from ethanol to give the compound X in 90 % yield (cf. Table 5).

Hydrolysis of IXb

Hydrochloric acid (50 ml 10 %) was added to IXb (1 g ; 0.03 mole) and the reaction mixture was stirred at room temperature for 3 hrs. The formed precipitate was filtered off and recrystallized from ethanol to give compound X in 65 % yield. The product was identified by m.p. and mixed m.p.

TABLE 5

Mannich bases derived from compound I

Compound	m.p. (°C)	Formula	Analysis % (Found/Calcd.) C	H	N	S
IXa	163	$C_{13}H_{14}ClN_3O_2S_2$	47.51 47.63	4.25 4.27	12.63 12.82	19.39 19.54
IXb	200	$C_{13}H_{14}N_4O_3S_2$	46.05 46.15	4.44 4.14	16.31 16.57	18.72 18.93
X	190 decomp	$C_9H_7N_3O_3S_2$	40.32 40.15	3.04 2.60	15.52 15.61	23.41 23.79

Action of morpholine on X

A solution of X (2.6 g ; 0.01 mole) in 50 ml ethanol and morpholine (1.3 g ; 0.015 mole) was heated under reflux for 1 hr. The reaction mixture was concentrated and cooled to ive IXb in 85 % yield. The product was identified by m.p. and mixed m.p.

REFERENCES

[1] W. R. Sherman, *J. Org. Chem.*, **26**, 88 (1961).

[2] M. A. Salama, F. A. Moti, A. A. G. Ghattas, *Bull. NRC, Egypt*, **3**, 87 (1978).

[3] J. R. Vishnu and H. N. Pandey, *Agr. Biol Chem.*, **37**, 1465 (1973).

[4] G. Maffii, E. Testa and R. Ettore, *Il Farmaco (Pavia) Ed. Sci.* **13**, 187 (1958).

[5] V. M. Artemov and U. P. Snaviaka, *Khim. Heterotsikl. Soedin.*, **7**, 905 (1971).

[6] A. A. El-Barbary, M. Anwar, A. A. G. Ghattas and A. F. Hashem., *Rev. Roumaine Chim.*, in print.

[7] A. Stempel, J. Zelauskas and J. A. Aeschlimann, *J. Org Chem.* **20**, 412 (1955).

[8] F. M. E. Abde-Megeid, M. A. F. Elkaschef and A. A. G. Ghattas, *Egypt, J. Chem.*, **20**, 235 (1977).

[9] R. Madhavan and V. Srinivasan, *Indian J. Chem.*, **7**, 760 (1969).

[10] A. R. Katritzky and A. J. Boulton, "Advances in Heterocyclic Chemistry" Vol. 9, Academic Press, New York, 1968, p. 208.

[11] Yu. N. Sheinker, I. Ya Postovskii and N. M. Varonina, *Zhur fiz. Khim.* **33**, 302 (1959).

[12] T. Radha and V. Srinivasan, *Indian J. Chem.*, **7**, 583 (1969).

[13] K. A. Jensen, and H. R. Baccaro O. Buchardt, G. E. Olsen, C. Pedersen and J. Toft, *Acta Chim. Acad. Sci. Hung.*, **15**, 1109 (1961).

[14] J. Sandströn, *Arkiv Kemi.*, **4**, 297 (1952).

[15] K. A. Jensen and C. Pedersen, *Acta Chim. Acad. Sci. Hung.*, **15**, 1124 (1961).

[16] C. Ainsworth *J. Amer. Chem. Soc.*, **80**, 5201 (1958).

Revue Roumaine de Chimie, **26**, *8*, 1135–1139 (1981)

STRUKTUR UND REAKTIVITÄT HETEROSUBSTITUIERTER NITRILE. XXXIII[1]

KINETIC UND MECHANISMUS DER 2-AMINOBENOXAZOLBILDUNG AUS *o*-AMINOPHENOL UND PHENYLCYANAT

ILSE BACALOGLU, TRUONG THE KY, HANS-HORST GLATT, CARMEN BOERIU, RADU BACALOGLU und DIETER MARTIN *

Laboratorium für Organische Chemie der Technischen Hochschule „Traian Vuia“, Str. Bocşa 6, Timişoara

*** Zentralinstitut für Organische Chemie der Akademie der Wissenschaften der DDR, 1199 Berlin. Rudower Chaussee 5, DDR**

Eingegangen am 21. Oktober 1980

Für die Reaktion von *o*-Aminophenol mit Phenylcyanat wurden die Reaktionsgeschwindigkeitskonstanten erster und zweiter Ordnung in Dioxan-Wasser bestimmt. Im ersten Schritt findet ein paralleler Angriff des Phenylcyanats an die Amino- und die Hydroxygruppe des *o*-Aminophenols statt, wobei sich cca. 10mal rascher N-(2-Hydroxyphenyl)-O-phenyl-isoharnstoff als O-(2-Aminophenyl)-O-phenylkohlensäureesterimid bildet. Der Isoharnstoff elimiert cca. 5mal schneller Phenol als das Kohlensäureesterimid, wobei sich das entsprechende Cyanamid und bzw. Cyanat bilden, die rasch zum 2-Aminobenzoxazol zyklisieren.

The first and second order rate constants of *o*-aminophenol phenylcyanate reaction in dioxane — water have been determined. A parallel phenylcyanate atack on the *o*-aminophenol amino- and hydroxy-group takes place in the first step of the reaction. The N-(2-hydroxyphenyl)-O-phenyl isoureea is formed about ten times faster than the O-(2-aminophenyl)-O-phenyl iminocarbonate. The isoureea eliminates phenol about five times faster than the iminocarbonate, the corresponding formed cyanamide and respectively cyanate undergo fast cyclization to 2-aminobenzoxazol.

o-Aminophenole reagieren mit heterosubstituierten Nitrilen zu 2-Aminobenzoxazolen :

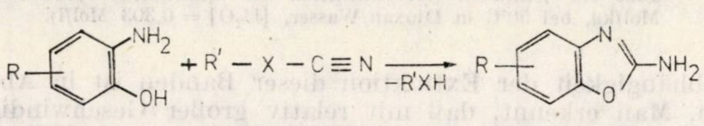

Als Zyklisierungsagentien können Salze der Thiocyansäure[2]. Arylcyanate[3]. Bromcyan[4–7] oder Cyanamide[5] verwendet werden.
In Verbindung mit unseren vorangehenden Arbeiten über die Reaktion von Arylcyanaten mit aromatischen Aminen und Phenolen[8,9] und unseren präparativen Versuchen[10] nach denen *o*-Aminophenole mit Arylcyanaten leicht zu 2-Aminobenzoxazolen zyklisieren, erschien es uns interessant, diese Reaktion auch vom Standpunkt ihrer Kinetik und ihres Mechanismus zu untersuchen.

Unsere Versuche ergaben, daß die Reaktionsgeschwindigkeit von *o*-Aminophenol mit Phenylcyanat in wässrigem Dioxan langsam genug ist, um IR-spektroskopisch verfolgt zu werden.

Durch den Vergleich der IR-Spektren mit denen authentischer Proben und mit Literaturangaben[8, 11] konnten Reaktanten, Zwischenstufen und Endprodukte identifiziert werden. Das Verschwinden des Phenylcyanats wurde anhand der ν-OCN-Bande (2250 cm^{-1}), das Erscheinen und Verschwinden des Isoharnstoffs bzw. Kohlensäurewesterimids anhand der C-N-Valenzschwingungsbande bei 1610 bzw. 1720 cm^{-1} verfolgt.

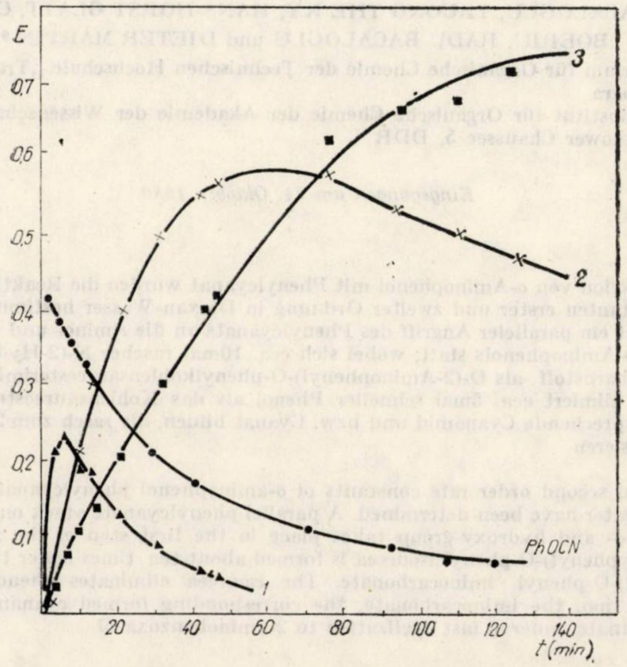

Abb. 1. — Extinktions-Zeit-Abhängigkeit der Phenylcyanat(PhOCN 2250 cm^{-1}). Isoharnstoff-(*1.* 1610 cm^{-1}). Kohlensäureesterimid-(*2*, 1720 cm^{-1}) und 2-Aminobenzoxazol-(*3*, 1660 cm^{-1})-Banden (Konzentration der Reaktanten 0,187 Mol/kg, bei 50°C in Dioxan/Wasser, $[H_2O] = 0{,}303$ Mol/l).

Die Zeitabhängigkeit der Extinktion dieser Banden ist in Abbildung 1 angegeben. Man erkennt, daß mit relativ großer Geschwindigkeit, zugleich mit dem Verschwinden des Phenylcyanats, der Isoharnstoff *1* erscheint, der ebenfalls mit großer Geschwindigkeit verschwindet. Zum Zeitpunkt des Verschwindens der gesamten Cyanatmenge ist im Reaktionsgemisch auch kein Isoharnstoff mehr vorzufinden. Parallel, aber viel langsamer als der Isoharnstoff, entsteht das Kohlensäureesterimid *2*, das dann langsam verschwindet. Das 2-Aminobenzoxazol *3* bildet sich zugleich mit dem Verschwinden des Isoharnstoffs und solange im Reaktionsgemisch Kohlensäureesterimid vorliegt. Die Reaktion verläuft also nach folgendem Schema:

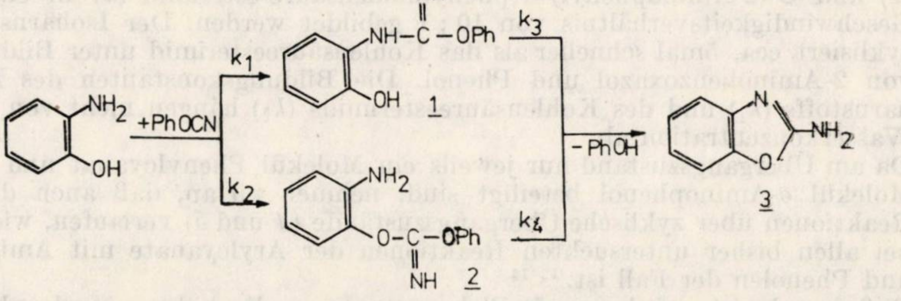

Aus der Zeitabhängigkeit der Extinktion des Phenylcyanats wurde die Summe der Geschwindigkeitskonstanten k_1 und k_2 berechnet, wobei festgestellt wurde, daß die Reaktionsgeschwindigkeit erster Ordnung in bezug auf Phenylcyanat und erster Ordnung in bezug auf *o*-Aminophenol ist. Das Verhältnis von k_1 und k_2 wurde aus dem Verhältnis der Extinktionen der C = N-Bande der Zwischenprodukte *1* und *2* bestimmt. Angesichts der strukturellen Ähnlichkeit der Zwischenstufen, wurden ihre molaren Extinktionskoeffizienten als gleich angenommen. Das Verschwinden der beiden Zwischenprodukte erfolgt nach einer Kinetik erster Ordnung.

Durch Auswerten der fallenden Teile der Extinktions-Zeitabhängigkeit nach der Guggenheim-Methode wurden k_3 und k_4 bestimmt. In Tabelle 1 sind die Mittelwerte der Reaktionsgeschwindigkeitskonstanten eingetragen.

TABELLE 1

Geschwindigkeitskonstanten der Reaktion von *o*-Aminophenol mit Phenylcyanat in Dioxan/Wasser bei 50°C

[PhOCN] Mol/kg	[*o*-AP] Mol/kg	[H_2O] Mol/l	k_1 kg/molmin	k_2 kg/Molmin	k_3 min^{-1}	k_4 min^{-1}
0.186	0.197	0.020	0.380	0.037	—	0.00794
0.186	0.222	0.020	0.322	0.025	—	0.0112
0.185	0.240	0.020	0.263	0.022	—	0.0109
0.186	0.258	0.020	0.163	0.020	—	0.00657
0.187	0.187	0.041	0.211	0.017	0.0367	—
0.186	0.185	0.280	—	—	0.0526	0.00699
0.187	0.187	0.301	0.227	0.017	0.0298	—
0.187	0.197	0.301	0.288	0.032	0.0452	0.00765
0.185	0.222	0.301	0.196	0.025	0.0266	0.00818
0.186	0.259	0.301	0.150	0.029	0.0454	0.00551
0.182	0.182	1.213	—	—	—	0.00602
Mittelwerte:			0.24 ± 0.03	0.025 ± 0.002	0.039 ± 0.004	0.0079 ± 0.0007

Die kinetischen Daten haben einen relativ hohen Fehler, da die Extinktionen nach dem Grundlinienverfahren im Falle von nur teilweise aufgelösten Banden bestimmt wurden. Aus den in Tabelle 1 zusammengestellten Daten ergibt sich, daß aus Phenylcyanat und *o*-Aminophenol in zwei parallelen Reaktionen N-(2-Hydroxyphenyl)-O-phenylisoharnstoff (*1*) und O-(2-Aminophenyl)-O-phenylkohlensäure-esterimid (*2*) in einem Geschwindigkeitsverhältnis von 10 : 1 gebildet werden. Der Isoharnstoff zyklisiert cca. 5mal schneller als das Kohlensäureesterimid unter Bildung von 2-Aminobenzoxazol und Phenol. Die Bildungskonstanten des Isoharnstoffs (k_1) und des Kohlensäureesterimids (k_2) hängen nicht von der Wasserkonzentration ab.

Da am Übergangszustand nur jeweils ein Molekül Phenylcyanat und ein Molekül *o*-Aminophenol beteiligt sind, nehmen wir an, daß auch diese Reaktionen über zyklische Übergangszustände (*4* und *5*) verlaufen, wie es bei allen bisher untersuchten Reaktionen der Arylcyanate mit Aminen und Phenolen der Fall ist.[12–14]

Daß $k_1 > k_2$ ist, wird verständlich, wenn man die höhere Nucleophilie der Aminogruppe und die größere Acidität der Hydroxygruppe in *4* mit der geringeren Nucleophilie der Hydroxygruppe und der kleineren Acidität der Aminogruppe in *5* vergleicht.

Die 5mal schnellere Zyklisierung des Isoharnstoffs *1* als die des Kohlensäureesterimids *2* ist zu verstehen, wenn man für den langsamen Schritt der Reaktionen eine Phenoleliminierung unter Bildung von Cyanamid bzw. Cyanat annimmt.

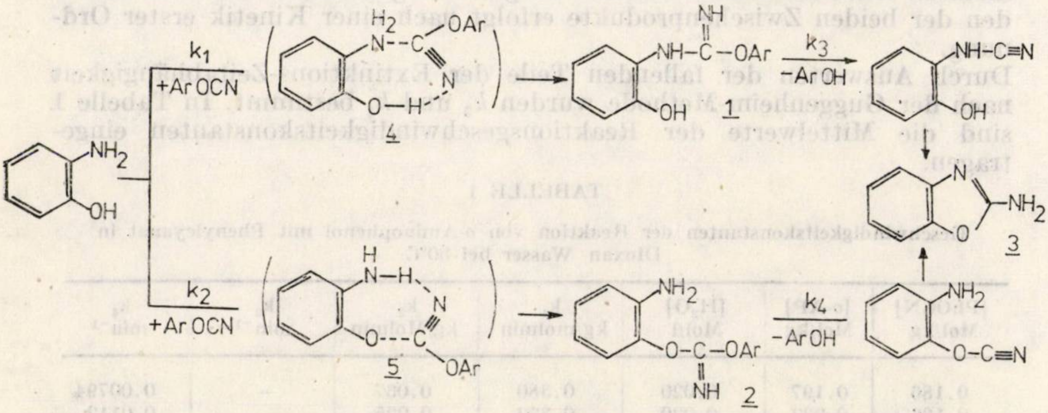

Bei diesen Eliminierungen muß die Reaktivität des Isoharnstoffs wegen der wichtigeren konjugativen Asisstenz des nichtbindenden Elektronenpaares des Stickstoffatoms größer sein als die des Kohlensäurediesterimids. Die Zyklisierung durch direkten nucleophilen Angriff der Amino- bzw. Hydroxygruppe an das sp^2-C-Atom in *1* oder *2* würde eine höhere Reaktivität des Kohlensäureesterimids erfordern.

BESCHREIBUNG DER VERSUCHE

SUBSTANZEN UND LÖSUNGSMITTEL

Phenylcyanat wurde nach bekannten Methoden[15,16] hergestellt, gereinigt und IR-spektroskopisch und gaschromatographisch auf Reinheit geprüft.

o-Aminophenol war ein Handelsprodukt (Fluka), das durch Sublimieren gereinigt wurde.

Dioxan wurde einige Stunden über Na unter Rückfluß gehalten und anschließend destilliert. Die Wasserkonzentration im Dioxan wurde nach Karl Fischer bestimmt.

KINETISCHE MESSUNGEN

Die kinetischen Bestimmungen wurden in mit Si-Fenster versehenen, thermostatierten Glasküvetten (Schichtdicke 0.015) durchgeführt. Zum Zeitpunkt Null wurde das in wässrigen Dioxan ($[H_2O] = 0{,}02 - 1{,}2$ Mol/l) gelöste Phenylcyanat ([PhOCN] = 0,182 – 0,187 Mol/L) und *o*-Aminophenol ([*o*-AP] = 0,182 – 0,259 Mol/l) kräftig vermischt und in die Küvette eingetragen. Von Zeit zu Zeit wurde das IR-Spektrum (650 — 4600 cm^{-1}) mit einem IR-Spektrophotometer SPECORD 71 (Carl Zeiss Jena) aufgezeichnet. Nach dem Grundlinienverfahren wurden die Extinktionen der den Reaktanten Zwischenstufen und Endprodukten entsprechenden Banden bestimmt. Ein Beispiel für die zeitabhängige Veränderung der Extinktionen dieser Banden ist in Abb. 1 angegeben.

Zur Berechnung von k_1 und k_2 aus dem Verschwinden des Phenylcyanats (PhOCN. Abb. 1) wurde folgendes Modell verwendet :

$$\frac{dx}{dt} = (k_1 + k_2) \cdot (a - x) \cdot (b - x)$$

wobei *a* und *b* die Anfangskonzentration des Phenylcyanats und *o*-Aminophenols sind und

$$x = \frac{E_0 - E_t}{E_0} \cdot a$$

(E_0 und E_t = Extinktionen am Anfang der Reaktion und zum Zeitpunkt *t*).

Das Verhältnis der RGK k_1 und k_2 wurde gleich dem Verhältnis der Extinktionen der beiden Zwischenprodukte gesetzt :

$$\frac{k_1}{k_2} = \frac{\varepsilon(2)\, E(2)}{\varepsilon(1)\, E(1)} = \frac{E(2)}{E(1)},$$

$$\text{da } \varepsilon(1) \approx \varepsilon(2).$$

Die Guggenheim-Methode wurde zum Berechnen von k_3 und k_4 für den fallenden Teil der Kurven *1* und *2* in Abb. 1 angewendet.

Zur Berechnung diente ein mit Plotter ausgerüsteter Hewlett Packard 9810.

LITERATURVERZEICHNIS

[1] 22 Mitt. : R. Bacaloglu, C. Antal, V. Pode und M. Divo *Bul. Inst Polit. „Traian Vuia" (Timişoara)* **1980**, im Druck.
[2] R. Passerini und L. Pentimalli, *Bull. Sci. Fac. chim. ind. Bologna* **12**, 165 (1954).
[3] E. Grigat, *Angew. Chem.*, **84**, 1015 (1972).
[4] T. Nagano, M. Itoh und K. Matsumura, *J. Amer. Chem. Soc.*, **75**, 2770 (1953).
[5] R. M. Acheson und N. F. Taylor, *J. Chem. Soc.*, **1956**, 4727.
[6] P. Biddle, E. S. Lane und J. L. Willans. *J. Chem. Soc.*, **1960** 2369.
[7] J. Sam und J. N. Plampin, *J. Pharm. Sci.*, **53**, 538 (1964).
[8] D. Martin, K. Nadolski, R. Bacaloglu und I. Bacaloglu. *J. prakt. Chem.*, **313**, 58 (1971).
[9] I. Bacaloglu, K. Nadolski, R. Bacaloglu und D. Martin. *J. prakt. Chem.*, **313**, 839 (1971).
[10] I. Bacaloglu, Truong The Ky. C. Boeriu, H. H. Glatt, H. Graubaum, R. Bacaloglu und D. Martin, *Bul. Inst. Polit. Iaşi*, im Druck.
[11] D. Martin, *Z. Chem.*, **7**, 123 (1967).
[12] I. Bacaloglu, R. Bacaloglu, D. Martin und K. Nadolski, *J. prakt. Chem.*, **316**, 526 (1974).
[13] I. Bacaloglu, R. Bacaloglu, D. Martin und H. J. Birkhahn, *J. prakt. Chem.*, **317**, 214 (1975).
[14] R. Bacaloglu, D. Martin, I. Bacaloglu und K. Oehler, *J. prakt. Chem.*, **317**, 601 (1975).
[15] D. Martin, *Chem. Ber.*, **97**, 2689 (1964).
[16] E. Grigat und R. Pütter, *Chem. Ber.*, **97**, 3012 (1964).

Revue Roumaine de Chimie, 26, 8, 1141–1148 (1981)

SYNTHESIS AND SOME REACTIONS OF 3-CYANO-4-PHENYL-6-[1'(2'-METHOXYNAPHTHALENYL)]-2-PYRIDONE

A. ESSAWY, M. El-GARBY YOUNES and A. Z. M. HEIKAL
Chemistry Department, Faculty of Science, Zagazig University, Zagazig, Egypt

Received April 10, 1980

Reactions of 3-cyano-4-phenyl-6-[1'(2'-methoxynaphthalenyl)]-2-pyridone (2) with alkylating agents, phosphorous oxychloride, amines and Grignard reagents are described.

In continuation of our studies on 6-substituted-3-cyano-4-phenyl-2-pyridone and related compounds, [1,2] we report here some reactions of 3-cyano-4-phenyl-6-[1'(2'-methoxynaphthalenyl)]-2-pyridone (**2**). Thus, ethyl cyanoacetate condenses with chalcone **1** in the presence of ammonium acetate to give compounds **2**, **3** and **4**. [3-5] Boiling **2** with conc. HCl affected hydrolysis of the cyano group and gave 4-phenyl-6-[1'(2'-methoxynaphthalenyl)]-2-pyridone-3-carboxylic acid (**5**). Hydrolysis of **4** with 10% alc. KOH yielded 2-amino-4-phenyl-6-[1'(2' methoxynaphthalenyl)] nicotinic acid (**6**).

The IR spectrum of **2** showed strong absorption bands at 2230, 1675, 3300 – 3200 and 1610 cm^{-1} attributable to $C \equiv N$, $C = O$, NH, OH and $C = N$ respectively. [6-8] The ^1H-NMR spectrum of **2** in $CDCl_3$ showed signals at 3.9 (*s*, 3H ; $-OCH_3$), 7.6–7.86 (*m*, 12 H ; Ar–H) and 7.8–8.16 (*s*, 1H ; N*H*).

The IR spectrum of **4** showed well defined absorption bands at 3290, 1690 and 1610 cm^{-1} attributable to NH, $C = O$ and $C = N$ respectively. The IR spectrum of **6** showed absorption bands for NH (3300), $C = O$ (1665) and $C = N$ (1605) cm^{-1}.

The reaction with chalcone, when carried out in benzene[1] gave only the 3-cyano-4-phenyl-6-[1'(2'-methoxynaphthalenyl)] -2-oxo-1, 2, 3, 4-tetrahydropyridine (**7**). This involved most probably the Michael addition and cyclization without dehydrogenation. In favour of this assumption is the fact that **2** can be prepared from **7** by heating at 160°C or by action of bromine via aromatization. The IR spectrum of **7** exhibited characteristic absorption bands for NH and OH (3450–3300), $C \equiv N$ (2230) and $C = O$ (1683) cm^{-1}. The ^1H-NMR spectrum of **7** in $CDCl_3$ showed signals at 3.9 (*s*, 3H ; $-OCH_3$), 7.03–7.73 (*m*, 14H ; Ar–H) and 8.0–8.1 (*s*, 1H ; $-NH$). The alkylation of the pyridone **2** was investigated. Thus, treatment of the sodium or potassium salts of **2** prepared by the method of Adams and Schrecker with dimethyl sulphate, diethyl sulphate, benzyl chloride and ethyl bromoacetate [9-12], gave 2-methoxy (**8a**), 2-ethoxy (**8b**), 2-benzyloxy -4-phenyl-6-[1′ (2′-methoxynaphthalenyl)], nicotinonitrile (**8c**) and 3-cyano-4-phenyl-6-[1′ (2′-methoxynaphthalenyl)]-pyridyl oxyacetic acid ethyl ester (**8d**). It has been found that the ester **8d** is easily hydrolysed under alkaline conditions to the acid **9**. Similarly, treatment of the sodium salt of **7** with dimethyl sulphate and/or benzyl chloride gave **10a** and **10b** respectively. The IR spectra of compounds **8a** and **8b** showed bands attributable to $C\equiv N$ (2230), $C=N$ (1600), $C\equiv C$ (1580), the ether linkage group (1260–1280) cm^{-1} and showed the absence of OH, NH, and CO groups.

The structure of **9** was proved from its solubility in sodium bicarbonate solution and through the IR bands at 1710 (ν_{CO} of carboxylic group), 3000 (ν_{OH}), 1605 ($\nu_{C=N}$), 2235 ($\nu_{C\equiv N}$) and 1590 cm^{-1} ($\nu_{C=C}$). The IR spectra of compounds **10** showed bands attributable to $C\equiv N$ (2228), $C=N$ (1610), $C=C$ (1590) and ether linkage (1257–1285) cm^{-1}. Compound **2** reacted with phosphorous oxychloride [1] and gave 2-chloro-4-phenyl-6-[1′ (2′-methoxynaphthalenyl)] nicotino nitrile (**11**). Treatment of the tetrahydropyridone derivative **7** with phosphorous oxychloride resulted in the replacement of hydroxyl group by chlorine accompanied by dehydrogenation and formation of **11**, which was identified by melting point and mixed melting point. Compound **11** reacted with sodium methoxide and sodium ethoxide and gave **8a** and **8b** identical with that obtained by alkylation of **2**, as shown by the IR spectra of the compounds. The easily replaceable chlorine at position 2, in compound **11** was reacted with various amines and gave 2-amino derivatives, **12a** – **f**, **13** and **14**. The infrared spectrum of compound **11** showed different characteristic bands attributable to $C\equiv N$ (2230), $C=N$ (1610–1585) and $C-Cl$ stretching (700) cm^{-1}. Compound **12a** showed IR bands at 3050 (ν_{NH}) and 2230 cm^{-1} ($\nu_{C\equiv N}$). The IR spectrum of **12d** showed bands at 3100 (ν_{NH}), 2240 ($\nu_{C\equiv N}$), 1695 (ν_{CO} of carboxylic group) and 2950 cm^{-1} (ν_{OH}). Compound **2** reacted with Grignard reagents [1, 2, 13, 14] with subsequent decomposition and hydrolysis to give 3-acyl and 3-aroyl-2-(1H)pyridones (**15a** – **e**). The best results were obtained using four moles of the Grignard reagent to one mole of the pyridone. Similarly, 3-cyanotetrahydropyridone derivative **7** reacted with Grignard reagents to give the 3-acyl and 3-aroyl tetrahydropyridone derivatives (**16a** – **e**). The IR spectrum of compound **15b** showed absorption bands at 3450, 1620, 1710 and 1660 cm^{-1} attributable to NH, $C=N$, $C=O$ (acetyl) and $C=O$ (amide) respectively.

The $^{-1}$H-NMR spectrum of compound **15b** in $CDCl_3$ showed signals at 0.54–1.4 (*t*, 3H, $-CH_2-CH_3$), 2.96–3.21 (*q*, 2H; $-CH_2-CH_3$), 3.75 (*s*, 3H; $-OCH_3$), 6.9–7.67 (*m*, 12H; ArH) and 7.78–8.1 (*s*, 1H; $-NH$). The IR spectrum of compound **16c** showed different characteristic bands for $C=N$, $C=O$ and amide $C=O$ groups at 1610, 1700 and 1600 cm^{-1} respectively.

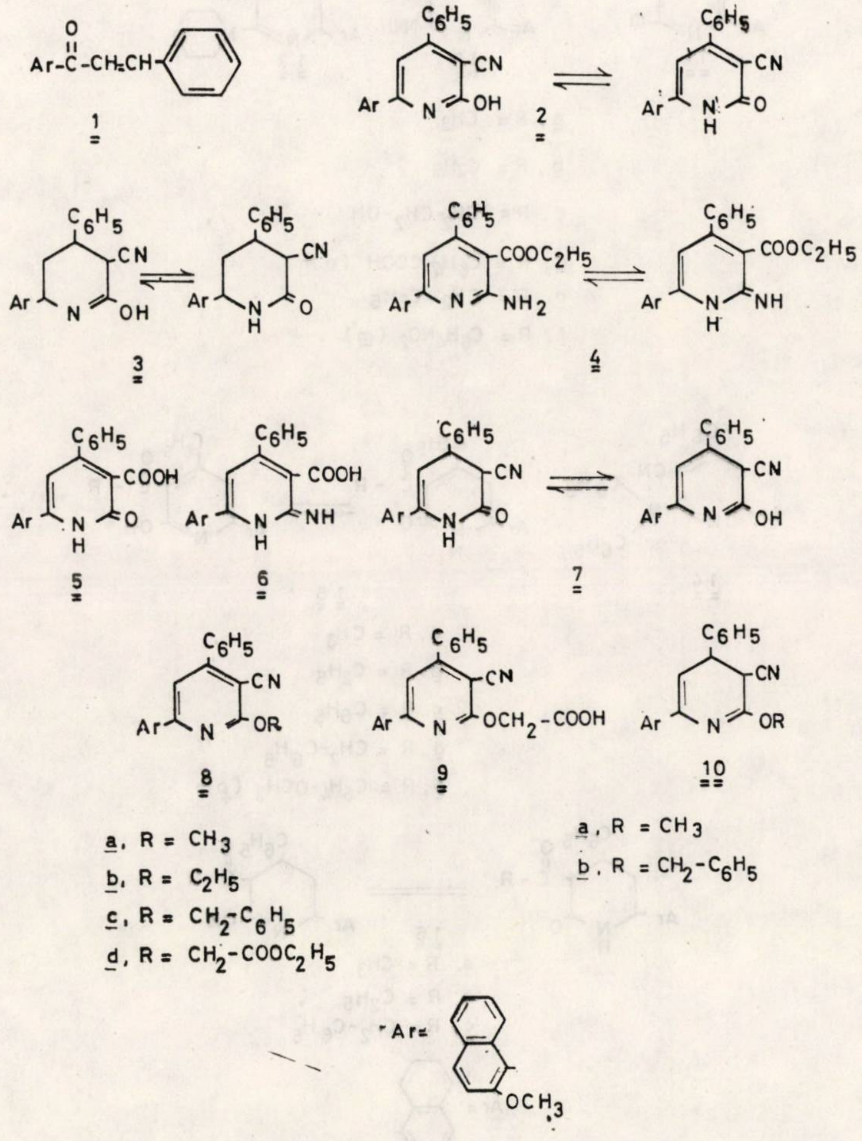
1
2
3
4
5
6
7
8
9
10
a, R = CH3
b, R = C2H5
c, R = CH2-C6H5
d, R = CH2-COOC2H5
a, R = CH3
b, R = CH2-C6H5
Ar=
OCH3

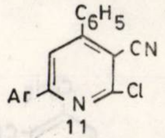

11

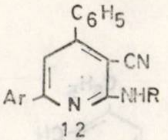

12

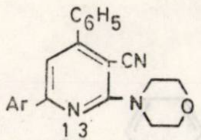

13

a, R = CH_3

b, R = C_2H_5

c, R = CH_2-CH_2-OH

d, R = C_6H_4-COOH (o)-

e, R = $CH_2-C_6H_5$

f, R = $C_6H_4NO_2$ (m)-

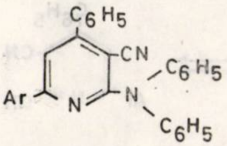

14

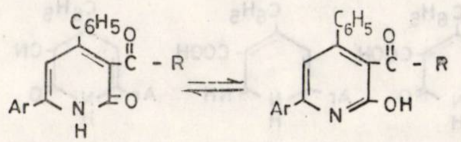

15

a, R = CH_3

b, R = C_2H_5

c, R = C_6H_5

d, R = $CH_2-C_6H_5$

e, R = $C_6H_4-OCH_3$ (p)-

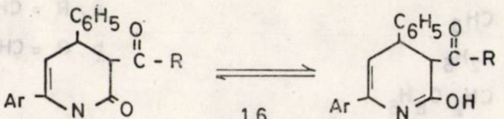

16

a, R = CH_3

b, R = C_2H_5

c, R = $CH_2-C_6H_5$

Ar =

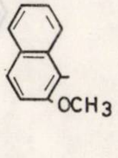

EXPERIMENTAL

Melting points are uncorrected. IR spectra in KBr were taken on a Unicam Sp 1200 spectrophotometer (ν_{max} in cm^{-1}). ^{1}H-NMR spectra were recorded on a Varian VN 1009 (S-60T) instrument using TMS as internal standard (chemical shifts in δ-scale).

The reaction of ethyl cyanoacetate with chalcone 1 without solvent

A mixture of ethylcyanoacetate (4.52 g ; 40 mmoles) ; the unsaturated ketone **1** (11.52 g ; 40 mmoles) and ammonium acetate (2.1 g ; 30 mmoles) was heated at 160°C for 6 hours, then allowed to cool. The yellowish oil obtained was washed with benzene. It was divided into two parts, a benzene soluble part and a benzene insoluble part. The benzene solution was concentrated after standing overnight at room temperature, colourless crystals which separated on recrystallizing from light petrol (60−80°) gave **4** (Table 1). The solid separated after addition

TABLE 1

Characterization of products **2**, **3**, **4**, **5**, **6**, **7** ; **8a** − **d**, **9**, **10a** and **10b**

Compound	m.p. (C°)	Solvent * yield (%)	Formula	Analysis (%) Found	Analysis (%) Calculated
2	130	E	$C_{23}H_{16}N_2O_2$	C 78.3	78.4
		55		H 4.6	4.5
				N 8.0	7.9
3	68	P (40−60°)	$C_{23}H_{20}N_2O_2$	C 77.5	77.5
		20		H 5.7	5.6
				N 7.7	7.8
4	120	P (60−80°)	$C_{25}H_{22}N_2O_3$	C 75.2	75.3
		20		H 5.4	5.5
				N 7.1	7.0
5	over 300	E	$C_{23}H_{17}NO_4$	C 74.21	74.3
		80		H 4.6	4.5
				N 3.5	3.7
6	140	E	$C_{23}H_{18}N_2O_3$	C 74.5	74.6
		75		H 4.9	4.8
				N 7.6	7.5
7	137	B	$C_{23}H_{18}N_2O_2$	C 77.8	77.9
		70		H 5.1	5.0
				N 8.0	7.9
8a	125	B/P (40−60°)	$C_{24}H_{18}N_2O_2$	C 78.8	78.6
		60		H 4.8	4.9
				N 7.5	7.6
8b	133	E	$C_{25}H_{20}N_2O_2$	C 78.8	78.9
		80		H 5.2	5.2
				N 7.2	7.2
8c	120	B/P (60−80°)	$C_{30}H_{22}N_2O_2$	C 81.5	81.4
		60		H 5.0	4.9
				N 6.3	6.3
8d	72	B	$C_{27}H_{22}N_2O_4$	C 73.8	73.9
		70		H 5.1	5.0
				N 6.3	6.3
9	180	E	$C_{25}H_{18}N_2O_4$	C 73.3	73.2
		70		H 4.5	4.4
				N 6.7	6.8
10a	165	B/P	$C_{24}H_{20}N_2O_2$	C 78.3	78.2
		(60−80°)		H 5.3	5.4
		75		N 7.5	7.6
10b	150	B/P (60−80°)	$C_{30}H_{24}N_2O_2$	C 81.1	81.08
		80		H 5.3	5.4
				N 6.2	6.3

* B = benzene ; P = light petrol ; E = ethanol.

of light petrol (40 – 60°C) to benzene filtrate was crystallized from light petrol (40 – 60°C) to give compound **3** (Table 1). The benzene insoluble part was crystallized from ethanol and gave compound **2** as yellow crystals (Table 1).

Hydrolysis of 2; Formation of 4-phenyl-6-[1′(2′-methoxynaphthalenyl)]-2-pyridone-3-carboxylic acid (5)

The compound **2** (1 g; 3 mmoles) was heated with concentrated hydrochloric acid (20 ml) for 10 hours. The solid obtained was washed with water and crystallized from ethanol to give **5** (Table 1).

Hydrolysis of ethyl 2-amino-4-phenyl-6-[1′(2′-methoxynaphthalenyl)] nicotinic acid (4); Formation of 6

The compound **4** (1 g; 3 mmoles) was heated with 10% alcoholic potassium hydroxide (20 ml) for 5 hours. The crystals which separated on cooling the reaction mixture and standing overnight, were filtered off and crystallized from the suitable solvent to give **6** (Table 1).

The reactions of ethylcyanoacetate with chalcone 1 in benzene; Formation of 7

A mixture of ethylcyanoacetate (5.65 g; 50 mmole) chalcone **1** (14.40 g; 50 mmole), and ammonium acetate (2.8 g; 40 mmole) in 60 ml benzene was refluxed for 10 hours. Water was added to the reaction and after standing overnight, a crystalline solid precipitated. It was treated with a small amount of dilute methanol to remove the unchanged chalcone and crystallized from benzene to give **7** (Table 1).

Alkylation of 3-cyano-4, 6-diaryl-2-pyridone 2; Formation of 8a – d

a) *Methylation*: A hot solution of 3-cyano-4,6-diaryl-2-pyridone **2**, (1 g; 3 mmole) in sodium hydroxide solution (50 ml; 20%) was treated with dimethylsulphate (3 ml; 8 mmole) and then warmed for one hour on a steam bath. The crystalline solid that separated after cooling was crystallized from benzene-light petrol (40 – 60°C) to give **8a** (Table 1).

b) *Ethylation*: 3-cyano-4,6-diaryl-2-pyridone (**2**) undergoes ethylation to give **8b** by using diethylsulphate in the same manner as described above for methylation (Table 1).

c) *Benzylation*: A mixture of the sodium or potassium salt of **2** (1 g; 3 mmole), absolute ethanol (50 ml), and benzyl chloride (3 ml; 8 mmole) was refluxed for 5 hours. The yellow crystals which separated upon cooling the reaction mixture were filtered off and recrystallized from benzene-light petrol (60 – 80°C) to give the compound **8c** (Table 1).

d) *Reaction with ethyl bromoacetate*: A mixture of the sodium or potassium salt of **2** (1 g, 3 mmole), absolute ethanol (50 ml); and ethyl bromoacetate (1 g; 6 mmole) was refluxed for 5 hours. The crystals which separated on cooling, were filtered off and crystallized from benzene to give the compound **8d** (Table 1).

Hydrolysis of 2-alkoxy derivative 8d to the corresponding monocarboxylic acid 9

A mixture of **8d** (4.06 g; 10 mmole) and KOH (0.56 g; 10 mmole) was dissolved in a mixture of ethanol (30 ml) and water (30 ml), and heated under reflux for three hours, cooled, acidified with dilute hydrochloric acid and extracted with ether.

The ethereal layer was washed with water, dried over anhydrous calcium chloride, evaporated and the residual oil was crystallized from ethanol to give **9** (Table 1).

Alkylation of 3-cyano-4-phenyl-6-[1′ (2′-methoxynaphthalenyl)]-2-oxo-1,2,3,4-tetrahydropyridine 7; formation of 10a and 10b

The tetrahydropyridone derivative **7** undergoes ethylation and benzylation in the same manner used on alkylation of compound **2** to give **10a** and **10b** (Table 1).

TABLE 2

Characterization of products **11**, **12a – f**, **13**, **14**, **15a – e** and **16a – c**

Com-pound	m.p (C°)	Solvent* yield (%)	Formula	Analysis (%)	
				Found	Calculated
11	over 300	B 70	$C_{23}H_{15}N_2ClO$	C 74.5 H 3.9 N 7.4	74.49 4.0 7.5
12a	over 300	B/P 80	$C_{24}H_{19}N_3O$	C 78.8 H 5.2 N 11.5	78.9 5.2 11.5
12b	292	B/P 70	$C_{25}H_{21}N_3O$	C 79.2 H 5.3 N 11.1	79.1 5.5 11.08
12c	290	B/P 80	$C_{25}H_{21}N_3O_2$	C 76.0 H 5.2 N 10.5	75.9 5.3 10.6
12d	224	B/P 70	$C_{30}H_{21}N_3O_3$	C 76.2 H 4.5 N 8.8	76.4 4.4 8.9
12e	295	E 80	$C_{30}H_{23}N_3O$	C 81.5 H 5.2 N 9.4	81.6 5.2 9.5
12f	297	B/P 80	$C_{29}H_{20}N_4O_3$	C 73.6 H 4.2 N 11.7	73.7 4.2 11.8
13	258	B/P 70	$C_{27}H_{23}N_3O_2$	C 77.0 H 5.3 N 10.0	76.9 5.4 9.98
14	105	B/P 65	$C_{35}H_{25}N_3O$	C 83.5 H 5.1 N 8.1	83.5 4.9 8.3
15a	190	B/P 70	$C_{24}H_{19}NO_3$	C 78.1 H 5.1 N 3.8	78.05 5.1 3.79
15b	69	P 70	$C_{25}H_{21}NO_3$	C 78.4 H 5.2 N 3.5	78.3 5.4 3.6
15c	170	B/P 70	$C_{29}H_{21}NO_3$	C 80.6 H 4.9 N 3.2	80.7 4.8 3.2
15d	135	B/P 75	$C_{30}H_{23}NO_3$	C 81.0 H 5.0 N 3.2	80.9 5.1 3.1
15e	105	B/P 60	$C_{30}H_{23}NO_4$	C 78.1 H 4.9 N 3.1	78.09 4.99 3.00
16a	155	B/P 60	$C_{24}H_{21}NO_3$	C 77.7 H 5.5 N 3.5	77.6 5.6 3.7
16b	255	E 70	$C_{25}H_{23}NO_3$	C 77.8 H 6.0 N 3.5	77.9 5.97 3.6
16c	108	P 70	$C_{30}H_{25}NO_3$	C 80.5 H 5.6 N 3.1	80.5 5.59 3.1

* B = benzene ; B/p = benzene/ light petrol (100/120°) ; P = light petrol (100/120°C) ; E = ethanol.

Action of phosphorous oxychloride on 2-pyridone 2; formation of 11

A suspension of 2 (1 g; 3 mmole) in phosphorous oxychloride (1.53 g; 10 mmole) was heated on a water bath for 2 hours, then the reaction mixture was poured gradually into crushed ice. The solid which separated was filtered off and crystallized from benzene to give **11** (Table 2).

The reaction was carried out as described above using the compound **7**, the product was proved to be identical with that of 2.

Reaction of 2-chloro-3-cyano-4,6-diaryl pyridine 11 with sodium methoxide and sodium ethoxide; formation of 8a and 8b.

A solution of **11** (1 g; 3 mmole) in methanol or ethanol (20 ml) was treated with sodium methoxide or sodium ethoxide, refluxed for 5 hours, then allowed to cool.

The reaction mixture was diluted with water, the solid formed was filtered off and crystallized from benzene/light petrol (40−60°C) or ethanol and proved to be identical with **8a** and **8b** respectively.

Reaction of 2-chloro -3-cyano-4,6-diaryl pyridine with amines; Formation of 12a – f, 13 and 14.

A suspension of **11** (50 mmole) and the appropriate amine (methyl amine, ethyl amine, ethanol amine, anthranilic acid, benzylamine, *m*-nitro aniline, morpholine, or diphenyl amine, (100 mmole) was refluxed for 2 hours and allowed to cool; the reaction was triturated with cold ethanol, and the solid was crystallized from a suitable solvent to give **12a – f, 13** and **14.** (Table 2).

Action of Grignard reagents on 2; Formation of 15a – e

To a suspension of 2 (2 g; 6 mmole) in dry benzene (50 ml) an ethereal solution of alkyl and/or arylmagnesium halide (prepared from 0.9 g magnesium, 7.0 g alkyl or aryl halide and 40 ml dry ether), was added. The reaction mixture was refluxed (steam-bath) for 2 hours, set aside at room temperature, then decomposed with a cold solution of hydrochloric acid (10%). The coloured solid was crystallized from the proper solvent (Table 2).

Action of Grignard reagents on 7; Formation of 16a – e

Tetrahydropyridone **7** reacted with alkyl and/or aryl magnesium halide in the same manner as above to give **16a – e** (Table 2).

REFERENCES

[1] M. Abdalla, A. Essawy and A. Deeb, *Pakistan J. Sci. Ind. Res.*, **20**, 139 (1977).
[2] M. Abdalla, A. Essawy and A. Deeb, *Indian J. Chem.*, **16**, 332 (1978).
[3] A. Sakurai and H. Midorikawa, *Bull. Chem. Soc. Japan*, **40**, 1680 (1967).
[4] A. Albert and E. Spinner, *J. Chem. Soc.*, **1960**, 1221.
[5] S. F. Mason, *J. Chem. Soc.*, **1957**, 4874.
[6] N. J. Lecnard and J. H. Boyer, *J. Amer. Chem. Soc.*, **72**, 2980 (1950).
[7] E. Spinner and J. C. B. White, *J. Chem. Soc.*, **1966**, 991.
[8] J. A. Gibson, W. Kynsaston and A. S. Lindsay, *J. Chem. Soc.*, **1955**, 4340.
[9] T. Takahashi and M. Kawashima, *J. Pharm. Soc. Japan*, **63**, 546 (1943).
[10] L. Gogalimaka, *Acta PO1, Pharm.*, **21**, 343 (1964).
[11] D. J. Cook, R. E. Bowen, P. Sorter and E. Doniels, *J. Org. Chem.*, **26**, 4949 (1961).
[12] J. T. Plati and W. Wenner, *J. Org. Chem.*, **14**, 447 (1949).
[13] R. I. Schriner and T. A. Turner, *J. Amer. Chem. Soc.*, **52**, 1267 (1930).
[14] R. L. Frank and C. Weatherbea, *J. Amer. Chem. Soc.*, **70**, 3282 (1948).

Revue Roumaine de Chimie, 26, *8*, 1149—1159 (1981)

NOUVEAUX THIO-ÉTHERS AROMATIQUES

M. IOVU et ELENA BĂDĂU
Faculté de pharmacie, str. Traian Vuia 6, Bucarest, Roumanie

Reçu le 14 juin 1980

Des composés contenant tant la fonction d'éther aromatique que la fonction de thioéther mixte ont été synthétisés, en utilisant la réaction de condensation d'un nombre d'arylchlorméthyle dérivés avec le di(*p*-thiolphényl)-éther, à la suite de la transformation de ce dernier à l'état de sel de sodium anhydre, par l'élimination azéotrope de l'eau résultée de la réaction avec l'hydroxyde de sodium. Les nouveaux bisthio-éthers synthétisés ont été transformés en sulfones correspondants par oxydation avec de l'H_2O_2 30%. Les thio-éthers et les sulfones obtenus ont été caractérisés par l'analyse spectrale en I.R., U.V. et R.M.N.

Compounds with aromatic ether as well as mixed thioethers functional groups were synthesized using the condensation reaction of the chloromethyl aryl derivatives with di(*p*-thiophenyl)ether, which was transformed into anhydrous sodium salt by the azeotropic elimination of water resulted from the reaction with sodium hydroxide. The new bisthioethers were transformed into the corresponding sulphones through oxidation with 30% H_2O_2. The thioethers and sulfones were caracterised by IR, UV and NMR spectral analysis.

Dans des études antérieures, nous avons synthétisé des benzylphényle thio-éthers [1] et des bisthio-éthers [2] aromatiques, en traitant les composés chlorméthylés avec des thiophénolates alcalins anhydres ; l'eau résultée de la réaction du thiophénol avec de l'hydroxyde alcalin a été éliminée par distillation azéotropique en employant un mélange d'éthanol-benzène.

Dans des études plus anciennes, d'autres auteurs ont obtenu le thiophénolate anhydre en traitant le thiophénol avec des alcoxydes de sodium. [3]

Brintzinger, Schrnahl et Witte [4] ont obtenu le phénylbenzylthioéther en traitant le chlorméthylsulfochlorure avec du benzène en présence de l'$AlCl_3$.

Dans un brevet américain [5] de 1967 est mentionnée la synthèse de quelques bis(α-arylthio-*p*-tolyl)éthers avec la formule générale

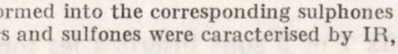

où Ar est un phényle, un halophényle, un tolyl ou un cumyl. Les composés ont une action pesticide. Conformément au brevet, on obtient les éthers par le chauffage du 4,4'-dichlorméthyl-diphényléther avec des thiophénols, dans un solvant inerte à 80—150°C.

En considérant l'importance de l'application de ces composés, qui contiennent la fonction mixte d'éther et de thio-éther, nous avons passé à la synthèse d'une nouvelle classe d'éthers-bisthio-éthers aromatiques dont la formule générale est :

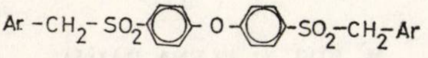

qui peuvent être isomères de ceux décrits par le brevet américain si les radicaux Ar sont identiques.

Pour synthétiser les nouveaux composés nous avons utilisé la méthode mentionnée au début, qui permet de travailler à des temperatures plus basses que celles prévues dans le brevet américain et qui, en même temps agrandit beaucoup la vitesse de réaction, grâce à la transformation de la réaction entre le composé chlorméthylé et le dithiol, à la suite du passage de celui-ci à l'état de sel de sodium, dans une réaction entre les ions.

Les éther-bisthio-éthers obtenus à la suite de cette réaction ont été soumis à l'oxydation avec de l'H_2O_2 30 % dans un milieu d'acide acétique glacial et chauffage pendant 2 heures. De cette manière, les sulfones correspondantes ont été obtenues.

RÉSULTATS ET DISCUSSIONS

Dans les tableaux 1 et 2 sont inscrites les formules de structure et les formules moléculaires des nouveaux éthers-bisthio-éthers aromatiques, respectivement des sulfones, les résultats de l'analyse élémentaire quantitative de C, H, S, les points de fusion et les rendements d'obtention.

Comme il était à supposer, la substitution du radical méthyle dans position *para* fait beaucoup monter le point de fusion.

Des données des tableaux on constate que les points de fusion montent beaucoup lors du passage des sulfures en sulfones. Les différences sont d'environ 100°. Les rendements à l'oxydation sont de 61% à 72% comme suite du fait qu'on a poursuivi l'obtention d'un produit pur à partir de solutions diluées.

CARACTÉRISATION SPECTRALE

SPECTRES DE ROTATION-VIBRATION

L'analyse des spectres I.R. exécutée chez des pastilles contenant du KBr indique l'existence des bandes caractéristiques aux vibrations de valence ν_{C-H}, qui se trouvent sur les noyaux aromatiques, dans la région des valeurs 3100—3000 cm^{-1}. Le nombre de bandes de cette région dépend du nombre de remplaçants qui se trouvent sur les noyaux aromatiques (tabl. 3).

TABLEAU 1

Éther-thio-éthers

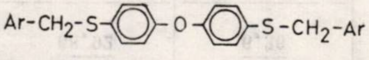

N°. crt.	Ar	Formule moléculaire	C % calculé/trouvé	H % calculé/trouvé	S % calculé/trouvé	P.f. °C	η %	λ_{nm}	ε_{max}
1	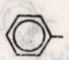	$C_{26}H_{22}OS_2$	75,32 75,02	5,34 5,54	15,46 15,20	129	91,7	266	17100
2	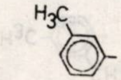	$C_{28}H_{26}OS_2$	75,97 76,20	5,92 5,95	14,48 14,56	64	65,8	266	19400
3	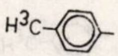	$C_{28}H_{26}OS_2$	75,97 76,20	5,92 5,78	14,48 14,30	147	87,8	266	19400
4	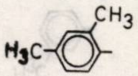	$C_{30}H_{30}OS_2$	76,55 76,06	6,42 6,70	13,70 13,84	145	72,3	268	18800
5	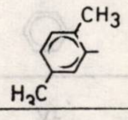	$C_{30}H_{30}OS_2$	76,55 77,02	6,42 6,21	13,70 13,50	77	87,2	268	18800
6	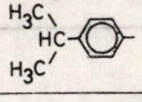	$C_{32}H_{34}OS_2$	77,28 77,68	6,87 7,02	12,85 12,45	89	88,3	266	21100
7	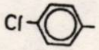	$C_{26}H_{29}Cl_2OS_2$	64,59 64,88	4,17 4,29	13,26 13,44	135	74,7	268 233	23100 38600

TABLEAU 2

Bissulfonyl-éthers

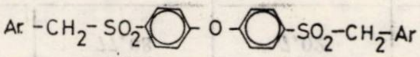

Nº. crt.	Ar	Formule moléculaire	C% calculé/trouvé	H% calculé/trouvé	S% calculé/trouvé	P.f. °C	η %	λ_{nm}	ε_{max}
1	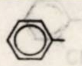	$C_{26}H_{22}O_5S_2$	65,28 64,75	4,63 4,45	13,40 13,28	249	72,1	249	21400
2	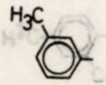	$C_{28}H_{26}O_5S_2$	66,11 66,09	5,15 5,02	12,60 12,56	275	60,9	249	24090
3	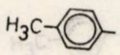	$C_{28}H_{26}O_5S_2$	66,11 65,77	5,15 5,07	12,60 12,17	249	61,8	248	24090
4	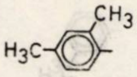	$C_{30}H_{30}O_5S_2$	67,38 66,04	5,65 5,77	11,99 12,04	236	64,91	250	22300
5	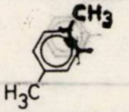	$C_{30}H_{30}O_5S_2$	67,38 67,47	5,65 5,78	11,99 12,19	202	63,8	251	22100
6	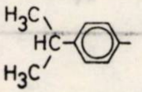	$C_{32}H_{34}O_5S_2$	68,29 68,92	6,09 6,36	11,36 11,47	233	62,7	251	22740
7	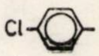	$C_{36}H_{20}Cl_2O_5S_2$	57,04 57,67	3,65 3,68	11,71 11,78	259	71,1	249	25100

TABLEAU 3

Les absorptions I.R. des éther-bisthio-éthers

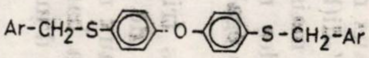

Nº. crt.	Ar	Nombre d'onde cm^{-1}							
		ν C–H	ν CH_3 asym	νCH_2 asym	νCH_2 sym.	νC=C	νC–O asym	νC–O sym	γC–H
1	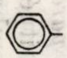	3085 3050 3020	—	2926	2845	1580 1480	1250 1270	1160	700 770 810
2	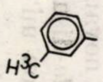	3085 3060 3020	2960	2926	2855	1580 1480	1255 1275	1160	700 810 825
3	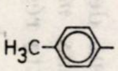	3080 3060 3020	2960	2926	2855	1580 1480	1255 1275	1165	820
4	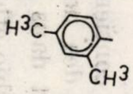	3090 3060 3020	2965	2926	2855	1580 1480	1250 1275	1165	870 820 810
5	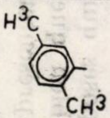	3090 3060 3020	2962	2926	2855	1580 1480	1255 1275	1165	885 820 810
6	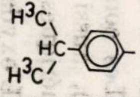	3080 3060 3020	2960	2926	2855	1580 1480	1255 1275	1185	820
7	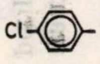	3080 3050 3028	—	2926	2855	1580 1480	1255 1275	1165	820

Les vibrations de valence des groupements CH_2, déterminent des absorptions à 2926 cm^{-1} pour la vibration antisymétrique et à 2845 ± 10 cm^{-1} pour la vibration symétrique. Dans cette région il y a également les bandes dues aux vibrations de valence des groupements CH_3 substitués sur les noyaux benzéniques.

La présence des anneaux benzéniques substitués est mise en évidence par l'existence des bandes dues aux vibrations de valence $C\overset{\cdots}{-}C$, à 1580 cm^{-1} et 1480 cm^{-1}.

Tous les composés absorbent grâce aux vibrations de valence $C-O$, éthérées. Ainsi, la bande de vibration ν_{C-O} antisymétrique apparaît à 1250 cm^{-1}, et la bande symétrique à 1160 cm^{-1}.

Les bandes d'absorption dues à la vibration γ_{C-H}, qui apparaissent dans la région 900—700 cm^{-1}, diffèrent quant à leur nombre et position du fait que les composés synthétisés contiennent en même temps des noyaux benzéniques à nombre variable de substituants.

La bande située à 810 ± 15 cm^{-1}, présente dans les spectres de tous les composés, à été attribuée aux noyaux aromatiques *para*-disubstitués centraux. Outre cette bande, il y a d'autres qui correspondent aux noyaux périphériques mono-, di- et trisubstitués. Par exemple le 4,4'-di(benzylthio)-diphényléther présente la bande intense de 810 cm^{-1}, mais aussi deux autres bandes à 700 cm^{-1} et 770 cm^{-1}, caractéristiques des noyaux aromatiques monosubstitués. Une bande à 700 cm^{-1} se trouve également dans le spectre du composé à noyaux *méta*-disubstitués.

Les composés qui contiennent des noyaux aromatiques trisubstitués asymétriques présentent la bande γ_{C-H} des deux atomes de hydrogènes adjacents à 825 cm^{-1}, presque commune avec celle due aux noyaux aromatiques *para*-disubstitués de 810 cm^{-1}, aussi bien que la bande de vibration de l'atome de l'hydrogène isolé à 870—885 cm^{-1}, d'intensité moyenne.

Ces bandes ont été mises en corrélation avec les harmoniques et leurs bandes de combinaison qui sont situées dans la région 2000—1660 cm^{-1}. Elles ont une intensité faible, c'est pourquoi les spectres ont été effectués sur des pastilles ayant une concentration trois fois supérieure.

Dans le spectre du 4,4'-di(benzylthio)diphényléther il y a dans cette région 4 bandes à 1950 cm^{-1}, 1870 cm^{-1}, 1800 cm^{-1} et 1750 cm^{-1}.

Dans le cas des composés qui ne contiennent que de noyaux *para*-disubstitués il y a deux bandes à 1940 cm^{-1} et 1870 cm^{-1}, caractéristiques de ces noyaux.

Les composés qui contiennent des noyaux *para*-disubstitués (centraux), aussi bien que des noyaux *méta*-disubstitués ou trisubstitués, périphériques, présentent dans cette région un nombre accru de bandes.

L'oxydation des thio-éthers chez les sulfones est marquée par l'apparition, dans le spectre I.R. de la bande due à la vibration de valence ν_{SO_2} antisymétrique, à 1310 cm^{-1} très intense et par l'apparition de la bande due à la vibration de valence ν_{SO_2} symétrique à 1145 cm^{-1} (tabl. 4).

TABLEAU 4

Les absorptions I.R. des bissulfonyl-éthers

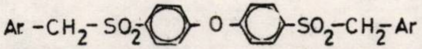

Ar –CH$_2$– SO$_2$–C$_6$H$_4$–O–C$_6$H$_4$–SO$_2$–CH$_2$–Ar

N°. crt.	Ar	Nombre d'onde cm^{-1}							
		ν_{C-H}	$\nu_{CH_3 asym.}$	$\nu_{CH_2 asym.}$	$\nu_{CH_2 sym.}$	$\nu_{C \cdots C}$	$\nu_{C-O\ asym.}$	$\nu_{C-O sym.}$ $\nu_{SO_2 sym.}$	$\nu_{SO_2 asym.}$
1	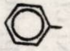	3090 3060 3030	—	2930	—	1580 1480	1260	1145	1310
2	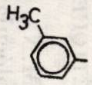	3090 3060 3030	2960	2930	2855	1580 1480	1250	1147	1310
3	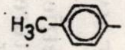	3090 3060 3030	2960	2926	2855	1580 1485	1250	1147	1310
4	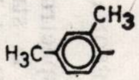	3085 3060 3025	2950	2926	2855	1580 1485	1250	1147	1310
5	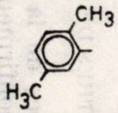	3080 3060 3030	2950	2926	2855	1580 1485	1250	1147	1310
6	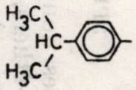	3090 3065 3030	2965	2930	2865	1575 1465	1245	1145	1310
7	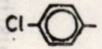	3090 3065 3030	—	2926	2855	1580 1480	1245	1150	1310

SPECTRES ÉLECTRONIQUES

Les composés synthétisés absorbent dans l'U.V. grâce aux transitions d'électrons caractéristiques des noyaux benzéniques substitués.

Chez les thio-éthers, la bande du type B (benzénoïde) est située à 266 nm (tableau 1) puisque déplacée par rapport à la bande du benzène monosubstitué (254 nm). La substitution du noyaux benzénique périphérique avec des radicaux méthyle a un faible effet batochrome, surtout dans le cas de la double substitution.

Un déplacement similaire est constaté également dans le cas de la substitution avec du chlore.

La transformation des thio-éthers dans des sulfones est accompagnée d'un puissant effet hypsochrome et en conséquence les sulfones absorbent à 249—250 nm (tableaux 1 et 2).

Pour mettre en évidence le déplacement hypsochrome, nous avons représenté, dans la figure 1, les spectres U.V. de 4,4'-di(benzylthio)-diphényléther et de 4,4'-di(benzylsulfonyl)-diphényléther.

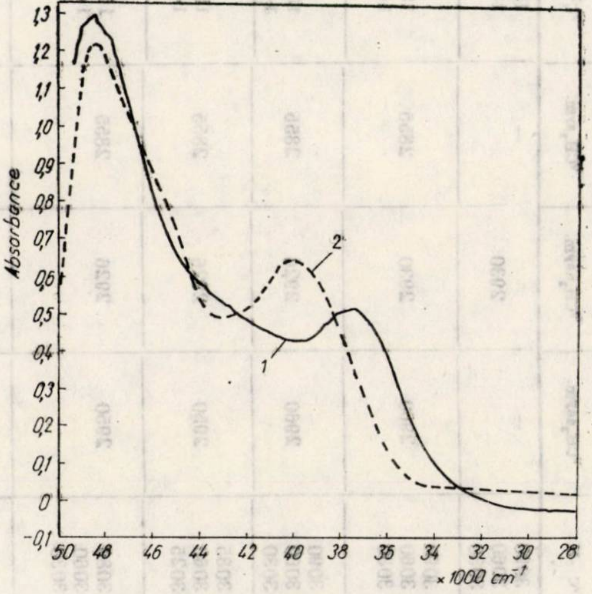

Fig. 1. — Les spectres en U.V. du :
1. 4,4'-di(benzylthio)-diphényléther ;
2. 4,4'-di(benzylsulfonyle)-diphényléther.

SPECTRES DE RÉSONANCE MAGNÉTIQUE NUCLÉAIRE

Les données de la spectrométrie R.M.N., appliquées à des étherbisthio-éthers, confirment la structure moléculaire déduite des données chimiques et spectrales I.R. et U.V.

Le tableau 5 comprend les déplacements chimiques, la multiplicité et l'attribution des signes du spectre aux protons du 4,4'-di(*p*-isopropylbenzylthio)-diphényléther.

Le doublet centré à 1,19 ppm est attribué aux groupements CH_3 des radicaux isopropyle qui ont les protons bien écranés dont l'épine est couplée avec l'épine du proton voisin appartenant au C tertiaire. Ce dernier est un peu plus désécrané, raison pour laquelle le centre du multiplet dû à l'accouplement avec les apines des protons voisins, appartenant aux groupements méthyle, se trouve à 2,90 ppm.

TABLEAU 5

Spectre R.M.N. du 4,4'-di (*p*-isopropylbenzylthio)-diphényléther

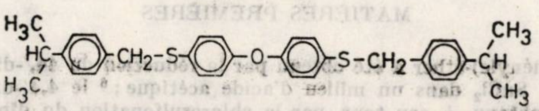

δppm	Signal	Intégration	Attribution
1,19	doublet	12	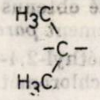
2,90	multiplet	2	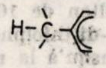
4,04	singlet	4	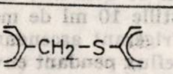
6,88	doublet	4	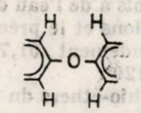
7,19	singlet	8	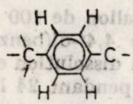
7,25	doublet	4	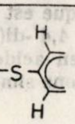

Pour les groupements CH_2 désécranés par la contiguïté du soufre et des anneaux aromatiques, on obtient un signal à 4,04 ppm.

Il y a, dans la molécule, deux types de noyaux benzéniques. Les noyaux benzéniques situés aux extrémités de la molécule, étant substitués avec des substituants alkyliques, émettent un singlet à 7,19 ppm.

Les noyaux benzéniques centraux, étant substitués de manières différentes, émettent des signaux à valeurs différentes du δ pour les protons de la contiguïté de l'oxygène (doublet à 6,88 ppm) et pour les protons de la contiguïté du soufre (à 7,25 ppm). A la suite des accouplements épine-épine, les deux signaux se trouvent en tant que doublet.

LA PARTIE EXPÉRIMENTALE

MATIÈRES PREMIÈRES

Le di(*p*-thiolphényle)-éther a été obtenu par la réduction du 44,'-disulfonylchlorure-diphényléther avec du $SnCl_2$ dans un milieu d'acide acétique ; [6] le 4,4'-disulfonylchlorure du diphényléther a été obtenu, à son tour, par la chlorosulfonation du diphényléther (produit commercial Riedel). [7]

Le chlorure de benzyle est un produit commercial Fluka. Le *p*-chlorbenzylchlorure est un produit commercial Merck. Le 1-chlorméthyl-3-méthylbenzène et le 1-chlorméthyl-4-méthyl-benzène ont été obtenus par la chloruration photochimique avec du chlorure de sulfuryle de *méta-*, respectivement *para-*xylène.

Le 1-chlorméthyl-2,4-diméthylbenzène et le 1-chlorméthyl-2,5-diméthylbenzène ont été obtenus par la chlorométhylation de *méta-* et respectivement *para-*xylène.

La synthèse du 4,4'-di(benzylthio)-diphényléther.

Dans un ballon de 100 ml muni d'un réfrigérant ascendant, sont introduits 2,34 g (0,01 moles) de 4,4'-di(thiolphényl)-éther, 0,8 g (2.0,01 moles) de NaOH et 20 ml d'éthanol, on chauffe à reflux jusqu'à la réaction complète du dithiol avec de l'hydroxyde de sodium. On ajoute 5 ml de benzène, on remplace le réfrigérant ascendant par un réfrigérant descendant et on distille 10 ml de mélange azéotrope ternaire (eau-éthanol-benzène). On monte à nouveau le réfrigérant ascendant et on ajoute 3,22 g (2.0,01 moles) de chlorure de benzyle. On chauffe à reflux pendant environ 4 heures, après quoi on refroidit et on filtre sur un filtre à plaque synthérisée de glace sur le vacuum. On lave en petites portions à un ml d'éthanol, ensuite plusieurs fois à de l'eau distillée (environ 3—4 ml). On ajoute de nouveau 2 ml d'éthanol en petites portions et le précipité est mis à sécher. Il résulte 3,6 g de 4,4'-di(benzylthio)-diphényléther. Rendement 91,7%. P.f. 124—125°. Après la recristallisation en alcool-benzène (1 : 1). P.f. 129°.

Les autres thio-éthers du tableau 1 ont été obtenus en conditions similaires.

La synthèse du 4,4'-di(benzylsulfonyl)-diphényléther.

Dans un ballon de 100 ml muni d'un réfrigerant ascendant, ont été introduits 2,07 g (0,005 moles) de 4,4'-di(benzylthio)-diphényléther et 50 ml d'acide acétique glacial. On chauffe jusqu'à la dissolution et on ajoute 20 ml de H_2O_2 30%. Après un reflux de 2 heures on laisse reposer pendant 24 heures.

L'acide acétique est écarté par distillation. La résidu est repris avec de l'eau et filtré. Il résulte 1,17 g de 4,4'-di(benzylsulfonyl)-diphényléther. Rendement 72,1%. P.f. 233° (Après la recristallisation en acide acétique P.f. = 249°). Les autres sulfones de la table 2 ont été obtenues en conditions similaires.

*

La détermination du soufre a été effectuée d'après Kasterina. [8] Les spectres I.R. ont été exécutés avec un spectrophotomètre Specord-75, Carl Zeiss-Jena, en utilisant la technique du pastillage avec du KBr.

Les spectres U.V. ont été exécutés avec un spectrographe Specord UV-Vis Carl Zeiss-Jena, pour des solutions en éthanol.

Les spectres R.M.N. ont été exécutés avec un appareil Varian A60A.

CONCLUSIONS

Nous avons synthétisé 7-éthers-bisthio-éthers d'une nouvelle classe, qui ont été oxydés aux sulfones correspondantes.

La pureté et la structure moléculaire des nouveaux composés ont été vérifiées à l'aide de l'analyse élémentaire quantitative et de la spectrométrie de I.R., U.V. et R.M.N.

BIBLIOGRAPHIE

[1] M. Iovu et A. Angelescu, *Rev. Roumaine Chim.*, **18**, 263 (1973).
[2] M. Iovu et A. Angelescu, *Rev. Roumaine Chim.* **19**, 1061 (1974).
[3] R. L. Schriner, H. G. Struck et W. Jorison, *J. Amer. Chem. Soc.*, **52**, 2060 (1930).
[4] H. Brintzinger, H. Schmahl et H. Witte, *Chem. Ber.*, **85**, 338 (1952).
[5] L. F. Sonnabend, brevet U.S. 3,338,976 ; *Chem. Abstr.*, **67**, 99850 (1967).
[6] C. M. Suter, *J. Amer. Chem. Soc.*, **13**, 1112 (1936).
[7] C. M. Suter, *J. Amer. Chem. Soc.* **58**, 54 (1936).
[8] T. N. Kasterina et L. S. Kalinina, « Analiza chimică a rășinilor sintetice și a materialelor plastice », Ed. tehnică, București, 1965, p. 42.

Revue Roumaine de Chimie, 26, 8, 1161–1167 (1981)

ACTION OF HYDRAZINES, AMINES AND THIOUREA UPON β(4-CHLORO-3-METHYL)-BENZOYLACRYLIC ACID

M. El-KADI, M. A. El-HASHASH and M. A. SAYED
Chemistry Department, Faculty of Science, Ain Shams University, Abbassia, Cairo, Egypt

Received May 16, 1980

β-Aroylacrylic acid 1 reacts with thiourea to give methyl thiazole 2a, and with hydrazine-hydrate, phenylhydrazine and/or hydroxylamine to give thiazolodihydropyridazine 3, phenylhydrazone 4 and thiazolo-oxazine 5 respectively. Compound 1 reacts with amines or hydrazines to give α-alkylamino β-aroylpropionic acid 6 and the corresponding hydrazones 8 and 10 respectively.

Previously,[1] it has been reported that thiourea reacts with ethyl-β-benzoylacrylate to give 2-amino-4-ethoxy-5-benzoyl-methylthiazole. This prompted us to extend the study of the behaviour of the olefinic double bond in β-aroylacrylic acid towards the same reagent. β-(4-Chloro-3-methyl)benzoylacrylic acid (**1**) reacts with thiourea and gives 2-amino-4-hydroxy-5(4′-chloro-3′-methylbenzoyl)methylthiazole **2a**.

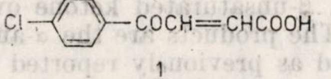

1

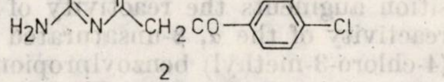

2

a, R=H **b**, R=$COCH_3$

The infrared spectrum of **2** shows well defined absorption bands attributable to ν(OH) and ν(NH) groups at 3350 and 3100 cm^{-1}, the carbonyl group band at 1690 cm^{-1} and ν(C = N) of the thiazole at 1600 cm^{-1}.[2,3] Compound **2a** gave a 4-acetoxy derivative **2b** on boiling with acetic anhydride. The IR spectrum of the acetoxy derivative exhibits absorptions at 1760 cm^{-1} and 1220 cm^{-1} attributable to stretching frequencies of ν(C = O) and ν(C—O) respectively.

Furthermore, the reaction of thiazole **2a** with hydrazines and hydroxylamine was investigated. In this way, polynuclear systems containing a thiazole ring fused with another heterocyclic ring are usually formed.[4] Condensation of **2a** with hydrazinehydrate in boiling alcohol gave thiazolodihydropyridazine derivative **3**. The infrared spectrum of **3** is characterized by strong absorptions at 3330 cm^{-1} due to ν(NH) (secondary); 3450 cm^{-1} ν(NH) (primary), 1670 cm^{-1} and 1620 cm^{-1} attributable to ν_{max} of two —C = N groups.

On the other hand, the reaction of **2a** with phenylhydrazine in warm acetic acid affected condensation with the carbonyl group with formation of the corresponding phenylhydrazone **4** without cyclization, due to the steric factor of phenyl group. Condensation of **2a** with hydroxylamine hydrochloride in alcoholic sodium hydroxide affected condensation with the carbonyl group and subsequent ring closure yielding the thiazolo-oxazine derivative **5**. The infrared spectrum of **5** shows well defined absorption bands attributed to ν(C = N) of thiazole at 1670 cm^{-1}, ν(C = N) of oxime at 1610 cm^{-1} and ν(NH) at 3440 cm^{-1} (primary).

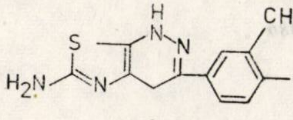

3

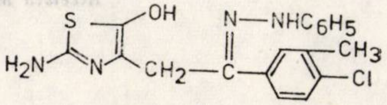

4

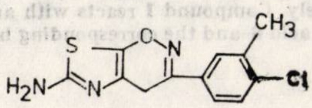

5

Reaction with amines. Several workers have investigated the addition of amines to the olefinic double bond in β-benzoylacrylic acids. Some workers [2,3] reported that the products are the corresponding β-amino-β-benzoylpropionic acids, but other investigators [5-7] reported that the products are the α-amino-β-benzoylpropionic acids. The present investigation deals with the behaviour of the β-(4-chloro-3-methyl)benzoylacrylic acid (**1**) towards the action of amines in which the chlorine atom in 4-position augments the reactivity of the α, β-unsaturated ketone over the reactivity of the α, β-unsaturated acid. The products are the α-amino-β-(4-chloro-3-methyl) benzoylpropionic acid as previously reported [5-7] and not β-amino-derivatives. The addition of the amine occurred alpha to the carboxyl group in these instances, the polarization of the double bond by the ketone group strongly outweighed that exhibited by the carboxyl group, i.e. α-carbon atom accepted the nucleophiles more readily than β-carbon. Thus, acid **1** resembles α, β-unsaturated ketones in its mode of addition.

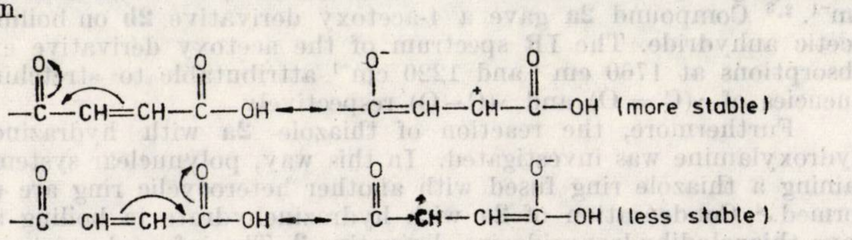

$$-\overset{O}{\overset{\|}{C}}-CH{=}CH-\overset{O}{\overset{\|}{C}}-OH \longleftrightarrow -\overset{O^-}{\overset{|}{C}}{=}CH-\overset{+}{C}H-\overset{O}{\overset{\|}{C}}-OH \quad \text{(more stable)}$$

$$-\overset{O}{\overset{\|}{C}}-CH{=}CH-\overset{O}{\overset{\|}{C}}-OH \longleftrightarrow -\overset{O}{\overset{\|}{C}}-\overset{+}{C}H-CH{=}\overset{O^-}{\overset{|}{C}}-OH \quad \text{(less stable)}$$

The treatment of benzene solution of acid **1** with amines, namely: piperidine, morpholine, 2-aminopyridine, aniline, benzylamine, *m*-chloroaniline, *p*-toluidine, *o*-anisidine 5-chloro-*o*-toluidine and 3,4-xylidine yielded the α-alkylamino-β-(4-chloro-3-methyl)-benzoyl propionic acids **6a** — **j** respectively. The infrared spectra of **6a** and **6b** show strong absorption bands in the region 1680 cm^{-1} and 1685 cm^{-1} attributable to ν(C = O) of aroylketone with other band in the region of 1610 — 1618 cm^{-1} which evidently stand for stretching frequencies of the carboxylate anion. The IR spectrum of **6d** shows well defined absorption bands at 1682 cm^{-1}, 1615 cm^{-1} attributable to ν_{max} of two carbonyl groups and another band at 3350 cm^{-1} due to ν(NH).

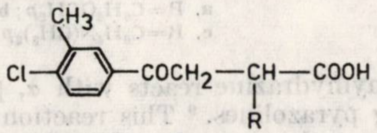

6

R = **a** NC_5H_{10}, **b** NC_4H_8O, **c** NHC_5H_4N-2, **d** NHC_6H_5, **e** $NHCH_2C_6H_5$, **f** NHC_6H_4Cl-*m*, **g** $NHC_6H_4CH_3$-*p*, **h** $NHC_6H_4OCH_3$-*o*, **i** $NHC_6H_3(Cl, CH_3)$5,2 **j** $NHC_6H_3(CH_3)_2$-3,4

The α-(*o*-anisyl)amino-β-(4-chloro-3-methyl)benzoyl propionic acid **(6h)** on treatment with ethyl chloroacetate in the presence of anhydrous potassium carbonate and dry acetone yields ethoxy-carbonyl methyl α(*o*-anisyl)amino-β-(4-chloro-3-methyl)benzoyl propionate (**7**). The IR spectrum of **7** shows well defined absorption bands at 1735 cm^{-1}, 1720 cm^{-1} attributable to ν_{max} of two carbonyl groups of ester, at 1680 cm^{-1} due to ν(CO) and another band at 3340 cm^{-1} due to ν(NH).

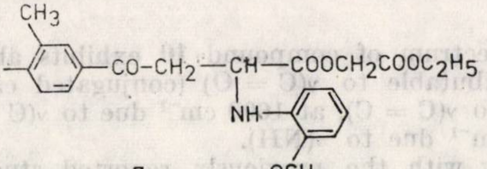

7

Reaction with hydrazines. Previously it was reported [8] that β-benzoyl-α-methylacrylic acid gives 2,3-dihydro-4-methyl-3-oxo-6-phenylhydrazine when heated for two hours with hydrazine sulphate in sodium hydroxide. The present investigation deals also with the behaviour of β(4-chloro-3-methyl)-benzoylacrylic acid **(1)** towards the action of hydrazines. Thus, the acid **1** reacts with hydrazinehydrate in warm alcohol and yields the corresponding hydrazone **8**. This is due to the deactivation effect caused by chlorine atom in our acid. The structure of the hydrazone **8** was inferred from the following data

a) IR-Spectrum of **8** shows strong absorptions at 1700 cm^{-1} due to ν(C = O), at 1640 cm^{-1} due to ν(C = N) and a broad band at 3420 cm^{-1}, attributable to ν(NH).

b) Chemically, the compound **8** condenses with aldehydes, namely : anisaldehyde, salicylaldehyde and N,N-dimethyl-*p*-aminobenzaldehyde yielding the corresponding arylidene-amino hydrazone **9a**, **9b** and **9c** respectively. The infrared spectra of the compound **9** lack the ν(NH) stretching frequency.

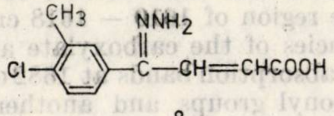

8

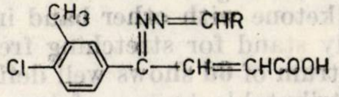

9

a, $R=C_6H_4OCH_3p$; **b**, $R=C_6H_4OH\text{-}o$
c, $R=C_6H_4N(CH_3)_2p$

In general, phenylhydrazine reacts with α, β-unsaturated carbonyl compounds producing pyrazolines.[9] This reaction has now been applied to **1**. The product is not the expected pyrazoline but the corresponding phenylhydrazone without the ring closure. This may be due to the smaller reactivity of the olefinic double bond in **1** than in unsaturated ketones. Thus, condensation of **1** with phenylhydrazine in acetic acid at room temperature gave the phenylhydrazone **10**. The phenylhydrazone **10** does not give the colour test of pyrazolines.[10]

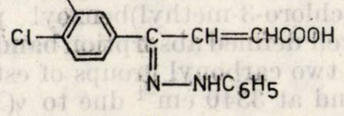

10

The IR-spectrum of compound **10** exhibits absorption bands at 1685 cm^{-1}, attributable to ν(C = O) (conjugated carbonyl group), at 1620 cm^{-1}, due to ν(C = C), at 1600 cm^{-1} due to ν(C = N) and a broad band at 3330 cm^{-1} due to ν(NH).

By analogy with the previously reported studies,[4] the phenylhydrazone **10** was obtained by the reaction of the α-morpholino-β(4-chloro-3-methyl)benzoyl propionic acid **(6b)** with phenylhydrazine in glacial acetic acid with elimination of the morpholino group.

EXPERIMENTAL

The infrared absorption spectra were determined with an Unicam SP 1200 Spectrophotometer using KBr wafer technique. All melting points are not corrected.

Reaction of β-(4-chloro-3-methyl) benzoylacrylic acid (1) with thiourea ; Formation of thiazole 2a

A mixture of **1** (0.01 mole), thiourea (0.02 mole), and ethanol (15 ml) was treated with 10 drops of glacial acetic acid. The mixture was then refluxed for 4 hrs. The solid separated after evaporation of the most of the solvent and cooling, was crystallized from acetic acid to give the 2-amino-4-hydroxy-5-(4-chloro-3-methylbenzoyl)methylthiazole **(2a)**, m.p. 235°C, yield 90%. Found : C, 50.20 ; H, 4.00 ; N, 10.20 ; S, 11.50 ; $C_{12}H_{11}ClN_2O_2S$ req. : C, 50.43 ; H, 3.85 ; N, 9.80 ; S, 11.20%.

Acetylation of 2a ; Formation of 2b

A solution of **2a** (2g) in acetic anhydride (15 ml) was heated for 2 hrs. on the water-bath. The cooled solution was poured into ice and the solid separated was crystallized from *n*-butanol to give the acetyl derivative **2b**, m.p. 227°C, yield 52 %.

Found : C, 52.10 ; H, 4.30 ; N, 8.80 ; $C_{14}H_{13}ClN_2O_3S$ req. : C, 51.77 ; H, 4.00 ; N, 8.62 %.

Condensation of 2a with hydrazine hydrate ; Formation of thiazolodihydropyridazine derivative 3

A solution of the thiazole **2a** (0.01 mole) in ethanol (20 ml) was treated with hydrazine hydrate (2 ml ; 85 %), and the solution was refluxed for 3 hrs. The solid that separated after cooling was crystallized from acetic acid to give the corresponding thiazolodihydropyridazine derivative, **3**, m.p.> 238°C, yield 60 %.

Found : C, 51.40 ; H, 3.80 ; S, 10.49 ; $C_{12}H_{11}ClN_4S$ req. : C, 51.70 ; H, 3.94 ; S, 11.49 %.

Reaction of 2a with phenylhydrazine ; Formation of phenylhydrazone 4

A solution of **2a** (0.01 mole) in glacial acetic acid was heated with phenylhydrazine (0.01 mole). The solution was heated on water-bath for one hr. and then left at room temperature for 12 hrs. The solution was poured into ice and the solid separated was crystallized from light petroleum (b.p. 100—120°C) to give the colourless phenylhydrazone **4**, m.p.134°C, yield 80 %.

Found : C, 58.10 ; H, 4.80 ; N, 14.30 ; $C_{18}H_{17}ClN_4OS$ req. : C, 57.52 ; H, 4.52 ; N, 14.91 %.

Reaction of 2a with hydroxylamine hydrochloride ; Formation of thiazolo-oxazine derivative 5

To a solution of **2a** (0.01 mole) in ethanol and a solution of sodium hydroxide (0.02 mole) in water, 15 ml hydroxylamine hydrochloride were added. The cooled mixture was shaken for one hour then left overnight. The solid separated was crystallized from ethanol to give the thiazolo-oxazine derivative **5** as colourless crystals, m.p. above 236°C, yield 70 %.

Found : C, 51.70 ; H, 3.20 ; N, 11.66 ; $C_{12}H_{10}ClN_3OS$ req.: C, 51.52 ; H, 3.57 ; N, 11.06 %.

Reaction of β-aroylacrylic acid 1 with amines ; Formation of α-alkylamino-β-(4-chloro-3-methyl) benzoylpropionic acids (6a — 6j)

To a solution of β-aroylacrylic acid **1** (0.01 mole) in benzene (100 ml) the appropriate amines were added, namely : piperidine, morpholine, 2-aminopyridine, aniline, benzylamine, *m*-chloroaniline, *p*-toluidine, *o*-anisidine, 5-chloro-*o*-toluidine and 3,4-xylidine (0.02 mole). After standing at room temperature (10—30 min) the separated products were crystallized from a suitable solvent to give the α-alkylamino-β-aroylpropionic acids (**6a— 6j**) respectively, as colourless crystals, yield 90 — 95 %. The results are listed in table 1.

Action of ethyl chloroacetate on 6h ; Formation of 7

To a solution of the α(*o*-anisyl)amino-β-(4-chloro-3-methyl)-benzoylpropionic acid **(6H)** (0.01 mole) in acetone (100 ml), ethyl chloroacetate (0.01 mole) and 5 g anhydrous potassium carbonate were added. The mixture was heated on water-bath for 72 hrs. The acetone was evaporated and the solid was poured into water, the solid separated was crystallized from light petrol (60 — 80°C) to give the ethoxy carbonyl methyl α(*o*-anisyl)amino-β-(4-chloro-3-methyl) benzoylpropionic acid (**7**), m.p. 106°C, yield 52 %.

Found : C, 60.90 ; H, 5.60 ; N, 3.50 ; $C_{22}H_{23}ClNO_6$ req. : C, 61.04 ; H, 5.31 ; N, 3.23 %.

Reaction of β(4-chloro-3-methyl)benzoylacrylic acid (1) with hydrazinehydrate ; Formation of the corresponding hydrazone 8

A hot solution of the β-aroylacrylic acid **1** (0.01 mole) in ethanol (20 ml) was treated with hydrazinehydrate (0.02 mole). The exothermic reaction was allowed to run its course.

TABLE 1

α-Alkylamino-β-aroylpropionic acids **6a**—**6j**

Compd.	m.p. (°C)	Solvent*	Formula	Analysis % Found	Analysis % Requd.
6a	121	T	$C_{16}H_{12}ClNO_3$	C 62.20 H 6.30 N 4.10	62.03 6.46 4.52
6b	156	E	$C_{15}H_{18}ClNO_4$	C 58.10 H 5.40 N 5.10	57.78 5.77 4.49
6c	230	T	$C_{16}H_{15}ClN_2O_3$	C 60.60 H 4.50 N 8.90	60.28 4.70 8.79
6d	197	P	$C_{17}H_{16}ClNO_3$	C 64.60 H 5.10 N 4.60	64.25 5.03 4.40
6e	>235	B	$C_{18}H_{18}ClNO_3$	C 64.90 H 5.70 N 3.80	65.15 5.42 4.22
6f	129	T	$C_{17}H_{15}Cl_2NO_3$	C 57.60 H 4.60 N 4.30	57.95 4.26 3.97
6g	141	B	$C_{18}H_{18}ClNO_3$	C 65.30 H 5.10 N 4.40	65.15 5.42 4.22
6h	183	B	$C_{18}H_{18}ClNO_4$	C 61.80 H 5.30 N 3.70	62.15 5.17 4.02
6i	143	B	$C_{18}H_{17}Cl_2NO_3$	C 59.40 H 4.30 N 4.10	59.01 4.64 3.82
6j	217	P	$C_{19}H_{20}ClNO_3$	C 66.20 H 5.40 N 3.90	65.99 5.78 4.05

*T = Toluene ; E = Ethanol ; P = Light petrol (b. p. 80 — 100°C) ; B = Benzene

The crystals separated were crystallized from ethanol to give the hydrazone **8**, m.p. above 237°C, yield 50 %.

Found : C, 55.60 ; H, 4.30 ; N, 12.00 ; $C_{11}H_{11}ClN_2O_2$ req. : C, 55.34 ; H, 4.61 ; N, 11.74 %.

Condensation of hydrazone 8 with aldehydes ; Formation of arylidene amino hydrazone 9a — 9c

A suspension of hydrazone **8** (0.005 mole) in ethanol (10 ml) was treated with aldehydes,, namely ; anisaldehyde, salicyaldehyde and N,N-dimethyl-*p*-aminobenzaldehyde (0.01 mole), and the mixture was refluxed for one hr. The crystals separated after cooling were recrystallized from a suitable solvent to give the corresponding arylidene aminohydrazone **9a** — **9c**, yields 50 — 60 %. The results are listed in table 2.

TABLE 2

Arylidene amino hydrazones **9a** — **9c**

Compd.	m.p. (°C) Colour	Solvent*	Formula	Analysis %		
					Found	Requd.
9a	232 Colourless	T	$C_{19}H_{17}ClN_2O_3$	C	64.10	63.95
				H	4.60	4.76
				N	8.20	7.85
9b	211 Yellowish	E	$C_{18}H_{15}ClN_2O_3$	C	63.40	63.06
				H	4.50	4.37
				N	8.30	8.17
9c	242 Reddish-brown	P	$C_{20}H_{20}ClN_3O_2$	C	65.10	64.95
				H	5.30	5.41
				N	11.70	11.36

*T = Toluene ; E = Ethanol ; P = Light petrol (b. p. 80 – 100°C).

Reaction of β-(4-chloro-3-methyl)benzoylacrylic acid (1) with phenylhydrazine ; Formation of phenylhydrazone 10

To a solution of β-aroylacrylic acid **1** (0.01 mole) in glacial acetic acid (20 ml) phenylhydrazine (0.02 mole) was added. A voluminous light yellow precipitate separated immediately which soon redissolved after standing at room temperature for 24 hrs. The reaction mixture was poured into ice and the solid separated was crystallised from benzene to give the phenylhydrazone **10** as yellow crystals, m.p. 190°C, yield 90 %.

Found : C, 65.10 ; H, 4.30 ; N, 9.30 ; $C_{17}H_{15}ClN_2O_2$ req. : C, 64.86 ; H, 4.76 ; N, 8.90 %.

Reaction of α-morpholino-β-(4-chloro-3-methyl)benzoyl propionic acid (6b) with phenylhydrazine ; Formation of 10

To a solution of **6b** (0.005 mole) in glacial acetic acid (10 ml), phenylhydrazine (0.01 mole) was added and after a treatment similar to that mentioned above, yellow crystals separated from benzene and were identified as phenylhydrazone **10** by melting point and mixed melting point determination.

REFERENCES

[1] R. Delaby, S. Danton, and P. Chabrier, *Bull. Soc. chim. France, 1961,* 2061 ; *Chem. Abstr.*, **56**, 14157 (1962).

[2] R. Moreau, and C. Dumant, *Compt. rend.*, **250**, 2383 (1960) ; *Chem. Abstr.*, **55**, 25843 (1961).

[3] J. Boughoult, and P. Chabrier, *Compt. rend.*, **230**, 212 (1950).

[4] A. Sammour, M. I. B. Selim, and E. A. Soliman *U.A.R. J. Chem.* **16**, 312 (1972).

[5] N. H. Cromwell, P. L. Crager and K. E. Cook, *J. Amer. Chem. Soc.*, **78**, 4412 (1956).

[6] N. H. Cromwell, and K. E. Cook, *J. Org. Chem.*, **23**, 1327 (1958).

[7] H. Kato, and M. Schiona, *Nippon Kagaku Zasshi*, **68**, 2274 (1957).

[8] S. Dixon, H. Gregory, and. L. F. Wiggins, *J. Chem. Soc.*, **1949**, 2139.

[9] A. Sammour, A. A. Afify, M. A. Hassan and A. R. Abdel Ghany, *Egypt J. Chem.*, **19**, 601 (1976).

[10] V. Knorr, *Liebigs Ann Chem.*, **238**, (1887).

Revue Roumaine de Chimie, 26, 8, 1169–1175 (1981)

THEORETICAL STUDY ON THE REGIOSELECTIVITY IN THE 1,3-DIPOLAR CYCLOADDITIONS OF PYRIDINIUM-YLIDES TO Z-SUBSTITUTED ALKENES

GH. SURPĂȚEANU *, M. CONSTANTINESCU **, C. LUCHIAN *,
M. PETROVANU *, I. ZUGRĂVESCU * and A. LABLACHE-COMBIER ***

* The Polytechnic "Gh. Asachi", Organic Chemistry Department, Jassy, 11, str. 23 August, Romania

** Computer Center of the University "Al. I. Cuza", Jassy, Romania

*** Physical Organic Chemistry Department, University of Lille, France

Received September 30, 1980

Perturbation and frontier orbital theories are applied to explain the regioselectivity of 1,3-dipolar cycloadditions of several pyridinium-ylides to Z-substituted alkenes. Molecular orbital calculations have been performed by CNDO/2 method. A survey of the molecular orbital parameters permitted the construction of the orbital correlation diagrams presented in Figs 1–4. Generally, the regioselectivity of 1,3-dipolar cycloadditions of pyridinium-ylides to the Z-substituted alkenes depends on the nature of both the addends. Theoretically, the first four ylides (Table 2) reacting with methyl acrylate and acrylonitrile give the cycloadducts of the type III, in agreement with the general accepted polarization of the dipoles and the double bond in the dipolarophiles. In the same cycloadditions, the ylides 7 and 8 (Table 2) give cycloadducts of the type IV.

The cycloimmonium-ylides participate in the 1,3-dipolar cycloadditions by their resonance structures Ib, which are 1,3-dipoles.$^{1-6}$

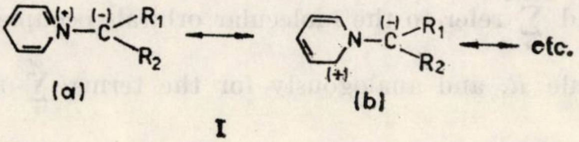

I

In the 1,3-dipolar cycloadditions of pyridinium-ylides to unsymmetrical alkenes, two regioisomers of type III and IV could be theoretically obtained :

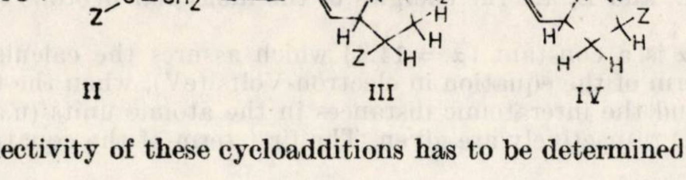

The regioselectivity of these cycloadditions has to be determined

The regioselectivity is controlled by the steric, electronical and orbital factors. There are many papers dealing with the influence of these factors on the regioselectivity. [7–10]

Moreover we present several aspects of the application of the frontier molecular orbital theory to the study of the regioselectivity.

Briefly, the regioselectivity of a cycloaddition could be predicted by the following sequence : 1) estimates the energies of the HOMO (the highest occupied molecular orbital) and the LUMO (the lowest unoccupied molecular orbital) of both components ; 2) identifies which HOMO/LUMO pair is closer in energy ; 3) using this HOMO/LUMO pair, estimates the relative size of the coefficients of the atomic orbitals on the atoms at which bonding is to take place ; 4) matches the larger coefficient on one component with the larger on the other. All these facts are the result of the "principle of narrowing the inter-frontier level separation" applied to the study of the chemical interactions. [11] The energy of the HOMO orbitals of the donor increases and the energy of the LUMO orbitals of the acceptor decreases versus the reaction co-ordinates.

Using the generalized perturbation theory of the second-order, Klopman [12] and Salem [13] proposed the following relation for the calculation of the interaction energy ΔE between two molecules R and S, by their two atoms k and l, respectively.

$$\Delta E = (q_a + q_b)\, \beta_{ab} S_{ab} + \frac{Q_k Q_l}{R_{kl} \cdot \varepsilon} \cdot \alpha - \left(\sum_{r}^{occ} \sum_{s}^{unocc} + \sum_{r}^{unocc} \sum_{s}^{occ} \right) \frac{2 (C_{ra} C_{sb} \beta_{ab})}{E_s \quad E_r} \qquad (1)$$

Equation (1) is adequate to the single side interactions between two shell systems.

— q_a and q_b are the electron populations in the atomic orbitals a and b beloging to the atoms k and l respectively ;

— β_{ab} and S_{ab} are the resonance and overlap integrals ;

— ε is the local dielectric constant ;

— $\sum_{r}^{occ}$ and $\sum_{r}^{unocc}$ refer to the molecular orbitals occupied and unoccupied in molecule R, and analogously for the terms $\sum_{s}^{occ}$ and $\sum_{s}^{unocc}$ in the molecule S ;

— Q_k and Q_l are the total charges on atoms k and l ;

— R_{kl} is the distance between the atoms k and l ;

— C_{ra} and C_{sb} are the coefficients of atomic orbitals a and b in the molecular orbitals r and s, where r refers to the molecular orbitals on one molecule and s refers to those on the other ;

— E_s and E_r are the energies of the molecular orbitals s and r respectively ;

— α is a constant ($\alpha = 14.4$) which assures the calculation of the second term of the equation in electron-Volts (eV), when the total atomic charges and the interatomic distances in the atomic units (u.a) and angströms (Å) respectively are given. The first term of the equation is a closed-shell repulsion term, the second term is a Coulombic repulsion (or attraction) term, and the third term is called variously the delocalization, overlap, or charge-transfer stabilization. This last term is the second-order perturbation term and is true only if $E_s \neq E_r$; it represents the interaction of all the filled orbitals with all the unfilled ones. (When $E_s \approx E_r$, the interaction is better described in charge-transfer terms, and the perturbation is then a first-order one of the form $2C_{ra}C_{sb}\beta_{ab}$). Here the interaction HOMO-LUMO is most important.

To summarize, we can see that the frontier molecular orbitals (HOMO and LUMO) are important from the energetic viewpoint and they are the stereodirecting orbitals which permit to establish stereochemistry of chemical reactions.

RESULTS AND DISCUSSION

In order to apply the frontier molecular orbital theory to the study of the regioselectivity in the cycloaddition reactions of pyridinium-ylides to Z-substituted alkenes, we calculated the molecular orbital (MO) energies, the total atomic charges and the coefficients of the atomic orbitals (AO). The calculations reported here were carried out by CNDO/2 method [14] adapted by us on a Felix C–256 computer.

In table 1 there are presented the 1,3-ylide-dipoles and the dipolarophiles taken into account in our investigation and the total atomic charges of the atoms participating in cycloadditions.

TABLE 1

The total atomic charges

No.	Compound	Total atomic charges		
	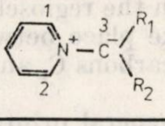	Q_{C_1}	Q_{C_2}	Q_{C_3}
1	$R_1 = H$; $R_2 = CN$	−0.0008	−0.0002	−0.2238
2	$R_1 = R_2 = CN$	+0.0118	+0.0118	−0.3823
3	$R_1 = H$; $R_2 = CO_2CH_3$	−0.0042	+0.0246	−0.2710
4	$R_1 = R_2 = CO_2CH_3$	+0.0190	+0.0478	−0.3672
5	$R_1 = H$; $R_2 = COC_6H_5$	−0.0015	+0.0181	−0.2246
6	$R_1 = H$; $R_2 = COCH_3$	+0.0147	−0.0143	−0.2875
	$\overset{1}{C}H_2 = \overset{2}{C}H-R$	Q_{C_1}	Q_{C_2}	
7	$R = CN$	−0.0306	+0.0622	
8	$R = CO_2CH_3$	+0.0163	−0.0724	

Carbons C_1 and C_2 in pyridinium-ylides, have small positive or negative charges and the difference between them is insignificant.

The pyridinium-ylides geometry considered in the calculations was previously presented. [15-17] The ylide carbon C_3 and the cyclic carbons

C_1 and C_2 in ylide molecules are approximately in the same plane. The geometry of the two dipolarophiles was already described. [18,19]

Table 2 gives the frontier orbital energies and the p_z atomic orbital coefficients of the carbons C_1, C_2 and C_3 of pyridinium-ylides and of the atoms C_1 and C_2 of dipolarophiles. In table 2 the same parameters for two nitrile oxides [8] are also shown.

Huisgen and Christl [20] show that the nitrile oxide V reacts with the methyl acrylate VII to give only one regioisomer of the type VIII ($R = H$). The acetonitrile oxide VI in the same reaction gives two regioisomers VIII ($R = CH_3$) 94.9% and IX ($R = CH_3$) 5.1%.

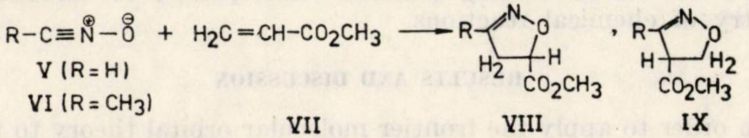

These experimental results permit to estimate that, despite the general accepted molecular polarization, the regioisomers of the type VIII are the major reaction products.

In other words, in such cycloadditions the electrostatic term of the equation (1) is insignificant because the total atomic charges on the atoms involved in the reaction are small. Usually, in these conditions, the orbital factors play the main role in the determination of the regioselectivity.

In pyridinium-ylides the ylide carbons are negatively charged and the carbons C_1 and C_2 in dipolarophiles have small negative or positive charges. Even in these reactions we can appreciate that the orbital factors play a dominant role. The values of the atomic orbital coefficients of the atoms C_1 and C_2 in ylides are very closed, and so we shall refer only to the atom C_1 in the next discussion on the regioselectivity.

We think that the cycloadditions take place between the p_z orbitals of 1,3 dipoles and the p_z orbitals of the carbons C_1 and C_2 in dipolarophiles.

Theoretically, we can construct two general orbital corelation diagrams :

(i) a diagram (Fig. 1), in which the cycloadditions are HOMO-controlled in respect to the pyridinium-ylides **1**–**4** (Table 2).

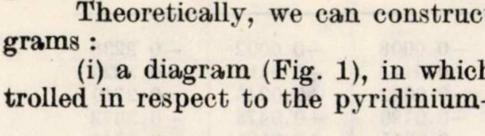

Fig. 1. — The orbital correlation diagrams between HOMO and LUMO orbitals of pyridinium-ylides **1**–**4** and dipolarophiles **9**, **10** (Table 2), respectively. ○ sign (+) ; ▨ sign (−).

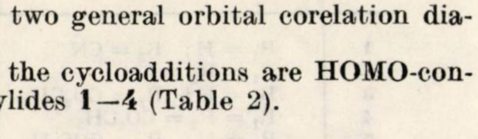

Fig. 2. — The orbital correlation diagrams between HOMO and LUMO orbitals of the compounds **5**–**8** and dipolarophiles **9**, **10** (Table 2) respectively. ○ sign (+) ; ▨ sign (−).

(ii) a diagram (Fig. 2), in which the cycloadditions are HOMO-controlled as well in respect to the dipoles (compounds **5**–**8** in Table 2).

The regioselectivity of the cycloadditions from figure 1 is in agreement with the general accepted polarization of the 1,3 dipole in ylides and the polarization of double bond in the Z-substituted alkenes. In these cycloadditions, cycloadducts of the type III are obtained.

TABLE 2

The frontier orbital energies and the p_z atomic orbital coefficients

No.	Compound	Frontier orbital	Orbital energy (eV)	Atomic orbital coefficients		
	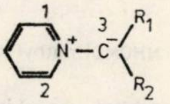			C_{C_1}	C_{C_2}	C_{C_3}
1	$R_1 = H$; $R_2 = CN$	HOMO	−8.52186	0.3264	0.3248	−0.7120
		LUMO	1.72130	0.3015	0.3013	0.3475
2	$R_1 = R_2 = CN$	HOMO	−10.37667	0.2600	0.2600	−0.6274
		LUMO	−1.66241	0.4200	0.4200	0.2986
3	$R_1 = H$; $R_2 = CO_2CH_3$	HOMO	−8.80487	0.3086	0.3116	−0.7252
		LUMO	1.89203	0.2777	0.3216	0.2685
4	$R_1 = R_2 = CO_2CH_3$	HOMO	−10.36980	0.2434	0.2435	−0.6411
		LUMO	0.29018	−0.4063	−0.4062	−0.2048
5	$R_1 = H$; $R_2 = COC_6H_5$	HOMO	−8.94658	−0.2979	−0.2963	0.6618
		LUMO	1.13297	−0.3133	−0.3628	−0.1917
6	$R_1 = H$; $R_2 = COCH_3$	HOMO	−8.79171	−0.3111	−0.3086	0.7271
		LUMO	2.04585	0.3575	0.2800	0.2542
	RCNO			C_C	C_O	
7	$R = H$	HOMO	−12.8950	−0.5600	0.802	
		LUMO	4.1330	0.6770	0.298	
8	$R = CH_3$	HOMO	−11.9540	−0.5240	0.764	
		LUMO	4.0520	0.6040	0.284	
	$\overset{1}{CH_2} = \overset{2}{CH}-R$			C_{C_1}	C_{C_2}	
9	$R = CN$	HOMO	−14.11488	0	0	
		LUMO	3.50279	−0.6531	−0.5241	
		NHOMO	−14.33695	−0.6046	−0.4934	
		NLUMO	4.03385	0	0	
10	$R = CO_2CH_3$	HOMO	−13.55033	0	0	
		LUMO	2.77134	−0.6194	0.4286	
		NHOMO	−13.81001	0.3708	0.2859	
		NLUMO	6.87399	0	0	

According to the regioselectivity of the cycloadditions inferred from figure 2, one obtains cycloadducts of the type IV despite the general polarizations of the atoms involved in these reactions.

The previously presented diagrams are energetically favoured because they involve the lowest energy differences between the frontier orbitals.

This paper presents two more orbital correlation diagrams allowed from the theoretical viewpoint (Figs 3 and 4).

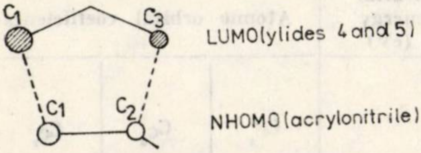

Fig. 3. — The orbital correlation diagrams between LUMO and HOMO orbitals of ylides, **4**, **5** and acrylonitrile respectively. ▨ sign (−).

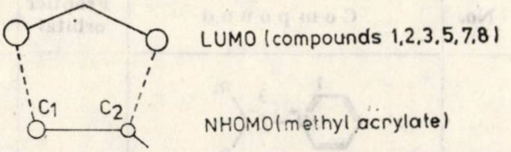

Fig. 4. — The orbital correlation diagrams between LUMO and NHOMO orbitals of compounds **1**, **2**, **3**, **5**, **7**, **8** and methyl acrylate, respectively. ○ sign (+).

As the atomic orbital coefficient values of the atoms C_1 and C_2 in the dipolarophiles **9** and **10** are zero, table 2 shows their values for the next highest occupied molecular orbital (NHOMO). These values lead to the diagrams of figures 3 and 4.

It is to be mentioned that only the reaction between nitrile oxide **VI** and methyl acrylate provided a small quantity of cycloadduct of the type **IX**. A survey of the cycloaddition reactions of nitrile oxides to methyl acrylate allows us to consider that it is a good agreement between the experimental and theoretical results.

A brief analysis of the orbital correlation diagrams of the cycloadditions of pyridinium-ylides to methyl acrylate or acrylonitrile (Figs 1 and 2), shows that in such reactions two types of regioisomers **III** and **IV** could be obtained. The structure of the ylides and the dipolarophiles plays the dominant role. The first four ylides in table 2, having cyano or carbomethoxy groups bonded to the ylide carbon, must form the cycloadducts of the type **III** according to the correlation diagram presented in figure 1. Ylides **5** and **6** having the acyle groups bonded to the ylide carbon, must form the cycloadducts of the type **IV**, according to the correlation diagram in figure 2.

Finally, it can be pointed out that it is difficult to establish a general rule on the regioselectivity of these cycloadditions in the case of pyridinium-ylides and the Z-substituted alkenes. It is necessary to construct the orbital correlation diagrams for each ylide-dipolarophile pair.

REFERENCES

[1] R. Huisgen, *Angew. Chem.*, **75**, 604 (1963).
[2] T. Sasaki, K. Kanematsu and Y. Yokimoto, *J. Chem. Soc.*, **1970**, 481.
[3] V. Boekelheide and N. A. Fedoruk, *J. Amer. Chem. Soc.*, **90**, 3830 (1968).
[4] L. Zirngible, *Tetrahedron Letters*, **1971**, 4189.
[5] M. Petrovanu, C. Luchian, Gh. Surpățeanu and V. Bărboiu, *Rev. Roumaine Chim.*, **24**, 1053 (1979).

[6] W. Friedrich, H. Kehr, F. Kröhnke and P. Schiller, *Chem. Ber.*, **98**, 3808 (1965).

[7] J. Fleming, "Frontier Orbitals and Organic Chemical Reactions", Wiley, London, 1976.

[8] K. N. Houk, J. Sims, R. E. Duke, Jr., R. W. Storzier and John K. George, *J. Amer. Chem. Soc.*, **95**, 7287 (1973).

[9] K. N. Houk, J. Sims, C. R. Watts and L. J. Luskus, *J. Amer. Chem. Soc.*, **95**, 7301 (1973).

[10] J. Bastide and O. Henri Rousseau, *Bull. Soc. chim. France*, **1974**, 1037.

[11] K. Fukui, "Theory of Orientation and Stereoselection" vol. 2, Springer Verlag, Berlin, 1975.

[12] G. Klopman, *J. Amer. Chem. Soc.*, **90**, 223 (1968).

[13] L. Salem, *J. Amer. Chem. Soc.*, **90**, 543 (1968)

[14] J. A. Pople and D. L. Beveridge, "Approximate Molecular Orbital Theory", McGraw-Hill, New York, 1970, QCPE 141.

[15] Gh. Surpăţeanu, J. P. Catteau, P. Karafiloglu and A. Lablache-Combier, *Tetrahedron*, **32**, 2647 (1976).

[16] Gh. Surpăţeanu, M. Constantinescu and I. Zugrăvescu, *Rev. Roumaine Chim.*, **23**, 1449 (1978).

[17] I. Zugrăvescu, M. Constantinescu, Gh. Surpăţeanu, A. Lablache Combier and L. Devos, *Rev. Roumaine Chim.*, **24**, 1089 (1979).

[18] W. S. Wilox, J. H. Goldstein and J. W. Simmons, *J. Chem. Phys.*, **22**, 516 (1954).

[19] J. S. Rollett, *Acta Cryst.*, **8**, 487 (1955).

[20] M. Christl and R. Huisgen, *Chem. Ber.*, **106**, 3345 (1973).

Revue Roumaine de Chimie **26**, *8*, 1177–1184 (1981)

LA RÉACTIVITÉ DU VERT DE MALACHITE SUBSTITUE, DANS LA RÉACTION AVEC L'ANION TÉTRACHLOROAURIQUE

GH. CONSTANTINESCU et CECILIA CONSTANTINESCU
Institut Polytechnique, Str. Polizu, 1, Bucarest, Roumanie

Reçu le 31 mars 1980

On a étudié l'influence des substituants métoxy et nitro placés en position *ortho- méta* ou *para* face de l'atome central de carbone dans la molécule de vert de malachite en réaction avec l'anion tétrachloroaurique. Les combinaisons ainsi obtenues ont été précipitées, ensuite extraites en benzène. Les meilleurs résultats ont été obtenus avec le réactif vert de paranitral, extractibilité d'environ 98%, $\varepsilon = 100\,000$ entre 0,2–0,8μg Au$\cdot$ml^{-1} à 657 nm. Les résultats s'expliquent bien par la participation des électrons π du substituant au système conjugué du réactif.

The influence of the metoxy- or nitro- substituent in *ortho-*, *meta-* or *para-* position of the central atom of malachite green in reaction with $H[AuCl_4]$ is studied. The obtained combinations were precipitated and/or extracted in benzene. The best results are obtained for the reagent *para-* Nitralgreen : extractibility above 98%, $\varepsilon = 100\,000$ between 0.2 and 8.0 μg Au$\cdot$ml^{-1} by 657 nm. The results are well explained through the participation of π electrons to delocalised system of the reagent.

Parmi les techniques modernes d'extraction des métaux se trouvent celles basées sur la formation de complexes organo-métalliques dans la phase aqueuse suivie par extraction liquide-liquide dans un solvant organique.

On a étudié particulièrement les réactions de l'anion tétrachloroaurique avec les colorants triphénylméthaniques de la classe du vert de malachite, réactions qui conduisent à la formation d'associations ioniques. On avait pour but deux importantes applications pratiques : l'extraction du métal et le dosage quantitatif de l'anion complexe.

Les conditions de réaction et surtout le pH de la solution aqueuse, la forme cationique sous laquelle se trouve le colorant dans la solution aqueuse, ainsi que le rapport de combinaison entre l'anion métallique et le cation organique sont les principaux problèmes qui doivent être d'abord étudiés. Dans ce but nous avons utilisé l'analyse élémentaire des combinaisons obtenues et l'étude analytique thermodifférentielle et on a comparé les résultats avec ceux obtenus dans l'étude spéctrophotométrique et conductimétrique des solutions organiques.

Les colorants choisis connus dans la littérature [1] sont : le vert de malachite et ses dérivés avec des groupes attrayants d'électrons comme $-NO_2$ ou des groupes répulsifs comme $-OCH_3$ en différentes positions face de l'atome de carbone central. Ces colorants sont assez faciles à préparer et bon marché.

PARTIE EXPÉRIMENTALE

Les réactifs étudiés sont les suivants :

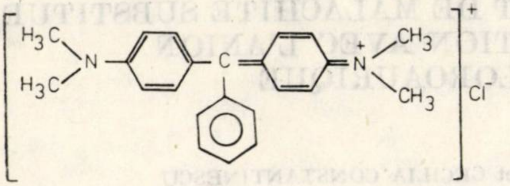
H₃C
N
H₃C
C
CH₃
N
CH₃
Cl

vert de malachite (étalon) **VM**

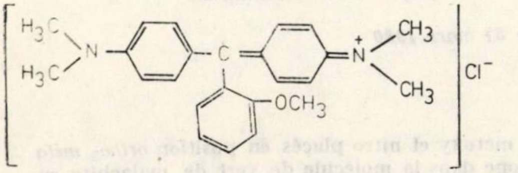
H₃C
N
H₃C
C
CH₃
N
CH₃
Cl⁻
OCH₃

vert d'*ortho*-anisidine ***o*-VA**

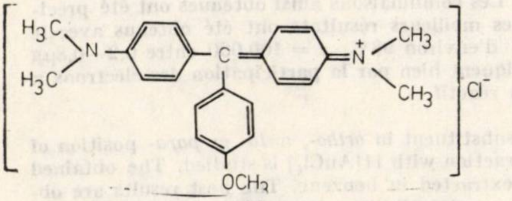
H₃C
N
H₃C
C
CH₃
N
CH₃
Cl⁻
OCH₃

vert de *para*-anisidine ***p*-VA**

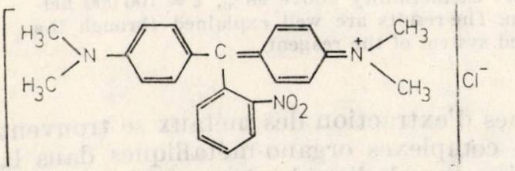
H₃C
N
H₃C
C
CH₃
N
CH₃
Cl⁻
NO₂

vert d'*ortho*-nitral ***o*-VN**

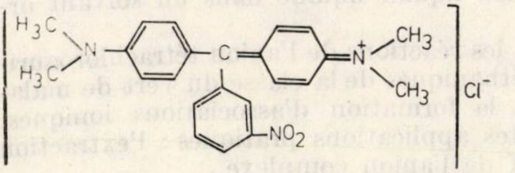
H₃C
N
H₃C
CH₃
N
CH₃
Cl⁻
NO₂

vert de *méta*-nitral ***m*-VN**

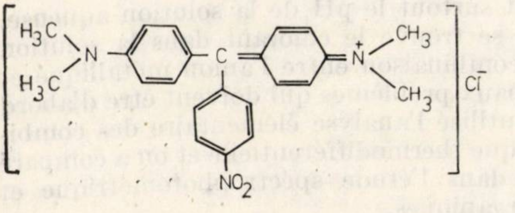
H₃C
N
H₃C
C
CH₃
N
CH₃
Cl⁻
NO₂

vert de *para*-nitral ***p*-VN**

SYNTHÈSE DES COLORANTS

Pour la synthèse des colorants on a employé la diméthylaniline et l'aldéhyde correspondant à chaque colorant : l'aldéhyde benzoïque, l'*ortho*-anisidine, *para*-anisidine, les aldéhydes *ortho-méta-* et *para*-nitrobenzoïques.

La condensation a été conduite de manière classique au bain-marie suivie d'un entraînement à vapeurs d'eau. Le résidu est dissous en alcool éthylique, la leucobase est précipitée et ensuite oxydée à dioxyde de plomb (noir) pour l'obtention du carbinol, lequel forme avec l'acide chlorhydrique le colorant respectif : [1]

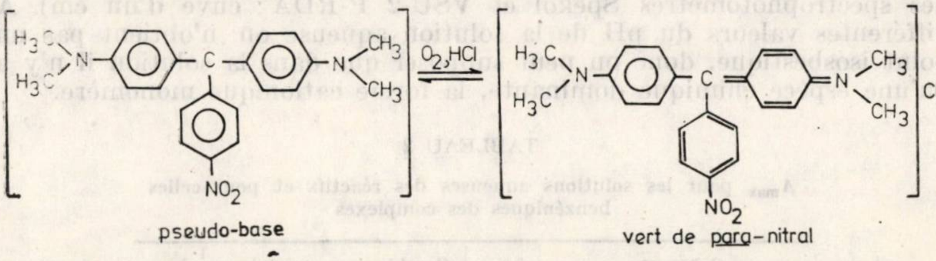

Les colorants obtenus ont été soumis à une purification par recristallisation de l'alcool éthylique. Leur pureté a été déterminée par la méthode du dichromate de potassium. [2] Les chromatogrammes à papier avec mélange d'alcool-méthylique-eau ont montré des compositions unitaires.

La solution aqueuse d'or ($c = 197\ \mu g\ Au.cm^{-3}$) a été préparée à partir de l'H $[Au\ Cl_4]$ (Merck) en ajoutant de l'acide chlorhydrique. Le titre a été déterminé par la méthode semi-micro volumétrique de Chow et Beamish. [3]

L'extraction des complexes a été opérée dans une ampoule à décanter ou dans un Erlenmayer. Dans ce but on a réalisé un volume de 10 ml de solution aqueuse avec de $l'H[AuCl_4]$ 1.10^{-4} m, HCl 6 n, H_2O bidistillée et d'une solution aqueuse de 1.10^{-3} m de colorant. On ajoute ensuite 10 ml de benzène.

L'équilibre entre les deux phases liquides est atteint après une agitation énergique (mécanique) pendant 1—2 minutes.

Dans le même intervalle de temps et de la même manière on prépare les essais à blanc.

RÉSULTATS ET DISCUSSIONS

Pour détérminer le coefficient de distribution et l'extractibilité des complexes on a conduit les extractions de la manière décrite et on a dosé les quantités d'or dans la solution benzénique amenée à sec (en y ajoutant de $l'H_2SO_4$ conc.) et aussi dans la solution aqueuse. Pour comparaison on a choisi la méthode spectrophotométrique à Rhodamine B. [4] Les résultats sont présentés dans la tableau 1.

TABLEAU 1

L'extraction de combinaisons complexes

Combinaison complexe	Coefficient de distribution, D	E% par une extraction
$(VM)^+[AuCl_4]^-$	5,29	84,20
$(o\text{-}VA)^+[AuCl_4]^-$	8,51	89,73
$(p\text{-}VA)^+[AuCl_4]^-$	8,68	90,36
$(o\text{-}VN)^+[AuCl_4]^-$	11,01	98,21
$(m\text{-}VN)^+[AuCl_4]^-$	10,58	91,50
$(p\text{-}VN)^+[AuCl_4]^-$	11,00	98,00

On suppose généralement que l'extraction est d'autant plus facile que les complexes sont plus stables.

Dans le tableau 2 on donne les longueurs d'onde pour lesquelles l'absorbance A passe par un maximum pour les solutions aqueuses de colorants purs et pour les solutions benzéniques d'associations ioniques.[5,6] A ces longueurs d'onde on a fait des dosages spectrophotométriques (avec des spectrophotomètres Spekol et VSU-2 P-RDA ; cuve d'un cm). A différentes valeurs du pH de la solution aqueuse on n'obtient pas un point isosbestique, donc on peut supposer que dans la solution il n'y a qu'une espèce chimique dominante, la forme cationique monomère.

TABLEAU 2

A_{max} pour les solutions aqueuses des réactifs et pour celles benzéniques des complexes

Colorant (solution aqueuse)	λ_{max} nm	Combinaison complexe (solution benzénique)	λ_{max} nm
Vert de malachite	620	$(VM)^+[AuCl_4]^-$	635
Vert de l'*ortho*-anisidine	606	$(o\text{-}VA)^+[AuCl_4]^-$	623
Vert de *para*-anisidine	606	$(p\text{-}VA)^+[AuCl_4]^-$	625
Vert de l'*ortho*-nitral	635	$(o\text{-}VN)^+[AuCl_4]^-$	645
Vert de *meta*-nitral	637	$(m\text{-}VN)^+[AuCl_4]^-$	650
Vert de *para*-nitral	640	$(p\text{-}VN)^+[AuCl_4]^-$	657

On a examiné aussi la capacité d'extraction d'autres solvants et aussi des mélanges de benzène avec des cétones, alcools ou éther. Les résultats sont présentés dans le tableau 3.

TABLEAU 3

Absorbances *A* en divers solvants

Solvant	$(VM)^+[AuCl_4]^-$ à 635 nm	$(o\text{-}VN)^+[AuCl_4]^-$ à 623 nm	$(p\text{-}VN)^+[AuCl_4]^-$ 625 nm	$(o\text{-}VA)^+[AuCl_4]^-$ à 645 nm	$(p\text{-}VA)^+[AuCl_4]^-$ à 657 nm
Benzène	0,34	0,82	0,84	0,69	0,71
Benzène-éther éthylique 2 : 1	0,14	0,08	0,10	6,16	0,17
Benzène-méthanol 2 :1	0,20	0,23	0,21	0,12	0,12
Benzène-éthanol 2 :1	0,16	0,28	0,25	0,18	0,18
Benzène-cyclohexanol 2 : 1	0,24	0,31	0,32	0,20	0,24
Benzène-acétone 3 : 1	0,12	0,26	0,25	0,28	0,30
Benzène-cyclohexanol 3 : 1	0,6	0,42	0,44	0,40	0,42
Benzène-méthyléthyl-cétone 4 : 1	0,28	0,63	0,70	0,38	0,42
Benzène-méthyléthyl-cétone 6 : 1	0,35	0,70	0,74	0,52	0,54
Benzène-méthyléthyl-cétone 8″1	0,38	0,88	0,90	0,73	0,77

Les mélanges benzène-méthyléthylcétone donnent de meilleurs résultats, mais ont l'incovénient d'extraire aussi le colorant libre. On a travaillé ensuite seulement avec des solutions à benzène.

La concentration molaire du réactif (colorant) en phase aqueuse, déterminée chaque fois pour que l'équilibre

$$H^+[AuCl_4]^- + (\text{col. basique})^+Cl^- \rightleftharpoons (\text{col. basique})^+ [AuCl_4]^- + H^+Cl^-$$

soit déplacé à droite, doit être au minimum 10 fois supérieure à celle stœquiométrique.

Le pH de la solution aqueuse exerce une grande influence sur les espèces existant dans la solution aqueuse. [7] En comparaison du vert de malachite qui a un maximum d'absorption prononcé à 0,15 n(HCl), les autres colorants étudiés ont des domaines plus larges de pH où l'absorption se maintient constante, en général entre 0,6 et 1,5 n (HCl). [8,9] Les acidités optimales ont été maintenues à tous les essais.

En utilisant la méthode de la variation continue de Job [10] et des solutions isomolaires on a déterminé les rapports de combinaison entre $H[AuCl_4]^-$ et les cations des colorants. Dans tous les cas le résultat a été le même 1 : 1. Un seul groupe $-NR_2$ des colorants réagit cationiquement, résultat qui concorde avec d'autres recherches. [7] Des associations ioniques $(R)^+[AuCl_4]^-$ sont donc formées où R^+ est le cation du colorant basique étudié.

Pour que les réactions soient applicables aux études spectrophotométriques on a aussi déterminé les limites de concentration dans lesquelles la loi de Lambert-Beer reste valable. Dans le tableau 4 sont donnés les résultats.

TABLEAU 4

Validité de la loi de Lambert-Beer et les coefficients molaires d'extinction

Combinaison	μg Au/cm³	ε
$(VM)^+[AuCl_4]^-$	10,0—100,0	5 700
$(o\text{-}VA)^+[AuCl_4]^-$	2,0— 10,0	37 500
$(p\text{-}VA)^+[AuCl_4]^-$	1,0— 12,0	55 000
$(o\text{-}VN)^+[AuCl_4]^-$	0,6— 10,0	81 000
$(m\text{-}VN)^+[AuCl_4]^-$	3,0— 36,0	52 500
$(p\text{-}VN)^+[AuCl_4]^-$	0,2— 8,0	100 000

La stabilité des solutions organiques est très bonne ; en contact avec l'air et la lumière, la plus faible stabilité ont montré les solutions benzéniques du complexe à vert de malachite. (1/2 heure), suivie de celles de vert de *para*-nitral (4 heures). Les autres solutions sont extrêmement stables (100 heures).

La conductibilité électrique des solutions benzéniques a été déterminée par comparaison avec celle du benzène pur et des épreuves à blanc (avec un appareil Megaohmmeter du type Tetralin Statron RDA). Les résultats présentés dans le tableau 5 ont conduit à la conclusion que les combinaisons se présentent sous forme d'associations ioniques non ionisées.

TABLEAU 5

Conductibilité électrique de solutions benzéniques

	$\rho = \frac{1}{R} (\Omega \cdot cm)$	$\gamma = \frac{1}{\rho} (\Omega^{-1} cm^{-1})$
Benzène pur	$0,82 \cdot 10^{11}$	$1,22 \cdot 10^{-11}$
Essai à blanc	$0,33 \cdot 10^{8}$	$3,0 \cdot 10^{-8}$
$(VM)^+[AuCl_4]^-$	$0,15 \cdot 10^{7}$	$6,8 \cdot 10^{-7}$
$(o\text{-}VA)^+[AuCl_4]^-$	$0,23 \cdot 10^{7}$	$0,46 \cdot 10^{-7}$
$(p\text{-}VA)^+[AuCl_4]^-$	$0,82 \cdot 10^{7}$	$1,25 \cdot 10^{-7}$
$(o\text{-}VN)^+[AuCl_4[^-$	$0,34 \cdot 10^{7}$	$3,0 \cdot 10^{-7}$
$(m\text{-}VN)^+[AuCl_4]^-$	$0,23 \cdot 10^{7}$	$4,4 \cdot 10^{-7}$
$(p\text{-}VN)^+[AuCl_4]^-$	$0,68 \cdot 10^{7}$	$1,5 \cdot 10^{-7}$

Pour obtenir le rapport molaire de combinaison en phase solide entre l'anion complexe et le cation du colorant, on a traité 0,025 g Au dissous dans 10 ml de solution chlorhydrique à la normalité optimale demandée par l'extraction liquide-liquide, avec 0,6 g de colorant dissous dans 25 ml de H_2O. On obtient un précipité vert bleuâtre en utilisant les colorants de l'anisidine et vert dans le cas des colorants *o*-, *m*, et *p*-nitral. Après le lavage à l'eau, on a dosé la teneur en or, [3] azote et chlore. [11,12] Les résultats sont présentés dans la tableau 6. On constate un rapport molaire de combinaison métal-colorant de 1 : 1.

TABLEAU 6

Analyse élémentaire des combinaisons complexes solides

Combinaison	Au%		N%		Cl%	
	calc.	dosé	calc.	dosé	calc.	dosé
$(VM)^+[AuCl_4]^-$	29,49	29,38	4,19	4,23	21,25	21,18
$(o\text{-}VA)^+[AuCl_4]^-$	28,22	28,28	4,25	2,21	20,31	20,36
$(o\text{-}VA)^+[AuCl_4]^-$	27,63	27,51	5,89	5,95	19,77	19,65
$(p\text{-}VN)^+[AuCl_4]^-$	27,63	27,04	5,89	5,79	19,77	19,20

La destruction thermo-oxydative des colorants et de leurs combinaisons avec $[AuCl_4]^-$ a été réalisée jusqu'à 900° avec un appareil du type MOM Budapest, à la vitesse de chauffage de 9°/mn dans 100 mn. Dans le tableau 7 on donne les étapes de la destruction thermique du colorant *ortho*-ansidine et son composé avec $[AuCl_4]$. Jusqu'à 350° le colorant est décomposé endothermiquement et à partir de 350° on constate un effet exothermique important dû à l'oxydation des produits de décomposition. A 620° le colorant est complètement détruit.

Le complexe solide avec du $[AuCl_4]^-$ montre un comportement analogue mais une autre répartition des pertes pendant la décomposition. L'effet exothermique remarqué à partir de 580° conduit ensuite probablement à l'Au_2O_3 qui rapporté à la quantité initiale concorde avec l'analyse élémentaire, c.-à-d., le rapport molaire de combinaison métal-colorant est toujours 1 : 1.

Les autres combinaisons ont un comportement identique.

TABLEAU 7

Destruction thermo-oxydative des produits

Composé	I		II		III		IV	
	°C	pertes %	°C	pertes %	°C	pertes %	°C	pertes %
o-VA (vert d'*ortho*-anisidine)	45—160	3	160—350	37	350—620	60	—	—
(*o*-VA) $[AuCl_4]^-$	45—160	4	160 350	9,5	350—580	52,2	580—900	1,1

Pour chaque réaction a été établié l'influence des ions gênants. Les ions V(V), Ge(IV), Mo(VI), Cu(II), Zn(II), Co(II), Ni(II) ne gênent pas, mais Tl(III), In(III), Ga(III), Bi(III), sont gênants par l'accroissement de l'absorption et le dosage doit être conduit en éliminant les ions gênants par les méthodes habituelles de la chimie analytique quantitative.

En ce qui concerne l'influence des substituants introduits dans la molécule de vert de malachite, les principales conclusions sont les suivantes :

— les colorants obtenus par substitution d'un atome d'hydrogène dans le cycle benzénique de la molécule de vert de malachite, quel que soit le substituant, ont une meilleure sensibilité et spécificité pour l'anion $[AuCl_4]^-$;

— l'introduction des groupes répulsifs d'électrons comme $-OCH_3$ conduit à des colorants qui réagissent brièvement et qui donnent des produits et des solutions benzéniques extrêmement stables, bien que la sensibilité de réaction ne soit pas exceptionnelle, mais la sélectivité s'accroît ;

— l'utilisation des groupes attrayants d'électrons comme le $-NO_2$ conduit à des colorants extrêmement sensibiles pour le $[AuCl_4]^-$ ayant une meilleure spécificité que la rhodamine B ou le violet de méthyle. [4,11] Cela s'explique bien par la participation, des électrons π du substituent au système conjugué du colorant (plus forte dans le cas de verte de l'*ortho*- et de *para*-nitral), comme ou peut constater dans les structures limite présentées sur les figures ci-dessus :

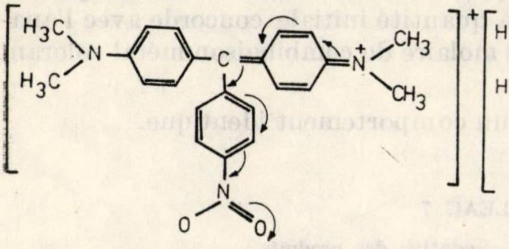

cas de vert de para-nitral

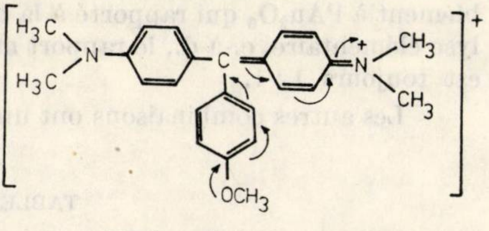

cas de vert de para-anisidine

REFERENCES

[1] C. Constantinescu, Thèse de doctorat, Univ. « Al. I. Cuza », Iaşi, Roumanie, 1974.
[2] R. P. Lastovschi et I. I. Vainstein, « Tekhnicheskii analiz v proizdvestvo promezhytochnykh i krasitelei », Tekhn. Izd. Khim. Lit., Moscova, 1958, p. 642.
[3] A. Chow et F. E. Beamish, *Talanta*, **10**, 883 (1963).
[4] H. Onishi, *Mikrochim, Acta*, **9**, p. 29 (1959).
[5] Gh. C. Constantinescu, *Bull. Inst. Pol.* Iaşi, **19** (**23**), Fasc 1—2, 109 (1973).
[6] Gh. C. Constantinescu *Rev. Roumaine Chim.*, **20**, 1267 (1975).
[7] O. F. Ginsburg et C. M. Zavlin, *Zhur. obshchei Khim.*, **32**, 3559 (1962).
[8] Gh. Constantinescu, *Rev. Roumaine Chim.*, **25**, 1249 (1980).
[9] Gh. C. Constantinescu, *Rev. Roumaine Chim.*, **25**, 1260 (1980).
[10] P. Job, *Ann. Chim. (France)*, **9**, 113 (1928).
[11] I. S. Lealicov, « Metode fizico-chimice de analiză », Editura tehnică, Bucureşti, 1961.
[12] N. H. Furman, « Standard Methods of Chemical Analysis », IIe Éd., Van Nostrand, New York, 1962—1963, p. 189.

Revue Roumaine de Chimie 26, 8, 1185–1193 (1981)

SYNTHESIS AND POLYMERIZATION OF POLYETHYLENE GLYCOL DIMETHACRYLATES. I.

STUDY OF SYNTHESIS PROCESS OF POLYETHYLENE GLYCOL DIMETHACRYLATES

GH. HUBCA, CR. OPRESCU, MARGARETA TOMESCU and M. DIMONIE
The Polytechnic, Laboratory of Macromolecular Technology, Calea Victoriei, no. 149,
Bucharest, Romania

Received February 10, 1981

The studies on the synthesis methods of polyethylene glycol dimethacrylates are comparatively presented. From the analysis of the results obtained, we reached the conclusion that the transesterification of methylmethacrylate with polyglycols is the most economical procedure. A detailed study on this synthesis method makes evident the main characteristic aspects of the transesterification reaction : secondary catalyst-inhibitor reactions ; influence of the polyglycol length and molar ratio of reagents on the transesterification rate ; influence of temperature on the purity of the products obtained.

INTRODUCTION

Polyetylene glycol dimethacrylates are the basic components of the anaerobic adhesive resins[1-4] which have been largely used in different fields of technology. [5]

The synthesis of these monomers can be achieved by one of the following procedures : [6,7]

1. Esterification of methacrylic acid with polyglycols

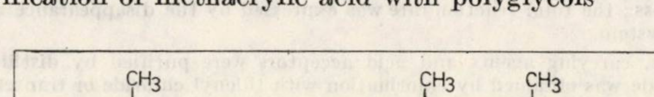

$$2CH_2=\underset{COOH}{\overset{CH_3}{C}} + HO-R-OH \rightleftharpoons CH_2=\underset{COO-R-OOC}{\overset{CH_3}{C}}\qquad\overset{CH_3}{C}=CH_2+2H_2O$$

2. Condensation of methacryloylchloride with polyglycols in the presence of an acid acceptor.

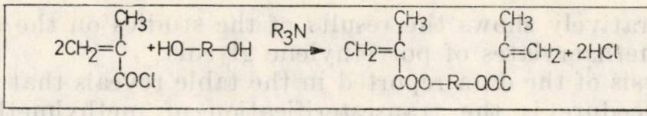

$$2CH_2=\underset{COCl}{\overset{CH_3}{C}} + HO-R-OH \xrightarrow{R_3N} CH_2=\underset{COO-R-OOC}{\overset{CH_3}{C}}\qquad\overset{CH_3}{C}=CH_2+2HCl$$

3. Transesterification of methyl methacrylate with polyglycols.

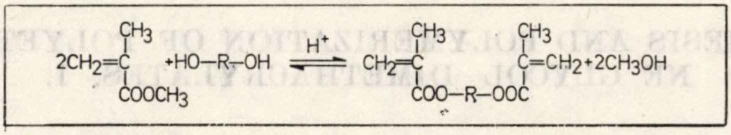

$$2CH_2=\underset{COOCH_3}{\overset{CH_3}{C}} + HO-R-OH \xrightleftharpoons{H^+} CH_2=\underset{COO-R-OOC}{\overset{CH_3}{C}}\!\!\!\!\quad\overset{CH_3}{C}=CH_2 + 2CH_3OH$$

The present paper reports on several aspects concerning the synthesis of ethylene dimethacrylate, diethylene glycol dimethacrylate, triethylene glycol dimethacrylate and tetraethylene glycol dimethacrylate by the above mentioned procedures, among which the transesterification of methyl methacrylate (MMA) with ethylene glycol (EG), diethylene glycol (DEG), triethylene glycol (TEG) and tetraethylene glycol (TTEG) holds an important place.

EXPERIMENTAL

The esterification of methacrylic acid with polyglycols was achieved in a glass sterilizer equipped with stirrer, bubbler for inert gas and device for recirculating the agent for removing water from the system and thermometer. The esterification reaction was performed at a molar ratio methacrylic acid : polyglycols = (2.5 – 3) ; volumetric ratio removing agent : reaction mixture = 0.5 – 1 ; in argon atmosphere, at a temperature of 80 – 120°C, in the presence of *p*-benzoquinone, phenothiazine or picric acid as inhibitors and sulfuric acid or *p*-toluenesulfonic acid as catalyst.

The resulted water was removed from the system by carrying with toluene, carbon tetrachloride or dichlorethane, the last ones being the best due to their complete and immediate separation from water. The recirculation device of the carrying agents differs as a function of its nature, due to the differences existing between water density and carrying agent.

The dosage of water in time allowed watching the kinetics of the esterification process.

The condensation of the methacryloylchloride with polyglycols took place in benzene medium at a molar ratio methacryloyl chloride : polyglycol = 2.5 : 1, methacryloyl chloride : acid acceptor = 1 : 1, at a temperature of 25 – 50°C. Pyridine, dimethylaniline or triethylamine were used as acid acceptors.

The transesterification of methylmethacrylate with polyglycols was effected in a glass sterilizer provided with stirrer, bubbler for inert gas, distillation column, thermometer and a device for dosig methylmethacrylate-methanol azeotrope resulted from the process.

The dosage in time of the methanol formed permitted watching the kinetics of the transesterification process ; the total reaction rate was expressed by the disappearance rate of the OH groups in the system.

The reagents, carrying agents and acid acceptors were purified by distillation, and methacryloyl chloride was obtained by chlorination with thionyl chloride or transchlorination with benzoyl chloride. The catalysts and inhibitors tested – pure chemical substances – were used as such.

The inert gas was set free of oxygen, by passing it over a copper catalyst (BTS) and then dried by passing it over potassium hydroxide, sulfuric acid and molecular sieves.

RESULTS AND DISCUSSIONS

Table 1 comparatively shows the results of the studies on the synthesis methods of dimethacrylates of polyethylene glycols.

The analysis of the data reported in the table reveals that the most economical procedure is the transesterification of methylmethacrylate

TABLE 1

Comparative results obtained on the synthesis procedures of polyethylene glycol dimethacrylates

	Esterification of methacrylic acid with polyglycols	Condensation of methacryloyl chloride with polyglycols	Transesterification of methylmethacrylate with polyglycols
1	2	3	4
Steps of the process	Esterification	Synthesis of methacryloyl chloride	Transesterification
	Neutralization and filtration	Condensation of methacryloyl chloride	Neutralization and filtration
	Distillation of carrying agent in the reaction mixture	Filtration of chlorhydrate	Distillation and recirculation of unreacted methylmethacrylate
	Recovery, purification and recirculation of methacrylic acid	Distillation and recirculation of benzene and unreacted methacryloyl chloride	Recovery of methylmethacrylate from azeotrope
	Purification and recirculation of carrying agent	Recovery and recirculation of amine used as acid acceptor	
Disadvantages	Slow recovery of unreacted methacrylic acid	Low yields at synthesis and recovery of methacryloyl chloride	Need of recovering methylmethacrylate from the azeotrope resulted from synthesis
	Need of using some large amounts of neutralization agents	Low yields at recovery of amine out of chlorhydrate	
	Wrong use of reactor capacity due to the introduction of removing agent	Need of using some reagents of high purity (complete lack of water)	
	Need of recovering and recirculating the solvent	Great number of phases	
	Slower reaction rate	High toxicity and strong corrosive character of chlorination agents, by-products resulted from chlorination, and methacryloyl chloride	
		High cost	
Advantages	Working in solvent the inhibition of the process is easier	Monomers of high purity are obtained	A few number of phases
		Condensation reaction takes place at low temperatures and problems concerning the inhibition of the process are not arisen	Unreacted methyl methacrylate distilled from the reaction mixture is of satisfying purity and is recirculated straight to the synthesis
			Easier processing of the reaction mass
			Low cost due to the use of polymethyl methacrylate waste
			High reaction rate

with polyglycols. That is why, a detailed study of this method is presented further down.

The transesterification of methylmethacrylate with polyglycols has the optimal rate at relatively high temperatures (~120°C) which cause a premature polymerization of the new formed monomer during synthesis. Due to this fact, the necessity of finding a suitable inhibitor becomes the main problem.

This inhibitor was found by testing a relatively large number of substances with inhibiting properties (more than 20). The main effects obtained are shown in table 2. The analysis of the results obtained points out that the largest part of the inhibitors is inefficient and the system polymerizes after a certain period of time.

TABLE 2

Influence of the inhibitor nature on the transesterification process of methylmethacrylate with diethyleneglycol

Molar ratio MMA : DEG = 5 :1, $t = 120$°C

Inhibitor	Conc.	Catalyst	The effect obtained expressed by the time after which the charge polymerization starts
Hydroquinone	1.0	H_2SO_4	2–3
p-Benzoquinone	2.0	H_2SO_4	6–7
p-Benzoquinone	1.0	$H_3C-C_6H_4SO_3H$	6–7
p-Benzoquinone	1.0	Na	Consumes the catalyst ; the reaction is limited to low conversions
p-*t*-Butylcatechol	1–2.5	H_2SO_4	3–5
Anthraquinone	1.7	H_2SO_4	1
2,6-di-t-Butyl-p-creosol	3.0	H_2SO_4	4–4.5
2,6-di-t-butyl-phenol	2.5	H_2SO_4	3.5–4
2,5-di-t-butyl-phenol	2.5	H_2SO_4	3–3.5
Methylene blue	1.65	H_2SO_4	Consumes the catalyst ; reaction is limited to low conversions
Methyl blue	1.0	H_2SO_4	2
Phenothiazine	1.0	H_2SO_4	Efficient but colours the product in dark green and it is difficult to be purified
Phenyl-naphtyl-amine	3.0	H_2SO_4	Consumes the catalyst ; reaction is limited to low conversions
Phenyl-naphthyl-amine	2.0	Na	Consumes the catalyst ; reaction is limited to low conversions
m-Dinitrobenzene	1.0	H_2SO_4	0.5
Picric acid	0.5–1	$CH_3C_6H_5SO_3H$	Highly efficient

The experiments performed for isolating the causes that generate the premature polymerization of the monomer during synthesis showed that they were due to the secondary reactions between inhibitor and catalyst. As a result of these reactions, inactive compounds appear as inhibitors and the system polymerizes, or as catalysts and the process is limited to small conversions.

When sulfuric acid was used as catalyst, sulfonation reactions (as in the case of hydroquinone, *p*-t-butylcatechol, 2,6-di-t-butyl-p-creosol, 2,6-di-t-butylphenol etc.) or reactions with some functional groups of inhibitors took place.

When using metallic sodium as catalyst, the share of the secondary reaction – catalyst-inhibitor – was larger. The low efficiency of the phenols substituted is also caused by the fact that they are efficient only in air, whereas in the presence of hydroquinone and p-benzoquinone they behave as retarders for methylmethacrylates.[8,9]

As a result of the researches undertaken on the inhibiting process of the system, picric acid[10] was found to be a highly efficient inhibitor (even in small concentrations in the system : 0.1–0.5%) when acid catalysts (H_2SO_4, *p*-toluenesulfonic acid) were used.

The high efficiency of the picric acid, as inhibitor, is due to the fact that it does not sulfonate in reaction conditions (the rate of the process is not influenced by the inhibitor concentration) (Fig. 1).

As seen in figure 2, small differences between the values of the transesterification rates appear at a conversion higher than 50%. This is probably due to the experimental errors that appear as a consequence of a smaller quantity of azeotrope formed and thus its more difficult elimination from the system.

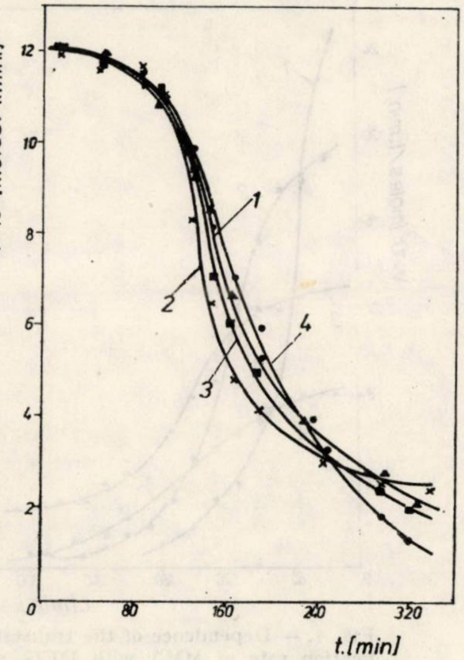

Fig. 1. – Variation of the transesterification rate of MMA with DEG in time as a function of the picric acid concentration. Molar ratio MMA : DEG = 5 : 1 ; $[H_2SO_4] = 1.7\%$; t = 120°C.
1 – 0.1% ; *2* – 0,25% ; *3* – 0.5% ; *4* – 2.8%.

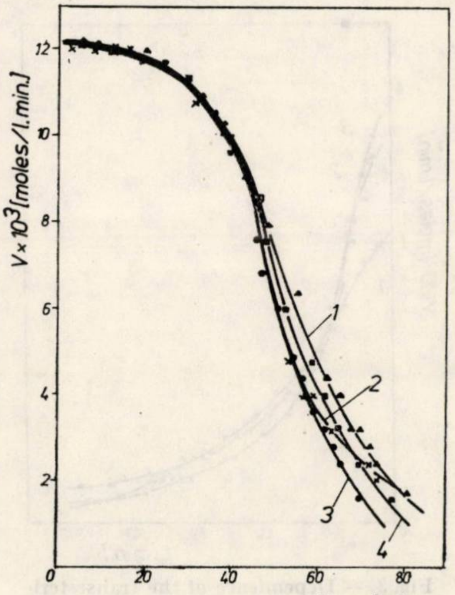

Fig. 2. – Dependence of the rate of transesterification reaction of MMA with DEG as a function of conversion, at different concentrations of picric acid.
Molar ratio MMA : DEG = 5 : 1 ; $[H_2SO_4] = 1.7\%$; t = 120°C.
1 – 0.1% ; *2* – 0.25% ; *3* – 0.5% ; *4* – 2.8%.

Transesterification reaction is a process that develops at equilibrium and that is the reason why an important role on the yield in diester is held by the molar ratio methylmethacrylate : polyglycol. The studies undertaken reveal that the molar ratio of reagents influences not only the shift of the chemical equilibrium but also the rate of the transesterification process. Figure 3 shows that the highest reaction rates are obtained at a molar ratio MMA : DEG = 6 : 1.

The attempts made to reduce the molar ratio of the reagents by introducing polyglycols in shares, did not give good results as, in that case, the rate of the process lowered and the reaction time got longer, a fact having an unfavourable influence on the system stability.

The nature of the catalyst influences the rate of the transesterification process and conversion. Both acid catalysts (perchloric acid, sulfuric acid, *p*-toluenesulfonic acid) and basic ones (metallic sodium) were used. The results obtained are given in figure 4.

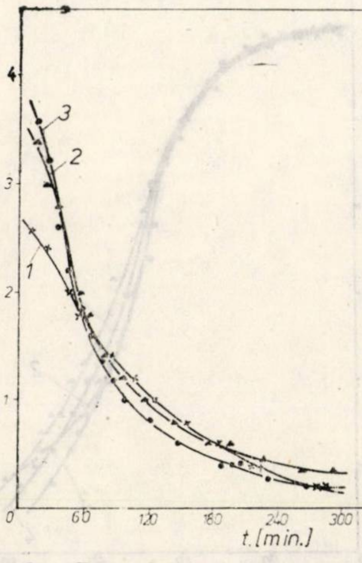

Fig. 3. — Dependence of the transesterification rate of MMA with DEG as a function of the molar ratio of reagents. $[H_2SO_4] = 2\%$; [Picric acid] = 1% ; t = 120°C.
1 — MMA/DEG = 4 : 1 ; *2* — MMA/DEG = 5 : 1 ; *3* — MMA/DEG = 6 : 1.

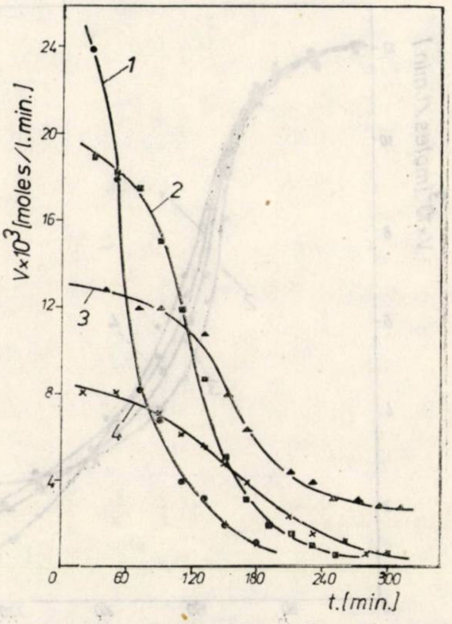

Fig. 4. — Dependence of the transesterification rate of MMA with DEG as a function of the catalyst nature.
Molar ratio MMA : DEG = 5 : 1, t = 120°C ; picric acid is used as inhibitor for acid catalyst and *p*-benzoquinone for metallic Na. *1* — metallic Na ; *2* — $HClO_4$; *3* — H_2SO_4 ; *4* — $CH_3C_6H_4-SO_3H$.

The highest reaction rates are obtained in the presence of metallic sodium and perchloric acid, but the rapid lowering of the reaction rate in time is the very proof of some intense secondary reactions that are caused by the high reactivity of sodium glycolate and the strong oxidative character of perchloric acid.

Due to these aspects, sulfuric acid and *p*-toluenesulfonic acid are preferred as catalysts. The former has the advantage of obtaining higher reaction rates, the latter of getting products of a higher purity.

When sulfuric acid was used as catalyst, products with a lower purity were obtained, due to the secondary reactions catalysed by HSO_4^- anion. This observation is the starting point for using some catalysts where HSO_4^- anion should be fixed on a support. Very good results were obtained when anion was fixed on an inorganic support. A new type of catalyst for the transesterification reaction was thus obtained with the general formula $Me_n(SO_4)_m \cdot H_2SO_4 \times H_2O$.[11] Using these catalysts, got by the interaction of sulfuric acid with a metal sulfate,[12-14] products of a high purity can be obtained at reaction rates superior to those obtained in the presence of *p*-toluenesulfonic acid and at the slight removal of the catalyst in the system.

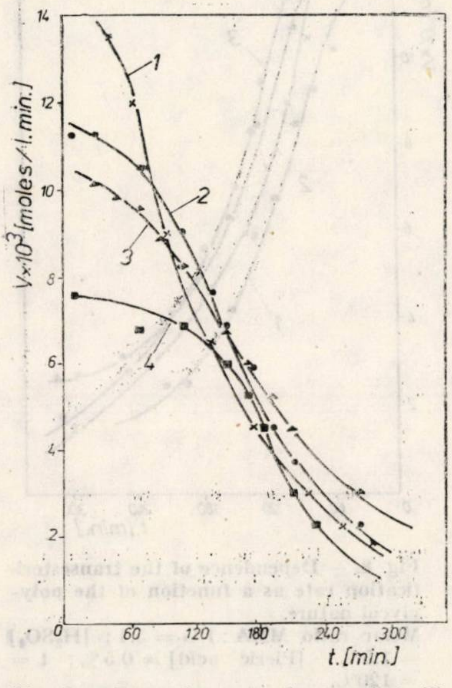

Fig. 5. — Dependence of the transesterification rate of methylmethacrylate with triethylene glycol as a function of the metal nature of catalytic complex. Molar ratio MMA : TEG = 5 : 1 ; [Picric acid] = 0.5 % ; t = 120°C ; [Catalyst] = = 4.6 % (for H_2SO_4 1.5 %). *1* — H_2SO_4 ; *2* — $Al_2(SO_4)_3 \cdot H_2SO_4 \times H_2O$; *3* — $Fe_2(SO_4)_3 \cdot H_2SO_4 \times H_2O$; *4* — $MgSO_4 \cdot H_2SO_4 \times H_2O$.

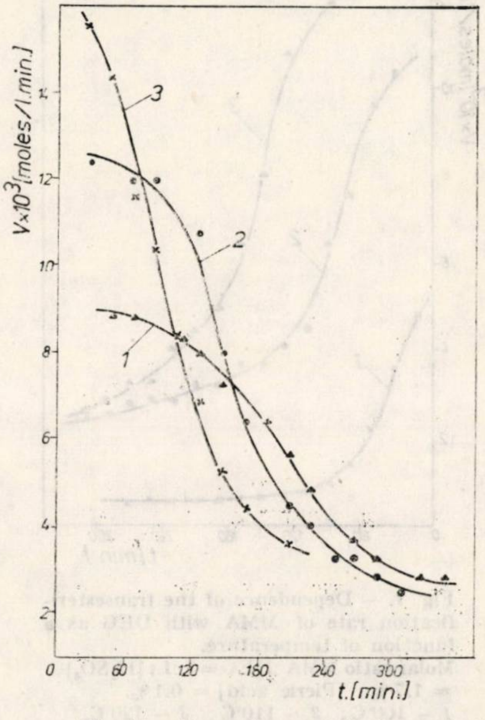

Fig. 6. — Dependence of the transesterification rate of MMA with DEG as a function of the sulfuric acid concentration. Molar ratio MMA : DEG = = 5 : 1 ; [Picric acid] = 0.1 % ; t = = 120°C. *1* — H_2SO_4 1 % ; *2* — H_2SO_4 1.7 % ; *3* — H_2SO_4 4 %.

The activity of these catalysts depends on the nature of the metal of catalytic complex, the most active among them being those on the basis of aluminium sulfate and ferric sulfate (Fig. 5).

The rate of the transesterification reaction increases with the increase of the catalyst concentration (Fig. 6) and temperature (Fig. 7) but this thing is unfavourably reflected on the system stability.

The studies of the influence of the polyglycol nature on the transesterification process showed that the reaction rate increased with length; the highest rates were recorded with tetraethylglycol (Fig. 8).

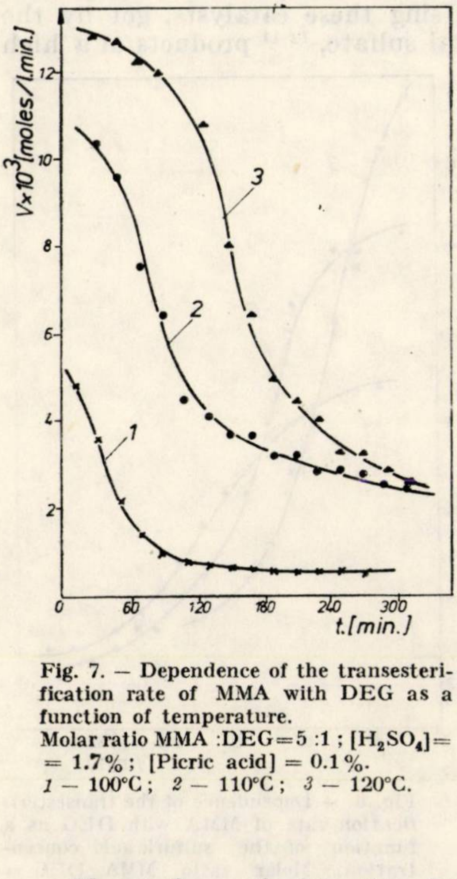

Fig. 7. — Dependence of the transesterification rate of MMA with DEG as a function of temperature.
Molar ratio MMA : DEG = 5 : 1 ; $[H_2SO_4] = 1.7\%$; [Picric acid] = 0.1 %.
1 — 100°C ; *2* — 110°C ; *3* — 120°C.

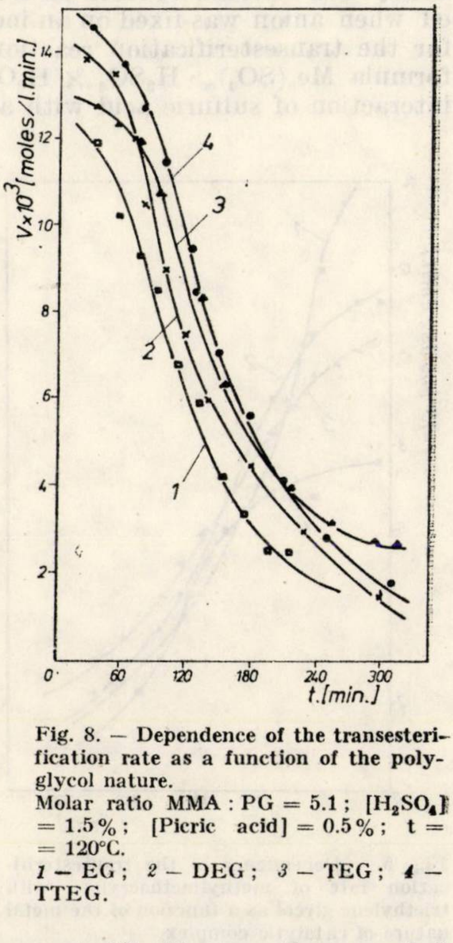

Fig. 8. — Dependence of the transesterification rate as a function of the polyglycol nature.
Molar ratio MMA : PG = 5.1 ; $[H_2SO_4] = 1.5\%$; [Picric acid] = 0.5 % ; t = 120°C.
1 — EG ; *2* — DEG ; *3* — TEG ; *4* — TTEG.

The study on the kinetics of the transesterification reaction revealed some quantitative data concerning the influence of polyglycol nature on the process. These data will be published in a future paper.

CONCLUSIONS

The possibilities of synthesis of ethylene dimethylmethacrylate, diethylene glycol dimethacrylate, triethylene glycol dimethacrylate and tetraethylene glycol dimethacrylate have been comparatively studied with the view of obtaining them. The most advantageous, from an economical point of view, proved to be methylmethacrylate transesterification with polyglycols.

2. The high reactivity of polyethylene glycol dimethacrylates determines their premature polymerization during synthesis. The prevention of this process is the decisive factor in the transesterification reaction.

The isolation of the factors that produce polymerization of monomers in reaction determined the finding of picric acid as inhibitor that, in low concentrations, achieves an adequate inhibition.

3. The nature and concentration of the catalyst influence the reaction rate, conversion and purity of the products, the best results being obtained in the presence of sulfuric acid.

For diminishing the secondary reactions (determined by HSO_4^- anion in the reaction conditions) the anion was fixed on an inorganic support and thus a new type catalyst for the transesterification reactions was found $[Me_n(SO_4)_m \cdot H_2SO_4 \times H_2O]$ whose activity depends on the nature of the metal of the catalytic complex.

4. The rate of the transesterification process depends on the nature of polyglycol and increases with the increase of the catalyst concentration and reaction temperature

REFERENCES

[1] V. K. Krieble, US Pat. 2.895.950 (1959), *Chem. Abstr.*, **53**, 18556 (1959).

[2] V. K. Krieble, US Pat. 3.218.305 (1965), *Chem. Abstr.*, **64**, 3795 (1966).

[3] Borden Chem. Comp. Br. Pat. 1.067.433 (1967) ; *Chem. Abstr.*, **67**, 2160 (1967).

[4] Intercontinental Chem. Comp. Jap. Pat. 7.624.537 (1976) ; *Chem. Abstr.*, **86**, 30559 (1977).

[5] Cr. Oprescu and R. Roșescu, *Mat. Plastice*, **11**, 285 (1974).

[6] C. D. Nenițescu, "Chimie organică", vol. I, Ed. Didactică și Pedagogică, București, VII, 1973.

[7] S. Nissan, US Pat. 3.639.459 (1972) ; *Chem. Abstr.*, **76**, 17 (1972).

[8] G. Caldwell and L. Ihring, *J. Polymer Sci.*, **46**, 507 (1960).

[9] Ch. Bamford, W. G. Barb, A. D. Jenkins and P. F. Onyon, "The Kinetics of Vinyl Polymerization by Radical Mechanisms", Butterworths, London, 1958, p. 249.

[10] M. Dimonie, Gh. Hubca, Gh. Dinu and Cr. Oprescu, Rom. Pat. **75**, 046 (1980).

[11] M. Dimonie, Gh. Hubca, Cr. Oprescu and Gh. Dinu, Rom.Pat. 75.047 (1980).

[12] J. Lal, US Pat. 3.062.789 (1962) ; *Chem. Abstr.*, **58**, 3524 (1963).

[13] J. Lal and J. E. McGrath, *J. Polymer Sci.*, **A2**, 3369 (1964).

Revue Roumaine de Chimie, **26**, *8*, 1195– 1196 (1981)

COMPTE RENDU

IUPAC — Pure and Applied Chemistry. Volume 52, No 6, (June) 1980

This volume contains the invited lectures presented at the International Symposium on Aromaticity, held in Dubrovnik (3–5 September, 1979).

Two characteristic features of the papers could be mentioned from the beginning : a) a trend to new positions in discussing aromaticity (e.g. graph theoretical approach, Randić's conjugated circuits concept, London susceptibility in connection with ring-current concepts, the topological resonance energy approach etc.) and b) the presence of many multi-disciplinar papers (including physical, chemical and mathematical problems integrated in unitary concepts).

From the 18 contributions at least 8 present different aspects of aromaticity developed with the aid of *quantum-mechanical calculations*. Thus, I. Agranat, B. A. Hess and L. J.Schaad calculated resonance energies of nonalternant annulenoannulenes and corannulenes, demonstrating that the aromatic character of the former is dominated by their periphery, whereas for the latter ones no simple correlation could be drawn. M. J. S. Dewar and M. L. Mc Kee discussed different aspects of cyclic conjugation reaching some interesting conclusions such as : a) parrafins are σ-conjugated molecules, isoconjugate with polyenes (it follows that cyclopropane should be aromatic like benzene and cyclobutane antiaromatic, like cyclooctatetraene), b) in the case of higher annulenes the determinant factor of aromaticity seems to be a special type of electron correlation, analogous to that postulated by Löwdin in the alternant orbital theory. B. M. Gimarc and N. Trinajstić discussed general aromatic properties of inorganic rings. B. A. Hess and L. J. Schaad examined possible reference structures or the computation of ion and radical resonance energies (numerous resonance energies for cyclic ions and radicals are given). P. Ilić and N. Trinajstić discussed the homoaromaticity of different systems (with the aid of a first-order perturbation treatment), simplifying the phenomenon to competitive tendencies of aromatic stabilization and minimal strain conformation, and underlining the importance of through-space interactions. J. Kruszewski demonstrated that aromaticity of polycyclic compounds can be treated most simply by applying the Randić's conjugated circuits concept. This concept is also applied by M. Randić himself (in his paper dedicated to E. Clar, "doyen of benzenoid chemistry") to different polycyclic benzenoid hydrocarbons, examined from a graph-theoretical position. G. Náray-Szabó studied some "strange molecules" (e.g. $S(SN)_2^+$, formazanes etc) on the basis of CNDO/2 quantum chemical calculations.

Some of the remaining contributions present *chemical aspects* of aromaticity and antiaromaticity. Thus, M. Rabinovitz and I. Willner discussed the synthesis and properties of novel aromatic cations and anions (e.g. dibenzononalenide dianion, cyclooctafluorene anion etc) and emphasized that the peripheral electron delocalization brings a significant contribution to the resultant aromatic nature of the system. M. Tishler made a survey of the chemistry of azaindolizines underlining that the stability and reactivity of such compounds is governed by the dual character of the bicycle (π-excessive and π-deficient parts). M. Torres, E. M. Lown and O. P. Strausz discussed some 4n π-electron antiaromatic species such as oxirene, thiirene (isolated as substance) and 2-azirine. *Ab initio* MO-calculations confirm the chemical conclusions. P. C. Vollhardt presented the syntheses and properties (physical, chemical and biological) of several new strained ring hydrocarbons (e.g. cyclobuta /1,2d/ benzyne, 2,3 : 5,6-dicyclobutapyridine, /2.2.2/ (1, 2, 4) cyclophanes etc.).

Another group of papers discusses the aromaticity as it results from the data furnished by different *physical methodes*. Thus, L. Klasinc presented photoelectron spectra of conjugated molecules, J. Michl discussed the electronic structure of aromatic π-electron systems as reflected in their magnetic circular dichroism spectra, and M. Simonetta presented the results of X-ray diffractometry of a number of bridged /10/-, /12/- and /14/- annulenes (of the Vogel type).

R. B. Mallion commented the use of the ring current concept in diagnosing and defining aromaticity. One important conclusion of the paper is that "the overall London magnetic susceptibility of a polycyclic species (see the recent papers of Haddon and Aihara)-rather than its individual ring-current — is the more appropriate quantity to be considered in the evaluation of aromaticity".

W. C. Herndon in his contribution "Resonance energies from photoelectron spectra" used PE spectroscopy to derive resonance energies (with the help of a graph-theoretical procedure). The results agree well with those of LCAO—MO—SCF—PPP calculations.

A. T. Balaban in his complex contribution, "Is aromaticity outmoded?" presented a brief but very comprehensive historical survey of aromaticity underlining the two important theoretical breakthroughs : Kekule's formula of benzene and Hückel's rule. The author showed the limitations of the Hückel method which "led to pace slackening in the last decade and to severe criticism toward the notion of aromaticity". The author argues, on the basis of his original research areas (pyrylium salts, graph-teoretical approach to predict all possible monocyclic aromatic systems with heteroatoms, measurement of ring-currents etc) that *"a reasonable balance of generality makes the concept of aromaticity extremely useful qualitatively ; however for quantitative determinations, narrower, more precisely defined areas of aromaticity are to be specified"*.

In my opinion the same is the conclusions of the entire book, which could by highly recommended to all chemists interested in this old but continuously fascinating domain : AROMATICITY.

M. Banciu

NOTE POUR LES AUTEURS

La Revue Roumaine de Chimie publie des articles en anglais, français, russe, allemand ou espagnol. Les auteurs sont priés d'envoyer des articles et des comptes rendus inédits.

Les manuscrits seront dactylographiés à deux intervalles. La bibliographie, les tableaux et la légende des figures seront placés après le texte.

Si l'article fait partie d'une série numérotée, la partie précédente sera donnée comme première référence.

Chaque article sera précédé d'un résumé comprenant quinze lignes au maximum.

Les références bibliographiques dans le texte seront faites par des exposants sans parenthèses et paraîtront à la fin de l'ouvrage.

Les publications périodiques mentionnées dans la bibliographie seront présentées suivant les prescriptions internationales ; le nom de l'auteur précédé de l'initiale du prénom, le titre du périodique abrégé conformément à « Chemical Abstracts » et souligné par une ligne, le numero du tome indiqué par des chiffres arabes et souligné par deux lignes, suivi de la première page de l'article : à la fin, l'année de la parution sera placée entre parenthèses. Le numéro de la revue ne sera pas indiqué, si les pages du volume sont numérotées consécutivement.

Les textes des livres ou traités inclueront : les noms des auteurs, précédé de l'initiale du prénom, le titre du livre entre guillemets et sans être souligné, le numéro du tome précédé par l'abréviation « vol » (ou « Bd. »), le numéro de l'édition, les éditions (the publisher), la localité de la parution du livre, l'année de la parution et la page de la référence précédée(s) par l'abréviation « p » (ou « S »).

Les brevets seront indiqués comme suit : l'auteur ou la firme, le pays et le numéro du brevet, la date et la revue (*Chem. Abstr.*). Par ex. : M. Jones (to Union Carbide Co.), Brit. Pat. 601 238, 2 Sept. 1959, *Chem. Abstr.*, **54**, 12808 (1960).

Si la référence n'a pas été lue en original, on indiquera aussi la revue de references consultée.

Les diagrammes seront tracés à l'encre de Chine sur papier calque. Les tableaux et les figures (en nombre strictement nécessaire) ainsi que les courbes dans les figures seront numérotés par des chiffres arabes. Leur explication sera donnée dans la légende des figures. Prière de ne pas inscrire les mêmes données dans les tableaux et les figures. Chaque tableau aura un titre. On indiquera dans le texte la place approximative des tableaux et des figures. Les formules chimiques seront incluses dans le texte : en outre, elle seront transcrites sur papier calque, à l'encre de Chine.

Les auteurs sont priés d'indiquer les caractères italiques (en soulignant les lettres au crayon), ainsi que tout autre caractère spécial : les préfixes *ortho*, *meta*, *para*, *cis*, *trans*, etc. seront soulignés pour indiquer leurs caractères italiques, et ne seront jamais écrits avec des majuscules.

Aucune correction à la main ne sera admise sur le manuscrit. Les corrections seront frappées à la machine. Les lettres grecques ou autres symboles spéciaux seront insérés à la main à l'encre clairement.

Le manuscrit sera signé par l'auteur.

Le colonne-titre aura 50 lettres au maximum.

L'entière responsabilité du contenu des articles appartient aux auteurs.

Sur demande on peut obtenir un note plus complète.

PRINTED IN ROMANIA

NOTE POUR LES AUTEURS

La Revue Roumaine de Chimie publie des articles en anglais, français, russe, allemand ou espagnol. Les auteurs sont priés d'envoyer des articles et des comptes rendus inédits.

Les manuscrits seront dactylographiés à deux intervalles. La bibliographie, les tableaux et la légende des figures seront placés après le texte.

Si l'article fait partie d'une série numérotée, la partie précédente sera donnée comme première référence.

Chaque article sera précédé d'un résumé comprenant quinze lignes au maximum.

Les références bibliographiques dans le texte seront faites par des exposants sans parenthèses et paraîtront à la fin de l'ouvrage.

Les publications périodiques mentionnées dans la bibliographie seront présentées suivant les prescriptions internationales : le nom de l'auteur précédé de l'initiale du prénom, le titre du périodique abrégé conformément à « Chemical Abstracts » et souligné par une ligne, le numéro du tome indiqué par des chiffres arabes et souligné par deux lignes, suivi de la première page de l'article ; à la fin, l'année de la parution sera placée entre parenthèses. Le numéro de la revue ne sera pas indiqué, si les pages du volume sont numérotées consécutivement.

Les textes des livres ou traités incluront : les noms des auteurs, précédé de l'initiale du prénom, le titre du livre entre guillemets et sans être souligné, le numéro du tome précédé par l'abréviation « vol » (ou « Bd. »), le numéro de l'édition, les éditions (the publisher), la localité de la parution du livre, l'année de la parution et la page de la référence précédée(s) par l'abréviation « p » (ou « S »).

Les brevets seront indiqués comme suit : l'auteur ou la firme, le pays et le numéro du brevet, la date et la revue (*Chem. Abstr.*). Par ex. : M. Jones (to Union Carbide Co.), Brit. Pat. 901 258, 2 Sept. 1959, *Chem. Abstr.*, 54, 12808 (1960).

Si la référence n'a pas été lue en original, on indiquera aussi la revue de références consultée.

Les diagrammes seront tracés à l'encre de Chine sur papier calque. Les tableaux et les figures (en nombre strictement nécessaire) ainsi que les courbes dans les figures seront numérotés par des chiffres arabes, leur explication sera donnée dans la légende des figures. Prière de ne pas inscrire les mêmes données dans les tableaux et les figures. Chaque tableau aura un titre. On indiquera dans le texte la place approximative des tableaux et des figures. Les formules chimiques seront incluses dans le texte ; en outre, elle seront transcrites sur papier calque, à l'encre de Chine.

Les auteurs sont priés d'indiquer les caractères italiques (en soulignant les lettres au crayon), ainsi que tout autre caractère spécial : les préfixes *orto, meta, para, cis, trans*, etc. seront soulignés pour indiquer leurs caractères italiques, et ne seront jamais écrits avec des majuscules.

Aucune correction à la main ne sera admise sur le manuscrit. Les corrections seront frappées à la machine. Les lettres grecques et autres symboles spéciaux seront insérés à la main à l'encre clairement.

Le manuscrit sera signé par l'auteur.

Le colonne titre aura 50 lettres au maximum.

L'entière responsabilité du contenu des articles appartient aux auteurs.

Sur demande on peut obtenir un note plus complète.

PRINTED IN ROMANIA

1983

[illegible]

TRAVAUX PARUS AUX ÉDITIONS DE L'ACADÉMIE DE LA RÉPUBLIQUE SOCIALISTE DE ROUMANIE

1982 MAR

- I. G. MURGULESCU, TATIANA ONCESCU și E. SEGAL, **Introducere în chimia fizică. Vol. II.2. Cinetică chimică și cataliză** (Introduction à la chimie physique. Vol. II.2. Cinétique chimique et catalyse), 1981, 1024 p.
- V. DRĂGUȚAN, A. T. BALABAN, M. DIMONIE, **Metateza olefinelor și polimerizarea prin deschidere de inel a cicloolefinelor** (La métathèse des oléfines et la polymérisation par ouverture annulaire des cyclo-oléfines), 1981, 254 p.
- O. IORDACHE, **Procese polistocastice aplicate la fenomenele de transfer** (Processus polystochastiques appliqués aux phénomènes de transfert), 1981, 187 p.
- CRISTOFOR SIMIONESCU, VALERIA GORDUZA, **Polimeri biocompatibili și biologic activi** (Polymères biocompatibles et biologiquement actifs), 1980, 479 p.
- Ș. MOLDOVEANU, A. SAVIN, **Aplicații în chimie ale metodelor semiempirice de orbitali moleculari** (Applications en chimie des méthodes semi-empiriques d'orbitaux moléculaires), 1980, 286 p.
- ELENA CEAUȘESCU, **Polimerizarea stereospecifică a izoprenului** (La polymérisation stéréospécifique de l'isoprène), 1979, 307 p.
- MIHAIL FLORESCU, **Metode științifice în dezvoltarea industriei chimice moderne** (Méthodes scientifiques dans le développement de l'industrie chimique moderne), 1979, 256 p.
- A. T. BALABAN, I. GALĂȚEANU, G. GEORGESCU, LIGIA SIMIONESCU, **Compuși marcați și radiofarmaceutici cu aplicații în medicina nucleară** (Composés marqués et radiopharmaceutiques à application en médecine nucléaire), 1979, 495 p.
- CONST. GH. MACAROVICI, *Analiza chimică cantitativă anorganică* (L'Analyse chimique quantitative inorganique), 1979, 457 p.
- I. G. MURGULESCU, E. SEGAL, **Introducere în chimia fizică, vol. II.1. Teoria molecular cinetică a materiei** (Introduction à la chimie physique, vol. II.1. La théorie moléculaire-cinétique de la matière), 1979, 1036 p.
- I. E. TEODORESCU, MARIA FITI, **Iradierea tehnologică** (L'Irradiation technologique), 1979, 216 p.
- S. STERNBERG, FL. DANEȘ, **Termodinamica chimică aplicată** (La thermodynamique chimique appliquée), 1978, 400 p.
- I. G. MURGULESCU, V. EM. SAHINI, **Introducere în chimia fizică, Vol. I.2. Structura și proprietățile moleculelor** (Introduction à la chimie physique. Vol. I.2. La structure et les propriétés des molécules), 1978, 604 p.
- C. DRĂGULESCU, E. PETROVICI, **Chimie structurală modernă. Chimia coordinanței 8** (La chimie structurale moderne. La chimie de la coordinence 8), 1977, 947 p.
- D. PURDELA (sous la direction de), **Nomenclatura chimiei anorganice** (La nomenclature de la chimie inorganique), 1977, 153 p.
- I. ZUGRĂVESCU, MAGDA PETROVANU, **N-ylid chemistry**, coédition avec McGraw Hill International Book Company, U.S.A., 1977, 396 p.
- I. G. MURGULESCU, **Introducere în chimia fizică. Vol. I.1. Atomi, molecule, legătură chimică** (Introduction à la chimie physique, vol. I.1. Atomes, molécules, liaison chimique), 1976, 560 p.
- CONST. GH. MACAROVICI, D. MACAROVICI, **Chimia oxizilor dubli și utilizările lor** (La chimie des oxydes doubles et leur utilisation), 1975, 195 p.
- ELENA CEAUȘESCU, **Research work on synthesis and characterization of macromolecular compounds. Contributions**, 1974, 251 p.
- CR. SIMIONESCU, VIORICA RUSAN, V. POPA, **Chimia algelor marine** (La chimie des algues marines), 1974, 212 p., 1 pl.

I. P. INFORMAȚIA c. 1293

43426

Lei 25.—

$ 55 (pour un abonnement annuel)

F 1103

Végl.

ACADÉMIE DE LA RÉPUBLIQUE SOCIALISTE DE ROUMANIE

REFERÁLVA

REVUE ROUMAINE DE CHIMIE

TOME 26

N°s 9—10

Septembre — Octobre 1981

EDITURA ACADEMIEI REPUBLICII SOCIALISTE ROMÂNIA

Rev. Roumaine Chim.

RRCHAX. **26**, *9—10*, p. 1197—1342 (1981), Bucarest

ACADÉMIE DE LA RÉPUBLIQUE SOCIALISTE DE ROUMANIE

COMITÉ DE RÉDACTION

Rédacteur en chef :

I. G. MURGULESCU, membre de l'Académie de la République Socialiste de Roumanie

Rédacteurs en chef adjoints:

A. T. BALABAN et V. EM. SAHINI, membres correspondants de l'Académie de la République Socialiste de Roumanie

Collège de rédaction:

EM. BRATU, ELENA CEAUŞESCU, ECATERINA CIORĂNESCU-NENITZESCU, CR. SIMIONESCU, membres de l'Académie de la République Socialiste de Roumanie; P. SPACU, membre correspondant de l'Académie de la République Socialiste de Roumanie; MARGARETA AVRAM, M. BANCIU, I. HAIDUC, D. I. MARCHIDAN, I. MOLDOVAN, G. NIAC et D. SĂNDULESCU

La Revue Roumaine de Chimie paraît 10 fois par an. Toute commande de l'étranger pour les travaux parus aux Editions de l'Académie de la République Socialiste de Roumanie sera adressée à ILEXIM, Departamentul Export-Import Carte (Livres)/Departamentul Export-Import Presă (Revues), P.O.B. 136—137, télex 11226, 3, str. 13 Decembrie, 79517-Bucarest, Roumanie.

Les manuscrits, les livres et les revues proposés en échange, ainsi que toute correspondance seront envoyés à la rédaction :

REVUE ROUMAINE DE CHIMIE

125, Calea Victoriei 79717 Bucarest, Roumanie, téléphone 50 76 80

EDITURA ACADEMIEI REPUBLICII SOCIALISTE ROMÂNIA
125, Calea Victoriei, 79717 Bucarest, Roumanie, téléphone 50 76 80

REVUE ROUMAINE DE CHIMIE

ORSZÁGOS MŰSZAKI KÖNYVTÁR ÉS DOKUMENTÁCIÓS KÖZPONT

Tome 26, N°s 9–10 Septembre–Octobre, 1981

M. M. GIRGIS, D. P. LAZĂR and E. I. SEGAL, Catalytic oxidation of ammonia. II. Low temperature oxidation on a $Fe_2O_3-Cr_2O_3$catalyst. Influence of the amount of the catalyst. Analysis of the reaction products . . . . 1199–1203 R

V. GOŞA, R. H. SCHUSTER, N. I. IONESCU, D. OANCEA and DOMNINA POPESCU, Explosive combustion of vinylacetylene-air mixtures initiated by hot platinum wire (in German) 1205–1212

I. TEOREANU, CECILIA HRIŢCU, N. BUTUCESCU and LIANA BUCEA, Electronomicroscopical researches and thermal differential analysis of $4CaO.Al_2O_3.Fe_2O_3$ and $2CaO.Al_2O_3$ hydration at high temperatures and pressures (in French) 1213–1220

MARIA BREZEANU, I. SEBE, MELANIA GUŢUL and IOANA JITARU, Cu(II) complex compounds with 1-(β-phenyl-β-amino) ethylcyclobutanol and 1-(β-*p*-chlorophenyl-β-amino) ethylcyclobutanol 1221–1230

A. C. BANCIU, A New bridged binuclear low-spin pentacoordinate Co(II) complex containing strongly electronegative donor atoms . . . . 1231–1243 R

MOHAMED ABDEL SALAM El ABSY, GH. MARCU, J. ZSAKÓ and CS. VÁRHELYI, Studies on some nitro-bis-acetylacetonato-cobalt (III) compounds . . . . 1245–1254 Bc

SILVIA BARBU and CONST. GH. MACAROVICI, The spectrophotometric study of some Cu(II)-thiocarbohydrazone systems in solution and their analytical application . . . . 1255–1259 Bc

VIORICA CIMPU, AURELIA MEGHEA and IOANA JITARU, Copper (II) complexes with 10-[2-(dimethylamino)propyl]-phenothiazine 1261–1270

J. ZSAKÓ, J. HORÁK and CS. VÁRHELYI, On the α-dioximine complexes of transition metals. LXIII. Spectrophotometric study on the stability of Fe(II) and Co(II) complexes of 1,2-cycloheptane- and 1,2-cyclooctanedione dioximes 1271–1277

R. AVRAM, L. PAPAHAGI and I. ILIUŢĂ, The oxidation of n-dodecane in liquid phase with molecular oxygen in the presence of aluminium, lanthanum and cerium naphthenates . . . . 1279–1283 R

A. ESSAWY, M. A. El-HASHASH, M. M. ABDALLA and A. M. El-GENDY, Some reactions of 6-[1′(2′-methyl naphthalenyl)]-2, 3, 4, 5 tetrahydropyridazin-3-one. 1285–1293

Revue Roumaine Chim. **26,*9* –*10*, p. 1197–1342 (1981), Bucarest**

A. AIRINEI, DANA DOROHOI and ANICA TOLEA, The influence of the solvent on the electronic absorption spectra of some n-substituted 2-nitroanilines **1295–1303**

J. RADHAKRISHNAN, Investigations on the synthesis of *cis*-9,10-disubstituted decalins **1305–1314**

GH. DRĂGAN, Amorphous-crystalline coupling in polyethylene. IX. Study of the transforming branches by step calorimetric system **1315–1326**

GH. HUBCA, D. RACOȚI, CR. OPRESCU and M. DIMONIE, Synthesis and polymerization of polyethyleneglycol dimethacrylate. II. Kinetics of the transesterification process of methylmethacrylate with polyglycols . . . **1327–1334**

M. MITTAL, KEEMTI LAL and S. P. GUPTA, Potentiometric studies on complexes of some transition metal ions with 4,5-dimethyl-2-hydroxy acetophenone and its oxime **1335–1340**

BOOK REVIEWS **1341–134**

Revue Roumaine de Chimie, **26**, *9–10*, 1199–1203 (1981)

CATALYTIC OXIDATION OF AMMONIA. II.[1]

LOW TEMPERATURE OXIDATION ON A $Fe_2O_3-Cr_2O_3$ CATALYST. INFLUENCE OF THE AMOUNT OF THE CATALYST. ANALYSIS OF THE REACTION PRODUCTS

M. M. GIRGIS*, D. P. LAZĂR** and E. I. SEGAL***

*** Faculty of Science, Department of Chemistry, University of Assiut, Egypt**
**** The Polytechnical Institute of Jassy, Department of Physical Chemistry, Romania**
***** National Institute of Chemistry Department, of Physical Chemistry and Electrochemical Technology, Bucharest, Romania.**

Received March 25, 1981

Continuing the morphological characterization of the ammonia oxidation process on an industrial catalyst $Fe_2O_3-Cr_2O_3$, in the present paper the influence of the thickness of the catalyst bed is reported. The gas chromatographic analysis of the reaction products is also reported within the experimental conditions previously described.

1. INFLUENCE OF THE THICKNESS OF THE CATALYST BED

In a previous paper,[1] some experimental results have been reported, using a quartz reactor (30 mm inner diameter and 175 mm length), completely filled with pelletized catalyst.

The present paper reports on some other experimental data using the same equipment and reactor as before, but this time the pelletized catalyst is placed inside the reactor only in a narrow central zone under the form of a disk composed of one, two or respectively four parallel layers of pellets. These experiments were carried out with two purposes in mind :

— the establishment of the minimum thickness of the catalyst bed which could ensure a complete conversion of ammonia (i.e. $\alpha = 1.0$),

— the determination of the minimum initial temperature $T_{i,\min.}$ of the reactor and of the $\Delta T_{\max.}$ value for a complete conversion of ammonia, as a function of the catalyst bed thickness.

Practically, the same reactor, previously described,[1] has been used, but some modifications have been accomplished to allow the building of catalyst bed in the cross-section of the reactor, using one, two or four parallel layers of pellets, each individual layer having 4 mm width (Fig. 1).

For testing these different catalyst beds, a standard gaseous reaction mixture was used, with a percentage composition of 11.09 % (v/v) NH_3, at a flow rate of 33.33 cm^3.s^{-1}.

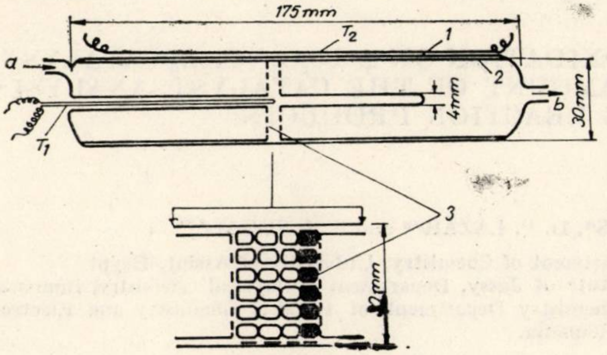

Fig. 1. — **The shape and dimensions of the reactor used for the determination of the influence of the catalyst bed thickness.** ***a.*** **initial reactant admission ;** ***b.*** **gaseous reaction products exit ;** ***1.*** **reactor ;** ***2.*** **cylindrical glass pieces for fastening the catalyst pellets ;** ***3.*** **catalyst layers ;** T_1 **— mobile thermocouple ;** T_2 **— fixed thermocouple.**

Influence of the monolayered catalyst bed (4 mm width)

Within the framework described before and having the reactor heated at an initial temperature, T_i = 195 °C, the oxidation process of ammonia on this monolayered catalyst bed (4 mm width) does not take place. It has been experimentally established that the oxidation process starts only when temperature of the reactor reaches 219°C; following this temperature limit, the oxidation of ammonia develops itself as a strong exothermal process. Kinetically, the reaction exhibits a very short induction period (approximately one minute) followed by an autoacceleration period of about 12 — 13 minutes (Fig. 2, curve 1).

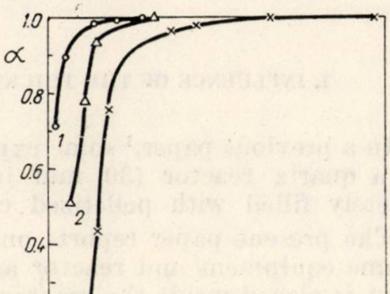

Fig. 2. — **The variation of the ammonia conversion, α, as a function of the reaction time, for different catalyst bed thickness (11.09 %, v/v, NH: content ; flow rate = 33.33 cm^3.s^{-1})$_3$** ***1.*** **one-layer catalyst bed ; 4 mm thickness ;** T_i **= 219°C ;** ***2.*** **two-layers catalyst bed ; 8 mm thickness ;** T_i**= 195°C ;** ***3.*** **four-layers catalyst bed ; 16 mm thickness ;** T_i **= 195°C.**

As soon as the steady state of the oxidation process has been set up, the temperature of the reaction system, in the catalyst bed zone, reaches the value of 557°C, therefore $\Delta T_{\max.} = 557° - 219° = 338°C$.

Using the viewing window of the reactor, an intense dark-red emission is observed. At the end of the autoacceleration period, the degree of ammonia conversion reaches its maximum value, $\alpha = 1.0$. This experiment has been repeated for $T_i = 227°C$ and it has been found that the induction period diminishes to a few seconds while the autoacceleration period reduces to several minutes.

Influence of the double-layered catalyst bed (8 mm width)

In this case, the experimental data prove that a complete conversion of ammonia can be reached only if the catalyst is heated at least to 195° C. The oxidation process is also strongly exothermal, with an induction period of about 3 minutes and an autoacceleration period of 14 minutes (Fig. 2, curve 2). During the steady state of the process development, the temperature of the reaction system raises up to 582°C, that makes $\Delta T_{max.} = 582° - 195° = 387°$ (with 50°C more than in the previous experiment, where a 4 mm catalyst bed has been used). During this experiment, both the reaction mixture and the catalyst bed exhibited the phenomenon of incandescence. In steady state conditions, the degree of the ammonia conversion has a maximum value, $\alpha = 1.0$.

Influence of the quadrupled catalyst bed (16 mm width)

In this experiment, the catalyst bed was built-up from four parallel layers of pellets, placed in the cross-section of the reactor, in its mediane zone.

The oxidation process began at $T_i = 195°C$, exhibiting an induction period of 4 — 5 minutes and an autoacceleration period of about 30 minutes. The relatively high values of the induction period has prompted us to establish — using the gas chromatographic analysis — the fact that the induction period is characterized by an adsorption process of the ammonia molecules which occurs firstly on the catalyst surface (initially α diminishes from 0.2 to 0.08).

The autoaccelerated development of the process starts only after the complete saturation of the catalyst surface with ammonia molecules; during this kinetic stage α increases again to its maximum value ($\alpha = 1.0$) (Fig. 2, curve 3).

In the two previous experiments where the catalyst beds of 4 and 8 mm respectively were used, it was not possible to make evident — gas chromatographically — the existence of the ammonia molecules sorption process on the catalyst surface because the corresponding induction periods (i.e. "sorption periods") were too short (1 — 3 minutes.)

After the set-up time of the steady state process, the temperature of the catalyst bed reached a value of 608°C, then $\Delta T_{max.} = 608° - 195° = 413°C$.

The direct visual observation of the reactor in the catalyst zone, permitted to establish that only the first two layers became incandescent.

2. GAS CHROMATOGRAPHIC ANALYSIS OF THE REACTION PRODUCTS

The gaseous reaction products were gas chromatographically analysed using a "CHROMATROM" instrument (made in G.D.R.), type H.F.G.C. 18.3, equipped with a katharometric detector. Actually, two types of columns were used : a 2 m stainless steel column packed with molecular sieves 5 Å, for the separation and quantitative determination of N_2 and O_2, and a 3 m stainless steel one filled with Porapak Q, 80 — 100 mesh, for the separation and dosage of nitrogen oxides.

The G. C. investigations were applied to the gaseous reaction mixtures having the following standardized volumetric compositions :

6.22 % NH_3 ($T_i = 201°$),
8.56 % NH_3 ($T_i = 195°$)
10.90 % NH_3 ($T_i = 195°$)
12.01 % NH_3 ($T_i = 186°$),
16.10 % NH_3 ($T_i = 186°$).

Figures inside the round brackets indicate the T_i value for each individual experiment was made at. For all experiments the flow rate was constant, namely 27.77 $cm^3.s^{-1}$.

It was established that after the achievement of the steady state of the oxidation process, the reaction products collected just near the reactor exit mainly consisted of N_2, NO and H_2O. The analysis of the experimental G.C. data proved that irrespective of the ammonia percentage composition in the initial reaction mixture, the same quota (i.e. 17.05 % v/v NH_3) was chemically converted to NO during the oxidation process (Table 1).

TABLE 1

The values of the NO/NH_3 ratio (%, v/v) as a function of the intial reaction mixture composition

% NH_3(v/v) in the initial reaction mixture	T_i (°C)	NO/NH_3 ratio (%, v/v)	Mean value (%)
6.22	201	17.05	17.05
8.56	195	17.10	
10.90	195	17.10	
12.01	186	16.90	
16.10	186	17.11	

A plot of O_2 content (in % v/v) variation in the gaseous mixture vs. the variable percentage composition of NH_3 in the different initial gaseous reaction mixtures reveals a linear dependence (Fig. 3).

This graphical representation proves that when using an iron—chromium catalyst it is advisable that the gaseous reaction mixtures should not exceed the composition of 18.8 % v/v NH_3, if a complete conversion of ammonia is desired.

The investigation of the flow rate influence on the final composition of the gaseous reaction products — during the steady state of the ammonia oxidation process — has been carried out using a gaseous reaction mixture with a composition of 10.43 % v/v NH_3; this initial reaction mixture has been used for different flow rates, ranging between 16.66 and 41.66 $cm^3.s^{-1}$ and for an initial temperature $T_i = 195°C$.

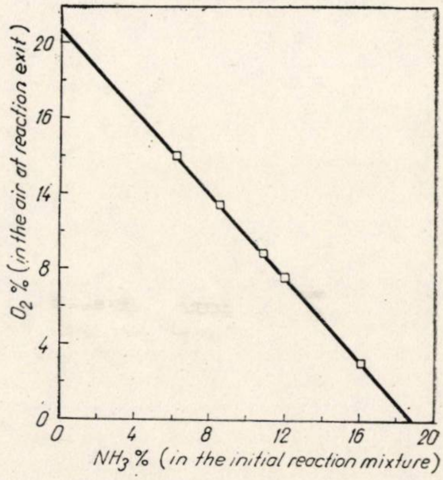

Fig. 3. — The variation of the O_2 content (v/v) in the gaseous mixture, at the reactor exist, vs. the ammonia content (v/v) in the initial reaction mixture. (The G. C. analysis of the reaction products has been carried out after the setting up of the steady state of the oxidation process).

Using the G.C. analysis method for the investigation of the reaction products composition, two conclusions have been ascertained:

1. during the development of the steady state regime of the catalytic amonia oxidation, the reaction products were also N_2, NO and H_2O.

2. irrespective of the flow rate of the reaction mixture, the same fraction of the initial amount of ammonia, i.e. about 17.00% v/v, is converted to NO.

Therefore, the selectivity of the catalyst relating to the conversion $NH_3 \longrightarrow NO$ is not a function of the flow rate variation.

The above reported results are in good agreement with those reported by Anokhin and Babankov.[2]

CONCLUSIONS

1. The gradual increasing of the catalyst bed thickness determines the decreasing of the minimum value of T_i for which the complete ammonia conversion is accomplished; also, an increase of both induction and autoacceleration periods and of the $\Delta T_{max.}$ values were evidenced.

2. The percentage content of NO, referred to the total amount of gaseous reaction products, is independent of the initial reaction mixture composition, as well as of the flow rate.

REFERENCES

[1] Part I, M.M. Girgis and D. P. Lazăr, *Rev. Roumaine Chim.*, **25**, 1293 (1980).
[2] V. N. Anokhin and V. P. Babankov, *Tr. Mosk. Khim. Tekhnol. Inst.*, **79**, 150 (1974).

The investigation of the flow rate influence on the final composition of the gaseous reaction products — during the steady state of the ammonia oxidation process — has been carried out using a gaseous reaction mixture with a composition of 10.10 % v/v NH_3; this initial reaction mixture has been used for different flow rates, ranging between 15.98 and 33.66 cm^3 s^{-1} and for an initial temperature T_i = 197°C.

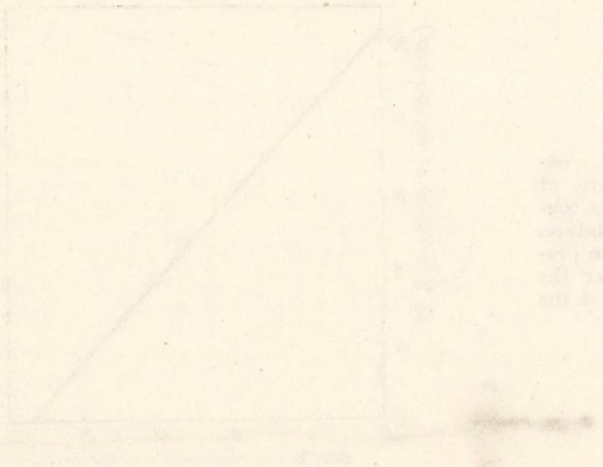

Fig. 3. – The variation of the C content in the gaseous mixture at the reactor outlet vs. the ammonia content in the initial reaction mixture. The [illegible] analysis of the reaction products has been carried out after the setting up of the steady state of the oxidation process.

Using the G.C. analysis method for the investigation of the reaction products composition, two conclusions have been ascertained:

1. During the development of the steady state regime of the catalytic ammonia oxidation, the reaction products were also N_2, NO and N_2O.

2. Irrespective of the flow rate of the reaction mixture, the same fraction of the initial amount of ammonia, i.e. about 11.60 % v/v, is converted in NO.

Therefore, the selectivity of the catalyst relating to the conversion $NH_3 \longrightarrow NO$ is not a function of the flow rate variation.

The above reported results are in good agreement with those reported by Andreev and Zubenko.[2]

CONCLUSIONS

1. The gradual increasing of the catalyst bed thickness determines the decreasing of the minimum value of T_i for which the complete ammonia conversion is accomplished; also an increase of both induction and steady-state periods and of the ΔT_{max} values were evidenced.

2. The percentage amount of NO, referred to the total amount of gaseous reaction products, is independent of the initial reaction mixture composition, as well as of the flow rate.

REFERENCES

1. [illegible], 43, 1295 (1969).
2. [illegible], 78, 18 (1970).

Revue Roumaine de Chimie, **26**, *9–10*, 1205–1212 (1981)

EXPLOSIVE VERBRENNUNG VON VINYLACETYLEN-LUFT-GEMISCHEN AN PLATINWENDEL GEZÜNDET

V. GOŞA*, R. H. SCHUSTER*, N. I. IONESCU*, D. OANCEA** und DOMNINA POPESCU*

* Zentrum für physikalische Chemie, Bukarest, Splaiul Independenţei 202, Bukarest, Rumänien

** Lehrstuhl für physikalische Chemie des Instituts für Chemie, Bd. Republicii 13, Bukarest, Rumänien

Eingegangen am 29. April 1980

Die Untersuchung der explosiven Verbrennung von Vinylacetylen-Luft-Gemischen, die mit heißen Platinwendel gezündet war, zeigt in einem weiten Konzentrationsbereich eine nichtmonotone Abhängigkeit der gemessenen Parameter von der Konzentration, die gut mit den innerhalb der Explosionsgrenzen gefundenen distinkten Brennbereichen im Einklang ist.

The study of the explosive combustion of vinylacetylene—air mixtures, initiated by hot platinum wire shows the dependence of the characteristic parameters of the explosion upon vinylacetylene concentration, in a large concentration range. This corelation changes for each of the domains observed in the flammability range of the vinylacetylene—air mixtures, as the nature of the reactive intermediates changes.

Die Diagramme die die Konzentrationsabhängigkeit der charakteristischen Parameter einer Explosion von Kohlenwasserstoff-Luft-Gemischen darstellen, sind bei der Untersuchung dieser Gemische wichtig.

Bei niederen Alkanen[1] und Olefinen[2] wurden gefächerte Diagramme in Koordinaten Anfangsdruck-Konzentration erhalten, die die Existenz verschiedener Brennbereiche aufzeigen. Eine ähnliche Situation wurde beim System Vinylacetylen-Luft festgestellt.[3] Als Folge untersuchen wir in der vorliegenden Arbeit einige Aspekte der explosiven Verbrennung des Systems Vinylacetylen-Luft eingehend.

EXPERIMENTELLES

Die Arbeitsvorrichtung und Durchführung der Versuche wurde anderweitig beschrieben.[4] Der Brennstoff mit der Zusammensetzung : 95,8 % Vinylacetylen ; 2,2 % Vinylchlorid ; Argon ; 0,3 % Acetylen und 0,5 % Butadien wird in der vorliegenden Arbeit als Vinylacetylen (VAz) bezeichnet. Zum Unterschied zu einer früheren Arbeit[3] wo eine Nickel-Chrom-Wendel verwendet wurde (die im Laufe der Versuche Umwandlungen erfuhr) ist in der vorliegenden Arbeit eine Platinwendel (Ø = 0,1 mm, L = 50 mm), mit Gleichstrom angeheitzt, zur Zündung verwendet worden.

ERGEBNISSE UND DISKUSSION

In der vorliegenden Arbeit wurde die explosive Verbrennung von VAz-Luft Gemischen bei Unterdruck bis zu einer oberen Konzentrationsgrenze von 30% VAz untersucht. Wie auch in vorangegangenen Arbeiten[3] wurden in Abhängigkeit der Konzentration bestimmt : die untere Explosionsgrenze, Mindestinitialdruck bei der die Explosion stattfindet, kritische Zündenergie, der Impuls der durch die Explosion der Verschlußplatte der Meßzelle übertragen wird.

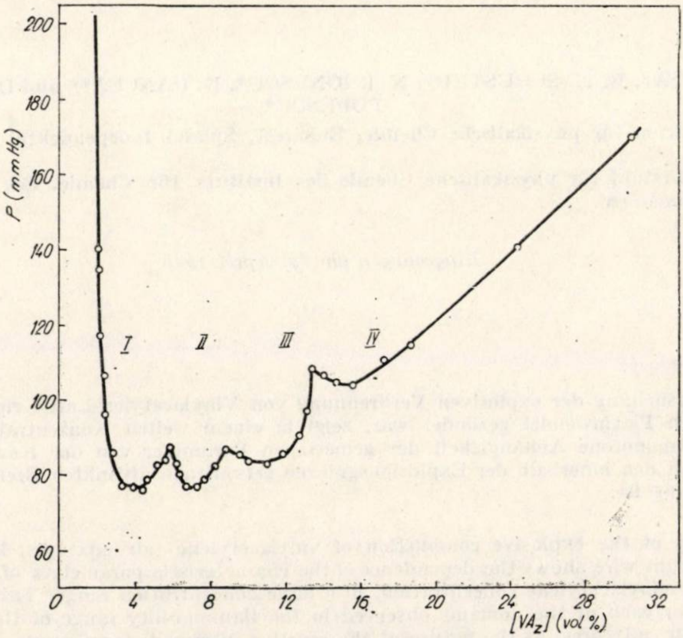

Abb.1. — Die Abhängigkeit des Mindestinitialdrucks der Explosion von der Vinylacetylenkonzentration in VAz-Luft-Gemisch.

Der Mindestinitialdruck bei dem die Explosion stattfindet ist in Abhängigkeit der VAz-Konzentration in Abbildung 1 dargestellt. Als Kriterium wurde bei dieser Kurve angenommen, daß die Explosion von einer Flamme beleitet wird, die sich in der ganzen Zelle ausbreitet.

Im untersuchten Konzentrationsbereich sind vier Brennbereiche eindeutig zu unterscheiden, wodurch der in einer vorangegangenen Arbeit[3] erhaltene Befund bestärkt wird. Der erste Bereich (I) ist durch die untere Explosionsgrenze bei 1,6 %VAz und durch die Konzentration 5,9% VAz begrenzt. Angefangen von der unteren Explosionsgrenze fällt der Mindestinitialdruck bis auf 75 mm Hg beim stoechiometrischen Gemisch ab und steigt anschließend auf 90 mm Hg an der oberen Grenze des ersten Bereiches (5,9% VAz). Der erste Brennbereich ist durch eine blaue Flamme mit schwacher Lumineszenz gekennzeichnet. Wie auch im Falle anderer brennbarer Gase, tritt diese Flamme bei brennstoffarmen Gemischen auf.[5] Bei Vinylacetylen tritt die blaue Flamme bis zu einer Zusammensetzung von etwa 1,5 mal die stoechiometrische Brennstoffmenge auf. Der zweite Brennbereich (II) ist von den Konzentrationen 5,9% und 8,8% VAz begrenzt. Die Mindestinistialdrücke haben wiederum niedere Werte mit einem Mindestwert von 75 mm Hg bei 7 % VAz (1,7 mal die stoechiometrische Brennstoffmenge). Die auftretende Flamme ist intensiv grün gefärbt und wurde wie auch bei anderen Brennstoff-Luftgemischen[6] als eine Übergangsflamme zur heißen gelben Flamme gedeutet. Bei dieser Flamme erlangen die Reaktionen des atomaren Sauerstoffes zur Bedeutung.[7] Als Quelle der grünen Flamme werden die Radikale C_2 (bei 5165 Å) und CH (bei 4135 Å) angesehen.[7] Da diese bei Acetylen-Sauerstoff Flammen[8] auftreten ist es naheliegend, daß auch bei Vinylacetylen-Luft ähnliche elementare Reaktionen determinant sind. Der dritte Brennbereich (III) liegt zwischen den Konzentrationen 8,8 und 13,4 % VAz. Im ersten Teil des Bereiches fällt der Mindestinitialdurck auf einen Wert von 82 mm Hg bei 10,9% VAz (2,8 mal die stoechiometrische Zusammensetzung) ab und steigt dann auf 108 mm Hg bei 13,4 % VAz. Die Flamme hat in diesem Bereich eine intensiv weiß-gelbe Farbe, die der Emission des Kohlenstoffs zugeschrieben wird.[7] Im letzten Brennbereich, oberhalb von 13,4% VAz, steigt praktisch der Mindestinitialdruck ständig mit der VAz-Konzentration an. In diesem Bereich tritt außer einer gelben Flamme auch eine immer stärker werdende Rußbildung auf.

In den ersten drei Brennbereichen wird sowohl eine aufsteigende als auch eine abfallende Flammenfortpflanzung beobachtet. Dagegen pflanzt sich die Flamme im letzten Brennbereich ausschließlich aufsteigend fort, im Sinne der Konvektionsströmung im Gas.

Die kritische Zündenergie der Explosion wurde wie anderweitig beschrieben,[4] aus der Heizperiode der Wendel und der elektrischen Leistung, bestimmt. Die berechneten Werte ergeben eine scheinbare Zündenergie, weil zwei Faktoren dabei nicht berücksichtigt wurden: die Widerstandsänderung der Wendel während des Anheizens und die Wärmeverluste an den Kontakten. Gleichfalls müssen die absoluten Zündenergien von verschiedenen Zündquellen nicht übereinstimmen.[9] Die erhaltenen Werte wurden um die Vinylacetylen-Luft-Gemische bei verschiedenen Initialdrucken und Konzentrationen zu vergleichen verwendet.

Die Änderung der Zündenergie in Abhängigkeit vom Initialdruck zeigt einen deutlichen Anstieg der Werte gegen den Mindestinitialdruck an (Abb. 2). Um die Konzentrationsabhängigkeit der Zündenergie zu verfolgen wurden die verschiedenen Gemische jeweils bei einem Druck P miteinander verglichen, für den der reduzierte Druck P/P_M (P_M = Mindestinitialdruck) konstant ist. Die erhaltenen Kurven besitzen keinen monotonen Charakter und sind durch zwei Bereiche gekennzeichnet (Abb. 3).

Der erste Bereich entspricht den ersten zwei Brennbereichen (I und II aus Abbildung 1) die nicht getrennt erscheinen. Ein Energiemaximum beim stoechiometrischen Gemisch, gefolgt von einem Minimum bei 7% VAz und einem zweiten wenig ausgeprägten Maximum bei 8,9% VAz kennzeichnen diesen Bereich. Der zweite Bereich der Kurve zeigt einen langsamen monotonen Abfall der Zündenergiewerte mit ansteigender

VAz Konzentration. Die nichtmonotone Konzentrationsabhängigkeit der Zündenergie im ersten Kurvenbereich ist erstaunlich, wurde aber auch von anderen Autoren beobachtet. So wurde ein Zündenergiemaximum bei der stoechiometrischen Zusammensetzung des Gemisches Methan-Luft dann beobachtet, wenn mit einer Platinwendel gezündet wurde.[10,11] Zur Erklärung wurde ein katalitischer Effekt der Platinwendel herangezogen.[12]

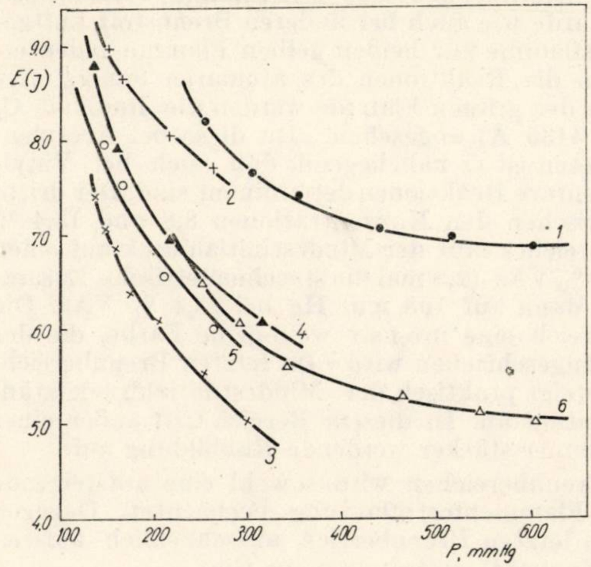

Abb. 2. – Die Abhängigkeit der Zündenergie vom Initialdruck für einige Vinylacetylenkonzentrationen des Gemisches VAz-Luft : *1.* 1,8 % ; *2.* 6,0 % ; *3.* 7,0 % ; *4.* 10,0 % ; *5.* 12,6 % ; *6.* 20,4 % VAz.

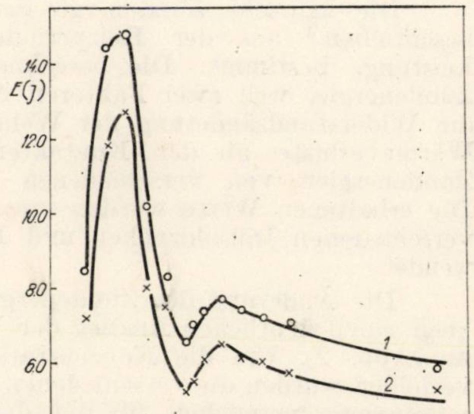

Abb. 3. – Die Abhängigkeit der Zündenergie von der Vinylacetylenkonzentration im VAz-Luft Gemisch bei verschiedenen Werten des „reduzierten Drucks" : *1.* $P_r = 2,10$; *2.* $P_r = 3,50$.

Die durch den Heizdraht ausgelöste chemische Reaktion, bewirkt einen Temperaturanstieg in den angrenzenden Gasschichten aufgrund der freiwerdenden Wärme, die, im Falle des Platins als Zündquelle vornehmlich an den Heizdraht abgegeben wird, wodurch dieser das verbrannte Gas abkühlt. Gleichzeitig bewirkt die Diffusion der Reaktionsprodukte gegen das Frischgas, ein Konzentrationsgefälle das eine kontinuierliche „Absorption“ des Frischgases in Richtung Heizdraht bestimmt, wodurch das Frischgas an der heißen Wendel katalytisch verbrannt wird. Als Folge dieser Vorgänge wird der Heizdraht durch eine Schicht von kaltem verbrannten Gas isoliert, was wiederum eine längere Anheizperiode erfordert und somit höhere Zündenergiewerte gemessen werden. Untersuchungen des katalitischen Effektes der Platinwendel bei der Verbrennung von Methan in Luft[13] haben gezeigt, daß dieser Effekt am größten bei der stoechiometrischen Zusammensetzung ist. Ein ähnlicher Effekt kann somit auch im Falle der Konzentrationsabhängigkeit der Zündenergie beim Gemisch Vinylacetylen-Luft angenommen werden.

In den gegebenen experimentellen Bedingungen[4] wurde die explosive Verbrennung durch zwei zusätzliche Aspekte gekennzeichnet :

a) „Nullimpuls“ – Kurve[3]

b) Impuls der der Verschlußplatte der Zelle durch die Explosion übertragen wird.[2,4]

Die „Nullimpuls“ – Kurve (Ab. 4) hat eine gefächerte Struktur die mit der Mindestinitialdruckkurve korreliert werden kann.

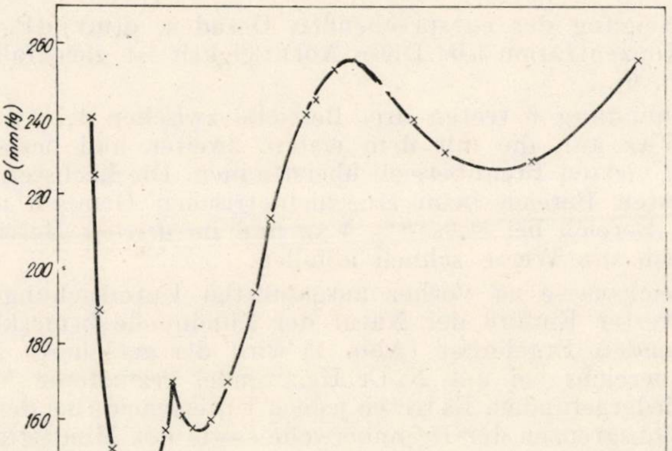

Abb. 4. – „Nullimpuls“ Kurve für das Gemisch Vinylacetylen-Luft.

Von der unteren Explosionsgrenze (1,6% VAz) angefangen, zeigt die Kurve einen Abfall und drei distinkte Bereiche treten im Diagram (Abb. 4), zwischen den Konzentrationen 2,5–6 ; 6–15,6 und oberhalb von 16 % VAz auf.

Aus der „Nullimpuls"-Kurve kann das nichtmonotone Verhalten des maximalen Explosionsdrucks in Abhängigkeit der VAz-Konzentration abgeleitet werden, wenn Rechnung getragen wird, daß das Verhältnis des atmosphärischen Drucks zum Anfangsdruck der Explosionen, die der Verschlußplatte der Zelle einen Impuls vom Wert Null übertragen, eine relative Druckerhöhung bedeutet. Die höchsten Werte der Druckerhöhung erhält man für Gemischzusammensetzungen im ersten Bereich, der mit dem ersten Brennbereich zusammenfällt. Im zweiten Bereich der Kurve, der mit dem zweiten Brennbereich übereinstimmt, wurde eine niedrigere Druckerhöhung gefunden. Ein Abfallen dieser Werte (vom 4,5-fachen auf den 3-fachen Anfangsdruck) ist im Bereich zwischen 7,5—15,6 % VAz bemerkbar. Für die Gemische im dritten Bereich steigt der Druck während der Explosion relativ wenig an. Die größte Druckerhöhung (5,5 mal) wird beim stoechiometrischen Gemisch registriert. Die Gemische mit hohem VAz-Gehalt die während der Explosion zur Rußbildung neigen, sind durch eine kleine Druckerhöhung gekennzeichnet.

Der Impuls, der der Verschlußplatte der Zelle übertragen wird, hängt im ganzen Konzentrationsbereich linear vom Anfangsdruck ab (Abb. 5).

Die Neigung der entsprechenden Geraden, d(mv)/dP, hängt von der VAz Konzentration ab. Diese Abhängigkeit ist gleichfalls nichtmonoton (Abb. 6).

In Abbildung 6 treten drei Bereiche zwischen 1,7—6; 6—9 und über 9% VAz auf, die mit dem ersten, zweiten und beziehungsweise dritten und vierten Brennbereich überstimmen. Die höchsten Neigungen sind im ersten Bereich beim stoechiometrischen Gemisch anzutreffen, im zweiten Bereich bei etwa 8% VAz und im dritten Bereich bei 11% VAz, wonach die Werte schnell abfallen.

Vergleichsweise zu vorher ausgeführten Untersuchungen[3] ist ein bemerkenswerter Einfluß der Natur der Zündquelle bemerkbar. Durch die vorliegenden Ergebnisse (Abb. 1) wird der gefächerte Aspekt des Exploisionsbereichs bei mit Ni-Cr Heizwendel gezündeten VAz-Luftgemischen[3] wiedergefunden. Es treten jedoch Unterscheide bei den jeweiligen Konzentrationsgrenzen der Brennbereiche sowie des Mindestinitialdrucks auf. Auf jeden Fall sind bei VAz Konzentrationen bis 9% die kleinsten Mindestinitialdrücke unabhängig von der Zündquelle. Der niedrigste Wert des Mindestinitaldrucks wird zweifellos für das stoechiometrische Gemisch gemessen. Bei VAz-reichen Gemischen erhält man höhere Mindestinitialdrücke und zum Teil wird auch Ruß gebildet. Die Konzentrationsabhängigkeit der Flammenfarbe wird jedoch nicht von der Zündquelle bestimmt. Die Änderung der Flammenfarbe kann durch das Auftreten einiger angeregten Spezies erklärt werden was wiederum auf verschiedene Reaktionsmechanismen in den jeweiligen Brennbereichen hinweist. Die Unterschiede die bei den Konzentrationsgrenzen und Mindestinitialdrucken im Falle der Zündung mit einer Ni—Cr oder einer Pt-Heizwendel auftreten, können daher dem katalitischen Effekt des Platins zugeschrieben werden, durch welchen die Bildung oder der Abbau einiger intermädiaren Spezies beeinflußt werden kann.

Die Abhängigkeit der Zündenergie vom Anfangsdruck in der Zelle hat bei beiden verwendeten Heizwendeln Pt und Ni—Cr[3] einen ähnlichen Aspekt. Im Falle beider Heizwendeln ist eine betonte Abhängigkeit der Zündenergie von der Zusammensetzung des VAz-Luft Gemisches zu bemerken, die jedoch für die versendeten Zündquellen Unterschiede aufweist. So durchläuft die Zündergie bei Verwendung einer Ni—Cr Heizwendel ein Minimum bei 6—8 % VAz und steigt danach langsam an[3], was auf das Fehlen eines katalitischen Effektes zurückzuführen ist. Unterschiede im Wert der Zündenergien hängen allem Anschein nach von der Geometrie der verwendeten Wendeln ab.

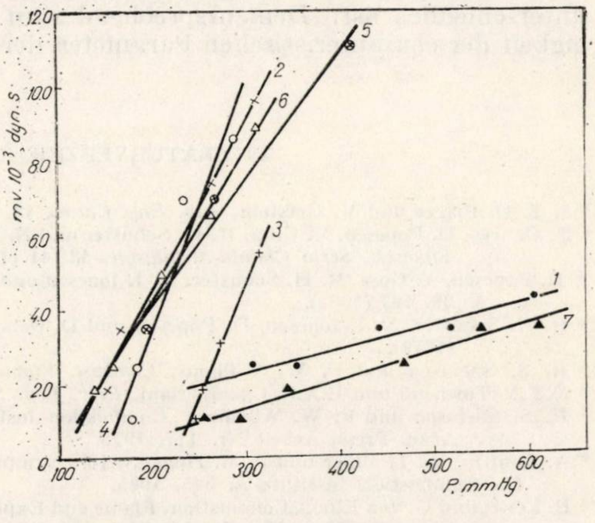

Abb. 5. — Die Abhängigkeit des Impulses der an die Verschluß-platte der Meßzelle durch die Explosion übertragen wird, von der Vinylacetylenkonzentration : *1.* 1,8 % ; *2.* 3,0 % ; *3.* 6,0 % ; *4.* 7,9 % *5.* 8,9 % ; *6.* 11,1 % ; *7.* 20,4 % VAz.

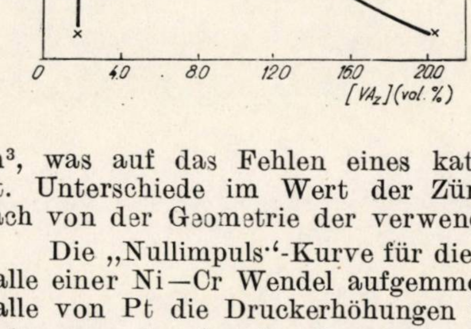

Abb. 6. — Die Abhängigkeit der Neigungen der Geraden Impuls — Anfangsdruck von der Vinylacetylenkonzentration im VAz-Luft-Gemisch.

Die „Nullimpuls"-Kurve für die Pt-Wendel (Abb. 4) gleicht der im Falle einer Ni—Cr Wendel aufgemmonen Kurve,[3] dabei sind jedoch im Falle von Pt die Druckerhöhungen relativ größer. Gleichfalls sind die Neigungen der Geraden Impuls-Druck höher im Falle der Platinwendel als im Falle einer Ni—Cr Wendel.

SCHLUßFOLGERUNGEN

Die Untersuchungen der explosiven Verbrennung der an Platinwendel gezündeten Vinylacetylen-Luft-Gemischen hat die Existenz von distinkten Brennbereichen gezeigt, für die der Verbrennungsmechanismus unterschiedlich ist. Dementsprechend wird eine nichtmonotone Abhängigkeit der charakteristischen Parameter der Explosion bemerkt.

LITERATURVERZEICHNICSS

[1] J. T. Di Piazza und M. Gerstein, *Ind. Eng. Chem.*, **43**, 2721 (1951).

[2] D. Oancea, D. Popescu, V. Goşa, R. H. Schuster und N. I. Ionescu, *Bull. Instit. Polytechnic Bukarest, Seria Chimie-Metalurgie*, **42**, 41 (1980).

[3] D. Popescu, V. Goşa, R. H. Schuster, N. I. Ionescu und D. Oancea, *Rev. Roumaine Chim.*, **26**, 197 (1981).

[4] R. H. Schuster, N. I. Ionescu, D. Popescu und D. Oancea, *Rev. Roumaine Chim.*, **24**, 531 (1979).

[5] R. S. Sheinson und F. W. Williams, *Combust. Flame*, **21**, 221 (1973).

[6] D.T.A. Townend und E.A.C. Chamberlain, *Proc. Roy. Soc.*, **A 158**, 415 (1937).

[7] R. S. Sheinson und F. W. Williams, „Combustion Institute European Symposium 1973", Acad. Press, Arbeit Nr. 117, 1973.

[8] A. Fontijn, W. T. Miller und J. M. Hogan, „10th Symposium on Combustion, Pittsburg, The Combustion Institute, s. 545, 1965.

[9] B. Lewis und G. von Elbe, „Combustion, Flame and Explosion of Gases, ", Second Edition, Academic Press, New York, 1961, cap. V.

[10] H. F. Coward und P. G. Guest, *J. Amer. Chem. Soc.*, **49**, 2479 (1972).

[11] P. G. Guest, U.S. Bur. Mines Techn. Paper 475 (1930).

[12] W. Jost, „Explosion and Combustion Processes in Gases", First Edition, McGraw Hill, New York, 1946, cap. I.

[13] O. C. Ellis, *Fuel*, **7**, 245 (1928).

Revue Roumaine de Chimie, 26, *9–10*, 1213–1220 (1981)

RECHERCHES ÉLECTRONOMICROSCOPIQUES ET PAR ANALYSE THERMIQUE SUR L'HYDRATATION DE $4CaO.Al_2O_3.Fe_2O_3$ ET $2CaO.Fe_2O_3$ À DES TEMPÉRATURES ET PRESSIONS ÉLEVÉES

I. TEOREANU*, CECILIA HRIȚCU*, N. BUTUCESCU** et LIANA BUCEA**

* Institut Polytechnique Bucarest, str. Polizu, n° 1

** Institut de Recherche et Projection pour l'Industrie des Liants et d'Amianteciment, Bucarest, Bul. Preciziei, n° 6.

Reçu le 9 février 1981

L'objet de ce travail sont les recherches électronomicroscopiques et par analyse thermique concernant l'hydratation-hydrolyse du ferroaluminate tétracalcique et de la ferrite dicalcique. Elles viennent compléter l'image du processus, en particulier en ce qui concerne la nature et la morphologie des phases hydratées, formées dans différentes conditions de température et de pression.

The subject of this paper refers to the electronomicroscopical researches and thermal differential analysis of tetracalcium ferritealuminate and dicalcic ferrite hydration and hydrolysis. These researches supplement the aspects of the process, especially of the nature and morphology of the hydrated phases, produced under different temperature and pressure conditions.

INTRODUCTION

L'interaction avec l'eau des composés contenant du fer $4CaO.Al_2O_3.Fe_2O_3$ et $2CaO.Fe_2O_3$, les constituants usuels du clinker portland pour forages profonds, est influencée évidemment par les conditions de traitement à des températures et pressions élevées.

Le mécanisme d'hydratation – hydrolyse de $4CaO.Al_2O_3.Fe_2O_3$ et de $2CaO.Fe_2O_3$ à des températures et pressions élevées (jusqu'à 150°C et 1325 at.), ainsi que l'influence de l'augmentation de la température et de la pression de traitement sur la cinétique de l'interaction de ces deux composés avec l'eau, déduits des résultats de diffractométrie X, spectrométrie Mössbauer, déterminations d'eau liée et de surface spécifique B E T , ont été présentés dans des travaux antérieurs.[1,2]

Les recherches électronomicroscopiques et par analyse thermique concernant l'hydratation – hydrolyse du ferroaluminate tétracalcique et de la ferrite dicalcique, qui font l'objet de cet article, viennent compléter l'image du processus, en particulier en ce qui concerne la nature et la morphologie des phases hydratées, formées, comme suite de l'interaction des deux composés mentionnés avec l'eau, dans différentes conditions de température et de pression.

CONDITIONS EXPÉRIMENTALES

Le ferroaluminate tétracalcique et la ferrite dicalcique ont été synthétisés par réaction en phase solide d'un mélange stoechiométrique de substances chimiquement pures : $CaCO_3$, Fe_2O_3 et Al_2O_3.

Les échantillons de $4CaO.Al_2O_3.Fe_2O_3$ et de $2CaO\ Fe_2O_3$ ont été hydratés pendant 6 heures en pâte préparée avec le rapport eau/solide = 0,4, tant à température et pression normales qu'à celles élevées (50°C et 390 at., 75°C et 650 at., 100°C et 920 at., 120°C et 1135 at. et 150°C et 1325 at.).

L'analyse thermique différentielle a été efectuée avec un dérivatographe de type M O M (four de 1000°C, vitesse de chauffage 10°/min.).

L'examen au microscope électronique a été effectué avec un appareil du type JEM 7A, par transmission, à une tension d'accélération des électrons de 80 Kv et par recherche directe de l'échantillon ; les préparations ont été obtenues par dépôt sur une pellicule — support, de poudre fine dispersée en alcool éthylique absolu.

INTERPRÉTATION DES RÉSULTATS

Les courbes A T D des échantillons de $4CaO.Al_2O_3.Fe_2O_3$ hydratés à des températures et pressions élevées (fig. 1) sont similaires à celles des échantillons hydratés en conditions normales. Dans tous les cas — excepté l'échantillon hydraté à 150°C et 1325 at. — trois effets endothermiques sont mis en évidence, situés à 200—260°C, 360—410°C et respectivement à 840—900°C. Le premier effet a été attribué à la deshydratation des formations hexagonales hydroaluminate-ferritiques (de type $4CaO.R_2O_3.13H_2O$), ainsi que du gel d'hydrate d'oxyde ferrique ($Fe_2O_3.nH_2O$). L'intensité de cet effet croît en même temps que la croissance de la température de traitement, jusqu'à 75°C et, ensuite, décroît avec la croissance de celle-ci jusqu'à 150°C, suggérant la diminution, jusqu'à la disparition, des hydroformations hexagonales et du produit gélique $Fe_2O_3.nH_2O$. Le deuxième effet endothermique, correspond à la déshydratation des hydrogranats ($3CaO.Al_2O_3.6H_2O - 3CaO.Fe_2O_3.6H_2O$) ; ce dernier effet se développe avec la croissance de la température et de la pression auxquelles a eu lieu l'hydratation de l'échantillon (jusqu'à 150°C et 1325 at.), illustrant la formation, avec prépondérance ou seulement, des hydroferroaluminates de type hydrogranat. Cette dernière conclusion est renforcée par le fait qu'à des températures de traitement supérieures à 50°C (et à pressions correspondantes) un nouveau effet endothermique est mis en évidence à 550—600°C, qui, de même, peut être attribué aux hydrogranats. Le dernier effet (à 840°—900°C) peut être attribué éventuellement à la décomposition des formations hydratées contaminées avec CO_2[3].

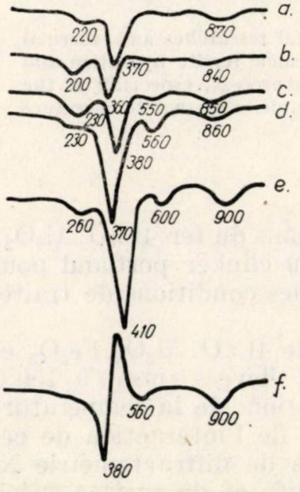

Fig. 1. — Courbes ATD de C_4AF hydraté (6 heures) à différentes températures et pressions : *a* — 20°C et 1 at ; *b* — 50°C et 390 at ; *c* — 75°C et 650 at ; *d* — 100°C et 920 at ; *e*—120°C et 1135 at ; *f*—150°C et 1325 at.

Sur la courbe ATD de l'échantillon hydraté à 150°C et 1325 at. on constate un puissant effet exothermique qui pourrait être attribué aux transformations structurelles de certains hydrocomposés en fer (caractéristiques pour les échantillons durcis à des températures et pressions plus élevées — la durée de durcissement étant très courte, ou pour les échantillons durcis en conditions normales de température et pression mais avec d'additions accélérateurs de durcissement[4] ou à des durées plus grandes de durcissement[5]).

En dehors des mutations intervenues dans la nature des phases, l'analyse thermique du $4CaO.Al_2O_3.Fe_2O_3$ hydraté met en évidence, de même, l'intensification de l'interaction avec l'eau de ce composé sous l'influence de la croissance de la température et de la pression de traitement.

Dans les micrographies électroniques des échantillons hydratés de $4CaO.Al_2O_3.Fe_2O_3$ (fig. 2), les composés crystallins prédominent : avec des contours hexagonaux (attribués aux produits de type $4CaO.R_2O_3.\,.nH_2O$) — en particulier dans les échantillons durcis à 50°C et moins fréquemment dans les échantillons durcis à des températures plus élevées, même dans ceux durcis à 75°C, et avec des contours cubiques (les hydrogranats) — en quantité plus grande lorsque la température et la pression de traitement s'accroissent (jusqu'à 150°C et 1325 at.). À températures de traitement moindres, on observe en plus, assez clairement, le produit gélique attribué à $Fe_2O_3.nH_2O$. Ces observations sont en bon accord avec les résultats de l'analyse thermique différentielle effectuée dans les mêmes conditions (qui illustrent la réduction substantielle de l'effet endothermique de 200°C), en confirmant clairement les résultats de spectrométrie Mössbauer qui ont conduit à présumer que, dans les échantillons de $4CaO.Al_2O_3.Fe_2O_3$ durcis à des températures plus élevées, le fer hydraté est lié prépondérant sous forme de solutions cubiques d'hydroaluminoferrite de calcium.[2]

La courbe ATD de l'échantillon de $2CaO.Fe_2O_3$, hydraté à 50°C et 390 at. (fig. 3), est similaire à cele réalisée avec l'échantillon hydraté en conditions normales de température et pression (pareillement au cas de $4CaO.Al_2O_3.Fe_2O_3$) ; le fait qui les distingue c'est que les effets thermiques sont plus grands dans le premier cas, en particulier l'effet situé à 150 — 170°C (attribué à la déshydratation du gel d'hydrate de l'oxyde ferrique, $Fe_2O_3.nH_2O$), ainsi que celui situé à 510—550°C (dû à la décomposition de $Ca(OH)_2$).

Sur les courbes ATD des échantillons de $2CaO.Fe_2O_3$, durcis à 100°C, 120°C et 150°C et à pressions correspondantes (fig. 3), le pic attribué à la décomposition de $Ca(OH)_2$ est plus aigu, ayant une plus grande intensité à cause de la quantité plus grande de ce composé et de son haut degré de cristalinité ; d'autre part, l'effet correspondant à des températures moins élevées (150 — 170°C) est plus réduit et en continuelle décroissance, ce qui exprime la diminution de la proportion de l'hydrate d'oxyde ferrique avec l'augmentation de la température et de la pression de traitement. La réduction de ce dernier effet se trouve en parfaite concordance avec les résultats d'analyse diffractométrique et de spectrométrie Mössbauer.[2] L'échantillon de $2CaO.Fe_2O_3$ hydraté à 75°C et 650 at. montre une courbe ATD aussi peu résolue que le spectre Mössbauer[2] ; les effets thermiques mis en évidence dans le cas de l'hydratation à des températures moins élevées (20°C et 50°C) sont, pour l'échantillon durci à 75°C et 650 at., beaucoup réduits.

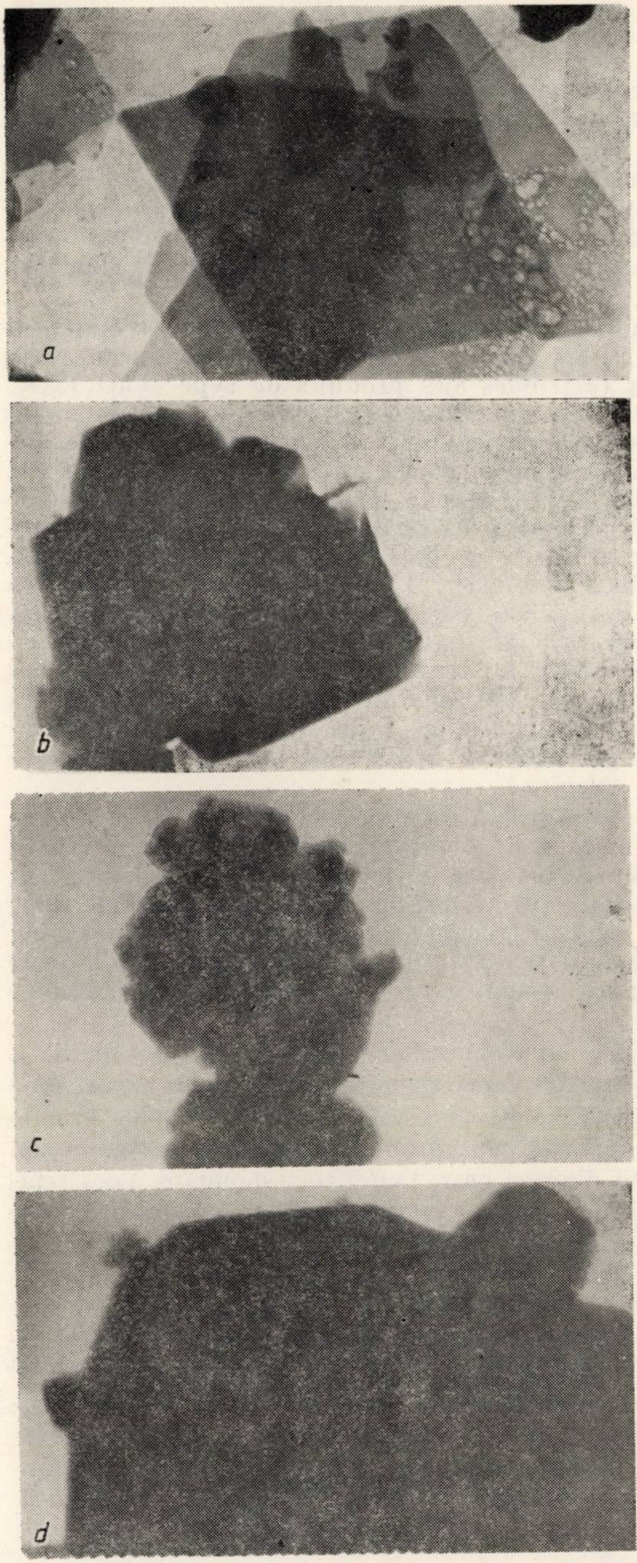

Fig. 2. — Images électronomicroscopiques de C_4AF hydraté (6 heures) à des températures et pressions élevées : *a* — 50°C et 390 at. (30.000 X) ; *b* — 75°C et 650 at. (30.000 X) ; *c* — 100°C et 920 at. (15.000 X) ; *d* — 120°C et 1135 at. (30.000X).

L'analyse thermique des échantillons de ferrite dicalcique hydratée, pareillement au échantillons de ferroaluminate tétracalcique hydraté, illustre en outre l'influence accélératrice de la croissance de la température et de la pression sur la cinétique de l'interaction avec l'eau de ce composé. En bon accord avec les résultats de diffraction X et d'eau liée,[1,2] l'effet endothermique de 510—550°C (dû à la déshydratation de $Ca(OH)_2$) croît intensément avec l'augmentation de la température et de la pression d'hydratation, depuis 20°C et la pression atmosphérique jusqu'à 100°C et 920 at. ; aux températures et pressions plus élevées (jusqu'à 150°C et 1325 at.) la grandeur de l'effet reste pratiquement constante.

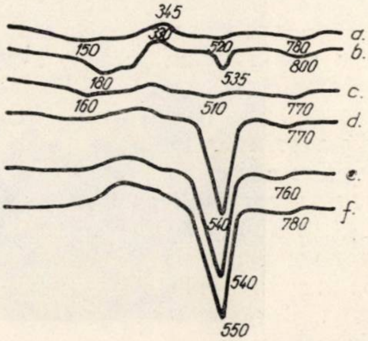

Fig. 3. — Courbes ATD de C_2F hydraté (6 heures) à différentes températures et pressions : *a* — 20°C et 1 at. ; *b* — 50°C et 390 at. ; *c* — 75°C et 650 at. *d* — 100°C et 920 at. ; 120°C et 1135 at. ; *f* — 150°C et 1325 at.

En ce qui concerne la morphologie des produits obtenus par l'hydratation de la ferrite dicalcique aux températures et pressions élevées, l'examen au microscope électronique (fig. 4) met en évidence des formations feuillues, transparentes (formes attribuées à l'hydroxyde de calcium) qui, en général, n'ont pas des contours polygonaux (seulement rarement elles ont des contours hexagonaux). On peut encore observer de petits sphérolithes colloïdaux (phase incipiente de transformation vers les feuillets d'hydroxyde de calcium). L'hydroxyde de fer se présente de même sous forme colloïdale, en particules fines qui bordent les granules de matériel anhydre.

Dans les échantillons de $2CaO.Fe_2O_3$ durcis aux températures de 120°C et de 150°C et à des pressions correspondantes, on observe des microparticules (inférieures à 0,1 µm) ayant des contours approximativement irréguliers (sans aspect géométrique), partiellement transparentes. Après les essais d'identification effectués par spectrométrie Mössbauer et diffraction Roentgen (v. le travail antérieur[2]) et en corrélation avec des données de la littérature,[6] elles peuvent être attribuées au composé $\alpha - Fe_2O_3$. Dans des cas très isolés on observe des formes cubiques de $\gamma - Fe_2O_3$ (fig. 4 d_1).

Les images électronomicroscopiques indiquent, elles aussi, un très avancé degré d'hydratation des échantillons durcis à des températures supérieures à 100°C (en bon accord avec les résultats de diffraction X, d'eau liée[1,2] et d'analyse thermique différentielle).

Fig. 4. — Images électronomicroscopiques de C_2F hydraté (6 heures) à des températures et pressions élevées (30.000X) : *a*— 50°C et 390 at. ; *b* — 75°C et 650 at. ; *c* — 100°C et 920 at. ; *d* — 120°C et 1135 at. ; d_0 — avec $\alpha - Fe_2O_3$: d_1 — avec $\gamma - Fe_2O_3$; *e* — 150°C et 1325 at.

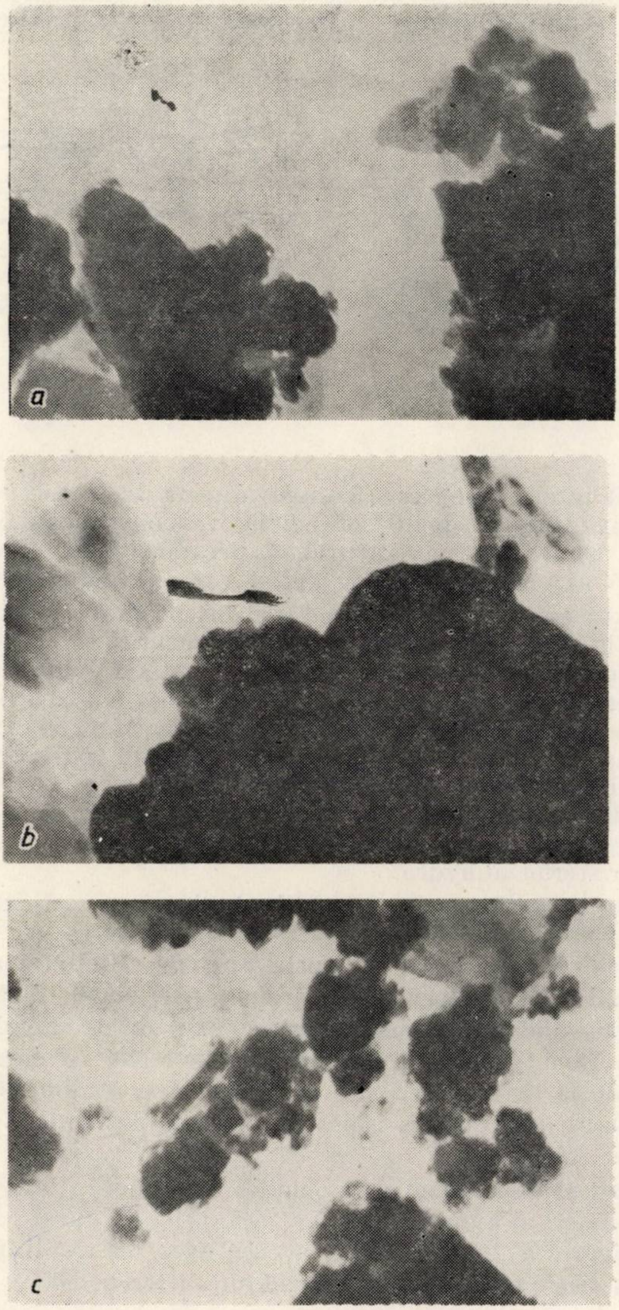

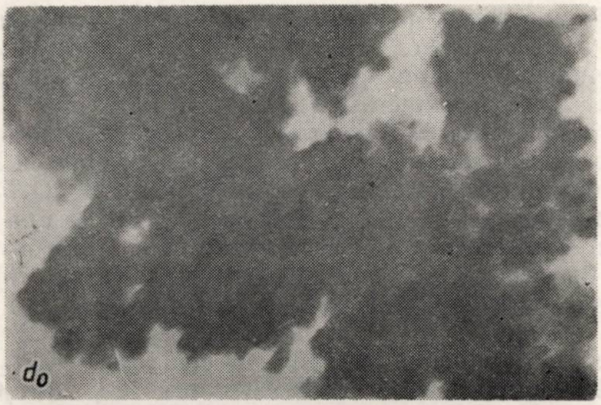

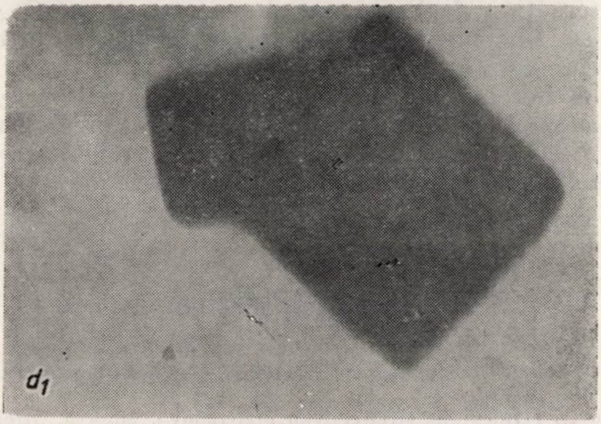

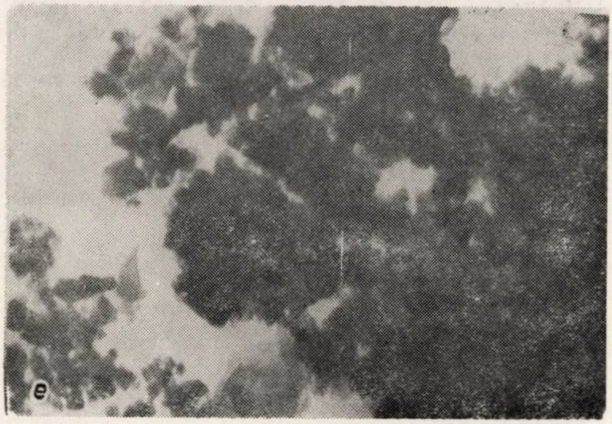

CONCLUSIONS

Les résultats présentés plus haut conduisent aux conclusions suivantes :

1. À l'hydratation — hydrolyse du $4CaO.Al_2O_3.Fe_2O_3$ en conditions de température et de pression jusqu'à 50°C et 390 at. — 75°C et

650 at., après une courte période d'interaction avec l'eau (6 heures), se forment des hydrocomposés de la série isomorphe des hydroferroaluminates de calcium hexagonaux plus riches en Al_2O_3 et du produit gélique $Fe_2O_3.nH_2O$. À des températures et pressions plus élevées (jusqu'à 150°C et 1325 at.), a lieu la formation avec prépondérance ou uniquement, des hydroferroaluminates de type cubique, plus riches en Fe_2O_3.

2. À l'interaction de l'eau avec le produit $2CaO.Fe_2O_3$, en conditions de températures et de pressions élevées, après une courte période d'hydratation — hydrolyse, a lieu la formation de l'hydroxyde de calcium cristallin et du produit gélique $Fe_2O_3.nH_2O$; la quantité maximale de produit gélique se forme à 50°C et 390 at. À températures et pressions de traitement plus élevées (120°C — 150°C et 1135 — 1325 at), ensemble avec l'hydroxyde de calcium cristallin, le composé $\alpha - Fe_2O_3$ est présent aussi (dans des cas très isolés on observe aussi le $\gamma - Fe_2O_3$).

3. L'interaction de l'eau avec les composés $4CaO.Al_2O_3.Fe_2O_3$ et $2CaO.Fe_2O_3$ est fortement accélérée par l'augmentation de la température et de la pression de traitement.

4. Les recherches effectuées par voie thermique et électronomicroscopique ont confirmé le mécanisme d'hydratation de $4CaO.Al_2O_3Fe_2O_3$ et de $2CaO.Fe_2O_3$, dans des conditions de températures et pressions élevées, qui a été présenté dans un travail antérieur.[2]

BIBLIOGRAPHIE

[1] I. Teoreanu et C. Hriţcu, *Materiale de Constr.*, **6**, 157 (1976).

[2] I. Teoreanu, G. Filoti, C. Hriţcu, L. Bucea, V. Spînu, S. Ciocănel et M. Ivaşcu, *Il. Cemento*, **76**, 19 (1979).

[3] V. S. Gorshkov, « Termografia stroitelinykh materialov », Moskva, Stroiizd, 1968.

[4] I. Teoreanu et M. Muntean, *Rev. des Mat. de Constr.*, **697**, 317 (1975).

[5] V. S. Ramachandran, « Application et Differential Thermal Analysis in Cement Chemistry », Chemical Publishing Company, Inc., New York, 1969.

[6] H. Bentelspacher et H. W. Van des Marel, « Atlas of Electron Microscopy of Clay Minerals and their Admixtures », Elsevier, Amsterdam, 1968.

Revue Roumaine de Chimie, **26**, *9–10*, 1221–1230 (1981)

Cu(II) COMPLEX COMPOUNDS WITH 1-(β-PHENYL-β-AMINO)ETHYLCYCLOBUTANOL AND 1-(β-*p*-CHLOROPHENYL-β-AMINO) ETHYLCYCLOBUTANOL

MARIA BREZEANU, I. SEBE, MELANIA GUŢUL and IOANA JITARU
The Polytechnic, Department of Chemistry, Laboratory of Inorganic Chemistry, 3–5 Polizu str., Bucharest Romania

Received April 22, 1980

A series of Cu(II) complexes with 1-(β-phenyl-β-amino)ethylcyclobutanol (AOH) and 1-(β-p-chlorophenyl-β-amino)ethylcyclobutanol (A'OH) have been obtained ; they are of the following general types : $[Cu(AOH)X_2].nH_2O$ and $[Cu(A'OH)X_2].n\ H_2O$ ($X = Cl$, $n=3$; $X=Br$, $n=2$) ; $[Cu(AOH)_2]X_2.n\ H_2O$ and $[Cu(A'OH)_2]X_2.n\ H_2O$ ($X=NO_3$, $n=0$; $X = 1/2\ SO_4$, $n = 1$) ; $[Cu(AOH)(AO)]\ CH_3COO$ and $[Cu\ (A'OH)\ (A'O)H_2O]\ CH_3COO$. These compounds have been characterized by elemental analysis, electric molecular conductivity measurements, electronic and vibrational spectra and thermal analysis. The most probable stereochemistry is then attributed to these compounds, on the basis of the results.

The paper belongs to a more extended area of research concerning the coordination ability of some superior aminoalcohols (namely propanol–amines).

Previous researches[1-3] in this field led to the conclusion that, in the presence of some metals, under well-defined experimental conditions, 3-amino-1-propanol exhibits its maximum coordination capacity, the tendency of coordination of the donor atoms being ordered as such : the nitrogen of the aminogroup, the oxygen of the deprotonated OH group, the oxygen of the hydroxyl.

From this point of view, the study of the coordination capacity of the propanolamines 1-(β-phenyl-β-amino)ethylcyclobutanol (C_6H_5- $-CHNH_2-CH_2-CB-OH$ where CB=1,1-cyclobutylene= 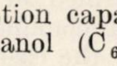)noted in this paper AOH and 1-(β-*p*-chlorophenyl-β-amino)ethylcyclobutanol (p-$Cl-C_6H_4-CHNH_2-CH_2-CB-OH$) noted in this paper A'OH, where one of the donor groups (OH) is directly bound to a saturated cycle, and the other donor group (NH_2) is indirectly bound to a benzene ring as to AOH, or to a substituted benzene ring as to A'OH, seems to be an interesting field of research.

The present paper reports on the results obtained in the synthesis and the characterization of some Cu(II) compounds with 1-(β-phenyl-β-amino) ethylcyclobutanol and 1-(β-*p*-chlorophenyl-β-amino) ethylcyclobutanol.

In order to establish the types of complexes which Cu(II) could form with these propanolamines, we studied the synthesis of complexes under different experimental conditions, changing the following parametres : — the molar ratio between Cu(II) salt and substituted propanolamine ;

— the nature of the Cu(II) salt anion ;

— the used solvent ;

— the pH of the reaction medium.

We could characterize in this way a series of complexes, belonging to the following general types : $[Cu(AOH)X_2].n\ H_2O$ and $[Cu(A'OH)X_2].n\ H_2O$ ($X = Cl$, $n = 3$ or $X = Br$, $n = 2$), $[Cu\ (AOH)_2]\ X_2.n\ H_2O$ and $[Cu(A'OH)_2]X_2.n\ H_2O$ ($X = NO_3$, $n = 0$; $X = 1/2SO_4$, $n = 1$); $[Cu(AOH)\ (AO)]CH_3COO$ and $[Cu\ (A'OH)\ (A'O)H_2O]\ CH_3COO$, where $AO = C_6H_5-CHNH_2-CH_2-CB-O^-$ and $A'O = p\text{-}Cl-C_6H_4-CHNH_2-CH_2-CB-O^-$.

RESULTS AND DISCUSSIONS

The synthesis of Cu(II) complexes with 1-(β-phenyl-β-amino)ethylcyclobutanol and 1-(β-*p*-chlorophenyl-β-amino)ethylcyclobutanol was carried out in alcohol or acetone solution (water was not a suitable solvent because of the insolubility of the used aminoalcohols in this medium), at values of the molar ratio $CuX_2(X = Cl, Br, NO_3, 1/2\ SO_4)$: propanolamine ranging from 1 :1 to 1 :5 ($pH \sim 5$); two different types of compounds were obtained, depending on the nature of Cu(II) salt anion, namely $[Cu(AOH)X_2].n\ H_2O$ when $X = Cl$, Br are characterized by a great tendency towards coordination and $[Cu(AOH)_2]X_2.n\ H_2O$ when $X = NO_3$, $1/2\ SO_4$ have a weak tendency towards coordination.

When the molar ratio of the components $Cu(CH_3COO)_2$: propanolamine is ranging from 1 :1 to 1 : 5, in alcohol or acetone solution, at $pH \sim 10$, compounds of the type $[Cu(AOH)\ (AO)]\ CH_3COO$ were obtained; in them, a molecule of propanolamine behaves as a neutral ligand, and another molecule as an anionic ligand. Although this kind of synthesis was performed in alkaline medium, complex compounds in which all the propanolamine molecules act as anionic ligands could not be separated, as in the case of 3-amino-l-propanol.

Molar electric conductivity measurements. The formulation assigned to the complex compounds investigated was confirmed by the determination of molar electric conductivities (Table 1).

The assignment of the electrolyte type was made by applying the procedure reported in the literature for dimethylformamide.[4]

Electronic spectra. In order to assign the most probable structure to these compounds their electronic spectra were registered.

Figure 1 and figure 2 show the electronic reflectance spectra, registered for such compounds as $[Cu(AOH)X_2].nH_2O$, $[Cu(A'OH)X_2].n\ H_2O$ ($X = Cl$, $n = 3$ or $X = Br$, $n = 2$), $[Cu(AOH)_2]X_2.n\ H_2O$ and $[Cu(A'OH)_2]$

TABLE 1

Molar electric conductivities of the studied compounds

Compound	Molar electric conductivity ($\Omega^{-1}cm^2mol^{-1}$)	Electrolyte type
$[Cu(AOH)Cl_2].3\ H_2O$*	25.70	nonelectrolyte
$[Cu(AOH)Br_2].2\ H_2O$*	20.30	nonelectrolyte
$[Cu(AO)\ (AOH)]\ CH_3COO$*	83.25	1 : 1
$[Cu(AOH)_2]\ (NO_3)_2$*	150.30	1 : 2
$[Cu(AOH)_2]SO_4 . H_2O$*	91.80	1 : 1
$[Cu(A'OH)_2]\ (NO_3)_2$**	155.20	1 : 2
$[Cu(A'OH)_2]\ SO_4 . H_2O$**	88.30	1 : 1
$[Cu(A'OH)Cl_2].3\ H_2O$**	17.30	nonelectrolyte
$[Cu(A'OH)Br_2].2\ H_2O$**	15.75	nonelectrolyte
$[Cu(A'O)\ (A'OH)H_2O]\ CH_3COO$**	85.70	1 : 1

10^{-3} M solutions, $t = 25°C$, solvent DMF
* $AOH = C_6H_5 - CHNH_2 - CH_2 - CB - OH$;
$AO = C_6H_5 - CHNH_2 - CH_2 - CB - O^-$
** $A'OH = p\text{-}Cl - C_6H_4 - CHNH_2 - CH_2 - CB - OH$;
$A'O = p\text{-}Cl - C_6H_4 - CHNH_2 - CH_2 - CB - O^-$ (where CB is 1,1-cyclobutylene).

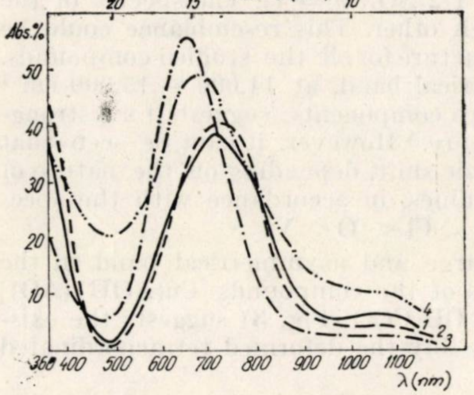

Fig. 1. — Electronic reflectance spectra of compounds : *1.* $[Cu(AOH)Cl_2].3\ H_2O$; *2.* $[Cu(AOH)Br_2].2\ H_2O$; *3.* $[Cu(AOH)_2]\ (NO_3)_2$; *4.* $[Cu(AOH)_2]\ SO_4.H_2O$ (where $AOH = C_6H_5 - CHNH_2 - CH_2 - CB - OH$)

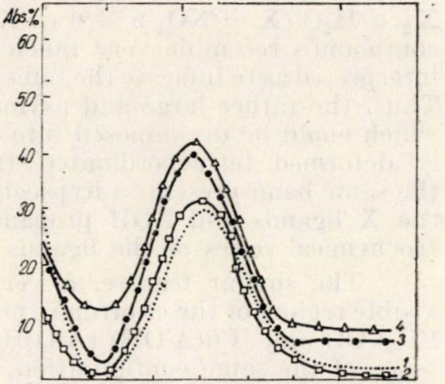

Fig. 2. — Electronic reflectance spectra of compounds : 1. $[Cu(A'OH)Cl_2].3\ H_2O$; 2. $[Cu(A'OH)Br_2].2\ H_2O$; 3. $[Cu(A'OH)_2]\ (NO_3)_2$; 4. $[Cu(A'OH)_2]\ SO_4.H_2O$. (where $A'OH = p\text{-}Cl - C_6H_4 - CHNH_2 - CH_2 - CB - OH$)

TABLE

IR frequencies (cm^{-1}) of Cu(II) complex compounds with 1-(β-

Compound	ν(OH)	ν(asNH) ν(sNH)	$\delta(NH_2) + \rho(NH_2)$
$AOH = C_6H_5-CHNH_2-CH_2-CB-OH$	3300	3300	895 1280
$[Cu(AOH)Cl_2] . 3H_2O$	3270	3225 3130	880 1240, 1260
$[Cu(AOH)\ (AO)]\ CH_3COO$	3250 3280	3220 3140	885 1220, *1255*, 1275
$[Cu(AOH)_2]\ (NO_3)_2$	3260 3270	3120 3170	885
$[Cu(AOH)_2]\ SO_4 . H_2O$	3290 3380	3240 3150	885

$X_2 . n\ H_2O$ ($X = NO_3$ $n = 0$ or $X = 1/2\ SO_4$, $n = 1$). The spectra of the compounds resemble very much each other. This resemblance could be interpreted as to indicate the same structure for all the studied compounds. Thus, the rather large and asymmetrical band, at 14.000 – 15.000 cm^{-1} which could be decomposed into more components, suggests for a strongly deformed tetracoordinated structure.[5] However, it can be seen that the same band presents a hypsochromic shift, depending on the nature of the X ligands and AOH propanolamines, in accordance with the spectrochemical series of the ligands $Br < Cl < O < N$.

The similar feature, a very large and asymmetrical band in the visible region, of the electronic spectra of the compounds $[Cu(AOH)(AO)]$ CH_3COO and $[Cu(A'OH)\ (A'O)H_2O]\ CH_3COO$ (Fig. 3) suggests the existence of the same configuration, possibly the deformed tetracoordinated structure.[6,7]

IR spectra. In order to supply additional data on their stereochemistry, particularly on the coordination manner of the ligand (neutral molecule, mono- or bidentate anion) and also on the behaviour of the anions (coordinated or in the ionization outer sphere), the IR spectra of these compounds were registered.

2

phenyl, β-amino)ethyl cyclobutanol and their probable assignments

ν(aryl)	ν(OCO) CH_3COO^-	ν(NO) NO_3^-	ν(SO) SO_4^{2-}	ν(OH) (water)
685, 704 1055, 1090 1153 1530 3090	—	—	—	—
630, 675, 705, 765 1035, 1060, 1085 1110, 1165 1500, 1580, 1610 3035, 3065, 3100	—	—	—	3490 3570
630, 675, 705, 735, 765 1035, 1050, 1070, 1080 1120, 1150, 1170, 1185 1500 3030, 3075	1400($_{sOCO}$) 1580 ($_{asOCO}$) (CH_3COO ionic)	—	—	—
650, 675, 710 1020, 1055, 1080 1125, 1170, 1185 1500, 1580 3050, 3080	—	1370 (ionic NO_3)	—	—
ionic SO_4 bands 705, 740 1030 ionic SO_4 bands 1505 3035, 3070	—	—	610, 630 1120 (ionic SO_4)	3565 3590

From this point of view, of interest are the O−H, ν(OH), C−O, ν(CO), stretching vibration and N−H, ν(asNH), ν(sNH), stretching vibration and δ(NH_2) bending vibration) of the ligands 1-(β-phenyl-β-amino)

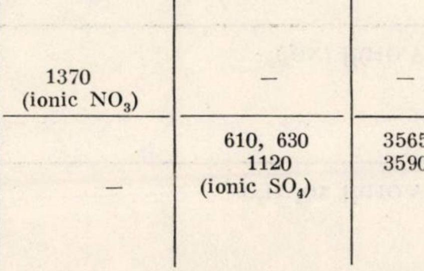

Fig. 3. — Electronic reflectance spectra of compounds : *1.* [Cu(A'OH) (A'O)H_2O] CH_3COO ; *2.* [Cu(AOH) (AO)] CH_3COO (where A'OH=p-Cl−C_6H_4−$CHNH_2$−CH_2−*CB*−OH, A'O = p-Cl−C_6H_4−$CHNH_2$−CH_2−*CB*−O^- and AOH = C_6H_5−$CHNH_2$−CH_2−*CB*−OH, AO = C_6H_5−$CHNH_2$−CH_2−*CB*−O^-).

TABLE

IR frequencies (cm^{-1}) of Cu(II) complex compounds with 1-(β-*p*-chlor

Compound	ν(OH)	ν(asNH) ν(sNH)	δ(NH_2) + ρ(NH_2)
A'OH = $p\text{-Cl}-C_6H_4-CHNH_2-CH_2-CB-OH$	3310	3310	895 1295
$[Cu(A'OH)Cl_2].3\ H_2O$	3265 3225	3310	880 1260
$[Cu(A'OH)(A'O)H_2O]CH_3COO$	3330 3225	3080	880 1250
$[Cu(A'OH)_2]\ (NO_3)_2$	3240 3285	3135	885 1260
$[Cu(A'OH)_2]\ SO_4.H_2O$	3250 3270	3150	885

ethylcyclobutanol and 1-(β-*p*-chlorophenyl-β-amino)ethylcyclobutanol, and on the other hand, the range where absorption can be assigned to the stretching modes of anions. For a more correct assignment, the spectra of the free ligands were registred too.

The frecquency of the O—H stretching vibration, ν(OH), in the spectra of 1-(β-phenyl-β-amino)ethylcyclobutanol and 1-(β-*p*-chlorophenyl-β-amino)ethylcyclobutanol appears at about 3300 cm^{-1} and at 3310 cm^{-1}, respectively.

Being compared to the stretching vibration frequency, ν(OH), from the primary alcohols (3600—3590 cm^{-1}) this value points to the presence of inter- and intramolecular hydrogen bonds in propanolamines.[8]

Tables 2 and 3 show the characteristic IR frequencies of some studied compounds and probable assignments.

An analysis of the data leads to the following conclusions, relative to the coordination manner of the aminoalcohols ligands :

—in all the studied compounds, the frecquency of the N—H stretching vibrations, ν(asNH), ν(sNH), and deformation vibrations, δ(NH_2),

3

phenyl, β-amino)ethylcyclobutanol and their probable assignments

ν(aryl)	ν(C−Cl)	ν(OCO) CH_3COO^-	ν(NO) NO_3^-	ν(SO) SO_4^{2-}	ν(OH) H_2O coord.	ν(OH) H_2O cryst.
845 1010, 1060, 1085 1160, 1185 1245 1550	1465	—	—	—	—	—
825, 850 1020, 1040, 1055 1110, 1175, 1190 1245 1580, 1615	1450	—	—	—	—	3500 3570
845 1020, 1055 1125, 1170, 1195 1240, 1258 CH_3COO bands	1460	1400 (ν_{sOCO}) 1575 (ν_{asOCO}) (ionic CH_3COO)	—	—	930, 970 1020	—
825, 855, 875 1018, 1050, 1075 1095, 1115, 1170, 1180 1275 1500, 1565, 1580, 1615	1470	—	1360 1390	—	—	—
840, 865 1020, 1050 1110, 1175 1245, 1280 1500, 1560, 1580	1470	—	—	620 1125 (ionic SO_4)	—	—

ρ(NH_2), shifted towards lower values, relative to the free ligands, indicate their coordination through the nitrogen of amino group;

— in the spectra of compounds $[Cu(AOH)X_2].n.H_2O$ and $[Cu(A'OH)X_2].n\ H_2O$ the absorption band assigned to the O−H stretching vibration appears at lower values (3285−3225 cm^{-1}), relative to the free ligands (3300 cm^{-1} and 3310 cm^{-1} respectively), which leads to the conclusion that the propanolamine ligands are coordinated as neutral bidentate molecules;

— the frequency of the O−H stretching vibration, ν(OH), appearing in the spectrum of $[Cu(A'OH)\ (A'O)H_2O]\ CH_3COO$ becomes visible in the same place with that for the free aminoalcohol, which indicates the presence of at least one propanolamine ligand coordinated as a neutral monodentate molecule, by means of the amino group;

— the absorption bands at ~3500 cm^{-1} from the $[Cu(AOH)X_2].n\ H_2O$ and $[Cu(AOH)_2]X_2.n\ H_2O$ spectra are probably due to the crystallization water.[9]

The IR spectra were also used to establish the anion function. Thus, the bands occurring in the ranges which can be assigned to the vibration modes of nitrate, sulphate and acetate anions show their presence in $[Cu(AOH)_2]X_2 . n\ H_2O$ ($X = NO_3$, $n = 0$; $X = 1/2SO_4$, $n = 1$), $[Cu(AOH)(AO)]\ CH_3COO$ and $[Cu(A'OH)(A'O)\ H_2O]\ CH_3COO$ respectively, as uncoordinated ionic species.[10-12]

Thermal analysis. In order to get information about the thermal stability of some studied complex compounds we carried out their thermogravimetric and thermodifferential analysis.

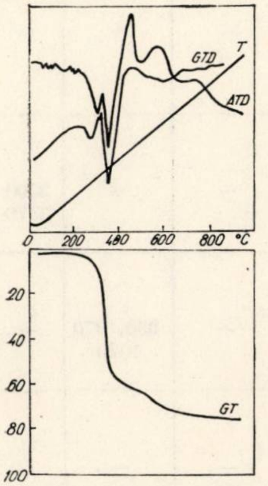

Fig. 4. — Derivatogramm of compound : $[Cu(A'OH)(A'O)H_2O]CH_3COO$ (where $A'OH) = p\text{-}Cl-C_6H_4-CHNH_2-CH_2-CB-OH$ and $AO = p\text{-}Cl-C_6H_4-CHNH_2-CH_2-CB-O^-$).

The obtained data were used to ellucidate the proposed structures and to establish the nature of the present water namely water of crystallisation or coordination.

From this point of view it is interesting to study the heating behaviour of $[Cu(A'OH)(A'O)H_2O]\ CH_3COO$ with coordination water. The DTA curve of $[Cu(A'OH)(A'O)H_2O]\ CH_3COO$, given in figure 4, presents two distinct effects, at 280° and 320°, respectively. The first endoeffect corresponds to a weight loss of about 2.75% (3.20% theoretically) and it could be due to the loss of water molecule from the coordination sphere.

The endoeffect at 320°C corresponds to the complete thermal decomposition of the compound. The absence of an endoeffect at temperature about 100°C, accompanied by a pronounced weight loss, proves the formulated structure with water of coordination.

Conclusions. By examination of all results obtained in this study we have come to the following conclusions :

— the both propanolamines, 1-(β-phenyl-β-amino) ethylcyclobutanol and 1-(β-*p*-chlorophenyl-β-amino)ethylcyclobutanol form, in similar conditions, the same general types of complex compounds ;

— the both propanolamines exhibit a high coordination capacity towards the Cu(II) salts, using both the nitrogen of the amino group and the oxygen of the hydroxyl group ;

— as well as 3-amino-l-propanol, the both studied propanolamines act as neutral bidentate ligands and as anionic bidentate ligands too ;

— however, in contrast with 3-amino-l-propanol, for which we could not obtain complex compounds with two propanolamine molecules as neutral ligands, 1-(β-phenyl-β-amino)ethylcyclobutanol and 1-(β-*p*-chlorophenyl-β-amino)ethylcyclobutanol ligands form such compounds, in weak acid medium ;

— the neutral and especially the alkaline medium favours the behaviour of propanolamine as anionic ligands whereas the acid medium favours their behaviour as neutral ligands ;

— the anion nature and its coordination capacity are very important too for the stabilization of the different types of the Cu(II) complex compounds ;

— although some of the syntheses were performed in strong alkaline solutions, we could not obtain complex compounds in which all the coordinated propanolamine molecules were deprotonated;

— the impossibility of obtaining such compounds is probably due to the fact that aqueous solution could not be used (the studied propanolamines were insoluble in water), a solution in which the most alkaline pH value can be achieved, being necessary to the deprotonation of all propanolamine ligands.

EXPERIMENTAL

I. *Synthesis of the complex compounds*

1. $[Cu(AOH)X_2].n\ H_2O$ *and* $Cu(A'OH)X_2].n\ H_2O$ (AOH = $C_6H_5-CHNH_2-CH_2-$ $-\mathit{CB}-OH$; A'OH = $p-Cl-C_6H_4-CHNH_2-CH_2-\mathit{CB}-OH$, X = Cl, n = 3 or X = Br, n = 2).

To a solution obtained by dissolving 0.1 g $CuX_2.n\ H_2O$ (X = Cl, Br, n = 2) in 5 ml acetone (or 10 ml alcohol) was added a solution of propanol-amine AOH or A'OH in acetone or ethyl alcohol, the corresponding molar ratio being CuX_2 :AOH = 1 :1.

By concentration of solution on a water bath, a light blue substance (AOH) or a light green one (A'OH) was separated, filtered, washed with a little amount of acetone or ethyl alcohol and then dried.

Calcd. for $CuC_{12}H_{17}NOCl_2.3H_2O$: Cu %, 16.73 ; C %, 37.94 ; N %, 3.69 ; Cl %, 18.71 ; H_2O %, 14.22.
Found : Cu %, 16.50 ; C %, 37.65 ; N %, 3.50 ; Cl %, 18.60 ; H_2O %, 13.95.
Calcd. for $CuC_{12}H_{17}NOBr_2 \cdot 2H_2O$: Cu %,14.11 ;C % 31.97 ; N %, 3.11 ; Br %, 35.48 ; H_2O %, 7.9
Found : Cu %, 14.28 ; C %, 31.30 ; N %, 3.25 ; Br %, 35.30 ; H_2O %, 7.55.
Calcd. for $CuC_{12}H_{16}NOCl_3.3H_2O$: Cu %, 15.34 ; C %, 34.79 ; N %, 3.38 ; Cl %, 25.69 ; H_2O %, 13.05
Found : Cu %, 15.10 ; C %, 34.53 ; N %, 3.75 ; Cl %, 25.50 ; H_2O %, 13.30.
Calcd. for $CuC_{12}C_{16}NOClBr_2.2H_2O$: Cu %, 13.07 ; C %, 29.64 ; N %, 2.88 ; H_2O %, 7.41 ;
Found : Cu %, 12.80 ; C %, 29.50 ; N %, 3.10 ; H_2O %, 7.50.

2. $[Cu(AOH)_2]\ X_2.n\ H_2O$ *and* $[Cu\ (A'OH)_2]\ X_2.n\ H_2O$ (AOH = $C_6H_5-CHNH_2-CH_2-\mathit{CB}-OH$, A'OH = $p\text{-}Cl-C_6H_4-CHNH_2-CH_2-\mathit{CB}-OH$, X = NO_3, n = 0 or X = 1/2 SO_4, n = 1).

To a solution of propanolamine (AOH or A'OH) in acetone was added the solution obtained by dissolving of 0.1 g $CuX_2.n\ H_2O$ (X = NO_3, n = 6 ; X = 1/2 SO_4, n = 5) in 10 ml acetone for nitrate or in 10 ml, 1 : 1 acetone : water mixture for sulphate, respectively (the corresponding molar ratio of CuX_2 : AOH = 1 : 2).

The rrection mixture was boiled (on a water bath) for two hours. When cooled, a crystalline blue substance (X = NO_3, 1/2 SO_4) was separated. It was filtered and washed with acetone or with 1 : 1 acetone : water mixture respectively.

Calcd. for $CuC_{24}H_{34}N_4O_8$: Cu %, 11.15 ; C %, 50.57 ; N %, 9.83
Found : Cu %, 11.25 ; C %, 50.80 ; N %, 9.55.
Calcd. for $CuC_{24}H_{34}N_2O_6S.H_2O$: Cu %, 11.34 ; C %, 51.47 ; N %, 5.00 ; SO_4 %, 17.16 ;
Found : Cu %, 11.10 ; C %, 51.47 ; N %, 4.75 ; SO_4 %, 16.84 ; H_2O %, 3.40.
Calcd. for $CuC_{24}H_{32}N_4O_8Cl_2$: Cu %, 9.91 ; C %, 44.97 ; N %, 8.74 ; Cl %, 11.08 ;
Found : Cu %, 9.56 ; C %, 44.50 ; N %, 8.90 ; Cl %, 10.87.
Calcd. for $CuC_{24}H_{32}N_2O_6SCl_2.H_2O$: Cu %, 10.07 ; C %, 45.68 ; N %, 4.44 ; Cl %, 11.26 ; SO_4 %, 15.23 ; H_2O %, 2.85 ;
Found : Cu %, 9.87 ; C %, 45.40 ; N %, 4.65 ; Cl %, 10.95 ; SO_4 %, 15.30 ; H_2O %, 3.10.

3. $[Cu(AOH)\ (AO)]\ CH_3COO$ *and* $[Cu(A'OH)\ (A'O)\ H_2O]\ CH_3COO$ (AOH = $C_6H_5-CHNH_2-CH_2-\mathit{CB}-OH$, AO = $C_6H_5-CHNH_2-CH_2-\mathit{CB}-O^-$, A'OH = $p\text{-}Cl-C_6H_4-CHNH_2-CH_2-\mathit{CB}-OH$, A'O = $p\text{-}Cl-C_6H_4-CHNH_2-CH_2-\mathit{CB}-O^-$)

To a concentrated solution of propanolamine in acetone was added, with a molar ratio Cu $(CH_3COO)_2$: AOH = 1 : 3, a concentrated solution of $Cu(CH_3COO)_2.H_2O$ in acetone (0.1 g $Cu(CH_3COO)_2.H_2O$ in 3 ml acetone). The obtained solution was cooled and the dark blue crystalline substance was immediately separated, filtered and washed with a little amount of acetone.

Calcd. for $CuC_{26}H_{39}N_2O_5$: Cu %, 12.15 ; C %, 59.71 ; N %, 5.36 ;
Found : Cu %, 12.50 ; C %, 60.10 ; N %, 5.20.
Calcd. for $CuC_{26}H_{27}N_2O_4Cl_2$: Cu %, 11.03 ; C %, 54.21 ; N %, 4.86 ; Cl %, 12.33 ;
Found : Cu %, 11.23 ; C %, 54.51 ; N %, 4.66 ; Cl %, 12.50.

II. *Molar electric conductivity measurements.* Molar electric conductivity determinations were performed on a C. Zeiss Jena type II conductometer, with the cell constant $k = 0.55$. 10^{-3}M dimethylformamide solutions were used, at a temperature of 25°C.

The assignment of the electrolyte type was made by applying the procedure reported in the literature for dimethylformamide.

III. *Electronic spectra.* Electronic reflectance spectra were recorded at room temperature using a C. Zeiss Jena VSU-1 spectrophotometer. The used reference material was magnesium oxide. The electronic spectra in solution were recorded at room temperature using a spectrophotometer VSU-2G, C. Zeiss Jena.

IV. *IR spectra.* IR spectra were recorded in KBr pellets by means of a Perkin Elmer spectrophotometer.

V. *Thermodifferential analysis.* The thermogravimetric and thermodifferential analysis was made with a Paulik-Paulik-Erdey derivatograph with a simultaneous registering of curves T, TG, DTG and DTA. The temperature ranged from 20°C to 1000°C. The curves were registered in air, the heating speed was 5°/min, the standard sample was calcinated Al_2O_3.

REFERENCES

[1] M. Brezeanu and I. Jitaru, *Rev. Roumaine Chim.*, **18,** 2039 (1973).
[2] M. Brezeanu and I. Jitaru, *Rev. Roumaine Chim.*, **22,** 371 (1977).
[3] M. Brezeanu and I. Jitaru, *Rev. Roumaine Chim.*, in press.
[4] J. F. Jonug, R. D. Gillord and G. Willkinson, *J. Chem. Soc. A*, **1964,** 2176.
[5] R. A. Palmer and T. S. Piper, *Inorg. Chem.*, **5,** 864 (1966).
[6] A. A. G. Tomlinson, *J. Chem. Soc. A*, **1969,** 65.
[7] L. Sacconi and M. Ciampolini, *J. Chem. Soc. A*, **1964,** 276.
[8] L. J. Bellamy, "The Infrared Spectra of Complex Molecules", Academic Press, London, 1958, p. 108.
[9] K. Nakamoto, *J. Amer. Chem. Soc.*, **78,** 1347 (1956).
[10] N. F. Curtis, *Bull. Chem. Soc. Japan*, **31,** 303 (1958).
[11] N. F. Curtis, *J. Chem. Soc.*, **1968,** 1579.
[12] K. Nakamoto, "Infrared Spectra of Inorganic and Coordination Compounds", Academic Press, London, 1963, p. 161.

Revue Roumaine de Chimie, **26**, *9–10*, 1231–1243 (1981)

A NEW BRIDGED BINUCLEAR LOW-SPIN PENTACOORDINATE Co(II) COMPLEX CONTAINING STRONGLY ELECTRONEGATIVE DONOR ATOMS

A. C. BANCIU

ICECHIM — Center of Physical Chemistry, Bucharest,
Spl. Independenţei 202, Romania

Received July 2, 1980

In the attempt to synthetize the tetracoordinate complex compound $Co(II)L_2$, (L = the conjugated anion of the C-carbethoxy-N,N'-di-*p*-tolyl-formazane), in methanol solution and in the presence of triethylamine, an unusual pentacoordinate low-spin Co(II) complex compound containing strongly electronegative donor atoms (N and O) has been surprisingly obtained. Based on the elemental chemical analysis, the IR spectrum (200–4000 cm^{-1}) and the electronic one (360 – 1200 nm), the lack of any ionic character of the complex in water solution, as well as on the electric conductivity and paramagnetic susceptibility measurements, to the new complex the bridged binuclear structure $L_2Co(II)\ (CH_3O)Co(II)L[N(C_2H_5)_3]_2$ may be ascribed. The value $\mu_{eff} = (1.50 \pm 0.10)$ B.M. per Co(II) ion (at 298 K) shows a certain metal—metal interaction in the complex.

INTRODUCTION

It is well known the ability of the formazanes to form, with bivalent transition metal ions, tetracoordinate chelate complexes of ML_2 type.[1] The Co(II) complexes of this type are either square-planar or tetrahedral.[2]

In the attempt to synthetize such a tetracoordonate chelate complex of Co(II), with C-carbethoxy-N,N′-di-*p*-tolyl-formazane, in methanol solution and in the presence of triethylamine, a new pentacoordinate complex compound of Co(II) has been surprisingly obtained. There are known at present numerous pentacoordinate complexes of Co(II), but the pentacoordination remains, nevertheless, exceptional for this ion[3] and is generally achieved with special classes of ligands (tripod, macrocyclic, etc.). For the Co(II) ion the pentacoordination with typically bidentate ligands (such as the formazanes) is much rarer. The cases of the pentacoordinate low-spin complexes of Co(II) where the donor atoms are strongly electronegative constitute very rare exceptions.

In the present paper we shall study the synthesis as well as the chemical and physical properties of this new and unusual pentacoordinate Co(II) complex compound, which is bridged, binuclear, low-spin, but contains strongly electronegative donor atoms (N and O).

EXPERIMENTAL

The synthesis of the organic ligand, the C-carbethoxy-N,N'-di-*p*-tolyl-formazane, has been performed according to a method reported in the literature,[1] by the azoic coupling reaction (in ethanol—water solution and in strongly alkaline medium) of the ethyl ester of the acetyl-acetic acid, **I**, with the diazonium salt of the *p*-toluidine (molar ratio ester : diazonium salt = 1 :2). By 1 :1 azoic coupling it is obtained the azoic compound **II**, which is unstable and isomerizes immediately to the phenylhydrazone of the dicetobutyric ester, **III**. In strongly alkaline medium **III** undergoes dezacylation and, from the formed intermediatet carboanion, the organic ligand, **IV**, is obtained, by 1 :1 azoic coupling with the diazonium sal of the *p*-toluidine.

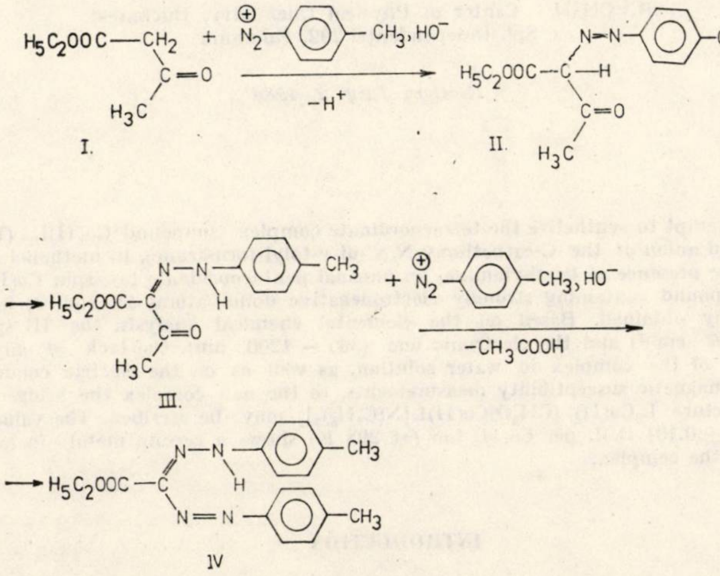

I. II. III. IV

The crude product is purified by crystallization from absolute ethanol in the presence of active charcoal. M.p. 116—119°C. *Anal.* C 66.40 % ; H 6.55 % ; (calculated for $C_{18}H_{20}N_4O_2$: C 66.63 % ; H 6.23 %).

The synthesis of the Co(II) complex. 1.30 g (4 mmol) organic ligand (formazane **IV**), 0.48 g (2 mmol) $CoCl_2 \cdot 6\,H_2O$ and 0.55ml (0.40 g = 4 mmol) triethylamine (as basic reagent for the deprotonation of the formazane) are boiled under reflux in 150—170 ml absolute ethanol. After 10 minutes boiling from the hot solution one precipitates the microcrystalline Co(II) complex which, after cooling of the reaction mixture, is filtered on a Büchner funnel. The crude complex is washed with 20 — 30 ml cooled methanol, then purified, in order to remove the unreacted inorganic salt, by impregnation with 50 — 60 ml 3 % acetic acid and heating under stirring, at 40°C, followed by filtration on a Büchner funcl. This procedure is repeated 3 times. Each washing with acetic acid is followed by a washing with cooled methanol (20 ml). The purified complex is finally washed with 25 — 30 ml hot (55—60°) absolute methanol and quickly filtered on the Büchner funnel. *Yield* : 0.60 — 0.70 g purified and dried (3 days in a vacuum desiccator, on P_4O_{10}) complex. *Properties* : microcrystals from dark indigo-brown color, m.p. 209—212°C. The complex is insoluble in (cooled or warm) water, and in methanol, less soluble in ethanol and acetone, soluble in benzene and easily soluble in DMF (dimethylformamide). The solutions in ethanol, acetone and benzene are red-brown, whereas the DMF solution is dark green, almost black. A solution of 0.0748 g complex in 100 ml ethanol has at 20°C a specific electric conductivity ($\varkappa$) of 13.3×10^{-6} ohm^{-1}cm^{-1}, and a solution of 0.0380 g complex in 100 ml DMF has at 20°C $\varkappa = 16.2 \times 10^{-6}$ohm^{-1}cm^{-1}. *Anal.* Co 8.50 % ; C 61.18 % ; H 6.29 %. Calculated for $L_2Co(II)\ (CH_3O)\ Co(II)\ L[N(C_2H_5)_3]_2$ (see below) : Co 8.91 % ; C 60.88 % ; H 6.87 %.

The elemental chemical analysis (C and H) of the organic ligand **IV** and of the complex has been made by means of usual micromethods. The Co content of the complex has been determined by atomic spectroscopy. By Schöniger combustion followed by mercurimetric titration it has been established that the complex does not contain chlorine.

The specific electric conductivities have been determined with an OK 102/1 Radelkis conductometer.

The IR spectra have been recorded within the 200 – 4000 cm^{-1} range on a Perkin-Elmer type 225 spectrophotometer.

The electronic diffuse reflectance spectra have been recorded within the 360 – 1200 nm range on a VSU-1 Carl Zeiss (Jena) spectrophotometer, using MgO as standard.

The paramagnetic susceptibility of the solid complex has been determined, at room temperature, by Faraday method, using $HgCo(SCN)_4$ as standard. It has the value $\chi_g = (0.95 \pm \pm 0.15) \times 10^{-6}$ c.g.s.u. per gramme of complex.

RESULTS AND DISCUSSIONS

The structure **IV** of the organic ligand agrees well with the IR spectral data (see Table 1). One observes numerous and intense bands of the substituted benzene rings and of the esteric group, $COOC_2H_5$. The presence of this group in the ligand molecule shows that during the synthesis neither the initial ester nor the intermediate ones undergo the decarboxylation reaction. If decarboxylation would take place, then in the strongly alkaline medium of the reaction mixture, C-diazo-*p*-tolyl-N,N′-di-*p*-tolyl-formazane[4] would be specially formed.

The conditions for the synthesis of the new Co(II) complex were those usual for the synthesis of a tetracoordinate chelate complex of $Co(II)L_2$ type (L = the conjugated anion of the C-carbethoxy-N,N'-di-*p*-tolyl-formazane, **IV**). Much more, the elemental chemical analysis of the new complex agrees with that expected for a tetracoordinate $Co(II)L_2$ complex (C 61.26% and H 5.43%). The obtained complex differs, however, obviously (by its dark indigo-brown color) from the common complexes of $Co(II)L_2$ type, synthetized with ligands from the class of formazanes (which are dark blue-green). The diffuse reflectance electronic spectrum of the new complex, recorded within the 360–1200 nm range, is *characteristic* for *a pentacoordinate Co(II) complex* (see below). On the other hand, even though the exact chemical formula and, therefore, the molecular weight and the diamagnetic correction are unknown, the weak paramagnetism, $\chi_g = (0.95 \pm 0.15) \times 10^{-6}$ c.g.s.u., shows that the complex must be of low-spin type.

The undoubtedfully pentacoordinated structure of the Co(II) ion (according to the electronic spectrum) and the structure of $Co(II)L_2$ type (according to the chemical analysis) would be put in concordance if a dimeric molecular structure of $(Co(II)L_2)_2$ type were assumed. The two formally possible structures for a dimeric arrangement must be nevertheless excluded. One of them would involve the existence in the dimeric molecule of two coordinative bonds between the two Co(II) ions and the oxygen atoms of esteric carbonyl group from the neighbour monomeric $Co(II)L_2$ unit. The IR spectrum excludes this structure, because the C=O stretching vibration occurs exactly as in the free ligand spectrum, at 1720 cm^{-1}. For coordinated C=O group the $\nu(C=O)$ band ought to occur strongly shifted,[5] at 1640–1670 cm^{-1}, which is obviously not the case.

The other dimeric pentacoordinated structure would involve the existence of a direct Co(II)—Co(II) bonding between the two monomeric Co(II)L_2 units. This structure must be rejected due to the steric requirements. In each monomeric Co(II)L_2 unit, on the four donor nitrogen atoms there are bonded bulky substituents (*p*-tolyl-groups), comparable in their size with the chelatic rings formed by the ligands L and the Co(II) ions. The Co(II)—Co(II) bonding is therefore not possible, what is easily to check on steric models.

The new complex under discussion cannot be also formulated as a monomeric pentacoordinate Co(II) complex. All monomeric pentacoordinate structures must be excluded since they do not lead to a simultaneous agreement between the elemental chemical analysis, the non-electrolyte character (unsoluble in water but soluble in benzene) and the IR data of the complex.

Because in the IR spectrum of the complex (Table 1) the intense band corresponding to the O—H stretching vibration (in the 3000—3500 cm^{-1} range) does not occur, the species H_2O, CH_3OH and HO^- cannot act as ligands. The chloride ion is excluded as ligand, based on the elemental chemical analysis.

Since the complex is still soluble in organic solvents, such as inferior alcohols (ethanol) it cannot have a high polymeric structure. Because the monomeric and dimeric structures of $(Co(II)L_2)_2$ type are excluded, it appears as very probable a bridged binuclear structure. In this case, the bridge must be formed by the CH_3O^- anion, since the other species able to form bridges and existent in the reaction mixture of the synthesis of the complexes, i.e. Cl^-, HO^-, H_2O and CH_3OH, are, as we have above seen, excluded.

The CH_3O^- anion (like the HO^- anion) occurs doubtless (to a certain concentration) in the reaction medium of the synthesis of the complex.

Indeed, triethylamine, NR_3, $(R=C_2H_5)$, may react not only with the formazane **IV**, (LH), but also with water (existent in $CoCl_2.6H_2O$) or with methanol (the main solvent).

The shift of the equilibrium

$$NR_3 + H_2O \rightleftharpoons [H\overset{\oplus}{N}R_3]^+ + HO^-$$

towards the right side is facilitated on one hand by the fact that water is a more acid reagent than methanol (pK = 14 and 16 for the autoprotolysis of water and methanol,[6] respectively) and on the other hand by the fact that it has a high dielectric constant[6] ($\varepsilon = 80$).

From these points of view (acidity and dielectric constant, both smaller) the shift of the equilibrium

$$NR_3 + CH_3OH \rightleftharpoons [H\overset{\oplus}{N}R_3]^+ + CH_3O^-$$

towards the right side is disadvantaged, compared with the first case. The shift towards the right side of the last equilibrium is nevertheless strongly favoured by the enormous excess of methanol, existent in the reaction medium of the complex synthesis (which contains only 12 mmol H_2O but 3.75—4.20 mol methanol!).

The only ligands which may exist in the new pentacoordinate Co(II) complex are L (the conjugated anion of the formazane **IV**), CH_3O^- and NR_3. The last two ones are difficult to be evidenced in the IR spectrum of the complex (Table 1), which does not, however, contain any other information against their presence in the complex.

Even though with this small number of possible ligands, there are many possibilities to formulate the new Co(II) complex as a bridged binuclear pentacoordinate complex. This is so because it is not necessary that both Co ions should be bivalent or both pentacoordinated. It is sufficient that only one of the Co ions fulfill simultaneously these conditions. For example, a binuclear complex with a CH_3O bridge between a pentacoordinated Co(II) ion and a hexacoordinated Co(III) ion may have almost all of the investigated physical and chemical properties of the new complex under discussion, such as the elemental chemical analysis, the non-ionic character, the IR spectrum and even the electronic one. The electronic spectrum of the hexacoordinated Co(III) ion would be practically completely obscured by the spectrum with numerous and strong absorption bands of the pentacoordinated Co(II) ion.

Among the different CH_3O-bridged binuclear formulations formally possible for the new Co complex, finally only two remain as pertinent. These are:

$$L_2Co(III)\ (OCH_3)\ Co(II)L_2 \qquad \textbf{(V)}$$

and

$$L_2Co(II)\ (OCH_3)\ Co(II)\ L\ [N(C_2H_5)_3]_2 \qquad \textbf{(VI)}$$

Both structures agree with the elemental chemical analysis, the IR spectrum, the non-ionic character (in water) of the complex, its dissociation in some organic solvents (ethanol, DMF) as well as the magnetic behaviour.

In the formulation **V**, which involves the partial oxidation of Co(II) to Co(III), under the conditions of the synthesis of the complex, the paramagnetism of the complex may be explained, assuming that the pentacoordinated Co(III) ion is diamagnetic (low-spin d^6 configuration in the C_{4v} symmetry). If the whole molecular paramagnetism is ascribed to the Co(II) ion, since $\chi_g = (0.95 \pm 0.15)\times10^{-6}$ c.g.s.u., M.W. = 1442.52 and the diamagnetic correction is $\chi_{dia} = 605\times10^{-6}$ c.g.s.u./mole, by means of the formula

$$\mu_{eff} = 2.828\sqrt{(\chi_g \text{M.W.} - \chi_{dia})T}\ \text{B.M.}$$

one obtains a magnetic moment of 2.17 ± 0.12 B.M. per Co(II) ion. This result seems reasonable, being in agreement with the data reported in the literature.[7] However, the formulation **V** arises some questions against it (1. why the partial oxidation of Co(II) to Co(III), since this oxidation does not occur in other very similar syntheses of Co(II) complexes with formazanes?; 2. why the pentacoordinated Co(III) ion does not influence the electronic spectrum of the complex compound, which is *characteristic* for *a pentacoordinate Co(II) complex*?; 3. why the Co(III) ion, which has a very pronounced tendency for hexacoordination, remains only pentacoordinated in this complex?).

Also, the assumed diamagnetism of the pentacoordinated Co(III) ion may be unrealistic. Eventhough there are some indications[8] that the pentacoordinated Co(III) ion may be diamagnetic (in the square-pyramidal geometry, but not in the trigonal-bipyramidal one!) there are other works[9] which show that *irrespective of the pentacoordinated geometry* the Co(III) ion *is* practically *always paramagnetic*.

The formulation **VI** avoids the questions of the structure **V**. For the structure **VI**, M.W. = 1321.57, $\chi_{dia} = 638 \times 10^{-6}$ c.g.s.u./mole (calculated from the Pascal constants) and using the experimental value $\chi_g = (0.95 \pm 0.15) \times 10^{-6}$ c.g.s.u. and the formula

$$[\mu_{eff} = 2.828\sqrt{\left(\frac{\chi_g \text{M.W.}}{2} - \frac{\chi_{dia}}{2}\right)T} \quad \text{B.M.}$$

one obtains a magnetic moment of 1.50 ± 0.10 B.M. per Co(II) ion. This μ_{eff} value, lower than the spin-only value for an unpaired electron (1.73 B.M.) may indicate a certain metal—metal magnetic interaction in the complex. There are known many pentacoordinate low-spin complexes of Co(II) which present magnetic moments lower than 1.73 B.M.,[10] at the room temperature.

The metal—metal interaction in the complex (formulated as **VI**) appears as possible from steric requirements too. It is known that not all binuclear complexes exhibit metal—metal interaction. From geometric reasons this interaction is possible only for five special cases.[11] One from these cases is "the complexes with one bridging atom or group and angular M-bridge-M bonding". In the structure **VI** the Co(II)—O—Co(II) bond is undoubtedfully angular. The oxygen atom of the OCH_3 bridge is (like in water and alcohols) to an important extent in the sp^3 hybridization state. The angle between the Co(II)—O bonds of the bridge should be close to the tetrahedral one (~110°).

The IR spectrum of the complex, summarized in Table 1, agrees well with the formula **VI**.

One observes some bands (325, 430, 447, 610 and 653 cm^{-1}) which do not occur in the free ligand **IV** spectrum and which are assigned to the metal—ligand bond vibrations.

Formula **VI** of the complex explains well its electrolytic behaviour. From the M.W. value of 1321.57 and the experimentally determined $\varkappa$ values one finds the molar electric conductivities $\Lambda_M = 24.0$ ohm^{-1} cm^2mol^{-1} (in ethanol) and $\Lambda_M = 56.0$ ohm^{-1} cm^2mol^{-1} (in DMF). They are lower than but close to those of a 1:1 electrolyte. A true 1:1 electrolyte has $\Lambda_M = 35-45$ ohm^{-1} cm^2mol^{-1} (in ethanol) and $\Lambda_M = 65-90$ ohm^{-1} cm^2mol^{-1} (in DMF).[12] If the new complex has the structure **VI**, eventhough nonionic (unsoluble) in water, it may, however, dissociate in organic solvents (such as ethanol), into the ionic species $[Co(II)\,L(N(C_2H_5)_3)_2]^{1+}$ and $[Co(II)L_2(OCH_3)]^{1-}$ or into the neutral species $[Co(II)\,(N(C_2H_5)_3)_2L\,(OCH_3)]$ and $[Co(II)L_2]$. If the first mentioned dissociation is complete,

TABLE 1

IR spectra [cm^{-1}] of the free organic ligand (formazane **IV**) and of the new pentacoordinate Co(II) complex **VI**

Free ligand **IV**	Complex **VI**	Assignments
	325 vw	metal-ligand stretching
340 vw	348 vw	
	430 sh(w)	metal-ligand stretching
	447 w	metal-ligand stretching
482 s	480 w	
510 m	510 m	
520 m	520 u(m)	
542 m	542 w	
585 w		
	610 w	metal-ligand stretching
622 w	630 w	
640 w	640 w	
	653 w	metal-ligand stretching
710 vw	703 w	
735 m	738 m	
760 sh		in-plane bending vibration for 1,4-disubst. benzene
768 m	775 sh(m)	
787 s	783 s	out-of-plane C—H bending vibration for 1,4-disubst. benzene
807 s	810 s	
820 vs	818 s	out-of-plane C—H bending vibration for 1,4-disubst. benzene
	825 sh	
830 s	833 sh	
840 m		
852 m		
860 m	858 w	
870—880 sh	875 w	
925 vw	912 m	
	930 vw	
940 w	940 sh(w)	
1007 m	990 sh	ring vibrations for 1,4-disubst. benzene
	1005 sh	
	1015 sh(s)	
1030 m	1022 s	
	1035 sh	
	1090 sh(m)	
1110 vs	1120 vs	asymm. O—CH$_2$—C stretching from ester group
1118 sh(s)		
1155 s		
1205 vs	1210 vs	different vibrations from ester group
1278 vs	1275 sh(s)	asymm. C—C—O stretching from ester group
	1287 vs	
	1303 vs	Ph-NH—, respectively
1315 vs	1312 vs	Ph-N$<$ stretching
	1325 vs	
1345 s-vs	1345 sh	
1370 s	1370 vs	OCH$_2$ wag + CH$_3$ symm. deformation from ester group

Table 1 (continued)

Free ligand **IV**	Complex **VI**	Assignments
1390 m	1395 m	
1410 s	1410vw	CH_2 and CH_3 deformation vibrations + ring stretching vibrations for 1,4-disubst. benzene
1440–1460 m	1450–1460 sh	aliphatic-CH_3 asymm. deformation, OCH_2 deformation vibration from ester group and ring stretching vibrations for 1,4-disubst. benzene ring
1478 m	1465 m	
1497 vs	1500 s	ring stretching vibrations for 1,4-disubst. benzene
1507–1515 vs	1510 sh	
	1580 vw	C= N asymm. stretching vibration and ring stretching vibrations for 1,4-disubst. benzene
1600 m	1600 m	
1720 vs	1720 vs	C = O stretching vibration from ester group
1900 vw	1890 vw	
2860 sh	2860–2880 sh	CH_2 stretching vibration
2900 m		CH_3 stretching vibration
2920 m	2920–2960 m	asymm. CH_2 stretching vibration
2980 s	2980 m	asymm. CH_3 stretching vibration
3020 m	3020 m	C–H stretching vibration of aromatic rings

w = weak ; vw = very weak ; s = strong ; vs = very strong ; sh = shoulder.

the complex should be a true 1 :1 electrolyte (in these solvents). The above calculated Λ_M values may be reasonably explained assuming that the complex only partially dissociates into the above mentioned ionic species and a partially dissociation into the mentioned non-ionic species takes also place. The dark green, almost black color of the complex solutions in DMF (compared with the brown-red color of the complex solutions in other solvents) may be well explained through the participation of this solvent to the coordination of the Co(II) ions and the removal of other ligands (such as OCH_3 or NR_3).

Figure 1 shows the diffuse reflectance electronic spectra of the complex **VI** and of the free organic ligand **IV**. One may observe that the band of the complex placed at 425 nm is of $\pi \rightarrow \pi^*$ type, proper to the free organic ligand, and it appears hypsochromically shifted in the complex spectrum. The band of the complex, placed at 550 nm, is most likely of CT-type, because is less probable to be the band (shoulder) placed at 520 nm in the free ligand spectrum, which appears bathochromically shifted in the complex spectrum. The band of the complex placed at 650 – 660 nm may be also of CT-type or due to the ligand field. The other two bands of the complex, placed at longer wavelengths, are most likely due to the ligand field.

Table 2 summarizes the electronic spectra and some magnetic and structural data of many pentacoordinate Co(II) complexes, together with the new Co(II) complex **VI**, herein discussed.

One may observe that practically all the pentacoordinate Co(II) complexes have bands in the following ranges: 5500 – 9500 cm^{-1} (1800–1050 nm); 10 000 – 13 000 cm^{-1} (1 000 – 770 nm); 14 000 – 16500 cm^{-1} (710 – 605 nm) and 19 300 – 21 500 cm^{-1} (520–465 nm). Some complexes present supplementary bands in the 17 000 – 18 000cm^{-1} (590–555 nm) and 23 000–26 000 cm^{-1} (435 – 380 nm) ranges.

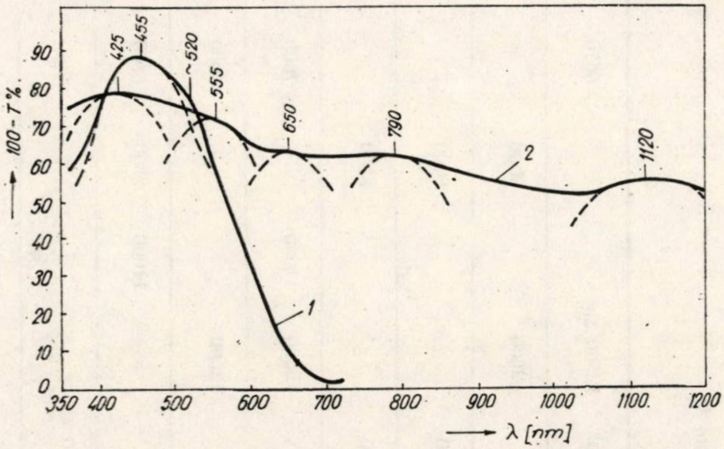

Fig. 1. — Electronic diffuse reflectance spectra of the pentacoordinate Co(II) complex **VI** and of the free organic ligand **IV** : 1 — free organic ligand (formazane **IV**) ; 2 — Co(II) complex **VI**.

These spectra, with numerous and intense bands, in the visible and near IR range, allow to identify the pentacoordinate Co(II) complexes. On the other hand, the similitude between them make *uncertain* the difference between the pentacoordinate complexes with trigonal-bipyramidal and those with square-pyramidal microsymmetry. For example, the spectra of the complexes nos. 5 and 6 (Table 2) are very similar. The similitude between these spectra is in fact more pronounced than shown by data summarized in Table 2; the only significant difference is the higher intensity of the band placed at ~15 000 cm^{-1} in the complex no. 5 spectrum.[13] Despite this pronounced similitude between their spectra, the microsymmetries of the two complexes are different.

The magnetic criterion does not allow the difference between the two possible microsymmetries of the pentacoordinate Co(II) complexes. Most of complexes summarized in Table 2 are of low-spin type, eventhough they belong to different microsymmetries. The complexes nos 1 and 13 (Table 2) are magnetically different, but their electronic spectra are very like and they possess the same microsymmetry.

From Table 2 one may see that from the 14 summarized complexes the complex no. 2 (that is the new complex **VI**) and no. 3 are very like. In their spectra there are 5 bands which practically coincide. Such a similitude is not observed with other complexes. Based on this analogy and on the physical and chemical properties a trigonal-bi pyramidal microsymmetry has been attributed to the new complex **VI**. This assignment

TABLE 2

Electronic absorption spectra of some pentacoordinate Co(II) complexes

No.	Complex	$\bar{\nu}_{max}$ [cm^{-1}]									Structure ; Magnetic type	References
1	$[Co(AP_2)Br]ClO_4$ [a]		21050			14600	12500 sh			6670	SP ; low	[14]
2	$L_2Co(II)(OCH_3)Co(II)-L[N(C_2H_5)_3]_2$	23500	21050	18000	15400		12600		9000		TB ; low	this paper
3	$Co(CR)Br_2 \cdot H_2O$ [b]	25000	20000	18000	16100	13900			9000		TB ; low	[10]
4	$Co(CR)Br(ClO_4)$ [b]		20000	18000	16400	14300			8600		TB ; low	[10]
5	$[Co(dpe)_2Cl]SnCl_3 . - C_6H_5Cl$ [c]	23000	20400sh		15400		13000	11000		7000	TB ; low	[13]
6	$[Co(dpe)_2Cl]\ SnCl_3$ [c]	25000 23000			15000		13000			7000	SP ; low	[13]
7	$Co(sacsac)_2L'$ [d]	23800	21600	17300	15200			11000	8300	6800	SP ; low	[15]
8	$CoBr_2[P(CH_3)_3]_3$	23500	19250		15400	13900 sh					TB ; low	[16]
9	$Co(dpe)_2Br_2$ [c]	22750			15400	14700				6850	SP ; low	[10]
10	$[Co(NO_3)(QP)]^+$ [e]		20000		15000			10000			TB ; low	[17]

11	$[CoCl(QP)][BPh_4]$	e		19600		16500		9600		TB ; low	18
12	$[Co(Me_6tren)Cl]^+$	f		19600		15800	12300		5500	TB ; high	19
13	β-$Co(paphy)Cl_2$	g		21000 sh	17500 sh	15500	12300			SP ; high	19
14	$Co(Ga\text{-}p-NO_2-h)_2$	h	26000	19400		15600	12500	9500		TB ; high	20

SP = square-pyramidal ; TB = trigonal-bipyramidal ; low = low-spin ; high = high-spin ; sh = shoulder

[a] AP = diphenyl (*o*-diphenylarsinophenyl) phosphine ;

[b] CR = 2,12-dimethyl-3,7,11,17-tetraazabicyclo 11.3.1 heptadeca-1(17),2,11,13,15-pentane ;

[c] dpe = 1,2-bis (diphenylphosphine)-ethane ;

[d] sacsac = thioacetylacetonate ; $L' = P(C_6H_5)_3$;

[e] QP = tris-(*o*-diphenylphosphinophenyl)-phosphine ;

[f] Me_6tren = tris-(2-dimethylaminoethyl) amine ;

[g] paphy = pyridine-2-aldehyde-2-pyridylhydrazone ;

[h] Ga-*p*-NO_2-h = 1-methyl-2-carbethoxy-glyoxalanil-(1)-*p*-NO_2-phenylhydrazone-(2).

for the Co (II)-ligand bonds in the new complex is supported by chemical and steric arguments. If one assume that the two Co(II) ions have a square-pyramidal coordination it should be difficult to explain why the Co(II) ions do not reach the hexacoordination, with yet a less bulky ligand (such as Cl^-, CH_3O^- or OH^-), coordinated in the opposite position to that of the CH_3O bridge. If one assumes a trigonal-bipyramidal structure for the two Co(II) ions, the lack of hexacoordination may be easily explained. In the trigonal—bipyramidal environment the space around the Co(II) ions is filled with bulky ligands, L and $N(C_2H_5)_3$. Under these circumstances the coordination yet of a ligand (even less bulky) is no more possible, what is easily checked on steric models.

One may see that *all physical and chemical properties herein investigated* of the new pentacoordinate Co(II) complex (elemental chemical analysis, electronic and IR spectra, electric conductivity measurements in different solvents and the paramagnetic behaviour of the complex in the solid state) *may be well explained* assuming that the complex has a bridged binuclear structure (formula **VI**), where the Co(II) ions are pentacoordinated, in a trigonal-bipyramidal microsymmetry. In my opinion this is the only structure which explains well all the investigated physical and chemical properties of the complex.

The new Co(II) complex **VI** is an interesting case of pentacoordination without special ligands (tripod, macrocyclic, etc.) which force the metal ions to pentacoordinate (the formazane **IV** used in the complex synthesis is a typically bidentate ligand).

The new complex **VI** is also interesting in what the magnetic behaviour is concerned. It is of low-spin type, eventhough it contains strongly electronegative donor atoms (N and O). There are extremely few complexes of such a type, as for example $Co(CR)Br_2.H_2O$,[10] the ligand being in that last case a special tetradentate macrocyclic one. The majority of the low-spin pentacoordinate Co(II) complexes have weakly electronegative donor atoms (P, As, Sb, S or Se), whereas almost all pentacoordinate Co(II) complexes with strongly electronegative donor atoms are of high-spin type.[3]

ACKNOWLEDGEMENT. I thank Mr. V. Mincu, lecturer at the Polytechnic, Bucharest, for the magnetic susceptibility measurements.

REFERENCES

[1] C. D. Nenițescu, "Chimie organică", vol. 2, Editura didactică și pedagogică, București, 1968, p. 77.

[2] R. H. Holm and M. J. O'C onnor, "Progress in Inorganic Chemistry", vol. 14, Wiley, New York, 1971, p. 241.

[3] P. L. Orioli, *Coord. Chem. Rev.*, **6**, 286 (1971).

[5] O. Wichterle, "Allgemeine organische Chemie", Deutscher Verlag der Wissenschaften, Berlin, 1959, p. 612.

[5] L. J. Bellamy, "The Infrared Spectra of Complex Molecules", Methuen, London, 1962, p. 184.

[6] C. D. Nenițescu, "Chimie organică", vol. 1, Editura didactică și pedagogică, București, 1966, p. 201—204.

[7] M. Ciampolini, *Stucture and Bonding*, **6**, 52 (1970).

[8] B. N. Figgis and J. Lewis, "Modern Coordination Chemistry", Interscience, New York, 1964, p. 422.

[9] G. Navon and H. Shinar, *Inorg. Chim. Acta*, **46**(B1), 51 (1980).

[10] K. M. Long and D. H. Busch, *Inorg. Chem.*, **9**, 505 (1970).

[11] B. Jezowska-Trzebiatowska and W. Wojciechowski, "Transition Metal Chemistry", vol. 6, Marcel Dekker, New York, 1970, p. 20.

[12] W. J. Geary, *Coord. Chem. Rev.*, **7**, 81 (1971).

[13] J. K. Stalik, R.W.R. Corfield and D. W. Meek, *Inorg. Chem.*, **12**, 1669 (1973).

[14] G. Dyer and D. W. Meek, *J. Amer. Chem. Soc.*, **89**, 3983 (1967).

[15] J. F. White and M. F. Farona, *Inorg. Chem.*, **10**, 1080 (1970).

[16] M. Bressan and P. Rigo, *Inorg. Chem.*, **14**, 38 (1975).

[17] M. J. Norgett, J.H.M. Thornley and L. M. Venanzi, *J. Chem. Soc.*, **A 1967**, 540.

[18] M. J. Norgett and L. M. Venanzi, *Inorg. Chim. Acta*, **2**, 107 (1968).

[19] A.B.P. Lever, "Inorganic Electronic Spectroscopy", Elsevier, Amsterdam, 1968, chap. 8—9.

[20] A. C. Banciu, *Rev. Roumaine Chim.*, **22**, 1353 (1977).

Revue Roumaine de Chimie, **26**, *9–10*, 1245–1254 (1981)

STUDIES ON SOME NITRO-bis-ACETYLACETONATO-COBALT (III) COMPOUNDS

MOHAMED ABDEL SALAM El ABSY*, GH. MARCU**, J. ZSAKÓ***
and CS. VÁRHELYI**

* Nuclear Research Center — Cairo, Egypt
** Faculty of Chemical Technology, "Babeş-Bolyai" University, 3400-Cluj-Napoca, str. Arany János 11, Romania

Received October 18, 1980

The substitution reaction of $Na_3[Co(NO_2)_6]$ with sodium acetylacetonate (Na acac) leads to the formation of $Na[Co(acac)_2(NO_2)_2]$. Some new complex salts of the type Cation. . $[Co(acac)_2 (NO_2)_2]$ were obtained by double exchange reactions (Cation : monovalent metals and various complexes of the diacido-tetramine series). Nonelectrolytes of the type $[Co(acac)_2 (NO_2) (amine)]$ are formed easily from the dinitro-salt by a ligand exchange reaction with aliphatic, heterocyclic and aromatic amines with pK_b values : 8–12. The kinetics of the thermal dehydration and the thermal stability of some nitro-complexes of these types were studied by derivatography. The IR and electronic spectra of these compounds are discussed.

INTRODUCTION

The β-diketones react in their enolic form with transition metal salts to form chelates of various types. These chelating agents function as bidentate ligands. The resulting six membered chelate rings are stable enough in neutral and weakly acid media.

The tervalent cobalt forms homogeneous (e.g. $[Co(acac)_3]$[1]) and various mixed chelates with these reagents. The $[Co(en)_2(acac)]^{2+}$ was obtained from $[Co(en)_2(H_2O)Cl]^{2+}$, $[Co(en)_2CO_3]^+$ and acetylacetone [2,3]. ($acac^- =$ acetylacetonate monoanion, en = ethylenediamine).

Rosenheim and Garfunkel[4] observed the sodium acetylacetonate to react with sodium hexanitro—cobaltiat according to equation (1).

$$Na_3[Co(NO_2)_6]+2\,Na.acac = Na[Co(acac)_2\,(NO_2)_2]+4\,NaNO_2 \qquad (1)$$

One of the co-ordinated nitro-groups can be substituted easily by water or by other neutral molecules, e.g. NH_3, pyridine bases. The nitro-aquo-nonelectrolyte : $[Co(acac)_2(NO_2)\,(H_2O)]$ appears during the hydrolysis of $[Co(acac)_2\,(NO_2)_2]$. Some $[Co(acac)_2\,(NO_2)-(amine)]$ nonelectrolytes with NH_3 and pyridine bases were described.[5,6] The second NO_2 can be substituted only in special conditions (in the presence of ammonia or pyridine and active coal)[7].

In the present paper a series of new salts of the dinitro-bis-acetylacetonato-cobalt(III)-anion were described and the thermal decomposition of some of these derivatives was studied by means of derivatography.

Further, a series of new substitution reactions of the dinitro-complex of this type with primary and tertiary aliphatic, aromatic and heterocyclic amines were carried out. Some of the resulting nonelectrolytes were also studied by derivatography and by IR and UV-spectroscopy.

RESULTS AND DISCUSSION

The $Na[Co(acac)_2(NO_2)_2] . 6\ H_2O$ was obtained following Rosenheim and Garfunkel's method from $Na_3[Co(NO_2)_6]$ and sodium acetylacetonate, in concentrated aqueous solution. The recrystallized sodium salt was dissolved in water and used for a series of double decomposition reactions with conc. aqueous solutions of NH_4Cl, KCl, $TlNO_3$, $AgNO_3$ and with various complex salts of the diacido-tetramine type, e.g. $[Co(en)_2X_2]X$, $[Co(ec)\,(amine)_2]X$ (ec. H_2 = ethylenediimino-bis-acetylacetone), $[Co(DH)_2\,(amine)_2]X$ (DH_2 = dimethylglyoxime, X = monovalent anion).

The formed binary complex salts are characteristic, well crystallized products. Some of these compounds are characterized in table 1.

TABLE 1

Binary complex salts of the type Cation. $[Co(acac)_2(NO_2)_2]$

Formula	Aspect	Analysis	
		Calcd.	Found
$Na[Co(acac)_2(NO_2)_2] . 6H_2O$	Brown prisms[4]	Co 12.27 H_2O 22.51	12.80 22.40
$K[Co(acac)_2(NO_2)_2] . 2\ H_2O$	Irregular brown cryst.	Co 13.89 H_2O 8.49	14.06 8.50
$NH_4[Co(acac)_2(NO_2)_2] . 3\ H_2O$	Irregular brown prisms[4]	Co 13.99 H_2O 12.83	14.20 12.50
$Ag[Co(acac)_2(NO_2)_2]$	brown prisms	Co 12.89 Ag 23.60	12.16 23.50
$[Co(DH)_2(pyridine)_2] . [Co(acac)_2(NO_2)_2] . H_2O$	golden-yellow irregular plates	Co 14.47 H_2O 2.21	14.58 2.54
$[Co(DH)_2\ (aniline)_2] . [Co(acac)_2(NO_2)_2] . 4\ H_2O$	golden-brown tetrahedral plates	Co 13.15 H_2O 8.04	13.26 8.05
$[Co(DH)_2(\beta\text{-}picoline)_2] . [Co(acac)_2(NO_2)_2] . 4\ H_2O$	brown prisms	Co 13.15 H_2O 8.04	13.35 7.60
$[Co(DH)_2\ (Thiourea)_2] . [Co(acac)_2(NO_2)_2] . 2\ H_2O$	brown plates	Co 14.26 S 7.76 H_2O 4.36	14.10 7.97 4.23
$[Co(ec)\ (pyridine)_2] . [Co(acac)_2(NO_2)_2] . H_2O$	brown prisms	Co 14.36 H_2O 2.23	14.57 1.30
$[Co(ec)\ (\beta\text{-}picoline)_2] . [Co(acac)_2(NO_2)_2] . H_2O$	irregular brown cryst.	Co 14.15	14.03

Co detn. with EDTA, S as $BaSO_4$, Co + Ag as Co_3O_4 + Ag

It is worth mentioning the bi- and trivalent transition metal cations, and the complex salts of hexamin- and monoacidopentamin-types to be not able of double decomposition reactions with $[Co(acac)_2(NO_2)_2]^-$.

In contrast with a series of monobazic complex acids of the tervalent transition metals, e.g. $H[Co(NCS)_4(NH_3)_2]$[8,9], $H[Cr(NCS)_4\ (aniline)_2]$[10], $H[Co(DH)_2X_2]$ ($X = Cl, Br, I, NCS, NCSe, N_3, NO_2$)[11-13], the $H[Co(acac)_2(NO_2)_2]$ cannot be obtained in free state and it does not form salts with the heterocyclic organic N-bases and alkaloids.

The substitution reaction of $[Co(acac)_2(NO_2)_2]^-$ with various organic amines takes place according to equation (2)

$$[Co(acac)_2(NO_2)_2]^- + amine = [Co(acac)_2(NO_2)\ (amine)] + NO_2^- \qquad (2)$$

Our systematic study upon this ligand exchange reaction with about 60 aliphatic, aromatic and heterocyclic primary and tertiary amines and some phosphines (diethyl-phenyl-phosphine, diethyl-p-tolyl-phosphine, etc.) shows the heterocyclic N-bases (pyridine, chinoleine, imidazole-derivatives) to form easily crystalline nonelectrolytes of this type. The aromatic primary amines with pK_b values $8-12$ co-ordinate also easily in the Co(III) ion under similar experimental conditions. The reactions products crystallize from the aqueous, or aqueous-alcoholic solutions. The non-electrolytic compounds with aliphatic amines and with the above mentioned phosphines are, generally, very slightly soluble in water or are present as oils and cannot be solidified.

TABLE 2

Nitro-amino-bis-acetylacetonato-cobalt (III) nonelectrolytes

Formula	Aspect	Analysis	
		Calcd.	Found
$[Co(acac)_2(NO_2)\ (NH_3)]$[7]	brown prisms	N 8.28	8.25
$[Co(acac)_2(NO_2)\ (pyridine)]$[7]	reddish-brown needles	Co 15.42	15.18
$[Co(acac)_2(NO_2)\ (aniline)]$	brown prisms	Co 14.87	14.98
$[Co(acac)_2(NO_2)\ (2\text{-}amino\text{-}pyridine)]$	brown needles	Co 14.83	14.68
$[Co(acac)_2(NO_2)\ (3,4\text{-}lutidine)]$	red-brown microcryst.	N 10.58 Co 14.36	10.96 14.15
$[Co(acac)_2(NO_2)\ (3\text{-}ethyl\text{-}pyridine)]$	red-brown irregular crystals	Co 14.36	14.40
$[Co(acac)_2(NO_2)\ (thiourea)].3H_2O$	red-brown microcryst.	Co 13.60 H_2O 12.47	13.59 12.90
$[Co(acac)_2(NO_2)\ (izobuthylamine)]$	yellow-brown microcryst.	N 7.48	7.66
$[Co(acac)_2(imidazole)\ (NO_2)].1/2H_2O$	thin brown needles	Co 15.47 N 11.26 H_2O 2.36	15.70 11.90 2.26
$[Co(acac)_2(NO_2)\ (phenylamine)]$	yellow-brown microcryst.	Co 13.89	13.70

Some compounds of this type are characterized in table 2. The non-electrolytic compounds are slightly soluble in some polar solvents, e.g. acetone, methylethylketone, dimethylformamide and pyridine, they are very sparingly soluble in unpolar solvents, e.g. CCl_4, $CHCl_3$, benzene, n-hexane.

The X-ray studies[5–7] show the $[Co(acac)_2(NO_2)_2]^-$-ion to have a *trans* geometrical configuration and the substitution of one nitro-group with a neutral molecule occurs with retention of the configuration.

The IR spectra of some nitro-bis-acetylacetonato-cobalt-(III)-complexes were taken in KBr pellets.

The spectral data are shown in table 3.

TABLE 3

Infrared spectral data of some acetylacetonato-Co(III)-complexes

Vibration	I.	II.	III.	IV.	V.	VI.	VII.
$\nu(O-H)$	—	3510 m	—	—	—	3340– 3400m	—
$\nu(N-H)$	—	—	—	3285m 3225m 3150m	3480vs 3380 vs 3245 vs	3165 vs	—
$\nu(C-H)$	2960 m 2920 m	2980 m 2940 m	2980 m	2980 m 2935 m	2930 w	2970 w 2930 m	2930 m
$\nu(C\overset{\cdots}{-}O)$	1575 s	1585 vs	1580 vs	1580 s	1570 vs	1585 vs	1580 s
$\nu(C\overset{\cdots}{-}C)$	1525 m		1535 vs	1525 vs	1535 s	1530 vs	1525 vs
$\delta(NH_2)$	—	—	—	1565 w	—	—	—
$\nu(C-O)+\delta$ + $\delta(C-H)$	1430 s	1460 vs	1450 w	1465 vs	1465 s 1450 s	1430 vs	1455 s
$\delta(CH_3)$	1390 m	1370 w	1380 s	1390 w	1380 vs	1390 vs	1380 s
$\nu(C\overset{\cdots}{-}C)$ + + $\nu(C-CH_3)$	1285 s	1300 s	1290 vs	1285 s	1295 s	1290 s 1260 s	1295 s
$\nu(NO_2)$	—	1420 vs	1415 vs	1425 vs	1440 s	1430 vs	1425 vs
$\nu(NO_2)$	—	1330 vs	1320 vs	1330 vs	1325 vs	1330 vs	1330 vs
$\delta(C-H)$	1195 m	1205 m	1200 s	1200 s	1200 s	1200 s	1200 s
$\delta(CH_3)$	1022 s	1040 vs	1035 vs	1025 s	1035 vs	1035 s	1035 vs
$\gamma(NH_2)$	—	845 vs					
$\gamma(OH_2)$		825 vs	855 vs	850 w	850 s	830 s	830 s
$\gamma(NO_2)$			815 vs	830 vs	830 s		
deform cycl-+		670 vs	700 vs	670m	670 m	690 s	670 vs
$\nu(C-O)$	690 m		670 vs			670 s	
$\nu(Co-N)$	500 m	510w	530 m	530 m	500 s	500 s	490 vs 530 m
$\nu(Co-O)$	460 m	475 vs	480 vs 425 w	480 vs	475 m	455 m	485 vs

vs. = very strong, s = strong, m = medium, w = weak

I. $[Co(acac)_3]$, II. $K[Co(acac)_2(NO_2)_2]\,.\ 2\,H_2O$; III. $Ag[Co(acac)_2(NO_2)_2]$;
IV. $[Co(acac)_2(NO_2)$ (phenetylamine] V. $[Co(acac)_2(NO_2)$ (2-amino-pyridine)] ;
VI. $[Co(acac)_2(NO_2)$ (imidazole)]$.1/2H_2O$, VII. $[Co(acac)_2(NO_2)$ (pyridine)]

The IR spectra of a great number of various deuterated, ^{13}C and ^{18}O labelled α-dicetonato-complexes of transition metals were thoroughly investigated.[14–18] In these spectra the different carbonyl bands, the $\nu(C\overset{\cdots}{-}C)$ bands and the M–O stretchingbands are the most important from the point of view of the stability and the bond strength of the corresponding complexes.

In our cases the ν(C—O) stretching and ν(C⩳C) stretching bands appear at 1560—1580 cm^{-1} and 1525 cm^{-1}, respectively. The coupled ν(C⩳O) and C—H in plane bending vibrations have been assigned to the band at 1430 — 1460 cm^{-1}. The band at 460 — 480 cm^{-1} has been noted to Co—O stretching. The position of these bands is generally not influenced by coordination effect.

The stretching vibrations of the NO_2-group and the O—N—O deformation vibrations appear at 1425 — 1440 cm^{-1} (v.s.), 1330 cm^{-1} (s) and 825 — 830 cm^{-1} (m), respectively, as in other nitro-cobalt (III)-complexes (e.g.$[Co(NH_3)_5NO_2]Cl_2$). Thus the Co-nitro bond is formed through the nitrogen atom and not with the participation of the oxygen atom, as in the case of nitrito-complexes (Co—O—N—O).[19,20]

The ν(N—H) vibration bands of the co-ordinated primary aromatic and aliphatic amines may be observed at about 3200 cm^{-1} (s) and 3080 — 3100 cm^{-1} (m), shifted by 200 — 250 cm^{-1} towards lower frequencies, as compared to the free, non co-ordinated amines. The above mentioned spectral data show that all Co-ligands bonds (Co-acac, Co—NO_2, Co-amine) have strongly covalent character.

It is worth mentioning that we could not obtain dinitro- and nitro-amino-complexes with other β-diketones, e.g. benzoylacetone, on an analogous way.

The visible and UV absorption spectra have been recorded by means of a Specord recording spectrophotometer in the region 12.000 — 50.000 cm^{-1} in the case of three non-electrolytic complexes : $[Co(acac)_2(NO_2)$ (amine)], with amine = aniline, pyridine and imidazole, by using methanol as solvent and concentrations of 10^{-2} — 10^{-4} M. The electronic absorption spectra are given in figure 1.

As seen from this figure, the complexes studied show in the vi sible region a single absorption band. Taking into account the molar absorption coefficient, this band can be presumed to correspond to a ligand field transition. In the UV region four bands seem to appear, some of them being marked by an inflexion (shoulder). These bands may be assigned to charge transfer and to ligand transitions.

The wave number of the ligand field transition denoted as A in table 4 is influenced by the nature of the amine molecule.

The position of the charge transfer bands in also given in table 4 (bands B — E). It is obvious that they are practically identical in the case of the derivatives of pyridine and imidazole, but the bands are slightly shifted towards the higher wave numbers in the case of the aniline derivative (i.e. in the opposite direction as compared to the ligand field transition).

The thermal decomposition of 6 nitro-acetylacetonato-complexes has been studied by means of a MOM Derivatograph (Budapest). 20 mg samples have been heated with a $q = 20$ K/min heating rate. The TG and DTA curves obtained are given in figures 2 and 3.

As seen from these curves, the hydration water is lost in a single stage, marked by an endothermic peak on the DTA curve ($Na[Co(acac)_2(NO_2)_2].6\ H_2O$, $K[Co(acac)_2(NO_2)_2].2H_2O$, $NH_4(Co(acac)_2(NO_2)_2]$. $3H_2O$ $[Co(acac)_2\ (NO_2)\ (thiourea)].3H_2O$)

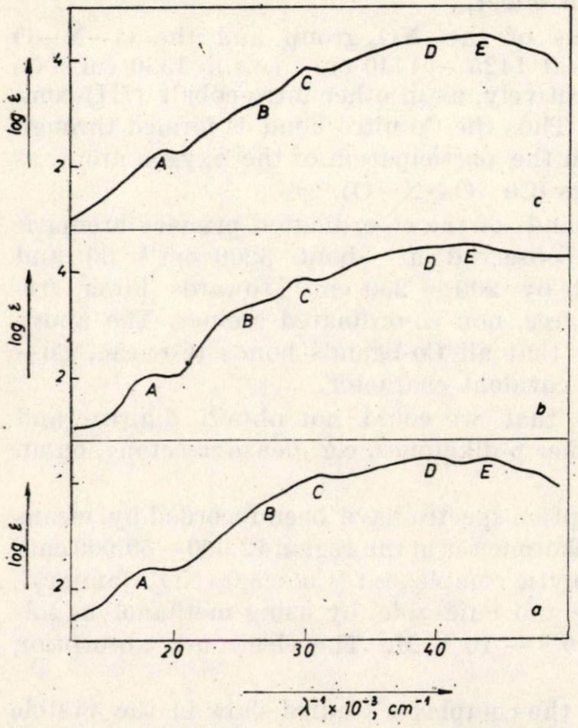

Fig. 1. — Visible and UV absorption spectra of some $[Co(acac)_2(NO_2)$ (amine)] type complexes: amine : *a* — aniline ; *b* — pyridine ; *c* — imidazole

The decomposition of the complex anion begins with a very rapid exothermic reaction, which frequently occurs explosion like. This is why the final weight of the sample at high temperature is sometimes less than the theoretical weight of the metal oxides. This stage is followed at higher temperatures by another, even more exothermic decomposition stage.

TABLE 4

Position of the absorption bands of $[Co(acac)_2\ (NO_2)$ (amine)] type complexes

Amine	λ^{-1}, cm^{-1}				
	A	B	C	D	E
aniline	18 200	27 000(i)	31 400	39 100	43 800
pyridine	18 640	26 200(i)	29 600	39 000(i)	43 900
imidazole	19 200	26 000(i)	29 800	38 700(i)	43 100

(i) denotes an influexion point of the absorption curve

The position of both exothermic peaks is very much influenced by the nature of the cation as seen in table 5. This influence might be presumed to be related to the polarizing effect of the cation. This hypothesis is in agreement with the melting point data[21] of fluorids and chlorids of the same cations, also given in table 5.

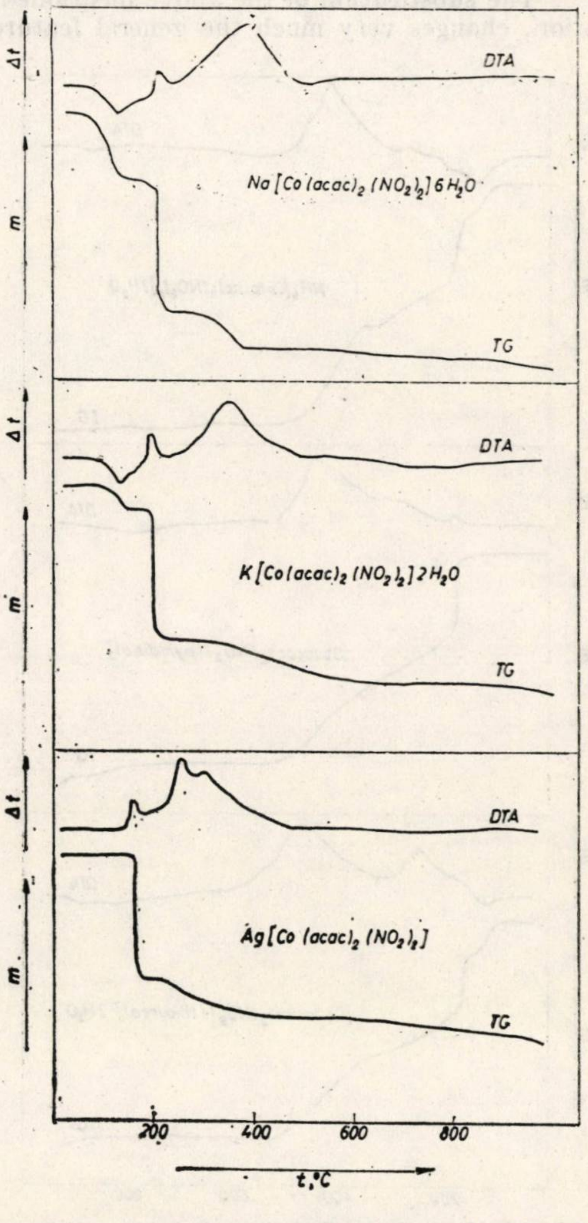

Fig. 2.—DTA and TG curves of compounds: $Na[Co(acac)_2(NO_2)_2]\cdot 6\ H_2O$ $K[(Co(acac)_2(NO_2)_2]\cdot 2\ H_2O$ $Ag[Co(acac)_2(NO_2)_2]$

It is worth mentioning that the weight loss stops after both exothermic decomposition stages correspond to no stoichiometric intermediates, i.e. nothing can be told on the nature of these decomposition reactions and it is not worth deriving kinetic parameters from these portions of the TG curves.

The substitution of the above mentioned cations by an ammonium cation, changes very much the general features of the thermolysis. The loss of the crystallization water is not so clearly separated from the first exothermic process as with the Na and K salts. Only an inflexion point appears on the TG curve instead of a well defined plateau. The first

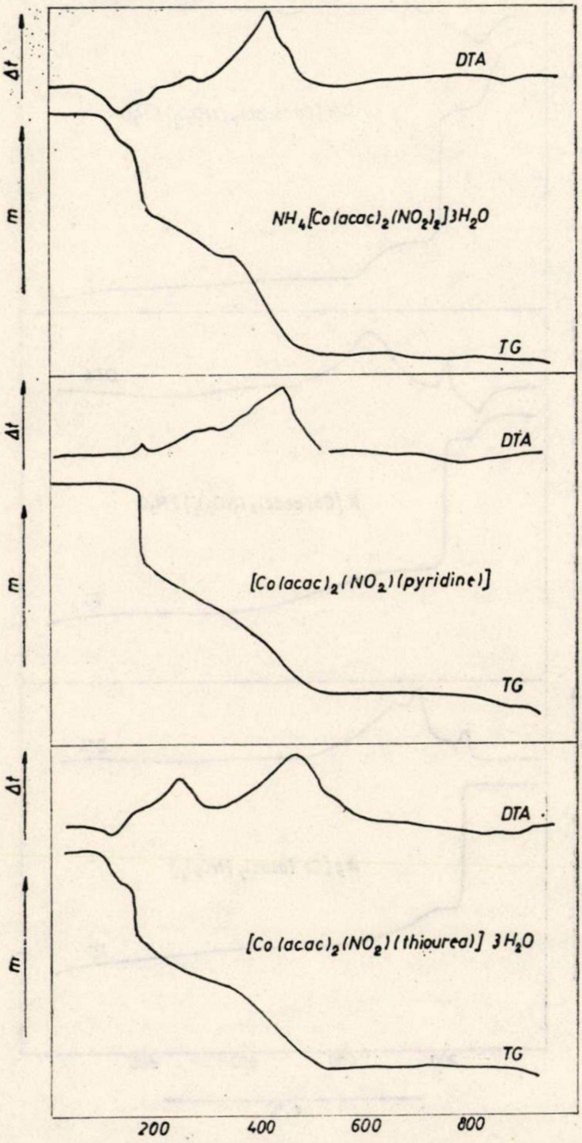

Fig. 3. — DTA and TG curves of compounds : $NH_4[Co(acac)_2(NO_2)_2] . 3\ H_2O$ $[Co(acac)_2(NO_2)(pyridine)]$ $[Co(acac)_2(NO_2)(thiourea)] . 3\ H_2O$

rapid decomposition stage of the anion begins at very low temperatures (140 – 150°C) and gives no clear exothermic peak. The weight loss in this stage is much less than with the Na, K and Ag-salts and is followed by a rather slow exothermic decomposition. The large exothermic peak of the last decomposition stage appears only at about 420°C. These important differences between the decomposition of the Na,K and Ag-salts on the one hand and of the NH_4-salt on the other hand, are due probably to some redox reactions of the ammonium ion with the NO_2-ligands.

TABLE 5

Position of the exothermic peaks at the thermal decomposition of some $M[Co(acac)_2(NO_2)_2]$ type salts and the melting points of the corresponding fluorides and chlorides

Cation	Exothermic peaks		Melting points, °C	
	first, °C	second, °C	MF	MCl
Na^+	208	397	993	800.4
K^+	199	362	856	770.3
Ag^+	157	280	435	457.5

The TG curves of the $[Co(acac)_2 (NO_2) (pyridine)]$ and $[Co(acac)_2 (NO_2) (thiourea)]$ non-electrolytic type compounds containing a single NO_2-ligand, ressemble the TG curve of the $NH_4[Co(acac)_2-(NO_2)_2]\cdot 3 H_2O$, but the relatively short very rapid decomposition stage gives a clear exothermic peak with $[Co(acac)_2(NO_2) (pyridine)]$. The last large exothermic peak appears at much higher temperatures as with the Na, K and Ag-salts, at 440 and 460°C, respectively. This is due probably to the absence of a polarizing cation in the crystal lattice of these non-electrolytic type complexes.

Since the only well defined intermediates are formed in the case of the crystallo-hydrates, viz. corresponding to the loss of all crystallization water, kinetic analysis of the TG curves has been made, only for the first decomposition stage of $Na[Co(acac)_2(NO_2)_2]\cdot 6 H_2O$, $K[Co(acac)_2 (NO_2)_2]\cdot 2 H_2O$, $NH_4[Co(acac)_2-(NO_2)_2].3 H_2O$ and $[Co(acac)_2(NO_2) (thiourea)]\cdot 3 H_2O$. Kinetic analysis has been performed by means of a computerized integral method, proposed in our earlier paper[22] as "method 3". On the base of the TG curves the temperature has been determined at which the conversion of the crystallohydrate attains the following values : $\alpha = 0.1, 0.2, 0.3...0.9$. The apparent kinetic parameters reaction order (n), activation energy (E) and pre-exponential factor (Z) as well as the standard decomposition temperature T_c, defined as the absolute temperature corresponding to $\alpha = 0.1$, are given in table 6 (Z values are calculated in s^{-1}).

The only conclusion which can be drawn from the kinetic parameter data is an increasing tendency of the apparent reaction order n with increasing number of the crystallization water molecules. The activation energy values are between the limits of the E_a values found in the case of dehydration of other complex molecules [23–25].

TABLE 6

Kinetic parameters and standard decomposition temperature for the thermal dehydration of some nitro-bis-acetylacetone-cobalt (III) complexes

Compound	n	E, k J/mol	log Z	T_c, K
$Na[Co(acac)_2\ (NO_2)_2]\cdot 6H_2O$	1.59	98.8	12.9	338
$K[Co(acac)_2(NO_2)_2].2\ H_2O$	0.86	73.5	8.1	361
$NH_4[Co(acac)_2(NO_2)].3H_2O$	1.33	92.7	10.7	366
$[Co(acac)_2(NO_2)$ (thiourea)]3 H_2O	1.41	99.5	12.0	358

n — reaction order, E-activation energy, Z-pre-exponential factor in s^{-1}, T_c— standard decomposition temperature

EXPERIMENTAL

$Na[Co(acac)_2(NO_2)_2]\cdot 6\ H_2O$ was obtained following Rosenheim and Garfunkel's method, from $Na_3[Co(NO_2)_6]$ and sodium acetylacetonate in concd. aqueous solution. The crude product was dissolved in water, treated with $NaNO_2$, and after standing of 1/2 hour cooled with ice. The sodium salt crystallizes in brown prisms. *Cation*. $[Co(acac)_2\ [NO_2)_2]$: 20 mmoles of $Na[Co(acac)_2(NO_2)_2]$ were dissolved in 100 ml water and treated with an excess of conc. aqueous solution of KCl, NH_4Cl, 0.1 mol $AgNO_3$, 0.1 mol $TlNO_3$ or 0.1 mol complex salts of the diacido-tetramine type, respectively, in water or in dil. alcohol (1 :2). The formed crystalline products were filtered and washed with ice cooled water and dried on air.

Synthesis of $[Co(acac)_2(NO_2)$ *(amine)*]. 10 mmoles of $Na[Co(acac)_2-(NO_2)_2]$ were treated in 100 ml water with 12—15 mmoles of the corresponding amine in 10—15 ml alcohol. The mixture wax stirred with a glass stick for 10—30 minutes. The crystalline precipitate formed was filtered off after 1—2 hours. The crude product can be purified, generally, by dissolving in alcohol and reprecipitating with an excess of water.

REFERENCES

[1] B. E. Bryant and W. C. Fernelius, *Inorg. Synth.*, **5**, 188 (1957).
[2] A. Werner, J. E. Schweizer and W. Karrer, *Helv. Chim. Acta*, **4**, 113 (1921).
[3] J. K. Reid and A. M. Sargeson, *Inorg. Synth.*, **9**, 167 (1967).
[4] A. Rosenheim and A. Garfunkel, *Ber. dtsch. chem. Ges.*, **44**, 1865 (1911).
[5] B. P. Cotsoradis and R. D. Archer, *J. Inorg. Chem.*, **6**, 800 (1967).
[6] R. D. Archer and B. P. Cotsoradis, *J. Inorg. Chem.*, **4**, 1584 (1965).
[7] L. J. Boucher and J. C. Bailar jr., *J. Inorg. Chem.*, **3**, 589 (1964).
[8] O. T. Christensen, *J. prakt. Chem.*, **45**, 213, 356 (1892).
[9] R. Coupechoux, *J. Pharm. Chim.*, **30**, 118 (1939).
[10] W. Bergmann, *J. Biol. Chem.*, **110**, 476 (1935).
[11] A. V. Ablov and G. P. Syrzova, *Zhur. obshchei Khim.*, **25**, 2053 (1955).
[12] A. V. Ablov and N. M. Samus, *Doklady Akad. Nauk S.S.S.R.*, **133**, 1327 (1960).
[13] Cs. Várhelyi, Z. Finta and S. Kiss, *Monatsh. Chem.*, **106**, 659 (1975).
[14] K. Nakamoto, J. Marimoto and A. E. Martell *J. Phys. Chem.*, **66**, 346 (1962).
[15] G. T. Behnke and K. Nakamoto, *J. Inorg Nuclear Chem.*, **6**, 433, 440 (1967).
[16] H. Junge and H. Musso, *Spectrochim. Acta, Part A*, **24**, 1219 (1968).
[17] L. J. Bellamy and R. F. Branch, *J. Chem. Soc.*, **1954**, 4491.
[18] S. Pindias, B. L. Silber and J. Laulicht, *J. Chem. Phys.*, **46**, 1506 (1967).
[19] J. R. Beattie and H. J. Tyrrel, *J. Chem. Soc.*, **1956**, 2849.
[20] R. B. Penland, T. J. Lane and J. V. Quagliano, *J. Amer. Chem. Soc.*, **78**, 887 (1956).
[21] I. Náray-Szabó „Szervetlen Kémia", Akadémiai Kiadó, Budapest, 1957—1958, Vol. II, p. 43, 44, 48, 51, Vol. III, p. 40, 44.
[22] J. Zsakó and J. Zsakó jr., *J. Thermal Anal.*, **19**, 333 (1980).
[23] J. Zsakó, Cs. Várhelyi, C. Liptay and K. Szilágyi, *J. Thermal Anal.*, **7**, 411 (1975).
[24] J. Zsakó, G. Brandt-Petrik, G. Liptay and Cs. Várhelyi, *J. Thermal. Anal.*, **12**, 421 (1977).
[25] J. Zsakó, M. Várhelyi and Cs. Várhelyi, *J. Thermal Anal.*, **17**, 123 (1979).

Revue Roumaine de Chimie, **26**, *9–10*, 1255–1259 (1981)

THE SPECTROPHOTOMETRIC STUDY OF SOME Cu(II)-THIOCARBOHYDRAZONE SYSTEMS IN SOLUTION AND THEIR ANALYTICAL APPLICATION

SILVIA BARBU* and CONST. GH. MACAROVICI**
* Faculty of Pharmacy Str. Ion Creangă Nr. 12, 3400 Cluj-Napoca
** Faculty of Chemical Technology Str. Arany Janos Nr. 11, 3400 Cluj-Napoca

Received May 23, 1980

A spectrophotometric study of the reaction of Cu(II) ion with the thiocarbohydrazones of salicyl-aldehyde, vanilline and nicotinaldehyde was performed in order to elaborate a quantitative spectrophotometric method for thiocarbohydrazone and Cu(II) ion determination. The metal to ligand combination ratio, the instability constants of the complexes and the application of the Lambert–Beer law were studied.

In some previous papers we have presented the results of our studies referring to the coordinating capacity of some monothiocarbohydrazones $H_2N-NH-CS-NH-N=CH-R$, where :

$$R = -C_6H_4OH;\ -C_6H_3(OH)\ (OCH_3);\ -C_5H_4N.$$

Their bidentate ligand character due to the azomethyne and thiocarbonyl group present in the molecule was established.[1-4]

In order to test the analytical use of complex compounds of these thiocarbohydrazones with ions of the transition metals, the results of the UV–VIS spectrophotometric study of the Cu(II)-salicylaldehyde thiocarbohydrazone (S-TCH), Cu(II-vanilline thiocarbohydrazone (V-TCH) and Cu(II)-nicotin aldehyde thiocarbohydrazone (N-TCH) are shown.

The variation of the extinctions dependent on the wavelength, the combination ratio metal to ligand, the instability constant and the Lambert-Beer law application were studied.

EXPERIMENTAL

The reagents used were alcoholic solutions of the ligand containing 10^{-4} M for Cu(II)–(S-TCH) and Cu(II)–(V-TCH) and 10^{-2}M for Cu(II)–(N-TCH) system, respectively alcoholic Cu(II) solutions for Cu(II)–(S-TCH) and aqueous Cu(II) solutions for Cu(II)–(V-TCH) and Cu(II)–(N-TCH) systems having the same molar concentrations with the solutions of ligands.

A VSU-2P spectrophotometer and a Spekol spectrophotometer were used. The blank was methanol for Cu(II)–(S-TCH) and Cu(II)–(V-TCH) systems and water for Cu(II)–(N-TCH) system.

RESULTS AND DISCUSSION

Cu^{+2} ion forms with S-TCH and V-TCH yellow complex compounds, stable in time, at pH = 5—6. The Cu(II)—(N-TCH) complex is green. The electronic spectra show a characteristic absorption maximum for Cu(II)—(S-TCH) and Cu(II)—(V-TCH) as compared with the absorption maximum of the ligand at wavelength 400 nm (Fig. 1).

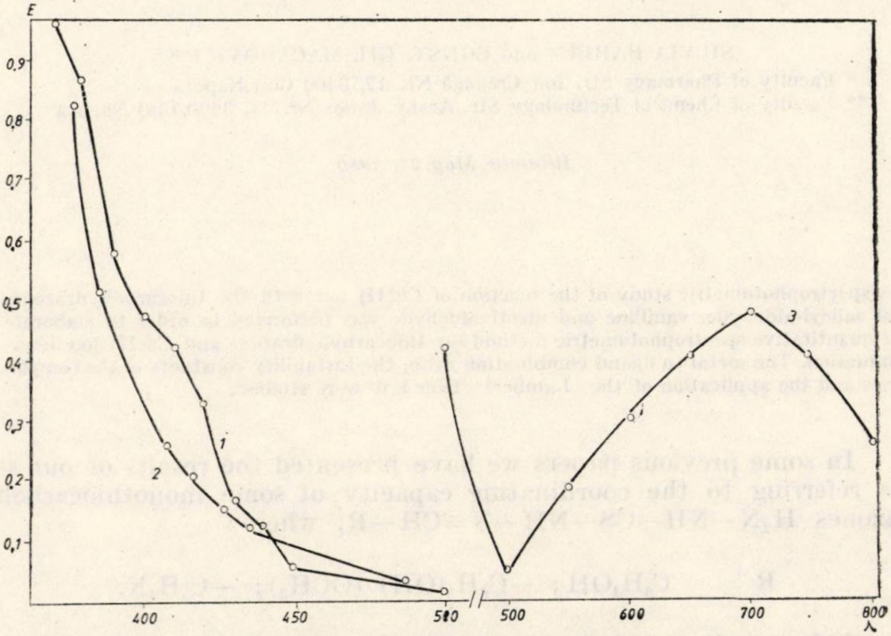

Fig. 1.—The extinction variation dependent on wavelength: 1. Cu(II)—(S-TCH) 2. Cu(II)—(V-TCH) 3. Cu(II)—(N-TCH)

The spectrum of Cu(II)—(N-TCH) complex shows a maximum at 700 nm (Fig. 1).

In order to establish the metal—ligand combination ratio, the extinction of some mixtures of equimolar solutions was determined (Fig. 2).

The instability constant was established by means of the Job method[5] following the extinction variation of non equimolar solutions mixtures.

The plot of the experimental data allowed the determination of the composition corresponding to the maximum extinction value (Fig. 3).

The results of the spectrophotometric study of Cu(II) thiocarbohydrazone systems in solutions are given in table 1.

The Cu^{2+} ion reactions with the above mentioned thiocarbohydrazones were applied in the spectrophotometric assay of the ligands and of Cu^{2+} ion. For this purpose the applicability of the Lambert—Beer law was verified. The extinction variation dependent on both the ligand concentration and the Cu^{2+} ion concentration was studied.

TABLE 1

The results of the spectrophotometric studies in solution

System	λnm	Colour	Combination ratio M :L	Sample	$K_{\text{inst.}}$					
					C_1	C_2	p	X	$K_{\text{inst.}}$	$K_{\text{inst.mean}}$
Cu(II)–(S-TCH)	400	yellow	1 : 1	1 2	2.32×10^{-4} 4.97×10^{-4}	6.21×10^{-4} 11.80×10^{-4}	2.67 2.37	0.45 0.41	5.00×10^{-4} 2.80×10^{-4}	2.90×10^{-4}
Cu(II)–(V-TCH)	400	yellow	1 : 2	1 2	2.10×10^{-4} 2.10×10^{-4}	5.00×10^{-4} 6.00×10^{-4}	2.50 3.00	0.54 0.50	0.93×10^{-8} $0.75 \times 10.^{-8}$	0.84×10^{-8}
Cu(II)–(N-TCH)	700	green	1 : 2	1 2	0.59×10^{-2} 0.59×10^{-2}	1.50×10^{-2} 1.27×10^{-2}	2.54 2.10	0.50 0.54	1.48×10^{-6} 1.50×10^{-6}	1.49×10^{-6}

C_1 = molar concentration of Cu^{2+}, C_2 = the molar concentration of the ligand, $p = \frac{C_2}{C_1}$,

X = the maximu m composition of the ligand corresponding to the highest extinction.

The experimental results obtained with the spectrophotometric dosage of ligands and Cu^{2+} ion were processed by regression analysis.[6]

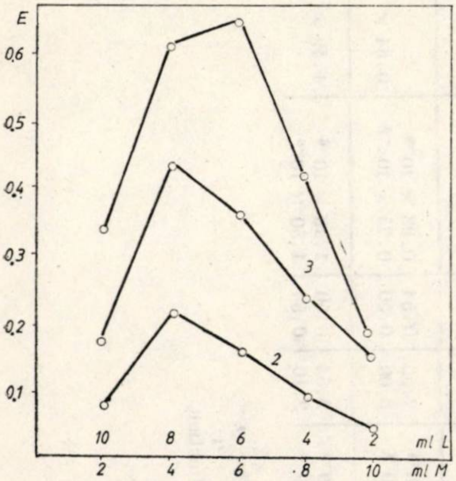

Fig. 2. — The extinction variation of the isomolar solution mixtures : *1.* Cu(II) and S-TCH. *2.* Cu(II) and V-TCH. *3.* Cu(II) and N-TCH.

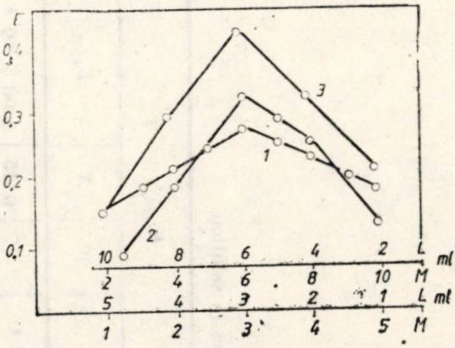

Fig. 3. — The extinction variation of the nonisomolar solution mixtures : *1.* Cu(II) and S-TCH. *2.* Cu(II) and V-TCH. *3.* Cu(II) and N-TCH.

TABLE 2

The results of the statistical calculus

Reagent	Ligand dosage		Cu(II) dosage	
	Concentration	Statistical calculus	Concentration	Statistical calculus
S-TCH	10^{-1}mg/ml	$r = 0.999$ $p < 0.001$ $a = 1.367$ $b = 0.0021$ $\varepsilon = 2\%$	10^{-3}mg/ml	$r = 0.999$ $p < 0.001$ $a = 0.5835$ $b = -0.00459$ $\varepsilon = 2\%$
V-TCH	10^{-1}mg/ml	$r = 0.999$ $p < 0.001$ $a = 0.0334$ $b = -0.00607$ $\varepsilon = 3\%$	10^{-2}mg/ml	$r = 0.999$ $p < 0.001$ $a = 0.0326$ $b = -0.00727$ $\varepsilon = 2\%$
N-TCH	1 mg/ml	$r = 0.999$ $p < 0.001$ $a = 0.0561$ $b = 0.0270$ $\varepsilon = 1.5\%$	1mg/ml	$r = 0.999$ $p < 0.001$ $a = 0.1760$ $b = 0.0166$ $\varepsilon = 1.3\%$

The results of the statistical calculus are given in table 2. The order of magnitude of the concentration is expressed in mg/ml; the linear correlation coefficient r, the statistical signification threshold of the correlation coefficient p, the regression coefficients a and b and the error ε are given.

The linear regression coefficient values show the practicability of the elaborated methods; the obtained data are in the range of the allowed error limit. The errors are obtained for N-TCH.

REFERENCES

[1] C. Gh. Macarovici and S. Barbu, *Rev. Roumaine Chim.*, **23**, 1035 (1978).
[2] C. Gh. Macarovici and S. Barbu, *Rev. Roumaine Chim.*, **24**, 1039 (1979).
[3] C. Ch. Macarovici and S. Barbu, *Rev. Roumaine Chim.*, **24**, 1291 (1979).
[4] S. Barbu and C. Gh. Macarovici, *Rev. Roumaine Chim.*, **25**, 207 (1980).
[5] P. Job, *Liebigs Ann. Chem.*, **9**, 113 (1928).
[6] K. Doerffel, "Statistica v analiticheskoi khimii", Perevod s nemetskogo Izdatelstvo Mir, 1969, p. 175.

Revue Roumaine de Chimie, **26,** *9–10,* 1261–1269 (1981)

COPPER (II) COMPLEXES WITH 10-[2-(DIMETHYLAMINO)PROPYL]-PHENOTHIAZINE

VIORICA CIMPU, AURELIA MEGHEA and IOANA JITARU
The Polytechnic, Department of Inorganic Chemistry, 1 Polizu str., Bucharest, Romania

Receveid March 10, 1980

The paper reports on the synthesis and structural characterization of some Cu(II) complex compounds with 10-[2-(dimethylamino) propyl]-phenothiazine (Romergan) corresponding to the following general types : $[CuRomX_2]\cdot n\ H_2O$ (X=Cl, n=2 ; X=SCN, n = 0), $[Cu_2Rom_2Cl_4]$ and $[CuRom_2]\ [Cu(SCN)_4]$, where Rom is Romergan. The compounds obtained were characterized by elemental analysis, molecular weight determinations, electric conductivity measurements, electronic, – ESR – and vibration spectra. The most probable stereochemistry of the compounds was ascribed on the basis of the data thus obtained.

The literature includes numerous papers that mention or study, under various aspects, the complex compounds of phenothiazines with different transitional ions. Researches in this fields are justified by the biological actitvity of these compounds in the human body.[1-7] Nevertheless, few systematic works referring to the structure of phenothiazine compounds are known. There is still controversy concerning the formulation of Cu(II) compounds. Some authors consider them Vauquelin salts, others charge-transfer complexes.[8,9]

The present paper mentions the results obtained in the synthesis and characterization of some Cu(II) compounds with 10-[2-(dimethylamino) propyl]-phenothiazine (Romergan) :

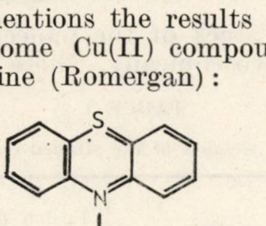

The compounds obtained correspond to the following general types :

- $[CuRomX_2]\cdot n\ H_2O$ (X :Cl, n = 2 ; X : SCN, n=0)
- $[Cu_2Rom_2Cl_4]$ and
- $[CuRom_2]\ [Cu(SCN)_4]$

The formulation proposed, that is the probable stereochemistry of these compounds, is established in keeping with the interpretation of molecular electric conductivity, electronic, ESR and vibration data.

RESULTS AND DISCUSSION

In order to obtain a great diversity of Cu(II) complex compounds with Romergan, the compounds were prepared varying:

- the ratio of the components (metallic salt–ligand);
- pH of the medium;
- temperature;
- nature of the Cu(II) salt anion.

Working at molar ratios of Cu(II) salt : Romergan = 2 :1 and 1 :1, the same type of complex compound was obtained at a Cu : Romergan ratio of 1 :1.

Cu(II) chloride and sulfocyanide behaviour with regard to Romergan was studied in neutral or slightly acidic medium. The same type of compound was obtained regardless of the reaction medium.

Romergan was used in the synthesis either as a free base or in the form of Romergan maleate (for pharmaceutical use).

The use of Romergan free base led to the formation of compounds with a higher degree of purity.

The compounds were synthesized either at 50°C or, in order to obtain dimeric compounds, at higher temperatures (80°C).

At 80°C, in the presence of Romergan maleate, the dimeric chloride $[Cu_2Rom_2Cl_4]$, and a sulfocynaide dimer of the $[CuRom_2]$ $[Cu(SCN)_4]$ type were obtained.

The synthesized compounds were characterized by elemental analysis, molecular weight and molecular electric conductivity measurements, electronic, ESR– and vibration spectra.

Molecular weight measurements

Table 1 gives the values of the molecular weight of the studied compounds determined cryoscopically. These values confirm the formulation, as monomers, of the complex compounds synthesized at 50°C in a slightly acidic medium using Romergan as free base, and the formulation, as dimers, of the compounds obtained at 80°C.

TABLE 1

Molecular weights of the studied compounds

Compound	Colour	Fusion point °C	Molecular weight	
			Calcd.	Found.
$[CuRomCl_2].2\ H_2O$	light green	92–106	455	449
$[CuRom(SCN)_2]$	olive-green	90–126	464	454
$[Cu_2Rom_2Cl_4]$	dark green	102–123	838	798
$[CuRom_2]$ $[Cu(SCN)_4]$	yellow	148–152	928	920

Molecular electrical conductivity measurements

The formulation attributed to the studied complex compounds, in which the electrolyte type was established, was confirmed by the determination of their molecular electrical conductivity (Table 2).

TABLE 2

Molecular electric conductivity

Compound	Molecular electric conductivities $\Omega^{-1}cm^2mol^{-1}$	Electrolyte type
$[CuRomCl_2].2\ H_2O$	15.10	non-electrolyte
$[CuRom(SCN)_2]$	10.70	non-electrolyte
$[Cu_2Rom_2Cl_4]$	20.30	non-electrolyte
$[CuRom_2]\ [Cu(SCN)_4]$	85.90	1 : 1

Thus, the conductivity values for compounds of the $[CuRomX_2]\cdot nH_2O$ and $[Cu_2Rom_2Cl_4]$ type show that they are of non-electrolytic nature, whereas the value for $[CuRom_2]\ [Cu(SCN)_4]$ indicates an electrolyte type 1 :1.

Electronic spectra

In order to establish the most probable stereochemistry of the studied compounds, their electronic reflectance spectra were recorded. These spectra were interpreted in correlation with the electronic spin resonance spectra.

Analysis of the electronic reflectance spectra recorded for $[CuRomX_2]\cdot nH_2O$ compounds and shown in figure 1 suggests that these compounds probably have a strongly distorted octahedral structure. The spectra of the two compounds are similar exhibiting the same structure.

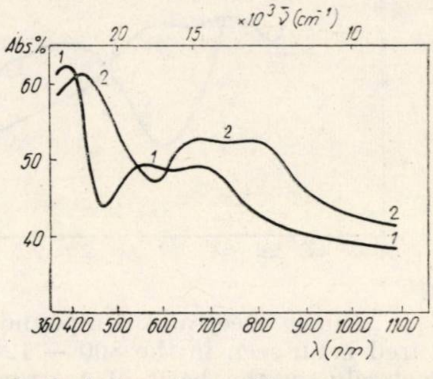

Fig. 1. — Electronic reflectance spectra of the compounds : 1 — $[CuRomCl_2].2H_2O$ and 2 — $[CuRom(SCN)_2]$.

Thus, the large asymmetrical band at about 700 nm (16,600 cm^{-1}) in the case of the thiocyanate complex and the split band in the case of the chlorocomplexes — which might be split into several components —

plead for the formulation suggested. The marked distortion of the octahedral symmetry is due to the non-equivalence of the donor atoms deriving from the ligand (if Romergan is considered to act as a bidentate ligand, probably through S and N) and from Cu(II) salt anions.[10,11]

In spite of its large and asymmetrical aspect the band indicates a hypsochromic shift going from chlorocomplex to the thiocyanate one (in terms of the nature of the ligand X); this shift is in accordance with the ligand positions in the spectrochemical series.[12]

In the nearly ultraviolet range, the studied compounds show a relatively intense band that might be interpreted as a charge transfer band, L—M.[13]

This band shows a bathochromic shift (in terms of the nature of X ligands, namely of their reducing character) (from 400 nm in the thiocyanate complex to 440 nm in the chlorocomplex).

The charge transfer band is more intense in the case of thiocyanate complex suggesting a stronger metal—ligand interaction, as confirmed also by ESR spectra.

The bands appearing at 300 nm and 250 nm are attributed to certain transitions characteristic of the Romergan ligand. These data are in agreement with the data published in the literature.[14]

The spectrum of compound $[Cu_2Rom_2Cl_4]$ (Fig. 2) pleads for a strongly distorted octahedral stereochemistry (axial symmetry).

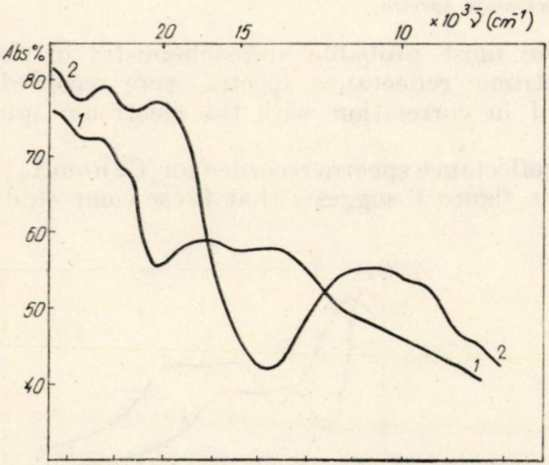

Fig. 2.—Electronic reflectance spectra of the compounds : 1—$[Cu_2Rom_2\ Cl_4]$ and 2 — $[CuRom_2]$ $[Cu(SCN)_4]$.

In the spectra of compound $[CuRom_2]$ $[Cu(SCH)_4]$, the large structured band seen in the 800 — 1200 nm range, may be interpreted satisfactorily on the basis of a strongly distorted tetrahedral configuration (the band is sufficiently structured to differentiate the three peaks corresponding to the three transitions theoretically foreseen) and the intense band in the nearly ultraviolet range may be attributed to a charge transfer L—M.[15]

Vibration spectra

The IR spectra of the compounds were studied in order to obtain additional data regarding their stereochemistry, especially the mode of coordination of the Romergan ligand (monodentate ligand, coordination through N or bidentate ligand, coordination through N and S) and the behaviour of anions (coordinated or in the ionization sphere).

From this point of view, the most interesting spectral ranges are, on the one hand, those in which absorption is attributed to stretching vibrations $\nu(C-S)$ and $\nu(C_{arom}-N)$ of the Romergan ligand, and on the other hand those attributed to the mode of vibration of anions.

For correct determination of the IR spectra of the studied complex compounds the free Romergan spectrum was recorded on the same apparatus and compared with the published data.[1,2,14,16] In the free Romergan spectrum the stretching vibration frequency, $\nu(C-S)$ appears in the 680 cm^{-1} range as a band of weak intensity, and the stretching vibration frequency, $\nu(C_{arom}-N)$ in 1330 cm^{-1} as a band of medium intensity.

Table 3 shows the IR frequencies characteristic of the studied compounds and their probable attributions.

TABLE 3

Characteristic IR frequencies (in cm^{-1}) of the studied complex compounds and their probable assignments*

Compound	$\nu(C-S)$	$\nu(C_{arom}-N)$	$\nu(OH)$	ν(CN) (SCN)	ν(CS) (SCN)
Romergan	680(w)	1330(m)	—	—	—
$[CuRomCl_2].2\ H_2O$	630(w)	1320(m)	3300(m)	—	—
$[Cu_2Rom_2Cl_4]$	680(w)	1315(m)	—	—	—
$[CuRom(SCN)_2]$	630(w)	1310(m)	—	2030 $2080^{(s)}$	890(w)
$[CuRom_2][Cu(SCN)_4]$	630(w)	1320(m)	—	2030 $2085^{(s)}$	885(w)

* w — weak band ; m — medium band ; s — strong band.

The data included in this table suggest the following :

— in the spectra of all the $[CuRomX_2].nH_2O$ and $[CuRom_2][Cu(SCN)_4]$ compounds the bands corresponding to the $\nu(C-S)$ and $\nu(C_{arom}-N)$ stretching vibrations shift towards lower frequencies, proving coordination of Romergan with the central metal ion through N and S (structural formulae a);

— in the spectra of $[Cu_2Rom_2Cl_4]$ compound, the band corresponding to stretching vibration $\nu(C-S)$ can be found within the same range as with free Romergan, whereas that corresponding to $\nu(C_{arom}-N)$ shifts towards lower frequencies showing that in this compound, Romergan acts as a monodentate ligand coordinating only through N (structural formulae b);

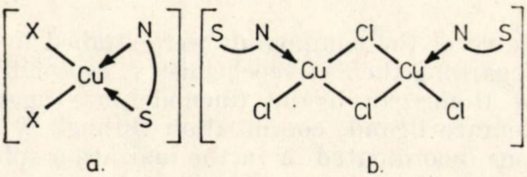

— in the spectra of $[CuRomCl_2].2H_2O$ compound a band corresponding to the modes of vibration of crystallization water appears (3300 cm^{-1}), whereas in the spectrum of $[CuRom(SCN)_2]$ compound this band lacks;

— the presence in the spectra of $[CuRom\ (SCN)_2]$ and $[CuRom_2][Cu(SCN)_4]$ compounds of a strongly sharp band, split in the 2030–2080 cm^{-1} (ν(CN) range) and of a weak band at about 890 cm^{-1} (ν(CS) range) suggests a structure with SCN coordinated with the central metal ion through S.

ESR spectra

Table 4 gives the parameters of the ESR spectra. The chlorocomplex synthesized at 50°C with free Romergan gives the spectrum in figure 3.1, presenting a 3rd order anisotropy; g tensor components have values close to those found for $CuCl_2.H_2O$ ($g_1=2.037$; $g_2=2.187$; $g_3=2.252$).[17] These data indicate a strongly distorted octahedral geometry according to a rhombic asymmetry, in agreement with its electronic spectra.

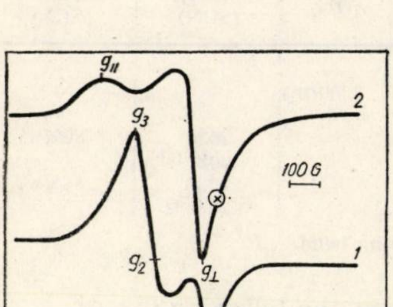

Fig. 3. — ESR spectra of the chlorocomplexes : 1 — $[CuRom\ Cl_2].2\ H_2O$ and 2 — $[Cu_2Cl_4Rom_2]$.

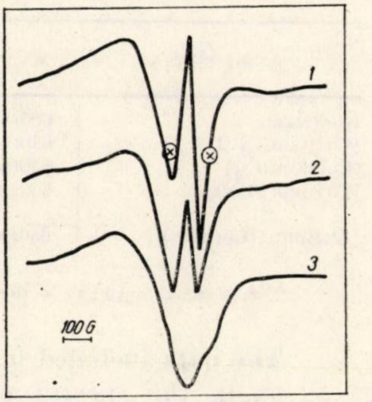

Fig. 4. — ESR spectra of $[CuRom(SCN)_2]$: 1 — prepared at 50°C with Romergan free base ; 2 — prepared at 50°C with Romergan maleate ; 3 — prepared at 80°C with Romergan maleate.

The chlorocomplex prepared at 80°C with Romergan maleate presented a completely different ESR spectra (Fig. 3.2) resulting from the Cu ion situated within a field of axial symmetry (distorted octahedron). Such a geometry would be in accordance with a dimer structure where Romergan coordinates monodentately. This hypothesis is confirmed by the IR spectrum, where only the vibration shift of the C—N band in Romergan can be noticed, ν(C—S) vibration being not affected.

With thiocyanate complex prepared at 50°C, a large, relatively symmetrical line (Fig. 4.1) characteristic of a less distorted octahedral complex is obtained. This symmetry is probably due to the fact that atoms of the same nature—nitrogen and sulphur—take part in coordination with both Romergan and SCN⁻.

TABLE 4

ESR spectrum parameters

Compound	g_1 or	g_2 $g\perp$	g_3 $g\|$	g_i	a_i Gauss	g_{CT}	a_{CT} Gauss
$[CuRomCl_2].2\ H_2O$	2.0417	2.1923	2.2534	—	—	—	—
$[Cu_2Cl_4Rom_2]$	—	2.1018	2.3469	—	—	—	—
$[CuRom(SCN)_2]$	—	—	—	2.0647	207.66	2.0035	46.62

Superposed over this large band, characteristic of Cu(II) ion with an octahedral coordination, there is another intense, narrow line, with g factor $= 2.0035$, very close to g factor of the free electron. This line can be attributed to a powerful donor-acceptor interaction, characteristic for charge-transfer complex, being also in accordance with the intense charge transfer band observed in the electronic spectrum of this complex.

Synthesis of a similar compound at 80°C resulted in the complex salt $[CuRom_2]$ $[Cu(SCN)_4]$ that did not exhibit the ESR signal. The absence of ESR spectrum might be due to the powerful ion-ion interactions which interfere in this case in spin-spin interactions (leading to a total spin $S = 1$).

Syntheses using the SCN⁻ anion and Romergan maleate (at 50°C and 80°C) gave impure compounds, with diminution of the charge transfer band in ESR spectra (Figs. 4.2, 4.3). Under these conditions, mixtures of complex thiocyanate and complex salt were obtained, as reported also in the literature.[1]

EXPERIMENTAL

Synthesis of compounds

$[CuRomCl_2].2\ H_2O$. To an HCl-acidulated aqueous solution 0.5 M of $CuCl_2.2\ H_2O$ an alcoholic Romergan solution (free base) (molar ratio Cu (II) : Romergan ≃ 2 :1) was added. The solution obtained was heated in a water bath at ≃ 50°C up to the concentration and formation of a light green compound. The filtered compound was purified by dissolving in dimethylformamide, precipitation with ether, and then dried in vacuum on P_4O_{10}.

Calculated for $CuC_{17}H_{20}N_2SCl_2.2\ H_2O$: Cu 14.06 ; C 44.83 ; H 5.27 ; N 6.15 ; S 7.03 ; Cl 15.60.

Found Cu 13.70 ; C 45.00 ; H 5.15 ; N 6.10 ; S 7.35 and Cl 15.67%.

The compound is highly soluble in water, acetone, chloroform, slightly soluble in ethanol and methanol dimethylformamide and hardly soluble in ether or benzene.

$[Cu_2Rom_2Cl_4]$. The compound obtained under similar condition (molar ratio Cu : Romergan maleate ≃ 2 :1) was maintained in a water bath at 80°C. The precipitate agglomerates and becomes darker. It is filtered and purified by dissolving in dimethylformamide and precipitation with ether, then dried in a vacuum desiccator on P_4O_{10}.

Calculated for $Cu_2C_{34}H_{40}N_4S_2Cl_4$: Cu 15.26 ; C 48.80 ; H 4.78 ; N 6.70 ; S 7.66 ; Cl 17.00.
Found Cu 14.80 ; C 49.05 ; H 5.05 ; N 6.95 ; S 7.35 and Cl 16.90%.

$[CuRom(SCN)_2]$. To an HCl-acidulated aqueous solutions 0.5 M of $CuCl_2 \cdot 2\ H_2O$, a Romergan (free base) solution in ethanol (molar ratio Cu(II) : Romergan = 1 :1) was added. The mixture was heated in a water bath at 50°C for 20–30 minutes then a concentrated aqueous KSCN solution (molar ratio Cu(II) : Rom : SCN = 1 :1 :4) was added over it. The mixture was maintained in a water bath at the same temperature for 15–20 minutes. The olive-green compound was filtered and washed with water and ether, then dried in vacuum desiccator on P_4O_{10}.

Calculated for $CuC_{19}H_{20}N_4S_3$: Cu 13.79 ; C 49.11 ; H 4.31 ; N 12.06 ; S 20.68.
Found Cu 14.00 ; C 49.23 ; H 4.41 ; N 12.10 and 20.26 %.

The thiocyanate complex is hardly soluble in water, ethanol and methanol, ethylic ether, methanol, ethylic ether, benzene ; it is soluble in acetone, dimethylformamide.

$[CuRom_2]$ $[Cu(SCH)_4]$. The olive green compound obtained under the afore mentioned conditions (molar ratio Cu(II) : Rom : SCN = 1 : 1 : 4) was maintained in a water bath at 70–80°C. The precipitate agglomerates and turns from green to yellow. It is filtered and purified by dissolving in dimethylformamide and precipitation with ether, then dried in a vacuum desiccator on P_4O_{10}.

Calculated for $Cu_2C_{38}H_{40}N_8S_6$: Cu 13.79 ; C 49.11 ; H 4.31 ; N 12.06 ; S 20.68.
Found Cu 13.73 ; C 49.06 ; H 4.44 ; N 12.18 and S 20.42%.

The dimer complex is sparingly soluble in water, insoluble in ether. It is slightly soluble in ethanol, methanol and dimethylformamide.

Molecular weight measurements

The molecular weights of the studied compounds were determined by the Rast method using camphor as solvent.

Molecular electric conductivity measurements

Measurements of molecular electric conductivity were carried out with a Radelkis conductometer (Hungary), cell constant $K = 0.52$, using 10^{-3}M dimethylformamide solutions at 25°C. Assignment of the electrolyte type was based on the published indications referring to the methods for determination of the electrolyte type in dimethylformamide solution.[18]

Electronic spectra

Electronic reflectance spectra were recorded at room temperature using a C. Zeiss Jena – VSU 1 spectrophotometer and magnesium oxide as reference material. Eectronic spectra in solution were recorded at room temperature with a VSU 2G spectrophotometer.

Vibration spectra

IR spectra were recorded with a Perkin Elmer spectrophotometer in Nujol solution or KBr pellets.

ESR spectra

Spectra of electronic spin resonance were recorded in polycrystalline powders with an ART 5 – IFA spectrometer (Bucharest) at X frequency band and magnetic field modulation 100 KC/s.

REFERENCES

[1] J. Barbe and J. Hurwic, *Compt. rend.*, **273**, 1481 (1971).
[2] J. Barbe, J. P. Galy and J. Hurwic, *Ann. pharm. franc.*, **30**, 665 (1972).
[3] J. Lagubeau and P. Mesnard, *Bull. Soc. chim. France*, **1965**, 2815.

[4] F. Gutmann and H. Kayzer, *J. Chem. Phys.*, **46**, 1969 (1967).
[5] J. Blazek, *Pharmazie*, **22**, 129 (1967).
[6] J. Blazek, V. Spinkova and E. Stejkal, *Ann. Farm. Hosp.*, **10**, 7 (1967).
[7] J. Blazek and E. Stejkal, *Pharmazie*, **27**, 506 (1972).
[8] J. Barbe and J. Hurwic, *Ann. pharm. franc.*, **31**, 227 (1973).
[9] M. Tarasiewicz, *Acta Pol. Pharm.*, **29**, 583 (1972).
[10] L. Sacconi and M. Ciampolini, *J. Chem. Soc.* (A), **1964**, 276.
[11] R. A. Palmer and T. S. Piper, *Inorg. Chem.*, **5**, 864 (1966).
[12] M. Brezeanu and P. Spacu "Chimia combinaţiilor complexe", Ed. didactică şi pedagogică, Bucureşti, 1974.
[13] A.B.P. Lever, "Inorganic Electronic Spectroscopy", Academic Press, New York, 1968, p. 309.
[14] R. J. Warren, J. B. Eisdorfer, W. E. Thompson and J. E. Zarembo, *J. Pharm. Sci.*, **55**, 144 (1966).
[15] A.A.G. Tomlinson, *J. Chem. Soc. (A)*, **1969**, 65.
[16] J. Blazek and J. Kraemar, *Cesk. Farm.*, **26**, 174 (1975).
[17] F. K. Kneubühl, *J. Chem. Phys.*, **33**, 1074 (1960).
[18] J. V. Quagliano, J. T. Summers, S. Kida and L. M. Vallarino, *Inorg. Chem.*, **3**, 1577 (1964).

[illegible] and [illegible] Phys. Rev. 26, [illegible]
[illegible] Physik 23, [illegible]
[illegible] 16, [illegible]
[illegible] 22, [illegible]
[illegible] 3, [illegible]
[illegible] 28, [illegible]
[illegible] 1934, [illegible]
[illegible] 8, [illegible]
[illegible] and [illegible]
[illegible] 1932
[illegible] New York, 1934,
[illegible]
[illegible] J. Chem. Phys.
[illegible]
[illegible] 1935, [illegible]
[illegible] 28, 177 [illegible]
[illegible] 30, [illegible]
[illegible]
[illegible]

Revue Roumaine de Chimie, **26**, *9–10*, 1271–1277 (1981)

ON THE α-DIOXIMINE COMPLEXES OF TRANSITION METALS. LXIII*

SPECTROPHOTOMETRIC STUDY ON THE STABILITY OF Fe(II) AND Co(II) COMPLEXES OF 1,2-CYCLOHEPTANE- AND 1,2-CYCLOOCTANEDIONE DIOXIMES

J. ZSAKÓ, J. HORÁK and CS. VÁRHELYI

Faculty of Chemical Technology, Babeş-Bolyai University, str. Arany János **11**,
3400-Cluj-Napoca, Romania

Received May 23, 1980

The complex formation of Co(II) and Fe(II) with heptoxime (1,2-cycloheptanedione dioxime) and octoxime (1,2-cyclooctanedione dioxime) has been studied spectrophotometrically. The formation of ML_2 type complexes is reported. The overall stability constants β_2 have been determined at 20°C in acetate buffer solutions, by using author's spectrophotometric approximation method. Heptoxime complexes have been found to be more stable than octoxime ones. Stability constants derived for the Co(II) complexes are in agreement with those found potentiometrically, but the Fe(II) complexes seem to be less stable than found earlier.

INTRODUCTION

In our previous paper[1] the formation of the water soluble Fe(II) and Co(II) complexes of 1,2-cycloheptanedione dioxime (Heptoxime, Heptox.H_2 : $C_7H_{12}N_2O_2$) and of 1,2-cyclooctanedione dioxime (Octoxime, Octox. H_2 :$C_8H_{14}N_2O_2$) was studied by means of potentiometric titration with NaOH. In all cases the formation of ML_2 type complexes has been observed (Fig. 1) at 20°C and ionic strength of $\mu = 0.1$. The stability constant values given in table 1 have been derived. The same table contains also the acidity constants of the corresponding dioximes.[2]

The possibility of deriving overall stability constants β_2 of ML_2 type complexes from spectrophotometric data has been discussed in our previous paper,[3] where a method has been proposed and the conditions of its applicability have been established. Since the dioximes are weak acids and only the anions Diox.H$^-$ participate in the complex formation equilibrium, their protolytic equilibrium must also be taken into account.

---

* Part LXII ; F. Mánok, E. Köszegi, Cs. Várhelyi, *Stud. Univ. Babeş-Bolyai, Chem.*, **26**, 000 (1981) in press

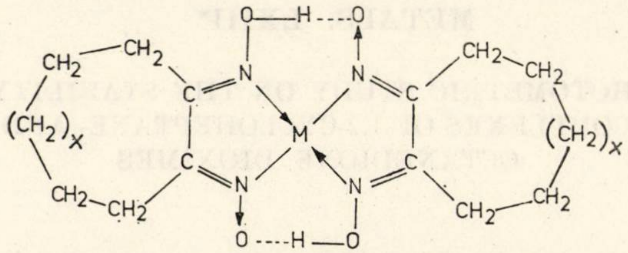

Fig. 1. — Structure of the ML_2 type complexes studied : M = Co(II), Fe(II) ; *a*, L = 1,2-cycloheptanedione dioxime (x = 1) ; *b*, L = 1,2- cyclooctanedione dioxime ($x = 2$).

TABLE 1

Stability constants of some M $(Diox.H)_2$ type complexes and the acidity constants of the corresponding dioximes

Complex	log β_1	log β_2	Ref.
$[Co(Heptox.H)_2]$	10.18	19.43	1
$[Co(Octox.H)_2]$	9.87	19.09	1
$[Fe(Heptox.H)_2]$	10.46	20.01	1
$[Fe(Octox.H)_2]$	10.21	19.70	1
Dioxime	p K_1	p K_2	
Heptox.H_2	10.65	11.74	2
Octox.H_2	10.54	11.60	2

By considering the protolytic equilibrium

$$HL \rightleftarrows H^+ + L^- \text{ with } K_a = \frac{[H^+][L^-]}{[HL]} \tag{1}$$

and the complex formation equilibria

$$\begin{aligned} M^{2+} + L^- &\rightleftarrows ML^+ \text{ with } \beta_1 = \frac{[ML^+]}{[M^{2+}][L^-]} \\ M^{2+} + 2\,L^- &\rightleftarrows ML_2 \text{ with } \beta_2 = \frac{[ML_2]}{[M^{2+}][L^-]^2} \end{aligned} \tag{2}$$

the following effective stability constants can be defined

$$\beta_1' = \frac{[ML^+]}{[M^+][LH]} = \beta_1 \frac{K_a}{[H^+]} \text{ and } \beta_2' = \frac{[ML_2]}{[M^+][LH]^2} = \beta_2 \frac{K_a^2}{[H^+]^2} \tag{3}$$

If $[L^-] \ll [LH]$, the conditions found for the applicability of our method are valid for these effective stability constants. Let us consider the formation of the above complexes in a solution with an overall metal concentration of $C_M = 10^{-4}$ mole/l, at pH = 5. By using the data given in table 1, one can calculate β_1' and β_2' and verify the conditions of applicability of our method.[3] These calculations show β_1' to be, in the case of Co(II) complexes, about 30—40 fold, in the case of Fe(II) complexes, about 40—50 fold higher than the maximum value admitted for an error below 10% in the β_2 value derived. On the basis of figure 2 given in our paper[3] it is obvious that in these conditions β_2 values given by our method can be expected to be lower than the real ones corresponding to an error of about $\Delta\log\beta_2 = 0.2\ldots0.3$.

Thus, our method can be applied only as a first approximation. The following notations will be used :

A for the absorption of the sample

A_∞ for the limiting value of the absorption at a high excess of the ligand

R for the ligand to metal ratio C_L/C_M

The appliation of our method involves the following presumptions :

$$[ML^+] \ll [ML_2] \text{ i.e. } [ML_2] = \frac{A}{A_\infty} C_M \text{ and } [M^{2+}] = \left(1 - \frac{A}{A_\infty}\right) C_M \quad (4)$$

$$[L^-] \ll [LH] \text{ i.e. } [LH] = C_L - 2\frac{A}{A_\infty} C_M = \left(R - \frac{A}{A_\infty}\right) C_M \quad (5)$$

From relations (3), (4) and (5) the following formula can be derived for the calculation of the overall stability constant :

$$\beta_2 = \frac{[H^+]^2 A A_\infty^2}{K_a^2 C_M^2 (A_\infty - A)(R A_\infty - 2A)^2} \quad (6)$$

SPECTROPHOTOMETRIC INVESTIGATIONS

In order to determine the most suitable wavelength for the investigation of the complex formation, the UV and visible spectra of solutions of M^{2+}. HL and their mixtures have been recorded. An example is given in figure 2 representing these curves in the case of the system Co^{2+} — Octox.H_2. As seen from this figure the absorption spectrum of the mixture (curve 3) is totally different from the sum of the spectra of the pure components. This shows complex formation in the system. The complex has an absorption band at $\lambda^{-1} = 3.45 \times 10^4$ cm^{-1} (marked by an arrow in Fig. 2), corresponding to $\lambda = 290$ nm. This wavelength has been chosen for the spectrophotometric investigations, since at this wavelength the absorption of the pure oxime is very low and the Co(II) salt practically does not absorb at all.

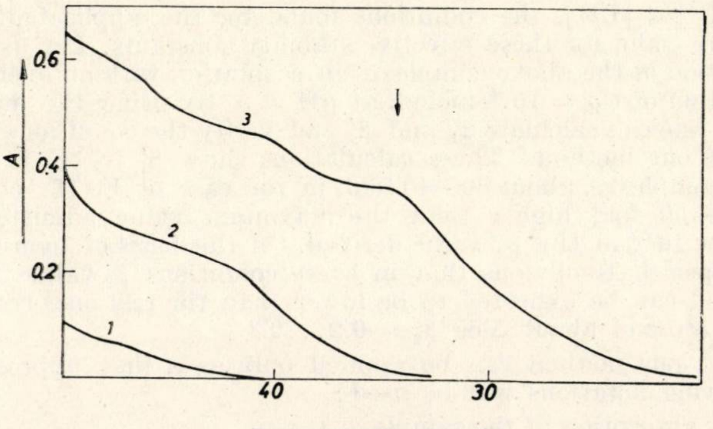

Fig. 2. – Absorption spectra of the system Co^{2+} – Octox. H_2 : *1* – $CoSO_4$, 10^{-4}M ; *2* – Octox. H_2, 10^{-4} M ; *3* – $CoSO_4$, 10^{-4}M + + Octox.H_2, 10^{-4} M.

Absorbtion spectra recorded in the system Co^{2+}—Heptox.H_2 indicated also $\lambda = 290$ nm, those of Fe^{2+} – Heptox.H_2 and Fe^{2+} – Octox.H_2 gave $\lambda = 350$ nm as most suitable for a spectrophotometric study.

The composition of the complexes formed has been established by using Job's method. Job's curves have been obtained in all the four systems studied, viz. at different pH values. As an example, figure 3 presents 2 curves obtained in the system Co^{2+} – Heptox.H_2 at two different pH values.

As seen, at higher pH values the complex formation is more pronounced, which is in perfect agreement with our presumption that only the

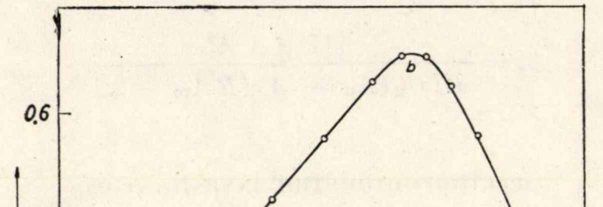

Fig. 3. – Curves Job in the system Co^{2+} – Heptox. H_2 : $C_M + C_L = 2 \times 10^{-4}$M ; $\lambda = 290$ nm ; *a*, pH = 4.80 ; *b*, pH = 5.73

anionic form L^- of the dioxime participates to the complex formation equilibrium. All the curves indicate a clear maximum at about $X = C_L/(C_L + C_M) = 0.67$, indicating the formation of ML_2 type complexes in all the systems studied.

The stability of the complexes has been studied by performing absorption measurements in samples having the same pH, the same overall metal concentration and corresponding to different ligand to metal ratios $R = C_L : C_M$.

Stability constants have been derived by means of formula (6). Since the direct determination of A_∞ presents some experimental difficulties, the following procedure has been used. For a given complex and a given pH value, β_2 values have been calculated by means of formula (6), for different R values, by presuming a reasonable A_∞ value. The standard deviation of the individual β_2 values from their arithmetical mean has been calculated. By performing a systematic variation of the presumed A_∞ value, the minimum of the standard deviation has been presumed to indicate the correct A_∞ value. This A_∞ value has been used for the calculation of the stability constant β_2.

An example is given in table 2. In this table the absorption values are presented for different ratios R, obtained in the system Co^{2+}—Heptox. H_2 at pH $= 4.72$. By calculating β_2 by means of formula (6) the minimum standard deviation is obtained with $A_\infty = 0.700$.

TABLE 2

Absorption of the Co(II)-samples containing various amounts of heptoxieme

R	2	4	6	8	12	16	20
A	0.094	0.285	0.440	0.559	0.603	0.635	0.644

$[CoSO_4]$: 5×10^{-5} M ; $t = 20°C$; pH $= 4.72$; $\lambda = 290$ nm

The corresponding log β_2 values are presented in table 3. The same table contains some other examples concerning the stability constants derived by means of the above procedure in the other three systems studied.

TABLE 3

Stability constants derived from the absorption of the samples corresponding to different ligands to metal ratios R

$[Co(Heptox.H)_2]$ pH = 4.7		$[Co(Octox.H)_2]$ pH = 5.6		$[Fe(Heptox.H)_2]$ pH = 5.2		$[Fe(Octix.H)_2]$ pH = 5.6	
R	log β_2	R	log β_2	R	log β_2	R	log β_2
2	19.18	2	18.89	1.6	16.55	1.6	16.40
4	19.20	4	18.77	3.2	16.57	3.2	16.24
6	19.34	6	19.19	4.8	16.58	4.8	16.42
8	19.45	8	19.08	6.4	16.62	6.4	16.25
12	19.23	12	18.75	8.0	16.58	8.0	16.37
16	19.15	16	18.68	9.6	16.48	9.6	16.26
20	19.00	20	18.62				

As seen from this table for a given complex and at a constant pH value one obtains practically the same stability constant by means of formula (6), irrespective of the ratio R. This shows the applicability of our method in the case of the complexes studied.

RESULTS AND DISCUSSION

For each complex, stability constants β_2 have been derived at two different pH-values. Results are given in table 4. Data presented in this table represent the arithmetical mean of 10–15 individual log β_2 values for each pH.

TABLE 4

Stability constants derived for different pH values and their arithmetical mean

Complex	pH	log β_2	pH	log β_2	log β_2 general mean
$[Co(Heptox.H)_2]$	4.7	19.24	5.6	19.13	19.19 ± 0.22
$[Co(Octox.H)_2]$	4.7	18.84	5.6	18.79	18.82 ± 0.35
$[Fe(Heptox.H)_2]$	5.2	16.73	5.6	16.51	16.62 ± 0.20
$[Fe(Octox.H)_2]$	5.2	16.58	5.6	16.29	16.44 ± 0.21

If one compares the results obtained with the data reported earlier and given in table 1, one can see the stability constants of the Co(II) complexes to be in agreement with those derived from potentiometric measurements although the log β_2 values are a little smaller than found earlier. Taking into account that β_1 values derived from potentiometric measurements are a little higher than admitted for the applicability of our spectrophotometric method, these low values are not surprising, they are exactly as expected, affected by an error of about -0.3.

The stability constants obtained for the Fe(II) complexes are much lower than found potentiometrically. This is hardly probable to be a consequence of the approximation method used, although this possibility cannot be excluded either, since higher β_1 values than those obtained potentiometrically could lead to a similar effect. But it is more likely this disagreement to be due to the instability of Fe(II) towards oxidation. In order to prevent the oxidation by atmospheric oxygen dissolved in the samples, methane has been bubbled through the solutions. Nevertheless, a variation of the absorbance could be observed in time, which was more important if the sample was in contact with air. Thus neither the potentiometric, nor the spectrophotometric data are trustful enough.

At any rate both with Co(II) and Fe(II) complexes the higher stability of the heptoxime derivatives as compared to the octoxime ones, has been proved again. As presumed earlier[1] this higher stability might be due to the higher nucleophilic character of the heptoxime as compared to the octoxime, reflected also in the value of their acidity constants.

EXPERIMENTAL

Synthesis of the dioximes has been performed as reported earlier.[2]

Absorption spectra have been recorded in the UV and visible region by means of a Specord recording spectrophotometer.

Absorbance measurements at constant wavelength were made with a VSU-2 spectrophotometer, with 1 cm cells, against the buffer solution as reference.

The constant pH value was ensured by acetate buffer solutions of an overall concentration of 4×10^{-2} M in the sample. The actual pH value was measured with a Radelkis -OP-205 precision pH-meter, by using a OPHJ-1/A type combined electrode.

All measurements were performed at 20°C.

In order to remove dissolved oxygen, methane was bubbled through the solutions, before and after mixing them.

REFERENCES

[1] C. Gh. Macarovici, J. Horák and Cs. Várhelyi, *Rev. Roumaine Chim.*, **25**, 805 (1980).
[2] J. Zsakó, J. Horák, Z. Finta, Cs. Várhelyi and J. Mitrache, *Mikrochim. Acta*, **1979**, 405.
[3] J. Zsakó, *Rev. Roumaine Chim.*, **25**, 1499 (1980).

EXPERIMENTAL

[illegible]

REFERENCES

[illegible]

Revue Roumaine de Chimie, **26**, *9–10*, 1279–1283 (1981)

THE OXIDATION OF n-DODECANE IN LIQUID PHASE WITH MOLECULAR OXYGEN IN THE PRESENCE OF ALUMINIUM, LANTHANUM AND CERIUM NAPHTHENATES

R. AVRAM, L. PAPAHAGI and I. ILIUŢĂ
National Institute of Chemistry, Calea Victoriei 149, Bucharest, Romania

Received October 24, 1980

The influence of aluminium, lanthanum and cerium naphthenates onto the oxidation process of n-dodecane, in liquid phase, with molecular oxygen has been studied ; one major concern was to find out the way in which these catalysts act on the initiation and the formation of acids and peroxy compounds. GLC measurements have been carried out for the fatty acids obtained by oxidation, in order to establish their structures.

INTRODUCTION

The oxidation of n-alkanes with molecular oxygen represents a process with important applications in the synthesis of fatty acids, secondary fatty alcohols,[1] peroxides[2] and dicarboxylic acids.[3, 4]

By using catalysts in the oxidation process of n-alkanes it becomes possible to carry out the reaction in milder conditions (i.e. – a lower temperature) ; this fact leads to the decrease of the amount of secondary degradation products, typical for profound oxidations.

The catalytic effect of some catalysts, based on alkali and earth-alkali metals has been studied by Tsyshkovski[5] and Zenailov.[6] The catalytic influence of mixtures, especially based on magnesium and potassium was reported by several authors.[7–10] Drimuş and his associates[11–13] have worked in the field of catalytic oxidation of n-alkanes in the presence of various metals.

The catalysts used in the above-mentioned papers have an intermediate position between the homogeneous and heterogeneous catalysts. This is the reason why Denisov and Emanuel[14] call them pseudohomogeneous catalysts.

EXPERIMENTAL

The naphthenates used in this work were prepared by double exchange reactions, between a water-soluble naphthenate (sodium naphthenate) and Al, La or Ce salt.

The oxidation reaction was carried out in a glass reactor, electrically heated, into which 40 g of n-dodecane were introduced ; oxygen was bubbled through a porous glass plate with a constant flow of 5 l/h. The catalytic oxidations were carried out at 140°C, while the thermal ones at 140°C and 155°C. The amount of catalysts used was 1 mole to 100 n-dodecane moles. The oxidation process was stopped when an acid number of 35–45 mg KOH/g was reached.

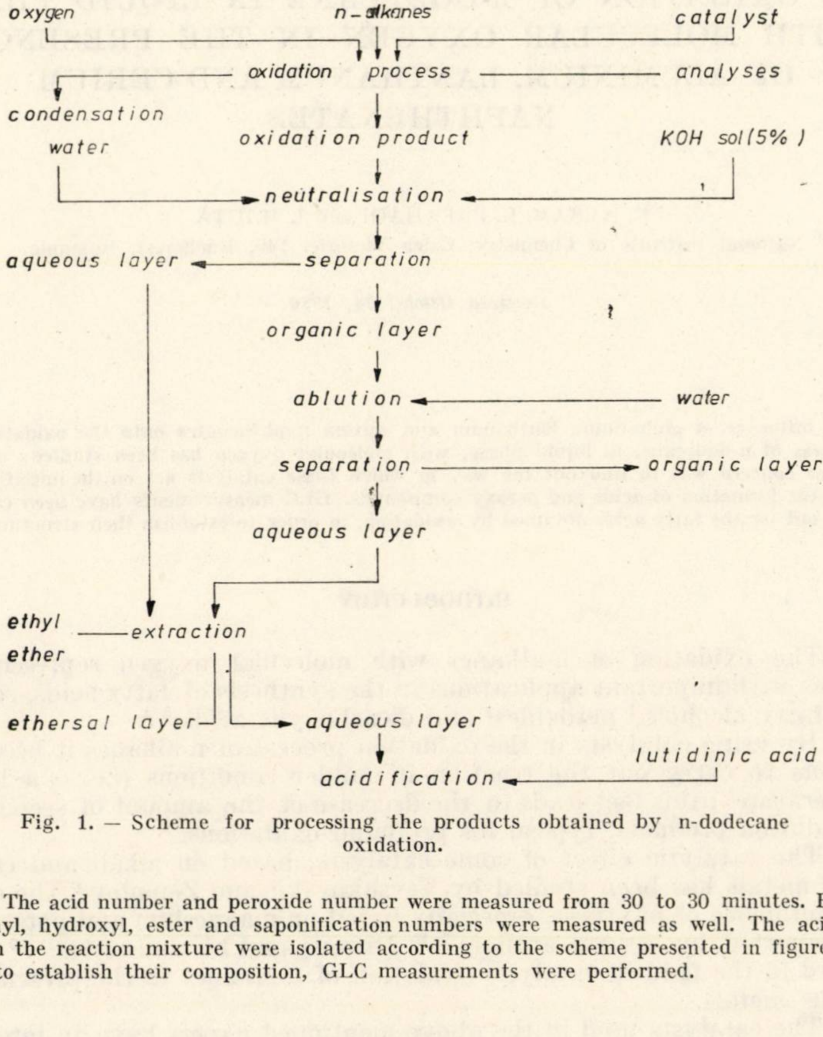
oxygen
n – alkanes
catalyst
oxidation process
analyses
condensation
water
oxidation product
KOH sol(5%)
neutralisation
aqueous layer
separation
organic layer
ablution
water
separation
organic layer
aqueous layer
ethyl
ether
extraction
ethersal layer
aqueous layer
lutidinic acid
acidification

Fig. 1. – Scheme for processing the products obtained by n-dodecane oxidation.

The acid number and peroxide number were measured from 30 to 30 minutes. Finally, carbonyl, hydroxyl, ester and saponification numbers were measured as well. The acids present in the reaction mixture were isolated according to the scheme presented in figure 1 ; in order to establish their composition, GLC measurements were performed.

RESULTS

The results obtained are presented in figures 2, 3 and tables 1, 2.

A comparison of values regarding the increase of acidity (Fig. 2) shows that the same acid number (40 mg KOH/g) is reached in short time, when the oxidation reaction is catalyzed by cerium and lanthanum naphthenates.

On the contrary, for aluminium, or in the case of thermal oxidations, three hours are necessary to reach an acid number of 40 mg KOH/g.

In the case of cerium and lanthanum, as well as for thermal oxidations, the peroxide numbers are higher than those obtained when using heavy metal naphthenates.[12]

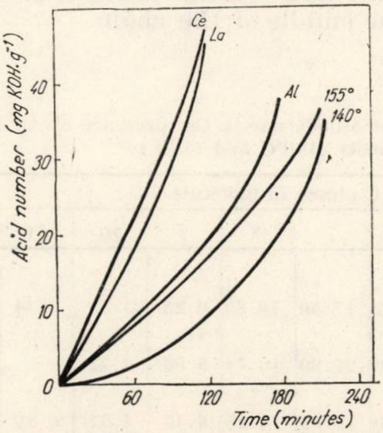

Fig. 2. — Evolution of acid numbers at n-dodecane oxidation in the presence of Al, La and Ce naphthenates and thermally (140°C and 155°C).

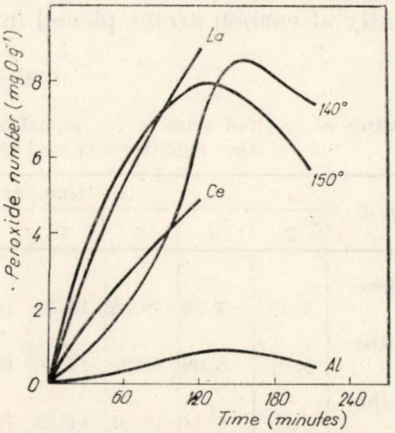

Fig. 3. — Evolution of peroxide numbers at n-dodecane oxidation in the presence of Al, La and Ce naphthenates and thermally (140°C and 155°C).

Aluminium naphthenate gives minimal values for peroxide accumulation, as for acidity.

By comparison of the values AN/EI (Table 1) it results that when the oxidation process is carried out in order to obtain acids, lanthanum and cerium naphthenates seem to be the most suitable; aluminium naphthenate favours the formation of aldehydes and ketones.

TABLE 1

Average values of acidity A. N. (mg KOH/g), saponification, S.N. (mg KOH/g), ester E.N. (mg KOH/g), hydroxyl OH.N. (mg KOH/g) and carbonyl CO.N. (mg 0/g) numbers

Catalyst	A.N.	S.N.	E.N.	CO.N.	OH.N.	A.N./E.N.
Al naphthenate	37.50	66.61	29.11	10.00	38.10	1.28
La naphthenate	45.10	67.25	22.15	5.80	34.54	2.03
Ce naphthenate	45.13	79.25	27.82	9.20	33.39	1.62
Without catalyst; 140°C	32.40	74.80	42.40	10.30	41.20	0.76
Without catalyst; 155°C	36.02	76.30	40.28	6.40	42.50	0.89

The acids were separated by processing the oxidation products according to the scheme presented in figure 1. The composition of acid mixtures was established by GLC and molar concentrations were calculated accordingly. The results are presented in table 2; as it can be seen from these figures, the maximal concentrations are reached for the acids containing 5, 6, 7 or 8 carbon atoms in molecule. This fact indicates that the attack of the oxygen on the hydrocarbon chain takes place especially at carbon atoms placed in the middle of the chain.

TABLE 2

Composition of resulted acids in the oxidation of n-dodecane in the presence of Al, La and Ce naphthenates and thermally (140°C and 155°C)

Catalyst	Number of C atoms in molecule										
	2	3	4	5	6	7	8	9	10	11	12
Al naphthenate	5.33	7.26	9.82	10.32	16.32	17.56	18.89	6.23	5.53	0.44	2.30
La naphthenate	5.01	6.09	9.20	14.60	17.20	21.30	15.74	5.96	3.72	—	1.18
Ce naphthenate	5.80	6.44	10.31	11.68	16.90	19.82	15.25	6.45	4.51	0.86	1.98
without catalyst at 140°C	6.00	10.30	14.90	15.80	21.00	18.50	7.10	3.50	1.50	0.50	0.90
without catalyst at 155°C	7.20	7.60	11.14	12.03	17.12	16.50	11.64	7.38	4.22	1.77	3.40

CONCLUSIONS

In the oxidation reaction of n-dodecane with molecular oxygen in the presence of Al, La and Ce naphthenates at 140°C or in the thermal one (at 140°C and 155°C) we have noticed the following features:

a) Cerium and lanthanum naphthenates allow the obtaining of good rates for the accumulation of acids.

b) The use of aluminium naphthenate is not suitable for the oxidation of n-alkanes in order to obtain monocarboxylic acids.

c) The concentration of peroxides is higher when using lanthanum or cerium naphthenates, in comparison with the use of heavy metal naphthenates.

d) When oxidizing n-dodecane in the presence of Al, La or Ce naphthenates, or thermally, the obtained acids contain mainly 5, 6, 7 or 8 carbon atoms in molecule.

REFERENCES

[1] I. Drimuş and F. Schenermann, *Bul. Inst. Polytechn. Bucureşti*, **20**, 129 (1958).
[2] I. Drimuş, *Studii, Cercetări Chim., Acad. R.P.R.*, **7**, 79 (1959).
[3] I. Drimuş and I. Manase, *Ind. Chim. belge*, **1960**, 151.

[4] I. Drimuş, A. Măcelaru, Th. Spindler, I. Ionescu and V. Poleacov, *Bul. Inst. Polytechn. Bucureşti*, **29**, 49 (1967).

[5] V. K. Tsyshkovski, B. G. Freidin and E. K. Prokofiev, *Zhur. priklad. Khim.*, **34**, 2586 (1961).

[6] "Okislenie uglevodorov v zhidkoi faze", Izd. Akad. Nauk S.S.S.R., Moscou, 1959, p. 168—182.

[7] N. K. Diakonova, *Neftekhim.*, **9**, 286 (1969).

[8] V. M. Goldberg, L. K. Obuhova and N. M. Emanuel, *Neftekhim.*, **2**, 229 (1962).

[9] A. A. Perchenko, *Maslozhirov. Prom.*, **26** (3), 23 (1960).

[10] I. Drimuş and A. Lupu, *Rev. Roumaine Chim.*, **17**, 1409 (1972).

[11]. I. Drimuş and L. Papahagi, *Rev. Roumaine Chim.*, **20**, 973 (1975).

[12] I. Drimuş and L. Papahagi, *Rev. Roumaine Chim.*, **23**, 209 (1978).

[13] I. Drimuş, L. Papahagi, and C. Cristescu, *Rev. Roumaine Chim.*, **23**, 407 (1978).

[14] E. T. Denisov and N. M. Emanuel, *Uspekhi Khim.*, **29**, 1409 (1960).

Revue Roumaine de Chimie, **26**, *9–10*, 1285–1293 (1981)

SOME REACTIONS OF 6-[1′(2′-METHYL NAPHTHALENYL)] -2,3,4,5 TETRAHYDROPYRIDAZIN-3-ONE

A. ESSAWY, M. A. El-HASHASH*, M. M. ABDALLA and A. M. El-GENDY
Faculties of Science, Zagazig and *Ain Shams Universities Egypt

Received February 4, 1980

The reactions of 6-[1′(2′-methyl naphthalenyl)]-2, 3,4,5-tetrahydropyridazin-3-one (**1**) with alkylating agents, phosphorous oxychloride, aryl diazonium chloride and phosphorous pentasulphide have been investigated. The 6-[1′(2′-methyl naphthalenyl)]-3-chloro-4,5-dihydropyridazine **6** reacted with amines and gave **7a**, **7b** and **7c**. The tetrahydropyridazin-3-one **1** reacted with ethyl bromoacetate and zinc dust and gave ethylacetate derivative **11**. On the other hand, the reactions of 11 with amines and hydrazines have been investigated. Alkaline hydrolysis of ester **2c** gave the corresponding acid **3a**. The ester **2c** reacted with hydrazine hydrate, benzylamine and benzaldehyde and gave compounds **3b**, **3e**, **4** and **5** respectively.

It was reported that 4,6-diaryl-2,3,4,5-tetrahydropyridazin-3-one reacted with dialkylsulphate and yielded 3-alkoxy-4,6-diaryl-4,5-dihydropyridazine.[1] The present investigation deals with some reactions of 6-[1′(2′--methyl naphthalenyl)] 2, 3, 4,5-tetrahydropyridazin-3 one (**1**) in which the reactivity of the carbonyl group has been studied towards many reagents.

Diethyl sulphate, dimethyl sulphate or ethyl chloroacetate reacted with **1** in the presence of anhydrous potassium carbonate and dry acetone and yielded 3-alkoxy-6-[1′(2′-methyl naphthalenyl)] -4,5-dihydropyridazine (**2a, 2b**) and 3-*o*-carboethoxymethyl-6- [1′(2′-methyl naphthalenyl)]-4,5- dihydropyridazine (**2c**) respectively. The IR spectra of **2a** and **2b** showed ν(C=N) at 1620 cm^{-1}, a characteristic value for conjugated cyclic compounds. They also lack the stretching frequency for ν(C=O) of cyclic amides ans also ν(NH). This fact explains that the pyridazinone **1** exists really in solution in a lactimic form. The IR spectrum of **2c** showed well defined absorption bands at 1740 cm^{-1} and 1625 cm^{-1} attributable to ν(C=O) of saturated ester and to ν(C=N) of conjugated cyclic compounds, respectively. The mass spectrum of **2c** showed molecular ion (I) M$^+$, at $m/e = 324$ which decomposes to give the intense high mass peak (III) $m/e = 238$ via loss of (CH_2=CH_2) by Mc-Lafferty rearrangement followed by loss of the neutral fragments (CO and CH_2O) by skeletal rearrangement. Ion (II) further decomposes by H-rearrangement and extrusion of the neutral fragment (NCO) to form (III) $m/e = 196$. The further decomposition of ion (III) takes place either via the retro Diels — Alder[2,3] type fragmentation mode resulting in the formation of the most abundant high stable peak (VIII) $m/e = 168$ or by loss of (CH_2) yielding (IV) $m/e = 182$ which undergoes loss of (H) to give (V) $m/e = 181$. Ion (V) undergoes further cleavage by loss of (CH_2) to give the intense high mass peak (VI) $m/e = 167$. Ion (VII) $m/e = 141$ corresponds to loss of (CN) from (VI). The previously mentioned ion (II) may also lose (H) to give (IX) $m/e = 237$. This ion (IX) further decomposes by rearrangement and loss of (N_2) to give (X) $m/e = 209$ which rearranges and decomposes to give (XI) $m/e = 170$ which losses (H) to give the most stable and high abundant (XII) $m/e = 169$. All the above fragments agree well with the proposed structure of compound **2c** (chart 1 and Fig. 1).

Alkaline hydrolysis of ester **2c** yielded the corresponding acid **3a**. Ester **2c** reacted with hydrazine hydrate in butanol or with benzyl amine in ethanol and yielded the corresponding acid hydrazide and N-benzyl amide, **3b** and **3c** respectively. Recently,[4] it has been shown that the ethyl -*p*-chlorophenoxyacetate could be easily condensed with benzaldehide. This reaction has been applied on the *O*-carboethoxymethyl-pyridazine derivative **2c**.

The reaction of benzaldehyde with **2c** in the presence of sodium ethoxide provided the crotonic condensation product **4**. On the other hand, when the reaction was carried out in the presence of potassium *tert*-butoxide as a base both Stobbe and Claisen condensation products **5** and **4** were obtained. By increasing the basicity of base catalyst by using sodium hydride in dry benzene instead of potassium *tert*-butoxide, the Stobbe condensation product **5** was obtained as a sole product. This can be explained by the fact that increase in the basicity of base catalysing agent favours the presence of the Stobbe type condensation. In the presence of potassium *tert*-butoxide as a base, the reaction possibly takes place via B-lactonic ring as intermediate which is less readily formed than the γ-lactonic ring produced in the Stobbe condensation of aldehyde with succinic esters. The IR spectra of products **4** and **5** gave support to the structures assigned: the ν(C=O) frequency of carbethoxy group appears at 1730 cm^{-1} (α, β-unsaturated ester) for **4** and ν(C=O) of carboxylic group at 1700 cm^{-1} (α, β-unsaturated acid). Alkaline hydrolysis of ester **4** afforded the corresponding acid **5**.

Reaction of tetrahydropyridazin-3-one (**1**) with phosphorous oxychloride produced 6-[1′(2′-methyl naphthalenyl)]-3-chloro-4,5-dihydropyridazine (**6**).

The IR spectrum of **6** showed an absorption characteristic for ν(C=N) at 1640 cm^{-1} and lacked the stretching frequency of carbonyl group. Treatment of chloro derivative **6** with ethylamine, benzylamine or morpholine in boiling benzene gave 3-N-ethylamino, 3-N-benzylamino and 3-morpholino-4,5-dihydropyridazines **7a**, **7b** and **7c** respectively. Compound **7** showed IR bands at 1630 cm^{-1} ν(C=N) and **7a** and **7b** also at 3200 cm^{-1} ν(NH).

The behaviour of compound **1** towards the action of aryl diazonium chloride has been investigated. It was found that this reaction gives the coupling products **8a** and **8b**. Their IR spectra showed bands in the region of 3200–3350 cm^{-1} attributable to ν(NH). Compound **1** reacted with phosphorous pentasulphide in refluxing xylene and gave 6-[1′(2′-methyl

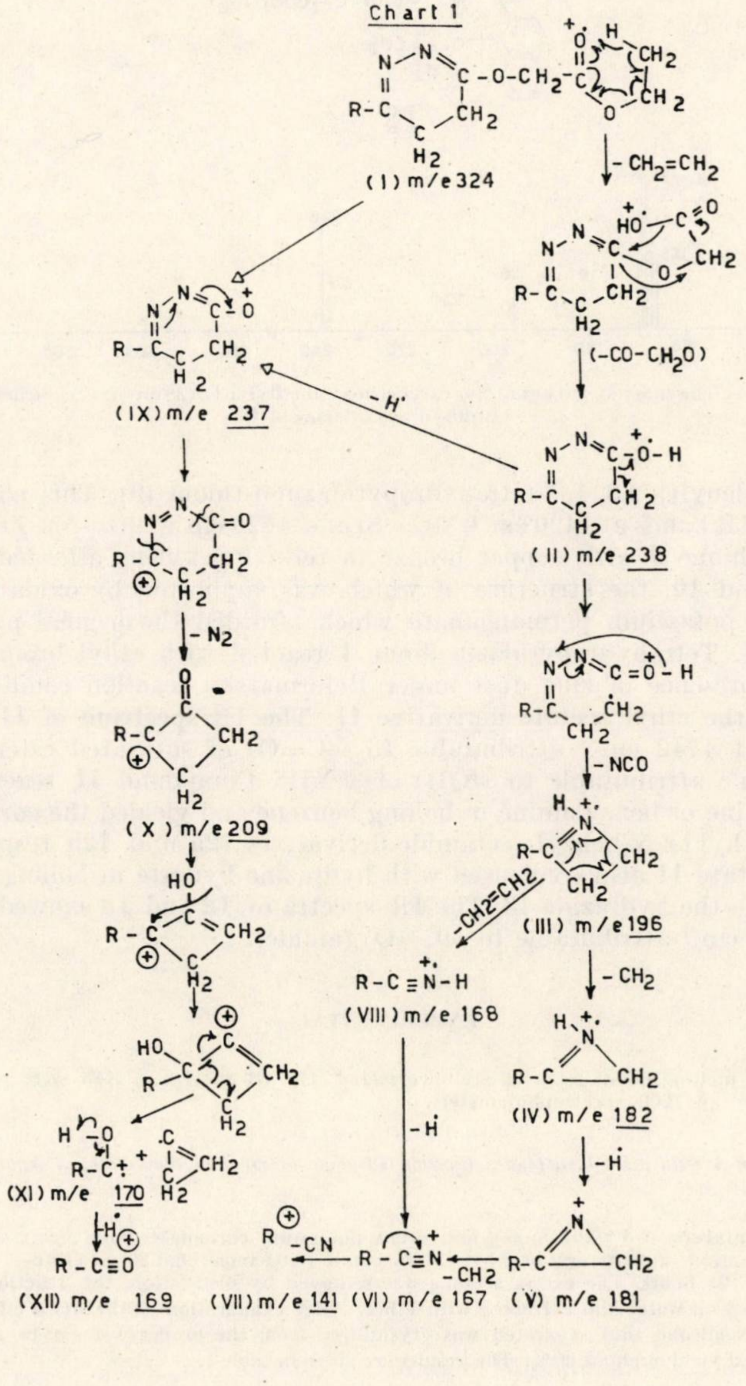

Chart 1

(I) m/e 324
− CH2=CH2
(−CO−CH2O)
(II) m/e 238
−H'
(IX) m/e 237
− N2
(X) m/e 209
− NCO
(III) m/e 196
−CH2=CH2
R−C≡N−H
(VIII) m/e 168
− CH2
(IV) m/e 182
−H
(XI) m/e 170
−H
R−C≡O
(XII) m/e 169
−CN
(VII) m/e 141
R−C≡N
(VI) m/e 167
−CH2
(V) m/e 181

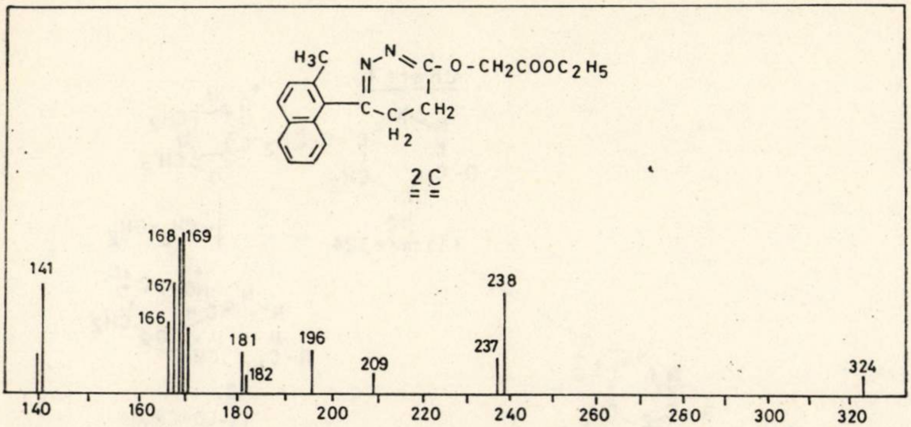

Fig. 1. — The mass spectrum of 3-*o*-carboethoxy methyl-6-[1′(2′-methyl naphthalenyl)]-4,5-dihydropyridazine **2 C.**

naphthalenyl)]- 2,3, 4, 5-tetrahydropyridazin-3-thione (**9**). This compound showed IR bands at 1420 cm^{-1}, ν(C=S) and 1620 cm^{-1}, ν(C=N). Treatment of the thione **9** with copper bronze in refluxing xylene afforded the bis compound **10**, the structure of which was supported by oxidation with alkaline potassium permanganate which afforded the original pyridazin-3-one **1**. Tetrahydropyridazin 3-one **1** reacted with ethyl bromoacetate in the presence of zinc dust under Reformatsky reaction condition and yielded the ethyl acetate derivative **11**. The IR spectrum of **11** showed bands at 1742 cm^{-1} attributable to ν(C=O) of saturated ester and at 3450 cm^{-1} attributable to ν(OH) or ν(NH). Compound **11** reacted with ethylamine or benzylamine in boiling benzene and yielded the corresponding N-ethyl or N-benzyl acetamide derivatives **12a** and **12b** respectively. The acetate **11** also condensed with hydrazine hydrate in boiling butanol and gave the hydrazide **13**. The IR spectra of **12** and **13** showed a band at 1650 cm^{-1} attributable to ν(C=O) (amide).

EXPERIMENTAL

All melting points reported are uncorrected. The IR spectra in KBr were recorded on a Unicam Sp 1200 spectrophotometer.

Reaction of **1** *with diethyl sulphate, dimethyl sulphate or ethyl chloroacetate*; *Formation of* **2a**, **2b** *and* **2c**.

A mixture of **1** (0.01 mole), anhydrous potassium carbonate (0.04 mole), diethyl sulphate, dimethyl sulphate and/or ethyl chloroacetate (0.04 mole) and 50 ml acetone was refluxed for 20—25 hours. The excess acetone was removed by distillation, the reaction mixture then poured on water and extracted with ether. After evaporation of the dried ethereal solution, the semisolid that separated was crystallized from the proper solvent to give **2a**, **2b** and **2c** in a yield of about 60%. The results are given in table 1.

Hydrolysis of the acetate **2c** ; *Formation of acid* **3a**.

Acetate **2c** (0.01 mole) was added to a solution containing sodium hydroxide (0.01 mole) dissolved in a mixture of ethanol (20 ml) and water (30 ml).The mixture was refluxed for 5 hours, cooled, ethanol was evaporated, the residue diluted with water and extracted with ether to get rid of unsaponified organic product. The aqueous layer was acidified with cold dilute hydrochloric acid then extracted with ether. Evaporation of the dried ethereal layer gave **3a**. The results are listed in table 1.

TABLE 1

Characterisation of compounds **2**—**5**

Compd.	Solvent yield (%)	m.p. (°C) colour	Formula	Analysis %	
				Found	Calcd.
2a	Ethanol	210	$C_{17}H_{18}N_2O$	C 76·25	76·69
	72	buff		H 6·65	6·77
				N 10·62	10·55
2b	Methanol	190	$C_{16}H_{16}N_2O$	C 76·40	76·20
	70	buff		H 6·21	6·30
				N 11·00	11·10
2c	Toluene	200	$C_{19}H_{20}N_2O_3$	C 70·30	70·40
	65	pale		H 6·31	6·20
		grey		N 8·65	8·64
3a	Glacial acetic	260	$C_{17}H_{16}N_2O_3$	C 68·78	68·92
	52	colourless		H 5·52	5·41
				N 9·52	9·46
3b	Butanol	216	$C_{17}H_{18}N_4O_2$	C 65·78	65·81
	70	yellow		H 5·91	5·81
				N 18·21	18·06
3c	Benzene	208	$C_{24}H_{23}N_3O_2$	C 74·78	74·81
	75	yellow		H 5·89	5·97
				N 10·93	10·91
4	Ethanol	105	$C_{26}H_{24}N_2O_3$	C 75·82	75·73
	30	yellow		H 5·92	5·83
				N 6·70	6·80
5	Benzene	167	$C_{24}H_{20}N_2O_3$	C 74·80	75·00
	50	pale		H 5·30	5·20
		yellow		N 7·29	7·29

Action of hydrazine on the acetate **2c**; *Formation of acid hydrazide* **3b**.

A solution of **2c** (0.01 mole) and hydrazine hydrate (0.01 mole) in butanol (40 ml) was heated under reflux for 5 hours. The product obtained after concentrating and cooling the reaction mixture was recrystallized from butanol to give **3b**. The results are given in table 1.

Action of benzyl amine on the acetate **2c**; *Formation of N-benzyl amide* **3c**.

A solution of **2c** (0.01 mole) and benzyl amine (0.01 mole) in ethanol or benzene (60 ml) was heated under reflux for 7 hours. The product obtained after concentration and cooling of the reaction mixture was crystallized from a proper solvent to give **3c**. The results are listed in table 1.

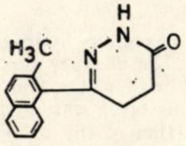

1

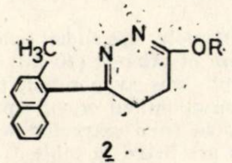

2

a, R = C_2H_5
b, R = CH_3
c, R = $CH_2-COOC_2H_5$

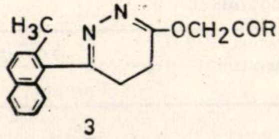

3

a, R = OH
b, R = $NHNH_2$
c, R = $NHCH_2C_6H_5$

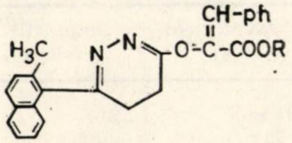

4; R = C_2H_5
5; R = H

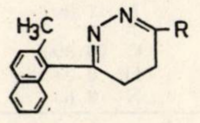

6; R = Cl
7a; R = $NH-C_2H_5$
7b; R = $NH-CH_2-C_6H_5$
7c; R =

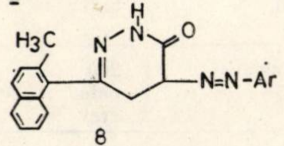

8

a, Ar = C_6H_5
b, Ar = o-C_6H_4-Cl

Action of benzaldehyde in the presence of sodium ethoxide on the acetate **2c**; *Formation of* **4**.

To a mixture of **2c** (0.01 mole) and sodium ethoxide (0.01 mole) in 50 ml ethanol, benzaldehyde (0.01 mole) was added and the reaction mixture was heated under reflux for about 8 hours. The oil obtained after concentration and cooling the reaction mixture was extracted with ether; the solid obtained after evaporation of the dried ethereal layer was crystallized from the proper solvent to give **4**. The results are given in table 1.

Action of benzaldehyde in the presence of potassium t-*butoxide on the acetate* **2c**; *Formation of* **4** *and* **5**.

A mixture of benzaldehyde (0.01 mole) and **2c** (0.015 mole) was added during 30 minutes to a stirred boiling solution of potassium *t*-butoxide (prepared from potassium 0.11 g atom, and 35 ml *t*-butanol for 1 g potassium); boiling and stirring were then continued for 3 hours. Most of the alcohol was then removed under reduced pressure, the cooled residue was poured in water, acidified with dil. HCl and extracted with ether (the organic material taken up in the ethereal layer), and the ethereal layer was washed with aqueous 10% sodium bicarbonate solution. The dried ethereal layer after evaporation left a yellow oil which was triturated with ethyl alcohol to give a yellow solid which was recrystallized from ethyl alcohol and was identified to be **4** by m.p. and mixed m.p. determination, yield 30%.

The aqueous layer was acidified with dil. HCl and extracted with ether; after evaporation of the dried ethereal layer a pale solid was obtained and recrystallized from the suitable solvent to give **5**. The results are listed in table 1.

Action of benzaldehyde in the presence of sodium hydride on the acetate **2c** ; *Formation of* **5.**

A mixture of benzaldehyde (0.01 mole) and **2c** (0.01 mole) in benzene was added to a stirred solution of NaH (0.03 mole) in 30 ml dry benzene. The reaction mixture was heated under reflux for about 3 hours. The excess solvent was removed by evaporation under reduced pressure, the cooled residue was poured upon water, acidified with dil. HCl and extracted with ether. The dried ethereal layer left after evaporation an oil which was then dissolved in sodium carbonate and extracted with ether. The aqueous layer was acidified with dil. HCl giving a pale yellow solid, crystallized from benzene and identified to be **5** by m.p. and mixed m.p. determination ; yield 70%.

Action of phosphorous oxychloride on the tetrahydropyridazin-3-one **1** ; *Formation of 6-[1' (2'-methyl-naphthalenyl)]-3-chloro-4,5-dihydropyridazine* **6.**

A mixture of **1** (0.01 mole) and phosphorous oxychloride (0.02 mole) was refluxed on a steam bath for 3 hours, then poured slowly into ice-cold water. The solid that separated was washed several times with water then filtered, dried and crystallized from ethanol to give **6** as grey crystals (m.p. 210°C) ; yield 60%.
Found : C, 70.01 ; H, 5.20 ; N, 10.83%. $C_{15}H_{13}ClN_2$, requires : C, 70.18 ; H, 5.07 ; N, 10.9%.

Action of ethylamine, benzylamine or morpholine on 6-[1'(2'-methyl naphthalenyl)]-3-chloro-4,5-dihydropyridazine **6** ; *Formation of* **7a, 7b** *and* **7c.**

A mixture of **6** (0.01 mole) and ethylamine, benzylamine or morpholine (0.01 mole) in 40 ml benzene was heated under reflux for 4—6 hours then the reaction mixture was concentrated by evaporation. The solid products obtained were crystallized from the proper solvent to give **7a, 7b** and **7c** (yields about 65%). The results were listed in table 2.

Reaction of benzene diazonium chloride or o-chlorobenzene diazonium chloride with **1** ; *Formation of* **8a** *and* **8b.**

A diazonium salt was prepared by direct addition of sodium nitrite solution (0.1 mole) to aniline or to *o*-chloroaniline (0.1 mole) dissolved in concentrated hydrochloric acid and water at 5°C. The obtained diazonium salt was added to a solution of **1** in 10% aqueous

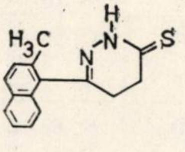

9

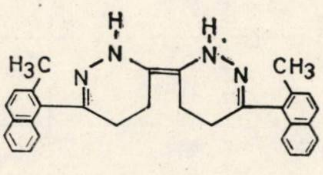

10

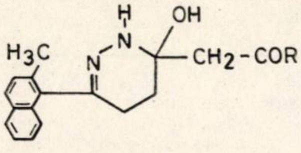

11 ; R = OC_2H_5
12a ; R = NHC_2H_5
12b ; R = $NH-CH_2C_6H_5$
13 ; R = $NH-NH_2$

sodium hydroxide while stirring and cooling. The coloured solid obtained was filtered and crystallized from the proper solvent to give **8a** and **8b** respectively. The results are given in table 2.

TABLE 2

Characterisation of compounds **7**–**13**

Compd	Solvent yield (%)	m.p. (°C) colour	Formula	Analysis % Found	Analysis % Calcd.
7a	Benzene 62	200 grey	$C_{17}H_{19}N_3$	C 76.82 H 7.18 N 15.83	76.98 7.17 15.85
7b	Benzene 65	190 buff	$C_{22}H_{21}N_3$	C 80.71 H 6.24 N 12.39	80.73 6.42 12.84
7c	Toluene 60	205 buff	$C_{19}H_{21}N_3O$	C 74.32 H 6.82 N 13.41	74.27 6.84 13.66
8a	Acetic acid 55	190 orange	$C_{21}H_{18}N_4O$	C 73.81 H 5.41 N 16.52	73.70 5.30 16.40
8b	Ethanol 60	200 red	$C_{21}H_{17}ClN_4O$	C 66.93 H 4.62 N 14.87	67.05 4.63 14.92
9	Xylene 50	115 pale yellow	$C_{15}H_{14}N_2S$	C 70.72 H 5.62 N 11.32	70.87 5.51 11.02
10	Butanol 55	130 buff	$C_{30}H_{28}N_4$	C 81.20 H 6.51 N 13.00	81.08 6.31 12.61
11	Benzene 42	217 yellow	$C_{19}H_{22}N_2O_3$	C 69.82 H 6.81 N 8.58	69.94 6.75 8.59
12a	Benzene 70	207 buff	$C_{19}H_{23}N_3O_2$	C 69.92 H 7.20 N 13.00	70.15 7.08 12.92
12b	Benzene 62	195 yellow	$C_{24}H_{25}N_3O_2$	C 74.42 H 6.46 N 10.85	74.45 6.52 10.92
13	Methanol 80	202 yellow	$C_{17}H_{20}N_4O_2$	C 65.41 H 6.52 N 18.10	65.39 6.41 17.95

Action of phosphorous pentasulphide on **1** ; *Formation of 6-[1'(2'-methyl naphthalenyl)]-2, 3,4,5-tetrahydropyridazin-3-thione* (**9**)

A solution of **1** (0.01 mole), phosphorous pentasulphide (0.02 mole) and dry xylene (100 ml) was heated under reflux for 6 hours. The reaction mixture was filtered hot and concentrated. The product that separated on cooling was crystallized from the proper solvent giving **9**. The results are listed in table 2.

Action of copper bronze on **9**; *Formation of the bis compound* **10**.

A mixture of **9** (0.01 mole) and 2 g of copper bronze in dry xylene (100 ml) was heated under reflux for 10 hours. The reaction mixture was filtered upon hot and the filtrate was concentrated. The product that separated on cooling was crystallized from a suitable solvent giving **10**. The results are given in table 2.

Oxidation of the bis compound **10**; *Formation of* **1**.

To a mixture of **10** (0.01 mole) and 30 % sodium carbonate solution (500 ml), 2 % potassium permanganate solution (350 ml) was added portionwise while stirring. After complete addition of potassium permanganate, stirring was continued for a further one hour, and the precipitated manganese dioxide was filtered; both precipitate and alkaline solution were throughly extracted with ether, then with benzene. Evaporation of the solvent gave a colourless solid which was crystallized from ethanol and was identified to be **1** by m.p. and mixed m.p. determination; yield 50 %.

Action of ethyl bromoacetate in the presence of zinc dust on **1**; *Formation of* **11**.

To a mixture of **1** (0.01 mole) and zinc powder (1 g) in 20 ml dry benzene, ethyl bromoacetate (0.01 mole) in 20 ml dry benzene was added with stirring. The reaction mixture was heated at 80°C for 4 hours and then refluxed for another 3 hours; benzene was evaporated and ethanol was added. The reaction mixture was left for few days, the yellow crystals which separated were crystallised from a suitable solvent to give **11**. The results are listed in table 2.

Action of ethyl amine or benzyl amine on **11**. *Formation of N-ethyl or N-benzyl acetamide derivatives* **12a** *and* **12b**.

A mixture of **11** (0.01 mole) and ethyl amine or benzyl amine (0.01 mole) in 60 ml dry benzene was heated under reflux for 4 – 6 hours. The reaction mixture was concentrated by evaporation. The solid products obtained were crystallized from the proper solvent to give **12a** and **12b**. The results obtained are listed in table 2.

Action of hydrazine on **11**; *Formation of acid hydrazide* **13**.

A solution of **11** (0.01 mole) and hydrazine (0.01 mole) in butanol (60 ml) was heated under reflux for 6 hours. The product obtained after concentration and cooling of the reaction mixture was crystallized from the proper solvent to give **13**. The results are given in table 2.

REFERENCES

[1] M.A. El-Hashash, M. M. Mohamed and M. El-Kady, *Indian J. Chem.*, **18**, 136 (1979).

[2] F. W. McLafferty, "Interpretation of Mass Spectra", W. A. Benjamin, Inc., 1977, p. 72–75.

[3] K. G. Das and E. P. James, "Organic Mass Spectrometry", Oxford and IBH Publishing Co., 1976, p. 69–75, 135.

[4] M. A. El Hashash, M. M. Mohamed, A. El-Naggar and O-El-Sayed, *Rev. Roumaine Chim.*, *24*, 1343 (1979).

[illegible]

[illegible]

[illegible]

[illegible]

[illegible]

[illegible]

[illegible]

[illegible]

[illegible]

[illegible]

[illegible]

[illegible]

REFERENCES

[illegible]

Revue Roumaine de Chimie **26**, *9–10*, 1295–1303 (1981)

THE INFLUENCE OF THE SOLVENT ON THE ELECTRONIC ABSORPTION SPECTRA OF SOME *N*-SUBSTITUTED 2-NITROANILINES

A. AIRINEI, DANA DOROHOI* and ANICA TOLEA
Institute of Macromolecular Chemistry "Petru Poni", Aleea Gr. Ghica Vodă 41A, 6600-Iaşi, Romania
* Spectroscopy Laboratory, "Al. I. Cuza" University, Calea 23 August 11, 6600–Iaşi, Romania

Received July 28, 1980

The solvent influence on the position of the electronic absorption bands of some N-substituted 2-nitro-anilines has been studied. The frequency of the $n \rightarrow \pi^*$ absorption bands in different solvents has been correlated with the solvent macroscopic parameters (refractive index, electric permittivity). The obtained results show that in solutions of N-substituted 2-nitroanilines, universal interactions occur.

The electronic absorption spectra are particularly characteristic of the molecules in gaseous state. In this case, the intermolecular interactions are negligible. In condensed media, as well as in solutions, the spectral-active molecule is affected by surrounding atomic systems (ions, molecules, molecular ions, etc.), the electronic absorption spectra being given by the solvent-solute system and offering in this way information on the nature and strength of intermolecular interactions in liquid state.

The shifts of the absorption bands, when the molecule passes from the gaseous state in solution, depend on the nature of the spectral-active molecule and on the solvent, as well as on the nature of the transition involving the appearance of the absorption band.

Some theoretical attempts have been made to determine quantomechanically[1-3] and semiclassically[4,5] the size and the sign of the shift of absorption bands and to elucidate the mechanism of intermolecular interactions in solution.

According to these theories, the shift of electronic absorption bands, $\Delta\nu^a = \nu^a_{\text{solv}} - \nu^a_{\text{vap}}$, for a given solvent (with the frequency ν^a_{solv}), regarding the vapour state (characterized by the frequency ν^a_{vap}), depends on the influence of the forces of universal nature (orientation, induction, dispersion and polarization), when the possible contribution of the forces of specific nature is negligible[3]:

$$\Delta\nu^a = \Delta\nu^a_{\text{orient}} + \Delta\nu^a_{\text{disp}} + \Delta\nu^a_{\text{ind}} + \Delta\nu^a_{\text{pol}} = \frac{1}{hc} f^a(n,\ \varepsilon) \qquad (1)$$

where : h is Planck's constant ; c is the light velocity : $f^a(n,\varepsilon)$ is the function of intermolecular interactions for the electronic absorption spectra.

According to Bachshiev's theory[6], $f^a(n, \varepsilon)$ has the following form :

$$f^a(n,\varepsilon) = \frac{2n^2+1}{n^2+1}\left[\frac{2\mu_g(\mu_g-\mu_e\cos\varphi)}{a^3}\left(\frac{\varepsilon-1}{\varepsilon+2}-\frac{n^2-1}{n^2+2}\right)+\right.$$
$$\left.+\frac{\mu_g^2-\mu_e^2}{a^3}\,\frac{n^2-1}{n^2+2}+P^a\,\frac{n^2-1}{n^2+2}+Q^a\,\frac{n^2-1}{2n^2-1}\right] \qquad (2)$$

where : n is the refractive index and ε is the electric permittivity of solvent ; μ_g and μ_e are the dipole moments of the molecule in the ground and excited states, respectively ; a is the radius of Onsager cavity and P^a, Q^a are parameters depending on the microscopical characteristics of the molecule.

The present investigation has been undertaken in order to study the influence of the nature of solvent on the position of electronic absorption bands for some N-substituted 2-nitroanilines, which correspond to the general formula :

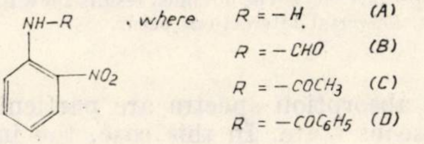

EXPERIMENTAL

The macroscopic parameters of the solvents were determined as follows. The refractive index, $n_{404.7}$, was established with a Rayleigh interferometer for $\lambda = 404.7$ nm, at 20°C. The electric permittivity, ε, was determined with an Oehme DK-meter of RL type, at 7MHz.

The electronic absorption spectra were recorded by means of a Unicam SP-800 spectrophotometer, at room temperature, using 10 mm cells. From a preliminary study, it was noticed that the frequency of absorption bands does not depend on concentration in the absorbance range.

Commerçial *o*-nitroaniline (A) was purified by crystallization. N-Formyl-2-nitroaniline (2-nitroformanilide) (B) was obtained by the formylation reaction of 2-nitroaniline with anhydrous formic acid.[7] N-acetyl-2-nitroaniline (2-nitroacetanilide) (C) was synthetized by acetylation with acetic anhydride and N-benzoyl-2-nitroaniline (2-nitrobenzanilide) (D) was prepared by benzoylation of 2-nitroaniline with benzoyl chloride.[8] The solvents were spectrograde or purified by known methods.

RESULTS AND DISCUSSION

Twenty seven binary solutions of N-substituted 2-nitroaniline derivatives (Table 1) have been studied. Comparing the electronic spectra in the same solvent, one observes that in the case of N-substituted 2-nitroanilines, the longer wavelength bands are less intense than of 2-nitroaniline and undergo hypsochromic shifts (Fig. 1), in the order : $B < C < D < A$. This order can be explained by the electron withdrawing effect of carbonyl group, whose action is diminished by the inductive, respectively electromer effects of the methyl and phenyl groups.

This order of hypsochromic shift does not hold for the following solvents : ethanol, ethylene glycol, N-methyl pyrrolidone, dimethylformamide and dimethyl sulfoxyde.

Also, the total shift of this absorption band, passing from a non-polar solvent to a polar one, is the largest for 2-nitroaniline and the smallest for 2-nitroformanilide.

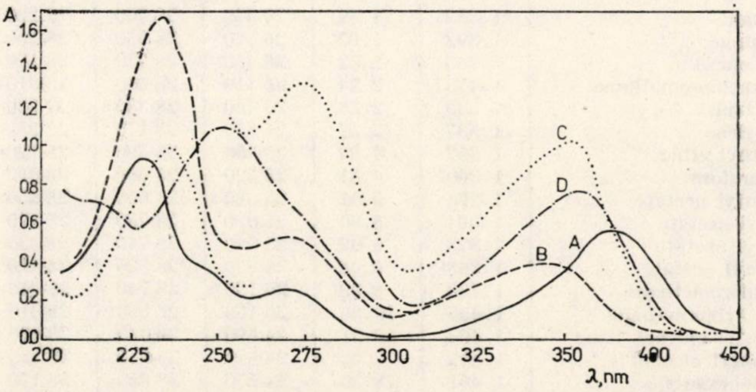

Fig. 1. — Electronic absorption spectra of N-substituted 2-nitroanilines (in hexane) : 2-nitroaniline(*A*) ; 2-nitroformanilide (*B*) ; 2-nitroacetanilide (*C*) ; 2-nitrobenzanilide (*D*).

Taking into account the general criteria of assigning the absorption bands to different transitions,[4,5] the longer wavelength bands in spectra of 2-nitroaniline are assigned as follows.[9-11]

The 378 nm absorption band is assigned to $n_{\mathrm{NH_2}} \rightarrow \pi^*_{\mathrm{NO_2}}$ transition with the charge transfer from the nonbonding orbital of the nitogen atom of amino group to the vacant orbital of nitro group. The 270 nm absorption band is assigned to a $\pi_{\mathrm{ring}} \rightarrow \pi^*_{\mathrm{NO_2}}$ transition, similar to the nitrobenzene band of 280 nm.[12,13]

In order to elucidate the nature of the interactions in solutions of compounds A, B, C, D, we have studied the behaviour of the longest wavelength band which is the most sensitive absorption band at the solvent influence.

Therefore, we correlated the frequency of the $n \rightarrow \pi^*$ absorption band in different solvents with the macroscopic parameters of solvents. In table 1, the frequency of the $n \rightarrow \pi^*$ absorption band and the macroscopic parameters of solvents are presented.

Relation (2) can be used especially when all types of interactions appear in solution, with the same strength. For non-polar solvents $\frac{\varepsilon - 1}{\varepsilon + 2} \approx \frac{n^2 - 1}{n^2 + 2}$, relation (2) points out in approximation $n^2 + 2 \approx 2n^2 + 1$, a relationship of type (3), between ν_{calc} and n :

$$\nu_{\mathrm{calc}} = C_1^a \frac{2n^2 + 1}{n^2 + 2} \cdot \frac{n^2 - 1}{n^2 + 2} + m \qquad (3)$$

where C_1^a and m are constants.

TABLE 1

Macroscopic parameters of solvents and $n \rightarrow \pi^*$ absorption band frequencies

No.	Solvent	n	ε	ν_A (cm^{-1})	ν_B (cm^{-1})	ν_C (cm^{-1})	ν_D (cm^{-1})
1.	Hexane	1.382	1.89	26 490	28 900	28 290	27 780
2.	Heptane	1.392	1.92	26 520	28 860	28 250	27 780
3.	Cyclohexane	1.433	2.02	26 450	28 730	28 170	27 780
4.	Tetrachloromethane	1.473	2.24	26 110	28 690	28 010	27 550
5.	Benzene	1.539	2.28	25 440	28 330	27 620	27 170
6.	*o*-Xylene	1.537	2.57	25 570	28 170	27 550	27 030
7.	Diethyl ether	1.352	4.34	25 250	28 780	28 170	27 620
8.	Chloroform	1.360	4.81	25 320	28 690	28 090	27 620
9.	n-Butyl acetate	1.395	5.01	25 060	28 650	28 250	27 780
10.	Vinyl acetate	1.394	5.90	25 030	28 780	28 170	27 700
11.	Ethyl acetate	1.373	6.02	25 030	28 740	28 330	27 820
12.	Methyl acetate	1.368	6.68	24 870	28 820	28 450	28 010
13.	Dichloromethane	1.430	8.93	25 120	28 740	28 010	27 320
14.	1,2-Dichloroethane	1.454	10.36	25 190	28 690	28 010	27 620
15.	n-Butyl alcohol	1.404	17.51	24 690	29 030	28 900	28 170
16.	Isobutyl alcohol	1.402	17.93	24 630	29 070	28 980	28 250
17.	Cyclohexanone	1.461	18.30	24 570	28 650	28 170	27 780
18.	Methyl ethyl ketone	1.379	18.51	24 690	28 740	28 330	28 170
19.	Isopropyl alcohol	1.383	19.92	24 630	29 280	29 150	28 330
20.	n-Propyl alcohol	1.393	20.33	24 690	29 200	29 030	28 330
21.	Acetone	1.367	20.70	26 870	28 820	28 570	28 090
22.	Ethanol	1.369	24.55	24 690	29 240	29 240	28 490
23.	N-Methylpyrrolidone	1.471	32.00	24 040	28 780	29 500	29 670
24.	Methanol	1.335	32.70	24 750	29 390	29 450	28 860
25.	Dimethylformamide	1.453	36.70	24 330	28 860	29 200	29 280
26.	Etylene glycol	1.440	37.70	24 210	29 070	29 540	29 980
27.	Dimethyl sulfoxide	1.492	48.90	23 980	28 860	29 980	30 260

In the case of polar molecules, dissolved in polar media, the spectral shift caused by the polarization and orientation—induction component of the local reactive field is expressed by function $\frac{(\varepsilon-1)(2\varepsilon+1)}{\varepsilon}$.[14,15]

In order to calculate the frequency of $n \rightarrow \pi^*$ absorption band of the 2-nitroanilines, we used relation (4):

$$\nu^{a}_{\text{calc}} = C^{a}_{1}\frac{2n^2+1}{n^2+2}\cdot\frac{n^2-1}{n^2+2} + C^{a}_{2}\,\frac{(\varepsilon-1)(2\varepsilon+1)}{\varepsilon} + C^{a}_{3} \qquad (4)$$

C^a_1, C^a_2, C^a_3 parameters depend on the nature of molecules. C^a_3 includes the frequency value of absorption band in gaseous state.

Relation (3) holds for our samples in nonpolar solvents (1–6, Table 1). The determination of C^a_1 and m parameters was done by means of the least square method, using a program written in JAL language for a JEC-6 computer.

In the (ν_{exp}, ν_{calc}) plots (ν_{calc} with relation (3)), the points corresponding to the non-polar solvents are placed in the proximity of the first bisectrix and those corresponding to polar solvents present deviations from this line. Measuring these deviations ($\Delta\nu = \nu_{\text{calc}} - \nu_{\text{exp}}$) for the polar solvents, an almost linear relationship between $\Delta\nu$ and ε can be observed (Fig. 2).

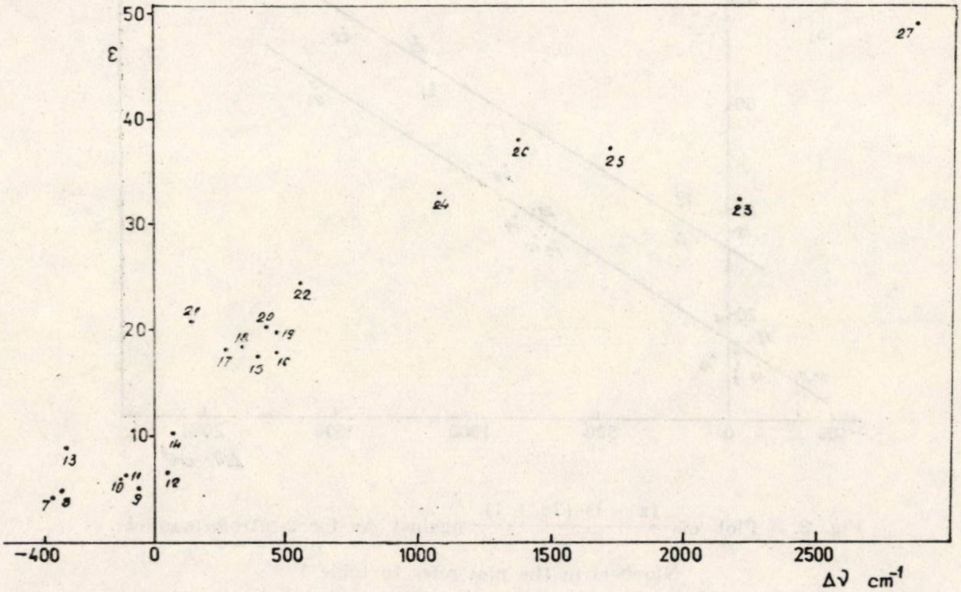

Fig. 2. — Variation of ε with $\Delta\nu$ for 2-nitrobenzanilide. Numbers in the plot refer to table 1.

Taking into account the relationship $\Delta\nu = f(\varepsilon)$ and the results obtained by Baur and Nicol,[14,15] we used expresion (5) to calculate $\Delta\nu$.

$$\Delta\nu = C_2^a \frac{(\varepsilon - 1)\ (2\varepsilon + 1)}{\varepsilon} + k \tag{5}$$

We obtained a satisfactorily linear relationship (Fig. 3). As can be seen from figure 3, the representative points for every compound are near two or three straight lines, grouping together solvents with the same action on the absorption band.

During statistical processing of experimental data we observed that some points deviated from the above-mentioned dependence, namely : 12 for 2-nitroaniline 23, 25, 27 for 2-nitrobenzanilide.

Since, in Bachshiev's theory, the contribution of forces of specific nature was not included, the mentioned points were eliminated during the statistical processing, considering that the deviations can occur due to the participation of the molecule to the specific interactions with these solvents.

In figures 4—7, the frequencies of $n \to \pi^*$ absorption band, calculated with (4), ν^a_{calc}, against the frequencies determined experimentally, ν_{exp}, are plotted.

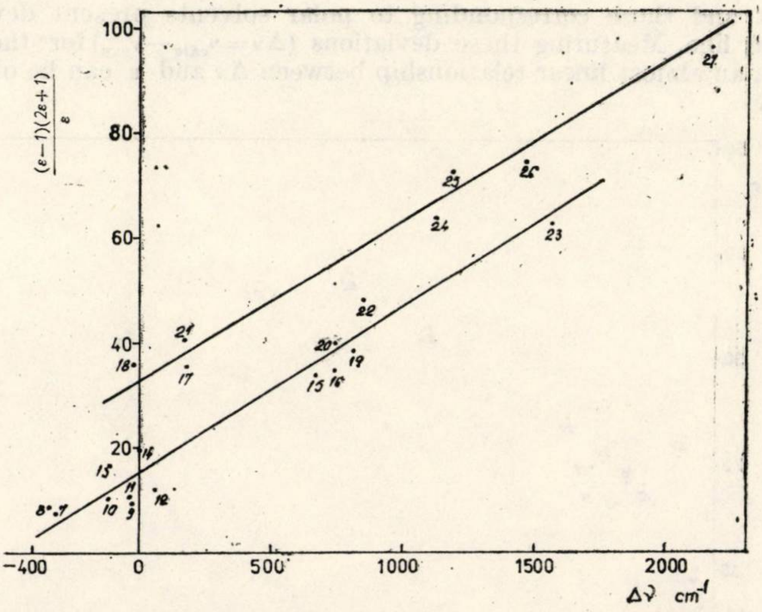

Fig. 3. – Plot of $\frac{(\varepsilon - 1)\ (2\varepsilon + 1)}{\varepsilon}$ against $\Delta\nu$ for 2-nitroformanilide. Numbers in the plot refer to table 1.

TABLE 2

Values of linearization parameters

Compound	C_1^a	m	C_2^a	k
A	−8534.9	29 071	−11.3 −10.7	−956.8 −1451.9
B	−5210.6	30429	10.8 12.7 13.6	−558.1 −373.8 −245.2
C	−5744.1	29 981	31.3 34.6	−466.8 −1174.4
D	−5809.7	29 536	15.8 20.5	−508.2 −308.5

Since the electronic absorption bands are wide and the determinations accuratelly made, we can conclude that relation (4) clearly expresses the frequency of the absorption-band maxima, for a given solvent characterized by the macroscopic parameters n and ε.

The parameters of linearization are presented in table 2.

The results obtained by a statistical processing of spectral data enable us to affirm that the universal interactions occur in the most of N-substituted 2-nitroanilines solutions, the orientation – induction interactions being predominant.

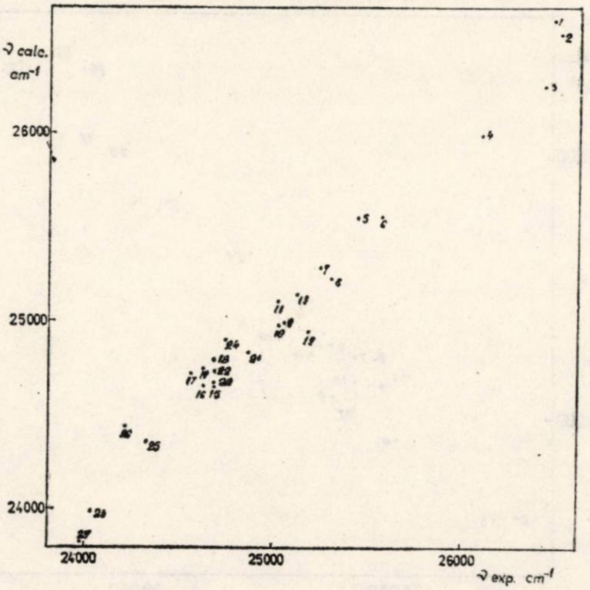

Fig. 4. — Plot of ν_{calc} against ν_{exp} for 2-nitroaniline. Numbers in the plot refer to table 1.

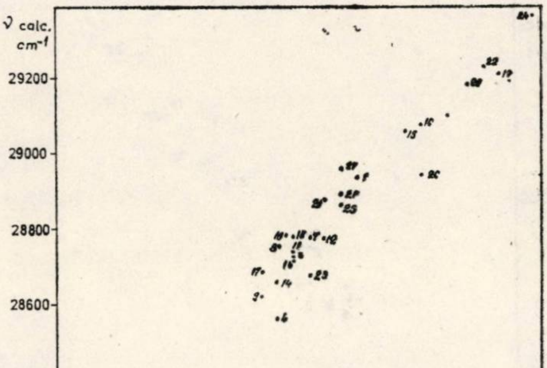

Fig. 5. — Plot of ν_{calc} against ν_{exp} for 2-nitroformanilide. Numbers in the plot refer to table 1.

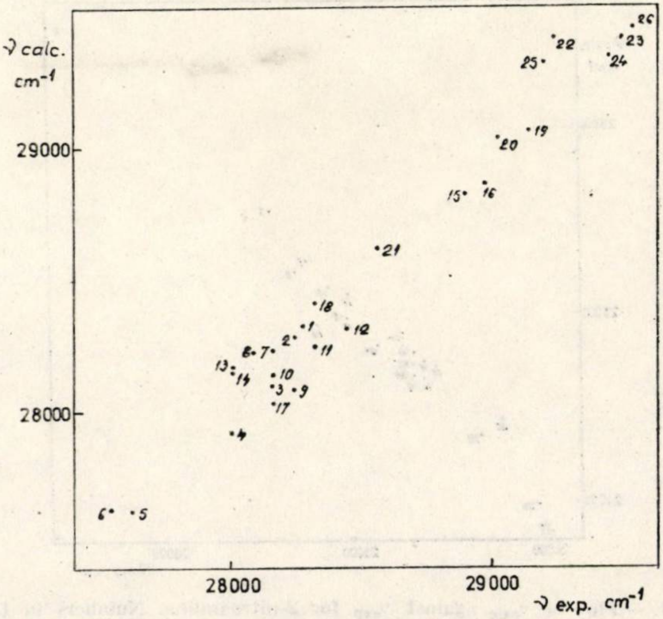

Fig. 6. — Plot of ν_{calc} against ν_{exp} for 2-nitroacetanilide. Numbers in the plot refer to table 1.

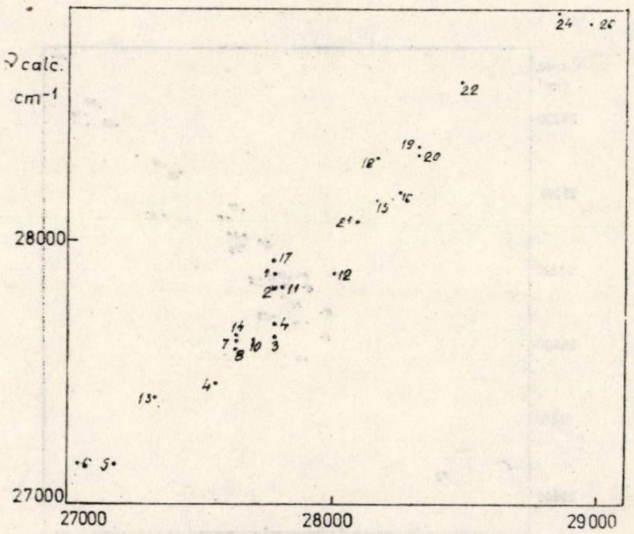

Fig. 7. — Plot of ν_{calc} against ν_{exp} for 2-nitrobenzanilide. Numbers in the plot refer to table 1.

REFERENCES

[1] E. McRae, *J. Phys. Chem.*, **61**, 562 (1957).
[2] Y. Ooshika, *J. Phys. Soc. Jap.*, **9**, 594 (1954).
[3] E. Lippert, *Z. Elektrochem.*, **61**, 962 (1957).
[4] N. G. Bachshiev, "Spektroskopiya mezhmolekulyarnov vzaimodeistvyakh", Izd. Nauka, Leningrad, 1973.
[5] O. V. Sverdlova, "Elektronnye spektry v organicheskoi khimii", Izd. Nauka Leningrad, 1973.
[6] N. G. Bachshiev, *Opt. Spektrosk.*, **16**, 821 (1964).
[7] S. von Niementowski, *Ber. dtsch. chem. Ges.*, **43**, 3018 (1910).
[8] P. Grammaticakis, *Bull. Soc. chim. France*, **1950**, 158.
[9] J. F. Corbett, *Spectrochim. Acta*, **23A**, 2315 (1967).
[10] A. E. Lutskii and N. I. Gorohova, *Opt. Spektrosk.*, **27**, 917 (1969).
[11] S. Millefiori, G. Favini, A. Millefiori and D. Grasso, *Spectrochim. Acta*, **33A**, 21 (1977).
[12] S. Nagakura, M. Kojima and I. Marujama, *J. Mol. Spectrosc.*, **13**, 174 (1964).
[13] V. Macovei, *Rev. Roumaine Chim.*, **21**, 1137 (1976).
[14] M. E. Baur and M. Nicol, *J. Chem. Phys.*, **44**, 3337 (1966).
[15] M. Nicol, J. Swain, Yin-Yan Shun, R. Merin and R. H. H. Chen, *J. Chem. Phys.*, **48**, 3587 (1968).

Revue Roumaine de Chimie, **26**, *9–10*, 1305–1314 (1981)

INVESTIGATIONS ON THE SYNTHESIS OF *CIS*-9,10-DISUBSTITUTED DECALINS

J. RADHAKRISHNAN
University of Connecticut Storrs, Connecticut 06268, U.S.A.

Received August 8, 1978
Revised March 30, 1981

Both 1-bromocyclohexene-2-carboxaldehyde and methyl 2-bromocyclohexenecarboxylate failed to undergo Diels-Alder reaction with 1,3-butadiene. Furan was converted to dimethyl 1,4-epoxy-*cis*-decalin-9,10-dicarboxylate (9) in four steps. However, 9 could not be deoxygenated to the decalin diester 10 under a variety of conditions. 1,2,3,6-Tetrahydrophthalic anhydride 11 was transformed into the diacid 18 in four steps. Several attempts to prepare the desired bromoester 4 proved largely unsuccessful. Synthesis of 11, 11-dichlorotricyclo-(4.4.1.0.)-undecane and 11, 11-dibromotricyclo-(4.4.1.0.)-undecane is described.

An investigation of the fragmentation of saturated β-haloacids (dehalogenative decarboxylations) was undertaken in these Laboratories[1] to ascertain, if, in any instance the reaction conforms completely to Grob's requirements[2] for synchronous heterolytic fragmentation. According to Grob's picture, a fragmentable system applied to β-haloacids may most simply be pictured as

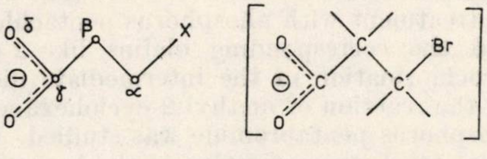

which might undergo two possible modes of fragmentation: a) a synchronous fragmentation involving frangomeric effect due to all bonds involved (including the δ-electron pair) lying in one plane (i.e., rotation about the β, γ-bond does not inhibit the synchronous process); b) a stepwise solvolysis in which fragmentation of the resultant cation is only one of two or more competing reactions.[3]

Since the dehalogenative decarboxylations of β-haloacids studied[1] did not fit in completely with Grob's synchronous fragmentation mechanism, thereby indicating conformational flexibility, an investigation of conformationally rigid (diaxial) β-bromo acids was undertaken. With this end in view, 10-bromodecalin-9-carboxylic acid was prepared[1] by the addition of hydrogen bromide in toluene to $\Delta^{4,10}$-octalin-9-carboxylic acid and its fragmentation studied, even though its stereochemistry was not unequivocally determined. Alkaline solvolysis of the aforesaid compound gave 9,10-octalin as the exclusive product.

In order to establish the stereochemistry of the above mentioned decalin bromo acid, the present investigations were undertaken in the hope of developing an unambiguous and stereospecific synthesis of *cis*-9-bromodecalin-10-carboxylic acid.

The contemplated steps in the envisaged synthesis of *cis*-9-bromodecalin-10-carboxylic acid are depicted in Chart I.

CHART I

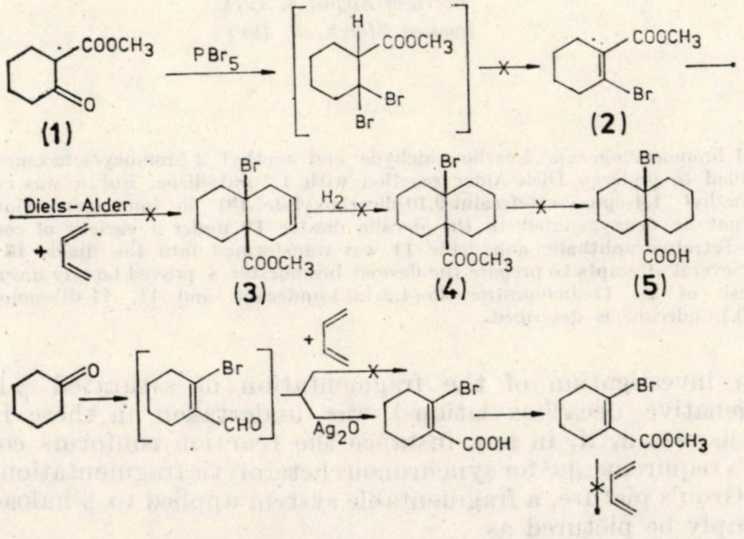

Newman and his associates [4] have reported that ketones like 4-phenyl-2-butanone on treatment with phosphorus pentachloride in methylene dichloride afforded the corresponding olefins like 2-chloro-4-phenyl-1-butene by dehydrochlorination of the intermediate dichloro compound.

Accordingly, the reaction of methyl 2-cyclohexanonecarboxylate (**1**) (Chart I) with phosphorus pentabromide was studied. However, under a variety of conditions tried, aromatization of the keto ester **1** was the predominant reaction and none of the desired bromoester **2** was isolated.

Following essentially the report of Paquette et al.[5] cyclohexanone was treated with PBr_5 in anhydrous dimethylformamide to afford 1-bromocyclohexene-2-carboxaldehyde in 40% yield, characterized as its semicarbazone. However, attempted Diels-Alder reaction of this aldehyde with 1,3-butadiene gave an intractable gum, which resisted all attempts at purification, evaporative distillation of which furnished a mixture of aromatic compounds.

Since the above mentioned bromoaldehyde was very unstable to thermal reactions, the corresponding ester, viz., methyl 2-bromocyclohexenecarboxylate (**2**) (Chart I) was prepared by the esterification of the intermediate bromo acid, obtained by the Ag_2O oxidation of 2-bromocyclohexene-1-carboxaldehyde, and its Diels-Alder reaction with 1,3-butadiene investigated.

Unfortunately, much difficulty was encountered during the attempted Diels-Alder reaction since the sealed tubes containing the reactants, methyl-2-bromocyclohexenecarboxylate (**2**), 1,3-butadiene, the solvent (absolute ethanol) and hydroquinone (added as a radical scavenger), exploded with violence each time. Nevertheless, in a single experiment using 0.02 mole of the bromoester **2**, a dark viscous gum was obtained, the only isolable material from which was found to be the starting ester **2**.

Interestingly enough, attempted Diels-Alder reaction of the bromoester **2** with 1,3-butadiene (generated *in situ* from butadienesulfone) resulted only in quantitative recovery of the unreacted starting bromoester **2**.

Stork and coworkers[6] reported the synthesis of the tricyclic diester **8** (Chart II) during their total synthesis of cantharidin. It was hoped that

CHART II

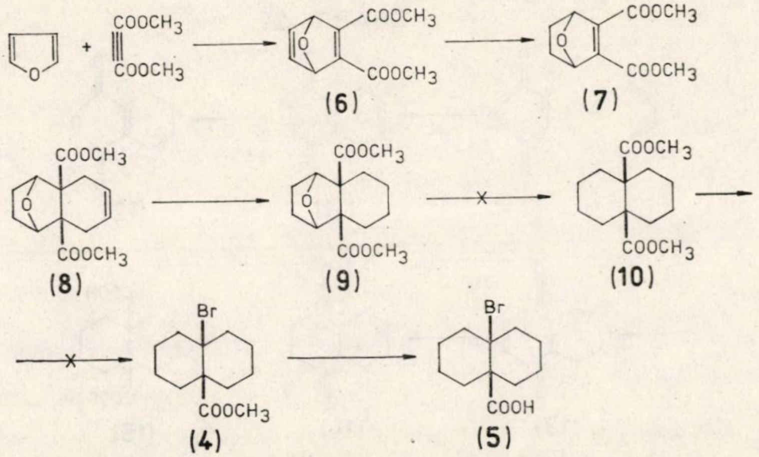

the deoxygenated decalin diester **10** could be manipulated to afford the desired decalin bromo ester **4**. The contemplated synthetic sequence is delineated in Chart II.

Diels-Alder reaction of furan with dimethylacetylenedicarboxylate furnished the adduct, dimethyl 3,6-dihydrophthalate **6**[7] which was found to undergo rapid decomposition. Consequently, the semi-hydrogenation of this diester **6** was carried out immediately after its preparation over 5 % Pd—C catalyst to afford dimethyl 3,6-epoxy-3,4,5,6-tetrahydrophthalate(**7**).[6] Attempted Diels-Alder reaction of the diester **7** with 1,3-butadiene generated from butadienesulfone *in situ*, in 2-butanone under vigorous reflux in a closed system over extended periods of time gave none of the desired product **8**, but only the unreacted starting diester **7** in quantitative yield.

However, Diels-Alder reaction of the bicyclic diester **7** with 1,3-butadiene in absolute ethanol gave the required adduct, viz., dimethyl 1,4-epoxy-$\Delta^{6,7}$-*cis*-decalin-9,10-dicarboxylate, **(8)**.[6] Catalytic hydrogenation of this diester **8** over 5% Pd—C catalyst in ethyl acetate afforded the corresponding, hitherto unknown, dihydro derivative, dimethyl 1,4-epoxy-*cis*-decalin-9,10-dicarboxylate **(9)** in quantitative yield as a liquid which solidified to a low melting solid.

The next step in our envisaged synthetic scheme (Chart II) involved the deoxygenation of the saturated tricyclic diester **9** to the bicyclic decalin diester **10**. Repeated attempts at this deoxygenation reaction proved largely unsuccessful in furnishing the desired decalin diester **10** and hence this route to *cis*-9,10-disubstituted decalins was discontinued. The following conditions were tried :

i) Attempted reduction of the tricyclic diester **9** with phosphorus and 48% hydroiodic acid following the procedure of Stephenson[8] led to intractable tarry products.

ii) When the same reaction was tried over 98% PtO_2 catalyst in absolute ethanol at a hydrogen pressure of 3—5 atmospheres over

CHART III

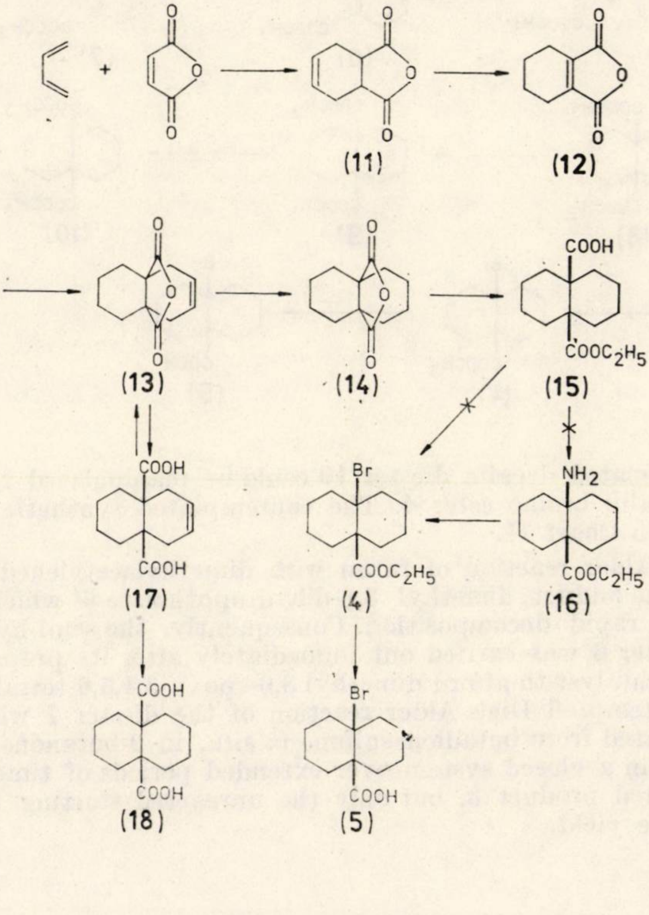

extended periods of time (8 hrs to 3 days), only the unchanged starting material was recovered. Use of 10% Pd—C catalyst at a hydrogen pressure of 3—5 atmospheres in absolute ethanol medium also produced similar results.

The conversion of *cis*-9,10-symmetrically disubstituted decalins to the required methyl *cis*-9-bromodecalin-10-carboxylate **(4)** was subsequently investigated as illustrated in Chart III. 1, 2, 3,6-Tetrahydrophthalic anhydride **(11)** was prepared following the procedure of Diels and Alder[9] and isomerized to $\Delta^{1,2}$-tetrahydrophthalic anhydride[10] by heating with phosphorus pentoxide. 1,4-Addition of 1,3-butadiene to $\Delta^{1,2}$-tetrahydrophthalic anhydride **(12)** followed by saponification of the intermediate Δ^2-decalin-*cis*-9,10-dicarboxylic anhydride **(13)**, furnished the desired Δ^2-decalin-*cis*-9,10-dicarboxylic acid **(17)**[11] as a white solid. Hydrogenation of **17** in glacial acetic acid over PtO_2 catalyst afforded the corresponding *cis*-decalin-9,10-dicarboxylic acid **(18)** in 75% yield.

Attempted Hunsdiecker reaction of the decalin dicarboxylic acid **18** adopting the procedure of Vaughan et al.[12] (see Experimental) led to the recovery of the starting material. However, attempted Cristol reaction[13] of the decalin dicarboxylic acid **18** gave the anhydride **14**. Presumably, the intermediate monohypobromite formed, eliminated elements of hypobromous acid to yield the decalin dicarboxylic anhydride **14**.

As the Hunsdiecker reaction or the Cristol modification on the decalin dicarboxylic anhydride **14** or the acid **18** (Chart III) failed to give the bromo acid **5**, consequently, investigation of the aforesaid reactions on the corresponding half-ester **15** was undertaken. Accordingly, the *cis*-half ethyl ester **15** was prepared by the ethanolysis of the decalin dicarboxylic anhydride **14** in 80% yield. Spectral and microanalytical data confirmed its structure. Contrary to expectations, attempted Cristol[13] and Hunsdiecker reactions on the half-ester **15** furnished only the decalin dicarboxylic anhydride **14**.

It was then supposed that the *cis*-9-aminodecalin-10-carboxylic acid **(20)** could be converted to the required decalin bromo acid **5** as shown in Chart IV. Ammonolysis of the decalin anhydride **14** gave,

CHART IV

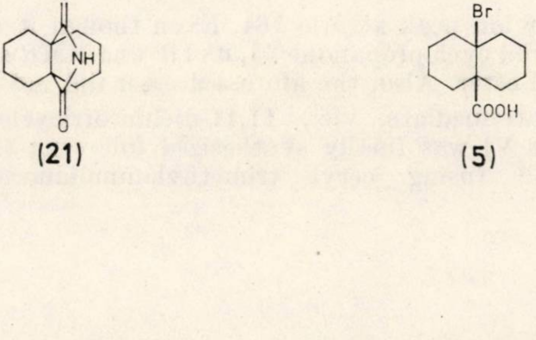

instead of the expected acid amide **19**, only the imide **21** as the exclusive product in 80 % yield. Its structure was confirmed by infrared NMR and mass spectral analyses. Treatment of the imide **21** with bromine and potassium hydroxide under Hoffman reaction conditions[14] gave back the starting material **21** quantitatively and thus failed to furnish any of the decalin amino acid **20**.

Consequently, a Schmidt reaction was tried on the decalin dicarboxylic anhydride **14**, but the starting material was recovered unaffected in quantitative yield. Similarly, attempted Curtius reaction of the decalin half-ester **15** also failed to afford any of the expected key-intermediate, the decalin amino acid **20**. It is worthwhile pointing out that the decalin imide **21** could not be hydrolysed to the decalin acid amine **19**.

An alternative approach to the synthesis of the key-intermediate, viz., *cis*-decalin-9-amino-10-carboxylic acid **(20)** was devised as illustrated in Chart V. Towards this end, naphthalene was reduced with lithium in a dimethylamine — ethylamine solvent mixture and the required octalin **22** isolated in 50 % yield following the procedure of Kaiser and Benkeser.[15] Reaction of $\Delta^{9,10}$-octalin **(22)** with chlorosulfonylisocyanate (prepared according to the procedure reported by Graf[16]) furnished the expected decalin lactam **23** in 1 % yield. In view of the depressingly low yield, this route was no longer pursued. Use of different solvents for the reaction like dimethylsulfoxide or liquid sulfur dioxide did not improve the yield of the lactam **23**.

Synthesis of the tricyclic β-lactam **23** (Chart V) was then attempted *via* the cyclopropanone **25**. Thus, dichlorocarbene (generated *in situ* from ethyl trichloroacetate and sodium methoxide) addition[17] to $\Delta^{9,10}$-octalin gave a yellow oil in 60 % yield whose mass spectrum exhibited a double molecular ion peak at m/e 164. Even though it corresponded to that of the required cyclopropanone **25**, its IR and NMR spectra indicated it to be an ethyl ester. Also, the aforesaid ester did not form an oxime.

CHART V

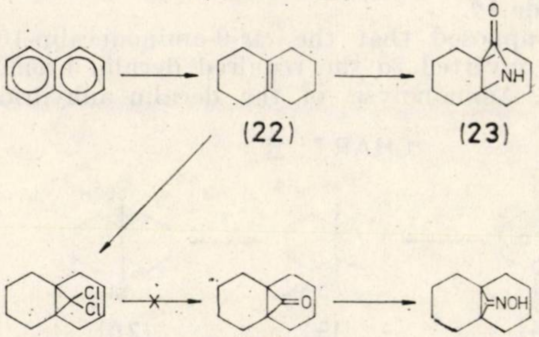

The key-intermediate, viz., 11,11-dichlorotricyclo-(4.4.1.0.)-undecane **(24)** (Chart V) was finally synthesized following the procedure of Devaprabhakara[18] (using cetyl trimethylammoniumbromide — cetrimide — as a phase transfer catalyst), but attempted hydrolysis of this dichloroundecane **24** using silver nitrate or silver acetate did not yield any of the cyclopropanone **25**.

Similarly, 11,11-dibromotricyclo-(4.4.1.0.)-undecane[18] was prepared in 75% yield by the dibromocarbene (generated *in situ* from bromoform and potassium tert. butoxide in pentane solvent) addition to 9,10-octalin (**22**). However, the dibromoundecane too could not be hydrolysed to the cyclopropanone **25**. It was inferred that the difficulty in these attempted hydrolyses could be due to the angle strain involved.

Further work is in progress.

EXPERIMENTAL

All melting points were determined in open capillaries and are uncorrected. Petroleum ether refers to the fraction boiling in the range 40 – 60°C. Infrared spectra were determined on a Perkin Elmer Model 237 Grating Infrared spectrophotometer. NMR spectra were run on a Varian A60 spectrometer using tetramethylsilane as internal standard. Mass spectra were obtained on an AEI double inlet MS9 Spectrometer. Microanalyses were performed by Baron Consulting Co., Orange, Connecticut. For some compounds, elemental analyses were determined by high resolution mass spectrometry ; they are indicated by an asterisk.

Reaction of methyl 2-cyclohexanonecarboxylate **1** *with phosphorus pentabromide*[4] :

A mixture of 17 g (0.109 mole) of methyl 2-cyclohexanone-carboxylate, 107 g (0.25 mole) of PBr_5 and 300 ml of dry benzene was refluxed under anhydrous conditions for 16 hrs. The reaction mixture was cooled, extracted with benzene (4 × 100 ml), the combined benzene extracts carefully washed with ice cold water (2 × 40 ml), 5% Na_2CO_3 (ice cold, 2 × 50 ml), ice water (2 × 40 ml), dried, solvent removed and the residue distilled. All fractions collected, exhibited aromatic protons.

Preparation of 2-bromo-1-cyclohexenecarboxaldehyde[5] *:**

To an ice cold solution of 22 g of dimethylformamide in 80 ml of dry $CHCl_3$ taken in a flame dried 500 ml 3-necked flask fitted with a mechanical stirrer, a pressure equalising dropping funnel with a dry nitrogen inlet and a water condenser, was added 60 g of freshly distilled PBr_5, followed by a solution of 10 g of pure cyclohexanone in 50 ml of dry $CHCl_3$. The green reaction mixture was stirred at 20 – 22°C for 18 hrs, at the end of which it turned brown. Chloroform was evaporated *in vacuo*, from the reaction mixture and 200 g of powdered ice added to it, followed immediately by solid $NaHCO_3$ to neutralize the reaction mixture. It was extracted with chloroform (3 × 200 ml), washed with water (2 × 100 ml), saturated K_2CO_3 solution (2 × 50 ml) and water (2 × 100 ml), dried, solvent stripped off to obtain 7.5 g of a yellow oil (40%). It gave a yellow semicarbazone, m.p. 222–223°C (rep.[5] 212–214°C). Mol. Wt. (mass spec.) : 245.0161. Calcd. for $C_8H_{12}BrN_3O$: 245.0161.

Attempted Diels-Alder reaction of 2-bromo-1-cyclohexenecarboxaldehyde:

1,3-Butadiene (50 ml) was condensed into a flame dried 500 ml 3-necked flask fitted with a mechanical stirrer, two dry ice condensers (one carrying a dry nitrogen inlet tube and the other a drying tube), containing a solution of 7 g of 2-bromo-1-cyclohexenecarboxaldehyde, in 50 ml of dry benzene, cooled to −20°C. It was stirred at this temperature for 3 hrs, and left overnight at room temperature. The crude residue was distilled at 55–57°/0.2 mm to furnish 4 g of a product, NMR spectrum of which exhibited proton signals in the aromatic region.

Preparation of methyl 2-bromocyclohexenecarboxylate **2*** :

To a pale brown solution of 47 g (0.25 mole) of the crude 2-bromocyclohexenecarboxaldehyde in 150 ml of aqueous ethyl alcohol was added 64 g (0.38 mole) of $AgNO_3$, followed by a solution of 40 g (1.0 mole) of NaOH in 500 ml of water and the mixture stirred overnight at room temperature. Usual work-up of the dark brown reaction mixture gave 25 g (48 % yield) of the desired 2-bromocyclohexenecarboxylic acid.

Esterification of this unsaturated bromo acid with diazomethane yielded the required 2-bromocyclohexenecarboxylate **2** as a colorless liquid (18 g., 85 % yield), b.p. 61–63°/ 0.03–0.04 mm. Found : 217.9942, Calcd : for $C_8H_{11}BrO_2$: 217.9940.

Hydrogenation of dimethyl 1,4-epoxy- $\Delta^{6,7}$ *-cis-decalin-9,10-dicarboxylate* **(8)*** :

A solution of 2.7 g (0.01 mole) of dimethyl 1,4-epoxy-$\Delta^{6,7}$-*cis*-decalin-9,10-dicarboxylate (prepared according to the method reported by Stork et al[6]) in 50 ml of ethyl acetate was hydrogenated over 0.1 g of 5 % Pd–C catalyst to obtain in 100 % yield, the corresponding dihydro derivative, viz., dimethyl 1,4-epoxy-*cis*-decalin-9,10-dicarboxylate **9** as a colorless oil, b.p. 100 – 102°/0.05 mm. IR, 1750 cm^{-1} (ester C=O). Mol. Wt. (mass spec) 268.1304. $C_{14}H_{20}O_5$ requires 268.1309.

Hydrolysis of $\Delta^{2,3}$ *-cis-decalin-9,10-dicarboxylic anhydride* **(13)**

Saponification of 20 g of the title compound gave a 70 % yield of $\Delta^{2,3}$-*cis*-decalin-9,10-dicarboxylic acid **(17)**, m.p. 201–203°C (rep.[11] 203°) (white crystals from methanol).

Hydrogenation of $\Delta^{2,3}$*-cis-decalin-9,10-dicarboxylic acid* **(17)** :

Hydrogenation of the octalin acid **17** over 98 % PtO_2 catalyst in glacial acetic acid afforded in 75 % yield, *cis*-decalin-9,10-dicarboxylic acid **(18)** as white crystals from methanol–benzene, m.p. 190–191°C.
Calcd. for $C_{12}H_{18}O_4$: C : 63.71 ; H : 7.96 % Found : C : 63.42 ; H : 8.13 %.

Hunsdiecker reaction of cis-decalin-9,10-dicarboxylic acid **(18)** :

Adopting the procedure of Vaughan and his associates,[12] Hunsdiecker reaction of the decalin dicarboxylic acid **18** (2.3 g, 0.01 mole), gave as the only isolable product, 1.4 g of a white solid identified as the starting material.

Cristol reaction[13] *of cis-decalin-9,10-dicarboxylic acid* **(18)** :

To a solution of 1.6 g of bromine (0.01 mole) in 100 ml of dry CCl_4 was added 2.0 g of red HgO (0.009 mole) followed by 2.3 g of (0.01 mole) the decalin acid **18** at room temperature and the reaction mixture stirred at room temperature for 1 hr, and at 60°C for 6 hrs. It was then cooled, filtered twice and the filtrate worked up to obtain 2.0 g of a product identified as *cis*-decalin-9,10-dicarboxylic anhydride **(14)**.

Hydrogenation of $\Delta^{2,3}$*-cis-decalin-9,10-dicarboxylic anhydride* **(13)** :

Hydrogenation of the octalin anhydride **13** (15 g, 0.07 mole) over 0.5 g of 84.8 % PtO catalyst in ethyl acetate furnished 14.2 g (94 %) of *cis*-9,10-decalindicarboxylic anhydride **14** as a colorless liquid (b.p. 120–122°/0.2 mm) which solidified to a colorless solid ; it was recrystallized twice from petroleum ether, m.p. 94–95°C.

Preparation of the half ethyl ester of cis-decalin-9,10-dicarboxylic acid **(15)*** :

Ethanolysis of 32 g of the decalin anhydride **14** gave after three crystallizations from chloroform–petroleum ether, the desired half ester **15** as colorless crystals, (yield 80 %), m.p. 108–109°C.
Mol. Wt. (mass spec.) : 254.1518 : Calcd. for $C_{14}H_{22}O_4$: 254.1536.

Ammonolysis of cis-decalin-9,10-dicarboxylic anhydride **(14)** :

A reaction mixture of 5 g (0.024 mole) of the decalin anhydride **14** and 100 ml of 30 % ammonium hydroxide was stirred at 85°C for 3 hrs. A careful work-up yielded a white solid, which, after three crystallizations from chloroform–petroleum ether gave 4.5 g (80 %) of *cis*-decalin-9,10-dicarboxylic imide **(21)** as colorless crystals, m.p. 190–191°C.
Analysis : Calcd. for $C_{12}H_{17}NO_2$:C :69.56, H : 8.21, N : 6.76 %.
Found : C : 69.52, H : 8.07, N : 6.72 %.

Reaction of $\Delta^{9,10}$*-octalin* **(22)**[15] *with chlorosulfonylisocyanate*[16] :*

To a mixture of $\Delta^{9,10}$ -octalin **22** (0.5 g. 0.004 mole) and anhydrous KCl (0.05 g, oven dried at 100°C for 2 hrs prior to the experiment) in 15 ml of dry CCl_4 cooled by a dry ice

bath was added 0.7 g (0.005 mole) of freshly distilled chlorosulfonylisocyanate in 10 ml of dry CCl_4 under a dry nitrogen atmosphere. It was then brought to room temperature and refluxed with vigorous stirring overnight. The reaction mixture was decomposed with 50 ml of ice and water, the solvent removed in a stream of nitrogen and neutralized with 5% ice cold NaOH till pH 7. Careful work up gave a brown oil, which was flash distilled to obtain 8 mg (about 1% yield) of the required β-lactam, **23**.
Mol. wt. (mass spec.): 179.1312; Calcd. for $C_{11}H_{17}NO$: 179.1311.

Dichlorocarbene addition to $\Delta^{9,10}$ *-octalin* **(22)** :

A solution of 6.8 g (0.05 mole) of $\Delta^{9,10}$-octalin **22** in 150 ml of dry CCl_4 was added to dry sodium methoxide (5.5 g, 0.1 mole) taken in a flame dried 300 ml 3-necked flask fitted with a dry nitrogen inlet, stopper, drying tube and a magnetic stirrer. After stirring at room temperature for 15 minutes, a solution of 14 g (0.75 mole) of freshly distilled ethyl trichloroacetate in 50 ml of dry CCl_4 was added and then the reaction mixture was stirred at room temperature overnight.

Work up of the reaction mixture followed by distillation at 90—95°/15 mm gave 5.5 g (67% yield) of a colorless oil which showed a double molecular ion peak at m/e 164. IR : 1755 cm^{-1} NMR : 8.85δ (triplet, 3H), 5.80δ (quartet, 2H).

Preparation of 11,11-*dichlorotricyclo*-(4.4.1.0.)-*undecane*[18] **(24)*** :

A solution of $\Delta^{9,10}$-octalin (2.7 g, 0.02 mole) in 13 g of dry $CHCl_3$ (0.08 mole) was deoxygenated with dry nitrogen and then cooled in dry ice. Cetyltrimethylammonium bromide (cetrimide, 73 mg, 0.0002 mole) was added to it followed by 100 ml of 4% sodium hydroxide solution in drops to obtain a clear solution, which was stirred at room temperature overnight. It was cooled in ice, acidified with 1 : 1 HCl and worked up. The resulting oily product was distilled to isolate 1.4 g (33% yield) of 11,11-dichlorotricyclo-(4.4.1.0.)-undecane **(24)**, b.p. 120—122°/15 mm as a colorless liquid. Mol. wt. (mass spec.) : 218.0630. Calcd. for $C_{11}H_{16}Cl_2$: 218.0630.

Preparation of 11,11-*dibromotricyclo*-(4.4.1.0.)-*undecane:* **(24a)**

To the dry white powder of potassium tert. butoxide (prepared from 0.8 g of potassium and 20 ml of tertiary butyl alcohol and dried at 100°C for half an hour at 1 mm pressure) was added a solution of 2.7 g (0.02 mole) of $\Delta^{9,10}$-octalin in 50 ml of anhydrous pentane and cooled to —10°C. Bromoform (5.1 g, 0.02 mole) was added in drops to the slurried mass and the mixture was then stirred at room temperature overnight in a nitrogen atmosphere and then worked up. The product was distilled to yield 4.9 g (75% yield) of 11,11-dibromotricyclo-(4.4.1.0.)-undecane[18] **(24a)** as a colorless liquid at 95—98°/0.3—0.4 mm. Mol. wt. : (mass spec) 308. Found : (M-Br) : 227.0427; Calcd. for $C_{11}H_{16}Br$: 227.0437.

REFERENCES

[1] W. R. Vaughan, W. F. Cartwright and B. Henzi, *J. Amer. Chem. Soc.*, **94**, 4978 (1972) and references cited therein.

[2a] C. A. Grob, *Experientia*, **13**, 126 (1957); [b] "Kekule Symposium on Theoretical Organic Chemistry", Butterworths, London, 1959, p. 114 ff.

[3] C. A. Grob, *Bull. Soc. chim. France*, **1960**, 1360.

[4] M. S. Newman, G. Fraenkel and W. N. Kirn, *J. Org. Chem.*, **28**, 1851 (1963).

[5] L. A. Paquette, B. A. Johnson and F. M. Hinga, *Org. Syn.*, **46**, 18 (1966).

[6] G. Stork, E. E. van Tamelen, L. J. Frieman and A. W. Burgstahler, *J. Amer. Chem. Soc.*, **75**, 384 (1953).

[7] O. Diels and S. Olsen, *J. prakt. chem.*, (2), **156**, 285 (1940).

[8] E. F. M. Stephenson, *Org. Syn. Coll. Vol.*, **3**, 475 (1955).

[9] O. Diels and K. Alder, *Leibigs Ann. Chem.*, **460,** 113 (1928).

[10] M. E. Bailey and E. D. Amstutz, *J. Amer. Chem. Soc.*, **78,** 3828 (1956).

[11] K. Alder and K. H. Backendorff, *Chem. Ber.*, **71,** 2199 (1938).

[12] W. R. Vaughan, R. Caple, J. Csapilla and P. Schneider, *J. Amer. Chem. Soc.*, **87,** 2204 (1965).

[13] S. J. Cristol and W. C. Firth, *J. Org. Chem.*, **26,** 280 (1961).

[14] C. M. Wynn and W. R. Vaughan, *J. Org. Chem.*, **33,** 2371 (1968).

[15] E. M. Kaiser and R. A. Benkeser, *Org. Syn.*, **50,** 88 (1970).

[16] R. Graf, *Org. Syn.*, **46,** 51 (1966).

[17a] W. E. Parham, E. E. Schweizer and S. A. Mierzwa, Jr., *Org. Syn.*, **41,** 76 (1966) ; [b] E.V. Couch, J. A. Landgrebe and E. T. Castaneda, *J. Org. Chem.*, **40,** 1529 (1975) ; [c] W. von E. Doering and A. K. Hoffmann, *J. Amer. Chem. Soc.*, **76,** 6162 (1954).

[18] D. Devaprabhakara and R. Vaidyanathaswamy, *Chem. Ind.*, **1968,** 515.

Revue Roumaine de Chimie, 26, *9–10*, 1315–1326 (1981)

AMORPHOUS-CRYSTALLINE COUPLING IN POLYETHYLENE. IX[1]

STUDY OF THE TRANSFORMING BRANCHES BY STEP CALORIMETRIC SYSTEM

GH. DRĂGAN
Institute of Chemical Research, ICECHIM, Spl. Independenţei 202, Bucharest 77208, Romania.

Received October 5, 1977
Revised March 25, 1981

The series of studies on the amorphous-crystalline coupling in the three types of polyethylenes and the derived chlorinated species, is continued by using the DSC system commanded by temperature steps. Comparing the energetic circuits both in dry and medium system, and for chlorinated samples in addition "in vivo" and "in vitro" systems, respectively, the property of additive composition of the transforming branches is perfectly observed. The composition diagram associated with the overall circuit shows its structure by purely dissipative coupled transforming branches and reveals a similar situation to the pyramidal composition of elementary particles according to quantum numbers.

INTRODUCTION

In two recent studies[2,3] some results were drawn for measuring systems whose transformation branches are purely dissipatively coupled to the boundary condition. Linear relationships may be established between measurables, so that for thermally driven processes these lead to additive relationships between the activation energies associated to the transformation branches purely dissipatively coupled to the laboratory reference system.[2] Theoretically, even for coupling reactances containing inductive elements,[4] it has been demonstrated that the overall relaxation function obeys an additive rule between the partial functions corresponding to the component branches.[3] The development of the working principles in energetic-topological terms for concrete tasks is possible by experimentally checking the partial theoretical results. In this way, formal principles initially introduced by Oster and Auslander[5] might be enriched in physical meaning and then successfully applied in the study of non-equilibrium systems.[6,7]

In the present study the calorimetric systems are considered again of differential type (DMS) and single type (SMS),[3] for overall energetic circuits in the linear polyethylene samples (LPE) and chlorinated species (CPE) which were studied in this series for the isothermal boundary condition. The response functions are expressed in units of specific heat, being possible to value the excess energy for the overall circuit or for a transformation branch. A similar study was performed on polycrystalline aluminium samples,[8] and the results were explained by topological principles.[2] Thus, it has been revealed that the activation energy associated to a transformation branch is an invariant against the response function, being an intrinsic characteristic for the energetic circuit relative to a temporar reference system. By using these results, the global energetic circuit may be decomposed in elementary transformation branches purely dissipatively coupled to the boundary condition. The main transformation process which is modified with secondary branches in LPE and CPE samples is T_m^0.[6] In present view of phase transitions it was already concluded that in critical range the energetic transfer in non-equilibrium systems may be expressed as a coupling between different energetic modes.[6,9] Initially,[10] with the first results and later when phase transitions were phenomenologically reconsidered,[6,11] it was considered that the transforming branch couples more and less with the "remaining inert lattice". The topological models offer the advantage of delimiting the transformation branches with purely dissipative coupling; this is achieved by selecting convenient measuring systems. Thus, even in superposed processes, *e.g.* crystallization from a multicomponent melt,[6] crosslinking-polymerization in epoxide systems,[7] thermal oxidation of amorphous phase in high and low density polyethylene samples[12] and many other intricate processes (see reference[2]), one can separate one of the transformation branches in the approximation of purely dissipative coupling.

The calorimetric method, which is the subject of this contribution and of a patent,[13] employs overall energy circuits for LPE and CPE samples (in dry form or blended with silicon oil),[1] decomposed into transformation branches coupled only dissipatively to the laboratory reference system (LabRS); the associated bond diagram[5] is replaced by another diagram which expresses the affinity relationships[2] among transformation branches.

These results have allowed the reconsideration of relativistic effects established for the formation of disclination states on simultaneous annealing; for this case a "scattering" diagram of energy circuits was established. Like this relativistic effect which is due to inductive element, the composition of branches by dissipative coupling is similar to the composition of elementary particles according to quantum numbers.

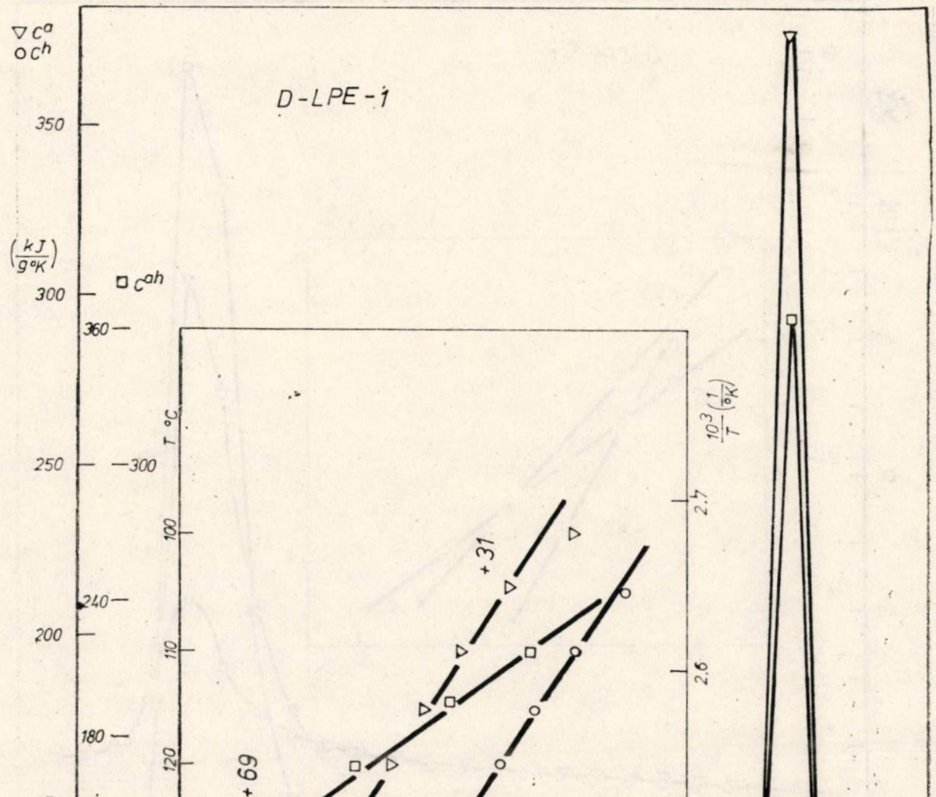

Fig. 1. — The plot of the response functions C^a, C^h and C^{ah} versus temperature and Arrhenius plots of the associated energies in excess for D-LPE-1 sample.

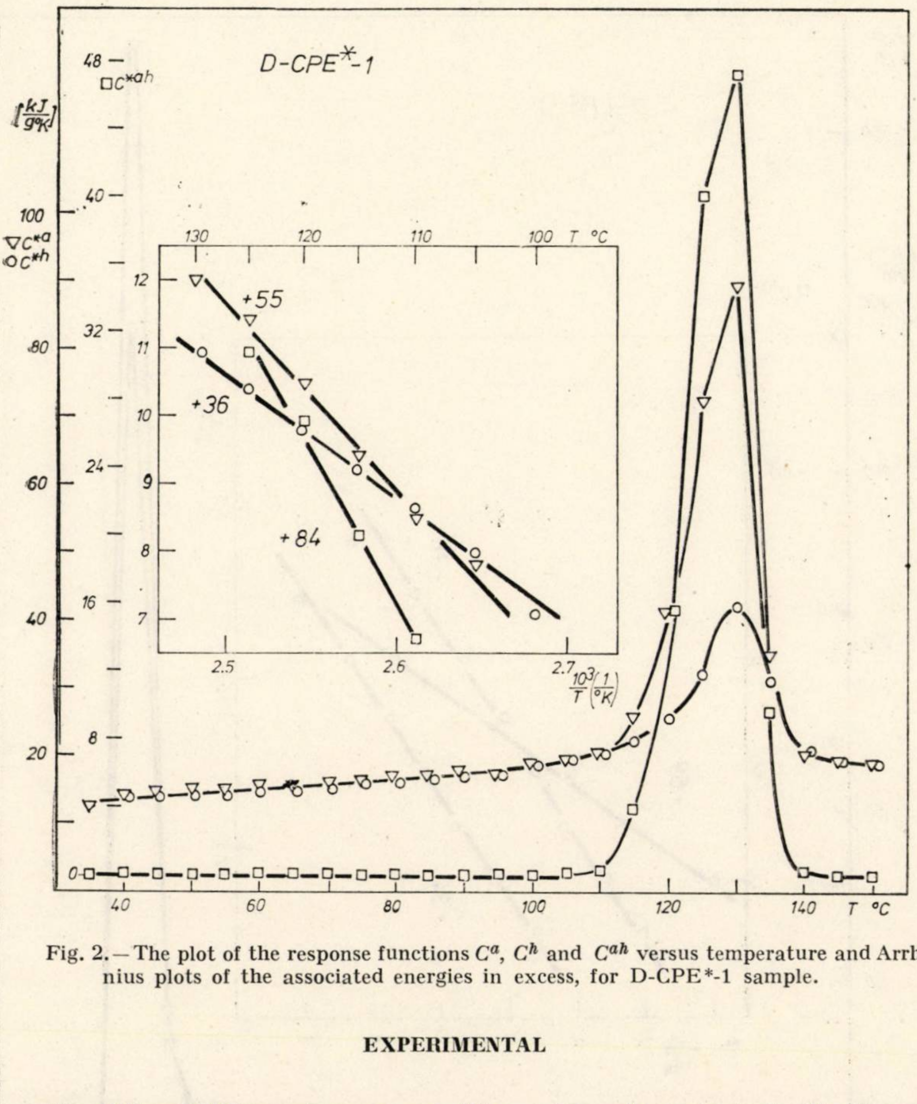

Fig. 2. — The plot of the response functions C^a, C^h and C^{ah} versus temperature and Arrhenius plots of the associated energies in excess, for D-CPE*-1 sample.

EXPERIMENTAL

The LPE and CPE samples were used either as dry systems or mixed with silicon oil (as annealing medium) as it was previously shown.[14] Du Pont 990 DSC apparatus was used for calorimetric analysis ; isothermal steps were of 5°, the sensitivity 0.5 mcal/s. in, the time base 2 min/in, Aluminium cells with lid have been employed (PN 900655—001, and 900656-001, respectively) filled up and compacted to ensure optimal thermal contact with the sensors. To standardize the thermograms in heat capacity units use has been made of saphire pellet supplied in the apparatus kit.

RESULTS AND DISCUSSIONS

A thermogram (endotherm) obtained for a heating step allows the determination of heat capacity of inert component C^h from the height of the peak and the total heat capacity of the material C^a from the area of

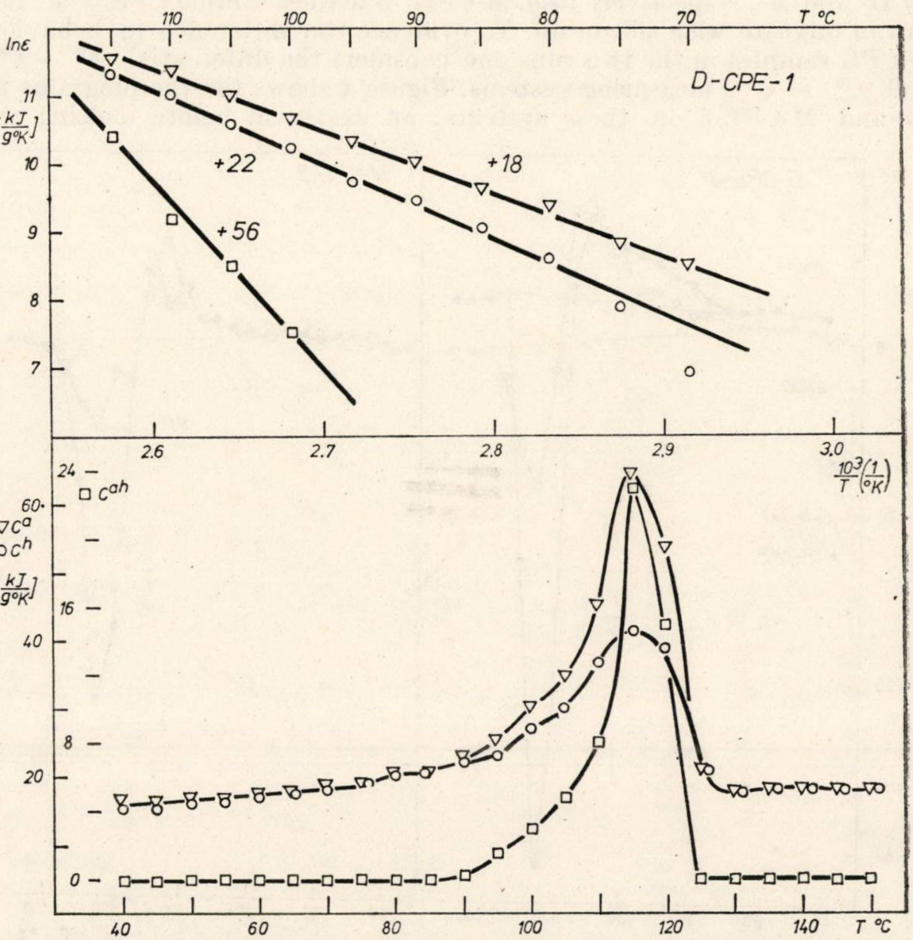

Fig. 3. — The plot of the response functions C^a, C^h and C^{ah} versus temperature and Arrhenius plots of the associated energies in excess, for D-CPE-1 sample.

the endotherm, both expressed in kJ/g.K.[13] These quantities in turn can be used to calculate the derived measurable $C^{ah} = C^a - C^h$ corresponding to DMS system with C^a as SMS. [3] Figures 1—3 show the plots of the three measurables as a function of temperature for LPE 1 and CPE 1 as dry system,[14] respectively, within 30—155° temperature range. Unlike LPE samples, the temperature dependence of CPE drastically changes at a subsequent calorimetric run which is due to transformation branches brought about by migration of grafted deffects and/or the medium, process which is more evident in this case.[1] To separate these branches, we consider the thermograms of the first run which make up an "in vivo" measuring system denoted by the index* and those of a subsequent run on the same sample which represents an "in vitro" measuring system.[2] On the other hand, the dry systems and those with medium are denoted by D- and M-, respectively : *e.g.* M-CPE*-3 defines sample CPE 3 at first run in mixture with silicon oil. To evidence the difference in behaviour of CPE samples in the two runs one considers the differential ($C^h - C^{*h}$) and ($C^a - C^{*a}$) measuring systems. Figure 4 shows the thermograms for D- and M-CPE-3 in these systems: an exotherm before melting and

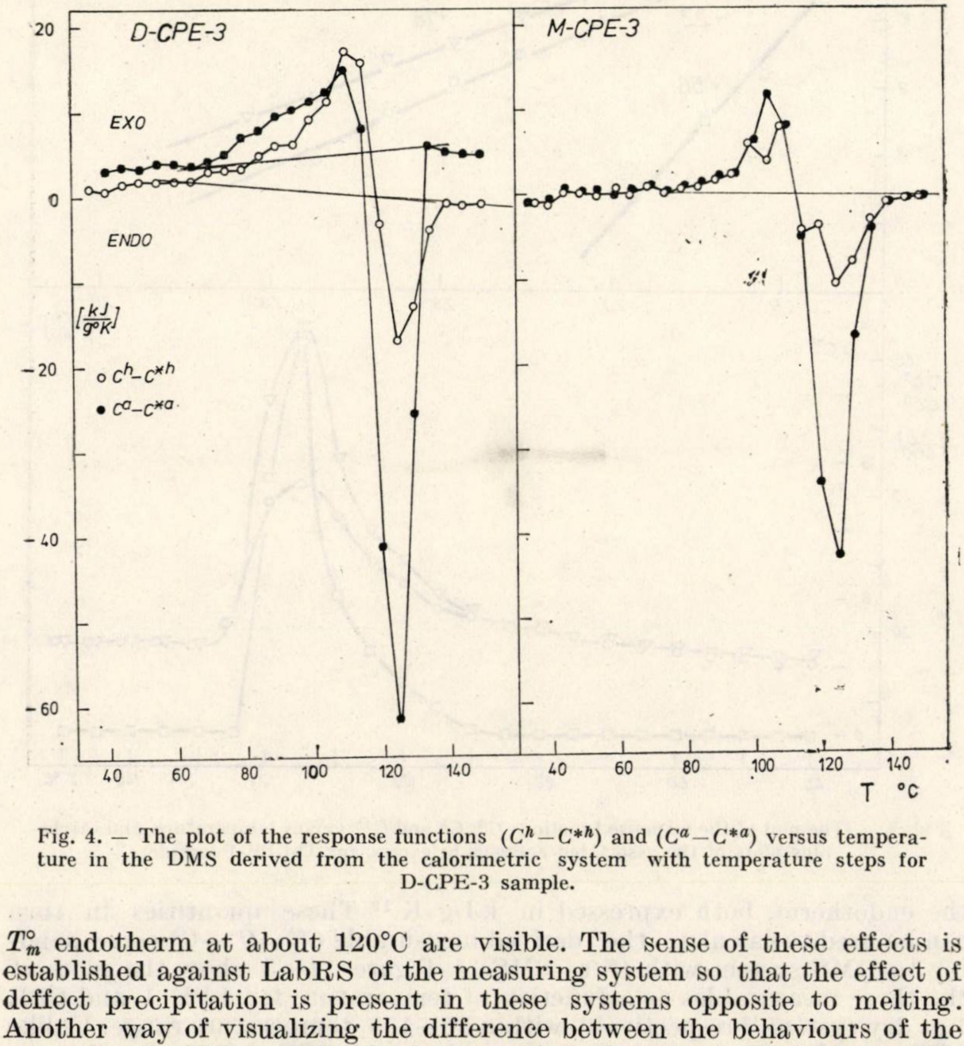

Fig. 4. — The plot of the response functions ($C^h - C^{*h}$) and ($C^a - C^{*a}$) versus temperature in the DMS derived from the calorimetric system with temperature steps for D-CPE-3 sample.

T_m° endotherm at about 120°C are visible. The sense of these effects is established against LabRS of the measuring system so that the effect of deffect precipitation is present in these systems opposite to melting. Another way of visualizing the difference between the behaviours of the two runs on CPE samples is the recording of various caloric fluxes for each temperature step of the two runs expressed for the same amount of samples : $\Delta w = w - w^*$.[13] These fluxes are represented in figure 5 for D-CPE-3 within 95–130°C. It is noteworthy that extent of these effects reproduces the behaviour given in figure 4 while, on the other hand, since steps are successive on the same sample, the durations of peaks of all fluxes[6] defined by the same differential measuring system are practically the same. Integration of these fluxes yields results in figure 7.

Regarding the bahaviour of samples in the three SMS systems (Figs. 1—3) one can notice firstly that while CPE samples exhibit an order-disorder process (which may be T_m^1) around 115°C, LPE and CPE samples exhibit a marked T_m° process centered around 130°C. On the other hand, the melting process is much more extensive in LPE than in CPE, proportional to crystalline phase. From the very beginning we have noticed[10,11] that the coupling of a phase transition with the "remaining lattice" may be evidenced by its broadening within the temperature range. Thus, figures 1 — 3 show that compared to T_m° process in LPE, in the samples which in addition posses other secondary branches as diffusion of the medium and/or grafted deffects, the overall transition processes of order-disorder type become much more broadened.

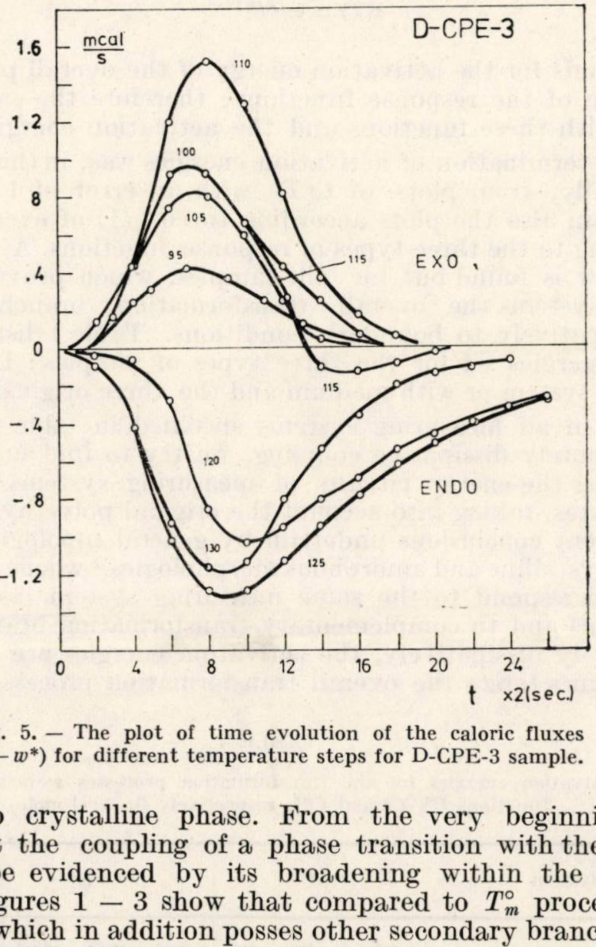

Fig. 5. — The plot of time evolution of the caloric fluxes $(w-w^*)$ for different temperature steps for D-CPE-3 sample.

Another finding which characterizes the coupling of the melting process T_m°, with other secondary branches, shows that the response functions, C^h and C^a behave more or less differently towards one another within the critical temperature range. We also consider D-LPE as reference sample which exhibits important differences between the two behaviours. The quantity C^h which characterizes the inert component, i.e. the rest of the network is small compared to C^a which practically stands for the branch in T_m° transformation. As more secondary branches are involved, C^h shows more extensive transitions.

Accurate studies of various processes of transformation based on this calorimetric technique have established that the magnitude of excess energy of the system for a certain temperature T in the critical range measured against the extrapolated base line for inert behaviour follows an Arrhenius-type relation.[15]

$$\varepsilon(T) \simeq e^{-E/RT} \tag{1}$$

where E stands for the activation energy of the overall process characterized by one of the response functions; therefore the same indexes are employed with these functions and the activation energies.

The determination of activation energies was, in this cases, performed graphically, from plots of $C(T)$ with an error of 1 – 5%. Figures 1 – 3 contain also the plots according to eq. (1) of excess energy, $\varepsilon(T)$ corresponding to the three types of response functions. A good agreement with this law is found out for all samples, which proves that in these measuring systems the overall transformation branches are coupled purely dissipatively to boundary conditions. Table 1 lists the values of activation energies set for the three types of samples: LPE, CPE* and CPE as dry system or with medium and the three original polyethylenes.

Since in all measuring systems specified in table 1 the processes reveal the purely dissipative coupling, we try to find out what relation exists among the energy circuits of measuring systems established by sample natures, taking into account the original polyethylenes. According to some recent conclusions underlain by general topologic considerations regarding crystalline and amorphous morphologies,[2] whenever two response functions correspond to the same measuring system (as temporal reference system) and to complementary transformation branches which are coupled purely dissipatively, the activation energies are composed additively to characterize the overall transformation process.

TABLE 1

The overall activation energies for the transformation processes associated to the response functions C^a, C^h and C^{ah}, respectively (in kcal/mole)

Dry system	D-LPE			D-CPE*			D-CPE		
Original PE	E^h	E^a	E^{ah}	E^{xh}	E^{xa}	E^{xah}	E^h	E^a	E^{ah}
LPE – 1	34	31	69	36	55	84	18	22	56
LPE – 2	30	18	48	27	15	30	22	22	(0)
LPE – 3	23	23	50	30	37	57	19	19	(0)
Medium system	M-CPE			M-CPE*			M-CPE		
LPE – 1	24	12	35	28	26	30	18	15	20
LPE – 2	31	14	46	32	27	46	19	14	46
LPE – 3	25	16	44	14	12	30	20	18	15

We test the linearity between pairs of activation energies for the same initial polyethylene with and without medium, and/or with or without grafted deffects by chlorination.

Let us assume for the beginning that the C^a(D-CPE*) circuit is composed of C^a(D-LPE) and the branch corresponding to precipitation of grafted deffects. We express this in the following way:

$$\begin{array}{c} C^a(\text{D-CPE}^*) \\ \mathbf{(55,\ 15,\ 37)} \end{array} \begin{array}{ll} \nearrow C^a(\text{D-LPE}) & \mathbf{(31,\ 18,\ 23)} \\ \searrow \text{D}-\text{Cl}^* & (24, -3, 14) \end{array} \tag{2}$$

where the figures associated to circuits denote the activation energies corresponding to samples derived from initial LPE 1,2 and 3 (the boldface figures stand for experimental values and the ordinary ones for those calculated additively). To check relation (2) we consider the DMS circuit

$$\begin{array}{c} C^a(\text{D}-\text{CPE}^*) - C^a(\text{D}-\text{LPE}) \\ \mathbf{(51,\ 30,\ 33)} \end{array} \begin{array}{ll} \nearrow 2C^a(\text{D}-\text{LPE}) & \mathbf{(62,\ 36,\ 46)} \\ \searrow \text{D}-\text{Cl}^* & (-11,\ -6, -13) \end{array} \tag{3}$$

The D-Cl* branch is not purely dissipatively coupled with D-LPE within D-CPE*. Let be now the similar case for M-CPE* circuit:

$$\begin{array}{c} C^a(\text{M-CPE}^*) \\ \mathbf{(26,\ 27,\ 12)} \end{array} \begin{array}{ll} \nearrow C^a(\text{M-LPE}) & \mathbf{(12,\ 14,\ 16)} \\ \searrow \text{M}-\text{Cl}^* & (14,\ 13,\ -4) \end{array} \tag{4}$$

and respectively:

$$\begin{array}{c} C^a(\text{M-CPE}^*) - C^a(\text{M-LPE}) \\ \mathbf{(38,\ 41,\ 28)} \end{array} \begin{array}{ll} \nearrow 2C^a\ (\text{M-LPE}) & (24,\ 28,\ 32) \\ \searrow \text{M}-\text{Cl}^* & (14,\ 13,\ -4) \end{array} \tag{5}$$

which proves that in the case of M-CPE* circuits the branches of relation (4) are purely dissipatively coupled.

Let be the DMS C^{ah} (D—CPE*) circuit:

$$\begin{array}{c} C^{ah}(\text{D-CPE}^*) \\ \mathbf{(84,\ 30,\ 57)} \end{array} \begin{array}{ll} \nearrow C^a(\text{D-CPE}^*) & \mathbf{(55,\ 15,\ 37)} \\ \searrow C^a(\text{D-LPE}) & \mathbf{(31,\ 18,\ 23)} \end{array} \tag{6}$$

This circuit is a differential of D-CPE* and therefore consists of a branch of chlorinated sample and one of initial polyethylene. Likewise, for the circuit with medium one can write:

$$\begin{array}{c} C^{ah}(\text{M-CPE}^*) \\ \mathbf{(30,\ 46,\ 30)} \end{array} \begin{array}{ll} \nearrow C^a(\text{M-CPE}^*) & \mathbf{(26,\ 27,\ 12)} \\ \searrow C^a(\text{M-LPE}) & \mathbf{(12,\ 14,\ 16)} \end{array} \tag{7}$$

In both cases the coupling of branches is purely dissipative. For the "in vitro" circuit we consider a similar summing up:

$$\begin{array}{c} C^{ah}(\text{D-CPE}) \\ \mathbf{(56,\ 0,\ 0)} \end{array} \begin{array}{ll} \nearrow C^a(\text{D}-\text{CPE}) & \mathbf{(18,\ 22,\ 19)} \\ \searrow C^a(\text{D-LPE}) & \mathbf{(31,\ 18,\ 23)} \end{array} \tag{8}$$

and

$$\underset{(\mathbf{20,\ 43,\ 15})}{C^{ah}(\text{M-CPE})}\begin{array}{l}\diagup\, C^{a}(\text{M-CPE})\ (\mathbf{15,\ 14,\ 18})\\ \diagdown\, C^{a}(\text{M-LPE})\ (\mathbf{12,\ 14,\ 16})\end{array} \tag{9}$$

which results as nonvalid relation. D-LPE may be replaced in (9) for M-LPE, and it does not work too. Two distinct cases may be noticed. The former refers to DMS in the presence of medium :

$$\underset{(\mathbf{38,\ 45,\ 22})}{C^{a}(\text{M-CPE*}) - C^{a}(\text{M-LPE})}\begin{array}{l}\diagup\, C^{a}(\text{M-CPE*})\ \ (\mathbf{26,\ 27,\ 12})\\ \diagdown\, C^{a}(\text{M-LPE})\ \ (\mathbf{12,\ 14,\ 16})\end{array} \tag{10}$$

If relation (4) is considered it turns out that they are commutative. This relation allows finding out the activation energies for M-Cl* branch as (14, 17, −9) (see Appendix). The latter case refers to the similar DMS circuit as dry system :

$$\underset{(\mathbf{51,\ 30,\ 33})}{C^{a}(\text{D-CPE*}) - C^{a}(\text{D-LPE})}\begin{array}{l}\diagup\, C^{a}(\text{D-CPE*})\quad (\mathbf{55,15,\ 37})\\ \diagdown\, C^{a}(\text{D-LPE})\quad (\mathbf{31,\ 18,\ 23})\end{array} \tag{11}$$

which holds only for D-CPE*-2 case which may verify the relation above so that :

$$C^{a}(\text{D-CPE*}-2) - C^{a}(\text{D-LPE-2})\begin{array}{l}\diagup\, C^{a}(\text{D-LPE-2})\\ \diagdown\, \text{D}-\text{Cl*}\end{array} = \begin{array}{l}\diagup\, 2C^{h}(\text{D}-\text{LPE-2})\\ \diagdown\, \text{D}-\text{Cl*}\end{array} \tag{12}$$

Thus, only for D-CPE*-2 one can separate the precipitation branch of D-Cl* grafted defects with an activation energy of −6 kcal/mole. The activation energies for DMS (10) and (11) circuits are determined from plots of these values. We resume the study of the circuit :

$$\underset{(\mathbf{26,\ 27,\ 12})}{C^{a}(\text{M}-\text{CPE*})}\begin{array}{l}\diagup\, C^{a}(\text{D-CPE*})\quad (\mathbf{55,\ 15,\ 37})\\ \diagdown\, \Delta(\text{M-CPE*})\ (-29,\ 12,\ -25)\end{array} \tag{13}$$

where Δ(M-CPE*) stands for the affine branch bonding C^a(M-CPE*) and C^a(D-CPE*) due exclusively to the presence of medium. This branch should be present in the differential circuit :

$$\underset{(\mathbf{30,\ 46,\ 30})}{C^{ah}(\text{M-CPE*})}\begin{array}{l}\diagup\, C^{ah}(\text{D-CPE*})\quad (\mathbf{84,\ 30,\ 57})\\ \diagdown\, \Delta(\text{M-CPE*})\quad (-54,\ 16,\ -27)\end{array} \tag{14}$$

One can notice that the affine relations (13) and (14) hold simultaneously only for the circuits of samples M-CPE*-2 and-3.

The relations established so far may be expressed partially by the affinity diagram of energy circuits :

$$\begin{tikzcd} C^{a}(\text{D-CPE*}) \arrow[r, "\text{M}", "1"'] \arrow[d, "C^{a}(\text{D-LPE})\ 2"'] & C^{a}(\text{M-CPE*}) \arrow[d, "4\ C^{a}(\text{M-LPE})"] \\ C^{ah}(\text{D-CPE*}) \arrow[r, "\text{M}", "3"'] & C^{ah}(\text{M-CPE*}) \end{tikzcd} \tag{15}$$

where the corners of the diagram are occupied by the circuits which on addition of the branches specified above the arrows, yield the circuits lying at arrowheads. The sides 3 and 4 of the diagram are valid for CPE*-1. Symbol M denotes the shift branch due to the medium.

Consideration of relations (4) and (5) yields the diagram:

$$\begin{tikzcd}
C^a(\text{D-CPE}^*) \arrow[r, "\text{M}"] & C^a(\text{M-CPE}^*) \arrow[dr] & \\
 & & C^a(\text{M-CPE}^*)-C^a(\text{M-LPE})\equiv \text{DMS}(\text{M-CPE}^*) \\
 & C^a(\text{M-LPE}) \arrow[uu, "\text{M}-\text{Cl}^*"'] \arrow[ur] &
\end{tikzcd} \tag{16}$$

Likewise, the C^h(D-LPE) circuit which defines the T_m^0 process has been found to be at the basis of the diagram

$$\begin{tikzcd}
 & C^h(\text{D-LPE}) \arrow[dl, "\Delta(\text{M-LPE})"'] \arrow[dr] & \\
C^a(\text{M-LPE}) & & C^a(\text{D-LPE}) \arrow[ll, "\text{M}"']
\end{tikzcd} \tag{17}$$

where Δ(M-LPE) is the right side of the medium contribution which is specific for LPE samples.

Finally the (15)–(17) diagrams may be written unitarily as:

$$\begin{tikzcd}
 & C^h(\text{D-LPE})\equiv T_m^0 \arrow[dl] \arrow[d, shift right, dash] \arrow[d, shift left, dashed] & & \\
C^a(\text{D-LPE}) \arrow[r, dash, "\text{M}"] & C^a(\text{M-LPE}) \arrow[r] \arrow[d, shift right, dash] \arrow[d, shift left, dashed] \arrow[dr, dash, "\text{M-Cl}^\times"] \arrow[dr, dashed, shift right, dash] & C^{ah}(\text{M-CPE}^*) \arrow[d, "C^{ah}(\text{M-LPE})"] & C^{ah}(\text{D-CPE}^*) \arrow[l, "\Delta(\text{M-CPE}^*)"'] \arrow[d, "C^a(\text{D-LPE})"] \\
 & \text{DMS}(\text{M-CPE}^*) \arrow[r, Rightarrow, dashed] & C^a(\text{M-CPE}^*) \arrow[r, equal, dashed] & C^a(\text{D-CPE}^*) \arrow[d, dashed, "C^h(\text{D-LPE})"] \\
 & & & C^a(\text{D-CPE})
\end{tikzcd} \tag{18}$$

This diagram shows the correlation between the elementary energy branches which are composed in LPE, CPE* and CPE samples and appear as "grafted" on the basic $T_m^0 = C^h$ (D-LPE) process. The dotted sides make up the diagram which is valid for samples derived from LPE-1 as well. This "pyramid" of composition of energy systems is similar to that established for structural correlation of elementary particles according to quantum numbers which define their behaviour in scattering measuring systems.[16]

APPENDIX

We determine the activation energies for M-Cl* branch against the measuring system of overall circuit :

$$\begin{tikzcd}[row sep=small] & C^a(\text{M-LPE}) \quad \mathbf{(12,\ 14,\ 16)} \\ C^a(\text{M-CPE}^*) \arrow[ur, dash] \arrow[dr, dash] & \\ \mathbf{(26,\ 27,\ 12)} & \text{M-Cl}^* \quad (14,\ 13,\ -4) \end{tikzcd}$$

This branch represents the process of formation of interlamellar disclination state as a result of precipitation of grafted defects, by chlorination, in the presence of the medium. We considered as in C^a(D-CPE*) that the complementary branch is C^a(M-LPE). Thus the (14, 13, −4) values result. To verify this composition of the circuit was consider the differential measuring system with C^a(M-LPE) as reference branch.

For calculation, the response function :

$$c_1 C^a(\text{M-CPE}^*) - \beta\, c_2 C^a(\text{M-LPE})$$

is plotted as in figures 1 − 3, where c_1 is the concentration of dry LPE in M-LPE, c_2 the concentration of D-CPE in M-CPE and β the degree of crystallinity of M-CPE against M-CPE. The plotting of this response function yields the behaviour of differential circuit :

$$\begin{tikzcd}[row sep=small] & 2C^a(\text{M-LPE}) \quad \mathbf{(24,\ 28,\ 32)} \\ C^a(\text{M-CPE}^*) - C^a(\text{M-LPE}) \arrow[ur, dash] \arrow[dr, dash] & \\ \mathbf{(38,\ 45,\ 23)} & \text{M-Cl}^* \quad \mathbf{(14,\ 17,\ -9)} \end{tikzcd}$$

REFERENCES

[1] Part VIII : Gh. Drăgan, *Rev. Roumaine Chim.*, **23,** 1313 (1978).

[2] Gh. Drăgan, *Rev. Roumaine Chim.*, **24,** 627 (1979).

[3] Gh. Drăgan, *J. Thermal Anal.*, **15,** 297 (1979).

[4] Gh. Drăgan, *Revista de Chimie*, **29,** 214 (1978).

[5] G. F. Oster and D. M. Auslander, *J. Franklin Inst.*, **292,** 1 (1971).

[6] Gh. Drăgan, *Rev. Roumaine Chim.*, **23,** 629 (1978).

[7] Gh. Drăgan and F. Stoenescu, *Rev. Roumaine Chim.*, **24,** 55 (1979).

[8] C. Guarini and G. M. Schiavini, *Phil. Mag.*, **14,** 47 (1966).

[9] L. P. Kadanoff and J. Swift, *Phys. Rev.*, **166,** 89 (1968).

[10] Gh. Drăgan, Proceedings of the III-th National Conference on Analytical Chemistry, Brașov, Romania, 22−26 September 1971, p. 351.

[11] Gh. Drăgan, *Rev. Roumaine Chim.*, **20,** 687 (1975).

[12] Gh. Drăgan, V. Dobrescu and N. Goldenberg, *J. Polymer Sci.*, in press.

[13] Gh. Drăgan, Romanian Patent No. 68690 (1977).

[14] Gh. Drăgan, *Rev. Roumaine Chim.*, **21,** 1381 (1976).

[15] Gh. Drăgan, *Acta Polym.*, **31,** 293 (1980).

[16] J. F. Chou, M. Gell-Mann and A. G. Rosenfeld, *Scientific American*, February 1964.

Revue Roumaine de Chimie, **26**, *9–10*, 1327–1334 (1981)

SYNTHESIS AND POLYMERIZATION OF POLYETHYLENEGLYCOL DIMETHACRYLATES. II[1]

KINETICS OF THE TRANSESTERIFICATION PROCESS OF METHYLMETHACRYLATE WITH POLYGLYCOLS

GH. HUBCA, D. RACOŢI, CR. OPRESCU and M. DIMONIE
The Polytechnic, Laboratory of Macromolecular Technology, Calea Victoriei, No. 149, Bucharest
Romania

Received February 13, 1981

The kinetics of the process of transesterification reaction of methylmethacrylate with polyglycols has been studied with the view of obtaining quantitative data. The results obtained show that the reactivity of the hydroxyl groups in polyglycols is different from that in monoester and this is the reason why the two stages of the process have different rates. The reactivity of the hydroxyl group in monoester depends on the length of the polyether chain and it increases at the same time with the latter. The calculation of the rate constants for the two stages of the process has allowed to find out the way in which the composition of the reaction mixture varies in time.

The transesterification reaction of methylmethacrylate with polyglycols is a reversible process described by two parallel consecutive equations :

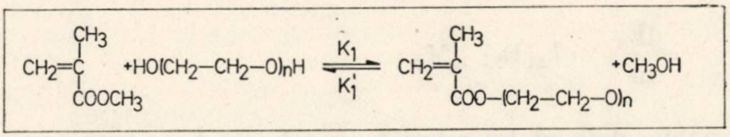

$$CH_2{=}\overset{\overset{\displaystyle CH_3}{|}}{\underset{\underset{\displaystyle COOCH_3}{|}}{C}} + HO(CH_2{-}CH_2{-}O)_nH \underset{K_1'}{\overset{K_1}{\rightleftharpoons}} CH_2{=}\overset{\overset{\displaystyle CH_3}{|}}{\underset{\underset{\displaystyle COO{-}(CH_2{-}CH_2{-}O)_n}{|}}{C}} + CH_3OH \qquad (1)$$

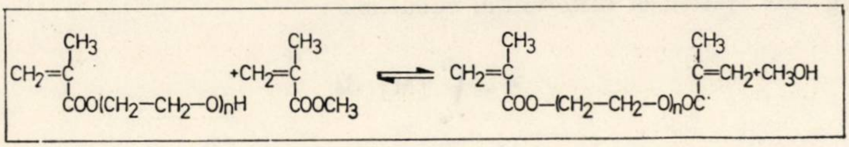

$$CH_2{=}\overset{\overset{\displaystyle CH_3}{|}}{\underset{\underset{\displaystyle COO(CH_2{-}CH_2{-}O)_nH}{|}}{C}} + CH_2{=}\overset{\overset{\displaystyle CH_3}{|}}{\underset{\underset{\displaystyle COOCH_3}{|}}{C}} \rightleftharpoons CH_2{=}\overset{\overset{\displaystyle CH_3}{|}}{\underset{\underset{\displaystyle COO{-}(CH_2{-}CH_2{-}O)_nOC}{|}}{C}} \overset{\overset{\displaystyle CH_3}{|}}{C}{=}CH_2 + CH_3OH \qquad (2)$$

where : $n = 1 - 4$.

Taking into account the two stages of the process, the question arises whether the reactivity of the hydroxyl groups in polyglycols is equal to the reactivity of the hydroxyl groups in monoester, or otherwise stated whether the formation rate of monoester is equal to the formation rate of diester.

The studies on the transesterification reaction[1] show that the total rate of the process depends on the polyglycol length.

In order to give an answer to the above-mentioned question and to obtain quantitative data on the influence of polyglycol length on the transesterification reaction, the kinetics of the process was studied, starting with the general case : $k_1 \neq k_2$.

The development of the transesterification reaction in excess of methylmethacrylate and the continuous removal of the methanol formed by distillation make, with a good enough approximation, equations (1) and (2) be considered irreversible reactions.

Thus, reactions (1) and (2) will be

$$\mathrm{M} + \mathrm{G} \xrightarrow{k_1} \mathrm{E}_1 + \mathrm{MeOH} \tag{3}$$

$$\mathrm{E}_1 + \mathrm{M} \xrightarrow{k_2} \mathrm{E}_2 + \mathrm{MeOH} \tag{4}$$

where : G — glycol ; M — methylmethacrylate ; E_1 — monoester ; E_2 — diester and MeOH — methanol.

According to these equations, the process is given by the following differential equations

$$\frac{\mathrm{d}M}{\mathrm{d}t} = k_1\,[\mathrm{M}]\,[\mathrm{G}] + k_2\,[\mathrm{M}]\,[\mathrm{E}_1] \tag{5}$$

$$\frac{\mathrm{dG}}{\mathrm{d}t} = k_1\,[\mathrm{M}]\,[\mathrm{G}] \tag{6}$$

$$\frac{\mathrm{dE}_1}{\mathrm{d}t} = k_1\,[\mathrm{M}]\,[\mathrm{G}] - k_2[\mathrm{E}_1]\,[\mathrm{M}] \tag{7}$$

$$\frac{\mathrm{dE}_2}{\mathrm{d}t} = k_2[\mathrm{E}_1]\,[\mathrm{M}] \tag{8}$$

A new variable, defined by relation (9), should be introduced for solving this system of differential equations :

$$\lambda = \int_{t_0}^{t_i} [\mathrm{M}]\ \mathrm{d}t \tag{9}$$

After combination of expression (9) with relations (5—8) and integration, the following is obtained :

$$[\mathrm{M}_i] = [\mathrm{M}_0] - 2[\mathrm{G}_0] + \frac{2k_2 - k_1}{k_2 - k_1}\cdot[\mathrm{G}_0]\cdot \mathrm{e}^{-k_1\lambda_i} - \frac{k_1}{k_2 - k_1}[\mathrm{G}_0]\cdot \mathrm{e}^{-k_2\lambda_i} \tag{10}$$

$$[\mathrm{G}] = [\mathrm{G_0}]\cdot \mathrm{e}^{-k_1\lambda_i} \tag{11}$$

$$[\mathrm{E_1}] = \frac{k_1}{k_2 - k_1}[\mathrm{G_0}]\,(\mathrm{e}^{-k_1\lambda_i} - \mathrm{e}^{-k_2\lambda_i}) \tag{12}$$

$$[\mathrm{E_2}] = [\mathrm{G_0}] - \frac{k_2}{k_2 - k_1}\cdot[\mathrm{G_0}]\cdot \mathrm{e}^{-k_1\lambda_i} + \frac{k_1}{k_2 - k_1}\cdot[\mathrm{G_0}]\cdot \mathrm{e}^{-k_2\lambda_i} \tag{13}$$

The kinetic treatment presented enables the calculation of the composition of the reaction mixture in time, if the values of the rate constants k_1 and k_2 are known.

The determination of the kinetic constants belongs to the general category of estimating the problems of the process parameters.[2]

Thus, by developing the experiments so that $[\mathrm{M_0}] = 5[\mathrm{G_0}]$, relation (10) becomes:

$$[\mathrm{M}_i] = [\mathrm{G_0}]\left[3 + \frac{2k_2 - k_1}{k_2 - k_1}\cdot \mathrm{e}^{-k_1\lambda_i} - \frac{k_1}{k_2 - k_1}\cdot \mathrm{e}^{-k_2\lambda_i}\right] \tag{14}$$

$[\mathrm{M}_i]$ values are experimentally determined at successive moments of the reaction, t_i, $i = 1, 2, \ldots$ NPE (NPE = number of experimental points).

By the numerical integration of function $M = f(t)$,[3] the values of parameter λ are obtained and constants k_1 and k_2 are determined from the experimental data, using relations (9) and (14) (inverse problem in the kinetics of elementary reactions).

A system of nonlinear algebraic equations, oversized in k_1 and k_2, is thus obtained, as defined by relation (15)

$$f_i(k_1,\ k_2) = [\mathrm{G_0}]\left[3 + \frac{2k_2 - k_1}{k_2 - k_1}\cdot \mathrm{e}^{-k_1\lambda_i} - \frac{k_1}{k_2 - k_1}\cdot \mathrm{e}^{-k_2\lambda_i}\right] - \mathrm{M}_i = 0 \tag{15}$$

In the general case these systems are inconsistent and that is why the solution must be obtained by the least square method,[4] a fact determining vector $\boldsymbol{k} = (k_1,\ k_2)^T$, that minimizes

$$H(k_1,\ k_2) = //\boldsymbol{f}(\boldsymbol{k})//^2 \tag{16}$$

where $//x// = \sqrt{\langle x,\ x\rangle}$ is the Euclidean norm.

Therefore, the problem of solving the system of nonlinear equations (15) is transformed into the equivalent problem[5] of nonlinear programming:

$$\min_{k_1,\ k_2} H(k_1,\ k_2) \tag{17}$$

with restrictions $k_1 > 0$, $k_2 > 0$

The problem with restriction (17) is transformed into a problem of nonlinear programming without restrictions

$$\min_{k_1^*,\, k_2^*} H^*(k_1^*,\, k_2^*) \tag{18}$$

by transforming the independent variables[6]

$$k_i = e_i + (u_i - e_i)\cdot \frac{e^{k_i^*}}{e^{k_i^*} + e^{-k_i^*}}\,, \quad i = 1{,}2 \tag{19}$$

where : e_i — lower limit for variable i

u_i — upper limit for variable i.

The minimum of the function in comparison with variable k_1^* was objectively calculated after operating these transformations.

The above-mentioned transformations do not introduce additional local minima owing to the fact that if any point k_1^* is transformed into k_i, then the vicinity of k_1^* in space k^* is transformed into a vicinity of k_i in space k.

The problem of nonlinear programming (18) was solved by using Davidon–Fletcher Powell algorithms[7,8] and Fletcher–Reeves algorithms[9,10] which are stronger[11] than the usual ones used for solving the least square problems[12–15] and have an increased convergence rate.

The results obtained for the values of the rate constants, k_1 and k_2, are given in table 1.

TABLE 1

The values k_1 and k_2 for the transesterification of methyl-methacrylate with polyglycols

Polyglycol	k_1,/l.mol^{-1}.min^{-1}/		k_2/mol^{-1}.min^{-1}/	
	Calcd.	Experimental	Calcd.	Experimental
Ethylene glycol	$0.111237.10^{-2}$	$0.13427.10^{-2}$	$0.164378\cdot10^{-3}$	$0.12276\cdot10^{-3}$
Diethylene glycol	$0.123266\cdot10^{-2}$	$0.13810\cdot10^{-2}$	$0.626384\cdot10^{-3}$	—
Triethylene glycol	$0.118923\cdot10^{-2}$	$0.15313\cdot10^{-2}$	$0.105857\cdot10^{-2}$	$0.10786\cdot10^{-2}$
Tetraethylene glycol	$0.094319\cdot10^{-2}$	$0.07134\cdot10^{-2}$	$0.293565\cdot10^{-2}$	—

The values obtained by calculation were experimentally checked. Constant k_1 was determined by studying the kinetics of the transesterification process of methylmethacrylate in excess of polyglycol (molar ratio OH/MMA = 5 :1) and constant k_2 by methylmethacrylate transesterification with the respective monoester in excess of methylmethacrylate (molar ratio MMA/OH = 5 : 1). A relatively good agreement is found between the values calculated and those experimentally determined, and the checkings carried out, taking into account the material balance, show that the calculated values are more exact (Table 1).

The analysis of the way of varying the rate constants as a function of polyglycol nature shows that the value of the formation rate constant of the monoester (k_1) is approximately equal for all the polyglycols studied. On the other hand, the formation rate constant of the diester (k_2) increases from ethylene glycol to tetraethylene glycol.

A comparison between the values k_1 and k_2 for each gylcol shows that for the transesterification of methylmethacrylate with ethylene glycol and diethylene glycol, the decisive rate stage is diester formation while for tetraethylene glycol is monoester formation.

This situation is probably determined by the factors influencing the reactivity of the OH groups. For the first stage, the formation of the hydrogen bonds among the molecules of polyglycols could lead to a diminishing of the reactivity of the OH groups, but as this situation is common for all polyglycols, no considerable differences are recorded.

In the second stage, hydroxyl groups in monoester can form both intramolecular hydrogen bonds (with ethereal oxygens or carbonyl oxygen in the ester group) and intermolecular hydrogen bonds. Intra- and intermolecular hydrogen bonds achieved by ethereal oxygens must be practically identical for all monoesters. On the other hand, the strength of the intramolecular hydrogen bonds, achieved between OH groups and carbonyl oxygens in the ester groups, depends on the distance between these groups and is probably decisive for the reactivity of the hydroxyl groups.

Figure 1 shows that in the case of β-hydroxyethylmethacrylate, a cycle of 7 atoms is formed as a consequence of these hydrogen bonds. This cycle is much stabler than the cycles formed by the other monoesters, and thus the reactivity of the hydroxyl group in it is lower.

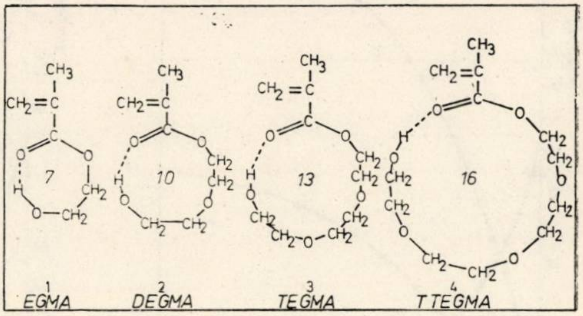

Fig. 1. — Formation of the intramolecular hydrogen bonds between OH groups and carbonyl oxygens in ester groups.

The way of varying in time the compositions of the reaction mixture was determined by relations (10—13) and the rate constants got by calculation (Fig. 2).

Figure 2 shows that for the same reaction time, significant differences exist between the compositions of the reaction mixture corresponding to the 4 systems, a fact determined by the values of the rate constants that are a measure of the reactivity of the polyglycols studied.

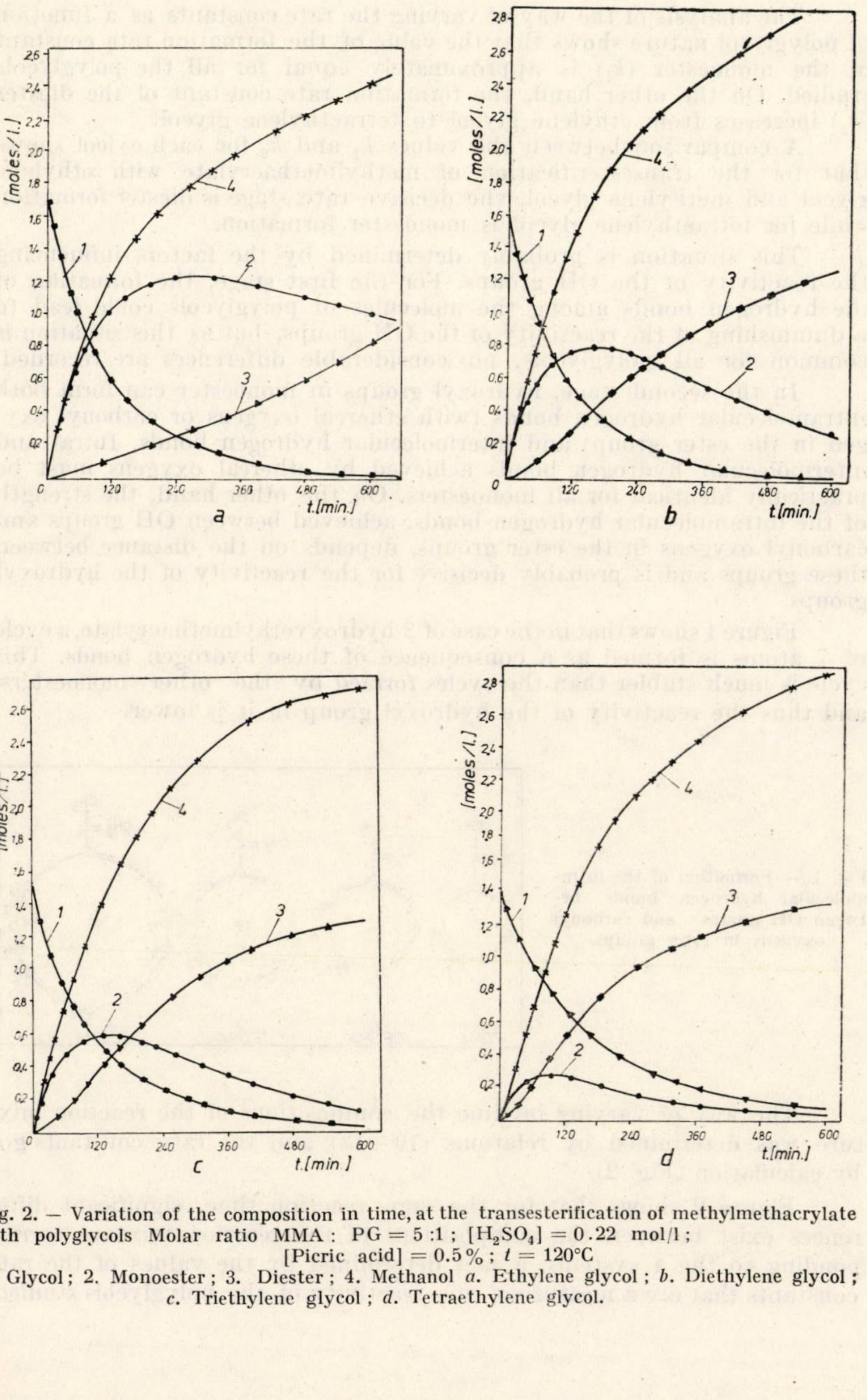

Fig. 2. — Variation of the composition in time, at the transesterification of methylmethacrylate with polyglycols Molar ratio MMA : PG = 5 :1 ; $[H_2SO_4] = 0.22$ mol/l ; [Picric acid] = 0.5 % ; $t = 120°C$

1. Glycol ; 2. Monoester ; 3. Diester ; 4. Methanol *a*. Ethylene glycol ; *b*. Diethylene glycol ; *c*. Triethylene glycol ; *d*. Tetraethylene glycol.

To underline this thing, the value of parameter λ was calculated, for which monoester reaches the highest value with relation (20) deriving from relation (12)

$$\lambda = \frac{\ln k_2/k_1}{k_2 - k_1} \tag{20}$$

The dependence of parameter λ and time at which the monoester reaches the highest value on the nature of polyglycol is presented in figure 3.

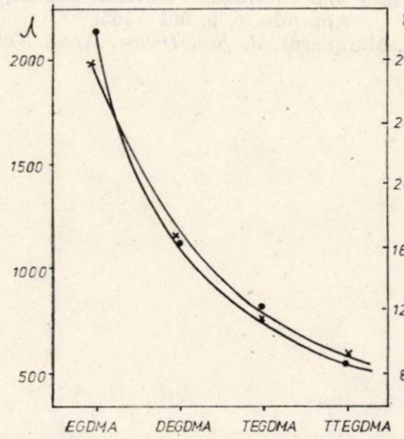

Fig. 3. — Dependence of parameter λ and time when monoester reaches the highest value as a function of polyglycol nature EGDMA = ethylene dimethacrylate, DEGDMA = diethylene glycol dimethacrylate, TEGDMA = triethylene glycol dimethacrylate, TTEGDMA = tetraethylene glycol dimethacrylate.

CONCLUSIONS

1. The study of the kinetics of the transesterification reaction of methylmethacrylate with polyglycols has shown that the rate of the formation of monoester is different from the rate of the formation of diester, therefore the reactivity of hydroxyl groups in polyglycols differs from the reactivity of the hydroxyl groups in monoesters.

2. The difference between the reactivity of the hydroxyl groups in monoesters decreases with the increase of the length of polyethereal chain, a fact pointing out that the intramolecular interactions diminish to the advantage of the intermolecular ones.

3. The calculation of the rate constants for the four systems studied enabled the determination of the way in which the composition of the reaction mixture varied in time.

REFERENCES

[1] Part. I: Gh. Hubca, Cr. Oprescu, M. Tomescu and M. Dimonie, *Rev. Roumaine Chim.* **8**, 1185 (1981).
[2] P. Eykhoff, "System Identification", Wiley, New York, 1974, p. 43–49.
[3] D. Racoţi, Particular Communication.

[4] Y. Kowalik and M. R. Osborn, "Methods for Enconstrained Optimization Problems", Elsevier, New York, 1973, p. 71–80.

[5] N. Bakhvalov, "Méthodes Numériques", Mir, Moscow, 1976, p. 390–391.

[6] M. J. Box, *Computer J.*, **8**, 67 (1966).

[7] R. Fletcher and M. J. D. Powell, *Computer J.*, **6**, 163 (1963).

[8] Subroutines FMFP and DFMFP, System/360, Scientific Subroutine Package, GH 20–0205-4, IBM, New York, 1973, p. 221–225.

[9] R. Fletcher and M. Reeves, *Computer J.*, **7**, 149 (1964).

[10] C.I.I., Bibliotheque Mathématique, 3460 E 2/FR, Sous-programme Geracomin, Lonveciennes France.

[11] V. Dumitru, "Programare neliniară", Ed. Academiei, Bucharest, 1975, p. 80–97.

[12] G. H. Golub, *Numer. Math.*, **9**, 139 (1966).

[13] M. J. D. Powell, *Computer J.*, **7**, 303 (1965).

[14] E. Henley and E. Rosen, "Material and Energy Balance Computations", New York, 1969, Appendix e, p. 561–565.

[15] D. W. Marquardt, *J. Soc. Indust. Appl. Nath.*, **11**, 431 (1963).

Revue Roumaine de Chimie, 26, *9–10*, 1335–1340 (1981)

POTENTIOMETRIC STUDIES ON COMPLEXES OF SOME TRANSITION METAL IONS WITH 4,5-DIMETHYL-2-HYDROXY ACETOPHENONE AND ITS OXIME

M. MITTAL, KEEMTI LAL and S. P. GUPTA
Chemical Laboratories, D.N. College, Meerut – 250002, India

Received March 22, 1980

Protonation and stepwise stability constants of 4,5-dimethyl-2-hydroxy acetophenone, its oxime and their complexes of some bivalent cations such as Mn(II), Fe(II), Co(II), Ni(II), Cu(II), Zn(II), Cd(II), VO(II) and UO_2 (II) have been calculated at various ionic strengths (0.01 M, 0.05 M, and 0.1 M $NaClO_4$) and 30°C in 75% (V/V) dioxane-water medium by Irving and Rossotti's method. The order of the stability constant has been found to be UO_2(II) > Cu(II) > VO(II) > Zn(II) > Ni(II) > Co(II) > Fe(II) > > Mn(II) > Cd(II) which is in good agreement with the Irving and Williams order of stability of bivalent metal complexes of 3d-transition metal series. The thermodynamic stabilization energy has also been calculated by George and McClure's method.

INTRODUCTION

o-Hydroxy keto-oximes have been successfully used as spectrophotometric and gravimetric reagent for a number of transition metals.[1–5] Gupta et al.[5–7] have reported the physico-chemical studies on the chelates of substituted hydroxy acetophenones and their oximes. In continuation of our earlier studies[7], on the transition metal complexes of 4,5-dimethyl-2-hydroxy acetophenone (DMHA) and its oxime (DMHAO) we now report the stepwise stability constants of UO_2(II), VO(II), Cd(II), Zn(II), Cu(II), Ni(II), Co(II), Fe(II) and Mn(II) complexes with DMHA and DMHAO in 75% (V/V) dioxane-water at different ionic strengths (0.01, 0.05 and 0.1 M $NaClO_4$) using Calving-Bjerrum technique as applied by Irving and Rossotti.[8] Thermodynamic stabilization energy (δH) for Fe(II), Co(II), Ni(II) and Cu(II) was also calculated by George and McClure's method.

EXPERIMENTAL

The ligands were prepared as described earlier.[7] Solutions of metal ions, sodium hydroxide and perchloric acid B.D.H. (AnalaR grade) were prepared and standardized as usual.[9] Sodium perchlorate (Riedel) was used to maintain the desired ionic strengths. Dioxane was purified by the method described by Vogel.[10] An inert atmosphere was maintained by bubbling nitrogen through the solution during titration.

Systronic digital pH-meter type 335 with a sensitivity of 0.01 unit was used for pH measurements. In aquo-dioxane mixtures the pH values were corrected by the use of Van Uitert and Haas equation.[11,12]

$$- \log\ [H^+] = B + \log U_H$$

where B = pH meter reading and log U_H is the conversion factor which was obtained from the difference between the B and the theoretical value $- \log\ [H^+]$.

Procedure

The experimental procedure of Irving and Rossotti[8] was used for potentiometric titrations against standard carbonate free sodium hydroxide (0.05 M) in a nitrogen atmosphere of the following solutions :

(A) : 2.0 ml $HClO_4$ (0.05 M)
(B) : A + 10.0 ml ligand (0.01 M)
(C) : B + 2.5 ml metal ion (0.008 M).

The ionic strengths 0.01 M, 0.05 M ($NaClO_4$) were maintained by addition of appropriate sodium perchlorate solution keeping total volume 40.0 ml in 75% (V/V) dioxane.

In view of very low concentration ($\sim 10^{-3}$M) of the metal ions used in the titrations, the possibility of formation of polynuclear complexes is ruled out. The metal to ligand ratio is taken 1 :5 to fulfil the maximum co-ordination number of the metal ions. The hydrolysis effect was ignored because the complex formation takes place at a lower B values than that of hydrolysis.

Calculations

The Irving and Rossotti's method[8] was used for the calculation of formation functions such as $\bar{n}_H$, $\bar{n}$ and pL. Log K_1^H was obtained from formation curve, between $\bar{n}_H$ and pH at $\bar{n}_H = 0.05$. The value was also calculated by pointwise calulation method and least square method. The average values of log K_1^H are reported in table 1 at different ionic strengths.

The formation curves of metal complexes were obtained by plotting $\bar{n}$ vs pL. The values of $\bar{n}$ were less than 2 showing the formation of only two complexes viz 1 :1 and 1 :2 (metal : ligand) under the experimental conditions. In cases where the values of $\bar{n}$ were even less than 1.5, log K_2 was calculated by the equation :

$$\log K_1K_2 = 2\ \text{pL}\ (\bar{n} = 1.0)$$

The values of log K_1 and log K_2 were calculated by various computational methods[8] such as half-integral method, mid point method, point wise calculation and least square method. The average values are reported in table 1.

The experimental accuracy of the stepwise stability constant values can be verified by comparing the values of $\bar{n}$ found experimentally and those calculated from the equation :

$$\sum_O^N (\bar{n} - n)\, \beta_n\, [L]^n = 0$$

where, $\beta_n = K_1.K_2.K_3.K_4\ldots\ldots K_n$; and $\beta_{0=1}$.
The difference between $\bar{n}$ (exp.) and $\bar{n}_{(cal.)}$ is found to be smaller than 8% in most of the cases.

RESULTS AND DISCUSSION

Kamat and Datar[13] obtained log K_1^H value 11.85 for *o*-hydroxy acet ophenone (HA) in 75% dioxane at ionic strength 0.1 M $NaClO_4$ at 30°C. Log K_1^H value 12.18 for DMHA is slightly higher than 11.85 for HA that may be due to the substitution with methyl groups at 4 and 5

TABLE 1

Stepwise stability constant of DMHA and DMHAO chelates (Temp. = 30°C, Dioxane = = 75%(V/V)

Cation	μ = 0.1M ($NaClO_4$)			μ = 0.05M ($NaClO_4$)			μ = 0.01 M ($NaClO_4$)		
	log K_1	log K_2	log β_n	log K_1	log K_2	log β_n	log K_1	log K_2	log β_n
	4,5-Dimethyl-2-hydroxy acetophenone (DMHA)								
H(I)	12.18	—	12.18	12.36	—	12.36	12.53	—	12.53
UO_2(II)	9.09	7.80	16.89	9.21	7.86	17.07	9.37	7.90	17.27
Cu(II)	8.50	6.70	15.20	8.58	6.75	15.33	8.69	6.90	15.59
VO(II)	7.54	6.06	13.60	7.64	6.16	13.80	7.92	6.28	14.20
Zn(II)	7.10	—	7.10	7.24	—	7.24	7.48	—	7.48
Ni(II)	6.27	5.03	11.30	6.31	5.09	11.40	6.55	5.15	11.70
Co(II)	5.79	4.20	9.99	5.83	4.37	10.20	6.13	4.47	10.60
Fe(II)	5.13	4.07	9.20	5.28	4.12	9.40	5.41	4.29	9.70
Mn(II)	4.64	—	4.64	4.66	—	4.66	4.85	—	4.85
Cd(II)	4.20	—	4.20	4.34	—	4.34	4.53	—	4.53
	4,5-Dimethyl-2-hydroxy acetophenone oxime (DMHAO)								
H(I)	10.76	—	10.76	10.87	—	10.87	11.12	—	11.12
UO_2(II)	11.76	10.17	21.93	11.82	10.27	22.09	12.00	10.35	22.35
Cu(II)	11.21	9.18	20.39	11.34	9.30	20.64	11.63	9.34	20.97
VO(II)	10.29	9.04	19.33	10.49	9.11	19.60	10.66	9.22	19.88
Zn(II)	9.93	8.61	18.54	10.07	8.65	18.72	10.31	8.69	19.00
Ni(II)	8.56	7.59	16.15	8.64	7.64	16.28	8.83	7.81	16.64
Co(II)	7.66	6.67	14.33	7.80	6.71	14.51	8.02	6.84	14.86
Fe(II)	7.30	6.11	13.41	7.36	6.19	13.55	7.58	6.31	13.89
Mn(II)	6.39	5.51	11.90	6.50	5.64	12.14	6.69	5.74	12.43
Cd(II)	5.59	4.72	10.31	5.72	4.77	10.49	5.83	4.88	10.71

positions in benzene ring. This effect is small due to the large distance from phenolic—OH group. The log K_1^H value 10.76 for DMHAO is still lower than DMHA. This may be due to the weaker hydrogen bond between hydrogen of the phenolic —OH and nitrogen of the oximino group than the hydrogen of the phenolic OH and the oxygen if the ketonic group. Consequently the release of the phenolic hydrogen of the oxime is facilitated.

The average values of log K_1 and log K_2 are reported in table 1. The order of stability constant is UO_2(II) > Cu(II) > VO(II) > Zn(II) > > Ni(II) > Co(II) > Fe(II) > Mn(II) > Cd(II), which is in agreement with Irving and Williams[14] order (Zn(II) < Cu(II) > Ni(II) > Co(II) > > Fe(II) > Mn(II)). The complexes of copper are found to be relatively more stable than those of nickel and zinc. This might be due to the difference in the configuration of copper complexes from those of nickel and zinc complexes. Probably the copper forms square planar complexes while nickel and zinc form tetrahedral or preferably octahedral complexes. The higher values of log K_1 for Zn(II) chelates as compared to those for Ni(II) chelates may be due to the greater M—L π-interaction between the π-orbital of Zn(II) and the ligands.

EFFECT OF IONIC STRENGTH

The values of log β_2 in Table 1 suggest that with an increase in the ionic strength of the medium, the value of log β_2 decreases. The relationship between activity coefficient of an ion and the ionic strength (μ) according to Hückel[14] for concentrations of 0.01 and higher is given below :

$$-\ln \gamma i = \frac{Zi^2\ \alpha\mu^{i/2}}{1+\beta_{ai}\mu^{1/2}} - b_i\mu$$

showing that the activity of the metal ion for its interaction with other molecular species decreases with the increase of the μ of the medium under study. Thus, the increasing μ of the medium decreases the formation constant of the transition metal ion complexes with both the ligands. These observations are in agreement with the finding of Debye.[16]

The thermodynamic stability constant was obtained by extrapolation of the plots of log β_n vs$\mu^{1/2}$ to zero ionic strength.[17] The values of log β_2^0 and change in free energy ($-\Delta G^\circ$ kcal mole^{-2}) at zero ionic strength were evaluated by usual expression at 30°C and reported in table 2.

TABLE 2

Thermodynamic formation constants δH and free energies (kcal mole^{-1}) of metal chelates of DMHA and DMHAO at 30°C

Cation	DMHA			DMHAO		
	log K°	$-\Delta G^\circ$	δH	log K°	$-\Delta G^\circ$	δH
H(I)	12.70	17.63	—	11.30	15.69	—
UO_2(II)	17.55	24.37	—	22.60	31.38	—
Cu(II)	15.80	21.94	26.75	21.30	29.58	26.88
VO(II)	14.45	20.06	—	20.15	27.98	—
Zn(II)	7.70	10.69	—	19.25	26.73	—
Ni(II)	11.90	16.52	34.00	16.90	23.47	33.75
Co(II)	11.00	15.27	24.52	15.15	21.04	24.04
Fe(II)	9.90	13.75	16.65	14.15	19.65	16.13
Mn(II)	4.95	6.87	—	12.70	17.63	—
Cd(II)	4.70	6.53	—	11.00	15.27	—

The thermodynamic stabilization energy (δH) for Fe(II), Co(II), Ni(II), and Cu(II) was calculated from log K_1^0 values by George and McClure's method,[18] the Er (Mn−Zn) values found to be 50.66, and 52.03 for DMHA and DMHAO respectively. The values are of the same order for the ligand having co-ordination through oxygen and nitrogen atoms.

This fact is further supported by a slight shift in the curve of ΔH_L (heat or complexation) as compared to the curve of ΔH_H (heat of hydration of the metal ion) against atomic number. The straight line joining Mn(II) and Zn(II) represents the situation in the absence of crystal field stabilization.

ACKNOWLEDGEMENT : One of the authors (M.M.) wish to express her thanks to U.G.C., New Delhi (India) for awarding Teacher's Fellowship.

REFERENCES

[1] S. N. Poddar, *Z. analyt. Chem.*, **154**, 254 (1957); **155**, 327 (1957); *Analyt. Chim. Acta.*, **28**, 586(1963); *Indian J. Chem.*, **1**, 496, 537 (1963).

[2] S. Prakash, Y. Dutt and R. P. Singh, *Indian J. Chem.*, **6**, 664 (1968).

[3] B. D. Gupta and W.U. Malik, *Indian J. Chem.*, **7**, 724, 922 (1969).

[4] J. R. Shah and R. P. Patel, *J. Indian Chem. Soc.*, **48**, 169, 1177 (1971).

[5] K. Lal and S. P. Gupta, *Curr. Sci.*, **44**, 178, 652 (1975); *Indian J. Chem.*, **13**, 297, 973 (1975), *Rev. Chem. (București)*, **27**,657 (1976).

[6] K. Lal, J. Singh and S. P. Gupta, *J. Inorg. Nuclear Chem.*, **40**, 359 (1978); *Acta Chim. Acad. Sci. Hung.*, **95**, 233 (1977); *Chim. Acta. Turcica*, **6**, 11 (1978).

[7] (Mrs) M. Mittal, K. Lal and S. P. Gupta, *Metals and Min. Review*, in press (1980).

[8] H. Irving and H. S. Rossotti, *J. Chem. Soc.*, **1953**, 3397; **1954**, 2904.

[9] A. I. Vogel, "A Text Book of Quantitative Inorganic Analysis", Longmans Green, London, 1962.

[10] A. I. Vogel, "A Text Book of Practical Organic Chemistry", Longmans Green, London, 1956, 177.

[11] L. G. Van Uitert and C. G. Hass, *J. Amer. Chem. Soc.*, **75**, 451 (1953).

[12] K. Lal, *Talanta*, **26**, 1171 (1979).

[13] P. V. Kamat and M. G. Datar, *J. Indian Chem. Soc.*, **47**, 409 (1970).

[14] H. Irving and R.J.P. Williams, *J. Chem. Soc.*, **1953**, 3192.

[15] E. Huckel, *Physik. Z.*, **26**, 93 (1925).

[16] P. Debye, *Trans. Electrochem Soc.*, **82**, 7 (1942).

[17] K. B. Yatsimirskii and V. P. Vasilev, "Instability Constants of Complex Compounds", D. Van Nostrand, London, 1966, 65.

[18] P. George and D. S. McClure, "Progress in Inorganic Chemistry", Editor F. A. Cotton, 1959, Vol. 1, 428.

REFERENCES

[1] S. N. Poddar, Z. anorg. Chem., 134, 34 (1963); 138, 137 (1963); Analyt. Chim. Acta, 30, 398 (1964); Indian J. Chem., 1, 496 (1963).

[2] S. Prakash, V. Dutt and P. P. Singh, Indian J. Chem., 6, 605 (1968).

[3] B. N. Gupta and S. L. Mathur, Indian J. Chem., 7, 124, 822 (1969).

[4] J. H. Shah and R. P. Patel, J. Indian Chem. Soc., 48, 103, 1317 (1971).

[5] K. Lal and S. P. Gupta, Curr. Sci., 41, 178, 652 (1972); Indian J. Chem., 11, 202, 273 (1973); Rev. Roum. Chim., 27, 257 (1973).

[6] K. Lal, R. Singh and S. P. Gupta, J. Inorg. Nuclear Chem., 40, 359 (1978); Bull. Acad. Pol. Sci., Chem., 25, 257 (1977); Chim. Acta Turcica, 5, 11 (1977).

[7] (Miss) M. Mittal, K. Lal and S. P. Gupta, Monatsh. Chem., in press (1980).

[8] H. Irving and H. S. Rossotti, J. Chem. Soc., 1953, 3397; 1954, 2904.

[9] A. I. Vogel, "A Text Book of Quantitative Inorganic Analysis", Longmans Green, London, 1962.

[10] A. I. Vogel, "A Text Book of Practical Organic Chemistry", Longmans Green, London, 1966.

[11] L. G. Van Uitert and C. G. Haas, J. Amer. Chem. Soc., 75, 451 (1953).

[12] K. Lal, Talanta, 20, 1178 (1973).

[13] S. V. Kamat and M. C. Dutta, J. Indian Chem. Soc., 47, 1004 (1970).

[14] H. Irving and R. J. P. Williams, J. Chem. Soc., 1953, 3192.

[15] E. Hückel, Physik. Z., 26, 93 (1925).

[16] P. Debye, Trans. Electrochem. Soc., 82, 7 (1942).

[17] K. B. Yatsimirskii and V. P. Vasil'ev, "Instability Constants of Complex Compounds", D. Van Nostrand, London, 1960, 95.

[18] P. George and D. S. McClure, "Progress in Inorganic Chemistry", Editor F. A. Cotton, 1959, Vol. 1, 381.

Revue Roumaine de Chimie, **26**, *9–10*, 1341–1342 (1981)

COMPTES RENDUS

K. VARMUZA, "Pattern Recognition in Chemistry" (Lecture Notes in Chemistry, No. 21), Springer-Verlag, Berlin, 1980, 217 pp., soft cover 35.60 DM (21.00 US $).

The topic of pattern recognition (to be abbreviated as PR) is becoming so popular that a comprehensive review for its chemical applications was timely. The book under discussion is not only the most recent and comprehensive one in this field, but probably also one of the best. By its conception, this review aims at providing both an introduction to PR methods for chemists who have no previous training in this area, and a comprehensive and exhaustive enumeration of chemical applications of PR.

The first part describes in its first chapter the basic concepts of pattern recognition. An attractive feature is a critically evaluated collection of literature sources on this topic of PR : general PR, and PR from the chemist's viewpoint. The following seven chapters describe non-exhaustively those methods which have been of most use in chemical applications. The last two chapters of the first part describe how to select features for PR, and how to evaluate classifiers for PR.

The second part of the book describes various applications of PR in chemistry. An exhaustive literature search is the avowed aim of this second part. Among the most successful applications of PR in chemical contexts one may cite : mass spectrometry, where considerable effort has been made (including publications by the author of the book), other spectroscopic methods (IR, Raman, NMR), chromatography, electrochemistry, classification of chemicals, clinical chemistry, environmental chemistry, relationships between chemical structure and biological activity. Each of the main chemical applications is treated in a separate chapter of the second part.

The 435 literature quotations are arranged alphabetically, and an author and a subject index facilitate locating any desired data.

A. T. Balaban

New Syntheses with Carbon Monoxide" (Reactivity and Structure Concepts in Organic Chemistry, No. 11), edited by J. FALBE, Springer-Verlag, Berlin, 1980, 465 pp.

More than ten years ago, Dr. J. Falbe had written for Springer a smaller book, "Carbon Monoxide in Organic Synthesis" (German version, 1967 ; English version, 1970). The present book edited by him, totally in English, contains the following chapters which update and complete the previous monograph (in order, the author(s), the title of the chapter, the number of pages and of references are indicated) :

1. Hydroformylation ; oxo reaction, Roelen reaction, by B. Cornils, 180 pp., 1970 refs.
2. Homologation of alcohols, by H. Bahrmann and B. Cornils, 15 pp., 77 refs.
3. Carbonylations catalyzed by metal carbonyls — Reppe reactions, by A. Mullen, 60 pp., 289 refs.
4. Hydrogenation of carbon monoxide, by C. Frohning, 60 pp., 262 refs.
5. Koch reactions, by H. Bahrmann, 35 pp., 221 refs.
6. Ring closure reactions with carbon monoxide, by A. Mullen, 25 pp., 96 refs.

The book has a detailed subject index.

In the context of the oil crisis, the chemistry of coal and of carbon monoxide has an all-pervading importance. The Fischer—Tropsch synthesis of alkanes, the Roelen reaction (oxo synthesis, i.e. the hydroformylation of alkanes to alkanols) and in a smaller measure the Koch reaction (synthesis of tertiary acids from alkenes and carbon monoxide in the presence of Brönsted acids, but also, as it had been prefigurated in Germany and Romania in 1930—1960, in the presence of Lewis acids) as well as the methanol synthesis (which is not covered in the volume discussed here) are economically important processes. Both the scientific and the technological aspects are well balanced in all chapters. Even economical data are present in every chapter of the book.

For all chemists and technologists interested in all features of these technologically important reactions of carbon monoxide, this book is an invaluable source of information, since it discusses critically and systematically all relevant literature data of the latest years. As already indicated, many chapters have hundreds, and one chapter has almost 2000, references. The quality of the printing and the clarity of formulae and diagrams are excellent.

A. T. Balaban

WING-SUM TSANG and G. W. GRIFFIN, "Metabolic Activation of Polynuclear Aromatic Hydrocarbons", Pergamon Press, Oxford, 1979, hard-cover edition 16.00 pounds, 125 pp.

The book is a brief, but very well documented and comprehensive review for the mode of action of the most important class of chemical carcinogens. Polycyclic aromatic hydrocarbons (to be abbreviated as PAH's) were the first chemical carcinogens to be discovered owing to their fluorescence as the cause of tar-induced skin cancer. It took almost fifty years to understand the chemical processes responsible for their action. Ironically, it is the enzymatic system of the host cell (cytochrome P and epoxide hydrase) which converts a restricted class of PAH's into potent carcinogens.

The book discusses in detail the recent results of chemical and biochemical research concernig the fate of PAH's : most of the discussion is centered around benzo[a]pyrene. The historical perspective is presented objectively taking into account that the manuscript was circulated to all interested parties prior to publication, and that suggestions were taken into account in the book as it now stands. The contributions of Borgen, Boyland, Sims, McCaustland and Jerina with his collaborators from the National Institutes of Health (Bethesda, Maryland, USA) are clearly delineated in elucidating the metabolic activation of PAH's.

All present chemical and biochemical data are in agreement with the "bay-region" theory of carcinogenic activity : the PAH is converted into a dihydrodiol (presumably *via* epoxidation) whose olefinic double bond is then epoxidated to a diolepoxide (alternatively, as the authors of the book intimate, the diolepoxide might be formed *via* a diepoxide). This diolepoxide seems to be the ultimate carcinogen, because it binds covalently weak nucleophiles such as guaninic amino groups. The epoxy ring of the diolepoxide, bordering the bay region, is readily opened due to anchimeric assistance of a hydroxy group placed in a sterically favourable situation so that a benzylic carbonium ion site is stabilized at the brink of the marginal benzenoid ring whose presence is a prerequisite for the bay region.

Though most data are on benzo[a]pyrene and its substituted derivatives, the data on benzo[a]anthracene and on benzo[a,h]anthracene and their derivatives also agree with the bay-region theory and with the same metabolic activation steps.

It is still not clear why the presence of a bay region is not a necessary and sufficient condition in a PAH for oncogenic activity. In fact, phenanthrene which has a bay region is non-carcinogenic, while cyclopenta [c,d] pyrene is mutagenic and carcinogenic in mice though it lacks a bay region. Also, the initiating/promoting carcinogenicities of PAH's are still incompletely understood.

The book is photoprinted after a typewritten manuscript, which made possible a speedy reproduction, so that from its 140 references many quotations dated 1978 are included. The style is highly readable. The author and subject indexes are detailed and extensive. The authors do not explain why they preferred to employ the less usual Clar-type formulae in preference to the classical Kekulé-type ones.

The book is recommended as well-informed, lucid exposition of the arguments and counter-arguments which led to the present-day view on metabolic activation of PAH's. Knowing that each year in the United States alone 1300 tones of benzo[a] pyrene are formed and released into the environment from incomplete pyrolysis of organic materials, exhaust gases and tobacco smoke, this most lethal human carcinogen is at least nowadays partly understood in its mode of action, allowing the hope that some day remedies would be found against it. The book can serve both as an introductory text, and as a rich, condensed source of information and key to the voluminous primary literature.

A. T. Balaban

NOTE POUR LES AUTEURS

La Revue Roumaine de Chimie publie des articles en anglais, français, russe, allemand ou espagnol. Les auteurs sont priés d'envoyer des articles et des comptes rendus inédits.

Les manuscrits seront dactylographiés à deux intervalles. La bibliographie, les tableaux et la légende des figures seront placés après le texte.

Si l'article fait partie d'une série numérotée, la partie précédente sera donnée comme première référence.

Chaque article sera précédé d'un résumé comprenant quinze lignes au maximum.

Les références bibliographiques dans le texte seront faites par des exposants sans parenthèses et paraîtront à la fin de l'ouvrage.

Les publications périodiques mentionnées dans la bibliographie seront présentées suivant les prescriptions internationales ; le nom de l'auteur précédé de l'initiale du prénom, le titre du périodique abrégé conformément à « Chemical Abstracts » et souligné par une ligne, le numéro du tome indiqué par des chiffres arabes et souligné par deux lignes, suivi de la première page de l'article : à la fin, l'année de la parution sera placée entre parenthèses. Le numéro de la revue ne sera pas indiqué si les pages du volume sont numérotées consécutivement.

Les textes des livres ou traités incluront : les noms des auteurs, précédés de l'initiale du prénom, le titre du livre entre guillemets at sans être souligné, le numéro du tome précédé par l'abréviation « vol » (ou« Bd.»), le numéro de l'édition, les éditions (the publisher), la localité de la parution du livre, l'année de la parution et la page de la référence précédée(s) par l'abréviation «p » (ou « S »).

Les brevets seront indiqués comme suit : L'auteur ou la firme, le pays et le numéro du brevet, la date et la revue *(Chem. Abstr.)*. Par ex. : M. Jones (to Union Carbide Co.), *Brit. Pat.* 601 238, 2 Sept. 1959, *Chem. Abstr.*, **54**, 12808 (1960).

Si la référence n'a pas été lue en original, on indiquera aussi la revue de références consultée.

Les diagrammes seront tracés à l'encre de Chine sur papier calque. Les tableaux et les figures (en nombre strictement nécessaire) ainsi que les courbes dans les figures seront numérotées par des chiffres arabes. Leur explication sera donnée dans la légende des figures. Prière de ne pas inscrire les mêmes données dans les tableaux et les figures. Chaque tableau aura un titre. On indiquera dans le texte la place approximative des tableaux et des figures. Les formules chimiques seront incluses dans le texte : en outre, elle seront transcrites sur papier calque, à l'encre de Chine.

Les auteurs sont priés d'indiquer les caractères italiques (en soulignant les lettres au crayon), ainsi que tout autre caractère spécial : les préfixes *ortho*, *meta*, *para*, *cis*, *trans*, etc. seront soulignés pour indiquer leurs caractères italiques et ne seront jamais écrits avec des majuscules.

Aucune correction à la main ne sera admise sur le manuscrit. Les corrections seront frappées à la machine. Les lettres grecques ou d'autres symboles spéciaux seront insérés à la main à l'encre clairement.

Le manuscrit sera signé par l'auteur.

Le colonne-titre aura 50 lettres au maximum.

L'entière responsabilité du contenu des articles appartient aux auteurs.

Sur demande on peut obtenir un note plus complète.

PRINTED IN ROMANIA

ORSZÁGOS MŰSZAKI KÖNYVTÁR ÉS DOKUMENTÁCIÓS KÖZPONT 1988

NOTE POUR LES AUTEURS

La Revue Roumaine de Chimie publie des articles en anglais, français, russe, allemand et espagnol. Les auteurs sont priés d'envoyer des articles et des comptes rendus inédits.

Les manuscrits seront dactylographiés à deux interlignes. La bibliographie, les tableaux et légendes des figures seront placés après le texte.

Si l'article fait partie d'une série numérotée, la partie précédente sera donnée comme première référence.

Chaque article sera précédé d'un résumé contenant quinze lignes au maximum.

Les références bibliographiques dans le texte seront faites par des exposants sans parenthèses et paraîtront à la fin de l'ouvrage.

Les publications périodiques mentionnées dans la bibliographie seront présentées suivant les normes internationales : le nom de l'auteur précédé de l'initiale du prénom, le titre du périodique abrégé conformément à « Chemical Abstracts » et souligné par une ligne, le numéro du tome indiqué par des chiffres arabes et souligné par deux lignes suivi de la première page de l'article ; à la fin, l'année de la parution sera placée entre parenthèses. Le numéro de la revue ne sera pas indiqué si les pages du volume sont numérotées consécutivement.

Les titres des livres ou traités incluront : les noms des auteurs, précédés de l'initiale du prénom, le titre du livre entier souligné [illegible] sans être souligné, le numéro du tome précédé par l'abréviation vol. (par ex. vol. 2), le numéro de l'édition, les éditeurs (ou publishers), la localité de la parution du livre, l'année de la parution et la page de la référence précédée par l'abréviation « p. » (ex. « p. 5 »).

Les brevets seront indiqués comme suit : L'auteur ou le titre, le pays et le numéro du brevet, la date et la revue d'abstracts. Par ex. : M. Jones (to Union Carbide Co.), Brit. Pat. 807,224, 2 Sept. 1958 ; Chem. Abstr., 53, 12055 (1959).

Si la référence n'a pas été lue en original, on indiquera aussi la revue de références consultée.

Les diagrammes seront tracés à l'encre de Chine sur papier calque. Les tableaux et les figures [illegible] strictement nécessaires. [illegible] dans les figures seront numérotées par des chiffres arabes. Leur explication sera donnée dans la légende des figures. Éviter de ne pas inscrire les mêmes données dans les tableaux et les figures. Chaque tableau aura un titre. On indiquera dans le texte la place approximative des tableaux et des figures. Les formules chimiques seront incluses dans le texte ; si non, elles seront dessinées sur papier calque, à l'encre de Chine.

Les auteurs sont priés de marquer les caractères italiques (en soulignant les lettres du texte), ainsi que tout autre caractère spécial : les préfixes ortho, meta, para, cis, trans, etc. seront soulignés pour marquer leurs caractères italiques et ne seront jamais écrits avec des majuscules.

Aucune correction à la main ne sera admise sur le manuscrit. Les corrections seront frappées à la machine. Les lettres grecques et d'autres symboles spéciaux seront inscrits à la main à l'encre clairement.

Le manuscrit sera signé par l'auteur.

Le [illegible] sera [illegible] manuscrits.

L'entière responsabilité du contenu des articles appartient aux auteurs.

Sur demande on peut obtenir une note plus complète.

PRINTED IN ROMANIA

1982 APR 29

TRAVAUX PARUS AUX ÉDITIONS DE L'ACADÉMIE DE LA RÉPUBLIQUE SOCIALISTE DE ROUMANIE

ELENA CEAUŞESCU, **Noi cercetări în domeniul compuşilor macromoleculari** (Nouvelles recherches dans le domaine des composés macromoléculaires), 1981, p. 536.

I. G. MURGULESCU, TATIANA ONCESCU, E. SEGAL, **Introducere în chimia fizică. Vol. II.2. Cinetică chimică şi cataliză** (Introduction à la chimie physique. Vol. II.2. Cinétique chimique et catalyse), 1981, 1024 p.

V. DRĂGUŢAN, A. T. BALABAN, M. DIMONIE, **Metateza olefinelor şi polimerizarea prin deschidere de inel a cicloolefinelor** (La métathèse des oléfines et la polymérisation par ouverture annulaire des cyclooléfines), 1981, 254 p.

O. IORDACHE, **Procese polistocastice aplicate la fenomenele de transfer** (Processus polystochastiques appliqués aux phénomènes de transfert), 1981, 187 p.

CR. SIMIONESCU, VALERIA GORDUZA, **Polimeri biocompatibili şi biologic activi** (Polymères biocompatibles et biologiquement actifs), 1980, 479 p.

Ş. MOLDOVEANU, A. SAVIN, **Aplicaţii în chimie ale metodelor semiempirice de orbitali moleculari** (Applications en chimie des méthodes semi-empiriques d'orbitaux moléculaires), 1980, 286 p.

ELENA CEAUŞESCU, **Polimerizarea stereospecifică a izoprenului** (La polymérisation stéréospecifique de l'isoprène), 1979, 307 p.

M. FLORESCU, **Metode ştiinţifice în dezvoltarea industriei chimice moderne** (Méthodes scientifiques dans le développement de l'industrie chimique moderne), 1979, 256 p.

A. T. BALABAN, I. GĂLĂŢEANU, G. GEORGESCU, LIGIA SIMIONESCU, **Compuşi marcaţi şi radiofarmaceutici cu aplicaţii în medicina nucleară** (Composés marqués et radiopharmaceutiques à application en médecine nucléaire), 1979, 495 p.

CONST. GH. MACAROVICI, **Analiza chimică cantitativă anorganică** (L'Analyse chimique quantitative inorganique), 1979, 457 p.

I. G. MURGULESCU, E. SEGAL, **Introducere în chimia fizică, vol. II.1. Teoria molecular cinetică a materiei** (Introduction à la chimie physique, vol. II. 1. La théorie moléculaire-cinétique de la matière), 1979, 1036 p.

I. E. TEODORESCU, MARIA FITI, **Iradierea tehnologică** (L'Irradiation technologique), 1979, 216 p.

S. STERNBERG, FL. DANES, **Termodinamica chimică aplicată** (La thermodynamique chimique appliquée), 1978, 400 p.

I. G. MURGULESCU, V. EM. SAHINI, **Introducere în chimia fizică, Vol. I.2. Structura şi proprietăţile moleculelor** (Introduction à la chimie physique. Vol. I.2. La structure et les propriétés des molécules), 1978, 604 p.

C. DRĂGULESCU, E. PETROVICI. **Chimie structurală modernă. Chimia coordinanţei 8** (La chimie structurale moderne. La chimie de la coordinence 8), 1977, 947 p.

D. PURDELA (sous la direction de), **Nomenclatura chimiei anorganice** (La nomenclature de la chimie inorganique), 1977, 153 p.

I. ZUGRĂVESCU, MAGDA PETROVANU, **N-ylid chemistry**, coédition avec McGraw-Hill International Book Company, U.S.A., 1977, 396 p.

I. G. MURGULESCU, **Introducere în chimia fizică. Vol. I.1. Atomi, molecule, legătură chimică** (Introduction à la chimie physique. Vol.I. 1. Atomes, molécules, liaison chimique), 1976, 560 p.

CONST. GH. MACAROVICI, D. MACAROVICI, **Chimia oxizilor dubli şi utilizările lor** (La chimie des oxydes doubles et leur utilisation), 1975, 195 p.

ELENA CEAUŞESCU, **Research work on synthesis and characterization of macromolecular compounds, Contributions**, 1974, 251 p.

CR. SIMIONESCU, VIORICA RUSAN, V. POPA, **Chimia algelor marine** (La chimie des algues marines), 1974, 212 p., 1 pl.

I. P. INFORMAŢIA c. 1311

43 426

Lei 25

$ 55 (pour un abonnement annuel)

F1103

ACADÉMIE DE LA RÉPUBLIQUE SOCIALISTE DE ROUMANIE

REFERÁLVA!

R

REVUE ROUMAINE DE CHIMIE

TOME 26

N°s 11–12

Novembre—Décembre 1981

EDITURA ACADEMIEI REPUBLICII SOCIALISTE ROMÂNIA

Rev. Roumaine Chim.

RRCHAX **26**, *11–12*, p. 1343–1522 (1981), Bucarest

ACADÉMIE DE LA RÉPUBLIQUE SOCIALISTE DE ROUMANIE

COMITÉ DÉ RÉDACTION

Rédacteur en chef :

I. G. MURGULESCU, membre de l'Académie de la République Socialiste de Roumanie

Rédacteur en chef adjoints :

A. T. BALABAN et V. EM. SAHINI, membres correspondants de l'Académie de la République Socialiste de Roumanie

Collège de rédaction :

EM. BRATU, ELENA CEAUŞESCU, ECATERINA CIORĂNESCU-NENITZESCU, CR. SIMIONESCU, membres de l'Académie de la République Socialiste de Roumanie ; P. SPACU, membre correspondant de l'Académie de la République Socialiste de Roumanie; MARGARETA AVRAM, M. BANCIU, I. HAIDUC, D. I. MARCHIDAN, I. MOLDOVAN, G. NIAC et D. SĂNDULESCU

La Revue Roumaine de Chimie parait 10 fois par an. Toute commande de l'étranger pour les travaux parus aux Editions de l'Académie de la République Socialiste de Roumanie sera adressée à ILEXIM,— Departamentul Export-Import Carte (Livres)/Departamentul Export-Import Presă (Revues) P.O.B. 136—137, télex 11226, 3, str. 13 Decembrie, 79517 Bucarest, Roumanie

Les manuscrits, les livres et les revues proposés en échange, ainsi que toute correspondance seront envoyés à la rédaction :

REVUE ROUMAINE DE CHIMIE

Calea Victoriei 125, 79717 Bucarest, Roumanie, téléphone 50 76 80

EDITURA ACADEMIEI REPUBLICII SOCIALISTE ROMÂNIA
125 Calea Victoriei, 79717 Bucarest, Roumanie, téléphone 50 76 80

REVUE ROUMAINE DE CHIMIE

ORSZÁGOS MŰSZAKI KÖNYVTÁR ÉS DOKUMENTÁCIÓS KÖZPONT 1983

Tome 26, N°s 11—12 **Novembre—Décembre, 1981**

E. CHIFU, Z. FINTA, M. SALAJAN and EUGENIA GAVRILĂ, Surface mobility of surfactant solutions. IX. Surface and capillary flow between drops linked by surface canals. . . . . 1345—1354

RODICA VÎLCU, A. CIOCHINĂ and GH. VASU, Absolute measurement of thermal conductivity of emulsions . . . . 1355—1364 R

D. GEANĂ and F. DANEŞ, An analysis of the effect of input data changes on the chemical equilibrium composition . . . . 1365—1376

F. DANEŞ, S. STERNBERG and SILVIA DANEŞ, An extension of the Staverman/Scatchard thermodynamic theory of membrane potential (in French) 1377—1386

IOANA DEMETRESCU and D. FĂTU, X-ray analysis of some carbon fibres 1387—1391

O. BUNESCU, P. ROTARU and S. I. BLEJOIU, Electrical conduction in nickel—alumina catalyst . . . . 1393—1399 R

R. P. VARMA and SMT. S. SHUKLA, Solubility of iron(III) carboxylate in mixed organic solvents . . . . 1401—1404 R

V. MACOVEI, Spectral solvent effects in aromatic compound solutions. VII. Solvent effects on the benzonitrile band at ~260 nm . . . . 1405—1412

F. Y. EL-KADY, Comparison between the hydrocracking activity of cobalt—molybdenum/alumina and nickel—molybdenum/alumina catalysts . . . 1413—1422 C

M. M. GIRGIS, D. P. LAZĂR and E. I. SEGAL, Catalytic oxidation of ammonia. III. Low temperature oxidation on a $Fe_2O_3-Cr_2O_3$ catalyst; evaluation of the experimental data in order to obtain kinetic parameters 1423—1429

ARUN SYAMAL and PRADIP K. MANDAL, New cobalt(III) complexes containing trimethylenediamine, propylenediamine and other ligands . . . 1431—1439 R

I. SILAGHI-DUMITRESCU, A simple topology-based method for estimating stretching force constants in AB_n molecules . . . . 1441—1445 R

S. CHORBADJIEV, Synthesis of medium and higher dialkyl disulphides . . . 1447—1450 R

M. CONSTANTINESCU, GH. SURPĂŢEANU, CRISTINA LUCHIAN, MAGDA PETROVANU and I. ZUGRĂVESCU, Theoretical aspects on the regioselectivity in the 1,3-dipolar cycloadditions of pyridinium—ylides to acetylenic dipolarophiles . . . . 1451—1456

S. D. SARAF, Reaction of thionyl bromide with thiophenols . . . . 1457—1459 B C

M. IOVU and EMANUELA IONESCU, N,N′-substituted trinitrophenylene diamines . . . . 1461—1467

M. ANWAR, F. I. ABDEL-HAY, A. A. ELBARBARY and M. El-BORAI, Some reactions of 4-chloro-quinazoline, 6-nitro- and 6-amino-4-3H-quinazolones . . . . 1469—1478

N. LUCHIAN, AGLAIA CIOBANU and M. BOSTAN, Cyclic organosilicon compounds. II. Reaction of 1,4-dilithium-1,1,4,4-tetraphenylbutane with organotrichlorosilanes 1479–1485

MARIA MIOȘCU, IOVANCA HAIDUC and D. C. CÖRMÖS, Potentiometric determination of L-alanine, L-serine, tyrosine and histidine with a Cu^{2+} sensitive electrode 1487–1491

GH. HUBCA, CR. OPRESCU and M. DIMONIE, Synthesis and polymerization of polyethylene glycol dimethacrylates. III. Analysis of kinetic data obtained by transesterification of methyl methacrylate with polyglycols 1493–1497

BOOK REVIEW 1499–1500

AUTHOR INDEX 1501–1513

SUBJECT INDEX 1515–1522

Revue Roumaine de Chimie, **26**, *11–12*, 1345–1354 (1981)

SURFACE MOBILITY OF SURFACTANT SOLUTIONS. IX[1]

SURFACE AND CAPILLARY FLOW BETWEEN DROPS LINKED BY SURFACE CANALS

E. CHIFU, Z. FINTA, M. SĂLĂJAN and EUGENIA GAVRILĂ
Department of Physical Chemistry, "Babeş-Bolyai" University,
Str. Arany J. 11, 3400 Cluj-Napoca, România

Received April 14, 1981

An experimental study is presented on the liquid flow between two drops found at neutral buoyancy (or at zero gravity) and linked by surface canal–slits. The flow is caused by the simultaneous action of the surface tension gradients (surface flow – Marangoni effect) and of the capillary pressure differences (capillary flow). The contribution of these two types of flow to the liquid transfer between the two drops is rendered evident.

INTRODUCTION

In a series of previous papers we have studied, theoretically and experimentally, the flow of surfactant solutions, caused by surface tension gradients, through "surface canal-slits" joining two plane liquid / gas interfaces.[1,7] This surface flow – the so-called Marangoni effect – acquires a major importance in the absence of weight;[2-3] the motivation consists in the fact that, at zero gravity, the only type of forces which act upon the liquids, determining their behaviour, are the intermolecular forces, exhibited in the surface tension.[4]

Yet, in zero gravity conditions, the equilibrium shape of the free liquid surfaces is the spherical, which requires the modelling of the above phenomenon as a surface flow through a canal joining two spherical liquid / gas interfaces (drops, see Figure 1).

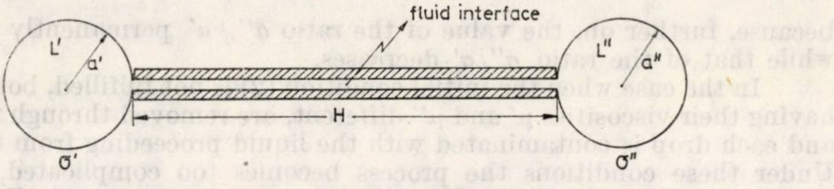

Fig. 1. – Model of the flow between two spherical liquid / gas interfaces linked by a surface canal – slit.

The analysis of this model leads to the conclusion that, if the surface tensions σ′ and σ″ of the two liquids L′ and L″ are different, there are two factors determining the motion of the liquid through the canal :

1. The surface tension difference $\sigma'' - \sigma'$ which causes the *surface flow* of the liquid from the drop having the lower surface tension to that with the higher one. Due to the finite value of the viscosity, this surface flow will be accompanied by a bulk flow, because adjacent liquid layers are carried by the surface layer removed under the action of the surface tension gradient.

2. The difference between the capillary pressures

$$p'' - p' = 2\,\sigma''/a'' - 2\sigma'/a' \tag{1}$$

which appear inside the two drops of radii a' and a'' due to the spherical shape of their surface; this difference determines a motion of the liquid through the whole section of the canal. In the following, this type of flow will be called *capillary flow*.

The theoretical treatment of the above-presented model constitutes the subject of some forthcoming papers. The aim of this preliminary work is to experimentally illustrate the described phenomenon, and to prove our hypothesis concerning the role of the two factors in the overall flow process.

The flow between two spherical liquid / gas interfaces cannot be experimentally performed under the conditions of terrestrial gravity. The behaviour of the liquids at zero gravity can be, however, approximated by simulating the zero gravity conditions with the aid of immiscible liquids of equal densities. It is obvious that in this case the interface will be a liquid / liquid one, and the model presented in Figure 1 will be experimentally achieved by immersing the entire system (the canal and the drops L′ and L″) in a third liquid L‴ (the continuous phase) immiscible with L′ and L″. The densities of the three liquids must be the same.

In the interpretation of the experimental data it will be necessary to take into account that the two above-described flow types may occur either in parallels or oppositely. Therefore, if $\sigma'' > \sigma'$, the direction of the surface flow will be always L′→ L″, as it results from the nature of the Marangoni effect. In this case, the condition for a capillary flow to be parallel with the surface flow is that $p' > p''$ all along the process. This condition will be fulfilled if at the initial moment we have

$$\sigma'/a' > \sigma''/a'', \text{ or } a''/a' > \sigma''/\sigma', \tag{2}$$

because, further on, the value of the ratio a'' / a' permanently increases while that of the ratio σ''/σ' decreases.

In the case when the initial condition (2) is not fulfilled, both liquids, having their viscosities μ' and μ'' different, are removed through the canal, and each drop is contaminated with the liquid proceeding from the other. Under these conditions the process becomes too complicated, and the quantitative interpretation of the experimental data is practically impossible.

Taking into account the above discussion, in this work we have confined ourselves to the analysis of those cases when the two types of flow are parallel (L′ → L″); so the liquid drained through the canal is L′ with the viscosity μ' and the interfacial tension $\sigma' < \sigma''$.

EXPERIMENTAL

APPARATUS AND METHOD

The experimental device used in the study of the above-modelled phenomenon (see Figure 1) consisted of a parallelepipedic glass vessel having a capacity of 3 dm,^{3} thermostatted at 20 ± 0.1°C and filled with distilled water which made up the continuous phase L'''. The canal was immersed into the phase L''' and fixed horizontally on an Inox rod.

Before placing the two drops at the extremities of the canal, the latter was filled with the corresponding liquid, in order to evaluate as exactly as possible the beginning of the flow, as well as the volume of the drops during the process. The drops L' and L'' were placed at the extremities of the canal by pipetting, and fixed in their correct position by adhesion to the liquid column existing in the canal.

The drain of the liquid was followed by measuring the radius of the smaller drop, with a horizontal catetometer (precision : 10^{-2} cm), in time.

The surface canal—slit used in this study had an equilateral triangular section with a height $\delta = 10^{-1}$ cm, the base of the triangle being marked by the L'/L''' interface on which the interfacial tension gradient was acting. In the conception of this canal the wetting properties of the used materials were taken into account. Therefore, the proper body (the solid walls) of the canal was made up of a hydrophobic material perfectly wetted by the liquids L' and L'', but limited by hydrophilic surfaces destined to hinder the overflow of these organic liquids and to assure a well-defined meniscus. Besides, the canal was equipped at its extremities with two hydrophilic barriers for maintaining the drops L' and L'' in their position, because in the absence of these barriers the drops tended to lay along the liquid/liquid interface. However, the barriers were open beyond the free surface of the canal, in order not to disturb the contact between the drop and the liquid in the canal. A sketch of the canal described above is presented in Figure 2.

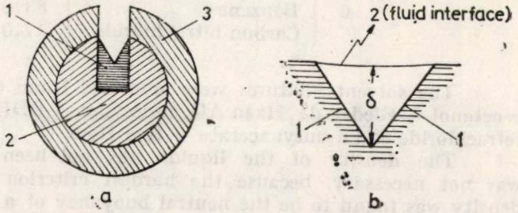

Fig. 2. — *a* — Transversal section of the canal body, at an extremity. *1* — Teflon, *2* — Inox steel, *3* — Inox barrier.
b — Transversal section of the canal. *1* — solid walls, *2* — L'/L''' interface, δ — height of the triangular section.

As a choosing criterion for the suitable materials, the value of the contact angle (at advance) at the interface between water and some representative organic solvents as components of the drops L' and L'' was considered. These values were determined by using the tilting plate method,[5] and some of them are presented in table 1. On the basis of these data,

TABLE 1

Contact angles (at advance) of various solid surfaces at the water / organic solvent interface, at 20°C

Interface	Contact angle		
	Glass	Inox steel	Teflon
Water / n-Octanol	65°	105°	145°
Water / Carbon tetrachloride	25°	45°	125°

and taking also into account the technical properties of the tested materials, a Teflon canal with Inox borders and terminal barriers has been conceived and manufactured.

THE L′/L″ LIQUID SYSTEMS

The L′/L″ systems were obtained by an adequate pairing of the solvents listed in table 2. These pairs of liquids do mix, but they are practically immiscible with water, and their density ρ is equal to that of the water at 20°C.

TABLE 2

Solvent mixtures equidense with water at 20°C ($\rho = 0.998$ g cm^{-3}), used for achieving the L′ / L″ liquid systems

Liquid	Composition	% vol.	μ, poise	σ, dyn. cm^{-1}
1	n-Octanol Carbon tetrachloride	77.4 22.6	0.0498	10.4 ± 0.1
2	n-Heptanol Nitrobenzene	53.1 46.9	0.0286	10.2 ± 0.1
3	n-Decanol Nitrobenzene	54.3 45.7	0.0429	12.3 ± 0.2
4	n-Butyl acetate Carbon tetrachloride	82.8 17.2	0.0079	16.5 ± 0.1
5	Toluene Nitrobenzene	61.4 38.6	0.0091	23.6 ± 0.2
6	Benzene Carbon tetrachloride	83.0 17.0	0.0070	34.9 ± 0.2

The solvent mixtures were obtained from analytical grade reagents: n-heptanol and n-octanol — Riedel de Haën AG, n-decanol — BDH, benzene, toluene, nitrobenzene, carbon tetrachloride and n-butyl acetate — Reactivul.

The density of the liquids has not been determined by direct measurements. This was not necessary, because the hardest criterion for establishing and controlling the equidensity was found to be the neutral buoyancy of a drop suspended in water and having the radius large enough (circ. 0.5 cm). Thus, the density of the mixtures presented in table 2 was adjusted to that of the water at 20°C (0.998 g cm^{-3}) by carefully altering their composition until the neutral buoyancy was reached. It is important to show that in the case of bicomponent mixtures this state could be maintained for at most a few minutes; further on, the drops began to remove, due probably to the different solubility of their components in water. The composition of the mixtures, corresponding to the equidensity with water, is given in table 2.

The viscosity μ of the mixtures (1) — (6) was determined at 20 ± 0.1°C with an Ubbelhode viscometer.

The interfacial tension σ against water of the organic solvent mixtures was measured by using a capillary method proposed by Mason and Clark [6] for liquid pairs of equal densities, and tested in our previous paper.[2] A satisfactory accuracy has been obtained with capillary tubes of diameters between 0.04 and 0.09 cm (see Table 2).

RESULTS AND DISCUSSION

DETERMINATION OF THE MARANGONI SURFACE FLUX

By plotting the volume V of the liquid drained through the canal versus time, curves of the type of that presented in Figure 3 are obtained. As it results from the model described in Introduction, the overall flux at a given moment represents the sum of the surface flux Q_s and the capillary one, Q_c:

$$Q = Q_s + Q_c\,, \tag{3}$$

determined, in their turn, by the momentary value of the interfacial tension difference $\sigma'' - \sigma'$, and of the capillary pressure difference $\Delta p = p' - p''$, respectively.

As concerns the interfacial tension difference, it cannot stay invariable during the flow because the L″/L‴ interface is continuously contaminated with the liquid L′ drained through the canal. So, instead of the initial interfacial tension σ_0'', we have at the L″/L‴ interface a value $\sigma'' < \sigma_0''$ which decreases monotonously with the increasing quantity of liquid L′ drained into the drop L″; therefore, we have implicitely $\sigma'' = \sigma''(t)$. The interfacial tension σ' remains, however, invariable if the inequality (2) is valid, and equal to its initial value σ_0' at the interface L′/L‴.

In these circumstances, the analysis of the flow process along its entire road was abandoned in a first step, and the initial value of the flux defined as

$$Q_0 = (\mathrm{d}V/\mathrm{d}t)_{t\to 0} \tag{4}$$

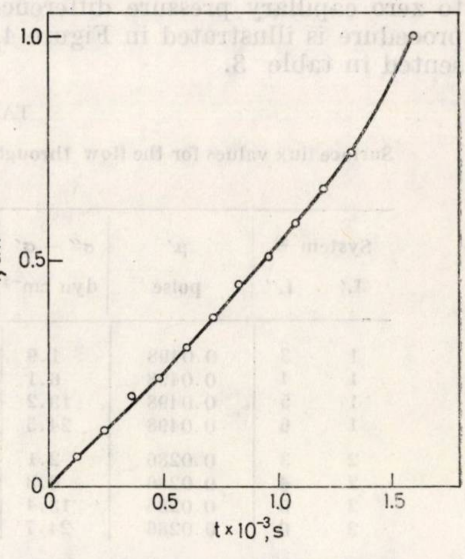

Fig. 3. — The variation in time of the liquid volume drained in the direction L′ → L″. L′ — liquid (1) in Table 2, L″ — liquid (4); the initial drop volumes: $V' = 1$ cm³, $V'' = 4$ cm³; the length of the canal: $H = 10$ cm, the height of the transversal section: $\delta = 0.1$ cm

has been estimated from the tangents at the origin of the $V(t)$ curves obtained for various initial interfacial tension differences $\sigma_0'' - \sigma_0'$. The latter values were achieved by an adequate pairing of the mixtures (1)—(6) presented in table 2, so that the liquid L′ draining through the canal could be always the same. In this way, two series of Q_0 values were obtained for two different viscosities μ' of the drained liquid. These Q_0 values were computed according to the empirical equations obtained for the $V(t)$

curves by non-linear regression based on the least squares method; the derivatives of these curves were evaluated for $t = 0$.

Yet, the obtained Q_0 values are not only dependent on the interfacial tension difference but are also influenced by the initial values of the capillary pressure difference $p_0' - p_0''$. In order to eliminate this factor, Q_0 values were calculated from experimental $V(t)$ curves obtained at various a_0''/a_0' ratios of the initial drop radii, and the Q_s value corresponding to zero capillary pressure difference was derived by extrapolation; this procedure is illustrated in Figure 4, and the obtained Q_s values are presented in table 3.

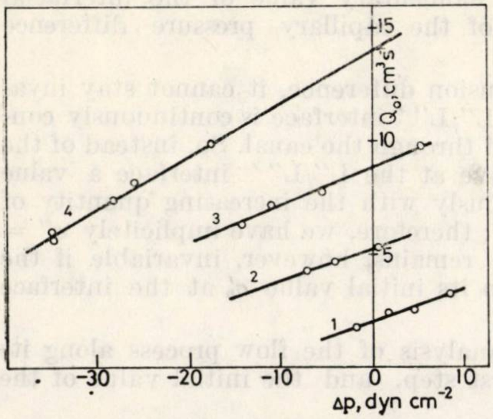

Fig. 4. — The graphical evaluation of the surface flux Q_s from the $Q_0 \times 10^4$ values of the overall flux at capillary pressure difference $\Delta p = 0$. The L′/L″ systems are: *1*—(1)/(3); *2* — (1)/(4); *3*—(1)/(5); *4* — (1)/(6).

TABLE 3

Surface flux values for the flow through a canal with H=10 cm and δ=0.1 cm, at 20°C

System [a)] L′	L″	μ′ poise	σ″ − σ′ dyn cm^{-1}	$Q_{s(\ \ )} \times 10^4$ cm^{3}s^{-1}	$Q_{s(calc)} \times 10^4$ cm^3 s^{-1}	$\frac{Q_{s(exp)}}{Q_{s(calc)}}$ %
1	3	0.0498	1.9	2.0	2.39	83
1	4	0.0498	6.1	5.2	7.67	68
1	5	0.0498	13.2	8.9	16.6	54
1	6	0.0498	24.5	14.0	30.8	45
2	3	0.0286	2.1	3.2	4.61	70
2	4	0.0286	6.3	7.4	13.8	54
2	5	0.0286	13.4	12.0	29.4	41
2	6	0.0286	24.7	18.9	54.3	35

[a)] Numbering as in Table 2

At large $\sigma_0'' - \sigma_0'$ differences, the extrapolation becomes uncertain due to the decreasing possibility of achieving a_0''/a_0' ratios close to that corresponding to zero capillary pressure difference; in this case the two flows are opposite and the viscosity of the drained liquid is indefinite. Nevertheless, in the examples presented in Figure 4 a good linearity can be still observed, which allows an extrapolation in acceptable conditions.

We think that — in the absence of a mathematical model of the studied process — the comparison of the experimental Q_s values listed in Table 3 with those calculated by the relation

$$Q_s = \frac{2\sqrt{2}(\sigma'' - \sigma')}{45\, \mu' H}\, \delta^2 \tag{5}$$

proposed in a previous paper [7] for the flow between two plane liquid / gas interfaces is meaningful, even if our data dwell on liquid/liquid interfaces.

The $Q_{s(\mathrm{calc})}$ values derived from equation (5) for the case of a canal with $H = 10$ cm and $\delta = 0.1$ cm are also included in table 3. As seen, the variation of the experimental surface flux $Q_{s(\mathrm{exp})}$ with the interfacial tension difference and with the viscosity of the liquid agrees with the qualitative picture resulting on the basis of equation (5). The quantitative agreement between the experimental and theoretical values also seems to be satisfactory (up to 80%) at low values of the flux, which are obtained at small interfacial tension differences and high viscosity of the drained liquid. With the increasing values of the surface flux the experimental data lag more and more behind of those calculated, their ratio decreasing up to 35 %. This fact may be explained — at least in part — by the stepwise leaving of the laminar flow regime with the increasing flux.

THE STUDY OF THE OVERALL FLOW

The above discussed data concerning the surface flow "isolated" from the contribution of the capillary flow can be useful in evaluating the role played by these two effects in the overall process described by the curve presented in Figure 3. In this purpose the momentary values of the interfacial tension difference $\sigma'' - \sigma'$ must be known. This value varies during the flow, as it has been shown earlier, but it can be approximated from the experimental data if the following conditions are respected :

— the liquid L′ drained through the canal is homogenized quickly enough in the bulk phase of the drop L″ ;

— the adsorption — desorption processes occurring at the (L′ + L″)/L‴ interface are sufficiently fast to ensure the establishment of an equilibrium between the homogenous (L′ + L″) bulk phase and the interface.

In these conditions, the composition of the drop L″ can be determined in any moment from the L′ liquid volume drained through the canal (which is given, in its turn, by the decrease of the radius a'), and the corresponding interfacial tension σ'' can be evaluated from the interfacial tension — composition isotherm of the (L′ + L″)/water system. In this manner, the curve presented in Figure 5 has been obtained for the time dependence of the interfacial tension σ'' during the flow process described by the curve in Figure 3.

The interfacial tension σ' being invariable, the difference $\sigma'' - \sigma'$ can be calculated in any moment of the flow, and the corresponding surface flux Q_s can be evaluated with the aid of the data listed in table 3.

Thus, on the basis of the above procedure the contribution of the surface flow to the overall process can be estimated. For the case presented in Figure 3, the surface flow is described by curve (1) in Figure 7.

The capillary flow can easily be realized in "pure state" by placing at the ends of the canal two drops of different radii, made up of the same liquid. In order to have capillary flow data corresponding to the overall flow illustrated in Figure 3, the liquid (1) (see Table 2) has been chosen for this measurement. By following the variation in time of the radius of one of the drops, the volume of the liquid drained from L′ in L″ till a given moment can be calculated, as well as the corresponding value $p = 2\sigma/a$ of the capillary pressure inside the two drops. As seen from Figure 6, the dependence of the capillary flux Q_c on the capillary pressure difference exhibits a relatively good linearity, in a sufficiently large Δp range (up to circ. 50 dyn cm^{-2}). The slope $dQ_c/d\Delta p = 1.42 \times 10^{-5}$ cm^5 dyn^{-1}s^{-1} of the obtained straight line, calculated by the least square method,

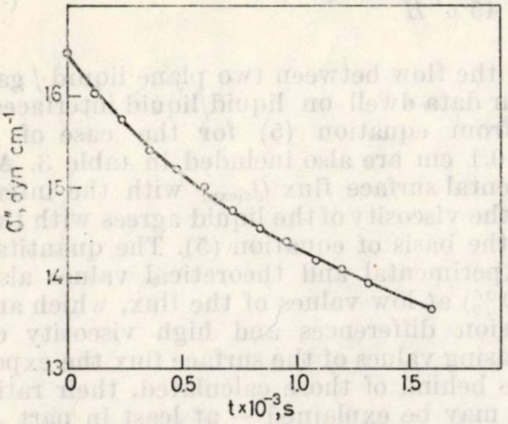

Fig. 5. — Variation of the interfacial tension σ″ at the (L′ + L″)/L″′ interface during the flow. The liquid pair: L′ liquid (1), L″ – liquid (4).

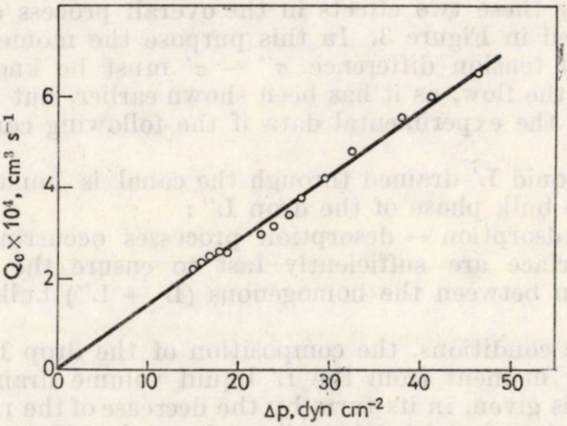

Fig. 6. — The dependence of the capillary flux Q_c on the capillary pressure difference between the drops L′ and L″. (L′ and L″ — liquid (1) in Table 2).

can be considered as an empirical parameter characterizing univocally the capillary flow of a liquid through a given canal. The importance of this fact consists in the possibility of calculating the capillary flux for any value of the capillary pressure difference situated in the linear portion of the curve in Figure 6, even if an interfacial tension difference is simultaneously established, which also influences — besides the ratio a''/a' — the capillary pressure difference $p' - p''$.

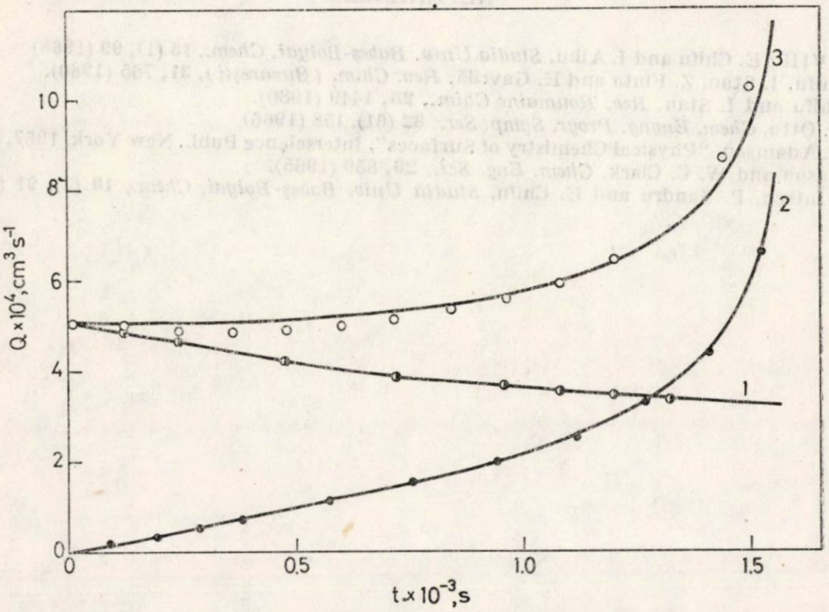

Fig. 7. — The contribution of the surface and capillary flow to the overall process, in the case of the liquid pair (1) / (4). Curve (*1*) : the surface flux ; curve (*2*) : the capillary flux ; curve (*3*) : the overall flux ($Q = Q_s + Q_c$) : the distinct points : the overall flux derived from the $V(t)$ curve in Fig. 3.

In possession of the above data, the capillary flux Q_c as a component of the overal flux Q can be evaluated, the a', a'', σ' and σ'' values being known in any moment. The variation in time of this flux for the case represented in Figure 3 is given by curve (2) in Figure 7.

Now, by setting up the sum of the Q_s and Q_c values corresponding to the same moment, given by the curves (1) and (2), the curve (3) is obtained, which—according to the model proposed—ought to give the overall flux Q derived from the $V(t)$ curve in Figure 3. By deriving this curve in various moments, the corresponding fluxes are obtained, and these are also presented in Figure 7 as separate points. As can be observed, these points fit quite satisfactorily the curve (3). This "reconstitution" of the flow process described by Figure 3 from independent data confirms our hypothesis concerning the manner in which the two effects — the interfacial tension difference $\sigma'' - \sigma'$ and the capillary pressure difference $p' - p''$ —

control the drain of the liquid through the canal. At the same time, these results also certify the good reproducibility of the experimental data reported in this paper.

REFERENCES

[1] Part VIII : E. Chifu and I. Albu, *Studia Univ. Babeş-Bolyai, Chem.*, **13** (1), 99 (1968).
[2] E. Chifu, I. Stan, Z. Finta and E. Gavrilă, *Rev. Chim. (Bucureşti)*, **31**, 765 (1980).
[3] E. Chifu and I. Stan, *Rev. Roumaine Chim.*, **25**, 1449 (1980).
[4] E. W. Otto, *Chem. Engng. Progr. Symp. Ser.*, **62** (61), 158 (1966).
[5] A. W. Adamson, "Physical Chemistry of Surfaces", Interscience Publ., New York, 1967, p. 355.
[6] G. Mason and W. C. Clark, *Chem. Eng. Sci.*, **20**, 859 (1965).
[7] R. Deutsch, P. Sandru and E. Chifu, *Studia Univ. Babeş-Bolyai, Chem.*, **10** (2), 91 (1965).

Revue Roumaine de Chimie, **26**, *11–12*, 1355–1364 (1981)

ABSOLUTE MEASUREMENT OF THERMAL CONDUCTIVITY OF EMULSIONS

RODICA VÎLCU*, A. CIOCHINĂ** and GH. VASU**

* The National Institute of Chemistry, Department of Physical Chemistry and Electrochemical Technology, Bd. Republicii 13, Bucharest, Romania

** ICECHIM, Centre of Physical Chemistry, Spl. Independenței 202, Bucharest, Romania 77208.

Received February 18, 1981

The classical procedure of the transient hot wire method for absolute measurement of thermal conductivity of electrically non-conductive liquids is extended to emulsions (electrically conductive liquids) by using a coated transducer. The theory of the method and the measuring principle of the apparatus are briefly described. Results on distilled water and seven O/W type emulsions, at 298.2 K, are presented. As estimated from both computation of phenomenological errors and comparison with the available data in the literature for thermal conductivity of distilled water as reference fluid, the accuracy of the measurements is better than 3 %.

1. INTRODUCTION

An emulsion is a heterogeneous system in which liquid droplets are distributed throughout an immiscible liquid. Estimation of the effective thermal conductivity of emulsions is frequently used by engineers in many fields, particularly in the chemical and petroleum industries, metallurgy (heat treatments, cooling and lubricating fluids), etc.

The effective thermal conductivity is a volume averaged property and its value depends upon the thermal conductivities, volume fractions and orientations of the constituent phases of the system. An expression which takes these factors into account, developed by Lal Chaurasia [1] for predicting the effective thermal conductivity of porous materials, was applied to suspensions and emulsions.

Another theoretical technique to predict the thermal conductivity of heterogeneous solid mixtures, derived by Cheng and Vachon, [2] has been applied to suspensions, emulsions and porous materials. Based on the scarce experimental data available in literature, both techniques are able to predict the values of thermal conductivity with an accuracy of 18 % for suspensions and 9 – 12 % for emulsions. A number of the other equations have also been proposed to predict thermal conductivity of emulsions. [3–11]

In our opinion, the accurate measurement remains the only alternative to both obtaining thermal conductivity values for emulsions and testing the estimation procedures. This statement is justified by the following reasons : — thermal conductivity values of the constituent phases of the emulsions are implied in all estimation methods, therefore they have to be measured ; — the calculated value of thermal conductivity for an emulsion has to be compared with the measured one ; — the literature offers only a few thermal conductivity data for emulsions and their components ; — due to the nature of components and their great variety, the emulsions represent complex heterogeneous systems with hardly predictable physicochemical proprieties ; — an estimation method for thermal conductivity generally applicable to the great variety of emulsions can not impose itself by the accuracy of the calculated values, unless these values stand the confrontation with accurate experimental data obtained on an as large as possible assortment of emulsions.

In steady state measurement methods, [12–14] reaching the steady state thermal regime is a slow process and natural convection is likely to appear within the measurement cell when temperature gradient through the liquid layer is too great.[15–18] A calculation of conditions for natural convection onset within the measurement cell can not be made because of lack in values of some physical properties of emulsions (density, viscosity, heat capacity, volumetric expansion coefficient), their temperature dependence and because of uncertainty of the Ra <1000 criterion validity (Ra — Rayleigh's number). Due to the difference in density between the two phases, a non-homogeneization of the emulsion could appear in time due to thermal diffusion effect.

Transient measurement methods allow for rapid determination of the thermal conductivity of liquids by applying a short-duration thermal pulse, avoiding thus the risk of natural convection onset and thermal diffusion effect.[12–14,19]

Among them, the transient hot wire method, intensively employed in thermal conductivity studies of electrically non-conductive liquids,[20–24] encounters experimental difficulties when used for electrically-conductive liquids in general and emulsions in special, due to electrical conductivity of liquid, polarization phenomena and adsorption at the wire / fluid interface. The electrical insulation of fluid from transducer, by coating the latter with an electro-insulating material, represents a simple experimental solution which permits the used of this method for emulsions, in general for electrically conductive fluids (electrolyte solutions, ionic melts), polarizable liquids, tenside solutions, suspensions, etc.

In the present contribution, after a brief discussion on clasical procedure of the transient coated hot wire method, experimental set up and measurement principle, the experimental values are given for thermal conductivity of some O/W type emulsions. The validity of the method and measurement accuracy have been proved by determinations on distilled water, whose thermal conductivity is known from literature.

2. THEORETICAL PRINCIPLE OF THE METHOD

The transient hot wire method determines the thermal conductivity, λ, of fluids by measuring the temperature rising rate as a function of time for a metalic wire vertically immersed into the fluid. The wire, electrically heated by a step-pulse of constant voltage, simulates a linear source of heat [19] with a constant heat flow per unit length, q, and develops within the fluid a temperature field which increases radially in time and is axially symmetrical.

Supposing that: — the wire of radius r_1 and of infinite length, L, is made of an homogeneous material of density ρ_1, specific heat c_1, (both temperature independent) and has infinite thermal conductivity, λ_1; — the fluid is homogeneous and unbounded with λ, ρ, c_p properties (temperature independent); —the heat flow per unit length, q, of the wire is constant; — there is no thermal resistances between the wire and the fluid, the temperature rise $\theta(r_1, t)$ of the wire at $r = r_1$ and the time t counted from the heating turning on $t = 0^+$, against the initial T_0 temperature of the cell at $t = 0^-$, is then given by the relation. [20-21]

$$\theta(r_1, t) = \frac{q}{4\pi\lambda}\left[\ln\frac{4\tau}{C} + \frac{1}{2\tau} + \frac{b-2}{b}\,\frac{1}{2\tau}\ln\frac{4\tau}{C} + \dots\right] =$$

$$= \frac{q}{4\pi\lambda}\left[\left(1 - \frac{\rho_1 c_1 - \rho c_p}{2\lambda t}\,r_1^2\right)\ln\frac{4\tau}{C} + \frac{1}{2\tau} + \dots\right] \tag{1}$$

where: $\tau = at/r_1^2$; $b = 2\rho c_p/(\rho_1 c_1)$; $a = \lambda/(\rho c_p)$ is thermal diffusivity of the fluid; $C = \exp\gamma = 1.781$ and $\gamma = 0.5772$ is Euler's constant.

After a certain time, t_A, from starting the step — pulse ($t = 0^+$), the product between time and rate of the wire temperature rise is inversely proportional to the fluid thermal conductivity. For $t \geqslant t_A$, the temperature rise $\theta(r_1, t)$ of the wire is described with an accuracy better than 0.1 % by the formula:

$$\theta(r_1, t) = \frac{q}{4\pi\lambda}\ln\frac{4\tau}{C} \tag{2}$$

In the $\theta(\ln t)$ plot, equation (2) represents a straight line with a slope inversely proportional to the thermal conductivity. This linear logarithmic law is obeyed only for $t_A \leqslant t \leqslant t_B$, systematic deviations occurring for both short ($t < t_A$) and long ($t > t_B$) times. The time t_A depends upon geometrical and physical finite constants of the wire and t_B is the critical time for natural convection onset, wall cell effect and heat losses at the wire ends. Equation (2) represents the wire temperature rise, with a close approximation, only for sufficiently large values of τ.

The classical procedure of the method is based on the validity of equation (2): thermal conductivity, $\lambda^{(0)}$, is calculated from the slope of (Δ) straight line fitted by the least square method with the experimental pairs $[\theta(r_1, t), \ln t]$, within the linear range of $\theta(\ln t)$ curve, i.e. $t_A \leqslant t \leqslant t_B$. The index $(^0)$ means that λ is obtained by classical procedure of the method. [24]

Let us consider a metallic wire with the characteristics r_1, ρ_1, c_1 and $\lambda_1 = \infty$, coated uniformly with an electro-insulating material having r_h, ρ_h, c_h, λ_h and a_h, which is immersed into a radially unbounded fluid of characteristics λ, ρ, c_p, and a. The three media (wire, its coating and fluid) are supposed infinite along the axial direction, are homogeneous and isotropic, their physical properties are not temperature dependent and there are no thermal resistances at their interface so that heat transfer is exclusively conductive.

If the uniform equilibrium temperature of the three media is T_0 at $t = 0^-$, then the temperature rise, $\theta_h(r_1, t)$ of the coated wire is given by the relation :[25]

$$\theta_h(r_1, t) = q\left[\frac{m}{2\pi}\left(\frac{1}{\lambda_h} - \frac{1}{\lambda}\right) + \frac{1}{4\pi\lambda}\ln\frac{4\tau}{C} - \frac{A}{t} + \frac{2B}{t}\ln\frac{4\tau}{C} + \ldots\right] \tag{3}$$

where :

$$m = \ln\frac{r_h}{r_1}; \quad A = \frac{C^*}{D} - \frac{E\times H + F\times G}{D^2}; \quad B = -\frac{F\times H}{D^2}$$

$$C^* = \frac{mr_h}{4}\left(\frac{\lambda_h}{a_h} - \frac{\lambda}{a}\right) - \frac{r_h}{8}\left(\frac{\lambda_h}{a_h} - \frac{\lambda_h}{a}\right) + \frac{r_1^2}{8r_h}\,\frac{\lambda_h}{a_h}$$

$$D = -\frac{2\pi\lambda\lambda_h}{r_h}; \quad E = \frac{m}{r_h}(\lambda_h - \lambda); \quad F = \frac{\lambda_h}{2r_h}$$

$$G = \frac{\lambda}{r_h}\left\{m\pi r_1^2\rho_h c_h + m\pi r_1^2\rho_1 c_1\left(\frac{\lambda_h}{\lambda} - 1\right) + [\pi(r_h^2 - r_1^2)\,\rho_h c_h]\times\right.$$
$$\left.\times\left(m\frac{\lambda_h}{\lambda} - \frac{1}{2}\right) + \frac{\pi r_h^2\rho c_p\lambda_h}{\lambda}\left(\frac{1}{2} - m\right)\right\}$$

$$H = \frac{\lambda_h}{2r_h}\left[\pi r_1^2\rho_1 c_1 + \pi(r_h^2 - r_1^2)\,\rho_h c_h - \pi r_h^2\rho c_p\right]$$

When $r_1 = r_h$, that is the wire is uncoated, one obtains :

$$\frac{m}{2\pi}\left(\frac{1}{\lambda_h} - \frac{1}{\lambda}\right) = 0; \quad A = -\frac{r_1^2\rho c_p}{8\pi\lambda^2}; \quad B = \frac{r_1^2(\rho c_p - \rho_1 c_1)}{16\pi\lambda^2} \tag{4}$$

and finds equation (1) again.

For times long enough, equation (3) becomes :

$$\theta_h(r_1, t) = \frac{q}{4\pi\lambda}\left[\left(2\ln\frac{r_h}{r_1}\right)\left(\frac{\lambda}{\lambda_h} - 1\right) + \ln\frac{4\tau}{C} + \ldots\right] \tag{5}$$

or :

$$\Phi = b + \lambda^{-1}(\ln t) \tag{6}$$

where : $\Phi = 4\pi\theta_h(r_1, t)/q$

$$b = \lambda^{-1}\left[\ln\frac{4a}{r_1^2C} + \left(2\ln\frac{r_h}{r_1}\right)\left(\frac{\lambda}{\lambda_h} - 1\right)\right]$$

Equation (5), as basic for the measurements, shows that in the case of a coated wire, an additive constant term appears but it does not alter the slope of $\theta_h(\ln t)$ curve. The straight line defined by equation (5) suffers a shift parallel to the straight line which would be obtained for the uncoated wire (equation (2)). The coating causes a small increase, constant in time, of the wire temperature and an increase in t_A by consuming some amount of time for establishing a constant temperature gradient (steady state regime) across the coating.

3. EXPERIMENTAL ASSEMBLY

The experimental set up consists of : measurement cell, thermostat, vacuum unit, thermal conductivimeter and electrical measurement apparatus. Details on the experimental assembly and working mode were given in a previous paper.[26]

3.1. MEASUREMENT CELL

The mesuring cell, made of Pyrex glass tube (30 mm i.d.) contains the investigated liquid. The transducer consists of a pure platinum wire (Heraeus Degussa) of a 0.015 mm diameter and 0.3 m length, soldered at the ends to thick copper leads. The transducer is coated with a polymeric resin. Briefly, the technique of coating consists in immersing the transducer in a polymeric liquid substance, operation followed by heat treatment. Unfortunately, the thickness of the coating was non-uniform, but the electrical insulation is yet ensured. The coated transducer is vertically immersed into the cell. The whole assembly is maintained at the constant temperature T_0 in a Dewar flask,[18] connected to a U – 10 type thermostat.

3.2. OPERATION PRINCIPLE OF THE APPARATUS

The platinum wire is calibrated as a thermoresistance, that is the electrical resistance variation is a measure for the temperature rise, $\theta(r_1, t)$, and it is measured on a Wheatstone bridge. At $t = 0^-$ and T_0, the bridge is either balanced or a known resistive unbalance is imposed ; the heating current is nil. At $t = 0^+$, a step pulse of D. C. constant voltage, E_p, is applied at the bridge input. The bridge is activated and, simultaneously, seven electronic timers are released. By Joule heating, the current in the bridge brings about a temperature rise, that is an increase in the wire electrical resistance. At the very moment when the (amplified) bridge output signal becomes successively equal to seven present voltage levels of the comparators, each of the comparators triggers a stopping signal to the corresponding timer. Thus, the time intervals are measured from $t = 0^+$ (START of the timers) till t_i instants ($i = 1, .., 7$) (successive STOP of the timers). The wire temperature rise between $t = 0^+$ and $t = t_i$ moments can be calculated from the bridge equation and temperature coefficient, α, of the wire electrical resistance. The heat flow, q, produced in the wire unit length is calculated from the measurable E_p, L and R_1^0 values, the last being the wire electrical resistance at $t = 0^-$ and T_0.

3.3. EMULSIONS PREPARATION

All emulsions employed are of O/W type and have a concentration of 5 % oil in water (in weight). The studied emulsions were prepared from seven assortments of oils containing emulsifier and stabilizer : E_I and E_{II} emulsions contain import oils and are as references and $E_1 - E_5$ emulsions have indigeneous oils (different qualitative and quantitative compositions depending on oil, emulsifier and stabilizer nature, respectively). Preparation procedure of emulsions is as follows : to obtain a 5 % oil in water emulsion, corresponding amounts of oil and water are weighed in two separate flasks. In the flask with oil, a small amount of water is added, the content being then stirred till the oil gets the consistency of mayonaise. The remainder of water is added gradually, under continuous stirring. In order to stabilize the emulsion properties, the determinations were carried out 24 hours after their preparation and repeated after 4 – 7 days. During this period of time no deposits were noticed and the precision of measurements was of 1 %.

4. EXPERIMENTAL RESULTS

In table 1 the experimental results t_i, x_i and Φ_i are presented, where $x_i = \ln t_i$ and $\Phi_i = 4\pi\theta_h(r_i, t)/q$.

TABLE 1

Experimental results

Water

$t_i(s)$	0.4486	0.7168	1.1526	1.8585	2.9533	4.6277	7.4621	11.8099
x_i	−0.8016	−0.3329	0.1421	0.6198	1.0829	1.5321	2.0098	2.4689
Φ_i	15.6346	16.3801	17.1267	17.8740	18.6203	19.3680	20.1167	20.8654

$\lambda_{exp} = 0.625 \pm 0.005$ W/(mK)

E_I emulsion

$t_i(s)$	0.5196	0.7939	1.2072	1.7867	2.7482	4.2507
x_i	−0.6548	−0.2308	0.1883	0.5804	1.0110	1.4471
Φ_i	16.1308	16.8741	17.6185	18.3635	19.1086	19.8544

E_{II} emulsion

$t_i(s)$	0.3090	0.4644	0.7319	1.0876	1.6502	2.4503	3.8381
x_i	−1.1744	−0.7670	−0.3121	0.0840	0.5009	0.8962	1.3450
Φ_i	15.3615	16.0973	16.8344	17.5726	18.3119	19.0559	19.8007

E_1 emulsion

$t_i(s)$	0.5295	0.8059	1.1941	1.8010	2.7594
x_t	−0.6359	−0.2157	0.1774	0.5883	1.0150
Φ_i	16.1816	16.9182	17.6564	18.3965	19.1394

E_2 emulsion

$r_i(s)$	0.3200	0.4899	0.7377	1.1583	1.7326	2.4885	3.6364
x_i	−1.1393	−0.7135	−0.3042	0.1469	0.5496	0.9117	1.2910
Φ_i	15.4011	16.1404	16.8804	17.6214	18.3656	19.1108	19.8546

E_3 emulsion

$t_i(s)$	0.3313	0.4989	0.7616	1.1364	1.7380	2.7624	4.2829	6.6027
x_i	−1.1047	−0.6953	−0.2724	0.1279	0.5527	1.0161	1.4546	1.8875
Φ_i	15.4228	16.1623	16.9023	17.6435	18.3867	19.1318	19.8795	20.6277

E_4 emulsion

$t_i(s)$	0.3205	0.4907	0.7503	1.1539	1.7436	2.7457	4.4144
x_i	−1.1379	−0.7118	−0.2873	0.1431	0.5559	1.0100	1.4849
Φ_i	15.5264	16.2667	17.0116	17.7584	18.5084	19.2593	20.0079

E_5 emulsion

$t_i(s)$	0.3136	0.4790	0.7311	1.0589	1.6973	2.4485	3.9209	6.4243
x_i	−1.1595	−0.7360	−0.3132	0.0572	0.5291	0.8955	1.3663	1.8601
Φ_i	15.5867	16.3308	17.0803	17.8319	18.5906	19.3420	20.0937	20.8436

In order to test the experimental method, thermal conductivity determinations were carried out on distilled water, at $T_0 = 298.2$ K. Between the obtained experimental value, $\lambda_{\mathrm{exp}} = 0.625$ W/(mK), and the mean value given in the literature,[27-29] $\lambda_{\mathrm{ref}} = 0.610$ W/(mK), there is a relative error of 2.5 %.

By regression analysis,[30] a straight line $\Phi = b + mx$ (where $m = \lambda^{-1}$) was calculated for each emulsion. The following data are listed, for each emulsion, in table 2 :

n — number of (Φ_i, x_i) pairs of experimental values,
r — correlation coefficient of the regression straight line,
b, m — intercept and slope of regression straight line,
$\overline{\Phi}$, $\bar{x}$ — mean values for Φ_i and x_i variables,

$$S_\Phi = [n \sum_i \Phi_i^2 - (\sum_i \Phi_i)^2]^{1/2} n^{-1/2} (n-1)^{-1/2}$$

$$S_x = [n \sum_i x_i^2 - (\sum_t x_i)^2]^{1/2} n^{-1/2} (n-1)^{-1/2}$$

$S_{\Phi|x}$ — standard deviation of Φ at a given x,
S_m — standard deviation in the slope m.

TABLE 2

Regression analysis of the experimental data

Emulsion	n	r	b	m	$\overline{\Phi}$	$\bar{x}$	S_Φ	S_x	$S_{\Phi\vert x}$	S_m
E_{I}	6	0.99990	17.2964	1.78172	17.9917	0.3902	1.39331	0.78192	0.02193	0.012541
E_{II}	7	0.99986	17.4315	1.77017	17.5763	0.0818	1.59799	0.90261	0.02932	0.013263
E_1	5	0.99990	17.3238	1.80056	17.6584	0.1858	1.16908	0.64924	0.01635	0.012588
E_2	7	0.99941	17.4317	1.82211	17.6249	0.1060	1.60371	0.87963	0.06013	0.027907
E_3	8	0.99985	17.3763	1.73490	18.0196	0.3708	1.82114	1.04955	0.03450	0.012426
E_4	7	0.99981	17.5028	1.72093	17.7627	0.1510	1.61451	0.93799	0.03410	0.014841
E_5	8	0.99942	17.6612	1.76524	18.2128	0.3124	1.84224	1.04302	0.06773	0.024545

From the slope m and standard deviation S_m, the thermal conductivity values together with the confidence untervals calculated for a significance level of 5 %, are presented in table 3.

Since all these emulsions have almost the same thermal conductivity, a statistical study was carried out to establish the extent to which the emulsions differ one from another. The differentiation of these emulsion, at a level of significance of 5 % and for the results presented in Table 2, has been checked by three statistical tests :[30]

— Test F, applied to the standard deviation around the regression straight line, $S^2_{\Phi|x}$, at a significance level of 5 %, $\mathrm{F}_{\mathrm{exp}} = 9.5$ results for E_5

and E_I emulsions, the comparison value, $F_{crit} = 9.2$, being lower. The difference being however small, the test is not conclusive and it only points out that E_5 differs statistically from E_I.

TABLE 3

The thermal conductivity values of emulsions

Emulsion	λ[W/(mK)]
E_I	0.561±0.011
E_{II}	0.565±0.011
E_1	0.555±0.012
E_2	0.549±0.022
E_3	0.576±0.010
E_4	0.581±0.013
E_5	0.567±0.019

— Test t for significance of the differences in $m = \lambda^{-1}$ slopes at a significance level of 5 %. According to this test one can state the existence of a significant difference in thermal conductivity only for the following pairs of emulsions :

E_3 and E_I $(t_{exp} = 2.30 > 2.23 = t_{crit})$

E_4 and E_I $(t_{exp} = 2.88 > 2.26 = t_{crit})$

E_4 and E_{II} $(t_{exp} = 2.47 > 2.23 = t_{crit})$

Even in this case the differences are still small.

— The test using the confidence band of the regression straight line at a significance level of 5 %. The regression straight lines of E_I emulsion (Fig. 1a) and E_{II} emulsion (Fig. 1b), respectively, were considered as reference and $\Phi(x)$ deviations of regression straight lines for the other emulsions were represented regarding E_I and E_{II}, as functions of $x = \ln t$ variable. The hachured regions in Fig. 1a and 1b represent the confidence band for the difference between two samples of regression of emulsion E_I (Fig. 1a) and respectively E_{II} (Fig. 1b).

From Fig. 1a, it results that E_1 is the emulsion with a thermal conductivity alike E_I, although the former has a distinctive behaviour (it is not completely located within the confidence band of E_I emulsion).

From Fig. 1b, one can see that E_2 emulsion has closest behaviour to E_{II} (the line for E_2 coincides with the limit of the confidence band for E_{II}).

In conclusion, from analysis of the obtained experimental data, we consider that the employed method and experimental set up allow for determining thermal conductivity of emulsions with an accuracy better than 3 %.

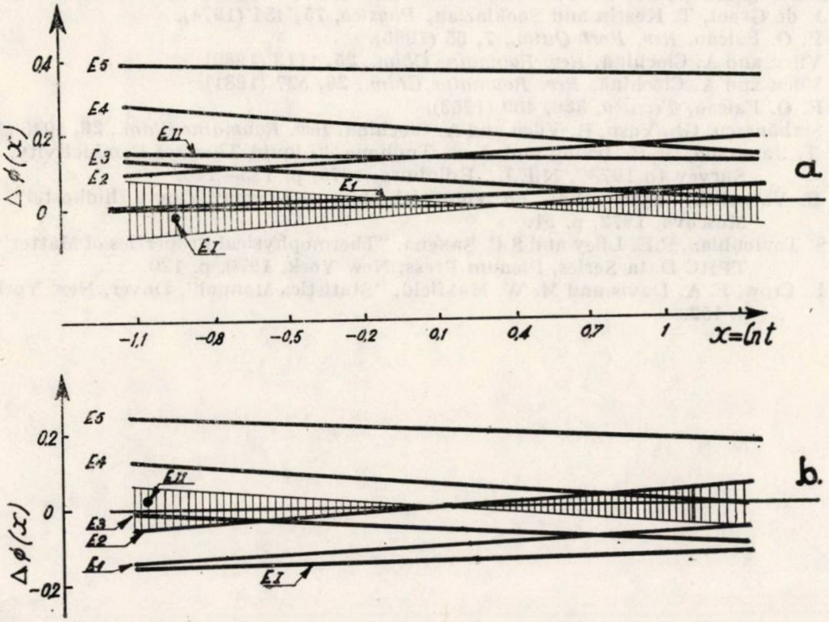

Fig. 1. — The $\Delta\Phi(x)$ deviations of regression straight lines of E_1-E_5 emulsions as a function of $x = \ln t$ variable.

REFERENCES

[1] P. B. Lal Chaurasia, D. R. Chaudhary and R. C. Bhandari, *J. Appl. Chem. Biotechnol.*, **25**, 881 (1975).

[2] S. C. Cheng and R. J. Vachon, *Internat. J. Heat Mass Transf.*, **13**, 537 (1970).

[3] R. H. Wang and J. G. Knudsen, *Ind. Eng. Chem.*, **50**, 1667 (1968).

[4] C. Mahas and J. R. Couper, "Res. Rept. Series N° 7, Engng, Exp. Station", Univ. of Arkansas, 1966.

[5] J. C. Maxwell, "A treatise on Electricity and Magnetism", vol. I, Dover, New York, 1954, p. 314.

[6] T. B. Jefferson, O. W. Witzell and W. L. Sibbitt, *Ind. Eng. Chem.*, **50**, 1589 (1958).

[7] D. A. G. Bruggeman, *Ann. Physique*, **24**, 636 (1935).

[8] R. L. Hamilton and O. K. Crosser, *Ind. Eng. Chem.*, **1**, 187 (1963).

[9] G. T. N. Tsao, *Ind. Eng. Chem.*, **53**, 395 (1961).

[10] H. W. Russell, *J. Amer. Ceram. Soc.*, **18**, 1 (1935).

[11] K. Lichtenecker, *Z. Physik*, **25**, 193 (1924).

[12] N. V. Tsederberg, "Thermal Conductivity of Gases and Liquids", Edward Arnold Ltd., London, 1965, p. 1—66.

[13] A. Missenard, "Conductivité thermique des solides, liquides, gas et de leurs mélanges", Eyrolles, Paris, 1965, p. 116—178.

[14] "Thermal Conductivity", ed. R. P. Tye, vol. II, Academic Press, London, 1969, p. 66—145.

[15] R. Vîlcu and A. Ciochină, *Rev. Roumaine Chim.*, **17**, 1679 (1972).

[16] R. Vîlcu and A. Ciochină, *Studii și cercetări Chim. Aacad. R.S.R.*, **21**, 571 (1973).
[17] R. Vîlcu and A. Ciochină, *Studii și cercetări Chim. Acad. R.S.R.*, **21**, 643 (1973).
[18] R. Vîlcu and A. Ciochină, *Rev. Roumaine Chim.*, **26**, 161 (1981).
[19] H. S. Carslaw and J. C. Jaeger, "Conduction of Heat in Solids", Clarendon Press, Oxford, 1959, p. 261.
[20] E. McLaughlin and J. F. T. Pittman, *Phil. Trans. Ray. Soc., London*, **270**, 557 (1971).
[21] J. J. de Groot, T. Kestin and Sookiazian, *Physica*, **75**, 454 (1974).
[22] A. F. O. Falcao, *Rev. Port. Quim.*, **7**, 65 (1965).
[23] R. Vîlcu and A. Ciochină, *Rev. Roumaine Chim.*, **25**, 1113 (1980).
[24] R. Vîlcu and A. Ciochină, *Rev. Roumaine Chim.*, **26**, 527 (1981).
[25] A. F. O. Falcao, *Tecnica*, **326**, 409 (1963).
[26] D. Șerbănescu, Gh. Vasu, R. Vîlcu and A. Ciochină, *Rev. Roumaine Chim.*, **26**, 1045 (1981).
[27] D. T. Jamieson, J. B. Irving and J. S. Tudhope, "Liquid Thermal Conductivity, A Data Survey to 1973", N.E.L., Edinburg, 1975, p. 133–140.
[28] N. B. Vargaftik, "Spravochnik po teplofizicheskim svoistvam gazov i zhidkostei", Nauka, Moscova, 1972, p. 51.
[29] Y. S. Toulouhian, P.E. Liley and S.C. Saxena, "Thermophysical Properties of Matter", vol. 3, TPRC Data Series, Plenum Press, New York, 1970, p. 120.
[30] E. L. Crow, F. A. Davis and M. W. Maxfield, "Statistics Manual", Dover, New York, 1975, p. 152.

Revue Roumaine de Chimie, 26, *11–12*, 1365–1376 (1981)

AN ANALYSIS OF THE EFFECT OF INPUT DATA CHANGES ON THE CHEMICAL EQUILIBRIUM COMPOSITION

D. GEANĂ and F. DANEȘ
The Polytechnic, Dept. Physical Chemistry
str. Polizu 1, Bucharest, Romania

Received November 12, 1980

The paper presents a treatment of the effect of changes in input data (μ_i^0, T, P, n_i^0) on the composition at chemical equilibrium. The analysis is presented in relation to a Newton's type procedure for the computation of chemical equilibrium. The system of catalytic reforming of methane by steam ($CH_4 + H_2O$) is considered as an example of application.

1. INTRODUCTION

In a previous paper[1] we have presented a transformation of the chemical equilibrium problem in multicomponent system. The transformation implies a change of variables, from mole numbers (n_i) to reaction extents (ξ_j). The last variables are also known as progress variables or De Donder variables.

For a system with N chemical species and $\mathscr{R}$ reactions, considered in gaseous phase and ideal, the transformation[1] leads to the formulation of chemical equilibrium problem :

$$\min g = \sum_i \Big(n_i^0 + \sum_j \nu_{ij}\xi_j\Big) g_i^0 + \sum_i \Big(n_i^0 + \sum_j \nu_{ij}\xi_j\Big) \cdot \ln \frac{n_i^0 + \sum_j \nu_{ij}\xi_j}{n^0 + \sum_j \nu_j \xi_j} \tag{1}$$

with constraints

$$n_i = n_i^0 + \sum_j \nu_{ij}\xi_j \geqslant 0 \tag{2}$$

The following notations were used :

$$n^0 = \sum_i n_i^0 \tag{3a}$$

$$\nu_j = \sum_i \nu_{ij} \tag{3b}$$

$$g = \frac{G}{RT} \tag{3c}$$

$$g_i^0 = \frac{\mu_i^0(T)}{RT} + \ln P \tag{3d}$$

with the index set

$$\begin{Bmatrix} i = 1,2 \ldots N \\ j = 1, 2 \ldots \mathscr{R} \end{Bmatrix} \tag{4}$$

The formulation (1,2) will be called "ξ formulation". A similar formulation was presented recently in a series of works [2-4] based on the geometric programming method (GP). It was shown [2,3] that chemical equilibrium problem is equivalent to a dual program in GP. The similar problem to that formulated here as (1,2) is obtained in GP by a Gauss — Jordan procedure and is called [2,3] a "transformed dual program". This transformed dual program was used by Dinkel and Lakshmanan [4] for an analysis of input data changes on the composition at chemical equilibrium.

It must be mentioned that similar analyses were previously advanced by Pings and co-workers, [5] Smith [6] and van Zeggeren and Storey.[7] In a recent paper we have presented a general treatment of the problem.[8]

In this paper we develop another treatment of the effect of changes in input data (μ_i^0, T, P, n_i^0) on the composition at chemical equilibrium. This treatment is presented in relation to a Newton's type procedure for the computation of chemical equilibrium composition. The final results are certainly similar to those obtained in the works.[4-6,8] Our treatment is more general as compared to[5] and is more directly related to chemical thermodynamics as compared to.[4] Other aspects in relation to the works[6,7] were discussed elsewhere.[8] It is noteworthy that our treatment as well as those from [4,6-8] are essentially forms of a general mathematical technique known as "sensivity analysis".

2. THE CALCULATION OF EQUILIBRIUM COMPOSITION USING "ξ FORMULATION"

In the formulation (1,2) the chemical equilibrium problem is a mathematical nonlinear program with inequality restrictions. Such a program can be solved by general methods.[9] A Newton's type method will be presented in what follows. In this type of methods the objective function of the nonlinear program (the function to be optimized) is developed in a Taylor series including second order terms. Thus :

$$g^{h+1} = g^h + \sum_j \frac{\partial g}{\partial \xi_j} \delta \xi_j + \frac{1}{2} \sum_{i,k} \frac{\partial^2 g}{\partial \xi_j \partial \xi_k} \delta \xi_j \delta \xi_k \tag{5a}$$

where

$$\delta \xi_j = \xi_j^{h+1} - \xi_j^h$$

and the derivatives from both sums are taken in the point ξ_j^h.

The function (5a) can be written in a matrix form :

$$g^{h+1} = g^h + \nabla g^h \cdot \| \delta \xi_j \| + \frac{1}{2} \| \delta \xi_j \|^T . \ \text{Hess}\ (g^h) \cdot \| \delta \xi_j \| \qquad (5b)$$

where $\| \delta \xi_j \|$ represents the vector of De Donder variables. ∇g^h is the gradient vector having as elements

$$\frac{\partial g}{\partial \xi_j} = \sum_i \nu_{ij} g_i^0 + \sum_i \nu_{ij} \ln \frac{n_i^0 + \sum\limits_j \nu_{ij} \xi_j}{n^0 + \sum\limits_j \nu_j \xi_j} \qquad (6)$$

Hεss (g^h) is the hessian matrix (of the second order partial derivatives) of elements :

$$\frac{\partial^2 g}{\partial \xi_j \partial \xi_k} = \sum_i \frac{\nu_{ij} \nu_{ik}}{n_i^0 + \sum\limits_j \nu_{ij} \xi_j} - \frac{\nu_j \nu_k}{n^0 + \sum\limits_j \nu_j \xi_j} \qquad (7)$$

The function (5a) is a quadratic form, the idea of the method of optimization being to approximate the program function with a quadratic form between two steps of the calculation.

Thus one solves the problem (1,2) iteratively by

$$\min g^{h+1} \qquad (8a)$$

with

$$n_i^0 + \sum_j \nu_{ij} \xi_j^{h+1} \geqslant 0 \qquad (8b)$$

The minimum conditions (without ,constraints) of the quadratic form (5b) are :[9,10]

$$\nabla g^{h+1}(\delta \xi_j) = 0 \qquad (9a)$$

$$\text{Hess}\ [g^{h+1}(\delta \xi_j)] > 0 \qquad (9b)$$

Because Hess (g^h) is a symmetrical matrix, it results :

$$\nabla g^h + \text{Hess}\ (y^h) \cdot \| \delta \xi_j \| = 0 \qquad (9c)$$

$$\text{Hess}\ (g^h) > 0 \qquad (9d)$$

The condition (9d) is the well known stability condition of equilibrium [11] and for ideal systems it is always fulfilled.

Equation (9c) can be solved by matrix inversion :

$$\| \delta \xi_j \| = - [\text{Hess}\ (g^h)]^{-1} \cdot \nabla g^h \qquad (10a)$$

or

$$\| \xi_j^{h+1} \| = \| \xi_j^h \| - [\text{Hess}\ (g^h)]^{-1} \cdot \nabla g^h \qquad (10b)$$

Taking into consideration the constraints (8b), one introduces the step length (parameter) $\lambda^h > 0$

$$\| \xi_j^{h+1} \| = \| \xi_j^h \| - \lambda^h [\text{Hess}\,(g^h)]^{-1} \cdot \nabla g^h \tag{10c}$$

which is obtained from

$$\lambda^h = \min \{\lambda_m^h, \lambda_{ad}^h\} \tag{11}$$

where λ_m^h is the unidimensional minimum [9,10] and λ_{ad}^h is the greatest value of λ for which the constraints (8b) are fulfilled.

The algorithm of calculation is:

(a) start with $\| \xi_j^h \|$, $h = 0$, an initial approximation of the solution which is feasible for (8b)

(b) calculation of ∇g^h, Hess (g^h) with eq. (6,7)

(c) calculation of descent direction vector

$$d^h = -[\text{Hess}\,(g^h)]^{-1} \cdot \nabla g^h$$

(d) calculation of λ_{ad}^h with (8b, 10b)

(e) calculation of unidimensional optimum λ_m^h with a corresponding procedure [9,10]

(f) calculation of step lenght λ^h with (11)

(g) calculation of the new values ξ_j^{h+1} with (10c)

(h) verification of stop criterion. If the criterion is not fulfilled one takes $h := h + 1$ and one repeats from (b).

A criterion of stop may be $|\xi_j^{h+1} - \xi_j^h| \leqslant \varepsilon$. Application of the above algorithm and the obtained results with different systems will be presented in another paper.

3. EQUILIBRIUM COMPOSITION SHIFT BY SMALL CHANGES IN INPUT DATA μ_i^0, T, P AND n_i^0

Let us consider a system for which the chemical equilibrium composition was calculated, being ξ_j (with corresponding n_i values) for initial data T, P and n_i^0. If one produces small changes (of the first order) in the input data, the system will reach a new equilibrium state of composition $\xi_j + \delta \xi_j$.

As can be observed from eq. (3d), the changes in μ_i^0, temperature and pressure are reflected as changes in the function g_i^0. There exists thus two types of changes which produce a shift of the equilibrium composition:

a) change in g_i^0, denoted δg_i^0, due to changes in T and (or) P. The changes in T will produce corresponding changes in $\mu_i^0(T)$, but one can consider also herein the errors in μ_i^0 (at unchanged T and P). The corrections for the real behaviour of systems can be also included by the function:

$$g_i^{\square} = \frac{\mu_i^0(T)}{RT} + \ln P + \ln \varphi_i(T, P, x_i) \tag{12}$$

b) changes in n_i^0, denoted δn_i^0. These may be due to errors but may be also made intentionally for obtaining a better conversion in a desired product. This last problem may be eventually posed in the sense of optimization of the equilibrium composition.[5] It must be mentioned that the changes δg_i^0 and δn_i^0 (and corresponding $\delta \xi_j$) will be considered small (of first order), but the treatment can be applied to large changes by using an incremental procedure.[4]

In what follows we present a treatment of both types of changes in input data based on a procedure suggested in [7] and correctly formulated by us. [8]

3.1. EQUILIBRIUM COMPOSITION SHIFT BY δg_i^0 CHANGES

As said, the δg_i^0 changes (of first order) lead to $\delta \xi_j$ changes in chemical equilibrium composition. The corresponding change in the Gibbs free energy is :

$$\Delta g = \sum_i \frac{\partial g}{\partial g_i^0} \delta g_i^0 + \sum_j \frac{\partial g}{\partial \xi_j} \delta \xi_j + \frac{1}{2} \Big[2 \sum_{i,j} \frac{\partial^2 g}{\partial g_i^0 \partial \xi_j} \delta g_i^0 \delta \xi_j + \sum_{j,k} \frac{\partial^2 g}{\partial \xi_j \partial \xi_k} \delta \xi_j \delta \xi_k + \sum_{i,l} \frac{\partial^2 g}{\partial g_i^0 \partial g_l^0} \delta g_i^0 \delta g_l^0 \Big] \tag{13}$$

including first and second order terms. The partial derivatives from (13) are taken in the initial equilibrium point. Because both states of the system are equilibrium states (g is minimum) it results that Δg must be minimum too. One obtains a quadratic program :

$$\min \Delta g(\delta \xi_j) \tag{14a}$$

with

$$n_i^0 + \sum_j \nu_{ij}(\xi_j + \delta \xi_j) \geqslant 0 \tag{14b}$$

It was shown [2,4] (theorem 5, lemma 1) that such a program can be formulated only for the so-called "well formed" chemical equilibrium problem, i.e. for equilibria when the constraints (2,14b) are fulfilled with "$>$". Because $\delta g_i^0 = \text{constant}$ ($i = 1,2 \ldots \mathrm{N}$) and $\partial g / \partial \xi_j = 0$ ($j = 1, 2, \ldots \mathscr{R}$) the program (14a) becomes :

$$\min \Delta g = \frac{1}{2} \Big[2 \sum_{i,j} \frac{\partial^2 g}{\partial g_i^0 \partial \xi_j} \delta g_i^0 \delta \xi_j + \sum_{j,k} \frac{\partial^2 g}{\partial \xi_j \partial \xi_k} \delta \xi_j \delta \xi_k + \sum_{i,l} \frac{\partial^2 g}{\partial g_i^0 \partial g_l^0} \delta g_i^0 \delta g_l^0 \Big] \tag{14c}$$

Certainly, the new function Δg is different from that of (13) $\left(\text{by } \sum_i \frac{\partial g}{\partial g_i^0} \delta g_i^0 \right)$, but the same notation is used for simplicity.

It results :

$$\frac{\partial g}{\partial g_i^0} = n_i^0 + \sum_j \nu_{ij}\,\xi_j \tag{15a}$$

$$\frac{\partial^2 g}{\partial g_i^0\,\partial \xi_j} = \frac{\partial^2 g}{\partial \xi_j\,\partial g_i^0} = \nu_{ij} \tag{15b}$$

$$\frac{\partial^2 g}{\partial g_i^0\,\partial g_i^0} = 0 \tag{15c}$$

Thus, problem (14c) becomes :

$$\min\,\Delta g = \sum_{i,j} \nu_{ij}\,\delta g_i^0\,\delta \xi_j + \frac{1}{2}\sum_{j,k} \frac{\partial^2 g}{\partial \xi_j\,\partial \xi_k}\,\delta \xi_j\,\delta \xi_k \tag{16a}$$

Noting :

$$\delta(\Delta g_j^0) = \sum_i \nu_{ij}\,\delta g_i^0 \tag{17}$$

which represents the change in the Gibbs standard free energy of a reaction j, including the effect of P and of real behaviour, the program (16a) can be written in matrix form :

$$\min\,\Delta g = \|\,\delta(\Delta g_j^0)\,\|^T \cdot \|\,\delta \xi_j\,\| + \frac{1}{2}\,\|\,\delta \xi_j\,\|^T \cdot \mathrm{Hess}\,(g) \cdot \|\,\delta \xi_j\,\| \tag{16b}$$

This program is a quadratic one [9,10] and implies :

$$\nabla\,[\Delta g(\delta \xi_j)] = 0 \tag{18a}$$

$$\mathrm{Hess}\,[\Delta g(\delta \xi_j)] > 0 \tag{18b}$$

Because Hess (g) is symmetrical, one obtains from (18a, b) :

$$\|\,\delta(\Delta g_j^0)\,\| + \mathrm{Hess}\,(g) \cdot \|\,\delta \xi_j\,\| = 0 \tag{18c}$$

$$\mathrm{Hess}\,(g) > 0 \tag{18d}$$

Eq. (18d) represents the stability condition [11] of the initial equilibrium state.

Solving eq. (18d) by matrix inversion, it results :

$$\|\delta \xi_j\| = -\,[\mathrm{Hess}\,(g)]^{-1} \cdot \|\,\delta(\Delta g_j^0)\,\| \tag{19}$$

Eq. (19) gives $\delta \xi_j$ values corresponding to the equilibrium shift by $\delta(\Delta g_i^0)$ changes. The corresponding changes in mole numbers are:

$$\delta n_i = \sum_j \nu_{ij} \delta \xi_j \tag{20}$$

The final results (eq. (19, 20)) are similar to those obtained in,[4] the difference being due to different functions in which the changes take place (herein g_i^0, but $c_i = \exp(-g_i^0)$ in [4]).

Eq. (19) allows to obtain expressions which give directly the effect of changes in T or P respectively. Thus

$$\delta(\Delta g_j^0) = -\frac{\Delta^r H_j^0}{RT^2} \delta T \tag{21}$$

and

$$\frac{1}{\delta T} \| \delta \xi_j \| = [\text{Hess}\,(g)]^{-1} \cdot \| \Delta^r H_j^0 / RT^2 \| \tag{22}$$

From eq. (20) one obtains the changes $\delta n_i / \delta T$. Similarly, for pressure P:

$$\delta(\Delta g_j^0) = \sum_j \nu_{ij} \delta \ln P = \nu_j \, \delta \ln P \tag{23}$$

for ideal behaviour of gases. Then:

$$\frac{1}{\delta \ln P} \| \delta \xi_j \| = -\,[\text{Hess}\,(g)^{-1} \cdot \| \nu_j \| \tag{24}$$

Eq. (22, 24) are similar to those in [5] for ideal behaviour of the system. It must be mentioned that in our treatment, the corrections for real behaviour are more easily introduced by eq. (19, 23) as compared to [5]. The changes δg_i^0 are in this case related to excess thermodynamic functions:

$$\delta g_i^0 = g_i^{\square} - g_i^0 = \ln \varphi_i(T, P, X_i) \equiv \mu_i^E / RT \tag{25}$$

Our experience [12] shows that for $\delta g_i^0 \ll g_i^0$ the reality corrections can be made directly by eq. (19) whereas in the case of large deviations from ideality the corrections must be made as follows:

(a) with the initial equilibrium composition (computed for an ideal behaviour) one calculates $\varphi_i(T, P, X_i)$ and $g_i^{\square}$

(b) a new equilibrium point is calculated (using for example the algorithm from § 2)

(c) a new vector $g_i^{\square}$ (new) is calculated. One obtains $\delta g_i^0 = g_i^{\square}$ (new) $-$ $g_i^{\square}$ (old). If $\delta g_i^0 \ll g_i$ (old) one makes directly the correction by eq. (19). Otherwise one repeats from (b).

3.2. EQUILIBRIUM COMPOSITION SHIFT BY δn_i^0 CHANGES

In this case the change in the Gibbs free energy corresponding to changes in initial mole numbers, δn_i^0, is :

$$\Delta g = \sum_i \frac{\partial g}{\partial n_i^0}\delta n_i^0 + \sum_j \frac{\partial g}{\partial \xi_j}\delta \xi_j + \frac{1}{2}\Bigg[2\sum_{i,j}\frac{\partial^2 g}{\partial n_i^0 \partial \xi_j}\delta n_i^0 \delta \xi_j + \sum_{j,k}\frac{\partial^2 g}{\partial \xi_j \partial \xi_k}\delta \xi_j \delta \xi_k + \sum_{i,l}\frac{\partial^2 g}{\partial n_i^0 \partial n_l^0}\delta n_i^0 \delta n_l^0\Bigg] \qquad (26)$$

including also second order terms in the series. The partial derivatives are taken in the initial equilibrium point. As in § 3.1 a nonlinear program results :

$$\min \Delta g(\delta \xi_j) \qquad (27a)$$

with

$$n_i^0 + \delta n_i^0 + \sum_i \nu_{ij}(\xi_j + \delta \xi_j) \geqslant 0 \qquad (27b)$$

The same considerations as in § 3.1 related to "well-formed" equilibrium must be made. Because $\delta n_i^0 = \text{constant}$ and $\partial g/\partial \xi_j = 0$, problem (27a) becomes :

$$\min \Delta g = \frac{1}{2}\Bigg[2\sum_{i,j}\frac{\partial^2 g}{\partial n_i^0 \partial \xi_j}\delta n_i^0 \delta \xi_j + \sum_{j,k}\frac{\partial^2 g}{\partial \xi_j \partial \xi_k}\delta \xi_j \delta \xi_k + \sum_{i,l}\frac{\partial^2 g}{\partial n_i^0 \partial n_l^0}\delta n_i^0 \delta n_l^0\Bigg] \qquad (27c)$$

The partial derivatives in (27c) are :

$$\frac{\partial g}{\partial n_i^0} = g_i^0 + \ln \frac{n_i^0 + \sum_j \nu_{ij}\xi_j}{n^0 + \sum_j \nu_j \xi_j} \qquad (28a)$$

$$\frac{\partial^2 g}{\partial n_i^0 \partial \xi_j} = \frac{\partial^2 g}{\partial \xi_j \partial n_i^0} = \frac{\nu_{ij}}{n_i^0 + \sum_j \nu_{ij}\xi_j} - \frac{\nu_j}{n^0 + \sum_j \nu_j \xi_j} \qquad (28b)$$

$$\frac{\partial^2 g}{\partial n_i^0 \partial n_1^0} = \frac{\delta_{il}}{n_i^0 + \sum_j \nu_{ij}\xi_j} - \frac{1}{n^0 + \sum_j \nu_j \xi_j} \qquad (28c)$$

with δ_{il} – Kronecker delta.

Problem (27c) becomes :

$$\min \Delta g = \sum_{i,j}\frac{\partial^2 g}{\partial n_i^0 \partial \xi_j}\delta n_i^0 \delta \xi_j + \frac{1}{2}\sum_{j,k}\frac{\partial^2 g}{\partial \xi_j \partial \xi_k}\delta \xi_j \delta \xi_k + \text{const.} \qquad (27d)$$

With the notation:

$$\sum_i \frac{\partial^2 g}{\partial n_i^0 \partial \xi_j} \delta n_i^0 = B_j \tag{29}$$

The program (27d) can be written in a matrix form:

$$\min \Delta g = \| B_j \|^T \cdot \| \delta \xi_j \| + \frac{1}{2} \| \delta \xi_j \|^T \cdot \mathrm{Hess}(g) \cdot \| \delta \xi_j \| + \text{const.} \tag{27e}$$

The minimum in (27e) implies:

$$\nabla [\Delta g(\delta \xi_j)] = 0 \tag{30a}$$

$$\mathrm{Hess}\,[\Delta g(\delta \xi_j)] > 0 \tag{30b}$$

Because Hess (g) is symmetrical, one obtains:

$$\| B_j \| + \mathrm{Hess}(g) \cdot \| \delta \xi_j \| = 0 \tag{30c}$$

$$\mathrm{Hess}(g) > 0 \tag{30d}$$

Solving (30c) by matrix inversion it results:

$$\| \delta \xi_j \| = - [\mathrm{Hess}(g)]^{-1} \cdot \| B_j \| \tag{31}$$

Eq. (31) gives $\delta \xi_j$ values corresponding to δn_i^0 changes (with corresponding B_j). This equation is similar to that obtained in [4] by GP method.

If the δn_i^0 changes are made methodically, namely one changes only the initial amount of a component, the other ones being unchanged, it results from eq. (31):

$$\frac{1}{\delta n^0_{i_{(k)}}} \| \delta \xi_j \| = - [\mathrm{Hess}(g)]^{-1} \cdot \| B'_j \| \tag{32}$$

where the notation $\delta n^0_{i_{(k)}}$ represents a change in n_i^0 for the species i the other n_k^0 $(k = 1, 2, \ldots N, k \neq i)$ being constant. From (29) it results for B'_j:

$$B'_j = \frac{\partial^2 g}{\partial n_i^0 \partial \xi_j} \quad (\delta n_k^0 = 0, k = 1, 2 \ldots N, k \neq i) \tag{33}$$

And

$$\delta n_i = \delta n_i^0 + \Sigma \nu_{ij} \delta \xi_j \tag{34}$$

4. EXAMPLE OF APPLICATION

One considers the system of catalytic reforming of methane by steam ($CH_4 + H_2O$) at $T = 1\,000$ K, $P = 1$ atm and initial amounts $n^0_{CH_4} = 1$, $n^0_{H_2O} = 4$ moles.

The stoechiometric matrix is:

$$\nu_{ij} = \begin{array}{ccccc} CH_4 & H_2O & CO & H_2 & CO_2 \\ -1 & -1 & 1 & 3 & 0 \\ 0 & -1 & -1 & 1 & 1 \end{array} \tag{35}$$

Table 1 presents the values of standard free enthalpies of formation $(\Delta^f G^0_{1000})_i$ calculated by the matrix method[13] and the chemical equilibrium composition. The reaction extents ξ_j, computed by Marquardt's method,[14] were $\xi_1 = 0.99357$ and $\xi_2 = 0.49286$. The matrix Hess (g) is:

TABLE 1

Standard free enthalpies of formation [13] and equilibrium composition. System $CH_4 + H_2O$. $T = 1000$ K, $P = 1$ atm., $n^0_{CH_4} = 1$ mole, $n^0_{H_2O} = 4$ moles

Compound	CH_4	H_2O	CO	H_2	CO_2
$(\Delta^f G^0_{1000})_i$, kcal/mole	4.5911	−46.034	−47.9623	0	−94.6077
g^0_i	2.3103	−23.1656	−24.1359	0	−47.615
n_i	0.00643	2.51356	0.50071	3.47358	0.49286

$$\text{Hess}\,(g) = \left\| \begin{array}{cc} 159.934507 & -0.73566 \\ -0.73566 & 4.711866 \end{array} \right\| \tag{36}$$

and

$$[\text{Hess}(g)]^{-1} = \left\| \begin{array}{cc} 6.257053 . 10^{-3} & 0.9769 . 10^{-3} \\ 0.9769 . 10^{-3} & 0.212383 \end{array} \right\| \tag{37}$$

a) The effect of temperature

The reaction enthalpies, $(\Delta^r H^0_{1000})_j$, are: 53.955699 and −9.3279309 kcal. At $T = 1000$ K one obtains:

$$\| \Delta^r H^0_j / R T^2 \| = \left\| \begin{array}{c} 0.027162555 \\ -4.6958976 . 10^{-3} \end{array} \right\| \tag{38}$$

Using equation (22) it results:

$$\frac{1}{\delta T} \| \delta \xi_j \| = \left\| \begin{array}{c} 0.16537 . 10^{-3} \\ -0.970792 . 10^{-3} \end{array} \right\| \tag{39}$$

The corresponding values $\delta n_i/\delta T$, calculated by equation (20) are given in table 2.

TABLE 2

The effect of input data changes on the equilibrium composition. System $CH_4 + H_2O$. $T = 1000$ K, $P = 1$ atm, $n^0_{C_4H} = 1$ mol, $n^0_{H_2O} = 4$ moles

Compound	CH_4	H_2O	CO	H_2	CO_2
$1000\ \delta n_i/\delta T$	−0.16537	0.805422	1.136162	−0.474682	−0.970792
$1000\ \delta n_i/\delta \ln P$	12.514105	14.467905	−10.560305	−39.496115	−1.9538
$\delta n_i/\delta n^0_{CH_4}(k)$	0.025108	−1.127099	0.822685	3 076883	0.152207
$\delta n_i/\delta n^0_{H_2O}(k)$	−0.004669	0.910449	−0.080213	0.098889	0.084882

b) The effect of pressure

The sums of stoichiometric coefficients of the reactions are $\nu_1 = 2$ and $\nu_2 = 0$ respectively. Using equation (24) one obtains:

$$\frac{1}{\delta \ln P} \| \delta \xi_j \| = \left\| \begin{matrix} -12.514105 . 10^{-3} \\ -1.9538 . 10^{-3} \end{matrix} \right\| \tag{40}$$

The corresponding values $\delta n_i/\delta \ln P$, calculated by equation (20) are also given in table 2.

c) The effect of initial amounts

This effect was firstly calculated for the simultaneous changes $\delta n^0_{CH_4} = 0.001$ and $\delta n^0_{H_2O} = -0.001$ (the other changes $\delta n^0_i = 0$, $i \neq CH_4, H_2O$). From equation (29) it results:

$$\| B_j \| = \left\| \begin{matrix} 0.1551231 \\ 0.3978 . 10^{-3} \end{matrix} \right\| \tag{41}$$

Using equation (31) one obtains:

$$\| \delta \xi_j \| = \left\| \begin{matrix} 9.702 . 10^{-4} \\ 6.7 . 10^{-5} \end{matrix} \right\| \tag{42}$$

The correspinging δn_i values are: $0.0298.10^{-3}$, $-2.0372.10^{-3}$, $0.9032.10^{-3}$, $2.9776.10^{-3}$, $0.067.10^{-3}$.

The effect of change in the initial amount of a component was calculated by equation (32). For a change in the initial amount of CH_4 it results

$$\| B'_j \| = \left\| \begin{matrix} -155.807235 \\ 0 \end{matrix} \right\| \tag{43}$$

and from (32) :

$$\frac{1}{\delta n^0_{CH_4(k)}} \| \delta \xi_j \| = \left\| \begin{matrix} 0.974892 \\ 0.152207 \end{matrix} \right\| \tag{44}$$

Similarly a change $\delta n^0_{H_2O(k)}$ gives :

$$\| B'_j \| = \left\| \begin{matrix} -0.68408 \\ -0.39784 \end{matrix} \right\| \tag{45}$$

and from (32) :

$$\frac{1}{\delta n^0_{H_2O(k)}} \| \delta \xi_j \| = \left\| \begin{matrix} 4.668973 . 10^{-3} \\ 0.084882 \end{matrix} \right\| \tag{46}$$

The corresponding values $\delta n_i / \delta n^0_{CH_4(k)}$ and $\delta n_i / \delta n^0_{H_2O(k)}$ are given in table 2.

Some results of the treatment advanced in this paper are similar to those obtained by the "theta" method.[8] Possible applications and the limits of "theta method" were largely discussed elsewhere[8] but the conclusions are valid for this work too.

REFERENCES

[1] D. Geană *Rev. Roumaine Chim.*, **26,** 43 (1981).

[2] R. J. Duffin, E. L. Peterson and C. Zener, "Geometric Programming Theory and Application", Wiley, New York, 1967.

[3] I. Marusciac, "Programare geometrică şi aplicaţii", Ed. Dacia, Cluj-Napoca, 1978.

[4] J. J. Dinkel and R. Lakshmanan, *Comput. Chem. Eng.*, **1,** 41 (1977) ; *J. Engng. Mathemat.*, **9,** 343 (1975).

[5] C. J. Pings, *Chem. Eng. Sci.* **16,** 181 (1961) ; A. H. Larsen, C. S. Lu and C. J. Pings, *ibid.*, **23,** 289 (1968).

[6] W. R. Smith, *Can J. Chem. Eng.*, **47,** 95 (1969) ; *Ind. Eng. Chem. Fundam.*, **17,** 69 (1978).

[7] F. van Zeggeren and S. H. Storey, "The Computation of Chemical Equilibrium", Cambridge Univ. Press, 1970, p. 47.

[8] F. Daneş and D. Geană, Bulet. Inst. Politehnic. Bucureşti, in press.

[9] V. Dumitru, "Programare Neliniară", Ed. Academiei, Bucueşti, 1975, cap. 1.

[10] M. Dragomirescu and M. Maliţa, "Programare neliniară", Ed. Ştiinţifică, Bucureşti, 1972, cap. 2, 3.

[11] I. Prigogine and R. Defay, "Chemische Thermodynamik", VEB Deutscher Vlg., Leipzig, 1962, cap. 15.

[12] F. Daneş and D. Geană, *Rev. Chim. (Bucureşti)*, **30,** 244 (1979).

[13] D. Geană, *Rev. Chim. (Bucureşti)*, **28,** 1058 (1977).

[14] E. J. Henley, and E. M. Rosen, "Material and Energy Balance Computations", Wiley, New York, 1969, p. 202.

Revue Roumaine de Chimie **26**, *11–12*, 1377–1386 (1981)

UNE EXTENSION DE LA THÉORIE THERMODYNAMYQUE STAVERMAN/SCATCHARD DU POTENTIEL DE MEMBRANE

F. DANEŞ, S. STERNBERG, SILVIA DANEŞ
Laborator Chimie Fizică, str. Polizu 1, 78126 Bucureşti

Reçu le 4 novembre 1980

En partant de la relation thermodynamique entre le potentiel de membrane et les nombres de transfert, on déduit des expressions générales pour la polarité des électrodes et pour la tension électromotrice de l'élément galvanique de concentration à membrane non ionogène ou échangeuse d'ions, expressions rendant aussi compte du déplacement du centre de masse du système. Les arguments sont les valences des ions, les concentrations de l'anolyte et du catolyte et quelques indicateurs à deux valeurs concernant le type d'électrode, le type de membrane et le sens du déplacement électro-osmotique. Les expressions obtenues lient la t.é.m. aux variations des nombres de transport à travers la membrane et à l'activité ionique en fonction de la concentration.

Starting from the thermodynamic relationship between membrane potential and transference number, general expressions are derived for the polarity of electrode and for the e.m.f. of the concentration galvanic cell with nonionic or ion exchanging membrane, taking into acount the displacement of mass centre of the system. Arguments are ion valences, concentrations of anolyte and catolyte and some two-value indicators concerning electrode type, membrane type and direction of the electroosmotic displacement. The expressions obtained relate the e.m.f. to the variations in the transfer numbers across membrane and in the ion activity, as functions of concentration.

1. THÉORIES ACTUELLES DU POTENTIEL DE MEMBRANE (PM)

Le potentiel de membrane PM représente la différence de potentiel électrique entre deux solutions séparées par une membrane, solutions formées par les mêmes constituants (un solvant – d'habitude l'eau – et un soluté électrolyte) mais différant par la concentration. L'importance pratique du PM [1-3] justifie l'emploi de plusieurs méthodes d'évaluation et de corrélation des PM, pouvant être classifiées [4-6] en :

I. Méthodes structurelles de Teorell (1935) ou de Mayer et Sievers (1936), les plus utilisées aujourd'hui ; [7]

II. Méthode thermodynamique statistique de Nagasawa [8] qui part de la théorie VAR d'Eyring ; et

III. Méthode thermodynamique phénoménologique de Staverman [9] et Scatchard [10], reliant le PM aux nombres de transport des ions et de l'eau dans la membrane.

Les deux premières méthodes manient des grandeurs difficilement mesurables (concentrations dans la membrane, en I), calculées à une marge d'erreur inévaluable (fonctions de partition, en II) ou mal définies (concentration « efficiente » des charges fixes, en I), de manière que pour l'instant l'approche phénoménologique est le seul opérationnel. Au prix du renoncement à l'explication du mécanisme de formation du PM, l'approche III s'avère ainsi nettement supérieure aux autres du point de vue prédictif. Introduits sur une base demi-empirique, des travaux de thermodynamique des processus irréversibles [11] ont montré ensuite que son équation fondamentale est rigoureusement correcte, la seule simplification étant [12] l'assimilation des centres des masses du système et du solvant (v. § 2). La vérification expérimentale – portant sur les nombres de transport chez Lorimer [13] et Hookway [14] ou sur les PM chez Lakshminarayanaiah [15] – est satisfaisante. Le dernier auteur trouve ainsi [16] une erreur moyenne de 0,5 mV pour les PM obtenues par III et de 6 mV si on les obtient par I, tandis que en [17] on trouve la déviation standard des PM calculée par III de 3–10 %, valeur acceptable par comparaison à la précision expérimentale de 5–8 % selon Novikov. [18]

D'autre part, le champ d'application de la théorie Staverman–Scatchard est encore assez étroit : solutés électrolytes 1–1, électrodes réversibles par rapport à l'anion, effet électro-osmotique « normal » (l'eau est transportée dans la direction de l'ion à nombre de transport plus grand [19]). La théorie n'est pas capable d'établir si c'est la plus concentrée des deux solutions qui joue le rôle de l'anolyte (électrolyte en contact avec l'anode) ou bien la plus diluée. Le but des paragraphes suivants sera l'extension de la théorie mentionnée aux ions de n'importe quelle valence, électrodes de toute sorte et transport d'eau « anormal ».

2. RELATION THERMODYNAMIQUE DU POTENTIEL DE MEMBRANE

L'expression de Scatchard et Staverman pour le PM

$$E_{m,\mathrm{ss}} = -(RT/F)\,\Sigma_i \int_{\ln a_i'}^{\ln a_i''} \tau_i \,\mathrm{d}(\ln a_i)$$

revient à

$$E_{m,\mathrm{ss}} = -(RT/F)\left[\int_{\ln a_\mathrm{A}'}^{\ln a_\mathrm{A}''} \tau_\mathrm{A}\,\mathrm{d}(\ln a_\mathrm{A}) + \right.$$

$$\left. + \int_{\ln a_\mathrm{C}'}^{\ln a_\mathrm{C}''} \tau_\mathrm{C}\,\mathrm{d}(\ln a_\mathrm{C}) + \int_{\ln a_\mathrm{W}'}^{\ln a_\mathrm{W}''} \tau_\mathrm{W}\,\mathrm{d}(\ln a_\mathrm{W})\right] \qquad (1a)$$

quand le solvant est l'eau (indice W) et le soluté électrolyte est totalement dissocié en formant l'anion A et le cation C. Ici R, F et T sont la constante du gaz parfait, celle de Faraday et la température, a_{A}, a_{C}, a_{W} — les activités des espèces A, C, W dans la solution d'une composition donnée tandis que τ_{A}, τ_{C} et τ_{W} sont les « nombres de transfert » des mêmes espèces à travers la membrane équilibrée avec la solution de concentration (molarité) m. Les limites d'intégration a'_{A}, a'_{C}, a'_{W} correspondent à l'anolyte et les limites a''_{A}, a''_{C} a''_{W} — au catolyte. Le nombre de transfert τ_i est défini comme le rapport entre le nombre des particules i et le nombre des charges élémentaires d'électricité positive qui traversent simultanément la membrane dans le même sens. Riandé[12] montre qu'au PM Staverman/Scatchard il faut ajouter la correction $E_{m,\mathrm{Ri}}$ rendant compte du déplacement différent des centres de masse du système total et de l'eau :

$$E_{m,\mathrm{Ri}} = (-RT/F)\int_{\ln a'_{\mathrm{W}}}^{\ln a''_{\mathrm{W}}} (\tau_{\mathrm{A}} + \tau_{\mathrm{C}})\,\mathrm{d}(\ln a_{\mathrm{W}}) \qquad (1b)$$

Le PM corrigé, E_m, sera ainsi $E_m = E_{m,\mathrm{ss}} + E_{m,\mathrm{Ri}}$ soit, avec $E_{m,\mathrm{ss}}$ et $E_{m,\mathrm{R}}$ de (1a), (1b) :

$$E_m = (-RT/F)\left[\int_{\ln a'_{\mathrm{A}}}^{\ln a''_{\mathrm{A}}} \tau_{\mathrm{A}}\,\mathrm{d}(\ln a_{\mathrm{A}}) + \int_{\ln a'_{\mathrm{C}}}^{\ln a''_{\mathrm{C}}} \tau_{\mathrm{C}}\,\mathrm{d}(\ln a_{\mathrm{C}}) + \right.$$

$$\left. + \int_{\ln a'_{\mathrm{W}}}^{\ln a''_{\mathrm{W}}} (\tau_{\mathrm{W}} + \tau_{\mathrm{A}} + \tau_{\mathrm{C}})\,\mathrm{d}(\ln a_{\mathrm{W}})\right]$$

On peut passer des « nombres de transfert » ioniques τ_{A}, τ_{C} aux « nombres de transport » de Hittorf, t_{A} et t_{C}, par les relations

$$t_{\mathrm{A}} = -Z_{\mathrm{A}}\tau_{\mathrm{A}}\,; \quad t_{\mathrm{C}} = Z_{\mathrm{C}}\tau_{\mathrm{C}}$$

Z_{A} et Z_{C} étant les valences (en module) des deux ions, et substituer d'autre part τ_{W} par

$$\tau_{\mathrm{W}} = \delta'_{\mathrm{W}} t_{\mathrm{W}}$$

où t_{W}, le « nombre de transport » de l'eau, représente la valeur absolue de son nombre de transfert et l'indicateur δ'_{W} du sens de déplacement de l'eau sera -1 si ce sens coïncide avec celui de l'anion et $+1$ si il coïncide avec celui du cation. En passant de τ_i au t_i :

$$E_m = (RT/F)\left[\int_{\ln a'_{\mathrm{A}}}^{\ln a''_{\mathrm{A}}} (t_{\mathrm{A}}/Z_{\mathrm{A}})\,\mathrm{d}(\ln a_{\mathrm{A}}) - \int_{\ln a'_{\mathrm{C}}}^{\ln a''_{\mathrm{C}}} (t_{\mathrm{C}}/Z_{\mathrm{C}})\,\mathrm{d}(\ln a_{\mathrm{C}}) - \right.$$

$$\left. - \int_{\ln a'_{\mathrm{W}}}^{\ln a''_{\mathrm{W}}} (\delta'_{\mathrm{W}} t_{\mathrm{W}} - t_{\mathrm{A}}/Z_{\mathrm{A}} + t_{\mathrm{C}}/Z_{\mathrm{C}})\,\mathrm{d}(\ln a_{\mathrm{W}})\right] \qquad (2)$$

La grandeur mesurable n'est pas le PM, mais la tension électromotrice (t.é.m.) E de l'élément galvanique de concentration (EGC) symbolisé par

$$(-)\ \mathrm{Me}'/\mathrm{Sol}'//\mathrm{Sol}''/\mathrm{Me}''\ (+) \tag{I}$$

où les constituants métalliques Me′ et Me″ de l'anode, respectivement du cathode, sont identiques, Sol′ représente l'anolyte. Sol″ — le catolyte et // — la membrane.

La composante électrodique E_{el} de la t.é.m. pour l'EGC (I) sera, selon Nernst :

$$E_{\mathrm{el}} = -\,(RT/FZ_{\mathrm{A}}) \ln (a''_{\mathrm{A}}/a'_{\mathrm{A}})$$

si les électrodes sont réversibles par rapport à l'anion et

$$E_{\mathrm{el}} = (RT/FZ_{\mathrm{C}}) \ln (a''_{\mathrm{C}}/a'_{\mathrm{C}})$$

pour des électrodes cation-réversibles, ou dans une seule expression

$$E_{\mathrm{el}} = (RT/2F)\,[Z_{\mathrm{A}}^{-1}(\delta_{\mathrm{E}} - 1) \ln (a''_{\mathrm{A}}/a'_{\mathrm{A}}) + Z_{\mathrm{C}}^{-1}(\delta_{\mathrm{E}} + 1) \ln (a''_{\mathrm{C}}/a'_{\mathrm{C}})]$$

où l'indicateur δ_{E} prend la valeur -1 pour des électrodes anion — réversibles et $+1$ si ils sont cation — réversibles. En tenant compte de la relation générale

$$\ln (x''/x') = \int_{\ln x'}^{\ln x''} \mathrm{d}(\ln x)$$

il s'ensuit que

$$E_{\mathrm{el}} = (RT/2F)\left[(\delta_{\mathrm{E}} - 1)\int_{\ln a'_{\mathrm{A}}}^{\ln a''_{\mathrm{A}}} Z_{\mathrm{A}}^{-1}\,\mathrm{d}(\ln a_{\mathrm{A}}) + (\delta_{\mathrm{E}} + 1)\int_{\ln a'_{\mathrm{C}}}^{\ln a''_{\mathrm{C}}} Z_{\mathrm{C}}^{-1}\,\mathrm{d}(\ln a_{\mathrm{C}})\right] \tag{3}$$

La t.é.m. sera la somme

$$E = E_m + E_{\mathrm{el}}$$

ou, avec E_m, E_{el} de (2) et (3) :

$$E = (RT/F)\left[\int_{\ln a'_{\mathrm{A}}}^{\ln a''_{\mathrm{A}}} \varphi_{\mathrm{A}}\,\mathrm{d}(\ln a_{\mathrm{A}}) + \int_{\ln a'_{\mathrm{C}}}^{\ln a''_{\mathrm{C}}} \varphi_{\mathrm{C}}\,\mathrm{d}(\ln a_{\mathrm{C}}) + \int_{\ln a'_{\mathrm{W}}}^{\ln a''_{\mathrm{W}}} \varphi_{\mathrm{W}}\,\mathrm{d}(\ln a_{\mathrm{W}})\right] \tag{4}$$

où :

$$\varphi_W = - t_W \delta'_W + t_A/Z_A - t_C/Z_C \tag{5a}$$

$$\varphi_A = (\delta_E/2 - 1/2 + t_A)/Z_A, \quad \varphi_C = (\delta_E/2 + 1/2 - t_C)/Z_C$$

Les deux dernières expressions deviennent, en substituant $1 = t_A + t_C$:

$$\varphi_A = (\delta_E + t_A - t_C)/2Z_A, \quad \varphi_C = (\delta_E + t_A - t_C)/2Z_C \tag{5b, 5c}$$

Les quantités (en moles) n_A, n_C, n_W des trois constituants dans une quantité de solution de molalité m et qui contient 1 kg d'eau seront :

$$n_A = \nu_A m\,; \quad n_C = \nu_C m\,; \quad n_W = 1/M_W \tag{6}$$

où M_W est la masse molaire de l'eau et ν_A, ν_C sont les nombres des anions et cations dans la formule conventionnelle du soluté électrolyte, c.-à-d. :

$$\nu_A = Z_C/\omega, \quad \nu_C = Z_A/\omega \tag{7a, 7b}$$

d'où on obtient :

$$n_A = Z_C m/\omega, \quad n_C = Z_A m/\omega \tag{8a, 8b}$$

ω étant le plus grand diviseur commun des nombres Z_A et Z_C. En substituant n_A, n_C, n_W de (8a, 8b, 6) dans la relation

$$n_A \, \mathrm{d}(\ln a_A) + n_C \, \mathrm{d}(\ln a_C) + n_W \, \mathrm{d}(\ln a_W) = 0$$

de Gibbs et Duhem, il résulte que

$$\mathrm{d}(\ln a_W) = - (M_W m/\omega)\,[Z_C \, \mathrm{d}(\ln a_A) + Z_A \, \mathrm{d}(\ln a_C)] \tag{9}$$

En substituant φ_W, φ_A, φ_C et $\mathrm{d}(\ln a_W)$ de (5a, 5b, 5c, 9) en (4), on obtient :

$$E = (RT/F)\left[\int_{\ln a'_A}^{\ln a''_A} (\psi/Z_A)\, \mathrm{d}(\ln a_A) + \int_{\ln a'_C}^{\ln a''_C} (\psi/Z_C)\, \mathrm{d}(\ln a_C)\right] \tag{10}$$

l'expression ψ représentant

$$\psi = (\delta_E + t_A - t_C)/2 + (M_W m Z_A Z_C/\omega)\,(\delta'_W t_W - t_A/Z_A + t_C/Z_C) \tag{11}$$

D'autre part, en substituant ν_A, ν_C de (7a, 7b) dans la définition

$$(a)^{\nu_A + \nu_C} = (a_A)^{\nu_A} (a_C)^{\nu_C}$$

de l'activité ionique moyenne a, on obtient après différentiation :

$$(Z_A^{-1} + Z_C^{-1})\,\mathrm{d}(\ln a) = Z_A^{-1}\,\mathrm{d}(\ln a_A) + Z_C^{-1}\,\mathrm{d}(\ln a_C)$$

de manière que (10) devient

$$E = (RT/F)\,(Z_A^{-1} + Z_C^{-1})\int_{\ln a'}^{\ln a''} \psi\,\mathrm{d}(\ln a_A)$$

a' et a'' étant les activités ioniques moyennes de l'anolyte et du catolyte. En substituant ψ de (11), on arrive à :

$$E = (RT/F)\,(Z_A + Z_C)\int_{\ln a'}^{\ln a''} [(\delta_E + t_A - t_C)/(2Z_AZ_C) +$$

$$+ (M_W m/\omega)\,(\delta'_W t_W - t_A/Z_A + t_C/Z_C)]\,\mathrm{d}(\ln a) \tag{12}$$

expression finale permettant de calculer E en fonction des molalités m' (anolyte) et m'' (catolyte), si on connaît les variations isothermes de t_A (ou t_C), de t_W et de a avec la molalité m.

L'expression (12) revient, pour des ions monovalents ($Z_A = Z_C = 1$, donc $\omega = 1$), électrodes anion-réversibles ($\delta_E = 1$) et déplacement de l'eau vers le catolyte (donc $\delta'_W = 1$), à :

$$E = (2RT/F)\int_{\ln a'}^{\ln a''} [(-1 + t_A - t_C)/2 - M_W m(-t_W - t_A + t_C)]\,\mathrm{d}(\ln a)$$

ou, en substituant $t_A = 1 - t_C$ et en négligeant t_A et t_C auprès de t_W ($|t_A - t_C| \ll t_W$) :

$$E = (2RT/F)\int_{\ln a''}^{\ln a'} (t_C - M_W m t_W)\,\mathrm{d}(\ln a)$$

ce qui représente la relation obtenue par Staverman et Scatchard.

3. POLARITÉ DE L'EGC

L'utilité de l'expression (12) augmente si on exprime a', a'' et E en fonction des molalités m_1 et m_2 de la plus diluée, respectivement de la plus concentrée des deux solutions. On a donc par définition

$$m_1 < m_2 \tag{13a}$$

d'où il s'ensuit que les activités correspondant à ces deux molalités seront aussi dans le rapport

$$a_1 < a_2 \tag{13b}$$

car toujours

$$da/\mathrm{d}m > 0 \tag{14}$$

(autrement le soluté sera précipité).

En mettant (12) dans la forme

$$E = \int_{\ln a'}^{\ln a''} G(a)\, \mathrm{d}(\ln a) \tag{15}$$

on remarquera que $G(a)$ ne change pas de signe pour aucune des valeurs a admissibles, (positives), sinon E augmentera quand la différence $(a_2 - a_1)$ diminue. Le signe de G doit être le même que celui de $(a'' - a')$ car autrement de (15) il s'ensuivra $E < 0$. Donc :

$$(a'' - a')\, G(a) > 0 \tag{16a}$$

D'autre part, en comparant (12) et (15) :

$$G = RT/(2Z_\mathrm{A}Z_\mathrm{C}F)\,(Z_\mathrm{A}+Z_\mathrm{C})\,[\delta_\mathrm{E}+t_\mathrm{A}-t_\mathrm{C}+2M_\mathrm{W}mZ_\mathrm{A}Z_\mathrm{C}\omega^{-1}(\delta'_\mathrm{W}t_\mathrm{W}-t_\mathrm{A}/Z_\mathrm{A}+t_\mathrm{C}/Z_\mathrm{C})],$$

le plus important terme de la parenthèse carrée étant δ_E (toujours $|t_\mathrm{A} - t_\mathrm{C}| < 1$) de manière que G et δ_E ont le même signe :

$$\delta_\mathrm{E} G(a) > 0 \tag{16b}$$

En combinant (15a, 16b) on a

$$(a'' - a')\, \delta_\mathrm{E} > 0$$

donc $a'' < a'$ si $\delta_\mathrm{E} = -1$ et $a'' > a'$ si $\delta_\mathrm{E} = 1$; ou bien, en vertu de (14) :

$$m'' < m', \quad \delta_\mathrm{E} = -1 \tag{17a}$$

$$m'' > m', \quad \delta_\mathrm{E} = 1 \tag{17b}$$

ce qu'on peut exprimer aussi par les relations

$$m' = [m_1 + m_2 + \delta_\mathrm{E}(m_1 - m_2)]/2 \tag{18a}$$

$$m'' = [m_2 + m_1 + \delta_\mathrm{E}(m_2 - m_1)]/2 \tag{18b}$$

tandis que l'expression (12) devient

$$E = \delta_\mathrm{E}(RT/F)\,(Z_\mathrm{A} + Z_\mathrm{C}) \int_{\ln a_1}^{\ln a_2} [(\delta_\mathrm{E} + t_\mathrm{A} - t_\mathrm{C})/(2Z_\mathrm{A}Z_\mathrm{C}) +$$

$$+ (M_\mathrm{W}m/\omega)\,(\delta'_\mathrm{W}t_\mathrm{W} - t_\mathrm{A}/Z_\mathrm{A} + t_\mathrm{C}/Z_\mathrm{C})]\, \mathrm{d}(\ln a)$$

ou, en remarquant que $(\delta_E)^2 = 1$:

$$E = (RT/F)\,(Z_A + Z_C)\int_{\ln a_1}^{\ln a_2} \{[1 + \delta_E(t_A - t_C)]/(2Z_AZ_C) +$$

$$+ (M_W m/\omega)\,[t_W \delta'_W \delta_E + \delta_E(-t_A/Z_A + t_C/Z_C)]\}\ \mathrm{d}\,(\ln a) \tag{19}$$

Forme alternative de l'équation (19) pour la t.é.m. : en notant par R_I le rapport $(n_A + n_C)/n_W$ entre le nombre total des ions et le nombre des molécules d'eau, on obtient de (6, 8a, 8b) :

$$R_I = M_W m(Z_A + Z_C)/\omega$$

On peut définir aussi la « valence moyenne » des ions comme moyenne harmonique, Z_h, des deux valences des ions

$$(Z_h)^{-1} = (Z_A^{-1} + Z_C^{-1})/2$$

La relation (19) devient, par introduction de R_I et Z_h :

$$E = (RT/F)\int_{\ln a_1}^{\ln a_2} \{[1 + \delta_E(t_A - t_C)]/Z_h + R_I\delta_E(\delta'_W t_W -$$

$$- t_A/Z_A + t_C/Z_C)\}\ \mathrm{d}(\ln a) \tag{20}$$

4. EGC À MEMBRANE ÉCHANGEUSE D'IONS

Pour la migration par des membranes échangeuses d'ions il faut distinguer entre le co-ion (ion ayant le même signe de la charge électrique que les groupes actifss fixés au réseau polymère) et le contre-ion (à signe opposé). Le co-ion sera le cation pour les membranes échangeuses d'anions (anioniques) et l'anion pour les membranes cationiques, échangeuses de cations. La propriété de la permsélectivité revient à un nombre de transport t_K du co-ion beaucoup moindre que celui du contre-ion, ou bien

$$t_K \ll 1$$

En introduisant l'indicateur δ_M du type de membrane ($\delta_M = -1$ pour une membrane anionique et $\delta_M = 1$ pour une membrane cationique), on aura $t_K = t_C$ si $\delta_M = -1$ et $t_K = t_A$ si $\delta_M = 1$. En tenant compte de la relation $t_A + t_C = 1$, il s'ensuit que

$$t_A = (1 - \delta_M)/2 + \delta_M t_K\,; \quad t_C = (1 + \delta_M)/2 - \delta_M t_K$$

la relation (19) devenant ainsi

$$E = (RT/F)\,(Z_A + Z_C)\int_{\ln a_1}^{\ln a_2} \{[1 + \delta_E\delta_M(2t_K - 1)]/(2Z_AZ_C) +$$

$$+(M_W m/\omega)[t_W \delta'_W \delta_E - \delta_E(1/Z_A - 1/Z_C)/2 + \delta_E\delta_M(1/2 - t_K)\,(1/Z_A + 1/Z_C)]\}\ \mathrm{d}(\ln a)$$

Il s'avère avantageux de remplacer les indicateurs δ'_W, δ_M par les nouveaux indicateurs δ_W, δ_S, définis par

$$\delta_W = \delta'_W \delta_M \tag{21a}$$

$$\delta_S = \delta_E \delta_M \tag{21b}$$

de manière que $\delta_W = -1$ pour l'électro-osmose anormale et $\delta_W = +1$ pour l'électro-osmose normale, tandis que $\delta_S = -1$ si les électrodes sont réversibles par rapport au co-ion et $\delta_S = 1$ s'ils sont réversibles par rapport au contre-ion. En combinant (21a, 21b) on obtient $\delta'_W = \delta_W \delta_E / \delta_S$ ou bien ($\delta_S^2 = 1$)

$$\delta'_W = \delta_W \delta_S \delta_E \tag{21c}$$

En introduisant δ_M et δ'_W (21b, 21c) dans l'expression pour E, celle-ci devient

$$E = (RT/F)\,(Z_A^{-1} + Z_C^{-1}) \int_{\ln a_1}^{\ln a_2} [(1 - \delta_S)/2 + \delta_S t_K + M_W m \omega^{-1} Z_A Z_C t_W \delta_S \delta_W +$$

$$+ M_W m \omega^{-1} \delta_E (Z_A - Z_C)/2 + (M_W m/\omega) \delta_S (Z_A + Z_C)\,(1/2 - t_K)]\, \mathrm{d}(\ln a) \tag{22}$$

L'expression pour la t.é.m. peut être scindée dans quelques contributions séparées, nommément :

a) la correction de Riandé pour le déplacement du centre de masse du système

$$E_{R1} = (RTM_W/2F\omega)\,(Z_A^{-1} + Z_C^{-1}) \int_{\ln a_1}^{\ln a_2} \mathrm{m}[\delta_E (Z_A - Z_C) +$$

$$+ \delta_S (Z_A + Z_C)\,(1 - 2t_K)]\, \mathrm{d}(\ln a) \tag{23a}$$

b) la contribution du déplacement de l'eau

$$E_W = (RTM_W \delta_S \delta_W / F\omega)\,(Z_A + Z_C) \int_{\ln a_1}^{\ln a_2} \mathrm{m} t_W\, \mathrm{d}(\ln a) \tag{23b}$$

c) la contribution de la migration du co-ion

$$E_K = RT \delta_S F^{-1} (Z_A^{-1} + Z_C^{-1}) \int_{\ln a_1}^{\ln a_2} t_K\, \mathrm{d}(\ln a) \tag{23c}$$

d) la contribution de la membrane « parfaite », où il n'y a pas déplacement du centre de masse, du co-ion et de l'eau :

$$E_p = (RT/2F)\,(Z_A^{-1} + Z_C^{-1})\,(1 - \delta_S)\ln(a_2/a_1) \tag{23d}$$

la relation (22) devenant ainsi :

$$E = E_p + E_k + E_W + E_{Ri}. \tag{24}$$

Si $\delta_S = -1$, les composantes E_k, E_W ont le signe opposé à celui de la composante principale E_p et sont moindres que celle-ci, sans être pour autant négligeables. Si $\delta_S = 1$, E_p s'annule et E_k, E_W deviennent les principales composantes de la t.é.m. Quant à E_{Ri}, cette contribution est généralement négligeable. Le signe de E_k et E_W coïncide pour l'électro-osmose normale.

5. CONCLUSIONS

On a développé des relations générales qui permettent de calculer la polarité des électrodes [17,18] et la tension électromotrice de l'élément galvanique de concentration à membrane, quelconque [19,20] ou échangeuse d'ions. [22,24] Les arguments y entrant sont : les valences des ions ; les nombres de transport et l'activité, comme fonction de la molalité de la solution ; une série d'indicateurs à deux valeurs, 1 et −1, rendant compte des différences qualitatives qui peuvent apparaître en ce qui concerne le sens de déplacement de l'eau, le type de membrane ou d'électrode, etc. En particularisant pour certains types d'ions et d'électrodes, on retrouve les expressions plus simples déduites précédemment : celle de la membrane parfaitement sélective, celles de Staverman et Scatchard, de Riandé, etc.

Les expressions déduites ont permis aux auteurs de vérifier pour la première fois [17] la théorie thermodynamique du PM en systèmes à soluté électrolyte constitué d'ions polyvalents.

BIBLIOGRAPHIE

[1] « Ionnoobmennye membrany v elektrodialize », red. K. M. Saldadze, izd. Khimya, Leningrad, 1970.

[2] R. Lacey, S. Loeb, « Industrial Processing with Membranes », Wiley, New York, 1972, 2nd chap.

[3] N. Lakshminarayanaiah, « Membrane Electrodes », Academic Press, New York, 1976, 3rd chap.

[4] S. Caplan, D. Miculescu, « Transport Processes in Membranes », vol. « Ion Exchange », 1st vol., red. J. Marinsky, ed. M. Dekker, New York, 1966, 8th chap.

[5] E. Riande, « Transport Phaenomena in Ion Exchange Membranes », vol. « Physics of Electrolytes », 1st vol., red. J. Hladik, Academic Press, New York, 1972, 11th chap.

[6] F. Siddiqi, M. Nasim Beg, S. Singh, A. Haque, *Electrochim. Acta*, **22**, 631 (1977).

[7] F. Siddiqi, M. Nasim Beg, A. Haque, S. Singh, *Electrochim. Acta*, **22**, 639 (1977).

[8] M. Nagasawa, Y. Kobatake, *J. Phys. Chem.*, **56**, 1017 (1952).

[9] A. Staverman, *Trans. Faraday Soc.*, **48**, 176 (1952).

[10] G. Scatchard, *J. Amer. Chem. Soc.*, **75**, 2883 (1953).

[11] G. Hills, P. Jacobs, N. Lakshminarayanaiah, *Proc. Roy. Soc.*, **A 262** ; 246 (1961).

[12] E. Riande, G. Guzman y M. Dominguez, *Anales de Quimica*, **66**, 57 (1970).

[13] J. Lorimer, E. Boterenbrood, J. Hermans, *Discuss. Faraday Soc.*, **21**, 141 (1956).

[14] H. Hookway, *Nat. Acad. Sci. Publ.*, **568**, 233 (1958).

[15] N. Lakshminarayanaiah, V. Subrahmanyan, *J. Polymer Sci.*, **A2**, 4491 (1964).

[16] N. Lakshminarayanaiah, *J. Phys. Chem.*, **70**, 1588 (1966).

[17] S. Sternberg, L. Shirshina, S. Daneş, F. Daneş, *Z. phys. Chem. (Leipzig)* (à paraître).

[18] P. D. Novikov, op. cit. [1], s. 108–120.

[19] F. Helfferich, « Ionenaustauscher », 1. Bd., Vlg. Chemie, Wienheim, 1959, 8. Kap.

Revue Roumaine de Chimie, **26**, *11–12*, 1387–1391 (1981)

X-RAY ANALYSIS OF SOME CARBON FIBRES

IOANA DEMETRESCU and D. FĂTU
Physical Chemistry Department, National Institute of Chemistry,
Bd. Republicii 13, Bucharest, Romania

Received August 1, 1980

Correlations between structure and texture of materials consisting of carbon fibres, on the one hand and the technology used to obtain fibres,[1-3] woven materials [4] or composite[5-6] were established. The study was done by X-ray analysis.

INTRODUCTION

One of the latest forms of carbon offered to the modern industry is the carbon fibre. Raw materials for fibres are organic synthetic fibres like polyacrylonitrile or aromatic residues and oil gudron. The material is thermally degraded in oxidative atmosphere and then in inert atmosphere[1-4] and finally fibres with great resistance at mechanical efforts and elasticity are obtained.

Depending on the utilization of carbon fibres, there are numerous subsequent technological processes by which a new material [5,6] (metal, resin, silicon) is included to be a support for the fibre, adding, at the same time, new properties and applications of the composite.

In this paper we have undertaken the X-ray analysis of three types of carbon fibres : fibre, woven material and composite. We have determined the correlation between the graphite content and fibres texture with various production technologies.

EXPERIMENTAL

In order to get diffraction maxima of carbon fibres by Debye–Scherer method, a Philips. X-ray difractometer with Cu-anticathode was used. The powder samples were studied using a cup-like sample support.

The fibre texture was studied by means of X-ray equipment, type TUR-M-60. An arrangement to render evident the prefferential orientation of (0002) planes with respect to fibre axis is presented in figure 1. The diffraction pattern was obtained after a 22 hour exposure. The radiation $K_{\alpha \mathrm{Ni}} = 1.658$ Å was used.

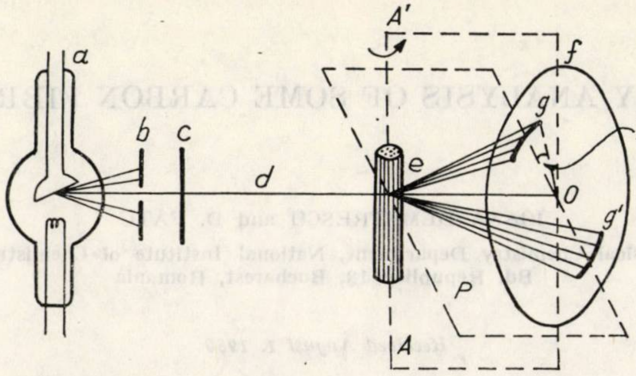

Fig. 1. — Experimental arrangement for getting fibre texture : *a* — X-ray tub ; *b* — slit ; *c* — filter ; *d* — monochromatic pencil of X rays ; *e* — sample (bunch of parallel carbon fibres fixed with colodium) ; *f* — film mounted in chamber Laue ; *eo* — distance between sample and film (30 mm) ; *P* — equatorial plane; *AA'* — fibre axis

RESULTS AND DISCUSSION

All studied materials have an intense diffraction maximum characteristic to Miller index (0002) planes. This shows that the fibre consists of amorphous carbon and graphite. Since two allotropic forms are present in this system and both have the same mass attenuation coefficient of X radiation, we can get the graphite molar fraction or weight fraction (W) using the linear relation :[7,8]

$$I/I_g = W \tag{1}$$

where I is the integrated intensity of (0002) diffraction maximum for the sample and I_g is the intensity of the same maximum in the case of pure graphite.

The linearity of eq. (1) was verified using amorphous carbon and graphite mixture in various proportions. The plot of the ratio I/I_g as a function of the graphite weight fraction is in a good agreement with eq. (1) (Fig. 2).

The intensities were determined both by measuring the height of the diffraction maximum and by evaluating the area delimited by the signal and its base line. The calibration curves were not significantly affected by the way the signal intensity was determined.

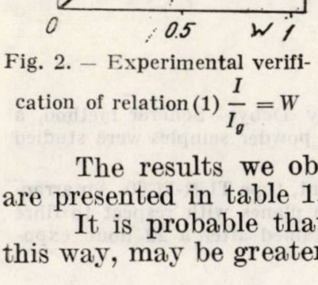

Fig. 2. — Experimental verification of relation (1) $\frac{I}{I_g} = W$

The results we obtained for fibre, woven material and composite are presented in table 1.

It is probable that the weight fraction of graphite, determined in this way, may be greater than the real one, because the (0002) diffraction maximum might be produced not only by crystalline graphite with a hexagonal lattice, but also by an intermediate phase with a structure characterized by partly unoriented and more distanced (0002) planes and missing $(hkil)l \neq 0$ planes.

TABLE 1

Weight fraction W of graphite phase in materials with carbon fibre

Material	W %
fibre	25
composite (superficial layer)	11
composite (in depth)	14
woven material	19
woven material (after calcination with constant temperature increase 10°/minute) up to 1000°C.	30

The data in table 1 also show that the thermal treatment leads to the increase in the graphite fraction. Thus, the graphite percentage in woven samples increased from 19 % to 30 % during calcination to 1000°C with a constant temperature increase of 10°/minute.

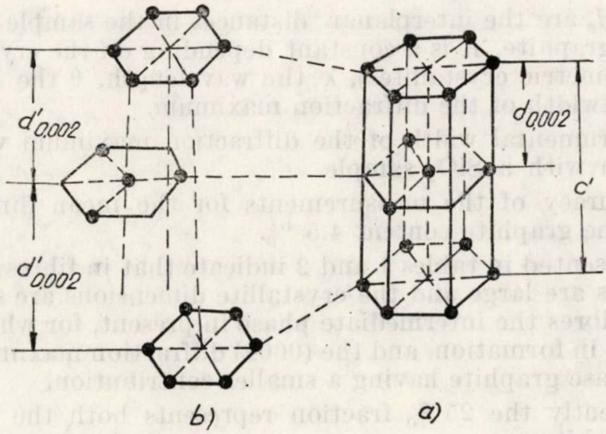

Fig. 3*a*. — Graphite hexagonal lattice; *b*. Planes 0002, partially unoriented and translated, of intermediate phase.

The interplanar distances and the crystallite dimensions of the studied carbon fibres, in comparison with pure graphite, are given in table 2.

In order to complete the comparative study, the distance d_{0002} between the (0002) planes, the relative variation $\Delta d/d$, and the average

TABLE 2

Interplanar distance and crystallite diameter

Material	d(Å) (0002)	$\frac{\Delta d}{d}$ %	D (Å)
fibre	3.460	2.5	45
composite	3.378	0.09	110
woven material	3.392	0.5	106
graphite etalon	3.375	—	>1000
graphite (literature)	3.38	—	>1000

dimension [9] D of crystallites were evaluated. The following equations were used :

$$\frac{\Delta d}{d} = \frac{d_p - d_g}{d_g} \tag{2}$$

$$D = \frac{K\lambda}{B\cos\theta} \tag{3}$$

where d_p and d_g are the interplanar distances in the sample and the reference powder graphite, K is a constant depending on the crystallite shape ($K = 1$ for isometric crystallites), λ the wavelength, θ the Bragg angle, and B the halfwidth of the diffraction maximum.

The instrumental width of the diffraction maximum was corrected by comparison with a SiO_2 sample.

The accuracy of the measurements for the mean dimension is of 8 % and for the graphite content 4.5 %.

Data presented in tables 1 and 2 indicate that in fibres the distances between planes are large and the crystallite dimensions are small. In this way, in such fibres the intermediate phase in present, for which the hexagonal lattice is in formation, and the (0002) diffraction maximum is mostly due to this phase graphite having a smaller contribution.

Consequently the 25 % fraction represents both the intermediate phase and graphite.

In carbon fibres which are termally treated and included in composite, crystallites have larger average dimensions, which shows a greater graphitization degree, even if the global proportion of intermediate phase and graphite is smaller than in the case of untreated fibres.

In figure 4 the image of the g and g' arcs is presented, corresponding to the X-ray diffraction on the 0002 planes, after 22 hour of exposure of a sample. The position of g and g' arcs in the equatorial plane shows that the (0002) planes have a preferential orientation parallel to the fibre axis AA'.

Measurements on films show an average half-angle of the equatorial dispersion arc $\varkappa_e$ (Fig. 1) of 32° and a Bragg angle $\theta K_{\alpha \mathrm{Ni}} = 14°20'$.

Using these data the angle of dispersion of (0002) planes with respect to the fibre axis AA' can be calculated[10], using equations of spherical trigonometry :

$$\sin \Phi = \cos \theta \sin \varkappa_e \qquad (4)$$

There results for this case $\Phi = 31°$.

Because $\theta < 20°$, $\cos \theta \cong 1$ and our data follow the simple relations $\sin \Phi \cong \sin \varkappa_e$ and $\Phi \cong \varkappa_e$.

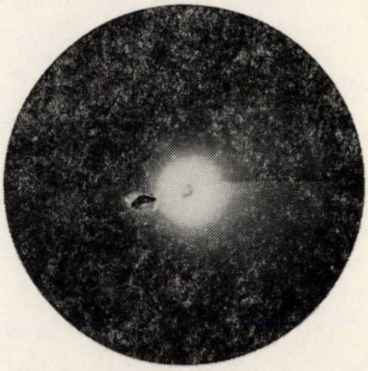

Fig 4. — Image of g and g' arcs corresponding to X-rays diffraction on (0002) planes after a 22 hour exposure of a sample.

CONCLUSIONS

1. X-ray analysis shows, for all materials consisting of carbon fibres, an intense diffraction maximum which can be due both to graphite and to an intermediate phase with (0002) planes translated from one another. Generally, the distance $d_{(0002)}$ is greater than the corresponding one for graphite.

2. X -ray phase analysis shows that by thermal treatment the intermediate phase and graphite percentage as well as the average crystallite dimensions are increased.

3. Texture studies show that the (0002) planes have a preferential orientation with respect to the fibre axis, the dispersion angle being of 31°.

4. The technology used to obtain the various kinds of carbon fibres does affect the graphitization degree and the mean dimension of crystallites.

ACKNOWLEDGEMENTS. We are grateful to Professor Dr. eng. D. Drimer (The Polytechnic Bucharest) for fibres and helpful discussions.

REFERENCES

[1] Patent specification, 1110791 (1970) (D01F 9/12).

[2] Patent specification, 1443935 (1972) (D01F 9/12).

[3] Patent specification, 1385213 (1972) (D01F 9/12).

[4] Patent specification, 1388789 (1973) (D01F 9/12).

[5] Patent specification, D01 F 9/12 1403863/1975.

[6] Patent specification, D01 F 9/12 1487947 (1974).

[7] A. Guinier, "Théorie et technique de la radiocristallographie", Dunod Paris 1964, p. 365.

[8] B. D. Cullity, "Elements of X-ray Diffraction", Addison Wesley Reading Massachussetts 1956, p. 391.

[9] H. P. Klug and L. E. Alexander "X-ray diffraction procedures for polycrystalline and amorphous material", J. Wiley Sons, Inc. New York, 1959.

[10] W. T. Astbury, *Proc. Roy. Soc., B*, **134**, 303 (1947)

Revue Roumaine de Chimie, **26**, *11–12*, 1393–1399 (1981)

ELECTRICAL CONDUCTION IN NICKEL–ALUMINA CATALYST

O. BUNESCU*, P. ROTARU* and S. I. BLEJOIU**

* University of Craiova, str. A. I. Cuza no. 13, Romania
** Chemical Works Craiova, Romania

Received March 20, 1981

The results of the electrical conductivity measurements in the temperature range 370–700 K and of Seebeck coefficient in the temperature range 550–700 K in nickel–alumina catalyst are presented. The effect of partial oxygen pressure on the electrical conductivity and influence of impurities is discussed.

1. INTRODUCTION

The nickel–alumina catalyst is used in ammonia industry. The charge carriers play an important part in the processes in which this catalyst participates. Thus, the chemisorption of different gases on catalyst surface implies the formation of certain bounds in which electrons or holes from the surface layer participate.

The charge carrier concentration in semiconductor oxide is dependent on the degree of nonstoichiometry. The electrical conduction type depends on the presence of an oxygen excess or deficit in the crystaline lattice; oxygen excess leads to *p*-type and oxygen deficit to *n*-type conduction. The presence of impurity ions having a different valence from that of the lattice ions leads to the appearance of certain charge carriers determined by the turning of a number of oxide cations into a valence state different from the valence corresponding to the chemical formula. We can easily remark that both the stoichiometry changes and those of impurity concentration will be reflected in the electrical conductivity variation.

In the nickel–alumina catalyst, the nickel oxide (NiO) is carried on the aluminium oxide (Al_2O_3). In order to discuss the experimental results of electrical conductivity and Seebek coefficient measurements in this catalyst, we are going to present in short the results obtained by different authors in studying the electrical transport properties of the two oxides.

2. ELECTRICAL CONDUCTION IN NiO AND Al_2O_3

NiO is a *p*-type semiconductor whose conduction is due both to nickel vacancies and to the presence in its lattice of some ions having a different valence from that of nickel ions.

The electrical conduction in Li-doped NiO was explained for the first time by Verwey and Boer [1] by $Li^+ - Ni^{3+}$ acceptor centre appearance. According to these authors the activation energy of the conductivity is equal to the energy necessary for detaching the holes from Li^+ ion and not for the exchange of electrons between the nickel ions.

In their studies on electrical conductivity and Seebeck effect in Li-doped NiO, Morin [2] and Heikes and Johnston [3] did not agree with the conduction model suggested by Verwey and de Boer. Supposing that the state density in NiO is constant and equal with the concentration of the lattice sites occupied by the cations and the transport term in the Seebeck coefficient expression is zero, Morin concluded that the charge carrier mobility increased exponentially with the temperature, having an activation energy of about 0.1 eV. According to Morin, the temperature dependence of NiO conductivity is mostly determined by the mobility variation with temperature and less by the variation of the charge carrier concentration. Morin, Heikes and Johnston have explained this fact, supposing that the electrical conduction in NiO is achieved by a thermal activated hopping mechanism. This model was also supported by the latest researches of van Houten,[4] Fujime, Murakami and Hirahara [5] and of Nachman, Cojocaru and Ribko.[6]

The electrical conductivity, the Seebeck and Hall effect studies of Ksendzov and his co-workers [7] on Li-doped NiO polycrystalline samples and of Roilos and Nagels [8] in NiO single crystals have demonstrated that the Hall mobility has values greater than those obtained by electrical conductivity and Seebeck effect data, based on hopping model and that above the room temperature the Hall mobility decreases when temperature increases. These results contradict the hopping conduction model and demonstrate that the hole transport in NiO implies a narrov band mechanism. This model has been sustained by the studies of Bosman and Crevecoeur [9] on the Li-doped NiO polycrystalline sample and by Austin and his co-workers [10] on Li-doped NiO single crystals.

There are different opinions concerning NiO energy level structure. According to some authors, such as Kröger [11] and Austin and Mott,[12] the 3*d* levels in NiO are localized or they form a narrow band in the Fermi level neighbourhood, and a small polarom conduction occurs. On the other hand Bosman and van Daal [13] and Alder and Feinleib [14] consider NiO a wide band semiconductor, the large polarom conduction implying the 2*p* oxygen band.

The electric transport properties of monocrystalline and polycrystalline Al_2O_3 have been studied by several authors, [15-17] who have found an exponential dependence of conductivity on temperature, having activation energies in the range $0.25 - 4$ eV.[18] These differences are attributed to the impurities existent in Al_2O_3 and to different preparation and measurement conditions. Peters [15] has studied the temperature dependence of electrical conductivity and Seebeck coefficient in Al_2O_3 single crystals in air in the temperature range 673—1273 K. The Seebeck coefficient is positive so that a *p*-type conduction exists. The great mobility values lead to the idea of hopping conduction. The high mobility may also be attributed to ionic conduction contribution whose part is not so important in the electrical conductivity measurements. Peters' results are in accord with those obtained by Champion.[16]

Pappins and Kingery[17] have studied the Al_2O_3 electrical conductivity dependence on oxygen pressure up to 2000 K. At pressures between 10^{-3} and 1 atm $\tau \sim p_{O_2}^{0.2}$ and between 10^{-10} and 10^{-7} atm $\sigma \sim p_{O_2}^{-0.17}$, in the intermediate pressure range σ being independent of pressure. Taking into consideration the Seebeck coefficient they established that at high oxygen pressures, Al_2O_3 conduction is of a *p*-type one, while at low pressures there is an n-type conduction.

3. ELECTRICAL CONDUCTIVITY AND SEEBECK COEFFICIENT MEASUREMENTS IN NICKEL—ALUMINA CATALYST

The electrical conductivity and Seebeck coefficient measurements have been made on the samples of nickel—alumina catalyst. The A sample contains 45 mol. % NiO carried on $\gamma - Al_2O_3$ and it has been obtained from nitrates by coprecipitation with alkali carbonate followed by the drying and the calcination of the precipitate. The B sample has been obtained by diluting A sample with gybbsite the result being a composition of 24 mol. % NiO carried on $\gamma - Al_2O_3$ and $K - Al_2O_3$, the latter resulting from the calcination of the gybbsite. The experimental details of electrical conductivity and Seebeck coefficient have been described in a previous paper.[19]

The variation of the electrical conductivity and Seebeck coefficient on temperature is illustrated in figures 1 and 2. Figure 1 shows the curves $\log \sigma$ as a function of the reciprocal absolute temperature in the temperature range 370—640 K for A sample and 450—700 K for B sample. For A and B samples the electrical conductivity measurements have been made in the air at three different pressures. These pressures are $p_1 = 1$ atm, $p_2 = 7 \times 10^{-3}$ Torr and $p_3 = 3 \times 10^{-4}$ Torr for A sample and $p_1' = 1$ atm, $p_2' = 5 \times 10^{-3}$ Torr and $p_3' = 7 \times 10^{-5}$ Torr for B sample. Each of the six curves has two well distinguished portions, the slopes of the straight lines in high temperature range being greater than in low temperature range. The slopes of the straight lines are changed between 460—490 K for A sample and 600—640 K for B sample. For these samples the lower the pressures, the higher the values of this temperature are.

The Seebeck coeffcient measurements have been made in the air at 1 atm, between 600—710 K for A sample and between 550—700 K for B sample. In the both samples the Seebeck coefficient is positive so that the electrical conduction in nickel—alumina catalyst is due to the holes.

Figure 2 illustrates the Seebeck coefficient dependence on absolute temperature; it is noticed that the two curves have the same shape, α values increasing slightly with the increase of temperature above 600 K.

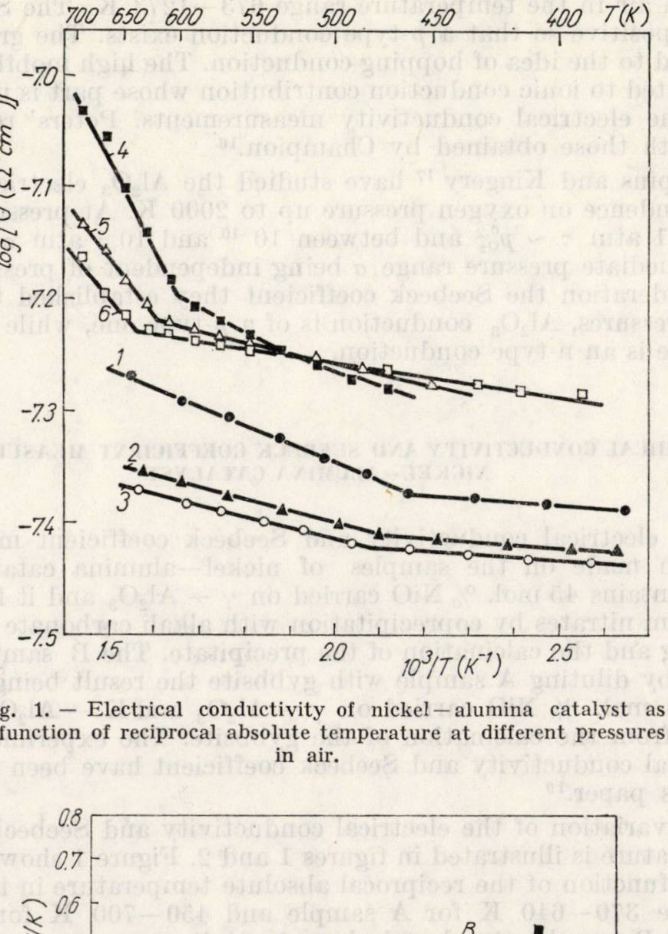

Fig. 1. — Electrical conductivity of nickel—alumina catalyst as a function of reciprocal absolute temperature at different pressures in air.

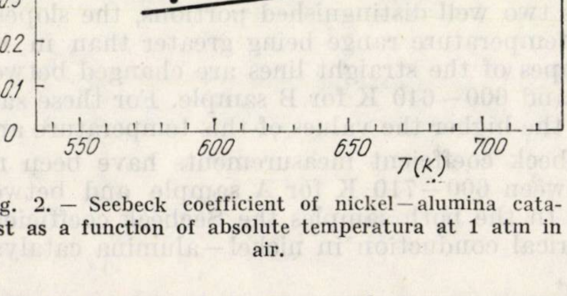

Fig. 2. — Seebeck coefficient of nickel—alumina catalyst as a function of absolute temperatura at 1 atm in air.

The Seebeck coefficient value of the B sample is twice greater than that of the A sample. At 700 K, $\alpha \sim 0.3$ mV/K in A sample and ~ 0.6 mV/K in B sample, near to $\alpha \sim 0.5$ mV/K, the values reported by Bosman and

Crevecoeur[9] in ceramic samples of NiO doped with 0.088 atomic. % Li. These values are however smaller compared to that of $\alpha \sim 8$ mV/K found by Peters in Al_2O_3 single crystal. The data reported by these authors show that between 600 and 700 K the Seebeck coefficient decreases with the increase of the temperature both in NiO and Al_2O_3.

p-Type conduction in nickel—alumina catalyst may be explained by taking into account the different mechanisms of hole appearance, depending in these samples on their compositions and the measurement condition. The first way of hole appearance is the oxygen excess which depends mainly on the way of sample preparation. The holes may also appear due to the doping with ions having a valence inferior to that of Ni^{2+} and Al^{3+} ions, in most cases with ions of alkali metals.

4. ELECTRICAL CONDUCTIVITY DEPENDENCE ON PARTIAL OXYGEN PRESSURE

Electrical conductivity measurements at different partial oxygen pressures may give information on the part played by excess oxygen atoms as a source of holes in the nickel—alumina catalyst. The experimental results are shown in figure 3 by the curves of conductivity logarithm dependence on the logarithm of partial oxygen pressures. The slopes of the straight lines obtained for A and B samples have the same value. The dependence of conductivity on partial oxygen pressure is described by the formula

$$\sigma \sim p_{O_2}^{0.017}, \qquad (1)$$

that follows the general form of dependence, $\sigma \sim p_{O_2}^{1/n}$, characteristic of the excess oxygen semiconductors.

In NiO, the oxygen excess is due to the absence in the cation sites of the lattice of a certain number of nickel atoms, that is to the existence of Ni vacancy. To compensate these vacancies, an equal number of Ni^{2+} ions turn into Ni^{3+} state. These ions form the holes generated by the excess oxygen atoms. The stoichiometry measurements and the studies concerning the defect influence lead us to the conclusion that at temperatures above 1 100 K, the nickel ionized vacancies are the predominant defects. [20] If the singly charged nickel vacancies (V'_{Ni}) predominate the doubly charged vacancies (V''_{Ni}), $\sigma \sim p_{O_2}^{1/4}$; otherwise $\sigma \sim p_{O_2}^{1/6}$. The value of n coefficient resulting from the slope of the straight lines in figure 3 is $n = 1/0.017 \approx 59$, much different from the above mentioned values (4 and 6). It is also different from the values in Al_2O_3 obtained by Pappins

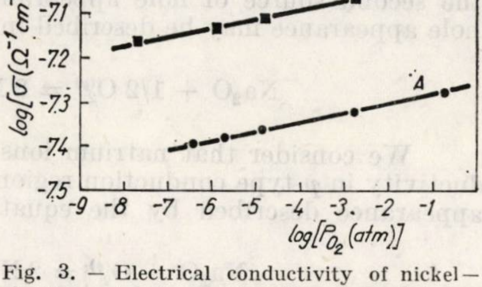

Fig. 3. — Electrical conductivity of nickel—alumina catalyst as a function of partial oxygen pressure at 640 K (A) and 690 K (B).

and Kingery[17] above 1500 K. It is obvious that the results obtained for the two oxides at high temperatures cannot have the same values as those obtained in the nickel—alumina catalyst at temperatures about 700 K.

The slight dependence of the catalyst conductivity on the partial oxygen pressure may be explained by the very slight oxygen diffusion in the crystalline lattice at such a low temperature or even by the absence of oxygen diffusion. Taking into account these assumptions the dependence described by the experimental formula (1) may be explained by supposing that the oxygen excess implied in conductivity variation does not enter the catalyst lattice but, on the one hand, it is bound to the crystal surface by chemisorption, and on the other hand, incorporated in the surface layer.

5. ELECTRICAL CONDUCTIVITY DEPENDENCE ON IMPURITIES

The second way of hole appearance in the nickel—alumina catalyst is the presence of lower valence ions, namely K^+ and Na^+. The presence of these ions depends on the preparation method, in this case coprecipitation with alkali carbonate. Thus, the A sample contains 0.21 mol. % K_2O and 0.16 mol. % Na_2O and the B sample contains 0.07 mol.K_2O and 0.24 mol. % Na_2O.

Verwey and de Boer[1] have assumed that the presence of Li atoms determines the appearance of Ni^{3+} ions which form the holes. According to Bielanski and co-workers,[21] the Li^+ ions increase the NiO conductivity by some orders of magnitude, while the K^+ ions slightly influence the conductivity. This may be explained by the fact that the size of lithium ions is almost equal with that of nickel ions, while the size of potassium ions is much different from that of nickel ions, so that a small number enters the lattice or they do not enter at all. The same authors show that the potassium ions increase NiO conductivity to a smaller extent than the lithium ions.

Taking into account these results we may say that the Na^+ ions are the second source of hole appearance in nickel—alumina catalyst. The hole appearance may be described in this case by the following equation:

$$Na_2O + 1/2\, O_2^{(g)} \rightleftarrows 2\, Na'_{Ni} + 2h^{\cdot} + 2\, NiO. \qquad (2)$$

We consider that natrium ions have a similar effect on Al_2O_3 conductivity in p-type conduction region, that is, at high pressures. The hole appearance described by the equation:

$$Na_2O + O_2^{(g)} \rightleftarrows 2\, Na'_{Al} + 2h^{\cdot} + Al_2O_3 \qquad (3)$$

leads to an electrical conductivity increase. At very low oxygen pressures, where Al_2O_3 has a contrary effect the phenomenon may be described by the equation

$$Na_2O + 2e' + O_2^{(g)} \rightleftarrows 2\, Na'_{Al} + Al_2O_3, \qquad (4)$$

in which $2e'$ term in the left part of the equation shows the decrease of electron concentration, that is, the decrease of electrical conductivity.

The different natrium and potassium contents in the two samples of nickel—alumina catalyst help us to estimate the effect of impurities on electrical conductivity. Figure 1 shows that at a certain temperature the conductivity of the B sample is greater than that of the A sample. We may explain this result by the fact that the B sample contains more Al_2O_3 and Na_2O than the A sample. We consider that the Na_2O contents in B sample increases with Al_2O_3 contents. This assumption is in accord with the above-mentioned supposition concerning the existence in Al_2O_3 of defect reaction of (3) and (4) type. Taking into account the fact that potassium oxide content is smaller in B sample than in A sample, we may assert that this oxide is present especially in NiO.

REFERENCES

[1] J. H. de Boer and J. W. Verwey, *Proc. Phys. Soc.*, **49**, 59 (1937).
[2] F. J. Morin, *Phys. Rev.*, **83**, 1005 (1951).
[3] R. R. Heikes and D. W. Johnston, *J. Chem. Phys.*, **26**, 582 (1957).
[4] S. van Houten, *J. Chem. Phys. Solids*, **17**, 7 (1960).
[5] S. Fujime, M. Murakami and E. Hirahara, *J. Phys. Soc. Japan*, **16**, 183 (1961).
[6] M. Nachman, L. N. Cojocaru and L. V. Ribko, *Phys. Status Solidi*, **8**, 773 (1965).
[7] Ya. M. Ksendzov, L. N. Anselm, L L. Vasileva and V. M. Latysheva, *Soviet Phys. Solid State*, **5**, 1116 (1963).
[8] M. Roilos and P. Nagels, *Solid State Commun.*, **2**, 285 (1964).
[9] A. J. Bosman and C. Crevecoeur, *Phys, Rev.*, **144**, 763 (1966).
[10] I. G. Austin, A. J. Springthorpe, B. A. Smith and C. E. Turner, *Proc. Phys. Soc.*, **90**, 157 (1967).
[11] F. A. Kröger, *J. Phys, Chem. Solids*, **32**, 1343 (1968).
[12] I. G. Austin and N. F. Mott, *Science*, **168**, 78 (1970).
[13] A. J. Bosman and H. J. van Daal, *Adv. Phys.*, **19**, 1 (1970).
[14] A. Alder and J. Feinleib, *Phys. Rev.*, **B**, **2**, 3112 (1970).
[15] D. W. Peters, *J. Phys. Chem. Solids*, **27**, 1560 (1966).
[16] J. A. Champion, *Brit. J. Appl. Phys.*, **15**, 633 (1964).
[17] J. Pappins and W. D. Kingery, *J. Amer. Ceram. Soc.*, **44**, 549 (1961).
[18] Z. M. Jarzebski, "Oxide Semiconductors", Pergamon Press, Oxford, 1973.
[19] O. Bunescu, S. I. Blejoiu and P. Rotaru, *Anal. Univ. Craiova, Ser. Mat., Fiz.—Chim.*, **9**, (1981).
[20] P. Kofstad, "Nonstoichiometry, Diffusion, and Electrical Conductivity in Binary Metal Oxides", Wiley, New York, 1972.
[21] A. Bielanski, J. Derén, J. Haber and I. Sloczynski, *Trans. Faraday Soc.*, **16**, 165 (1962).

Revue Roumaine de Chimie, 26, 11–12, 1401–1404 (1981)

SOLUBILITY OF IRON(III) CARBOXYLATE IN MIXED ORGANIC SOLVENTS

R. P. VARMA* and SMT. S. SHUKLA
Department of Chemistry, D.A.V. College, Muzaffarnagar — 251001, India

Received June 21, 1979
Revised April 20, 1981

The solubilities of iron(III) carboxylates of general composition Fe $(O_2CR)_3$ (where $R = C_5H_{11}$, C_7H_{15}, C_9H_{19}) have been measured in mixed organic solvents at temperatures of 30—55°C. The solubility, apparent heat of solution and the entropy of solution confirm the existence of micellar aggregates of carboxylates above the Krafft point. The effect of compositions of mixed solvents on these parameters has been discussed.

INTRODUCTION

Nonaqueous solvents are almost innumerable and vary from highly polar to the nonpolar saturated hydrocarbons. This wide range of solvent characteristic leads to differences in solubility and micelle formation. Studies on solubility of various transition metal carboxylates in nonaqueous solvents have been a field of interest for several groups of workers.[1-7] Recently, the solubility of some iron and cobalt carboxylates has been measured[8] in alcohols. In the present communication an effort has been made to study the solubility of iron(III) carboxylates i.e. caproate, caprylate and caprate in mixed solvents in order to study the micellar aggregation by varying the solvent characteristics at different temperatures (30—55°C).

EXPERIMENTAL

Merck or B.D.H. reagent grade iron chloride, n-caproic, caprylic, capric acids and solvents were used. The fatty acids were purified by distillation under reduced pressure.

Iron(III) carboxylates were prepared by adding a hot solution of sodium carboxylate to an aqueous solution of iron chloride, the former being added dropwise with stirring at 50—55°C. The precipitate was filtered off and washed with hot water. After initial drying in an air oven (100—5°C), final drying was carried out under reduced pressure. The carboxylates were characterised by the method described earlier.[8] The elemental analysis shows the percentage of iron(III) in different soaps as follows: caprate 9.80% (calc. 9.82%); caprylate, 11.50% (calc. 11.84%) and caproate 13.90% (calc. 13.92%). Soaps are free from water of crystallization. This observation is supported by IR spectra of soaps which show no peak in between 3590–3650 cm^{-1} due to the absence of water crystallization.

---

* Author to whom correspondence should be addressed.

Each saturated solution was prepared by agitation of an excess of iron(III) carboxylate in a 25 ml stoppered wide mouth bottle and placed in a thermostatic bath at the required temperature. Clear supernatant saturated solution was taken only when the equilibrium was attained (after 3–5 hrs.) with pipette, evaporated, dried and weighed.

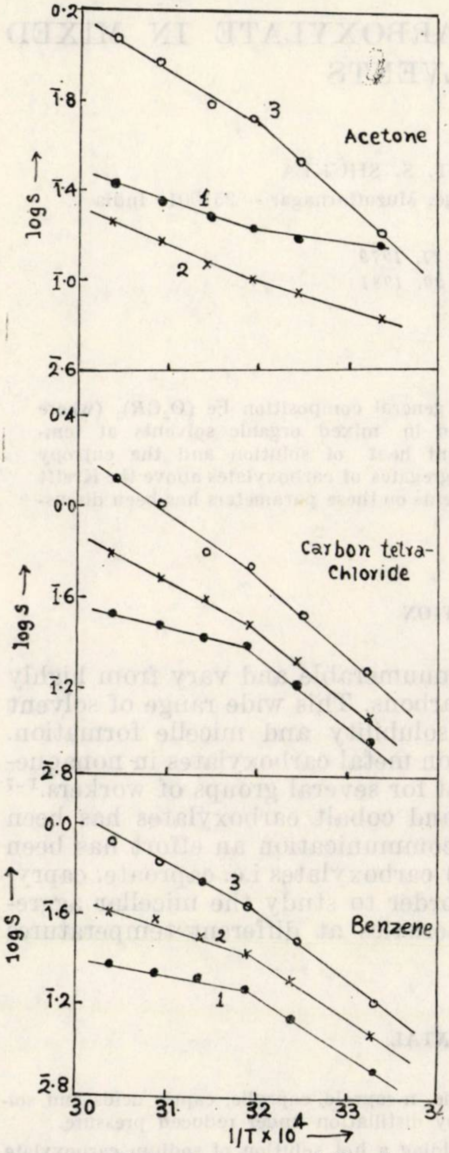

Fig. 1. Plot of logs vs. $1/T$ of iron (III) carboxylates in n-butanol in the presence of 10% benzene, carbon tetrachloride and acetone. *1.* ● Caprate; *2.* × Caprylate; *3.* ○ Caproate.

RESULTS AND DISCUSSION

Solubility varies with composition of solvent mixture in a very remarkable manner. It increases with increasing concentration of benzene and carbon tetrachloride in the mixed solvent but decreases with increasing concentration of acetone. An increase in solubility with increase in chain length of carboxylates is found in n-butanol–benzene and n-butanol–carbon tetrachloride mixtures but this behaviour is not observed in n-butanol–acetone mixtures. A comparison of these values of iron(III) carboxylates in different mixed solvents shows the following order: n-butanol–carbon tetrachloride > n-butanol–benzene > n-butanol–acetone.

Solubility of carboxylates increases with increasing temperature. The plots of solubility vs. temperature are not exponential in nature but show a marked change at 45° C indicating the existence of micellar aggregates above this temperature known as the Krafft point.

The apparent heat of solution, ΔH_S can be calculated by

$$\Delta H_S = RT^2 \frac{d \ln S}{dT}$$

Where S is the solubility in moles $litre^{-1}$ and the other terms have their usual significance.

The plots (Fig. 1) of $\log S$ vs. $1/T$ are characterised by an intersection of two straight lines at a point which corresponds to the Krafft point.[6,9] The values of apparent heat of solution, ΔH_S, calculated from the slopes of the linear plots, are recorded in table 1. The values of ΔH_S are found to

TABLE 1

Average values of apparent heat of solution, ΔH_S in kcal. mole^{-1} below and above the Krafft point of iron soaps in mixed solvents

Volume % of solvents in n-butanol	Caprate		Caprylate		Caproate	
	Above	Below	Above	Below	Above	Below
Benzene						
10	3.20	11.91	5.49	12.83	10.08	13.74
20	2.75	9.16	5.04	11.45	9.16	12.83
30	2.29	7.33	4.58	10.99	7.79	11.91
Carbon tetrachloride						
10	5.49	12.74	9.62	13.74	10.19	14.66
20	4.58	10.99	8.24	12.83	10.08	13.74
30	3.20	10.08	5.95	11.45	8.24	12.83
Acetone						
10	6.48	2.43	7.29	5.67	9.72	11.34
20	8.91	3.24	9.72	6.07	12.15	14.99
30	9.72	6.48	11.34	10.53	12.96	17.01

differ appreciably below and above the Krafft point which confirms the micelle formation of these compounds in mixed solvents. It is found that ΔH_S increases with increase in acetone concentration in n-butanol—acetone mixture where these values decrease with the increase in benzene and carbon tetrachloride concentration in other mixed solvents. When the carboxylates dissolve in n-butanol—benzene and n-butanol—carbon tetrachloride mixture the values of ΔH_S decrease above the Krafft point but in acetone mixture the otherwise behaviour is noted. However, the values of ΔH_S are found to increase with decrease in chain length of carboxylic acid in the compound.

Since the process of solution of the carboxylates in these solvent mixtures can be considered an isothermal equilibrium reaction, the free energy change is zero and the entropy of solution, ΔS_{sol}

$$\Delta S_{\text{sol}} = \frac{\Delta H_S}{T}$$

The values of ΔS_{sol} have been calculated and are recorded in table 2. An examination of the effect of temperature on these values reveals an attractive point of departure at the Krafft point at which ΔS_{sol} decreases abruptly and remains almost constant with further increase in temperature. This change in behaviour confirms the micelle formation in these solvents. However, the entropy changes with concentration of benzene, carbon tetrachloride and acetone and with chain length of carboxylate similarly as ΔH_S values change.

ACKNOWLEDGEMENT. We appreciate the laboratory facilities provided by College authorities and the advice given by Dr. K. N. Mehrotra.

TABLE 2

Values of entropy, $\Delta S_{sol} \times 10^2$ in kcal mole^{-1} deg^{-1}, of iron(III) carboxylates in mixed solvents at different temperatures

Vol. % of solvent in 1-butanol	n-butanol—benzene			n-butanol—carbon tetrachloride			n-butanol—acetone		
	Caprate	Caprylate	Caproate	Caprate	Caprylate	Caproate	Caprate	Caprylate	Caproate
10%									
30°	393	4.23	4.53	4.20	4.53	4.83	0.80	1.87	3.77
35°	386	4.16	4.46	4.13	4.46	4.75	0.78	1.84	3.68
45°	100	1.72	3.16	1.72	3.02	3.45	2.03	2.28	3.05
50°	99	1.69	3.12	1.69	2.97	3.40	2.00	2.25	3.01
55°	97	1.67	3.07	1.67	2.93	3.35	1.97	2.21	2.96
20%									
30°	302	3.78	4.23	3.62	4.23	4.53	1.06	2.00	4.94
35°	297	3.71	4.16	3.56	4.16	4.46	1.05	1.97	4.86
45°	86	1.58	2.88	1.44	2.59	3.16	2.80	3.05	3.82
50°	85	1.56	2.83	1.42	2.55	3.12	2.75	3.70	3.76
55°	83	1.53	2.79	1.39	2.51	3.07	2.71	2.96	3.69
30%									
30°	241	3.62	3.93	3.32	3.78	4.23	2.13	3.47	5.61
35°	238	3.56	3.85	3.27	3.71	4.16	2.10	3.42	5.52
45°	72	1.44	2.44	1.00	1.87	2.59	3.05	3.56	4.07
50°	70	1.41	2.40	0.99	1.84	2.55	3.01	3.51	4.01
55°	69	1.39	2.38	0.97	1.81	2.51	2.96	3.45	3.95

REFERENCES

[1] E. P. Martin and R. C. Pink, *J. Chem. Soc.*, **1948**, 1750.

[2] W. V. Ostwald and R. Riedel, *Koll. Zeit.*, **69**, 185 (1934).

[3] A. S. C. Lawrence, *Trans. Faraday Soc.*, **34**, 660 (1938).

[4] S. M. Nelson and R. C. Pink, *J. Chem. Soc.*, **1952**, 1744.

[5] R. C. Mehrotra, *Nature*, **172**, 74 (1953).

[6] W. U. Malik and S. I. Ahmad, *J. Am. Oil Chem. Soc.*, **42**, 454 (1965).

[7] K. N. Mehrotra, V. P. Mehta and T. N. Nagar, *J. prakt. Chem.*, **313**, 607 (1971).

[8] R. P. Varma and H. K. Bhargava, *Ann. Chim.*, **66**, 773 (1976).

[9] F. Krafft, *Ber. dtsch. chem. Ges.*, **27**, 1747, 1755 (1894) ; **32**, 1584 (1899) .

Revue Roumaine de Chimie, **26**, *11–12*, 1405–1412 (1981)

SPECTRAL SOLVENT EFFECTS IN AROMATIC COMPOUND SOLUTIONS. VII[1]

SOLVENT EFFECTS ON THE BENZONITRILE BAND AT ~260 nm

V. MACOVEI

Physical Chemistry Laboratory, The Faculty of Chemistry and Engineering Chemistry, Splai Bahlui – stînga Street, 71, Iassy, Romania

Received October 8, 1977
Revised July 25, 1980

The effects of the solvents on the position and intensity of benzonitrile electronic band at ~260 nm are investigated and the dipole moment of the solute molecule in the excited state is evaluated with the aim of contributing to the elucidation of the intermolecular interactions of the solute and the surrounding solvent medium.

I. INTRODUCTION

The examination of the effects of the intermolecular interactions in solutions on the position, intensities and the fine structure of the electronic spectral bands leads to valuable information concerning the molecular excited states and particularly the dipole moment of the solute molecule, giving an important orientation on the molecular reactivity.[2] With this end in view, the influence of the solvents on the spectra of benzene and of monosubstituted benzene with substituents of the first and second order [1,3–7] was investigated. The generalization of the conclusions requires the study of several molecules. Thus, after the examination of the nitrobenzene [5] and benzaldehyde,[7] the effects of the solvents on the benzonitrile spectrum were investigated. Benzonitrile has a dipole moment [8] of 4.05 D in the ground state, close to that of nitrobenzene[9] (4.28 D in the gaseous state). Therefore, one can expect a behaviour of the benzonitrile spectrum in solution similar to that of nitrobenzene.[5]

II. RESULTS AND DISCUSSION

The electronic spectral band of benzonitrile at ~260 nm, in different solvents, exhibits a substantial preservation of the vibrational structure, even if the –CN group is a strongly polar substituent [10] of the second order. This fact is obvious in figure 1, which shows the benzonitrile spectrum in some used solvents. (The numbers in figure 1 correspond to the solvents in table 1, notation used throughout the paper). The vibrational structure of the benzonitrile spectrum is some more blurred on the side of the great wave numbers, as compared with the previous investigated compounds [1,3,4,6] The retention to a great extent of the vibrational structure shows that the band corresponds to the benzonitrile ${}^1A_1 \longrightarrow {}^1B_1$ transition, originating in the forbidden transition ${}^1A_{1g} \longrightarrow {}^1B_{2u}$ of benzene.[11] The unsignificant distorsion of benzene skeleton by the substituent [12,13] explains the retention of the vibrational structure. Assuming the same symmetry[14,15] C_{2v} for both the ground and excited states of the benzonitrile planar molecule, the observed spectrum corresponds to the ${}^1A_1 \longrightarrow {}^1B_1$ transition. The

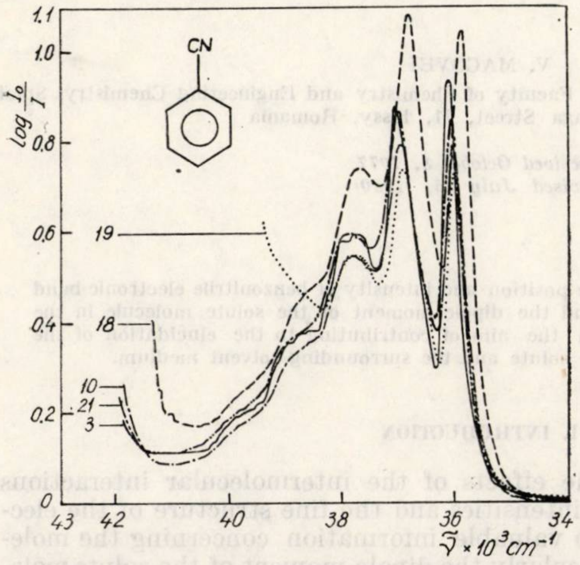

Fig. 1. — The benzonitrile spectrum in: 3. Cyclohexane; 10. Ethanol; 18. Chloroform; 19. Carbon tetrachloride; 21. Acetonitrile.

(0, 0) electrono-vibrational component is distinctly detached from the remainder spectrum, and its examination will represent the behaviour of the spectrum as a whole, in solution. [3] The position of the (0, 0) component in the vapour spectrum of benzonitrile was established [16] at 37,516 cm^{-1} and was adopted as reference to establish the shifts $\Delta\tilde{\nu}$ (cm^{-1}) in solutions. These shifts are listed in table 1. The obtained values are greater than those of the previously studied molecules [1,3,4,6] but only approximate halves in comparison with the nitrobenzene shifts.[5] The spectra of the compounds with close polarities must behave alike under the influence of the solvents.[17] In contrast to nitrobenzene,[5] the spectrum of benzonitrile shows small shifts and preserves to a great extent the vibrational structure in solutions. However, the only property of solvents showing *any* correlation with the spectral shifts [1-7] is the function of the dielectric constant $f(D) = (D-1)/(D+2)$, as seen in figure 2. The explanation of the *approximate* correlation, in figure 2, is the following: during the absorption process the dipole moment of the solute molecule may vary, but the part of the *reaction field*[18] determined by the orientation polarization remains unaltered because the permanent dipoles of the solvent do not have the necessary time for reorientation. At the same time, the electron polarization of the solvent molecules may follow the variation of the dipole moment, practically, without inertia. Taking into account the considerations of Lippert,[19] one utilises the equation of McRae [20] for the

TABLE 1
The principal characteristics of the electronic absorption of the benzonitrile, at 38,477 cm^{-1} (259.9 nm)

No.	Solvent	$\tilde{\nu}_{max}$ (cm^{-1})	$\tilde{\nu}_{oo}$ (cm^{-1})	$\Delta\tilde{\nu}_{abs}(cm^{-1}) = \tilde{\nu}_{vap} - \tilde{\nu}_{sol}$		$\delta\tilde{\nu}_{oo}$ (cm^{-1})	$\varepsilon(l.mol^{-1}cm^{-1})$		$f.10^3$
				Experim.	Calcd.		$\tilde{\nu}_{max}$	$\tilde{\nu}_{oo}$	
0	Vapour[16]		37,516	—	—	0	—	—	—
1	Cyclopentane	37,035	36,065	1,451	1,451	0	376.5	410.0	3.93
2	n-Pentane	37,100	36,145	1,371	1,296	+ 75	353.5	375.0	7.64
3	Cyclohexane	37,065	36,110	1,406	1,477	− 71	436.5	466.5	4.71
4	n-Hexane	37,070	36,120	1,396	1,347	+ 49	455.0	482.5	4.78
5	n-Heptane	37,085	36,130	1,386	1,376	+ 10	407.5	423.5	4.54
6	n-Octane	37,135	36,185	1,331	1,405	− 74	475.0	402.5	3.99
7	n-Decane	37,045	36,065	1,451	1,441	+ 10	620.0	657.0	9.03
8	n-Dodecane	37,030	36,065	1,451	1,470	− 19	617.0	647.0	6.94
9	Methanol	36,950	35,990	1,526	1,432	+ 94	805.0	789.0	9.31
10	Ethanol	36,980	36,030	1,486	1,496	− 10	786.0	763.0	9.04
11	1-Propanol	36,955	36,000	1,516	1,546	− 30	946.0	920.0	10.46
12	2-Propanol	36,965	36,000	1,516	1,547	− 31	820.0	796.0	8.98
13	1-Butanol	37,160	36,205	1,311	1,571	−260	842.0	816.0	9.62
14	3-Methyl-1-butanol	36,840	35,905	1,611	1,579	+ 32	1050.0	972.0	11.07
15	Ethyl ether	37,030	36,070	1,446	1,335	+111	820.0	853.0	9.08
16	Isoamyl ether	37,045	36,080	1,436	1,445	− 9	790.0	800.0	—
17	Methylene chloride	36,907	35,937	1,579	1,575	+ 4	1006.0	975.0	11.37
18	Chloroform	36,875	35,922	1,594	1,563	+ 31	1070.0	1043.0	12.20
19	Carbon tetrachloride	36,952	36,005	1,511	1,558	− 47	737.0	731.0	—
20	1,2-Dichloroethane	36,885	35,932	1,584	1,625	− 41	831.0	803.0	9.25
21	Acetonitrile	37,000	36,042	1,474	1,475	− 1	855.0	841.0	10.09
22	Methyl acetate	37,027	36,075	1,441	1,399	+ 42	950.0	988.0	10.08
23	Ethyl acetate	37,088	36,068	1,448	1,413	+ 35	898.0	920.0	9.95
24	Butyl acetate	37,012	36,057	1,459	1,496	− 37	870.0	895.0	9.67
25	n-Amyl acetate	37,012	36,065	1,451	1,466	− 15	827.0	848.0	9.11
26	1,4-Dioxane	36,962	35,997	1,519	1,471	+ 48	831.0	827.0	9.45
27	Water	36,922	35,940	1,576	1,471	+105	1053.0	973.0	12.20

theoretical calculation of the spectral shifts in solutions, in the following simplified form:

$$\Delta\tilde{\nu}_{\text{abs.}}(\text{cm}^{-1}) = (A + B + C)(n^2 - 1)/(2n^2 + 1) + + E[(D - 1)/(D + 2) - (n^2 - 1)/(n^2 + 2)] + + F[(D - 1)/(D + 2) - (n^2 - 1)/(n^2 + 2)]^2 \qquad (1)$$

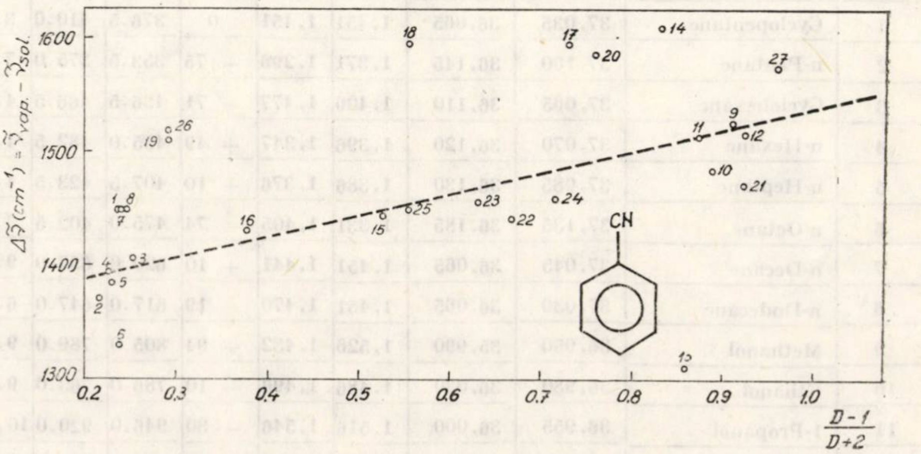

Fig. 2. — The shift dependence of the (0,0) electrono-vibrational component in the benzonitrile spectrum of the $f(D)$ function of the solvent.

where A, B, C, E and F are characteristic constants for the solute molecule, n and D are the refractive index and the dielectric constant of the solvent, respectively. In relation (1) the terms containing the function of the refractive index $f(n^2)$ may be considered constants because the refractive index varies little from one solvent to another, while the dielectric constant varies much from solvent to solvent. (Indeed, the range of variation of the refractive indices is from 1.331 for methanol to 1.460 for carbontetrachloride, that is a difference of 0.127 unities, while the range of variation of the dielectric constants is from 1.844 for n-pentane to 80.360 for water, that is a difference of 74.516 unities). The separation of the two terms in the polarity function,[10] $f(D)$ and $f(n^2)$, results [21] from the theory of Onsager.[18] In the spectral shift in solutions, the dispersion forces [22] intervene in all the systems, but our results indicate a substantial contribution of the dipolar forces. The characteristic constants, in equation (1), were evaluated * by the least square method,[23] and have the values: $(A + B + C) = 7241.18$ cm^{-1}, $E = 38.91$ cm^{-1} and $F = 354.92$ cm^{-1}. Inserting these constants, as well as n_D^{20} and D, in equation (1) we have calculated the spectral displacements and the values are listed in table 1, together with the differences between the experimental and the theoretical

---

* The calculation program has been established at the Territorial Center of Electronic Computation, Iassy.

shifts $\delta\tilde{\nu}_{oo}$. The apparatus accuracy is of ± 50 cm^{-1}. The experimental shift deviations, either smaller or greater than the apparatus accuracy, in comparison with the theoretical values may be explained in terms of *strain state*[17] of the solute molecule in its solvent cage. The solvent cavity radius, in the excited state of the solute molecule, is identical with that of the cavity in the ground state, because the molecular volume does not change appreciably on excitation. Equation (1) is not modified by the variation of the cavity radius. The orientation of the solvent dipoles remains unchanged, but this will introduce the solvent cavity strain and consequently the variation of the excitation energy.[21] Here, the number and the geometry of the solvent molecules surrounding the solute molecule must play an important role.

The theoretical substantiation of the preservation of the vibrational structure of the benzonitrile spectrum in solution is found in the assumption[10] that the lower vacant π^*-orbital of the CN group lies at an enough high energy level, determining a negligible charge transfer character for the benzonitrile electronic state. The benzonitrile dipole moment is chiefly concentrated in the CN group and consequently, the *local specific interactions*[1,4-7] intervene in the spectral shifts.

According to the Franck – Condon principle[24] one may interpret the spectral shift by the variation of the dipole moment between the ground and excited states of the solute molecule. The dipole moment of the excited state is evaluated using the calculated value of the parameter E and its explicit form from the equation of McRae,[20] that is :

$$E = (2/hc)M_{oo}(M_{oo} - M_{ii})/a^3 \tag{2}$$

where h and c have the known significations ; M_{oo} and M_{ii} are the dipole moment in the ground and excited states, respectively, and a is the radius of the solvent cavity, evaluated[25] according to the expression :

$$a^3 = 3\mathrm{M}/4\pi N\rho \tag{3}$$

where M is the molecular weight, N is the Avogadro's number, and ρ is the material density. Using the values[26] of M and ρ (at 20°C) one calculates $a^3(10^{-10}\ m) = 40.69$, and consequently $M_{ii} = 4.011$ D. The diminution of the dipole moment with 0.039 D has not important effects on the solvation energy in the excited state. In the ground state, the dipole moment of the benzonitrile is built up from the structures[27-29] of the type :

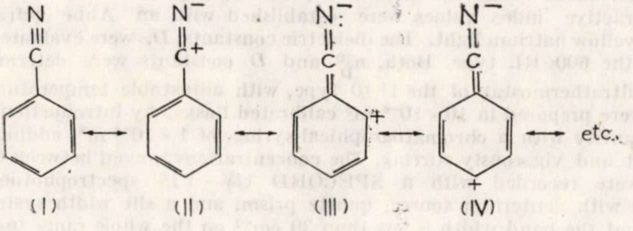

and the theoretical value [29] of M_{oo} is 3.65 D. If the most polar structures, such as (III) and (IV), are stabilised preferentially in the excited state [30] the molecular sizes decrease. Indeed, the calculation of the distance between the aromatic ring and the nitrogen atom of the CN group with the covalent radii [31] involved in single, double and triple bond gives, for the corresponding structures: (I) $2.691 \cdot 10^{-10}$ m, (II) $2.807 \cdot 10^{-10}$ m and (III) and (IV) $2.595 \cdot 10^{-10}$ m. The cumulation of both effects, the diminution of molecular sizes and of the dipole moment, determines a small reduction of the number of solvent molecules which interact with the solute molecule, and a tiny lowering of the *orientation strain* [17] in the excited state, hence a decrease of the solvation energy and the spectrum is shifted a little to the blue. This shift opposes to the general red shift, thus explaining the smaller values of the spectral displacements of the benzonitrile in solutions, as compared with those of nitrobenzene.[5]

The spectral band intensity increases in solutions as compared with the value in the vapour spectrum.[3,24] Usually, the comparison is made in terms of the *molar extinction coefficients*,[32] ε_ν, or better in terms of the *oscillator strengths*,[33] f, which contain the *integrated (absolute) intensities*.[32] There is in the literature[34] a single value of the intensity of the benzonitrile spectral band at 270 nm, $\varepsilon_\nu = 600.00\,\mathrm{l \cdot mol^{-1} \cdot cm^{-1}}$, in *n*-heptane. We find for 269.6 nm, in the same solvent, $\varepsilon_\nu = 407.50\,\mathrm{l \cdot mol^{-1} \cdot cm^{-1}}$. Our result shows that the part of the spectral band on the great wave numbers side cannot be subjected to a thorough vibrational analysis because in the spectrum the envelopes of some groups of bands appear. But in the part of the spectral band of the small wavenumbers side, a redistribution of the intensities [35,36] among the electrono-vibrational components $\tilde{\nu}_{oo}$ and $\tilde{\nu}_{\max.}$ takes place. The ε_ν and f values are listed in table 1. In such solvents as the hydrocarbons, ethers, esters, the value of ε_ν is greater for the $\tilde{\nu}_{oo}$ component while in the other solvents the situation is reversed. The changes of the intensity from a solvent to another must be related to the geometrical requirements of the solvent—solute system. All the previous results [1-7] have demonstrated the spectral intensity increase under the solvent influence, hence the phenomenon takes place also in the case of benzonitrile.

III. EXPERIMENTAL

The purification of benzonitrile and solvents was performed by the known methods,[26] the purity criteria being the refractive indices, n_D^{20}, the boiling points, b.p., and the dielectric constants, D, whose values are given in a preceding paper. [3]

The refractive index values were established with an Abbé refractometer, of the G type, for the yellow natrium light. The dielectric constants, D, were evaluated with an Oehme apparatus, of the 600 RL type. Both, n_D^{20} and D constants were determined at 20°C by means of an ultrathermostat of the U 10 type, with adjustable temperature, at 20 ± 0.1°C. The solutions were prepared in 10×10^{-6} m^3 calibrated flasks, by introduction of the necessary benzonitrile quantity with a chromatographical syringe of 1×10^{-8} m^3, adding then small portions of solvent and vigorously stirring. The concentrations ranged between 0.01 and 0.008 M. The spectra were recorded with a SPECORD UV—VIS spectrophotometer, Carl Zeiss, Jena, equipped with deuterium source, quartz prism, and a slit width system automatically adjustable so that the band width is less than 30 cm^{-1} on the whole range used. The employed cells were of $1 \cdot 10^{-3}$ and $1 \cdot 10^{-2}$ m thickness. The position of each band and the spectral intensities are the mean of at least three measurements. The integrated intensities were evaluated by cutting up and weighing, having as integration limits the onset of the spectral band, from the small wave numbers, to the deepest minimum at great wave numbers.

REFERENCES

[1] Part. VI. V. Macovei, *Rev. Roumaine Chim.*, **25**, 651 (1980).
[2] V. Macovei, Doctoral Thesis, Faculty of Chemistry, The Chemistry Institute, The Polytechnic, Bucharest, 1974.
[3] V. Macovei, *Rev. Roumaine Chim.*, **20**, 1357 (1975).
[4] V. Macovei, *Rev. Roumaine Chim.*, **21**, 193 (1976).
[5] V. Macovei, *Rev. Roumaine Chim.*, **21**, 1137 (1976).
[6] V. Macovei, *Anal. Sti., Univ. "Al. I. Cuza", Iaşi. Sect. I, b*, **22**, 51 (1976).
[7] V. Macovei, *Anal. Sti., Univ. "Al. I. Cuza", Iaşi, Sect. I, b*, **22**, 61 (1976).
[8] O. A. Osipov, V.J. Minkin, and A. D. Garnovskii, "Spravochinik po Dipolnym Momentam", Izd. Vysshaia Shkola, Moskva, 1971.
[9] A. L. McClellan, "Tables of Experimental Dipole Moments", W. H. Freeman, San-Francisco, 1963.
[10] P. Suppan, *Spectrochim. Acta*, **24 A**, 1161 (1968).
[11] P. C. Upadhya, G. D. Baruah, K. N. Upadhya, and D. K. Rai, *Isr. J. Chem.*, **9**, 7 (1971).
[12] D. R. Lide, *J. Chem. Phys.*, **22**, 1577 (1954).
[13] G. Erlandsson, *Arkiv. Phys.*, **9**, 399 (1955).
[14] J. Kahane-Paillous, *J. Chim. phys.*, **57**, 581 (1960).
[15] H. Sponer and S. H. Wollam, *J. Chem. Phys.*, **9**, 816 (1941).
[16] H. Sponer and E. Teller, *Rev. Mod. Phys.*, **13**, 76, (1941).
[17] N. S. Bayliss and E. G. McRae, *J. Phys. Chem.*, **58**, 1002 (1964).
[18] L. Onsager, *J. Amer. Chem. Soc.*, **58**, 1486 (1936).
[19] E. Lippert, *Z. Elektrochem.*, **61**, 562 (1957).
[20] E. G. McRae, *J. Phys. Chem.*, **61**, 562 (1957).
[21] P. Suppan, *J. Chem. Soc.*, **A 1968**, 3125.
[22] F. London, *Z. Physik*, **63**, 245 (1930).
[23] D. York, *Canad. J. Phys.*, **44**, 1079 (1966).
[24] H. H. Jaffé and M. Orchin, "Theory and Applications of Ultraviolet Spectroscopy", Wiley, New York, 1964.
[25] M. Lamotte, G. A. Gerhold, and J. Joussot-Dubien, *J. Chim. phys.* **67**, 2006, (1970).
[26] A. Weissberger. E. S. Proskauer, J. A. Riddick and E. E. Toops, Jr., "Technique of Organic Chemistry. Vol. VII, Organic Solvents", 2nd ed., Interscience, New York, 1955.
[27] J. A. Pople and M. S. Gordon, *J. Amer. Chem. Soc.*, **89**, 4253 (1967).
[28] W. J. Hehre and J. A. Pople, *J. Amer. Chem. Soc.*, **92**, 2191 (1970).
[29] W. J. Hehre, L. Radom and J. A. Pople, *J. Amer. Chem. Soc.*, **94**, 1496 (1972).
[30] H. E. Ungnade, *J. Amer. Chem. Soc.*, **75**, 432 (1953).
[31] O. A. Reutov, "Probleme Teoretice ale Chimiei Organice", Ed. Academiei R.P.R., Bucureşti, 1964.
[32] H. H. Willard, L. L. Merritt, Jr., and J. A. Dean, "Instrumental Methods of Analysis", 3rd ed., D. Van Nostrand, Princeton, 1960.
[33] R. S. Mulliken, *J. Chem. Phys.*, **7**, 14 (1939).
[34] P. P. Shoryghin, V. A. Petukhov, A. H. Khomenko, and E. A. Chernyshev, *Zhur. fiz. Khim.*, **42**, 1057 (1968).
[35] V. Macovei and C. Ghirvu, *Anal. Sti., Univ. "Al. I. Cuza", Iaşi. Sect. I. c*, **15**, 1 (1969).
[36] V. Macovei and C. Ghirvu, *Anal. Sti., Univ. "Al. I. Cuza", Iaşi. Sect. I, c*, **15**, 7 (1969).

Revue Roumaine de Chimie, **26**, *11–12*, 1413–1422 (1981)

COMPARISON BETWEEN THE HYDROCRACKING ACTIVITY OF COBALT – MOLYBDENUM/ALUMINA AND NICKEL – MOLYBDENUM/ALUMINA CATALYSTS

F. Y. EL-KADY
Refining Division, Egyptian Petroleum Research Institute, Nasr City, Cairo, Egypt

Received May 14, 1977
Revised April 17, 1981

The hydrocracking activities of nickel—molybdenum and cobalt—molybdenum catalysts, supported on the same alumina carrier were compared in a static phase, using medium wax distillate fraction (b.p. 331°—472°C) at different working temperatures (400°, 425°, and 450°C) and different reaction periods (1, 2, 4 and 6 hours). The initial hydrogen pressure (75 atm) and catalyst/feed ratio (1/10) were kept constant throughout the experiments. The hydrocracking activities of both catalysts increase with increasing working temperature and/or reaction period. Cobalt—molybdenum/alumina catalyst possesses higher h ydrocracking activity, lower hydrodesulphurization efficiency and hydrogen consumption.

INTRODUCTION

The progress of the hydrocracking process is directly related to the development of catalysts of high activity and selectivity. Hydrocracking catalysts are usually termed dual function catalysts since they are composed of a hydrogenating site (active catalyst component), and a cracking site (the active centers of the support).[1–7] The interaction between these two sites changes the acid—hydrogenation balance and affects the behaviour of the catalyst system.[8–13]

The present study aims to compare the hydrocracking and hydrodesulphurization activities of nickel—molybdenum/alumina and cobalt — molybdenum/alumina catalysts under the hydrocracking conditions. The effect caused by the interaction between acid sites (support active centers) and hydrogenation—dehydrogenation sites (active catalyst components) is eliminated by using the same alumina carrier.

EXPERIMENTAL

Charge stock : The charge stock employed is a technical vacuum wax distillate fraction, b.p. 331°—472°C, obtained from Ras Tannora crude oil. The most important characteristics of the charge stock are given in table 1.

Catalyst used: Low density Ketjenfine catalysts, composed of synthetic, purified alumina oxide carrier and combination of nickel—molybdenum oxides and cobalt—molybdenum oxides as hydrogenation compounds have been used in this investigation. Characteristics of the used catalysts are given in table 2.

TABLE 1
Characteristics of the charge stock

Characteristics	
Gravity, 60/60°F, API	25.3
Density, 70°C, g/ml	0.8703
Refractive index, 70°C	1.4860
Mean molecular weight	420
Pour point, °C	25
Total sulphur content, wt. %	2.35
Bromine number	13
ASTM Distillation, °C	
IBP	331
10 vol % recovered	395
30 " " "	433
50 " " "	441
70 " " "	453
90 " " "	468
F B P	472
Elementary analysis, wt.%	
Carbon	85.45
Hydrogen	12.20
Nitrogen	0.0048

TABLE 2
Physical and analytical data on nickel—molybdenum and cobalt—molybdenum/alumina catalysts

Catalyst type / Characteristics	A	B
Loss on ignition (650°C), wt.%	0.65	1.46
Chemical composition, wt.%		
MoO_3	11.62	11.95
CoO		4.11
NiO	5.00	
Na_2O	0.07	0.05
SiO_2	1.10	1.21
SO_4	2.28	2.03
Bulk density, g/ml	0.78	0.77
Average length, mm	3.70	4.30
Crushing strength, kg/mm	1.36	1.36
Surface area, m²/g	256	248
Pore volume, ml/g	0.46	0.47

Apparatus and procedure: The hydrogenation experiments are carried out in a static phase. A sample of 300 grams of the charge stock is charged with 30 grams of the catalyst under investigation in a two-litre tubular rocking Andreas Hofer autoclave. The performance of the catalysts has been investigated at different working temperatures (400°C, 425°C and 450°C) and reaction periods (1, 2, 4 and 6 hours). An initial hydrogen pressure of 75 atm and a catalyst/feed ratio of 1/10 are kept constant throughout the investigation.

Samples of gases are collected after removal of H_2S and NH_3 through scrubbing with a 10% NaOH solution. The hydrogen consumption, as well as the weight per cent of hydrocarbon gases are determined using an F & M Model 500 gas chromatograph. The liquid hydrogenates are subjected to fractional distillation. An atmospheric gasoline fraction, up to 160°C, is collected. Further fractionation is carried out at 10 mmHg to get kerosine fraction (160° —250°C) and at 2 mmHg for gas oil fraction (250°C—350°C).

Expression of the results: Total conversion signifies the total gaseous and liquid products distilling up to 350°C in wt.% per charge stock.

$$\text{Selectivity} = \frac{\text{Wt.\% of middle distillate fraction } (160^\circ\text{C} - 350^\circ\text{C})}{\text{Total conversion}} \times 100$$

RESULTS AND DISCUSSION

The effect of the nickel—molybdenum and cobalt—molybdenum catalysts on the yield of the cracked products, conversion, selectivity and hydrogen consumption at different working temperatures and reaction periods, are given in tables 3 and 4 respectively.

Data given in tables 3 and 4 show clearly that the cracking—hydrogenation activities of the two catalysts increase with the increase of working temperature and/or reaction period as indicated by total conversion, gas yield and liquid hydrogenate fractions. Meanwhile, the rate of increase of the cracking activity as represented by total conversion and product distribution is specific for each catalyst. The effect of process variables on the cracking—hydrogenation activity of the investigated catalysts can be discussed as follows :

1 — *Liquid hydrogenates:* The yield of liquid hydrogenates and their fractions vary with the variation of the operating conditions (tables 3 and 4), decrease or increase with the increase of working temperatures and/or reaction periods. These variations are more influenced by raising the working temperature rather than by increasing the reaction period for a given set of conditions.

Higher gasoline and kerosine yields are obtained by cobalt—molybdenum/alumina catalyst.

2 — *Middle distillate fractions (kerosine and gas oil):* The yield of kerosine increases with temperature and/or reaction period for the two catalysts. For gas oil fraction, the yield is increased under relatively low temperatures (up to 425°C), with the increase of the reaction period for the two catalysts.

At 450°C, the yield remains nearly constant irrespective of the reaction period in the case of nickel—molybdenum/alumina catalyst and decreases in the case of cobalt—molybdenum/alumina catalyst. This is mainly attributed to the increase in the cracking—hydrogenation activities of the two catalysts under this set of conditions.

Nearly, under all the same experimental conditions, cobalt—molybdenum/alumina catalyst produces higher kerosine and lower gas oil yields than those observed with the nickel—molybdenum/alumina catalyst. Compared with kerosine, higher yields of gas oil are produced up to 450°C and 4 hours reaction period. At 450°C and 6 hours, gas oil yields diminish and an approximate equipartition of the two components is attained by

TABLE 3

Product distribution in wt. %/charge stock at different working temperatures and reaction periods using nickel–molybdenum/alumina catalyst

Temperature, °C	400				425				450			
Reaction period, hr / Yield, wt. %	1	2	4	6	1	2	4	6	1	2	4	6
Total gas yield	2.05	3.77	5.19	7.71	4.82	6.11	7.98	9.33	5.73	7.16	9.74	12.69
Total liquid yield	97.42	95.73	94.43	93.39	95.05	93.89	92.05	91.89	94.25	93.01	90.60	87.93
$H_2S + NH_3 + H_2O$ + Losses	1.43	1.52	1.80	2.51	2.01	2.19	2.45	2.57	2.14	2.35	2.46	3.30
Hydrogen consumption	0.90	1.02	1.42	3.61	1.88	2.19	2.48	3.79	2.12	2.52	2.80	3.92
Gasoline fr., up to 160°C	0.41	0.54	0.68	1.03	0.89	1.12	1.89	3.67	6.52	7.39	8.41	11.35
Kerosine fr., 160°–250°C	1.03	1.81	2.99	4.09	5.97	8.10	10.18	11.45	15.64	18.22	21.83	25.58
Gas oil fr., 250°–350°C	6.78	7.61	9.17	10.69	14.01	15.41	16.95	20.30	25.73	26.82	27.69	26.47
Middle distillate fr., 160–350°C	7.81	9.42	12.16	14.78	19.98	23.51	27.13	31.75	41.37	45.04	49.52	52 05
Fuel oil fr., >350°C	89.20	85.77	81.59	77.58	74.18	69.26	63 03	56.47	46.36	40.58	32.67	24.53
Total conversion up to 350°C	11.70	15.25	19.83	26.03	27.70	32.93	39.45	47.32	55.76	61.94	70.03	79.39
Selectivity for middle distillate fr., 160–350°C	66.75	61.77	61.32	56.78	72.13	71.39	68.77	67.10	74.19	72.72	70.61	65.56

TABLE 4

Product distribution in wt. %/charge stock at different working temperatures and reaction periods using cobalt–molybdenum/alumina catalyst

Working temperature, °C	400				425				450			
Reaction period, hr Yield, wt. %	1	2	4	6	1	2	4	6	1	2	4	6
Total gas yield	2.24	3.52	6.11	8.94	5.14	7.69	9.81	12.78	8.33	10.85	12.36	14.08
Total liquid yield	97.53	95.96	93.25	89.81	94.59	91.96	89.83	86.99	90.79	88.23	87.05	85.40
$H_2S + NH_3 + H_2O$ + Losses	1.08	1.43	1.69	2.43	1.90	2.10	2.54	2.63	2.79	3.10	3.42	3.94
Hydrogen consumption	0.85	0.91	1.05	1.18	1.63	1.75	2.18	2.40	1.91	2.18	2.83	3.42
Gasoline fr., up to 160°C	0.62	1.09	1.83	2.00	0.93	2.65	4.41	5.13	10.76	14.01	16.92	18.20
Kerosine fr., 160°–250°C	1.12	2.81	5.45	6.31	5.34	7.65	10.60	12.25	16.60	19.34	24.07	27.00
Gas oil fr., 250°–350°C	5.03	5.94	7.62	10.82	10.58	11.24	13.22	16.19	27.71	25.48	24.51	23.80
Middle distillate fr., 160°–350°C	6.15	8.75	13.07	17.13	15.92	18.89	23.82	28.44	44.31	44.82	48.58	50.80
Fuel oil fr., > 350°C	90.76	86.12	78.35	70.68	77.74	70.42	61.60	53.42	35.72	29.40	21.55	16.40
Total conversion, up to 350°C	10.09	14.79	22.70	30.50	23.89	31.33	40.58	48.98	66.19	72.78	81.28	87.02
Selectivity for middle distillate fr., 160°–350°C	60.95	59.16	57.57	56.16	66.64	60.29	58.70	58.06	66.94	61.58	59.77	58.38

N.B. fr., means fraction

using nickel—molybdenum alumina catalyst, while low gas oil kerosine ratio is reported with the cobalt—molybdenum alumina catalyst.

3 — *Fuel oil residue:* Although fuel oil yield (> 350°C) decreases continuously as a function of the process severity, yet the decrease is remarkably high at 450°C at all the reaction periods.

4 — *Hydrocarbon gases:* Tables 5 and 6 represent the hydrocarbon gas analysis and their distribution. It could be noted that the process is mainly catalytic, whereby C_1 and C_2 are produced is small or rather negligible amounts. Although, C_3 and C_4 form the major gas constituents, C_4 is produced in remarkably higher amounts than C_3. The difference between both nickel—molybdenum/alumina and cobalt—molybdenum/alumina catalysts is markedly evident in the percentage of the gas constituents. C_1, C_2 and C_3 produced by cobalt—molybdenum/alumina catalyst are always much higher than those produced by nickel—molybdenum/alumina catalyst, while the reverse is true with regard to C_4. The selectivity for liquified petroleum gas production, as determined by the ratio $(C_3 + C_4)/(C_1 + C_2)$ is almost always higher for nickel—molybdenum/alumina catalyst than for cobalt—molybdenum/alumina catalyst.

Conversion and selectivity

The total conversion increases continuously in the line with the increase in the craking—hydrogenation activities. Conversions at 400°C and 425°C (at lower reaction periods) are mainly resulted into the production of middle distillates.

Selectivity, on the other hand, decreases as a function of the reaction period due to the remarkable increase in the hydrocarbon gases and gasolines on the account of middle distillate and heavier fractions. Meanwhile, as the working temperature goes up, the hydrocracking activities of the investigated catalysts increase, hence the increase in the gases and gasolines is counterbalanced by a remarkable increase in the middle distillate, therefore the selectivity is slightly affected or increased.

Results obtained with cobalt—molybdenum/alumina catalyst indicate higher conversions and lower selectivities as compared with nickel—molybdenum/alumina catalyst due to the higher hydrocracking activity of the former catalyst.

Effect of the process variables on the refining—hydrogenation activities of the utilized catalysts "hydrodesulphurization"

The sulphur level indicated for the liquid hydrogenates produced with each of the investigated catalysts under all operating conditions attains a minimum at 450°C and 6 hours reaction period, as shown in table 7.

Sulphur level is not only a function of the reaction period, but also of the working temperature. It is also indicated that nickel—molybdenum/alumina catalyst induces higher refining—hydrogenation activity, namely, hydrodesulphurization is compared with cobalt—molybdenum/alumina catalyst which is mainly attributed to the higher hydrogenation activity of the nickel—molybdenum/alumina catalysts under the above selected operating conditons.

TABLE 5

Hydrocarbon gas production and distribution at different working temperatures and reaction periods using nickel–molybdenum/alumina catalyst

Working temperature, °C	400				425				450			
Reaction period, hr / Hydrocarbon gas, wt. %	1	2	4	6	1	2	4	6	1	2	4	6
Yield, wt. % on charge stock												
Methane, C_1	0.21	0.28	0.52	0.79	0.63	0.71	0.83	1.00	0.82	0.90	1.03	1.52
Ethane, C_2	0.05	0.08	0.17	0.32	0.18	0.24	0.36	0.54	0.29	0.37	0.56	0.96
Propane, C_3	0.42	0.74	1.29	1.95	0.82	1.15	1.73	2.15	1.22	1.63	2.33	3.11
Butane, C_4	1.37	2.67	3.21	4.65	3.19	4.01	5.06	5.64	3.40	4.26	5.82	7.10
Distribution, wt. %												
Methane, C_1	10.24	7.43	10.02	10.25	13.07	11.62	10.40	10.72	14.31	12.57	10.58	11.98
Ethane, C_2	2.44	2.12	3.28	4.15	3.73	3.93	4.51	5.79	5.06	5.16	5.75	7.56
Propane, C_3	20.49	19.63	24.85	25.29	17.01	18.82	21.67	23.04	21.29	22.77	23.92	24.51
Butane, C_4	66.83	70.82	61.85	60.31	66.19	65.63	63.42	60.45	59.34	59.50	59.75	55.95
$(C_3 + C_4)/(C_1 + C_2)$	6.66	9.47	6.52	5.95	4.95	5.43	5.70	5.06	4.16	4.64	5.13	4.08

TABLE 6

Hydrocarbon gas production and distribution at different working temeperatures and reaction periods using cobalt—molybdenum/alumina catalyst

Working temperature, °C	400				425				450			
Reaction period, hr / Hydrocarbon gas, wt. %	1	2	4	6	1	2	4	6	1	2	4	6
Yield, wt% on charge stock												
Methane, C_1	0.52	0.73	1.02	1.70	0.92	1.22	1.42	2.06	1.39	1.68	1.91	2.46
Ethane, C_2	0.21	0.41	0.83	1.30	0.49	0.98	1.36	1.95	0.88	1.55	1.84	2.16
Propane, C_3	0.59	0.98	1.95	2.88	1.65	2.59	3.41	3.99	2.80	3.77	4.33	4.59
Butane, C_4	0.92	1.40	2.31	3.06	2.08	2.90	3.62	4.78	3.26	3.85	4.28	4.87
Distribution, wt. %												
Methane, C_1	23.21	20.74	16.69	19.02	17.90	15.87	14.48	16.12	16.69	15.48	15.43	17.47
Ethane, C_2	9.38	11.65	13.58	14.54	9.53	12.74	13.86	15.26	10.56	14.29	15.89	15.34
Propane, C_3	26.34	27.84	31.92	32.18	32.10	33.68	34.76	31.22	33.61	34.79	35.01	32.60
Butane, C_4	41.07	39.77	37.81	34.26	40.47	37.71	36.90	37.40	39.14	35.44	34.67	34.59
$(C_3 + C_4)/(C_1 + C_2)$	2.07	2.09	2.30	1.98	2.65	2.50	2.53	2.19	2.67	2.36	2.30	2.05

TABLE 7

Sulphur content (wt %) and per cent removal in liquid hydrogenate at different operating conditions

Reaction period, hr		1		2		4		6	
Catalyst type / Temperature, °C		A	B	A	B	A	B	A	B
400°	wt. %	1.12	1.95	0.96	1.62	0.86	1.16	0.53	1.08
	% removal	52.34	17.02	59.15	31.06	63.40	50.64	77.45	54.04
425°	wt. %	0.55	0.84	0.38	0.57	0.20	0.31	0.14	0.22
	% removal	76.60	64.26	83.83	75.74	91.49	86.81	94.04	90.64
450°	wt. %	0.31	0.46	0.18	0.30	0.07	0.08	0.05	0.06
	% removal	86.80	80.43	92.34	87.23	97.02	96.60	97.87	97.45

However, at 450°C and 6 hours, the two catalysts induce approximately the same hydrodesulphurization activity, which may be attributed to equal hydrogenation activity of the two catalysts at this temperature.

Effects of process variables on the external hydrogen consumption

In all catalytic hydrogenation processes, hydrogen is chemically consumed to saturate the cracked products, to saturate aromatic structures and in the hydrogenation—refining reactions as well.

Results given in tables 3 and 4 indicate that the external hydrogen consumption increases continuously under all the operating variables (temperature and reaction period); or in other words as the cracking—hydrogenation activity, refining—hydrogenation efficiency and saturation—hydrogenation ability increase.

At a reaction period of 6 hours and in the temperature range between 400°C and 450°C the highest external hydrogen consumption is reported for the two catalysts.

Under all the experimental conditions, hydrogen consumption of the two catalysts declines in the following order:

nickel—molybdenum/alumina > cobalt—molybdenum/alumina

REFERENCES

[1] R. C. Archibald, B. S. Greensfelder, G. Holzmann and D. H. Rowe, *Ind. Eng. Chem.*, **52**, 745 (1960).

[2] H. L. Coonradt F. G. Ciapetta, W. E. Garwood, W. K. Leaman and J. N. Miale, *Ind. Eng. Chem.*, **53**, 727 (1961).

[3] A. Voorhies, W. M. Smith, and D. D. MacLaren, "Proceeding of the 6th World Petroleum Congress", Sec. III, P. 219, Frankfurt/Main, 1963.

[4] R. A. Flinn, O. A. Larson and H. Beuther, *Ind. Eng. Chem.*, **52**, 153 (1960).

[5] S. A. Qader and G. R. Hill, *Ind. Eng. Chem., Proc. Des. Develop.*, **8**, 450, 456, 462 (1969).

[6] P. B. Weisz and C.D. Prater, in "Advances in Catalysis and Related Subjects", Ed. Farkas, A., Vol. 9, Academic Press, New York, 1957, P. 575.

[7] C. G. Myers, W. E. Garwood, B. W. Rope, R. L. Wadlinger and W. P. Hawthorne, *J. Chem. Eng. Data*, **7**, 257 (1962).

[8] A. Voorhies and W. M. Smith, *Preprints, Div. Petrol. Chem., Am. Chem. Soc.*, **7**, 187 (1962).

[9] O. A. Larson, D. S. MacIver, H. H. Tobin and R. A. Flinn, *Ind. Eng. Chem., Proc. Des. Develop.*, **1**, 300 (1962).

[10] R. P. Baddour and M. C. Deibert, *J. Phys. Chem.*, **70**, 2173 (1966).

[11] F. Solymosi, *Catal. Rev.*, **1**, 233 (1967).

[12] L. A. Moddox and H. F. Rase, *Ind. Eng. Chem., Prod. Res. Develop.*, **10**, 32 (1971).

[13] S. P. Ahuja, M. L. Derrian and J. F. Le Page, *Ind. Eng. Chem., Prod. Res. Develop.*, **9**, 272 (1970).

Revue Roumaine de Chimie, **26**, *11–12*, 1423–1429 (1981)

CATALYTIC OXIDATION OF AMMONIA. III. [1,2]

LOW TEMPERATURE OXIDATION ON A Fe_2O_3—Cr_2O_3 CATALYST; EVALUATION OF THE EXPERIMENTAL DATA IN ORDER TO OBTAIN KINETIC PARAMETERS

M. M. GIRGIS *, D. P. LAZĂR ** and E. I. SEGAL ***
* Faculty of Science, Department of Chemistry, University of Assiut, Egypt
** The Polytechnical Institute of Jassy, Department of Physical Chemistry, Romania
*** Department of Physical Chemistry and Electrochemical Technology, National Institute of Chemistry, Bucharest, Romania

Received March 25, 1981

The overall kinetic parameters of the catalytic oxidation of ammonia, using a Fe_2O_3 — Cr_2O_3 catalyst have been evaluated through the estimation of the "temperature peak" exhibited by the exothermal oxidation process. The quantitative data used in this purpose have been experimentally obtained as it was reported in a previous paper.

1. INTRODUCTION

In some earlier papers [1,2] the investigation procedure, the technical equipment and the detailed experimental conditions used for the flow oxidation process of ammonia have been described. It was there pointed out that for the ammonia conversion to reaction products, atmospheric oxygen at normal pressure was used, together with an industral Fe_2O_3—Cr_2O_3 catalyst The main experimental results and the phenomenology of the oxidation process have been also described in detail.

In the present paper, both results and conclusions of the kinetic study are reported, referring to ammonia oxidation within the experimental conditions previously mentioned.[1,2]

2. EXPERIMENTAL

It has been phenomenologically established that the complete oxidation of ammonia using the industrial pelletized catalyst Fe_2O_3—Cr_2O_3 occurs only if the reactor reaches a minimum initial temperature $T_{i,\min}$. Within the framework in which these experiments were carried out, $T_{i,\min}$. values ranged between 186°C and 219 °C.

The upper concentration limit of the gaseous reaction mixture was 18.8% (v/v) NH_3 in air; the flow rates did not exceed 33.33 $cm^3 \cdot s^{-1}$ whereas the catalyst bed thickness varied between 4 and 175 mm.

Thus, using a reaction mixture having a 10.27% (v/v) NH_3 in air at a constant flow rate of 22.22 $cm^3 \cdot s^{-1}$, it was established that, for an initial temperature of the reactor equal to 195°C, the ammonia oxidation process exhibited a strong exothermal effect. After about 18 minutes following the reaction mixture admission into the reactor, the initial temperature distribution inside the reactor was markedly disturbed by the appearance of a "temperature peak" (shaped as a sharp pulse temperature), characterized by a given width and a certain height (expressed in temperature degrees) over the initial temperature distribution inside the reactor (Fig. 1).

The temperature peak makes its first appearance around the central zone of the reactor, just immediately after the "induction period" of the process. Then, during the next kinetic period (the so-called "autoacceleration period") the "temperature peak" slowly moves against the gas stream, toward the reactor entrance. Simultaneously, the "temperature peak" becomes narrower and higher (Fig. 1, curves 1–8). Finally, the "temperature peak" becomes stabilized at about 2–4 cm away from the gas entrance inside the reactor, reaching there its maximum value.

It has been observed that the position of the "temperature peak" and also its specific dimensions preserve their values provided that the initial temperature of the reactor ($T_{i,\mathrm{min}}$) and the flow rate of the reaction mixture are strictly maintained at constant values.

It has been also found that during the slow displacement of the "temperature peak" toward the reactor entrance, the temperature of the reactor behind the "temperature peak" quickly comes back to the initial value $T_{i,\mathrm{min}}$.

It is important to specify that outside the "temperature peak" it was not possible to record any temperature increase during development of the oxidation process, irrespective of how long this process was kept in action.

Therefore, the "temperature peak" can be considered to be similar to the "cool flame" phenomenon observed during the chain oxidation (process of hydrocarbons).

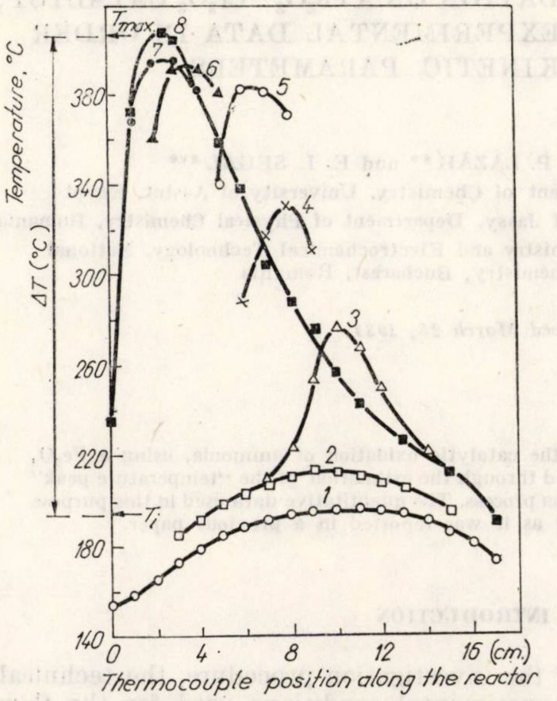

Fig. 1. — Time evolution of the maximum temperatures (for $T_i = 195$°C, flow rate 22.22 $\mathrm{cm^3 \cdot s^{-1}}$ ammonia content 10.27 %(v/v))
1. initial temperature distribution; *2.* temperature distribution after 18 min; *3.* temperature distribution after 40.5 min; *4.* after 43.5 min.; *5.* after 48 min.; *6.* after 50 min.; *7.* after 58 min.; *8.* after 64 min.

The influence of the reaction mixture flow rate on both position and value of the "temperature peak" is illustrated in figure 2, where ii can be observed that, owing to the increase of the flow rate, the "temperature peak" is dsplaced from the initial position (near the reactor entrance) back to the middle zone of the reactor. Simultaneously, an increase of the "temperature peak" value is observed: from 396°C for a flow rate of 16.66 $\mathrm{cm^3 \cdot s^{-1}}$, to about 472°C corresponding to a flow rate of 41.66 $\mathrm{cm^3 \cdot s^{-1}}$.

The composition of the reaction mixture substantially affects both shape and value of the "temperature peak", as it is shown in figure 3.

Also, it has been established that the increase of the volumetric percentage content of ammonia from 6.22% to 16.10% determined an increase of the "temperature peak" value from 392°C to 458°C. Positionally, the "temperature peak" is less affected by the ammonia content increase, than was expected.

When the ammonia content in the reaction mixture was somewhat increased, a certain narrowing of the "temperature peak" was observed.

Fig. 2. — Influence of the reaction mixture flow rate on the temperature distribution in the steady state ($T_i = 195$°C; ammonia content 10.43 %, v/v). Flow rate : *1.* 16.66 $\mathrm{cm^3 \cdot s^{-1}}$; *2.* 22.22 $\mathrm{cm^3 \cdot s^{-1}}$; *3.* 27.77 $\mathrm{cm^3 \cdot s^{-1}}$; *4.* 33.33 $\mathrm{cm^3 \cdot s^{-1}}$; *5.* 41.66 $\mathrm{cm^3 \cdot s^{-1}}$.

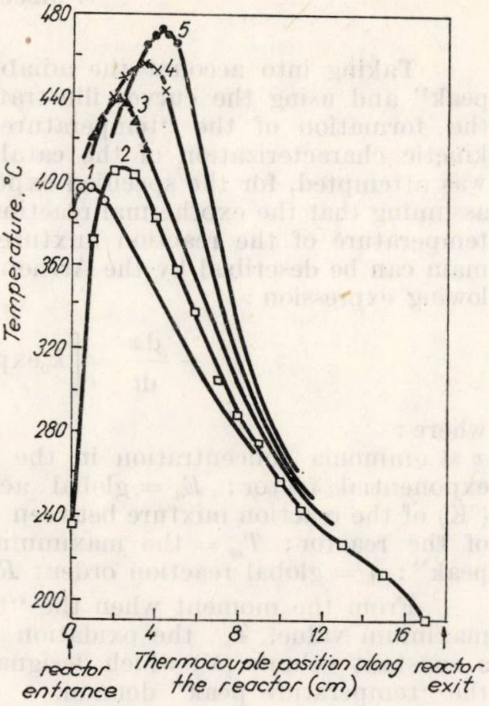

Fig. 3. — Influence of reaction mixture composition on the temperature distribution in the steady state (flow rate 27.77 $\mathrm{cm^3 \cdot s^{-1}}$) ammonia content (%, v/v) : *1.* 6.22 % ($T_i = 201$°C) ; *2.* 8.56 % ($T_i = 195$°C) ; *3.* 10.90 % ($T_i = 195$°C) ; *4.* 12.01 % ($T_i = 186$°C) ; *5.* 16.10 % ($T_i = 186$°C). *a.* Initial temperature distribution : *I.* 186°C ; II. 195°C ; III. 201°C.

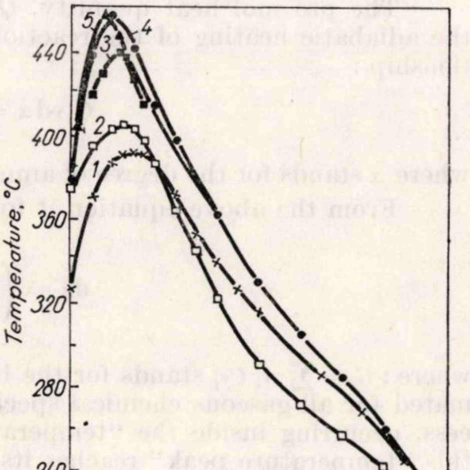

3. DISCUSSIONS

Taking into account the adiabatic character of the "temperature peak" and using the curves illustrating the temperature increase during the formation of the "temperature peak" maximum, a quantitative kinetic characterization of the catalytic oxidation process of ammonia was attempted, for the specified experimental conditions reported. Thus, assuming that the exothermal reaction, responsible for the increase of the temperature of the reaction mixture over the "temperature peak" domain can be described by the Arrhenius equation, one may write the following expression :

$$-\frac{\mathrm{d}x}{\mathrm{d}t} = \left[k_0 \exp.\left(-\frac{E_a}{RT}\right)\right]x^n \tag{1}$$

where :
x = ammonia concentration in the initial reaction mixture; k_0 = pre-exponential factor; E_a = global activation energy; T = temperature (°K) of the reaction mixture between T_i and T_m; T_i = initial temperature of the reactor; T_m = the maximum value of the stable "temperature peak"; n = global reaction order; R = gas constant.

From the moment when the "temperature peak" settles its stable maximum value, T_m, the oxidation process of ammonia takes place at a constant volume (V) which designates the proper volume occupied by the "temperature peak" domain.

The pro mol heat quantity, Q_v, consumed at constant volume, for the adiabatic heating of the reaction mixture, will be given by the relationship :

$$Q_v \cdot \mathrm{d}\alpha = C_v \cdot \mathrm{d}T \tag{2}$$

where α stands for the degree of ammonia conversion to reaction products.

From the above equation it follows that :

$$\mathrm{d}\alpha = \left(\frac{C_v}{Q_v}\right)\mathrm{d}T \tag{3}$$

where : $C_v = \sum n_i C_{v_i}$ stands for the heat capacity at constant volume, summated for all gaseous chemical species participating to the chemical process, occurring inside the "temperature peak" domain of emission, when this "temperature peak" reaches its maximum value, T_m.

The ammonia percentage content in the reaction mixture, corresponding to the conversion degree α is given by equation

$$x = x_0(1 - \alpha) \tag{4}$$

x_0 defining the ammonia percentage content into the reaction mixture just at the reactor entrance.

From (4), by differentiating, we get:

$$\mathrm{d}x = -\,x_0\,\mathrm{d}\alpha \tag{5}$$

From (3) and (5) the following differential expression can be written:

$$-\,\mathrm{d}x = x_0\frac{C_v}{Q_v}\,\mathrm{d}T \tag{6}$$

which by integration leads to:

$$x = x_0\frac{C_v}{Q_v}\,(T_m - T_x) \tag{7}$$

where: T_x is an arbitrarily selected temperature next to T_m.

Consequently, the time variation of the "temperature peak" between T_i and T_m values can be quantitatively described by the following equation:

$$\frac{\mathrm{d}T_x}{\mathrm{d}t} = \left[k_0\left(x_0\,\frac{C_v}{Q_v}\right)^{n-1}\right](T_m - T_x)^n\cdot\exp.\left(-\,\frac{E_a}{RT_x}\right) \tag{8}$$

which is similar to that proposed by Kondratiev [3] for the quantitative kinetic description of the reaction rate of the adiabatic oxidation process occurring in gas phase.

Taking decimal logarithms of equation (8), the result can be used for plotting a kinetic curve whose main parameters can be used to estimate the total reaction order (n) and total activation energy (E_a):

$$\begin{aligned}\log\left(\frac{\mathrm{d}T_x}{\mathrm{d}t}\right) &= \log\left[k_0\left(x_0\cdot\frac{C_v}{Q_v}\right)^{n-1}\right] + \\ &+ n\log(T_m - T_x) - \frac{E_a}{2.303\,R}\left(\frac{1}{T_x}\right)\end{aligned} \tag{9}$$

If equation (9) is successively applied to two adjoining points, T_{x_1} and T_{x_2}, located on the temperature curve, so that the $\left(x_0\,\frac{C_v}{Q_v}\right)$ ratio may be practically temperature independent, after the rearrangement of the terms, the following equation will be obtained:

$$\frac{\Delta\log\left(\dfrac{\mathrm{d}T_x}{\mathrm{d}t}\right)}{\Delta\log(T_m - T_x)} = n - \frac{E_a}{2.303\,R}\,\frac{\Delta\left(\dfrac{1}{T_x}\right)}{\Delta\log(T_m - T_x)} \tag{10}$$

Equation (10) can be restricted to a simpler form:

$$A = n - \frac{E_a}{2.303\,R} \cdot B \tag{10a}$$

where:

$$A = \frac{\Delta \log \left(\dfrac{\mathrm{d}T_x}{\mathrm{d}t}\right)}{\Delta \log T_m - T_x)} \text{ and } B = \frac{\Delta \left(\dfrac{1}{T_x}\right)}{\Delta \log (T_m - T_x)}$$

According to equation (10a), the linear dependence of A values upon B values can be used to plot a straight line, the slope of which will give the value of Arrhenius activation energy and the intercept the value of the global reaction order, n.

The only difficulty concerning the practical application of equation (10a) is connected with graphical differentiation of the curves representing the temperature increase inside the "temperature peak" domain.

The application of equation (10a) to the real case of the catalytic oxidation of ammonia — within the experimental conditions already mentioned — leads to the straight line shown in figure 4.

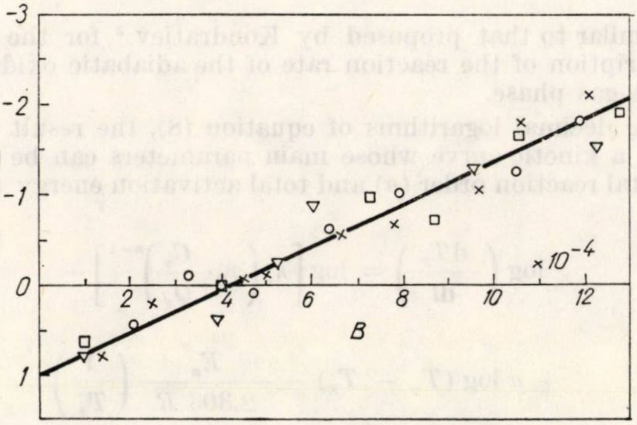

Fig. 4. — Graphical illustration of eqn. (10a) for the stationary "temperature peak", in different experimental conditions.
(□) 12.01 % (v/v) NH_3 and $T_i = 186°C$;
(▽) 16.10 % (v/v) NH_3 and $T_i = 186°C$;
(×) 33.33 $cm^3 \cdot s^{-1}$ and $T_i = 195°C$;
(○) 27.77 $cm^3 \cdot s^{-1}$ and $T_i = 195°C$; 10.43 % (v/v) NH_3.

It is obvious that, in spite of a certain spreading of the experimental data (due to the well known imprecision of the graphical differentiation), a straight line is obtained; the slope will give the value of the activation energy, i.e. 45.56 KJ.mol^{-1}, and the intercept will give the total reaction order, $n = 1$.

In order to find the best straight line through the set of the experimental points, the least-square method has been applied for computing the main kinetic parameters of the ammonia oxidation process; the results were $n = 0.95$ and $E_a = 43.8$ KJ.mol^{-1}.

As it can be seen the values of the main parameters n and E_a, as they were computed by means of the two different methods, are in good agreement. Moreover, the above results are in accordance also with those reported by other authors.[4-8]

Using equation (9) and the numerical values $n = 1$ and $E_a = 45.56$ KJ.mol^{-1}, the preexponential factor k_0 has been determined and a value of $2.52 \cdot 10^4$ min.$^{-1}$ was obtained.

CONCLUSIONS

The global kinetic parameters of the catalytic oxidation of ammonia, on a $Fe_2O_3 - Cr_2O_3$ catalyst, have been determined using the quantitative properties of the "temperature peak", the main characteristic phenomenological feature of the ammonia catalytic oxidation.

REFERENCES

[1] Part I, M. M. Girgis and D. P. Lazăr, *Rev. Roumaine Chim.*, **25**, 1293 (1980).
[2] Part II, M. M. Girgis, D. P. Lazăr and E. I. Segal, *Rev. Roumaine Chim.*, **26**, 1199 (1981).
[3] V. N. Kondratiev, "Kinetika Himiceskih Gazovyh Reaktsii", Izd. Akad. Nauk. Moskow 1958, p. 548.
[4] A. P. Zasorin and V. I. Atroshchenko, *Khim. Tekhnol.*, **12**, 139 (1969).
[5] L. L. Holbrook and H. Wise, *J. Catalysis*, **27**, 322 (1972).
[6] A. P. Zasorin, V. I. Atroshchenko and N. F. Kleshchev, *Kinetika i Katalis*, **9**, 22 (1972).
[7] J. N. Bradley, R. N. Butlin and D. Lewis, *Trans. Faraday Soc.*, **64**, 71 (1968).
[8] A. P. Zasorin, V. N. Cherkashin and V. I. Atroshchenko, *Izv. Vyssh. Ucheb. Zaved. Khim. Tekhnol.*, **11**, 1361 (1968).

evue Roumaine de Chimie, **26**, *11–12*, 1431–1439 (1981)

NEW COBALT(III) COMPLEXES CONTAINING TRIMETHYLENEDIAMINE, PROPYLENEDIAMINE AND OTHER LIGANDS

ARUN SYAMAL * and PRADIP K. MANDAL

Department of Applied Sciences and Humanities, Kurukshetra University, Kurukshetra, Haryana and Department of Chemistry, Regional Engineering College, Kurukshetra 132119, Haryana, India

Received April 24, 1980

Several new cobalt(III) complexes of the $[CoL_2(pn)(tn)]L$ and $[Co(pn)(tn)(AA)]X_n$ types (where pn = propylenediamine, tn = trimethylenediamine, $X = Cl^-, Br^-, I^-$, $L = Cl^-, NO_2^-$, AA = *ortho*-phenanthroline, ethylenediamine and acetoacetanilide, $n = 2-3$) have been synthesized and characterized by elemental analysis, paper chromatography, electronic and IR spectral studies, magnetic susceptibility measurements and molecular weight determination. The electronic spectra are typical of octahedral cobalt (III) complex. The complexes are diamagnetic and octahedral. The IR data indicate the *trans* configuration of $[CoCl_2(pn)(tn)]Cl$ and $[Co(NO_2)_2(pn)(tn)]NO_2$.

INTRODUCTION

In recent years there has been considerable research interest on the syntheses of cobalt (III) complexes containing ethylenediamine (en) and monodentate and other bidentate ligands.[1-4] Relatively little is known on similar cobalt (III) complexes containing propylenediamine (pn) and trimethylenediamine (tn). The cobalt (III) heterochelates of the $[Co(AA)(BB)(CC)]^{n+}$ type (where $AA \neq BB \neq CC$ = bidentate ligand) are novel in the sense that they contain three different bidentate ligands in the same coordination zone. These compounds may serve as model compounds for naturally occurring metal-ternary or quarternary systems. So far only the complexes viz. $[Co(en)(tn)(tetramethylenediamine)]^{3+}$, $[Co(en)(tn)\ neopentanediamine)]^{3+}$ and $[Co(en)(glycine)(C_2O_4)]$ have been reported in the literature. [5-7] Also there is no report on the mixed complexes of the type $[Co(NO_2)_2(pn)(tn)]NO_2$ and $[CoCl_2(pn)(tn)]Cl$. In this paper we report on the syntheses of the hitherto unknown complexes *trans*-$[Co(NO_2)_2(pn)(tn)]NO_2$ and *trans*-$[CoCl_2(pn)(tn)]Cl$. The reactivity of *trans*-$[CoCl_2(pn)(tn)]Cl$ towards bidentate ligands is tested and, as a result, the complexes of the $[Co(pn)(tn)(AA)]X_n$ type (where AA = en, *ortho*-phenanthroline and acetoacetanilide, $X = Cl^-, Br^-$ and I^-, n = 2,3) have been synthesized. The complexes have been characterized on the basis of elemental analysis, chromatogrophy, I.R. and electronic spectra, molecular weight, conductance and magnetic susceptibility measurements.

EXPERIMENTAL

MATERIALS

$Co(NO_3)_2 \cdot 6H_2O$ was BDH reagent grade. The ligands trimethylenediamine and acetoacetanilide (Aldrich Chemical Co.) were used. *Ortho*-phenanthroline and propylenediamine were purchased from Lobacheme Wien-Fischamend and Riedel (AG) respectively. $NaNO_2$ and ethylenediamine were the products of Sarabhai M. Chemicals. *Trans*-$[Co(NO_2)_2(en)_2]NO_2$ and *trans*-$[Co(NO_2)_2(tn)_2]NO_2$ were prepared by following the literature procedures.[8,9]

PHYSICAL MEASUREMENTS

The conductivity measurements were made on freshly prepared aqueous solutions at 30° with a Philips Conductivity Bridge and a dip type cell. Magnetic susceptibility was measured at room temperature by the Gouy method using $Hg[Co(NCS)_4]$ as the calibrant. IR spectra were recorded on a Perkin Elmer 237 spetrophotometer. Each spectrum was calibrated with a polystyrene film and the KBr disk technique was used. Electronic spectra were recorded with a Beckman DU2 spectrophotometer using 10 mm matched quartz cells. Microanalyses were done by Ciba Geigy Research Centre, Bombay. Cobalt content was determined by decomposing the complex to cobalt oxide by ignition and then treating with analar concentrated H_2SO_4 and finally titrating with standard EDTA solution using xylenol orange as indicator. Halide analysis was done gravimetrically precipitating as silver halide. Equivalent weight was determined by passing an aqueous solution of the complex through an anion exchange resin (Amberlite IR 120, H^+ form) column and then titrating the eluate with standard 0.05 M NaOH solution. Paper chromatography was carried out in aqueous solution by the ascending chromatographic technique[10] using the solvent mixture (1 : 1) of 0.01 M KCl and 95% ethanol as developer. A spot of the solution of the complex was placed on a strip of filter paper (46 cm × 2.5 cm). The distance of the spot from the end was 3 cm. The time of the experiment was 3 h. After drying the paper, the developed spot was identified by spraying an aqueous solution of sodium sulphide.

PREPARATION OF THE COMPLEXES

Trans-dinitro (propylenediamine) (trimethylenediamine) cobalt(III) nitrite

To a hot solution of $Co(NO_3)_2 \cdot 6H_2O$ (11.65 g, 0.04 mol) and sodium nitrite (6 g, 0.085 mol) in H_2O (20 cm^3) a hot solution of concentrated analar HNO_3 (1.5 cm^3), propylenediamine (3.3 cm^3, 0 04 mol) and trimethylenediamine (3.3 cm^3, 0.04 mol) in H_2O (10 cm^3) was added with vigorous stirring. A stream of air was passed through the reaction mixture for 3 h. After that the solution was treated with H_2O (*ca.* 50 cm^3) and heated on a waterbath for 30 min. The hot solution was filtered and washed with H_2O. The filtrate was evaporated to a small volume (*ca.* 30 cm^3) and cooled in icebath for 3 h. The separated golden yellow compound was filtered, washed with icecold water followed by acetone and dried *in vacuo*. This was recrystallized from minimum of H_2O. The yield was 40%.

Trans-dichloro (propylenediamine) (trimethylenediamine) cobalt(III) chloride

To the *trans*- $[Co(NO_2)_2(pn)(tn)]NO_2 \cdot H_2O$ (6g), concentrated HCl (25 cm^3) was added with vigorous stirring. At this stage the evolution of nitrous fumes was noticed. The solution was heated on a waterbath for 1 h with occasional stirring. The initial yellow colour of the solution changed to red and finally to green. The green solution was evaporated on the waterbath until the solution was covered with green crystals. The mixture was kept in a refrigerator overnight. The separated green shining crystalline compound was filtered, washed with conc. HCl followed by 95% ethanol and acetone, and dried *in vacuo*. The complex was recrystallized from minimum of conc. HCl. The yield was 30%.

Acetoacetanilido (propylenediamine) (trimethylenediamine) cobalt(III) chloride

Trans-$[CoCl_2(pn)(tn)]Cl$ (1.5 g, 0.005 mol) was dissolved in minimum of H_2O (ca. 3 cm^3). The pH of the solution was adjusted to 7 by 2N NaOH solution. Acetoacetanilide (0.85 g, 0.005 mol) was dissolved in 95% ethanol (20 cm^3) and was added to the above neutral solution with stirring. The mixture was heated on a waterbath till the volume was reduced to ca. 4 cm^3. The pH of the solution was adjusted to 6.5 by 2M HCl solution and then was cooled in icebath for 1 h. The separated precipitate was filtered, washed with ice cold water followed by 95% ethanol and finally dried *in vacuo*. The compound was recrystallized from minimum of H_2O. The yield was 20%.

Acetoacetanilido(propylenediamine) (trimethylenediamine) cobalt(III) bromide and iodide

These complexes were prepared by the metathetic reaction between [Co (pn) (tn) (acan)]Cl_2 and KBr and KI respectively.

Ortho-phenanthroline(propylenediamine) (trimethylenediamine) cobalt(III) chloride

Trans-[$CoCl_2$ (pn) (tn)]Cl (1.5 g, 0.005 mol) was dissolved in minimum of H_2O (*ca.* 3 cm^3) and the pH was adjusted to 7 by 2N NaOH solution. *Ortho*-phenanthroline (0.90 g, 0.005 mol) was dissolved in 95% ethanol (20 cm^3) and was added to the above solution. The mixture was heated on a waterbath until the volume was reduced to ca. 4 cm^3. The pH of the solution was adjusted to 6.5 by 2M HCl after cooling the solution to room temperature. This was then cooled in ice for 1 h. and the separated precipitate was filtered, washed with ice cold water followed by 95% ethanol and dried *in vacuo*. The compound was recrystallized from minimum of H_2O. The yield was 20%.

Ortho-phenanthroline (propylenediamine) (trimethylenediamine) cobalt(III) bromide and iodide

These were prepared by metathetic reaction between [Co(pn) (tn) (ophen)]Cl_3 and KBr and KI respectively.

Ethylenediamine (propylenediamine) (trimethylenediamine) cobalt(III) iodide

Trans-[$CoCl_2$(pn) (tn)] Cl (3.1 g, 0.01 mol) was dissolved in H_2O (20 cm^3). Ethylenediamine (0.6 g, 0.01 mol) was mixed with H_2O (5 cm^3) and added to the above solution with stirring. The pH of the mixture was adjusted to 7 by adding 2M HCl solution. The mixture was heated on a waterbath till the volume was reduced to 10 cm^3. The pH of the solution was adjusted to 6.5 by 2M HCl solution. The solution was cooled to room temperature and to this a saturated solution of KI was added. The mixture was allowed to stand for 30 min. The separated precipitate was filtered, washed with icecold water and dried *in vacuo*. The yield was 15%.

RESULTS AND DISCUSSIONS

The air oxidation of a mixture of aqueous solution of cobalt (II) nitrate, sodium nitrite, nitric acid, pn and tn leads to the synthesis of the golden yellow compound dinitro (trimethylenediamine) (propylenediamine) cobalt (III) nitrite. The equivalent weight and molecular weight of the complex as determined by the ion exchange method agree well with the theoretical value (Table 1). The complex exhibits the molar conductance value of 80.7 and 115.5 ohm^{-1} cm^2 mole^{-1} in 0.001N solutions in methanol and water respectively. The conductance data indicate 1:1 electrolytic nature of the complex.[11,12] The equivalent weight and conductance data indicate that the complex does not undergo aquation in aqueous solution. The electronic spectrum of the complex exhibits two bands at 22,730 and 28,985 cm^{-1} due to the $^1A_{1g} \rightarrow {}^1T_{1g}$ (band I) and $^1A_{1g} \rightarrow {}^1T_{2g}$ (band II) transitions respectively.[13,14] Several investigators [4,9,15] have observed that the band II due to the $^1A_{1g} \rightarrow {}^1T_{1g}$ transi-

TABLE 1

Analytical and equivalent weight data of cobalt(III) mixed ligand complexes [a]

Complex	Found (Calcd.) %						Equivalent weight
	Co	C	H	N	anion	H_2O[b]	
trans- $[Co(NO_2)_2(pn)(tn)]NO_2.H_2O$	15.9(16.2)	19.3(19.8)	5.7(6.1)	27.4(27.0)	—	4.8(5.0)	344(363)
trans- $[CoCl_2(pn)(tn)]Cl$	18.5(18.8)	22.4(23.0)	6.4(6.4)	17.7(17.9)	32.9(33.9)		
$[Co(pn)(tn)(acan)]Cl_2.2H_2O$	12.1(12.0)	40.3(39.2)	6.9(6.9)	14.0(14.3)	14.1(14.5)	7.2(7.3)	235(245)
$[Co(pn)(tn)(acan)]Br_2$	10.6(10.9)	35.5(35.4)	5.1(5.5)	12.6(12.9)	29.3(29.5)		
$[Co(pn)(tn)(acan)]I_2$	9.0(9.3)	30.1(30.1)	4.6(4.7)	10.8(11.0)	39.6(39.9)		
$[Co(pn)(tn)(ophen)]Cl_3$	11.8(12.0)	42.9(43.8)	5.7(5.9)	16.9(17.0)	21.4(21.6)		160(164.5)
$[Co(pn)(tn)(ophen)]Br_3$	9.0(9.4)	34.6(34.4)	4.2(4.5)	13.1(13.4)	38.2(38.3)		
$[Co(pn)(tn)(ophen)]I_3$	7.5(7.7)	27.9(28.1)	3.4(3.6)	10.6(10.9)	49.1(49.6)		
$[Co(pn)(tn)(en)]I_3$	9.0(9.1)	14.6(14.8)	4.1(4.3)	12.9(13.0)	57.2(58.8)		

[a] Abbreviations : acan = deprotonated anion of acetoacetanilide, ophen = *ortho*-phenanthroline and en = ethylenediamine.

[b] H_2O analysis was done heating at 110°C for 1h.

tion in the *trans*-dinitro cobalt (III) complexes occurs at lower energy than that of the *cis*-form. The band II in the *trans*-dinitro cobalt (III) complex is usually observed in the range 28,570 – 28,850 cm^{-1} and in the *cis*-dinitro complexes in the range 29,850 – 31,250 cm^{-1}.[15] The observed band II position at 28,985 cm^{-1} in the complex $[Co(NO_2)_2 (pn) (tn)]NO_2$ indicates a *trans*-structure.[16] The absorption maximum of the band II in the complex *trans*-$[Co(NO_2)_2 (pn) (tn)]NO_2$ (28,985 cm^{-1}) lies between the values of *trans*-$[Co(NO_2)_2 (pn)_2]NO_2$ (29,410 cm^{-1}) and *trans*-$[Co (NO_2)_2(tn)_2]NO_2$ (28,570 cm^{-1}). This is in agreement with the *trans*-structure of the complex, $[Co(NO)_2)_2 (pn) (tn)]NO_2$.[7,8] Usually in Co^{III} A_4B_2 type complexes the band I splits in *trans*-complexes when A and B are widely spaced in the spectrochemical series.[14] No such splitting was noticed in *trans*-$[Co(NO_2)_2 (pn) (tn)]NO_2$. The infrared spectral data have been used for the confirmation of the *trans*-structure of the complex. Because of low symmetry, the *cis*-isomer is expected to give more absorption peaks than the *trans*-isomer since the latter has a centre of symmetry while the former does not. Several workers [17-18] have noted that the bands near 1300 cm^{-1} due to the NO_2 symmetric stretching and near 800 cm^{-1} due to the NO_2 bending split into two bands in the *cis*-complexes but do not split in the *trans*-isomers. The infrared spectrum of $[Co(NO_2)_2 (pn) (tn)]NO_2$ exhibits only one band in the range 1290 – 1325 cm^{-1} and one band in the range 790–830 cm^{-1} and no splitting of the bands due to NO_2 symmetric stretch and NO_2 bending mode was observed. The infrared data are indicative of the *trans*-structure of the complex, $[Co(NO_2)_2 (pn) (tn)]NO_2$. In the *cis*-cobalt (III) complexes with diamines the asymmetric NH_2 deformation vibration at around 1600 cm^{-1} is known to split; on the other hand this absorption does not split in the *trans*-cobalt (III) complexes.[3] In the present complex also no such splitting was observed thus corroborating the *trans*-structure. The absence of a band arround 1050 cm^{-1} indicates that NO_2 is not bonded to cobalt through oxygen atom (ONO) and hence it is coordinated through the nitrogen atom (NO_2).[18] The NO_2 asymmetric stretch is located at 1415 cm^{-1} in *trans*-$[Co(NO_2)_2(pn) (tn)]NO_2$.[19]

The paper chromatographic studies of the complexes *trans*-$[Co(NO_2)_2 (pn)(tn)]NO_2$, *trans*-$[Co(NO_2)_2 (pn)_2]NO_2$ and *trans*-$[Co (NO)_2 (tn)_2]NO_2$ have been carried out using the 1 :1 mixture of 0.01 N KCl(15 cm^3) and 95 % ethanol (15 cm^3) as the developer. The R_f values of the complexes lie in the order: *trans*-$[Co(NO_2)_2 (pn)_2] NO_2$, 0.97 > *trans*-$[Co(NO_2)_2 (pn) (tn)]NO_2$, 0.95 > *trans*-$[Co(NO_2)_2(tn)_2] NO_2$, 0.87. This shows that the property of *trans*-$[Co(NO_2)_2 (pn) (tn)]NO_2$ is intermediate between *trans*-$[Co(NO_2)_2 (pn)_2]NO_2$ and *trans*-$[Co(NO_2)_2 (tn)_2] NO_2$. The similar trend in R_f values has been reported[19] in the complexes *trans*-$[Co(NO_2)_2 (en)_2]NO_2$, *trans*-$[Co(NO_2)_2(en) (tn)]NO_2$ and *trans*- $[Co(NO_2)_2 (tn)_2]NO_2$. The R_f value of the *trans*-$[Co(NO_2)_2(en)(tn)]NO_2$ ($R_f=0.74$) lies between the R_f values of *trans*-$[Co(NO_2)_2(en)_2]NO_2$ ($R_f = 0.66$) and *trans*-$[Co(NO_2)_2(tn)]NO_2$ ($R_f= 0.81$) in the solvent mixture: water (20 cm^3), acetone (75 cm^3) and conc. HNO_3 (5 cm^3).[19] The paper chromatographic data also indicate a *trans*-structure rather than the *cis* structure.[19] It is of interest to compare the R_f values of *trans*-$[Co(NO_2)_2 (en)_2] NO_2$ (0.76), *trans*-$[Co(NO_2)_2 (pn)_2]NO_2$ (0.97) and *trans*-$[Co(NO_2)_2 (tn)_2] NO_2$ (0.87). Propylenediamine ($H_2NCH_2 CH(CH_3) NH_2$) contains one electron donating methyl group. The electron donation by the methyl group to the chelate ring reduces the effective positive charge and this results in higher R_f value of *trans*-$[Co(NO_2)_2](pn)_2]NO_2$ in comparison to *trans*-$[Co(NO_2)_2(en)_2]NO_2$. As no such electronic effect is present in the complexes *trans*-$[Co(NO_2)_2(en)_2]NO_2$ and *trans*-$[Co(NO_2)_2(tn)_2]NO_2$ one would expect the R_f value in these two complexes to be the same. However, the latter complex exhibits a higher R_f value (0.87) in comparison to the former (0.76). This trend has also been observed by Celap et al.[19] We are unable to offer any explanation for this trend.

The treatment of the golden yellow *trans*-$[Co(NO_2)_2(pn)(tn)]NO_2$ with conc. HCl at the temperature of a steambath leads to the synthesis of the green coloured compound $[CoCl_2(pn)(tn)]Cl$. The complex does not undergo aquation in concentrated hydroclorie acid solution. However, when the solid complex is treated with water the colour changes immediately to pink due to aquation. The equivalent weight determination in aqueous solution by the ionexchange resin method reveals that $[Co(H_2O)_2(pn)(tn)]Cl_3$ is formed during aquation. The calculated equivalent weight of $[CoCl_2(pn)(tn)]Cl$ is 313.5 but we observed the equivalent weight value of 110 which agrees well with the theoretical value of 116.5 expected for $[Co(H_2O)_2(pn)(tn)]Cl_3$. This is also supported by the conductance data in aqueous medium; the complex behaves as a tri-univalent electrolyte (Table 2) in aqueous medium. In methanol the complex shows the behaviour of 1 :1 electrolyte[11] (Table 2). The characteristic green colour of this dichloro complex indicates a *trans* structure. This is confirmed by the electronic and infrared spectral data. The com-

TABLE 2

Molar conductance (30°C) and electronic spectral data of cobalt(III) mixed ligand complexes

Complex	Molar conductance (ohm^{-1} cm^2. $mole^{-1}$)	$\nu_{max}(\varepsilon)$, cm^{-1}
trans-$[Co(NO_2)_2(pn)(tn)]NO_2.H_2O$	100.5[a] 80.7[b]	22730 (235), 28985 (350)[a]
trans-$[CoCl_2(pn)(tn)]Cl$	392.3[a] 83.8[b]	15385, 24390,30 580[c] 16000 (15), 25380 (21), 3790 (428)[d] 20200 (273), 28330 (294)[e]
$[Co(acan)(pn)(tn)]Cl_2.2H_2O$	235[a]	20360 (190), 36875 (16580)[e]
$[Co(ophen)(pn)(tn)]Cl_3$	421[a]	20100 (120), 28640 (170)[e]
$[Co(en)(pn)(tn)]I_3$	430[a]	20410 (100), 38460 (19270)[e]

a Conductance is measured in water.
b Conductance is measured in methanol (0.001M)
c Electronic spectrum in solid state.
d Electronic spectrum in methanol.
e Electronic spectrum in water (0.0013M)
f *trans*-$[Co(NO_2)_2(en)_2]NO_2(\nu_{max})^8 = = 23100, 28820\ cm^{-1}$, *trans*-$[Co(NO_2)_2(pn)_2NO_2\ (\nu_{max})^8 = = 22990, 29410\ cm^{-1}$, *trans*-$[Co(NO_2)_2(tn)_2]NO_2\ \nu_{max}) = = 22, 420, 28570\ cm^{-1})^9$, *trans*-$[Co(NO_2)_2(en)(tn)]NO_2\ (\nu_{max})^{19} = = 22880, 28990\ cm^{-1}$, *trans*-$[CoCl_2(en)_2]Cl\ (\nu_{max}) = = 16000, 22220, 25970\ cm^{-1})^8$, *trans*-$[CoCl_2(pn)_2]Cl\ (\nu_{max})^8 = = 16390, 22220, 26320\ cm^{-1})$.

plex exhibits three electronic spectral bands at around 16000, 24,000 and 30,000 cm^{-1} in methanol solution and in solid state. The first two bands arise due to the splitting of the $^1T_{1g}$ state and are assigned to the transitions $^1A_{1g} \to A_{2g}$ and $^1A_{1g} \to {'E_g}$ respectively.[20] The third band at 30,000 cm^{-1} is assigned to the $^1A_{1g} \to {^1T_{2g}}$ transition. The splitting of the $^1A_{1g} \to {^1T_{1g}}$ transition conclusively proves the *trans*-structure for the complex. In the complex *trans*-[$CoCl_2(en)_2Cl$, similar splitting of the $^1A_{1g} \to {^1T_{1g}}$ transition has been observed.[8] The aqueous solution spectrum of the complex is different from the spectra in methanol solution and in solid state. The aqueous solution spectrum shows two bands at 20,000 and 28,330 cm^{-1} due to the $^1A_{1g} \to {^1T_{1g}}$ and $^1A_{1g} \to {^1T_{2g}}$ transitions respectively.[13-14] The aqueous solution spectrum [21] is comparable to the electronic spectrum of $[Co(H_2O)_2(en)_2]^{3+}$. Work is initiated in our laboratory for the isolation and assignment of geometrical configuration of $[Co(H_2O)_2(pn)(tn)Cl_3$. [22] In the case of *cis*-dichlorodiamine cobalt (III) complexes it has been observed that the NH_2 asymmetric deformation vibration at *ca.* 1600 cm^{-1} and CH_2 rocking vibration at *ca.* 900 cm^{-1} undergo splitting but the corresponding *trans*-complexes do not show the splitting of these bands.[23] The absence of splitting of the NH_2 deformation vibration at 1560 cm^{-1} and CH_2 rocking vibration at 910 cm^{-1} in $[CoCl_2(pn)(tn)]Cl$ indicates a *trans*-structure. [23] The bands at 3200 and 800 cm^{-1} are assigned to the NH_2 stretch (symmetric and asymmetric) and NH_2 rocking vibrations respectively. [3]

The complex *trans*-$[CoCl_2(pn)(tn)]Cl$ reacts with the bidentate ligands like en, *ortho*-phenanthroline and acetoacetanilide in aqueous—ethanol medium at pH 7 at the temperature of the steambath and the complexes of the type $[Co(AA)(pn)(tn)]^{n+}$ (where AA = bidentate ligand) are formed. These complexes are novel in the sense that three different bidentate ligands are inside the same coordination zone. The complex $[Co(en)(pn)(tn)]I_3$ is unique in having three different diamines in the coordination zone. These heterochelates are highly soluble in water and in some case the complex cation can only be isolated using the bulkier anion like I^-. The complexes are strongly absorbed by the cation exchange resin (Amberlite IR 120, H^+ form) thus verifying their cationic nature. The equivalent and molecular weights as determined by running aqueous solution of the complexes through the ion-exchange resin agree with the theoretical values (Table 2). The conductance measurements of the complexes were done in aqueous solution at several concentrations (N/64, N/128, N/256, N/512 and N/1024) and mean molar conductance values are given in table 2. The Λ_M values of $[Co(AA)(pn)(tn)]X_3$ (where AA = en, *ortho*-phenanthroline, $X = Cl^-$, I^-) and [Co(acetoacetanilide) (pn) (tn)] Cl_2 occur at 420 — 430 and 235 $ohm^{-1}\ cm^2\ mole^{-1}$ respectively indicating the triunivalent and biunivalent nature of the complex cations respectively (expected $\Lambda_M = 380 - 432$ for 1 : 3 electrolytes and 225—270 $ohm^{-1} \cdot cm^2 \cdot mole^{-1}$ for 1:2 electrolytes[12]). The Λ_v values increase steadily with dilution and Λ_α was calculated using the equation

$\Lambda_\alpha = \Lambda_v(1 + 0.692\ n_1 n_2 v^{\frac{1}{2}})$ where n_1 and n_2 are the valence of the cation and anion respectively. Λ_M values were calculated from mean Λ_α values. The electronic spectra of the complexes exhibit two bands at around

20, 000 and 29,000 cm^{-1} due to the $^1A_{1g} \rightarrow {}^1T_{1g}$ and $^1A_{1g} \rightarrow {}^1T_{2g}$ transitions respectively.[13-14] In some complexes the band II due to the $^1A_{1g} \rightarrow {}^1T_{2g}$ transition cannot be located as this band is presumably buried underneath the strong metal ligand charge transfer transitions.[20] The infrared spectral data of the ligands and the complexes are given in Table 3.

TABLE 3

IR spectral data (cm^{-1}) of ligands and cobalt(III) mixed ligand complexes

Probable assignments	tn. 2HCl (pn. 2HCl)	ophen	[Co(ophen) (pn)(tn)]Cl$_3$	[Co(NO$_2$)$_2$ (pn) (tn)] NO$_2$.H$_2$O	[Co(en)(pn) (tn)]I$_3$
NH$_2$ def.	1600 1590		1570	1590	1550
ν (C=N)		1558	1610		
NO$_2$asym. str.				1415	
NO$_2$sym.str.				1320	
NO$_2$ def.				815	

	acan	[Co(acan)(pn)(tn)]Cl$_2$.2H$_2$O	[CoCl$_2$(pn)(tn)]Cl
ν (C=O)	1730	1570	
Amide I	1660	1600	
NH$_2$ def.		1570	1560
Amide II	1540	1525	

Trimethylenediaminedihydrochloride and propylenediaminedihydrochloride exhibit a strong band at 1600 and 1590 cm^{-1} respectively which is assigned to the N—H bending vibration. This band is lowered in cobalt (III) mixed ligand complexes indicating the nitrogen coordination of tn and pn. The ν(C = O) vibration of acetoacetanilide shifts to lower frequency in the cobalt(III) heterochetate complex and this is indicative of the oxygen coordination of acetoacetanilide. The ν (C = N) frequency of *ortho*-phenanthroline is shifted to higher frequency in [Co(*ortho*-phenanthroline) (pn) (tn)]Cl$_3$ and this is indicative of nitrogen coordination of *ortho*-phenanthroline.[24] The other details of the spectral band assignments are given in table 3. The paper chromatography of the complexes [Co(*ortho*-phenanthroline (pn) (tn)]Cl$_3$ and [Co(acetoacetanilide) (pn) (tn)]Cl$_2$ was first done in distilled water. In distilled water the complex remains near the starting point and does not move. This indicates that the spots of the complex cations are strongly attracted by the negatively charged filter paper in distilled water. In order to reduce the strong attraction between the complex and filter paper and to observe the effect of the different ionic charge on the R_f values, the development was carried out with aqueous solutions containing different amount of KCl. In KCl solutions the complex cations move more compared to distilled water. Using the 1 :1 mixture of 0.01 M KCl (15 cm^3) and 95 % ethanol (15 cm^3) as the developer we observed the R_f values in the following order : [Co(*ortho*-phenanthroline) (pn) (tn)]Cl$_3$, 0.50 <[Co(acetoacetanilide) (pn) (tn)]Cl$_2$, 0.61. This indicates that the tripositive cation is attracted by the paper more in comparison to the dipositive cation. Thus the R_f values increase as the positive charge on the complex cations decreases.[25]

ACKNOWLEDGEMENTS. The authors are indebted to the University Grants Commission, New Delhi 110002 and the faculty research fund of Regional Engineering College, Kurukshetra 132119 for supporting this research.

REFERENCES

[1] F. P. Dwyer, T. E. MacDermott and A. M. Sargeson, *J. Amer. Chem. Soc.*, **85**, 2913 (1963).

[2] Y. Kojima and M. Shibata, *Inorg. Chem.*, **12**, 1009 (1973).

[3] M. L. Morris and D. H. Busch, *J. Amer. Chem. Soc.*, **82**, 1523 (1960).

[4] Y. Shimura, *J. Amer. Chem. Soc.*, **73**, 5079 (1951).

[5] J. C. Bailar, Jr., and J. B. Work, *J. Amer. Chem. Soc.*, **68**, 232 (1946).

[6] M. Kojima, Y. Yamada, H. Ogino and J. Fujita, *Bull. Chem. Soc., Japan*, **50**, 2325 (1977).

[7] N. Matsuska, J. Hidaka and Y. Shimura, *Bull. Chem. Soc. Japan*, **40**, 1868 (1967).

[8] F. Basolo, *J. Amer. Chem. Soc.*, **72**, 4393 (1950).

[9] M. B. Celap, M. J. Malinar and P. N. Radivojsa, *Inorg. Chem.*, **14**, 2965 (1975).

[10] A. I. Vogel, "Quantitative Inorganic Analysis", 3rd Edit., Longman, London, 1961, p. 724.

[11] R. A. Krause and D. H. Busch, *J. Amer. Chem. Soc.*, **82**, 4830 (1960).

[12] M. M. Jones, "Elementary Coordination Chemistry", Prentice Hall, Englewood Cliff, 1964, p. 524.

[13] A. B. P. Lever, "Inorganic Electronic Spectroscopy", Elsevier, Amsterdam, 1968, p. 306.

[14] F. A. Cotton and G. Wilkinson, "Advanced Inorganic Chemistry", 3rd Edit., Interscience Publishers, New York, 1972, p. 884.

[15] H. Kawaguchi and S. Kawaguchi, *Bull. Chem. Soc. Japan.*, **43**, 2103 (1970).

[16] N. Matsuoka, J. Hidaka and Y. Shimura, *Bull. Chem. Soc. Japan*, **39**, 1257 (1966).

[17] J. P. Faust and J. V. Quagliano, *J. Amer. Chem. Soc.*, **76**, 5346 (1954).

[18] R. L. Dutta and A. Syamal, *J. Indian Chem. Soc.*, **45**, 138 (1968).

[19] M. J. Celap, M. J. Malinar and T. J. Jangic, *Rev. Chim. Min.*, **13**, 278 (1976).

[20] B. N. Figgis, "Introduction to Ligand Fields", Wiley Eastern, New Delhi, 1976, p. 248.

[21] J. Y. Tong and P. E. Yankwich, *J. Amer. Chem. Soc.*, **80**, 2664 (1958).

[22] A. Syamal, unpublished data.

[23] M. L. Morris and D. H. Busch, *J. Amer. Chem. Soc.*, **82**, 1523 (1960); J. M. Figg and E. Sharwin, *J. Inorg. Nucl Chem.*, **27**, 653 (1965).

[24] A. A. Schilt and R. C. Taylor, *J. Inorg. Nuclear. Chem.*, **9**, 211 (1959).

[25] B. C. Bag and A. Syamal, *J. Indian Chem. Soc.*, **47**, 475 (1970).

Revue Roumaine de Chimie, **26**, *11–12*, 1441–1445 (1981)

A SIMPLE TOPOLOGY-BASED METHOD FOR ESTIMATING STRETCHING FORCE CONSTANTS OF AB_n MOLECULES

I. SILAGHI-DUMITRESCU

Chemistry Department, Babeș–Bolyai University, R–3400 Cluj-Napoca, Romania

Received February 6, 1981

A simple method based on the topological features of AB_n ($n = 2-6$) molecular systems is suggested for the calculation of the stretching force constants of isolated A–B bonds. These force constants are in good agreement with those calculated by normal coordinate analyses. In the case of larger molecules, AB_n groups can be separated and approximate stretching force constants can be derived for each A–B bond. These force constants are good starting points in the least squares refinements or even in the kinematic coupling methods of molecular force field determinations.

INTRODUCTION

The average sum rule, suggested by Lehmann[1] for the vibrational frequencies of simple molecules is well established. This is a pure consequence of the topology of the molecular constituents (i.e. the relative position of different bonds in the molecule) as pointed out by Jotham.[2]

In connection with these works we report some calculations of the stretching force constants for the AB_n type molecules.

PRESENTATION OF THE METHOD

The energy related to the stretching motions of an AB_n system can be described in terms of the energies of the separated A–B units and an interaction part which depends on the relative positions of the A–B bonds.

Mathematically, we can transcribe this picture in a matrix form in which the diagonal elements (V_{ii}) represent the energy of the separated A–B vibrations (or the corresponding frequencies) [2] and the off diagonal terms (V_{ij}) represent the interaction between different A–B stretching modes. These interaction terms show how the stretching frequency of an isolated A–B bond is changed as a consequence of the presence of the other A–B bonds.

For an AB_3-C_{3v} symmetry molecule, for instance, the interaction matrix shown in figure 1 can be set up.

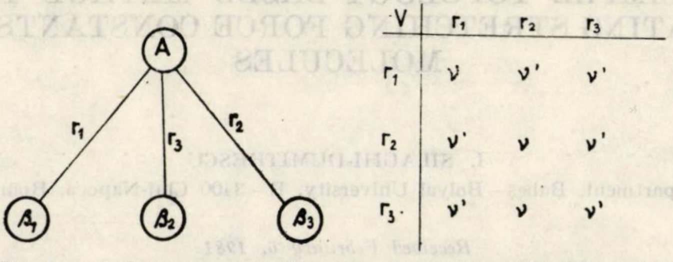

Fig. 1. — A C_{3v} symmetry AB_3 molecule and the related V matrix.

These matrices can be easily diagonalized by a standard coordinate transformation in accordance with the symmetry properties of the system, or directly by solving the Hückel type secular equation :

$$|V - E\,X| = 0 \tag{1}$$

For the AB_3 type pyramidal molecules, the following eigenvalues are obtained :

$$x_1 = \nu + 2\nu'$$

$$x_{2,3} = \nu - \nu'$$

These two eigenvalues are identified with the frequencies of the A_1 and E symmetry stretchings respectively, whence ν and ν' are easily obtained.

It must be pointed out that x_i are not exactly equal with the frequencies of the normal modes because of the coupling between the stretching and bending modes but in the first approximation the contribution from other than stretching modes is neglected.

Now, the force constant of the isolated A—B bond is calculated using the formula

$$K_{AB}^{\text{isolated}} = \frac{0.588851 \cdot \nu^2}{\mu_A + \mu_B} \cdot 10^{-6}\ \text{mdyne/Å} \tag{6}$$

where μ_A and μ_B are the reciprocal of the atomic masses of A and B. The following example illustrates the calculation procedure. For the PH_3 molecule, the observed A_1 and E frequencies are 2323 and 2328 cm^{-1} respectively. From (2) the following is calculated :

$$\nu = (x_1 + x_2 + x_3)/3 = 2326\ cm^{-1}$$

and $K_{PH} = 3.11$ mdyne/Å (literature value = 3.10 mdyne/Å)[3]

In Tables 1, 2, 3 and 4 the force constants calculated according to the procedure described, are compared with literature data, obtained with more sophisticated methods. Where differences are noticed, they stem from the mixing of the stretching with bending modes, since the stretching—stretching interactions were implicitly taken into account in setting up the V matrix.

TABLE 1

A—B force constants for the AB_2 type molecules

Molecule	Eigenvalues cm^{-1}		ν cm^{-1}	Force constants mdyne/Å	
	(1)	(2)		this work	lit. value[3]
H_2O	3657	3756	3706.5	7.67	7.67
H_2S	2615	2628	2621.5	3.95	3.95
H_2Se	2345	2358	2351.5	3.24	3.24
O_3	1110	1042	1076	5.45	5.70
SO_2	1151	1362	1265.5	10.06	10.02
ClO_2	945	1111	1028	6.86	7.01

TABLE 2

A—B force constants for the AB_3 type molecules

Molecule	Eigenvalues cm^{-1}		ν cm^{-1}	Force constants mdyne/Å	
	(1)	(2,3)		this work	lit. value[3]
NH_3	3337	3443	3407	6.43	6.54
PH_3	2323	2328	2326	3.11	3.10
AsH_3	2116	2123	2120	2.63	2.60
SbH_3	1891	1894	1893	2.10	2.05
PCl_3	511	484	493	2.36	2.32
$AsCl_3$	405	370	382	2.06	2.02
$SbCl_3$	360	320	333	1.79	1.78
ClO_3^-	932	982	965	6.05	5.87
BrO_3^-	805	830	821	5.30	5.28
SO_3^{2-}	967	933	944	5.60	5.42
SeO_3^{2-}	810	740	763	4.56	4.55
TeO_3^{2-}	758	703	720	4.34	4.36

In the case of more complex (and less symmetric) molecules it is possible (provided other vibrational modes do not mix to a great extent with the stretching modes) to isolate, closed or approximately closed AB_n groups for which the above scheme could be applied. This way, an internal source of approximate stretching force constants is available, when no suitable force constants can be transferred from other molecules. This approximate set can be used further in least squares refinement or in progressive coupling methods of the molecular force field determination.

TABLE 3

A—B force constants for the AB_4 type molecules

Molecule	Eigenvalues cm^{-1}		ν cm^{-1}	Force constants mdyne/Å	
	(1)	(2, 3, 4)		this work	lit. value[3]
CH_4	2917	3019	2993	4.87	4.95
CD_4	2109	2259	2221	4.90	
SiH_4	2187	2190	2189	2.74	2.77
GeH_4	1504	1522	1517	2.61	2.61
NH_4^+	3233	3314	3293	6.00	6.00
PH_4^+	2306	2372	2355	3.19	3.19
AsH_4^+	2119	2225	2198	2.83	2.83
$SnCl_4$	366	403	393	2.48	2.47
$SnBr_4$	221	280	265	1.97	2.00
SnI_4	149	216	199	1.43	1.48
$InCl_4^-$	321	237	333	1.76	1.76
$InBr_4^-$	197	239	228	1.44	1.48
InJ_4^-	139	185	174	1.06	1.04
PO_4^{3-}	938	1017	997	6.17	6.16
AsO_4^{3-}	810	810	810	5.09	5.07
SeO_4^{2-}	837	873	864	5.84	5.81
CrO_4^{2-}	847	884	875	5.52	5.52
MoO_4^{2-}	997	841	860	5.97	5.92
RuO_4^{2-}	880	913	905	6.57	6.65

TABLE 4

A—B force constants for the AB_6 type molecules

Molecule	Eigenvalues cm^{-1}			ν cm^{-1}	Force constants	
	(6)	(4, 5)	(1, 2, 3)		this work	lit. value[3]
SF_6	775	694	940	814	4.65	4.89
SeF_6	708	662	780	728	4.78	4.75
TeF_6	701	674	752	717	5.01	5.01
PF_6^-	735	563	840	730	3.69	3.99
AsF_6^-	679	565	700	651	3.78	3.77
SiF_6^{2-}	646	466	741	633	2.67	2.94
GeF_6^{2-}	627	454	598	555	2.73	2.74
NbF_6^-	683	562	580	591	3.24	3.38
MoF_6	741	644	741	709	4.69	4.74
WF_6	769	670	712	708	5.08	5.11
TcF_6	705	551	748	673	4.25	4.29
ReF_6	755	596	715	681	4.70	4.75
PtF_6^{2-}	600	576	571	577	3.39	3.42
PCl_6^-	360	281	449	378	1.39	1.62
$SbCl_6^-$	337	277	336	316	1.61	1.66
$SnCl_6^{2-}$	311	229	313	284	1.29	1.33
$PbCl_6^{2-}$	285	215	265	251	1.12	1.14

As an example we give a system in which we are particulary interested, namely the dithiophosphinato chelate ring shown in figure 2.

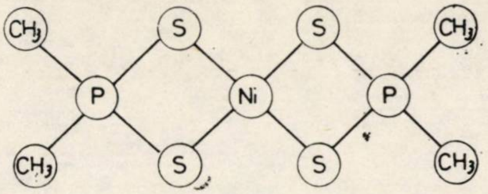

Fig. 2. — The Ni dithiophosphinato chelate ring.

The following approximate closed groups can be considered : NiS_2, PS_2, and PC_2. In table 5 the corresponding frequencies and force constants are given. It can be seen that even in this relatively complicated system the predicted A—B (isolated) force constants have suitable values for an improvement by the least squares procedure.[4]

TABLE 5

Predicted and refined force constants in $Ni[S_2P(CH_3)_2]_2$

Bond	Eigenvalues cm^{-1}	ν cm^{-1}	K_{A-B} mdyne/Å	Refined[4] values
NiS	350 281	315	1.21	1.12
PS	585 511	548	2.79	2.99
PC	732 736	734	2.74	2.82

REFERENCES

[1] W. J. Lehmann, *J. Mol. Spectrosc.*, **7**, 261 (1961).

[2] R. W. Jotham, *Chem. Soc. Rev.*, **2**, 457 (1973).

[3] H. Siebert "Anwendungen der Schwingungsspektroskopie in der anorganischen Chemie", Springer-Verlag, Berlin, 1966.

[4] I. Silaghi-Dumitrescu and I. Haiduc, *Rev. Roumaine Chim.*, **25**, 823 (1980).

Revue Roumaine de Chimie, 26, *11–12*, 1447–1450 (1981)

SYNTHESIS OF MEDIUM AND HIGHER DIALKYL DISULPHIDES

S. CHORBADJIEV

Faculty of Chemistry, University of Sofia, Sofia 1126, 1 Anton Ivanov avenue, Bulgaria

Received September 13, 1980

By means of the interaction of medium and higher alkyl bromides with the sodium hydroxide—sulphur combination the corresponding dialkyl disulphides are obtained.

INTRODUCTION

Medium and higher, as well as lower, dialkyl disulphides are usually obtained by the interaction of sodium (or potassium) disulphide with alkyl bromide[1] or with alkyl tosylate[2] in alcohol medium. Another possibility of preparing dialkyl disulphides is when alkyl halide interacts with sodium sulphide and sulphur[3] or with sodium thiosulphate followed by the treatment with iodine, hydrogen peroxide, or alkali hydroxide.[4] A series of medium and higher dialkyl disulphides is also obtained by the oxidation (with iodine, bromine, hydrogen peroxide etc.) of the corresponding mercaptans or their derivatives.[5] Alkyl rhodanides[6] and trialkyl boron compounds[7] are used in some cases for the preparation of dialkyl disulphides.

In one of our previous papers[8] we showed that lower dialkyl disulphides could be obtained successfully by the interaction of alkyl bromide with the sodium hydroxide—sulphur combination in ethanol medium. Different ratios alkyl bromide : sodium hydroxide : sulphur were used, the most favourable being the ratio 2 :3 :3. In this way, twelve dialkyl disulphides were synthesized with good yields (60—70 %). It is interesting to see the scope of this method and how far it could be applied for the preparation of dialkyl disulphides with longer aliphatic carbon chain. Moreover, the data in the literature for some of these disulphides are controversial, some disulphides being not prepared (e.g. diundecyl disulphide), and some being prepared in lower yield.

In this work we examined the possibility of preparing medium and higher dialkyl disulphides by means of the interaction of the corresponding alkyl bromide with the sodium hydroxide—sulphur combination in ethanol medium. The dialkyl disulphides with alkyls from C_7 to C_{18} were synthesized. The way of purifying the compounds was also worked out.

EXPERIMENTAL

The following alkyl bromides were used for the interaction : n-heptyl, n-octyl, n-nonyl n-decyl, n-undecyl, n-dodecyl, n-tetradecyl, n-hexadecyl, and n-octadecyl bromide. They were obtained from the corresponding alcohols with red phosphorus and bromine. The ratio alkyl bromide : sodium hydroxide : sulphur 2 : 3 : 3 was used. The boiling and melting points of the compounds synthesized were not corrected.

The interaction of alkyl bromide, sodium hydroxide, and sulphur was carried out in the following *general procedure* : The mixture of 0.075 mol (3.00 g) of sodium hydroxide, 0.075 mol (2.40 g) of powdered sulphur and 30 ml of 95% ethanol is refluxed for one hour with stirring. In this way the so-called "sodium hydroxide—sulphur combination" is prepared. After cooling to room temperature 0.05 mol of the corresponding alkyl bromide is added and the reaction mixture is refluxed for four hours with frequent stirring. The content of the flask is then poured out into 400—500 ml of cold water and the product is extracted with ether or hexane. The solution is dried with sodium sulphate, the ether is distilled off, and the final product isolated. The product of the interaction of hexadecyl and octadecyl bromide with sodium hydroxide—sulphur combination is solid and as there are some difficulties in extracting it, it was filtered off, washed with water and dried in air. The isolation of diheptyl, dioctyl and dinonyl disulphide from the reaction mixture can be carried out by steam distillation, thus quite a pure product being obtained. The applying of steam distillation for the isolation of higher disulphides is not advisable because of their low volatility with steam.

The purification of the compounds isolated was fulfilled by means of vacuum distillation (for the compounds from diheptyl disulphide to didodecyl disulphide) or by recrystallization from acetic acid or benzene (for ditetradecyl, dihexadecyl and dioctadecyl disulphide).

The purification of the disulphides was achieved much easier by chromatographic filtration through silicagel. For 2 g of substance, 25 g of silicagel were used, the elution completed with 50—70 ml of hexane. All the disulphides synthesized were purified in this way.

The purity of the products obtained was checked by means of qualitative analysis for bromine (impurity of alkyl bromide) and infrared spectra — for the presence of alkyl alcohol (due to the hydrolysis of the alkyl bromide). Actually, the alcohol impurity is removed during the chromatographic filtration through silicagel.

TABLE 1

Dialkyl disulphides obtained by the interaction between alkyl bromides and sodium hydroxide—sulphur combination

Dialkyl disulphide	Yield, %	B.p., °C/mmHg	M.p., °C	n_D^{20}
Diheptyl disulphide	68.5	165—167/12	—	1.4870
Dioctyl disulphide	67.4	198—203/13	—	1.4858
Dinonyl disulphide	69.1	208—211/9	—	1.4835
Didecyl disulphide	64.9	213—216/10	—	1.4830
Diundecyl disulphide	77.4	210—213/8	26—27	1.4840
Didodecyl disulphide	62.8	212—216/5	29—30	1.4838
Ditetradecyl disulphide	77.5	—	43—45	1.4800*
Dihexadecyl disulphide	69.2	—	49—50	—
Dioctadecyl disulphide	66.3	—	59—60	—

* The compound gives overcooled liquid that crystallizes with difficulty, so it is possilbe to determine the refractive index at a temperature much lower than its m.p.

The medium and higher dialkyl disulphides synthesized were identified by means of their melting and boiling points, refractive index (Table 1) and quantitative analysis (Table 2).

TABLE 2

Quantitative analysis of the compounds synthesized

Dialkyl disulphide	Found		Calculated	
	%C	%H	%C	%H
Diheptyl disulphide	63·84	11.07	64.12	11.45
Dioctyl disulphide	66.29	12.02	66.10	11.80
Dinonyl disulphide	68.36	11.49	67.92	11.95
Didecyl disulphide	69.05	12.17	69.36	12.14
Diundecyl disulphide	69.97	12.21	70.59	12.30
Didodecyl disulphide	71.30	12.50	71.64	12.44
Ditetradecyl disulphide	73.61	12.05	73.36	12.66
Dihexadecyl disulphide	74.25	12.42	74.71	12.84
Dioctadecyl disulphide	75·32	12·42	75·79	12.98

DECOMPOSITION OF THE SODIUM HYDROXIDE – SULPHUR COMBINATION

The combination of sodium hydroxide—sulphur was prepared from 0.075 mol (3.00 g) of sodium hydroxide, 0.075 mol (2.40 g) of sulphur and 30 ml of 95% ethanol. After cooling it, 60 ml of diluted (1 : 1) hydrochloric acid (0.3 mol HCl) were added dropwise. The yellow precipitate of sulphur was filtered, washed with water and dried ; the yield was 1.55 g (64.5%). The gas evolved during the decomposition with hydrochloric acid was passed through two washing bottles each containing 0.1 mol (37.94 g) of lead acetate dissolved in 100 ml of water. Black precipitate of lead sulphide (0.25 g, 1.375% of the initially used sulphur) was obtained in the first bottle only.

RESULTS AND DISCUSSION

By means of interaction of the sodium hydroxide—sulphur combination with different alkyl bromides (ratio alkyl bromide : sodium hydroxide : sulphur 2 : 3 :3) in ethanol medium, nine medium and higher dialkyl disulphides are obtained. The results of the experiments are summarized in table 1 and table 2. The yields of the products are within the range of 60—70 %. It is necessary to remark that during the interaction, the whole amount of the initial alkyl bromide is consumed entirely as even the raw reaction product does not show the presence of bromine. On the other hand, after the separation of the product from the water layer the water solution shows only slight alkaline reaction, pH about 8.

In all cases the interaction was carried out with comparatively small amounts of alkyl bromide, 0.05 mol. In several cases however, larger amounts of alkyl bromide were used (about 1—1.5 mol). Increase of the amounts of the reactants does not lead to complications in carrying out the interaction and in the isolation and purification of the products. Generally, the yields increase to some extent. Difficulties may arise in chromatographic filtration of larger amounts of dialkyl disulphide. When working with larger amounts the isolation of the raw product can be fulfilled only by separation of the upper layer after pouring the reaction mixture into water (for liquid disulphides) or by filtration (for solid disulphides) without extraction.

The method described in this paper, as well as in the previous one,[8] gives the possibility of preparing dialkyl disulphides with different alkyl groups (from C_2 to C_{18}) on a laboratory or even a larger scale. Obviously, the interaction between alkyl bromide and sodium hydroxide—sulphur combination has a general character and can be used as a preparative method of synthesis.

As to the sodium hydroxide—sulphur combination itself little definite can be said. All the amount of the sulphur in it is in a combined state as when the combination is poured out into 500 ml of water, a transparent dark yellow solution is obtained with pH about 11. It is after the interaction with alkyl bromide that pH diminishes to about 8. If the water solution is acidified, only 64.6 % of the sulphur separates in elemental state. If the sodium hydroxide—sulphur combination (without dilution in water) is decomposed with hydrochloric acid, 64.5 % of the sulphur separates in elemental state and only 1.38 % of it evolves as hydrogen sulphide. Evidently, the remaining 34 % of sulphur are under other forms (probably sulphate, sulphite etc.).

Inclusion of sulphur in organic compounds can be achieved only after its preliminary interaction with sodium hydroxide and formation of the "sodium hydroxide—sulphur combination" for alkyl halides do not react with elemental sulphur. For instance, after a one-and-a-half hour refluxing of butyl chloride and sulphur (3 :2), the reactants were isolated unchanged (sulphur 98.9 %, butyl chloride 84.3 %). The same was the case of the "interaction" between propyl bromide and sulphur.

On the other hand, the sodium hydroxide—sulphur system does not interact with aryl bromides which contain less reactive halogen. Thus, for instance, bromobenzene, or α-bromonaphthalene were isolated unchanged from the reaction mixture with sodium hydroxide and sulphur (78.3 % of bromobenzene, resp. 94.2 % of α-bromonaphthalene). The solutions, after pouring out the reaction mixtures in water, did not contain bromide ions (there were only sulphide ions).

REFERENCES

[1] N. N. Melnikow and L. G. Wol'fson, *Zhur. obshchei Khim.*, **20**, 2085 (1950) ; C. R. Noller and J. J. Gordon, *J. Amer. Chem. Soc.*, **55**, 1091 (1933).

[2] F. Drahowzal and D. Klamann, *Monatsh.*, **82**, 970 (1951).

[3] Houben-Weyl, "Methoden der organischen Chemie", 4. Aufl., Bd. IX, Georg-Thieme-Verlag. Stuttgart 1955, S. 65 ; R. Hueter (to Unichem. A. G.) *Amer. Pat.* 2 277 325 (1939) ; *Chem. Abstr.*, **36**, 4831 (1942).

[4] H. E. Westlake and G. Dougherty, *J. Amer. Chem. Soc.*, **64**, 149 (1942) ; I. N. Tiz-Skworzowa, S. Y. Levina, A. I. Leonova and E. A. Karaseva, *Zhur. obshchei Khim.*, **21**, 242 (1951) ; R. D. Obolentsev, S. V. Netupskaya, A. V. Mashkina and L. K. Gladkova, *Izvest. Vostoch. Filialov Akad. Nauk S. S. S. R.*, **1957**, 60 ; *Chem. Abstr.*, **53**, 272 (1959) ; W. Davey and E. D. Edwards, *Wear*, **1**, 291 (1957/1958) ; *Chem. Abstr.*, **52**, 15040 (1958).

[5] F. H. McMillan and J. A. King, *J. Amer. Chem. Soc.*, **70**, 4148 (1948) ; S. Bezzi and P. Lanza, *Gaz. chim. Ital.*, **80**, 180 (1950) ; *Chem. Abstr.*, **45**, 3798 (1951) ; Collin, Hilditch, Marsh and McLeod, *J. Soc. Chem. Ind.*, **52** T, 272 (1933) ; D. Fore and R. W. Bost, *J. Amer. Chem. Soc.*, **59**, 2558 (1937) ; G. S. Hartley, *J. Amer. Chem. Soc.*, **58**, 2348 (1936).

[6] E. Hoggarth and W. A. Sexton, *J. Chem. Soc.*, **1947**, 816.

[7] Z. Yoshida, T. Okushi and O. Manabe, *Tetrahedron Letters*, **1970**, 1641 ; T. Okushi, O. Manabe and Z. Yoshida, *Kogyo Kagaku Zasshi*, **73**, 2006 (1970).

[8] S. Chorbadjiev, C. Roumain and P. Markov, *J. prak. Chem.*, **319**, 1036 (1977) ; *Bulg. Pat.* 20 899, Nov. 14, 1974.

Revue Roumaine de Chimie, 26, 11–12, 1451–1456 (1981)

THEORETICAL ASPECTS ON THE REGIOSELECTIVITY IN THE 1,3-DIPOLAR CYCLOADDITIONS OF PYRIDINIUM—YLIDES TO ACETYLENIC DIPOLAROPHILES

M. CONSTANTINESCU*, GH. SURPĂŢEANU**, CRISTINA LUCHIAN**,
MAGDA PETROVANU** and I. ZUGRĂVESCU**

* Computer Center of the University "Al. I. Cuza", Jassy

** The Polytechnic "GH. Asachi", Organic Chemistry Department, Jassy, 11, str. 23 August, Romania

Received September 23, 1980

Perturbation and frontier orbital theories are applied to explain the regioselectivity in the 1,3-dipolar cycloadditions of pyridinium—ylides to methyl propiolate and cyanoacetylene. Molecular orbital calculations were carried out by CNDO/2 method. A survey of the molecular orbital parameters permitted the drawing of the orbital correlation diagrams presented in figures 1—8. The energetically favoured regioisomers are those corresponding to the orbital correlation diagrams in figures 3—6. Theoretically, it is possible to obtain only one regioisomer in the cycloadditions of ylide 5 to methyl propiolate and of ylide 1, 2, 3, 6 (Table 3) to cyanoacetylene. There is no possibility to give a general rule of the regioselectivity of the cycloadditions of pyridinium—ylides to methyl propiolate or cyano-acetylene.

In a previous paper[1] the regioselectivity of the 1,3-dipolar cycloadditions of pyridinium—ylides to methyl acrylate and acrylonitrile was theoretically investigated. Those investigations were performed on the basis of frontier orbital theory.[2,3] The obtained theoretical results allowed the conclusion that the orbital correlation diagrams have to be constructed for each ylide—dipolarophile pair. In such cycloadditions it is possible to obtain two types of regioisomers.

In this paper we applied the frontier orbital theory to the investigation of the cycloadditions of pyridinium—ylides to the acetylenic dipolarophiles (cyanoacetylene and methyl propiolate).

RESULTS AND DISCUSSION

As the experimental data are already available, the regioselectivity of 1,3-dipolar cycloadditions of several nitrile oxides to methyl propiolate will be firstly discussed.

Table 1 shows the frontier orbital energies and the atomic orbital coefficients of the carbon and the oxygen in the group —CNO of three nitrile oxides.

The data in table 1 were calculated by CNDO/2 method and are taken from the literature.[4]

TABLE 1

The frontier orbital energies and the p_z atomic orbital coefficients for nitrile oxides

No.	Nitrile oxide (RCNO), R	Frontier orbital	Orbital energy (eV)	Atomic orbital coefficients	
				C_c	C_o
1	$-H$	HOMO LUMO	−12.895 4.133	−0.560 0.677	0.802 0.298
2	$-CH_3$	HOMO LUMO	−11.954 4.052	−0.524 0.604	0.764 0.284
3	$-C_6H_5$	HOMO LUMO	−12.090 2.193	−0.438 0.326	0.602 0.253

Taking into account our previous paper,[1] it can be supposed that the electrostatic interactions between the atoms involved in cycloadditions are insignificant. We suggested that in cycloadditions the orbital factors played a dominant role and the orbital interactions took place by the p_z orbitals of atoms C and O in dipole (RCNO) and C_1 and C_2 in dipolarophile.

The nitrile oxides of the type I react with methyl propiolate giving two regioisomers III and IV.

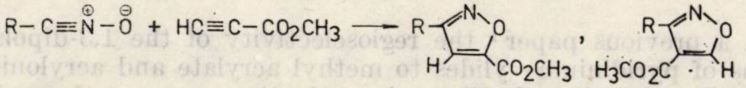

I II III IV

If the signs of the atomic orbital coefficients are taken into account it is possible to construct two orbital correlation diagrams (Figs 1 and 2).

The formation of the regioisomers of the type III is orbitally and energetically favoured by the diagrams in figures 1 and 2. That is not in agreement with the nitrile oxide dipole and methyl propiolate polariza-

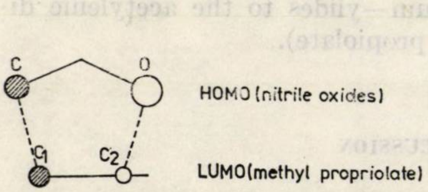

Fig. 1. — The orbital correlation diagrams between HOMO of nitrile oxides and LUMO of methyl propiolate. ○ sign (+), ◍ sign (−).

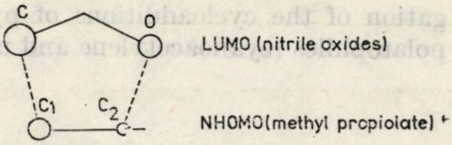

Fig. 2. — The orbital correlation diagrams between LUMO of nitrile oxides and NHOMO of methyl propiolate. ○ sign (+).

tion. As the diagrams in figure 2 show that all the orbital coefficients of the atoms implied in the reactions are positive, the formation of cycloadducts of the type IV is theoretically less possible.

Table 2 shows the percentages of the experimentally obtained cycloadducts III and IV in the analysed reactions.[5]

TABLE 2

The percentages of the cycloadducts III and IV

No.	Nitrile oxide (RCNO), R	Cycloadduct III %	Cycloadduct IV %
1	$-H$	84	16
2	$-CH_3$	69	31
3	$-C_6H_5$	72	28

As shown in table 2, the yield in cycloadduct III is larger than the yield in cycloadduct IV. Thus, we consider that a very good agreement exists between experimental and theoretical results.

Next the same investigation is developed on the regioselectivity of the cycloadditions of pyridinium–ylides to methyl propiolate and cyanoacetylene. In such cycloadditions two types of regioisomers VII and VIII could be obtained.

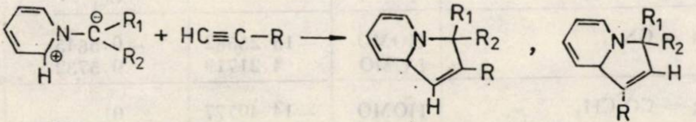

V VI VII VIII

Table 3 shows the frontier orbital energies and the atomic orbital coefficients for six pyridinium–ylides and the dipolarophiles (cyanoacetylene and methyl propiolate). The same parameters are also given for the next HOMO (NHOMO) and the next LUMO (NLUMO) oι the methyl propiolate. The data in table 3 were calculated by CNDO/2 method,[6] adapted by us on a Felix C–256 computer.

The values of the atomic orbitals of the atoms C_1 and C_2 in ylides are very closed, and so we shall refer only to the atom C_1.

The pyridinium–ylides geometry considered in the calculations was previously presented.[7–9] The geometry of the cyanoacetylene and the methyl propiolate was already described.[10,11]

Using all the data of Table 3, the following orbital correlation diagrams can be drawn (Figs 3–6) :

It is to be pointed out that even in these cases the orbital interactions take place between the p_z orbitals of the atoms involved in reactions.

TABLE 3

The frontier orbital energies and the p_z atomic orbital coefficients

No.	Compound	Frontier orbital	Orbital energy (eV)	Atomic orbital coefficients		
	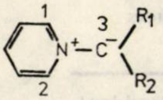			C_{C_1}	C_{C_2}	C_{C_3}
1	$R_1 = H ; R_2 = CN$	HOMO LUMO	− 8.52186 1.72130	0.3264 0.3015	0.3248 0.3013	−0.7120 0.3475
2	$R_1 = R_2 = CN$	HOMO LUMO	−10.37667 − 1.66241	0.2600 0.4200	0.2600 0.4200	−0.6247 0.2986
3	$R_1 = H ; R_2 = CO_2CH_3$	HOMO LUMO	− 8.80487 1.89203	0.3086 0.2777	0.3116 0.3216	−0.7252 0.2685
4	$R_1 = R_2 = CO_2CH_3$	HOMO LUMO	−10.36980 0.29018	0.2434 −0.4063	0.2435 −0.4062	−0.6411 −0.2048
5	$R_1 = H ; R_2 = COC_6H_5$	HOMO LUMO	− 8.94658 1.13297	−0.2977 −0.3133	−0.2963 −0.3628	0.6618 −0.1917
6	$R_1 = H ; R_2 = COCH_3$	HOMO LUMO	− 8.79171 2.04585	−0.3111 0.3575	−0.3086 0.2800	0.7271 0.2542
	1 2 $CH \equiv C - R$			C_{C_1}	C_{C_2}	
7	$R = CN$	HOMO LUMO	−15.25562 4.21719	−0.5645 0.5732	−0.4361 −0.4186	
8	$R = CO_2CH_3$	HOMO NHOMO LUMO NLUMO	−14.40777 −14.57747 3.15969 5.89403	0 0.2858 −0.5010 0	0 0.2092 0.2896 0	

The regioisomers of the type VII correspond to a cycloaddition occurring despite the general accepted polarization of the dipoles and dipolarophiles. The formation of the type VIII cycloadducts is in agreement with the general accepted polarization of the two addends.

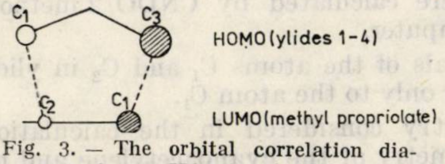

Fig. 3. — The orbital correlation diagrams between HOMO of ylides 1−4 and LUMO of methyl propiolate. ○ sign (+) ; sign(−).

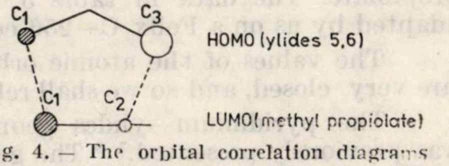

Fig. 4. — The orbital correlation diagrams between HOMO of ylides 5 and 6 and LUMO of methyl propiolate. ○ sign (+); ▥ sign (−).

According to the orbital diagram in figure 3, the ylides 1—4 react with methyl propiolate giving the cycloadducts of the type VIII ($R = CO_2CH_3$). According to the orbital diagram in figure 4, the ylides 5 and 6 react with methyl propiolate giving cycloadducts of the type VII ($R = CO_2CH_3$).

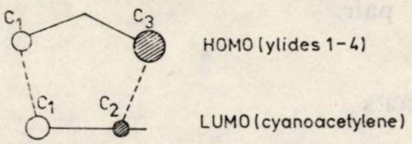

Fig. 5. — The orbital correlation diagrams between HOMO of ylides 1—4 and LUMO of cyanoacetylene. ○ sign (+); ▨ sign (—).

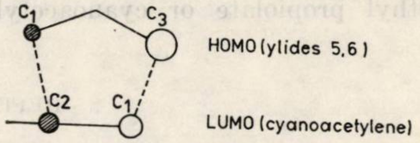

Fig. 6. — The orbital correlation diagrams between HOMO of ylides 5 and 6 and LUMO of cyanoacetylene. ○ sign (+); ▨ sign (—).

The cycloadditions of pyridinium—ylides to cyanoacetylene take place in a different manner. According to the orbital diagram in figure 5, the ylides 1—4 react with cyanoacetylene giving cycloadducts of the type VII ($R = CN$). The diagram in figure 6 shows that the cycloadditions of ylides 5 and 6 to cyanoacetylene form cycloadducts of the type VIII ($R = CN$).

All the cycloadditions presented in figures 3—6 are HOMO—controlled in respect to the ylide.

Theoretically, it is possible to construct two more orbital correlation diagrams (Figs 7 and 8), where the cycloadditions are LUMO—controlled as related to ylide.

According to the orbital correlation diagrams of figures 7 and 8, the cycloadditions which are allowed to form cycloadducts of the type VII are energetically favoured. Taking into account that in figure 7 as well as in figure 8 the atomic orbital coefficients have the same signs, the cycloadduct formation of the type VIII is energetically less possible but not excluded.

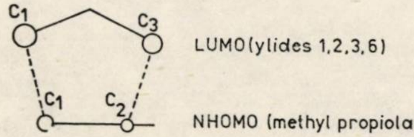

Fig. 7. — The orbital correlation diagrams between LUMO of ylides 1, 2, 3 and 6 and NHOMO of methyl propiolate. ○ sign (+).

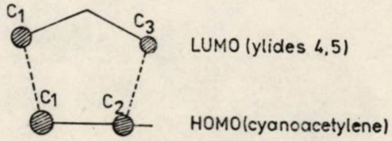

Fig. 8. — The orbital correlation diagrams between LUMO of ylides 4 and 5 and HOMO of cyanoacetylene. ▨ sign (—).

A survey of all the orbital diagrams leads to the conclusion that the energetically more favoured cycloadducts are those presented in figure 3—6. From the theoretical viewpoint it is possible to obtain only one regioisomer in cycloadditions of ylide 5 to methyl propiolate or of ylides 1—4 to cyanoacetylene.

As a general conclusion we can appreciate that it is not possible to establish a general rule on the regioselectivity of the cycloaddition reactions of pyridinium—ylides to methyl propiolate or cyanoacetylene. The orbital correlation diagrams have to be constructed for each ylide dipole—methyl propiolate or cyanoacetylene pair.

REFERENCES

[1] Gh. Surpăţeanu, M. Constantinescu, C. Luchian, M. Petrovanu, I. Zugrăvescu and A. Lablache-Combier, part. I, *Rev. Roumaine Chim.*, **26**, 1169 (1981).

[2] K. Fukui, "Theory of Orientation and Stereoselection", Vol. 2, Springer-Verlag, Berlin, 1975.

[3] K. N. Houk, *Acc. Chem. Res.*, **8**, 361 (1975).

[4] K. N. Houk, J. Sims, R. E. Duke, Jr., R. W. Storzier and J. K. George, *J. Amer. Chem. Soc.*, **95**, 7287 (1973).

[5] M. Christl and R. Huisgen, *Chem. Ber.*, **106**, 3345 (1973).

[6] J. A. Pople, and D. L. Beveridge, "Approximate Molecular Orbital Theory", McGraw-Hill, New York, 1970, QCPE 141.

[7] Gh. Surpăţeanu, J. P. Catteau, P. Karafiloglu and A. Lablache-Combier, *Tetrahedron*, **32**, 2647 (1976).

[8] Gh. Surpăţeanu, M. Constantinescu and I. Zugrăvescu, *Rev. Roumaine Chim.*, **23**, 1449 (1978).

[9] I. Zugrăvescu, M. Constantinescu, Gh. Surpăţeanu, A. Lablache-Combier and L. Devos, *Rev. Roumaine Chim.*, **24**, 1089 (1979).

[10] A. A. Westenberg and E. B. Wilson, *J. Amer. Chem. Soc.*, **72**, 1899 (1950).

[11] J. S. Rollet, *Acta Cryst.*, **8**, 487 (1955).

Revue Roumaine de Chimie, **26**, *11–12*, 1457–1459 (1981)

REACTION OF THIONYL BROMIDE WITH THIOPHENOLS

S. D. SARAF
Chemistry Department, Kuwait University, Kuwait

Received June 12, 1980

Thionyl bromide reacts with thiophenol to yield diphenyl sulphide, whereas *p*-thiocresol and *p*-halogenothiophenols gave the corresponding disulphides in high yield.

It has already been reported that thionyl bromide reacts with phenol and tropolone to yield 2,4-dibromophenol and 3,7-dibromotropolone.[1] However, no mechanism for the formation of such compounds was suggested. Recently we have shown that aromatic aldehydes are converted into the corresponding acid bromides for which a free radical mechanism has been proposed.[2] This suggested mechanism was further supported by the isolation of 4-bromomethylbenzal bromide, the formation of which could only be explained by free radical bromination of 4-methylbenzaldehyde.[3]

This paper deals with the reactions of thionyl bromide with thiophenols in order to find out the nature of the products and also the reaction path which might support the suggested free radical mechanism for thionyl bromide.

Treatment of thionyl chloride with thiophenols has been shown to yield two products, namely diphenyl disulphide and diphenyl tetrasulphide.[4] On the other hand *p*-substituted halogenothiophenols have been converted into the corresponding disulphides with nitric acid [5] or by adding sulphur to the corresponding Grigard reagent.[6] It has been reported that passing air stream through 4-bromo and 4-iodothiophenols also gives the corresponding disulphides.[6,7]

Addition of thionyl bromide to thiophenol in dry benzene gave a red solution, which was refluxed on a water bath for three hours. Distillation of benzene followed by the product gave a yellow solution of diphenyl sulphide b.p. 290–292°C in 90 % yield. However, the separation of the dissolved sulphur proved difficult. Repeated chromatography on alumina (neutral) in petroleum ether gave the pure product, b.p. 292°C.

Repeating the reaction with *p*-thiocresol and halogenothiophenols at room temperature in neat resulted in a vigorous reaction with the evolution of sulphur dioxide and hydrogen bromide and precipitation of sulphur. The oils thus obtained solidified on cooling. All these compounds were chromatographed on silica gel columns. Elution with petroleum ether gave yellow solid, which was proved to be elemental sulphur. Further elution with petroleum ether and benzene (3 :1, v/v) gave the corresponding disulphides as oils which crystallised from ethanol as white needles. The yields of the disulphides ranged from 80—90 %.

The identities of these compounds were confirmed by IR, NMR (where possible) and by correct elemental analysis.

The undermentioned mechanism is proposed for the formation of diphenyl sulphide.

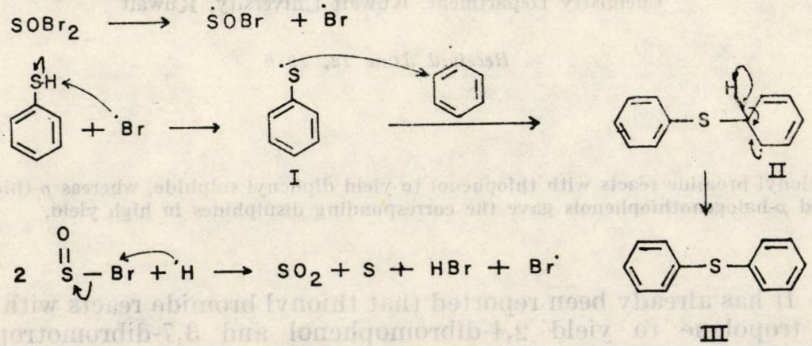

This mechanism postulates the formation of a stable radical intermediate I which attacks benzene present in large excess to yield II. Loss of $\dot{H}$ then gives the desired product III. The decomposition of SOBr radical releases the Br radical and therefore the cyclic process continues till the completion of the reaction. However, the formation of substituted diphenyl sulphides could be obtained by this method.

The formation of corresponding disulphides arises by the dimerisation of the radical I as given below.

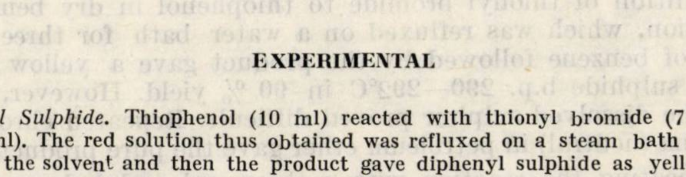

X = H, Cl, Br, I, CH_3

EXPERIMENTAL

Diphenyl Sulphide. Thiophenol (10 ml) reacted with thionyl bromide (7 ml) in dry benzene (200 ml). The red solution thus obtained was refluxed on a steam bath for 3 hours. Distillation of the solvent and then the product gave diphenyl sulphide as yellow oil b.p. 290—292°C/750 mm. yield 90 %. It was repeatedly chromatographed on neutral alumine in petroleum ether. Elution petroleum ether (30—40) gave elemental sulphur as yellow crystals (benzene) m.p. 115—116°C (55 mg). Further elution with petroleum ether—benzene (9 :1,v/v) gave diphenyl sulphide b.p. 292°C, IR 1590, 1475, 1440, 1080, 1070, 1000, 735, and 690 cm^{-1}.

4,4-Dimethyldiphenyl disulphide. *p*-Thiocresol (10g) was reacted with thionyl bromide (7 ml) at room temperature. An immediate brisk reaction occurred with the evolution of sulphur dioxide and hydrogen bromide. After about an hour the resulting oil was chromatographed on a silica gel column. Elution with petroleum (30–40°C) gave elemental sulphur m.p. 115–116°C (40 mg). Further elution with petroleum ether–benzene (3 :1, v/v) gave an oil which solidified on cooling. Crystallisation from ethanol gave white plate m.p. 40°C yield (78%) NMR ($CDCl_3$) 2.5–2.4 (4H. aromatic) 2.9–3 (4H, aromatic) 7.5 (6H, $2CH_3$).

Result of this and the other compounds are given in table 1.

TABLE 1

Analysis of compounds

Starting material	Compound isolated	m.p/b.p	Formula	Req.			Found			Yield
				C	H	S	C	H	S	
1. Thiophenol	Diphenyl sulphide	292/755	$C_{12}H_{10}S$	74.0	6.1	19.7	73.65	6.4	19.69	90%
2. Thiophenol	Diphenyl disulphide	60°	$C_{12}H_{10}S$	66.0	4.6	29.4	65.93	4.61	29.22	85%
3.4-Chlorothiophenol	4,4-Dichlorodiphenyl disulphide	70–71°	$C_{12}H_8S_2Cl_2$	50.1	2.7	22.3	49.72	2.55	22.0	90%
4.4-Bromothiophenol	4,4′-Dibromodiphenyl disulphide	94–95°	$C_{12}H_8S_2Br_2$	38.3	2.1	17.0	38.15	2.10	16.8	85%
5. 4-Iodothiophenol	4,4′-Diiododiphenyl disulphide	124–125°	$C_{12}H_8S_2I_2$	33.0	1.83	7.3	32.7	1.74	7.0	75%
6. 4-Methyl thiophenol	4,4-Dimethyldiphenyl disulphide	48–49°	$C_{14}H_{14}S_2$	68.28	5.28	26.0	68.22	5.65	25.9	90%

REFERENCES

[1] S. D. Saraf, *Canad. J. Chem.* **47**, 2803 (1969).
[2] S. D. Saraf, *J. prakt. Chem.*, in print.
[3] S. D. Saraf, *Organic Preparation and Procedures*, in print.
[4] S. H. Tasker and O. H. Jones, *J. Chem. Soc.*, **32**, 1911 (1910).
[5] O. Otto, *Liebigs Ann. Chem.*, **143**, 111 (1851).
[6] H. Alsberg, *Liebigs, Ann. Chem.*, **156**, 328 (1862).

Revue Roumaine de Chimie, 26, *11–12*, 1461–1467 (1981)

N,N′-SUBSTITUTED TRINITROPHENYLENE DIAMINES

M. IOVU* and EMANUELA IONESCU**
* Institute of Medicine and Pharmacy, Faculty of Pharmacy, Bucharest, Romania
** "N. Bălcescu" Agronomic Institute, Department of Chemistry, Bucharest, Romania

Received August 20, 1980

Some N,N′-disubstituted trinitrophenylene diamines were synthesized by condensation of 2,4,6-trinitro-1,3-chlorobenzene with diethylamine, diisobutylamine, pyrrolidine, piperidine, 2-methylpiperidine, morpholine, dimethylmorpholine, hexamethylenimine and benzylpiperidine. The purity and molecular structure of the new compounds were checked by means of elemental quantitative analysis, physical constants and spectral properties.

In a previous paper[1] we have presented the synthesis of 2,4,6-trinitrophenyl tertiary amines of general formula :

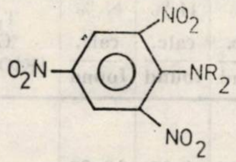

which possess fungistatic and cytostatic action.

Trinitrophenyl N-substituted amines have been synthesized by condensation of picryl chloride with cyclic or acyclic secondary amines. These substances are characterized by the presence of three nitro groups on the benzenic ring, whose strong – E effect results in a decreased basicity of amino group.

In the present paper we report the results concerning the synthesis of N,N′-disubstituted trinitrophenylene diamines obtained by condensation of 2,4,6-trinitro-1,3-dichlorobenzene with diethylamine, diisobutylamine, pyrrolidine, piperidine, 2-methylpiperidine, morpholine, dimethylmorpholine, hexamethylenimine and benzylpiperidine.

The synthesized bis-amines have not been described so far. The synthesis of new trinitrophenylene diamines was performed by a previously described method.[1]

Dichloro-trinitrobenzene in ethanol was treated with different amines in the presence of $Na_2CO_3 \cdot 10\ H_2O$:

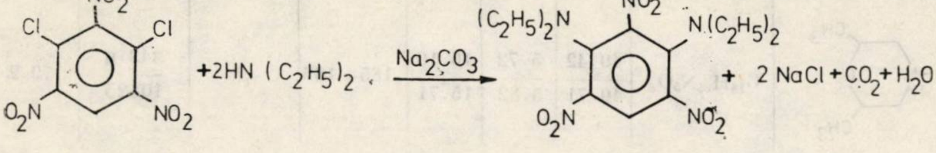

The obtained trinitrophenylene diamines were crystallized from ethanol, separated by filtration and washed with water to remove natrium chloride and unreacted reagents.

RESULTS AND DISCUSSION

The structural and molecular formulae of the new trinitrophenylene diamines, the results of their semimicro-analysis of carbon, hydrogen and nitrogen, their melting points, the yields, the wavelengths corresponding to the absorption peaks in ultraviolet and visible and their molar coefficients of extinction are listed in table 1.

TABLE 1

N,N′-disubstituted trinitrophenylene diamines

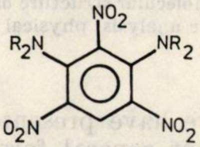

NR₂	Formula	C % calc. found	H % calc. found	N % calc. found	T_t °C (EtOH)	UV–vis λ_{max}. nm ε_{max}		η %
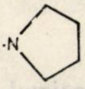	$C_{14}H_{17}N_5O_6$	47.85 48.08	4.87 5.22	19.93 19.38	181.5*	465.0 2343	363.6 9844	85.3
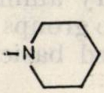	$C_{16}H_{21}N_5O_6$	50.65 50.32	5.66 5.09	18.64 18.38	104.5*	383.1 13125	344.8 10312	82.3
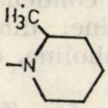	$C_{18}H_{25}N_5O_6$	53.06 53.49	6.18 6.26	17.19 16.87	223–224		357.0 4843	39.1
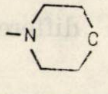	$C_{14}H_{17}N_5O_8$	43.86 44.25	4.47 4.92	18.27 18.63	186–187		341.3 10169	72.0
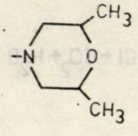	$C_{18}H_{25}N_5O_8$	49.42 49.71	5.72 5.82	16.10 15.71	185–186		343.6 10625	79.2

Table 1 (continued)

NR_2	Formula	C % calc. found	H % calc. found	N % calc. found	T_t °C (EtOH)	UV−vis λ_{max} nm ε_{max}	η %
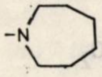	$C_{18}H_{25}N_5O_6$	53.00 53.81	6.18 6.19	17.24 17.01	153−154	353.4 9531	81.0
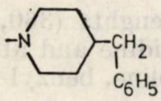	$C_{30}H_{33}N_5O_6$	64.20 64.15	5.94 5.85	12.51 12.51	164	347.2 9062	54.1
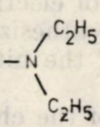	$C_{14}H_{21}N_5O_6$	47.34 46.62	5.91 6.42	19.71 19.72	115.5	355.9 9531	94.3
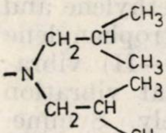	$C_{22}H_{37}N_5O_6$	56.50 56.81	7.97 8.29	14.98 15.22	117*	352.1 10625	75.3

* from $CHCl_3$

All the synthesised compounds resulted as yellow crystals. The compounds obtained by condensation with the pyrrolidine, piperidine, diethylamine and diisobutylamine melt at higher temperatures in comparison with those of the corresponding trinitro- and dinitrophenyl amines while condensation with morpholine, dimethylmorpholine and benzylpiperidine yields compounds whose melting points are lower than those of the corresponding trinitro- and dinitrophenyl amines.[1-13]

The UV and visible absorption spectra evidence the presence of the chromophore N = O groups grafted on the benzenic ring of bis-amine molecule; the spectra also show the presence of auxochromic $-N<$ groups of secondary amines substituted in *ortho* and *para* positions with respect to nitro groups of benzenic nuclei.

Strong absorption due to $\pi \rightarrow \pi^*$ transitions in N=O bond are noticeable at lower wavelengths within 209−213 nm range. The presence of two electron donor amino groups and three electron acceptor nitro groups on the benzenic ring causes E_2 type bands to shift bathochromously and to overlap on weak absorption bands at 218−231 nm due to $n \rightarrow \pi^*$ transitions of $-N=O$ groups.

The absorption at higher wavelenghts, from 340—465 nm to visible is probably due to the formation of chinoidic structures :

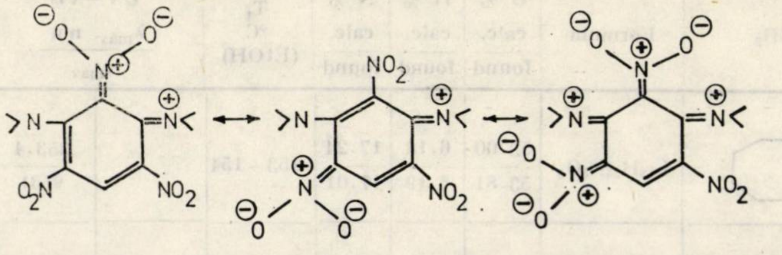

The absorption in UV region occurs at higher wavelenghts (360, 350 nm) for compounds obtained from pyrrolidine and piperidine and at lower ones (341, 347, 343 nm) for those obtained from morpholine, benzylpiperidine and dimethylmorpholine.

The hypsochromic effect is probably due to the presence of electronegative oxygen in the ring of the secondary amine. In the synthesized compounds, the basicity of the amino group is low because of the nitro group. No salt is formed in the presence of HCl.

Examination of the infrared spectra shows the presence of the characteristic band for the in-plane vibrations of the C—H bond in the aromatic ring and for the valence vibrations ν (C—H) of the methylene and methyl groups (whenever present). In N,N′-diisobutyl trinitrophenylene diamine the weak band at 3075 cm^{-1} corresponds to ν C(Ar—H) vibration. For methyl groups, antisymmetrical and symmetrical vibration $\nu(CH_3)$ are centered at 2960 cm^{-1} and 2870 cm^{-1} respectively. Symmetrical vibration $\nu\,(CH_2)$ are centered at 2855 ; the band assigned to antisymmetrical vibration $\nu\,(CH_2)$ superposes over that corresponding to symmetrical vibration of $-CH_3$ group.

The very weak band assigned to valence vibration of C—H group is hardly detectable among the other very strong bands[14] mentioned.

The presence of $-CH_3$ groups is signaled by the band at 1460 cm^{-1} assigned to the bending vibration ; this band overlaps on that assigned to shear vibration of $>CH_2$.

The symmetrical bending vibration of $>CH_2$ group is assigned for the band at 1326 cm^{-1}.

The valence vibrations of benzenic rings substituted with nitro and amino groups cause the occurrence of two bands at 1580 and 1500 cm^{-1}. The two very strong bands (1550 and 1330 cm^{-1}) assigned to vibration of NO_2 groups, lie within the same range.

Simpler spectra were recorded for the compounds originating in secondary cyclic amines without methyl groups. The IR spectrum of bis (N-morpholino)trinitrobenzene exhibits a band at 1105 cm^{-1} assigned to antisymmetrical valence vibrations of C—O—C group. This band was not found in compounds yielded by cyclic or acyclic amines.

^1H—NMR spectra show both the presence of protons from residue cyclic or acyclic tertiary amine and of protons from benzenic rings substituted with nitro groups. The aromatic proton gives a signal at δ =

= 8.40—8.54 ppm, a range which is very narrow and independent of the nature of substituted amino group in the aromatic ring.

The ^1H-NMR spectra confirm the molecular structure advanced for the synthesized compounds (Table 2).

TABLE 2

NMR spectral data

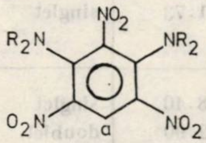

NR_2	δ ppm	Multiplicity	Assignment
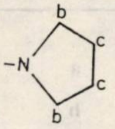	8.50	singlet	a
	3.33	quintet	b
	1.98	quintet	c
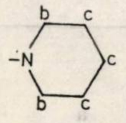	8.50	singlet	a
	3.15	singlet	b
	1.73	singlet	c
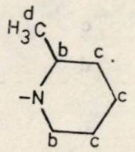	8.33	doublet	a
	3.11	multiplet	b
	1.55	multiplet	c
	0.92	doublet	d
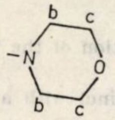	8.50	singlet	a
	3.25	triplet	b
	3.75	triplet	c
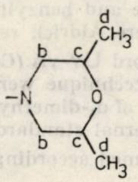	8.47	singlet	a
	2.63—3.14	multiplet	b
	3.68	multiplet	c
	1.16	doublet	d

Table 2 (continued)

NR_2	δ ppm	Multiplicity	Assignment
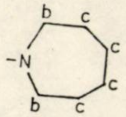	8.54	singlet	a
	3.31	singlet	b
	1.73	singlet	c
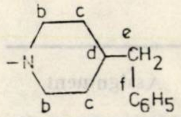	8.40	singlet	a
	2.90	doublet	b
	1.68	doublet	c
	1.56	multiplet	d
	2.58	doublet	e
	7.15	singlet	f
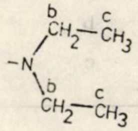	8.51	singlet	a
	3.23	quadruplet	b
	1.10	triplet	d
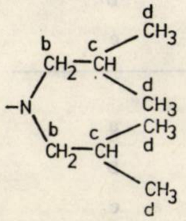	8.40	singlet	a
	2.91	doublet	b
	1.98	multiplet	c
	0.85	doublet	d

EXPERIMENTAL

2,4,6-Trinitro-1,3-dichlorobenzene was obtained by chlorination of the trinitroresorcino in the presence of pyridine.[15]

2,4,6-Trinitroresorcinol was obtained by nitration of resorcinol with a mixture of sulfuric and nitric acids.[16]

Diethylamine was a UCR reagent. Pyrrolidine was a Merck reagent. Piperidine was Prolabo reagent. Diisobutylamine, morpholine, 2-methylpiperidine and benzylpiperidine wer Fluka reagents. Hexamethylenimine and dimethylmorpholine were Aldrich reagents.

The UV spectra (in ethanol) were carried out with a Specord UV-vis (Carl Zeiss Jena spectrometer. A Specord IR—75 and the pelletting in KBr technique were employed i recording IR spectra. The ^1H-NMR spectra in deuterochloroform of d_6-dimethylsulfoxide wer carried out with a Varian A—60A spectrometer using TMS as internal standard.

The analyses of carbon, hydrogen and nitrogen were performed according to semimicr techniques.

CONDENSATION OF DIETHYLAMINE WITH 2,4,6-TRINITRO-1,3-DICHLOROBENZENE

In a 100 ml double-necked flask equipped with a reflux condenser 1.41 g (1/200 mole) 2,4,6-trinitro-1,3-dichlorobenzene, 15 ml ethanol, 5.42 g $Na_2CO_3 \cdot 10\,H_2O$ (1/50 mole) and 0.73 (1/100 mole) diethylamine were introduced. The content of the flask was heated to completion of reaction (about 3 hrs). The product was vacuum filtered and washed several times with water (to remove sodium chloride and finaly the traces of reactants) then with 2—3 ml anhydrous ethanol. After drying 1.67 g (94.3 %) of bis(diethyl—trinitrophenyl) amine resulted. The pure product crystallized from ethanol had the melting point of 115.5°C. The other bis(trinitrophenyl)amines given in table 1 were obtained in a similar way and were crystallized from ethanol and chloroform.

CONCLUSIONS

In the present paper we have shown that N,N'-substituted trinitrophenylene diamines may be obtained starting from 2,4,6-trinitro-1,3-dichlorobenzene and tertiary amines. By condensation of the above mentioned reactants in the presence of Na_2CO_3, nine new compounds were synthesized (Table 1) and characterised by determining their physical constants.

The UV-vis, IR and ^1H—NMR spectra support the structure advanced for all the obtained compounds.

ACKNOWLEDGEMENT. The authors are grateful to Dr. F. Chiraleu (Center of Organic Chemistry) for providing facility to carry out ^1H—NMR spectra.

REFERENCES

[1] M. Iovu and Em. Ionescu, *Rev. Chim. (Bucureşti)*, **31**, 957 (1980).

[2] E. Jeney und T. Zsolnai, *Zentr. Bakteriol. Parasitenk. Abt. I, orig.*, **193**, 535 (1964).

[3] I. L. Rosenfeld, V. P. Persanteva, M. N. Polteva and P. B. Terentev, *Ann. Univ. Ferrara*, **3**, 528 (1961); *Chem. Abstr.*, **56**, 1867 (1962).

[4] P. van Romburg, *Rec. Trav. chim.*, **14**, 68 (1885).

[5] M. Ionescu and M. Vagonescu, *Studia Univ. Babeş-Bolyai*, Ser. I, **2**, 135 (1960).

[6] P. van Romburg, *Rec. Trav. chim.*, **2**, 40 (1883).

[7] S. D. Ross and M. Finkelstein, *J. Amer. Chem. Soc.*, **79**, 6547 (1957).

[8] E. Sellmann and W. Gelles, *Ber. dtsch. chem. Ges.*, **21**, 2283 (1888).

[9] H. von Brāniger and K. Spyngenberg, *Pharmazie*, **12**, 335 (1957).

[10] R. H. Harradence and F. Lions, *J. Proc. Roy. Soc., New South Wales*, **70**, 406 (1937); *Chem. Abstr.*, **31**, 6662 (1937).

[11] M. D. Naiv and R. Adams, *J. Amer. Chem. Soc.*, **83**, 3518 (1961).

[12] V. Prelog and Z. Blazec, *Coll. Czech. Chem. Comm.*, **6**, 549 (1934); *Chem. Abstr.*, **29**, 2959 (1935).

[13] M. E. Mulder, *Rec. Trav. chim.*, **25**, 108 (1906).

[14] M. Avram and Gh. D. Mateescu, "Spectroscopia în infraroşu — aplicaţii în chimia organică", Ed. Tehnică, Bucureşti, 1966.

[15] G. P. Sarin, B. I. Buzikin, V. V. Iugatin and I. E. Moisak, *Zhur. org. Khim.*, **3**, 82 (1967).

[16] H. Merz and G. Zetter, *Ber. dtsch. chem. Ges.*, **12**, 2037 (1879).

Revue Roumaine de Chimie, **26**, *11–12*, 1469–1478 (1981)

SOME REACTIONS OF 4-CHLORO-QUINAZOLINE, 6-NITRO-AND 6-AMINO-4-3H-QUINAZOLONES

M. ANWAR, F.I. ABDEL-HAY, A. A. ELBARBARY and M. El-BORAI
Chemistry Department, Faculty of Science, Tanta University, Tanta-Egypt

Received Mai 29, 1980

4-Chloroquinazoline (I) reacts with amides, anilides and hydrazines to give 4-substituted quinazolines II–IV. 4-3H-Quinazolones V react with amines in the presence of formaldehyde yielding compounds VI. 6-Amino-4-quinazolone (Vc) reacts with some halocompounds and ethylacetoacetate forming the compounds VII–IX.

2,3-Disubstituted-4-3H-quinazolinones were previously studied in many separate papers. The reactivity of methyl-, amino-, styryl- and N-arylidene substituted 4-quinazolones was already explored.[1–5]

In the present investigation a trial was made to study some 4- and/or 6-substituted quinazolones.

4-Cloroquinazoline (I) was prepared by the recommended methods.[6,7] Reaction of I with urea, formamide and acetamide gives the compounds II a–c

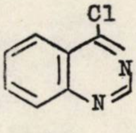

(I)

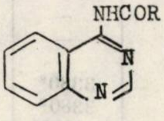

(II)

a, R= NH_2

b, R= H

c, R= CH_3.

The structures of compounds II were established by :

(i) IR-Spectral studies. Compounds II show the three skeletal quinazoline bands[4,8] in the regions of 1605–1590 cm^{-1}, 1580–1560 cm^{-1} and 1515–1475 cm^{-1}. The other functional groups are listed in table 1.

(ii) UV-Spectral studies. Compounds II show three main absorption bands in the regions : 230–225 nm, 280–262 nm and 310–300 nm. This bands may be assigned to the ^1L_a, ^1L_b and C = O, the third band may be the charge transfer band. These data are similar to that obtained at the 2,3-disubstituted-4-quinazolones (the lack of one band may be due to the absence of substituents in the 2 and 3 positions[5]).

(iii) The ^{1}H-NMR-spectra cf. table 2.

Compounds I react with some anilides or hydrazines to form the compounds IIIa-d and IVa, b.

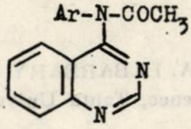

(III)

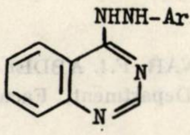

(IV)

a, Ar= C_6H_5

b, Ar= $C_6H_4CH_3$-o

c, Ar= $C_6H_4CH_3$-p

d, Ar= $C_{10}H_7$-1

a, Ar= $C_6H_4NO_2$-p

b, Ar= $C_6H_3(NO_2)_2$ -2,4

The structures of compounds III and IV were confirmed by:—

(i) IR-Spectral studies (cf. Table 1).

(ii) The C.T. band in compounds IV shows a red shift due to the presence of nitro group, the band appearing at 500—475 nm.

TABLE 1

IR spectral data of compounds II—IX* (KBr; cm^{-1})

Compound	ν(OH)	ν(NH)	ν(C=O)	ν(C=N)
IIa	—	3200^{br}	1720^{s}	1640^{m}
IIb	—	3220^{br}	1730^{s}	1635^{m}
IIc	—	3220^{br}	1720^{s}	1640^{w}
IIIa	3380^{s}	—	1670^{s}	1630^{sh}
IIIb	3380^{s}	—	1665^{s}	1620^{m}
IIIc	3400^{br}	—	1680^{s}	1620^{sh}
IVa	—	3400^{br}	—	1640^{m}
IVb	—	3450^{m}	—	1625^{m}
VIa	—	—	1695^{s}	1650^{m}
VIb	—	—	1695^{s}	1650^{m}
VIc	—	3460^{br}	1690^{s}	1650^{m}
VId	—	3440^{br}	1695^{s}	1645^{m}
VIe	—	—	1665^{m}	1610^{m}
VIf	—	—	1665^{s}	1610^{sh}
VIg	—	3400^{w}	1660^{m}	1605^{m}
VII	—	3360^{br}	1685^{s}	1635^{m}
VIIa	—	3490^{br}	1700^{s}	1630^{m}
VIIb	—	3520^{br}	1730^{s}	1650^{m}
VIII	3480—3500^{br}		1700^{s} (quinazol.) 1750^{sh} (6-subst.)	1640^{m}
IXa	3500^{m}	3320^{br}	1700^{vs} (quinazol.) 1750^{sh} (6-sub.)	1635^{m}
IXc	3480^{w}	3385^{br}	1720^{vs} (quinazol.) 1770^{m} (6-sub.)	1630^{m}

* s = strong, vs = very strong, sh = shoulder, br = broad, m=medium.

(iii) ^{1}H-NMR-Spectra (cf. Table 2).

4-3H-Quinazolinones (Va—d) were prepared by the recommended methods.[9-12] Reaction of the compounds Va, b, d with secondary and primary amines in the presence of formaldehyde in acidic medium (Mannich reaction) gave the corresponding condensation products, VIa—j.[13,14]

Compound VIa reacts with butylamine to give compound VIi.[13] Oxidation of VIi with potassium permanganate in acetic acid medium afforded Va (m.p. and mixed m.p. undepressed).

The structures of compounds VI were established by:

(i) IR-Spectral studies. Compounds VI showed absorption bands attributable to δ-CH_2 in the region 1455—1435 cm^{-1}. Compounds VIe—h showed absorption bands attributable to the antisymmetric and symmetric stretching of NO_2 group in the region 1570—1560 cm^{-1} and at 1340 cm^{-1}. Compounds VIi—k showed absorption bands attributable to the ν (C=S) at 1320—1305 cm^{-1}

(ii) ^{1}H-NMR-spectra; the data for compounds VIa and VIh are depicted in table 2.

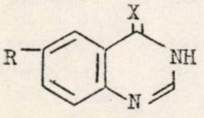

(V)

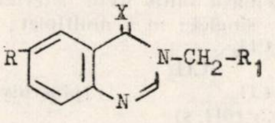

(VI)

	R	X
a,	H	O
b,	NO_2	O
c,	NH_2	O
d,	H	S

	R	R$_1$	X		R	R$_1$	X
a,	H	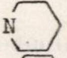	O	g,	NO_2	$NHC_6H_4CH_3$-p	O
b,	H	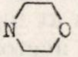	O	h,	NO_2	NHC_5H_4N (pyridyl)	O
c,	H	$NHC_6H_4CH_3$p	O	i,	H	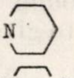	S
d,	H	NHC_5H_4N	O	j,	H	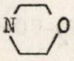	S
e,	NO_2	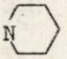	O	k,	H	$NHC_6H_4CH_3$-p	S
f,	NO_2	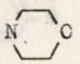	O	l,	H	NHC_4H_9	O

6-Amino-4-3H-quinazolone Vc reacts with some halocompounds, namely 1-chloro-2,4-dinitrobenzene and toluene sulphonyl chloride to form compounds (VIIa, b).

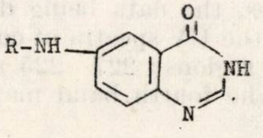

(VII)

a, R = $C_6H_3(NO_2)_2$-2,4 ; b, R = SO_2-CH_2-C_6H_4-CH_3-p

TABLE 2

The ^1H-NMR spectral data for compounds II–IX *, **

Compound	Aromatic and quinazolone	$-CH_3$	$-CH_2-$	$-NH$
IIc	6.8–7.4 (5H, m)	2.5 (3H, d)	—	1.5 (1H, s)
IIIa	6.8–7.4 (10 H, m)	2.45 (3H, s)	—	—
IVa	7.1–8.0 (10 H, m)	—	—	5.7 (2H, s) NH–NH
VIa***	6.8–7.4 (5H, m)	—	5.0 (2H,s)	—
VIb	7.3–8.1 (8H, m)	—	5.5 (2H, s)	3.0 (1H, s)
VIIb	6.8–7.4 (8H, m)	2.45 (3H, s)		2.0 (1H, s) $NH-SO_2-$ 4.6 (1H, s) NH-quin.
VIII	6.9–7.5 (4H, m)	2.2 (3H, d)	5.4 (2H, d)	1.5 (1H, s) CO–NH–R 4.3 (1H, s) NH-quin.
IXb	6.8–7.4 (9H, m)	3.9 (3H, d) $H_3C-\underset{\substack{\vert\\ OH}}{C}=$ 2.2 (3H, s) H_3C-arom.	—	1.9 (1H, s) NH-quin. 1.4 (1H, s) R–NHCO–

* Chemical shifts were determined as δ (ppm) in DMS O.

** s = singlet ; m = multiplet ; d = doublet

***

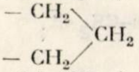

δ = 1.5 (6H, s)

(piperidyl)

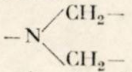

δ = 2.8 (4H, s)

The structures of compounds VII were established by infrared and ^1H-NMR-spectral studies; the data are depicted in table 1 and table 2, respectively.

Acetoarylides containing the quinazolone moiety are hitherto unknown. It is now shown that Vc condenses at high temperature with ethyl acetoacetate to yield the corresponding acetoarylide (VIII).

Compound VIII was coupled with diazotised aniline, p-toluidine and p-anisidine to give the corresponding azo dyes (IXa–c).

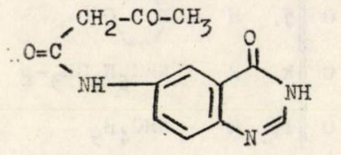

(VIII)

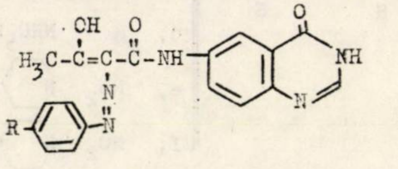

(IX)

a, R= H ; b, R= CH_3 ; c, R= OCH_3

The structures of compounds VIII and IX were established by infrared and ^1H-NMR-spectral studies, the data being depicted in table 1 and table 2, respectively. Moreover the UV spectra of compounds IX show four main absorption bands in the regions : 227–225 nm, 290–275 nm, 340–315 nm and 465–462 nm. The fourth band may be attributed to the N = N group.

Further confirmation for these structures was attained by a mass spectral study of compounds VIII and IXb. The ratios of *m/e* are given in the following scheme :

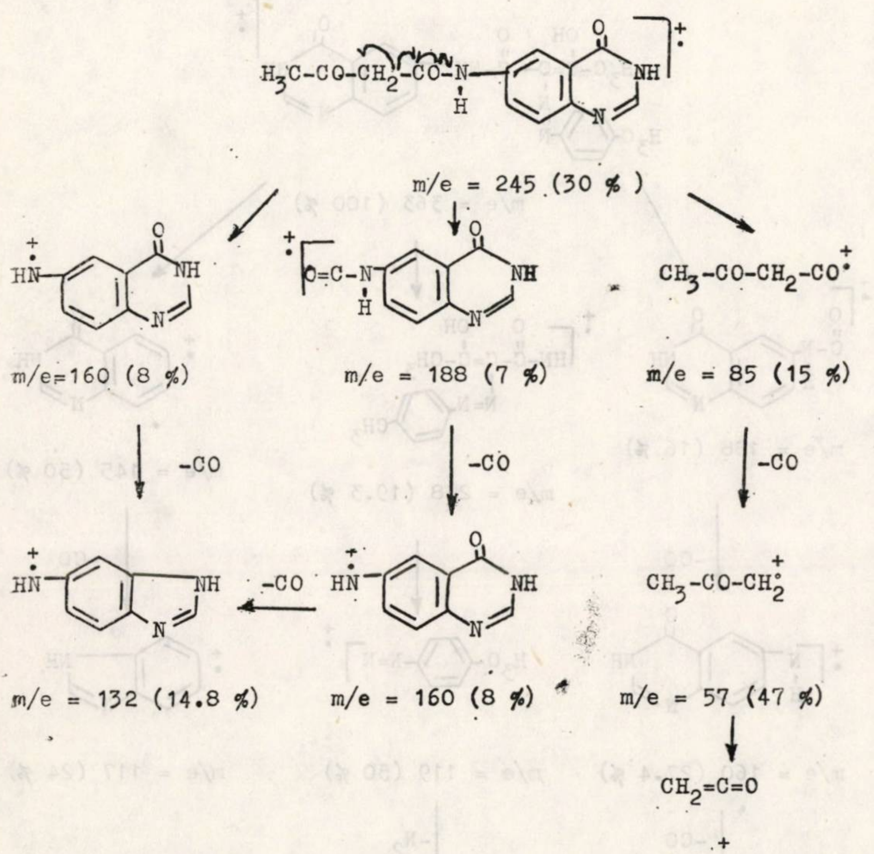
m/e = 245 (30 %)
m/e=160 (8 %)
m/e = 188 (7 %)
m/e = 85 (15 %)
CH3-CO-CH2-CO
-CO
-CO
-CO
-CO
m/e = 132 (14.8 %)
m/e = 160 (8 %)
CH3-CO-CH2
m/e = 57 (47 %)
CH2=C=O
H3C
m/e = 15 (25.6 %)

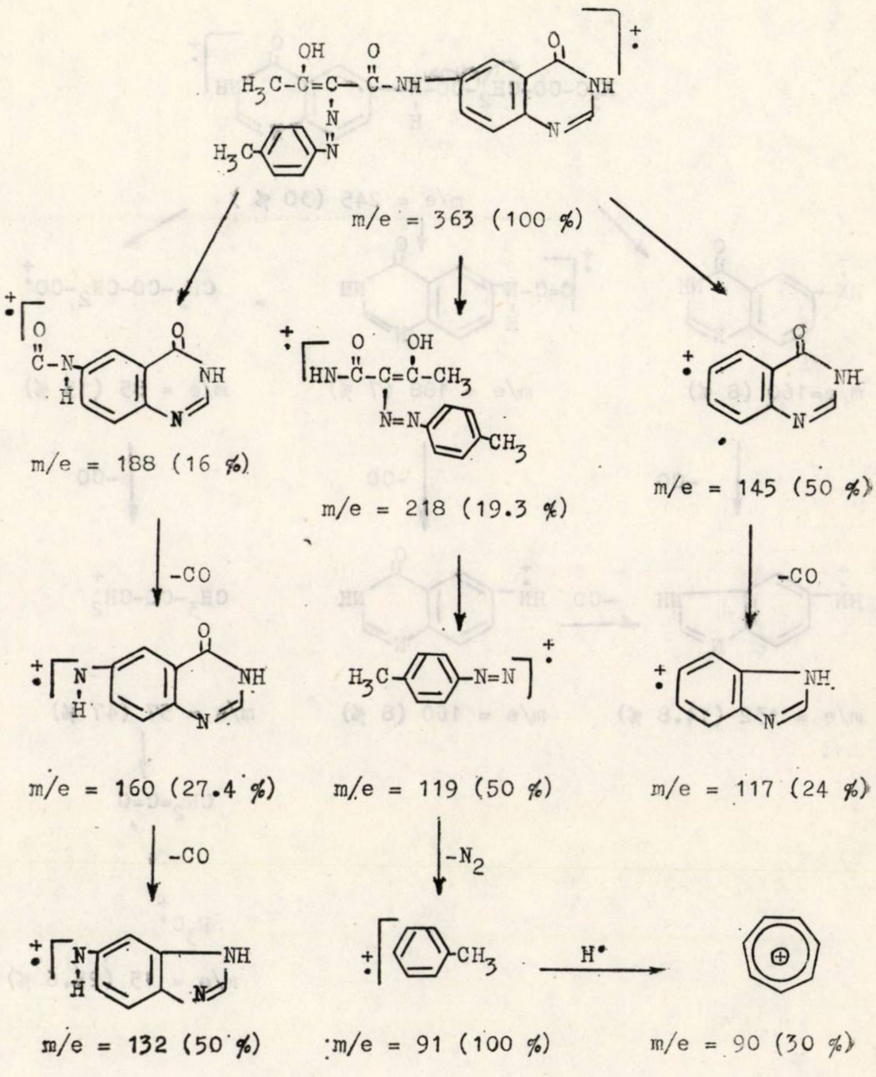
m/e = 363 (100 %)
m/e = 188 (16 %)
m/e = 218 (19.3 %)
m/e = 145 (50 %)
-CO
-CO
m/e = 160 (27.4 %)
m/e = 119 (50 %)
m/e = 117 (24 %)
-CO
$-N_2$
H•
m/e = 132 (50 %)
m/e = 91 (100 %)
m/e = 90 (30 %)

EXPERIMENTAL

The IR spectra were recorded with a Unicam S.P. 1200 spectrophotometer. The KBr pellet technique was used.

The absorption spectra in the UV region were recorded with a Unicam S.P. 800 spectrophotometer. The ethanol was used as solved in 1 cm matched cells. $^1H-NMR-$spectra were recorded at 60 MHz on a Varian A—60 spectrometer. Mass spectra were recorded on a V.G. micromass 7070 F spectrometer operating at 70 eV using direct inlet.

All melting points are uncorrected.

REACTION OF 4-CHLOROQUINAZOLINE I WITH UREA AND AMIDES FORMATION OF 4-SUBSTITUTED QUINAZOLINES, IIa—c

A mixture of 4-chloroquinazoline I (1.7 g, 0.01 mole) and urea and/ or amide (0.01 mole) in 50 ml absolute ethanol was heated under reflux for 1 hr. After concentration and cooling the coloureless solid obtained was crystallised from benzene to give IIa—c, yield 80—85 %. (The results are listed in table 3).

REACTION OF I WITH ANILIDES. FORMATION OF IIIa—d

A mixture of I (1.7 g; 0.01 mole) and anilide (0.01 mole) in 50 ml benzene was heated under reflux for 3 hrs. After concentration and cooling the colourless solid obtained was crystallised from benzene to give IIIa—d, yield 75—80 %. The physical data are given in table 3.

REACTION OF I WITH HYDRAZINES. FORMATION OF IVa, b

A mixture of I (1.7 g; 0.01 mole) and hydrazine (0.015 mole) in 50 ml absolute ethanol was heated under reflux for 3 hrs. After concentration and cooling the solid obtained was crystallised from benzene to give IVa, b; yield about 75 % (See Table 3).

TABLE 3

Condensation products of 4-chloroquinazoline with amides, anilides and hydrazines

Compound	M.p. (°C)	Formula	Analysis % (Found/Calcd.)		
			C	H	N
IIa	172	$C_9H_8N_4O$	57.45 57.21	4.26 4.37	29.78 29.46
IIb	212	$C_9H_7N_3O$	62.43 62.07	4.05 4.32	24.28 24.20
IIc	207	$C_{10}H_9N_3O$	64.17 63.92	4.81 4.63	22.46 22.07
IIIa	105	$C_{16}H_{13}N_3O$	73.00 73.06	4.94 4.61	15.97 16.00
IIIb	107	$C_{17}H_{15}N_3O$	73.65 73.45	5.42 5.70	15.16 15.22
IIIc	140	$C_{17}H_{15}N_3O$	73.65 73.60	5.42 5.60	15.16 15.04
IIId	135	$C_{20}H_{15}N_3O$	76.68 76.22	4.79 4.61	13.42 13.27
IVa	155	$C_{14}H_{11}N_5O_2$	59.79 59.54	3.91 4.13	24.91 24.77
IVb	192	$C_{14}H_{10}N_6O_4$	51.53 51.34	3.07 3.39	25.77 25.39

MANNICH REACTION ON Va, b, d. FORMATION OF 3-SUBSTITUTED QUINAZOLONES

A mixture of Va, b, d (0.01 mole), formaldehyde or paraformaldehyde (0.6 g ; 0.02 mole) and secondary amine (0.012 mole) in 20 % hydrochloric acid, was dissolved in 50 ml ethanol. The reaction mixture was heated under reflux for 6 hrs. and left to stand overnight. A dilute solution of sodium hydroxide was added to the reaction mixture till alkaline and then extracted with ether. The alkaline solution was stirred with charcoal and filtered, then acidified with 50 % acetic acid. The resulted solid was crystallised from ethanol to give VIa – k, yield 70 – 75 %. The results are listed in table 4.

REACTION OF BUTYLAMINE WITH VIa. FORMATION OF VIi

A mixture of VIa (2.3 g, 0.01 mole) and butylamine (1.1 g, 0.015 mole) in 50 ml ethanol was heated under reflux for 3 hrs. After concentration and cooling the obtained solid VIi was crystallised from ethanol, yield 60 % (Table 4).

TABLE 4

Mannich bases derived from 4-quinazolones

Compound	M.p (°C)	Formula	Analysis % (Found/Calcd). C	H	N	S
VIa	217	$C_{14}H_{17}N_3O$	69·14 69·01	7.00 6·85	17·28 17·04	—
VIb	237	$C_{13}H_{15}N_3O_2$	63·73 63·54	6·12 6·00	17·14 17.01	—
VIc	232	$C_{16}H_{15}N_3O$	72.45 72·32	5·66 5·72	15·85 15·51	—
VId	225	$C_{14}H_{12}N_4O$	66·67 66·41	4·76 4·64	22·22 22.00	—
VIe	275	$C_{14}H_{16}N_4O_3$	58·33 58.02	5·56 5·71	19.44 19·22	—
VIf	266	$C_{13}H_{14}N_4O_4$	53·79 53·42	4.83 5·12	19.31 19.01	—
VIg	285	$C_{16}H_{14}N_4O_3$	61.94 61·72	4.52 5·00	18.06 18·17	—
VIh	278	$C_{14}H_{11}N_5O_3$	56·57 56·23	3·70 4.10	23·57 23·21	—
VIi	182	$C_{14}H_{17}N_3S$	64.86 64.41	6·56 6·50	16·22 15·97	12·36 12.11
VIj	206	$C_{13}H_{15}N_3OS$	59.43 59·77	5.81 5·75	16·09 15·64	12·26 12.00
VIk	209	$C_{16}H_{15}N_3S$	68.33 67.88	5·34 5·51	14.95 14.66	11·39 11.42
VIl	213	$C_{13}H_{17}N_3O$	67·53 67·34	7·36 6·96	18.18 18.00	—

OXIDATION OF VIi. FORMATION OF VIa

Potassium permanganate solution (46 g, 0.003 mole) in the least amount of water was gradually added to a solution of VIi (1 g) in acetic acid (50 ml.). The reaction mixture was heated on a water-bath for 12 hrs, concentrated and cooled. The reaction mixture was poured on ice-cold water, the formed precipitate was filtered and recrystallised from ethanol to give VIa ; m.p. and mixed m.p. were undepressed.

REACTION OF Vd WITH SOME HALO-COMPOUNDS. FORMATION OF VIIa, b

A mixture of Vd (1.6 g, 0.01 mole), 2-4-dinitrochlorobenzene and/or *p*-toluenesulphonyl chloride (0.02 mole) and 1g potassium hydroxide in 40 ml ethanol was refluxed for 2 hrs. The cooled solution was acidified with dilute hydrochloric acid and the solid obtained was crystallised from ethanol to give VIIa,b (yield about 85 %). The physical data are given in table 5.

TABLE 5

6-Substituted-4-quinazolones

Compound	M.p. (°C)	Formula	Analysis % (Found/Calcd). C	H	N
VIIa	275	$C_{14}H_{9}N_{5}O_{5}$	51.38 51.72	2.75 2.54	21.41 21.00
VIIb	253	$C_{15}H_{13}N_{3}O_{3}S$	57.14 57.01	4.13 4.37	13.33 13.04
VIII	255	$C_{12}H_{11}N_{3}O_{3}$	58.78 58.54	4.49 4.52	17.14 16.88
IXa	over 300	$C_{18}H_{15}N_{5}O_{3}$	61.89 61.62	4.30 4.26	20.06 20.02
IXb	over 300	$C_{19}H_{17}N_{5}O_{3}$	60.15 60.00	4.49 4.58	18.47 18.16
IXc	over 300	$C_{19}H_{17}N_{5}O_{4}$	57.72 57.42	4.30 4.59	17.72 17.39

REACTION OF Vd WITH ETHYL ACETOACETATE. FORMATION OF VIII

A mixture of Vd (1.6 g, 0.01 mole), pure ethyl acetoacetate (2.6 g, 0.02 mole) was heated in an oil-bath at 200–220°C for 3 hrs. The reaction mixture was then colled and triturated with ethanol to give pale yellow crystals of VII in 85 % yield (See Table 5).

REACTION OF VIII WITH SOME DIAZONIUM SALTS. FORMATION OF IXa–c.

Compound VIII (2.5 g, 0.01 mole) was dissolved in ethanol (20 ml) and cooled to 0–5°C. A solution of the corresponding diazotised amine (0.01 mole) was added slowly with constant stirring. The pH of the mixture was adjusted to 6 by careful addition of sodium acetate solution. The precipitate azo-dye was cooled and crystallised from ethanol. Yields are almost quantitative and the resulted dyes are listed in table 5.

REFERENCES

[1] A. Sammour, T. Zimaity and M. Anwar, *Egypt. J. Chem.*, **16**, 215 (1873).

[2] M. Anwar, F. I. Abdel-Hay and M. Fahmy, *Rev. Roumaine Chim.*, **23**, 1085 (1978).

[3] M. Anwar, M. Omara, F. I. Abdel-Hay and A. A. Saafan, "Proceedings of XIV Egyptian Conference of Pharmaceutical Science", 1975, p. 69.

[4] A. Abbady M. Anwar, F. I. Abdel-Hay and M. F. Abdel-Megeed, *Egypt. J. Chem.*, **18,** 1063 (1975).

[5] A. Abbady, M. Anwar and M. F. Abdel-Megeed, *Acta Chim. Acad. Sci.* Hung., **91,** 341 (1976).

[6] E. Wick, *J. Amer. Chem. Soc.*, **68,** 1299 (1949).

[7] W. P. Armarego, *J. Chem. Soc.*, **1962,** 561.

[8] M. Anwar and M. F. Abdel-Megeed, *Pakistan J. Sci. Res.*, **31,** 128 (1979).

[9] M. T. Bogert and E. M. McColm, *J. Amer. Chem. Soc.*, **49,** 2650 (1927).

[10] M. T. Bogert and G. A. Geiger, *J. Amer. Chem. Soc.*, **34,** 524 (1912).

[11] L. Legrand and N. Lozach. *Bull. Soc. Chim. France*, **1961,** 1400.

[12] N. Leonard and D. Y. Curtin, *J. Org. Chem.*, **11,** 349 (1946).

[13] T. Zimaity, M. Anwar and M. F. Abdel-Megeed, *Indian J. Chem.*, **15B,** 750 (1977).

[14] M. Anwar M. M. Abou-Sekkina and A. A. Saafan "Proceedings of XIV Egyptian Conference of Pharmaceutical Science", 1975, p. 81.

Revue Roumaine de Chimie, 26, 11–12, 1479–1485 (1981)

CYCLIC ORGANOSILICON COMPOUNDS. II[+]

REACTION OF 1,4-DILITHIUM-1,1,4,4-TETRAPHENYLBUTANE WITH ORGANOTRICHLOROSILANES

N. LUCHIAN, AGLAIA CIOBANU and M. BOSTAN
Institute of Macromolecular Chemistry "Petru Poni"
Aleea Gr. Ghica Vodă 41 A Iassy, Romania

Received Mai 29, 1980

New cyclic organosilicon compounds were obtained by reaction between 1,4-dilithium-1,1,4,4-tetraphenylbutane and trichlorosilane, trichloromethylsilane and trichlorophenylsilane. The chemical analysis, molecular mass determination and the IR spectra have shown that the new compounds have been formed by ring closure through siloxane bonds between two 1,1,4,4-tetraphenylbutanediyl-1,4 groups in 1 and 4 positions.

The reaction of dichlorodialkyl- or dichlorodiarylsilanes in the presence of olefines, alkyl- or arylolefines, with lithium in tetrahydrofuran has been intensely investigated, especially by Nefedov et al.[1–11] The introduction of a mixture of dichlorodiorganosilanes and olefines in the lithium containing tetrahydrofuran leads to the intermediate diorganosylilenes which will add to the ethylenic double bond, giving substituted organosilacyclopentanes or organodisilacyclohexanes, as well as macromolecular products of the general formula $[(CH_3)_2Si]_n$, n being greater than three.

Much less investigated were the reactions of trichlorosilane, trichloroalkyl- and trichloroarylsilane with lithium which led to the formation of bis-silacyclopentanes in small yields and cross-linked polymers.[3,4]

Following our investigations on the reaction of 1,4-dilithium-1,1,4,4-tetraphenylbutane with chloroorganosilanes,[12] the present paper presents the synthesis and some physico-chemical characteristics of the compounds resulted from the reaction of the dilithium derivative with trichlorosilane, trichloromethylsilane and trichlorophenylsilane.

EXPERIMENTAL

1,1-Diphenylethylene was prepared according to the method reported in the literature.[13] By reaction with lithium metal in diethyl ether, the 1,4-dilithium–1,1,4,4-tetraphenylbutane was obtained.

Trichlorosilane, trichloromethylsilane and trichlorophenylsilane were of 98–99 % purity.

Diethyl ether was dried and distilled over sodium and other solvents were purified by distillation.

The IR spectra were recorded by a Perkin—Elmer spectrophotometer model 577, within the 4000—200 cm^{-1}, on KBr pelleted samples.

DTA and TG curves were recorded using a MOM Paulik-Paulik—Erdey Derivatograph with 9°/min. heating rate, within a temperature range of 20—900°C.

1,3,8,10-tetrahydro-4,4,7,7,11,11,14,14-octaphenyl-,1,3,8,10-tetrasila-2,9,15, 16-tetraoxa-tricyclo [8.3.1·1.^{3,8}] hexadecane (I)

The synthesis method was described in a previous work.[12] There were used 10 g freshly prepared 1,1-diphenylethylene, 350 ml anhydrous ethyl ether and 1.5 g lithium in small pieces. After the formation of the 1,4-dilithium—1,1,4,4-tetraphenylbutane 4.7 g trichlorosilane were added. The exothermic reaction is completed after 40 hours. The lithium chloride precipitate has deposited and the ethereal solution was clear. The yellow compound left after the distillation of diethyl ether was solved in acetone and precipitated with ethyl alcohol. The product was purified by solving in acetone and precipitating with ethyl alcohol. A crystalline, white slightly yellowish product was obtained, m.p. 131—132°C; yield 3 g (24 %). The compound is soluble in benzene, acetone and carbon tetrachloride.

Anal. Calcd. for $C_{56}H_{52}O_4Si_4$: C, 74.67 ; H, 5.78 ; Si, 12.44 ; mol. wt. 900. Found : C, 76.28 ; H, 6.05 ; Si, 12.78 ; mol. wt. 901 (determined cryoscopically in benzene).

1,3,8,10-tetramethyl-4,4,7,7,11,11,14,14-octaphenyl-1,3,8,10-tetrasila-2,9,15, 16-tetraoxa-tricyclo[8.3.1.1.^{3,8}] hexadecane (II)

The mode of the preparation was similar ; 4.1 g trichloromethylsilane were used and the reaction time was 40 hours. The compound obtained was a white-yellowish microcrystalline product, m.p. 210°C, yield 1 g (7.53 %).

Anal. Calcd. for $C_{60}H_{60}O_4Si_4$: C, 75.31 ; H, 6.27 ; Si, 11.71 ; mol. wt. 956. Found : C,76.03 ; H. 6.30 ; Si, 11.54 ; mol. wt. 942 (determined cryoscopically in benzene).

1,3,8,10-tetraphenyl-4,4,7,7,11,11,14,14-octaphenyl-1,3,8,10-tetrasila-2,9,15, 16-tetraoxa-tricyclo[8.3.1.1.^{3,8}] hexadecane (III)

The same way of synthesis was used ; the amount of trichlorophenylsilane was 5.06 g, the reaction time being 40 hours. A white yellowish microcrystalline product was separated ; m.p. 170—171°C, yield 2.85 g (17 %).

Anal. Calcd. for $C_{80}H_{68}O_4Si_4$: C, 79.83 ; H, 5.64 ; Si, 9.30 ; mol. wt.1204. Found : C,79.65 ; H. 5.43 ; Si, 9.25 ; mol.wt .1190 (determined cryoscopically in benzene).

RESULTS AND DISCUSSIONS

As in the case of dichlorodiorganosilanes,[12] the reaction between 1,4-dilithium-1,1,4,4-tetraphenylbutane and trichlorosilanes was carried out in two stages. In the first step the substitution of lithium atoms by two dicloroorganosilyl and dichlorosilyl groups respectively occurred, probably according to the following reaction :

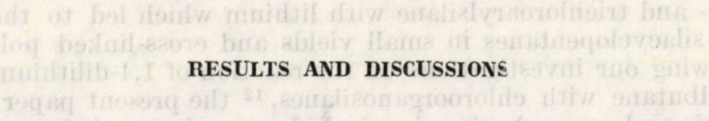

$$\underset{Li}{Ph_2C}-CH_2-CH_2-\underset{Li}{CPh_2} + RSiCl_3 \xrightarrow[-LiCl]{} \underset{R-\underset{Cl}{Si}-Cl}{Ph_2C}-CH_2-CH_2-\underset{Cl-\underset{Cl}{Si}-R}{CPh_2}$$

R = H, Me, Ph

In the second step, the wet ethanol promoted hydrolysis of the Si-Cl groups, with ring closure :

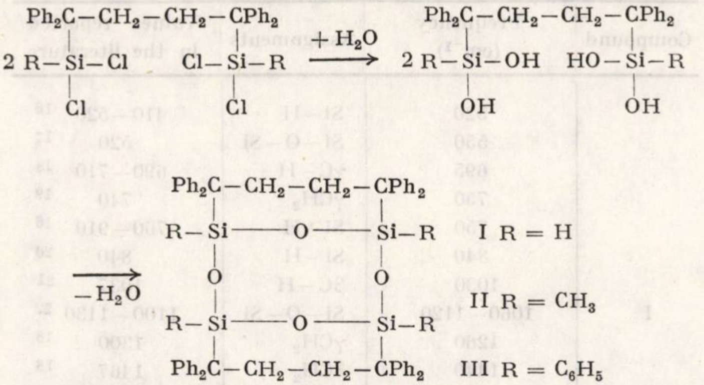

I R = H

II R = CH_3

III R = C_6H_5

Small yields of up to 10 % low molecular products were also obtained in the reactions of trichlorophenylsilane and trichlorosilane with lithium and styrene [3] or the trichlorosilane reaction with arylethylenes. [4] Besides low molecular crystalline compounds, cross-linked polymers were also obtained, which are under investigation.

The IR spectra of the new compounds, compared to that of 1,1,4,4-tetraphenylbutane, present absorption bands at lower wavelengths ($5-50$ cm^{-1}), as do the previously reported dichlorodiorganosilane derivatives.[12] This was explained by the decrease of silicon electronegativity.[14] It was shown [15] that the position of the Si—H bond vibrations depends on the inductive ability of the groups bonded to silicon, the groups with a stronger electron-repelling effect causing a shift to higher frequencies. A $10-35$ cm^{-1} lower band shift is also observed in the case of compound I, due to the $(C_6H_5)_2C-CH_2-$ groups bonded to the silicon atom (Table 1).

The TG and DTA curves indicate that the compound III, with phenyl group bonded to silicon, has a better thermal stability than compounds II and I, with methyl group or hydrogen substituents at silicon.

The weight loss takes place in three steps ; the last step corresponds to the product decomposition. The slopes of the curves are more accentuated in the case of products II and I, therefore they indicate a greater transformation rate, than for the product III. The starting temperatures of the transformation reaction, t_1 and t_2, the starting decomposition, t_3 and the weight loss, expressed in percentage and phenyl groups number, are given in table 2.

From the data obtained, the following order of thermal stability of the products was established III > I > II.

The synthesized compounds were heated at temperatures coresponding to the transformation steps, during two hours, then the samples were taken out and their IR spectra measured. The absorption frequencies are presented in table 3, compared to those of compounds prior heating.

TABLE 1

IR absorption spectra of the new compounds

Compound	Frequency (cm^{-1})	Assignments	Values reported in the literature
I	520	Si–H	410–520 [16]
	550	Si–O–Si	520 [17]
	695	γC–H	690–710 [18]
	750	γCH$_2$	740 [19]
	750	Si–H	760–910 [16]
	840	Si–H	840 [20]
	1030	βC–H	1037 [21]
	1060–1120	Si–O–Si	1100–1130 [22]
	1260	γCH$_2$	1300 [18]
	1440	δCH$_2$	1467 [18]
	1490	νCC	1475–1525 [23]
	1595	νCC	1580–1600 [24]
	2140	Si–H	2175 [25]
	2240	Si–H	2080–2270 [26]
	3020 and 3045	νC–H	3027–3039 [27]
II	550	Si–O–Si	520 [17]
	690	γC–H	690–710 [18]
	775	Si–CH$_3$	775 [20]
	1020–1100	Si–O–Si	1100–1130 [22]
	1250	Si–CH$_3$	1240–1280 [28]
	1390 and 1440	Si–CH$_3$	1390–1440 [20]
	1485	νCC	1475–1525 [23]
	2950	νC–H	2962 [18]
	3020 and 3045	νC–H	3027–3039 [27]
III	520	Si–O–Si	520 [17]
	695	γC–H	690–710 [18]
	735	Si–C$_6$H$_5$	700–740 [29]
	1025	δC–H	1037 [21]
	1070–1100	Si–O–Si	1100–1130 [22]
	1425	Si–C$_6$H$_5$	1430 [30]
	1485	νC–C	1475–1525 [23]
	1590	νC–C	1580–1600 [24]
	3020 and 3040	νC–H	3027–3039 [27]
1,1,4,4-tetraphenylbutane	710	γC–H	690–710 [18]
	760	γCH$_2$	740 [19]
	1040	δC–H	1037 [21]
	1260	γCH$_2$	1300 [18]
	1460	δCH$_2$	1467 [18]
	1500	νC–C	1475–1525 [23]
	1600	νC–C	1580–1600 [24]
	2900	νC–H	2962 [18]
	3010	νC–H	3027–3039 [27]

TABLE 2

The starting temperature of the transformation reactions t_1 and t_2, the decomposition temperature t_3 and the phenyl group losses

Compound	Temperature °C			Phenyl group loss		
	t_1	t_2	t_3	Number of phenyl groups	% exp.	% calcd.
I	110			4	35·56	34·22
		410	542	7	60·62	59·98
II	80			4	32·05	32·21
		355	425	7	57·00	56·38
III	130			2	13·26	12·79
		340	460	5	32·14	31·97

According to table 2 the weight losses observed after heating at temperatures of 110°C, 80°C and 130°C respectively, indicate the splitting of four (I), four (II) and two phenyl groups from the 1,1,4,4-tetraphenylbutanediyl-1,4 chain, with the formation of double bonds evidenced by the IR absorption bands at 1665 cm^{-1} (I) and 1660 cm^{-1} (II and III). The presence of the absorption bands at 746 and 1425 cm^{-1} characteristic of the Si$-$C$_6$H$_5$ bonds shows that the phenyl groups were split from the substituted butane chain.

In the second transformation step, the weight losses of seven (I), seven (II) and respectively five phenyl groups (III) lead to a new molecule transformation where both the tetraphenylbutanediyl chain and the Si$-$R bonds (R = H, CH$_3$, C$_6$H$_5$) are affected by the weakening, the disappearance of some characteristic bands, or the broadening of siloxane bond band (Table 3).

TABLE 3

IR absorption spectra before and after heating of the new compounds

Compound	Unheated sample Frequency (cm^{-1})	Heated sample at t_1 Frequency (cm^{-1})	Heated sample at t_2 Frequency (cm^{-1})	Assignment
I	520	— t_1=110°C	— t_2=410°C	Si$-$H
	550	590w	—	Si$-$O$-$Si
	695	695	695	γC$-$H
	750	745	745	γCH$_2$
	840	840	—	Si$-$H
	1030	1030vw	—	βC$-$H
	1060$-$1120	1050$-$1100	1010$-$1100	Si$-$O$-$Si
	1260	1260	1260	γCH$_2$
	1440	1440	1440	δ CH$_2$
	1490	1485	1485	ν C$-$C
	1595	1590	1590	ν C$-$C

Table 3 (*continued*)

Compound	Unheated sample	Heated sample at t_1	Heated sample at t_2	Assignment
	Frequency (cm^{-1})	Frequency (cm^{-1})	Frequency (cm^{-1})	
I	—	1655	1660vw	ν C=C
	2140	2140	—	Si—H
	2240	2240	—	Si—H
	3020 and 3045	3020w	—	ν C—H arom.
II	550	520 $t_1=80$°C	— $t_2=355$°C	Si—O—Si
	690	700	700sh	γ C—H
	775	760 and 780	765	Si—CH_3
	—	820	820sh	γ CH (alkene)
	—	900	—	γ=CH_2
	1020—1100	1035—1100	1000—1100	Si—O—Si
	—	1160	1150w	γ CH vinyl
	1250	1250	1170	Si—CH_3
	1390	1390 w	1340sh	Si—CH_3
	1440	1440	1470vw	Si—CH_3
	1485	1485	1480vw	ν C—C
	1590	1590	1590w	ν C—C
	—	1660	1660vw	ν C=C
	2950	2930	2975	ν C—H
	3020 and 3045	3020 and 3035w	—	ν C—H arom.
III	520	480—530 $t_1=130$°	440—480 $t_2=340$°	Si—O—Si
	695	695	695vw	γ C—H phenyl
	735	740	740vw	Si—C_6H_5
	1025	1010vw	—	δ C—H
	1070—1100	1040—1130	1010—1130	Si—O—Si
	1425	1425	1430vw	Si—C_6H_5
	1485	1490	—	ν C—C
	1590	1590	1590	ν C—C
	—	1660	—	ν C—C
	3020 and 3040	3020 and 3040	—	ν C—H arom.

The analytical data, the determined molecular weight values, together with the IR data of the new compounds support the proposed structures.

REFERENCENS

* Part I : see reference 12.

[1] O. M. Nefedov, M. M. Manakov, and A. D. Petrov, *Izvest. Akad. Nauk S.S.S.R., Otdel. khim. Nauk*, **1961**, 1717.

[2] O. M. Nefedov, M. N. Manakov and A. D. Petrov, *Izvest. Akad. Nauk S.S.S.R., Otdel. khim. Nauk*, **1962**, 1228.

[3] O. M. Nefedov, M. N. Manakov and A. D. Petrov, "Sintez i svoistva monomerov", Akad. Nauk S.S.S.R., Inst. Neftekhim. Sinteza Sb. Rabot XXXI-oi Konf. po Vysokomolekul. Soedin., 1962, 67—74 ; *Chem. Abstr.*, **62**, 6502 f (1965).

[4] O. M. Nefedov, M. N. Manakov and A. D. Petrov, *Plaste und Kautschuk*, **10**, 721 (1963).

[5] O. M. Nefedov, M. N. Manakov and A. D. Petrov, *Doklady Akad. Nauk. S.S.S.R.*, **154**, 395 (1964).

[6] O. M. Nefedov and M. N. Manakov, *Angew. Chem.*, **76**, 270 (1964).

[7] O. M. Nefedov and M. N. Manakov, *Zhur. obshchei Khim.*, **34**, 2465 (1964).

[8] O. M. Nefedov, G. Garzó, T. Székely and V. I. Shiryaev, *Doklady Akad. Nauk S.S.S.R.*, **164**, 822 (1965).

[9] O. M. Nefedov, T. Székely, G. Garzó, S. P. Kolesnikov, M. N. Manakov and V. I. Shiryaev, "International Symposium on Organosilicon Chemistry. Scientific Communications", Prague, 1965 ; *Chem. Abstr.*, **65**, 12298 b (1966).

[10] O. M. Nefedov, M. N. Manakov, V. N. Medvedev, A. S. Khachaturov and V. I. Shiryaev, *Khim. Geterotsikl. Soedin. Latv. S.S.R.*, **2**, 299 (1966) ; *Chem. Abstr.*, **65**, 2287d (1966).

[11] O. M. Nefedov and M. N. Manakov, *Angew. Chem.*, 78, 1039 (1966).

[12] A. Ciobanu, N. Luchian and V. Hamciuc, *Rev. Roumaine Chim.*, **23**, 943 (1978).

[13] M. Tissier and V. Grignard, *Compt. rend.*, **132**, 1182 (1901).

[14] T. Srivastava and M. Onyszchuk, *Canad. J. Chem.*, **41**, 1244 (1963).

[15] A. L. Smith and C. Angelotti, *Spectrochim. Acta*, 15, 412 (1959).

[16] A. L. Smith "Analysis of Silicones", Wiley, New York, 1974, p. 259.

[17] H. Kriegsmann, *Z. Elektrochem.*, **61**, 1088 (1957).

[18] N. Sheppard and D. M. Simpson, *Quart. Rev.*, **7**, 19 (1953)

[19] M. Avram and Gh. Mateescu "Spectroscopia în infraroşu. Aplicaţi iîn chimia organică", Ed. Tehnică, Bucureşti, 1966, p. 201

[20] A. L. Smith, loc. cit. (ref. 16) p. 261.

[21] M. Avram and Gh. Mateescu, loc. cit. (ref. 19) p. 267.

[22] A. L. Smith, loc. cit. (ref. 16) p. 275.

[23] L. J. Bellamy, "The Infrared Spectra of Complex Molecules", Methuen, London, 1959, p. 69.

[24] L. J. Bellamy, loc. cit. (ref. 23), p. 72.

[25] A. L. Smith, loc. cit. (ref. 16) p. 257.

[26] S. E. Westermark, *Acta Chem. Scand.*, **9**, 947 (1955)

[27] S. E. Wiberley, S. C. Bunce and W. H. Bauer, *Analyt. Chem.*, **32**, 217 (1960).

[28] N. Wright and M. H. Hunter, *J. Amer. Chem. Soc.*, **69**, 803 (1947).

[29] L. Spialter, D. C. Priest and C. W. Harris, *J. Amer. Chem. Soc.*, **77**, 6227 (1955).

[30] C. W. Young, P. C. Servais, C. C. Currie and M. J. Hunter, *J. Amer. Chem. Soc.*, **70**, 3758 (1948).

Revue Roumaine de Chimie, **26**, *11–12*, 1487–1491 (1981)

POTENTIOMETRIC DETERMINATION OF L-ALANINE, L-SERINE, TYROSINE AND HISTIDINE WITH A Cu^{2+} SENSITIVE ELECTRODE

MARIA MIOŞCU, IOVANCA HAIDUC and D. C. CÖRMÖS

Babeş-Bolyai University, Chemistry Department, Arany Janos 11, 3400, Cluj-Napoca, Romania

Received December 29, 1980

A direct potentiometric titration method for the determination of milligram quantities of the following amino-acids : L-alanine, L-serine, tyrosine and histidine, was elaborated. A $CuSO_4$ solution was used with a Cu(II) sensitive indicator electrode. The titrations were performed at pH = 9 ($Na_2B_4O_7.10H_2O$ buffer solution). The method is applicable for amino-acid quantities between 2.5–40 mg/sample with a 0.2–2.7 % error. The repeatability of the determinations gives a standard deviation of 1×10^{-3} – -1.5×10^{-2} mg.

INTRODUCTION

There is a small number of substances as important for the living world as amino-acids. This fact justifies the need of their determination in the biologic and medical laboratories and in the pharmaceutical industry.

Though there exists a great number of determination methods in this field, the volumetric ones, still maintain their actuality due to the simple equipment needed, being fast and easily automatizable. The classic chemical methods use the titration either of the carboxyl or of the amino group.[1-3] Among the titration methods of the amino group, the complexing methods have been recently remarked. These methods use standard solutions of some cations, e.g. : Cu(II),[4] Cd(II),[5] Zn(II),[6] Be(II),[7] Hg(II),[8,6] Nd(III)[9] and W(IV).[9]

Another series of titrimetric methods are based on the oxidative decomposition of amino-acids with various oxidizers of medium strengths : $HAuCl_4$,[10] H_2PtCl_6,[11] Ce(IV)[11] etc.

The volumetric methods using the instrumental reading of the end point are among the others : the potentiometric method,[12-15] dead-stop method,[16] calorimetry,[17] fluorometry,[18] coulometric method.[19]

The practicability of the potentiometric method for the amino-acid determination was considerably extended using the I.S.E.[12,20]

The present work continues our researches on the potentiometric determination of amino-acids,[21] with a $CuSO_4$ standard solution, using a monocrystal of PbSe as Cu(II) sensitive indicator electrode.[22] L-Alanine, L-serine, tyrosine and histidine were thus determined.

EXPERIMENTAL

REAGENTS AND EQUIPMENT

Standard M/50 $CuSO_4 \cdot 5H_2O$ solution (standardized against complexone III, using murexid as indicator).

Buffer solution of pH = 9.0 was obtained dissolving 19.09 g $Na_2B_4O_7 \cdot 10H_2O$ in 1 l bidistilled water.

Amino-acid solutions were obtained dissolving the aminoacids in water or in a suitable volume of buffer, pH = 9.

Monocrystal PbSe electrode.
SCE (saturated calomel electrode)
pH-meter Radelkis OP—208 having a ± 0.1 mV sensitivity
Magnetical stirrer
Microburette 3—5 ml

PROCEDURE

Transfer 10 ml amino-acid solution into a 100 ml beaker, add 5—15 ml buffer solution, up to pH approx. 9. Titrate under continuous stirring. The volume of the Cu(II) solution corresponding to the end of the titration was determined by computation.

During the titration the e.m.f. of the following electrochemical cell was determined.

SCE	**KCl saturated solution**	**Test amino-acid solution**	**Monocrystal PbSe electrode**

RESULTS AND DISCUSSION

The determination of the following amino-acids : L-alanine, L-Serine, tyrosine, and histidine is based on the formation of complexes of the type CuL_x ($x = 1, 2$) having the maximum stability at pH = 9. In order to verify their stability, the absorbance of $Cu(al)_2$ (al = alanine) complex was measured at various pH values. The maximum absorbance was obtained at pH = 9 (curve 5, Fig. 1)

The titration curve has the classic form of the potentiometric titration curves, the potential jump being near to the equivalence point (± 0.5 ml) between 50 mV (curve 1, Fig. 2) and 180 mV (curve 4, Fig. 2).

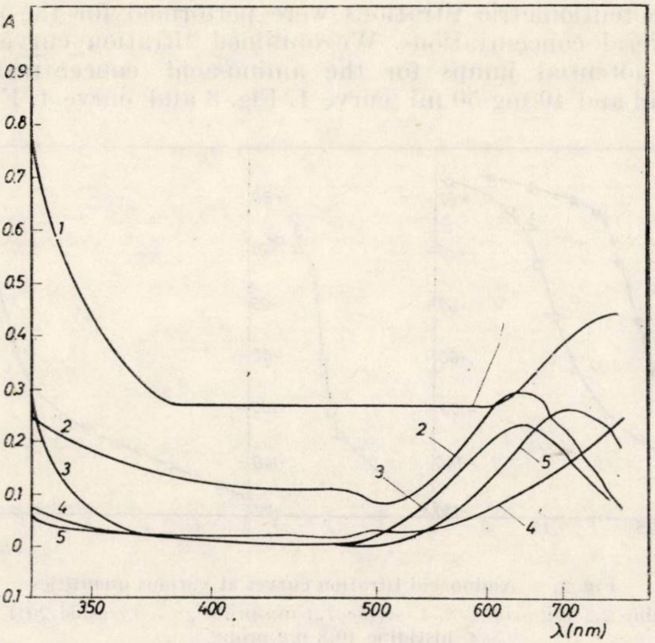

Fig. 1. — CuL_x complex stability as a function of pH:
1. pH = 5; *2.* pH = 6; *3.* pH = 7; *4.* pH = 8;
5. pH = 9.

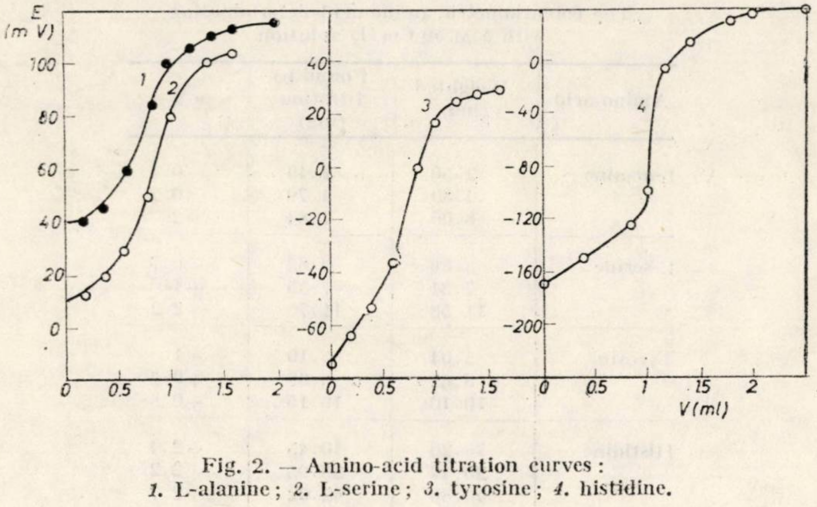

Fig. 2. — Amino-acid titration curves:
1. L-alanine; *2.* L-serine; *3.* tyrosine; *4.* histidine.

The potentiometric titrations were performed for the same amino-acid at several concentrations. We obtained titration curves with easy detectable potential jumps for the amino-acid concentration between 2.5 mg/50 ml and 40 mg/50 ml (curve 1, Fig. 3 and curve 4, Fig. 3).

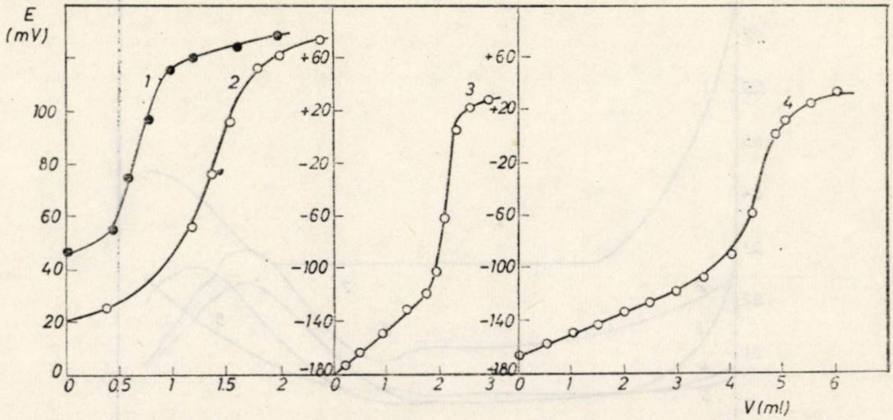

Fig. 3. — Aminoacid titration curves at various quantities : *1.* L-alanine 2.5 mg/probe ; *2.* L-serine 7.3 mg/probe ; *3.* tyrosine 20.4 mg/probe ; *4.* histidine 40.8 mg/probe.

The results of the titration of L-alanine, L-serine and tyrosine denote a CuL_2 complexing, whereas for histidine the titrations indicate a CuL_3 complexing.

The results for the titrations made for different amino-acid quantities are given in table 1. The percentage errors were calculated referring to the analytical grade amino-acid titrated.

TABLE 1

The potentiometric amino-acid determination with a M/50 Cu(II) solution

Amino-acid	Weighted (mg)	Found by titration (mg)	e%
L-alanine	2.50	2.49	−0.4
	4.80	4.79	−0.2
	8.00	7.84	−2
L-serine	3.86	3.83	−0.7
	7.31	7.39	+1
	11.58	11.70	+2.2
Tyrosine	5.04	5.10	+1
	8.65	8.69	+0.5
	10.10	10.15	+0.5
Histidine	10.20	10.45	+2.4
	20.40	20.95	+2.2
	40.80	42.02	+2.7

Table 2 shows the repeatability of the determinations at the same concentration levels. The repeatability is good, the standard deviation of the results being between 1.10^{-3} and 1.5×10^{-2} mg.

TABLE 2

The repeatability of the determination at the same concentration levels

Amino-acid	Weighted (mg)	Found (mg)	Standard deviation (mg)
L-alanine	2.50	2.49 2.50 2.47	1.5×10^{-2}
L-serine	3.86	3.83 3.82 3.81	1×10^{-2}
Tyrosine	8.65	8.71 8.69 8.70	1×10^{-2}
Histidine	40.80	42.0 42.03 42.04	1×10^{-3}

The potentiometric titration with a Cu(II) solution of the above-mentioned amino-acids can be applied especially to small quantities (in the range of milligrams) with a 0.2 – 2.7 % error.

REFERENCES

[1] A. K. Saxena, H. N. Strivastava and B. B. L. Saxena, *Microchem. J.*, **14**, 361 (1969).
[2] A. K. Saxena, *Microchem. J.*, **53**, 757 (1971).
[3] A. K. Saxena, *Chim. analyt.*, **17**, 91 (1972).
[4] Y. A. Gawargious, A. Besada and M. E. M. Hassouna, *Mikrochim. Acta*, **1974**, 45, 1003.
[5] K. Bahadur and I. Saxena, *Microchem, J.*, **18**, 358 (1973).
[6] O. C. Saxena, *Microchem. J.*, **18**, 652 (1973).
[7] O. C. Saxena, *Microchem. J.* **17**, 512 (1972).
[8] K. Bahadur and P. Sen, *Microchem. J.*, **18**, 694 (1973)
[9] O. C. Saxena, *Microchem. J.*, **17**, 462 (1972).
[10] A. K. Saxena, *Microchem. J.*, **13**, 316 (1968).
[11] I. Takahas, *Analyt. Chim. Acta*, **25**, 136 (1961).
[12] M. Matsui and H. Freiser, *Analyt. Lett.*, **3**, 161 (1970).
[13] P. K. Norkus and G. S. Shimkyavichute, *Zhur. analit. Khim.*, **26**, 2002 (1971).
[14] V. V. Rubler, L. M. Makarova, and S. V. Sukhanov, *Zhur. analit. Khim.*, **30**, 1801 (1975).
[15] G. G. Guilbault and E. Krabankova, *Analyt. Lett.*, **3**, 53 (1970).
[16] G. G. Guilbault and G. J. Subeano, *Analyt. Chim. Acta*, **69**, 183 (1974).
[17] L. D. Hansen and E. A. Lewis, *Analyt. Chem.*, **43**, 1393 (1971).
[18] P. D. Frazier Murphy and G. K. Summer, *Analyt. Biochem.*, **44**, 66 (1971).
[19] T. Yoshinori, K. Takeshi and M. Güchi, *Analyst*, **17**, 1491 (1968).
[20] D. C. Cörmös, I. Haiduc and P. Stețiu, *Rev. Roumaine Chim.*, **19**, 1949 (1974).
[21] I. Haiduc, M. Mioșcu and D. Cörmös, *Stud. Univ. Babeş-Bolyai, Chim.*, **24**, 59 (1979).
[22] I. Haiduc, D. C. Cörmöş and M. Nandrea, *Stud. Univ. Babeş-Bolyai, Chim.*, **21**, 56 (1976).

Revue Roumaine de Chimie, **26**, *11–12*, 1493–1497 (1981)

SYNTHESIS AND POLYMERIZATION OF POLYETHYLENE GLYCOL DIMETHACRYLATES. III.[1]

ANALYSIS OF KINETIC DATA OBTAINED BY TRANSESTERIFICATION OF METHYL METHACRYLATE WITH POLYGLYCOLS

GH. HUBCA, CR. OPRESCU and M. DIMONIE

Polytechnic Institute of Bucharest, Laboratory of Macromolecular Technology,
Calea Victoriei, nr. 149, Bucharest, Romania

Received February 13, 1981

The kinetic data obtained by transesterification of methyl methacrylate with polyglycols using the method of hyperbolas are presented. As a result of the performed analysis the equations of hyperbolas which describe the transesterification of the studied processes were found .On this basis, the composition of the reaction mixture may be determined in every moment.

The synthesis of polyethylene glycol dimetacrylates by transesterification of methyl methacrylate is the result of some parallel-consecutive reactions, whose kinetic parameters were presented in a previous paper.[1]

The calculation of rate constants for each stage enabled the determination of the way in which the composition of the reaction varies.[1]

For a suitable leading of the process it is also important to know the way in which the composition of the reaction mixtures varies with conversion. This was realized by analyzing the kinetic data using the method of hyperbolas.[2] Thus, the reaction components existing at one time in the system are classified into : (a) reactants ; (b) wanted products (diester), (c) unwanted products (monoester). The experimental data are plotted on a triangular diagram and the line connecting them is a hyperbola described by equation (1)

$$y = \frac{x(1-x)}{a+bx} \tag{1}$$

in which :

y = the weight or mole fraction of the reactants turned to unwanted products (monoester)
x = the weight or mole fraction of the reactants turned to wanted products (diester)
a, b = constants

The constants *a* and *b* are determined according to the experimental data by plotting the expression : $x(1-x)/y = f(x)$. The data obtained by transesterification of methyl methacrylate with ethylene glycol are shown in table 1 and the plot of the function $x(1-x)/y = f(x)$ (Fig. 1)

TABLE 1

Hyperbolic analysis of kinetic data obtained by transesterification of methyl methacrylate with ethylene glycol ($/EG/ = 1.7013$ moles/l ; $/H_2SO_4 = 0.22$ moles/*l* ; $t = 120$°C)

Experimental data			Calculatet data				
$y^* = \frac{E_1}{1.7013}$	$x^{**} = \frac{E_2}{1.7013}$	$\frac{x(1-x)}{y}$	x	$y = \frac{x(1-x)}{0.024 + 1.033}$	$x_A = x + y$	$\varphi_x = \frac{x}{x_A}$	$\varphi_y = \frac{y}{y_A}$
0.32551	0.010646	0.0324	0.025	0.48950	0.51450	0.0486	0.9514
0.38145		0.0405	0.050	0.62790	0.67790	0.0738	0.9262
0.46205	0.025895	0.0546	0.100	0.70699	0.80699	0.1239	0.8761
0.51372	0.035021	0.0658	0.200	0.69380	0.89380	0.2238	0.7762
0.55660	0.044856	0.0770	0.300	0.62890	0.92890	0.3230	0.6770
0.59209	0.055244	0.0880	0.400	0.54890	0.94890	0.4215	0.5785
0.64683	0.078037	0.1112	0.500	0.46250	0.96250	0.5195	0.4805
0.67048	0.092605	0.1253	0.600	0.37280	0.97280	0.6168	0.3832
0.69268	0.112140	0.1437	0.700	0.28110	0.98110	0.7135	0.2865
0.70202	0.123990	0.1547	0.800	0.18810	0.98810	0.8096	0.1904
0.71361	0.147820	0.1765	0.900	0.09540	0.99437	0.9050	0.0949
0.71772	0.171670	0.1981	0.925	0.07080	0.99437	0.9289	0.0949
0.71466	0.203200	0.2266	0.950	0.04720	0.99720	0.9527	0.0473

y^* = molar fraction of ethylene glycol turned to monoester (E_1)
x^{**} = molar fraction of ethylene glycol turned to diester (E_2)

is a straight line whose parameters, calculated by the method of the least squares, have the following values : $a = 0.024$ (intercept) and $b = 1.033$ (slope).

The parameters of hyperbolas that describe the four studied systems are presented in table 2 and the plot of hyperbolas in figure 2.

TABLE 2

Values of parameters *a.b* for the studied systems

Polyglycol	*a*	*b*
Ethylene glycol	0.024	1.033
Diethylene-glycol	0.100	1.045
Triethylene-glycol	0.135	1.357
Tetraethylene glycol	0.240	2.933

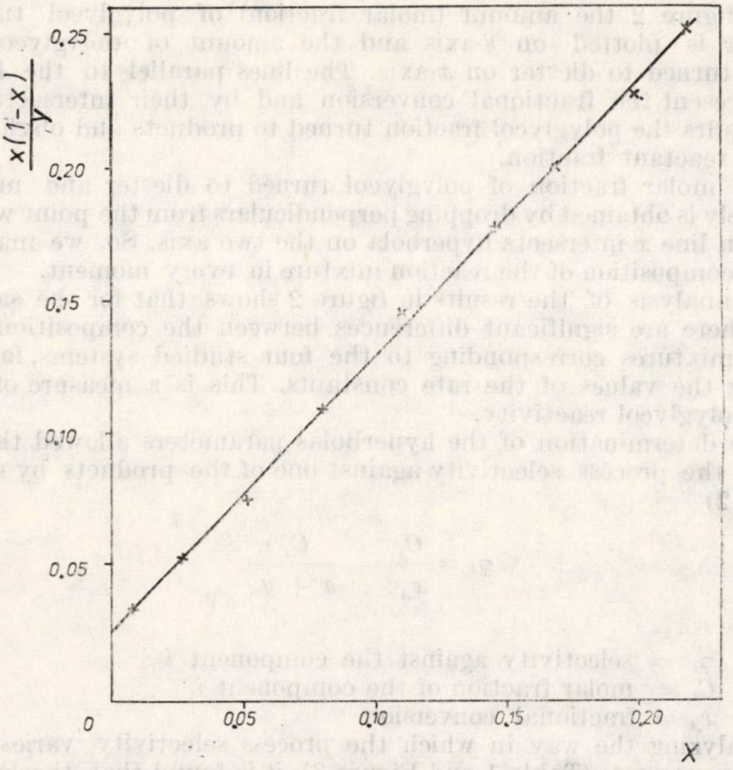

Fig. 1. — The plot of the function $x(1-x)/y = f(x)$ for transesterification of methyl methycrylate with ethylene glycol.

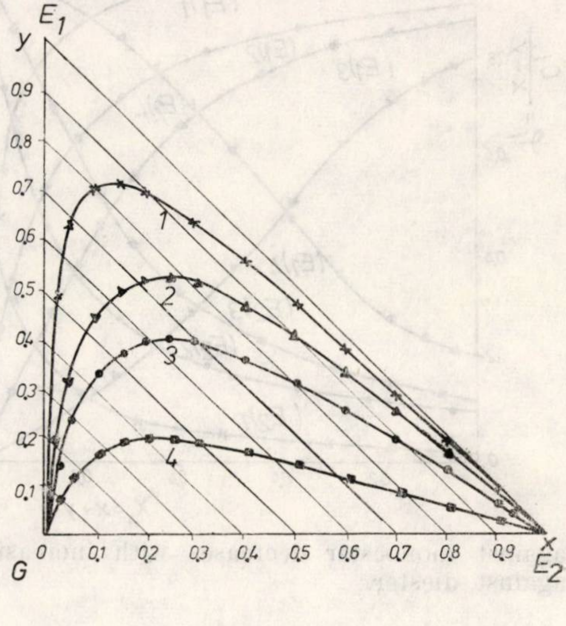

Fig. 2. — The plot of hyperbolas that describe the transesterification processes of methyl methycrylate with polyglycols.
1 — Ethylene glycol; *2* — Diethylene glycol; *3* — Triethylene glycol; *4* — Tetraethylene glycol.

In figure 2 the amount (molar fraction) of polyglycol turned to monoester is plotted on y-axis and the amount of polyglycol (molar fraction) turned to diester on x-axis. The lines parallel to the hypothenuse represent the fractional conversion and by their intersection with x-axis results the polyglycol fraction turned to products and obviously the unturned reactant fraction.

The molar fraction of polyglycol turned to diester and monoester respectively is obtained by dropping perpendiculars from the point where the conversion line x intersects hyperbola on the two axis. So, we may determine the composition of the reaction mixture in every moment.

An analysis of the results in figure 2 shows that for the same conversion there are significant differences between the compositions of the reaction mixtures corresponding to the four studied systems, fact determined by the values of the rate constants. This is a measure of the respective polyglycol reactivity.

The determination of the hyperbolas parameters allowed the calculation of the process selectivity against one of the products by means of relation (2)

$$\varphi_i = \frac{C_i}{x_A} = \frac{C_i}{x + y} \tag{2}$$

where :

φ_i = selectivity against the component i
C_i = molar fraction of the component i
x_A = fractional conversion

Analyzing the way in which the process selectivity varies against one of the products (Table 1 and Figure 3), it is found that the selectivity against monoester decreases with increasing conversion and increases against diester.

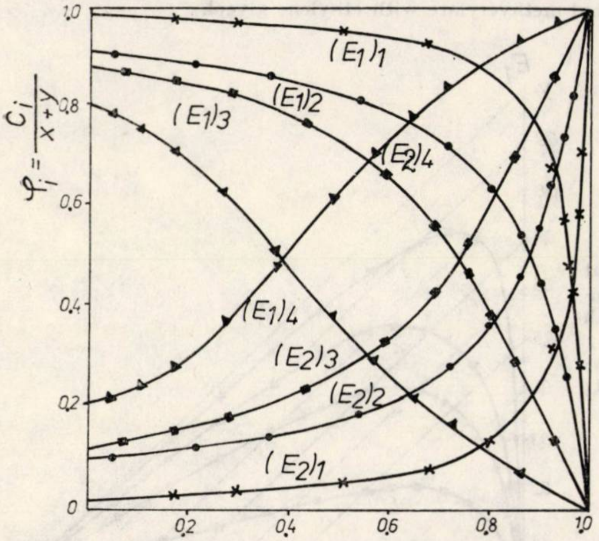

Fig. 3. — Dependence of transesterification selectivity process of methyl methacrylate with polyglycols on the polyglycol nature. $(E_1)_1$ = Ethylene glycol monomethacrylate, $(E_1)_2$ = Diethylene glycol monomethacrylate, $(E_1)_3$ = Triethylene glycol monomethacrylate, $(E_1)_4$ = Tetraethylene glycol monomethacrylate, $(E_2)_1$ = Ethylene dimethacrylate, $(E_2)_2$ = Diethylene glycol dimethacrylate, $(E_2)_3$ = Triethylene glycol dimethacrylate, $(E_2)_4$ = Tetraethylene glycol dimethacrylate.

Taking into account the facts mentioned above and that the transesterification reaction is made in well-stirred reactors where the maximum yield of diester is represented by the area of a rectangle whose upper right corner touches the selectivity curve and whose base is equal to the difference $x_A - x_{A_0}$[2], it is found that these are significant differences between the selectivities of the four studied systems. It means that for obtaining greater productivities in diester by transesterification of methyl methacrylate with ethylene glycols and diethylene glycols, greater conversions and thus greater reaction times are necessary.

CONCLUSIONS

1. The analysis of the kinetic data obtained by transesterification of methyl methacrylate with polyglycols determined the finding of equations of hyperbolas that describe the studied processes on whose bases we may determine, in every moment, the composition of the mixture.

2. Studying the influence of polyglycol nature upon the composition of the reaction mixture and the processes selectivity, it has been found that for obtaining great productivities in diester, the greater conversions and reaction times are necessary the smaller the length of polyglycol is.

REFERENCES

[1] Part. II : Gh. Hubca, D. Racoţi, Cr. Oprescu and M. Dimonie, *Rev. Roumaine Chim*, 2, 1327(1981).

[2] V. Kafarov, "Cybernetic Methods in Chemistry and Chemical Engineering", Translated from the Russian, MIR Publishers, Moscow, 1976.

Revue Roumaine de Chimie, **26**, *11–12*, 1499 (1981)

COMPTE RENDU

ADVANCES IN POLYMER SCIEMCE. VOLUME 37 S. Penczek, P. Kubisa and K. Matyjaszewski, "Cationic Ring-Opening Polymerization of Heterocyclic Monomers", Springer Verlag, Berlin, Heidelberg, New York, 1980, 156 pages.

The book is written by three Polish authors (from Centre of Macromolecular Studies, Polish Academy of Science, Lodz), which are active investigators in the title area.

In a short introduction the characteristic features of the oxonium ions which allowed the discovery of systems behaving as living systems are stressed (especially their high stability, making them immune to some reactions which cannot be avoided at carbenium ions).

Being the most studied monomers, the living systems like tetrahydrofuran are mainly detailes throughout the book.

After a short presentation of the essential factors affecting reactivities of heterocyclic monomers, the remaining part of the book is divided after three main headings, corresponding to the chemistry of the process : initiation, propagation and termination.

In chapter 3 ("Initiation" ; 30 pages) all the major classes of initiators are presented, namely : 1) protonic acids ; 2) carbenium ions ; 3) alcoxy carbenium ions ; 4) dioxolenium salts ; 5) oxocarbenium ions ; 6) onium ions ; 7) "hidden cations" (e.g. esters or anhydrides of strong protonic acids — "superacids" — which give tise to ion pairs) ; 8) Friedel-Crafts initiators ; 9) cations formed by electron transfer and 10) organometallic initiators.

A special section is devoted to kinetics of initiation (a tubular presentation of rate constants and activation parameters is given) underlining the importance of ^{1}H— ; ^{19}F— ; ^{14}C-NMR spectroscopy in such studies.

In chapter 4 ("Propagation", 38 pages) the following important aspects are developed : 1) chemical structure of the growing species, exemplified for polymerization of cyclic acetals under the influence of different initiators, of 1,3-dioxolane, lactams etc. ; 2) macroions and macroion pairs in propagation (including dissociation reactivities and solvent effects) ; 3) rate constants of propagation and structure of monomers and 4) stereochemistry of the cationic ring opening propagation (including a discussion of the usual is version of configuration during cationic polymerizations of heterocycles). Kinetic data are alo given and the utility of NMR in investigation of such reactions is again stressed.

Chapter 5 ("Termination and transfer processes" ; 49 pages) presents : 1) temporary termination (involving covalent and ionic species) ; 2) termination by irreversible collapse of the macroion pair ; 3) transfer and termination involving the polymer backbone (inter- and intramolecular chain transfer, kinetic and stereochemical aspects, tables with basic kinetic equations in nonstationary kinetics with chain transfer) and 4) hydride ion, proton and carbocation transfer to monomers.

A ten pages addenda (including the literature up to december 1979), a reference list (with 312 references) and a short subject index end this interesting book which will be useful to macromolecular and organic chemists.

M. Banciu

Revue Roumaine de Chimie, 26, 11–12, [illegible] (1981)

COMPTE RENDU

ADVANCES IN POLYMER SCIENCE, VOLUME 37 S. Penczek, P. Kubisa and K. Matyjaszewski, "Cationic Ring-Opening Polymerization of Heterocyclic Monomers", Springer Verlag, Berlin, Heidelberg, New York, 1980, 156 pages.

The book is written by three Polish authors (from Centre of Macromolecular Studies, Polish Academy of Sciences, Lodz), which are active investigators in the title area.

In a short introduction the characteristic features of the oxonium ions which allowed the discovery of systems behaving as living systems are stressed (especially their high stability making them immune to some reactions which cannot be avoided at carbenium ions).

Being the most studied monomers, the living systems like tetrahydrofuran are mainly detailed throughout the book.

After a short presentation of the essential factors affecting reactivities of heterocyclic monomers, the remaining part of the book is divided after three main headings, corresponding to the chemistry of the process: initiation, propagation and termination.

In chapter 3 ("Initiation", 34 pages) all the major classes of initiators are presented, namely: 1) protonic acids; 2) carbenium ions; 3) stable carbenium ions; 4) dioxolenium salts; 5) oxocarbenium ions; 6) onium ions; 7) "hidden cations" (e.g., esters or anhydrides of strong protonic acids); 8) "superacids" which give rise to ion pairs); 9) halide Lewis initiators; 9) cations formed by electron transfer and 10) organometallic initiators.

A special section is devoted to kinetics of initiation in tabular presentation of rate constants and activation parameters is given, underlining the importance of ^{1}H-, ^{19}F-, ^{13}C-NMR spectroscopy in such studies.

In chapter 4 ("Propagation", 38 pages) the following important aspects are developed: 1) chemical structure of the growing species, exemplified for polymerization of cyclic acetals under the influence of different initiators, of 1,3-dioxolane, lactams etc.; 2) macroions and macroion pairs in propagation (including dissociation reactivities and solvent effects); 3) rate constants of propagation and structure of monomers and 4) stereochemistry of the cationic ring opening propagation (including a discussion on the usual inversion of configuration during cationic polymerizations of heterocycles). Kinetic data are also given and the utility of NMR in investigation of such reactions is again stressed.

Chapter 5 ("Termination and transfer processes", 19 pages) presents: 1) temporary termination (involving covalent and ionic species); 2) termination by irreversible collapse of the ion pair; 3) transfer and termination involving the polymer backbone (inter- and intramolecular chain transfer). Kinetic and stereochemical aspects, tables with basic kinetic equations in nonstationary kinetics with chain transfer) and 4) hydride ion, proton and carbocation transfer to monomers.

A few pages addenda (including the literature up to december 1979), a reference list (with 312 references) and a short subject index end this interesting book which will be useful to macromolecular and organic chemists.

M. Puiu

F 1103

INDEX DES AUTEURS

A

ABDALLA M. and A. ESSAWY, M. A. EL-HASHASH, A. M. EL-GENDY, Action of aromatic hydrocarbons, active methylene compounds and Grignard reagents on α-3-benzylidene-5-[1′(2′-methylnaphthalenyl)]-2(3H) furanone and 4-benzylidene-1-*p*-tolyl-2-[1′(2′-methylnaphthalenyl)]-2-pyrroline-5-one 95
— , voir ESSAWY A. 601
— , voir ESSAWY A. 1285
ABDEL-GHANI N. T., voir ISSA R. M. 667
ABDEL HALIM F. M., voir SIDAHMED I. M. 37
ABDEL-HAY F. I., voir ANWAR M. 993
— , voir ANWAR M. 1127
— , voir ANWAR M. 1149
ABO-BAKER O. A., voir MOHAMED M. M. 441
ABRAHAM M., The activity of one salt at high concentrations in pure water (in French) 829
AIRINEI A. and D. DOROHOI, A. TOLEA, The influence of the solvent on the electronic absorption spectra of some n-substituted 2-nitroanilines 1295
ANIL K., voir SRIVASTAVA S. P. 939
ANWAR M., Reactions of some 4(3H) quinazolinones 639
— and F. I. ABDEL-HAY, Reactions of 1-phenyl-3,5-pyrazolidinedione 993
— and F. I. ABDEL-HAY, A. A. EL-BARBARY, M. EL-BORAI, Reactions of some 5-aryl-2-thiono-1,3,4-thiadiazoles 1127
— and F. I. ABDEL-HAY, A. A. EL-BARBARY, M. EL-BORAI, Some reactions of 4-chloro-quinazoline, 6-nitro- and 6-amino-4-3H-quinazolones 1469
— , voir EL-BARBARY A. A. 449
ARRANZ A., voir SENENT S. 377
ARVAY ZS., voir RĂZUȘ A. C. 457
AVRAM R. and L. PAPAHAGI, I. ILIUȚĂ, The oxidation of n-dodecane in liquid phase with molecular oxygen in the presence of aluminium, lanthanum and certain naphthenates 1279
AVRAMESCU D., voir MARCU GH. 575
AWAD A. and F. EL-CHEIKH, A. ABD EL-GABER, Adsorption effects of some natural and synthetic macromolecules at charged interfaces 1025
— , voir THARWAT M. 491

B

BACALOGLU I. and TRUONG THE KY, HANS-HORST GLATT, C. BOERIU, R. BACALOGLU, D. MARTIN, Structure and reactivity of hetero-substituted nitriles. XXIII. Kinetics and mechanism of the formation of 2-aminobenzoxazole from *o*-aminophenol and phenylcyanate (in German) 1135
— , voir BACALOGLU R. 611
BACALOGLU R., voir CHICU A. 435
— and A. CHICU, ILSE BACALOGLU, I. COTÂRCĂ, Nucleophilic substitutions at carbonic acid derivatives. XVIII. Kinetics and mechanism of the alcoholysis of N,N,N′-trisubstituted carbonic acid chloramidines (in German) 611
— , voir BACALOGLU I. 1135
BACIU I., voir HILLEBRAND M. 17
BADEA F., voir RĂZUȘ A. C. 457

— and A. M. GLATZ, A. C. RĂZUŞ, Ring opening in benzo [b] bicyclo[3.1.0] hexyl cations 629

BĂDĂU E., voir IOVU M. 1149

BADRAN M. M., voir ESSAWY A. 245

BAHADUR P., voir SINGH P. 389

BALABAN A. T., Chemical graphs. XXXVII. A simple rule for classifying *peri*-condensed benzenoid hydrocarbons as closed-shell or open-shell (polyradicalic) systems using dualist (characteristic) graphs 407

— voir MOŢOC I. 593

BĂLĂ E. and M. S. IONESCU, C. STOICESCU, Copper(II) complexes of threonine and allothreonine 861

BĂLĂNESCU M., voir CEAUŞESCU E. 509

BALINT A., voir NIMARĂ A. 967

BALLESTEROS J. SÁNCHEZ and F. HERNANDEZ HERNANDEZ, D. J. McPHEE, Study and transformations of the condensation products of isopropylidene-D-glyceraldehyde with active methylenes 705

— and D. J. McPHEE, F. HERNANDEZ HERNANDEZ, Preparation of polyfunctional furanic derivatives from trioses 899

BANCIU A. C., A new bridged binuclear low-spin pentacoordinate Co(II) complex containing strongly electronegative donor atoms 1231

BANCIU M., and PHAN LE THUY, M. ELIAN, C. DRĂGHICI, E. CIORĂNESCU, A rearrangement of dibenzo[*c*, *e*]tricyclo [$5.3.0.0^{2,10}$] deca-3,5-dien-9-ol into triphenylene derivatives 1115

BANYAI P., voir IONESCU N. I. 681

— , voir CĂLDĂRARU M. 837

BARBU S. and CONST. GH. MACAROVICI, The spectrophotometric study of some Cu(II)-thiocarbohydrazone systems in solution and their analytical application 1255

BENTIA T., voir MATEESCU M. A. 117

BEZAK E., voir LENARCIK B. 229

BHANDARI C. S., voir CALLA S. 1033

BLEJOIU I., voir BUNESCU O. 1393

BOERIU C., voir BACALOGLU I. 1135

BONCHEV D. and O. MEKENYAN An estimate of the upper limit of the periodic table based on the Eddington number 349

BOOK REVIEWS . . . 155, 327, 503, 655, 801, 1041, 1195, 1341, 1499

BORDEIANU R., voir CEAUŞESCU E. 509

BOSTAN M., voir LUCHIAN N. 1479

BRĂCĂCESCU D., voir URSEANU F. 755

BRĂILEANU A., voir ZAHARESCU M. 1063

BREZEANU M. and I. JITARU, M. DINCULESCU Co(III) complex compounds with 3-amino-1-propanol and dimethylglyoxime 1097

— and I. SEBE, M. GUŢUL, I. JITARU, Cu(II) complex compounds with 1-(β-phenyl-β-amino)ethylcyclobutanol and 1-(β-*p*-chlorophenyl-β-amino) ethylcyclobutanol 1221

BRUMĂ M. and G. NEAMŢU, Poly-1,3,4-oxadiazoles. IX. Ordered poly-1,3,4-oxadiazole-amide-imides 87

BUCEA L., voir TEOREANU I. 1213

BUCUR I., voir STEINBRECHER G. 1077

BUDIU T., voir VĂŢULESCU R. 851

— , voir VĂŢULESCU R. 971

BUNESCU O., voir STEINBRECHER G. 1077

— and P. ROTARU, S. I. BLEJOIU, Electrical conduction in nickel-alumina catalyst 1393

BURGUERA J. L., voir BURGUERA M. 761

BURGUERA M. and J. L. BURGUERA, A. TOWNSHEND, Analysis by molecular emission in cavity for the determination of nonmetals using volatilization systems (in Spanish) 761

BUTUCESCU N., voir TEOREANU I. 1213

BYOUK BLOURI, voir GIRAUD J. 397

C

CALLA S. and S. P. MATHUR, R. S. THAKUR, C. S. BHANDARI, Direct photometric determination of cerium(IV) with 3-phenylazohydroxylamine 1033
— , voir JAIMAN R. D. 1111
CĂLDĂRARU M., voir IONESCU N. I. 681
— and BANYAI P., N. I. IONESCU, Electrical conductivity of a complex bismuth—molybdenum catalyst in the reaction of propylene oxidation . . 837
CALU C. and N. CALU, A. ONU, Ion exchange in the system Na_2WO_4 (solution) — Amberlite IR 120 (H^+). II. Polytungstic acid T (in French) . . . 955
CALU N. and O. VICOL, New aspects in the spectrophotometric analysis. I. Computational equations for the dosage of some dyestuffs in mixtures 783
— , voir CALU C. 955
CAMPELO J. M. and D. LUNA, M. MARINAS, Liquid-phase reduction of cyclohexene in the presence of new systems of supported nickel catalysts (in Spanish) . . 867
CEAUŞESCU E. and R. BORDEIANU, I. CERCHEZ, M. BĂLĂNESCU, P. GHIOCA, Kinetics of anionic polymerization of butadiene and styrene with organolithium catalysts in toluene 509
CERCASOV C. voir CIUREANU M. 659
CERCHEZ I., voir CEAUŞESCU E. 509
CERCHEZ M. V., voir DINESCU R. 545
CHATZOPOULOS M. and J. P. MONTHEARD, Radicalic cyclizations of unsaturated aldehydes (in French) 275
CHAWLA R. S., voir SINHA P. P. 917
CHICU A. and R. BACALOGLU, Nucleophilic substitutions to carbonic acid derivatives. XVII. Kinetics and mechanism of the hydrolysis of N,N,N′-trisubstituted carbonic acid chloramide (in German) 435
— , voir BACALOGLU R. 611
CHIFU E., and Z. FINTA, M. SĂLĂJAN, E. GAVRILĂ, Surface mobility of surfactant solutions. IX. Surface and capillary flow between drops linked by surface canals 1345
CHIRALEU F., voir GEORGESCU FL. 879
CHIRCĂ M., voir IONESCU N. I. 681
CHIRIAC C. I., A convenient new method for synthesis of aromatic amides under mild conditions 1001
CHITHAMBARATHANU PILLAI G. and J. RAJARAM, J. C. KURIACOSE, The oxidation of butan-2-one by vanadium (V) in aqueous perchlorate media. Kinetics and mechanism 21
CHORBADJIEV S., Synthesis of medium and higher dialkyl disulphides 1447
CIMPU V. and A. MEGHEA, I. JITARU, Copper (II) complexes with 10-[2-(dimethylamino)propyl]-phenothiazine 1261
CIOBANU A., voir LUCHIAN N. 1479
CIOCHINĂ A., voir VÎLCU R. 161
— , voir VÎLCU R. 527
— , voir ŞERBĂNESCU D. 1047
— , voir VÎLCU R. 1255
CIORĂNESCU E., voir BANCIU M. 1115
CIUREANU M. and F. CORNEA, C. CERCASOV, M. CONTINEANU, Internal rotation in charge transfer complexes 659
CÎRJALIU F., voir OANCEA D. 933
COLDEA M., voir COLDEA V. 71
COLDEA V. and M. COLDEA, I. HAIDUC, Proton magnetic resonance spectra of some di- and triorganotion mono- and dithiocarboxylates 71
COLŢEA P., voir MATEI S. 985
CONSTANTINESCU C., voir CONSTANTINESCU GH. 1177
CONSTANTINESCU GH. and C. CONSTANTINESCU, Reactivity of substituted malachite green in the reaction with the tetrachloroauric anion (in French) . 1177
CONSTANTINESCU M., voir SURPĂŢEANU GH. 1169
— and GH. SURPĂŢEANU, C. LUCHIAN, M. PETROVANU, I. ZUGRĂVESCU, Theoretical aspects on the regioselectivity in the 1,3-dipolar cycloadditions of pyridinium-ylides to acetylenic dipolarophiles 1451
CONTINEANU M., voir CIUREANU M. 659

CONȚESCU CR. and M. I. VASS, FEM study of silver layers adsorbed on tungsten. II. Surface structure and surface migration 175
— , FEM study of silver layers adsorbed on tungsten. III. Silver layer growth modes 355
CÖRMÖS D. C., voir MIOȘCU M. 1487
CORNEA F., voir CIUREANU M. 659
CORPACIUS A. J., Quantitative analysis of chromatographic observations. 315
COTARCĂ L., voir BACALOGLU R. 611
COUTURIER D., voir RICART G. 253

D

DANEȘ F. E. and D. GEANĂ, Computation of chemical equilibrium of methanol synthesis using state equations of gases at high pressure (in French). . . 947
— , voir GEANĂ D. 1365
— and S. STERNBERG, S. DANEȘ, An extension of the Staverman/Scatchard thermodynamic theory of membrane potential (in French) . . . 1377
DANEȘ S., voir DANEȘ F. 1377
DĂNEȚ A. FL., Study of extraction and complexing of palladium (II) with 1- *p*-nitrophenyl)-3-*p'*-azobenzene)-triazene and 1- *p*-nitronaphthyl), 3- *p'*-azobenzene)-triazene 141
DAVID V. and Ș. MOLDOVEANU, Interaction between two charge distributions situated into a continuum, infinite and isotropic medium 333
— and Ș. MOLDOVEANU, The long-range interaction of two molecules in the presence of a *Kirkwood* perturbational field. 805
DEEB A., voir ESSAWY A. 601
DEMETRESCU I., voir TOMESCU M. 793
— and D. FĂTU, X-ray analysis of some carbon fibres. 1387
DEMIAN A. M. and W. SCHMIDT, Rapid photometric determination of absorbing substances in mixtures (in German) 769
DIMA M. and S. OPREA, E. DUMITRIU, Reactivity of acrylic monomers. III. Copolymerization of N,N-dimethylaminoethyl-methacrylate with N,N-diethylacrylamide 131
DIMITRIU C., voir MATEESCU M. A. 117
DIMONIE M., voir MATEESCU M. A. 117
— , voir HUBCA GH. 1185
— , voir HUBCA GH. 1327
— , voir HUBCA GH. 1493
DINCULESCU M., voir BREZEANU M. 1097
DINESCU R. and M. V. CERCHEZ, Kinetics and reaction mechanism of chemical compounds in mixtures belonging to the $Na_2O-CaO-Al_2O_3-SiO_2-CO_3$ system (in German) 545
DIUDEA M. V., Phenazathionium cations. III. The selective nucleophilic substitutions on phenazathionium cations 725
— , Phenazathionium cations. IV. Demonstration on the structure of 1,3,7-trisubstituted derivatives of phenothiazine by mass spectrometry and ^1H- NMR. 887
DOMKA F. and M. ŁANIECKI, The effect of synthesis conditions on the activity of iron-chromium oxide catalysts for water gas shift reaction (in French). 211
— and J. MICIUKIEWICZ, W. ZMIERCZAK, Catalytic properties of $Fe_2O_3-Nd_2O_3$ system (in French) 203
— et M. LANIECKI, Influence of alkali metal oxides on the formation of a ferro-chromic catalyst for conversion of carbon monoxide by steam (in French) 1085
DOROHOI D., voir AIRINEI A. 1295
DOSS S. H. and F. A. RASHID, Identification of two organic sultam compounds . . 623
DRĂGAN GH., Amorphous-crystalline coupling in polyethylene. IX. Study of the transforming branches by step calorimetric system 1315
DRĂGHICI C., voir BANCIU M. 1115
DRUȚĂ I., voir GEORGESCU EM. 109
DUMITRIU E., voir DIMA M. 131

E

EL ABSY M. A. S., and GH. MARCU, J. ZSAKÓ, VS. VÁRHELYI, Studies on some nitro-bis-acetylacetonato-cobalt (III) compounds 1245
EL-ANSARY A. L., voir ISSA R. M. 667
EL-BARBARY A. A., and M. ANWAR, A. A. GHATTAS, A. F. HASHEM, Reaction of 5-aryl-2-thiono-1,3,4-oxadiazoles with some amino- and halo-compounds . 449
— , voir ANWAR M. 1127
— , voir ANWAR M. 1169
EL-BORAI M., voir ANWAR M. 1127
— , voir ANWAR M. 1169
EL-CHEIKH F., voir AWAD A. 1025
EL-DEEK M. and M. A. I. SALEM, A. A. HAMED, M. SAMAAN, Studies on pyridones. I. Synthesis and reactions of 3-acetyl-(3,4-dichlorophenyl)-2-(1H)-pyridones 647
— and M. A. I. SALEM, A. A. HAMED, M. SAMAAN, Studies on pyridones. II. Synthesis and reactions of 6-(3,4-dichlorophenyl)-3-(substituted cinnamcyl)-4-aryl-2(1*H*)-pyridones. 775
EL-GABER A. A., voir AWAD A. 1025
EL-GARBY YOUNES M., voir ESSAWY A. 245
— , voir ESSAWY A. 1141
EL-GENDY A. M., voir ABDALLA M. 95
— , voir ESSAWY A. 1285
EL-HASHASH M. A., voir ABDALLA M. 95
— and M. E. SHABAN, M. M. HABASHY, Some reactions of 3,4-methylenedioxybenzylidene-*p*-isopropylacetophenone 101
— , voir MOHAMED M. M. 441
— , voir EL-KADI M. 1161
— , voit ESSAWY A. 1285
ELIAN M., voir BANCIU M. 1115
EL-KADI M., and M .A. EL-HASHASH and M. A. SAYED, Action of hydrazines, amines and thiourea upon β(4-chloro-3-methyl)-benzoylacrylic acid 1161
EL-KADY F. Y., Comparison between the hydrocracking activity of cobalt-molybden/alumina and nickel—molibdyenum/alumina catalysts 1413
ELKASABY M. A. and M. A. I. SALEM, Synthesis and reactions of 6,7(4′-alkyl-α-pyrano)4-alkyl coumarins 717
EL-KHAWAGA M. A. A., voir KHALAF A. A.. 739
EL-NAGGAR H. A., voir MASOUD M. S. 961
ESSAWY A., voir ABDALLA M. 95
— and M. EL-GARBY YOUNES, M. M. BADRAN, A. Z. M. HEIKAL, Synthesis and reactions of 3-cinnamoyl-4-phenyl-6-[1′(2′-methoxynaphthalenyl]-2-pyridone and of 2-methyl-(b)-2′-[α(β-methoxynaphthalenyl)-4′-phenyl-3′-4′-dihydropyridyl]-azachromone. 245
— , voir HABASHY M. M. 283
— and M. ABDALLA, A. DEEB, Some reactions with Michael adducts of bromobenzoyl acrylic acid and its amides 601
— and M. EL-GARBY YOUNES, A. Z. M. HEIKAL, Synthesis and some reactions of 3-cyano-4-phenyl-6-[1′(2′-methoxynaphthalenyl)]-2-pyridone. 1141
— and M. A. EL-HASHASH, M. M. ABDALLA, A. M. EL-GENDY, Some reactions of 6-[1′(2′-methyl naphthalenyl)]-2,3,4,5 tetrahydropyridazin-3-one 1285

F

FASIHUDDIN K., voir SINHA P. P.. 917
FĂTU D., voir DEMETRESCU I. 1387
FERRARI L., voir SENENT S. 377
FERRO D., and V. PIACENTE, M. PELINO, Measurements of the vapour pressure of β-bromonaphthalene 9
FINTA Z., voir CHIFU E.. 1345
FIŞEL S., voir ODOCHIAN L.. 383

G

GANOVICI L., voir PETRESCU N. 55
— , voir PETRESCU N. 843
GAVRILĂ D., Experimental studies bearing upon the behaviour of polyvinyl chloride in heavy fields of nuclear radiations 125
GAVRILĂ E., voir CHIFU E. 1345
GAYOSO J. and OURIDA OUAMERALI, A new aromaticity index based on the exaltation of diamagnetic susceptibility (in French) 1035
GEANĂ D., Chemical equilibrium in multicomponent reaction systems 43
— , On the problem of phase equilibrium in chemical reaction systems . . . 363
— , voir DANEŞ F. E. 947
— , and DANEŞ, F. An analysis of the effect of input data changes on the chemical equilibrium composition 1365
GEORGESCU E., voir GEORGESCU FL. 879
GEORGESCU FL. and F. CHIRALEU, E. GEORGESCU, I. ZUGRĂVESCU, Pyridinium-ylids. II. The reactions of some carbanion-monosubstituted 4-phenylpyridinium-ylids with activated acetylenes (in French) 879
GEORGESCU E. and I. DRUTA, M. PETROVANU, Dipolar derivatives in the quinazoline series. I. Synthesis of pyrrolo [1,2-c] quinazolines (in French) . . . 109
GHATTAS A. A., voir EL-BARBARY A. A. 449
GHIOCA P., voir CEAUŞESCU E. 509
GIRAUD J., and S. NOURI, B. BLOURI, On the steam cracking of 6-methyleicosane (in French) 397
GIRGIS M. M. and D. P. LAZĂR, E. I. SEGAL, Catalytic oxidation of ammonia. II. Low temperature oxidation on a $Fe_2O_3-Cr_2O_3$ catalyst. Influence of the amount of the catalyst. Analysis of the reaction products 1199
— and D. P. LAZĂR, E. I. SEGAL, Catalytic oxidation of ammonia. III. Low temperature oxidation on a $Fe_2O_3-Cr_2O_3$ catalyst; evaluation of the experimental data in order to obtain kinetic parameters 1425
GLACET CH., voir RICART G. 253
GLATT H. H., voir BACALOGLU I. 1135
GLATZ A. M., voir RĂZUŞ A. C. 457
— , voir BADEA F. 629
GOŞA V., voir POPESCU D. 197
— , voir SCHUSTER R. H. 819
— , voir POPESCU D. 927
— , voir OANCEA D. 933
— and R. S. SCHUSTER, N. I. IONESCU, D. OANCEA, D. POPESCU, Explosive combustion of vinylacetylene-air mixtures initiated by hot platinum wire (in German) 1205
GUPTA B. K., voir SYAMAL A. 857
GUPTA S. P., voir MITTAL M. 1335
GUPTA V. K., voir SRIVASTAVA S. P. 939
GUŢUL M., voir BREZEANU M. 1221

H

HABASHY M. M., voir EL-HASHASH M. A. 101
— and A. ESSAWY, M. M. M. HAMAD, Epoxidation of 2,6-diarylidenecyclohexanones and some reactions of the corresponding epoxides 283
HAIDUC I., voir COLDEA V. 71
— , voir MIOŞCU M. 1487
HAMAD M. M. M., voir HABASHY M. M. 283
HAMED A. A., voir EL-DEEK M. 647
— , voir EL-DEEK M. 775
HASHEM A. F., voir EL-BARBARY A. A. 449
HASSAN KH. M., voir YOUSSEF M. S. K. 81
HASSAN M. and A. R. O. ABDEL NOUR, A. M. SATTI, I. A. WAKEEL, Studies of the reactions of aryl propene oxides in basic media. II. Reactions of some *o*-substituted epoxides compared to *p*- and *m*-substituted analogues . . . 979

HEIKAL A. Z. M., voir ESSAWY A. 245
— , voir ESSAWY A. 1141
HERNANDEZ HERNANDEZ F., voir BALLESTEROS SÁNCHEZ J. 705
— , voir BALLESTEROS SÁNCHEZ J. 899
HILLEBRAND M. and I. BACIU, G. MAXIM, ESR and electronic study of the 1,4-benzo-*p*-dioxin[2,3,-b] thioxanthone anion-radical 17
HORÁK J., voir ZSAKÓ J. 1271
HRIŢCU C., voir TEOREANU I. 1213
HUBCA GH. and CR. OPRESCU, M. TOMESCU, M. DIMONIE, Synthesis and polymerization of polyethylene glycol dimethacrylates. I. Study of synthesis process of polyethylene glycol dimethacrylates 1185
— and D. RACOŢI, CR. OPRESCU, M. DIMONIE, Synthesis and polymerization of polyethyleneglycol dimethacrylate. II. Kinetics of the transesterification process of methylmethacrylate with polyglycols 1327
— and CR. OPRESCU, M. DIMONIE, Synthesis and polymerization of polyethylene glycol dimethacrylates. III. Analysis of kinetic data obtained by transesterification of methyl methacrylate with polyglycols 1493

I

ILIUŢĂ J., voir AVRAM R. 1279
IONESCU E., voir IOVU M. 1461
IONESCU M., voir VÂNTU V. 269
IONESCU N. I., voir POPESCU D. 197
— and P. BANYAI, M. CĂLDĂRARU, M. CHIRCĂ, The reduction of a complex molybdenum—bismuth oxide catalyst with propylene 681
— , Concerning a recently proposed equation for the adsorption of gases on solids 815
— , voir SCHUSTER R. H. 819
— , voir CĂLDĂRARU M. 837
— , voir POPESCU D. 927
— , voir OANCEA D. 933
— , voir GOŞA V. 1205
IONESCU S. M., voir BĂLĂ E. 861
IOVU M. and E. BĂDĂU, Novel aromatic thioethers (in French) 1149
— and E. IONESCU, N. N′-substituted trinitrophenylene diamines 1461
ISSA R. M. and N. T. ABDEL-GHANI, A. L. EL-ANSARY, A. F. SHOUKRY, Charge transfer complexes of some pyridine derivatives with aromatic tri- and di-nitrocompounds 667
ISAC D. and M. MRACEC, N. PROŞTEANU, Z. SIMON, The kinetics of thermal and photochemical decomposition of aromatic diazonium salts 29
ISAC D. and M. MRACEC, Z. SIMON, Structure and reactivity in diazotization reaction. Electronic spectra and molecular orbital calculations for aromatic diazonium salts 341

J

JADON S. P. S., Kinetics of self-decomposition of tin(IV) peroxydichromate 1107
JAIMAN R. D. and S. CALLA, S. P. MATHUR, R. S. THAKUR, Spectrophotometric investigations of iron(III)-N-acetyl-N-m-tolylhydroxylamine-complexes 1111
JAIN R. K., voir TAMBI S. B. 477
— , voir SINGH C. P. 1011
JITARU I., voir BREZEANU M. 1097
— , voir BREZEANU M. 1221
— , voir CIMPU V. 1261
JOSHI B. C., voir PANDE R. K. 875
JOSYULU O. S. and J. SOBHANADRI, B. VISWANTHAN, Lattice constant and saturation magnetization of cobalt zinc ferrites and magnesium zinc ferrite . . 687

K

KHALAF A. A. and AHMED M. A., EL-KHAWAGA, Modern Friedel-Crafts chemistry. IX. On the cycloalkylation of aryl alkenyl ketones and other related systems 739

KOKKINOS K. and CHR. MARKOPOULOS, Attempts towards the synthesis of 10-methyl-9-methylene-dihydroacridine-ω-aldehyde (in German) 733

KURIACOSE J. C., voir CHITHAMBARATHANU PILLAI G. 21

KRIZA A. and M. NASTA, Complex compounds of zirconium (IV) with azomethine . . 693

L

LAL K., voir MITTAL M. 1335

LABLACHE-COMBIER A., voir SURPĂŢEANU GH. 1169

LANIECKI M., voir DOMKA F. 1085

— , voir DOMKA F. 211

LÁSZLÓ T., voir ZSAKÓ J. 237

LAZĂR D. P., voir GIRGIS M. M. 1425

— , voir GIRGIS M. M. 1199

LENARCIK B. and E. BEZAK, A study for optimum conditions of extraction of transition metal complexes with pyridine derivatives. Extraction of the Co(II), Ni(II) and Zn(II) complexes of 3,5-dimethylpyridine 229

LITEANU C. and I. I. PANOVICI, Frequentometric detection in different stability conditions of IR analytic systems 909

LLAVINA J., voir SINISTERRA J. V. 415

LUCHIAN C., vir SURPĂŢEANU GH. 1169

— , voir CONSTANTINESCU M. 1457

LUCHIAN N. and A. CIOBANU, M. BOSTAN, Cyclic organosilicon compounds. II. Reaction of 1,4-dilithium,1,1,4,4-tetraphenylbutane with organotrichlorosilanes 1479

LUNA D., voir CAMPELO J. M. 867

M

MACAROVICI CONST. GH., voir BARBU S. 1255

MACOVEI V., Spectral solvent effects in aromatic compound solutions. VII. Solvent effects in the benzonitrile band at 260 nm 1405

MAHADEVAPPA D. S., voir SWAMY R. 565

MAIOR O., voir MATEESCU M. A. 117

MARC M. and A. UNGUREANU, Nickel(II) and manganese (II) complexes of cystine. 587

MARCU GH. and CS. VÁRHELYI, M. SOMAY, D. AVRAMESCU, New cobalt(III) complex compounds with methylisopropyl-glyoxime (in German) 575

MARCU GH., voir VĂŢULESCU R. 851

— , voir VĂŢULESCU R. 971

— , voir MOHAMED ABDEL SALAM EL-ABSY 1245

MARINAS J. M., voir SINISTERRA J. V. 415

MARINAS M., voir CAMPELO J. M. 867

MARKOPOULOS CHR., voir KOKKINOS KONST. 733

MARTIN D., voir BACALOGLU I. 1135

MASOUD M. S. and M. M. OSMAN, H. A. EL-NAGGAR, Studies on osmium-quinisatine oxime reaction 961

MATEESCU M. A. and H. C. SCHELL, M. DIMONIE, T. BENŢIA, C. DIMITRIU, O. MAIOR, Cationic beaded PVA ion exchangers. I. Reticulation, derivatisation and some physical-chemical properties (in German) 117

MATEI S. and J. RUSSU, P. COLŢEA, The synthesis and the electronic spectra of some *trans*-α-cyano-2-styrylbenzimidazoles 985

MATHUR S. P., voir S. CALLA 1033

— , voir JAIMAN R. D. 1111

MAXIM G., voir HILLEBRAND M. 17

McPHEE D. J., voir BALLESTEROS SÁNCHEZ J. 705

McPHEE D. J., voir BALLESTEROS SÁNCHEZ J. 899

MEGHEA A., voir CIMPU V. 1261
MEKENYAN O., voir BONCHEV D. 349
MICIUKIEWICZ J., voir DOMKA F.. 203
MIHAI E., voir ODOCHIAN L. 383
MIOȘCU M. and I. HAIDUC, C. D. CÖRMÖS, Potentiometric determination of L-alanine- L-serine, tyrosins and histidine with a Cu^{2+} sensitive electrode. . . 1487
MITAL R. L., voir TAMBI S. B. 477
MITTAL M. and K. LAL, S. P. GUPTA, Potentiometric studies on complexes of some transition metal ions with 4,5-dimethyl-2-hydroxyacetophenone and its oxime 1335
MITOȘERIU O., voir ODOCHIAN L.. 383
MOHAMED M. M. and M. A. EL-HASHASH, M. A. SAYED, O. A. ABO-BAKER, Studies on the cyclisation of the products of Stobbe condensation with 2,4-dimethylacetophenone 441
MOLDOVEANU Ș., voir DAVID V. 333
— , voir DAVID V. 805
MONTHEARD J. P., voir CHATZOPOULOS M. 275
MOREY J.- voir SINISTERRA J. V.. 415
MOȚOC I. and A. T. BALABAN, Topological indices : intercorrelations, physical meaning, correlational ability 593
MRACEC M., voir ISAC D. 29
— , voir ISAC D. 341
MUREȘAN N., voir STEINBRECHER G. 1077

N

NASTA M., voir KRIZA A. 693
NEAMȚU G., voir BRUMĂ M. 87
NICOLESCU I. V. and I. SĂNDULESCU, Relations between the methods of preparation, properties and activity of Bi—Mo—Fe—O catalyst in oxidative dehydrogenation of n-butenes in butadiene 217
NIMARĂ A. and E. PRINCZ, A. BALINT, Bismuth(III)-ethylenediaminetetraacetic acid complexes. III. Exchange reaction of Bi(III) from BiEDTA with Fe(III) 967
NOUR ABDEL A. R. O., voir HASSAN M. 979

O

OANCEA D., voir POPESCU D. 197
— , voir SCHUSTER R. H. 819
— and D. POPESCU, V. GOȘA, R. H. SCHUSTER, N. I. IONESCU, F. CÎRJALIU, Overall activation energy of explosive combustion of methane — air mixtures 933
— , voir POPESCU D. 927
— , voir GOȘA V. 1205
ODOCHIAN L. and E. MIHAI, S. FIȘEL, O. MITOȘERIU, Thermogravimetrical analysis of some complex compounds of thiobisnaphthol (in French). . . 383
OJHA A. C., voir SINGH C. P. 1011
OLTEANU T., voir URSEANU F. 755
ONU A., voir CALU C. 955
OPREA S., voir DIMA M. 131
OPRESCU CR., voir HUBCA GH. 1185
— , voir HUBCA GH. 1327
— , voir HUBCA GH. 1493
OSMAN M. M., voir MASOUD M. S. 961
OUAMERALI O., voir GAYOSO J. 1035

P

PANDE R. K. and R. SHARMA, B. C. JOSHI, A novel route for the synthesis of keto-benzoic acid derivatives, auxin transport inhibitors 875
PANDEY R. P. and T. UPRETI, Extension and comparison of collision factor theory and free length theory in liquid ternary mixtures 1071

PANOVICI I. I., voir LITEANU C. . . . 909
PAPAHAGI L., voir AVRAM R. . . . 1279
PATEL A. N., voir QURESHI A. M. . . . 151
PELINO M., voir FERRO D. . . . 9
PETRESCU N. and L. GANOVICI, Self-diffusion of tellurium in liquid Tl$_2$Te alloy . . . 55
— and L. GANOVICI, Self-diffusion of tellurium in the liquid Pb—Te eutectic alloy . . . 843
PETROVANU M., voir GEORGESCU EM. . . . 109
—, voir SURPĂŢEANU GH. . . . 1169
—, voir CONSTANTINESCU M. . . . 1451
PIACENTE V., voir FERRO D. . . . 9
PLOŞTINARU S. and P. SPACU, Mixed ligand compounds of lanthanides with neutral ligands containing donor oxygen atoms. III. Chlorosalicylates of lanthanides with 2,2′-dipyridyl-1,1′-dioxide . . . 65
POP C. D. M., voir VLĂDESCU L. . . . 1019
POPA M., voir VASILIU-OPREA C. . . . 291
POPA V. T. and E. SEGAL, Adsorption on heterogeneous surfaces: on the "Condensation approximation" . . . 185
POPESCU D. and V. GOŞA, R. H. SCHUSTER, N. I. IONESCU, D. OANCEA, The explosive combustion of the vinylacetylene-air mixtures initiated by a hot nickel—chromium wire . . . 197
—, voir URSEANU F. . . . 755
—, voir SCHUSTER R. H. . . . 819
—, and V. GOŞA, R. H. SCHUSTER, N. I. IONESCU, D. OANCEA, The explosive combustion of propylene. I. The explosion limits of propylene in air . . . 927
—, voir OANCEA D. . . . 933
—, voir GOŞA V. . . . 1205
PRADIP MANDAL K., voir SYAMAL A. . . . 1431
PRINCZ E., voir NIMARĂ A. . . . 967
PROŞTEANU N., voir ISAC D. . . . 29

Q

QURESHI A. M. and A. N. PATEL, A new acid-base indicator . . . 151

R

RACOŢI D., voir HUBCA GH. . . . 1327
RADHAKRISHNAN J., Investigations on the synthesis of *cis*-9,10-disubstituted decalins . . . 1305
RAJARAM J., voir CHITHAMBARATHANU PILLAI G. . . . 21
RASHID F. A., voir DOSS S. H. . . . 623
RASHWAN F., voir THARWAT M. . . . 491
RĂDULESCU N., voir VÂNTU V. . . . 269
RĂZUŞ A. C. and V. WERTHEIMER, A. M. GLATZ, ZS. ARVAY, F. BADEA, Kinetics of the thermal rearrangement of benzo[b]bicyclo[3.1.0]hex-2-en-4-yl derivatives . . . 457
—, voir BADEA F. . . . 629
RICART G. and G. GLACET, D. COUTURIER, Synthesis and stereochemistry of 2-dialkylamino-3-(2-tetrahydropyranyl)-tetrahydropyrans (in French) . . . 253
ROTARU P., voir STEINBRECHER G. . . . 1077
—, voir BUNESCU O. . . . 1393
RUSSU J., voir MATEI S. . . . 985

S

SAHINI V. E. and L. TELEA, CNDO/2 calculations of anisidine isomers . . . 3
SAHINI V. EM., voir WEINBERG J. . . . 521
SALEM S. M., voir SIDAHMED I. M. . . . 37
SALEM M. A. I., voir EL-DEEK M. . . . 647

— , voir ELKASABY M.A. 717
— , voir EL-DEEK M. 775
SALIU L., voir STEINBRECHER G. 1077
SĂLĂJAN M., voir CHIFU E. 1345
SAMAAN M., voir EL-DEEK M. 647
— , voir EL-DEEK M. 775
SĂNDULESCU I., voir NICOLESCU I. V. 217
SARAF S. D., Reaction of thionyl bromide with thiophenols 1457
SÂRBU C., voir VÂNTU V. 269
SATTI A. M., voir HASAN M. 979
SAYED A. M., voir MOHAMED M. M. 441
— , voir EL-KADI M. 1161
SCHELL H. C., voir MATEESCU M. A. 117
SCHMIDT W., voir DEMIAN A. M. 769
SCHUSTER R. H., voir POPESCU D. 197
— , Influence of medium on the solvolysis of alkyl halides. IX. Temperature dependence of linear salt effects in methanol-water ($X_{H_2O} = 0.359$) (in German) 675
SCHUSTER R. H. and N. I. IONESCU, D. OANCEA, D. POPESCU, V. GOȘA, The explosive combustion of propylene. II. Flame speed determination in tubes by photographic methods 819
— , voir POPESCU D. 927
— , voir OANCEA D. 933
— , Influence of the medium in the solvolysis of alkyl halides. VIII. Salt effects in the hydrolysis of *t*-butyl chloride (in German) 1091
— , voir GOȘA V. 1205
SEBE I., voir BREZEANU M. 1221
THE SECOND NATIONAL CONGRESS OF CHEMISTRY 1045
SEGAL E., voir V. T. POPA 185
— , voir TOMESCU M. 793
— , voir GIRGIS M. M. 1199
— , voir GIRGIS M. M. 1425
SENENT S. and L. FERRARI, A. ARRANZ, Kinetic study of the reduction of Cr(VI) by hydroxylamine (in Spanish) 377
SEOANE F., Temperature effect on the kinetics of the α-chimotrypsin-catalyzed hydrolysis of the ethyl ester of N-benzoyl-L-tyrosine (in Spanish) 539
SHABAN M. E., voir EL-HASHASH M.A. 101
SHARMA R., voir PANDE R. K. 875
SHOURKY A. F., voir ISSA R. M. 667
SHUKLA S. SMT., voir VARMA R. P. 1401
SIDAHMED I. M. and S. M. SALEM, F. M. ABDEL HALIM, Alkaline hydrolysis of formamide in water-organic solvent mixtures 37
SILAGHI-DUMITRESCU I., A simple topology-based method for estimating stretching force constants in AB_n molecules 1441
SIMON Z., voir ISAC D. 29
— , voir ISAC D. 341
SINDHWANI S. K., voir SINHA P. P. 917
SINGH K. and P. BAHADUR, P. BAHADUR, Effect of added salt on the colloidal behaviour of alkaline earth metal caprylates 389
SINGH C. P. and R. JAIN, A. C. OJHA, Synthesis of N^1-(substituted phenyl)-3-methyl-4-(substituted phenylazo)-2-pyrazolin-5-one 1011
SINHA P. P. and R. S. CHAWLA, S. K. SINDHWANI, F. KAMIL, Thiovioluric acid as an analytical reagent. Spectrophotometric and complexometric determination of copper (II) 917
SINISTERRA J. V. and J. LLAVINA, J. MOREY, J. M. MARINAS, Contribution to mechanism determination of esterification of aliphatic carboxylic acids, catalyzed by $ALPO_4$ and related systems (in Spanish) 415
SIROUSSE NOURI, voir GIRAUD J. 397
SOBHANADRI J., voir JOSYULU O. S. 687
SOLIMAN E. A., Some reactions of 2-[3-(3,4-dichlorophenyl)-2-pyrazolin-5-yl]-4*H*-benzoxazin-4-one 699
SOMAY M., voir MARCU GH. 575

SPACU P., voir PLOŞTINARU S. 65
SRIVASTAVA S. P. and A. KUMAR, V. K. GUPTA, Kinetics and mechanism of Ag(I) catalysed oxidation of hexane-1,6-diol by peroxydisulphate ion. 939
STEINBRECHER G. and P. ROTARU, L. SALIU, O. BUNESCU, N. MUREŞAN, I. BUCUR, Method for determining effective diffusion coefficient of gases in catalyst pellets 1077
STERNBERG S., voir DANES F. 1377
STOICESCU C., voir BĂLĂ C.. 861
SURPĂŢEANU GH. and M. CONSTANTINESCU, C. LUCHIAN, M. PETROVANU, I. ZUGRĂVESCU, A. LABLACHE-COMBIER, Theoretical study on the regioselectivity in the 1,3-dipolar cycloadditions of pyridinium-ylides to Z-substituted alkenes. 1169
— , voir CONSTANTINESCU M. 1451
SWAMY R. and H. S. YATHIRAJAN, D. S. MAHADEVAPPA, Kinetics and mechanism of oxidation of phenyl allyl alcohol by sodium N-chloro-benzene sulphonamide in hydrochloric acid medium 565
SYAMAL A., B. K. GUPTA, New dioxouranium (VI) complexes with bidentate ON donor Schiff bases derived from salicylaldehyde or substituted salicylaldehyde and benzoylhydrazide 857
SYAMAL A. and P. K. MANDAL, New cobalt (III) complexes containing trimethylenediamine, propylenediamine and other ligands 1431
ŞERBĂNESCU D. and GH. VASU, R. VÎLCU, A. CIOCHINĂ, Transient hot wire thermal conductivimeter for absolute measurements in fluids. 1047

T

TAMBI S. B. and R. K. JAIN, R. L. MITAL, Synthesis of some new fluorosubstituted tricyclic heterocyclics 477
TELEA L., voir SAHINI V. E. 3
TEOREANU I. and C. HRIŢCU, N. BUTUCESCU, L. BUCEA, Electronomicroscopical researches and thermal differential analysis of $4CaO \cdot Al_2O_3 \cdot Fe_2O_3$ and $2CaO \cdot Al_2O_3$ hydration at high temperatures and pressures (in French). 1213
THAKUR R. S., voir S. CALLA 1033
— , voir JAIMAN R. D. 1111
THARWAT M. and A. AWAD, F. RASHWAN, Effect of surfactants on kinetics of reduction of V(V) in universal buffer solutions at the dropping mercury electrode 491
THUY P. L., voir BANCIU M. 1115
TOLEA A., voir AIRINEI A. 1295
TOMESCU M., voir HUBCA GH. 1185
— and I. DEMETRESCU, E. SEGAL, Study on the thermal degradation of acrylic copolymers 793
TOTIR N. D., Kinetic studies of electrode processes using the method of half-lives. . . 811
TOWNSHEND A., voir BURGUERA M. 761
TRUONG THE KY, voir BACALOGLU I. 1135

U

UNGUREANU A., voir MARC M. 587
UPRETI T., voir PANDEY R. P. 1071
URSEANU F. and D. POPESCU, D. BRĂCĂCESCU, T. OLTEANU, Synthesis of dyes with dibenzo [*f*, *ij*] isoquinoline [2,3-b] quinazoline-5,10-dione structure 755

V

VÁRHELYI CS., voir MARCU GH. 575
— , voir MOHAMED ABDEL SALAM EL ABSY 1245
— , voir ZSAKÓ J. 1271
VARMA R. P. and SMT. S. SHUKLA, Solubility of iron (III) carboxylate in mixed organic solvents 1401

VASS M. I., voir CONŢESCU CR. . . . 175

VASILESCU D. S., Alternating tendency in copolymerization. V. Equimolecular copolymers and dimers of 1,1-diphenylethylene . . . 305

— , Alternating tendency in copolymerization. VI. Chain transfer for complexed monomers . . . 481

VASILIU-OPREA C. and M. POPA, Mechano-chemical reactions of poly(vinyl chloride). 9. Characterization of the obtained products by mixing PVC-S with aromatic diamines (in German) . . . 291

VASU GH., voir ŞERBĂNESCU D. . . . 1047

— , voir VÎLCU R. . . . 1355

VÂNTU V. and N. RĂDULESCU, M. IONESCU, C. SÂRBU, Leaving group effect in the reaction of 5-substituted-2-pentanones with sodium methoxide . . . 269

VĂŢULESCU R. and T. BUDIU, GH. MARCU, Heteropolytungstates with Ti(IV) and Ni(II). I. The formation of two new heteropolyanions with Ti(IV) and Ni(II) in solution . . . 851

— and T. BUDIU, GH. MARCU, Heteropolytungstates with Ti(IV) and Ni(II). II. The synthesis and basicity of heteropolyanions $[H_2ONiTiW_{11}O_{39}]^{6-}$ and $[H_2ONiTiW_5O_{20}]^{4-}$ . . . 971

VICOL O., voir CALU N. . . . 783

VISWANATHAN B., voir JOSYULU O. S. . . . 687

VÎLCU R. and A. CIOCHINĂ, Steady state hot wire thermal conductivity set-up for fluids . . . 161

— and A. CIOCHINĂ, Absolute measurement of thermal conductivity and thermal diffusivity of liquids by classical procedure of the transient hot-wire method . . . 527

— , voir ŞERBĂNESCU D. . . . 1047

— and A. CIOCHINĂ, GH. VASU, Absolute measurement of thermal conductivity of emulsions . . . 1355

VLĂDESCU L. and C. D. M. POP, Utilization of Ferron in separation and concentration of iron with ion exchange resins . . . 1019

W

WAKEEL I. A., voir HASSAN M. . . . 979

WEINBERG J. and V. EM. SAHINI, Xylidine isomers. V. Molecular complex spectra of iodine with xylidines . . . 521

WERTHEIMER V., voir RĂZUŞ A. C. . . . 457

Y

YATHIRAJAN H. S., voir SWAMY R. . . . 565

YOUSSEF M. S. K. and KH. M. HASSAN, Synthesis of some new thienylazetidin-2-ones and thienylthiazolidin-4-ones . . . 81

— , Synthesis of some new styryl oxazolophenoxazine cyanines . . . 427

— , Reaction of diazomethane with anils and mixed azines of thiophene aldehyde or isatin . . . 471

— , Cyclocondensation of mercaptoacetic acid with thienylidene anils . . . 1005

Z

ZAHARESCU M. and A. BRĂILEANU, The formation mechanism of the compounds in the $MgO-V_2O_5$ system . . . 1063

ZMIERCZAK W., voir DOMKA F. . . . 203

ZSAKÓ J. and T. LÁSZLÓ, Complex compounds of some diosphenolic type carotenoids. Astacene complexes. Spectrophotometric study of the system Fe(III)-astacene . . . 237

ZSAKÓ I., voir MOHAMED ABDEL SALAM EL ABSY . . . 1245

— and J. HORÁK, CS. VÁRHELYI, On the α-dioximine complexes of transition metals. LXIII. Spectrophotometric study on the stability of Fe(II) and Co(II) complexes of 1,2-cyclo-heptane and 1,2-cyclooctanedione dioximes . . . 1271

ZUGRĂVESCU I., voir GEORGESCU FL. . . . 879

— , voir SURPĂŢEANU GH. . . . 1169

INDEX DES SUJETS

Absolute measurement of thermal conductivity and thermal diffusivity of liquids by classical procedure of the transient hot-wire method, R. VÎLCU and A. CIOCHINĂ 527

Acid-base indicator, A new —, A. M. QURESHI and A. N. PATEL 151

Acrylic copolymers, Study on the thermal degradation of —, M. TOMESCU, I. DEMETRESCU and E. SEGAL 793

Acrylic monomers. III. Copolymerization of N,N-dimethylaminoethyl-methacrylate with N,N-diethylacrylamide, Reactivity of —, M. DIMA, S. OPREA and E. DUMITRIU 131

Adsorption of gases on solids, Concerning a recently proposed equation for the —, N. I. IONESCU 815

Adsorption on heterogeneous surfaces : on the "Condensation approximation", V. T. POPA and E. SEGAL 185

Alkaline hydrolysis of formamide in water — organic solvent mixtures, I. M. SIDAHMED, S. M. SALEM and F. M. ABDEL HALIM 37

Alkyl halides. VIII. Salt effects in the hydrolysis of *t*-butyl chloride, Influence of the medium in the solvolysis of — (in German), R. H. SCHUSTER 1091

Alternating tendency in copolymerization. VI. Chain transfer for complexed monomers, D. S. VASILESCU 481

Ammonia. II. Low temperature oxidation on a $Fe_2O_3-Cr_2O_3$ catalyst. Influence of the amount of the catalyst. Analysis of the reaction products, Catalytic oxidation of —, M. M. GIRGIS, D. P. LAZĂR and E. I. SEGAL 1199

Ammonia III. Low temperature oxidation on a $Fe_2O_3-Cr_2O_3$ catalyst ; evaluation of the experimental data in order to obtain kinetic parameters, Catalytic oxidation of —, M. M. GIRGIS, D. P. LAZĂR and E. I. SEGAL 1423

Anisidine isomers, CNDO/2 calculations of —, V. E. SAHINI and L. TELEA 3

Aromatic amides under mild conditions, A convenient new method for synthesis of —, C. I. CHIRIAC 1001

Aromatic hydrocarbons, active methylene compounds and Grignard reagents on α-3-benzylidene-5-[1′(2′-methylnaphthalenyl)]-2(3H) furanone and 4-benzylidene-1-*p*-tolyl-2-[1′(2′-methylnaphthalenyl)]-2-pyrroline-5-one, M. ABDALLA, A. ESSAWY, M. A. EL-HASHASH and A. M. EL-GENDY 95

Aromaticity index based on the exaltation of diamagnetic susceptibility, A new — (in French), J. GAYOSO and O. OUAMERALI 1035

Aryl propene oxides in basic media. II. Reactions of some *o*-substituted epoxides compared to *p*- and *m*-substituted analogues, Studies of the reactions of —, M. HASSAN, A.R.O. ABDEL NOUR, A. M. SATTI and I. A. WAKEEL 979

5-Aryl-2-thiono-1,3,4-oxadiazoles with some amino- and halo-compounds, Reaction of —, A. A. EL-BARBARY, M. ANWAR, A. A. GHATTAS and A. F. HASHEM 449

5-Aryl-2-thiono-1,3,4-thiadiazoles, Reactions of some —, M. ANWAR, F. I. ABDEL-HAY, A. A. EL-BARBARY and M. EL-BORAI 1127

Bismuth(III)-ethylenediaminetetraacetic acid complexes. III. Exchange reaction of Bi(III) from BiEDTA with Fe(III), A. NIMARA, E. PRINCZ and A. BALINT 967

BOOK REVIEWS 155, 156, 327, 328, 329, 330, 503, 504, 655, 801, 801, 1041, 1042, 1195, 1341, 1341, 1342, 1499

Bromobenzoyl acrylic acid and its amides, Some reactions with Michael adducts of —, A. ESSAWY, M. ABDALLA and a. DEEB 601

Butadiene and styrene with organolithium catalysts in toluene, Kinetics of anionic polymerization of —, E. CEAUȘESCU, R. BORDEIANU, I. CERCHEZ, M. BĂLĂNESCU and P. GHIOCA 509

Butan-2-one by vanadium(V) in aqueous perchlorate media. Kinetics and mechanism, The oxidation of —, G. CHITHAMBARATHANU PILLAI, J. RAJARAM and J. C. KURIACOSE 21

Carbon fibres, X-ray analysis of some —, I. DEMETRESCU and D. FĂTU 1387
Catalytic properties of $Fe_2O_3-Nd_2O_3$ system (in French), F. DOMKA, J. MICIUKIEWICZ and W. ZMIERCZAK 203
Cationic beaded PVA ion exchangers. I. Reticulation, derivatisation and some physical-chemical properties (in German), M. A. MATEESCU, H. C. SCHELL, M. DIMONIE, T. BENŢIA, C. DIMITRIU and O. MAIOR 117
Cerium (IV) with 3-phenylazohydroxylamine, Direct photometric determination of —, S. CALLA, S. P. MATHUR, R. S. THAKUR and C. S. BHANDARI 1033
Charge distributions situated into a continuum, infinite and isotropic medium, Interaction between two —, V. DAVID and Ş. MOLDOVEANU 333
Charge transfer complexes, Internal rotation in —, M. CIUREANU, F. CORNEA, C. CERCASOV and M. CONTINEANU 659
Charge transfer complexes of some pyridine derivatives with aromatic tri- and di-nitrocompounds, R. M. ISSA, N. T. ABDEL-GHANI, A. L. EL-ANSARY and A. F. SHOUKRY 667
Chemical equilibrium composition, An analysis of the effect of input data changes on the —, D. GEANĂ and F. DANEŞ 1365
Chemical equilibrium of methanol synthesis using state equations of gases at high pressure, Computation of —, F. E. DANEŞ and D. GEANĂ 947
Chemical equilibrium in multicomponent reaction systems, D. GEANĂ 43
Chemical graphs. XXXVII. A simple rule for classifying *peri*-condensed benzenoid hydrocarbons as closed-shell or open-shell (polyradicalic) systems using dualist (characteristic) graphs, A. T. BALABAN 407
Chemistry, The Second National Congress of —, ... 1045
α-Chimotrypsin-catalyzed hydrolysis of the ethyl ester of N-benzoyl-L-tyrosine, Temperature effect on the kinetics of the — (in Spanish), F. SEOANE 539
4-Chloro-quinazoline, 6-nitro- and 6-amino-4-3H-quinazolones, Some reactions of —, M. ANWAR, F. I. ABDEL-HAY, A. A. ELBARBARY and M. EL-BORAI . . 1469
Chromatographic observations, Quantitative analysis of —, A. J. CORPACIUS . . . 315
3-Cinnamoyl-4-phenyl-6-[1′(2′-methoxynaphtholenyl]-2-pyridone and of 2-methyl-(b)-2′-[α(β-methoxynaphthalenyl)-4′-phenyl-3′,4′-dihydropyridyl]-azochromone, Synthesis and reactions of—, A. ESSAWY, M. EL-GARBY YOUNES, M. M. BADRAN and A. Z. M. HEIKAL 245
Co(III) complex compounds with 3-amino-1-propanol and dimethylglyoxime, M. BREZEANU, J. JITARU and M. DINCULESCU 1097
Co(II) complex containing strongly electronegative donor atoms, A new bridged binuclear low-spin pentacoordinate, — A. C. BANCIU 1231
Cobalt(III) complex compounds with methylisopropyl-glyoxime, New —, GH. MARCU, CS. VÁRHELYI, M. SOMAY and D. AVRAMESCU 575
Cobalt(III) complexes containing trimethylenediamine, propylenediamine and other ligands, New —, A. SYAMAL and P. K. MANDAL 1431
Collision factor theory and free length theory in liquid ternary mixtures, Extension and comparison of —, R. P. PANDEY and T. UPRETI 1071
Colloidal behaviour of alkaline earth metal caprylates, Effect of added salt on the —, K. SINGH, P. BAHADUR and P. BAHADUR 389
Complex compounds of some diosphenolic type carotenoids. Astacene complexes. Spectrophotometric study of the system Fe(III) — astacene, J. ZSAKÓ and T. LÁSZLÓ . 237
Complex compounds of zirconium (IV) with azomethine, A. KRIZA and M. NASTA . . 693
Complex molybdenum—bismuth oxide catalyst with propylene, The reduction of a —, N. I. IONESCU, P. BANYAI, M. CĂLDĂRARU and M. CHIRCA 681
Complex of some transition metal ions with 4,5-dimethyl-2-hydroxy acetophenone and its oxime, Potentiometric studies on —, M. MITTAL, K. LAL and S. P. GUPTA . 1335
Conductivimeter for absolute measurements in fluids, Transient hot wire thermal —, D. ŞERBĂNESCU, GH. VASU, R. VÎLCU and A. CIOCHINĂ 1047
Copolymerization. V. Equimolecular copolymers and dimers of 1,1-diphenylethylene, Alternating tendency in —, D. S. VASILESCU 305
Copper(II) complexes with 10-[2-(dimethylamino)propyl]-phenothiazine, V. CIMPU, A. MEGHEA and I. JITARU 1261
Copper(II) complexes of threonine and allothreonine, E. BĂLĂ, M. S. IONESCU and C. STOICESCU 861
Coumarins, Synthesis and reactions of 6,7(4′-alkyl-α-pyrano)4-alkyl —, M. A. ELKASABY and M. A. I. SALEM 717

Cu(II) complex compounds with 1-(β-phenyl-β-amino) ethylcyclobutanol and 1-(β-*p*-chlorphenyl-β-amino) ethylcyclobutanol, M. BREZEANU, I. SEBE, M. GUŢUL and I. JITARU 1221

Cu(II)-thiocarbohydrazone systems in solution and their analytical application, The spectrophotometric study of some — , S. BARBU and C. GH. MACAROVICI . . 1255

3-Cyano-4-phenyl-6-[1′(2′-methoxynaphthalenyl)]-2-pyridone, Synthesis and some reactions of — , A. ESSAWY, M. EL-GARBY YOUNES and A. Z. M. HEIKAL . . 1141

Cyclic organosilicon compounds. II. Reaction of 1,4-dilithium-1,1,4-tetraphenylbutane with organotrichlorosilanes, N. LUCHIAN, A. CIOBANU and M. BOSTAN . . 1479

Cyclisation of the products of Stobbe condensation with 2,4-dimethylacetophenone, Studies on the — , M. M. MOHAMED, M. A. EL-HASHASH, M. A. SAYED and O. A. ABO-BAKER 441

Cyclocondensation of mercaptoacetic acid with thienylidene anils, M. S. K. YOUSSEF . 1005

Cyclohexene in the presence of new systems of supported nickel catalysts, Liquid-phase reduction of — , J. M. CAMPELO, D. LUNA and M. MARINAS 867

Decalins, Investigations on the synthesis of *cis*-9,10-disubstituted — , J. RADHAKRISHNAN 1305

2-Dialkylamino-3-(2-tetrahydropyranyl)-tetrahydropyrans, Synthesis and stereochemistry of — (in French), G. RICART, C. GLACET and D. COUTURIER . . . 253

Dialkyl disulphides, Synthesis of medium and higher — , S. CHORBADJIEV 1447

Diazomethane with anils and mixed azines of thiophene aldehyde or isatin, Reaction of — , M. S. K. YOUSSEF 471

Diazotiazion reaction. Electronic spectra and molecular orbital calculations for aromatic diazonium salts, Structure and reactivity in — , D. ISAC, M. MRACEC and Z. SIMON 341

Dibenzo[*c*, *e*] tricycl [$5.3.0.0^{2,10}$] deca-3,5-dien-9-ol into triphenylene derivatives, A rearrangement of — , M. BANCIU, PHAN LE THUY, M. ELIAN, C. DRĂGHICI and E. CIORĂNESCU 1115

2-[3-(3,4-Dichlorophenyl)-2-pyrazolin-5-yl]-4*H*-benzoxazin-4-one, Some reactions of —, E. A. SOLIMAN 699

Diffusion coefficient of gases in catalyst pellets, Method for determining effective — , G. STEINBRECHER, P. ROTARU, L. SALIU, O. BUNESCU, N. MUREŞAN and I. BUCUR 1077

α-Dioximine complexes of transition metals. LXIII. Spectrophotometric study on the stability of Fe(II) and Co(II) complexes of 1,2-cycloheptane- and 1,2-cyclooctanedione dioximes, On the — , J. ZSAKÓ, J. HORÁK and CS. VÁRHELYI 1271

Dioxouranium (VI) complexes with bidentate ON donor Schiff bases derived from salicylaldehyde or substituted salicylaldehyde and benzoylhydrazide, New — , A. SYAMAL and B. K. GUPTA 857

n-Dodecane in liquid phase with molecular oxygen in the presence of aluminium, lanthanum and cerium naphthenates, The oxidation of — , R. AVRAM, L. PAPAHAGI and I. ILIUŢĂ 1279

Dyes with dibenzo [*f*, *ij*] isoquinoline [2,3-b] quinazoline-5,10-dione structure, Synthesis of — , F. URSEANU, D. POPESCU, D. BRĂCĂCESCU and T. OLTEANU . . 755

Electrical conduction in nickel—alumina catalyst, O. BUNESCU, P. ROTARU and S. I. BLEJOIU 1393

Electrical conductivity of a complex bismuth—molybdenum catalyst in the reaction of propylene oxidation, M. CĂLDĂRARU, P. BANYAI and N. I. IONESCU . . . 837

Electrode processes using the method of half-lives, Kinetic studies of — , N. D. TOTIR . 811

Electronic spectra of some *trans*-α-cyno-2-styrylbenzimidazoles, The synthesis and the —, S. MATEI, J. RUSSU and P. COLŢEA 985

Electronomicroscopical researches and thermal differential analysis of $4CaO.Al_2O_3.Fe_2O_3$ and $2CaO.Al_2O_3$ hydration at high temperatures and pressures (in French), I. TEOREANU, C. HRIŢCU, N. BUTUCESCU and L. BUCEA 1213

Epoxidation of 2,6-diarylidenecyclohexanones and some reactions of the corresponding epoxides, M. M. HABASHY, A. ESSAWY and M. M. M. HAMAD 283

ESR and electronic study of the 1,4-benzo-*p*-dioxin[2,3-b] thioxanthone anion-radical, M. HILLEBRAND, I. BACIU and G. MAXIM 17

Esterification of aliphatic carboxylic acids, catalyzed by $AlPO_4$ and related systems, Contribution to mechanism determination of — , J. V. SINISTERRA, J. LLAVINA, J. MOREY and J. MARINAS 415

Explosive combustion of methane—air mixtures, Overall activation energy of —, D. OANCEA, D. POPESCU, V. GOȘA, R. H. SCHUSTER, N. I. IONESCU and F. CÎRJALIU 933

Explosive combustion of propylene. I. The explosion limits of propylene in air, The —, D. POPESCU, V. GOȘA, R. H. SCHUSTER, N. I. IONESCU and D. OANCEA. 927

Explosive combustion of propylene. II. Flame speed determination in tubes by photographic methods, The —, R. H. SCHUSTER, N. I. IONESCU, D. OANCEA, D. POPESCU and V. GOȘA 819

Explosive combustion of the vinylacetylene—air mixtures initiated by a hot nickel—chromium wire, The —, D. POPESCU, V. GOȘA, R. H. SCHUSTER, N. I. IONESCU and D. OANCEA 197

Explosive combustion of vinylacetylene-air mixtures initiated by hot platinum wire (in German), V. GOȘA, R. H. SCHUSTER, N. I. IONESCU, D. OANCEA and D. POPESCU 1205

Ferro-chromic catalyst for conversion of carbon monoxide by steam, Influence of alkali metal oxides on the formation of a —, F. DOMKA and M. LANIECKI 1085

Fluorosubstituted trycyclic heterocyclics, Synthesis of some new —, S. B. TAMBI, R. K. JAIN and R. L. MITAL 477

Frequentometric detection in different stability conditions of IR analytic systems, C. LITEANU and I. I. PANOVICI 909

Furanic derivatives from trioses, Preparation of polyfunctional —, J. SÁNCHEZ BALLESTEROS, D. J. McPHEE and F. HERNANDEZ HERNANDEZ . . 899

Heteropolytungstates with Ti(IV) and Ni(II). II. The synthesis and basicity of heteropolyanions $[H_2ONiTiW_{11}O_{39}]^{6-}$ and $[H_2ONiTiW_5O_{20}]^{4-}$, R. VĂȚULESCU, T. BUDIU and GH. MARCU 971

Heteropolytungstates with Ti(IV) and Ti(II). I. The formation of two new heteropolyanions with Ti(IV) and Ni(II) in solution, R. VĂȚULESCU, T. BUDIU and GH. MARCU 851

Hexane-1,6-diol by peroxydisulphate ion, Kinetics and mechanism of Ag(I) catalysed oxidation of —, S. P. SRIVASTAVA, A. KUMAR and V. K. GUPTA 939

Hydrazines, amines and thiourea upon β(4-chloro-3-methyl)-benzoylacrylic acid, Action of —, M. EL-KADI, M. A. EL-HASHASH and M. A. SAYED 1161

Hydrocracking activity of cobalt—molybden, alumina and nickel—molybdenum/alumina catalysts, Comparison between the —, F. Y. EL-KADY 1413

Ion exchange in the system Na_2WO_4 (solution)-Amberlite IR 120(H^+). II. Polytungstic acid T (in French), C. CALU, N. CALU and A. ONU 955

Iron(III) carboxylate in mixed organic solvents, Solubility of —, R. P. VARMA and S. S. SHUKLA 1401

Iron(III)-N-acetyl-N-m-tolylhydroxylamine-complexes, R. D. JAIMAN, S. CALLA, S. P. MATHUR and R. S. THAKUR 1111

Iron with ion exchange resins, Utilization of Ferron in separation and concentration of —, L. VLĂDESCU and C. D. M. POP 1019

Isopropylidene-D-glyceraldehyde with active methylenes, Study and transformations of the condensation products of —, J. SÁNCHEZ BALLESTEROS, F. HERNANDEZ HERNANDEZ and D. J. McPHEE 705

Iron-chromium oxide catalysts for water gas shift reaction, The effect of synthesis conditions on the activity of —, F. DOMKA and M. ŁANIECKI 211

Keto-benzoic acid derivatives, auxin transport inhibitors, A novel route for the synthesis of —, R. K. PANDE, R. SHARMA and B. C. JOSHI 875

L-alanine, L-serine, tyrosine and histidine with a Cu^{2+} sensitive electrode, Potentiometric determination of —, M. MIOȘCU, I. HAIDUC and D. C. CÖRMÖS . . . 1487

Lanthanides with neutral ligands containing donor oxygen atoms. III. Chlorosalicylates of lanthanides with 2,2′-dipyridyl-1,1′-dioxide, Mixed ligand compounds of —, S. PLOȘTINARU and P. SPACU 65

Lattice constant and saturation magnetization of cobalt zinc ferrites and magnesium zinc ferrite, O. S. JOSYULU, J. SOBHANDRI and B. VISWANATHAN . . 687

Leaving group effect in the reaction of 5-substituted-2-pentanones with sodium methoxide, V. VÂNTU, N. RĂDULESCU, M. IONESCU and C. SÂRBU 269

Long-range interaction of two molecules in the presence of a *Kirkwood* perturbational field, The —, V. DAVID and Ș. MOLDOVEANU 805

Macromolecules at charged interfaces, Adsorption effects of some natural and synthetic —, A. AWAD, F. EL-CHEICH and A. ABD EL-GABER 1025

Malachite green in the reaction with the tetrachloroauric anion, Reactivity of substituted (in French) — , GH. CONSTANTINESCU and C. CONSTANTINESCU . . . 1177
Membrane potential, An extension of the Staverman/Scatchard thermodynamic theory of — , F. DANEŞ, S. STERNBERG and S. DANEŞ 1377
6-[1′(2′-Methyl naphthenyl)]-2,3,4,5 tetrahydropyridazin-3-one, Some reactions of —, A. ESSAWY, M. A. EL-HASHASH, M. M. ABDALLA and A. M. EL-GENDY 1285
10-Methyl-9 methylene-dihydroacridine-ω-aldehyde, Attempts towards the synthesis of — (in German), K. KOKKINOS and C. MARKOPOULOS 733
3,4-Methylenedioxybenzylidene-*p*-isopropylacetophenone, Some reactions of —, M. A. EL-HASHASH, M. E. SHABAN and M. M. HABASHY 101
$MgO-V_2O_5$ system, The formation mechanism of the compounds in the — , M. ZAHARESCU and A. BRĂILEANU 1063
Mixtures belonging to the $Na_2O-CaO-Al_2O_3-SiO_2-CO_2$ system, Kinetics and reaction mechanism of chemical compounds in — , R. DINESCU and V. M. CERCHEZ . . 545
Mixtures, Rapid photometric determination of absorbing substances in — (in German), A. M. DEMIAN and W. SCHMIDT 769
Modern Friedel-Crafts chemistry. IX. On the cycloalkylation of aryl alkenyl ketones and other related systems, A. A. KHALAF and A. M. A. EL-KHAWAGA. 739
Nickel(II) and manganese(II) complexes of cystine, M. MARC and A. UNGUREANU . . 587
Nitriles. XXIII. Kinetics and mechanism of the formation of 2-aminobenzoxazole from *o*-aminophenol and phenylcyanate. Structure and reactivity of hetero-substituted — , (in German), I. BACALOGLU, TRUONG THE KY, H. H. GLATT, C. BOERIU, R. BACALOGLU and D. MARTIN 1135
2-Nitroanilines, The influence of the solvent on the electronic absorption spectra of some n-substituted — , A. AIRINEI, D. DOROHOI and A. TOLEA 1295
Nitro-bis-acetylacetonato-cobalt (III) compounds, Studies on some — ,M. A. S. EL ABSY, GH. MARCU, J. ZSAKÓ and CS. VÁRHELYI 1245
Nonmetals using volatilization systems, Analysis by molecular emission in cavity for the determination of — (in Spanish), M. BURGUERA, J. L. BURGUERA and A. TOWNSHEND. 761
Nucleophilic substitutions at carbonic acid derivatives. XVIII. Kinetics and mechanism of the alcoholysis of N,N,N′-trisubstituted carbonic acid chloramidines, R. BACALOGLU, A. CHICU, I. BACALOGLU and I. COTARCĂ 611
Nucleophilic substitutions to carbonic acid derivatives. XVII. Kinetics and mechanism of the hydrolysis of N,N,N′-trisubstituted carbonic acid chloramide, A. CHICU and R. BACALOGLU 435
Osmium—quinisatine oxime reaction, Studies on — , M. S. MASOUD, M. M. OSMAN and H. A. EL-NAGGAR 961
Oxidation of phenyl allyl alcohol by sodium N-chloro-benzene sulphonamide in hydrochloric acid medium, Kinetics and mechanism of — , R. SWAMY, H. S. YATHIRAJAN and D. S. MAHADEVAPPA 565
Oxidative dehydrogenation of n-butenes in butadiene, Relations between the methods of preparation, properties and activity of Bi—Mo—Fe—O catalyst in — , I. V. NICOLESCU and I. SĂNDULESCU 217
Palladium (II) with 1-(*p*-nitrophenyl), 3-(*p′*-azobenzene)-triazene and 1-(*p*-nitronaphthyl), 3-(*p′*-azobenzene)-triazene, Study of extraction and complexing of — , A. FL. DĂNEŢ 141
Periodic table based on the Eddington number, An estimate of the cupper limit of the — , D. BONCHEV and O. MEKENYAN 349
Phase equilibrium in chemical reaction systems, On the problem of — , D. GEANĂ . . . 363
Phenazathionium cations. III. The selective nucleophilic substitutions on phenazathionium cations, M. V. DIUDEA 725
Phenazathionium cations. IV. Demonstration on the structure of 1,3,7-trisubstituted derivatives of phenothiazine by mass spectrometry and ^1H-NMR, M. V. DIUDEA 887
1-Phenyl-3,5-pyrazolidinedione, Reactions of — , M. ANWAR and F. I. ABDEL-HAY . 993
Polyethylene. IX. Study of the transforming branches by step calorimetric system, Amorphous-crystalline coupling in — , GH. DRĂGAN 1315
Polyethylene glycol dimethacrylates. I. Study of synthesis process of polyethylene glycol dimethacrylates, Synthesis and polymerization of — , GH. HUBCA, CR. OPRESCU, M. TOMESCU and M. DIMONIE 1185
Polyethylene glycol dimethacrylate. II. Kinetics of the transesterification process of methylmethacrylate with polyglycols, Synthesis and polymerization of — , GH. HUBCA, D. RACOŢI, CR. OPRESCU and M. DIMONIE 1327

Polyethylene glycol dimethacrylates. III. Analysis of kinetic data obtained by transesterification of methyl methacrylate with polyglycols, Synthesis and polymerization of — , GH. HUBCA, CR. OPRESCU and M. DIMONIE 1493

Poly-1,3,4-oxadiazoles. IX. Ordered poly-1,3,4-oxadiazole-amide-imides, M. BRUMĂ and G. NEAMŢU 87

Poly(vinyl chloride).9. Characterization of the obtained products by mixing PVC—S with aromatic diamines, Mechano-chemical reactions of — (in German), C. VASILIU-OPREA and M. POPA 291

Polyvinyl chloride in heavy fields of nuclear radiations, Experimental studies bearing upon the behaviour of — , D. GAVRILĂ 125

Proton magnetic resonance spectra of some di- and triorganotion mono- and dithiocarboxylates, V. COLDEA, M. COLDEA and I. HAIDUC 71

2-Pyrozolin-5-one, Synthesis of N^1-(substituted phenyl)-3-methyl-4-(substituted phenylazo)-2-pyrazolin-5-one, G. P. SINGH, R. JAIN and A. C. OJHA 1011

Pyridinium-ylids. II. The reactions of some carbanion-monosubstituted 4-phenylpyridinium-ylids with activated acetylenes (in French), F. GEORGESCU, F. CHIRALEU, E. GEORGESCU and I. ZUGRĂVESCU 879

Pyridinium-ylides to Z-substituted alkenes, Theoretical study on the regioselectivity in the 1,3-dipolar cycloadditions of —, GH. SURPĂŢEANU, M. CONSTANTINESCU, C. LUCHIAN, M. PETROVANU, I. ZUGRĂVESCU and A. LABLACHE-COMBIER 1169

Pyridones. I. Synthesis and reactions of 3-acetyl-(3,4-dichlorophenyl)-2-(1H)-pyridones, M. EL-DEEK, M. A. I. SALEM, A. A. HAMED and M. SAMAAN. 647

Pyridones. II. Synthesis and reactions of 6-(3,4-dichlorophenyl)-3-(substituted cinnamoyl)-4-aryl-2(1*H*)-pyridones, Studies on — , M. EL-DEEK, M. A. I. SALEM, A. A. HAMED and M. SAMAAN 775

Quinazoline series. I. Synthesis of pyrrolo[1,2-c] quinazolines, Dipolar derivatives in the — (in French), EM. GEORGESCU, I. DRUŢĂ and M. PETROVANU. . . 109

4(3H) Quinazolinones, Reactions of some — , M. ANWAR 639

Radicalic cyclizations of unsaturated aldehydes (in French), M. CHATZOPOULOS and J. P. MONTHEARD 275

Reduction of Cr(VI) by hydroxylamine, Kinetic study of the — (in Spanish), S. SENENT, L. FERRARI and A. ARRANZ 377

Reduction of V(V) in universal buffer solutions at the dropping mercury electrode, Effect of surfactants on kinetics of — , M. THARWAT, A. AWAD and F. RASHWAN. 491

Regioselectivity in 1,3-dipolar cycloadditions of pyridinium-ylides to acetylenic dipolarophiles, Theoretical aspects on the — , M. CONSTANTINESCU, GH. SURPĂŢEANU, C. LUCHIAN, M. PETROVANU and I. ZUGRĂVESCU 1451

Ring opening in benzo[b] bicyclo[3.1.0] hexyl cations, F. BADEA, A. M. GLATZ and A. C. RĂZUŞ 629

Salt at high concentrations in pure water, The activity of one — (in French), M. A. ABRAHAM 829

Self-diffusion of tellurium in the liquid Pb—Te eutectic alloy, N. PETRESCU and L. GANOVICI 843

Self-diffusion of tellurium in liquid Tl_2Te alloy, N. PETRESCU and L. GANOVICI. . . 55

Silver layers adsorbed on tungsten. II. Surface structure and surface migration, FEM study of — , CR. CONŢESCU and M. I. VASS 175

Silver layers adsorbed on tungsten. III. Silver layer growth modes, FEM study of — , CR. CONŢESCU 355

Solvolysis of alkyl halides. IX. Temperature dependence of linear salt effects in methanol-water ($X_{H_2O} = 0.359$), Influence of medium on the — (in German), R. H. SCHUSTER 675

Spectral solvent effects in aromatic compound solutions. VII. Solvent effects on the benzonitrile band at $\sim$ 260 nm, V. MACOVEI 1405

Spectrophotometric analysis. I. Computational equations for the dosage of some dyestuffs in mixtures, New aspects in the — , N. CALU and O. VICOL. 783

Steam cracking of 6-methyleicosane, On the — , J. GIRAUD, S. NOURI and B. BLOURI 397

Styryl oxazolophenoxazine cyanines, Synthesis of some new — , M. S. K. YOUSSEF. . 427

Sultam compounds, Identification of two organic—, S. H. DOSS and F. A. RASHID. . 623

Surface mobility of surfactant solutions. IX. Surface and capillary flow between drops linked by surface canals, E. CHIFU, Z. FINŢA, M. SALAJAN and E. GAVRILĂ 1345

Thermal conductivity of emulsions, Absolute measurement of — , R. VÎLCU, A. CIOCHINĂ and GH. VASU 1355

Thermal conductivity set-up for fluids, Steady stat hot wire — , R. VÎLCU and A. CIOCHINĂ 161

Thermal and photochemical decomposition of aromatic diazonium salts, The kinetics of — , D. ISAC, M. MRACEC, N. PROŞTEANU and Z. SIMON 29

Thermal rearrangement of benzo[b]bicyclo[3.1.0] hex-2-en-4-yl derivatives, Kinetics of the — , A. C. RĂZUŞ, V. WERTHEIMER, A. M. GLATZ, ZS. ARVAY and F. BADEA 457

Thermogravimetrical analysis of some complex compounds of thiobisnaphtol (in French), L. ODOCHIAN, E. MIHAI, S. FIŞEL and O. MITOŞERIU 383

Thienylazetidin-2-ones and thienylthiazolidin-4-ones, Synthesis of some new — , M. S. K. YOUSSEF and KH. M. HASSAN 81

Thioethers, Novel aromatic — (in French), M. IOVU and E. BĂDĂU 1149

Thiophenols, Reaction of thionyl bromide with — , S. M. SARAF 1457

Thiovioluric acid as an analytical reagent. Spectrophotometric and complexometric determination of copper (II), P. P. SINHA, R. S. CHAWLA, S. K. SINDWANI and F. KAMIL 917

Tin(IV) peroxydichromate, Kinetics of self-decomposition of — , S. P. S. JADON. . . 1107

Topological indices intercorrelations, physical meaning, correlational ability, I. MOŢOC and A. T. BALABAN 593

Topology-based method for estimating stretching force constants in AB_n molecules, A simple — , I. SILAGHI-DUMITRESCU 1441

Transition metal complexes with pyridine derivatives. Extraction of the Co(II), Ni(II) and Zn(II) complexes of 3,5-dimethylpyridine, A study for optimum conditions of extraction of — , B. LENARCIK and E. BEZAK 229

Trinitrophenylene diamines, N,N′-substituted — , M. IOVU and E. IONESCU. . . . 1461

Vapour pressure of β-bromonaphthalene, Measurements of the — , D. FERRO, V. PIACENTE and M. PELINO 9

Xylidine isomers. V. Molecular complex spectra of iodine with xylidines, J. WEINBERG and V. EM. SAHINI 521

NOTE POUR LES AUTEURS

La Revue Roumaine de Chimie publie des articles en anglais, français, russe, allemand ou espagnol. Les auteurs sont priés d'envoyer des articles et des comptes rendus inédits.

Les manuscrits seront dactylographiés à deux intervalles. La bibliographie, les tableaux et la légende des figures seront placés après le texte.

Si l'article fait partie d'une serie numérotée, la partie précédente sera donnée comme première référence.

Chaque article sera précédé d'un résumé comprenant quinze lignes au maximum.

Les références bibliographiques dans le texte seront faites par des exposants sans parenthèses et paraîtront à la fin de l'ouvrage.

Les publications périodiques mentionnées dans la bibliographie seront présentées suivant les prescriptions internationales ; le nom de l'auteur précédé des l'initiale du prénom, le titre du périodique abrégé conformément à « Chemical Abstracts » et souligné par une ligne, le numéro du tome indiqué par des chiffres arabes et souligné par deux lignes, suivi de la première page de l'article : à la fin, l'année de la parution sera placée entre parenthèses. Le numéro de la revue ne sera pas indiqué si les pages du volume sont numérotées consécutivement.

Les textes des livres ou traités inclueront : les noms des auteurs, précédé des l'initiales du prénom, le titre du livre entre guillements et sans être souligné, le numéro du tome précédé par l'abréviation « vol » (ou « Bd »), le numéro de l'édition, les éditions (the publisher), la localité de la parution du livre, l'année de la parution et la page de la référence précédée(s) par l'abréviation « p » (ou « S »).

Les brevets seront indiqués comme suit : L'auteur ou la firme, le pays et le numéro du brevet, la date et la revue *(Chem. Abstr.)* . Par ex. : M. Jones (to Union Carbide Co.), *Brit. Pat.* 601 238, 2 Sept. 1959, *Chem. Abstr.*, **54**, 12808 (1960).

Si la référence n'a pas été lue en original, on indiquera aussi la revue de références consultée.

Les diagrammes seront tracés à l'encre de Chine sur papier calque. Les tableaux et les figures (en nombre strictement nécessaire) ainsi que les courbes dans les figures seront numérotés par des chiffres arabes. Leur explication sera donnée dans la légende des figures. Prière de ne pas inscrire les même données dans les tableaux et les figures. Chaque tableau aura un titre. On indiquera dans le texte la place approximative des tableaux et des figures. Les formules chimiques seront incluses dans le texte : en outre, elle seront transcrites sur papier calque, à l'encre de Chine.

Les auteurs sont priés d'indiquer les caractères italiques (en soulignant les lettres au crayon), ainsi que tout autre caractère spécial : les préfixes *ortho*, *meta*, *para*, *cis*, *trans*, etc. seront soulignés pour indiquer leurs caractères italiques et ne seront jamais écrits avec des majuscules.

Aucune correction à la main ne sera admise sur le manuscrit. Les corrections seront frappées à la machine. Les lettres grecques ou d'autres symboles spéciaux seront insérés à la main à l'encre clairement.

Le manuscrit sera signé par l'auteur.

Le collone-titre aura 50 lettres au maximum.

L'entière responsabilité du contenu des articles appartient aux auteurs.

Sur demande on peut obtenir un note plus complète.

PRINTED IN ROMANIA

1982 APR 29

TRAVAUX PARUS AUX ÉDITIONS DE L'ACADÉMIE DE LA RÉPUBLIQUE SOCIALISTE DE ROUMANIE

ELENA CEAUŞESCU, **Noi cercetări în domeniul compuşilor macromoleculari** (Nouvelles recherches dans le domaine des composés macromoléculaires), 1981, 536 p.

I. G. MURGULESCU, TATIANA ONCESCU, E. SEGAL, **Introducere în chimia fizică. Vol. II.2. Cinetică chimică şi cataliză** (Introduction à la chimie physique. Vol. II.2. Cinétique chimique et catalyse), 1981, 1024 p.

V. DRĂGUŢAN, A. T. BALABAN, M. DIMONIE, **Metateza olefinelor şi polimerizarea prin deschidere de inel a cicloolefinelor** (La métathése des oléfines et la polymérisation par ouverture annulaire des cyclooléfines), 1981, 254 p.

O. IORDACHE, **Procese polistocastice aplicate la fenomenele de transfer** (Processus polystochastiques appliqués aux phénomènes de transfert), 1981, 187 p.

ELENA CEAUŞESCU, **Polimerizarea stereospecifică a izoprenului** (La polymérisation stéréospécifique de l'isoprène), 1979, 307 p.

CR. SIMIONESCU, VALERIA GORDUZA, **Polimeri biocompatibili şi biologic activi** (Polyméres biocompatibles et biologiquement actifs), 1980, 497 p.

Ş. MOLDOVEANU, A. SAVIN, **Aplicaţii în chimie ale metodelor semiempirice de orbitali moleculari** (Applications en chimie des méthodes semi-empiriques d'orbitaux moléculaires), 1980, 286 p.

M. FLORESCU, **Metode ştiinţifice în dezvoltarea industriei chimice moderne** (Méthodes scientifiques dans le développement de l'industrie chimique moderne), 1979, 256 p.

A. T. BALABAN, I. GĂLĂŢEANU, G. GEORGESCU, LIGIA SIMIONESCU, **Compuşi marcaţi şi radiofarmaceutici cu aplicaţii în medicina nucleară** (Composés marqués et radiopharmaceutiques à application en médicine nucléaire), 1979, 495 p.

CONST. GH. MACAROVICI, **Analiza chimică cantitativă anorganică** (L'Analyse chimique quantitative inorganique), 1979, 457 p.

I. G. MURGULESCU, E. SEGAL, **Introducere în chimia fizică, vol. II. 1. Teoria moleculară cinetică a materiei** (Introduction à la chimie physique, IIe vol. 1. La théorie moléculaire-cinétique de la matière), 1979, 1036 p.

I. E. TEODORESCU, MARIA FITI, **Iradierea tehnologică** (L'Irradiation technologique), 1979, 216 p.

S. STERNBERG, FL. DANEŞ. **Termodinamica chimică aplicată** (La thermodynamique chimique appliquée), 1978, 400 p.

I. G. MURGULESCU, V. EM. SAHINI, **Introducere în chimia fizică, Vol. I.2. Structura şi proprietăţile moleculelor** (Introduction à la chimie physique. Vol. I.2. La structure et les propriétés des molècules), 1978, 604 p.

C. DRĂGULESCU, E. PETROVICI, **Chimie structurală modernă. Chimia coordinanţei 8** (La chimie structurale moderne. La chimie de la coordinence 8), 1977, 947 p.

D. PURDELA (sous la direction de), **Nomenclatura chimiei anorganice** (La nomenclature de la chimie inorganique), 1977, 153 p.

I. ZUGRĂVESCU, MAGDA PETROVANU, **N-ylid chemistry,** coédition avec McGraw Hill International Book Company, U.S.A., 1977, 396 p.

I. G. MURGULESCU, **Introducere în chimia fizică. Vol. I.1. Atomi, molecule, legătură chimică** (Introduction à la chimie physique, Ier vol. 1. Atomes, molécules, liaison chimique), 1976, 560 p.

CONST. GH. MACAROVICI, D. MACAROVICI, **Chimia oxizilor dubli şi utilizările lor** (La chimie des oxydes doubles et leur utilisation), 1975, 195 p.

ELENA CEAUŞESCU, **Research work on synthesis and characterization of macromolecular compounds. Contributions,** 1974, 251 p.

CR. SIMIONESCU, VIORICA RUSAN, V. POPA, **Chimia algelor marine** (La chimie des algues marines), 1974, 212 p., 1 pl.

I. P. „INFORMAŢIA" c. 1418

43 426

Lei 25.—

$ 55 (price per year)